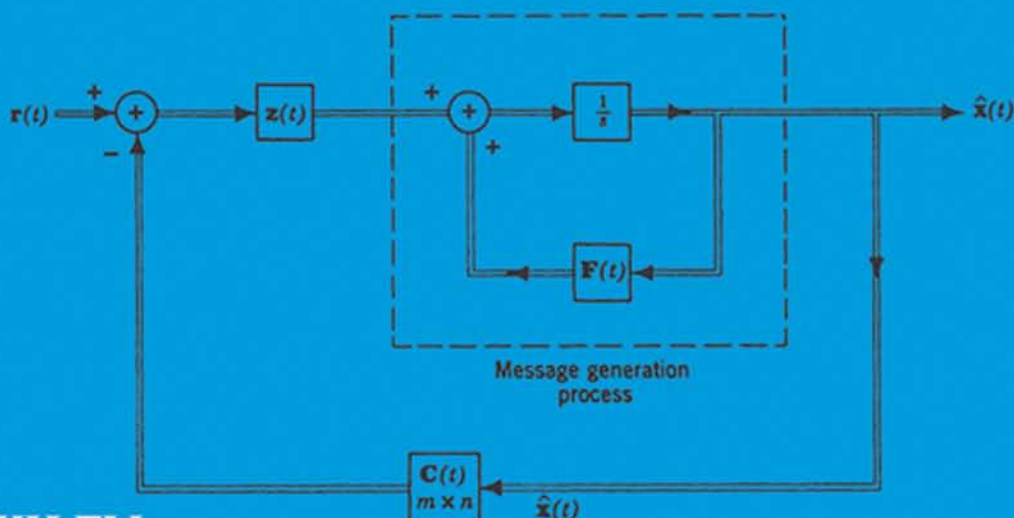
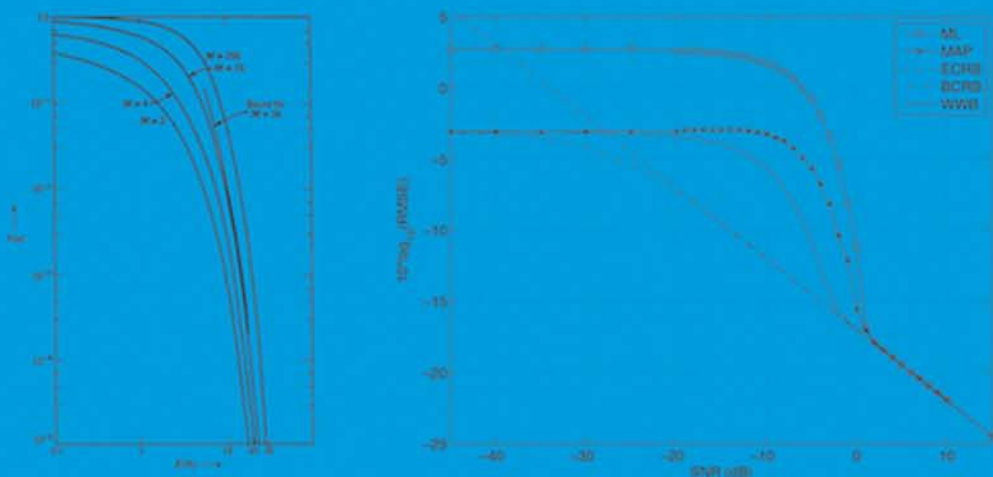


DETECTION, ESTIMATION, AND MODULATION THEORY

PART 1 - Detection, Estimation, and Filtering Theory

HARRY L. VAN TREES • KRISTINE L. BELL
with ZHI TIAN



Detection, Estimation, and Modulation Theory

Part I: Detection, Estimation, and Filtering Theory

Second Edition

Detection, Estimation, and Modulation Theory

Part I: Detection, Estimation, and Filtering Theory

Second Edition

**HARRY L. VAN TREES
KRISTINE L. BELL
with
ZHI TIAN**

WILEY

Copyright © 2013 by John Wiley & Sons, Inc. All rights reserved.

Published by John Wiley & Sons, Inc., Hoboken, New Jersey.

Published simultaneously in Canada.

No part of this publication may be reproduced, stored in a retrieval system, or transmitted in any form or by any means, electronic, mechanical, photocopying, recording, scanning, or otherwise, except as permitted under Section 107 or 108 of the 1976 United States Copyright Act, without either the prior written permission of the Publisher, or authorization through payment of the appropriate per-copy fee to the Copyright Clearance Center, Inc., 222 Rosewood Drive, Danvers, MA 01923, (978) 750-8400, fax (978) 750-4470, or on the web at www.copyright.com. Requests to the Publisher for permission should be addressed to the Permissions Department, John Wiley & Sons, Inc., 111 River Street, Hoboken, NJ 07030, (201) 748-6011, fax (201) 748-6008, or online at <http://www.wiley.com/go/permission>.

Limit of Liability/Disclaimer of Warranty: While the publisher and author have used their best efforts in preparing this book, they make no representations or warranties with respect to the accuracy or completeness of the contents of this book and specifically disclaim any implied warranties of merchantability or fitness for a particular purpose. No warranty may be created or extended by sales representatives or written sales materials. The advice and strategies contained herein may not be suitable for your situation. You should consult with a professional where appropriate. Neither the publisher nor author shall be liable for any loss of profit or any other commercial damages, including but not limited to special, incidental, consequential, or other damages.

For general information on our other products and services or for technical support, please contact our Customer Care Department within the United States at (800) 762-2974, outside the United States at (317) 572-3993 or fax (317) 572-4002.

Wiley also publishes its books in a variety of electronic formats. Some content that appears in print may not be available in electronic formats. For more information about Wiley products, visit our web site at www.wiley.com.

Library of Congress Cataloging-in-Publication Data:

Van Trees, Harry L.

Detection estimation and modulation theory. – Second edition / Harry L. Van Trees, Kristine L. Bell, Zhi Tian.

pages cm

Includes bibliographical references and index.

ISBN 978-0-470-54296-5 (cloth)

1. Signal theory (Telecommunication)
2. Modulation (Electronics)
3. Estimation theory. I. Bell, Kristine L. II. Tian, Zhi, 1972- III. Title.

TK5102.5.V3 2013

621.382'2–dc23

2012036672

Printed in the United States of America

10 9 8 7 6 5 4 3 2 1

To my mentors at Massachusetts Institute of Technology; Professors Yuk Wing Lee, Norbert Weiner, Wilbur Davenport, and Amar Bose; to my colleagues at M.I.T., Arthur Baggeroer, Lewis Collins, Estil Hoversten, and Donald Snyder whose critiques and contributions greatly enhanced the first edition; and to my wife, Diane Enright Van Trees who has patiently accommodated the time that I have spent over the years on DEMT.

Harry Van Trees

To Harry Van Trees, whose knowledge and guidance have shaped my professional development in immeasurable ways for nearly 30 years. It has been an honor to collaborate on this second edition of a truly classic textbook. And to my husband Jamie, my daughters Julie and Lisa, and parents Richard and Jean LaCroix, who are my foundation.

Kristine L. Bell

Contents

Preface	xv
Preface to the First Edition	xix
1 Introduction	1
1.1 Introduction	1
1.2 Topical Outline	1
1.3 Possible Approaches	11
1.4 Organization	14
2 Classical Detection Theory	17
2.1 Introduction	17
2.2 Simple Binary Hypothesis Tests	20
2.2.1 Decision Criteria	20
2.2.2 Performance: Receiver Operating Characteristic	35
2.3 M Hypotheses	51
2.4 Performance Bounds and Approximations	63
2.5 Monte Carlo Simulation	80
2.5.1 Monte Carlo Simulation Techniques	80
2.5.2 Importance Sampling	86
2.5.2.1 Simulation of P_F	87
2.5.2.2 Simulation of P_M	91
2.5.2.3 Independent Observations	94
2.5.2.4 Simulation of the ROC	94
2.5.2.5 Examples	96
2.5.2.6 Iterative Importance Sampling	106
2.5.3 Summary	108
2.6 Summary	109
2.7 Problems	110
3 General Gaussian Detection	125
3.1 Detection of Gaussian Random Vectors	126
3.1.1 Real Gaussian Random Vectors	126
3.1.2 Circular Complex Gaussian Random Vectors	127

3.1.3	General Gaussian Detection	132
3.1.3.1	Real Gaussian Vectors	132
3.1.3.2	Circular Complex Gaussian Vectors	136
3.1.3.3	Summary	137
3.2	Equal Covariance Matrices	138
3.2.1	Independent Components with Equal Variance	142
3.2.2	Independent Components with Unequal Variances	146
3.2.3	General Case: Eigendecomposition	147
3.2.4	Optimum Signal Design	156
3.2.5	Interference Matrix: Estimator–Subtractor	160
3.2.6	Low-Rank Models	165
3.2.7	Summary	173
3.3	Equal Mean Vectors	174
3.3.1	Diagonal Covariance Matrix on H_0 : Equal Variance	175
3.3.1.1	Independent, Identically Distributed Signal Components	177
3.3.1.2	Independent Signal Components: Unequal Variances	178
3.3.1.3	Correlated Signal Components	179
3.3.1.4	Low-Rank Signal Model	184
3.3.1.5	Symmetric Hypotheses, Uncorrelated Noise	186
3.3.2	Nondiagonal Covariance Matrix on H_0	191
3.3.2.1	Signal on H_1 Only	191
3.3.2.2	Signal on Both Hypotheses	195
3.3.3	Summary	196
3.4	General Gaussian	197
3.4.1	Real Gaussian Model	197
3.4.2	Circular Complex Gaussian Model	198
3.4.3	Single Quadratic Form	201
3.4.4	Summary	208
3.5	M Hypotheses	209
3.6	Summary	213
3.7	Problems	215
4	Classical Parameter Estimation	230
4.1	Introduction	230
4.2	Scalar Parameter Estimation	232
4.2.1	Random Parameters: Bayes Estimation	232
4.2.2	Nonrandom Parameter Estimation	246
4.2.3	Bayesian Bounds	261
4.2.3.1	Lower Bound on the MSE	261
4.2.3.2	Asymptotic Behavior	265
4.2.4	Case Study	268
4.2.5	Exponential Family	279
4.2.5.1	Nonrandom Parameters	279
4.2.5.2	Random Parameters	287
4.2.6	Summary of Scalar Parameter Estimation	292

4.3	Multiple Parameter Estimation	293
4.3.1	Estimation Procedures	293
4.3.1.1	Random Parameters	293
4.3.1.2	Nonrandom Parameters	296
4.3.2	Measures of Error	296
4.3.2.1	Nonrandom Parameters	296
4.3.2.2	Random Parameters	299
4.3.3	Bounds on Estimation Error	299
4.3.3.1	Nonrandom Parameters	299
4.3.3.2	Random Parameters	316
4.3.4	Exponential Family	321
4.3.4.1	Nonrandom Parameters	321
4.3.4.2	Random Parameters	324
4.3.5	Nuisance Parameters	325
4.3.5.1	Nonrandom Parameters	325
4.3.5.2	Random Parameters	326
4.3.5.3	Hybrid Parameters	328
4.3.6	Hybrid Parameters	328
4.3.6.1	Joint ML and MAP Estimation	329
4.3.6.2	Nuisance Parameters	331
4.3.7	Summary of Multiple Parameter Estimation	331
4.4	Global Bayesian Bounds	332
4.4.1	Covariance Inequality Bounds	333
4.4.1.1	Covariance Inequality	333
4.4.1.2	Bayesian Bounds	334
4.4.1.3	Scalar Parameters	334
4.4.1.4	Vector Parameters	340
4.4.1.5	Combined Bayesian Bounds	341
4.4.1.6	Functions of the Parameter Vector	342
4.4.1.7	Summary of Covariance Inequality Bounds	344
4.4.2	Method of Interval Estimation	345
4.4.3	Summary of Global Bayesian Bounds	348
4.5	Composite Hypotheses	348
4.5.1	Introduction	348
4.5.2	Random Parameters	350
4.5.3	Nonrandom Parameters	352
4.5.4	Simulation	372
4.5.5	Summary of Composite Hypotheses	375
4.6	Summary	375
4.7	Problems	377
5	General Gaussian Estimation	400
5.1	Introduction	400
5.2	Nonrandom Parameters	401
5.2.1	General Gaussian Estimation Model	401
5.2.2	Maximum Likelihood Estimation	407
5.2.3	Cramér–Rao Bound	409

5.2.4	Fisher Linear Gaussian Model	412
5.2.4.1	Introduction	412
5.2.4.2	White Noise	418
5.2.4.3	Low-Rank Interference	424
5.2.5	Separable Models for Mean Parameters	429
5.2.6	Covariance Matrix Parameters	442
5.2.6.1	White Noise	443
5.2.6.2	Colored Noise	444
5.2.6.3	Rank One Signal Matrix Plus White Noise	445
5.2.6.4	Rank One Signal Matrix Plus Colored Noise	450
5.2.7	Linear Gaussian Mean and Covariance Matrix Parameters	450
5.2.7.1	White Noise	450
5.2.7.2	Colored Noise	451
5.2.7.3	General Covariance Matrix	452
5.2.8	Computational Algorithms	452
5.2.8.1	Introduction	452
5.2.8.2	Gradient Techniques	453
5.2.8.3	Alternating Projection Algorithm	457
5.2.8.4	Expectation–Maximization Algorithm	461
5.2.8.5	Summary	469
5.2.9	Equivalent Estimation Algorithms	469
5.2.9.1	Least Squares	470
5.2.9.2	Minimum Variance Distortionless Response	470
5.2.9.3	Summary	472
5.2.10	Sensitivity, Mismatch, and Diagonal Loading	473
5.2.10.1	Sensitivity and Array Perturbations	474
5.2.10.2	Diagonal Loading	477
5.2.11	Summary	481
5.3	Random Parameters	483
5.3.1	Model, MAP Estimation, and the BCRB	483
5.3.2	Bayesian Linear Gaussian Model	487
5.3.3	Summary	494
5.4	Sequential Estimation	495
5.4.1	Sequential Bayes Estimation	495
5.4.2	Recursive Maximum Likelihood	504
5.4.3	Summary	506
5.5	Summary	507
5.6	Problems	510
6	Representation of Random Processes	519
6.1	Introduction	519
6.2	Orthonormal Expansions: Deterministic Signals	520
6.3	Random Process Characterization	528
6.3.1	Random Processes: Conventional Characterizations	528
6.3.2	Series Representation of Sample Functions of Random Processes	532
6.3.3	Gaussian Processes	536

6.4	Homogeneous Integral Equations and Eigenfunctions	540
6.4.1	Rational Spectra	540
6.4.2	Bandlimited Spectra	545
6.4.3	Nonstationary Processes	548
6.4.4	White Noise Processes	550
6.4.5	Low Rank Kernels	552
6.4.6	The Optimum Linear Filter	553
6.4.7	Properties of Eigenfunctions and Eigenvalues	559
6.4.7.1	Monotonic Property	559
6.4.7.2	Asymptotic Behavior Properties	560
6.5	Vector Random Processes	564
6.6	Summary	568
6.7	Problems	569
7	Detection of Signals—Estimation of Signal Parameters	584
7.1	Introduction	584
7.1.1	Models	584
7.1.1.1	Detection	584
7.1.1.2	Estimation	587
7.1.2	Format	589
7.2	Detection and Estimation in White Gaussian Noise	591
7.2.1	Detection of Signals in Additive White Gaussian Noise	591
7.2.1.1	Simple Binary Detection	591
7.2.1.2	General Binary Detection in White Gaussian Noise	597
7.2.1.3	M -ary Detection in White Gaussian Noise	601
7.2.1.4	Sensitivity	611
7.2.2	Linear Estimation	614
7.2.3	Nonlinear Estimation	616
7.2.4	Summary of Known Signals in White Gaussian Noise	628
7.2.4.1	Detection	628
7.2.4.2	Estimation	628
7.3	Detection and Estimation in Nonwhite Gaussian Noise	629
7.3.1	“Whitening” Approach	632
7.3.1.1	Structures	632
7.3.1.2	Construction of $Q_n(t, u)$ and $g(t)$	635
7.3.1.3	Summary	639
7.3.2	A Direct Derivation Using the Karhunen-Loève Expansion	639
7.3.3	A Direct Derivation with a Sufficient Statistic	641
7.3.4	Detection Performance	643
7.3.4.1	Performance: Simple Binary Detection Problem	643
7.3.4.2	Optimum Signal Design: Coincident Intervals	644
7.3.4.3	Singularity	645
7.3.4.4	General Binary Receivers	647
7.3.5	Estimation	648
7.3.6	Solution Techniques for Integral Equations	650
7.3.6.1	Infinite Observation Interval: Stationary Noise	650

7.3.6.2	Finite Observation Interval: Rational Spectra	654
7.3.6.3	Finite Observation Time: Separable Kernels	662
7.3.7	Sensitivity, Mismatch, and Diagonal Loading	667
7.3.7.1	Sensitivity	667
7.3.7.2	Mismatch and Diagonal Loading	673
7.3.8	Known Linear Channels	673
7.3.8.1	Summary	675
7.4	Signals with Unwanted Parameters: The Composite Hypothesis Problem	675
7.4.1	Random Phase Angles	677
7.4.2	Random Amplitude and Phase	694
7.4.3	Other Target Models	706
7.4.4	Nonrandom Parameters	709
7.4.4.1	Summary	711
7.5	Multiple Channels	712
7.5.1	Vector Karhunen–Loëve	712
7.5.1.1	Application	714
7.6	Multiple Parameter Estimation	716
7.6.1	Known Signal in Additive White Gaussian Noise	717
7.6.2	Separable Models	718
7.6.3	Summary	720
7.7	Summary	721
7.8	Problems	722
8	Estimation of Continuous-Time Random Processes	771
8.1	Optimum Linear Processors	771
8.2	Realizable Linear Filters: Stationary Processes, Infinite Past: Wiener Filters	787
8.2.1	Solution of Wiener–Hopf Equation	788
8.2.2	Errors in Optimum Systems	798
8.2.3	Unrealizable Filters	801
8.2.4	Closed-Form Error Expressions	803
8.3	Gaussian–Markov Processes: Kalman Filter	807
8.3.1	Differential Equation Representation of Linear Systems and Random Process Generation	808
8.3.2	Kalman Filter	825
8.3.3	Realizable Whitening Filter	839
8.3.4	Generalizations	841
8.3.5	Implementation Issues	842
8.4	Bayesian Estimation of Non-Gaussian Models	842
8.4.1	The Extended Kalman Filter	843
8.4.1.1	Linear AWGN Process and Observations	844
8.4.1.2	Linear AWGN Process, Nonlinear AWGN Observations	845
8.4.1.3	Nonlinear AWGN Process and Observations	848
8.4.1.4	General Nonlinear Process and Observations	849
8.4.2	Bayesian Cramér–Rao Bounds: Continuous-Time	849
8.4.3	Summary	852

8.5 Summary	852
8.6 Problems	855
9 Estimation of Discrete-Time Random Processes	880
9.1 Introduction	880
9.2 Discrete-Time Wiener Filtering	882
9.2.1 Model	882
9.2.2 Random Process Models	883
9.2.3 Optimum FIR Filters	894
9.2.4 Unrealizable IIR Wiener Filters	900
9.2.5 Realizable IIR Wiener Filters	904
9.2.6 Summary: Discrete-Time Wiener Filter	918
9.3 Discrete-Time Kalman Filter	919
9.3.1 Random Process Models	920
9.3.2 Kalman Filter	926
9.3.2.1 Derivation	927
9.3.2.2 Reduced Dimension Implementations	934
9.3.2.3 Applications	939
9.3.2.4 Estimation in Nonwhite Noise	954
9.3.2.5 Sequential Processing of Estimators	955
9.3.2.6 Square-Root Filters	958
9.3.2.7 Divergence	962
9.3.2.8 Sensitivity and Model Mismatch	966
9.3.2.9 Summary: Kalman Filters	972
9.3.3 Kalman Predictors	973
9.3.3.1 Fixed-Lead Prediction	974
9.3.3.2 Fixed-Point Prediction	975
9.3.3.3 Fixed-Interval Prediction	977
9.3.3.4 Summary: Kalman Predictors	977
9.3.4 Kalman Smoothing	978
9.3.4.1 Fixed-Interval Smoothing	978
9.3.4.2 Fixed-Lag Smoothing	979
9.3.4.3 Summary: Kalman Smoothing	982
9.3.5 Bayesian Estimation of Nonlinear Models	982
9.3.5.1 General Nonlinear Model: MMSE and MAP Estimation	983
9.3.5.2 Extended Kalman Filter	985
9.3.5.3 Recursive Bayesian Cramér–Rao Bounds	987
9.3.5.4 Applications	992
9.3.5.5 Joint State and Parameter Estimation	1005
9.3.5.6 Continuous-Time Processes and Discrete-Time Observations	1009
9.3.5.7 Summary	1013
9.3.6 Summary: Kalman Filters	1013
9.4 Summary	1016
9.5 Problems	1016

10 Detection of Gaussian Signals	1030
10.1 Introduction	1030
10.2 Detection of Continuous-Time Gaussian Processes	1030
10.2.1 Sampling	1032
10.2.2 Optimum Continuous-Time Receivers	1034
10.2.3 Performance of Optimum Receivers	1046
10.2.4 State-Variable Realization	1049
10.2.5 Stationary Process-Long Observation Time (SPLIT) Receiver	1051
10.2.6 Low-Rank Kernels	1061
10.2.7 Summary	1066
10.3 Detection of Discrete-Time Gaussian Processes	1067
10.3.1 Second Moment Characterization	1067
10.3.1.1 Known Means and Covariance Matrices	1067
10.3.1.2 Means and Covariance Matrices with Unknown Parameters	1068
10.3.2 State Variable Characterization	1070
10.3.3 Summary	1076
10.4 Summary	1076
10.5 Problems	1077
11 Epilogue	1084
11.1 Classical Detection and Estimation Theory	1084
11.1.1 Classical Detection Theory	1084
11.1.2 General Gaussian Detection	1086
11.1.3 Classical Parameter Estimation	1088
11.1.4 General Gaussian Estimation	1089
11.2 Representation of Random Processes	1093
11.3 Detection of Signals and Estimation of Signal Parameters	1095
11.4 Linear Estimation of Random Processes	1098
11.5 Observations	1105
11.5.1 Models and Mismatch	1105
11.5.2 Bayes vis-a-vis Fisher	1105
11.5.3 Bayesian and Fisher Bounds	1105
11.5.4 Eigenspace	1106
11.5.5 Whitening	1106
11.5.6 The Gaussian Model	1106
11.6 Conclusion	1106
Appendix A: Probability Distributions and Mathematical Functions	1107
Appendix B: Example Index	1119
References	1125
Index	1145

Preface

We have included the preface to the first edition in order to provide a context for the original work. For readers who are not familiar with Part I of Detection, Estimation, and Modulation Theory (DEMT), it may be useful to read it first.

In 1968, Part I of DEMT was published. It turned out to be a reasonably successful book that has been widely used by several generations of engineers. There were 28 printings, but the last printing was in 1996. Parts II and III were published in 1971 and focused on specific applications areas such as analog modulation, Gaussian signals and noise, and the radar–sonar problem. Part II had a short life span due to the shift from analog modulation to digital modulation. Part III is still widely used as a reference and as a supplementary text. In 2002, the fourth volume in the sequence, *Optimum Array Processing*, was published. In conjunction with the publication of *Optimum Array Processing*, paperback versions of Parts I, II, and III were published. In 2007, in order to expand on the performance bounds that played an important role in Parts I–IV, Dr. Kristine Bell and I edited a book, *Bayesian Bounds for Parameter Estimation and Nonlinear Filtering/Tracking*.

In the 44 years since the publication of Part I, there have been a large number of changes:

1. The basic detection and estimation theory has remained the same but numerous new results have been obtained.
2. The exponential growth in computational capability has enabled us to implement algorithms there were only of theoretical interest in 1968. The results from detection and estimation theory were applied in operational systems.
3. Simulation became more widely used in system design and analysis, research, and teaching.
4. Matlab became an essential tool.

If I had stayed at MIT and continued working in this area, then presumably a new edition would have come out every 10 years and evolved along with the field and this might be the fifth edition.

A few comments on my career may help explain the long delay between editions. In 1972, MIT loaned me to the Defense Communications Agency in Washington, DC, where I spent 3 years as the Chief Scientist and the Associate Director of Technology. At the end of the tour, I decided, for personal reasons, to stay in Washington, DC. I spent the next 3 years as an Assistant Vice President at Comsat where my group did the advanced planning for the INTELSAT satellites. In 1978, I became the Chief Scientist of the United States Air Force. In 1979, Dr. Gerald Dinneen, the former director of Lincoln Laboratory,

was serving as Assistant Secretary of Defense for Command, Control, Communications, and Intelligence (C3I). He asked me to become his Principal Deputy and I spent 2 years in that position. In 1981, I joined M/A-COM Linkabit. This is the company that Irwin Jacobs and Andrew Viterbi had started in 1969 and sold to M/A-COM in 1979. I started an Eastern Operation that grew to about 200 people in 3 years. After Irwin and Andy left M/A-COM and started Qualcomm, I was responsible for the government operations in San Diego as well as Washington, DC. In 1988, M/A-COM sold the division and at that point I decided to return to the academic world.

I joined George Mason University (GMU) in September 1988. One of my priorities was to restart my research in detection and estimation theory and finish the book on *Optimum Array Processing*. However, I found that I needed to build up a research center in order to attract young research-oriented faculty and doctoral students. One of my first students was Dr. Bell, who had worked for me at M/A-COM. She joined the doctoral program in 1990, graduated in 1995, and joined the GMU faculty in the Statistics Department. The process of growing a research center took about 6 years. The Center for Excellence in C3I has been very successful and has generated over 30 million dollars in research funding during its existence. During this growth phase, I spent some time on my research but a concentrated effort was not possible.

After I retired from teaching and serving as Director of the C3I Center in 2005, I could devote full time to consulting and writing. After the publication of *Bayesian Bounds* in 2007, Dr. Bell and I started work on the second edition of Part I. There were a number of factors that had to be considered:

1. The first edition was written during a period that is sometimes referred to as the “Golden Age of Communications Theory.” Norbert Wiener, Claude Shannon, and Y. W. Lee were on the MIT faculty and a number of the future leaders in the field were graduate students. Detection and estimation theory was an exciting new research area. It has evolved into a mature discipline that is applied in a number of areas.
2. The audience for the book has changed. The first edition was designed for my course at MIT in which the audience was 40–50 graduate students, many of whom planned to do research in the area. This allowed me to leave out the implementation details and incorporate new derivations in the problems (the best example was the derivation of the discrete-time Kalman filter as a problem in Chapter 2). To make the second edition more readable to a larger audience, we have expanded the explanations in many areas.
3. There have been a large number of new results. We have tried to select the ones that are most suitable for an introductory textbook.
4. The first edition emphasized closed-form analytic solutions wherever possible. The second edition retains that focus but incorporates iterative solutions, simulations, and extensive use of Matlab.

Some of the specific new features in the second edition include:

1. Chapter 2 in the first edition has been expanded into Chapters 2–5 in the second edition. The new Chapter 2 develops classical detection theory (Sections 2.1–2.3 and 2.7 in the first edition) and adds a section on importance sampling as a logical extension of the tilted densities in the performance bounds section. Chapter 3, “Gaussian Detection,” is a significant expansion of Section 2.6 in the first edition and derives

a number of explicit results that will be used later in the book. Chapter 4, “Classical Parameter Estimation,” is a significant expansion of Sections 2.4 and 2.5 in the first edition. It introduces several new topics and includes a detailed development of global Bayesian bounds based on the introductory material in *Bayesian Bounds*. Chapter 5, “General Gaussian Estimation,” is new material. It introduces the Fisher linear Gaussian model and the Bayesian linear Gaussian model. It discusses computational algorithms, equivalent estimation algorithms (ML, least squares, MVDR), sensitivity and mismatch, and introduces sequential estimation.

2. Chapters 6, 7, and 8 in the second edition correspond to Chapters 3, 4, and 6 in the first edition. There are minor changes but the basic material is the same.
3. Chapter 9, “Linear Estimation of Discrete-Time Random Processes,” is a new chapter. It develops the discrete-time Wiener filter and the discrete-time Kalman filter. In addition to developing the various algorithms, it discusses the various problems that may arise in the numerical implementation of the algorithms and techniques for avoiding these problems as well as reducing the computational complexity.
4. Chapter 10, “Detection of Gaussian Signals,” treats both continuous-time and discrete-time processes. The discussion of continuous-time processes is taken from Chapters 2 and 4 of DEMT, Part III. The discussion of discrete-time processing is divided into block processing and sequential processing. For block processing, we provide tables to show where in Chapters 3–5 we have already solved the problem. For sequential processing, we show how the detection statistics can be generated from the outputs of an FIR Wiener filter or a discrete-time Kalman filter.

For readers familiar with the first edition of DEMT, Part I or other detection theory or estimation theory texts, it may be useful to scan Chapter 11, “Epilogue,” to see a summary of the material covered in the second edition.

The addition of a significant amount of material on filtering and the deletion of the chapter on modulation theory motivated the addition of a subtitle for Part I, *Detection, Estimation, and Filtering Theory*.

From the standpoint of specific background, little advanced material is required. A thorough knowledge of elementary probability theory and random processes is assumed. In particular, the reader needs to have worked with second-moment characterizations of random processes and Gaussian random processes. The reader should have worked with matrices and be comfortable in eigenspace. In later chapters, experience with state variable representations is useful. Our teaching experience with a wide variety of audiences shows that many students understand the basic results in detection and estimation theory but have trouble implementing them because of a weak background in random processes and/or matrix theory. The level of mathematical rigor is moderate, although in most sections the results could be rigorously proved by simply being more careful in our derivations. We have adopted this approach in order not to obscure the important ideas with a lot of detail and to make the material readable for the kind of engineering audience that will find it useful. Fortunately, in almost all cases, we can verify that our answers are intuitively logical. It is worthwhile to observe that the ability to check our answers intuitively would be necessary even if our derivations were rigorous, because our ultimate objective is to obtain answers that correspond to some physical system of interest. It is easy to find physical problems in which a plausible mathematical model and correct mathematics lead to an unrealistic answer for the original problem.

We need to reemphasize the necessity for the reader to solve problems to understand the material fully. Throughout the course of the book, we emphasize the development of the ability to work problems. At the end of each chapter are problems that range from routine manipulations to significant extensions of the material in the text. Only by working a fair number is it possible to appreciate the significance and generality of the results. A solution manual is available (email: demt2013@gmail.com). It contains solutions to about 25% of the problems in the text. In addition, it contains the Matlab scripts for most of the figures that are new in the second edition.

The actual authorship of the book has evolved as we worked our way through the manuscript. Originally Dr. Bell and I were to be coauthors of the entire book. After Dr. Bell left GMU in 2009 to join Metron, we agreed that she would complete her responsibilities for the first five chapters and I would continue to develop the remaining six chapters. I was the only author of Chapters 6–8, 10, and 11. However, in order to complete Chapter 9, I recruited Dr. Zhi Tian, a former doctoral student at GMU and currently a Professor of ECE at Michigan Technological University, to be a coauthor of the chapter. It is important to recognize the contributions of these coauthors. They brought excellent analytical and mathematical skills to the project and an ability to work with Matlab, which was essential to the completion of the book. In addition, Dr. Bell also developed the two appendices and did a careful proof reading of the entire book. Their contribution is gratefully acknowledged.

The actual production of the draft manuscript was challenging because the first edition was published in the pre-LaTeX era. Some financial support was provided by Norma Corrales and Fred Rainbow of AFCEA and Prof. Mark Pullen, the current director of the C4I Center at GMU. The manuscript was put into LaTeX by three graduate students: Seyed Rizi, Awais Khawar, and Khalid Al-Muhanna. They devoted an enormous amount of time to repeated drafts even though the material was not in their research area. Seyed Rizi oversaw the entire process and deserves special recognition for his dedication to the project. Vibhu Dubey and his staff at Thomson Digital did an excellent job of typesetting the final manuscript.

Harry L. Van Trees

Preface to the First Edition

The area of detection and estimation theory that we shall study in this book represents a combination of the classical techniques of statistical inference and the random process characterization of communication, radar, sonar, and other modern data processing systems. The two major areas of statistical inference are decision theory and estimation theory. In the first case we observe an output that has a random character and decide which of two possible causes produced it. This type of problem was studied in the middle of the eighteenth century by Thomas Bayes [1]. In the estimation theory case the output is related to the value of some parameter of interest, and we try to estimate the value of this parameter. Work in this area was published by Legendre [2] and Gauss [3] in the early nineteenth century. Significant contributions to the classical theory that we use as background were developed by Fisher [4] and Neyman and Pearson [5] more than 30 years ago. In 1941 and 1942 Kolmogoroff [6] and Wiener [7] applied statistical techniques to the solution of the optimum linear filtering problem. Since that time the application of statistical techniques to the synthesis and analysis of all types of systems has grown rapidly. The application of these techniques and the resulting implications are the subject of this book.

This book and the subsequent volume, Detection, Estimation, and Modulation Theory, Part II, are based on notes prepared for a course entitled "Detection, Estimation, and Modulation Theory," which is taught as a second-level graduate course at M.I.T. My original interest in the material grew out of my research activities in the area of analog modulation theory. A preliminary version of the material that deals with modulation theory was used as a text for a summer course presented at M.I.T. in 1964. It turned out that our viewpoint on modulation theory could best be understood by an audience with a clear understanding of modern detection and estimation theory. At that time there was no suitable text available to cover the material of interest and emphasize the points that I felt were important, so I started writing notes. It was clear that in order to present the material to graduate students in a reasonable amount of time it would be necessary to develop a unified presentation of the three topics: detection, estimation, and modulation theory, and exploit the fundamental ideas that connected them. As the development proceeded, it grew in size until the material that was originally intended to be background for modulation theory occupies the entire contents of this book. The original material on modulation theory starts at the beginning of the second book. Collectively, the two books provide a unified coverage of the three topics and their application to many important physical problems.

For the last three years I have presented successively revised versions of the material in my course. The audience consists typically of 40 to 50 students who have completed a graduate course in random processes which covered most of the material in Davenport and

Root [8]. In general, they have a good understanding of random process theory and a fair amount of practice with the routine manipulation required to solve problems. In addition, many of them are interested in doing research in this general area or closely related areas. This interest provides a great deal of motivation which I exploit by requiring them to develop many of the important ideas as problems. It is for this audience that the book is primarily intended. The appendix contains a detailed outline of the course.

On the other hand, many practicing engineers deal with systems that have been or should have been designed and analyzed with the techniques developed in this book. I have attempted to make the book useful to them. An earlier version was used successfully as a text for an in-plant course for graduate engineers.

From the standpoint of specific background little advanced material is required. A knowledge of elementary probability theory and second moment characterization of random processes is assumed. Some familiarity with matrix theory and linear algebra is helpful but certainly not necessary. The level of mathematical rigor is low, although in most sections the results could be rigorously proved by simply being more careful in our derivations. We have adopted this approach in order not to obscure the important ideas with a lot of detail and to make the material readable for the kind of engineering audience that will find it useful. Fortunately, in almost all cases we can verify that our answers are intuitively logical. It is worthwhile to observe that this ability to check our answers intuitively would be necessary even if our derivations were rigorous, because our ultimate objective is to obtain an answer that corresponds to some physical system of interest. It is easy to find physical problems in which a plausible mathematical model and correct mathematics lead to an unrealistic answer for the original problem.

We have several idiosyncrasies that it might be appropriate to mention. In general, we look at a problem in a fair amount of detail. Many times we look at the same problem in several different ways in order to gain a better understanding of the meaning of the result. Teaching students a number of ways of doing things helps them to be more flexible in their approach to new problems. A second feature is the necessity for the reader to solve problems to understand the material fully. Throughout the course and the book we emphasize the development of an ability to work problems. At the end of each chapter are problems that range from routine manipulations to significant extensions of the material in the text. In many cases they are equivalent to journal articles currently being published. Only by working a fair number of them is it possible to appreciate the significance and generality of the results. Solutions for an individual problem will be supplied on request, and a book containing solutions to about one third of the problems is available to faculty members teaching the course. We are continually generating new problems in conjunction with the course and will send them to anyone who is using the book as a course text. A third issue is the abundance of block diagrams, outlines, and pictures. The diagrams are included because most engineers (including myself) are more at home with these items than with the corresponding equations.

One problem always encountered is the amount of notation needed to cover the large range of subjects. We have tried to choose the notation in a logical manner and to make it mnemonic. All the notation is summarized in the glossary at the end of the book. We have tried to make our list of references as complete as possible and to acknowledge any ideas due to other people.

A number of people have contributed in many ways and it is a pleasure to acknowledge them. Professors W. B. Davenport and W. M. Siebert have provided continual encouragement and technical comments on the various chapters. Professors Estil Hoversten and

Donald Snyder of the M.I.T. faculty and Lewis Collins, Arthur Baggeroer, and Michael Austin, three of my doctoral students, have carefully read and criticized the various chapters. Their suggestions have improved the manuscript appreciably. In addition, Baggeroer and Collins contributed a number of the problems in the various chapters and Baggeroer did the programming necessary for many of the graphical results. Lt. David Wright read and criticized Chapter 2. L. A. Frasco and H. D. Goldfein, two of my teaching assistants, worked all of the problems in the book. Dr. Howard Yudkin of Lincoln Laboratory read the entire manuscript and offered a number of important criticisms. In addition, various graduate students taking the course have made suggestions which have been incorporated. Most of the final draft was typed by Miss Aina Sils. Her patience with the innumerable changes is sincerely appreciated. Several other secretaries, including Mrs. Jarmila Hrbek, Mrs. Joan Bauer, and Miss Camille Tortorici, typed sections of the various drafts.

As pointed out earlier, the books are an outgrowth of my research interests. This research is a continuing effort, and I shall be glad to send our current work to people working in this area on a regular reciprocal basis. My early work in modulation theory was supported by Lincoln Laboratory as a summer employee and consultant in groups directed by Dr. Herbert Sherman and Dr. Barney Reiffen. My research at M.I.T. was partly supported by the Joint Services and the National Aeronautics and Space Administration under the auspices of the Research Laboratory of Electronics. This support is gratefully acknowledged.

Harry L. Van Trees

Cambridge, Massachusetts
October, 1967

REFERENCES

- [1] Thomas Bayes, "An Essay Towards Solving a Problem in the Doctrine of Chances," *Phil. Trans.*, **53**, 370–418 (1764).
- [2] A. M. Legendre, *Nouvelles Méthodes pour La Détermination ces Orbites des Comètes*, Paris, 1806.
- [3] K. F. Gauss, *Theory of Motion of the Heavenly Bodies Moving About the Sun in Conic Sections*, reprinted by Dover, New York, 1963.
- [4] R. A. Fisher, "Theory of Statistical Estimation," *Proc. Cambridge Philos. Soc.*, **22**, 700 (1925).
- [5] J. Neyman and E. S. Pearson, "On the Problem of the Most Efficient Tests of Statistical Hypotheses," *Phil. Trans. Roy. Soc. London*, **A 231**, 289, (1933).
- [6] A. Kolmogoroff, "Interpolation and Extrapolation von Stationären Zufälligen Folgen," *Bull. Acad. Sci. USSR, Ser. Math.* **5**, 1941.
- [7] N. Wiener, *Extrapolation, Interpolation, and Smoothing of Stationary Time Series*, Tech. Press of M.I.T. and Wiley, New York, 1949 (originally published as a classified report in 1942).
- [8] W. B. Davenport and W. L. Root, *Random Signals and Noise*, McGraw-Hill, New York, 1958.

1

Introduction

1.1 INTRODUCTION

This book is the second edition of Part I of the four-volume series on “Detection, Estimation, and Modulation Theory.” It is a significant expansion of the original Part I [Van68, Van01a]. It includes many of the important results that have occurred in the 44 years since the first edition was published. It expands upon many of the original areas from the first edition and introduces a large number of new areas. In addition, some of the material from the original Part III is moved into this edition.

In this book, we shall study three areas of statistical theory, which we have labeled detection theory, estimation theory, and filtering theory. The goal is to develop these theories in a common mathematical framework and demonstrate how they can be used to solve a wealth of practical problems in many diverse physical situations.

In this chapter, we present three outlines of the material. The first is a topical outline in which we develop a qualitative understanding of the three areas by examining some typical problems of interest. The second is a logical outline in which we explore the various methods of attacking the problems. The third is a chronological outline in which we explain the structure of the book.

1.2 TOPICAL OUTLINE

An easy way to explain what is meant by detection theory is to examine several physical situations that lead to detection theory problems.

A simple digital communication system is shown in Figure 1.1. The source puts out a binary digit every T seconds. Our objective is to transmit this sequence of digits to some other location. The channel available for transmitting the sequence depends on the particular situation. Typically, it could be a telephone line, a radio link, or an acoustical channel. For purposes of illustration, we shall consider a radio link. In order to transmit the information, we must put it into a form suitable for propagating over the channel. A straightforward method would be to build a device that generates a sine wave,

$$s_1(t) = \sin \omega_1 t, \quad (1.1)$$



Figure 1.1: Digital communication system.

for T seconds if the source generated a “one” in the preceding interval, and a sine wave of a different frequency,

$$s_0(t) = \sin \omega_0 t, \quad (1.2)$$

for T seconds if the source generated a “zero” in the preceding interval. The frequencies are chosen so that the signals $s_0(t)$ and $s_1(t)$ will propagate over the particular radio link of concern. The output of the device is fed into an antenna and transmitted over the channel. Typical source and transmitted signal sequences are shown in Figure 1.2.

In the simplest kind of channel the signal sequence arrives at the receiving antenna attenuated but essentially undistorted. To process the received signal, we pass it through the antenna and some stages of rf amplification, in the course of which a thermal noise $n(t)$ is added to the message sequence. Thus in any T -second interval, we have available a waveform $r(t)$ in which

$$r(t) = s_1(t) + n(t), \quad 0 \leq t \leq T, \quad (1.3)$$

if $s_1(t)$ was transmitted and

$$r(t) = s_0(t) + n(t), \quad 0 \leq t \leq T, \quad (1.4)$$

if $s_0(t)$ was transmitted. We are now faced with the problem of deciding which of the two possible signals was transmitted. We label the device that does this a decision device. It is simply a processor that observes $r(t)$ and guesses whether $s_1(t)$ or $s_0(t)$ was sent according to some set of rules. This is equivalent to guessing what the source output was in the preceding interval. We refer to designing and evaluating the processor as a detection theory problem. In this particular case, the only possible source of error in making a decision is the additive noise. If it were not present, the input would be completely known and we could make decisions without errors. We denote this type of problem as the *known signal in noise problem*. It corresponds to the lowest level (i.e., simplest) of the detection problems of interest.

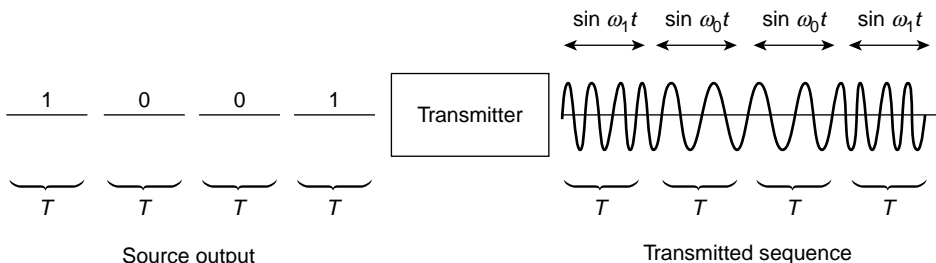


Figure 1.2: Typical sequences.

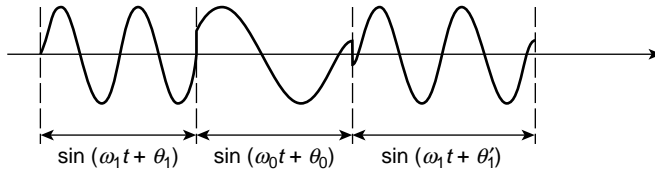


Figure 1.3: Sequence with phase shifts.

An example of the next level of detection problem is shown in Figure 1.3. The oscillators used to generate $s_1(t)$ and $s_0(t)$ in the preceding example have a phase drift. Therefore in a particular T -second interval, the received signal corresponding to a “one” is

$$r(t) = \sin(\omega_1 t + \theta_1) + n(t), \quad 0 \leq t \leq T, \quad (1.5)$$

and the received signal corresponding to a “zero” is

$$r(t) = \sin(\omega_0 t + \theta_0) + n(t), \quad 0 \leq t \leq T, \quad (1.6)$$

where θ_0 and θ_1 are unknown constant phase angles. Thus, even in the absence of noise the input waveform is not completely known. In a practical system the receiver may include auxiliary equipment to measure the oscillator phase. If the phase varies slowly enough, we shall see that essentially perfect measurement is possible. If this is true, the problem is the same as above. However, if the measurement is not perfect, we must incorporate the signal uncertainty in our model.

A corresponding problem arises in the radar and sonar areas. A conventional radar transmits a pulse at some frequency ω_c with a rectangular envelope:

$$s_t(t) = \sin \omega_c t, \quad 0 \leq t \leq T. \quad (1.7)$$

If a target is present, the pulse is reflected. Even the simplest target will introduce an attenuation and phase shift in the transmitted signal. Thus, the signal available for processing in the interval of interest is

$$\begin{aligned} r(t) &= V_r \sin[\omega_c(t - \tau) + \theta_r] + n(t), & \tau \leq t \leq \tau + T, \\ &= n(t), & 0 \leq t < \tau, \tau + T < t < \infty, \end{aligned} \quad (1.8)$$

if a target is present and

$$r(t) = n(t), \quad 0 \leq t < \infty, \quad (1.9)$$

if a target is absent. We see that in the absence of noise the signal still contains three unknown quantities: V_r , the amplitude, θ_r , the phase, and τ , the round-trip travel time to the target.

These two examples represent the second level of detection problems. We classify them as *signal with unknown parameters in noise problems*.

Detection problems of a third level appear in several areas. In a passive sonar detection system, the receiver listens for noise generated by enemy vessels. The engines, propellers, and other elements in the vessel generate acoustical signals that travel through the ocean to the hydrophones in the detection system. This composite signal can best be characterized as

a sample function from a random process. In addition, the hydrophone generates self-noise and picks up sea noise. Thus, a suitable model for the detection problem might be

$$r(t) = s_{\Omega}(t) + n(t) \quad (1.10)$$

if the target is present and

$$r(t) = n(t) \quad (1.11)$$

if it is not. In the absence of noise, the signal is a sample function from a random process (indicated by the subscript Ω).

In the communications field, a large number of systems employ channels in which randomness is inherent. Typical systems are tropospheric scatter links, orbiting dipole links, and chaff systems. A common technique is to transmit one of two signals separated in frequency. (We denote these frequencies as ω_1 and ω_0 .) The resulting received signal is

$$r(t) = s_{\Omega_1}(t) + n(t) \quad (1.12)$$

if $s_1(t)$ was transmitted and

$$r(t) = s_{\Omega_0}(t) + n(t) \quad (1.13)$$

if $s_0(t)$ was transmitted. Here, $s_{\Omega_1}(t)$ is a sample function from a random process centered at ω_1 and $s_{\Omega_0}(t)$ is a sample function from a random process centered at ω_0 . These examples are characterized by the lack of any deterministic signal component. Any decision procedure that we design will have to be based on the difference in the statistical properties of the two random processes from which $s_{\Omega_0}(t)$ and $s_{\Omega_1}(t)$ are obtained. This is the third level of detection problem and is referred to as a *random signal in noise problem*.

In our examination of representative examples, we have seen that detection theory problems are characterized by the fact that we must decide which of several alternatives is true. There were only two alternatives in the examples cited; therefore, we refer to them as binary detection problems. Later we will encounter problems in which there are M alternatives available (the M -ary detection problem). Our hierarchy of detection problems is presented graphically in Table 1.1.

Table 1.1: Detection theory hierarchy

Detection Theory	
Level 1. Known signals in noise	1. Synchronous digital communication 2. Pattern recognition problems
Level 2. Signals with unknown parameters in noise	1. Conventional pulsed radar or sonar, target detection 2. Target classification (orientation of target unknown) 3. Digital communication systems without phase reference 4. Digital communication over slowly fading channels
Level 3. Random signals in noise	1. Digital communication over scatter link, orbiting dipole channel, or chaff link 2. Passive sonar 3. Seismic detection system 4. Radio astronomy (detection of noise sources)

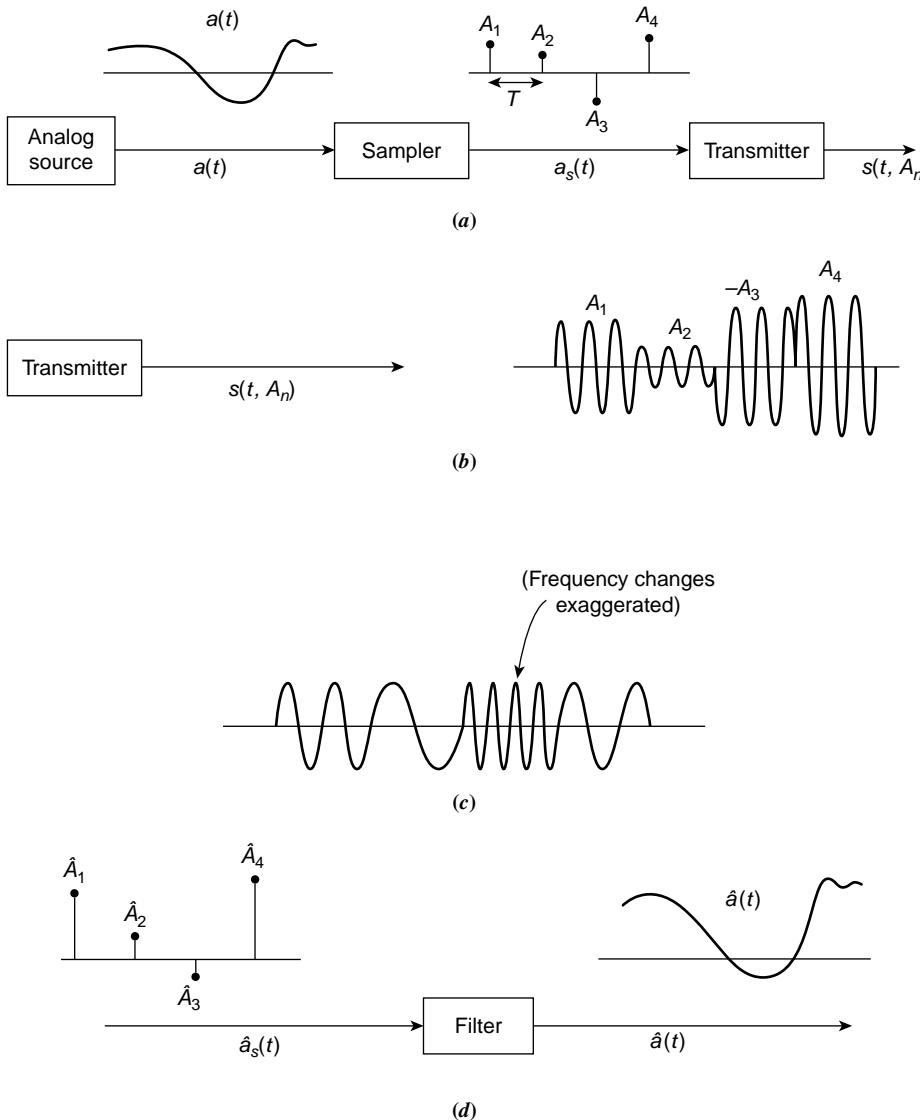


Figure 1.4: (a) Sampling an analog source; (b) pulse-amplitude modulation; (c) pulse-frequency modulation; (d) waveform reconstruction.

There is a parallel set of problems in the estimation theory area. A simple example is given in Figure 1.4, in which the source puts out an analog message $a(t)$ (Figure 1.4a). To transmit the message we first sample it every T seconds. Then, every T seconds we transmit a signal that contains a parameter that is uniquely related to the last sample value. In Figure 1.4b, the signal is a sinusoid whose amplitude depends on the last sample value. Thus, if the sample at time nT is A_n , the signal in the interval $[nT, (n + 1)T]$ is

$$s(t, A_n) = A_n \sin \omega_c t, \quad nT \leq t \leq (n + 1)T. \quad (1.14)$$

A system of this type is called a pulse amplitude modulation (PAM) system. In Figure 1.4c, the signal is a sinusoid whose frequency in the interval differs from the reference frequency ω_c by an amount proportional to the preceding sample value,

$$s(t, A_n) = \sin(\omega_c t + A_n t), \quad nT \leq t \leq (n+1)T. \quad (1.15)$$

A system of this type is called a pulse-frequency modulation (PFM) system. Once again there is additive noise. The received waveform, given that A_n was the sample value, is

$$r(t) = s(t, A_n) + n(t), \quad nT \leq t \leq (n+1)T. \quad (1.16)$$

During each interval, the receiver tries to estimate A_n . We denote these estimates as \hat{A}_n . Over a period of time we obtain a sequence of estimates, as shown in Figure 1.4d, which is passed into a device whose output is an estimate of the original message $a(t)$. If $a(t)$ is a band-limited signal, the device is just an ideal low-pass filter. For other cases, it is more involved.

If, however, the parameters in this example were known and the noise were absent, the received signal would be completely known. We refer to problems in this category as *known signal in noise problems*. If we assume that the mapping from A_n to $s(t, A_n)$ in the transmitter has an inverse, we see that if the noise were not present we could determine A_n unambiguously. (Clearly, if we were allowed to design the transmitter, we should always choose a mapping with an inverse.) The *known signal in noise problem* is the first level of the estimation problem hierarchy.

Returning to the area of radar, we consider a somewhat different problem. We assume that we know a target is present but do not know its range or velocity. Then the received signal is

$$\begin{aligned} r(t) &= V_r \sin[(\omega_c + \omega_d)(t - \tau) + \theta_r] + n(t), \quad \tau \leq t \leq \tau + T, \\ &= n(t), \quad 0 \leq t < \tau, \tau + T < t < \infty, \end{aligned} \quad (1.17)$$

where ω_d denotes a Doppler shift caused by the target's motion. We want to estimate τ and ω_d . Now, even if the noise were absent and τ and ω_d were known, the signal would still contain the unknown parameters V_r and θ_r . This is a typical second-level estimation problem. As in detection theory, we refer to problems in this category as *signal with unknown parameters in noise problems*.

At the third level, the signal component is a random process whose statistical characteristics contain parameters we want to estimate. The received signal is of the form

$$r(t) = s_\Omega(t, A) + n(t), \quad (1.18)$$

where $s_\Omega(t, A)$ is a sample function from a random process. In a simple case it might be a stationary process with the narrow-band spectrum shown in Figure 1.5. The shape of the spectrum is known but the center frequency is not. The receiver must observe $r(t)$ and, using the statistical properties of $s_\Omega(t, A)$ and $n(t)$, estimate the value of A . This particular example could arise in either radio astronomy or passive sonar. The general class of problem in which the signal containing the parameters is a sample function from a random process is referred to as the *random signal in noise problem*. The hierarchy of estimation theory problems is shown in Table 1.2.

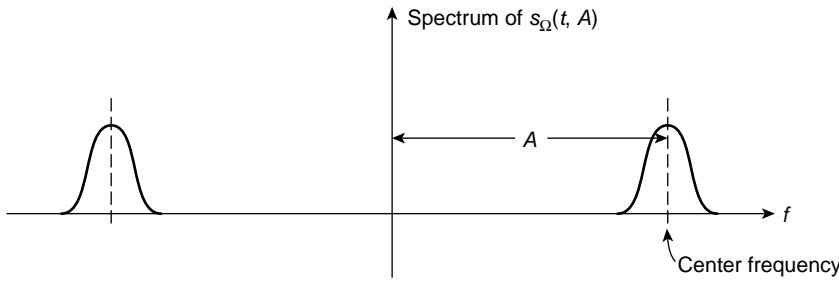


Figure 1.5: Spectrum of random signal.

When we develop the estimation theory model in detail, we will find the parameters can be modeled as unknown nonrandom parameters or random parameters. Thus, the estimation theory hierarchy in Table 1.2 will have two parallel tracks.

The two hierarchies emphasize increasing signal complexity and, in our initial models, assume that the statistical characteristics of the noise, $n(t)$, are known. In many applications, we may know that the noise has a flat spectrum but the spectrum height is unknown. We may know that it has an exponential covariance function,

$$K_n(\tau) = \sigma_n^2 \exp(-\alpha\tau), \quad -\infty \leq \tau \leq \infty, \quad (1.19)$$

but σ_n^2 and α are unknown. The partially known noise model adds another dimension to the hierarchies.

We note that there appears to be considerable parallelism in the detection and estimation theory problems. We shall frequently exploit these parallels to reduce the work, but there is a basic difference that should be emphasized. In binary detection, the receiver is either “right” or “wrong.” In the estimation of a continuous parameter, the receiver will seldom

Table 1.2: Estimation theory hierarchy

Estimation Theory	
Level 1. Known signals in noise	<ol style="list-style-type: none"> 1. PAM, PFM, and PPM communication systems with phase synchronization 2. Inaccuracies in inertial systems (e.g., drift angle measurement)
Level 2. Signals with unknown parameters in noise	<ol style="list-style-type: none"> 1. Range, velocity, or angle measurement in radar/sonar problems 2. Discrete time, continuous amplitude communication system (with unknown amplitude or phase in channel)
Level 3. Random signals in noise	<ol style="list-style-type: none"> 1. Power spectrum parameter estimation 2. Range or Doppler spread target parameters in radar/sonar problem 3. Velocity measurement in radio astronomy 4. Target parameter estimation: passive sonar 5. Ground mapping radars

be exactly right, but it can try to be close most of the time. This difference will be reflected in the manner in which we judge system performance.

The third area of interest is filtering theory. We consider several examples. A simple example is

$$r(t) = a(t) + n(t), \quad 0 \leq t \leq T, \quad (1.20)$$

where $a(t)$ is a sample function of a message random process and $n(t)$ is a sample function of a noise process. The message could correspond to speech or music. We want to estimate the value of $a(t)$ at every time in the interval $0 \leq t \leq T$. If we want to base that estimate on $r(u)$, $0 \leq u \leq t$, this is referred to as a *realizable filtering problem*. If we are willing to wait until $r(t)$ is observed from $0 \leq t \leq T$, this is referred to as a *smoothing problem*. If we want to estimate $a(t + \alpha)$, $\alpha > 0$ based on $r(t)$, $0 \leq u \leq t$, then it is referred to as a *prediction problem*.

This example can be put into the communication context as shown in Figure 1.6. In Figure 1.6a, we show the analog message source whose output is $a(t)$. To convey the message over the channel, we transform it by using a modulation scheme to get it into a form suitable for propagation. The transmitted signal is a continuous waveform that depends on $a(t)$ in some deterministic manner. In Figure 1.6b, it is an amplitude-modulated waveform:

$$s[t, a(t)] = [1 + ma(t)] \sin(\omega_c t). \quad (1.21)$$

(This is conventional double-sideband AM with modulation index m .) In Figure 1.6c, the transmitted signal is a frequency-modulated (FM) waveform:

$$s[t, a(t)] = \sin \left[\omega_c t + \int_{-\infty}^t a(u) du \right]. \quad (1.22)$$

When noise is added, the received signal is

$$r(t) = s[t, a(t)] + n(t). \quad (1.23)$$

Now the receiver must observe $r(t)$ and put out a continuous estimate of the message $a(t)$, as shown in Figure 1.6d. We refer to this as a *modulation problem* and treat modulation as a special case of filtering.

There is an important difference between the model in (1.20) and the model in (1.23). In the first case, the signal is a linear function of $a(t)$, so we refer to it as a *linear filtering problem*. In the second case, the signal is a nonlinear function of $a(t)$, so we refer to it as a *nonlinear filtering problem*.

A simple example of a tracking problem is shown in Figure 1.7. The observer is located at the origin and can estimate the range and bearing to the target. Thus,

$$\mathbf{r}(t) = \begin{bmatrix} \sqrt{x^2(t) + y^2(t)} \\ \tan^{-1} \left(\frac{y(t)}{x(t)} \right) \end{bmatrix} + \begin{bmatrix} n_1(t) \\ n_2(t) \end{bmatrix} \quad (1.24)$$

is a 2×1 vector and $n_1(t)$ and $n_2(t)$ represent the estimation errors. This is an example of a nonlinear tracking problem. The target trajectory is a simple function of a random process whose statistics are known. We will refer to this category of problems as *estimation of the sample function of a random process with known statistics* or with a

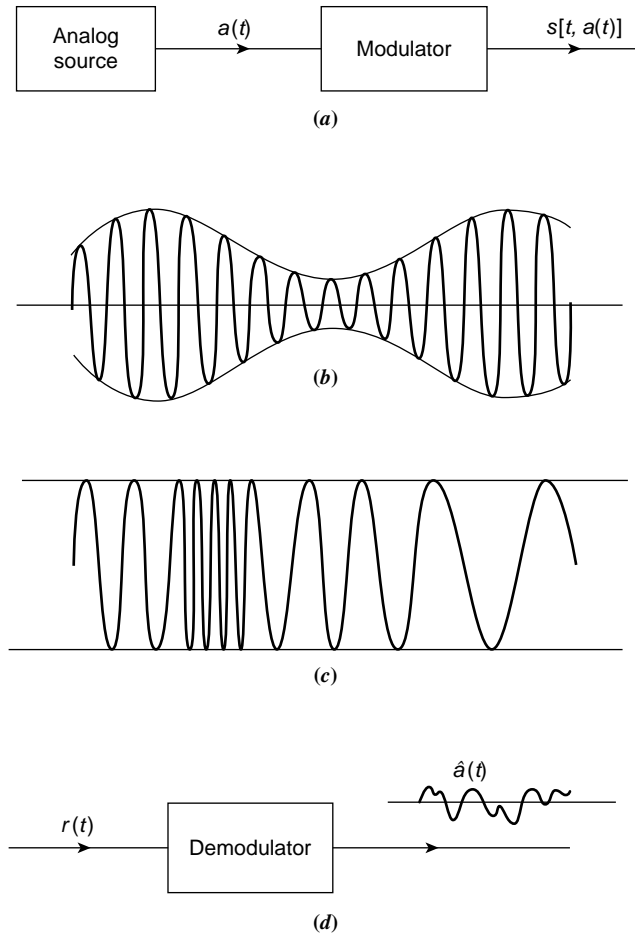


Figure 1.6: A modulation theory example: (a) analog transmission system; (b) amplitude-modulated signal; (c) frequency-modulated signal; (d) demodulator.

shorter term *random signals in noise; known statistics*. Our ability to solve this type of problem will depend on the process model (linear or nonlinear) and observation model (linear or nonlinear).

The other levels of the filtering theory problem follow by direct analogy. In the amplitude modulation system shown in Figure 1.6b, the receiver frequently does not know the phase angle of the carrier. In this case a suitable model is

$$r(t) = [1 + ma(t)] \sin(\omega_c t + \theta) + n(t), \quad (1.25)$$

where θ is an unknown parameter. This is an example of a *random signal with unknown parameter problem* in the filtering theory area.

A simple example of a third-level problem is one in which we transmit a frequency-modulated signal over a radio link whose gain and phase characteristics are time varying.

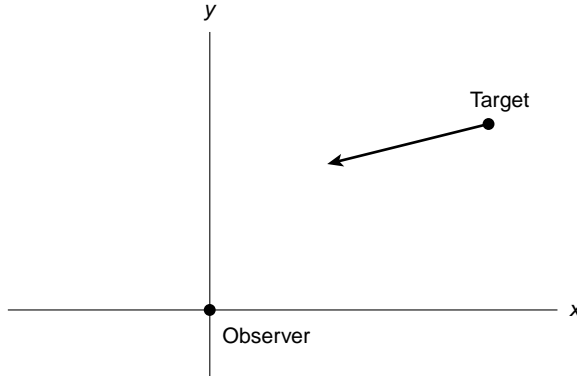


Figure 1.7: Two-dimensional tracking problem.

We shall find that if we transmit the signal in (1.22) over this channel, the received waveform will be

$$r(t) = V(t) \sin \left[\omega_c t + \int_{-\infty}^t a(u) du + \theta(t) \right] + n(t), \quad (1.26)$$

where $V(t)$ and $\theta(t)$ are sample functions from random processes whose statistics are unknown. We refer to this level as *random signals with unknown waveforms in noise*. Thus, even if $a(u)$ were known and the noise $n(t)$ were absent, the received signal would still be a random process. An overall outline of the problems of interest to us appears in Table 1.3. Additional examples included in the table to indicate the breadth of the problems that fit into the outline are discussed in more detail in the text.

Table 1.3: Filtering theory hierarchy

Filtering Theory	
Level 1. Random signals in noise; known statistics	<ol style="list-style-type: none"> 1. Conventional communication systems such as AM (DSB-AM, SSB), FM, and PM with phase synchronization 2. Optimum filter theory 3. Optimum feedback systems 4. Target tracking in radar/sonar problems 5. Orbital estimation for satellites 6. Signal estimation in seismic and sonar classification systems 7. Synchronization in digital systems
Level 2. Random signals with unknown parameters in noise	<ol style="list-style-type: none"> 1. Conventional communication systems without phase synchronization 2. Estimation of channel characteristics when phase of input signal is unknown
Level 3. Random signals with unknown waveforms in noise	<ol style="list-style-type: none"> 1. Analog communication over randomly varying channels 2. Estimation of statistics of time-varying processes 3. Estimation of plant characteristics

Now that we have outlined the areas of interest it is appropriate to determine how to go about solving them.

1.3 POSSIBLE APPROACHES

From the examples we have discussed it is obvious that an inherent feature of all the problems is randomness of source, channel, or noise (often all three). Thus, our approach must be statistical in nature. Even assuming that we are using a statistical model, there are many different ways to approach the problem. We can divide the possible approaches into two categories, which we denote as “structured” and “nonstructured.” Some simple examples will illustrate what we mean by a structured approach.

Example 1.1. The input to a linear time-invariant system is $r(t)$:

$$\begin{aligned} r(t) &= s(t) + n(t), \quad 0 \leq t \leq T, \\ &= 0, \quad \text{elsewhere.} \end{aligned} \quad (1.27)$$

The impulse response of the system is $h(\tau)$. The signal $s(t)$ is a known function with energy E_s ,

$$E_s = \int_0^T s^2(t) dt, \quad (1.28)$$

and $n(t)$ is a sample function from a zero-mean random process with a covariance function:

$$K_n(t, u) = \frac{N_0}{2} \delta(t - u). \quad (1.29)$$

We are concerned with the output of the system at time T . The output due to the signal is a deterministic quantity:

$$s_0(T) = \int_0^T h(\tau) s(T - \tau) d\tau. \quad (1.30)$$

The output due to the noise is a random variable:

$$n_0(T) = \int_0^T h(\tau) n(T - \tau) d\tau. \quad (1.31)$$

We can define the output signal-to-noise ratio at time T as

$$\frac{S}{N} \triangleq \frac{s_0^2(T)}{E[n_0^2(T)]}, \quad (1.32)$$

where $E[\cdot]$ denotes expectation.

Substituting (1.30) and (1.31) into (1.32), we obtain

$$\frac{S}{N} = \frac{\left[\int_0^T h(\tau) s(T - \tau) d\tau \right]^2}{E \left[\int_0^T \int_0^T h(\tau) h(u) n(T - \tau) n(T - u) d\tau du \right]}. \quad (1.33)$$

By bringing the expectation inside the integral, using (1.29), and performing the integration with respect to u , we have

$$\frac{S}{N} = \frac{\left[\int_0^T h(\tau) s(T - \tau) d\tau \right]^2}{N_0/2 \int_0^T h^2(\tau) d\tau}. \quad (1.34)$$

The problem of interest is to choose $h(\tau)$ to maximize the signal-to-noise ratio. The solution follows easily, but it is not important for our present discussion (see Problem 6.3.1). ■

This example illustrates the three essential features of the structured approach to a statistical optimization problem:

Structure. The processor was required to be a linear time-invariant filter. We wanted to choose the best system in this class. Systems that were not in this class (e.g., nonlinear or time varying) were not allowed.

Criterion. In this case, we wanted to maximize a quantity that we called the signal-to-noise ratio.

Information. To write the expression for S/N , we had to know the signal shape and the covariance function of the noise process.

If we knew more about the process (e.g., its first-order probability density), we could not use it, and if we knew less, we could not solve the problem. Clearly, if we changed the criterion, the information required might be different. For example, to maximize x

$$x = \frac{s_0^4(T)}{E[n_0^4(T)]}, \quad (1.35)$$

the covariance function of the noise process would not be adequate. Alternatively, if we changed the structure, the information required might change. Thus, the three ideas of structure, criterion, and information are closely related. It is important to emphasize that the structured approach does not imply a linear system, as illustrated by Example 1.2.

Example 1.2. The input to the nonlinear no-memory device shown in Figure 1.8 is $r(t)$, where

$$r(t) = s(t) + n(t), \quad -\infty < t < \infty. \quad (1.36)$$

At any time t , $s(t)$ is the value of a random variable s with known probability density function (pdf) $p_s(S)$. Similarly, $n(t)$ is the value of a statistically independent random variable n with known density $p_n(N)$. The output of the device is $y(t)$, where

$$y(t) = a_0 + a_1[r(t)] + a_2[r(t)]^2 \quad (1.37)$$

is a quadratic no-memory function of $r(t)$. The adjective no-memory emphasizes that the value of $y(t_0)$ depends *only* on $r(t_0)$. We want to choose the coefficients a_0 , a_1 , and a_2 so that $y(t)$ is the minimum mean-square error estimate of $s(t)$. The mean-square error is

$$\begin{aligned} \xi(t) &\triangleq E\{[y(t) - s(t)^2]\} \\ &= E\left\{(a_0 + a_1[r(t)] + a_2[r^2(t)]) - s(t)^2\right\} \end{aligned} \quad (1.38)$$

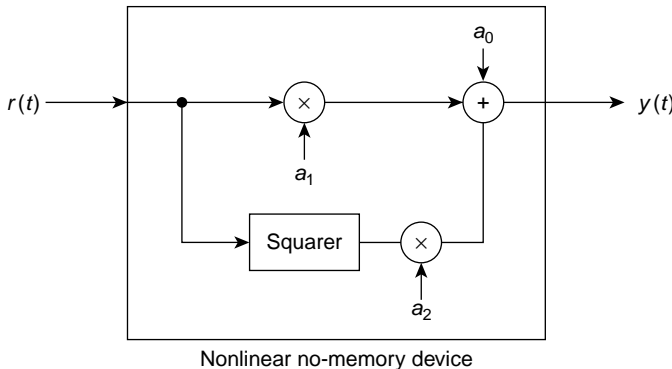


Figure 1.8: A structured nonlinear device.

and a_0 , a_1 , and a_2 are chosen to minimize $\xi(t)$. The solution to this particular problem is given in Chapter 6. ■

The technique for solving structured problems is conceptually straightforward. We allow the structure to vary within the allowed class and choose the particular system that maximizes (or minimizes) the criterion of interest.

An obvious advantage to the structured approach is that it usually requires only a partial characterization of the processes. This is important because, in practice, we must measure or calculate the process properties needed.

An obvious disadvantage is that it is often impossible to tell if the structure chosen is correct. In Example 1.1, a simple nonlinear system might be far superior to the best linear system. Similarly, in Example 1.2, some other nonlinear system might be far superior to the quadratic system. Once a class of structure is chosen, we are committed. A number of trivial examples demonstrate the effect of choosing the wrong structure.

At first glance it appears that one way to get around the problem of choosing the proper structure is to let the structure be an arbitrary nonlinear time-varying system. In other words, the class of structure is chosen to be so large that every possible system will be included in it. The difficulty is that there is no convenient tool, such as the convolution integral, to express the output of a nonlinear system in terms of its input. This means that there is no convenient way to investigate all possible systems by using a structured approach.

The alternative to the structured approach is a nonstructured approach. Here, we refuse to make any *a priori* guesses about what structure the processor should have. We establish a criterion, solve the problem, and implement whatever processing procedure is indicated.

A simple example of the nonstructured approach can be obtained by modifying Example 1.2. Instead of assigning characteristics to the device, we denote the estimate by $y(t)$. Letting

$$\xi(t) \triangleq E \{ [y(t) - s(t)]^2 \}, \quad (1.39)$$

we solve for the $y(t)$ that is obtained from $r(t)$ in *any* manner to minimize ξ . The obvious advantage is that if we can solve the problem we know that our answer is, *with respect to the chosen criterion*, the best processor of all possible processors. The obvious disadvantage is that we must completely characterize all the signals, channels, and noises that enter into

the problem. Fortunately, it turns out that there are a large number of problems of practical importance in which this complete characterization is possible. We will utilize both the nonstructured and structured approach in the book.

In the nonstructured approach to continuous-time processing, we will emphasize two random processes in which a complete characterization is possible:

1. Gaussian processes
2. Markov processes.

These processes allow us to obtain analytical results and also are realistic models in a number of applications. For discrete-time processing, we use the discrete version of these two processes. In addition, we consider discrete-time processes with non-Gaussian statistically independent samples.

We use a structured approach to the linear estimation problem by restricting our processor to be linear. However, we will also show that if the processes are Gaussian, then a linear processor is the solution to the nonstructured approach.

1.4 ORGANIZATION

The material covered in this book is organized into 11 chapters that can be grouped into four topical areas.

The first can be labeled *Classical Detection and Estimation Theory* and consists of Chapters 2–5. Here, we deal with problems in which the observations are sets of random variables instead of random waveforms. The theory needed to solve problems of this type has been studied by statisticians for many years. We therefore use the adjective classical to describe it. The purpose of these chapters is twofold: first, to derive all the basic statistical results we need in the remainder of the chapters; second, to provide a general background in detection and estimation theory that can be extended into various areas that we do not discuss in detail. To accomplish the second purpose we keep the discussion as general as possible.

In Chapter 2, we consider in detail the binary and M -ary hypothesis testing problem. We find the optimum test using both a Bayes criterion and Neyman–Pearson criterion and show that they have an identical structure. In order to analyze the performance, we develop analytical techniques to find the exact performance and methods to bound the performance. We also introduce importance sampling that plays a key role in efficient simulation.

In Chapter 3, we study the general Gaussian detection problem. The Gaussian model is applicable in many important applications. We are able to obtain analytical results for the performance of the optimum detectors in almost all cases of interest. In addition, by working in an eigenspace, we can develop a better understanding of the important factors in the model.

In Chapter 4, we study the problem of estimating random and nonrandom parameters. We develop Bayes estimators for random parameters and maximum likelihood estimators for nonrandom parameters. We consider both scalar and vector parameters and develop bounds on the performance of the estimators. We will find that when the parameter is embedded nonlinearly in the observation, a threshold phenomenon occurs as the signal-to-noise ratio decreases and the performance degrades rapidly. We develop a family of global bounds to

predict this behavior. We also revisit the detection problem to study composite hypothesis testing in which unknown parameters appear in the hypotheses.

In Chapter 5, we study the general Gaussian estimation problem for random and non-random parameters. We develop explicit solutions for the models in which the parameters appear in the mean and covariance matrix of a Gaussian random vector. We develop performance bounds on the performance of the estimators. In many cases, the optimum estimate is the maximum of a D -dimensional surface. We develop computational algorithms to find the maximum. We introduce the sequential estimation model and develop the optimum solution.

All of the basic results in these four chapters apply to a wide variety of physical situations outside the context of communications, radar, sonar, and seismology. Examples include medical device technology, financial engineering, and patient diagnosis techniques. However, to motivate our core reader, we have motivated many of our examples by assuming we obtained the observation vector by sampling a continuous-time random process.¹

The second topical area bridges the gap between the classical case and the waveform problems discussed in Section 1.2. Chapter 6 develops the necessary techniques. The key to the transition is a suitable method for characterizing random processes. When the observation interval is finite, the most useful characterization is by a series expansion of the random process using a Karhunen–Loëve expansion that is a generalization of the conventional Fourier series. When the observation interval is infinite, a transform characterization, which is a generalization of the usual Fourier transform, is needed. In the process of developing these characterizations, we encounter integral equations and we digress briefly to develop methods of solution. Just as in Chapters 2–5, our discussion is general and provides background for other areas of application.

With these five chapters as a foundation, we are prepared to work our way through the hierarchy of problems outlined in Tables 1.1–1.3. The third topical area consists of Chapters 7 and 10. Chapter 7 is entitled “Detection of Signals—Estimation of Signal Parameters.” Here, we develop the first two levels described in Section 1.2. (This material corresponds to the upper two levels in Tables 1.1 and 1.2.) We begin by looking at the simple binary digital communication system described in Figure 1.1 and then proceed to more complicated problems in the communications, radar, and sonar area involving M -ary communication, random phase channels, random amplitude and phase channels, and colored noise interference. By exploiting the parallel nature of the estimation problem, results are obtained easily for the estimation problem outlined in Figure 1.4 and other more complex systems. The extension of the results to include the multiple channel (e.g., frequency diversity systems or arrays) and multiple parameter (e.g., range and Doppler) problems completes our discussion. The results in this chapter are fundamental to the understanding of modern communication and radar/sonar systems. Chapter 10 completes this topical area and we will discuss it after we discuss the fourth topical area.

The fourth topical area consists of Chapters 8 and 9 and studies the problem of linear estimation of a random process. Chapter 8 deals with continuous-time processes, and Chapter 9 deals with discrete-time processes. In Chapter 8, we first derive the integral equations that specify the optimum realizable filter and then derive the optimum filter itself, where “optimum” denotes that it minimizes the mean-square error. We next discuss the special

¹We should note that if one is willing to assume that the sampling process does not lose any information, then we have solved the problems in the upper two levels of hierarchies in Tables 1.1 and 1.2.

case in which the processes are stationary and the infinite past is available. This case, the Wiener problem, leads to straightforward solution techniques. The original work of Wiener is extended to obtain some important closed-form error expressions. In the next section we discuss the case in which the processes can be characterized by using state-variable techniques. This case, the Kalman–Bucy problem, enables us to deal with nonstationary, finite-interval problems and adds considerable insight to the results of the preceding section. We show that if the processes are Gaussian, then the optimum linear estimator is the optimum Bayes estimator for a mean-square error cost function. We also provide an introduction to the problem of Bayesian estimation of random processes in which both the process model and the observation model may be nonlinear. We provide brief discussions of the currently available processors, but our emphasis is on recursive Bayesian bounds that provide a lower bound on the performance of any processor.

In Chapter 9, we study linear estimation of discrete-time random processes. We develop the finite impulse response (FIR) Wiener filter, the infinite impulse response (IIR) unrealizable Wiener filter, and the IIR realizable Wiener filter. We next develop the discrete-time Kalman filter. A number of issues arise when implementing the Kalman filter in actual applications. We develop alternate implementation algorithms to reduce computational complexity and decrease sensitivity to round-off errors. We provide an introduction to Bayesian estimation of discrete-time non-Gaussian random processes and develop the extended Kalman filter and recursive Bayesian Cramér–Rao bound. Chapters 8 and 9 may be read independently.

We return to detection theory in Chapter 10. We revisit the detection theory model and study the problem of detecting a sample function from a Gaussian random process in the presence of additive Gaussian noise. We consider the continuous-time problem first and develop three canonical receiver structures whose key components are the optimum linear filters developed in Chapter 8. We consider state-variable models and stationary-process long-observation time models where we can obtain explicit solutions and evaluate the performance. Next, we consider discrete-time processes and develop detectors using the filters derived in Chapter 9.

Finally, in Chapter 11, we summarize some of the more important results and offer some concluding comments.

In the course of our development, we will work with a variety of statistical distributions and mathematical functions. These are summarized in Appendix A. Numerical evaluation of these mathematical functions can be easily accomplished using computer software such as Matlab. Where appropriate, we indicate the Matlab functions that apply. We will demonstrate results through numerous examples, many of which are interrelated. Appendix B contains an index to the examples for reference.

2

Classical Detection Theory

2.1 INTRODUCTION

In this chapter, we develop in detail the basic ideas of classical detection theory. The first step is to define the various terms.

The basic components of a simple decision theory problem are shown in Figure 2.1.

The first is a *source* that generates an output. In the simplest case, this output is one of two choices. We refer to them as hypotheses and label them H_0 and H_1 in the two-choice case. More generally, the output might be one of M hypotheses, which we label H_0, H_1, \dots, H_{M-1} . Some typical source mechanisms are the following:

1. A digital communication system transmits information by sending ones and zeros. When “one” is sent, we call it H_1 , and when “zero” is sent, we call it H_0 .
2. In a radar system, we look at a particular range and azimuth and try to decide whether a target is present; H_1 corresponds to the presence of a target and H_0 corresponds to no target.
3. In a medical diagnosis problem, we examine an electrocardiogram. Here H_1 could correspond to the patient having had a heart attack and H_0 to the absence of one.

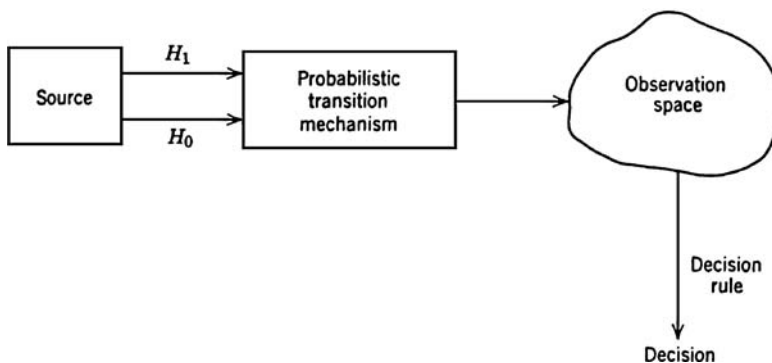


Figure 2.1: Components of a decision theory problem.

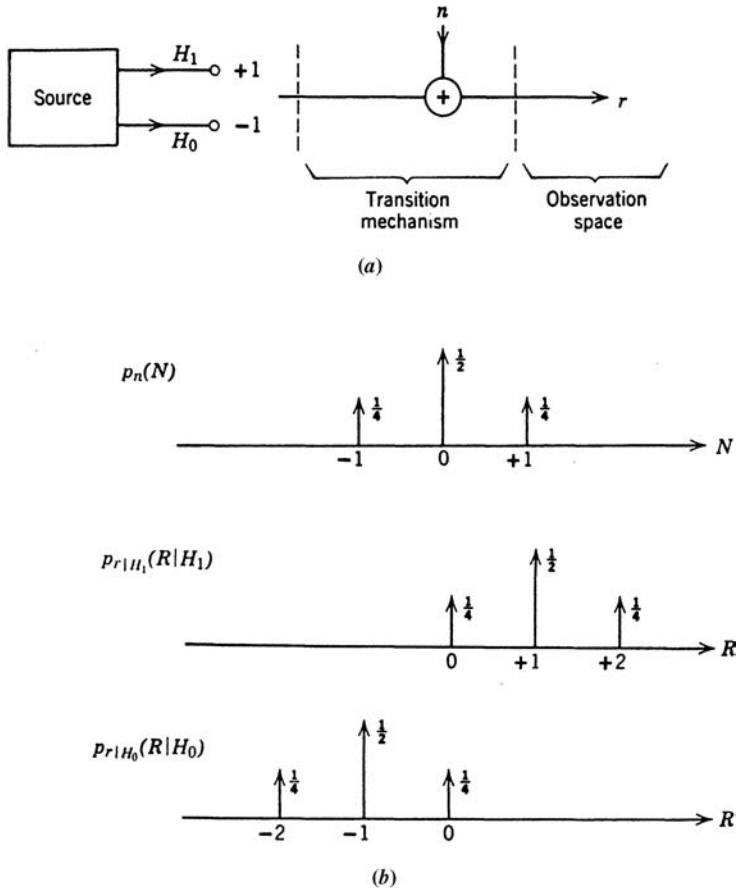


Figure 2.2: A simple decision problem: (a) model; (b) probability densities.

4. In a speaker classification problem we know the speaker is German, British, or American and either male or female. There are six possible hypotheses.

In the cases of interest to us, we do not know which hypothesis is true.

The second component of the problem is a probabilistic transition mechanism; the third is an observation space. The transition mechanism can be viewed as a device that knows which hypothesis is true. Based on this knowledge, it generates a point in the observation space according to some probability law. A simple example to illustrate these ideas is given in Figure 2.2. When H_1 is true, the source generates +1. When H_0 is true, the source generates -1. An independent discrete random variable n whose probability density is shown in Figure 2.2b is added to the source output. The sum of the source output and n is the observed variable r .

Under the two hypotheses, we have

$$\begin{aligned} H_1 : r &= 1 + n, \\ H_0 : r &= -1 + n. \end{aligned} \tag{2.1}$$

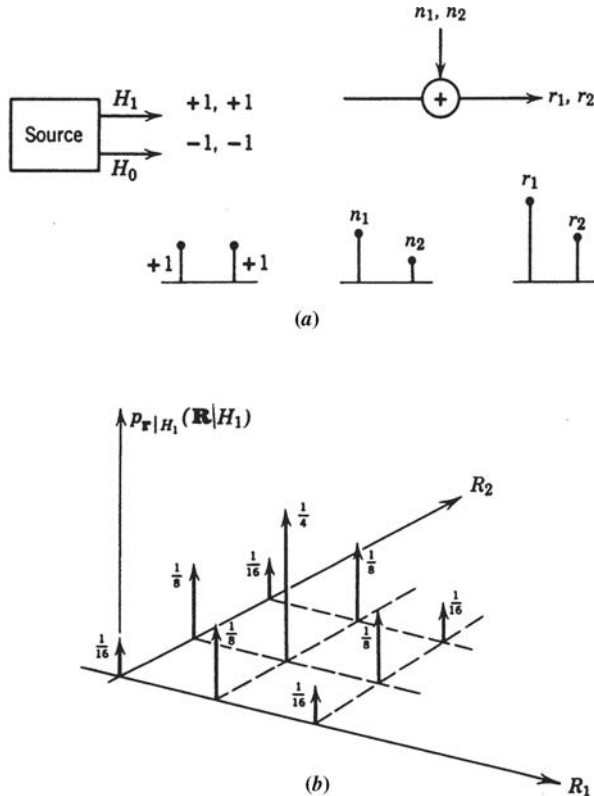


Figure 2.3: A two-dimensional problem: (a) model; (b) probability density.

The probability densities of r on the two hypotheses are shown in Figure 2.2b. The observation space is one dimensional, for any output can be plotted on a line.

A related example is shown in Figure 2.3a in which the source generates two numbers in sequence. A random variable n_1 is added to the first number and an independent random variable n_2 is added to the second.

Thus,

$$\begin{aligned}
 H_1 : r_1 &= 1 + n_1, \\
 r_2 &= 1 + n_2, \\
 H_0 : r_1 &= -1 + n_1, \\
 r_2 &= -1 + n_2.
 \end{aligned} \tag{2.2}$$

The joint probability density of r_1 and r_2 when H_1 is true is shown in Figure 2.3b. The observation space is two dimensional and any observation can be represented as a point in a plane.

In this chapter, we confine our discussion to problems in which the observation space is finite dimensional. In other words, the observations consist of a set of N numbers and can be represented as a point in an N -dimensional space. This is the class of problem that

statisticians have treated for many years. For this reason, we refer to it as the *classical* decision problem.

The fourth component of the detection problem is a decision rule. After observing the outcome in the observation space we shall guess which hypothesis was true, and to accomplish this we develop a decision rule that assigns each point to one of the hypotheses. Suitable choices for decision rules will depend on several factors that we discuss in detail later. Our study will demonstrate how these four components fit together to form the total decision (or hypothesis testing) problem.

Organization. This chapter is organized in the following sections. In Section 2.2, we study the binary hypothesis testing problem. Then in Section 2.3, we extend the results to the case of M hypotheses.

In many cases of practical importance, we can develop the “optimum” decision rule according to certain criteria but cannot evaluate how well the test will work. In Section 2.4, we develop bounds and approximate expressions for the performance that will be necessary for some of the later chapters. In Section 2.5, we discuss Monte Carlo simulation and introduce a simulation technique using importance sampling. Finally, in Section 2.6, we summarize our results and indicate some of the topics that we have omitted.

2.2 SIMPLE BINARY HYPOTHESIS TESTS

As a starting point, we consider the decision problem in which each of two source outputs corresponds to a hypothesis. Each hypothesis maps into a point in the observation space. We assume that the observation space corresponds to a set of N observations: $r_1, r_2, r_3, \dots, r_N$. Thus, each set can be thought of as a point in an N -dimensional space and can be denoted by a vector \mathbf{r} :

$$\mathbf{r} \triangleq \begin{bmatrix} r_1 \\ r_2 \\ \vdots \\ r_N \end{bmatrix}. \quad (2.3)$$

The probabilistic transition mechanism generates points in accord with the two known conditional probability densities $p_{\mathbf{r}|H_1}(\mathbf{R}|H_1)$ and $p_{\mathbf{r}|H_0}(\mathbf{R}|H_0)$. The object is to use this information to develop a suitable decision rule. To do this, we must look at various criteria for making decisions.

2.2.1 Decision Criteria

In the binary hypothesis problem, we know that either H_0 or H_1 is true. We shall confine our discussion to decision rules that are required to make a choice. (An alternative procedure would be to allow decision rules with three outputs: (a) H_0 true, (b) H_1 true, (c) do not know.) Thus, each time the experiment is conducted one of four things can happen:

1. H_0 true; choose H_0 .
2. H_0 true; choose H_1 .

3. H_1 true; choose H_1 .
4. H_1 true; choose H_0 .

The first and third alternatives correspond to correct choices. The second and fourth alternatives correspond to errors. The purpose of a decision criterion is to attach some relative importance to the four possible courses of action. It might be expected that the method of processing the received data (\mathbf{r}) would depend on the decision criterion we select. In this section, we show that for the two criteria of most interest, the Bayes and the Neyman–Pearson, the operations on \mathbf{r} are identical.

Bayes Criterion. A Bayes test is based on two assumptions. The first is that the source outputs are governed by probability assignments, which are denoted by P_1 and P_0 , respectively, and called the *a priori* probabilities. These probabilities represent the observer's information about the source before the experiment is conducted. The second assumption is that a cost is assigned to each possible course of action. We denote the cost for the four courses of action as C_{00} , C_{10} , C_{11} , C_{01} , respectively. The first subscript indicates the hypothesis chosen and the second, the hypothesis that is true. Each time the experiment is conducted, a certain cost will be incurred. We should like to design our decision rule so that *on the average* the cost will be as small as possible. To do this, we first write an expression for the expected value of the cost. We see that there are two probabilities that we must average over; the *a priori* probability and the probability that a particular course of action will be taken. Denoting the expected value of the cost as the risk \mathcal{R} , we have

$$\begin{aligned}\mathcal{R} = & C_{00} P_0 \Pr(\text{say } H_0 | H_0 \text{ is true}) \\ & + C_{10} P_0 \Pr(\text{say } H_1 | H_0 \text{ is true}) \\ & + C_{11} P_1 \Pr(\text{say } H_1 | H_1 \text{ is true}) \\ & + C_{01} P_1 \Pr(\text{say } H_0 | H_1 \text{ is true}).\end{aligned}\quad (2.4)$$

Because we have assumed that the decision rule must say either H_1 or H_0 , we can view it as a rule for dividing the total observation space Z into two parts, Z_0 and Z_1 , as shown in Figure 2.4. Whenever an observation falls in Z_0 we say H_0 , and whenever an observation falls in Z_1 we say H_1 .

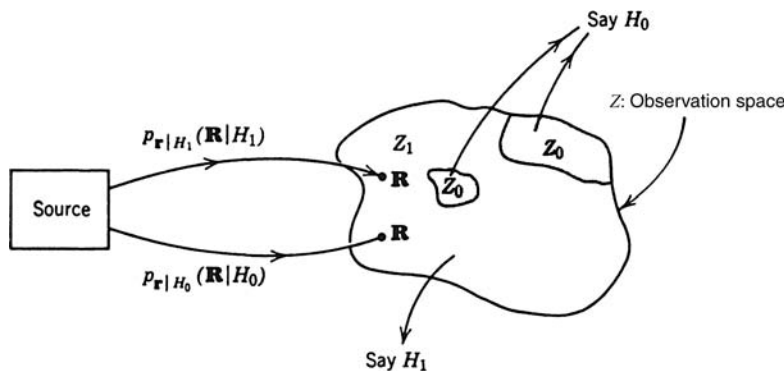


Figure 2.4: Decision regions.

We can now write the expression for the risk in terms of the transition probabilities and the decision regions:

$$\begin{aligned}\mathcal{R} &= C_{00} P_0 \int_{Z_0} p_{\mathbf{r}|H_0}(\mathbf{R}|H_0) d\mathbf{R} \\ &\quad + C_{10} P_0 \int_{Z_1} p_{\mathbf{r}|H_0}(\mathbf{R}|H_0) d\mathbf{R} \\ &\quad + C_{11} P_1 \int_{Z_1} p_{\mathbf{r}|H_1}(\mathbf{R}|H_1) d\mathbf{R} \\ &\quad + C_{01} P_1 \int_{Z_0} p_{\mathbf{r}|H_1}(\mathbf{R}|H_1) d\mathbf{R}. \end{aligned} \quad (2.5)$$

For an N -dimensional observation space, the integrals in (2.5) are N -fold integrals. We shall assume throughout our work that the cost of a wrong decision is higher than the cost of a correct decision. In other words,

$$\begin{aligned}C_{10} &> C_{00}, \\ C_{01} &> C_{11}. \end{aligned} \quad (2.6)$$

Now, to find the Bayes test we must choose the decision regions Z_0 and Z_1 in such a manner that the risk will be minimized. Because we require that a decision be made, this means that we must assign each point \mathbf{R} in the observation space Z to Z_0 or Z_1 .

Thus,

$$Z = Z_0 + Z_1 \triangleq Z_0 \cup Z_1. \quad (2.7)$$

Rewriting (2.5), we have

$$\begin{aligned}\mathcal{R} &= P_0 C_{00} \int_{Z_0} p_{\mathbf{r}|H_0}(\mathbf{R}|H_0) d\mathbf{R} + P_0 C_{10} \int_{Z-Z_0} p_{\mathbf{r}|H_0}(\mathbf{R}|H_0) d\mathbf{R} \\ &\quad + P_1 C_{01} \int_{Z_0} p_{\mathbf{r}|H_1}(\mathbf{R}|H_1) d\mathbf{R} + P_1 C_{11} \int_{Z-Z_0} p_{\mathbf{r}|H_1}(\mathbf{R}|H_1) d\mathbf{R}. \end{aligned} \quad (2.8)$$

Observing that

$$\int_Z p_{\mathbf{r}|H_0}(\mathbf{R}|H_0) d\mathbf{R} = \int_Z p_{\mathbf{r}|H_1}(\mathbf{R}|H_1) d\mathbf{R} = 1, \quad (2.9)$$

(2.8) reduces to

$$\mathcal{R} = P_0 C_{10} + P_1 C_{11} + \int_{Z_0} \left[(P_1(C_{01} - C_{11}) p_{\mathbf{r}|H_1}(\mathbf{R}|H_1)) - (P_0(C_{10} - C_{00}) p_{\mathbf{r}|H_0}(\mathbf{R}|H_0)) \right] d\mathbf{R}. \quad (2.10)$$

The first two terms represent the fixed cost. The integral represents the cost controlled by those points \mathbf{R} that we assign to Z_0 . The assumption in (2.6) implies that the two terms

inside the brackets are positive. Therefore, all values of \mathbf{R} where the second term is larger than the first should be included in Z_0 because they contribute a negative amount to the integral. Similarly, all values of \mathbf{R} where the first term is larger than the second should be excluded from Z_0 (assigned to Z_1) because they would contribute a positive amount to the integral. Values of \mathbf{R} where the two terms are equal have no effect on the cost and may be assigned arbitrarily. We shall assume that these points are assigned to H_1 and ignore them in our subsequent discussion. Thus, the decision regions are defined by the statement: If

$$P_1(C_{01} - C_{11})p_{\mathbf{r}|H_1}(\mathbf{R}|H_1) \geq P_0(C_{10} - C_{00})p_{\mathbf{r}|H_0}(\mathbf{R}|H_0), \quad (2.11)$$

assign \mathbf{R} to Z_1 and consequently say that H_1 is true. Otherwise assign \mathbf{R} to Z_0 and say H_0 is true.

Alternatively, we may write

$$\frac{p_{\mathbf{r}|H_1}(\mathbf{R}|H_1)}{p_{\mathbf{r}|H_0}(\mathbf{R}|H_0)} \stackrel{H_1}{\gtrless} \frac{P_0(C_{10} - C_{00})}{P_1(C_{01} - C_{11})}. \quad (2.12)$$

The quantity on the left-hand side is called the *likelihood ratio* and denoted by $\Lambda(\mathbf{R})$

$$\boxed{\Lambda(\mathbf{R}) \triangleq \frac{p_{\mathbf{r}|H_1}(\mathbf{R}|H_1)}{p_{\mathbf{r}|H_0}(\mathbf{R}|H_0)}}. \quad (2.13)$$

Because it is the ratio of two functions of a random variable, it is a random variable. We see that regardless of the dimensionality of \mathbf{R} , $\Lambda(\mathbf{R})$ is a one-dimensional variable.

The quantity on the right-hand side of (2.12) is the threshold of the test and is denoted by η :

$$\eta \triangleq \frac{P_0(C_{10} - C_{00})}{P_1(C_{01} - C_{11})}. \quad (2.14)$$

Thus, Bayes criterion leads us to a *likelihood ratio test* (LRT)

$$\Lambda(\mathbf{R}) \stackrel{H_1}{\gtrless} \eta. \quad (2.15)$$

We see that all the data processing is involved in computing $\Lambda(\mathbf{R})$ and is not affected by *a priori* probabilities or cost assignments. This invariance of the data processing is of considerable practical importance. Frequently, the costs and *a priori* probabilities are merely educated guesses. The result in (2.15) enables us to build the entire processor and leave η as a variable threshold to accommodate changes in our estimates of *a priori* probabilities and costs.

Because the natural logarithm is a monotonic function, and both sides of (2.15) are positive, an equivalent test is

$$\ln \Lambda(\mathbf{R}) \stackrel{H_1}{\gtrless} \ln \eta. \quad (2.16)$$

Two forms of a processor to implement a likelihood ratio test are shown in Figure 2.5. Before proceeding to other criteria, we consider three simple examples.

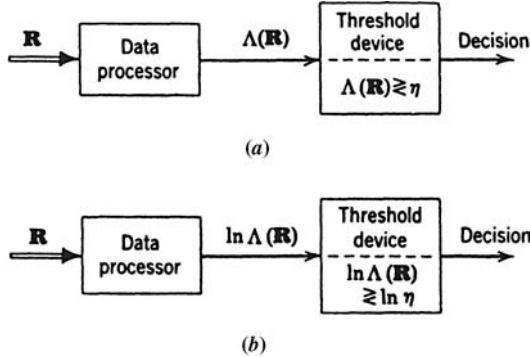


Figure 2.5: Likelihood ratio processors.

Example 2.1. We assume that under H_1 the source output is a constant voltage m . Under H_0 , the source output is zero. Before observation, the voltage is corrupted by an additive noise. We sample the output waveform each second and obtain N samples. Each noise sample is a zero-mean Gaussian random variable n with variance σ^2 . The noise samples at various instants are independent random variables and are independent of the source output. Looking at Figure 2.6, we see that the observations under the two hypotheses are

$$\begin{aligned} H_1 : r_i &= m + n_i, \quad i = 1, 2, \dots, N, \\ H_0 : r_i &= n_i, \quad i = 1, 2, \dots, N, \end{aligned} \quad (2.17)$$

and

$$p_{n_i}(X) = \frac{1}{\sqrt{2\pi}\sigma} \exp\left(-\frac{X^2}{2\sigma^2}\right), \quad (2.18)$$

because the noise samples are Gaussian.

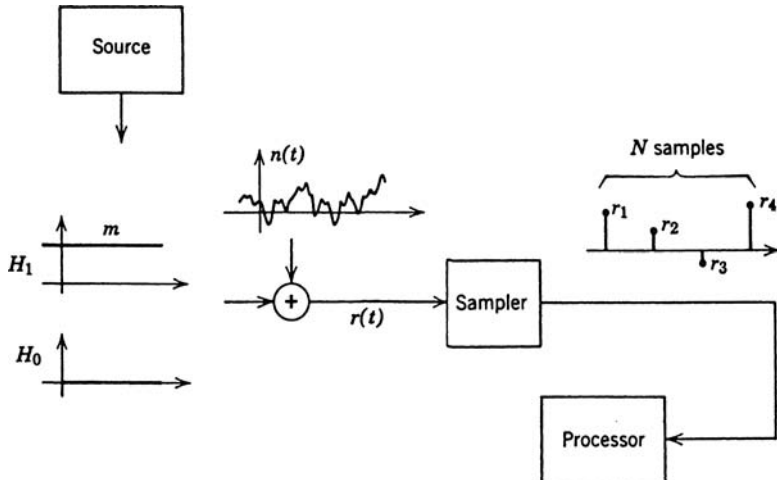


Figure 2.6: Model for Example 2.1.

The probability density of r_i under each hypothesis follows easily:

$$p_{r_i|H_1}(R_i|H_1) = p_{n_i}(R_i - m) = \frac{1}{\sqrt{2\pi}\sigma} \exp\left(-\frac{(R_i - m)^2}{2\sigma^2}\right) \quad (2.19)$$

and

$$p_{r_i|H_0}(R_i|H_0) = p_{n_i}(R_i) = \frac{1}{\sqrt{2\pi}\sigma} \exp\left(-\frac{R_i^2}{2\sigma^2}\right). \quad (2.20)$$

Because the n_i are statistically independent, the joint probability density of the r_i (or, equivalently, of the vector \mathbf{r}) is simply the product of the individual probability densities. Thus,

$$p_{\mathbf{r}|H_1}(\mathbf{R}|H_1) = \prod_{i=1}^N \frac{1}{\sqrt{2\pi}\sigma} \exp\left(-\frac{(R_i - m)^2}{2\sigma^2}\right) \quad (2.21)$$

and

$$p_{\mathbf{r}|H_0}(\mathbf{R}|H_0) = \prod_{i=1}^N \frac{1}{\sqrt{2\pi}\sigma} \exp\left(-\frac{R_i^2}{2\sigma^2}\right). \quad (2.22)$$

Substituting into (2.13), we have

$$\Lambda(\mathbf{R}) = \frac{\prod_{i=1}^N \frac{1}{\sqrt{2\pi}\sigma} \exp\left(-\frac{(R_i - m)^2}{2\sigma^2}\right)}{\prod_{i=1}^N \frac{1}{\sqrt{2\pi}\sigma} \exp\left(-\frac{R_i^2}{2\sigma^2}\right)}. \quad (2.23)$$

After canceling common terms and taking the logarithm, we have

$$\ln \Lambda(\mathbf{R}) = \frac{m}{\sigma^2} \sum_{i=1}^N R_i - \frac{Nm^2}{2\sigma^2}. \quad (2.24)$$

Thus, the likelihood ratio test is

$$\frac{m}{\sigma^2} \sum_{i=1}^N R_i - \frac{Nm^2}{2\sigma^2} \stackrel{H_1}{\underset{H_0}{\gtrless}} \ln \eta \quad (2.25)$$

or, equivalently,

$$\sum_{i=1}^N R_i \stackrel{H_1}{\underset{H_0}{\gtrless}} \frac{\sigma^2}{m} \ln \eta + \frac{Nm}{2} \triangleq \gamma. \quad (2.26)$$

We see that the processor simply adds the observations and compares them with a threshold. ■

In this example, the only way the data appear in the likelihood ratio test is in a sum. This is an example of a *sufficient statistic*, which we denote by $l(\mathbf{R})$ (or simply l when the argument is obvious). It is just a function of the received data, which has the property that $\Lambda(\mathbf{R})$ can be written as a function of l . In other words, when making a decision, knowing the value of the sufficient statistic is just as good as knowing \mathbf{R} . In Example 2.1, l is a linear function of the R_i . A case in which this is not true is illustrated in Example 2.2.

Example 2.2. Several different physical situations lead to the mathematical model of interest in this example. The observations consist of a set of N values: $r_1, r_2, r_3, \dots, r_N$. Under both hypotheses,

the r_i are independent, identically distributed, zero-mean Gaussian random variables. Under H_1 , each r_i has a variance σ_1^2 . Under H_0 , each r_i has a variance σ_0^2 . Because the variables are independent, the joint density is simply the product of the individual densities. Therefore

$$p_{\mathbf{r}|H_1}(\mathbf{R}|H_1) = \prod_{i=1}^N \frac{1}{\sqrt{2\pi}\sigma_1} \exp\left(-\frac{R_i^2}{2\sigma_1^2}\right) \quad (2.27)$$

and

$$p_{\mathbf{r}|H_0}(\mathbf{R}|H_0) = \prod_{i=1}^N \frac{1}{\sqrt{2\pi}\sigma_0} \exp\left(-\frac{R_i^2}{2\sigma_0^2}\right). \quad (2.28)$$

Substituting (2.27) and (2.28) into (2.13) and taking the logarithm, we have

$$\frac{1}{2}\left(\frac{1}{\sigma_0^2} - \frac{1}{\sigma_1^2}\right) \sum_{i=1}^N R_i^2 + N \ln \frac{\sigma_0}{\sigma_1} \stackrel{H_1}{\gtrless} \ln \eta. \quad (2.29)$$

In this case, the sufficient statistic is the sum of the squares of the observations

$$l(\mathbf{R}) = \sum_{i=1}^N R_i^2, \quad (2.30)$$

and an equivalent test for $\sigma_1^2 > \sigma_0^2$ is

$$l(\mathbf{R}) \stackrel{H_1}{\gtrless} \frac{2\sigma_0^2\sigma_1^2}{\sigma_1^2 - \sigma_0^2} \left(\ln \eta - N \ln \frac{\sigma_0}{\sigma_1} \right) \triangleq \gamma. \quad (2.31)$$

For $\sigma_1^2 < \sigma_0^2$, the inequality is reversed because we are multiplying by a negative number:

$$l(\mathbf{R}) \stackrel{H_0}{\gtrless} \frac{2\sigma_0^2\sigma_1^2}{\sigma_0^2 - \sigma_1^2} \left(N \ln \frac{\sigma_0}{\sigma_1} - \ln \eta \right) \triangleq \gamma'; \quad \sigma_1^2 < \sigma_0^2. \quad (2.32)$$

■

These two examples have emphasized Gaussian variables. In the next example, we consider a different type of distribution.

Example 2.3. The Poisson distribution of events is encountered frequently as a model of shot noise and other diverse phenomena (e.g., [DR58c] or [BR60]). Each time the experiment is conducted, a certain number of events occur. Our observation is just this number that ranges from 0 to ∞ and obeys a Poisson distribution on both hypotheses; that is,

$$\Pr(n \text{ events}) = \frac{(m_i)^n}{n!} e^{-m_i}, \quad n = 0, 1, 2, \dots; i = 0, 1. \quad (2.33)$$

where m_i is the parameter that specifies the average number of events:

$$E(n) = m_i. \quad (2.34)$$

It is this parameter m_i that is different in the two hypotheses. Rewriting (2.33) to emphasize this point, we have for the two Poisson distributions

$$H_1 : \Pr(n \text{ events}) = \frac{(m_1)^n}{n!} e^{-m_1}, \quad n = 0, 1, 2, \dots, \quad (2.35)$$

$$H_0 : \Pr(n \text{ events}) = \frac{(m_0)^n}{n!} e^{-m_0}, \quad n = 0, 1, 2, \dots. \quad (2.36)$$

Then, the likelihood ratio test is

$$\Lambda(n) = \left(\frac{m_1}{m_0} \right)^n e^{-(m_1 - m_0)} \stackrel{H_1}{\gtrless} \eta \quad (2.37)$$

or, equivalently,

$$\begin{aligned} n &\stackrel{H_1}{\gtrless} \frac{\ln \eta + m_1 - m_0}{\ln m_1 - \ln m_0}, & \text{if } m_1 > m_0, \\ n &\stackrel{H_0}{\gtrless} \frac{\ln \eta + m_1 - m_0}{\ln m_1 - \ln m_0}, & \text{if } m_0 > m_1. \end{aligned} \quad (2.38)$$

This example illustrates how the likelihood ratio test that we originally wrote in terms of probability densities can be simply adapted to accommodate observations that are discrete random variables. ■

Independent Distribution (ID) Model. In Examples 2.1 and 2.2, the components of the vector \mathbf{r} are statistically independent and have identical probability distributions. This is referred to as an IID (independent identical distribution) model. In Examples 2.1 and 2.2, the probability densities are Gaussian but that is not necessary for an ID or IID model.

The likelihood ratio is given in (2.13). If the components are statistically independent (but not necessarily identically distributed), then

$$\begin{aligned} \Lambda(\mathbf{R}) &= \frac{p_{\mathbf{r}|H_1}(\mathbf{R}|H_1)}{p_{\mathbf{r}|H_0}(\mathbf{R}|H_0)} = \frac{\prod_{i=1}^N p_{r_i|H_1}(R_i|H_1)}{\prod_{i=1}^N p_{r_i|H_0}(R_i|H_0)} \\ &\triangleq \prod_{i=1}^N \Lambda_i(R_i), \end{aligned} \quad (2.39)$$

and the ID log-likelihood ratio is

$$\ln \Lambda(\mathbf{R}) = \sum_{i=1}^N \ln \Lambda_i(R_i). \quad (2.40)$$

If the components have identical probability densities,

$$p_{r_i|H_j}(R_i|H_j) = p_{r|H_j}(R_i|H_j) \quad j = 0, 1, \quad (2.41)$$

then (2.40) reduces to the IID log-likelihood ratio,

$$\ln \Lambda(\mathbf{R}) = \sum_{i=1}^N \ln \Lambda(R_i), \quad (2.42)$$

where

$$\ln \Lambda(R_i) \triangleq \ln \frac{p_{r|H_1}(R_i|H_1)}{p_{r|H_0}(R_i|H_0)} \quad (2.43)$$

is the marginal log-likelihood ratio. The log-likelihood ratio processor for the IID case is shown in Figure 2.7.

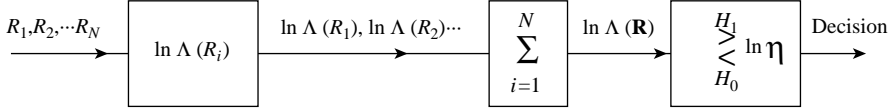


Figure 2.7: Likelihood ratio test for the IID model.

In Example 2.1, from (2.24)

$$\ln \Lambda(R_i) = \frac{m R_i}{\sigma^2} - \frac{m^2}{2\sigma^2}. \quad (2.44)$$

In Example 2.2, from (2.29)

$$\ln \Lambda(R_i) = \frac{1}{2} \left(\frac{\sigma_1^2 - \sigma_0^2}{\sigma_0^2 \sigma_1^2} \right) R_i^2 - \frac{1}{2} \ln \left(\frac{\sigma_1^2}{\sigma_0^2} \right). \quad (2.45)$$

We now consider an IID model where $p_{\mathbf{r}|H_j}(\mathbf{r}|H_j); j = 0, 1$ are non-Gaussian.

Example 2.4. The observations under the two hypotheses are

$$\begin{aligned} H_1 : r_i &= -\frac{m}{2} + n_i, \quad i = 1, 2, \dots, N, \\ H_0 : r_i &= \frac{m}{2} + n_i, \quad i = 1, 2, \dots, N. \end{aligned} \quad (2.46)$$

The noise n_i is modeled as a zero-mean Generalized Gaussian random variable. The n_i are statistically independent random variables.

The Generalized Gaussian random variable family is defined as

$$p_n(X) = c \exp \left(- \left| \frac{X}{b} \right|^{\alpha} \right), \quad -\infty < X < \infty, \quad (2.47)$$

where α denotes a particular density in the family, b defines the spread of the density, and c normalizes the density. For $\alpha = 2$, we have a Gaussian random variable. For $\alpha = 1$, we have a Laplacian random variable.

The parameter b and constant c depend on the variance of the density,

$$b = \sigma \sqrt{\frac{\Gamma(1/\alpha)}{\Gamma(3/\alpha)}}, \quad (2.48)$$

$$c = \frac{\alpha}{2b\Gamma(1/\alpha)}, \quad (2.49)$$

where $\Gamma(\cdot)$ is the Gamma function.¹

The probability densities for $\alpha = 1, 2$, and 3 , and $\sigma = 1$ are shown in Figure 2.8. We see that as α decreases the densities decay more slowly.²

¹The Gamma function is defined as $\Gamma(a) = \int_0^\infty x^{a-1} e^{-x} dx$. It can be computed in Matlab using the function `gamma`. See Appendix A.

²Later, when we study clutter, we will see that these are referred to as heavy-tailed distributions.

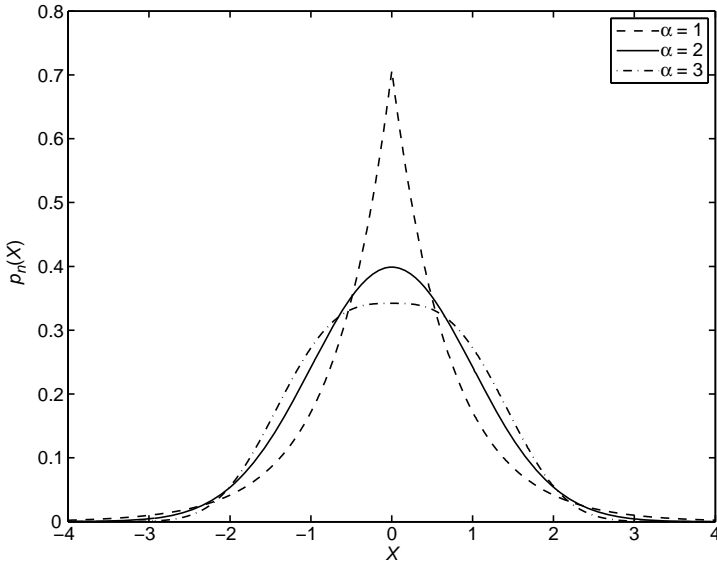


Figure 2.8: Probability densities; Generalized Gaussian random variable, $\alpha = 1, 2$, and 3 .

The probability densities of the r_i on the two hypotheses are

$$p_{r|H_0}(R_i|H_0) = c \exp\left(-\left|\frac{R_i + m/2}{b}\right|^\alpha\right), \quad i = 1, 2, \dots, N, \quad (2.50)$$

$$p_{r|H_1}(R_i|H_1) = c \exp\left(-\left|\frac{R_i - m/2}{b}\right|^\alpha\right), \quad i = 1, 2, \dots, N. \quad (2.51)$$

The marginal log-likelihood ratio is found by substituting (2.50) and (2.51) in (2.43),

$$\begin{aligned} \ln \Lambda(R_i) &= \ln \left(\frac{c \exp\left(-\left|\frac{R_i - m/2}{b}\right|^\alpha\right)}{c \exp\left(-\left|\frac{R_i + m/2}{b}\right|^\alpha\right)} \right) \\ &= \frac{1}{b^\alpha} \left(\left|R_i - \frac{m}{2}\right|^\alpha - \left|R_i + \frac{m}{2}\right|^\alpha \right). \end{aligned} \quad (2.52)$$

In Figure 2.9, we plot $\ln \Lambda(R_i)$ for $\alpha = 1, 2$, and 3 . As α increases, the weighting of large values of R_i increases. ■

The LRT processor in Figure 2.7 is an important result because we can always find $\ln \Lambda(R_i)$ as defined in (2.43). In addition, since $\ln \Lambda(R_i)$ is a single variable-to-single variable mapping, we can always find the probability density of the output of the first box. This step will be important when we analyze the performance of the LRT.

We consider the IID model because it occurs frequently in practice. For the ID case when the components are statistically independent but have different probability densities, we obtain the more general model that is given in (2.39) and (2.40).

We now return to our general discussion of Bayes tests. There are several special kinds of Bayes test that are frequently used and that should be mentioned explicitly.

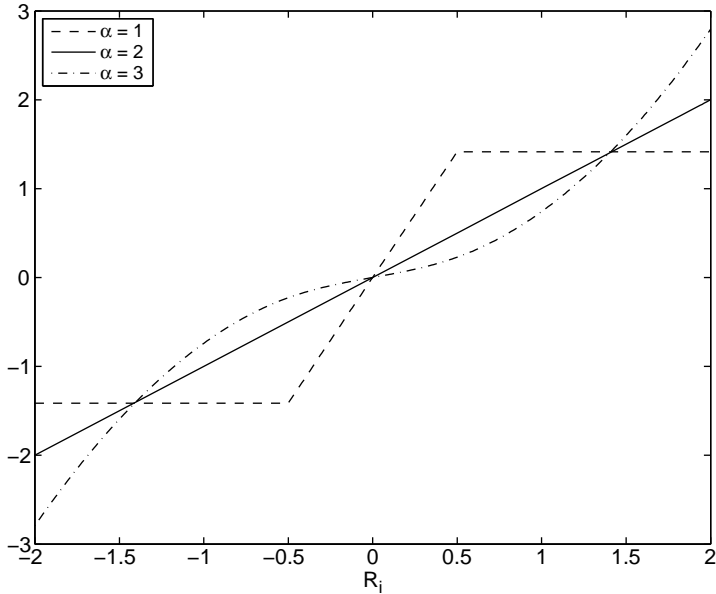


Figure 2.9: $\ln \Lambda(R_i)$; $\alpha = 1, 2$, and 3 .

If we assume that C_{00} and C_{11} are zero and $C_{01} = C_{10} = 1$, the expression for the risk in (2.8) reduces to

$$\mathcal{R} = P_0 \int_{Z_1} p_{\mathbf{r}|H_0}(\mathbf{R}|H_0) d\mathbf{R} + P_1 \int_{Z_0} p_{\mathbf{r}|H_1}(\mathbf{R}|H_1) d\mathbf{R}. \quad (2.53)$$

We see that (2.53) is just the total probability of making an error. Therefore, for this cost assignment the Bayes test is minimizing the total probability of error. The test is

$$\ln \Lambda(\mathbf{R}) \stackrel{H_0}{\gtrless} \ln \frac{P_0}{P_1} = \ln P_0 - \ln(1 - P_0). \quad (2.54)$$

These processors are commonly referred to as minimum probability of error receivers. When the two hypotheses are equally likely, the threshold is zero. This assumption is normally true in digital communications systems.

We can also write the likelihood ratio test as

$$P_1 p_{\mathbf{r}|H_1}(\mathbf{R}|H_1) \stackrel{H_1}{\gtrless} \stackrel{H_0}{\gtrless} P_0 p_{\mathbf{r}|H_0}(\mathbf{R}|H_0) \quad (2.55)$$

or

$$\frac{P_1 p_{\mathbf{r}|H_1}(\mathbf{R}|H_1)}{p_{\mathbf{r}}(\mathbf{R})} \stackrel{H_1}{\gtrless} \stackrel{H_0}{\gtrless} \frac{P_0 p_{\mathbf{r}|H_0}(\mathbf{R}|H_0)}{p_{\mathbf{r}}(\mathbf{R})}. \quad (2.56)$$

The terms in (2.56) are the *a posteriori* probabilities of the two hypotheses,

$$\Pr_{H_0}^{H_1}(\mathbf{R}) \geq \Pr_{H_0}(\mathbf{R}). \quad (2.57)$$

Therefore, a minimum probability of error test is computing *a posteriori* probabilities of the two hypotheses and choosing the largest. It is frequently referred to as a maximum *a posteriori* probability (MAP) test.

A second special case of interest arises when the *a priori* probabilities are unknown. To investigate this case, we look at (2.8) again. We observe that once the decision regions Z_0 and Z_1 are chosen, the values of the integrals are determined. We denote these values in the following manner:

$$\begin{aligned} P_F &= \int_{Z_1} p_{\mathbf{r}|H_0}(\mathbf{R}|H_0) d\mathbf{R}, \\ P_D &= \int_{Z_1} p_{\mathbf{r}|H_1}(\mathbf{R}|H_1) d\mathbf{R}, \\ P_M &= \int_{Z_0} p_{\mathbf{r}|H_1}(\mathbf{R}|H_1) d\mathbf{R} = 1 - P_D. \end{aligned} \quad (2.58)$$

We see that these quantities are *conditional probabilities*. The subscripts are mnemonic and chosen from the radar problem in which hypothesis H_1 corresponds to the presence of a target and hypothesis H_0 corresponds to its absence. P_F is the probability of a false alarm (i.e., we say the target is present when it is not); P_D is the probability of detection (i.e., we say the target is present when it is); P_M is the probability of a miss (we say the target is absent when it is present). Although we are interested in a much larger class of problems than this notation implies, we shall use it for convenience.

For any choice of decision regions, the risk expression in (2.8) can be written in the notation of (2.58):

$$\mathcal{R} = P_0 C_{10} + P_1 C_{11} + P_1(C_{01} - C_{11})P_M - P_0(C_{10} - C_{00})(1 - P_F). \quad (2.59)$$

Because

$$P_0 = 1 - P_1, \quad (2.60)$$

(2.59) becomes

$$\mathcal{R}(P_1) = C_{00}(1 - P_F) + C_{10}P_F + P_1[(C_{11} - C_{00}) + (C_{01} - C_{11})P_M - (C_{10} - C_{00})P_F]. \quad (2.61)$$

Now, if all the costs and *a priori* probabilities are known, we can find a Bayes test. In Figure 2.10a, we plot the Bayes risk, $\mathcal{R}_B(P_1)$, as a function of P_1 . Observe that as P_1 changes the decision regions for the Bayes test change and therefore P_F and P_M change.

Now consider the situation in which a certain P_1 (say $P_1 = P_1^*$) is assumed and the corresponding Bayes test designed. We now fix the threshold and assume that P_1 is allowed to change. We denote the risk for this fixed threshold test as $\mathcal{R}_F(P_1^*, P_1)$. Because the threshold is fixed, P_F and P_M are fixed, and (2.61) is just a straight line. Because it is a Bayes test for $P_1 = P_1^*$, it touches the $\mathcal{R}_B(P_1)$ curve at that point. Looking at (2.14), we

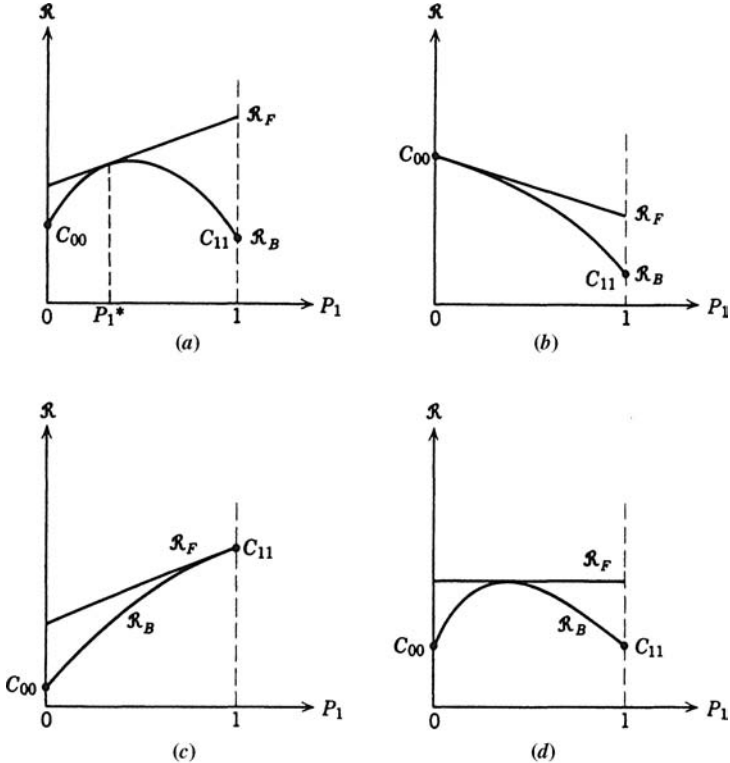


Figure 2.10: Risk curves: (a) fixed risk versus typical Bayes risk; (b) maximum value of \mathcal{R}_1 at $P_1 = 0$; (c) maximum value of \mathcal{R}_1 at $P_1 = 1$; (d) maximum value of \mathcal{R}_1 interior to $[0, 1]$.

see that the threshold changes continuously with P_1 . Therefore, whenever $P_1 \neq P_1^*$, the threshold in the Bayes test will be different. Because the Bayes test minimizes the risk,

$$\mathcal{R}_F(P_1^*, P_1) \geq \mathcal{R}_B(P_1). \quad (2.62)$$

If $\Lambda(\mathbf{R})$ is a continuous random variable with a probability distribution function that is strictly monotonic, then changing η always changes the risk. $\mathcal{R}_B(P_1)$ is strictly concave downward and the inequality in (2.62) is strict. This case, which is one of the particular interest to us, is illustrated in Figure 2.10a. We see that $\mathcal{R}_F(P_1^*, P_1)$ is tangent to $\mathcal{R}_B(P_1)$ at $P_1 = P_1^*$. These curves demonstrate the effect of incorrect knowledge of the *a priori* probabilities.

An interesting problem is encountered if we assume that the *a priori* probabilities are chosen to make our performance as bad as possible. In other words, P_1 is chosen to maximize our risk $\mathcal{R}_F(P_1^*, P_1)$. Three possible examples are given in Figures 2.10b, 2.10c, and 2.10d. In Figure 2.10b, the maximum of $\mathcal{R}_B(P_1)$ occurs at $P_1 = 0$. To minimize the maximum risk, we use a Bayes test designed assuming $P_1 = 0$. In Figure 2.10c, the maximum of $\mathcal{R}_B(P_1)$ occurs at $P_1 = 1$. To minimize the maximum risk, we use a Bayes test designed assuming $P_1 = 1$. In Figure 2.10d, the maximum occurs inside the interval $[0, 1]$, and we

choose \mathcal{R}_F to be the horizontal line. This implies that the coefficient of P_1 in (2.61) must be zero:

$$(C_{11} - C_{00}) + (C_{01} - C_{11})P_M - (C_{10} - C_{00})P_F = 0. \quad (2.63)$$

A Bayes test designed to minimize the maximum possible risk is called a *minimax test*. Equation (2.63) is referred to as the minimax equation and is useful whenever the maximum of $\mathcal{R}_B(P_1)$ is interior to the interval.

A special cost assignment that is frequently logical is

$$C_{00} = C_{11} = 0. \quad (2.64)$$

(This guarantees the maximum is interior.)

Denoting,

$$\begin{aligned} C_{01} &= C_M, \\ C_{10} &= C_F, \end{aligned} \quad (2.65)$$

the risk is,

$$\begin{aligned} \mathcal{R} &= C_F P_F + P_1(C_M P_M - C_F P_F) \\ &= P_0 C_F P_F + P_1 C_M P_M, \end{aligned} \quad (2.66)$$

and the minimax equation is

$$C_M P_M = C_F P_F. \quad (2.67)$$

Before continuing our discussion of likelihood ratio tests we shall discuss a second criterion and prove that it also leads to a likelihood ratio test.

Neyman–Pearson Tests. In many physical situations, it is difficult to assign realistic costs or *a priori* probabilities. A simple procedure to bypass this difficulty is to work with the conditional probabilities P_F and P_D . In general, we should like to make P_F as small as possible and P_D as large as possible. For most problems of practical importance, these are conflicting objectives. An obvious criterion is to constrain one of the probabilities and maximize (or minimize) the other. A specific statement of this criterion is the following:

Neyman–Pearson Criterion. Constrain $P_F = \alpha' \leq \alpha$ and design a test to maximize P_D (or minimize P_M) under this constraint.

The solution is obtained easily by using Lagrange multipliers. We construct the function f ,

$$f = P_M + \lambda(P_F - \alpha'), \quad (2.68)$$

or

$$f = \int_{Z_0} p_{\mathbf{r}|H_1}(\mathbf{R}|H_1) d\mathbf{R} + \lambda \left(\int_{Z_1} p_{\mathbf{r}|H_0}(\mathbf{R}|H_0) d\mathbf{R} - \alpha' \right). \quad (2.69)$$

Clearly, if $P_F = \alpha'$, then minimizing f minimizes P_M . We rewrite (2.69) as

$$f = \lambda(1 - \alpha') + \int_{Z_0} [p_{\mathbf{r}|H_1}(\mathbf{R}|H_1) - p_{\mathbf{r}|H_0}(\mathbf{R}|H_0)] d\mathbf{R}. \quad (2.70)$$

Now, observe that for any positive value of λ an LRT will minimize f . (A negative value of λ gives an LRT with the inequalities reversed.)

This follows directly, because to minimize f we assign a point \mathbf{R} to Z_0 only when the term in the bracket is negative. This is equivalent to the test

$$\frac{p_{\mathbf{r}|H_1}(\mathbf{R}|H_1)}{p_{\mathbf{r}|H_0}(\mathbf{R}|H_0)} < \lambda, \quad \text{assign point to } Z_0 \text{ or say } H_0. \quad (2.71)$$

The quantity on the left is just the likelihood ratio. Thus, f is minimized by the likelihood ratio test

$$\Lambda(\mathbf{R}) \stackrel{H_1}{\underset{H_0}{\gtrless}} \lambda. \quad (2.72)$$

To satisfy the constraint, we choose λ so that $P_F = \alpha$. If we denote the density of Λ when H_0 is true as $p_{\Lambda|H_0}(\Lambda|H_0)$, then we require

$$P_F = \int_{\lambda}^{\infty} p_{\Lambda|H_0}(\Lambda|H_0) d\Lambda = \alpha'. \quad (2.73)$$

Solving (2.73) for λ gives the threshold. The value of λ given by (2.73) will be nonnegative because $p_{\Lambda|H_0}(\Lambda|H_0)$ is zero for negative values of λ . Observe that decreasing λ is equivalent to increasing Z_1 , the region where we say H_1 . Thus, P_D increases as λ decreases. Therefore, we decrease λ until we obtain the largest possible $\alpha' \leq \alpha$. In most cases of interest to us, P_F is a continuous function of λ and we have $P_F = \alpha$. We shall assume this continuity in all subsequent discussions. Under this assumption, the Neyman–Pearson criterion leads to a likelihood ratio test. Later, we shall see the effect of the continuity assumption not being valid.

Summary. In this section, we have developed two ideas of fundamental importance in hypothesis testing. The first result is the demonstration that for a Bayes or a Neyman–Pearson criterion the optimum test consists of processing the observation \mathbf{R} to find the likelihood ratio $\Lambda(\mathbf{R})$ and then comparing $\Lambda(\mathbf{R})$ to a threshold in order to make a decision. Thus, regardless of the dimensionality of the observation space, the decision space is one dimensional.

The second idea is that of a sufficient statistic $l(\mathbf{R})$. The idea of a sufficient statistic originated when we constructed the likelihood ratio and saw that it depended explicitly only on $l(\mathbf{R})$. If we actually construct $\Lambda(\mathbf{R})$, and then recognize $l(\mathbf{R})$, the notion of a sufficient statistic is perhaps of secondary value. A more important case is when we can recognize $l(\mathbf{R})$ directly. An easy way to do this is to examine the geometric interpretation of a sufficient statistic. We considered the observations r_1, r_2, \dots, r_N as a point \mathbf{r} in an N -dimensional space, and one way to describe this point is to use these coordinates. When we choose a sufficient statistic, we are simply describing the point in a coordinate system that is more useful for the decision problem. We denote the first coordinate in this system by l , the

sufficient statistic, and the remaining $N - 1$ coordinates which will not affect our decision by the $(N - 1)$ -dimensional vector \mathbf{y} . Thus,

$$\Lambda(\mathbf{R}) = \Lambda(L, \mathbf{Y}) = \frac{p_{l,y|H_1}(L, \mathbf{Y}|H_1)}{p_{l,y|H_0}(L, \mathbf{Y}|H_0)}. \quad (2.74)$$

Now, the expression on the right can be written as

$$\Lambda(L, \mathbf{Y}) = \frac{p_{l|H_1}(L|H_1) p_{y|l,H_1}(\mathbf{Y}|L, H_1)}{p_{l|H_0}(L|H_0) p_{y|l,H_0}(\mathbf{Y}|L, H_0)}. \quad (2.75)$$

If l is a sufficient statistic, then $\Lambda(\mathbf{R})$ must reduce to $\Lambda(L)$. This implies that the second terms in the numerator and denominator must be equal. In other words,

$$p_{y|l,H_0}(\mathbf{Y}|L, H_0) = p_{y|l,H_1}(\mathbf{Y}|L, H_1) \quad (2.76)$$

because the density of \mathbf{y} cannot depend on which hypothesis is true. We see that choosing a sufficient statistic simply amounts to picking a coordinate system in which one coordinate contains all the information necessary to making a decision. The other coordinates contain no information and can be disregarded for the purpose of making a decision.

In Example 2.1, the new coordinate system could be obtained by a simple rotation. For example, when $N = 2$,

$$\begin{aligned} L &= \frac{1}{\sqrt{2}}(R_1 + R_2), \\ Y &= \frac{1}{\sqrt{2}}(R_1 - R_2). \end{aligned} \quad (2.77)$$

In Example 2.2, the new coordinate system corresponded to changing to polar coordinates. For $N = 2$,

$$\begin{aligned} L &= R_1^2 + R_2^2, \\ Y &= \tan^{-1} \frac{R_2}{R_1}. \end{aligned} \quad (2.78)$$

Notice that the vector \mathbf{y} can be chosen in order to make the demonstration of the condition in (2.76) as simple as possible. The only requirement is that the pair (l, \mathbf{y}) must describe any point in the observation space. We should also observe that the condition

$$p_{y|H_1}(\mathbf{Y}|H_1) = p_{y|H_0}(\mathbf{Y}|H_0), \quad (2.79)$$

does not imply (2.76) unless l and \mathbf{y} are independent under H_1 and H_0 . Frequently, we will choose \mathbf{y} to obtain this independence and then use (2.79) to verify that l is a sufficient statistic.

In the examples considered so far, the sufficient statistic has been a scalar quantity, but it may be multidimensional in general (see Problem 2.2.19).

2.2.2 Performance: Receiver Operating Characteristic

To complete our discussion of the simple binary problem, we must evaluate the performance of the likelihood ratio test. For a Neyman–Pearson test, the values of P_F and P_D completely

specify the test performance. Looking at (2.59), we see that the Bayes risk \mathcal{R}_B follows easily if P_F and P_D are known. Thus, we can concentrate our efforts on calculating P_F and P_D .

We begin by considering Example 2.1 in Section 2.2.1.

Example 2.5 (continuation of Example 2.1). From (2.25), we see that an equivalent test is

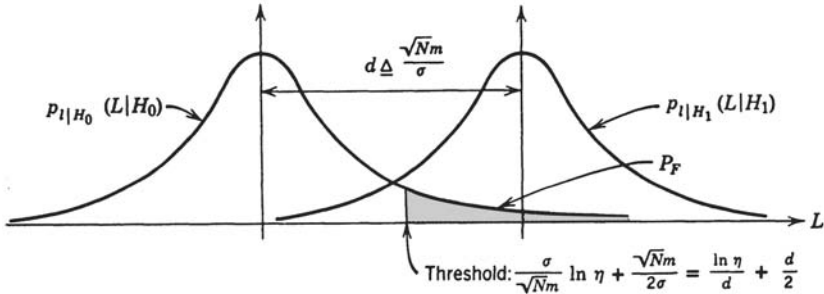
$$l(\mathbf{R}) = \frac{1}{\sqrt{N}\sigma} \sum_{i=1}^N R_i \stackrel{H_1}{\gtrless} \frac{\sigma}{\sqrt{Nm}} \ln \eta + \frac{\sqrt{Nm}}{2\sigma}. \quad (2.80)$$

We have multiplied (2.25) by σ/\sqrt{Nm} to normalize the next calculation. Under H_0 , l is obtained by adding N independent zero-mean Gaussian variables with variance σ^2 and then dividing by \sqrt{Nm} . Therefore l is $N(0, 1)$.

Under H_1 , l is $N(\sqrt{Nm}/\sigma, 1)$. The probability densities on the two hypotheses are sketched in Figure 2.11a. The threshold is also shown. Now, P_F is simply the integral of $p_{l|H_0}(L|H_0)$ to the right of the threshold.

Thus,

$$P_F = \int_{(\ln \eta)/d+d/2}^{\infty} \frac{1}{\sqrt{2\pi}} \exp\left(-\frac{x^2}{2}\right) dx, \quad (2.81)$$



(a)

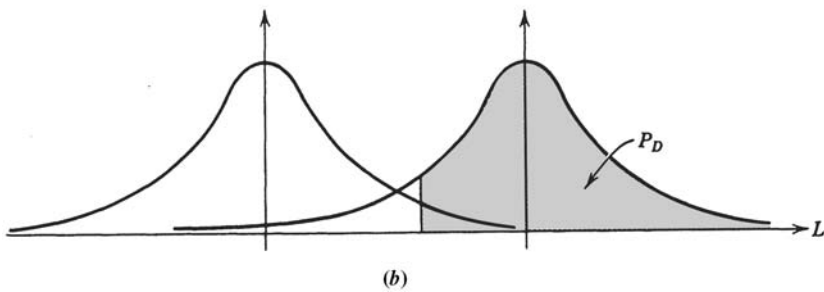


Figure 2.11: Error probabilities: (a) P_F calculation; (b) P_D calculation.

where

$$d \triangleq \frac{\sqrt{Nm}}{\sigma}, \quad (2.82)$$

is the distance between the means of the two densities. The integral in (2.81) is called the complementary error function and is tabulated in many references (e.g., [AS64] or [GH62]). We use a modified version of the standard definition that we denote as³

$$\text{erfc}_*(X) \triangleq \int_X^\infty \frac{1}{\sqrt{2\pi}} \exp\left(-\frac{x^2}{2}\right) dx. \quad (2.83)$$

In this notation,

$$P_F = \text{erfc}_*\left(\frac{\ln \eta}{d} + \frac{d}{2}\right). \quad (2.84)$$

Similarly, P_D is the integral of $p_{l|H_1}(L|H_1)$ to the right of the threshold, as shown in Figure 2.11b:

$$\begin{aligned} P_D &= \int_{(\ln \eta)/d+d/2}^\infty \frac{1}{\sqrt{2\pi}} \exp\left(-\frac{(x-d)^2}{2}\right) dx \\ &= \int_{(\ln \eta)/d-d/2}^\infty \frac{1}{\sqrt{2\pi}} \exp\left(-\frac{y^2}{2}\right) dy \triangleq \text{erfc}_*\left(\frac{\ln \eta}{d} - \frac{d}{2}\right). \end{aligned} \quad (2.85)$$

In Figure 2.12a, we have plotted P_D versus P_F for various values of d with η as the varying parameter. For $\eta = 0$, $\ln \eta = -\infty$, and the processor always guesses H_1 . Thus, $P_F = 1$ and $P_D = 1$. As η increases, P_F and P_D decrease. When $\eta = \infty$, the processor always guesses H_0 and $P_F = P_D = 0$.

As we would expect from Figure 2.11, the performance increases monotonically with d . In Figure 2.12b, we have replotted the results to give P_D versus d with P_F as a parameter on the curves. For a particular d , we can obtain any point on the curve by choosing η appropriately $(0, \infty)$.

The result in Figure 2.12a is referred to as the receiver operating characteristic (ROC). It completely describes the performance of the test as a function of the parameter of interest.

A special case that will be important when we look at communication systems is the case in which we want to minimize the total probability of error

$$\Pr(\epsilon) \triangleq P_0 P_F + P_1 P_M. \quad (2.86)$$

The threshold for this criterion was given in (2.54). For the special case in which $P_0 = P_1$ the threshold η equals one and

$$\Pr(\epsilon) = \frac{1}{2} (P_F + P_M). \quad (2.87)$$

Using (2.84) and (2.85) in (2.87), we have

$$\Pr(\epsilon) = \int_{d/2}^\infty \frac{1}{\sqrt{2\pi}} \exp\left(-\frac{x^2}{2}\right) dx = \text{erfc}_*\left(\frac{d}{2}\right). \quad (2.88)$$

³The standard complementary error function is defined as $\text{erfc}(X) = (2/\sqrt{\pi}) \int_X^\infty e^{-x^2} dx$. Our modified version can be computed using the `normcdf` function in the Matlab Statistics Toolbox. See Appendix A.

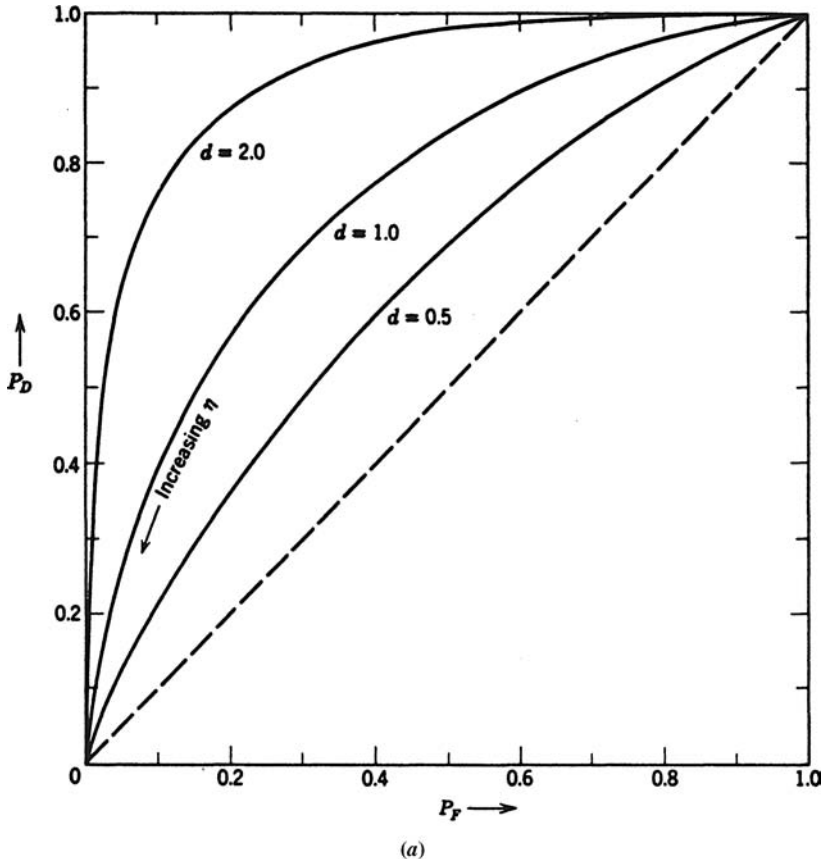


Figure 2.12: (a) Receiver operating characteristic: Gaussian variables with unequal means.

It is obvious from (2.88) that we could also obtain the $\Pr(\epsilon)$ from the ROC. However, if this is the only threshold setting of interest, it is generally easier to calculate the $\Pr(\epsilon)$ directly. ■

Before calculating the performance of the other two examples, it is worthwhile to point out two simple bounds on $\text{erfc}_*(X)$. They will enable us to discuss its approximate behavior analytically. For $X > 0$,

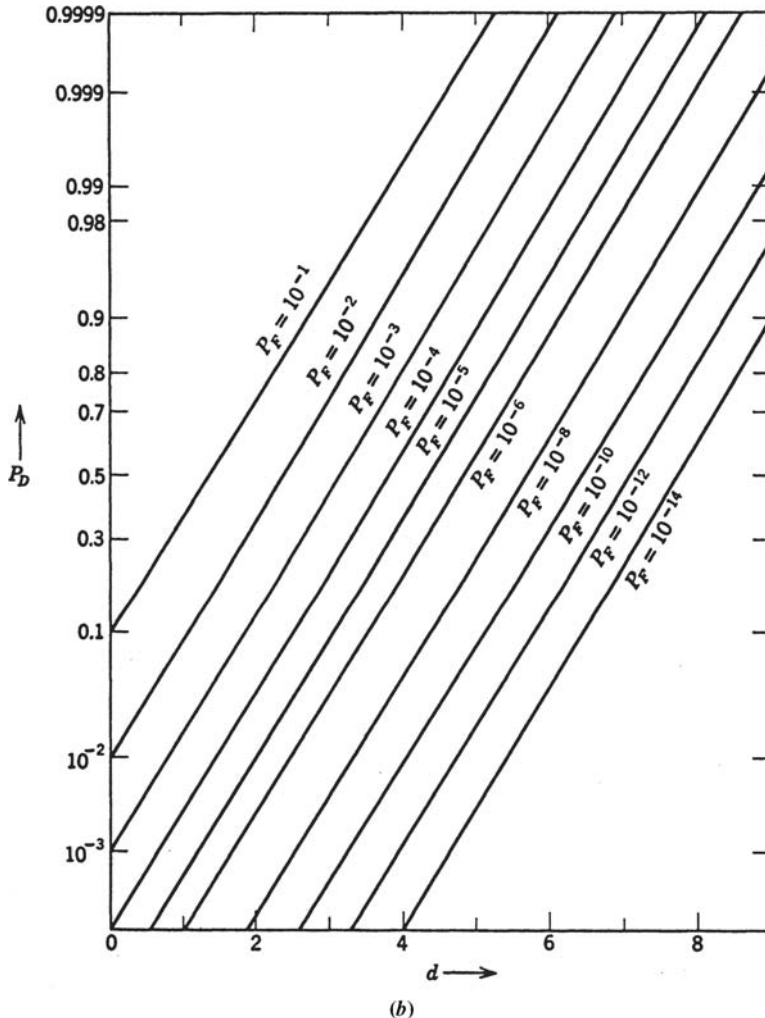
$$\frac{1}{\sqrt{2\pi}X} \left(1 - \frac{1}{X^2}\right) \exp\left(-\frac{X^2}{2}\right) < \text{erfc}_*(X) < \frac{1}{\sqrt{2\pi}X} \exp\left(-\frac{X^2}{2}\right). \quad (2.89)$$

This can be derived by integrating by parts (see Problem 2.2.15 or Feller [Fel57]). A second bound is

$$\text{erfc}_*(X) < \frac{1}{2} \exp\left(-\frac{X^2}{2}\right), \quad x > 0, \quad (2.90)$$

which can also be derived easily (see Problem 2.2.16). The four curves are plotted in Figure 2.13. We note that $\text{erfc}_*(X)$ decreases exponentially.

The receiver operating characteristics for the other two examples are also of interest.

Figure 2.12: (b) Detection probability versus d .

Example 2.6 (continuation of Example 2.2). In this case, the test is

$$l(\mathbf{R}) = \sum_{i=1}^N R_i^2 \stackrel{H_1}{\geqslant} \frac{2\sigma_0^2\sigma_1^2}{\sigma_1^2 - \sigma_0^2} \left(\ln \eta - N \ln \frac{\sigma_0}{\sigma_1} \right) = \gamma, \quad \sigma_1 > \sigma_0. \quad (2.91)$$

A particularly simple case appearing frequently in practice is $N = 2$. Under H_0 the r_i are independent zero-mean Gaussian variables with variances equal to σ_0^2 :

$$P_F = \Pr(l \geqslant \gamma | H_0) = \Pr(r_1^2 + r_2^2 \geqslant \gamma | H_0). \quad (2.92)$$

To evaluate the expression on the right, we change to polar coordinates:

$$\begin{aligned} r_1 &= z \cos \theta, & z &= \sqrt{r_1^2 + r_2^2} \\ r_2 &= z \sin \theta, & \theta &= \tan^{-1} \frac{r_2}{r_1}. \end{aligned} \quad (2.93)$$

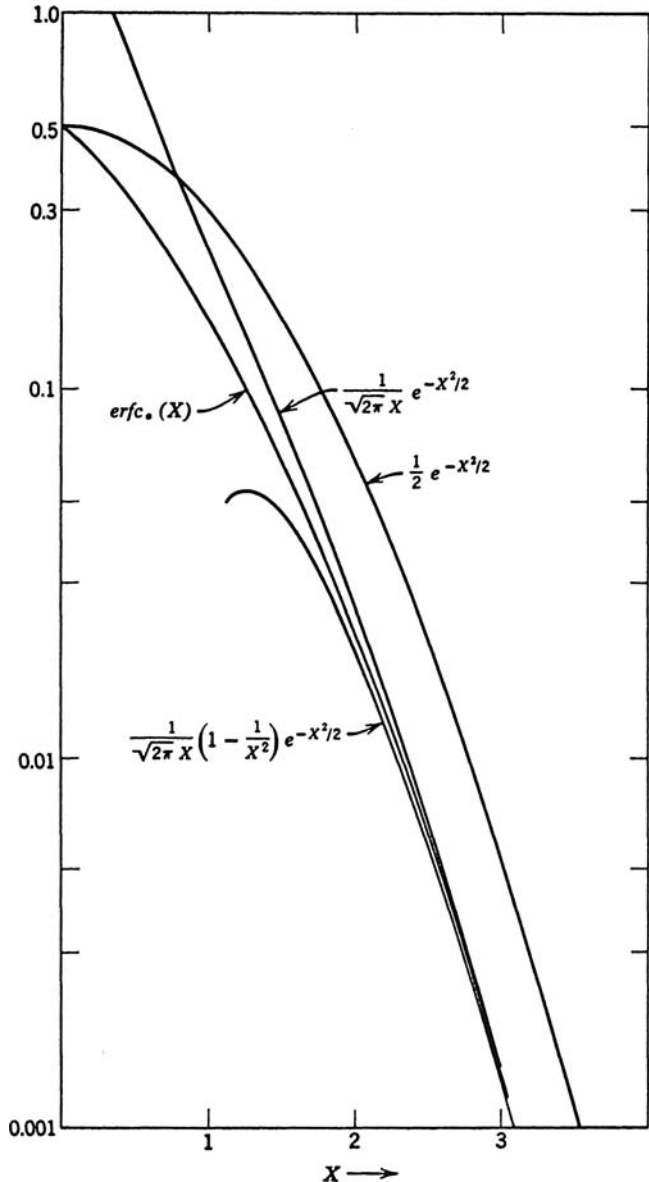


Figure 2.13: Plot of $\text{erfc}_*(X)$ and related functions.

Then,

$$\Pr(z^2 \geq \gamma | H_0) = \int_0^{2\pi} d\theta \int_{\sqrt{\gamma}}^{\infty} Z \frac{1}{2\pi\sigma_0^2} \exp\left(-\frac{Z^2}{2\sigma_0^2}\right) dZ. \quad (2.94)$$

Integrating with respect to θ , we have

$$P_F = \int_{\sqrt{\gamma}}^{\infty} Z \frac{1}{2\sigma_0^2} \exp\left(-\frac{Z^2}{2\sigma_0^2}\right) dZ. \quad (2.95)$$

We observe that l , the sufficient statistic, equals z^2 . Changing variables, we have

$$P_F = \int_{-\infty}^{\infty} \frac{1}{2\sigma_0^2} \exp\left(-\frac{L}{2\sigma_0^2}\right) dL = \exp\left(-\frac{\gamma}{2\sigma_0^2}\right). \quad (2.96)$$

(Note that the probability density of the sufficient statistic is exponential.)

Similarly,

$$P_D = \exp\left(-\frac{\gamma}{2\sigma_1^2}\right). \quad (2.97)$$

To construct the ROC, we can combine (2.96) and (2.97) to eliminate the threshold γ . This gives

$$P_D = (P_F)^{\sigma_0^2/\sigma_1^2}. \quad (2.98)$$

In terms of logarithms,

$$\ln P_D = \frac{\sigma_0^2}{\sigma_1^2} \ln P_F. \quad (2.99)$$

As expected, the performance improves monotonically as the ratio σ_1^2/σ_0^2 increases.

We now calculate the performance for arbitrary N . On both hypotheses, $l(\mathbf{R})$ is the sum of the squares of N Gaussian variables. The difference in the hypotheses is in the variance of the Gaussian variables.

To find $p_{l|H_0}(L|H_0)$, we observe that the characteristic function (CF) of each R_i^2 is

$$\begin{aligned} M_{R_i^2|H_0}(jv) &\triangleq E\left\{e^{jvR_i^2} \mid H_0\right\} = \int_{-\infty}^{\infty} e^{jvR_i^2} \frac{1}{\sqrt{2\pi}\sigma_0} e^{-R_i^2/2\sigma_0^2} dR_i \\ &= (1 - 2jv\sigma_0^2)^{-1/2}. \end{aligned} \quad (2.100)$$

Because of the independence of the variables, $M_{l|H_0}(jv)$ can be written as a product. Therefore,

$$M_{l|H_0}(jv) = (1 - 2jv\sigma_0^2)^{-N/2}. \quad (2.101)$$

Taking the inverse transform, we obtain $p_{l|H_0}(L|H_0)$:

$$p_{l|H_0}(L|H_0) = \frac{L^{N/2-1} e^{-L/2\sigma_0^2}}{2^{N/2} \sigma_0^N \Gamma\left(\frac{N}{2}\right)} \quad L \geq 0, \quad (2.102)$$

which is familiar as the Gamma probability density function with shape parameter $a = N/2$ and scale parameter $b = 2\sigma_0^2$. The properties of the Gamma density are available in many sources (e.g., [JKB94]) and are summarized in Appendix A. Plots of the probability density are shown in Figure 2.14. When $\sigma_0^2 = 1$, the Gamma density in (2.102) is identical to a Chi-squared density with N degrees of freedom. For $N = 2$, it is easy to check that it is the simple Exponential density in (2.96).

Similarly, for H_1 we have,

$$p_{l|H_1}(L|H_1) = \frac{L^{N/2-1} e^{-L/2\sigma_1^2}}{2^{N/2} \sigma_1^N \Gamma\left(\frac{N}{2}\right)} \quad L \geq 0. \quad (2.103)$$

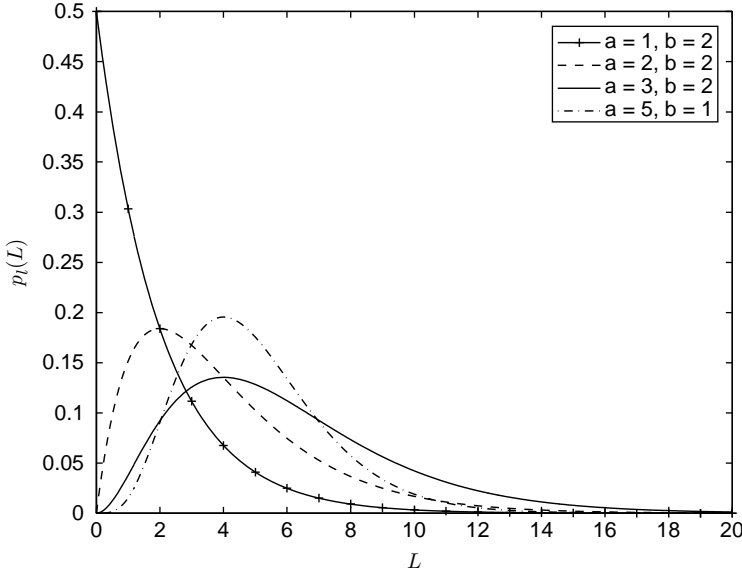


Figure 2.14: Gamma probability density for various a and b .

The expressions for P_D and P_F are,

$$P_D = \int_{\gamma}^{\infty} \left[2^{N/2} \sigma_1^N \Gamma \left(\frac{N}{2} \right) \right]^{-1} L^{N/2-1} e^{-L/2\sigma_1^2} dL, \quad (2.104)$$

and

$$P_F = \int_{\gamma}^{\infty} \left[2^{N/2} \sigma_0^N \Gamma \left(\frac{N}{2} \right) \right]^{-1} L^{N/2-1} e^{-L/2\sigma_0^2} dL. \quad (2.105)$$

Making the substitution,

$$X_1 = \frac{L}{2\sigma_1^2}, \quad (2.106)$$

in (2.104), and

$$X_0 = \frac{L}{2\sigma_0^2}, \quad (2.107)$$

in (2.105), the integrals are incomplete Gamma functions, where the normalized incomplete Gamma function is defined as⁴

$$\Gamma_a(x) \triangleq \frac{1}{\Gamma(a)} \int_0^x t^{a-1} e^{-t} dt. \quad (2.108)$$

⁴The incomplete Gamma function is tabulated in several references (e.g., [FY53] or [AS64]) and can be computed in Matlab using the `gammainc` function. See Appendix A.

Therefore,

$$P_D = 1 - \Gamma_{N/2} \left(\frac{\gamma}{2\sigma_1^2} \right), \quad (2.109)$$

and

$$P_F = 1 - \Gamma_{N/2} \left(\frac{\gamma}{2\sigma_0^2} \right). \quad (2.110)$$

We see that, for $N = 2$, P_F and P_D reduce to (2.96) and (2.97).

Consider the physical situation in which there is "noise" only on H_0 ,

$$\sigma_0^2 = \sigma_n^2, \quad (2.111)$$

and "signal" plus "noise" on H_1 ,

$$\sigma_1^2 = \sigma_s^2 + \sigma_n^2. \quad (2.112)$$

In Figure 2.15, we have plotted the receiver operating characteristic for some representative values of N and σ_s^2/σ_n^2 .

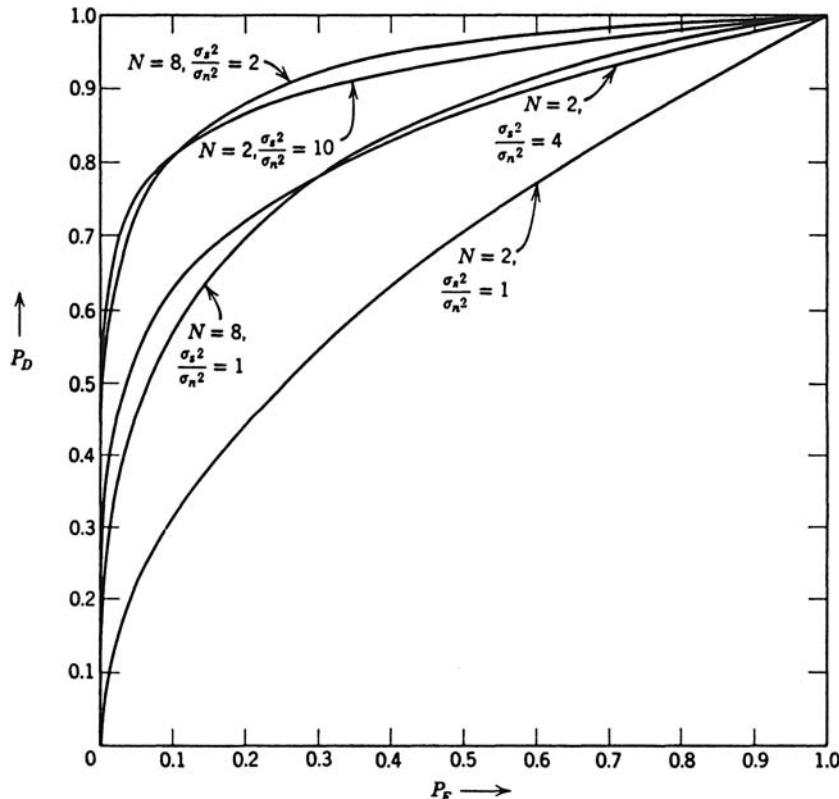


Figure 2.15: Receiver operating characteristic: Gaussian variables with identical means and unequal variances on the two hypotheses.

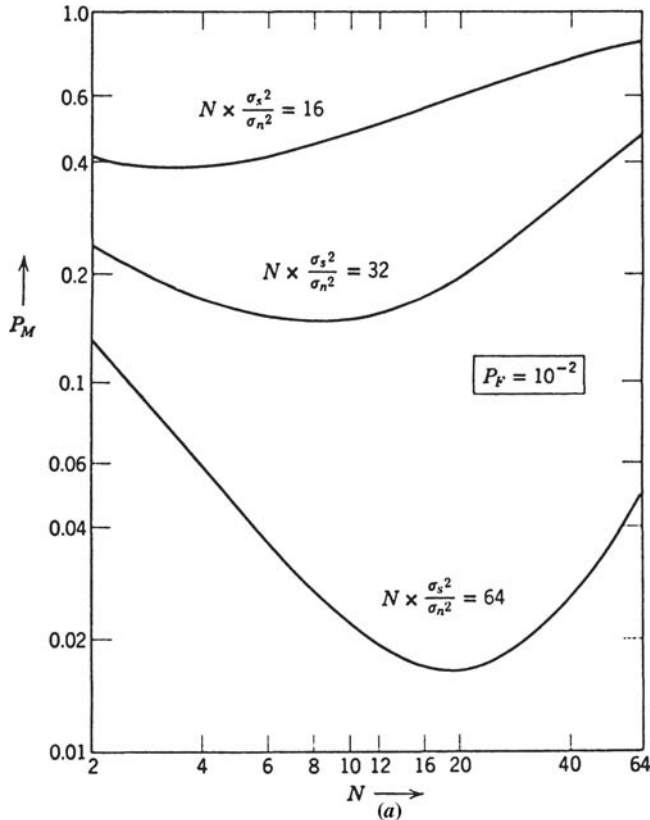


Figure 2.16: (a) P_M as a function of N [$P_F = 10^{-2}$].

Two particularly interesting curves are those for $N = 8$, $\sigma_s^2/\sigma_n^2 = 1$, and $N = 2$, $\sigma_s^2/\sigma_n^2 = 4$. In both cases, the product $N\sigma_s^2/\sigma_n^2 = 8$. We see that when the desired P_F is greater than 0.3, P_D is higher if the available “signal strength” is divided into more components. This suggests that for each P_F and $N\sigma_s^2/\sigma_n^2$ there should be an optimum N . In Chapter 7, we shall see that this problem corresponds to optimum diversity in communication systems and the optimum energy per pulse in radars. In Figures 2.16a and b, we have plotted P_M as a function of N for $P_F = 10^{-2}$ and 10^{-4} , respectively, and various $N\sigma_s^2/\sigma_n^2$ products. We discuss the physical implications of these results in Chapters 7 and 10. ■

The two Poisson distributions are the third example.

Example 2.7 (continuation of Example 2.3). From (2.38), the likelihood ratio test is

$$n \stackrel{H_1}{\gtrless} \frac{\ln \eta + m_1 - m_0}{\ln m_1 - \ln m_0} = \gamma, \quad m_1 > m_0. \quad (2.113)$$

Because n takes on only integer values, it is more convenient to rewrite (2.113) as

$$n \stackrel{H_1}{\gtrless} \gamma_1, \quad \gamma_1 = 1, 2, \dots \quad (2.114)$$

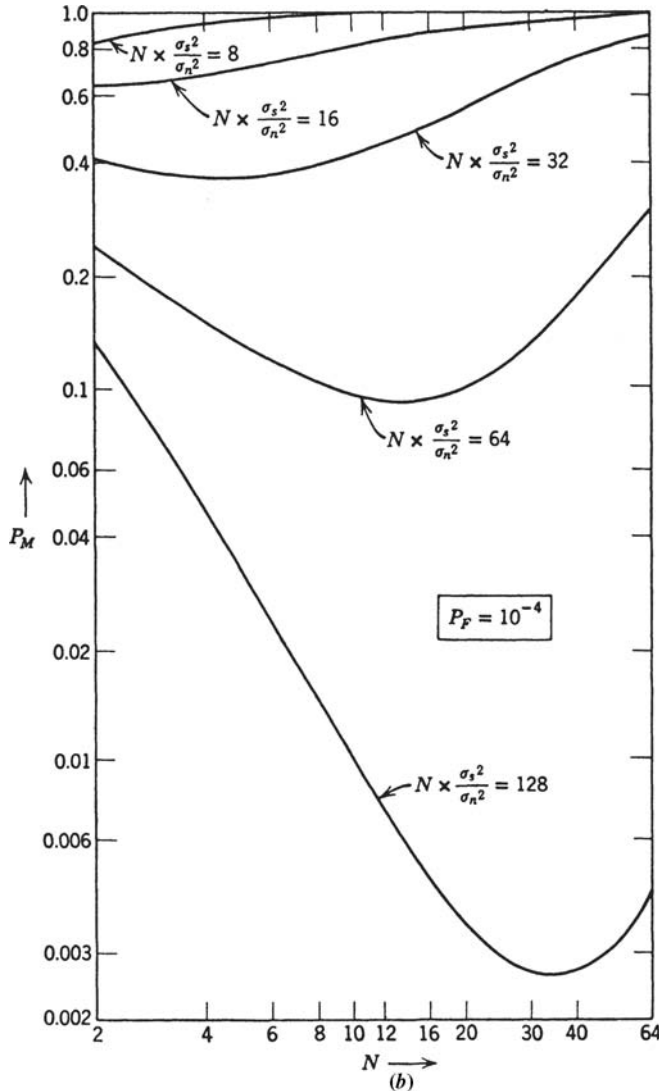


Figure 2.16: (b) P_M as a function of N [$P_F = 10^{-4}$].

where γ_I takes on only integer values. Using (2.35),

$$P_D = 1 - e^{-m_1} \sum_{n=0}^{\gamma_I-1} \frac{(m_1)^n}{n!}, \quad \gamma_I = 0, 1, 2, \dots, \quad (2.115)$$

and from (2.36)

$$P_F = 1 - e^{-m_0} \sum_{n=0}^{\gamma_I-1} \frac{(m_0)^n}{n!}, \quad \gamma_I = 0, 1, 2, \dots. \quad (2.116)$$

The resulting ROC is plotted in Figure 2.17a for some representative values of m_0 and m_1 .

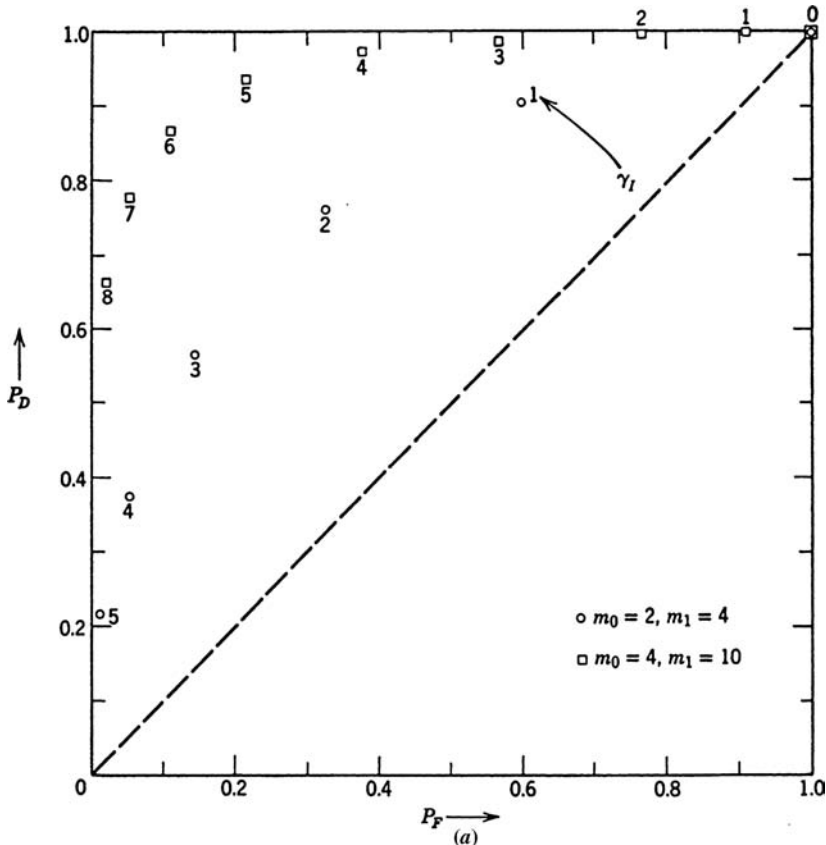


Figure 2.17: (a) Receiver operating characteristic, Poisson problem.

We see that it consists of a series of points and that P_F goes from 1 to $1 - e^{-m_0}$ when the threshold is changed from 0 to 1. Now suppose we wanted P_F to have an intermediate value, say $1 - \frac{1}{2}e^{-m_0}$. To achieve this performance, we proceed in the following manner. Denoting the LRT with $\gamma_I = 0$ as LRT No. 0 and the LRT with $\gamma_I = 1$ as LRT No. 1, we have the following table:

LRT	γ_I	P_F	P_D
0	0	1	1
1	1	$1 - e^{-m_0}$	$1 - e^{-m_1}$

To get the desired value of P_F , we use LRT No. 0 with probability $\frac{1}{2}$ and LRT No. 1 with probability $\frac{1}{2}$. The test is

If $n = 0$, say H_1 with probability $\frac{1}{2}$,
say H_0 with probability $\frac{1}{2}$,
If $n \geq 1$, say H_1 .

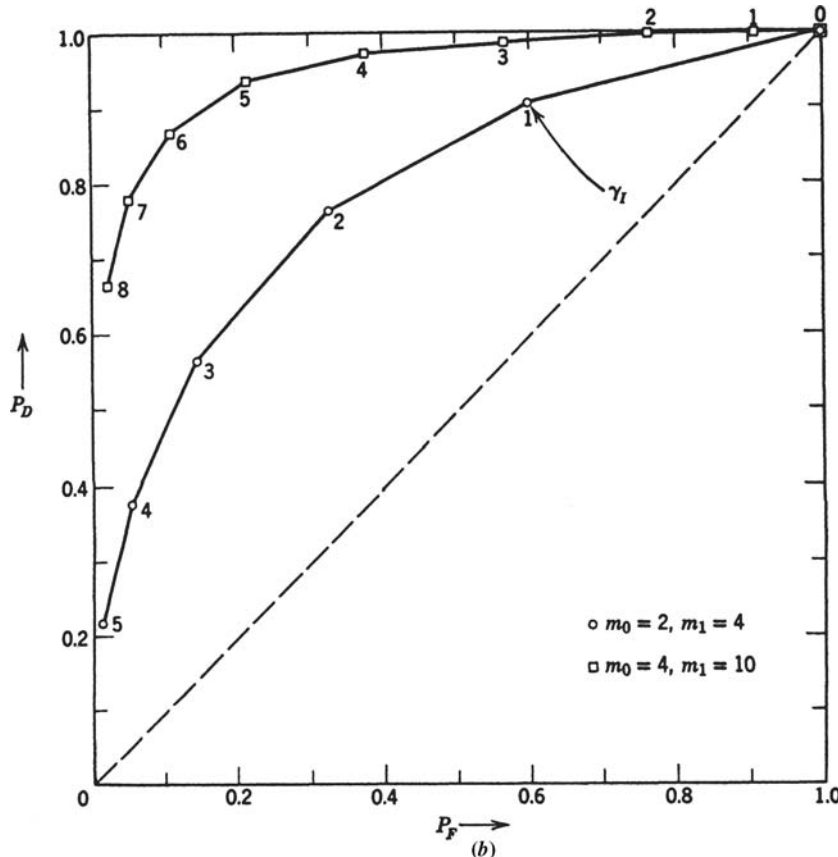


Figure 2.17: (b) Receiver operating characteristic with randomized decision rule.

This procedure, in which we mix two likelihood ratio tests in some probabilistic manner, is called a *randomized decision rule*. The resulting P_D is simply a weighted combination of detection probabilities for the two tests.

$$P_D = 0.5(1) + 0.5(1 - e^{-m_1}) = 1 - 0.5e^{-m_1}. \quad (2.117)$$

We see that the ROC for randomized tests consists of straight lines which connect the points in Figure 2.17a, as shown in Figure 2.17b. The reason that we encounter a randomized test is that the observed random variables are discrete. Therefore, $\Lambda(\mathbf{R})$ is a discrete random variable and, using an ordinary likelihood ratio test, only certain values of P_F are possible. ■

Looking at the expression for P_F in (2.73) and denoting the threshold by η , we have

$$P_F(\eta) = \int_{\eta}^{\infty} p_{\Delta|H_0}(X|H_0) dX. \quad (2.118)$$

If $P_F(\eta)$ is a continuous function of η , we can achieve a desired value from 0 to 1 by a suitable choice of η and a randomized test will never be needed. This is the only case of interest to us in the sequel (see Problem 2.2.12).

In each of the first three examples, we were able to compute the probability density of the sufficient statistic on H_0 and H_1 . However, in Example 2.4, this is difficult to do for arbitrary α . For observations that are IID, a Matlab-based approach provides a good alternative. We discuss this case briefly. From (2.39) and (2.42),

$$\Lambda(\mathbf{R}) = \frac{p_{\mathbf{r}|H_1}(\mathbf{R}|H_1)}{p_{\mathbf{r}|H_0}(\mathbf{R}|H_0)} = \prod_{i=1}^N \frac{p_{r|H_1}(R_i|H_1)}{p_{r|H_0}(R_i|H_0)} \stackrel{H_1}{\gtrless} \stackrel{H_0}{\lessdot} \eta, \quad (2.119)$$

$$l(\mathbf{R}) = \ln \Lambda(\mathbf{R}) = \sum_{i=1}^N \ln \Lambda(R_i), \quad (2.120)$$

where

$$\ln \Lambda(R_i) \triangleq \ln \frac{p_{r|H_1}(R_i|H_1)}{p_{r|H_0}(R_i|H_0)}. \quad (2.121)$$

To evaluate performance, we need to compute

$$P_D = \int_{\ln \eta}^{\infty} p_{l|H_1}(L|H_1) dL \quad (2.122)$$

and

$$P_F = \int_{\ln \eta}^{\infty} p_{l|H_0}(L|H_0) dL. \quad (2.123)$$

In many cases, we can compute the probability density of $\ln \Lambda(R_i)$ on H_0 and H_1 , but an analytic formula for the density of $l(\mathbf{R})$ is hard to find. However, we know that it is an $(N - 1)$ -fold convolution of identical densities. This is straightforward to carry out using Matlab. We then perform numerical integration to obtain P_D and P_F .

Example 2.8 (continuation of Example 2.4). In Figure 2.18, we plot the ROC for $m = 1$, $\sigma = 0.5$, $N = 10$, and $\alpha = 1.1, 1.5$, and 2.0 . For $\alpha = 2$, the density is Gaussian, so the result is the same as Example 2.5. ■

With these examples as a background, we now derive a few general properties of receiver operating characteristics. We confine our discussion to continuous likelihood ratio tests.

Two properties of all ROC's follow immediately from this example.

Property 1. All continuous likelihood ratio tests have ROC's that are concave downward. If they were not, a randomized test would be better. This would contradict our proof that a LRT is optimum (see Problem 2.2.12).

Property 2. All continuous likelihood ratio tests have ROC's that are above the $P_D = P_F$ line. This is just a special case of Property 1 because the points $(P_F = 0, P_D = 0)$ and $(P_F = 1, P_D = 1)$ are contained on all ROC's.

Property 3. The slope of a curve in a ROC at a particular point is equal to the value of the threshold η required to achieve the P_D and P_F of that point.

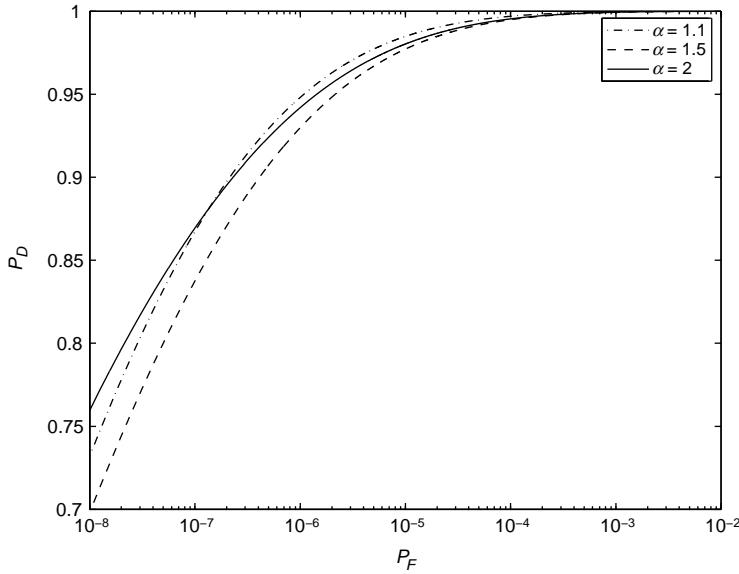


Figure 2.18: P_D versus P_F for Generalized Gaussian probability density: $m = 1, \sigma = 0.5, N = 10; \alpha = 1.1, 1.5, 2.0$.

Proof.

$$\begin{aligned} P_D &= \int_{\eta}^{\infty} p_{\Lambda|H_1}(\Lambda|H_1) d\Lambda, \\ P_F &= \int_{\eta}^{\infty} p_{\Lambda|H_0}(\Lambda|H_0) d\Lambda. \end{aligned} \quad (2.124)$$

Differentiating both expressions with respect to η and writing the results as a quotient, we have

$$\frac{dP_D/d\eta}{dP_F/d\eta} = \frac{-p_{\Lambda|H_1}(\Lambda|H_1)}{-p_{\Lambda|H_0}(\Lambda|H_0)} = \frac{dP_D}{dP_F}. \quad (2.125)$$

We now show that

$$\frac{p_{\Lambda|H_1}(\Lambda|H_1)}{p_{\Lambda|H_0}(\Lambda|H_0)} = \eta. \quad (2.126)$$

Let

$$\Omega(\eta) \triangleq \{\mathbf{R} | \Lambda(\mathbf{R}) \geq \eta\} = \left[\mathbf{R} \left| \frac{p_{\mathbf{r}|H_1}(\mathbf{R}|H_1)}{p_{\mathbf{r}|H_0}(\mathbf{R}|H_0)} \geq \eta \right. \right]. \quad (2.127)$$

Then,

$$\begin{aligned} P_D(\eta) \triangleq \Pr \{ \Lambda(\mathbf{R}) \geq \eta | H_1 \} &= \int_{\Omega(\eta)} p_{\mathbf{r}|H_1}(\mathbf{R}|H_1) d\mathbf{R} \\ &= \int_{\Omega(\eta)} \Lambda(\mathbf{R}) p_{\mathbf{r}|H_0}(\mathbf{R}|H_0) d\mathbf{R}, \end{aligned} \quad (2.128)$$

where the last equality follows from the definition of the likelihood ratio. Using the definition of $\Omega(\eta)$, we can rewrite the last integral

$$P_D(\eta) = \int_{\Omega(\eta)} \Lambda(\mathbf{R}) p_{\mathbf{r}|H_0}(\mathbf{R}|H_0) d\mathbf{R} = \int_{\eta}^{\infty} X p_{\Lambda|H_0}(X|H_0) dX. \quad (2.129)$$

Differentiating (2.129) with respect to η , we obtain

$$\frac{dP_D(\eta)}{d\eta} = -\eta p_{\Lambda|H_0}(X|H_0). \quad (2.130)$$

Equating the expression for $dP_D(\eta)/d\eta$ in the numerator of (2.125) to the right side of (2.130) gives the desired result.

We see that this result is consistent with Example 2.5. In Figure 2.12a, the curves for nonzero d have zero slope at $P_F = P_D = 1$ ($\eta = 0$) and infinite slope at $P_F = P_D = 0$ ($\eta = \infty$).

Property 4. Whenever the maximum value of the Bayes risk is interior to the interval $(0, 1)$ on the P_1 axis, the minimax operating point is the intersection of the line

$$(C_{11} - C_{00}) + (C_{01} - C_{11})(1 - P_D) - (C_{10} - C_{00})P_F = 0 \quad (2.131)$$

and the appropriate curve of the ROC (see (2.63)). In Figure 2.19, we show the special case defined by (2.67),

$$C_F P_F = C_M P_M = C_M(1 - P_D), \quad (2.132)$$

superimposed on the ROC of Example 2.5. We see that it starts at the point $P_F = 0, P_D = 1$, and intersects the $P_F = 1$ line at

$$P_F = 1 - \frac{C_F}{C_M}. \quad (2.133)$$

This completes our discussion of the binary hypothesis testing problem. Several key ideas should be re-emphasized:

1. Using either a Bayes criterion or a Neyman–Pearson criterion, we find that the optimum test is a likelihood ratio test. Thus, regardless of the dimensionality of the observation space, the test consists of comparing a scalar variable $\Lambda(\mathbf{R})$ with a threshold. (We assume $P_F(\eta)$ is continuous.)
2. In many cases, construction of the LRT can be simplified if we can identify a sufficient statistic. Geometrically, this statistic is just that coordinate in a suitable coordinate

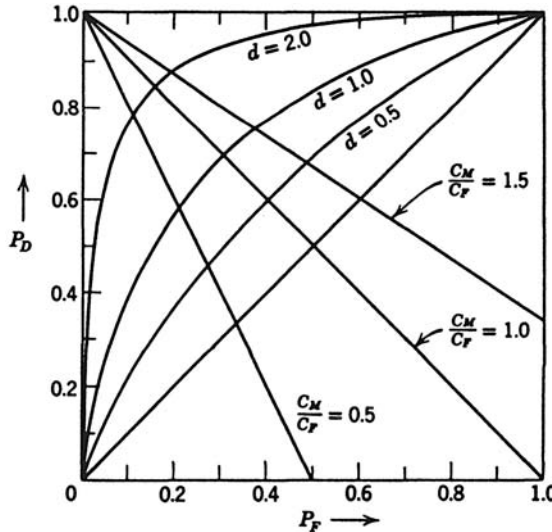


Figure 2.19: Determination of minimax operating point.

system that describes the observation space that contains *all* the information necessary to make a decision.

3. A complete description of the LRT performance was obtained by plotting the conditional probabilities P_D and P_F as the threshold η was varied. The resulting ROC could be used to calculate the Bayes risk for any set of costs. In many cases only one value of the threshold is of interest and a complete ROC is not necessary.

A number of interesting binary tests are developed in the problems.

2.3 M HYPOTHESES

The next case of interest is one in which we must choose one of M hypotheses. In the simple binary hypothesis test, there were two source outputs, each of which corresponded to a single hypothesis. In the simple M -ary test, there are M source outputs, each of which corresponds to one of M hypotheses. As before, we assume that we are forced to make a decision. Thus, there are M^2 alternatives that may occur each time the experiment is conducted. The Bayes criterion assigns a cost to each of these alternatives, assumes a set of *a priori* probabilities P_0, \dots, P_{M-1} , and minimizes the risk. The generalization of the Neyman–Pearson criterion to M hypotheses is also possible. Because it is not widely used in practice, we shall discuss only the Bayes criterion in the text.

Bayes Criterion. To find a Bayes test, we denote that cost of each course of action as C_{ij} . The first subscript signifies that the i th hypothesis is chosen. The second subscript signifies that the j th hypothesis is true. We denote the region of the observation space in which we choose H_i as Z_i and the *a priori* probabilities are P_i . The model is shown in Figure 2.20. The expression for the risk is

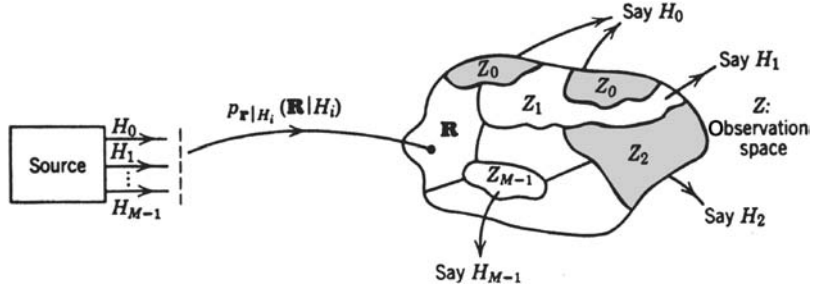


Figure 2.20: M hypothesis problem.

$$\mathcal{R} = \sum_{i=0}^{M-1} \sum_{j=0}^{M-1} P_j C_{ij} \int_{Z_i} p_{\mathbf{r}|H_j}(\mathbf{R}|H_j) d\mathbf{R}. \quad (2.134)$$

To find the optimum Bayes test, we simply vary the Z_i to minimize \mathcal{R} . This is a straightforward extension of the technique used in the binary case.

Noting that $Z_0 = Z - Z_1 - Z_2$, because the regions are disjoint, we obtain

$$\begin{aligned} \mathcal{R} &= P_0 C_{00} \int_{Z-Z_1-Z_2} p_{\mathbf{r}|H_0}(\mathbf{R}|H_0) d\mathbf{R} + P_0 C_{10} \int_{Z_1} p_{\mathbf{r}|H_0}(\mathbf{R}|H_0) d\mathbf{R} \\ &\quad + P_0 C_{20} \int_{Z_2} p_{\mathbf{r}|H_0}(\mathbf{R}|H_0) d\mathbf{R} + P_1 C_{11} \int_{Z-Z_0-Z_2} p_{\mathbf{r}|H_1}(\mathbf{R}|H_1) d\mathbf{R} \\ &\quad + P_1 C_{01} \int_{Z_0} p_{\mathbf{r}|H_1}(\mathbf{R}|H_1) d\mathbf{R} + P_1 C_{21} \int_{Z_2} p_{\mathbf{r}|H_1}(\mathbf{R}|H_1) d\mathbf{R} \\ &\quad + P_2 C_{22} \int_{Z-Z_0-Z_1} p_{\mathbf{r}|H_2}(\mathbf{R}|H_2) d\mathbf{R} + P_2 C_{02} \int_{Z_0} p_{\mathbf{r}|H_2}(\mathbf{R}|H_2) d\mathbf{R} \\ &\quad + P_2 C_{12} \int_{Z_1} p_{\mathbf{r}|H_2}(\mathbf{R}|H_2) d\mathbf{R}. \end{aligned} \quad (2.135)$$

This reduces to

$$\begin{aligned} \mathcal{R} &= P_0 C_{00} + P_1 C_{11} + P_2 C_{22} \\ &\quad + \int_{Z_0} [P_2(C_{02} - C_{22}) p_{\mathbf{r}|H_2}(\mathbf{R}|H_2) + P_1(C_{01} - C_{11}) p_{\mathbf{r}|H_1}(\mathbf{R}|H_1)] d\mathbf{R} \\ &\quad + \int_{Z_1} [P_0(C_{10} - C_{00}) p_{\mathbf{r}|H_0}(\mathbf{R}|H_0) + P_2(C_{12} - C_{22}) p_{\mathbf{r}|H_2}(\mathbf{R}|H_2)] d\mathbf{R} \\ &\quad + \int_{Z_2} [P_0(C_{20} - C_{00}) p_{\mathbf{r}|H_0}(\mathbf{R}|H_0) + P_1(C_{21} - C_{11}) p_{\mathbf{r}|H_1}(\mathbf{R}|H_1)] d\mathbf{R}. \end{aligned} \quad (2.136)$$

As before, the first three terms represent the fixed cost and the integrals represent the variable cost that depends on our choice of Z_0, Z_1, Z_2 . Clearly, we assign each \mathbf{R} to the region in which the value of the integrand is the smallest. Labeling these integrands $I_0(\mathbf{R}), I_1(\mathbf{R})$, and $I_2(\mathbf{R})$, we have the following rule:

$$\begin{aligned} &\text{if } I_0(\mathbf{R}) < I_1(\mathbf{R}) \text{ and } I_2(\mathbf{R}), \text{ choose } H_0, \\ &\text{if } I_1(\mathbf{R}) < I_0(\mathbf{R}) \text{ and } I_2(\mathbf{R}), \text{ choose } H_1, \\ &\text{if } I_2(\mathbf{R}) < I_0(\mathbf{R}) \text{ and } I_1(\mathbf{R}), \text{ choose } H_2. \end{aligned} \quad (2.137)$$

We can write terms in terms of likelihood ratios by defining

$$\begin{aligned} \Lambda_1(\mathbf{R}) &\triangleq \frac{p_{\mathbf{r}|H_1}(\mathbf{R}|H_1)}{p_{\mathbf{r}|H_0}(\mathbf{R}|H_0)}, \\ \Lambda_2(\mathbf{R}) &\triangleq \frac{p_{\mathbf{r}|H_2}(\mathbf{R}|H_2)}{p_{\mathbf{r}|H_0}(\mathbf{R}|H_0)}. \end{aligned} \quad (2.138)$$

Using (2.138) in (2.136) and (2.137), we have

$$P_1(C_{01} - C_{11})\Lambda_1(\mathbf{R}) \underset{H_0 \text{ or } H_2}{\gtrless} P_0(C_{10} - C_{00}) + P_2(C_{12} - C_{02})\Lambda_2(\mathbf{R}), \quad (2.139)$$

$$P_2(C_{02} - C_{22})\Lambda_2(\mathbf{R}) \underset{H_0 \text{ or } H_1}{\gtrless} P_0(C_{20} - C_{00}) + P_1(C_{21} - C_{01})\Lambda_1(\mathbf{R}), \quad (2.140)$$

$$P_2(C_{12} - C_{22})\Lambda_2(\mathbf{R}) \underset{H_1 \text{ or } H_0}{\gtrless} P_0(C_{20} - C_{10}) + P_1(C_{21} - C_{11})\Lambda_1(\mathbf{R}). \quad (2.141)$$

We see that the decision rules correspond to three lines in the (Λ_1, Λ_2) plane. It is easy to verify that these lines intersect at a common point and therefore uniquely define three decision regions, as shown in Figure 2.21. The decision space is two dimensional for the three-hypothesis problem. It is easy to verify that M hypotheses *always* lead to a decision space that has, at most, $(M - 1)$ dimensions.

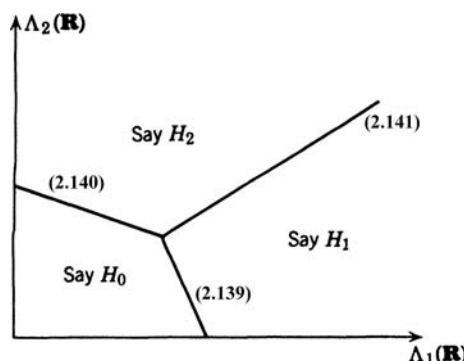


Figure 2.21: Decision space.

Several special cases will be useful in our later work. The first is defined by the assumptions

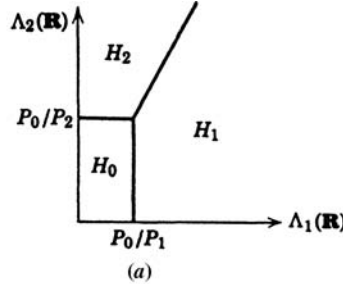
$$\begin{aligned} C_{00} &= C_{11} = C_{22} = 0, \\ C_{ij} &= 1, \quad i \neq j. \end{aligned} \quad (2.142)$$

These equations indicate that any error is of equal importance. Looking at (2.134), we see that this corresponds to minimizing the total probability of error.

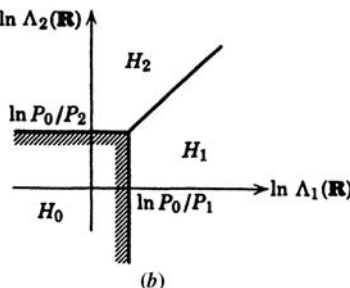
Substituting into (2.139)–(2.141), we have

$$\begin{aligned} P_1 \Lambda_1(\mathbf{R}) &\stackrel{H_1 \text{ or } H_2}{\gtrless} P_0, \\ P_2 \Lambda_2(\mathbf{R}) &\stackrel{H_2 \text{ or } H_1}{\gtrless} P_0, \\ P_2 \Lambda_2(\mathbf{R}) &\stackrel{H_2 \text{ or } H_0}{\gtrless} P_1 \Lambda_1(\mathbf{R}). \end{aligned} \quad (2.143)$$

The decision regions in the (Λ_1, Λ_2) plane are shown in Figure 2.22a. In this particular case, the transition to the $(\ln \Lambda_1, \ln \Lambda_2)$ plane is straightforward (Figure 2.22b). The equations are



(a)



(b)

Figure 2.22: Decision spaces.

$$\begin{aligned} \ln \Lambda_1(\mathbf{R}) &\stackrel{\substack{H_1 \text{ or } H_2 \\ H_0 \text{ or } H_2}}{\gtrless} \ln \frac{P_0}{P_1}, \\ \ln \Lambda_2(\mathbf{R}) &\stackrel{\substack{H_2 \text{ or } H_1 \\ H_0 \text{ or } H_1}}{\gtrless} \ln \frac{P_0}{P_2}, \\ \ln \Lambda_2(\mathbf{R}) &\stackrel{\substack{H_2 \text{ or } H_0 \\ H_1 \text{ or } H_0}}{\gtrless} \ln \Lambda_1(\mathbf{R}) + \ln \frac{P_1}{P_2}. \end{aligned} \quad (2.144)$$

The expressions in (2.143) and (2.144) are adequate, but they obscure an important interpretation of the processor. The desired interpretation is obtained by a little manipulation.

Substituting (2.138) into (2.139)–(2.141) and multiplying both sides by $p_{\mathbf{r}|H_0}(\mathbf{R}|H_0)$, we have

$$\begin{aligned} P_1 p_{\mathbf{r}|H_1}(\mathbf{R}|H_1) &\stackrel{\substack{H_1 \text{ or } H_2 \\ H_0 \text{ or } H_2}}{\gtrless} P_0 p_{\mathbf{r}|H_0}(\mathbf{R}|H_0), \\ P_2 p_{\mathbf{r}|H_2}(\mathbf{R}|H_2) &\stackrel{\substack{H_2 \text{ or } H_1 \\ H_0 \text{ or } H_1}}{\gtrless} P_0 p_{\mathbf{r}|H_0}(\mathbf{R}|H_0), \\ P_2 p_{\mathbf{r}|H_2}(\mathbf{R}|H_2) &\stackrel{\substack{H_2 \text{ or } H_0 \\ H_1 \text{ or } H_0}}{\gtrless} P_1 p_{\mathbf{r}|H_1}(\mathbf{R}|H_1). \end{aligned} \quad (2.145)$$

Looking at (2.145), we see that an equivalent test is to compute *a posteriori* probabilities $\Pr(H_0|\mathbf{R})$, $\Pr(H_1|\mathbf{R})$, and $\Pr(H_2|\mathbf{R})$ and choose the largest. (Simply divide both sides of each equation by $p_{\mathbf{r}}(\mathbf{R})$ and examine the resulting test.) For this reason, the processor for the minimum probability of error criterion is frequently referred to as a *maximum a posterior probability computer*.

The next two topics deal with degenerate tests. Both results will be useful in later applications. A case of interest is a degenerate one in which we combine H_1 and H_2 . Then,

$$C_{12} = C_{21} = 0, \quad (2.146)$$

and, for simplicity, we can let

$$C_{01} = C_{10} = C_{20} = C_{02} \quad (2.147)$$

and

$$C_{00} = C_{11} = C_{22} = 0. \quad (2.148)$$

Then (2.139) and (2.140) both reduce to

$$P_1 \Lambda_1(\mathbf{R}) + P_2 \Lambda_2(\mathbf{R}) \stackrel{\substack{H_1 \text{ or } H_2 \\ H_0}}{\gtrless} P_0 \quad (2.149)$$

and (2.141) becomes an identity.

The decision regions are shown in Figure 2.23. Because we have eliminated all of the cost effect of a decision between H_1 and H_2 , we have reduced it to a binary problem.

We next consider the dummy hypothesis technique. A simple example illustrates the idea. The actual problem has two hypotheses, H_1 and H_2 , but occasionally we can simplify

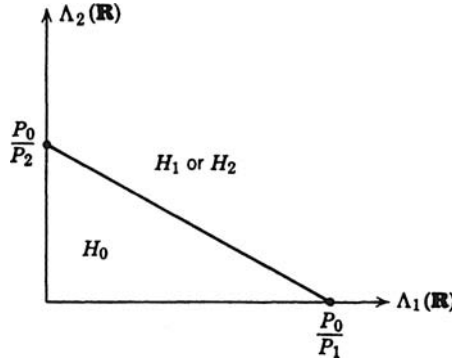


Figure 2.23: Decision spaces.

the calculations by introducing a dummy hypothesis H_0 that occurs with zero probability. We let

$$\begin{aligned} P_0 &= 0, \quad P_1 + P_2 = 1, \\ C_{12} &= C_{02}, \quad C_{21} = C_{01}. \end{aligned} \quad (2.150)$$

Substituting these values into (2.139)–(2.141), we find that (2.139) and (2.140) imply that we always choose H_1 or H_2 and the test reduces to

$$P_2(C_{12} - C_{22})\Lambda_2(\mathbf{R}) \stackrel{H_2}{\underset{H_1}{\gtrless}} P_1(C_{21} - C_{11})\Lambda_1(\mathbf{R}). \quad (2.151)$$

Looking at (2.12) and recalling the definition of $\Lambda_1(\mathbf{R})$ and $\Lambda_2(\mathbf{R})$, we see that this result is exactly what we would expect. [Just divide both sides of (2.12) by $p_{\mathbf{r}|H_0}(\mathbf{R}|H_0)$.] On the surface this technique seems absurd, but it will turn out to be useful when the ratio

$$\frac{p_{\mathbf{r}|H_2}(\mathbf{R}|H_2)}{p_{\mathbf{r}|H_1}(\mathbf{R}|H_1)}$$

is difficult to work with and the ratios $\Lambda_1(\mathbf{R})$ and $\Lambda_2(\mathbf{R})$ can be made simple by a proper choice of $p_{\mathbf{r}|H_0}(\mathbf{R}|H_0)$.

The formulation of the M hypothesis problem in (2.134)–(2.141) leads to an efficient decision space but loses some of the symmetry. The optimum Bayes test can be written in a different manner by defining a function

$$\beta_i(\mathbf{R}) = \sum_{j=0}^{M-1} C_{ij} \Pr(H_j|\mathbf{R}), \quad i = 0, 1, \dots, M-1. \quad (2.152)$$

Using Bayes rule, we can rewrite (2.134) as

$$\begin{aligned}
 \mathcal{R} &= \sum_{i=0}^{M-1} \sum_{j=0}^{M-1} P_j C_{ij} \int_{Z_i} p_{\mathbf{r}|H_j}(\mathbf{R}|H_j) d\mathbf{R} \\
 &= \sum_{i=0}^{M-1} \sum_{j=0}^{M-1} C_{ij} \int_{Z_i} p_{\mathbf{r}|H_j}(\mathbf{R}|H_j) P_j d\mathbf{R} \\
 &= \sum_{i=0}^{M-1} \sum_{j=0}^{M-1} C_{ij} \int_{Z_i} \Pr(H_j|\mathbf{R}) p_{\mathbf{r}}(\mathbf{R}) d\mathbf{R} \\
 &= \sum_{i=0}^{M-1} \int_{Z_i} \left(\sum_{j=0}^{M-1} C_{ij} \Pr(H_j|\mathbf{R}) \right) p_{\mathbf{r}}(\mathbf{R}) d\mathbf{R}.
 \end{aligned} \tag{2.153}$$

Substituting (2.152) into (2.153)

$$\mathcal{R} = \sum_{i=0}^{M-1} \int_{Z_i} \beta_i(\mathbf{R}) p_{\mathbf{r}}(\mathbf{R}) d\mathbf{R}. \tag{2.154}$$

Evaluating (2.154) gives,

$$\mathcal{R} = \int_{Z_0} \beta_0(\mathbf{R}) p_{\mathbf{r}}(\mathbf{R}) d\mathbf{R} + \int_{Z_1} \beta_1(\mathbf{R}) p_{\mathbf{r}}(\mathbf{R}) d\mathbf{R} + \cdots + \int_{Z_{M-1}} \beta_{M-1}(\mathbf{R}) p_{\mathbf{r}}(\mathbf{R}) d\mathbf{R}. \tag{2.155}$$

Each particular \mathbf{R} will be included in only one integral. We want to assign it to the region Z_i where it will make the smallest contribution to \mathcal{R} . Clearly this is done by choosing the smallest $\beta_i(\mathbf{R})$ and assigning \mathbf{R} to that region. Thus, the optimum Bayes test is, compute

$$\boxed{\beta_i(\mathbf{R}) = \sum_{j=0}^{M-1} C_{ij} \Pr(H_j|\mathbf{R}), \quad i = 0, 1, \dots, M-1} \tag{2.156}$$

and choose the smallest.

For a minimum probability of error test, we consider the costs,

$$\begin{aligned}
 C_{ii} &= 0, \quad i = 0, 1, \dots, M-1, \\
 C_{ij} &= C, \quad i \neq j; i, j = 0, 1, \dots, M-1.
 \end{aligned} \tag{2.157}$$

Substituting into (2.152),

$$\beta_i(\mathbf{R}) = \sum_{j=0}^{M-1} C_{ij} \Pr(H_j|\mathbf{R}) = C \sum_{\substack{j=0 \\ j \neq i}}^{M-1} \Pr(H_j|\mathbf{R}), \tag{2.158}$$

or

$$\beta_i(\mathbf{R}) = C[1 - \Pr(H_i|\mathbf{R})]. \tag{2.159}$$

From (2.159), it is clear that choosing the largest $\Pr(H_j|\mathbf{R})$ is equivalent to choosing the smallest $\beta_i(\mathbf{R})$. This is the *maximum a posteriori* test that we previously encountered in (2.145) for $M = 3$. Thus, the optimum Bayes test is, compute

$$l_j(\mathbf{R}) = \Pr(H_j|\mathbf{R}), \quad j = 0, 1, \dots, M - 1, \quad (2.160)$$

and choose the largest.

A special case that occurs frequently in practice is equal *a priori* probabilities.

$$P_j = \frac{1}{M}, \quad j = 0, 1, \dots, M - 1. \quad (2.161)$$

Then, since

$$\begin{aligned} \Pr(H_j|\mathbf{R}) &= \frac{P_j p_{\mathbf{r}|H_j}(\mathbf{R}|H_j)}{p_{\mathbf{r}}(\mathbf{R})} \\ &= \left(\frac{1}{M p_{\mathbf{r}}(\mathbf{R})} \right) p_{\mathbf{r}|H_j}(\mathbf{R}|H_j), \quad j = 0, 1, \dots, M - 1, \end{aligned} \quad (2.162)$$

we can compute

$$l_j(\mathbf{R}) = p_{\mathbf{r}|H_j}(\mathbf{R}|H_j), \quad j = 0, 1, \dots, M - 1, \quad (2.163)$$

and choose the largest. Thus the maximum a posteriori test involves computing M sufficient statistics.

We now consider several examples.

Example 2.9. The observed random variable is Gaussian on each of five hypotheses.

$$p_{r|H_j}(R|H_j) = \frac{1}{\sqrt{2\pi}\sigma} \exp\left(-\frac{(R-m_j)^2}{2\sigma^2}\right), \quad -\infty < R < \infty; j = 1, 2, \dots, 5, \quad (2.164)$$

where

$$\begin{aligned} m_1 &= -2m, \\ m_2 &= -m, \\ m_3 &= 0, \\ m_4 &= m, \\ m_5 &= 2m. \end{aligned} \quad (2.165)$$

The hypotheses are equally likely and the criterion is minimum $\Pr(\epsilon)$.

In this case, $M = 5$ and the decision space is one dimensional. From (2.160), we know that to minimize the $\Pr(\epsilon)$, we choose the H_j with the largest *a posteriori* probability.

$$\Pr(H_j|R) = \Pr(R|H_j) \frac{P_j}{p_r(R)}. \quad (2.166)$$

Since the H_j are equally likely, this is equivalent to choosing the H_j for which,

$$p_{r|H_j}(R|H_j) = \frac{1}{\sqrt{2\pi}\sigma} \exp\left(-\frac{(R-m_j)^2}{2\sigma^2}\right), \quad j = 1, 2, \dots, 5, \quad (2.167)$$

is the largest. This, in turn, is equivalent to choosing the H_j for which

$$l_j(R) = |R - m_j|, \quad j = 1, 2, \dots, 5, \quad (2.168)$$

is the smallest. The decision space and the boundaries are shown in Figure 2.24.

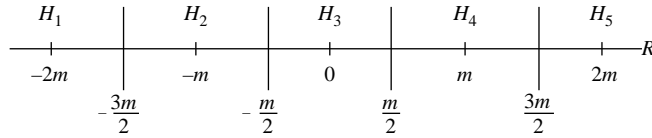


Figure 2.24: Decision space.

The probability of error is

$$\Pr(\epsilon) = \frac{1}{5} \left[\Pr(\epsilon|H_1) + \cdots + \Pr(\epsilon|H_5) \right]. \quad (2.169)$$

By comparing Figure 2.24 to Figure 2.11, we have

$$\Pr(\epsilon|H_j) = 2 \operatorname{erfc}_* \left(\frac{m}{2\sigma} \right), \quad j = 2, 3, 4, \quad (2.170)$$

and

$$\Pr(\epsilon|H_j) = \operatorname{erfc}_* \left(\frac{m}{2\sigma} \right), \quad j = 1, 5, \quad (2.171)$$

so

$$\Pr(\epsilon) = \frac{8}{5} \operatorname{erfc}_* \left(\frac{m}{2\sigma} \right). \quad (2.172)$$

■

Example 2.10. Consider the case where $M = 4$ and $N = 2$

$$\begin{aligned} r_1 &= m_{1j} + n_1, \quad j = 0, 1, 2, 3 \\ r_2 &= m_{2j} + n_2, \quad j = 0, 1, 2, 3. \end{aligned} \quad (2.173)$$

The n_1 and n_2 are statistically independent, zero-mean Gaussian random variables with variance σ^2 . The m_{1j} and m_{2j} form a two-dimensional vector whose components are

$$\begin{aligned} \mathbf{m}_0 &= [m \quad 0]^T, \\ \mathbf{m}_1 &= [0 \quad m]^T, \\ \mathbf{m}_2 &= [-m \quad 0]^T, \\ \mathbf{m}_3 &= [0 \quad m]^T. \end{aligned} \quad (2.174)$$

The hypotheses are equally likely and the criteria is minimum probability of error.

The joint probability density of r_1 and r_2 on H_j is

$$p_{r_1, r_2|H_j}(R_1, R_2|H_j) = \frac{1}{2\pi\sigma^2} \exp \left(-\frac{1}{2\sigma^2} [(R_1 - m_{1j})^2 + (R_2 - m_{2j})^2] \right). \quad (2.175)$$

From (2.163), we take the logarithm of (2.175) and choose the largest. Dropping terms that do not depend on the hypotheses gives

$$l_j(R_1, R_2) = -[(R_1 - m_{1j})^2 + (R_2 - m_{2j})^2], \quad j = 0, 1, 2, 3. \quad (2.176)$$

Choosing the largest in (2.176) is equivalent to choosing the smallest of

$$D_j = [(R_1 - m_{1j})^2 + (R_2 - m_{2j})^2], \quad j = 0, 1, 2, 3, \quad (2.177)$$

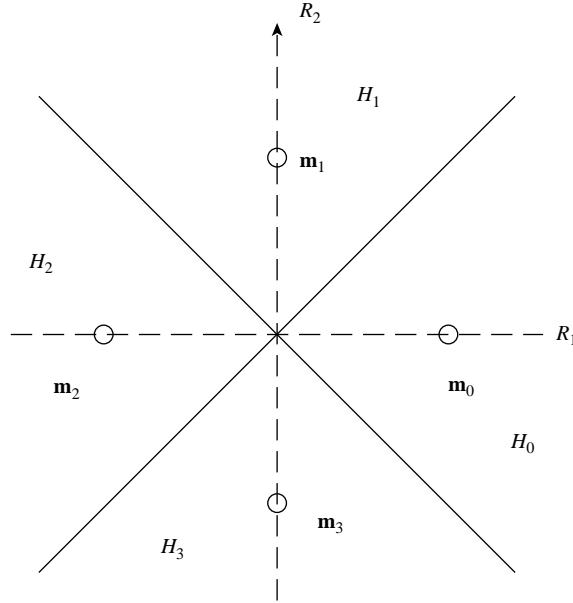


Figure 2.25: Decision space.

which is just the distance between the observations \$(R_1, R_2)\$ and \$\mathbf{m}_j\$ in the two-dimensional space shown in Figure 2.25. The result is an example of a *minimum distance decision rule*. We choose the hypothesis corresponding to the mean vector that the observation is closest to.

Note that the minimum distance test applies to any set of \$\mathbf{m}_j\$. We can also write

$$D_j = -2(R_1 m_{1j} + R_2 m_{2j}) + R_1^2 + R_2^2 + m_{1j}^2 + m_{2j}^2, \quad j = 0, 1, 2, 3, \quad (2.178)$$

and observe that for the \$\mathbf{m}_j\$ in (2.174) only the first term depends on the hypotheses. Thus, we can compute

$$\mathbf{R}^T \mathbf{m}_j = R_1 m_{1j} + R_2 m_{2j}, \quad j = 0, 1, 2, 3, \quad (2.179)$$

and choose the largest. This is a *correlation test*.

To compute the \$\Pr(\epsilon)\$, we observe that

$$\Pr(\epsilon) = \frac{1}{4} \sum_{j=0}^3 \Pr(\epsilon|H_j) \quad (2.180)$$

and that, from the symmetry of the decision space, all of the \$\Pr(\epsilon|H_j)\$ are identical.

We also observe that the answer would be invariant to a \$45^\circ\$ rotation of the signal set because the noise is circularly symmetric.

Thus, the problem of interest reduces to the simple diagram shown in Figure 2.26. The \$\Pr(\epsilon)\$ is simply the probability that \$\mathbf{r}\$ lies outside the first quadrant when \$H_1\$ is true.

Now \$r_1\$ and \$r_2\$ are independent Gaussian variables with identical means and variances:

$$\begin{aligned} E(r_1|H_1) &= E(r_2|H_1) = m/\sqrt{2}, \\ \text{Var}(r_1|H_1) &= \text{Var}(r_2|H_1) = \sigma^2. \end{aligned} \quad (2.181)$$

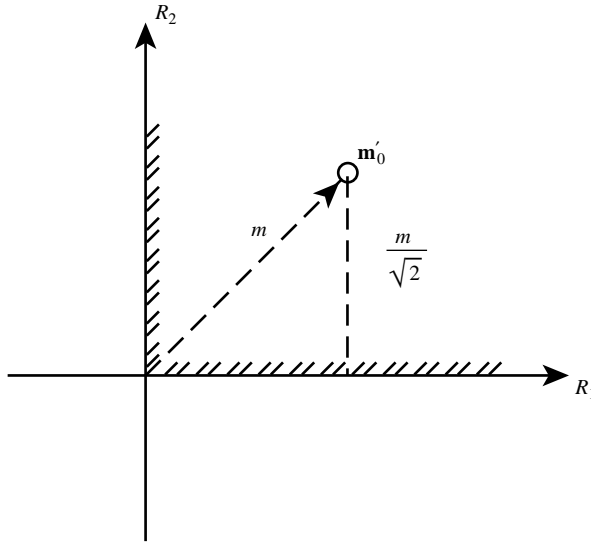


Figure 2.26: Rotation of signal.

The $\text{Pr}(\epsilon)$ can be obtained by integrating $p_{r_1, r_2 | H_1}(R_1, R_2 | H_1)$ over the area outside the first quadrant. Equivalently, $\text{Pr}(\epsilon)$ is the integral over the first quadrant subtracted from unity,

$$\text{Pr}(\epsilon) = 1 - \left[\int_0^{\infty} (2\pi\sigma^2)^{-1/2} \exp\left(-\frac{(R_1 - m/\sqrt{2})^2}{2\sigma^2}\right) dR_1 \right] \left[\int_0^{\infty} (2\pi\sigma^2)^{-1/2} \exp\left(-\frac{(R_2 - m/\sqrt{2})^2}{2\sigma^2}\right) dR_2 \right]. \quad (2.182)$$

Changing variables, we have

$$\text{Pr}(\epsilon) = 1 - \left(\int_{-m/\sqrt{2}\sigma}^{\infty} \frac{1}{\sqrt{2\pi}} \exp\left(-\frac{x^2}{2}\right) dx \right)^2 = 1 - \left[\text{erfc}_* \left(-\frac{m}{\sqrt{2}\sigma} \right) \right]^2, \quad (2.183)$$

which is the desired result. ■

Example 2.11. In this example, we consider a non-Gaussian density with M hypotheses. We consider the Generalized Gaussian probability density introduced in Example 2.4. We assume that α is the same on all hypotheses. The mean is zero on all hypotheses but the variances σ_j^2 are different. The probability densities are

$$p_{r_i | H_j}(R_i | H_j) = c_j \exp\left(-\left|\frac{R_i}{b_j}\right|^\alpha\right), \quad j = 0, 1, \dots, M-1, \quad (2.184)$$

where b_j and c_j were defined in (2.48) and (2.49). To simplify notation, we define

$$\beta(\alpha) = \sqrt{\frac{\Gamma(1/\alpha)}{\Gamma(3/\alpha)}} = \frac{b_j}{\sigma_j} \quad (2.185)$$

and

$$\gamma(\alpha) = \frac{1}{2\beta(\alpha)\Gamma(1+1/\alpha)} = c_j\sigma_j. \quad (2.186)$$

Then, (2.184) can be rewritten as

$$p_{r_i|H_j}(R_i|H_j) = \frac{1}{\sigma_j} \gamma(\alpha) \exp\left(-\left|\frac{R_i}{\sigma_j\beta(\alpha)}\right|^\alpha\right) \quad (2.187)$$

and

$$p_{\mathbf{r}|H_j}(\mathbf{R}|H_j) = \prod_{i=1}^N p_{r_i|H_j}(R_i|H_j). \quad (2.188)$$

We assume that the hypotheses are equally likely, so we choose the H_j for which $p_{\mathbf{r}|H_j}(\mathbf{R}|H_j)$ is the largest.

$$\begin{aligned} \ln p_{\mathbf{r}|H_j}(\mathbf{R}|H_j) &= N \ln \gamma(\alpha) - N \ln \sigma_j - \sum_{i=1}^N \left| \frac{R_i}{\sigma_j\beta(\alpha)} \right|^\alpha \\ &= N \ln \gamma(\alpha) - N \ln \sigma_j - \frac{1}{[\sigma_j\beta(\alpha)]^\alpha} \sum_{i=1}^N |R_i|^\alpha. \end{aligned} \quad (2.189)$$

We can see that a sufficient statistic is

$$l_N(\mathbf{R}) = \sum_{i=1}^N |R_i|^\alpha. \quad (2.190)$$

We define

$$\bar{l}_N(\mathbf{R}) = \frac{1}{N} \sum_{i=1}^N |R_i|^\alpha \quad (2.191)$$

and choose the largest of

$$l_j(\mathbf{R}) = -\ln \sigma_j - \frac{1}{[\sigma_j\beta(\alpha)]^\alpha} \bar{l}_N(\mathbf{R}), \quad j = 0, 1, \dots, M-1. \quad (2.192)$$

In Figure 2.27, we plot $l_j(\mathbf{R})$ versus $\bar{l}_N(\mathbf{R})$ for $M = 4$ hypotheses with $\alpha = 1$, $\sigma_1 = 1$, $\sigma_2 = 2$, $\sigma_3 = 5$, and $\sigma_4 = 10$. We see that there are four distinct regions where each of the $l_j(\mathbf{R})$ is largest. The performance can be evaluated, but it is tedious. ■

In this section, we have developed the basic results needed for the M hypothesis problem. Several important points should be emphasized.

1. The dimension of the decision space is no more than $M - 1$. The boundaries of the decision regions are hyperplanes in the $(\Lambda_1, \dots, \Lambda_{M-1})$ plane.
2. The optimum Bayes test is straightforward to find. We compute

$$\beta_i(\mathbf{R}) = \sum_{j=0}^{M-1} C_{ij} \Pr(H_j|\mathbf{R}), \quad i = 0, 1, \dots, M-1, \quad (2.193)$$

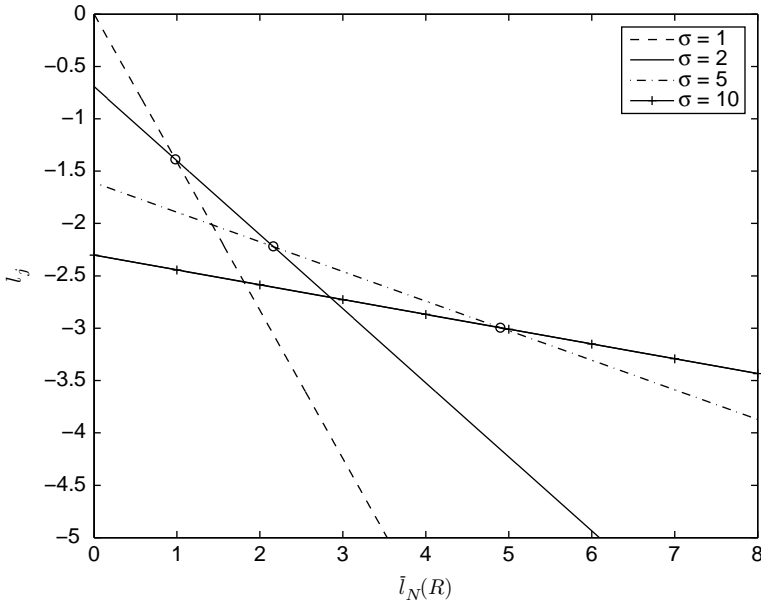


Figure 2.27: l_j versus $\bar{l}_N(\mathbf{R})$.

or

$$\beta'_i(\mathbf{R}) = \sum_{j=0}^{M-1} C_{ij} P_j p_{\mathbf{r}|H_j}(\mathbf{R}|H_j), \quad i = 0, 1, \dots, M-1, \quad (2.194)$$

and choose the smallest. We shall find however, when we consider specific examples, that the error probabilities are frequently difficult to compute.

3. A particular test of importance is the minimum total probability of error test. Here we compute the *a posteriori* probability of each hypothesis $\Pr(H_i|\mathbf{R})$ and choose the largest.

These points will be appreciated more fully as we proceed through various applications.

2.4 PERFORMANCE BOUNDS AND APPROXIMATIONS

Up to this point, we have dealt primarily with problems in which we could derive the structure of the optimum receiver and obtain relatively simple expressions for the receiver operating characteristic or the error probability.

In many cases of interest, the optimum test can be derived but an exact analytic performance calculation is difficult or impossible. For these cases, we must resort to bounds on the error probabilities or approximate expressions for these probabilities. In this section, we derive some simple bounds and approximations that are useful in many problems of practical importance. The basic results, due to Chernoff [Che62], were extended initially by Shannon [Sha56]. They have been further extended by Fano [Fan61], Shannon, Gallager, and Berlekamp [SGB67], and Gallager [Gal65] and applied to a problem of interest to us by Jacobs [Jac66]. Our approach is based on the last two references. Because the latter part

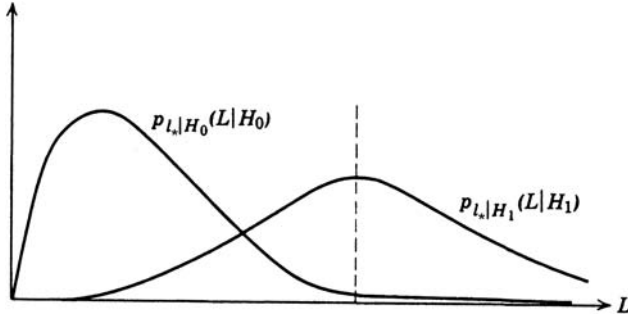


Figure 2.28: Typical densities.

of the development is heuristic in nature, the interested reader should consult the references given for more careful derivations.

The problem of interest is the general binary hypothesis test outlined in Section 2.2. From our results in that section we know that it will reduce to a likelihood ratio test. We begin our discussion at this point.

The likelihood ratio test is

$$l_*(\mathbf{R}) \triangleq \ln \Lambda(\mathbf{R}) = \ln \left[\frac{p_{\mathbf{r}|H_1}(\mathbf{R}|H_1)}{p_{\mathbf{r}|H_0}(\mathbf{R}|H_0)} \right] \stackrel{H_1}{\underset{H_0}{\gtrless}} \ln \eta \triangleq \gamma_*. \quad (2.195)$$

We use the notation $l_*(\mathbf{R})$ to denote the sufficient statistic that is equal to the log-likelihood ratio and γ_* to denote the threshold for this statistic. The variable $l_*(\mathbf{R})$ is a random variable whose probability density depends on which hypothesis is true. In Figure 2.28, we show a typical $p_{l_*|H_1}(L|H_1)$ and $p_{l_*|H_0}(L|H_0)$.

If the two densities are known, then P_F and P_D are given by

$$P_D(\gamma_*) = \int_{\gamma_*}^{\infty} p_{l_*|H_1}(L|H_1) dL, \quad (2.196)$$

$$P_F(\gamma_*) = \int_{\gamma_*}^{\infty} p_{l_*|H_0}(L|H_0) dL, \quad (2.197)$$

where we have used the notation $P_D(\gamma_*)$ and $P_F(\gamma_*)$ to emphasize the dependence of these probabilities on the value of the threshold γ_* . The difficulty is that it is often hard to find $p_{l_*|H_j}(L|H_j)$; $j = 0, 1$. A common case in practice occurs when the components of \mathbf{R} are statistically independent but are non-Gaussian. In a few cases, analytic expressions for $p_{l_*|H_j}(L|H_j)$; $j = 0, 1$ can be obtained, but in most cases, an $(N - 1)$ -fold convolution is required. On the other hand, if we set out to synthesize a system, it is inefficient (if not impossible) to try successive systems and evaluate each numerically. Therefore, we should like to find some simpler approximate expressions for the error probabilities.

When we discuss simulation in Section 2.5, we will find that the approximate expressions we derive in this section are the key to efficient simulation.

In this section, we derive some simple expressions that we shall use in the sequel. We first focus our attention on cases in which $l_*(\mathbf{R})$ is a sum of independent random variables. This suggests that its characteristic function may be useful, for it will be the product of the

individual characteristic functions of the R_i . Similarly, the moment-generating function will be the product of the individual moment-generating functions. Therefore, an approximate expression based on one of these functions should be relatively easy to evaluate. The first part of our discussion develops bounds on the error probabilities in terms of the moment-generating function of $l_*(\mathbf{R})$.

In the second part, we consider the case in which $l_*(\mathbf{R})$ is sum of a *large* number of independent random variables. By the use of the central limit theorem, we improve on the results obtained in the first part of the discussion.

We begin by deriving a simple upper bound on $P_F(\gamma_*)$ in terms of the moment-generating function. The moment-generating function of $l_*(\mathbf{R})$ on hypothesis H_0 is

$$\phi_{l_*|H_0}(s) \triangleq E(e^{sL}|H_0) = \int_{-\infty}^{\infty} e^{sL} p_{l_*|H_0}(L|H_0) dL, \quad (2.198)$$

where s is a real variable. (The range of s corresponds to those values for which the integral exists.) We shall see shortly that it is more useful to write

$$\phi_{l_*|H_0}(s) \triangleq \exp[\mu(s)], \quad (2.199)$$

so that

$$\mu(s) = \ln \int_{-\infty}^{\infty} e^{sL} p_{l_*|H_0}(L|H_0) dL. \quad (2.200)$$

We may also express $\mu(s)$ in terms of $p_{\mathbf{r}|H_1}(\mathbf{R}|H_1)$ and $p_{\mathbf{r}|H_0}(\mathbf{R}|H_0)$. Because l_* is just a function of \mathbf{r} , we can write (2.198) as

$$\phi_{l_*|H_0}(s) = \int_{-\infty}^{\infty} e^{s l_*(\mathbf{R})} p_{\mathbf{r}|H_0}(\mathbf{R}|H_0) d\mathbf{R}. \quad (2.201)$$

Then,

$$\mu(s) = \ln \int_{-\infty}^{\infty} e^{s l_*(\mathbf{R})} p_{\mathbf{r}|H_0}(\mathbf{R}|H_0) d\mathbf{R}. \quad (2.202)$$

Using (2.195),

$$\mu(s) = \ln \int_{-\infty}^{\infty} \left(\frac{p_{\mathbf{r}|H_1}(\mathbf{R}|H_1)}{p_{\mathbf{r}|H_0}(\mathbf{R}|H_0)} \right)^s p_{\mathbf{r}|H_0}(\mathbf{R}|H_0) d\mathbf{R}, \quad (2.203)$$

or

$$\mu(s) = \ln \int_{-\infty}^{\infty} [p_{\mathbf{r}|H_1}(\mathbf{R}|H_1)]^s [p_{\mathbf{r}|H_0}(\mathbf{R}|H_0)]^{1-s} d\mathbf{R}. \quad (2.204)$$

The function $\mu(s)$ plays a central role in the succeeding discussion. It is now convenient to rewrite the error expressions in terms of a new random variable whose mean is in the vicinity of the threshold. The reason for this step is that we shall use the central limit theorem in the

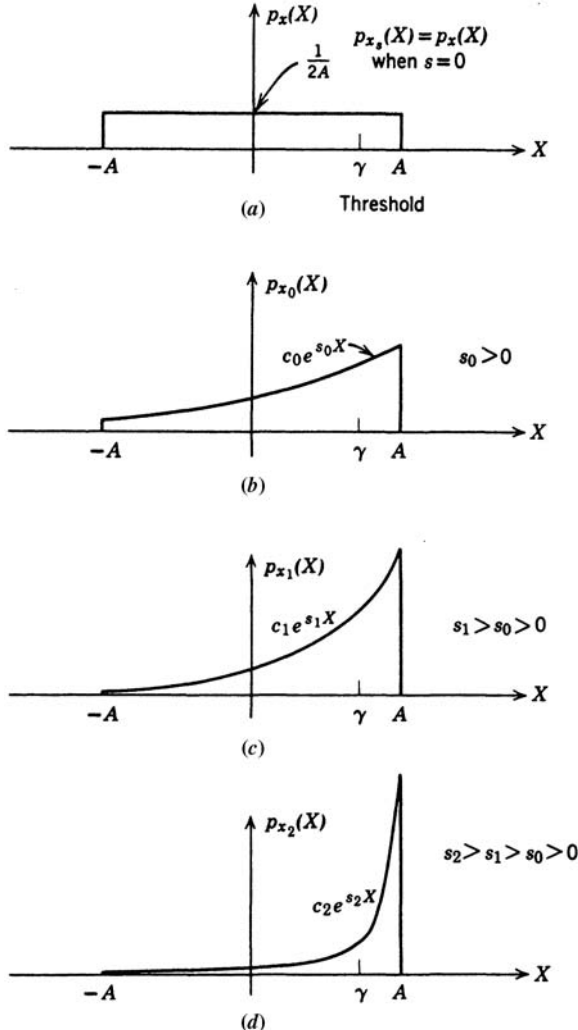


Figure 2.29: Tilted probability densities.

second part of our derivation. This is most effective near the mean of the random variable of interest. Consider the simple probability density shown in Figure 2.29a. To get the new family of densities shown in Figure 2.29, we multiply $p_x(X)$ by e^{sX} for various values of s (and normalize to obtain a unit area). We see that for $s > 0$ the mean is shifted to the right. For the moment, we leave s as a parameter. We see that increasing s “tilts” the density more.

Denoting this new variable as x_s , we have

$$p_{x_s}(X) \triangleq \frac{e^{sX} p_{l^*|H_0}(X|H_0)}{\int_{-\infty}^{\infty} e^{sL} p_{l^*|H_0}(L|H_0) dL} = \frac{e^{sX} p_{l^*|H_0}(X|H_0)}{e^{\mu(s)}} = e^{sX - \mu(s)} p_{l^*|H_0}(X|H_0). \quad (2.205)$$

Observe that we define x_s in terms of its density function, for that is what we are interested in. Equation (2.205) is a general definition. For the density shown in Figure 2.29, the limits would be $(-A, A)$.

We now find the mean and variance of x_s :

$$E(x_s) = \int_{-\infty}^{\infty} X p_{x_s}(X) dX = \frac{\int_{-\infty}^{\infty} X e^{sX} p_{l_*|H_0}(X|H_0) dX}{\int_{-\infty}^{\infty} e^{sL} p_{l_*|H_0}(L|H_0) dL}. \quad (2.206)$$

Comparing (2.206) and (2.200), we see that

$$E(x_s) = \frac{d\mu(s)}{ds} \triangleq \dot{\mu}(s). \quad (2.207)$$

Similarly, we find

$$\text{Var}(x_s) = \ddot{\mu}(s). \quad (2.208)$$

[Observe that (2.208) implies that $\mu(s)$ is convex.]

We now rewrite $P_F(\gamma_*)$ in terms of this tilted variable x_s :

$$\begin{aligned} P_F(\gamma_*) &= \int_{\gamma_*}^{\infty} p_{l_*|H_0}(L|H_0) dL = \int_{\gamma_*}^{\infty} e^{\mu(s)-sX} p_{x_s}(X) dX \\ &= e^{\mu(s)} \int_{\gamma_*}^{\infty} e^{-sX} p_{x_s}(X) dX. \end{aligned} \quad (2.209)$$

We can now find a simple upper bound on $P_F(\gamma_*)$. For values of $s \geq 0$,

$$e^{-sX} \leq e^{-s\gamma_*}, \quad \text{for } X \geq \gamma_*. \quad (2.210)$$

Thus,

$$P_F(\gamma_*) \leq e^{\mu(s)-s\gamma_*} \int_{\gamma_*}^{\infty} p_{x_s}(X) dX, \quad s \geq 0. \quad (2.211)$$

Clearly the integral is less than one. Thus,

$$P_F(\gamma_*) \leq e^{\mu(s)-s\gamma_*}, \quad s \geq 0. \quad (2.212)$$

To get the best bound, we minimize the right-hand side of (2.212) with respect to s . Differentiating the exponent and setting the result equal to zero, we obtain

$$\dot{\mu}(s) = \gamma_*. \quad (2.213)$$

Because $\dot{\mu}(s)$ is nonnegative, a solution will exist if

$$\dot{\mu}(0) \leq \gamma_* \leq \dot{\mu}(\infty). \quad (2.214)$$

Because

$$\dot{\mu}(0) = E(l_*|H_0), \quad (2.215)$$

the left inequality implies that the threshold must be to the right of the mean of l_* on H_0 . If $\gamma_* < \dot{\mu}(0)$, the value of s that minimizes the bound in (2.212) will be $s_* = 0$, which gives the bound $P_F(\gamma_*) \leq 1$.

Let s_* denote the value of s that is the solution to (2.213),

$$s_* : \dot{\mu}(s_*) = \gamma_*. \quad (2.216)$$

The resulting bound is:

$$P_F(\gamma_*) \leq \begin{cases} e^{\mu(s_*) - s_* \dot{\mu}(s_*)}, & \gamma_* \geq \dot{\mu}(0) \\ 1 & \gamma_* < \dot{\mu}(0). \end{cases} \quad (2.217)$$

(Note that we have assumed $\mu(s)$ exists for the desired s_* .)

Equation (2.217) is commonly referred to as the Chernoff bound [Che62]. Comparing (2.216) and (2.207), we observe that s_* is chosen so that the mean of the tilted variable x_s is at the threshold γ_* .

The next step is to find a bound on $P_M(\gamma_*)$, the probability of a miss:

$$P_M(\gamma_*) = \int_{-\infty}^{\gamma_*} p_{l_*|H_1}(X|H_1) dX, \quad (2.218)$$

which we want to express in terms of the tilted variable x_s .

Using an argument identical to that in (2.124) through (2.130), we see that

$$p_{l_*|H_1}(X|H_1) = e^X p_{l_*|H_0}(X|H_0). \quad (2.219)$$

Substituting (2.219) into the right side of (2.205), we have

$$p_{l_*|H_1}(X|H_1) = e^{\mu(s)+(1-s)X} p_{x_s}(X). \quad (2.220)$$

Substituting into (2.218),

$$P_M(\gamma_*) = e^{\mu(s)} \int_{-\infty}^{\gamma_*} e^{(1-s)X} p_{x_s}(X) dX. \quad (2.221)$$

For $s \leq 1$,

$$e^{(1-s)X} \leq e^{(1-s)\gamma_*}, \quad \text{for } X \leq \gamma_*. \quad (2.222)$$

Thus,

$$\begin{aligned} P_M(\gamma_*) &\leq e^{\mu(s)+(1-s)\gamma_*} \int_{-\infty}^{\gamma_*} p_{x_s}(X) dX \\ &\leq e^{\mu(s)+(1-s)\gamma_*}, \quad s \leq 1. \end{aligned} \quad (2.223)$$

Once again the bound is minimized for

$$\gamma_* = \dot{\mu}(s) \quad (2.224)$$

if a solution exists for $s \leq 1$. Observing that

$$\dot{\mu}(1) = E(l_*|H_1), \quad (2.225)$$

we see that this requires that threshold to be to the left of the mean of l_* on H_1 . If $\gamma_* > \dot{\mu}(1)$, then the value of s that minimizes the bound in (2.223) will be $s_* = 1$, which gives the bound $P_M(\gamma_*) \leq 1$.

Combining (2.217) and (2.223), we have

$$\begin{aligned} P_F(\gamma_*) &\leq \exp[\mu(s_*) - s_*\dot{\mu}(s_*)], & s_* \geq 0 \Rightarrow \gamma_* &\geq \dot{\mu}(0), \\ P_M(\gamma_*) &\leq \exp[\mu(s_*) + (1 - s_*)\dot{\mu}(s_*)], & s_* \leq 1 \Rightarrow \gamma_* &\leq \dot{\mu}(1), \end{aligned} \quad (2.226)$$

where

$$s_* : \dot{\mu}(s_*) = \gamma_* \quad (2.227)$$

Confining $s_* \geq 0$ (and therefore $\gamma_* \geq \dot{\mu}(0)$) for the $P_F(\gamma_*)$ bound and $s_* \leq 1$ (therefore $\gamma_* \leq \dot{\mu}(1)$) for the $P_M(\gamma_*)$ bound is not too restrictive because if the threshold is not between the means then one of the error probabilities will be large (greater than one half if the median coincides with the mean).

As pointed out in [SGB67], the exponents have a simple graphical interpretation. A typical $\mu(s)$ is shown in Figure 2.30. We draw a tangent at the point at which $\dot{\mu}(s) = \gamma_*$. This tangent intersects vertical lines at $s = 0$ and $s = 1$. The value of the intercept at $s = 0$ is the exponent in the $P_F(\gamma_*)$ bound. The value of the intercept at $s = 1$ is the exponent in the $P_M(\gamma_*)$ bound.

For the special case in which the hypotheses are equally likely and the error costs are equal we know that $\gamma_* = 0$. Therefore to minimize the bound we choose that value of s where $\dot{\mu}(s) = 0$.

The probability of error $\Pr(\epsilon)$ is

$$\Pr(\epsilon) = \frac{1}{2} P_F(\gamma_* = 0) + \frac{1}{2} P_M(\gamma_* = 0). \quad (2.228)$$

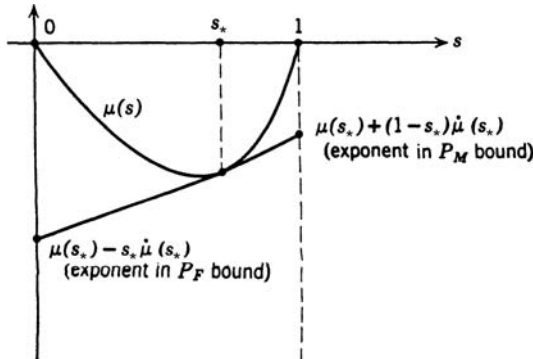


Figure 2.30: Exponents in bounds.

Substituting (2.211) and (2.223) into (2.228) and denoting the value s for which $\dot{\mu}(s) = 0$ as s_m , we have

$$\Pr(\epsilon) \leq \frac{1}{2} e^{\mu(s_m)} \int_0^\infty p_{x_s}(X) dX + \frac{1}{2} e^{\mu(s_m)} \int_{-\infty}^0 p_{x_s}(X) dX, \quad (2.229)$$

or

$$\boxed{\Pr(\epsilon) \leq \frac{1}{2} e^{\mu(s_m)}}. \quad (2.230)$$

where

$$s_m : \dot{\mu}(s_m) = 0. \quad (2.231)$$

Up to this point we have considered arbitrary binary hypothesis tests. The bounds in (2.226) and (2.230) are always valid if $\mu(s)$ exists. In many cases of interest, $l_*(\mathbf{R})$ consists of a sum of a large number of independent random variables, and we can obtain a simple approximate expression for $P_F(\gamma_*)$ and $P_M(\gamma_*)$ that provides a much closer estimate of their actual value than the above bounds. The exponent in this expression is the same, but the multiplicative factor will often be appreciably smaller than unity.

We start the derivation with the expression for $P_F(\gamma_*)$ given in (2.209). Motivated by our result in (2.213) in the bound derivation, we choose s_* so that

$$\dot{\mu}(s_*) = \gamma_*. \quad (2.232)$$

Then, (2.209) becomes

$$P_F(\gamma_*) = e^{\mu(s_*)} \int_{\dot{\mu}(s_*)}^\infty e^{-s_* X} p_{x_s}(X) dX. \quad (2.233)$$

This can be written as

$$P_F(\gamma_*) = e^{\mu(s_*) - s_* \dot{\mu}(s_*)} \int_{\dot{\mu}(s_*)}^\infty e^{+s_* [\dot{\mu}(s_*) - X]} p_{x_s}(X) dX. \quad (2.234)$$

The term outside is just the bound in (2.217). We now use a central limit theorem argument to evaluate the integral. First, define a standardized variable:

$$y \triangleq \frac{x_s - E(x_s)}{[\text{Var}(x_s)]^{1/2}} = \frac{x_s - \dot{\mu}(s_*)}{\sqrt{\ddot{\mu}(s_*)}}. \quad (2.235)$$

Substituting (2.235) into (2.234), we have

$$P_F(\gamma_*) = e^{\mu(s_*) - s_* \dot{\mu}(s_*)} \int_0^\infty e^{-s_* \sqrt{\ddot{\mu}(s_*)} Y} p_y(Y) dY. \quad (2.236)$$

In many cases, the probability density governing \mathbf{r} is such that y approaches a Gaussian random variable as N (the number of components of \mathbf{r}) approaches infinity.⁵ A simple case in which this is true is the case in which the r_i are independent, identically distributed random variables with finite means and variances. In such cases, y approaches a zero-mean Gaussian random variable with unit variance and the integral in (2.236) can be evaluated by substituting the limiting density,

$$\int_0^\infty e^{-s_*\sqrt{\mu(s_*)}Y} \frac{1}{\sqrt{2\pi}} e^{-(Y^2/2)} dY = e^{s_*^2 \dot{\mu}(s_*)/2} \operatorname{erfc}_* \left[s_* \sqrt{\dot{\mu}(s_*)} \right]. \quad (2.237)$$

Then,

$$P_F(\gamma_*) \approx \left\{ \exp \left[\mu(s_*) - s_* \dot{\mu}(s_*) + \frac{s_*^2}{2} \ddot{\mu}(s_*) \right] \right\} \operatorname{erfc}_* \left[s_* \sqrt{\dot{\mu}(s_*)} \right]. \quad (2.238)$$

The approximation arises because y is only approximately Gaussian for finite N . For values of $s_* \sqrt{\dot{\mu}(s_*)} > 3$, we can approximate $\operatorname{erfc}_*(\cdot)$ by the upper bound in (2.89). Using this approximation,

$$P_F(\gamma_*) \approx \frac{1}{\sqrt{2\pi s_*^2 \ddot{\mu}(s_*)}} \exp [\mu(s_*) - s_* \dot{\mu}(s_*)], \quad s_* > 0. \quad (2.239)$$

It is easy to verify that the approximate expression in (2.239) can also be obtained by letting

$$p_y(Y) \approx p_y(0) \approx \frac{1}{\sqrt{2\pi}}. \quad (2.240)$$

Looking at Figure 2.31, we see that this is valid when the exponential function decreases to a small value while $Y \ll 1$.

In exactly the same manner, we obtain

$$P_M(\gamma_*) \approx \left\{ \exp \left[\mu(s_*) + (1 - s_*) \dot{\mu}(s_*) + \frac{(s_* - 1)^2}{2} \ddot{\mu}(s_*) \right] \right\} \operatorname{erfc}_* \left[(1 - s_*) \sqrt{\dot{\mu}(s_*)} \right]. \quad (2.241)$$

For $(1 - s_*) \sqrt{\dot{\mu}(s_*)} > 3$, this reduces to

$$P_M(\gamma_*) \approx \frac{1}{\sqrt{2\pi(1 - s_*)^2 \ddot{\mu}(s_*)}} \exp [\mu(s_*) + (1 - s_*) \dot{\mu}(s_*)], \quad s_* < 1. \quad (2.242)$$

Observe that the exponents in (2.239) and (2.242) are identical to those obtained by using the Chernoff bound. The central limit theorem argument has provided a multiplicative factor that will be significant in many of the applications of interest to us. In practice, we will normally use (2.238) and (2.241) in our numerical evaluations.

⁵An excellent discussion is contained in Feller [Fel66], pp. 517–520.

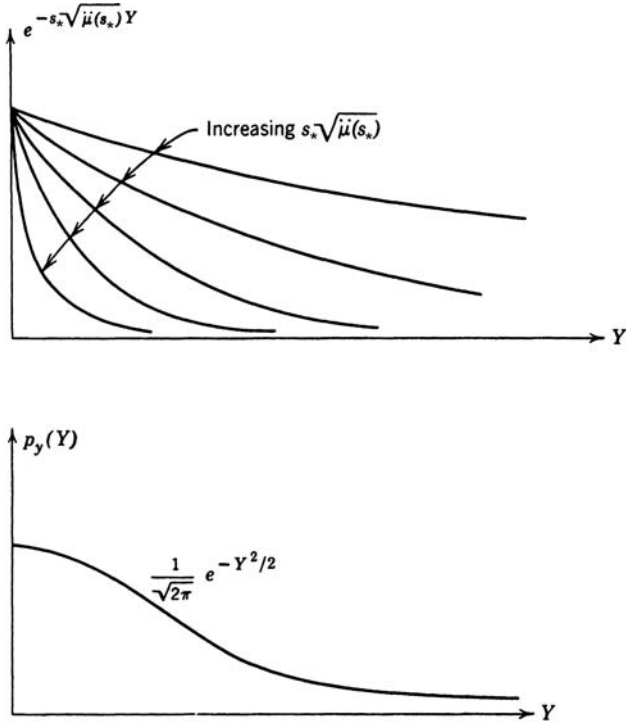


Figure 2.31: Behavior of functions.

For the case in which $\Pr(\epsilon)$ is the criterion and the hypotheses are equally likely we have

$$\begin{aligned}\Pr(\epsilon) &= \frac{1}{2} P_F(0) + \frac{1}{2} P_M(0) \\ &= \frac{1}{2} \exp \left[\mu(s_m) + \frac{s_m^2}{2} \dot{\mu}(s_m) \right] \operatorname{erfc}_* \left[s_m \sqrt{\ddot{\mu}(s_m)} \right] \\ &\quad + \frac{1}{2} \exp \left[\mu(s_m) + \frac{(1-s_m)^2}{2} \dot{\mu}(s_m) \right] \operatorname{erfc}_* \left[(1-s_m) \sqrt{\ddot{\mu}(s_m)} \right],\end{aligned}\quad (2.243)$$

where s_m is defined in (2.231) [i.e., $\dot{\mu}(s_m) = 0 = \gamma_*$]. When both $s_m \sqrt{\ddot{\mu}(s_m)} > 3$ and $(1-s_m) \sqrt{\ddot{\mu}(s_m)} > 3$, this reduces to

$$\Pr(\epsilon) \approx \frac{1}{2 [2\pi \dot{\mu}(s_m)]^{1/2} s_m (1-s_m)} \exp \mu(s_m).$$

(2.244)

Independent Observations. The function $\mu(s)$ defined in (2.204) and its derivatives $\dot{\mu}(s)$ and $\ddot{\mu}(s)$ are the key quantities in the bounds and approximations derived in this section. We now show that their expressions can be simplified in the case where the observation vector \mathbf{r} consists of N statistically independent components. In many cases, the probability

densities of the observation components are identical, but that is not necessary for the current derivation. For independent observations, we have

$$p_{\mathbf{r}|H_j}(\mathbf{R}|H_j) = \prod_{i=1}^N p_{r_i|H_j}(R_i|H_j) \quad j = 0, 1. \quad (2.245)$$

From (2.204),

$$\mu(s) = \ln \int_{-\infty}^{\infty} [p_{\mathbf{r}|H_1}(\mathbf{R}|H_1)]^s [p_{\mathbf{r}|H_0}(\mathbf{R}|H_0)]^{1-s} d\mathbf{R}. \quad (2.246)$$

Using (2.245) in (2.246), for the ID model, we have

$$\begin{aligned} \mu(s) &= \sum_{i=1}^N \ln \int [p_{r_i|H_1}(R_i|H_1)]^s [p_{r_i|H_0}(R_i|H_0)]^{1-s} dR_i \\ &= \sum_{i=1}^N \mu_i(s), \end{aligned} \quad (2.247)$$

where

$$\mu_i(s) = \ln \int [p_{r_i|H_1}(R_i|H_1)]^s [p_{r_i|H_0}(R_i|H_0)]^{1-s} dR_i. \quad (2.248)$$

Taking derivatives with respect to s yields

$$\dot{\mu}(s) = \sum_{i=1}^N \dot{\mu}_i(s), \quad (2.249)$$

$$\ddot{\mu}(s) = \sum_{i=1}^N \ddot{\mu}_i(s). \quad (2.250)$$

If the components of \mathbf{r} are IID, then $\mu_i(s)$ is the same for all $i = 1, \dots, N$, and we have

$$\mu(s) = N\mu_i(s), \quad (2.251)$$

$$\dot{\mu}(s) = N\dot{\mu}_i(s), \quad (2.252)$$

$$\ddot{\mu}(s) = N\ddot{\mu}_i(s). \quad (2.253)$$

We now consider several examples to illustrate the application of these ideas. The first is one in which the exact performance is known. We go through the bounds and approximations to illustrate the manipulations involved.

Example 2.12 (continuation of Examples 2.1 and 2.5). In this example, we consider the simple Gaussian problem first introduced in Example 2.1:

$$p_{\mathbf{r}|H_1}(\mathbf{R}|H_1) = \prod_{i=1}^N \frac{1}{\sqrt{2\pi}\sigma} \exp \left[-\frac{(R_i - m)^2}{2\sigma^2} \right] \quad (2.254)$$

and

$$p_{\mathbf{r}|H_0}(\mathbf{R}|H_0) = \prod_{i=1}^N \frac{1}{\sqrt{2\pi}\sigma} \exp\left(-\frac{R_i^2}{2\sigma^2}\right). \quad (2.255)$$

Then, using (2.246)

$$\mu(s) = \ln \int_{-\infty}^{\infty} \cdots \int_{-\infty}^{\infty} \prod_{i=1}^N \frac{1}{\sqrt{2\pi}\sigma} \exp\left[-\frac{(R_i - m)^2 s + R_i^2(1-s)}{2\sigma^2}\right] dR_i. \quad (2.256)$$

Because the observations are IID, all the integrals are identical, and

$$\mu(s) = N\mu_i(s) = N \ln \int_{-\infty}^{\infty} \frac{1}{\sqrt{2\pi}\sigma} \exp\left[-\frac{(R - m)^2 s + R^2(1-s)}{2\sigma^2}\right] dR. \quad (2.257)$$

Integrating we have

$$\mu(s) = Ns(s-1) \frac{m^2}{2\sigma^2} = \frac{s(s-1)d^2}{2}, \quad (2.258)$$

where d was defined in (2.82). The curve is shown in Figure 2.32.

Taking the derivative with respect to s gives:

$$\dot{\mu}(s) = \frac{(2s-1)d^2}{2}. \quad (2.259)$$

Evaluating $\dot{\mu}(s)$, we obtain

$$\dot{\mu}(s) = d^2. \quad (2.260)$$

Using (2.227), the value of s_* is found from:

$$s_* = \frac{\gamma_*}{d^2} + \frac{1}{2}. \quad (2.261)$$

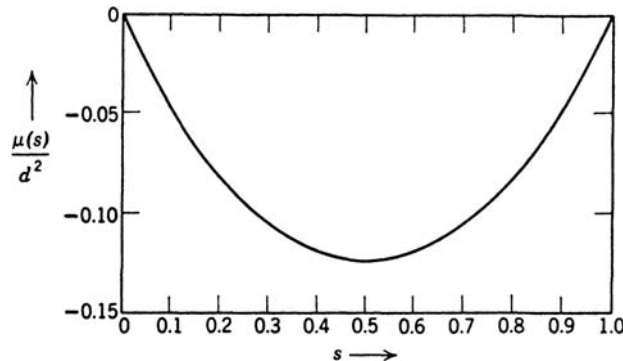


Figure 2.32: $\mu(s)$ for Gaussian variables with unequal means.

Using the bounds in (2.226), we have

$$\begin{aligned} P_F(\gamma_*) &\leq \exp\left(\frac{-s_*^2 d^2}{2}\right); \quad s_* \geq 0 \implies \gamma_* \geq -\frac{d^2}{2}, \\ P_M(\gamma_*) &\leq \exp\left[-\frac{(1-s_*)^2 d^2}{2}\right]; \quad s_* \leq 1 \implies \gamma_* \leq \frac{d^2}{2}. \end{aligned} \quad (2.262)$$

Because $l(\mathbf{R})$ is the sum of Gaussian random variables, the expressions in (2.238) and (2.241) are exact. Substituting (2.258)–(2.261) into (2.238) and (2.241), we have

$$P_F(\gamma_*) = \text{erfc}_* \left[s_* \sqrt{\dot{\mu}(s_*)} \right] = \text{erfc}_*(s_* d) = \text{erfc}_* \left(\frac{\gamma_*}{d} + \frac{d}{2} \right) \quad (2.263)$$

and

$$P_M(\gamma_*) = \text{erfc}_* \left[(1-s_*) \sqrt{\dot{\mu}(s_*)} \right] = \text{erfc}_*[(1-s_*)d] = \text{erfc}_* \left(-\frac{\gamma_*}{d} + \frac{d}{2} \right). \quad (2.264)$$

These expressions are identical to (2.84) and (2.85).

An even simpler case is one in which the total probability of error is the criterion. Then, we choose s_m such that $\dot{\mu}(s_m) = 0$. From Figure 2.32, we see that $s_m = \frac{1}{2}$. Using (2.243) and (2.244), we have

$$\Pr(\epsilon) = \text{erfc}_* \left(\frac{d}{2} \right) \approx \left(\frac{2}{\pi d^2} \right)^{1/2} \exp \left(-\frac{d^2}{8} \right). \quad (2.265)$$

The first expression is exact and identical to (2.88) and the second approximate expression is very good for $d > 6$.

This example is a special case of the binary symmetric hypothesis problem in which $\mu(s)$ is symmetric about $\frac{1}{2}$. When this is true and the criterion is minimum $\Pr(\epsilon)$, then $\mu\left(\frac{1}{2}\right)$ is the important quantity.

$$\mu\left(\frac{1}{2}\right) = \ln \int_{-\infty}^{\infty} [p_{\mathbf{r}|H_1}(\mathbf{R}|H_1)]^{1/2} [p_{\mathbf{r}|H_0}(\mathbf{R}|H_0)]^{1/2} d\mathbf{R}. \quad (2.266)$$

The negative of this quantity is frequently referred to as the Bhattacharyya distance (e.g., [Bha43]). It is important to note that it is the significant quantity only when $s_m = \frac{1}{2}$. ■

The next example also considers a case in which we have exact expressions for $P_D(\gamma_*)$ and $P_F(\gamma_*)$. However, it serves as useful lead into the case where the σ_j^2 ; $j = 0, 1$ are different on each component (i.e., we have σ_{ij}^2 ; $j = 0, 1$; $i = 1, 2, \dots, N$) that we will encounter in Chapter 3.

Example 2.13 (continuation of Examples 2.2 and 2.6). From (2.27) and (2.28),

$$\begin{aligned} p_{\mathbf{r}|H_1}(\mathbf{R}|H_1) &= \prod_{i=1}^N \frac{1}{\sqrt{2\pi}\sigma_1} \exp\left(-\frac{R_i^2}{2\sigma_1^2}\right), \\ p_{\mathbf{r}|H_0}(\mathbf{R}|H_0) &= \prod_{i=1}^N \frac{1}{\sqrt{2\pi}\sigma_0} \exp\left(-\frac{R_i^2}{2\sigma_0^2}\right). \end{aligned} \quad (2.267)$$

Substituting (2.267) into (2.246) and using the IID property gives,

$$\mu(s) = N\mu_i(s) = N \ln \int_{-\infty}^{\infty} \frac{1}{\sqrt{2\pi}\sigma_1^s\sigma_0^{1-s}} \exp\left[-\frac{sR^2}{2\sigma_1^2} - \frac{(1-s)R^2}{2\sigma_0^2}\right] dR \quad (2.268)$$

or

$$\mu(s) = \frac{N}{2} \ln \left[\frac{(\sigma_0^2)^s(\sigma_1^2)^{1-s}}{s\sigma_0^2 + (1-s)\sigma_1^2} \right]. \quad (2.269)$$

A case that will be of interest in the sequel is

$$\begin{aligned} \sigma_1^2 &= \sigma_n^2 + \sigma_s^2, \\ \sigma_0^2 &= \sigma_n^2. \end{aligned} \quad (2.270)$$

Substituting (2.270) into (2.269) gives

$$\frac{\mu(s)}{N/2} = \left\{ (1-s) \ln \left(1 + \frac{\sigma_s^2}{\sigma_n^2} \right) - \ln \left[1 + (1-s) \frac{\sigma_s^2}{\sigma_n^2} \right] \right\}. \quad (2.271)$$

This function is shown in Figure 2.33. Taking derivatives,

$$\dot{\mu}(s) = \frac{N}{2} \left[-\ln \left(1 + \frac{\sigma_s^2}{\sigma_n^2} \right) + \frac{\sigma_s^2/\sigma_n^2}{1 + (1-s)\sigma_s^2/\sigma_n^2} \right] \quad (2.272)$$

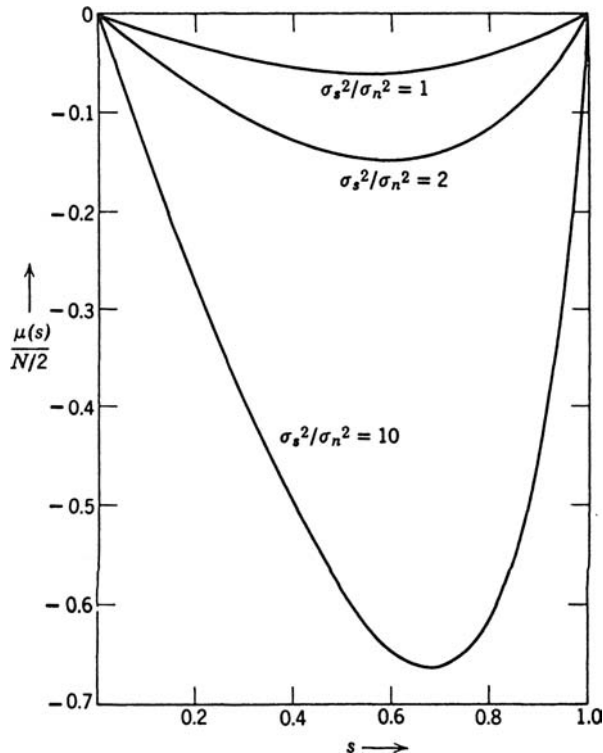


Figure 2.33: $\mu(s)$ for Gaussian variables with unequal variances.

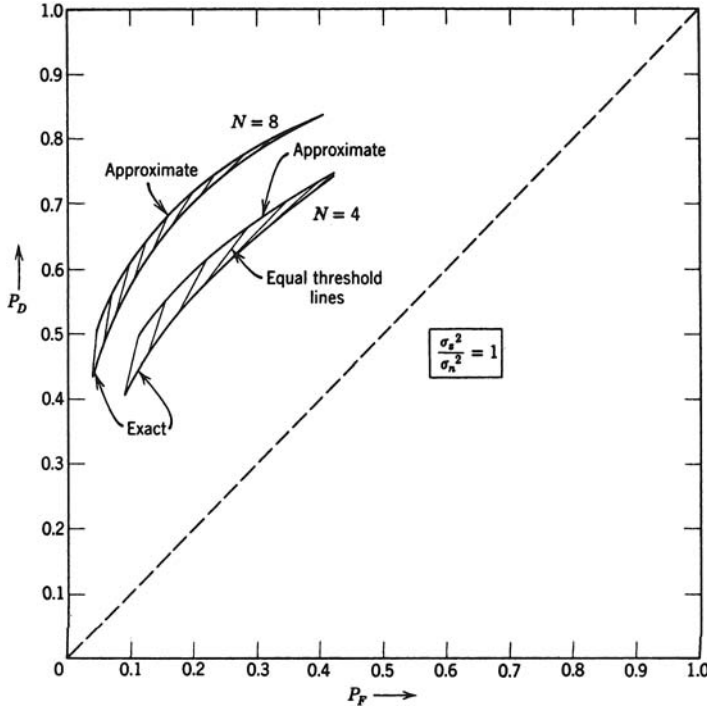


Figure 2.34: Approximate receiver operating characteristics.

and

$$\bar{\mu}(s) = \frac{N}{2} \left[\frac{\sigma_s^2 / \sigma_n^2}{1 + (1-s)\sigma_s^2 / \sigma_n^2} \right]^2. \quad (2.273)$$

By substituting (2.271), (2.272), and (2.273) into (2.238) and (2.241), we can plot an approximate receiver operating characteristic. This can be compared with the exact ROC in Figure 2.15 to estimate the accuracy of the approximation. In Figure 2.34, we show the comparison for $N = 4$ and 8 , and $\sigma_s^2 / \sigma_n^2 = 1$. The lines connect the equal threshold points. We see that the approximation is good. For larger N , the exact and approximate ROC are identical for all practical purposes. ■

Examples 2.12 and 2.13 allowed us to compare the P_D and P_F approximations to exact expressions. In the next example analytic solutions are not available for P_D and P_F .

Example 2.14. The observations on the two hypotheses are statistically independent samples from Weibull probability densities with different parameters,

$$p_{r_i|H_j}(R_i|H_j) = \frac{\alpha_j}{b_j} \left(\frac{R_i}{b_j} \right)^{\alpha_j-1} e^{-(R_i/b_j)^{\alpha_j}}, \quad i = 1, 2, \dots, N; j = 0, 1. \quad (2.274)$$

When we study radar applications later in the text, we will find that the Weibull probability density is a good model for clutter in many applications. The parameter $\alpha_j > 0$ controls the shape and the parameter $b_j > 0$ controls the scale. The mean is

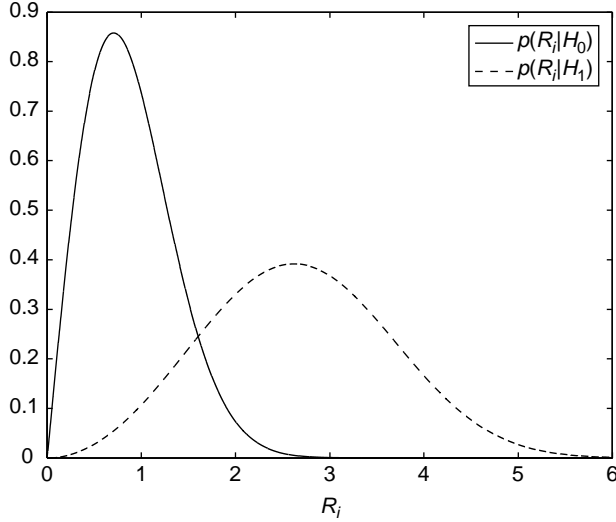


Figure 2.35: Weibull densities on H_0 and H_1 , $\alpha_0 = 2$, $b_0 = 1$, $\alpha_1 = 3$, $b_1 = 3$.

$$E(r_i|H_j) = b_j \Gamma\left(1 + \frac{1}{\alpha_j}\right) \quad (2.275)$$

and the variance is

$$\text{Var}(r_i|H_j) = b_j^2 \left[\Gamma\left(1 + \frac{2}{\alpha_j}\right) - \Gamma^2\left(1 + \frac{1}{\alpha_j}\right) \right]. \quad (2.276)$$

We consider the following specific values: $\alpha_0 = 2$, $b_0 = 1$, $\alpha_1 = 3$, $b_1 = 3$. The resulting probability densities on the two hypotheses are shown in Figure 2.35.

The functions $\mu(s)$, $\dot{\mu}(s)$, and $\ddot{\mu}(s)$ are computed numerically. We use (2.274) to obtain $\mu_i(s)$ and then differentiate numerically to obtain $\dot{\mu}_i(s)$, and $\ddot{\mu}_i(s)$. The results are shown in Figure 2.36. We obtain $\mu(s)$, $\dot{\mu}(s)$, and $\ddot{\mu}(s)$ from (2.251)–(2.253) by multiplying by N . In order to construct an approximate ROC using (2.238) and (2.241), we let s_* vary from 0 to 1. The $\dot{\mu}_i(s)$ curve in Figure 2.36 specifies the threshold $\gamma_* = N\dot{\mu}_i(s_*)$. The results are shown in Figure 2.37. As expected, the performance improves as N increases. In the problems, we will investigate the behavior for various α_j and b_j . We do not have an analytic result to verify the approximation, but in Section 2.5 we will discuss techniques for simulating the LRT to validate the results. ■

Summary. The principal results of this section were the bounds on P_F , P_M , and $\Pr(\epsilon)$ given in (2.226) and (2.230), and the approximate error expressions given in (2.238), (2.239), (2.241), (2.242), (2.243), and (2.244). These expressions will enable us to find performance results for a number of cases of physical interest.

The first two examples considered Gaussian densities on both hypotheses and analytic results were available. The results play a much more important role when we have statistically independent observations and the probability densities are non-Gaussian. Then,

$$\mu(s) = \sum_{i=1}^N \mu_i(s)$$

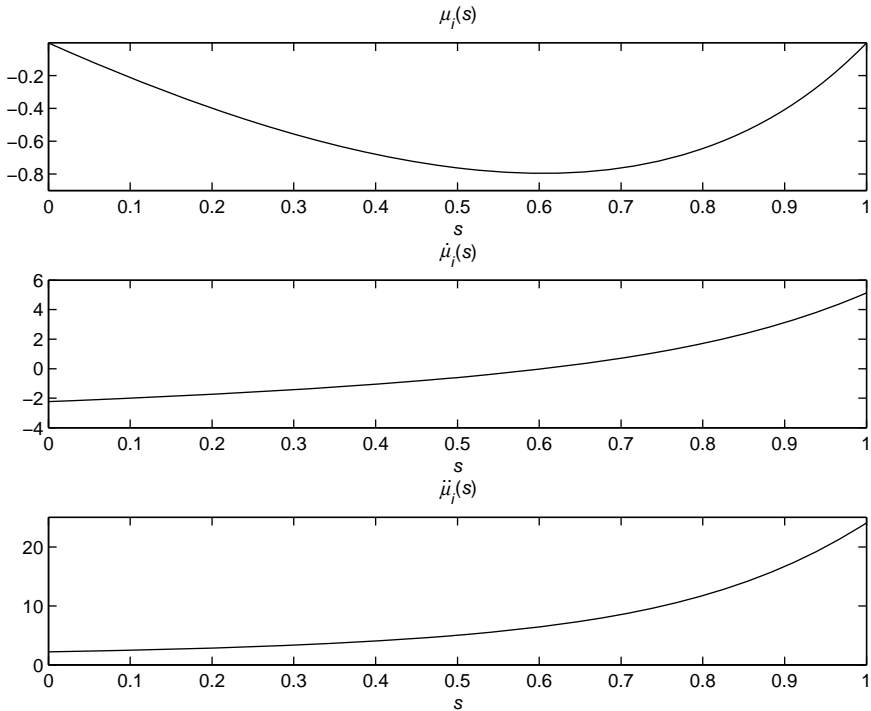


Figure 2.36: Weibull densities; $\mu_i(s)$, $\dot{\mu}_i(s)$, and $\ddot{\mu}_i(s)$.

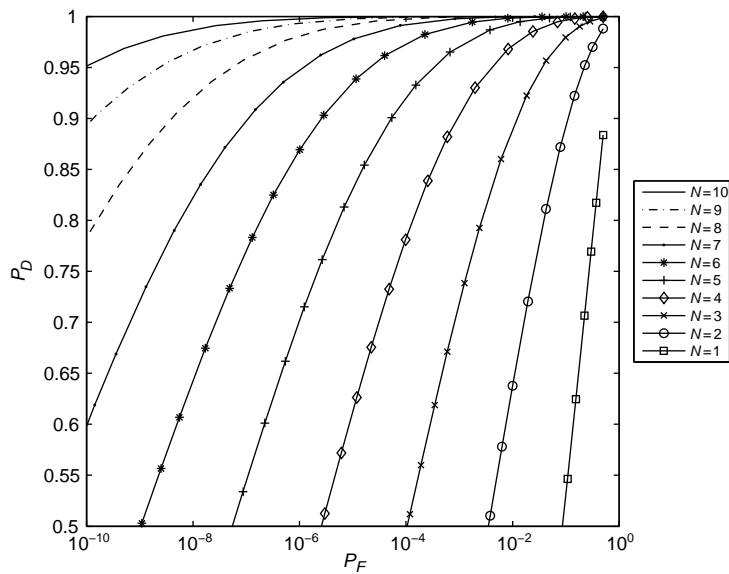


Figure 2.37: Receiver operating characteristic; Weibull densities, $N = 1, 2, \dots, 10$.

and we can find $\mu_i(s)$ by a numerical one-dimensional integration of (2.248) if an analytic result is not available. We can then construct an approximate ROC as in Example 2.14. Thus, for an ID, non-Gaussian model, the results in Section 2.2 specify the optimum test and the results in this section allow us to bound the performance and construct approximate ROCs.

In the next section, we will discuss Monte Carlo simulation techniques and will find that the $\mu(s)$ function plays the central role in designing optimum simulations.

2.5 MONTE CARLO SIMULATION

In many of the applications of interest, it is necessary to simulate the detection algorithm in order to evaluate the performance. In Section 2.5.1, we give a brief introduction to Monte Carlo (MC) simulation. A key issue is the number of trials needed to have a desired level of confidence in the result. In most systems of interest, the desired P_F is very small (e.g., $P_F \leq 10^{-6}$ is frequently required). In these cases, the number of trials required to obtain a reasonable confidence level is prohibitively large.

In Section 2.4, we introduced the Chernoff bound and various extensions in order to obtain bounds on the performance and approximate expressions for the performance. The key idea was that, by defining a $\mu(s)$ function, we could tilt the relevant probability densities so that the mass of the tilted density was near the threshold. We can apply the same idea to the simulation problem. The resulting technique is called “importance sampling” in the literature. We develop the key results in Section 2.5.2 and apply them to several of the examples introduced earlier in the chapter.

In Section 2.5.3, we summarize our results.

2.5.1 Monte Carlo Simulation Techniques

The log-likelihood ratio test consists of comparing the log-likelihood ratio to a threshold. From (2.195),

$$l_*(\mathbf{R}) \triangleq \Lambda(\mathbf{R}) \stackrel{H_1}{\gtrless} \stackrel{H_0}{\lessdot} \gamma_* \quad (2.277)$$

From (2.75), the log-likelihood ratio and the corresponding error probabilities can equivalently be expressed in terms of any sufficient statistic \mathbf{x} ,

$$l_*(\mathbf{X}) \triangleq \ln \frac{p_{\mathbf{x}|H_1}(\mathbf{X}|H_1)}{p_{\mathbf{x}|H_0}(\mathbf{X}|H_0)} \quad (2.278)$$

The expressions for $P_F(\gamma_*)$ and $P_M(\gamma_*)$ in terms of \mathbf{x} are

$$P_F(\gamma_*) = \Pr(l_*(\mathbf{X}) \geq \gamma_* | H_0) = \int_{l_*(\mathbf{X}) \geq \gamma_*} p_{\mathbf{x}|H_0}(\mathbf{X}|H_0) d\mathbf{X} \quad (2.279)$$

and

$$P_M(\gamma_*) = 1 - P_D(\gamma_*) = \Pr(l_*(\mathbf{X}) < \gamma_* | H_1) = \int_{l_*(\mathbf{X}) < \gamma_*} p_{\mathbf{x}|H_1}(\mathbf{X}|H_1) d\mathbf{X}. \quad (2.280)$$

At one extreme, the sufficient statistic may be the scalar log-likelihood ratio itself or a scalar function of the observations that is related to the log-likelihood ratio in a straightforward (invertible) manner. At the other extreme, it may be the N -dimensional observation vector \mathbf{r} . In other cases, \mathbf{x} may be multidimensional with dimension less than N . The latter two cases are important when it is difficult to find $p_{l_*|H_0}(L|H_0)$ and $p_{l_*|H_1}(L|H_1)$. As in the previous sections, we will find it useful to work with a variety of sufficient statistics.

For this discussion, we will make use of the indicator function $\mathbb{I}(\cdot)$, which is equal to one when its argument is true and zero otherwise. The indicator function allows us to express probabilities as expected values. For example,

$$\mathbb{I}(l_*(\mathbf{X}) \geq \gamma_*) = \begin{cases} 1 & l_*(\mathbf{X}) \geq \gamma_* \\ 0 & l_*(\mathbf{X}) < \gamma_* \end{cases} \quad (2.281)$$

With this definition, $P_F(\gamma_*)$ in (2.279) may be written as

$$P_F(\gamma_*) = \int \mathbb{I}(l_*(\mathbf{X}) \geq \gamma_*) p_{\mathbf{x}|H_0}(\mathbf{X}|H_0) d\mathbf{X} = E_0 [\mathbb{I}(l_*(\mathbf{X}) \geq \gamma_*)], \quad (2.282)$$

where $E_0[\cdot]$ denotes expectation on H_0 . Similarly,

$$P_M(\gamma_*) = E_1 [\mathbb{I}(l_*(\mathbf{X}) < \gamma_*)], \quad (2.283)$$

where $E_1[\cdot]$ denotes expectation on H_1 .

The procedure for estimating P_F is to simulate a random sample of the sufficient statistic \mathbf{x} and estimate the expected value in (2.282) by computing the sample mean of the indicator function. To generate the random sample, we conduct a set of K_F independent trials. On each trial, we generate a realization of \mathbf{x} from the probability density $p_{\mathbf{x}|H_0}(\mathbf{X}|H_0)$. Our choice of sufficient statistic \mathbf{x} will often be driven by the ease in which we can generate random samples from the specified distribution. There are a variety of techniques for generating random samples that are discussed in [DeV86] and [BFS87].

If the sufficient statistic is the scalar x and its cumulative distribution function (CDF) $P_x(X)$ is known, then we can use the inversion method. In this method, we generate a sample of a random variable y with a uniform probability density

$$p_y(Y) = \begin{cases} 1 & 0 \leq Y \leq 1 \\ 0 & \text{elsewhere} \end{cases} \quad (2.284)$$

and transform Y to X by the inverse of the CDF,

$$X = P_x^{-1}(Y). \quad (2.285)$$

Then,

$$Y = P_x(X). \quad (2.286)$$

To verify that X is a sample from $p_x(X)$, and the Jacobian of the transformation in (2.285) is

$$J = \frac{dY}{dX} = \frac{dP_x(X)}{dX} = p_x(X) \quad (2.287)$$

and

$$p_x(X) = p_y(P_x(X))|J| = 1 \cdot p_x(X). \quad (2.288)$$

Thus, we can generate $U(0, 1)$ random samples and transform them with $P_x^{-1}(Y)$.

If the inverse of the CDF is not known explicitly, then we may use other methods such as numerical inversion or the rejection method [DeV86, BFS87].⁶

We denote the simulated sufficient statistic generated on the k th trial as \mathbf{X}_k and the value of the log-likelihood ratio as $l_*(\mathbf{X}_k; H_0)$. On each trial, we compute $l_*(\mathbf{X}_k; H_0)$ and count the number of times that it exceeds the threshold γ_* . We denote this count by the random variable n_{γ_*} , which is defined as⁷

$$n_{\gamma_*} = \sum_{k=1}^{K_F} \mathbb{I}(l_*(\mathbf{X}_k; H_0) \geq \gamma_*). \quad (2.289)$$

It is a Binomial(K_F, P_F) random variable with probability mass function,

$$\Pr(n_{\gamma_*} = n) = \binom{K_F}{n} P_F^n (1 - P_F)^{K_F - n} \quad n = 0, 1, \dots, K_F. \quad (2.290)$$

Given n_{γ_*} , we estimate $P_F(\gamma_*)$ as⁸

$$\hat{P}_F(\gamma_*) = \frac{n_{\gamma_*}}{K_F} = \frac{1}{K_F} \sum_{k=1}^{K_F} \mathbb{I}(l_*(\mathbf{X}_k; H_0) \geq \gamma_*). \quad (2.291)$$

The expectation of the estimate is

$$E[\hat{P}_F] = \frac{1}{K_F} E[n_{\gamma_*}] = \frac{K_F P_F}{K_F} = P_F, \quad (2.292)$$

which is an unbiased estimate. The variance of the estimate is

$$\text{Var}(\hat{P}_F) = \frac{1}{K_F^2} \text{Var}(n_{\gamma_*}) = \frac{K_F P_F (1 - P_F)}{K_F^2} = \frac{P_F (1 - P_F)}{K_F}. \quad (2.293)$$

The variance of the estimate decreases as the number of trials increases and we would like to determine how many trials we need to get a good estimate. We do this in terms of a confidence interval $\hat{P}_F \in [(1 - \alpha)P_F, (1 + \alpha)P_F]$, where

⁶The Matlab Statistics Toolbox has random number generators for many standard distributions, including all of the distributions listed in Appendix A except for the Generalized Gaussian. The inversion or rejection methods could be used for that case.

⁷Our development is similar to a number of references (e.g., [Ech91] or [Sri02]).

⁸In Chapter 4, when we study estimation theory, we will see that \hat{P}_F is the maximum likelihood estimate of P_F .

$$\Pr\left(\frac{|\hat{P}_F - P_F|}{P_F} \leq \alpha\right) = p_c, \quad (2.294)$$

where p_c is the confidence probability (e.g., 0.95) and α is the percent deviation tolerance (e.g., 0.1). Then, (2.294) can be written as

$$\Pr\left(|\hat{P}_F - P_F| \leq \alpha P_F\right) = p_c. \quad (2.295)$$

For large K_F , the probability density of \hat{P}_F approaches a Gaussian density with mean and variance given by (2.292) and (2.293), that is,

$$\hat{P}_F \sim N\left(P_F, \frac{P_F(1 - P_F)}{K_F}\right). \quad (2.296)$$

For a Gaussian random variable $z \sim N(\mu_z, \sigma_z^2)$, the probability that z has a value within c standard deviations of its mean is

$$\Pr(|z - \mu_z| \leq c \sigma_z) = p_c, \quad (2.297)$$

where c is given in Table 2.1 for several values of p_c . Using the Gaussian approximation for \hat{P}_F from (2.296) in (2.297), we have

$$\Pr\left(|\hat{P}_F - P_F| \leq c \sqrt{\frac{P_F(1 - P_F)}{K_F}}\right) = p_c. \quad (2.298)$$

Comparing this expression to (2.295), we can achieve the desired confidence level if

$$\alpha P_F = c \sqrt{\frac{P_F(1 - P_F)}{K_F}}. \quad (2.299)$$

This occurs when

$$K_F = \frac{c^2}{\alpha^2} \frac{1 - P_F}{P_F}. \quad (2.300)$$

The preceding analysis is valid when P_F is small (less than 0.5). In some cases, we may want to simulate a scenario where $P_F > 0.5$. In this case, we want the tolerance to be a fraction of $1 - P_F$. To cover both cases, we express the tolerance as a fraction of the smaller of P_F and $1 - P_F$, that is,

$$\Pr\left(|\hat{P}_F - P_F| \leq \alpha \min(P_F, 1 - P_F)\right) = p_c. \quad (2.301)$$

Table 2.1: Confidence interval probabilities from the Gaussian distribution

p_c	0.900	0.950	0.954	0.990	0.997
c	1.645	1.960	2.000	2.576	3.000

Then, (2.299) becomes

$$\alpha \min(P_F, 1 - P_F) = c \sqrt{\frac{P_F(1 - P_F)}{K_F}}. \quad (2.302)$$

and the more general formula for the required number of trials is:

$$K_F = \frac{c^2}{\alpha^2} \frac{P_F(1 - P_F)}{\min(P_F, 1 - P_F)^2}. \quad (2.303)$$

For example, if $p_c = 0.954$, then $c = 2$. When $\alpha = 0.1$ and P_F is small, we have

$$K_F \approx \frac{4}{0.01} \frac{1}{P_F} = \frac{400}{P_F}. \quad (2.304)$$

Since false alarms occur with probability P_F , we would expect to observe one false alarm in about every $1/P_F$ trials. The result above tells us that we need to observe at least 400 false alarms to get a good estimate of P_F , which requires at least $400/P_F$ trials. If we want a higher confidence probability or lower tolerance factor, even more trials would be required.

To simulate an entire ROC curve, we need to estimate both P_F and P_D (or P_M) at various thresholds. To estimate P_M , we conduct a set of K_M independent trials in which we generate a realization of \mathbf{x} from the probability density $p_{\mathbf{x}|H_1}(\mathbf{X}|H_1)$ and count the number of times that $l_*(\mathbf{X}_k; H_1)$ falls below the threshold γ_* . Following a similar argument, the required number of trials is:

$$K_M = \frac{c^2}{\alpha^2} \frac{P_M(1 - P_M)}{\min(P_M, 1 - P_M)^2}, \quad (2.305)$$

and the estimate of $P_M(\gamma_*)$ is:

$$\hat{P}_M(\gamma_*) = \frac{1}{K_M} \sum_{k=1}^{K_M} \mathbb{I}(l_*(\mathbf{X}_k; H_1) < \gamma_*). \quad (2.306)$$

We consider the following example to demonstrate the results. It is a continuation of Examples 2.1 and 2.5. Because we have analytic results, we probably would not simulate this model in practice, but it is useful to introduce the simulation procedure.

Example 2.15 (continuation of Examples 2.1, 2.5, and 2.12). From (2.19) and (2.20),

$$\begin{aligned} H_1 : r_i &\sim N(m, \sigma^2) & i = 1, 2, \dots, N \\ H_0 : r_i &\sim N(0, \sigma^2) & i = 1, 2, \dots, N, \end{aligned} \quad (2.307)$$

and from (2.84) and (2.85),

$$P_F(\gamma_*) = \text{erfc}_* \left(\frac{\gamma_*}{d} + \frac{d}{2} \right), \quad (2.308)$$

$$P_M(\gamma_*) = 1 - \text{erfc}_* \left(\frac{\gamma_*}{d} - \frac{d}{2} \right), \quad (2.309)$$

where

$$d = \frac{\sqrt{Nm}}{\sigma}. \quad (2.310)$$

Table 2.2: Simulation values for $d = \sqrt{40}$, $p_c = 0.954$, and $\alpha = 0.1$

P_F	Z_F	γ_*	P_M	K_F	K_M
10^{-2}	2.33	-5.29	3.2×10^{-5}	4×10^4	1.3×10^7
10^{-4}	3.72	3.52	0.0046	4×10^6	8.7×10^4
10^{-6}	4.75	10.06	0.0581	4×10^8	6488
10^{-8}	5.61	15.49	0.2381	4×10^{10}	1281
10^{-10}	6.36	20.23	0.5147	4×10^{12}	425
10^{-12}	7.03	24.49	0.7611	4×10^{14}	1275

We define Z_F as the argument of $\text{erfc}_*(\cdot)$ that corresponds to the value of P_F that we want to simulate.⁹ We rewrite (2.308) as

$$P_F = \text{erfc}_*(Z_F). \quad (2.311)$$

Therefore,

$$Z_F = \frac{\gamma_*}{d} + \frac{d}{2} \quad (2.312)$$

and we calculate the threshold from

$$\gamma_* = Z_F d - \frac{d^2}{2} \quad (2.313)$$

and then calculate $P_M(\gamma_*)$ from (2.309). The required number of trials is obtained from (2.303) and (2.305). A summary is given in Table 2.2 for $d = \sqrt{40}$, $p_c = 0.954$ ($c = 2$), $\alpha = 0.1$, and a variety of ROC points. We observe that as P_F decreases, K_F increases correspondingly. At the same time, P_M is increasing and K_M is decreasing until P_M becomes greater than 0.5. Then $1 - P_M < P_M$, and K_M begins increasing.

To implement the simulation, we need to pick a sufficient statistic to simulate. We could choose the statistic to be the original observations, $\mathbf{x} = \mathbf{r}$. Then for each trial, we would generate N IID observations from the densities in (2.307). Alternatively, we could choose the statistic to be the log-likelihood ratio, $\mathbf{x} = l_*$, which is given in (2.24). Then, from (2.307) and (2.310),

$$H_1 : l_* \sim N\left(\frac{d}{2}, d^2\right) \quad (2.314)$$

$$H_0 : l_* \sim N\left(-\frac{d}{2}, d^2\right), \quad (2.315)$$

and for each trial, we would generate a scalar random variable from these densities.

To simulate the ROC curves in Figure 2.12b, for each point on the curve, we would determine the threshold γ_* from P_F and d , and calculate the required K_F and K_M . We would generate K_F trials from $p_{\mathbf{x}|H_0}(\mathbf{X}|H_0)$ and compute $\hat{P}_F(\gamma_*)$ using (2.291), then generate K_M trials from $p_{\mathbf{x}|H_1}(\mathbf{X}|H_1)$ and compute $\hat{P}_M(\gamma_*)$ using (2.306).

To simulate the curves in 2.12a, we could follow the same procedure. However, in this case only the threshold varies along each curve while the densities remain the same, and we can use a simpler procedure. We first determine the maximum number of trials needed over all points on the curve and denote these by \bar{K}_F and \bar{K}_M . We then generate \bar{K}_F trials from $p_{\mathbf{x}|H_0}(\mathbf{X}|H_0)$ and compute $\hat{P}_F(\gamma_*)$ using (2.291) by varying γ_* , and do the same using \bar{K}_M trials from $p_{\mathbf{x}|H_1}(\mathbf{X}|H_1)$ to calculate $\hat{P}_M(\gamma_*)$. This

⁹For a specified P_F , Z_F can be computed in Matlab using the `norminv` function. See Appendix A.

method has the advantage that only one set of data is generated. The worst-case accuracy will be as specified by α and p_c ; however, many of the points will have significantly better accuracy since the number of trials generated will be larger than required. ■

In the previous example, the simulation method was straightforward, however the number of trials was very large for the small values of P_F considered. Clearly, we need to find a better technique in order to reduce the number of trials required to achieve the desired accuracy and confidence level.

2.5.2 Importance Sampling

Our development of importance sampling is based on our discussion of tilted densities, $\mu(s)$, and the Chernoff bound in Section 2.4.

We introduced a new random variable x_s whose probability density was related to $p_{l|H_0}(L|H_0)$ by (2.205)

$$p_{x_s}(X) = e^{sX - \mu(s)} p_{l|H_0}(X|H_0), \quad (2.316)$$

where $s \geq 0$. In Figure 2.29, we saw that as s increased, more of the density was moved to the right of the threshold. The tightest bound on P_F was obtained by choosing s so that the mean of the tilted variable x_s was at the threshold.

In Section 2.5.1, we found that a key issue in MC simulation was that if P_F (or P_M) was very small, then the number of trials was prohibitively large. However, if we could run the simulation using the tilted density, then the probability of exceeding the threshold would be on the order of 0.5. (It would be exactly 0.5 if the median and mean were equal.) If we could relate this probability to the desired P_F (or P_M), then presumably the required number of trials would be significantly smaller.

There is an extensive literature on tilted densities and importance sampling. The earliest use of tilted densities appears in a paper by Esscher [Ess32]. His results are still widely used in the financial community and are referred to as the Esscher transformation (e.g., [The84]). Siegmund [Sie76] applied the technique to sequential detection. The first application to communications was by Cottrell et al. [CFM83]. The technique started to be referred to as *large deviation theory* and a number of applications, books, and journal articles began to appear.

Importance sampling was discussed in the early work of Kahn and Marshall [KM53] and the book by Hammersley and Handscomb [HH64]. The early work developed various techniques to modify the probability density for simulation purposes but did not utilize tilted densities. Papers by Sadowsky and Bucklew [SB90] and Sadowsky [Sad93] showed the optimality of tilted densities and the technique became more widely used.

The paper by Smith et al. [SSG97] provides an excellent review of the history and status of the area (circa 1997). It contains an extensive list of references. The book by Srinivasan [Sri02] provides a good development of importance sampling at a mathematical level similar to our discussion. Other books include Bucklew [Buc90] and Jeruchim et al. [JBS92].

Our objective in this section is to introduce the reader to the application of tilted densities (large deviation theory) to a specific set of problems:

1. We restrict our attention to the problem of estimating $\Pr(l_*(\mathbf{X}) \geq \gamma_*)$ and $\Pr(l_*(\mathbf{X}) < \gamma_*)$ by simulation, where $l_*(\mathbf{X})$ is the log-likelihood ratio in (2.278). This enables us to find $\hat{P}_F(\gamma_*)$ and $\hat{P}_M(\gamma_*)$.
2. We restrict our development to finding the “optimum” tilted density to use in the simulation. We do not discuss other importance sampling techniques that involve other types of biasing densities that may be simpler to implement (but may not perform as well).
3. We assume that the components of \mathbf{r} are statistically independent, but not necessarily IID.

The approach should provide the necessary background so that students and practicing engineers can effectively simulate the algorithms that we develop in the text and problems.

The initial part of our discussion follows Srinivasan’s book on importance sampling [Sri02]. However, after establishing some preliminary results we can proceed directly to the tilted densities of Section 2.4.

2.5.2.1 Simulation of P_F

First, consider P_F . We introduce a biasing probability density $p_{\mathbf{x}|0^*}(\mathbf{X})^{10}$ that is related to $p_{\mathbf{x}|H_0}(\mathbf{X}|H_0)$ in a manner yet to be determined, and write $P_F(\gamma_*)$ as:

$$\begin{aligned} P_F(\gamma_*) &= \int \mathbb{I}(l_*(\mathbf{X}) \geq \gamma_*) p_{\mathbf{x}|H_0}(\mathbf{X}|H_0) d\mathbf{X} \\ &= \int \mathbb{I}(l_*(\mathbf{X}) \geq \gamma_*) \frac{p_{\mathbf{x}|H_0}(\mathbf{X}|H_0)}{p_{\mathbf{x}|0^*}(\mathbf{X})} p_{\mathbf{x}|0^*}(\mathbf{X}) d\mathbf{X}. \end{aligned} \quad (2.317)$$

Defining,

$$W_0(\mathbf{X}) \triangleq \frac{p_{\mathbf{x}|H_0}(\mathbf{X}|H_0)}{p_{\mathbf{x}|0^*}(\mathbf{X})}, \quad (2.318)$$

we can write

$$\begin{aligned} P_F(\gamma_*) &= \int \mathbb{I}(l_*(\mathbf{X}) \geq \gamma_*) W_0(\mathbf{X}) p_{\mathbf{x}|0^*}(\mathbf{X}) d\mathbf{X} \\ &= E_{0^*} [\mathbb{I}(l_*(\mathbf{X}) \geq \gamma_*) W_0(\mathbf{X})]. \end{aligned} \quad (2.319)$$

Note that in general, that for any function $f(\mathbf{X})$,

$$E_0 [f(\mathbf{X})] = E_{0^*} [f(\mathbf{X}) W_0(\mathbf{X})]. \quad (2.320)$$

We will simulate the test, choosing \mathbf{X}_k from the biasing density $p_{\mathbf{x}|0^*}(\mathbf{X})$. Then,

$$\hat{P}_F(\gamma_*) = \frac{1}{K_F} \sum_{k=1}^{K_F} \mathbb{I}(l_*(\mathbf{X}_k; H_0^*) \geq \gamma_*) W_0(\mathbf{X}_k; H_0^*). \quad (2.321)$$

¹⁰We used $p_{x_s}(X)$ in Section 2.4. We need different notation because \mathbf{X} may be a vector and, even if it is a scalar, the biasing density may be different.

The expectation of the estimate is

$$E_{0^*} [\hat{P}_F] = \frac{K_F}{K_F} E_{0^*} [\mathbb{I}(l_*(\mathbf{x}) \geq \gamma_*) W_0(\mathbf{x})] = E_0 [\mathbb{I}(l_*(\mathbf{x}) \geq \gamma_*)] = P_F, \quad (2.322)$$

and the variance is

$$\text{Var}_{0^*}(\hat{P}_F) = \frac{K_F}{K_F^2} \text{Var}_{0^*} [\mathbb{I}(l_*(\mathbf{x}) \geq \gamma_*) W_0(\mathbf{x})] = \frac{1}{K_F} (I_F - P_F^2), \quad (2.323)$$

where

$$I_F(\gamma_*) \triangleq E_{0^*} [\mathbb{I}^2(l_*(\mathbf{x}) \geq \gamma_*) W_0^2(\mathbf{x})]. \quad (2.324)$$

Noting that $\mathbb{I}^2(\cdot) = \mathbb{I}(\cdot)$, and using the property in (2.320), we may also write $I_F(\gamma_*)$ as:

$$I_F(\gamma_*) = E_0 [\mathbb{I}(l_*(\mathbf{x}) \geq \gamma_*) W_0(\mathbf{x})]. \quad (2.325)$$

Comparing (2.323) to (2.293), if $I_F < P_F$, then the variance of the importance sampling estimate is less than the variance of the conventional estimate for the same number of trials. Therefore, the number of trials can be reduced to get the same level of accuracy in the estimate. For the importance sampling estimate, (2.302) becomes

$$\alpha \min(P_F, 1 - P_F) = c \sqrt{\frac{(I_F - P_F^2)}{K_F}}, \quad (2.326)$$

and the required number of trials is:

$$K_{F,IS} = \frac{c^2}{\alpha^2} \frac{(I_F - P_F^2)}{\min(P_F, 1 - P_F)^2}. \quad (2.327)$$

We would like to find the biasing probability density $p_{\mathbf{x}|0^*}(\mathbf{X})$ that minimizes I_F . This is difficult, so instead we find an upper bound on I_F similar to the Chernoff bound and find the biasing density that minimizes the bound. We observe that for $s \geq 0$,

$$\mathbb{I}(l_*(\mathbf{X}) \geq \gamma_*) \leq e^{s[l_*(\mathbf{X}) - \gamma_*]} \quad s \geq 0. \quad (2.328)$$

This is illustrated in Figure 2.38.

Using (2.328) in (2.324),

$$I_F(\gamma_*) \leq E_{0^*} [e^{2s[l_*(\mathbf{x}) - \gamma_*]} W_0^2(\mathbf{x})] \triangleq \bar{I}_F(\gamma_*). \quad (2.329)$$

We now apply Jensen's inequality, which states that for any nonnegative function $f(\mathbf{X})$,

$$E[f^2(\mathbf{X})] \geq E^2[f(\mathbf{X})], \quad (2.330)$$

with equality iff $f(\mathbf{X}) = E[f(\mathbf{X})]$. For the quantities in (2.329), $\bar{I}_F(\gamma_*)$ will be minimized iff

$$\begin{aligned} e^{s[l_*(\mathbf{X}) - \gamma_*]} W_0(\mathbf{X}) &= E_{0^*} [e^{s[l_*(\mathbf{X}) - \gamma_*]} W_0(\mathbf{x})] \\ &= E_0 [e^{s[l_*(\mathbf{X}) - \gamma_*]}] \\ &= e^{\mu(s) - s\gamma_*}, \end{aligned} \quad (2.331)$$

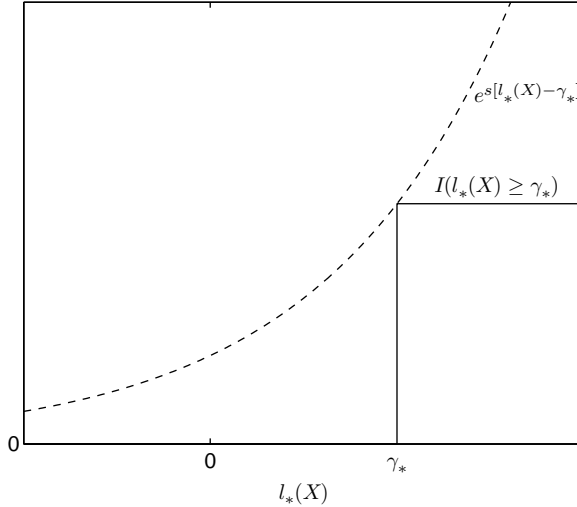


Figure 2.38: Upper bound on $\mathbb{I}(l_*(\mathbf{X}) \geq \gamma_*)$.

where $\mu(s)$ was defined in (2.200) in Section 2.4, and can be expressed in terms of any sufficient statistic as:

$$\mu(s) \triangleq \ln E_0 [e^{sl_*(\mathbf{X})}] = \ln \int [p_{\mathbf{X}|H_1}(\mathbf{X}|H_1)]^s [p_{\mathbf{X}|H_0}(\mathbf{X}|H_0)]^{1-s} d\mathbf{X}. \quad (2.332)$$

Using (2.318) in (2.331) gives

$$e^{s[l_*(\mathbf{X}) - \gamma_*]} \frac{p_{\mathbf{X}|H_0}(\mathbf{X}|H_0)}{p_{\mathbf{X}|0^*}(\mathbf{X})} = e^{\mu(s) - s\gamma_*} \quad (2.333)$$

or

$$p_{\mathbf{X}|0^*}(\mathbf{X}; s) = e^{s[l_*(\mathbf{X}) - \mu(s)]} p_{\mathbf{X}|H_0}(\mathbf{X}|H_0). \quad (2.334)$$

Not surprisingly, the biasing density in (2.334) is the same as the tilted density in (2.205).

Substituting (2.334) into (2.318) gives

$$W_0(\mathbf{X}; s) = e^{-s[l_*(\mathbf{X}) + \mu(s)]}. \quad (2.335)$$

These results are essentially the same as the results in [Sri02 equations (2.18) and (2.19)]. However, there are two differences that will be important in our later development. The results developed in [Sri02] are for a generic scalar statistic being compared to a threshold, while we are specifically considering the log-likelihood ratio expressed as a function of a multidimensional sufficient statistic \mathbf{X} ,

$$l_*(\mathbf{X}) = \ln \frac{p_{\mathbf{X}|H_1}(\mathbf{X}|H_1)}{p_{\mathbf{X}|H_0}(\mathbf{X}|H_0)} \quad (2.336)$$

so that

$$e^{s[l_*(\mathbf{X})]} = \left(\frac{p_{\mathbf{X}|H_1}(\mathbf{X}|H_1)}{p_{\mathbf{X}|H_0}(\mathbf{X}|H_0)} \right)^s. \quad (2.337)$$

In our case, $\mu(s)$ is defined as in (2.332) and the tilted density has the form

$$p_{\mathbf{x}|0^*}(\mathbf{X}; s) = e^{-\mu(s)} p_{\mathbf{x}|H_0}(\mathbf{X}|H_0)^{1-s} p_{\mathbf{x}|H_1}(\mathbf{X}|H_1)^s. \quad (2.338)$$

The tilted density is specified in terms of the sufficient statistic \mathbf{x} , rather than the log-likelihood ratio l_* , and it can be found directly from the original densities $p_{\mathbf{x}|H_0}(\mathbf{X}|H_0)$ and $p_{\mathbf{x}|H_1}(\mathbf{X}|H_1)$. This is a key result, because in many, if not most, of the cases when we need to use this in practice, analytical expressions for $p_{l_*|H_0}(L|H_0)$ and $p_{l_*|H_1}(L|H_1)$ are not available. In addition, we will find that the optimum tilted density for estimating P_M is identical to $p_{\mathbf{x}|0^*}(\mathbf{X}; s)$. In many cases we use $\mathbf{x} = \mathbf{r}$, corresponding to the original observations, and we tilt the N -dimensional densities $p_{\mathbf{r}|H_0}(\mathbf{R}|H_0)$ and $p_{\mathbf{r}|H_1}(\mathbf{R}|H_1)$. In practice, the case of most interest will be when the r_i are statistically independent (not necessarily identical) and we tilt the marginal probability densities. Thus, this more general approach enables us to find the tilted densities for a large number of useful applications. A final note is that although $W_0(\mathbf{X}; s)$ is defined in terms of $p_{\mathbf{x}|H_0}(\mathbf{X}|H_0)$ and $p_{\mathbf{x}|0^*}(\mathbf{X}; s)$, the expression in (2.335) can be evaluated without specifying these densities.

From (2.330) and (2.331), the optimized upper bound is

$$\bar{I}_F(\gamma_*; s) \triangleq e^{2[\mu(s) - s\gamma_*]} \quad s \geq 0. \quad (2.339)$$

Comparing (2.339) to (2.212), we see that $\bar{I}_F(\gamma_*; s)$ is the square of the Chernoff bound. As with the Chernoff bound, we can get the tightest bound by minimizing it with respect to s . The optimum s is the same as for the Chernoff bound and is given by

$$s_* : \dot{\mu}(s_*) = \gamma_*, \quad (2.340)$$

as long as $\gamma_* \geq \dot{\mu}(0)$. If $\gamma_* < \dot{\mu}(0)$, the optimum value is $s_* = 0$, which gives the bound $\bar{I}_F(\gamma_*; 0) = 1$.

The upper bound $\bar{I}_F(\gamma_*; s)$ was useful for showing that the optimal biasing density has the form of the tilted density given in (2.338) and for finding the value of s_* that minimizes the estimation variance. However, the bound is too weak to be used in (2.327) to determine the required number of trials. For this calculation, we would prefer to compute I_F itself. Substituting (2.335) in (2.325) gives an expression for I_F when the biasing density is the tilted density in (2.334),

$$I_F(\gamma_*; s) \triangleq e^{\mu(s)} \int \mathbb{I}(l_*(\mathbf{X}) \geq \gamma_*) e^{-s l_*(\mathbf{X})} p_{\mathbf{x}|H_0}(\mathbf{X}|H_0) d\mathbf{X}. \quad (2.341)$$

Note that when $s = 0$, $I_F(\gamma_*; 0) = P_F(\gamma_*)$ because $p_{\mathbf{x}|0^*}(\mathbf{X}; 0) = p_{\mathbf{x}|H_0}(\mathbf{X}|H_0)$, and we do not get any advantage from importance sampling.

In problems where we can find an analytical expression for P_F , we will generally also be able to evaluate (2.341) to find an analytical expression for I_F . In cases where the evaluation is intractable, we can approximate I_F using the technique developed in Section 2.4 for approximating P_F . If we let $x = l_*$ and note that $p_{x|0^*}(x; s) = p_{x_s}(x)$, then substituting (2.335) into (2.324) and using the optimum s_* from (2.340) gives the following expression,

$$I_F(\gamma_*; s_*) = \int_{\dot{\mu}(s_*)}^{\infty} e^{2[\mu(s_*) - s_* X]} p_{x_s}(X) dX. \quad (2.342)$$

In Section 2.4, we started with a similar expression for P_F in (2.233) and derived the approximate expression in (2.238). Noting that (2.342) and (2.233) differ only in a factor of two in the exponent, we may follow the same argument and obtain an approximate expression for I_F ,

$$I_F(\gamma_*; s_*) \approx \left\{ \exp \left[2\mu(s_*) - 2s_*\dot{\mu}(s_*) + 2s_*^2\ddot{\mu}(s_*) \right] \right\} \operatorname{erfc}_* \left[2s_*\sqrt{\dot{\mu}(s_*)} \right]. \quad (2.343)$$

2.5.2.2 Simulation of P_M

The next step is to find the optimum biasing density to estimate P_M . The arguments are identical, so we omit some of the intermediate equations. We begin from

$$\begin{aligned} P_M(\gamma_*) &= \int \mathbb{I}(l_*(\mathbf{X}) < \gamma_*) p_{\mathbf{x}|H_1}(\mathbf{X}|H_1) d\mathbf{X} \\ &= \int \mathbb{I}(l_*(\mathbf{X}) < \gamma_*) W_1(\mathbf{X}) p_{\mathbf{x}|1^*}(\mathbf{X}) d\mathbf{X}, \end{aligned} \quad (2.344)$$

where

$$W_1(\mathbf{X}) \triangleq \frac{p_{\mathbf{x}|H_1}(\mathbf{X}|H_1)}{p_{\mathbf{x}|1^*}(\mathbf{X})}. \quad (2.345)$$

The expression in (2.344) can be written as

$$P_M(\gamma_*) = E_{1^*} [\mathbb{I}(l_*(\mathbf{X}) < \gamma_*) W_1(\mathbf{X})]. \quad (2.346)$$

We define

$$I_M(\gamma_*) \triangleq E_{1^*} [\mathbb{I}^2(l_*(\mathbf{X}) < \gamma_*) W_1^2(\mathbf{X})] \quad (2.347)$$

$$= E_1 [\mathbb{I}(l_*(\mathbf{X}) < \gamma_*) W_1(\mathbf{X})]. \quad (2.348)$$

Then,

$$\operatorname{Var}_{1^*} (\hat{P}_M) = \frac{1}{K_M} (I_M - P_M^2) \quad (2.349)$$

and

$$K_{M,IS} = \frac{c^2}{\alpha^2} \frac{(I_M - P_M^2)}{\min(P_M, 1 - P_M)^2}. \quad (2.350)$$

We can upper bound $\mathbb{I}(l_*(\mathbf{X}) < \gamma_*)$ as shown in Figure 2.39,

$$\mathbb{I}(l_*(\mathbf{X}) < \gamma_*) \leq e^{-t[l_*(\mathbf{X}) - \gamma_*]} \quad t \geq 0. \quad (2.351)$$

Then,

$$I_M(\gamma_*) \leq E_{1^*} [e^{-2t[l_*(\mathbf{X}) - \gamma_*]} W_1^2(\mathbf{X})] \triangleq \bar{I}_M(\gamma_*), \quad (2.352)$$

which is minimized when

$$e^{-t[l_*(\mathbf{X}) - \gamma_*]} W_1(\mathbf{X}) = E_1 [e^{-t[l_*(\mathbf{X}) - \gamma_*]}]. \quad (2.353)$$

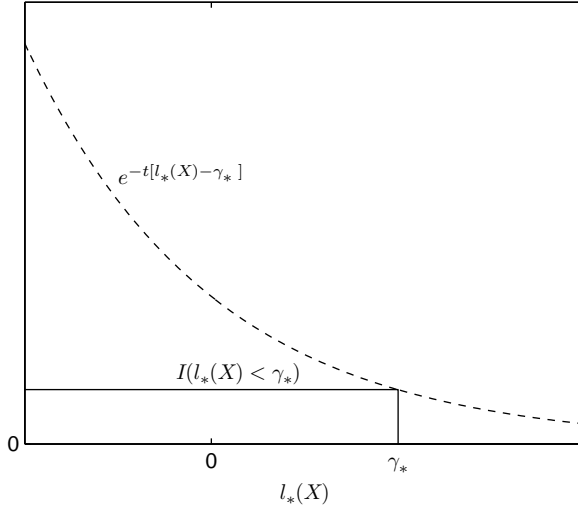


Figure 2.39: Upper bound on $\mathbb{I}(l_*(\mathbf{X}) < \gamma_*)$.

Now note that

$$e^{-tl_*(\mathbf{X})} = \left(\frac{p_{\mathbf{x}|H_1}(\mathbf{X}|H_1)}{p_{\mathbf{x}|H_0}(\mathbf{X}|H_0)} \right)^{-t} = \left(\frac{p_{\mathbf{x}|H_0}(\mathbf{X}|H_0)}{p_{\mathbf{x}|H_1}(\mathbf{X}|H_1)} \right)^t, \quad (2.354)$$

so

$$\begin{aligned} E_1 [e^{-tl_*(\mathbf{X})}] &= \int p_{\mathbf{x}|H_0}(\mathbf{X}|H_0)^t p_{\mathbf{x}|H_1}(\mathbf{X}|H_1)^{1-t} d\mathbf{X} \\ &= e^{\mu(1-t)}. \end{aligned} \quad (2.355)$$

From (2.353), $\bar{I}_M(\gamma_*)$ is minimized when

$$e^{-t[l_*(\mathbf{X}) - \gamma_*]} \frac{p_{\mathbf{x}|H_1}(\mathbf{X}|H_1)}{p_{\mathbf{x}|1^*}(\mathbf{X})} = e^{\mu(1-t)+t\gamma_*} \quad (2.356)$$

or

$$p_{\mathbf{x}|1^*}(\mathbf{X}; t) = e^{-tl_*(\mathbf{X}) - \mu(1-t)} p_{\mathbf{x}|H_1}(\mathbf{X}|H_1). \quad (2.357)$$

Substituting (2.357) into (2.345), we obtain

$$W_1(\mathbf{X}; t) = e^{tl_*(\mathbf{X}) + \mu(1-t)}. \quad (2.358)$$

The optimized upper bound is

$$\bar{I}_M(\gamma_*; t) = e^{2[\mu(1-t)+t\gamma_*]} \quad t \geq 0. \quad (2.359)$$

Minimizing $\bar{I}_M(\gamma_*; t)$ with respect to t , we obtain

$$t_* : \dot{\mu}(1 - t_*) = \gamma_*, \quad (2.360)$$

for $\gamma_* \leq \dot{\mu}(1)$. If $\gamma_* > \dot{\mu}(1)$, the optimum value is $t_* = 0$, which gives the bound $\bar{I}_M(\gamma_*; 0) = 1$.

Substituting (2.358) in (2.348) gives the following expression for I_M ,

$$I_M(\gamma_*; t) = e^{\mu(1-t)} \int \mathbb{I}(l_*(\mathbf{X}) < \gamma_*) e^{tl_*(\mathbf{X})} p_{\mathbf{x}|H_1}(\mathbf{X}|H_1) d\mathbf{X}. \quad (2.361)$$

In this case when $t = 0$, $I_M(\gamma_*; 0) = P_M(\gamma_*)$, and $p_{\mathbf{x}|1^*}(\mathbf{X}; 0) = p_{\mathbf{x}|H_1}(\mathbf{X}|H_1)$, and there is no importance sampling gain.

If we let

$$s = 1 - t \quad s \leq 1, \quad (2.362)$$

and use the expression for $l_*(\mathbf{X})$ in (2.336), the tilted density in (2.357) becomes

$$\boxed{p_{\mathbf{x}|1^*}(\mathbf{X}; s) = e^{-\mu(s)} p_{\mathbf{x}|H_0}(\mathbf{X}|H_0)^{1-s} p_{\mathbf{x}|H_1}(\mathbf{X}|H_1)^s} \quad (2.363)$$

which is the same as the tilted density in (2.338). We use the following notation for the optimum tilted density for estimating both P_F and P_M ,

$$\boxed{p_{\mathbf{x}|s_*}(\mathbf{X}) = e^{-\mu(s_*)} p_{\mathbf{x}|H_0}(\mathbf{X}|H_0)^{1-s_*} p_{\mathbf{x}|H_1}(\mathbf{X}|H_1)^{s_*}.} \quad (2.364)$$

In terms of s , (2.358)–(2.361) become

$$\boxed{W_1(\mathbf{X}; s) = e^{(1-s)l_*(\mathbf{X}) + \mu(s)}} \quad (2.365)$$

$$\boxed{\bar{I}_M(\gamma_*; s) = e^{2[\mu(s) + (1-s)\gamma_*]} \quad s \leq 1.} \quad (2.366)$$

$$s_* : \dot{\mu}(s_*) = \gamma_*, \quad (2.367)$$

$$I_M(\gamma_*; s) = e^{\mu(s)} \int \mathbb{I}(l_*(\mathbf{X}) < \gamma_*) e^{(1-s)l_*(\mathbf{X})} p_{\mathbf{x}|H_1}(\mathbf{X}|H_1) d\mathbf{X}. \quad (2.368)$$

From (2.367) and (2.340), we see that the optimum tilting specified by s_* is the same for both P_M and P_F .

If we let $x = l_*$ and note that $p_{x|1^*}(x; s) = p_{x_s}(x)$, then substituting (2.365) into (2.347) and using the optimum s_* from (2.367) gives the following expression,

$$I_M(\gamma_*; s_*) = \int_{-\infty}^{\dot{\mu}(s_*)} e^{2[\mu(s_*) + (1-s_*)X]} p_{x_s}(X) dX, \quad (2.369)$$

from which we can derive the approximate expression for $I_M(\gamma_*; s_*)$:

$$\boxed{I_M(\gamma_*; s_*) \approx \left\{ \exp \left[2\mu(s_*) + 2(1-s_*)\dot{\mu}(s_*) + 2(1-s_*)^2 \ddot{\mu}(s_*) \right] \right\} \operatorname{erfc}_* \left[2(1-s_*)\sqrt{\dot{\mu}(s_*)} \right].} \quad (2.370)$$

2.5.2.3 Independent Observations

The optimum tilted density in terms of the original observations is found by letting $\mathbf{X} = \mathbf{R}$ in (2.364),

$$p_{\mathbf{r}|s_*}(\mathbf{R}) = e^{-\mu(s_*)} p_{\mathbf{r}|H_0}(\mathbf{R}|H_0)^{1-s_*} p_{\mathbf{r}|H_1}(\mathbf{R}|H_1)^{s_*}. \quad (2.371)$$

If the observations are independent, we substitute (2.245) and (2.247) in (2.371) to obtain

$$\begin{aligned} p_{\mathbf{r}|s_*}(\mathbf{R}) &= \exp\left(-\sum_{i=1}^N \mu_i(s)\right) \left(\prod_{i=1}^N p_{r_i|H_0}(R_i|H_0)\right)^{1-s_*} \left(\prod_{i=1}^N p_{r_i|H_1}(R_i|H_1)\right)^{s_*} \\ &= \prod_{i=1}^N (e^{-\mu_i(s_*)} p_{r_i|H_0}(R_i|H_0)^{1-s_*} p_{r_i|H_1}(R_i|H_1)^{s_*}) \end{aligned} \quad (2.372)$$

that can be written as

$$p_{\mathbf{r}|s_*}(\mathbf{R}) = \prod_{i=1}^N p_{r_i|s_*}(R_i) \quad (2.373)$$

where the tilted marginal probability density is defined as

$$p_{r_i|s_*}(R_i) \triangleq e^{-\mu_i(s_*)} p_{r_i|H_0}(R_i|H_0)^{1-s_*} p_{r_i|H_1}(R_i|H_1)^{s_*}. \quad (2.374)$$

This is a key result for the cases in which it is difficult to compute $p_{l_*|H_0}(L|H_0)$ and $p_{l_*|H_1}(L|H_1)$. Most applications with non-Gaussian observations fall into this category. We can use the tilted marginal probability densities to simulate the r_i .

2.5.2.4 Simulation of the ROC

To summarize our results, we have the following procedure for simulating a (P_F , P_D) point on the ROC curve:

1. Compute $\mu(s)$ from (2.332),

$$\mu(s) = \ln \int [p_{\mathbf{x}|H_1}(\mathbf{X}|H_1)]^s [p_{\mathbf{x}|H_0}(\mathbf{X}|H_0)]^{1-s} d\mathbf{X}. \quad (2.375)$$

For an ID model, we can compute $\mu_i(s)$ from (2.248) and $\mu(s)$ from (2.247),

$$\mu_i(s) = \ln \int [p_{r_i|H_1}(R_i|H_1)]^s [p_{r_i|H_0}(R_i|H_0)]^{1-s} dR_i \quad (2.376)$$

$$\mu(s) = \sum_{i=1}^N \mu_i(s). \quad (2.377)$$

Differentiate $\mu(s)$ to obtain $\dot{\mu}(s)$ and $\ddot{\mu}(s)$. Note that $\ddot{\mu}(s)$ is only needed if we are computing approximate expressions in step 3.

2. Find s_* using

$$s_* = \begin{cases} 0 & \gamma_* < \dot{\mu}(0) \\ s_* : \dot{\mu}(s_*) = \gamma_* & \dot{\mu}(0) \leq \gamma_* \leq \dot{\mu}(1) \\ 1 & \gamma_* > \dot{\mu}(1) \end{cases} \quad (2.378)$$

3. Find $P_F(\gamma_*)$, $P_M(\gamma_*)$, $I_F(\gamma_*; s)$, and $I_M(\gamma_*; s)$. Exact analytical expressions can be obtained from (2.317), (2.344), (2.341), and (2.368), when they can be evaluated.

$$P_F(\gamma_*) = \int \mathbb{I}(l_*(\mathbf{X}) \geq \gamma_*) p_{\mathbf{x}|H_0}(\mathbf{X}|H_0) d\mathbf{X}, \quad (2.379)$$

$$P_M(\gamma_*) = \int \mathbb{I}(l_*(\mathbf{X}) < \gamma_*) p_{\mathbf{x}|H_1}(\mathbf{X}|H_1) d\mathbf{X}, \quad (2.380)$$

$$I_F(\gamma_*; s) = e^{\mu(s)} \int \mathbb{I}(l_*(\mathbf{X}) \geq \gamma_*) e^{-s l_*(\mathbf{X})} p_{\mathbf{x}|H_0}(\mathbf{X}|H_0) d\mathbf{X}, \quad (2.381)$$

$$I_M(\gamma_*; s) = e^{\mu(s)} \int \mathbb{I}(l_*(\mathbf{X}) < \gamma_*) e^{(1-s)l_*(\mathbf{X})} p_{\mathbf{x}|H_1}(\mathbf{X}|H_1) d\mathbf{X}. \quad (2.382)$$

Alternatively, use the approximate expressions in (2.238), (2.241), (2.343), and (2.370),

$$\begin{aligned} P_F(\gamma_*) &\approx \left\{ \exp \left[\mu(s_*) - s_* \dot{\mu}(s_*) + \frac{s_*^2}{2} \ddot{\mu}(s_*) \right] \right\} \\ &\quad \times \operatorname{erfc}_* \left[s_* \sqrt{\dot{\mu}(s_*)} \right], \end{aligned} \quad (2.383)$$

$$\begin{aligned} P_M(\gamma_*) &\approx \left\{ \exp \left[\mu(s_*) + (1-s_*) \dot{\mu}(s_*) + \frac{(s_* - 1)^2}{2} \ddot{\mu}(s_*) \right] \right\} \\ &\quad \times \operatorname{erfc}_* \left[(1-s_*) \sqrt{\dot{\mu}(s_*)} \right], \end{aligned} \quad (2.384)$$

$$I_F(\gamma_*; s_*) \approx \left\{ \exp \left[2\mu(s_*) - 2s_* \dot{\mu}(s_*) + 2s_*^2 \ddot{\mu}(s_*) \right] \right\} \operatorname{erfc}_* \left[2s_* \sqrt{\dot{\mu}(s_*)} \right], \quad (2.385)$$

$$\begin{aligned} I_M(\gamma_*; s_*) &\approx \left\{ \exp \left[2\mu(s_*) + 2(1-s_*) \dot{\mu}(s_*) + 2(1-s_*)^2 \ddot{\mu}(s_*) \right] \right\} \\ &\quad \times \operatorname{erfc}_* \left[2(1-s_*) \sqrt{\dot{\mu}(s_*)} \right]. \end{aligned} \quad (2.386)$$

Note that we can only use the approximate expressions for thresholds that satisfy $\dot{\mu}(0) \leq \gamma_* \leq \dot{\mu}(1)$, while the exact expressions are valid for any γ_* .

4. Pick a sufficient statistic \mathbf{x} to be used in the simulation and evaluate (2.278) to find an expression for $l_*(\mathbf{X})$,

$$l_*(\mathbf{X}) = \ln \frac{p_{\mathbf{x}|H_1}(\mathbf{X}|H_1)}{p_{\mathbf{x}|H_0}(\mathbf{X}|H_0)}. \quad (2.387)$$

5. Find the optimum tilted density from (2.364),

$$p_{\mathbf{x}|s_*}(\mathbf{X}) = e^{-\mu(s_*)} p_{\mathbf{x}|H_0}(\mathbf{X}|H_0)^{1-s_*} p_{\mathbf{x}|H_1}(\mathbf{X}|H_1)^{s_*}. \quad (2.388)$$

For an ID model, the optimum tilted marginal densities are found from (2.374),

$$p_{r_i|s_*}(R_i) = e^{-\mu_i(s_*)} p_{r_i|H_0}(R_i|H_0)^{1-s_*} p_{r_i|H_1}(R_i|H_1)^{s_*}. \quad (2.389)$$

6. Find the weighting functions from (2.335) and (2.365),

$$W_0(\mathbf{X}; s_*) = e^{-s_* l_*(\mathbf{X}) + \mu(s_*)}, \quad (2.390)$$

$$W_1(\mathbf{X}; s_*) = e^{(1-s_*) l_*(\mathbf{X}) + \mu(s_*)}. \quad (2.391)$$

7. Specify the confidence interval parameters α and c and compute $K_{F,IS}$ and $K_{M,IS}$ from using (2.327) and (2.350),

$$K_{F,IS} = \frac{c^2}{\alpha^2} \frac{I_F(\gamma_*; s_*) - P_F(\gamma_*)^2}{\min [P_F(\gamma_*), 1 - P_F(\gamma_*)]^2} \quad (2.392)$$

$$K_{M,IS} = \frac{c^2}{\alpha^2} \frac{I_M(\gamma_*; s_*) - P_M(\gamma_*)^2}{\min [P_M(\gamma_*), 1 - P_M(\gamma_*)]^2}. \quad (2.393)$$

Select the larger value for the simulation,

$$K_{IS} = \max (K_{F,IS}, K_{M,IS}). \quad (2.394)$$

8. Generate K_{IS} independent realizations of \mathbf{x} from $p_{\mathbf{x}|s_*}(\mathbf{X})$ and compute the estimates

$$\hat{P}_F(\gamma_*) = \frac{1}{K_{IS}} \sum_{k=1}^{K_{IS}} \mathbb{I}(l_*(\mathbf{X}_k; s_*) \geq \gamma_*) W_0(\mathbf{X}_k; s_*) \quad (2.395)$$

$$\hat{P}_M(\gamma_*) = \frac{1}{K_{IS}} \sum_{k=1}^{K_{IS}} \mathbb{I}(l_*(\mathbf{X}_k; s_*) < \gamma_*) W_1(\mathbf{X}_k; s_*.). \quad (2.396)$$

An estimate of $P_D(\gamma_*)$ can be found from

$$\hat{P}_D(\gamma_*) = 1 - \hat{P}_M(\gamma_*) = \frac{1}{K_{IS}} \sum_{k=1}^{K_{IS}} \mathbb{I}(l_*(\mathbf{X}_k; s_*) \geq \gamma_*) W_1(\mathbf{X}_k; s_*.). \quad (2.397)$$

It is important to note that $\mu(s)$, $P_F(\gamma_*)$, $P_M(\gamma_*)$, $I_F(\gamma_*; s)$, $I_M(\gamma_*; s)$, $W_0(\mathbf{X}; s)$, and $W_1(\mathbf{X}; s)$ are all defined in terms of a sufficient statistic \mathbf{X} . When computing these quantities, we do not need to use the same statistic, and in fact we will usually find it convenient to use different statistics.

2.5.2.5 Examples

In this section, we apply importance sampling using the optimum tilted density. The first two examples are continuations of Examples 2.1 and 2.2. Because we have analytic results, we probably would not simulate these models in practice, but they are useful to introduce the simulation procedure. The third example illustrates the case where we can find an analytic expression for $\mu(s)$, but cannot find $p_{l_*|H_0}(L|H_0)$ and $p_{l_*|H_1}(L|H_1)$ and cannot evaluate P_F and P_M . We use importance sampling with the approximate expressions and develop an iterative importance sampling scheme in Section 2.5.2.6 to solve this case.

Example 2.16 (continuation of Examples 2.1, 2.5, 2.12, and 2.15). For this model, $\mu(s)$, $\dot{\mu}(s)$, and $\ddot{\mu}(s)$ were computed in Example 2.12. Recall from (2.257)–(2.259) that

$$\mu_i(s) = \frac{s(s-1)d^2}{2N}, \quad (2.398)$$

$$\mu(s) = \frac{s(s-1)d^2}{2}, \quad (2.399)$$

$$\dot{\mu}(s) = \frac{(2s-1)d^2}{2}. \quad (2.400)$$

To find s_* , we solve $\dot{\mu}(s) = \gamma_*$. The result is

$$s_* = \begin{cases} 0 & \gamma_* < -\frac{d^2}{2} \\ \frac{\gamma_*}{d^2} + \frac{1}{2} & -\frac{d^2}{2} \leq \gamma_* \leq \frac{d^2}{2} \\ 1 & \gamma_* > \frac{d^2}{2}. \end{cases} \quad (2.401)$$

$P_F(\gamma_*)$ and $P_M(\gamma_*)$ were found in Examples 2.5 and 2.15 and are given in (2.308) and (2.309).

We next compute $I_F(\gamma_*; s)$ using (2.381). It is convenient to use

$$x_0 = \frac{1}{\sigma\sqrt{N}} \sum_{i=1}^N r_i, \quad (2.402)$$

which is $N(0, 1)$ on H_0 . Then, from (2.24)

$$l_*(X_0) = dX_0 - \frac{d^2}{2} \quad (2.403)$$

and $l_*(X_0) \geq \gamma_*$ when $X_0 \geq Z_F$, where Z_F was defined in (2.312). Thus,

$$I_F(\gamma_*; s) = e^{\frac{s(s-1)d^2}{2}} \int_{Z_F}^{\infty} e^{-sdX_0 + \frac{sd^2}{2}} \frac{1}{\sqrt{2\pi}} e^{-\frac{x_0^2}{2}} dX_0, \quad (2.404)$$

which reduces to

$$I_F(\gamma_*; s) = e^{s^2 d^2} \operatorname{erfc}_*(Z_F + sd) = e^{(sd)^2} \operatorname{erfc}_*\left(\frac{\gamma_*}{d} + \frac{d}{2} + sd\right). \quad (2.405)$$

To calculate $I_M(\gamma_*; s)$, we proceed in a similar manner. We define

$$x_1 = \frac{1}{\sigma\sqrt{N}} \sum_{i=1}^N r_i - d, \quad (2.406)$$

which is $N(0, 1)$ on H_1 . In this case,

$$l_*(X_1) = dX_1 + \frac{d^2}{2} \quad (2.407)$$

and $l_*(X_1) < \gamma_*$ when $X_1 < Z_F - d$. Evaluating (2.382), we obtain

$$I_M(\gamma_*; s) = e^{[(s-1)d]^2} \left[1 - \operatorname{erfc}_*\left(\frac{\gamma_*}{d} - \frac{d}{2} + (s-1)d\right) \right]. \quad (2.408)$$

Table 2.3: Importance sampling simulation values for $d = 6$, $p_c = 0.954$, and $\alpha = 0.1$

P_F	γ_*	s_*	P_M	I_F	I_M	$K_{F,IS}$	$K_{M,IS}$
10^{-2}	-5.29	0.37	3.2×10^{-5}	3.7×10^{-4}	5.6×10^{-9}	1069	1804
10^{-4}	3.52	0.59	0.0046	5.2×10^{-8}	8.3×10^{-5}	1676	1185
10^{-6}	10.06	0.75	0.0581	6.4×10^{-12}	0.0099	2155	774
10^{-8}	15.49	0.89	0.2381	7.4×10^{-16}	0.1281	2562	504
10^{-10}	20.23	1	0.5147	8.3×10^{-20}	0.5147	2934	425
10^{-12}	24.49	1	0.7611	1.2×10^{-23}	0.7611	4539	1275

For the simulation, we choose our sufficient statistic to be the original data $\mathbf{x} = \mathbf{r}$, which are IID. From (2.24),

$$l_*(\mathbf{R}) = \left(\frac{1}{\sqrt{N}\sigma} \sum_{i=1}^N R_i \right) d - \frac{d^2}{2}. \quad (2.409)$$

The tilted marginal densities are given by (2.389). Substituting (2.19), (2.20), and (2.398) into (2.389) and simplifying gives

$$p_{r_i|s_*}(R_i) \sim N(s_* m, \sigma^2). \quad (2.410)$$

We see that the tilted density corresponds to a Gaussian density with the same variance but with a mean value of $s_* m$ that varies between 0 and m . When $s_* = 0$, $p_{r_i|s_*}(R_i) = p_{r_i|H_0}(R_i|H_0)$, and when $s_* = 1$, $p_{r_i|s_*}(R_i) = p_{r_i|H_1}(R_i|H_1)$.

From (2.390) and (2.391), the weighting functions are

$$W_0(\mathbf{R}; s_*) = e^{-s_* l_*(\mathbf{R})} e^{\mu(s_*)} = e^{-s_* l_*(\mathbf{R})} e^{s_*(s_* - 1) \frac{d^2}{2}}, \quad (2.411)$$

$$W_1(\mathbf{R}; s_*) = e^{(1-s_*) l_*(\mathbf{R})} e^{\mu(s_*)} = e^{(1-s_*) l_*(\mathbf{R})} e^{s_*(s_* - 1) \frac{d^2}{2}}. \quad (2.412)$$

We consider the parameter values used in Table 2.2: $d = \sqrt{40}$, $c = 2$, $\alpha = 0.1$, and a variety of ROC points. For $d = \sqrt{40}$, $\dot{\mu}(0) = -20$, and $\dot{\mu}(1) = 20$. We compute s_* , $I_F(\gamma_*; s_*)$, $I_M(\gamma_*; s_*)$, $K_{F,IS}$, and $K_{M,IS}$. The results are summarized in Table 2.3. We see that in all cases $I_F < P_F$ and $K_{F,IS}$ is significantly smaller than the corresponding K_F in Table 2.2. In the last two rows of the table, we have $\gamma_* > \dot{\mu}(1)$ and the optimum $s_* = 1$. For these cases, $I_M = P_M$ and $K_{M,IS} = K_M$. For the other rows, $I_M < P_M$ and $K_{M,IS} < K_M$. We see that importance sampling has dramatically reduced the required number of trials when P_F or P_M is very small.

We run the simulation for $P_F = 10^{-6}$, choosing $N = 40$, $m = 1$, and $\sigma^2 = 1$. From Table 2.3, $P_M = 0.0581$ and $P_D = 0.9419$, and the required number of trials is $K_{IS} = \max(2155, 774) = 2155$. The confidence intervals are:

$$\hat{P}_F \in [0.9, 1.1] \times 10^{-6},$$

$$\hat{P}_D \in [0.9384, 0.9454].$$

We generate the required number of trials using the tilted marginal density¹¹ and compute \hat{P}_F and \hat{P}_D from (2.395) and (2.397). (Without importance sampling, we would have had to run two separate

¹¹The random samples are generated using the Matlab function `randn`.

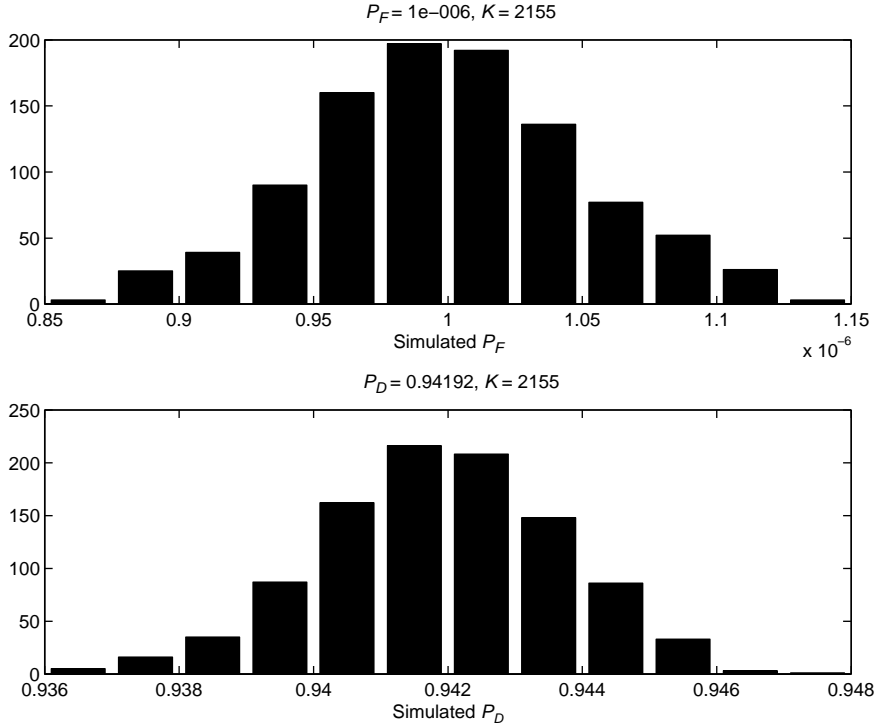


Figure 2.40: Histograms of \hat{P}_F and \hat{P}_D .

simulations to estimate \hat{P}_F and \hat{P}_D requiring $K_F = 4 \times 10^8$ and $K_M = 6488$ trials, respectively.) We repeat the simulation 1000 times. Histograms of \hat{P}_F and \hat{P}_D are shown in Figure 2.40. We see that the results are consistent with the confidence interval specifications.

We next consider the ROC curves plotted in Figure 2.12b. We run the simulation for various values of d and P_F and plot the simulation results on top of the analytic results in Figure 2.41. We see that there is excellent agreement between the simulation and the analytic results. ■

Example 2.17 (continuation of Examples 2.2, 2.6, and 2.13). In this example, the r_i are IID zero-mean Gaussian random variables with different variances on the two hypotheses:¹²

$$p_{r_i|H_j}(R_i|H_j) = \frac{1}{\sqrt{2\pi}\sigma_j} \exp\left\{-\frac{1}{2}\frac{R_i^2}{\sigma_j^2}\right\}, \quad i = 1, 2, \dots, N \text{ and } j = 0, 1. \quad (2.413)$$

We assume $\sigma_1^2 > \sigma_0^2$.

We computed P_F and P_D in Example 2.6. From (2.109) and (2.110),¹³

$$P_F(\gamma) = 1 - \Gamma_{N/2}\left(\frac{\gamma}{2\sigma_0^2}\right), \quad (2.414)$$

¹²This example also has an analytic solution for P_D and P_F . However, it serves as an introduction to the problem whose σ_j^2 is different on each observation and an analytic solution is not available.

¹³For a specified P_F or P_M , γ can be computed in Matlab using the `gaminv` function. See Appendix A.

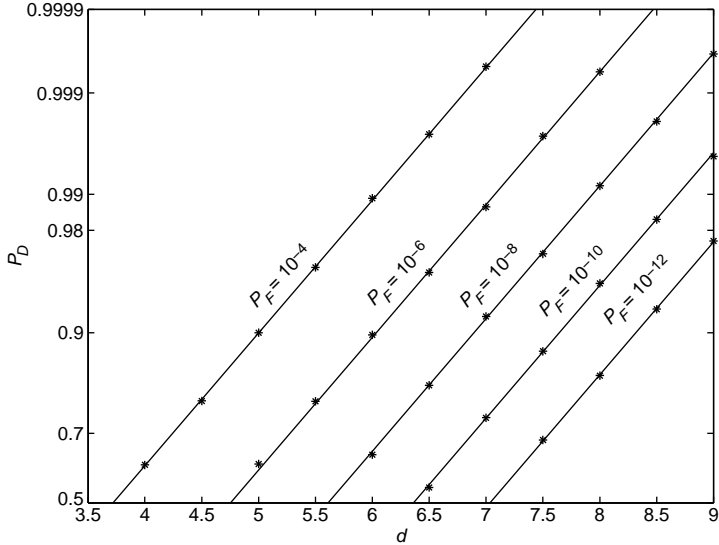


Figure 2.41: Simulated P_D versus d for various P_F using optimum tilted density.

$$P_M(\gamma) = \Gamma_{N/2} \left(\frac{\gamma}{2\sigma_1^2} \right), \quad (2.415)$$

where γ was defined in terms of $\gamma_* = \ln \eta$ in (2.91),

$$\gamma = \frac{2\sigma_0^2\sigma_1^2}{\sigma_1^2 - \sigma_0^2} \left[\gamma_* - \frac{N}{2} \ln \left(\frac{\sigma_0^2}{\sigma_1^2} \right) \right]. \quad (2.416)$$

For notational simplicity, it will be easier to work with γ instead of γ_* . We can easily convert the results back to γ_* by rearranging (2.416) to obtain,

$$\gamma_* = \frac{\gamma(\sigma_1^2 - \sigma_0^2)}{2\sigma_0^2\sigma_1^2} + \frac{N}{2} \ln \left(\frac{\sigma_0^2}{\sigma_1^2} \right). \quad (2.417)$$

We computed $\mu_i(s)$ and $\mu(s)$ in Example 2.13. Recall from (2.268) and (2.269),

$$\mu(s) = N\mu_i(s) = \frac{N}{2} \ln \left[\frac{(\sigma_0^2)^s (\sigma_1^2)^{1-s}}{s\sigma_0^2 + (1-s)\sigma_1^2} \right]. \quad (2.418)$$

Differentiating gives

$$\dot{\mu}(s) = \frac{N}{2} \left[\ln \left(\frac{\sigma_0^2}{\sigma_1^2} \right) + \frac{\sigma_1^2 - \sigma_0^2}{s\sigma_0^2 + (1-s)\sigma_1^2} \right]. \quad (2.419)$$

To find s_* we solve $\dot{\mu}(s) = \gamma_*$ for $\dot{\mu}(0) \leq \gamma_* \leq \dot{\mu}(1)$ and then use (2.417) to express the results in terms of γ . The result is

$$s_* = \begin{cases} 0 & \gamma < N\sigma_0^2 \\ \frac{\sigma_1^2}{\sigma_1^2 - \sigma_0^2} \left(1 - \frac{N\sigma_0^2}{\gamma} \right) & N\sigma_0^2 \leq \gamma \leq N\sigma_1^2 \\ 1 & \gamma > N\sigma_1^2. \end{cases} \quad (2.420)$$

To find $I_F(\gamma; s)$, we define

$$x = \sum_{i=1}^N R_i^2 \quad (2.421)$$

and evaluate (2.381) using an analysis similar to Example 2.6 to obtain¹⁴

$$I_F(\gamma; s) = \left[\frac{\sigma_1^2}{s\sigma_0^2 + (1-s)\sigma_1^2} \right]^{\frac{N}{2}} \left[\frac{\sigma_1^2}{-s\sigma_0^2 + (1+s)\sigma_1^2} \right]^{\frac{N}{2}} \left(1 - \Gamma_{N/2} \left[\gamma \frac{-s\sigma_0^2 + (1+s)\sigma_1^2}{2\sigma_0^2\sigma_1^2} \right] \right). \quad (2.422)$$

Similarly,

$$I_M(\gamma; s) = \left[\frac{\sigma_0^2}{s\sigma_0^2 + (1-s)\sigma_1^2} \right]^{\frac{N}{2}} \left[\frac{\sigma_0^2}{(2-s)\sigma_0^2 + (s-1)\sigma_1^2} \right]^{\frac{N}{2}} \Gamma_{N/2} \left[\gamma \frac{(2-s)\sigma_0^2 + (s-1)\sigma_1^2}{2\sigma_0^2\sigma_1^2} \right]. \quad (2.423)$$

For the simulation, we choose our sufficient statistic to be the original data $\mathbf{x} = \mathbf{r}$, which are IID. From (2.29), the log-likelihood ratio is

$$l_*(\mathbf{R}) = \frac{1}{2} \left(\frac{1}{\sigma_0^2} - \frac{1}{\sigma_1^2} \right) \sum_{i=1}^N R_i^2 + N \ln \frac{\sigma_0}{\sigma_1} = \left(\frac{\sigma_1^2 - \sigma_0^2}{2\sigma_1^2\sigma_0^2} \right) \sum_{i=1}^N R_i^2 + \frac{N}{2} \ln \left(\frac{\sigma_0^2}{\sigma_1^2} \right). \quad (2.424)$$

To find the tilted marginal densities, we use (2.413) and (2.418) in (2.389) to obtain

$$p_{r_i|s_*}(R_i) = \left[\frac{(\sigma_0^2)^{s_*} (\sigma_1^2)^{1-s_*}}{s_*\sigma_0^2 + (1-s_*)\sigma_1^2} \right]^{-1/2} \left(\frac{1}{\sqrt{2\pi\sigma_0^2}} e^{-R_i^2/2\sigma_0^2} \right)^{1-s_*} \left(\frac{1}{\sqrt{2\pi\sigma_1^2}} e^{-R_i^2/2\sigma_1^2} \right)^{s_*} \quad (2.425)$$

which reduces to

$$p_{r_i|s_*}(R_i) \sim N(0, \sigma_{s_*}^2) \quad (2.426)$$

where

$$\sigma_{s_*}^2 \triangleq \frac{\sigma_0^2\sigma_1^2}{s_*\sigma_0^2 + (1-s_*)\sigma_1^2}. \quad (2.427)$$

We see that the tilted marginal density is a zero-mean Gaussian density with variance $\sigma_{s_*}^2$. When $s_* = 0$, $\sigma_{s_*}^2 = \sigma_0^2$, and when $s_* = 1$, $\sigma_{s_*}^2 = \sigma_1^2$.

The weighting functions are

$$W_0(\mathbf{R}; s_*) = e^{-s_* l_*(\mathbf{R})} e^{\mu(s_*)} = e^{-s_* l_*(\mathbf{R})} \left[\frac{(\sigma_0^2)^{s_*} (\sigma_1^2)^{1-s_*}}{s_*\sigma_0^2 + (1-s_*)\sigma_1^2} \right]^{\frac{N}{2}}, \quad (2.428)$$

$$W_1(\mathbf{R}; s_*) = e^{(1-s_*) l_*(\mathbf{R})} e^{\mu(s_*)} = e^{(1-s_*) l_*(\mathbf{R})} \left[\frac{(\sigma_0^2)^{s_*} (\sigma_1^2)^{1-s_*}}{s_*\sigma_0^2 + (1-s_*)\sigma_1^2} \right]^{\frac{N}{2}}. \quad (2.429)$$

We consider the following parameter values: $N = 8$, $\sigma_0^2 = 1$, $\sigma_1^2 = 21$, $p_c = 0.954$ ($c = 2$), and $\alpha = 0.1$, and a variety of ROC points. We compute the quantities of interest and summarize the results in Table 2.4. In this example, $I_F < P_F$ for all the ROC points and $K_{F,IS} < K_F$. Also, $I_M < P_M$ and

¹⁴The analysis is straightforward but tedious.

Table 2.4: Importance sampling simulation values for $N = 8$, $\sigma_0^2 = 1$, $\sigma_1^2 = 21$, $p_c = 0.954$, and $\alpha = 0.1$

P_F	γ	s_*	P_M	I_F	I_M	K_F	$K_{F,IS}$	K_M	$K_{M,IS}$
10^{-4}	31.8	0.79	0.0076	8.8×10^{-8}	0.0001	4×10^6	3129	5.3×10^4	573
10^{-6}	42.7	0.85	0.0200	1.2×10^{-11}	0.0009	4×10^8	4495	2.0×10^4	536
10^{-8}	53.2	0.89	0.0398	1.6×10^{-15}	0.0036	4×10^{10}	5820	9658	503
10^{-10}	63.4	0.92	0.0668	1.9×10^{-19}	0.0097	4×10^{12}	7120	5585	472
10^{-12}	73.5	0.94	0.1007	2.2×10^{-23}	0.0214	4×10^{14}	8401	3573	444

$K_{M,IS} < K_M$. Again, importance sampling has significantly reduced the required number of trials when P_F and P_M are very small.

Next we let $\sigma_1^2 = \sigma_s^2 + \sigma_n^2$ and study the behavior as a function of σ_s^2/σ_n^2 . We run the simulation for various values of σ_s^2/σ_n^2 and P_F by generating the required number of trials using the tilted marginal density and computing \hat{P}_F and \hat{P}_D using (2.395) and (2.397). In Figure 2.42, we plot the analytic results and simulation results for P_D versus σ_s^2/σ_n^2 for various P_F . Once again, the agreement is excellent. ■

In Examples 2.16 and 2.17, we had analytic expressions for P_F and P_D , so we could specify the desired P_F and solve for threshold γ_* . In this case, we do not really need to simulate the likelihood ratio test. A more realistic case is when we do not have an analytic expression relating P_F and γ_* . We consider this case in the next example.

Example 2.18. The observations on H_0 and H_1 are statistically independent draws from a Beta probability density,

$$p_{r_i|H_j}(R_i|H_j) = \frac{1}{B(a_j, b_j)} R_i^{a_j-1} (1-R_i)^{b_j-1}, \quad 0 \leq r_i \leq 1; i = 1, 2, \dots, N; j = 0, 1, \quad (2.430)$$

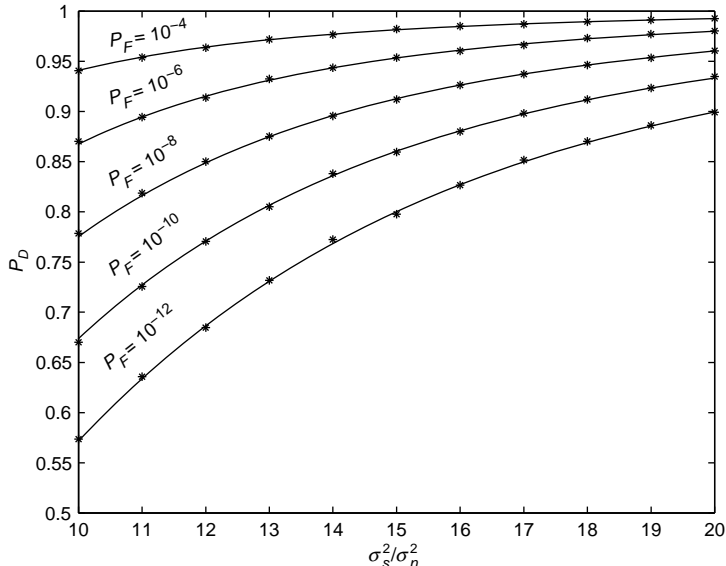


Figure 2.42: Simulated P_D versus σ_s^2/σ_n^2 for various P_F using optimum tilted density.

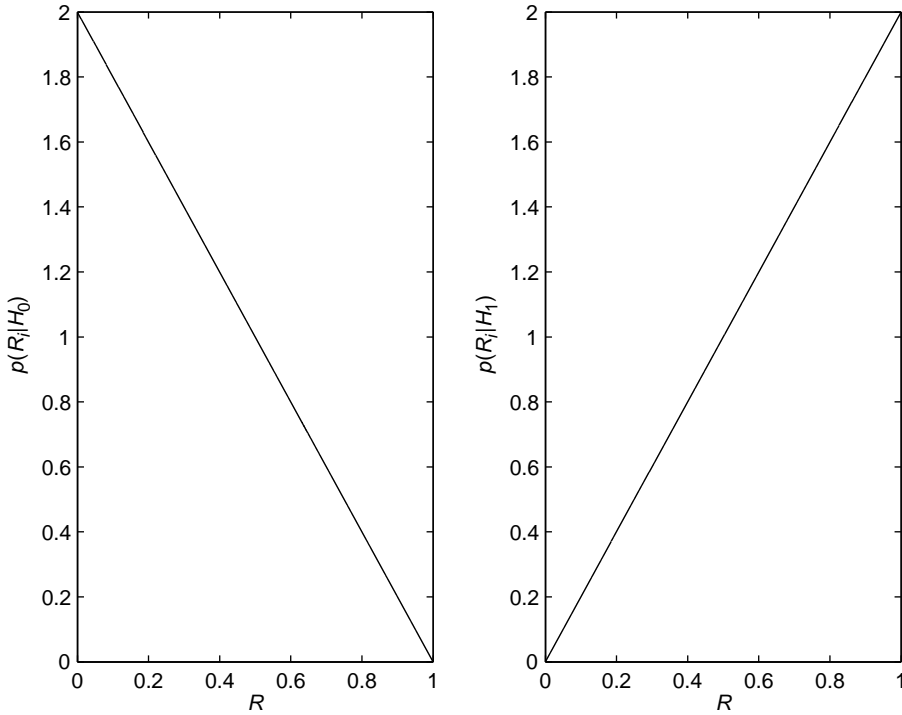


Figure 2.43: Probability densities; $p_{r_i|H_0}(R_i|H_0)$ and $p_{r_i|H_1}(R_i|H_1)$.

where $B(a, b)$ is the Beta function:¹⁵

$$B(a, b) \triangleq \int_0^1 x^{a-1} (1-x)^{b-1} dx = \frac{\Gamma(a)\Gamma(b)}{\Gamma(a+b)}. \quad (2.431)$$

On H_0 we have $a_0 = 1, b_0 = 2$ and on H_1 we have $a_1 = 2, b_1 = 1$, which gives the following densities

$$\begin{aligned} H_0 : p_{r_i|H_0}(R_i|H_0) &= 2(1-R_i) \quad 0 \leq R_i \leq 1; i = 1, 2, \dots, N, \\ H_1 : p_{r_i|H_1}(R_i|H_1) &= 2R_i \quad 0 \leq R_i \leq 1; i = 1, 2, \dots, N. \end{aligned} \quad (2.432)$$

The densities on the two hypotheses are shown in Figure 2.43.

The log-likelihood ratio is

$$l_*(\mathbf{R}) = \ln \prod_{i=1}^N \frac{R_i}{1-R_i} = \sum_{i=1}^N \ln \frac{R_i}{1-R_i}. \quad (2.433)$$

We do not know how to evaluate $p_{l_*|H_0}(L|H_0)$ and $p_{l_*|H_1}(L|H_1)$, therefore we do not have analytical expressions for P_F and P_M . However we can find $\mu_i(s)$. Substituting (2.432) into (2.376), we have

$$e^{\mu_i(s)} = \int_0^1 p_{r_i|H_1}(R_i|H_1)^s p_{r_i|H_0}(R_i|H_0)^{1-s} dR_i = 2 \int_0^1 R_i^s (1-R_i)^{1-s} dR_i. \quad (2.434)$$

¹⁵The Beta function can be computed in Matlab using the `beta` function. See Appendix A.

The integral can be evaluated using (2.431), which gives

$$e^{\mu_i(s)} = \frac{2\Gamma(s+1)\Gamma(2-s)}{\Gamma(3)} = \Gamma(s+1)\Gamma(2-s), \quad (2.435)$$

therefore,

$$\mu_i(s) = \ln \Gamma(s+1) + \ln \Gamma(2-s). \quad (2.436)$$

Differentiating yields

$$\dot{\mu}_i(s) = \frac{\Gamma'(s+1)}{\Gamma(s+1)} - \frac{\Gamma'(2-s)}{\Gamma(2-s)} = \psi_0(s+1) - \psi_0(2-s), \quad (2.437)$$

$$\ddot{\mu}_i(s) = \psi'_0(s+1) - \psi'_0(2-s) = \psi_1(s+1) + \psi_1(2-s), \quad (2.438)$$

where $\psi_0(\cdot)$ and $\psi_1(\cdot)$ are the Digamma and Trigamma functions defined as¹⁶

$$\psi_0(z) = \frac{\Gamma'(z)}{\Gamma(z)}, \quad (2.439)$$

$$\psi_1(z) = -\frac{d}{dz} \psi_0(z). \quad (2.440)$$

The samples are IID, so

$$\mu(s) = N\mu_i(s) = N \ln \Gamma(s+1) + N \ln \Gamma(2-s), \quad (2.441)$$

$$\dot{\mu}(s) = N\dot{\mu}_i(s) = N\psi_0(s+1) - N\psi_0(2-s), \quad (2.442)$$

$$\ddot{\mu}(s) = N\ddot{\mu}_i(s) = N\psi_1(s+1) + N\psi_1(2-s). \quad (2.443)$$

We want to run a simulation to estimate P_F and P_D and compare the results to the approximate expressions. We start by choosing a set of ROC points to simulate by choosing some values for s_* that satisfy $0 \leq s_* \leq 1$. We then find the corresponding threshold using

$$\gamma_* = \dot{\mu}(s_*) = N\psi_0(s_*+1) - N\psi_0(2-s_*). \quad (2.444)$$

We compute $P_F(\gamma_*)$, $P_M(\gamma_*)$, $I_F(\gamma_*; s_*)$, and $I_M(\gamma_*; s_*)$ using (2.383)–(2.386).

For the simulation, we choose $\mathbf{x} = \mathbf{r}$. The log-likelihood ratio is given in (2.433) and the tilted marginal density is found by substituting (2.432) into (2.389). The result is

$$\begin{aligned} p_{ri|s_*}(R_i) &= \frac{1}{\Gamma(s_*+1)\Gamma(2-s_*)} 2^{s_*} R_i^{s_*} 2^{1-s_*} (1-R_i)^{1-s_*}, \quad 0 \leq R_i \leq 1, \\ &= \frac{1}{B(s_*+1, 2-s_*)} R_i^{s_*} (1-R_i)^{1-s_*}, \quad 0 \leq R_i \leq 1, \end{aligned} \quad (2.445)$$

which is a Beta($s_*+1, 2-s_*$) probability density. In Figure 2.44, we show the tilted density for $s_* = 0.7$. We see that, although it is still a Beta probability density, it has a significantly different shape than the original densities.

The weighting functions are evaluated by substituting (2.433) and (2.441) into (2.390) and (2.391). We specify $\alpha = 0.1$ and $c = 3$ and calculate $K_{F,IS}$, $K_{M,IS}$, and K_{IS} using (2.392)–(2.394). We generate the random samples from the tilted marginal density¹⁷ and compute the estimates $\hat{P}_F(\gamma_*)$ and $\hat{P}_D(\gamma_*)$ using (2.395) and (2.397). We plot the approximate ROC curve and the simulation estimates in Figure 2.45 for $N = 20$. The results show that the approximation is quite accurate for this example. ■

¹⁶The Digamma and Trigamma functions can be computed in Matlab using the `psi` function. See Appendix A.

¹⁷The random samples are generated using the Matlab function `betarnd`.

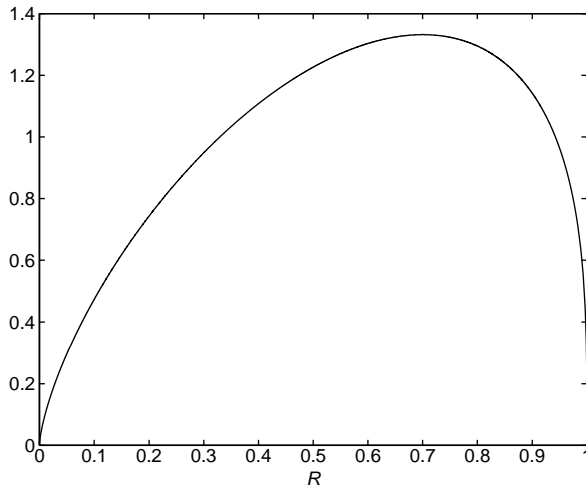


Figure 2.44: Tilted probability density for $s_* = 0.7$.

These three examples provide interesting results for the optimum “tilted” density. In Example 2.16, the original Gaussian density is translated so that its mean is s_*m and its variance is unchanged. Example 2.17, the variance of the original Gaussian density is modified. This is equivalent to scaling the density. In neither case is the density actually tilted as shown in Figure 2.29. In Example 2.18, the parameters of the Beta density are modified so that another Beta density is obtained. The operation is not a scaling or shifting operation and “tilting” is a more appropriate description.

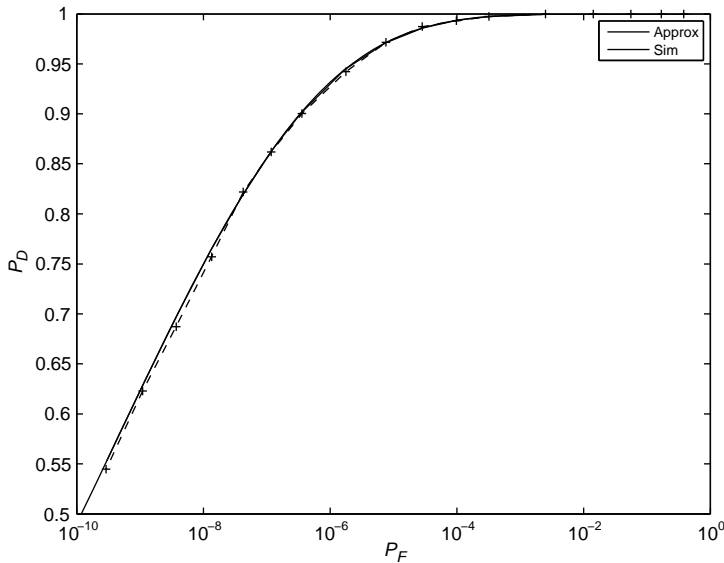


Figure 2.45: Approximate and simulated P_D versus P_F for $N = 20$.

Srinivasan [Sri02] and other references (e.g., [Mit81]) consider an approach that restricts $p_{x|0*}(X)$ to be a scaled transformation,

$$p_{x|0*}(X) = \frac{1}{a} p_{x|H_0}\left(\frac{X}{a}\right) \quad (2.446)$$

or a translated density

$$p_{x|0*}(X) = p_{x|H_0}(X - b) \quad (2.447)$$

and chooses a or b to minimize the variance. The disadvantage is that it is not clear which form is appropriate for a given problem. In addition, in many cases, the optimum tilted density will not be the same form as the original density.

Example 2.18 illustrated how simulation can be used to validate theoretical results. To make the comparison, we needed a representative set of points on the two ROC curves, but the specific values were not important. It turned out that the simulated P_F and P_D were quite close to the approximate values, however this is not always the case. If we are trying to simulate a particular value of P_F , such as when producing curves similar to those in Figures 2.41 and 2.42, the threshold γ_* corresponding to the approximate $P_F(\gamma_*)$ may produce an estimate \hat{P}_F that is not within the specified confidence interval. We develop an iterative technique to handle this situation in the next section.

2.5.2.6 Iterative Importance Sampling

In this section, we consider the model in which we do not have an exact analytic expression relating P_F and γ_* and want to simulate a particular value of P_F , which we denote as P_F^* . We develop an iterative algorithm for solving this problem.¹⁸

We assume that we can find $\mu(s)$, either analytically or numerically, and can then find $\dot{\mu}(s)$ and $\ddot{\mu}(s)$. We use (2.383) to specify an approximate expression for P_F as a function of s ,

$$P_F(s) \approx \left\{ \exp \left[\mu(s) - s\dot{\mu}(s) + \frac{s^2}{2}\ddot{\mu}(s) \right] \right\} \operatorname{erfc}_* \left[s\sqrt{\dot{\mu}(s)} \right]. \quad (2.448)$$

We solve (2.448) to find s (usually numerically) for the desired P_F^* , that is,

$$s : P_F(s) = P_F^*. \quad (2.449)$$

We then find the corresponding threshold using

$$\gamma = \dot{\mu}(s). \quad (2.450)$$

Note that we can only use this technique for values of P_F^* where $0 \leq s \leq 1$ or equivalently $\dot{\mu}(0) \leq \gamma \leq \dot{\mu}(1)$. We run the simulation and compute the estimate \hat{P}_F using (2.395). If the estimate falls within our confidence interval, that is,

$$(1 - \alpha)P_F^* \leq \hat{P}_F \leq (1 + \alpha)P_F^* \quad (2.451)$$

then we accept the simulation results. If not, we adjust s and γ iteratively.

¹⁸Srinivasan [Sri02] (p. 55) also discusses this problem but our approach is significantly different. [SSG97] also discusses various adaptive techniques and gives references.

Our iterative procedure is a gradient approach based on a Taylor series expansion of $\ln P_F(s)$,

$$\ln P_F(s) \approx \ln P_F(s_0) + (s - s_0) \frac{d \ln P_F(s)}{ds} \Big|_{s=s_0}. \quad (2.452)$$

To evaluate the derivative in (2.452) we use the Chernoff bound in (2.217), which we denote as $\bar{P}_F(s)$,

$$\bar{P}_F(s) \triangleq e^{\mu(s) - s\dot{\mu}(s)}. \quad (2.453)$$

Although the Chernoff bound can be weak compared to the approximation $P_F(s)$, they have similar derivatives, that is,

$$\frac{d \ln \bar{P}_F(s)}{ds} \approx \frac{d \ln P_F(s)}{ds}. \quad (2.454)$$

Differentiating the log of (2.453) gives

$$\frac{d \ln \bar{P}_F(s)}{ds} = \frac{d}{ds} \left(\mu(s) - s\dot{\mu}(s) \right) = -s\ddot{\mu}(s). \quad (2.455)$$

Let $s^{(n)}$ and $\hat{P}_F^{(n)}$ denote the values of s and \hat{P}_F at the n th iteration. In (2.452), we set $s_0 = s^{(n)}$, $s = s^{(n+1)}$, $P_F(s_0) = \hat{P}_F^{(n)}$, and $P_F(s) = P_F^*$. Then s can be updated as follows

$$s^{(n+1)} = s^{(n)} + \frac{\ln P_F^* - \ln \hat{P}_F^{(n)}}{s^{(n)} \ddot{\mu}(s^{(n)})}, \quad (2.456)$$

and $\gamma^{(n+1)}$ is given by

$$\gamma^{(n+1)} = \dot{\mu}(s^{(n+1)}). \quad (2.457)$$

We iterate until convergence in \hat{P}_F as specified in (2.451).

Note that, at each step in the iteration, the tilt in the marginal density changes per (2.456). Also note that we have used several approximations, so there is no guarantee that the algorithm will converge.

Example 2.19 (continuation of Example 2.18). We consider the same model as in Example 2.18. We specify $\alpha = 0.1$, $c = 2$, $N = 20$, and $P_F^* = 10^{-8}$. In Figure 2.46, we show the iteration for one trial. The simulated values are slightly less than the approximate values and it converges in three iterations. ■

Examples 2.18 and 2.19 are representative of the class of problems where we can find an analytic expression for $\mu(s)$ but we do not know how to find $p_{l_*|H_0}(L|H_0)$ and $p_{l_*|H_1}(L|H_1)$, and therefore cannot evaluate P_F and P_M . The approximate expressions used in Example 2.18 and the iterative algorithm used in Example 2.19 appear to provide efficient techniques for simulating this class of problems.

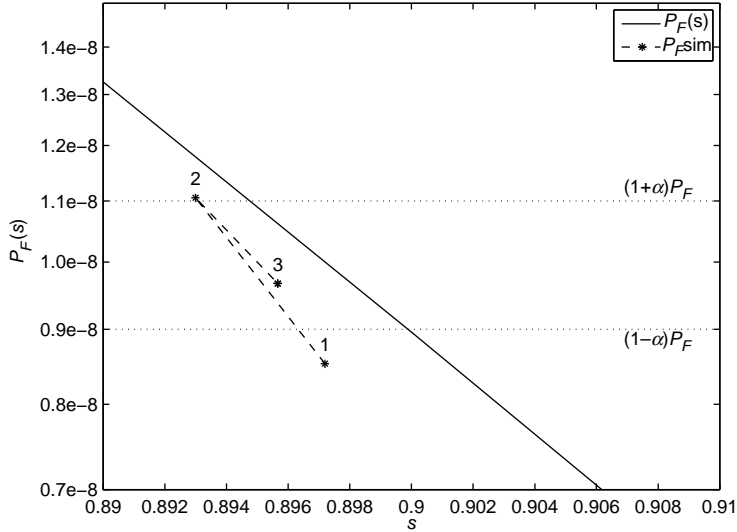


Figure 2.46: Convergence of iterative algorithm.

Example 2.14 in Section 2.4 is representative of the class of problems where we have to find $\mu(s)$ numerically. The approximate and iterative algorithms are also applicable to this class of problems (see Problem 2.5.6).

There are a number of references on adaptive importance sampling techniques. Srinivasan [Sri02] and Smith et al. [SSG97] have a discussion of various techniques and a list of references.

2.5.3 Summary

In this section, we have developed an approach to importance sampling that utilizes tilted densities to specify the probability density to be used for simulation. The technique is also referred to as exponential twisting or large deviation theory in the literature. Although we did not include the derivation, one can show that this approach is asymptotically efficient as $N \rightarrow \infty$ or $P_F \rightarrow 0$ (e.g., [SB90]).

By focusing on the log-likelihood ratio (which is optimal for our model), we were able to find $\mu(s)$ using the probability densities of a sufficient statistic \mathbf{X} on H_0 and H_1 . This enabled us to solve problems where $p_{l_*|H_0}(L|H_0)$ and $p_{l_*|H_1}(L|H_1)$ were difficult to find. This result was exceedingly useful when the components of \mathbf{R} were statistically independent and we could tilt the marginal probability densities. This approach allowed us to achieve the required accuracy and confidence intervals with K_{IS} values that were typically lower by factors of up to 10^{10} compared with classical Monte Carlo techniques.

We did not consider the simulation of suboptimal tests or tests that simply compared an arbitrary statistic to a threshold. All of the tilting ideas carry over, but the $\mu(s)$ relation in (2.375) no longer applies.

Our goal in this section was to provide an introduction to importance sampling that focused on the use of tilted densities. It provides adequate background to simulate most of the detection problems that we will encounter in the text.

2.6 SUMMARY

In this chapter, we have derived the essential detection theory results that provide the basis for much of our work in the remainder of the book.

We began our discussion in Section 2.2 by considering the simple binary hypothesis testing problem. There were several key results:

1. Using either a Bayes criterion or a Neyman–Pearson criterion, we find that the optimum test is a likelihood ratio test,

$$\Lambda(\mathbf{R}) = \frac{p_{\mathbf{r}|H_1}(\mathbf{R}|H_1)}{p_{\mathbf{r}|H_0}(\mathbf{R}|H_0)} \stackrel{H_1}{\geq} \eta.$$

Thus, regardless of the dimensionality of the observation space, the test consists of comparing a scalar variable $\Lambda(\mathbf{R})$ with a threshold.

2. In many cases, construction of the LRT can be simplified if we can identify a sufficient statistic. Geometrically, this statistic is just that coordinate in a suitable coordinate system that describes the observation space that contains *all* the information necessary to make a decision (see (2.74)–(2.76)).
3. A complete description of the LRT performance was obtained by plotting the conditional probabilities P_D and P_F as the threshold η was varied. The resulting ROC could be used to calculate the Bayes risk for any set of costs. In many cases, only one value of the threshold is of interest and a complete ROC is not necessary.

In Section 2.3, we introduced the M hypotheses problem. The key results were

1. The dimension of the decision space is no more than $M - 1$. The boundaries of the decision regions are hyperplanes in the $(\Lambda_1, \dots, \Lambda_{M-1})$ plane.
2. The optimum test is straightforward to find. From (2.156), we compute

$$\beta_i(\mathbf{R}) = \sum_{j=0}^{M-1} C_{ij} \Pr(H_j|\mathbf{R}), \quad i = 0, 1, \dots, M-1,$$

and choose the smallest. We shall find however, when we consider specific examples that the error probabilities are frequently difficult to compute.

3. A particular test of importance is the minimum total probability of error test. Here we compute the *a posteriori* probability of each hypothesis $\Pr(H_i|\mathbf{R})$ and choose the largest.

In Sections 2.2 and 2.3, we dealt primarily with problems in which we could derive the structure of the optimum test and obtain relatively simple analytic expressions for the receiver operating characteristic or the error probability. In Section 2.4, we developed bounds and approximate expressions for the error probabilities for the large group of problems where an exact solution is difficult. The key function in these results was the logarithm of the moment generating function of the likelihood ratio. From (2.204)

$$\mu(s) = \ln \int_{-\infty}^{\infty} [p_{\mathbf{r}|H_1}(\mathbf{R}|H_1)]^s [p_{\mathbf{r}|H_0}(\mathbf{R}|H_0)]^{1-s} d\mathbf{R}.$$

The function $\mu(s)$ plays a central role in all of the bounds and approximate expressions that are derived in Section 2.4. It is straightforward to calculate when the components of \mathbf{r} on the two hypotheses are statistically independent. Then,

$$\mu_i(s) = \ln \int_{-\infty}^{\infty} [p_{r_i|H_1}(R_i|H_1)]^s [p_{r_i|H_0}(R_i|H_0)]^{1-s} dR_i, \quad i = 1, \dots, N,$$

and

$$\mu(s) = \sum_{i=1}^N \mu_i(s).$$

We have introduced $\mu(s)$ early in the text because of the central role it plays in the analysis of non-Gaussian models.

In many applications of interest, it is necessary to simulate the detection algorithm in order to evaluate the performance. In Section 2.5, we gave a brief introduction to Monte Carlo simulation. A key issue is the number of trials needed to have a desired level of confidence in the result. In most systems of interest, the desired P_F is very small (e.g., $P_F \leq 10^{-6}$ is frequently required). In these cases, the number of trials required to obtain a reasonable confidence level is prohibitively large. We introduced a technique called “importance sampling” that provided a dramatic reduction in the number of trials. The key function in our approach was $\mu(s)$ developed in Section 2.4.

In this chapter, we confined our discussion to the decision problem in which the transition probabilities $p_{\mathbf{r}|H_j}(\mathbf{R}|H_j)$ were known. This is referred to as *simple* hypothesis testing. In many applications, $p_{\mathbf{r}|H_j, \theta}(\mathbf{R}|H_j, \theta)$ depends on an unknown vector parameter θ that may be random or nonrandom. This is referred to as *composite* hypothesis testing and we study it in Chapter 4.

In this chapter, we have developed many of the key results in detection theory. All of our discussion dealt with arbitrary probability densities. A large number of important signal processing applications in communications, radar and sonar can be modeled assuming that $p_{\mathbf{r}|H_j}(\mathbf{R}|H_j)$, $j = 0, \dots, M - 1$ is a multivariate Gaussian probability density. In Chapter 3, we consider this model in detail.

2.7 PROBLEMS

The problems are divided into sections corresponding to the major sections in the chapter. For example, section P2.2 pertains to text material in Section 2.2. In sections in which it is appropriate the problems are divided into topical groups.

P2.2 Simple Binary Hypothesis Tests

SIMPLE BINARY TESTS

Problem 2.2.1. Consider the following binary hypothesis testing problem:

$$\begin{aligned} H_1 &: r = s + n, \\ H_0 &: r = n, \end{aligned}$$

where s and n are independent random variables:

$$p_s(S) = \begin{cases} ae^{-as} & S \geq 0 \\ 0 & S < 0 \end{cases}$$

and

$$p_n(N) = \begin{cases} be^{-bN} & N \geq 0 \\ 0 & N < 0. \end{cases}$$

1. Prove that the likelihood ratio test reduces to

$$R \stackrel{H_1}{\gtrless} \stackrel{H_0}{\gamma}.$$

2. Find γ for the optimum Bayes test as a function of the costs and *a priori* probabilities.
3. Now assume that we need a Neyman–Pearson test. Find γ as a function of P_F , where

$$P_F \triangleq \Pr(\text{say } H_1 | H_0 \text{ is true}).$$

Problem 2.2.2. The two hypotheses are

$$\begin{aligned} H_1 &: p_r(R) = \frac{1}{2} \exp(-|R|), \\ H_0 &: p_r(R) = \frac{1}{\sqrt{2\pi}} \exp\left(-\frac{1}{2} R^2\right). \end{aligned}$$

(This is an example of the Generalized Gaussian density with $\alpha_0 = 1$, $b_0 = 1$, and $\alpha_1 = 2$, $b_1 = \sqrt{2}$.)

1. Find the likelihood ratio $\Lambda(R)$.
2. The test is

$$\Lambda(R) \stackrel{H_1}{\gtrless} \stackrel{H_0}{\eta}.$$

Compute the decision regions for various values of η .

Problem 2.2.3. The random variable x is $N(0, \sigma^2)$. It is passed through one of two nonlinear transformations.

$$\begin{aligned} H_1 &: y = x^2 \\ H_0 &: y = x^3. \end{aligned}$$

Find the LRT.

Problem 2.2.4. The random variable x is $N(m, \sigma^2)$. It is passed through one of two nonlinear transformations.

$$\begin{aligned} H_1 : y &= e^x, \\ H_0 : y &= x^2. \end{aligned}$$

Find the LRT.

Problem 2.2.5. Consider the following hypothesis testing problem. There are K independent observations:

$$\begin{aligned} H_1 : r_i &\text{ is Gaussian, } N(0, \sigma_1^2) \quad i = 1, 2, \dots, K \\ H_0 : r_i &\text{ is Gaussian, } N(0, \sigma_0^2) \quad i = 1, 2, \dots, K, \end{aligned}$$

where $\sigma_0^2 < \sigma_1^2$.

1. Compute the likelihood ratio.
2. Assume that the threshold is η :

$$\Lambda(\mathbf{R}) \stackrel{H_1}{\underset{H_0}{\gtrless}} \eta.$$

Show that a sufficient statistic is $l(\mathbf{R}) = \sum_{i=1}^K R_i^2$. Compute the threshold γ for the test

$$l(\mathbf{R}) \stackrel{H_1}{\underset{H_0}{\gtrless}} \gamma$$

in terms of η , σ_0^2 , and σ_1^2 .

3. Define

$$\begin{aligned} P_F &= \Pr(\text{choose } H_1 | H_0 \text{ is true}), \\ P_M &= \Pr(\text{choose } H_0 | H_1 \text{ is true}). \end{aligned}$$

Find an expression for P_F and P_M .

4. Plot the ROC for $K = 1$, $\sigma_1^2 = 2$, and $\sigma_0^2 = 1$.
5. What is the threshold for the minimax criterion when $C_M = C_F$ and $C_{00} = C_{11} = 0$?

Problem 2.2.6. The observation r is defined in the following manner:

$$\begin{aligned} H_1 : r &= bm_1 + n, \\ H_0 : r &= n, \end{aligned}$$

where b and n are independent zero-mean Gaussian variables with variances σ_b^2 and σ_n^2 , respectively.

1. Find the LRT and draw a block diagram of the optimum processor.
2. Draw the ROC.
3. Assume that the two hypotheses are equally likely. Use the criterion of minimum probability of error. What is the $\Pr(\epsilon)$?

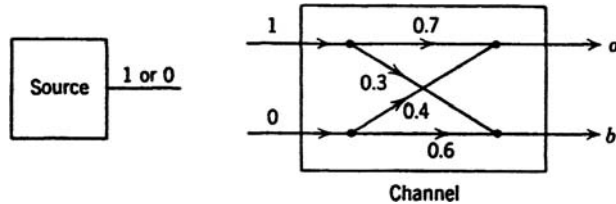


Figure P2.1: Binary communication channel.

Problem 2.2.7. One of two possible sources supplies the inputs to the simple communication channel as shown in Figure P2.1.

Both sources put out either 1 or 0. The numbers on the line are the channel transition probabilities; that is,

$$\Pr(a \text{ out} | 1 \text{ in}) = 0.7.$$

The source characteristics are

$$\text{Source 1: } \Pr(1) = 0.5 \quad \Pr(0) = 0.5$$

$$\text{Source 2: } \Pr(1) = 0.6 \quad \Pr(0) = 0.4.$$

To put the problem in familiar notation, define

- (a) False alarm—say source 2 when source 1 is present;
- (b) Detection—say source 2 when source 2 is present.

1. Compute the ROC of a test that maximizes P_D subject to the constraint that $P_F = \alpha$.
2. Describe the test procedure in detail for $\alpha = 0.25$.

Problem 2.2.8. The probability densities on the two hypotheses are

$$H_i : p_{x|H_i}(X|H_i) = \frac{1}{\pi [1 + (X - a_i)^2]} \quad i = 0, 1; -\infty < X < \infty.$$

where $a_0 = 0$ and $a_1 = 1$.

1. Find the LRT.
2. Plot the ROC.

Problem 2.2.9. Consider a simple coin tossing problem:

$$H_1 : \text{heads are up: } \Pr[H_1] \triangleq P_1,$$

$$H_0 : \text{tails are up: } \Pr[H_0] \triangleq P_0 < P_1.$$

N independent tosses of the coin are made. Show that the number of observed heads N_H is a sufficient statistic for making a decision between the two hypotheses.

Problem 2.2.10. A sample function of a simple Poisson counting process $N(t)$ is observed over the interval T :

$$\begin{aligned} H_1 &: \text{The mean rate is } k_1 : \Pr(H_1) = \frac{1}{2}, \\ H_0 &: \text{The mean rate is } k_0 : \Pr(H_0) = \frac{1}{2}. \end{aligned}$$

1. Prove that the number of events in the interval T is a “sufficient statistic” to choose hypothesis H_0 or H_1 .
2. Assuming equal costs for the possible errors, derive the appropriate likelihood ratio test and the threshold.
3. Find an expression for the probability of error.

Problem 2.2.11. Let

$$y = \sum_{i=0}^n x_i,$$

where the x_i are statistically independent random variables with a Gaussian density $N(0, \sigma^2)$. The number of variables in the sum is a random variable with a Poisson distribution:

$$\Pr(n = k) = \frac{\lambda^k}{k!} e^{-\lambda}, \quad k = 0, 1, \dots$$

We want to decide between the two hypotheses,

$$\begin{aligned} H_1 &: n \leq 1 \\ H_0 &: n > 1. \end{aligned}$$

Write an expression for the LRT.

Problem 2.2.12. Randomized tests. Our basic model of the decision problem in the text did not permit randomized decision rules. We can incorporate them by assuming that at each point \mathbf{R} in Z we say H_1 with probability $\phi(\mathbf{R})$ and say H_0 with probability $1 - \phi(\mathbf{R})$. The model in the text is equivalent to setting $\phi(\mathbf{R}) = 1$ for all \mathbf{R} in Z_1 and $\phi(\mathbf{R}) = 0$ for all \mathbf{R} in Z_0 .

1. We consider the Bayes criterion first. Write the risk for the above decision model.
2. Prove that an LRT minimizes the risk and a randomized test is *never* necessary.
3. Prove that the risk is constant over the interior of any straight-line segment on an ROC. Because straight-line segments are generated by randomized tests, this is an alternate proof of the result in Part 2.
4. Consider the Neyman–Pearson criterion. Prove that the optimum test always consists of either
 - (i) an ordinary LRT with $P_F = \alpha$ or
 - (ii) a probabilistic mixture of *two* ordinary likelihood ratio tests constructed as follows: Test 1: $\Lambda(\mathbf{R}) \stackrel{H_1}{\geq} \eta$ gives $P_F = \alpha^+$. Test 2: $\Lambda(\mathbf{R}) \stackrel{H_1}{>} \eta$ gives $P_F = \alpha^-$, where $[\alpha^-, \alpha^+]$ is the smallest interval containing α . $\phi(\mathbf{R})$ is 0 or 1 except for those \mathbf{R} where $\phi(\mathbf{R}) = \eta$. (Find $\phi(\mathbf{R})$ for this set.)

MATHEMATICAL PROPERTIES

Problem 2.2.13. The random variable $\Lambda(\mathbf{R})$ is defined by (2.13) and has a different probability density on H_1 and H_0 . Prove the following:

1. $E(\Lambda^n | H_1) = E(\Lambda^{n+1} | H_0)$.
2. $E(\Lambda | H_0) = 1$.
3. $E(\Lambda | H_1) - E(\Lambda | H_0) = \text{Var}(\Lambda | H_0)$.

Problem 2.2.14. Consider the random variable Λ . In (2.128)–(2.129), we showed that

$$p_{\Lambda|H_1}(X|H_1) = X p_{\Lambda|H_0}(X|H_0).$$

1. Verify this relation by direct calculation of $p_{\Lambda|H_1}(\cdot)$ and $p_{\Lambda|H_0}(\cdot)$ for the densities in Examples 2.1 and 2.5.
2. We saw that the performance of the test in Example 2.5 was completely characterized by d^2 . Show that

$$d^2 = \ln[1 + \text{Var}(\Lambda | H_0)].$$

Problem 2.2.15. The function $\text{erfc}_*(X)$ is defined in (2.83).

1. Integrate by parts to establish the bound

$$\frac{1}{\sqrt{2\pi}X} \left(1 - \frac{1}{X^2}\right) \exp\left(-\frac{X^2}{2}\right) < \text{erfc}_*(X) < \frac{1}{\sqrt{2\pi}X} \exp\left(-\frac{X^2}{2}\right) \quad X > 0.$$

2. Generalize part 1 to obtain the asymptotic series

$$\text{erfc}_*(X) = \frac{1}{\sqrt{2\pi}X} e^{-X^2/2} \left[1 + \sum_{m=1}^{n-1} (-1)^m \frac{1 \cdot 3 \cdots (2m-1)}{X^{2m}} + R_n \right].$$

The remainder is less than the magnitude of the $n+1$ term and is the same sign. *Hint:* Show that the remainder is

$$R_n = \left[(-1)^{n+1} \frac{1 \cdot 3 \cdots (2n-1)}{X^{2n+2}} \right] \theta,$$

where

$$\theta = \int_0^\infty e^{-t} \left(1 + \frac{2t}{X^2}\right)^{-n-\frac{1}{2}} dt < 1.$$

3. Assume that $X = 3$. Calculate a simple bound on the *percentage* error when $\text{erfc}_*(3)$ is approximated by the first n terms in the asymptotic series. Evaluate this percentage error for $n = 2, 3, 4$ and compare the results. Repeat for $X = 5$.

Problem 2.2.16.

1. Prove

$$\text{erfc}_*(X) < \frac{1}{2} \exp\left(-\frac{X^2}{2}\right) \quad X > 0.$$

Hint: Show

$$[\text{erfc}_*(X)]^2 = \Pr(x \geq X, y \geq Y) < \Pr(x^2 + y^2 \geq 2X^2),$$

where x and y are independent zero-mean Gaussian variables with unit variance.

2. For what values of X is this bound better than (2.89)?

HIGHER DIMENSIONAL DECISION REGIONS

A simple binary test can always be reduced to a one-dimensional decision region. In many cases, the results are easier to interpret in two or three dimensions. Some typical examples are illustrated in this section.

Problem 2.2.17. The joint probability density of the random variables x_1 and x_2 on H_1 and H_0 is

$$\begin{aligned} H_1 : p_{x_1, x_2 | H_1}(X_1, X_2 | H_1) &= \frac{1}{4\pi\sigma_1\sigma_0} \left[\exp\left(-\frac{X_1^2}{2\sigma_1^2} - \frac{X_2^2}{2\sigma_0^2}\right) + \exp\left(-\frac{X_1^2}{2\sigma_0^2} - \frac{X_2^2}{2\sigma_1^2}\right) \right], \\ H_0 : p_{x_1, x_2 | H_0}(X_1, X_2 | H_0) &= \frac{1}{2\pi\sigma_0^2} \exp\left(-\frac{X_1^2}{2\sigma_0^2} - \frac{X_2^2}{2\sigma_0^2}\right), \end{aligned}$$

where $-\infty < X_1, X_2 < \infty$.

1. Find the LRT.
2. Write an exact expression for P_D and P_F . Upper and lower bound P_D and P_F by modifying the region of integration in the exact expression.

Problem 2.2.18. The joint probability density of the random variables $x_i; i = 1, 2, \dots, M$ on H_1 and H_0 is

$$\begin{aligned} H_1 : p_{\mathbf{x}|H_1}(\mathbf{X}|H_1) &= \sum_{k=1}^M p_k \frac{1}{(2\pi\sigma^2)^{M/2}} \exp\left[-\frac{(X_k - m)^2}{2\sigma^2}\right] \prod_{i \neq k}^M \exp\left(-\frac{X_i^2}{2\sigma^2}\right), \\ H_0 : p_{\mathbf{x}|H_0}(\mathbf{X}|H_0) &= \prod_{i=1}^M \frac{1}{\sqrt{2\pi}\sigma} \exp\left(-\frac{X_i^2}{2\sigma^2}\right), \end{aligned}$$

where $-\infty < X_i < \infty$, and

$$\sum_{k=1}^M p_k = 1.$$

1. Find the LRT.
2. Draw the decision regions for various values of η in the X_1, X_2 -plane for the special case in which $M = 2$ and $p_1 = p_2 = \frac{1}{2}$.
3. Find an upper and lower bound to P_F and P_D by modifying the regions of integration.

Problem 2.2.19. The probability density of r_i on the two hypotheses is

$$p_{r_i|H_k}(R_i | H_k) = \frac{1}{\sqrt{2\pi}\sigma_k} \exp\left[-\frac{(R_i - m_k)^2}{2\sigma_k^2}\right] \quad \begin{array}{ll} i = 1, 2, \dots, N \\ k = 0, 1. \end{array}$$

The observations are independent.

1. Find the LRT. Express the test in terms of the following quantities:

$$l_\alpha = \sum_{i=1}^N R_i,$$

$$l_\beta = \sum_{i=1}^N R_i^2.$$

2. Draw the decision regions in the l_α, l_β -plane for the case in which

$$2m_0 = m_1 > 0$$

$$2\sigma_1 = \sigma_0.$$

Problem 2.2.20 (continuation of Problem 2.2.19).

1. Consider the special case

$$m_0 = 0,$$

$$\sigma_0 = \sigma_1.$$

Draw the decision regions and compute the ROC.

2. Consider the special case

$$m_0 = m_1 = 0,$$

$$\sigma_1^2 = \sigma_s^2 + \sigma_n^2,$$

$$\sigma_0 = \sigma_n.$$

Draw the decision regions.

Problem 2.2.21. A shell is fired at one of two targets: Under H_1 the point of aim has coordinates x_1, y_1, z_1 ; under H_0 it has coordinates x_0, y_0, z_0 . The distance of the actual landing point from the point of aim is a zero-mean Gaussian variable, $N(0, \sigma^2)$, in each coordinate. The variables are independent. We wish to observe the point of impact and guess which hypothesis is true.

1. Formulate this as a hypothesis testing problem and compute the likelihood ratio. What is the simplest sufficient statistic? Is the ROC in Figure 2.12a applicable? If so, what value of d^2 do we use?
2. Now include the effect of time. Under H_k the desired explosion time is $t_k; k = 1, 2$. The distribution of the actual explosion time is

$$p_{\tau|H_k}(\tau) = \frac{1}{\sqrt{2\pi}\sigma_t} \exp\left(-\frac{(\tau - t_k)^2}{2\sigma_t^2}\right) \quad -\infty < \tau < \infty \quad k = 1, 2.$$

Find the LRT and compute the ROC.

Problem 2.2.22. Consider the model in Examples 2.2 and 2.6.

1. Plot P_M versus N for $P_F = 10^{-6}$.
2. Define N_{opt} as the value of N that gives the minimum P_M for a given

$$\text{SNR}_T \triangleq N\sigma_s^2/\sigma_n^2.$$

Plot N_{opt} versus SNR_T for $P_F = 10^{-2}, 10^{-4}$, and 10^{-6} .

3. Plot $P_M(N_{\text{opt}})$ versus SNR_T for $P_F = 10^{-2}, 10^{-4}$, and 10^{-6} .

IID MODEL

The following problems assume the IID model in (2.39)–(2.43) and Figure 2.7.

Problem 2.2.23. Consider the Generalized Gaussian model in Example 2.4. Plot $\ln \Lambda(R_i)$ for $\alpha = 1, 1.1, 1.2, \dots, 1.9$.

Problem 2.2.24. [Kay98] The observations on the two hypotheses are

$$\begin{aligned} H_1 : r_i &= m + n_i & i = 1, \dots, N \\ H_0 : r_i &= n_i & i = 1, \dots, N, \end{aligned}$$

where $p_{n_i}(N_i)$ is Cauchy

$$p_{n_i}(N_i) = \frac{1}{\pi(1 + N_i^2)} \quad -\infty < N_i < \infty.$$

Plot $\ln \Lambda(R_i)$.

Problem 2.2.25. The observations on the two hypotheses are

$$\begin{aligned} H_1 : r_i &= m + n_i, & i = 1, \dots, N, \\ H_0 : r_i &= n_i, & i = 1, \dots, N, \end{aligned}$$

where n_i is a sample from a Gaussian mixture density

$$p_{n_i}(N_i) = \alpha \frac{1}{\sqrt{2\pi}\sigma_1} \exp\left(-\frac{1}{2} \frac{N_i^2}{\sigma_1^2}\right) + (1 - \alpha) \frac{1}{\sqrt{2\pi}\sigma_2} \exp\left(-\frac{1}{2} \frac{N_i^2}{\sigma_2^2}\right)$$

for $0 \leq \alpha \leq 1$.

(a) Assume $m = 1, \sigma_1^2 = 1$, and three values of σ_2^2 : 2, 10, and 20. Plot $\ln \Lambda(R_i)$ for $\alpha = 0, 0.1, \dots, 1.0$.

(b) Fix $\alpha = 0.5, m = 1, \sigma_1^2 = 1$. Plot $\ln \Lambda(R_i)$ for various σ_2^2/σ_1^2 .

Problem 2.2.26. The observations on the two hypotheses are:

$$\begin{aligned} H_1 : r_i &= m + n_i, & i = 1, \dots, N, \\ H_0 : r_i &= n_i & i = 1, \dots, N. \end{aligned}$$

The noise n_i is a sum of two statistically independent noise terms

$$n_i = w_i + x_i, \quad i = 1, \dots, N,$$

where w_i has a Weibull density, defined in (2.274),

$$p_{w_i}(W_i) = \frac{\alpha}{b} \left(\frac{W_i}{b}\right)^{\alpha-1} e^{-(W_i/b)^\alpha}, \quad W_i \geq 0; i = 1, 2, \dots, N,$$

and x_i has a Rayleigh density

$$p_{x_i}(X_i) = \frac{X_i}{\sigma_x^2} \exp\left(-\frac{X_i^2}{2\sigma_x^2}\right), \quad X_i \geq 0; i = 1, 2, \dots, N.$$

The n_i are statistically independent.

Notice that the Weibull density corresponds to the Rayleigh density when $\alpha = 2$ and $b = \sqrt{2}\sigma_x$. The variance of w_i is given by (2.276). We will encounter this model later when we sample the output of a bandpass square-law detector.

- (a) Assume $\alpha = b = 3$. The resulting density is shown in Figure 2.35. Assume $m/\sigma_x^2 = 10$. Find $p_{n_i}(N_i)$ by numerically convolving $p_{r_i}(R_i)$ and $p_{x_i}(X_i)$ for three variance ratios, $\frac{\sigma_w^2}{\sigma_x^2} = 0.1, 1.0, 10.0$.
- (b) Plot $\ln \Lambda(R_i)$ for the values in part (a).

Problem 2.2.27. Consider the Generalized Gaussian model in Example 2.4. Plot $\ln \Lambda(R_i)$ for $\alpha < 1$. Explain your results.

Problem 2.2.28. Extend the results in (2.42)–(2.43) where the observations are vectors \mathbf{R}_i that are IID. Explain your results.

P2.3 M Hypotheses

Problem 2.3.1.

1. Verify that the M hypothesis Bayes test always leads to a decision space whose dimension is less than or equal to $M - 1$.
2. Assume that the coordinates of the decision space are

$$\Lambda_k(\mathbf{R}) \triangleq \frac{p_{\mathbf{r}|H_k}(\mathbf{R}|H_k)}{p_{\mathbf{r}|H_0}(\mathbf{R}|H_0)} \quad k = 1, 2, \dots, M - 1.$$

Verify that the decision boundaries are hyperplanes.

Problem 2.3.2. The observed random variable r has a Gaussian density on the three hypotheses,

$$p_{r|H_k}(R|H_k) = \frac{1}{\sqrt{2\pi}\sigma_k} \exp\left[-\frac{(R - m_k)^2}{2\sigma_k^2}\right] \quad -\infty < R < \infty \quad k = 1, 2, 3,$$

where the parameter values on the three hypotheses are,

$$\begin{aligned} H_1 : m_1 &= 0, & \sigma_1^2 &= \sigma_\alpha^2, \\ H_2 : m_2 &= m, & \sigma_2^2 &= \sigma_\alpha^2 \quad (m > 0), \\ H_3 : m_3 &= 0, & \sigma_3^2 &= \sigma_\beta^2 \quad (\sigma_\beta^2 > \sigma_\alpha^2). \end{aligned}$$

The three hypotheses are equally likely and the criterion is minimum $\Pr(\epsilon)$.

1. Find the optimum Bayes test.
2. Draw the decision regions on the R -axis for the special case,

$$\begin{aligned} \sigma_\beta^2 &= 2\sigma_\alpha^2, \\ \sigma_\alpha^2 &= m^2. \end{aligned}$$

3. Compute the $\Pr(\epsilon)$ for this special case.

Problem 2.3.3. The probability density of \mathbf{r} on the three hypotheses is

$$p_{r_1, r_2 | H_k}(R_1, R_2 | H_k) = (2\pi\sigma_{1k}\sigma_{2k})^{-1} \exp\left[-\frac{1}{2}\left(\frac{R_1^2}{\sigma_{1k}^2} + \frac{R_2^2}{\sigma_{2k}^2}\right)\right] \quad -\infty < R_1, R_2 < \infty \quad k = 1, 2, 3,$$

where

$$\begin{aligned} \sigma_{11}^2 &= \sigma_n^2, & \sigma_{21}^2 &= \sigma_n^2, \\ \sigma_{12}^2 &= \sigma_s^2 + \sigma_n^2, & \sigma_{22}^2 &= \sigma_n^2, \\ \sigma_{13}^2 &= \sigma_n^2, & \sigma_{23}^2 &= \sigma_s^2 + \sigma_n^2. \end{aligned}$$

The cost matrix is

$$\begin{bmatrix} 0 & 1 & 1 \\ 1 & 0 & \alpha \\ 1 & \alpha & 0 \end{bmatrix},$$

where $0 \leq \alpha < 1$ and $\Pr(H_2) = \Pr(H_3) \triangleq p$. Define $l_1 = R_1^2$ and $l_2 = R_2^2$.

1. Find the optimum test and indicate the decision regions in the l_1, l_2 -plane.
2. Write an expression for the error probabilities. (Do not evaluate the integrals.)
3. Verify that for $\alpha = 0$ this problem reduces to Problem 2.2.17.

Problem 2.3.4. On H_k the observation is the value of a Poisson random variable

$$\Pr(r = n) = \frac{k_m^n}{n!} e^{-k_m}, \quad m = 1, 2, \dots, M,$$

where $k_m = mk$. The hypotheses are equally likely and the criterion is minimum $\Pr(\epsilon)$.

1. Find the optimum test.
2. Find a simple expression for the boundaries of the decision regions and indicate how you would compute the $\Pr(\epsilon)$.

Problem 2.3.5. Assume that the received vector on each of the three hypotheses is

$$\begin{aligned} H_0 : \mathbf{r} &= \mathbf{m}_0 + \mathbf{n}, \\ H_1 : \mathbf{r} &= \mathbf{m}_1 + \mathbf{n}, \\ H_2 : \mathbf{r} &= \mathbf{m}_2 + \mathbf{n}, \end{aligned}$$

where

$$\mathbf{r} \triangleq \begin{bmatrix} r_1 \\ r_2 \\ r_3 \end{bmatrix} \quad \mathbf{m}_i \triangleq \begin{bmatrix} m_{i1} \\ m_{i2} \\ m_{i3} \end{bmatrix} \quad \mathbf{n} \triangleq \begin{bmatrix} n_1 \\ n_2 \\ n_3 \end{bmatrix}.$$

The \mathbf{m}_i are known vectors, and the components of \mathbf{n} are statistically independent, zero-mean Gaussian random variables with variance σ^2 .

1. Using the results in the text, express the Bayes test in terms of two sufficient statistics:

$$l_1 = \sum_{i=1}^3 c_i r_i,$$

$$l_2 = \sum_{i=1}^3 d_i r_i.$$

Find explicit expressions for c_i and d_i . Is the solution unique?

2. Sketch the decision regions in the l_1, l_2 -plane for the particular cost assignment:

$$C_{00} = C_{11} = C_{22} = 0,$$

$$C_{12} = C_{21} = C_{01} = C_{10} = \frac{1}{2}C_{02} = \frac{1}{2}C_{20} > 0.$$

P2.4 Performance Bounds and Approximations

Problem 2.4.1. Consider the binary test with N independent observations r_i , where

$$p_{r_i|H_k}(R_i|H_k) = N(m_k, \sigma_k^2) \quad k = 0, 1 \\ i = 1, 2, \dots, N.$$

Find $\mu(s)$, $\dot{\mu}(s)$, and $\ddot{\mu}(s)$.

Problem 2.4.2 (continuation of Problem 2.4.1). Consider the special case in which

$$m_0 = 0, \\ \sigma_0^2 = \sigma_n^2,$$

and

$$\sigma_1^2 = \sigma_s^2 + \sigma_n^2.$$

1. Find $\mu(s)$, $\dot{\mu}(s)$, and $\ddot{\mu}(s)$.
2. Assuming equally likely hypotheses, find an upper bound on the minimum $\Pr(\epsilon)$.
3. With the assumption in part 2, find an approximate expression for the $\Pr(\epsilon)$ that is valid for large N .

Problem 2.4.3. We derived the Chernoff bound in (2.217) by using tilted densities. This approach prepared us for the central limit theorem argument in the second part of our discussion. If we are interested only in (2.217), a much simpler derivation is possible.

1. Consider a function of the random variable x that we denote as $f(x)$. Assume

$$f(x) \geq 0, \quad \text{all } x \\ f(x) \geq f(X_0) > 0, \quad \text{all } x \geq X_0.$$

Prove

$$\Pr[x \geq X_0] \leq \frac{E[f(x)]}{f(X_0)}.$$

2. Now let

$$f(x) = e^{sx}, \quad s \geq 0,$$

and

$$X_0 = \gamma.$$

Use the result in part 1 to derive (2.212). What restrictions on γ are needed to obtain (2.217)?

Problem 2.4.4. The reason for using tilted densities and Chernoff bounds is that a straightforward application of the central limit theorem gives misleading results when the region of interest is on the tail of the density. A trivial example taken from [WJ65] illustrates this point.

Consider a set of statistically independent random variables x_i that assume values 0 and 1 with equal probability. We are interested in the probability

$$\Pr \left[y_N = \frac{1}{N} \sum_{i=1}^N x_i \geq 1 \right] \triangleq \Pr[A_N].$$

(a) Define a standardized variable

$$z \triangleq \frac{y_N - \bar{y}_N}{\sigma_{y_N}}.$$

Use a central limit theorem argument to estimate $\Pr[A_N]$. Denote this estimate as $\hat{\Pr}[A_N]$.

(b) Calculate $\Pr[A_N]$ exactly.

(c) Verify that the fractional error is

$$\frac{\hat{\Pr}[A_N]}{\Pr[A_N]} \propto e^{0.19N}$$

Observe that the fractional error grows exponentially with N .

(d) Estimate $\Pr[A_N]$ using the Chernoff bound of Problem 2.4.6. Denote this estimate as $\Pr_c[A_N]$. Compute $\frac{\Pr_c[A_N]}{\Pr[A_N]}$.

Problem 2.4.5.

(a) Find $\mu(s)$, $\dot{\mu}(s)$, and $\ddot{\mu}(s)$ for the model in Problem 2.2.1.

(b) Plot an approximate ROC.

Problem 2.4.6.

(a) Find $\mu(s)$, $\dot{\mu}(s)$, and $\ddot{\mu}(s)$ for the model in Problem 2.2.23.

(b) Plot an approximate ROC.

Problem 2.4.7.

(a) Find $\mu(s)$, $\dot{\mu}(s)$, and $\ddot{\mu}(s)$ for the model in Problem 2.2.24.

(b) Plot an approximate ROC.

P2.5 Monte Carlo Simulation

Problem 2.5.1. This problem is a continuation of Example 2.16. The observations on the two hypotheses are:

$$\begin{aligned} H_1 : r_i &\sim N(m_{1i}, \sigma^2), \quad i = 1, 2, \dots, N, \\ H_0 : r_i &\sim N(m_{0i}, \sigma^2), \quad i = 1, 2, \dots, N, \end{aligned}$$

where

$$\begin{aligned} m_{1i} &= m(1 + 0.2i), \\ m_{0i} &= m(1 - 0.2i). \end{aligned}$$

Simulate the optimum detector for $N = 40$, $m = 1$, and $\sigma^2 = 1$ and compare your results to the analytic solution.

Problem 2.5.2. This problem is a continuation of Example 2.16. The observations on the two hypotheses are:

$$\begin{aligned} H_1 : r_i &\sim N(m, \sigma_i^2), \quad i = 1, 2, \dots, N, \\ H_0 : r_i &\sim N(0, \sigma_i^2), \quad i = 1, 2, \dots, N, \end{aligned}$$

where

$$\sigma_i^2 = \sigma^2(1 + 0.05i) \quad i = 1, 2, \dots, N.$$

Simulate the optimum detector for $N = 40$, $m = 1$, and $\sigma^2 = 1$ and compare your results to the analytic solution.

Problem 2.5.3. This problem is a continuation of Example 2.17. The observations on the two hypotheses are:

$$\begin{aligned} H_1 : r_i &\sim N(0, \sigma_{s_i}^2 + \sigma_n^2), \quad i = 1, 2, \dots, N, \\ H_0 : r_i &\sim N(0, \sigma_n^2), \quad i = 1, 2, \dots, N, \end{aligned}$$

where

$$\sigma_{s_i}^2 = \sigma_s^2(1 + 0.05i) \quad i = 1, 2, \dots, N$$

Simulate the optimum detector and generate a curve similar to Figure 2.42.

Problem 2.5.4. This problem is a continuation of Examples 2.16 and 2.17. The observations on the two hypotheses are:

$$\begin{aligned} H_1 : r_i &\sim N(m, \sigma_s^2 + \sigma_n^2), \quad i = 1, 2, \dots, N, \\ H_0 : r_i &\sim N(0, \sigma_s^2), \quad i = 1, 2, \dots, N. \end{aligned}$$

- (a) Find the LRT.
- (b) Simulate the optimum detector for $N = 40$ and $m = 1$. Plot a figure similar to Figure 2.42 versus σ_s^2/σ_n^2 .

Problem 2.5.5. This problem is a continuation of Example 2.14.

- (a) Find the LRT for the model in Example 2.14.
- (b) Simulate the optimum detector and compare your results to the approximate ROC computed in Example 2.14.

Problem 2.5.6. This problem is a continuation of Example 2.18.

- (a) Generalize the results in (2.436)–(2.438) to other values of a_j and b_j ; $j = 0, 1$.
- (b) Plot the results corresponding to Figures 2.43–2.45.

Problem 2.5.7. Simulate the model developed in Problems 2.2.23 and 2.4.6.

Problem 2.5.8. Simulate the model developed in Problems 2.2.24 and 2.4.7.

3

General Gaussian Detection

All of our discussion up to this point has dealt with arbitrary probability densities. In the binary detection case, $p_{\mathbf{r}|H_1}(\mathbf{R}|H_1)$ and $p_{\mathbf{r}|H_0}(\mathbf{R}|H_0)$ were not constrained to have any particular form. The models in Examples 2.1 and 2.2 were Gaussian random variables and we saw that the resulting likelihood ratio tests were easy to implement and analyze. When we begin our discussion of the waveform problem, we shall find that most of our discussions concentrate on problems in which the conditional density of \mathbf{r} is Gaussian.

A large number of important signal processing applications in communications, radar, and sonar can be modeled with Gaussian assumptions. We discuss this class of problems in detail in this chapter. The material in this chapter and the problems associated with it lay the groundwork for many of the results in the sequel.¹

In Section 3.1, we first define Gaussian random vectors. We have already used real Gaussian vectors in Chapter 2. We now introduce circular complex Gaussian vectors. We then solve the general binary Gaussian detection problem.

In Section 3.2, we consider the special case in which the covariance matrices are equal on the two hypotheses. The resulting detector is linear and an analytical expression for the performance is easy to derive. We introduce an eigendecomposition to analyze the performance and better understand the detector behavior.

In Section 3.3, we consider the special case in which the means on the two hypotheses are equal and the covariance matrices are unequal. This model leads to a quadratic detector. The eigendecomposition plays a central role in the performance analysis. For the real vector case, a numerical solution is required for the arbitrary covariance matrix case. For the circular complex vector case, an analytical solution is available.

In Section 3.4, we return to the general case in which both the means and the covariances are unequal. We can always find the optimum detector but the performance analysis is difficult.

In Section 3.5, we consider the M hypothesis problem and in Section 3.6, we summarize our results.

The chapter is long but we have tried to motivate each model by indicating where it might appear in practice.

¹This chapter is a greatly expanded version of Section 2.6 in DEMT-I. Many of the results were included in the problems in DEMT-I. Other results are special cases of results in Chapters 2–5 of DEMT-III.

3.1 DETECTION OF GAUSSIAN RANDOM VECTORS

In Sections 3.1.1 and 3.1.2, we define real Gaussian random vectors and circular complex Gaussian random vectors, respectively. In Section 3.1.3, we solve the binary detection problem for real and complex Gaussian vectors.

3.1.1 Real Gaussian Random Vectors

A real scalar Gaussian random variable has the probability density function (pdf)

$$p_r(R) = \frac{1}{\sqrt{2\pi}\sigma_r} \exp\left(-\frac{(R - m_r)^2}{2\sigma_r^2}\right), \quad (3.1)$$

and the characteristic function (CF)

$$M_r(jv) \triangleq E[e^{jvr}] = \exp\left(jvm_r - \frac{v^2\sigma_r^2}{2}\right). \quad (3.2)$$

Definition. A set of random variables r_1, r_2, \dots, r_N is defined as jointly Gaussian if all their linear combinations are Gaussian random variables.

Definition. A vector \mathbf{r}

$$\mathbf{r} = [r_1 \ r_2 \ \dots \ r_N]^T \quad (3.3)$$

is a Gaussian random vector when its components r_1, r_2, \dots, r_N are jointly Gaussian random variables. In other words if

$$z = \sum_{i=1}^N g_i r_i \triangleq \mathbf{g}^T \mathbf{r} \quad (3.4)$$

is a Gaussian random variable for all finite \mathbf{g} , then \mathbf{r} is a Gaussian random vector.

A real $N \times 1$ Gaussian random vector \mathbf{r} has a mean

$$\mathbf{m}_r \triangleq E[\mathbf{r}] \quad (3.5)$$

and a covariance matrix

$$\mathbf{K}_r \triangleq E[(\mathbf{r} - \mathbf{m}_r)(\mathbf{r} - \mathbf{m}_r)^T]. \quad (3.6)$$

The covariance matrix \mathbf{K}_r is a symmetric, rank N , positive definite matrix. The probability density function of \mathbf{r} is

$$p_r(\mathbf{R}) = \left((2\pi)^{N/2} |\mathbf{K}_r|^{1/2}\right)^{-1} \exp\left[-\frac{1}{2}(\mathbf{R} - \mathbf{m}_r)^T \mathbf{K}_r^{-1} (\mathbf{R} - \mathbf{m}_r)\right] \quad (3.7)$$

and the characteristic function is

$$M_r(j\mathbf{v}) \triangleq E[e^{j\mathbf{v}^T \mathbf{r}}] = \exp\left(j\mathbf{v}^T \mathbf{m}_r - \frac{1}{2} \mathbf{v}^T \mathbf{K}_r \mathbf{v}\right). \quad (3.8)$$

We also define a new $K \times 1$ vector \mathbf{y} that is obtained by a linear transformation of \mathbf{r} ,

$$\mathbf{y} = \mathbf{B} \mathbf{r} \quad (3.9)$$

where \mathbf{B} is a $K \times N$ matrix. The mean of \mathbf{y} is

$$\mathbf{m}_y = E[\mathbf{y}] = \mathbf{B} E[\mathbf{r}] = \mathbf{B} \mathbf{m}_r \quad (3.10)$$

and the covariance matrix is

$$\begin{aligned} \mathbf{K}_y &\triangleq E\left[(\mathbf{y} - \mathbf{m}_y)(\mathbf{y} - \mathbf{m}_y)^T\right] \\ &= E\left[(\mathbf{B} \mathbf{r} - \mathbf{B} \mathbf{m}_r)(\mathbf{r}^T \mathbf{B}^T - \mathbf{m}_r^T \mathbf{B}^T)\right] \\ &= \mathbf{B} \left(E\left[(\mathbf{r} - \mathbf{m}_r)(\mathbf{r}^T - \mathbf{m}_r^T)\right] \right) \mathbf{B}^T \\ &= \mathbf{B} \mathbf{K}_r \mathbf{B}^T. \end{aligned} \quad (3.11)$$

The characteristic function of \mathbf{y} is

$$\begin{aligned} M_y(j\mathbf{v}) &= E\left[e^{j\mathbf{v}^T \mathbf{y}}\right] = E\left[e^{j\mathbf{v}^T \mathbf{B} \mathbf{r}}\right] \\ &= \exp\left(j\mathbf{v}^T \mathbf{B} \mathbf{m}_r - \frac{1}{2}\mathbf{v}^T \mathbf{B} \mathbf{K}_r \mathbf{B}^T \mathbf{v}\right) \\ &= \exp\left(j\mathbf{v}^T \mathbf{m}_r - \frac{1}{2}\mathbf{v}^T \mathbf{K}_y \mathbf{v}\right) \end{aligned} \quad (3.12)$$

which is the characteristic function of a Gaussian random vector. Therefore, the output of a linear transformation of a Gaussian random vector is a Gaussian random vector.

3.1.2 Circular Complex Gaussian Random Vectors

In many cases, the observations are complex random variables. We denote complex quantities with a tilde $\tilde{\cdot}$, for example, \tilde{R} . We define an $N \times 1$ complex vector,

$$\tilde{\mathbf{r}} = \mathbf{r}_R + j \mathbf{r}_I. \quad (3.13)$$

If \mathbf{r}_R and \mathbf{r}_I are joint Gaussian random vectors, then the probability density of $\tilde{\mathbf{r}}$ is a $2N$ -dimensional Gaussian joint probability density. To characterize that probability density, we define a real $2N \times 1$ vector \mathbf{r}_{2N}

$$\mathbf{r}_{2N} \triangleq \begin{bmatrix} \mathbf{r}_R \\ \mathbf{r}_I \end{bmatrix}. \quad (3.14)$$

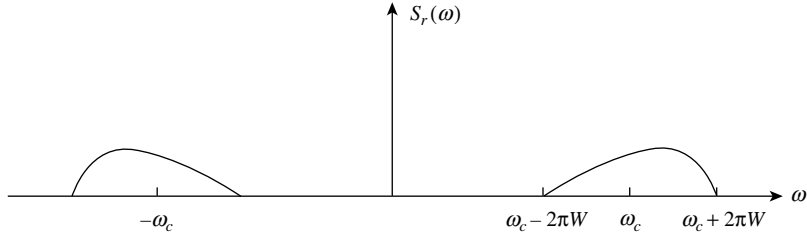


Figure 3.1: Typical spectrum for bandpass process.

We assume that \mathbf{r}_R and \mathbf{r}_I are zero-mean Gaussian random vectors with covariance matrices

$$\mathbf{K}_R \triangleq E[\mathbf{r}_R \mathbf{r}_R^T], \quad (3.15)$$

$$\mathbf{K}_I \triangleq E[\mathbf{r}_I \mathbf{r}_I^T], \quad (3.16)$$

$$\mathbf{K}_{RI} \triangleq E[\mathbf{r}_R \mathbf{r}_I^T], \quad (3.17)$$

$$\mathbf{K}_{IR} \triangleq E[\mathbf{r}_I \mathbf{r}_R^T] = \mathbf{K}_{RI}^T. \quad (3.18)$$

Then

$$\mathbf{K}_{\mathbf{r}_{2N}} = \begin{bmatrix} \mathbf{K}_R & \mathbf{K}_{RI} \\ \mathbf{K}_{IR} & \mathbf{K}_I \end{bmatrix} \quad (3.19)$$

and

$$p_{\mathbf{r}_{2N}}(\mathbf{R}_{2N}) = \frac{1}{(2\pi)^N |\mathbf{K}_{\mathbf{r}_{2N}}|^{1/2}} \exp\left(-\frac{1}{2} \mathbf{R}_{2N}^T \mathbf{K}_{\mathbf{r}_{2N}}^{-1} \mathbf{R}_{2N}\right). \quad (3.20)$$

In the general case, we must work with this probability density.

An application that occurs frequently in practice that allows for significant simplification is quadrature decomposition of a bandpass Gaussian random process followed by sampling.

We assume that the waveform is a stationary, zero-mean, bandpass Gaussian random process $r(t)$ with spectrum $S_r(\omega)$ as shown in Figure 3.1.² We perform quadrature demodulation as shown in Figure 3.2 and obtain two low-pass processes $r_c(t)$ and $r_s(t)$. We define a complex process

$$\tilde{r}(t) = r_c(t) - jr_s(t) \quad (3.21)$$

and sample it to obtain a set of N complex samples. It leads us to the definition of a circular complex Gaussian random vector that will play an important role in many applications.

²For the purposes of this discussion, we assume the reader is familiar with bandpass processes and Gaussian processes. Our goal is for the reader to understand the motivation for the definition of a circular complex Gaussian random vector. Readers without this background can simply accept the definition and will understand the rest of the chapter.

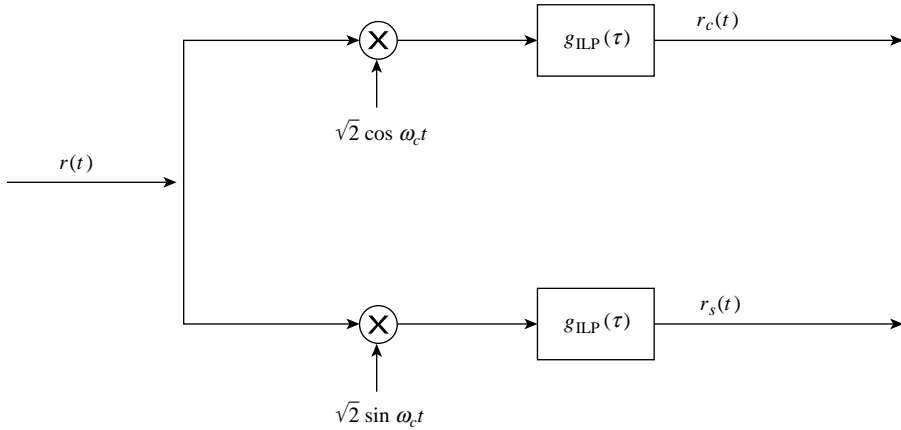


Figure 3.2: Generation of quadrature components.

If we sample the complex process $\tilde{r}(t)$ defined in (3.21), we obtain a set of N complex samples that we denote by the vector $\tilde{\mathbf{r}}$,

$$\tilde{\mathbf{r}} = [\tilde{r}_1 \quad \tilde{r}_2 \quad \dots \quad \tilde{r}_N]^T. \quad (3.22)$$

The real and imaginary parts have the following properties³:

$$\mathbf{K}_R = \mathbf{K}_I, \quad (3.23)$$

$$\mathbf{K}_{IR} = -\mathbf{K}_{RI}. \quad (3.24)$$

The \mathbf{K}_{IR} matrix must have zeros on the diagonal from (3.24). A necessary and sufficient condition for $\mathbf{K}_{IR} = \mathbf{0}$ is that the spectrum in Figure 3.1 be symmetric around the carrier frequency.

First, consider a single sample \tilde{r}_i . Suppressing the subscript, we write

$$\tilde{r} = r_R + j r_I. \quad (3.25)$$

From (3.23), the real part r_R and the imaginary part r_I have the same variance σ_r^2 . From (3.24), the covariance of r_R and r_I is zero, therefore, r_R and r_I are statistically independent. The mean and variance of \tilde{r} are

$$E[\tilde{r}] = E[r_R] + j E[r_I] = 0, \quad (3.26)$$

$$\sigma_{\tilde{r}}^2 = E[|\tilde{r}|^2] = E[r_R^2 + r_I^2] = 2\sigma_r^2. \quad (3.27)$$

We can write the joint probability density of r_R and r_I as

$$p_{r_R, r_I}(R_R, R_I) = \frac{1}{2\pi\sigma_r^2} \exp\left(-\frac{1}{2} \frac{R_R^2 + R_I^2}{\sigma_r^2}\right). \quad (3.28)$$

³We derive the properties of bandpass random processes in Appendix A of DEMT-III and summarize the results here.

This can be expressed in terms of \tilde{r} as

$$p_{\tilde{r}}(\tilde{R}) = \frac{1}{\pi\sigma_{\tilde{r}}^2} \exp\left(-\frac{|\tilde{R}|^2}{\sigma_{\tilde{r}}^2}\right), \quad (3.29)$$

which is defined to be the probability density of \tilde{r} . It is important to note that although it appears like the probability density of a scalar random variable, it should be interpreted as compact notation for the two-dimensional probability density in (3.28). The probability density in (3.28) is circularly symmetric so we refer to \tilde{r} as a *circular complex Gaussian random variable*.

The characteristic function of \tilde{r} is

$$M_{\tilde{r}}(j\tilde{v}) \triangleq E\left[\exp\left\{j\Re(\tilde{v}^*\tilde{r})\right\}\right] = \exp\left(-\frac{1}{4}|\tilde{v}|^2\sigma_{\tilde{r}}^2\right). \quad (3.30)$$

Now consider the complex vector $\tilde{\mathbf{r}} = \mathbf{r}_R + j\mathbf{r}_I$. The real and imaginary parts have the properties given in (3.23) and (3.24). The mean of $\tilde{\mathbf{r}}$ is

$$E[\tilde{\mathbf{r}}] = E[\mathbf{r}_R] + jE[\mathbf{r}_I] = \mathbf{0}, \quad (3.31)$$

and its covariance matrix is

$$\begin{aligned} \tilde{\mathbf{K}}_{\tilde{\mathbf{r}}} &= E[\tilde{\mathbf{r}}\tilde{\mathbf{r}}^H] = E[(\mathbf{r}_R + j\mathbf{r}_I)(\mathbf{r}_R^T - j\mathbf{r}_I^T)] \\ &= \mathbf{K}_R + j\mathbf{K}_{IR} - j\mathbf{K}_{RI} + \mathbf{K}_I \\ &= 2[\mathbf{K}_R + j\mathbf{K}_{IR}]. \end{aligned} \quad (3.32)$$

Note that

$$\mathbf{K}_R = \mathbf{K}_I = \frac{1}{2} \Re[\tilde{\mathbf{K}}_{\tilde{\mathbf{r}}}] \quad (3.33)$$

and

$$\mathbf{K}_{IR} = \frac{1}{2} \Im[\tilde{\mathbf{K}}_{\tilde{\mathbf{r}}}] \quad (3.34)$$

Circular complex Gaussian random vectors also have the property

$$\begin{aligned} E[\tilde{\mathbf{r}}\tilde{\mathbf{r}}^T] &= E[(\mathbf{r}_R + j\mathbf{r}_I)(\mathbf{r}_R^T + j\mathbf{r}_I^T)] \\ &= \mathbf{K}_R + j\mathbf{K}_{IR} + j\mathbf{K}_{RI} - \mathbf{K}_I \\ &= \mathbf{0}. \end{aligned} \quad (3.35)$$

The probability density function is

$$p_{\tilde{\mathbf{r}}}(\tilde{\mathbf{R}}) = \frac{1}{\pi^N |\tilde{\mathbf{K}}_{\tilde{\mathbf{r}}}|} \exp\left(-\tilde{\mathbf{R}}^H \tilde{\mathbf{K}}_{\tilde{\mathbf{r}}}^{-1} \tilde{\mathbf{R}}\right). \quad (3.36)$$

Once again $p_{\tilde{\mathbf{r}}}(\tilde{\mathbf{R}})$ is interpreted as compact notation for the $2N$ -dimensional density in (3.20).

The characteristic function is defined as

$$M_{\tilde{\mathbf{r}}}(j\tilde{\mathbf{v}}) \triangleq E\left[e^{j\Re(\tilde{\mathbf{v}}^H \tilde{\mathbf{r}})}\right] = \exp\left(-\frac{1}{4} \tilde{\mathbf{v}}^H \tilde{\mathbf{K}}_{\tilde{\mathbf{r}}} \tilde{\mathbf{v}}\right). \quad (3.37)$$

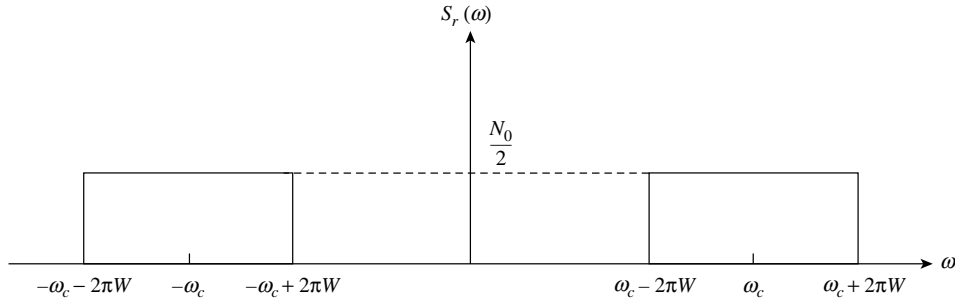


Figure 3.3: Spectrum of bandpass white noise.

If the bandpass process has the spectrum shown in Figure 3.3, then

$$\tilde{\mathbf{K}}_{\tilde{\mathbf{r}}} = \sigma_{\tilde{r}}^2 \mathbf{I}, \quad (3.38)$$

where $\sigma_{\tilde{r}}^2 = N_0$.

If there are deterministic bandpass signals, then the circular complex Gaussian random vector will have mean $\tilde{\mathbf{m}}_{\tilde{\mathbf{r}}}$. The probability density function is

$$p_{\tilde{\mathbf{r}}}(\tilde{\mathbf{R}}) = \frac{1}{\pi^N |\tilde{\mathbf{K}}_{\tilde{\mathbf{r}}}|} \exp\left(-[\tilde{\mathbf{R}} - \tilde{\mathbf{m}}_{\tilde{\mathbf{r}}}]^H \tilde{\mathbf{K}}_{\tilde{\mathbf{r}}}^{-1} [\tilde{\mathbf{R}} - \tilde{\mathbf{m}}_{\tilde{\mathbf{r}}}]^H\right) \quad (3.39)$$

and the characteristic function is

$$M_{\tilde{\mathbf{r}}}(j\tilde{\mathbf{v}}) = \exp\left(j \Re(\tilde{\mathbf{v}}^H \tilde{\mathbf{m}}_{\tilde{\mathbf{r}}}) - \frac{1}{4} \tilde{\mathbf{v}}^H \tilde{\mathbf{K}}_{\tilde{\mathbf{r}}} \tilde{\mathbf{v}}\right). \quad (3.40)$$

We denote the probability density in (3.39) as $\tilde{\mathbf{R}} \sim \mathcal{CN}(\tilde{\mathbf{m}}_{\tilde{\mathbf{r}}}, \tilde{\mathbf{K}}_{\tilde{\mathbf{r}}})$.

A linear transformation of a circular complex Gaussian random vector is another circular complex Gaussian random vector. Define the new $K \times 1$ vector as

$$\tilde{\mathbf{y}} = \tilde{\mathbf{B}} \tilde{\mathbf{r}}, \quad (3.41)$$

where

$$\tilde{\mathbf{B}} = \mathbf{A} + j\mathbf{B} \quad (3.42)$$

is a $K \times N$ matrix. Then

$$\begin{aligned} \tilde{\mathbf{y}} &= (\mathbf{A} + j\mathbf{B})(\mathbf{r}_R + j\mathbf{r}_I) \\ &= (\mathbf{A}\mathbf{r}_R - \mathbf{B}\mathbf{r}_I) + j(\mathbf{B}\mathbf{r}_R + \mathbf{A}\mathbf{r}_I) \\ &= \mathbf{y}_R + j\mathbf{y}_I. \end{aligned} \quad (3.43)$$

The mean of $\tilde{\mathbf{y}}$ is

$$\tilde{\mathbf{m}}_{\tilde{\mathbf{y}}} = \tilde{\mathbf{B}} \tilde{\mathbf{m}}_{\tilde{\mathbf{r}}} = (\mathbf{A}\mathbf{m}_R - \mathbf{B}\mathbf{m}_I) + j(\mathbf{B}\mathbf{m}_R + \mathbf{A}\mathbf{m}_I). \quad (3.44)$$

We need to verify that the properties in (3.23) and (3.24) hold for $\tilde{\mathbf{y}}$.

$$\begin{aligned}\mathbf{K}_{\mathbf{y}R} &= E[(\mathbf{y}_R - \mathbf{m}_{\mathbf{y}R})(\mathbf{y}_R - \mathbf{m}_{\mathbf{y}R})^T] \\ &= E\left\{\left[\mathbf{A}(\mathbf{r}_R - \mathbf{m}_R) - \mathbf{B}(\mathbf{r}_I - \mathbf{m}_I)\right]\left[\mathbf{A}(\mathbf{r}_R - \mathbf{m}_R) - \mathbf{B}(\mathbf{r}_I - \mathbf{m}_I)\right]^T\right\} \\ &= \mathbf{A}\mathbf{K}_R\mathbf{A}^T - \mathbf{B}\mathbf{K}_{IR}\mathbf{A}^T - \mathbf{A}\mathbf{K}_{RI}\mathbf{B}^T + \mathbf{B}\mathbf{K}_I\mathbf{B}^T,\end{aligned}\quad (3.45)$$

$$\begin{aligned}\mathbf{K}_{\mathbf{y}I} &= E[(\mathbf{y}_I - \mathbf{m}_{\mathbf{y}I})(\mathbf{y}_I - \mathbf{m}_{\mathbf{y}I})^T] \\ &= E\left\{\left[\mathbf{B}(\mathbf{r}_R - \mathbf{m}_R) + \mathbf{A}(\mathbf{r}_I - \mathbf{m}_I)\right]\left[\mathbf{B}(\mathbf{r}_R - \mathbf{m}_R) + \mathbf{A}(\mathbf{r}_I - \mathbf{m}_I)\right]^T\right\} \\ &= \mathbf{B}\mathbf{K}_R\mathbf{B}^T + \mathbf{A}\mathbf{K}_{IR}\mathbf{B}^T + \mathbf{B}\mathbf{K}_{RI}\mathbf{A}^T + \mathbf{A}\mathbf{K}_I\mathbf{A}^T,\end{aligned}\quad (3.46)$$

$$\begin{aligned}\mathbf{K}_{\mathbf{y}RI} &= E[(\mathbf{y}_R - \mathbf{m}_{\mathbf{y}R})(\mathbf{y}_I - \mathbf{m}_{\mathbf{y}I})^T] \\ &= E\left\{\left[\mathbf{A}(\mathbf{r}_R - \mathbf{m}_R) - \mathbf{B}(\mathbf{r}_I - \mathbf{m}_I)\right]\left[\mathbf{B}(\mathbf{r}_R - \mathbf{m}_R) + \mathbf{A}(\mathbf{r}_I - \mathbf{m}_I)\right]^T\right\} \\ &= \mathbf{A}\mathbf{K}_R\mathbf{B}^T - \mathbf{B}\mathbf{K}_{IR}\mathbf{B}^T + \mathbf{A}\mathbf{K}_{RI}\mathbf{A}^T - \mathbf{B}\mathbf{K}_I\mathbf{A}^T.\end{aligned}\quad (3.47)$$

Using the properties in (3.23) and (3.24) for $\tilde{\mathbf{r}}$, we have

$$\mathbf{K}_{\mathbf{y}R} = \mathbf{K}_{\mathbf{y}I} = \mathbf{A}\mathbf{K}_R\mathbf{A}^T + \mathbf{B}\mathbf{K}_R\mathbf{B}^T + \mathbf{A}\mathbf{K}_{IR}\mathbf{B}^T - \mathbf{B}\mathbf{K}_{IR}\mathbf{A}^T \quad (3.48)$$

and

$$\mathbf{K}_{\mathbf{y}RI} = -\mathbf{K}_{\mathbf{y}IR} = \mathbf{A}\mathbf{K}_R\mathbf{B}^T - \mathbf{B}\mathbf{K}_R\mathbf{A}^T - \mathbf{B}\mathbf{K}_{IR}\mathbf{B}^T - \mathbf{A}\mathbf{K}_{IR}\mathbf{A}^T. \quad (3.49)$$

Thus, $\tilde{\mathbf{y}}$ is a circular complex Gaussian random vector.

We have introduced circular complex Gaussian random vectors early in our development because they play a central role in most communication and radar applications. As a side benefit, the circular constraint that has a physical basis induces a mathematical property that allows us to obtain analytical results for the complex model that are not available in the real case. There are discussions of noncircular complex Gaussian vectors in the literature, but we will not consider them in the text. All further references to complex Gaussian variables or vectors are assumed to be circular.

3.1.3 General Gaussian Detection

An hypothesis testing problem is called a general Gaussian detection problem if $p_{\mathbf{r}|H_i}(\mathbf{R}|H_i)$ is a Gaussian density on all hypotheses. We formulate the general Gaussian detection problem for binary hypotheses in this section and develop it in detail in Sections 3.2, 3.3, and 3.4. We develop the M hypotheses problem in Section 3.5.

3.1.3.1 Real Gaussian Vectors

The basic model for the binary detection problem is straightforward. We assume that the observation space is N -dimensional. Points in the space are denoted by the N -dimensional vector \mathbf{r} .

Under the first hypothesis H_1 , we assume that \mathbf{r} is a Gaussian random vector, which is completely specified by its mean vector and covariance matrix. We denote these quantities as

$$E[\mathbf{r}|H_1] = \begin{bmatrix} E(r_1|H_1) \\ E(r_2|H_1) \\ \vdots \\ E(r_N|H_1) \end{bmatrix} \triangleq \begin{bmatrix} m_{11} \\ m_{12} \\ \vdots \\ m_{1N} \end{bmatrix} \triangleq \mathbf{m}_1. \quad (3.50)$$

The covariance matrix is

$$\begin{aligned} \mathbf{K}_1 &\triangleq E[(\mathbf{r} - \mathbf{m}_1)(\mathbf{r}^T - \mathbf{m}_1^T)|H_1] \\ &= \begin{bmatrix} {}_1K_{11} & {}_1K_{12} & \dots & {}_1K_{1N} \\ {}_1K_{21} & {}_1K_{22} & \dots & {}_1K_{2N} \\ \vdots & \vdots & \ddots & \vdots \\ {}_1K_{N1} & {}_1K_{N2} & \dots & {}_1K_{NN} \end{bmatrix}. \end{aligned} \quad (3.51)$$

We define the inverse of \mathbf{K}_1 as \mathbf{Q}_1

$$\mathbf{Q}_1 \triangleq \mathbf{K}_1^{-1}, \quad (3.52)$$

$$\mathbf{Q}_1 \mathbf{K}_1 = \mathbf{K}_1 \mathbf{Q}_1 = \mathbf{I}, \quad (3.53)$$

where \mathbf{I} is the identity matrix with ones on the diagonal and zeros elsewhere. Using (3.50), (3.51), (3.52), and (3.53), we may write the probability density of \mathbf{r} on H_1 ,

$$p_{\mathbf{r}|H_1}(\mathbf{R}|H_1) = \left((2\pi)^{N/2} |\mathbf{K}_1|^{1/2} \right)^{-1} \exp \left[-\frac{1}{2} (\mathbf{R} - \mathbf{m}_1)^T \mathbf{Q}_1 (\mathbf{R} - \mathbf{m}_1) \right]. \quad (3.54)$$

Going through a similar set of definitions for H_0 , we obtain the probability density

$$p_{\mathbf{r}|H_0}(\mathbf{R}|H_0) = \left((2\pi)^{N/2} |\mathbf{K}_0|^{1/2} \right)^{-1} \exp \left[-\frac{1}{2} (\mathbf{R} - \mathbf{m}_0)^T \mathbf{Q}_0 (\mathbf{R} - \mathbf{m}_0) \right]. \quad (3.55)$$

Using the definition in (2.13), the likelihood ratio test follows easily:

$$\Lambda(\mathbf{R}) \triangleq \frac{p_{\mathbf{r}|H_1}(\mathbf{R}|H_1)}{p_{\mathbf{r}|H_0}(\mathbf{R}|H_0)} = \frac{|\mathbf{K}_0|^{1/2} \exp \left[-\frac{1}{2} (\mathbf{R} - \mathbf{m}_1)^T \mathbf{Q}_1 (\mathbf{R} - \mathbf{m}_1) \right]}{|\mathbf{K}_1|^{1/2} \exp \left[-\frac{1}{2} (\mathbf{R} - \mathbf{m}_0)^T \mathbf{Q}_0 (\mathbf{R} - \mathbf{m}_0) \right]} \stackrel{H_1}{\gtrless} \eta. \quad (3.56)$$

Taking logarithms, we obtain

$$\begin{aligned} l(\mathbf{R}) &= \frac{1}{2} (\mathbf{R} - \mathbf{m}_0)^T \mathbf{Q}_0 (\mathbf{R} - \mathbf{m}_0) - \frac{1}{2} (\mathbf{R} - \mathbf{m}_1)^T \mathbf{Q}_1 (\mathbf{R} - \mathbf{m}_1) \\ &\stackrel{H_1}{\gtrless} \ln \eta + \frac{1}{2} \ln |\mathbf{K}_1| - \frac{1}{2} \ln |\mathbf{K}_0| \triangleq \gamma_1. \end{aligned} \quad (3.57)$$

We see that the test consists of finding the difference between two *quadratic forms*. The result in (3.57) is basic to many of our later discussions. For this reason, we treat various cases of the general Gaussian problem in some detail.

In many of these cases, we can find an analytical expression for P_D and P_F or the probability of error. We also have available the bounds and approximate expressions developed in Section 2.4. These rely on the function $\mu(s)$ and its derivatives with respect to s , where

$$\mu(s) \triangleq \ln \int_{-\infty}^{\infty} [p_{\mathbf{r}|H_1}(\mathbf{R}|H_1)]^s [p_{\mathbf{r}|H_0}(\mathbf{R}|H_0)]^{1-s} d\mathbf{R}. \quad (3.58)$$

For the general Gaussian model, we have

$$\begin{aligned} e^{\mu(s)} &= \int_{-\infty}^{\infty} (2\pi)^{-N/2} |\mathbf{K}_1|^{-s/2} |\mathbf{K}_0|^{-(1-s)/2} \cdot \\ &\quad \exp \left\{ -\frac{s}{2} (\mathbf{R} - \mathbf{m}_1)^T \mathbf{K}_1^{-1} (\mathbf{R} - \mathbf{m}_1) - \frac{1-s}{2} (\mathbf{R} - \mathbf{m}_0)^T \mathbf{K}_0^{-1} (\mathbf{R} - \mathbf{m}_0) \right\} d\mathbf{R} \\ &= B \exp\{A\} \int_{-\infty}^{\infty} (2\pi)^{-N/2} |\mathbf{K}|^{-1/2} \exp \left\{ -\frac{1}{2} (\mathbf{R} - \mathbf{m})^T \mathbf{K}^{-1} (\mathbf{R} - \mathbf{m}) \right\} d\mathbf{R}, \end{aligned} \quad (3.59)$$

where

$$\mathbf{K}^{-1} = s\mathbf{K}_1^{-1} + (1-s)\mathbf{K}_0^{-1} = \mathbf{K}_1^{-1}\mathbf{K}_0^{-1} [s\mathbf{K}_0 + (1-s)\mathbf{K}_1], \quad (3.60)$$

$$\mathbf{m} = \mathbf{K} [s\mathbf{K}_1^{-1}\mathbf{m}_1 + (1-s)\mathbf{K}_0^{-1}\mathbf{m}_0], \quad (3.61)$$

$$B = |\mathbf{K}_1|^{(1-s)/2} |\mathbf{K}_0|^{s/2} |s\mathbf{K}_0 + (1-s)\mathbf{K}_1|^{-1/2}, \quad (3.62)$$

$$A = \frac{-s(1-s)}{2} (\mathbf{m}_1 - \mathbf{m}_0)^T [s\mathbf{K}_0 + (1-s)\mathbf{K}_1]^{-1} (\mathbf{m}_1 - \mathbf{m}_0). \quad (3.63)$$

The integral in (3.59) is unity, therefore

$$e^{\mu(s)} = B \exp\{A\}, \quad (3.64)$$

so⁴

$$\begin{aligned} \mu(s) &= \frac{-s(1-s)}{2} (\mathbf{m}_1 - \mathbf{m}_0)^T [s\mathbf{K}_0 + (1-s)\mathbf{K}_1]^{-1} (\mathbf{m}_1 - \mathbf{m}_0) \\ &\quad - \frac{1}{2} \ln \left(|\mathbf{K}_1|^{s-1} |\mathbf{K}_0|^{-s} |s\mathbf{K}_0 + (1-s)\mathbf{K}_1| \right). \end{aligned} \quad (3.65)$$

Now define $\Delta\mathbf{m}$ as the difference between the mean vectors on the two hypotheses

$$\Delta\mathbf{m} \triangleq \mathbf{m}_1 - \mathbf{m}_0 \quad (3.66)$$

⁴This is the solution to Problem 2.7.6 in DEMT-I. The derivation is given in terms of eigenvalues on pp. 35–36 of DEMT-III.

and define the matrix $\mathbf{K}(s)$ as

$$\mathbf{K}(s) \triangleq s\mathbf{K}_0 + (1-s)\mathbf{K}_1. \quad (3.67)$$

Then

$$\boxed{\mu(s) = \frac{s(s-1)}{2} \Delta\mathbf{m}^T \mathbf{K}(s)^{-1} \Delta\mathbf{m} + \frac{s}{2} \ln|\mathbf{K}_0| + \frac{1-s}{2} \ln|\mathbf{K}_1| - \frac{1}{2} \ln|\mathbf{K}(s)|.} \quad (3.68)$$

To find $\dot{\mu}(s)$ and $\ddot{\mu}(s)$, we need the following properties. If $\mathbf{X}(s)$ is an $N \times N$ invertible matrix, then⁵

$$\frac{\partial}{\partial s} \ln|\mathbf{X}(s)| = \text{tr} \left\{ \mathbf{X}^{-1}(s) \frac{\partial \mathbf{X}(s)}{\partial s} \right\}, \quad (3.69)$$

$$\frac{\partial}{\partial s} \mathbf{X}^{-1}(s) = -\mathbf{X}^{-1}(s) \frac{\partial \mathbf{X}(s)}{\partial s} \mathbf{X}^{-1}(s), \quad (3.70)$$

$$\frac{\partial}{\partial s} \text{tr} \left\{ \mathbf{X}^{-1}(s) \mathbf{Y} \right\} = -\text{tr} \left\{ \mathbf{X}^{-1}(s) \frac{\partial \mathbf{X}(s)}{\partial s} \mathbf{X}^{-1}(s) \mathbf{Y} \right\}. \quad (3.71)$$

Using these properties and the derivative of $\mathbf{K}(s)$ with respect to s , which is given by,

$$\frac{\partial \mathbf{K}(s)}{\partial s} = \mathbf{K}_0 - \mathbf{K}_1, \quad (3.72)$$

we have

$$\begin{aligned} \dot{\mu}(s) &= \frac{2s-1}{2} \Delta\mathbf{m}^T \mathbf{K}(s)^{-1} \Delta\mathbf{m} - \frac{s^2-s}{2} \Delta\mathbf{m}^T \mathbf{K}(s)^{-1} (\mathbf{K}_0 - \mathbf{K}_1) \mathbf{K}(s)^{-1} \Delta\mathbf{m} \\ &\quad + \frac{1}{2} \ln|\mathbf{K}_0| - \frac{1}{2} \ln|\mathbf{K}_1| - \frac{1}{2} \text{tr} \left\{ \mathbf{K}(s)^{-1} (\mathbf{K}_0 - \mathbf{K}_1) \right\}. \end{aligned} \quad (3.73)$$

This can be simplified to

$$\boxed{\begin{aligned} \dot{\mu}(s) &= \frac{1}{2} \Delta\mathbf{m}^T \mathbf{K}(s)^{-1} \left[s^2 \mathbf{K}_0 - (1-s)^2 \mathbf{K}_1 \right] \mathbf{K}(s)^{-1} \Delta\mathbf{m} + \frac{1}{2} \ln|\mathbf{K}_0| \\ &\quad - \frac{1}{2} \ln|\mathbf{K}_1| + \frac{1}{2} \text{tr} \left\{ \mathbf{K}(s)^{-1} (\mathbf{K}_1 - \mathbf{K}_0) \right\}. \end{aligned}} \quad (3.74)$$

Taking the derivative again and combining terms, we obtain

$$\boxed{\begin{aligned} \ddot{\mu}(s) &= \Delta\mathbf{m}^T \mathbf{K}(s)^{-1} \mathbf{K}_1 \mathbf{K}(s)^{-1} \mathbf{K}_0 \mathbf{K}(s)^{-1} \Delta\mathbf{m} \\ &\quad + \frac{1}{2} \text{tr} \left\{ \mathbf{K}(s)^{-1} (\mathbf{K}_1 - \mathbf{K}_0) \mathbf{K}(s)^{-1} (\mathbf{K}_1 - \mathbf{K}_0) \right\}. \end{aligned}} \quad (3.75)$$

We now find the corresponding result for complex Gaussian vectors.

⁵See [Van02], Appendix A.

3.1.3.2 Circular Complex Gaussian Vectors

The complex Gaussian model is a straightforward modification to the real Gaussian model. Points in the space are denoted by the N -dimensional vector $\tilde{\mathbf{r}}$. The mean vector and covariance matrix on H_1 are

$$\tilde{\mathbf{m}}_1 \triangleq E[\tilde{\mathbf{r}}|H_1] \quad (3.76)$$

$$\tilde{\mathbf{K}}_1 \triangleq E[(\tilde{\mathbf{r}} - \tilde{\mathbf{m}}_1)(\tilde{\mathbf{r}}^H - \tilde{\mathbf{m}}_1^H)|H_1]. \quad (3.77)$$

The inverse of $\tilde{\mathbf{K}}_1$ is $\tilde{\mathbf{Q}}_1$:

$$\tilde{\mathbf{Q}}_1 \triangleq \tilde{\mathbf{K}}_1^{-1} \quad (3.78)$$

and

$$\tilde{\mathbf{Q}}_1 \tilde{\mathbf{K}}_1 = \tilde{\mathbf{K}}_1 \tilde{\mathbf{Q}}_1 = \mathbf{I}. \quad (3.79)$$

The probability density on H_1 is

$$p_{\tilde{\mathbf{r}}|H_1}(\tilde{\mathbf{R}}|H_1) = \frac{1}{\pi^N |\tilde{\mathbf{K}}_1|} \exp\left[-(\tilde{\mathbf{R}} - \tilde{\mathbf{m}}_1)^H \tilde{\mathbf{Q}}_1 (\tilde{\mathbf{R}} - \tilde{\mathbf{m}}_1)\right]. \quad (3.80)$$

Using a similar set of definitions for H_0 , we obtain the probability density

$$p_{\tilde{\mathbf{r}}|H_0}(\tilde{\mathbf{R}}|H_0) = \frac{1}{\pi^N |\tilde{\mathbf{K}}_0|} \exp\left[-(\tilde{\mathbf{R}} - \tilde{\mathbf{m}}_0)^H \tilde{\mathbf{Q}}_0 (\tilde{\mathbf{R}} - \tilde{\mathbf{m}}_0)\right]. \quad (3.81)$$

The likelihood ratio test is

$$\begin{aligned} \Lambda(\tilde{\mathbf{R}}) &\triangleq \frac{p_{\tilde{\mathbf{r}}|H_1}(\tilde{\mathbf{R}}|H_1)}{p_{\tilde{\mathbf{r}}|H_0}(\tilde{\mathbf{R}}|H_0)} \\ &= \frac{|\tilde{\mathbf{K}}_0|}{|\tilde{\mathbf{K}}_1|} \frac{\exp\left[-(\tilde{\mathbf{R}} - \tilde{\mathbf{m}}_1)^H \tilde{\mathbf{Q}}_1 (\tilde{\mathbf{R}} - \tilde{\mathbf{m}}_1)\right]}{\exp\left[-(\tilde{\mathbf{R}} - \tilde{\mathbf{m}}_0)^H \tilde{\mathbf{Q}}_0 (\tilde{\mathbf{R}} - \tilde{\mathbf{m}}_0)\right]}. \end{aligned} \quad (3.82)$$

Taking logarithms, we obtain

$$\begin{aligned} l(\tilde{\mathbf{R}}) &= (\tilde{\mathbf{R}} - \tilde{\mathbf{m}}_0)^H \tilde{\mathbf{Q}}_0 (\tilde{\mathbf{R}} - \tilde{\mathbf{m}}_0) - (\tilde{\mathbf{R}} - \tilde{\mathbf{m}}_1)^H \tilde{\mathbf{Q}}_1 (\tilde{\mathbf{R}} - \tilde{\mathbf{m}}_1) \\ &\stackrel[H_1]{>} H_0 \ln \eta + \ln |\tilde{\mathbf{K}}_1| - \ln |\tilde{\mathbf{K}}_0| \triangleq \gamma'_1. \end{aligned} \quad (3.83)$$

The $\mu(s)$, $\dot{\mu}(s)$, and $\ddot{\mu}(s)$ functions are

$$\begin{aligned}\mu(s) &= s(s-1)\Delta\tilde{\mathbf{m}}^H\tilde{\mathbf{K}}(s)^{-1}\Delta\tilde{\mathbf{m}} + s \ln|\tilde{\mathbf{K}}_0| \\ &\quad + (1-s) \ln|\tilde{\mathbf{K}}_1| - \ln|\tilde{\mathbf{K}}(s)|,\end{aligned}\tag{3.84}$$

$$\begin{aligned}\dot{\mu}(s) &= \Delta\tilde{\mathbf{m}}^H\tilde{\mathbf{K}}(s)^{-1} \left[s^2\tilde{\mathbf{K}}_0 - (1-s)^2\tilde{\mathbf{K}}_1 \right] \tilde{\mathbf{K}}(s)^{-1}\Delta\tilde{\mathbf{m}} + \ln|\tilde{\mathbf{K}}_0| \\ &\quad - \ln|\tilde{\mathbf{K}}_1| + \text{tr}\left\{\tilde{\mathbf{K}}(s)^{-1}(\tilde{\mathbf{K}}_1 - \tilde{\mathbf{K}}_0)\right\},\end{aligned}\tag{3.85}$$

$$\begin{aligned}\ddot{\mu}(s) &= 2\Delta\tilde{\mathbf{m}}^H\tilde{\mathbf{K}}(s)^{-1}\tilde{\mathbf{K}}_1\tilde{\mathbf{K}}(s)^{-1}\tilde{\mathbf{K}}_0\tilde{\mathbf{K}}(s)^{-1}\Delta\tilde{\mathbf{m}} \\ &\quad + \text{tr}\left\{\tilde{\mathbf{K}}(s)^{-1}(\tilde{\mathbf{K}}_1 - \tilde{\mathbf{K}}_0)\tilde{\mathbf{K}}(s)^{-1}(\tilde{\mathbf{K}}_1 - \tilde{\mathbf{K}}_0)\right\},\end{aligned}\tag{3.86}$$

where

$$\Delta\tilde{\mathbf{m}} \triangleq \tilde{\mathbf{m}}_1 - \tilde{\mathbf{m}}_0,\tag{3.87}$$

$$\tilde{\mathbf{K}}(s) \triangleq s\tilde{\mathbf{K}}_0 + (1-s)\tilde{\mathbf{K}}_1.\tag{3.88}$$

3.1.3.3 Summary

In the next three sections, we will consider a sequence of models that correspond to the physical applications that we encounter later in the text.

In Section 3.2, we consider the case in which the covariance matrices on the two hypotheses are equal. We will find that the sufficient statistic is Gaussian and that the performance of the likelihood ratio test is completely determined by a d^2 term that is a generalization of the d^2 term we first encountered in Example 2.5. This model will be encountered in communication systems in which the means represent the signal transmitted on the two hypotheses and the transmission channel attenuates the signal and adds interference and noise. We can find analytical performance results and can design optimum signals for a specific interference. We introduce eigendecomposition in order to better understand our analytical results.

In Section 3.3, we consider the case in which the mean vectors on the hypotheses are equal. We will find that the sufficient statistic is a quadratic form. In order to analyze the performance we do an eigendecomposition. For the real Gaussian case we can find the characteristic function of l on both hypotheses but need to do a numerical integration to find the probability densities needed to calculate P_D , P_F , or $\Pr(\epsilon)$. For the complex case, we find a closed form expression for the probability densities and calculate P_D and P_F using standard mathematical functions. This model will be encountered in communications and radar systems where the channel (or target) introduces a complex Gaussian multiplier onto the transmitted signals (referred to as the Rayleigh model). We will also encounter it in radar, sonar, and radio astronomy where we are trying to detect a sample from a Gaussian random process (either real or complex) in the presence of Gaussian interference and noise.

In Section 3.4, we return to the general Gaussian case. We will find that the sufficient statistic is the sum of a linear term and a quadratic term that are correlated in most cases. Except for some special cases, we cannot find analytical expressions for the performance. We resort to the bounds and approximations using $\mu(s)$ developed in Section 2.4 and to the simulations using importance sampling developed in Section 2.5. The closed form expression for $\mu(s)$ enables us to find the appropriate tilted density. This model will be encountered in communications and radar systems where the channel (or target) introduces

a complex Gaussian multiplier with a nonzero mean (the specular component) onto the transmitted signals (referred to as the Rician model).

In Section 3.5, we extend these models to the M hypotheses case. We can always find the optimum Bayes test. Except for special cases, the performance is difficult to evaluate and we resort to bounds on the $\Pr(\epsilon)$.

It is important to note that the likelihood ratio test can be implemented using (3.57) or (3.83). By studying the various models, we can find analytical performance results that enable us to understand how the components of the model affect performance. The closed form expressions for $\mu(s)$ and its derivatives ((3.68), (3.74), (3.75), and (3.84)–(3.86)) give the expressions we need to find the optimum tilted density to use in an importance sampling simulation.

3.2 EQUAL COVARIANCE MATRICES

The first special case of interest is the model where the observations under the two hypotheses are

$$\begin{aligned} H_0 : \mathbf{r} &= \mathbf{m}_0 + \mathbf{n}, \\ H_1 : \mathbf{r} &= \mathbf{m}_1 + \mathbf{n}. \end{aligned} \quad (3.89)$$

The \mathbf{m}_j vectors ($j = 0, 1$) correspond to a deterministic signal and \mathbf{n} is a zero-mean Gaussian noise vector with covariance matrix \mathbf{K} . We will encounter this model in communications systems where the mean vectors result from sampling deterministic signals that are transmitted over a channel that adds Gaussian noise.

Thus, the model in (3.57) applies with equal covariance matrices

$$\mathbf{K}_1 = \mathbf{K}_0 \triangleq \mathbf{K}, \quad (3.90)$$

and different means.

Denote the inverse of \mathbf{K} as \mathbf{Q} :

$$\mathbf{Q} = \mathbf{K}^{-1}. \quad (3.91)$$

Substituting into (3.57), multiplying the matrices, canceling common terms, and using the symmetry of \mathbf{Q} , we have

$$(\mathbf{m}_1^T - \mathbf{m}_0^T)\mathbf{QR} \stackrel[H_1]{H_0}{\gtrless} \ln \eta + \frac{1}{2}(\mathbf{m}_1^T \mathbf{Q} \mathbf{m}_1 - \mathbf{m}_0^T \mathbf{Q} \mathbf{m}_0) \triangleq \gamma_2, \quad (3.92)$$

which can be written as

$$l(\mathbf{R}) \triangleq \Delta \mathbf{m}^T \mathbf{QR} \stackrel[H_1]{H_0}{\gtrless} \gamma_2$$

(3.93)

or, equivalently,

$$l(\mathbf{R}) \triangleq \mathbf{R}^T \mathbf{Q} \Delta \mathbf{m} \stackrel[H_1]{H_0}{\gtrless} \gamma_2. \quad (3.94)$$

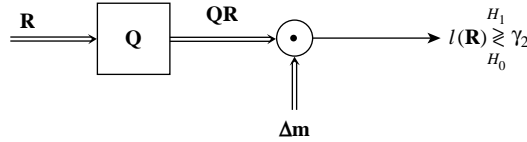


Figure 3.4: Optimum detection: Gaussian model with equal covariance matrices on H_0 and H_1 .

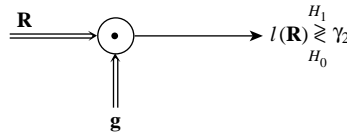


Figure 3.5: Optimum detection: correlation implementation.

This implementation is shown in Figure 3.4.⁶

It is useful to define the vector

$$\mathbf{g} \triangleq \mathbf{Q} \Delta \mathbf{m} \quad (3.95)$$

and write (3.93) as

$$l(\mathbf{R}) = \mathbf{g}^T \mathbf{R} \stackrel{H_1}{\geqslant} \gamma_2. \quad (3.96)$$

This implementation is shown in Figure 3.5.

The quantity on the left-hand side of (3.93) and (3.96) is a *scalar* Gaussian random variable, for it was obtained by a linear transformation of jointly Gaussian random variables. Therefore, as we discussed in Example 2.5, we can completely characterize the performance of the test by the quantity d^2 . In that example, we defined d as the distance between the means on the two hypotheses when the variance was normalized to one. An identical definition is,

$$d^2 \triangleq \frac{[E(l|H_1) - E(l|H_0)]^2}{\text{Var}(l|H_0)}, \quad (3.97)$$

which is often referred to as the deflection ratio.

Using (3.54) and (3.55) with the definition of l , we have

$$E(l|H_1) = \Delta \mathbf{m}^T \mathbf{Q} \mathbf{m}_1 \quad (3.98)$$

and

$$E(l|H_0) = \Delta \mathbf{m}^T \mathbf{Q} \mathbf{m}_0. \quad (3.99)$$

⁶The box denotes a matrix multiply \mathbf{QR} . The \odot denotes the dot product, $\Delta \mathbf{m}^T \mathbf{QR}$. The vertical input is transposed.

Using (3.93), (3.94), and (3.99), we have

$$\text{Var}[l|H_0] = E\left\{\left[\Delta \mathbf{m}^T \mathbf{Q}(\mathbf{R} - \mathbf{m}_0)\right]\left[(\mathbf{R} - \mathbf{m}_0)^T \mathbf{Q} \Delta \mathbf{m}\right]\right\}. \quad (3.100)$$

Using (3.51) to evaluate the expectation and then (3.53), we have

$$\text{Var}[l|H_0] = \Delta \mathbf{m}^T \mathbf{Q} \Delta \mathbf{m}. \quad (3.101)$$

Substituting (3.98), (3.99), and (3.101) into (3.97), we obtain

$$d^2 = \Delta \mathbf{m}^T \mathbf{Q} \Delta \mathbf{m}. \quad (3.102)$$

Thus, the performance for the equal covariance Gaussian case is completely determined by the quadratic form in (3.102). This can also be written as

$$d^2 = \mathbf{g}^T \Delta \mathbf{m}. \quad (3.103)$$

We now derive the analogous result for the circular complex Gaussian case. We have

$$\tilde{\mathbf{K}}_1 = \tilde{\mathbf{K}}_0 \triangleq \tilde{\mathbf{K}}. \quad (3.104)$$

The inverse is

$$\tilde{\mathbf{Q}} = \tilde{\mathbf{K}}^{-1}. \quad (3.105)$$

Substituting into (3.83), multiplying the matrices, canceling common terms, and using the fact that $\tilde{\mathbf{Q}}$ is Hermitian, $\tilde{\mathbf{Q}}^H = \tilde{\mathbf{Q}}$, we have

$$\begin{aligned} (\tilde{\mathbf{m}}_1 - \tilde{\mathbf{m}}_0)^H \tilde{\mathbf{Q}} \tilde{\mathbf{R}} + \tilde{\mathbf{R}}^H \tilde{\mathbf{Q}} (\tilde{\mathbf{m}}_1 - \tilde{\mathbf{m}}_0) &= 2\Re\left[(\tilde{\mathbf{m}}_1 - \tilde{\mathbf{m}}_0)^H \tilde{\mathbf{Q}} \tilde{\mathbf{R}}\right] \\ &\stackrel[H_1]{\gtrless}_{H_0} \ln \eta + \tilde{\mathbf{m}}_1^H \tilde{\mathbf{Q}} \tilde{\mathbf{m}}_1 - \tilde{\mathbf{m}}_0^H \tilde{\mathbf{Q}} \tilde{\mathbf{m}}_0 \triangleq 2\gamma'_2. \end{aligned} \quad (3.106)$$

Defining

$$\Delta \tilde{\mathbf{m}} = \tilde{\mathbf{m}}_1 - \tilde{\mathbf{m}}_0, \quad (3.107)$$

(3.106) can be written as

$$l(\tilde{\mathbf{R}}) \triangleq \Re\left\{\Delta \tilde{\mathbf{m}}^H \tilde{\mathbf{Q}} \tilde{\mathbf{R}}\right\} = \Re\left\{\tilde{\mathbf{R}}^H \tilde{\mathbf{Q}} \Delta \tilde{\mathbf{m}}\right\} \stackrel[H_1]{\gtrless}_{H_0} \gamma'_2. \quad (3.108)$$

This test is shown in Figure 3.6.⁷

We can define

$$\tilde{\mathbf{g}} \triangleq \tilde{\mathbf{Q}} \Delta \tilde{\mathbf{m}} \quad (3.109)$$

⁷For complex inputs, \odot denotes the dot product, $\Delta \tilde{\mathbf{m}}^H \tilde{\mathbf{Q}} \tilde{\mathbf{R}}$. The vertical input is Hermitian transposed. The box $\Re\{\cdot\}$ takes the real part of the input.

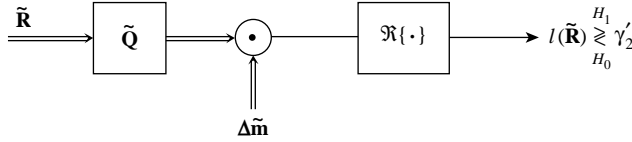


Figure 3.6: Optimum detection: complex Gaussian model with equal covariance matrices on H_0 and H_1 .

and write $l(\tilde{\mathbf{R}})$ as

$$l(\tilde{\mathbf{R}}) = \Re \left\{ \tilde{\mathbf{g}}^H \tilde{\mathbf{R}} \right\} \stackrel{H_1}{\gtrless} \stackrel{H_0}{\gamma'_2}, \quad (3.110)$$

which can be implemented as shown in Figure 3.7.

The random variable at the output of the correlator is defined as

$$\tilde{l}(\tilde{\mathbf{R}}) \triangleq \tilde{\mathbf{g}}^H \tilde{\mathbf{R}} = \Delta\tilde{\mathbf{m}}^H \tilde{\mathbf{Q}} \tilde{\mathbf{R}}. \quad (3.111)$$

Then

$$l(\tilde{\mathbf{R}}) = \Re \{ \tilde{l}(\tilde{\mathbf{R}}) \}. \quad (3.112)$$

The output of the correlator is a linear transformation of a circular complex Gaussian random vector; therefore, it is a scalar circular complex Gaussian random variable. The first step is to compute the mean and variance of \tilde{l} on the two hypotheses.

$$E(\tilde{l}|H_0) = \Delta\tilde{\mathbf{m}}^H \tilde{\mathbf{Q}} \tilde{\mathbf{m}}_0 \quad (3.113)$$

$$E(\tilde{l}|H_1) = \Delta\tilde{\mathbf{m}}^H \tilde{\mathbf{Q}} \tilde{\mathbf{m}}_1 \quad (3.114)$$

and

$$\begin{aligned} \text{Var}(\tilde{l}|H_0) &= E \left\{ \Delta\tilde{\mathbf{m}}^H \tilde{\mathbf{Q}} (\tilde{\mathbf{R}} - \tilde{\mathbf{m}}_0) (\tilde{\mathbf{R}} - \tilde{\mathbf{m}}_0)^H \tilde{\mathbf{Q}} \Delta\tilde{\mathbf{m}} \right\} \\ &= \Delta\tilde{\mathbf{m}}^H \tilde{\mathbf{Q}} \tilde{\mathbf{K}} \tilde{\mathbf{Q}} \Delta\tilde{\mathbf{m}} \\ &= \Delta\tilde{\mathbf{m}}^H \tilde{\mathbf{Q}} \Delta\tilde{\mathbf{m}}, \end{aligned} \quad (3.115)$$

which is real because $\tilde{\mathbf{Q}}$ is Hermitian.

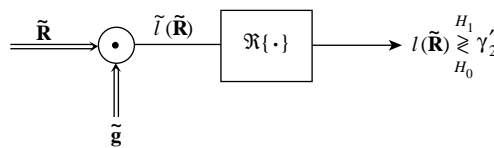


Figure 3.7: Optimum detection: correlation implementation.

From Section 3.1.2, the real and imaginary parts of \tilde{l} are independent real Gaussian random variables with variance equal to one-half of $\text{Var}(\tilde{l}|H_0)$. Thus, the probability densities of l on the two hypotheses are

$$p_{l|H_0}(L|H_0) \sim N\left(\Re\{\Delta\tilde{\mathbf{m}}^H\tilde{\mathbf{Q}}\tilde{\mathbf{m}}_0\}, \frac{1}{2}\Delta\tilde{\mathbf{m}}^H\tilde{\mathbf{Q}}\Delta\tilde{\mathbf{m}}\right) \quad (3.116)$$

and

$$p_{l|H_1}(L|H_1) \sim N\left(\Re\{\Delta\tilde{\mathbf{m}}^H\tilde{\mathbf{Q}}\tilde{\mathbf{m}}_1\}, \frac{1}{2}\Delta\tilde{\mathbf{m}}^H\tilde{\mathbf{Q}}\Delta\tilde{\mathbf{m}}\right) \quad (3.117)$$

and

$$d^2 = \frac{2\left(\Re\{\Delta\tilde{\mathbf{m}}^H\tilde{\mathbf{Q}}\tilde{\mathbf{m}}_0\} - \Re\{\Delta\tilde{\mathbf{m}}^H\tilde{\mathbf{Q}}\tilde{\mathbf{m}}_1\}\right)^2}{\Delta\tilde{\mathbf{m}}^H\tilde{\mathbf{Q}}\Delta\tilde{\mathbf{m}}} = 2\Delta\tilde{\mathbf{m}}^H\tilde{\mathbf{Q}}\Delta\tilde{\mathbf{m}} \quad (3.118)$$

or

$$d^2 = 2\tilde{\mathbf{g}}^H\Delta\tilde{\mathbf{m}}. \quad (3.119)$$

It is important to note that for the real Gaussian detection model, (3.93) or (3.96) completely defines the likelihood ratio test and the performance is completely defined by d^2 in (3.102) or (3.103). We use P_F and P_D as in Chapter 2 ((2.84) and (2.85)) and the ROC and $\text{Pr}(\epsilon)$ curves are applicable. For the complex Gaussian detection model, the analogous results are given in (3.108), (3.110), (3.118), and (3.119).

What is missing is an understanding of how \mathbf{m} and \mathbf{K} interact with each other to produce the results. In most signal processing problems of interest to us, \mathbf{m} corresponds to a signal that we have some freedom to design, so it is important to know how \mathbf{K} affects that choice. The rest of this section is devoted to developing an understanding of the models.

Many of the techniques discussed here are applicable in Sections 3.3 and 3.4, where we discuss unequal covariances. In those models, the techniques will be necessary to define performance.

We now interpret the results for some cases of interest.

3.2.1 Independent Components with Equal Variance

For the real Gaussian case, each r_i has the same variance σ^2 and is statistically independent. Thus,

$$\mathbf{K} = \sigma^2\mathbf{I} \quad (3.120)$$

and

$$\mathbf{Q} = \frac{1}{\sigma^2}\mathbf{I}. \quad (3.121)$$

Substituting (3.121) into (3.102), we obtain

$$d^2 = \Delta\mathbf{m}^T \frac{1}{\sigma^2} \mathbf{I} \Delta\mathbf{m} = \frac{1}{\sigma^2} \Delta\mathbf{m}^T \Delta\mathbf{m} = \frac{1}{\sigma^2} \|\Delta\mathbf{m}\|^2 \quad (3.122)$$

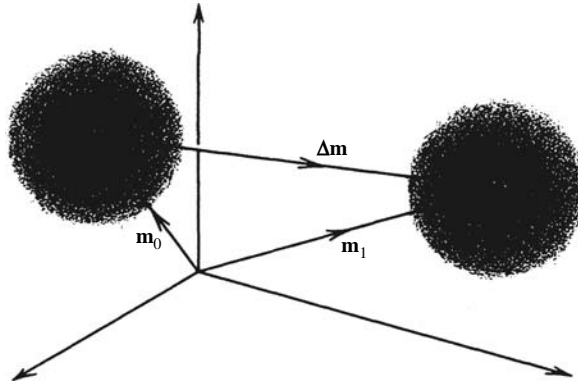


Figure 3.8: Mean vectors.

or

$$d = \frac{\|\Delta \mathbf{m}\|}{\sigma}. \quad (3.123)$$

We see that d corresponds to the *distance* between the two mean vectors divided by the standard deviation of r_i . This is shown in Figure 3.8.

In (3.93), we see that

$$l(\mathbf{R}) = \frac{1}{\sigma^2} \Delta \mathbf{m}^T \mathbf{R}. \quad (3.124)$$

Thus, the sufficient statistic is just the dot (or scalar) product of the observed vector \mathbf{R} and the mean difference vector $\Delta \mathbf{m}$. Note that this case corresponds to Example 2.1 in Chapter 2 with a mean vector \mathbf{m}_0 added on H_0 .

For the complex Gaussian case,

$$\tilde{\mathbf{K}} = \sigma_r^2 \mathbf{I} \quad (3.125)$$

$$l(\mathbf{R}) = \Re \left\{ \frac{\Delta \tilde{\mathbf{m}}^H \tilde{\mathbf{R}}}{\sigma_r^2} \right\}, \quad (3.126)$$

and

$$d^2 = 2 \frac{\|\Delta \tilde{\mathbf{m}}\|^2}{\sigma_r^2}. \quad (3.127)$$

Example 3.1. A case that occurs frequently in practice is when we receive a deterministic signal that is a complex exponential of known frequency ω that is corrupted by white bandpass noise (see Figure 3.3). We sample it and the resulting mean vector is

$$[\tilde{\mathbf{m}}_1]_n = \tilde{b}_n e^{j\omega n}, \quad n = 0, 1, \dots, N - 1, \quad (3.128)$$

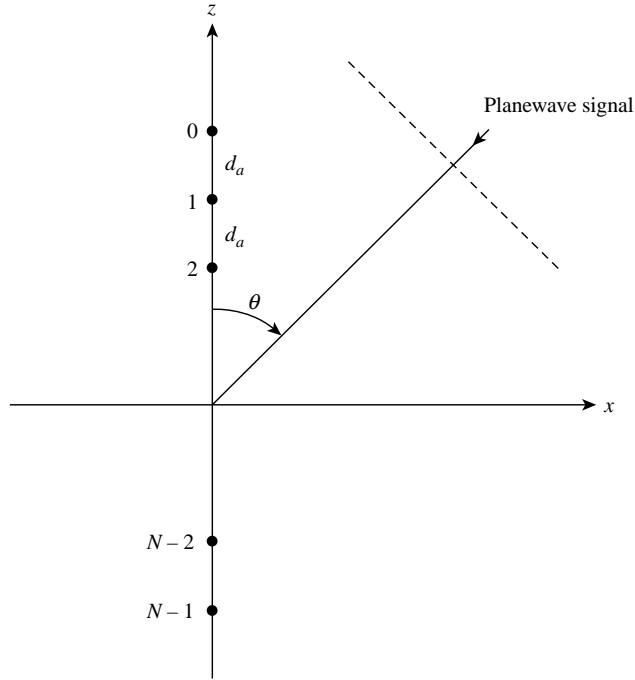


Figure 3.9: Uniform linear array with planewave input.

where \tilde{b}_n is a known complex parameter and

$$d^2 = \frac{2}{\sigma_r^2} \sum_{n=0}^{N-1} |\tilde{b}_n|^2. \quad (3.129)$$

■

Example 3.2. A different physical problem that leads to the same model is shown in Figure 3.9. A planewave at frequency ω_c impinges on a linear uniformly spaced array of omni-directional sensors. The angle of arrival measured from the \$z\$-axis is θ . The signal at sensor 0 is

$$\tilde{s}_0(t) = \tilde{b} e^{j\omega_c t}. \quad (3.130)$$

The signal at sensor \$n\$ is

$$\tilde{s}_n(t) = \tilde{b} e^{j\omega_c(t-\tau_n)} = \tilde{b} e^{j\omega_c t} e^{-j\omega_c \tau_n}, \quad (3.131)$$

where τ_n is the time delay from sensor 0. Now

$$\tau_n = \frac{d_a \cos(\theta)}{c} n, \quad (3.132)$$

where d_a is the interelement spacing and c is the velocity of propagation.

We now define the directional cosine as

$$u \triangleq \cos(\theta), \quad -1 \leq u \leq 1. \quad (3.133)$$

Conventional arrays have half-wavelength spacing, $d_a = \lambda/2$, where $\lambda = 2\pi c/\omega_c$. Therefore, we can write

$$\omega_c \tau_n = \frac{2\pi c}{\lambda} \frac{\lambda}{2} \frac{u}{c} n = \pi u n. \quad (3.134)$$

Finally, we define the wavenumber as⁸

$$\psi = \pi u, \quad -\pi \leq \psi \leq \pi. \quad (3.135)$$

We can write the N signals as a vector

$$\tilde{\mathbf{s}}(t) = \tilde{s}_0(t) \begin{bmatrix} 1 & e^{-j\psi} & e^{-j2\psi} & \dots & e^{-jn\psi} & \dots & e^{-j(N-1)\psi} \end{bmatrix}^T. \quad (3.136)$$

The vector in (3.136) is referred to as the array manifold vector, which is defined as

$$\tilde{\mathbf{v}}(\psi) \triangleq \begin{bmatrix} 1 & e^{-j\psi} & e^{-j2\psi} & \dots & e^{-j(N-1)\psi} \end{bmatrix}^T. \quad (3.137)$$

If we sample at $t = 0$, the result is a vector whose elements are

$$[\tilde{\mathbf{m}}_1]_n = [\tilde{\mathbf{s}}(0)]_n = \tilde{b} e^{-j\psi n}, \quad n = 0, 1, \dots, N-1. \quad (3.138)$$

Thus, a sample of the array output produces the same mean vector $\tilde{\mathbf{m}}_1$ as in (3.128) with

$$\omega = -\psi \quad (3.139)$$

and

$$\tilde{b}_n = \tilde{b}. \quad (3.140)$$

Thus, frequency in the complex exponential signal case corresponds to the wavenumber in the array case. If we assume that the noise is sensor noise that is statistically independent from sensor to sensor then we have an identical model to the complex frequency model.

If we take successive samples at $t = t_k, k = 1, 2, \dots, K$ then the signal vectors are

$$\tilde{\mathbf{s}}(t_k) = \tilde{b} e^{j\omega_c t_k} \tilde{\mathbf{v}}(\psi), \quad k = 1, 2, \dots, K. \quad (3.141)$$

We can multiply the observed sample vectors by $e^{-j\omega_c t_k}$ to remove the complex phase from the signal term. This does not change the statistical properties of the circular complex Gaussian noise, so the mean vectors at each sample have the same form as in (3.138), which can be written in vector form as

$$\tilde{\mathbf{m}}_1 = \tilde{b} \tilde{\mathbf{v}}(\psi). \quad (3.142)$$

We assume the noise at successive samples is independent so we have an IID model.

The duality between the two applications is important because it means we are solving two problems at once. ■

⁸ ψ is the wavenumber whose significance is discussed in various references, for example [Van02].

3.2.2 Independent Components with Unequal Variances

Here, the r_i are statistically independent but have unequal variances. Thus,

$$\mathbf{K} = \begin{bmatrix} \sigma_1^2 & & & \mathbf{0} \\ & \sigma_2^2 & & \\ & & \sigma_3^2 & \\ & & & \ddots \\ \mathbf{0} & & & \sigma_N^2 \end{bmatrix} \quad (3.143)$$

and

$$\mathbf{Q} = \begin{bmatrix} \frac{1}{\sigma_1^2} & & & \mathbf{0} \\ & \frac{1}{\sigma_2^2} & & \\ & & \frac{1}{\sigma_3^2} & \\ & & & \ddots \\ \mathbf{0} & & & \frac{1}{\sigma_N^2} \end{bmatrix}. \quad (3.144)$$

Substituting into (3.102) and performing the multiplication, we have

$$d^2 = \sum_{i=1}^N \frac{(\Delta m_i)^2}{\sigma_i^2}. \quad (3.145)$$

Now the various difference components contribute to d^2 with weighting that is inversely proportional to the variance along that coordinate. We can also interpret the result as distance in a new coordinate system.

Let

$$\Delta \mathbf{m}' = \begin{bmatrix} \frac{1}{\sigma_1} \Delta m_1 \\ \frac{1}{\sigma_2} \Delta m_2 \\ \vdots \\ \frac{1}{\sigma_N} \Delta m_N \end{bmatrix} \quad (3.146)$$

and

$$R'_i = \frac{1}{\sigma_i} R_i. \quad (3.147)$$

This transformation changes the scale on each axis so that the variances are equal to one. We see that d corresponds exactly to the difference vector in this “scaled” coordinate system.

The sufficient statistic is

$$l(\mathbf{R}) = \sum_{i=1}^N \frac{\Delta m_i \cdot R_i}{\sigma_i^2}. \quad (3.148)$$

In the scaled coordinate system it is the dot product of the two vectors

$$l(\mathbf{R}') = \Delta \mathbf{m}'^T \mathbf{R}' \quad (3.149)$$

and

$$d^2 = \Delta \mathbf{m}'^T \Delta \mathbf{m}' = \|\Delta \mathbf{m}'\|^2. \quad (3.150)$$

For the complex case

$$\tilde{\mathbf{K}} = \begin{bmatrix} \sigma_{\tilde{r}_1}^2 & & & \mathbf{0} \\ & \sigma_{\tilde{r}_2}^2 & & \\ & & \sigma_{\tilde{r}_3}^2 & \\ & & & \ddots \\ \mathbf{0} & & & \sigma_{\tilde{r}_N}^2 \end{bmatrix} \quad (3.151)$$

and

$$\Delta \tilde{\mathbf{m}}' = \left[\frac{\Delta \tilde{m}_1}{\sigma_{\tilde{r}_1}} \quad \frac{\Delta \tilde{m}_2}{\sigma_{\tilde{r}_2}} \quad \dots \quad \frac{\Delta \tilde{m}_N}{\sigma_{\tilde{r}_N}} \right]^T. \quad (3.152)$$

For the mean vector in (3.152),

$$d^2 = 2 \|\Delta \tilde{\mathbf{m}}'\|^2. \quad (3.153)$$

3.2.3 General Case: Eigendecomposition

This is the general case. A satisfactory answer for l and d is already available in (3.93) and (3.102):

$$l(\mathbf{R}) = \Delta \mathbf{m}^T \mathbf{Q} \mathbf{R} \quad (3.154)$$

and

$$d^2 = \Delta \mathbf{m}^T \mathbf{Q} \Delta \mathbf{m}. \quad (3.155)$$

Valuable insight into the important features of the problem can be gained by looking at it in a different manner.

The key to the simplicity in the first two cases was the diagonal covariance matrix. This suggests that we try to represent \mathbf{r} in a new coordinate system in which the components are statistically independent random variables. In Figure 3.10a, we show the observation in the original coordinate system. In Figure 3.10b, we show a new set of coordinate axes, which we denote by the orthogonal unit vectors $\phi_1, \phi_2, \dots, \phi_N$:

$$\phi_i^T \phi_j = \delta_{ij}. \quad (3.156)$$

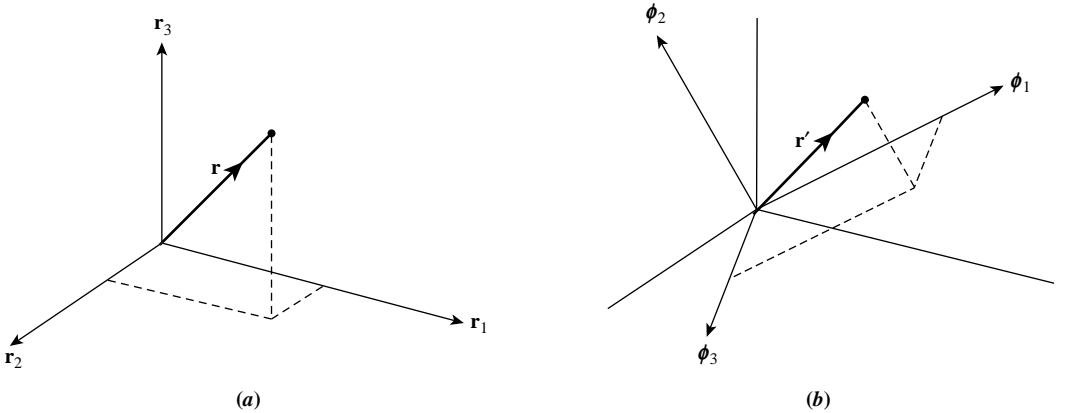


Figure 3.10: Coordinate systems: (a) original coordinate system; (b) new coordinate system.

We denote the observation in the new coordinate system by \mathbf{r}' . We want to choose the orientation of the new system so that the components r'_i and r'_j are uncorrelated (and therefore statistically independent, for they are Gaussian) for all $i \neq j$. In other words,

$$E[(r'_i - m'_i)(r'_j - m'_j)] = \lambda_i \delta_{ij}, \quad (3.157)$$

where

$$E(r'_i) \triangleq m'_i \quad (3.158)$$

and

$$\text{Var}(r'_i) \triangleq \lambda_i. \quad (3.159)$$

Now the components of \mathbf{r}' can be expressed simply in terms of the dot product of the original vector \mathbf{r} and the various unit vectors

$$r'_i = \mathbf{r}^T \boldsymbol{\phi}_i = \boldsymbol{\phi}_i^T \mathbf{r}. \quad (3.160)$$

Using (3.160) in (3.157), we obtain

$$E[\boldsymbol{\phi}_i^T (\mathbf{r} - \mathbf{m})(\mathbf{r} - \mathbf{m})^T \boldsymbol{\phi}_j] = \lambda_i \delta_{ij}. \quad (3.161)$$

The expectation of the random part is just \mathbf{K} (see (3.51) and (3.90)). Therefore, (3.161) becomes

$$\lambda_i \delta_{ij} = \boldsymbol{\phi}_i^T \mathbf{K} \boldsymbol{\phi}_j. \quad (3.162)$$

This will be satisfied if and only if

$$\lambda_j \boldsymbol{\phi}_j = \mathbf{K} \boldsymbol{\phi}_j, \quad \text{for } j = 1, 2, \dots, N. \quad (3.163)$$

To check the “if” part of this result, substitute (3.163) into (3.162):

$$\lambda_i \delta_{ij} = \boldsymbol{\phi}_i^T \lambda_j \boldsymbol{\phi}_j = \lambda_i \delta_{ij}, \quad (3.164)$$

where the right equality follows from (3.156). The “only if” part follows using a simple proof by contradiction. Now (3.163) can be written with the j subscript suppressed:

$$\lambda \boldsymbol{\phi} = \mathbf{K} \boldsymbol{\phi}. \quad (3.165)$$

We see that the question of finding the proper coordinate system reduces to the question of whether we can find N solutions to (3.165) that satisfy (3.156).

It is instructive to write (3.165) out in detail. Each $\boldsymbol{\phi}$ is a vector with N components:

$$\boldsymbol{\phi} = [\phi_1 \ \phi_2 \ \phi_3 \ \cdots \ \phi_N]^T. \quad (3.166)$$

Substituting (3.166) into (3.165), we have

$$\begin{aligned} K_{11}\phi_1 + K_{12}\phi_2 + \cdots + K_{1N}\phi_N &= \lambda\phi_1 \\ K_{21}\phi_1 + K_{22}\phi_2 + \cdots + K_{2N}\phi_N &= \lambda\phi_2 \\ K_{31}\phi_1 + K_{32}\phi_2 + \cdots + K_{3N}\phi_N &= \lambda\phi_3 \\ &\vdots \\ K_{N1}\phi_1 + K_{N2}\phi_2 + \cdots + K_{NN}\phi_N &= \lambda\phi_N. \end{aligned} \quad (3.167)$$

We see that (3.167) corresponds to a set of N homogeneous simultaneous equations. A nontrivial solution will exist if and only if the determinant of the coefficient matrix is zero. In other words if and only if

$$|\mathbf{K} - \lambda \mathbf{I}| = \begin{vmatrix} K_{11} - \lambda & K_{12} & K_{13} & \cdots & K_{1N} \\ K_{21} & K_{22} - \lambda & K_{23} & \cdots & K_{2N} \\ K_{31} & K_{32} & K_{33} - \lambda & \cdots & K_{3N} \\ \vdots & \vdots & \vdots & \ddots & \vdots \\ K_{N1} & K_{N2} & K_{N3} & \cdots & K_{NN} - \lambda \end{vmatrix} = 0. \quad (3.168)$$

We see that this is an N th-order polynomial in λ . The N roots, denoted by $\lambda_1, \lambda_2, \dots, \lambda_N$, are called the *eigenvalues* of the covariance matrix \mathbf{K} . It can be shown that the following properties are true (e.g. [Bel60] or [Hil52]):

1. Because \mathbf{K} is symmetric, the eigenvalues are real.
2. Because \mathbf{K} is a covariance matrix, the eigenvalues are nonnegative. (Otherwise we would have random variables with negative variances.) If \mathbf{K} is rank N , then all N eigenvalues will be positive. If \mathbf{K} is rank $D < N$, then D eigenvalues will be positive and $N - D$ will be zero.

For each λ_i we can find a solution $\boldsymbol{\phi}_i$ to (3.165). Because there is an arbitrary constant associated with each solution to (3.165), we may choose $\boldsymbol{\phi}_i$ to have unit length.

$$\boldsymbol{\phi}_i^T \boldsymbol{\phi}_i = 1. \quad (3.169)$$

These solutions are called the normalized *eigenvectors* of \mathbf{K} . Several other properties may also be shown for symmetric matrices.

3. If the roots λ_i are distinct, the corresponding eigenvectors are orthogonal.

4. If a particular root λ_i is of multiplicity M , the M associated eigenvectors are linearly independent. They can be chosen to be orthonormal.
5. If we define an $N \times N$ matrix

$$\mathbf{u}_\phi = [\boldsymbol{\phi}_1 \quad \boldsymbol{\phi}_2 \quad \cdots \quad \boldsymbol{\phi}_N]. \quad (3.170)$$

and an $N \times N$ diagonal matrix,

$$\Lambda_\phi = \text{diag}[\lambda_1 \quad \lambda_2 \quad \cdots \quad \lambda_N], \quad (3.171)$$

then we can write \mathbf{K} as

$$\mathbf{K} = \mathbf{u}_\phi \Lambda_\phi \mathbf{u}_\phi^T = \sum_{i=1}^N \lambda_i \boldsymbol{\phi}_i \boldsymbol{\phi}_i^T. \quad (3.172)$$

6. The \mathbf{u}_ϕ matrix is orthogonal

$$\mathbf{u}_\phi^{-1} = \mathbf{u}_\phi^T \quad (3.173)$$

and

$$\mathbf{u}_\phi \mathbf{u}_\phi^T = \mathbf{u}_\phi^T \mathbf{u}_\phi = \mathbf{I}. \quad (3.174)$$

We refer to \mathbf{u}_ϕ as the *diagonalization matrix* because premultiplying \mathbf{r} by \mathbf{u}_ϕ^T diagonalizes the covariance matrix.

7. If \mathbf{K} is nonsingular, then

$$\mathbf{Q} = \mathbf{K}^{-1} = \mathbf{u}_\phi \Lambda_\phi^{-1} \mathbf{u}_\phi^T = \sum_{i=1}^N \frac{1}{\lambda_i} \boldsymbol{\phi}_i \boldsymbol{\phi}_i^T. \quad (3.175)$$

We have now described a coordinate system in which the observations are statistically independent. The mean difference vector can be expressed

$$\begin{aligned} \Delta m'_1 &= \boldsymbol{\phi}_1^T \Delta \mathbf{m} \\ \Delta m'_2 &= \boldsymbol{\phi}_2^T \Delta \mathbf{m} \\ &\vdots \\ \Delta m'_N &= \boldsymbol{\phi}_N^T \Delta \mathbf{m} \end{aligned} \quad (3.176)$$

or in vector notation

$$\Delta \mathbf{m}' = \begin{bmatrix} \boldsymbol{\phi}_1^T \\ \boldsymbol{\phi}_2^T \\ \boldsymbol{\phi}_3^T \\ \vdots \\ \boldsymbol{\phi}_N^T \end{bmatrix} \Delta \mathbf{m} \triangleq \mathbf{u}_\phi^T \Delta \mathbf{m} \quad (3.177)$$

and

$$\mathbf{R}' = \mathbf{u}_\phi^T \mathbf{R}. \quad (3.178)$$

The resulting sufficient statistic in the new coordinate system is

$$l(\mathbf{R}') = \sum_{i=1}^N \frac{\Delta m'_i \cdot R'_i}{\lambda_i} \quad (3.179)$$

or

$$l(\mathbf{R}') = \Delta \mathbf{m}^T \mathbf{u}_\phi \Lambda_\phi^{-1} \mathbf{u}_\phi^T \mathbf{R}' = \Delta \mathbf{m}'^T \Lambda_\phi^{-1} \mathbf{R}' \quad (3.180)$$

and

$$d^2 = \sum_{i=1}^N \frac{(\Delta m'_i)^2}{\lambda_i} = \Delta \mathbf{m}'^T \Lambda_\phi^{-1} \Delta \mathbf{m}'.$$

(3.181)

Note that if

$$\mathbf{K} = \sigma_n^2 \mathbf{I} \quad (3.182)$$

then (3.165) becomes

$$\lambda \boldsymbol{\phi} = \sigma_n^2 \mathbf{I} \boldsymbol{\phi}, \quad (3.183)$$

so any set of orthonormal vectors are suitable eigenvectors and all of the eigenvalues are equal to σ_n^2 . Thus, we can write

$$\sigma_n^2 \mathbf{I} = \sigma_n^2 \sum_{i=1}^N \boldsymbol{\phi}_i \boldsymbol{\phi}_i^T \quad (3.184)$$

for any set of orthonormal vectors.

There are several ways to implement the optimum detector that offer different insights.

Diagonalization Detection. In this implementation, we use (3.177) and (3.180) directly. The resulting likelihood ratio processor is shown in Figure 3.11.

Note that this implementation reduces the general case to the model in Section 3.2.2, independent components with unequal variances.

Whitening Detection. A second implementation is obtained by using (3.175) in (3.154). Define the $N \times N$ matrix

$$\Lambda_\phi^{-\frac{1}{2}} = \text{diag} \left[\frac{1}{\sqrt{\lambda_1}} \quad \frac{1}{\sqrt{\lambda_2}} \quad \cdots \quad \frac{1}{\sqrt{\lambda_N}} \right], \quad (3.185)$$

Then (3.154) may be written as

$$l(\mathbf{R}) = \Delta \mathbf{m}^T \mathbf{u}_\phi \Lambda_\phi^{-\frac{1}{2}} \Lambda_\phi^{-\frac{1}{2}} \mathbf{u}_\phi^T \mathbf{R}. \quad (3.186)$$

We define a whitening transformation \mathbf{W}^T , where

$$\mathbf{W}^T = \Lambda_\phi^{-\frac{1}{2}} \mathbf{u}_\phi^T. \quad (3.187)$$

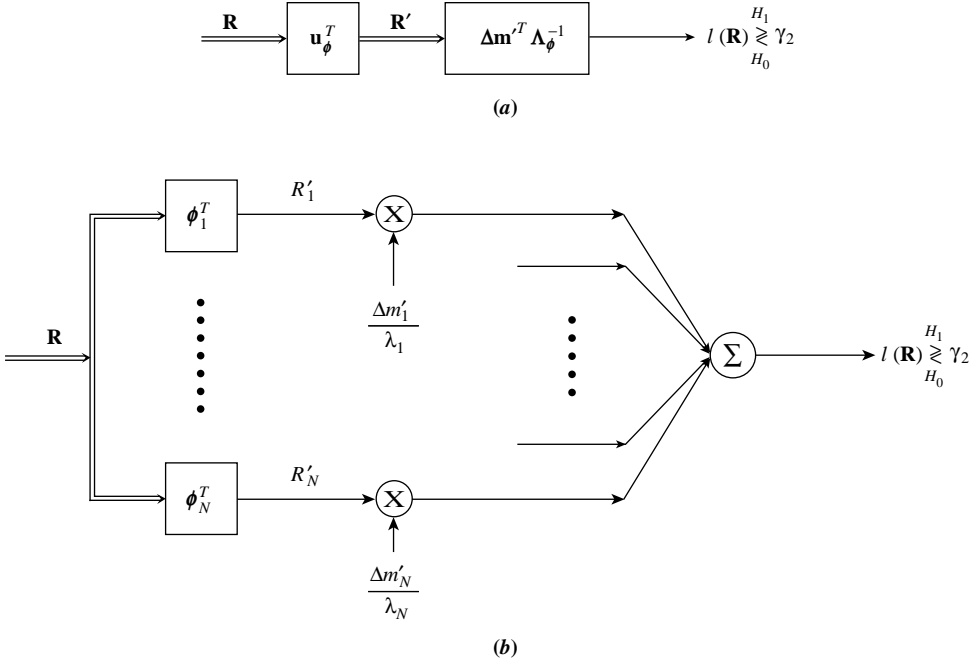


Figure 3.11: Diagonal detection: (a) vector representation; (b) scalar representation.

Then

$$l(\mathbf{R}) = \Delta \mathbf{m}^T \mathbf{W} \mathbf{W}^T \mathbf{R} = \Delta \mathbf{m}_W^T \mathbf{R}_W \quad (3.188)$$

where

$$\mathbf{R}_W = \mathbf{W}^T \mathbf{R} \quad (3.189)$$

and

$$\Delta \mathbf{m}_W = \mathbf{W}^T \Delta \mathbf{m}. \quad (3.190)$$

Note that

$$\begin{aligned} \text{Cov}[\mathbf{R}_W | H_i] &= E\left[\mathbf{W}^T (\mathbf{R} - \mathbf{m}_i)(\mathbf{R} - \mathbf{m}_i)^T \mathbf{W}\right] \\ &= \mathbf{W}^T \mathbf{K} \mathbf{W} \\ &= \Lambda_\phi^{-\frac{1}{2}} \mathbf{u}_\phi^T \mathbf{u}_\phi \Lambda_\phi \mathbf{u}_\phi^T \mathbf{u}_\phi \Lambda_\phi^{-\frac{1}{2}} = \mathbf{I}. \end{aligned} \quad (3.191)$$

A whitening transformation results in an identity matrix as the covariance matrix at its output. The whitening implementation is shown in Figure 3.12.

Note that this implementation reduces the general case to the model in Section 3.2.1, independent components with equal variances. To be consistent, we always whiten so the

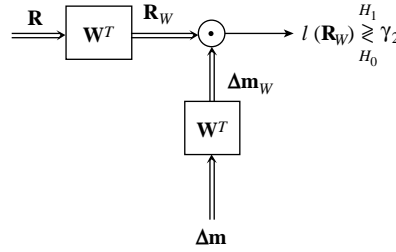


Figure 3.12: Whitening detection.

output covariance matrix is \mathbf{I} . The same result can be obtained by whitening so the output covariance matrix is $\sigma^2\mathbf{I}$, where $\sigma^2 > 0$ is an arbitrary constant.

Correlation Detection. The third implementation is simply the correlation detector shown in Figure 3.5.

The derivation leading to (3.179) and (3.181) is somewhat involved, but the result is of fundamental importance, for it demonstrates that there always exists a coordinate system in which the random variables are uncorrelated and that the new system is related to the old system by a linear transformation. To illustrate the technique we consider a simple example.⁹

Example 3.3. For simplicity we let $N = 2$ and $\mathbf{m}_0 = \mathbf{0}$. Let

$$\mathbf{K} = \begin{bmatrix} 1 & \rho \\ \rho & 1 \end{bmatrix} \quad (3.192)$$

and

$$\mathbf{m}_1 = \begin{bmatrix} m_{11} \\ m_{12} \end{bmatrix}. \quad (3.193)$$

To find the eigenvalues, we solve

$$\begin{vmatrix} 1 - \lambda & \rho \\ \rho & 1 - \lambda \end{vmatrix} = 0 \quad (3.194)$$

or

$$(1 - \lambda)^2 - \rho^2 = 0. \quad (3.195)$$

Solving,

$$\begin{aligned} \lambda_1 &= 1 + \rho, \\ \lambda_2 &= 1 - \rho. \end{aligned} \quad (3.196)$$

⁹We carry out the solution analytically to gain some insight. In practice, we will use Matlab to find the eigenvectors and eigenvalues.

To find ϕ_1 , we substitute λ_1 into (3.167),

$$\begin{bmatrix} 1 & \rho \\ \rho & 1 \end{bmatrix} \begin{bmatrix} \phi_{11} \\ \phi_{12} \end{bmatrix} = \begin{bmatrix} (1 + \rho)\phi_{11} \\ (1 + \rho)\phi_{12} \end{bmatrix}. \quad (3.197)$$

Solving, we obtain

$$\phi_{11} = \phi_{12}. \quad (3.198)$$

Normalizing gives

$$\phi_1 = \begin{bmatrix} +\frac{1}{\sqrt{2}} \\ +\frac{1}{\sqrt{2}} \end{bmatrix}. \quad (3.199)$$

Similarly,

$$\phi_2 = \begin{bmatrix} +\frac{1}{\sqrt{2}} \\ -\frac{1}{\sqrt{2}} \end{bmatrix}. \quad (3.200)$$

The old and new axes are shown in Figure 3.13. The transformation is

$$\mathbf{u}_\phi = [\phi_1 \quad \phi_2] = \begin{bmatrix} +\frac{1}{\sqrt{2}} & +\frac{1}{\sqrt{2}} \\ +\frac{1}{\sqrt{2}} & -\frac{1}{\sqrt{2}} \end{bmatrix} \quad (3.201)$$

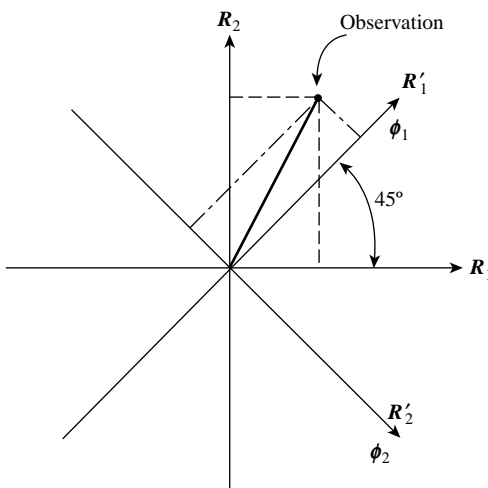


Figure 3.13: Rotation of axes.

and

$$\begin{aligned} R'_1 &= \frac{R_1 + R_2}{\sqrt{2}}, \\ R'_2 &= \frac{R_1 - R_2}{\sqrt{2}}, \\ m'_{11} &= \frac{m_{11} + m_{12}}{\sqrt{2}}, \\ m'_{12} &= \frac{m_{11} - m_{12}}{\sqrt{2}}. \end{aligned} \quad (3.202)$$

The sufficient statistic is obtained by using (3.202) in (3.179),

$$l(\mathbf{R}') = \frac{1}{1+\rho} \frac{(R_1 + R_2)(m_{11} + m_{12})}{2} + \frac{1}{1-\rho} \frac{(R_1 - R_2)(m_{11} - m_{12})}{2} \quad (3.203)$$

and d^2 is

$$d^2 = \frac{(m_{11} + m_{12})^2}{2(1+\rho)} + \frac{(m_{11} - m_{12})^2}{2(1-\rho)} = \frac{(m'_{11})^2}{1+\rho} + \frac{(m'_{12})^2}{1-\rho}. \quad (3.204)$$

To illustrate a typical application in which the transformation is important, we consider a simple optimization problem. The length of the mean vector is constrained,

$$\|\mathbf{m}_1\|^2 = 1. \quad (3.205)$$

We want to choose m_{11} and m_{12} to maximize d^2 . Because our transformation is a rotation, it preserves lengths

$$\|\mathbf{m}'_1\|^2 = 1. \quad (3.206)$$

Looking at (3.204), we obtain the solution by inspection:

- If $\rho > 0$, choose $m'_{11} = 0$ and $m'_{12} = 1$.
- If $\rho < 0$, choose $m'_{11} = 1$ and $m'_{12} = 0$.
- If $\rho = 0$, all vectors satisfying (3.205) give the same d^2 .

We see that this corresponds to choosing the mean vector to be equal to the eigenvector with the smallest eigenvalue. This result can be easily extended to N dimensions.

The result in this example is characteristic of a wide class of optimization problems in which the solution corresponds to an eigenvector (or the waveform analog to it). ■

The complex Gaussian case follows in a similar manner. The covariance matrix $\tilde{\mathbf{K}}$ is Hermitian, $\tilde{\mathbf{K}}^H = \tilde{\mathbf{K}}$, and positive semidefinite and the eigendecomposition is

$$\lambda \tilde{\boldsymbol{\phi}} = \tilde{\mathbf{K}} \tilde{\boldsymbol{\phi}}. \quad (3.207)$$

The eigenvalues are real and nonnegative and the eigenvectors are complex.

We define

$$\tilde{\mathbf{u}}_{\tilde{\boldsymbol{\phi}}} = \begin{bmatrix} \tilde{\boldsymbol{\phi}}_1 & \tilde{\boldsymbol{\phi}}_2 & \cdots & \tilde{\boldsymbol{\phi}}_N \end{bmatrix} \quad (3.208)$$

and

$$\Lambda_{\tilde{\boldsymbol{\phi}}} = \text{diag}[\lambda_1 \ \lambda_2 \ \cdots \ \lambda_N]. \quad (3.209)$$

The $\tilde{\mathbf{u}}_{\tilde{\phi}}$ matrix is unitary

$$\tilde{\mathbf{u}}_{\tilde{\phi}}^{-1} = \tilde{\mathbf{u}}_{\tilde{\phi}}^H \quad (3.210)$$

and

$$\tilde{\mathbf{u}}_{\tilde{\phi}} \tilde{\mathbf{u}}_{\tilde{\phi}}^H = \tilde{\mathbf{u}}_{\tilde{\phi}}^H \tilde{\mathbf{u}}_{\tilde{\phi}} = \mathbf{I}. \quad (3.211)$$

Thus,

$$\tilde{\mathbf{K}} = \tilde{\mathbf{u}}_{\tilde{\phi}} \Lambda_{\tilde{\phi}} \tilde{\mathbf{u}}_{\tilde{\phi}}^H = \sum_{i=1}^N \lambda_i \tilde{\mathbf{u}}_{\tilde{\phi}} \tilde{\phi}_i \tilde{\phi}_i^H \quad (3.212)$$

and if $\tilde{\mathbf{K}}$ is nonsingular,

$$\tilde{\mathbf{Q}} = \tilde{\mathbf{K}}^{-1} = \tilde{\mathbf{u}}_{\tilde{\phi}} \Lambda_{\tilde{\phi}}^{-1} \tilde{\mathbf{u}}_{\tilde{\phi}}^H = \sum_{i=1}^N \frac{1}{\lambda_i} \tilde{\phi}_i \tilde{\phi}_i^H. \quad (3.213)$$

In the transformed coordinate system

$$\Delta \tilde{\mathbf{m}}' = \tilde{\mathbf{u}}_{\tilde{\phi}}^H \Delta \tilde{\mathbf{m}} \quad (3.214)$$

$$\tilde{\mathbf{R}}' = \tilde{\mathbf{u}}_{\tilde{\phi}}^H \tilde{\mathbf{R}} \quad (3.215)$$

$$l(\tilde{\mathbf{R}}) = \Re \left\{ \Delta \tilde{\mathbf{m}}'^H \Lambda_{\tilde{\phi}}^{-1} \tilde{\mathbf{R}}' \right\} \quad (3.216)$$

$$d^2 = 2 \sum_{i=1}^N \frac{|\Delta \tilde{m}'_i|^2}{\lambda_i} = 2 \Delta \tilde{\mathbf{m}}'^H \Lambda_{\tilde{\phi}}^{-1} \Delta \tilde{\mathbf{m}}'. \quad (3.217)$$

The whitening matrix is

$$\tilde{\mathbf{W}}^H = \Lambda_{\tilde{\phi}}^{-\frac{1}{2}} \tilde{\mathbf{u}}_{\tilde{\phi}}^H \quad (3.218)$$

and

$$\Delta \tilde{\mathbf{m}}_W = \tilde{\mathbf{W}}^H \Delta \tilde{\mathbf{m}} \quad (3.219)$$

$$\tilde{\mathbf{R}}_W = \tilde{\mathbf{W}}^H \tilde{\mathbf{R}} \quad (3.220)$$

$$l(\tilde{\mathbf{R}}) = \Re \left\{ \Delta \tilde{\mathbf{m}}_W^H \tilde{\mathbf{R}}_W \right\}. \quad (3.221)$$

All of the canonical detectors in Figures 3.5, 3.11, and 3.12 have the same structure and the output is $\tilde{l}(\tilde{\mathbf{R}})$. We then take the real part to obtain $l(\tilde{\mathbf{R}})$.

In the next section, we generalize the optimum signal design result in Example 3.3.

3.2.4 Optimum Signal Design

From (3.181), we know that

$$d^2 = \sum_{i=1}^N \frac{(\Delta m'_i)^2}{\lambda_i}. \quad (3.222)$$

Later, we will see that $\|\mathbf{m}_1\|^2$ and $\|\mathbf{m}_0\|^2$ correspond to the energy in the deterministic component in the received waveform. Suppose that this is constrained, for example,

$$\|\mathbf{m}_j\|^2 \leq E, \quad j = 0, 1. \quad (3.223)$$

We want to choose \mathbf{m}_0 and \mathbf{m}_1 to maximize d^2 .

We assume that the eigenvalues are ordered,

$$\lambda_1 \geq \lambda_2 \geq \lambda_3 \geq \cdots \geq \lambda_N. \quad (3.224)$$

Thus, it is obvious from (3.222) that we choose

$$\Delta\mathbf{m}' = \alpha \begin{bmatrix} 0 & 0 & \cdots & 1 \end{bmatrix}^T, \quad (3.225)$$

where α is a parameter to be optimized. Now

$$\Delta\mathbf{m}' = \mathbf{u}_\phi^T \Delta\mathbf{m}. \quad (3.226)$$

Using (3.174)

$$\Delta\mathbf{m} = \mathbf{u}_\phi \Delta\mathbf{m}', \quad (3.227)$$

so

$$\Delta\mathbf{m} = \alpha \begin{bmatrix} \phi_1 & \phi_2 & \phi_3 & \cdots & \phi_N \end{bmatrix} \begin{bmatrix} 0 \\ 0 \\ 0 \\ \vdots \\ 1 \end{bmatrix} \quad (3.228)$$

or

$$\Delta\mathbf{m} = \alpha \phi_N. \quad (3.229)$$

All of the signal energy is along the eigenvector with the smallest eigenvalue. Then

$$d^2 = \frac{\alpha^2}{\lambda_N} = \frac{\|\Delta\mathbf{m}\|^2}{\lambda_N}. \quad (3.230)$$

Before proceeding, it should be noted that while choosing $\Delta\mathbf{m} = \alpha \phi_N$ maximizes d^2 , choosing $\Delta\mathbf{m} = \alpha \phi_1$ minimizes d^2 . Thus, we have the following bounds on d^2 for any choice of $\Delta\mathbf{m}$.

$$\frac{\|\Delta\mathbf{m}\|^2}{\lambda_1} \leq d^2 \leq \frac{\|\Delta\mathbf{m}\|^2}{\lambda_N}. \quad (3.231)$$

We must now maximize $\alpha^2 = \|\Delta\mathbf{m}\|^2$ subject to the energy constraint in (3.223). This is done by choosing

$$\|\Delta\mathbf{m}_j\|^2 = E \quad (3.232)$$

and

$$\mathbf{m}_1 = -\mathbf{m}_0 = \sqrt{E}\phi_N. \quad (3.233)$$

Then

$$\Delta \mathbf{m} = 2\sqrt{E}\phi_N, \quad (3.234)$$

$$\|\Delta \mathbf{m}\|^2 = 4E, \quad (3.235)$$

$$d^2 = \frac{4E}{\lambda_N}. \quad (3.236)$$

In the complex case, we have

$$\frac{2 \|\Delta \tilde{\mathbf{m}}\|^2}{\lambda_1} \leq d^2 \leq \frac{2 \|\Delta \tilde{\mathbf{m}}\|^2}{\lambda_N} \quad (3.237)$$

$$\tilde{\mathbf{m}}_1 = -\tilde{\mathbf{m}}_0 = \sqrt{E}\tilde{\phi}_N, \quad (3.238)$$

$$\Delta \tilde{\mathbf{m}} = 2\sqrt{E}\tilde{\phi}_N, \quad (3.239)$$

$$\|\Delta \tilde{\mathbf{m}}\|^2 = 4E, \quad (3.240)$$

$$d^2 = \frac{8E}{\lambda_N}. \quad (3.241)$$

We will find that this result that is obvious in eigenspace will be the key to a large number of signal design applications.

Example 3.4. Consider the case where $N \geq 2$ and \mathbf{K} is the Toeplitz matrix,¹⁰

$$\mathbf{K} = \begin{bmatrix} 1 & \rho & \rho^2 & \cdots & \rho^{N-1} \\ \rho & 1 & \rho & \cdots & \rho^{N-2} \\ \vdots & \vdots & \vdots & \ddots & \vdots \\ \rho^{N-1} & \rho^{N-2} & \rho^{N-3} & \cdots & 1 \end{bmatrix}. \quad (3.242)$$

For $N = 2$, we saw in Example 3.3 that the largest eigenvalue was $\lambda_1 = 1 + |\rho|$ and the smallest eigenvalue was $\lambda_2 = 1 - |\rho|$. The eigenvectors were the same for all ρ with $\phi_1 = \frac{1}{\sqrt{2}} [1 \ 1]^T$ when $\rho > 0$ and $\phi_1 = \frac{1}{\sqrt{2}} [1 \ -1]^T$ when $\rho < 0$. When $N > 2$, it is difficult to obtain analytical expressions for the eigenvalues and eigenvectors except in special cases, and we use Matlab to find them numerically. In the limiting case of $\rho = 0$, $\mathbf{K} = \mathbf{I}$, and $\lambda_i = 1$, $i = 1, 2, \dots, N$.

When $\rho = 1$

$$\mathbf{K} = \begin{bmatrix} 1 & 1 & 1 & \cdots & 1 \\ 1 & 1 & 1 & \cdots & 1 \\ \vdots & \vdots & \vdots & \ddots & \vdots \\ 1 & 1 & 1 & \cdots & 1 \end{bmatrix} = \mathbf{1}\mathbf{1}^T, \quad (3.243)$$

¹⁰This \mathbf{K} matrix would occur if we sampled a stationary random process whose covariance function is $K(\tau) = \exp(-\beta|\tau|)$ at 1 s intervals, where $\rho = e^{-\beta}$ and $\beta \geq 0$.

where

$$\mathbf{1} \triangleq [1 \ 1 \ 1 \ \cdots \ 1]^T. \quad (3.244)$$

\mathbf{K} is a rank 1 matrix with one nonzero eigenvalue $\lambda_1 = N$ and corresponding eigenvector¹¹

$$\phi_1 = \frac{1}{\sqrt{N}} \mathbf{1}. \quad (3.245)$$

Similarly when $\rho = -1$,

$$\mathbf{K} = \begin{bmatrix} 1 & -1 & 1 & \cdots & (-1)^{N-1} \\ -1 & 1 & -1 & \cdots & (-1)^{N-2} \\ \vdots & \vdots & \vdots & \ddots & \vdots \\ (-1)^{N-1} & (-1)^{N-2} & (-1)^{N-3} & \cdots & 1 \end{bmatrix} = \mathbf{1}_{(-)} \mathbf{1}_{(-)}^T \quad (3.246)$$

where

$$\mathbf{1}_{(-)} \triangleq [1 \ -1 \ 1 \ \cdots \ (-1)^{N-1}]^T. \quad (3.247)$$

Again, $\lambda_1 = N$ and $\lambda_2 = \cdots = \lambda_N = 0$ with

$$\phi_1 = \frac{1}{\sqrt{N}} \mathbf{1}_{(-)}. \quad (3.248)$$

For any ρ ,

$$\sum_{i=1}^N \lambda_i = \text{tr}(\mathbf{K}) = N. \quad (3.249)$$

A plot of the eigenvalues versus ρ for $N = 4$ is shown in Figure 3.14. All of the eigenvalues are equal to one for $\rho = 0$. As $|\rho|$ approaches one, the largest eigenvalue goes to N and the remaining eigenvalues go to zero.

The upper and lower bounds on d^2 in (3.231) are plotted against N for several values of $|\rho|$ for $\|\Delta\mathbf{m}\|^2 = 1$ in Figure 3.15. We see that the upper bound increases with $|\rho|$ since λ_N decreases, and it levels out at about $N = 6$ for all values of ρ . The lower bound decreases with both N and $|\rho|$.

In Figure 3.16, the upper and lower bounds on d^2 are plotted versus $|\rho|$ for $N = 10$ and $\|\Delta\mathbf{m}\|^2 = 1$. When $|\rho|$ is small, the noise energy is distributed fairly equally among the eigenvectors in the N -dimensional space and there is not much difference between the upper and lower bounds. As $|\rho|$ increases, the noise energy becomes more concentrated along the dominant eigenvectors and eventually is confined to a one-dimensional subspace when $|\rho| = 1$. The difference between the upper and lower bounds indicates that more performance gain can be achieved by aligning the signal energy along the eigenvector containing the least noise and more performance degradation will occur when the signal energy is aligned with the eigenvector containing the most noise. ■

There are two special cases of the eigendecomposition that occur in several situations. We discuss them in the next two sections.

¹¹Note that our development assumed that \mathbf{K} is nonsingular. In our applications, we will always assume that there is a nonzero white noise component $\sigma_w^2 \mathbf{I}$ added to \mathbf{K} to avoid the singular case.

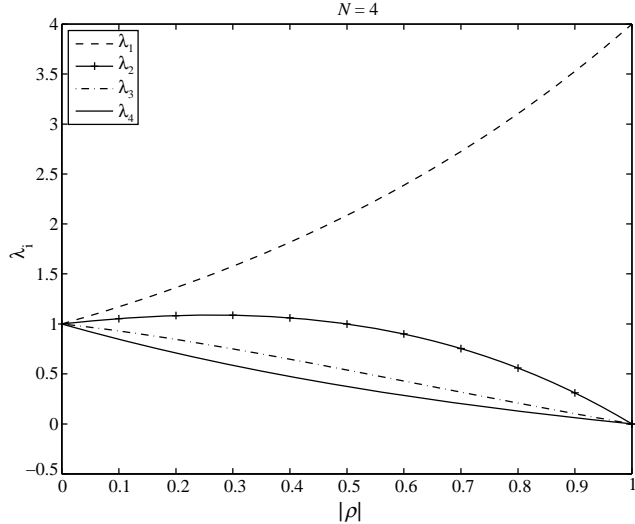


Figure 3.14: Eigenvalues of \mathbf{K} versus $|\rho|$.

3.2.5 Interference Matrix: Estimator–Subtractor

A case that occurs frequently in practice is when the observations contain a component due to white noise and a component due to interference. Thus,

$$\begin{aligned} H_0 : \mathbf{r} &= \mathbf{m}_0 + \mathbf{n}_I + \mathbf{w}, \\ H_1 : \mathbf{r} &= \mathbf{m}_1 + \mathbf{n}_I + \mathbf{w}, \end{aligned} \quad (3.250)$$

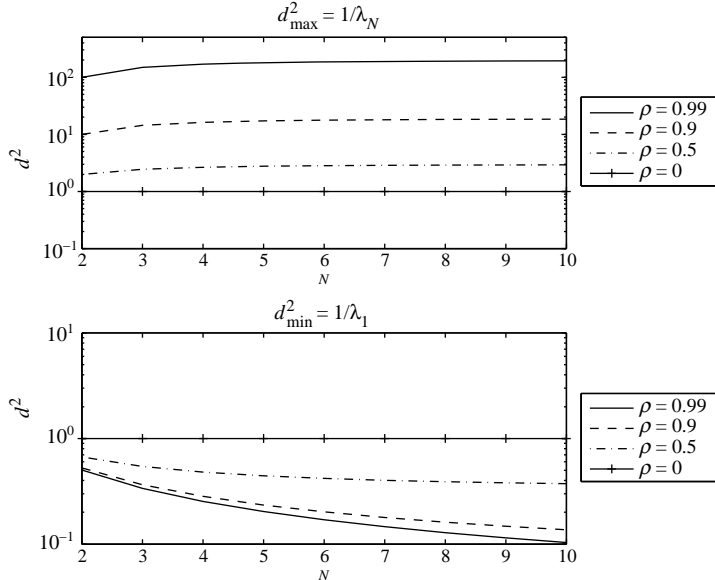


Figure 3.15: Upper and lower bounds on d^2 versus N for $\|\Delta\mathbf{m}\|^2 = 1$.

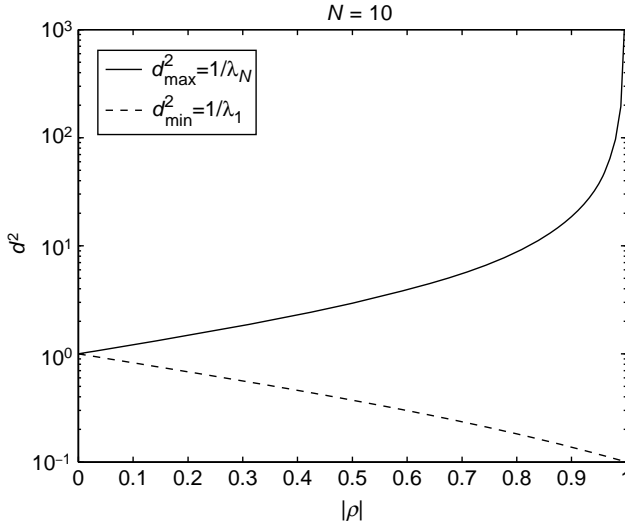


Figure 3.16: Upper and lower bounds on d^2 versus $|\rho|$ for $N = 10$ and $\|\Delta\mathbf{m}\|^2 = 1$.

where \mathbf{n}_I and \mathbf{w} are zero-mean, statistically independent N -dimensional random vectors,

$$\mathbf{w} \sim N(\mathbf{0}, \sigma_w^2 \mathbf{I}) \quad (3.251)$$

where \mathbf{I} is an N -dimensional identity matrix, and

$$\mathbf{n}_I \sim N(\mathbf{0}, \mathbf{K}_I). \quad (3.252)$$

The interference covariance matrix \mathbf{K}_I does not have to be of rank N .

The covariance matrix is

$$\mathbf{K} = \sigma_w^2 \mathbf{I} + \mathbf{K}_I \quad (3.253)$$

and

$$\mathbf{Q} = [\sigma_w^2 \mathbf{I} + \mathbf{K}_I]^{-1} = \frac{1}{\sigma_w^2} \left[\mathbf{I} + \frac{1}{\sigma_w^2} \mathbf{K}_I \right]^{-1}. \quad (3.254)$$

To do an eigendecomposition, we substitute (3.253) into (3.165).

$$\lambda \boldsymbol{\phi} = [\sigma_w^2 \mathbf{I} + \mathbf{K}_I] \boldsymbol{\phi} \quad (3.255)$$

or

$$(\lambda - \sigma_w^2) \boldsymbol{\phi} = \mathbf{K}_I \boldsymbol{\phi} \quad (3.256)$$

or

$$\lambda^I \boldsymbol{\phi} = \mathbf{K}_I \boldsymbol{\phi}, \quad (3.257)$$

where

$$\lambda^I \triangleq \lambda - \sigma_w^2. \quad (3.258)$$

So the decomposition is done with respect to the interference covariance matrix. However, the Λ_ϕ matrix uses the total eigenvalue $\lambda = \lambda^I + \sigma_w^2$,

$$\Lambda_\phi = \text{diag} \begin{bmatrix} \lambda_1^I + \sigma_w^2 & \lambda_2^I + \sigma_w^2 & \dots & \lambda_N^I + \sigma_w^2 \end{bmatrix}. \quad (3.259)$$

We can implement the optimum detector in any of the canonical forms in Section 3.2.3. We can obtain an interesting interpretation of the optimum detector by writing

$$\begin{aligned} \mathbf{Q} &= \sum_{i=1}^N \frac{1}{\sigma_w^2 + \lambda_i^I} \boldsymbol{\phi}_i \boldsymbol{\phi}_i^T \\ &= \frac{1}{\sigma_w^2} \sum_{i=1}^N \left[1 - \frac{\lambda_i^I}{\sigma_w^2 + \lambda_i^I} \right] \boldsymbol{\phi}_i \boldsymbol{\phi}_i^T \\ &= \frac{1}{\sigma_w^2} \left[\sum_{i=1}^N \boldsymbol{\phi}_i \boldsymbol{\phi}_i^T - \sum_{i=1}^N \frac{\lambda_i^I}{\sigma_w^2 + \lambda_i^I} \boldsymbol{\phi}_i \boldsymbol{\phi}_i^T \right] \\ &= \frac{1}{\sigma_w^2} [\mathbf{I} - \mathbf{H}], \end{aligned} \quad (3.260)$$

where

$$\mathbf{H} \triangleq \sum_{i=1}^N \frac{\lambda_i^I}{\sigma_w^2 + \lambda_i^I} \boldsymbol{\phi}_i \boldsymbol{\phi}_i^T. \quad (3.261)$$

Using (3.260) in (3.93), the optimum detector is

$$\begin{aligned} l(\mathbf{R}) &= \Delta \mathbf{m}^T \mathbf{Q} \mathbf{R} \\ &= \frac{1}{\sigma_w^2} \Delta \mathbf{m}^T [\mathbf{I} - \mathbf{H}] \mathbf{R}. \end{aligned} \quad (3.262)$$

The performance is given by

$$\begin{aligned} d^2 &= \frac{1}{\sigma_w^2} \Delta \mathbf{m}^T [\mathbf{I} - \mathbf{H}] \Delta \mathbf{m} \\ &= \frac{1}{\sigma_w^2} \left\{ \|\Delta \mathbf{m}\|^2 - \Delta \mathbf{m}^T \mathbf{H} \Delta \mathbf{m} \right\}. \end{aligned} \quad (3.263)$$

Using (3.261) in (3.263), we can write d^2 as

$$d^2 = \frac{1}{\sigma_w^2} \left\{ \|\Delta \mathbf{m}\|^2 - \Delta \mathbf{m}^T \left(\sum_{i=1}^N \boldsymbol{\phi}_i \left(\frac{\lambda_i^I / \sigma_w^2}{1 + \lambda_i^I / \sigma_w^2} \right) \boldsymbol{\phi}_i^T \right) \Delta \mathbf{m} \right\}. \quad (3.264)$$

Since from (3.176)

$$\Delta m'_i = \boldsymbol{\phi}_i^T \Delta \mathbf{m}, \quad (3.265)$$

d^2 can be written as

$$d^2 = \frac{1}{\sigma_w^2} \left\{ \|\Delta \mathbf{m}\|^2 - \sum_{i=1}^N (\Delta m'_i)^2 \left(\frac{\lambda_i^I / \sigma_w^2}{1 + \lambda_i^I / \sigma_w^2} \right) \right\}. \quad (3.266)$$

It is important to understand the geometric interpretation of this result. We have developed an eigenspace whose coordinate axes are orthogonal. The total disturbances along these axes (interference and noise) are statistically independent Gaussian random variables. The total “signal” strength is $\|\Delta\mathbf{m}\|^2$ and the signal component along the i th axis is $\Delta m'_i$, where

$$\sum_{i=1}^N (\Delta m'_i)^2 = \|\Delta\mathbf{m}\|^2. \quad (3.267)$$

The $\Delta m'_i$ describes how the signal strength is distributed along the axes in eigenspace. If the λ_i^I were all zero, then

$$d^2 = \frac{\|\Delta\mathbf{m}\|^2}{\sigma_w^2}, \quad (3.268)$$

which is the independent components with equal variance case in Section 3.2.1. When the λ_i^I are not zero, d^2 is decreased by subtracting $(\Delta m'_i)^2$ multiplied by a term that depends on the λ_i^I/σ_w^2 ratio. As

$$\frac{\lambda_i^I}{\sigma_w^2} \rightarrow \infty,$$

the entire $(\Delta m'_i)^2$ is subtracted because the i th signal component is not contributing to performance. As

$$\frac{\lambda_i^I}{\sigma_w^2} \rightarrow 0,$$

nothing is subtracted out.

We can also combine the terms in (3.266) to obtain

$$d^2 = \frac{1}{\sigma_w^2} \sum_{i=1}^N \frac{(\Delta m'_i)^2}{1 + \lambda_i^I/\sigma_w^2}. \quad (3.269)$$

The optimum LRT can be implemented as shown in Figure 3.17.

In Chapter 5, when we study Gaussian estimation, we will show that, in the absence of \mathbf{m}_0 and \mathbf{m}_1 , the minimum mean-square error (MMSE) estimate of \mathbf{n}_l is

$$\hat{\mathbf{n}}_l = \mathbf{H}\mathbf{R}, \quad (3.270)$$

so the LRT can be interpreted as an estimator–subtractor.

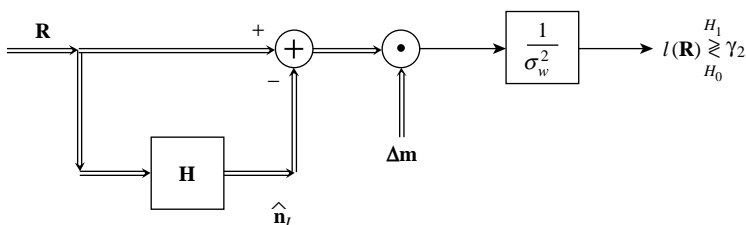


Figure 3.17: Estimator–subtractor implementation.

In the complex Gaussian case, we have

$$\tilde{\mathbf{K}} = \sigma_{\tilde{w}}^2 \mathbf{I} + \tilde{\mathbf{K}}_I, \quad (3.271)$$

$$\tilde{\mathbf{Q}} = \sum_{i=1}^N \frac{1}{\sigma_w^2 + \lambda_i^I} \tilde{\boldsymbol{\phi}}_i \tilde{\boldsymbol{\phi}}_i^H, \quad (3.272)$$

$$\tilde{\mathbf{H}} = \sum_{i=1}^N \frac{\lambda_i^I}{\sigma_w^2 + \lambda_i^I} \tilde{\boldsymbol{\phi}}_i \tilde{\boldsymbol{\phi}}_i^H, \quad (3.273)$$

$$\Delta \tilde{\mathbf{m}}' = \tilde{\boldsymbol{\phi}}_i^H \Delta \tilde{\mathbf{m}}, \quad (3.274)$$

$$l(\tilde{\mathbf{R}}) = \frac{1}{\sigma_w^2} \Re \{ \Delta \tilde{\mathbf{m}}^H [\mathbf{I} - \tilde{\mathbf{H}}] \tilde{\mathbf{R}} \}, \quad (3.275)$$

$$d^2 = \frac{2}{\sigma_w^2} \left\{ \|\Delta \tilde{\mathbf{m}}\|^2 - \sum_{i=1}^N |\Delta \tilde{m}'_i|^2 \left(\frac{\lambda_i^I / \sigma_w^2}{1 + \lambda_i^I / \sigma_w^2} \right) \right\}. \quad (3.276)$$

Example 3.5 (continuation of Example 3.4). Now we assume

$$\mathbf{K} = \sigma_I^2 \begin{bmatrix} 1 & \rho & \rho^2 & \cdots & \rho^{N-1} \\ \rho & 1 & \rho & \cdots & \rho^{N-2} \\ \rho^2 & \rho & 1 & \cdots & \rho^{N-3} \\ \vdots & \vdots & \vdots & \ddots & \vdots \\ \rho^{N-1} & \rho^{N-2} & \rho^{N-3} & \cdots & 1 \end{bmatrix} + \sigma_w^2 \mathbf{I}. \quad (3.277)$$

The important properties are in (3.257) and (3.259). We do an eigendecomposition of \mathbf{K}_I to determine its eigenvectors and eigenvalues. The eigenvectors of \mathbf{K} are the same as the eigenvectors of \mathbf{K}_I (\mathbf{K} in Example 3.4) and the eigenvalues are

$$\lambda_i = \lambda_i^I + \sigma_w^2 = \sigma_I^2 \xi_i + \sigma_w^2, \quad i = 1, 2, \dots, N, \quad (3.278)$$

where the ξ_i are the eigenvalues of \mathbf{K} in Example 3.4.

The upper and lower bounds on d^2 are

$$\frac{\|\Delta \mathbf{m}\|^2}{\sigma_w^2 + \lambda_1^I} \leq d^2 \leq \frac{\|\Delta \mathbf{m}\|^2}{\sigma_w^2 + \lambda_N^I} \quad (3.279)$$

or

$$\frac{\|\Delta \mathbf{m}\|^2}{\sigma_w^2 + \sigma_I^2} \cdot \frac{1}{(1-\alpha) + \alpha \xi_1} \leq d^2 \leq \frac{\|\Delta \mathbf{m}\|^2}{\sigma_w^2 + \sigma_I^2} \cdot \frac{1}{(1-\alpha) + \alpha \xi_N}, \quad (3.280)$$

where

$$\alpha = \frac{\sigma_I^2}{\sigma_w^2 + \sigma_I^2} = \frac{\sigma_I^2 / \sigma_w^2}{1 + \sigma_I^2 / \sigma_w^2} \quad (3.281)$$

is the fraction of the total noise due to interference and $1 - \alpha$ is the fraction of total noise due to white noise. In Figure 3.18, the upper and lower bounds are plotted versus $|\rho|$ for $N = 10$ and $\|\Delta \mathbf{m}\|^2 / (\sigma_w^2 + \sigma_I^2) = 1$ for several values of σ_I^2 / σ_w^2 . As $\sigma_I^2 / \sigma_w^2 \rightarrow 0$, the noise is mostly white noise

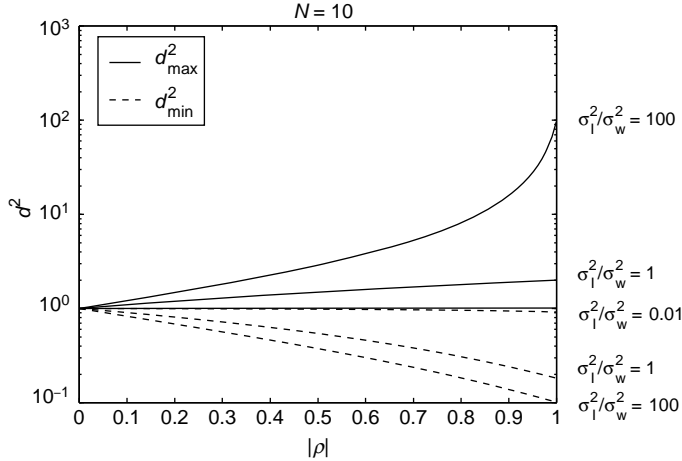


Figure 3.18: Upper and lower bounds on d^2 versus $|\rho|$ for $N = 10$ and $\|\Delta\mathbf{m}\|^2 / (\sigma_w^2 + \sigma_I^2) = 1$.

and d^2 is close to one for all $|\rho|$. As $\sigma_I^2/\sigma_w^2 \rightarrow \infty$, the bounds in Example 3.4, Figure 3.16 are obtained.

Although the interference becomes more concentrated along the dominant eigenvectors as $|\rho|$ increases, the white noise is always uniformly distributed across the eigenvectors. As the white noise is increased, there is less difference between the maximum and minimum eigenvalues, and less performance gain or loss from aligning the signal energy along the eigenvectors with the most or least interference. ■

3.2.6 Low-Rank Models

In many applications, the interference can be modeled as a sum of known vectors multiplied by Gaussian random variables.

In Example 3.1, we introduced a model in which the mean vector was defined by sampling a known complex exponential. In many applications, the received signal consists of this desired signal plus a set of D complex exponentials whose frequency is known but their amplitude and phase must be modeled as random variables.

In the array processing application, we encounter the same model. The desired signal is a planewave that is represented by the array manifold vector $\tilde{\mathbf{v}}_s$. The interferences are D planewaves whose directions are known and characterized by the array manifold vectors vector $\tilde{\mathbf{v}}_i$, $i = 1, \dots, D$.

We begin with the real Gaussian model. We use the model in (3.250) with

$$\mathbf{n}_I = \sum_{i=1}^D \mathbf{v}_i a_i = \mathbf{V} \mathbf{a}, \quad (3.282)$$

where

$$\mathbf{V} \triangleq \begin{bmatrix} \mathbf{v}_1 & \mathbf{v}_2 & \cdots & \mathbf{v}_D \end{bmatrix} \quad (3.283)$$

and

$$\mathbf{a} \triangleq [a_1 \ a_2 \ \cdots \ a_D]^T. \quad (3.284)$$

The $a_i, i = 1, 2, \dots, D$ are zero-mean Gaussian random variables with covariance matrix \mathbf{K}_a .

We can write the model in (3.250) as

$$\begin{aligned} H_1 : \mathbf{r} &= \mathbf{m}_1 + \mathbf{V}\mathbf{a} + \mathbf{w}, \\ H_0 : \mathbf{r} &= \mathbf{m}_0 + \mathbf{V}\mathbf{a} + \mathbf{w}, \end{aligned} \quad (3.285)$$

where \mathbf{V} is a known $N \times D$ matrix and \mathbf{a} is a $D \times 1$ zero-mean Gaussian random vector $N(\mathbf{0}, \mathbf{K}_a)$.

The covariance matrix of \mathbf{n}_I is

$$\mathbf{K}_I = E[\mathbf{V}\mathbf{a}\mathbf{a}^T\mathbf{V}^T] = \mathbf{V}\mathbf{K}_a\mathbf{V}^T. \quad (3.286)$$

From (3.253),

$$\mathbf{K} = \sigma_w^2 \mathbf{I} + \mathbf{V}\mathbf{K}_a\mathbf{V}^T. \quad (3.287)$$

In order to implement the optimum detector in Figure 3.17 we find the eigenvalues and eigenvectors of \mathbf{K}_I . However, we know that the columns of \mathbf{V} define a D -dimensional subspace that contains all of the interference. There will be D positive eigenvalues and $N - D$ eigenvalues equal to zero. We denote the D eigenvectors associated with the nonzero eigenvalues as $\phi_i; i = 1, 2, \dots, D$. These eigenvectors provide an orthonormal basis for the interference subspace.

Now (3.261) becomes

$$\mathbf{H} = \sum_{i=1}^D \frac{\lambda_i^I}{\sigma_w^2 + \lambda_i^I} \phi_i \phi_i^T, \quad (3.288)$$

so we can implement the LRT in Figure 3.17 and analyze the problem in the D -dimensional interference subspace and do not have to generate the rest of the eigenspace. The optimum detector is implemented using (3.288) in (3.262)

$$\begin{aligned} l(\mathbf{R}) &= \frac{1}{\sigma_w^2} \Delta \mathbf{m}^T [\mathbf{I} - \mathbf{H}] \mathbf{R} \\ &= \frac{1}{\sigma_w^2} \left[\Delta \mathbf{m}^T \mathbf{R} - \sum_{i=1}^D (\Delta m'_i \cdot R'_i) \left(\frac{\lambda_i^I / \sigma_w^2}{1 + \lambda_i^I / \sigma_w^2} \right) \right], \end{aligned} \quad (3.289)$$

and is shown in Figure 3.19.

The performance is given by (3.266), which becomes

$$d^2 = \frac{1}{\sigma_w^2} \left\{ \|\Delta \mathbf{m}\|^2 - \sum_{i=1}^D (\Delta m'_i)^2 \left(\frac{\lambda_i^I / \sigma_w^2}{1 + \lambda_i^I / \sigma_w^2} \right) \right\}. \quad (3.290)$$

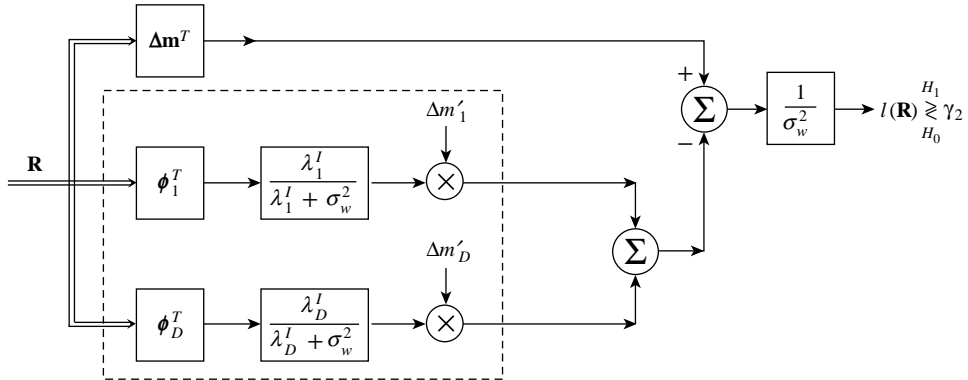


Figure 3.19: Optimum detection: low-rank model.

The complex version of the low-rank model follows in a similar manner. The model analogous to (3.285) is

$$\begin{aligned} H_1 : \tilde{\mathbf{r}} &= \tilde{\mathbf{m}}_1 + \tilde{\mathbf{V}}\tilde{\mathbf{a}} + \tilde{\mathbf{w}} \\ H_0 : \tilde{\mathbf{r}} &= \tilde{\mathbf{m}}_0 + \tilde{\mathbf{V}}\tilde{\mathbf{a}} + \tilde{\mathbf{w}} \end{aligned} \quad (3.291)$$

with

$$\tilde{\mathbf{H}} = \sum_{i=1}^D \frac{\lambda_i^I}{\sigma_{\tilde{w}}^2 + \lambda_i^I} \tilde{\boldsymbol{\phi}}_i \tilde{\boldsymbol{\phi}}_i^H \quad (3.292)$$

and

$$\begin{aligned} l(\tilde{\mathbf{R}}) &= \frac{1}{\sigma_{\tilde{w}}^2} \Re \left\{ \Delta \tilde{\mathbf{m}}^H [\mathbf{I} - \tilde{\mathbf{H}}] \tilde{\mathbf{R}} \right\} \\ &= \frac{1}{\sigma_{\tilde{w}}^2} \Re \left\{ \Delta \tilde{\mathbf{m}}^H \tilde{\mathbf{R}} - \sum_{i=1}^D (\Delta \tilde{m}_i'^* \cdot \tilde{R}_i) \left(\frac{\lambda_i^I}{\sigma_{\tilde{w}}^2 + \lambda_i^I} \right) \right\} \end{aligned} \quad (3.293)$$

and

$$d^2 = \frac{2}{\sigma_{\tilde{w}}^2} \left\{ \|\Delta \tilde{\mathbf{m}}\|^2 - \sum_{i=1}^D |\Delta \tilde{m}_i'|^2 \left(\frac{\lambda_i^I / \sigma_{\tilde{w}}^2}{1 + \lambda_i^I / \sigma_{\tilde{w}}^2} \right) \right\}. \quad (3.294)$$

Note that the optimum choice of $\Delta \mathbf{m}$ or $(\Delta \tilde{\mathbf{m}})$ is not unique in the low-rank interference case. Whenever \mathbf{K}_I has at least one zero eigenvalue, then any $\Delta \mathbf{m}$ that is orthogonal to the interference subspace is optimum.

We illustrate typical applications with two examples.

Example 3.6 (continuation of Example 3.1). Consider the complex exponential model in Example 3.1. The signal on H_1 is a complex exponential with frequency ω_s . For simplicity, we assume that the known complex amplitude is constant across samples, that is, $\tilde{b}_n = \tilde{b}$, $n = 0, 1, \dots, N - 1$.

The interference is a complex exponential with frequency ω_I and random complex amplitude \tilde{a} that is constant across samples. Thus,

$$[\tilde{\mathbf{m}}_1]_n = \tilde{b} e^{j\omega_s n}, \quad n = 0, 1, \dots, N-1, \quad (3.295)$$

$$[\tilde{\mathbf{v}}]_n = e^{j\omega_I n}, \quad n = 0, 1, \dots, N-1. \quad (3.296)$$

We assume that $\mathbf{m}_0 = \mathbf{0}$, so we are trying to detect a complex exponential in the presence of white noise and a single complex exponential interferer.

The observations on the two hypotheses are

$$\begin{aligned} H_1 : \tilde{\mathbf{r}} &= \tilde{\mathbf{m}}_1 + \tilde{\mathbf{v}}\tilde{a} + \tilde{\mathbf{w}}, \\ H_0 : \tilde{\mathbf{r}} &= \tilde{\mathbf{v}}\tilde{a} + \tilde{\mathbf{w}} \end{aligned} \quad (3.297)$$

with

$$\tilde{\mathbf{K}}_{\tilde{a}} = \sigma_I^2 \quad (3.298)$$

and

$$\tilde{\mathbf{K}}_{\tilde{\mathbf{w}}} = \sigma_w^2 \mathbf{I}. \quad (3.299)$$

The interference covariance matrix is

$$\tilde{\mathbf{K}}_I = \sigma_I^2 \tilde{\mathbf{v}} \tilde{\mathbf{v}}^H. \quad (3.300)$$

It is a rank $D = 1$ matrix with

$$\lambda_1^I = N\sigma_I^2, \quad (3.301)$$

$$\tilde{\phi}_1 = \frac{1}{\sqrt{N}} \tilde{\mathbf{v}}. \quad (3.302)$$

To evaluate performance, we use (3.294) with $D = 1$, $\Delta\tilde{\mathbf{m}} = \tilde{\mathbf{m}}_1$, and

$$\begin{aligned} \Delta\tilde{m}'_1 &= \tilde{\phi}_1^H \Delta\tilde{\mathbf{m}} = \frac{\tilde{b}}{\sqrt{N}} \sum_{n=0}^{N-1} e^{-j\omega_I n} e^{j\omega_s n} \\ &= \frac{\tilde{b}}{\sqrt{N}} \sum_{n=0}^{N-1} e^{j\Delta\omega n}, \end{aligned} \quad (3.303)$$

where

$$\Delta\omega \triangleq \omega_s - \omega_I. \quad (3.304)$$

To evaluate (3.303), we need the following identities:

$$\sum_{n=0}^{N-1} z^n = \frac{1 - z^N}{1 - z} \quad (3.305)$$

and

$$\sin(x) = \frac{e^{jx} - e^{-jx}}{2j}. \quad (3.306)$$

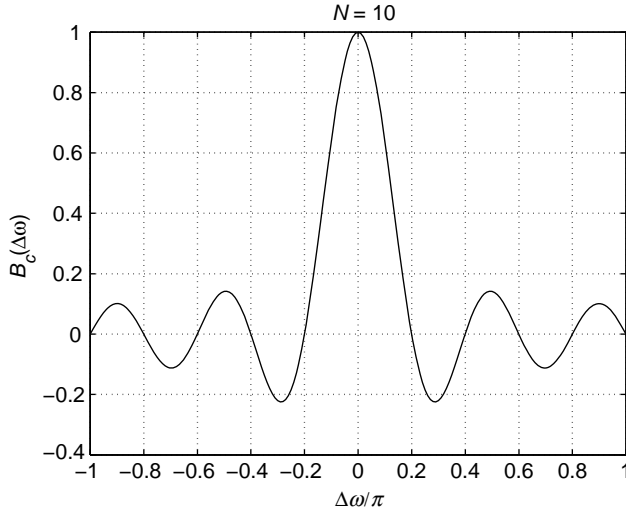


Figure 3.20: $B_c(\Delta\omega)$ versus $\Delta\omega/\pi$; $N = 10$.

We define

$$\tilde{\rho}_{Is}(\Delta\omega) \triangleq \frac{1}{N} \sum_{n=0}^{N-1} e^{j\Delta\omega n}. \quad (3.307)$$

It is the response of a complex correlator tuned to ω_I when the input is a complex exponential at $\omega_s = \omega_I + \Delta\omega$. Using (3.305) and (3.306) in (3.307), we obtain

$$\begin{aligned} \tilde{\rho}_{Is}(\Delta\omega) &= \frac{1}{N} \frac{1 - e^{j\Delta\omega N}}{1 - e^{j\Delta\omega}} \\ &= \frac{1}{N} \frac{e^{j\Delta\omega N/2}}{e^{j\Delta\omega/2}} \frac{e^{-j\Delta\omega N/2} - e^{j\Delta\omega N/2}}{e^{-j\Delta\omega/2} - e^{j\Delta\omega/2}} \\ &= e^{j\Delta\omega((N-1)/2)} \frac{1}{N} \frac{\sin(\frac{N\Delta\omega}{2})}{\sin(\frac{\Delta\omega}{2})} \\ &= e^{j\Delta\omega((N-1)/2)} B_c(\Delta\omega), \end{aligned} \quad (3.308)$$

where¹²

$$B_c(\Delta\omega) \triangleq \frac{1}{N} \frac{\sin(\frac{N\Delta\omega}{2})}{\sin(\frac{\Delta\omega}{2})}. \quad (3.309)$$

$B_c(\Delta\omega)$ is a real, symmetric function and is plotted in Figure 3.20 for $N = 10$. It is equal to one when $\Delta\omega = 0$, and equal to zero when $\Delta\omega$ is an integer multiple of $2\pi/N$.

¹²The notation $B_c(\cdot)$ comes from the array processing model that follows in Example 3.7, where this function is called the *conventional beampattern* of the array.

Substituting (3.307) and (3.308) into (3.303), we have

$$\Delta \tilde{m}'_1 = \tilde{b} \sqrt{N} e^{j\Delta\omega((N-1)/2)} B_c(\Delta\omega) \quad (3.310)$$

and

$$|\Delta \tilde{m}'_1|^2 = N |\tilde{b}|^2 B_c^2(\Delta\omega). \quad (3.311)$$

The mean vector norm term in (3.294) is

$$\|\Delta \tilde{\mathbf{m}}\|^2 = |\tilde{b}|^2 \sum_{n=0}^{N-1} |e^{j\omega_s n}|^2 = N |\tilde{b}|^2 \quad (3.312)$$

and d^2 is

$$\begin{aligned} d^2 &= \frac{2N|\tilde{b}|^2}{\sigma_w^2} \left\{ 1 - \left| \frac{\sin\left(\frac{N\Delta\omega}{2}\right)}{N \sin\left(\frac{\Delta\omega}{2}\right)} \right|^2 \left(\frac{N\sigma_I^2/\sigma_w^2}{1 + N\sigma_I^2/\sigma_w^2} \right) \right\} \\ &= 2N \cdot \text{SNR} \left\{ 1 - B_c^2(\Delta\omega) \frac{N \cdot \text{INR}}{1 + N \cdot \text{INR}} \right\}, \end{aligned} \quad (3.313)$$

where the signal-to-noise ratio (SNR) is defined as

$$\text{SNR} \triangleq \frac{|\tilde{b}|^2}{\sigma_w^2} \quad (3.314)$$

and the interference-to-noise ratio (INR) is defined as

$$\text{INR} \triangleq \frac{\sigma_I^2}{\sigma_w^2}. \quad (3.315)$$

In Figure 3.21, we plot d^2 versus $\Delta\omega$ for $N = 5$, $\text{SNR} = 1$, and several values of INR. For $\Delta\omega$ close to zero (when the interferer is close to the signal we are trying to detect), $d^2 \rightarrow 0$ as $\text{INR} \rightarrow \infty$. As $|\Delta\omega|$ increases, d^2 increases to a maximum value of $2N$ and exhibits a ripple behavior across $\Delta\omega$. The maximum value of $2N$ is obtained at the $N - 1 = 4$ points where the signal vector is orthogonal to the interference eigenvector and $B_c(\Delta\omega) = 0$. In Figure 3.22, we plot d^2 versus $\Delta\omega$ for $\text{INR} = 0.2$, $\text{SNR} = 1$, and several values of N . In each plot, d^2 has its minimum value at $\Delta\omega = 0$, and its maximum value of $2N$ at the $N - 1$ points where $\tilde{\mathbf{m}}_1$ and $\tilde{\phi}_1$ are orthogonal. ■

The dual model in array processing is discussed in Example 3.7.

Example 3.7 (continuation of Example 3.2). Consider the array processing model in Example 3.2. The mean $\tilde{\mathbf{m}}_1$ corresponds to the desired signal that is arriving from broadside, $\theta_s = \pi/2$. Thus, $\psi_s = 0$ and

$$\tilde{\mathbf{m}}_1 = \mathbf{1}\tilde{b}. \quad (3.316)$$

There is an interfering planewave arriving from $\psi_I = \pi \cos(\theta_I)$ as shown in Figure 3.23. Therefore, $\tilde{\mathbf{v}}$ is the array manifold vector given in (3.137)

$$\tilde{\mathbf{v}} = \mathbf{v}(\psi_I) = \begin{bmatrix} 1 & e^{-j\psi_I} & e^{-j2\psi_I} & \dots & e^{-j(N-1)\psi_I} \end{bmatrix}^T. \quad (3.317)$$

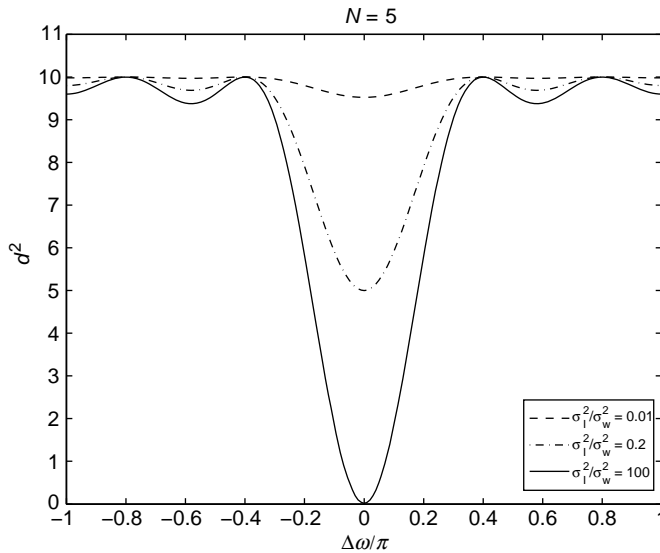


Figure 3.21: d^2 versus $\Delta\omega/\pi$ for $N = 5$ and $\text{SNR} = 1$.

The k th sample is an $N \times 1$ vector

$$\begin{aligned} H_1 : \mathbf{r}_k &= \tilde{\mathbf{m}}_1 + \tilde{\mathbf{v}}\tilde{a}_k + \tilde{\mathbf{w}}_k, & k &= 1, 2, \dots, K, \\ H_0 : \mathbf{r}_k &= \tilde{\mathbf{v}}\tilde{a}_k + \tilde{\mathbf{w}}_k, & k &= 1, 2, \dots, K. \end{aligned} \quad (3.318)$$

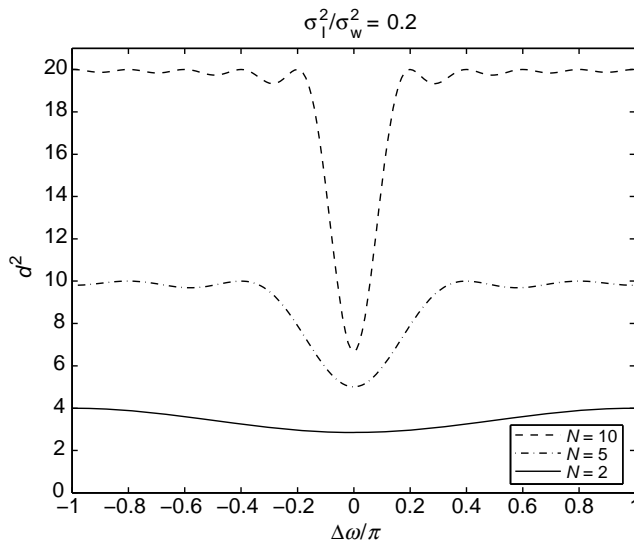


Figure 3.22: d^2 versus $\Delta\omega/\pi$ for $\text{INR} = 0.2$ and $\text{SNR} = 1$.

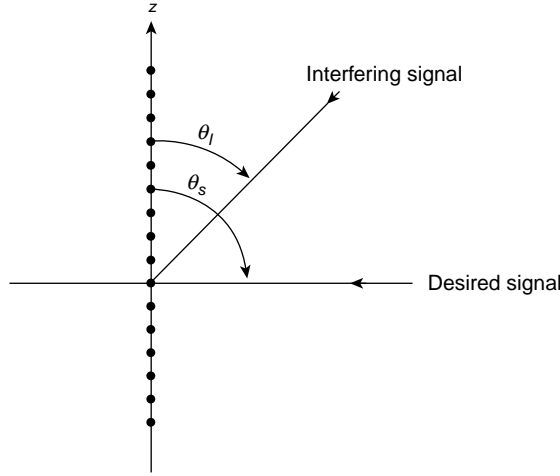


Figure 3.23: Uniform linear array with planewave interference.

We assume the \tilde{a}_k are zero-mean, IID complex Gaussian random variables with variance σ_l^2 . The white noise is independent across sensors and samples so

$$E[\tilde{\mathbf{w}}_k \tilde{\mathbf{w}}_l^H] = \sigma_w^2 \mathbf{I} \delta_{kl}, \quad (3.319)$$

and \tilde{a}_k and $\tilde{\mathbf{w}}_l$ are statistically independent. On each sample

$$\tilde{\mathbf{K}}_{lk} = \tilde{\mathbf{K}}_l = \sigma_l^2 \tilde{\mathbf{v}} \tilde{\mathbf{v}}^H. \quad (3.320)$$

We see that the model is the same as in Example 3.6 if we let $K = 1$ and

$$\Delta\psi \triangleq \psi_s - \psi_I = -\Delta\omega. \quad (3.321)$$

The resulting receiver is shown in Figure 3.24. We perform the same processing for each snapshot as in the complex exponential case, and then sum the snapshots. In this case we have

$$d^2 = 2KN \cdot \text{SNR} \left\{ 1 - B_c^2(\Delta\psi) \left(\frac{N \cdot \text{INR}}{1 + N \cdot \text{INR}} \right) \right\} \quad (3.322)$$

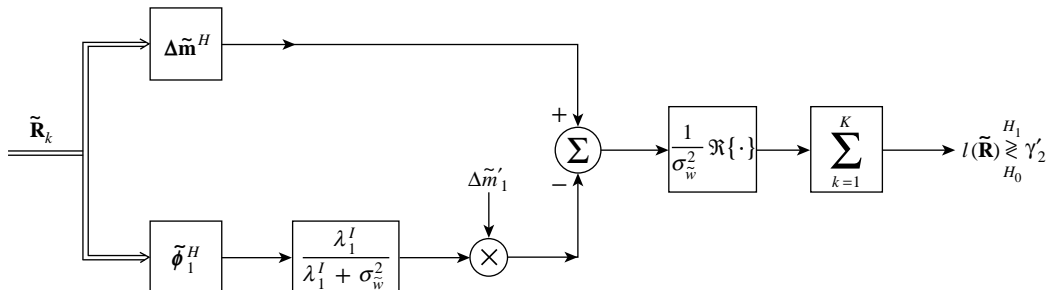


Figure 3.24: Optimum detection: linear array with single interfering planewave.

and we see that d^2 is increased by a factor of K . For the array processing problem, $\rho_{Is}(\Delta\psi)$ is the response of a beamformer pointed at ψ_I to a planewave at $\psi_s = 0$, and $B_c^2(\Delta\psi)$ is the conventional beampattern. ■

We consider further examples in the problems.

3.2.7 Summary

In this section, we have studied the Gaussian binary hypothesis testing problem for the special case in which the covariance matrices are identical on the hypotheses. The LRT follows easily. From (3.93)

$$l(\mathbf{R}) \triangleq \mathbf{\Delta m}^T \mathbf{Q} \mathbf{R} \stackrel{H_1}{\gtrless} \stackrel{H_0}{\lessdot} \gamma_2. \quad (3.323)$$

The sufficient statistic is a Gaussian random variable so the performance is completely determined by d^2 , where

$$d^2 = \mathbf{\Delta m}^T \mathbf{Q} \mathbf{\Delta m} \quad (3.324)$$

and P_D , P_F , and $\Pr(\epsilon)$ follow from (2.84), (2.85), and (2.86).

In order to understand the important issues in the model, we did an eigendecomposition of the \mathbf{K} matrix. This maps the model into an eigenspace where the component Gaussian random variables are statistically independent and the resulting covariance matrix is diagonal. Working in eigenspace enables us to understand the problem from a more fundamental basis.

When \mathbf{K} is nonsingular, d^2 can be written as

$$d^2 = \sum_{i=1}^N \frac{(\Delta m'_i)^2}{\lambda_i}, \quad (3.325)$$

where $\Delta m'_i$ is the projection of $\mathbf{\Delta m}$ along the i th eigenvector and λ_i is the i th eigenvalue. Note that we always include a white noise component $N(\mathbf{0}, \sigma_w^2 \mathbf{I})$ in \mathbf{K} , so it is always nonsingular.

Thus, the performance is bounded by

$$\frac{\|\mathbf{\Delta m}\|^2}{\lambda_{\max}} \leq d^2 \leq \frac{\|\mathbf{\Delta m}\|^2}{\lambda_{\min}} \quad (3.326)$$

and the optimum signal design follows easily, with

$$d^2 = \frac{4E}{\lambda_{\min}}. \quad (3.327)$$

Similar results were given for the complex case.

In many applications, we encounter interference that can be modeled as a sum of known vectors multiplied by Gaussian random variables. This leads to a low-rank model that was analyzed in Section 3.2.6. Two important examples, detection of a complex exponential and detection of a planewave, were analyzed.

3.3 EQUAL MEAN VECTORS

In the second special case of interest, the mean vectors on the two hypotheses are equal. In other words,

$$\mathbf{m}_1 = \mathbf{m}_0 \triangleq \mathbf{m}. \quad (3.328)$$

Substituting (3.328) into (3.57), we have

$$\frac{1}{2}(\mathbf{R} - \mathbf{m})^T(\mathbf{Q}_0 - \mathbf{Q}_1)(\mathbf{R} - \mathbf{m}) \stackrel{H_1}{\underset{H_0}{\gtrless}} \ln \eta + \frac{1}{2} \ln |\mathbf{K}_1| - \frac{1}{2} \ln |\mathbf{K}_0| = \gamma_1. \quad (3.329)$$

Because the mean vectors contain no information that will tell us which hypothesis is true, the likelihood test subtracts them from the received vector. Therefore, without loss of generality, we may assume that $\mathbf{m} = \mathbf{0}$.

We denote the difference of the inverse matrices as $\Delta \mathbf{Q}$:

$$\Delta \mathbf{Q} \triangleq \mathbf{Q}_0 - \mathbf{Q}_1. \quad (3.330)$$

The likelihood ratio test may be written as

$$l(\mathbf{R}) \triangleq \mathbf{R}^T \Delta \mathbf{Q} \mathbf{R} \stackrel{H_1}{\underset{H_0}{\gtrless}} 2 \ln \eta + \ln |\mathbf{K}_1| - \ln |\mathbf{K}_0| \triangleq \gamma_3.$$

(3.331)

Note that l is the dot product of two Gaussian vectors, \mathbf{r} and $\Delta \mathbf{Q} \mathbf{r}$. Thus, l is not a Gaussian random variable.

Both \mathbf{K}_0 and \mathbf{K}_1 are nonsingular in our definition of a Gaussian random vector. Therefore, we can always find \mathbf{Q}_0 , \mathbf{Q}_1 , and $\Delta \mathbf{Q}$. The important issue is determining the performance of the likelihood ratio test. In this section, we will study a number of interesting cases that are motivated by signal processing models that occur frequently in practice. In many of these cases, we can find an analytical expression for P_D and P_F or the probability of error. We also have available the bounds and approximate expressions developed in Section 2.4. For the general Gaussian model with $\mathbf{m}_0 = \mathbf{m}_1 = \mathbf{0}$, (3.68) reduces to

$$\mu(s) = \frac{s}{2} \ln |\mathbf{K}_0| + \frac{1-s}{2} \ln |\mathbf{K}_1| - \frac{1}{2} \ln |s\mathbf{K}_0 + (1-s)\mathbf{K}_1|. \quad (3.332)$$

Similarly, for the complex Gaussian case the LRT in (3.83) reduces to

$$l(\tilde{\mathbf{R}}) \triangleq \tilde{\mathbf{R}}^H \Delta \tilde{\mathbf{Q}} \tilde{\mathbf{R}} \stackrel{H_1}{\underset{H_0}{\gtrless}} \ln \eta + \ln |\tilde{\mathbf{K}}_1| - \ln |\tilde{\mathbf{K}}_0| \triangleq \gamma'_3,$$

(3.333)

where

$$\Delta \tilde{\mathbf{Q}} \triangleq \tilde{\mathbf{Q}}_0 - \tilde{\mathbf{Q}}_1, \quad (3.334)$$

and the $\mu(s)$ function in (3.84) becomes

$$\mu(s) = s \ln |\tilde{\mathbf{K}}_0| + (1-s) \ln |\tilde{\mathbf{K}}_1| - \ln |s\tilde{\mathbf{K}}_0 + (1-s)\tilde{\mathbf{K}}_1|. \quad (3.335)$$

We now consider the behavior of the likelihood ratio test for some interesting special cases.

3.3.1 Diagonal Covariance Matrix on H_0 : Equal Variance

Here, the r_i on H_0 are statistically independent variables with equal variances:

$$\mathbf{K}_0 = \sigma_w^2 \mathbf{I}. \quad (3.336)$$

We shall see later that (3.336) corresponds to the physical situation in which there is “white noise” only on H_0 . On H_1 the r_i contain the same noise as on H_0 , plus additional signal components that may be correlated. The model is

$$\begin{aligned} H_1 : \mathbf{r} &= \mathbf{w}, \\ H_0 : \mathbf{r} &= \mathbf{s} + \mathbf{w}. \end{aligned} \quad (3.337)$$

On H_1 the covariance matrix is

$$\mathbf{K}_1 = \mathbf{K}_s + \sigma_w^2 \mathbf{I}, \quad (3.338)$$

where the matrix \mathbf{K}_s represents the covariance matrix of the signal components. Then

$$\mathbf{Q}_0 = \frac{1}{\sigma_w^2} \mathbf{I} \quad (3.339)$$

and

$$\mathbf{Q}_1 = \frac{1}{\sigma_w^2} \left(\mathbf{I} + \frac{1}{\sigma_w^2} \mathbf{K}_s \right)^{-1}. \quad (3.340)$$

As in (3.260), it is convenient to write (3.340) as

$$\mathbf{Q}_1 = \frac{1}{\sigma_w^2} [\mathbf{I} - \mathbf{H}],$$

which implies that

$$\mathbf{H} = (\sigma_w^2 \mathbf{I} + \mathbf{K}_s)^{-1} \mathbf{K}_s = \mathbf{K}_s (\sigma_w^2 \mathbf{I} + \mathbf{K}_s)^{-1} = \sigma_w^2 (\mathbf{Q}_0 - \mathbf{Q}_1) = \sigma_w^2 \Delta \mathbf{Q}. \quad (3.341)$$

Using the matrix inversion lemma, we can also write

$$\mathbf{H} = \frac{1}{\sigma_w^2} \left[\frac{1}{\sigma_w^2} \mathbf{I} + \mathbf{K}_s^{-1} \right]^{-1}. \quad (3.342)$$

Substituting (3.341) into (3.331), we have

$$l(\mathbf{R}) \triangleq \frac{1}{\sigma_w^2} \mathbf{R}^T \mathbf{H} \mathbf{R} \stackrel{H_1}{\gtrless} \stackrel{H_0}{\gtrless} \gamma_3. \quad (3.343)$$

In Chapter 5, we will show that the MMSE estimate of the signal vector \mathbf{s} is,

$$\hat{\mathbf{s}} = \mathbf{H} \mathbf{R}, \quad (3.344)$$

so that the optimum detector can be written as

$$l(\mathbf{R}) = \mathbf{R}^T \hat{\mathbf{s}} = \hat{\mathbf{s}}^T \mathbf{R} \stackrel{H_1}{\gtrless} \stackrel{H_0}{\gtrless} \sigma_w^2 \gamma_3. \quad (3.345)$$

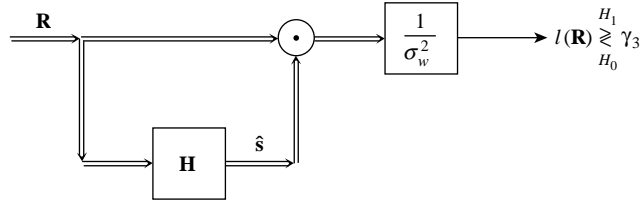


Figure 3.25: Estimator–correlator.

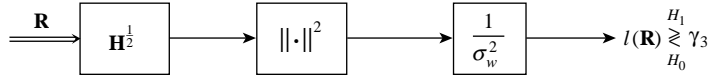


Figure 3.26: Squaring implementation.

The implementation in (3.345) is referred to as an estimator–correlator and is shown in Figure 3.25.

The matrix \mathbf{H} is symmetric and positive definite, so we can write,

$$\mathbf{H} = \mathbf{H}^{1/2} \mathbf{H}^{T/2} \quad (3.346)$$

and write (3.343) as

$$l(\mathbf{R}) = \frac{1}{\sigma_w^2} (\mathbf{R}^T \mathbf{H}^{1/2}) (\mathbf{H}^{T/2} \mathbf{R}) \stackrel{H_1}{\underset{H_0}{\gtrless}} \gamma_3, \quad (3.347)$$

which can be implemented as shown in Figure 3.26. The factorization in (3.346) is not unique. Later, in some applications we will impose the restriction that $\mathbf{H}^{1/2}$ be lower triangular. Then (3.346) is a Cholesky decomposition and is unique.¹³

The complex model follows in a similar fashion

$$\tilde{\mathbf{Q}}_0 = \frac{1}{\sigma_{\tilde{w}}^2} \mathbf{I}, \quad (3.348)$$

$$\tilde{\mathbf{H}} = \frac{1}{\sigma_{\tilde{w}}^2} \left(\frac{1}{\sigma_{\tilde{w}}^2} \mathbf{I} + \tilde{\mathbf{K}}_{\tilde{s}} \right)^{-1}, \quad (3.349)$$

and

$$l(\tilde{\mathbf{R}}) = \frac{1}{\sigma_{\tilde{w}}^2} \tilde{\mathbf{R}}^H \tilde{\mathbf{H}} \tilde{\mathbf{R}} \stackrel{H_1}{\underset{H_0}{\gtrless}} \gamma'_3. \quad (3.350)$$

$\tilde{\mathbf{H}}$ is a positive definite Hermitian matrix, so a Cholesky decomposition can be used.

Several subclasses are important.

¹³The Cholesky decomposition can be performed using the Matlab function chol.

3.3.1.1 Independent, Identically Distributed Signal Components

In this case the signal components s_i are independent variables with identical variances:

$$\mathbf{K}_s = \sigma_s^2 \mathbf{I}. \quad (3.351)$$

Then

$$\mathbf{H} = \left(\sigma_w^2 \mathbf{I} + \sigma_s^2 \mathbf{I} \right)^{-1} \sigma_s^2 \mathbf{I}, \quad (3.352)$$

or

$$\mathbf{H} = \frac{\sigma_s^2}{\sigma_w^2 + \sigma_s^2} \mathbf{I}. \quad (3.353)$$

The LRT is

$$l(\mathbf{R}) = \frac{1}{\sigma_w^2} \frac{\sigma_s^2}{\sigma_w^2 + \sigma_s^2} \mathbf{R}^T \mathbf{R} = \frac{1}{\sigma_w^2} \frac{\sigma_s^2}{\sigma_w^2 + \sigma_s^2} \sum_{i=1}^N R_i^2. \quad (3.354)$$

The constant can be incorporated in the threshold to give

$$l(\mathbf{R}) \triangleq \sum_{i=1}^N R_i^2 \stackrel{H_1}{\gtrless} \frac{\sigma_w^2(\sigma_w^2 + \sigma_s^2)}{\sigma_s^2} \gamma_3 \triangleq \gamma. \quad (3.355)$$

Note that this is just Example 2.2 with $\sigma_0^2 = \sigma_w^2$ and $\sigma_1^2 = \sigma_s^2 + \sigma_w^2$. We derived exact expressions for P_D and P_F in (2.109) and (2.110),

$$P_D = 1 - \Gamma_{N/2} \left(\frac{\gamma}{2(\sigma_s^2 + \sigma_w^2)} \right), \quad (3.356)$$

$$P_F = 1 - \Gamma_{N/2} \left(\frac{\gamma}{2\sigma_w^2} \right). \quad (3.357)$$

We also calculated $\mu(s)$ in (2.271).

The complex version of (3.355) is

$$\begin{aligned} l(\tilde{\mathbf{R}}) &\triangleq \sum_{i=1}^N |\tilde{R}_i|^2 \\ &= \sum_{i=1}^N R_{R_i}^2 + R_{I_i}^2. \end{aligned} \quad (3.358)$$

If

$$\tilde{\mathbf{K}}_0 = \sigma_{\tilde{w}}^2 \mathbf{I} \quad (3.359)$$

and

$$\tilde{\mathbf{K}}_1 = (\sigma_{\tilde{s}}^2 + \sigma_{\tilde{w}}^2) \mathbf{I} \quad (3.360)$$

then r_{R_i} and r_{I_i} are statistically independent real Gaussian random variables with variances equal to $\sigma_{\tilde{w}}^2/2$ on H_0 and $(\sigma_{\tilde{s}}^2 + \sigma_{\tilde{w}}^2)/2$ on H_1 . Therefore, the performance of the complex

model is equivalent to the real model with $2N$ observations and variances of one-half the complex model variance, that is,

$$P_D = 1 - \Gamma_N \left(\frac{\gamma'}{\sigma_s^2 + \sigma_w^2} \right), \quad (3.361)$$

$$P_F = 1 - \Gamma_N \left(\frac{\gamma'}{\sigma_{\tilde{w}}^2} \right), \quad (3.362)$$

where

$$\gamma' = \frac{\sigma_{\tilde{w}}^2(\sigma_s^2 + \sigma_{\tilde{w}}^2)}{\sigma_s^2} \gamma_3' = \frac{\sigma_{\tilde{w}}^2(\sigma_s^2 + \sigma_{\tilde{w}}^2)}{\sigma_s^2} \left(\ln \eta - N \ln \frac{\sigma_{\tilde{w}}^2}{\sigma_s^2 + \sigma_{\tilde{w}}^2} \right). \quad (3.363)$$

3.3.1.2 Independent Signal Components: Unequal Variances

In this case the signal components s_i are independent variables with variances $\sigma_{s_i}^2$:

$$\mathbf{K}_s = \begin{bmatrix} \sigma_{s_1}^2 & & & \mathbf{0} \\ & \sigma_{s_2}^2 & & \\ & & \sigma_{s_3}^2 & \\ & & & \ddots \\ \mathbf{0} & & & \sigma_{s_N}^2 \end{bmatrix}. \quad (3.364)$$

Then

$$\mathbf{H} = \begin{bmatrix} \frac{\sigma_{s_1}^2}{\sigma_w^2 + \sigma_{s_1}^2} & & & \mathbf{0} \\ & \frac{\sigma_{s_2}^2}{\sigma_w^2 + \sigma_{s_2}^2} & & \\ & & \frac{\sigma_{s_3}^2}{\sigma_w^2 + \sigma_{s_3}^2} & \\ & & & \ddots \\ \mathbf{0} & & & \frac{\sigma_{s_N}^2}{\sigma_w^2 + \sigma_{s_N}^2} \end{bmatrix}. \quad (3.365)$$

and

$$l(\mathbf{R}) = \frac{1}{\sigma_w^2} \sum_{i=1}^N \frac{\sigma_{s_i}^2}{\sigma_w^2 + \sigma_{s_i}^2} R_i^2 \stackrel{H_1}{\gtrless} \stackrel{H_0}{\gtrless} \gamma'. \quad (3.366)$$

The characteristic function of l follows easily, but the calculation of P_F and P_D are difficult.

For the complex case,

$$\tilde{\mathbf{K}}_{\tilde{s}} = \text{diag} \left[\sigma_{\tilde{s}_1}^2 \quad \sigma_{\tilde{s}_2}^2 \quad \sigma_{\tilde{s}_3}^2 \quad \dots \quad \sigma_{\tilde{s}_N}^2 \right] \quad (3.367)$$

and

$$\tilde{\mathbf{H}} = \text{diag} \left[\frac{\sigma_{\tilde{s}_1}^2}{\sigma_{\tilde{w}}^2 + \sigma_{\tilde{s}_1}^2} \quad \frac{\sigma_{\tilde{s}_2}^2}{\sigma_{\tilde{w}}^2 + \sigma_{\tilde{s}_2}^2} \quad \frac{\sigma_{\tilde{s}_3}^2}{\sigma_{\tilde{w}}^2 + \sigma_{\tilde{s}_3}^2} \quad \dots \quad \frac{\sigma_{\tilde{s}_N}^2}{\sigma_{\tilde{w}}^2 + \sigma_{\tilde{s}_N}^2} \right] \quad (3.368)$$

and

$$\begin{aligned} l(\tilde{\mathbf{R}}) &= \frac{1}{\sigma_w^2} \tilde{\mathbf{R}}^H \tilde{\mathbf{H}} \tilde{\mathbf{R}} \\ &= \frac{1}{\sigma_w^2} \sum_{i=1}^N \frac{\sigma_{\tilde{s}_i}^2}{\sigma_w^2 + \sigma_{\tilde{s}_i}^2} |\tilde{R}_i|^2. \end{aligned} \quad (3.369)$$

We defer the performance analysis until we study the general case in the next section.

3.3.1.3 Correlated Signal Components

This is of course, the general equal-mean case. However, we found in Section 3.2.3 that we can reduce it to the diagonal case by doing eigendecomposition. We repeat the relevant equations.

We write

$$\mathbf{K}_s = \mathbf{u}_\phi \Lambda_s \mathbf{u}_\phi^T, \quad (3.370)$$

where \mathbf{u}_ϕ is the $N \times N$ orthogonal matrix of the eigenvectors of \mathbf{K}_s ,

$$\mathbf{u}_\phi = [\phi_1 \quad \phi_2 \quad \cdots \quad \phi_N] \quad (3.371)$$

and Λ_s is the diagonal matrix of the eigenvalues,

$$\Lambda_s = \text{diag}[\lambda_{s1} \quad \lambda_{s2} \quad \cdots \quad \lambda_{sN}]. \quad (3.372)$$

Substituting into the second term on the right-hand side of (3.341)

$$\begin{aligned} \mathbf{H} &= \mathbf{u}_\phi \Lambda_s \mathbf{u}_\phi^T \left(\sigma_w^2 \mathbf{I} + \mathbf{u}_\phi \Lambda_s \mathbf{u}_\phi^T \right)^{-1} \\ &= \mathbf{u}_\phi \Lambda_s \mathbf{u}_\phi^T \left(\mathbf{u}_\phi (\sigma_w^2 \mathbf{I} + \Lambda_s) \mathbf{u}_\phi^T \right)^{-1} \\ &= \mathbf{u}_\phi \Lambda_s (\sigma_w^2 \mathbf{I} + \Lambda_s)^{-1} \mathbf{u}_\phi^T. \end{aligned} \quad (3.373)$$

Substituting into (3.343), the LRT is

$$l(\mathbf{R}) = \frac{1}{\sigma_w^2} \mathbf{R}^T \mathbf{u}_\phi \Lambda_s (\sigma_w^2 \mathbf{I} + \Lambda_s)^{-1} \mathbf{u}_\phi^T \mathbf{R} \stackrel{H_1}{\gtrless} \gamma_3. \quad (3.374)$$

Define the vector \mathbf{r}' whose covariance matrix is diagonal

$$\mathbf{r}' = \mathbf{u}_\phi^T \mathbf{r}. \quad (3.375)$$

Denoting the signal component of \mathbf{r}' on H_1 as \mathbf{s}' , then

$$\text{Cov}(\mathbf{s}') = \text{diag}[\lambda_{s1} \quad \lambda_{s2} \quad \cdots \quad \lambda_{sN}]. \quad (3.376)$$

The optimum detector is given by (3.366) with R'_i replacing R_i . Then

$$l(\mathbf{R}) = \frac{1}{\sigma_w^2} \sum_{i=1}^N \frac{\lambda_{s_i}}{\lambda_{s_i} + \sigma_w^2} (R'_i)^2. \quad (3.377)$$

The optimum detector is shown in Figure 3.27.

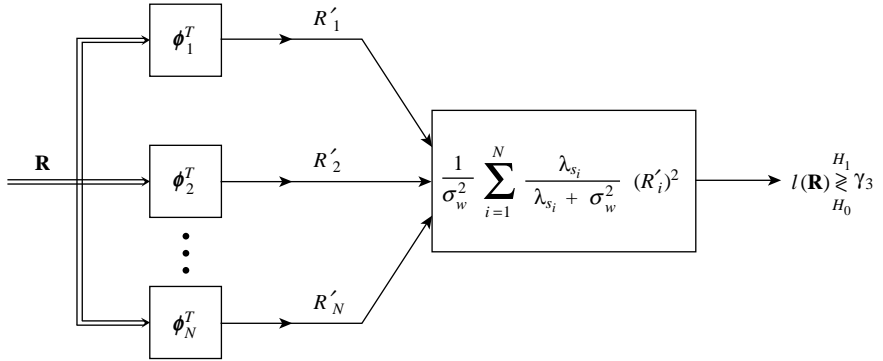


Figure 3.27: Optimum detector.

Note that we diagonalized the signal component but did not whiten it. If we had tried to whiten the signal, we would have “unwhitened” the noise.

To evaluate the performance, we find the characteristic functions on H_0 and H_1 . On H_0 , the random variables $(r'_i)^2$ are independent Gamma $(1/2, 2\sigma_w^2)$ random variables with characteristic function given in (2.100). Now define

$$\alpha_i \triangleq \frac{\lambda_{s_i}}{\lambda_{s_i} + \sigma_w^2}. \quad (3.378)$$

In the LRT, each $(r'_i)^2$ is multiplied by the factor α_i/σ_w^2 and then summed. Therefore, the characteristic function of l on H_0 is

$$M_{l|H_0}(jv) = \prod_{i=1}^N (1 - 2j\alpha_i v)^{-\frac{1}{2}}. \quad (3.379)$$

On H_1 , each $(r'_i)^2$ is a Gamma $(1/2, 2(\lambda_{s_i}^2 + \sigma_w^2))$ random variable; therefore, the characteristic function of l on H_1 is

$$M_{l|H_1}(jv) = \prod_{i=1}^N \left(1 - 2jv \frac{\lambda_{s_i}}{\sigma_w^2}\right)^{-\frac{1}{2}}. \quad (3.380)$$

We need to take the inverse Fourier transform to find $p_{l|H_0}(L|H_0)$ and $p_{l|H_1}(L|H_1)$ and then integrate to find P_F and P_D . In general, this must be done numerically. However, we can also use $\mu(s)$ in (3.332) to obtain bounds and approximate results.

The complex case follows in similar manner. The optimum test is given in (3.350),

$$l(\tilde{\mathbf{R}}) = \frac{1}{\sigma_{\tilde{w}}^2} \tilde{\mathbf{R}}^H \tilde{\mathbf{H}} \tilde{\mathbf{R}} \stackrel{H_1}{\geqslant} \stackrel{H_0}{\gamma_3}, \quad (3.381)$$

where

$$\tilde{\mathbf{H}} = \tilde{\mathbf{K}}_{\tilde{s}} \left(\sigma_{\tilde{w}}^2 \mathbf{I} + \tilde{\mathbf{K}}_{\tilde{s}} \right)^{-1}. \quad (3.382)$$

We perform an eigendecomposition of $\tilde{\mathbf{K}}_{\tilde{s}}$. Then

$$\tilde{\mathbf{K}}_{\tilde{s}} = \tilde{\mathbf{u}}_{\tilde{\phi}} \Lambda_{\tilde{s}} \tilde{\mathbf{u}}_{\tilde{\phi}}^H, \quad (3.383)$$

where

$$\tilde{\mathbf{u}}_{\tilde{\phi}} = [\tilde{\boldsymbol{\phi}}_1 \quad \tilde{\boldsymbol{\phi}}_2 \quad \cdots \quad \tilde{\boldsymbol{\phi}}_N] \quad (3.384)$$

is a unitary matrix whose columns are the complex eigenvectors of $\tilde{\mathbf{K}}_{\tilde{s}}$.

$$\Lambda_{\tilde{s}} = \text{diag}[\lambda_{\tilde{s}_1} \quad \lambda_{\tilde{s}_2} \quad \cdots \quad \lambda_{\tilde{s}_N}] \quad (3.385)$$

is a real diagonal matrix whose elements are the real eigenvalues of $\tilde{\mathbf{K}}_{\tilde{s}}$.

Then, $\tilde{\mathbf{H}}$ can be written as

$$\begin{aligned} \tilde{\mathbf{H}} &= \tilde{\mathbf{u}}_{\tilde{\phi}} \Lambda_{\tilde{s}} \tilde{\mathbf{u}}_{\tilde{\phi}}^H \tilde{\mathbf{u}}_{\tilde{\phi}} \left(\sigma_w^2 \mathbf{I} + \Lambda_{\tilde{s}} \right)^{-1} \tilde{\mathbf{u}}_{\tilde{\phi}}^H \\ &= \tilde{\mathbf{u}}_{\tilde{\phi}} \left[\tilde{\Lambda}_{\tilde{s}} \left(\sigma_w^2 \mathbf{I} + \tilde{\Lambda}_{\tilde{s}} \right)^{-1} \right] \tilde{\mathbf{u}}_{\tilde{\phi}}^H. \end{aligned} \quad (3.386)$$

The LRT can be written as

$$\begin{aligned} l(\tilde{\mathbf{R}}) &= \tilde{\mathbf{R}}^H \tilde{\mathbf{u}}_{\tilde{\phi}} \left[\tilde{\Lambda}_{\tilde{s}} \left(\sigma_w^2 \mathbf{I} + \Lambda_{\tilde{s}} \right)^{-1} \right] \tilde{\mathbf{u}}_{\tilde{\phi}}^H \tilde{\mathbf{R}} \\ &= \frac{1}{\sigma_w^2} (\tilde{\mathbf{R}}')^H \left[\Lambda_{\tilde{s}} \left(\sigma_w^2 \mathbf{I} + \Lambda_{\tilde{s}} \right)^{-1} \right] \tilde{\mathbf{R}}', \end{aligned} \quad (3.387)$$

where $\tilde{\mathbf{r}}' = \tilde{\mathbf{u}}_{\tilde{\phi}}^H \tilde{\mathbf{r}}$ is a complex vector with a diagonal covariance matrix. Then

$$l(\tilde{\mathbf{R}}') = \frac{1}{\sigma_w^2} \sum_{i=1}^N \frac{\lambda_{\tilde{s}_i}}{\lambda_{\tilde{s}_i} + \sigma_w^2} |\tilde{R}'_i|^2 = \frac{1}{\sigma_w^2} \sum_{i=1}^N \alpha_i |\tilde{R}'_i|^2, \quad (3.388)$$

where

$$\alpha_i = \frac{\lambda_{\tilde{s}_i}}{\lambda_{\tilde{s}_i} + \sigma_w^2}. \quad (3.389)$$

Each $|\tilde{r}'_i|^2$ is the sum of the squares of two IID, zero-mean Gaussian random variables with variance $\sigma_w^2/2$. We showed in Example 2.6 that this is an Exponential random variable. On H_0 , its characteristic function is

$$M_{|\tilde{R}'_i|^2|H_0}(jv) = (1 - jv\sigma_w^2)^{-1}. \quad (3.390)$$

Then¹⁴

$$M_{l|H_0}(jv) = \prod_{i=1}^N (1 - jv\alpha_i)^{-1}. \quad (3.391)$$

¹⁴This can also be obtained from the solution to Problem 2.6.4 in DEMT-I using paired sequences for the real Gaussian model. It is on page 52 of Van Trees and Goldfein [VTG68].

We assume the α_i are distinct and use a partial fraction expansion of (3.391) to obtain

$$M_{l|H_0}(jv) = \sum_{i=1}^N c_i (1 - jv\alpha_i)^{-1}, \quad (3.392)$$

where

$$c_i = \prod_{\substack{k=1 \\ k \neq i}}^N \frac{\alpha_i}{\alpha_i - \alpha_k}. \quad (3.393)$$

The characteristic function in (3.392) is a weighted sum of Exponential characteristic functions, so the corresponding probability density is a weighted sum of Exponential probability densities,

$$p_{l|H_0}(L|H_0) = \sum_{i=1}^N c_i \frac{1}{\alpha_i} \exp\left(-\frac{L}{\alpha_i}\right). \quad (3.394)$$

We can now integrate to find P_F ,

$$\begin{aligned} P_F &= \int_{\gamma'_3}^{\infty} p_{l|H_0}(L|H_0) dL \\ &= \sum_{i=1}^N \left[\prod_{\substack{k=1 \\ k \neq i}}^N \frac{\alpha_i}{\alpha_i - \alpha_k} \right] \exp\left(-\frac{\gamma'_3}{\alpha_i}\right). \end{aligned} \quad (3.395)$$

Similarly, to find P_D we have

$$M_{l|H_1}(jv) = \prod_{i=1}^N \left(1 - jv \frac{\lambda_{\tilde{s}_i}}{\sigma_{\tilde{w}}^2}\right)^{-1}. \quad (3.396)$$

Following the same steps

$$P_D = \sum_{i=1}^N \left[\prod_{\substack{k=1 \\ k \neq i}}^N \frac{\lambda_{\tilde{s}_i}}{\lambda_{\tilde{s}_i} - \lambda_{\tilde{s}_k}} \right] \exp\left(-\frac{\gamma'_3 \sigma_{\tilde{w}}^2}{\lambda_{\tilde{s}_i}}\right). \quad (3.397)$$

This result enables us to analyze the performance of the optimum detector for the complex equal-mean Gaussian detection problem for arbitrary signal covariance matrix. The key to obtaining a closed form solution is that the complex eigenvalue corresponds to two identical real eigenvalues.

We consider a simple example to illustrate the result.

Example 3.8. The signal covariance matrix is given by the $N \times N$ complex Toeplitz matrix

$$\tilde{\mathbf{K}}_{\tilde{s}} = \sigma_{\tilde{s}}^2 \begin{bmatrix} 1 & \tilde{\rho}^* & (\tilde{\rho}^*)^2 & \cdots & (\tilde{\rho}^*)^{N-1} \\ \tilde{\rho} & 1 & \tilde{\rho}^* & \cdots & (\tilde{\rho}^*)^{N-2} \\ \tilde{\rho}^2 & \tilde{\rho} & 1 & \cdots & (\tilde{\rho}^*)^{N-3} \\ \vdots & \vdots & \vdots & \ddots & \vdots \\ \tilde{\rho}^{N-1} & \tilde{\rho}^{N-2} & \tilde{\rho}^{N-3} & \cdots & 1 \end{bmatrix}. \quad (3.398)$$

This is the complex version of the matrix in Examples 3.4 and 3.5, but now it corresponds to the signal. Then,

$$\tilde{\mathbf{K}}_0 = \sigma_{\tilde{w}}^2 \mathbf{I}, \quad (3.399)$$

$$\tilde{\mathbf{K}}_1 = \tilde{\mathbf{K}}_{\tilde{s}} + \sigma_{\tilde{w}}^2 \mathbf{I}. \quad (3.400)$$

Let $\xi_i; i = 1, 2, \dots, N$ denote the eigenvalues of the normalized matrix $\frac{1}{\sigma_{\tilde{s}}^2} \tilde{\mathbf{K}}_{\tilde{s}}$. They are the same as in Example 3.4 and depend only on $|\tilde{\rho}|$. Figure 3.14 showed a plot of the eigenvalues versus $|\tilde{\rho}|$ for $N = 4$. The eigenvalues of $\tilde{\mathbf{K}}_{\tilde{s}}$ are $\lambda_{\tilde{s}_i} = \sigma_{\tilde{s}}^2 \xi_i$. The eigenvectors of $\tilde{\mathbf{K}}_{\tilde{s}}$ depend on the phase of $\tilde{\rho}$ and will be different from those in the real case.

For $|\tilde{\rho}| = 0$,

$$\tilde{\mathbf{K}}_{\tilde{s}} = \sigma_{\tilde{s}}^2 \mathbf{I} \quad (3.401)$$

and $\xi_i; i = 1, 2, \dots, N$. Thus, we have repeated eigenvalues with $\lambda_{\tilde{s}_i} = \sigma_{\tilde{s}}^2$ and $\alpha_i = \sigma_{\tilde{s}}^2 / (\sigma_{\tilde{s}}^2 + \sigma_{\tilde{w}}^2)$ and (3.390) and (3.396) become

$$M_{l|H_0}(jv) = \left(1 - jv \frac{\sigma_{\tilde{s}}^2}{\sigma_{\tilde{s}}^2 + \sigma_{\tilde{w}}^2} \right)^{-N}, \quad (3.402)$$

$$M_{l|H_1}(jv) = \left(1 - jv \frac{\sigma_{\tilde{s}}^2}{\sigma_{\tilde{w}}^2} \right)^{-N}. \quad (3.403)$$

Thus, l has a Gamma distribution on both hypotheses and P_F and P_D are given by

$$P_F = 1 - \Gamma_N \left(\gamma'_3 \left[\frac{\sigma_{\tilde{s}}^2 + \sigma_{\tilde{w}}^2}{\sigma_{\tilde{s}}^2} \right] \right) = 1 - \Gamma_N \left(\frac{\gamma'}{\sigma_{\tilde{w}}^2} \right), \quad (3.404)$$

$$P_D = 1 - \Gamma_N \left(\gamma'_3 \frac{\sigma_{\tilde{w}}^2}{\sigma_{\tilde{s}}^2} \right) = 1 - \Gamma_N \left(\frac{\gamma'}{\sigma_{\tilde{s}}^2 + \sigma_{\tilde{w}}^2} \right). \quad (3.405)$$

This is the IID case studied in Section 3.3.1.1 and the expressions in (3.404) and (3.405) are the same as (3.361) and (3.362).

For $|\tilde{\rho}| = 1$,

$$\tilde{\mathbf{K}}_{\tilde{s}} = \sigma_{\tilde{s}}^2 \tilde{\rho} \tilde{\rho}^H, \quad (3.406)$$

where¹⁵

$$\tilde{\rho} = \begin{bmatrix} 1 \\ \tilde{\rho} \\ \tilde{\rho}^2 \\ \vdots \\ \tilde{\rho}^{N-1} \end{bmatrix}. \quad (3.407)$$

For this case, $\xi_1 = N$ while $\xi_2 = \dots = \xi_N = 0$. Thus, $\lambda_{\tilde{s}_1} = N\sigma_{\tilde{s}}^2$ and $\alpha_1 = N\sigma_{\tilde{s}}^2/(N\sigma_{\tilde{s}}^2 + \sigma_{\tilde{w}}^2)$ and the remaining eigenvalues are zero. In this case (3.390) and (3.396) are given by

$$M_{l|H_0}(jv) = \left(1 - jv \frac{N\sigma_{\tilde{s}}^2}{N\sigma_{\tilde{s}}^2 + \sigma_{\tilde{w}}^2}\right)^{-1}, \quad (3.408)$$

$$M_{l|H_1}(jv) = \left(1 - jv \frac{N\sigma_{\tilde{s}}^2}{\sigma_{\tilde{w}}^2}\right)^{-1}. \quad (3.409)$$

Now l has an Exponential distribution on both hypotheses and P_F and P_D are

$$P_F = \exp \left\{ -\gamma'_3 \left[\frac{N\sigma_{\tilde{s}}^2 + \sigma_{\tilde{w}}^2}{N\sigma_{\tilde{s}}^2} \right] \right\}, \quad (3.410)$$

$$P_D = \exp \left\{ -\gamma'_3 \frac{\sigma_{\tilde{w}}^2}{N\sigma_{\tilde{s}}^2} \right\}. \quad (3.411)$$

For $0 < |\tilde{\rho}| < 1$, the eigenvalues are distinct and must be found numerically. To evaluate performance, we use (3.395) and (3.397) with

$$\alpha_i = \frac{\sigma_{\tilde{s}}^2 \xi_i}{\sigma_{\tilde{s}}^2 \xi_i + \sigma_{\tilde{w}}^2}. \quad (3.412)$$

Note that $|\tilde{\rho}| = 0$ and $|\tilde{\rho}| = 1$ are both special cases of the model in Examples 2.2 and 2.6, where the sufficient statistic was the sum of squared IID, zero-mean Gaussian random variables. $|\tilde{\rho}| = 0$ corresponds to $2N$ real observations with signal-to-noise ratio $\text{SNR} = \sigma_s^2/\sigma_{\tilde{w}}^2$ while $|\tilde{\rho}| = 1$ corresponds to two real observations with $\text{SNR} = N\sigma_{\tilde{s}}^2/\sigma_{\tilde{w}}^2$.

In Figure 3.28, we plot ROC curves for $N = 4$ and several values of $|\rho|$ and $\text{SNR} = \sigma_{\tilde{s}}^2/\sigma_{\tilde{w}}^2$. The behavior is similar to Figure 2.15. In Figure 3.29, we plot P_D versus SNR for $N = 4$ and several values of $|\rho|$ and P_F . For high SNR, better P_D performance is achieved as $|\rho| \rightarrow 0$ and the signal is more evenly distributed throughout the N -dimensional observation space. For low SNR, better performance is achieved as $|\rho| \rightarrow 1$ and the signal is more concentrated in a lower dimensional subspace. ■

3.3.1.4 Low-Rank Signal Model

In many applications of interest the observed vector on the two hypotheses can be written as

$$\begin{aligned} H_1 : \mathbf{r} &= \mathbf{v}a + \mathbf{w}, \\ H_0 : \mathbf{r} &= \mathbf{w}, \end{aligned} \quad (3.413)$$

where \mathbf{v} corresponds to a known signal that was transmitted and a corresponds to a $N(0, \sigma_a^2)$ Gaussian random variable that was introduced by the transmission channel.

¹⁵We saw an example of this model in Examples 3.6 and 3.7, where $\tilde{\rho} = \tilde{\mathbf{v}}$ and $\tilde{\rho} = e^{j\omega t}$ or $\tilde{\rho} = e^{-j\psi t}$.

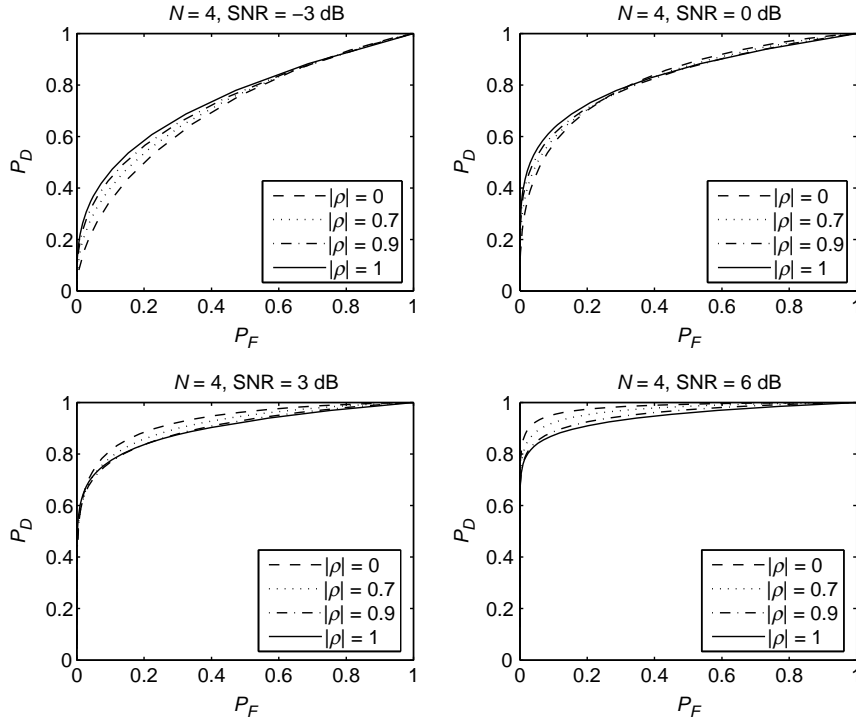


Figure 3.28: ROC curves for $N = 4$.

The corresponding complex model is

$$\begin{aligned} H_1 : \tilde{\mathbf{r}} &= \tilde{\mathbf{v}}\tilde{\mathbf{a}} + \tilde{\mathbf{w}}, \\ H_0 : \tilde{\mathbf{r}} &= \tilde{\mathbf{w}}, \end{aligned} \quad (3.414)$$

where $\tilde{\mathbf{a}}$ is $CN(0, \sigma_{\tilde{a}}^2)$.

A more general model for the observation on H_1 that we will also encounter in practice is

$$H_1 : \mathbf{r} = \mathbf{V}\mathbf{a} + \mathbf{w}, \quad (3.415)$$

where

$$\mathbf{V} = [\mathbf{v}_1 \quad \mathbf{v}_2 \quad \cdots \quad \mathbf{v}_D] \quad (3.416)$$

and

$$\mathbf{a} = [a_1 \quad a_2 \quad \cdots \quad a_D]^T, \quad (3.417)$$

where \mathbf{a} is $N(\mathbf{0}, \mathbf{K}_a)$.

The corresponding complex model is

$$H_1 : \tilde{\mathbf{r}} = \tilde{\mathbf{V}}\tilde{\mathbf{a}} + \tilde{\mathbf{w}}, \quad (3.418)$$

where $\tilde{\mathbf{a}}$ is $CN(\mathbf{0}, \tilde{\mathbf{K}}_{\tilde{a}})$.

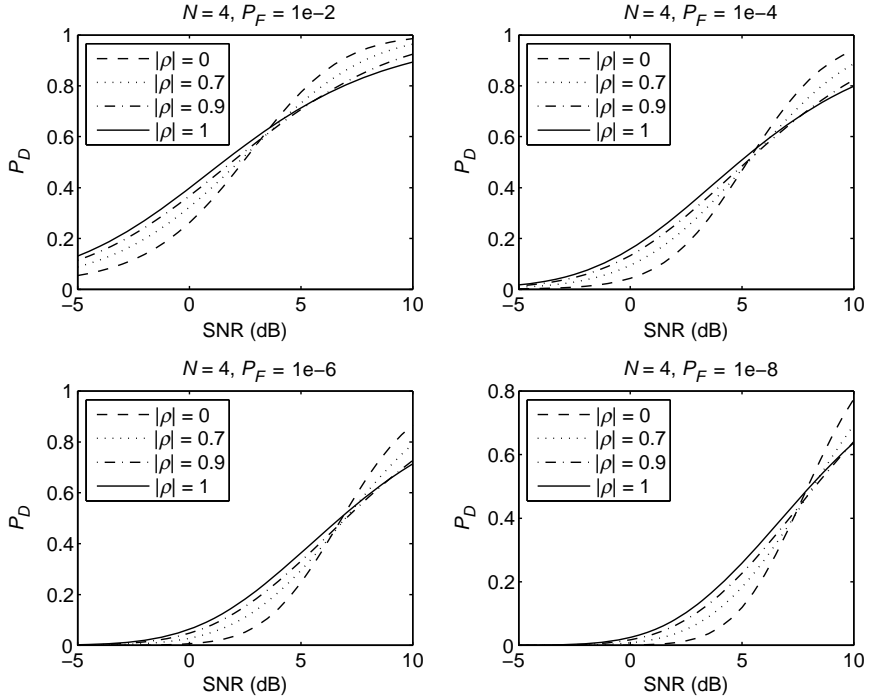


Figure 3.29: P_D versus SNR for $N = 4$.

One application where we will encounter this model is a radar system where we transmit a sequence of pulses modeled by $\tilde{\mathbf{v}}_1, \tilde{\mathbf{v}}_2, \dots, \tilde{\mathbf{v}}_D$ and the signal reflected from the target multiplies each pulse by a different realization of complex Gaussian random variable denoted by $\tilde{a}_1, \tilde{a}_2, \dots, \tilde{a}_D$.

Note that this model is a special case of the model in Section 3.3.1.3. All of the results apply by letting $\lambda_{s_i} = 0$, $i = D + 1, \dots, N$. In particular, for the complex Gaussian case, the closed form expression for P_F and P_D in (3.395) and (3.397) apply. Several examples are considered in the problems.

3.3.1.5 Symmetric Hypotheses, Uncorrelated Noise

The previous cases were unsymmetric because of the noise-only hypothesis. Here, we have the following hypotheses:

$$\begin{aligned} H_1 : r_i &= s_i + w_i, & i &= 1, 2, \dots, N, \\ &w_i, & i &= N + 1, N + 2, \dots, 2N, \\ H_0 : r_i &= s_i + w_i, & i &= N + 1, N + 2, \dots, 2N, \\ &w_i, & i &= 1, 2, \dots, N, \end{aligned} \tag{3.419}$$

where the w_i are independent random variables with variance σ_w^2 and the s_i have a covariance matrix \mathbf{K}_s . Then

$$\mathbf{K}_1 = \left[\begin{array}{c|c} \sigma_w^2 \mathbf{I} + \mathbf{K}_s & \mathbf{0} \\ \hline \mathbf{0} & \sigma_w^2 \mathbf{I} \end{array} \right] \tag{3.420}$$

and

$$\mathbf{K}_0 = \begin{bmatrix} \sigma_w^2 \mathbf{I} & \mathbf{0} \\ \mathbf{0} & \sigma_w^2 \mathbf{I} + \mathbf{K}_s \end{bmatrix}, \quad (3.421)$$

where we have partitioned the $2N \times 2N$ matrices into $N \times N$ submatrices. Then

$$\Delta \mathbf{Q} = \begin{bmatrix} \frac{1}{\sigma_w^2} \mathbf{I} & \mathbf{0} \\ \mathbf{0} & (\sigma_w^2 \mathbf{I} + \mathbf{K}_s)^{-1} \end{bmatrix} - \begin{bmatrix} (\sigma_w^2 \mathbf{I} + \mathbf{K}_s)^{-1} & \mathbf{0} \\ \mathbf{0} & \frac{1}{\sigma_w^2} \mathbf{I} \end{bmatrix}. \quad (3.422)$$

Using (3.341), we have

$$\Delta \mathbf{Q} = \frac{1}{\sigma_w^2} \begin{bmatrix} \mathbf{H} & \mathbf{0} \\ \mathbf{0} & -\mathbf{H} \end{bmatrix}, \quad (3.423)$$

where, as previously defined in (3.341), \mathbf{H} is

$$\mathbf{H} \triangleq (\sigma_w^2 \mathbf{I} + \mathbf{K}_s)^{-1} \mathbf{K}_s. \quad (3.424)$$

If we partition \mathbf{R} into two $N \times 1$ matrices,

$$\mathbf{R} = \begin{bmatrix} \mathbf{R}_1 \\ \mathbf{R}_2 \end{bmatrix}, \quad (3.425)$$

then

$$l(\mathbf{R}) = \frac{1}{\sigma_w^2} (\mathbf{R}_1^T \mathbf{H} \mathbf{R}_1 - \mathbf{R}_2^T \mathbf{H} \mathbf{R}_2) \stackrel{H_1}{\underset{H_0}{\gtrless}} \gamma_3. \quad (3.426)$$

The special cases analogous to those in Sections 3.3.1.1 and 3.3.1.2 follow easily.

Case 1: Uncorrelated, Identically Distributed Signal Components.

Let

$$\mathbf{K}_s = \sigma_s^2 \mathbf{I}; \quad (3.427)$$

then

$$l(\mathbf{R}) = \sum_{i=1}^N R_i^2 - \sum_{i=N+1}^{2N} R_i^2 \stackrel{H_1}{\underset{H_0}{\gtrless}} \gamma. \quad (3.428)$$

If the hypotheses are equally likely and the criterion is minimum $\Pr(\epsilon)$, the threshold η in the LRT is unity (see 2.87). From (3.331) and (3.355), we see that this will result in $\gamma = 0$. We assume that N is even. This case occurs frequently and leads to a simple error calculation. The test then becomes

$$l_1(\mathbf{R}) \triangleq \sum_{i=1}^N R_i^2 \stackrel{H_1}{\underset{H_0}{\gtrless}} \sum_{i=N+1}^{2N} R_i^2 \triangleq l_0(\mathbf{R}). \quad (3.429)$$

The probability of error given that H_1 is true is the probability that l_0 is greater than l_1 . Because the test is symmetric with respect to the two hypotheses,

$$\Pr(\epsilon) = \frac{1}{2} \Pr(\epsilon|H_0) + \frac{1}{2} \Pr(\epsilon|H_1) = \Pr(\epsilon|H_1). \quad (3.430)$$

Thus,

$$\Pr(\epsilon) = \int_0^\infty dL_1 p_{l_1|H_1}(L_1|H_1) \int_{L_1}^\infty p_{l_0|H_1}(L_0|H_1) dL_0. \quad (3.431)$$

Substituting (2.102) and (2.103) in (3.431), recalling that N is even, and evaluating the inner integral, we have

$$\Pr(\epsilon) = \int_0^\infty \frac{1}{2^{N/2} \sigma_1^N \Gamma(N/2)} L_1^{N/2-1} e^{-L_1/2\sigma_1^2} \times \left[e^{-L_1/2\sigma_w^2} \sum_{k=0}^{N/2-1} \frac{(L_1/2\sigma_w^2)^k}{k!} \right] dL_1. \quad (3.432)$$

Defining

$$\alpha = \frac{\sigma_w^2}{\sigma_1^2 + \sigma_w^2} = \frac{\sigma_w^2}{\sigma_s^2 + 2\sigma_w^2}, \quad (3.433)$$

and integrating, (3.432) reduces to

$$\Pr(\epsilon) = \alpha^{N/2} \sum_{j=0}^{N/2-1} \binom{\frac{N}{2} + j - 1}{j} (1 - \alpha)^j. \quad (3.434)$$

This result is due to Pierce [Pie58]. It is a closed form expression.

It is also useful to compute the $\Pr(\epsilon)$ using $\mu(s)$ because we have already done most of the work. Each of the submatrices in (3.420) and (3.421) corresponds to the model in Example 2.13.

From (2.269),

$$\mu(s) = \frac{N}{2} \ln \left[\frac{(\sigma_0^2)^s (\sigma_1^2)^{1-s}}{s\sigma_0^2 + (1-s)\sigma_1^2} \right]. \quad (3.435)$$

The $\mu(s)$ for the binary symmetric model corresponds to the sum of the $\mu(s)$ in (3.435) and a $\mu(s)$ with σ_1^2 and σ_0^2 interchanged. Thus,

$$\mu_{BS}(s) = \frac{N}{2} \left\{ \ln \left[\frac{(\sigma_0^2)^s (\sigma_1^2)^{1-s}}{s\sigma_0^2 + (1-s)\sigma_1^2} \right] + \ln \left[\frac{(\sigma_1^2)^s (\sigma_0^2)^{1-s}}{s\sigma_1^2 + (1-s)\sigma_0^2} \right] \right\}, \quad (3.436)$$

where

$$\begin{aligned} \sigma_1^2 &= \sigma_s^2 + \sigma_w^2, \\ \sigma_0^2 &= \sigma_w^2. \end{aligned} \quad (3.437)$$

Then

$$\mu_{BS}(s) = \frac{N}{2} \left(s \ln \sigma_w^2 + (1-s) \ln(\sigma_w^2 + \sigma_s^2) - \ln(\sigma_w^2 + s\sigma_s^2) \right) \quad (3.438)$$

$$\begin{aligned} &+ (1-s) \ln \sigma_w^2 + s \ln(\sigma_w^2 + \sigma_s^2) - \ln [\sigma_w^2 + (1-s)\sigma_s^2] \Big) \\ &= \frac{N}{2} \left(\ln \left(1 + \frac{\sigma_s^2}{\sigma_w^2} \right) - \ln \left[\left(1 + \frac{s\sigma_s^2}{\sigma_w^2} \right) \left(1 + \frac{(1-s)\sigma_s^2}{\sigma_w^2} \right) \right] \right). \end{aligned} \quad (3.439)$$

The function $\mu_{BS}(s)/(N/2)$ is plotted in Figure 3.30. The minimum is at $s = \frac{1}{2}$. This is the point of interest at which minimum $\Pr(\epsilon)$ is the criterion.

Taking derivatives of (3.439), we have

$$\dot{\mu}_{BS}(s) = -\frac{N}{2} \left(\frac{\sigma_s^2}{\sigma_w^2 + s\sigma_s^2} - \frac{\sigma_s^2}{\sigma_w^2 + (1-s)\sigma_s^2} \right) \quad (3.440)$$

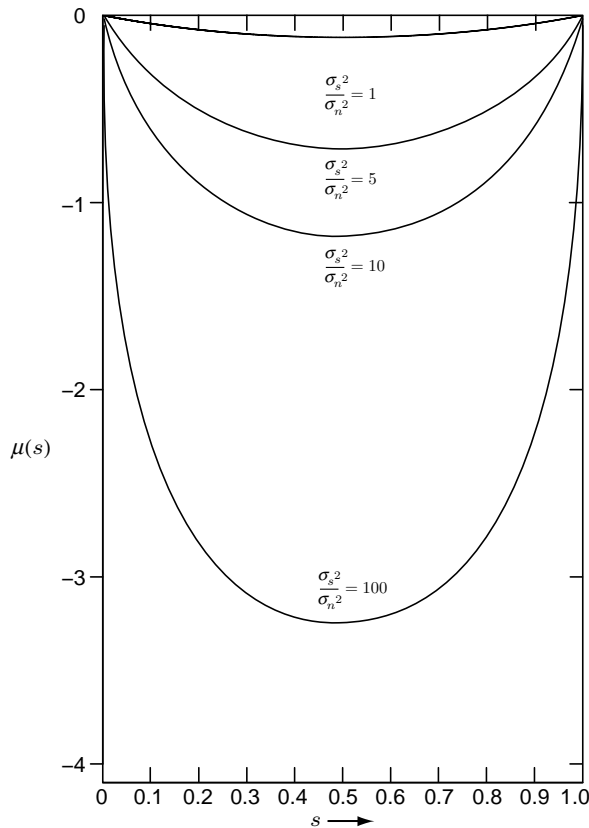


Figure 3.30: $\mu_{BS}(s)/(N/2)$ for the binary symmetric hypothesis problem.

and

$$\bar{\mu}_{BS}(s) = \frac{N}{2} \left(\frac{\sigma_s^4}{(\sigma_w^2 + s\sigma_s^2)^2} + \frac{\sigma_s^4}{(\sigma_w^2 + (1-s)\sigma_s^2)^2} \right). \quad (3.441)$$

Using (2.244), we have

$$\Pr(\epsilon) \approx \left[\pi \frac{N}{2} \frac{\sigma_s^4}{(\sigma_w^2 + \sigma_s^2/2)^2} \right]^{-1/2} \exp \left(\frac{N}{2} \ln \left(1 + \frac{\sigma_s^2}{\sigma_w^2} \right) - N \ln \left(1 + \frac{\sigma_s^2}{2\sigma_w^2} \right) \right) \quad (3.442)$$

or

$$\Pr(\epsilon) \approx \left[\pi \frac{N}{2} \frac{\sigma_s^4}{(\sigma_w^2 + \sigma_s^2/2)^2} \right]^{-1/2} \left(\frac{1 + \sigma_s^2/\sigma_w^2}{(1 + \sigma_s^2/2\sigma_w^2)^2} \right)^{N/2}, \quad (3.443)$$

which reduces to

$$\Pr(\epsilon) \approx \sqrt{\frac{2}{\pi N}} \frac{(1 + \sigma_s^2/\sigma_w^2)^{N/2}}{(\sigma_s^2/\sigma_w^2)(1 + \sigma_s^2/2\sigma_w^2)^{N-1}}. \quad (3.444)$$

Alternatively, we can use the approximation given by (2.243). For this case it reduces to

$$\Pr(\epsilon) \approx \left[\frac{1 + \sigma_s^2/\sigma_w^2}{(1 + \sigma_s^2/2\sigma_w^2)^2} \right]^{N/2} \exp \left[\frac{N}{8} \left(\frac{\sigma_s^2/\sigma_w^2}{1 + \sigma_s^2/2\sigma_w^2} \right)^2 \right] \operatorname{erfc}_* \left[\left(\frac{N}{4} \right)^{1/2} \left(\frac{\sigma_s^2/\sigma_w^2}{1 + \sigma_s^2/2\sigma_w^2} \right) \right]. \quad (3.445)$$

In Figure 3.31, we have plotted the approximate $\Pr(\epsilon)$ using (3.445) and the exact $\Pr(\epsilon)$ that was given by (3.434). We see that the approximation is excellent.

Case 2: Uncorrelated Signal Components: Unequal Variances.

Now

$$\mathbf{K}_s = \begin{bmatrix} \sigma_{s_1}^2 & & & \mathbf{0} \\ & \sigma_{s_2}^2 & & \\ & & \sigma_{s_3}^2 & \\ & & & \ddots \\ \mathbf{0} & & & \sigma_{s_N}^2 \end{bmatrix}. \quad (3.446)$$

It follows that

$$l(\mathbf{R}) = \frac{1}{\sigma_w^2} \left[\sum_{i=1}^N \frac{\sigma_{s_i}^2}{\sigma_w^2 + \sigma_{s_i}^2} R_i^2 - \sum_{i=N+1}^{2N} \frac{\sigma_{s_{i-N}}^2}{\sigma_w^2 + \sigma_{s_{i-N}}^2} R_i^2 \right]_{H_0}^{H_1} \gtrless \gamma_3. \quad (3.447)$$

The $\Pr(\epsilon)$ is difficult to compute. However, we can get an approximate expression using $\mu(s)$ and its derivatives. This approach is carried out in the problems. The model for arbitrary \mathbf{K}_s reduces to this case via an eigendecomposition.

The circular complex Gaussian models for either Case 1 or Case 2 are obvious modifications. We can compute the $\Pr(\epsilon)$ using the same approach as in (3.445).

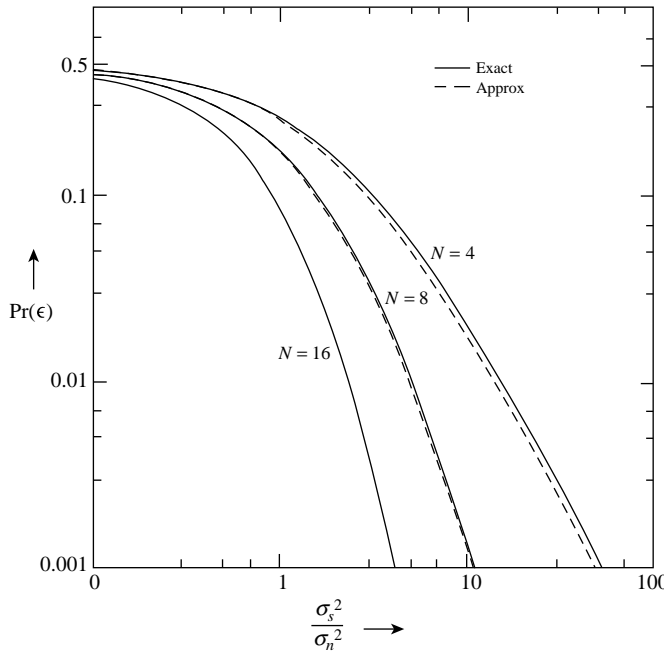


Figure 3.31: Exact and approximate error expressions for the binary symmetric hypothesis case.

3.3.2 Nondiagonal Covariance Matrix on H_0

The general Gaussian model has arbitrary covariance matrices on H_0 and H_1 . The sufficient statistic is given by (3.331),

$$l(\mathbf{R}) = \mathbf{R}^T \Delta \mathbf{Q} \mathbf{R}, \quad (3.448)$$

where $\Delta \mathbf{Q}$ was defined in (3.330).

In this section, we consider two special cases that occur frequently in practice.

3.3.2.1 Signal on H_1 Only

In this model, the signal is a zero-mean Gaussian vector that occurs only on H_1 . The received vectors on the two hypotheses are

$$H_1 : \mathbf{r} = \mathbf{s} + \mathbf{n}, \quad (3.449)$$

$$H_0 : \mathbf{r} = \mathbf{n}. \quad (3.450)$$

There is a noise component with a nondiagonal covariance matrix on each hypothesis

$$\mathbf{K}_0 = \mathbf{K}_n, \quad (3.451)$$

$$\mathbf{K}_1 = \mathbf{K}_n + \mathbf{K}_s, \quad (3.452)$$

where \mathbf{K}_n is the total noise matrix that consists of two terms,

$$\mathbf{K}_n = \mathbf{K}_I + \sigma_w^2 \mathbf{I}. \quad (3.453)$$

The LRT is given by (3.331) with

$$\begin{aligned}\Delta \mathbf{Q} &= \mathbf{Q}_0 - \mathbf{Q}_1 \\ &= \mathbf{K}_n^{-1} - \left[\mathbf{K}_n + \mathbf{K}_s \right]^{-1} \\ &= \mathbf{K}_n^{-1} \mathbf{K}_s \left[\mathbf{K}_n + \mathbf{K}_s \right]^{-1}.\end{aligned}\quad (3.454)$$

Then (3.331) can be written as

$$\begin{aligned}l(\mathbf{R}) &= \mathbf{R}^T \mathbf{K}_n^{-1} \left(\mathbf{K}_s \left[\mathbf{K}_n + \mathbf{K}_s \right]^{-1} \mathbf{R} \right) \\ &= \mathbf{R}^T \mathbf{K}_n^{-1} \hat{\mathbf{s}},\end{aligned}\quad (3.455)$$

where $\hat{\mathbf{s}}$ is the MMSE estimate of \mathbf{s} , so the detection still has an estimator–correlator interpretation.

To analyze the behavior we need to put it in the form of Figure 3.27. The simplest way is to do a two-step whitening transformation.

First, do an eigendecomposition of \mathbf{K}_I ,

$$\mathbf{K}_I = \mathbf{u}_0 \Lambda_I \mathbf{u}_0^T, \quad (3.456)$$

where

$$\Lambda_I = \text{diag}[\lambda_{I_1} \quad \lambda_{I_2} \quad \cdots \quad \lambda_{I_N}]. \quad (3.457)$$

Note that, if \mathbf{K}_I is rank D , where $D < N$, we have to augment its eigenvectors with $N - D$ orthogonal vectors so that \mathbf{u}_0 is an $N \times N$ matrix. The eigendecomposition of \mathbf{K}_n is

$$\mathbf{K}_n = \mathbf{u}_0 [\Lambda_I + \sigma_w^2 \mathbf{I}] \mathbf{u}_0^T = \mathbf{u}_0 \Lambda_n \mathbf{u}_0^T. \quad (3.458)$$

The diagonal white noise matrix guarantees that Λ_n is rank N . Then we define the whitening transformation

$$\mathbf{W}_0^T \triangleq [\Lambda_n]^{-1/2} \mathbf{u}_0^T = [\Lambda_I + \sigma_w^2 \mathbf{I}]^{-1/2} \mathbf{u}_0^T, \quad (3.459)$$

and apply it to \mathbf{R} to obtain

$$\mathbf{R}_W = \mathbf{W}_0^T \mathbf{R}. \quad (3.460)$$

This step is shown in Figure 3.32.

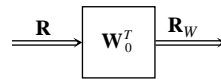


Figure 3.32: Whitening the H_0 hypothesis.

The covariance matrix of \mathbf{r}_W on H_0 is \mathbf{I} . On H_1 , its covariance matrix is

$$\begin{aligned}\mathbf{K}_{W_1} &= \mathbf{W}_0^T [\mathbf{K}_s + \mathbf{K}_n] \mathbf{W}_0 \\ &= \mathbf{W}_0^T \mathbf{K}_s \mathbf{W}_0 + \mathbf{I} \\ &\triangleq \mathbf{K}_{sW} + \mathbf{I}.\end{aligned}\quad (3.461)$$

We now do an eigendecomposition of \mathbf{K}_{sW} :

$$\mathbf{K}_{sW} = \mathbf{u}_{sW} \boldsymbol{\Lambda}_{sW} \mathbf{u}_{sW}^T. \quad (3.462)$$

Once again, we augment the eigenvectors if \mathbf{K}_{sW} is not rank N . The eigendecomposition of the \mathbf{K}_{W_1} matrix is

$$\mathbf{K}_{W_1} = \mathbf{u}_{sW} [\lambda_{sW} + \mathbf{I}] \mathbf{u}_{sW}^T = \mathbf{u}_{sW} \boldsymbol{\Lambda}_{W_1} \mathbf{u}_{sW}^T, \quad (3.463)$$

where

$$\begin{aligned}\boldsymbol{\Lambda}_{W_1} &= \text{diag}[\lambda_{sW_1} + 1 \quad \lambda_{sW_2} + 1 \quad \cdots \quad \lambda_{sW_N} + 1] \\ &= \text{diag}[\lambda_{W_1} \quad \lambda_{W_2} \quad \cdots \quad \lambda_{W_N}].\end{aligned}\quad (3.464)$$

We next define a diagonalization operation

$$\mathbf{D}_1^T \triangleq \mathbf{u}_{sW}^T. \quad (3.465)$$

The second diagonalizing operation is shown in Figure 3.33. The output is denoted by

$$\mathbf{R}_{WD} = \mathbf{D}_1^T \mathbf{R}_W = \mathbf{D}_1^T \mathbf{W}_0^T \mathbf{R}. \quad (3.466)$$

We check the covariance matrix of \mathbf{r}_{WD} on H_0 and H_1 . On H_0 ,

$$\begin{aligned}\text{Cov}(\mathbf{r}_{WD}|H_0) &= E(\mathbf{r}_{WD} \mathbf{r}_{WD}^T | H_0) \\ &= E(\mathbf{D}_1^T \mathbf{r}_W \mathbf{r}_W^T \mathbf{D}_1 | H_0) \\ &= \mathbf{D}_1^T \mathbf{I} \mathbf{D}_1 = \mathbf{I}.\end{aligned}\quad (3.467)$$

Similarly, on H_1

$$\begin{aligned}\text{Cov}(\mathbf{r}_{WD}|H_1) &= E(\mathbf{r}_{WD} \mathbf{r}_{WD}^T | H_1) \\ &= E(\mathbf{D}_1^T \mathbf{r}_W \mathbf{r}_W^T \mathbf{D}_1 | H_1) \\ &= \mathbf{D}_1^T \mathbf{K}_{W_1} \mathbf{D}_1 \\ &= \mathbf{u}_{sW}^T \mathbf{u}_{sW} [\lambda_{sW} + \mathbf{I}] \mathbf{u}_{sW}^T \mathbf{u}_{sW} \\ &= \boldsymbol{\Lambda}_{sW} + \mathbf{I}.\end{aligned}\quad (3.468)$$

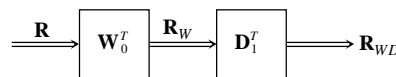


Figure 3.33: Diagonalizing H_1 .

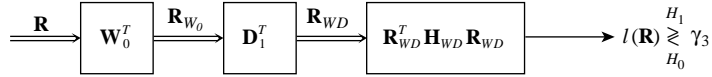


Figure 3.34: Likelihood ratio test.

We define a diagonal matrix \mathbf{H}_{WD}

$$\mathbf{H}_{WD} \triangleq \text{diag} \left[\frac{\lambda_{sW_1}}{\lambda_{sW_1} + 1} \quad \frac{\lambda_{sW_2}}{\lambda_{sW_2} + 1} \quad \dots \quad \frac{\lambda_{sW_N}}{\lambda_{sW_N} + 1} \right]. \quad (3.469)$$

Then, from (3.377)

$$\begin{aligned} l(\mathbf{R}) &= l(\mathbf{R}_{WD}) = \mathbf{R}_{WD}^T \mathbf{H}_{WD} \mathbf{R}_{WD} \\ &= \sum_{i=1}^N \frac{\lambda_{sW_i}}{\lambda_{sW_i} + 1} (R_{WD_i})^2 \end{aligned} \quad (3.470)$$

and the complete LRT is shown in Figure 3.34.

This reduces the problem to the model in Figure 3.27. The characteristic functions on the two hypotheses are given by (3.379) and (3.380) but the probability densities are difficult to evaluate.

However, as in Section 3.3.1.3, the expression for $\mu(s)$ follows easily. From (3.435),

$$\mu(s) = \frac{1}{2} \sum_{i=1}^N \left[(1-s) \ln(\lambda_{sW_i}) - \ln \left(1 + (1-s)\lambda_{sW_i} \right) \right] \quad (3.471)$$

and we can compute approximate ROCs. Note that we can also use (3.332) directly to evaluate $\mu(s)$ so that the eigendecomposition is not necessary.

The complex case follows in a similar manner. However, we can evaluate the performance for this case. The equations are

$$l(\tilde{\mathbf{R}}) = \tilde{\mathbf{R}}^H \tilde{\mathbf{K}}_{\tilde{n}}^{-1} \left(\tilde{\mathbf{K}}_{\tilde{s}} [\tilde{\mathbf{K}}_{\tilde{s}} + \tilde{\mathbf{K}}_{\tilde{n}}]^{-1} \right) \tilde{\mathbf{R}} = \tilde{\mathbf{R}}^H \tilde{\mathbf{K}}_{\tilde{n}}^{-1} \hat{\mathbf{s}}, \quad (3.472)$$

$$\tilde{\mathbf{K}}_{\tilde{n}} = \tilde{\mathbf{u}}_0 \Lambda_{\tilde{n}} \tilde{\mathbf{u}}_0^H, \quad (3.473)$$

$$\tilde{\mathbf{W}}_0^H = \Lambda_{\tilde{n}}^{-1/2} \tilde{\mathbf{u}}_0^H, \quad (3.474)$$

$$\tilde{\mathbf{R}}_W = \tilde{\mathbf{W}}_0^H \tilde{\mathbf{R}}, \quad (3.475)$$

$$\tilde{\mathbf{K}}_{W_1} = \tilde{\mathbf{u}}_{sW} \Lambda_{\tilde{W}_1} \tilde{\mathbf{u}}_{sW}^H, \quad (3.476)$$

$$\tilde{\mathbf{D}}_1^H = \tilde{\mathbf{u}}_{sW}^H, \quad (3.477)$$

$$\tilde{\mathbf{R}}_{WD} = \tilde{\mathbf{D}}_1^H \tilde{\mathbf{R}}_W = \tilde{\mathbf{D}}_1^H \tilde{\mathbf{W}}_0^H \tilde{\mathbf{R}}, \quad (3.478)$$

and

$$\tilde{\mathbf{H}}_{WD} = \text{diag} \left[\frac{\lambda_{s\tilde{W}_1}}{\lambda_{s\tilde{W}_1} + 1} \quad \frac{\lambda_{s\tilde{W}_2}}{\lambda_{s\tilde{W}_2} + 1} \quad \dots \quad \frac{\lambda_{s\tilde{W}_N}}{\lambda_{s\tilde{W}_N} + 1} \right]. \quad (3.479)$$

The LRT is shown in Figure 3.35.

We can now evaluate the performance using equations (3.388)–(3.397). The closed form expressions for P_F in (3.395) and P_D in (3.397) are the principal advantages of doing

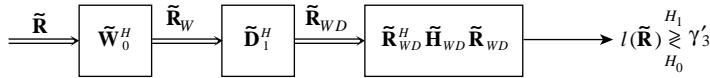


Figure 3.35: Likelihood ratio test for complex observations.

the eigendecomposition. The combination of the whitening and diagonalization operations make it difficult to track the physical significance of the eigenvalues. Alternatively, we can calculate an approximate ROC using $\mu(s)$. For the complex case, $\mu(s)$ is

$$\mu(s) = \sum_{i=1}^N \left[(1-s) \ln(\lambda_{s\tilde{W}_i}) - \ln \left(1 + (1-s)\lambda_{s\tilde{W}_i} \right) \right]. \quad (3.480)$$

Once again, we can also find $\mu(s)$ using (3.332) without doing an eigendecomposition.

Several examples are included in the problems.

3.3.2.2 Signal on Both Hypotheses

In this model, signals appear on both hypotheses. We will consider the complex case in the text. The received vectors on the two hypotheses are

$$H_1 : \tilde{\mathbf{r}} = \tilde{\mathbf{s}}_1 + \tilde{\mathbf{w}}, \quad (3.481)$$

$$H_0 : \tilde{\mathbf{r}} = \tilde{\mathbf{s}}_0 + \tilde{\mathbf{w}}, \quad (3.482)$$

and the covariance matrices on the two hypotheses are

$$\tilde{\mathbf{K}}_0 = \tilde{\mathbf{K}}_{\tilde{\mathbf{s}}_0} + \sigma_w^2 \mathbf{I}, \quad (3.483)$$

$$\tilde{\mathbf{K}}_1 = \tilde{\mathbf{K}}_{\tilde{\mathbf{s}}_1} + \sigma_w^2 \mathbf{I}. \quad (3.484)$$

We proceed in a similar manner to the previous section. We first do an eigendecomposition of $\tilde{\mathbf{K}}_{\tilde{\mathbf{s}}_0}$

$$\tilde{\mathbf{K}}_{\tilde{\mathbf{s}}_0} = \tilde{\mathbf{u}}_0 \Lambda_{\tilde{\mathbf{s}}_0} \tilde{\mathbf{u}}_0^H. \quad (3.485)$$

Then we can write

$$\tilde{\mathbf{K}}_0 = \tilde{\mathbf{u}}_0 \left[\Lambda_{\tilde{\mathbf{s}}_0} + \sigma_w^2 \mathbf{I} \right] \tilde{\mathbf{u}}_0^H. \quad (3.486)$$

We diagonalize $\tilde{\mathbf{R}}$ with the matrix,

$$\tilde{\mathbf{D}}_0^H = \tilde{\mathbf{u}}_0^H. \quad (3.487)$$

The resulting covariance matrix on H_0 is

$$\begin{aligned} \tilde{\mathbf{K}}_{\tilde{\mathbf{D}}_0} &= \tilde{\mathbf{u}}_0^H \tilde{\mathbf{K}}_0 \tilde{\mathbf{u}}_0 \\ &= \Lambda_{\tilde{\mathbf{s}}_0} + \sigma_w^2 \mathbf{I}. \end{aligned} \quad (3.488)$$

The covariance matrix on H_1 is

$$\begin{aligned}\tilde{\mathbf{K}}_{\tilde{D}_1} &= \tilde{\mathbf{u}}_0^H \tilde{\mathbf{K}}_1 \tilde{\mathbf{u}}_0 \\ &= \tilde{\mathbf{u}}_0^H \tilde{\mathbf{K}}_{\tilde{s}_1} \tilde{\mathbf{u}}_0 + \sigma_w^2 \mathbf{I} \\ &\triangleq \tilde{\mathbf{K}}_{\tilde{D}_s} + \sigma_w^2 \mathbf{I}.\end{aligned}\quad (3.489)$$

We do an eigendecomposition of $\tilde{\mathbf{K}}_{\tilde{D}_s}$

$$\tilde{\mathbf{K}}_{\tilde{D}_s} = \tilde{\mathbf{u}}_1 \Lambda_{\tilde{D}_s} \tilde{\mathbf{u}}_1^H \quad (3.490)$$

and write

$$\tilde{\mathbf{K}}_{\tilde{D}_1} = \tilde{\mathbf{u}}_1 (\Lambda_{\tilde{D}_s} + \sigma_w^2 \mathbf{I}) \tilde{\mathbf{u}}_1^H. \quad (3.491)$$

We then diagonalize with the matrix

$$\tilde{\mathbf{D}}_1^H = \tilde{\mathbf{u}}_1^H \quad (3.492)$$

to obtain

$$\tilde{\mathbf{R}}_D = \tilde{\mathbf{D}}_1^H \tilde{\mathbf{D}}_0^H \tilde{\mathbf{R}}. \quad (3.493)$$

The covariance matrices of $\tilde{\mathbf{r}}_D$ on the two hypotheses are

$$\begin{aligned}\tilde{\mathbf{K}}_{\tilde{r}_D|H_0} &= \tilde{\mathbf{u}}_1^H \tilde{\mathbf{K}}_{\tilde{D}_0} \tilde{\mathbf{u}}_1 \\ &= \tilde{\mathbf{u}}_1^H \Lambda_{\tilde{s}_0} \tilde{\mathbf{u}}_1 + \sigma_w^2 \mathbf{I} \triangleq \Lambda_{\tilde{r}_{D_0}}\end{aligned}\quad (3.494)$$

and

$$\begin{aligned}\tilde{\mathbf{K}}_{\tilde{r}_D|H_1} &= \tilde{\mathbf{u}}_1^H \tilde{\mathbf{K}}_{\tilde{D}_1} \tilde{\mathbf{u}}_1 \\ &= \Lambda_{\tilde{D}_s} + \sigma_w^2 \mathbf{I} \triangleq \Lambda_{\tilde{r}_{D_1}}.\end{aligned}\quad (3.495)$$

Then

$$\Delta \tilde{\mathbf{Q}} = \Lambda_{\tilde{r}_{D_0}}^{-1} - \Lambda_{\tilde{r}_{D_1}}^{-1}. \quad (3.496)$$

We can proceed as in Section 3.3.2.1 to compute the performance.

3.3.3 Summary

In this section, we considered the case in which the means were the same on both hypotheses and the covariance matrices were different. The likelihood ratio test reduced to a quadratic form (3.331),

$$l(\mathbf{R}) \triangleq \mathbf{R}^T \Delta \mathbf{Q} \mathbf{R} \stackrel{H_1}{\gtrless} \gamma_3 \stackrel{H_0}{\gtrless}$$

and (3.333)

$$l(\tilde{\mathbf{R}}) \triangleq \tilde{\mathbf{R}}^H \Delta \tilde{\mathbf{Q}} \tilde{\mathbf{R}} \stackrel{H_1}{\gtrless} \gamma'_3 \stackrel{H_0}{\gtrless}$$

We will encounter this model in communication, radar, and sonar systems in which the signal component has a random amplitude (Gaussian or circular complex Gaussian). The complex version will be referred to as the Rayleigh model when we discuss physical applications. We will also encounter the model when the signal of interest is a sampled realization of a Gaussian random process.

By using an eigendecomposition and a diagonalizing transformation we could reduce $\Delta\tilde{\mathbf{Q}}$ to a diagonal matrix. To evaluate the performance we have to take the inverse transform of a characteristic function containing an N -fold product. For the real case, this required a numerical integration so a more practical approach was to use the bounds and approximations containing the $\mu(s)$ function (3.332),

$$\mu(s) = \frac{s}{2} \ln|\mathbf{K}_0| + \frac{1-s}{2} \ln|\mathbf{K}_1| - \frac{1}{2} \ln|s\mathbf{K}_0 + (1-s)\mathbf{K}_1|$$

and its derivative. For the complex case, the “pairs of equal eigenvalues” property enabled us to obtain analytical solutions for P_D and P_F .

3.4 GENERAL GAUSSIAN

In this case, both the mean and covariance matrices are different on the hypotheses. In Section 3.4.1, we study the likelihood ratio for real variables. In Section 3.4.2, we consider the complex version of the same model. In Section 3.4.3, we consider a special case where we can reduce the detector to a single quadratic form. In Section 3.4.4, we summarize our results.

3.4.1 Real Gaussian Model

The likelihood ratio test for the general Gaussian model was given in (3.57)

$$\begin{aligned} l(\mathbf{R}) &= \frac{1}{2}(\mathbf{R} - \mathbf{m}_0)^T \mathbf{Q}_0 (\mathbf{R} - \mathbf{m}_0) - \frac{1}{2}(\mathbf{R} - \mathbf{m}_1)^T \mathbf{Q}_1 (\mathbf{R} - \mathbf{m}_1) \\ &\stackrel{H_1}{\gtrless} \ln \eta + \frac{1}{2} \ln|\mathbf{K}_1| - \frac{1}{2} \ln|\mathbf{K}_0| \triangleq \gamma_1, \end{aligned} \quad (3.497)$$

which can be rewritten as

$$l(\mathbf{R}) = \frac{1}{2} \left\{ \mathbf{R}^T \Delta \mathbf{Q} \mathbf{R} - 2\mathbf{m}_0^T \mathbf{Q}_0 \mathbf{R} + 2\mathbf{m}_1^T \mathbf{Q}_1 \mathbf{R} \right\} \stackrel{H_1}{\gtrless} \gamma_1 - \frac{1}{2} \mathbf{m}_0^T \mathbf{Q}_0 \mathbf{m}_0 + \frac{1}{2} \mathbf{m}_1^T \mathbf{Q}_1 \mathbf{m}_1 \triangleq \gamma_4, \quad (3.498)$$

where

$$\Delta \mathbf{Q} \triangleq \mathbf{Q}_0 - \mathbf{Q}_1. \quad (3.499)$$

Now define

$$\mathbf{g}_0^T = \mathbf{m}_0^T \mathbf{Q}_0, \quad (3.500)$$

$$\mathbf{g}_1^T = \mathbf{m}_1^T \mathbf{Q}_1, \quad (3.501)$$

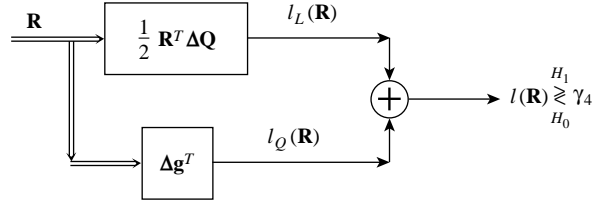


Figure 3.36: Optimum detector: general Gaussian.

and

$$\Delta \mathbf{g}^T = \mathbf{g}_1^T - \mathbf{g}_0^T = \mathbf{m}_1^T \mathbf{Q}_1 - \mathbf{m}_0^T \mathbf{Q}_0. \quad (3.502)$$

Then

$$l(\mathbf{R}) = \frac{1}{2} \mathbf{R}^T \Delta \mathbf{Q} \mathbf{R} + \Delta \mathbf{g}^T \mathbf{R}. \quad (3.503)$$

Defining

$$l_Q(\mathbf{R}) = \frac{1}{2} \mathbf{R}^T \Delta \mathbf{Q} \mathbf{R} \quad (3.504)$$

and

$$l_L(\mathbf{R}) = \Delta \mathbf{g}^T \mathbf{R}, \quad (3.505)$$

we can write

$$l(\mathbf{R}) = l_Q(\mathbf{R}) + l_L(\mathbf{R}). \quad (3.506)$$

Thus, the likelihood ratio generates two sufficient statistics corresponding to a quadratic component $l_Q(\mathbf{R})$ and a linear component $l_L(\mathbf{R})$. The LRT is shown in Figure 3.36.

To analyze the performance, we need the probability density function of l . From Section 3.2, we know that l_L is a Gaussian random variable. In Section 3.3, we developed the probability density of l_Q for a number of interesting cases. Unfortunately, l_L and l_Q are correlated so in general we cannot simply convolve their densities.¹⁶

3.4.2 Circular Complex Gaussian Model

The circular complex Gaussian model follows in a similar manner. Starting with (3.83), we obtain

$$l_Q(\tilde{\mathbf{R}}) = \tilde{\mathbf{R}}^H \Delta \tilde{\mathbf{Q}} \tilde{\mathbf{R}} \quad (3.507)$$

and

$$l_L(\tilde{\mathbf{R}}) = 2\Re \left\{ \Delta \tilde{\mathbf{g}}^H \tilde{\mathbf{R}} \right\}, \quad (3.508)$$

¹⁶The two statistics are uncorrelated iff $\mathbf{m}_i^T \Delta \mathbf{Q} \mathbf{K}_i \Delta \mathbf{g} = 0$, $i = 0, 1$.

where

$$\Delta \tilde{\mathbf{g}}^H = \tilde{\mathbf{m}}_1^H \tilde{\mathbf{Q}}_1 - \tilde{\mathbf{m}}_0^H \tilde{\mathbf{Q}}_0. \quad (3.509)$$

The LRT is

$$l(\tilde{\mathbf{R}}) = l_Q(\tilde{\mathbf{R}}) + l_L(\tilde{\mathbf{R}}) \stackrel[H_1]{\geqslant} \gamma'_1 - \tilde{\mathbf{m}}_0^H \tilde{\mathbf{Q}}_0 \tilde{\mathbf{m}}_0 + \tilde{\mathbf{m}}_1^H \tilde{\mathbf{Q}}_1 \tilde{\mathbf{m}}_1 \triangleq \gamma'_4. \quad (3.510)$$

The block diagram has the same structure and l_Q and l_L are correlated in most applications.¹⁷

To illustrate the issues involved in analyzing the performance of the optimum detector in the general Gaussian model, we consider a generalization of the low-rank signal model in Section 3.3.1.4.

Example 3.9. Consider

$$H_1 : \tilde{\mathbf{r}} = \tilde{\mathbf{v}}\tilde{a} + \tilde{\mathbf{w}}, \quad (3.511)$$

$$H_0 : \tilde{\mathbf{r}} = \tilde{\mathbf{w}}, \quad (3.512)$$

where $\tilde{\mathbf{w}}$ is $CN(\mathbf{0}, \sigma_w^2 \mathbf{I})$ and \tilde{a} is $CN(\tilde{a}_s, \sigma_s^2)$. We assume that

$$\|\tilde{\mathbf{v}}\|^2 = N. \quad (3.513)$$

This model corresponds to an application where the transmitted signal is modeled by $\tilde{\mathbf{v}}$ and the channel (or target) causes a constant known attenuation \tilde{a}_s (known as the specular component) and a random component modeled with the σ_s^2 variance.

Then

$$\tilde{\mathbf{m}}_0 = \mathbf{0}, \quad (3.514)$$

$$\tilde{\mathbf{m}}_1 = \tilde{a}_s \tilde{\mathbf{v}}, \quad (3.515)$$

$$\tilde{\mathbf{K}}_0 = \sigma_w^2 \mathbf{I}, \quad (3.516)$$

$$\tilde{\mathbf{K}}_1 = \sigma_s^2 \tilde{\mathbf{v}} \tilde{\mathbf{v}}^H + \sigma_w^2 \mathbf{I}. \quad (3.517)$$

The inverses are

$$\tilde{\mathbf{Q}}_0 = \frac{1}{\sigma_w^2} \mathbf{I}, \quad (3.518)$$

$$\tilde{\mathbf{Q}}_1 = \frac{1}{\sigma_w^2} \mathbf{I} - \frac{\sigma_s^2}{\sigma_w^2 (\sigma_w^2 + N\sigma_s^2)} \tilde{\mathbf{v}} \tilde{\mathbf{v}}^H. \quad (3.519)$$

Then

$$\Delta \tilde{\mathbf{Q}} = \frac{\sigma_s^2}{\sigma_w^2 (\sigma_w^2 + N\sigma_s^2)} \tilde{\mathbf{v}} \tilde{\mathbf{v}}^H, \quad (3.520)$$

$$\Delta \tilde{\mathbf{g}}^H = \tilde{\mathbf{m}}_1^H \tilde{\mathbf{Q}}_1 = \frac{\tilde{a}_s^*}{\sigma_w^2 + N\sigma_s^2} \tilde{\mathbf{v}}^H, \quad (3.521)$$

¹⁷For the complex case, l_Q and l_L are uncorrelated iff $\Re \{ \tilde{\mathbf{m}}_i^H \Delta \tilde{\mathbf{Q}} \tilde{\mathbf{K}}_i \Delta \tilde{\mathbf{g}} \} = 0, i = 0, 1$.

and

$$l_Q(\tilde{\mathbf{R}}) = \frac{\sigma_s^2}{\sigma_w^2(\sigma_w^2 + N\sigma_s^2)} |\tilde{\mathbf{v}}^H \tilde{\mathbf{R}}|^2, \quad (3.522)$$

$$l_L(\tilde{\mathbf{R}}) = 2\Re \left\{ \frac{\tilde{a}_s^*}{\sigma_w^2 + N\sigma_s^2} \tilde{\mathbf{v}}^H \tilde{\mathbf{R}} \right\}. \quad (3.523)$$

The quantity $\tilde{\mathbf{v}}^H \tilde{\mathbf{r}}$ is a scalar complex Gaussian random variable, so l_L is a scalar real Gaussian random variable on both hypotheses. On H_0 , $\tilde{\mathbf{v}}^H \tilde{\mathbf{r}}$ has a zero mean and l_Q is an Exponential random variable that is uncorrelated with l_L . On H_1 , $\tilde{\mathbf{v}}^H \tilde{\mathbf{r}}$ has a nonzero mean and l_Q is a scaled Noncentral Chi-squared random variable that is correlated with l_L .

To analyze the performance, we find $\mu(s)$, $\dot{\mu}(s)$, and $\ddot{\mu}(s)$ using (3.84)–(3.86) and the approximate expressions for P_F and P_M in (2.238) and (2.241). Defining

$$\alpha \triangleq \frac{|\tilde{a}_s|^2}{\sigma_w^2}, \quad (3.524)$$

$$\beta \triangleq \frac{\sigma_s^2}{\sigma_w^2}, \quad (3.525)$$

$$c(s) \triangleq 1 + (1 - s)N\beta, \quad (3.526)$$

we can derive the following expressions:

$$\mu(s) = N\alpha \frac{(s^2 - s)}{c(s)} + (1 - s) \ln(1 + N\beta) - \ln c(s), \quad (3.527)$$

$$\dot{\mu}(s) = \frac{N\alpha}{c(s)^2} [s - (1 - s)c(s)] - \ln(1 + N\beta) + \frac{N\beta}{c(s)}, \quad (3.528)$$

$$\ddot{\mu}(s) = \frac{2N\alpha(1 + N\beta)}{c(s)^3} + \left(\frac{N\beta}{c(s)} \right)^2. \quad (3.529)$$

Define the total signal-to-noise ratio as

$$\zeta = \alpha + \beta = \frac{|\tilde{a}_s|^2 + \sigma_s^2}{\sigma_w^2} \quad (3.530)$$

and let ν denote the fraction of signal energy in the mean

$$\nu \triangleq \frac{|\tilde{a}_s|^2}{|\tilde{a}_s|^2 + \sigma_s^2} = \frac{\alpha}{\alpha + \beta}. \quad (3.531)$$

For $\nu = 1$, all of the signal energy is on the mean and $\sigma_s^2 = 0$, $\beta = 0$, and $\alpha = \zeta$. This is the equal covariance, unequal mean case studied in Section 3.2.1. In this case, $l_Q = 0$ and l_L is Gaussian. We have closed form expressions for P_F and P_D in (2.84) and (2.85) with d^2 defined in (3.118),

$$d^2 = 2\Delta \tilde{\mathbf{m}}^H \tilde{\mathbf{Q}} \Delta \tilde{\mathbf{m}} = 2 \frac{\tilde{\mathbf{v}}^H \tilde{\mathbf{v}} |\tilde{a}_s|^2}{\sigma_w^2} = 2N\alpha. \quad (3.532)$$

We showed in Example 2.12 that the approximate P_F and P_D obtained using (3.527)–(3.529) in (2.238) and (2.241) are equal to the exact P_F and P_D in (2.84) and (2.85).

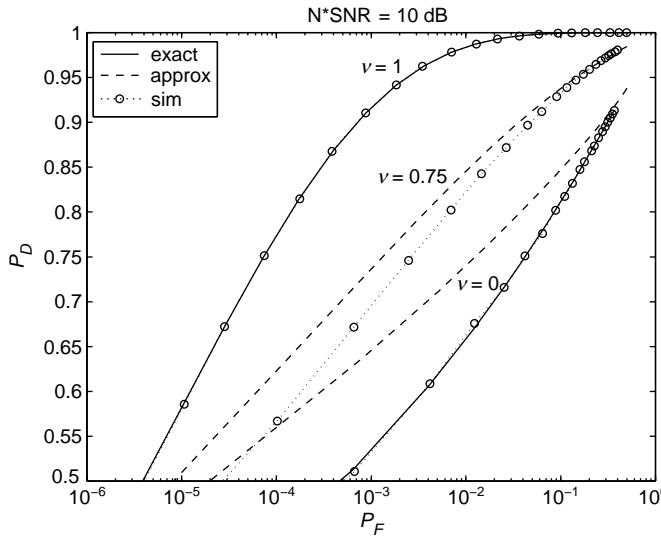


Figure 3.37: ROC curves for $N\xi = 10$ and several values of ν .

For $\nu = 0$, all of the signal energy is in the covariance matrix and $|\tilde{a}_s|^2 = 0$, $\alpha = 0$, and $\beta = \zeta$. This is the equal mean, unequal covariance case studied in Section 3.3.1.3. In this case, $l_L = 0$ and l_Q is an Exponential random variable on both hypotheses. In Example 3.8, we derived closed form expressions for P_F and P_D in (3.410) and (3.411). In this case, the approximate expressions are not the same as the exact expressions. The approximate expressions assume that the LRT statistic is approximately Gaussian, when it is actually Exponential.

For $0 < \nu < 1$, we expect the approximation to be better for ν closer to one, where the LRT statistic is dominated by the Gaussian term $l_L(\tilde{\mathbf{R}})$. In Figure 3.37, we plot approximate ROC curves for fixed $N\xi = 10$ and several values of ν . We also plot simulated ROC curves obtained using the importance sampling technique developed in Section 2.5, and the exact ROC curves for $\nu = 0$ and $\nu = 1$. We see excellent agreement between the simulation results and the exact curves for the $\nu = 0$ and $\nu = 1$ cases. The approximate and exact ROC curves are quite different for $\nu = 0$, but the simulation results show that the approximation improves as ν increases, as expected. Overall, performance improves as ν increases and more of the signal energy is in the mean. ■

The example illustrates the techniques necessary to evaluate performance in the general Gaussian model. In a later chapter, we will find some cases where the binary symmetric model allows analytical expressions for the $\Pr(\epsilon)$.

In the next section, we consider a special case of $\Delta\mathbf{Q}$ that allows us to write the LRT as a single quadratic form.

3.4.3 Single Quadratic Form

Because of the correlation between l_Q and l_L , it is useful to express $l(\mathbf{R})$ as single quadratic form. This representation requires $\Delta\mathbf{Q}$ to be nonsingular. This excludes many important cases, including all cases that have a common white noise covariance matrix on both

hypotheses and a low-rank interference matrix on one or both hypotheses, but there are a number of interesting applications when the technique is useful. We write

$$l(\mathbf{R}) = \frac{1}{2} \left\{ [\mathbf{R} - \mathbf{m}_c]^T \Delta \mathbf{Q} [\mathbf{R} - \mathbf{m}_c] \right\}. \quad (3.533)$$

Expanding terms, we have

$$l(\mathbf{R}) = \frac{1}{2} \left\{ \mathbf{R}^T \Delta \mathbf{Q} \mathbf{R} - 2\mathbf{m}_c^T \Delta \mathbf{Q} \mathbf{R} + \mathbf{m}_c^T \Delta \mathbf{Q} \mathbf{m}_c \right\}. \quad (3.534)$$

Now we choose \mathbf{m}_c so that the linear term in (3.534) is equal to the linear terms in (3.498). Define

$$\mathbf{m}_c^T \Delta \mathbf{Q} = \mathbf{m}_0^T \mathbf{Q}_0 - \mathbf{m}_1^T \mathbf{Q}_1 = \mathbf{g}_0^T - \mathbf{g}_1^T = -\Delta \mathbf{g}^T. \quad (3.535)$$

Assuming $\Delta \mathbf{Q}$ is invertible,

$$\mathbf{m}_c = -\Delta \mathbf{Q}^{-1} \Delta \mathbf{g} \quad (3.536)$$

and the single quadratic form LRT is

$$l(\mathbf{R}) \stackrel{H_1}{\geqslant} \gamma_4 + \frac{1}{2} \mathbf{m}_c^T \Delta \mathbf{Q} \mathbf{m}_c \triangleq \gamma_c. \quad (3.537)$$

Note that by reducing the likelihood ratio test to the form in (3.533), many of the results in Section 3.3 can be adopted. It is not the same case because the $p(l|H_1)$ and $p(l|H_0)$ will be different. Once again, the $\mu(s)$ function can play an important role.

For the circular complex Gaussian case, the single quadratic form version is

$$l(\tilde{\mathbf{R}}) = \left[\tilde{\mathbf{R}}^H - \tilde{\mathbf{m}}_c^H \right] \Delta \tilde{\mathbf{Q}} \left[\tilde{\mathbf{R}} - \tilde{\mathbf{m}}_c \right] \stackrel{H_1}{\geqslant} \gamma'_4 + \tilde{\mathbf{m}}_c^H \Delta \tilde{\mathbf{Q}} \tilde{\mathbf{m}}_c \triangleq \gamma'_c, \quad (3.538)$$

where

$$\tilde{\mathbf{m}}_c = \Delta \tilde{\mathbf{Q}}^{-1} \left[\tilde{\mathbf{Q}}_0 \tilde{\mathbf{m}}_0 - \tilde{\mathbf{Q}}_1 \tilde{\mathbf{m}}_1 \right]. \quad (3.539)$$

To illustrate the technique, we consider the case in which there is white noise with unequal variances on the hypotheses and $\mathbf{m}_0 \neq \mathbf{m}_1$.

$$H_1 : \mathbf{r} = \mathbf{m}_1 + \mathbf{w}_1, \quad (3.540)$$

$$H_0 : \mathbf{r} = \mathbf{m}_0 + \mathbf{w}_0, \quad (3.541)$$

where

$$\mathbf{w}_1 \sim N(\mathbf{0}, \sigma_1^2 \mathbf{I}), \quad (3.542)$$

$$\mathbf{w}_0 \sim N(\mathbf{0}, \sigma_0^2 \mathbf{I}), \quad (3.543)$$

and $\sigma_1^2 > \sigma_0^2$. The vectors are $N \times 1$. Then

$$\mathbf{Q}_0 = \frac{1}{\sigma_0^2} \mathbf{I}, \quad (3.544)$$

$$\mathbf{Q}_1 = \frac{1}{\sigma_1^2} \mathbf{I}, \quad (3.545)$$

and

$$\Delta \mathbf{Q} = \left(\frac{1}{\sigma_0^2} - \frac{1}{\sigma_1^2} \right) \mathbf{I} = \frac{\sigma_1^2 - \sigma_0^2}{\sigma_0^2 \sigma_1^2} \mathbf{I} \triangleq \frac{1}{\sigma_c^2} \mathbf{I}, \quad (3.546)$$

where

$$\sigma_c^2 = \frac{\sigma_0^2 \sigma_1^2}{\sigma_1^2 - \sigma_0^2}. \quad (3.547)$$

Then

$$l(\mathbf{R}) = \frac{1}{2} \left[\mathbf{R}^T - \mathbf{m}_c^T \right] \frac{1}{\sigma_c^2} \left[\mathbf{R} - \mathbf{m}_c \right]_{H_0}^{H_1} \gtrless \gamma_c, \quad (3.548)$$

where

$$\mathbf{m}_c = \sigma_c^2 \left[\frac{1}{\sigma_0^2} \mathbf{m}_0 - \frac{1}{\sigma_1^2} \mathbf{m}_1 \right]. \quad (3.549)$$

We rewrite $l(\mathbf{R})$ as

$$l(\mathbf{R}_\Delta) = \frac{1}{2} \mathbf{R}_\Delta^T \mathbf{R}_\Delta, \quad (3.550)$$

where

$$\mathbf{R}_\Delta = \frac{\mathbf{R} - \mathbf{m}_c}{\sigma_c}. \quad (3.551)$$

We see that we are summing the squares of N IID Gaussian random variables with nonzero means, so $p_{l|H_0}(L|H_0)$ and $p_{l|H_1}(L|H_1)$ will be scaled Noncentral Chi-squared densities of order N . We find the mean and covariance of \mathbf{r}_Δ on the two hypotheses.

On H_0 ,

$$E[\mathbf{r}_\Delta | H_0] = E \left[\frac{\mathbf{r} - \mathbf{m}_c}{\sigma_c} \middle| H_0 \right] = \frac{\mathbf{m}_0 - \mathbf{m}_c}{\sigma_c} \quad (3.552)$$

and

$$\begin{aligned} \text{Cov}(\mathbf{r}_\Delta | H_0) &= E \left\{ \left[\mathbf{r}_\Delta - \frac{\mathbf{m}_0 - \mathbf{m}_c}{\sigma_c} \right] \left[\mathbf{r}_\Delta^T - \left(\frac{\mathbf{m}_0 - \mathbf{m}_c}{\sigma_c} \right)^T \right] \middle| H_0 \right\} \\ &= E \left\{ \left[\frac{\mathbf{r} - \mathbf{m}_c}{\sigma_c} - \frac{\mathbf{m}_0 - \mathbf{m}_c}{\sigma_c} \right] \left[\left(\frac{\mathbf{r} - \mathbf{m}_c}{\sigma_c} \right)^T - \left(\frac{\mathbf{m}_0 - \mathbf{m}_c}{\sigma_c} \right)^T \right] \middle| H_0 \right\} \\ &= \frac{1}{\sigma_c^2} E \{ (\mathbf{r} - \mathbf{m}_0)(\mathbf{r} - \mathbf{m}_0)^T | H_0 \} = \frac{\sigma_0^2}{\sigma_c^2} \mathbf{I}. \end{aligned} \quad (3.553)$$

In the standard form of a Noncentral Chi-squared density, the terms are $N(m_i, 1)$. Define

$$\mathbf{r}_{u_0} = \frac{\sigma_c}{\sigma_0} \mathbf{r}_\Delta. \quad (3.554)$$

Then

$$E[\mathbf{r}_{u_0}|H_0] = \frac{\mathbf{m}_0 - \mathbf{m}_c}{\sigma_0} \triangleq \mathbf{m}_{u_0} \quad (3.555)$$

and

$$\text{Cov}(\mathbf{r}_{u_0}|H_0) = \mathbf{I}. \quad (3.556)$$

On H_1 , we use the same steps and define

$$\mathbf{r}_{u_1} = \frac{\sigma_c}{\sigma_1} \mathbf{r}_\Delta. \quad (3.557)$$

Then

$$E[\mathbf{r}_{u_1}|H_1] = \frac{\mathbf{m}_1 - \mathbf{m}_c}{\sigma_1} \triangleq \mathbf{m}_{u_1} \quad (3.558)$$

and

$$\text{Cov}(\mathbf{r}_{u_1}|H_1) = \mathbf{I}. \quad (3.559)$$

Then

$$l_0(\mathbf{R}) \triangleq \frac{2\sigma_c^2}{\sigma_0^2} l(\mathbf{R}) = \sum_{i=1}^N (R_{u_0i})^2 \quad (3.560)$$

is the sum of N squared independent $N(m_{0i}, 1)$ random variables on H_0 and

$$l_1(\mathbf{R}) \triangleq \frac{2\sigma_c^2}{\sigma_1^2} l(\mathbf{R}) = \sum_{i=1}^N (R_{u_1i})^2 \quad (3.561)$$

is the sum of N squared independent $N(m_{1i}, 1)$ random variables on H_1 . l_0 and l_1 have Noncentral Chi-squared densities of order N ,

$$p_{l_j|H_j}(L|H_j) = \frac{1}{2} \left(\frac{L}{\lambda_j} \right)^{(N-2)/4} \exp\left(-\frac{1}{2}(L + \lambda_j)\right) I_{(N/2)-1}\left(\sqrt{L\lambda_j}\right), \quad L \geq 0; j = 0, 1. \quad (3.562)$$

Here, $I_\nu(x)$ is a modified Bessel function of the first kind and order ν . The parameter λ_j is called the noncentrality parameter

$$\lambda_j \triangleq \mathbf{m}_{uj}^T \mathbf{m}_{uj}, \quad j = 0, 1. \quad (3.563)$$

The mean of l_j is

$$E(l_j|H_j) = N + \lambda_j, \quad j = 0, 1 \quad (3.564)$$

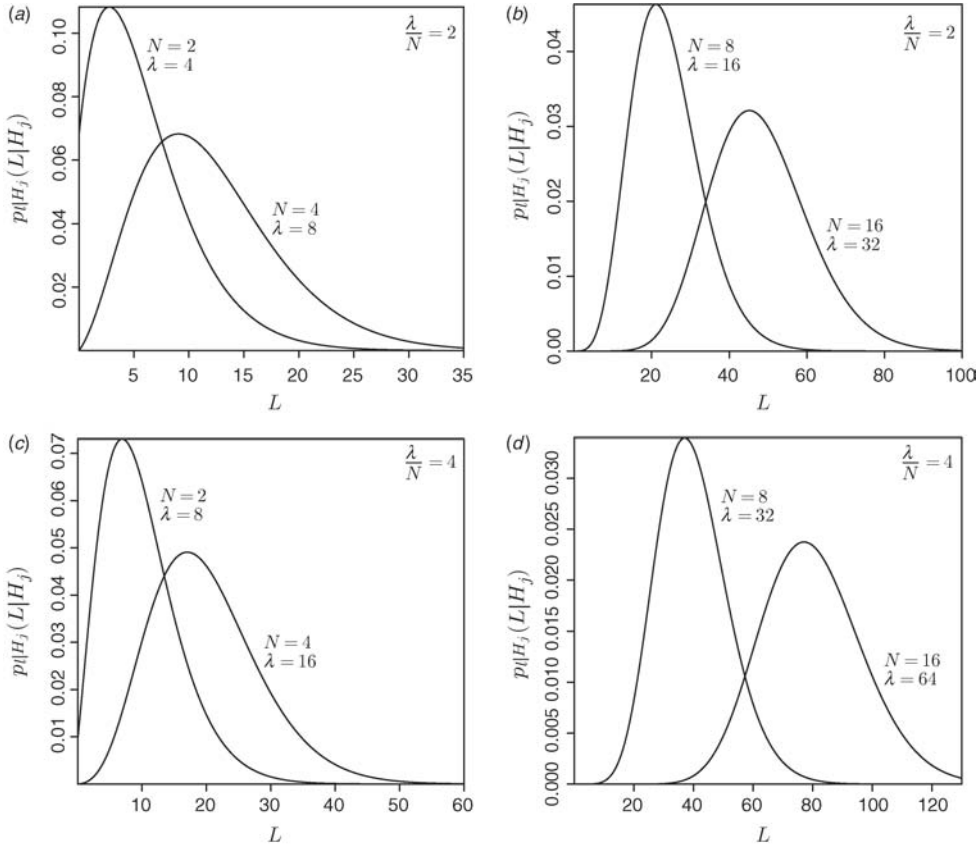


Figure 3.38: The Noncentral Chi-squared density.

and the variance is

$$\text{Var}_j(l|H_j) = 2N + 4\lambda_j, \quad j = 0, 1. \quad (3.565)$$

Some typical probability densities are shown in Figure 3.38. Note that the densities approach a Gaussian density with the same mean and variance reasonably quickly.

Then¹⁸

$$\begin{aligned} P_F &= \Pr(l \geq \gamma_c | H_0) = \Pr(l_0 \geq \gamma_{c0} | H_0) \\ &= \int_{\gamma_{c0}}^{\infty} p_{l_0|H_0}(L|H_0) dL, \end{aligned} \quad (3.566)$$

¹⁸This integral can be evaluated in Matlab using the function ncx2cdf or marcumq. See Appendix A.

where

$$\gamma_{c0} \triangleq \frac{2\sigma_c^2}{\sigma_0^2} \gamma_c = \frac{2\sigma_1^2}{\sigma_1^2 - \sigma_0^2} \gamma_c. \quad (3.567)$$

Similarly,

$$\begin{aligned} P_D &= \Pr(l \geq \gamma_c | H_1) = \Pr(l_1 \geq \gamma_{c1} | H_1) \\ &= \int_{\gamma_{c1}}^{\infty} p_{l_1|H_1}(L | H_1) dL, \end{aligned} \quad (3.568)$$

where

$$\gamma_{c1} \triangleq \frac{2\sigma_c^2}{\sigma_1^2} \gamma_c = \frac{2\sigma_0^2}{\sigma_1^2 - \sigma_0^2} \gamma_c. \quad (3.569)$$

In the complex case, l_0 and l_1 have Noncentral Chi-squared densities with $2N$ degrees of freedom and

$$\lambda_j = \tilde{\mathbf{m}}_{uj}^H \tilde{\mathbf{m}}_{uj}. \quad (3.570)$$

The thresholds for calculating P_F and P_D are analogous to (3.567) and (3.569)

$$\gamma'_{c0} \triangleq \frac{\sigma_c^2}{\sigma_0^2} \gamma'_c = \frac{\sigma_1^2}{\sigma_1^2 - \sigma_0^2} \gamma'_c, \quad (3.571)$$

$$\gamma'_{c1} \triangleq \frac{\sigma_c^2}{\sigma_1^2} \gamma'_c = \frac{\sigma_0^2}{\sigma_1^2 - \sigma_0^2} \gamma'_c. \quad (3.572)$$

We consider a simple example to illustrate the behavior.

Example 3.10. We assume the magnitudes of the means are constrained

$$\|\mathbf{m}_j\|^2 \leq E, \quad j = 0, 1, \quad (3.573)$$

and let

$$\sigma_1^2 = \beta \sigma_0^2, \quad \text{where } \beta > 1. \quad (3.574)$$

We assume a minimum probability of error criterion with equally likely hypotheses, so that

$$\gamma_c = 0 + \frac{N}{2} \ln(\sigma_1^2) - \frac{N}{2} \ln(\sigma_0^2) - \frac{1}{2\sigma_0^2} \|\mathbf{m}_0\|^2 + \frac{1}{2\sigma_1^2} \|\mathbf{m}_1\|^2 + \frac{1}{2\sigma_c^2} \|\mathbf{m}_c\|^2. \quad (3.575)$$

Then

$$\sigma_c^2 = \frac{\sigma_0^2 \sigma_1^2}{\sigma_1^2 - \sigma_0^2} = \frac{\beta \sigma_0^2}{(\beta - 1)}, \quad (3.576)$$

$$\mathbf{m}_c = \sigma_c^2 \left[\frac{\mathbf{m}_0}{\sigma_0^2} - \frac{\mathbf{m}_1}{\sigma_1^2} \right] = \frac{\beta \mathbf{m}_0 - \mathbf{m}_1}{\beta - 1}, \quad (3.577)$$

$$\mathbf{m}_{u_0} = \frac{\mathbf{m}_0 - \mathbf{m}_c}{\sigma_0} = \frac{\mathbf{m}_1 - \mathbf{m}_0}{\sigma_0(\beta - 1)}, \quad (3.578)$$

$$\mathbf{m}_{u_1} = \frac{\mathbf{m}_1 - \mathbf{m}_c}{\sigma_1} = \frac{\beta^{1/2}(\mathbf{m}_1 - \mathbf{m}_0)}{\sigma_0(\beta - 1)}. \quad (3.579)$$

The noncentrality parameters are

$$\lambda_0 = \|\mathbf{m}_{u_0}\|^2 = \frac{\|\mathbf{m}_1 - \mathbf{m}_0\|^2}{\sigma_0^2(\beta - 1)^2}, \quad (3.580)$$

$$\lambda_1 = \|\mathbf{m}_{u_1}\|^2 = \frac{\beta \|\mathbf{m}_1 - \mathbf{m}_0\|^2}{\sigma_0^2(\beta - 1)^2}. \quad (3.581)$$

On H_0 , l has a scaled Noncentral Chi-squared density with mean

$$E[l|H_0] = \frac{\sigma_0^2}{2\sigma_c^2} E[l_0|H_0] = \frac{\beta - 1}{2\beta} (N + \lambda_0) \quad (3.582)$$

and on H_1 ,

$$E[l|H_1] = \frac{\sigma_1^2}{2\sigma_c^2} E[l_1|H_1] = \frac{\beta - 1}{2} (N + \lambda_1). \quad (3.583)$$

The probability of error will be the smallest when the densities are separated as much as possible, that is, when the difference between the means is largest. Now

$$E[l|H_1] - E[l|H_0] = \frac{(\beta - 1)^2}{2\beta} N + \frac{(\beta + 1)}{2\beta} \frac{\|\mathbf{m}_1 - \mathbf{m}_0\|^2}{\sigma_0^2} \quad (3.584)$$

and the difference is maximized when $\|\mathbf{m}_1 - \mathbf{m}_0\|^2$ is maximized, so we choose

$$\mathbf{m}_1 = -\mathbf{m}_0 \quad (3.585)$$

and

$$\|\mathbf{m}_1\|^2 = \|\mathbf{m}_0\|^2 = E. \quad (3.586)$$

Then

$$\|\mathbf{m}_1 - \mathbf{m}_0\|^2 = 4E, \quad (3.587)$$

$$\mathbf{m}_c = \frac{\beta + 1}{\beta - 1} \mathbf{m}_0, \quad (3.588)$$

$$\|\mathbf{m}_c\|^2 = \left(\frac{\beta + 1}{\beta - 1} \right)^2 E \quad (3.589)$$

and

$$\lambda_0 = \frac{4}{(\beta - 1)^2} \frac{E}{\sigma_0^2}, \quad (3.590)$$

$$\lambda_1 = \frac{4\beta}{(\beta - 1)^2} \frac{E}{\sigma_0^2}. \quad (3.591)$$

The threshold is

$$\begin{aligned} \gamma_c &= 0 + \frac{N}{2} \ln(\beta\sigma_0^2) - \frac{N}{2} \ln(\sigma_0^2) - \frac{E}{2\sigma_0^2} + \frac{E}{2\beta\sigma_0^2} + \frac{(\beta + 1)^2 E}{2\beta(\beta - 1)\sigma_0^2} \\ &= \frac{1}{2} \left[N \ln(\beta) + \frac{4}{\beta - 1} \frac{E}{\sigma_0^2} \right] \end{aligned} \quad (3.592)$$

and the scaled thresholds are

$$\gamma_{c0} = \frac{\beta}{\beta - 1} \left[N \ln(\beta) + \frac{4}{\beta - 1} \frac{E}{\sigma_0^2} \right], \quad (3.593)$$

$$\gamma_{c1} = \frac{1}{\beta - 1} \left[N \ln(\beta) + \frac{4}{\beta - 1} \frac{E}{\sigma_0^2} \right]. \quad (3.594)$$

We find the probability of error from

$$\Pr(\epsilon) = \frac{1}{2} P_F + \frac{1}{2} (1 - P_D) \quad (3.595)$$

with P_F and P_D given by (3.566) and (3.568). These results are valid for $\beta > 1$.

When $\beta = 1$, $\Delta\mathbf{Q}$ becomes singular (in fact all zeros) and the problem reduces to the equal variance, unequal mean case studied in Section 3.2.1. In this case, $\Pr(\epsilon)$ is obtained from (2.88) and (3.123),

$$\Pr(\epsilon) = \text{erfc}_* \left(\frac{d}{2} \right) \quad (3.596)$$

with

$$d^2 = \frac{\|\mathbf{m}_1 - \mathbf{m}_0\|^2}{\sigma_0^2} = \frac{4E}{\sigma_0^2}. \quad (3.597)$$

$\Pr(\epsilon)$ is plotted versus E/σ_0^2 for $N = 10$ and several values of β in Figure 3.39. ■

3.4.4 Summary

In this section, we considered the general Gaussian case and the LRT was given by (3.498) or (3.503). For the real case, the LRT could be written as the sum of two components,

$$\begin{aligned} l(\mathbf{R}) &= \frac{1}{2} \mathbf{R}^T \Delta \mathbf{Q} \mathbf{R} + \Delta \mathbf{g}^T \mathbf{R} \\ &= l_Q(\mathbf{R}) + l_L(\mathbf{R}). \end{aligned} \quad (3.598)$$

A similar result was obtained for the complex case in (3.507)–(3.510).

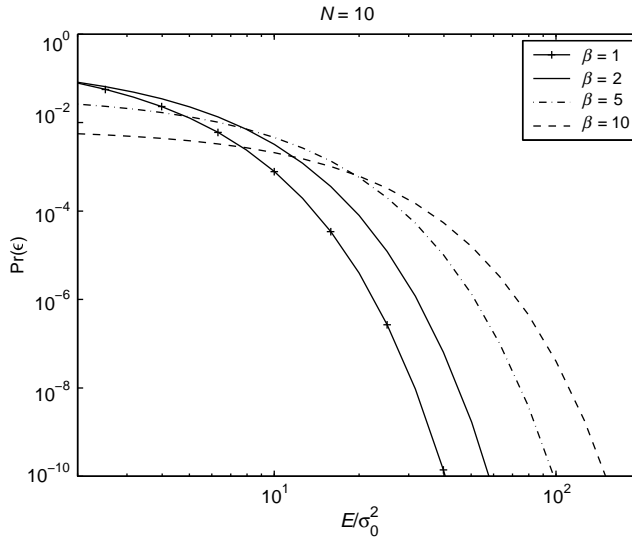


Figure 3.39: $\text{Pr}(\epsilon)$ versus E/σ_0^2 for $N = 10$ and several values of β .

For arbitrary $\Delta\mathbf{Q}$, the performance is difficult to derive. The $\mu(s)$ function was derived in (3.68) and (3.84), so we can find bounds and approximations to P_D and P_F using the expressions in Section 2.4.

In Example 3.9, we found that the approximations were not accurate enough and we resorted to simulation. The closed form expressions for $\mu(s)$ allowed us to use the importance sampling technique in Section 2.5.

For the special case when $\Delta\mathbf{Q}$ is nonsingular, we were able to transform (3.503) into a single quadratic form test and obtain analytical results for some special cases.

3.5 M HYPOTHESES

In this section, we discuss the case in which the transition probabilities have a Gaussian probability density on each hypothesis. For $j = 0, 1, \dots, M - 1$,

$$p_{\mathbf{r}|H_j}(\mathbf{R}|H_j) = \frac{1}{(2\pi)^{N/2} |\mathbf{K}_j|^{1/2}} \exp\left\{-\frac{1}{2} (\mathbf{R}^T - \mathbf{m}_j^T)(\mathbf{K}_j)^{-1}(\mathbf{R} - \mathbf{m}_j)\right\}. \quad (3.599)$$

From (2.156) in Section 2.3, the optimum Bayes test is to compute¹⁹

$$\begin{aligned} \beta_i(\mathbf{R}) &= \sum_{j=0}^{M-1} C_{ij} \Pr(H_j|\mathbf{R}) \\ &= \sum_{j=0}^{M-1} C_{ij} p_{\mathbf{r}|H_j}(\mathbf{R}|H_j) \frac{\Pr(H_j)}{p_{\mathbf{r}}(\mathbf{R})}, \quad i = 0, 1, \dots, M - 1 \end{aligned} \quad (3.600)$$

¹⁹This discussion corresponds to Problems 2.6.1–2.6.3 in DEMT-I and the solutions on pp. 47–50 of Van Trees and Goldfein [VTG68].

and choose the smallest. Since $p_{\mathbf{r}}(\mathbf{R})$ is common to all terms, an equivalent test is to compute

$$\beta'_i(\mathbf{R}) = \sum_{j=0}^{M-1} C_{ij} \Pr(H_j) p_{\mathbf{r}|H_j}(\mathbf{R}|H_j), \quad i = 0, 1, \dots, M-1 \quad (3.601)$$

and choose the smallest.

Using (3.599) and letting $P_j = \Pr(H_j)$ gives

$$\beta'_i(\mathbf{R}) = \sum_{j=0}^{M-1} C_{ij} P_j \frac{1}{(2\pi)^{N/2} |\mathbf{K}_j|^{1/2}} \exp\left\{-\frac{1}{2} (\mathbf{R}^T - \mathbf{m}_j^T) \mathbf{Q}_j (\mathbf{R} - \mathbf{m}_j)\right\}. \quad (3.602)$$

For the general cost assignment, further simplification is usually not possible. For the minimum $\Pr(\epsilon)$ criterion, we can compute

$$P_i p_{\mathbf{r}|H_i}(\mathbf{R}|H_i) = \frac{P_i}{(2\pi)^{N/2} |\mathbf{K}_i|^{1/2}} \exp\left\{-\frac{1}{2} (\mathbf{R}^T - \mathbf{m}_i^T) \mathbf{Q}_i (\mathbf{R} - \mathbf{m}_i)\right\} \quad (3.603)$$

and choose the largest. Taking the logarithm of (3.603) and ignoring constant terms, we have

$$l_i(\mathbf{R}) = \ln P_i - \frac{1}{2} \ln |\mathbf{K}_i| - \frac{1}{2} (\mathbf{R}^T - \mathbf{m}_i^T) \mathbf{Q}_i (\mathbf{R} - \mathbf{m}_i) \quad (3.604)$$

and choose the largest.

The resulting $\Pr(\epsilon)$ is given by

$$\begin{aligned} \Pr(\epsilon) &= \sum_{i=0}^{M-1} P_i \Pr(\epsilon|H_i \text{ is true}) \\ &\triangleq \sum_{i=0}^{M-1} P_i \Pr(\epsilon|H_i). \end{aligned} \quad (3.605)$$

If H_i is true, then an error occurs if any $l_j; j \neq i$ is larger than l_i . We can write this as

$$\Pr(\epsilon|H_i) = 1 - \Pr(\text{all } l_j < l_i : j \neq i | H_i) \quad (3.606)$$

or

$$\Pr(\epsilon|H_i) = 1 - \int_{-\infty}^{\infty} p_{l_i|H_i}(L_i|H_i) \left(\prod_{\substack{j=0 \\ j \neq i}}^{M-1} \int_{-\infty}^{L_i} p_{l_j|H_i}(L_j|H_i) dL_j \right) dL_i. \quad (3.607)$$

Using the results from Sections 3.2–3.4, we can compute $p_{l_j|H_i}(L_j|H_i)$ for a large number of interesting cases. Therefore, we can calculate $\Pr(\epsilon|H_i)$ via a collection of single variable integrations.

Before considering some special cases, we derive an upper bound on $\Pr(\epsilon|H_i)$. We can rewrite (3.606) as

$$\Pr(\epsilon|H_i) = \Pr(\text{any } l_j > l_i : j \neq i | H_i) \quad (3.608)$$

$$= \Pr(l_1 > l_i \text{ or } l_2 > l_i \text{ or } \dots \text{ or } l_{M-1} > l_i | H_i). \quad (3.609)$$

Now, several l_j can be greater than l_i , because the events are not mutually exclusive. Thus,

$$\Pr(\epsilon|H_i) \leq \sum_{\substack{j=0 \\ j \neq i}}^{M-1} \Pr(l_j > l_i|H_i) \quad (3.610)$$

or

$$\Pr(\epsilon|H_i) \leq \int_{-\infty}^{\infty} p_{l_i|H_i}(L_i|H_i) \left(\sum_{\substack{j=0 \\ j \neq i}}^{M-1} \int_{L_i}^{\infty} p_{l_j|H_i}(L_j|H_i) dL_j \right) dL_i. \quad (3.611)$$

We consider several special cases that occur in applications of interest.

In communications systems, the signal of interest often corresponds to the means and the covariance is the same on each hypothesis. Thus,

$$\mathbf{r} = \mathbf{m}_j + \mathbf{n}, \quad j = 0, 1, \dots, M - 1 \quad (3.612)$$

and

$$\mathbf{n} = N(\mathbf{0}, \mathbf{K}). \quad (3.613)$$

We assume that the $\mathbf{m}_j : j = 0, 1, \dots, M - 1$ are orthogonal and have the same magnitude

$$\mathbf{m}_i^T \mathbf{m}_j = \|\mathbf{m}\|^2 \delta_{ij}. \quad (3.614)$$

A physical application where this will occur is the case where the means correspond to samples of sinusoids at orthogonal frequencies.

We assume that $\mathbf{K} = \sigma_w^2 \mathbf{I}$. Thus, (3.607) reduces to

$$\Pr(\epsilon|H_i) = 1 - \int_{-\infty}^{\infty} \frac{1}{\sqrt{2\pi}\sigma_w} \exp\left(-\frac{1}{2\sigma_w^2}(L_i - \|\mathbf{m}\|)^2\right) \left(\int_{-\infty}^{L_i} \frac{1}{\sqrt{2\pi}\sigma_w} \exp\left(-\frac{L_j^2}{2\sigma_w^2}\right) dL_j \right)^{M-1} dL_i. \quad (3.615)$$

Normalizing the variables, we have

$$\Pr(\epsilon|H_i) = 1 - \int_{-\infty}^{\infty} dx \frac{1}{\sqrt{2\pi}} \exp\left(-\frac{(x - \|\mathbf{m}\|/\sigma_w)^2}{2}\right) \left(\int_{-\infty}^x \frac{1}{\sqrt{2\pi}} \exp\left(-\frac{y^2}{2}\right) dy \right)^{M-1}, \quad (3.616)$$

which can be written as

$$\Pr(\epsilon|H_i) = 1 - \int_{-\infty}^x dx \frac{1}{\sqrt{2\pi}} \exp\left(-\frac{(x - \|\mathbf{m}\|/\sigma_w)^2}{2}\right) \left(1 - \text{erfc}_*(x)\right)^{M-1} \quad (3.617)$$

and can be integrated numerically.²⁰ For the case when the hypotheses are equally likely

$$\Pr(\epsilon) = \Pr(\epsilon|H_i). \quad (3.618)$$

²⁰In DEMT-I, we used tabulated results from [Urb55]. Now we use Matlab.

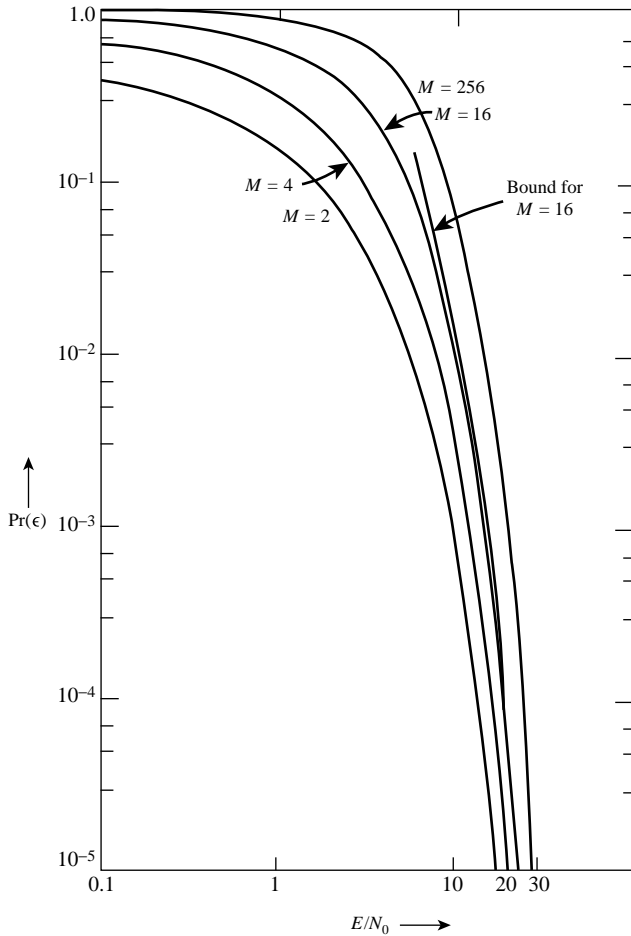


Figure 3.40: Error probability for M orthogonal signals.

The $\Pr(\epsilon)$ is plotted in Figure 3.40 versus $\|\mathbf{m}\|^2 / \sigma_w^2$. We also show the bound from (3.611) for $M = 16$. We see that for the values of $\Pr(\epsilon)$ that are of most interest, the bound is essentially equal to the exact result.

Similar results follow for the complex case. We leave this derivation as an exercise for the reader (see Problem 3.5.2).

An important case in the complex Gaussian model is one where the probability densities on all hypotheses are zero-mean complex Gaussian. The covariance matrices are

$$\text{Cov}(\tilde{\mathbf{r}}|H_j) = \sigma_s^2 \tilde{\mathbf{v}}_j \tilde{\mathbf{v}}_j^H + \sigma_w^2 \mathbf{I}, \quad j = 0, 1, \dots, M-1, \quad (3.619)$$

where

$$\tilde{\mathbf{v}}_i^H \tilde{\mathbf{v}}_j = N\delta_{ij}. \quad (3.620)$$

This is the M -ary version of the binary low-rank model in Section 3.3.

We will show later that this corresponds to transmitting orthogonal signals over a Rayleigh fading channel. This model is analyzed in Problem 3.5.5.

We have not considered an example where both the means and the covariances are different on different hypotheses. The techniques in Section 3.4.1 carry over to this case. An interesting example for this case is

$$\tilde{\mathbf{r}} = \tilde{\mathbf{v}}_j \tilde{a}_j + \tilde{\mathbf{w}}, \quad j = 0, 1, \dots, M - 1, \quad (3.621)$$

where \tilde{a}_j is a complex Gaussian random variable with

$$E(\tilde{a}_{jR}) = \alpha, \quad (3.622)$$

$$E(\tilde{a}_{jI}) = 0, \quad (3.623)$$

and

$$\text{Var}(\tilde{a}_j) = \sigma_{\tilde{a}}^2. \quad (3.624)$$

The noise vector $\tilde{\mathbf{w}}$ is zero-mean complex Gaussian

$$\text{Cov}(\tilde{\mathbf{w}}) = \sigma_{\tilde{w}}^2 \mathbf{I} \quad (3.625)$$

and (3.620) applies. We will show later that this corresponds to transmitting orthogonal signals over a Rician fading channel.

3.6 SUMMARY

In this chapter, we have done a comprehensive study of the general Gaussian detection problem that is an accurate model for a large number of applications. Our emphasis has been on using the model to solve a wide variety of communications, radar, and sonar problems.

In Section 3.1, we derived the likelihood ratio for the real and circular complex Gaussian models. From (3.57)

$$\begin{aligned} l(\mathbf{R}) &= \frac{1}{2}(\mathbf{R} - \mathbf{m}_0)^T \mathbf{Q}_0 (\mathbf{R} - \mathbf{m}_0) - \frac{1}{2}(\mathbf{R} - \mathbf{m}_1)^T \mathbf{Q}_1 (\mathbf{R} - \mathbf{m}_1) \\ &\stackrel{H_1}{\gtrless} \ln \eta + \frac{1}{2} \ln |\mathbf{K}_1| - \frac{1}{2} \ln |\mathbf{K}_0| \triangleq \gamma_1 \end{aligned}$$

for the real case, and from (3.83)

$$l(\tilde{\mathbf{R}}) = (\tilde{\mathbf{R}} - \tilde{\mathbf{m}}_0)^H \tilde{\mathbf{Q}}_0 (\tilde{\mathbf{R}} - \tilde{\mathbf{m}}_0) - (\tilde{\mathbf{R}} - \tilde{\mathbf{m}}_1)^H \tilde{\mathbf{Q}}_1 (\tilde{\mathbf{R}} - \tilde{\mathbf{m}}_1) \stackrel{H_1}{\gtrless} \ln \eta + \ln |\tilde{\mathbf{K}}_1| - \ln |\tilde{\mathbf{K}}_0| \triangleq \gamma'_1$$

for the circular complex case.

We derived the $\mu(s)$ function that was the key to performance bounds and simulation using importance sampling. From (3.68),

$$\mu(s) = \frac{s(s-1)}{2} \Delta \mathbf{m}^T \mathbf{K}(s)^{-1} \Delta \mathbf{m} + \frac{s}{2} \ln |\mathbf{K}_0| + \frac{1-s}{2} \ln |\mathbf{K}_1| - \frac{1}{2} \ln |\mathbf{K}(s)|$$

for the real case, and from (3.84),

$$\mu(s) = s(s - 1)\Delta\tilde{\mathbf{m}}^H\tilde{\mathbf{K}}(s)^{-1}\Delta\tilde{\mathbf{m}} + s \ln|\tilde{\mathbf{K}}_0| + (1 - s) \ln|\tilde{\mathbf{K}}_1| - \ln|\tilde{\mathbf{K}}(s)|$$

for the circular complex case.

These results gave us everything needed to implement the optimum test and to simulate its performance. The next three sections developed a sequence of models corresponding to important applications. By studying various models, we can find analytical performance results that enable us to understand how the components of the models affect performance.

In Section 3.2, we considered the case in which the covariance matrices on the two hypotheses are equal. We found that the likelihood ratio test was

$$l(\mathbf{R}) \triangleq \Delta\mathbf{m}^T \mathbf{Q} \mathbf{R} \begin{matrix} H_1 \\ \gtrless \\ H_0 \end{matrix} \gamma_2$$

for the real case. It is a linear transformation of the observed Gaussian vector so it is a scalar Gaussian variable and the performance was completely determined by using

$$d^2 = \Delta\mathbf{m}^T \mathbf{Q} \Delta\mathbf{m}$$

in (2.84) and in (2.85). Similar results were obtained for the circular complex case in (3.108) and (3.118).

This model will be encountered in communication systems in which the means represent the signal transmitted on the two hypotheses and the transmission channel attenuates the signal and adds interference and noise. We found analytical performance results and showed how to design optimum signals for a specific interference. We introduced eigendecomposition in order to better understand our analytical results.

In Section 3.3, we considered the case in which the mean vectors on the hypotheses are equal. We found that the sufficient statistic was a quadratic form. From (3.331)

$$l(\mathbf{R}) \triangleq \mathbf{R}^T \Delta \mathbf{Q} \mathbf{R} \begin{matrix} H_1 \\ \gtrless \\ H_0 \end{matrix} \gamma_3$$

for the real case, and from (3.333)

$$l(\tilde{\mathbf{R}}) \triangleq \tilde{\mathbf{R}}^H \Delta \tilde{\mathbf{Q}} \tilde{\mathbf{R}} \begin{matrix} H_1 \\ \gtrless \\ H_0 \end{matrix} \gamma'_3$$

for the circular complex case.

In order to analyze the performance, we did an eigendecomposition. We showed that by a sequence of whitening and diagonalizing transformations we could change any model to the case where $\Delta\mathbf{Q}$ was a diagonal matrix whose components were functions of the eigenvalues.

For the real Gaussian case, we found the characteristic function of l on both hypotheses but had to do a numerical integration to find the probability densities needed to calculate P_D , P_F , or $\Pr(\epsilon)$. For the complex case, we found a closed form expression for the probability densities and calculated P_D and P_F using standard mathematical functions. This model will be encountered in communications and radar systems where the channel (or target) introduces a complex Gaussian multiplier onto the transmitted signals (referred to as the Rayleigh model). We will also encounter it in radar, sonar, and radio astronomy where we

are trying to detect a sample from a Gaussian random process (either real or complex) in the presence of Gaussian interference and noise.

In Section 3.4, we returned to the general Gaussian case. We found that the sufficient statistic was the sum of a quadratic term and a linear term that are correlated in most cases. From (3.503)

$$l(\mathbf{R}) = \frac{1}{2} \mathbf{R}^T \Delta \mathbf{Q} \mathbf{R} + \Delta \mathbf{g}^T \mathbf{R}.$$

Except for some special cases, we could not find analytical expressions for the performance. We resorted to the bounds and approximations using $\mu(s)$ developed in Section 2.4 and to the simulations using importance sampling developed in Section 2.5. The closed form expression for $\mu(s)$ enabled us to find the appropriate tilted density. This model will be encountered in communications and radar systems where the channel (or target) introduces a complex Gaussian multiplier with a nonzero mean (the specular component) onto the transmitted signals (referred to as the Rician model).

In Section 3.5, we extended these models to the M hypotheses case. We could always find the optimum Bayes test. Except for special cases, the performance was difficult to evaluate and we resorted to bounds on the $\Pr(\epsilon)$.

This completes our discussion of the classical general Gaussian detection problem for simple hypothesis testing. In Section 4.5, we will revisit the Gaussian model in the context of composite hypothesis testing where \mathbf{m}_j and/or \mathbf{K}_j ; $j = 0, 1$ contain unknown parameters.

This chapter has been long and it is probably not until we get to physical applications in Chapter 7 that the reader will appreciate how many important applications reduce to one of the models in this chapter.

In Chapters 4 and 5, we develop classical estimation theory and the general Gaussian estimation model.

3.7 PROBLEMS

The problems are divided into sections corresponding to the major sections in the chapter. For example, Section P3.2 pertains to text material in Section 3.2. In sections in which it is appropriate the problems are divided into topical groups. Many of the problems ask for plots of P_D or $\Pr(\epsilon)$. It is important that in addition to the plots, a discussion of the results is included in the solution.

P3.2 Equal Covariance Matrices

P3.2.1 Independent Components with Equal Variance

Problem 3.2.1. The received vectors on the two hypotheses are

$$\begin{aligned} H_0 : \tilde{\mathbf{r}} &= \tilde{\mathbf{w}} \\ H_1 : \tilde{\mathbf{r}} &= \sqrt{E} \tilde{\mathbf{s}} + \tilde{\mathbf{w}} \end{aligned}$$

where $\tilde{\mathbf{w}}$ is a zero-mean, circular complex Gaussian random vector $CN(\mathbf{0}, \sigma_w^2 \mathbf{I})$ and $\tilde{\mathbf{s}}$ is a known deterministic vector that is normalized

$$\tilde{\mathbf{s}}^H \tilde{\mathbf{s}} = 1$$

and E is a known parameter.

- (a) Find the optimum detector.
- (b) Plot P_D versus $d = 2E/\sigma_w^2$ for various P_F . Compare to Figure 2.12b.

Problem 3.2.2. The received vectors on the two hypotheses are

$$\begin{aligned} H_0 : \tilde{\mathbf{r}} &= \sqrt{E} \tilde{\mathbf{s}}_0 + \tilde{\mathbf{w}}, \\ H_1 : \tilde{\mathbf{r}} &= \sqrt{E} \tilde{\mathbf{s}}_1 + \tilde{\mathbf{w}}, \end{aligned}$$

where $\tilde{\mathbf{w}}$ is a zero-mean, circular complex Gaussian random vector $CN(\mathbf{0}, \sigma_w^2 \mathbf{I})$ and $\tilde{\mathbf{s}}_0$ and $\tilde{\mathbf{s}}_1$ are known deterministic complex orthonormal signals,

$$\tilde{\mathbf{s}}_i^H \tilde{\mathbf{s}}_j = \delta_{ij}, \quad i, j = 0, 1,$$

and E is a known parameter. The criterion is minimum $\Pr(\epsilon)$.

- (a) Find the optimum detector.
- (b) Plot $\Pr(\epsilon)$ versus E/σ_w^2 .

ARRAY PROCESSING

Problem 3.2.3. Consider the array model in Example 3.2. From (3.142), the mean vector is

$$\tilde{\mathbf{m}}_1 = \tilde{b} \tilde{\mathbf{v}}(\psi). \quad (\text{P.1})$$

- (a) Show that

$$l(\mathbf{R}) = \Re \left\{ \frac{\tilde{b} \tilde{\mathbf{v}}^H(\psi) \tilde{\mathbf{R}}}{\sigma_w^2} \right\} \quad (\text{P.2})$$

and

$$d^2 = \frac{2|\tilde{b}|^2}{\sigma_w^2} \tilde{\mathbf{v}}^H(\psi) \tilde{\mathbf{v}}(\psi) = \frac{2|\tilde{b}|^2}{\sigma_w^2} N. \quad (\text{P.3})$$

The effect of the array is completely characterized by the array gain, which is the ratio of the value in (P.3) divided by the value of (P.3) with $N = 1$. In this case

$$A_w(\psi) = N,$$

where the subscript w denotes white sensor noise (statistically independent among sensors).

- (b) Define SNRs as

$$\begin{aligned} \text{SNR}_{\text{out}} &= \frac{|\tilde{b}|^2 N}{\sigma_w^2}, \\ \text{SNR}_{\text{in}} &= \frac{|\tilde{b}|^2}{\sigma_w^2}. \end{aligned}$$

Show that

$$A_w(\psi) = \frac{\text{SNR}_{\text{out}}}{\text{SNR}_{\text{in}}}.$$

Note that $A_w(\psi)$ is independent of ψ .

Problem 3.2.4. Now assume that the processor is fixed as in (P.2). The signal actually arrives from ψ_a , so its array manifold vector is $\tilde{\mathbf{v}}(\psi_a)$.

- (a) Plot d^2 as a function of ψ_a , $-\pi \leq \psi_a \leq \pi$.
- (b) The normalized version of this result is called the *beampattern*.

$$B_c(\psi_a, \psi_s) = \frac{1}{N} \mathbf{v}^H(\psi_s) \mathbf{v}(\psi_a).$$

Problem 3.2.5. Consider the array model in Figure 3.9. Now assume that the sensors are located at $p_x(0), p_x(1), \dots, p_x(N-1)$. Assume $N = 5$ with the following spacing

$$1 \cdot 3 \cdot 5 \cdot 2.$$

Repeat Problems 3.2.3 and 3.2.4.

POLYNOMIAL FITTING

Problem 3.2.6. Consider the model of a constant-velocity target moving in one dimension. The position of the target on the two hypotheses is

$$p_j(i) = x(0) + v_j(0) iT, \quad i = 0, 1, \dots, N,$$

where $x(0)$ and $v_j(0)$ are the position and velocity, respectively, at $i = 0$ and T is the time between observations. We observe

$$r(i) = p_j(i) + w(i), \quad i = 0, 1, \dots, N,$$

where $w(i)$ are IID $N(0, \sigma_w^2)$. The criterion is minimum $\Pr(\epsilon)$.

- (a) Find the LRT.
- (b) Find d^2 .
- (c) Plot $\Pr(\epsilon)$ versus N for several values of

$$\frac{\Delta v}{\sigma_w} \triangleq \frac{v_1(0) - v_0(0)}{\sigma_w}.$$

Problem 3.2.7. Generalize the model in Problem 3.2.6 to a constant acceleration model, where

$$p_j(i) = x(0) + v_j(0) iT + a_j(0) \frac{(iT)^2}{2}, \quad j = 0, 1.$$

Repeat Problem 3.2.6. In part (c), choose the appropriate parameters.

Problem 3.2.8 (continuation). Generalize the model in Problem 3.2.6 to

$$p_j(i) = x(0) + v_j(0) iT + a_j(0) \frac{(iT)^2}{2} + c_j(0) \frac{(iT)^3}{6}, \quad j = 0, 1.$$

Repeat Problem 3.2.6.

Problem 3.2.9 (continuation). The general polynomial case is

$$p_j(i) = \sum_{k=0}^K c_{jk}(0) \frac{(iT)^k}{k!},$$

where

$$c_{jk}(t) = \left[\frac{d^k}{dt^k} x(t) \right]_{t=0}.$$

Repeat parts (a) and (b) of Problem 3.2.6.

Problem 3.2.10. Modify Problem 3.2.9 to a model in which the target is only present on H_1 and

$$r(i) = w(i)$$

on H_0 .

Consider values of $K = 1, 2$, and 3 . Plot P_D versus the appropriate parameters for $P_F = 10^{-4}$ and 10^{-6} .

P3.2.3 General Case: Eigendecomposition

Problem 3.2.11. Consider the model in (3.89) with $\mathbf{m}_0 = \mathbf{0}$, $\|\mathbf{m}_1\|^2 = 1$, and

$$\mathbf{K} = \sigma_I^2 \begin{bmatrix} 1 & \rho & \rho^2 \\ \rho & 1 & \rho \\ \rho^2 & \rho & 1 \end{bmatrix} + \sigma_w^2 \mathbf{I}.$$

(a) Assume $\mathbf{m}_1 = \frac{1}{\sqrt{3}} \mathbf{1}$. The SNR is

$$\text{SNR} \triangleq \frac{\|\mathbf{m}_1\|^2}{\sigma_I^2 + \sigma_w^2}.$$

Plot d^2 versus SNR for various $\rho \in [-1, 1]$.

(b) Choose \mathbf{m}_1 to maximize d^2 subject to the constraint $\|\mathbf{m}_1\|^2 = 1$. Plot d_{opt}^2 versus SNR for various $\rho \in [-1, 1]$.

Problem 3.2.12. Consider the same model as in Problem 3.2.11 except that $N = 10$ and

$$\mathbf{K} = \sigma_I^2 \begin{bmatrix} 1 & \rho & \rho^2 & 0 & 0 & 0 & 0 & 0 & 0 & 0 \\ \rho & 1 & \rho & \rho^2 & 0 & 0 & 0 & 0 & 0 & 0 \\ \rho^2 & \rho & 1 & \rho & \rho^2 & 0 & 0 & 0 & 0 & 0 \\ 0 & \rho^2 & \rho & 1 & \rho & \rho^2 & 0 & 0 & 0 & 0 \\ 0 & 0 & \rho^2 & \rho & 1 & \rho & \rho^2 & 0 & 0 & 0 \\ 0 & 0 & 0 & \rho^2 & \rho & 1 & \rho & \rho^2 & 0 & 0 \\ 0 & 0 & 0 & 0 & \rho^2 & \rho & 1 & \rho & \rho^2 & 0 \\ 0 & 0 & 0 & 0 & 0 & \rho^2 & \rho & 1 & \rho & \rho^2 \\ 0 & 0 & 0 & 0 & 0 & 0 & \rho^2 & \rho & 1 & \rho \\ 0 & 0 & 0 & 0 & 0 & 0 & 0 & \rho^2 & \rho & 1 \end{bmatrix} + \sigma_w^2 \mathbf{I}.$$

Repeat Problem 3.2.11.

P3.2.5 Interference Matrix: Estimator–Subtractor

Problem 3.2.13. The received vectors on the two hypotheses are

$$\begin{aligned} H_0 : \mathbf{r} &= \mathbf{m}_0 + \mathbf{n}_I + \mathbf{w}, \\ H_1 : \mathbf{r} &= \mathbf{m}_1 + \mathbf{n}_I + \mathbf{w}, \end{aligned}$$

where the model is described in (3.250)–(3.254). The vectors are all $N \times 1$. However, $\mathbf{m}_i; i = 0, 1$ only has $N_s \leq N$ nonzero components.

$$\mathbf{m}_j = \begin{bmatrix} \mathbf{m}_{s_j} \\ \mathbf{0} \end{bmatrix}.$$

The received vectors are identical on the last $N - N_s$ observations.

The covariance matrix is given in Example 3.5 (3.277). The upper and lower bounds on d^2 are given in Figure 3.18 for $N_s = N = 10$.

Now consider the case where $\sigma_I^2/\sigma_w^2 = 100$ and $N_s = 10$. Consider three values of $|\rho| : 0.1, 0.5$, and 0.9.

- (a) Plot the upper and lower bounds on d^2 for $N = 10, 11, 12, \dots$
- (b) Give an intuitive explanation for your results.

P3.2.6 Low-Rank Models

Problem 3.2.14. Consider the generalization of Example 3.6 where the received vectors are

$$\begin{aligned} H_0 : \tilde{\mathbf{r}} &= \tilde{\mathbf{V}}\tilde{\mathbf{a}} + \tilde{\mathbf{w}}, \\ H_1 : \tilde{\mathbf{r}} &= \tilde{\mathbf{m}} + \tilde{\mathbf{V}}\tilde{\mathbf{a}} + \tilde{\mathbf{w}}, \end{aligned}$$

where $\tilde{\mathbf{V}}$ is $N \times D$ and $\tilde{\mathbf{a}}$ is a $D \times 1$ vector that is $CN(\mathbf{0}, \sigma_a^2 \mathbf{I})$.

Assume $D = 2$ and

$$\begin{aligned} [\tilde{\mathbf{v}}_1]_n &= e^{j\omega_I n}, & n = 0, 1, \dots, N-1, \\ [\tilde{\mathbf{v}}_2]_n &= e^{-j\omega_I n}, & n = 0, 1, \dots, N-1. \end{aligned}$$

Plot d^2 versus $\Delta\omega/\pi = (\omega_s - \omega_I)/\pi$ for $N = 5$ and $|\tilde{b}|^2/\sigma_w^2 = 1$.

Problem 3.2.15. Consider the model in Problem 3.2.14 with $D = 4$ and

$$\begin{aligned} [\tilde{\mathbf{v}}_1]_n &= e^{j\omega_I n}, & n = 0, 1, \dots, N-1, \\ [\tilde{\mathbf{v}}_2]_n &= e^{-j\omega_I n}, & n = 0, 1, \dots, N-1, \\ [\tilde{\mathbf{v}}_3]_n &= e^{j2\omega_I n}, & n = 0, 1, \dots, N-1, \\ [\tilde{\mathbf{v}}_4]_n &= e^{-j2\omega_I n}, & n = 0, 1, \dots, N-1. \end{aligned}$$

Repeat Problem 3.2.14 with $N = 10$.

ARRAY PROCESSING

Problem 3.2.16. Consider the model in Problem 3.2.14 and the uniform linear array in Example 3.7. Assume $D = 2$ and

$$\begin{aligned} [\tilde{\mathbf{v}}_1]_n &= e^{j\psi_1 n}, & n = 0, 1, \dots, N-1, \\ [\tilde{\mathbf{v}}_2]_n &= e^{-j\psi_1 n}, & n = 0, 1, \dots, N-1, \end{aligned}$$

and that $\tilde{\mathbf{a}}$ is a 2×1 vector that is $CN(\mathbf{0}, \sigma_{\tilde{a}}^2 \mathbf{I})$. Let

$$\sigma_{\tilde{s}}^2 \triangleq |\tilde{b}|^2.$$

Plot d^2 versus ψ_1 for $N = 10$ and various combinations of

$$\begin{aligned} \text{INR} &\triangleq \frac{\sigma_{\tilde{a}}^2}{\sigma_{\tilde{w}}^2}, \\ \text{SNR} &\triangleq \frac{\sigma_{\tilde{s}}^2}{\sigma_{\tilde{w}}^2}. \end{aligned}$$

Problem 3.2.17. Repeat Problem 3.2.16 for the case in which the interferers are correlated

$$\tilde{\mathbf{a}} \sim CN(\mathbf{0}, \tilde{\mathbf{K}}_{\tilde{a}}),$$

where

$$\tilde{\mathbf{K}}_{\tilde{a}} = \sigma_{\tilde{a}}^2 \begin{bmatrix} 1 & \tilde{\rho}^* \\ \tilde{\rho} & 1 \end{bmatrix}.$$

Plot d^2 for $\tilde{\rho} = 0.5$ and 0.9 .

Problem 3.2.18. Consider the uniform linear array in Example 3.7. Repeat Example 3.7 for the case in which

$$[\tilde{\mathbf{m}}_1]_n = \tilde{b} e^{-j\psi_s n}, \quad n = 0, 1, \dots, N-1$$

or

$$\tilde{\mathbf{m}}_1 = \tilde{\mathbf{v}}(\psi_s) \tilde{b}.$$

P3.3 Equal Mean Vectors

P3.3.1 Diagonal Covariance Matrix on H_0 : Equal Variance

Problem 3.3.1. Consider the optimum detector in Figure 3.27 and assume the signal and noise are real Gaussian variables.

- (a) Find $\mu(s)$, $\dot{\mu}(s)$, and $\ddot{\mu}(s)$, using (3.332), (3.74), and (3.75) for $N = 10$ and \mathbf{K}_s equal to the real version of (3.398).
- (b) Plot approximate ROCs for $\rho = 0.3, 0.7$, and 0.9 and $\sigma_s^2/\sigma_w^2 = 1, 3$, and 10 .

Problem 3.3.2. The reason we could obtain an analytical solution to the complex model was that the eigenvalues corresponded to paired equal eigenvalues in the real model. Try to find an

approximate solution to the real problem by constructing equal eigenvalue pairs. Assume N is even. Let

- (a) $\lambda_{s_i}^c = \lambda_{s_{i+1}}^c = \frac{1}{2}(\lambda_{s_i} + \lambda_{s_{i+1}})$, $i = 1, 3, \dots, N - 1$,
- (b) $\lambda_{s_i}^c = \lambda_{s_{i+1}}^c = (\lambda_{s_i} \lambda_{s_{i+1}})^{1/2}$, $i = 1, 3, \dots, N - 1$,
- (c) $\lambda_{s_i}^c = \lambda_{s_{i+1}}^c = \frac{1}{2}(\lambda_{s_{i+1}})$, $i = 1, 3, \dots, N - 1$,
- (d) $\lambda_{s_i}^c = \lambda_{s_{i+1}}^c = \frac{1}{2}(\lambda_{s_i})$, $i = 1, 3, \dots, N - 1$.

Plot ROCs for the parameters in Problem 3.3.1.

LOW-RANK SIGNAL MODELS

Problem 3.3.3. Consider the circular complex Gaussian model where the observed $N \times 1$ vectors on the two hypotheses are

$$\begin{aligned} H_0 : \tilde{\mathbf{r}} &= \tilde{\mathbf{w}}, \\ H_1 : \tilde{\mathbf{r}} &= \tilde{b}\tilde{\mathbf{s}} + \tilde{\mathbf{w}}. \end{aligned}$$

The noise $\tilde{\mathbf{w}}$ is $CN(\mathbf{0}, \sigma_w^2 \mathbf{I})$. The signal $\tilde{\mathbf{s}}$ is a known deterministic vector that is normalized,

$$\tilde{\mathbf{s}}^H \tilde{\mathbf{s}} = 1.$$

The scalar multiplier \tilde{b} is $CN(0, \sigma_b^2)$.

We define a unitary $N \times N$ matrix

$$\tilde{\mathbf{u}}_{\tilde{\phi}} = [\tilde{\mathbf{s}} \quad \tilde{\phi}_2 \quad \tilde{\phi}_3 \quad \cdots \quad \tilde{\phi}_N],$$

where $\tilde{\phi}_i$; $i = 2, 3, \dots, N$ are an arbitrary orthonormal set such that

$$\tilde{\mathbf{s}}^H \tilde{\phi}_i = 0, \quad i = 2, 3, \dots, N.$$

- (a) Verify that $\tilde{\mathbf{K}}_{\tilde{\mathbf{s}}}$ can be written as

$$\tilde{\mathbf{K}}_{\tilde{\mathbf{s}}} = \tilde{\mathbf{u}}_{\tilde{\phi}} [\Lambda_{\tilde{\mathbf{s}}} + \sigma_w^2 \mathbf{I}] \tilde{\mathbf{u}}_{\tilde{\phi}}^H,$$

where

$$\Lambda_{\tilde{\mathbf{s}}} = \text{diag} [\sigma_b^2 \quad 0 \quad 0 \quad \cdots \quad 0].$$

- (b) Find the optimum detector.
- (c) Find analytical expressions for P_D and P_F .
- (d) Plot P_D versus σ_b^2/σ_w^2 for $P_F = 10^{-4}$ and 10^{-6} .
- (e) Find $\mu(s)$ and the approximate expressions for P_D and P_F . Plot the results and compare them to the results in part (d).

Problem 3.3.4. Consider the following generalization,

$$\begin{aligned} H_0 : \tilde{\mathbf{r}} &= \tilde{\mathbf{w}}, \\ H_1 : \tilde{\mathbf{r}} &= \sum_{i=1}^D \tilde{b}_i \tilde{\mathbf{s}}_i + \tilde{\mathbf{w}}. \end{aligned}$$

The observed vector on H_1 can be written as

$$\tilde{\mathbf{r}} = \tilde{\mathbf{S}} \tilde{\mathbf{b}} + \tilde{\mathbf{w}},$$

where

$$\tilde{\mathbf{S}} = [\tilde{\mathbf{s}}_1 \quad \tilde{\mathbf{s}}_2 \quad \cdots \quad \tilde{\mathbf{s}}_D]$$

is a known deterministic $N \times D$ matrix and $\tilde{\mathbf{b}}$ is a $D \times 1$ zero-mean circular complex Gaussian vector, $CN(\mathbf{0}, \sigma_b^2 \mathbf{I})$. We assume the signal vectors are orthonormal

$$\tilde{\mathbf{S}}^H \tilde{\mathbf{S}} = \mathbf{I}.$$

- (a) Generalize the results in part (a) of Problem 3.3.3. Explain your results in terms of subspaces.
- (b) Repeat parts (b) through (e) of Problem 3.3.3.

Problem 3.3.5. Consider the model in Problem 3.3.4 with nonorthogonal signals

$$\tilde{\mathbf{S}}^H \tilde{\mathbf{S}} = \tilde{\rho}_{\tilde{\mathbf{s}}},$$

where

$$\tilde{\mathbf{s}}_i^H \tilde{\mathbf{s}}_i = 1, \quad i = 1, 2, \dots, D.$$

- (a) Generalize parts (a) through (c) of Problem 3.3.3. Explain your results in terms of subspaces.
- (b) Now assume $D = 4$ and

$$\tilde{\rho}_{\tilde{\mathbf{s}}} = \begin{bmatrix} 1 & 0.75 & 0.50 & 0.25 \\ 0.75 & 1 & 0.75 & 0.50 \\ 0.50 & 0.75 & 1 & 0.75 \\ 0.25 & 0.50 & 0.75 & 1 \end{bmatrix}.$$

Repeat parts (d) and (e) of Problem 3.3.3.

Problem 3.3.6. Consider the model in Problem 3.3.4 with orthogonal signals and correlated $\tilde{\mathbf{b}}$:

$$E[\tilde{\mathbf{b}} \tilde{\mathbf{b}}^H] = \tilde{\mathbf{K}}_{\tilde{\mathbf{b}}}.$$

- (a) Generalize parts (a)–(c) of Problem 3.3.3. Explain your results in terms of subspaces.
- (b) Now assume that $\tilde{\mathbf{K}}_{\tilde{\mathbf{b}}}$ is a $D \times D$ matrix of the form of (3.398).
- (c) Plot P_D versus $\text{SNR} = \sigma_b^2 / \sigma_w^2$ (in dB) for $|\rho| = 0.7, 0.9$; $P_F = 10^{-4}$ and 10^{-6} , and $D = 4, N = 10$.
- (d) Repeat part (e) of Problem 3.3.3.

Problem 3.3.7. Consider the model in Problem 3.3.4. Assume that

$$E_r \triangleq D\sigma_b^2$$

is fixed. We want to choose D to maximize P_D for a given value of P_F . Assume $N = 16$.

Plot P_D versus E_r / σ_w^2 (in dB) for $P_F = 10^{-6}$ and $D = 1, 2, \dots, 16$ and discuss your results.

ARRAY PROCESSING

Problem 3.3.8. Consider the uniform linear array in Example 3.2. The k th sample on the two hypotheses is

$$\begin{aligned} H_1 : \tilde{\mathbf{r}}_k &= \tilde{b}_k \tilde{\mathbf{v}}(\psi_s) + \tilde{\mathbf{w}}_k, & k = 0, 1, \dots, K-1, \\ H_0 : \tilde{\mathbf{r}}_k &= \tilde{\mathbf{w}}_k, & k = 0, 1, \dots, K-1. \end{aligned}$$

The noise model is the same as in Example 3.2. The \tilde{b}_k are $CN(0, \sigma_b^2)$ and are statistically independent of $\tilde{\mathbf{w}}_k$.

- (a) Find the optimum detector.
- (b) Show that the optimum detector is separable into two components, an array processing term that is the same as the result in Example 3.2 and a scalar processing term.
- (c) Plot P_D and P_F curves as a function of σ_b^2/σ_w^2 .

Problem 3.3.9. Repeat Problem 3.3.8 for the case of a signal with multiple components and $K = 1$,

$$\begin{aligned} H_1 : \tilde{\mathbf{r}}_k &= \sum_{i=1}^D \tilde{b}_{ik} \tilde{\mathbf{v}}(\psi_{s_i}) + \tilde{\mathbf{w}}_k, \\ H_0 : \tilde{\mathbf{r}}_k &= \tilde{\mathbf{w}}_k. \end{aligned}$$

Define

$$\tilde{\mathbf{b}}_k \triangleq [\tilde{b}_{1k} \quad \tilde{b}_{2k} \quad \dots \quad \tilde{b}_{Dk}]^T$$

and

$$\tilde{\mathbf{V}} \triangleq [\tilde{\mathbf{v}}(\psi_{s_1}) \quad \tilde{\mathbf{v}}(\psi_{s_2}) \quad \dots \quad \tilde{\mathbf{v}}(\psi_{s_D})].$$

Then the signal can be written as

$$\tilde{\mathbf{s}}_k = \tilde{\mathbf{V}} \tilde{\mathbf{b}}_k.$$

The $\tilde{\mathbf{b}}_k$ are IID $CN(\mathbf{0}, \tilde{\mathbf{K}}_{\tilde{\mathbf{b}}})$. In this problem, we consider the case when

$$\tilde{\mathbf{K}}_{\tilde{\mathbf{b}}} = \sigma_b^2 \mathbf{I}.$$

- (a) Find the optimum detector.
- (b) Plot P_D and P_F curves for $D = 2$ as a function of σ_b^2/σ_w^2 for various values of $\Delta\psi = \psi_2 - \psi_1$.

Problem 3.3.10. Repeat Problem 3.3.9 for

$$\tilde{\mathbf{K}}_{\tilde{\mathbf{b}}} = \sigma_b^2 \begin{bmatrix} 1 & \tilde{\rho}^* \\ \tilde{\rho} & 1 \end{bmatrix}.$$

P3.3.2 Nondiagonal Covariance Matrix on H_0

LOW-RANK INTERFERENCE MODELS

Problem 3.3.11. Consider the circular complex Gaussian model where the observed $N \times 1$ vectors on the two hypotheses are

$$\begin{aligned} H_1 : \tilde{\mathbf{r}} &= \tilde{b}\tilde{\mathbf{s}} + \tilde{a}\tilde{\mathbf{s}}_I + \tilde{\mathbf{w}}, \\ H_0 : \tilde{\mathbf{r}} &= \tilde{a}\tilde{\mathbf{s}}_I + \tilde{\mathbf{w}}. \end{aligned}$$

The noise $\tilde{\mathbf{w}}$ is $CN(\mathbf{0}, \sigma_w^2 \mathbf{I})$. The signal $\tilde{\mathbf{s}}$ is a known deterministic vector that is normalized,

$$\tilde{\mathbf{s}}^H \tilde{\mathbf{s}} = 1.$$

The scalar multiplier \tilde{b} is $CN(0, \sigma_b^2)$. The interference is a known deterministic signal that is normalized,

$$\tilde{\mathbf{s}}_I^H \tilde{\mathbf{s}}_I = 1$$

and

$$\tilde{\mathbf{s}}^H \tilde{\mathbf{s}}_I \triangleq \tilde{\rho}_{sI}.$$

The scalar multiplier \tilde{a} is $CN(0, \sigma_a^2)$.

Using the same approach as in Section 3.2.2 and Problem 3.3.3,

- (a) Find the optimum detector.
- (b) Find analytical expressions for P_D and P_F .
- (c) Construct plots of P_D for various combinations of P_F , σ_b^2 , σ_a^2 , σ_w^2 , and ρ_{sI} . Check that as $\sigma_a^2 \rightarrow 0$, the results approach those in Problem 3.3.3.
- (d) Find $\mu(s)$ and the approximate expressions for P_D and P_F . Compare your results to those in part (c).

Problem 3.3.12. Consider the following generalization of Problem 3.3.11

$$\begin{aligned} H_1 : \tilde{\mathbf{r}} &= \tilde{b}\tilde{\mathbf{s}} + \tilde{\mathbf{S}}_I \tilde{\mathbf{a}} + \tilde{\mathbf{w}}, \\ H_0 : \tilde{\mathbf{r}} &= \tilde{\mathbf{S}}_I \tilde{\mathbf{a}} + \tilde{\mathbf{w}}, \end{aligned}$$

where $\tilde{\mathbf{a}}$ is a $D_I \times 1$ vector

$$\tilde{\mathbf{a}} = [\tilde{a}_1 \quad \tilde{a}_2 \quad \cdots \quad \tilde{a}_{D_I}]^T$$

and

$$\tilde{\mathbf{S}}_I = [\tilde{\mathbf{s}}_{I1} \quad \tilde{\mathbf{s}}_{I2} \quad \cdots \quad \tilde{\mathbf{s}}_{ID_I}^T]$$

is an $N \times D_I$ matrix.

The $\tilde{\mathbf{a}}$ are statistically independent of each other, $\tilde{\mathbf{b}}$, and $\tilde{\mathbf{w}}$ with density $CN(\mathbf{0}, \sigma_a^2 \mathbf{I})$. The $\tilde{\mathbf{s}}_{Ii}$ are normalized but not necessarily orthogonal

$$\tilde{\mathbf{s}}_{Ii}^H \tilde{\mathbf{s}}_{Ij} = \tilde{\rho}_{ij}, \quad -1 \leq |\tilde{\rho}_{ij}| \leq 1.$$

Repeat parts (a) through (c) of Problem 3.3.11.

Problem 3.3.13. Repeat Problem 3.3.12 for the case where $\tilde{\mathbf{a}} \sim CN(\mathbf{0}, \tilde{\mathbf{K}}_{\tilde{\mathbf{a}}})$ and

$$\tilde{\mathbf{K}}_{\tilde{\mathbf{a}}} = \sigma_{\tilde{a}}^2 \begin{bmatrix} 1 & \tilde{\rho}^* \\ \tilde{\rho} & 1 \end{bmatrix}.$$

Problem 3.3.14. Generalize Problem 3.3.12 to the case where

$$\begin{aligned} H_1 : \tilde{\mathbf{r}} &= \tilde{\mathbf{S}}\tilde{\mathbf{b}} + \tilde{\mathbf{S}}_I\tilde{\mathbf{a}} + \tilde{\mathbf{w}}, \\ H_0 : \tilde{\mathbf{r}} &= \tilde{\mathbf{S}}_I\tilde{\mathbf{a}} + \tilde{\mathbf{w}}, \end{aligned}$$

where $\tilde{\mathbf{b}}$ is $D_s \times 1$, $\tilde{\mathbf{S}}$ is $N \times D_s$, $\tilde{\mathbf{a}}$ is $D_I \times 1$, $\tilde{\mathbf{S}}_I$ is $N \times D_I$

$$\begin{aligned} \tilde{\mathbf{b}} &\sim CN(\mathbf{0}, \tilde{\mathbf{K}}_{\tilde{\mathbf{b}}}), \\ \tilde{\mathbf{a}} &\sim CN(\mathbf{0}, \tilde{\mathbf{K}}_{\tilde{\mathbf{a}}}). \end{aligned}$$

The optimum detector is specified in (3.472)–(3.479) and the performance can be calculated using (3.395) and (3.397). Find the optimum detector and plot P_D and P_F for the following special cases.

- (a) $D_s = 1, D_I = 1, \tilde{\mathbf{K}}_{\tilde{\mathbf{a}}} = \sigma_{\tilde{a}}^2, \tilde{\mathbf{K}}_{\tilde{\mathbf{b}}} = \sigma_b^2$.
- (b) $D_s = 1, D_I = 2, \tilde{\mathbf{K}}_{\tilde{\mathbf{b}}} = \sigma_b^2$, and

$$\tilde{\mathbf{K}}_{\tilde{\mathbf{a}}} = \sigma_{\tilde{a}}^2 \begin{bmatrix} 1 & \tilde{\rho}^* \\ \tilde{\rho} & 1 \end{bmatrix}, \quad -1 \leq |\tilde{\rho}| \leq 1.$$

- (c) $D_s = 1, D_I = 3, \tilde{\mathbf{K}}_{\tilde{\mathbf{b}}} = \sigma_b^2$, and

$$\tilde{\mathbf{K}}_{\tilde{\mathbf{a}}} = \sigma_{\tilde{a}}^2 \begin{bmatrix} 1 & \tilde{\rho}^* & (\tilde{\rho}^*)^2 \\ \tilde{\rho} & 1 & \tilde{\rho}^* \\ \tilde{\rho}^2 & \tilde{\rho} & 1 \end{bmatrix}, \quad -1 \leq |\tilde{\rho}| \leq 1.$$

- (d) $D_s = 2, D_I = 1, \tilde{\mathbf{K}}_{\tilde{\mathbf{a}}} = \sigma_{\tilde{a}}^2$, and

$$\tilde{\mathbf{K}}_{\tilde{\mathbf{b}}} = \sigma_b^2 \begin{bmatrix} 1 & \tilde{\rho}_s^* \\ \tilde{\rho}_s & 1 \end{bmatrix}, \quad -1 \leq |\tilde{\rho}_s| \leq 1.$$

- (e) $D_s = 2, D_I = 2$, the covariances are given in parts (b) and (d).

- (f) $D_s = 2, D_I = 2, \tilde{\mathbf{K}}_{\tilde{\mathbf{b}}} = \sigma_b^2 \mathbf{I}$, and

$$\tilde{\mathbf{K}}_{\tilde{\mathbf{a}}} = \text{diag} [\sigma_{\tilde{a}_1}^2 \quad \sigma_{\tilde{a}_2}^2].$$

ARRAY PROCESSING

Problem 3.3.15. Consider the uniform linear array in Figure 3.9. We can generalize the signal and interference model to match Problem 3.3.14. The samples on the two hypotheses are

$$\begin{aligned} H_1 : \tilde{\mathbf{r}} &= \tilde{\mathbf{V}}_s \tilde{\mathbf{b}} + \tilde{\mathbf{V}}_I \tilde{\mathbf{a}} + \tilde{\mathbf{w}}, \\ H_0 : \tilde{\mathbf{r}} &= \tilde{\mathbf{V}}_I \tilde{\mathbf{a}} + \tilde{\mathbf{w}}, \end{aligned}$$

where $\tilde{\mathbf{V}}_s$ and $\tilde{\mathbf{V}}_I$ are the signal and interference array manifold matrices, respectively.

Repeat Problem 3.3.14 but interpret your answers in terms of the various directions of arrival.

SYMMETRIC HYPOTHESES

Problem 3.3.16. Consider the circular complex Gaussian model where the observed $N \times 1$ vectors on the two hypotheses are

$$\begin{aligned} H_0 : \tilde{\mathbf{r}} &= \tilde{a}_0 \tilde{\mathbf{s}}_0 + \tilde{\mathbf{w}}, \\ H_1 : \tilde{\mathbf{r}} &= \tilde{a}_1 \tilde{\mathbf{s}}_1 + \tilde{\mathbf{w}}. \end{aligned}$$

The noise $\tilde{\mathbf{w}}$ is $CN(\mathbf{0}, \sigma_w^2 \mathbf{I})$. The signals $\tilde{\mathbf{s}}_0$ and $\tilde{\mathbf{s}}_1$ are known deterministic orthonormal signals,

$$\tilde{\mathbf{s}}_i^H \tilde{\mathbf{s}}_j = \delta_{ij}.$$

The scalar multipliers \tilde{a}_0 and \tilde{a}_1 are zero-mean, statistically independent circular complex Gaussian random variables $CN(0, \sigma_a^2)$. The hypotheses are equally likely and the criterion is minimum $\Pr(\epsilon)$.

- (a) Find the optimum detector.
- (b) Compute $\Pr(\epsilon)$ and plot it versus σ_a^2 / σ_w^2 (in dB). Compare it to the case in Section 3.2, where

$$\tilde{a}_0 = \tilde{a}_1 = \sigma_a$$

are nonrandom.

- (c) Compute $\mu(s)$ and the approximate expression for $\Pr(\epsilon)$. Compare the approximate expression to the exact expression in part (b).

Problem 3.3.17 (continuation). Generalize the results in Problem 3.3.16 to the case, where

$$\begin{aligned} H_0 : \tilde{\mathbf{r}} &= \tilde{\mathbf{S}}_0 \tilde{\mathbf{a}}_0 + \tilde{\mathbf{w}}, \\ H_1 : \tilde{\mathbf{r}} &= \tilde{\mathbf{S}}_1 \tilde{\mathbf{a}}_1 + \tilde{\mathbf{w}}, \end{aligned}$$

where $\tilde{\mathbf{S}}_0$ and $\tilde{\mathbf{S}}_1$ are $N \times K$ matrices, where

$$\tilde{\mathbf{S}}_0^H \tilde{\mathbf{S}}_0 = \tilde{\mathbf{S}}_1^H \tilde{\mathbf{S}}_1 = \mathbf{I}$$

and

$$\tilde{\mathbf{S}}_0^H \tilde{\mathbf{S}}_1 = \mathbf{0}.$$

The multipliers $\tilde{\mathbf{a}}_0$ and $\tilde{\mathbf{a}}_1$ are zero-mean, statistically independent circular complex Gaussian random vectors $CN(\mathbf{0}, \sigma_a^2 \mathbf{I})$.

Repeat Problem 3.3.16. Compare your results to those in Problem 3.3.16 and explain the difference.

P3.4 General Gaussian

LOW-RANK MODELS

Note: In order to generate low-rank models for the general Gaussian case, we can use Problems 3.3.3, 3.3.4, 3.3.8, 3.3.9, 3.3.11–3.3.15 and let the mean of $\tilde{\mathbf{b}}$ or $\tilde{\mathbf{b}}$ be nonzero. We will be able to derive the optimum detector but will have to resort to bounds and simulation to evaluate the performance.

Problem 3.4.1. Repeat Problem 3.3.9 with

$$\tilde{\mathbf{b}} \sim CN(\tilde{\mathbf{m}}_{\tilde{\mathbf{b}}}, \tilde{\mathbf{K}}_{\tilde{\mathbf{b}}})$$

for the following special cases

- (a) $D = 1, \tilde{b} \sim CN(\tilde{m}_{\tilde{b}}, \sigma_{\tilde{b}}^2)$.
- (b) $D = 2, \tilde{\mathbf{b}} \sim CN(\tilde{\mathbf{m}}_{\tilde{b}}, \sigma_{\tilde{b}}^2 \mathbf{I})$.
- (c) $D = 2$, and

$$\tilde{\mathbf{K}}_{\tilde{b}} = \sigma_{\tilde{b}}^2 \begin{bmatrix} 1 & \tilde{\rho}^* \\ \tilde{\rho} & 1 \end{bmatrix}.$$

In each part, use $\mu(s)$ to bound the performance and approximate the performance and use the iterative importance sampling algorithm to simulate the performance. Study the performance as the ratio of the specular component to the changes in the random component.

Problem 3.4.2. Repeat the six parts of Problem 3.3.14 with nonzero means.

In each part, use $\mu(s)$ to bound the performance and approximate the performance and use the iterative importance sampling algorithm to simulate the performance. Study the performance as the ratio of the specular component to the changes in the random component.

P3.5 M Hypotheses

Problem 3.5.1. Verify that (3.603) follows from (3.602).

Problem 3.5.2. Find the results analogous to (3.602) and (3.603) for the circular complex Gaussian model.

Problem 3.5.3. The observed vectors are

$$\mathbf{r} = \mathbf{m}_j + \mathbf{w}, \quad j = 0, 1, \dots, M - 1,$$

where

$$\mathbf{w} \sim N(\mathbf{0}, \sigma_w^2 \mathbf{I})$$

and

$$\mathbf{m}_j = a(M) \cos \theta_j \mathbf{m}$$

with

$$\cos \theta_j = \frac{360^\circ}{M} j,$$

$a(M)$ is a known constant, and $\|\mathbf{m}\|^2 = 1$.

- (a) Assume the hypotheses are equally likely. Find the minimum $\Pr(\epsilon)$ test.
- (b) Compute the $\Pr(\epsilon)$ for $M = 4$. Compare to the case when $M = 2$ and

$$a^2(4) = 2a^2(2).$$

Problem 3.5.4. Generalize the results in Problem 3.5.3(b) to the case, where

$$M = 2^n, \quad n = 0, 1, \dots$$

and $a^2(M) = \log_2 M \cdot a^2(2)$. Find the $\Pr(\epsilon)$ for $M = 8$ and 16 and plot versus $a^2(2)/\sigma_w^2$. This will require a numerical integration.

Problem 3.5.5. Consider the M -ary signaling model

$$H_j : \tilde{\mathbf{r}} = \tilde{a}_j \tilde{\mathbf{v}}_j + \tilde{\mathbf{w}}, \quad j = 0, 1, \dots, M-1,$$

where \tilde{a}_j is a circular complex Gaussian random variable with $\text{Cov}(\tilde{\mathbf{r}}|H_j)$ is given by (3.619) and the $\tilde{\mathbf{v}}$ are orthonormal. The hypotheses are equally likely and the criterion is minimum $\Pr(\epsilon)$.

- (a) Find the bound on the $\Pr(\epsilon)$ given by (3.611).
- (b) Find the exact $\Pr(\epsilon)$.
- (c) Plot the results versus $\sigma_{\tilde{a}}^2/\sigma_{\tilde{w}}^2$.

Problem 3.5.6. The M hypothesis, general Gaussian problem is

$$p_{\mathbf{r}|H_i}(\mathbf{R}|H_i) = [(2\pi)^{N/2} |\mathbf{K}_i|^{1/2}]^{-1} \exp \left[-\frac{1}{2} (\mathbf{R} - \mathbf{m}_i)^T \mathbf{Q}_i (\mathbf{R} - \mathbf{m}_i) \right], \quad i = 1, 2, \dots, M.$$

- (a) Find the Bayes test for this problem.
- (b) For the particular case in which the cost of a correct decision is zero and the cost of any wrong decision is equal, show that the test reduces to the following:

Compute

$$l_i(\mathbf{R}) = \ln P_i - \frac{1}{2} \ln |\mathbf{K}_i| - \frac{1}{2} (\mathbf{R} - \mathbf{m}_i)^T \mathbf{Q}_i (\mathbf{R} - \mathbf{m}_i)$$

and choose the largest.

Problem 3.5.7 (continuation). Consider the special case in which all $\mathbf{K}_i = \sigma_w^2 \mathbf{I}$ and the hypotheses are equally likely. Use the costs in part (b) of Problem 3.5.6.

- (a) What determines the dimension of the decision space? Draw some typical decision spaces to illustrate the various alternatives.
- (b) Interpret the processor as a minimum-distance decision rule.

Problem 3.5.8. Consider the special case in which all $\mathbf{m}_i = \mathbf{0}$, $i = 1, 2, \dots, M$, and the hypotheses are equally likely. Use the costs in part (b) Problem 3.5.6.

- (a) Show that the test reduces to the following:

Compute

$$l_i(\mathbf{R}) = \mathbf{R}^T \mathbf{Q}_i \mathbf{R} + \ln |\mathbf{K}_i|$$

and choose the *smallest*.

- (b) Write an expression for the $\Pr(\epsilon)$ in terms of $p_{\mathbf{l}|H_i}(\mathbf{l}|H_i)$, where

$$\mathbf{l} \triangleq \begin{bmatrix} l_1 \\ l_2 \\ \vdots \\ l_M \end{bmatrix}.$$

Problem 3.5.9. Consider the M -ary hypothesis testing problem. *Each* observation is a three-dimensional vector.

$$\begin{aligned} H_0 : \mathbf{r} &= \mathbf{m}_0 + \mathbf{w}, \\ H_1 : \mathbf{r} &= \mathbf{m}_1 + \mathbf{w}, \\ H_2 : \mathbf{r} &= \mathbf{m}_2 + \mathbf{w}, \\ H_3 : \mathbf{r} &= \mathbf{m}_3 + \mathbf{w}, \\ \mathbf{m}_0 &= +A, 0, B, \\ \mathbf{m}_1 &= 0, +A, B, \\ \mathbf{m}_2 &= -A, 0, B, \\ \mathbf{m}_3 &= 0, -A, B. \end{aligned}$$

The components in the noise vector are independent, identically distributed Gaussian variables, $N(0, \sigma_w^2)$. We have K independent observations. Assume a minimum $\text{Pr}(\epsilon)$ criterion and equally likely hypotheses. Sketch the decision region and compute the $\text{Pr}(\epsilon)$.

4

Classical Parameter Estimation

4.1 INTRODUCTION

In Chapters 2 and 3, we have considered a problem in which one of several hypotheses occurred. As the result of a particular hypothesis, a vector random variable \mathbf{r} was observed. Based on our observation, we shall try to choose the true hypothesis.

In Chapters 4 and 5, we discuss the problem of parameter estimation. In Chapter 4, we develop classic parameter estimation theory. In Chapter 5, we study the general Gaussian estimation model.

Before formulating the general problem, let us consider a simple example.

Example 4.1 Gaussian. We want to measure a voltage a at a single time instant. From physical considerations, we know that the voltage is between $-V$ and $+V$ volts. The measurement is corrupted by noise that may be modeled as an independent additive zero-mean Gaussian random variable n . The observed variable is r . Thus,

$$r = a + n. \quad (4.1)$$

The probability density governing the observation process is $p_{r|a}(R|A)$. In this case

$$p_{r|a}(R|A) = p_n(R - A) = \frac{1}{\sqrt{2\pi}\sigma_n} \exp\left(-\frac{(R - A)^2}{2\sigma_n^2}\right). \quad (4.2)$$

The problem is to observe r and estimate a . ■

This example illustrates the basic features of the estimation problem. A model of the general estimation problem is shown in Figure 4.1. The model has the following four components:

Parameter Space. The output of the source is a parameter (or variable). We view this output as a point in a parameter space. For the single-parameter case, which we shall study first, this will correspond to segments of the line $-\infty < A < \infty$. In the example considered above the segment is $(-V, V)$.

Probabilistic Mapping from Parameter Space to Observation Space. This is the probability law that governs the effect of a on the observation.

Detection, Estimation, and Modulation Theory, Second Edition. Harry L. Van Trees, Kristine L. Bell with Zhi Tian. © 2013 John Wiley & Sons, Inc. Published 2013 by John Wiley & Sons, Inc.

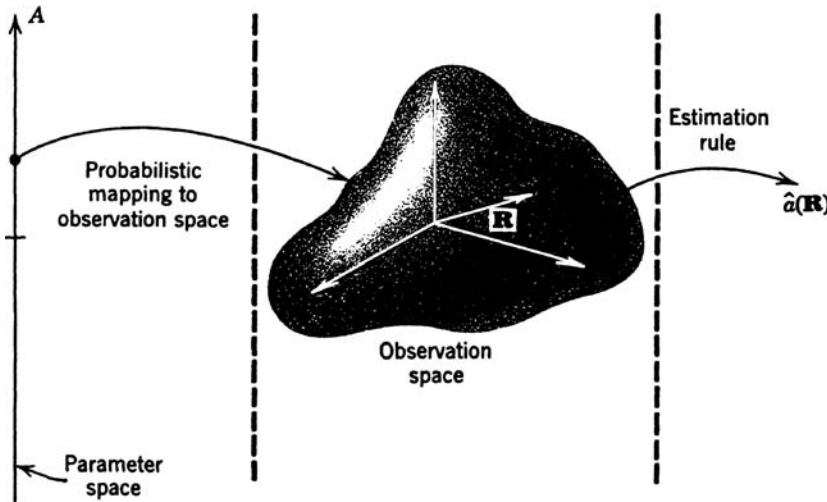


Figure 4.1: Estimation model.

Observation Space. In the classical problem this is a finite-dimensional space. We denote a point in it by the vector \mathbf{R} .

Estimation Rule. After observing \mathbf{R} , we shall want to estimate the value of a . We denote this estimate as $\hat{a}(\mathbf{R})$. This mapping of the observation space into an estimate is called the estimation rule. The purpose of this section is to investigate various estimation rules and their implementations.

The second and third components are familiar from the detection problem. The new features are the parameter space and the estimation rule. When we try to describe the parameter space, we find that two cases arise. In the first case, the parameter is a random variable whose behavior is governed by a probability density. In the second case, the parameter is an unknown quantity but not a random variable. These two cases are analogous to the source models we encountered in the hypothesis testing problem. To correspond with each of these models of the parameter space, we shall develop suitable estimation rules.

The chapter is organized in the following manner. In Section 4.2, we consider scalar parameter estimation. In the case of random parameters, we find the optimum Bayes estimator for various cost functions. For the case of nonrandom parameters, we utilize an estimator called the maximum likelihood (ML) estimator and analyze its performance. In many applications, we can find the desired estimator but cannot analyze its performance. For nonrandom parameters, we develop the Cramér–Rao bound (CRB) on the variance of the error of any unbiased estimate. For random parameters, we develop the Bayesian Cramér–Rao bound (BCRB) on the mean-square error (MSE) of any estimate.

In Section 4.3, we extend these results to vector parameters. For the case in which we want to estimate all of the unknown parameters in the model, the results are straightforward extensions of the scalar case. We also consider the case where some of the unknown parameters are not of interest. This is referred to as the nuisance parameter case. A third case of interest is one in which some of the parameters are random and some are nonrandom.

This is referred to as the hybrid parameter case. We develop estimators and bounds for these cases.

As we analyze various applications in Sections 4.2 and 4.3, we find that whenever the parameters appear in a nonlinear manner in the signal, as the SNR or number of observations decrease, the MSE or error variance exhibits a threshold where the performance degrades rapidly. The CRB and BCRB no longer provide a useful indication of the actual performance. In Section 4.4, we develop a family of global Bayesian bounds that provide more accurate prediction of the actual performance. This section is somewhat more involved and can be omitted without loss of continuity.

In Section 4.5, we study the composite hypothesis testing problem where the probability densities on the two hypotheses depend on an unknown vector parameter θ that may be random or nonrandom. We introduce a test called the generalized likelihood ratio test (GLRT) and study its performance.

In Section 4.6, we summarize our results.

4.2 SCALAR PARAMETER ESTIMATION

In Section 4.2.1, we study Bayesian estimation of scalar random parameters. In Section 4.2.2, we study nonrandom parameters and develop maximum likelihood estimators and the Cramér–Rao bound. In Section 4.2.3, we revisit Bayesian estimation and derive the Bayesian Cramér–Rao bound. In Section 4.2.4, we introduce a case study on frequency and phase estimation that we utilize throughout the chapter. In Section 4.2.5, we introduce exponential families and study their properties. In Section 4.2.6, we summarize our results.

4.2.1 Random Parameters: Bayes Estimation

In the Bayes detection problem we saw that the two quantities we had to specify were the set of costs C_{ij} and the *a priori* probabilities P_i . The cost matrix assigned a cost to each possible course of action. Because there were M hypotheses and M possible decisions, there were M^2 costs. In the estimation problem, a and $\hat{a}(\mathbf{R})$ are continuous variables. Thus, we must assign a cost to all pairs $[a, \hat{a}(\mathbf{R})]$ over the range of interest. This is a function of two variables that we denote as $C(a, \hat{a}(\mathbf{R}))$. In many cases of interest it is realistic to assume that the cost depends only on the error of the estimate. We define this error as

$$a_\epsilon(\mathbf{R}) \triangleq \hat{a}(\mathbf{R}) - a. \quad (4.3)$$

The cost function $C(a_\epsilon)$ is a function of a single variable. Some typical cost functions are shown in Figure 4.2. In Figure 4.2a, the cost function is simply the square of the error:

$$C(a_\epsilon) = a_\epsilon^2. \quad (4.4)$$

This cost is commonly referred to as the squared error cost function. We see that it accentuates the effects of large errors. In Figure 4.2b, the cost function is the absolute value of the error:

$$C(a_\epsilon) = |a_\epsilon|. \quad (4.5)$$

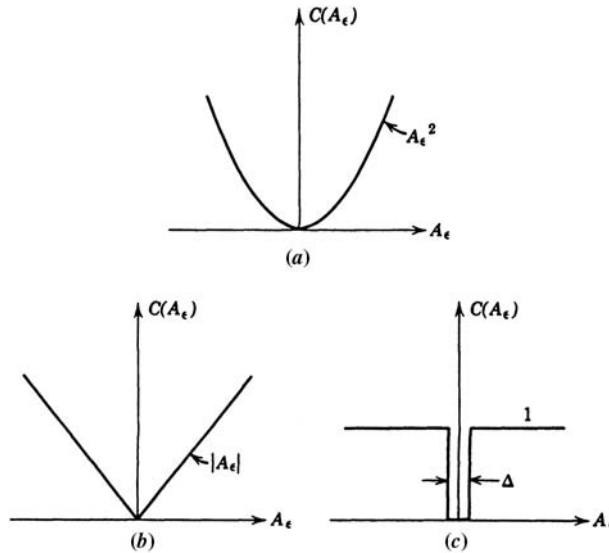


Figure 4.2: Typical cost functions: (a) mean-square error; (b) absolute error; (c) uniform cost function.

In Figure 4.2c, we assign zero cost to all errors less than $\pm\Delta/2$. In other words, an error less than $\Delta/2$ in magnitude is as good as no error. If $a_\epsilon > \Delta/2$, we assign a uniform value:

$$\begin{aligned} C(a_\epsilon) &= 0, & |a_\epsilon| &\leq \frac{\Delta}{2}, \\ &= 1, & |a_\epsilon| &> \frac{\Delta}{2}. \end{aligned} \quad (4.6)$$

In a given problem we choose a cost function to accomplish two objectives. First, we should like the cost function to measure user satisfaction adequately. Frequently it is difficult to assign an analytical measure to what basically may be a subjective quality.

Our goal is to find an estimate that minimizes that expected value of the cost. Thus, our second objective in choosing a cost function is to assign one that results in a tractable problem. In practice, cost functions are usually some compromise between these two objectives. Fortunately, in many problems of interest the same estimate will be optimum for a large class of cost functions.

Corresponding to the *a priori* probabilities in the detection problem, we have an *a priori* probability density $p_a(A)$ in the random parameter estimation problem. In all of our discussions we assume that $p_a(A)$ is known. If $p_a(A)$ is not known, a procedure analogous to the minimax test may be used.

Once we have specified the cost function and the *a priori* probability, we may write an expression for the risk:

$$\mathcal{R} \triangleq E[C(a, \hat{a}(\mathbf{R}))] = \int_{-\infty}^{\infty} dA \int_{-\infty}^{\infty} C(A, \hat{a}(\mathbf{R})) p_{a,\mathbf{R}}(A, \mathbf{R}) d\mathbf{R}. \quad (4.7)$$

The expectation is over the random variable a and the observed variables \mathbf{r} . For costs that are functions of one variable only (4.7) becomes

$$\mathcal{R} = \int_{-\infty}^{\infty} dA \int_{-\infty}^{\infty} C(A - \hat{a}(\mathbf{R})) p_{a,\mathbf{r}}(A, \mathbf{R}) d\mathbf{R}. \quad (4.8)$$

The Bayes estimate is the estimate that minimizes the risk. It is straightforward to find the Bayes estimates for the cost functions in Figure 4.2. For the cost function in Figure 4.2a, the risk corresponds to mean-square error. We denote the risk for the mean-square error criterion as \mathcal{R}_{ms} . Substituting (4.4) into (4.8), we have

$$\mathcal{R}_{\text{ms}} = \int_{-\infty}^{\infty} dA \int_{-\infty}^{\infty} d\mathbf{R} (A - \hat{a}(\mathbf{R}))^2 p_{a,\mathbf{r}}(A, \mathbf{R}). \quad (4.9)$$

The joint density can be rewritten as

$$p_{a,\mathbf{r}}(A, \mathbf{R}) = p_{\mathbf{r}}(\mathbf{R}) p_{a|\mathbf{r}}(A|\mathbf{R}). \quad (4.10)$$

Using (4.10) in (4.9), we have

$$\mathcal{R}_{\text{ms}} = \int_{-\infty}^{\infty} d\mathbf{R} p_{\mathbf{r}}(\mathbf{R}) \int_{-\infty}^{\infty} dA (A - \hat{a}(\mathbf{R}))^2 p_{a|\mathbf{r}}(A|\mathbf{R}). \quad (4.11)$$

Now the inner integral and $p_{\mathbf{r}}(\mathbf{R})$ are nonnegative. Therefore, we can minimize \mathcal{R}_{ms} by minimizing the inner integral. We denote this estimate as $\hat{a}_{\text{ms}}(\mathbf{R})$ and refer to it as the minimum MSE (MMSE) estimate. To find it we differentiate the inner integral with respect to $\hat{a}(\mathbf{R})$ and set the result equal to zero:

$$\frac{d}{d\hat{a}(\mathbf{R})} \int_{-\infty}^{\infty} dA (A - \hat{a}(\mathbf{R}))^2 p_{a|\mathbf{r}}(A|\mathbf{R}) = -2 \int_{-\infty}^{\infty} A p_{a|\mathbf{r}}(A|\mathbf{R}) dA + 2\hat{a}(\mathbf{R}) \int_{-\infty}^{\infty} p_{a|\mathbf{r}}(A|\mathbf{R}) dA. \quad (4.12)$$

Setting the result equal to zero and observing that the second integral equals one, we have

$$\hat{a}_{\text{ms}}(\mathbf{R}) = \int_{-\infty}^{\infty} dA A p_{a|\mathbf{r}}(A|\mathbf{R}). \quad (4.13)$$

This is a unique minimum, for the second derivative equals two. The term on the right-hand side of (4.13) is familiar as the mean of the *a posteriori* density (or the conditional mean).

Looking at (4.11), we see that if $\hat{a}(\mathbf{R})$ is the conditional mean the inner integral is just the *a posteriori* variance (or the conditional variance). Therefore, the minimum value of \mathcal{R}_{ms} is just the average of the conditional variance over all observations \mathbf{R} .

To find the Bayes estimate for the absolute value criterion in Figure 4.2b we write

$$\mathcal{R}_{\text{abs}} = \int_{-\infty}^{\infty} d\mathbf{R} p_{\mathbf{r}}(\mathbf{R}) \int_{-\infty}^{\infty} dA (|A - \hat{a}(\mathbf{R})|) p_{a|\mathbf{r}}(A|\mathbf{R}). \quad (4.14)$$

To minimize the inner integral we write

$$I(\mathbf{R}) = \int_{-\infty}^{\hat{a}(\mathbf{R})} dA (\hat{a}(\mathbf{R}) - A) p_{a|\mathbf{r}}(A|\mathbf{R}) + \int_{\hat{a}(\mathbf{R})}^{\infty} dA (A - \hat{a}(\mathbf{R})) p_{a|\mathbf{r}}(A|\mathbf{R}). \quad (4.15)$$

Differentiating with respect to $\hat{a}(\mathbf{R})$ and setting the result equal to zero, we have

$$\int_{-\infty}^{\hat{a}_{\text{abs}}(\mathbf{R})} dA p_{a|\mathbf{r}}(A|\mathbf{R}) = \int_{\hat{a}_{\text{abs}}(\mathbf{R})}^{\infty} dA p_{a|\mathbf{r}}(A|\mathbf{R}). \quad (4.16)$$

This is just the definition of the median of the *a posteriori* density.

The third criterion is the uniform cost function in Figure 4.2c. The risk expression follows easily:

$$\mathcal{R}_{\text{unf}} = \int_{-\infty}^{\infty} d\mathbf{R} p_{\mathbf{r}}(\mathbf{R}) \left[1 - \int_{\hat{a}_{\text{unf}}(\mathbf{R}) - \Delta/2}^{\hat{a}_{\text{unf}}(\mathbf{R}) + \Delta/2} p_{a|\mathbf{r}}(A|\mathbf{R}) dA \right]. \quad (4.17)$$

To minimize this equation we maximize the inner integral. Of particular interest to us is the case in which Δ is an arbitrarily small but nonzero number. A typical *a posteriori* density is shown in Figure 4.3. We see that for small Δ the best choice for $\hat{a}(\mathbf{R})$ is the value of A at which the *a posteriori* density has its maximum. This is the *mode* of the *a posteriori* density. We denote the estimate for this special case as $\hat{a}_{\text{map}}(\mathbf{R})$, the maximum *a posteriori* (MAP) estimate. In the sequel we use $\hat{a}_{\text{map}}(\mathbf{R})$ without further reference to the uniform cost function.

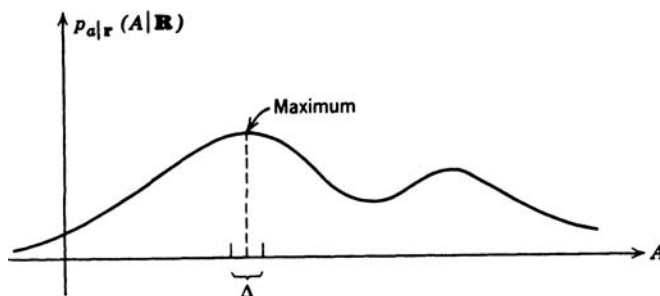


Figure 4.3: An *a posteriori* density.

To find $\hat{a}_{\text{map}}(\mathbf{R})$, we must have the location of the maximum of $p_{a|\mathbf{r}}(A|\mathbf{R})$. Because the logarithm is a monotone function, we can find the location of the maximum of $\ln p_{a|\mathbf{r}}(A|\mathbf{R})$ equally well. As we saw in the detection problem, this is frequently more convenient.

If the maximum is interior to the allowable range of A and $\ln p_{a|\mathbf{r}}(A|\mathbf{R})$ has a continuous first derivative then a necessary, but not sufficient, condition for a maximum can be obtained by differentiating $\ln p_{a|\mathbf{r}}(A|\mathbf{R})$ with respect to A and setting the result equal to zero:

$$\left. \frac{\partial \ln p_{a|\mathbf{r}}(A|\mathbf{R})}{\partial A} \right|_{A=\hat{a}(\mathbf{R})} = 0. \quad (4.18)$$

We refer to (4.18) as the MAP equation. In each case we must check to see if the solution is the absolute maximum. For a scalar parameter, we can plot $p_{a|\mathbf{r}}(A|\mathbf{R})$ and find the maximum.

We may rewrite the expression for $p_{a|\mathbf{r}}(A|\mathbf{R})$ to separate the role of the observed vector \mathbf{R} and the *a priori* knowledge:

$$p_{a|\mathbf{r}}(A|\mathbf{R}) = \frac{p_{\mathbf{r}|a}(\mathbf{R}|A) p_a(A)}{p_{\mathbf{r}}(\mathbf{R})}. \quad (4.19)$$

Taking logarithms,

$$\ln p_{a|\mathbf{r}}(A|\mathbf{R}) = \ln p_{\mathbf{r}|a}(\mathbf{R}|A) + \ln p_a(A) - \ln p_{\mathbf{r}}(\mathbf{R}). \quad (4.20)$$

For MAP estimation we are interested only in finding the value of A where the left-hand side is maximum. Because the last term on the right-hand side is not a function of A , we can consider just the function

$$l_B(A; \mathbf{R}) \triangleq \ln p_{\mathbf{r}|a}(\mathbf{R}|A) + \ln p_a(A), \quad (4.21)$$

which we refer to as the *Bayesian log-likelihood function*. The first term in (4.21) gives the probabilistic dependence of \mathbf{R} on A and is called the *log-likelihood function*,

$$l(A; \mathbf{R}) \triangleq \ln p_{\mathbf{r}|a}(\mathbf{R}|A). \quad (4.22)$$

The second term in (4.21) describes *a priori* knowledge.

The MAP equation can be written as

$$\left. \frac{\partial l_B(A; \mathbf{R})}{\partial A} \right|_{A=\hat{a}(\mathbf{R})} = \left. \frac{\partial \ln p_{\mathbf{r}|a}(\mathbf{R}|A)}{\partial A} \right|_{A=\hat{a}(\mathbf{R})} + \left. \frac{\partial \ln p_a(A)}{\partial A} \right|_{A=\hat{a}(\mathbf{R})} = 0. \quad (4.23)$$

Our discussion in the remainder of the book emphasizes minimum mean-square error and maximum *a posteriori* estimates for random parameter estimation.

To study the implications of these two estimation procedures, we consider several examples.

Example 4.2 (continuation of Example 4.1) Gaussian. Let

$$r_i = a + n_i, \quad i = 1, 2, \dots, N. \quad (4.24)$$

We assume that a is Gaussian, $N(0, \sigma_a^2)$, and that the n_i are each independent Gaussian variables $N(0, \sigma_n^2)$. Then

$$\begin{aligned} p_{\mathbf{r}|a}(\mathbf{R}|A) &= \prod_{i=1}^N \frac{1}{\sqrt{2\pi}\sigma_n} \exp\left(-\frac{(R_i - A)^2}{2\sigma_n^2}\right), \\ p_a(A) &= \frac{1}{\sqrt{2\pi}\sigma_a} \exp\left(-\frac{A^2}{2\sigma_a^2}\right). \end{aligned} \quad (4.25)$$

To find $\hat{a}_{\text{ms}}(\mathbf{R})$, we need to know $p_{a|\mathbf{r}}(A|\mathbf{R})$. One approach is to find $p_{\mathbf{r}}(\mathbf{R})$ and substitute it into (4.19), but this procedure is algebraically tedious. It is easier to observe that $p_{a|\mathbf{r}}(A|\mathbf{R})$ is a probability density with respect to a for any \mathbf{R} . Thus, $p_{\mathbf{r}}(\mathbf{R})$ just contributes to the constant needed to make

$$\int_{-\infty}^{\infty} p_{a|\mathbf{r}}(A|\mathbf{R}) dA = 1. \quad (4.26)$$

(In other words, $p_{\mathbf{r}}(\mathbf{R})$ is simply a normalization constant.) Thus,

$$p_{a|\mathbf{r}}(A|\mathbf{R}) = \left[\frac{\left(\prod_{i=1}^N \frac{1}{\sqrt{2\pi}\sigma_n} \right) \frac{1}{\sqrt{2\pi}\sigma_a}}{p_{\mathbf{r}}(\mathbf{R})} \right] \exp \left\{ -\frac{1}{2} \left[\frac{\sum_{i=1}^N (R_i - A)^2}{\sigma_n^2} + \frac{A^2}{\sigma_a^2} \right] \right\}. \quad (4.27)$$

Rearranging the exponent, completing the square, and absorbing terms depending only on R_i^2 into the constant, we have

$$p_{a|\mathbf{r}}(A|\mathbf{R}) = k(\mathbf{R}) \exp \left\{ -\frac{1}{2\sigma_p^2} \left[A - \frac{\sigma_a^2}{\sigma_a^2 + \sigma_n^2/N} \left(\frac{1}{N} \sum_{i=1}^N R_i \right) \right]^2 \right\}, \quad (4.28)$$

where

$$\sigma_p^2 \triangleq \left(\frac{1}{\sigma_a^2} + \frac{N}{\sigma_n^2} \right)^{-1} = \frac{\sigma_a^2 \sigma_n^2}{N\sigma_a^2 + \sigma_n^2} \quad (4.29)$$

is the *a posteriori* variance.

We see that $p_{a|\mathbf{r}}(A|\mathbf{R})$ is just a Gaussian density. The estimate $\hat{a}_{\text{ms}}(\mathbf{R})$ is just the conditional mean

$$\hat{a}_{\text{ms}}(\mathbf{R}) = \frac{\sigma_a^2}{\sigma_a^2 + \sigma_n^2/N} \left(\frac{1}{N} \sum_{i=1}^N R_i \right). \quad (4.30)$$

Because the *a posteriori* variance is not a function of \mathbf{R} , the mean-square risk equals the *a posteriori* variance [see (4.11)].

Two observations are useful:

1. The R_i enter into the *a posteriori* density only through their sum. Thus,

$$S(\mathbf{R}) = \sum_{i=1}^N R_i \quad (4.31)$$

is a *sufficient statistic*. This idea of a sufficient statistic is identical to that in the detection problem.¹ For the estimation problem, a statistic $S(\mathbf{R})$ is said to be sufficient for estimating a if the conditional density of \mathbf{R} given $S(\mathbf{R})$ is not a function of a . According to the Neyman–Pearson factorization theorem, a necessary and sufficient condition for $S(\mathbf{R})$ to be a sufficient statistic is that $p_{\mathbf{r}|a}(\mathbf{R}|A)$ can be factored as²

$$p_{\mathbf{r}|a}(\mathbf{R}|A) = h_1(\mathbf{R}) h_2(S(\mathbf{R}), A), \quad (4.32)$$

where $h_1(\mathbf{R})$ does not depend on A and $h_2(S(\mathbf{R}), A)$ depends on \mathbf{R} only through $S(\mathbf{R})$. In this example, one possible factorization is

$$h_1(\mathbf{R}) = \frac{1}{(\sqrt{2\pi}\sigma_n)^N} \exp \left\{ -\frac{1}{2\sigma_n^2} \sum_{i=1}^N R_i^2 \right\}, \quad (4.33)$$

$$h_2(S(\mathbf{R}), A) = \exp \left\{ \frac{A}{\sigma_n^2} \sum_{i=1}^N R_i - \frac{NA^2}{\sigma_n^2} \right\}. \quad (4.34)$$

It should be noted that the sufficient statistic is defined relative to a particular parameter a , and that it is not unique. Two sufficient statistics are said to be equivalent if they are related by a one-to-one mapping.

2. The estimation rule uses the information available in an intuitively logical manner. If $\sigma_a^2 \ll \sigma_n^2/N$, the *a priori* knowledge is much better than the observed data and the estimate is very close to the *a priori* mean. (In this case, the *a priori* mean is zero.) On the other hand, if $\sigma_a^2 \gg \sigma_n^2/N$, the *a priori* knowledge is of little value and the estimate uses primarily the received data. In the limit $\hat{a}_{\text{ms}}(\mathbf{R})$ is just the arithmetic average of the R_i .

$$\lim_{\frac{\sigma_a^2}{N\sigma_n^2} \rightarrow 0} \hat{a}_{\text{ms}}(\mathbf{R}) = \frac{1}{N} \sum_{i=1}^N R_i \triangleq \bar{R}. \quad (4.35)$$

The MAP estimate for this case follows easily. Looking at (4.28), we see that because the density is Gaussian the maximum value of $p_{a|\mathbf{r}}(A|\mathbf{R})$ occurs at the conditional mean. Thus,

$$\hat{a}_{\text{map}}(\mathbf{R}) = \hat{a}_{\text{ms}}(\mathbf{R}). \quad (4.36)$$

Because the conditional median of a Gaussian density occurs at the conditional mean, we also have

$$\hat{a}_{\text{abs}}(\mathbf{R}) = \hat{a}_{\text{ms}}(\mathbf{R}). \quad (4.37)$$

■

¹In this chapter, we will use the notation $S(\mathbf{R})$ rather than $l(\mathbf{R})$ to denote the sufficient statistic for estimation to avoid confusion with the log-likelihood functions $l(A; \mathbf{R})$ and $l_B(A; \mathbf{R})$.

²This is discussed in [Leh83] and proven in [Leh59].

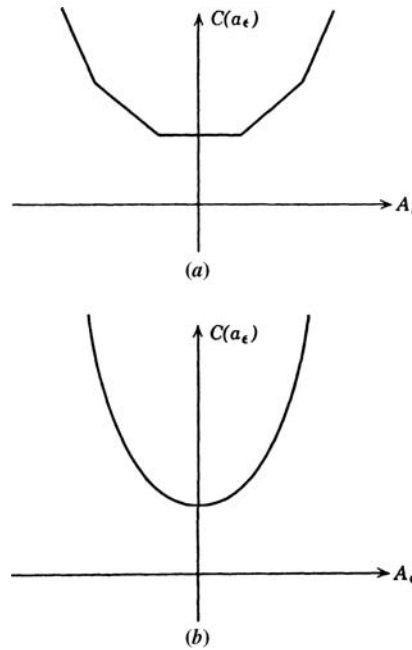


Figure 4.4: Symmetric convex cost functions: (a) convex; (b) strictly convex.

Thus, we see that for this particular example all three cost functions in Figure 4.2 lead to the same estimate. This invariance to the choice of a cost function is obviously a useful feature because of the subjective judgments that are frequently involved in choosing $C(a_\epsilon)$. Some conditions under which this invariance holds are developed in the next two properties.³

Property 1. We assume that the cost function $C(a_\epsilon)$ is a symmetric, convex-upward function and that the *a posteriori* density $p_{a|\mathbf{r}}(A|\mathbf{R})$ is symmetric about its conditional mean; that is,

$$C(a_\epsilon) = C(-a_\epsilon) \quad (\text{symmetry}), \quad (4.38)$$

$$C(bx_1 + (1 - b)x_2) \leq bC(x_1) + (1 - b)C(x_2) \quad (\text{convexity}) \quad (4.39)$$

for any b inside the range $(0, 1)$ and for all x_1 and x_2 . Equation (4.39) simply says that all chords lie above or on the cost function.

This condition is shown in Figure 4.4a. If the inequality is strict whenever $x_1 \neq x_2$, we say the cost function is strictly convex (upward) as in Figure 4.4b. Defining

$$z \triangleq a - \hat{a}_{\text{ms}}(\mathbf{R}) = a - E(a|\mathbf{R}), \quad (4.40)$$

the symmetry of the *a posteriori* density implies

$$p_{z|\mathbf{r}}(Z|\mathbf{R}) = p_{z|\mathbf{r}}(-Z|\mathbf{R}). \quad (4.41)$$

³These properties are due to Sherman [She58]. Our derivation is similar to that given by Viterbi [Vit66].

The estimate \hat{a} that minimizes any cost function in this class is identical to $\hat{a}_{\text{ms}}(\mathbf{R})$ (which is conditional mean).

Proof. As before we can minimize the conditional risk [see (4.11)]. Define

$$\mathcal{R}_B(\hat{a}|\mathbf{R}) \triangleq E_a[C(\hat{a} - a)|\mathbf{R}] = E_a[C(a - \hat{a})|\mathbf{R}], \quad (4.42)$$

where the second equality follows from (4.38). We now write four equivalent expressions for $\mathcal{R}_B(\hat{a}|\mathbf{R})$:

$$\mathcal{R}_B(\hat{a}|\mathbf{R}) = \int_{-\infty}^{\infty} C(\hat{a} - \hat{a}_{\text{ms}}(\mathbf{R}) - Z) p_{z|\mathbf{r}}(Z|\mathbf{R}) dZ \quad (4.43)$$

[Use (4.40) in (4.42)]

$$= \int_{-\infty}^{\infty} C(\hat{a} - \hat{a}_{\text{ms}}(\mathbf{R}) + Z) p_{z|\mathbf{r}}(Z|\mathbf{R}) dZ \quad (4.44)$$

[(4.41) implies this equality]

$$= \int_{-\infty}^{\infty} C(\hat{a}_{\text{ms}}(\mathbf{R}) - \hat{a} - Z) p_{z|\mathbf{r}}(Z|\mathbf{R}) dZ \quad (4.45)$$

[(4.38) implies this equality]

$$= \int_{-\infty}^{\infty} C(\hat{a}_{\text{ms}}(\mathbf{R}) - \hat{a} + Z) p_{z|\mathbf{r}}(Z|\mathbf{R}) dZ \quad (4.46)$$

[(4.41) implies this equality].

We now use the convexity condition (4.39) with the terms in (4.44) and (4.46):

$$\begin{aligned} \mathcal{R}_B(\hat{a}|\mathbf{R}) &= \frac{1}{2} E \left([C(Z + (\hat{a}_{\text{ms}}(\mathbf{R}) - \hat{a})) + C(Z - (\hat{a}_{\text{ms}}(\mathbf{R}) - \hat{a}))] |\mathbf{R} \right) \\ &\geq E \left(C \left[\frac{1}{2}(Z + (\hat{a}_{\text{ms}}(\mathbf{R}) - \hat{a})) + \frac{1}{2}(Z - (\hat{a}_{\text{ms}}(\mathbf{R}) - \hat{a})) \right] |\mathbf{R} \right) \\ &= E(C(Z)|\mathbf{R}). \end{aligned} \quad (4.47)$$

Equality will be achieved in (4.47) if $\hat{a}_{\text{ms}}(\mathbf{R}) = \hat{a}$. This completes the proof. If $C(a_\epsilon)$ is strictly convex, we will have the additional result that the minimizing estimate \hat{a} is unique and equals $\hat{a}_{\text{ms}}(\mathbf{R})$.

To include cost functions like the uniform cost functions that are not convex we need a second property.

Property 2. We assume that the cost function is a symmetric, nondecreasing function and that the *a posteriori* density $p_{a|\mathbf{r}}(A|\mathbf{R})$ is a symmetric (about the conditional mean), unimodal function that satisfies the condition

$$\lim_{x \rightarrow \infty} C(x) p_{a|\mathbf{r}}(A|\mathbf{R}) = 0.$$

The estimate \hat{a} that minimizes any cost function in this class is identical to $\hat{a}_{\text{ms}}(\mathbf{R})$. The proof of this property is similar to the above proof [Vit66].

The significance of these two properties should not be underemphasized. Throughout the book we consider only minimum mean-square error and maximum *a posteriori* probability estimators. Properties 1 and 2 ensure that whenever the *a posteriori* densities satisfy the assumptions given above the estimates that we obtain will be optimum for a large class of cost functions. Clearly, if the *a posteriori* density is Gaussian, it will satisfy the above assumptions.

We now consider two examples of a different type.

Example 4.3 (continuation of Example 4.2) Gaussian. The variable a appears in the signal in a nonlinear manner. We denote this dependence by $s(A)$. Each observation r_i consists of $s(A)$ plus a Gaussian random variable n_i , $N(0, \sigma_n^2)$. The n_i are statistically independent of each other and a . Thus,

$$r_i = s(A) + n_i. \quad (4.48)$$

Therefore,

$$p_{a|\mathbf{r}}(A|\mathbf{R}) = k(\mathbf{R}) \exp \left(-\frac{1}{2} \left\{ \frac{\sum_{i=1}^N (R_i - s(A))^2}{\sigma_n^2} + \frac{A^2}{\sigma_a^2} \right\} \right). \quad (4.49)$$

This expression cannot be further simplified without specifying $s(A)$ explicitly.

The MAP equation is obtained by substituting (4.49) into (4.23)

$$\hat{a}_{\text{map}}(\mathbf{R}) = \frac{\sigma_a^2}{\sigma_n^2} \sum_{i=1}^N (R_i - s(A)) \left. \frac{\partial s(A)}{\partial A} \right|_{A=\hat{a}_{\text{map}}(\mathbf{R})}. \quad (4.50)$$

To solve this explicitly we must specify $s(A)$. We shall find that an analytical solution is generally not possible when $s(A)$ is a nonlinear function of A . We see that $S(\mathbf{R}) = \sum_{i=1}^N R_i$ is again the sufficient statistic for estimating A . ■

Another type of problem that frequently arises is the estimation of a parameter in a probability density.

Example 4.4 Poisson. The number of events in an experiment obey a Poisson law with mean value a . Thus,

$$\Pr(n \text{ events} | a = A) = \frac{A^n}{n!} \exp(-A), \quad n = 0, 1, \dots \quad (4.51)$$

We want to observe the number of events and estimate the parameter a of the Poisson law. We shall assume that a is a random variable with an exponential density

$$p_a(A) = \begin{cases} \lambda \exp(-\lambda A), & A > 0, \\ 0, & \text{elsewhere.} \end{cases} \quad (4.52)$$

The *a posteriori* density of a is

$$p_{a|n}(A|N) = \frac{\Pr(n = N|a = A) p_a(A)}{\Pr(n = N)}. \quad (4.53)$$

Substituting (4.51) and (4.52) into (4.53), we have

$$p_{a|n}(A|N) = k(N) \left[A^N \exp(-A(1 + \lambda)) \right], \quad A \geq 0, \quad (4.54)$$

where

$$k(N) = \frac{(1 + \lambda)^{N+1}}{N!} \quad (4.55)$$

in order for the density to integrate to 1. (As already pointed out, the constant is unimportant for MAP estimation but is needed if we find the MMSE estimate by integrating over the conditional density.)

The MMSE estimate is the conditional mean:

$$\begin{aligned} \hat{a}_{\text{ms}}(N) &= \frac{(1 + \lambda)^{N+1}}{N!} \int_0^\infty A^{N+1} \exp(-A(1 + \lambda)) dA \\ &= \frac{(1 + \lambda)^{N+1}}{(1 + \lambda)^{N+2}} (N + 1) = \frac{N + 1}{1 + \lambda}. \end{aligned} \quad (4.56)$$

To find $\hat{a}_{\text{map}}(N)$ we take the logarithm of (4.54)

$$\ln p_{a|n}(A|N) = N \ln A - A(1 + \lambda) + \ln k(N). \quad (4.57)$$

By differentiating with respect to A , setting the result equal to zero, and solving, we obtain

$$\hat{a}_{\text{map}}(N) = \frac{N}{1 + \lambda}. \quad (4.58)$$

Observe that $\hat{a}_{\text{map}}(N)$ is not equal to $\hat{a}_{\text{ms}}(N)$. For this example, the sufficient statistic is simply N . ■

In Example 4.4, the prior density in (4.52) is an Exponential density with rate λ , which is a special case of a Gamma probability density with shape parameter $a = 1$ and scale parameter $b = \lambda^{-1}$. The posterior density in (4.54) is also a Gamma density with $a = N + 1$ and $b = (1 + \lambda)^{-1}$. We encountered the Gamma density previously in Examples 2.6 and 3.8.

We observe that in Examples 4.2 and 4.4, the *a posteriori* density, $p_{a|R}(A|R)$ or $p_{a|n}(A|N)$, had the same form as the *a priori* density $p_a(A)$ with different parameter values. Whenever this relationship occurs, we refer to the prior density as a *conjugate prior density* or *reproducing density*. These densities play an important role in Bayesian estimation theory because they simplify the analysis. The prior is chosen to characterize our knowledge of the parameter based on the phenomenon we are modeling. In many cases, it is reasonable to use a conjugate prior to model that knowledge. In the terminology of reproducing densities, the probability density of the observations conditioned on the unknown parameter is referred to as the *likelihood function*.

We revisit Examples 4.2 and 4.4 to introduce the use of conjugate prior densities.

Example 4.5 (continuation of Example 4.2) Gaussian. In Example 4.2, the likelihood function $p_{\mathbf{r}|a}(\mathbf{R}|A)$ is $N(a\mathbf{1}, \sigma_n^2 \mathbf{I})$. The conjugate prior is

$$p_a(A) \sim N(m_a, \sigma_a^2). \quad (4.59)$$

Following the same steps as in Example 4.2, one can show that

$$p_{a|\mathbf{r}}(A|\mathbf{R}) \sim N(m_p, \sigma_p^2), \quad (4.60)$$

where

$$m_p = \left(\frac{m_a}{\sigma_a^2} + \frac{\sum_{i=1}^N R_i}{\sigma_n^2} \right) \sigma_p^2 \quad (4.61)$$

and

$$\sigma_p^2 = \left(\frac{1}{\sigma_a^2} + \frac{N}{\sigma_n^2} \right)^{-1}. \quad (4.62)$$

The parameters, m_a and σ_a^2 are called the *prior hyperparameters* and the parameters m_p and σ_p^2 are called the *posterior hyperparameters*. Since m_p is the mean, median, and mode of the *a posteriori* density, we have

$$\hat{a}_{\text{ms}}(\mathbf{R}) = \hat{a}_{\text{abs}}(\mathbf{R}) = \hat{a}_{\text{map}}(\mathbf{R}) = m_p = \left(\frac{m_a}{\sigma_a^2} + \frac{N\bar{R}}{\sigma_n^2} \right) \sigma_p^2 = \frac{\sigma_n^2 m_a + \sigma_a^2 N \bar{R}}{\sigma_n^2 + \sigma_a^2 N} \quad (4.63)$$

and the mean-square error is σ_p^2 . ■

Example 4.4 can be generalized by assuming that we conduct multiple trials.

Example 4.6 (continuation of Example 4.4) Poisson. We assume that we conduct M trials of the experiment. Then,

$$\Pr(\mathbf{n} = \mathbf{N}|a = A) = \prod_{i=1}^M \Pr(n_i = N_i|a = A) = \prod_{i=1}^M \left[\frac{A^{N_i}}{N_i!} \exp(-A) \right], \quad N_i = 0, 1, \dots \quad (4.64)$$

A more general conjugate prior for the Poisson likelihood function is the Gamma probability density,

$$p_a(A) = \frac{A^{\alpha-1} e^{-A/b}}{b^\alpha \Gamma(\alpha)}, \quad A \geq 0 \quad (4.65)$$

where α is the shape parameter and b is the scale parameter.⁴

We first verify that the Gamma prior density and Poisson likelihood function result in a Gamma posterior density for a . The posterior density is

$$p_{a|\mathbf{n}}(A|\mathbf{N}) = \frac{\Pr(\mathbf{n} = \mathbf{N}|a = A)p_a(A)}{\Pr(\mathbf{n} = \mathbf{N})}, \quad (4.66)$$

⁴We use α and α_p to denote the prior and posterior shape hyperparameters to avoid confusion with the Poisson parameter a .

where

$$\begin{aligned}
\Pr(\mathbf{n} = \mathbf{N}) &= \int_0^\infty \Pr(\mathbf{n} = \mathbf{N}|a = A)p_a(A)dA \\
&= \int_0^\infty \prod_{i=1}^M \left[\frac{A^{N_i}}{N_i!} \exp(-A) \right] \frac{A^{\alpha-1} e^{-A/b}}{b^\alpha \Gamma(\alpha)} dA \\
&= \int_0^\infty \frac{A^{\left(\sum_{i=1}^M N_i\right)}}{\prod_{i=1}^M N_i!} \exp(-MA) \frac{A^{\alpha-1} e^{-A/b}}{b^\alpha \Gamma(\alpha)} dA \\
&= \frac{1}{\left(\prod_{i=1}^M N_i!\right) b^\alpha \Gamma(\alpha)} \int_0^\infty A^{\left(\alpha + \sum_{i=1}^M N_i\right) - 1} \exp\left\{-A\left(M + \frac{1}{b}\right)\right\} dA \\
&= \frac{b_p^{\alpha_p} \Gamma(\alpha_p)}{\left(\prod_{i=1}^M N_i!\right) b^\alpha \Gamma(\alpha)}, \tag{4.67}
\end{aligned}$$

where

$$\alpha_p = \alpha + \sum_{i=1}^M N_i \tag{4.68}$$

and

$$b_p = \left(M + \frac{1}{b}\right)^{-1} = \frac{b}{Mb + 1}. \tag{4.69}$$

Thus,

$$p_{a|\mathbf{n}}(A|\mathbf{N}) = \frac{A^{\alpha_p-1} e^{-A/b_p}}{b_p^{\alpha_p} \Gamma(\alpha_p)}. \tag{4.70}$$

We recognize this as a Gamma density with posterior hyperparameters α_p and b_p . The properties of the Gamma density are summarized in Appendix A. In particular, the mean is $\alpha_p b_p$, the mode is $(\alpha_p - 1)b_p$ for $\alpha_p \geq 1$, and the variance is $\alpha_p b_p^2$.

The MMSE estimate is the posterior mean

$$\hat{a}_{\text{ms}}(\mathbf{N}) = \alpha_p b_p = \left(\alpha + \sum_{i=1}^M N_i\right) \left(\frac{b}{Mb + 1}\right), \tag{4.71}$$

and the sufficient statistic is now $S(\mathbf{R}) = \sum_{i=1}^M N_i$.

The conditional variance is

$$E\{(\hat{a}_{\text{ms}}(\mathbf{N}) - a)^2 | \mathbf{N}\} = \alpha_p b_p^2 = \left(\alpha + \sum_{i=1}^M N_i\right) \left(\frac{b}{Mb + 1}\right)^2. \tag{4.72}$$

We must average over the joint density of \mathbf{n} to obtain the MSE

$$\text{MSE}[\hat{a}_{\text{ms}}(\mathbf{N})] = E_{\mathbf{n}} \left\{ \left(\alpha + \sum_{i=1}^M N_i \right) \left(\frac{b}{Mb+1} \right)^2 \right\} = \left(\alpha + \sum_{i=1}^M E_{\mathbf{n}} \{ N_i \} \right) \left(\frac{b}{Mb+1} \right)^2. \quad (4.73)$$

To compute the expected value, we use

$$E_{\mathbf{n}} \{ N_i \} = E_a \{ E_{\mathbf{n}|a} (N_i) \} = E_a \{ a \} = \alpha b. \quad (4.74)$$

The MSE is, therefore,

$$\text{MSE}[\hat{a}_{\text{ms}}(\mathbf{N})] = (\alpha + \alpha b M) \left(\frac{b}{Mb+1} \right)^2 = \frac{\alpha b^2}{Mb+1}. \quad (4.75)$$

For large M , the MSE approaches

$$\lim_{M \rightarrow \infty} \text{MSE}[\hat{a}_{\text{ms}}(\mathbf{N})] = \frac{\alpha b}{M}. \quad (4.76)$$

The MAP estimate is the posterior mode,

$$\hat{a}_{\text{map}}(\mathbf{N}) = (\alpha_p - 1)b_p = \left(\alpha - 1 + \sum_{i=1}^M N_i \right) \left(\frac{b}{Mb+1} \right). \quad (4.77)$$

The results in Example 4.4 are a special case of these results obtained by setting $M = 1$, $\alpha = 1$, and $b = 1/\lambda$. As in Example 4.4, $\hat{a}_{\text{map}}(\mathbf{N})$ is not equal to $\hat{a}_{\text{ms}}(\mathbf{N})$. ■

Other examples of conjugate priors are developed in the problems. They require that we have IID observations. In this section, we considered scalar observations. In later sections, we will consider vector observations and multiple parameters.

Later, we will consider models in which the observations arrive sequentially. After each observation, we estimate the parameter. We then update the estimate when the next observation arrives. Using a conjugate prior makes the updating algorithm straightforward.

Unfortunately, for arbitrary likelihood functions, a conjugate prior does not exist. We will discuss this issue in Section 4.2.5.

The principal results of this section are the following:

1. The MMSE estimate is always the mean of the *a posteriori* density (the conditional mean).
2. The maximum absolute error estimate is the median of the *a posteriori* density (the conditional median).
3. The MAP estimate is the value of A at which the *a posteriori* density has its maximum (the conditional mode).
4. For a large class of cost functions, the optimum estimate is the conditional mean whenever the *a posteriori* density is a unimodal function that is symmetric about the conditional mean.
5. If we can incorporate our prior knowledge using a conjugate prior then the posterior density reproduces the prior with new parameters.

These results are the basis of most of our estimation work. As we study more complicated problems, the only difficulty we shall encounter is the actual evaluation of the conditional

mean or conditional maximum. In many cases of interest the MAP and MMSE estimates will turn out to be equal.

We now turn to the second class of estimation problems described in the introduction.

4.2.2 Nonrandom Parameter Estimation

In many cases it is unrealistic to treat the unknown parameter as a random variable. The problem formulation in Section 4.1 is still appropriate. Now, however, the parameter is assumed to be nonrandom, and we want to design an estimation procedure that is good in some sense.⁵

A logical first approach is to try to modify the Bayes procedure in the last section to eliminate the average over $p_a(A)$. As an example, consider a mean-square error criterion,

$$\mathcal{R}(A) \triangleq \int_{-\infty}^{\infty} [\hat{a}(\mathbf{R}) - A]^2 p_{\mathbf{r}|a}(\mathbf{R}|A) d\mathbf{R}, \quad (4.78)$$

where the expectation is only over \mathbf{R} , for it is the only random variable in the model. Minimizing $\mathcal{R}(A)$, we obtain

$$\hat{a}_{\text{ms}}(\mathbf{R}) = A. \quad (4.79)$$

The answer is correct, but not of any value, for A is the unknown quantity that we are trying to find. Thus, we see that this direct approach is not fruitful. A more useful method in the nonrandom parameter case is to examine other possible measures of quality of estimation procedures and then to see whether we can find estimates that are good in terms of these measures.

The first measure of quality to be considered is the expectation of the estimate

$$E[\hat{a}(\mathbf{R})] \triangleq \int_{-\infty}^{\infty} \hat{a}(\mathbf{R}) p_{\mathbf{r}|a}(\mathbf{R}|A) d\mathbf{R}. \quad (4.80)$$

The possible values of the expectation can be grouped into three classes:

1. If $E[\hat{a}(\mathbf{R})] = A$, for all values of A , we say that the estimate is *unbiased*. This statement means that the average value of the estimates equals the quantity we are trying to estimate.
2. If $E[\hat{a}(\mathbf{R})] = A + B$, where B is not a function of A , we say that the estimate has a *known bias*. We can always obtain an unbiased estimate by subtracting B from $\hat{a}(\mathbf{R})$.
3. If $E[\hat{a}(\mathbf{R})] = A + B(A)$, we say that the estimate has an *unknown bias*. Because the bias depends on the unknown parameter, we cannot simply subtract it out.

Clearly, even an unbiased estimate may give a bad result on a particular trial. A simple example is shown in Figure 4.5. The probability density of the estimate is centered around A , but the variance of this density is large enough that big errors are probable.

⁵The beginning of nonrandom parameter estimation theory can be attributed to Fisher [Fis22, Fis25, Fis34, Fis35]. Many discussions of the basic ideas are now available (e.g. [Cra46, Wil62], or [KS61]).

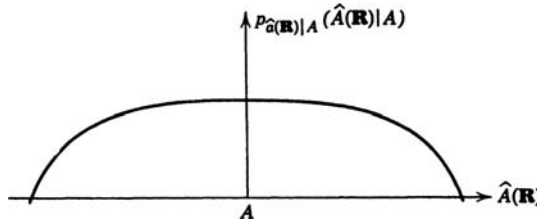


Figure 4.5: Probability density for an estimate.

A second measure of quality is the variance of the estimation error:⁶

$$\text{Var}[\hat{A}(\mathbf{R}) - A] = E[(\hat{A}(\mathbf{R}) - A)^2] - B^2(A). \quad (4.81)$$

This provides a measure of the spread of the error. In general, we shall try to find unbiased estimates with small variances. There is no straightforward minimization procedure that will lead us to the minimum variance unbiased estimate. Therefore, we are forced to try an estimation procedure to see how well it works.

Maximum Likelihood Estimation. There are several ways to motivate the estimation procedure that we shall use. Consider the simple estimation problem outlined in Example 4.1. Recall that

$$r = A + n, \quad (4.82)$$

$$p_{r|a}(R|A) = \left(\sqrt{2\pi}\sigma_n\right)^{-1} \exp\left[-\frac{1}{2\sigma_n^2}(R - A)^2\right]. \quad (4.83)$$

We choose as our estimate that value of A that most likely caused a given value of R to occur. In this simple additive case we see that this is the same as choosing that most probable value of the noise ($N = 0$) and subtracting it from R . We denote the value obtained by using this procedure as a *maximum likelihood estimate*.

$$\hat{a}_{\text{ml}}(R) = R. \quad (4.84)$$

The maximum likelihood estimate $\hat{a}_{\text{ml}}(\mathbf{R})$ is the value of A at which the likelihood function $p_{r|a}(\mathbf{R}|A)$ is a maximum. If the maximum is interior to the range of A , and the log-likelihood function $\ln p_{r|a}(\mathbf{R}|A)$ has a continuous first derivative, then a necessary condition on $\hat{a}_{\text{ml}}(\mathbf{R})$ is obtained by differentiating $\ln p_{r|a}(\mathbf{R}|A)$ with respect to A and setting the result equal to zero:

$$\left. \frac{\partial \ln p_{r|a}(\mathbf{R}|A)}{\partial A} \right|_{A=\hat{a}_{\text{ml}}(\mathbf{R})} = 0. \quad (4.85)$$

This equation is called the *likelihood equation*. Comparing (4.23) and (4.85), we see that the ML estimate corresponds mathematically to the limiting case of a MAP estimate in which the *a priori* knowledge approaches zero.

⁶Since A is a nonrandom parameter, $\text{Var}[\hat{a}(\mathbf{R}) - A] = \text{Var}[\hat{a}(\mathbf{R})]$. Therefore, the variance of the *estimation error* and the variance of the *estimator* are the same and may be used interchangeably to measure estimation performance.

In general, we must plot $\ln p_{\mathbf{r}|a}(\mathbf{R}|A)$ and find the maximum. In order to see how effective the ML procedure is we can compute the bias and the variance. Frequently this is difficult to do. Rather than approach the problem directly, we shall first derive a lower bound on the variance on *any* unbiased estimate. Then we shall see how the variance of $\hat{a}_{\text{ml}}(\mathbf{R})$ compares with this lower bound.

Cramér–Rao Inequality: Nonrandom Parameters. We now want to consider the variance of *any* estimate $\hat{a}(\mathbf{R})$ of the real variable A . We shall prove the following statement.

Theorem. (a) If $\hat{a}(\mathbf{R})$ is any unbiased estimate of A , then

$$\text{Var}[\hat{a}(\mathbf{R}) - A] \geq \left(E \left\{ \left[\frac{\partial \ln p_{\mathbf{r}|a}(\mathbf{R}|A)}{\partial A} \right]^2 \right\} \right)^{-1} \quad (4.86)$$

or, equivalently,

(b)

$$\text{Var}[\hat{a}(\mathbf{R}) - A] \geq \left\{ -E \left[\frac{\partial^2 \ln p_{\mathbf{r}|a}(\mathbf{R}|A)}{\partial A^2} \right] \right\}^{-1}, \quad (4.87)$$

where the following conditions are assumed to be satisfied:

(c)

$$\frac{\partial \ln p_{\mathbf{r}|a}(\mathbf{R}|A)}{\partial A} \text{ and } \frac{\partial^2 \ln p_{\mathbf{r}|a}(\mathbf{R}|A)}{\partial A^2}$$

exist and are absolutely integrable.

The inequalities were first stated by Fisher [Fis22] and proved by Dugué [Dug37]. They were also derived by Cramér [Cra46] and Rao [Rao45] and are usually referred to as the Cramér–Rao bound. Any estimate that satisfies the bound with an equality is called an *efficient* estimate.

The proof is a simple application of the Schwarz inequality. Because $\hat{a}(\mathbf{R})$ is unbiased,

$$E[\hat{a}(\mathbf{R}) - A] \triangleq \int_{-\infty}^{\infty} p_{\mathbf{r}|a}(\mathbf{R}|A)[\hat{a}(\mathbf{R}) - A] d\mathbf{R} = 0. \quad (4.88)$$

Differentiating both sides with respect to A , we have

$$\frac{d}{dA} \int_{-\infty}^{\infty} p_{\mathbf{r}|a}(\mathbf{R}|A)[\hat{a}(\mathbf{R}) - A] d\mathbf{R} = \int_{-\infty}^{\infty} \frac{d}{dA} \{ p_{\mathbf{r}|a}(\mathbf{R}|A)[\hat{a}(\mathbf{R}) - A] \} d\mathbf{R} = 0, \quad (4.89)$$

where condition (c) allows us to bring the differentiation inside the integral. Then

$$- \int_{-\infty}^{\infty} p_{\mathbf{r}|a}(\mathbf{R}|A) d\mathbf{R} + \int_{-\infty}^{\infty} \frac{\partial p_{\mathbf{r}|a}(\mathbf{R}|A)}{\partial A} [\hat{a}(\mathbf{R}) - A] d\mathbf{R} = 0. \quad (4.90)$$

The first integral is just +1. Now observe that

$$\frac{\partial p_{\mathbf{r}|a}(\mathbf{R}|A)}{\partial A} = \frac{\partial \ln p_{\mathbf{r}|a}(\mathbf{R}|A)}{\partial A} p_{\mathbf{r}|a}(\mathbf{R}|A). \quad (4.91)$$

Substituting (4.91) into (4.90), we have

$$\int_{-\infty}^{\infty} \frac{\partial \ln p_{\mathbf{r}|a}(\mathbf{R}|A)}{\partial A} p_{\mathbf{r}|a}(\mathbf{R}|A) [\hat{a}(\mathbf{R}) - A] d\mathbf{R} = 1. \quad (4.92)$$

Rewriting, we have

$$\int_{-\infty}^{\infty} \left[\frac{\partial \ln p_{\mathbf{r}|a}(\mathbf{R}|A)}{\partial A} \sqrt{p_{\mathbf{r}|a}(\mathbf{R}|A)} \right] \left[\sqrt{p_{\mathbf{r}|a}(\mathbf{R}|A)} [\hat{a}(\mathbf{R}) - A] \right] d\mathbf{R} = 1, \quad (4.93)$$

and, using the Schwarz inequality, we have

$$\left\{ \int_{-\infty}^{\infty} \left[\frac{\partial \ln p_{\mathbf{r}|a}(\mathbf{R}|A)}{\partial A} \right]^2 p_{\mathbf{r}|a}(\mathbf{R}|A) d\mathbf{R} \right\} \times \left\{ \int_{-\infty}^{\infty} [\hat{a}(\mathbf{R}) - A]^2 p_{\mathbf{r}|a}(\mathbf{R}|A) d\mathbf{R} \right\} \geq 1, \quad (4.94)$$

where we recall from the derivation of the Schwarz inequality that equality holds if and only if

$$\frac{\partial \ln p_{\mathbf{r}|a}(\mathbf{R}|A)}{\partial A} = [\hat{a}(\mathbf{R}) - A] k(A), \quad (4.95)$$

for all \mathbf{R} and A . We see that the two terms of the left-hand side of (4.94) are the expectations in statement (a) of (4.86). Thus,

$$E \left\{ [\hat{a}(\mathbf{R}) - A]^2 \right\} \geq \left\{ E \left[\frac{\partial \ln p_{\mathbf{r}|a}(\mathbf{R}|A)}{\partial A} \right]^2 \right\}^{-1}. \quad (4.96)$$

To prove statement (b), we observe

$$\int_{-\infty}^{\infty} p_{\mathbf{r}|a}(\mathbf{R}|A) d\mathbf{R} = 1. \quad (4.97)$$

Differentiating with respect to A , we have

$$\int_{-\infty}^{\infty} \frac{\partial p_{\mathbf{r}|a}(\mathbf{R}|A)}{\partial A} d\mathbf{R} = \int_{-\infty}^{\infty} \frac{\partial \ln p_{\mathbf{r}|a}(\mathbf{R}|A)}{\partial A} p_{\mathbf{r}|a}(\mathbf{R}|A) d\mathbf{R} = 0. \quad (4.98)$$

Differentiating again with respect to A and applying (4.91), we obtain

$$\int_{-\infty}^{\infty} \frac{\partial^2 \ln p_{\mathbf{r}|a}(\mathbf{R}|A)}{\partial A^2} p_{\mathbf{r}|a}(\mathbf{R}|A) d\mathbf{R} + \int_{-\infty}^{\infty} \left(\frac{\partial \ln p_{\mathbf{r}|a}(\mathbf{R}|A)}{\partial A} \right)^2 p_{\mathbf{r}|a}(\mathbf{R}|A) d\mathbf{R} = 0. \quad (4.99)$$

or

$$\boxed{E \left[\frac{\partial^2 \ln p_{\mathbf{r}|a}(\mathbf{R}|A)}{\partial A^2} \right] = -E \left[\frac{\partial \ln p_{\mathbf{r}|a}(\mathbf{R}|A)}{\partial A} \right]^2 \triangleq J_F(A)}, \quad (4.100)$$

which together with (4.96) gives condition (b). The terms in (4.100) are called the *Fisher information* and are denoted by $J_F(A)$.

We revisit the condition for equality in (4.95). Differentiating (4.95) with respect to A gives

$$\frac{\partial^2 \ln p_{\mathbf{r}|a}(\mathbf{R}|A)}{\partial A^2} = -k(A) + [\hat{a}(\mathbf{R}) - A] \frac{\partial k(A)}{\partial A}. \quad (4.101)$$

Taking the expectation with respect to \mathbf{r} gives

$$\boxed{E \left\{ \frac{\partial^2 \ln p_{\mathbf{r}|a}(\mathbf{R}|A)}{\partial A^2} \right\} = -k(A) + E[\hat{a}(\mathbf{R}) - A] \frac{\partial k(A)}{\partial A}}. \quad (4.102)$$

The expectation in the second term on the right-hand side of (4.102) is zero because the estimate is unbiased. The term on the left-hand side is $-J_F(A)$, so

$$k(A) = J_F(A) \quad (4.103)$$

and the equality condition can be written as

$$\boxed{\frac{\partial \ln p_{\mathbf{r}|a}(\mathbf{R}|A)}{\partial A} = J_F(A)[\hat{a}(\mathbf{R}) - A]}. \quad (4.104)$$

Several important observations should be made about these results.

1. It shows that any unbiased estimate must have a variance greater than a certain number.
2. From (4.81), the variance is the conditional mean-square error minus the bias squared. The estimate is unbiased so the CRB is also a bound on the mean-square error.
3. If (4.104) is satisfied, the estimate $\hat{a}_{\text{ml}}(\mathbf{R})$ will satisfy the bound with an equality. We show this by combining (4.104) and (4.85). The left equality is the maximum likelihood equation. The right equality is (4.104):

$$0 = \frac{\partial \ln p_{\mathbf{r}|a}(\mathbf{R}|A)}{\partial A} \Big|_{A=\hat{a}_{\text{ml}}(\mathbf{R})} = (\hat{a}(\mathbf{R}) - A) J_F(A) \Big|_{A=\hat{a}_{\text{ml}}(\mathbf{R})}. \quad (4.105)$$

In order for the right-hand side to equal zero either

$$\hat{a}(\mathbf{R}) = \hat{a}_{\text{ml}}(\mathbf{R}) \quad (4.106)$$

or

$$J_F(\hat{a}_{\text{ml}}) = 0. \quad (4.107)$$

Because we want a solution that depends on the data, we eliminate (4.107) and require (4.106) to hold.

Thus, if an efficient estimate exists, it is $\hat{a}_{\text{ml}}(\mathbf{R})$ and can be obtained as a unique solution to the likelihood equation.

4. If an efficient estimate does not exist [i.e., $\partial \ln p_{\mathbf{r}|a}(\mathbf{R}|A)/\partial A$ cannot be put into form of (4.104)], we do not know how good $\hat{a}_{\text{ml}}(\mathbf{R})$ is. Further, we do not know how close the variance of any estimate will approach the bound.
5. In order to use the bound, we must verify that the estimate of concern is unbiased. A similar bound can be derived simply for biased estimates (Problem 4.2.22). If

$$E(\hat{a}(\mathbf{R})) = A + B(A), \quad (4.108)$$

then

$$\text{Var}(\hat{a}(\mathbf{R}) - A) \geq J_F^{-1}(A) \left(1 + \frac{dB(A)}{dA}\right)^2 \quad (4.109)$$

and

$$\mathcal{R}(A) \geq J_F^{-1}(A) \left(1 + \frac{dB(A)}{dA}\right)^2 + B^2(A). \quad (4.110)$$

To evaluate these bounds, we must have an expression for $B(A)$.

6. If we want to estimate a function a ,

$$d = \gamma(a), \quad (4.111)$$

where $\gamma(a)$ is one to one and monotonically increasing or decreasing so that

$$a = \gamma^{-1}(d) \quad (4.112)$$

exists, then the likelihood function for d can be expressed as

$$p_{\mathbf{r}|d}(\mathbf{R}|D) = p_{\mathbf{r}|a}(\mathbf{R}|A)\gamma^{-1}(D). \quad (4.113)$$

From (4.113), we can see that if $\hat{a}_{\text{ml}}(\mathbf{R})$ is the estimate that maximizes $p_{\mathbf{r}|a}(\mathbf{R}|A)$, then the estimate that maximizes $p_{\mathbf{r}|d}(\mathbf{R}|D)$ satisfies

$$\gamma^{-1}[\hat{d}_{\text{ml}}(\mathbf{R})] = \hat{a}_{\text{ml}}(\mathbf{R}), \quad (4.114)$$

or

$$\hat{d}_{\text{ml}}(\mathbf{R}) = \gamma[\hat{a}_{\text{ml}}(\mathbf{R})]. \quad (4.115)$$

Thus, ML estimation commutes over linear and nonlinear transformations. However, unbiasedness and efficiency only commute over linear transformations. In fact, if $\hat{a}_{\text{ml}}(\mathbf{R})$ is unbiased and efficient, then $\hat{d}_{\text{ml}}(\mathbf{R})$ will be unbiased and efficient iff $\gamma(a)$ is a linear transformation.

7. The Fisher information for d is related to the Fisher information for a by

$$J_F(D) = \left(\frac{\partial \gamma(A)}{\partial A}\right)^{-2} J_F(A) \Big|_{A=\gamma^{-1}(D)}. \quad (4.116)$$

Therefore, if $\hat{d}_{\text{ml}}(\mathbf{R})$ is unbiased,

$$\text{Var}[\hat{d}_{\text{ml}}(\mathbf{R}) - D] \geq J_F^{-1}(D) = \left(\frac{\partial \gamma(A)}{\partial A} \right)^2 J_F^{-1}(A) \Big|_{A=\gamma^{-1}(D)}. \quad (4.117)$$

Conversely,

$$J_F(A) = \left(\frac{\partial \gamma(A)}{\partial A} \right)^2 J_F(D) \Big|_{D=\gamma(A)}, \quad (4.118)$$

and if $\hat{a}_{\text{ml}}(\mathbf{R})$ is unbiased,

$$\text{Var}[\hat{a}_{\text{ml}}(\mathbf{R}) - A] \geq J_F^{-1}(A) = \left(\frac{\partial \gamma(A)}{\partial A} \right)^{-2} J_F^{-1}(D) \Big|_{D=\gamma(A)}. \quad (4.119)$$

These relationships may be expressed in several equivalent forms (see Problem 4.2.23).

We can illustrate the application of ML estimation and the Cramér–Rao inequality by considering Examples 4.2, 4.3, and 4.6. The observation models are identical. We now assume, however, that the parameters to be estimated are *nonrandom variables*.

Example 4.7 (continuation of Examples 4.2 and 4.5) Gaussian. From (4.24) we have

$$r_i = A + n_i, \quad i = 1, 2, \dots, N. \quad (4.120)$$

Taking the logarithm of (4.25) and differentiating, we have

$$\frac{\partial \ln p_{\mathbf{r}|a}(\mathbf{R}|A)}{\partial A} = \frac{N}{\sigma_n^2} \left(\frac{1}{N} \sum_{i=1}^N R_i - A \right). \quad (4.121)$$

Thus,

$$\hat{a}_{\text{ml}}(\mathbf{R}) = \frac{1}{N} \sum_{i=1}^N R_i = \bar{R}. \quad (4.122)$$

To find the bias we take the expectation of both sides,

$$E[\hat{a}_{\text{ml}}(\mathbf{R})] = \frac{1}{N} \sum_{i=1}^N E(R_i) = \frac{1}{N} \sum_{i=1}^N A = A, \quad (4.123)$$

so that $\hat{a}_{\text{ml}}(\mathbf{R})$ is unbiased.

Because the expression in (4.121) has the form required by (4.95) and (4.104), we know that $\hat{a}_{\text{ml}}(\mathbf{R})$ is an efficient estimate. To evaluate the variance we differentiate (4.121)⁷

$$\frac{\partial^2 \ln p_{\mathbf{r}|a}(\mathbf{R}|A)}{\partial A^2} = -\frac{N}{\sigma_n^2}. \quad (4.124)$$

⁷For efficient estimates, this is usually the easiest way to find the variance.

Using (4.87) and the efficiency result, we have

$$\text{Var}[\hat{a}_{\text{ml}}(\mathbf{R}) - A] = \frac{\sigma_n^2}{N}. \quad (4.125)$$

Note that we could have obtained this result directly using (4.121) and (4.104) and concluding that

$$J_F(A) = \frac{N}{\sigma_n^2} \quad (4.126)$$

by inspection. ■

Skipping Example 4.3 for the moment, we go to Example 4.6.

Example 4.8 (continuation of Examples 4.4 and 4.6) Poisson. Differentiating the logarithm of (4.64), we have

$$\begin{aligned} \frac{\partial \ln \Pr(\mathbf{n} = \mathbf{N}|A)}{\partial A} &= \frac{\partial}{\partial A} \left[\left(\sum_{i=1}^M N_i \right) \ln A - MA - \sum_{i=1}^M \ln N_i! \right] \\ &= \frac{1}{A} \sum_{i=1}^M N_i - M = \frac{M}{A} \left[\frac{1}{M} \sum_{i=1}^M N_i - A \right]. \end{aligned} \quad (4.127)$$

The ML estimate is

$$\hat{a}_{\text{ml}}(\mathbf{N}) = \frac{1}{M} \sum_{i=1}^M N_i = \bar{N}. \quad (4.128)$$

It is clearly unbiased and efficient. To obtain the variance we differentiate (4.127);

$$\frac{\partial^2 \ln \Pr(\mathbf{n} = \mathbf{N}|A)}{\partial A^2} = -\frac{1}{A^2} \sum_{i=1}^M N_i. \quad (4.129)$$

Thus,

$$\text{Var}[\hat{a}_{\text{ml}}(\mathbf{N}) - A] = \frac{A^2}{\sum_{i=1}^M E(N_i)} = \frac{A^2}{MA} = \frac{A}{M}. \quad (4.130)$$

Again, this could have been obtained directly using (4.127) and (4.104) and observing that

$$J_F(A) = \frac{M}{A}. \quad (4.131)$$
■

In Example 4.7, $\hat{a}_{\text{ml}}(\mathbf{R})$ in (4.122) is obtained by letting $N \rightarrow \infty$ in $\hat{a}_{\text{map}}(\mathbf{R})$ in (4.63). Similarly, in Example 4.8 The ML estimate in (4.128) is obtained from the MAP estimate in (4.77) by letting $M \rightarrow \infty$. This is true in general, that is,

$$\hat{a}_{\text{map}}(\mathbf{R}) \rightarrow \hat{a}_{\text{ml}}(\mathbf{R}) \quad (4.132)$$

as the number of observations approach infinity.

In Examples 4.7 and 4.8, we see that the ML estimates could also have been obtained from the MAP estimates by a suitable choice of the prior parameters. In Example 4.7, let $\sigma_a \rightarrow \infty$ in (4.63), and in Example 4.8, let $\alpha = 1$ and $b \rightarrow \infty$ in (4.77). We refer to these as *noninformative* priors.

We now return to Example 4.3.

Example 4.9 (continuation of Examples 4.3 and 4.7) Gaussian. From the first term in the exponent in (4.49), we have

$$\frac{\partial \ln p_{\mathbf{r}|a}(\mathbf{R}|A)}{\partial A} = \frac{1}{\sigma_n^2} \sum_{i=1}^N [R_i - s(A)] \frac{\partial s(A)}{\partial A}. \quad (4.133)$$

In general, the right-hand side cannot be written in the form required by (4.104), and therefore an unbiased efficient estimate does not exist.

The likelihood equation is

$$\left[\frac{\partial s(A)}{\partial A} \frac{1}{\sigma_n^2} \right] \left[\frac{1}{N} \sum_{i=1}^N R_i - s(A) \right] \Big|_{A=\hat{a}_{\text{ml}}(\mathbf{R})} = 0. \quad (4.134)$$

If the range of $s(A)$ includes $(1/N) \sum_{i=1}^N R_i$, a solution exists:

$$s[\hat{a}_{\text{ml}}(\mathbf{R})] = \frac{1}{N} \sum_{i=1}^N R_i. \quad (4.135)$$

If (4.135) can be satisfied, then

$$\hat{a}_{\text{ml}}(\mathbf{R}) = s^{-1} \left(\frac{1}{N} \sum_{i=1}^N R_i \right). \quad (4.136)$$

[Observe that (4.136) tacitly assumes that $s^{-1}(\cdot)$ exists. If it does not, then even in the absence of noise we shall be unable to determine A unambiguously. If we were designing a system, we would always choose an $s(\cdot)$ that allows us to find A unambiguously in the absence of noise.] If the range of $s(A)$ does not include $(1/N) \sum_{i=1}^N R_i$, the maximum is at the end point of the range.

As shown in (4.114), the ML estimate commutes over nonlinear operations.⁸ (This is *not* true for MMSE or MAP estimation.) If it is unbiased, we evaluate the bound on the variance by differentiating (4.133):

$$\frac{\partial^2 \ln p_{\mathbf{r}|a}(\mathbf{R}|A)}{\partial A^2} = \frac{1}{\sigma_n^2} \sum_{i=1}^N [R_i - s(A)] \frac{\partial^2 s(A)}{\partial A^2} - \frac{N}{\sigma_n^2} \left[\frac{\partial s(A)}{\partial A} \right]^2. \quad (4.137)$$

Observing that

$$E[r_i - s(A)] = E(n_i) = 0, \quad (4.138)$$

we obtain the following bound for any unbiased estimate,

$$\text{Var}[\hat{a}(\mathbf{R}) - A] \geq \frac{\sigma_n^2}{N[\partial s(A)/\partial A]^2}. \quad (4.139)$$

This has the form of (4.119) where $D = s(A)$ and $J_F(D) = N/\sigma_n^2$ from Example 4.7. The intuitive reason for the factor $[\partial s(A)/\partial A]^2$ and also some feeling for the conditions under which the bound will be useful may be obtained by inspecting the typical function shown in Figure 4.6. Define

$$Y = s(A). \quad (4.140)$$

⁸Let $d = s(a) = \gamma(a)$.

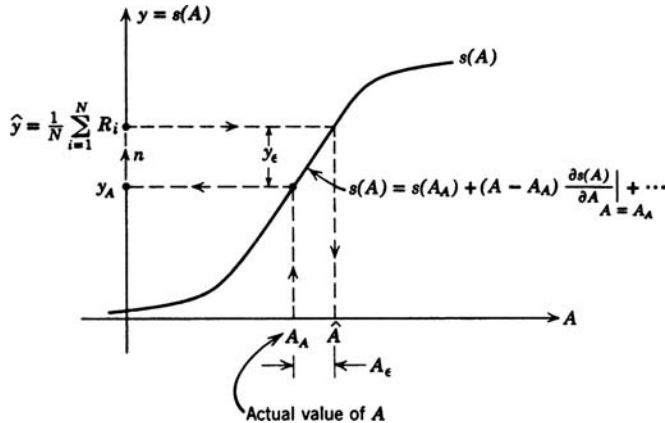


Figure 4.6: Behavior of error variance in the presence of small errors.

Then

$$r_i = Y + n_i. \quad (4.141)$$

The variance in estimating Y is just σ_n^2/N . However, if y_ϵ , the error in estimating Y , is small enough so that the slope is constant, then

$$A_\epsilon \approx \frac{Y_\epsilon}{\left. \frac{\partial s(A)}{\partial A} \right|_{A=\hat{a}(R)}} \quad (4.142)$$

and

$$\text{Var}(a_\epsilon) \approx \frac{\text{Var}(y_\epsilon)}{N[\partial s(A)/\partial A]^2}. \quad (4.143)$$

We observe that if a_ϵ is large there will no longer be a simple linear relation between y_ϵ and a_ϵ . This tells us when we expect the Cramér–Rao bound to give an accurate answer in the case in which the parameter enters the problem in a nonlinear manner. Specifically, whenever the estimation error is small, relative to $A \partial^2 s(A)/\partial A^2$, we should expect the actual variance to be close to the variance bound given by the Cramér–Rao inequality. ■

In Example 4.6, we encountered the Gamma density both as a prior and as a posterior density. In many applications, it is a reasonable model for A . We consider various aspects of it in the next three examples.

Example 4.10 Gamma. Consider the case where we observe N statistically independent r_i that have a $\text{Gamma}(a, b)$ probability density. The shape parameter a is fixed and the scale parameter b is to be estimated; therefore,

$$p_{r_i|b}(R_i|B) = R_i^{a-1} \frac{e^{-R_i/B}}{B^a \Gamma(a)}, \quad R_i \geq 0. \quad (4.144)$$

Then,

$$p_{\mathbf{r}|b}(\mathbf{R}|B) = \left(\prod_{i=1}^N R_i^{a-1} \right) \frac{\exp \left\{ -\frac{1}{B} \sum_{i=1}^N R_i \right\}}{B^{Na} \Gamma^N(a)}. \quad (4.145)$$

The log-likelihood function is

$$\ln p_{\mathbf{r}|b}(\mathbf{R}|B) = (a-1) \sum_{i=1}^N \ln R_i - \frac{1}{B} \sum_{i=1}^N R_i - Na \ln B - N \ln \Gamma(a). \quad (4.146)$$

Differentiating with respect to B and setting the result equal to zero gives

$$\frac{\partial \ln p_{\mathbf{r}|b}(\mathbf{R}|B)}{\partial B} = \left[\frac{N \bar{R}}{B^2} - \frac{Na}{B} \right] \Big|_{B=\hat{b}_{\text{ml}}(\mathbf{R})} = 0. \quad (4.147)$$

Solving (4.147) gives

$$\hat{b}_{\text{ml}}(\mathbf{R}) = \frac{1}{a} \bar{R}, \quad (4.148)$$

thus, the sufficient statistic for estimating B is \bar{R} . We check the bias,

$$E[\hat{b}_{\text{ml}}(\mathbf{R})] = \frac{1}{a} \frac{1}{N} \sum_{i=1}^N E(R_i) = \frac{1}{aN} \cdot N \cdot aB = B, \quad (4.149)$$

so the estimate is unbiased.

Taking the second derivative with respect to B gives

$$\frac{\partial^2 \ln p_{\mathbf{r}|b}(\mathbf{R}|B)}{\partial B^2} = -\frac{2}{B^3} N \bar{R} + \frac{Na}{B^2}, \quad (4.150)$$

and the Fisher information is

$$J_F(B) = E \left\{ \frac{2}{B^3} N \bar{R} - \frac{Na}{B^2} \right\} = \frac{2Na}{B^2} - \frac{Na}{B^2} = \frac{Na}{B^2}. \quad (4.151)$$

To check efficiency, we rewrite (4.147) as

$$\frac{\partial \ln p_{\mathbf{r}|b}(\mathbf{R}|B)}{\partial B} = \frac{Na}{B^2} \left[\frac{1}{a} \bar{R} - B \right] = J_F(B) [\hat{b}_{\text{ml}}(\mathbf{R}) - B]. \quad (4.152)$$

The equality in (4.104) is satisfied, so $\hat{b}_{\text{ml}}(\mathbf{R})$ is efficient and

$$\text{Var}[\hat{b}_{\text{ml}}(\mathbf{R}) - B] = J_F^{-1}(B) = \frac{B^2}{Na}. \quad (4.153)$$

■

Example 4.11 (continuation of Example 4.10) Gamma. We now consider the case in which we parameterize the Gamma density with the shape parameter a and inverse scale parameter $\beta = 1/b$. We assume a is known and β is unknown. The Gamma probability density in (4.144) can now be written as

$$p_{r_i|\beta}(R_i|\beta) = \frac{R_i^{a-1} \beta^a e^{-\beta R_i}}{\Gamma(a)}, \quad (4.154)$$

and the log-likelihood function is

$$\ln p_{\mathbf{r}|\beta}(\mathbf{R}|\beta) = (a - 1) \sum_{i=1}^N \ln R_i - \beta \sum_{i=1}^N R_i + Na \ln \beta - N \ln \Gamma(a). \quad (4.155)$$

Differentiating with respect to β and setting the result equal to zero gives,

$$\frac{\partial \ln p_{\mathbf{r}|\beta}(\mathbf{R}|\beta)}{\partial \beta} = \left[- \sum_{i=1}^N R_i + \frac{Na}{\beta} \right] \Big|_{\beta=\hat{\beta}_{\text{ml}}(\mathbf{R})} = 0 \quad (4.156)$$

or

$$\hat{\beta}_{\text{ml}}(\mathbf{R}) = \frac{a}{\bar{R}} = \frac{1}{\hat{b}_{\text{ml}}(\mathbf{R})}, \quad (4.157)$$

thus, \bar{R} is also the sufficient statistic for estimating β , and we see that ML estimation commutes over the nonlinear transformation $\beta = 1/b$. Since \bar{R} is a weighted sum of IID Gamma random variables, it has a $\text{Gamma}(Na, 1/N\beta)$ probability density. To find the expected value of $\hat{\beta}_{\text{ml}}(\mathbf{R})$, we first evaluate the expected value of \bar{R}^{-1} .

$$\begin{aligned} E\{\bar{R}^{-1}\} &= \int_0^\infty \frac{1}{X} \frac{X^{Na-1} (N\beta)^{Na-1} e^{-N\beta X}}{\Gamma(Na)} dX \\ &= \frac{N\beta \Gamma(Na-1)}{\Gamma(Na)} \int_0^\infty \frac{X^{(Na-1)-1} (N\beta)^{(Na-1)-1} e^{-N\beta X}}{\Gamma(Na-1)} dX \\ &= \frac{N\beta \Gamma(Na-1)}{\Gamma(Na)} = \frac{N\beta}{Na-1}, \end{aligned} \quad (4.158)$$

since the integral equals one.⁹

Thus,

$$E\{\hat{\beta}_{\text{ml}}(\mathbf{R})\} = \frac{Na\beta}{Na-1} = \beta + \frac{\beta}{Na-1}. \quad (4.159)$$

The estimate is biased but converges to β as $N \rightarrow \infty$, so it is asymptotically unbiased.

Using similar steps, one can show that the variance is

$$\text{Var}\{\hat{\beta}_{\text{ml}}(\mathbf{R}) - B\} = \text{Var}\{\hat{\beta}_{\text{ml}}(\mathbf{R})\} = \frac{(Na\beta)^2}{(Na-1)^2(Na-2)} = \frac{\beta^2}{Na \left(1 - \frac{1}{Na}\right)^2 \left(1 - \frac{2}{Na}\right)}. \quad (4.160)$$

The Fisher information is

$$J_F(\beta) = -E\left\{\frac{\partial^2 \ln p_{\mathbf{r}|\beta}(\mathbf{R}; a|\beta)}{\partial \beta^2}\right\} = \frac{Na}{\beta^2}. \quad (4.161)$$

We could also obtain $J_F(\beta)$ from $J_F(B)$ using (4.151) in (4.116) with

$$\beta = \gamma(B) = B^{-1}. \quad (4.162)$$

⁹ An alternative approach to obtaining (4.159) and (4.160) is to recognize that $\hat{b}_{\text{ml}}(\mathbf{R}) = a/\bar{R}$ has an Inverse Gamma density and use the tabulated values of the mean and variance in Appendix A.

Then

$$J_F(\beta) = (-B^{-2})^{-2} \frac{Na}{B^2} \Big|_{B=\beta^{-1}} = \frac{Na}{\beta^2}. \quad (4.163)$$

From (4.159), we see that $\hat{\beta}_{\text{ml}}(\mathbf{R})$ is biased with bias function¹⁰

$$\text{Bias}(\beta) = \frac{\beta}{Na - 1}. \quad (4.164)$$

Since the bias function is known, we can compute the CRB for biased estimators given in (4.109),

$$\text{CRB}(\beta) = J_F^{-1}(\beta) \left(1 + \frac{d \text{Bias}(\beta)}{d\beta} \right)^2 = \frac{Na\beta^2}{(Na - 1)^2}. \quad (4.165)$$

It is straightforward to verify that the variance in (4.160) is greater than the biased CRB in (4.165) and that both converge to $J_F^{-1}(\beta)$ as $N \rightarrow \infty$ so $\hat{\beta}_{\text{ml}}(\mathbf{R})$ is asymptotically efficient. ■

Examples 4.10 and 4.11 illustrated the relationships between ML estimates of parameters related by a nonlinear transformation. The ML estimate of the parameter B was unbiased, while the ML estimate of the parameter $\beta = 1/B$ was only asymptotically unbiased. For B we computed the CRB for unbiased estimators and showed that the ML estimate was efficient, and for β we computed the CRB for biased estimators and showed that the ML estimate was asymptotically efficient.

Example 4.12 Gamma. Now consider the case where the shape parameter a is unknown and the scale parameter b is known. The Gamma probability density in (4.144) can now be written as

$$p_{r_i|a}(R_i|A) = R_i^{A-1} \frac{e^{-R_i/b}}{b^A \Gamma(A)}, \quad R_i \geq 0 \quad (4.166)$$

and the log-likelihood function is

$$\ln p_{\mathbf{r}|a}(\mathbf{R}|A) = (A - 1) \sum_{i=1}^N \ln R_i - \frac{1}{b} \sum_{i=1}^N R_i - NA \ln b - N \ln \Gamma(A). \quad (4.167)$$

Differentiating (4.167) with respect to A gives

$$\frac{\partial \ln p_{\mathbf{r}|a}(\mathbf{R}|A)}{\partial A} = \sum_{i=1}^N \ln R_i - N \ln b - N \psi_0(A), \quad (4.168)$$

where

$$\psi_0(A) = \frac{\Gamma'(A)}{\Gamma(A)} \quad (4.169)$$

is the Digamma function.

Setting (4.168) equal to zero gives

$$\psi_0(\hat{a}_{\text{ml}}(\mathbf{R})) = \frac{1}{N} \sum_{i=1}^N \ln R_i - \ln b = \frac{1}{N} \sum_{i=1}^N \ln \left(\frac{R_i}{b} \right) \quad (4.170)$$

¹⁰We use $\text{Bias}(\beta)$ to denote the bias function to avoid confusion with the parameter B .

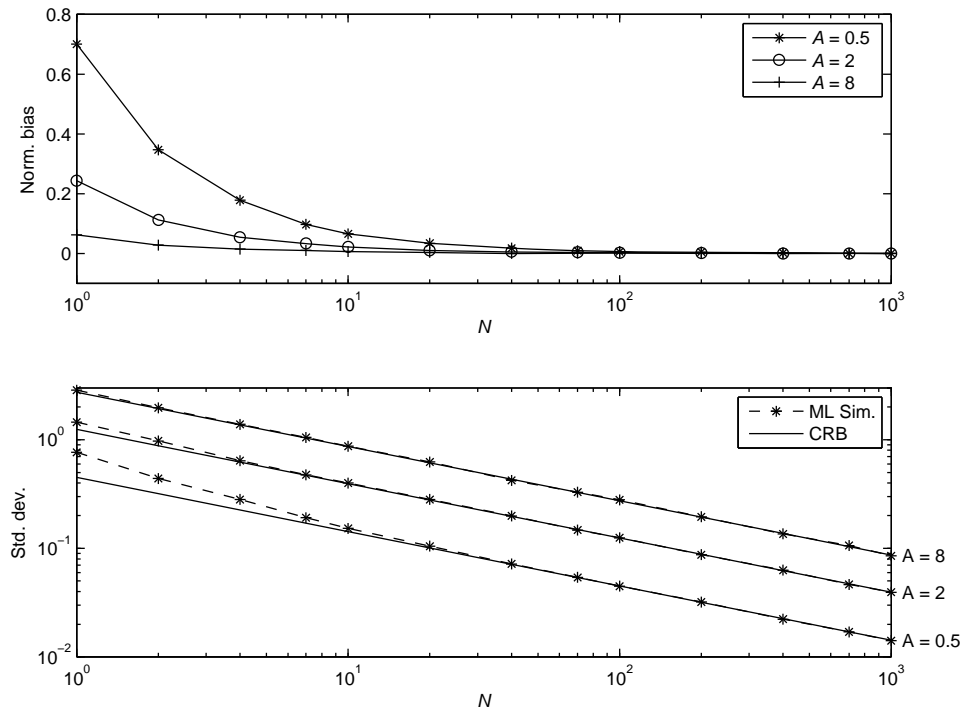


Figure 4.7: Normalized bias and standard deviation; $b = 1$, $A = 0.5, 2$, and 8 .

or

$$\hat{a}_{\text{ml}}(\mathbf{R}) = \psi_0^{-1} \left[\frac{1}{N} \sum_{i=1}^N \ln \left(\frac{R_i}{b} \right) \right]. \quad (4.171)$$

We solve (4.171) numerically to find $\hat{a}_{\text{ml}}(\mathbf{R})$.¹¹ In this case, the sufficient statistic for a is $\sum_{i=1}^N \ln R_i$ or $\sum_{i=1}^N \ln(R_i/b)$.

The Fisher information is obtained by differentiating (4.168) with respect to A and taking the expected value. The result is

$$J_F(A) = N\psi_1(A), \quad (4.172)$$

where $\psi_1(A) = \psi'_0(A)$ is the Trigamma function.

It is difficult to evaluate the bias and variance of $\hat{a}_{\text{ml}}(\mathbf{R})$ analytically, however, since the expression in (4.168) does not satisfy (4.104), we know that the ML estimate is not efficient. To study the bias and variance, we simulate the estimation for $b = 1$ and several values of A . The results are shown in Figure 4.7. The top plot shows the normalized bias, $\text{Bias}(A)/A$, and the bottom plot shows the square root of the variance and CRB versus N . The ML estimate is asymptotically unbiased and efficient.

¹¹We use linear interpolation of the Matlab `psi` function.

For small values of N , however, there is a positive bias and the variance exceeds the (unbiased) CRB. The effect is more pronounced for smaller values of A . ■

We now consider the case in which \mathbf{R} consists of a set of N statistically independent, identically distributed random variables. Then,

$$p_{\mathbf{r}|a}(\mathbf{R}|A) = \prod_{i=1}^N p_{r|a}(R_i|A). \quad (4.173)$$

We want to investigate the properties of the ML estimate as $N \rightarrow \infty$. This behavior is referred to as the asymptotic behavior. Under reasonably general conditions the following may be proved (e.g. [Cra46], pp. 500–504).

1. The solution of the likelihood equation (4.85) converges in probability to the correct value of A as $N \rightarrow \infty$. Any estimate with this property is called *consistent*. Thus, the ML estimate is consistent.
2. The ML estimate is asymptotically efficient; that is,

$$\lim_{N \rightarrow \infty} \frac{\text{Var}[\hat{a}_{\text{ml}}(\mathbf{R}) - A]}{\left(-E\left[\frac{\partial^2 \ln p_{\mathbf{r}|a}(\mathbf{R}|A)}{\partial A^2}\right]\right)^{-1}} = 1. \quad (4.174)$$

3. The ML estimate is asymptotically Gaussian, $N(A, \sigma_{a_e}^2)$.

These properties all deal with the behavior of ML estimates for large N . They provide some motivation for using the ML estimate even when an efficient estimate does not exist. A key question in applying this result is “How large does N have to be in order for the asymptotic results to be an accurate prediction of the performance of the ML estimation?” We will revisit that question in Section 4.4.

At this point a logical question is “Do better estimation procedures than the maximum likelihood procedure exist?” Certainly if an efficient estimate does not exist, there may be unbiased estimates with lower variances. The difficulty is that there is no general rule for finding them. In a particular situation we can try to improve on the ML estimate. In almost all cases, however, the resulting estimation rule is more complex, and therefore we emphasize the maximum likelihood technique in all of our work with nonrandom variables.

In many applications (particularly when we consider the multiple parameter case), the ML estimate may be difficult to compute. In this situation we may look for suboptimal algorithms that are computationally simpler. These suboptimal schemes are usually model specific. We will encounter a few examples in the sequel but will not emphasize them. The interested reader can find a number of examples in the literature.

One of the problems associated with using the CRB in (4.86) is that you must verify that the estimator is unbiased (or asymptotically unbiased) in order to use it. For biased estimates, we obtained a bound on the conditional MSE,

$$\mathcal{R}(A) \geq \frac{\left(1 + \frac{\partial B(A)}{\partial A}\right)^2}{E\left\{\left[\frac{\partial \ln p_{\mathbf{r}|a}(\mathbf{R}|A)}{\partial A}\right]^2\right\}} + B^2(A). \quad (4.175)$$

One of the difficulties of using (4.175) is that it depends on the bias of the estimator, $B(A)$, which may be difficult to find and varies from estimator to estimator. There are a number of papers that discuss techniques for trading bias and variance to minimize the mean-square error (e.g. [HFU96, Eld04], and [SM90]).

A second logical question is “Do better lower bounds than the Cramér–Rao inequality exist?” One straightforward but computationally tedious procedure is the Bhattacharyya bound. The Cramér–Rao bound uses $\partial^2 p_{\mathbf{r}|a}(\mathbf{R}|A)/\partial A^2$. Whenever an efficient estimate does not exist, a larger bound that involves the higher partial derivatives can be obtained. Simple derivations are given in [Bha48] and [Van66a] and in Problems 4.2.28 and 4.2.29. A second bound is the Barankin bound (e.g. [Bar49]). Its two major advantages are that it does not require the probability density to be differentiable and it gives the greatest lower bound. Its disadvantages are that it requires a maximization over a function to obtain the bound and the procedure for finding this maximum is usually not straightforward. Some simple examples are given in Problems 4.2.24 and 4.2.25.

We will revisit the question of improved bounds in Section 4.4.

4.2.3 Bayesian Bounds

4.2.3.1 Lower Bound on the MSE

In this section, we prove the following theorem.

Theorem. Let a be a random variable and \mathbf{r} , the observation vector. The mean-square error of any estimate $\hat{a}(\mathbf{R})$ satisfies the inequality

$$\begin{aligned} E \{ [\hat{a}(\mathbf{R}) - a]^2 \} &\geq \left(E \left\{ \left[\frac{\partial \ln p_{\mathbf{r},a}(\mathbf{R}, A)}{\partial A} \right]^2 \right\} \right)^{-1} \\ &= \left\{ -E \left[\frac{\partial^2 \ln p_{\mathbf{r},a}(\mathbf{R}, A)}{\partial A^2} \right] \right\}^{-1}. \end{aligned} \quad (4.176)$$

Observe that the probability density is a joint density and that the expectation is over both a and \mathbf{r} . The following conditions are assumed to exist:

1. $\frac{\partial \ln p_{\mathbf{r},a}(\mathbf{R}, A)}{\partial A}$ is absolutely integrable with respect to \mathbf{R} and A .
2. $\frac{\partial^2 \ln p_{\mathbf{r},a}(\mathbf{R}, A)}{\partial A^2}$ is absolutely integrable with respect to \mathbf{R} and A .
3. The conditional expectation of the error, given A , is

$$B(A) = \int_{-\infty}^{\infty} [\hat{a}(\mathbf{R}) - A] p_{\mathbf{r}|a}(\mathbf{R}|A) d\mathbf{R}. \quad (4.177)$$

We assume that

$$\lim_{A \rightarrow \infty} B(A) p_a(A) = 0, \quad (4.178)$$

$$\lim_{A \rightarrow -\infty} B(A) p_a(A) = 0. \quad (4.179)$$

The proof is a simple modification of the derivation of the CRB. Multiply both sides of (4.177) by $p_a(A)$ and then differentiate with respect to A :

$$\frac{d}{dA}[p_a(A)B(A)] = - \int_{-\infty}^{\infty} p_{r,a}(\mathbf{R}, A) d\mathbf{R} + \int_{-\infty}^{\infty} \frac{\partial p_{r,a}(\mathbf{R}, A)}{\partial A} [\hat{a}(\mathbf{R}) - A] d\mathbf{R}. \quad (4.180)$$

Now integrate with respect to A :

$$p_a(A)B(A) \Big|_{-\infty}^{\infty} = -1 + \int_{-\infty}^{\infty} \int_{-\infty}^{\infty} \frac{\partial p_{r,a}(\mathbf{R}, A)}{\partial A} [\hat{a}(\mathbf{R}) - A] dA d\mathbf{R}. \quad (4.181)$$

The assumption in Condition 3 makes the left-hand side zero. The remaining steps are identical. The result is

$$E \{[\hat{a}(\mathbf{R}) - a]^2\} \geq \left\{ E \left[\left(\frac{\partial \ln p_{r,a}(\mathbf{R}, A)}{\partial A} \right)^2 \right] \right\}^{-1} \quad (4.182)$$

or, equivalently,

$$E \{[\hat{a}(\mathbf{R}) - a]^2\} \geq \left\{ -E \left[\frac{\partial^2 \ln p_{r,a}(\mathbf{R}|A)}{\partial A^2} \right] - E \left[\frac{\partial^2 \ln p_a(A)}{\partial A^2} \right] \right\}^{-1} \quad (4.183)$$

with equality if and only if

$$\frac{\partial \ln p_{r,a}(\mathbf{R}, A)}{\partial A} = k[\hat{a}(\mathbf{R}) - A], \quad (4.184)$$

for all \mathbf{R} and all A . (In the nonrandom variable case we used the Schwarz inequality on an integral over \mathbf{R} so that the constant $k(A)$ could be a function of A . Now the integration is over both \mathbf{R} and A so that k cannot be a function of A .) Differentiating again gives an equivalent condition

$$\frac{\partial^2 \ln p_{r,a}(\mathbf{R}, A)}{\partial A^2} = -k. \quad (4.185)$$

Observe that (4.185) may be written in terms of the *a posteriori* density,

$$\frac{\partial^2 \ln p_{a|\mathbf{r}}(A|\mathbf{R})}{\partial A^2} = -k. \quad (4.186)$$

Integrating (4.186) twice and putting the result in the exponent, we have

$$p_{a|\mathbf{r}}(A|\mathbf{R}) = \exp(-kA^2 + C_1 A + C_2) \quad (4.187)$$

for all \mathbf{R} and A ; but (4.187) is simply a statement that the *a posteriori* probability density of a must be Gaussian for all \mathbf{R} in order for an efficient estimate to exist. (Note that C_1 and C_2 are functions of \mathbf{R}).

We define the following information quantities

$$\begin{aligned} J_B &\triangleq E \left\{ \left[\frac{\partial \ln p_{\mathbf{r},a}(\mathbf{R}, A)}{\partial A} \right]^2 \right\} \\ &= -E \left\{ \left[\frac{\partial^2 \ln p_{\mathbf{r},a}(\mathbf{R}, A)}{\partial A^2} \right] \right\}, \end{aligned} \quad (4.188)$$

where the expectation is over \mathbf{r} and a . J_B is called the *Bayesian information*. We define two components of J_B as

$$\begin{aligned} J_D &\triangleq E \left\{ \left[\frac{\partial \ln p_{\mathbf{r}|a}(\mathbf{R}|A)}{\partial A} \right]^2 \right\} \\ &= -E \left\{ \left[\frac{\partial^2 \ln p_{\mathbf{r}|a}(\mathbf{R}|A)}{\partial A^2} \right] \right\}, \end{aligned} \quad (4.189)$$

or

$$J_D = E_a \{ J_F(A) \}, \quad (4.190)$$

where $J_F(A)$ is the Fisher information. The subscript “ D ” denotes data.

The second component is

$$J_P \triangleq E_a \left\{ \left[\frac{\partial \ln p_a(A)}{\partial A} \right]^2 \right\} = -E_a \left\{ \left[\frac{\partial^2 \ln p_a(A)}{\partial A^2} \right] \right\}. \quad (4.191)$$

The subscript “ P ” denotes prior.

Then,

$$\begin{aligned} J_B &= J_D + J_P \\ &= E_a \{ J_F(A) \} + J_P \end{aligned} \quad (4.192)$$

and the Bayesian CRB defined in (4.183) is¹²

$E \{ (\hat{a}(\mathbf{R}) - a)^2 \} \geq J_B^{-1}.$

(4.193)

¹²The Bayesian Cramér–Rao bound was derived by Van Trees [Van68, Van01a]. It was derived independently by Shutzbenberger [Shu57]. This latter derivation is a model of economy (1/3 of a page) but does not appear to have been noticed by either the engineering or statistical community. The bound in (4.193) goes by different names in the literature. The engineering papers in the early 1970s (e.g. [BMZ87, BZ75]) referred to it as the Van Trees version of the CRB. The statistics literature (e.g. [GL95]) referred to it as the Van Trees inequality. More recent papers in the engineering literature refer to it as the Bayesian version of the CRB (e.g. [WW88]) and the posterior CRB (e.g. [TMN98]).

The condition for equality in (4.184) can be written as

$$\frac{\partial \ln p_{\mathbf{R}|a}(\mathbf{R}|A)}{\partial A} = J_B[\hat{a}(\mathbf{R}) - A]. \quad (4.194)$$

We refer to an estimate that satisfies the BCRB as a *Bayesian efficient estimate*.

Arguing as in (4.105)–(4.107), we see that if (4.184) is satisfied, the MAP estimate will be efficient. Because the MMSE estimate cannot have a larger error, this tells us that $\hat{a}_{\text{ms}}(\mathbf{R}) = \hat{a}_{\text{map}}(\mathbf{R})$ whenever an efficient estimate exists. As a matter of technique, when an efficient estimate does exist, it is usually computationally easier to solve the MAP equation than it is to find the conditional mean. When an efficient estimate does not exist, we do not know how closely the mean-square error, using either $\hat{a}_{\text{map}}(\mathbf{R})$ or $\hat{a}_{\text{ms}}(\mathbf{R})$, approaches the lower bound.

We revisit Examples 4.2 and 4.5 for the case when the parameters are modeled as random variables.

Example 4.13 (continuation of Examples 4.2, 4.5, and 4.7) Gaussian. From (4.30) and (4.63),

$$\hat{a}_{\text{ms}}(\mathbf{R}) = \hat{a}_{\text{map}}(\mathbf{R}) = \frac{\sigma_a^2}{\sigma_a^2 + \sigma_n^2/N} \left(\frac{1}{N} \sum_{i=1}^N R_i \right). \quad (4.195)$$

From (4.126),

$$J_F = \frac{N}{\sigma_n^2}, \quad (4.196)$$

which does not depend on A . From (4.25),

$$\ln p_a(A) = -\frac{1}{2} \ln(2\pi\sigma_a^2) - \frac{A^2}{2\sigma_a^2} \quad (4.197)$$

and

$$J_P = -E \left\{ \frac{\partial^2}{\partial A^2} \ln p_a(A) \right\} = \frac{1}{\sigma_a^2}. \quad (4.198)$$

Then, using (4.196) and (4.198) in (4.192), we have

$$J_B = \frac{N}{\sigma_n^2} + \frac{1}{\sigma_a^2}. \quad (4.199)$$

The equality in (4.185) is satisfied, so

$$\text{MSE}[\hat{a}_{\text{map}}(\mathbf{R})] = \text{MSE}[\hat{a}_{\text{ms}}(\mathbf{R})] = \left(\frac{N}{\sigma_n^2} + \frac{1}{\sigma_a^2} \right)^{-1} = \frac{\sigma_a^2 \sigma_n^2}{N \sigma_a^2 + \sigma_n^2}, \quad (4.200)$$

which we found previously in (4.29).

As N increases, the prior knowledge becomes less important and

$$\lim_{N \rightarrow \infty} \hat{a}_{\text{map}}(\mathbf{R}) = \hat{a}_{\text{ml}}(\mathbf{R}) = \frac{1}{N} \sum_{i=1}^N R_i \quad (4.201)$$

and

$$\lim_{N \rightarrow \infty} \text{BCRB} = \text{CRB} = \frac{\sigma_n^2}{N}. \quad (4.202)$$

■

We will consider several other examples after we study the asymptotic behavior as $N \rightarrow \infty$.

4.2.3.2 Asymptotic Behavior

We now examine the asymptotic behavior of $\hat{a}_{\text{map}}(\mathbf{R})$ and $\hat{a}_{\text{ms}}(\mathbf{R})$ for the data model in (4.173). Recall

$$\begin{aligned} \hat{a}_{\text{map}}(\mathbf{R}) &= \underset{A}{\operatorname{argmax}} \left\{ \ln p_{\mathbf{r},a}(\mathbf{R}, A) \right\} \\ &= \underset{A}{\operatorname{argmax}} \left\{ \ln p_{\mathbf{r}|a}(\mathbf{R}|A) + \ln p_a(A) \right\}. \end{aligned} \quad (4.203)$$

For the model in (4.173), (4.203) reduces to

$$\hat{a}_{\text{map}}(\mathbf{R}) = \underset{A}{\operatorname{argmax}} \left\{ \sum_{i=1}^N \ln p_{r|a}(R_i|A) + \ln p_a(A) \right\}. \quad (4.204)$$

As $N \rightarrow \infty$, the first term in braces will dominate and

$$\lim_{N \rightarrow \infty} \hat{a}_{\text{map}}(\mathbf{R}) = \underset{A}{\operatorname{argmax}} \left\{ \sum_{i=1}^N \ln p_{r|a}(R_i|A) \right\} = \hat{a}_{\text{ml}}(\mathbf{R}). \quad (4.205)$$

As we would expect, the effect of prior knowledge decreases and asymptotically goes to zero as we get more data. It can be shown that the posterior density $p_{a|\mathbf{r}}(A|\mathbf{R})$ is asymptotically Gaussian with variance equal to the inverse of the Fisher information,¹³ therefore, the MAP and MMSE estimates will be the same asymptotically and their MSE will satisfy

$$\lim_{N \rightarrow \infty} \text{MSE}[\hat{a}_{\text{ms}}(\mathbf{R})] = \lim_{N \rightarrow \infty} \text{MSE}[\hat{a}_{\text{map}}(\mathbf{R})] = \lim_{N \rightarrow \infty} \text{MSE}[\hat{a}_{\text{ml}}(\mathbf{R})] = E_a \{ J_F^{-1}(A) \}. \quad (4.206)$$

We can substitute the CRB into the right-hand side of (4.206). The asymptotic performance of $\hat{a}_{\text{ms}}(\mathbf{R})$ and $\hat{a}_{\text{map}}(\mathbf{R})$ are found by taking the expectation of the conditional CRB with respect to a ,

$$\lim_{N \rightarrow \infty} \text{MSE}[\hat{a}_{\text{ms}}(\mathbf{R})] = \lim_{N \rightarrow \infty} \text{MSE}[\hat{a}_{\text{map}}(\mathbf{R})] = E_a \{ \text{CRB}(A) \} \triangleq \text{ECRB}. \quad (4.207)$$

From Jensen's Inequality and (4.192),

$$\text{ECRB} = E_a \{ J_F^{-1}(A) \} \geq [E_a \{ J_F(A) \}]^{-1} \geq [J_D + J_P]^{-1} = \text{BCRB}. \quad (4.208)$$

The second inequality is satisfied asymptotically and the first inequality is satisfied with equality if and only if $J_F(A)$ is not a function of A . Thus, asymptotically, the ECRB (and therefore the MSE of $\hat{a}_{\text{ms}}(\mathbf{R})$ and $\hat{a}_{\text{map}}(\mathbf{R})$) in (4.207) may be greater than the BCRB in (4.208). In many applications of interest, $J_F(A)$ does not depend on A (as in Example 4.13),

¹³This is discussed in [Leh59].

and $\hat{a}_{\text{ms}}(\mathbf{R})$ and $\hat{a}_{\text{map}}(\mathbf{R})$ achieve the BCRB asymptotically. However, when $J_F(A)$ does depend on A (as in Examples 4.8–4.12), the BCRB may not be a tight bound asymptotically (see Example 4.14).

Note that in order to use (4.207) in the nonasymptotic regime, we have to show that the estimate is conditionally unbiased for all A , that is, $E_{\mathbf{r}|a}\{\hat{a}_{\text{ms}}(\mathbf{R})\} = A$ or $E_{\mathbf{r}|a}\{\hat{a}_{\text{map}}(\mathbf{R})\} = A$. In most applications, this is not true for the estimate, because of the effect of the prior. We illustrate these properties with an example.

Example 4.14 (continuation of Examples 4.4, 4.6, and 4.8) Poisson. The MMSE, MAP, and ML estimates are given in (4.71), (4.77), and (4.128), respectively. The MSE of $\hat{a}_{\text{ms}}(\mathbf{R})$ is given in (4.75),

$$\text{MSE}[\hat{a}_{\text{ms}}(\mathbf{N})] = \frac{\alpha b^2}{Mb + 1}. \quad (4.209)$$

It is the minimum MSE achievable by any estimator. The Fisher information was given in (4.131),

$$J_F(A) = \frac{M}{A}. \quad (4.210)$$

For this problem, the Fisher information and CRB depend on the value of A .

In order to compute the BCRB, we need to evaluate the J_D and J_P terms in (4.190) and (4.191). The J_D term is given by

$$J_D = E_a\{J_F(A)\} = M E_a\{A^{-1}\}. \quad (4.211)$$

Recognizing that a^{-1} has an Inverse Gamma density (with mean and variance given in Appendix A), we have

$$J_D = \frac{M}{b(\alpha - 1)}. \quad (4.212)$$

The J_P term is

$$\begin{aligned} J_P &= E_a\left\{-\frac{\partial^2 \ln p_a(A)}{\partial^2 A}\right\} = E_a\{(\alpha - 1)A^{-2}\} \\ &= \frac{1}{b^2(\alpha - 2)}. \end{aligned} \quad (4.213)$$

Putting these terms together, we have

$$J_B = \frac{1}{b^2} \left[\frac{Mb}{\alpha - 1} + \frac{1}{\alpha - 2} \right]. \quad (4.214)$$

We can see that the inverse of J_B in (4.214) is strictly less than the minimum MSE in (4.209).

For small M , the J_P term dominates, and we have

$$\begin{aligned} \lim_{M \rightarrow 0} J_B^{-1} &= J_P^{-1} = (\alpha - 2)b^2 \\ &= \frac{\alpha - 2}{\alpha} \sigma_a^2, \end{aligned} \quad (4.215)$$

where $\sigma_a^2 = \alpha b^2$ is the *a priori* variance. For large α , the BCRB approaches σ_a^2 in the limit of no data.

For large M , the J_D term dominates, and we have

$$\lim_{M \rightarrow \infty} J_B^{-1} = J_D^{-1} = \frac{(\alpha - 1)b}{M}. \quad (4.216)$$

To find the asymptotic MSE of the MMSE, MAP and ML estimates, we evaluate the ECRB

$$\begin{aligned} \text{ECRB} &= E_a \left\{ J_F^{-1}(A) \right\} \\ &= E_a \left\{ \frac{A}{M} \right\} \\ &= \frac{\alpha b}{M}, \end{aligned} \quad (4.217)$$

which agrees with the asymptotic MSE in (4.76). The ECRB in (4.217) is strictly greater than the asymptotic BCRB in (4.216), however the difference diminishes as α increases.

To illustrate these results, we ran a Monte Carlo simulation for various values of M . On each trial, a random sample of the parameter a was drawn from a Gamma density with $b = 0.1$ and $\alpha = 3$. M observations were generated, and the ML, MAP, and MMSE estimates calculated. In Figure 4.8, we show the results from 5000 trials. The root MSE (RMSE) for the estimates averaged over trials is plotted as a function of M , as well as the square roots of the bounds. These are plotted on a log–log scale so that the $1/M$ decrease appears linear. For all M , the MMSE estimator achieves the MSE in (4.209). By definition of the MMSE estimator, this is the best possible performance of any estimator. The MAP estimate has slightly higher MSE for small M . For large M , the MAP, MMSE, and ML estimates coincide and their MSE is equal to the ECRB. Asymptotically, the BCRB is two-thirds of the ECRB; therefore, it is not a tight lower bound in the asymptotic region. The ML estimator is conditionally unbiased for all M and its performance is still predicted by the ECRB for small M . However, as M decreases and the prior information dominates the observations, the MAP and MMSE

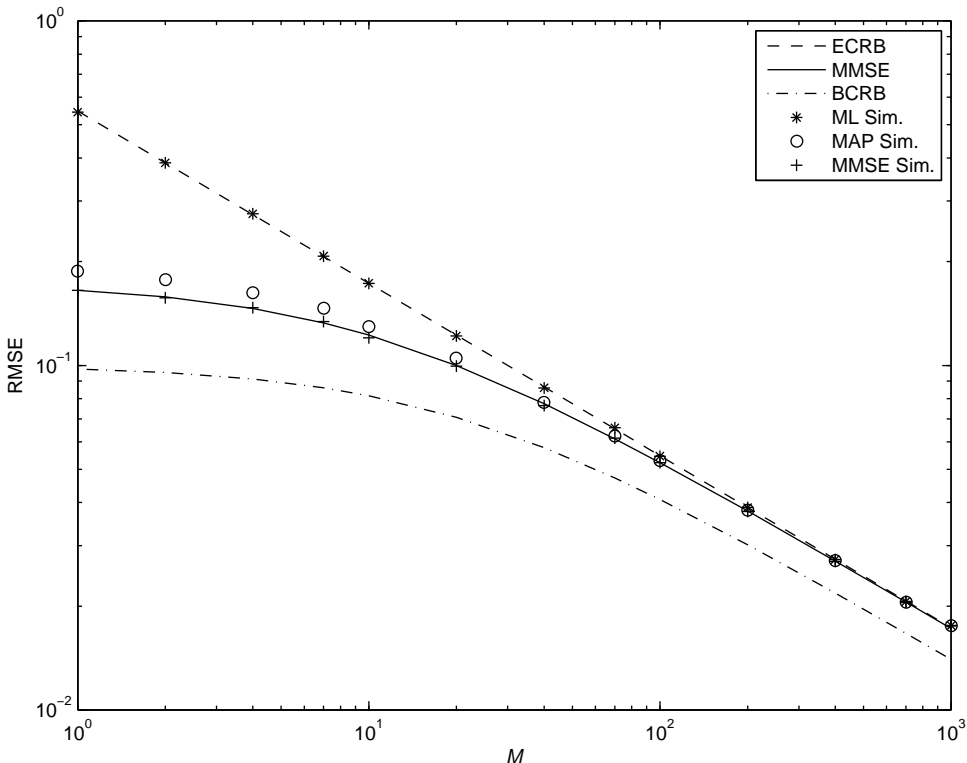


Figure 4.8: MSE, BCRB, and ECRB in estimating a versus M ; $b = 0.1$ and $\alpha = 3$.

estimates are drawn closer to the prior mean and are no longer conditionally unbiased. Their MSE becomes smaller and approaches the *a priori* variance. The ECRB is no longer a valid predictor of their performance. The BCRB incorporates the effect of the prior and is a valid (though not tight) lower bound for all three estimators for all M . ■

4.2.4 Case Study

In this section, we introduce a case study that we will follow throughout the chapter. Although it deals with a specific problem, it illustrates the techniques involved in actual application and the issues that must be studied.

Example 4.15 Frequency estimation. We want to estimate the frequency of a complex exponential observed in the presence of circular complex Gaussian noise.¹⁴ The signal of interest is

$$\tilde{s}(t) = b e^{j(\omega_c t + \theta)}, \quad (4.218)$$

where b is the real, positive amplitude, ω_c is the frequency, and θ is the phase. It is the complex representation of the output of a quadrature demodulator when the input is a bandpass process with carrier frequency ω_c . The signal and noise processes are bandlimited to $\pm 2\pi W$. They are sampled every $T_s = 1/W$ seconds to obtain the sequence

$$\tilde{r}_n = b e^{j(\omega_c n T_s + \theta)} + \tilde{w}_n, \quad n = 0, \dots, N - 1, \quad (4.219)$$

where the noise \tilde{w}_n is a zero-mean circular complex Gaussian random variable with variance $\sigma_{\tilde{w}}^2$. The SNR of the observed data is defined as

$$\text{SNR} \triangleq \frac{b^2}{\sigma_{\tilde{w}}^2}. \quad (4.220)$$

In this example, we assume the amplitude and phase are known and the frequency is an unknown, nonrandom parameter we wish to estimate. It is convenient to define a sampled (or digital) frequency,

$$\omega \triangleq \omega_c T_s. \quad (4.221)$$

Then the observations may be written as

$$\tilde{r}_n = b e^{j\theta} e^{j\omega n} + \tilde{w}_n, \quad n = 0, \dots, N - 1. \quad (4.222)$$

This is the same model as in Examples 3.1 and 3.6, with $\tilde{b} = b e^{j\theta}$. The observation vector $\tilde{\mathbf{r}}$ is $CN(\tilde{\mathbf{m}}, \sigma_{\tilde{w}}^2 \mathbf{I})$ with

$$[\tilde{\mathbf{m}}]_n = b e^{j\theta} e^{j\omega n}. \quad (4.223)$$

¹⁴This example appears in Rife and Boorstyn [RB74]. It is the discrete-time version of the example in Chapter 4 of Van Trees [Van68, Van01a]. The continuous-time version is also discussed in Slepian [Sle57].

The log-likelihood function is

$$\begin{aligned} l(\omega; \tilde{\mathbf{R}}) &= \ln p_{\tilde{\mathbf{r}}|\omega}(\tilde{\mathbf{R}}|\omega) \\ &= -\frac{N}{\sigma_w^2} \left[\frac{1}{N} \sum_{n=0}^{N-1} |\tilde{R}_n - b e^{j\theta} e^{j\omega n}|^2 \right] - N \ln(\pi \sigma_w^2) \\ &= (2N) \left(\frac{b}{\sigma_w^2} \right) \Re \left[e^{-j\theta} \frac{1}{N} \sum_{n=0}^{N-1} \tilde{R}_n e^{-j\omega n} \right] + \zeta, \end{aligned} \quad (4.224)$$

where ζ represents terms that do not depend on ω . We denote the term containing the data as $A(\omega; \tilde{\mathbf{R}})$,

$$A(\omega; \tilde{\mathbf{R}}) \triangleq \Re \left[e^{-j\theta} F(\omega; \tilde{\mathbf{R}}) \right], \quad (4.225)$$

where the function

$$F(\omega; \tilde{\mathbf{R}}) \triangleq \frac{1}{N} \sum_{n=0}^{N-1} \tilde{R}_n e^{-j\omega n} \quad (4.226)$$

is proportional to the discrete Fourier transform (DFT) of the data. The ML estimate is

$$\hat{\omega}_{\text{ml}}(\tilde{\mathbf{R}}) = \underset{\omega}{\operatorname{argmax}} \{ A(\omega; \tilde{\mathbf{R}}) \}. \quad (4.227)$$

Suppose \tilde{R}_n is noise free and contains only a signal component, that is,

$$\tilde{R}_n = b e^{j\theta} e^{j\omega_a n}, \quad (4.228)$$

where ω_a is the actual frequency value. Substituting (4.226) and (4.228) into (4.225) and following the derivation in (3.307)–(3.309), in the absence of noise $A(\omega; \tilde{\mathbf{R}})$ has the form

$$\begin{aligned} A_s(\omega) &= \Re \left[e^{-j\theta} \frac{1}{N} \sum_{n=0}^{N-1} b e^{j\theta} e^{j\omega_a n} e^{-j\omega n} \right] \\ &= \Re \left[\frac{b}{N} \sum_{n=0}^{N-1} e^{j(\omega_a - \omega)n} \right] \\ &= b \Re \left[e^{j(\omega_a - \omega)\frac{N-1}{2}} \right] \frac{\sin \left[(\omega_a - \omega) \frac{N}{2} \right]}{N \sin \left[(\omega_a - \omega) \frac{1}{2} \right]} \\ &= b \cos \left[(\omega - \omega_a) \frac{N-1}{2} \right] B_c(\omega - \omega_a), \end{aligned} \quad (4.229)$$

where $B_c(\cdot)$ was defined in (3.309), and we have used the symmetry property to obtain the final expression in (4.229). The function $A_s(\omega)$ is periodic with period 2π , but since the signal is bandlimited, we focus only on the $-\pi \leq \omega \leq \pi$ region. We define the normalized function

$$A_{sn}(\omega) \triangleq \frac{1}{b} A_s(\omega) = \cos \left[(\omega - \omega_a) \frac{N-1}{2} \right] B_c(\omega - \omega_a), \quad (4.230)$$

and refer to it the *normalized ambiguity surface*.¹⁵ $A_{sn}(\omega)$ is plotted in Figure 4.9. It has a peak at ω_a and also has smaller peaks or “sidelobes” on either side of ω_a .

¹⁵We do not use “ambiguity function” because it is widely used in the engineering literature for a specific parameter set and signal model (e.g. [Van71a, Van01b]).

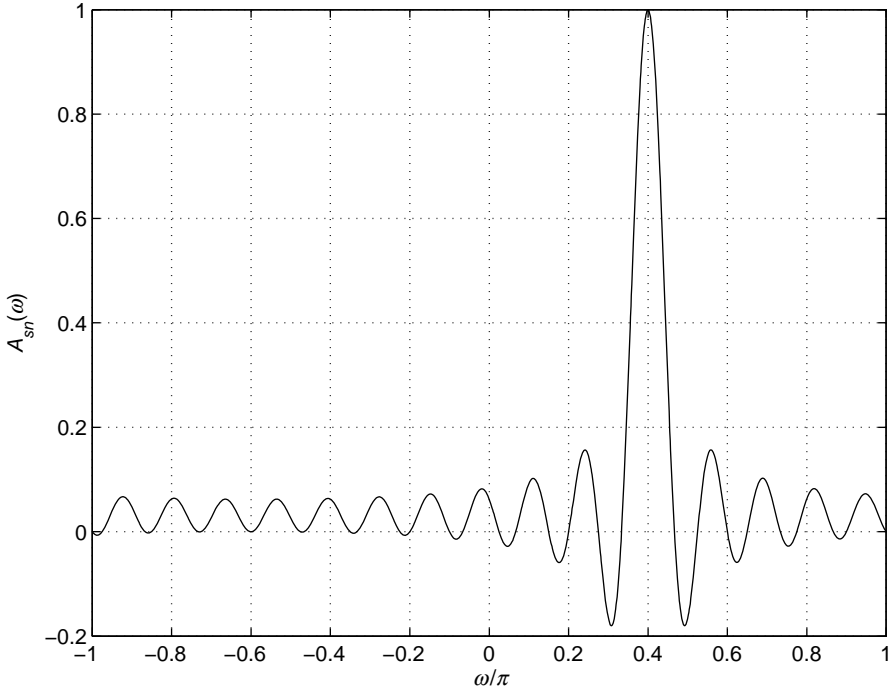


Figure 4.9: Normalized signal ambiguity surface, $A_{sn}(\omega)$, known phase. $N = 16$, $\omega_a = 0.4\pi$, $\theta = \pi/6$.

In practice, we observe the noisy ambiguity surface $A(\omega; \tilde{\mathbf{R}})$. To illustrate the behavior in the presence of noise, we ran Monte Carlo simulations for various values of SNR. In Figure 4.10, we show three realizations of $A(\omega; \tilde{\mathbf{R}})$ for $N = 16$ and three values of SNR (5, -10, and -25 dB). We see that for SNR = 5 dB, the peaks of the ambiguity surfaces are in the close vicinity of the correct value and the estimation error is small. For SNR = -10 dB, the noise has caused the peak of one of the ambiguity surfaces to be in the vicinity of the second sidelobe and the error is significantly larger. For SNR = -25 dB, one ambiguity surface has a peak near the true value. The other two ambiguity surfaces have peaks due to noise and the estimates have no relation to the actual frequency. The estimation errors are very large. Figure 4.11 shows the distribution of the frequency estimates for 10,000 trials. For high SNR (5 dB), the distribution is tightly clustered around the true value $\omega_a = 0.4\pi$. As SNR decreases (-10 dB), the clustering around the true value becomes more spread out, and subsidiary clusters at the sidelobes as well as a uniform distribution of random estimates appear. For low SNR (-25 dB), the uniform distribution of random estimates becomes the dominant component of the distribution.

In Figures 4.12 and 4.13, we show the bias and RMSE as a function of SNR for 10,000 trials of a Monte Carlo simulation. The CRB is also plotted for comparison with the RMSE. The Fisher information for estimating ω is

$$\begin{aligned} J_F(\omega) &= -E \left\{ \frac{\partial^2}{\partial \omega^2} l(\omega; \tilde{\mathbf{R}}) \right\} \\ &= (2N) \left(\frac{b}{\sigma_w^2} \right) \Re \left[e^{-j\theta} \frac{1}{N} \sum_{n=0}^{N-1} E \{ \tilde{\mathbf{R}}_n \} e^{-j\omega n} n^2 \right] \end{aligned}$$

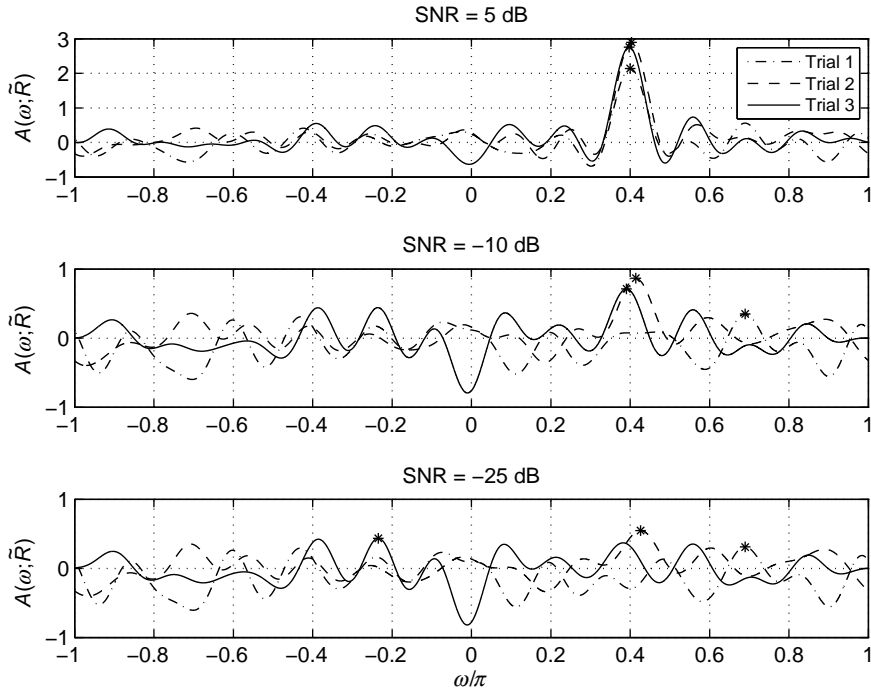


Figure 4.10: Noisy ambiguity surface, $A(\omega; \tilde{\mathbf{R}})$, known phase. $N = 16$, $\omega_a = 0.4\pi$, $\theta = \pi/6$.

$$\begin{aligned}
 &= 2 \left(\frac{b^2}{\sigma_w^2} \right) \sum_{n=0}^{N-1} n^2 \\
 &= \text{SNR} \frac{N(N-1)(2N-1)}{3}.
 \end{aligned} \tag{4.231}$$

Note that $J_F(\omega)$ is a function of SNR and N , but does not depend on ω . Inverting $J_F(\omega)$, we obtain a bound on the variance of any unbiased estimator,

$$\text{Var} [\hat{\omega}(\tilde{\mathbf{R}}) - \omega] \geq \frac{1}{\text{SNR}} \frac{3}{N(N-1)(2N-1)}. \tag{4.232}$$

For high SNR, the bias approaches zero and the RMSE is equal to the CRB. There is a sharp threshold at about SNR = 1 dB, where the RMSE increases significantly above the CRB. This is due to the presence of large estimation errors obtained when the peak of the noisy ambiguity surface is at a sidelobe or another random point. The bias also begins to deviate from zero at the threshold. As SNR decreases, the RMSE increases and eventually levels out and the bias becomes more significant. ■

We now consider the Bayesian version of Example 4.15.

Example 4.16 (continuation of Example 4.15) Frequency estimation. The data model in Example 4.15 is still valid. The parameter ω is now modeled as a random variable with known *a priori*

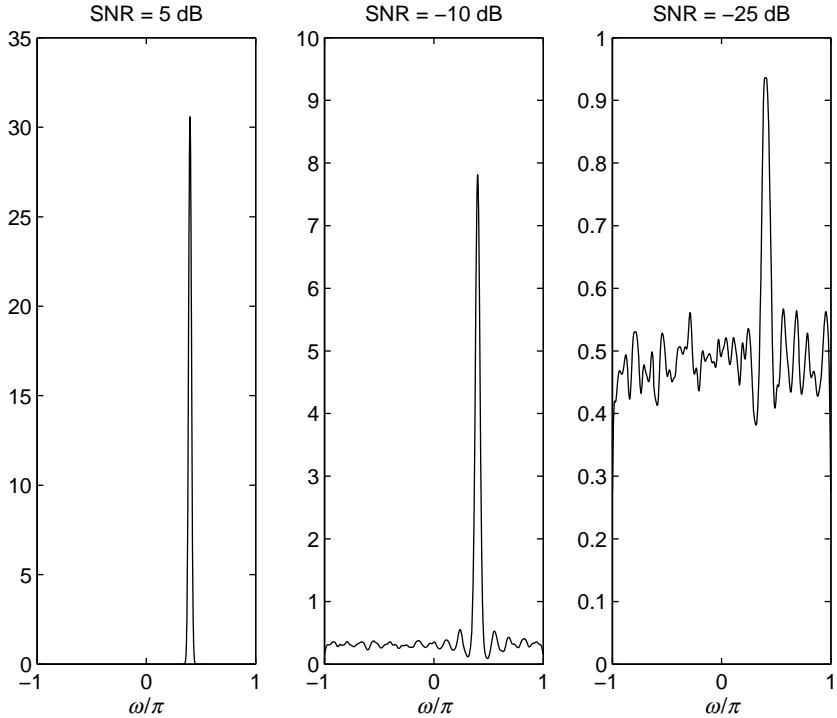


Figure 4.11: Distribution of $\hat{\omega}_{\text{ml}}(\tilde{\mathbf{R}})$ for known phase, SNR = 5, -10, and -25 dB. $N = 16$, $\omega_a = 0.4\pi$, $\theta = \pi/6$.

density. We consider a family of probability densities based on the symmetric Beta density ($a = b$) that has been shifted and scaled to the interval $-\pi \leq \omega \leq \pi$. The prior pdf is

$$p_\omega(\omega) = \frac{1}{2\pi B(a, a)} \left(\frac{\pi + \omega}{2\pi} \right)^{a-1} \left(\frac{\pi - \omega}{2\pi} \right)^{a-1}, \quad -\pi \leq \omega \leq \pi, \quad (4.233)$$

This pdf is symmetric with mean $\mu_\omega = 0$ and variance $\sigma_\omega^2 = \pi^2/(2a+1)$. It is shown in Figure 4.14 for several values of a .

To find $\hat{\omega}_{\text{map}}(\tilde{\mathbf{R}})$, we find the maximum of $l_B(\omega; \tilde{\mathbf{R}})$. The first term in (4.21) is given by (4.224). The second term is

$$\ln p_\omega(\omega) = (a-1) \ln \left(\frac{\pi + \omega}{2\pi} \right) + (a-1) \ln \left(\frac{\pi - \omega}{2\pi} \right) - \ln [2\pi B(a, a)]. \quad (4.234)$$

Combining the terms, the Bayesian log-likelihood function is

$$l_B(\omega; \tilde{\mathbf{R}}) = (2N) \left(\frac{b}{\sigma_{\tilde{w}}^2} \right) \Re [e^{-j\theta} F(\omega; \tilde{\mathbf{R}})] + (a-1) \ln \left(\frac{\pi + \omega}{2\pi} \right) + (a-1) \ln \left(\frac{\pi - \omega}{2\pi} \right) + \zeta, \quad (4.235)$$

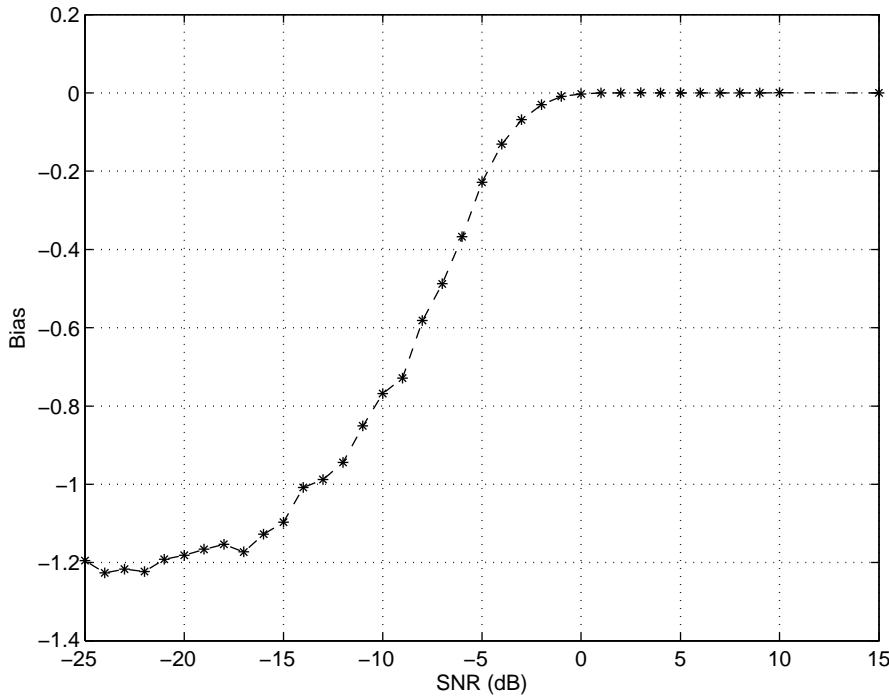


Figure 4.12: Frequency estimation bias versus SNR, known phase. $N = 16$, $\omega_a = 0.4\pi$, $\theta = \pi/6$.

and

$$\hat{\omega}_{\text{map}}(\tilde{\mathbf{R}}) = \underset{\omega}{\operatorname{argmax}} \{l_B(\omega; \tilde{\mathbf{R}})\}. \quad (4.236)$$

We refer to the noise-free component of (4.235) as the *posterior ambiguity surface*. It has the form

$$\begin{aligned} A_{ps}(\omega) &= (2N \text{SNR}) \cos \left[(\omega - \omega_a) \frac{N-1}{2} \right] B_c(\omega - \omega_a) \\ &\quad + (a-1) \ln \left(\frac{\pi + \omega}{2\pi} \right) + (a-1) \ln \left(\frac{\pi - \omega}{2\pi} \right) - \ln [2\pi B(a, a)]. \end{aligned} \quad (4.237)$$

The first term is proportional to the normalized signal ambiguity surface in (4.230), and the remaining terms are due to the prior. The relative importance of the data and prior terms will depend on the relative values of N , SNR, and a . The posterior ambiguity surface is shown in Figure 4.15 for $a = 20$ and three values of SNR. The prior terms add a weighting that is largest at the peak of the prior pdf ($\omega = 0$) and tapers off as $\omega \rightarrow \pm\pi$. For high SNR, the data component dominates and the peak of the posterior ambiguity surface is at the actual frequency, whereas for low SNR, the prior term dominates and the peak is at zero.

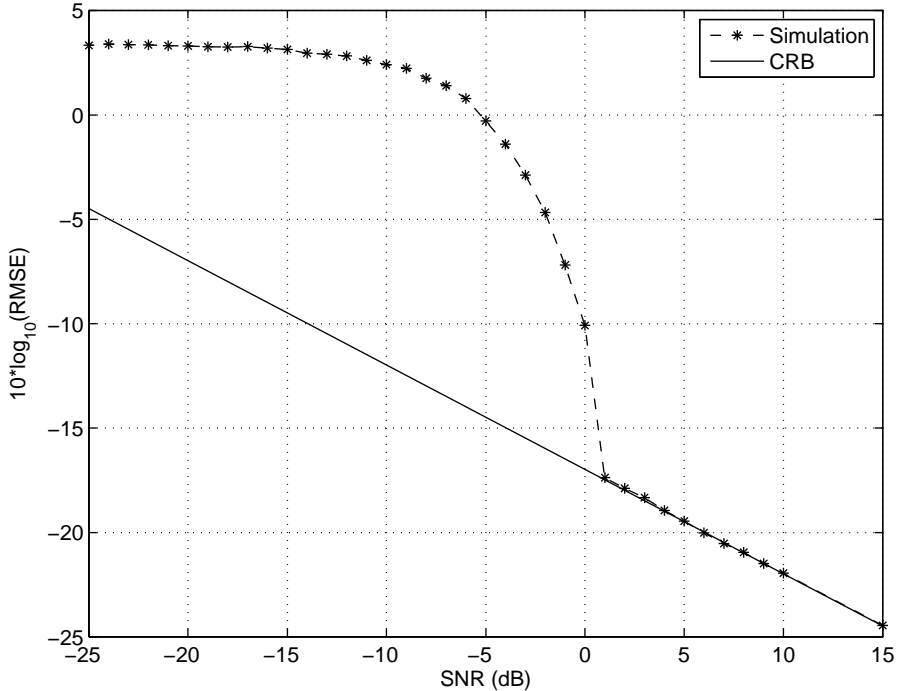


Figure 4.13: Frequency estimation RMSE versus SNR, known phase. $N = 16$, $\omega_a = 0.4\pi$, $\theta = \pi/6$.

In order to compute the BCRB, we need to evaluate the J_D and J_P terms in (4.190) and (4.191). The J_D term is equal to J_F in (4.231) because J_F does not depend on ω . The J_P term is

$$\begin{aligned}
 J_P &= E \left\{ -\frac{\partial^2 \ln p_\omega(\omega)}{\partial \omega^2} \right\} \\
 &= E \left\{ (a-1)(\pi + \omega)^{-2} + (a-1)(\pi - \omega)^{-2} \right\} \\
 &= \frac{a-1}{4\pi^2} \left[\frac{B(a-2, a)}{B(a, a)} + \frac{B(a, a-2)}{B(a, a)} \right] \\
 &= \frac{(a-1)(2a-1)}{\pi^2(a-2)}, \tag{4.238}
 \end{aligned}$$

which is valid for $a > 2$. Combining the two terms, the total Bayesian information is

$$J_B = \text{SNR} \frac{N(N-1)(2N-1)}{3} + \frac{(a-1)(2a-1)}{\pi^2(a-2)}. \tag{4.239}$$

The ECRB for this problem is equal to J_F^{-1} since J_F is not a function of ω . The BCRB is plotted versus SNR for several values of a in Figure 4.16, along with the ECRB. For large SNR, the BCRB converges to the ECRB, whereas for low SNR, it flattens out at the prior variance.

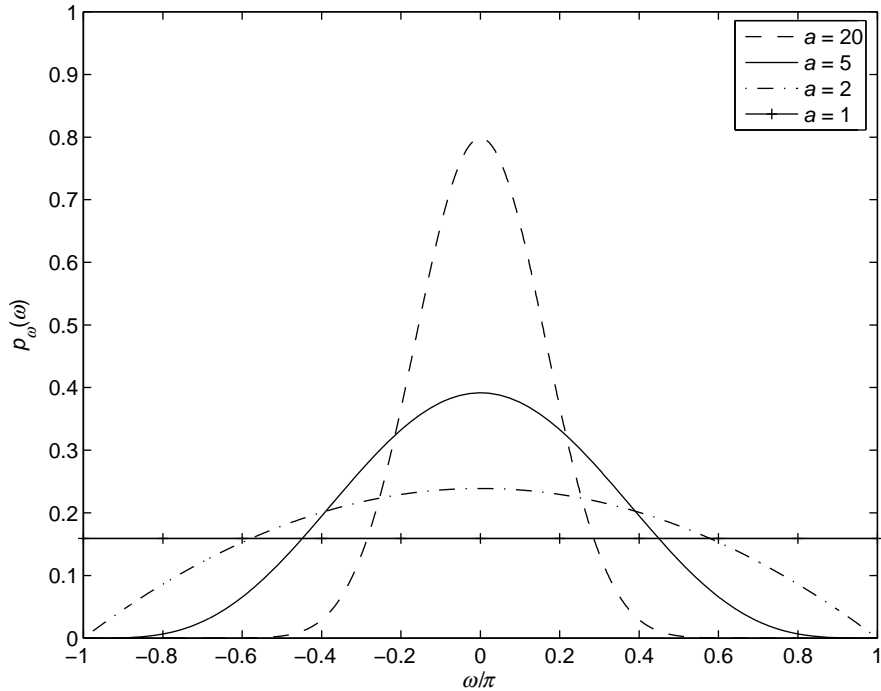


Figure 4.14: Family of probability densities $p_\omega(\omega)$.

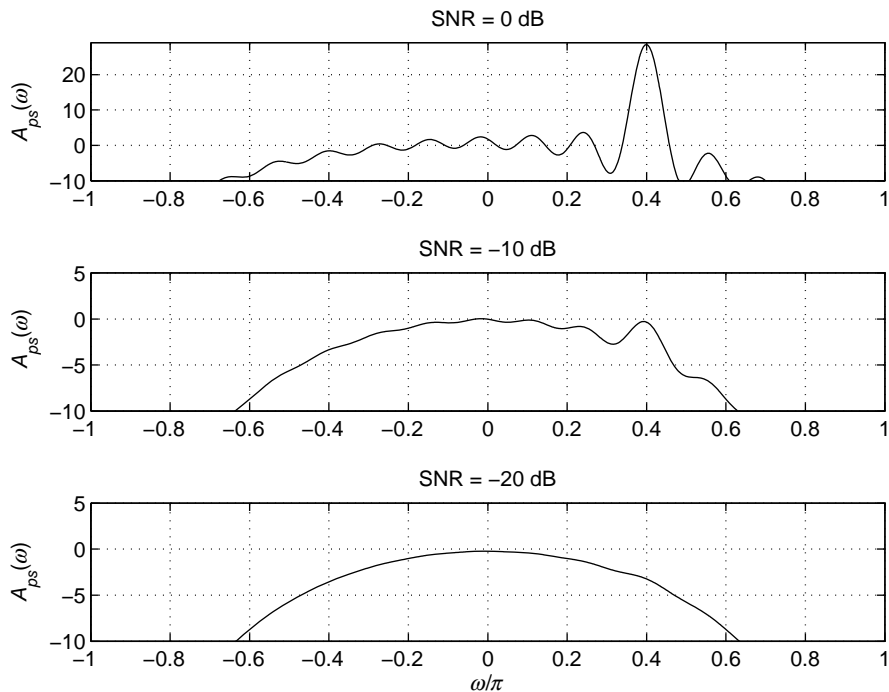


Figure 4.15: Posterior signal ambiguity surface, $A_{ps}(\omega)$. $a = 20$, $N = 16$, $\omega_a = 0.4\pi$, $\theta = \pi/6$.

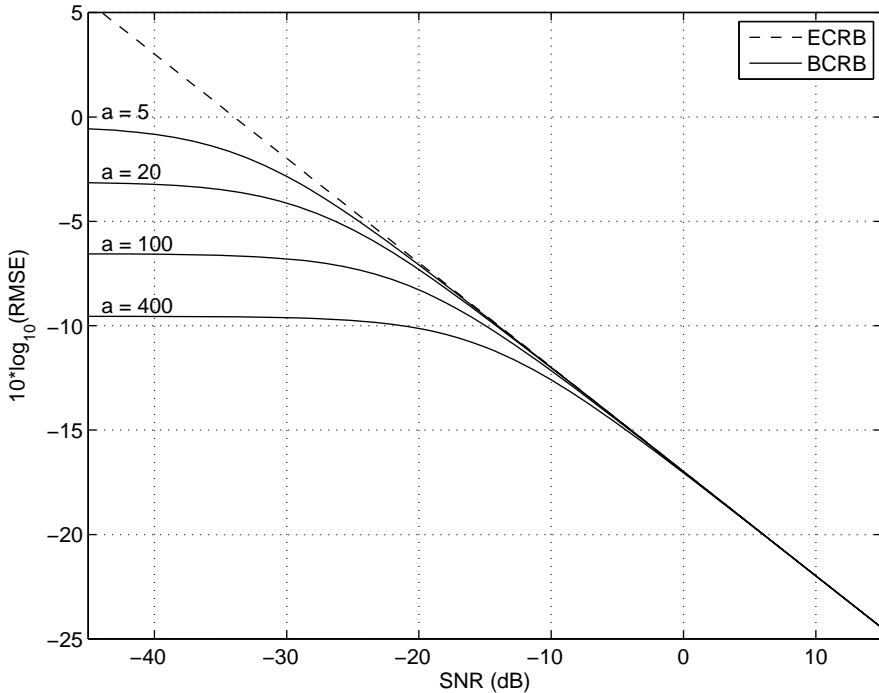


Figure 4.16: Bayesian Cramér–Rao bound versus SNR. $N = 16$.

The MAP and ML algorithms were simulated for $a = 20$ and various values of SNR. On each trial, the value of ω was drawn from the probability density in (4.233). The results from 10,000 trials are shown in Figure 4.17. The asymptotic performance of $\hat{\omega}_{\text{map}}(\tilde{\mathbf{R}})$ is the same as $\hat{\omega}_{\text{ml}}(\tilde{\mathbf{R}})$ and both converge to the BCRB/ECRB. The threshold occurs at the same SNR for both estimators, but for low SNR, prior knowledge keeps the MAP estimates close to the peak of the *a priori* density ($\omega = 0$) and $\hat{\omega}_{\text{map}}(\tilde{\mathbf{R}})$ has a lower MSE than $\hat{\omega}_{\text{ml}}(\tilde{\mathbf{R}})$. For low SNR, the ECRB exceeds the actual MSE of the ML estimate. It is not valid in this region because the ML estimate is biased. Like the CRB in Example 4.15, the BCRB does not predict the threshold and is a weak bound in the threshold region. However, it is a valid bound for all SNR because there is no unbiasedness assumption as in the CRB. ■

These examples show most of the important issues in the general nonlinear parameter estimation problem:

1. For high SNR, the estimate will, with high probability, be on the correct peak of the log-likelihood function and the error will be small.
2. As the SNR decreases, the estimator reaches a threshold and some of the estimates are near a subsidiary peak (sidelobe) in the ambiguity surface while others are randomly distributed due to noise.
3. As the SNR continues to decrease, the peaks are only due to noise and provide no useful information about the parameters.

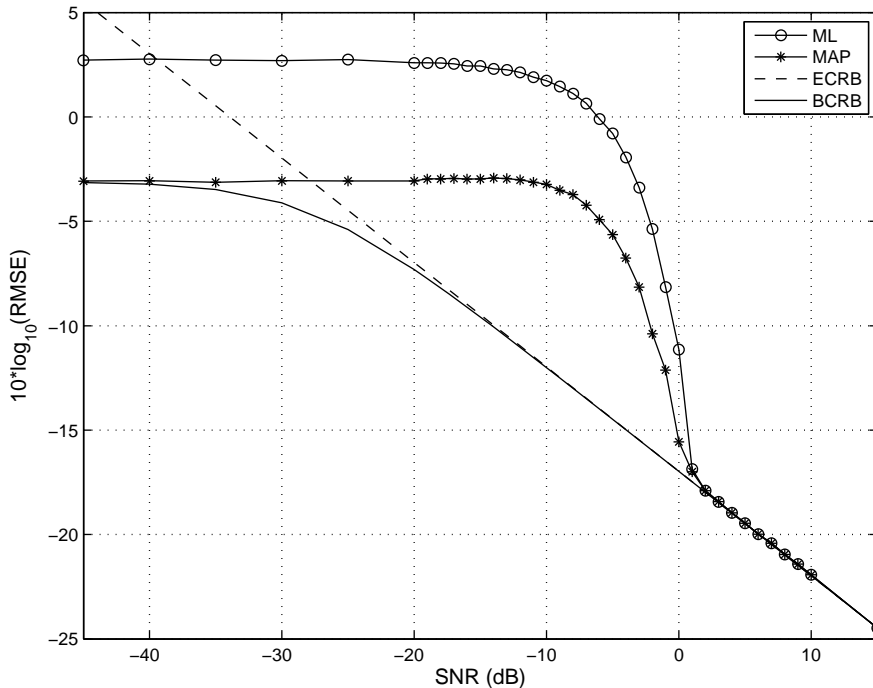


Figure 4.17: Frequency RMSE and BCRB versus SNR. $N = 16, \theta = \pi/6, a = 20$.

Accordingly, it is useful to consider three regions of operation in parameter estimation problems:

1. Small error or asymptotic region.
2. Threshold region.
3. Prior (no information, data irrelevant) region.

These regions are shown in Figures 4.18 and 4.19 using the results from Example 4.15.

The small error region generally corresponds to the case of high SNR (whose definition will depend on the specific problem) or a large number of independent observations (high N for the discrete-time case or long T for the continuous case).¹⁶ In the engineering literature, both cases are often referred to as the “asymptotic” region. In the statistical literature, only the high N /long T case is referred to as asymptotic. It is important to note that the behavior is due to two different phenomena and the analysis may be different (e.g. [IH81]).

As the SNR (or N) decreases, a point is reached at which ambiguous errors (or outliers) start to occur. These errors are usually large enough that even a few errors will cause an abrupt increase in the MSE. The location of this transition is called the threshold. The precise definition may depend on the problem but in most cases a suitable choice will be clear. When SNR and/or observation time are very small, the observations provide very

¹⁶In the continuous case, T is the length of the observation interval.

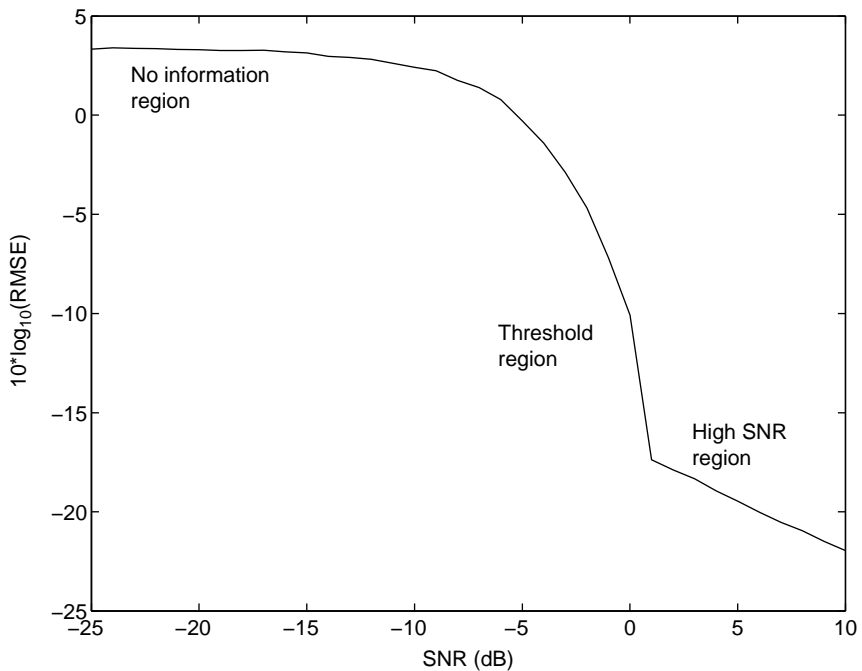


Figure 4.18: Frequency RMSE versus SNR. $N = 16$, $\omega_a = 0.4\pi$, $\theta = \pi/6$.

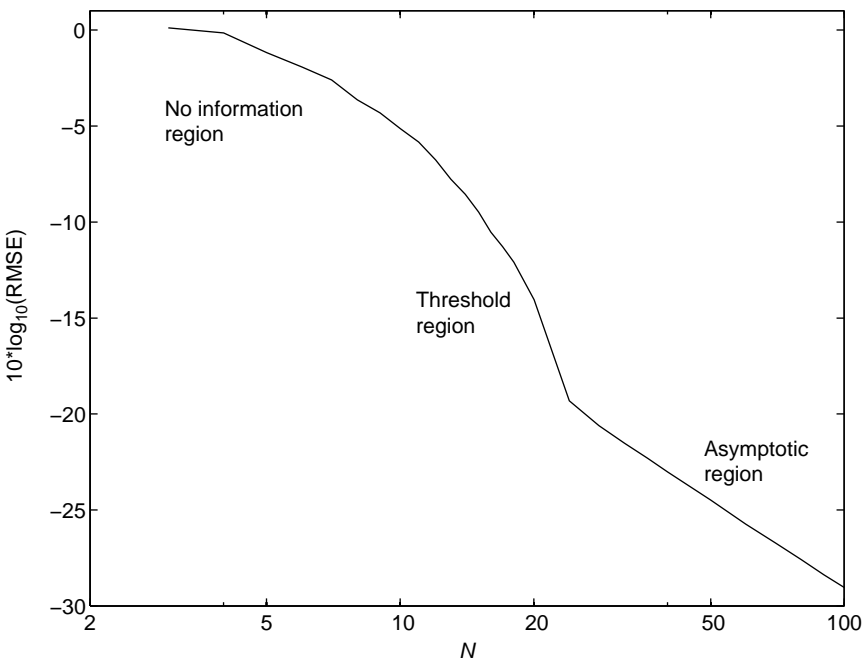


Figure 4.19: Frequency RMSE versus N . SNR = 0 dB, $\omega_a = 0.4\pi$, $\theta = \pi/6$.

little information and the RMSE is close to that obtained from prior knowledge about the problem (e.g., in Example 4.16, we know that $-\pi \leq \omega \leq \pi$).

Unfortunately, in almost all cases, it is difficult to evaluate the MSE and we must resort to simulation. In Section 4.4, we will develop lower bounds on the MSE that closely characterize performance in both the asymptotic and threshold regions, and accurately predict the location of the threshold.

4.2.5 Exponential Family

In this section, we introduce the exponential family of probability densities. Many of the probability densities that we encounter in practice belong to the exponential family and have a number of important properties. In the first section, we consider nonrandom parameters; in the second section, we consider random parameters.

4.2.5.1 Nonrandom Parameters

The exponential family is defined in terms of the likelihood function. We assume that we have N IID observations. The likelihood function for a single observation can be written the following form:

$$p_{r|a}(R|A) = C(R) \exp \{ \phi(A)S(R) - T(A) \}. \quad (4.240)$$

Note that $T(A)$ is just a normalization factor. The integral of $p_{r|a}(R|A)$ with respect to R is unity because it is a probability density. Thus,

$$\exp \{-T(A)\} \int C(R) \exp \{ \phi(A)S(R) \} dR = 1 \quad (4.241)$$

so

$$T(A) = \ln \left\{ \int C(R) \exp \{ \phi(A)S(R) \} dR \right\}. \quad (4.242)$$

The model is defined for the range of A where the integral in (4.241) is finite. Thus, the effect of A on the probability density is completely specified by $\phi(A)$.

The likelihood function for N IID observations is

$$p_{\mathbf{r}|a}(\mathbf{R}|A) = \left(\prod_{i=1}^N C(R_i) \right) \exp \left\{ \phi(A) \sum_{i=1}^N S(R_i) - NT(A) \right\}. \quad (4.243)$$

If we define the sufficient statistic as

$$S(\mathbf{R}) \triangleq \sum_{i=1}^N S(R_i) \quad (4.244)$$

and

$$C_N(\mathbf{R}) \triangleq \left(\prod_{i=1}^N C(R_i) \right), \quad (4.245)$$

then

$$p_{\mathbf{r}|a}(\mathbf{R}|A) = C_N(\mathbf{R}) \exp \{ \phi(A)S(\mathbf{R}) - NT(A) \}. \quad (4.246)$$

A special case occurs when

$$\phi(A) = A. \quad (4.247)$$

In this case, the parameter is referred to as a *natural parameter* of the density, which we will denote by θ . Then (4.246) can be written as

$$p_{\mathbf{R}|\theta}(\mathbf{R}|\theta) = C_N(\mathbf{R}) \exp \left\{ \theta S(\mathbf{R}) - NT(\theta) \right\}. \quad (4.248)$$

We refer to (4.248) as a *canonical form*.

We illustrate the notation with several examples.

Example 4.17 (continuation of Examples 4.2, 4.5, 4.7, and 4.13) Gaussian. Consider the Gaussian likelihood function where the variance σ_n^2 is known and the mean is the unknown parameter A . From (4.25),

$$p_{\mathbf{R}|a}(\mathbf{R}|A) = \frac{1}{(2\pi\sigma_n^2)^{N/2}} \exp \left\{ -\frac{1}{2\sigma_n^2} \left(\sum_{i=1}^N R_i^2 - 2A \sum_{i=1}^N R_i + NA^2 \right) \right\}. \quad (4.249)$$

Comparing (4.249) and (4.246), we have

$$C_N(\mathbf{R}) = \frac{1}{(2\pi\sigma_n^2)^{N/2}} \exp \left\{ -\frac{1}{2\sigma_n^2} \sum_{i=1}^N R_i^2 \right\}, \quad (4.250)$$

$$\phi(A) = A, \quad (4.251)$$

$$S(\mathbf{R}) = \frac{1}{\sigma_n^2} \sum_{i=1}^N R_i, \quad (4.252)$$

$$T(A) = \frac{A^2}{2\sigma_n^2}, \quad (4.253)$$

which results in a canonical form; thus, the mean is a natural parameter of the Gaussian density.

This representation is not unique because constant terms may be allocated arbitrarily. For instance we could also choose

$$\phi(A) = \frac{A}{\sigma_n^2}, \quad (4.254)$$

$$S(\mathbf{R}) = \sum_{i=1}^N R_i \quad (4.255)$$

and/or

$$C_N(\mathbf{R}) = \exp \left\{ -\frac{1}{2\sigma_n^2} \sum_{i=1}^N R_i^2 \right\}, \quad (4.256)$$

$$T(A) = \frac{A^2}{2\sigma_n^2} + \frac{1}{2} \ln (2\pi\sigma_n^2). \quad (4.257)$$

We generally try to choose a representation where $\phi(A)$ and $T(A)$ are as simple as possible. ■

Example 4.18 (continuation of Examples 4.4, 4.6, 4.8, and 4.14) Poisson. Consider the Poisson distribution where the rate is the unknown parameter. From (4.64),

$$\Pr(\mathbf{N}|A) = \frac{A^{\left(\sum_{i=1}^M N_i\right)}}{\prod_{i=1}^M N_i!} \exp\{-MA\}, \quad (4.258)$$

which can be rewritten as

$$\Pr(\mathbf{N}|A) = \frac{1}{\prod_{i=1}^M N_i!} \exp \left\{ (\ln A) \sum_{i=1}^M N_i \right\} \exp\{-MA\}. \quad (4.259)$$

Then

$$C_M(\mathbf{N}) = \left(\prod_{i=1}^M N_i! \right)^{-1}, \quad (4.260)$$

$$\phi(A) = \ln A, \quad (4.261)$$

$$S(\mathbf{N}) = \sum_{i=1}^M N_i, \quad (4.262)$$

$$T(A) = A. \quad (4.263)$$

Note that this is not in canonical form; therefore, the rate is not a natural parameter of the distribution. ■

Example 4.19 (continuation of Examples 4.10 and 4.11) Gamma. Consider the Gamma probability density where the shape parameter a is known and the scale parameter b is to be estimated. From (4.145),

$$\begin{aligned} p_{r|b}(\mathbf{R}|B) &= \left(\prod_{i=1}^N R_i^{a-1} \right) \left(\frac{1}{B^a \Gamma(a)} \right)^N \exp \left\{ -\frac{1}{B} \sum_{i=1}^N R_i \right\} \\ &= \left(\prod_{i=1}^N R_i^{a-1} \right) (\Gamma(a))^{-N} \exp \left\{ -\frac{1}{B} \sum_{i=1}^N R_i - Na \ln B \right\} \end{aligned} \quad (4.264)$$

The terms in the exponential family notation are

$$C_N(\mathbf{R}) = \frac{1}{\Gamma(a)^N} \left(\prod_{i=1}^N R_i^{a-1} \right), \quad (4.265)$$

$$\phi(B) = -\frac{1}{B}, \quad (4.266)$$

$$S(\mathbf{R}) = \sum_{i=1}^N R_i, \quad (4.267)$$

$$T(B) = a \ln B. \quad (4.268)$$

This is not in canonical form, however, we can put it into canonical form by choosing the parameter to be the inverse scale parameter

$$\beta = \frac{1}{B}. \quad (4.269)$$

Then $C_N(\mathbf{R})$ remains the same and

$$\phi(\beta) = \beta, \quad (4.270)$$

$$S(\mathbf{R}) = -\sum_{i=1}^N R_i, \quad (4.271)$$

$$T(\beta) = -a \ln \beta. \quad (4.272)$$

In general, we can always put the density in canonical form by transforming the parameter A to the natural parameter θ using

$$\theta = \phi(A). \quad (4.273)$$

■

Example 4.20 Weibull. Consider the Weibull density with known shape parameter α and unknown scale parameter b . We encountered the Weibull density previously in Example 2.14. The probability density function is

$$\begin{aligned} p_{\mathbf{r}|b}(\mathbf{R}|B) &= \left(\frac{\alpha}{B}\right)^N \prod_{i=1}^N \left(\frac{R_i}{B}\right)^{\alpha-1} \exp\left\{-\sum_{i=1}^N \left(\frac{R_i}{B}\right)^\alpha\right\} \\ &= \alpha^N \prod_{i=1}^N R_i^{\alpha-1} \exp\left\{-B^{-\alpha} \sum_{i=1}^N R_i^\alpha - N\alpha \ln B\right\}, \end{aligned} \quad (4.274)$$

and the exponential family representation is

$$C_N(\mathbf{R}) = \alpha^N \prod_{i=1}^N R_i^{\alpha-1}, \quad (4.275)$$

$$\phi(B) = -B^{-\alpha}, \quad (4.276)$$

$$S(\mathbf{R}) = \sum_{i=1}^N R_i^\alpha, \quad (4.277)$$

$$T(B) = \alpha \ln B. \quad (4.278)$$

■

The exponential family includes many of the probability densities that we will encounter in our applications. Continuous probability densities in the exponential family include Gaussian, Gamma (and therefore Exponential and Chi-squared), Beta, Weibull, and Inverse Gamma. Discrete probability densities include Poisson, Binomial (and therefore Bernoulli), and Negative Binomial (and therefore Geometric). We develop the exponential family form of some of these other densities in the problems.

We now develop several properties of the exponential family.

Property 1: Cumulants of $S(\mathbf{R})$. If the exponential family is written in canonical form (perhaps by transforming the original parameter), then the probability density has the form given in (4.248). The mean and variance (first two cumulants) of $S(\mathbf{R})$ given θ are

$$E\{S(\mathbf{R})|\theta\} = N \frac{dT(\theta)}{d\theta}, \quad (4.279)$$

$$\text{Var}\{S(\mathbf{R})|\theta\} = N \frac{d^2 T(\theta)}{d\theta^2}. \quad (4.280)$$

Proof. The moment generating function of $S(\mathbf{R})$ is

$$\begin{aligned} M_{S(\mathbf{R})}(t) &\triangleq E \left\{ e^{tS(\mathbf{R})} \right\} \\ &= \int C_N(\mathbf{R}) \exp \{(\theta + t)S(\mathbf{R}) - NT(\theta)\} d\mathbf{R} \\ &= \frac{e^{-NT(\theta)}}{e^{-NT(\theta+t)}} \int C_N(\mathbf{R}) \exp \{(\theta + t)S(\mathbf{R}) - NT(\theta + t)\} d\mathbf{R}. \end{aligned} \quad (4.281)$$

The integral is one, so

$$M_{S(\mathbf{R})}(t) = \exp \{-NT(\theta) + NT(\theta + t)\}. \quad (4.282)$$

Then

$$\begin{aligned} E \{ S(\mathbf{R}) | \theta \} &= \frac{d}{dt} M_{S(\mathbf{R})}(t) \Big|_{t=0} \\ &= \exp \{-NT(\theta) + NT(\theta + t)\} NT'(\theta + t) \Big|_{t=0} \\ &= NT'(\theta) \end{aligned} \quad (4.283)$$

$$\begin{aligned} E \{ S^2(\mathbf{R}) | \theta \} &= \frac{d^2}{dt^2} M_{S(\mathbf{R})}(t) \Big|_{t=0} \\ &= \exp \{-NT(\theta) + NT(\theta + t)\} [(NT'(\theta + t))^2 + NT''(\theta + t)] \Big|_{t=0} \\ &= (NT'(\theta))^2 + NT''(\theta), \end{aligned} \quad (4.284)$$

so

$$\text{Var} \{ S(\mathbf{R}) | \theta \} = E \{ S^2(\mathbf{R}) | \theta \} - [E \{ S(\mathbf{R}) | \theta \}]^2 = NT''(\theta). \quad (4.285)$$

We illustrate Property 1 with the following examples.

Example 4.21 (continuation of Examples 4.2, 4.5, 4.7, 4.13, and 4.17) Gaussian. This model is in canonical form with $\theta = a$. Using (4.253)

$$\frac{dT(A)}{dA} = \frac{A}{\sigma_n^2} \quad (4.286)$$

and

$$\frac{d^2T(A)}{dA^2} = \frac{1}{\sigma_n^2}. \quad (4.287)$$

Therefore,

$$\begin{aligned} E \{ S(\mathbf{R}) | A \} &= \frac{NA}{\sigma_n^2}, \\ \text{Var} \{ S(\mathbf{R}) | A \} &= \frac{N}{\sigma_n^2}. \end{aligned} \quad (4.288)$$

■

Example 4.22 (continuation of Examples 4.11 and 4.19) Gamma. This model is in canonical form if $\theta = \beta = B^{-1}$. From (4.272),

$$\frac{dT(\beta)}{d\beta} = -\frac{a}{\beta} \quad (4.289)$$

and

$$\frac{d^2T(\beta)}{d\beta^2} = \frac{a}{\beta^2}, \quad (4.290)$$

so the cumulants of the sufficient statistic defined in (4.271) are

$$E \{S(\mathbf{R})|\beta\} = -\frac{Na}{\beta} \quad (4.291)$$

and

$$\text{Var} \{S(\mathbf{R})|\beta\} = \frac{Na}{\beta^2}. \quad (4.292)$$

■

Property 2: Maximum likelihood estimate. The maximum likelihood estimate of A is given by

$$\left. \frac{T'(A)}{\phi'(A)} \right|_{A=\hat{a}_{\text{ml}}(\mathbf{R})} = \frac{S(\mathbf{R})}{N} \triangleq \bar{S}(\mathbf{R}). \quad (4.293)$$

Proof. The log of (4.246) is

$$\ln p_{\mathbf{R}|a}(\mathbf{R}|A) = \ln C_N(\mathbf{R}) + \phi(A)S(\mathbf{R}) - NT(A). \quad (4.294)$$

Differentiating with respect to A and setting the result equal to zero gives

$$\phi'(A) \frac{S(\mathbf{R})}{N} = T'(A) \quad (4.295)$$

or

$$\left. \frac{T'(A)}{\phi'(A)} \right|_{A=\hat{a}_{\text{ml}}(\mathbf{R})} = \frac{S(\mathbf{R})}{N} = \bar{S}(\mathbf{R}), \quad (4.296)$$

which must be solved to find $\hat{a}_{\text{ml}}(\mathbf{R})$.

In the canonical form,

$$\phi'(\theta) = 1. \quad (4.297)$$

Then, because of Property 1, $T'(\theta) = E \{S(R_i)|\theta\}$, and (4.296) may be written as

$$E \{S(R_i)|\theta\}|_{\theta=\hat{\theta}_{\text{ml}}(\mathbf{R})} = \bar{S}(\mathbf{R}). \quad (4.298)$$

Thus, the ML estimate is setting the statistical mean of $S(R_i)$ equal to the sample mean $\bar{S}(\mathbf{R})$.

Property 3: Cramér–Rao bound. The Cramér–Rao bound on any unbiased estimate is $J_F^{-1}(A)$, where

$$J_F(A) = N \frac{d^2 T(A)}{dA^2} - \frac{d^2 \phi(A)}{dA^2} E \{S(\mathbf{R})|A\}, \quad (4.299)$$

and, if the density is in canonical form

$$J_F(\theta) = N \frac{d^2 T(\theta)}{d\theta^2}. \quad (4.300)$$

Proof.

$$\begin{aligned} J_F(A) &= -E \left\{ \frac{d^2 \ln p_{\mathbf{r}|a}(\mathbf{R}|A)}{dA^2} \right\} \\ &= -E \left\{ \frac{d^2 \phi(A)}{dA^2} S(\mathbf{R}) - N \frac{d^2 T(A)}{dA^2} \right\} \\ &= N \frac{d^2 T(A)}{dA^2} - \frac{d^2 \phi(A)}{dA^2} E \{S(\mathbf{R})|A\}. \end{aligned} \quad (4.301)$$

In the canonical form,

$$\frac{d^2 \phi(\theta)}{d\theta^2} = 0, \quad (4.302)$$

so

$$J_F(\theta) = N \frac{d^2 T(\theta)}{d\theta^2}. \quad (4.303)$$

Property 4: Efficiency. The condition for equality in (4.95) and (4.104)

$$\frac{\partial \ln p_{\mathbf{r}|a}(\mathbf{R}|A)}{\partial A} = [\hat{a}_{\text{ml}}(\mathbf{R}) - A] J_F(A) \quad (4.304)$$

imposes a requirement on the structure of any $p_{\mathbf{r}|a}(\mathbf{R}|A)$ that satisfies the CRB with equality. Under suitable regularity conditions, one can show that $p_{\mathbf{r}|a}(\mathbf{R}|A)$ must be a member of the exponential family.

These results are due to Fend [Fen59]. His derivation is similar to the steps in (4.101)–(4.104) and the reader is referred to that reference for the detailed derivation. In the derivation, he requires that $\hat{a}_{\text{ml}}(\mathbf{R})$ must be a linear function of the sufficient statistic $S(\mathbf{R})$. Thus, being a member of the exponential family, or even having a canonical form, does not imply that an unbiased efficient estimate exists. Other references include [Wij73] and [Jos76] that discuss conditions on the densities.

Example 4.23 (continuation of Examples 4.2, 4.5, 4.7, 4.13, 4.17, and 4.21) Gaussian. This is in canonical form with $\phi'(A) = 1$ and

$$\frac{dT(A)}{dA} = \frac{A}{\sigma_n^2}, \quad (4.305)$$

so (4.293) reduces to

$$\frac{\hat{a}_{\text{ml}}(\mathbf{R})}{\sigma_n^2} = \frac{S(\mathbf{R})}{N} = \frac{1}{\sigma_n^2} \left(\frac{1}{N} \sum_{i=1}^N R_i \right) \quad (4.306)$$

or

$$\hat{a}_{\text{ml}}(\mathbf{R}) = \frac{1}{N} \sum_{i=1}^N R_i = \bar{R}, \quad (4.307)$$

which is familiar from Example 4.7, equation (4.122).

The Fisher information is

$$J_F(A) = N \frac{d^2 T(A)}{dA^2} = \frac{N}{\sigma_n^2} \quad (4.308)$$

which is familiar from (4.126). From (4.306), we see that the ML estimate is a linear function of the sufficient statistic, therefore it is an efficient estimate. \blacksquare

Example 4.24 (continuation of Examples 4.10, 4.11, 4.19, and 4.22) Gamma. In terms of the scale parameter b ,

$$\frac{d\phi(B)}{dB} = \frac{1}{B^2}, \quad (4.309)$$

$$\frac{d^2\phi(B)}{dB^2} = \frac{-2}{B^3}, \quad (4.310)$$

$$\frac{dT(B)}{dB} = \frac{a}{B}, \quad (4.311)$$

$$\frac{d^2T(B)}{dB^2} = \frac{-a}{B^2}, \quad (4.312)$$

and the ML estimate is found from (4.293),

$$\left. \frac{aB^{-1}}{B^{-2}} \right|_{B=\hat{b}_{\text{ml}}(\mathbf{R})} = \frac{S(\mathbf{R})}{N} \quad (4.313)$$

or

$$\hat{b}_{\text{ml}}(\mathbf{R}) = \frac{1}{Na} S(\mathbf{R}) = \frac{1}{Na} \sum_{i=1}^N R_i = \frac{\bar{R}}{a}, \quad (4.314)$$

which is familiar from Example 4.10, equation (4.148). From (4.299),

$$J_F(B) = -\frac{Na}{B^2} + \frac{2}{B^3} E\{S(\mathbf{R})|B\}. \quad (4.315)$$

The expectation is

$$E\{S(\mathbf{R})|B\} = E\left\{\sum_{i=1}^N R_i\right\} = NaB. \quad (4.316)$$

Using (4.316) in (4.315) gives

$$J_F(B) = \frac{Na}{B^2}, \quad (4.317)$$

which is the same as (4.151). From (4.314), we see that the ML estimate of b is a linear function of its sufficient statistic, therefore it is an efficient estimate.

In terms of the inverse scale parameter β , we use $\phi'(\beta) = 1$, (4.289), and (4.271) in (4.293) to obtain

$$\hat{\beta}_{\text{ml}}(\mathbf{R}) = \frac{-a}{S(\mathbf{R})} = \frac{a}{\frac{1}{N} \sum_{i=1}^N R_i} = \frac{a}{\bar{R}}, \quad (4.318)$$

which is the same as (4.157) in Example 4.11.

The Fisher information for β is obtained by substituting (4.290) into (4.303), which gives

$$J_F(\beta) = N \frac{d^2 T(\beta)}{d\beta^2} = \frac{Na}{\beta^2}, \quad (4.319)$$

which agrees with (4.161). In this case, the ML estimate in (4.318) is not a linear function of the sufficient statistic, therefore it is not an efficient estimate. ■

4.2.5.2 Random Parameters

In this section, we discuss exponential family models where the parameter a or θ is a random variable. The relations in (4.240)–(4.248) apply except that a or θ is a random variable with an *a priori* density $p_a(A)$ or $p_\theta(\theta)$.

Our first result is to show how to determine the conjugate prior from the likelihood function when it is written in the exponential family form.

Property 5: Conjugate prior. From (4.246), the likelihood function can be written as

$$p_{\mathbf{r}|a}(\mathbf{R}|A) = C_N(\mathbf{R}) \exp \{ \phi(A) S(\mathbf{R}) - NT(A) \}. \quad (4.320)$$

If we assume the prior has the form

$$p_a(A) = C_0 \exp \{ \phi(A) S_0 - N_0 T(A) \}, \quad (4.321)$$

then the posterior density is given by

$$\begin{aligned} p_{a|\mathbf{r}}(A|\mathbf{R}) &= \frac{p_{\mathbf{r}|a}(\mathbf{R}|A)p_a(A)}{p_{\mathbf{r}}(\mathbf{R})} \\ &= \frac{C_N(\mathbf{R})C_0}{p_{\mathbf{r}}(\mathbf{R})} \exp \{ \phi(A)[S(\mathbf{R}) + S_0] - (N + N_0)T(A) \} \\ &= C_p(\mathbf{R}) \exp \{ \phi(A)S_p(\mathbf{R}) - N_p T(A) \}, \end{aligned} \quad (4.322)$$

where

$$C_p(\mathbf{R}) \triangleq \frac{C_N(\mathbf{R})C_0}{p_{\mathbf{r}}(\mathbf{R})}, \quad (4.323)$$

$$S_p(\mathbf{R}) \triangleq S(\mathbf{R}) + S_0, \quad (4.324)$$

$$N_p \triangleq N + N_0. \quad (4.325)$$

We see that the posterior density has the same form as the prior density with respect to the parameter A . The functions $\phi(A)$ and $T(A)$ determine the form of the prior and posterior densities. The prior hyperparameters will be a function of S_0 and N_0 and the posterior hyperparameters will be a function of $S_p(\mathbf{R})$ and N_p .

The posterior density also has the same form as the likelihood function with respect to the parameter A . We can interpret $S_p(\mathbf{R})$ as an *a posteriori* sufficient statistic and N_p as an increase in the effective number of observations.

Property 6: MAP estimate. The MAP estimate of a is given by

$$\left. \frac{T'(A)}{\phi'(A)} \right|_{A=\hat{a}_{\text{map}}(\mathbf{R})} = \frac{1}{N_p} S_p(\mathbf{R}) \triangleq \bar{S}_p(\mathbf{R}). \quad (4.326)$$

Proof. The proof is the same as for the ML estimate in Property 2 with $p_{a|\mathbf{r}}(A|\mathbf{R})$ replacing $p_{\mathbf{r}|a}(\mathbf{R}|A)$, $S_p(\mathbf{R})$ replacing $S(\mathbf{R})$, and N_p replacing N .

Property 7: Bayesian Cramér–Rao bound. The Bayesian information is given by

$$J_B = E_a \left\{ N_p \frac{d^2 T(A)}{dA^2} - \frac{d^2 \phi(A)}{dA^2} E[S_p(\mathbf{R})|A] \right\} \quad (4.327)$$

and, if the density is in canonical form

$$J_B = N_p E_\theta \left\{ \frac{d^2 T(\theta)}{d\theta^2} \right\}. \quad (4.328)$$

Proof.

$$\begin{aligned} J_B &= -E_{\mathbf{r},a} \left\{ \frac{d^2 \ln p_{\mathbf{r},a}(\mathbf{R}, A)}{dA^2} \right\} \\ &= -E_{\mathbf{r},a} \left\{ \frac{d^2 \ln p_{a|\mathbf{r}}(A|\mathbf{R})}{dA^2} + \frac{d^2 \ln p_{\mathbf{r}}(\mathbf{R})}{dA^2} \right\} \\ &= -E_{\mathbf{r},a} \left\{ \frac{d^2 \phi(A)}{dA^2} S_p(\mathbf{R}) - N_p \frac{d^2 T(A)}{dA^2} \right\} \\ &= E_a \left\{ N_p \frac{d^2 T(A)}{dA^2} - \frac{d^2 \phi(A)}{dA^2} E[S_p(\mathbf{R})|A] \right\}. \end{aligned} \quad (4.329)$$

In the canonical form

$$\frac{d^2 \phi(\theta)}{d\theta^2} = 0, \quad (4.330)$$

so

$$J_B = N_p E_\theta \left\{ \frac{d^2 T(\theta)}{d\theta^2} \right\}. \quad (4.331)$$

We illustrate these properties with the Gamma likelihood function that we encountered in Example 4.19.

Example 4.25 (continuation of Examples 4.10, 4.19, and 4.24) Gamma. We consider the Gamma likelihood function in Example 4.19 with known shape parameter a and unknown

scale parameter b . From (4.266)–(4.268),

$$\phi(B) = -\frac{1}{B}, \quad (4.332)$$

$$T(B) = a \ln B, \quad (4.333)$$

$$S(\mathbf{R}) = \sum_{i=1}^N R_i = N\bar{R}. \quad (4.334)$$

Using (4.321), the conjugate prior density has the form

$$p_b(B) = C_0 \exp \left\{ -\frac{1}{B} S_0 - N_0 a \ln B \right\} = C_0 B^{-aN_0} \exp \left\{ -\frac{S_0}{B} \right\}. \quad (4.335)$$

We recognize this as an Inverse Gamma probability density. The standard form is

$$p_x(X) = \frac{1}{b_0^{\alpha_0} \Gamma(\alpha_0)} X^{-\alpha_0-1} \exp \left\{ -\frac{1}{X b_0} \right\}, \quad (4.336)$$

with shape parameter α_0 and scale parameter b_0 , where $\alpha_0 > 0, b_0 > 0$. In Figure 4.20, we show the Inverse Gamma density for several values of α_0 . The parameter b_0 just scales the density.

Thus, the prior hyperparameters are

$$\alpha_0 = aN_0 - 1 \quad (4.337)$$

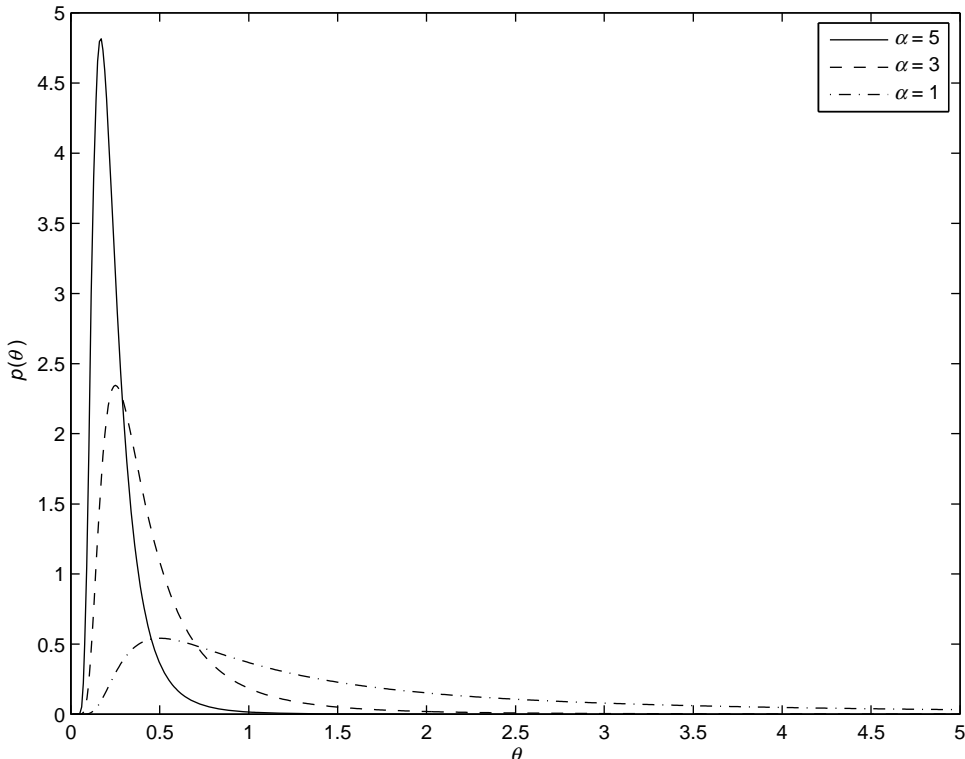


Figure 4.20: Inverse Gamma probability density: $b_0 = 1$; $\alpha_0 = 1, 3$, and 5 .

and

$$b_0 = S_0^{-1}, \quad (4.338)$$

and the normalizing constant in (4.335) is

$$C_0 = \frac{1}{b_0^{\alpha_0} \Gamma(\alpha_0)}. \quad (4.339)$$

Using (4.322), the *a posteriori* density is

$$\begin{aligned} p_{b|\mathbf{R}}(B|\mathbf{R}) &= C_p(\mathbf{R}) \exp \left\{ -\frac{1}{B} S_p(\mathbf{R}) - N_p a \ln B \right\} \\ &= C_p(\mathbf{R}) B^{-aN_p} \exp \left\{ -\frac{S_p(\mathbf{R})}{B} \right\}, \end{aligned} \quad (4.340)$$

which is an Inverse Gamma density with posterior hyperparameters

$$\alpha_p = aN_p - 1 = a(N + N_0) - 1 = \alpha_0 + aN \quad (4.341)$$

and

$$b_p(\mathbf{R}) = S_p(\mathbf{R})^{-1} = (S(\mathbf{R}) + S_0)^{-1} = (N\bar{R} + b_0^{-1})^{-1}. \quad (4.342)$$

Using Properties 2 and 6, the MAP estimate has the same form as the ML estimate with $\bar{S}_p(\mathbf{R})$ replacing $\bar{S}(\mathbf{R})$ and N_p replacing N in (4.314). Thus,

$$\hat{b}_{\text{map}}(\mathbf{R}) = \frac{1}{N_p a} S_p(\mathbf{R}) = \frac{N\bar{R} + b_0^{-1}}{Na + \alpha_0 + 1} = \frac{1}{b_p(\mathbf{R})(\alpha_p + 1)}, \quad (4.343)$$

which is the mode of the posterior density. We see that as $N \rightarrow \infty$, $\hat{b}_{\text{map}}(\mathbf{R}) \rightarrow \hat{b}_{\text{ml}}(\mathbf{R}) = \bar{R}/a$ and as $N \rightarrow 0$, $\hat{b}_{\text{map}}(\mathbf{R}) \rightarrow 1/b_0(\alpha_0 + 1)$, the mode of the prior density.

In this case, the moments of the *a posteriori* density are available, so we can find $\hat{b}_{\text{ms}}(\mathbf{R})$ and the mean-square error. The MMSE estimate is the conditional mean,

$$\hat{b}_{\text{ms}}(\mathbf{R}) = \frac{1}{b_p(\mathbf{R})(\alpha_p - 1)}, \quad \text{for } \alpha_p > 1 \quad (4.344)$$

$$= \frac{N\bar{R} + b_0^{-1}}{Na + \alpha_0 - 1}. \quad (4.345)$$

As $N \rightarrow \infty$, $\hat{b}_{\text{ms}}(\mathbf{R}) \rightarrow \hat{b}_{\text{ml}}(\mathbf{R}) = \bar{R}/a$ and as $N \rightarrow 0$, $\hat{b}_{\text{ms}}(\mathbf{R}) \rightarrow 1/b_0(\alpha_0 - 1)$, the mean of the prior density.

The mean-square error is the expected value of the conditional variance,

$$\begin{aligned} \text{MSE} \{ \hat{b}_{\text{ms}}(\mathbf{R}) \} &= E_{\mathbf{r}} \left\{ \frac{1}{b_p(\mathbf{R})^2 (\alpha_p - 1)^2 (\alpha_p - 2)} \right\}, \quad \text{for } \alpha_p > 2 \\ &= \frac{E_{\mathbf{r}} \{ S_p(\mathbf{R})^2 \}}{(Na + \alpha_0 - 1)^2 (Na + \alpha_0 - 2)}. \end{aligned} \quad (4.346)$$

To evaluate this expression, we note that from (4.342), $S_p(\mathbf{R}) = S(\mathbf{R}) + b_0^{-1}$ and from (4.334), $S(\mathbf{R})$ is the sum of N IID Gamma(a, b) random variables, therefore it is a Gamma(Na, b) random variable. Then

$$E_{\mathbf{r}|b} \{S_p(\mathbf{R})|B\} = E_{\mathbf{r}|b} \{S(\mathbf{R})|B\} + b_0^{-1} = NaB + b_0^{-1}. \quad (4.347)$$

$$\begin{aligned} E_{\mathbf{r}|b} \{S_p(\mathbf{R})^2|B\} &= E_{\mathbf{r}|b} \{S(\mathbf{R})^2|B\} + 2b_0^{-1}E_{\mathbf{r}|b} \{S(\mathbf{R})|B\} + b_0^{-2} \\ &= (Na + N^2a^2)B^2 + 2b_0^{-1}NaB + b_0^{-2}. \end{aligned} \quad (4.348)$$

Next we use the properties of the Inverse Gamma density to obtain the first two moments of b ,

$$E_b \{B\} = \frac{1}{b_0(\alpha_0 - 1)}, \quad (4.349)$$

$$E_b \{B^2\} = \frac{1}{b_0^2(\alpha_0 - 1)(\alpha_0 - 2)}. \quad (4.350)$$

Then

$$\begin{aligned} E_{\mathbf{r}} \{S_p(\mathbf{R})^2\} &= E_b \{E_{\mathbf{r}|b} \{S_p(\mathbf{R})^2|B\}\} \\ &= (Na + N^2a^2)E_b \{B^2\} + 2b_0^{-1}NaE_b \{B\} + b_0^{-2} \\ &= \frac{(Na + \alpha_0 - 1)(Na + \alpha_0 - 2)}{b_0^2(\alpha_0 - 1)(\alpha_0 - 2)}. \end{aligned} \quad (4.351)$$

Substituting (4.351) into (4.346), we have

$$\text{MSE} \{\hat{b}_{\text{ms}}(\mathbf{R})\} = \frac{1}{b_0^2(Na + \alpha_0 - 1)(\alpha_0 - 1)(\alpha_0 - 2)}. \quad (4.352)$$

To find the BCRB, we use Property 7,

$$J_B = E_b \left\{ N_p \frac{d^2 T(B)}{dB^2} - \frac{d^2 \phi(B)}{dB^2} E \{S_p(\mathbf{R})|B\} \right\}. \quad (4.353)$$

Using (4.310), (4.312), and (4.347), we have

$$\begin{aligned} J_B &= E_b \left\{ -\frac{N_p a}{B^2} + \frac{2}{B^3}(NaB + b_0^{-1}) \right\} \\ &= (Na - \alpha_0 - 1)E_b \{B^{-2}\} + 2b_0^{-1}E_b \{B^{-3}\}. \end{aligned} \quad (4.354)$$

We note that b^{-1} is a Gamma(α_0, b_0) random variable, so

$$E \{B^{-2}\} = \alpha_0(\alpha_0 + 1)b_0^2, \quad (4.355)$$

$$E \{B^{-3}\} = \alpha_0(\alpha_0 + 1)(\alpha_0 + 2)b_0^3. \quad (4.356)$$

Substituting (4.355) and (4.356) in (4.354), the Bayesian information is

$$J_B = b_0^2(Na + \alpha_0 + 3)\alpha_0(\alpha_0 + 1). \quad (4.357)$$

Using the expression for $J_F(B)$ in (4.151), the ECRB is

$$\begin{aligned} \text{ECRB} &= E_b \{J_F^{-1}(B)\} \\ &= E_b \left\{ \frac{B^2}{Na} \right\} \\ &= \frac{1}{b_0^2 Na(\alpha_0 - 1)(\alpha_0 - 2)}. \end{aligned} \quad (4.358)$$

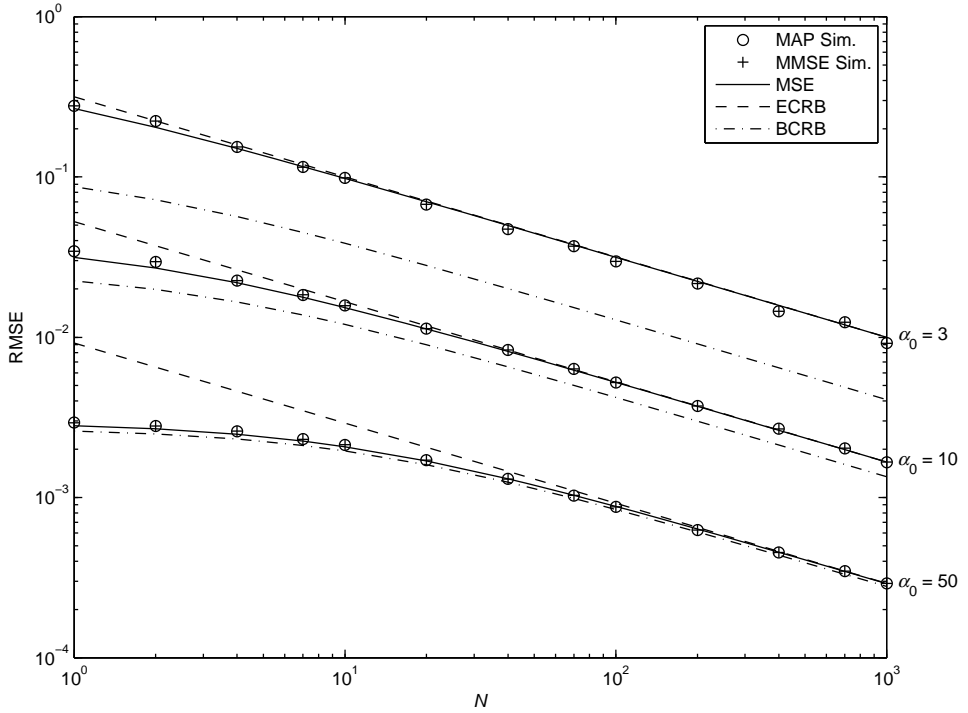


Figure 4.21: Mean-square error of MAP and MMSE estimates and BCRB versus N ; $\alpha_0 = 3, 10, 50$, $b_0 = 1$, and $a = 5$.

It can easily be seen that minimum MSE in (4.352) is strictly greater than J_B^{-1} in (4.357) and approaches the ECRB in (4.358) as $N \rightarrow \infty$.

In Figure 4.21, we plot the MSE, BCRB, and ECRB for $\alpha_0 = 3, 10$, and 50 , $b_0 = 1$, and $a = 5$. We also plot the simulated MSE for $\hat{b}_{\text{map}}(\mathbf{R})$ and $\hat{b}_{\text{ms}}(\mathbf{R})$. In this case, the two estimators have essentially identical MSE, as given in (4.352). The BCRB is less than the MSE, but it is closer for larger α_0 . ■

This example illustrates the relationship of the exponential family and the conjugate prior. A number of references give the conjugate priors for various likelihood functions (e.g. [GCSR04]). In Appendix A, we provide a partial list of conjugate prior densities for distributions in the exponential family.

4.2.6 Summary of Scalar Parameter Estimation

For nonrandom parameter estimation the key results are as follows:

1. The maximum likelihood estimate $\hat{a}_{\text{ml}}(\mathbf{R})$ is the value of A where the likelihood function $p_{\mathbf{r}|a}(\mathbf{R}|A)$ achieves its maximum.
2. The variance of any unbiased estimate of A is lower bounded by the Cramér–Rao bound.

3. Under suitable regularity conditions, $\hat{a}_{\text{ml}}(\mathbf{R})$ is unbiased and approaches the CRB asymptotically.
4. If the parameter is embedded in the signal in a nonlinear manner, then a threshold behavior will occur as the SNR or number of observations decreases.
5. If the likelihood function is in the exponential family, then a number of useful properties are available.

For Bayesian estimation, the key results are as follows:

1. For a quadratic cost function, the MMSE estimate is the mean of the *a posteriori* density.
2. The MAP estimate is the mode of the *a posteriori* density. We often use it when $\hat{a}_{\text{ms}}(\mathbf{R})$ is difficult to find.
3. The MSE of any Bayesian estimator is lower bounded by the Bayesian Cramér–Rao bound.
4. The MMSE estimate and the MAP estimate approach the ML estimate asymptotically and their MSE approaches the ECRB.
5. Bayesian estimates exhibit a similar threshold behavior to ML estimates as the SNR or the number of observations decreases.
6. The conjugate prior may be determined explicitly when the likelihood function is in the exponential family.

In the next section, we consider the vector parameter estimation problem.

4.3 MULTIPLE PARAMETER ESTIMATION

In many problems of interest we shall want to estimate more than one parameter. A familiar example is the radar problem in which we shall estimate the range and velocity of a target. Most of the ideas and techniques developed for scalar parameter estimation can be extended to the multiple parameter case in a straightforward manner. The model is shown in Figure 4.22. If there are K parameters, a_1, a_2, \dots, a_K , we describe them by a parameter vector \mathbf{a} in a K -dimensional space. The other elements of the model are the same as before. We shall consider both the case in which \mathbf{a} is a random parameter vector and that in which \mathbf{a} is a nonrandom parameter vector. Three issues are of interest. In each the result is the vector analog to a result in the scalar case.

1. Estimation procedures
2. Measures of error
3. Bounds on performance.

4.3.1 Estimation Procedures

4.3.1.1 Random Parameters

For random variables we could consider the general case of Bayes estimation in which we minimize the risk for some arbitrary scalar cost function $C(\mathbf{a}, \hat{\mathbf{a}})$, but for our purposes it is

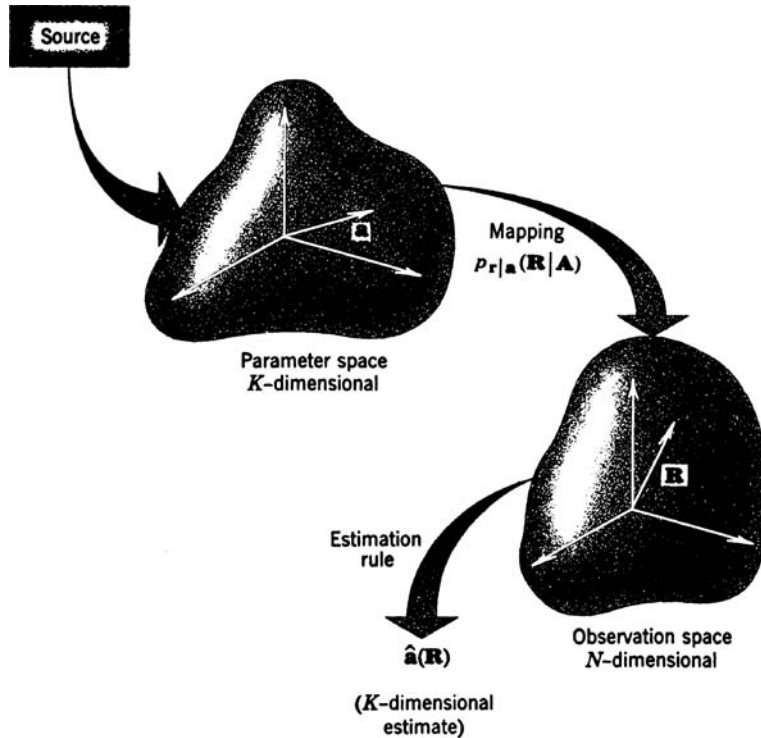


Figure 4.22: Multiple parameter estimation model.

adequate to consider only cost functions that depend on the error. We define the error vector as

$$\mathbf{a}_\epsilon(\mathbf{R}) = \begin{bmatrix} \hat{a}_1(\mathbf{R}) - a_1 \\ \hat{a}_2(\mathbf{R}) - a_2 \\ \vdots \\ \hat{a}_K(\mathbf{R}) - a_K \end{bmatrix} = \hat{\mathbf{a}}(\mathbf{R}) - \mathbf{a}. \quad (4.359)$$

For a mean-square error criterion, the cost function is simply

$$C(\mathbf{a}_\epsilon(\mathbf{R})) \triangleq \sum_{i=1}^K a_{\epsilon_i}^2(\mathbf{R}) = \mathbf{a}_\epsilon(\mathbf{R})^T \mathbf{a}_\epsilon(\mathbf{R}). \quad (4.360)$$

This is just the sum of the squares of the errors. The risk is

$$\mathcal{R}_{\text{ms}} = \int_{-\infty}^{\infty} \int_{-\infty}^{\infty} C(\mathbf{a}_\epsilon(\mathbf{R})) p_{r,a}(\mathbf{R}, \mathbf{A}) d\mathbf{R} d\mathbf{A} \quad (4.361)$$

or

$$\mathcal{R}_{\text{ms}} = \int_{-\infty}^{\infty} p_r(\mathbf{R}) d\mathbf{R} \int_{-\infty}^{\infty} \left[\sum_{i=1}^K (\hat{a}_i(\mathbf{R}) - a_i)^2 \right] p_{r|a}(\mathbf{R}|\mathbf{A}) d\mathbf{A}. \quad (4.362)$$

As before, we can minimize the inner integral for each \mathbf{R} . Because the terms in the sum are positive, we minimize them separately. This gives

$$\hat{a}_{ms_i}(\mathbf{R}) = \int_{-\infty}^{\infty} A_i p_{\mathbf{a}|\mathbf{r}}(\mathbf{A}|\mathbf{R}) d\mathbf{A} \quad (4.363)$$

or

$$\hat{\mathbf{a}}_{ms}(\mathbf{R}) = \int_{-\infty}^{\infty} \mathbf{A} p_{\mathbf{a}|\mathbf{r}}(\mathbf{A}|\mathbf{R}) d\mathbf{A}. \quad (4.364)$$

It is easy to show that MMSE estimation commutes over *linear transformations*. Thus, if

$$\mathbf{d} = \mathbf{\Gamma}\mathbf{a}, \quad (4.365)$$

where $\mathbf{\Gamma}$ is an $L \times K$ matrix, and we want to minimize

$$E[\mathbf{d}_e(\mathbf{R})^T \mathbf{d}_e(\mathbf{R})] = E \left[\sum_{i=1}^L d_{\epsilon_i}^2(\mathbf{R}) \right], \quad (4.366)$$

the result will be,

$$\hat{\mathbf{d}}_{ms}(\mathbf{R}) = \mathbf{\Gamma}\hat{\mathbf{a}}_{ms}(\mathbf{R}). \quad (4.367)$$

For MAP estimation, we must find the value of \mathbf{A} that maximizes the *a posteriori* probability density $p_{\mathbf{a}|\mathbf{r}}(\mathbf{A}|\mathbf{R})$

$$\hat{\mathbf{a}}_{map}(\mathbf{R}) = \underset{\mathbf{A}}{\operatorname{argmax}} \{ p_{\mathbf{a}|\mathbf{r}}(\mathbf{A}|\mathbf{R}) \}. \quad (4.368)$$

Note that we have to search over a K -dimensional space to find the maximum. Later in the text, we will discuss efficient search techniques. If the maximum is interior and $\partial \ln p_{\mathbf{a}|\mathbf{r}}(\mathbf{A}|\mathbf{R}) / \partial A_i$ exists at the maximum then a necessary condition is obtained from the MAP equations. We take the logarithm of $p_{\mathbf{a}|\mathbf{r}}(\mathbf{A}|\mathbf{R})$, differentiate with respect to each parameter A_i , $i = 1, 2, \dots, K$, and set the result equal to zero. This gives a set of K simultaneous equations:

$$\frac{\partial \ln p_{\mathbf{a}|\mathbf{r}}(\mathbf{A}|\mathbf{R})}{\partial A_i} \Big|_{\mathbf{A}=\hat{\mathbf{a}}_{map}(\mathbf{R})} = 0, \quad i = 1, 2, \dots, K. \quad (4.369)$$

We can write (4.369) in a more compact manner by defining a partial derivative matrix operator

$$\nabla_{\mathbf{A}} \triangleq \begin{bmatrix} \frac{\partial}{\partial A_1} \\ \frac{\partial}{\partial A_2} \\ \vdots \\ \frac{\partial}{\partial A_K} \end{bmatrix}. \quad (4.370)$$

This operator can be applied only to $1 \times m$ matrices; for example,

$$\nabla_{\mathbf{A}} \mathbf{G} = \begin{bmatrix} \frac{\partial G_1}{\partial A_1} & \frac{\partial G_2}{\partial A_1} & \dots & \frac{\partial G_m}{\partial A_1} \\ \vdots & \vdots & \dots & \vdots \\ \frac{\partial G_1}{\partial A_K} & \frac{\partial G_2}{\partial A_K} & \dots & \frac{\partial G_m}{\partial A_K} \end{bmatrix}. \quad (4.371)$$

Several useful properties of $\nabla_{\mathbf{A}}$ are developed in Problems 4.3.1–4.3.2. In our case (4.369) becomes a single vector equation,

$$[\nabla_{\mathbf{A}} \ln p_{\mathbf{a}|\mathbf{r}}(\mathbf{A}|\mathbf{R})] \Big|_{\mathbf{A}=\hat{\mathbf{a}}_{\text{map}}(\mathbf{R})} = \mathbf{0}. \quad (4.372)$$

4.3.1.2 Nonrandom Parameters

Similarity, for ML estimates we must find the value of \mathbf{A} that maximizes $p_{\mathbf{r}|\mathbf{a}}(\mathbf{R}|\mathbf{A})$.

$$\hat{\mathbf{a}}_{\text{ml}}(\mathbf{R}) = \underset{\mathbf{A}}{\operatorname{argmax}} \{p_{\mathbf{r}|\mathbf{a}}(\mathbf{R}|\mathbf{A})\}. \quad (4.373)$$

Once again, we have to search over a K -dimensional space to find the maximum. If the maximum is interior and $\partial \ln p_{\mathbf{r}|\mathbf{a}}(\mathbf{R}|\mathbf{A})/\partial A_i$ exists at the maximum then a necessary condition is obtained from the likelihood equations:

$$[\nabla_{\mathbf{A}} \ln p_{\mathbf{r}|\mathbf{a}}(\mathbf{R}|\mathbf{A})] \Big|_{\mathbf{A}=\hat{\mathbf{a}}_{\text{ml}}(\mathbf{R})} = \mathbf{0}. \quad (4.374)$$

4.3.2 Measures of Error

For scalar parameters, we used the mean-square error, $E[a_\epsilon^2]$ as the measure of error for random parameters and the bias, $E[a_\epsilon]$, and the variance, $\text{Var}[a_\epsilon]$, as the measures of error for nonrandom parameters. In this section, we extend these measures to vector parameters.

4.3.2.1 Nonrandom Parameters

For nonrandom variables the first measure of interest is the bias. Now the bias is a vector,

$$\mathbf{B}(\mathbf{A}) \triangleq E[\mathbf{a}_\epsilon(\mathbf{R})] = E[\hat{\mathbf{a}}(\mathbf{R})] - \mathbf{A}. \quad (4.375)$$

If each component of the bias vector is zero for every \mathbf{A} , we say that the estimate is unbiased.

In the single parameter case, a rough measure of the spread of the error was given by the variance of the estimate. In the special case in which $a_\epsilon(\mathbf{R})$ was Gaussian this provided a complete description:

$$p_{a_\epsilon}(A_\epsilon) = \frac{1}{\sqrt{2\pi}\sigma_{a_\epsilon}} \exp\left(-\frac{A_\epsilon^2}{2\sigma_{a_\epsilon}^2}\right). \quad (4.376)$$

For a vector variable the quantity analogous to the variance is the covariance matrix

$$\Lambda_\epsilon \triangleq E[(\mathbf{a}_\epsilon - \bar{\mathbf{a}}_\epsilon)(\mathbf{a}_\epsilon^T - \bar{\mathbf{a}}_\epsilon^T)], \quad (4.377)$$

where

$$\bar{\mathbf{a}}_\epsilon \triangleq E(\mathbf{a}_\epsilon) = \mathbf{B}(\mathbf{A}) \quad (4.378)$$

and the expectation is with respect to $p_{\mathbf{r}|\mathbf{a}}(\mathbf{R}|\mathbf{A})$.

The best way to determine how the covariance matrix provides a measure of spread is to consider the special case in which the a_{ϵ_i} are jointly Gaussian. For algebraic simplicity, we let $E(\mathbf{a}_\epsilon) = \mathbf{0}$. The joint probability density for a set of K jointly Gaussian variables is

$$p_{\mathbf{a}_\epsilon}(\mathbf{A}_\epsilon) = (|2\pi|^{K/2} |\Lambda_\epsilon|^{1/2})^{-1} \exp\left(-\frac{1}{2}\mathbf{A}_\epsilon^T \Lambda_\epsilon^{-1} \mathbf{A}_\epsilon\right). \quad (4.379)$$

The probability density for $K = 2$ is shown in Figure 4.23a. In Figure 4.23b and c, we have shown the equal-probability contours of two typical densities. From (4.379), we

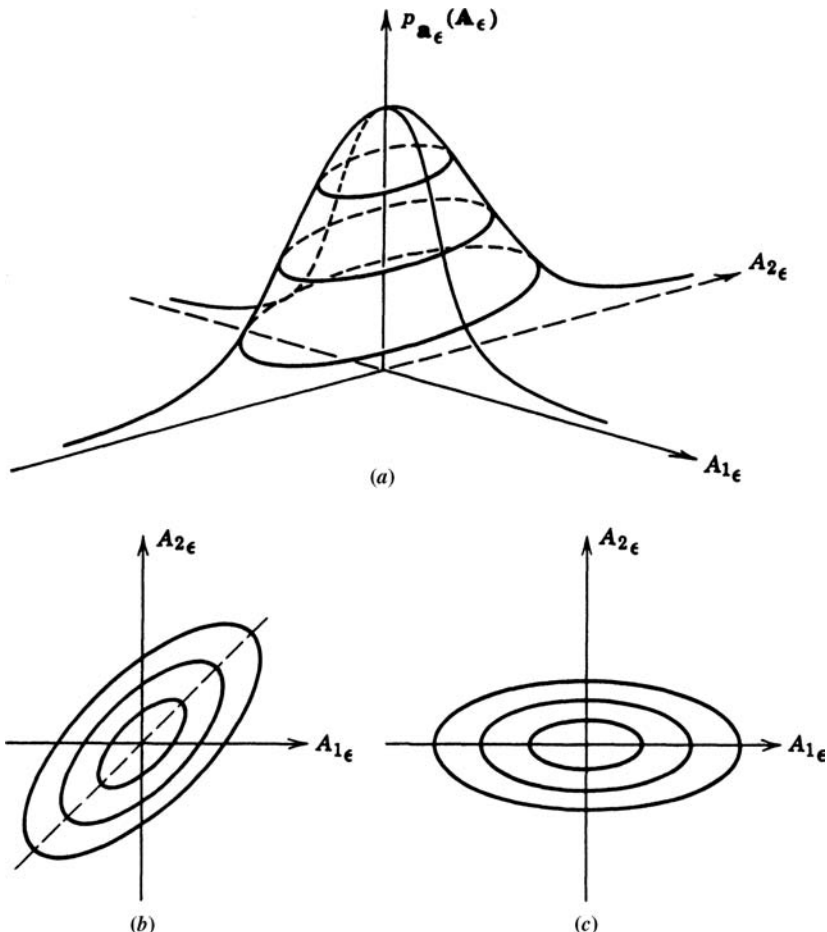


Figure 4.23: Gaussian densities: (a) two-dimensional Gaussian density; (b) equal-height contours; (c) equal-height contours, uncorrelated variables.

observe that the equal-height contours are defined by the relation,

$$\mathbf{A}_\epsilon^T \mathbf{\Lambda}_\epsilon^{-1} \mathbf{A}_\epsilon = C^2, \quad (4.380)$$

which is the equation for an ellipse when $K = 2$. The ellipses move out monotonically with increasing C . They also have the interesting property that the probability of being inside the ellipse is only a function of C^2 .

Property. For $K = 2$, the probability that the error vector lies inside an ellipse whose equation is

$$\mathbf{A}_\epsilon^T \mathbf{\Lambda}_\epsilon^{-1} \mathbf{A}_\epsilon = C^2, \quad (4.381)$$

is

$$P = 1 - \exp\left(-\frac{C^2}{2}\right). \quad (4.382)$$

Proof. The area inside the ellipse defined by (4.381) is

$$\mathcal{A} = |\mathbf{\Lambda}_\epsilon|^{1/2} \pi C^2. \quad (4.383)$$

The differential area between ellipses corresponding to C and $C + dC$, respectively, is

$$d\mathcal{A} = |\mathbf{\Lambda}_\epsilon|^{1/2} 2\pi C dC. \quad (4.384)$$

The height of the probability density in this differential area is

$$(2\pi|\mathbf{\Lambda}_\epsilon|^{1/2})^{-1} \exp\left(-\frac{C^2}{2}\right). \quad (4.385)$$

We can compute the probability of a point lying outside the ellipse by multiplying (4.384) by (4.385) and integrating from C to ∞ .

$$1 - P = \int_C^\infty X \exp\left(-\frac{X^2}{2}\right) dX = \exp\left(-\frac{C^2}{2}\right), \quad (4.386)$$

which is the desired result.

For this reason the ellipses described by (4.380) are referred to as *concentration ellipses* because they provide a measure of the concentration of the density.

A similar result holds for arbitrary K . Now (4.380) describes an ellipsoid. Here, the differential¹⁷ volume in K -dimensional space is

$$dv = |\mathbf{\Lambda}_\epsilon|^{1/2} \frac{\pi^{K/2}}{\Gamma(K/2 + 1)} KC^{K-1} dC. \quad (4.387)$$

The value of the probability density on the ellipsoid is

$$[(2\pi)^{K/2} |\mathbf{\Lambda}_\epsilon|^{1/2}]^{-1} \exp\left(-\frac{C^2}{2}\right). \quad (4.388)$$

¹⁷For example, Cramér [Cra46], p. 120 or Sommerfeld [Som29].

Therefore,

$$\begin{aligned}
1 - P &= \frac{K}{2^{K/2} \Gamma(K/2 + 1)} \int_C^\infty X^{K-1} e^{-X^2/2} dX, \\
&= \frac{1}{\Gamma(K/2)} \int_{C^2/2}^\infty t^{K/2-1} e^{-t} dt \\
&= 1 - \Gamma_{K/2} \left(\frac{C^2}{2} \right),
\end{aligned} \tag{4.389}$$

which is the desired result. We refer to these ellipsoids as *concentration ellipsoids*.

When the probability density of the error is *not* Gaussian, the concentration ellipsoid no longer specifies a unique probability. This is directly analogous to the one-dimensional case in which the variance of a non-Gaussian zero-mean random variable does not determine the probability density. We can still interpret the concentration ellipsoid as a rough measure of the spread of the errors. When the concentration ellipsoids of a given density lie wholly outside the concentration ellipsoids of a second density, we say that the second density is more concentrated than the first. With this motivation, we will derive some properties and bounds pertaining to concentration ellipsoids in Section 4.3.3.

4.3.2.2 Random Parameters

For random parameters, the measure of error is a *mean-square error matrix*

$$\Sigma_\epsilon = \text{MSE}(\hat{\mathbf{a}}(\mathbf{R})) \triangleq E \{ \mathbf{a}_\epsilon(\mathbf{R}) \mathbf{a}_\epsilon(\mathbf{R})^T \}, \tag{4.390}$$

where the expectation is over \mathbf{r} and \mathbf{a} . The diagonal elements represent the mean-square errors and the off-diagonal elements are the cross-correlations.

All of the discussion in the previous section applies except it applies to the MSE matrix instead of the covariance matrix.

4.3.3 Bounds on Estimation Error

In this section, we derive the CRB for nonrandom parameters and the Bayesian CRB for random parameters.

4.3.3.1 Nonrandom Parameters

In this section, we derive a bound on the covariance matrix of the errors of any unbiased estimate. We assume that

$$\frac{\partial \ln p_{\mathbf{r}|\mathbf{a}}(\mathbf{R}|\mathbf{A})}{\partial A_i} \quad \text{and} \quad \frac{\partial^2 \ln p_{\mathbf{r}|\mathbf{a}}(\mathbf{R}|\mathbf{A})}{\partial A_i \partial A_j}, \quad i, j = 1, 2, \dots, K \tag{4.391}$$

exist and are absolutely integrable.

We define a $K \times K$ matrix $\mathbf{J}_F(\mathbf{A})$. The ij elements are

$$\begin{aligned}
J_{F_{ij}}(\mathbf{A}) &\triangleq E \left[\frac{\partial \ln p_{\mathbf{r}|\mathbf{a}}(\mathbf{R}|\mathbf{A})}{\partial A_i} \cdot \frac{\partial \ln p_{\mathbf{r}|\mathbf{a}}(\mathbf{R}|\mathbf{A})}{\partial A_j} \right] \\
&= -E \left[\frac{\partial^2 \ln p_{\mathbf{r}|\mathbf{a}}(\mathbf{R}|\mathbf{A})}{\partial A_i \partial A_j} \right]
\end{aligned} \tag{4.392}$$

or, in matrix notation

$$\begin{aligned}\mathbf{J}_F(\mathbf{A}) &\triangleq E\left(\left[\nabla_{\mathbf{A}} \ln p_{\mathbf{r}|\mathbf{a}}(\mathbf{R}|\mathbf{A})\right]\left[\nabla_{\mathbf{A}} \ln p_{\mathbf{r}|\mathbf{a}}(\mathbf{R}|\mathbf{A})\right]^T\right) \\ &= -E\left(\nabla_{\mathbf{A}}\left[\nabla_{\mathbf{A}} \ln p_{\mathbf{r}|\mathbf{a}}(\mathbf{R}|\mathbf{A})\right]^T\right).\end{aligned}\quad (4.393)$$

The $\mathbf{J}_F(\mathbf{A})$ matrix is commonly called *Fisher's information matrix (FIM)*.

Property 1. The vector CRB is

$$\boldsymbol{\Lambda}_{\epsilon} - \mathbf{J}_F^{-1}(\mathbf{A}) \geq 0, \quad (4.394)$$

where the matrix inequality means that matrix is nonnegative definite.

The inequality in (4.394) implies that all submatrices are nonnegative definite and, in particular,

$$\sigma_{\epsilon_i}^2 \triangleq \text{Var}[\hat{a}_i(\mathbf{R}) - A_i] \geq J_F^{ii}(\mathbf{A}), \quad (4.395)$$

where $J_F^{ii}(\mathbf{A})$ is the i th diagonal element of $\mathbf{J}_F^{-1}(\mathbf{A})$.

The equality in (4.394) holds if and only if

$$\hat{a}_i(\mathbf{R}) - A_i = \sum_{j=1}^N k_{ij}(\mathbf{A}) \frac{\partial \ln p_{\mathbf{r}|\mathbf{a}}(\mathbf{R}|\mathbf{A})}{\partial A_j} \quad (4.396)$$

for all values of A_i and \mathbf{R} .

In other words, the estimation error can be expressed as the weighted sum of the partial derivatives of $\ln p_{\mathbf{r}|\mathbf{a}}(\mathbf{R}|\mathbf{A})$ with respect to the various parameters.

The requirement in (4.396) can be written in matrix notation as

$$\hat{\mathbf{a}}(\mathbf{R}) - \mathbf{A} = \mathbf{k}(\mathbf{A}) \left[\nabla_{\mathbf{A}} \ln p_{\mathbf{r}|\mathbf{a}}(\mathbf{R}|\mathbf{A}) \right], \quad (4.397)$$

where

$$\mathbf{k}(\mathbf{A}) = \mathbf{J}_F^{-1}(\mathbf{A}). \quad (4.398)$$

Proof. Because $\hat{a}_i(\mathbf{R})$ is unbiased,

$$\int_{-\infty}^{\infty} [\hat{a}_i(\mathbf{R}) - A_i] p_{\mathbf{r}|\mathbf{a}}(\mathbf{R}|\mathbf{A}) d\mathbf{R} = 0. \quad (4.399)$$

Differentiating with respect to A_j gives

$$-\delta_{ij} \int_{-\infty}^{\infty} p_{\mathbf{r}|\mathbf{a}}(\mathbf{R}|\mathbf{A}) d\mathbf{R} + \int_{-\infty}^{\infty} [\hat{a}_i(\mathbf{R}) - A_i] \frac{\partial p_{\mathbf{r}|\mathbf{a}}(\mathbf{R}|\mathbf{A})}{\partial A_j} d\mathbf{R} = 0. \quad (4.400)$$

The first integral equals unity and

$$\frac{\partial p_{\mathbf{r}|\mathbf{a}}(\mathbf{R}|\mathbf{A})}{\partial A_j} = \frac{\partial \ln p_{\mathbf{r}|\mathbf{a}}(\mathbf{R}|\mathbf{A})}{\partial A_j} p_{\mathbf{r}|\mathbf{a}}(\mathbf{R}|\mathbf{A}). \quad (4.401)$$

So (4.400) can be rewritten as

$$\int_{-\infty}^{\infty} \left\{ [\hat{a}_i(\mathbf{R}) - A_i] \sqrt{p_{\mathbf{r}|\mathbf{a}}(\mathbf{R}|\mathbf{A})} \right\} \left\{ \sqrt{p_{\mathbf{r}|\mathbf{a}}(\mathbf{R}|\mathbf{A})} \frac{\partial \ln p_{\mathbf{r}|\mathbf{a}}(\mathbf{R}|\mathbf{A})}{\partial A_j} \right\} d\mathbf{R} = \delta_{ij} \quad (4.402)$$

or, in matrix notation,

$$\int_{-\infty}^{\infty} \left\{ [\hat{\mathbf{a}}(\mathbf{R}) - \mathbf{A}] \sqrt{p_{\mathbf{r}|\mathbf{a}}(\mathbf{R}|\mathbf{A})} \right\} \left\{ \sqrt{p_{\mathbf{r}|\mathbf{a}}(\mathbf{R}|\mathbf{A})} [\nabla_{\mathbf{A}} \ln p_{\mathbf{r}|\mathbf{a}}(\mathbf{R}|\mathbf{A})]^T \right\} d\mathbf{R} = \mathbf{I}. \quad (4.403)$$

We need to put (4.403) in a form where we can use the Schwarz inequality. We define two arbitrary $K \times 1$ vectors, \mathbf{b}_1 and \mathbf{b}_2 , that do not depend on \mathbf{R} . We premultiply by \mathbf{b}_1^T and postmultiply by \mathbf{b}_2 ,

$$\int_{-\infty}^{\infty} \left\{ \mathbf{b}_1^T [\hat{\mathbf{a}}(\mathbf{R}) - \mathbf{A}] \sqrt{p_{\mathbf{r}|\mathbf{a}}(\mathbf{R}|\mathbf{A})} \right\} \left\{ \sqrt{p_{\mathbf{r}|\mathbf{a}}(\mathbf{R}|\mathbf{A})} [\nabla_{\mathbf{A}} \ln p_{\mathbf{r}|\mathbf{a}}(\mathbf{R}|\mathbf{A})]^T \mathbf{b}_2 \right\} d\mathbf{R} = \mathbf{b}_1^T \mathbf{b}_2. \quad (4.404)$$

The terms in the braces are scalars, so we can use the Schwarz inequality to obtain

$$\begin{aligned} (\mathbf{b}_1^T \mathbf{b}_2)^2 &\leq \int_{-\infty}^{\infty} \mathbf{b}_1^T [\hat{\mathbf{a}}(\mathbf{R}) - \mathbf{A}] [\hat{\mathbf{a}}(\mathbf{R}) - \mathbf{A}]^T \mathbf{b}_1 p_{\mathbf{r}|\mathbf{a}}(\mathbf{R}|\mathbf{A}) d\mathbf{R} \\ &\bullet \int_{-\infty}^{\infty} \mathbf{b}_2^T [\nabla_{\mathbf{A}} \ln p_{\mathbf{r}|\mathbf{a}}(\mathbf{R}|\mathbf{A})] [\nabla_{\mathbf{A}} \ln p_{\mathbf{r}|\mathbf{a}}(\mathbf{R}|\mathbf{A})]^T \mathbf{b}_2 p_{\mathbf{r}|\mathbf{a}}(\mathbf{R}|\mathbf{A}) d\mathbf{R}, \end{aligned} \quad (4.405)$$

with equality iff

$$\mathbf{b}_1^T [\hat{\mathbf{a}}(\mathbf{R}) - \mathbf{A}] = C(\mathbf{A}) [\nabla_{\mathbf{A}} \ln p_{\mathbf{r}|\mathbf{a}}(\mathbf{R}|\mathbf{A})]^T \mathbf{b}_2. \quad (4.406)$$

Recognizing the integrals as Λ_ϵ and $\mathbf{J}_F(\mathbf{A})$, (4.405) reduces to

$$(\mathbf{b}_1^T \mathbf{b}_2)^2 \leq [\mathbf{b}_1^T \Lambda_\epsilon \mathbf{b}_1] [\mathbf{b}_2^T \mathbf{J}_F(\mathbf{A}) \mathbf{b}_2]. \quad (4.407)$$

Because (4.406) is valid for arbitrary \mathbf{b}_2 , we let

$$\mathbf{b}_2 = \mathbf{J}_F^{-1}(\mathbf{A}) \mathbf{b}_1 \quad (4.408)$$

and (4.407) reduces to

$$[\mathbf{b}_1^T \Lambda_\epsilon \mathbf{b}_1] [\mathbf{b}_1^T \mathbf{J}_F^{-1}(\mathbf{A}) \mathbf{b}_1] \geq (\mathbf{b}_1^T \mathbf{J}_F^{-1}(\mathbf{A}) \mathbf{b}_1)^2. \quad (4.409)$$

Then

$$\mathbf{b}_1^T \Lambda_\epsilon \mathbf{b}_1 \geq \mathbf{b}_1^T \mathbf{J}_F^{-1}(\mathbf{A}) \mathbf{b}_1 \quad (4.410)$$

or

$$\mathbf{b}_1^T [\Lambda_\epsilon - \mathbf{J}_F^{-1}(\mathbf{A})] \mathbf{b}_1 \geq 0. \quad (4.411)$$

Because \mathbf{b}_1 is arbitrary, this implies

$$\Lambda_\epsilon - \mathbf{J}_F^{-1}(\mathbf{A}) \geq 0, \quad (4.412)$$

where the inequality means that the matrix is nonnegative definite.

Substituting (4.408) into (4.406), the condition for equality becomes

$$\mathbf{b}_1^T [\hat{\mathbf{a}}(\mathbf{R}) - \mathbf{A}] = C(\mathbf{A}) [\nabla_{\mathbf{A}} \ln p_{\mathbf{r}|\mathbf{a}}(\mathbf{R}|\mathbf{A})]^T \mathbf{J}_F^{-1}(\mathbf{A}) \mathbf{b}_1. \quad (4.413)$$

Because \mathbf{b}_1 is arbitrary, (4.413) reduces to

$$[\hat{\mathbf{a}}(\mathbf{R}) - \mathbf{A}]^T = C(\mathbf{A}) [\nabla_{\mathbf{A}} \ln p_{\mathbf{r}|\mathbf{a}}(\mathbf{R}|\mathbf{A})]^T \mathbf{J}_F^{-1}(\mathbf{A}). \quad (4.414)$$

We rewrite this as,

$$[\nabla_{\mathbf{A}} \ln p_{\mathbf{r}|\mathbf{a}}(\mathbf{R}|\mathbf{A})]^T = [\hat{\mathbf{a}}(\mathbf{R}) - \mathbf{A}]^T \frac{\mathbf{J}_F(\mathbf{A})}{C(\mathbf{A})}. \quad (4.415)$$

Taking the gradient with respect to \mathbf{A} gives

$$\nabla_{\mathbf{A}} [\nabla_{\mathbf{A}} \ln p_{\mathbf{r}|\mathbf{a}}(\mathbf{R}|\mathbf{A})]^T = -\mathbf{I} \frac{\mathbf{J}_F(\mathbf{A})}{C(\mathbf{A})} + [\hat{\mathbf{a}}(\mathbf{R}) - \mathbf{A}]^T \nabla_{\mathbf{A}} \left\{ \frac{\mathbf{J}_F^{-1}(\mathbf{A})}{C(\mathbf{A})} \right\}, \quad i = 1, 2, \dots, K. \quad (4.416)$$

Multiplying by -1 and taking the expectation on both sides, the second term is equal to zero because the estimate is unbiased, and we have

$$\mathbf{J}_F(\mathbf{A}) = \frac{1}{C(\mathbf{A})} \mathbf{J}_F(\mathbf{A}), \quad (4.417)$$

so $C(\mathbf{A}) = 1$ and (4.414) reduces to

$$\hat{\mathbf{a}}(\mathbf{R}) - \mathbf{A} = \mathbf{J}_F^{-1}(\mathbf{A}) [\nabla_{\mathbf{A}} \ln p_{\mathbf{r}|\mathbf{a}}(\mathbf{R}|\mathbf{A})] \quad (4.418)$$

or equivalently,

$$\nabla_{\mathbf{A}} \ln p_{\mathbf{r}|\mathbf{a}}(\mathbf{R}|\mathbf{A}) = \mathbf{J}_F(\mathbf{A}) [\hat{\mathbf{a}}(\mathbf{R}) - \mathbf{A}] \quad (4.419)$$

as the necessary condition for equality.

Frequently we want to estimate functions of the K basic parameters rather than the parameters themselves. We denote the desired estimates as

$$\begin{aligned} d_1 &= \gamma_1(\mathbf{a}), \\ d_2 &= \gamma_2(\mathbf{a}), \\ &\vdots \\ d_M &= \gamma_M(\mathbf{a}) \end{aligned} \quad (4.420)$$

or

$$\mathbf{d} = \boldsymbol{\gamma}(\mathbf{a}).$$

The number of estimates M is not related to K in general. The functions may be nonlinear. The estimation error is

$$\hat{d}_i(\mathbf{R}) - \gamma_i(\mathbf{A}) \triangleq d_{\epsilon_i}. \quad (4.421)$$

If we assume that the estimates are unbiased and denote the error covariance matrix as $\Lambda_\epsilon(\mathbf{D})$, then by using methods identical to those above we can prove the following properties.

Property 2.

$$\Lambda_\epsilon(\mathbf{D}) - (\nabla_{\mathbf{A}}[\gamma^T(\mathbf{A})])^T \mathbf{J}_F^{-1}(\mathbf{A}) (\nabla_{\mathbf{A}}[\gamma^T(\mathbf{A})]) \geq 0. \quad (4.422)$$

This implies the following property (just multiply the second matrix out and recall that all diagonal elements of a nonnegative definite matrix are nonnegative).

Property 3.

$$\text{Var}(d_{\epsilon_i}) \geq \sum_{k=1}^K \sum_{j=1}^K \frac{\partial \gamma_i(\mathbf{A})}{\partial A_k} J_F^{kj}(\mathbf{A}) \frac{\partial \gamma_i(\mathbf{A})}{\partial A_j}. \quad (4.423)$$

For the special case in which the desired functions are linear, the result in (4.423) can be written in a simpler form.

Property 4. Assume that

$$\gamma(\mathbf{A}) \triangleq \boldsymbol{\Gamma} \mathbf{A}, \quad (4.424)$$

where $\boldsymbol{\Gamma}$ is an $M \times K$ matrix. If the estimates are unbiased, then

$$\Lambda_\epsilon(\mathbf{D}) - \boldsymbol{\Gamma} \mathbf{J}_F^{-1}(\mathbf{A}) \boldsymbol{\Gamma}^T \geq 0. \quad (4.425)$$

Property 5. Efficiency commutes with linear transformations but does not commute with nonlinear transformations. In other words, if $\hat{\mathbf{a}}(\mathbf{R})$ is efficient, then $\hat{\mathbf{d}}(\mathbf{R})$ will be efficient if and only if $\gamma(\mathbf{a})$ is a linear transformation.

We consider several examples to illustrate these properties.

Example 4.26 (continuation of Examples 4.2, 4.5, 4.7, 4.13, 4.17, 4.21, and 4.23)
Gaussian. The observations consist of N IID Gaussian random variables whose mean and variance are unknown nonrandom parameters. We define

$$\mathbf{a} \triangleq [m \quad \sigma^2]^T \quad (4.426)$$

and

$$p_{\mathbf{r}|\mathbf{a}}(\mathbf{R}|\mathbf{A}) = \prod_{i=1}^N \frac{1}{\sqrt{2\pi\sigma^2}} \exp\left\{-\frac{(R_i - m)^2}{2\sigma^2}\right\}. \quad (4.427)$$

Then

$$l(\mathbf{A}; \mathbf{R}) \triangleq \ln p_{\mathbf{r}|\mathbf{a}}(\mathbf{R}|\mathbf{A}) = -\frac{N}{2} \ln (2\pi\sigma^2)^2 - \frac{1}{2\sigma^2} \sum_{i=1}^N (R_i - m)^2. \quad (4.428)$$

Taking the derivative with respect to m ,

$$\frac{\partial l(\mathbf{A}; \mathbf{R})}{\partial m} = \frac{1}{2\sigma^2} \sum_{i=1}^N 2(R_i - m) = 0 \quad (4.429)$$

or

$$\sum_{i=1}^N R_i = Nm. \quad (4.430)$$

The ML estimate of m is, therefore,

$$\hat{m}_{\text{ml}}(\mathbf{R}) = \frac{1}{N} \sum_{i=1}^N R_i \triangleq \bar{R}. \quad (4.431)$$

Note that this is the same estimate as in Example 4.7, equation (4.122), thus, estimation of the mean is the same regardless of whether σ^2 is known or unknown.

Differentiating $l(\mathbf{A}; \mathbf{R})$ with respect to σ^2 gives

$$\frac{\partial l(\mathbf{A}; \mathbf{R})}{\partial \sigma^2} = -\frac{N}{2\sigma^2} + \frac{1}{2(\sigma^2)^2} \sum_{i=1}^N (R_i - m)^2 = 0 \quad (4.432)$$

or

$$\hat{\sigma}_{\text{ml}}^2(\mathbf{R}, m) = \frac{1}{N} \sum_{i=1}^N (R_i - m)^2. \quad (4.433)$$

This is the ML estimator of the variance when the mean m is known. Substituting $\hat{m}_{\text{ml}}(\mathbf{R})$ from (4.431) into (4.433) gives

$$\hat{\sigma}_{\text{ml}}^2(\mathbf{R}) = \frac{1}{N} \sum_{i=1}^N (R_i - \hat{m}_{\text{ml}}(\mathbf{R}))^2 = \frac{1}{N} \sum_{i=1}^N (R_i - \bar{R})^2, \quad (4.434)$$

which is the sample variance. Thus, ML estimation is equating the sample mean and variance to the theoretical mean and variance.

To find the Fisher information matrix, we first differentiate (4.429) with respect to m :

$$\frac{\partial^2 l(\mathbf{A}; \mathbf{R})}{\partial m^2} = -\frac{N}{\sigma^2}, \quad (4.435)$$

so

$$J_{F_{mm}} = \frac{N}{\sigma^2}. \quad (4.436)$$

We next differentiate (4.432) with respect to σ^2 ,

$$\frac{\partial^2 l(\mathbf{A}; \mathbf{R})}{\partial (\sigma^2)^2} = \frac{N}{2}(\sigma^2)^{-2} - (\sigma^2)^{-3} \sum_{i=1}^N (R_i - m)^2, \quad (4.437)$$

so

$$J_{F_{\sigma^2 \sigma^2}} = -E \left\{ \frac{N}{2}(\sigma^2)^{-2} - (\sigma^2)^{-3} \sum_{i=1}^N (R_i - m)^2 \right\} = \frac{-N}{2\sigma^4} + \frac{N\sigma^2}{\sigma^6} = \frac{N}{2\sigma^4}. \quad (4.438)$$

The off-diagonal terms are

$$\frac{\partial^2 l(\mathbf{A}; \mathbf{R})}{\partial m \partial \sigma^2} = -\sigma^4 \sum_{i=1}^N (R_i - m), \quad (4.439)$$

so

$$J_{F_{m,\sigma^2}} = -E \left\{ -\sigma^4 \sum_{i=1}^N (R_i - m) \right\} = 0. \quad (4.440)$$

The Fisher information matrix is

$$\mathbf{J}_F(\mathbf{A}) = \begin{bmatrix} \frac{N}{\sigma^2} & 0 \\ 0 & \frac{N}{2\sigma^4} \end{bmatrix} \quad (4.441)$$

and the CRB is

$$\text{CRB}(\mathbf{A}) = \mathbf{J}_F(\mathbf{A})^{-1} = \frac{1}{N} \begin{bmatrix} \sigma^2 & 0 \\ 0 & 2\sigma^4 \end{bmatrix}. \quad (4.442)$$

Note that the diagonal term $J_{F_{mm}}$ is the Fisher information for estimating m when σ^2 is known, the term $J_{F_{\sigma^2\sigma^2}}$ is the Fisher information for estimating σ^2 when m is known. Because the off-diagonal terms are zero,

$$J_F^{mm} \triangleq [\mathbf{J}(\mathbf{A})^{-1}]_{mm} = \frac{\sigma^2}{N} \quad (4.443)$$

and

$$J_F^{\sigma^2\sigma^2} \triangleq [\mathbf{J}_F(\mathbf{A})^{-1}]_{\sigma^2\sigma^2} = \frac{2\sigma^4}{N} \quad (4.444)$$

and the CRBs for joint estimation of m and σ^2 are the same as for estimation of the parameters individually.

In Example 4.7, we computed the bias and variance of $\hat{m}_{\text{ml}}(\mathbf{R})$ and showed that it was an unbiased, efficient estimator. For $\hat{\sigma}_{\text{ml}}^2(\mathbf{R})$, one can show that $N\hat{\sigma}_{\text{ml}}^2(\mathbf{R})/\sigma^2$ has a Chi-squared($N - 1$) density, so its mean and variance are

$$E \left\{ \frac{N\hat{\sigma}_{\text{ml}}^2(\mathbf{R})}{\sigma^2} \right\} = N - 1, \quad (4.445)$$

$$\text{Var} \left\{ \frac{N\hat{\sigma}_{\text{ml}}^2(\mathbf{R})}{\sigma^2} \right\} = 2(N - 1). \quad (4.446)$$

Then

$$E \{ \hat{\sigma}_{\text{ml}}^2(\mathbf{R}) \} = \frac{N-1}{N} \sigma^2 = \sigma^2 - \frac{1}{N} \sigma^2. \quad (4.447)$$

It is a biased estimator with bias function

$$B_{\text{ml}}(\sigma^2) = -\frac{1}{N} \sigma^2. \quad (4.448)$$

The variance is

$$\text{Var}\{\hat{\sigma}_{\text{ml}}^2(\mathbf{R})\} = \frac{2\sigma^4}{N} \frac{N-1}{N} < \frac{2\sigma^4}{N}. \quad (4.449)$$

The inequality in (4.449) does not violate the CRB because the estimate is biased. The CRB for biased estimators with bias function given by (4.448) is given by

$$\text{CRB}_B(\sigma^2) = \left(\frac{N-1}{N}\right)^2 \frac{2\sigma^4}{N} < \text{Var}\{\hat{\sigma}_{\text{ml}}^2(\mathbf{R})\}. \quad (4.450)$$

As $N \rightarrow \infty$, $\hat{\sigma}_{\text{ml}}^2(\mathbf{R})$ becomes an asymptotically unbiased and efficient estimate.

An unbiased estimator of σ^2 is

$$\hat{\sigma}_{\text{u}}^2(\mathbf{R}) = \frac{N}{N-1} \hat{\sigma}_{\text{ml}}^2(\mathbf{R}) = \frac{1}{N-1} \sum_{i=1}^N (R_i - \bar{R})^2. \quad (4.451)$$

The variance of this estimator is

$$\text{Var}\{\hat{\sigma}_{\text{u}}^2(\mathbf{R})\} = \left(\frac{N}{N-1}\right)^2 \text{Var}\{\hat{\sigma}_{\text{ml}}^2(\mathbf{R})\} = \frac{2\sigma^4}{N-1} > \frac{2\sigma^4}{N}. \quad (4.452)$$

These two estimators of σ^2 illustrate the trade-off between bias and variance. The unbiased estimator has a smaller bias but a larger variance than the ML estimator. The conditional MSE defined in (4.78) combines the effect of bias and variance and provides a way to compare the estimators based on a single measure,

$$\text{MSE}(\hat{\sigma}^2(\mathbf{R})|\sigma^2) \triangleq E\left\{(\hat{\sigma}^2(\mathbf{R}) - \sigma^2)^2\right\} = \text{Var}\{\hat{\sigma}^2(\mathbf{R})\} + B^2(\sigma^2). \quad (4.453)$$

The conditional MSE of the ML and unbiased estimators are

$$\text{MSE}(\hat{\sigma}_{\text{ml}}^2(\mathbf{R})|\sigma^2) = \sigma^4 \frac{2N-1}{N^2}, \quad (4.454)$$

$$\text{MSE}(\hat{\sigma}_{\text{u}}^2(\mathbf{R})|\sigma^2) = \sigma^4 \frac{2}{N}, \quad (4.455)$$

thus, the ML estimator has a smaller conditional MSE than the unbiased estimator. The estimator that has the minimum conditional MSE is

$$\hat{\sigma}_{\text{m}}^2(\mathbf{R}) = \frac{1}{N+1} \sum_{i=1}^N (R_i - \bar{R})^2, \quad (4.456)$$

and its conditional MSE is

$$\text{MSE}(\hat{\sigma}_{\text{m}}^2(\mathbf{R})|\sigma^2) = \sigma^4 \frac{2}{N+1}. \quad (4.457)$$

■

Example 4.27 Multivariate Gaussian. We consider the case where the likelihood function is multivariate Gaussian with known covariance matrix \mathbf{K}_n and unknown mean vector \mathbf{m} . The observations are

$$\mathbf{r}_i = \mathbf{m} + \mathbf{n}_i, \quad i = 1, 2, \dots, N, \quad (4.458)$$

where \mathbf{m} is a K -dimensional nonrandom parameter vector that we want to estimate and \mathbf{n}_i is a zero-mean Gaussian random vector,

$$p_{\mathbf{n}_i}(\mathbf{N}_i) = \frac{1}{(2\pi)^{M/2} |\mathbf{K}_{\mathbf{n}}|^{1/2}} \exp \left\{ -\frac{1}{2} \mathbf{N}_i^T \mathbf{K}_{\mathbf{n}}^{-1} \mathbf{N}_i \right\}, \quad (4.459)$$

where $\mathbf{K}_{\mathbf{n}}$ is known. The conditional probability density is

$$p_{\mathbf{r}_1, \dots, \mathbf{r}_N | \mathbf{m}}(\mathbf{R}_1, \dots, \mathbf{R}_N | \mathbf{M}) = \prod_{i=1}^N \frac{1}{(2\pi)^{M/2} |\mathbf{K}_{\mathbf{n}}|^{1/2}} \exp \left\{ -\frac{1}{2} (\mathbf{R}_i - \mathbf{M})^T \mathbf{K}_{\mathbf{n}}^{-1} (\mathbf{R}_i - \mathbf{M}) \right\}. \quad (4.460)$$

The log-likelihood function is

$$l(\mathbf{M}; \mathbf{R}_1, \dots, \mathbf{R}_N) = -\frac{1}{2} \sum_{i=1}^N (\mathbf{R}_i - \mathbf{M})^T \mathbf{K}_{\mathbf{n}}^{-1} (\mathbf{R}_i - \mathbf{M}) + \zeta, \quad (4.461)$$

where ζ represents terms that are not a function of \mathbf{m} . Taking the gradient with respect to \mathbf{m} gives

$$\nabla_{\mathbf{M}} l(\mathbf{M}; \mathbf{R}_1, \dots, \mathbf{R}_N) = \mathbf{K}_{\mathbf{n}}^{-1} \sum_{i=1}^N (\mathbf{R}_i - \mathbf{M}) = N \mathbf{K}_{\mathbf{n}}^{-1} \left[\frac{1}{N} \sum_{i=1}^N \mathbf{R}_i - \mathbf{M} \right] = \mathbf{0}. \quad (4.462)$$

The ML estimate is

$$\hat{\mathbf{m}}_{\text{ml}}(\mathbf{R}) = \frac{1}{N} \sum_{i=1}^N \mathbf{R}_i \triangleq \bar{\mathbf{R}}, \quad (4.463)$$

which is the vector version of (4.122).

We differentiate (4.462) with respect to \mathbf{M} and take the expected value to find $\mathbf{J}_F(\mathbf{M})$. The result is

$$\mathbf{J}_F(\mathbf{M}) = N \mathbf{K}_{\mathbf{n}}^{-1}, \quad (4.464)$$

which is the matrix version of (4.126).

To find the bias, we have

$$E \{ \hat{\mathbf{m}}_{\text{ml}}(\mathbf{R}) \} = \frac{1}{N} \sum_{i=1}^N E \{ \mathbf{R}_i \} = \mathbf{m}, \quad (4.465)$$

so the estimate is unbiased.

Because (4.462) satisfies (4.419), the ML estimate is efficient and its covariance matrix equals the CRB

$$\Lambda_{\epsilon} = \mathbf{J}_F(\mathbf{M})^{-1} = \frac{1}{N} \mathbf{K}_{\mathbf{n}}. \quad (4.466)$$

■

Example 4.28 (continuation of Examples 4.10 and 4.12) Gamma. We considered the Gamma probability density in Examples 4.10 and 4.12 under the assumption that one of the parameters was known and the other parameter was to be estimated. In this example, we assume that the observations consist of N IID random variables with a Gamma probability density where both the shape parameter a and the scale parameter b are unknown,

$$p_{\mathbf{r}|a,b}(\mathbf{R}|A, B) = \prod_{i=1}^N R_i^{A-1} \frac{e^{-R_i/B}}{B^A \Gamma(A)}. \quad (4.467)$$

We define

$$\mathbf{a} \triangleq [a \quad b]^T. \quad (4.468)$$

The log-likelihood function is

$$l(\mathbf{A}; \mathbf{R}) = l(A, B; \mathbf{R}) = (A - 1) \sum_{i=1}^N \ln R_i - \sum_{i=1}^N \frac{R_i}{B} - NA \ln B - N \ln \Gamma(A). \quad (4.469)$$

Differentiating with respect to B gives

$$\frac{\partial l(A, B; \mathbf{R})}{\partial B} = \frac{1}{B^2} \sum_{i=1}^N R_i - \frac{NA}{B} = 0 \quad (4.470)$$

or

$$\hat{b}_{ml}(\mathbf{R}, A) = \frac{1}{AN} \sum_{i=1}^N R_i = \frac{\bar{R}}{A} \quad (4.471)$$

which is the same as (4.148) in Example 4.10.

Differentiating (4.469) with respect to A gives

$$\frac{\partial l(A, B; \mathbf{R})}{\partial A} = \sum_{i=1}^N \ln R_i - N \ln B - N\psi_0(A) = 0. \quad (4.472)$$

We now substitute $\hat{b}_{ml}(\mathbf{R}, A)$ from (4.471) for B in (4.472) to obtain

$$\sum_{i=1}^N \ln R_i - N \ln \bar{R} + N \ln A - N\psi_0(A) = 0 \quad (4.473)$$

or

$$\{\psi_0(A) - \ln A\}|_{A=\hat{a}_{ml}(\mathbf{R})} = \frac{1}{N} \sum_{i=1}^N \ln R_i - \ln \bar{R}. \quad (4.474)$$

This equation has to be solved numerically. Once we find $\hat{a}_{ml}(\mathbf{R})$, we substitute it into (4.471) so that

$$\hat{b}_{ml}(\mathbf{R}) = \frac{\bar{R}}{\hat{a}_{ml}(\mathbf{R})}. \quad (4.475)$$

We obtain the Fisher information matrix by differentiating (4.470) with respect to B and taking the expectation to obtain $J_{F_{BB}}$, differentiating (4.472) with respect to A and taking the expectation to obtain $J_{F_{AA}}$, and differentiating (4.470) with respect to A and taking the expectation to obtain $J_{F_{AB}} = J_{F_{BA}}$. $J_{F_{BB}}$ and $J_{F_{AA}}$ were computed in Example 4.10, equation (4.151) and Example 4.12, equation (4.172). $J_{F_{AB}}$ is given by

$$J_{F_{AB}} = -E \left\{ \frac{\partial l(A, B; \mathbf{R})}{\partial B \partial A} \right\} = \frac{N}{B}. \quad (4.476)$$

The FIM is

$$\mathbf{J}_F(A, B) = N \begin{bmatrix} \psi_1(A) & \frac{1}{B} \\ \frac{1}{B} & \frac{A}{B^2} \end{bmatrix} \quad (4.477)$$

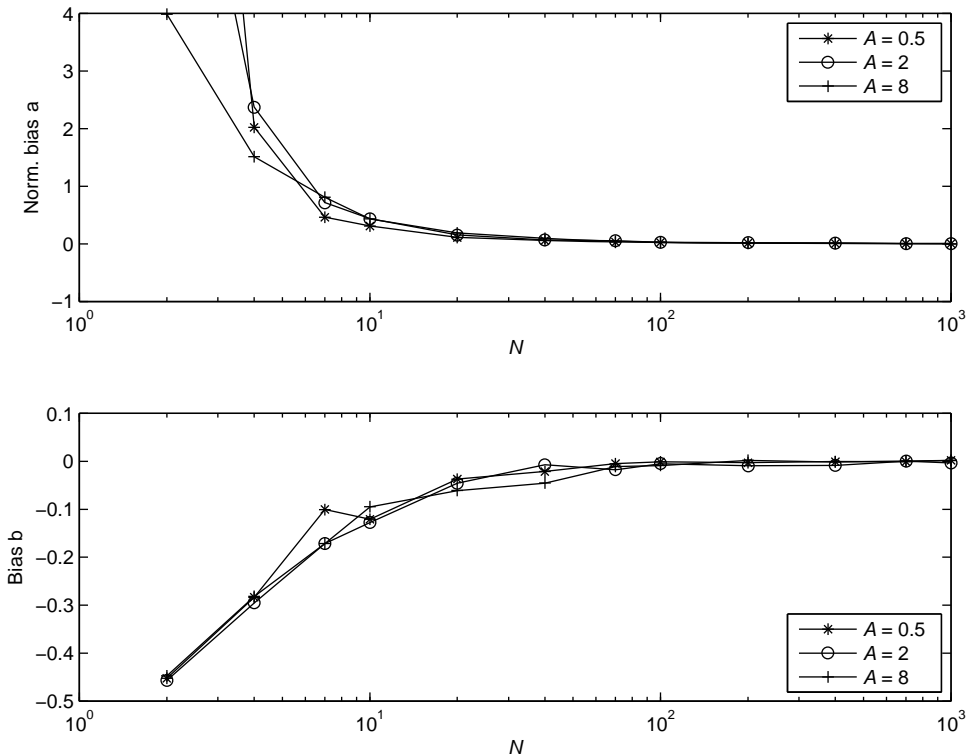


Figure 4.24: Normalized bias in estimating Gamma parameters; $A = 0.5, 2, 8, B = 1$.

and the CRB is

$$\text{CRB}(A, B) = \frac{A\psi_1(A)}{A\psi_1(A) - 1} \cdot \frac{1}{N} \begin{bmatrix} \frac{1}{\psi_1(A)} & -\frac{B}{\psi_1(A)} \\ -\frac{B}{\psi_1(A)} & \frac{B^2}{A} \end{bmatrix}. \quad (4.478)$$

Comparing the diagonal terms to the individual CRBs in (4.153) and (4.172), the joint CRBs are larger by a factor of $A\psi_1(A)/(A\psi_1(A) - 1)$, so estimation performance suffers when both parameters are unknown.

It is difficult to evaluate the bias and variance of the estimates analytically, therefore we simulate ML estimation for the case when $A = 0.5, 2$, and 8 , and $B = 1$. In Figure 4.24, we plot the normalized bias $\text{Bias}(A)/A$ and the bias $\text{Bias}(B)$. We see that both estimates are biased, but asymptotically unbiased. In Example 4.10 when a was known, $\hat{b}_{\text{ml}}(\mathbf{R})$ was unbiased, and in Example 4.12 when b was known, the bias of $\hat{a}_{\text{ml}}(\mathbf{R})$ shown in Figure 4.7 was smaller than the bias shown in Figure 4.24.

Because the estimates are biased in the nonasymptotic region, the unbiased CRB is not a valid lower bound, however we do not have analytical expressions for the bias so we cannot compute the biased CRB. This occurs often in practice. The best we can do is compare the estimation variance to the unbiased CRB with the understanding that it is not a valid lower bound in the nonasymptotic region. In Figure 4.25, we plot the standard deviation and the square root of the CRB. We see that both estimates are asymptotically efficient. The variance of $\hat{a}_{\text{ml}}(\mathbf{R})$ exceeds the unbiased CRB in the nonasymptotic region, while the variance of $\hat{b}_{\text{ml}}(\mathbf{R})$ is less than the unbiased CRB in the nonasymptotic region. ■

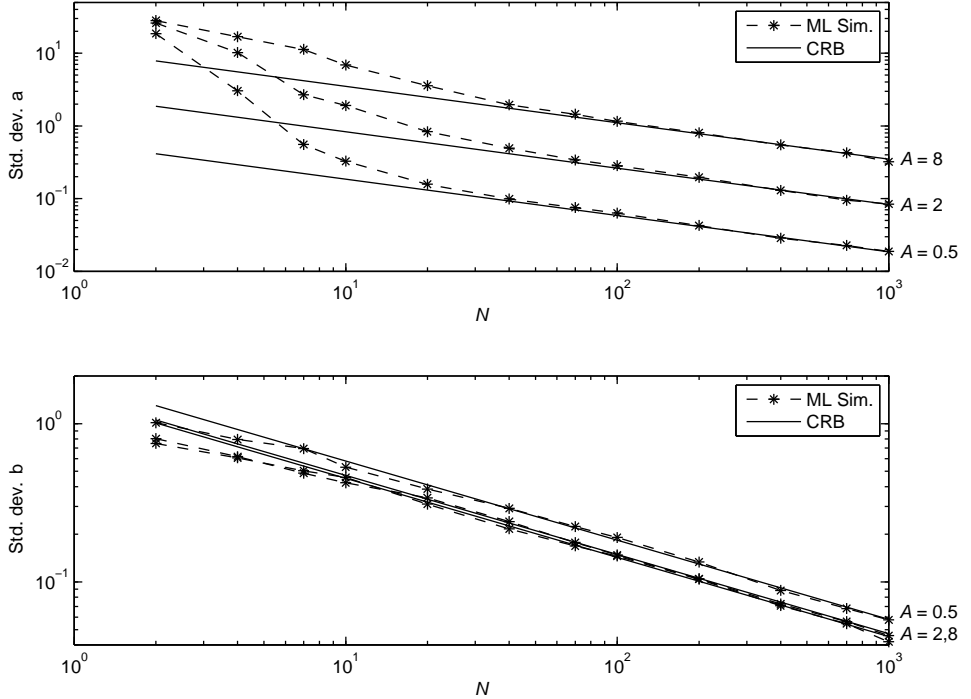


Figure 4.25: Standard deviation and root CRB in estimating Gamma parameters; $A = 0.5, 2, 8$, $B = 1$.

We now return to our frequency estimation case study.

Example 4.29 (continuation of Examples 4.15 and 4.16) Frequency and phase estimation. Suppose that we now want to estimate both the frequency and the phase. The unknown parameter vector is

$$\mathbf{a} \triangleq \begin{bmatrix} \omega \\ \theta \end{bmatrix}, \quad (4.479)$$

and the log-likelihood function is given by (4.224),

$$\begin{aligned} l(\mathbf{A}; \tilde{\mathbf{R}}) &= l(\omega, \theta; \tilde{\mathbf{R}}) = 2N \left(\frac{b}{\sigma_w^2} \right) \Re \left[e^{-j\theta} \frac{1}{N} \sum_{n=0}^{N-1} \tilde{R}_n e^{-j\omega n} \right] + \zeta \\ &= 2N \left(\frac{b}{\sigma_w^2} \right) \Re [e^{-j\theta} F(\omega; \tilde{\mathbf{R}})] + \zeta \end{aligned} \quad (4.480)$$

where $F(\omega; \tilde{\mathbf{R}})$ was defined in (4.226) and ζ represents terms that do not depend on ω or θ . Taking the derivative with respect to θ , setting the result equal to zero and solving, the ML estimate for the phase is

$$\hat{\theta}_{\text{ml}}(\tilde{\mathbf{R}}, \omega) = \arg \{F(\omega; \tilde{\mathbf{R}})\}. \quad (4.481)$$

Since we have an analytical solution for the ML estimate of θ as a function of $\tilde{\mathbf{R}}$ and ω , we can substitute it into the log-likelihood function in (4.480) to create a *compressed log-likelihood function* that is only a function of ω and $\tilde{\mathbf{R}}$,

$$\begin{aligned} l(\omega; \tilde{\mathbf{R}}) &= 2N \left(\frac{b}{\sigma_w^2} \right) \Re \left[e^{-j\hat{\theta}_{\text{ml}}(\tilde{\mathbf{R}}, \omega)} F(\omega; \tilde{\mathbf{R}}) \right] + \zeta \\ &= 2N \left(\frac{b}{\sigma_w^2} \right) |F(\omega; \tilde{\mathbf{R}})| + \zeta. \end{aligned} \quad (4.482)$$

Thus, the ML estimate of the frequency when the phase is unknown is

$$\hat{\omega}_{\text{ml}}(\tilde{\mathbf{R}}) = \underset{\omega}{\operatorname{argmax}} \{ |F(\omega; \tilde{\mathbf{R}})| \} \quad (4.483)$$

and the phase estimate is

$$\hat{\theta}_{\text{ml}}(\tilde{\mathbf{R}}) = \arg \{ F(\hat{\omega}_{\text{ml}}(\tilde{\mathbf{R}}); \tilde{\mathbf{R}}) \}. \quad (4.484)$$

For this problem, the noisy ambiguity surface is

$$A(\omega; \tilde{\mathbf{R}}) = |F(\omega; \tilde{\mathbf{R}})|. \quad (4.485)$$

The square of the right-hand side is familiar as the periodogram. The normalized signal ambiguity surface has the form

$$A_{sn}(\omega) = |B_c(\omega - \omega_a)|. \quad (4.486)$$

$A_{sn}(\omega)$ is plotted in Figure 4.26. It is similar to the known phase ambiguity surface in Figure 4.9 except the “mainlobe” around the peak at ω_a is wider and the sidelobes have a different structure.

The Fisher information matrix for joint estimation of ω and θ is (e.g. [RB74] or Problem 4.3.7),

$$\mathbf{J}(\omega, \theta) = \text{SNR} \begin{bmatrix} \frac{N(N-1)(2N-1)}{3} & N(N-1) \\ N(N-1) & 2N \end{bmatrix}. \quad (4.487)$$

Again, it depends on SNR and N , but not ω or θ . Taking the inverse of (4.487), we obtain bounds on the variances of any unbiased estimators:

$$\text{Var} [\hat{\omega}(\tilde{\mathbf{R}}) - \omega] \geq \frac{1}{\text{SNR}} \left(\frac{6}{N(N^2-1)} \right), \quad (4.488)$$

$$\text{Var} [\hat{\theta}(\tilde{\mathbf{R}}) - \theta] \geq \frac{1}{\text{SNR}} \left(\frac{2N-1}{N(N+1)} \right). \quad (4.489)$$

In Figures 4.27 and 4.28, we show the results from 10,000 trials of a Monte Carlo simulation. The frequency bias is similar to Example 4.15. Both the frequency and the phase are asymptotically unbiased. The frequency RMSE again exhibits a sharp threshold at 1 dB, whereas the phase RMSE increases more gradually below the same threshold. Both approach their respective CRBs as the SNR increases. For low SNR, the phase CRB exceeds the actual MSE. It is not a valid bound in this region because the estimator is biased. For comparison, the frequency RMSE and CRB for the known phase

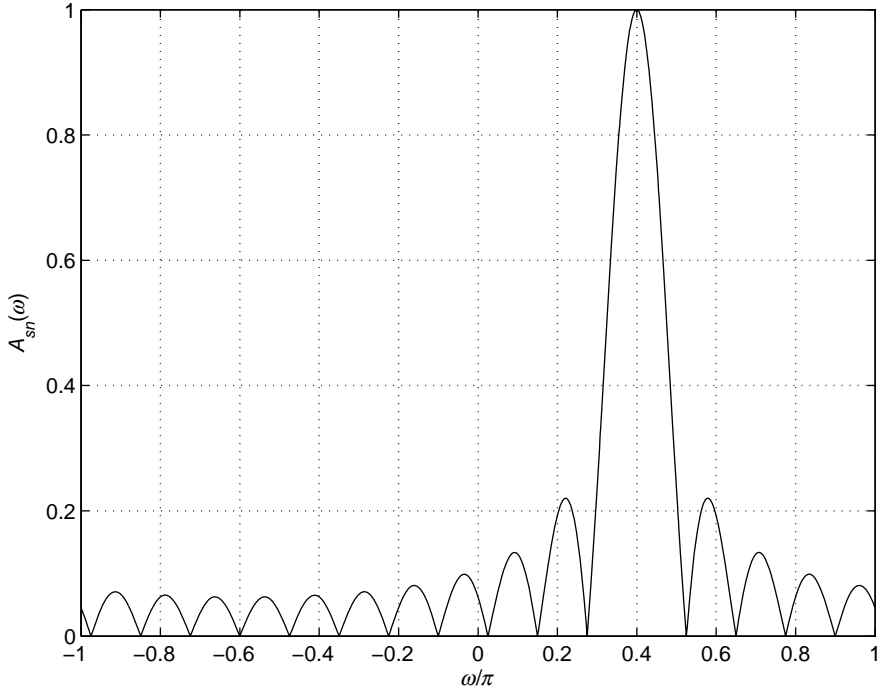


Figure 4.26: Signal ambiguity surface, $A_{sn}(\omega)$, unknown phase. $N = 16$, $\omega_a = 0.4\pi$, $\theta = \pi/6$.

case are also plotted in Figure 4.28. The asymptotic RMSE is better by about a factor of two (3 dB) when the phase is known. ■

A similar model arises in the array processing problem introduced in Examples 3.2 and 3.7 in the context of a detection problem. We now revisit it in the context of an estimation problem.

Example 4.30 DOA estimation. The physical model of interest is described in Example 3.2 (Figure 3.9 and equations (3.130)–(3.142)). The output from a single sample is

$$\tilde{\mathbf{r}}_k = \tilde{b} \tilde{\mathbf{v}}(\psi) + \tilde{\mathbf{w}}_k, \quad k = 1, 2, \dots, K, \quad (4.490)$$

where $\tilde{\mathbf{v}}(\psi)$ was defined in (3.137). We assume that

$$E [\tilde{\mathbf{w}}_k^H \tilde{\mathbf{w}}_l] = \sigma_w^2 \mathbf{I} \delta_{kl}. \quad (4.491)$$

We want to estimate ψ and \tilde{b} , where

$$\tilde{b} = b e^{j\phi}, \quad (4.492)$$

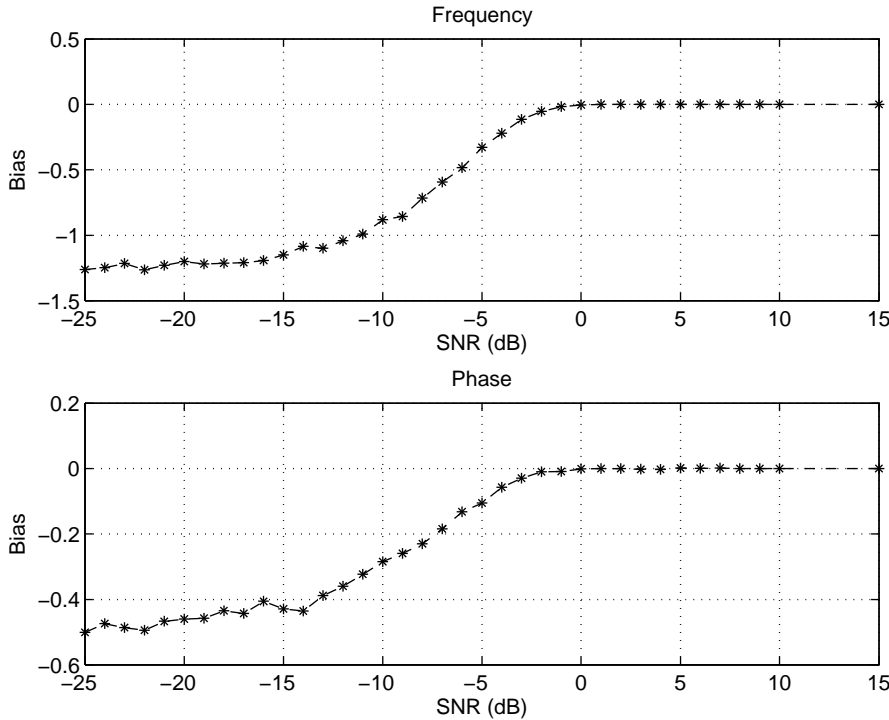


Figure 4.27: Frequency and phase bias versus SNR. $N = 16$, $\omega_a = 0.4\pi$, $\theta = \pi/6$.

so the parameter vector is¹⁸

$$\mathbf{a} \triangleq \begin{bmatrix} b \\ \psi \\ \phi \end{bmatrix}. \quad (4.493)$$

We can also write the parameter vector as

$$\tilde{\mathbf{a}} = \begin{bmatrix} \tilde{b} \\ \psi \end{bmatrix}, \quad (4.494)$$

as a short-hand notation for (4.493).

The joint probability density is

$$p_{\tilde{\mathbf{r}}_1, \tilde{\mathbf{r}}_2, \dots, \tilde{\mathbf{r}}_K | \mathbf{a}} (\tilde{\mathbf{R}}_1, \tilde{\mathbf{R}}_2, \dots, \tilde{\mathbf{R}}_K | \mathbf{A}) = \prod_{k=1}^K \frac{1}{(\pi \sigma_w^2)^N} \exp \left\{ -\frac{1}{\sigma_w^2} (\tilde{\mathbf{R}}_k - \tilde{b} \tilde{\mathbf{v}}(\psi))^H (\tilde{\mathbf{R}}_k - \tilde{b} \tilde{\mathbf{v}}(\psi)) \right\}, \quad (4.495)$$

¹⁸We use ϕ to denote the phase of \tilde{b} to avoid confusion with the angle of arrival θ defined in Example 3.2. We use K to denote the number of samples. This should not be confused with the number of unknown parameters, which is three for this problem.

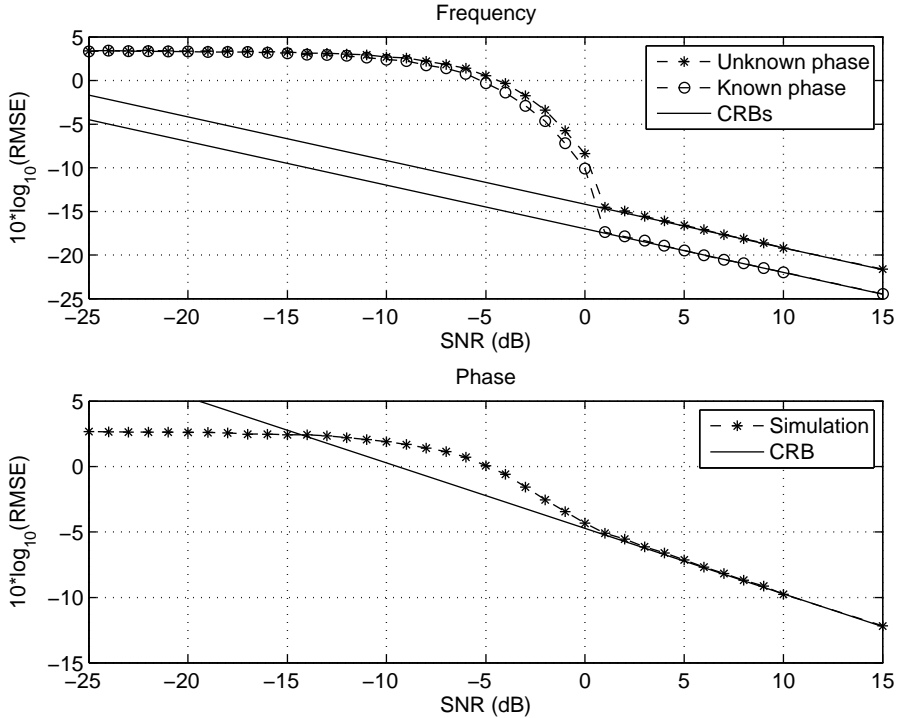


Figure 4.28: Frequency and phase RMSE versus SNR. $N = 16$, $\omega_a = 0.4\pi$, $\theta = \pi/6$.

and the log-likelihood function is¹⁹

$$l(\mathbf{A}; \tilde{\mathbf{R}}) = l(\tilde{b}, \psi; \tilde{\mathbf{R}}) = -KN \ln(\pi \sigma_w^2) - \frac{1}{\sigma_w^2} \sum_{k=1}^K (\tilde{\mathbf{R}}_k - \tilde{b} \tilde{\mathbf{v}}(\psi))^H (\tilde{\mathbf{R}}_k - \tilde{b} \tilde{\mathbf{v}}(\psi)). \quad (4.496)$$

To find $\hat{\mathbf{a}}_{\text{ml}}(\tilde{\mathbf{R}})$, we find the maximum of $l(\tilde{b}, \psi; \tilde{\mathbf{R}})$. Taking the complex gradient with respect to \tilde{b}^* and putting the result equal to zero gives²⁰

$$\sum_{k=1}^K \frac{\tilde{\mathbf{v}}(\psi)^H}{\sigma_w^2} (\tilde{\mathbf{R}}_k - \tilde{b} \tilde{\mathbf{v}}(\psi)) = 0. \quad (4.497)$$

Solving gives the maximum likelihood estimate of \tilde{b} ,

$$\hat{\tilde{b}}_{\text{ml}}(\tilde{\mathbf{R}}, \psi) = \frac{\tilde{\mathbf{v}}(\psi)^H}{\tilde{\mathbf{v}}(\psi)^H \tilde{\mathbf{v}}(\psi)} \left(\frac{1}{K} \sum_{k=1}^K \tilde{\mathbf{R}}_k \right). \quad (4.498)$$

¹⁹Note that this model is different from the models in Section 8.4 of *Optimum Array Processing* [Van02]. In those models, \tilde{b} is a function of k and is modeled as either a zero-mean complex Gaussian variable or an unknown nonrandom parameter. Those models also include multiple planewaves. The same techniques apply but the results are more complicated.

²⁰A discussion of complex gradients is given in Section 5.2.4.1 and p. 1404 of [Van02], based on Brandwood [Bra83].

Noting that the first term in (4.498) is the Moore–Penrose pseudo-inverse,

$$\tilde{\mathbf{v}}(\psi)^\dagger \triangleq (\tilde{\mathbf{v}}(\psi)^H \tilde{\mathbf{v}}(\psi))^{-1} \tilde{\mathbf{v}}(\psi)^H, \quad (4.499)$$

and defining the sample mean vector to be

$$\tilde{\mathbf{R}} \triangleq \frac{1}{K} \sum_{k=1}^K \tilde{\mathbf{R}}_k, \quad (4.500)$$

(4.498) reduces to

$$\hat{b}_{\text{ml}}(\tilde{\mathbf{R}}, \psi) = \tilde{\mathbf{v}}(\psi)^\dagger \tilde{\mathbf{R}}. \quad (4.501)$$

The processor $\tilde{\mathbf{v}}(\psi)^\dagger$ is called the *conventional beamformer*.

Substituting (4.501) into (4.496) gives the compressed log-likelihood function

$$l(\psi; \tilde{\mathbf{R}}) = -\frac{1}{\sigma_w^2} \sum_{k=1}^K \left[\tilde{\mathbf{R}}_k^H - \tilde{\mathbf{R}}^H \tilde{\mathbf{v}}(\psi) \tilde{\mathbf{v}}(\psi)^\dagger \right] \left[\tilde{\mathbf{R}}_k - \mathbf{v}(\psi) \mathbf{v}(\psi)^\dagger \tilde{\mathbf{R}} \right] + \zeta_1, \quad (4.502)$$

where ζ_1 represents terms that do not depend on ψ . Multiplying the terms out and noting that the $\tilde{\mathbf{R}}_k^H \tilde{\mathbf{R}}_k$ term does not depends on ψ gives

$$l(\psi; \tilde{\mathbf{R}}) = \frac{K}{\sigma_w^2} |\tilde{\mathbf{v}}(\psi)^\dagger \tilde{\mathbf{R}}|^2 + \zeta_2. \quad (4.503)$$

Therefore,

$$\hat{\psi}_{\text{ml}}(\tilde{\mathbf{R}}) = \underset{\psi}{\operatorname{argmax}} |\tilde{\mathbf{v}}(\psi)^\dagger \tilde{\mathbf{R}}|, \quad (4.504)$$

which is identical to (4.483) with the sample mean vector $\tilde{\mathbf{R}}$ replacing the observation vector $\tilde{\mathbf{R}}$ and $-\psi$ replacing ω . Thus, all of the results in Example 4.29 (Figures 4.26–4.28) for frequency estimation are applicable with

$$N_{DOA} = N_F, \quad (4.505)$$

$$K \operatorname{SNR}_{DOA} = \operatorname{SNR}_F, \quad (4.506)$$

where

$$\operatorname{SNR}_{DOA} \triangleq \frac{b^2}{\sigma_w^2}. \quad (4.507)$$

In order to find the Fisher information matrix, we must use the parameter vector in (4.493). The FIM for joint estimation of b , ψ , and ϕ is (e.g. [RB74] or Problem 4.3.7),

$$\mathbf{J}_F(\mathbf{A}) = K \operatorname{SNR}_{DOA} \begin{bmatrix} 2N & 0 & 0 \\ 0 & \frac{N(N-1)(2N-1)}{3} & N(N-1) \\ 0 & N(N-1) & 2N \end{bmatrix}. \quad (4.508)$$

The bound on b is uncoupled so the results in (4.488) and (4.489) hold. In particular

$$\operatorname{Var} [\hat{\psi}(\tilde{\mathbf{R}}) - \psi] \geq \frac{1}{K \operatorname{SNR}_{DOA}} \left(\frac{6}{N(N^2-1)} \right). \quad (4.509)$$

■

Other examples of ML estimation of nonrandom parameters are developed in the problems. The key steps are as follows:

(1) Find

$$\hat{a}_{\text{ml}}(\mathbf{R}) = \underset{\mathbf{A}}{\operatorname{argmax}} \left\{ \ln p_{\mathbf{r}|\mathbf{a}}(\mathbf{R}|\mathbf{A}) \right\}. \quad (4.510)$$

(a) Assuming the maximum is interior, use the likelihood equation,

$$\frac{\partial}{\partial A_i} \left[\ln p_{\mathbf{r}|\mathbf{a}}(\mathbf{R}|\mathbf{A}) \right] = 0, \quad i = 1, 2, \dots, K. \quad (4.511)$$

If there is a single solution, check that the maximum is interior. If there are multiple solutions, evaluate (4.510) and choose the solution that gives the maximum. Note that in many applications, there are too many solutions to (4.511) that step 1(a) is not practical (recall Figure 4.10) and we must do the search in step 1.

(b) If (4.511) has an analytical solution for some subset of \mathbf{A} , say \mathbf{A}_1 , substitute these solutions into $l(\mathbf{A}_1, \mathbf{A}_2; \mathbf{R})$ to create a compressed log-likelihood function $l(\mathbf{A}_2; \mathbf{R})$, then

$$\hat{\mathbf{a}}_{2\text{ml}}(\mathbf{R}) = \underset{\mathbf{A}_2}{\operatorname{argmax}} l(\mathbf{A}_2; \mathbf{R}). \quad (4.512)$$

- (2) Check the bias of estimates.
- (3) Evaluate the CRB and check for efficiency using (4.395).
- (4) Simulate the estimation algorithm and check both the asymptotic performance and the threshold behavior.

We consider random parameters in the next section.

4.3.3.2 Random Parameters

The extension of the Bayesian Cramér–Rao bound to the multiple parameter case is straightforward. We first state the bound and then derive it.

We define a $K \times K$ *Bayesian information matrix* (BIM) \mathbf{J}_B , whose elements are

$$\begin{aligned} J_{Bij} &\triangleq E_{\mathbf{r}, \mathbf{a}} \left\{ \frac{\partial \ln p_{\mathbf{r}, \mathbf{a}}(\mathbf{R}, \mathbf{A})}{\partial A_i} \cdot \frac{\partial \ln p_{\mathbf{r}, \mathbf{a}}(\mathbf{R}, \mathbf{A})}{\partial A_j} \right\} \\ &= -E_{\mathbf{r}, \mathbf{a}} \left\{ \frac{\partial^2 \ln p_{\mathbf{r}, \mathbf{a}}(\mathbf{R}, \mathbf{A})}{\partial A_i \partial A_j} \right\}, \end{aligned} \quad (4.513)$$

which can be written in matrix notation as

$$\begin{aligned} \mathbf{J}_B &= E \left([\nabla_{\mathbf{A}} \ln p_{\mathbf{r}, \mathbf{a}}(\mathbf{R}, \mathbf{A})] [\nabla_{\mathbf{A}} \ln p_{\mathbf{r}, \mathbf{a}}(\mathbf{R}, \mathbf{A})]^T \right) \\ &= -E_{\mathbf{r}, \mathbf{a}} \left(\nabla_{\mathbf{A}} [\nabla_{\mathbf{A}} \ln p_{\mathbf{r}, \mathbf{a}}(\mathbf{R}, \mathbf{A})]^T \right). \end{aligned} \quad (4.514)$$

Note that the expectation is over the joint density $p_{\mathbf{r}, \mathbf{a}}(\mathbf{R}, \mathbf{A})$.

The BIM can be divided into two parts

$$\mathbf{J}_B = \mathbf{J}_D + \mathbf{J}_P, \quad (4.515)$$

where

$$\begin{aligned}
J_{D_{ij}} &\triangleq E_{\mathbf{r}, \mathbf{a}} \left\{ \frac{\partial \ln p_{\mathbf{r}|\mathbf{a}}(\mathbf{R}|\mathbf{A})}{\partial A_i} \cdot \frac{\partial \ln p_{\mathbf{r}|\mathbf{a}}(\mathbf{R}|\mathbf{A})}{\partial A_j} \right\} \\
&= -E_{\mathbf{r}, \mathbf{a}} \left\{ \frac{\partial^2 \ln p_{\mathbf{r}|\mathbf{a}}(\mathbf{R}|\mathbf{A})}{\partial A_i \partial A_j} \right\} \\
&= E_{\mathbf{a}} \left\{ -E_{\mathbf{r}|\mathbf{a}} \frac{\partial^2 \ln p_{\mathbf{r}|\mathbf{a}}(\mathbf{R}|\mathbf{A})}{\partial A_i \partial A_j} \right\} \\
&= E_{\mathbf{a}} \{ J_{F_{ij}}(\mathbf{A}) \},
\end{aligned} \tag{4.516}$$

or, in matrix notation

$$\mathbf{J}_D = E_{\mathbf{a}} \{ \mathbf{J}_F(\mathbf{A}) \}, \tag{4.517}$$

and

$$\begin{aligned}
J_{P_{ij}} &\triangleq E_{\mathbf{a}} \left\{ \frac{\partial \ln p_{\mathbf{a}}(\mathbf{A})}{\partial A_i} \cdot \frac{\partial \ln p_{\mathbf{a}}(\mathbf{A})}{\partial A_j} \right\} \\
&= -E_{\mathbf{a}} \left\{ \frac{\partial^2 \ln p_{\mathbf{a}}(\mathbf{A})}{\partial A_i \partial A_j} \right\}
\end{aligned} \tag{4.518}$$

or, in matrix notation

$$\begin{aligned}
\mathbf{J}_P &= E \left([\nabla_{\mathbf{A}} \ln p_{\mathbf{a}}(\mathbf{A})] [\nabla_{\mathbf{A}} \ln p_{\mathbf{a}}(\mathbf{A})]^T \right) \\
&= -E_{\mathbf{a}} \left\{ \nabla_{\mathbf{A}} [\nabla_{\mathbf{A}} \ln p_{\mathbf{a}}(\mathbf{A})]^T \right\}.
\end{aligned} \tag{4.519}$$

The \mathbf{J}_D term in (4.517) represents the contribution of the data and the \mathbf{J}_P term in (4.519) represents the contribution of the prior information.

The Bayesian Cramér–Rao bound states that

$$\boldsymbol{\Sigma}_{\epsilon} - \mathbf{J}_B^{-1} \geqslant 0, \tag{4.520}$$

where $\boldsymbol{\Sigma}_{\epsilon}$ is the MSE matrix defined in (4.390) and \mathbf{J}_B is the BIM defined in (4.514).

Proof. The following conditions are assumed to exist:

1. $\frac{\partial p_{\mathbf{r}, \mathbf{a}}(\mathbf{R}, \mathbf{A})}{\partial A_i}$ is absolutely integrable with respect to \mathbf{R} and \mathbf{A} for $i = 1, 2, \dots, K$.
2. $\frac{\partial^2 p_{\mathbf{r}, \mathbf{a}}(\mathbf{R}, \mathbf{A})}{\partial A_i \partial A_j}$ is absolutely integrable with respect to \mathbf{R} and \mathbf{A} for $i, j = 1, 2, \dots, K$.
3. The conditional expectation of the error, given \mathbf{A} , is

$$\mathbf{B}(\mathbf{A}) = \int_{-\infty}^{\infty} [\hat{\mathbf{a}}(\mathbf{R}) - \mathbf{A}] p_{\mathbf{r}|\mathbf{a}}(\mathbf{R}|\mathbf{A}) d\mathbf{R}. \tag{4.521}$$

We assume that

$$\begin{aligned} \lim_{A_i \rightarrow \infty} \mathbf{B}(\mathbf{A}) p_{\mathbf{a}}(\mathbf{A}) &= \mathbf{0}, \\ \lim_{A_i \rightarrow -\infty} \mathbf{B}(\mathbf{A}) p_{\mathbf{a}}(\mathbf{A}) &= \mathbf{0}, \end{aligned} \quad \text{for } i = 1, 2, \dots, K. \quad (4.522)$$

Multiply both sides of (4.521) by $p_{\mathbf{a}}(\mathbf{A})$ and then differentiate with respect to \mathbf{A} :

$$p_{\mathbf{a}}(\mathbf{A}) \mathbf{B}^T(\mathbf{A}) = \int_{-\infty}^{\infty} p_{\mathbf{r}, \mathbf{a}}(\mathbf{R}, \mathbf{A}) [\hat{\mathbf{a}}(\mathbf{R}) - \mathbf{A}]^T d\mathbf{R}, \quad (4.523)$$

$$\nabla_{\mathbf{A}} \{ p_{\mathbf{a}}(\mathbf{A}) \mathbf{B}^T(\mathbf{A}) \} = \int_{-\infty}^{\infty} \nabla_{\mathbf{A}} \{ p_{\mathbf{r}, \mathbf{a}}(\mathbf{R}, \mathbf{A}) \} [\hat{\mathbf{a}}(\mathbf{R}) - \mathbf{A}]^T d\mathbf{R} - \mathbf{I} \int_{-\infty}^{\infty} p_{\mathbf{r}, \mathbf{a}}(\mathbf{R}, \mathbf{A}) d\mathbf{R}. \quad (4.524)$$

Now integrate with respect to \mathbf{A} . The ij th element of the left-hand side is

$$\begin{aligned} \left[\int_{-\infty}^{\infty} \nabla_{\mathbf{A}} \{ p_{\mathbf{a}}(\mathbf{A}) \mathbf{B}^T(\mathbf{A}) \} d\mathbf{A} \right]_{ij} &= \int_{-\infty}^{\infty} \frac{\partial p_{\mathbf{a}}(\mathbf{A}) B_j(\mathbf{A})}{\partial A_i} d\mathbf{A} \\ &= \int_{-\infty}^{\infty} \cdots \int_{-\infty}^{\infty} \left(p_{\mathbf{a}}(\mathbf{A}) B_j(\mathbf{A}) \Big|_{A_i=-\infty}^{\infty} \right) \\ &\quad \times dA_1 \cdots dA_{i-1} dA_{i+1} \cdots dA_K. \end{aligned} \quad (4.525)$$

The assumption in Condition 3 makes (4.525) equal to zero for all i and j . Setting the integral of the right-hand side equal to $\mathbf{0}$ gives

$$\mathbf{0} = \int_{-\infty}^{\infty} \int_{-\infty}^{\infty} \nabla_{\mathbf{A}} \{ p_{\mathbf{r}, \mathbf{a}}(\mathbf{R}, \mathbf{A}) \} [\hat{\mathbf{a}}(\mathbf{R}) - \mathbf{A}]^T d\mathbf{R} d\mathbf{A} - \mathbf{I}, \quad (4.526)$$

which may be written as

$$\int_{-\infty}^{\infty} \int_{-\infty}^{\infty} \left\{ [\hat{\mathbf{a}}(\mathbf{R}) - \mathbf{A}] \sqrt{p_{\mathbf{r}, \mathbf{a}}(\mathbf{R}, \mathbf{A})} \right\} \left\{ \sqrt{p_{\mathbf{r}, \mathbf{a}}(\mathbf{R}, \mathbf{A})} [\nabla_{\mathbf{A}} \ln p_{\mathbf{r}, \mathbf{a}}(\mathbf{R}, \mathbf{A})]^T \right\} d\mathbf{R} d\mathbf{A} = \mathbf{I}. \quad (4.527)$$

We see that (4.527) is in exactly the same form as (4.403). We repeat the steps in (4.404) through (4.412) and obtain

$$\boldsymbol{\Sigma}_{\epsilon} - \mathbf{J}_B^{-1} \geqslant 0, \quad (4.528)$$

where the inequality means the matrix is nonnegative definite. We have equality in (4.528) iff

$$\nabla_{\mathbf{A}} \ln p_{\mathbf{r}, \mathbf{a}}(\mathbf{R}, \mathbf{A}) = \mathbf{k}[\hat{\mathbf{a}}(\mathbf{R}) - \mathbf{A}] \quad (4.529)$$

or equivalently, in terms of *a posteriori* density

$$\nabla_{\mathbf{A}} \ln p_{\mathbf{a}|\mathbf{r}}(\mathbf{A}|\mathbf{R}) = \mathbf{k}[\hat{\mathbf{a}}(\mathbf{R}) - \mathbf{A}]. \quad (4.530)$$

As in the scalar case, this implies that the *a posteriori* density must be a multivariate Gaussian density. Note that \mathbf{k} is not a function of \mathbf{A} . Repeating the steps in (4.413)–(4.419),

we find that $\mathbf{k} = \mathbf{J}_B$. Whenever (4.529) is satisfied, we call the estimate a Bayesian efficient estimate.²¹

Several properties follow easily:

Property 1.

$$E[a_{\epsilon_i}^2] \geq J_B^{ii}. \quad (4.531)$$

In other words, the diagonal elements in the inverse of the Bayesian information matrix are lower bounds on the corresponding mean-square errors.

Property 2: Functions of the parameter vector. Define

$$\mathbf{d} = \gamma(\mathbf{a}). \quad (4.532)$$

The estimation error is

$$d_{\epsilon_i} \triangleq \hat{d}_i(\mathbf{R}) - \gamma_i(\mathbf{A}) \quad (4.533)$$

and the MSE matrix is²²

$$\Sigma_{\epsilon} \{\mathbf{d}\} \triangleq E_{\mathbf{r}, \mathbf{a}} \{ \mathbf{d}_{\epsilon} \mathbf{d}_{\epsilon}^T \}. \quad (4.534)$$

The BCRB is

$$\Sigma_{\epsilon} \{\mathbf{d}\} - E_{\mathbf{a}} \{ \nabla_{\mathbf{A}} [\gamma^T(\mathbf{A})] \}^T \mathbf{J}_B^{-1} E_{\mathbf{a}} \{ \nabla_{\mathbf{A}} [\gamma^T(\mathbf{A})] \} \geq 0. \quad (4.535)$$

This is proved in Section 4.4.1.6 when we discuss global Bayesian bounds.

Property 3. Assume that

$$\gamma(\mathbf{A}) \triangleq \boldsymbol{\Gamma} \mathbf{A}, \quad (4.536)$$

where $\boldsymbol{\Gamma}$ is an $M \times K$ matrix. Then

$$\Sigma_{\epsilon} \{\mathbf{d}\} - \boldsymbol{\Gamma} \mathbf{J}_B^{-1} \boldsymbol{\Gamma}^T \geq 0. \quad (4.537)$$

Property 4: Asymptotic behavior. The asymptotic behavior for the vector parameter case is the same as in the scalar parameter case. The MMSE and MAP estimates approach the ML estimate

$$\lim_{N \rightarrow \infty} \hat{\mathbf{a}}_{\text{ms}}(\mathbf{R}) = \lim_{N \rightarrow \infty} \hat{\mathbf{a}}_{\text{map}}(\mathbf{R}) = \hat{\mathbf{a}}_{\text{ml}}(\mathbf{R}). \quad (4.538)$$

Under suitable regularity conditions $\hat{\mathbf{a}}_{\text{ml}}(\mathbf{R})$ is asymptotically unbiased, so that the ECRB applies.

²¹The vector Bayesian Cramér–Rao bound was derived by Van Trees [Van68, Van01a]. It was derived independently by Shutzenberger [Shu57].

²²We use the notation $\Sigma_{\epsilon} \{\mathbf{d}\}$ to indicate that the MSE matrix is with respect to the parameter vector \mathbf{d} . It is not a function of \mathbf{d} , since we take the expected value over both \mathbf{r} and $\mathbf{a} = \gamma^{-1}(\mathbf{d})$.

The lower bounds are

$$\text{ECRB} = E_{\mathbf{a}} \{ \mathbf{J}_F^{-1}(\mathbf{A}) \} \geq [E_{\mathbf{a}} \{ \mathbf{J}_F(\mathbf{A}) \}]^{-1} \geq [\mathbf{J}_D + \mathbf{J}_P]^{-1} = \text{BCRB} \quad (4.539)$$

and the mean-square error matrix Σ_ϵ approaches the ECRB as $N \rightarrow \infty$.

There is parallelism between the Cramér–Rao bounds for nonrandom parameters and Bayesian Cramér–Rao bounds for random parameters but there are also significant differences. In both cases, they are bounds that closely predict performance of realizable estimators in the asymptotic or the high SNR region, under suitable regularity conditions. However, for nonrandom parameters the bounds will usually be on the variance of the error of any unbiased estimator and will depend on the actual value of \mathbf{a} . In the random parameter case, the bound will be for the MSE averaged over the prior distribution and there is no requirement for the estimator to be unbiased. The theory and application of these “small error” bounds is well understood and there are numerous examples in the literature.

Property 5: Conjugate priors. Conjugate priors are available for many of the likelihood functions that we will encounter in our applications. Tables of conjugate priors are available in Gelman et al. [GCSR04]. In Appendix A, we provide a partial list of conjugate prior densities for distributions in the exponential family. Some cases of particular interest are as follows:

- (a) Likelihood function $N(m, \sigma^2)$ with both parameters unknown; conjugate prior is Normal-Inverse Gamma $(m_0, \sigma_0^2, a_0, b_0)$.
- (b) Likelihood function $N(\mathbf{m}, \mathbf{K})$ with \mathbf{K} known; conjugate prior is $N(\mathbf{m}_0, \mathbf{K}_0)$.
- (c) Likelihood function $N(\mathbf{m}, \mathbf{K})$ with \mathbf{m} known; conjugate prior is Inverse Wishart (n_0, \mathbf{Q}_0) .
- (d) Likelihood function $N(\mathbf{m}, \mathbf{K})$ with both parameters unknown; conjugate prior is Normal-Inverse Wishart $(\mathbf{m}_0, \sigma_0^2, n_0, \mathbf{Q}_0)$.

We consider an example to illustrate the concepts.

Example 4.31 (continuation of Example 4.27) Multivariate Gaussian. The likelihood function is given in (4.460). Now the unknown mean vector \mathbf{m} is a random vector with *a priori* density

$$p_{\mathbf{m}}(\mathbf{M}) = \frac{1}{(2\pi)^{M/2} |\mathbf{K}_0|^{1/2}} \exp \left\{ -\frac{1}{2} (\mathbf{M} - \mathbf{m}_0)^T \mathbf{K}_0^{-1} (\mathbf{M} - \mathbf{m}_0) \right\}. \quad (4.540)$$

The Bayesian log-likelihood function is

$$l_B(\mathbf{M}; \mathbf{R}_1, \mathbf{R}_2, \dots, \mathbf{R}_N) = -\frac{1}{2} \sum_{i=1}^N (\mathbf{R}_i - \mathbf{M})^T \mathbf{K}_n^{-1} (\mathbf{R}_i - \mathbf{M}) - \frac{1}{2} (\mathbf{M} - \mathbf{m}_0)^T \mathbf{K}_0^{-1} (\mathbf{M} - \mathbf{m}_0) + \zeta, \quad (4.541)$$

where ζ represents terms that are not a function of \mathbf{M} . Taking the gradient with respect to \mathbf{M} gives

$$\nabla_{\mathbf{M}} l_B(\mathbf{M}; \mathbf{R}_1, \dots, \mathbf{R}_N) = \mathbf{K}_n^{-1} \sum_{i=1}^N (\mathbf{R}_i - \mathbf{M}) - \mathbf{K}_0^{-1} (\mathbf{M} - \mathbf{m}_0) = \mathbf{0}, \quad (4.542)$$

and the MAP estimate is

$$\hat{\mathbf{m}}_{\text{map}}(\mathbf{R}) = [\mathbf{K}_0^{-1} + N\mathbf{K}_{\mathbf{n}}^{-1}]^{-1} [\mathbf{K}_0^{-1}\mathbf{m}_0 + N\mathbf{K}_{\mathbf{n}}^{-1}\bar{\mathbf{R}}], \quad (4.543)$$

which is the vector version of (4.63).

We differentiate (4.542) with respect to \mathbf{M} to find \mathbf{J}_B . The result is

$$\mathbf{J}_B = N\mathbf{K}_{\mathbf{n}}^{-1} + \mathbf{K}_0^{-1}, \quad (4.544)$$

which is the matrix version of (4.199).

The Bayesian log-likelihood function in (4.541) can be rewritten in the following form:

$$\begin{aligned} l_B(\mathbf{M}; \mathbf{R}_1, \mathbf{R}_2, \dots, \mathbf{R}_N) &= -\frac{1}{2} \left\{ \mathbf{M}^T [N\mathbf{K}_{\mathbf{n}}^{-1} + \mathbf{K}_0^{-1}] \mathbf{M} - 2\mathbf{M}^T \left(\mathbf{K}_{\mathbf{n}}^{-1} \sum_{i=1}^N \mathbf{R}_i + \mathbf{K}_0^{-1}\mathbf{m}_0 \right) \right\} + \zeta' \\ &= -\frac{1}{2} \{ \mathbf{M}^T \mathbf{K}_p^{-1} \mathbf{M} - 2\mathbf{M}^T \mathbf{K}_p^{-1} \mathbf{m}_p \} + \zeta'', \end{aligned} \quad (4.545)$$

where

$$\mathbf{K}_p \triangleq [N\mathbf{K}_{\mathbf{n}}^{-1} + \mathbf{K}_0^{-1}]^{-1}, \quad (4.546)$$

$$\mathbf{m}_p \triangleq \mathbf{K}_p (N\mathbf{K}_{\mathbf{n}}^{-1}\bar{\mathbf{R}} + \mathbf{K}_0^{-1}\mathbf{m}_0). \quad (4.547)$$

This corresponds to a multivariate Gaussian density with mean \mathbf{m}_p and covariance matrix \mathbf{K}_p ; thus, the prior density in (4.540) is a conjugate prior with prior hyperparameters \mathbf{m}_0 and \mathbf{K}_0 , and the posterior hyperparameters are \mathbf{m}_p and \mathbf{K}_p . Since \mathbf{m}_p is the mean and mode of the posterior density, the MMSE and MAP estimates are the same and are given by (4.543), with MSE matrix equal to \mathbf{K}_p . Thus, the MMSE and MAP estimates are Bayesian efficient, that is,

$$\Sigma_\epsilon = \mathbf{K}_p = [N\mathbf{K}_{\mathbf{n}}^{-1} + \mathbf{K}_0^{-1}]^{-1} = \mathbf{J}_B^{-1}. \quad (4.548)$$

Note that, as $N \rightarrow \infty$,

$$\lim_{N \rightarrow \infty} \hat{\mathbf{m}}_{\text{ms}}(\mathbf{R}) = \lim_{N \rightarrow \infty} \hat{\mathbf{m}}_{\text{map}}(\mathbf{R}) = \hat{\mathbf{m}}_{\text{ml}}(\mathbf{R}) = \bar{\mathbf{R}} \quad (4.549)$$

and

$$\lim_{N \rightarrow \infty} \Sigma_\epsilon = \mathbf{J}_F^{-1} = \frac{1}{N} \mathbf{K}_{\mathbf{n}}, \quad (4.550)$$

where $\hat{\mathbf{m}}_{\text{ml}}(\mathbf{R})$ and \mathbf{J}_F were found in Example 4.27, equations (4.463) and (4.464). ■

In the next section, we consider the exponential family.

4.3.4 Exponential Family

4.3.4.1 Nonrandom Parameters

The exponential family for vector parameters is a straightforward generalization of the scalar model. We assume that \mathbf{A} is a $K \times 1$ vector. We assume that we have N IID observations of an $M \times 1$ vector \mathbf{R} . The probability density of a single observation has the form

$$p_{\mathbf{r}_i|\mathbf{a}}(\mathbf{R}_i|\mathbf{A}) = C(\mathbf{R}_i) \exp \{ \boldsymbol{\phi}^T(\mathbf{A}) \mathbf{S}(\mathbf{R}_i) - T(\mathbf{A}) \}, \quad (4.551)$$

where $\mathbf{S}(\mathbf{R}_i)$ is a $K \times 1$ sufficient statistic and $\boldsymbol{\phi}(\mathbf{A})$ is a $K \times 1$ vector that is a function of the parameter vector \mathbf{A} . If

$$\boldsymbol{\phi}(\mathbf{A}) = \mathbf{A} \quad (4.552)$$

then the form is canonical.

The joint probability density function is

$$\begin{aligned} p_{\mathbf{r}_1, \mathbf{r}_2, \dots, \mathbf{r}_N | \mathbf{a}}(\mathbf{R}_1, \mathbf{R}_2, \dots, \mathbf{R}_N | \mathbf{A}) &= \prod_{i=1}^N p_{\mathbf{r}_i | \mathbf{a}}(\mathbf{R}_i | \mathbf{A}) \\ &= \left(\prod_{i=1}^N C(\mathbf{R}_i) \right) \exp \left\{ \boldsymbol{\phi}^T(\mathbf{A}) \sum_{i=1}^N \mathbf{S}(\mathbf{R}_i) - NT(\mathbf{A}) \right\} \\ &= C_N(\mathbf{R}) \exp \left\{ \boldsymbol{\phi}^T(\mathbf{A}) \mathbf{S}(\mathbf{R}) - NT(\mathbf{A}) \right\}, \end{aligned} \quad (4.553)$$

where

$$\mathbf{S}(\mathbf{R}) \triangleq \sum_{i=1}^N \mathbf{S}(\mathbf{R}_i) \quad (4.554)$$

is the $K \times 1$ sufficient statistic.

Property 1: Cumulants of $\mathbf{S}(\mathbf{R})$. We denote the components of $\mathbf{S}(\mathbf{R})$ by $S_k(\mathbf{R})$; $k = 1, 2, \dots, K$. Then, if the density is in the canonical form,

$$E \{ S_k(\mathbf{R}) | \boldsymbol{\theta} \} = N \frac{\partial T(\boldsymbol{\theta})}{\partial \theta_k}, \quad k = 1, 2, \dots, K \quad (4.555)$$

and

$$\text{Cov} \{ S_k(\mathbf{R}), S_j(\mathbf{R}) | \boldsymbol{\theta} \} = N \frac{\partial^2 T(\boldsymbol{\theta})}{\partial \theta_k \partial \theta_j}, \quad j, k = 1, 2, \dots, K. \quad (4.556)$$

Property 2: Maximum likelihood estimate. The maximum likelihood estimate of \mathbf{A} is given by

$$\left[\nabla_{\mathbf{A}} \boldsymbol{\phi}^T(\mathbf{A}) \right]^{-1} \nabla_{\mathbf{A}} T(\mathbf{A}) \Big|_{\mathbf{A}=\hat{\mathbf{a}}_{\text{ml}}(\mathbf{R})} = \frac{1}{N} \mathbf{S}(\mathbf{R}) \triangleq \bar{\mathbf{S}}(\mathbf{R}). \quad (4.557)$$

Proof. The log of (4.553) is

$$\ln p_{\mathbf{r}_1, \mathbf{r}_2, \dots, \mathbf{r}_N | \mathbf{a}}(\mathbf{R}_1, \mathbf{R}_2, \dots, \mathbf{R}_N | \mathbf{A}) = \boldsymbol{\phi}^T(\mathbf{A}) \mathbf{S}(\mathbf{R}) - NT(\mathbf{A}) + \zeta. \quad (4.558)$$

Taking the gradient with respect to \mathbf{A} and setting the result equal to zero gives

$$\nabla_{\mathbf{A}} \{ \boldsymbol{\phi}^T(\mathbf{A}) \} \frac{\mathbf{S}(\mathbf{R})}{N} = \nabla_{\mathbf{A}} \{ T(\mathbf{A}) \}, \quad (4.559)$$

which is the vector version of (4.295). Inverting the matrix on the left gives (4.557).

Property 3: Cramér–Rao bound. The Fisher information matrix is

$$\mathbf{J}_F(\mathbf{A}) = N \nabla_{\mathbf{A}} [\nabla_{\mathbf{A}} T(\mathbf{A})]^T - \sum_{k=1}^K (\nabla_{\mathbf{A}} [\nabla_{\mathbf{A}} \phi_k(\mathbf{A})]^T) E \{S_k(\mathbf{R})|\mathbf{A}\} \quad (4.560)$$

and if the density is in canonical form

$$\mathbf{J}_F(\boldsymbol{\theta}) = N \nabla_{\boldsymbol{\theta}} [\nabla_{\boldsymbol{\theta}} T(\boldsymbol{\theta})]^T. \quad (4.561)$$

Example 4.32 (continuation of Examples 4.17, 4.21, 4.23, and 4.26) Gaussian. The model is given in Example 4.26. The observations consist of N IID $N(m, \sigma^2)$ random variables where both m and σ^2 are unknown. From (4.427), the likelihood function is

$$\begin{aligned} p_{\mathbf{r}|\mathbf{a}}(\mathbf{R}|\mathbf{A}) &= \prod_{i=1}^N \frac{1}{\sqrt{2\pi\sigma^2}} \exp \left\{ -\frac{(R_i - m)^2}{2\sigma^2} \right\} \\ &= \frac{1}{(2\pi)^{N/2}} \exp \left\{ -\frac{1}{2\sigma^2} \sum_{i=1}^N R_i^2 + \frac{m}{\sigma^2} \sum_{i=1}^N R_i - \frac{Nm^2}{2\sigma^2} - \frac{N}{2} \ln \sigma^2 \right\}. \end{aligned} \quad (4.562)$$

Comparing (4.562) and (4.553) gives

$$C_N(\mathbf{R}) = \frac{1}{(2\pi)^{N/2}}, \quad (4.563)$$

$$\mathbf{S}(\mathbf{R}) = \begin{bmatrix} \sum_{i=1}^N R_i & \sum_{i=1}^N R_i^2 \end{bmatrix}^T, \quad (4.564)$$

$$\boldsymbol{\phi}^T(\mathbf{A}) = \begin{bmatrix} \frac{m}{\sigma^2} & -\frac{1}{2\sigma^2} \end{bmatrix}, \quad (4.565)$$

$$T(\mathbf{A}) = \frac{m^2}{2\sigma^2} + \frac{\ln \sigma^2}{2}. \quad (4.566)$$

Taking gradients

$$\nabla_{\mathbf{A}} \boldsymbol{\phi}^T(\mathbf{A}) = \begin{bmatrix} \frac{1}{\sigma^2} & 0 \\ \frac{-m}{\sigma^4} & \frac{1}{2\sigma^4} \end{bmatrix}, \quad (4.567)$$

$$\nabla_{\mathbf{A}} T(\mathbf{A}) = \begin{bmatrix} \frac{m}{\sigma^2} \\ \frac{-m^2}{2\sigma^4} + \frac{1}{2\sigma^2} \end{bmatrix}. \quad (4.568)$$

Using (4.567), (4.568), and (4.564) in (4.557), we obtain

$$\begin{bmatrix} m \\ m^2 + \sigma^2 \end{bmatrix} \Big|_{\mathbf{a}=\hat{\mathbf{a}}_{ml}(\mathbf{R})} = \begin{bmatrix} \frac{1}{N} \sum_{i=1}^N R_i \\ \frac{1}{N} \sum_{i=1}^N R_i^2 \end{bmatrix}, \quad (4.569)$$

which yields

$$\hat{m}_{\text{ml}}(\mathbf{R}) = \frac{1}{N} \sum_{i=1}^N R_i = \bar{R}, \quad (4.570)$$

$$\hat{\sigma}_{\text{ml}}^2(\mathbf{R}) = \frac{1}{N} \sum_{i=1}^N (R_i - \bar{R})^2, \quad (4.571)$$

which agree with (4.431) and (4.434).

To calculate the Fisher information matrix, we compute

$$\nabla_{\mathbf{A}} [\nabla_{\mathbf{A}} T(\mathbf{A})]^T = \begin{bmatrix} \frac{1}{\sigma^2} & \frac{-m}{\sigma^4} \\ \frac{-m}{\sigma^4} & \frac{m^2}{\sigma^6} - \frac{1}{2\sigma^4} \end{bmatrix}, \quad (4.572)$$

$$\nabla_{\mathbf{A}} [\nabla_{\mathbf{A}} \phi_1(\mathbf{A})]^T = \begin{bmatrix} 0 & \frac{-1}{\sigma^4} \\ \frac{-1}{\sigma^4} & \frac{2m}{\sigma^6} \end{bmatrix}, \quad (4.573)$$

$$\nabla_{\mathbf{A}} [\nabla_{\mathbf{A}} \phi_2(\mathbf{A})]^T = \begin{bmatrix} 0 & 0 \\ 0 & -\frac{1}{\sigma^6} \end{bmatrix}, \quad (4.574)$$

$$E \{ \mathbf{S}(\mathbf{R}) | \mathbf{A} \} = \begin{bmatrix} Nm \\ N(m^2 + \sigma^2) \end{bmatrix}. \quad (4.575)$$

We substitute (4.572)–(4.575) into (4.560) to obtain

$$\mathbf{J}_F(\mathbf{A}) = \begin{bmatrix} \frac{N}{\sigma^2} & \frac{-Nm}{\sigma^4} \\ \frac{-Nm}{\sigma^4} & \frac{Nm^2}{\sigma^6} - \frac{N}{2\sigma^4} \end{bmatrix} - \begin{bmatrix} 0 & \frac{-Nm}{\sigma^4} \\ \frac{-Nm}{\sigma^4} & \frac{2Nm}{\sigma^6} \end{bmatrix} - \begin{bmatrix} 0 & 0 \\ 0 & \frac{-N(m^2 + \sigma^2)}{\sigma^6} \end{bmatrix} = \begin{bmatrix} \frac{N}{\sigma^2} & 0 \\ 0 & \frac{N}{2\sigma^4} \end{bmatrix}, \quad (4.576)$$

which agrees with (4.441). ■

4.3.4.2 Random Parameters

Property 4: Conjugate prior. In the vector case, the conjugate prior has the form

$$p_{\mathbf{a}}(\mathbf{A}) = C_0 \exp \{ \boldsymbol{\phi}^T(\mathbf{A}) \mathbf{S}_0 - N_0 T(\mathbf{A}) \} \quad (4.577)$$

and the posterior density is

$$p_{\mathbf{a}|\mathbf{r}}(\mathbf{A}|\mathbf{R}) = C_p(\mathbf{R}) \exp \{ \boldsymbol{\phi}^T(\mathbf{A}) \mathbf{S}_p(\mathbf{R}) - N_p T(\mathbf{A}) \}, \quad (4.578)$$

where

$$N_p \triangleq N + N_0 \quad (4.579)$$

and

$$\mathbf{S}_p \triangleq \mathbf{S}(\mathbf{R}) + \mathbf{S}_0 \quad (4.580)$$

is the *a posteriori* sufficient statistic.

Property 5: MAP estimate. The MAP estimate of \mathbf{A} is given by

$$\left[\nabla_{\mathbf{A}} \phi^T(\mathbf{A}) \right]^{-1} \nabla_{\mathbf{A}} T(\mathbf{A}) \Big|_{\mathbf{A}=\hat{\mathbf{a}}_{\text{map}}(\mathbf{R})} = \frac{1}{N_p} \mathbf{S}_p(\mathbf{R}) \triangleq \bar{\mathbf{S}}_p(\mathbf{R}). \quad (4.581)$$

Property 6: Bayesian Cramér–Rao bound. The BIM is

$$\mathbf{J}_B = E_{\mathbf{a}} \left\{ N_p \nabla_{\mathbf{A}} [\nabla_{\mathbf{A}} T(\mathbf{A})]^T - \sum_{k=1}^K (\nabla_{\mathbf{A}} [\nabla_{\mathbf{A}} \phi_k(\mathbf{A})]^T) E [S_{p,k}(\mathbf{R}) | \mathbf{A}] \right\} \quad (4.582)$$

and if the density is in canonical form

$$\mathbf{J}_B = N_p E_{\theta} \{ \nabla_{\theta} [\nabla_{\theta} T(\theta)]^T \}. \quad (4.583)$$

4.3.5 Nuisance Parameters

Up to this point, we have assumed that all of the components of \mathbf{a} are of interest. We then developed estimation procedures and bounds on the MSE matrix in the Bayesian case and the error covariance matrix into the nonrandom parameter case. In many applications, the parameter vector contains the parameters of interest to us as well as other unwanted parameters.

We partition \mathbf{a} into two vectors,

$$\mathbf{a} = \begin{bmatrix} \mathbf{a}_w \\ \mathbf{a}_u \end{bmatrix}, \quad (4.584)$$

where \mathbf{a}_w is a $K_1 \times 1$ vector containing the wanted parameters and \mathbf{a}_u is a $K_2 \times 1$ vector containing the unwanted parameters, with $K_1 + K_2 = K$.

There are three cases of interest.

- (i) \mathbf{a}_w and \mathbf{a}_u are nonrandom vectors.
- (ii) \mathbf{a}_w and \mathbf{a}_u are random vectors.
- (iii) \mathbf{a} is a hybrid vector in which some elements are nonrandom and some elements are random.

We discuss these cases in the next three subsections.

4.3.5.1 Nonrandom Parameters

In this case, \mathbf{a}_w is a $K_1 \times 1$ nonrandom vector containing the wanted parameters and \mathbf{a}_u is a $K_2 \times 1$ nonrandom vector containing the unwanted parameters. To find the maximum likelihood estimate of \mathbf{a}_w , we must find the ML estimate of the entire vector \mathbf{a} :

$$\hat{\mathbf{a}}_{\text{ml}}(\mathbf{R}) = \underset{\mathbf{A}}{\operatorname{argmax}} \{ \ln p_{\mathbf{r}|\mathbf{a}}(\mathbf{R} | \mathbf{A}) \}. \quad (4.585)$$

Note that we do not have any way to eliminate \mathbf{a}_u so the fact that it is “unwanted” does not affect the estimator or the bound.

We can compute the Cramér–Rao bound on \mathbf{a}_w to determine how the unwanted parameters affect the bound. We write the Fisher information matrix as a partitioned matrix.

$$\mathbf{J}_F(\mathbf{A}) = \begin{bmatrix} \mathbf{J}_F(\mathbf{A}_w, \mathbf{A}_w) & \mathbf{J}_F(\mathbf{A}_w, \mathbf{A}_u) \\ \mathbf{J}_F(\mathbf{A}_u, \mathbf{A}_w) & \mathbf{J}_F(\mathbf{A}_u, \mathbf{A}_u) \end{bmatrix}, \quad (4.586)$$

where

$$[\mathbf{J}_F(\mathbf{A}_w, \mathbf{A}_w)]_{ij} = -E_{\mathbf{r}|\mathbf{a}} \left\{ \frac{\partial^2 \ln p_{\mathbf{r}|\mathbf{a}}(\mathbf{R}|\mathbf{A})}{\partial A_i \partial A_j} \right\}, \quad \begin{array}{l} i = 1, 2, \dots, K_1 \\ j = 1, 2, \dots, K_1 \end{array}, \quad (4.587)$$

$$[\mathbf{J}_F(\mathbf{A}_w, \mathbf{A}_u)]_{ij} = -E_{\mathbf{r}|\mathbf{a}} \left\{ \frac{\partial^2 \ln p_{\mathbf{r}|\mathbf{a}}(\mathbf{R}|\mathbf{A})}{\partial A_i \partial A_j} \right\}, \quad \begin{array}{l} i = 1, 2, \dots, K_1 \\ j = K_1 + 1, K_1 + 2, \dots, K \end{array}, \quad (4.588)$$

$$[\mathbf{J}_F(\mathbf{A}_u, \mathbf{A}_u)]_{ij} = -E_{\mathbf{r}|\mathbf{a}} \left\{ \frac{\partial^2 \ln p_{\mathbf{r}|\mathbf{a}}(\mathbf{R}|\mathbf{A})}{\partial A_i \partial A_j} \right\}, \quad \begin{array}{l} i = K_1 + 1, K_1 + 2, \dots, K \\ j = K_1 + 1, K_1 + 2, \dots, K \end{array}, \quad (4.589)$$

and

$$\mathbf{J}_F(\mathbf{A}_u, \mathbf{A}_w) = \mathbf{J}_F^T(\mathbf{A}_w, \mathbf{A}_u). \quad (4.590)$$

We partition the CRB in a similar manner:

$$\text{CRB}(\mathbf{A}) = \begin{bmatrix} \text{CRB}(\mathbf{A}_w) & \text{CRB}(\mathbf{A}_w, \mathbf{A}_u) \\ \text{CRB}(\mathbf{A}_u, \mathbf{A}_w) & \text{CRB}(\mathbf{A}_u) \end{bmatrix}. \quad (4.591)$$

We use the formula for the inverse of a block partitioned matrix to obtain

$$\text{CRB}(\mathbf{A}_w) = [\mathbf{J}_F(\mathbf{A}_w, \mathbf{A}_w) - \mathbf{J}_F(\mathbf{A}_w, \mathbf{A}_u)\mathbf{J}_F^{-1}(\mathbf{A}_u, \mathbf{A}_u)\mathbf{J}_F(\mathbf{A}_u, \mathbf{A}_w)]^{-1}. \quad (4.592)$$

The first term is the FIM for the wanted parameters when the unwanted parameters are known. The second term represents the effect of the unwanted parameters on the estimation error of the wanted parameters. It is always nonnegative definite. It will be zero when $\mathbf{J}_F(\mathbf{A}_w, \mathbf{A}_u)$ is zero, which corresponds to uncoupled parameters. If $\mathbf{J}_F(\mathbf{A}_w, \mathbf{A}_u)$ is nonzero, the minus sign before the second term causes $\text{CRB}(\mathbf{A}_w)$ to be larger than it would be when the unwanted parameters are known, that is,

$$\text{CRB}(\mathbf{A}_w) \geq J_F(\mathbf{A}_w, \mathbf{A}_w)^{-1}. \quad (4.593)$$

4.3.5.2 Random Parameters

We consider the same model as in the previous section except that \mathbf{a} is a random vector parameter with known *a priori* probability density. In order to find the MMSE or MAP estimate of \mathbf{a}_w , we find the posterior density of \mathbf{a}_w given \mathbf{r} :

$$p_{\mathbf{a}_w|\mathbf{r}}(\mathbf{A}_w|\mathbf{R}) = \frac{p_{\mathbf{r}, \mathbf{a}_w}(\mathbf{R}, \mathbf{A}_w)}{p_{\mathbf{r}}(\mathbf{R})}. \quad (4.594)$$

To find $p_{\mathbf{r}, \mathbf{a}_w}(\mathbf{R}, \mathbf{A}_w)$, we integrate out the unwanted parameters \mathbf{a}_u from the joint density $p_{\mathbf{r}, \mathbf{a}}(\mathbf{R}, \mathbf{A})$.

$$\begin{aligned} p_{\mathbf{r}, \mathbf{a}_w}(\mathbf{R}, \mathbf{A}_w) &= \int p_{\mathbf{r}, \mathbf{a}}(\mathbf{R}, \mathbf{A}) d\mathbf{A}_u \\ &= \int p_{\mathbf{r}|\mathbf{a}_w, \mathbf{a}_u}(\mathbf{R}|\mathbf{A}_w, \mathbf{A}_u) p_{\mathbf{a}_w, \mathbf{a}_u}(\mathbf{A}_w, \mathbf{A}_u) d\mathbf{A}_u. \end{aligned} \quad (4.595)$$

To find $\hat{\mathbf{a}}_{w, \text{map}}(\mathbf{R})$, we find the maximum of $\ln p_{\mathbf{r}, \mathbf{a}_w}(\mathbf{R}, \mathbf{A}_w)$.

$$\begin{aligned} \hat{\mathbf{a}}_{w, \text{map}}(\mathbf{R}) &= \underset{\mathbf{A}_w}{\operatorname{argmax}} \left\{ \ln p_{\mathbf{r}, \mathbf{a}_w}(\mathbf{R}, \mathbf{A}_w) \right\} \\ &= \underset{\mathbf{A}_w}{\operatorname{argmax}} \left\{ \ln p_{\mathbf{a}_w|\mathbf{r}}(\mathbf{A}_w|\mathbf{R}) \right\}. \end{aligned} \quad (4.596)$$

In order to find $\hat{\mathbf{a}}_{w, \text{map}}(\mathbf{R})$ using (4.596), we must perform the integration in (4.595). In many applications, this is difficult to do. An alternative approach is to jointly estimate \mathbf{a}_w and \mathbf{a}_u as in the nonrandom case. In order to compare the resulting performance, we study various Bayesian Cramér–Rao bounds on the MSE matrix.²³ The first bound is the BCRB on \mathbf{a}_w . The BIM is²⁴

$$\mathbf{J}_B \{ \mathbf{a}_w \} = -E_{\mathbf{r}, \mathbf{a}_w} \left\{ \nabla_{\mathbf{A}_w} \left[\nabla_{\mathbf{A}_w} \ln p_{\mathbf{r}, \mathbf{a}_w}(\mathbf{R}, \mathbf{A}_w) \right]^T \right\}. \quad (4.597)$$

We refer to the inverse of $\mathbf{J}_B \{ \mathbf{a}_w \}$ as Bound 1 (\mathbf{B}_1):

$$\mathbf{B}_1 = \mathbf{J}_B^{-1} \{ \mathbf{a}_w \}. \quad (4.598)$$

A second bound can be obtained by assuming we jointly estimated both \mathbf{a}_w and \mathbf{a}_u instead of integrating \mathbf{a}_u out. In this case, we compute $\mathbf{J}_B^{-1} \{ \mathbf{a} \}$ and use the $K_1 \times K_1$ matrix in the upper left corner as a bound on the MSE matrix of \mathbf{a}_w . Thus,

$$\begin{aligned} \mathbf{B}_2 &= [\mathbf{J}_B^{-1} \{ \mathbf{a} \}]_{\mathbf{a}_w, \mathbf{a}_w} \\ &= \left([\mathbf{J}_B \{ \mathbf{a} \}]_{\mathbf{a}_w, \mathbf{a}_w} - [\mathbf{J}_B \{ \mathbf{a} \}]_{\mathbf{a}_w, \mathbf{a}_u} ([\mathbf{J}_B \{ \mathbf{a} \}]_{\mathbf{a}_u, \mathbf{a}_u})^{-1} [\mathbf{J}_B \{ \mathbf{a} \}]_{\mathbf{a}_u, \mathbf{a}_w} \right)^{-1}. \end{aligned} \quad (4.599)$$

This bound has the same structure as (4.592); however, the \mathbf{J}_B terms are obtained by derivatives and expectations over $p_{\mathbf{r}, \mathbf{a}}(\mathbf{R}, \mathbf{A})$.

A third bound is obtained by inverting the upper left matrix in $\mathbf{J}_B \{ \mathbf{a} \}$:

$$\mathbf{B}_3 = ([\mathbf{J}_B \{ \mathbf{a} \}]_{\mathbf{a}_w, \mathbf{a}_w})^{-1}. \quad (4.600)$$

These bounds are ordered:

$$\mathbf{B}_1 \geq \mathbf{B}_2 \geq \mathbf{B}_3. \quad (4.601)$$

The order relation between \mathbf{B}_1 and \mathbf{B}_2 is proved in [BMZ87]. The order relation between \mathbf{B}_2 and \mathbf{B}_3 follows from (4.599).

²³This discussion follows Bobrovsky et al. [BMZ87].

²⁴We use the notation $\mathbf{J}_B \{ \mathbf{a}_w \}$ to indicate that BIM is with respect to the parameter vector \mathbf{a}_w . The BIM is not a function of \mathbf{a}_w , since we take the expected value over both \mathbf{r} and \mathbf{a}_w .

A different bound was derived by Miller and Chang [MC78]. They compute the Bayesian bound on \mathbf{a}_w conditioned on \mathbf{a}_u and take the expected value with respect to \mathbf{a}_u . We denote the conditional bound as $\mathbf{J}_B^{-1}\{\mathbf{a}_w|\mathbf{a}_u\}$. It is important to note that the conditional bound is a bound on the MSE matrix of \mathbf{a}_w and does not require that the estimate be unbiased for each value of \mathbf{a}_u . Then,

$$\mathbf{B}_4 = E_{\mathbf{a}_u} [\mathbf{J}_B^{-1}\{\mathbf{a}_w|\mathbf{a}_u\}]. \quad (4.602)$$

Note that

$$[\mathbf{J}_B\{\mathbf{a}\}]_{\mathbf{a}_w, \mathbf{a}_w} = E_{\mathbf{a}_u} [\mathbf{J}_B\{\mathbf{a}_w|\mathbf{a}_u\}], \quad (4.603)$$

and, therefore from Jensen's inequality

$$\mathbf{B}_4 \geq \mathbf{B}_3. \quad (4.604)$$

Bobrovsky et al. [BMZ87] give two examples to show that no further ordering is possible. In the first example, $\mathbf{B}_2 > \mathbf{B}_4$ and in the second example $\mathbf{B}_4 > \mathbf{B}_1$. In Miller and Chang [MC78], an example is analyzed and \mathbf{B}_4 provides the tightest bound.

Several comments are useful:

1. In many cases, the integration in (4.595) is difficult and/or the resulting expression is hard to analyze.
2. In several applications of interest, the first inequality in (4.601) reduces to an equality.
3. By partitioning \mathbf{a} differently (e.g., consider each $\mathbf{a}_{w_i}; i = 1, 2, \dots, K_1$, separately), different bounds are obtained.

4.3.5.3 Hybrid Parameters

In the most general model, the wanted parameter vector can be written as a hybrid vector

$$\mathbf{a}_w = \begin{bmatrix} \mathbf{a}_{w,nr} \\ \mathbf{a}_{w,r} \end{bmatrix}, \quad (4.605)$$

where $\mathbf{a}_{w,nr}$ is a $K_{11} \times 1$ nonrandom parameter vector and $\mathbf{a}_{w,r}$ is a $K_{12} \times 1$ random vector, where $K_{11} + K_{12} = K_1$. Similarly, the unwanted parameter vector can be written as a hybrid vector

$$\mathbf{a}_u = \begin{bmatrix} \mathbf{a}_{u,nr} \\ \mathbf{a}_{u,r} \end{bmatrix}, \quad (4.606)$$

where $\mathbf{a}_{u,nr}$ is a $K_{21} \times 1$ nonrandom parameter vector and $\mathbf{a}_{u,r}$ is a $K_{22} \times 1$ random vector, where $K_{21} + K_{22} = K_2$. We defer discussion of this case until the next section.

4.3.6 Hybrid Parameters

In the next case of interest, the parameter vector is

$$\mathbf{a} = \begin{bmatrix} \mathbf{a}_{nr} \\ \mathbf{a}_r \end{bmatrix}, \quad (4.607)$$

where \mathbf{a}_{nr} is a $K_1 \times 1$ nonrandom parameter vector and \mathbf{a}_r is a $K_2 \times 1$ random parameter vector with probability density $p_{\mathbf{a}_r|\mathbf{a}_{nr}}(\mathbf{A}_r|\mathbf{A}_{nr})$ and $K = K_1 + K_2$. We first consider the case in which we want to estimate the entire \mathbf{a} vector.

4.3.6.1 Joint ML and MAP Estimation

The probability density of interest is $p_{\mathbf{r},\mathbf{a}_r|\mathbf{a}_{nr}}(\mathbf{R}, \mathbf{A}_r|\mathbf{A}_{nr})$. The hybrid ML/MAP estimator is

$$\begin{aligned}\hat{\mathbf{a}}_{\text{hb}}(\mathbf{R}) &= \begin{bmatrix} \hat{\mathbf{a}}_{nr,\text{ml}}(\mathbf{R}) \\ \hat{\mathbf{a}}_{r,\text{map}}(\mathbf{R}) \end{bmatrix} \\ &= \underset{\mathbf{A}}{\operatorname{argmax}} \left\{ \ln p_{\mathbf{r},\mathbf{a}_r|\mathbf{a}_{nr}}(\mathbf{R}, \mathbf{A}_r|\mathbf{A}_{nr}) \right\} \\ &= \underset{\mathbf{A}}{\operatorname{argmax}} \left\{ \ln p_{\mathbf{r}|\mathbf{a}_r,\mathbf{a}_{nr}}(\mathbf{R}|\mathbf{A}_r, \mathbf{A}_{nr}) + \ln p_{\mathbf{a}_r|\mathbf{a}_{nr}}(\mathbf{A}_r|\mathbf{A}_{nr}) \right\}. \end{aligned} \quad (4.608)$$

To find a hybrid CRB/BCRB, we define a $K \times K$ hybrid information matrix \mathbf{J}_H , whose elements are

$$\begin{aligned}J_{Hij}(\mathbf{A}_{nr}) &\triangleq E_{\mathbf{r},\mathbf{a}_r|\mathbf{a}_{nr}} \left\{ \frac{\partial \ln p_{\mathbf{r},\mathbf{a}_r|\mathbf{a}_{nr}}(\mathbf{R}, \mathbf{A}_r|\mathbf{A}_{nr})}{\partial A_i} \cdot \frac{\partial \ln p_{\mathbf{r},\mathbf{a}_r|\mathbf{a}_{nr}}(\mathbf{R}, \mathbf{A}_r|\mathbf{A}_{nr})}{\partial A_j} \right\} \\ &= -E_{\mathbf{r},\mathbf{a}_r|\mathbf{a}_{nr}} \left\{ \frac{\partial^2 \ln p_{\mathbf{r},\mathbf{a}_r|\mathbf{a}_{nr}}(\mathbf{R}, \mathbf{A}_r|\mathbf{A}_{nr})}{\partial A_i \partial A_j} \right\},\end{aligned} \quad (4.609)$$

and the hybrid CRB is

$$\text{HCRB} \triangleq \mathbf{J}_H(\mathbf{A}_{nr})^{-1}. \quad (4.610)$$

Like \mathbf{J}_B , $\mathbf{J}_H(\mathbf{A}_{nr})$ can be expressed as the sum

$$\mathbf{J}_H(\mathbf{A}_{nr}) = \mathbf{J}_D(\mathbf{A}_{nr}) + \mathbf{J}_P(\mathbf{A}_{nr}), \quad (4.611)$$

where

$$\begin{aligned}J_{Dij}(\mathbf{A}_{nr}) &\triangleq E_{\mathbf{r},\mathbf{a}_r|\mathbf{a}_{nr}} \left\{ \frac{\partial \ln p_{\mathbf{r}|\mathbf{a}_r,\mathbf{a}_{nr}}(\mathbf{R}|\mathbf{A}_r, \mathbf{A}_{nr})}{\partial A_i} \cdot \frac{\partial \ln p_{\mathbf{r}|\mathbf{a}_r,\mathbf{a}_{nr}}(\mathbf{R}|\mathbf{A}_r, \mathbf{A}_{nr})}{\partial A_j} \right\} \\ &= -E_{\mathbf{r},\mathbf{a}_r|\mathbf{a}_{nr}} \left\{ \frac{\partial^2 \ln p_{\mathbf{r}|\mathbf{a}_r,\mathbf{a}_{nr}}(\mathbf{R}|\mathbf{A}_r, \mathbf{A}_{nr})}{\partial A_i \partial A_j} \right\} \\ &= E_{\mathbf{a}_r|\mathbf{a}_{nr}} \left\{ -E_{\mathbf{r}|\mathbf{a}_r,\mathbf{a}_{nr}} \left[\frac{\partial^2 \ln p_{\mathbf{r}|\mathbf{a}_r,\mathbf{a}_{nr}}(\mathbf{R}|\mathbf{A}_r, \mathbf{A}_{nr})}{\partial A_i \partial A_j} \right] \right\} \\ &= E_{\mathbf{a}_r|\mathbf{a}_{nr}} \left\{ J_{F_{ij}}(\mathbf{A}_r, \mathbf{A}_{nr}) \right\}\end{aligned} \quad (4.612)$$

and

$$\begin{aligned}J_{Pij}(\mathbf{A}_{nr}) &\triangleq E_{\mathbf{a}_r|\mathbf{a}_{nr}} \left\{ \frac{\partial \ln p_{\mathbf{a}_r|\mathbf{a}_{nr}}(\mathbf{A}_r|\mathbf{A}_{nr})}{\partial A_i} \cdot \frac{\partial \ln p_{\mathbf{a}_r|\mathbf{a}_{nr}}(\mathbf{A}_r|\mathbf{A}_{nr})}{\partial A_j} \right\} \\ &= -E_{\mathbf{a}_r|\mathbf{a}_{nr}} \left\{ \frac{\partial^2 \ln p_{\mathbf{a}_r|\mathbf{a}_{nr}}(\mathbf{A}_r|\mathbf{A}_{nr})}{\partial A_i \partial A_j} \right\}.\end{aligned} \quad (4.613)$$

In many cases, $p_{\mathbf{a}_r|\mathbf{a}_{nr}}(\mathbf{A}_r|\mathbf{A}_{nr})$ does not depend on \mathbf{A}_{nr} , that is,

$$p_{\mathbf{a}_r|\mathbf{a}_{nr}}(\mathbf{A}_r|\mathbf{A}_{nr}) = p_{\mathbf{a}_r}(\mathbf{A}_r). \quad (4.614)$$

Then we have

$$\hat{\mathbf{a}}(\mathbf{R}) \triangleq \begin{bmatrix} \hat{\mathbf{a}}_{nr,\text{ml}}(\mathbf{R}) \\ \hat{\mathbf{a}}_{r,\text{map}}(\mathbf{R}) \end{bmatrix} = \begin{bmatrix} \underset{\mathbf{A}_{nr}}{\operatorname{argmax}} \left\{ \ln p_{\mathbf{r}|\mathbf{a}_r, \mathbf{a}_{nr}}(\mathbf{R}|\mathbf{A}_r, \mathbf{A}_{nr}) \right\} \\ \underset{\mathbf{A}_r}{\operatorname{argmax}} \left\{ \ln p_{\mathbf{r}|\mathbf{a}_r, \mathbf{a}_{nr}}(\mathbf{R}|\mathbf{A}_r, \mathbf{A}_{nr}) + \ln p_{\mathbf{a}_r}(\mathbf{A}_r) \right\} \end{bmatrix} \quad (4.615)$$

and

$$\mathbf{J}_D(\mathbf{A}_{nr}) = E_{\mathbf{a}_r} \{ \mathbf{J}_F(\mathbf{A}_r, \mathbf{A}_{nr}) \}, \quad (4.616)$$

$$\mathbf{J}_P = \begin{bmatrix} \mathbf{0} & \mathbf{0} \\ \mathbf{0} & -E_{\mathbf{a}_r} \left\{ \nabla_{\mathbf{A}_r} [\nabla_{\mathbf{A}_r} \ln p_{\mathbf{a}_r}(\mathbf{A}_r)]^T \right\} \end{bmatrix}, \quad (4.617)$$

where only the $K_2 \times K_2$ lower right corner of \mathbf{J}_P corresponding to the random parameters contains nonzero entries. Most of the results for Bayesian CRBs and classical CRBs carry over to the hybrid model. Rockah and Schultheiss [RS87] and Reuven and Messer [RM97] discuss applications.

1. The $K_1 \times K_1$ matrix in the upper left corner is a lower bound on the variance of any unbiased estimate of \mathbf{a}_{nr} .
2. The $K_2 \times K_2$ matrix in the lower right corner is a lower bound on the mean-square error of any estimate of \mathbf{a}_r .
3. The asymptotic properties of the hybrid estimate are the same as the components that were discussed earlier.

We revisit the DOA estimation problem to show a typical example of hybrid estimation.

Example 4.33 (continuation of Example 4.30) DOA estimation. Consider the same model as in Example 4.30, except that the array elements are perturbed from their nominal position. For notational simplicity, we assume the perturbation is only in the z -direction.²⁵ The element locations are

$$d_n = \frac{\lambda}{2} (n + v_n), \quad n = 0, 1, \dots, N-1, \quad (4.618)$$

where the v_n are IID zero-mean Gaussian random variables with variance σ_d^2 . We define an $N \times 1$ perturbation vector \mathbf{v} ,

$$\mathbf{v} \triangleq \begin{bmatrix} v_0 \\ v_1 \\ \vdots \\ v_{N-1} \end{bmatrix}, \quad (4.619)$$

with *a priori* pdf

$$p_{\mathbf{v}}(\mathbf{v}) = \frac{1}{(2\pi\sigma_d^2)^{N/2}} \exp \left\{ -\frac{1}{2\sigma_d^2} \mathbf{v}^T \mathbf{v} \right\}. \quad (4.620)$$

²⁵The general case is discussed in Chapter 2 of [Van02].

The unknown parameter vector is a $(3 + N) \times 1$ hybrid vector

$$\mathbf{a} = [b \quad \psi \quad \phi \quad v_0 \quad v_1 \quad \cdots \quad v_{N-1}]^T = [b \quad \psi \quad \phi \quad \mathbf{v}^T]^T. \quad (4.621)$$

We want to jointly estimate the parameters.

The Bayesian likelihood function is

$$l_B(\mathbf{A}; \tilde{\mathbf{R}}) = -\frac{1}{\sigma_w^2} \sum_{k=1}^K (\tilde{\mathbf{R}}_k - \tilde{b} \tilde{\mathbf{v}}(\psi, \mathbf{v}))^H (\tilde{\mathbf{R}}_k - \tilde{b} \tilde{\mathbf{v}}(\psi, \mathbf{v})) - \frac{1}{2\sigma_d^2} \mathbf{v}^T \mathbf{v} + \zeta, \quad (4.622)$$

where

$$[\tilde{\mathbf{v}}(\psi, \mathbf{v})]_n = \exp \{-j\psi(n + v_n)\}, \quad n = 0, 1, \dots, N-1. \quad (4.623)$$

Following Example 4.30, (4.622) reduces to

$$l_B(\psi, \mathbf{v}; \tilde{\mathbf{R}}) = \frac{K}{N\sigma_w^2} \left| \tilde{\mathbf{v}}(\psi, \mathbf{v})^H \tilde{\mathbf{R}} \right|^2 - \frac{1}{2\sigma_d^2} \mathbf{v}^T \mathbf{v} + \zeta_3. \quad (4.624)$$

Then

$$\begin{bmatrix} \hat{\psi}_{\text{ml}}(\tilde{\mathbf{R}}) \\ \hat{\mathbf{v}}_{\text{map}}(\tilde{\mathbf{R}}) \end{bmatrix} = \underset{\psi, \mathbf{v}}{\text{argmax}} \{ l_B(\psi, \mathbf{v}; \tilde{\mathbf{R}}) \}. \quad (4.625)$$

Rockah and Schultheiss [RS87] discuss the generalized version of this model and derive the hybrid CRB. This example is representative of an important class of problems called *model uncertainty*. Another example is given in Xu et al. [XBR04]. The Bayesian formulation plays a central role. ■

4.3.6.2 Nuisance Parameters

Similar estimators and bounds can be written for the model in Section 4.3.5.3 but, because of the various combinations, the results are cumbersome.

A particular case that we will encounter in applications is when \mathbf{a}_w is nonrandom and \mathbf{a}_u is random. This case arises in applications where we want to investigate *model uncertainty* or *environmental mismatch*. Note that Example 4.33 could have been formulated this way by saying that \mathbf{v} was unwanted.

We discuss some examples in the problems.

4.3.7 Summary of Multiple Parameter Estimation

In this section, we have developed estimators for nonrandom and random parameter vectors. The results were extensions of the results for scalar parameters in Section 4.2.

The difficulty arises in implementing the estimation procedures. In the case of a K -dimensional nonrandom parameter vector, we must search over a K -dimensional space to find $\hat{\mathbf{a}}_{\text{ml}}(\mathbf{R})$. For a K -dimensional random parameter, a similar search is required to find $\hat{\mathbf{a}}_{\text{map}}(\mathbf{R})$ and a K -fold integration is required to find $\hat{\mathbf{a}}_{\text{ms}}(\mathbf{R})$. In Chapter 5, we will discuss several iterative techniques that can be used in certain applications.

For nonrandom parameters, the CRB provides a lower bound on the covariance matrix of any unbiased estimate. If the components of the observation \mathbf{r} are statistically independent given \mathbf{a} ,

$$p_{\mathbf{r}|\mathbf{a}}(\mathbf{R}|\mathbf{A}) = \prod_{i=1}^N p_{r_i|\mathbf{a}}(R_i|\mathbf{A}) \quad (4.626)$$

then the CRB can be evaluated by one-dimensional integrations. In the special case where $p_{\mathbf{r}|\mathbf{a}}(\mathbf{R}|\mathbf{A})$ is multivariate Gaussian, we can always achieve independence by a whitening transformation.

For random parameters, the BCRB provides a lower bound on the mean-square error matrix of any estimator and the ECRB provides the asymptotic value of the mean-square error matrix. These bounds require the integration of $\mathbf{J}_F(\mathbf{A})$ or $\mathbf{J}_F^{-1}(\mathbf{A})$ over $p_{\mathbf{a}}(\mathbf{A})$.

In many applications, some of the parameters in the vector are unwanted and can be treated as nuisance parameters. We developed various techniques to solve this problem that depend on how \mathbf{a}_w and \mathbf{a}_u are modeled (random or nonrandom).

In other applications, the parameter vector contains random and nonrandom components, \mathbf{a}_r and \mathbf{a}_{nr} . We develop a hybrid estimator and a hybrid bound.

We expanded our case study to include joint frequency and phase estimation. As expected, we also observed the threshold behavior when we jointly estimated frequency and phase. In the next section, we develop a family of bounds that more accurately characterize the behavior in nonlinear estimation problems.

4.4 GLOBAL BAYESIAN BOUNDS

Our discussion of estimation theory has emphasized the Cramér–Rao bound and the Bayesian Cramér–Rao bound as the method of bounding the performance of the estimators. However, we saw in the frequency estimation problem in Examples 4.15, 4.16, and 4.29 that as the SNR decreased, the estimator encountered a threshold and the performance deteriorated dramatically. The CRB and BCRB no longer provided useful information about the performance. We need to develop new bounds that can accurately predict where the threshold will occur and the resulting performance. We refer to these bounds as global bounds.

We have included the discussion of global bounds in an introductory text because we feel strongly that the CRB and BCRB do not adequately characterize the performance of estimators. Unless the estimators are efficient (in the Bayesian case, this requires a Gaussian model), the performance will approach the bounds *asymptotically* (as $N \rightarrow \infty$) or for high SNR (as $\text{SNR} \rightarrow \infty$).²⁶ A key question is, “How large does N or SNR have to be for the asymptotic results to give a realistic measure of performance?” Alternatively, “Where is the threshold and how does the performance degrade?”

We have focused our attention on Bayesian bounds because they can be extended to the nonlinear filtering or tracking problem [VB07]. In Section 4.4.1.7, we give some references to comparable bounds for nonrandom parameters.

²⁶For $\hat{\mathbf{a}}_{\text{ml}}(\mathbf{R})$, the covariance matrix approaches the CRB. For $\hat{\mathbf{a}}_{\text{map}}(\mathbf{R})$, the MSE matrix approaches the ECRB.

Finding global bounds that accurately predict the location of the threshold and the performance in the ambiguity region is challenging. The current global bounds can be divided into three families:

1. Bounds that are derived from the *covariance inequality*.
2. Bounds that relate the MSE in the estimation problem to the probability of error in a binary hypothesis problem. We refer to these bounds as the *Ziv-Zakai family*.
3. Approximations that utilize a two-step process called the *method of interval estimation* (MIE).

We will discuss the bounds and approximations in the first and third families. A discussion of the Ziv-Zakai family is contained in Van Trees and Bell [VB07].

4.4.1 Covariance Inequality Bounds

The bounds in this family are all special cases of the covariance inequality (e.g. [Leh83] or [IH81]). The covariance inequality is the vector extension of the familiar Schwarz inequality. We first derive the Bayesian covariance inequality and then derive the Weiss–Weinstein bound (WWB).²⁷ A series of additional bounds are derived in [VB07], and a recent generalization of this family of bounds for both random and nonrandom parameters can be found in [TT10a] and [TT10b].

4.4.1.1 Covariance Inequality

The parameter \mathbf{a} is a $K \times 1$ random vector with probability density $p_{\mathbf{a}}(\mathbf{A})$. The observation \mathbf{R} is an $N \times 1$ vector. The joint density is $p_{\mathbf{r},\mathbf{a}}(\mathbf{R}, \mathbf{A})$. Let $\mathbf{f}(\mathbf{R}, \mathbf{A})$ be a real $K \times 1$ vector function, $\mathbf{g}(\mathbf{R}, \mathbf{A})$ be a real $M \times 1$ vector function, and \mathbf{B} be a real $K \times M$ matrix. Then

$$E_{\mathbf{r},\mathbf{a}} \left\{ [\mathbf{f}(\mathbf{R}, \mathbf{A}) - \mathbf{B}\mathbf{g}(\mathbf{R}, \mathbf{A})] [\mathbf{f}(\mathbf{R}, \mathbf{A}) - \mathbf{B}\mathbf{g}(\mathbf{R}, \mathbf{A})]^T \right\} \geq 0. \quad (4.627)$$

Define

$$\mathbf{T} \triangleq E_{\mathbf{r},\mathbf{a}} \left\{ \mathbf{f}(\mathbf{R}, \mathbf{A}) \mathbf{g}(\mathbf{R}, \mathbf{A})^T \right\}, \quad (4.628)$$

$$\mathbf{G} \triangleq E_{\mathbf{r},\mathbf{a}} \left\{ \mathbf{g}(\mathbf{R}, \mathbf{A}) \mathbf{g}(\mathbf{R}, \mathbf{A})^T \right\}, \quad (4.629)$$

and (4.627) becomes

$$E_{\mathbf{r},\mathbf{a}} \left\{ \mathbf{f}(\mathbf{R}, \mathbf{A}) \mathbf{f}(\mathbf{R}, \mathbf{A})^T \right\} \geq \mathbf{B} \mathbf{T}^T + \mathbf{T} \mathbf{B}^T - \mathbf{B} \mathbf{G} \mathbf{B}^T. \quad (4.630)$$

To maximize²⁸ the right-hand side of (4.630), we choose

$$\mathbf{B} = \mathbf{T} \mathbf{G}^{-1}. \quad (4.631)$$

Substituting (4.631) into (4.630) gives

$$E_{\mathbf{r},\mathbf{a}} \left\{ \mathbf{f}(\mathbf{R}, \mathbf{A}) \mathbf{f}(\mathbf{R}, \mathbf{A})^T \right\} \geq \mathbf{T} \mathbf{G}^{-1} \mathbf{T}^T. \quad (4.632)$$

²⁷Our derivation is similar to that in Weiss and Weinstein [WW88] and Abel [Abe93].

²⁸We say that a matrix \mathbf{M} is maximized when the scalar quantity $\mathbf{b}^T \mathbf{M} \mathbf{b}$ is maximized for any nonzero \mathbf{b} .

4.4.1.2 Bayesian Bounds

We can use the covariance inequality to derive a family of Bayesian bounds. First let

$$\mathbf{f}(\mathbf{R}, \mathbf{A}) = -[\hat{\mathbf{a}}(\mathbf{R}) - \mathbf{A}], \quad (4.633)$$

where $\hat{\mathbf{a}}(\mathbf{R})$ and \mathbf{A} are $K \times 1$ vectors. The vector $\hat{\mathbf{a}}(\mathbf{R})$ is any estimate of \mathbf{a} (not necessarily $\hat{\mathbf{a}}_{\text{ms}}(\mathbf{R})$ or $\hat{\mathbf{a}}_{\text{map}}(\mathbf{R})$, but they are included). Then the left-hand side of (4.632) is the MSE matrix

$$\begin{aligned} E_{\mathbf{r}, \mathbf{a}} \{ \mathbf{f}(\mathbf{R}, \mathbf{A}) \mathbf{f}(\mathbf{R}, \mathbf{A})^T \} &= E_{\mathbf{r}, \mathbf{a}} \{ [\hat{\mathbf{a}}(\mathbf{R}) - \mathbf{A}] [\hat{\mathbf{a}}(\mathbf{R}) - \mathbf{A}]^T \} \\ &= \boldsymbol{\Sigma}_\epsilon. \end{aligned} \quad (4.634)$$

Next consider $\mathbf{g}(\mathbf{R}, \mathbf{A})$ functions that satisfy

$$E_{\mathbf{a}|\mathbf{r}} \{ \mathbf{g}(\mathbf{R}, \mathbf{A}) \} = \mathbf{0}. \quad (4.635)$$

Then

$$\begin{aligned} \mathbf{T} &= -E_{\mathbf{r}, \mathbf{a}} \{ [\hat{\mathbf{a}}(\mathbf{R}) - \mathbf{A}] \mathbf{g}(\mathbf{R}, \mathbf{A})^T \} \\ &= -E_{\mathbf{r}, \mathbf{a}} \{ \hat{\mathbf{a}}(\mathbf{R}) \mathbf{g}(\mathbf{R}, \mathbf{A})^T \} + E_{\mathbf{r}, \mathbf{a}} \{ \mathbf{A} \mathbf{g}(\mathbf{R}, \mathbf{A})^T \} \\ &= -E_{\mathbf{r}} \{ \hat{\mathbf{a}}(\mathbf{R}) E_{\mathbf{a}|\mathbf{r}} \{ \mathbf{g}(\mathbf{R}, \mathbf{A})^T \} \} + E_{\mathbf{r}, \mathbf{a}} \{ \mathbf{A} \mathbf{g}(\mathbf{R}, \mathbf{A})^T \}. \end{aligned} \quad (4.636)$$

From the restriction in (4.635), the first term in (4.636) is zero, and we have

$$\mathbf{T} = E_{\mathbf{r}, \mathbf{a}} \{ \mathbf{A} \mathbf{g}(\mathbf{R}, \mathbf{A})^T \}. \quad (4.637)$$

Thus, the mean-square error matrix is bounded by

$$\boldsymbol{\Sigma}_\epsilon \geq \mathbf{T} \mathbf{G}^{-1} \mathbf{T}^T, \quad (4.638)$$

where \mathbf{T} is given by (4.637) and \mathbf{G} is given by (4.629). Note that the right-hand side of (4.638) does not depend on $\hat{\mathbf{a}}(\mathbf{R})$, and is therefore a bound on the MSE matrix of any estimator. Furthermore, no assumptions about the estimator, such as unbiasedness, were required. By choosing various $\mathbf{g}(\mathbf{R}, \mathbf{A})$, we can obtain a family of Bayesian bounds.

4.4.1.3 Scalar Parameters

We first consider the case of scalar parameters ($K = 1$) and develop bounds on the MSE

$$\sigma_\epsilon^2 \triangleq E_{\mathbf{r}, \mathbf{a}} \{ (\hat{a}(\mathbf{R}) - A)^2 \}. \quad (4.639)$$

Bayesian Cramér–Rao Bound.²⁹ The Bayesian Cramér–Rao bound is obtained by letting

$$g(\mathbf{R}, A) = \frac{\partial \ln p_{\mathbf{r}, \mathbf{a}}(\mathbf{R}, A)}{\partial A}. \quad (4.640)$$

Note that, unlike the classic Cramér–Rao bound, the function is the derivative of the joint probability density. We assume that

²⁹We derived the scalar BCRB in Section 4.2.3.1, equation (4.193). We include it here to show how it fits into the global Bayesian bounds family.

1. $\frac{\partial \ln p_{\mathbf{r},a}(\mathbf{R}, A)}{\partial A}$ exists and is absolutely integrable,
2. $\frac{\partial^2 \ln p_{\mathbf{r},a}(\mathbf{R}, A)}{\partial A^2}$ exists and is absolutely integrable.

In addition, in order to evaluate \mathbf{T} , we assume that

3. $\lim_{A \rightarrow \pm\infty} A p_{\mathbf{r},a}(A|\mathbf{R}) = 0$ for all \mathbf{R} .

First we verify that the condition in (4.635) is satisfied. We can write $g(\mathbf{R}, A)$ as

$$g(\mathbf{R}, A) = \frac{\partial \ln p_{a|\mathbf{r}}(A|\mathbf{R})}{\partial A} + \frac{\partial \ln p_{\mathbf{r}}(\mathbf{R})}{\partial A} = \frac{1}{p_{a|\mathbf{r}}(A|\mathbf{R})} \frac{\partial p_{a|\mathbf{r}}(A|\mathbf{R})}{\partial A}. \quad (4.641)$$

Then

$$\begin{aligned} E_{a|\mathbf{r}} \{ g(\mathbf{R}, A) \} &= \int_{-\infty}^{\infty} \frac{\partial p_{a|\mathbf{r}}(A|\mathbf{R})}{\partial A} \frac{p_{a|\mathbf{r}}(A|\mathbf{R})}{p_{a|\mathbf{r}}(A|\mathbf{R})} dA \\ &= \int_{-\infty}^{\infty} \frac{\partial p_{a|\mathbf{r}}(A|\mathbf{R})}{\partial A} dA \\ &= p_{a|\mathbf{r}}(A|\mathbf{R})|_{-\infty}^{\infty} \\ &= 0, \end{aligned} \quad (4.642)$$

where the last equality is guaranteed by condition 3, which is a stronger condition.

To evaluate T , we have

$$\begin{aligned} T &= E_{\mathbf{r},a} \{ A g(\mathbf{R}, A) \} \\ &= E_{\mathbf{r}} \left\{ E_{a|\mathbf{r}} \left\{ \frac{A}{p_{a|\mathbf{r}}(A|\mathbf{R})} \frac{\partial p_{a|\mathbf{r}}(A|\mathbf{R})}{\partial A} \right\} \right\} \\ &= E_{\mathbf{r}} \left\{ \int_{-\infty}^{\infty} A \frac{\partial p_{a|\mathbf{r}}(A|\mathbf{R})}{\partial A} dA \right\}. \end{aligned} \quad (4.643)$$

The integral can be evaluated using integration by parts,

$$T = E_{\mathbf{r}} \left\{ A p_{a|\mathbf{r}}(A|\mathbf{R})|_{-\infty}^{\infty} - \int_{-\infty}^{\infty} p_{a|\mathbf{r}}(A|\mathbf{R}) dA \right\}. \quad (4.644)$$

The first term is zero from condition 3, and the second term is one. Therefore,

$$T = E_{\mathbf{r}} \{ 0 - 1 \} = -1. \quad (4.645)$$

To evaluate G , we substitute (4.640) into (4.629) to obtain

$$G = E_{\mathbf{r},a} \left\{ \left(\frac{\partial \ln p_{\mathbf{r},a}(\mathbf{R}, A)}{\partial A} \right)^2 \right\}. \quad (4.646)$$

We observe that $G = J_B$ is the *Bayesian information* defined in (4.188). For the single-parameter case, it is a scalar. Using (4.645) and (4.646) in (4.638) gives

$$\sigma_{\epsilon}^2 \geq J_B^{-1}. \quad (4.647)$$

The inequality in (4.647) is the Bayesian Cramér–Rao bound that we introduced in (4.193).

A number of global Bayesian bounds can be derived from the covariance inequality. They are discussed in Van Trees and Bell [VB07]. In the next section, we develop the Weiss–Weinstein bound that produces a reasonably tight bound in the threshold area in many applications.

Weiss–Weinstein Bound. Weiss and Weinstein [WW85] proposed the M -dimensional vector $\mathbf{g}(\mathbf{R}, A)$ whose i th element is

$$g_i(\mathbf{R}, A) = L^{s_i}(\mathbf{R}; A + h_i, A) - L^{1-s_i}(\mathbf{R}; A - h_i, A), \quad i = 1, 2, \dots, M, \quad (4.648)$$

where $0 < s_i < 1$ and $L(\mathbf{R}; A_1, A_2)$ is the (joint) likelihood ratio:

$$L(\mathbf{R}; A_1, A_2) \triangleq \frac{p_{\mathbf{r}, a_1}(\mathbf{R}, A_1)}{p_{\mathbf{r}, a_2}(\mathbf{R}, A_2)}. \quad (4.649)$$

For this case,

$$[\mathbf{T}]_i = -h_i E_{\mathbf{r}, a} \{ L^{s_i}(\mathbf{R}; A + h_i, A) \}, \quad (4.650)$$

$$\begin{aligned} [\mathbf{G}]_{ij} &= E_{\mathbf{r}, a} \{ [L^{s_i}(\mathbf{R}; A + h_i, A) - L^{1-s_i}(\mathbf{R}; A - h_i, A)] \\ &\quad \times [L^{s_j}(\mathbf{R}; A + h_j, A) - L^{1-s_j}(\mathbf{R}; A - h_j, A)] \}, \end{aligned} \quad (4.651)$$

and the WWB is

$$\sigma_\epsilon^2 \geq \mathbf{T}\mathbf{G}^{-1}\mathbf{T}^T. \quad (4.652)$$

The bound can also be written as

$$\sigma_\epsilon^2 \geq \mathbf{h}\mathbf{Q}^{-1}\mathbf{h}^T, \quad (4.653)$$

where \mathbf{h} is defined as

$$\mathbf{h} = [h_1 \quad h_2 \quad \cdots \quad h_M] \quad (4.654)$$

and

$$[\mathbf{Q}]_{ij} = \frac{E_{\mathbf{r}, a} \{ [L^{s_i}(\mathbf{R}; A + h_i, A) - L^{1-s_i}(\mathbf{R}; A - h_i, A)] [L^{s_j}(\mathbf{R}; A + h_j, A) - L^{1-s_j}(\mathbf{R}; A - h_j, A)] \}}{E_{\mathbf{r}, a} \{ L^{s_i}(\mathbf{R}; A + h_i, A) \} E_{\mathbf{r}, a} \{ L^{s_j}(\mathbf{R}; A + h_j, A) \}}. \quad (4.655)$$

The WWB must be optimized over the free variables: s_i and h_i ; $i = 1, 2, \dots, M$.

When a single test point is used ($M = 1$), the WWB has the form

$$\sigma_\epsilon^2 \geq \frac{h^2 (E_{\mathbf{r}, a} \{ L^s(\mathbf{R}; A + h, A) \})^2}{E_{\mathbf{r}, a} \{ [L^s(\mathbf{R}; A + h, A) - L^{1-s}(\mathbf{R}; A - h, A)]^2 \}}. \quad (4.656)$$

The bound in (4.656) can be written in terms of the function

$$\begin{aligned}
 \eta(s; h) &\triangleq \ln E_{\mathbf{r}, a} \{ L^s(\mathbf{R}; A + h, A) \} \\
 &= \ln \int \int p_{\mathbf{r}, a}(\mathbf{R}, A + h)^s p_{\mathbf{r}, a}(\mathbf{R}, A)^{1-s} d\mathbf{R} dA \\
 &= \ln \int p_a(A + h)^s p_a(A)^{1-s} \left\{ \int p_{\mathbf{r}|a}(\mathbf{R}|A + h)^s p_{\mathbf{r}|a}(\mathbf{R}|A)^{1-s} d\mathbf{R} \right\} dA \\
 &= \ln \int p_a(A + h)^s p_a(A)^{1-s} e^{\mu(s; A + h, A)} dA,
 \end{aligned} \tag{4.657}$$

where

$$\mu(s; A_1, A_2) \triangleq \ln \int p_{\mathbf{r}|a}(\mathbf{R}|A_1)^s p_{\mathbf{r}|a}(\mathbf{R}|A_2)^{1-s} d\mathbf{R}. \tag{4.658}$$

It is important to note that in order to avoid singularities, the integration with respect to A in (4.657) is performed over the region $A = \{A : p_a(A) > 0\}$. The function $\mu(s; A_1, A_2)$ is the same $\mu(s)$ that we introduced in Section 2.4.³⁰ Then

$$\sigma_\epsilon^2 \geq \max_{s, h} \frac{h^2 e^{2\eta(s, h)}}{e^{\eta(2s, h)} + e^{\eta(2-2s, -h)} - 2e^{\eta(s, 2h)}}. \tag{4.659}$$

The BCRB is a special case of this bound obtained in the limit when $h \rightarrow 0$ for any s . Although valid for any $s \in (0, 1)$, the WWB is generally computed using $s = \frac{1}{2}$, for which the single test point bound simplifies to³¹

$$\sigma_\epsilon^2 \geq \max_h \frac{h^2 e^{2\eta(\frac{1}{2}, h)}}{2 \left(1 - e^{\eta(\frac{1}{2}, 2h)} \right)}. \tag{4.660}$$

In most applications, multiple test points are required to obtain a tight bound. When the WWB is plotted versus SNR (or N), the best set will vary with SNR (or N). An efficient technique is to choose the test points to coincide with the sidelobes of the log-likelihood surface plus several small values of decreasing order of magnitude (e.g., $h = 0.01, 0.001, 0.0001, \dots$). Increasing the number of test points always improves the bound (although the improvement may be slight), so another approach is to use a dense set of points in the sidelobe region in addition to the sidelobe points. Theoretically, the WWB can be evaluated for any number of distinct test points, but closely spaced test points may cause numerical difficulties in inverting \mathbf{Q} .

To illustrate the Weiss–Weinstein bound we revisit the frequency estimation case study.

Example 4.34 (continuation of Examples 4.15 and 4.16) Frequency estimation. We use the model in Example 4.16, however, we no longer need the assumption that $a > 2$ in the *a priori* density. In order to compute the WWB, we need to evaluate the terms $\mu(s; \omega + h, \omega)$ and $\eta(s; h)$

³⁰Our notation is different from [WW85]. We define $\mu(s; A + h, A)$ using a conditional expectation so we can use $\mu(s)$ functions available in the literature. Our $\eta(s; h)$ corresponds to the $\mu(s, h)$ in [WW85].

³¹Note that if the WWB is optimized over s and h , then it has to be greater than or equal to the BCRB because it is a special case. When we set $s = \frac{1}{2}$, this ordering still appears to be true but has not been proven.

defined in (4.657) and (4.658). Evaluating $\mu(s; \omega + h, \omega)$ is straightforward and the result is

$$\begin{aligned}\mu(s; \omega + h, \omega) &= -s(1-s)2N \text{SNR} \left[1 - \frac{1}{N} \frac{\cos\left(\frac{h(N-1)}{2}\right) \sin\left(\frac{hN}{2}\right)}{\sin\left(\frac{h}{2}\right)} \right] \\ &\triangleq \mu(s; h).\end{aligned}\quad (4.661)$$

Note that the expression is only a function of s and h and not a function of ω . We use the notation $\mu(s; h)$ to emphasize this property, which greatly simplifies the subsequent analysis. Note also that $\mu(s; h)$ has a term with the same form as the normalized ambiguity surface in (4.230).

To evaluate $\eta(s; h)$, we have

$$\begin{aligned}\eta(s; h) &= \ln \int_{-\pi}^{\pi} p_{\omega}(\omega + h)^s p_{\omega}(\omega)^{1-s} e^{\mu(s; h)} d\omega \\ &= \ln \left\{ e^{\mu(s; h)} \int_{-\pi}^{\pi} p_{\omega}(\omega + h)^s p_{\omega}(\omega)^{1-s} d\omega \right\} \\ &= \mu(s; h) + \ln \int_{-\pi}^{\pi} p_{\omega}(\omega + h)^s p_{\omega}(\omega)^{1-s} d\omega \\ &= \mu(s; h) + \rho(s; h),\end{aligned}\quad (4.662)$$

where

$$\rho(s; h) \triangleq \ln \int_{-\pi}^{\pi} p_{\omega}(\omega + h)^s p_{\omega}(\omega)^{1-s} d\omega.\quad (4.663)$$

The integral in (4.663) has a closed form expression only in some special cases. One of the special cases is when $a = 1$, where

$$\begin{aligned}e^{\rho_1(s; h)} &= \int_{-\pi}^{\pi} \frac{1}{2\pi} d\omega \\ &= \begin{cases} 1 - \frac{|h|}{\pi}, & |h| \leq \pi, \\ 0, & \text{otherwise.} \end{cases}\end{aligned}\quad (4.664)$$

For any a , when $s = \frac{1}{2}$, $e^{\rho(\frac{1}{2}; h)}$ has a maximum value of one when $h = 0$ and is a nonnegative, monotonically decreasing function of $|h|$, which can be evaluated using numerical integration.

We evaluate the multiple test point bound in (4.653)–(4.655) using $s = \frac{1}{2}$ and $h = 0.01\pi, 0.001\pi$, and the seven sidelobes to the right of the mainlobe in the normalized ambiguity surface shown in Figure 4.9. Figure 4.29 shows the results for several values of a , including $a = 1$ and $a = 2$, where we were not able to calculate the BCRB. Also plotted are the ECRB and BCRBs, where they exist ($a > 2$). We see that in all cases the WWB converges to the ECRB for high SNR and to the *a priori* variance for low SNR. The WWB is greater than or equal to the BCRB for all SNR, and significantly larger in the threshold region. The WWB is close to the BCRB for all SNR only when a gets so large that the *a priori* pdf is within the main peak of the ambiguity surface (e.g., $a = 400$). In Figure 4.30, we plot the WWB for $a = 20$ with the simulation results from Example 4.16, Figure 4.17. The WWB is much closer to the MSE of the MAP estimator, but there is still a gap in the threshold region. The WWB provides a good indication of the location of the threshold region, predicting that it begins at about -2 dB SNR, whereas the MAP estimator exhibits a threshold at about 2 dB, a difference of approximately 4 dB. ■

Applications of the WWB to DOA estimation problems are contained in Bell [Bel95], Nguyen and Van Trees [NV94], and DeLong [DeL93]. Applications to range estimation are contained in Weiss and Weinstein [WW85].

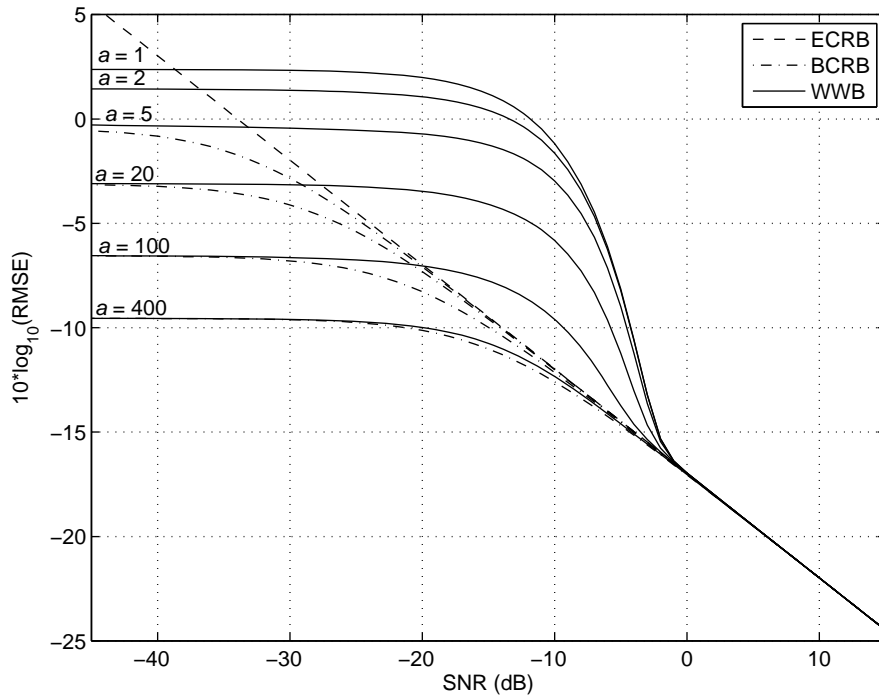


Figure 4.29: Weiss–Weinstein bound versus SNR, $N = 16$.

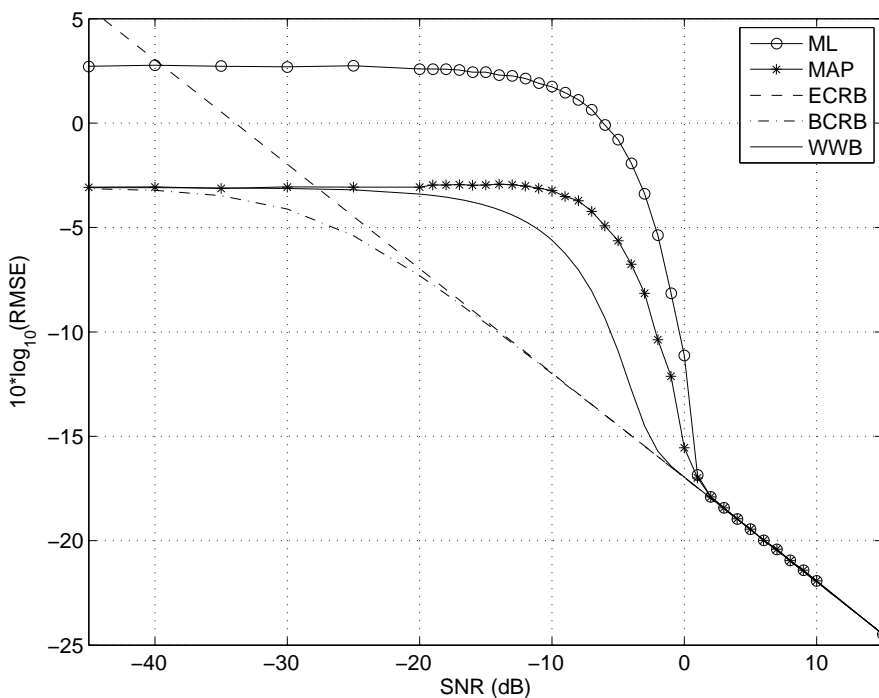


Figure 4.30: Frequency RMSE and WWB versus SNR. $N = 16$, $\theta = \pi/6$, $a = 20$.

4.4.1.4 Vector Parameters

We now consider the case of vector parameters ($K > 1$). The mean-square error matrix bound is given in (4.638) with \mathbf{T} defined in (4.637) and \mathbf{G} defined in (4.629). In order for the bound matrix to be full rank, we require that the dimension M of the vector $\mathbf{g}(\mathbf{R}, \mathbf{A})$ be at least K . We confine our discussion in the text to the Weiss–Weinstein bound.

The vector WWB is obtained by choosing

$$g_i(\mathbf{R}, \mathbf{A}) = L^{s_i}(\mathbf{R}; \mathbf{A} + \mathbf{h}_i, \mathbf{A}) - L^{1-s_i}(\mathbf{R}; \mathbf{A} - \mathbf{h}_i, \mathbf{A}), \quad i = 0, 1, \dots, M, \quad (4.665)$$

where $M \geq K$ and the set of test point vectors must have rank K . Analogous to the scalar case, the i th column of \mathbf{T} is

$$[\mathbf{T}]_{\cdot, i} = -\mathbf{h}_i E_{\mathbf{r}, \mathbf{a}} \{L^{s_i}(\mathbf{R}; \mathbf{A} + \mathbf{h}_i, \mathbf{A})\} \quad (4.666)$$

and

$$[\mathbf{G}]_{ij} = E_{\mathbf{r}, \mathbf{a}} \{ [L^{s_i}(\mathbf{R}; \mathbf{A} + \mathbf{h}_i, \mathbf{A}) - L^{1-s_i}(\mathbf{R}; \mathbf{A} - \mathbf{h}_i, \mathbf{A})] \\ \times [L^{s_j}(\mathbf{R}; \mathbf{A} + \mathbf{h}_j, \mathbf{A}) - L^{1-s_j}(\mathbf{R}; \mathbf{A} - \mathbf{h}_j, \mathbf{A})] \}, \quad (4.667)$$

and the bound is given by (4.638). It can also be written as

$$\Sigma_\epsilon \geq \mathbf{H} \mathbf{Q}^{-1} \mathbf{H}^T, \quad (4.668)$$

where \mathbf{h} is defined as

$$\mathbf{H} \triangleq [\mathbf{h}_1 \quad \mathbf{h}_2 \quad \cdots \quad \mathbf{h}_M] \quad (4.669)$$

and

$$[\mathbf{Q}]_{ij} = \frac{E_{\mathbf{r}, \mathbf{a}} \{ [L^{s_i}(\mathbf{R}; \mathbf{A} + \mathbf{h}_i, \mathbf{A}) - L^{1-s_i}(\mathbf{R}; \mathbf{A} - \mathbf{h}_i, \mathbf{A})] [L^{s_j}(\mathbf{R}; \mathbf{A} + \mathbf{h}_j, \mathbf{A}) - L^{1-s_j}(\mathbf{R}; \mathbf{A} - \mathbf{h}_j, \mathbf{A})] \}}{E_{\mathbf{r}, \mathbf{a}} \{L^{s_i}(\mathbf{R}; \mathbf{A} + \mathbf{h}_i, \mathbf{A})\} E_{\mathbf{r}, \mathbf{a}} \{L^{s_j}(\mathbf{R}; \mathbf{A} + \mathbf{h}_j, \mathbf{A})\}}. \quad (4.670)$$

In this general form, the WWB requires maximization over a large number of free variables. A practical form of the bound with $s_i = \frac{1}{2}; i = 1, \dots, M$ has been used in several applications. For this case, (4.670) reduces to

$$[\mathbf{Q}]_{ij} = \frac{2 \left[e^{\eta(\frac{1}{2}; \mathbf{h}_i, \mathbf{h}_j)} - e^{\eta(\frac{1}{2}; \mathbf{h}_i, -\mathbf{h}_j)} \right]}{e^{\eta(\frac{1}{2}; \mathbf{h}_i, \mathbf{0})} e^{\eta(\frac{1}{2}; \mathbf{h}_j, \mathbf{0})}}, \quad (4.671)$$

where

$$\begin{aligned} \eta\left(\frac{1}{2}; \mathbf{h}_i, \mathbf{h}_j\right) &= \ln E_{\mathbf{r}, \mathbf{a}} \left\{ \sqrt{\frac{p_{\mathbf{r}, \mathbf{a}}(\mathbf{R}, \mathbf{A} + \mathbf{h}_i)}{p_{\mathbf{r}, \mathbf{a}}(\mathbf{R}, \mathbf{A})} \frac{p_{\mathbf{r}, \mathbf{a}}(\mathbf{R}, \mathbf{A} + \mathbf{h}_j)}{p_{\mathbf{r}, \mathbf{a}}(\mathbf{R}, \mathbf{A})}} \right\} \\ &= \ln \int \sqrt{p_{\mathbf{a}}(\mathbf{A} + \mathbf{h}_i) p_{\mathbf{a}}(\mathbf{A} + \mathbf{h}_j)} \left\{ \int \sqrt{p_{\mathbf{r}|\mathbf{a}}(\mathbf{R}|\mathbf{A} + \mathbf{h}_i) p_{\mathbf{r}|\mathbf{a}}(\mathbf{R}|\mathbf{A} + \mathbf{h}_j)} d\mathbf{R} \right\} d\mathbf{A} \\ &= \ln \int \sqrt{p_{\mathbf{a}}(\mathbf{A} + \mathbf{h}_i) p_{\mathbf{a}}(\mathbf{A} + \mathbf{h}_j)} e^{\mu(\frac{1}{2}; \mathbf{A} + \mathbf{h}_i, \mathbf{A} + \mathbf{h}_j)} d\mathbf{A}. \end{aligned} \quad (4.672)$$

Again, integration with respect to \mathbf{A} is over the region $\mathbf{A} = \{\mathbf{A} : p_{\mathbf{a}}(\mathbf{A}) > 0\}$. The WWB has been shown to be a useful bound for all regions of operation [Wei85, Wei86, Wei87, DeL93, BEV96].

4.4.1.5 Combined Bayesian Bounds

The final type of Bayesian covariance inequality bounds are referred to as mixed or combined bounds. They are obtained by concatenating $\mathbf{g}(\mathbf{R}, \mathbf{A})$ from two or more of the Bayesian bounds discussed above. This approach was used by Abel [Abe93] for nonrandom parameters. The technique was used much earlier by McAulay and Hofstetter [MH71] when they combined the Cramér–Rao bound and the Barankin bound and applied the result to the radar range estimation problem. The technique has been applied to Bayesian bounds by Weiss in his thesis [Wei85] and by Renaux et al. [RFLR06]. To illustrate the approach, we consider a combined BCRB and WWB. It is a special case of the recursive bound in Bell and Van Trees [BV06].

Consider the case of a $K \times 1$ parameter vector. We define a $K \times 1$ vector $\mathbf{g}^C(\mathbf{R}, \mathbf{A})$ whose i th element is

$$\mathbf{g}_i^C(\mathbf{R}, \mathbf{A}) = \frac{\partial \ln p_{\mathbf{r}, \mathbf{a}}(\mathbf{R}, \mathbf{A})}{\partial A_i}, \quad i = 1, 2, \dots, K. \quad (4.673)$$

The superscript C denotes Bayesian Cramér–Rao. We define an $S \times 1$ vector $\mathbf{g}^W(\mathbf{R}, \mathbf{A})$ whose i th element is

$$\mathbf{g}_i^W(\mathbf{R}, \mathbf{A}) = L^{\frac{1}{2}}(\mathbf{R}; \mathbf{A} + \mathbf{h}_i, \mathbf{A}) - L^{\frac{1}{2}}(\mathbf{R}; \mathbf{A} - \mathbf{h}_i, \mathbf{A}), \quad i = 1, 2, \dots, S. \quad (4.674)$$

The superscript W denotes Weiss–Weinstein. The total $\mathbf{g}(\mathbf{R}, \mathbf{A})$ vector is an $M \times 1$ vector, where $M = K + S$,

$$\mathbf{g}(\mathbf{R}, \mathbf{A}) = \begin{bmatrix} \mathbf{g}^C(\mathbf{R}, \mathbf{A}) \\ \mathbf{g}^W(\mathbf{R}, \mathbf{A}) \end{bmatrix}. \quad (4.675)$$

Then

$$\begin{aligned} \mathbf{T} &= E_{\mathbf{r}, \mathbf{a}} \left\{ \left[\mathbf{A} [\mathbf{g}^C(\mathbf{R}, \mathbf{A})]^T \quad \mathbf{A} [\mathbf{g}^W(\mathbf{R}, \mathbf{A})]^T \right] \right\} \\ &\triangleq \begin{bmatrix} \mathbf{T}_C & \mathbf{T}_W \end{bmatrix}, \end{aligned} \quad (4.676)$$

where $\mathbf{T}_C = -\mathbf{I}_D$ and \mathbf{T}_W was defined in (4.666), and

$$\begin{aligned} \mathbf{G} &= E_{\mathbf{r}, \mathbf{a}} \{ \mathbf{g}(\mathbf{R}, \mathbf{A}) \mathbf{g}^T(\mathbf{R}, \mathbf{A}) \} \\ &= E_{\mathbf{r}, \mathbf{a}} \left\{ \begin{bmatrix} \mathbf{g}^C(\mathbf{R}, \mathbf{A}) [\mathbf{g}^C(\mathbf{R}, \mathbf{A})]^T & \mathbf{g}^C(\mathbf{R}, \mathbf{A}) [\mathbf{g}^W(\mathbf{R}, \mathbf{A})]^T \\ \mathbf{g}^W(\mathbf{R}, \mathbf{A}) [\mathbf{g}^C(\mathbf{R}, \mathbf{A})]^T & \mathbf{g}^W(\mathbf{R}, \mathbf{A}) [\mathbf{g}^W(\mathbf{R}, \mathbf{A})]^T \end{bmatrix} \right\} \\ &= \begin{bmatrix} \mathbf{G}_C & \mathbf{G}_{CW} \\ \mathbf{G}_{CW}^T & \mathbf{G}_W \end{bmatrix}. \end{aligned} \quad (4.677)$$

In (4.677), \mathbf{G}_C is the \mathbf{G} matrix for the Bayesian CRB. It is also the Bayesian information matrix. Similarly, \mathbf{G}_W is the \mathbf{G} matrix in the WWB (4.667). The new term is the $K \times S$ cross matrix \mathbf{G}_{CW} , whose ij element is

$$[\mathbf{G}_{CW}]_{ij} = E_{\mathbf{r}, \mathbf{a}} \left\{ \frac{\partial \ln p_{\mathbf{r}, \mathbf{a}}(\mathbf{R}, \mathbf{A})}{\partial A_i} \left(L^{\frac{1}{2}}(\mathbf{R}; \mathbf{A} + \mathbf{h}_j, \mathbf{A}) - L^{\frac{1}{2}}(\mathbf{R}; \mathbf{A} - \mathbf{h}_j, \mathbf{A}) \right) \right\}. \quad (4.678)$$

For this bound, the \mathbf{T} matrix will always be full rank regardless of the test point vectors chosen; therefore, the set of test point vectors can be chosen arbitrarily. Note that we could have accomplished a similar result with a pure WWB by setting the first K test point vectors to be

$$[\mathbf{h}_1 \quad \mathbf{h}_2 \quad \cdots \quad \mathbf{h}_K] = h \mathbf{I}_K, \quad (4.679)$$

and letting $h \rightarrow 0$. The difficulty with this approach is in evaluating the WWB terms and choosing test points for all of the parameters. It is often the case that the BCRB is a good predictor of MSE performance for some of the parameters, but is a weak bound for other components. The combined bound using nonzero test points only for a subset of the parameters can provide as tight a bound as the WWB while keeping the complexity manageable.

4.4.1.6 Functions of the Parameter Vector

In many applications, we want to estimate a function of the parameter vector \mathbf{A} .³² We denote the desired function by the K_d -dimensional vector $\gamma(\mathbf{A})$ and the transformed parameter vector as \mathbf{d} ,

$$\mathbf{d} = \gamma(\mathbf{A}), \quad (4.680)$$

or

$$d_i = \gamma_i(\mathbf{A}), \quad i = 1, 2, \dots, K_d. \quad (4.681)$$

A simple example occurs in the DOA estimation problem in Example 4.30. Recall that θ is the angle from the z -axis. The “original” parameter A is

$$A = \psi = \pi \cos \theta. \quad (4.682)$$

The desired parameter d is θ ,

$$d = \theta = \cos^{-1}(\psi/\pi). \quad (4.683)$$

Scalar Parameters. We consider the scalar parameter case first. By defining $f(\mathbf{R}, A)$ as

$$f(\mathbf{R}, A) = \hat{d}(\mathbf{R}) - \gamma(A) \quad (4.684)$$

and following the same steps as in (4.633)–(4.638), we obtain

$$E_{\mathbf{r}, a} \left\{ (\hat{d}(\mathbf{R}) - \gamma(A))^2 \right\} \geq \mathbf{T}_\gamma \mathbf{G}^{-1} \mathbf{T}_\gamma^T, \quad (4.685)$$

³²Our discussion follows Weiss [Wei85].

where

$$\mathbf{T}_\gamma = E_{\mathbf{r},a} \left\{ \gamma(A) \mathbf{g}(\mathbf{R}, A)^T \right\}, \quad (4.686)$$

and \mathbf{G} was defined in (4.629). First, consider the BCRB. Then, using (4.640), the required expectation is

$$\begin{aligned} T_\gamma &= E_{\mathbf{r},a} \left\{ \gamma(A) \frac{\partial \ln p(\mathbf{R}, A)}{\partial A} \right\} \\ &= \int \int \gamma(A) \frac{\partial \ln p_{\mathbf{r},a}(\mathbf{R}, A)}{\partial A} p_{\mathbf{r},a}(\mathbf{R}, A) d\mathbf{R} dA \\ &= \int \left(\int \gamma(A) \frac{\partial p_{\mathbf{r},a}(\mathbf{R}, A)}{\partial A} dA \right) d\mathbf{R} \\ &= \int p_{\mathbf{r}}(\mathbf{R}) \left(\int \gamma(A) \frac{\partial p_{a|\mathbf{r}}(A|\mathbf{R})}{\partial A} dA \right) d\mathbf{R}. \end{aligned} \quad (4.687)$$

Evaluating the inner integral gives

$$\int \gamma(A) \frac{\partial p_{a|\mathbf{r}}(A|\mathbf{R})}{\partial A} dA = \gamma(A) p(A|\mathbf{R}) \Big|_{-\infty}^{\infty} - \int \frac{\partial \gamma(A)}{\partial A} p_{a|\mathbf{r}}(A|\mathbf{R}) dA. \quad (4.688)$$

Assuming

$$\lim_{A \rightarrow \pm\infty} \gamma(A) p_{a|\mathbf{r}}(A|\mathbf{R}) = 0, \quad \text{for all } \mathbf{R}, \quad (4.689)$$

we have

$$\begin{aligned} T_\gamma &= - \int \int \frac{\partial \gamma(A)}{\partial A} p_{\mathbf{r},a}(\mathbf{R}, A) d\mathbf{R} dA \\ &= -E_a \left\{ \frac{\partial \gamma(A)}{\partial A} \right\}. \end{aligned} \quad (4.690)$$

Therefore, the BCRB is

$$E \left\{ (\hat{d}(\mathbf{R}) - \gamma(A))^2 \right\} \geq \frac{\left(E_a \left\{ \frac{\partial \gamma(A)}{\partial A} \right\} \right)^2}{J_B}. \quad (4.691)$$

This is the Bayesian analog to the nonrandom parameter result in (4.117).

For the Weiss–Weinstein bound with multiple test points, the required expectation is

$$[\mathbf{T}_\gamma]_j = E_{\mathbf{r},a} \left\{ \gamma(A) [L^{s_j}(\mathbf{R}; A + h_j, A) - L^{1-s_j}(\mathbf{R}; A - h_j, A)] \right\}. \quad (4.692)$$

Defining $\beta = A - h_j$, the second term can be written as

$$\begin{aligned} E_{\mathbf{r},a} \left\{ \gamma(A) L^{1-s_j}(\mathbf{R}; A - h_j, A) \right\} &= \int \int \gamma(A) \left(\frac{p_{\mathbf{r},a}(\mathbf{R}, A - h_j)}{p_{\mathbf{r},a}(\mathbf{R}, A)} \right)^{1-s_j} p_{\mathbf{r},a}(\mathbf{R}, A) d\mathbf{R} dA \\ &= \int \int \gamma(\beta + h_j) \left(\frac{p_{\mathbf{r},a}(\mathbf{R}, \beta + h_j)}{p_{\mathbf{r},a}(\mathbf{R}, \beta)} \right)^{s_j} p_{\mathbf{r},a}(\mathbf{R}, \beta) d\mathbf{R} d\beta \\ &= E_{\mathbf{r},a} \left\{ \gamma(A + h_j) L^{s_j}(\mathbf{R}; A + h_j, A) \right\}. \end{aligned} \quad (4.693)$$

Thus,

$$\begin{aligned}
[\mathbf{T}_\gamma]_j &= E_{\mathbf{r},a} \{ (\gamma(A) - \gamma(A + h_j)) L^{s_j}(\mathbf{R}; A + h_j, A) \} \\
&= \iint (\gamma(A) - \gamma(A + h_j)) p_{\mathbf{r},a}(\mathbf{R}, A + h_j)^{s_j} p_{\mathbf{r},a}(\mathbf{R}, A)^{1-s_j} d\mathbf{R} dA \\
&= \int (\gamma(A) - \gamma(A + h_j)) p_a(A + h_j)^{s_j} p_a(A)^{1-s_j} \left(\int p_{\mathbf{r}|a}(\mathbf{R}|A + h_j)^{s_j} p_{\mathbf{r}|a}(\mathbf{R}|A)^{1-s_j} d\mathbf{R} \right) dA. \\
&= \int (\gamma(A) - \gamma(A + h_j)) p_a(A + h_j)^{s_j} p_a(A)^{1-s_j} e^{\mu(s_j; A + h_j, A)} dA. \tag{4.694}
\end{aligned}$$

The function $\mu(s_j; A + h_j, A)$ does not depend on the transformation, $\gamma(A)$. The \mathbf{G} matrix is given by (4.651) and the bound is

$$E \left\{ (\hat{d}(\mathbf{R}))^2 \right\} \geq \mathbf{T}_\gamma \mathbf{G}^{-1} \mathbf{T}_\gamma^T. \tag{4.695}$$

Vector Parameters. The vector parameter case follows in a similar manner. We assume \mathbf{A} is a $K \times 1$ vector and that $\gamma(\mathbf{A})$ is a $K_d \times 1$ vector. We define

$$\mathbf{f}(\mathbf{R}, \mathbf{A}) = \hat{\mathbf{d}}(\mathbf{R}) - \gamma(\mathbf{A}). \tag{4.696}$$

Then

$$\mathbf{T}_\gamma = E_{\mathbf{r},a} \{ \gamma(\mathbf{A}) \mathbf{g}^T(\mathbf{R}, \mathbf{A}) \}. \tag{4.697}$$

The Bayesian bound is

$$E \left\{ [\hat{\mathbf{d}}(\mathbf{R}) - \gamma(\mathbf{A})] [\hat{\mathbf{d}}(\mathbf{R}) - \gamma(\mathbf{A})]^T \right\} \geq \mathbf{T}_\gamma \mathbf{G}^{-1} \mathbf{T}_\gamma^T. \tag{4.698}$$

For the vector BCRB, $\mathbf{G} = \mathbf{J}_B$ and \mathbf{T}_γ is the $K_d \times K$ matrix

$$\mathbf{T}_\gamma = -E_{\mathbf{a}} \left\{ [\nabla_{\mathbf{A}} \gamma^T(\mathbf{A})]^T \right\}, \tag{4.699}$$

which proves the bound stated in (4.535).

For the vector parameter WWB, \mathbf{G} is given by (4.667) and

$$[\mathbf{T}_\gamma]_{ij} = E_{\mathbf{r},a} \{ \gamma_i(\mathbf{A}) [L^{s_j}(\mathbf{R}; \mathbf{A} + \mathbf{h}_j, \mathbf{A}) - L^{1-s_j}(\mathbf{R}; \mathbf{A} - h_j, \mathbf{A})] \}. \tag{4.700}$$

Using the same approach as in (4.694) gives

$$[\mathbf{T}_\gamma]_{ij} = \int (\gamma_i(\mathbf{A}) - \gamma_i(\mathbf{A} + \mathbf{h}_j)) p_{\mathbf{a}}(\mathbf{A} + \mathbf{h}_j)^{s_j} p_{\mathbf{a}}(\mathbf{A})^{1-s_j} e^{\mu(s_j; \mathbf{A} + \mathbf{h}_j, \mathbf{A})} d\mathbf{A}. \tag{4.701}$$

Similar results can be derived for the other bounds in the covariance inequality family.

4.4.1.7 Summary of Covariance Inequality Bounds

In this section, we have provided the necessary framework to derive a family of global Bayesian bounds based on the covariance inequality. We then discussed the Weiss–Weinstein bound in detail. Other Bayesian bounds are developed in the problems. The techniques of combined bounds and bounds on transformed parameters were also discussed.

An analogous covariance inequality is available for the case of nonrandom parameters and a set of bounds can be derived from it. In Table 4.1, we show the covariance inequality

Table 4.1: The covariance inequality bound hierarchy

	Nonrandom: Classical	Random: Bayesian
1	<i>Cramér–Rao</i> Fisher [Fis22] Dugué [Dug37] Cramér [Cra46] Rao [Rao45] Fréchet [Fré43]	<i>Bayesian Cramér–Rao</i> Van Trees [Van68, Van01a] Shutzenberger [Shu57]
2		<i>Weighted Bayesian Cramér–Rao</i> Bobrovsky et al. [BMZ87]
3	<i>Bhattacharyya</i> Bhattacharyya [Bha43]	<i>Bayesian Bhattacharyya</i> Van Trees [Van68, Van01a]
4	<i>Barankin</i> Barankin [Bar49] McAulay and Hofstetter [MH71]	<i>Bobrovsky–Zakai</i> Bobrovsky and Zakai [BZ76] Bobrovsky et al. [BMZ87] Reuven and Messer [RM97]
5		<i>Weiss–Weinstein</i> Weiss and Weinstein [WW85]
6	<i>Combined</i> McAulay and Hofstetter [MH71] Abel [Abe93]	<i>Combined</i> Weiss [Wei85] Renaux et al. [RFLR06] Bell and Van Trees [BV06]

hierarchy. Note that there is no nonrandom bound corresponding to the Bayesian Weiss–Weinstein bound.

The advantage of the global Bayesian bounds is that they provide reasonably tight bounds over a wide range of SNR or N . The disadvantage is that choosing the appropriate test points require some experience.

4.4.2 Method of Interval Estimation

The method of interval estimation (MIE) provides an approximation to the performance of the ML estimator and can be an excellent indicator of the threshold location. We explain the technique in the context of the frequency estimation problem in Example 4.15. In Figure 4.10, we showed plots of the noisy ambiguity surface computed on a fine grid from $-\pi$ to π . We then chose the maximum and denoted it as $\hat{\omega}_{\text{ml}}(\mathbf{R})$. We observed that there were two types of errors. The first type occurred when the estimate was in the vicinity of the correct peak of the log-likelihood function. In this case, the error was small and the MSE was equal to the CRB. The second type of error occurred when the estimate was in the vicinity of an incorrect peak of the log-likelihood function.

This behavior can be modeled by considering an alternative estimation approach that uses a two-step procedure. We first do a coarse search over ω by computing the ambiguity surface on a coarse grid,

$$\omega_m = \frac{2\pi m}{M}, \quad m = 0, 1, \dots, M - 1, \quad (4.702)$$

where $M \geq N$ and is a power of 2. This gives us a set of M values instead of a continuous function. We select the largest value and then do a local maximization around the selected point. This technique is computationally simpler than the technique used in Example 4.15, and analysis of its performance is the basis of the MIE technique. The continuous version of this analysis is given in [Van68, Van01a]. The discrete-time version is given in [RB74]. The same techniques were used earlier by Woodward (radar range measurement) [Woo52] and Kotelnikov (PPM and PFM) [Kot59]. Various modifications have been used by various authors (e.g., Wozencraft and Jacobs [WJ65], Darlington [Dar64], and Akima [Aki63]).

There are two types of errors. The first type is a coarse error (or outlier). We also refer to this as an interval error, since we have incorrectly localized the value to the wrong interval on the coarse grid. The second type is a local error about the correct coarse estimate. Thus, we approximate the conditional MSE of the ML estimator as

$$\begin{aligned} \text{MSE}(\hat{\omega}_{\text{ml}}(\tilde{\mathbf{R}})|\omega) &\approx E_{\tilde{\mathbf{r}}|\omega} \left\{ (\hat{\omega}_{\text{ml}}(\tilde{\mathbf{R}}) - \omega)^2 \middle| \text{interval error} \right\} \Pr(\text{interval error}) \\ &\quad + E_{\tilde{\mathbf{r}}|\omega} \left\{ (\hat{\omega}_{\text{ml}}(\tilde{\mathbf{R}}) - \omega)^2 \middle| \text{no interval error} \right\} \Pr(\text{no interval error}). \end{aligned} \quad (4.703)$$

Example 4.35 (continuation of Example 4.15) Frequency estimation. Our analysis is similar to [RB74], which was for joint frequency and phase estimation. From (4.703), the conditional MSE for a particular value of ω is approximated as

$$\text{MSE}(\hat{\omega}_{\text{ml}}(\tilde{\mathbf{R}})|\omega) \approx q\sigma_I^2(\omega) + (1-q)J_F^{-1}(\omega), \quad (4.704)$$

where q is the probability of making an interval error, $\sigma_I^2(\omega)$ is the MSE when an interval error is made, and $J_F^{-1}(\omega)$ is the small error MSE, given in (4.231). In this example, it is not a function of ω .

We saw in Example 4.15 that for low SNR, large error frequency estimates were approximately uniformly distributed in the *a priori* interval $(-\pi, \pi)$. We would expect that the two-step estimation procedure would result in a similar distribution of errors. For a fixed ω , the conditional MSE of these errors is

$$\begin{aligned} \sigma_I^2(\omega) &= E_{\hat{\omega}} \{ (\hat{\omega}_{\text{ml}} - \omega)^2 \} \\ &= E_{\hat{\omega}} \{ \hat{\omega}_{\text{ml}}^2 \} - 2\omega E_{\hat{\omega}} \{ \hat{\omega}_{\text{ml}} \} + \omega^2 \\ &= \frac{(2\pi)^2}{12} + \omega^2. \end{aligned} \quad (4.705)$$

To find q , it is easier to first find $1 - q$, the probability of not making an interval error. When the phase is known, the ambiguity surface is proportional to the real part of the DFT of the data. If the DFT is implemented on the frequency grid in (4.702) with $M = N$ and ω is one of the DFT frequencies, then the ambiguity surface values are independent Gaussian random variables with variance σ^2/N . The mean of the ambiguity surface at the correct frequency point is the signal amplitude b , and the remaining terms have zero mean. Let z be the value of the ambiguity surface at the correct frequency. The probability of choosing the correct frequency is the probability that all of the ambiguity surface values at the incorrect frequencies are less than z . The probability that any one of them is less than z is $1 - \text{erfc}_*(zN/\sigma)$, and since they are independent, the probability that they are all less than z is the

product of the individual probabilities. Integrating this probability over the pdf of z , the probability of choosing the correct interval is

$$1 - q = \int_{-\infty}^{\infty} \left[1 - \text{erfc}_* \left(\frac{zN}{\sigma} \right) \right]^{N-1} \sqrt{\frac{N}{2\pi\sigma^2}} \exp \left\{ -\frac{N(z-b)^2}{2\sigma^2} \right\} dz, \quad (4.706)$$

which must be evaluated using numerical integration and is not a function of ω . ■

Example 4.36 (continuation of Examples 4.16, 4.34, and 4.35) Frequency estimation. When ω is a random variable with pdf $p_\omega(\omega)$, the global MSE is found by evaluating the expected value of the conditional MSE in (4.704) with respect to the prior $p_\omega(\omega)$. Only the $\sigma_t^2(\omega)$ term depends on ω , so the expectation is straightforward. The result is no longer a function of ω and is given by,

$$\sigma_\epsilon^2 = E_\omega \{ \text{MSE}(\hat{\omega}_{\text{ml}}(\tilde{\mathbf{R}})|\omega) \} \approx q \left(\frac{(2\pi)^2}{12} + \sigma_\omega^2 \right) + (1-q)J_F^{-1}. \quad (4.707)$$

In Figure 4.31, we plot the MIE MSE in (4.707) for $a = 20$ with the bounds and simulation results from Example 4.16. The MIE approximations are quite close to the MSE of the ML and MAP estimators, and give an excellent prediction of the threshold location. ■

In the previous example, all interval errors had the same probability. This was true because $M = N$ and the actual frequency was one of the coarse grid points. If we use $M > N$, then looking at Figure 4.11, we see that as SNR decreases and the estimator moves into the threshold region, the outliers initially tend to be at the sidelobes of the signal component of the ambiguity surface, thus some interval errors are more likely than others.

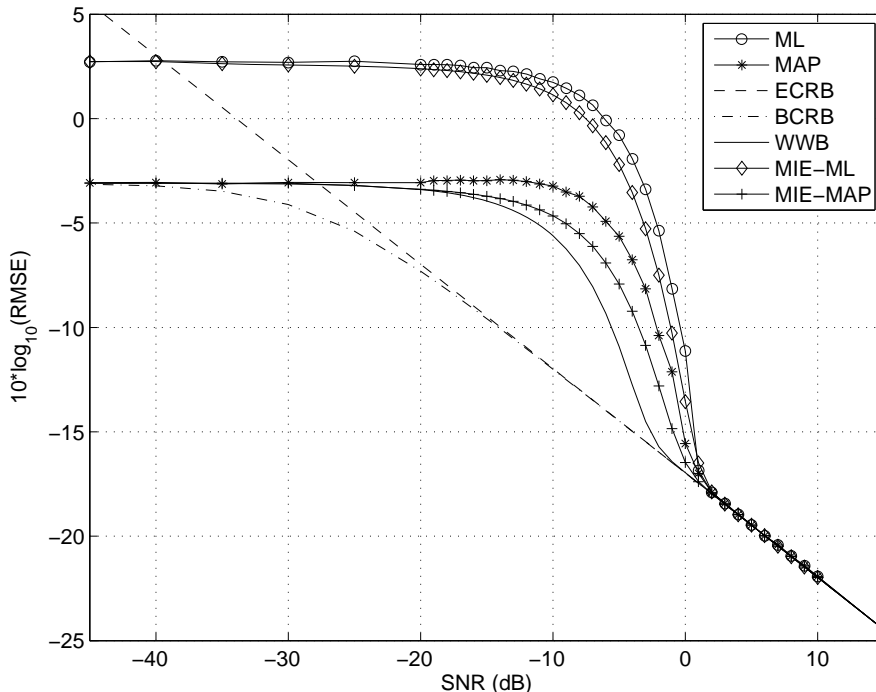


Figure 4.31: Frequency RMSE and MIE versus SNR. $N = 16$, $\theta = \pi/6$, $a = 20$.

A more informative way to write the first term in (4.703) is

$$\sigma_{\epsilon,IE}^2 = \sum_{m=0}^{M-1} p_m \left(\omega - \frac{2\pi m}{M} \right)^2, \quad (4.708)$$

where p_m is the probability that the m th interval is chosen and $\left(\omega - \frac{2\pi m}{M} \right)^2$ is the squared error for this choice. The difficulty in computing this quantity is computing the $p_m; m = 0, \dots, M-1$.

References [Van68, Van01a, RB74], and [Van71b, Van01b] represent earlier work using the technique. There have been several applications of the MIE by a number of authors. Richmond in [Ric05] provides a good history of various applications and applies the MIE to a Capon estimator. Athley [Ath05] and Najjar-Atallah et al. [NALF05] apply the MIE to investigate threshold behavior for various estimation problems.

It is important to note that MIE is an approximation and depends on the algorithm being used. It is not a bound. In many applications, it provides a good indication of the threshold performance.

4.4.3 Summary of Global Bayesian Bounds

In this section, we developed the framework for a family of global Bayesian bounds based on the covariance inequality. We derived the Weiss–Weinstein bound and applied it to our frequency estimation case study. The WWB or a combined BCRB–WWB appear to provide the best prediction of performance for bounds in the covariance inequality family. As demonstrated by the example, choosing the test points to use in the bound requires some skill.

The method of interval estimation is an approximation rather than a bound. It is motivated by an algorithm that could be used to find the maximum of the *a posteriori* density. It appears to provide good results in many applications.

Readers who plan to pursue the global bounds area should also read the discussion of Ziv-Zakai bounds in Van Trees and Bell [VB07].

4.5 COMPOSITE HYPOTHESES

4.5.1 Introduction

In Chapter 2, we confined our discussion to the decision problem in which the hypotheses were simple. We now have the necessary estimation theory background to extend our discussion to the case in which the hypotheses are composite. The term composite is most easily explained by a simple example.

Example 4.37 (continuation of Examples 2.1 and 2.5) Gaussian. Under hypothesis H_0 the observed variable r is Gaussian with zero mean and variance σ^2 . Under hypothesis H_1 the observed variable r is Gaussian with mean m and variance σ^2 . The value of m can be anywhere in the interval $[M_L, M_U]$. Thus,

$$\begin{aligned} H_0 : p_{r|H_0}(R|H_0) &= \frac{1}{\sqrt{2\pi}\sigma} \exp\left(-\frac{R^2}{2\sigma^2}\right), \\ H_1 : p_{r|H_1,m}(R|H_1, M) &= \frac{1}{\sqrt{2\pi}\sigma} \exp\left(-\frac{(R-M)^2}{2\sigma^2}\right), \quad M_L \leq M \leq M_U. \end{aligned} \quad (4.709)$$

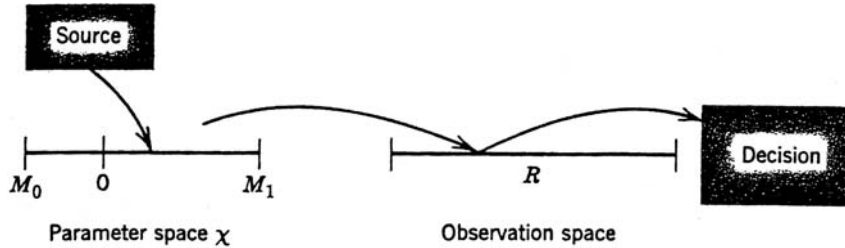


Figure 4.32: Composite hypothesis testing problem for the single-parameter example.

We refer to H_1 as a composite hypothesis because the parameter value M , which characterizes the hypothesis, ranges over a set of values. A model of this decision problem is shown in Figure 4.32. The output of the source is a parameter value M , which we view as a point in a parameter space χ . We then define the hypotheses as subspaces of χ . In this case, H_0 corresponds to the point $M = 0$ and H_1 corresponds to the interval $[M_L, M_U]$. We assume that the probability density governing the mapping from the parameter space to the observation space, $p_{r|m}(R|M)$, is known for all values of M in χ .

The final component is a decision rule that divides the observation space into two parts that correspond to the two possible decisions. It is important to observe that we are interested *solely* in making a decision and that the actual value M is not of interest to us. ■

The extension of these ideas to the general composite hypothesis testing problem is straightforward. The model is shown in Figure 4.33. The output of the source is a set of parameters. We view it as a point in a parameter space χ and denote it by the vector θ . The hypotheses are subspaces of χ . (In Figure 4.33, we have indicated nonoverlapping spaces for convenience.) The probability density governing the mapping from the parameter space to the observation space is denoted by $p_{r|\theta}(\mathbf{R}|\theta)$ and is assumed to be known for all values of θ in χ . Once again, the final component is a decision rule.

The composite hypothesis problem that we will consider can be written as

$$H_0 : p_{\mathbf{r}|H_0, \theta_0}(\mathbf{R}|H_0, \theta_0) \quad (4.710)$$

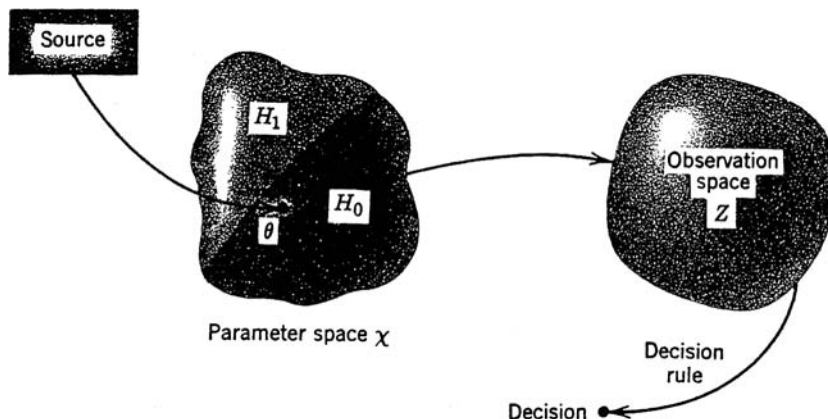


Figure 4.33: Composite hypothesis testing problem for the multiple-parameter example.

and

$$H_1 : p_{\mathbf{r}|H_1, \boldsymbol{\theta}_1}(\mathbf{R}|H_1, \boldsymbol{\theta}_1), \quad (4.711)$$

where $\boldsymbol{\theta}_0$ is an $N_0 \times 1$ vector and $\boldsymbol{\theta}_1$ is an $N_1 \times 1$ vector.

In some cases, some of the components of $\boldsymbol{\theta}_0$ and $\boldsymbol{\theta}_1$ are the same on both hypotheses and it is useful to partition the vector,

$$\boldsymbol{\theta}_0 = \begin{bmatrix} \boldsymbol{\theta}_{w_0} \\ \boldsymbol{\theta}_u \end{bmatrix} \quad (4.712)$$

and

$$\boldsymbol{\theta}_1 = \begin{bmatrix} \boldsymbol{\theta}_{w_1} \\ \boldsymbol{\theta}_u \end{bmatrix}, \quad (4.713)$$

where, as in Section 4.3.5, “ w ” denotes wanted and “ u ” denotes the unwanted parameters that are the same on both hypotheses.

To complete the formulation, we must characterize the parameter $\boldsymbol{\theta}$. The parameter $\boldsymbol{\theta}$ may be a random parameter vector or an unknown nonrandom parameter vector or a hybrid parameter vector. We first consider the random parameter case.

4.5.2 Random Parameters

If $\boldsymbol{\theta}$ is a random vector with a known probability density, the procedure is straightforward. Denoting the probability density of $\boldsymbol{\theta}$ on the two hypotheses as $p_{\boldsymbol{\theta}_0|H_0}(\boldsymbol{\theta}_0|H_0)$ and $p_{\boldsymbol{\theta}_1|H_1}(\boldsymbol{\theta}_1|H_1)$, the likelihood ratio is

$$\Lambda(\mathbf{R}) \triangleq \frac{p_{\mathbf{r}|H_1}(\mathbf{R}|H_1)}{p_{\mathbf{r}|H_0}(\mathbf{R}|H_0)} = \frac{\int_{\chi_1}^{\chi_1} p_{\mathbf{r}|\boldsymbol{\theta}_1}(\mathbf{R}|\boldsymbol{\theta}_1, H_1) p_{\boldsymbol{\theta}_1|H_1}(\boldsymbol{\theta}_1|H_1) d\boldsymbol{\theta}_1}{\int_{\chi_0}^{\chi_0} p_{\mathbf{r}|\boldsymbol{\theta}_0}(\mathbf{R}|\boldsymbol{\theta}_0, H_0) p_{\boldsymbol{\theta}_0|H_0}(\boldsymbol{\theta}_0|H_0) d\boldsymbol{\theta}_0}. \quad (4.714)$$

The reason for this simplicity is that the known probability density on $\boldsymbol{\theta}$ enables us to reduce the problem to a simple hypothesis testing problem by integrating over $\boldsymbol{\theta}$. We can illustrate this procedure for a generalization of the model in Example 4.37.

Example 4.38 (continuation of Examples 4.2 and 4.37) Gaussian. The received vectors on the two hypotheses are

$$H_1 : \mathbf{r} = m \mathbf{v} + \mathbf{n}, \quad (4.715)$$

$$H_0 : \mathbf{r} = \mathbf{n}, \quad (4.716)$$

where \mathbf{v} is a known $N \times 1$ vector and \mathbf{n} is an $N \times 1$ zero-mean Gaussian vector $N(\mathbf{0}, \sigma_n^2 \mathbf{I})$.

The parameter m is a zero-mean Gaussian random variable $N(0, \sigma_m^2)$ that is statistically independent of \mathbf{n} . Then

$$p_{\mathbf{r}|H_1}(\mathbf{R}|H_1) = \int_{-\infty}^{\infty} \frac{1}{(2\pi\sigma_n^2)^{N/2}} \exp \left\{ -\frac{1}{2\sigma_n^2} [\mathbf{R} - M \mathbf{v}]^T [\mathbf{R} - M \mathbf{v}] \right\} \cdot \frac{1}{\sqrt{2\pi}\sigma_m} \exp \left\{ -\frac{M^2}{2\sigma_m^2} \right\} dM \quad (4.717)$$

and

$$p_{\mathbf{r}|H_0}(\mathbf{R}|H_0) = \frac{1}{(2\pi\sigma_n^2)^{N/2}} \exp \left\{ -\frac{1}{2\sigma_n^2} \mathbf{R}^T \mathbf{R} \right\}. \quad (4.718)$$

Integrating (4.717), substituting into the likelihood ratio in (4.714) and taking the logarithm gives

$$\frac{1}{2} \ln \sigma_p^2 - \frac{1}{2} \ln \sigma_m^2 + \frac{\sigma_p^2}{2\sigma_n^2} |\mathbf{v}^T \mathbf{R}|^2 \stackrel{H_1}{\underset{H_0}{\gtrless}} \ln \eta, \quad (4.719)$$

where

$$\sigma_p^2 = \frac{\sigma_n^2 \sigma_m^2}{\sigma_m^2 \mathbf{v}^T \mathbf{v} + \sigma_n^2}. \quad (4.720)$$

This reduces to

$$\frac{1}{\sigma_n^2} |\mathbf{v}^T \mathbf{R}|^2 \stackrel{H_1}{\underset{H_0}{\gtrless}} 2 \frac{(\sigma_m^2 \mathbf{v}^T \mathbf{v} + \sigma_n^2)}{\sigma_m^2} \left\{ \ln \eta + \frac{1}{2} \ln \left(1 + \frac{\sigma_m^2 \mathbf{v}^T \mathbf{v}}{\sigma_n^2} \right) \right\} \triangleq \gamma. \quad (4.721)$$

Note that when $\mathbf{v} = \mathbf{1}$, the model on H_1 corresponds to the model in Example 4.2. Following the steps in Example 4.2, we can show that

$$\hat{m}_{\text{map}}(\mathbf{R}) = \frac{\sigma_p^2}{\sigma_n^2} \mathbf{v}^T \mathbf{R}, \quad (4.722)$$

so that the test in (4.719) can also be written as

$$\frac{\hat{m}_{\text{map}}(\mathbf{R}) \mathbf{v}^T \mathbf{R}}{\sigma_n^2} \stackrel{H_1}{\underset{H_0}{\gtrless}} 2 \ln \eta - \ln \left(\frac{\sigma_p^2}{\sigma_m^2} \right) \triangleq \gamma'. \quad (4.723)$$

We see that this is just the known signal result in Section 3.2.1, equation (3.124) with m replaced by its MAP (also MMSE) estimate.

Note that we can also view this a simple hypothesis test of two Gaussian densities with zero mean on both hypotheses and covariance matrices

$$\mathbf{K}_0 = \sigma_n^2 \mathbf{I}, \quad (4.724)$$

$$\mathbf{K}_1 = \sigma_m^2 \mathbf{v} \mathbf{v}^T + \sigma_n^2 \mathbf{I}. \quad (4.725)$$

Then the results in Section 3.3.1 apply. ■

This example can be generalized to the following case.

Example 4.39 (continuation of Examples 4.37 and 4.38) Gaussian. The received vectors on the two hypotheses are

$$H_1 : \mathbf{r} = \mathbf{V}\boldsymbol{\theta} + \mathbf{n}, \quad (4.726)$$

$$H_0 : \mathbf{r} = \mathbf{n}, \quad (4.727)$$

where \mathbf{V} is a known $N \times D$ matrix and \mathbf{n} is $N(\mathbf{0}, \sigma_n^2 \mathbf{I})$. The parameter vector $\boldsymbol{\theta}$ is a $D \times 1$ zero-mean Gaussian random vector $N(\mathbf{0}, \mathbf{K}_{\boldsymbol{\theta}})$. Then

$$\begin{aligned} p_{\mathbf{r}|H_1}(\mathbf{R}|H_1) &= \int_{-\infty}^{\infty} \frac{1}{(2\pi\sigma_n^2)^{N/2}} \exp \left\{ -\frac{1}{2\sigma_n^2} [\mathbf{R} - \mathbf{V}\boldsymbol{\theta}]^T [\mathbf{R} - \mathbf{V}\boldsymbol{\theta}] \right\} \\ &\quad \cdot \frac{1}{(2\pi)^{D/2} |\mathbf{K}_{\boldsymbol{\theta}}|^{1/2}} \exp \left\{ -\frac{1}{2} [\boldsymbol{\theta}^T \mathbf{K}_{\boldsymbol{\theta}}^{-1} \boldsymbol{\theta}] \right\} d\boldsymbol{\theta} \end{aligned} \quad (4.728)$$

and $p_{\mathbf{r}|H_0}(\mathbf{R}|H_0)$ is given by (4.718).

Substituting (4.728) and (4.718) into (4.714) and proceeding as in Example 4.38 (see Problem 4.5.9), we obtain

$$\frac{1}{\sigma_n^2} \mathbf{R}^T \mathbf{H} \mathbf{R} \stackrel{H_1}{\gtrless} \stackrel{H_0}{\lss} \gamma, \quad (4.729)$$

where

$$\mathbf{H} = \mathbf{V} \mathbf{K}_\theta \mathbf{V}^T (\mathbf{V} \mathbf{K}_\theta \mathbf{V}^T + \sigma_n^2 \mathbf{I})^{-1}. \quad (4.730)$$

In this case, it is simpler to treat it as simple hypotheses test with zero-mean and covariance matrices

$$\mathbf{K}_0 = \sigma_n^2 \mathbf{I}, \quad (4.731)$$

$$\mathbf{K}_1 = \mathbf{V} \mathbf{K}_\theta \mathbf{V}^T + \sigma_n^2 \mathbf{I}. \quad (4.732)$$

Then, the results in Section 3.3.1 apply. ■

In these examples, the integrals were easy to evaluate because the densities were Gaussian. For the general case given in (4.714) the actual calculation may be more involved, but the desired procedure is well defined.

When θ is a random variable with an unknown density, the best test procedure is not clearly specified. One possible approach is a minimax test over the unknown density. An alternate approach is to try several densities based on any partial knowledge of θ that is available. In many cases the test structure will be insensitive to the detailed behavior of the probability density.

The more challenging case occurs when the unknown parameters are modeled as non-random parameters. We develop that case in the next section.

4.5.3 Nonrandom Parameters

The second case of interest is the case in which θ is a nonrandom vector. We shall try a procedure and investigate the results. A first observation is that, because θ has no probability density over which to average, a Bayes test is not meaningful. Thus, we can devote our time to Neyman–Pearson tests.

We begin our discussion by examining what we call a *perfect measurement bound* on the test performance. We illustrate this idea for the problem in Example 4.37.

Example 4.40 (continuation of Examples 2.1, 2.5, and 4.37) Gaussian. In this case, $\theta = m$ is an unknown nonrandom parameter. From (4.709),

$$\begin{aligned} H_1 : p_{r|H_1, m}(R|H_1, M) &= \frac{1}{\sqrt{2\pi}\sigma} \exp\left(-\frac{(R-M)^2}{2\sigma^2}\right), & M_L \leq M \leq M_U, \\ H_0 : p_{r|H_0, m}(R|H_0, M) &= \frac{1}{\sqrt{2\pi}\sigma} \exp\left(-\frac{R^2}{2\sigma^2}\right). \end{aligned} \quad (4.733)$$

It is clear that whatever test we design can never be better than a hypothetical test in which the receiver first measures M perfectly (or, alternately, it is told M) and then designs that optimum likelihood ratio test. Thus, we can bound the ROC of any test by the ROC of this fictitious perfect measurement test. For this example we could use the ROCs in Example 2.5, Figure 2.12a by letting $d^2 = M^2/\sigma^2$. Because we are interested in the behavior versus M , the format in Figure 2.12b is more useful. This is shown in Figure 4.34. Such a curve is called a *power function*. It is simply a plot of

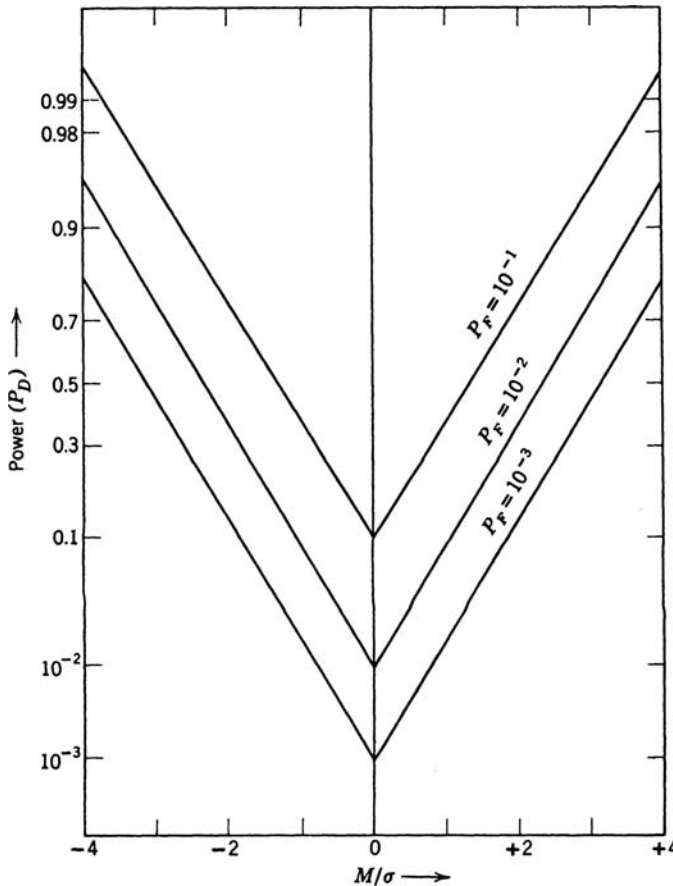


Figure 4.34: Power function for perfect measurement test.

P_D for all values for M (more generally θ) for various values of P_F . Because $H_0 = H_1$ for $M = 0$, $P_D = P_F$. The curves in Figure 4.34 represent a bound on how well any test could do. We now want to see how close the actual test performance comes to this bound.

The best performance we could achieve would be obtained if an actual test's curves equaled the bound for all $M \in \chi$. We call such tests *uniformly most powerful* (UMP). In other words, for a given P_F a UMP test has a P_D greater than or equal to any other test for all $M \in \chi$. The conditions for a UMP test to exist can be seen in Figure 4.35. We first construct the perfect measurement bound. We next consider other possible tests and their performances. Test A is an ordinary likelihood ratio test designed under the assumption that $M = 1$. The first observation is that the power of this test equals the bound at $M = 1$, which follows from the manner in which we constructed the bound. For other values of M , the power of test A may or may not equal the bound. Similarly, test B is a likelihood ratio test designed under the assumption that $M = 2$, and test C is a likelihood ratio test designed under the assumption that $M = -1$. In each case their power equals the bound at their design points. (The power functions in Figure 4.35 are drawn to emphasize this and are not quantitatively correct away from the design point.) They may also equal the bound at other points. The conditions for a UMP test are now obvious. We must be able to design a complete likelihood ratio test (including the threshold) for every $M \in \chi$ without knowing M . ■

The analogous result for the general case follows easily.

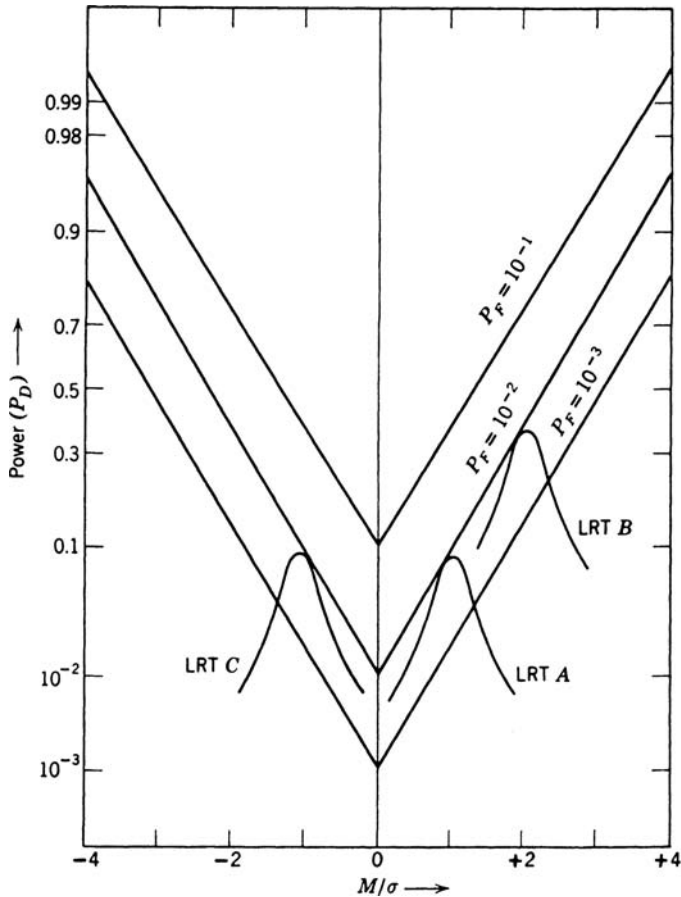


Figure 4.35: Power functions for various likelihood ratio tests.

It is clear that in general the bound can be reached for any particular θ simply by designing an ordinary LRT for that particular θ . Now a UMP test must be as good as any other test for every θ . This gives us a necessary and sufficient condition for its existence.

Property. A UMP test exists if and only if the likelihood ratio test for every $\theta \in \chi$ can be completely defined (including threshold) without knowledge of θ .

The “if” part of the property is obvious. The “only if” follows directly from our discussion in the preceding paragraph. If there exists some $\theta \in \chi$ for which we cannot find the LRT without knowing θ , we should have to use some other test, because we do not know θ . This test will necessarily be inferior for that particular θ to a LRT test designed for that particular θ and therefore is not *uniformly* most powerful.

Example 4.40 (continued). Returning to Example 4.40 and using the results in Example 2.5, Figure 2.11, we know that the likelihood ratio test for $M > 0$ is

$$R \stackrel[H_1]{\geqslant} \gamma^+ \quad (4.734)$$

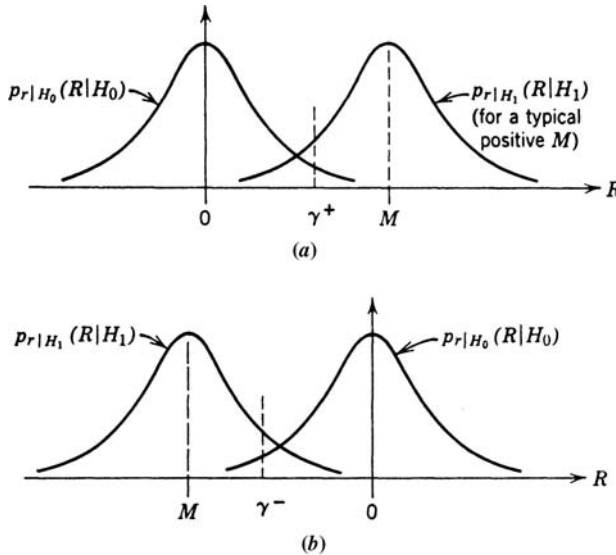


Figure 4.36: Effect of sign of M : (a) threshold for positive M ; (b) threshold for negative M .

and

$$P_F = \int_{\gamma^+}^{\infty} \frac{1}{\sqrt{2\pi}\sigma} \exp\left(-\frac{R^2}{2\sigma^2}\right) dR, \quad \text{if } M > 0. \quad (4.735)$$

(The superscript + emphasizes the test assumes $M > 0$. The value of γ^+ may be negative.) This is shown in Figure 4.36a.

Similarly, for the case in which $M < 0$ the likelihood ratio test is

$$R \stackrel[H_1]{\stackrel[H_0]{\gtrless}}{\gamma^-}, \quad (4.736)$$

where

$$P_F = \int_{-\infty}^{\gamma^-} \frac{1}{\sqrt{2\pi}\sigma} \exp\left(-\frac{R^2}{2\sigma^2}\right) dR, \quad \text{if } M < 0. \quad (4.737)$$

This is shown in Figure 4.36b. We see that the threshold is just the negative of the threshold for $M > 0$. This reversal is done to get the largest portion of $p_{r|H_1}(R|H_1)$ inside the H_1 region (and therefore maximize P_D). Thus, with respect to this example, we draw the following conclusions:

1. If M can take on *only* nonnegative values (i.e., $M_L \geq 0$), a UMP test exists [use (4.734)].
2. If M can take on *only* nonpositive values (i.e., $M_U \leq 0$), a UMP test exists [use (4.736)].
3. If M can take on both negative and positive values (i.e., $M_L < 0$ and $M_U > 0$), then a UMP test does not exist. In Figure 4.37, we show the power function for a likelihood ratio test designed under the assumption that M was positive. For negative values of M , P_D is less than P_F because the threshold is on the wrong side.

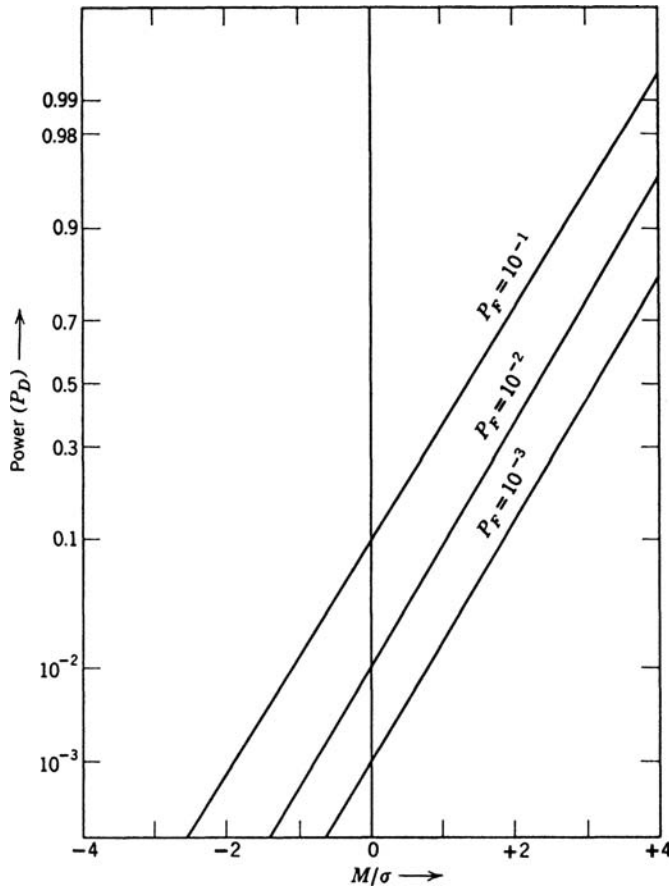


Figure 4.37: Performance of LRT assuming positive M .

The test corresponding to conclusions 1 and 2 can be written in terms of the probability density $p_{r|m}(R|M)$ as

$$\begin{aligned} H_0 : M &= 0, \\ H_1 : M &> 0 \end{aligned} \quad (4.738)$$

and

$$\begin{aligned} H_0 : M &= 0, \\ H_1 : M &< 0. \end{aligned} \quad (4.739)$$

These are called one-sided tests. A two-sided test has the form

$$\begin{aligned} H_0 : M &= 0, \\ H_1 : M &\neq 0. \end{aligned} \quad (4.740)$$

where M can be positive or negative. A UMP test will only exist if the problem can be written as a one-sided test [KS79]. ■

For scalar parameters there is a theorem due to Karlin and Rubin [KR56] that defines a class of probability densities that will result in a one-sided UMP test.

Consider a vector parameter \mathbf{r} whose probability density is parameterized by the scalar parameter θ . If the likelihood ratio

$$\Lambda(\mathbf{R}; \theta_1, \theta_0) = \frac{p_{\mathbf{r}|H_1}(\mathbf{R}|H_1)}{p_{\mathbf{r}|H_0}(\mathbf{R}|H_0)} = \frac{p_{\mathbf{r}|\theta_1}(\mathbf{R}|\theta_1)}{p_{\mathbf{r}|\theta_0}(\mathbf{R}|\theta_0)} \quad (4.741)$$

is a *nondecreasing function* of a scalar sufficient statistic $S(\mathbf{R})$ for any pair (θ_1, θ_0) where $\theta_1 > \theta_0$, it is said to be a *monotone likelihood ratio* (MLR). When the MLR criterion is satisfied, then a UMP test exists for testing

$$\begin{aligned} H_0 : \theta &\leq \theta_0, \\ H_1 : \theta &> \theta_0, \end{aligned} \quad (4.742)$$

and it has the form³³

$$S(\mathbf{R}) \stackrel[H_1]{H_0}{\gtrless} \gamma. \quad (4.743)$$

This result allows for a one-sided composite hypothesis on H_0 as well as H_1 . When there is a composite hypothesis on H_0 , the P_F of the test is the worst-case P_F over all possible values of θ on H_0 . In an MLR test, the worst case occurs on the boundary, so

$$P_F = \sup_{\theta \leq \theta_0} \Pr \{ S(\mathbf{R}) > \gamma | \theta \} = \Pr \{ S(\mathbf{R}) > \gamma | \theta_0 \}. \quad (4.744)$$

The P_D (or power) depends on the value of θ ,

$$P_D(\theta) = \Pr \{ S(\mathbf{R}) > \gamma | \theta \}, \quad \theta > \theta_0. \quad (4.745)$$

Because of the MLR property, it is an increasing function of θ , so performance improves monotonically as the separation between θ and θ_0 increases.

Example 4.41 (continuation of Example 4.40) Gaussian. In Example 4.40, $\theta = m$ and

$$\begin{aligned} \Lambda(R; M_1, M_0) &= \frac{\exp \left\{ -\frac{(R - M_1)^2}{2\sigma^2} \right\}}{\exp \left\{ -\frac{(R - M_0)^2}{2\sigma^2} \right\}} \\ &= \exp \left\{ R \frac{(M_1 - M_0)}{\sigma^2} - \frac{(M_1^2 - M_0^2)}{2\sigma^2} \right\}. \end{aligned} \quad (4.746)$$

Since $M_1 > M_0$, this is an MLR with

$$S(R) = R. \quad (4.747)$$

³³Proofs are given in Scharf [Sch91] and Levy [Lev08]. The statistical theory behind these discussions appears in Ferguson [Fer67] and Lehmann [Leh59].

The test

$$R \stackrel{H_1}{\underset{H_0}{\gtrless}} \gamma^+ \quad (4.748)$$

is a UMP test for testing $H_0 : M \leq M_0$ versus $H_1 : M > M_0$. Example 4.40 was a special case with $M_0 = 0$ and a simple hypothesis on H_0 . ■

A second example is the Poisson distribution that we introduced in Example 2.3.

Example 4.42³⁴ (continuation of Example 2.3) Poisson. The probability distribution is

$$\Pr(n|\theta) = \frac{e^{-\theta}\theta^n}{n!}, \quad n = 0, 1, \dots \quad (4.749)$$

The likelihood ratio is

$$\Lambda(n;\theta_1, \theta_0) = \frac{\Pr(n|\theta_1)}{\Pr(n|\theta_0)} = \left(\frac{\theta_1}{\theta_0}\right)^n \exp(-(\theta_1 - \theta_0)), \quad (4.750)$$

which is monotone with

$$S(n) = n. \quad (4.751)$$

Therefore, the test

$$n \stackrel{H_1}{\underset{H_0}{\gtrless}} \gamma \quad (4.752)$$

is UMP for $H_0 : \theta \leq \theta_0$ versus $H_1 : \theta > \theta_0$. ■

For the one-parameter exponential family of probability densities introduced in Section 4.2.5, the test for a monotone likelihood ratio can be simplified.³⁵ We assume that the observation on both hypotheses consist of N IID random variables and that³⁶

$$p_{\mathbf{r}|\theta}(\mathbf{R}|\theta) = C_N(\mathbf{R}) \exp\{\phi(\theta) S(\mathbf{R}) - NT(\theta)\} \quad (4.753)$$

where $S(\mathbf{R})$ is a scalar sufficient statistic. Then, if $\phi(\theta)$ is nondecreasing function of θ , there exists a UMP test of the one-sided hypothesis $H_0 : \theta \leq \theta_0$ versus $H_1 : \theta > \theta_0$.

A simple example illustrates the result.

Example 4.43 (continuation of Example 4.19) Gamma. From (4.264)–(4.268), the Gamma probability density with known shape parameter a and unknown scale parameter b can be written in exponential family form as

$$p_{\mathbf{r}|b}(\mathbf{R}|B) = \frac{1}{\Gamma(a)^N} \left(\prod_{i=1}^N R_i^{a-1} \right) \exp \left\{ -\frac{1}{B} \sum_{i=1}^N R_i - Na \ln B \right\} \quad (4.754)$$

³⁴From Scharf [Sch91].

³⁵This is taken from Scharf [Sch91] but is originally due to Lehmann [Leh59].

³⁶In this model θ is not necessarily a natural parameter and the model is not necessarily in canonical form.

with

$$\phi(B) = -\frac{1}{B} \quad (4.755)$$

and

$$S(\mathbf{R}) = \sum_{i=1}^N R_i. \quad (4.756)$$

The function $\phi(B)$ is monotone increasing so a UMP test exists. To find the UMP test, we write the LRT for the simple hypothesis test $H_0 : B = B_0$ versus $H_1 : B = B_1$, as

$$\Lambda(\mathbf{R}; B_1, B_0) = \exp \left\{ - \left(\frac{1}{B_1} - \frac{1}{B_0} \right) \sum_{i=1}^N R_i - Na \ln \left(\frac{B_1}{B_0} \right) \right\} \geq \eta, \quad (4.757)$$

which reduces to

$$S(\mathbf{R}) \triangleq \sum_{i=1}^N R_i \stackrel{H_1}{\underset{H_0}{\gtrless}} \frac{B_0 B_1}{B_1 - B_0} \left\{ \ln \eta + Na \ln \left(\frac{B_1}{B_0} \right) \right\} \triangleq \gamma. \quad (4.758)$$

We find γ by solving

$$P_F = \int_{\gamma}^{\infty} p_{S(\mathbf{R})|b}(X|B) dX, \quad (4.759)$$

where $S(\mathbf{R})$ has a Gamma(Na, b) distribution. ■

Unfortunately, in a number of applications we have multiple unknown parameters so the results are not directly applicable. In addition, one often finds that a UMP test does not exist. In these cases we try some logical tests and see how close they come to the perfect measurement bound.

The perfect measurement bound suggests that a logical procedure is to estimate $\boldsymbol{\theta}$ assuming H_1 is true, then estimate $\boldsymbol{\theta}$ assuming H_0 is true, and use these estimates in a likelihood ratio test as if they were correct. If the maximum likelihood estimates are used, the result is called a *generalized likelihood ratio test* (GLRT). Specifically,

$$\Lambda_g(\mathbf{R}) = \frac{\sup_{\boldsymbol{\theta}_1 \in \chi_1} p_{\mathbf{r}|\boldsymbol{\theta}_1}(\mathbf{R}|\boldsymbol{\theta}_1)}{\sup_{\boldsymbol{\theta}_0 \in \chi_0} p_{\mathbf{r}|\boldsymbol{\theta}_0}(\mathbf{R}|\boldsymbol{\theta}_0)} \stackrel{H_1}{\underset{H_0}{\gtrless}} \gamma, \quad (4.760)$$

where $\boldsymbol{\theta}_1$ ranges over all $\boldsymbol{\theta}$ in χ_1 and $\boldsymbol{\theta}_0$ ranges over all $\boldsymbol{\theta}$ in χ_0 . In other words, we make an ML estimate of $\boldsymbol{\theta}_1$, assuming that H_1 is true. We then evaluate $p_{\mathbf{r}|\boldsymbol{\theta}_1}(\mathbf{R}|\boldsymbol{\theta}_1)$ for $\boldsymbol{\theta}_1 = \hat{\boldsymbol{\theta}}_1(\mathbf{R})$ and use this value in the numerator. A similar procedure gives the denominator.

We consider several examples to illustrate the behavior of the GLRT.

Example 4.44 (continuation of Examples 4.7, 4.37, and 4.40) Gaussian. The basic probabilities are the same as in Example 4.40. Once again, $\theta = m$. Instead of one, we have N independent observations, which we denote by the vector \mathbf{R} . The probability densities are

$$p_{\mathbf{r}|H_1,m}(\mathbf{R}|H_1, M) = \prod_{i=1}^N \frac{1}{\sqrt{2\pi}\sigma} \exp \left\{ -\frac{(R_i - M)^2}{2\sigma^2} \right\},$$

$$p_{\mathbf{r}|H_0}(\mathbf{R}|H_0) = \prod_{i=1}^N \frac{1}{\sqrt{2\pi}\sigma} \exp \left\{ -\frac{R_i^2}{2\sigma^2} \right\}. \quad (4.761)$$

In this example H_1 is a composite hypothesis and H_0 , a simple hypothesis. From (4.122) in Example 4.7, the ML estimate of m is

$$\hat{m}_1(\mathbf{R}) = \hat{m}_{\text{ml}}(\mathbf{R}) = \frac{1}{N} \sum_{i=1}^N R_i. \quad (4.762)$$

Then

$$\Lambda_g(\mathbf{R}) = \frac{\prod_{i=1}^N \frac{1}{\sqrt{2\pi}\sigma} \exp\left\{-\left[R_i - \frac{1}{N} \sum_{j=1}^N R_j\right]^2 / 2\sigma^2\right\}}{\prod_{i=1}^N \frac{1}{\sqrt{2\pi}\sigma} \exp\left\{-\frac{R_i^2}{2\sigma^2}\right\}} \stackrel{H_1}{\gtrless} \stackrel{H_0}{\gtrless} \eta. \quad (4.763)$$

Cancelling common terms and taking the logarithm, we have

$$\ln \Lambda_g(\mathbf{R}) = \frac{1}{2\sigma^2 N} \left(\sum_{i=1}^N R_i \right)^2 \stackrel{H_1}{\gtrless} \stackrel{H_0}{\gtrless} \ln \eta. \quad (4.764)$$

The left-hand side of (4.764) is always greater than or equal to zero. Thus, η can always be chosen greater than or equal to one. Therefore, an equivalent test is

$$\left(\frac{1}{\sqrt{N}} \sum_{i=1}^N R_i \right)^2 \stackrel{H_1}{\gtrless} \stackrel{H_0}{\gtrless} \gamma_1^2, \quad (4.765)$$

where $\gamma_1 \geq 0$. Equivalently,

$$|z| \triangleq \left| \frac{1}{\sqrt{N}} \sum_{i=1}^N R_i \right| \stackrel{H_1}{\gtrless} \stackrel{H_0}{\gtrless} \gamma_1. \quad (4.766)$$

The power function of this test follows easily. The variable z has a variance equal to σ^2 . On H_0 its mean is zero and on H_1 its mean is $M\sqrt{N}$. The densities are sketched in Figure 4.38.

$$\begin{aligned} P_F &= \int_{-\infty}^{-\gamma_1} \frac{1}{\sqrt{2\pi}\sigma} \exp\left\{-\frac{Z}{2\sigma^2}\right\} dZ + \int_{\gamma_1}^{\infty} \frac{1}{\sqrt{2\pi}\sigma} \exp\left\{-\frac{Z}{2\sigma^2}\right\} dZ \\ &= 2 \operatorname{erfc}_*(\frac{\gamma_1}{\sigma}) \end{aligned} \quad (4.767)$$

and

$$\begin{aligned} P_D(M) &= \int_{-\infty}^{-\gamma_1} \frac{1}{\sqrt{2\pi}\sigma} \exp\left\{-\frac{(Z - M\sqrt{N})^2}{2\sigma^2}\right\} dZ + \int_{\gamma_1}^{\infty} \frac{1}{\sqrt{2\pi}\sigma} \exp\left\{-\frac{(Z - M\sqrt{N})^2}{2\sigma^2}\right\} dZ \\ &= \operatorname{erfc}_*\left(\frac{\gamma_1 + M\sqrt{N}}{\sigma}\right) + \operatorname{erfc}_*\left(\frac{\gamma_1 - M\sqrt{N}}{\sigma}\right). \end{aligned} \quad (4.768)$$

The resulting power function is plotted in Figure 4.39. The perfect measurement bound is shown for comparison purposes.

The difference between the GLRT power function and the perfect measurement bound becomes smaller as P_F decreases, but does not approach zero as $\sqrt{NM}/\sigma \rightarrow \infty$. This is similar to the behavior seen in Example 4.29 where frequency estimation performance suffered a degradation when the phase had to be estimated as compared to when it was known. ■

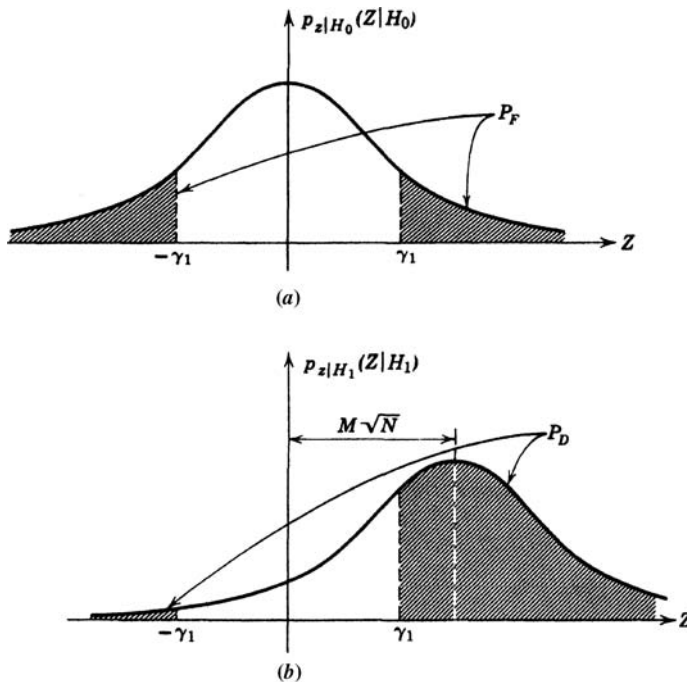


Figure 4.38: Errors in generalized likelihood ratio test: (a) P_F calculation; (b) P_D calculation.

The next example is a straightforward generalization of Example 4.44. It is the same model as in Example 4.38, except that m is nonrandom.

Example 4.45 (continuation of Examples 4.38 and 4.44) Gaussian. This model corresponds to a deterministic signal with an unknown amplitude plus white Gaussian noise on H_1 and white noise only on H_0 . From Example 4.38, the observations are

$$H_1 : \mathbf{r} = m\mathbf{v} + \mathbf{n}, \quad (4.769)$$

$$H_0 : \mathbf{r} = \mathbf{n}, \quad (4.770)$$

where \mathbf{v} is a known signal vector. We assume that $|\mathbf{v}|^2 = E_v$, so the energy in the signal is $M^2 E_v$. The model in Example 4.44 is a special case of this model with $\mathbf{v} = \mathbf{1}$ and $E_v = N$. The noise \mathbf{n} is a zero-mean Gaussian vector $N(\mathbf{0}, \sigma_n^2 \mathbf{I})$. The probability density on H_1 is

$$p_{\mathbf{r}|H_1,m}(\mathbf{R}|H_1, M) = \frac{1}{(2\pi\sigma_n^2)^{N/2}} \exp \left\{ -\frac{1}{2\sigma_n^2} [\mathbf{R} - M\mathbf{v}]^T [\mathbf{R} - M\mathbf{v}] \right\}. \quad (4.771)$$

Taking the log, differentiating with respect to M and setting the result equal to zero gives

$$\hat{m}_1(\mathbf{R}) = [\mathbf{v}^T \mathbf{v}]^{-1} \mathbf{v}^T \mathbf{R}, \quad (4.772)$$

which reduces to

$$\hat{m}_1(\mathbf{R}) = \frac{\mathbf{v}^T \mathbf{R}}{E_v}. \quad (4.773)$$

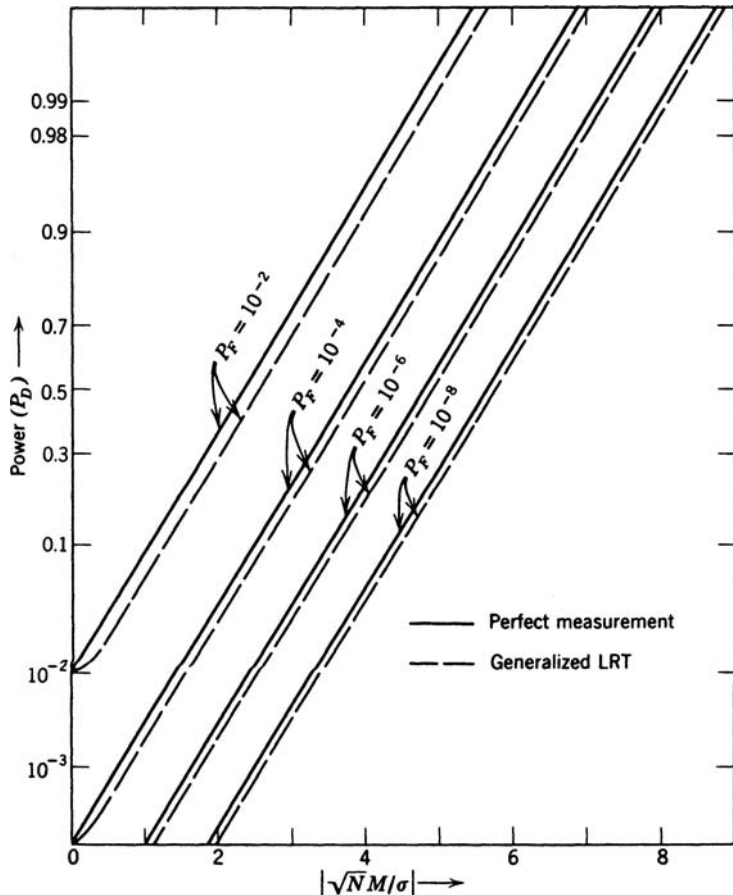


Figure 4.39: Power function: generalized likelihood ratio tests.

The GLR is

$$\Lambda_g(\mathbf{R}) = \frac{p_{\mathbf{r}|H_1,m}(\mathbf{R}|H_1, \hat{m}_1(\mathbf{R}))}{p_{\mathbf{r}|H_0}(\mathbf{R}|H_0)}. \quad (4.774)$$

Twice the log of $\Lambda_g(\mathbf{R})$ is

$$2 \ln \Lambda_g(\mathbf{R}) = \frac{1}{\sigma_n^2} \left\{ \mathbf{R}^T \mathbf{R} - \left\{ \left[\mathbf{R} - \frac{\mathbf{v}^T \mathbf{R}}{E_v} \mathbf{v} \right]^T \left[\mathbf{R} - \frac{\mathbf{v}^T \mathbf{R}}{E_v} \mathbf{v} \right] \right\}_{H_0}^{H_1} \right\} \geq 2 \ln \eta \quad (4.775)$$

or

$$\frac{|\mathbf{v}^T \mathbf{R}|^2}{\sigma_n^2 E_v} \stackrel{H_1}{\gtrless} 2 \ln \eta, \quad (4.776)$$

which can be written as

$$|\mathbf{v}^T \mathbf{R}|^2 \stackrel{H_1}{\gtrless} 2 \sigma_n^2 E_v \ln \eta \triangleq \gamma'. \quad (4.777)$$

We see that it is the same test as in Example 4.38, equation (4.721), where we modeled m as a Gaussian random variable. We can adjust the threshold to achieve the desired P_F .

The expression in (4.776) can also be written in the same form as (4.765). The performance is given in Figure 4.39 with \sqrt{NM}/σ replaced by $\sqrt{E_v M}/\sigma_n$.

The result in (4.775) can also be written as

$$2 \ln \Lambda_g(\mathbf{R}) = \frac{1}{\sigma_n^2} \left\{ \mathbf{R}^T \mathbf{R} - \mathbf{R}^T \left[\mathbf{I} - \mathbf{v} [\mathbf{v}^T \mathbf{v}]^{-1} \mathbf{v}^T \right] \left[\mathbf{I} - \mathbf{v} [\mathbf{v}^T \mathbf{v}]^{-1} \mathbf{v}^T \right] \mathbf{R} \right\}_{H_0}^{H_1} \gtrless 2 \ln \eta. \quad (4.778)$$

The projection matrix onto the signal subspace define by \mathbf{v} is³⁷

$$\mathbf{P}_v \triangleq \mathbf{v} [\mathbf{v}^T \mathbf{v}]^{-1} \mathbf{v}^T. \quad (4.779)$$

Using (4.779) in (4.778) gives

$$\frac{1}{\sigma_n^2} \left\{ \mathbf{R}^T \mathbf{P}_v \mathbf{R} \right\} = \frac{1}{\sigma_n^2} \|\mathbf{P}_v \mathbf{R}\|^2_{H_0}^{H_1} \gtrless 2 \ln \eta. \quad (4.780)$$

This form of the result will be useful later. We see that we are comparing the ratio of the energy in the signal subspace to σ_n^2 . ■

In Example 4.45, the GLRT led to the same test as the case where m was modeled as a Gaussian random variable. This resulted because m was embedded linearly in the likelihood function. In the general case, the GLRT will lead to a different test. However, in many cases, the ML estimation required in the GLRT is easier than the integration required in Section 4.5.2, so we use the GLRT for random θ . In some of the literature, the estimation is referred to as a conditional ML (CML) estimate $\hat{\theta}_{\text{cml}}(\mathbf{R})$. We obtain the performance by averaging $P_D(\theta)$ over $p_\theta(\theta)$.

We now want to generalize Example 4.45 to the case where σ_n^2 is unknown. In this case σ_n^2 is a nuisance parameter that is unknown under both hypotheses.

Example 4.46³⁸ (continuation of Example 4.45) Gaussian. The probability densities on the two hypotheses are

$$p_{\mathbf{R}|H_1, m, \sigma_n^2}(\mathbf{R}|H_1, M, \sigma_n^2) = \frac{1}{(2\pi\sigma_n^2)^{N/2}} \exp \left\{ -\frac{1}{2\sigma_n^2} [\mathbf{R} - M\mathbf{v}]^T [\mathbf{R} - M\mathbf{v}] \right\} \quad (4.781)$$

and

$$p_{\mathbf{R}|H_0, \sigma_n^2}(\mathbf{R}|H_0, \sigma_n^2) = \frac{1}{(2\pi\sigma_n^2)^{N/2}} \exp \left\{ -\frac{1}{2\sigma_n^2} \mathbf{R}^T \mathbf{R} \right\}, \quad (4.782)$$

where both m and σ_n^2 are unknown nonrandom parameters.

On H_0 , we obtain the log-likelihood function for σ_n^2 by taking the log of (4.782),

$$l(\sigma_n^2; \mathbf{R}) = -\frac{N}{2} \ln (\sigma_n^2) - \frac{1}{2\sigma_n^2} \mathbf{R}^T \mathbf{R} + \zeta, \quad (4.783)$$

where ζ does not depend on σ_n^2 . Differentiating with respect to σ_n^2 and setting the result equal to zero gives

$$-\frac{N}{2} \frac{1}{\sigma_n^2} + \frac{1}{2} \frac{\|\mathbf{R}\|^2}{(\sigma_n^2)^2} = 0 \quad (4.784)$$

³⁷Note that $\mathbf{P}_v \mathbf{P}_v = \mathbf{P}_v$.

³⁸This example is essentially the same as Problem 2.5.7 (CFAR receivers) in DEMT-I, first edition [Van68, Van01a].

or

$$\hat{\sigma}_0^2(\mathbf{R}) \triangleq \hat{\sigma}_{n,\text{ml}}^2(\mathbf{R}|H_0) = \frac{\|\mathbf{R}\|^2}{N}. \quad (4.785)$$

From (4.781), the log-likelihood function on H_1 is

$$l_1(M, \sigma_n^2; \mathbf{R}) = -\frac{N}{2} \ln(\sigma_n^2) - \frac{1}{2\sigma_n^2} [\mathbf{R} - M\mathbf{v}]^T [\mathbf{R} - M\mathbf{v}] + \xi. \quad (4.786)$$

We obtain a compressed log-likelihood function for σ_n^2 by substituting in the estimate $\hat{m}_1(\mathbf{R})$ given in (4.773) for M . This gives

$$\begin{aligned} l_1(\sigma_n^2; \mathbf{R}) &= -\frac{N}{2} \ln(\sigma_n^2) - \frac{1}{2\sigma_n^2} \left[\mathbf{R} - \frac{\mathbf{v}^T \mathbf{R}}{E_v} \mathbf{v} \right]^T \left[\mathbf{R} - \frac{\mathbf{v}^T \mathbf{R}}{E_v} \mathbf{v} \right] + \xi \\ &= -\frac{N}{2} \ln(\sigma_n^2) - \frac{1}{2\sigma_n^2} \left\{ \|\mathbf{R}\|^2 - \frac{|\mathbf{v}^T \mathbf{R}|^2}{E_v} \right\} + \xi. \end{aligned} \quad (4.787)$$

Differentiating and setting the result equal to zero gives

$$\hat{\sigma}_1^2(\mathbf{R}) \triangleq \hat{\sigma}_{n,\text{ml}}^2(\mathbf{R}|H_1) = \frac{1}{N} \left\{ \|\mathbf{R}\|^2 - \frac{|\mathbf{v}^T \mathbf{R}|^2}{E_v} \right\}, \quad (4.788)$$

which can also be written as

$$\hat{\sigma}_1^2(\mathbf{R}) = \frac{1}{N} \|\mathbf{P}_v^\perp \mathbf{R}\|^2 = \frac{1}{N} \mathbf{R}^T \mathbf{P}_v^\perp \mathbf{R}, \quad (4.789)$$

where \mathbf{P}_v^\perp is the projection matrix onto the subspace that does not contain \mathbf{v} ,

$$\mathbf{P}_v^\perp \triangleq \mathbf{I} - \mathbf{P}_v. \quad (4.790)$$

The result in (4.789) is logical. We project \mathbf{R} into a subspace that does not contain any signal and then compute the sample energy.

Then, the GLRT is

$$\Lambda_g(\mathbf{R}) = \frac{p_{\mathbf{r}|H_1, m, \sigma_n^2}(\mathbf{R}|H_1, \hat{m}_1(\mathbf{R}), \hat{\sigma}_1^2(\mathbf{R}))}{p_{\mathbf{r}|H_0, \sigma_n^2}(\mathbf{R}|H_0, \hat{\sigma}_0^2(\mathbf{R}))} = \left(\frac{\hat{\sigma}_0^2(\mathbf{R})}{\hat{\sigma}_1^2(\mathbf{R})} \right)^{N/2} \stackrel{H_1}{\gtrless} \eta. \quad (4.791)$$

Note that $\eta > 1$ or we would always choose H_1 . Therefore, we can rewrite (4.791) as

$$S_1(\mathbf{R}) \triangleq (\Lambda_g(\mathbf{R}))^{2/N} - 1 \stackrel{H_1}{\gtrless} \left(\eta^{2/N} - 1 \right) \triangleq \gamma_1. \quad (4.792)$$

Using (4.791) in (4.792) gives

$$S_1(\mathbf{R}) = \frac{\hat{\sigma}_0^2(\mathbf{R}) - \hat{\sigma}_1^2(\mathbf{R})}{\hat{\sigma}_1^2(\mathbf{R})} = \frac{\|\mathbf{R}\|^2 - \mathbf{R}^T \mathbf{P}_v^\perp \mathbf{R}}{\mathbf{R}^T \mathbf{P}_v^\perp \mathbf{R}} \stackrel{H_1}{\gtrless} \gamma_1, \quad (4.793)$$

which can be written as

$$S_1(\mathbf{R}) \triangleq \frac{\mathbf{R}^T \mathbf{P}_v \mathbf{R}}{\mathbf{R}^T \mathbf{P}_v^\perp \mathbf{R}} = \frac{\|\mathbf{P}_v \mathbf{R}\|^2}{\|\mathbf{P}_v^\perp \mathbf{R}\|^2} \stackrel{H_1}{\gtrless} \gamma_1. \quad (4.794)$$

We see that the GLRT is comparing the ratio of the energy in the signal subspace to the energy in the noise only subspace.³⁹ It is referred to as a *matched subspace detector*.

A second form of the GLRT⁴⁰ is obtained by inverting (4.791). Since $\eta > 1$,

$$\Lambda_g(\mathbf{R})^{-2/N} = \frac{\hat{\sigma}_1^2(\mathbf{R})}{\hat{\sigma}_0^2(\mathbf{R})} \stackrel{H_0}{\gtrless} \eta^{-2/N}. \quad (4.795)$$

Substituting (4.785) and (4.788) into (4.795) gives,

$$\frac{\hat{\sigma}_1^2(\mathbf{R})}{\hat{\sigma}_0^2(\mathbf{R})} = 1 - \frac{|\mathbf{v}^T \mathbf{R}|^2}{E_v \|\mathbf{R}\|^2} \stackrel{H_0}{\gtrless} \eta^{-2/N} \quad (4.796)$$

which reduces to

$$S_2(\mathbf{R}) \triangleq \frac{|\mathbf{v}^T \mathbf{R}|^2}{E_v \|\mathbf{R}\|^2} \stackrel{H_1}{\gtrless} (1 - \eta^{-2/N}) \triangleq \gamma_2. \quad (4.797)$$

The GLRT has the important property that the probability of false alarm, P_F , does not depend on the actual value of σ_n^2 . To demonstrate this result, we let $\sigma_n^2 = 1$ in (4.769) and (4.770). Now consider the scaled model in which

$$\mathbf{r}' = c \mathbf{r} \quad (4.798)$$

on both hypotheses.

The sufficient statistic for the scaled model on H_0 is

$$S_2(\mathbf{R}') = \frac{|\mathbf{v}^T \mathbf{R}'|^2}{E_v \|\mathbf{R}'\|^2} = \frac{|\mathbf{v}^T c \mathbf{R}|^2}{E_v \|c \mathbf{R}\|^2} = \frac{|\mathbf{v}^T \mathbf{R}|^2}{E_v \|\mathbf{R}\|^2} = S_2(\mathbf{R}), \quad (4.799)$$

so the sufficient statistic does not depend on the variance of \mathbf{n} . Tests that exhibit the property are called *constant false alarm rate* (CFAR) and they play an important role in most radar and sonar systems.

The test in (4.797) can also be written as

$$|\mathbf{v}^T \mathbf{R}|^2 \stackrel{H_1}{\gtrless} \{N E_v (1 - \eta^{-2/N})\} \frac{\|\mathbf{R}\|^2}{N}. \quad (4.800)$$

The term on the left-hand side is just the sufficient statistic from Example 4.45, equation (4.777) for the case of unknown m and known σ_n^2 . The fixed threshold in (4.777) that depends on the known σ_n^2 has been replaced by an adaptive threshold containing the ML estimate of σ_n^2 on H_0 . The test in (4.800) is referred to as an *adaptive matched filter*.

In order to evaluate the performance, we use (4.794). We observe that it is a ratio of two quadratic forms. In the numerator \mathbf{P}_v has rank one and, in the denominator, \mathbf{P}_v^\perp has rank $N - 1$. The two vectors, $\mathbf{P}_v \mathbf{r}$ and $\mathbf{P}_v^\perp \mathbf{r}$ are statistically independent Gaussian random vectors on both hypotheses because \mathbf{P}_v and \mathbf{P}_v^\perp are orthogonal,

$$\begin{aligned} E \left\{ (\mathbf{P}_v \mathbf{r} - E[\mathbf{P}_v \mathbf{r}]) (\mathbf{P}_v^\perp \mathbf{r} - E[\mathbf{P}_v^\perp \mathbf{r}])^T \right\} &= \mathbf{P}_v E \{(\mathbf{r} - E[\mathbf{r}]) (\mathbf{r} - E[\mathbf{r}])^T\} \mathbf{P}_v^\perp \\ &= \mathbf{P}_v \sigma_n^2 \mathbf{I} \mathbf{P}_v^\perp = \sigma_n^2 \mathbf{P}_v \mathbf{P}_v^\perp = \mathbf{0}. \end{aligned} \quad (4.801)$$

³⁹This result and interpretation are due to Scharf [Sch91].

⁴⁰This form of the GLRT is contained in [Kay98].

Now define

$$N(\mathbf{R}) \triangleq \frac{\|\mathbf{P}_v \mathbf{R}\|^2}{\sigma_n^2}, \quad (4.802)$$

$$D(\mathbf{R}) \triangleq \frac{\|\mathbf{P}_v^\perp \mathbf{R}\|^2}{\sigma_n^2} \quad (4.803)$$

and write (4.794) as

$$S_1(\mathbf{R}) = \frac{N(\mathbf{R})}{D(\mathbf{R})} \stackrel{H_1}{\gtrless} \gamma_1. \quad (4.804)$$

The numerator $N(\mathbf{R})$ and the denominator $D(\mathbf{R})$ are statistically independent Chi-squared random variables on both hypotheses.

Since $\mathbf{P}_v^\perp \mathbf{v} = \mathbf{0}$, the probability density of $D(\mathbf{R})$ is the same on both hypotheses and is Chi-squared with $N - 1$ degrees of freedom.

$$H_0, H_1 : D(\mathbf{R}) \sim \chi_{N-1}^2. \quad (4.805)$$

On H_0 , $N(\mathbf{R})$ is Chi-squared with one degree of freedom, and on H_1 , $N(\mathbf{R})$ is Noncentral Chi-squared with one degree of freedom and noncentrality parameter

$$\begin{aligned} \lambda &= \frac{(E[\mathbf{r}|H_1])^T \mathbf{P}_v (E[\mathbf{r}|H_1])}{\sigma_n^2} \\ &= M \mathbf{v}^T (\mathbf{v}(\mathbf{v}^T \mathbf{v})^{-1} \mathbf{v}^T) \mathbf{v} M \\ &= \frac{M^2 E_v}{\sigma_n^2} \triangleq \frac{E_s}{\sigma_n^2}. \end{aligned} \quad (4.806)$$

Thus,

$$\begin{aligned} H_0 : N(\mathbf{R}) &\sim \chi_1^2, \\ H_1 : N(\mathbf{R}) &\sim \chi_1^2(\lambda). \end{aligned} \quad (4.807)$$

We can write the test in (4.794) as

$$S_3(\mathbf{R}) = \frac{N(\mathbf{R})}{D(\mathbf{R})/(N-1)} \stackrel{H_1}{\gtrless} (N-1)\gamma_1 \triangleq \gamma_3. \quad (4.808)$$

The resulting probability density of $S_3(\mathbf{R})$ is a Central F -density on H_0 and a Noncentral F -density on H_1 ,

$$\begin{aligned} H_0 : S_3(\mathbf{R}) &\sim F_{1,N-1}, \\ H_1 : S_3(\mathbf{R}) &\sim F'_{1,N-1}(\lambda). \end{aligned} \quad (4.809)$$

The densities are defined in Appendix A. In Figure 4.40, we show plots of the Central and Noncentral F -densities for various values of $\sqrt{\lambda} = \sqrt{E_s}/\sigma_n$.

The P_F and P_D are given by

$$P_F = \int_{\gamma_3}^{\infty} p_{1,N-1}(X) dX \quad (4.810)$$

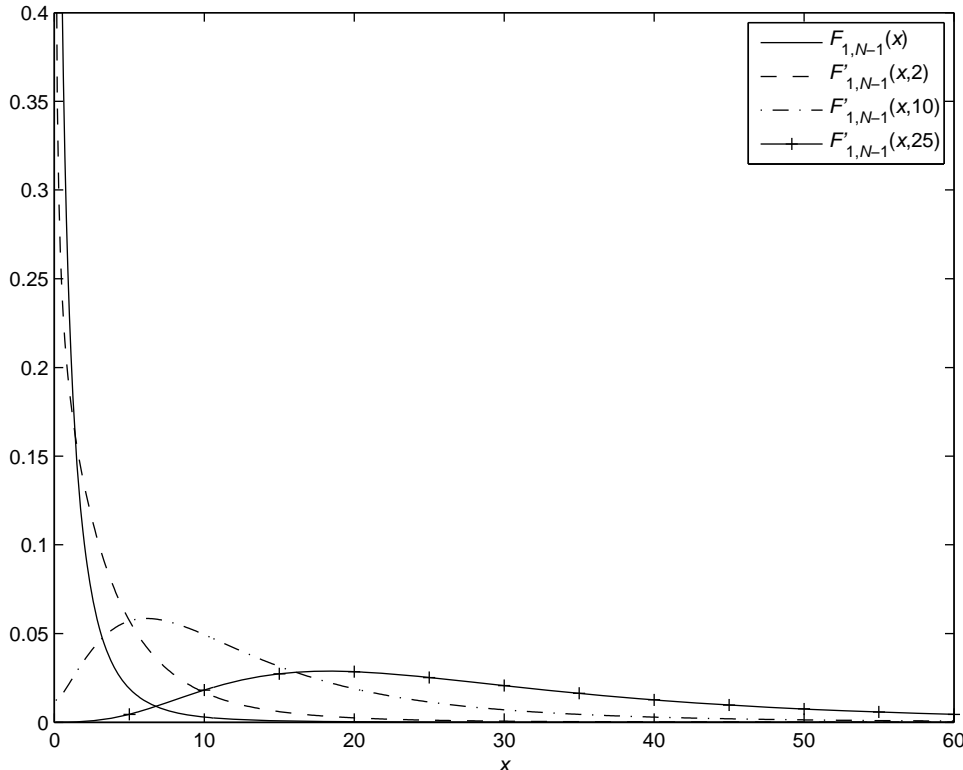


Figure 4.40: Central and Noncentral F -distribution for $N = 10$.

and

$$P_D = \int_{\gamma_3}^{\infty} p'_{1,N-1}(X; \lambda) dX. \quad (4.811)$$

The power function is plotted in Figure 4.41 for several values of N . Also plotted is the perfect measurement bound. When $N \rightarrow \infty$, the F -distributions approach Chi-squared distributions and the performance approaches the known noise variance case in Example 4.44, equations (4.767) and (4.768), with $\sqrt{N}M/\sigma$ replaced by $\sqrt{\lambda}$.

The GLRT in this example has the important property that the probability of the false alarm given in (4.810) does not depend on the actual value of the unknown parameters M and σ_n^2 .

We should point that, although the GLRT is CFAR, its performance is not adequate for an actual radar system. In a typical radar system the model in this example would correspond to the processing in a particular range-Doppler cell. Other range-Doppler cells are being processed simultaneously. If we assume that it is unlikely that targets are in nearby cells, then we can use their outputs to get a better estimate of σ_n^2 . We discuss this in more detail in Chapter 7. ■

Example 4.46 is a special case of the following model.

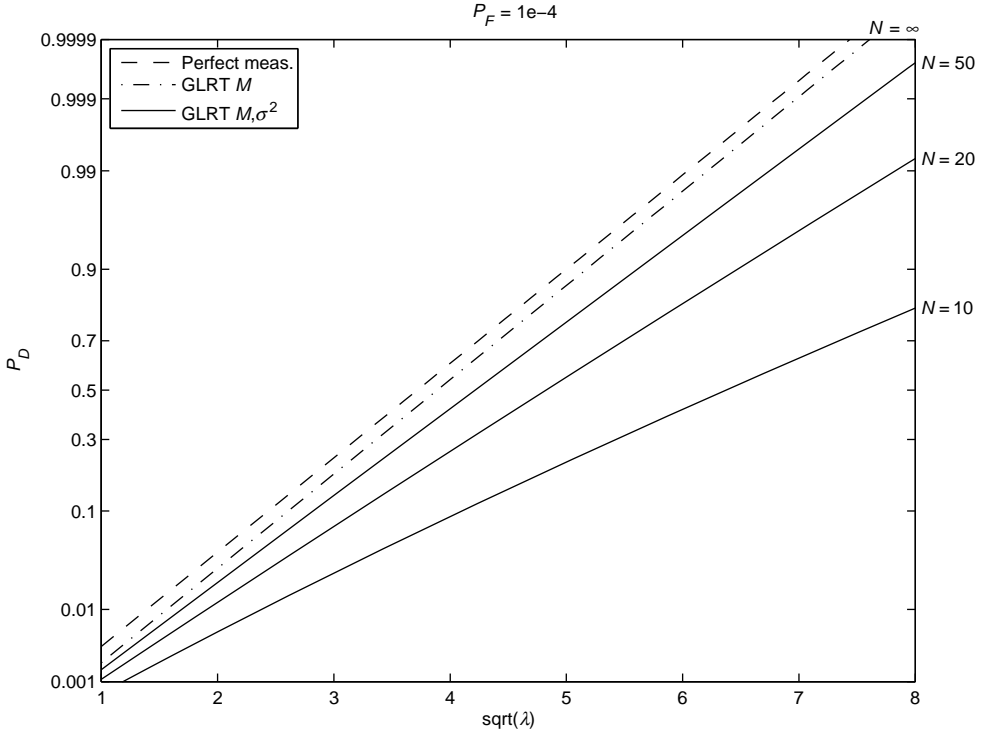


Figure 4.41: The power function for GLRT when both M and σ_n^2 are unknown.

Example 4.47⁴¹ (continuation of Examples 4.39 and 4.46) Gaussian. As in Example 4.39, we assume the received data have the form,

$$\mathbf{r} = \mathbf{V}\boldsymbol{\theta} + \mathbf{n}, \quad (4.812)$$

where \mathbf{V} is a known $N \times D$ matrix of rank D with $N > D$; $\boldsymbol{\theta}$ is a $D \times 1$ vector of parameters, and \mathbf{n} is an $N \times 1$ zero-mean Gaussian random vector $N(\mathbf{0}, \sigma_n^2 \mathbf{I})$. Here, we assume $\boldsymbol{\theta}$ and σ_n^2 are unknown nonrandom parameters.

The hypothesis testing problem is

$$H_1 : \boldsymbol{\theta} \neq \mathbf{0}, \sigma_n^2 > 0, \quad (4.813)$$

$$H_0 : \boldsymbol{\theta} = \mathbf{0}, \sigma_n^2 > 0. \quad (4.814)$$

We proceed in exactly the same manner as in Example 4.45 and obtain the following estimates:

$$\hat{\boldsymbol{\theta}}_1(\mathbf{R}) = [\mathbf{V}^T \mathbf{V}]^{-1} \mathbf{V}^T \mathbf{R}, \quad (4.815)$$

$$\hat{\sigma}_0^2(\mathbf{R}) = \frac{1}{N} \|\mathbf{R}\|^2, \quad (4.816)$$

$$\hat{\sigma}_1^2(\mathbf{R}) = \frac{1}{N} \|\mathbf{P}_{\mathbf{V}}^\perp \mathbf{R}\|^2, \quad (4.817)$$

⁴¹This example is due to Scharf (e.g., pp. 148–153 of [Sch91]). His work originally appeared in Scharf and Lytle [SL71]. Kay [Kay98] did a slightly more general model using the GLRT. Both approaches lead to the same test.

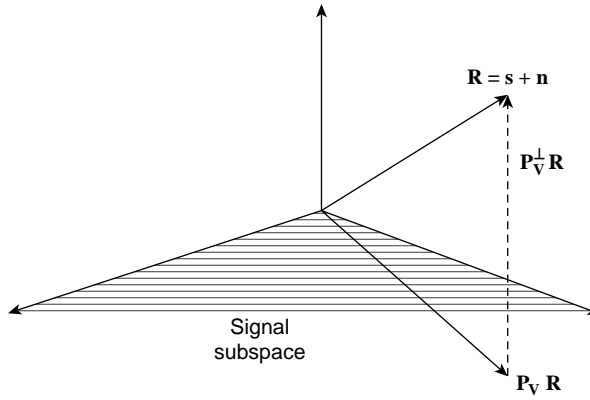


Figure 4.42: Matched subspace detectors.

where

$$\mathbf{P}_V \triangleq \mathbf{V} [\mathbf{V}^T \mathbf{V}]^{-1} \mathbf{V}^T \quad (4.818)$$

is the projection matrix onto the signal subspace and

$$\mathbf{P}_V^\perp \triangleq \mathbf{I} - \mathbf{P}_V \quad (4.819)$$

is the projection matrix onto the orthogonal (noise only) subspace.

The generalized likelihood ratio test is

$$S_1(\mathbf{R}) = (\Lambda_g(\mathbf{R})^{2/N} - 1) \stackrel{H_1}{\underset{H_0}{\gtrless}} \gamma_1, \quad (4.820)$$

where

$$S_1(\mathbf{R}) = \frac{\mathbf{R}^T \mathbf{P}_V \mathbf{R}}{\mathbf{R}^T \mathbf{P}_V^\perp \mathbf{R}} = \frac{\|\mathbf{P}_V \mathbf{R}\|^2 / \sigma_n^2}{\|\mathbf{P}_V^\perp \mathbf{R}\|^2 / \sigma_n^2} = \frac{N(\mathbf{R})}{D(\mathbf{R})}. \quad (4.821)$$

We project \mathbf{R} onto the signal subspace and onto the noise subspace as shown in Figure 4.42 and calculate the magnitudes squared.⁴²

The random vectors $\mathbf{P}_V \mathbf{r}$ and $\mathbf{P}_V^\perp \mathbf{r}$ are statistically independent Gaussian random vectors so the numerator and denominator are independent Chi-squared random variables. The denominator $D(\mathbf{R})$ has a probability density that is Chi-squared with $N - D$ degrees of freedom under both hypotheses. The numerator $N(\mathbf{R})$ has a probability density that is Chi-squared with D degrees of freedom under H_0 , and Noncentral Chi-squared with D degrees of freedom and noncentrality parameter λ under H_1 , where

$$\lambda = \frac{\boldsymbol{\theta}^T \mathbf{V}^T \mathbf{V} \boldsymbol{\theta}}{\sigma_n^2} \triangleq \frac{E_s}{\sigma_n^2}. \quad (4.822)$$

We can normalize $S_1(\mathbf{R})$ so the test becomes

$$S_3(\mathbf{R}) = \frac{N(\mathbf{R})/D}{D(\mathbf{R})/(N - D)} \stackrel{H_1}{\underset{H_0}{\gtrless}} \gamma_3. \quad (4.823)$$

The detector is shown in Figure 4.43.⁴³

⁴²This subspace interpretation is due to Scharf and Friedlander [SF94].

⁴³This is the equivalent to Figure 4.29 in [Sch91].

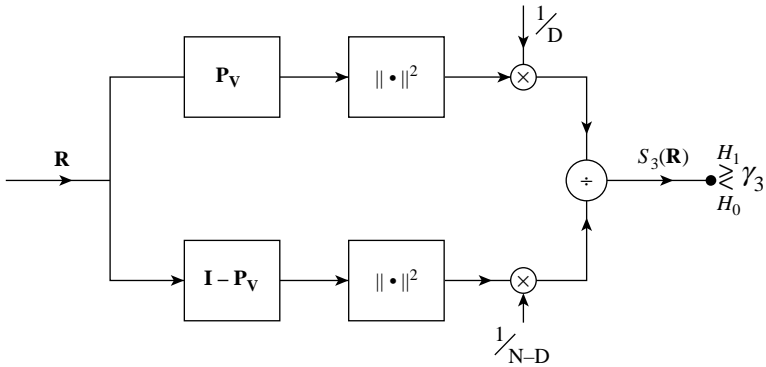


Figure 4.43: Subspace projections.

The probability density of $S_3(\mathbf{R})$ is a Central $F_{D,N-D}$ -distribution on H_0 , and a Noncentral $F'_{D,N-D}(\lambda)$ -distribution on H_1 . P_F and P_D are found from

$$P_F = \int_{\gamma_3}^{\infty} p_{D,N-D}(X) dX \quad (4.824)$$

and

$$P_D = \int_{\gamma_3}^{\infty} p'_{D,N-D}(X; \lambda) dX. \quad (4.825)$$

Again, P_F does not depend on any of the unknown parameters, so this is a CFAR test.

Note that for a given P_F , the performance P_D is a function of three quantities:

- (a) N , the number of samples.
- (b) D , the dimension of signal subspace.
- (c) $\lambda = \frac{\theta^T \mathbf{V}^T \mathbf{V} \theta}{\sigma_n^2} \triangleq \frac{E_s}{\sigma_n^2}$, the signal energy-to-noise ratio.

Therefore, we can plot the results for various D as shown in Figure 4.44. We also show the perfect measurement bound. The $D = 1$ case was shown in Figure 4.41 for various N .

For any value of N , the best performance is achieved when $D = 1$. As D increases, we pay an increasing penalty for not knowing how the signal is distributed across the signal subspace. As $N \rightarrow \infty$, performance converges to the known variance case. The penalty for not knowing θ is still present but is not as severe as for smaller N . ■

An important issue arises out of Examples 4.46 and 4.47. In these examples we derived the GLRT and it turned out to be CFAR. In other words, its performance was *invariant* to the scaling of the noise. This invariance is an important property. An alternate approach would be to require the test to be invariant to the scaling of the noise. This requirement would define a class of tests and we could investigate if UMP tests existed for this class of tests.

Invariant tests for hypothesis testing are widely used in the statistics literature. A series of papers and books by E. L. Lehmann (e.g. [Leh50, Leh59, LC98, LS53, LR05]) treat invariant tests in detail. Chapter 6 of [LR05] contains a comprehensive discussion of his work. Ferguson's book [Fer67] also contains an extensive discussion.

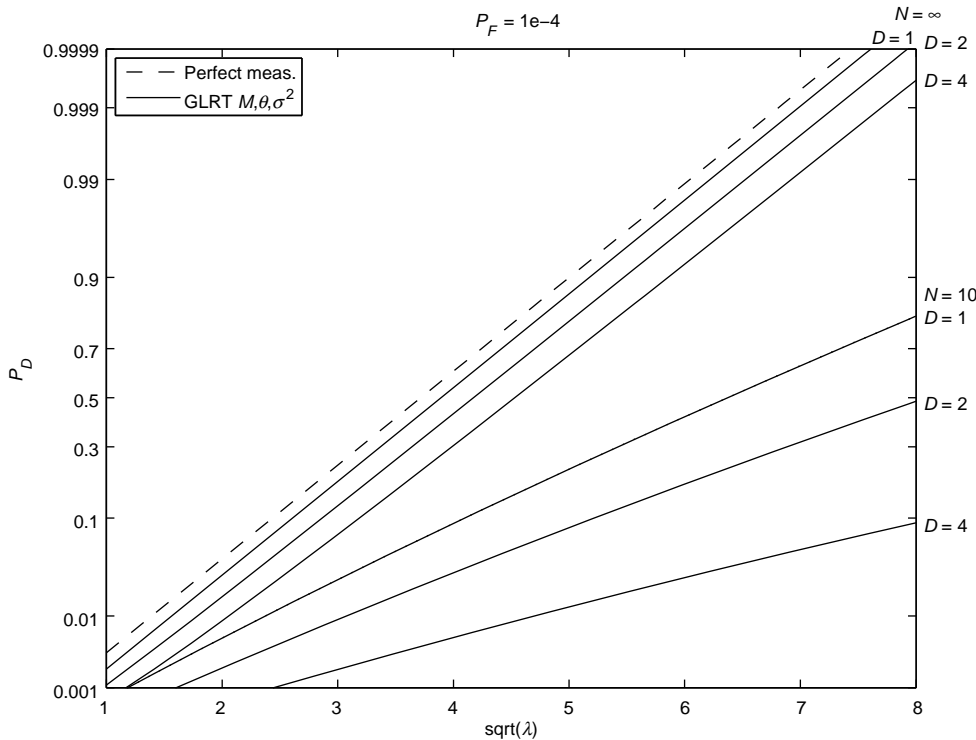


Figure 4.44: Power function for GLRT when M , θ , and σ_n^2 are unknown.

Invariant tests were introduced into signal detection theory and practice by Scharf and Lytle in their 1971 paper [SL71]. Scharf continued to develop the theory and application (e.g. [Dun86, Sch87].) Chapter 4 of Scharf's book [Sch91] has a tutorial. Chapter 5 of Levy's book [Lev08] contains a good discussion.

The basic idea of invariant tests is straightforward. Many statistical applications exhibit symmetries or other characteristics that provide natural restrictions on the type of test we can use. One tries to derive tests that accommodate these restrictions and then check to see if they are UMP among all tests in this class.

The approach consists of four steps

- (i) Find a transformation $g(\mathbf{R})$ of the observation vector \mathbf{R} that incorporates the physical constraints on the model and results in a new test that is invariant to the transformation.
- (ii) Find a sufficient statistic that is invariant to the transformation.
- (iii) Write the likelihood ratio as a function of the sufficient statistic. Check to see if the likelihood ratio is monotone increasing. If so, the test is UMP invariant (UMPI).
- (iv) Analyze the performance of the invariant test and compare its performance to the perfect measurement bound.

The reader is referred to either [Sch91] or [Lev08] for a complete discussion.

4.5.4 Simulation

In order to simulate the GLRT detectors using importance sampling we need to revisit our discussion in Sections 2.5.2.1 and 2.5.2.2. The derivations in those sections assumed that the detector was comparing the log-likelihood ratio $l_*(\mathbf{R})$ to the threshold γ_* . In this section, we compare a test statistic $S(\mathbf{R})$ to a threshold γ , where $S(\mathbf{R})$ is not necessarily the log-likelihood ratio $l_*(\mathbf{R})$.

Recall that the analysis in Section 2.5 was expressed in terms of a statistic \mathbf{X} , which may or may not be equal to \mathbf{R} . All of the analysis applies if we make the substitutions $l_*(\mathbf{X}) \rightarrow S(\mathbf{X})$ and $\gamma_* \rightarrow \gamma$ and replace $\mu(s)$ with appropriately modified functions. Rather than repeat the equations, we go through the derivation and show which equations are applicable to $S(\mathbf{X})$ and which are specific to $l_*(\mathbf{X})$. We then provide the necessary replacement equations. To begin, (2.277) becomes

$$S(\mathbf{X}) \stackrel[H_1]{\gtrless}_{H_0} \gamma. \quad (4.826)$$

For simulating P_F , the analysis in Section 2.5.2.1, equations (2.317)–(2.335), applies, except we replace $\mu(s)$ with $\ln M_S^{(0)}(s)$, where

$$M_S^{(0)}(s) \triangleq E_0 \{ e^{sS(\mathbf{X})} \} \quad (4.827)$$

is the MGF of $S(\mathbf{X})$ on H_0 .

Equations (2.279) and (2.317) become

$$P_F(\gamma) = \Pr(S(\mathbf{X}) \geq \gamma | H_0) = \int \mathbb{I}(S(\mathbf{X}) \geq \gamma) p_{\mathbf{X}|H_0}(\mathbf{X}|H_0) d\mathbf{X}, \quad (4.828)$$

and (2.334) and (2.335) become

$$p_{\mathbf{X}|0^*}(\mathbf{X}; s) = \exp \left\{ sS(\mathbf{X}) - \ln M_S^{(0)}(s) \right\} p_{\mathbf{X}|H_0}(\mathbf{X}|H_0), \quad (4.829)$$

$$W_0(\mathbf{X}; s) = \frac{p_{\mathbf{X}|H_0}(\mathbf{X}|H_0)}{p_{\mathbf{X}|0^*}(\mathbf{X})} = e^{-sS(\mathbf{X}) + \ln M_S^{(0)}(s)}. \quad (4.830)$$

Equations (2.336)–(2.338) are specific to $l_*(\mathbf{X})$. Equations (2.339)–(2.341) are valid and become

$$\bar{I}_F(\gamma; s) = e^{2[\ln M_S^{(0)}(s) - s\gamma]}, \quad s \geq 0, \quad (4.831)$$

$$s_0 : \left. \frac{\partial}{\partial s} \ln M_S^{(0)}(s) \right|_{s=s_0} = \frac{\dot{M}_S^{(0)}(s_0)}{M_S^{(0)}(s_0)} = \gamma, \quad (4.832)$$

$$I_F(\gamma; s) = e^{\ln M_S^{(0)}(s)} \int \mathbb{I}(S(\mathbf{X}) \geq \gamma) e^{-sS(\mathbf{X})} p_{\mathbf{X}|H_0}(\mathbf{X}|H_0) d\mathbf{X}, \quad (4.833)$$

where γ is the threshold in (4.826).

For P_M , the analysis in Section 2.5.2.2 applies, but now we need to replace $\mu(1 - t)$ with $\ln M_S^{(1)}(-t)$, where

$$M_S^{(1)}(t) \triangleq E_1 \{ e^{tS(\mathbf{X})} \} \quad (4.834)$$

is the MGF of $S(\mathbf{X})$ on H_1 . Equations (2.344)–(2.361) are valid, and (2.280) and (2.344) become

$$P_M(\gamma) = 1 - P_D(\gamma) = \Pr(S(\mathbf{X}) < \gamma | H_1) = \int \mathbb{I}(S(\mathbf{X}) < \gamma) p_{\mathbf{x}|H_1}(\mathbf{X}|H_1) d\mathbf{X}. \quad (4.835)$$

Equations (2.355) and (2.357)–(2.361) become

$$E_1 \{ e^{-tS(\mathbf{X})} \} = M_S^{(1)}(-t), \quad (4.836)$$

$$p_{\mathbf{x}|1^*}(\mathbf{X}; t) = \exp \left\{ -tS(\mathbf{X}) - \ln M_S^{(1)}(-t) \right\} p_{\mathbf{x}|H_1}(\mathbf{X}|H_1), \quad (4.837)$$

$$W_1(\mathbf{X}; t) = \frac{p_{\mathbf{x}|H_1}(\mathbf{X}|H_1)}{p_{\mathbf{x}|1^*}(\mathbf{X})} = e^{tS(\mathbf{X}) + \ln M_S^{(1)}(-t)}, \quad (4.838)$$

$$\bar{I}_M(\gamma; t) = e^{2[\ln M_S^{(1)}(-t) + t\gamma]}, \quad t \geq 0, \quad (4.839)$$

$$t_1 : -\frac{\partial}{\partial t} \ln M_S^{(1)}(-t) \Big|_{t=t_1} = \frac{\dot{M}_S^{(1)}(-t_1)}{M_S^{(1)}(-t_1)} = \gamma, \quad (4.840)$$

$$I_M(\gamma; t) = e^{\ln M_S^{(1)}(-t)} \int \mathbb{I}(S(\mathbf{X}) < \gamma) e^{tS(\mathbf{X})} p_{\mathbf{x}|H_1}(\mathbf{X}|H_1) d\mathbf{X}. \quad (4.841)$$

When the test statistic is not the log-likelihood ratio, the tilted densities in (4.829) and (4.837) will not be the same in general, and we must simulate P_F and P_M separately.

For an ID model, if the sufficient statistic $S(\mathbf{R})$ can be expressed as a sum of marginal statistics of the form

$$S(\mathbf{R}) = \sum_{i=1}^N S_i(R_i), \quad (4.842)$$

then the MGFs in (4.827) and (4.834) can be expressed as a product of marginal MGFs

$$M_S^{(0)}(s) = \prod_{i=1}^N M_{S_i}^{(0)}(s), \quad (4.843)$$

$$M_S^{(1)}(t) = \prod_{i=1}^N M_{S_i}^{(1)}(t), \quad (4.844)$$

where

$$M_{S_i}^{(0)}(s) = E_0 \{ e^{sS_i(R_i)} \}, \quad (4.845)$$

$$M_{S_i}^{(1)}(t) = E_1 \{ e^{tS_i(R_i)} \}, \quad (4.846)$$

and the tilted densities in (4.829) and (4.837) can be expressed as a product of tilted marginal densities,

$$p_{\mathbf{r}|0^*}(\mathbf{R}; s) = \prod_{i=1}^N p_{r_i|0^*}(R_i; s), \quad (4.847)$$

$$p_{\mathbf{r}|1^*}(\mathbf{R}; t) = \prod_{i=1}^N p_{r_i|1^*}(R_i; t), \quad (4.848)$$

where

$$p_{r_i|0^*}(R_i; s) = \exp \left\{ s S_i(R_i) - \ln M_{S_i}^{(0)}(s) \right\} p_{r_i|H_0}(R_i | H_0), \quad (4.849)$$

$$p_{r_i|1^*}(R_i; t) = \exp \left\{ -t S_i(R_i) - \ln M_{S_i}^{(1)}(-t) \right\} p_{r_i|H_1}(R_i | H_1). \quad (4.850)$$

To summarize our results, we have the following procedure for simulating a (P_F, P_D) point on the ROC curve:

1. Specify the sufficient statistic $S(\mathbf{X})$ and threshold γ .
2. Compute $M_S^{(0)}(s)$ and $M_S^{(1)}(t)$ from (4.827) and (4.834) or (4.843)–(4.846).
3. Find s_0 and t_1 using

$$s_0 = \max \left(0, s : \frac{\dot{M}_S^{(0)}(s)}{M_S^{(0)}(s)} = \gamma \right), \quad (4.851)$$

$$t_1 = \max \left(0, t : \frac{\dot{M}_S^{(1)}(-t)}{M_S^{(1)}(-t)} = \gamma \right). \quad (4.852)$$

4. Find $P_F(\gamma)$, $P_M(\gamma)$, $I_F(\gamma; s)$, and $I_M(\gamma; t)$ using the analytical expressions in (4.828), (4.835), (4.833), and (4.841).
5. Find the tilted densities from (4.829) and (4.837) or (4.847)–(4.850).
6. Find the weighting functions from (4.830) and (4.838).
7. Specify the confidence interval parameters α and c and compute $K_{F,IS}$ and $K_{M,IS}$ from using (2.392) and (2.393),

$$K_{F,IS} = \frac{c^2}{\alpha^2} \frac{I_F(\gamma; s_0) - P_F(\gamma)^2}{\min [P_F(\gamma), 1 - P_F(\gamma)]^2}, \quad (4.853)$$

$$K_{M,IS} = \frac{c^2}{\alpha^2} \frac{I_M(\gamma; t_1) - P_M(\gamma)^2}{\min [P_M(\gamma), 1 - P_M(\gamma)]^2}. \quad (4.854)$$

8. Generate $K_{F,IS}$ independent realizations of \mathbf{x} from $p_{\mathbf{x}|0^*}(\mathbf{X}; s_0)$ and compute the estimate

$$\hat{P}_F(\gamma) = \frac{1}{K_{F,IS}} \sum_{k=1}^{K_{F,IS}} \mathbb{I}(S(\mathbf{X}_k; s_0) \geq \gamma) W_0(\mathbf{X}_k; s_0). \quad (4.855)$$

9. Generate $K_{F,IM}$ independent realizations of \mathbf{x} from $p_{\mathbf{x}|1^*}(\mathbf{X}; t_1)$ and compute the estimate

$$\hat{P}_M(\gamma) = \frac{1}{K_{M,IS}} \sum_{k=1}^{K_{M,IS}} \mathbb{I}(S(\mathbf{X}_k; t_1) < \gamma) W_1(\mathbf{X}_k; t_1). \quad (4.856)$$

An estimate of $P_D(\gamma)$ can be found from

$$\hat{P}_D(\gamma) = 1 - \hat{P}_M(\gamma) = \frac{1}{K_{M,IS}} \sum_{k=1}^{K_{M,IS}} \mathbb{I}(S(\mathbf{X}_k; t_1) \geq \gamma) W_1(\mathbf{X}_k; t_1). \quad (4.857)$$

A simulation of Example 4.45 is developed in the problems.

4.5.5 Summary of Composite Hypotheses

In this section, we discussed the composite hypothesis problem that we encounter frequently in practice. For random parameters with known densities, the optimum procedure is easy to formulate but may be hard to implement in practice.

For nonrandom parameters, we introduced the idea of UMP tests and the conditions for their existence. We developed the GLRT and will use it in many subsequent applications. We considered the linear Gaussian model in which the white noise variance was unknown and found that the GLRT had a CFAR character. This result led to a brief discussion of invariant tests, but we did not pursue the topic.

The examples we studied correspond to models in applications that we will encounter in practice. We have focused on a Gaussian model because it is frequently a good approximation to reality and we can get analytical answers. The basic ideas of the GLRT apply to the case of non-Gaussian noise and we will study it in a later chapter.

The GLRT is a logical test, but, for finite N , it has no claim for optimality unless it is UMP. From our discussion of the behavior of ML estimates, we might expect that the performance would approach the perfect measurement bound; however, this is not always the case. In Examples 4.46 and 4.47, as $N \rightarrow \infty$, performance converged to the case of known noise variance but did not converge to the case of known signal parameters.

4.6 SUMMARY

In this chapter, we discussed parameter estimation for nonrandom and random parameters. For nonrandom parameters we emphasized maximum likelihood estimates and the Cramér–Rao bound. For random parameters we emphasized Bayesian estimates and the Bayesian Cramér–Rao bound.

In Section 4.2, we considered scalar parameters. For nonrandom parameter estimation the key results were as follows:

1. The maximum likelihood estimate $\hat{a}_{ml}(\mathbf{R})$ is the value of A where the likelihood function $p_{\mathbf{r}|a}(\mathbf{R}|A)$ achieves its maximum.
2. The variance of any unbiased estimate of A is lower bounded by the CRB.

3. Under suitable regularity conditions, $\hat{a}_{ml}(\mathbf{R})$ is unbiased and approaches the CRB asymptotically.
4. If the parameter is embedded in the signal in a nonlinear manner, then a threshold behavior will occur as the SNR or number of observations decreases.
5. If the likelihood function is in the exponential family, then a number of useful properties are available.

For Bayesian estimation, the key results are as follows:

1. For a quadratic cost function, the MMSE estimate is the conditional mean of the *a posteriori* density.
2. The MAP estimate is the mode of the *a posteriori* density. We often use it when $\hat{a}_{ms}(\mathbf{R})$ is difficult to find.
3. The MSE of any Bayesian estimator is lower bounded by the Bayesian Cramér–Rao bound.
4. The MMSE estimate and the MAP estimate approach the ML estimate asymptotically and their MSE approaches the ECRB.
5. Bayesian estimates exhibit a similar threshold behavior to ML estimates as the SNR or the number of observations decreases.
6. The exponential family plays a key role in specifying the conjugate prior.

In Section 4.3, we developed estimators for nonrandom and random parameter vectors. The results were extensions of the results for scalar parameters in Section 4.2, and all of the comments in the preceding paragraph can be adapted to the vector case.

The difficulty arises in implementing the estimation procedures. In the case of a K -dimensional nonrandom parameter vector, we must search over a K -dimensional space to find $\hat{\mathbf{a}}_{ml}(\mathbf{R})$. For a K -dimensional random parameter, a similar search is required to find $\hat{\mathbf{a}}_{map}(\mathbf{R})$ and a K -fold integration is required to find $\hat{\mathbf{a}}_{ms}(\mathbf{R})$. In Chapter 5, we will discuss several iterative techniques that can be used in certain applications.

For nonrandom parameters, the CRB provides a lower bound on the covariance matrix of any unbiased estimate. If the components of the observation \mathbf{r} are statistically independent given \mathbf{a} ,

$$p_{\mathbf{r}|\mathbf{a}}(\mathbf{R}|\mathbf{A}) = \prod_{i=1}^N p_{r_i|\mathbf{a}}(R_i|\mathbf{A}), \quad (4.858)$$

then the CRB can be evaluated by one-dimensional integrations. In the special case where $p_{\mathbf{r}|\mathbf{a}}(\mathbf{R}|\mathbf{A})$ is multivariate Gaussian we can always achieve independence by a whitening transformation.

For random parameters, the BCRB provides a lower bound on the mean-square error matrix of any estimator and the ECRB provides the asymptotic value of the mean-square error matrix. These bounds require the integration of $\mathbf{J}_F(\mathbf{A})$ or $\mathbf{J}_F^{-1}(\mathbf{A})$ over $p_{\mathbf{a}}(\mathbf{A})$.

In many applications, some of the parameters in the vector are unwanted and can be treated as nuisance parameters. We developed various techniques to solve this problem that depended on how \mathbf{a}_w and \mathbf{a}_u were modeled (random or nonrandom).

In other applications, the parameter vector contains random and nonrandom components, \mathbf{a}_r and \mathbf{a}_{nr} . We developed a hybrid estimator and a hybrid bound.

We expanded our case study of frequency estimation introduced in Section 4.2 to include joint frequency and phase estimation. As expected, we also observed the threshold behavior when we jointly estimated frequency and phase. This motivated our development of global Bayesian bounds in Section 4.4.

In Section 4.4, we developed the framework for a family of global Bayesian bounds based on the covariance inequality. We derived the Weiss–Weinstein bound and applied it to our frequency estimation case study. The WWB or a combined BCRB–WWB appear to provide the best prediction of performance for bounds in the covariance inequality family. As demonstrated by the example, choosing the test points to use in the bound requires some skill.

We also discussed the method of interval estimation, which is an approximation rather than a bound. It is motivated by an algorithm that could be used to find the maximum of the *a posteriori* density. It appears to provide good results in many applications.

We have included this discussion of global bounds in this introductory text because we feel that understanding the threshold effect and the effect of “outliers” on the system performance is an essential part of the system design problem. In addition, the issue seems to be ignored in much of the literature.^{44,45}

In Section 4.5, we discussed the composite hypothesis problem that we encounter frequently in practice. For random parameters with known densities, the optimum procedure is easy to formulate but may be hard to implement in practice.

For nonrandom parameters, we introduced the idea of UMP tests and the conditions for their existence. We developed the GLRT and will use it in many subsequent applications. We considered the linear Gaussian model in which the white noise variance was unknown and found that the GLRT had a CFAR character. This result led to a brief discussion of invariant tests, but we did not pursue the topic.

In Chapter 5, we focus our attention on Gaussian random processes.

4.7 PROBLEMS

P4.2 Scalar Parameter Estimation

BAYES ESTIMATION

Problem 4.2.1. Let

$$r = ab + n,$$

where a , b , and n are independent zero-mean Gaussian variables with variances σ_a^2 , σ_b^2 , and σ_n^2 .

1. What is $\hat{a}_{\text{map}}(\mathbf{R})$?
2. Is this equivalent to simultaneously finding $\hat{a}_{\text{map}}(\mathbf{R})$, $\hat{b}_{\text{map}}(\mathbf{R})$?
3. Now consider the case in which

$$r = a + \sum_{i=1}^k b_i + n,$$

⁴⁴Many of the early references addressed the problem (e.g. [Woo52, Kot59, WJ65, Dar64, Aki63, WW85, Wei85, MH71]) but many other papers emphasize CRB without mentioning its region of applicability.

⁴⁵More recently, the financial world has discovered the importance of outliers (e.g., “The Black Swan” [Tal07].)

where the b_i are independent zero-mean Gaussian variables with variances $\sigma_{b_i}^2$.

- (a) What is $\hat{a}_{\text{map}}(\mathbf{R})$?
- (b) Is this equivalent to simultaneously finding $\hat{a}_{\text{map}}(\mathbf{R}), \hat{b}_{i,\text{map}}(\mathbf{R})$?
- (c) Explain intuitively why the answers to part 2 and part 3(b) are different.

Problem 4.2.2. We make K observations: R_1, \dots, R_K , where

$$r_i = a + n_i.$$

The random variable a has a Gaussian density $N(0, \sigma_a^2)$. The n_i are independent Gaussian variables $N(0, \sigma_n^2)$.

1. Find the MMSE estimate $\hat{a}_{\text{ms}}(\mathbf{R})$.
2. Find the MAP estimate $\hat{a}_{\text{map}}(\mathbf{R})$.
3. Compute the mean-square error.
4. Consider an alternate procedure using the same r_i .
 - (a) Estimate a after each observation using a MMSE criterion.
 - This gives a sequence of estimates $\hat{a}_1(R_1), \hat{a}_2(R_1, R_2), \dots, \hat{a}_j(R_1, \dots, R_j), \dots, \hat{a}_K(R_1, \dots, R_K)$. Denote the corresponding variances as $\sigma_1^2, \sigma_2^2, \dots, \sigma_K^2$.
 - (b) Express $\hat{a}_j(R_1, \dots, R_j)$ as a function of $\hat{a}_{j-1}(R_1, \dots, R_{j-1}), \sigma_{j-1}^2$, and R_j .
 - (c) Show that

$$\frac{1}{\sigma_j^2} = \frac{1}{\sigma_a^2} + \frac{j}{\sigma_n^2}.$$

Problem 4.2.3 [Vit66]. In this problem we outline the proof of Property 2 in Section 4.2.1. The assumptions are the following:

- (a) The cost function is a symmetric, nondecreasing function. Thus,

$$\begin{aligned} C(X) &= C(-X), \\ C(X_1) &\geq C(X_2), \quad \text{for} \quad X_1 \geq X_2 \geq 0, \end{aligned} \tag{P.1}$$

which implies

$$\frac{dC(X)}{dX} \geq 0, \quad \text{for} \quad X \geq 0. \tag{P.2}$$

- (b) The *a posteriori* probability density is symmetric about its conditional mean and is nonincreasing.
- (c)

$$\lim_{X \rightarrow \infty} C(X)p_{x|\mathbf{r}}(X|\mathbf{R}) = 0. \tag{P.3}$$

We use the same notation as in Property 1 in Section 4.2.1. Verify the following steps:

1. The conditional risk using the estimate \hat{a} is

$$\mathcal{R}(\hat{a}|\mathbf{R}) = \int_{-\infty}^{\infty} C(Z)p_{z|\mathbf{r}}(Z + \hat{a} - \hat{a}_{\text{ms}}(\mathbf{R})|\mathbf{R})dZ. \tag{P.4}$$

2. The difference in conditional risks is

$$\Delta \mathcal{R} = \mathcal{R}(\hat{a}|\mathbf{R}) - \mathcal{R}(\hat{a}_{\text{ms}}(\mathbf{R})|\mathbf{R}) = \int_0^{\infty} C(Z) [p_{z|\mathbf{r}}(Z + \hat{a} - \hat{a}_{\text{ms}}(\mathbf{R})|\mathbf{R}) p_{z|\mathbf{r}}(Z - \hat{a} + \hat{a}_{\text{ms}}(\mathbf{R})|\mathbf{R}) - 2p_{z|\mathbf{r}}(Z|\mathbf{R})] dZ. \quad (\text{P.5})$$

3. For $\hat{a} > \hat{a}_{\text{ms}}(\mathbf{R})$, the integral of the terms in the bracket with respect to Z from 0 to Z_0 is

$$\int_0^{\hat{a}-\hat{a}_{\text{ms}}(\mathbf{R})} [p_{z|\mathbf{r}}(Z_0 + Y|\mathbf{R}) - p_{z|\mathbf{r}}(Z_0 - Y|\mathbf{R})] dY \triangleq g(Z_0). \quad (\text{P.6})$$

4. Integrate (P.5) by parts to obtain

$$\Delta \mathcal{R} = C(Z)g(Z) \Big|_0^{\infty} - \int_0^{\infty} \frac{dC(Z)}{dZ} g(Z) dZ, \quad \hat{a} > \hat{a}_{\text{ms}}(\mathbf{R}). \quad (\text{P.7})$$

5. Show that the assumptions imply that the first term is zero and the second term is nonnegative.
6. Repeat Steps 3–5 with appropriate modifications for $\hat{a} < \hat{a}_{\text{ms}}(\mathbf{R})$.
7. Observe that these steps prove that $\hat{a}_{\text{ms}}(\mathbf{R})$ minimizes the Bayes risk under the above assumptions. Under what conditions will the Bayes estimate be unique?

CONJUGATE PRIORS

In the following set of problems, the observation consists of N IID continuous random variables: $r_i, i = 1, \dots, N$. The likelihood function $p_{r_i|a}(R_i|A)$ is specified and a conjugate prior is suggested. Do the following:

- (a) Identify the prior hyperparameters, confirm that the suggested conjugate prior is correct, and find the posterior hyperparameters.
- (b) Find $\hat{a}_{\text{ms}}(\mathbf{R})$ and the MSE.
- (c) Find $\hat{a}_{\text{map}}(\mathbf{R})$ and compare to $\hat{a}_{\text{ms}}(\mathbf{R})$.
- (d) Find the BCRB.
- (e) Plot the MSE and the BCRB versus N for several values of the prior hyperparameters.

Note: The probability densities and their mean, mode, and variance are defined in Appendix A.

Problem 4.2.4.

Likelihood Function	Parameter	Conjugate Prior Distribution	Prior Hyperparameters	Posterior Hyperparameters
Gaussian with known mean μ	Variance σ^2	Inverse Gamma	a_0, b_0	$a_p = a_0 + \frac{N}{2},$ $b_p = \left(\frac{1}{b_0} + \frac{1}{2} \sum_{i=1}^N (R_i - \mu)^2 \right)^{-1}$

Problem 4.2.5.

Likelihood Function	Parameter	Conjugate Prior Distribution	Prior Hyperparameters	Posterior Hyperparameters
Gaussian with known mean μ	Precision $\tau = \frac{1}{\sigma^2}$	Gamma	a_0, b_0	$a_p = a_0 + \frac{N}{2},$ $b_p = \left(\frac{1}{b_0} + \frac{1}{2} \sum_{i=1}^N (R_i - \mu)^2 \right)^{-1}$

Problem 4.2.6.

Likelihood Function	Parameter	Conjugate Prior Distribution	Prior Hyperparameters	Posterior Hyperparameters
Log-normal with known variance σ^2	Mean μ	Gaussian	μ_0, σ_0^2	$\mu_p = \sigma_p^2 \left(\frac{\mu_0}{\sigma_0^2} + \frac{1}{\sigma^2} \sum_{i=1}^N \ln R_i \right),$ $\sigma_p^2 = \left(\frac{1}{\sigma_0^2} + \frac{N}{\sigma^2} \right)^{-1}$

Problem 4.2.7.

Likelihood Function	Parameter	Conjugate Prior Distribution	Prior Hyperparameters	Posterior Hyperparameters
Gamma with known shape a	Scale b	Inverse Gamma	a_0, b_0	$a_p = a_0 + Na, b_p = \left(\frac{1}{b_0} + N\bar{R} \right)^{-1}$

Problem 4.2.8.

Likelihood Function	Parameter	Conjugate Prior Distribution	Prior Hyperparameters	Posterior Hyperparameters
Gamma with known shape a	Inverse scale $\beta = \frac{1}{b}$	Gamma	a_0, β_0	$a_p = a_0 + Na, \beta_p = \beta_0 + N\bar{R}$

Problem 4.2.9.

Likelihood Function	Parameter	Conjugate Prior Distribution	Prior Hyperparameters	Posterior Hyperparameters
Gamma with known scale b	Shape a	$\frac{C_0 p_0^{X-1}}{b^{X r_0} \Gamma(X)^{s_0}}$	p_0, r_0, s_0	$p_p = p_0 \prod_{i=1}^N R_i, r_p = r_0 + N, s_p = s_0 + N$

Problem 4.2.10.

Likelihood Function	Parameter	Conjugate Prior Distribution	Prior Hyperparameters	Posterior Hyperparameters
Inverse Gamma with known shape a	Inverse scale $\beta = \frac{1}{b}$	Gamma	a_0, β_0	$a_p = a_0 + Na, \beta_p = \beta_0 + \sum_{i=1}^N R_i^{-1}$

In the following set of problems, the observation consists of M IID discrete random variables: $n_i, i = 1, \dots, M$. The likelihood function $\Pr(n_i = N_i | a = A)$ is specified and a conjugate prior is suggested. Do the following:

- (a) Identify the prior hyperparameters, confirm that the suggested conjugate prior is correct, and find the posterior hyperparameters.
- (b) Find $\hat{a}_{\text{ms}}(\mathbf{N})$ and the MSE.
- (c) Find $\hat{a}_{\text{map}}(\mathbf{N})$ and compare to $\hat{a}_{\text{ms}}(\mathbf{N})$.
- (d) Find the BCRB.
- (e) Plot the MSE and the BCRB versus M for several values of the prior hyperparameters.

Note: The probability distributions and their mean, mode, and variance are defined in Appendix A.

Problem 4.2.11.

Likelihood Function	Parameter	Conjugate Prior Distribution	Prior Hyperparameters	Posterior Hyperparameters
Binomial with known N	Probability p	Beta	a_0, b_0	$a_0 + \sum_{i=1}^M N_i, b_0 + MN - \sum_{i=1}^M N_i$

Problem 4.2.12.

Likelihood Function	Parameter	Conjugate Prior Distribution	Prior Hyperparameters	Posterior Hyperparameters
Negative Binomial with known r	Probability p	Beta	a_0, b_0	$a_0 + Mr, b_0 - Mr + \sum_{i=1}^M N_i$

NONRANDOM PARAMETER ESTIMATION

Problem 4.2.13. We make n statistically independent observations: r_1, r_2, \dots, r_n , with mean m and variance σ^2 . Define the sample variance as

$$V = \frac{1}{n} \sum_{j=1}^n \left(R_j - \sum_{i=1}^n \frac{R_i}{n} \right)^2.$$

Is it an unbiased estimator of the actual variance?

Problem 4.2.14. We want to estimate a in a binomial distribution by using n observations.

$$\Pr(r \text{ events}|a) = \binom{n}{r} a^r (1-a)^{n-r}, \quad r = 0, 1, 2, \dots, n.$$

- (a) Find the ML estimate of a and compute its variance.
- (b) Is it efficient?

Problem 4.2.15.

- (a) Does an efficient estimate of the standard deviation σ of a zero-mean Gaussian density exist?
- (b) Does an efficient estimate of the variance σ^2 of a zero-mean Gaussian density exist?

Problem 4.2.16 (continuation). The results of Problem 4.2.15 suggest the general question. Consider the problem of estimating some function of the parameter A , say, $f_1(A)$. The observed quantity is R and $p_{r|a}(R|A)$ is known. Assume that A is a nonrandom variable.

- (a) What are the conditions for an efficient estimate $\hat{f}_1(A)$ to exist?
- (b) What is the lower bound on the variance of the error of any unbiased estimate of $f_1(A)$?
- (c) Assume that an efficient estimate of $f_1(A)$ exists. When can an efficient estimate of some other function $f_2(A)$ exist?

Problem 4.2.17. Let

$$y = \sum_{i=1}^N x_i,$$

where the x_i are independent, zero-mean Gaussian random variables with variance σ_x^2 . We observe y . In parts (a) through (d) treat N as a continuous variable.

- (a) Find the maximum likelihood estimate of N .
- (b) Is $\hat{n}_{\text{ml}}(Y)$ unbiased?
- (c) What is the variance of $\hat{n}_{\text{ml}}(Y)$?
- (d) Is $\hat{n}_{\text{ml}}(Y)$ efficient?
- (e) Discuss qualitatively how you would modify part (a) to take into account that N is discrete.

Problem 4.2.18. We observe a value of the discrete random variable x .

$$\Pr(x = i|A) = \frac{A^i}{i!} e^{-A}, \quad i = 0, 1, 2, \dots,$$

where A is nonrandom.

- (a) What is the lower bound on the variance of any unbiased estimate, $\hat{a}(X)$?
- (b) Assuming n independent observations, find an $\hat{a}(\mathbf{X})$ that is efficient.

Problem 4.2.19. Consider the Cauchy distribution

$$p_{x|a}(X|A) = \left\{ \pi [1 + (X - A)^2] \right\}^{-1}.$$

Assume that we make n independent observations in order to estimate A .

- (a) Use the Cramér–Rao inequality to show that the variance of any unbiased estimate of A has a variance greater than $2/n$.
- (b) Is the sample mean a consistent estimate?
- (c) We can show that the sample median is asymptotically normal, $N(A, \pi/\sqrt{4n})$ (see pp. 367–369 of Cramér [Cra46]). What is the asymptotic efficiency of the sample median as an estimator?

Problem 4.2.20. Assume that

$$p_{r_1, r_2 | \rho}(R_1, R_2 | \rho) = \frac{1}{2\pi(1-\rho^2)^{1/2}} \exp \left\{ -\frac{R_1^2 - 2\rho R_1 R_2 + R_2^2}{2(1-\rho^2)} \right\}.$$

We want to estimate the correlation coefficient ρ by using n independent observations of (R_1, R_2) .

- (a) Find the equation for the ML estimate $\hat{\rho}(\mathbf{R})$.
- (b) Find a lower bound on the variance of any unbiased estimate of ρ .

Problem 4.2.21 (continuation). Extend the result to the case where \mathbf{R} is an $N \times 1$ zero-mean Gaussian vector $N(\mathbf{0}, \mathbf{K}_r)$, where

$$\mathbf{K}_r = \begin{bmatrix} 1 & \rho & \rho^2 & \cdots & \rho^{N-1} \\ \rho & 1 & \cdots & \cdots & \rho^{N-2} \\ \dots & \dots & \ddots & \dots & \dots \\ \rho^{N-2} & \dots & \dots & 1 & \rho \\ \rho^{N-1} & \dots & \dots & \rho & 1 \end{bmatrix}$$

- (a) Find $\hat{\rho}_{\text{ml}}(\mathbf{R})$.
- (b) Find the Cramér–Rao bound.

LOCAL BOUNDS

These problems consider bounds that are most useful when the errors are small.

Problem 4.2.22. Consider the biased estimate $\hat{a}(\mathbf{R})$ of the *nonrandom* parameter A .

$$E[\hat{a}(\mathbf{R})] = A + B(A).$$

Show that

$$\text{Var}[\hat{a}(\mathbf{R}) - A] \geq \frac{(1 + dB(A)/dA)^2}{E \left\{ \left[\frac{\partial \ln p_{\mathbf{r}|a}(\mathbf{R}|A)}{\partial A} \right]^2 \right\}}.$$

This is the Cramér–Rao inequality for biased estimates. Show that a bound on the mean-square error is

$$\mathcal{R}(A) \geq \frac{(1 + dB(A)/dA)^2}{E \left\{ \left[\frac{\partial \ln p_{\mathbf{r}|a}(\mathbf{R}|A)}{\partial A} \right]^2 \right\}} + B^2(A).$$

Problem 4.2.23. Consider estimation of a function of a parameter $d = \gamma(a)$ with inverse transformation $a = \gamma^{-1}(d)$. Use the properties

$$\left[\frac{\partial \gamma(A)}{\partial A} \right] \Big|_{A=\gamma^{-1}(D)} = \left[\frac{\partial \gamma^{-1}(D)}{\partial D} \right]^{-1}$$

and

$$\frac{\partial \gamma(A)}{\partial A} = \left[\frac{\partial \gamma^{-1}(D)}{\partial D} \right]^{-1} \Big|_{D=\gamma(A)}$$

to show that (4.117) and (4.119) may equivalently be expressed as

$$\text{Var}[\hat{d}_{\text{ml}}(\mathbf{R}) - D] \geq \left(\frac{\partial \gamma^{-1}(D)}{\partial D} \right)^{-2} J_F^{-1}(A) \Big|_{A=\gamma^{-1}(D)}$$

and

$$\text{Var}[\hat{a}_{\text{ml}}(\mathbf{R}) - A] \geq \left(\frac{\partial \gamma^{-1}(D)}{\partial D} \right)^2 J_F^{-1}(D) \Big|_{D=\gamma(A)}.$$

Problem 4.2.24. Barankin bound. Let $p_{\mathbf{r}|a}(\mathbf{R}|A)$ be the probability density of \mathbf{r} , given A . Let h be an arbitrary random variable that is independent of \mathbf{r} defined so that $A + h$ ranges over all possible values of A . Assume that $p_{h_1}(H)$ and $p_{h_2}(H)$ are two arbitrary probability densities for h . Assuming that $\hat{a}(\mathbf{R})$ is unbiased, we have

$$\int [\hat{a}(\mathbf{R}) - (A + H)] p_{\mathbf{r}|a}(\mathbf{R}|A + H) d\mathbf{R} = 0.$$

Multiplying by $p_{h_i}(H)$ and integrating over H , we have

$$\int dH p_{h_i}(H) \int [\hat{a}(\mathbf{R}) - (A + H)] p_{\mathbf{r}|a}(\mathbf{R}|A + H) d\mathbf{R} = 0.$$

Show that

$$\text{Var}[\hat{a}(\mathbf{R}) - A] \geq \frac{[E_1(h) - E_2(h)]^2}{\int \left[\frac{\left(\int p_{\mathbf{r}|a}(\mathbf{R}|A + H) [p_{h_1}(H) - p_{h_2}(H)] dH \right)^2}{p_{\mathbf{r}|a}(\mathbf{R}|A)} \right] d\mathbf{R}}$$

for any $p_{h_1}(H)$ and $p_{h_2}(H)$. Observe that because this is true for all $p_{h_1}(H)$ and $p_{h_2}(H)$, we may write

$$\text{Var}[\hat{a}(\mathbf{R}) - A] \geq \sup_{p_{h_1}, p_{h_2}} (\text{right-hand side of above equation}).$$

Comment. Observe that this bound does not require any regularity conditions. Barankin [Bar49] has shown that this is the greatest lower bound.

Problem 4.2.25 (continuation). We now derive two special cases.

- (a) First, let $p_{h_2}(H) = \delta(H)$. What is the resulting bound?
- (b) Second, let $p_{h_1}(H) = \delta(H - H_0)$, where $H_0 \neq 0$. Show that

$$\text{Var}[\hat{a}(\mathbf{R}) - A] \geq \left(\inf_{H_0} \left\{ \frac{1}{H_0^2} \left[\int \frac{p_{r|a}^2(\mathbf{R}|A + H_0)}{p_{r|a}(\mathbf{R}|A)} d\mathbf{R} - 1 \right] \right\} \right)^{-1}.$$

The infimum being over all $H_0 \neq 0$ such that $p_{r|a}(\mathbf{R}|A) = 0$ implies

$$p_{r|a}(\mathbf{R}|A + H_0) = 0.$$

- (c) Show that the bound given in part (b) is always as good as the Cramér–Rao inequality when the latter applies.

Problem 4.2.26. An alternate way to derive the Cramér–Rao inequality is developed in this problem. First, construct the vector \mathbf{z} .

$$\mathbf{z} \triangleq \begin{bmatrix} \hat{a}(\mathbf{R}) - A \\ \frac{\partial \ln p_{r|a}(\mathbf{R}|A)}{\partial A} \end{bmatrix}.$$

- (a) Verify that for unbiased estimates $E(\mathbf{z}) = \mathbf{0}$.
- (b) Assuming that $E(\mathbf{z}) = \mathbf{0}$, the covariance matrix is

$$\boldsymbol{\Lambda}_{\mathbf{z}} = E(\mathbf{z}\mathbf{z}^T).$$

Using the fact that $\boldsymbol{\Lambda}_{\mathbf{z}}$ is nonnegative definite, derive the Cramér–Rao inequality. If the equality holds, what does this imply about $|\boldsymbol{\Lambda}_{\mathbf{z}}|$?

Problem 4.2.27. Repeat Problem 4.2.26 for the case in which a is a random variable. Define

$$\mathbf{z} = \begin{bmatrix} \hat{a}(\mathbf{R}) - a \\ \frac{\partial \ln p_{r,a}(\mathbf{R}, A)}{\partial A} \end{bmatrix}$$

and proceed as before.

Problem 4.2.28. Bhattacharyya bound. Whenever an efficient estimate does not exist, we can improve on the Cramér–Rao inequality. In this problem, we develop a conceptually simple but algebraically tedious bound for unbiased estimates of nonrandom variables.

- (a) Define an $(N + 1)$ -dimensional vector,

$$\mathbf{z} \triangleq \begin{bmatrix} \hat{a}(\mathbf{R}) - A \\ \frac{1}{p_{\mathbf{r}|a}(\mathbf{R}|A)} \frac{\partial p_{\mathbf{r}|a}(\mathbf{R}|A)}{\partial A} \\ \frac{1}{p_{\mathbf{r}|a}(\mathbf{R}|A)} \frac{\partial^2 p_{\mathbf{r}|a}(\mathbf{R}|A)}{\partial A^2} \\ \vdots \\ \frac{1}{p_{\mathbf{r}|a}(\mathbf{R}|A)} \frac{\partial^N p_{\mathbf{r}|a}(\mathbf{R}|A)}{\partial A^N} \end{bmatrix}.$$

Verify that

$$\mathbf{\Lambda}_z \triangleq E(\mathbf{zz}^T) = \begin{bmatrix} \sigma_\epsilon^2 & 1 & \mathbf{0} \\ 1 & \tilde{\mathbf{J}} & \\ \mathbf{0} & & \end{bmatrix}.$$

What are the elements in $\tilde{\mathbf{J}}$? Is $\mathbf{\Lambda}_z$ nonnegative definite? Assume that $\tilde{\mathbf{J}}$ is positive definite. When is $\mathbf{\Lambda}_z$ not positive definite?

- (b) Verify that the results in part (a) imply

$$\sigma_\epsilon^2 \geq \tilde{J}^{11}.$$

This is the Bhattacharyya bound. Under what conditions does the equality hold?

- (c) Verify that for $N = 1$, the Bhattacharyya bound reduces to Cramér–Rao inequality.
(d) Does the Bhattacharyya bound always improve as N increases?

Comment. In part (b) the condition for equality is

$$\hat{a}(\mathbf{R}) - A = \sum_{i=1}^N c_i(A) \frac{1}{p_{\mathbf{r}|a}(\mathbf{R}|A)} \frac{\partial^i p_{\mathbf{r}|a}(\mathbf{R}|A)}{\partial A^i}.$$

This condition could be termed N th-order efficiency but does not seem to occur in many problems of interest.

- (e) Frequently it is easier to work with

$$\frac{\partial^i \ln p_{\mathbf{r}|a}(\mathbf{R}|A)}{\partial A^i}.$$

Rewrite the elements \tilde{J}_{ij} in terms of expectations of combinations of these quantities for $N = 1$ and 2.

Problem 4.2.29 (continuation). Let $N = 2$ in the preceding problem.

- (a) Verify that

$$\sigma_\epsilon^2 \geq \frac{1}{\tilde{J}_{11}} + \frac{\tilde{J}_{12}^2}{\tilde{J}_{11}(\tilde{J}_{11}\tilde{J}_{22} - \tilde{J}_{12}^2)}.$$

The second term represents the improvement in the bound.

- (b) Consider the case in which \mathbf{r} consists of M independent observations with identical densities and finite conditional means and variances. Denote the elements of $\tilde{\mathbf{J}}$ due to M observations as $\tilde{J}_{ij}(M)$. Show that $\tilde{J}_{11}(M) = M\tilde{J}_{11}(1)$. Derive similar relations for $\tilde{J}_{12}(M)$ and $\tilde{J}_{22}(M)$. Show that

$$\sigma_\epsilon^2 \geq \frac{1}{M\tilde{J}_{11}(1)} + \frac{\tilde{J}_{12}^2(1)}{2M^2\tilde{J}_{11}^4(1)} + o\left(\frac{1}{M^2}\right).$$

Problem 4.2.30 [KS61]. Generalize the result in Problem 4.2.28 to the case in which we are estimating a function of A , say $f(A)$. Assume that the estimate is unbiased. Define

$$\mathbf{z} = \begin{bmatrix} \hat{a}(\mathbf{R}) - f(A) \\ k_1 \frac{1}{p_{\mathbf{r}|a}(\mathbf{R}|A)} \frac{\partial p_{\mathbf{r}|a}(\mathbf{R}|A)}{\partial A} \\ k_2 \frac{1}{p_{\mathbf{r}|a}(\mathbf{R}|A)} \frac{\partial^2 p_{\mathbf{r}|a}(\mathbf{R}|A)}{\partial A^2} \\ \vdots \\ k_N \frac{1}{p_{\mathbf{r}|a}(\mathbf{R}|A)} \frac{\partial^N p_{\mathbf{r}|a}(\mathbf{R}|A)}{\partial A^N} \end{bmatrix}.$$

Let

$$y = [\hat{a}(\mathbf{R}) - f(A)] - \sum_{i=1}^N k_i \frac{1}{p_{\mathbf{r}|a}(\mathbf{R}|A)} \cdot \frac{\partial^i p_{\mathbf{r}|a}(\mathbf{R}|A)}{\partial A^i}.$$

- (a) Find an expression for $\xi_y = E[y^2]$. Minimize ξ_y by choosing the k_i appropriately.
 (b) Using these values of k_i , find a bound on $\text{Var}[\hat{a}(\mathbf{R}) - f(A)]$.
 (c) Verify that the result in Problem 4.2.28 is obtained by letting $f(A) = A$ in (b).

Problem 4.2.31.

- (a) Generalize the result in Problem 4.2.28 to establish a bound on the mean-square error in estimating a random variable.
 (b) Verify that the matrix of concern is

$$\Lambda_z = \begin{bmatrix} E(a_\epsilon^2) & 1 & \mathbf{0} \\ 1 & \tilde{\mathbf{J}}_T & \\ \mathbf{0} & & \end{bmatrix}.$$

What are the elements in $\tilde{\mathbf{J}}_T$?

- (c) Find Λ_z for the special case in which a is $N(0, \sigma_a^2)$.

EXPONENTIAL FAMILY

The next set of problems consider various probability densities that can be expressed as an exponential family. For each density we assume N IID observations. The densities are defined in Appendix A.

- (a) Write the density in the form of (4.246) and define the four terms.
- (b) Put in a canonical form by transforming the parameters, if necessary.
- (c) Find the cumulants of $S(\mathbf{R})$.
- (d) Find the ML estimate of the parameter.
- (e) Find the Cramér–Rao bound.
- (f) Now assume that the parameter is random. Find the conjugate prior.

Problem 4.2.32. Gaussian. The observation R_i is $N(m, \sigma^2)$, where m is known and σ^2 is unknown.

Problem 4.2.33. Gamma. The observation R_i is $\text{Gamma}(a, b)$, where the scale parameter b is known and the shape parameter a is unknown.

Problem 4.2.34. Beta. The observation R_i is $\text{Beta}(a, b)$, where b is known and a is unknown.

Problem 4.2.35. Log-normal. The observation R_i is Log-normal(μ, σ^2), where the variance σ^2 is known and the mean μ is unknown.

Problem 4.2.36. Inverse Gamma. The observation R_i is Inverse Gamma(a, b), where the shape parameter a is known and the scale parameter b is unknown.

P4.3 Multiple Parameter Estimation

MATHEMATICAL PROPERTIES

Problem 4.3.1. In (4.370), we defined the partial derivative matrix $\nabla_{\mathbf{x}}$.

$$\nabla_{\mathbf{x}} \triangleq \begin{bmatrix} \frac{\partial}{\partial x_1} \\ \frac{\partial}{\partial x_2} \\ \vdots \\ \frac{\partial}{\partial x_n} \end{bmatrix}.$$

Verify the following properties.

- (a) The matrix \mathbf{A} is $n \times 1$ and the matrix \mathbf{B} is $n \times 1$. Show that

$$\nabla_{\mathbf{x}}(\mathbf{A}^T \mathbf{B}) = (\nabla_{\mathbf{x}} \mathbf{A}^T) \mathbf{B} + (\nabla_{\mathbf{x}} \mathbf{B}^T) \mathbf{A}.$$

- (b) If the $n \times 1$ matrix \mathbf{B} is not a function of \mathbf{x} , show that

$$\nabla_{\mathbf{x}}(\mathbf{B}^T \mathbf{x}) = \mathbf{B}.$$

(c) Let \mathbf{C} be an $n \times m$ constant matrix,

$$\nabla_{\mathbf{x}} (\mathbf{x}^T \mathbf{C}) = \mathbf{C}.$$

$$(d) \quad \nabla_{\mathbf{x}} (\mathbf{x}^T) = \mathbf{I}.$$

Problem 4.3.2. A problem that occurs frequently is the differentiation of a quadratic form.

$$\mathbf{Q} = \mathbf{A}^T(\mathbf{x}) \mathbf{\Lambda} \mathbf{A}(\mathbf{x}),$$

where $\mathbf{A}(\mathbf{x})$ is an $m \times 1$ matrix whose elements are a function of \mathbf{x} and $\mathbf{\Lambda}$ is a symmetric nonnegative definite $m \times m$ matrix. Recall that this implies that we can write

$$\mathbf{\Lambda} = \mathbf{\Lambda}^{1/2} \mathbf{\Lambda}^{1/2}.$$

(a) Prove

$$\nabla_{\mathbf{x}} \mathbf{Q} = 2 (\nabla_{\mathbf{x}} \mathbf{A}^T(\mathbf{x})) \mathbf{\Lambda} \mathbf{A}(\mathbf{x}).$$

(b) For the special case

$$\mathbf{A}(\mathbf{x}) = \mathbf{B}\mathbf{x},$$

prove

$$\nabla_{\mathbf{x}} \mathbf{Q} = 2\mathbf{B}^T \mathbf{\Lambda} \mathbf{B}\mathbf{x}.$$

(c) For the special case

$$\mathbf{Q} = \mathbf{x}^T \mathbf{\Lambda} \mathbf{x},$$

prove

$$\nabla_{\mathbf{x}} \mathbf{Q} = 2\mathbf{\Lambda} \mathbf{x}.$$

Problem 4.3.3. As discussed in (4.420), we frequently estimate,

$$\mathbf{d} \triangleq \gamma(\mathbf{a}).$$

Assume the estimates are unbiased. Derive (4.422).

Problem 4.3.4. The cost function, $C(\mathbf{a}_e)$ is a scalar-valued function of the vector \mathbf{a}_e . Assume that it is symmetric and convex,

1. $C(\mathbf{a}_e) = C(-\mathbf{a}_e),$
2. $C(b\mathbf{x}_1 + (1 - b)\mathbf{x}_2) \leq bC(\mathbf{x}_1) + (1 - b)C(\mathbf{x}_2), \quad 0 \leq b \leq 1.$

Assume that the *a posteriori* density is symmetric about its conditional mean. Prove that the conditional mean of \mathbf{a}_e minimizes the Bayes risk.

Problem 4.3.5. Assume that we want to estimate K nonrandom parameters A_1, A_2, \dots, A_K , denoted by \mathbf{A} . The probability density $p_{\mathbf{r}|\mathbf{a}}(\mathbf{R}|\mathbf{A})$ is known. Consider the biased estimates $\hat{\mathbf{a}}(\mathbf{R})$ in which

$$\mathbf{B}(a_i) \triangleq \int [\hat{a}_i(\mathbf{R}) - A_i] p_{\mathbf{r}|\mathbf{a}}(\mathbf{R}|\mathbf{A}) d\mathbf{R}.$$

- (a) Derive a bound on the mean-square error in estimating A_i .
(b) The conditional MSE matrix is

$$\mathcal{R}(\mathbf{A}) \triangleq E[(\hat{\mathbf{a}}(\mathbf{R}) - \mathbf{A})(\hat{\mathbf{a}}^T(\mathbf{R}) - \mathbf{A}^T)].$$

Find a matrix $\mathbf{J}_{F,B}(\mathbf{A})$ such that, $\mathcal{R}(\mathbf{A}) - \mathbf{J}_{F,B}(\mathbf{A})^{-1}$ is nonnegative definite.

Problem 4.3.6. Let

$$\mathbf{d} = \boldsymbol{\Gamma}\mathbf{a},$$

where $\boldsymbol{\Gamma}$ is a nonsingular matrix and \mathbf{a} and \mathbf{d} are vector random variables. Prove that

$$\begin{aligned}\hat{\mathbf{d}}_{\text{map}} &= \boldsymbol{\Gamma}\hat{\mathbf{a}}_{\text{map}}, \\ \hat{\mathbf{d}}_{\text{ms}} &= \boldsymbol{\Gamma}\hat{\mathbf{a}}_{\text{ms}}.\end{aligned}$$

NONRANDOM PARAMETER ESTIMATION

Problem 4.3.7. Derive the Fisher information matrices in (4.487) and (4.508) (see [RB74]).

Problem 4.3.8. The observation is an $N \times 1$ vector \mathbf{r} , where

$$\mathbf{r} = \mathbf{V}\boldsymbol{\theta} + \mathbf{w},$$

where \mathbf{V} is a known $N \times D$ matrix, $\boldsymbol{\theta}$ is a $D \times 1$ nonrandom parameter, and $\mathbf{w} \sim N(\mathbf{0}, \sigma_w^2 \mathbf{I})$.

- (a) Find $\hat{\boldsymbol{\theta}}_{\text{ml}}(\mathbf{R})$.
(b) Is $\hat{\boldsymbol{\theta}}_{\text{ml}}(\mathbf{R})$ unbiased and efficient?
(c) Find the Cramér–Rao bound.

Problem 4.3.9 (continuation). Assume σ_w^2 is an unknown nonrandom parameter. Define

$$\boldsymbol{\theta}_a = [\boldsymbol{\theta}^T \sigma_w^2]^T.$$

- (a) Find $\hat{\boldsymbol{\theta}}_{a,\text{ml}}(\mathbf{R})$.
(b) Is $\hat{\boldsymbol{\theta}}_{a,\text{ml}}(\mathbf{R})$ unbiased and efficient?
(c) Find the Cramér–Rao bound.

Problem 4.3.10 (continuation). The complex version of the model in Problem 4.3.8 is

$$\tilde{\mathbf{r}} = \tilde{\mathbf{V}}\tilde{\boldsymbol{\theta}} + \tilde{\mathbf{w}},$$

where $\tilde{\mathbf{V}}$ is a known $N \times D$ matrix, $\tilde{\boldsymbol{\theta}}$ is a complex nonrandom parameter,

$$\tilde{\theta}_i = b_i e^{j\phi_i},$$

and $\tilde{\mathbf{w}} \sim CN(\mathbf{0}, \sigma_{\tilde{w}}^2 \mathbf{I})$. Repeat problem 4.3.9.

Problem 4.3.11 (continuation of Example 4.30). Modify the model in Example 4.30 to assume there are two planewaves arriving from known ψ_1 and ψ_2 . Put this model into the notation of Problem 4.3.10.

- (a) Find $\hat{\theta}_{\text{ml}}(\tilde{\mathbf{R}})$ and the Cramér–Rao bound.
- (b) Assume $\psi_1 = 0$. Plot $\text{Var}[\hat{b}_{1,\text{ml}}(\tilde{\mathbf{R}})]$ versus ψ_2 and SNR for $K = 10$.

Problem 4.3.12. Inverse Gamma. The Inverse Gamma density has the form

$$p_{r_i|a,b}(R_i|A, B) = \frac{1}{B^A \Gamma(A)} \left(\frac{1}{R_i} \right)^{A+1} \exp \left(-\frac{1}{BR_i} \right),$$

where a is the shape parameter and b is the scale parameter. The Inverse Gamma density arises when $y = 1/x$ and x has a Gamma(a, b) density.

- (a) Find $\hat{a}_{\text{ml}}(\mathbf{R}), \hat{b}_{\text{ml}}(\mathbf{R})$, and the Cramér–Rao bound.
- (b) Use the results of Example 4.28 to find $\hat{a}_{\text{ml}}(\mathbf{R}), \hat{b}_{\text{ml}}(\mathbf{R})$, and the Cramér–Rao bound.

Problem 4.3.13. Log-normal. The Log-normal density has the form

$$p_{r_i|\mu,\sigma^2}(R_i|\mu, \sigma^2) = \frac{1}{\sqrt{2\pi}\sigma R_i} \exp \left(-\frac{(\ln R_i - \mu)^2}{2\sigma^2} \right), \quad R_i > 0.$$

Use the fact that $\ln R_i \sim N(\mu, \sigma^2)$ to find $\hat{\mu}_{\text{ml}}(\mathbf{R}), \hat{\sigma}_{\text{ml}}^2(\mathbf{R})$, and the Cramér–Rao bound.

Problem 4.3.14. Weibull. The observation R_i is Weibull(α, b), where both the shape parameter α and the scale parameter b are unknown. Define

$$\mathbf{a} = [\alpha \ b]^T.$$

- (a) Find $\hat{\mathbf{a}}_{\text{ml}}(\mathbf{R})$.
- (b) Find the Cramér–Rao bound.
- (c) Assuming N IID observations, plot the bias, variance, and CRB versus N .

RANDOM PARAMETER ESTIMATION

Problem 4.3.15 (continuation of Problem 4.3.8). Consider the same model as in Problem 4.3.8 except that θ is modeled as Gaussian random vector with prior density $N(\mathbf{m}_\theta, \mathbf{K}_\theta)$.

- (a) Find $\hat{\theta}_{\text{map}}(\mathbf{R})$.
- (b) Is it Bayesian efficient?
- (c) Find the BCRB.

CONJUGATE PRIORS

In the following set of problems, the observation consists of N IID random variables; $r_i; i = 1, \dots, N$. The likelihood function $p_{r_i|\mathbf{a}}(R_i|\mathbf{A})$ is specified and a conjugate prior is suggested. Do the following:

- (a) Identify the prior hyperparameters, confirm that the suggested conjugate prior is correct, and find the posteriori hyperparameters.
- (b) Find $\hat{\mathbf{a}}_{\text{ms}}(\mathbf{R})$ and the MSE.
- (c) Find $\hat{\mathbf{a}}_{\text{map}}(\mathbf{R})$ and compare to $\hat{\mathbf{a}}_{\text{ms}}(\mathbf{R})$.
- (d) Find the BCRB.
- (e) Plot the MSE and the BCRB versus N for several values of the prior hyperparameters.

Note: The probability distributions and their mean, mode, and variance are defined in Appendix A.

Problem 4.3.16.

Likelihood Function	Parameters	Conjugate Prior Distribution	Prior Hyperparameters	Posterior Hyperparameters
Gaussian	Mean μ and variance σ^2	Normal-Inverse Gamma	$\mu_0, \sigma_0^2, a_0, b_0$	$\mu_p = \sigma_p^2 \left(\frac{\mu_0}{\sigma_0^2} + N \bar{R} \right),$ $\sigma_p^2 = \left(\frac{1}{\sigma_0^2} + N \right)^{-1}, \quad a_p = a_0 + \frac{N}{2},$ $b_p = \left(\frac{1}{b_0} + \frac{N}{2} V + \frac{N \sigma_p^2}{2 \sigma_0^2} (\bar{R} - \mu_0)^2 \right)^{-1}$

Problem 4.3.17.

Likelihood Function	Parameters	Conjugate Prior Distribution	Prior Hyperparameters	Posterior Hyperparameters
Gaussian	Mean μ and precision $\tau = \frac{1}{\sigma^2}$	Normal-Gamma	$\mu_0, \sigma_0^2, a_0, b_0$	$\mu_p = \sigma_p^2 \left(\frac{\mu_0}{\sigma_0^2} + N \bar{R} \right),$ $\sigma_p^2 = \left(\frac{1}{\sigma_0^2} + N \right)^{-1}, \quad a_p = a_0 + \frac{N}{2},$ $b_p = \left(\frac{1}{b_0} + \frac{N}{2} V + \frac{N \sigma_p^2}{2 \sigma_0^2} (\bar{R} - \mu_0)^2 \right)^{-1}$

Problem 4.3.18.

Likelihood Function	Parameters	Conjugate Prior Distribution	Prior Hyperparameters	Posterior Hyperparameters
Gamma	Shape a and scale b	$\frac{C_0 p_0^{X-1} e^{-q/Y}}{Y^{X r_0} \Gamma(X)^{s_0}}$	p_0, q_0, r_0, s_0	$p_p = p_0 \prod_{i=1}^N R_i, q_p = q_0 + N \bar{R},$ $r_p = r_0 + N, s_p = s_0 + N$

Problem 4.3.19.

Likelihood Function	Parameters	Conjugate Prior Distribution	Prior Hyperparameters	Posterior Hyperparameters
Multivariate Gaussian with known mean μ	Covariance \mathbf{K}	Inverse Wishart	n_0, \mathbf{Q}_0	$n_p = n_0 + N$ $\mathbf{Q}_p = \mathbf{Q}_0 + \sum_{i=1}^N (\mathbf{R}_i - \mu)(\mathbf{R}_i - \mu)^T$

Problem 4.3.20.

Likelihood Function	Parameters	Conjugate Prior Distribution	Prior Hyperparameters	Posterior Hyperparameters
Multivariate Gaussian with known mean μ	Precision $\mathbf{Q} = \mathbf{K}^{-1}$	Wishart	n_0, \mathbf{K}_0	$n_p = n_0 + N,$ $\mathbf{K}_p = \left[\mathbf{K}_0^{-1} + \sum_{i=1}^N (\mathbf{R}_i - \mu)(\mathbf{R}_i - \mu)^T \right]^{-1}$

Problem 4.3.21.

Likelihood Function	Parameters	Conjugate Prior Distribution	Prior Hyperparameters	Posterior Hyperparameters
Multivariate Gaussian	Mean μ and covariance \mathbf{K}	Normal-Inverse Wishart	$\mu_0, \sigma_0^2, n_0, \mathbf{Q}_0$	$\mu_p = \sigma_p^2 \left(\frac{\mu_0}{\sigma_0^2} + N \bar{\mathbf{R}} \right), \sigma_p^2 = \left(\frac{1}{\sigma_0^2} + N \right)^{-1},$ $n_p = n_0 + N,$ $\mathbf{Q}_p = \mathbf{Q}_0 + NV + \frac{N\sigma_p^2}{\sigma_0^2} (\bar{\mathbf{R}} - \mu_0)(\bar{\mathbf{R}} - \mu_0)^T$

Problem 4.3.22.

Likelihood Function	Parameters	Conjugate Prior Distribution	Prior Hyperparameters	Posterior Hyperparameters
Multivariate Gaussian	Mean μ and precision \mathbf{Q}	Normal-Wishart	$\mu_0, \sigma_0^2, n_0, \mathbf{K}_0$	$\mu_p = \sigma_p^2 \left(\frac{\mu_0}{\sigma_0^2} + N \bar{\mathbf{R}} \right),$ $\sigma_p^2 = \left(\frac{1}{\sigma_0^2} + N \right)^{-1}, \quad n_p = n_0 + N,$ $\mathbf{K}_p^{-1} = \mathbf{K}_0^{-1} + NV + \frac{N\sigma_p^2}{\sigma_0^2} (\bar{\mathbf{R}} - \mu_0)(\bar{\mathbf{R}} - \mu_0)^T$

EXPONENTIAL FAMILY

The next set of problems consider various probability densities that can be expressed as an exponential family. For each density, we assume N IID observations. The densities are defined in Appendix A.

- (a) Write the density in the form of (4.553) and define the four terms.
- (b) Put in a canonical form by transforming the parameters, if necessary.
- (c) Find the cumulants of $\mathbf{S}(\mathbf{R})$.
- (d) Find the ML estimate of the parameter.
- (e) Find the Cramér–Rao bound.
- (f) Now assume that the parameter is random. Find the conjugate prior.

Problem 4.3.23. Gamma. The observation R_i is $\text{Gamma}(a, b)$, where both a and b are unknown.

Problem 4.3.24. Beta. The observation R_i is $\text{Beta}(a, b)$, where both a and b are unknown.

HYBRID AND NUISANCE PARAMETERS

Problem 4.3.25. Consider the Gaussian model in Example 4.26. Assume that that σ^2 is nonrandom and m is a Gaussian random variable $N(m_0, \sigma_0^2)$. Find $\hat{m}_{\text{map}}(\mathbf{R})$ and $\hat{\sigma}_{\text{ml}}^2(\mathbf{R})$. Evaluate the hybrid CRB.

Problem 4.3.26. Consider the Gaussian model in Example 4.26. Assume that m is nonrandom and that σ^2 is a random variable with a prior density that is an Inverse Gamma(a_0, b_0). Find $\hat{m}_{\text{ml}}(\mathbf{R})$ and $\hat{\sigma}_{\text{map}}^2(\mathbf{R})$. Evaluate the hybrid CRB.

Problem 4.3.27 (continuation). Compare the results with Example 4.26.

Problem 4.3.28. Consider the Gamma models in Examples 4.10 and 4.11. Assume that the inverse scale parameter β has a Gamma density, $\text{Gamma}(a_0, \beta_0)$ and that a is an unknown nonrandom variable. Find $\hat{\beta}_{\text{map}}(\mathbf{R})$ and $\hat{a}_{\text{ml}}(\mathbf{R})$. Evaluate the hybrid CRB.

Problem 4.3.29. Consider the DOA estimation model in Example 4.33. Evaluate the hybrid CRB for the case when $N = 10$, $K = 100$, and σ_λ is 0.1 the sensor element spacing. Plot the bound for ψ versus the SNR = b^2/σ_w^2 .

Problem 4.3.30. Consider the DOA estimation model in Example 4.30. Assume that \tilde{b} is a complex Gaussian random variable $\tilde{b} \sim \mathcal{CN}(0, \sigma_{\tilde{b}}^2)$.

- (a) Assume that we treat it as a nuisance parameter. Find $\hat{\psi}_{\text{ml}}(\mathbf{R})$ and the CRB for $N = 10$ and $M = 100$. Plot the CRB versus the SNR = $\sigma_{\tilde{b}}^2/\sigma_w^2$.
- (b) Assume that we want to estimate \tilde{b} . Find $\hat{\psi}_{\text{ml}}(\mathbf{R})$ and $\hat{\tilde{b}}_{\text{map}}(\mathbf{R})$. Evaluate the hybrid CRB and plot it versus the SNR.

Problem 4.3.31 (continuation). Evaluate the four bounds in Section 4.3.5.2 for the model in Problem 4.3.30.

MISCELLANEOUS

Problem 4.3.32. Another method of estimating nonrandom parameters is called the method of moments (Pearson [Pea02]). If there are K parameters to estimate, the first K sample moments are equated to the actual moments (which are functions of the parameters of interest). Solving these K equations gives the desired estimates. To illustrate this procedure, consider the following example. Let

$$p_{r|a}(R|A) = \begin{cases} \frac{1}{\Gamma(A)} R^{A-1} e^{-R}, & R \geq 0 \\ 0, & R < 0. \end{cases}$$

This is a $\text{Gamma}(a, 1)$ density. We have N independent observations of r .

- (a) Find a lower bound on the variance of any unbiased estimate.
- (b) Denote the method of moments estimate as $\hat{a}_{\text{mm}}(\mathbf{R})$. Show

$$\hat{a}_{\text{mm}}(\mathbf{R}) = \frac{1}{N} \sum_{i=1}^N R_i,$$

and compute $E[\hat{a}_{\text{mm}}(\mathbf{R})]$ and $\text{Var}[\hat{a}_{\text{mm}}(\mathbf{R})]$.

Comment. In [Cra46], the efficiency of $\hat{a}_{\text{mm}}(\mathbf{R})$ is computed. It is less than 1 and tends to zero as $N \rightarrow \infty$.

Problem 4.3.33. Assume that we have N independent observations from a Gaussian density $N(m, \sigma^2)$. Verify that the method of moments estimates of m and σ^2 are identical to the maximum likelihood estimates.

P4.4 Global Bayesian Bounds

Problem 4.4.1. Bobrovsky–Zakai bound. Let

$$g(\mathbf{R}, A) = \frac{1}{h} \left(\frac{p_{\mathbf{r},a}(\mathbf{R}, A+h)}{p_{\mathbf{r},a}(\mathbf{R}, A)} - 1 \right).$$

- (a) Show that the condition in (4.635) is satisfied, that is, $E_{a|\mathbf{r}} \{g(\mathbf{R}, A)\} = 0$.
- (b) Evaluate T and G using (4.637) and (4.629) and show that the bound in (4.638) is equal to

$$\sigma_\epsilon^2 \geq \frac{h^2}{E_{\mathbf{r},a} \left\{ \left(\frac{p_{\mathbf{r},a}(\mathbf{R}, A+h)}{p_{\mathbf{r},a}(\mathbf{R}, A)} - 1 \right)^2 \right\}}.$$

This bound was derived by Bobrovsky and Zakai in [BZ76] and is discussed in [BMZ87] and [RM97].

- (c) Write $g(\mathbf{R}, A)$ as

$$g(\mathbf{R}, A) = \frac{1}{p_{\mathbf{r},a}(\mathbf{R}, A)} \left(\frac{p_{\mathbf{r},a}(\mathbf{R}, A+h) - p_{\mathbf{r},a}(\mathbf{R}, A)}{h} \right)$$

and show that this converges to the $g(\mathbf{R}, A)$ given in (4.640) for the BCRB as $h \rightarrow 0$. Use this property to show that the Bobrovsky–Zakai bound converges to the BCRB as $h \rightarrow 0$.

Problem 4.4.2. Reuven–Messer bound. Let $\mathbf{g}(\mathbf{R}, A)$ be an M -dimensional vector whose m th element is

$$g_m(\mathbf{R}, A) = \frac{1}{h_m} \left(\frac{p_{\mathbf{r},a}(\mathbf{R}, A+h_m)}{p_{\mathbf{r},a}(\mathbf{R}, A)} - 1 \right).$$

- (a) Show that the condition in (4.635) is satisfied, that is, $E_{a|\mathbf{r}} \{\mathbf{g}(\mathbf{R}, A)\} = \mathbf{0}$.
- (b) Evaluate \mathbf{T} and \mathbf{G} using (4.637) and (4.629) and show that the bound in (4.638) can be written as

$$\sigma_\epsilon^2 \geq \mathbf{h} [\mathbf{P} - \mathbf{1}\mathbf{1}^T] \mathbf{h}^T,$$

where

$$\mathbf{h} = [h_1 \quad h_2 \quad \cdots \quad h_M]$$

and

$$[\mathbf{P}]_{ij} = E_{\mathbf{r},a} \left\{ \frac{p_{\mathbf{r},a}(\mathbf{R}, A+h_i)p_{\mathbf{r},a}(\mathbf{R}, A+h_j)}{p_{\mathbf{r},a}(\mathbf{R}, A)^2} \right\}.$$

This is the multiple test point version of the Bobrovsky–Zakai bound and was derived by Reuven and Messer [RM97].

Problem 4.4.3. Bayesian Bhattacharyya bound. Let $\mathbf{g}(\mathbf{R}, A)$ be an M -dimensional vector whose m th element is

$$g_m(\mathbf{R}, A) = \frac{\partial^m \ln p_{\mathbf{r}, a}(\mathbf{R}, A)}{\partial A^m}.$$

- (a) Show that the condition in (4.635) is satisfied, that is, $E_{a|\mathbf{r}}\{\mathbf{g}(\mathbf{R}, A)\} = \mathbf{0}$.
- (b) Evaluate \mathbf{T} and \mathbf{G} using (4.637) and (4.629) and show that the bound in (4.638) is the Bayesian Bhattacharyya bound derived in Problem 4.2.31.

Problem 4.4.4. Show that the BCRB is obtained from the single test-point WWB in (4.659) in the limit when $h \rightarrow 0$ for any s .

P4.5 Composite Hypotheses

Problem 4.5.1. Consider the following composite hypothesis testing problem,

$$H_0 : p_r(R) = \frac{1}{\sqrt{2\pi}\sigma_0} \exp\left(-\frac{R^2}{2\sigma_0^2}\right),$$

where σ_0^2 is known,

$$H_1 : p_r(R) = \frac{1}{\sqrt{2\pi}\sigma_1} \exp\left(-\frac{R^2}{2\sigma_1^2}\right),$$

where $\sigma_1^2 > \sigma_0^2$. Assume that we require $P_F = 10^{-2}$.

- (a) Construct an upper bound on the power function by assuming a perfect measurement scheme coupled with a likelihood ratio test.
- (b) Does a uniformly most powerful test exist?
- (c) If the answer to part (b) is negative, construct the power function of a generalized likelihood ratio test.

Problem 4.5.2. Consider the following composite hypothesis testing problem. Two statistically independent observations are received. Denote the observations as R_1 and R_2 . Their probability densities on the two hypotheses are

$$H_0 : p_{r_i}(R_i) = \frac{1}{\sqrt{2\pi}\sigma_0} \exp\left(-\frac{R_i^2}{2\sigma_0^2}\right), \quad i = 1, 2,$$

where σ_0^2 is known,

$$H_1 : p_{r_i}(R_i) = \frac{1}{\sqrt{2\pi}\sigma_1} \exp\left(-\frac{R_i^2}{2\sigma_1^2}\right), \quad i = 1, 2,$$

where $\sigma_1^2 > \sigma_0^2$. Assume that we require a $P_F = \alpha$.

- (a) Construct an upper bound on the power function by assuming a perfect measurement scheme coupled with a likelihood ratio test.
- (b) Does a uniformly most powerful test exist?
- (c) If the answer to part (b) is negative, construct the power function of a generalized likelihood ratio test.

Problem 4.5.3. The observation consists of a set of values of the random variables, r_1, r_2, \dots, r_M .

$$\begin{aligned} H_1 : r_i &= s_i + n_i, & i = 1, 2, \dots, M, \\ H_0 : r_i &= n_i, & i = 1, 2, \dots, M. \end{aligned}$$

The s_i and n_i are independent, identically distributed random variables with densities $N(0, \sigma_s^2)$ and $N(0, \sigma_n^2)$, respectively, where σ_n^2 is known and σ_s^2 is unknown.

- (a) Does a UMP test exist?
- (b) If the answer to part (a) is negative, find a GLRT.

Problem 4.5.4. The observation consists of a set of values of the random variables r_1, r_2, \dots, r_M , which we denote by the vector \mathbf{r} . Under H_0 the r_i are statistically independent, with densities

$$p_{r_i}(R_i) = \frac{1}{\sqrt{2\pi\lambda_i^0}} \exp\left(-\frac{R_i^2}{2\lambda_i^0}\right)$$

in which the λ_i^0 are known. Under H_1 the r_i are statistically independent, with densities

$$p_{r_i}(R_i) = \frac{1}{\sqrt{2\pi\lambda_i^1}} \exp\left(-\frac{R_i^2}{2\lambda_i^1}\right)$$

in which $\lambda_i^1 > \lambda_i^0$ for all i . Repeat Problem 4.5.3.

Problem 4.5.5. Consider the following hypothesis testing problem. Two statistically independent observations are received. Denote the observations R_1 and R_2 . The probability densities on the two hypotheses are

$$\begin{aligned} H_0 : p_{r_i}(R_i) &= \frac{1}{\sqrt{2\pi\sigma}} \exp\left(-\frac{R_i^2}{2\sigma^2}\right), & i = 1, 2, \\ H_1 : p_{r_i}(R_i) &= \frac{1}{\sqrt{2\pi\sigma}} \exp\left[-\frac{(R_i - m)^2}{2\sigma^2}\right], & i = 1, 2, \end{aligned}$$

where m can be any nonzero number. Assume that we require $P_F = \alpha$.

- (a) Construct an upper bound on the power function by assuming a perfect measurement scheme coupled with a likelihood ratio test.
- (b) Does a uniformly most powerful test exist?
- (c) If the answer to part (b) is negative, construct the power function of a generalized likelihood ratio test.

Problem 4.5.6. Consider the following hypothesis testing problem.

Under H_1 a nonrandom variable $\theta \in (-\infty, \infty)$ is transmitted. It is multiplied by the random variable m . A noise n is added to the result to give r . Under H_0 nothing is transmitted, and the output is just n . Thus,

$$\begin{aligned} H_1 : r &= m\theta + n, \\ H_0 : r &= n. \end{aligned}$$

The random variables m and n are independent.

$$p_n(N) = \frac{1}{\sqrt{2\pi}\sigma_n} \exp\left(-\frac{N^2}{2\sigma_n^2}\right),$$

$$p_m(M) = \frac{1}{2}\delta(M-1) + \frac{1}{2}\delta(M+1).$$

- (a) Does a uniformly most powerful test exist? If it does, describe the test and give an expression for its power function. If it does not, indicate why.
- (b) Do one of the following:
 1. If a UMP test exists for this example, derive a necessary and sufficient condition on $p_m(M)$ for a UMP test to exist. (The rest of the model is unchanged.)
 2. If a UMP test does not exist, derive a generalized likelihood ratio test and an expression for its power function.

Problem 4.5.7. How are the results to Problem 4.5.2 changed if we know that $\sigma_0^2 < \sigma_c^2$ and $\sigma_1^2 > \sigma_c^2$, where σ_c^2 is known. Neither σ_0^2 or σ_1^2 , however, is known. If a UMP test does not exist, what test procedure (other than a GLRT) would be logical?

Problem 4.5.8. The model in Examples 4.39 and 4.47 is a special case of the Fisher Linear Gaussian model that we will introduce in Section 5.2.4. The observation is

$$\mathbf{r} = \mathbf{V}\boldsymbol{\theta} + \mathbf{n},$$

where \mathbf{V} is a known $N \times D$ matrix, $\boldsymbol{\theta}$ is a $D \times 1$ nonrandom parameter, and $\mathbf{n} \sim N(\mathbf{0}, \sigma_n^2 \mathbf{I})$. The composite hypothesis test is

$$H_1 : \boldsymbol{\theta} = \mathbf{0},$$

$$H_0 : \boldsymbol{\theta} \neq \mathbf{0}.$$

Derive the following results.⁴⁶

- (a) Show that the ML estimate of $\boldsymbol{\theta}$ is

$$\hat{\boldsymbol{\theta}}_1(\mathbf{R}) = [\mathbf{V}^T \mathbf{V}]^{-1} \mathbf{V}^T \mathbf{R}.$$

- (b) Show that the GLRT has the form

$$S(\mathbf{R}) \triangleq 2 \ln \Lambda_g(\mathbf{R}) = \frac{\hat{\boldsymbol{\theta}}_1(\mathbf{R})^T [\mathbf{V}^T \mathbf{V}] \hat{\boldsymbol{\theta}}_1(\mathbf{R})}{\sigma_n^2} \stackrel{H_1}{\gtrless} \stackrel{H_0}{\gtrless} \gamma.$$

- (c) Show that on H_0 , $S(\mathbf{R})$ is a Chi-squared random variable with D degrees of freedom, and on H_1 , it is a Noncentral Chi-squared random variable with D degrees of freedom and noncentrality parameter

$$\lambda = \frac{\boldsymbol{\theta}^T [\mathbf{V}^T \mathbf{V}] \boldsymbol{\theta}}{\sigma_n^2}.$$

Problem 4.5.9. Derive the result in (4.729). Compare your result to the one obtained using (4.731) and (4.732). Derive P_D and P_F . Compare your results to the result in Problem 4.5.8.

⁴⁶See [Kay98].

Problem 4.5.10. Consider the model in Example 4.45. It is a special case of the model in Problem 4.5.8 with $D = 1$ and $\theta = m$.

- (a) From (4.776), we define the test statistic and threshold to be

$$S(\mathbf{R}) \triangleq \frac{|\mathbf{v}^T \mathbf{R}|^2}{E_v \sigma_n^2} \stackrel{H_1}{\gtrless} \gamma.$$

Define $X \triangleq S(\mathbf{R})$, so $S(\mathbf{X}) = X$. Show that on H_0 , X is a central Chi-squared random variable with one degree of freedom, that is,

$$p_{x|H_0}(X|H_0) = \frac{X^{-\frac{1}{2}} e^{-X/2}}{\sqrt{2\Gamma(\frac{1}{2})}}.$$

- (b) Find the moment generating function $M_S^{(0)}(s)$ using (4.827). Evaluate the derivative with respect to s and find an expression for s_0 as a function of γ using (4.851).
- (c) Using (4.828) and (4.833), show that

$$P_F(\gamma) = \int_{\gamma}^{\infty} p_{x|H_0}(X|H_0) dX = 1 - \Gamma_{\frac{1}{2}}\left(\frac{\gamma}{2}\right),$$

$$I_F(\gamma; s) = e^{\ln M_S^{(0)}(s)} \int_{\gamma}^{\infty} e^{-sX} p_{x|H_0}(X|H_0) dX = \frac{1}{\sqrt{1-4s^2}} \left[1 - \Gamma_{\frac{1}{2}}\left\{\gamma\left(s + \frac{1}{2}\right)\right\} \right].$$

Plot $P_F(\gamma)$ versus γ .

- (d) Show that the tilted density for X , given by

$$p_{x|0^*}(X; s) = e^{sX - \ln M_S^{(0)}(s)} p_{x|H_0}(X|H_0)$$

is a Gamma($\frac{1}{2}, \frac{2}{1-2s}$) density.

- (e) Find the weighting function $W_0(X; s)$ using (4.830).
- (f) For $\alpha = 0.1$ and $c = 2$, simulate several values of P_F using the procedure in Section 4.5.4 and plot with the results of part (c).

5

General Gaussian Estimation

5.1 INTRODUCTION

In this chapter, we revisit the parameter estimation problem that we studied in Chapter 4. We consider the special case in which the likelihood function is a multivariate Gaussian density whose mean and covariance matrix depend on parameters that we want to estimate. We consider both real and complex models.

We encountered models of this type in many of the examples of Chapter 4. The problem of estimating the amplitude, phase, and frequency of a complex exponential in Gaussian noise is in this family. The dual problem of estimating the complex amplitude and wavenumber of a planewave impinging on a linear array is in this family. The problem of estimating the variance of the additive white noise in the CFAR model is in this family.

Our goal in this chapter is to develop a set of results that apply to the general Gaussian estimation model so that when we encounter a model that belongs to the family we can utilize the general result and not have to solve the problem from basic principles.

For real observations, the general Gaussian estimation model for nonrandom parameters is defined by the probability density

$$p_{\mathbf{r}|\boldsymbol{\theta}}(\mathbf{R}|\boldsymbol{\theta}) = \frac{1}{(2\pi)^{N/2} |\mathbf{K}(\boldsymbol{\theta})|^{1/2}} \exp \left\{ -\frac{1}{2} [\mathbf{R} - \mathbf{m}(\boldsymbol{\theta})]^T \mathbf{K}^{-1}(\boldsymbol{\theta}) [\mathbf{R} - \mathbf{m}(\boldsymbol{\theta})] \right\}, \quad (5.1)$$

where $\boldsymbol{\theta}$ is a parameter we want to estimate.

In Section 5.2, we consider nonrandom parameter vectors. In Section 5.2.1, we define the general Gaussian estimation problem in more detail and provide examples of the model. In Section 5.2.2, we derive the maximum likelihood estimate and in Section 5.2.3, the Cramér–Rao bound. In Sections 5.2.4 and 5.2.5, we study the case where only the mean depends on the unknown parameters. In Section 5.2.4, we study the linear Gaussian model that plays a central role in many applications. In Section 5.2.5, we introduce separable models in which we can find an explicit solution for the linear parameters and use it to create a compressed likelihood function that only depends on the nonlinear parameters. In Section 5.2.6, we focus on the case where only the covariance matrix is a function of the parameter vector. This model will apply in many practical applications. In Section 5.2.7, we revisit the general problem in which the parameter vector appears in both the mean and covariance matrix.

Detection, Estimation, and Modulation Theory, Second Edition. Harry L. Van Trees, Kristine L. Bell with Zhi Tian. © 2013 John Wiley & Sons, Inc. Published 2013 by John Wiley & Sons, Inc.

As we saw in Chapter 4, many interesting problems require finding the absolute maximum or minimum of a multidimensional surface. In Chapter 4, we considered problems that had explicit solutions for some of the parameters and required maximization over at most one parameter, so we could use a grid search. In Section 5.2.8, we develop computational algorithms for maximizing a multidimensional function. In Section 5.2.9, we discuss other estimation techniques, such as least squares, and show how they relate to maximum likelihood. In Section 5.2.10, we provide an introduction to the problem of sensitivity of the optimum estimator to the case where the actual model is different from the assumed model. We develop a technique called diagonal loading that reduces sensitivity to model mismatch. In Section 5.2.11, we summarize the results for nonrandom parameters.

In Section 5.3, we consider random parameters. In addition to the likelihood function in (5.1) we must specify a prior probability density $p_{\theta}(\theta)$. In Section 5.3.1, we develop the model and derive the MAP estimate and the Bayesian Cramér–Rao bound. In Section 5.3.2, we study the Bayesian linear Gaussian model. In Section 5.3.3, we summarize our results.

In Section 5.4, we develop sequential versions of the MAP (also MMSE) and ML estimates. In Section 5.4.1, we develop a sequential estimator for the Bayes linear Gaussian model. In Section 5.4.2, we develop a recursive maximum likelihood algorithm (which is also recursive least squares) and show that, except for the initialization step, it is identical to the sequential Bayes algorithm.

In Section 5.5, we summarize our results.

5.2 NONRANDOM PARAMETERS

5.2.1 General Gaussian Estimation Model

In this section, we define the general Gaussian estimation model. We first give the definition of the model for the real and complex cases and then discuss a large number of examples to illustrate the widespread applicability of the model. Most of these examples are generalizations of models that we have encountered in Chapters 3 and 4.

For real observations, we assume the probability density of the $N \times 1$ observed vector \mathbf{r} is $N(\mathbf{m}(\theta_m), \mathbf{K}(\theta_c))$, where θ_m is an $M \times 1$ nonrandom parameter vector and θ_c is a $C \times 1$ nonrandom parameter vector. The subscript “ m ” denotes that the parameter is associated with the mean vector. The subscript “ c ” denotes that the parameter is associated with the covariance matrix.

Thus,

$$p_{\mathbf{r}|\theta_m, \theta_c}(\mathbf{R}|\theta_m, \theta_c) = \frac{1}{(2\pi)^{N/2} |\mathbf{K}(\theta_c)|^{1/2}} \exp \left\{ -\frac{1}{2} [\mathbf{R} - \mathbf{m}(\theta_m)]^T \mathbf{K}^{-1}(\theta_c) [\mathbf{R} - \mathbf{m}(\theta_c)] \right\}. \quad (5.2)$$

For complex observations, we assume the probability density of the $N \times 1$ observed vector is $CN(\tilde{\mathbf{m}}(\theta_m), \tilde{\mathbf{K}}(\theta_c))$, where θ_m is a nonrandom $M \times 1$ real parameter vector and θ_c is a $C \times 1$ nonrandom real parameter vector. In some models, it will be useful to combine one or more pairs of components in θ_m or θ_c into a single complex component and we use $\tilde{\theta}_m$ or $\tilde{\theta}_c$ to denote this pairing.

The probability density is

$$p_{\tilde{\mathbf{r}}|\theta_m, \theta_c}(\tilde{\mathbf{R}}|\theta_m, \theta_c) = \frac{1}{\pi^N |\tilde{\mathbf{K}}(\theta_c)|} \exp \left\{ - [\tilde{\mathbf{R}} - \tilde{\mathbf{m}}(\theta_m)]^H \tilde{\mathbf{K}}^{-1}(\theta_c) [\tilde{\mathbf{R}} - \tilde{\mathbf{m}}(\theta_c)] \right\}. \quad (5.3)$$

We can also define

$$\boldsymbol{\theta} \triangleq [\boldsymbol{\theta}_m^T \quad \boldsymbol{\theta}_c^T]^T \quad (5.4)$$

and write (5.2) in the form of (5.1)

$$p_{\mathbf{r}|\boldsymbol{\theta}}(\mathbf{R}|\boldsymbol{\theta}) = \frac{1}{(2\pi)^{N/2} |\mathbf{K}(\boldsymbol{\theta})|^{1/2}} \exp \left\{ -\frac{1}{2} [\mathbf{R} - \mathbf{m}(\boldsymbol{\theta})]^T \mathbf{K}^{-1}(\boldsymbol{\theta}) [\mathbf{R} - \mathbf{m}(\boldsymbol{\theta})] \right\}. \quad (5.5)$$

The physical model that led to the models in (5.2) and (5.3) occurred when we had a set of N scalar observations that we collected into an N -dimensional observation vector. As we saw in the array processing model in Examples 3.2, 3.7, 4.30, and 4.33, there are important problems where each observation is an N -dimensional vector and we have K observations. We can include that case in our model by stacking vectors to create an NK -dimensional model. This does not require any new concepts but requires more notation. In the text, we will focus our attention on the case where the \mathbf{r}_k are statistically independent, but not necessarily identically distributed. Then for $k = 1, 2, \dots, K$,

$$p_{\mathbf{r}_k|\boldsymbol{\theta}}(\mathbf{R}_k|\boldsymbol{\theta}) = \frac{1}{(2\pi)^{N/2} |\mathbf{K}_k(\boldsymbol{\theta})|^{1/2}} \exp \left\{ -\frac{1}{2} [\mathbf{R}_k - \mathbf{m}_k(\boldsymbol{\theta})]^T \mathbf{K}_k^{-1}(\boldsymbol{\theta}) [\mathbf{R}_k - \mathbf{m}_k(\boldsymbol{\theta})] \right\} \quad (5.6)$$

and

$$p_{\mathbf{r}_1, \mathbf{r}_2, \dots, \mathbf{r}_K|\boldsymbol{\theta}}(\mathbf{R}_1, \mathbf{R}_2, \dots, \mathbf{R}_K|\boldsymbol{\theta}) = \prod_{k=1}^K p_{\mathbf{r}_k|\boldsymbol{\theta}}(\mathbf{R}_k|\boldsymbol{\theta}). \quad (5.7)$$

We now develop a sequence of examples that we will revisit in later sections. The first group assumes that \mathbf{K} is known. Therefore, we can always assume $\mathbf{K} = \sigma_w^2 \mathbf{I}$ because of a prewhitening transformation.

Example 5.1. The first example was introduced in Section 3.3.1.4. The N -dimensional observation vector is

$$\mathbf{r} = \sum_{i=1}^D \mathbf{v}_i \theta_{m_i} + \mathbf{n} = \mathbf{V}\boldsymbol{\theta}_m + \mathbf{n}, \quad (5.8)$$

where $\boldsymbol{\theta}_m$ is the $D \times 1$ vector

$$\boldsymbol{\theta}_m \triangleq [\theta_{m_1} \quad \theta_{m_2} \quad \dots \quad \theta_{m_D}]^T, \quad (5.9)$$

\mathbf{V} is the known $N \times D$ matrix

$$\mathbf{V} \triangleq [\mathbf{v}_1 \quad \mathbf{v}_2 \quad \dots \quad \mathbf{v}_D], \quad (5.10)$$

and $\mathbf{n} \sim N(\mathbf{0}, \mathbf{K})$. Therefore, \mathbf{r} is $N(\mathbf{V}\boldsymbol{\theta}_m, \mathbf{K})$. ■

A special case of this model is given in the following example.

Example 5.1a Target tracking. Consider the following target tracking model where the target position at time $t_n = nT$ is denoted by $x(n)$. The track is deterministic and completely specified by the initial position x_0 and initial velocity v_0 that are unknown nonrandom parameters. The position at time t_n is

$$x(n) = x_0 + v_0 nT. \quad (5.11)$$

The observations are

$$\begin{aligned} r_n &= x(n) + w_n \\ &= x_0 + v_0 nT + w_n, \quad n = 1, 2, \dots, N. \end{aligned} \quad (5.12)$$

The noise is IID $N(0, \sigma_w^2)$ and σ_w^2 is known, thus the unknown parameter vector is

$$\boldsymbol{\theta}_m \triangleq [x_0 \quad v_0]^T. \quad (5.13)$$

The position at time t_n may then be written as

$$x(n) = [1 \quad nT] \boldsymbol{\theta}_m. \quad (5.14)$$

We define the N -dimensional vectors \mathbf{v}_1 and \mathbf{v}_2 as follows:

$$[\mathbf{v}_1]_n = 1, \quad (5.15)$$

$$[\mathbf{v}_2]_n = nT, \quad (5.16)$$

and the $N \times 2$ matrix

$$\mathbf{V} = [\mathbf{v}_1 \quad \mathbf{v}_2]. \quad (5.17)$$

Then, we can write (5.12) in vector form as

$$\mathbf{r} = \mathbf{V}\boldsymbol{\theta}_m + \mathbf{w}. \quad (5.18)$$

Therefore, \mathbf{r} is $N(\mathbf{V}\boldsymbol{\theta}_m, \sigma_w^2 \mathbf{I})$. ■

The complex version of the model in Example 5.1 is given in Example 5.2.

Example 5.2. The N -dimensional complex observation vector is

$$\tilde{\mathbf{r}} = \sum_{i=1}^D \tilde{\mathbf{v}}_i \tilde{\boldsymbol{\theta}}_{m_i} + \tilde{\mathbf{n}} = \tilde{\mathbf{V}} \tilde{\boldsymbol{\theta}}_m + \tilde{\mathbf{n}}, \quad (5.19)$$

where $\tilde{\boldsymbol{\theta}}_m$ is the $D \times 1$ vector

$$\tilde{\boldsymbol{\theta}}_m \triangleq [\tilde{\theta}_{m_1} \quad \tilde{\theta}_{m_2} \quad \cdots \quad \tilde{\theta}_{m_D}]^T, \quad (5.20)$$

$\tilde{\mathbf{V}}$ is the known $N \times D$ matrix

$$\tilde{\mathbf{V}} \triangleq [\tilde{\mathbf{v}}_1 \quad \tilde{\mathbf{v}}_2 \quad \cdots \quad \tilde{\mathbf{v}}_D], \quad (5.21)$$

and $\tilde{\mathbf{n}} \sim CN(\mathbf{0}, \tilde{\mathbf{K}})$. Therefore, $\tilde{\mathbf{r}}$ is $CN(\tilde{\mathbf{V}} \tilde{\boldsymbol{\theta}}_m, \tilde{\mathbf{K}})$. ■

Two specific cases of Example 5.2 that are generalizations of the frequency and DOA estimation models introduced in Chapters 3 and 4 illustrate this model.

Example 5.2a Complex exponentials. We observe D complex exponentials in the presence of circular complex white Gaussian noise. This is a generalization of the models in Examples 3.1, 3.6, and 4.15. The frequency of each exponential is known but the amplitude and phase need to be estimated. The complex observation vector is

$$\tilde{\mathbf{r}} = \sum_{i=1}^D \tilde{\mathbf{v}}(\omega_i) \tilde{b}_i + \tilde{\mathbf{n}}, \quad (5.22)$$

where, from (3.296),

$$\tilde{\mathbf{v}}(\omega_i) = [1 \quad e^{j\omega_i} \quad \dots \quad e^{j(N-1)\omega_i}]^T. \quad (5.23)$$

The complex unknown parameter vector is

$$\tilde{\boldsymbol{\theta}}_m \triangleq [\tilde{b}_1 \quad \tilde{b}_2 \quad \dots \quad \tilde{b}_D]^T, \quad (5.24)$$

where

$$\tilde{b}_i = b_i e^{j\theta_i} = b_{R_i} + j b_{I_i}. \quad (5.25)$$

This can also be written as a real parameter vector in two ways:

$$\boldsymbol{\theta}_m \triangleq [b_1 \quad \theta_1 \quad b_2 \quad \theta_2 \quad \dots \quad b_D \quad \theta_D]^T \quad (5.26)$$

or

$$\boldsymbol{\theta}_m \triangleq [b_{R_1} \quad b_{I_1} \quad b_{R_2} \quad b_{I_2} \quad \dots \quad b_{R_D} \quad b_{I_D}]^T. \quad (5.27)$$

In either case, there are two real parameters for each i . ■

The dual problem of observing D planewaves using a linear array with equally spaced elements is described in Example 5.2b.

Example 5.2b Array processing. We observe D planewaves impinging on a linear array in the presence of circular complex white Gaussian noise. This is a generalization of the models in Examples 3.2, 3.7, and 4.30. The wavenumber of each planewave is known but the amplitude and phase need to be estimated. The complex observation vector is

$$\tilde{\mathbf{r}}_k = \sum_{i=1}^D \tilde{b}_i \tilde{\mathbf{v}}(\psi_i) + \tilde{\mathbf{n}}_k, \quad k = 1, 2, \dots, K, \quad (5.28)$$

where $\tilde{\mathbf{v}}(\psi_i)$ is the array manifold vector defined in (3.137),

$$\tilde{\mathbf{v}}(\psi_i) = [1 \quad e^{-j\psi_i} \quad \dots \quad e^{-j(N-1)\psi_i}]^T. \quad (5.29)$$

The unknown parameter vector for this model is the same as (5.24):

$$\tilde{\boldsymbol{\theta}}_m \triangleq [\tilde{b}_1 \quad \tilde{b}_2 \quad \dots \quad \tilde{b}_D]^T. \quad (5.30)$$

The mean vector can be written as

$$\mathbf{m}(\tilde{\boldsymbol{\theta}}_m) = \tilde{\mathbf{V}} \tilde{\boldsymbol{\theta}}_m, \quad (5.31)$$

where

$$\tilde{\mathbf{V}} \triangleq [\tilde{\mathbf{v}}(\psi_1) \quad \tilde{\mathbf{v}}(\psi_2) \quad \dots \quad \tilde{\mathbf{v}}(\psi_D)]. \quad (5.32)$$

We assume that

$$E [\tilde{\mathbf{n}}_k^H \tilde{\mathbf{n}}_l] = \tilde{\mathbf{K}} \delta_{kl}. \quad (5.33)$$

The observed samples are IID, so

$$p_{\tilde{\mathbf{r}}_1, \tilde{\mathbf{r}}_2, \dots, \tilde{\mathbf{r}}_K | \tilde{\boldsymbol{\theta}}_m} (\tilde{\mathbf{R}}_1, \tilde{\mathbf{R}}_2, \dots, \tilde{\mathbf{R}}_K | \tilde{\boldsymbol{\theta}}_m) = \prod_{k=1}^K \frac{1}{\pi^N |\tilde{\mathbf{K}}|} \exp \left\{ - [\tilde{\mathbf{R}}_k - \tilde{\mathbf{V}} \tilde{\boldsymbol{\theta}}_m]^H \tilde{\mathbf{K}}^{-1} [\tilde{\mathbf{R}}_k - \tilde{\mathbf{V}} \tilde{\boldsymbol{\theta}}_m] \right\}. \quad (5.34)$$

■

Examples 5.1–5.2b are all linear estimation problems because the mean is a linear function of $\boldsymbol{\theta}_m$ or $\tilde{\boldsymbol{\theta}}_m$. A model that we encounter more often in practice is given in Examples 5.3 and 5.4.

Example 5.3. In this model, the mean vector is

$$\mathbf{m}(\boldsymbol{\theta}_m) = \mathbf{V}(\boldsymbol{\theta}_{m,nl}) \boldsymbol{\theta}_{m,l}, \quad (5.35)$$

where $\mathbf{V}(\boldsymbol{\theta}_{m,nl})$ is a $N \times D$ matrix that depends on $\boldsymbol{\theta}_{m,nl}$ in a nonlinear manner. The total parameter vector is

$$\boldsymbol{\theta}_m \triangleq \begin{bmatrix} \boldsymbol{\theta}_{m,l} \\ \boldsymbol{\theta}_{m,nl} \end{bmatrix}. \quad (5.36)$$

The dimensions of $\boldsymbol{\theta}_{m,l}$ and $\boldsymbol{\theta}_{m,nl}$ are not necessarily the same. ■

Example 5.4. This model is the complex version of Example 5.3. The mean vector is

$$\tilde{\mathbf{m}}(\tilde{\boldsymbol{\theta}}_m) = \tilde{\mathbf{V}}(\boldsymbol{\theta}_{m,nl}) \tilde{\boldsymbol{\theta}}_{m,l}, \quad (5.37)$$

and the total parameter vector is

$$\tilde{\boldsymbol{\theta}}_m \triangleq \begin{bmatrix} \tilde{\boldsymbol{\theta}}_{m,l} \\ \boldsymbol{\theta}_{m,nl} \end{bmatrix}. \quad (5.38)$$

■

In Examples 5.4a and 5.4b, we expand the models in Examples 5.2a and 5.2b to fit this model.

Example 5.4a Complex exponentials. We use the same model as in Example 5.2a except we assume that the ω_i in (5.22) are unknown nonrandom parameters. Then,

$$\boldsymbol{\theta}_{m,nl} = [\omega_1 \quad \omega_2 \quad \cdots \quad \omega_D]^T \quad (5.39)$$

and

$$\tilde{\boldsymbol{\theta}}_{m,l} = [\tilde{b}_1 \quad \tilde{b}_2 \quad \cdots \quad \tilde{b}_D]^T, \quad (5.40)$$

which can be written as a real parameter vector as in (5.26) or (5.27), so there are a total of $3D$ parameters to estimate. ■

Example 5.4b Array processing. The dual model for array processing is obtained from Example 5.2b by letting the ψ_i in (5.28) be unknown nonrandom parameters. Then,

$$\boldsymbol{\theta}_{m,nl} = [\psi_1 \quad \psi_2 \quad \cdots \quad \psi_D]^T \quad (5.41)$$

and $\tilde{\boldsymbol{\theta}}_{m,l}$ is the same as (5.40). ■

In Section 5.2.2, we will develop maximum likelihood estimation for the models described by (5.35) and (5.37). We will find that we can always find an analytic expression for $\hat{\theta}_{m,l}(\mathbf{R})$ (or $\hat{\theta}_{m,l}(\widetilde{\mathbf{R}})$). We substitute that into the likelihood function and obtain a compressed likelihood function that we must maximize over $\theta_{m,nl}$. This reduces the dimension of the problem, which is an important computational advantage. We refer to the models in (5.35) and (5.37) as *separable Gaussian models*.

We next develop a set of examples to illustrate θ_c .

Example 5.5. In this model, $\mathbf{r} \sim N(\mathbf{0}, \sigma_n^2 \mathbf{K}_n)$ and σ_n^2 is unknown. Thus,

$$\mathbf{K}(\theta_c) = \sigma_n^2 \mathbf{K}_n \quad (5.42)$$

and

$$\theta_c = \sigma_n^2 \quad (5.43)$$

is a scalar to be estimated. ■

A special case of Example 5.5 corresponds to white noise with unknown variance.

Example 5.5w. In this model, $\mathbf{r} \sim N(\mathbf{0}, \sigma_w^2 \mathbf{I})$ and σ_w^2 is unknown. Thus,

$$\mathbf{K}(\theta_c) = \sigma_w^2 \mathbf{I} \quad (5.44)$$

and

$$\theta_c = \sigma_w^2 \quad (5.45)$$

is a scalar to be estimated. This model is familiar from the H_0 model in the CFAR composite hypothesis testing problem in Example 4.46. ■

Another case where the covariance matrix is parameterized with a small set of parameters comes from the low rank models in Section 3.2.6. We consider the complex case.

Example 5.6. In this model, the observation vector is an $N \times 1$ circular complex Gaussian vector

$$\tilde{\mathbf{r}} = \sum_{i=1}^D \tilde{\mathbf{v}}_i \tilde{b}_i + \tilde{\mathbf{w}}, \quad (5.46)$$

where $\tilde{\mathbf{v}}_i$ is known and the \tilde{b}_i are statistically independent zero-mean circular complex Gaussian random variables $CN(0, \sigma_i^2)$. Therefore,

$$\widetilde{\mathbf{K}}(\theta_c) = \sum_{i=1}^D \sigma_i^2 \tilde{\mathbf{v}}_i \tilde{\mathbf{v}}_i^H + \sigma_{\tilde{w}}^2 \mathbf{I} \quad (5.47)$$

and

$$\theta_c = [\sigma_1^2 \ \sigma_2^2 \ \cdots \ \sigma_D^2 \ \sigma_{\tilde{w}}^2]^T \quad (5.48)$$

is a $D + 1$ parameter vector. ■

Example 5.6a Complex exponentials. A special case of this model comes from the problem in Example 5.2a with D complex exponentials, except we assume that the \tilde{b}_i are IID $CN(0, \sigma_i^2)$. Then, $\tilde{\mathbf{v}}_i = \tilde{\mathbf{v}}(\omega_i)$ defined in (5.23), $\widetilde{\mathbf{K}}(\theta_c)$ is given by (5.47), and θ_c is given by (5.48). ■

A generalization of Example 5.6a leads to the next model.

Example 5.7 Complex exponentials. This is the same model as Example 5.6a with D complex exponentials, except we assume that the ω_i are unknown nonrandom parameters. Thus,

$$\tilde{\mathbf{K}}(\boldsymbol{\theta}_c) = \sum_{i=1}^D \sigma_i^2 \tilde{\mathbf{v}}(\omega_i) \tilde{\mathbf{v}}^H(\omega_i) + \sigma_w^2 \mathbf{I} \quad (5.49)$$

and

$$\boldsymbol{\theta}_c = [\sigma_1^2 \ \sigma_2^2 \ \cdots \ \sigma_D^2 \ \sigma_w^2 \ \omega_1 \ \cdots \ \omega_D]^T \quad (5.50)$$

is a $(2D + 1)$ -dimensional vector. \blacksquare

Models from the group parameterized by $\boldsymbol{\theta}_m$ and the group parameterized by $\boldsymbol{\theta}_c$ can be combined to create models with both $\boldsymbol{\theta}_m$ and $\boldsymbol{\theta}_c$ as unknown parameter vectors.

5.2.2 Maximum Likelihood Estimation

In Chapter 4, we discussed maximum likelihood estimation for nonrandom parameters. In this section, we specialize those results to the case in which the likelihood function is a multivariate Gaussian probability density. We derive the results for a real parameter vector and real observations. We give the results for the case of complex observations.

The model is given in (5.5). The probability density of the observations is

$$p_{\mathbf{r}|\boldsymbol{\theta}}(\mathbf{R}|\boldsymbol{\theta}) = \frac{1}{(2\pi)^{N/2} |\mathbf{K}(\boldsymbol{\theta})|^{1/2}} \exp \left\{ -\frac{1}{2} [\mathbf{R} - \mathbf{m}(\boldsymbol{\theta})]^T \mathbf{K}^{-1}(\boldsymbol{\theta}) [\mathbf{R} - \mathbf{m}(\boldsymbol{\theta})] \right\}, \quad (5.51)$$

where $\boldsymbol{\theta}$ is a $D \times 1$ real nonrandom vector that we want to estimate and \mathbf{r} is a real $N \times 1$ observation vector. The mean vector $\mathbf{m}(\boldsymbol{\theta})$ and the covariance matrix $\mathbf{K}(\boldsymbol{\theta})$ are known functions of $\boldsymbol{\theta}$.

The log-likelihood function is

$$l(\boldsymbol{\theta}; \mathbf{R}) = -\frac{1}{2} \ln |\mathbf{K}(\boldsymbol{\theta})| - \frac{1}{2} [\mathbf{R} - \mathbf{m}(\boldsymbol{\theta})]^T \mathbf{K}^{-1}(\boldsymbol{\theta}) [\mathbf{R} - \mathbf{m}(\boldsymbol{\theta})] + \zeta, \quad (5.52)$$

where ζ does not depend on $\boldsymbol{\theta}$. The ML estimate is the value of $\boldsymbol{\theta}$ that maximizes $l(\boldsymbol{\theta}; \mathbf{R})$,

$$\hat{\boldsymbol{\theta}}_{\text{ml}}(\mathbf{R}) = \underset{\boldsymbol{\theta}}{\operatorname{argmax}} \{ l(\boldsymbol{\theta}; \mathbf{R}) \} \quad (5.53)$$

or

$$\boxed{\hat{\boldsymbol{\theta}}_{\text{ml}}(\mathbf{R}) = \underset{\boldsymbol{\theta}}{\operatorname{argmin}} \left\{ \ln |\mathbf{K}(\boldsymbol{\theta})| + [\mathbf{R} - \mathbf{m}(\boldsymbol{\theta})]^T \mathbf{K}^{-1}(\boldsymbol{\theta}) [\mathbf{R} - \mathbf{m}(\boldsymbol{\theta})] \right\}.} \quad (5.54)$$

If the maximum is interior, then a necessary, but not sufficient, condition on $\hat{\boldsymbol{\theta}}_{\text{ml}}(\mathbf{R})$ is

$$\left. \frac{\partial}{\partial \theta_i} l(\boldsymbol{\theta}; \mathbf{R}) \right|_{\boldsymbol{\theta}=\hat{\boldsymbol{\theta}}_{\text{ml}}(\mathbf{R})} = 0, \quad i = 1, 2, \dots, D. \quad (5.55)$$

This can be written in more compact form as

$$\left[\nabla_{\theta} l(\theta; \mathbf{R}) \right] \Big|_{\theta=\hat{\theta}_{\text{ml}}(\mathbf{R})} = \mathbf{0}, \quad (5.56)$$

where ∇_{θ} is the $D \times 1$ gradient vector operator defined in (4.370).

To evaluate the derivative of the log-likelihood function in (5.52), we use the formulas given in (3.69) and (3.70) to obtain

$$\begin{aligned} \frac{\partial l(\theta; \mathbf{R})}{\partial \theta_i} &= -\frac{1}{2} \text{tr} \left[\mathbf{K}^{-1}(\theta) \frac{\partial \mathbf{K}(\theta)}{\partial \theta_i} \right] + \frac{1}{2} \left\{ \frac{\partial \mathbf{m}^T(\theta)}{\partial \theta_i} \mathbf{K}^{-1}(\theta) [\mathbf{R} - \mathbf{m}(\theta)] \right. \\ &\quad + [\mathbf{R} - \mathbf{m}(\theta)]^T \left[\mathbf{K}^{-1}(\theta) \frac{\partial \mathbf{K}(\theta)}{\partial \theta_i} \mathbf{K}^{-1}(\theta) \right] [\mathbf{R} - \mathbf{m}(\theta)] \\ &\quad \left. + [\mathbf{R} - \mathbf{m}(\theta)]^T \mathbf{K}^{-1}(\theta) \left[\frac{\partial \mathbf{m}(\theta)}{\partial \theta_i} \right] \right\}, i = 1, 2, \dots, D. \end{aligned} \quad (5.57)$$

Setting the right-hand side of (5.57) equal to zero provides a set of necessary conditions that may be solved to find $\hat{\theta}_{\text{ml}}(\mathbf{R})$. However, in many cases a closed form solution does not exist.

In general, we must search over a D -dimensional surface to find the minimum of (5.54). In some cases, we use a grid search to get a coarse estimate and then a gradient search to find the minimum. Unless D is small, this procedure is not tractable. A large amount of research has been devoted to finding algorithms that find the minimum without doing a grid search. We discuss some of these techniques in Section 5.2.8.

In many cases of interest either $\mathbf{K}(\theta)$ or $\mathbf{m}(\theta)$ is a function of θ , but not both. For example, if $\mathbf{m}(\theta) = \mathbf{m}$, then (5.57) reduces to

$$\begin{aligned} \text{tr} \left[\mathbf{K}^{-1}(\theta) \frac{\partial \mathbf{K}(\theta)}{\partial \theta_i} \right] - [\mathbf{R} - \mathbf{m}]^T \left[\mathbf{K}^{-1}(\theta) \frac{\partial \mathbf{K}(\theta)}{\partial \theta_i} \mathbf{K}^{-1}(\theta) \right] [\mathbf{R} - \mathbf{m}] \Big|_{\theta=\hat{\theta}_{\text{ml}}(\mathbf{R})} &= 0, \\ i = 1, 2, \dots, D. \end{aligned} \quad (5.58)$$

Defining the sample covariance matrix as

$$\hat{\mathbf{K}}(\mathbf{R}) \triangleq [\mathbf{R} - \mathbf{m}] [\mathbf{R} - \mathbf{m}]^T, \quad (5.59)$$

and using the properties of the trace, we have

$$\text{tr} \left(\left[\mathbf{K}^{-1}(\theta) \hat{\mathbf{K}}(\mathbf{R}) \mathbf{K}^{-1}(\theta) - \mathbf{K}^{-1}(\theta) \right] \frac{\partial \mathbf{K}(\theta)}{\partial \theta_i} \right) \Big|_{\theta=\hat{\theta}_{\text{ml}}(\mathbf{R})} = 0, \quad i = 1, 2, \dots, D, \quad (5.60)$$

as a necessary condition.

If $\mathbf{K}(\theta) = \mathbf{K}$, then (5.57) reduces to

$$\left\{ \frac{\partial \mathbf{m}^T(\theta)}{\partial \theta_i} \mathbf{K}^{-1} [\mathbf{R} - \mathbf{m}(\theta)] \right\} \Big|_{\theta=\hat{\theta}_{\text{ml}}(\mathbf{R})} = 0, \quad i = 1, 2, \dots, D. \quad (5.61)$$

The corresponding results for complex observations and real parameters are

$$\hat{\boldsymbol{\theta}}_{\text{ml}}(\tilde{\mathbf{R}}) = \underset{\boldsymbol{\theta}}{\operatorname{argmin}} \left\{ \ln |\tilde{\mathbf{K}}(\boldsymbol{\theta})| + [\tilde{\mathbf{R}} - \tilde{\mathbf{m}}(\boldsymbol{\theta})]^H \tilde{\mathbf{K}}^{-1}(\boldsymbol{\theta}) [\tilde{\mathbf{R}} - \tilde{\mathbf{m}}(\boldsymbol{\theta})] \right\}. \quad (5.62)$$

If $\tilde{\mathbf{m}}(\boldsymbol{\theta}) = \tilde{\mathbf{m}}$, a necessary condition is

$$\operatorname{tr} \left(\left[\tilde{\mathbf{K}}^{-1}(\boldsymbol{\theta}) \tilde{\mathbf{K}}(\tilde{\mathbf{R}}) \tilde{\mathbf{K}}^{-1}(\boldsymbol{\theta}) - \tilde{\mathbf{K}}^{-1}(\boldsymbol{\theta}) \right] \frac{\partial \tilde{\mathbf{K}}(\boldsymbol{\theta})}{\partial \theta_i} \right) \Big|_{\boldsymbol{\theta}=\hat{\boldsymbol{\theta}}_{\text{ml}}(\tilde{\mathbf{R}})} = 0, \quad i = 1, 2, \dots, D. \quad (5.63)$$

where

$$\hat{\tilde{\mathbf{K}}}(\tilde{\mathbf{R}}) \triangleq [\tilde{\mathbf{R}} - \tilde{\mathbf{m}}][\tilde{\mathbf{R}} - \tilde{\mathbf{m}}]^H. \quad (5.64)$$

If $\tilde{\mathbf{K}}(\boldsymbol{\theta}) = \tilde{\mathbf{K}}$, a necessary condition is

$$\Re \left(\frac{\partial \tilde{\mathbf{m}}^H(\boldsymbol{\theta})}{\partial \theta_i} \tilde{\mathbf{K}}^{-1} [\tilde{\mathbf{R}} - \tilde{\mathbf{m}}(\boldsymbol{\theta})] \right) \Big|_{\boldsymbol{\theta}=\hat{\boldsymbol{\theta}}_{\text{ml}}(\tilde{\mathbf{R}})} = 0, \quad i = 1, 2, \dots, D. \quad (5.65)$$

5.2.3 Cramér–Rao Bound

In this section, we derive the Cramér–Rao bound for the general Gaussian estimation model. It is a special case of the CRB derived in Section 4.3.3.1. The CRB provides a bound on the covariance matrix of any *unbiased* estimate of $\boldsymbol{\theta}$. We denote the covariance matrix of the estimation errors by $\boldsymbol{\Lambda}_\epsilon$.

From (4.394), the multiple parameter CRB states that for any unbiased estimate of $\boldsymbol{\theta}$,

$$\boldsymbol{\Lambda}_\epsilon \geq \mathbf{J}_F^{-1}(\boldsymbol{\theta}), \quad (5.66)$$

where $\mathbf{J}_F(\boldsymbol{\theta})$ is the Fisher information matrix (FIM) defined (4.392) and (4.393).

The elements in $\mathbf{J}_F(\boldsymbol{\theta})$ are

$$\begin{aligned} J_{F_{ij}}(\boldsymbol{\theta}) &\triangleq E \left[\frac{\partial l(\boldsymbol{\theta}; \mathbf{R})}{\partial \theta_i} \cdot \frac{\partial l(\boldsymbol{\theta}; \mathbf{R})}{\partial \theta_j} \right] \\ &= -E \left[\frac{\partial^2 l(\boldsymbol{\theta}; \mathbf{R})}{\partial \theta_i \partial \theta_j} \right], \end{aligned} \quad (5.67)$$

or

$$\mathbf{J}_F(\boldsymbol{\theta}) = -E \left(\nabla_{\boldsymbol{\theta}} [\nabla_{\boldsymbol{\theta}} l(\boldsymbol{\theta}; \mathbf{R})]^T \right). \quad (5.68)$$

The first derivative needed in (5.67) is given by (5.57). We differentiate (5.57) using the formulas in (3.70) and (3.71) and take the expectation. The derivative of (5.57) is given in (5.69), except, terms containing a single $[\mathbf{R} - \mathbf{m}]$ term or its transpose are omitted because

their expectation will be zero in the next step. The θ argument is suppressed.

$$\begin{aligned} \frac{\partial^2 l(\theta; \mathbf{R})}{\partial \theta_i \partial \theta_j} &= -\frac{1}{2} \operatorname{tr} \left[-\mathbf{K}^{-1} \frac{\partial \mathbf{K}}{\partial \theta_j} \mathbf{K}^{-1} \frac{\partial \mathbf{K}}{\partial \theta_i} + \mathbf{K}^{-1} \frac{\partial^2 \mathbf{K}}{\partial \theta_i \partial \theta_j} \right] \\ &\quad - \frac{1}{2} \left\{ (\mathbf{R} - \mathbf{m})^T \left[\mathbf{K}^{-1} \frac{\partial \mathbf{K}}{\partial \theta_j} \mathbf{K}^{-1} \frac{\partial \mathbf{K}}{\partial \theta_i} \mathbf{K}^{-1} - \mathbf{K}^{-1} \frac{\partial^2 \mathbf{K}}{\partial \theta_i \partial \theta_j} \mathbf{K}^{-1} \right. \right. \\ &\quad \left. \left. + \mathbf{K}^{-1} \frac{\partial \mathbf{K}}{\partial \theta_i} \mathbf{K}^{-1} \frac{\partial \mathbf{K}}{\partial \theta_j} \mathbf{K}^{-1} \right] (\mathbf{R} - \mathbf{m}) \right\} \\ &\quad - \frac{1}{2} \left\{ 2 \frac{\partial \mathbf{m}^T}{\partial \theta_i} \mathbf{K}^{-1} \frac{\partial \mathbf{m}}{\partial \theta_j} \right\} + \text{omitted terms.} \end{aligned} \quad (5.69)$$

To evaluate the expectation in the middle term, we write

$$\begin{aligned} E \{ (\mathbf{R} - \mathbf{m})^T (\dots) (\mathbf{R} - \mathbf{m}) \} &= E \{ \operatorname{tr} [(\dots) (\mathbf{R} - \mathbf{m}) (\mathbf{R} - \mathbf{m})^T] \} \\ &= \operatorname{tr} [(\dots) \mathbf{K}]. \end{aligned} \quad (5.70)$$

Then,

$$\begin{aligned} -E \left[\frac{\partial^2 l(\theta; \mathbf{R})}{\partial \theta_i \partial \theta_j} \right] &= \frac{1}{2} \operatorname{tr} \left[-\mathbf{K}^{-1} \frac{\partial \mathbf{K}}{\partial \theta_j} \mathbf{K}^{-1} \frac{\partial \mathbf{K}}{\partial \theta_i} + \mathbf{K}^{-1} \frac{\partial^2 \mathbf{K}}{\partial \theta_i \partial \theta_j} \right. \\ &\quad \left. + \mathbf{K}^{-1} \frac{\partial \mathbf{K}}{\partial \theta_j} \mathbf{K}^{-1} \frac{\partial \mathbf{K}}{\partial \theta_i} - \mathbf{K}^{-1} \frac{\partial^2 \mathbf{K}}{\partial \theta_i \partial \theta_j} + \mathbf{K}^{-1} \frac{\partial \mathbf{K}}{\partial \theta_i} \mathbf{K}^{-1} \frac{\partial \mathbf{K}}{\partial \theta_j} \right] \\ &\quad + \left[\frac{\partial \mathbf{m}^T}{\partial \theta_i} \mathbf{K}^{-1} \frac{\partial \mathbf{m}}{\partial \theta_j} \right]. \end{aligned} \quad (5.71)$$

The first four terms inside the trace sum to zero. Thus,¹

$$J_{F_{ij}}(\theta) = \frac{1}{2} \operatorname{tr} \left[\mathbf{K}^{-1}(\theta) \frac{\partial \mathbf{K}(\theta)}{\partial \theta_i} \mathbf{K}^{-1}(\theta) \frac{\partial \mathbf{K}(\theta)}{\partial \theta_j} \right] + \left[\frac{\partial \mathbf{m}^T(\theta)}{\partial \theta_i} \mathbf{K}^{-1}(\theta) \frac{\partial \mathbf{m}(\theta)}{\partial \theta_j} \right]. \quad (5.72)$$

If the parameter vector θ is partitioned into a mean parameter vector θ_m and a covariance parameter vector θ_c as in (5.4), the FIM will have the following block matrix form,

$$\mathbf{J}_F(\theta) = \begin{bmatrix} \mathbf{J}_F(\theta_m) & \mathbf{J}_F(\theta_m, \theta_c) \\ \mathbf{J}_F(\theta_c, \theta_m) & \mathbf{J}_F(\theta_c) \end{bmatrix}. \quad (5.73)$$

For the θ_m block, the first term in (5.72) is zero, therefore,

$$\mathbf{J}_{F_{ij}}(\theta_m) = \frac{\partial \mathbf{m}^T(\theta_m)}{\partial \theta_i} \mathbf{K}^{-1}(\theta_c) \frac{\partial \mathbf{m}(\theta_m)}{\partial \theta_j}, \quad (5.74)$$

which can be written in matrix notation as

$$\mathbf{J}_F(\theta_m) = \nabla_{\theta_m} [\mathbf{m}^T(\theta_m)] \mathbf{K}^{-1}(\theta_c) (\nabla_{\theta_m} [\mathbf{m}^T(\theta_m)])^T. \quad (5.75)$$

¹This result was first published by Bangs [Ban71].

For the $\boldsymbol{\theta}_c$ block, the second term in (5.72) is zero, therefore,

$$J_{F_{ij}}(\boldsymbol{\theta}_c) = \frac{1}{2} \operatorname{tr} \left[\mathbf{K}^{-1}(\boldsymbol{\theta}_c) \frac{\partial \mathbf{K}(\boldsymbol{\theta}_c)}{\partial \theta_i} \mathbf{K}^{-1}(\boldsymbol{\theta}_c) \frac{\partial \mathbf{K}(\boldsymbol{\theta}_c)}{\partial \theta_j} \right]. \quad (5.76)$$

A second form of (5.76) that is often easier to calculate is found by using (3.70) in (5.76) to obtain:

$$J_{F_{ij}}(\boldsymbol{\theta}_c) = -\frac{1}{2} \operatorname{tr} \left[\frac{\partial \mathbf{K}^{-1}(\boldsymbol{\theta}_c)}{\partial \theta_i} \frac{\partial \mathbf{K}(\boldsymbol{\theta}_c)}{\partial \theta_j} \right]. \quad (5.77)$$

For the $(\boldsymbol{\theta}_m, \boldsymbol{\theta}_c)$ block, both terms in (5.72) are zero, so

$$\mathbf{J}_F(\boldsymbol{\theta}_m, \boldsymbol{\theta}_c) = \mathbf{0}. \quad (5.78)$$

Thus, the FIM in (5.73) has the form

$$\mathbf{J}_F(\boldsymbol{\theta}) = \begin{bmatrix} \mathbf{J}_F(\boldsymbol{\theta}_m) & \mathbf{0} \\ \mathbf{0} & \mathbf{J}_F(\boldsymbol{\theta}_c) \end{bmatrix}. \quad (5.79)$$

We see that estimation performance is decoupled for mean and covariance matrix parameters.

For the special case in which $\boldsymbol{\theta}$ is the scalar θ , (5.72) reduces to

$$J_F(\theta) = \left\{ \frac{1}{2} \operatorname{tr} \left(\left[\mathbf{K}^{-1}(\theta) \frac{\partial \mathbf{K}(\theta)}{\partial \theta} \right]^2 \right) + \left[\frac{\partial \mathbf{m}^T(\theta)}{\partial \theta} \mathbf{K}^{-1}(\theta) \frac{\partial \mathbf{m}(\theta)}{\partial \theta} \right] \right\}^{-1}, \quad (5.80)$$

or equivalently,

$$J_F(\theta) = \left\{ -\frac{1}{2} \operatorname{tr} \left(\frac{\partial \mathbf{K}^{-1}(\theta)}{\partial \theta} \frac{\partial \mathbf{K}(\theta)}{\partial \theta} \right) + \left[\frac{\partial \mathbf{m}^T(\theta)}{\partial \theta} \mathbf{K}^{-1}(\theta) \frac{\partial \mathbf{m}(\theta)}{\partial \theta} \right] \right\}^{-1}. \quad (5.81)$$

Note that the results in (5.72)–(5.81) are quite general and provide a starting point for many subsequent derivations. They apply whenever the observation is a Gaussian random vector whose mean and covariance matrices are functions of the parameters of interest.

If the observation is a complex Gaussian random vector the derivation is similar and the result is

$$J_{F_{ij}}(\boldsymbol{\theta}) = \operatorname{tr} \left[\tilde{\mathbf{K}}^{-1}(\boldsymbol{\theta}) \frac{\partial \tilde{\mathbf{K}}(\boldsymbol{\theta})}{\partial \theta_i} \tilde{\mathbf{K}}^{-1}(\boldsymbol{\theta}) \frac{\partial \tilde{\mathbf{K}}(\boldsymbol{\theta})}{\partial \theta_j} \right] + 2\Re \left[\frac{\partial \tilde{\mathbf{m}}^H(\boldsymbol{\theta})}{\partial \theta_i} \tilde{\mathbf{K}}^{-1}(\boldsymbol{\theta}) \frac{\partial \tilde{\mathbf{m}}(\boldsymbol{\theta})}{\partial \theta_j} \right]. \quad (5.82)$$

Note that the parameter vector $\boldsymbol{\theta}$ is real in this formulation.

For the case in which the individual observations are vectors and we have K independent observations, we denote the FIM for the k th observation as $\mathbf{J}_F(\boldsymbol{\theta}; k)$. To total FIM for all K observations is the sum of the single observation FIMs,

$$\mathbf{J}_F(\boldsymbol{\theta}) = \sum_{k=1}^K \mathbf{J}_F(\boldsymbol{\theta}; k). \quad (5.83)$$

If the observations have identical densities, then the single observation FIMs are all the same and

$$\mathbf{J}_F(\boldsymbol{\theta}) = K \mathbf{J}_F(\boldsymbol{\theta}; k). \quad (5.84)$$

5.2.4 Fisher Linear Gaussian Model

5.2.4.1 Introduction

In this section, we consider the models that were introduced in Examples 5.1 and 5.2. For real observations,

$$\mathbf{r} \sim N(\mathbf{V}\boldsymbol{\theta}_m, \mathbf{K}). \quad (5.85)$$

The \mathbf{V} matrix is a known $N \times D$ matrix and the covariance matrix \mathbf{K} is known. The parameter vector $\boldsymbol{\theta}_m$ is a $D \times 1$ vector that we want to estimate. For the complex case,

$$\tilde{\mathbf{r}} \sim CN(\tilde{\mathbf{V}}\tilde{\boldsymbol{\theta}}_m, \tilde{\mathbf{K}}). \quad (5.86)$$

The $\tilde{\mathbf{V}}$ matrix is a known $N \times D$ matrix and the covariance matrix $\tilde{\mathbf{K}}$ is known. The parameter vector $\tilde{\boldsymbol{\theta}}_m$ is a $D \times 1$ complex vector that we want to estimate.

We refer to this model as the Fisher linear Gaussian model to denote that it deals with nonrandom parameters.² The covariance matrix is known, so we can suppress the “ m ” subscript on $\boldsymbol{\theta}$. Substituting

$$\mathbf{m}(\boldsymbol{\theta}) = \mathbf{V}\boldsymbol{\theta} \quad (5.87)$$

into (5.52), the log-likelihood function is

$$l(\boldsymbol{\theta}; \mathbf{R}) = -\frac{1}{2} \ln|\mathbf{K}| - \frac{1}{2} [\mathbf{R} - \mathbf{V}\boldsymbol{\theta}]^T \mathbf{K}^{-1} [\mathbf{R} - \mathbf{V}\boldsymbol{\theta}] + \zeta, \quad (5.88)$$

which can be written as:

$$\begin{aligned} l(\boldsymbol{\theta}; \mathbf{R}) &= -\frac{1}{2} \boldsymbol{\theta}^T \mathbf{V}^T \mathbf{K}^{-1} \mathbf{V}\boldsymbol{\theta} + \frac{1}{2} \{ \boldsymbol{\theta}^T \mathbf{V}^T \mathbf{K}^{-1} \mathbf{R} + \mathbf{R}^T \mathbf{K}^{-1} \mathbf{V}\boldsymbol{\theta} \} - \frac{1}{2} \mathbf{R}^T \mathbf{K}^{-1} \mathbf{R} - \frac{1}{2} \ln|\mathbf{K}| + \zeta \\ &= -\frac{1}{2} \boldsymbol{\theta}^T \mathbf{V}^T \mathbf{K}^{-1} \mathbf{V}\boldsymbol{\theta} + \boldsymbol{\theta}^T \mathbf{V}^T \mathbf{K}^{-1} \mathbf{R} + \zeta. \end{aligned} \quad (5.89)$$

Equation (5.89) consists of a term that is quadratic in $\boldsymbol{\theta}$, a term that is linear in $\boldsymbol{\theta}$, and some terms that do not involve $\boldsymbol{\theta}$.

At this point it is useful to present some general properties of gradients of these terms with respect to $\boldsymbol{\theta}$. First define

$$\nabla_{\boldsymbol{\theta}^T} \equiv \nabla_{\boldsymbol{\theta}} = \begin{bmatrix} \frac{\partial}{\partial \theta_1} \\ \vdots \\ \frac{\partial}{\partial \theta_D} \end{bmatrix}. \quad (5.90)$$

²Fisher developed maximum likelihood estimation in 1912.

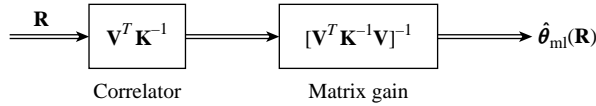


Figure 5.1: Correlator implementation of the ML estimator.

If \mathbf{b} is a real $D \times 1$ vector, then [Van02]

$$\nabla_{\theta^T}(\theta^T \mathbf{b}) = \nabla_{\theta}(\theta^T \mathbf{b}) = \mathbf{b}, \quad (5.91)$$

$$\nabla_{\theta^T}(\mathbf{b}^T \theta) = \nabla_{\theta}(\mathbf{b}^T \theta) = \mathbf{b}. \quad (5.92)$$

If \mathbf{A} is a real, symmetric matrix (i.e. $\mathbf{A}^T = \mathbf{A}$), then

$$\nabla_{\theta^T}(\theta^T \mathbf{A} \theta) = \nabla_{\theta}(\theta^T \mathbf{A} \theta) = 2\mathbf{A}\theta. \quad (5.93)$$

Differentiating (5.89) with respect to θ^T gives

$$\begin{aligned} \nabla_{\theta^T} l(\theta; \mathbf{R}) &= -\mathbf{V}^T \mathbf{K}^{-1} \mathbf{V} \theta + \mathbf{V}^T \mathbf{K}^{-1} \mathbf{R} \\ &= \mathbf{V}^T \mathbf{K}^{-1} [\mathbf{R} - \mathbf{V} \theta]. \end{aligned} \quad (5.94)$$

Setting the result equal to zero and solving gives

$$\hat{\theta}_{\text{ml}}(\mathbf{R}) = [\mathbf{V}^T \mathbf{K}^{-1} \mathbf{V}]^{-1} \mathbf{V}^T \mathbf{K}^{-1} \mathbf{R}. \quad (5.95)$$

The structure of the ML estimator follows from (5.95). The estimator correlates the received vector with the \mathbf{V} matrix to generate a $D \times 1$ vector. The $D \times 1$ vector is multiplied by a $D \times D$ gain matrix to obtain $\hat{\theta}_{\text{ml}}(\mathbf{R})$, as shown in Figure 5.1.

The ML estimate is an unbiased estimate,

$$E[\hat{\theta}_{\text{ml}}(\mathbf{R})] = \theta. \quad (5.96)$$

The Cramér–Rao bound is given by (5.75) with

$$\nabla_{\theta}[\mathbf{m}^T(\theta)] = \mathbf{V}^T. \quad (5.97)$$

Thus, Fisher information matrix is

$$\mathbf{J}_F(\theta) = \mathbf{V}^T \mathbf{K}^{-1} \mathbf{V}. \quad (5.98)$$

For this model, the FIM does not depend on the value of θ .

$\hat{\theta}_{\text{ml}}(\mathbf{R})$ satisfies (4.419), therefore it is an efficient estimate with error covariance matrix equal to the CRB,

$$\Lambda_{\epsilon} = \text{CRB}(\theta) = [\mathbf{V}^T \mathbf{K}^{-1} \mathbf{V}]^{-1}. \quad (5.99)$$

The ML estimate is a linear transformation of a Gaussian random vector, so it is a $N(\theta, [\mathbf{V}^T \mathbf{K}^{-1} \mathbf{V}]^{-1})$ Gaussian random vector.

For the special case in which the additive noise is white,

$$\mathbf{K} = \sigma_w^2 \mathbf{I} \quad (5.100)$$

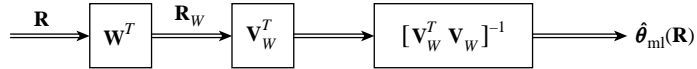


Figure 5.2: Whitening filter implementation of the ML estimator.

and (5.95) reduces to

$$\hat{\theta}_{\text{ml}}(\mathbf{R}) = [\mathbf{V}^T \mathbf{V}]^{-1} \mathbf{V}^T \mathbf{R} = \mathbf{V}^\dagger \mathbf{R}, \quad (5.101)$$

where \mathbf{V}^\dagger is the Moore–Penrose pseudo-inverse

$$\mathbf{V}^\dagger \triangleq [\mathbf{V}^T \mathbf{V}]^{-1} \mathbf{V}^T. \quad (5.102)$$

The Fisher information matrix is

$$\mathbf{J}_F(\boldsymbol{\theta}) = \frac{1}{\sigma_w^2} \mathbf{V}^T \mathbf{V} \quad (5.103)$$

and the error covariance matrix is

$$\boldsymbol{\Lambda}_\epsilon = \text{CRB}(\boldsymbol{\theta}) = \sigma_w^2 [\mathbf{V}^T \mathbf{V}]^{-1}. \quad (5.104)$$

For the nonwhite noise case, we obtain a similar structure by prewhitening \mathbf{R} . We use the square-root matrix \mathbf{W}^T that we defined in (3.187), where

$$\mathbf{K}^{-1} = \mathbf{W} \mathbf{W}^T, \quad (5.105)$$

Now, define

$$\mathbf{V}_W \triangleq \mathbf{W}^T \mathbf{V} \quad (5.106)$$

and

$$\mathbf{R}_W \triangleq \mathbf{W}^T \mathbf{R}. \quad (5.107)$$

Then (5.95) can be implemented as in Figure 5.2. The estimator maps the input into a new space where the noise is white and then operates in the whitened space. Thus, just as in Chapter 3, we can always use the white noise model when the covariance matrix \mathbf{K} is known.

For the complex observation case, we are usually interested in the model in (5.86) where $\tilde{\boldsymbol{\theta}}$ is complex. However, we begin our discussion with the case when $\boldsymbol{\theta}$ is real and the observations are complex, that is,

$$\tilde{\mathbf{r}} \sim \mathcal{CN}(\tilde{\mathbf{V}}\boldsymbol{\theta}, \tilde{\mathbf{K}}). \quad (5.108)$$

For this case,

$$l(\boldsymbol{\theta}; \tilde{\mathbf{R}}) = -\boldsymbol{\theta}^T \tilde{\mathbf{V}}^H \tilde{\mathbf{K}}^{-1} \tilde{\mathbf{V}} \boldsymbol{\theta} + [\boldsymbol{\theta}^T \tilde{\mathbf{V}}^H \tilde{\mathbf{K}}^{-1} \tilde{\mathbf{R}} + \tilde{\mathbf{R}}^H \tilde{\mathbf{K}}^{-1} \tilde{\mathbf{V}} \boldsymbol{\theta}] - \tilde{\mathbf{R}}^H \tilde{\mathbf{K}}^{-1} \tilde{\mathbf{R}} - \ln |\tilde{\mathbf{K}}| + \zeta. \quad (5.109)$$

The matrix $\tilde{\mathbf{V}}^H \tilde{\mathbf{K}}^{-1} \tilde{\mathbf{V}}$ is a Hermitian matrix. Any Hermitian matrix $\tilde{\mathbf{A}}$ can be written in terms of its real and imaginary components

$$\tilde{\mathbf{A}} = \mathbf{A}_R + j\mathbf{A}_I. \quad (5.110)$$

Since $\tilde{\mathbf{A}}^H = \tilde{\mathbf{A}}$, the components have the following properties

$$\mathbf{A}_R^T = \mathbf{A}_R, \quad (5.111)$$

$$\mathbf{A}_I^T = -\mathbf{A}_I. \quad (5.112)$$

Then, for real $\boldsymbol{\theta}$

$$\begin{aligned} \boldsymbol{\theta}^T \mathbf{A}_I \boldsymbol{\theta} &= (\boldsymbol{\theta}^T \mathbf{A}_I \boldsymbol{\theta})^T \\ &= \boldsymbol{\theta}^T \mathbf{A}_I^T \boldsymbol{\theta} \\ &= -\boldsymbol{\theta}^T \mathbf{A}_I \boldsymbol{\theta} \\ &= 0. \end{aligned} \quad (5.113)$$

This means that for real $\boldsymbol{\theta}$,

$$\begin{aligned} \boldsymbol{\theta}^T \tilde{\mathbf{A}} \boldsymbol{\theta} &= \boldsymbol{\theta}^T (\mathbf{A}_R + j\mathbf{A}_I) \boldsymbol{\theta} \\ &= \boldsymbol{\theta}^T \mathbf{A}_R \boldsymbol{\theta}. \end{aligned} \quad (5.114)$$

The likelihood function in (5.109) can be written as

$$l(\boldsymbol{\theta}; \tilde{\mathbf{R}}) = -\boldsymbol{\theta}^T \Re\{\tilde{\mathbf{V}}^H \tilde{\mathbf{K}}^{-1} \tilde{\mathbf{V}}\} \boldsymbol{\theta} + 2\boldsymbol{\theta}^T \Re\{\tilde{\mathbf{V}}^H \tilde{\mathbf{K}}^{-1} \tilde{\mathbf{R}}\} + \zeta. \quad (5.115)$$

Differentiating with respect to $\boldsymbol{\theta}^T$ and setting the result equal to zero gives

$$\hat{\boldsymbol{\theta}}_{\text{ml}}(\tilde{\mathbf{R}}) = (\Re[\tilde{\mathbf{V}}^H \tilde{\mathbf{K}}^{-1} \tilde{\mathbf{V}}])^{-1} (\Re[\tilde{\mathbf{V}}^H \tilde{\mathbf{K}}^{-1} \tilde{\mathbf{R}}]), \quad (5.116)$$

which is an unbiased efficient estimate. The Fisher information matrix is

$$\mathbf{J}_F(\boldsymbol{\theta}) = 2\Re[\tilde{\mathbf{V}}^H \tilde{\mathbf{K}}^{-1} \tilde{\mathbf{V}}]. \quad (5.117)$$

For white noise,

$$\hat{\boldsymbol{\theta}}_{\text{ml}}(\tilde{\mathbf{R}}) = (\Re[\tilde{\mathbf{V}}^H \tilde{\mathbf{V}}])^{-1} (\Re[\tilde{\mathbf{V}}^H \tilde{\mathbf{R}}]) \quad (5.118)$$

and

$$\mathbf{J}_F(\boldsymbol{\theta}) = \frac{2}{\sigma_w^2} \Re[\tilde{\mathbf{V}}^H \tilde{\mathbf{V}}]. \quad (5.119)$$

For the complex parameter model in (5.86), the log-likelihood function is

$$\begin{aligned} l(\tilde{\boldsymbol{\theta}}; \tilde{\mathbf{R}}) &= -\left[\tilde{\mathbf{R}}^H - \tilde{\boldsymbol{\theta}}^H \tilde{\mathbf{V}}^H\right] \tilde{\mathbf{K}}^{-1} [\tilde{\mathbf{R}} - \tilde{\mathbf{V}} \tilde{\boldsymbol{\theta}}] - \ln|\tilde{\mathbf{K}}| + \zeta \\ &= -\tilde{\boldsymbol{\theta}}^H \tilde{\mathbf{V}}^H \tilde{\mathbf{K}}^{-1} \tilde{\mathbf{V}} \tilde{\boldsymbol{\theta}} + \tilde{\boldsymbol{\theta}}^H \tilde{\mathbf{V}}^H \tilde{\mathbf{K}}^{-1} \tilde{\mathbf{R}} + \tilde{\mathbf{R}}^H \tilde{\mathbf{K}}^{-1} \tilde{\mathbf{V}} \tilde{\boldsymbol{\theta}} + \zeta. \end{aligned} \quad (5.120)$$

For this model, we will work with the real parameters $\boldsymbol{\theta}_R \triangleq \Re[\tilde{\boldsymbol{\theta}}]$ and $\boldsymbol{\theta}_I \triangleq \Im[\tilde{\boldsymbol{\theta}}]$, where

$$\tilde{\boldsymbol{\theta}} = \boldsymbol{\theta}_R + j\boldsymbol{\theta}_I. \quad (5.121)$$

We now define complex gradients as follows [Bra83, Van02]:

$$\nabla_{\tilde{\theta}} \triangleq \frac{1}{2} \left\{ \nabla_{\theta_R} - j \nabla_{\theta_I} \right\}, \quad (5.122)$$

$$\nabla_{\tilde{\theta}^H} \triangleq \frac{1}{2} \left\{ \nabla_{\theta_R} + j \nabla_{\theta_I} \right\}, \quad (5.123)$$

Then, we have for complex vector $\tilde{\mathbf{b}}$ and Hermitian matrix $\tilde{\mathbf{A}}$,

$$\nabla_{\tilde{\theta}} (\tilde{\theta}^H \tilde{\mathbf{b}}) = \mathbf{0}, \quad (5.124)$$

$$\nabla_{\tilde{\theta}} (\tilde{\mathbf{b}}^H \tilde{\theta}) = \tilde{\mathbf{b}}^*, \quad (5.125)$$

$$\nabla_{\tilde{\theta}^H} (\tilde{\theta}^H \tilde{\mathbf{b}}) = \tilde{\mathbf{b}}, \quad (5.126)$$

$$\nabla_{\tilde{\theta}^H} (\tilde{\mathbf{b}}^H \tilde{\theta}) = \mathbf{0}, \quad (5.127)$$

$$\nabla_{\tilde{\theta}} (\tilde{\theta}^H \tilde{\mathbf{A}} \tilde{\theta}) = (\tilde{\mathbf{A}} \tilde{\theta})^*, \quad (5.128)$$

$$\nabla_{\tilde{\theta}^H} (\tilde{\theta}^H \tilde{\mathbf{A}} \tilde{\theta}) = \tilde{\mathbf{A}} \tilde{\theta}. \quad (5.129)$$

It will be most convenient to work with $\nabla_{\tilde{\theta}^H}$.

Differentiating (5.120) with respect to $\tilde{\theta}^H$ and setting the result equal to zero gives

$$\hat{\theta}_{\text{ml}}(\tilde{\mathbf{R}}) = [\tilde{\mathbf{V}}^H \tilde{\mathbf{K}}^{-1} \tilde{\mathbf{V}}]^{-1} \tilde{\mathbf{V}}^H \tilde{\mathbf{K}}^{-1} \tilde{\mathbf{R}}. \quad (5.130)$$

To derive the CRB, we define the real $2D \times 1$ vector

$$\boldsymbol{\theta} \triangleq [\theta_R^T \quad \theta_I^T]^T. \quad (5.131)$$

The Fisher information matrix is

$$\mathbf{J}_F(\boldsymbol{\theta}) = \begin{bmatrix} \mathbf{J}_F(\theta_R) & \mathbf{J}_F(\theta_R, \theta_I) \\ \mathbf{J}_F(\theta_I, \theta_R) & \mathbf{J}_F(\theta_I) \end{bmatrix}. \quad (5.132)$$

The submatrices are obtained from (5.82) with

$$\nabla_{\theta_R} [\tilde{\mathbf{m}}^H(\boldsymbol{\theta})] = \nabla_{\theta_R} [\tilde{\mathbf{V}}(\theta_R + j\theta_I)]^H = \tilde{\mathbf{V}}^H, \quad (5.133)$$

$$\nabla_{\theta_I} [\tilde{\mathbf{m}}^H(\boldsymbol{\theta})] = \nabla_{\theta_I} [\tilde{\mathbf{V}}(\theta_R + j\theta_I)]^H = -j\tilde{\mathbf{V}}^H. \quad (5.134)$$

Then,

$$\mathbf{J}_F(\theta_R) = 2\Re[\tilde{\mathbf{V}}^H \tilde{\mathbf{K}}^{-1} \tilde{\mathbf{V}}] \quad (5.135)$$

and

$$\begin{aligned} \mathbf{J}_F(\theta_R, \theta_I) &= 2\Re[\tilde{\mathbf{V}}^H \tilde{\mathbf{K}}^{-1}(j\tilde{\mathbf{V}})] \\ &= -2\Im[\tilde{\mathbf{V}}^H \tilde{\mathbf{K}}^{-1}\tilde{\mathbf{V}}]. \end{aligned} \quad (5.136)$$

Similarly,

$$\mathbf{J}_F(\theta_I) = 2\Re[(-j\tilde{\mathbf{V}})^H \tilde{\mathbf{K}}^{-1}(j\tilde{\mathbf{V}})] = 2\Re[\tilde{\mathbf{V}}^H \tilde{\mathbf{K}}^{-1}\tilde{\mathbf{V}}] \quad (5.137)$$

and

$$\mathbf{J}_F(\boldsymbol{\theta}_I, \boldsymbol{\theta}_R) = 2\Im[\tilde{\mathbf{V}}^H \tilde{\mathbf{K}}^{-1} \tilde{\mathbf{V}}]. \quad (5.138)$$

Thus,

$$\mathbf{J}_F(\boldsymbol{\theta}) = 2 \begin{bmatrix} \Re[\tilde{\mathbf{V}}^H \tilde{\mathbf{K}}^{-1} \tilde{\mathbf{V}}] & -\Im[\tilde{\mathbf{V}}^H \tilde{\mathbf{K}}^{-1} \tilde{\mathbf{V}}] \\ \Im[\tilde{\mathbf{V}}^H \tilde{\mathbf{K}}^{-1} \tilde{\mathbf{V}}] & \Re[\tilde{\mathbf{V}}^H \tilde{\mathbf{K}}^{-1} \tilde{\mathbf{V}}] \end{bmatrix}. \quad (5.139)$$

Due to the special form of $\mathbf{J}_F(\boldsymbol{\theta})$ in (5.139), one can show that the resulting CRB is

$$\text{CRB}(\boldsymbol{\theta}) = \frac{1}{2} \begin{bmatrix} \Re[(\tilde{\mathbf{V}}^H \tilde{\mathbf{K}}^{-1} \tilde{\mathbf{V}})^{-1}] & -\Im[(\tilde{\mathbf{V}}^H \tilde{\mathbf{K}}^{-1} \tilde{\mathbf{V}})^{-1}] \\ \Im[(\tilde{\mathbf{V}}^H \tilde{\mathbf{K}}^{-1} \tilde{\mathbf{V}})^{-1}] & \Re[(\tilde{\mathbf{V}}^H \tilde{\mathbf{K}}^{-1} \tilde{\mathbf{V}})^{-1}] \end{bmatrix}. \quad (5.140)$$

Now, since

$$\tilde{\boldsymbol{\theta}} = [\mathbf{I} \quad j\mathbf{I}] \begin{bmatrix} \boldsymbol{\theta}_R \\ \boldsymbol{\theta}_I \end{bmatrix} = \boldsymbol{\theta}_R + j\boldsymbol{\theta}_I, \quad (5.141)$$

we can use the property in (4.425) for linear transformations,³ which yields

$$\begin{aligned} \text{CRB}(\tilde{\boldsymbol{\theta}}) &= [\mathbf{I} \quad j\mathbf{I}] \text{CRB}(\boldsymbol{\theta}) \begin{bmatrix} \mathbf{I} \\ -j\mathbf{I} \end{bmatrix} \\ &= (\tilde{\mathbf{V}}^H \tilde{\mathbf{K}}^{-1} \tilde{\mathbf{V}})^{-1}. \end{aligned} \quad (5.142)$$

The ML estimator is an unbiased, efficient estimator. The ML estimate is linear transformation of a circular complex Gaussian random vector, therefore it is a circular complex Gaussian random vector with mean $\tilde{\boldsymbol{\theta}}$ and covariance matrix

$$\boxed{\Lambda_\epsilon = \text{CRB}(\tilde{\boldsymbol{\theta}}) = (\tilde{\mathbf{V}}^H \tilde{\mathbf{K}}^{-1} \tilde{\mathbf{V}})^{-1}}. \quad (5.143)$$

Thus, it is an efficient estimate.

For white noise, (5.130) becomes

$$\boxed{\hat{\boldsymbol{\theta}}_{\text{ml}}(\tilde{\mathbf{R}}) = [\tilde{\mathbf{V}}^H \tilde{\mathbf{V}}]^{-1} \tilde{\mathbf{V}}^H \tilde{\mathbf{R}} = \tilde{\mathbf{V}}^\dagger \tilde{\mathbf{R}}}, \quad (5.144)$$

where the complex pseudo-inverse is defined as

$$\tilde{\mathbf{V}}^\dagger \triangleq [\tilde{\mathbf{V}}^H \tilde{\mathbf{V}}]^{-1} \tilde{\mathbf{V}}^H, \quad (5.145)$$

and (5.143) becomes

$$\boxed{\Lambda_\epsilon = \text{CRB}(\tilde{\boldsymbol{\theta}}) = \sigma_w^2 (\tilde{\mathbf{V}}^H \tilde{\mathbf{V}})^{-1}}. \quad (5.146)$$

³For complex linear transformations, the transpose $(\cdot)^T$ in (4.425) becomes Hermitian transpose $(\cdot)^H$.

When we have K independent vector samples, then we can write (5.88) as

$$l(\boldsymbol{\theta}; \mathbf{R}) = -\frac{1}{2} \sum_{k=1}^K [\mathbf{R}_k - \mathbf{V}_k \boldsymbol{\theta}]^T \mathbf{K}^{-1} [\mathbf{R}_k - \mathbf{V}_k \boldsymbol{\theta}] + \zeta, \quad (5.147)$$

where \mathbf{V}_k may be different on each k , but \mathbf{K} is the same. Proceeding as in (5.89)–(5.95) gives

$$\hat{\boldsymbol{\theta}}_{\text{ml}}(\mathbf{R}) = \left[\sum_{k=1}^K \mathbf{V}_k^T \mathbf{K}^{-1} \mathbf{V}_k \right]^{-1} \sum_{k=1}^K \mathbf{V}_k^T \mathbf{K}^{-1} \mathbf{R}_k \quad (5.148)$$

and, as in (5.97)–(5.98),

$$\mathbf{J}_F(\boldsymbol{\theta}) = \sum_{k=1}^K \mathbf{V}_k^T \mathbf{K}^{-1} \mathbf{V}_k. \quad (5.149)$$

For the complex case, we have

$$\hat{\tilde{\boldsymbol{\theta}}}_{\text{ml}}(\tilde{\mathbf{R}}) = \left[\sum_{k=1}^K \tilde{\mathbf{V}}_k^H \tilde{\mathbf{K}}^{-1} \tilde{\mathbf{V}}_k \right]^{-1} \sum_{k=1}^K \tilde{\mathbf{V}}_k^H \tilde{\mathbf{K}}^{-1} \tilde{\mathbf{R}}_k \quad (5.150)$$

and

$$\mathbf{J}_F(\tilde{\boldsymbol{\theta}}) = \sum_{k=1}^K \tilde{\mathbf{V}}_k^H \tilde{\mathbf{K}}^{-1} \tilde{\mathbf{V}}_k. \quad (5.151)$$

5.2.4.2 White Noise

We now consider four examples to illustrate the technique for the case when \mathbf{K} or $\tilde{\mathbf{K}}$ is a white noise matrix.

Example 5.8 (continuation of Example 5.1a) Target tracking. For the target tracking model in Example 5.1a,

$$\boldsymbol{\theta} \triangleq [x_0 \ v_0]^T, \quad (5.152)$$

and \mathbf{V} is defined in (5.15)–(5.17).

The ML estimate is given by (5.101),

$$\hat{\boldsymbol{\theta}}_{\text{ml}}(\mathbf{R}) = [\mathbf{V}^T \mathbf{V}]^{-1} \mathbf{V}^T \mathbf{R}, \quad (5.153)$$

and the Fisher information matrix is given by (5.103),

$$\mathbf{J}_F(\boldsymbol{\theta}) = \frac{1}{\sigma_w^2} \mathbf{V}^T \mathbf{V}. \quad (5.154)$$

Using (5.15)–(5.17) in (5.154) gives

$$\mathbf{J}_F(\boldsymbol{\theta}) = \frac{1}{\sigma_w^2} \mathbf{V}^T \mathbf{V} = \frac{1}{\sigma_w^2} \begin{bmatrix} \sum_{n=1}^N 1 & \sum_{n=1}^N nT \\ \sum_{n=1}^N nT & \sum_{n=1}^N (nT)^2 \end{bmatrix} = \frac{1}{\sigma_w^2} \begin{bmatrix} N & \frac{1}{2}N(N+1)T \\ \frac{1}{2}N(N+1)T & \frac{1}{6}N(N+1)(2N+1)T^2 \end{bmatrix}. \quad (5.155)$$

From (5.104), the error covariance matrix for estimating x_0 and v_0 is

$$\mathbf{A}_\epsilon = \sigma_w^2 (\mathbf{V}^T \mathbf{V})^{-1} = \frac{12\sigma_w^2}{T^2 N(N^2 - 1)} \begin{bmatrix} \frac{1}{6}(N+1)(2N+1)T^2 & -\frac{1}{2}(N+1)T \\ -\frac{1}{2}(N+1)T & 1 \end{bmatrix}. \quad (5.156)$$

The position of the target at any time n is given by (5.14), therefore the estimated position is

$$\hat{x}_{\text{ml}}(n) = [1 \ nT] \hat{\boldsymbol{\theta}}_{\text{ml}}(\mathbf{R}), \quad (5.157)$$

with error variance given by

$$\text{Var}(\hat{x}_{\text{ml}}(n)) = [1 \ nT] \mathbf{A}_\epsilon \begin{bmatrix} 1 \\ nT \end{bmatrix}. \quad (5.158)$$

Substituting (5.156) into (5.158), we have

$$\text{Var}(\hat{x}_{\text{ml}}(n)) = \frac{2\sigma_w^2}{N(N^2 - 1)} [6n^2 - 6n(N+1) + (N+1)(2N+1)]. \quad (5.159)$$

The variance is only a function of σ_w^2 , N , and n . It is not a function of x_0 or v_0 . It is a quadratic function of n with a minimum when $n = \frac{N+1}{2}$.

In Figure 5.3, we plot the variance of $\hat{x}_{\text{ml}}(n)$ versus n for several values of N . Note that n can be greater than N . The best estimation of target position occurs at the midpoint of the observation interval and the variance increases symmetrically out to end the points of the observation interval. When $n > N$, we are estimating the position without observations and the estimation error variance increases quadratically in n . ■

Example 5.9 (continuation of Example 5.2). Consider the model in Example 5.2 with $D = 2$ and $\tilde{\mathbf{n}} = \tilde{\mathbf{w}} \sim CN(\mathbf{0}, \sigma_w^2 \mathbf{I})$. The observation vector is

$$\tilde{\mathbf{r}} = \sum_{i=1}^2 \tilde{\mathbf{v}}_i \tilde{\theta}_i + \tilde{\mathbf{w}} = \tilde{\mathbf{V}} \tilde{\boldsymbol{\theta}} + \tilde{\mathbf{w}}, \quad (5.160)$$

where

$$\tilde{\mathbf{V}} = [\tilde{\mathbf{v}}_1 \ \tilde{\mathbf{v}}_2] \quad (5.161)$$

and

$$\tilde{\boldsymbol{\theta}} = [\tilde{\theta}_1 \ \tilde{\theta}_2]^T. \quad (5.162)$$

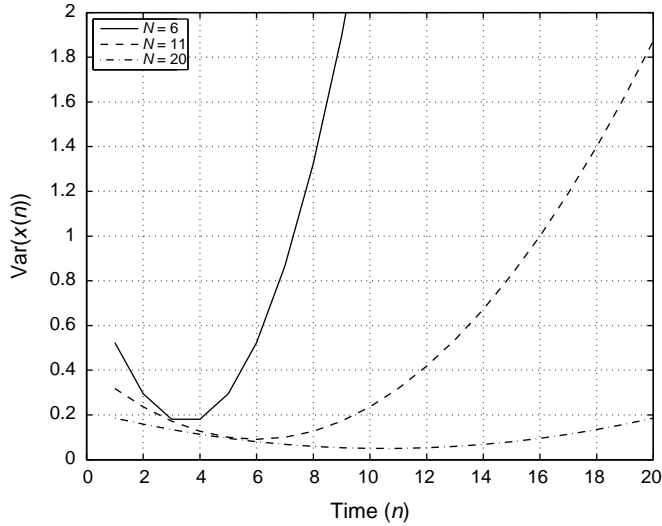


Figure 5.3: Variance of $\hat{x}_{\text{ml}}(n)$ versus n for $N = 6, 11, 20$.

The ML estimate is given by (5.144) and the error covariance matrix by (5.146). To evaluate these expressions, we first evaluate $\tilde{\mathbf{V}}^H \tilde{\mathbf{V}}$, which has the form

$$\tilde{\mathbf{V}}^H \tilde{\mathbf{V}} = \begin{bmatrix} \tilde{\mathbf{v}}_1^H \tilde{\mathbf{v}}_1 & \tilde{\mathbf{v}}_1^H \tilde{\mathbf{v}}_2 \\ \tilde{\mathbf{v}}_2^H \tilde{\mathbf{v}}_1 & \tilde{\mathbf{v}}_2^H \tilde{\mathbf{v}}_2 \end{bmatrix}. \quad (5.163)$$

Defining the complex correlation between $\tilde{\mathbf{v}}_1$ and $\tilde{\mathbf{v}}_2$ to be

$$\tilde{\rho}_{12} \triangleq \frac{\tilde{\mathbf{v}}_1^H \tilde{\mathbf{v}}_2}{\|\tilde{\mathbf{v}}_1\| \|\tilde{\mathbf{v}}_2\|}, \quad (5.164)$$

the inverse of $\tilde{\mathbf{V}}^H \tilde{\mathbf{V}}$ is given by

$$[\tilde{\mathbf{V}}^H \tilde{\mathbf{V}}]^{-1} = \frac{1}{(1 - |\tilde{\rho}_{12}|^2)} \begin{bmatrix} [\tilde{\mathbf{v}}_1^H \tilde{\mathbf{v}}_1]^{-1} & -\frac{\tilde{\rho}_{12}}{\|\tilde{\mathbf{v}}_1\| \|\tilde{\mathbf{v}}_2\|} \\ -\frac{\tilde{\rho}_{12}^*}{\|\tilde{\mathbf{v}}_1\| \|\tilde{\mathbf{v}}_2\|} & [\tilde{\mathbf{v}}_2^H \tilde{\mathbf{v}}_2]^{-1} \end{bmatrix}. \quad (5.165)$$

Substituting (5.165) into (5.144), the ML estimate is

$$\hat{\theta}_{\text{ml}}(\tilde{\mathbf{R}}) = \frac{1}{(1 - |\tilde{\rho}_{12}|^2)} \begin{bmatrix} \tilde{\mathbf{v}}_1^\dagger \tilde{\mathbf{R}} - \frac{\tilde{\rho}_{12} \|\tilde{\mathbf{v}}_2\|}{\|\tilde{\mathbf{v}}_1\|} \tilde{\mathbf{v}}_2^\dagger \tilde{\mathbf{R}} \\ \tilde{\mathbf{v}}_2^\dagger \tilde{\mathbf{R}} - \frac{\tilde{\rho}_{12}^* \|\tilde{\mathbf{v}}_1\|}{\|\tilde{\mathbf{v}}_2\|} \tilde{\mathbf{v}}_1^\dagger \tilde{\mathbf{R}} \end{bmatrix}. \quad (5.166)$$

The ML estimator for $\hat{\theta}_{1,\text{ml}}(\tilde{\mathbf{R}})$ is shown in Figure 5.4. The estimator contains the two single signal estimators $\tilde{\mathbf{v}}_1^\dagger \tilde{\mathbf{R}}$ and $\tilde{\mathbf{v}}_2^\dagger \tilde{\mathbf{R}}$. The single signal estimate of $\tilde{\theta}_2$ is multiplied by the complex correlation factor $\tilde{\rho}_{12} \|\tilde{\mathbf{v}}_2\| / \|\tilde{\mathbf{v}}_1\|$ and subtracted from the single signal estimate of $\tilde{\theta}_1$. This removes the second signal component in $\tilde{\mathbf{R}}$. Then, the result is scaled so that the estimate of $\tilde{\theta}_1$ is unbiased. If the signals are uncorrelated and $\tilde{\rho}_{12} = 0$, the estimate reduces to the single signal estimate of $\tilde{\theta}_1$.

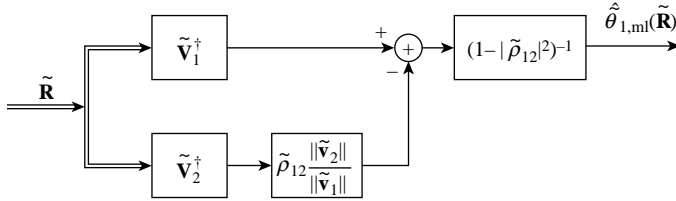


Figure 5.4: ML estimator: two signals.

Substituting (5.165) into (5.146), the error covariance matrix is

$$\Lambda_\epsilon = \text{CRB}(\tilde{\theta}) = \frac{\sigma_w^2}{(1 - |\tilde{\rho}_{12}|^2)} \begin{bmatrix} [\tilde{\mathbf{v}}_1^H \tilde{\mathbf{v}}_1]^{-1} & -\frac{\tilde{\rho}_{12}}{\|\tilde{\mathbf{v}}_1\| \|\tilde{\mathbf{v}}_2\|} \\ -\frac{\tilde{\rho}_{12}^*}{\|\tilde{\mathbf{v}}_2\| \|\tilde{\mathbf{v}}_1\|} & [\tilde{\mathbf{v}}_2^H \tilde{\mathbf{v}}_2]^{-1} \end{bmatrix}. \quad (5.167)$$

Looking at the diagonal components, we see that the error variance is increased by the factor $(1 - |\tilde{\rho}_{12}|^2)^{-1}$ over the error variance in the single signal case. If $\tilde{\rho}_{12} = 0$, the single signal error variance is obtained. ■

We now specialize these results for the complex exponential and array processing models.

Example 5.9a (continuation of Examples 5.2a and 5.9) Complex exponentials. Consider the model in Example 5.2a with $D = 2$ and $\tilde{\mathbf{w}} = \tilde{\mathbf{w}} \sim \mathcal{CN}(\mathbf{0}, \sigma_w^2 \mathbf{I})$. There are two complex exponentials with known frequencies in complex white Gaussian noise. The observation vector is

$$\tilde{\mathbf{r}} = \sum_{i=1}^2 \tilde{\mathbf{v}}(\omega_i) \tilde{b}_i + \tilde{\mathbf{w}} = \tilde{\mathbf{V}} \tilde{\mathbf{b}} + \tilde{\mathbf{w}}, \quad (5.168)$$

where

$$\tilde{\mathbf{V}} = [\tilde{\mathbf{v}}(\omega_1) \quad \tilde{\mathbf{v}}(\omega_2)] \quad (5.169)$$

and

$$\tilde{\mathbf{b}} = [\tilde{b}_1 \quad \tilde{b}_2]^T. \quad (5.170)$$

For this model $\tilde{\mathbf{v}}(\omega_1)^H \tilde{\mathbf{v}}(\omega_1) = \tilde{\mathbf{v}}(\omega_2)^H \tilde{\mathbf{v}}(\omega_2) = N$ and the single signal estimators are

$$\tilde{\mathbf{v}}(\omega_i)^\dagger \tilde{\mathbf{R}} = \frac{1}{N} \sum_{n=0}^{N-1} \tilde{\mathbf{R}}_n e^{-j\omega_i n} = F(\omega_i; \tilde{\mathbf{R}}); \quad i = 1, 2, \quad (5.171)$$

where $F(\omega_i; \tilde{\mathbf{R}})$ was defined in Example 4.15, equation (4.226).

The complex correlation is

$$\tilde{\rho}_c(\Delta\omega) \triangleq \frac{1}{N} \tilde{\mathbf{v}}(\omega_1)^H \tilde{\mathbf{v}}(\omega_2) = \frac{1}{N} \sum_{n=0}^{N-1} e^{j(\omega_2 - \omega_1)n}, \quad (5.172)$$

where

$$\Delta\omega \triangleq \omega_2 - \omega_1. \quad (5.173)$$

From (3.307)–(3.309),

$$\tilde{\rho}_c(\Delta\omega) = e^{j\Delta\omega \frac{N-1}{2}} B_c(\Delta\omega), \quad (5.174)$$

where

$$B_c(\Delta\omega) = \frac{\sin\left(\frac{N\Delta\omega}{2}\right)}{N \sin\left(\frac{\Delta\omega}{2}\right)}. \quad (5.175)$$

Note that

$$\tilde{\rho}_c^*(\Delta\omega) = \tilde{\rho}_c(-\Delta\omega). \quad (5.176)$$

Substituting (5.171) and (5.174) into (5.166) and (5.167), the ML estimates of \tilde{b}_1 and \tilde{b}_2 are

$$\hat{b}_{1,\text{ml}}(\tilde{\mathbf{R}}) = \frac{1}{(1 - B_c^2(\Delta\omega))} [F(\omega_1; \tilde{\mathbf{R}}) - \tilde{\rho}_c(\Delta\omega) F(\omega_2; \tilde{\mathbf{R}})], \quad (5.177)$$

$$\hat{b}_{2,\text{ml}}(\tilde{\mathbf{R}}) = \frac{1}{(1 - B_c^2(\Delta\omega))} [F(\omega_2; \tilde{\mathbf{R}}) - \tilde{\rho}_c^*(\Delta\omega) F(\omega_1; \tilde{\mathbf{R}})], \quad (5.178)$$

and the error covariance matrix is

$$\Lambda_{\epsilon} = \text{CRB}(\tilde{\mathbf{b}}) = \frac{\sigma_w^2}{N(1 - B_c^2(\Delta\omega))} \begin{bmatrix} 1 & -\tilde{\rho}_c(\Delta\omega) \\ -\tilde{\rho}_c^*(\Delta\omega) & 1 \end{bmatrix}. \quad (5.179)$$

In Figure 5.5, we plot the error variance of $\hat{b}_{1,\text{ml}}(\tilde{\mathbf{R}})$ versus $\Delta\omega$. When $B_c(\Delta\omega) = 0$, the error variance reduces to the variance in the single signal case. If $|\Delta\omega| > 2\pi/N$, $B_c(\Delta\omega)$ will be less than 0.23 (or -13 dB), so the error variance will be close to the single signal case. However, if $\Delta\omega$ is inside the mainlobe, then $B_c(\Delta\omega) \rightarrow 1$ as $\Delta\omega \rightarrow 0$ and the variance approaches infinity. ■

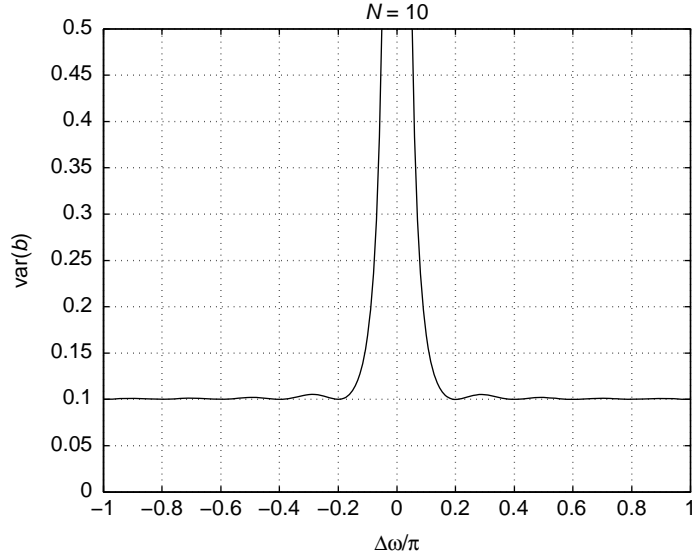


Figure 5.5: Error variance of $\hat{b}_{1,\text{ml}}(\tilde{\mathbf{R}})$ versus $\Delta\omega$.

Example 5.9b (continuation of Examples 5.2b, 5.9, and 5.9a) Array processing. Consider the model in Example 5.2b with $D = 2$ and $\tilde{\mathbf{n}} = \tilde{\mathbf{w}} \sim CN(\mathbf{0}, \sigma_w^2 \mathbf{I})$. This is the array processing dual to Example 5.9a. There are two planewaves with known wavenumber in complex white Gaussian noise. The observation vectors are

$$\tilde{\mathbf{r}}_k = \tilde{\mathbf{V}}\tilde{\mathbf{b}} + \tilde{\mathbf{w}}_k, \quad k = 1, 2, \dots, K, \quad (5.180)$$

where

$$\tilde{\mathbf{V}} = [\tilde{\mathbf{v}}(\psi_1) \ \tilde{\mathbf{v}}(\psi_2)], \quad (5.181)$$

and $\tilde{\mathbf{b}}$ is defined in (5.170).

The ML estimate and Fisher information matrix are given by (5.150) and (5.151) with $\tilde{\mathbf{V}}_k = \tilde{\mathbf{V}}$ and $\tilde{\mathbf{K}} = \sigma_w^2 \mathbf{I}$, thus

$$\hat{\mathbf{b}}_{\text{ml}}(\tilde{\mathbf{R}}) = \tilde{\mathbf{V}}^\dagger \left(\frac{1}{K} \sum_{k=0}^{K-1} \tilde{\mathbf{R}}_k \right) = \tilde{\mathbf{V}}^\dagger \tilde{\mathbf{R}}, \quad (5.182)$$

where $\tilde{\mathbf{R}}$ is the sample mean vector defined in (4.500), and

$$\mathbf{J}_F(\tilde{\mathbf{b}}) = \frac{K}{\sigma_w^2} \tilde{\mathbf{V}}^H \tilde{\mathbf{V}}. \quad (5.183)$$

For this model,

$$\tilde{\rho}_c(\Delta\psi) \triangleq \frac{1}{N} \tilde{\mathbf{v}}(\psi_1)^H \tilde{\mathbf{v}}(\psi_2) = \frac{1}{N} \sum_{n=0}^{N-1} e^{-j(\psi_2 - \psi_1)n} \quad (5.184)$$

and

$$\Delta\psi \triangleq \psi_2 - \psi_1. \quad (5.185)$$

In this case, the sign in the exponential term is negative and

$$\tilde{\rho}_c(\Delta\psi) = e^{-j\Delta\psi \frac{N-1}{2}} B_c(\Delta\psi). \quad (5.186)$$

As in the single signal case considered in Example 4.30, the results for complex exponentials in Example 5.9a apply with $\tilde{\mathbf{R}}$ replacing \mathbf{R} and $-\psi$ replacing ω . The error covariance is reduced by a factor of K . The single signal estimator for this model is the conventional beamformer defined in (4.501). ■

These examples illustrate the importance of the correlation between the columns of the $\tilde{\mathbf{V}}$ matrix. Although we require them to be linearly independent, if for some $i \neq j$,

$$\tilde{\rho}_{ij} = \frac{\tilde{\mathbf{v}}_i^H \tilde{\mathbf{v}}_j}{\|\tilde{\mathbf{v}}_i\| \|\tilde{\mathbf{v}}_j\|}, \quad (5.187)$$

is close to one, then $\tilde{\mathbf{V}}^H \tilde{\mathbf{V}}$ will be ill-conditioned. In the sinusoidal signal model, this corresponds to closely-spaced frequencies. In the array processing model, it corresponds to planewave directions that are close to each other. To explore this quantitatively, we would do an eigendecomposition of $\tilde{\mathbf{V}}^H \tilde{\mathbf{V}}$. If the ratio of the eigenvalues $\lambda_{\max}/\lambda_{\min}$ is large then the matrix will be ill-conditioned.

5.2.4.3 Low-Rank Interference

In this section, we consider the case where there is a single desired signal and $\tilde{\mathbf{r}} \sim CN(\tilde{\mathbf{v}}_s \tilde{\theta}, \tilde{\mathbf{K}})$, where the noise covariance matrix has the form

$$\tilde{\mathbf{K}} = \tilde{\mathbf{K}}_I + \sigma_{\tilde{w}}^2 \mathbf{I}, \quad (5.188)$$

where $\tilde{\mathbf{K}}_I$ has rank $D_I < N$.

We first perform an eigendecomposition of $\tilde{\mathbf{K}}_I$,

$$\tilde{\mathbf{K}}_I = \sum_{i=1}^{D_I} \lambda_i \tilde{\boldsymbol{\phi}}_i \tilde{\boldsymbol{\phi}}_i^H. \quad (5.189)$$

We define an $N \times D_I$ matrix $\tilde{\mathbf{V}}_{eig}$ as

$$\tilde{\mathbf{V}}_{eig} \triangleq [\tilde{\boldsymbol{\phi}}_1 \quad \tilde{\boldsymbol{\phi}}_2 \quad \dots \quad \tilde{\boldsymbol{\phi}}_{D_I}] \quad (5.190)$$

and a $D_I \times D_I$ diagonal matrix Λ_{eig} as

$$\Lambda_{eig} \triangleq \text{diag} [\lambda_1 \quad \lambda_2 \quad \dots \quad \lambda_{D_I}]. \quad (5.191)$$

Thus, the covariance matrix can be written as

$$\tilde{\mathbf{K}} = \tilde{\mathbf{V}}_{eig} \Lambda_{eig} \tilde{\mathbf{V}}_{eig}^H + \sigma_{\tilde{w}}^2 \mathbf{I}. \quad (5.192)$$

Using the matrix inversion lemma, the inverse is

$$\tilde{\mathbf{K}}^{-1} = \frac{1}{\sigma_{\tilde{w}}^2} \left[\mathbf{I} - \tilde{\mathbf{V}}_{eig} (\tilde{\mathbf{V}}_{eig}^H \tilde{\mathbf{V}}_{eig} + \sigma_{\tilde{w}}^2 \Lambda_{eig}^{-1})^{-1} \tilde{\mathbf{V}}_{eig}^H \right]. \quad (5.193)$$

The inner matrix is a $D_I \times D_I$ diagonal matrix

$$(\tilde{\mathbf{V}}_{eig}^H \tilde{\mathbf{V}}_{eig} + \sigma_{\tilde{w}}^2 \Lambda_{eig}^{-1}) = \mathbf{I} + \sigma_{\tilde{w}}^2 \Lambda_{eig}^{-1}. \quad (5.194)$$

The i th diagonal entry is

$$\begin{aligned} [\tilde{\mathbf{V}}_{eig}^H \tilde{\mathbf{V}}_{eig} + \sigma_{\tilde{w}}^2 \Lambda_{eig}^{-1}]_{ii} &= 1 + \frac{\sigma_{\tilde{w}}^2}{\lambda_i} \\ &= \frac{\lambda_i / \sigma_{\tilde{w}}^2 + 1}{\lambda_i / \sigma_{\tilde{w}}^2} \\ &= \frac{\text{INR}_{ei} + 1}{\text{INR}_{ei}}, \end{aligned} \quad (5.195)$$

where the eigenvalue-to-noise ratio of the i th eigenvector is defined as

$$\text{INR}_{ei} \triangleq \frac{\lambda_i}{\sigma_{\tilde{w}}^2}. \quad (5.196)$$

Then (5.193) may be written as

$$\tilde{\mathbf{K}}^{-1} = \frac{1}{\sigma_{\tilde{w}}^2} \left[\mathbf{I} - \sum_{i=1}^{D_I} \tilde{\boldsymbol{\phi}}_i \tilde{\boldsymbol{\phi}}_i^H \frac{\text{INR}_{ei}}{\text{INR}_{ei} + 1} \right]. \quad (5.197)$$

From (5.130), the ML estimate is

$$\hat{\theta}_{\text{ml}}(\tilde{\mathbf{R}}) = [\tilde{\mathbf{v}}_s^H \tilde{\mathbf{K}}^{-1} \tilde{\mathbf{v}}_s]^{-1} \tilde{\mathbf{v}}_s^H \tilde{\mathbf{K}}^{-1} \tilde{\mathbf{R}}. \quad (5.198)$$

The first term in (5.198) is

$$\begin{aligned} [\tilde{\mathbf{v}}_s^H \tilde{\mathbf{K}}^{-1} \tilde{\mathbf{v}}_s]^{-1} &= \left[\frac{1}{\sigma_w^2} \left(\tilde{\mathbf{v}}_s^H \tilde{\mathbf{v}}_s - \sum_{i=1}^{D_I} |\tilde{\mathbf{v}}_s^H \tilde{\boldsymbol{\phi}}_i|^2 \frac{\text{INR}_{ei}}{\text{INR}_{ei} + 1} \right) \right]^{-1} \\ &= \frac{\sigma_w^2}{\tilde{\mathbf{v}}_s^H \tilde{\mathbf{v}}_s} \left(1 - \sum_{i=1}^{D_I} |\tilde{\rho}_{si}|^2 \frac{\text{INR}_{ei}}{\text{INR}_{ei} + 1} \right)^{-1}, \end{aligned} \quad (5.199)$$

where

$$\tilde{\rho}_{si} \triangleq \frac{\tilde{\mathbf{v}}_s^H \tilde{\boldsymbol{\phi}}_i}{\|\tilde{\mathbf{v}}_s\| \|\tilde{\boldsymbol{\phi}}_i\|} = \frac{\tilde{\mathbf{v}}_s^H \tilde{\boldsymbol{\phi}}_i}{\|\tilde{\mathbf{v}}_s\|}. \quad (5.200)$$

The second term in (5.198) is

$$\tilde{\mathbf{v}}_s^H \tilde{\mathbf{K}}^{-1} \tilde{\mathbf{R}} = \frac{\tilde{\mathbf{v}}_s^H \tilde{\mathbf{v}}_s}{\sigma_w^2} \left[\tilde{\mathbf{v}}_s^\dagger \tilde{\mathbf{R}} - \sum_{i=1}^{D_I} \tilde{\rho}_{si} \frac{\text{INR}_{ei}}{\text{INR}_{ei} + 1} \frac{\tilde{\boldsymbol{\phi}}_i^H}{\|\tilde{\mathbf{v}}_s\|} \tilde{\mathbf{R}} \right]. \quad (5.201)$$

Thus, the ML estimate is

$$\hat{\theta}_{\text{ml}}(\tilde{\mathbf{R}}) = \left(1 - \sum_{i=1}^{D_I} |\tilde{\rho}_{si}|^2 \frac{\text{INR}_{ei}}{\text{INR}_{ei} + 1} \right)^{-1} \left[\tilde{\mathbf{v}}_s^\dagger \tilde{\mathbf{R}} - \sum_{i=1}^{D_I} \tilde{\rho}_{si} \frac{\text{INR}_{ei}}{\text{INR}_{ei} + 1} \frac{\tilde{\boldsymbol{\phi}}_i^H}{\|\tilde{\mathbf{v}}_s\|} \tilde{\mathbf{R}} \right]. \quad (5.202)$$

The ML processor is shown in Figure 5.6.

From (5.143), the error variance and Cramér–Rao bound are given by (5.199),

$$\Lambda_\epsilon = \text{CRB}(\tilde{\theta}) = \frac{\sigma_w^2}{\tilde{\mathbf{v}}_s^H \tilde{\mathbf{v}}_s} \left(1 - \sum_{i=1}^{D_I} |\tilde{\rho}_{si}|^2 \frac{\text{INR}_{ei}}{\text{INR}_{ei} + 1} \right)^{-1}. \quad (5.203)$$

If there are K IID observations, then the results apply with the sample mean $\tilde{\mathbf{R}}$ replacing $\tilde{\mathbf{R}}$ and the error covariance reduced by a factor of K .

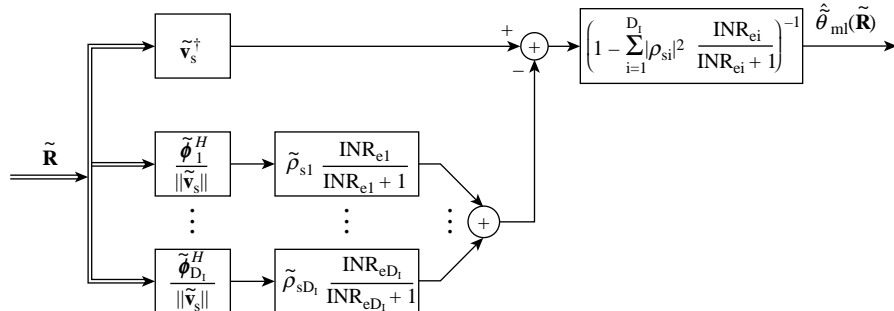


Figure 5.6: ML estimator: single signal and rank D_I interference.

We consider an example in which there is a single interferer to illustrate the behavior.

Example 5.10 (continuation of Example 5.2b) Array processing. We consider the model in Example 5.2b with $D = 1$ and additive noise $\tilde{\mathbf{n}}$ consisting of white noise and interference with rank $D_I = 1$. The K IID observation vectors are

$$\tilde{\mathbf{r}}_k = \tilde{\mathbf{v}}(\psi_s)\tilde{b}_s + \tilde{\mathbf{n}}_k, \quad k = 1, 2, \dots, K, \quad (5.204)$$

where $\tilde{\mathbf{v}}(\psi_s)$ is given by (5.29) with $\psi_i = \psi_s$. The covariance matrix of $\tilde{\mathbf{n}}_k$ is

$$\tilde{\mathbf{K}} = E\{\tilde{\mathbf{n}}_k \tilde{\mathbf{n}}_k^H\} = \sigma_I^2 \tilde{\mathbf{v}}(\psi_I) \tilde{\mathbf{v}}(\psi_I)^H + \sigma_w^2 \mathbf{I}, \quad (5.205)$$

where $\tilde{\mathbf{v}}(\psi_I)$ is given by (5.29) with $\psi_i = \psi_I$.

Then,

$$\tilde{\mathbf{v}}_s = \tilde{\mathbf{v}}(\psi_s) \quad (5.206)$$

$$\tilde{\theta} = \tilde{b}_s \quad (5.207)$$

$$\|\tilde{\mathbf{v}}(\psi_s)\| = \|\tilde{\mathbf{v}}(\psi_I)\| = \sqrt{N} \quad (5.208)$$

$$\tilde{\phi}_1 = \frac{\tilde{\mathbf{v}}(\psi_I)}{\sqrt{N}} \quad (5.209)$$

$$\lambda_1 = N\sigma_I^2 \quad (5.210)$$

$$\text{INR}_{e1} = N \cdot \text{INR} = N \frac{\sigma_I^2}{\sigma_w^2} \quad (5.211)$$

$$\tilde{\rho}_{s1} = \tilde{\rho}_c(\Delta\psi_{Is}) = e^{-j\Delta\psi_{Is}\frac{N-1}{2}} B_c(\Delta\psi_{Is}), \quad (5.212)$$

where

$$\Delta\psi_{Is} \triangleq \psi_I - \psi_s. \quad (5.213)$$

Substituting (5.206)–(5.212) into (5.202) and replacing $\tilde{\mathbf{R}}$ with $\tilde{\mathbf{R}}$, the ML estimate is given by

$$\hat{b}_{s,\text{ml}}(\tilde{\mathbf{R}}) = \left(1 - B_c^2(\Delta\psi_{Is}) \frac{N \cdot \text{INR}}{N \cdot \text{INR} + 1}\right)^{-1} \left\{ \tilde{\mathbf{v}}(\psi_s)^\dagger - \left(\tilde{\rho}_c(\Delta\psi_{Is}) \frac{N \cdot \text{INR}}{N \cdot \text{INR} + 1} \right) \tilde{\mathbf{v}}(\psi_I)^\dagger \right\} \tilde{\mathbf{R}}. \quad (5.214)$$

The estimator is shown in Figure 5.7. It consists of two conventional beamformers, one pointed to ψ_s and one pointed to ψ_I . The output of the beamformer pointed to ψ_I is multiplied by a gain term that depends on its location in the beampattern of the beamformer pointed to ψ_s and its strength (INR). The output is subtracted from the output of the beamformer pointed to ψ_s . The result is then scaled so that the output of the overall processor is equal to one for a signal at ψ_s and the estimator is unbiased. In the limit that $\text{INR} \rightarrow \infty$, we obtain the processor in Example 5.9b.

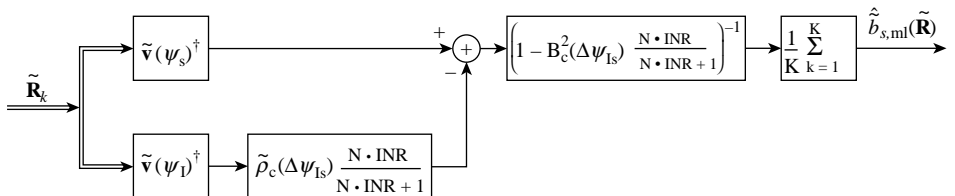


Figure 5.7: ML estimator: single signal and single interferer.

The error variance and CRB are found by substituting (5.206)–(5.212) into (5.203) and dividing by K to obtain

$$\Lambda_\epsilon = \text{CRB}(\tilde{b}_s) = \frac{\sigma_w^2}{KN} \left(1 - B_c^2(\Delta\psi_{Is}) \frac{N \cdot \text{INR}}{N \cdot \text{INR} + 1} \right)^{-1}. \quad (5.215)$$

The conventional beampattern $B_c(\Delta\psi_{Is})$ was plotted in Figure 3.20 for $N = 10$. It is equal to zero when $\Delta\psi_{Is}$ is an integer multiple of $2\pi/N$ and is relatively small outside the mainbeam; thus, the interferer has no effect on the CRB when $\Delta\psi_{Is}$ is at the zeros (or nulls) of the conventional beampattern, has some effect at the sidelobes, and has a significant effect inside the mainlobe where $B_c(\Delta\psi_{Is})$ is large.

The same model was used in a detection problem in Example 3.7. Comparing the processor in Figure 5.7 to the processor in Figure 3.24, we see that the structure is the same. Comparing the CRB in (5.215) to d^2 in (3.322), we see that d^2 is proportional to the inverse of the CRB, which is the Fisher information.

To analyze the ML processor, we compute the output of the processor to a planewave with DOA ψ ,

$$\begin{aligned} \tilde{\rho}_{\text{ml}}(\psi) &= \left(1 - B_c^2(\Delta\psi_{Is}) \frac{N \cdot \text{INR}}{N \cdot \text{INR} + 1} \right)^{-1} \left\{ \tilde{\mathbf{v}}(\psi_s)^\dagger - \left(\tilde{\rho}_c(\Delta\psi_{Is}) \frac{N \cdot \text{INR}}{N \cdot \text{INR} + 1} \right) \tilde{\mathbf{v}}(\psi_I)^\dagger \right\} \tilde{\mathbf{v}}(\psi) \\ &= \left(1 - B_c^2(\Delta\psi_{Is}) \frac{N \cdot \text{INR}}{N \cdot \text{INR} + 1} \right)^{-1} \left\{ \tilde{\rho}_c(\psi - \psi_s) - \left(\tilde{\rho}_c(\Delta\psi_{Is}) \frac{N \cdot \text{INR}}{N \cdot \text{INR} + 1} \right) \tilde{\rho}_c(\psi - \psi_I) \right\} \\ &= e^{-j\Delta\psi \frac{N-1}{2}} \left(1 - B_c^2(\Delta\psi_{Is}) \frac{N \cdot \text{INR}}{N \cdot \text{INR} + 1} \right)^{-1} \{B_c(\Delta\psi) - B_I(\Delta\psi)\}, \end{aligned} \quad (5.216)$$

where

$$\Delta\psi \triangleq \psi - \psi_s \quad (5.217)$$

and

$$B_I(\Delta\psi) \triangleq B_c(\psi - \psi_I) B_c(\Delta\psi_{Is}) \frac{N \cdot \text{INR}}{N \cdot \text{INR} + 1}. \quad (5.218)$$

Note that $B_I(\Delta\psi)$ is a conventional beampattern pointed to ψ_I multiplied by a scaling factor that is less than or equal to one. Ignoring the initial phase term in (5.216), we define the beampattern of the ML processor as

$$B_{\text{ml}}(\Delta\psi) = \left(1 - B_c^2(\Delta\psi_{Is}) \frac{N \cdot \text{INR}}{N \cdot \text{INR} + 1} \right)^{-1} \{B_c(\Delta\psi) - B_I(\Delta\psi)\}. \quad (5.219)$$

We are mainly interested in the output value of the ML beamformer when $\Delta\psi = 0$ ($\psi = \psi_s$) and $\Delta\psi = \Delta\psi_{Is}$ ($\psi = \psi_I$); however, it is useful to plot the beampatterns for all $\Delta\psi$. We consider $N = 10$ and four cases of interference: INR = 10 and 0.1 with $\Delta\psi_{Is} = 0.5\pi$ and 0.1π . These correspond to strong and weak interference, with the interferer being at a sidelobe or in the mainbeam. In Figures 5.8 and 5.9, we show $B_c(\Delta\psi)$, $B_I(\Delta\psi)$, and $B_{\text{ml}}(\Delta\psi)$ versus $\Delta\psi/\pi$. $B_{\text{ml}}(\Delta\psi)$ is shown in both standard and dB scale.

$B_c(\Delta\psi)$ is the beampattern of the conventional beamformer estimate,

$$\hat{b}_{s,c}(\tilde{\mathbf{R}}) \triangleq \tilde{\mathbf{v}}(\psi_s)^\dagger \tilde{\mathbf{R}}. \quad (5.220)$$

This is the optimum estimator when there is no interference. Since $B_c(\Delta\psi)$ is equal to one when $\Delta\psi = 0$, the estimate is unbiased with error variance

$$\text{Var}(\hat{b}_{s,c}(\tilde{\mathbf{R}})) = \frac{\sigma_w^2}{KN} (1 + B_c^2(\Delta\psi) N \cdot \text{INR}). \quad (5.221)$$

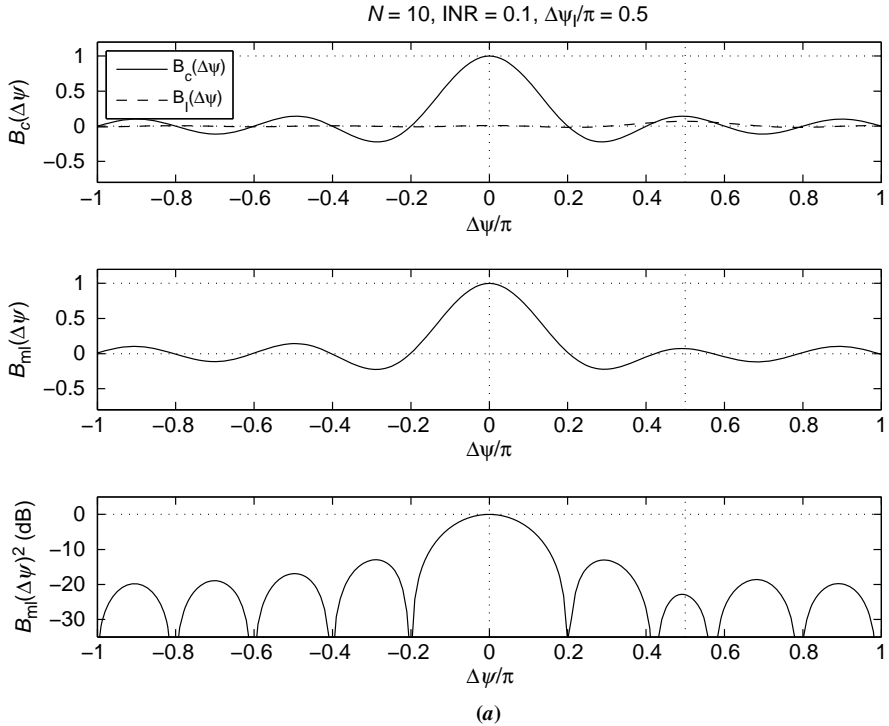


Figure 5.8: (a) Conventional beampattern, ML beampattern, and ML power pattern; $N = 10$, $\text{INR} = 0.1$, $\Delta\psi_{I_s} = 0.5\pi$.

In Figures 5.8a and 5.8b, $\Delta\psi_{I_s} = 0.5\pi$. Thus, the interferer is close to the second sidelobe in the conventional beampattern pointed to ψ_s . $B_{ml}(\Delta\psi)$ is equal to one when $\Delta\psi = 0$. For $\text{INR} = 0.1$, the effect is to lower the sidelobe at the interferer's location by about 8 dB. For $\text{INR} = 10$, the ML beampattern has a deep null (>30 dB) at the interferer's location.

In Figures 5.9a and 5.9b, $\Delta\psi_{I_s} = 0.1\pi$. Thus, the interferer is inside the mainlobe. The ML beamformer attempts to suppress the interference while maintaining a value of one at $\Delta\psi = 0$. For $\text{INR} = 0.1$, the effect on the ML beamformer is to shift the peak of the mainlobe away from the interferer by a small amount. For $\text{INR} = 10$, the effect is to put a deep null (>30 dB) at the interferer's location and move the maximum of the beampattern further away from the signal direction.

In Figure 5.10, we plot the variance of the ML and conventional processors versus $\Delta\psi_{I_s}/\pi$ for $\sigma_w^2/K = 1$, $N = 10$, and $\text{INR} = 0.1, 1.0$, and 10.0 . We see that for large INR the optimum ML processor offers significant improvement over the conventional processor in most of the main lobe region ($\Delta\psi_{I_s} < \sim 0.02\pi$) and near the peaks of the sidelobes. This is due to the ability of the ML processor to adapt its beampattern and place a null at the location of the interferer. As we would expect, the improvement decreases as the INR decreases. ■

The results of this example provide insight into the general ML estimator in Figure 5.6. Since the eigenvectors are a linear combination of the array manifold vectors of the interferers, each of the eigenvector correlators creates an eigenbeam that corresponds to a weighted sum of conventional beams tuned to $\tilde{\mathbf{v}}(\psi_i)$, $i = 1, \dots, D_I$. The output of the i th correlator is weighted by

$$\tilde{\rho}_{si} \frac{\text{INR}_{ei}}{\text{INR}_{ei} + 1}, \quad (5.222)$$

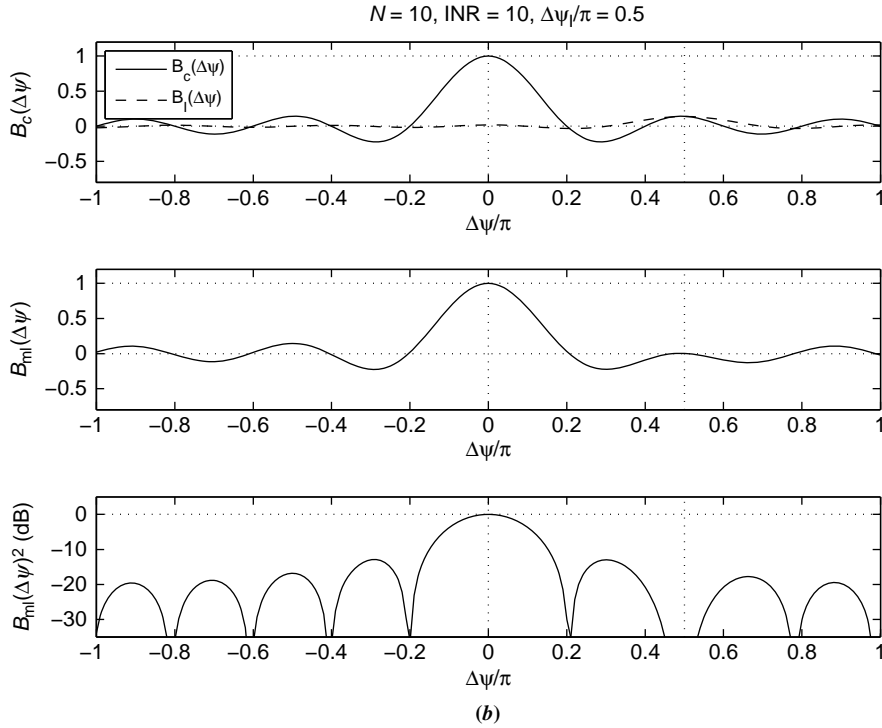


Figure 5.8: (b) Conventional beampattern, ML beampattern, and ML power pattern; $N = 10$, $\text{INR} = 10$, $\Delta\psi_{Is} = 0.5\pi$.

therefore, we can consider a suboptimum approximation that eliminates the eigenbeamformers where the $\tilde{\rho}_{si}$ or INR_{ei} is small.

The matrix portion of the ML processor (i.e. the beamformer) is called an *eigenspace beamformer* in the literature. It is discussed in detail in Section 6.8 of DEMT-IV [Van02].⁴ The generalization to planar arrays with two-dimensional wavenumber follows in a straightforward manner.

We have spent a fair amount of time studying the array processing problem because it is an important application. The results for the complex exponential model follow immediately and the interpretation with the beampattern is identical. However, it is important to remember that the eigenspace realization of the ML estimator applies to any low-rank interference model.

We next consider separable models.

5.2.5 Separable Models for Mean Parameters

In this section, we consider separable Gaussian models where the mean parameters are unknown. This model was introduced in Examples 5.3 and 5.4. The covariance matrices

⁴Under the eigendecomposition label, there are algorithms proposed by Hung and Turner [HT83], Citron and Kailath [CK84], Owsley [Ows85], Gabriel [Gab86], Van Veen [VV88], Chang and Yeh [CY92], Youn and Un [YU94], Yu and Yeh [YY95], and Kirsteins and Tufts [KT85].

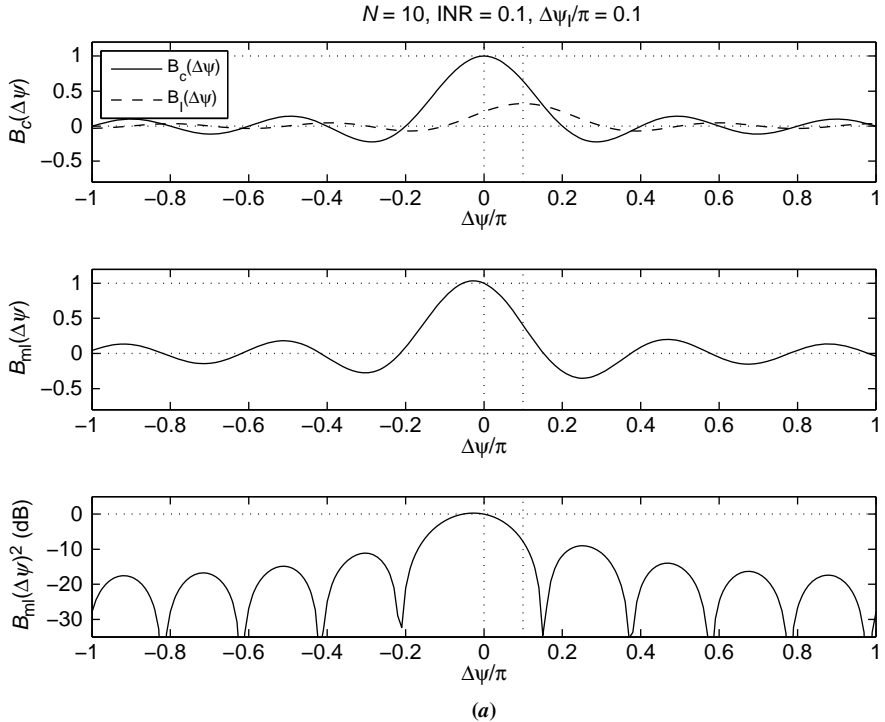


Figure 5.9: (a) Conventional beampattern, ML beampattern, and ML power pattern; $N = 10$, $\text{INR} = 0.1$, $\Delta\psi_{Is} = 0.1\pi$.

are known, so we can suppress the “ m ” subscript on θ . For real observations,

$$\mathbf{r} \sim N(\mathbf{V}(\boldsymbol{\theta}_{nl})\boldsymbol{\theta}_l, \mathbf{K}) \quad (5.223)$$

and the log-likelihood function is

$$l(\boldsymbol{\theta}; \mathbf{R}) = -\frac{1}{2} [\mathbf{R} - \mathbf{V}(\boldsymbol{\theta}_{nl})\boldsymbol{\theta}_l]^T \mathbf{K}^{-1} [\mathbf{R} - \mathbf{V}(\boldsymbol{\theta}_{nl})\boldsymbol{\theta}_l] + \zeta. \quad (5.224)$$

For complex observations and parameters,

$$\tilde{\mathbf{r}} \sim CN(\tilde{\mathbf{V}}(\boldsymbol{\theta}_{nl})\tilde{\boldsymbol{\theta}}_l, \tilde{\mathbf{K}}) \quad (5.225)$$

and the log-likelihood function is

$$l(\tilde{\boldsymbol{\theta}}; \tilde{\mathbf{R}}) = -[\tilde{\mathbf{R}} - \tilde{\mathbf{V}}(\boldsymbol{\theta}_{nl})\tilde{\boldsymbol{\theta}}_l]^H \tilde{\mathbf{K}}^{-1} [\tilde{\mathbf{R}} - \tilde{\mathbf{V}}(\boldsymbol{\theta}_{nl})\tilde{\boldsymbol{\theta}}_l] + \zeta. \quad (5.226)$$

First we consider the real case with

$$\mathbf{K} = \sigma_w^2 \mathbf{I}, \quad (5.227)$$

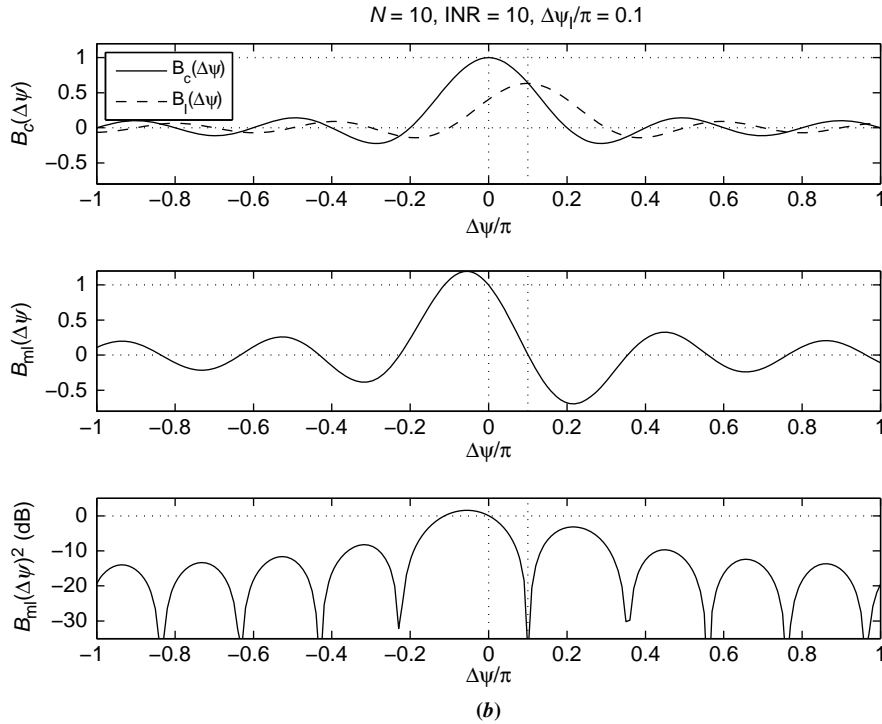


Figure 5.9: (b) Conventional beampattern, ML beampattern, and ML power pattern; $N = 10$, $\text{INR} = 10$, $\Delta\psi_I = 0.1\pi$.

because we can whiten the input. We retain σ_w^2 in the whitened output, so we can more easily keep track of the noise variance. Then, (5.224) can be written as

$$l(\theta_{nl}, \theta_l; \mathbf{R}) = -\frac{1}{2\sigma_w^2} [\mathbf{R} - \mathbf{V}(\theta_{nl})\theta_l]^T [\mathbf{R} - \mathbf{V}(\theta_{nl})\theta_l] + \zeta. \quad (5.228)$$

Differentiating with respect to θ_l and setting the result equal to zero gives the result in (5.101):⁵

$$\hat{\theta}_l(\mathbf{R}, \theta_{nl}) = [\mathbf{V}^T(\theta_{nl})\mathbf{V}(\theta_{nl})]^{-1} \mathbf{V}^T(\theta_{nl})\mathbf{R} = \mathbf{V}^\dagger(\theta_{nl})\mathbf{R}. \quad (5.229)$$

We now substitute (5.229) into (5.228) to create a compressed log-likelihood function for θ_{nl} ,

$$l(\theta_{nl}; \mathbf{R}) = l(\theta_{nl}, \hat{\theta}_l(\mathbf{R}, \theta_{nl}); \mathbf{R}) = -\frac{1}{2\sigma_w^2} [\mathbf{R} - \mathbf{V}(\theta_{nl})\mathbf{V}^\dagger(\theta_{nl})\mathbf{R}]^T [\mathbf{R} - \mathbf{V}(\theta_{nl})\mathbf{V}^\dagger(\theta_{nl})\mathbf{R}] + \zeta. \quad (5.230)$$

⁵We drop the “ml” subscript to reduce notation.

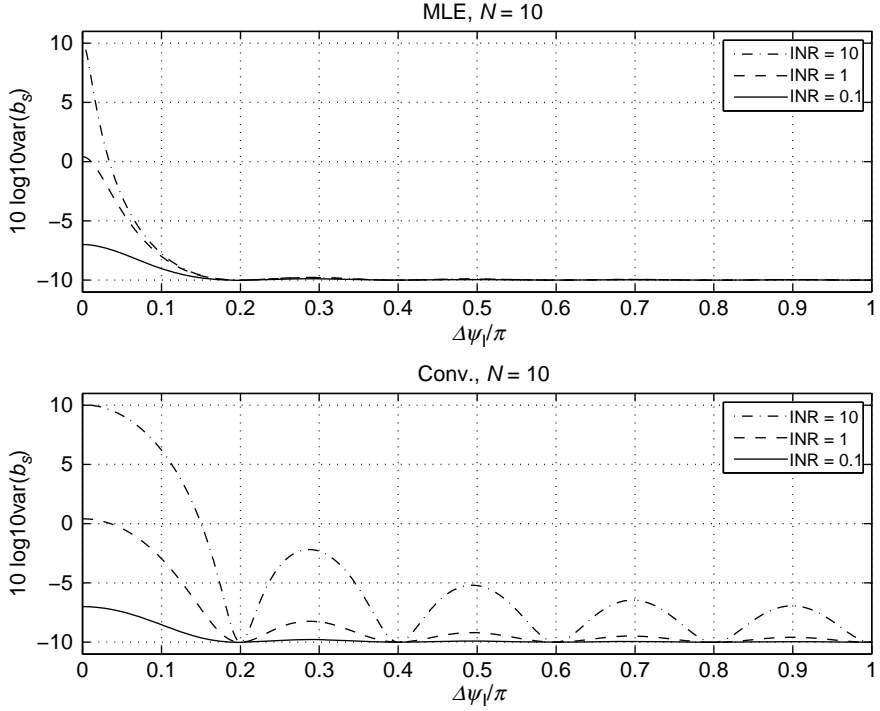


Figure 5.10: Variance of ML and conventional processors versus $\Delta\psi_{is}/\pi$.

We recognize the matrix multiplying \mathbf{R} as the projection matrix defined in (4.779),

$$\mathbf{P}_{\mathbf{V}(\theta_{nl})} = \mathbf{V}(\theta_{nl}) [\mathbf{V}^T(\theta_{nl}) \mathbf{V}(\theta_{nl})]^{-1} \mathbf{V}^T(\theta_{nl}). \quad (5.231)$$

Then,

$$l(\theta_{nl}; \mathbf{R}) = -\frac{1}{2\sigma_w^2} [\mathbf{R} - \mathbf{P}_{\mathbf{V}(\theta_{nl})} \mathbf{R}]^T [\mathbf{R} - \mathbf{P}_{\mathbf{V}(\theta_{nl})} \mathbf{R}] + \zeta. \quad (5.232)$$

The orthogonal projection matrix was defined in (4.790) as

$$\mathbf{P}_{\mathbf{V}(\theta_{nl})}^\perp \triangleq \mathbf{I} - \mathbf{P}_{\mathbf{V}(\theta_{nl})}. \quad (5.233)$$

Therefore, (5.232) may be written as

$$l(\theta_{nl}; \mathbf{R}) = -\frac{1}{2\sigma_w^2} \left\| \mathbf{P}_{\mathbf{V}(\theta_{nl})}^\perp \mathbf{R} \right\|^2 + \zeta. \quad (5.234)$$

The ML estimate of θ_{nl} is obtained by finding the value of θ_{nl} that maximizes $l(\theta_{nl}; \mathbf{R})$. Thus,

$$\hat{\theta}_{nl}(\mathbf{R}) = \underset{\theta_{nl}}{\operatorname{argmin}} \left\{ \left\| \mathbf{P}_{\mathbf{V}(\theta_{nl})}^\perp \mathbf{R} \right\|^2 \right\} \quad (5.235)$$

or, equivalently,

$$\hat{\theta}_{nl}(\mathbf{R}) = \operatorname{argmax}_{\theta_{nl}} \left\{ \|\mathbf{P}_{\mathbf{V}(\theta_{nl})}\mathbf{R}\|^2 \right\} = \operatorname{argmax}_{\theta_{nl}} \left\{ \mathbf{R}^T \mathbf{P}_{\mathbf{V}(\theta_{nl})} \mathbf{R} \right\}. \quad (5.236)$$

We encountered this type of result in Example 4.45. The expression in braces in (5.236) corresponds to the energy in the signal subspace, which is parameterized by θ_{nl} . In order to find $\hat{\theta}_{nl}(\mathbf{R})$, we find the value of θ_{nl} that maximizes the energy in the resulting signal subspace.

Once the estimate $\hat{\theta}_{nl}(\mathbf{R})$ is obtained, we substitute it back into (5.229) to obtain the estimate $\hat{\theta}_l(\mathbf{R})$,

$$\hat{\theta}_l(\mathbf{R}) = \mathbf{V}^\dagger \left(\hat{\theta}_{nl}(\mathbf{R}) \right) \mathbf{R}. \quad (5.237)$$

In order to find the Fisher information matrix, we use (5.75). We partition θ into

$$\theta = \begin{bmatrix} \theta_l \\ \theta_{nl} \end{bmatrix}. \quad (5.238)$$

For simplicity in notation, we assume that θ_l and θ_{nl} are both $D \times 1$. The generalization is straightforward.⁶

The Fisher information matrix is

$$\mathbf{J}_F(\theta) = \begin{bmatrix} \mathbf{J}_F(\theta_l) & \mathbf{J}_F(\theta_l, \theta_{nl}) \\ \mathbf{J}_F(\theta_{nl}, \theta_l) & \mathbf{J}_F(\theta_{nl}) \end{bmatrix}. \quad (5.239)$$

The necessary gradients are

$$\nabla_{\theta_l} [\mathbf{m}^T(\theta)] = \nabla_{\theta_l} [\theta_l^T \mathbf{V}^T(\theta_{nl})] = \mathbf{V}^T(\theta_{nl}), \quad (5.240)$$

$$\nabla_{\theta_{nl}} [\mathbf{m}^T(\theta)] = \nabla_{\theta_{nl}} [\theta_l^T \mathbf{V}^T(\theta_{nl})], \quad (5.241)$$

and the blocks in $J_F(\theta)$ are

$$\mathbf{J}_F(\theta_l) = \frac{1}{\sigma_w^2} \mathbf{V}^T(\theta_{nl}) \mathbf{V}(\theta_{nl}), \quad (5.242)$$

$$\mathbf{J}_F(\theta_l, \theta_{nl}) = \frac{1}{\sigma_w^2} \mathbf{V}^T(\theta_{nl}) (\nabla_{\theta_{nl}} [\theta_l^T \mathbf{V}^T(\theta_{nl})])^T, \quad (5.243)$$

$$\mathbf{J}_F(\theta_{nl}) = \frac{1}{\sigma_w^2} (\nabla_{\theta_{nl}} [\theta_l^T \mathbf{V}^T(\theta_{nl})]) (\nabla_{\theta_{nl}} [\theta_l^T \mathbf{V}^T(\theta_{nl})])^T. \quad (5.244)$$

We next consider the case where the observations are complex and

$$\tilde{\mathbf{K}} = \sigma_{\tilde{w}}^2 \mathbf{I}. \quad (5.245)$$

If both θ_l and θ_{nl} are real, then (5.226) becomes

$$l(\theta_{nl}, \theta_l; \tilde{\mathbf{R}}) = -\frac{1}{\sigma_{\tilde{w}}^2} [\tilde{\mathbf{R}} - \tilde{\mathbf{V}}(\theta_{nl})\theta_l]^H [\tilde{\mathbf{R}} - \tilde{\mathbf{V}}(\theta_{nl})\theta_l] + \zeta. \quad (5.246)$$

⁶A simple example where θ_{nl} is $2D \times 1$ is the model where we estimate the direction of arrival of a planewave using a planar array. The DOA is a 2×1 vector.

The solution for $\hat{\theta}_l(\tilde{\mathbf{R}}, \theta_{nl})$ is given by (5.118):

$$\hat{\theta}_l(\tilde{\mathbf{R}}, \theta_{nl}) = \left(\Re[\tilde{\mathbf{V}}^H(\theta_{nl})\tilde{\mathbf{V}}(\theta_{nl})] \right)^{-1} \left(\Re[\tilde{\mathbf{V}}^H(\theta_{nl})\tilde{\mathbf{R}}] \right). \quad (5.247)$$

Substituting (5.247) back into (5.246), we obtain a compressed log-likelihood function and the ML estimate of θ_{nl} is

$$\begin{aligned} \hat{\theta}_{nl}(\tilde{\mathbf{R}}) &= \underset{\theta_{nl}}{\operatorname{argmin}} \left\{ \left\| \tilde{\mathbf{R}} - \tilde{\mathbf{V}}(\theta_{nl}) \left(\Re[\tilde{\mathbf{V}}^H(\theta_{nl})\tilde{\mathbf{V}}(\theta_{nl})] \right)^{-1} \left(\Re[\tilde{\mathbf{V}}^H(\theta_{nl})\tilde{\mathbf{R}}] \right) \right\|^2 \right\} \\ &= \underset{\theta_{nl}}{\operatorname{argmax}} \left\{ \left(\Re[\tilde{\mathbf{R}}^H\tilde{\mathbf{V}}(\theta_{nl})] \right) \left(\Re[\tilde{\mathbf{V}}^H(\theta_{nl})\tilde{\mathbf{V}}(\theta_{nl})] \right)^{-1} \left(\Re[\tilde{\mathbf{V}}^H(\theta_{nl})\tilde{\mathbf{R}}] \right) \right\}. \end{aligned} \quad (5.248)$$

The Fisher information matrix is obtained from (5.82) and has the form

$$J_F(\theta) = \frac{2}{\sigma_w^2} \Re \left[\left(\nabla_{\theta} [\tilde{\mathbf{m}}^H(\theta)] \right) \left(\nabla_{\theta} [\tilde{\mathbf{m}}^H(\theta)] \right)^H \right]. \quad (5.249)$$

It has the same block structure as (5.239).

The required gradients are

$$\begin{aligned} \nabla_{\theta_l} [\tilde{\mathbf{m}}^H(\theta)] &= \nabla_{\theta_l} [\theta_l^T \tilde{\mathbf{V}}^H(\theta_{nl})] = \tilde{\mathbf{V}}^H(\theta_{nl}), \\ \nabla_{\theta_{nl}} [\tilde{\mathbf{m}}^H(\theta)] &= \nabla_{\theta_{nl}} [\theta_l^T \tilde{\mathbf{V}}^H(\theta_{nl})]. \end{aligned} \quad (5.250)$$

The blocks in $\mathbf{J}_F(\theta)$ are then

$$\mathbf{J}_F(\theta_l) = \frac{2}{\sigma_w^2} \Re \left[\tilde{\mathbf{V}}^H(\theta_{nl}) \tilde{\mathbf{V}}(\theta_{nl}) \right], \quad (5.251)$$

$$\mathbf{J}_F(\theta_l, \theta_{nl}) = \frac{2}{\sigma_w^2} \Re \left[\tilde{\mathbf{V}}^H(\theta_{nl}) \left(\nabla_{\theta_{nl}} [\theta_l^T \tilde{\mathbf{V}}^H(\theta_{nl})] \right)^H \right], \quad (5.252)$$

$$\mathbf{J}_F(\theta_{nl}) = \frac{2}{\sigma_w^2} \Re \left[\left(\nabla_{\theta_{nl}} [\theta_l^T \tilde{\mathbf{V}}^H(\theta_{nl})] \right) \left(\nabla_{\theta_{nl}} [\theta_l^T \tilde{\mathbf{V}}^H(\theta_{nl})] \right)^H \right], \quad (5.253)$$

and

$$\mathbf{J}_F(\theta_{nl}, \theta_l) = [\mathbf{J}_F(\theta_l, \theta_{nl})]^T. \quad (5.254)$$

For complex $\tilde{\theta}_l$ and real θ_{nl} , (5.226) becomes

$$l(\tilde{\theta}_l, \theta_{nl}; \tilde{\mathbf{R}}) = -\frac{1}{\sigma_w^2} \left[\tilde{\mathbf{R}} - \tilde{\mathbf{V}}(\theta_{nl}) \tilde{\theta}_l \right]^H \left[\tilde{\mathbf{R}} - \tilde{\mathbf{V}}(\theta_{nl}) \tilde{\theta}_l \right] + \zeta. \quad (5.255)$$

The solution for $\hat{\tilde{\theta}}_l(\tilde{\mathbf{R}}, \theta_{nl})$ is found from (5.144):

$$\hat{\tilde{\theta}}_l(\tilde{\mathbf{R}}, \theta_{nl}) = \left[\tilde{\mathbf{V}}^H(\theta_{nl}) \tilde{\mathbf{V}}(\theta_{nl}) \right]^{-1} \tilde{\mathbf{V}}^H(\theta_{nl}) \tilde{\mathbf{R}} = \tilde{\mathbf{V}}^\dagger(\theta_{nl}) \tilde{\mathbf{R}}, \quad (5.256)$$

and the ML estimate of θ_{nl} is given by

$$\hat{\theta}_{nl}(\tilde{\mathbf{R}}) = \underset{\theta_{nl}}{\operatorname{argmin}} \left\{ \|\mathbf{P}_{\tilde{\mathbf{V}}(\theta_{nl})} \tilde{\mathbf{R}}\|^2 \right\}, \quad (5.257)$$

where the complex projection matrix is defined as

$$\mathbf{P}_{\tilde{\mathbf{V}}(\theta_{nl})} \triangleq \tilde{\mathbf{V}}(\theta_{nl}) [\tilde{\mathbf{V}}^H(\theta_{nl}) \tilde{\mathbf{V}}(\theta_{nl})]^{-1} \tilde{\mathbf{V}}^H(\theta_{nl}). \quad (5.258)$$

To find the Fisher information matrix, we use the approach in Section 5.2.4.1 and write $\tilde{\theta}_l$ in terms of its real and imaginary components. We define $\theta_{lR} = \Re[\tilde{\theta}_l]$ and $\theta_{lI} = \Im[\tilde{\theta}_l]$. $J_F(\theta)$ is now partitioned into a 3×3 block matrix

$$J_F(\theta) = \begin{bmatrix} J_F(\theta_{lR}) & J_F(\theta_{lR}, \theta_{lI}) & J_F(\theta_{lR}, \theta_{nl}) \\ J_F(\theta_{lI}, \theta_{lR}) & J_F(\theta_{lI}) & J_F(\theta_{lI}, \theta_{nl}) \\ J_F(\theta_{nl}, \theta_{lR}) & J_F(\theta_{nl}, \theta_{lI}) & J_F(\theta_{nl}) \end{bmatrix}. \quad (5.259)$$

The gradients are

$$\nabla_{\theta_{lR}}[\tilde{\mathbf{m}}^H(\theta)] = \nabla_{\theta_{lR}}[(\theta_{lR}^T - j\theta_{lI}^T) \tilde{\mathbf{V}}^H(\theta_{nl})] = \tilde{\mathbf{V}}^H(\theta_{nl}), \quad (5.260)$$

$$\nabla_{\theta_{lI}}[\tilde{\mathbf{m}}^H(\theta)] = -j\tilde{\mathbf{V}}^H(\theta_{nl}), \quad (5.261)$$

$$\nabla_{\theta_{nl}}[\tilde{\mathbf{m}}^H(\theta)] = \left(\nabla_{\theta_{nl}} \left[\tilde{\theta}_l^H \tilde{\mathbf{V}}^H(\theta_{nl}) \right] \right), \quad (5.262)$$

and the blocks are

$$J_F(\theta_{lR}) = \frac{2}{\sigma_w^2} \Re \left[\tilde{\mathbf{V}}^H(\theta_{nl}) \tilde{\mathbf{V}}(\theta_{nl}) \right]. \quad (5.263)$$

$$J_F(\theta_{lR}, \theta_{lI}) = -\frac{2}{\sigma_w^2} \Im \left[\tilde{\mathbf{V}}^H(\theta_{nl}) \tilde{\mathbf{V}}(\theta_{nl}) \right], \quad (5.264)$$

$$J_F(\theta_{lR}, \theta_{nl}) = \frac{2}{\sigma_w^2} \Re \left[\tilde{\mathbf{V}}^H(\theta_{nl}) \left(\nabla_{\theta_{nl}} \left[\tilde{\theta}_l^H \tilde{\mathbf{V}}^H(\theta_{nl}) \right] \right)^H \right], \quad (5.265)$$

$$J_F(\theta_{lI}, \theta_{lR}) = \frac{2}{\sigma_w^2} \Im \left[\tilde{\mathbf{V}}^H(\theta_{nl}) \tilde{\mathbf{V}}(\theta_{nl}) \right], \quad (5.266)$$

$$J_F(\theta_{lI}) = \frac{2}{\sigma_w^2} \Re \left[\tilde{\mathbf{V}}^H(\theta_{nl}) \tilde{\mathbf{V}}(\theta_{nl}) \right], \quad (5.267)$$

$$J_F(\theta_{lI}, \theta_{nl}) = \frac{2}{\sigma_w^2} \Im \left[\tilde{\mathbf{V}}^H(\theta_{nl}) \left(\nabla_{\theta_{nl}} \left[\tilde{\theta}_l^H \tilde{\mathbf{V}}^H(\theta_{nl}) \right] \right)^H \right], \quad (5.268)$$

$$J_F(\theta_{nl}, \theta_{lR}) = \frac{2}{\sigma_w^2} \Re \left[\left(\nabla_{\theta_{nl}} \left[\tilde{\theta}_l^H \tilde{\mathbf{V}}^H(\theta_{nl}) \right] \right) \tilde{\mathbf{V}}(\theta_{nl}) \right], \quad (5.269)$$

$$J_F(\theta_{nl}, \theta_{lI}) = -\frac{2}{\sigma_w^2} \Im \left[\left(\nabla_{\theta_{nl}} \left[\tilde{\theta}_l^H \tilde{\mathbf{V}}^H(\theta_{nl}) \right] \right) \tilde{\mathbf{V}}(\theta_{nl}) \right], \quad (5.270)$$

$$J_F(\theta_{nl}) = \frac{2}{\sigma_w^2} \Re \left[\left(\nabla_{\theta_{nl}} \left[\theta_l^H \tilde{\mathbf{V}}^H(\theta_{nl}) \right] \right) \left(\nabla_{\theta_{nl}} \left[\tilde{\theta}_l^H \tilde{\mathbf{V}}^H(\theta_{nl}) \right] \right)^H \right]. \quad (5.271)$$

We consider several examples to illustrate the results. In the first example, we estimate the complex amplitude and frequency of a single complex exponential observed in the presence of additive white Gaussian noise. This is an extension of the Example 4.29, where we estimated the frequency and phase of a single complex exponential. It is the dual of Example 4.30, where we estimated the complex amplitude and wavenumber in the array processing problem, but the approach is slightly different. It also provides an introduction to the model with D complex exponentials.

Example 5.11 (continuation of Examples 4.29, 5.4a, and 5.9a) Complex exponentials. We consider the model in Example 5.4a with $D = 1$ and $\tilde{\mathbf{w}} = \tilde{\mathbf{w}} \sim \mathcal{CN}(\mathbf{0}, \sigma_w^2 \mathbf{I})$. There is a single complex exponential signal in complex white Gaussian noise. The received vector is

$$\tilde{\mathbf{r}} = \tilde{\mathbf{v}}(\omega) \tilde{b} + \tilde{\mathbf{w}}. \quad (5.272)$$

Both the frequency and complex amplitude are unknown, so the parameter vector $\tilde{\boldsymbol{\theta}}$ is

$$\tilde{\boldsymbol{\theta}} = \begin{bmatrix} \tilde{\theta}_l \\ \theta_{nl} \end{bmatrix} = \begin{bmatrix} \tilde{b} \\ \omega \end{bmatrix}. \quad (5.273)$$

From (5.256) and (5.171), the ML estimate of \tilde{b} given ω is

$$\hat{\tilde{b}}_{\text{ml}}(\tilde{\mathbf{R}}, \omega) = \tilde{\mathbf{v}}^\dagger(\omega) \tilde{\mathbf{R}} = F(\omega; \tilde{\mathbf{R}}), \quad (5.274)$$

and from (5.257), the ML estimate of ω is

$$\hat{\omega}_{\text{ml}}(\tilde{\mathbf{R}}) = \underset{\omega}{\operatorname{argmax}} \left\{ \| \mathbf{P}_{\tilde{\mathbf{v}}(\omega)} \tilde{\mathbf{R}} \|^2 \right\}, \quad (5.275)$$

which may be simplified to

$$\hat{\omega}_{\text{ml}}(\tilde{\mathbf{R}}) = \underset{\omega}{\operatorname{argmax}} \left\{ |F(\omega; \tilde{\mathbf{R}})| \right\}. \quad (5.276)$$

After $\hat{\omega}_{\text{ml}}(\tilde{\mathbf{R}})$ is found, the ML estimate of \tilde{b} is given by

$$\hat{\tilde{b}}_{\text{ml}}(\tilde{\mathbf{R}}) = \tilde{\mathbf{v}}^\dagger(\hat{\omega}_{\text{ml}}(\tilde{\mathbf{R}})) \tilde{\mathbf{R}} = F(\hat{\omega}_{\text{ml}}(\tilde{\mathbf{R}}); \tilde{\mathbf{R}}). \quad (5.277)$$

We obtained the same estimates for the frequency and phase in Example 4.29, and the equivalent estimates for the wavenumber and complex amplitude in Example 4.30. In those examples, we found the Fisher information matrix in terms of the magnitude and phase of \tilde{b} . Here we find the FIM in terms of the real and imaginary components of \tilde{b} .

To find the Fisher information matrix, we define

$$\mathbf{b} \triangleq \begin{bmatrix} \Re(\tilde{b}) \\ \Im(\tilde{b}) \end{bmatrix} = \begin{bmatrix} b_R \\ b_I \end{bmatrix} \quad (5.278)$$

and

$$\boldsymbol{\theta} = \begin{bmatrix} \mathbf{b} \\ \omega \end{bmatrix}, \quad (5.279)$$

and write the FIM in partitioned form as

$$\mathbf{J}_F(\boldsymbol{\theta}) = \begin{bmatrix} \mathbf{J}_F(\mathbf{b}) & \mathbf{J}_F(\mathbf{b}, \omega) \\ \mathbf{J}_F(\omega, \mathbf{b}) & \mathbf{J}_F(\omega) \end{bmatrix}. \quad (5.280)$$

From (5.263)–(5.267) or (5.139)

$$\mathbf{J}_F(\mathbf{b}) = \frac{2}{\sigma_w^2} \begin{bmatrix} \Re[\tilde{\mathbf{v}}^H(\omega) \tilde{\mathbf{v}}(\omega)] & -\Im[\tilde{\mathbf{v}}^H(\omega) \tilde{\mathbf{v}}(\omega)] \\ \Im[\tilde{\mathbf{v}}^H(\omega) \tilde{\mathbf{v}}(\omega)] & \Re[\tilde{\mathbf{v}}^H(\omega) \tilde{\mathbf{v}}(\omega)] \end{bmatrix} = \frac{2N}{\sigma_w^2} \mathbf{I}. \quad (5.281)$$

To use (5.265)–(5.271), we need

$$\frac{\partial \tilde{\mathbf{v}}^H(\omega)}{\partial \omega} = -j \begin{bmatrix} 0 & e^{-j\omega} & 2e^{-j2\omega} & \cdots & (N-1)e^{-j(N-1)\omega} \end{bmatrix}. \quad (5.282)$$

Then,

$$\mathbf{J}_F(\omega) = \frac{2}{\sigma_{\tilde{w}}^2} \Re \left[|\tilde{b}|^2 \frac{\partial \tilde{\mathbf{v}}^H(\omega)}{\partial \omega} \left(\frac{\partial \tilde{\mathbf{v}}^H(\omega)}{\partial \omega} \right)^H \right] = \frac{2|\tilde{b}|^2}{\sigma_{\tilde{w}}^2} \frac{N(N-1)(2N-1)}{6} \quad (5.283)$$

and

$$\mathbf{J}_F(\mathbf{b}, \omega) = \frac{2}{\sigma_{\tilde{w}}^2} \begin{bmatrix} \Re \left[\tilde{b} \tilde{\mathbf{v}}^H(\omega) \left(\frac{\partial \tilde{\mathbf{v}}^H(\omega)}{\partial \omega} \right)^H \right] \\ -\Im \left[\tilde{b} \tilde{\mathbf{v}}^H(\omega) \left(\frac{\partial \tilde{\mathbf{v}}^H(\omega)}{\partial \omega} \right)^H \right] \end{bmatrix} = \frac{2}{\sigma_{\tilde{w}}^2} \frac{N(N-1)}{2} \begin{bmatrix} -b_I \\ b_R \end{bmatrix}. \quad (5.284)$$

The total FIM is

$$\mathbf{J}_F = \frac{2N}{\sigma_{\tilde{w}}^2} \begin{bmatrix} \mathbf{I} & \frac{N-1}{2} \begin{bmatrix} -b_I \\ b_R \end{bmatrix} \\ \frac{N-1}{2} \begin{bmatrix} -b_I & b_R \end{bmatrix} & |\tilde{b}|^2 \frac{(N-1)(2N-1)}{6} \end{bmatrix}. \quad (5.285)$$

The CRB for ω is found using the formula for the inverse of a partitioned matrix [Van02],

$$\begin{aligned} \text{CRB}(\omega) &= (\mathbf{J}_F(\omega) - \mathbf{J}_F(\omega, \mathbf{b}) \mathbf{J}_F(\mathbf{b})^{-1} \mathbf{J}_F(\mathbf{b}, \omega))^{-1} \\ &= \frac{\sigma_{\tilde{w}}^2}{|\tilde{b}|^2} \cdot \frac{6}{N(N^2-1)}. \end{aligned} \quad (5.286)$$

This is the same as in Example 4.29. When \tilde{b} is known, the CRB for ω is the inverse of $J_F(\omega)$. Not knowing the complex amplitude has increased the bound by about a factor of 4 for large N .

Similarly, the CRB for \mathbf{b} is

$$\begin{aligned} \text{CRB}(\mathbf{b}) &= (\mathbf{J}_F(\mathbf{b}) - \mathbf{J}_F(\mathbf{b}, \omega) \mathbf{J}_F(\omega)^{-1} \mathbf{J}_F(\omega, \mathbf{b}))^{-1} \\ &= \frac{\sigma_{\tilde{w}}^2}{2N} \left(\mathbf{I} + \frac{1}{|\tilde{b}|^2} \frac{3(N-1)}{(N+1)} \begin{bmatrix} b_I^2 & -b_R b_I \\ -b_R b_I & b_R^2 \end{bmatrix} \right) \end{aligned} \quad (5.287)$$

and the CRB for \tilde{b} is

$$\begin{aligned} \text{CRB}(\tilde{b}) &= [1 \quad j] \text{CRB}(\mathbf{b}) \begin{bmatrix} 1 \\ -j \end{bmatrix} \\ &= \frac{\sigma_{\tilde{w}}^2}{N} \cdot \frac{5N-1}{2N+2}. \end{aligned} \quad (5.288)$$

For the case of known frequency,

$$\text{CRB}(\tilde{b}) = \sigma_{\tilde{w}}^2 (\tilde{\mathbf{v}}^H(\omega) \tilde{\mathbf{v}}(\omega))^{-1} = \frac{\sigma_{\tilde{w}}^2}{N}, \quad (5.289)$$

so not knowing the frequency has increased the bound by a factor of about 2.5 for large N . ■

Example 5.12 (continuation of Examples 4.29, 5.4a, 5.9a, and 5.11) Complex exponentials. We consider the model for D complex exponentials in Example 5.4a with

$\tilde{\mathbf{n}} = \tilde{\mathbf{w}} \sim CN(\mathbf{0}, \sigma_{\tilde{w}}^2 \mathbf{I})$. The received vector is

$$\tilde{\mathbf{r}} = \sum_{i=1}^D \tilde{\mathbf{v}}(\omega_i) \tilde{b}_i + \tilde{\mathbf{w}} = \tilde{\mathbf{V}}(\boldsymbol{\omega}) \tilde{\mathbf{b}} + \tilde{\mathbf{w}}, \quad (5.290)$$

where

$$\boldsymbol{\omega} = [\omega_1 \quad \omega_2 \quad \cdots \quad \omega_D]^T = \boldsymbol{\theta}_{nl}, \quad (5.291)$$

$$\tilde{\mathbf{V}}(\boldsymbol{\omega}) = [\tilde{\mathbf{v}}(\omega_1) \quad \tilde{\mathbf{v}}(\omega_2) \quad \cdots \quad \tilde{\mathbf{v}}(\omega_D)], \quad (5.292)$$

and

$$\tilde{\mathbf{b}} = [\tilde{b}_1 \quad \tilde{b}_2 \quad \cdots \quad \tilde{b}_D]^T = \tilde{\boldsymbol{\beta}}_l. \quad (5.293)$$

We also define the $2D \times 1$ real vector

$$\mathbf{b} \triangleq \begin{bmatrix} \Re(\tilde{\mathbf{b}}) \\ \Im(\tilde{\mathbf{b}}) \end{bmatrix}. \quad (5.294)$$

From (5.256) and (5.257), the ML estimates are

$$\hat{\boldsymbol{\omega}}_{ml}(\tilde{\mathbf{R}}) = \underset{\boldsymbol{\omega}}{\operatorname{argmax}} \left\{ \|\mathbf{P}_{\tilde{\mathbf{V}}(\boldsymbol{\omega})} \tilde{\mathbf{R}}\|^2 \right\}, \quad (5.295)$$

$$\hat{\mathbf{b}}_{ml}(\tilde{\mathbf{R}}) = \tilde{\mathbf{V}}(\hat{\boldsymbol{\omega}}_{ml}(\tilde{\mathbf{R}}))^\dagger \tilde{\mathbf{R}}. \quad (5.296)$$

The blocks in the Fisher information matrix are

$$\mathbf{J}_F(\mathbf{b}) = \frac{2}{\sigma_{\tilde{w}}^2} \begin{bmatrix} \Re[\tilde{\mathbf{V}}(\boldsymbol{\omega})^H \tilde{\mathbf{V}}(\boldsymbol{\omega})] - \Im[\tilde{\mathbf{V}}(\boldsymbol{\omega})^H \tilde{\mathbf{V}}(\boldsymbol{\omega})] \\ \Im[\tilde{\mathbf{V}}(\boldsymbol{\omega})^H \tilde{\mathbf{V}}(\boldsymbol{\omega})] \quad \Re[\tilde{\mathbf{V}}(\boldsymbol{\omega})^H \tilde{\mathbf{V}}(\boldsymbol{\omega})] \end{bmatrix}, \quad (5.297)$$

$$\mathbf{J}_F(\mathbf{b}, \boldsymbol{\omega}) = \frac{2}{\sigma_{\tilde{w}}^2} \begin{bmatrix} \Re[\tilde{\mathbf{V}}(\boldsymbol{\omega})^H \tilde{\mathbf{D}}(\boldsymbol{\omega}) \tilde{\boldsymbol{\beta}}] \\ \Im[\tilde{\mathbf{V}}(\boldsymbol{\omega})^H \tilde{\mathbf{D}}(\boldsymbol{\omega}) \tilde{\boldsymbol{\beta}}] \end{bmatrix}, \quad (5.298)$$

$$\mathbf{J}_F(\boldsymbol{\omega}) = \frac{2}{\sigma_{\tilde{w}}^2} \Re \left[\tilde{\boldsymbol{\beta}}^H \tilde{\mathbf{D}}(\boldsymbol{\omega})^H \tilde{\mathbf{D}}(\boldsymbol{\omega}) \tilde{\boldsymbol{\beta}} \right], \quad (5.299)$$

where

$$\tilde{\mathbf{D}}(\boldsymbol{\omega}) \triangleq \begin{bmatrix} \frac{\partial \tilde{\mathbf{v}}(\omega_1)}{\partial \omega_1} & \frac{\partial \tilde{\mathbf{v}}(\omega_2)}{\partial \omega_2} & \cdots & \frac{\partial \tilde{\mathbf{v}}(\omega_D)}{\partial \omega_D} \end{bmatrix} \quad (5.300)$$

and

$$\tilde{\boldsymbol{\beta}} = \operatorname{diag}(\tilde{\mathbf{b}}) = \begin{bmatrix} \tilde{b}_1 & 0 & \cdots & 0 \\ 0 & \tilde{b}_2 & \cdots & 0 \\ \vdots & \vdots & \ddots & \vdots \\ 0 & 0 & \cdots & \tilde{b}_D \end{bmatrix}. \quad (5.301)$$

After some manipulations, we obtain

$$\operatorname{CRB}(\boldsymbol{\omega}) = \frac{\sigma_{\tilde{w}}^2}{2} \left\{ \Re \left[\tilde{\mathbf{H}} \odot \tilde{\mathbf{B}}^T \right] \right\}^{-1}, \quad (5.302)$$

where

$$\tilde{\mathbf{H}} \triangleq \tilde{\mathbf{D}}^H(\omega) \mathbf{P}_{\tilde{\mathbf{V}}(\omega)}^\perp \tilde{\mathbf{D}}(\omega), \quad (5.303)$$

$$\tilde{\mathbf{B}} \triangleq \tilde{\mathbf{b}} \tilde{\mathbf{b}}^H, \quad (5.304)$$

and

$$\text{CRB}(\tilde{\mathbf{b}}) = \sigma_{\tilde{w}}^2 \tilde{\mathbf{V}}^H(\omega) \tilde{\mathbf{V}}(\omega) + \tilde{\mathbf{V}}^\dagger(\omega) \tilde{\mathbf{D}}(\omega) [\text{CRB}(\omega) \odot \tilde{\mathbf{B}}] \tilde{\mathbf{D}}^H(\omega) (\tilde{\mathbf{V}}^\dagger(\omega))^H. \quad (5.305)$$

■

Example 5.13 (continuation of Examples 4.29, 5.4a, 5.9a, 5.11, and 5.12) Two complex exponentials. We consider the model in Example 5.12 with $D = 2$. Then

$$\boldsymbol{\omega} = \begin{bmatrix} \omega_1 \\ \omega_2 \end{bmatrix}, \quad (5.306)$$

$$\tilde{\mathbf{V}}(\boldsymbol{\omega}) = [\tilde{\mathbf{v}}(\omega_1) \ \tilde{\mathbf{v}}(\omega_2)], \quad (5.307)$$

$$\tilde{\mathbf{b}} = \begin{bmatrix} \tilde{b}_1 \\ \tilde{b}_2 \end{bmatrix} = \begin{bmatrix} b_1 e^{j\theta_1} \\ b_2 e^{j\theta_2} \end{bmatrix}. \quad (5.308)$$

From Example 5.9a, the ML estimate of $\tilde{\mathbf{b}}$ given $\boldsymbol{\omega}$ is

$$\hat{\mathbf{b}}_{\text{ml}}(\tilde{\mathbf{R}}, \boldsymbol{\omega}) = \tilde{\mathbf{V}}^\dagger(\boldsymbol{\omega}) \tilde{\mathbf{R}} = \frac{1}{(1 - B_c^2(\Delta\omega))} \begin{bmatrix} F(\omega_1; \tilde{\mathbf{R}}) - \tilde{\rho}_c(\Delta\omega) F(\omega_2; \tilde{\mathbf{R}}) \\ F(\omega_2; \tilde{\mathbf{R}}) - \tilde{\rho}_c^*(\Delta\omega) F(\omega_1; \tilde{\mathbf{R}}) \end{bmatrix}. \quad (5.309)$$

The ML estimate of $\boldsymbol{\omega}$ is found using (5.295), which may also be written as

$$\begin{aligned} \hat{\boldsymbol{\omega}}_{\text{ml}}(\tilde{\mathbf{R}}) &= \underset{\boldsymbol{\omega}}{\operatorname{argmax}} \left\{ \tilde{\mathbf{R}}^H \mathbf{P}_{\tilde{\mathbf{V}}(\boldsymbol{\omega})} \tilde{\mathbf{R}} \right\} \\ &= \underset{\boldsymbol{\omega}}{\operatorname{argmax}} \left\{ \tilde{\mathbf{R}}^H \tilde{\mathbf{V}}(\boldsymbol{\omega}) \tilde{\mathbf{V}}^\dagger(\boldsymbol{\omega}) \tilde{\mathbf{R}} \right\} \\ &= \underset{\boldsymbol{\omega}}{\operatorname{argmax}} \left\{ \frac{1}{(1 - B_c^2(\Delta\omega))} \begin{bmatrix} NF^*(\omega_1; \tilde{\mathbf{R}}) & NF^*(\omega_2; \tilde{\mathbf{R}}) \end{bmatrix} \begin{bmatrix} F(\omega_1; \tilde{\mathbf{R}}) - \tilde{\rho}_c(\Delta\omega) F(\omega_2; \tilde{\mathbf{R}}) \\ F(\omega_2; \tilde{\mathbf{R}}) - \tilde{\rho}_c^*(\Delta\omega) F(\omega_1; \tilde{\mathbf{R}}) \end{bmatrix} \right\} \\ &= \underset{\boldsymbol{\omega}}{\operatorname{argmax}} \left\{ \frac{N}{(1 - B_c^2(\Delta\omega))} \left[|F(\omega_1; \tilde{\mathbf{R}})|^2 + |F(\omega_2; \tilde{\mathbf{R}})|^2 - 2\Re \left\{ \rho_c^*(\Delta\omega) F^*(\omega_2; \tilde{\mathbf{R}}) F(\omega_1; \tilde{\mathbf{R}}) \right\} \right] \right\}. \end{aligned} \quad (5.310)$$

This is straightforward to implement using the DFT. A brute-force method would take the DFT on a fine grid, construct a 2D surface in ω_1, ω_2 using (5.310) and find the maximum. The ML estimate of $\tilde{\mathbf{b}}$ is then found by substituting $\hat{\boldsymbol{\omega}}_{\text{ml}}(\tilde{\mathbf{R}})$ into (5.309).

This technique is straightforward but computationally demanding to implement even for $D = 2$. It becomes very cumbersome for larger D . In Section 5.2.8, we discuss computational techniques for finding the solution.

The CRB for the $D = 2$ case may be evaluated using (5.302)–(5.305). We consider equal amplitude signals, so $b_1 = b_2 = b$. We examine the CRB for $\boldsymbol{\omega}$, which depends on the number of observations N , the SNR,

$$\text{SNR} = \frac{b^2}{\sigma_{\tilde{w}}^2}, \quad (5.311)$$

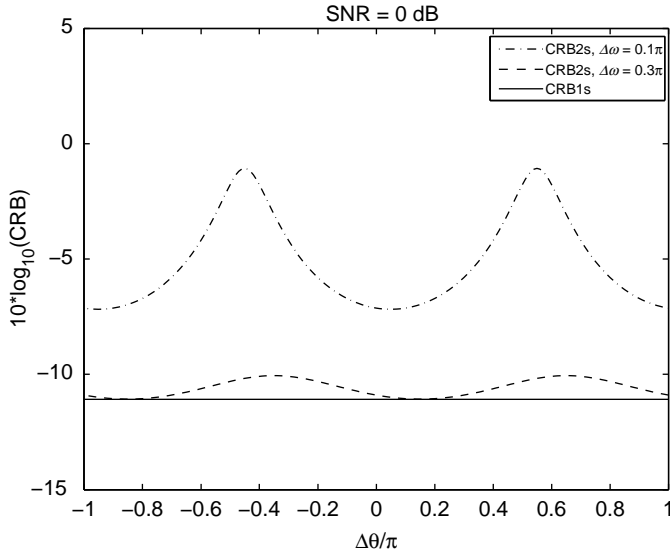


Figure 5.11: CRB(ω_i) versus $\Delta\theta$, SNR = 0 dB, $N = 10$.

the frequency separation

$$\Delta\omega = \omega_2 - \omega_1 \quad (5.312)$$

and the phase difference

$$\Delta\theta \triangleq \theta_2 - \theta_1. \quad (5.313)$$

In this case, the CRB for ω_1 and ω_2 are the same. In Figure 5.11, we show the CRB versus the phase difference $\Delta\theta$ for $N = 10$, SNR= 0 dB, and two frequency separations $\Delta\omega = 0.1\pi$ and $\Delta\omega = 0.3\pi$. We also plot the CRB for estimating a single frequency given in (5.286). It can be shown that the worst case (wc) phase difference occurs when

$$\Delta\theta_{\text{wc}} = \text{angle}(\tilde{H}_{12}) \pm \pi \quad (5.314)$$

where \tilde{H}_{12} is the upper right entry in the $\tilde{\mathbf{H}}$ matrix defined in (5.303). The phase of this component depends on the frequency separation $\Delta\omega$. The best case (bc) occurs when

$$\Delta\theta_{\text{bc}} = \text{angle}(\tilde{H}_{12}) \pm \frac{\pi}{2}. \quad (5.315)$$

This is apparent in Figure 5.11. The effect is more pronounced for smaller frequency separations.

In Figure 5.12, we show the CRB versus $\Delta\omega$ for $N = 10$, SNR= 0 dB, and the best-case and worst-case $\Delta\theta$ for each $\Delta\omega$. We see that for $\Delta\omega > 0.4\pi$, the two-signal CRB is practically the same as the one-signal CRB regardless of the phase. As the frequency separation decreases, the two-signal CRB becomes much larger than the single-signal case, indicating that it is harder to estimate the frequencies the closer they are. We also see that the phase separation has a bigger impact as $\Delta\omega$ decreases.

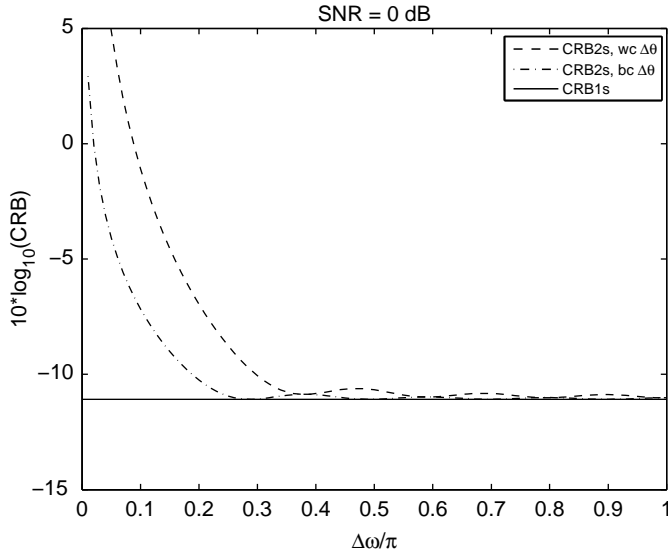


Figure 5.12: $\text{CRB}(\omega_i)$ versus $\Delta\omega$, $\text{SNR} = 0 \text{ dB}$, $N = 10$.

In Figure 5.13, we show the CRB versus SNR for $N = 10$, $\Delta\omega = 0.3\pi$, and the best and worst case $\Delta\theta$. The best case CRB is the same as the single source CRB for all SNR, while the worst-case CRB is about 1 dB larger for all SNR.

In Figure 5.14, we show estimation performance of the ML estimator for the worst-case $\Delta\theta$ versus SNR. Like the single-source case studied in Example 4.29, the ML estimator achieves the CRB for high SNR, but exhibits threshold behavior for low SNR. ■

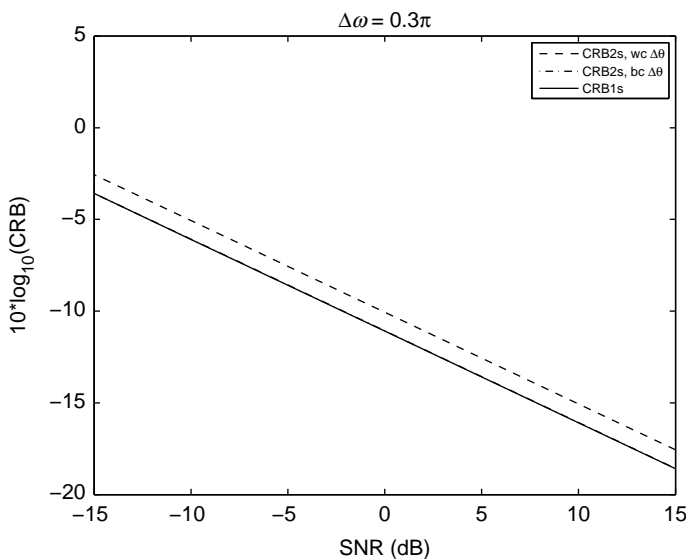


Figure 5.13: $\text{CRB}(\omega_i)$ versus SNR, $N = 10$, $\Delta\omega = 0.3\pi$.

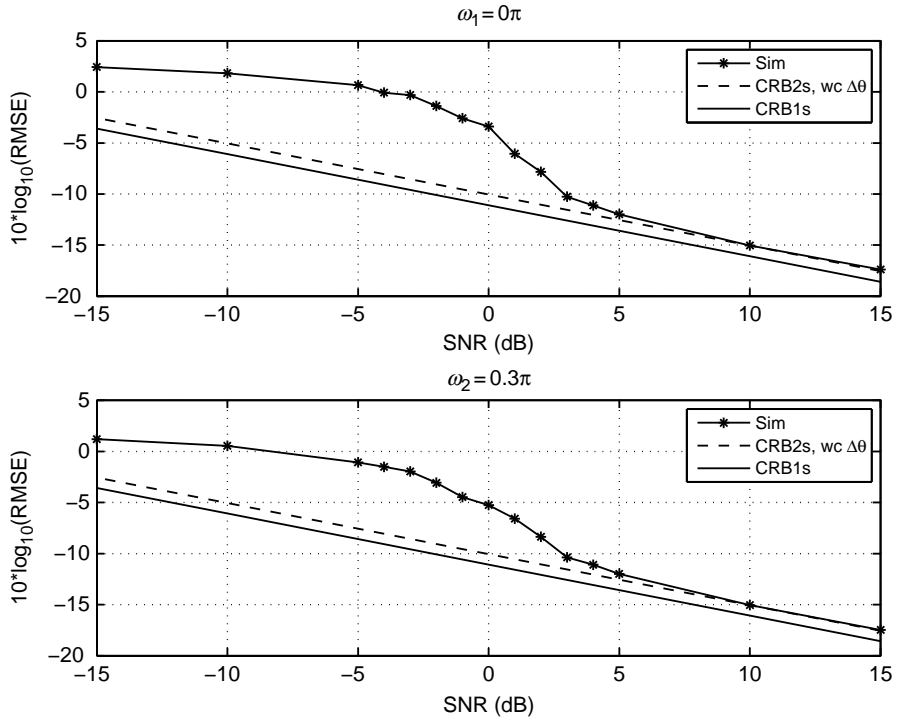


Figure 5.14: Frequency estimation RMSE versus SNR, $N = 10$, $\Delta\omega = 0.3\pi$, worst-case $\Delta\theta$.

5.2.6 Covariance Matrix Parameters

In this section, we study the models introduced in Examples 5.5–5.7 in which

$$\boldsymbol{\theta} = \boldsymbol{\theta}_c, \quad (5.316)$$

so that $\mathbf{m}(\boldsymbol{\theta}_m) = \mathbf{m}$ and is known. Without loss of generality we can let $\mathbf{m} = \mathbf{0}$. Then in the real observation, real $\boldsymbol{\theta}$ case,

$$l(\boldsymbol{\theta}; \mathbf{R}) = -\frac{1}{2} \ln |\mathbf{K}(\boldsymbol{\theta})| - \frac{1}{2} \mathbf{R}^T \mathbf{K}^{-1}(\boldsymbol{\theta}) \mathbf{R} + \zeta, \quad (5.317)$$

and in the complex observation, real $\boldsymbol{\theta}$, case,

$$l(\boldsymbol{\theta}; \widetilde{\mathbf{R}}) = -\ln |\widetilde{\mathbf{K}}(\boldsymbol{\theta})| - \widetilde{\mathbf{R}}^H \widetilde{\mathbf{K}}^{-1}(\boldsymbol{\theta}) \widetilde{\mathbf{R}} + \zeta. \quad (5.318)$$

Our approach is

1. Compute $\partial l(\boldsymbol{\theta}; \mathbf{R}) / \partial \theta_i$ and see if there is a solution to the likelihood equation for any of the θ_i .
2. If so, solve for $\hat{\theta}_i(\mathbf{R})$ and generate a compressed likelihood function. If not, solve (5.54).
3. Compute the Cramér–Rao bound.

From (5.57)–(5.58)

$$\frac{\partial l(\boldsymbol{\theta}; \mathbf{R})}{\partial \theta_i} = \frac{1}{2} \text{tr} \left[\mathbf{K}^{-1}(\boldsymbol{\theta}) \frac{\partial \mathbf{K}(\boldsymbol{\theta})}{\partial \theta_i} \right] - \frac{1}{2} \mathbf{R}^T \left[\mathbf{K}^{-1}(\boldsymbol{\theta}) \frac{\partial \mathbf{K}(\boldsymbol{\theta})}{\partial \theta_i} \mathbf{K}^{-1}(\boldsymbol{\theta}) \right] \mathbf{R}, \quad i = 1, 2, \dots, D, \quad (5.319)$$

and, from (5.76),

$$J_{F_{ij}}(\boldsymbol{\theta}) = \frac{1}{2} \text{tr} \left[\mathbf{K}^{-1}(\boldsymbol{\theta}) \frac{\partial \mathbf{K}(\boldsymbol{\theta})}{\partial \theta_i} \mathbf{K}^{-1}(\boldsymbol{\theta}) \frac{\partial \mathbf{K}(\boldsymbol{\theta})}{\partial \theta_j} \right], \quad i, j = 1, 2, \dots, D. \quad (5.320)$$

If there are K IID observations \mathbf{R}_k , $k = 1, \dots, K$, then (5.317), (5.319), and (5.320) become

$$l(\boldsymbol{\theta}; \mathbf{R}) = -\frac{K}{2} \ln |\mathbf{K}(\boldsymbol{\theta})| - \frac{1}{2} \sum_{k=1}^K \mathbf{R}_k^T \mathbf{K}^{-1}(\boldsymbol{\theta}) \mathbf{R}_k + \zeta, \quad (5.321)$$

$$\begin{aligned} \frac{\partial l(\boldsymbol{\theta}; \mathbf{R})}{\partial \theta_i} &= \frac{K}{2} \text{tr} \left[\mathbf{K}^{-1}(\boldsymbol{\theta}) \frac{\partial \mathbf{K}(\boldsymbol{\theta})}{\partial \theta_i} \right] - \frac{1}{2} \sum_{k=1}^K \mathbf{R}_k^T \left[\mathbf{K}^{-1}(\boldsymbol{\theta}) \frac{\partial \mathbf{K}(\boldsymbol{\theta})}{\partial \theta_i} \mathbf{K}^{-1}(\boldsymbol{\theta}) \right] \mathbf{R}_k, \\ i &= 1, 2, \dots, D, \end{aligned} \quad (5.322)$$

$$J_{F_{ij}}(\boldsymbol{\theta}) = \frac{K}{2} \text{tr} \left[\mathbf{K}^{-1}(\boldsymbol{\theta}) \frac{\partial \mathbf{K}(\boldsymbol{\theta})}{\partial \theta_i} \mathbf{K}^{-1}(\boldsymbol{\theta}) \frac{\partial \mathbf{K}(\boldsymbol{\theta})}{\partial \theta_j} \right]. \quad (5.323)$$

The complex versions follow in a similar manner.

We consider four models for $\mathbf{K}(\boldsymbol{\theta})$:

- (a) White noise
- (b) Colored noise
- (c) Rank one signal or interference plus white noise
- (d) Rank one signal or interference plus colored noise.

5.2.6.1 White Noise

We consider the model in Example 5.5w in which

$$\mathbf{K}(\boldsymbol{\theta}) = \sigma_w^2 \mathbf{I}, \quad (5.324)$$

$$\theta = \sigma_w^2. \quad (5.325)$$

We have already encountered this model in Example 4.46. From (4.784),

$$\frac{\partial l(\sigma_w^2; \mathbf{R})}{\partial \sigma_w^2} = -\frac{N}{2\sigma_w^2} + \frac{1}{2} \frac{\|\mathbf{R}\|^2}{(\sigma_w^2)^2}. \quad (5.326)$$

Setting (5.326) equal to zero gives

$$\hat{\sigma}_{w,\text{ml}}^2(\mathbf{R}) = \frac{\|\mathbf{R}\|^2}{N}. \quad (5.327)$$

From (5.320)

$$J_F(\sigma_w^2) = \frac{N}{2\sigma_w^4} \quad (5.328)$$

and the CRB is

$$\text{CRB}(\sigma_w^2) = \frac{2\sigma_w^4}{N}. \quad (5.329)$$

The estimate is unbiased and efficient.

5.2.6.2 Colored Noise

We next consider the more general model in Example 5.5 in which

$$\mathbf{K}(\theta) = \sigma_n^2 \mathbf{K}_n, \quad (5.330)$$

$$\theta = \sigma_n^2. \quad (5.331)$$

For this model, we have

$$\frac{\partial \mathbf{K}(\theta)}{\partial \theta} = \mathbf{K}_n, \quad (5.332)$$

$$\mathbf{K}^{-1}(\theta) = \frac{1}{\sigma_n^2} \mathbf{K}_n^{-1}. \quad (5.333)$$

Substituting (5.332)–(5.333) into (5.319) and setting the result equal to zero yields

$$\frac{N}{2\sigma_n^2} - \frac{\mathbf{R}^T \mathbf{K}_n^{-1} \mathbf{R}}{2(\sigma_n^2)^2} = 0, \quad (5.334)$$

so the ML estimate is

$$\hat{\sigma}_{n,\text{ml}}^2(\mathbf{R}) = \frac{\mathbf{R}^T \mathbf{K}_n^{-1} \mathbf{R}}{N}. \quad (5.335)$$

The Fisher information is

$$J_F(\sigma_n^2) = \frac{N}{2\sigma_n^4}. \quad (5.336)$$

Note that we could have obtained these results by whitening the data to obtain

$$\mathbf{R}_W = \mathbf{K}_n^{-\frac{1}{2}} \mathbf{R}, \quad (5.337)$$

which is $N(\mathbf{0}, \mathbf{K}_W(\theta))$, where

$$\begin{aligned} \mathbf{K}_W(\theta) &= \mathbf{K}_n^{-\frac{1}{2}} \mathbf{K}(\theta) \mathbf{K}_n^{-\frac{1}{2}} \\ &= \sigma_n^2 \mathbf{I}, \end{aligned} \quad (5.338)$$

and using (5.327) with \mathbf{R}_W replacing \mathbf{R} , that is,

$$\hat{\sigma}_{n,\text{ml}}^2(\mathbf{R}) = \frac{\|\mathbf{R}_W\|^2}{N} = \frac{\mathbf{R}^T \mathbf{K}_n^{-1} \mathbf{R}}{N}. \quad (5.339)$$

The Fisher information is obtained from (5.328) with σ_n^2 replacing σ_w^2 .

5.2.6.3 Rank One Signal Matrix Plus White Noise

In this section, we discuss the model in Example 5.6 with $D = 1$. The covariance matrix contains a rank one signal matrix plus white noise,⁷

$$\mathbf{K}(\boldsymbol{\theta}) = \sigma_s^2 \mathbf{v}_s \mathbf{v}_s^T + \sigma_w^2 \mathbf{I}, \quad (5.340)$$

$$\boldsymbol{\theta} = [\sigma_s^2 \ \sigma_w^2]^T. \quad (5.341)$$

We do an eigendecomposition of $\mathbf{K}(\boldsymbol{\theta})$. The eigenvector matrix is

$$\mathbf{u} = [\boldsymbol{\phi}_1 \ \boldsymbol{\phi}_2 \ \cdots \ \boldsymbol{\phi}_N]. \quad (5.342)$$

The first eigenvector is proportional to the signal vector \mathbf{v}_s ,

$$\boldsymbol{\phi}_1 = \frac{1}{\|\mathbf{v}_s\|} \mathbf{v}_s, \quad (5.343)$$

and the other eigenvectors are an arbitrary orthonormal set that spans an $N - 1$ dimensional noise subspace that is orthogonal to $\boldsymbol{\phi}_1$. We define

$$\mathbf{u}_1 \triangleq \boldsymbol{\phi}_1 \quad (5.344)$$

and

$$\mathbf{u}_{N-1} \triangleq [\boldsymbol{\phi}_2 \ \cdots \ \boldsymbol{\phi}_N], \quad (5.345)$$

so that

$$\mathbf{u} = [\mathbf{u}_1 \ \mathbf{u}_{N-1}]. \quad (5.346)$$

The projection matrices for the signal and noise subspaces are

$$\mathbf{P}_s = \mathbf{u}_1 \mathbf{u}_1^T = \boldsymbol{\phi}_1 \boldsymbol{\phi}_1^T, \quad (5.347)$$

$$\mathbf{P}_s^\perp = \mathbf{u}_{N-1} \mathbf{u}_{N-1}^T = \sum_{i=2}^N \boldsymbol{\phi}_i \boldsymbol{\phi}_i^T. \quad (5.348)$$

We can then write $\mathbf{K}(\boldsymbol{\theta})$ as

$$\begin{aligned} \mathbf{K}(\boldsymbol{\theta}) &= \lambda_s \boldsymbol{\phi}_1 \boldsymbol{\phi}_1^T + \sigma_w^2 \sum_{i=1}^N \boldsymbol{\phi}_i \boldsymbol{\phi}_i^T \\ &= (\lambda_s + \sigma_w^2) \boldsymbol{\phi}_1 \boldsymbol{\phi}_1^T + \sigma_w^2 \sum_{i=2}^N \boldsymbol{\phi}_i \boldsymbol{\phi}_i^T \\ &= \mathbf{u} (\Lambda_s + \sigma_w^2 \mathbf{I}) \mathbf{u}^T, \end{aligned} \quad (5.349)$$

where λ_s is the eigenvalue of the rank one signal matrix $\sigma_s^2 \mathbf{v}_s \mathbf{v}_s^T$ and is given by

$$\lambda_s = \sigma_s^2 \|\mathbf{v}_s\|^2, \quad (5.350)$$

⁷Our discussion follows pp. 260–266 of Scharf [Sch91].

and Λ_s is the $N \times N$ diagonal matrix

$$\Lambda_s = \text{diag} [\lambda_s \ 0 \ \dots \ 0]. \quad (5.351)$$

We will find it more convenient to find the ML estimates of σ_w^2 and λ_s . The ML estimate of σ_s^2 can then be obtained from ML estimate of λ_s using

$$\hat{\sigma}_{s,\text{ml}}^2(\mathbf{R}) = \frac{1}{\|\mathbf{v}_s\|^2} \hat{\lambda}_{s,\text{ml}}(\mathbf{R}). \quad (5.352)$$

We define a new parameter vector

$$\boldsymbol{\theta}' \triangleq [\lambda_s \ \sigma_w^2]^T. \quad (5.353)$$

In order to find the ML estimates, we need $\mathbf{K}^{-1}(\boldsymbol{\theta}')$, $\partial\mathbf{K}(\boldsymbol{\theta}')/\partial\lambda_s$, and $\partial\mathbf{K}(\boldsymbol{\theta}')/\partial\sigma_w^2$. From (3.175),

$$\mathbf{K}^{-1}(\boldsymbol{\theta}') = \mathbf{u} (\Lambda_s + \sigma_w^2 \mathbf{I})^{-1} \mathbf{u}^T = \frac{1}{(\lambda_s + \sigma_w^2)} \boldsymbol{\phi}_1 \boldsymbol{\phi}_1^T + \frac{1}{\sigma_w^2} \sum_{i=2}^N \boldsymbol{\phi}_i \boldsymbol{\phi}_i^T. \quad (5.354)$$

The partials with respect to λ_s and σ_w^2 are

$$\frac{\partial\mathbf{K}(\boldsymbol{\theta}')}{\partial\lambda_s} = \boldsymbol{\phi}_1 \boldsymbol{\phi}_1^T = \mathbf{P}_s \quad (5.355)$$

and

$$\frac{\partial\mathbf{K}(\boldsymbol{\theta}')}{\partial\sigma_w^2} = \mathbf{I}. \quad (5.356)$$

Substituting (5.354)–(5.356) into (5.319) and using the properties of the $\text{tr}\{\cdot\}$,⁸ we obtain two equations:

$$\frac{1}{\lambda_s + \sigma_w^2} - \frac{\mathbf{R}^T \mathbf{P}_s \mathbf{R}}{(\lambda_s + \sigma_w^2)^2} = 0 \quad (5.357)$$

and

$$\frac{1}{\lambda_s + \sigma_w^2} + \frac{N-1}{\sigma_w^2} - \frac{\mathbf{R}^T \mathbf{P}_s \mathbf{R}}{(\lambda_s + \sigma_w^2)^2} - \frac{\mathbf{R}^T \mathbf{P}_s^\perp \mathbf{R}}{(\sigma_w^2)^2} = 0. \quad (5.358)$$

Solving (5.357) gives

$$\lambda_s + \sigma_w^2 = \mathbf{R}^T \mathbf{P}_s \mathbf{R} = \|\mathbf{P}_s \mathbf{R}\|^2. \quad (5.359)$$

Substituting (5.359) into (5.358) gives

$$\frac{N-1}{\sigma_w^2} - \frac{\mathbf{R}^T \mathbf{P}_s^\perp \mathbf{R}}{(\sigma_w^2)^2} = 0 \quad (5.360)$$

⁸ $\text{tr}\{ABC\} = \text{tr}\{BCA\} = \text{tr}\{CAB\}$.

or

$$\hat{\sigma}_{w,\text{ml}}^2(\mathbf{R}) = \frac{1}{N-1} \mathbf{R}^T \mathbf{P}_s^\perp \mathbf{R} = \frac{\|\mathbf{P}_s^\perp \mathbf{R}\|^2}{N-1} \quad (5.361)$$

and

$$\hat{\lambda}_{s,\text{ml}}(\mathbf{R}) = \|\mathbf{P}_s \mathbf{R}\|^2 - \hat{\sigma}_{w,\text{ml}}^2(\mathbf{R}), \quad (5.362)$$

so

$$\hat{\sigma}_{s,\text{ml}}^2(\mathbf{R}) = \frac{1}{\|\mathbf{v}_s\|^2} \left(\|\mathbf{P}_s \mathbf{R}\|^2 - \hat{\sigma}_{w,\text{ml}}^2(\mathbf{R}) \right). \quad (5.363)$$

If there are K IID observations $\mathbf{R}_1, \dots, \mathbf{R}_K$, we follow the same steps using (5.321)–(5.323) to obtain

$$\hat{\sigma}_{w,\text{ml}}^2(\mathbf{R}) = \frac{1}{N-1} \cdot \frac{1}{K} \sum_{k=1}^K \|\mathbf{P}_s^\perp \mathbf{R}_k\|^2 = \frac{1}{N-1} \text{tr}\{\mathbf{P}_s^\perp \widehat{\mathbf{K}}(\mathbf{R})\}, \quad (5.364)$$

where

$$\widehat{\mathbf{K}}(\mathbf{R}) = \frac{1}{K} \sum_{k=1}^K \mathbf{R}_k \mathbf{R}_k^T \quad (5.365)$$

is the sample covariance matrix.

Thus, the ML estimator projects each \mathbf{R}_k onto the noise subspace, takes the magnitude squared, averages over the K observations, and divides by the dimension of the noise subspace ($N-1$). This is similar to the result in Example 4.46,⁹ except the estimate in Example 4.46 was divided by N rather than $N-1$.

Similarly,

$$\hat{\lambda}_{s,\text{ml}}(\mathbf{R}) = \frac{1}{K} \sum_{k=1}^K |\mathbf{P}_s \mathbf{R}_k|^2 - \hat{\sigma}_{w,\text{ml}}^2(\mathbf{R}) = \text{tr}\{\mathbf{P}_s \widehat{\mathbf{K}}(\mathbf{R})\} - \hat{\sigma}_{w,\text{ml}}^2(\mathbf{R}), \quad (5.366)$$

and

$$\hat{\sigma}_{s,\text{ml}}^2(\mathbf{R}) = \frac{1}{\|\mathbf{v}_s\|^2} \left(\text{tr}\{\mathbf{P}_s \widehat{\mathbf{K}}(\mathbf{R})\} - \hat{\sigma}_{w,\text{ml}}^2(\mathbf{R}) \right), \quad (5.367)$$

which have a similar interpretation. The ML estimate of σ_s^2 is the estimate of the power in the signal subspace.

Using the properties that

$$E\{\widehat{\mathbf{K}}(\mathbf{R})\} = \mathbf{K}(\boldsymbol{\theta}) \quad (5.368)$$

⁹Example 4.46 used a different model in which the signal on H_0 was modeled by the mean vector and the covariance matrix was white noise.

and

$$\text{tr}\{\mathbf{P}_s \mathbf{K}(\boldsymbol{\theta})\} = \lambda_s + \sigma_w^2, \quad (5.369)$$

$$\text{tr}\{\mathbf{P}_s^\perp \mathbf{K}(\boldsymbol{\theta})\} = (N - 1)\sigma_w^2, \quad (5.370)$$

we can show that the estimates are unbiased

$$E\{\hat{\sigma}_{w,\text{ml}}^2(\mathbf{R})\} = \frac{1}{N-1}(N-1)\sigma_w^2 = \sigma_w^2, \quad (5.371)$$

$$E\{\hat{\lambda}_{s,\text{ml}}(\mathbf{R})\} = \lambda_s + \sigma_w^2 - E\{\hat{\sigma}_{w,\text{ml}}^2(\mathbf{R})\} = \lambda_s, \quad (5.372)$$

$$E\{\hat{\sigma}_{s,\text{ml}}^2(\mathbf{R})\} = \frac{1}{\|\mathbf{v}_s\|^2} E\{\hat{\lambda}_{s,\text{ml}}(\mathbf{R})\} = \sigma_s^2. \quad (5.373)$$

The Fisher information matrix is given by (5.323). Using (5.354) and (5.355) in (5.323) gives

$$\begin{aligned} J(\lambda_s) &= \frac{K}{2} \text{tr} \left\{ \mathbf{u} (\Lambda_s + \sigma_w^2 \mathbf{I})^{-1} \mathbf{u}^T \boldsymbol{\phi}_1 \boldsymbol{\phi}_1^T \mathbf{u} (\Lambda_s + \sigma_w^2 \mathbf{I})^{-1} \mathbf{u}^T \boldsymbol{\phi}_1 \boldsymbol{\phi}_1^T \right\} \\ &= \frac{K}{2} (\lambda_s + \sigma_w^2)^{-2}. \end{aligned} \quad (5.374)$$

Similarly, using (5.354) and (5.356) in (5.323), we have

$$\begin{aligned} J(\sigma_w^2) &= \frac{K}{2} \text{tr} \left\{ \mathbf{u} (\Lambda_s + \sigma_w^2 \mathbf{I})^{-1} \mathbf{u}^T \mathbf{u} (\Lambda_s + \sigma_w^2 \mathbf{I})^{-1} \mathbf{u}^T \right\} \\ &= \frac{K}{2} \left\{ (\lambda_s + \sigma_w^2)^{-2} + (N-1)(\sigma_w^2)^{-2} \right\}. \end{aligned} \quad (5.375)$$

Finally, using (5.354), (5.355), and (5.356) in (5.323) yields

$$\begin{aligned} J(\lambda_s, \sigma_n^2) &= \frac{K}{2} \text{tr} \left\{ \mathbf{u} (\Lambda_s + \sigma_w^2 \mathbf{I})^{-1} \mathbf{u}^T \boldsymbol{\phi}_1 \boldsymbol{\phi}_1^T \mathbf{u} (\Lambda_s + \sigma_w^2 \mathbf{I})^{-1} \mathbf{u}^T \right\} \\ &= \frac{K}{2} (\lambda_s + \sigma_w^2)^{-2}. \end{aligned} \quad (5.376)$$

Putting these together, we have

$$\mathbf{J}_F(\boldsymbol{\theta}') = \frac{K}{2} \begin{bmatrix} (\lambda_s + \sigma_w^2)^{-2} & (\lambda_s + \sigma_w^2)^{-2} \\ (\lambda_s + \sigma_w^2)^{-2} & \{(\lambda_s + \sigma_w^2)^{-2} + (N-1)(\sigma_w^2)^{-2}\} \end{bmatrix}. \quad (5.377)$$

The inverse is

$$\mathbf{J}_F^{-1}(\boldsymbol{\theta}') = \frac{2}{K} \begin{bmatrix} \left\{ (\lambda_s + \sigma_w^2)^2 + \frac{\sigma_w^4}{N-1} \right\} & -\frac{\sigma_w^4}{N-1} \\ -\frac{\sigma_w^4}{N-1} & \frac{\sigma_w^4}{N-1} \end{bmatrix}. \quad (5.378)$$

The resulting CRBs are

$$\text{CRB}(\sigma_w^2) = \frac{2\sigma_w^4}{K(N-1)}, \quad (5.379)$$

$$\text{CRB}(\lambda_s) = \frac{2}{K} \left\{ (\lambda_s + \sigma_w^2)^2 + \frac{\sigma_w^4}{N-1} \right\}, \quad (5.380)$$

and from (5.350),

$$\text{CRB}(\sigma_s^2) = \frac{1}{\|\mathbf{v}_s\|^4} \frac{2}{K} \left\{ (\|\mathbf{v}_s\|^2 \sigma_s^2 + \sigma_w^2)^2 + \frac{\sigma_w^4}{N-1} \right\}. \quad (5.381)$$

For high SNR where $\sigma_s^2 \gg \sigma_w^2$, the CRB for σ_s^2 converges to

$$\text{CRB}(\sigma_s^2) \xrightarrow[\frac{\sigma_s^2}{\sigma_w^2} \rightarrow \infty]{} \frac{2\sigma_s^4}{K}. \quad (5.382)$$

For low SNR where $\sigma_s^2 \ll \sigma_w^2$, the CRB for σ_s^2 converges to

$$\text{CRB}(\sigma_s^2) \xrightarrow[\frac{\sigma_s^2}{\sigma_w^2} \rightarrow 0]{} \frac{2N\sigma_w^4}{K(N-1)\|\mathbf{v}_s\|^4}. \quad (5.383)$$

Thus, the noise level determines the estimation variance for low SNR.

All of these results carry over to the complex observation case with real parameters, except the factor of two in the Cramér–Rao bound is omitted.

We now consider an example to illustrate the behavior.

Example 5.14 (continuation of Example 5.6a) Complex exponentials. We consider the model in Example 5.6a with $D = 1$ complex exponential. The covariance matrix is

$$\tilde{\mathbf{K}}(\boldsymbol{\theta}) = \sigma_{\tilde{s}}^2 \tilde{\mathbf{v}}(\omega) \tilde{\mathbf{v}}(\omega)^H + \sigma_{\tilde{w}}^2 \mathbf{I}, \quad (5.384)$$

where ω is known, so the unknown parameter vector is

$$\boldsymbol{\theta} = [\sigma_{\tilde{s}}^2 \quad \sigma_{\tilde{w}}^2]^T. \quad (5.385)$$

The ML estimates are the complex equivalents of (5.361) and (5.363),

$$\hat{\sigma}_{\tilde{w},\text{ml}}^2(\tilde{\mathbf{R}}) = \frac{\|\mathbf{P}_{\tilde{\mathbf{v}}(\omega)}^\perp \tilde{\mathbf{R}}\|^2}{N-1}, \quad (5.386)$$

$$\hat{\sigma}_{\tilde{s},\text{ml}}^2(\tilde{\mathbf{R}}) = \frac{1}{N} \left(\|\mathbf{P}_{\tilde{\mathbf{v}}(\omega)} \tilde{\mathbf{R}}\|^2 - \hat{\sigma}_{\tilde{w},\text{ml}}^2(\tilde{\mathbf{R}}) \right). \quad (5.387)$$

The CRBs are given by (5.379) and (5.381), with $K = 1$ and the factor of two omitted for the complex case,

$$\text{CRB}(\sigma_{\tilde{w}}^2) = \frac{\sigma_{\tilde{w}}^4}{N-1}, \quad (5.388)$$

$$\text{CRB}(\sigma_{\tilde{s}}^2) = \frac{1}{N^2} \left\{ (N\sigma_{\tilde{s}}^2 + \sigma_{\tilde{w}}^2)^2 + \frac{\sigma_{\tilde{w}}^4}{N-1} \right\}. \quad (5.389)$$

■

5.2.6.4 Rank One Signal Matrix Plus Colored Noise

In this section, we generalize the model in the previous section to the case of colored noise. The covariance matrix is

$$\mathbf{K}(\boldsymbol{\theta}) = \sigma_s^2 \mathbf{v}_s \mathbf{v}_s^T + \sigma_n^2 \mathbf{K}_n. \quad (5.390)$$

The noise covariance matrix \mathbf{K}_n is known but the scale factor σ_n^2 is unknown. The parameter vector is

$$\boldsymbol{\theta} = [\sigma_s^2 \quad \sigma_n^2]^T. \quad (5.391)$$

We first whiten the data to obtain

$$\mathbf{R}_W = \mathbf{K}_n^{-\frac{1}{2}} \mathbf{R}. \quad (5.392)$$

Then

$$\begin{aligned} \mathbf{K}_W(\boldsymbol{\theta}) &= \sigma_s^2 \mathbf{K}_n^{-\frac{1}{2}} \mathbf{v}_s \mathbf{v}_s^T \mathbf{K}_n^{-\frac{1}{2}} + \sigma_n^2 \mathbf{I} \\ &= \sigma_s^2 \mathbf{v}_W \mathbf{v}_W^T + \sigma_n^2 \mathbf{I}, \end{aligned} \quad (5.393)$$

where

$$\mathbf{v}_W \triangleq \mathbf{K}_n^{-\frac{1}{2}} \mathbf{v}_s. \quad (5.394)$$

We now have the same model as in the previous section. All of the results apply, substituting \mathbf{R}_W for \mathbf{R} , \mathbf{v}_W for \mathbf{v}_s , and σ_n^2 for σ_w^2 .

5.2.7 Linear Gaussian Mean and Covariance Matrix Parameters

In this section, we discuss the model in which

$$\mathbf{m}(\boldsymbol{\theta}_m) = \mathbf{V}\boldsymbol{\theta}_m, \quad (5.395)$$

where \mathbf{V} is a known $N \times D$ matrix and $\boldsymbol{\theta}_m$ is a $D \times 1$ vector that we want to estimate. The covariance matrix $\mathbf{K}(\boldsymbol{\theta}_c)$ corresponds to one of the models in Section 5.2.6.

5.2.7.1 White Noise

We first consider the case where $\boldsymbol{\theta}_c = \sigma_w^2$ and

$$\mathbf{K}(\boldsymbol{\theta}_c) = \sigma_w^2 \mathbf{I}. \quad (5.396)$$

We have already solved this problem in Example 4.47. We repeat the results and compute the CRB.

The log-likelihood function is

$$l(\boldsymbol{\theta}_m, \sigma_w^2; \mathbf{R}) = -\frac{N}{2} \ln \sigma_w^2 - \frac{1}{2\sigma_w^2} [\mathbf{R} - \mathbf{V}\boldsymbol{\theta}_m]^T [\mathbf{R} - \mathbf{V}\boldsymbol{\theta}_m]. \quad (5.397)$$

We first consider $\boldsymbol{\theta}_m$. From (5.101) and (4.815),

$$\hat{\boldsymbol{\theta}}_{m,\text{ml}}(\mathbf{R}) = \mathbf{V}^\dagger \mathbf{R}. \quad (5.398)$$

This estimate is the same whether σ_w^2 is known or not. We now substitute $\hat{\theta}_{m,\text{ml}}(\mathbf{R})$ from (5.398) into (5.397) to create a compressed log-likelihood function. The result is

$$l(\sigma_w^2; \mathbf{R}) = l(\hat{\theta}_{m,\text{ml}}(\mathbf{R}), \sigma_w^2; \mathbf{R}) = -\frac{N}{2} \ln \sigma_w^2 - \frac{1}{2\sigma_w^2} \{[\mathbf{P}_V^\perp \mathbf{R}]^T [\mathbf{P}_V^\perp \mathbf{R}]\}. \quad (5.399)$$

We observe that (5.399) is identical to (5.317) if we replace \mathbf{R} in (5.317) with $\mathbf{P}_V^\perp \mathbf{R}$ and $\mathbf{K}(\boldsymbol{\theta})$ with $\sigma_w^2 \mathbf{I}$; thus, the results in Section 5.2.6.1 can be applied directly if we first project \mathbf{R} into a space that is orthogonal to \mathbf{V} . Thus, from (5.327), we have

$$\hat{\sigma}_{w,\text{ml}}^2(\mathbf{R}) = \frac{\|\mathbf{P}_V^\perp \mathbf{R}\|^2}{N}, \quad (5.400)$$

which is the result obtained in (4.817).

The Fisher information matrix has the block diagonal structure in (5.79),

$$\mathbf{J}_F(\boldsymbol{\theta}) = \begin{bmatrix} \mathbf{J}_F(\boldsymbol{\theta}_m) & \mathbf{0} \\ \mathbf{0} & J_F(\boldsymbol{\theta}_c) \end{bmatrix}, \quad (5.401)$$

with $\mathbf{J}_F(\boldsymbol{\theta}_m)$ computed from (5.75) and $J_F(\boldsymbol{\theta}_c)$ computed from (5.76). $\mathbf{J}_F(\boldsymbol{\theta}_m)$ was derived in Section 5.2.4.1, and is given by (5.103),

$$\mathbf{J}_F(\boldsymbol{\theta}_m) = \frac{1}{\sigma_w^2} \mathbf{V}^T \mathbf{V}. \quad (5.402)$$

$J_F(\boldsymbol{\theta}_c)$ was computed in Section 5.2.6.1 and is given by (5.328),

$$J_F(\boldsymbol{\theta}_c) = \frac{N}{2\sigma_w^4}. \quad (5.403)$$

Substituting (5.402) and (5.403) into (5.401), the FIM is

$$\mathbf{J}_F(\boldsymbol{\theta}) = \begin{bmatrix} \frac{1}{\sigma_w^2} \mathbf{V}^T \mathbf{V} & \mathbf{0} \\ \mathbf{0} & \frac{N}{2\sigma_w^4} \end{bmatrix}. \quad (5.404)$$

5.2.7.2 Colored Noise

We now consider the case where $\boldsymbol{\theta}_c = \sigma_n^2$ and

$$\mathbf{K}(\boldsymbol{\theta}_c) = \sigma_n^2 \mathbf{K}_n. \quad (5.405)$$

We first whiten the data using (5.392). Now $\mathbf{R}_W \sim N(\mathbf{V}_W \boldsymbol{\theta}, \sigma_n^2 \mathbf{I})$, where

$$\mathbf{V}_W \triangleq \mathbf{K}_n^{-\frac{1}{2}} \mathbf{V}. \quad (5.406)$$

Applying the results of Section 5.2.7.1, we have

$$\hat{\boldsymbol{\theta}}_{m,\text{ml}}(\mathbf{R}) = [\mathbf{V}_W^T \mathbf{V}_W]^{-1} \mathbf{V}_W^T \mathbf{R}_W = [\mathbf{V}^T \mathbf{K}_n^{-1} \mathbf{V}]^{-1} \mathbf{V}^T \mathbf{K}_n^{-1} \mathbf{R}, \quad (5.407)$$

which is familiar from (5.95). We note that this estimate does not require knowledge of σ_n^2 . The noise power estimate is

$$\hat{\sigma}_{n,\text{ml}}^2(\mathbf{R}) = \frac{\|\mathbf{P}_{\mathbf{V}_W}^\perp \mathbf{R}_W\|^2}{N}. \quad (5.408)$$

The Fisher information terms are given by (5.98) and (5.336),

$$\mathbf{J}_F(\boldsymbol{\theta}_m) = \frac{1}{\sigma_n^2} \mathbf{V}^T \mathbf{K}_n^{-1} \mathbf{V}, \quad (5.409)$$

$$J_F(\theta_c) = \frac{N}{2\sigma_n^4}. \quad (5.410)$$

5.2.7.3 General Covariance Matrix

In order to investigate the general case, we start with the log-likelihood function in (5.52) with $\mathbf{m}(\boldsymbol{\theta}) = \mathbf{V}\boldsymbol{\theta}_m$,

$$l(\boldsymbol{\theta}_m, \boldsymbol{\theta}_c; \mathbf{R}) = -\frac{1}{2} \ln |\mathbf{K}(\boldsymbol{\theta}_c)| - \frac{1}{2} \{ [\mathbf{R} - \mathbf{V}\boldsymbol{\theta}_m]^T \mathbf{K}^{-1}(\boldsymbol{\theta}_c) [\mathbf{R} - \mathbf{V}\boldsymbol{\theta}_m] \}. \quad (5.411)$$

We whiten with $\mathbf{K}(\boldsymbol{\theta}_c)$ and obtain

$$\hat{\boldsymbol{\theta}}_{m,\text{ml}}(\mathbf{R}, \boldsymbol{\theta}_c) = [\mathbf{V}^T \mathbf{K}^{-1}(\boldsymbol{\theta}_c) \mathbf{V}]^{-1} \mathbf{V}^T \mathbf{K}^{-1}(\boldsymbol{\theta}_c) \mathbf{R}. \quad (5.412)$$

Substituting this back into (5.411), the compressed log-likelihood function becomes

$$\begin{aligned} l(\boldsymbol{\theta}_c; \mathbf{R}) &= l(\hat{\boldsymbol{\theta}}_{m,\text{ml}}(\mathbf{R}, \boldsymbol{\theta}_c), \boldsymbol{\theta}_c; \mathbf{R}) \\ &= -\frac{1}{2} \ln |\mathbf{K}(\boldsymbol{\theta}_c)| - \frac{1}{2} \mathbf{R}^T \left\{ \mathbf{K}^{-1}(\boldsymbol{\theta}_c) - \mathbf{K}^{-1}(\boldsymbol{\theta}_c) \mathbf{V} [\mathbf{V}^T \mathbf{K}^{-1}(\boldsymbol{\theta}_c) \mathbf{V}]^{-1} \mathbf{V}^T \mathbf{K}^{-1}(\boldsymbol{\theta}_c) \right\} \mathbf{R}. \end{aligned} \quad (5.413)$$

This can then be minimized with respect to the parameter vector $\boldsymbol{\theta}_c$.

We consider other models in the problems.

5.2.8 Computational Algorithms

5.2.8.1 Introduction

In this section, we give a brief description of various computational algorithms that can be used to solve the minimization problem in (5.54) and the complex counterpart in (5.62),

$$\hat{\boldsymbol{\theta}}_{\text{ml}}(\tilde{\mathbf{R}}) = \underset{\boldsymbol{\theta}}{\operatorname{argmin}} \left\{ \ln |\tilde{\mathbf{K}}(\boldsymbol{\theta})| + [\tilde{\mathbf{R}} - \tilde{\mathbf{m}}(\boldsymbol{\theta})]^H \tilde{\mathbf{K}}^{-1}(\boldsymbol{\theta}) [\tilde{\mathbf{R}} - \tilde{\mathbf{m}}(\boldsymbol{\theta})] \right\}. \quad (5.414)$$

Some of our discussion will be applicable to the general model but most of results will emphasize the separable complex observation model in Section 5.2.5 where $\tilde{\mathbf{K}}$ is known and $\tilde{\mathbf{V}}(\boldsymbol{\theta}_{nl})$ is an $N \times D$ matrix of the form

$$\tilde{\mathbf{V}}(\boldsymbol{\theta}_{nl}) \triangleq [\tilde{\mathbf{v}}(\theta_{nl,1}) \quad \tilde{\mathbf{v}}(\theta_{nl,2}) \quad \cdots \quad \tilde{\mathbf{v}}(\theta_{nl,D})], \quad (5.415)$$

and we find a compressed log-likelihood function. To find the ML estimate of the (real) nonlinear parameter vector, we solve (5.257):

$$\hat{\theta}_{nl}(\tilde{\mathbf{R}}) = \underset{\theta_{nl}}{\operatorname{argmax}} \left\{ \|\mathbf{P}_{\tilde{\mathbf{V}}(\theta_{nl})}^{\perp} \tilde{\mathbf{R}}\|^2 \right\}, \quad (5.416)$$

or equivalently

$$\hat{\theta}_{nl}(\tilde{\mathbf{R}}) = \underset{\theta_{nl}}{\operatorname{argmin}} \left\{ \|\mathbf{P}_{\tilde{\mathbf{V}}(\theta_{nl})}^{\perp} \tilde{\mathbf{R}}\|^2 \right\}. \quad (5.417)$$

To simplify notation, we write the separable problem in (5.417) as

$$\hat{\theta} = \underset{\theta}{\operatorname{argmin}} \{f(\theta)\}, \quad (5.418)$$

where

$$f(\theta) = \|\mathbf{P}_{\tilde{\mathbf{V}}(\theta)}^{\perp} \tilde{\mathbf{R}}\|^2. \quad (5.419)$$

5.2.8.2 Gradient Techniques

In this section, we give a brief discussion of search techniques that can be used to solve the minimization problem,

$$\hat{\theta} = \underset{\theta}{\operatorname{argmin}} \{f(\theta)\}. \quad (5.420)$$

Most of the techniques that we discuss in this section originated in the nonlinear optimization area and are adapted to solve our estimation problems. The reader needs to explore some the optimization sources, such as Dennis and Schnabel [DS83], Gill et al. [GMW81], or Nash and Sofer [NS96] to get a comprehensive discussion. These sources have been utilized for ML estimation by Ottersten et al. [OVSN93] and several of our results are from that reference.

We utilize a search technique to find the value of θ that minimizes $f(\theta)$. The basic idea is to model $f(\theta)$ as a quadratic function in the vicinity of the minimum. We select a starting point $\hat{\theta}^{(0)}$. We then find a descent direction that will cause $f(\theta)$ to decrease and calculate a step size to determine how far to move in the descent direction. We discuss techniques for choosing $\hat{\theta}^{(0)}$ in Section 5.2.8.3.

At the first iteration,

$$\hat{\theta}^{(1)} = \hat{\theta}^{(0)} + \mathbf{a}_0 \left[\nabla_{\theta} f(\theta) \right] \Big|_{\theta=\hat{\theta}^{(0)}}. \quad (5.421)$$

In (5.421), $\hat{\theta}^{(0)}$ and $\hat{\theta}^{(1)}$ are $D \times 1$ vectors, $\nabla_{\theta} f(\theta)$ is the $D \times 1$ gradient vector,

$$\nabla_{\theta} f(\theta) = \mathbf{f}'(\theta) \triangleq \begin{bmatrix} \frac{\partial f(\theta)}{\partial \theta_1} & \frac{\partial f(\theta)}{\partial \theta_2} & \dots & \frac{\partial f(\theta)}{\partial \theta_D} \end{bmatrix}^T, \quad (5.422)$$

and \mathbf{a}_0 is a $D \times D$ matrix. The gradient vector will be equal to $\mathbf{0}$ at a stationary point and

$$\nabla_{\theta} f(\theta) = \mathbf{0} \quad (5.423)$$

is a necessary but not sufficient condition for a minimum. The matrix \mathbf{a}_0 determines both the descent direction and the step size. We will separate \mathbf{a}_0 into two terms in subsequent equations.

At the n th iteration,

$$\hat{\boldsymbol{\theta}}^{(n+1)} = \hat{\boldsymbol{\theta}}^{(n)} + \mathbf{a}_n \mathbf{f}'(\hat{\boldsymbol{\theta}}^{(n)}), \quad (5.424)$$

where $\mathbf{f}'(\hat{\boldsymbol{\theta}}^{(n)})$ is the gradient defined in (5.422), evaluated at $\boldsymbol{\theta} = \hat{\boldsymbol{\theta}}^{(n)}$.

We continue the iteration until we satisfy a stopping rule of the form,

$$|f(\hat{\boldsymbol{\theta}}^{(n+1)}) - f(\hat{\boldsymbol{\theta}}^{(n)})| < \delta_1, \quad (5.425)$$

or

$$\|\hat{\boldsymbol{\theta}}^{(n+1)} - \hat{\boldsymbol{\theta}}^{(n)}\| < \delta_2. \quad (5.426)$$

In the classical Newton method,

$$\mathbf{a}_n = -\left[\nabla_{\boldsymbol{\theta}}^2 f(\boldsymbol{\theta})\right]^{-1}_{\boldsymbol{\theta}=\hat{\boldsymbol{\theta}}^{(n)}}, \quad (5.427)$$

where $\nabla_{\boldsymbol{\theta}}^2 f(\boldsymbol{\theta})$ is the Hessian matrix

$$\left[\nabla_{\boldsymbol{\theta}}^2 f(\boldsymbol{\theta})\right]_{ij} \triangleq [\mathbf{H}(\boldsymbol{\theta})]_{ij} = \frac{\partial^2 f(\boldsymbol{\theta})}{\partial \theta_i \partial \theta_j}. \quad (5.428)$$

The classical Newton algorithm is then

$$\hat{\boldsymbol{\theta}}^{(n+1)} = \hat{\boldsymbol{\theta}}^{(n)} - \mathbf{H}^{-1}(\hat{\boldsymbol{\theta}}^{(n)}) \mathbf{f}'(\hat{\boldsymbol{\theta}}^{(n)}). \quad (5.429)$$

In order for $-\mathbf{H}^{-1}(\hat{\boldsymbol{\theta}}^{(n)}) \mathbf{f}'(\hat{\boldsymbol{\theta}}^{(n)})$ to be a descent direction, $\mathbf{H}(\hat{\boldsymbol{\theta}}^{(n)})$ must be positive definite. This may not be true if we are too far from the minimum, because $f(\boldsymbol{\theta})$ may not be quadratic. There are different techniques for modifying $\mathbf{H}(\hat{\boldsymbol{\theta}}^{(n)})$ to make it positive definite. One approach is to use diagonal loading,

$$\widehat{\mathbf{H}}(\hat{\boldsymbol{\theta}}^{(n)}) = \mathbf{H}(\hat{\boldsymbol{\theta}}^{(n)}) + \sigma_n^2 \mathbf{I}, \quad (5.430)$$

where σ_n^2 is chosen at each step to make $\widehat{\mathbf{H}}(\hat{\boldsymbol{\theta}}^{(n)})$ both positive definite and well conditioned. This technique is discussed in Chapter 5 of [DS96].

In practice, we want to adjust the step size, so we use a damped Newton algorithm (e.g., [GMW81, DS83, DS96]):

$$\hat{\boldsymbol{\theta}}^{(n+1)} = \hat{\boldsymbol{\theta}}^{(n)} - \mu_n \mathbf{H}^{-1}(\hat{\boldsymbol{\theta}}^{(n)}) \mathbf{f}'(\hat{\boldsymbol{\theta}}^{(n)}). \quad (5.431)$$

In order to choose the step length μ_n , we choose a $\mu < 1$ and let

$$\mu_n = \mu^{i_n}, \quad i_n \geq 0. \quad (5.432)$$

At each step in the iteration, we try successive values of i_n starting at $i_n = 0$ and use the smallest i_n that causes an adequate decrease in $f(\boldsymbol{\theta})$. For example, if $\mu = 0.5$, we would try

$$\mu_n = 1, \frac{1}{2}, \left(\frac{1}{2}\right)^2, \left(\frac{1}{2}\right)^3, \dots \quad (5.433)$$

until we obtain a satisfactory decrease in $f(\boldsymbol{\theta})$. Quadratic convergence is obtained if the step length converges to unity.

The advantage of the Newton algorithm is that one can show quadratic convergence. However, in order to implement the Newton method, we must compute a matrix of second derivatives and invert a $D \times D$ matrix. In most applications, we try to find a computationally simpler approximation to the Newton method that still converges at an adequate rate.

One approach is to replace the Hessian by an approximate Hessian that has the same form as the asymptotic form of the Hessian matrix. This approach is referred to in the statistical literature as the *scoring* method.

There are a number of other algorithms that attempt to retain some of the good properties of the Newton algorithm, but with a reduced computational cost. In this section, we present one of these algorithms that is effective for separable models.

The starting point for the methods in this section is the Newton algorithm. Once again, we choose an initial estimate $\hat{\boldsymbol{\theta}}^{(0)}$. The iteration is

$$\hat{\boldsymbol{\theta}}^{(n+1)} = \hat{\boldsymbol{\theta}}^{(n)} - \mu_n \mathbf{H}_G^{-1}(\hat{\boldsymbol{\theta}}^{(n)}) \mathbf{f}'(\hat{\boldsymbol{\theta}}^{(n)}). \quad (5.434)$$

We use a modified form of the Newton algorithm that is referred to as the *modified variable projection algorithm* (e.g. [Kau75, RW80, GP73]). The algorithm was applied to the array processing problem by Viberg et al. [VOK91], and our discussion follows that reference. We consider the separable estimation model. We write $f(\boldsymbol{\theta})$ as

$$\begin{aligned} f(\boldsymbol{\theta}) &= \|\mathbf{P}_{\tilde{\mathbf{V}}(\boldsymbol{\theta})}^\perp \tilde{\mathbf{R}}\|^2 \\ &= \|\tilde{\mathbf{x}}\|^2, \end{aligned} \quad (5.435)$$

where we define the vector $\tilde{\mathbf{x}}$ as

$$\tilde{\mathbf{x}} \triangleq \mathbf{P}_{\tilde{\mathbf{V}}(\boldsymbol{\theta})}^\perp \tilde{\mathbf{R}}. \quad (5.436)$$

The gradient of $f(\boldsymbol{\theta})$ with respect to θ_i is

$$\frac{\partial}{\partial \theta_i} f(\boldsymbol{\theta}) = 2\Re \left\{ \left(\frac{\partial \tilde{\mathbf{x}}}{\partial \theta_i} \right)^H \tilde{\mathbf{x}} \right\} = 2\Re \{ \tilde{\mathbf{x}}_i^H \tilde{\mathbf{x}} \}, \quad (5.437)$$

where

$$\tilde{\mathbf{x}}_i \triangleq \frac{\partial \tilde{\mathbf{x}}}{\partial \theta_i} = \frac{\partial}{\partial \theta_i} \mathbf{P}_{\tilde{\mathbf{V}}(\boldsymbol{\theta})}^\perp \tilde{\mathbf{R}}. \quad (5.438)$$

The derivative of the projection matrix is

$$\frac{\partial}{\partial \theta_i} \mathbf{P}_{\tilde{\mathbf{V}}(\boldsymbol{\theta})}^\perp = -\frac{\partial}{\partial \theta_i} \mathbf{P}_{\tilde{\mathbf{V}}(\boldsymbol{\theta})} = -\mathbf{P}_{\tilde{\mathbf{V}}(\boldsymbol{\theta})}^\perp \tilde{\mathbf{V}}_i(\boldsymbol{\theta}) \tilde{\mathbf{V}}_i^\dagger(\boldsymbol{\theta}) - \left(\mathbf{P}_{\tilde{\mathbf{V}}(\boldsymbol{\theta})}^\perp \tilde{\mathbf{V}}_i(\boldsymbol{\theta}) \tilde{\mathbf{V}}_i^\dagger(\boldsymbol{\theta}) \right)^H, \quad (5.439)$$

where

$$\tilde{\mathbf{V}}_i(\boldsymbol{\theta}) \triangleq \frac{\partial \tilde{\mathbf{V}}(\boldsymbol{\theta})}{\partial \theta_i} = \begin{bmatrix} \mathbf{0} & \mathbf{0} & \dots & \frac{\partial \tilde{\mathbf{v}}(\theta_i)}{\partial \theta_i} & \dots & \mathbf{0} \end{bmatrix}. \quad (5.440)$$

Using (5.438) and (5.439) in (5.437) gives

$$\mathbf{f}'(\boldsymbol{\theta}) = -2\Re \left\{ \text{diag} \left[\tilde{\mathbf{V}}^\dagger(\boldsymbol{\theta}) \tilde{\mathbf{R}} \tilde{\mathbf{R}}^H \mathbf{P}_{\tilde{\mathbf{V}}(\boldsymbol{\theta})}^\perp \tilde{\mathbf{D}}(\boldsymbol{\theta}) \right] \right\}, \quad (5.441)$$

where

$$\tilde{\mathbf{D}}(\boldsymbol{\theta}) \triangleq \begin{bmatrix} \frac{\partial \tilde{\mathbf{v}}(\theta_1)}{\partial \theta_1} & \frac{\partial \tilde{\mathbf{v}}(\theta_2)}{\partial \theta_2} & \dots & \frac{\partial \tilde{\mathbf{v}}(\theta_D)}{\partial \theta_D} \end{bmatrix}. \quad (5.442)$$

and $\text{diag}[\mathbf{A}]$ is a column vector containing the diagonal elements of \mathbf{A} .

The next step is to derive the Hessian, whose elements are

$$\frac{\partial^2}{\partial \theta_i \partial \theta_j} f(\boldsymbol{\theta}) = 2\Re \left\{ \tilde{\mathbf{x}}_i^H \tilde{\mathbf{x}}_j + \tilde{\mathbf{x}}_{ij}^H \tilde{\mathbf{x}}_j \right\}. \quad (5.443)$$

The Gaussian modification of the Newton method assumes that the second term in (5.443) is small and approximates the Hessian by

$$[\mathbf{H}_G(\boldsymbol{\theta})]_{ij} = 2\Re \left\{ \tilde{\mathbf{x}}_i^H \tilde{\mathbf{x}}_j \right\}. \quad (5.444)$$

Discarding the second derivative guarantees that (5.434) is a descent method because $\mathbf{H}_G(\boldsymbol{\theta})$ is nonnegative definite. The resulting algorithm is the variable projection algorithm of Golub and Pereyra [GP73]. Using (5.439) in (5.438) and observing that $\tilde{\mathbf{V}}^\dagger(\boldsymbol{\theta}) \mathbf{P}_{\tilde{\mathbf{V}}}^\perp(\boldsymbol{\theta}) = \mathbf{0}$, we obtain

$$\begin{aligned} \tilde{\mathbf{x}}_i^H \tilde{\mathbf{x}}_j &= \tilde{\mathbf{R}}^H \left[\left(\tilde{\mathbf{V}}^\dagger(\boldsymbol{\theta}) \right)^H \tilde{\mathbf{V}}_i(\boldsymbol{\theta})^H \mathbf{P}_{\tilde{\mathbf{V}}(\boldsymbol{\theta})}^\perp \tilde{\mathbf{V}}_j(\boldsymbol{\theta}) \tilde{\mathbf{V}}^\dagger(\boldsymbol{\theta}) \right. \\ &\quad \left. + \mathbf{P}_{\tilde{\mathbf{V}}(\boldsymbol{\theta})}^\perp \tilde{\mathbf{V}}_i(\boldsymbol{\theta}) \tilde{\mathbf{V}}^\dagger(\boldsymbol{\theta}) \left(\tilde{\mathbf{V}}^\dagger(\boldsymbol{\theta}) \right)^H \tilde{\mathbf{V}}_j(\boldsymbol{\theta})^H \mathbf{P}_{\tilde{\mathbf{V}}(\boldsymbol{\theta})}^\perp \right] \tilde{\mathbf{R}}. \end{aligned} \quad (5.445)$$

Kaufman [Kau75] modifies the Gauss–Newton algorithm by deleting the second term in (5.445). With this modification,

$$[\mathbf{H}_G(\boldsymbol{\theta})]_{ij} = 2\Re \left\{ \tilde{\mathbf{R}}^H \left(\tilde{\mathbf{V}}^\dagger(\boldsymbol{\theta}) \right)^H \tilde{\mathbf{V}}_i(\boldsymbol{\theta})^H \mathbf{P}_{\tilde{\mathbf{V}}(\boldsymbol{\theta})}^\perp \tilde{\mathbf{V}}_j(\boldsymbol{\theta}) \tilde{\mathbf{V}}^\dagger(\boldsymbol{\theta}) \tilde{\mathbf{R}} \right\}, \quad (5.446)$$

which can be expressed in matrix notation as,

$$\mathbf{H}_G(\boldsymbol{\theta}) = 2\Re \left\{ \left[\tilde{\mathbf{D}}(\boldsymbol{\theta})^H \mathbf{P}_{\tilde{\mathbf{V}}(\boldsymbol{\theta})}^\perp \tilde{\mathbf{D}}(\boldsymbol{\theta}) \right] \odot \left[\tilde{\mathbf{V}}^\dagger(\boldsymbol{\theta}) \tilde{\mathbf{R}} \tilde{\mathbf{R}}^H \left(\tilde{\mathbf{V}}^\dagger(\boldsymbol{\theta}) \right)^H \right]^T \right\}. \quad (5.447)$$

The iterative algorithm is defined by (5.434), (5.441), and (5.447).

In order to obtain convergence to a global minimum, we must initialize the algorithm appropriately. In Section 5.2.8.3, we develop the alternating projection algorithm that we use to initialize the modified Gauss–Newton algorithm. In [OVSN93], examples are given to show the effect of initialization accuracy.

In this section, we have provided a brief discussion of gradient techniques for solving ML estimation problems. The reader is referred to the various references, particularly [OVSN93] for further discussion.

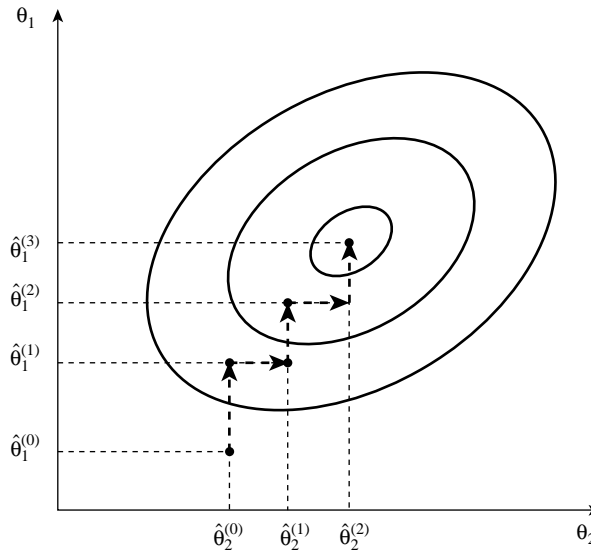


Figure 5.15: AP Algorithm: Successive iterations.

5.2.8.3 Alternating Projection Algorithm

In this section, we develop a technique that is sometimes referred to in the optimization literature as the relaxation method. The basic idea is straightforward. We have a function of D variables, $f(\theta)$. We want to find the value of θ that maximizes $f(\theta)$. We accomplish this by solving a sequence of one-dimensional maximization problems using an iterative technique in which, at each step of the iteration, we hold $D - 1$ parameter values constant and maximize over a single parameter.

The graphical behavior of the algorithm is shown in Figure 5.15. The algorithm moves to the peak in steps parallel to the axes. Since the value of $f(\theta)$ is maximized at each step, convergence to a local maximum is guaranteed. The initial condition is key to convergence to the global maximum.

From (5.416), the D -dimensional maximization problem is

$$\hat{\theta} = \operatorname{argmax}_{\theta} \left\{ \|\mathbf{P}_{\tilde{\mathbf{V}}(\theta)} \tilde{\mathbf{R}}\|^2 \right\}. \quad (5.448)$$

Ziskind and Wax [ZW88] developed the alternating projection (AP) algorithm to solve this problem. Our discussion follows [ZW88]. Holding $D - 1$ parameters fixed, the estimate of θ_i is obtained from

$$\hat{\theta}_i = \operatorname{argmax}_{\theta_i} \left\{ \|\mathbf{P}_{\tilde{\mathbf{V}}(\theta_{(i)})} \tilde{\mathbf{R}}\|^2 \right\}, \quad (5.449)$$

where the notation $\mathbf{P}_{\mathbf{B}, \mathbf{C}}$ denotes the projection matrix for the composite matrix $[\mathbf{B} \quad \mathbf{C}]$, and $\theta_{(i)}$ denotes the $(D - 1) \times 1$ vector obtained by removing the i th component of θ , that is,

$$\theta_{(i)} = [\theta_1 \quad \cdots \quad \theta_{i-1} \quad \theta_{i+1} \quad \cdots \quad \theta_D]^T. \quad (5.450)$$

Note that we have separated the space of the projection matrix into a $(D - 1)$ -dimensional fixed component and a one-dimensional component that is allowed to vary.

The algorithm maximizes the θ_i in order, starting at $i = 1$, using the current estimates of the remaining parameters for the components of $\hat{\theta}_{(i)}$ in (5.449). Thus, the value of θ_i at the $(n + 1)$ -th iteration is obtained by the following one-dimensional maximization problem,

$$\hat{\theta}_i^{(n+1)} = \underset{\theta_i}{\operatorname{argmax}} \left\{ \left\| \mathbf{P}_{\tilde{\mathbf{V}}(\hat{\theta}_{(i)}^{(n)})} \tilde{\mathbf{R}} \right\|^2 \right\}, \quad (5.451)$$

where

$$\hat{\theta}_{(i)}^{(n)} = [\hat{\theta}_1^{(n+1)} \quad \dots \quad \hat{\theta}_{i-1}^{(n+1)} \quad \hat{\theta}_{i+1}^{(n)} \quad \dots \quad \hat{\theta}_D^{(n)}]. \quad (5.452)$$

The estimates of θ_r for $r < i$ are the results of the $(n + 1)$ -th iteration and the estimates for $r > i$ are the results of the n th iteration.

The AP algorithm is based on a property of projection matrices referred to as the projection matrix update formula that simplifies the computation at each iteration.

Property. Let \mathbf{B} and \mathbf{C} be arbitrary matrices with the same number of rows (N) and define the composite matrix $[\mathbf{B} \ \mathbf{C}]$ and its projection matrix as

$$\mathbf{P}_{\mathbf{B}, \mathbf{C}} \triangleq \mathbf{P}_{[\mathbf{B} \ \mathbf{C}]} \quad (5.453)$$

If \mathbf{B} and \mathbf{C} were orthogonal, then

$$\mathbf{P}_{\mathbf{B}, \mathbf{C}} = \mathbf{P}_{\mathbf{B}} + \mathbf{P}_{\mathbf{C}}. \quad (5.454)$$

However, since they are not orthogonal, we define $\mathbf{C}[\mathbf{B}]$ to be the residual of the columns of \mathbf{C} , when \mathbf{C} is projected on \mathbf{B} ,

$$\mathbf{C}[\mathbf{B}] = [\mathbf{I} - \mathbf{P}_{\mathbf{B}}]\mathbf{C} = \mathbf{P}_{\mathbf{B}}^{\perp}\mathbf{C}. \quad (5.455)$$

Then, the projection matrix onto the column space of $[\mathbf{B} \ \mathbf{C}]$ is

$$\mathbf{P}_{\mathbf{B}, \mathbf{C}} = \mathbf{P}_{\mathbf{B}} + \mathbf{P}_{\mathbf{C}[\mathbf{B}]} \quad (5.456)$$

Now assume \mathbf{C} is an $N \times 1$ vector and define a normalized vector

$$\mathbf{c} \triangleq \frac{\mathbf{C}[\mathbf{B}]}{\|\mathbf{C}[\mathbf{B}]\|} = \frac{\mathbf{P}_{\mathbf{B}}^{\perp}\mathbf{C}}{\|\mathbf{P}_{\mathbf{B}}^{\perp}\mathbf{C}\|}. \quad (5.457)$$

Then

$$\mathbf{P}_{\mathbf{C}[\mathbf{B}]} = \mathbf{c}\mathbf{c}^H \quad (5.458)$$

and

$$\mathbf{P}_{\mathbf{B}, \mathbf{C}} = \mathbf{P}_{\mathbf{B}} + \mathbf{c}\mathbf{c}^H. \quad (5.459)$$

To utilize this result, we let

$$\mathbf{B} = \tilde{\mathbf{V}}(\hat{\theta}_{(i)}^{(n)}) \quad (5.460)$$

and

$$\mathbf{C} = \tilde{\mathbf{v}}(\theta_i). \quad (5.461)$$

Then,

$$\mathbf{c}\left(\theta_i, \hat{\boldsymbol{\theta}}_{(i)}^{(n)}\right) = \frac{\mathbf{P}_{\tilde{\mathbf{v}}(\hat{\boldsymbol{\theta}}_{(i)}^{(n)})}^{\perp} \tilde{\mathbf{v}}(\theta_i)}{\left\|\mathbf{P}_{\tilde{\mathbf{v}}(\hat{\boldsymbol{\theta}}_{(i)}^{(n)})}^{\perp} \tilde{\mathbf{v}}(\theta_i)\right\|} \quad (5.462)$$

and

$$\mathbf{P}_{\tilde{\mathbf{v}}(\theta_i)}[\tilde{\mathbf{v}}(\hat{\boldsymbol{\theta}}_{(i)}^{(n)})] = \mathbf{c}\left(\theta_i, \hat{\boldsymbol{\theta}}_{(i)}^{(n)}\right) \mathbf{c}^H\left(\theta_i, \hat{\boldsymbol{\theta}}_{(i)}^{(n)}\right). \quad (5.463)$$

From (5.456), we can write

$$\mathbf{P}_{\tilde{\mathbf{v}}(\hat{\boldsymbol{\theta}}_{(i)}^{(n)})}, \tilde{\mathbf{v}}(\theta_i) = \mathbf{P}_{\tilde{\mathbf{v}}(\hat{\boldsymbol{\theta}}_{(i)}^{(n)})} + \mathbf{P}_{\tilde{\mathbf{v}}(\theta_i)}[\tilde{\mathbf{v}}(\hat{\boldsymbol{\theta}}_{(i)}^{(n)})]. \quad (5.464)$$

Since the first term in (5.464) is not a function of θ_i , it can be dropped. Thus, (5.451) reduces to

$$\begin{aligned} \hat{\theta}_i^{(n+1)} &= \operatorname{argmax}_{\theta_i} \left\{ \left\| \mathbf{P}_{\tilde{\mathbf{v}}(\theta_i)}[\tilde{\mathbf{v}}(\hat{\boldsymbol{\theta}}_{(i)}^{(n)})] \tilde{\mathbf{R}} \right\|^2 \right\} \\ &= \operatorname{argmax}_{\theta_i} \left\{ \left| \mathbf{c}^H\left(\theta_i, \hat{\boldsymbol{\theta}}_{(i)}^{(n)}\right) \tilde{\mathbf{R}} \right|^2 \right\}. \end{aligned} \quad (5.465)$$

We continue the iteration across i and n until

$$\left| \hat{\theta}_i^{(n+1)} - \hat{\theta}_i^{(n)} \right| \leq \delta, \quad i = 1, 2, \dots, D, \quad (5.466)$$

where δ is a function of the desired accuracy.

Ziskind and Wax [ZW88] use the following initialization procedure. First solve the problem for a single source θ_1 . Thus,

$$\hat{\theta}_1^{(0)} = \operatorname{argmax}_{\theta_1} \left\{ \left\| \mathbf{P}_{\tilde{\mathbf{v}}(\theta_1)} \tilde{\mathbf{R}} \right\|^2 \right\}. \quad (5.467)$$

This is equivalent to assuming there is a single source. Then solve for the second source assuming the first source is at $\hat{\theta}_1^{(0)}$. Thus,

$$\hat{\theta}_2^{(0)} = \operatorname{argmax}_{\theta_2} \left\{ \left\| \mathbf{P}_{\tilde{\mathbf{v}}(\hat{\theta}_1^{(0)})}, \tilde{\mathbf{v}}(\theta_2) \tilde{\mathbf{R}} \right\|^2 \right\}. \quad (5.468)$$

We then find the third source assuming two sources at $\hat{\theta}_1^{(0)}$ and $\hat{\theta}_2^{(0)}$,

$$\hat{\theta}_3^{(0)} = \operatorname{argmax}_{\theta_3} \left\{ \left\| \mathbf{P}_{\tilde{\mathbf{v}}([\hat{\theta}_1^{(0)}, \hat{\theta}_2^{(0)}])}, \tilde{\mathbf{v}}(\theta_3) \tilde{\mathbf{R}} \right\|^2 \right\}. \quad (5.469)$$

We continue this procedure until we obtain the D initial estimated values, $\hat{\theta}_1^{(0)}, \hat{\theta}_2^{(0)}, \dots, \hat{\theta}_D^{(0)}$. At each step, we assume that all preceding initial values are known. With these initial values, we then carry out the optimization in (5.465).

The AP algorithm can be summarized:

- (i) Initialize the algorithm using the procedure in (5.467)–(5.469) to obtain $\hat{\theta}_1^{(0)}, \hat{\theta}_2^{(0)}, \dots, \hat{\theta}_D^{(0)}$.
- (ii) For $i = 1, 2, \dots, D$, and $n = 0$, use (5.465) to obtain $\hat{\theta}_1^{(1)}, \hat{\theta}_2^{(1)}, \dots, \hat{\theta}_D^{(1)}$.
- (iii) Iterate (5.465) for $n = 1, 2, \dots$
- (iv) Repeat until (5.466) is satisfied for all $i = 1, 2, \dots, D$.

The issues of interest with respect to the AP algorithm are:

- (i) What are the conditions on signal geometry, SNR_i , and N that will cause the initial conditions to be such that the AP algorithm converges to a global maximum?
- (ii) What is the rate of convergence?
- (iii) Is the rate of convergence improved by using the AP algorithm for the first several iterations and then switching to a gradient procedure?

We consider an example to illustrate the behavior of the AP algorithm.

Example 5.15 (continuation of Example 5.13) Two complex exponentials.

We develop the AP algorithm for the two complex exponentials model in Example 5.13. Suppose we want to estimate $\hat{\omega}_1^{(n+1)}$ at the $(n + 1)$ -th iteration. Then,

$$\hat{\theta}_{(1)}^{(n)} = \hat{\omega}_{(1)}^{(n)} = \hat{\omega}_2^{(n)}, \quad (5.470)$$

$$\mathbf{P}_{\tilde{\mathbf{v}}(\hat{\theta}_{(i)}^{(n)})} = \mathbf{P}_{\tilde{\mathbf{v}}(\hat{\omega}_2^{(n)})} = \frac{1}{N} \tilde{\mathbf{v}}(\hat{\omega}_2^{(n)}) \tilde{\mathbf{v}}^H(\hat{\omega}_2^{(n)}), \quad (5.471)$$

$$\begin{aligned} \tilde{\mathbf{v}}(\theta_i) \left[\tilde{\mathbf{V}} \left(\hat{\theta}_{(i)}^{(n)} \right) \right] &= \tilde{\mathbf{v}}(\hat{\omega}_1) \left[\tilde{\mathbf{v}}(\hat{\omega}_2^{(n)}) \right] \\ &= \mathbf{P}_{\tilde{\mathbf{v}}(\hat{\omega}_2^{(n)})}^\perp \tilde{\mathbf{v}}(\omega_1) \\ &= \left(\mathbf{I} - \frac{1}{N} \tilde{\mathbf{v}}(\hat{\omega}_2^{(n)}) \tilde{\mathbf{v}}^H(\hat{\omega}_2^{(n)}) \right) \tilde{\mathbf{v}}(\omega_1) \\ &= \tilde{\mathbf{v}}(\omega_1) - \tilde{\rho}_c^* \left(\hat{\omega}_2^{(n)} - \omega_1 \right) \tilde{\mathbf{v}}(\hat{\omega}_2^{(n)}), \end{aligned} \quad (5.472)$$

where $\tilde{\rho}_c(\Delta\omega)$ was defined in (5.172),

$$\begin{aligned} \left\| \tilde{\mathbf{v}}(\theta_i) \left[\tilde{\mathbf{V}} \left(\hat{\theta}_{(i)}^{(n)} \right) \right] \right\|^2 &= \tilde{\mathbf{v}}^H(\omega_1) \tilde{\mathbf{v}}(\omega_1) - \tilde{\rho}_c \left(\hat{\omega}_2^{(n)} - \omega_1 \right) \tilde{\mathbf{v}}^H(\hat{\omega}_2^{(n)}) \tilde{\mathbf{v}}(\omega_1) \\ &\quad - \tilde{\rho}_c^* \left(\hat{\omega}_2^{(n)} - \omega_1 \right) \tilde{\mathbf{v}}(\omega_1)^H \tilde{\mathbf{v}}(\hat{\omega}_2^{(n)}) + \left| \tilde{\rho}_c \left(\hat{\omega}_2^{(n)} - \omega_1 \right) \right|^2 \tilde{\mathbf{v}}^H(\hat{\omega}_2^{(n)}) \tilde{\mathbf{v}}(\hat{\omega}_2^{(n)}) \\ &= N \left(1 - \left| \tilde{\rho}_c \left(\hat{\omega}_2^{(n)} - \omega_1 \right) \right|^2 \right) \\ &= N \left(1 - B_c^2 \left(\hat{\omega}_2^{(n)} - \omega_1 \right) \right), \end{aligned} \quad (5.473)$$

$$\mathbf{c}\left(\theta_i, \hat{\theta}_{(i)}^{(n)}\right) = \mathbf{c}\left(\omega_1, \hat{\omega}_2^{(n)}\right) = \frac{\tilde{\mathbf{v}}(\omega_1) - \tilde{\rho}_c^* \left(\hat{\omega}_2^{(n)} - \omega_1\right) \tilde{\mathbf{v}}(\hat{\omega}_2^{(n)})}{\sqrt{N \left(1 - B_c^2 \left(\hat{\omega}_2^{(n)} - \omega_1\right)\right)}}. \quad (5.474)$$

Then, substituting (5.474) into (5.465), the estimate is

$$\hat{\omega}_1^{(n+1)} = \operatorname{argmax}_{\omega_1} \left\{ \frac{\left| \tilde{\mathbf{v}}^H(\omega_1) \tilde{\mathbf{R}} - \tilde{\rho}_c^* \left(\hat{\omega}_2^{(n)} - \omega_1\right) \tilde{\mathbf{v}}^H(\hat{\omega}_2^{(n)}) \tilde{\mathbf{R}} \right|^2}{N \left(1 - B_c^2 \left(\hat{\omega}_2^{(n)} - \omega_1\right)\right)} \right\}. \quad (5.475)$$

Using the definition of $F(\omega; \tilde{\mathbf{R}})$ in (5.171), we can write (5.475) as

$$\begin{aligned} \hat{\omega}_1^{(n+1)} = \operatorname{argmax}_{\omega_1} & \left\{ \frac{N}{\left(1 - B_c^2 \left(\hat{\omega}_2^{(n)} - \omega_1\right)\right)} \right. \\ & \left(\left| F(\omega_1; \tilde{\mathbf{R}}) \right|^2 - 2\Re \left[\tilde{\rho}_c^* \left(\hat{\omega}_2^{(n)} - \omega_1\right) F^*(\hat{\omega}_2^{(n)}; \tilde{\mathbf{R}}) F(\omega_1; \tilde{\mathbf{R}}) \right] \right. \\ & \left. \left. + B_c^2 \left(\hat{\omega}_2^{(n)} - \omega_1\right) \left| F(\hat{\omega}_2^{(n)}; \tilde{\mathbf{R}}) \right|^2 \right) \right\}. \end{aligned} \quad (5.476)$$

Note that if we add in the following term (which is not a function of ω_1)

$$\tilde{\mathbf{R}}^H \mathbf{P}_{\tilde{\mathbf{v}}(\hat{\omega}_2^{(n)})} \tilde{\mathbf{R}} = N \left| F(\hat{\omega}_2^{(n)}; \tilde{\mathbf{R}}) \right|^2 = \frac{N \left(1 - B_c^2 \left(\hat{\omega}_2^{(n)} - \omega_1\right)\right)}{\left(1 - B_c^2 \left(\hat{\omega}_2^{(n)} - \omega_1\right)\right)} \left| F(\hat{\omega}_2^{(n)}; \tilde{\mathbf{R}}) \right|^2, \quad (5.477)$$

then (5.476) becomes

$$\begin{aligned} \hat{\omega}_1^{(n+1)} = \operatorname{argmax}_{\omega_1} & \left\{ \frac{N}{\left(1 - B_c^2 \left(\hat{\omega}_2^{(n)} - \omega_1\right)\right)} \right. \\ & \left(\left| F(\omega_1; \tilde{\mathbf{R}}) \right|^2 - 2\Re \left[\tilde{\rho}_c^* \left(\hat{\omega}_2^{(n)} - \omega_1\right) F^*(\hat{\omega}_2^{(n)}; \tilde{\mathbf{R}}) F(\omega_1; \tilde{\mathbf{R}}) \right] + \left| F(\hat{\omega}_2^{(n)}; \tilde{\mathbf{R}}) \right|^2 \right) \right\}, \end{aligned} \quad (5.478)$$

which is (5.310) evaluated with $\omega_2 = \hat{\omega}_2^{(n)}$.

The AP algorithm is initialized with

$$\begin{aligned} \hat{\omega}_1^{(0)} &= \operatorname{argmax}_{\omega_1} \left\{ \left\| \mathbf{P}_{\tilde{\mathbf{v}}(\omega_1)} \tilde{\mathbf{R}} \right\|^2 \right\} \\ &= \operatorname{argmax}_{\omega_1} \left\{ N \left| F(\omega_1; \tilde{\mathbf{R}}) \right|^2 \right\}. \end{aligned} \quad (5.479)$$

Then $\hat{\omega}_2^{(0)}$ is obtained using (5.476) or (5.478), replacing ω_1 with ω_2 and, $\hat{\omega}_2^{(n)}$ with $\hat{\omega}_1^{(0)}$.

The algorithm is then iterated using (5.476) or (5.478) for ω_1 . For ω_2 , we use (5.476) or (5.478), replacing ω_1 with ω_2 and, $\hat{\omega}_2^{(n)}$ with $\hat{\omega}_1^{(n+1)}$.

In Figure 5.16, we show the estimates obtained from a typical iteration of the AP algorithm for the same scenario used in Example 5.13, Figure 5.14 with $\text{SNR}_1 = \text{SNR}_2 = 5\text{dB}$. In this example, it converged in four iterations to the value obtained by direct 2D maximization. ■

5.2.8.4 Expectation–Maximization Algorithm

In this section we develop the expectation–maximization (EM) algorithm and apply it to the separable model in Section 5.2.5. The basis for the name will become clear when the algorithm is developed.

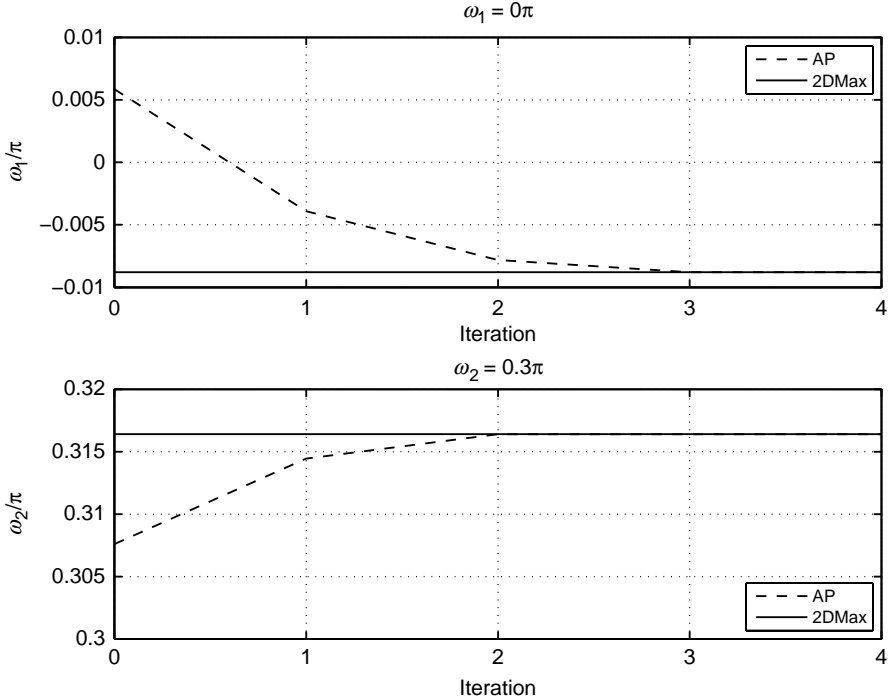


Figure 5.16: Convergence of the AP algorithm.

The original derivation of the EM algorithm is due to Dempster et al. [DLR77]. It has been applied to the array processing problem by Feder and Weinstein [FW88] and Miller and Fuhrmann [MF90]. A tutorial article by Moon [Moo96] discusses various other applications. Our discussion follows these references. We begin with a general discussion of the EM algorithm and then apply it to the problem of interest.

The basic idea of the EM algorithm is straightforward. We assume our observations are of the form

$$\tilde{\mathbf{r}} = \mathbf{V}(\boldsymbol{\theta}_{nl})\tilde{\boldsymbol{\theta}}_l + \tilde{\mathbf{w}}, \quad (5.480)$$

and want to find $\hat{\boldsymbol{\theta}}(\tilde{\mathbf{R}})$. Now suppose that, instead of $\tilde{\mathbf{r}}$, we could observe

$$\tilde{\mathbf{y}}_i = \tilde{\mathbf{v}}(\boldsymbol{\theta}_{nl,i})\tilde{\boldsymbol{\theta}}_{l,i} + \tilde{\mathbf{w}}_i, \quad i = 1, 2, \dots, D. \quad (5.481)$$

Then we would have set of D uncoupled one-dimensional maximization problems that are reasonably easy to solve. We refer to the transformation between $\tilde{\mathbf{r}}$ and the $\tilde{\mathbf{y}}_i$ as \mathbf{T} ,

$$\tilde{\mathbf{r}} = \mathbf{T}(\tilde{\mathbf{y}}_1, \tilde{\mathbf{y}}_2, \dots, \tilde{\mathbf{y}}_D), \quad (5.482)$$

and refer to the $\tilde{\mathbf{y}}_i; i = 1, 2, \dots, D$ as the “complete” or synthetic data and $\tilde{\mathbf{r}}$ as the “incomplete” or observed data. The EM algorithm is a technique for inferring the complete data from the incomplete data and using this inferred data to find the ML estimate of $\boldsymbol{\theta}$.

We denote the observed (“incomplete”) data by the vector $\tilde{\mathbf{r}}$ whose probability density $p_{\tilde{\mathbf{r}}}(\tilde{\mathbf{R}} : \boldsymbol{\theta})$ ¹⁰ depends on the vector parameter $\boldsymbol{\theta}$. We denote the complete data by the vector $\tilde{\mathbf{y}}$, which is related to $\tilde{\mathbf{r}}$ by the many-to-one (noninvertible) transformation $\mathbf{T}(\cdot)$

$$\tilde{\mathbf{r}} = \mathbf{T}(\tilde{\mathbf{y}}). \quad (5.483)$$

Note that the choice of $\tilde{\mathbf{y}}$ and therefore $\mathbf{T}(\cdot)$ is not unique, and one of the keys to successful application of the EM algorithm is an appropriate choice of $\tilde{\mathbf{y}}$ and $\mathbf{T}(\cdot)$.

We assume that the estimate of $\boldsymbol{\theta}$ at step n of the iteration is $\hat{\boldsymbol{\theta}}^{(n)}$. We denote the log-likelihood function of $\tilde{\mathbf{y}}$ as,

$$l(\boldsymbol{\theta}; \tilde{\mathbf{Y}}) \triangleq \ln p_{\tilde{\mathbf{y}}|\boldsymbol{\theta}}(\tilde{\mathbf{Y}}|\boldsymbol{\theta}) = \ln p_{\tilde{\mathbf{y}}}(\tilde{\mathbf{Y}} : \boldsymbol{\theta}). \quad (5.484)$$

If $\tilde{\mathbf{y}}$ were available, we would maximize $l(\boldsymbol{\theta}; \tilde{\mathbf{Y}})$. As only $\tilde{\mathbf{R}}$ is available, we find the expectation of $l(\boldsymbol{\theta}; \tilde{\mathbf{Y}})$, given that we have observed $\tilde{\mathbf{R}}$ and that our current parameter estimate is $\hat{\boldsymbol{\theta}}^{(n)}$.

We define the resulting expectation as $U(\boldsymbol{\theta}; \hat{\boldsymbol{\theta}}^{(n)})$:

$$U(\boldsymbol{\theta}; \hat{\boldsymbol{\theta}}^{(n)}) \triangleq E \left\{ \ln p_{\tilde{\mathbf{y}}}(\tilde{\mathbf{Y}} : \boldsymbol{\theta} | \tilde{\mathbf{R}}, \hat{\boldsymbol{\theta}}^{(n)}) \right\}. \quad (5.485)$$

This is the expectation step. Note that it is a conditional expectation with respect to $\tilde{\mathbf{R}}$ and $\hat{\boldsymbol{\theta}}^{(n)}$.

The next step is to maximize $U(\boldsymbol{\theta}; \hat{\boldsymbol{\theta}}^{(n)})$ with respect to $\boldsymbol{\theta}$. The resulting estimate is $\hat{\boldsymbol{\theta}}^{(n+1)}$. Thus,

$$\hat{\boldsymbol{\theta}}^{(n+1)} = \underset{\boldsymbol{\theta}}{\operatorname{argmax}} \left\{ U(\boldsymbol{\theta}; \hat{\boldsymbol{\theta}}^{(n)}) \right\}. \quad (5.486)$$

The steps in (5.485) and (5.486) define the EM algorithm.

The algorithm starts with an initial estimate $\hat{\boldsymbol{\theta}}^{(0)}$. The procedure described in (5.467)–(5.469) can be used to obtain this initial estimate. The iteration proceeds until

$$\left\| \hat{\boldsymbol{\theta}}^{(n+1)} - \hat{\boldsymbol{\theta}}^{(n)} \right\| < \delta. \quad (5.487)$$

The maximization step ensures that $U(\boldsymbol{\theta}; \hat{\boldsymbol{\theta}}^{(n)})$ increases on each iteration cycle. Wu [Wu83] shows that if $U(\boldsymbol{\theta}; \hat{\boldsymbol{\theta}}^{(n)})$ is continuous in both variables, then the algorithm converges to a stationary point.

We now apply the EM algorithm to solve for $\hat{\boldsymbol{\theta}}(\tilde{\mathbf{R}})$. From (5.480), the observation model is

$$\tilde{\mathbf{r}} = \tilde{\mathbf{V}}(\boldsymbol{\theta}_{nl})\tilde{\boldsymbol{\theta}}_l + \tilde{\mathbf{w}}, \quad (5.488)$$

¹⁰We use $p_{\tilde{\mathbf{r}}}(\tilde{\mathbf{R}} : \boldsymbol{\theta})$ instead of $p_{\tilde{\mathbf{r}}|\boldsymbol{\theta}}(\tilde{\mathbf{R}}|\boldsymbol{\theta})$ to minimize the use of double subscripts in the derivation.

where $\tilde{\mathbf{w}} \sim CN(\mathbf{0}, \sigma_w^2 \mathbf{I})$ and we assume the white noise level σ_w^2 is known. The unknown parameters are the $D \times 1$ vector θ_{nl} and the $D \times 1$ complex vector $\tilde{\theta}_l$. Thus,

$$\boldsymbol{\theta} = \begin{bmatrix} \boldsymbol{\theta}_{nl}^T & \tilde{\boldsymbol{\theta}}_l^T \end{bmatrix}^T. \quad (5.489)$$

The log-likelihood function is

$$l(\boldsymbol{\theta}; \tilde{\mathbf{R}}) = -\|\tilde{\mathbf{R}} - \tilde{\mathbf{V}}(\boldsymbol{\theta}_{nl})\tilde{\boldsymbol{\theta}}_l\|^2 \quad (5.490)$$

where we have discarded constant terms and scale factors. The incomplete data is $\tilde{\mathbf{r}}$. A logical choice for the complete data would be the observation of each component of $\tilde{\mathbf{V}}(\boldsymbol{\theta}_{nl})\tilde{\boldsymbol{\theta}}_l$ by itself in the presence of noise. Thus,

$$\tilde{\mathbf{y}}_i = \tilde{\mathbf{v}}(\boldsymbol{\theta}_{nl,i})\tilde{\boldsymbol{\theta}}_{l,i} + \tilde{\mathbf{w}}_i, \quad i = 1, 2, \dots, D, \quad (5.491)$$

where

$$E[\tilde{\mathbf{w}}_i \tilde{\mathbf{w}}_i^H] = \beta_i \sigma_w^2 \mathbf{I}, \quad (5.492)$$

and

$$\sum_{i=1}^D \beta_i = 1. \quad (5.493)$$

For simplicity, we will use

$$\beta_i = \frac{1}{D}. \quad (5.494)$$

Then, we can write $\tilde{\mathbf{r}}$ as

$$\tilde{\mathbf{r}} = \sum_{i=1}^D \tilde{\mathbf{y}}_i \triangleq \mathbf{T} \begin{bmatrix} \tilde{\mathbf{y}}_1 \\ \tilde{\mathbf{y}}_2 \\ \vdots \\ \tilde{\mathbf{y}}_D \end{bmatrix}. \quad (5.495)$$

We see that \mathbf{T} is a linear transformation so that $\tilde{\mathbf{r}}$ and $\tilde{\mathbf{y}}_i; i = 1, 2, \dots, D$ are jointly Gaussian.

Using (5.489) in (5.485), we can write

$$\begin{aligned} U\left(\boldsymbol{\theta}; \hat{\boldsymbol{\theta}}^{(n)}\right) &= U\left(\boldsymbol{\theta}_{nl}, \tilde{\boldsymbol{\theta}}_l; \hat{\boldsymbol{\theta}}_{nl}^{(n)}, \hat{\tilde{\boldsymbol{\theta}}}_l^{(n)}\right) \\ &= E\left\{\ln p_{\tilde{\mathbf{y}}}(\tilde{\mathbf{Y}} : \boldsymbol{\theta}_{nl}, \tilde{\boldsymbol{\theta}}_l | \tilde{\mathbf{R}}, \hat{\boldsymbol{\theta}}_{nl}^{(n)}, \hat{\tilde{\boldsymbol{\theta}}}_l^{(n)})\right\}. \end{aligned} \quad (5.496)$$

Neglecting constant terms, we can write the log-likelihood function as

$$l(\boldsymbol{\theta}_{nl}, \tilde{\boldsymbol{\theta}}_l; \tilde{\mathbf{Y}}) = -\sum_{i=1}^D \|\tilde{\mathbf{Y}}_i - \tilde{\mathbf{v}}(\boldsymbol{\theta}_{nl,i})\tilde{\boldsymbol{\theta}}_{l,i}\|^2. \quad (5.497)$$

Following [FW88] and [MF90], evaluating (5.496) reduces to finding the conditional mean,

$$\hat{\tilde{\mathbf{Y}}}^{(n)}_i \triangleq E\left\{\tilde{\mathbf{y}}_i | \tilde{\mathbf{R}}, \hat{\boldsymbol{\theta}}_{nl}^{(n)}, \hat{\tilde{\boldsymbol{\theta}}}_l^{(n)}\right\}. \quad (5.498)$$

Because $\tilde{\mathbf{y}}_i$ and $\tilde{\mathbf{r}}$ are jointly Gaussian, this is a classical estimation result (we will derive it in Section 5.3.2). We use Bayes rule to obtain $p_{\tilde{\mathbf{y}}|\tilde{\mathbf{r}}}(\cdot)$ from $p_{\tilde{\mathbf{r}}|\tilde{\mathbf{y}}}(\cdot)$ and find the mean by inspection,

$$\hat{\mathbf{Y}}_i^{(n)} - \tilde{\mathbf{v}}\left(\hat{\theta}_{nl,i}^{(n)}\right)\hat{\theta}_{l,i}^{(n)} = \frac{1}{D}\left[\tilde{\mathbf{R}} - \tilde{\mathbf{V}}\left(\hat{\theta}_{nl}^{(n)}\right)\hat{\theta}_l^{(n)}\right], \quad (5.499)$$

or

$$\hat{\mathbf{Y}}_i^{(n)} = \tilde{\mathbf{v}}\left(\hat{\theta}_{nl,i}^{(n)}\right)\hat{\theta}_{l,i}^{(n)} + \frac{1}{D}\left[\tilde{\mathbf{R}} - \tilde{\mathbf{V}}\left(\hat{\theta}_{nl}^{(n)}\right)\hat{\theta}_l^{(n)}\right]. \quad (5.500)$$

The conditional mean is the signal component from the n th iteration plus a portion ($1/D$) of the component of the current observation vector that is orthogonal to the estimated signal subspace. The result in (5.500) is the expectation step. We observe that the expectation result is also an estimation result, so the EM algorithm is sometimes referred to as the “estimation maximization” algorithm.

To define the maximization step, we recall from (5.256) and (5.257) that

$$\hat{\theta}_{nl} = \underset{\theta_{nl}}{\operatorname{argmax}} \left\{ \left\| \tilde{\mathbf{V}}(\theta_{nl}) [\tilde{\mathbf{V}}^H(\theta_{nl})\tilde{\mathbf{V}}(\theta_{nl})]^{-1} \tilde{\mathbf{V}}^H(\theta_{nl})\tilde{\mathbf{R}} \right\|^2 \right\} \quad (5.501)$$

and

$$\hat{\theta}_l = \tilde{\mathbf{V}}\left(\hat{\theta}_{nl}\right)^{\dagger} \tilde{\mathbf{R}}. \quad (5.502)$$

The corresponding one-dimensional relation for the complete data is

$$\hat{\theta}_{nl,i}^{(n+1)} = \underset{\theta_{nl,i}}{\operatorname{argmax}} \left\{ \frac{\left| \tilde{\mathbf{v}}^H(\theta_{nl,i})\hat{\mathbf{Y}}_i^{(n)} \right|^2}{\left\| \tilde{\mathbf{v}}(\theta_{nl,i}) \right\|^2} \right\}, \quad i = 1, 2, \dots, D, \quad (5.503)$$

and the one-dimensional version of (5.502) is

$$\hat{\theta}_{l,i}^{(n+1)} = \tilde{\mathbf{v}}\left(\hat{\theta}_{nl,i}^{(n+1)}\right)^{\dagger} \hat{\mathbf{Y}}_i^{(n)}, \quad i = 1, 2, \dots, D. \quad (5.504)$$

The EM algorithm is defined by (5.500), (5.503), and (5.504). This leads to the block diagram of the iteration process shown in Figure 5.17.¹¹ Note that all of the maximizations are done in parallel.

¹¹This figure is similar to Figure 1 in [FW88], but their model assumed a known signal rather than an unknown nonrandom signal.

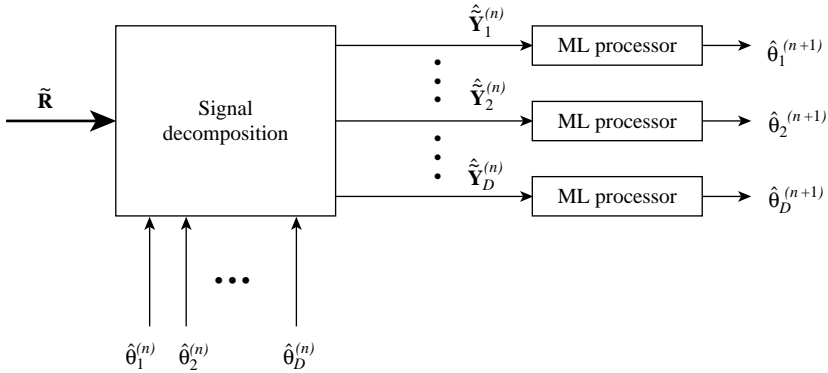


Figure 5.17: Implementation of EM algorithm.

Summarizing, the EM algorithm for the ML estimate is

- (i) Initialize the algorithm with $\hat{\theta}_{nl}^{(0)}$ (from (5.467)–(5.469)) and $\hat{\theta}_l^{(0)}$ from (5.502).
- (ii) Estimate $\hat{\mathbf{Y}}_i^{(n)}; i = 1, 2, \dots, D$, using (5.500).
- (iii) Maximize

$$\hat{\theta}_{nl,i}^{(n+1)} = \underset{\theta_{nl,i}}{\operatorname{argmax}} \left\{ \frac{\left| \tilde{\mathbf{v}}^H(\theta_{nl,i}) \hat{\mathbf{Y}}_i^{(n)} \right|^2}{\left\| \tilde{\mathbf{v}}(\theta_{nl,i}) \right\|^2} \right\}, \quad i = 1, 2, \dots, D. \quad (5.505)$$

- (iv) Compute

$$\hat{\theta}_{l,i}^{(n+1)} = \tilde{\mathbf{v}} \left(\hat{\theta}_{nl,i}^{(n+1)} \right)^{\dagger} \hat{\mathbf{Y}}_i^{(n)}, \quad i = 1, 2, \dots, D. \quad (5.506)$$

- (v) Iterate through steps (ii)–(iv) until

$$\left\| \hat{\theta}_{nl}^{(n+1)} - \hat{\theta}_{nl}^{(n)} \right\| \leq \delta. \quad (5.507)$$

The EM algorithm provides an alternative procedure to the AP algorithm for solving the ML problem. Fessler and Hero [FH94] develop a space-alternating generalized EM algorithm (SAGE), and demonstrate that it converges significantly faster than the conventional EM algorithm. The reader is referred to that reference for the details.

The SAGE algorithm for this problem differs from EM algorithm only in step (ii), and can be summarized as follows:

- (i) Initialize the algorithm with $\hat{\theta}_{nl}^{(0)}$ (from (5.467)–(5.469)) and $\hat{\theta}_l^{(0)}$ from (5.502).
- (ii) Estimate $\hat{\mathbf{Y}}_i^{(n)}; i = 1, 2, \dots, D$ using

$$\hat{\mathbf{Y}}_i^{(n)} = \tilde{\mathbf{v}} \left(\hat{\theta}_{nl,i}^{(n)} \right) \hat{\theta}_{l,i}^{(n)} + [\tilde{\mathbf{R}} - \tilde{\mathbf{V}} \left(\hat{\theta}_{nl}^{(n,i)} \right) \hat{\theta}_l^{(n,i)}], \quad (5.508)$$

where

$$\hat{\theta}_{nl}^{(n,i)} = \begin{bmatrix} \hat{\theta}_{nl,1}^{(n+1)} & \dots & \hat{\theta}_{nl,i-1}^{(n+1)} & \hat{\theta}_{nl,i}^{(n)} & \dots & \hat{\theta}_{nl,D}^{(n)} \end{bmatrix} \quad (5.509)$$

$$\hat{\theta}_l^{(n,i)} = \begin{bmatrix} \hat{\theta}_{l,1}^{(n+1)} & \dots & \hat{\theta}_{l,i-1}^{(n+1)} & \hat{\theta}_{l,i}^{(n)} & \dots & \hat{\theta}_{l,D}^{(n)} \end{bmatrix} \quad (5.510)$$

are the parameter vector estimates that contain the estimates of $\theta_{nl,r}$ and $\tilde{\theta}_{l,r}$ for $r < i$ from the current $(n + 1)$ -th iteration.

(iii) Maximize

$$\hat{\theta}_{nl,i}^{(n+1)} = \underset{\theta_{nl,i}}{\operatorname{argmax}} \left\{ \frac{\left| \tilde{\mathbf{v}}^H(\theta_{nl,i}) \tilde{\mathbf{Y}}_i^{(n)} \right|^2}{\left\| \tilde{\mathbf{v}}(\theta_{nl,i}) \right\|^2} \right\} \quad i = 1, 2, \dots, D. \quad (5.511)$$

(iv) Compute

$$\hat{\theta}_{l,i}^{(n+1)} = \frac{\tilde{\mathbf{v}}^H(\hat{\theta}_{nl,i}^{(n+1)}) \tilde{\mathbf{Y}}_i^{(n)}}{\left\| \tilde{\mathbf{v}}(\hat{\theta}_{nl,i}^{(n+1)}) \right\|^2} \quad i = 1, 2, \dots, D. \quad (5.512)$$

(v) Iterate through steps (ii)–(iv) until

$$\left\| \hat{\theta}_{nl}^{(n+1)} - \hat{\theta}_{nl}^{(n)} \right\| \leq \delta. \quad (5.513)$$

Example 5.16 (continuation of Examples 5.13 and 5.15) Two complex exponentials. We develop the EM and SAGE algorithms for the two complex exponentials model. We initialize both algorithms as in the AP algorithm using (5.479) to obtain $\hat{\omega}_1^{(0)}$, and (5.476) or (5.478), replacing ω_1 with ω_2 and $\hat{\omega}_2^{(n)}$ with $\hat{\omega}_1^{(0)}$, to obtain $\hat{\omega}_2^{(0)}$. Then, using (5.296)

$$\hat{\theta}_l^{(0)} = \hat{\mathbf{b}}^{(0)} = \tilde{\mathbf{V}}^\dagger(\hat{\omega}^{(0)}) \tilde{\mathbf{R}}. \quad (5.514)$$

For the EM algorithm, at the $(n + 1)$ -th iteration we compute

$$\tilde{\mathbf{W}}^{(n)} = \tilde{\mathbf{R}} - \tilde{\mathbf{V}}(\hat{\omega}^{(n)}) \hat{\mathbf{b}}^{(n)}, \quad (5.515)$$

$$\tilde{\mathbf{Y}}_1^{(n)} = \tilde{\mathbf{v}}(\hat{\omega}_1^{(n)}) \hat{b}_1^{(n)} + \frac{1}{2} \tilde{\mathbf{W}}^{(n)}, \quad (5.516)$$

$$\tilde{\mathbf{Y}}_2^{(n)} = \tilde{\mathbf{v}}(\hat{\omega}_2^{(n)}) \hat{b}_2^{(n)} + \frac{1}{2} \tilde{\mathbf{W}}^{(n)}, \quad (5.517)$$

$$\hat{\omega}_1^{(n+1)} = \underset{\omega_1}{\operatorname{argmax}} \left\{ N \left| F\left(\omega_1; \tilde{\mathbf{Y}}_1^{(n)}\right) \right|^2 \right\}, \quad (5.518)$$

$$\hat{\omega}_2^{(n+1)} = \underset{\omega_2}{\operatorname{argmax}} \left\{ N \left| F\left(\omega_2; \tilde{\mathbf{Y}}_2^{(n)}\right) \right|^2 \right\}, \quad (5.519)$$

$$\hat{b}_1^{(n+1)} = F\left(\hat{\omega}_1^{(n+1)}; \tilde{\mathbf{Y}}_1^{(n)}\right), \quad (5.520)$$

$$\hat{b}_2^{(n+1)} = F\left(\hat{\omega}_2^{(n+1)}; \tilde{\mathbf{Y}}_2^{(n)}\right). \quad (5.521)$$

For the SAGE algorithm, at the $(n + 1)$ -th iteration, we compute

$$\tilde{\mathbf{W}}_1^{(n)} = \tilde{\mathbf{R}} - \tilde{\mathbf{v}} \left(\hat{\omega}_1^{(n)} \right) \hat{b}_1^{(n)} - \tilde{\mathbf{v}} \left(\hat{\omega}_2^{(n)} \right) \hat{b}_2^{(n)}, \quad (5.522)$$

$$\tilde{\mathbf{Y}}_1^{(n)} = \tilde{\mathbf{v}} \left(\hat{\omega}_1^{(n)} \right) \hat{b}_1^{(n)} + \tilde{\mathbf{W}}_1^{(n)}, \quad (5.523)$$

$$\hat{\omega}_1^{(n+1)} = \operatorname{argmax}_{\omega_1} \left\{ N \left| F \left(\omega_1; \tilde{\mathbf{Y}}_1^{(n)} \right) \right|^2 \right\}, \quad (5.524)$$

$$\hat{b}_1^{(n+1)} = F \left(\hat{\omega}_1^{(n+1)}; \tilde{\mathbf{Y}}_1^{(n)} \right), \quad (5.525)$$

$$\tilde{\mathbf{W}}_2^{(n)} = \tilde{\mathbf{R}} - \tilde{\mathbf{v}} \left(\hat{\omega}_1^{(n+1)} \right) \hat{b}_1^{(n+1)} - \tilde{\mathbf{v}} \left(\hat{\omega}_2^{(n)} \right) \hat{b}_2^{(n)}, \quad (5.526)$$

$$\tilde{\mathbf{Y}}_2^{(n)} = \tilde{\mathbf{v}} \left(\hat{\omega}_2^{(n)} \right) \hat{b}_2^{(n)} + \tilde{\mathbf{W}}_2^{(n)}, \quad (5.527)$$

$$\hat{\omega}_2^{(n+1)} = \operatorname{argmax}_{\omega_2} \left\{ N \left| F \left(\omega_2; \tilde{\mathbf{Y}}_2^{(n)} \right) \right|^2 \right\}, \quad (5.528)$$

$$\hat{b}_2^{(n+1)} = F \left(\hat{\omega}_2^{(n+1)}; \tilde{\mathbf{Y}}_2^{(n)} \right). \quad (5.529)$$

In Figure 5.18, we show the estimates obtained from the same data as used in Example 5.15, Figure 5.16. The SAGE algorithm converged in five iterations while the EM algorithm took ten iterations to converge. We note that the EM algorithm has converged to a slightly different value than the other algorithms.

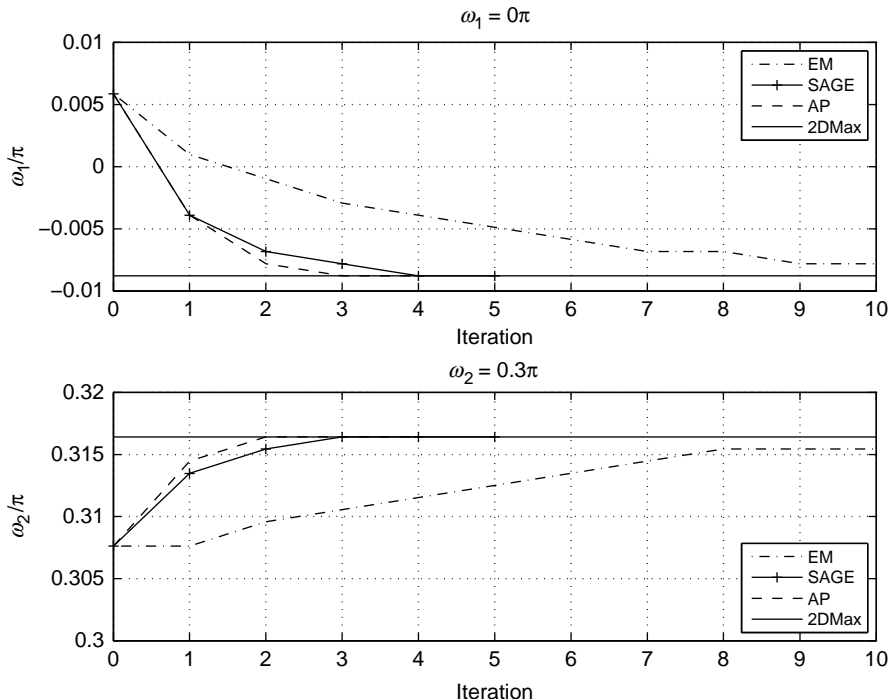


Figure 5.18: EM, SAGE, and AP algorithm convergence.

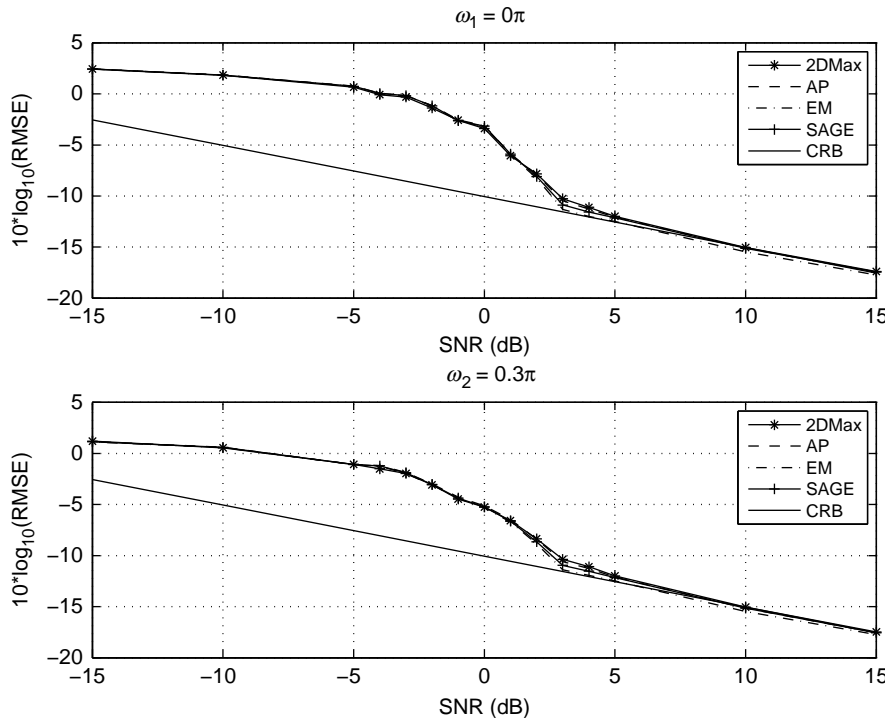


Figure 5.19: Frequency estimation RMSE versus SNR for 2D maximization using AP, EM, and SAGE algorithms, $N = 10$, $\Delta\omega = 0.3\pi$, worst-case $\Delta\theta$.

In Figure 5.19, we show the RMSE of the estimators obtained using the AP, EM, and SAGE algorithms as well as the 2D-maximization technique in Example 5.13 for the same data as in Figure 5.14. We see that they have nearly identical performance, as expected. ■

5.2.8.5 Summary

In this section, we have developed several techniques for solving the ML estimation problem. The most efficient approach in terms of both computation and speed of convergence appears to consist of the following steps:

- (i) Initialize the algorithm by using the procedure in (5.467)–(5.469).
- (ii) Use the iterative methods (either AP, EM, or SAGE, as appropriate) to get closer to the maximum.
- (iii) Use a search technique such as a quasi-Newton algorithm to achieve the final convergence to the estimate.

5.2.9 Equivalent Estimation Algorithms

In Section 5.2.2, we developed the maximum likelihood estimation algorithm and in Section 5.2.4 we considered the special case of the Fisher linear Gaussian estimation model. In this section, we study two other estimation algorithms and show their equivalence to the ML algorithm.

5.2.9.1 Least Squares

The method of least squares estimation was invented by Gauss in 1795 in his studies of the motion of heavenly bodies. The basic idea is straightforward. We have a set of vector observations

$$\mathbf{r}_k = \mathbf{m}_k(\boldsymbol{\theta}) + \mathbf{n}_k, \quad k = 1, 2, \dots, K, \quad (5.530)$$

where $\mathbf{m}_k(\boldsymbol{\theta})$ is an $N \times 1$ vector, which is a known function of a $D \times 1$ unknown parameter vector $\boldsymbol{\theta}$. The \mathbf{n}_k are $N \times 1$ noise vectors, which model the uncertainty in the observation. We make no assumptions about \mathbf{n}_k .

We define a cost function

$$f(\boldsymbol{\theta}; \mathbf{R}) = \sum_{k=1}^K [\mathbf{R}_k - \mathbf{m}_k(\boldsymbol{\theta})]^T [\mathbf{R}_k - \mathbf{m}_k(\boldsymbol{\theta})]. \quad (5.531)$$

The least squares estimator is defined to be

$$\hat{\boldsymbol{\theta}}_{\text{ls}}(\mathbf{R}) = \underset{\boldsymbol{\theta}}{\operatorname{argmin}} \{ f(\boldsymbol{\theta}; \mathbf{R}) \}. \quad (5.532)$$

We see that the $f(\boldsymbol{\theta}; \mathbf{R})$ we are minimizing is identical to the log-likelihood function if we model the \mathbf{n}_k as IID Gaussian $N(\mathbf{0}, \sigma_w^2 \mathbf{I})$. Thus,

$$\hat{\boldsymbol{\theta}}_{\text{ls}}(\mathbf{R}) = \hat{\boldsymbol{\theta}}_{\text{ml}}(\mathbf{R}), \quad (5.533)$$

so we can think of least squares estimation as a “closet ML algorithm.”

If

$$\mathbf{m}_k(\boldsymbol{\theta}) = \mathbf{V}_k \boldsymbol{\theta}, \quad (5.534)$$

we have a linear least squares problem.

If

$$\mathbf{m}_k(\boldsymbol{\theta}) = \mathbf{V}_k(\boldsymbol{\theta}_{nl}) \boldsymbol{\theta}_l, \quad (5.535)$$

we have a separable least squares problem.

If we believe that some of observations are more valuable than others, we can define a weighted cost function,

$$f(\boldsymbol{\theta}; \mathbf{R}) = \sum_{k=1}^K [\mathbf{R}_k - \mathbf{m}_k(\boldsymbol{\theta})]^T \mathbf{Q}_k [\mathbf{m}_k - \mathbf{s}_k(\boldsymbol{\theta})], \quad (5.536)$$

which is identical to the log-likelihood function if \mathbf{n}_k is modeled as IID Gaussian $N(\mathbf{0}, \mathbf{Q}_k^{-1})$.

In view of the identical structure, we will not discuss least squares further.

5.2.9.2 Minimum Variance Distortionless Response

We assume the data can be modeled with the linear model

$$\mathbf{r} = \mathbf{V}\boldsymbol{\theta} + \mathbf{n}, \quad (5.537)$$

where \mathbf{V} is the known $N \times D$ matrix

$$\mathbf{V} = [\mathbf{v}_1 \ \mathbf{v}_2 \ \cdots \ \mathbf{v}_D], \quad (5.538)$$

and $\boldsymbol{\theta}$ is the $D \times 1$ vector that we want to estimate. We assume that we know that the mean of \mathbf{n} is zero and that the covariance matrix is \mathbf{K} , but we do not assume that the noise is Gaussian.

We restrict our estimator to be a linear estimator,

$$\hat{\boldsymbol{\theta}}(\mathbf{R}) = \mathbf{H}^T \mathbf{R}, \quad (5.539)$$

where \mathbf{H} is an $N \times D$ matrix of the form

$$\mathbf{H} = [\mathbf{h}_1 \ \mathbf{h}_2 \ \cdots \ \mathbf{h}_D]. \quad (5.540)$$

We impose the constraint that, *in the absence of noise*, the estimate $\hat{\boldsymbol{\theta}}(\mathbf{R})$ must be equal to $\boldsymbol{\theta}$. We refer to this as the *distortionless response* (DR) constraint. Substituting (5.537) into (5.539), we have

$$\hat{\boldsymbol{\theta}}(\mathbf{R}) = \mathbf{H}^T \mathbf{V} \boldsymbol{\theta} + \mathbf{H}^T \mathbf{N}. \quad (5.541)$$

The DR constraint therefore requires that

$$\mathbf{H}^T \mathbf{V} = \mathbf{I}, \quad (5.542)$$

or, in terms of the column vectors

$$\mathbf{h}_i^T \mathbf{v}_j = \delta_{ij}, \quad i, j = 1, 2, \dots, D, \quad (5.543)$$

so we have a total of D^2 constraints. Assuming the DR constraints are satisfied, the estimate of $\theta_i; i = 1, 2, \dots, D$, can be written as

$$\hat{\theta}_i(\mathbf{R}) = \theta_i + \mathbf{h}_i^T \mathbf{N}, \quad (5.544)$$

and the variance of the estimation error is

$$\sigma_{\epsilon_i}^2 = E \{ \mathbf{h}_i^T \mathbf{n} \mathbf{n}^T \mathbf{h}_i \} = \mathbf{h}_i^T \mathbf{K} \mathbf{h}_i. \quad (5.545)$$

Subject to the constraints in (5.543), we choose the $\mathbf{h}_i; i = 1, 2, \dots, D$ to minimize the variance $\sigma_{\epsilon_i}^2; i = 1, 2, \dots, D$, thus our optimization criterion is minimum variance distortionless response (MVDR).

We use Lagrange multipliers. The function to be minimized is

$$f_i = \mathbf{h}_i^T \mathbf{K} \mathbf{h}_i + \sum_{j=1}^D \lambda_{ij} (\mathbf{h}_i^T \mathbf{v}_j - \delta_{ij}), \quad i = 1, 2, \dots, D. \quad (5.546)$$

Taking the gradient with respect to \mathbf{h}_i and gives

$$\nabla_{\mathbf{h}_i} f_i = 2 \mathbf{K} \mathbf{h}_i + \sum_{j=1}^D \lambda_{ij} \mathbf{v}_j. \quad (5.547)$$

Defining $\boldsymbol{\lambda}_i = [\lambda_{i1} \ \lambda_{i2} \ \cdots \ \lambda_{iD}]^T$ and setting (5.547) equal to zero gives

$$\mathbf{h}_i = -\frac{1}{2} \mathbf{K}^{-1} \mathbf{V} \boldsymbol{\lambda}_i. \quad (5.548)$$

To find the λ_i vector, we use the constraints in (5.543), which can be rewritten as

$$\mathbf{V}^T \mathbf{h}_i = \mathbf{e}_i, \quad (5.549)$$

where \mathbf{e}_i is the unit vector with a one in the i th position and zeros elsewhere. Using (5.548) in (5.549) gives

$$\mathbf{V}^T \mathbf{h}_i = \mathbf{V}^T \left[-\frac{1}{2} \mathbf{K}^{-1} \mathbf{V} \right] \lambda_i = \mathbf{e}_i \quad (5.550)$$

or

$$-\frac{1}{2} \lambda_i = [\mathbf{V}^T \mathbf{K}^{-1} \mathbf{V}]^{-1} \mathbf{e}_i. \quad (5.551)$$

Using (5.551) in (5.548) gives

$$\mathbf{h}_i = \mathbf{K}^{-1} \mathbf{V} [\mathbf{V}^T \mathbf{K}^{-1} \mathbf{V}]^{-1} \mathbf{e}_i. \quad (5.552)$$

The operation $\mathbf{A}\mathbf{e}_i$ selects the i th column of the matrix \mathbf{A} , therefore

$$\mathbf{H} = \mathbf{K}^{-1} \mathbf{V} [\mathbf{V}^T \mathbf{K}^{-1} \mathbf{V}]^{-1} \quad (5.553)$$

and

$$\hat{\theta}_{\text{mvdr}}(\mathbf{R}) = [\mathbf{V}^T \mathbf{K}^{-1} \mathbf{V}]^{-1} \mathbf{V}^T \mathbf{K}^{-1} \mathbf{R}, \quad (5.554)$$

which is identical to the maximum likelihood estimate $\hat{\theta}_{\text{ml}}(\mathbf{R})$ in (5.95).

Before leaving the linear estimator in (5.541), we consider a different criterion. We require that the estimator be unbiased, that is,

$$E \left\{ \hat{\theta}(\mathbf{R}) \right\} = \theta. \quad (5.555)$$

Taking the expectation of both sides of (5.541) we have

$$E \left\{ \hat{\theta}(\mathbf{R}) \right\} = \mathbf{H}^T \mathbf{V} \theta, \quad (5.556)$$

which requires

$$\mathbf{H}^T \mathbf{V} = \mathbf{I}. \quad (5.557)$$

This is identical to the distortionless response criterion. Subject to the constraint in (5.557), we minimize the error variances. This is the same problem as MVDR. Linear estimators based on this criterion are referred to as minimum variance unbiased estimators (MVUB) or best linear unbiased estimators (BLUE) in the literature.

Note that MVDR does not assume a Gaussian model.

5.2.9.3 Summary

In this section, we have discussed two different types of estimators and shown their equivalence to maximum likelihood. The most widely used is the method of least squares, which has a long history. It minimizes a quadratic cost function without specifying any underlying statistical model. The resulting cost function is identical to the log-likelihood function in our additive white Gaussian noise model.

The MVDR criterion assumes a linear data model and requires that the output in the absence of noise be distortionless. The minimum variance estimate subject to this constraint equals $\hat{\theta}_{\text{ml}}(\mathbf{R})$.

These equivalences reinforce the widespread use of ML estimates.

5.2.10 Sensitivity, Mismatch, and Diagonal Loading

In this section, we provide a brief introduction to the problem of estimating the performance degradation when our mathematical model is mismatched with the actual physical system. We then look at a simple technique to make the processor more robust to model mismatch. It is an area that is widely studied in the literature and we only provide an introduction.

We focus our attention on the Fisher linear Gaussian model in Section 5.2.4 but the general idea can be applied to most of the models in this chapter. The model of interest is given in (5.86):

$$\tilde{\mathbf{r}} = \tilde{\mathbf{V}}\tilde{\boldsymbol{\theta}} + \tilde{\mathbf{n}}, \quad (5.558)$$

where $\tilde{\mathbf{n}} \sim \mathcal{CN}(\mathbf{0}, \tilde{\mathbf{K}})$. From (5.130), the ML estimator is

$$\hat{\boldsymbol{\theta}}_{\text{ml}}(\tilde{\mathbf{R}}) = [\tilde{\mathbf{V}}^H \tilde{\mathbf{K}}^{-1} \tilde{\mathbf{V}}]^{-1} \tilde{\mathbf{V}}^H \tilde{\mathbf{K}}^{-1} \tilde{\mathbf{R}}. \quad (5.559)$$

All of our analyses so far have assumed that $\tilde{\mathbf{V}}$ and $\tilde{\mathbf{K}}$ are known. In a given application, they may be imperfectly known or may have to be measured. A common example is the case where we make observations in a noise-only environment and estimate $\tilde{\mathbf{K}}$,

$$\hat{\mathbf{K}} = \frac{1}{K} \sum_{k=1}^K \tilde{\mathbf{n}}_k \tilde{\mathbf{n}}_k^H. \quad (5.560)$$

In other cases, the columns in the modeled $\tilde{\mathbf{V}}$ matrix might be different than the actual matrix, which we denote as $\tilde{\mathbf{V}}_a$. For example, in Example 5.10, $\tilde{\mathbf{V}}$ is an $N \times 1$ matrix corresponding the signal's array manifold vector $\tilde{\mathbf{v}}(\psi_s)$. This vector depends on the direction-of-arrival of the signal and the position of the array elements. Perturbations in either of these will cause $\tilde{\mathbf{V}}_a \neq \tilde{\mathbf{v}}(\psi_s)$.

We want to study how this *mismatch* between the nominal model and the actual model affect the performance. We then want to study how to modify the ML estimator to make it more *robust* to model mismatch. We will find that we generally have to trade off optimum nominal performance versus suboptimum nominal, but robust, performance.

This is an important area and a significant amount of research has been devoted to it. A general study is beyond the scope of the book. We introduce the topic and go through a representative example. Our result is specific to our example but it turns out to be applicable to a wide variety of problems.

In order to keep the discussion manageable, we focus on a single problem, the array processing model we have encountered in Example 5.10. As discussed above, the nominal array manifold vector could be in error because the actual signal arrives from a different direction or because the array elements are in a different location. We restrict our attention to the latter case.

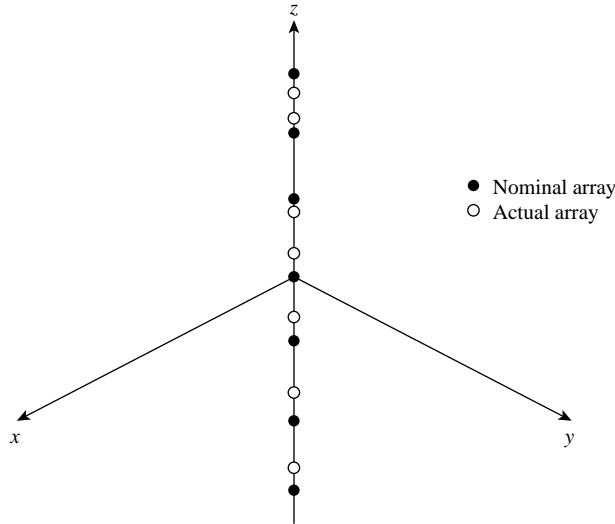


Figure 5.20: Linear array with perturbations.

5.2.10.1 Sensitivity and Array Perturbations

Consider the array shown in Figure 5.20. The nominal uniform linear array is on the z -axis. The actual array elements are perturbed from their nominal positions. In actual practice, they might be perturbed off of the z -axis but that is an unnecessary complication. We want to analyze the effect of the array perturbations on the performance of the ML estimator.

This problem has been analyzed using various perturbation models in a number of references (e.g., Nitzberg [Nit76], Kleinberg [Kle80], Mucci and Pridham [MP81], Farrier [Far83], Quazi [Qua82], Godara [God85, God86], and Youn and Un [YU94]). Our approach follows Gilbert and Morgan [GM55] and is a modified version of Section 2.6.3.2 of DEMT-IV [Van02].

Example 5.17 (continuation of Examples 4.33 and 5.10) Array processing. We consider the model in Example 5.10. The observation vector is

$$\tilde{\mathbf{r}}_k = \tilde{\mathbf{v}}(\psi_s)\tilde{b}_s + \tilde{\mathbf{n}}_k, \quad k = 1, 2, \dots, K, \quad (5.561)$$

where $\tilde{\mathbf{n}}_k \sim CN(\mathbf{0}, \tilde{\mathbf{K}})$ and

$$\tilde{\mathbf{K}} = \sigma_I^2 \tilde{\mathbf{v}}(\psi_I) \tilde{\mathbf{v}}(\psi_I)^H + \sigma_w^2 \mathbf{I}. \quad (5.562)$$

The unknown parameter is \tilde{b}_s .

From (5.214), the ML estimate is

$$\hat{b}_{s,\text{ml}}(\tilde{\mathbf{R}}) = \tilde{\mathbf{h}}_{\text{ml}}^H \tilde{\mathbf{R}}, \quad (5.563)$$

where

$$\tilde{\mathbf{h}}_{\text{ml}}^H = (1 - B_c^2(\Delta\psi_{Is})\alpha)^{-1} \left\{ \tilde{\mathbf{v}}(\psi_s)^\dagger - \tilde{\rho}_c(\Delta\psi_{Is})\alpha \tilde{\mathbf{v}}(\psi_I)^\dagger \right\}, \quad (5.564)$$

where

$$\alpha \triangleq \frac{N \cdot \text{INR}}{N \cdot \text{INR} + 1}. \quad (5.565)$$

The ML processor is a linear processor and is the same as the MVDR processor derived in Section 5.2.9.2.

From (5.220), the conventional beamformer (CBF) estimate is

$$\hat{b}_{s,c}(\tilde{\mathbf{R}}) = \tilde{\mathbf{h}}_c^H \tilde{\mathbf{R}}, \quad (5.566)$$

where

$$\tilde{\mathbf{h}}_c^H = \tilde{\mathbf{v}}(\psi_s)^\dagger. \quad (5.567)$$

It is also a linear processor.

The array elements are perturbed as in Example 4.33. We assume that the nominal element locations are

$$d_n^n = \frac{\lambda}{2} n, \quad n = 0, 1, \dots, N - 1, \quad (5.568)$$

and that the actual element locations are

$$d_n = \frac{\lambda}{2} (n + v_n), \quad n = 0, 1, \dots, N - 1, \quad (5.569)$$

where the v_n are IID zero-mean Gaussian random variables with variance σ_d^2 . We define an $N \times 1$ perturbation vector \mathbf{v} ,

$$\mathbf{v} \triangleq \begin{bmatrix} v_0 \\ v_1 \\ \vdots \\ v_{N-1} \end{bmatrix}. \quad (5.570)$$

The nominal array manifold vector $\tilde{\mathbf{v}}(\psi)$ is defined in (3.137). The actual array manifold vector is

$$\tilde{\mathbf{v}}(\psi, \mathbf{v}) = [e^{-j\psi v_0} \quad e^{-j\psi(1+v_1)} \quad \dots \quad e^{-j\psi(N-1+v_{N-1})}]^T. \quad (5.571)$$

It is a function of the random vector \mathbf{v} , therefore it is a random vector. We analyze the behavior of the estimators in the presence of these variations.

Under nominal conditions, both the ML and CBF processors are distortionless, that is,

$$\tilde{\mathbf{h}}_{ml}^H \tilde{\mathbf{v}}(\psi_s) = \tilde{\mathbf{h}}_c^H \tilde{\mathbf{v}}(\psi_s) = 1. \quad (5.572)$$

When there are perturbations, this property may be violated.

For any linear estimator (beamformer) with weight vector $\tilde{\mathbf{h}}$ that satisfies the distortionless criterion, the estimation error variance is

$$\begin{aligned} \sigma_\epsilon^2 &= \tilde{\mathbf{h}}^H \tilde{\mathbf{K}} \tilde{\mathbf{h}} \\ &= \sigma_I^2 |\tilde{\mathbf{h}}^H \tilde{\mathbf{v}}(\psi_I, \mathbf{v})|^2 + \sigma_n^2 \|\tilde{\mathbf{h}}\|^2 \\ &= \sigma_I^2 |B(\psi_I)|^2 + \sigma_n^2 \|\tilde{\mathbf{h}}\|^2, \end{aligned} \quad (5.573)$$

where

$$B(\psi) \triangleq \tilde{\mathbf{h}}^H \tilde{\mathbf{v}}(\psi, \mathbf{v}) = \sum_{n=0}^{N-1} \tilde{h}_n^* \exp \{-j\psi(n + v_n)\} \quad (5.574)$$

is the beampattern of the perturbed array. Thus, the variance depends on the norm of the weight vector and the beampattern of the processor at the location of the interferer.

The beampattern is a random function. The expectation of its magnitude squared can be written as

$$\begin{aligned} \overline{|B(\psi)|^2} &= E \left[|B(\psi)|^2 \right] \\ &= E \left[\sum_{n=0}^{N-1} \sum_{m=0}^{N-1} \tilde{h}_n^* \tilde{h}_m \exp \{j\psi(m + v_m - n - v_n)\} \right]. \end{aligned} \quad (5.575)$$

Then, taking the expectation in (5.575) and performing some algebraic manipulation,¹² we obtain

$$\overline{|B(\psi)|^2} = |B^n(\psi)|^2 e^{-\sigma_d^2 \psi^2} + \overline{|B_{\tilde{\mathbf{h}}}(\psi)|^2}, \quad (5.576)$$

where $B^n(\psi)$ is the nominal beampattern obtained when $\mathbf{v} = \mathbf{0}$ and

$$\overline{|B_{\tilde{\mathbf{h}}}(\psi)|^2} \triangleq \left\{ 1 - e^{-\sigma_d^2 \psi^2} \right\} \|\tilde{\mathbf{h}}\|^2. \quad (5.577)$$

The random variation has two effects. The first term in (5.576) attenuates the beampattern as a function of ψ . It means that the beampattern has a statistical bias. The expected value of the pattern along the signal direction is less than unity and the attenuation is stronger at endfire than at broadside. The second term is more critical. The effect of the second term is to raise the expected value by creating a floor across the entire range of ψ so that the nulls placed on the interferers are no longer as effective.¹³ The height of this floor is a function of σ_d^2 , $\|\tilde{\mathbf{h}}\|^2$, and ψ .

For the CBF estimator in (5.567),

$$\|\tilde{\mathbf{h}}_c\|^2 = \frac{1}{N}, \quad (5.578)$$

and for the ML estimator in (5.564), we have

$$\|\tilde{\mathbf{h}}_{ml}\|^2 = \frac{1 - (2\alpha - \alpha^2) B_c^2(\Delta\psi_I)}{N (1 - \alpha B_c^2(\Delta\psi_I))^2}. \quad (5.579)$$

For large INR, $\alpha \rightarrow 1$ and

$$\|\tilde{\mathbf{h}}_{ml}\|^2 \sim \frac{1}{N (1 - B_c^2(\Delta\psi_I))}. \quad (5.580)$$

It can be shown that the minimum value of $\|\tilde{\mathbf{h}}\|^2$ subject to the distortionless constraint is $1/N$, which is achieved by the CBF.

In Figures 5.21a and 5.21b, we plot $\overline{|B(\psi)|^2}$, $|B^n(\psi)|^2$, and $\overline{|B_{\tilde{\mathbf{h}}}(\psi)|^2}$ for the ML estimator for $\sigma_d = 0.15$, $\psi_s = 0$ and 0.8π , $\Delta\psi_I = 0.1\pi$, and INR = 30 dB. In Example 5.10, the ML processor achieved a reduction in variance over the CBF processor by putting a deep null on the interferer. The floor of the perturbed beampattern reduces the nulling ability and causes an increase in the variance. The effect is more pronounced when the signal and interferer are closer to broadside. Note that this case is more difficult than the four studied in Example 5.10 because the INR is larger.

¹²See [GM55], Section 2.6.3.2 of [Van02]

¹³Review Figures 5.8 and 5.9 to see the nulling property of the ML estimator.

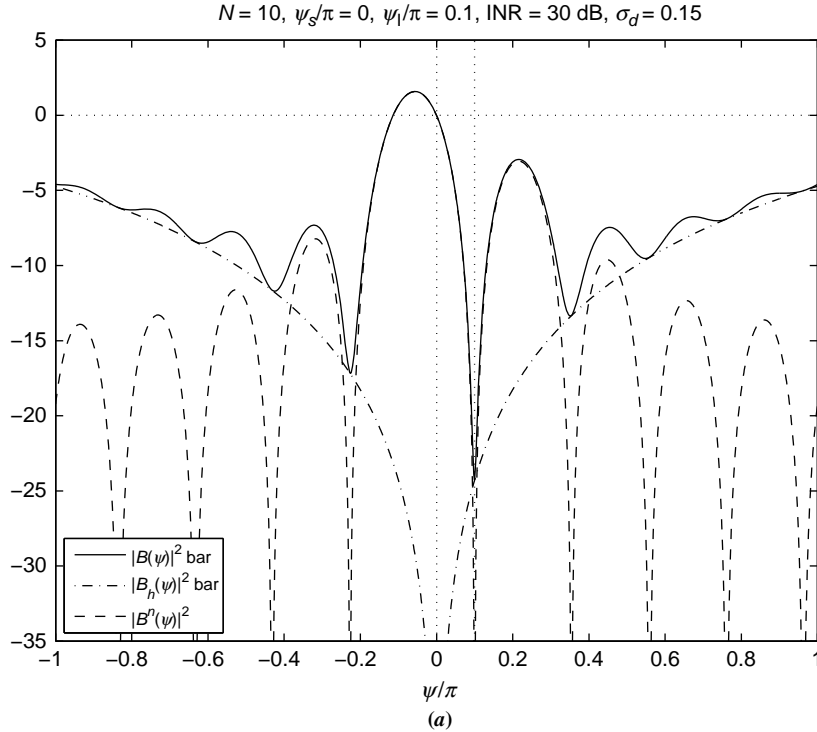


Figure 5.21: (a) Beamformer components for $\psi_s = 0$.

In Figure 5.22, we show the variance and $\|\tilde{\mathbf{h}}\|^2$ of the ML and CBF estimators as a function of interference direction ψ_I when $\psi_s = 0.8\pi$. When the interferer is outside the mainbeam, $\|\tilde{\mathbf{h}}\|^2 \approx 1/N$ for both processors. The variance is subject to an angle dependent floor that is detrimental to both processors. When the interferer is close to the signal, the weight vector norm increases significantly for the ML processor causing a corresponding increase in variance. ■

5.2.10.2 Diagonal Loading

We observed that the sensitivity of a linear estimator to array perturbations increases as $\|\tilde{\mathbf{h}}\|^2$ increases. This suggests the use of a quadratic constraint (QC),

$$\tilde{\mathbf{h}}^H \tilde{\mathbf{h}} \leq T_0, \quad (5.581)$$

where T_0 is a design parameter. Since $\|\tilde{\mathbf{h}}\|^2 \geq 1/N$, we must have

$$T_0 \geq \frac{1}{N}. \quad (5.582)$$

We show how the imposition of a quadratic constraint leads to a procedure that we refer to as *diagonal loading* (DL).

We assume the model in Section 5.2.4.3, where

$$\tilde{\mathbf{r}} = \tilde{\mathbf{v}}_s \tilde{\theta} + \tilde{\mathbf{n}}. \quad (5.583)$$

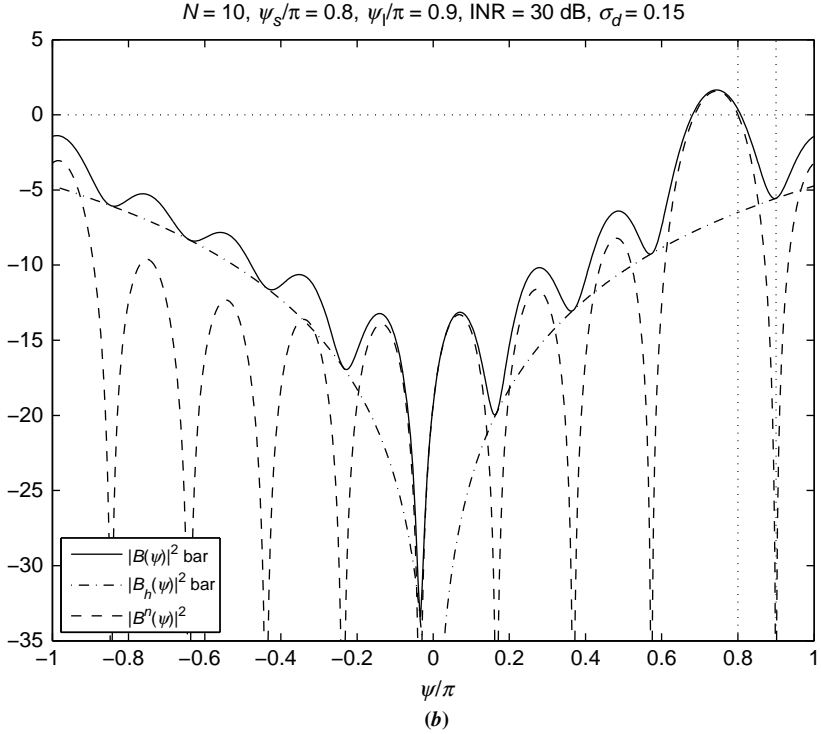


Figure 5.21: (b) Beamformer components for $\psi_s = 0.8\pi$.

The noise is $\tilde{\mathbf{n}} \sim \mathcal{CN}(\mathbf{0}, \tilde{\mathbf{K}})$ with covariance matrix

$$\tilde{\mathbf{K}} = \tilde{\mathbf{K}}_I + \sigma_w^2 \mathbf{I}. \quad (5.584)$$

From (5.198) and (5.554), the ML and MVDR processors are

$$\tilde{\mathbf{h}}_{\text{ml}}^H = \tilde{\mathbf{h}}_{\text{mvdr}}^H = [\tilde{\mathbf{v}}_s^H \tilde{\mathbf{K}}^{-1} \tilde{\mathbf{v}}_s]^{-1} \tilde{\mathbf{v}}_s^H \tilde{\mathbf{K}}^{-1}. \quad (5.585)$$

We develop a robust processor by incorporating a quadratic constraint in the MVDR formulation. The MVDR-QC optimization problem is:

$$\text{Minimize } \tilde{\mathbf{h}}^H \tilde{\mathbf{K}} \tilde{\mathbf{h}}, \quad (5.586)$$

subject to the distortionless constraint,

$$\tilde{\mathbf{h}}^H \tilde{\mathbf{v}}_s = 1 \quad (5.587)$$

and the quadratic constraint,

$$\tilde{\mathbf{h}}^H \tilde{\mathbf{h}} = T_0. \quad (5.588)$$

The function to minimize is

$$f \triangleq \tilde{\mathbf{h}}^H \tilde{\mathbf{K}} \tilde{\mathbf{h}} + \lambda_1 [\tilde{\mathbf{h}}^H \tilde{\mathbf{h}} - T_0] + \tilde{\lambda}_2 [\tilde{\mathbf{h}}^H \tilde{\mathbf{v}}_s - 1] + \tilde{\lambda}_2^* [\tilde{\mathbf{v}}_s^H \tilde{\mathbf{h}} - 1]. \quad (5.589)$$

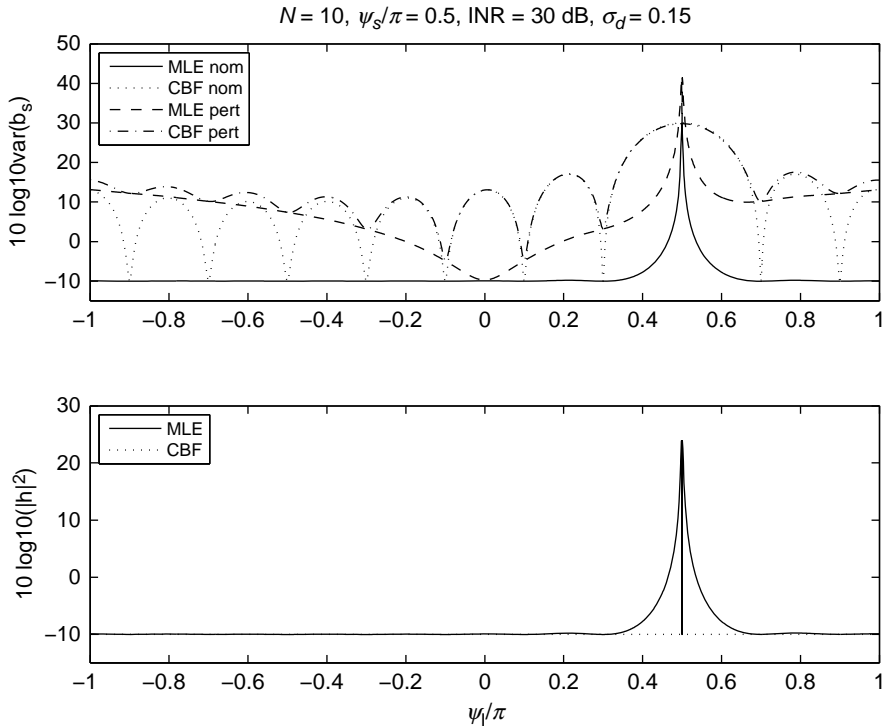


Figure 5.22: Estimator variance versus angle.

Differentiating with respect to $\tilde{\mathbf{h}}$ and setting the result equal to zero gives

$$\tilde{\mathbf{h}}^H \tilde{\mathbf{K}} + \lambda_1 \tilde{\mathbf{h}}^H + \tilde{\lambda}_2^* \tilde{\mathbf{v}}_s^H = \mathbf{0}. \quad (5.590)$$

Solving for $\tilde{\mathbf{h}}^H$ gives

$$\tilde{\mathbf{h}}^H = -\lambda_2^* \tilde{\mathbf{v}}_s^H [\tilde{\mathbf{K}} + \lambda_1 \mathbf{I}]^{-1}. \quad (5.591)$$

Substituting (5.591) into (5.587) gives

$$-\lambda_2^* \tilde{\mathbf{v}}_s^H [\tilde{\mathbf{K}} + \lambda_1 \mathbf{I}]^{-1} \tilde{\mathbf{v}}_s = 1 \quad (5.592)$$

or

$$\lambda_2^* = \left[\tilde{\mathbf{v}}_s^H [\tilde{\mathbf{K}} + \lambda_1 \mathbf{I}]^{-1} \tilde{\mathbf{v}}_s \right]^{-1}. \quad (5.593)$$

Thus,

$$\tilde{\mathbf{h}}^H = \left[\tilde{\mathbf{v}}_s^H (\tilde{\mathbf{K}} + \lambda_1 \mathbf{I})^{-1} \tilde{\mathbf{v}}_s \right]^{-1} \tilde{\mathbf{v}}_s^H [\tilde{\mathbf{K}} + \lambda_1 \mathbf{I}]^{-1}. \quad (5.594)$$

We see that the effect of the quadratic constraint is to add a diagonal matrix $\lambda_1 \mathbf{I}$ to the covariance matrix $\tilde{\mathbf{K}}$ in the formula for the optimum processor in (5.585). In effect, the MVDR-QC weight vector is designed for a higher white noise level than is actually

present. The technique is called *diagonal loading* in the engineering literature. The value of λ_1 depends on the choice of T_0 . We can substitute $\tilde{\mathbf{h}}^H$ from (5.594) into (5.588) and solve for λ_1 . However, since T_0 is arbitrary, we may also just specify $\lambda_1 = \sigma_L^2$ directly. Then, we can write

$$\tilde{\mathbf{h}}^H = [\tilde{\mathbf{v}}_s^H (\tilde{\mathbf{K}} + \sigma_L^2 \mathbf{I}) \tilde{\mathbf{v}}_s]^{-1} \tilde{\mathbf{v}}_s^H [\tilde{\mathbf{K}} + \sigma_L^2 \mathbf{I}]^{-1}. \quad (5.595)$$

Substituting (5.584) into (5.595), we obtain

$$\tilde{\mathbf{h}}^H = \left[\tilde{\mathbf{v}}_s^H (\tilde{\mathbf{K}}_I + \sigma_{\tilde{w}}^2 (1 + \text{LNR}) \mathbf{I})^{-1} \tilde{\mathbf{v}}_s \right]^{-1} \tilde{\mathbf{v}}_s^H [\tilde{\mathbf{K}}_I + \sigma_{\tilde{w}}^2 (1 + \text{LNR}) \mathbf{I}]^{-1}, \quad (5.596)$$

where LNR is the diagonal loading-to-noise ratio,

$$\text{LNR} \triangleq \frac{\sigma_L^2}{\sigma_{\tilde{w}}^2}. \quad (5.597)$$

Thus, the optimum quadratically constrained processor is just the ML processor designed for artificially increased white noise level. As $\text{LNR} \rightarrow 0$, we have the ML estimator. As $\text{LNR} \rightarrow \infty$, we approach the ML estimator designed for a white noise background, which is the CBF estimator.

Example 5.18 (continuation of Examples 4.33, 5.10, and 5.17) Array processing. We reexamine the model in Example 5.17 and impose the constraint

$$\mathbf{h}^H \mathbf{h} = \frac{3}{N \left(1 - e^{-\sigma_d^2 \psi_I^2} \right)} \leq T_0. \quad (5.598)$$

When $\|\tilde{\mathbf{h}}\|^2 < T_0$, the standard ML/MVDR processor is used. When $\|\tilde{\mathbf{h}}\|^2 > T_0$, the diagonal loading level is computed to satisfy the constraint.

The variance and weight vector norm are shown in Figure 5.23. Outside the mainbeam, the performance is the same as the ML processor shown in Figure 5.22. When the weight vector norm exceeds the constraint, the diagonal loading reduces the variance to approximately the CBF level. ■

One can also show that diagonal loading reduces the degradation due to errors in the signal's direction-of-arrival that causes a mismatched array manifold vector. A key question is how to choose the correct value of the LNR. There are significant number of references in this area. Many of the references introduced other types of constraints to augment the DL. Most of the early work used *ad hoc* methods to choose the LNR but recent efforts have provided a theoretical basis for some models. A partial list of early references includes Cox [Cox73], Frost [Fro72], Cox et al. [CZO87], and Carlson [Car88]. Recent papers by Li et al. [LSW03], Pezeshki et al. [PVS⁺08], Chen and Vaidyanathan [CV07] as well as the book by Li and Stoica, *Robust Adaptive Beamforming* [LS05], provide an extensive list of references.

The papers by Li et al. [LSW03], Vorobyov et al. [VGL03], and Lorenz and Boyd [LB05] make use of an uncertainty set of the array manifold vector to derive an analytic answer for the optimum LNR. The paper by Richmond et al. [RNE05] uses random matrix theory to derive the asymptotic performance of the MVDR-DL processor.

We have discussed diagonal loading in the context of array processing. It is widely used in a number of areas. In statistics, it is a regularization technique (sometimes called Tikhonov regularization) that occurs when taking the inverse of an ill-conditioned matrix.

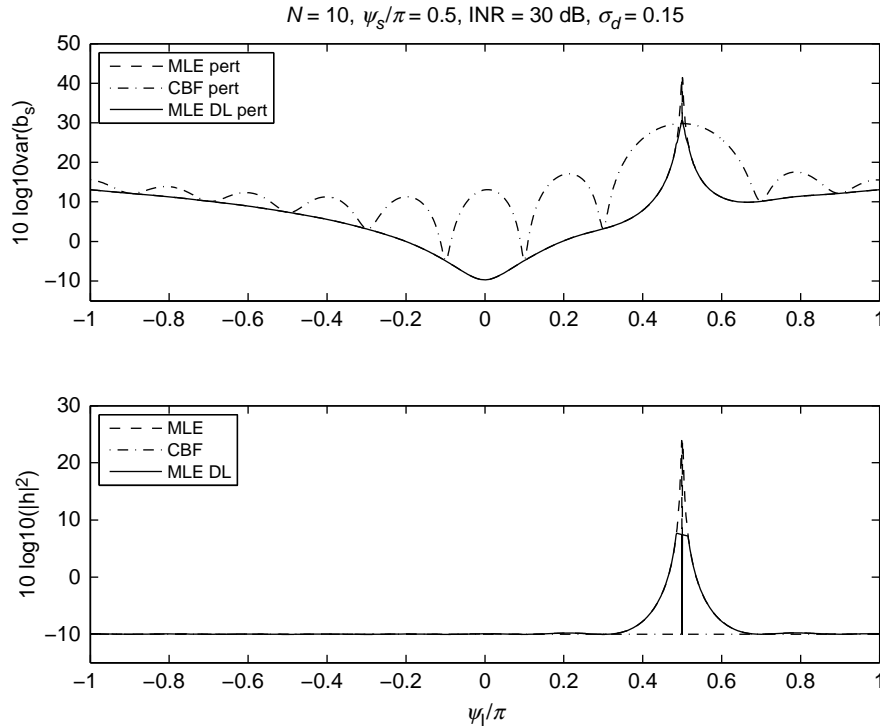


Figure 5.23: Estimator variance with quadratic constraint versus angle.

A key point that the reader should take away from this discussion is that the optimum processor should be checked to see how sensitive it is to mismatches with actual environment.

5.2.11 Summary

In this section we considered nonrandom parameter vectors. In Section 5.2.1, we defined the general Gaussian estimation model for real and complex vectors. For the real case, the probability density is given by (5.1),

$$p_{\mathbf{r}|\theta}(\mathbf{R}|\theta) = \frac{1}{(2\pi)^{N/2} |\mathbf{K}(\theta)|^{1/2}} \cdot \exp \left\{ -\frac{1}{2} [\mathbf{R} - \mathbf{m}(\theta)]^T \mathbf{K}^{-1}(\theta) [\mathbf{R} - \mathbf{m}(\theta)] \right\}.$$

We developed a large number of examples to show the widespread applicability of the model.

In Section 5.2.2, we derived the ML estimate in (5.54),

$$\hat{\theta}_{\text{ml}}(\mathbf{R}) = \underset{\theta}{\operatorname{argmin}} \left\{ \ln |\mathbf{K}(\theta)| + [\mathbf{R} - \mathbf{m}(\theta)]^T \mathbf{K}^{-1}(\theta) [\mathbf{R} - \mathbf{m}(\theta)] \right\}.$$

In general, we must search over a D -dimensional surface to find $\hat{\theta}_{\text{ml}}(\mathbf{R})$.

In Section 5.2.3, we derived the Cramér-Rao bound. For real parameters, the Fisher information matrix is given by (5.72),

$$J_{F_{ij}}(\boldsymbol{\theta}) = \frac{1}{2} \operatorname{tr} \left[\mathbf{K}^{-1}(\boldsymbol{\theta}) \frac{\partial \mathbf{K}(\boldsymbol{\theta})}{\partial \theta_i} \mathbf{K}^{-1}(\boldsymbol{\theta}) \frac{\partial \mathbf{K}(\boldsymbol{\theta})}{\partial \theta_j} \right] + \left[\frac{\partial \mathbf{m}^T(\boldsymbol{\theta})}{\partial \theta_i} \mathbf{K}^{-1}(\boldsymbol{\theta}) \frac{\partial \mathbf{m}(\boldsymbol{\theta})}{\partial \theta_j} \right].$$

In Section 5.2.4, we studied the Fisher linear Gaussian model where the parameter vector appears linearly in the mean vector and the covariance matrix is known. Then the ML estimate is given by (5.95),

$$\hat{\boldsymbol{\theta}}_{\text{ml}}(\mathbf{R}) = [\mathbf{V}^T \mathbf{K}^{-1} \mathbf{V}]^{-1} \mathbf{V}^T \mathbf{K}^{-1} \mathbf{R}.$$

It is an unbiased, efficient estimator whose error covariance matrix is given by (5.99),

$$\Lambda \epsilon = \operatorname{CRB}(\boldsymbol{\theta}) = [\mathbf{V}^T \mathbf{K}^{-1} \mathbf{V}]^{-1}.$$

In Section 5.2.5, we introduced separable Gaussian models in which we could find an explicit solution for the linear parameter $\boldsymbol{\theta}_l$ and use it to construct a compressed log-likelihood function for the nonlinear parameter $\boldsymbol{\theta}_{nl}$. The resulting ML estimates were given in (5.236) and (5.237),

$$\hat{\boldsymbol{\theta}}_{nl}(\mathbf{R}) = \underset{\boldsymbol{\theta}_{nl}}{\operatorname{argmax}} \left\{ \|\mathbf{P}_{\mathbf{V}(\boldsymbol{\theta}_{nl})} \mathbf{R}\|^2 \right\}$$

and

$$\hat{\boldsymbol{\theta}}_l(\mathbf{R}) = \mathbf{V}^\dagger (\hat{\boldsymbol{\theta}}_{nl}(\mathbf{R})) \mathbf{R}.$$

The Fisher information matrix was given in (5.239)–(5.244). It could be written in partitioned form as:

$$\mathbf{J}_F(\boldsymbol{\theta}) = \begin{bmatrix} \mathbf{J}_F(\boldsymbol{\theta}_l) & \mathbf{J}_F(\boldsymbol{\theta}_l, \boldsymbol{\theta}_{nl}) \\ \mathbf{J}_F(\boldsymbol{\theta}_{nl}, \boldsymbol{\theta}_l) & \mathbf{J}_F(\boldsymbol{\theta}_{nl}) \end{bmatrix},$$

where

$$\begin{aligned} \mathbf{J}_F(\boldsymbol{\theta}_l) &= \frac{1}{\sigma_w^2} \mathbf{V}^T(\boldsymbol{\theta}_{nl}) \mathbf{V}(\boldsymbol{\theta}_{nl}), \\ \mathbf{J}_F(\boldsymbol{\theta}_l, \boldsymbol{\theta}_{nl}) &= \frac{1}{\sigma_w^2} \mathbf{V}^T(\boldsymbol{\theta}_{nl}) (\nabla_{\boldsymbol{\theta}_{nl}} [\boldsymbol{\theta}_l^T \mathbf{V}^T(\boldsymbol{\theta}_{nl})])^T, \\ \mathbf{J}_F(\boldsymbol{\theta}_{nl}) &= \frac{1}{\sigma_w^2} (\nabla_{\boldsymbol{\theta}_{nl}} [\boldsymbol{\theta}_l^T \mathbf{V}^T(\boldsymbol{\theta}_{nl})]) (\nabla_{\boldsymbol{\theta}_{nl}} [\boldsymbol{\theta}_l^T \mathbf{V}^T(\boldsymbol{\theta}_{nl})])^T. \end{aligned}$$

In Section 5.2.6, we studied the case in which the parameter $\boldsymbol{\theta}_c$ appeared in the covariance matrix. Results for several special cases were derived.

In Section 5.2.7, we studied the case of a linear Gaussian mean vector,

$$\mathbf{m}(\boldsymbol{\theta}_m) = \mathbf{V} \boldsymbol{\theta}_m,$$

and several covariance matrix models parameterized by the vector $\boldsymbol{\theta}_c$. We obtained an explicit solution for $\boldsymbol{\theta}_m$ and a compressed log-likelihood function that could be solved for $\boldsymbol{\theta}_c$.

In Section 5.2.8, we studied various computational algorithms for finding the minimum of a D -dimensional surface. We discussed gradient techniques, the alternating projection algorithm, and the expectation–maximization algorithm.

In Section 5.2.9, we discussed the least squares algorithm and the MVDR algorithm and showed their relation to the ML algorithm.

In Section 5.2.10, we provided an introduction to the important problem of the sensitivity of optimum processor to the case where the actual model is different from the assumed model. We considered a specific example and showed that by imposing a quadratic constraint on the linear estimation vector,

$$\tilde{\mathbf{h}}^H \tilde{\mathbf{h}} \leq T_0,$$

we obtained a new linear estimator that included diagonal loading of the covariance matrix. Diagonal loading is widely used to develop robust processors. We provided several good references for further study.

5.3 RANDOM PARAMETERS

5.3.1 Model, MAP Estimation, and the BCRB

The mapping from the parameter space to the observation space is the same as in the nonrandom parameter model. The conditional probability density is

$$p_{\mathbf{r}|\theta}(\mathbf{R}|\theta) = \frac{1}{(2\pi)^{N/2} |\mathbf{K}(\theta_c)|^{1/2}} \exp \left\{ -\frac{1}{2} [\mathbf{R} - \mathbf{m}(\theta_m)]^T \mathbf{K}^{-1}(\theta_c) [\mathbf{R} - \mathbf{m}(\theta_m)] \right\}, \quad (5.599)$$

where

$$\boldsymbol{\theta} \triangleq [\boldsymbol{\theta}_m^T \quad \boldsymbol{\theta}_c^T]^T. \quad (5.600)$$

However, now $\boldsymbol{\theta}$ is a random parameter vector with known *a priori* probability density $p_{\boldsymbol{\theta}}(\boldsymbol{\theta})$. In most cases, $\boldsymbol{\theta}_m$ and $\boldsymbol{\theta}_c$ are independent but that is not required. The *a priori* density is chosen to model our prior knowledge about $\boldsymbol{\theta}_m$ and $\boldsymbol{\theta}_c$. Whenever possible, we will use the conjugate prior but that is not required and is often not available.

We refer to this model as the general Gaussian estimation problem for random parameters. We will focus our attention on MAP estimation but will also find the MMSE estimate when it is feasible. The MAP estimate requires finding the peak of the *a posteriori* probability density, or equivalently, the logarithm of $p_{\boldsymbol{\theta}|\mathbf{r}}(\boldsymbol{\theta}|\mathbf{R})$. In (4.21), we defined the Bayesian log-likelihood function as

$$l_B(\boldsymbol{\theta}; \mathbf{R}) \equiv \ln p_{\mathbf{r},\boldsymbol{\theta}}(\mathbf{R}, \boldsymbol{\theta}) = \ln p_{\mathbf{r}|\boldsymbol{\theta}}(\mathbf{R}|\boldsymbol{\theta}) + \ln p_{\boldsymbol{\theta}}(\boldsymbol{\theta}). \quad (5.601)$$

Using (5.599) gives

$$l_B(\boldsymbol{\theta}; \mathbf{R}) = -\frac{1}{2} \ln |\mathbf{K}(\boldsymbol{\theta}_c)| - \frac{1}{2} \{ [\mathbf{R} - \mathbf{m}(\boldsymbol{\theta}_m)]^T \mathbf{K}^{-1}(\boldsymbol{\theta}_c) [\mathbf{R} - \mathbf{m}(\boldsymbol{\theta}_m)] \} + \ln p_{\boldsymbol{\theta}}(\boldsymbol{\theta}) + \zeta. \quad (5.602)$$

Then,

$$\hat{\boldsymbol{\theta}}_{\text{map}}(\mathbf{R}) = \underset{\boldsymbol{\theta}}{\operatorname{argmax}} \{l_B(\boldsymbol{\theta}; \mathbf{R})\}. \quad (5.603)$$

From equations (4.515), (4.517), and (4.518) the Bayesian information matrix is given by

$$\mathbf{J}_B = \mathbf{J}_D + \mathbf{J}_P, \quad (5.604)$$

where

$$\begin{aligned} J_{P_{ij}} &= E_{\boldsymbol{\theta}} \left\{ \frac{\partial \ln p_{\boldsymbol{\theta}}(\boldsymbol{\theta})}{\partial \theta_i} \frac{\partial \ln p_{\boldsymbol{\theta}}(\boldsymbol{\theta})}{\partial \theta_j} \right\} \\ &= -E_{\boldsymbol{\theta}} \left\{ \frac{\partial^2 \ln p_{\boldsymbol{\theta}}(\boldsymbol{\theta})}{\partial \theta_i \partial \theta_j} \right\} \end{aligned} \quad (5.605)$$

and

$$\mathbf{J}_D = E_{\boldsymbol{\theta}} \{ \mathbf{J}_F(\boldsymbol{\theta}) \} \quad (5.606)$$

and $\mathbf{J}_F(\boldsymbol{\theta})$ is given by (5.72).

We consider several simple examples to illustrate some of the techniques.

Example 5.19. Consider the model in which we have N IID scalar observations that are $N(m, \sigma^2)$, where

$$\theta = m \quad (5.607)$$

is an unknown random parameter and σ^2 is known. The conjugate prior for m is $N(m_0, \sigma_0^2)$. As in Example 4.5, the *a posteriori* density is $N(m_p, \sigma_p^2)$, where

$$m_p = \left(\frac{m_0}{\sigma_0^2} + \frac{N\bar{R}}{\sigma^2} \right) \sigma_p^2 \quad (5.608)$$

and

$$\sigma_p^2 = \left(\frac{1}{\sigma_0^2} + \frac{N}{\sigma^2} \right)^{-1}. \quad (5.609)$$

Because the *a posteriori* density is Gaussian, the peak occurs at the mean and

$$\hat{m}_{\text{map}}(\mathbf{R}) = \hat{m}_{\text{ms}}(\mathbf{R}) = m_p = \left(\frac{m_0}{\sigma_0^2} + \frac{N\bar{R}}{\sigma^2} \right) \sigma_p^2 \quad (5.610)$$

and the MSE is σ_p^2 . The estimate is Bayesian efficient. ■

Example 5.20. Consider the model in which we have N IID scalar observations that are $N(m, \sigma^2)$. We assume the mean is known and $\theta = \sigma^2$ is unknown. The conjugate prior is an Inverse Gamma density with shape parameter a_0 and scale parameter b_0 . The Inverse Gamma density has the form

$$p_{\theta|a,b}(\theta|a, b) = \frac{1}{b^a \Gamma(a)} \left(\frac{1}{\theta} \right)^{a+1} \exp \left\{ -\frac{1}{\theta b} \right\}, \quad \theta \geq 0. \quad (5.611)$$

The posterior hyperparameters are (see Appendix A)

$$a_p = a_0 + \frac{N}{2} \quad (5.612)$$

$$b_p = \left(b_0^{-1} + \frac{1}{2} \sum_{i=1}^N (R_i - m)^2 \right)^{-1}. \quad (5.613)$$

The log of the *a posteriori* density is

$$l_P(\theta; \mathbf{R}) \triangleq \ln p_{\theta|\mathbf{R}}(\theta|\mathbf{R}) = -(a_p + 1) \ln \theta - \frac{1}{\theta b_p} + \zeta. \quad (5.614)$$

Differentiating with respect to θ gives

$$\frac{\partial l_P(\theta; \mathbf{R})}{\partial \theta} = -\frac{a_p + 1}{\theta} + \frac{1}{\theta^2 b_p}. \quad (5.615)$$

Setting the result equal to zero and solving gives

$$\hat{\theta}_{\text{map}}(\mathbf{R}) = \hat{\sigma}_{\text{map}}^2(\mathbf{R}) = \frac{1}{b_p(a_p + 1)} = \frac{\left(b_0^{-1} + \frac{1}{2} \sum_{i=1}^N (R_i - m)^2 \right)}{\left(a_0 + \frac{N}{2} + 1 \right)}. \quad (5.616)$$

In this case, we can also find the *a posteriori* mean, which is the minimum mean-square error estimate. From Appendix A,

$$\hat{\theta}_{\text{ms}}(\mathbf{R}) = \hat{\sigma}_{\text{ms}}^2(\mathbf{R}) = \frac{1}{b_p(a_p - 1)} = \frac{\left(b_0^{-1} + \frac{1}{2} \sum_{i=1}^N (R_i - m)^2 \right)}{\left(a_0 + \frac{N}{2} - 1 \right)}, \quad \text{for } a_0 + \frac{N}{2} > 1. \quad (5.617)$$

From Example 4.26, equation (4.433), the ML estimate when the mean m is known is

$$\hat{\theta}_{\text{ml}}(\mathbf{R}) = \hat{\sigma}_{\text{ml}}^2(\mathbf{R}) = \frac{1}{N} \sum_{i=1}^N (R_i - m)^2. \quad (5.618)$$

Rewriting (5.616) and (5.617) in terms of $\hat{\theta}_{\text{ml}}(\mathbf{R})$, we have

$$\hat{\theta}_{\text{map}}(\mathbf{R}) = \frac{\hat{\theta}_{\text{ml}}(\mathbf{R}) + \frac{2}{Nb_0}}{1 + \frac{2(a_0 + 1)}{N}} \xrightarrow{N \rightarrow \infty} \hat{\theta}_{\text{ml}}(\mathbf{R}), \quad (5.619)$$

$$\hat{\theta}_{\text{ms}}(\mathbf{R}) = \frac{\hat{\theta}_{\text{ml}}(\mathbf{R}) + \frac{2}{Nb_0}}{1 + \frac{2(a_0 - 1)}{N}} \xrightarrow{N \rightarrow \infty} \hat{\theta}_{\text{ml}}(\mathbf{R}). \quad (5.620)$$

Both the MAP and MMSE estimates converge to the ML estimate for large N . Also, the MAP and MMSE estimates differ only in a scale factor, with the MMSE estimate being slightly larger than the MAP estimate.

From Example 4.26, equation (4.438), we have

$$J_F(\theta) = \frac{N}{2\theta^2}. \quad (5.621)$$

Taking the expected value with respect to $p_{\theta|a_0,b_0}(\theta|a_0, b_0)$ we obtain

$$J_D = E_\theta\{J_F(\theta)\} = \frac{N}{2}a_0(a_0 + 1)b_0^2. \quad (5.622)$$

To find J_P , we evaluate (5.605) to obtain

$$J_P = a_0(a_0 + 1)(a_0 + 3)b_0^2. \quad (5.623)$$

Thus,

$$J_B = J_D + J_P = a_0(a_0 + 1) \left(a_0 + 3 + \frac{N}{2} \right) b_0^2 \quad (5.624)$$

and

$$\text{BCRB} = J_B^{-1} = \frac{1}{a_0(a_0 + 1) \left(a_0 + 3 + \frac{N}{2} \right) b_0^2}. \quad (5.625)$$

We can also find the ECRB

$$\text{ECRB} = E\{J_F^{-1}(\theta)\} = \frac{2}{N(a_0 - 1)(a_0 - 2)b_0^2}. \quad (5.626)$$

In Figure 5.24, we plot the RMSE of the MAP, MMSE, and ML estimators from 5000 simulation trials with the BCRB and ECRB. All three estimators achieve the ECRB as $N \rightarrow \infty$. The BCRB is a weak lower bound. ■

Similar results can be derived for the cases where both the mean and variance are unknown and the conjugate priors are used. The results can be extended to IID vector observations with appropriate conjugate priors.

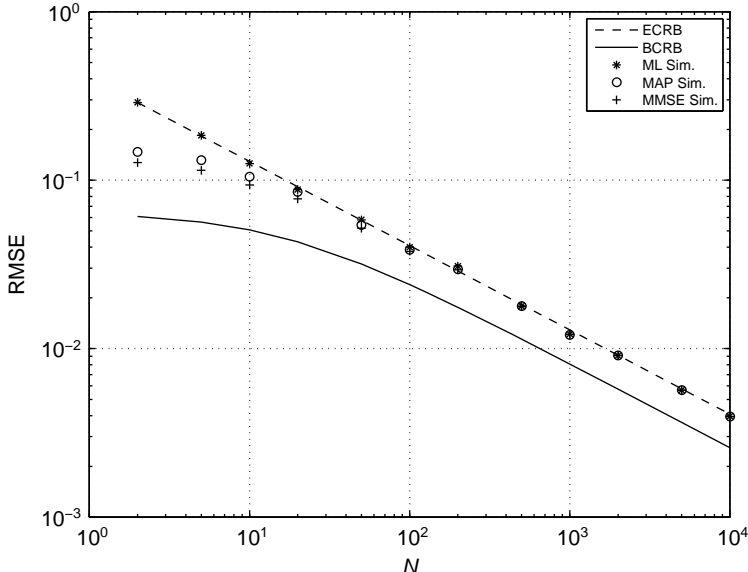


Figure 5.24: RMSE for MAP, MMSE, and ML Estimators, BCRB and ECRB.

The model for complex observations follows easily. For real parameters,

$$p_{\tilde{\mathbf{r}}|\theta}(\tilde{\mathbf{R}}|\theta) = \frac{1}{\pi^N |\tilde{\mathbf{K}}(\theta_c)|} \exp \left\{ - [\tilde{\mathbf{R}} - \tilde{\mathbf{m}}(\theta_m)]^H \tilde{\mathbf{K}}^{-1}(\theta_c) [\tilde{\mathbf{R}} - \tilde{\mathbf{m}}(\theta_m)] \right\} \quad (5.627)$$

and the a prior density is $p_\theta(\theta)$.

5.3.2 Bayesian Linear Gaussian Model

An important special case is the linear Gaussian model. The simplest version of the linear Gaussian model for random parameters is given by,

$$\mathbf{r} = \mathbf{V}\theta + \mathbf{n}, \quad (5.628)$$

where θ is a $D \times 1$ Gaussian random vector $N(\mathbf{m}_\theta, \mathbf{K}_\theta)$, \mathbf{n} is an $N \times 1$ Gaussian random vector $N(\mathbf{0}, \mathbf{K}_n)$, and the two vectors θ and \mathbf{n} are statistically independent. The matrix \mathbf{V} is a known $N \times D$ matrix.

We will show that whenever θ and \mathbf{r} have a multivariate Gaussian density, \mathbf{r} can be written in the form of (5.628) with θ and \mathbf{n} statistically independent. Therefore, the model in (5.628) is the general case.

Note that we have imposed two constraints on the model in Section 5.3.1.

1. The *a priori* density is Gaussian $N(\mathbf{m}_\theta, \mathbf{K}_\theta)$, which is the conjugate prior.
2. The covariance matrix \mathbf{K}_n is known.

The Bayesian log-likelihood function is

$$l_B(\theta; \mathbf{R}) = -\frac{1}{2} \{ [\mathbf{R} - \mathbf{V}\theta]^T \mathbf{K}_n^{-1} [\mathbf{R} - \mathbf{V}\theta] \} - \frac{1}{2} (\theta - \mathbf{m}_\theta)^T \mathbf{K}_\theta^{-1} (\theta - \mathbf{m}_\theta) + \zeta. \quad (5.629)$$

Differentiating with respect to θ and setting the result equal to zero gives

$$\nabla_\theta l_B(\theta; \mathbf{R}) = \mathbf{V}^T \mathbf{K}_n^{-1} \mathbf{R} - \mathbf{V}^T \mathbf{K}_n^{-1} \mathbf{V} \theta + \mathbf{K}_\theta^{-1} \mathbf{m}_\theta - \mathbf{K}_\theta^{-1} \theta = \mathbf{0}. \quad (5.630)$$

Solving for $\hat{\theta}_{\text{map}}(\mathbf{R})$ gives

$$\hat{\theta}_{\text{map}}(\mathbf{R}) = \mathbf{m}_\theta + [\mathbf{K}_\theta^{-1} + \mathbf{V}^T \mathbf{K}_n^{-1} \mathbf{V}]^{-1} \mathbf{V}^T \mathbf{K}_n^{-1} [\mathbf{R} - \mathbf{V}\mathbf{m}_\theta].$$

(5.631)

Using the matrix inversion lemma we can write (5.631) as

$$\hat{\theta}_{\text{map}}(\mathbf{R}) = \mathbf{m}_\theta + \mathbf{K}_\theta \mathbf{V}^T [\mathbf{V} \mathbf{K}_\theta \mathbf{V}^T + \mathbf{K}_n]^{-1} [\mathbf{R} - \mathbf{V}\mathbf{m}_\theta]. \quad (5.632)$$

To get a bound on the mean-square error, we differentiate (5.630) with respect to θ and take the expectation

$$\begin{aligned} \mathbf{J}_B &= -E_\theta \left[\nabla_\theta (\nabla_\theta l_B(\theta; \mathbf{R}))^T \right] = E_\theta [\mathbf{K}_\theta^{-1} + \mathbf{V}^T \mathbf{K}_n^{-1} \mathbf{V}] \\ &= \mathbf{K}_\theta^{-1} + \mathbf{V}^T \mathbf{K}_n^{-1} \mathbf{V}. \end{aligned} \quad (5.633)$$

The matrix is not a function of θ , so the expectation is trivial. Note that

$$\mathbf{J}_B = \mathbf{J}_P + \mathbf{J}_D, \quad (5.634)$$

where \mathbf{J}_P is the contribution due to the *a priori* knowledge and always equals \mathbf{K}_θ^{-1} for a Gaussian prior, and \mathbf{J}_D is the contribution due to the data and is the same term as in the ML model. From (5.98),

$$\mathbf{J}_D = \mathbf{J}_F = \mathbf{V}^T \mathbf{K}_n^{-1} \mathbf{V}. \quad (5.635)$$

The expressions in (5.630)–(5.631) satisfy the condition for Bayesian efficiency in (4.529), so $\hat{\boldsymbol{\theta}}_{\text{map}}(\mathbf{R})$ is Bayesian efficient and

$$\boxed{\boldsymbol{\Sigma}_\epsilon = \mathbf{J}_B^{-1} = [\mathbf{K}_\theta^{-1} + \mathbf{V}^T \mathbf{K}_n^{-1} \mathbf{V}]^{-1}.} \quad (5.636)$$

We can also write $\boldsymbol{\Sigma}_\epsilon$ as

$$\boxed{\boldsymbol{\Sigma}_\epsilon = \mathbf{K}_\theta - \mathbf{K}_\theta \mathbf{V}^T [\mathbf{V} \mathbf{K}_\theta \mathbf{V}^T + \mathbf{K}_n]^{-1} \mathbf{V} \mathbf{K}_\theta} \quad (5.637)$$

by using the matrix inversion lemma on (5.636).

We can also write $\hat{\boldsymbol{\theta}}_{\text{map}}(\mathbf{R})$ as

$$\hat{\boldsymbol{\theta}}_{\text{map}}(\mathbf{R}) = \mathbf{m}_\theta + \boldsymbol{\Sigma}_\epsilon \mathbf{V}^T \mathbf{K}_n^{-1} [\mathbf{R} - \mathbf{V} \mathbf{m}_\theta]. \quad (5.638)$$

Since the *a posteriori* density is Gaussian, the conditional mean equals the conditional mode and

$$\hat{\boldsymbol{\theta}}_{\text{ms}}(\mathbf{R}) = \hat{\boldsymbol{\theta}}_{\text{map}}(\mathbf{R}). \quad (5.639)$$

The corresponding results for complex observations are

$$\boxed{\hat{\boldsymbol{\theta}}_{\text{map}}(\tilde{\mathbf{R}}) = \tilde{\mathbf{m}}_{\tilde{\theta}} + \tilde{\boldsymbol{\Sigma}}_\epsilon \tilde{\mathbf{V}}^H \tilde{\mathbf{K}}_n^{-1} [\tilde{\mathbf{R}} - \tilde{\mathbf{V}} \tilde{\mathbf{m}}_{\tilde{\theta}}],} \quad (5.640)$$

and

$$\boxed{\tilde{\boldsymbol{\Sigma}}_\epsilon = [\tilde{\mathbf{K}}_{\tilde{\theta}}^{-1} + \tilde{\mathbf{V}}^H \tilde{\mathbf{K}}_n^{-1} \tilde{\mathbf{V}}]^{-1}.} \quad (5.641)$$

Note that because \mathbf{K}_n is known we can always reduce the real parameter model to

$$\mathbf{K}_n = \sigma_w^2 \mathbf{I} \quad (5.642)$$

by a whitening transformation. Then, (5.638) reduces to

$$\boxed{\hat{\boldsymbol{\theta}}_{\text{map}}(\mathbf{R}) = \mathbf{m}_\theta + \frac{1}{\sigma_w^2} \boldsymbol{\Sigma}_\epsilon \mathbf{V}^T [\mathbf{R} - \mathbf{V} \mathbf{m}_\theta],} \quad (5.643)$$

and (5.636) reduces to

$$\boxed{\boldsymbol{\Sigma}_\epsilon = \left[\mathbf{K}_\theta^{-1} + \frac{1}{\sigma_w^2} \mathbf{V}^T \mathbf{V} \right]^{-1}.} \quad (5.644)$$

The MAP/MMSE estimator can be implemented as shown in Figure 5.25 for the zero-mean white noise case. The first box maps \mathbf{R} into a D -dimensional subspace and the second box multiplies it by $\boldsymbol{\Sigma}_\epsilon$.

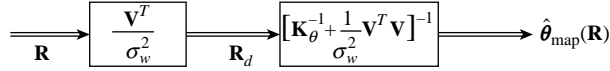


Figure 5.25: Correlator implementation of MAP estimator.

The corresponding result for complex white noise $CN(\mathbf{0}, \sigma_{\tilde{w}}^2 \mathbf{I})$ is,

$$\hat{\theta}_{\text{map}}(\tilde{\mathbf{R}}) = \tilde{\mathbf{m}}_{\tilde{\theta}} + \frac{1}{\sigma_{\tilde{w}}^2} \tilde{\Sigma}_{\epsilon} \tilde{\mathbf{V}}^H [\tilde{\mathbf{R}} - \tilde{\mathbf{V}} \tilde{\mathbf{m}}_{\tilde{\theta}}], \quad (5.645)$$

and

$$\tilde{\Sigma}_{\epsilon} = \left[\tilde{\mathbf{K}}_{\tilde{\theta}}^{-1} + \frac{1}{\sigma_{\tilde{w}}^2} \tilde{\mathbf{V}}^H \tilde{\mathbf{V}} \right]^{-1}. \quad (5.646)$$

In many cases of interest, we have a sequence of independent vector observations \mathbf{r}_k , $k = 1, 2, \dots, K$, where both \mathbf{V} and \mathbf{K}_n are a function of k , that is,

$$\mathbf{r}_k \sim N(\mathbf{V}_k \boldsymbol{\theta}, \mathbf{K}_{n_k}). \quad (5.647)$$

Then,

$$l_B(\boldsymbol{\theta}; \mathbf{R}) = -\frac{1}{2} \sum_{k=1}^K \left\{ [\mathbf{R}_k - \mathbf{V}_k \boldsymbol{\theta}]^T \mathbf{K}_{n_k}^{-1} [\mathbf{R}_k - \mathbf{V}_k \boldsymbol{\theta}] \right\} - \frac{1}{2} (\boldsymbol{\theta} - \mathbf{m}_{\boldsymbol{\theta}})^T \mathbf{K}_{\boldsymbol{\theta}}^{-1} (\boldsymbol{\theta} - \mathbf{m}_{\boldsymbol{\theta}}) + \zeta. \quad (5.648)$$

Then,

$$\hat{\boldsymbol{\theta}}_{\text{map}}(\mathbf{R}) = \mathbf{m}_{\boldsymbol{\theta}} + \left[\mathbf{K}_{\boldsymbol{\theta}}^{-1} + \sum_{k=1}^K \mathbf{V}_k^T \mathbf{K}_{n_k}^{-1} \mathbf{V}_k \right]^{-1} \sum_{k=1}^K \mathbf{V}_k^T \mathbf{K}_{n_k}^{-1} [\mathbf{R}_k - \mathbf{V}_k \mathbf{m}_{\boldsymbol{\theta}}] \quad (5.649)$$

and

$$\Sigma_{\epsilon} = \left[\mathbf{K}_{\boldsymbol{\theta}}^{-1} + \sum_{k=1}^K \mathbf{V}_k^T \mathbf{K}_{n_k}^{-1} \mathbf{V}_k \right]^{-1}. \quad (5.650)$$

In many applications, the model is specified in terms of $\mathbf{K}_{\boldsymbol{\theta}}$, $\mathbf{K}_{\mathbf{r}}$, and $\mathbf{K}_{\boldsymbol{\theta}, \mathbf{r}}$ instead of the form in (5.628). We derive the MAP equations and MSE matrix in terms of these quantities and show the equivalence of the two models. We need to find the posterior probability density,

$$p_{\boldsymbol{\theta}|\mathbf{r}}(\boldsymbol{\theta}|\mathbf{R}) = \frac{p_{\boldsymbol{\theta}, \mathbf{r}}(\boldsymbol{\theta}, \mathbf{R})}{p_{\mathbf{r}}(\mathbf{R})} = \frac{p_{\mathbf{r}|\boldsymbol{\theta}}(\mathbf{R}|\boldsymbol{\theta}) p_{\boldsymbol{\theta}}(\boldsymbol{\theta})}{p_{\mathbf{r}}(\mathbf{R})}. \quad (5.651)$$

We begin by defining $p_{\boldsymbol{\theta}, \mathbf{r}}(\boldsymbol{\theta}, \mathbf{R})$. We assume that $\boldsymbol{\theta}$ and \mathbf{R} are real, jointly Gaussian random vectors. The random vector $\boldsymbol{\theta}$ is distributed $N(\mathbf{m}_{\boldsymbol{\theta}}, \mathbf{K}_{\boldsymbol{\theta}})$ and the random vector \mathbf{r} is distributed

$N(\mathbf{m}_r, \mathbf{K}_r)$. Thus,

$$\begin{aligned} p_{\theta,r}(\boldsymbol{\theta}, \mathbf{R}) &= \frac{1}{(2\pi)^{N/2}(2\pi)^{D/2}|\mathbf{K}_{\theta,r}|^{1/2}} \\ &\times \exp \left\{ -\frac{1}{2} [(\boldsymbol{\theta} - \mathbf{m}_\theta)^T \quad (\mathbf{R} - \mathbf{m}_r)^T] \mathbf{K}_{\theta,r}^{-1} \begin{bmatrix} \boldsymbol{\theta} - \mathbf{m}_\theta \\ \mathbf{R} - \mathbf{m}_r \end{bmatrix} \right\}, \end{aligned} \quad (5.652)$$

where

$$\mathbf{K}_{\theta,r} = E \left\{ \begin{bmatrix} \boldsymbol{\theta} - \mathbf{m}_\theta \\ \mathbf{R} - \mathbf{m}_r \end{bmatrix} \begin{bmatrix} (\boldsymbol{\theta} - \mathbf{m}_\theta)^T & (\mathbf{R} - \mathbf{m}_r)^T \end{bmatrix} \right\} = \begin{bmatrix} \mathbf{K}_\theta & \mathbf{K}_{\theta r} \\ \mathbf{K}_{r \theta} & \mathbf{K}_r \end{bmatrix}. \quad (5.653)$$

The conditional density of interest is the *a posteriori* probability of $\boldsymbol{\theta}$ given \mathbf{r} ,

$$p_{\theta|r}(\boldsymbol{\theta}|\mathbf{R}) = \frac{(2\pi)^{N/2}|\mathbf{K}_r|^{1/2} \exp \left\{ -\frac{1}{2} [(\boldsymbol{\theta} - \mathbf{m}_\theta)^T \quad (\mathbf{R} - \mathbf{m}_r)^T] \mathbf{K}_{\theta,r}^{-1} \begin{bmatrix} \boldsymbol{\theta} - \mathbf{m}_\theta \\ \mathbf{R} - \mathbf{m}_r \end{bmatrix} \right\}}{(2\pi)^{N/2}(2\pi)^{D/2}|\mathbf{K}_{\theta,r}|^{1/2} \exp \left\{ -\frac{1}{2} (\mathbf{R} - \mathbf{m}_r)^T \mathbf{K}_r^{-1} (\mathbf{R} - \mathbf{m}_r) \right\}}. \quad (5.654)$$

To evaluate (5.654), we use the partitioned matrix inverse,

$$\begin{bmatrix} \mathbf{K}_\theta & \mathbf{K}_{\theta r} \\ \mathbf{K}_{r \theta} & \mathbf{K}_r \end{bmatrix}^{-1} = \begin{bmatrix} \mathbf{0} & \mathbf{0} \\ \mathbf{0} & \mathbf{K}_r^{-1} \end{bmatrix} + \begin{bmatrix} \mathbf{I} \\ \mathbf{K}_r^{-1} \mathbf{K}_{r \theta} \end{bmatrix} \boldsymbol{\Omega}^{-1} \begin{bmatrix} \mathbf{I} & -\mathbf{K}_{\theta r} \mathbf{K}_r^{-1} \end{bmatrix}, \quad (5.655)$$

where

$$\boldsymbol{\Omega} = \mathbf{K}_\theta - \mathbf{K}_{\theta r} \mathbf{K}_r^{-1} \mathbf{K}_{r \theta}, \quad (5.656)$$

and the property

$$\det[\mathbf{K}_{\theta,r}] = \det[\mathbf{K}_r] \det[\boldsymbol{\Omega}]. \quad (5.657)$$

Using (5.655), (5.656), and (5.657) in (5.654) gives

$$\begin{aligned} p_{\theta|r}(\boldsymbol{\theta}|\mathbf{R}) &= \frac{1}{(2\pi)^{D/2}|\boldsymbol{\Omega}|^{1/2}} \\ &\times \exp \left\{ -\frac{1}{2} [\boldsymbol{\theta} - \mathbf{m}_\theta - \mathbf{K}_{\theta r} \mathbf{K}_r^{-1} (\mathbf{R} - \mathbf{m}_r)]^T \boldsymbol{\Omega}^{-1} [\boldsymbol{\theta} - \mathbf{m}_\theta - \mathbf{K}_{\theta r} \mathbf{K}_r^{-1} (\mathbf{R} - \mathbf{m}_r)] \right\}, \end{aligned} \quad (5.658)$$

which is a Gaussian density with mean $\mathbf{m}_\theta + \mathbf{K}_{\theta r} \mathbf{K}_r^{-1} (\mathbf{R} - \mathbf{m}_r)$ and covariance matrix $\boldsymbol{\Omega}$.

Therefore,

$$\boxed{\hat{\boldsymbol{\theta}}_{\text{map}}(\mathbf{R}) = \hat{\boldsymbol{\theta}}_{\text{ms}}(\mathbf{R}) = \mathbf{m}_\theta + \mathbf{K}_{\theta r} \mathbf{K}_r^{-1} (\mathbf{R} - \mathbf{m}_r)} \quad (5.659)$$

and the MSE matrix is

$$\boxed{\boldsymbol{\Sigma}_\epsilon = \mathbf{K}_\theta - \mathbf{K}_{\theta r} \mathbf{K}_r^{-1} \mathbf{K}_{r \theta}}. \quad (5.660)$$

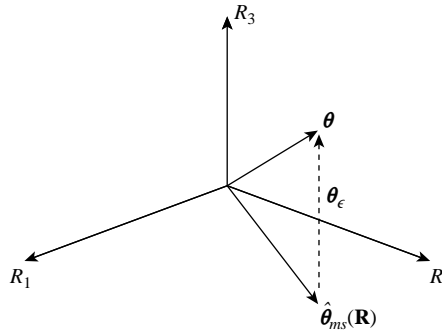


Figure 5.26: Orthogonality of estimation error.

The estimation error is

$$\theta_\epsilon(\mathbf{R}) = \hat{\theta}_{ms}(\mathbf{R}) - \theta = \mathbf{K}_{\theta\mathbf{r}} \mathbf{K}_\mathbf{r}^{-1} (\mathbf{R} - \mathbf{m}_\mathbf{r}) - (\theta - \mathbf{m}_\theta). \quad (5.661)$$

It is orthogonal to the space defined by linear transformation of \$\mathbf{R}\$

$$E \{ [\mathbf{K}_{\theta\mathbf{r}} \mathbf{K}_\mathbf{r}^{-1} (\mathbf{R} - \mathbf{m}_\mathbf{r}) - (\theta - \mathbf{m}_\theta)] (\mathbf{R} - \mathbf{m}_\mathbf{r})^T \mathbf{T} \} = (\mathbf{K}_{\theta\mathbf{r}} \mathbf{K}_\mathbf{r}^{-1} \mathbf{K}_\mathbf{r} - \mathbf{K}_{\theta\mathbf{r}}) \mathbf{T} = \mathbf{0}. \quad (5.662)$$

The orthogonality is shown in Figure 5.26.

For the model in (5.628), we have

$$\mathbf{m}_\mathbf{r} = \mathbf{V} \mathbf{m}_\theta, \quad (5.663)$$

$$\mathbf{K}_{\theta\mathbf{r}} = \mathbf{K}_\theta \mathbf{V}^T, \quad (5.664)$$

$$\mathbf{K}_\mathbf{r} = \mathbf{V} \mathbf{K}_\theta \mathbf{V}^T + \mathbf{K}_n. \quad (5.665)$$

Using (5.663)–(5.665) in (5.659) and (5.660), we obtain (5.632) and (5.637).

We now consider several examples. The first is a special case of the Bayesian linear Gaussian model that we encountered in Chapter 3 that is useful to revisit.

Example 5.21. Consider the signal model in Section 3.3,

$$\mathbf{r} = \mathbf{s} + \mathbf{n}, \quad (5.666)$$

where \$\mathbf{s}\$ is an \$N \times 1\$ zero-mean Gaussian random vector \$N(\mathbf{0}, \mathbf{K}_s)\$ and \$\mathbf{n}\$ is an \$N \times 1\$ zero-mean Gaussian random vector \$N(\mathbf{0}, \mathbf{K}_n)\$ that is statistically independent of \$\mathbf{s}\$. This is a special case of (5.628) with \$\mathbf{s} = \theta\$ and \$\mathbf{V} = \mathbf{I}\$. Then from (5.631),

$$\hat{\mathbf{s}}_{map}(\mathbf{R}) = \hat{\mathbf{s}}_{ms}(\mathbf{R}) = [\mathbf{K}_s^{-1} + \mathbf{K}_n^{-1}]^{-1} \mathbf{K}_n^{-1} \mathbf{R}. \quad (5.667)$$

When

$$\mathbf{K}_n = \sigma_w^2 \mathbf{I}, \quad (5.668)$$

this reduces to

$$\hat{\mathbf{s}}_{ms}(\mathbf{R}) = \left\{ \frac{1}{\sigma_w^2} \left[\frac{1}{\sigma_w^2} \mathbf{I} + \mathbf{K}_s^{-1} \right]^{-1} \right\} \mathbf{R}. \quad (5.669)$$

The term in the braces is the \mathbf{H} matrix that we encountered in our estimator–correlator interpretation of the optimum detector in (3.342).

For the general case, we can use (5.632) to write

$$\hat{\mathbf{s}}_{\text{ms}}(\mathbf{R}) = \left\{ \mathbf{K}_s [\mathbf{K}_n + \mathbf{K}_s]^{-1} \right\} \mathbf{R}, \quad (5.670)$$

and the term in braces corresponds to the \mathbf{H} matrix in (3.455). ■

The next two examples demonstrate that the MAP and MMSE estimates approach the ML estimate asymptotically. We first derive a general result and then revisit the target tracking problem.

Example 5.22. Consider the model where the observations are IID Gaussian vectors $N(\mathbf{V}\boldsymbol{\theta}, \sigma_w^2 \mathbf{I})$ and the *a priori* density is $N(\mathbf{0}, \sigma_s^2 \mathbf{I})$. There are K observations. Thus,

$$\mathbf{r}_k = \mathbf{V}\boldsymbol{\theta} + \mathbf{n}_k, \quad k = 1, 2, \dots, K. \quad (5.671)$$

From (5.649),

$$\hat{\boldsymbol{\theta}}_{\text{map}}(\mathbf{R}) = \left\{ \left[\frac{\mathbf{I}}{K\sigma_s^2} + \frac{\mathbf{V}^T \mathbf{V}}{\sigma_w^2} \right]^{-1} \frac{\mathbf{V}^T}{\sigma_w^2} \right\} \left\{ \frac{1}{K} \sum_{k=1}^K \mathbf{R}_k \right\} \quad (5.672)$$

and from (5.650)

$$\boldsymbol{\Sigma}_e = \frac{1}{K} \left[\frac{\mathbf{V}^T \mathbf{V}}{\sigma_w^2} + \frac{\mathbf{I}}{K\sigma_s^2} \right]^{-1}. \quad (5.673)$$

Note that as $K \rightarrow \infty$,

$$\lim_{K \rightarrow \infty} \hat{\boldsymbol{\theta}}_{\text{map}}(\mathbf{R}) = [\mathbf{V}^T \mathbf{V}]^{-1} \mathbf{V}^T \left\{ \frac{1}{K} \sum_{k=1}^K \mathbf{R}_k \right\} = \hat{\boldsymbol{\theta}}_{\text{ml}}(\mathbf{R}). \quad (5.674)$$

and

$$\lim_{K \rightarrow \infty} \boldsymbol{\Sigma}_e = \frac{\mathbf{V}^T \mathbf{V}}{K\sigma_w^2} = \mathbf{J}_F(\boldsymbol{\theta})^{-1}. \quad (5.675)$$

The rate at which $\hat{\boldsymbol{\theta}}_{\text{map}}(\mathbf{R})$ approaches $\hat{\boldsymbol{\theta}}_{\text{ml}}(\mathbf{R})$ will depend on

$$K \frac{\sigma_s^2}{\sigma_w^2} \triangleq K \text{ SNR}. \quad (5.676)$$

■

Example 5.23 (continuation of Examples 5.1a and 5.8) Target tracking. Consider the target tracking problem in Example 5.1a where

$$r_n = x_0 + v_0 nT + w_n, \quad n = 1, 2, \dots, N \quad (5.677)$$

where the initial position x_0 is $N(0, \sigma_x^2)$, the initial velocity v_0 is $N(0, \sigma_v^2)$, and the variables are statistically independent. The noise w_n is IID $N(0, \sigma_w^2)$.

We define $\boldsymbol{\theta}$, \mathbf{V} , and \mathbf{r} as in (5.13), (5.17), and (5.18). Then from (5.631),

$$\hat{\boldsymbol{\theta}}_{\text{map}}(\mathbf{R}) = \left[\mathbf{K}_{\boldsymbol{\theta}}^{-1} + \frac{1}{\sigma_w^2} \mathbf{V}^T \mathbf{V} \right]^{-1} \frac{\mathbf{V}^T}{\sigma_w^2} \mathbf{R}, \quad (5.678)$$

where

$$\mathbf{K}_\theta = \begin{bmatrix} \sigma_x^2 & 0 \\ 0 & \sigma_v^2 \end{bmatrix}. \quad (5.679)$$

The second term in (5.678) can be written as

$$\frac{\mathbf{V}^T \mathbf{R}}{\sigma_w^2} = \frac{1}{\sigma_w^2} \begin{bmatrix} \sum_{n=1}^N R_n \\ \sum_{n=1}^N nT R_n \end{bmatrix}. \quad (5.680)$$

Using (5.679), (5.680), and (5.155) in (5.678) gives

$$\hat{\theta}_{\text{map}}(\mathbf{R}) = \left[\begin{bmatrix} \frac{1}{\sigma_x^2} & 0 \\ 0 & \frac{1}{\sigma_v^2} \end{bmatrix} + \frac{1}{\sigma_w^2} \begin{bmatrix} N & \frac{1}{2}N(N+1)T \\ \frac{1}{2}N(N+1)T & \frac{1}{6}N(N+1)(2N+1)T^2 \end{bmatrix} \right]^{-1} \frac{1}{\sigma_w^2} \begin{bmatrix} \sum_{n=0}^N R_n \\ \sum_{n=0}^N nT R_n \end{bmatrix}. \quad (5.681)$$

The Bayesian information matrix is given by (5.633),

$$\mathbf{J}_B = \left[\begin{bmatrix} \frac{1}{\sigma_x^2} & 0 \\ 0 & \frac{1}{\sigma_v^2} \end{bmatrix} + \frac{1}{\sigma_w^2} \begin{bmatrix} N & \frac{1}{2}N(N+1)T \\ \frac{1}{2}N(N+1)T & \frac{1}{6}N(N+1)(2N+1)T^2 \end{bmatrix} \right], \quad (5.682)$$

where the second term is the Fisher information matrix $\mathbf{J}_F(\theta)$ derived in Example 5.8, equation (5.155). The MSE matrix of θ satisfies the bound \mathbf{J}_B^{-1} .

The estimated position of the target at any time n is given by

$$\hat{x}_{\text{map}}(n) = [1 \ nT] \hat{\theta}_{\text{map}}(\mathbf{R}). \quad (5.683)$$

Therefore,

$$\text{MSE}(\hat{x}_{\text{map}}(n)) = [1 \ nT] \mathbf{J}_B^{-1} \begin{bmatrix} 1 \\ nT \end{bmatrix}. \quad (5.684)$$

In Figure 5.27, we plot the MSE of $\hat{x}(n)$ for $N = 11$ and various values of σ_x^2 and σ_v^2 . When σ_x^2 and σ_v^2 are large, $\mathbf{J}_B \rightarrow \mathbf{J}_F(\theta)$ and we obtain the same performance as for the ML estimator shown in Figure 5.3. As the *a priori* variances σ_x^2 and/or σ_v^2 decrease, this helps the MAP estimator and its variance decreases. Decreasing the prior uncertainty in the position (σ_x^2) has a bigger impact than decreasing the uncertainty in the velocity (σ_v^2). ■

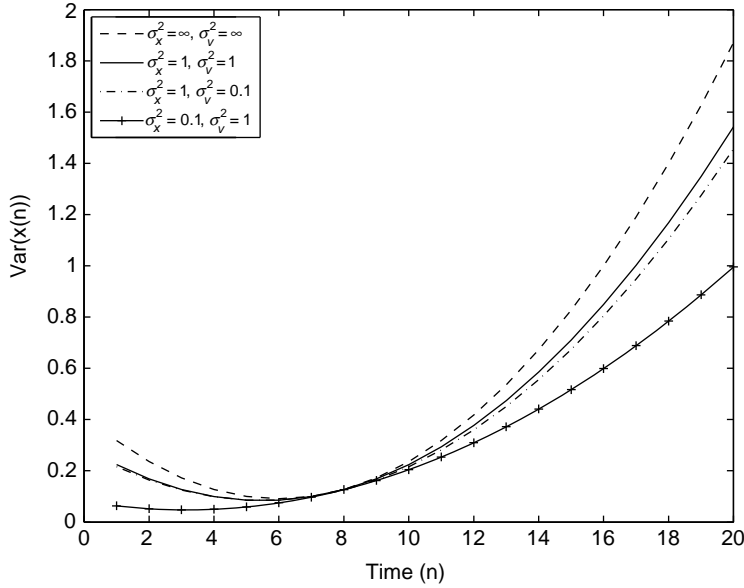


Figure 5.27: MSE of $\hat{x}_{\text{map}}(n)$ versus n for $N = 11$.

5.3.3 Summary

In this section, we have discussed Bayesian estimation of random parameters. For real parameters, the Bayesian log-likelihood function for the general Gaussian model was given in (5.602),

$$l_B(\boldsymbol{\theta}; \mathbf{R}) = -\frac{1}{2} \ln |\mathbf{K}(\boldsymbol{\theta}_c)| - \frac{1}{2} \{[\mathbf{R} - \mathbf{m}(\boldsymbol{\theta}_m)]^T \mathbf{K}^{-1}(\boldsymbol{\theta}_c) [\mathbf{R} - \mathbf{m}(\boldsymbol{\theta}_m)]\} + \ln p_{\boldsymbol{\theta}}(\boldsymbol{\theta}) + \zeta.$$

The MAP estimate was given by (5.603),

$$\hat{\boldsymbol{\theta}}_{\text{map}}(\mathbf{R}) = \underset{\boldsymbol{\theta}}{\operatorname{argmax}} \{l_B(\boldsymbol{\theta}; \mathbf{R})\}.$$

We used the BCRB and ECRB to bound the performance and predict asymptotic behavior. Whenever they were available, we used conjugate priors for the prior density of the parameters. We showed that as the number of samples increases, the MAP and MMSE estimates approach the ML estimate.

The Bayesian linear Gaussian model was discussed in Section 5.3.2. Here the unknown parameter appeared linearly in the observation,

$$\mathbf{r} = \mathbf{V}\boldsymbol{\theta} + \mathbf{n},$$

and the conjugate prior was $N(\mathbf{m}_{\boldsymbol{\theta}}, \mathbf{K}_{\boldsymbol{\theta}})$.

The Bayesian log-likelihood function was given by (5.629),

$$l_B(\boldsymbol{\theta}; \mathbf{R}) = -\frac{1}{2} \{[\mathbf{R} - \mathbf{V}\boldsymbol{\theta}]^T \mathbf{K}_{\mathbf{n}}^{-1} [\mathbf{R} - \mathbf{V}\boldsymbol{\theta}]\} - \frac{1}{2} (\boldsymbol{\theta} - \mathbf{m}_{\boldsymbol{\theta}})^T \mathbf{K}_{\boldsymbol{\theta}}^{-1} (\boldsymbol{\theta} - \mathbf{m}_{\boldsymbol{\theta}}) + \zeta,$$

and $\hat{\theta}_{\text{map}}(\mathbf{R})$, which is equal to $\hat{\theta}_{\text{ms}}(\mathbf{R})$, was given by (5.631),

$$\hat{\theta}_{\text{map}}(\mathbf{R}) = \mathbf{m}_\theta + [\mathbf{K}_\theta^{-1} + \mathbf{V}^T \mathbf{K}_n^{-1} \mathbf{V}]^{-1} \mathbf{V}^T \mathbf{K}_n^{-1} [\mathbf{R} - \mathbf{V} \mathbf{m}_\theta].$$

The estimate is efficient and satisfies the BCRB given in (5.636),

$$\Sigma_\epsilon = \mathbf{J}_B^{-1} = [\mathbf{K}_\theta^{-1} + \mathbf{V}^T \mathbf{K}_n^{-1} \mathbf{V}]^{-1}.$$

5.4 SEQUENTIAL ESTIMATION

All of our models in Chapters 4 and 5 have assumed that we received all of the data and did block processing. In many applications, the data is observed sequentially and we would like to generate an updated estimate as each new observation arrives. This approach is referred to as “sequential” or “recursive” estimation.

In Section 5.4.1, we derive the sequential version of Bayes estimation for the Bayesian linear Gaussian model. In Section 5.4.2, we derive the sequential version of maximum likelihood estimation for the Fisher linear Gaussian model. It will turn out to be the same algorithm except for the initialization. From our discussion in Section 5.2.9, we know that this algorithm will also be the recursive least squares algorithm.

5.4.1 Sequential Bayes Estimation

In this section, we derive a sequential Bayes estimator that computes θ recursively.¹⁴ We do the scalar observation case first. The model is

$$r(n) = \mathbf{v}(n)\theta + w(n), \quad n = 1, 2, \dots, N, \quad (5.685)$$

where $\mathbf{v}(n)$ is $1 \times D$, and θ is $D \times 1$ and $w(n) \sim N(0, \sigma_w^2)$. We write this as an N -dimensional vector,

$$\mathbf{r} = \mathbf{V}\theta + \mathbf{n}, \quad (5.686)$$

where

$$\mathbf{V} \triangleq \begin{bmatrix} \mathbf{v}(1) \\ \mathbf{v}(2) \\ \vdots \\ \mathbf{v}(N) \end{bmatrix}. \quad (5.687)$$

We want to rewrite the model to emphasize that we first solve the problem with one observation, then two observations and so forth. We define the $k \times 1$ vectors \mathbf{r}_k and \mathbf{w}_k ,

¹⁴This is Problem 2.6.13 on p. 158 of DEMT-I.

whose dimension corresponds to the current number of samples, as

$$\mathbf{r}_k \triangleq [r(1) \ r(2) \ \cdots \ r(k)]^T, \quad k = 1, 2, \dots, \quad (5.688)$$

$$\mathbf{w}_k \triangleq [w(1) \ w(2) \ \cdots \ w(k)]^T, \quad k = 1, 2, \dots. \quad (5.689)$$

The noise \mathbf{w}_k is a zero-mean real Gaussian random vector whose elements are uncorrelated $N(0, \sigma_w^2)$, so

$$\mathbf{K}_{\mathbf{w}_k} = \sigma_w^2 \mathbf{I}_{k \times k}. \quad (5.690)$$

We define the matrix \mathbf{V}_k to be the $k \times D$ matrix whose column length equals the number of samples, k ,

$$\mathbf{V}_k = \begin{bmatrix} \mathbf{v}(1) \\ \mathbf{v}(2) \\ \vdots \\ \mathbf{v}(k) \end{bmatrix}. \quad (5.691)$$

The parameter $\boldsymbol{\theta}$ is a real $D \times 1$ Gaussian random vector $N(\mathbf{m}_{\boldsymbol{\theta}}, \mathbf{K}_{\boldsymbol{\theta}})$ that is fixed over the observation interval. Then,

$$\mathbf{r}_k = \mathbf{V}_k \boldsymbol{\theta} + \mathbf{w}_k, \quad k = 1, 2, \dots. \quad (5.692)$$

We have already solved this problem using block processing. The MAP/MMSE estimate $\hat{\boldsymbol{\theta}}(k)$ and its covariance matrix $\Sigma(k)$ for any value of k are given by (5.643) and (5.644),

$$\hat{\boldsymbol{\theta}}(k) = \mathbf{m}_{\boldsymbol{\theta}} + \frac{1}{\sigma_w^2} \Sigma(k) \mathbf{V}_k^T [\mathbf{R}_k - \mathbf{V}_k \mathbf{m}_{\boldsymbol{\theta}}], \quad (5.693)$$

and

$$\Sigma^{-1}(k) = \mathbf{K}_{\boldsymbol{\theta}}^{-1} + \frac{1}{\sigma_w^2} \mathbf{V}_k^T \mathbf{V}_k, \quad (5.694)$$

where we have suppressed the subscripts on $\hat{\boldsymbol{\theta}}(k)$ and $\Sigma(k)$.

We now derive the sequential Bayes estimator. We start with $\hat{\boldsymbol{\theta}}(1)$, the MAP/MMSE estimate based on the first observation $R(1)$. The *a priori* density of $\boldsymbol{\theta}$ is $N(\mathbf{m}_{\boldsymbol{\theta}}, \mathbf{K}_{\boldsymbol{\theta}})$. The estimate is given by

$$\hat{\boldsymbol{\theta}}(1) = \mathbf{m}_{\boldsymbol{\theta}} + \frac{1}{\sigma_w^2} \Sigma(1) \mathbf{v}^T(1) [R(1) - \mathbf{v}(1) \mathbf{m}_{\boldsymbol{\theta}}], \quad (5.695)$$

where

$$\Sigma^{-1}(1) = \mathbf{K}_{\boldsymbol{\theta}}^{-1} + \frac{1}{\sigma_w^2} \mathbf{v}^T(1) \mathbf{v}(1). \quad (5.696)$$

Now $R(2)$ is observed. The block estimate is found using (5.693) and (5.694) with $k = 2$,

$$\begin{aligned}\hat{\theta}(2) &= \mathbf{m}_\theta + \frac{1}{\sigma_w^2} \Sigma(2) \mathbf{V}_2^T [\mathbf{R}_2 - \mathbf{V}_2 \mathbf{m}_\theta] \\ &= \mathbf{m}_\theta + \frac{1}{\sigma_w^2} \Sigma(2) \{ \mathbf{v}^T(1)[R(1) - \mathbf{v}(1)\mathbf{m}_\theta] + \mathbf{v}^T(2)[R(2) - \mathbf{v}(2)\mathbf{m}_\theta] \}. \quad (5.697)\end{aligned}$$

and

$$\begin{aligned}\Sigma^{-1}(2) &= \mathbf{K}_\theta^{-1} + \frac{1}{\sigma_w^2} \mathbf{V}_2^T \mathbf{V}_2 \\ &= \mathbf{K}_\theta^{-1} + \frac{1}{\sigma_w^2} \mathbf{v}^T(1) \mathbf{v}(1) + \frac{1}{\sigma_w^2} \mathbf{v}^T(2) \mathbf{v}(2). \quad (5.698)\end{aligned}$$

From (5.696), we have

$$\Sigma^{-1}(2) = \Sigma^{-1}(1) + \frac{1}{\sigma_w^2} \mathbf{v}^T(2) \mathbf{v}(2). \quad (5.699)$$

Using the matrix inversion lemma on (5.699) yields

$$\Sigma(2) = \Sigma(1) - \Sigma(1) \mathbf{v}^T(2) [\mathbf{v}(2) \Sigma(1) \mathbf{v}^T(2) + \sigma_w^2]^{-1} \mathbf{v}(2) \Sigma(1). \quad (5.700)$$

Substituting (5.700) into (5.697) and rearranging terms yields

$$\hat{\theta}(2) = \hat{\theta}(1) + \frac{1}{\sigma_w^2} \Sigma(2) \mathbf{v}^T(2) [R(2) - \mathbf{v}(2) \hat{\theta}(1)]. \quad (5.701)$$

The results in (5.699) and (5.701) may also be derived by recognizing that the posterior density $p_{\theta|r_1}(\theta|R_1)$ acts as the prior density for the second observation $r(2)$. Its mean and covariance matrix are $\hat{\theta}(1)$ and $\Sigma(1)$.

The term in brackets in (5.701) has an important interpretation. Using (5.659), we can write $\hat{\theta}(1)$ as

$$\hat{\theta}(1) = \mathbf{m}_\theta + \frac{E\{[\theta - \mathbf{m}_\theta][r(1) - m_1]\}}{E\{[r(1) - m_1]^2\}} [R(1) - m_1], \quad (5.702)$$

where

$$m_1 \triangleq E\{r(1)\} = \mathbf{v}(1)\mathbf{m}_\theta. \quad (5.703)$$

We now define $\hat{r}(2|1)$ to be the MMSE estimate of $r(2)$ given $r(1)$,

$$\hat{r}(2|1) = m_2 + \frac{E\{[r(2) - m_2][r(1) - m_1]\}}{E\{[r(1) - m_1]^2\}} [R(1) - m_1], \quad (5.704)$$

where

$$m_2 \triangleq E\{r(2)\} = \mathbf{v}(2)\mathbf{m}_\theta. \quad (5.705)$$

Substituting (5.685) and (5.705) into (5.704) yields

$$\begin{aligned}\hat{r}(2|1) &= \mathbf{v}(2)\mathbf{m}_\theta + \frac{E\{[\mathbf{v}(2)(\boldsymbol{\theta} - \mathbf{m}_\theta) + w(2)][r(1) - m_1]\}}{E\{[r(1) - m_1]^2\}}[R(1) - m_1] \\ &= \mathbf{v}(2) \left[\mathbf{m}_\theta + \frac{E\{[\boldsymbol{\theta} - \mathbf{m}_\theta][r(1) - m_1]\}}{E\{[r(1) - m_1]^2\}}[R(1) - m_1] \right] \\ &= \mathbf{v}(2)\hat{\boldsymbol{\theta}}(1).\end{aligned}\quad (5.706)$$

Thus, the term in the brackets in (5.701) is the residual error

$$R_\epsilon(2) \triangleq R(2) - \hat{r}(2|1). \quad (5.707)$$

From (5.662), we know that $r_\epsilon(2)$ is orthogonal (uncorrelated) with $r(1)$, and because they are Gaussian, they are statistically independent. The residual represents the new information in the data and is referred to as an *innovation*.

After observation $k - 1$, the posterior density of $\boldsymbol{\theta}$ given \mathbf{r}_{k-1} will be Gaussian with mean $\hat{\boldsymbol{\theta}}(k - 1)$ and covariance matrix $\boldsymbol{\Sigma}(k - 1)$. After observing $r(k)$, the new estimate will be

$$\hat{\boldsymbol{\theta}}(k) = \hat{\boldsymbol{\theta}}(k - 1) + \frac{1}{\sigma_w^2} \boldsymbol{\Sigma}(k) \mathbf{v}^T(k) [R(k) - \mathbf{v}(k)\hat{\boldsymbol{\theta}}(k - 1)], \quad (5.708)$$

or, defining a gain vector

$$\mathbf{G}(k) \triangleq \frac{1}{\sigma_w^2} \boldsymbol{\Sigma}(k) \mathbf{v}^T(k), \quad (5.709)$$

(5.708) can be written as

$$\hat{\boldsymbol{\theta}}(k) = \hat{\boldsymbol{\theta}}(k - 1) + \mathbf{G}(k) [R(k) - \mathbf{v}(k)\hat{\boldsymbol{\theta}}(k - 1)], \quad k = 1, 2, \dots, \quad (5.710)$$

or, in terms of innovations,

$$\hat{\boldsymbol{\theta}}(k) = \hat{\boldsymbol{\theta}}(k - 1) + \mathbf{G}(k)R_\epsilon(k), \quad (5.711)$$

where

$$\begin{aligned}R_\epsilon(k) &\triangleq R(k) - \hat{r}(k|k - 1) \\ &= R(k) - \mathbf{v}(k)\hat{\boldsymbol{\theta}}(k - 1).\end{aligned}\quad (5.712)$$

The MSE matrix is

$$\boldsymbol{\Sigma}^{-1}(k) = \boldsymbol{\Sigma}^{-1}(k - 1) + \frac{1}{\sigma_w^2} \mathbf{v}^T(k) \mathbf{v}(k), \quad k = 1, 2, \dots. \quad (5.713)$$

We initialize the algorithm with

$$\boldsymbol{\theta}(0) = \mathbf{m}_\theta \quad (5.714)$$

and

$$\boldsymbol{\Sigma}^{-1}(0) = \mathbf{K}_\theta^{-1}. \quad (5.715)$$

These six equations ((5.709) and (5.711)–(5.715)) specify the sequential Bayes estimator for scalar observations. Note that the $\Sigma(k)$ matrix is $D \times D$ and that $\Sigma^{-1}(k)$ can be precomputed.

As a by-product of the sequential estimation process, we have created an innovation sequence, $r(1) - \hat{r}(1|0)$, $r(2) - \hat{r}(2|1)$, $r(3) - \hat{r}(3|2)$, which are statistically independent, zero-mean Gaussian random variables with variance

$$\sigma_{r_\epsilon}^2(k) = \mathbf{v}(k)\Sigma(k-1)\mathbf{v}^T(k) + \sigma_w^2. \quad (5.716)$$

We will discuss the importance of this result later.

The extension to the case in which each observation is an N -dimensional vector is straightforward. The n th observation vector is

$$\mathbf{r}(n) = \mathbf{V}(n)\boldsymbol{\theta} + \mathbf{n}(n), \quad (5.717)$$

where $\mathbf{V}(n)$ is a known $N \times D$ matrix. As before, $\boldsymbol{\theta}$ is $N(\mathbf{m}_\theta, \mathbf{K}_\theta)$. The noise vector, $\mathbf{n}(n)$ is $N(\mathbf{0}, \mathbf{K}_n)$ and the noise vectors for different n are IID.

Then, using the same technique as in the scalar case gives

$$\hat{\boldsymbol{\theta}}(k) = \hat{\boldsymbol{\theta}}(k-1) + \mathbf{G}(k) \left[\mathbf{R}(k) - \mathbf{V}(k)\hat{\boldsymbol{\theta}}(k-1) \right], \quad (5.718)$$

where

$$\mathbf{G}(k) = \Sigma(k)\mathbf{V}^T(k)\mathbf{K}_n^{-1} \quad (5.719)$$

and

$$\Sigma^{-1}(k) = \Sigma^{-1}(k-1) + \mathbf{V}^T(k)\mathbf{K}_n^{-1}\mathbf{V}(k) \quad k = 1, 2, \dots \quad (5.720)$$

The algorithm is initialized with

$$\boldsymbol{\theta}(0) = \mathbf{m}_\theta, \quad (5.721)$$

$$\Sigma^{-1}(0) = \mathbf{K}_\theta^{-1}. \quad (5.722)$$

The last step in the derivation is to put the $\Sigma(k)$ recursion into a more efficient form. Using the matrix inversion lemma gives

$$\Sigma(k) = \Sigma(k-1) - \Sigma(k-1)\mathbf{V}^T(k) \left[\mathbf{V}(k)\Sigma(k-1)\mathbf{V}^T(k) + \mathbf{K}_n \right]^{-1} \mathbf{V}(k)\Sigma(k-1). \quad (5.723)$$

Substituting (5.723) into (5.719)

$$\begin{aligned} \mathbf{G}(k) &= \left[\Sigma(k-1) - \Sigma(k-1)\mathbf{V}^T(k) \left[\mathbf{V}(k)\Sigma(k-1)\mathbf{V}^T(k) + \mathbf{K}_n \right]^{-1} \mathbf{V}(k)\Sigma(k-1) \right] \mathbf{V}^T(k)\mathbf{K}_n^{-1} \\ &= \Sigma(k-1)\mathbf{V}^T(k) \left[\mathbf{I} - \left[\mathbf{V}(k)\Sigma(k-1)\mathbf{V}^T(k) + \mathbf{K}_n \right]^{-1} \mathbf{V}(k)\Sigma(k-1)\mathbf{V}^T(k) \right] \mathbf{K}_n^{-1} \\ &= \Sigma(k-1)\mathbf{V}^T(k) \left[\left[\mathbf{V}(k)\Sigma(k-1)\mathbf{V}^T(k) + \mathbf{K}_n \right]^{-1} \left[\mathbf{V}(k)\Sigma(k-1)\mathbf{V}^T(k) + \mathbf{K}_n \right] \right. \\ &\quad \left. - \left[\mathbf{V}(k)\Sigma(k-1)\mathbf{V}^T(k) + \mathbf{K}_n \right]^{-1} \mathbf{V}(k)\Sigma(k-1)\mathbf{V}^T(k) \right] \mathbf{K}_n^{-1} \\ &= \Sigma(k-1)\mathbf{V}^T(k) \left[\mathbf{V}(k)\Sigma(k-1)\mathbf{V}^T(k) + \mathbf{K}_n \right]^{-1}. \end{aligned} \quad (5.724)$$

We note that the term in brackets in (5.724),

$$\mathbf{S}_{\mathbf{r}_e}(k) \triangleq \mathbf{V}(k)\Sigma(k-1)\mathbf{V}^T(k) + \mathbf{K}_n \quad (5.725)$$

is the MSE matrix of the residual $\mathbf{r}_e(k)$ and is the matrix equivalent of (5.716).

Using (5.724) in (5.723) gives

$$\Sigma(k) = [\mathbf{I} - \mathbf{G}(k)\mathbf{V}(k)]\Sigma(k-1), \quad (5.726)$$

which is the desired result.

The steps in the sequential MAP/MMSE algorithm are

- (1) Initialize the algorithm with

$$\hat{\theta}(0) = \mathbf{m}_\theta \quad (5.727)$$

and

$$\Sigma(0) = \mathbf{K}_\theta. \quad (5.728)$$

- (2) For $k = 1, 2, \dots$, compute $\mathbf{G}(k)$, $\hat{\theta}(k)$, and $\Sigma(k)$ using (5.724), (5.718), and (5.726),

$$\mathbf{G}(k) = \Sigma(k-1)\mathbf{V}^T(k) [\mathbf{V}(k)\Sigma(k-1)\mathbf{V}^T(k) + \mathbf{K}_n]^{-1}. \quad (5.729)$$

$$\hat{\theta}(k) = \hat{\theta}(k-1) + \mathbf{G}(k) [\mathbf{R}(k) - \mathbf{V}(k)\hat{\theta}(k-1)]. \quad (5.730)$$

$$\Sigma(k) = [\mathbf{I} - \mathbf{G}(k)\mathbf{V}(k)]\Sigma(k-1). \quad (5.731)$$

A flow diagram of the sequential Bayes estimation algorithm is shown in Figure 5.28. The experienced reader will notice that we are just one step away from the Kalman filter. We will develop the continuous time version in Chapter 8 and the discrete time version in Chapter 9 (see also Problem 2.6.15 in [Van68, Van01a]).

Note that $\mathbf{G}(k)$ and $\Sigma(k)$ can be precomputed before any data is received. Note that, because θ is a fixed parameter, $[\Sigma(k)]_{ii}$, $i = 1, 2, \dots, D$ are nonincreasing functions of k .

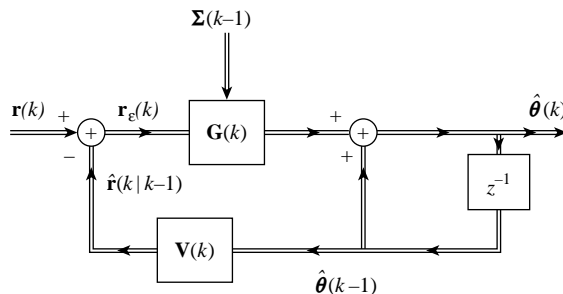


Figure 5.28: Sequential Bayes estimation.

An update of $\Sigma^{-1}(k)$ is given in (5.720). We recognize that

$$\Sigma^{-1}(k) = \mathbf{J}_B(k), \quad (5.732)$$

where $\mathbf{J}_B(k)$ is the Bayesian information matrix. Then (5.720) can be written as

$$\mathbf{J}_B(k) = \mathbf{J}_B(k-1) + \mathbf{V}^T(k)\mathbf{K}_n^{-1}\mathbf{V}(k). \quad (5.733)$$

This is referred to as the “information” implementation of the sequential estimator. We discuss it briefly in the problems and in more detail in Section 9.3.2.2. It can offer computational advantages when the dimension of the observation vector \mathbf{r} is much larger than the dimension of the parameter vector θ .

The algorithm for complex observations is a straightforward modification.

(1) Initialize the algorithm with

$$\hat{\theta}(0) = \tilde{\mathbf{m}}_{\hat{\theta}}, \quad (5.734)$$

$$\tilde{\Sigma}(0) = \tilde{\mathbf{K}}_{\hat{\theta}} \quad (5.735)$$

(2) For $k = 1, 2, \dots$, compute

$$\tilde{\mathbf{G}}(k) = \tilde{\Sigma}(k-1)\tilde{\mathbf{V}}^H(k)[\tilde{\mathbf{V}}(k)\tilde{\Sigma}(k-1)\tilde{\mathbf{V}}^H(k) + \tilde{\mathbf{K}}_n]^{-1}, \quad (5.736)$$

$$\hat{\theta}(k) = \hat{\theta}(k-1) + \tilde{\mathbf{G}}(k)[\tilde{\mathbf{R}}(k) - \tilde{\mathbf{V}}(k)\hat{\theta}(k-1)], \quad (5.737)$$

$$\tilde{\Sigma}(k) = [\mathbf{I} - \tilde{\mathbf{G}}(k)\tilde{\mathbf{V}}(k)]\tilde{\Sigma}(k-1). \quad (5.738)$$

We consider an example to illustrate the sequential Bayes estimation algorithm.

Example 5.24. Consider the simple model in which the observation is a scalar

$$r(k) = \theta + w(k), \quad k = 1, 2, 3, \dots, \quad (5.739)$$

where the $w(k)$ are Gaussian noise samples $N(0, \sigma_w^2)$ and θ is a scalar Gaussian random variable $N(0, \sigma_s^2)$.

We initialize the algorithm with

$$\hat{\theta}(0) = 0, \quad (5.740)$$

$$\Sigma(0) = \sigma_s^2. \quad (5.741)$$

Then for $k = 1, 2, \dots$, we compute

$$G(k) = \Sigma(k-1)[\Sigma(k-1) + \sigma_w^2]^{-1}, \quad (5.742)$$

$$\hat{\theta}(k) = \hat{\theta}(k-1) + G(k)[R(k) - \hat{\theta}(k-1)], \quad (5.743)$$

$$\Sigma(k) = [1 - G(k)]\Sigma(k-1). \quad (5.744)$$

Note that this is the same model as Example 5.19, so we know that $\Sigma(k)$ can be found in closed form to be

$$\Sigma(k) = \frac{\sigma_w^2 \sigma_s^2}{k\sigma_s^2 + \sigma_w^2}. \quad (5.745)$$

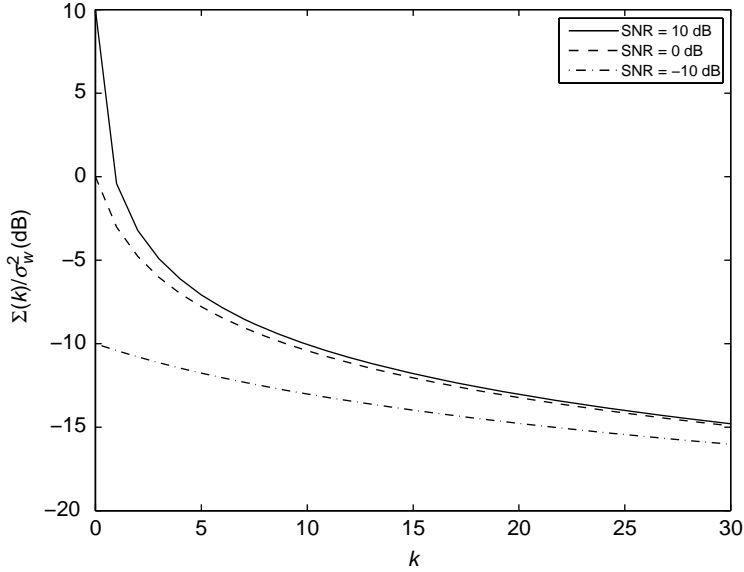


Figure 5.29: Normalized MSE versus k ; SNR = −10 dB, 0 dB, 10 dB.

Thus for large k

$$\lim_{k \rightarrow \infty} \Sigma(k) = \frac{\sigma_w^2}{k}. \quad (5.746)$$

In Figure 5.29, we plot $\Sigma(k)/\sigma_w^2$ versus k for $\sigma_s^2/\sigma_w^2 = -10$ dB, 0 dB, and 10 dB. As k increases, the MSE decreases to a reasonable level so that accurate estimation is possible even for low SNR. ■

Example 5.25 (continuation of Examples 5.1a, 5.8, and 5.23) Target tracking. Consider the model in Example 5.23. We now implement a sequential version of it.¹⁵ Recall that the track is completely specified by x_0 and v_0 , which are statistically independent Gaussian random variables $N(0, \sigma_x^2)$ and $N(0, \sigma_v^2)$, respectively. We want to find

$$\hat{\theta}(k) = \begin{bmatrix} \hat{x}_0(k) \\ \hat{v}_0(k) \end{bmatrix}. \quad (5.747)$$

We can precompute $\Sigma(k)$ using (5.682)

$$\Sigma(k) = \mathbf{J}_B(k)^{-1} = \left\{ \begin{bmatrix} \frac{1}{\sigma_x^2} & 0 \\ 0 & \frac{1}{\sigma_v^2} \end{bmatrix} + \frac{1}{\sigma_w^2} \begin{bmatrix} k & \frac{1}{2}k(k+1)T \\ \frac{1}{2}k(k+1)T & \frac{1}{6}k(k+1)(2k+1)T^2 \end{bmatrix} \right\}^{-1} \quad (5.748)$$

¹⁵This example follows Section 3.5.1 of Bar-Shalom et al. [BSLK01]. A similar model is discussed in Chapter 8 of [Kay93].

or we can compute it sequentially using (5.731). We use (5.730) to compute $\hat{\theta}(k)$. The position estimate at time k is

$$\hat{x}(k) = [1 \quad kT] \hat{\theta}(k) \quad (5.749)$$

and its MSE is

$$\text{MSE}(\hat{x}(k)) = [1 \quad kT] \Sigma(k) \begin{bmatrix} 1 \\ kT \end{bmatrix}. \quad (5.750)$$

This estimate is different from the block processing case considered in Example 5.23. There the entire block of N samples was used to compute $\hat{\theta}_{\text{map}}(\mathbf{R})$ and the position estimates for time before and after N . Here, we only use data samples up to time k to compute the parameter and position estimates at time k .

If we have received k observations, we can also predict where the target will be at time $q + k$. The position estimate is

$$\hat{x}(q+k|k) = [1 \quad (q+k)T] \hat{\theta}(k). \quad (5.751)$$

Its MSE is

$$\text{MSE}(\hat{x}(q+k|k)) = [1 \quad (q+k)T] \Sigma(k) \begin{bmatrix} 1 \\ (q+k)T \end{bmatrix}. \quad (5.752)$$

In Figure 5.30, we plot the MSE of the position estimate obtained using sequential estimation up to time $k = 11$, and prediction using (5.751) for times after $k = 11$. Also plotted are the ML estimator variance using $N = 11$ observations and the block estimation MSE using $N = 11$ from Example 5.23.

We see that the sequential estimator initially has a higher variance, but it gradually decreases and achieves the same performance as the block estimator at $k = N = 11$. For $k > 11$, the performance of the block and sequential estimators is the same. ■

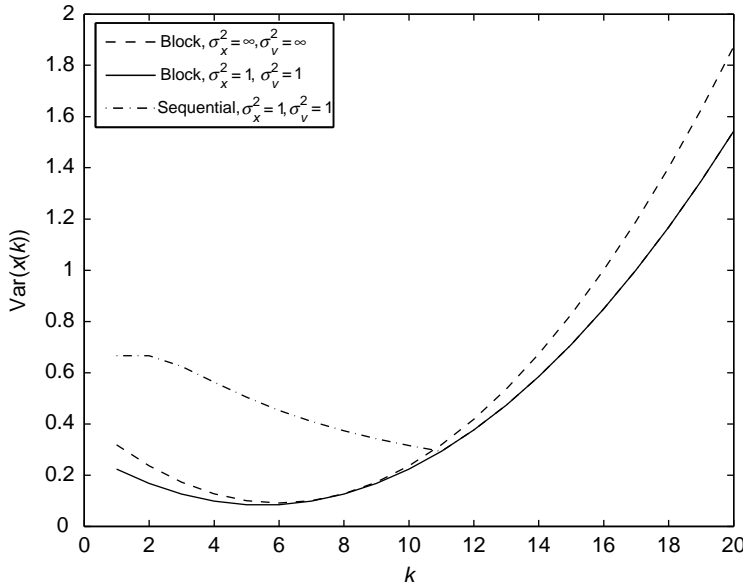


Figure 5.30: MSE of $\hat{x}(k)$; observations from $k=1$ to 11.

5.4.2 Recursive Maximum Likelihood

In this section, we discuss recursive maximum likelihood. In Section 5.2.9.1, we showed that least squares was identical to maximum likelihood with a Gaussian white noise assumption. Therefore, the algorithm developed in this section is also a recursive least squares algorithm. We have used the term “recursive” rather than “sequential” because it is more consistent with the literature.

The model is identical to the one in Section 5.4.1 except θ is a $D \times 1$ nonrandom parameter so that we do not have an *a priori* density $p_\theta(\theta)$. Therefore, in order to initiate a recursive ML algorithm, we must first do block processing on the first D observations. The block processing result for maximum likelihood is given by (5.148) and (5.149)

$$\hat{\theta}_{\text{ml}}(D) = \left[\sum_{k=1}^D \mathbf{V}^T(k) \mathbf{K}_n^{-1} \mathbf{V}(k) \right]^{-1} \sum_{k=1}^D \mathbf{V}^T(k) \mathbf{K}_n^{-1} \mathbf{R}_k, \quad (5.753)$$

$$\Sigma_{\text{ml}}(D) = \left[\sum_{k=1}^D \mathbf{V}^T(k) \mathbf{K}_n^{-1} \mathbf{V}(k) \right]^{-1}. \quad (5.754)$$

The output of the block processing is an estimate $\hat{\theta}(D)$ and a covariance matrix $\Sigma(D)$ that we can use to initiate the recursion. The remaining recursion is identical to the sequential Bayes algorithm.

We can summarize the recursive ML algorithm as follows:

- (1) Initialize the algorithm with $\hat{\theta}_{\text{ml}}(D)$ and $\Sigma_{\text{ml}}(D)$ obtained from (5.753) and (5.754).
- (2) For $k = D + 1, D + 2, \dots$, compute

$$\mathbf{G}_{\text{ml}}(k) = \Sigma_{\text{ml}}(k) \mathbf{V}^T(k) [\mathbf{V}(k) \Sigma_{\text{ml}}(k-1) \mathbf{V}^T(k) + \mathbf{K}_n]^{-1}, \quad (5.755)$$

$$\hat{\theta}_{\text{ml}}(k) = \hat{\theta}_{\text{ml}}(k-1) + \mathbf{G}_{\text{ml}}(k) [\mathbf{R}(k) - \mathbf{V}(k) \hat{\theta}_{\text{ml}}(k-1)], \quad (5.756)$$

$$\Sigma_{\text{ml}}(k) = [\mathbf{I} - \mathbf{G}_{\text{ml}}(k) \mathbf{V}(k)] \Sigma_{\text{ml}}(k-1). \quad (5.757)$$

The block diagram is identical to the Bayes block diagram in Figure 5.28 except for the initialization. As k increases the output of the sequential Bayes estimator will approach the output of the recursive ML estimator.

We consider an example to illustrate the algorithm.

Example 5.26 (continuation of Examples 5.1a, 5.8, 5.23, and 5.25) Target tracking. Consider the model in Examples 5.23 and 5.25. In this case, we have no prior mean and covariance to initialize the algorithm, so we get initial estimates for $D = 2$ parameters using block processing with $N = 2$. From (5.153), the ML estimate is

$$\hat{\theta}_{\text{ml}}(2) = [\mathbf{V}^T \mathbf{V}]^{-1} \mathbf{V}^T \mathbf{R}, \quad (5.758)$$

where

$$\mathbf{V} = \begin{bmatrix} 1 & T \\ 1 & 2T \end{bmatrix} \quad (5.759)$$

and

$$\mathbf{R} = \begin{bmatrix} R_1 \\ R_2 \end{bmatrix}. \quad (5.760)$$

Then,

$$\mathbf{V}^T \mathbf{R} = \begin{bmatrix} R_1 + R_2 \\ T(R_1 + 2R_2) \end{bmatrix} \quad (5.761)$$

and

$$\mathbf{V}^T \mathbf{V} = \begin{bmatrix} 2 & 3T \\ 3T & 5T^2 \end{bmatrix}, \quad (5.762)$$

so

$$(\mathbf{V}^T \mathbf{V})^{-1} = \frac{1}{T^2} \begin{bmatrix} 5T^2 & -3T \\ -3T & 2 \end{bmatrix}. \quad (5.763)$$

Therefore, our initial estimate is

$$\hat{\theta}_{\text{ml}}(2) = \begin{bmatrix} \hat{x}_0(2) \\ \hat{v}_0(2) \end{bmatrix} = \begin{bmatrix} 2R_1 - R_2 \\ \frac{1}{T}(R_2 - R_1) \end{bmatrix} = \begin{bmatrix} R_1 - T\hat{v}_0(2) \\ \frac{1}{T}(R_2 - R_1) \end{bmatrix}. \quad (5.764)$$

The initial velocity estimate is the difference in the observed positions divided by the time interval, and the initial position estimate is the first position observation less the distance traveled in the time interval using the velocity estimate.

The covariance matrix is given by (5.156)

$$\Sigma_{\text{ml}}(2) = \sigma_w^2 (\mathbf{V}^T \mathbf{V})^{-1} = \frac{\sigma_w^2}{T^2} \begin{bmatrix} 5T^2 & -3T \\ -3T & 2 \end{bmatrix}. \quad (5.765)$$

We then use (5.755)–(5.757) to generate $\hat{\theta}_{\text{ml}}(k)$ and $\Sigma_{\text{ml}}(k)$. As in Example 5.25, the sequential position estimate and its variance are given by (5.749) and (5.750). Position predictions for time $q + k$ are given by (5.751) and (5.752).

In Figure 5.31, we plot the position estimate versus k for the same scenario as in Example 5.25. The ML variance is higher than the Bayesian MSE because there is no prior information. The variance decreases until $k = N = 11$, when the recursive ML estimator variance is equal to the block ML estimator variance. ■

Example 5.27. The general target tracking/polynomial /fitting problem is¹⁶

$$x(n) = \sum_{j=0}^D \theta_j \frac{n^j}{j!}, \quad (5.766)$$

where the coefficients of the polynomial $\theta_1, \theta_2, \dots, \theta_D$ are to be estimated. For the tracking problem, θ_1 is the position at some reference time, θ_2 is the velocity at the same reference time, θ_3 is the acceleration at the same reference time, and so on.

¹⁶Our discussion follows pp. 149–152 of Bar-Shalom, Li, and Kirubarajan [BSLK01].

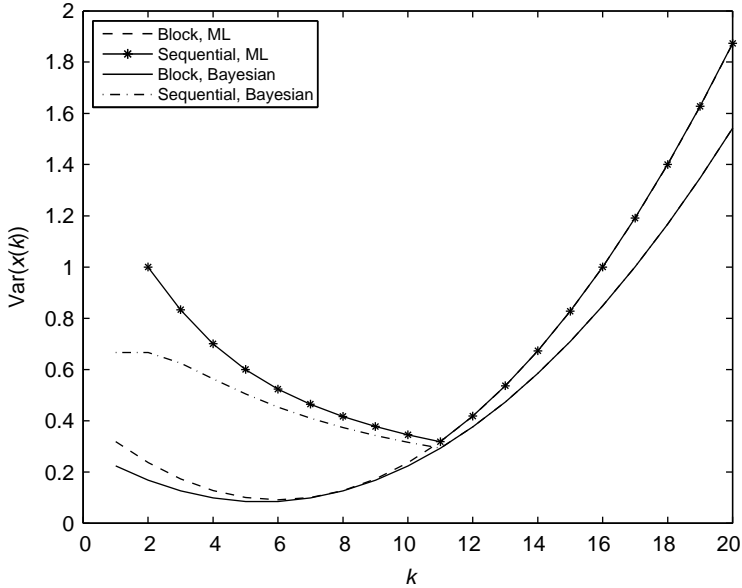


Figure 5.31: Variance of $\hat{x}(k)$: observations from $k = 1$ to 11; sequential Bayesian and recursive ML.

The noisy measurements are

$$r(n) = \mathbf{v}(n)\boldsymbol{\theta} + w(n), \quad n = 1, 2, \dots, k, \quad (5.767)$$

where

$$\boldsymbol{\theta} = [\theta_0 \ \theta_1 \ \theta_2 \ \dots \ \theta_D]^T \quad (5.768)$$

and

$$\mathbf{v}(n) = \left[1 \ n \ \frac{n^2}{2!} \ \dots \ \frac{n^D}{D!} \right]. \quad (5.769)$$

The $w(n)$ are IID $N(0, \sigma_w^2)$.

We can then proceed as in Example 5.26. Once again we must do block processing on the first D observations to initialize the algorithm. We consider some of these cases in the problems. ■

5.4.3 Summary

In this section, we have developed sequential versions of Bayes estimators and maximum likelihood (least squares) estimators. Both estimators are widely used in applications. In addition, the Bayes sequential estimator provides a useful precursor to discrete-time Kalman filter that we will study in Chapter 9.

All of our examples considered reasonably simple problems. In practice, we may deal with much larger observation vectors and parameter vectors. We must consider the actual numerical implementation of the algorithms and the effect of errors. In particular, numerical problems may cause $\Sigma(k)$ to lose its nonnegative definite property. We will need to modify

the algorithm to avoid this problem. We will discuss numerical issues in more detail in Chapter 9.

5.5 SUMMARY

In this chapter, we have studied the general Gaussian estimation problem in detail. The model is defined by the probability density in (5.1),

$$p_{\mathbf{r}|\boldsymbol{\theta}}(\mathbf{R}|\boldsymbol{\theta}) = \frac{1}{(2\pi)^{N/2} |\mathbf{K}(\boldsymbol{\theta})|^{1/2}} \exp \left\{ -\frac{1}{2} [\mathbf{R} - \mathbf{m}(\boldsymbol{\theta})]^T \mathbf{K}^{-1}(\boldsymbol{\theta}) [\mathbf{R} - \mathbf{m}(\boldsymbol{\theta})] \right\}.$$

In Section 5.2, we considered nonrandom parameters. For the general case, this required a minimization over a D -dimensional space as shown in (5.54)

$$\hat{\boldsymbol{\theta}}_{\text{ml}}(\mathbf{R}) = \underset{\boldsymbol{\theta}}{\operatorname{argmin}} \left\{ \ln |\mathbf{K}(\boldsymbol{\theta})| + [\mathbf{R} - \mathbf{m}(\boldsymbol{\theta})]^T \mathbf{K}^{-1}(\boldsymbol{\theta}) [\mathbf{R} - \mathbf{m}(\boldsymbol{\theta})] \right\}.$$

Before considering the solution to the minimization problem we developed compact expressions for the Cramér–Rao bound. For real observations and real parameters, the information matrix, $\mathbf{J}_F(\boldsymbol{\theta})$ was given by (5.72)

$$J_{F_{ij}}(\boldsymbol{\theta}) = \frac{1}{2} \operatorname{tr} \left[\mathbf{K}^{-1}(\boldsymbol{\theta}) \frac{\partial \mathbf{K}(\boldsymbol{\theta})}{\partial \theta_i} \mathbf{K}^{-1}(\boldsymbol{\theta}) \frac{\partial \mathbf{K}(\boldsymbol{\theta})}{\partial \theta_j} \right] + \left[\frac{\partial \mathbf{m}^T(\boldsymbol{\theta})}{\partial \theta_i} \mathbf{K}^{-1}(\boldsymbol{\theta}) \frac{\partial \mathbf{m}(\boldsymbol{\theta})}{\partial \theta_j} \right].$$

and the CRB equaled $\mathbf{J}_F^{-1}(\boldsymbol{\theta})$.

For complex observations and real parameters, $\mathbf{J}_F(\boldsymbol{\theta})$ was given by (5.82)

$$J_{F_{ij}}(\boldsymbol{\theta}) = \operatorname{tr} \left[\tilde{\mathbf{K}}^{-1}(\boldsymbol{\theta}) \frac{\partial \tilde{\mathbf{K}}(\boldsymbol{\theta})}{\partial \theta_i} \tilde{\mathbf{K}}^{-1}(\boldsymbol{\theta}) \frac{\partial \tilde{\mathbf{K}}(\boldsymbol{\theta})}{\partial \theta_j} \right] + 2\Re \left[\frac{\partial \tilde{\mathbf{m}}^H(\boldsymbol{\theta})}{\partial \theta_i} \tilde{\mathbf{K}}^{-1}(\boldsymbol{\theta}) \frac{\partial \tilde{\mathbf{m}}(\boldsymbol{\theta})}{\partial \theta_j} \right].$$

For multiple IID observations, $\mathbf{J}_F(\boldsymbol{\theta})$ was given by (5.84)

$$\mathbf{J}_F(\boldsymbol{\theta}) = K \mathbf{J}_F(\boldsymbol{\theta}; k).$$

It is important to remember that the CRBs are bounds on the covariance matrix and assume an unbiased estimate. For biased estimates, we must add the additional term in (4.109), which assumes that the bias is known. There are two topics that we did not pursue:

1. Estimators that trade off bias and variance to minimize the mean-square error matrix. References that discuss this problem include [HFU96, Eld04], and [SM90].
2. In some models, there are physical constraints on the parameter vector. For example,

$$\theta_{i,\min} \leq \theta_i \leq \theta_{i,\max}.$$

We can develop *constrained* CRBs to study this problem. References that discuss this problem include [GH90, Mar93, SN98], and [MSK02].

In Section 5.2.4, we studied the Fisher linear Gaussian model that is defined by (5.85) for real parameters (or (5.86) for the complex case),

$$\mathbf{r} \sim N(\mathbf{V}\boldsymbol{\theta}_m, \mathbf{K}),$$

where the covariance matrix \mathbf{K} is known.

Then, the ML estimate is given by (5.95) for the real case

$$\hat{\boldsymbol{\theta}}_{\text{ml}}(\mathbf{R}) = [\mathbf{V}^T \mathbf{K}^{-1} \mathbf{V}]^{-1} \mathbf{V}^T \mathbf{K}^{-1} \mathbf{R} \quad (5.770)$$

and (5.130) for the complex case. The estimates are unbiased and efficient. Their error covariance matrix satisfies the CRB with equality.

We considered several important examples to illustrate the behavior. In Section 5.2.4.3, we considered low-rank interference and developed an eigenspace version of the ML estimator shown in Figure 5.6. The structure provides an efficient implementation and also allows us to implement suboptimum reduced-rank estimators.

In Section 5.2.5, we considered separable models. These models are defined by (5.223) for the real observation and the real parameter case

$$\mathbf{r} \sim N(\mathbf{V}(\boldsymbol{\theta}_{nl})\boldsymbol{\theta}_l, \mathbf{K})$$

and (5.225) for the complex observation case.

We found an explicit expression for $\hat{\boldsymbol{\theta}}_l(\mathbf{R})$ and used it to create a compressed log-likelihood function. Thus, $\hat{\boldsymbol{\theta}}_{nl}(\mathbf{R})$ is given by (5.236)

$$\hat{\boldsymbol{\theta}}_{nl}(\mathbf{R}) = \underset{\boldsymbol{\theta}_{nl}}{\operatorname{argmax}} \left\{ \|\mathbf{P}_{\mathbf{V}(\boldsymbol{\theta}_{nl})} \mathbf{R}\|^2 \right\},$$

so we have reduced the problem to a maximization of a D -dimensional space instead of a $2D$ -dimensional space.

In Section 5.2.6, we considered the problem where the mean was known and the unknown parameters were in the covariance matrix. In general, $\hat{\boldsymbol{\theta}}_c$ is given by maximizing (5.317)

$$\hat{\boldsymbol{\theta}}_{c,\text{ml}}(\mathbf{R}) = \underset{\boldsymbol{\theta}_c}{\operatorname{argmax}} \left\{ -\frac{1}{2} \ln |\mathbf{K}(\boldsymbol{\theta}_c)| - \frac{1}{2} \mathbf{R}^T \mathbf{K}^{-1}(\boldsymbol{\theta}_c) \mathbf{R} \right\}.$$

We considered several cases in which the single parameter $\boldsymbol{\theta}_c$ corresponded to the noise power or the 2×1 vector $\boldsymbol{\theta}_c$ corresponded to the signal and noise powers. We were able to obtain closed form expressions for the ML estimates.

In Section 5.2.7, we studied the model in which the observations satisfied the linear Gaussian model but the covariance matrix also contained unknown parameters. We found that we could project \mathbf{R} into the signal subspace to create a compressed log-likelihood function. For the white noise case with unknown variance σ_w^2 , the compressed log-likelihood function was given by (5.399)

$$l(\hat{\boldsymbol{\theta}}_{m,\text{ml}}(\mathbf{R}), \sigma_w^2; \mathbf{R}) = -\frac{N}{2} \ln \sigma_w^2 - \frac{1}{2} \left\{ \frac{1}{\sigma_w^2} [\mathbf{P}_{\mathbf{V}}^\perp \mathbf{R}]^T [\mathbf{P}_{\mathbf{V}}^\perp \mathbf{R}] \right\}$$

and we could obtain an explicit answer for $\hat{\boldsymbol{\theta}}_{m,\text{ml}}(\mathbf{R})$ and $\hat{\sigma}_{w,\text{ml}}^2(\mathbf{R})$.

For the general case, we had to find the maximum of $l(\hat{\theta}_{m,\text{ml}}(\mathbf{R}, \boldsymbol{\theta}_c), \boldsymbol{\theta}_c; \mathbf{R})$ as given by (5.413)

$$\begin{aligned} l(\hat{\theta}_{m,\text{ml}}(\mathbf{R}, \boldsymbol{\theta}_c), \boldsymbol{\theta}_c; \mathbf{R}) &= -\frac{1}{2} \ln |\mathbf{K}(\boldsymbol{\theta}_c)| \\ &\quad - \frac{1}{2} \mathbf{R}^T \left\{ \mathbf{K}^{-1}(\boldsymbol{\theta}_c) - \mathbf{K}^{-1}(\boldsymbol{\theta}_c) \mathbf{V} [\mathbf{V}^T \mathbf{K}^{-1}(\boldsymbol{\theta}_c) \mathbf{V}]^{-1} \mathbf{V}^T \mathbf{K}^{-1}(\boldsymbol{\theta}_c) \right\} \mathbf{R}. \end{aligned}$$

In Section 5.2.8, we developed computational algorithms to solve minimization or maximization problems such as the one in (5.416). We developed three algorithms: gradient techniques, the alternating projection (AP) algorithm, and the expectation–maximization (EM) algorithm, and gave examples to illustrate their performance. The key to good performance is to start with a good set of initial conditions so that we do not converge to an incorrect local maximum or minimum.

In Section 5.2.9, we discussed equivalent algorithms and showed that minimum variance distortionless response (MVDR) algorithm and the least squares algorithm invented by Gauss are equivalent to the ML estimator when the Fisher linear Gaussian model is applicable.

In Section 5.2.10, we provided an introduction to the important problem of the sensitivity of the optimum processor to the case where the actual model is different from the assumed model. We considered a specific example and showed that by imposing a quadratic constraint on the weight vector

$$\tilde{\mathbf{h}}^H \tilde{\mathbf{h}} \leq T_0,$$

we obtain a new estimator that introduces an artificially high noise level by loading the diagonal matrix. The resulting estimator is given in (5.595),

$$\tilde{\mathbf{h}}^H = [\tilde{\mathbf{v}}_s^H (\tilde{\mathbf{K}} + \sigma_L^2 \mathbf{I}) \tilde{\mathbf{v}}_s]^{-1} \tilde{\mathbf{v}}_s^H [\tilde{\mathbf{K}} + \sigma_L^2 \mathbf{I}]^{-1}.$$

Diagonal loading is widely used to develop robust processors. We provided several good references for further study.

In Section 5.3.1, we considered random parameters and developed MAP and MMSE estimators, the BCRB and the ECRB. The Bayesian log-likelihood function is given by (5.602)

$$l_B(\boldsymbol{\theta}; \mathbf{R}) = -\frac{1}{2} \ln |\mathbf{K}(\boldsymbol{\theta}_c)| - \frac{1}{2} \{[\mathbf{R} - \mathbf{m}(\boldsymbol{\theta}_m)]^T \mathbf{K}^{-1}(\boldsymbol{\theta}_c) [\mathbf{R} - \mathbf{m}(\boldsymbol{\theta}_m)]\} + \ln p_{\boldsymbol{\theta}}(\boldsymbol{\theta}) + \zeta,$$

which is just the nonrandom $l(\boldsymbol{\theta}; \mathbf{R})$ plus the log of the prior density. The Bayesian information matrix is

$$\mathbf{J}_B = E_{\boldsymbol{\theta}} \{\mathbf{J}_F(\boldsymbol{\theta})\} + \mathbf{J}_P,$$

where \mathbf{J}_P is given by (5.605). The expected CRB is given by

$$\text{ECRB} = E_{\boldsymbol{\theta}} \{\mathbf{J}_F^{-1}(\boldsymbol{\theta})\} \geq \mathbf{J}_B^{-1} = \text{BCRB}.$$

The ECRB is important in the asymptotic case where

$$\lim_{K \rightarrow \infty} \hat{\boldsymbol{\theta}}_{\text{map}}(\mathbf{R}) \rightarrow \hat{\boldsymbol{\theta}}_{\text{ml}}(\mathbf{R}).$$

We considered several examples where the conjugate priors were applicable and found explicit solutions.

In Section 5.3.2, we considered the Bayesian linear Gaussian model defined by (5.628)

$$\mathbf{r} = \mathbf{V}\boldsymbol{\theta} + \mathbf{n}.$$

This expression has the same form as the Fisher linear Gaussian model. However, the parameter $\boldsymbol{\theta}$ is a random $D \times 1$ vector and the *a priori* density is the conjugate prior which is $N(\mathbf{m}_\theta, \mathbf{K}_\theta)$. We developed the MAP estimator in (5.631)

$$\hat{\boldsymbol{\theta}}_{\text{map}}(\mathbf{R}) = \mathbf{m}_\theta + [\mathbf{K}_\theta^{-1} + \mathbf{V}^T \mathbf{K}_n^{-1} \mathbf{V}]^{-1} \mathbf{V}^T \mathbf{K}_n^{-1} [\mathbf{R} - \mathbf{Vm}_\theta].$$

We also showed that if we defined the Bayesian linear Gaussian problem by requiring $p_{\theta|\mathbf{r}}(\boldsymbol{\theta}|\mathbf{R})$ to be Gaussian, then the MAP estimator had the form in (5.659)

$$\hat{\boldsymbol{\theta}}_{\text{map}}(\mathbf{R}) = \hat{\boldsymbol{\theta}}_{\text{ms}}(\mathbf{R}) = \mathbf{m}_\theta + \mathbf{K}_{\theta\mathbf{r}} \mathbf{K}_{\mathbf{r}}^{-1} (\mathbf{R} - \mathbf{m}_{\mathbf{r}}),$$

which is equivalent to the model in (5.628).

In Section 5.4, we developed sequential estimation. The result was the sequential MAP/MMSE estimator shown in Figure 5.28 and specified by (5.727)–(5.731). This sequential MAP/MMSE algorithm is important when the observations are received sequentially.

We also showed that the recursive ML algorithm had the same structure but required an initial block estimate using D samples to initialize the algorithm.

Chapters 2–5 complete our study of classical detection and estimation theory. Our examples emphasized models corresponding to applications in communications, radar, and sonar but the theory is applicable in a wide variety of areas.

The remainder of the book discusses how to apply this theory to communications, radar, and sonar problems.

5.6 PROBLEMS

P5.2 Nonrandom Parameters

P5.2.4 Fisher Linear Gaussian Model

Problem 5.2.1. Consider the model in Example 5.2a with $D = 3$ and $\tilde{\mathbf{n}} = \tilde{\mathbf{w}}$. Repeat Example 5.9a.

Problem 5.2.2. Consider the model in Example 5.2b with $D = 3$ and $\tilde{\mathbf{n}} = \tilde{\mathbf{w}}$. Repeat Example 5.9b.

Problem 5.2.3. Consider a generalization of the target tracking model in Example 5.1a where the target position at time $t_n = nT$ is denoted by $x(n)$. The track is deterministic and completely specified by x_0 , v_0 , and the constant acceleration a_0 ,

$$x(n) = x_0 + \sum_{k=0}^{n-1} v(k)T,$$

$$v(k) = v_0 + ka_0 T.$$

The observations are

$$r_n = x(n) + w_n, \quad n = 1, 2, \dots, N,$$

and the unknown parameters are

$$\boldsymbol{\theta} = [x_0 \quad v_0 \quad a_0]^T.$$

Repeat Example 5.8.

- a. Find $\hat{\boldsymbol{\theta}}_{\text{ml}}(\mathbf{R})$.
- b. Find the FIM.
- c. Verify that your results reduce to Example 5.8 when $a_0 = 0$.
- d. Plot the variance of $\hat{x}_{\text{ml}}(n)$ versus n for several values of N .
- e. Discuss your results.

Problem 5.2.4. Consider the array processing model in Example 5.10. Assume that

$$\tilde{\mathbf{K}} = E\{\tilde{\mathbf{n}}_k \tilde{\mathbf{n}}_k^H\} = \sum_{i=1}^2 \sigma_i^2 \tilde{\mathbf{v}}(\psi_i) \tilde{\mathbf{v}}(\psi_i)^H + \sigma_w^2 \mathbf{I}.$$

- a. Formulate the problem using the eigenvector approach that leads to the ML estimator in Figure 5.6.
- b. Repeat Example 5.10 and study the effects of ψ_1 and ψ_2 on the variance of $\hat{b}_{s,\text{ml}}(\tilde{\mathbf{R}})$. In particular study, the case where $\psi_2 = -\psi_1$.

Problem 5.2.5. Repeat Problem 5.2.4 for the case where

$$\tilde{\mathbf{V}}_I \triangleq [\tilde{\mathbf{v}}(\psi_1) \quad \tilde{\mathbf{v}}(\psi_2)]$$

and

$$\tilde{\mathbf{K}} = \tilde{\mathbf{V}}_I \tilde{\mathbf{K}}_I \tilde{\mathbf{V}}_I^H + \sigma_w^2 \mathbf{I},$$

where

$$\tilde{\mathbf{K}}_I = \sigma_I^2 \begin{bmatrix} 1 & \tilde{\rho}^* \\ \tilde{\rho} & 1 \end{bmatrix}.$$

Problem 5.2.6. Consider the model in which

$$\tilde{\mathbf{r}} = \tilde{\mathbf{v}}_s \tilde{\boldsymbol{\theta}} + \tilde{\mathbf{n}},$$

where the vectors are $N \times 1$ with $N = 10$. Assume

$$\tilde{\mathbf{K}} = \tilde{\mathbf{K}}_I + \sigma_w^2 \mathbf{I},$$

where

$$\tilde{\mathbf{K}}_I = \sigma_I^2 \begin{bmatrix} 1 & \tilde{\rho}^* & (\tilde{\rho}^*)^2 & \dots & (\tilde{\rho}^*)^{N-1} \\ \tilde{\rho} & 1 & \tilde{\rho}^* & \dots & \vdots \\ \vdots & & \ddots & & \\ \tilde{\rho}^{N-1} & & & & 1 \end{bmatrix}, \quad 0 < |\tilde{\rho}| < 1,$$

- a. Derive the processor in Figure 5.6 and the corresponding CRB. Analyze the effects of $\tilde{\rho}$ for various σ_I^2/σ_w^2 assuming $\tilde{\mathbf{v}}_s = \mathbf{1}$ and $|\tilde{\theta}|^2/\sigma_w^2 = 1$.
- b. Consider a suboptimum reduced-rank processor that eliminates the correlators with the lowest weights. Assuming that we require

$$\text{Var}(\hat{\theta}_{\text{ml}}(\tilde{\mathbf{R}})) \leq 1.03 \text{CRB}(\tilde{\theta}),$$

plot the number of correlators needed versus $\tilde{\rho}$.

Problem 5.2.7. Consider a generalization of the model in Example 5.10 with a 10-element uniform linear array and $\psi_s = 0$. The interference consists of a Gaussian emitter spread uniformly over a region of ψ -space

$$.25\pi \leq \psi_I \leq .35\pi \quad (5.771)$$

and the emissions from different values of ψ_I are statistically independent.

- a. Determine the $\tilde{\mathbf{K}}_I$ matrix and develop a reduced-rank eigenspace implementation of the ML estimator. (Hint: The eigenvectors are prolate spheroidal functions that are discussed in Chapter 6.)
- b. Evaluate the Cramér–Rao bound.

P5.2.5 Separable Models for Mean Parameters

Problem 5.2.8. Simulate the performance of the ML estimator in Example 5.11 and plot the results and the Cramér–Rao bound in a format similar to Figures 4.27 and 4.28.

Problem 5.2.9. Example 5.11 is the dual of Example 4.30 in Chapter 4. Use the results of Problem 5.2.8 to generate bias, variance, and CRB results for the array processing model.

Problem 5.2.10. Generalize the model in Problem 5.2.9 for low-rank interference. The observations are

$$\mathbf{r}_k = \tilde{\mathbf{v}}(\psi_s)\tilde{\mathbf{b}} + \tilde{\mathbf{n}}_k,$$

where

$$\tilde{\mathbf{K}} = E\{\tilde{\mathbf{n}}_k \tilde{\mathbf{n}}_k^H\} = \sigma_I^2 \tilde{\mathbf{v}}(\psi_I) \tilde{\mathbf{v}}(\psi_I)^H + \sigma_w^2 \mathbf{I}.$$

- a. Find $\hat{\theta}_{\text{ml}}(\tilde{\mathbf{R}})$.
- b. Find the expression that must be maximized to find $\hat{\psi}_{s,\text{ml}}(\tilde{\mathbf{R}})$.
- c. Derive the CRB and plot the results for $\psi_s = 0$ as a function of ψ_I . Assume $|\tilde{\mathbf{b}}|^2/\sigma_w^2 = 1$ and consider several values of σ_I^2/σ_w^2 .

P5.2.6 Covariance Matrix Parameters

Problem 5.2.11. Consider the model in Section 5.2.6.3 with a rank two signal matrix

$$\mathbf{K}(\theta) = \sigma_1^2 \mathbf{v}_1 \mathbf{v}_1^T + \sigma_2^2 \mathbf{v}_2 \mathbf{v}_2^T + \sigma_w^2 \mathbf{I},$$

where $\mathbf{v}_1^T \mathbf{v}_2 = 0$. The unknown parameters are

$$\theta = [\sigma_1^2 \ \sigma_2^2 \ \sigma_w^2]^T.$$

The eigenvector matrix is

$$\mathbf{u} = [\phi_1 \ \phi_2 \ \dots \ \phi_N] \triangleq [\mathbf{u}_1 \ \mathbf{u}_2 \ \mathbf{u}_{N-2}],$$

where

$$\begin{aligned}\phi_1 &= \frac{1}{\|\mathbf{v}_1\|} \mathbf{v}_1, \\ \phi_2 &= \frac{1}{\|\mathbf{v}_2\|} \mathbf{v}_2.\end{aligned}$$

- a. Find $\hat{\sigma}_1^2$, $\hat{\sigma}_2^2$, and $\hat{\sigma}_w^2$.
- b. Find the Cramér–Rao bound.

Problem 5.2.12. Consider a combination of the models in Sections 5.2.6.1 and 5.2.6.2. Assume

$$\mathbf{K}(\theta) = \sigma_n^2 \mathbf{K}_n + \sigma_w^2 \mathbf{I}.$$

The unknown parameters are

$$\theta = [\sigma_n^2 \ \sigma_w^2]^T.$$

Find $\hat{\sigma}_{n,\text{ml}}^2(\mathbf{R})$ and $\hat{\sigma}_{w,\text{ml}}^2(\mathbf{R})$.

Problem 5.2.13. For the model in Problem 5.2.12, let

$$\mathbf{K}_n(\rho) = \begin{bmatrix} 1 & \rho & & & & \\ \rho & 1 & & & & \\ & & \ddots & & & \mathbf{0} \\ & & & \rho & 1 & \\ & & & & & \ddots \\ \mathbf{0} & & & & & \rho \\ & & & & & & 1 \end{bmatrix}.$$

Now the unknown parameters are

$$\theta = [\rho \ \sigma_n^2 \ \sigma_w^2]^T.$$

Find $\hat{\rho}_{\text{ml}}(\mathbf{R})$, $\hat{\sigma}_{n,\text{ml}}^2(\mathbf{R})$, and $\hat{\sigma}_{w,\text{ml}}^2(\mathbf{R})$.

P5.2.7 Linear Gaussian Mean and Covariance Matrix Parameters

Problem 5.2.14. Assume

$$\tilde{\mathbf{r}} = \tilde{\mathbf{V}} \tilde{\boldsymbol{\theta}}_m + \tilde{\mathbf{n}},$$

where $\tilde{\mathbf{V}}$ is an $N \times D$ known matrix, $\tilde{\boldsymbol{\theta}}_m$ is a $D \times 1$ unknown nonrandom vector, and

$$\tilde{\mathbf{K}}(\boldsymbol{\theta}_c) = \sigma_I^2 \tilde{\mathbf{v}}_I \tilde{\mathbf{v}}_I^T + \sigma_w^2 \mathbf{I},$$

where $\tilde{\mathbf{v}}_I$ is known and

$$\boldsymbol{\theta}_c = [\sigma_I^2 \quad \sigma_w^2]^T.$$

The total parameter vector to be estimated is the $(2D + 2)$ -dimensional vector

$$\tilde{\boldsymbol{\theta}} = [\tilde{\boldsymbol{\theta}}_m^T \quad \boldsymbol{\theta}_c^T]^T.$$

- a. Find the ML estimates and the Cramér–Rao bound.
- b. Assume $D = 1$ and $\tilde{\mathbf{V}} = \mathbf{I}$. Evaluate the CRB and discuss your results.

P5.2.9 Equivalent Estimation Algorithms

Problem 5.2.15. Consider the model in Section 5.2.9.2. Assume we want to minimize

$$\text{tr}[\mathbf{H}^T \mathbf{K} \mathbf{H}]$$

subject to the constraint $\mathbf{H}^T \mathbf{V} = \mathbf{I}$. Find $\hat{\boldsymbol{\theta}}(\mathbf{R})$. Discuss your results.

Problem 5.2.16. Repeat the derivation of the MVDR estimator in Section 5.2.9.2 for the analogous complex observation, complex parameter model.

Problem 5.2.17. Linearly Constrained Minimum Variance (LCMV). The MVDR processor minimizes the variance of the estimation error of each component of $\boldsymbol{\theta}$, subject to the constraint, $\mathbf{H}^T \mathbf{V} = \mathbf{I}$. In some applications, we need to impose additional linear constraints due to the physical relationships between parameters or to improve robustness. We impose a general linear constraint of the form

$$\mathbf{H}^T \mathbf{C} = \mathbf{g}^T \tag{P1}$$

or equivalently

$$\mathbf{C}^T \mathbf{H} = \mathbf{g},$$

where \mathbf{C} is an $N \times N_c$ constraint matrix whose columns are linearly independent and \mathbf{g} is an $N_c \times D$ matrix of constraint values.

The LCMV processor minimizes

$$\sigma_{e_i}^2 = \mathbf{h}_i^T \mathbf{K} \mathbf{h}_i \quad i = 1, 2, \dots, D,$$

subject to the constraint in (P1).

Find $\hat{\boldsymbol{\theta}}_{\text{LCMV}}(\mathbf{R})$.

P5.2.10 Sensitivity, Mismatch, and Diagonal Loading

Problem 5.2.18. Consider the array processing model in Example 5.10,

$$\tilde{\mathbf{r}}_k = \tilde{\mathbf{v}}(\psi_s) \tilde{\mathbf{b}}_s + \tilde{\mathbf{n}}_k, \quad k = 1, 2, \dots, K,$$

but write the covariance matrix as

$$\tilde{\mathbf{K}} = \sigma_n^2 \tilde{\mathbf{K}}_{\mathbf{n}}.$$

Then, the conventional processor is

$$\tilde{\mathbf{h}}_c^H = \tilde{\mathbf{v}}(\psi_s)^\dagger,$$

the MVDR/ML processor is

$$\tilde{\mathbf{h}}_{\text{mvdr}}^H = \frac{\tilde{\mathbf{v}}(\psi_s)^H \tilde{\mathbf{K}}^{-1}}{\tilde{\mathbf{v}}(\psi_s)^H \tilde{\mathbf{K}}^{-1} \tilde{\mathbf{v}}(\psi_s)},$$

the MVDR-DL processor is

$$\tilde{\mathbf{h}}_{\text{mvdr-dl}}^H = \frac{\tilde{\mathbf{v}}(\psi_s)^H (\tilde{\mathbf{K}} + \sigma_L^2 \mathbf{I})^{-1}}{\tilde{\mathbf{v}}(\psi_s)^H (\tilde{\mathbf{K}} + \sigma_L^2 \mathbf{I})^{-1} \tilde{\mathbf{v}}(\psi_s)}.$$

The *actual* array manifold vector is $\tilde{\mathbf{v}}(\psi_a)$ due to the signal arriving from a different value of ψ . We want to investigate the effect of this signal mismatch on the performance.

We define the array gain for a linear processor as

$$A(\psi; \tilde{\mathbf{h}}) \triangleq \frac{\text{SNR}_{\text{out}}(\psi; \tilde{\mathbf{h}})}{\text{SNR}_{\text{in}}},$$

where

$$\text{SNR}_{\text{in}} \triangleq \frac{|\tilde{b}_s|^2}{\sigma_n^2}$$

and

$$\text{SNR}_{\text{out}}(\psi; \tilde{\mathbf{h}}) \triangleq \frac{|\tilde{\mathbf{h}}^H \tilde{\mathbf{v}}(\psi) \tilde{b}_s|^2}{\tilde{\mathbf{h}}^H \tilde{\mathbf{K}} \tilde{\mathbf{h}}}.$$

a. Show that

$$A(\psi; \tilde{\mathbf{h}}) = \frac{|\tilde{\mathbf{h}}^H \tilde{\mathbf{v}}(\psi)|^2}{\tilde{\mathbf{h}}^H \tilde{\mathbf{K}}_{\mathbf{n}} \tilde{\mathbf{h}}}.$$

b. Show that

$$A_c(\psi_a) \triangleq A(\psi_a; \tilde{\mathbf{h}}_c) = \frac{N^2 |B_c(\psi_a - \psi_s)|^2}{\tilde{\mathbf{v}}(\psi_s)^H \tilde{\mathbf{K}}_{\mathbf{n}} \tilde{\mathbf{v}}(\psi_s)}$$

and therefore

$$\frac{A_c(\psi_a)}{A_c(\psi_s)} = |B_c(\psi_a - \psi_s)|^2,$$

which is intuitively obvious.

c. Show that

$$\frac{A_{\text{mvdr}}(\psi_a)}{A_{\text{mvdr}}(\psi_s)} = |B_{\text{mvdr}}(\psi_a - \psi_s)|^2.$$

d. Use the model for $\tilde{\mathbf{K}}_{\mathbf{n}}$ in Example 5.10 and plot the ratio in part (c) versus ψ_a/π for $\psi_s = 0$ for several INR.

e. Repeat (c) for $\tilde{\mathbf{h}}_{\text{mvdr-dl}}$. Plot the variance of $\hat{b}_s(\tilde{\mathbf{R}})$ versus ψ_a/π for $\psi_s = 0$.

Problem 5.2.19. Read the paper by Li et al. [LSW03] and derive the optimum diagonal loading for an ellipsoidal uncertainty set of the array manifold vector.

P5.3 Random Parameters

P5.3.1 Model, MAP Estimation, and the BCRB

Problem 5.3.1. Consider the model in Examples 5.19 and 5.20 and assume that both m and σ^2 are unknown. The conjugate prior is the Normal-Inverse Gamma($m_0, \sigma_0^2, a_0, b_0$) density given in Appendix A.

- a. Find $\hat{m}_{\text{map}}(\mathbf{R})$ and $\hat{\sigma}_{\text{map}}^2(\mathbf{R})$.
- b. Find the BCRB and the ECRB.
- c. Compare the results to Examples 4.26, 5.19, and 5.20.

Problem 5.3.2. (continuation). Now assume that σ^2 is an unknown nonrandom parameter.

- a. Find the hybrid estimate

$$\hat{\theta}(\mathbf{R}) = \begin{bmatrix} \tilde{m}_{\text{map}}(\mathbf{R}) \\ \hat{\sigma}_{w,\text{ml}}^2(\mathbf{R}) \end{bmatrix}.$$

- b. Derive the hybrid Cramér–Rao bound.
- c. Compare your answer to the results in Problem 5.3.1.

Problem 5.3.3. Consider the complex version of Example 5.19. Then $\tilde{\mathbf{r}} \sim \mathcal{CN}(\tilde{m}, \sigma_w^2)$ and

$$\tilde{\theta} = \tilde{m}.$$

Repeat Example 5.19.

Problem 5.3.4. Consider the model

$$\mathbf{r} = \mathbf{v}\theta + \mathbf{w},$$

where $\mathbf{w} \sim N(\mathbf{0}, \sigma_w^2 \mathbf{I})$. The prior density for θ is $N(0, \sigma_0^2)$. Assume that \mathbf{v} is known and that σ_w^2 is an unknown nonrandom parameter.

- a. Find

$$\hat{\theta}(\mathbf{R}) = \begin{bmatrix} \hat{\theta}_{\text{map}}(\mathbf{R}) \\ \hat{\sigma}_{w,\text{ml}}^2(\mathbf{R}) \end{bmatrix}.$$

- b. Find the hybrid CRB.

P5.3.2 Bayesian Linear Gaussian Model

Problem 5.3.5. Consider the generalization of Example 5.22. We have K IID vector observations,

$$\mathbf{r}_k = \mathbf{V}\theta + \mathbf{n}_k \quad k = 1, 2, \dots, K,$$

where $\mathbf{n}_k \sim N(\mathbf{0}, \mathbf{K}_n)$ and $\boldsymbol{\theta} \sim N(\mathbf{m}_{\theta}, \mathbf{K}_{\theta})$, and \mathbf{V} and \mathbf{K}_n are known.

- a. Find $\hat{\boldsymbol{\theta}}_{\text{map}}(\mathbf{R})$.
- b. Find the MSE matrix.
- c. Verify that the MAP estimate converges to the ML estimate as $K \rightarrow \infty$.

Problem 5.3.6. Repeat Problem 5.3.5 for complex observations and complex $\tilde{\boldsymbol{\theta}}$. Express it in the context of the complex exponential and array processing models.

Problem 5.3.7. Consider the target tracking model in Problem 5.2.3. Now assume $\boldsymbol{\theta}$ is a random vector with

$$\mathbf{m}_{\theta} = [\bar{x}_0 \quad \bar{v}_0 \quad \bar{a}_0]^T,$$

$$\mathbf{K}_{\theta} = \text{diag} [\sigma_x^2 \quad \sigma_v^2 \quad \sigma_a^2].$$

Repeat Example 5.23.

- a. Find $\hat{\boldsymbol{\theta}}_{\text{map}}(\mathbf{R})$.
- b. Find the BIM.
- c. Plot the MSE of $\hat{x}_{\text{map}}(n)$ versus n for several values of N .
- d. Discuss your results.

Problem 5.3.8. Consider the $D = 2$ complex exponentials model in Example 5.9a,

$$\begin{aligned}\tilde{\mathbf{r}} &= \sum_{i=1}^2 \tilde{\mathbf{v}}(\omega_i) \tilde{b}_i + \tilde{\mathbf{w}} \\ &= \tilde{\mathbf{V}} \tilde{\mathbf{b}} + \tilde{\mathbf{w}}.\end{aligned}$$

The prior density is $CN(\mathbf{0}, \sigma_b^2 \mathbf{I})$.

- a. Find the joint MAP estimate of \tilde{b}_1 and \tilde{b}_2 .
- b. Now assume that \tilde{b}_1 is a wanted parameter and that \tilde{b}_2 is an unwanted parameter. Express $\tilde{\mathbf{r}}$ as

$$\begin{aligned}\tilde{\mathbf{r}} &= \tilde{\mathbf{v}}(\omega_1) \tilde{b}_1 + \tilde{\mathbf{v}}(\omega_2) \tilde{b}_2 + \tilde{\mathbf{w}} \\ &= \tilde{\mathbf{v}}(\omega_1) \tilde{b}_1 + \tilde{\mathbf{w}},\end{aligned}$$

where

$$\begin{aligned}\tilde{\mathbf{K}}_{\tilde{\mathbf{n}}} &= E [\tilde{\mathbf{n}} \tilde{\mathbf{n}}^H] \\ &= \sigma_b^2 \tilde{\mathbf{v}}(\omega_2) \tilde{\mathbf{v}}(\omega_2)^H + \sigma_w^2 \mathbf{I}.\end{aligned}$$

Find $\hat{\tilde{b}}_{1,\text{map}}(\mathbf{R})$.

- c. Verify that the two estimates of \tilde{b}_1 are equal.

Problem 5.3.9. Extend the results of Problem 5.3.8 to the case of D complex exponentials. The conclusion is that if you want to jointly estimate D statistically independent signals, then the result is identical to finding D single estimates treating the other $D - 1$ signals as interferers.

Problem 5.3.10. Consider the $D = 2$ array processing model in Example 5.9b. Repeat Problem 5.3.8.

P5.4 Sequential Estimation

P5.4.1 Sequential Bayes Estimation

Problem 5.4.1. Consider the target tracking model in Problem 5.3.7. Now repeat Example 5.25 and develop the sequential Bayes estimate.

- a. Find $\hat{\theta}(k)$.
- b. Plot the MSE of $\hat{x}(k)$ versus k .
- c. Discuss your results.

Problem 5.4.2. Repeat problem 5.4.1 for the model in which we measure both position and velocity

$$\begin{aligned}r_1(n) &= x(n) + w_1(n), \\r_2(n) &= v(n) + w_2(n).\end{aligned}$$

P5.4.2 Recursive Maximum Likelihood

Problem 5.4.3. Repeat Problem 5.4.1 for the case where θ is modeled as a nonrandom variable. Compare your results.

Problem 5.4.4. Repeat Problem 5.4.2 for the case where θ is modeled as a nonrandom variable. Compare your results.

6

Representation of Random Processes

6.1 INTRODUCTION

In Chapters 2–5, we have discussed classical detection and estimation theory. In both the detection and estimation problems, the observations were modeled as finite-dimensional vectors. In the parameter estimation problem, the parameters were categorized by a finite-dimensional vector. Our focus in this book is on physical applications, where the processes that we are observing are continuous functions of time (and space in some cases). We need to find a technique to transform the problem into a model where the observations are vectors (perhaps with countably infinite dimensions) and the sufficient statistics are finite-dimensional vectors. We can then use all of our results from Chapters 2–5.

In this chapter, we assume that the random processes are real Gaussian random processes. The extension to circular complex Gaussian random processes is carried out in the problems. There are many alternative ways of characterizing waveforms and random processes, but the best choice depends heavily on the problem that we are trying to solve. We focus on two techniques to obtain a vector model. The first technique is an eigendecomposition that leads to a vector model in which components are statistically independent Gaussian random variables. The result is referred to as a Karhunen–Loëve expansion of the process. The second technique models the random processes as Gaussian Markov processes that can be generated by exciting a linear (possibly time-varying) system with Gaussian white noise. We develop the first technique in this chapter and the second in Chapter 8.

We have already introduced another technique in Chapter 3 in order to motivate some of the examples that we wanted to consider. We assumed that the waveforms (both signal and noise) were bandlimited about a center frequency. We did a quadrature demodulation followed by sampling to obtain a complex-valued finite-dimensional vector.

If we assume the waveforms are bandlimited to W cps and sample the input at $T = 1/W$ seconds we obtain a real-valued finite-dimentional vector. The technique has the advantage that the transformation to vector space only requires knowledge of the bandwidth in order to select the sampling rate.¹ However, we need a complete description of the process in order to

¹In many applications, such as a radar doing scanning and tracking, the sampling rate is constrained by asset allocation and not a Nyquist criterion. In other applications such as array processing, the Nyquist rate does not allow adequate beamforming.

know the probability density of the resulting vector. If our subsequent processing is limited to linear operations, then we need to know the mean value function and covariance function of the input. The technique has the disadvantage that it does not exploit the available statistical knowledge about the input to find the most efficient mapping into a finite-dimensional vector.

In this chapter, we develop a technique that exploits the statistics of the signal and noise to develop a mapping that provides the minimum dimensional model and relates that model directly to the original continuous signals and interferers.

In Chapter 3, we found that a key to understanding many problems was an eigendecomposition. In order to find eigenvalues and eigenvectors, we had to solve a matrix equation. We will find that a decomposition into eigenvalues and eigenfunctions is a key to understanding the waveform problem. This will require solving an integral equation whose structure is identical to the matrix equations that we are familiar with.

The choice of coordinate functions will depend on the covariance function of the process through the integral equation

$$\lambda \phi(t) = \int_{T_i}^{T_f} K(t, u)\phi(u) du, \quad T_i \leq t \leq T_f. \quad (6.1)$$

The eigenvalue λ corresponds physically to the expected value of the energy along a particular coordinate function $\phi(t)$. This representation will be useful for both theoretical and practical purposes.

In Section 6.2, we motivate our approach with some simple examples and develop orthogonal representations for deterministic functions. In Section 6.3, we discuss random process characterizations and develop the Karhunen–Loève expansion.

In Section 6.4, we discuss the properties of the integral equation and study several classes of processes for which solutions to (6.1) can be obtained. One example, the simple Wiener process, leads us logically to the idea of a white noise process. As we proceed, we shall find that this white noise process plays a central role in many of our studies.

We introduce the case of stationary processes and long observation time (the SPLOT model). We will find that the eigenvalues of a stationary random process approach the power spectrum of the process and the eigenfunctions become sinusoids. Thus, for this class of problem, the expansion could be interpreted in terms of familiar quantities.

In Section 6.5, we extend the eigendecomposition to vector random processes.

We should note that all of discussion considers real random processes. The extension of eigendecomposition to complex processes is straightforward. As expected from our work in Chapter 3, we have complex eigenfunctions and real eigenvalues.

In Chapter 7, we apply these techniques to solve the detection and estimation problem.

6.2 ORTHONORMAL EXPANSIONS: DETERMINISTIC SIGNALS

We begin this section with a brief motivation discussion.

Several methods of characterizing signals come immediately to mind. The first is a time-domain characterization. A typical signal made up of pulses of various heights is shown in Figure 6.1. A time-domain characterization describes the signal shape clearly.

Is it a good representation? To answer this question, we must specify what we are going to do with the signal. In Figure 6.2, we illustrate two possible cases. In the first, we pass the signal through a limiter and want to calculate the output. The time-domain characterization enables us to find the output by inspection. In the second, we pass the signal through an ideal

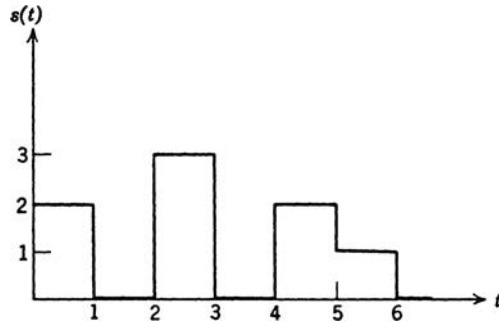


Figure 6.1: A typical signal.

low-pass filter and want to calculate the energy in the output. In this case, a time-domain approach is difficult. If, however, we take the Fourier transform of $s(t)$,

$$S(j\omega) = \int_{-\infty}^{\infty} s(t)e^{-j\omega t} dt, \quad (6.2)$$

the resulting problem is straightforward. The energy in $y(t)$ is E_y , where

$$E_y = 2 \int_0^{2\pi W} |S(j\omega)|^2 \frac{d\omega}{2\pi}. \quad (6.3)$$

Thus, as we well know, both the time-domain and frequency-domain descriptions play an important role in system analysis. The point of the example is that the most efficient characterization depends on the problem of interest.

To motivate another method of characterization, consider the simple communication systems shown in Figure 6.3. When hypothesis 1 is true, the deterministic signal $s_1(t)$

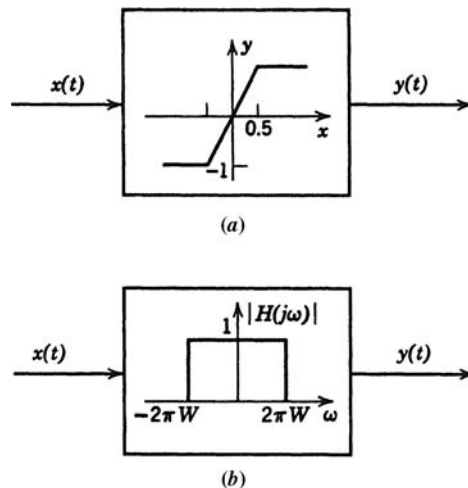


Figure 6.2: Operations on signals.

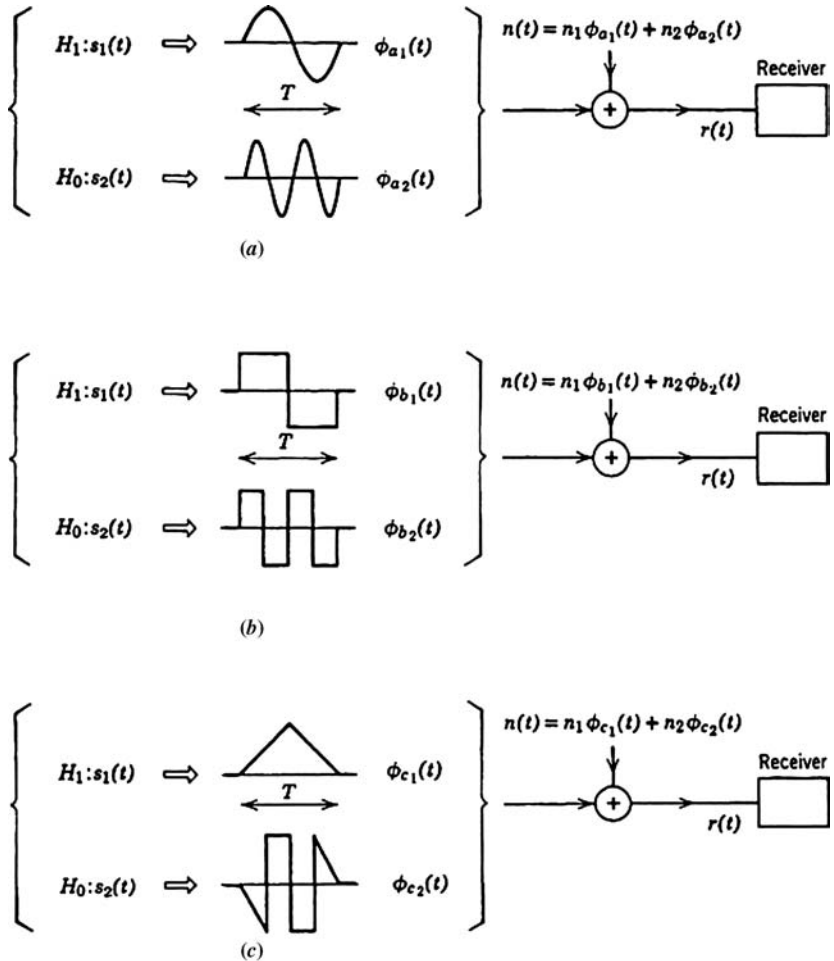


Figure 6.3: Three hypothetical communication systems.

is transmitted. When hypothesis 0 is true, the signal $s_2(t)$ is transmitted. The particular transmitted waveforms are different in systems A, B, and C. The noise in each idealized system is constructed by multiplying the two deterministic waveforms by independent, zero-mean Gaussian random variables and adding the resulting waveforms. The noise waveform will have a different shape in each system. The receiver wants to decide which hypothesis is true. We see that the transmitted signal and additive noise are appreciably different waveforms in systems A, B, and C. In all cases, however, they can be written as

$$\begin{aligned} s_1(t) &= s_1\phi_1(t), & 0 \leq t \leq T, \\ s_2(t) &= s_2\phi_2(t), & 0 \leq t \leq T, \\ n(t) &= n_1\phi_1(t) + n_2\phi_2(t), & 0 \leq t \leq T, \end{aligned} \quad (6.4)$$

where the functions $\phi_1(t)$ and $\phi_2(t)$ are *orthonormal*; that is,

$$\int_0^T \phi_i(t) \phi_j(t) dt = \delta_{ij}, \quad i, j = 1, 2. \quad (6.5)$$

The functions $\phi_1(t)$ and $\phi_2(t)$ are different in the three systems. It is clear that because

$$\begin{aligned} H_1 : r(t) &= (s_1 + n_1)\phi_1(t) + n_2\phi_2(t), & 0 \leq t \leq T, \\ H_0 : r(t) &= n_1\phi_1(t) + (s_2 + n_2)\phi_2(t), & 0 \leq t \leq T, \end{aligned} \quad (6.6)$$

we must base our decision on the observed value of the coefficients of the two functions. Thus, the test can be viewed as

$$H_1 : \mathbf{r} \triangleq \begin{bmatrix} r_1 \\ r_2 \end{bmatrix} = \begin{bmatrix} s_1 \\ 0 \end{bmatrix} + \begin{bmatrix} n_1 \\ n_2 \end{bmatrix}, \quad (6.7)$$

$$H_0 : \mathbf{r} \triangleq \begin{bmatrix} r_1 \\ r_2 \end{bmatrix} = \begin{bmatrix} 0 \\ s_2 \end{bmatrix} + \begin{bmatrix} n_1 \\ n_2 \end{bmatrix}. \quad (6.8)$$

This, however, is just a problem in classical detection that we encountered in Chapter 2.

The important observation is that any pair of orthonormal functions $\phi_1(t)$ and $\phi_2(t)$ will give the same detection performance. Therefore, either a time-domain or frequency-domain characterization will tend to obscure the significant features of this particular problem. We refer to this third method of characterization as an *orthogonal series* representation.

We develop this method of characterizing both deterministic signals and random processes in this chapter. In this section, we discuss deterministic signals.

Deterministic Functions: Orthogonal Representations. Consider the function $x(t)$ that is defined over the interval $[0, T]$ as shown in Figure 6.4. We assume that the energy in the function has some finite value E_x .

$$E_x = \int_0^T x^2(t) dt < \infty. \quad (6.9)$$

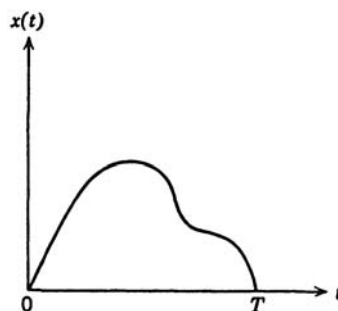


Figure 6.4: A time-limited function.

Now the sketch implies one way of specifying $x(t)$. For every t , we know the value of the function $x(t)$. Alternately, we may wish to specify $x(t)$ by a countable set of numbers.

The previous example suggests writing

$$x(t) = \sum_{i=1}^{\infty} x_i \phi_i(t), \quad (6.10)$$

where the $\phi_i(t)$ are some set of orthonormal functions.² For example, we could choose a set of sines and cosines

$$\begin{aligned} \phi_1(t) &= \left(\frac{1}{T}\right)^{1/2}, \\ \phi_2(t) &= \left(\frac{2}{T}\right)^{1/2} \cos\left(\frac{2\pi}{T}t\right), \\ \phi_3(t) &= \left(\frac{2}{T}\right)^{1/2} \sin\left(\frac{2\pi}{T}t\right), \quad 0 \leq t \leq T, \\ &\vdots \\ \phi_{2n}(t) &= \left(\frac{2}{T}\right)^{1/2} \cos\left(\frac{2\pi}{T}nt\right). \end{aligned} \quad (6.11)$$

Several mathematical and practical questions come to mind. The mathematical questions are the following:

1. Because it is only practical to use a finite number (N) of coefficients, how should we choose the coefficients to minimize the mean-square approximation (or representation) error?
2. As N increases, we would like the mean-square approximation error to go to zero. When does this happen?

The practical question is this:

If we receive $x(t)$ as a voltage waveform, how can we generate the coefficients experimentally?

First we consider the mathematical questions. The representation error is

$$e_N(t) = x(t) - \sum_{i=1}^N x_i \phi_i(t), \quad (6.12)$$

when we use N terms. The energy in the error is

$$E_e(N) \triangleq \int_0^T e_N^2(t) dt = \int_0^T \left[x(t) - \sum_{i=1}^N x_i \phi_i(t) \right]^2 dt. \quad (6.13)$$

²Throughout most of our discussion in this chapter, we are concerned with expanding real waveforms using real orthonormal functions and real coefficients. The modifications to include complex orthonormal functions and coefficients are straightforward.

We want to minimize this energy for any N by choosing the x_i appropriately. By differentiating with respect to some particular x_j , setting the result equal to zero, and solving, we obtain

$$x_j = \int_0^T x(t)\phi_j(t) dt. \quad (6.14)$$

Because the second derivative is a positive constant, the x_j given by (6.14) provides an absolute minimum. The choice of coefficient does not change as N is increased because of the orthonormality of the functions.

Finally, we look at the energy in the representation error as $N \rightarrow \infty$.

$$\begin{aligned} E_e(N) &\triangleq \int_0^T e_N^2(t) dt = \int_0^T \left[x(t) - \sum_{i=1}^N x_i \phi_i(t) \right]^2 dt \\ &= E_x - 2 \sum_{i=1}^N \int_0^T x(t)x_i \phi_i(t) dt + \int_0^T \sum_{i=1}^N \sum_{j=1}^N x_i x_j \phi_i(t) \phi_j(t) dt \\ &= E_x - \sum_{i=1}^N x_i^2. \end{aligned} \quad (6.15)$$

Because the x_i^2 are nonnegative, the error is a monotone-decreasing function of N .

If

$$\lim_{N \rightarrow \infty} E_e(N) = 0, \quad (6.16)$$

for all $x(t)$ with finite energy, we say that the $\phi_i(t)$, $i = 1, 2, \dots$, are a *complete orthonormal (CON) set* over the interval $[0, T]$ for the class of functions with finite energy. The importance of completeness is clear. If we are willing to use more coefficients, the representation error decreases. In general, we want to be able to decrease the energy in the error to any desired value by letting N become large enough.

We observe that for CON sets

$$E_x = \sum_{i=1}^{\infty} x_i^2. \quad (6.17)$$

Equation (6.17) is just Parseval's theorem. We also observe that x_i^2 represents the energy in a particular component of the signal.

Two possible ways of generating the coefficients are shown in Figure 6.5. In the first system, we multiply $x(t)$ by $\phi_i(t)$ and integrate over $[0, T]$. This is referred to as a correlation operation. In the second, we pass $x(t)$ into a set of linear filters with impulse responses $h_i(\tau) = \phi_i(T - \tau)$ and observe the outputs at time T . We see that the sampled output of the i th filter is

$$\int_0^T x(\tau) h_i(T - \tau) d\tau.$$

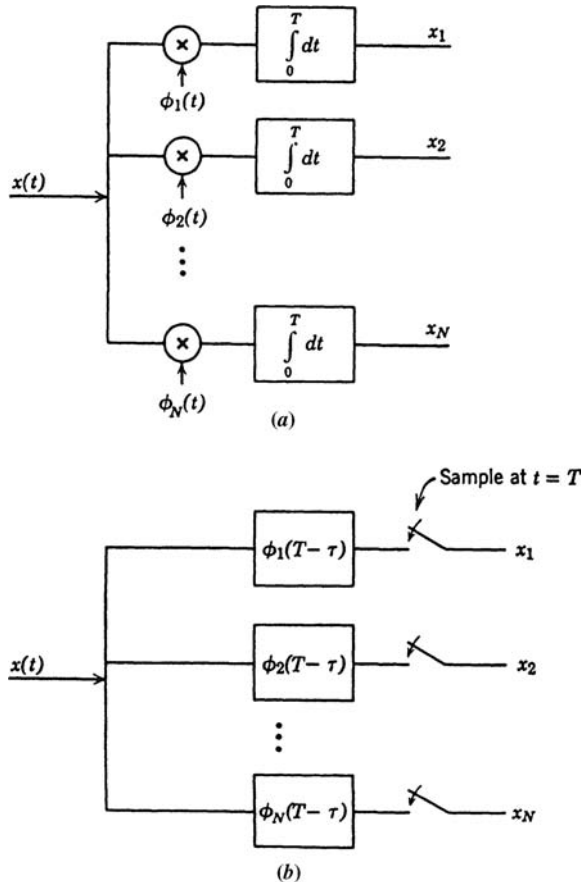


Figure 6.5: Generation of expansion coefficients: (a) correlation operation; (b) filter operation.

For the particular impulse response used this is x_i ,

$$x_i = \int_0^T x(\tau) \phi_i(\tau) d\tau, \quad i = 1, 2, \dots, N. \quad (6.18)$$

In Chapter 2, we saw that it was convenient to consider N observations as a point in an N -dimensional space. We shall find that it is equally useful to think of the N coefficients as defining a point in a space. For arbitrary signals, we may need an infinite dimensional space. Thus any finite energy signal can be represented as a vector. In Figure 6.6, we show two signals— $s_1(t)$ and $s_2(t)$:

$$\begin{aligned} s_1(t) &= \sum_{i=1}^3 s_{1i} \phi_i(t) \\ s_2(t) &= \sum_{i=1}^3 s_{2i} \phi_i(t). \end{aligned} \quad (6.19)$$

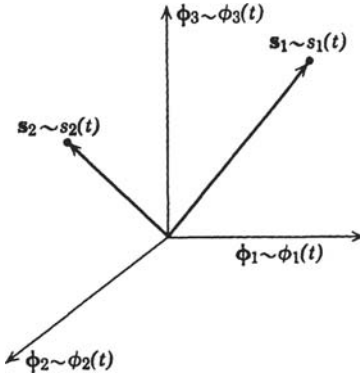


Figure 6.6: Representation of a signal as a vector.

The corresponding signal vectors are

$$\begin{aligned} \mathbf{s}_1 &\triangleq \begin{bmatrix} s_{11} \\ s_{12} \\ s_{13} \end{bmatrix} = \sum_{i=1}^3 s_{1i} \boldsymbol{\phi}_i \\ \mathbf{s}_2 &\triangleq \begin{bmatrix} s_{21} \\ s_{22} \\ s_{23} \end{bmatrix} = \sum_{i=1}^3 s_{2i} \boldsymbol{\phi}_i. \end{aligned} \quad (6.20)$$

Several observations follow immediately:

1. The length of the signal vector squared equals the energy in the signal.

$$\begin{aligned} \|\mathbf{s}_1\|^2 &= E_1, \\ \|\mathbf{s}_2\|^2 &= E_2. \end{aligned} \quad (6.21)$$

2. The correlation coefficient between two signals is defined as

$$\rho_{12} \triangleq \frac{\int_0^T s_1(t)s_2(t) dt}{\sqrt{E_1 E_2}}. \quad (6.22)$$

Substituting (6.19) into (6.22), we have

$$\rho_{12} = \frac{\int_0^T \left[\sum_{i=1}^3 s_{1i} \phi_i(t) \right] \left[\sum_{j=1}^3 s_{2j} \phi_j(t) \right] dt}{\sqrt{E_1 E_2}}. \quad (6.23)$$

Using the orthonormality of the coordinate functions the integral reduces to

$$\rho_{12} = \frac{\sum_{i=1}^3 s_{1i} s_{2i}}{\sqrt{E_1 E_2}}. \quad (6.24)$$

The numerator is just the dot product of \mathbf{s}_1 and \mathbf{s}_2 . Using (6.21) in the denominator, we obtain,

$$\rho_{12} = \frac{\mathbf{s}_1 \cdot \mathbf{s}_2}{\|\mathbf{s}_1\| \|\mathbf{s}_2\|}. \quad (6.25)$$

The obvious advantage of the vector space interpretation is that it enables us to use familiar geometric ideas in dealing with waveforms.

We now extend these ideas to random waveforms.

6.3 RANDOM PROCESS CHARACTERIZATION

We begin our discussion in this section by reviewing briefly how random processes are conventionally defined and characterized.

6.3.1 Random Processes: Conventional Characterizations

The basic idea of a random process is familiar. Each time we conduct an experiment, the outcome is a function over an interval of time instead of just a single number. Our mathematical model is illustrated in Figure 6.7. Each point in the sample space Ω maps into a time function. We could write the function that came from ω_i as $x(t, \omega_i)$ to emphasize its origin, but it is easier to denote it simply as $x(t)$. The collection of waveforms generated from the points in Ω are referred to as an *ensemble*. If we look down the ensemble at any

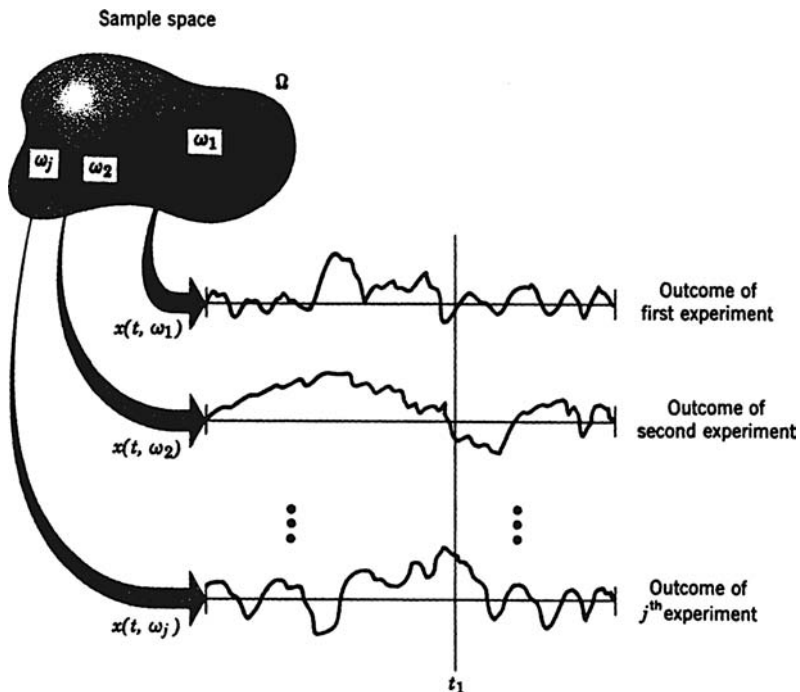


Figure 6.7: An ensemble of sample functions.

one time, say t_1 , we will have a random variable $x_{t_1} \triangleq x(t_1, \omega)$. Similarly, at other times t_i we have random variables x_{t_i} .

Clearly, we could characterize any particular random variable x_{t_i} by its probability density. A more difficult question is how to characterize the entire process. There is an obvious property that this characterization should have. If we consider a set of times t_1, t_2, \dots, t_n in the interval in which the process is defined, there are n random variables $x_{t_1}, x_{t_2}, x_{t_3}, \dots, x_{t_n}$. Any *complete* characterization should be able to specify the joint density $p_{x_{t_1}, x_{t_2}, \dots, x_{t_n}}(X_1, X_2, \dots, X_n)$. Furthermore, it should be able to specify this density for any set of n times in the interval (for any finite n).

Unfortunately, it is not obvious that a characterization of this kind will be adequate to answer all questions of interest about a random process. Even if it does turn out to be adequate, there is a practical difficulty in actually specifying these densities for an arbitrary random process.

There are two common ways of handling this difficulty in specifying the n th-order density. The first approach is to restrict our interest to problems that do not require a complete characterization, so we can work with only a partial characterization. We discuss this approach briefly and then return to the question of complete characterization.

A large number of partial characterizations are possible. Two of the most widely used are the following:

1. Single-time characterizations
2. Second-moment characterizations.

In a single-time characterization, we specify only $p_{x_t}(X)$, the first-order probability density at time t . In general, it will be a function of time. A simple example illustrates the usefulness of this characterization.

Example 6.1. Let

$$r(t) = x(t) + n(t). \quad (6.26)$$

Assume that x_t and n_t are statistically independent and $p_{x_t}(X)$ and $p_{n_t}(N)$ are known. We operate on $r(t)$ with a no-memory nonlinear device to obtain a minimum mean square error estimate of $x(t)$, which we denote by $\hat{x}(t)$.

From Chapter 2, $\hat{x}(t)$ is just the conditional mean. Because we are constrained to a no-memory operation, we can use only $r(t)$. Then

$$\hat{x}(t) = \int_{-\infty}^{\infty} X_t p_{x_t|r_t}(X_t|R_t) dX_t \triangleq f(R_t). \quad (6.27)$$

If x_t is Gaussian, $N(0, \sigma_x^2)$, and n_t is Gaussian, $N(0, \sigma_n^2)$, it is a simple exercise (Cf. Problem 6.3.2) to show that

$$f(R_t) = \frac{\sigma_x^2}{\sigma_x^2 + \sigma_n^2} R_t, \quad (6.28)$$

so that the no-memory device happens to be linear. Observe that because we allowed only a no-memory device a complete characterization of the process was not necessary. ■

In a second-moment characterization we specify only the first and second moments of the process. We define the mean value function of the process as

$$m_x(t) \triangleq E(x_t) = \int_{-\infty}^{\infty} X_t p_{x_t}(X_t) dX_t. \quad (6.29)$$

In general, this is a function of time. The correlation function is defined as

$$R_x(t, u) \triangleq E(x_t x_u) = \iint_{(-\infty, \infty)} X_t X_u p_{x_t x_u}(X_t, X_u) dX_t dX_u. \quad (6.30)$$

The covariance function is defined as

$$\begin{aligned} K_x(t, u) &\triangleq E\{[x_t - m_x(t)][x_u - m_x(u)]\} \\ &= R_x(t, u) - m_x(t)m_x(u). \end{aligned} \quad (6.31)$$

This partial characterization is well suited to *linear* operations on random processes. This type of application is familiar (e.g., [DR58], pp. 171–185).

The covariance function has several properties of interest to us. Looking at the definition in (6.31), we see that it is symmetric:

$$K_x(t, u) = K_x(u, t). \quad (6.32)$$

If we multiply a sample function $x(t)$ by some deterministic square-integrable function $f(t)$ and integrate over the interval $[0, T]$, we obtain a random variable:

$$x_f \triangleq \int_0^T x(t) f(t) dt. \quad (6.33)$$

The mean of this random variable is

$$E(x_f) = \bar{x}_f \triangleq E \int_0^T x(t) f(t) dt = \int_0^T m_x(t) f(t) dt, \quad (6.34)$$

and the variance is

$$\begin{aligned} \text{Var}(x_f) &\triangleq E[(x_f - \bar{x}_f)^2] \\ &= E \left\{ \int_0^T [x(t) - m_x(t)] f(t) dt \int_0^T [x(u) - m_x(u)] f(u) du \right\}. \end{aligned} \quad (6.35)$$

Bringing the expectation inside the integral, we have

$$\text{Var}(x_f) = \iint_{[0, T]} f(t) K_x(t, u) f(u) dt du. \quad (6.36)$$

The variance must be greater than or equal to zero. Thus, we have shown that

$$\iint_{[0,T]} f(t) K_x(t, u) f(u) dt du \geq 0 \quad (6.37)$$

for any $f(t)$ with finite energy. We call this property nonnegative definiteness. If the inequality is strict for every $f(t)$ with nonzero finite energy, we say that $K_x(t, u)$ is positive definite. We shall need the two properties in (6.32) and (6.37) in the next section.

If the process is defined over an infinite interval and the covariance function depends only on $|t - u|$ and not t or u individually, we say that the process is *covariance-stationary* and write³

$$K_x(t, u) = K_x(t - u) = K_x(\tau). \quad (6.38)$$

Similarly, if the correlation function depends only on $|t - u|$, we say that the process is *correlation-stationary* and write

$$R_x(t, u) = R_x(t - u) = R_x(\tau). \quad (6.39)$$

For stationary processes, a characterization using the power density spectrum $S_x(\omega)$ is equivalent to the correlation function characterization

$$S_x(\omega) \triangleq \int_{-\infty}^{\infty} R_x(\tau) e^{-j\omega\tau} d\tau,$$

and

$$R_x(\tau) = \int_{-\infty}^{\infty} S_x(\omega) e^{j\omega\tau} \frac{d\omega}{2\pi}. \quad (6.40)$$

As already pointed out, these partial characterizations are useful only when the operations performed on the random process are constrained to have a certain form.

Complete Characterization. In the second approach, we restrict our models to processes that have structure that allow to construct the n th order density from either a lower order density or from the second moment characteristics. The two most widely used models are Gaussian random processes and Markov processes.

In a Gaussian random process, the n th order density is completely specified by the mean of the process $m_x(t)$ and the covariance function $K_x(t, u)$. We will discuss this model in detail in Section 6.3.3 and focus our attention on it for the remainder of the book.

In a Markov process, we consider the probability density at the ordered set of times

$$t_1 < t_2 < t_3 < \dots < t_{n-1} < t_n.$$

³It is important to observe that although $K_x(t, u)$ is a function of two variables and $K_x(\tau)$ of only one variable, we use the same notation for both. This economizes on symbols and should cause no confusion.

If

$$p_{x_{t_n} | x_{t_{n-1}}, \dots, x_{t_1}}(X_{t_n} | X_{t_{n-1}}, \dots, X_{t_1}) = p_{x_{t_n} | x_{t_{n-1}}}(X_{t_n} | X_{t_{n-1}}), \quad (6.41)$$

the process is called a Markov process. Here knowledge of the second-order density enables us to construct the n th order density (e.g. [Mid60a] or Problems 6.3.9 and 6.3.10) and a special case of a Markov process occurs when $p_{x_{t_n} | x_{t_{n-1}}}(X_{t_n} | X_{t_{n-1}})$ is Gaussian. We will study a Gaussian Markov model in Chapters 8 and 9. For Gaussian random processes a useful representation for many of the problems of interest to us is a characterization in terms of an orthogonal series expansion. In the next section, we use a series expansion to develop a second-moment characterization. In the succeeding section, we extend it to provide a complete characterization for a Gaussian random process.

6.3.2 Series Representation of Sample Functions of Random Processes

In Section 6.2, we saw how we could represent a deterministic waveform with finite energy in terms of a series expansion. We now want to extend these ideas to include sample functions of a random process. We start off by choosing an arbitrary complete orthonormal set: $\phi_1(t), \phi_2(t), \dots$. For the moment we shall not specify the exact form of the $\phi_i(t)$. To expand $x(t)$, we write

$$x(t) = \lim_{N \rightarrow \infty} \sum_{i=1}^N x_i \phi_i(t), \quad 0 \leq t \leq T, \quad (6.42)$$

where

$$x_i \triangleq \int_0^T x(t) \phi_i(t) dt. \quad (6.43)$$

We have not yet specified the type of convergence required of the sum on the right-hand side. Various types of convergence for sequences of random variables are discussed in the prerequisite references ([DR58], p. 63 or [Pap65]).

An ordinary limit is not useful because this would require establishing conditions on the process to guarantee that *every* sample function could be represented in this manner.

A more practical type of convergence is mean-square convergence:

$$x(t) = \text{l.i.m.}_{N \rightarrow \infty} \sum_{i=1}^N x_i \phi_i(t), \quad 0 \leq t \leq T. \quad (6.44)$$

The notation l.i.m denotes limit in the mean (e.g., [DR58], p. 63), which is defined as,

$$\lim_{N \rightarrow \infty} E \left[\left(x_t - \sum_{i=1}^N x_i \phi_i(t) \right)^2 \right] = 0 \quad 0 \leq t \leq T. \quad (6.45)$$

For the moment, we assume that we can find conditions on the process to guarantee the convergence indicated in (6.45).

Before doing so, we discuss an appropriate choice for the orthonormal set. In our discussions of classical detection theory, our observation space was finite dimensional and

usually came with a built-in coordinate system. In Chapter 3, we found that problems were frequently easier to solve if we used a new coordinate system in which the random variables were uncorrelated (if they happened to be Gaussian variables, they were also statistically independent). In dealing with continuous waveforms, we have the advantage that there is no specified coordinate system, and therefore we can choose one to suit our purposes. From our previous results, a logical choice is a set of $\phi_i(t)$ that leads to *uncorrelated* coefficients.

If

$$E(x_i) \triangleq m_i, \quad (6.46)$$

we would like

$$E[(x_i - m_i)(x_j - m_j)] = \lambda_i \delta_{ij}. \quad (6.47)$$

For simplicity, we assume that $m_i = 0$ for all i . Several observations are worthwhile:

1. The value x_i^2 has a simple physical interpretation. It corresponds to the *energy* along the coordinate function $\phi_i(t)$ in a particular sample function.
2. Similarly, $E(x_i^2) = \lambda_i$ corresponds to the *expected* value of the energy along $\phi_i(t)$, assuming that $m_i = 0$. Clearly, $\lambda_i \geq 0$ for all i .
3. If $K_x(t, u)$ is positive definite, every λ_i is greater than zero. This follows directly from (6.37). A little later it will be easy to show that if $K_x(t, u)$ is not positive definite, at least one λ_i must equal zero.

We now want to determine what the requirement in (6.47) implies about the complete orthogonal set. Substituting (6.43) into (6.47) and bringing the expectation inside the integral, we obtain

$$\begin{aligned} \lambda_i \delta_{ij} &= E(x_i x_j) = E \left[\int_0^T x(t) \phi_i(t) dt \int_0^T x(u) \phi_j(u) du \right] \\ &= \int_0^T \phi_i(t) dt \int_0^T K_x(t, u) \phi_j(u) du, \quad \text{for all } i \text{ and } j. \end{aligned} \quad (6.48)$$

In order that (6.48) may hold for all choices of i and a particular j , it is necessary and sufficient that the inner integral equal $\lambda_j \phi_j(t)$:

$$\lambda_j \phi_j(t) = \int_0^T K_x(t, u) \phi_j(u) du, \quad 0 \leq t \leq T. \quad (6.49)$$

The functions $\phi_i(t)$ are called eigenfunctions and the numbers λ_i are called eigenvalues.

Therefore, we want to demonstrate that for some useful class of random processes there exist solutions to (6.49) with the desired properties. The form of (6.49) is reminiscent of the equation that specified the eigenvectors and eigenvalues in Chapter 3,

$$\lambda \phi = \mathbf{K}_x \phi, \quad (6.50)$$

where \mathbf{K}_x was a symmetric, nonnegative definite matrix. This was a set of N simultaneous homogeneous linear equations, where N was the dimensionality of the observation space. Using results from linear equation theory, we saw that there were N real, nonnegative values of λ for which (6.50) had a nontrivial solution. Now the coordinate space is infinite and we have a homogeneous linear integral equation to solve.

The function $K_x(t, u)$ is called the kernel of the integral equation, and because it is a covariance function it is symmetric and nonnegative definite. We restrict our attention to processes with a finite mean-square value $[E(x^2(t)) < \infty]$. Their covariance functions satisfy the restriction

$$\iint_{[0, T]} K_x^2(t, u) dt du \leq \left\{ \int_0^T E[x^2(t)] dt \right\}^2 < \infty, \quad (6.51)$$

where T is a finite number.

The restrictions in the last paragraph enable us to employ standard results from linear integral equation theory⁴ (e.g., [CH53], Chapter 3; [RN55]; [Lov24]; or [Tri57]).

Properties of Integral Equations

1. There exist *at least one* square-integrable function $\phi(t)$ and real number $\lambda \neq 0$ that satisfy (6.49).

It is clear that there may not be more than one solution. For example,

$$K_x(t, u) = \sigma_f^2 f(t)f(u), \quad 0 \leq t, u \leq T \quad (6.52)$$

has only one nonzero eigenvalue and one normalized eigenfunction.

2. By looking at (6.49) we see that if $\phi_j(t)$ is a solution, then $c\phi_j(t)$ is also a solution. Therefore we can always normalize the eigenfunctions.
3. If $\phi_1(t)$ and $\phi_2(t)$ are eigenfunctions associated with the same eigenvalue λ , then $c_1\phi_1(t) + c_2\phi_2(t)$ is also an eigenfunction associated with λ .
4. The eigenfunctions corresponding to different eigenvalues are orthogonal.
5. There is at most a countably infinite set of eigenvalues and all are bounded.
6. For any particular λ , there is at most a *finite* number of linearly independent eigenfunctions. [Observe that we mean algebraic linear independence; $f(t)$ is linearly independent of the set $\phi_i(t)$, $i = 1, 2, \dots, K$, if it cannot be written as a weighted sum of the $\phi_i(t)$.] These can always be orthonormalized (e.g., by the Gram–Schmidt procedure; see Problem 7.2.7 in Chapter 7).
7. Because $K_x(t, u)$ is nonnegative definite, the kernel $K_x(t, u)$ can be expanded in the series

$$K_x(t, u) = \sum_{i=1}^{\infty} \lambda_i \phi_i(t) \phi_i(u), \quad 0 \leq t, u \leq T, \quad (6.53)$$

where the convergence is uniform for $0 \leq t, u \leq T$. (This is called Mercer's theorem.)

⁴Here we follow [DR58], p. 373.

8. If $K_x(t, u)$ is positive definite, the eigenfunctions form a complete orthonormal set. From our results in Section 6.2, this implies that we can expand any deterministic function with finite energy in terms of the eigenfunctions.
9. If $K_x(t, u)$ is not positive definite, the eigenfunctions cannot form a complete orthonormal set. [This follows directly from (6.37) and (6.43).] Frequently, we augment the eigenfunctions with enough additional orthogonal functions to obtain a complete set. We occasionally refer to these additional functions as eigenfunctions with zero eigenvalues.
10. The sum of the eigenvalues is the expected value of the energy of the process in the interval $(0, T)$, that is,

$$E \left[\int_0^T x^2(t) dt \right] = \int_0^T K_x(t, t) dt = \sum_{i=1}^{\infty} \lambda_i.$$

(Recall that $x(t)$ is assumed to be zero mean.)

These properties guarantee that we can find a set of $\phi_i(t)$ that leads to uncorrelated coefficients. It remains to verify the assumption that we made in (6.45). We denote the expected value of the error if $x(t)$ is approximated by the first N terms as $\xi_N(t)$:

$$\xi_N(t) \triangleq E \left[\left(x(t) - \sum_{i=1}^N x_i \phi_i(t) \right)^2 \right]. \quad (6.54)$$

Evaluating the expectation, we have

$$\xi_N(t) = K_x(t, t) - 2E \left[x(t) \sum_{i=1}^N x_i \phi_i(t) \right] + E \left[\sum_{i=1}^N \sum_{j=1}^N x_i x_j \phi_i(t) \phi_j(t) \right] \quad (6.55)$$

$$\xi_N(t) = K_x(t, t) - 2E \left[x(t) \sum_{i=1}^N \left(\int_0^T x(u) \phi_i(u) du \right) \phi_i(t) \right] + \sum_{i=1}^N \lambda_i \phi_i(t) \phi_i(t) \quad (6.56)$$

$$\xi_N(t) = K_x(t, t) - 2 \sum_{i=1}^N \left(\int_0^T K_x(t, u) \phi_i(u) du \right) \phi_i(t) + \sum_{i=1}^N \lambda_i \phi_i(t) \phi_i(t) \quad (6.57)$$

$$\xi_N(t) = K_x(t, t) - \sum_{i=1}^N \lambda_i \phi_i(t) \phi_i(t). \quad (6.58)$$

Property 7 guarantees that the sum will converge uniformly to $K_x(t, t)$ as $N \rightarrow \infty$. Therefore,

$$\lim_{N \rightarrow \infty} \xi_N(t) = 0, \quad 0 \leq t \leq T, \quad (6.59)$$

which is the desired result. (Observe that the convergence in Property 7 implies that for any $\epsilon > 0$ there exists an N_1 independent of t such that $\xi_N(t) < \epsilon$ for all $N > N_1$).

The series expansion we have developed in this section is generally referred to as the Karhunen–Loëve expansion ([Kar47, Loe55], p. 478, and [Loe45]). It provides a second-moment characterization in terms of uncorrelated random variables. In the next section,

we shall find that for a particular process of interest, the Gaussian random process, the coefficients in the expansion are statistically independent Gaussian random variables. It is in this case that the expansion finds its most important application.

6.3.3 Gaussian Processes

We now return to the question of a suitable complete characterization of a random process. We shall confine our attention to Gaussian random processes. Recall that the random variables x_1, x_2, \dots, x_N are jointly Gaussian if

$$y = \sum_{i=1}^N g_i x_i \quad (6.60)$$

is a Gaussian random variable for any set of g_i . In Chapter 3, N was finite and we required the g_i to be finite. If N is countably infinite, we require the g_i to be such that $E[y^2] < \infty$. In the random process, instead of a linear transformation on a set of random variables, we are interested in a linear functional of a random function. This suggests the following definition:

Definition. Let $x(t)$ be a random process defined over some interval $[T_\alpha, T_\beta]$ with a mean-value $m_x(t)$ and covariance function $K_x(t, u)$. If every linear functional of $x(t)$ is a Gaussian random variable, then $x(t)$ is a Gaussian random process. In other words, if

$$y = \int_{T_\alpha}^{T_\beta} g(u) x(u) du, \quad (6.61)$$

and $g(u)$ is any function such that $E[y^2] < \infty$. Then, in order for $x(u)$ to be a Gaussian random process, y must be a Gaussian random variable for every $g(u)$ in the above class.

Several properties follow immediately from this definition.

Property 1. The output of a linear system is a particular linear functional of interest. We denote the impulse response as $h(t, u)$, the output at time t due to a unit impulse input at time u . If the input is $x(t)$, which is a sample function from a Gaussian random process, the output $y(t)$ is also.

Proof.

$$y(t) = \int_{T_\alpha}^{T_\beta} h(t, u) x(u) du, \quad T_\gamma \leq t \leq T_\Delta. \quad (6.62)$$

The interval $[T_\gamma, T_\Delta]$ is simply the range over which $y(t)$ is defined. We assume that $h(t, u)$ is such that $E[y^2(t)] < \infty$ for all t in $[T_\gamma, T_\Delta]$. From the definition it is clear that y_t is a Gaussian random variable. To show that $y(t)$ is a Gaussian random process we must show

that any linear functional of it is a Gaussian random variable. Thus,

$$z \triangleq \int_{T_\gamma}^{T_\Delta} g_y(t) y(t) dt, \quad (6.63)$$

or

$$z = \int_{T_\gamma}^{T_\Delta} g_y(t) dt \int_{T_\alpha}^{T_\beta} h(t, u) x(u) du, \quad (6.64)$$

must be Gaussian for every $g_y(t)$ [such that $E[z^2] < \infty$]. Integrating with respect to t and defining the result as

$$g(u) \triangleq \int_{T_\gamma}^{T_\Delta} g_y(t) h(t, u) dt, \quad (6.65)$$

we have

$$z = \int_{T_\alpha}^{T_\beta} g(u) x(u) du, \quad (6.66)$$

which is Gaussian by definition.

Thus, we have shown that if the input to a linear system is a Gaussian random process the output is a Gaussian random process.

Property 2. If

$$y_1 = \int_{T_\alpha}^{T_\beta} g_1(u) x(u) du, \quad (6.67)$$

and

$$y_2 = \int_{T_\alpha}^{T_\beta} g_2(u) x(u) du, \quad (6.68)$$

where $x(u)$ is a Gaussian random process, then y_1 and y_2 are jointly Gaussian. (The proof is obvious in light of (6.60).)

Property 3. If

$$x_i = \int_{T_\alpha}^{T_\beta} \phi_i(u) x(u) du, \quad (6.69)$$

and

$$x_j = \int_{T_\alpha}^{T_\beta} \phi_j(u) x(u) du, \quad (6.70)$$

where $\phi_i(u)$ and $\phi_j(u)$ are orthonormalized eigenfunctions of (6.49) [now the interval of interest is (T_α, T_β) instead of $(0, T)$] then x_i and x_j are statistically independent Gaussian random variables ($i \neq j$). Thus,

$$p_{x_i}(X_i) = \frac{1}{\sqrt{2\pi\lambda_i}} \exp\left[-\frac{(X_i - m_i)^2}{2\lambda_i}\right], \quad (6.71)$$

where

$$m_i \triangleq \int_{T_\alpha}^{T_\beta} m_x(t) \phi_i(t) dt. \quad (6.72)$$

This property follows from Property 2 and (6.48).

Property 4. For any set of times $t_1, t_2, t_3, \dots, t_n$ in the interval $[T_\alpha, T_\beta]$, the random variables $x_{t_1}, x_{t_2}, \dots, x_{t_n}$ are jointly Gaussian random variables.

Proof. If we denote the set by the vector \mathbf{x}_t ,

$$\mathbf{x}_t \triangleq \begin{bmatrix} x_{t_1} \\ x_{t_2} \\ \vdots \\ x_{t_n} \end{bmatrix}, \quad (6.73)$$

whose mean is \mathbf{m}_x ,

$$\mathbf{m}_x \triangleq E \begin{bmatrix} x_{t_1} \\ x_{t_2} \\ \vdots \\ x_{t_n} \end{bmatrix} = \begin{bmatrix} m_x(t_1) \\ m_x(t_2) \\ \vdots \\ m_x(t_n) \end{bmatrix}, \quad (6.74)$$

then the joint probability density is

$$p_{\mathbf{x}_t}(\mathbf{X}) = \left[(2\pi)^{n/2} |\Lambda_x|^{1/2} \right]^{-1} \exp \left[-\frac{1}{2} (\mathbf{X} - \mathbf{m}_x)^T \Lambda_x^{-1} (\mathbf{X} - \mathbf{m}_x) \right], \quad (6.75)$$

and the joint characteristic function is

$$M_{\mathbf{x}_t}(j\mathbf{v}) = \exp \left(j\mathbf{v}^T \mathbf{m}_x - \frac{1}{2} \mathbf{v}^T \Lambda_x \mathbf{v} \right), \quad (6.76)$$

where Λ_x is the covariance matrix of the random variables $x_{t_1}, x_{t_2}, \dots, x_{t_n}$. (We assume Λ_x is nonsingular.) The ij th element is

$$\Lambda_{x,ij} = E[(x_{t_i} - m_x(t_i))(x_{t_j} - m_x(t_j))]. \quad (6.77)$$

This property follows by using the function

$$g(u) = \sum_{i=1}^n g_i \delta(u - t_i) \quad (6.78)$$

in (6.61) and the result in (6.60). Thus we see that our definition has the desirable property suggested in Section 6.3.1, for it uniquely specifies the joint density at any set of times. Frequently Property 4 is used as the basic definition. The disadvantage of this approach is that it is more difficult to prove that our definition and Properties 1–3 follow from (6.75) than vice versa.

The Gaussian process we have defined has two main virtues:

1. The physical mechanisms that produce many processes are such that a Gaussian model is appropriate.
2. The Gaussian process has many properties that make analytical results feasible.

Discussions of physical mechanisms that lead logically to Gaussian processes are available in [Ric44] and [Van54]. Other properties of the Gaussian process which are not necessary for our main discussion, are developed in the problems (Cf. Problems 6.3.12–6.3.18).

We shall encounter multiple processes that are jointly Gaussian. The definition is a straightforward extension of the preceding one.

Definition. Let $x_1(t), x_2(t), \dots, x_N(t)$ be a set of random processes defined over the intervals $(T_{\alpha_1}, T_{\beta_1}), (T_{\alpha_2}, T_{\beta_2}), \dots, (T_{\alpha_N}, T_{\beta_N})$, respectively. If every sum of arbitrary functionals of $x_i(t)$, $i = 1, 2, \dots, N$, is a Gaussian random variable, then the processes $x_1(t), x_2(t), \dots, x_N(t)$ are defined to be jointly Gaussian random processes. In other words,

$$y = \sum_{i=1}^N \int_{T_{\alpha_i}}^{T_{\beta_i}} g_i(u) x_i(u) du$$

must be Gaussian for every set of $g_i(u)$ such that $E[y^2] < \infty$.

Other properties of jointly Gaussian processes are discussed in the problems.

Property 3 is the reason for our emphasis on the Karhunen–Loëve expansion. It enables us to characterize a Gaussian process in terms of an at most countably infinite set of statistically independent Gaussian random variables. The significance of this will perhaps be best appreciated when we see how easy it makes our ensuing work. Observe that if we had chosen to emphasize Markov processes the orthogonal expansion method of characterization would not have been particularly useful. In Section 8.3, we discuss characterizations that emphasize the Markovian structure.

The Karhunen–Loëve expansion is useful in two ways:

1. Many of our theoretical derivations use it as a tool. In the majority of these cases the eigenfunctions and eigenvalues do not appear in the final result. The integral equation that specifies them (6.49) need never be solved.
2. In other cases, the result requires an explicit solution for one or more eigenfunctions and eigenvalues. Here we must be able to solve the equation exactly or find good approximate solutions.

In the next section, we consider some useful situations in which solutions can be obtained.

6.4 HOMOGENEOUS INTEGRAL EQUATIONS AND EIGENFUNCTIONS

In this section, we shall study in some detail the behavior of the solutions to (6.49). In addition to the obvious benefit of being able to solve for an eigenfunction when it is necessary, the discussion serves several other purposes:

1. By looking at several typical cases and finding the eigenvalues and eigenfunctions, the idea of a coordinate expansion becomes somewhat easier to visualize.
2. In many cases, we shall have to make approximations to get to the final result. We need to develop some feeling for what can be neglected and what is important.
3. We want to relate the behavior of the eigenvalues and eigenfunctions to more familiar ideas such as the power density spectrum.

In Section 6.4.1, we illustrate a technique that is useful whenever the random process is stationary and has a rational power density spectrum. In Section 6.4.2, we consider band-limited stationary processes, and in Section 6.4.3 we look at an important nonstationary process. Next in Section 6.4.4, we introduce the idea of a “white” process. In Section 6.4.5, we consider low rank models. In Section 6.4.6, we derive the optimum linear filter for estimating a message corrupted by noise. Finally, in Section 6.4.7, we examine the asymptotic behavior of the eigenfunctions and eigenvalues for large time intervals.

The discussions in Sections 6.4.1–6.4.4 provide a set of models in which analytical solutions are available. They provide insight into the behavior of the eigenvalues and eigenfunctions in some interesting cases. However, it is important to remember that we can find a numerical solution by sampling the functions in (6.49) to obtain a matrix equation containing ϕ and \mathbf{K}_x that can be solved using Matlab.

6.4.1 Rational Spectra

The first set of random processes of interest are stationary and have spectra that can be written as a ratio of two polynomials in ω^2 .

$$S_x(\omega) = \frac{N(\omega^2)}{D(\omega^2)}, \quad (6.79)$$

where $N(\omega^2)$ is a polynomial of order q in ω^2 and $D(\omega^2)$ is a polynomial of order p in ω^2 . Because we assume that $x(t)$ has a finite mean-square value, $q < p$. We refer to these spectra as rational. There is a routine but tedious method of solution. The basic

idea is straightforward. We convert the integral equation to a differential equation whose solution can be easily found. Then we substitute the solution back into the integral equation to satisfy the boundary conditions. We first demonstrate the technique by considering a simple example and then return to the general case and formalize the solution procedure. (Detailed discussions of similar problems are contained in [Sle54, You57, DR58, LB56, Dar58, Hel60, Hel65], or [ZR52].)

Example 6.2. Let

$$S_x(\omega) = \frac{2\alpha P}{\omega^2 + \alpha_2}, \quad -\infty < \omega < \infty, \quad (6.80)$$

or

$$R_x(\tau) = P \exp(-\alpha|\tau|), \quad -\infty < \tau < \infty. \quad (6.81)$$

The mean-square value of $x(t)$ is P . The integral equation of interest is

$$\int_{-T}^T P \exp(-\alpha|t-u|) \phi(u) du = \lambda \phi(t) \quad -T \leq t \leq T. \quad (6.82)$$

(The algebra becomes less tedious with a symmetric interval.)

As indicated above, we solve the integral equation by finding the corresponding differential equation, solving it, and substituting it back into the integral equation. First, we rewrite (6.82) to eliminate the magnitude sign.

$$\lambda \phi(t) = \int_{-T}^t P \exp[-\alpha(t-u)] \phi(u) du + \int_t^T P \exp[-\alpha(u-t)] \phi(u) du. \quad (6.83)$$

Differentiating once, we have

$$\lambda \dot{\phi}(t) = -P\alpha e^{-\alpha t} \int_{-T}^t e^{+\alpha u} \phi(u) du + P\alpha e^{+\alpha t} \int_t^T e^{-\alpha u} \phi(u) du. \quad (6.84)$$

Differentiating a second time gives

$$\lambda \ddot{\phi}(t) = P\alpha^2 \int_{-T}^t e^{-\alpha|t-u|} \phi(u) du - 2P\alpha \phi(t), \quad (6.85)$$

but the first term on the right-hand side is just $\alpha^2 \lambda \phi(t)$. Therefore,

$$\lambda \ddot{\phi}(t) = \alpha^2 \lambda \phi(t) - 2P\alpha \phi(t), \quad (6.86)$$

or, for $\lambda \neq 0$,

$$\ddot{\phi}(t) = \frac{\alpha^2(\lambda - 2P/\alpha)}{\lambda} \phi(t). \quad (6.87)$$

The solution to (6.86) has four possible forms corresponding to

$$\begin{aligned} (i) \quad & \lambda = 0 \\ (ii) \quad & 0 < \lambda < \frac{2P}{\alpha} \\ (iii) \quad & \lambda = \frac{2P}{\alpha} \\ (iv) \quad & \lambda > \frac{2P}{\alpha}. \end{aligned} \quad (6.88)$$

We can show that the integral equation cannot be satisfied for (i), (iii), and (iv). (Cf. Problem 6.4.1.)

For (ii) we may write

$$b^2 = \frac{-\alpha^2(\lambda - 2P/\alpha)}{\lambda}, \quad 0 < b^2 < \infty. \quad (6.89)$$

Then

$$\phi(t) = c_1 e^{ibt} + c_2 e^{-ibt}. \quad (6.90)$$

Substituting (6.90) into (6.83) and performing the integration, we obtain

$$0 = e^{-\alpha t} \left[\frac{c_1 e^{-(\alpha+jb)t}}{\alpha+jb} + \frac{c_2 e^{-(\alpha-jb)t}}{\alpha-jb} \right] - e^{+\alpha t} \left[\frac{c_1 e^{-(\alpha-jb)t}}{-\alpha+jb} + \frac{c_2 e^{-(\alpha+jb)t}}{-\alpha-jb} \right]. \quad (6.91)$$

We can easily verify that if $c_1 \neq \pm c_2$, (6.91) cannot be satisfied for all time. For $c_1 = -c_2$, we require that $\tan bT = -b/\alpha$. For $c_1 = c_2$, we require $\tan bT = \alpha/b$. Combining these two equations, we have

$$\left(\tan bT + \frac{b}{\alpha} \right) \left(\tan bT - \frac{\alpha}{b} \right) = 0. \quad (6.92)$$

The values of b that satisfy (6.92) can be determined graphically as shown in Figure 6.8. The upper set of intersections correspond to the second term in (6.92) and the lower set to the first term. The corresponding eigenvalues are

$$\lambda_i = \frac{2P\alpha}{\alpha^2 + b_i^2}, \quad i = 1, 2, \dots. \quad (6.93)$$

Observe that we have ordered the solutions to (6.92), $b_1 < b_2 < b_3 < \dots$. From (6.93), we see that this orders the eigenvalues $\lambda_1 > \lambda_2 > \lambda_3 > \dots$. The odd-numbered solutions correspond to $c_1 = c_2$ and, therefore,

$$\phi_i(t) = \frac{1}{T^{1/2} \left(1 + \frac{\sin 2b_i T}{2b_i T} \right)^{1/2}} \cos b_i t, \quad -T \leq t \leq T \quad (i \text{ odd}). \quad (6.94)$$

The even-numbered solutions correspond to $c_1 = -c_2$ and, therefore,

$$\phi_i(t) = \frac{1}{T^{1/2} \left(1 - \frac{\sin 2b_i T}{2b_i T} \right)^{1/2}} \sin b_i t, \quad -T \leq t \leq T \quad (i \text{ even}). \quad (6.95)$$

We see that the eigenfunctions are cosines and sines whose frequencies are *not* harmonically related. ■

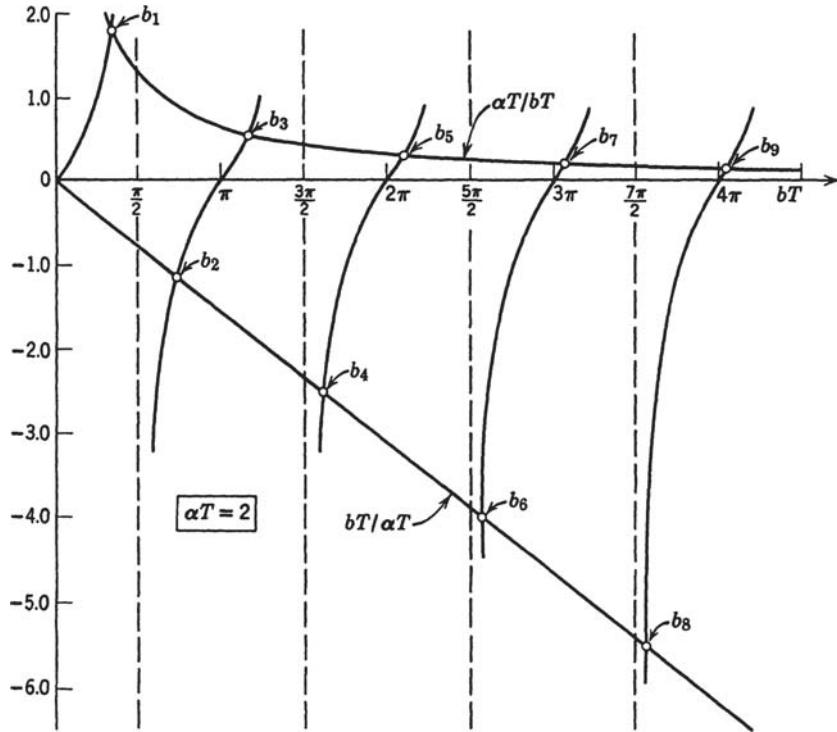


Figure 6.8: Graphical solution of transcendental equation.

Several interesting observations may be made with respect to this example:

1. The eigenvalue corresponding to a particular eigenfunction is equal to the height of the power density spectrum at that frequency.
2. As T increases, b_n decreases monotonically and therefore λ_n increases monotonically.
3. As bT increases, the upper intersections occur at approximately $(i - 1)\pi/2$ [i odd] and the lower intersections occur at approximately $(i - 1)\pi/2$ [i even]. From (6.94) and (6.95), we see that the higher index eigenfunctions are approximately a set of periodic sines and cosines.

$$\phi_i(t) \cong \begin{cases} \frac{1}{T^{1/2} \left(1 + \frac{\sin 2b_i T}{2b_i T}\right)^{1/2}} \cos \left[\frac{(i-1)\pi}{2T} t \right] & -T \leq t \leq T \quad (i \text{ odd}), \\ \frac{1}{T^{1/2} \left(1 - \frac{\sin 2b_i T}{2b_i T}\right)^{1/2}} \sin \left[\frac{(i-1)\pi}{2T} t \right] & -T \leq t \leq T \quad (i \text{ even}). \end{cases}$$

This behavior is referred to as the asymptotic behavior.

The first observation is not true in general. In Section 6.4.7, we shall show that the λ_n are always monotonically increasing functions of T . We shall also show that the asymptotic behavior seen in this example is typical of stationary processes.

Our discussion up to this point has dealt with a particular spectrum. We now return to the general case.

It is easy to generalize the technique to arbitrary rational spectra. First we write $S_x(\omega)$ as a ratio of two polynomials,

$$S_x(\omega) = \frac{N(\omega^2)}{D(\omega^2)}. \quad (6.96)$$

Looking at (6.86), we see that the differential equation does *not* depend explicitly on T . This independence is true whenever the spectrum has the form in (6.96). Therefore, we would obtain the same differential equation if we started with the integral equation

$$\lambda\phi(t) = \int_{-\infty}^{\infty} K_x(t-u)\phi(u) du \quad -\infty < t < \infty. \quad (6.97)$$

By use of Fourier transforms, a formal solution to this equation follows immediately:

$$\lambda\Phi(j\omega) = S_x(\omega)\Phi(j\omega) = \frac{N(\omega^2)}{D(\omega^2)}\Phi(j\omega) \quad (6.98)$$

or

$$0 = [\lambda D(\omega^2) - N(\omega^2)]\Phi(j\omega). \quad (6.99)$$

There are $2p$ homogeneous solutions to the differential equation corresponding to (6.99) for every value of λ (corresponding to the roots of the polynomial in the bracket). We denote them as $\phi_{h_i}(t, \lambda)$, $i = 1, 2, \dots, 2p$. To find the solution to (6.49), we substitute

$$\phi(t) = \sum_{i=1}^{2p} a_i \phi_{h_i}(t, \lambda) \quad (6.100)$$

into the integral equation and solve for those values of λ and a_i that lead to a solution. There are no conceptual difficulties, but the procedure is tedious. Because of these implementation difficulties, we launched a research effort in the late 1960s to find more efficient techniques. The basic idea was to model the random process using a state variable description and use the description to derive the differential equations for representing the kernel operator. The result was reported in *A State-Variable Approach to the Solution of the Fredholm Integral Equation* by Arthur Baggeroer [Bag69]. The work had been reported earlier in [Bag67a, Bag67b], and [Bag68]. Results of L. D. Collins were reported in [Col68c] and [Col68b]. A comprehensive discussion of this work is contained in the appendix of DEMT-II [Van71a, Van03]. The reader is referred to these references for a discussion of the technique.

One particular family of spectra serves as a useful model for many physical processes and also leads to tractable solutions to the integral equation for the problem under discussion. This is the family described by the equation

$$S_x(\omega : n) = \left(\frac{2n P}{\alpha} \right) \frac{\sin(\pi/2n)}{1 + (\omega/\alpha)^{2n}}. \quad (6.101)$$

It is referred to as the Butterworth family and is shown in Figure 6.9. When $n = 1$, we have the simple one-pole spectrum. As n increases, the attenuation versus frequency for $\omega > \alpha$

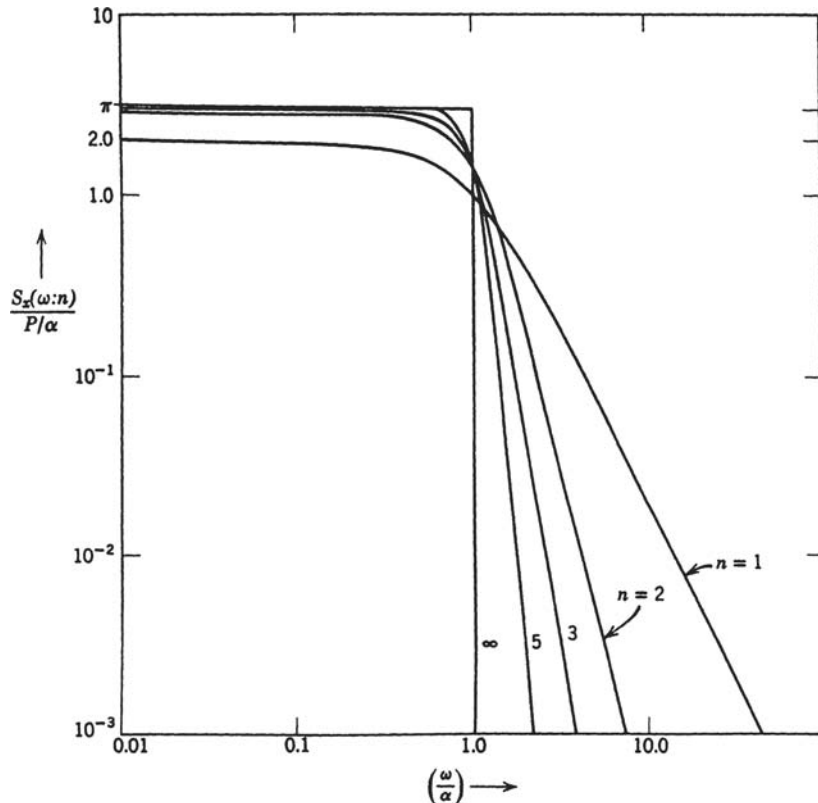


Figure 6.9: Butterworth spectra.

increases more rapidly. In the limit, as $n \rightarrow \infty$, we have an ideal bandlimited spectrum. In the next section we discuss the eigenfunctions and eigenvalues for the bandlimited spectrum.

6.4.2 Bandlimited Spectra

When the spectrum is not rational, the differential equation corresponding to the integral equation will usually have time-varying coefficients. Fortunately, in many cases of interest the resulting differential equation is some canonical type whose solutions have been tabulated. An example in this category is the bandlimited spectrum shown in Figure 6.10. In

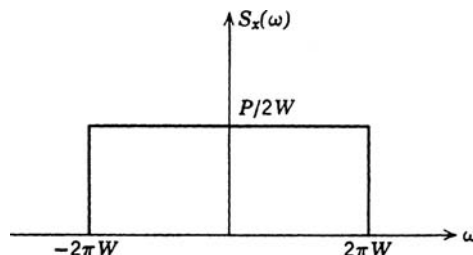


Figure 6.10: Bandlimited spectrum.

this case

$$S_x(\omega) = \begin{cases} \frac{\pi P}{\alpha} & |\omega| \leq \alpha \\ 0 & |\omega| > \alpha, \end{cases} \quad (6.102)$$

or, in cycles per second,

$$S_x(\omega) = \begin{cases} \frac{P}{2W} & |f| \leq W \\ 0 & |f| > W, \end{cases} \quad (6.103)$$

where

$$2\pi W = \alpha. \quad (6.104)$$

The corresponding covariance function is

$$K_x(t, u) = P \frac{\sin \alpha(t-u)}{\alpha(t-u)}. \quad (6.105)$$

The integral equation of interest becomes

$$\lambda \phi(t) = \int_{-T/2}^{+T/2} P \frac{\sin \alpha(t-u)}{\alpha(t-u)} \phi(u) du. \quad (6.106)$$

[This is just (6.49) with the interval shifted to simplify notation.]

Once again the procedure is to find a related differential equation and to examine its solution. We are, however, more interested in the results than the detailed techniques; therefore, we merely state them ([Sle54, SP61, LP61, LP62], and [Fla57] are useful for further study).

The related differential equation over a normalized interval is

$$(1-t^2) \ddot{f}(t) - 2t \dot{f}(t) + (\mu - c^2 t^2) f(t) = 0 \quad -1 < t < 1, \quad (6.107)$$

where

$$c = \frac{\alpha T}{2} = \pi W T, \quad (6.108)$$

and μ is the eigenvalue. This equation has continuous solutions for certain values of $\mu(c)$. These solutions are called *angular prolate spheroidal functions* and are denoted by $S_{0n}(c, t)$, $n = 0, 1, 2, \dots$. A plot of typical $S_{0n}(c, t)$ is contained in [SP61, LP61], and [LP62]. These functions also satisfy the integral equation

$$2 \left[R_{0n}^{(1)}(c, 1) \right]^2 S_{0n}(c, t) = \int_{-1}^{+1} \frac{\sin c(t-u)}{c(t-u)} S_{0n}(c, u) du, \quad -1 \leq t \leq 1, \quad (6.109)$$

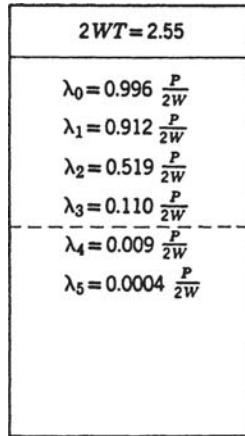


Figure 6.11: Eigenvalues for a bandlimited spectrum ($2WT = 2.55$).

or changing variables

$$PT \left[R_{0n}^{(1)} \left(\frac{\alpha T}{2}, 1 \right) \right]^2 S_{0n} \left(\frac{\alpha T}{2}, \frac{2t}{T} \right) = \int_{-T/2}^{T/2} \frac{P \sin \alpha(t-u)}{\alpha(t-u)} S_{0n} \left(\frac{\alpha T}{2}, \frac{2u}{T} \right) du,$$

$$-\frac{T}{2} \leq t \leq \frac{T}{2}, \quad (6.110)$$

where $R_{0n}^{(1)}(\alpha T/2, 1)$ is a *radial prolate spheroidal function*. Thus the eigenvalues are

$$\lambda_n = PT \left[R_{0n}^{(1)} \left(\frac{\alpha T}{2}, 1 \right) \right]^2, \quad n = 0, 1, 2, \dots$$

These functions are tabulated in several references (e.g. [Fla57] or [SMC⁺56]).

The first several eigenvalues for various values of WT are shown in Figures 6.11 and 6.12. We observe a very interesting phenomenon. For values of $n > (2WT + 1)$, the values of λ_n rapidly approach zero. We can check the total energy in the remaining eigenvalues, for

$$\sum_{i=0}^{\infty} \lambda_i = \int_{-T/2}^{+T/2} K_x(t, t) dt = PT. \quad (6.111)$$

In Figure 6.11, $2WT = 2.55$ and the first four eigenvalues sum to $(2.54/2.55)PT$. In Figure 6.12, $2WT = 5.10$ and the first six eigenvalues sum to $(5.09/5.10)PT$. This behavior is discussed in detail in [LP62]. Our example suggests that the following statement is plausible. When a bandlimited process $[-W, W]$ cps is observed over a T -second interval, there are only $(2TW + 1)$ significant eigenvalues. This result will be important to us in later chapters when we obtain approximate solutions by neglecting the higher eigenfunctions. More precise statements about the behavior are contained in [SP61, LP61], and [LP62].

2WT = 5.10	
λ_0	= 1.000 $\frac{P}{2W}$
λ_1	= 0.999 $\frac{P}{2W}$
λ_2	= 0.997 $\frac{P}{2W}$
λ_3	= 0.961 $\frac{P}{2W}$
λ_4	= 0.748 $\frac{P}{2W}$
λ_5	= 0.321 $\frac{P}{2W}$
λ_6	= 0.061 $\frac{P}{2W}$
λ_7	= 0.006 $\frac{P}{2W}$
λ_8	= 0.0004 $\frac{P}{2W}$

Figure 6.12: Eigenvalues of a bandlimited spectrum ($2WT = 5.10$).

6.4.3 Nonstationary Processes

The process of interest is the simple Wiener process. It was developed as a model for Brownian motion and is discussed in detail in [Par62] and [Ros62]. A typical sample function is shown in Figure 6.13.

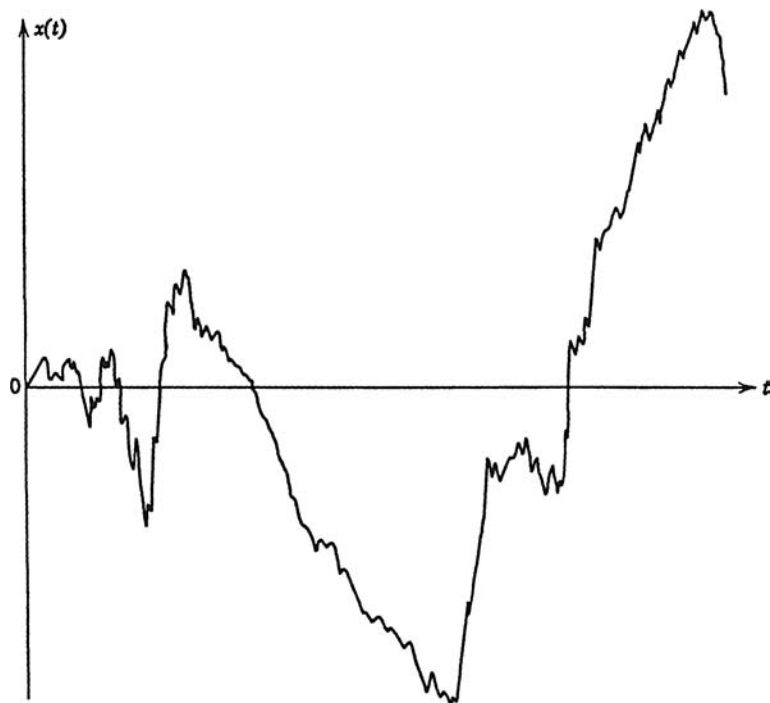


Figure 6.13: Sample function of a Wiener process.

This process is defined for $t \geq 0$ and is characterized by the following properties:

$$x(0) = 0 \quad (6.112)$$

$$E[x(t)] = 0 \quad (6.112)$$

$$E[x^2(t)] = \sigma^2 t \quad (6.113)$$

$$p_{x_t}(X_t) = \frac{1}{\sqrt{2\pi\sigma^2 t}} \exp\left(-\frac{X_t^2}{2\sigma^2 t}\right). \quad (6.114)$$

The increment variables are independent; that is, if $t_3 > t_2 > t_1$, then $(x_{t_3} - x_{t_2})$ and $(x_{t_2} - x_{t_1})$ are statistically independent. In the next example, we solve (6.49) for the Wiener process.

Example 6.3. Wiener Process. Using the properties of the Wiener process, we can show that

$$K_x(t, u) = \sigma^2 \min(u, t) = \begin{cases} \sigma^2 u & u \leq t \\ \sigma^2 t & t \leq u. \end{cases} \quad (6.115)$$

In this case, (6.49) becomes

$$\lambda\phi(t) = \int_0^T K_x(t, u) \phi(u) du \quad 0 \leq t \leq T. \quad (6.116)$$

Substituting (6.115) into (6.116)

$$\lambda\phi(t) = \sigma^2 \int_0^t u\phi(u) du + \sigma^2 t \int_t^T \phi(u) du. \quad (6.117)$$

Proceeding as in Section 6.4.1, we differentiate (6.117) and obtain,

$$\lambda\dot{\phi}(t) = \sigma^2 \int_t^T \phi(u) du. \quad (6.118)$$

Differentiating again, we obtain

$$\lambda\ddot{\phi}(t) = -\sigma^2 \phi(t), \quad (6.119)$$

or, for $\lambda \neq 0$,

$$\ddot{\phi}(t) + \frac{\sigma^2}{\lambda} \phi(t) = 0. \quad (6.120)$$

There are three possible ranges for λ :

- (i) $\lambda < 0$
- (ii) $\lambda = 0$
- (iii) $\lambda > 0$.

We can easily verify (Cf. Problem 6.4.3) that (i) and (ii) do not provide solutions that will satisfy the integral equation. For $\lambda > 0$ we proceed exactly as in the preceding section and find

$$\lambda_n = \frac{\sigma^2 T^2}{\left(n - \frac{1}{2}\right)^2 \pi^2} \quad n = 1, 2, \dots, \quad (6.122)$$

and

$$\phi_n(t) = \left(\frac{2}{T}\right)^{1/2} \sin\left[\left(n - \frac{1}{2}\right)\frac{\pi}{T}t\right] \quad 0 \leq t \leq T. \quad (6.123)$$

Once again the eigenfunctions are sinusoids. ■

The Wiener process is important for several reasons.

1. A large class of processes can be transformed into the Wiener process.
2. A large class of processes can be generated by passing a Wiener process through a linear or nonlinear system. (We discuss this in detail later.)

6.4.4 White Noise Processes

Another interesting process can be derived from the Wiener process. Using (6.44) and (6.123), we can expand $x(t)$ in a series.

$$x(t) = \text{l.i.m.}_{K \rightarrow \infty} \sum_{n=1}^K x_n \left(\frac{2}{T}\right)^{1/2} \sin\left[\left(n - \frac{1}{2}\right)\frac{\pi}{T}t\right], \quad (6.124)$$

where the mean-square value of the coefficient is given by (6.122):

$$E[x_n^2] = \frac{\sigma^2 T^2}{\left(n - \frac{1}{2}\right)^2 \pi^2}. \quad (6.125)$$

We denote the K -term approximation as $x_K(t)$.

Now, let us determine what happens when we differentiate $x_K(t)$:

$$\dot{x}_K(t) = \sum_{n=1}^K x_n \left(n - \frac{1}{2}\right) \frac{\pi}{T} \left\{ \left(\frac{2}{T}\right)^{1/2} \cos\left[\left(n - \frac{1}{2}\right)\frac{\pi}{T}t\right] \right\}. \quad (6.126)$$

We see that the time function inside the braces is still normalized. Thus, we may write

$$\dot{x}_K(t) = \sum_{n=1}^K w_n \left(\frac{2}{T}\right)^{1/2} \cos\left(n - \frac{1}{2}\right) \frac{\pi}{T} t, \quad (6.127)$$

where

$$E(w_n^2) = \sigma^2.$$

We observe that we have generated a process in which every eigenvalue is *equal*. Clearly, if we let $K \rightarrow \infty$, the series would not converge. If it did, it would correspond to a process with infinite energy over $[0, T]$.

We can *formally* obtain the covariance function of this resulting process by differentiating $K_x(t, u)$:

$$K_{\dot{x}}(t, u) = \frac{\partial^2}{\partial t \partial u} K_x(t, u) = \frac{\partial^2}{\partial t \partial u} [\sigma^2 \min(t, u)] = \sigma^2 \delta(t - u), \quad 0 \leq t, u \leq T. \quad (6.128)$$

We see that the covariance function is an impulse. Still proceeding formally, we can look at the solution to the integral equation (6.49) for an impulse covariance function:

$$\lambda \phi(t) = \sigma^2 \int_0^T \delta(t - u) \phi(u) du, \quad 0 < t < T. \quad (6.129)$$

The equation is satisfied for any $\phi(t)$ with $\lambda = \sigma^2$. Thus, *any* set of orthonormal functions is suitable for decomposing this process. The reason for the nonuniqueness is that the impulse kernel is not square-integrable. The properties stated earlier assumed square-integrability.

We shall find the resulting process to be a useful artifice for many models. We summarize its properties in the following definitions.

Definition. A *Gaussian* white noise process is a Gaussian process whose covariance function is $\sigma^2 \delta(t - u)$. It may be decomposed over the interval $[0, T]$ by using *any* set of orthonormal functions $\phi_i(t)$. The coefficients along *each* coordinate function are statistically independent Gaussian variables with equal variance σ^2 .

Some related notions follow easily.

Property. We can write, formally

$$\sigma^2 \delta(t - u) = \sum_{i=1}^{\infty} \sigma^2 \phi_i(t) \phi_i(u) \quad 0 \leq t, u \leq T, \quad (6.130)$$

or, equivalently,

$$\delta(t - u) = \sum_{i=1}^{\infty} \phi_i(t) \phi_i(u) \quad 0 \leq t, u \leq T. \quad (6.131)$$

Property. If the coefficients are uncorrelated, with equal variances, but *not* Gaussian, the process is referred to as a white process.

Property. If the process is defined over the infinite interval, its spectrum is

$$S_x(\omega) = \sigma^2; \quad (6.132)$$

that is, it is constant over all frequencies. The value of each eigenvalue corresponds to the spectral height σ^2 .

The utility of a white noise process is parallel to that of an impulse input in the analysis of linear systems. Just as we can observe an impulse only after it has been through a system

with some finite bandwidth, we can observe white noise only after it has passed through a similar system. Therefore, as long as the bandwidth of the noise is appreciably larger than that of the system, it can be considered as having an infinite bandwidth.

6.4.5 Low Rank Kernels

In a number of important applications

$$\begin{aligned} x(t) &= \sum_{i=1}^N a_i s_i(t) + w(t) \quad 0 \leq t \leq T \\ &\triangleq s(t) + w(t), \end{aligned} \quad (6.133)$$

where the $s_i(t)$ are known deterministic functions which are linearly independent, the a_i are zero-mean Gaussian random variables with covariance $K_{a_{ij}} = E[a_i a_j]$, and $w(t)$ is a white noise process with covariance $\sigma^2 \delta(t - u)$. We want to do an eigendecomposition of $K_s(t, u)$ by solving

$$\lambda_i \phi_i(t) = \int_0^T K_s(t, u) \phi_i(u) du, \quad 0 \leq t \leq T. \quad (6.134)$$

We define

$$\mathbf{s}(t) = [s_1(t) \quad s_2(t) \quad \cdots \quad s_N(t)]^T \quad (6.135)$$

and a coefficient vector

$$\mathbf{a} = [a_1 \quad a_2 \quad \cdots \quad a_N]^T. \quad (6.136)$$

Then

$$\begin{aligned} K_s(t, u) &= E\{s(t)s(u)\} \\ &= E\{\mathbf{s}^T(t) \mathbf{a} \mathbf{a}^T \mathbf{s}(u)\} \\ &= \mathbf{s}^T(t) \mathbf{K}_a \mathbf{s}(u). \end{aligned} \quad (6.137)$$

Then (6.134) can be written as

$$\lambda_i \phi_i(t) = \mathbf{s}^T(t) \mathbf{K}_a \int_0^T \mathbf{s}(u) \phi_i(u) du, \quad 0 \leq t \leq T. \quad (6.138)$$

We recognize that the $s_i(t)$, $i = 1, 2, \dots, N$ define our N -dimensional subspace so that $\phi_i(t)$ must be a linear transformation in that subspace. Therefore, we can write

$$\begin{aligned} \phi_i(t) &= \mathbf{c}_i^T \mathbf{s}(t) \\ &= \mathbf{s}^T(t) \mathbf{c}_i, \end{aligned} \quad (6.139)$$

where \mathbf{c}_i is an $N \times 1$ vector. Substituting (6.139) into (6.138) gives

$$\lambda_i \mathbf{s}^T(t) \mathbf{c}_i = \mathbf{s}^T(t) \mathbf{K}_a \int_0^T \mathbf{s}(u) \mathbf{s}^T(u) du \mathbf{c}_i, \quad i = 1, 2, \dots, N. \quad (6.140)$$

Defining,

$$\rho_s \triangleq \int_0^T \mathbf{s}(u) \mathbf{s}^T(u) du, \quad (6.141)$$

(6.140) reduces to

$$\lambda_i \mathbf{c}_i = \mathbf{K}_a \rho_s \mathbf{c}_i \quad i = 1, 2, \dots, N, \quad (6.142)$$

which is a formula from Chapter 2 for a classic eigendecomposition.

Thus we solve (6.142) for $i = 1, 2, \dots, N$ to obtain the eigenvalues and the \mathbf{c}_i vectors. We then use (6.139) to find the eigenfunctions. Several examples are developed in the problems and in Chapter 7.

6.4.6 The Optimum Linear Filter

In this section, we consider the problem of trying to estimate a message in the presence of interfering noise. Our treatment at this point is reasonably brief. We return to this problem and study it in detail in Chapter 8. Here we have three objectives in mind:

1. The introduction of time-varying linear filters and simple minimization techniques.
2. The development of a specific result to be used in subsequent chapters; specifically, the integral equation whose solution is the optimum linear filter.
3. The illustration of how the orthogonal expansion techniques we have just developed will enable us to obtain a formal solution to an integral equation.

The system of interest is shown in Figure 6.14. The message $a(t)$ is a sample function from a zero-mean random process with a finite mean-square value and a covariance function $K_a(t, u)$. It is corrupted by an uncorrelated additive zero-mean noise $n(t)$ with covariance function $K_n(t, u)$. We observe the sum of these two processes,

$$r(t) = a(t) + n(t), \quad 0 \leq t \leq T. \quad (6.143)$$

We pass $r(t)$ through a linear filter to obtain an estimate of $a(t)$ denoted by $\hat{a}(t)$.

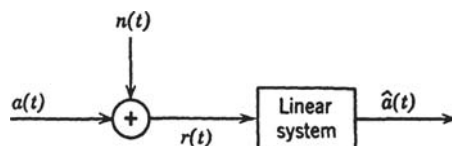


Figure 6.14: Linear filter problem.

Because $a(t)$ is not necessarily stationary and the observation interval is finite, we anticipate that to obtain the best estimate we may require a time-varying filter. We characterize the filter by its impulse response $h(t, u)$, which is the value of the output at time t when the input is an impulse at time u . If the system is physically realizable, then

$$h(t, u) = 0 \quad t < u,$$

for the output cannot precede the input. If the system is time-invariant, then $h(t, u)$ depends only on the difference $(t - u)$. We assume that $r(t)$ equals zero for $t < 0$ and $t > T$. Because the system is linear, the output due to $r(t)$, $0 \leq t \leq T$, can be written as

$$\hat{a}(t) = \int_0^T h(t, u) r(u) du, \quad (6.144)$$

which is an obvious generalization of the convolution integral.

We want to choose $h(t, u)$ to minimize the mean of the squared error integrated over the interval $[0, T]$. In other words, we want to choose $h(t, u)$ to minimize the quantity

$$\begin{aligned} \xi_I &\triangleq E \left\{ \frac{1}{T} \int_0^T [a(t) - \hat{a}(t)]^2 dt \right\} \\ &= E \left\{ \frac{1}{T} \int_0^T \left[a(t) - \int_0^T h(t, u) r(u) du \right]^2 dt \right\}. \end{aligned} \quad (6.145)$$

Thus, we are minimizing the mean-square error integrated over the interval. We refer to ξ_I as the *interval estimation error*.

Similarly, we can define a *point estimation error*:

$$\xi_P(t) = E \left\{ \left[a(t) - \int_0^T h(t, u) r(u) du \right]^2 \right\} \quad 0 \leq t \leq T. \quad (6.146)$$

Clearly, if we minimize the point error at each time, the total interval error will be minimized. One way to solve this minimization problem is to use standard variational techniques (e.g., [Hil52], Chapter 2). Our approach is less formal and leads directly to a necessary and sufficient condition. We require the filter $h(t, u)$ to be a continuous function in both variables over the area $0 \leq t, u \leq T$ and denote the $h(t, u)$ that minimizes $\xi_P(t)$ as $h_o(t, u)$. Any other filter function $h(t, u)$ in the allowed class can be written as

$$h(t, u) = h_o(t, u) + \epsilon h_\epsilon(t, u), \quad 0 \leq t, u \leq T, \quad (6.147)$$

where ϵ is a real parameter and $h_\epsilon(t, u)$ is in the allowable class of filters. Taking the expectation of (6.146), substituting (6.147) into the result, and grouping terms according to

the power of ϵ , we obtain

$$\xi_P(t : \epsilon) = K_a(t, t) - 2 \int_0^T h(t, u) K_a(t, u) du + \int_0^T dv \int_0^T du h(t, v) h(t, u) K_r(u, v), \quad (6.148)$$

or

$$\begin{aligned} \xi_P(t : \epsilon) &= K_a(t, t) - 2 \int_0^T h_o(t, u) K_a(t, u) du \\ &\quad + \int_0^T dv \int_0^T du h_o(t, u) h_o(t, v) K_r(u, v) \\ &\quad - 2\epsilon \int_0^T du h_\epsilon(t, u) \left[K_a(t, u) - \int_0^T h_o(t, v) K_r(u, v) dv \right] \\ &\quad + \epsilon^2 \iint_{[0,T]} h_\epsilon(t, v) h_\epsilon(t, u) K_r(u, v) du dv. \end{aligned} \quad (6.149)$$

If we denote the first three terms as $\xi_{P_o}(t)$ and the last two terms as $\Delta\xi(t : \epsilon)$, then (6.149) becomes

$$\xi_P(t : \epsilon) = \xi_{P_o}(t) + \Delta\xi(t : \epsilon). \quad (6.150)$$

Now, if $h_o(t, u)$ is the optimum filter, then $\Delta\xi(t : \epsilon)$ must be greater than or equal to zero for all allowable $h_\epsilon(t, u)$ and all $\epsilon \neq 0$. We show that a necessary and sufficient condition for this to be true is that

$$K_a(t, u) - \int_0^T h_o(t, v) K_r(u, v) dv = 0 \quad \begin{cases} 0 \leq t \leq T \\ 0 < u < T. \end{cases}$$

(6.151)

The equation for $\Delta\xi(t : \epsilon)$ is

$$\begin{aligned} \Delta\xi(t : \epsilon) &= -2\epsilon \int_0^T du h_\epsilon(t, u) \left[K_a(t, u) - \int_0^T h_o(t, v) K_r(u, v) dv \right] \\ &\quad + \epsilon^2 \iint_{[0,T]} h_\epsilon(t, v) h_\epsilon(t, u) K_r(u, v) du dv. \end{aligned} \quad (6.152)$$

Three observations are needed:

1. The second term is nonnegative for any choice of $h_\epsilon(t, v)$ and ϵ because $K_r(t, u)$ is nonnegative definite.

2. Unless

$$\int_0^T h_\epsilon(t, u) \left[K_a(t, u) - \int_0^T h_o(t, v) K_r(u, v) dv \right] du = 0, \quad (6.153)$$

there exists for every continuous $h_\epsilon(t, u)$ a range of values of ϵ that will cause $\Delta\xi(t : \epsilon)$ to be negative. Specifically, $\Delta\xi(t : \epsilon) < 0$ for all

$$0 < \epsilon < \frac{2 \int_0^T h_\epsilon(t, u) \left[K_a(t, u) - \int_0^T h_o(t, v) K_r(u, v) dv \right] du}{\iint_{[0,T]} h_\epsilon(t, v) h_\epsilon(t, u) K_r(u, v) du dv}, \quad (6.154)$$

if the numerator on the right side of (6.154) is positive. $\Delta\xi(t : \epsilon)$ is negative for all negative ϵ greater than the right side of (6.154) if the numerator is negative.

3. In order that (6.153) may hold, it is necessary and sufficient that the term in the bracket be identically zero for all $0 < u < T$. Thus,

$$K_a(t, u) - \int_0^T h_o(t, v) K_r(u, v) dv = 0, \quad \begin{aligned} 0 &\leq t \leq T \\ 0 &< u < T. \end{aligned} \quad (6.155)$$

The inequality on u is strict if there is a white noise component in $r(t)$ because the second term is discontinuous at $u = 0$ and $u = T$. If (6.155) is not true, we can make the left side of (6.153) positive by choosing $h_\epsilon(t, u) > 0$ for those values of u in which the left side of (6.155) is greater than zero and $h_\epsilon(t, u) < 0$ elsewhere. These three observations complete the proof of (6.151).

The result in (6.151) is fundamental to many of our later problems. For the case of current interest we assume that the additive noise is white. Then

$$K_r(t, u) = \frac{N_0}{2} \delta(t - u) + K_a(t, u). \quad (6.156a)$$

Substituting (6.156a) into (6.151), we obtain

$$\frac{N_0}{2} h_o(t, u) + \int_0^T h_o(t, v) K_a(u, v) dv = K_a(t, u) \quad \begin{aligned} 0 &\leq t \leq T \\ 0 &< u < T. \end{aligned} \quad (6.156b)$$

Observe that $h_o(t, 0)$ and $h_o(t, T)$ are uniquely specified by the continuity requirement

$$h_o(t, 0) = \lim_{u \rightarrow 0^+} h_o(t, u) \quad (6.157a)$$

$$h_o(t, T) = \lim_{u \rightarrow T^-} h_o(t, u). \quad (6.157b)$$

Because $a(t)$ has a finite mean-square value, (6.157a) and (6.157b) imply that (6.156b) is also valid for $u = 0$ and $u = T$.

The resulting error for the optimum processor follows easily. It is simply the first term in (6.150).

$$\begin{aligned}\xi_{P_o}(t) &= K_a(t, t) - 2 \int_0^T h_o(t, u) K_a(t, u) du \\ &\quad + \int_0^T \int h_o(t, u) h_o(t, v) K_r(u, v) du dv,\end{aligned}\quad (6.158)$$

or

$$\begin{aligned}\xi_{P_o}(t) &= K_a(t, t) - \int_0^T h_o(t, u) K_a(t, u) du \\ &\quad - \int_0^T h_o(t, u) \left[K_a(t, u) - \int_0^T h_o(t, v) K_r(u, v) dv \right] du.\end{aligned}\quad (6.159)$$

But (6.151) implies that the term in brackets is zero. Therefore,

$$\xi_{P_o}(t) = K_a(t, t) - \int_0^T h_o(t, u) K_a(t, u) du. \quad (6.160)$$

For the white noise case, substitution of (6.156b) into (6.160) gives

$$\boxed{\xi_{P_o}(t) = \frac{N_0}{2} h_o(t, t).} \quad (6.161)$$

As a final result in our present discussion of optimum linear filters, we demonstrate how to obtain a solution to (6.156b) in terms of the eigenvalues and eigenfunctions of $K_a(t, u)$. We begin by expanding the message covariance function in a series,

$$K_a(t, u) = \sum_{i=1}^{\infty} \lambda_i \phi_i(t) \phi_i(u), \quad (6.162)$$

where λ_i and $\phi_i(t)$ are solutions to (6.49) when the kernel is $K_a(t, u)$. Using (6.130), we can expand the white noise component in (6.156a)

$$K_w(t, u) = \frac{N_0}{2} \delta(t - u) = \sum_{i=1}^{\infty} \frac{N_0}{2} \phi_i(t) \phi_i(u). \quad (6.163)$$

To expand the white noise we need a CON set. If $K_a(t, u)$ is not positive definite we augment its eigenfunctions to obtain a CON set. (See Property 9 in Section 6.3.2).

Then

$$K_r(t, u) = \sum_{i=1}^{\infty} \left(\lambda_i + \frac{N_0}{2} \right) \phi_i(t) \phi_i(u). \quad (6.164)$$

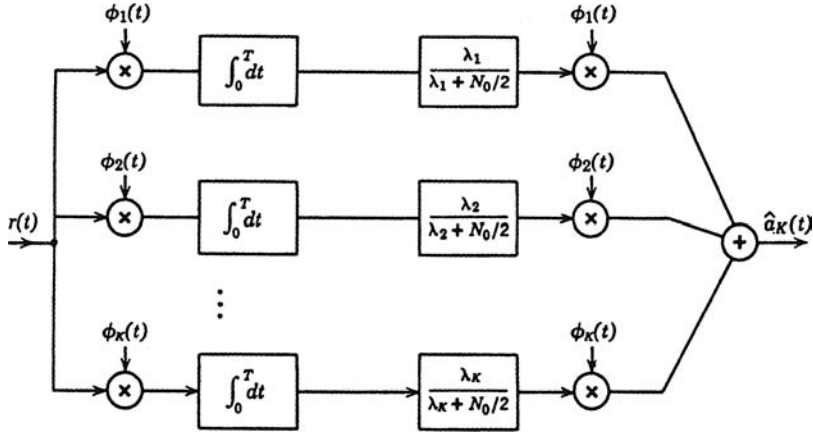


Figure 6.15: Optimum Filter.

Because the $\phi_i(t)$ are a CON set, we try a solution of the form

$$h_o(t, u) = \sum_{i=1}^{\infty} h_i \phi_i(t) \phi_i(u). \quad (6.165)$$

Substituting (6.162), (6.164), and (6.165) into (6.156b), we find

$$h_o(t, u) = \sum_{i=1}^{\infty} \frac{\lambda_i}{\lambda_i + N_0/2} \phi_i(t) \phi_i(u). \quad (6.166)$$

Thus the optimum linear filter can be expressed in terms of the eigenfunctions and eigenvalues of the message covariance function. A K -term approximation is shown in Figure 6.15.

The nonrealizability could be eliminated by a T -second delay in the second multiplication. Observe that (6.166) represents a practical solution only when the number of significant eigenvalues is small. In most cases, the solution in terms of eigenfunctions will be useful only for theoretical purposes. When we study filtering and estimation in detail in later chapters, we shall find more practical solutions.

The error can also be expressed easily in terms of eigenvalues and eigenfunctions. Substitution of (6.166) into (6.161) gives

$$\xi_{P_o}(t) = \frac{N_0}{2} \sum_{i=1}^{\infty} \frac{\lambda_i}{\lambda_i + N_0/2} \phi_i^2(t) \quad 0 \leq t \leq T, \quad (6.167)$$

and

$$\xi_I = \frac{1}{T} \int_0^T \xi_{P_o}(t) dt = \frac{N_0}{2T} \sum_{i=1}^{\infty} \frac{\lambda_i}{\lambda_i + N_0/2}. \quad (6.168)$$

In addition to the development of a useful result, this problem has provided an excellent example of the use of eigenfunctions and eigenvalues in finding a series solution to an integral equation. It is worthwhile to re-emphasize that all the results in this section were based on the original constraint of a linear processor and that a Gaussian assumption was not needed. We now return to the general discussion and develop several properties of interest.

6.4.7 Properties of Eigenfunctions and Eigenvalues

In this section, we derive two interesting properties that will be useful in the sequel.

6.4.7.1 Monotonic Property⁵

Consider the integral equation

$$\lambda_i(T)\phi_i(t : T) = \int_0^T K_x(t, u)\phi_i(u : T) du, \quad 0 \leq t \leq T, \quad (6.169)$$

where $K_x(t, u)$ is a square-integrable covariance function. [This is just (6.49) rewritten to emphasize the dependence of the solution on T .] Every eigenvalue $\lambda_i(T)$ is a monotone-increasing function of the length of the interval T .

Proof. Multiplying both sides by $\phi_i(t : T)$ and integrating with respect to t over the interval $[0, T]$, we have,

$$\lambda_i(T) = \iint_{[0, T]} \phi_i(t : T) K_x(t, u) \phi_i(u : T) dt du. \quad (6.170)$$

Differentiating with respect to T we have,

$$\begin{aligned} \frac{\partial \lambda_i(T)}{\partial T} &= 2 \int_0^T \frac{\partial \phi_i(t : T)}{\partial T} dt \int_0^T K_x(t, u) \phi_i(u : T) du \\ &\quad + 2\phi_i(T : T) \int_0^T K_x(T, u) \phi_i(u : T) du. \end{aligned} \quad (6.171)$$

Using (6.169), we obtain

$$\frac{\partial \lambda_i(T)}{\partial T} = 2\lambda_i(T) \int_0^T \frac{\partial \phi_i(t : T)}{\partial T} \phi_i(t : T) dt + 2\lambda_i(T) \phi_i^2(T : T). \quad (6.172)$$

To reduce this equation, recall that

$$\int_0^T \phi_i^2(t : T) dt = 1. \quad (6.173)$$

⁵This result is due to Huang and Johnson [HJ63].

Differentiation of (6.173) gives

$$2 \int_0^T \frac{\partial \phi_i(t : T)}{\partial T} \phi_i(t : T) dt + \phi_i^2(T : T) = 0. \quad (6.174)$$

By substituting (6.174) into (6.172), we obtain

$$\frac{\partial \lambda_i(T)}{\partial T} = \lambda_i(T) \phi_i^2(T : T) \geq 0, \quad (6.175)$$

which is the desired result.

The second property of interest is the behavior of the eigenfunctions and eigenvalues of stationary processes for *large* T .

6.4.7.2 Asymptotic Behavior Properties

In many cases we are dealing with stationary processes and are interested in characterizing them over an infinite interval. To study the behavior of the eigenfunctions and eigenvalues, we return to (6.49); we assume that the process is stationary and that the observation interval is infinite. Then (6.49) becomes

$$\lambda \phi(t) = \int_{-\infty}^{\infty} K_x(t-u) \phi(u) du, \quad -\infty < t < \infty. \quad (6.176)$$

In order to complete the solution by inspection, we recall the simple linear filtering problem shown in Figure 6.16. The input is $y(t)$, the impulse response is $h(\tau)$, and the output is $z(t)$. They are related by the convolution integral:

$$z(t) = \int_{-\infty}^{\infty} h(t-u) y(u) du, \quad -\infty < t < \infty. \quad (6.177)$$

In a comparison of (6.176) and (6.177), we see that the solution to (6.176) is simply a function that, when put into a linear system with impulse response $K_x(\tau)$, will come out of the system unaltered except for a gain change. It is well known from elementary linear circuit theory that complex exponentials meet this requirement. Thus,

$$\phi(t) = e^{j\omega t} \quad -\infty < \omega < \infty, \quad (6.178)$$

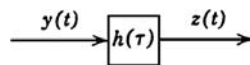


Figure 6.16: Linear filter.

is an eigenfunction for any ω on the real line.⁶ Substituting into (6.176), we have

$$\lambda e^{j\omega t} = \int_{-\infty}^{\infty} K_x(t-u) e^{j\omega u} du, \quad (6.179)$$

or

$$\lambda = \int_{-\infty}^{\infty} K_x(t-u) e^{-j\omega(t-u)} du = S_x(\omega). \quad (6.180)$$

Thus, the eigenvalue for a particular ω is the value of the power density spectrum of the process at that ω . Now the only difficulty with this discussion is that we no longer have a countable set of eigenvalues and eigenfunctions to deal with and the idea of a series expansion of the sample function loses its meaning. There are two possible ways to get out of this difficulty.

1. Instead of trying to use a series representation of the sample functions, we could try to find some integral representation. The transition would be analogous to the Fourier series–Fourier integral transition for deterministic functions.
2. Instead of starting with the infinite interval, we could consider a finite interval and investigate the behavior as the length increases. This might lead to some simple approximate expressions for large T .

In Sections 3.5 and 3.6 of the first edition of DEMT–I we developed the first approach. It is an approach for dealing with the infinite interval that can be made rigorous. In this edition, we will only include the second approach. We refer to this problem as the SPLOT (stationary process, long observation time) problem. This approach is definitely heuristic but leads to the correct results and is easy to apply.

We start with (6.49) and assume that the limits are $-T/2$ and $+T/2$:

$$\lambda \phi(t) = \int_{-T/2}^{+T/2} K_x(t-u) \phi(u) du, \quad -\frac{T}{2} \leq t \leq \frac{T}{2}. \quad (6.181)$$

We define

$$f_0 = \frac{1}{T}, \quad (6.182)$$

and try a solution of the form,

$$\phi_n(u) = e^{+j2\pi f_0 n u}, \quad -\frac{T}{2} \leq u \leq \frac{T}{2}, \quad (6.183)$$

where $n = 0, \pm 1, \pm 2, \dots$ (We index over both positive and negative integers for convenience).

⁶The function $e^{(\sigma+j\omega)t}$ also satisfies (6.177) for values of σ where the exponential transform of $h(\tau)$ exists. The family of exponentials with $\sigma = 0$ is adequate for our purposes. This is our first use of a complex eigenfunction. As indicated at the beginning of Section 6.2, the modifications should be clear. (See Problems 6.4.12–6.4.15)

Define

$$f_n = nf_0. \quad (6.184)$$

Substituting (6.183) into (6.181), we have

$$\lambda_n \phi_n(t) = \int_{-T/2}^{T/2} K_x(t-u) e^{+j2\pi f_n u} du. \quad (6.185)$$

Now,

$$K_x(t-u) = \int_{-\infty}^{\infty} S_x(f) e^{+j2\pi f(t-u)} df. \quad (6.186)$$

Substituting (6.186) into (6.185) and integrating with respect to u , we obtain

$$\lambda_n \phi_n(t) = \int_{-\infty}^{\infty} S_x(f) e^{+j2\pi ft} \left[\frac{\sin \pi T(f_n - f)}{\pi(f_n - f)} \right] df. \quad (6.187)$$

The function in the bracket, shown in Figure 6.17, is centered at $f = f_n$ where its height is T . Its width is inversely proportional to T and its area equals one for all values of T . We see that for large T the function in the bracket is approximately an impulse at f_n . Thus,

$$\lambda_n \phi_n(t) \simeq \int_{-\infty}^{\infty} S_x(f) e^{+j2\pi ft} \delta(f - f_n) df = S_x(f_n) e^{+j2\pi f_n t}. \quad (6.188)$$

Therefore

$$\boxed{\lambda_n \simeq S_x(f_n) = S_x(nf_0)} \quad (6.189)$$

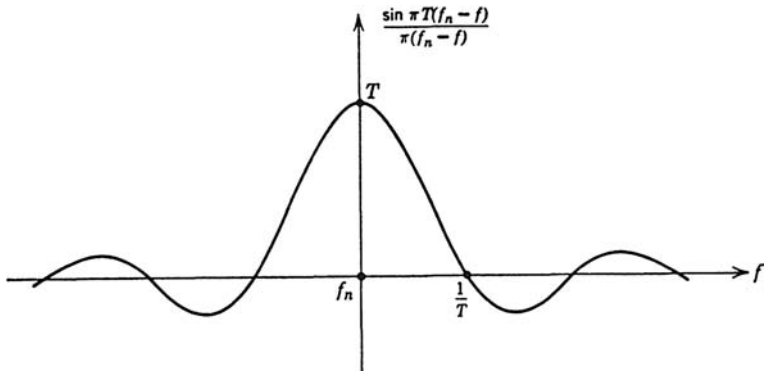


Figure 6.17: Weighting function in (6.187).

and

$$\boxed{\phi_n(t) \simeq \frac{1}{\sqrt{T}} e^{+j2\pi f_n t} \quad -\frac{T}{2} \leq t \leq \frac{T}{2}}, \quad (6.190)$$

for large T .

From (6.187), we see that the magnitude of T needed for the approximation to be valid depends on how quickly $S_x(f)$ varies near f_n .

In Section 6.4.6 we encountered the infinite sum of a function of the eigenvalues. For example,

$$\xi_I = \frac{N_0}{2T} \sum_{i=1}^{\infty} \frac{\lambda_i}{\lambda_i + N_0/2} \quad (6.191)$$

is the mean-square error in the filtering problem that we developed in (6.168). More generally we encounter sums of the form

$$g_\lambda \triangleq \sum_{i=1}^{\infty} g(\lambda_i). \quad (6.192)$$

An approximate expression for g_λ useful for large T follows directly from the above results. In Figure 6.18, we sketch a typical spectrum and the approximate eigenvalues based on (6.189). We see that

$$g_\lambda \simeq \sum_{n=-\infty}^{+\infty} g(S_x(nf_0)) = T \sum_{n=-\infty}^{+\infty} g(S_x(nf_0)) f_0, \quad (6.193)$$

where the second equality follows from the definition in (6.182). Now, for large T we can approximate the sum by an integral,

$$\boxed{g_\lambda \cong T \int_{-\infty}^{\infty} g(S_x(f)) df}, \quad (6.194)$$

which is the desired result.

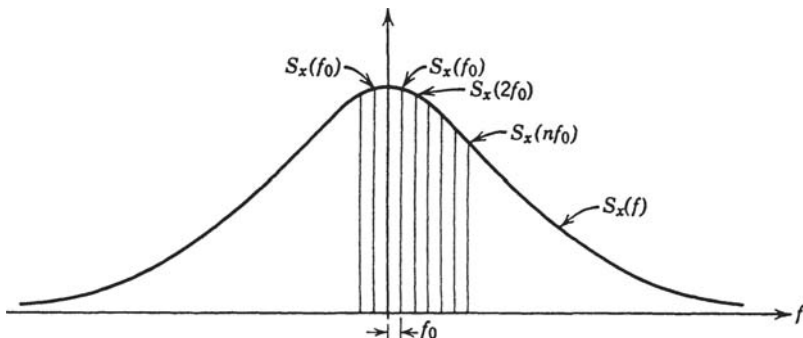


Figure 6.18: Approximate eigenvalues; large T .

The next properties concern the size of the largest eigenvalue.

Maximum and Minimum Properties. Let $x(t)$ be a stationary random process represented over an interval of length T . The largest eigenvalue $\lambda_{\max}(T)$ satisfies the inequality

$$\lambda_{\max}(T) \leq \max_f S_x(f) \quad (6.195)$$

for any interval T . This result is obtained by combining (6.189) with the monotonicity property.

Another bound on the maximum eigenvalue follows directly from Property 10 in Section 6.3.2.

$$\lambda_{\max}(T) \leq \int_{-T/2}^{T/2} K_x(t, t) dt = T \int_{-\infty}^{\infty} S_x(f) df. \quad (6.196)$$

A lower bound is derived in Problem 6.4.4,

$$\lambda_{\max}(T) \geq \iint_{[-T/2, T/2]} f(t) K_x(t, u) f(u) dt du,$$

where $f(t)$ is any function with unit energy in the interval $(-T/2, T/2)$.

These asymptotic properties are adequate for most of our work.

6.5 VECTOR RANDOM PROCESSES

In many cases of practical importance, we are concerned with more than one random process at the same time; for example, in the phased arrays used in radar systems the input at each element must be considered. Analogous problems are present in sonar arrays and seismic arrays in which the received signal has a number of components. In telemetry systems, a number of messages are sent simultaneously.

In all of these cases, it is convenient to work with a single vector random process $\mathbf{x}(t)$ where components are the processes of interest. If there are N processes, $x_1(t), x_2(t), \dots, x_N(t)$, we define $\mathbf{x}(t)$ as a column matrix,

$$\mathbf{x}(t) \triangleq \begin{bmatrix} x_1(t) \\ x_2(t) \\ \vdots \\ x_N(t) \end{bmatrix}. \quad (6.197)$$

The dimension N may be finite or countably infinite. Just as in the single process case, the second moment properties are described by the process means and covariance functions. In addition, the cross-covariance functions between the various processes must be known.

The mean value function is a vector

$$\mathbf{m}_x(t) \triangleq E \begin{bmatrix} x_1(t) \\ x_2(t) \\ \vdots \\ x_N(t) \end{bmatrix} = \begin{bmatrix} m_1(t) \\ m_2(t) \\ \vdots \\ m_N(t) \end{bmatrix}, \quad (6.198)$$

and the covariances may be described by an $N \times N$ matrix, $\mathbf{K}_x(t, u)$, whose elements are

$$K_{ij}(t, u) \triangleq E \{ [x_i(t) - m_i(t)][x_j(u) - m_j(u)] \}. \quad (6.199)$$

We want to derive a series expansion for the vector random process $\mathbf{x}(t)$. There are several possible representations, but two seem particularly efficient. In the first method, we use a set of vector functions as coordinate functions and have scalar coefficients. In the second method, we use a set of scalar functions as coordinate functions and have vector coefficients. For the first method and finite N , the modification of the properties developed for the scalar case are straightforward. For infinite N , we must be more careful. A detailed derivation that is valid for infinite N is given by Kelly and Root in [KR60]. In the text, we go through some of the details for finite N . The second method is only useful for the SPLOT model. Once again we consider zero-mean processes.

Method 1. Vector Eigenfunctions, Scalar Eigenvalues. Let

$$\mathbf{x}(t) = \underset{M \rightarrow \infty}{\text{l.i.m.}} \sum_{i=1}^M x_i \phi_i(t), \quad (6.200)$$

where

$$x_i = \int_0^T \phi_i^T(t) \mathbf{x}(t) dt = \int_0^T \mathbf{x}^T(t) \phi_i(t) dt = \sum_{k=1}^N \int_0^T x_k(t) \phi_i^k(t) dt, \quad (6.201)$$

and

$$\phi_i(t) \triangleq \begin{bmatrix} \phi_i^1(t) \\ \phi_i^2(t) \\ \vdots \\ \phi_i^N(t) \end{bmatrix} \quad (6.202)$$

is chosen to satisfy

$$\lambda_i \phi_i(t) = \int_0^T \mathbf{K}_x(t, u) \phi_i(u) du, \quad 0 \leq t \leq T. \quad (6.203)$$

Observe that the eigenfunctions are *vectors* but that the eigenvalues are still scalars.

Equation (6.203) can also be written as,

$$\sum_{j=1}^N \int_0^T K_{kj}(t, u) \phi_i^j(u) du = \lambda_i \phi_i^k(t), \quad k = 1, 2, \dots, N \quad 0 \leq t \leq T. \quad (6.204)$$

The scalar properties carry over directly. In particular,

$$E(x_i x_j) = \lambda_i \delta_{ij}, \quad (6.205)$$

and the coordinate functions are orthonormal; that is,

$$\int_0^T \phi_i^T(t) \phi_j(t) dt = \delta_{ij}, \quad (6.206)$$

or

$$\sum_{k=1}^N \int_0^T \phi_i^k(t) \phi_j^k(t) dt = \delta_{ij}. \quad (6.207)$$

The matrix

$$\mathbf{K}_x(t, u) = E[\mathbf{x}(t)\mathbf{x}^T(u)] - \mathbf{m}_x(t)\mathbf{m}_x^T(u) \quad (6.208)$$

$$= \sum_{i=1}^{\infty} \sum_{j=1}^{\infty} \text{Cov}[x_i x_j] \phi_i(t) \phi_j^T(u) \quad (6.209)$$

$$= \sum_{i=1}^{\infty} \lambda_i \phi_i(t) \phi_i^T(u), \quad (6.210)$$

or

$$K_{kj}(t, u) = \sum_{i=1}^{\infty} \lambda_i \phi_i^k(t) \phi_i^j(u) \quad k, j = 1, 2, \dots, N. \quad (6.211)$$

This is the multidimensional analog of (6.53).

One property that makes the expansion useful is that the coefficient is a scalar variable and not a vector. A simple example illustrates the approach.

Example 6.4. Let

$$x_j(t) = a_j s_j(t), \quad j = 1, 2, \dots, N, \quad (6.212)$$

where $s_j(t)$ are normalized linearly independent but not necessarily orthogonal. The a_j are the elements of a zero-mean Gaussian random vector

$$\mathbf{a} = [a_1 \quad a_2 \quad \cdots \quad a_N]^T \quad (6.213)$$

whose covariance matrix is \mathbf{K}_a . Then,

$$K_{kj}(t, u) = K_{a,kj} s_k(t) s_j(u) \quad k, j = 1, 2, \dots, N. \quad (6.214)$$

The eigenequations are

$$\lambda_i \phi_i^k(t) = \sum_{j=1}^N \int_0^T K_{a,kj} s_k(t) s_j(u) \phi_i^j(u) du \quad k = 1, 2, \dots, N. \quad (6.215)$$

From the definition in (6.212), we assume

$$\phi_i^j(t) = c_{ij} s_j(t). \quad (6.216)$$

Using (6.216) in (6.215) and performing the integration gives

$$\lambda_i s_k(t) c_{ik} = s_k(t) \sum_{j=1}^N K_{a,kj} c_{ij} \quad (6.217)$$

or

$$\lambda_i c_i = \mathbf{K}_a \mathbf{c}_i, \quad (6.218)$$

where \mathbf{c}_i is an $N \times 1$ vector whose j th entry is c_{ij} . We find the eigenvalues and eigenvectors of (6.218) and then use (6.216) to find the eigenvectors. ■

A second method of representation is obtained by incorporating the complexity into the eigenvalues.

Method 2. Matrix Eigenvalues, Scalar Eigenfunctions. In this approach we let

$$\mathbf{x}(t) = \sum_{i=1}^{\infty} \mathbf{x}_i \psi_i(t), \quad 0 \leq t \leq T, \quad (6.219)$$

and

$$\mathbf{x}_i = \int_0^T \mathbf{x}(t) \psi_i(t) dt. \quad (6.220)$$

We would like to find a set of Λ_i and $\psi_i(t)$ such that

$$E [\mathbf{x}_i \mathbf{x}_j^T] = \Lambda_i \delta_{ij}, \quad (6.221)$$

and

$$\int_0^T \psi_i(t) \psi_j(t) dt = \delta_{ij}. \quad (6.222)$$

These requirements lead to the equation

$$\Lambda_i \psi_i(t) = \int_0^T \mathbf{K}_x(t, u) \psi_i(u) du, \quad 0 \leq t \leq T. \quad (6.223)$$

For arbitrary time intervals, (6.223) does *not* have a solution except for a few trivial cases. However, if we restrict our attention to stationary processes and *large* time intervals (the

SPLOT model), then certain asymptotic results may be obtained. Defining

$$\mathbf{S}_x(\omega) \triangleq \int_{-\infty}^{\infty} \mathbf{K}_x(\tau) e^{j\omega\tau} d\tau, \quad (6.224)$$

and assuming the interval is large, we find

$$\psi_i(t) \simeq \frac{1}{\sqrt{T}} e^{j\omega_i t} \quad (6.225)$$

and

$$\Lambda_i \simeq \mathbf{S}_x(\omega_i). \quad (6.226)$$

The second method of representation has a great deal of intuitive appeal in the large time interval case where it is valid, but the first method enables us to treat a more general class of problems. For this reason, we shall utilize the first representation in the text and relegate the second to the problems. In Part IV of DEMT, “Optimum Array Processing,” we use the second representation extensively [Van02].

It is difficult to appreciate the importance of the first expansion until we get to some applications. We shall then find that it enables us to obtain results for multidimensional problems almost by inspection. The key to the simplicity is that we can still deal with *scalar* statistically independent random variables.

It is worthwhile to re-emphasize that we did not *prove* that the expansions had the desired properties. Specifically, we did not demonstrate that solutions to (6.203) existed and had the desired properties, that the multidimensional analog for Mercer’s theorem was valid, or that the expansion converged in the mean-square sense ([KR60] does this for the first expansion).

6.6 SUMMARY

In this chapter, we developed means for characterizing random processes. The emphasis was on a method of representation that was particularly well suited to solving detection and estimation problems in which the random processes were Gaussian. For non-Gaussian processes, the representation provides an adequate second-moment characterization but may not be particularly useful as a complete characterization method.

For finite time intervals, the desired representation was a series of orthonormal functions whose coefficients were uncorrelated random variables. The choice of coordinate functions depended on the covariance function of the process through the integral equation

$$\lambda\phi(t) = \int_{T_i}^{T_f} K(t, u)\phi(u) du \quad T_i \leq t \leq T_f. \quad (6.227)$$

The eigenvalues λ corresponded physically to the expected value of the energy along a particular coordinate function $\phi(t)$. We indicated that this representation was useful for both theoretical and practical purposes. Several classes of processes for which solutions to (6.227) could be obtained were discussed in detail. One example, the simple Wiener

process, led us logically to the idea of a white noise process with which we were already familiar.

We considered the case of stationary processes and long observation time (the SPLOT model). We found that the eigenvalues of a stationary process approached the power spectrum of the process and the eigenfunctions became sinusoids. Thus, for this class of problems the expansion could be interpreted in terms of familiar quantities.

Finally, we extended the eigendecomposition to vector random processes. The significant result here was the ability to describe the process in terms of *scalar* coefficients.

We should note that all of discussion consider real random processes. The extension of eigendecomposition to complex processes is straightforward. As expected from our work in Chapter 3, we will have complex eigenfunctions and real eigenvalues.

In Chapter 7, we apply these representation techniques to solve the detection and estimation problem.

6.7 PROBLEMS

Many of the problems in Section P6.3 are of a review nature and may be omitted by the reader with an adequate random process background. Problems 6.3.19–23 present an approach to the continuous problem based on sampling. We have already used these ideas in Chapters 2–5.

P6.3 Random Process Characterizations

SECOND MOMENT CHARACTERIZATIONS

Problem 6.3.1. In Chapter 1, we formulated the problem of choosing a linear filter to maximize the output signal-to-noise ratio.

$$\left(\frac{S}{N}\right)_o \triangleq \frac{\left[\int_0^T h(T-\tau)s(\tau)d\tau\right]^2}{N_0/2 \int_0^T h^2(\tau)d\tau}.$$

- (a) Use the Schwarz inequality to find the $h(\tau)$ that maximizes $(S/N)_o$.
- (b) Sketch $h(\tau)$ for some typical $s(t)$.

Comment. The resulting filter is called a matched filter and was first derived by North [Nor63].

Problem 6.3.2. Verify the result in (6.28).

Problem 6.3.3 [DR58]. The input to a stable linear system with a transfer function $H(j\omega)$ is a zero-mean process $x(t)$ whose correlation function is

$$R_x(\tau) = \frac{N_0}{2} \delta(\tau).$$

- (a) Find an expression for the variance of the output $y(t)$.
- (b) The noise bandwidth of a network is defined as

$$B_N \triangleq \frac{\int_{-\infty}^{\infty} |H(j\omega)|^2 d(\omega/2\pi)}{|H_{\max}|^2} \quad (\text{double-sided in cps}).$$

Verify that

$$\sigma_y^2 = \frac{N_0 B_N |H_{\max}|^2}{2}.$$

Problem 6.3.4 [DR58]. Consider the fixed-parameter linear system defined by the equations

$$v(t) = x(t - \delta) - x(t)$$

and

$$y(t) = \int_{-\infty}^T v(u) du.$$

- (a) Determine the impulse response relating the input $x(t)$ and output $y(t)$.
- (b) Determine the system function.
- (c) Determine whether the system is stable.
- (d) Find B_N .

Problem 6.3.5 [DR58]. The transfer function of an RC network is

$$\frac{Y(j\omega)}{X(j\omega)} = \frac{1}{1 + RCj\omega}.$$

The input consists of a noise which is a sample function of a stationary random process with a flat spectral density of height $N_0/2$, plus a signal which is a sequence of constant-amplitude rectangular pulses. The pulse duration is δ and the minimum interval between pulses is T , where $\delta \ll T$.

A signal-to-noise ratio at the system output is defined here as the ratio of the maximum amplitude of the output signal with no noise at the input to the rms value of the output noise.

- (a) Derive an expression relating the output signal-to-noise ratio as defined above to the input pulse duration and the effective noise bandwidth of the network.
- (b) Determine what relation should exist between the input pulse duration and the effective noise bandwidth of the network to obtain the maximum output signal-to-noise.

ALTERNATE REPRESENTATIONS AND NON-GAUSSIAN PROCESSES

Problem 6.3.6 (sampling representation). When the observation interval is infinite and the processes of concern are bandlimited, it is sometimes convenient to use a sampled representation of the process. Consider the stationary process $x(t)$ with the spectrum shown in Figure P6.1. Assume that $x(t)$ is sampled every $1/2W$ seconds. Denote the samples as $x(i/2W)$, $i = -\infty, \dots, 0, \dots$

- (a) Prove

$$x(t) = \lim_{K \rightarrow \infty} \sum_{-K}^K x\left(\frac{i}{2W}\right) \frac{\sin 2\pi W(t - i/2W)}{2\pi W(t - i/2W)}.$$

- (b) Find $E[x(i/2W)x(j/2W)]$.

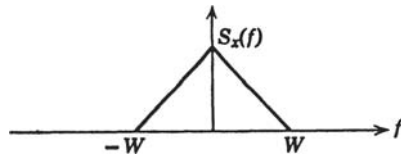


Figure P6.1

Problem 6.3.7 (continuation). Let

$$\phi_i(t) = \sqrt{2W} \frac{\sin 2\pi W(t - i/2W)}{2\pi W(t - i/2W)}, \quad -\infty < t < \infty.$$

Define

$$x(t) = \text{l.i.m.}_{K \rightarrow \infty} \sum_{i=-K}^K x_i \phi_i(t).$$

Prove that if

$$E(x_i x_j) = P \delta_{ij} \quad \text{for all } i, j,$$

then

$$S_x(f) = \frac{P}{2W} \quad |f| \leq W.$$

Problem 6.3.8. Let $x(t)$ be a bandpass process “centered” around f_c .

$$S_x(f) = 0 \quad \begin{cases} |f - f_c| > W & f > 0 \\ |f + f_c| > W & f < 0. \end{cases}$$

We want to represent $x(t)$ in terms of two low-pass processes $x_c(t)$ and $x_s(t)$. Define

$$\hat{x}(t) = \sqrt{2} x_c(t) \cos(2\pi f_c t) + \sqrt{2} x_s(t) \sin(2\pi f_c t),$$

where $x_c(t)$ and $x_s(t)$ are obtained physically as shown in Figure P6.2.

(a) Prove

$$E \{ [x(t) - \hat{x}(t)]^2 \} = 0.$$

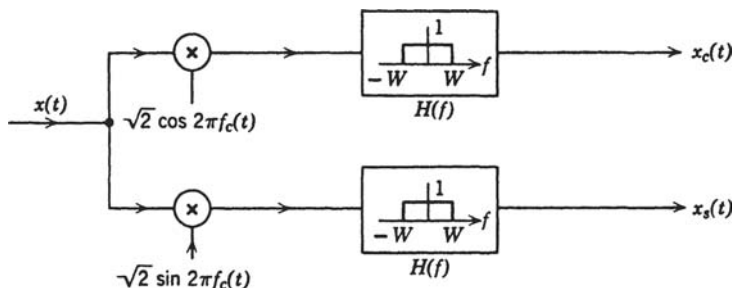


Figure P6.2

- (b) Find $S_{x_c}(f)$, $S_{x_s}(f)$, and $S_{x_c x_s}(f)$.
(c) What is a necessary and sufficient condition for $S_{x_c x_s}(f) = 0$?

Observe that this enables us to replace any bandpass process by *two* low-pass processes or a vector low-pass process.

$$\mathbf{x}(t) = \begin{bmatrix} x_c(t) \\ x_s(t) \end{bmatrix}.$$

Problem 6.3.9. Show that the n -dimensional probability density of a Markov process can be expressed as

$$p_{x_{t_1}, x_{t_2}, \dots, x_{t_n}}(X_{t_1}, X_{t_2}, \dots, X_{t_n}) = \frac{\prod_{k=2}^n p_{x_{t_{k-1}}, x_{t_k}}(X_{t_{k-1}}, X_{t_k})}{\prod_{k=2}^{n-1} p_{x_{t_k}}(X_{t_k})} \quad n \geq 3.$$

Problem 6.3.10. Consider a Markov process at three ordered time instants, $t_1 < t_2 < t_3$. Show that the conditional density relating the first and third time must satisfy the following equation:

$$p_{x_{t_3}|x_{t_1}}(X_{t_3}|X_{t_1}) = \int dX_{t_2} p_{x_{t_3}|x_{t_2}}(X_{t_3}|X_{t_2})p_{x_{t_2}|x_{t_1}}(X_{t_2}|X_{t_1}).$$

Problem 6.3.11. A continuous-parameter random process is said to have independent increments if, for all choices of indices $t_0 < t_1 < \dots < t_n$, the n random variables

$$x(t_1) - x(t_0), \dots, x(t_n) - x(t_{n-1})$$

are independent. Assuming that $x(t_0) = 0$, show that

$$M_{x_{t_1}, x_{t_2}, \dots, x_{t_n}}(jv_1, jv_2, \dots, jv_n) = M_{x_{t_1}}(jv_1 + jv_2 + \dots + jv_n) \times \prod_{k=0}^{n-1} M_{x_{t_k}-x_{t_{k+1}}}(jv_k + jv_{k+1} + \dots + jv_n).$$

GAUSSIAN PROCESSES

Problem 6.3.12 (Factoring of higher order moments). Let $x(t)$, $t \in T$ be a Gaussian process with zero-mean value function

$$E[x(t)] = 0.$$

- (a) Show that all odd-order moments of $x(t)$ vanish and that the even-order moments may be expressed in terms of the second-order moments by the following formula: Let n be an even integer and let t_1, t_2, \dots, t_n be points in T , some of which may coincide. Then

$$E[x(t_1)x(t_2)\cdots x(t_n)] = \sum E[x(t_{i_1})x(t_{i_2})] E[x(t_{i_3})x(t_{i_4})]\cdots E[x(t_{i_{n-1}})x(t_{i_n})],$$

in which the sum is taken over all possible ways of dividing the n points into $n/2$ combinations of pairs. The number of terms in the sum is equal to

$$1 \cdot 3 \cdot 5 \cdots (n-3)(n-1);$$

for example,

$$\begin{aligned} E[x(t_1)x(t_2)x(t_3)x(t_4)] &= E[x(t_1)x(t_2)]E[x(t_3)x(t_4)] + E[x(t_1)x(t_3)]E[x(t_2)x(t_4)] \\ &\quad + E[x(t_1)x(t_4)]E[x(t_2)x(t_3)]. \end{aligned}$$

Hint: Differentiate the characteristic function.

- (b) Use your result to find the fourth-order correlation function

$$R_x(t_1, t_2, t_3, t_4) = E[x(t_1)x(t_2)x(t_3)x(t_4)]$$

of a stationary Gaussian process whose spectral density is

$$S_x(f) = \begin{cases} \frac{N_0}{2} & |f| \leq W \\ 0 & \text{Elsewhere.} \end{cases}$$

What is $\lim_{W \rightarrow \infty} R_x(t_1, t_2, t_3, t_4)$?

Problem 6.3.13. Let $x(t)$ be a sample function of a stationary real Gaussian random process with a zero mean and finite mean-square value. Let a new random process be defined with the sample functions

$$y(t) = x^2(t).$$

Show that

$$R_y(\tau) = R_x^2(0) + 2R_x^2(\tau).$$

Problem 6.3.14 [DR58]. Consider the system shown in Figure P6.3. Let the input $e_0(t)$ be a sample function of stationary real Gaussian process with zero mean and *flat* spectral density at all frequencies of interest; that is, we may assume that

$$S_{e_0}(f) = N_0/2.$$

- (a) Determine the autocorrelation function or the spectral density of $e_2(t)$.
(b) Sketch the autocorrelation function or the spectral density of $e_0(t)$, $e_1(t)$, and $e_2(t)$.

Problem 6.3.15. The system of interest is shown in Figure P6.4, in which $x(t)$ is a sample function from an ergodic Gaussian random process.

$$R_x(\tau) = \frac{N_0}{2} \delta(\tau).$$

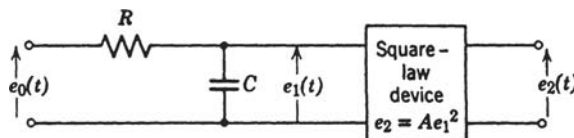


Figure P6.3

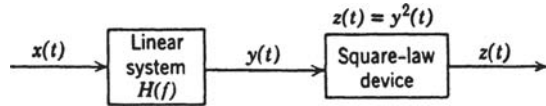


Figure P6.4

The transfer function of the linear system is

$$H(f) = \begin{cases} e^{2if} & |f| \leq W \\ 0 & \text{Elsewhere.} \end{cases}$$

- (a) Find the dc power in $z(t)$.
- (b) Find the ac power in $z(t)$.

Problem 6.3.16. The output of a linear system is $y(t)$, where

$$y(t) = \int_0^\infty h(\tau)x(t-\tau)d\tau.$$

The input $x(t)$ is a sample function from a *stationary* Gaussian process with correlation function

$$R_x(\tau) = \delta(\tau).$$

We should like the output at a particular time t_1 to be statistically independent of the input at that time. Find a necessary and sufficient condition on $h(\tau)$ for $x(t_1)$ and $y(t_1)$ to be statistically independent.

Problem 6.3.17. Let $x(t)$ be a real, wide-sense stationary, Gaussian random process with zero mean. The process $x(t)$ is passed through an ideal limiter. The output of the limiter is the process $y(t)$,

$$y(t) = L[x(t)],$$

where

$$L(u) = \begin{cases} +1 & u \geq 0 \\ -1 & u < 0. \end{cases}$$

Show that the autocorrelation functions of the two processes are related by the formula

$$R_y(\tau) = \frac{2}{\pi} \sin^{-1} \left[\frac{R_x(\tau)}{R_x(0)} \right].$$

Problem 6.3.18. Consider the bandlimited Gaussian process whose spectrum is shown in Figure P6.5. Write

$$x(t) = v(t) \cos [2\pi f_c t + \theta(t)].$$

- (a) Find $p_{v(t)}(V)$ and $p_{\theta(t)}(\theta)$.
- (b) Are $v(t)$ and $\theta(t)$ independent random variables?

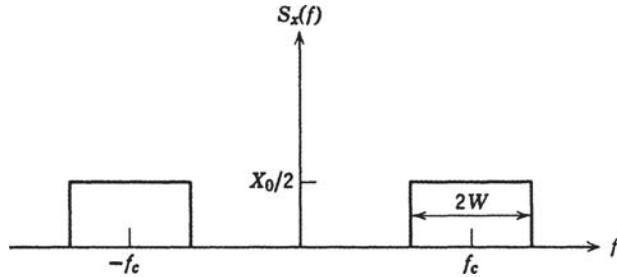


Figure P6.5

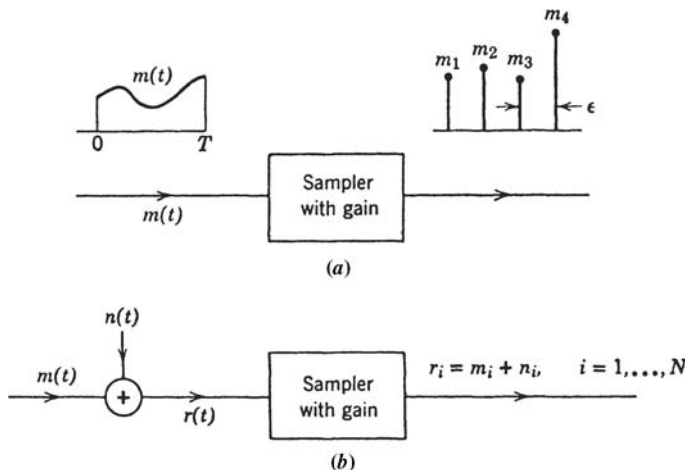


Figure P6.6

SAMPLING APPROACH TO CONTINUOUS GAUSSIAN PROCESSES

In Chapter 7, we extend the classical results to the waveform case by using the Karhunen–Loëve expansion. If, however, we are willing to use a heuristic argument, most of the results that we obtained Chapters 3 and 5 for the general Gaussian problem can be extended easily to the waveform case in the following manner.⁷

The processes and signals are sampled every ϵ seconds as shown in Figure P6.6a. The gain in the sampling device is chosen so that

$$\int_0^T m^2(t) dt = \lim_{\epsilon \rightarrow 0} \sum_{i=1}^{T/\epsilon} m_i^2. \quad (\text{P.1})$$

This requires

$$m_i = \sqrt{\epsilon} m(t_i). \quad (\text{P.2})$$

⁷We introduced the sampling approach in Chapter 3 in order to motivate some of the examples that we developed in classical detection and estimation theory. The next five problems show how to extend the sampling approach to the continuous time model. All of these results will be derived in Chapter 7 using the Karhunen–Loëve expansion.

Similarly, for a random process,

$$n_i = \sqrt{\epsilon}n(t_i), \quad (\text{P.3})$$

and

$$E[n_i n_j] = \epsilon E[n(t_i) n(t_j)] = \epsilon K_n(t_i, t_j). \quad (\text{P.4})$$

To illustrate the procedure consider the simple model shown in Figure P6.6b. The continuous waveforms are

$$\begin{aligned} H_1 : r(t) &= m(t) + n(t) & 0 \leq t \leq T \\ H_0 : r(t) &= n(t) & 0 \leq t \leq T, \end{aligned} \quad (\text{P.5})$$

where $m(t)$ is a known function and $n(t)$ is a sample function from a Gaussian random process.

The corresponding sampled problem is

$$\begin{aligned} H_1 : \mathbf{r} &= \mathbf{m} + \mathbf{n} \\ H_0 : \mathbf{r} &= \mathbf{n}, \end{aligned} \quad (\text{P.6})$$

where

$$\mathbf{r} \triangleq \sqrt{\epsilon} \begin{bmatrix} r(t_1) \\ r(t_2) \\ \vdots \\ r(t_N) \end{bmatrix},$$

and $N = T/\epsilon$. Assuming that the noise $n(t)$ is bandlimited to $1/\epsilon$ (double-sided, cps) and has a flat spectrum of $N_0/2$, the samples are statistically independent Gaussian variables (Problem 6.3.7).

$$E[\mathbf{n}\mathbf{n}^T] = E[n^2(t)]\mathbf{I} = \frac{N_0}{2}\mathbf{I} \triangleq \sigma^2\mathbf{I}. \quad (\text{P.7})$$

The vector problem in (P.6) is familiar from Chapter 3. From (3.124), the sufficient statistic is

$$l(\mathbf{R}) = \frac{1}{\sigma^2} \sum_{i=1}^N m_i R_i. \quad (\text{P.8})$$

Using (P.2) and (P.3) in (P.8), we have

$$l(\mathbf{R}) = \frac{2}{N_0} \sum_{i=1}^{T/\epsilon} \sqrt{\epsilon}m(t_i) \cdot \sqrt{\epsilon}r(t_i).$$

As $\epsilon \rightarrow 0$, we have (letting $dt = \epsilon$)

$$\lim_{\epsilon \rightarrow 0} l(\mathbf{R}) = \frac{2}{N_0} \int_0^T m(t)r(t) dt \triangleq l(r(t))$$

which is the desired result. Some typical problems of interest are developed below.

Problem 6.3.19. Consider the simple example described in the introduction.

- (a) Show that

$$d^2 = \frac{2E}{N_0},$$

where E is the energy in $m(t)$.

- (b) Draw a block diagram of the receiver and compare it with the result in Problem 6.3.1.

Problem 6.3.20. Consider the discrete case defined in Section 3.2. Here

$$E [\mathbf{n}\mathbf{n}^T] = \mathbf{K},$$

and

$$\mathbf{Q} = \mathbf{K}^{-1}.$$

- (a) Sample the bandlimited noise process $n(t)$ every ϵ seconds to obtain $n(t_1), n(t_2), \dots, n(t_k)$. Verify that in the limit \mathbf{Q} becomes a function with two arguments defined by the equation

$$\int_0^T Q(t, u) K(u, z) du = \delta(t - z).$$

Hint: Define a function $Q(t_i, t_j) = (1/\epsilon)Q_{ij}$.

- (b) Use this result to show that

$$l = \iint_{[0, T]} m_\Delta(t) Q(t, u) r(u) dt du$$

in the limit.

- (c) What is d^2 ?

Problem 6.3.21. In Section 3.3, the means are equal but the covariance matrices are different. Consider the continuous waveform analog to this and show that

$$l = \iint_{[0, T]} r(t) h_\Delta(t, u) r(u) dt du,$$

where

$$h_\Delta(t, u) = Q_0(t, u) - Q_1(t, u).$$

Problem 6.3.22. Consider the linear estimation problem in which the received vector is

$$\mathbf{r} = \mathbf{a} + \mathbf{n}.$$

Then, the MAP estimate of \mathbf{a} is

$$\begin{aligned} \mathbf{K}_a^{-1} \hat{\mathbf{a}} &= \mathbf{K}_r^{-1} \mathbf{R} \\ \hat{\mathbf{a}} &= \mathbf{K}_a \mathbf{K}_r^{-1} \mathbf{R}. \end{aligned}$$

Verify that the continuous analog to this result is

$$\hat{a}(t) = \int_0^T K_a(t, \sigma) d\sigma \int_0^T K_r^{-1}(\sigma, u) r(u) du \quad 0 \leq t \leq T.$$

Problem 6.3.23. Let

$$r(t) = a(t) + n(t) \quad 0 \leq t \leq T,$$

where $a(t)$ and $n(t)$ are independent zero-mean Gaussian processes with covariance functions $K_a(t, u)$ and $K_n(t, u)$, respectively. Consider a specific time t_1 in the interval. Find

$$P_{a(t_1)|r(t)} [A(t_1)|r(t)] \quad 0 \leq t \leq T.$$

Hint: Sample $r(t)$ every ϵ seconds and then let $\epsilon \rightarrow 0$.

P6.4 Integral equations

Problem 6.4.1. Consider the integral equation

$$\int_{-T}^T du P \exp(-\alpha|t-u|) \phi_i(u) = \lambda_i \phi_i(t) \quad -T \leq t \leq T.$$

- (a) Prove that $\lambda = 0$ and $\lambda = 2P/\alpha$ are not eigenvalues.
- (b) Prove that all values of $\lambda > 2P/\alpha$ cannot be eigenvalues of the above integral equation.

Problem 6.4.2. Plot the behavior of the largest eigenvalue of the integral equation in Problem 6.4.1 as a function of αT .

Problem 6.4.3. Consider the integral equation (6.117)

$$\lambda \phi(t) = \sigma^2 \int_0^t u \phi(u) du + \sigma^2 t \int_t^T \phi(u) du, \quad 0 \leq t \leq T.$$

Prove that values of $\lambda \leq 0$ are not eigenvalues of the equation.

Problem 6.4.4. Prove that the largest eigenvalue of the integral equation

$$\lambda \phi(t) = \int_{-T}^T K_n(t, u) \phi(u) du \quad -T \leq t \leq T$$

satisfies the inequality.

$$\lambda_1 \geq \iint_{[-T,T]} f(t) K_n(t, u) f(u) dt du,$$

where $f(t)$ is any function with unit energy in $[-T, T]$.

Problem 6.4.5. Compare the bound in Problem 6.4.4, using the function

$$f(t) = \frac{1}{\sqrt{2T}} \quad -T \leq t \leq T,$$

with the actual value found in Problem 6.4.2.

Problem 6.4.6 [SP61]. Consider a function whose total energy in the interval $-\infty < t < \infty$ is E .

$$E = \int_{-\infty}^{\infty} |f(t)|^2 dt.$$

Now, time-limit $f(t)$, $-T/2 \leq t \leq T/2$ and then bandlimit the result to $(-W, W)$ cps. Call this resulting function $f_{DB}(t)$. Denote the energy in $f_{DB}(t)$ as E_{DB} .

$$E_{DB} = \int_{-\infty}^{\infty} |f_{DB}(t)|^2 dt.$$

(a) Choose $f(t)$ to maximize

$$\gamma \triangleq \frac{E_{DB}}{E}.$$

(b) What is the resulting value of γ when $WT = 2.55$?

Problem 6.4.7 [SP61]. Assume that $f(t)$ is first bandlimited.

$$f_B(t) = \int_{-2\pi W}^{2\pi W} F(\omega) e^{j\omega t} \frac{d\omega}{2\pi}.$$

Now, time-limit $f_B(t)$, $-T/2 \leq t \leq T/2$ and bandlimit the result to $(-W, W)$ to obtain $f_{BDB}(t)$. Repeat Problem 6.4.6 with BDB replacing DB.

Problem 6.4.8 [Kai66]. Consider the triangular correlation function

$$K_n(t-u) = \begin{cases} 1 - |t-u| & |t-u| \leq 1 \\ 0 & \text{Elsewhere.} \end{cases}$$

Find the eigenfunctions and eigenvalues over the interval $(0, T)$ when $T < 1$.

Problem 6.4.9. Consider the integral equation

$$\lambda \phi(t) = \int_{T_i}^{T_f} K_n(t, u) \phi(u) du \quad T_i \leq t \leq T_f,$$

where

$$K_n(t, u) = \sum_{i=1}^6 \sigma_i^2 \cos\left(\frac{2\pi i t}{T}\right) \cos\left(\frac{2\pi i u}{T}\right),$$

and

$$T \triangleq T_f - T_i.$$

Find the eigenfunctions and eigenvalues of this equation.

Problem 6.4.10. The input to an unrealizable linear time-invariant system is $x(t)$ and the output is $y(t)$. Thus, we can write

$$y(t) = \int_{-\infty}^{\infty} h(\tau)x(t - \tau)d\tau.$$

We assume that

(i)

$$\int_{-\infty}^{\infty} x^2(t)dt = 1.$$

(ii)

$$h(\tau) = \frac{1}{\sqrt{2\pi}\sigma_c} \exp\left(-\frac{\tau^2}{2\sigma_c^2}\right), \quad -\infty < \tau < \infty.$$

(iii)

$$E_y \triangleq \int_{-\infty}^{\infty} y^2(t)dt.$$

- (a) What is the maximum value of E_y that can be obtained by using an $x(t)$ that satisfies the above constraints?
- (b) Find an $x(t)$ that gives an E_y arbitrarily close to the maximum E_y .
- (c) Generalize your answers to (a) and (b) to include an arbitrary $H(j\omega)$.

Problem 6.4.11. In (6.192), we considered a function

$$g_\lambda \triangleq \sum_{i=1}^{\infty} g(\lambda_i),$$

and derived its asymptotic value (6.194). Now consider the finite energy signal $s(t)$ and define

$$s_i \triangleq \int_{-T/2}^{T/2} s(t)\phi_i(t)dt,$$

where the $\phi_i(t)$ are the same eigenfunctions used to define (6.192). The function of interest is

$$g'_\lambda \triangleq \sum_{i=1}^{\infty} s_i^2 g(\lambda_i).$$

Show that

$$g'_\lambda \simeq \int_{-\infty}^{\infty} |S(j\omega)|^2 g(S_x(\omega)) \frac{d\omega}{2\pi}$$

for large T , where the function $S(j\omega)$ is the Fourier transform of $s(t)$.

COMPLEX GAUSSIAN PROCESSES

In the next set of problems, we consider circularly complex Gaussian random processes as discussed at the beginning of Chapter 3. We want to develop an analogous set of results for these processes.

Problem 6.4.12. We assume $\tilde{x}(t)$ is a deterministic signal such that

$$E_x = \int_0^T |\tilde{x}(t)|^2 dt < \infty$$

We want to expand

$$\tilde{x}(t) = \sum_{i=1}^N \tilde{x}_i \tilde{\phi}_i(t) \quad 0 < t < T,$$

where the $\tilde{\phi}_i(t)$ are orthonormal.

- (a) What choice of \tilde{x}_i minimizes the representation error in (6.15)?
- (b) Show how to map the coefficients into a vector space.

We now assume $\tilde{x}(t)$ is a zero-mean circularly complex Gaussian random process with covariance function

$$\tilde{K}_{\tilde{x}}(t, u) = E \{ \tilde{x}(t) \tilde{x}^*(u) \}$$

Problem 6.4.13. Expand $\tilde{x}(t)$ using a CON set

$$\tilde{x}(t) = \sum_{i=1}^{\infty} \tilde{x}_i \tilde{\phi}_i(t)$$

Show that the $\tilde{\phi}_i(t)$ are solutions to the integral equation

$$\lambda_i \tilde{\phi}_i(t) = \int_0^T \tilde{K}_{\tilde{x}}(t, u) \tilde{\phi}_i(u) du$$

where

$$\tilde{K}_{\tilde{x}}(t, u) = E \{ \tilde{x}(t) \tilde{x}^*(u) \}$$

and that

$$E \{ |\tilde{x}_i|^2 \} = \lambda_i.$$

Problem 6.4.14. Derive the analogous results to (6.142) for complex processes.

Problem 6.4.15. Assume that

$$\tilde{x}(t) = \sum_{i=1}^N \tilde{b}_i e^{j\omega_i t},$$

where the ω_i are known,

$$\omega_i = \omega_o + \Delta\omega i,$$

where

$$\Delta\omega = \alpha \frac{2\pi}{T}$$

with α a known positive constant that controls the spacing. The \tilde{b}_i are statistically independent circularly complex Gaussian random variables with $E\{|\tilde{b}_i|\} = \sigma_i^2$.

- (a) Formulate the problem using the complex version of (6.142).
- (b) Assume $N = 5$ and $\sigma_i^2 = 1$, $i = 1, 2, \dots, N$. Plot the eigenvalues as a function of α . Discuss your results.

Problem 6.4.16. Assume

$$x(t) = \sum_{i=1}^4 a_i s_i(t) \quad -\frac{T}{2} \leq t \leq \frac{T}{2},$$

where

$$s_1(t) = \sqrt{\frac{2}{T}} \cos \frac{2\pi}{T} t$$

and

$$s_i(t) = s_1 \left[t - (i-1) \frac{T}{4} \right] \quad i = 2, 3, 4.$$

The a_i are Gaussian random variables with covariance matrix

$$\mathbf{K}_a = \sigma_a^2 \begin{bmatrix} 1 & \rho & \rho^2 & \rho^3 \\ \rho & 1 & \rho & \rho^2 \\ \rho^2 & \rho & 1 & \rho \\ \rho^3 & \rho^2 & \rho & 1 \end{bmatrix}.$$

Find the eigenvalues and eigenfunctions of the Fredholm equation with $K_x(t, u)$ as its kernel.

Problem 6.4.17. Consider the model in Example 6.2. Replace the integral equation in (6.82) by a matrix equation by sampling the t and u variables. Compute the eigenvalues and eigenvectors using Matlab.

Compare your results to the results of Example 6.2. Discuss how to choose the sampling interval.

P6.5 Vector Random Processes

Problem 6.5.1. Consider the spectral matrix

$$\mathbf{S}(\omega) = \begin{bmatrix} 2 & \frac{\sqrt{2k}}{j\omega + k} \\ -\frac{\sqrt{2k}}{j\omega + k} & \frac{2k}{\omega^2 + k^2} \end{bmatrix}.$$

Extend the techniques in Section 6.4 to find the vector eigenfunctions and eigenvalues for Method 1.

Problem 6.5.2. Investigate the asymptotic behavior (i.e., as T becomes large) of the eigenvalues and eigenfunctions in Method 1 for an arbitrary stationary matrix kernel.

Problem 6.5.3. Let $x_1(t)$ and $x_2(t)$ be statistically independent zero-mean random processes with covariance functions $K_{x_1}(t, u)$ and $K_{x_2}(t, u)$, respectively. The eigenfunctions and eigenvalues are

$$\begin{aligned} K_{x_1}(t, u) : \lambda_i, \phi_i(t) &\quad i = 1, 2, \dots \\ K_{x_2}(t, u) : \mu_i, \psi_i(t) &\quad i = 1, 2, \dots \end{aligned}$$

Prove that the vector eigenfunctions and scalar eigenvalues can always be written as

$$\lambda_1, \begin{bmatrix} \phi_1(t) \\ 0 \end{bmatrix} : \mu_1, \begin{bmatrix} 0 \\ \psi_1(t) \end{bmatrix} : \lambda_2, \begin{bmatrix} \phi_2(t) \\ 0 \end{bmatrix} : \dots .$$

7

Detection of Signals–Estimation of Signal Parameters

7.1 INTRODUCTION

In Chapters 2–5, we formulated the detection and estimation problems in the classical context. In order to provide background for several areas, we first examined a reasonably general problem. Then, in Chapters 3 and 5, we investigated the more precise results that were available in the general Gaussian case.

In Chapter 6, we developed techniques for representing continuous processes by sets of numbers. The particular representation that we considered in detail was appropriate primarily for Gaussian processes.

We now want to use these representations to extend the results of the classical theory to the case in which the observations consist of *continuous waveforms*.

7.1.1 Models

The problems of interest to us in this chapter may be divided into two categories. The first is the detection problem that arises in three broad areas: digital communications, radar/sonar, and pattern recognition and classification. The second is the signal parameter estimation problem that also arises in these three areas.

7.1.1.1 Detection

The conventional model of a simple digital communication system is shown in Figure 7.1. The source puts out a binary digit (either 0 or 1) every T seconds. The most straightforward system would transmit either $\sqrt{E_0}s_0(t)$ or $\sqrt{E_1}s_1(t)$ during each interval. In a typical space communication system, an attenuated version of the transmitted signal would be received with negligible distortion. The received signal consists of $\sqrt{E_0}s_0(t)$ or $\sqrt{E_1}s_1(t)$ plus an additive noise component.

The characterization of the noise depends on the particular application. One source, always present, is thermal noise in the receiver front end. This noise can be modeled as a sample function from a Gaussian random process. As we proceed to more complicated models, we shall encounter other sources of interference that may turn out to be more important than the thermal noise. In many cases we can redesign the system to eliminate

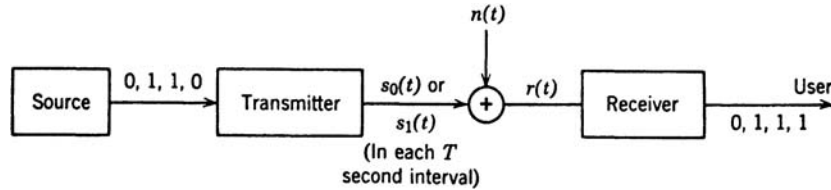


Figure 7.1: A digital communication system.

these other interference effects almost entirely. Then the thermal noise will be the disturbance that limits the system performance. In most systems the spectrum of the thermal noise is flat over the frequency range of interest, and we may characterize it in terms of a spectral height of $N_0/2$ joules. An alternate characterization commonly used is effective noise temperature T_e (e.g., Valley and Wallman [VW48] or Davenport and Root [DR58, DR87] Chapter 10). The two are related simply by

$$N_0 = kT_e, \quad (7.1)$$

where k is Boltzmann's constant, 1.38×10^{-23} J/K and T_e is the effective noise temperature, K.

Thus, in this particular case we could categorize the receiver design as a problem of detecting one of two *known signals in the presence of additive white Gaussian noise*.

If we look into a possible system in more detail, a typical transmitter could be as shown in Figure 7.2. The transmitter has an oscillator with nominal center frequency of ω_c . It is biphase modulated according to whether the source output is 1 (0°) or 0 (180°). The oscillator's instantaneous phase varies slowly, and the receiver must include some auxiliary equipment to measure the oscillator phase. If the phase varies slowly enough, we shall see that accurate measurement is possible. If this is true, the problem may be modeled as above. If the measurement is not accurate, however, we must incorporate the phase uncertainty in our model.

A second type of communication system is the point-to-point ionospheric scatter system shown in Figure 7.3 in which the transmitted signal is scattered by the layers in the

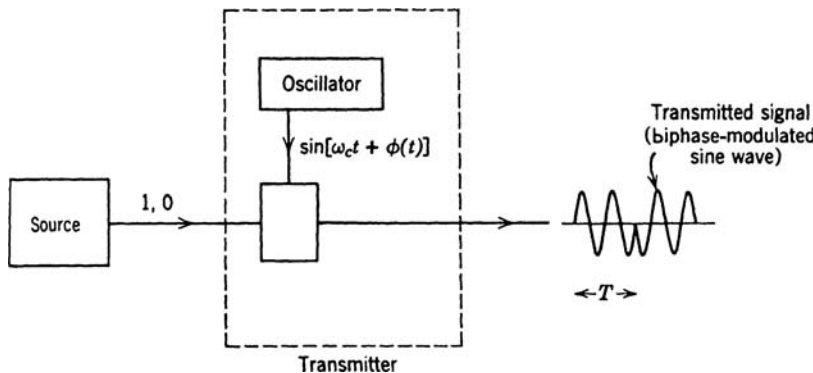


Figure 7.2: Details of typical system.

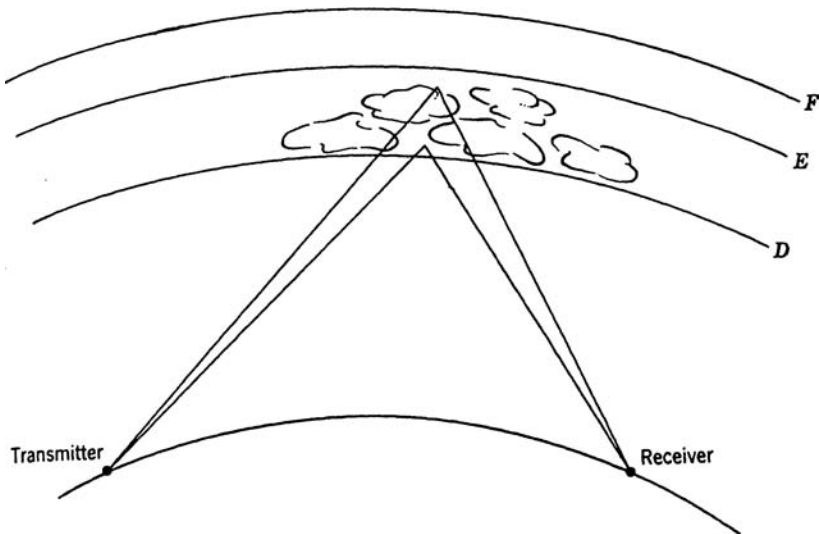


Figure 7.3: Ionospheric scatter link.

ionosphere. In a typical system we can transmit a “one” by sending a sine wave of a given frequency and a “zero” by a sine wave of another frequency. The receiver signal may vary as shown in Figure 7.4. Now, the receiver has a signal that fluctuates in amplitude and phase. In the commonly used frequency range most of the additive noise is Gaussian.

Corresponding problems are present in the radar context. A conventional pulsed radar transmits a signal as shown in Figure 7.5. If a target is present, the sequence of pulses is reflected. As the target fluctuates, the amplitude and phase of the reflected pulses change. The returned signal consists of a sequence of pulses whose amplitude and phase are unknown. The problem is to examine this sequence in the presence of receiver noise and decide whether a target is present.

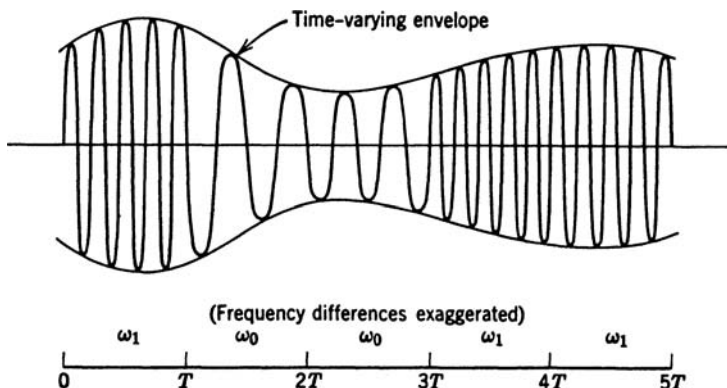


Figure 7.4: Signal component in time-varying channel.

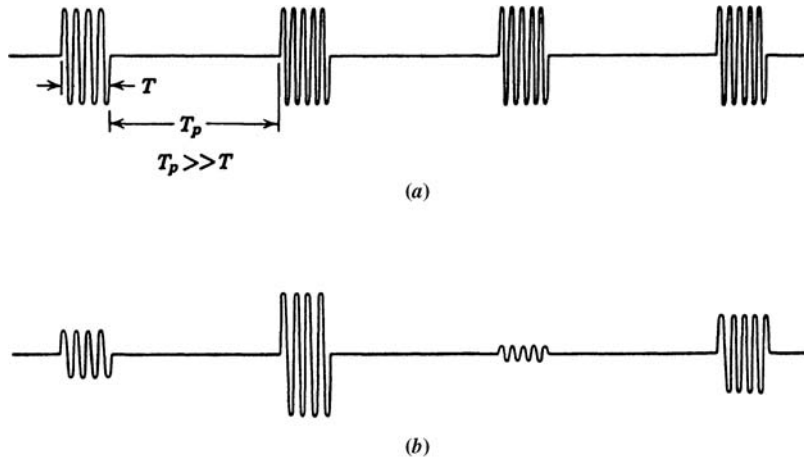


Figure 7.5: Signals in radar model: (a) transmitted sequence of rf pulses; (b) received sequence [amplified (time-shift not shown)].

There are obvious similarities between the two areas, but there are also some differences:

1. In a digital communication system the two types of error (say 1, when 0 was sent, and vice versa) are usually of equal importance. Furthermore, a signal may be present on both hypotheses. This gives a symmetry to the problem that can be exploited. In a radar/sonar system the two types of error are almost always of unequal importance. In addition, a signal is present only on one hypothesis. This means that the problem is generally nonsymmetric.
2. In a digital communication system the probability of error is usually an adequate measure of system performance. Normally, in radar/sonar a reasonably complete ROC is needed.
3. In a digital system we are sending a sequence of digits. Thus, we can correct digit errors by putting some structures into the sequence. In the radar/sonar case this is not an available alternative.

In spite of these differences, a great many of the basic results will be useful for both areas.

The above examples were “active” systems in which the user transmitted a signal. An important application in radar and sonar is the detection of a signal that is generated by a noisy target. In general, this signal can best be modeled as a random process so we will study how to detect a Gaussian random process in the presence of Gaussian noise.

7.1.1.2 Estimation

The second problem of interest is the estimation of signal parameters, which is encountered in both the communications and radar/sonar areas. We discuss a communication problem first.

Consider the analog message source shown in Figure 7.6a. For simplicity we assume that it is a sample function from a bandlimited random process ($2W$ cps; double sided). We could then sample it every $1/2W$ seconds without losing any information. In other

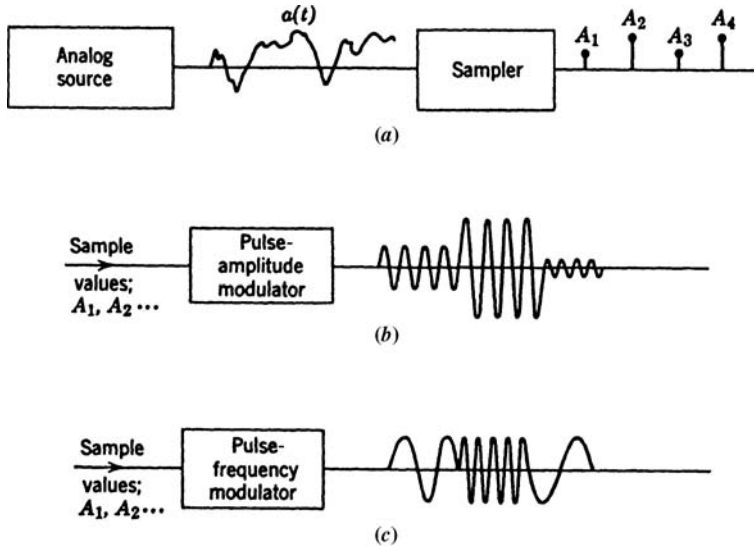


Figure 7.6: Analog message transmission.

words, given these samples at the receiver, we could reconstruct the message exactly (e.g., Nyquist [Nyg24] or Problem 6.3.6). Every T seconds ($T = 1/2W$) we transmit a signal that depends on the particular value A_i at the last sampling time. In the system in Figure 7.6b, the amplitude of a sinusoid depends on the value of A_i . This system is referred to as a pulse-amplitude modulation (PAM) system. In the system in Figure 7.6c, the frequency of the sinusoid depends on the sample value. This system is referred to as a pulse-frequency modulation (PFM) system. The signal is transmitted over a channel and is corrupted by noise (Figure 7.7). The received signal in the i th interval is

$$r(t) = s(t, A_i) + n(t), \quad T_i \leq t \leq T_{i+1}. \quad (7.2)$$

The purpose of the receiver is to estimate the values of the successive A_i and use these estimates to reconstruct the message.

A typical radar system is shown in Figure 7.8. In a simple pulsed radar, the transmitted signal is a sinusoid with a rectangular envelope.

$$s_t(t) = \begin{cases} \sqrt{2E_t} \sin \omega_c t, & 0 \leq t \leq T, \\ 0, & \text{Elsewhere.} \end{cases} \quad (7.3)$$

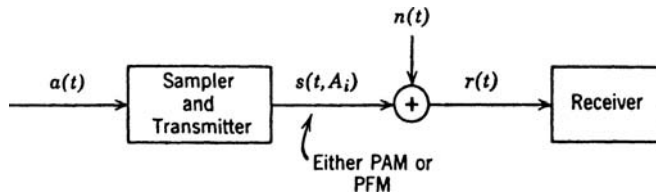


Figure 7.7: A parameter transmission system.

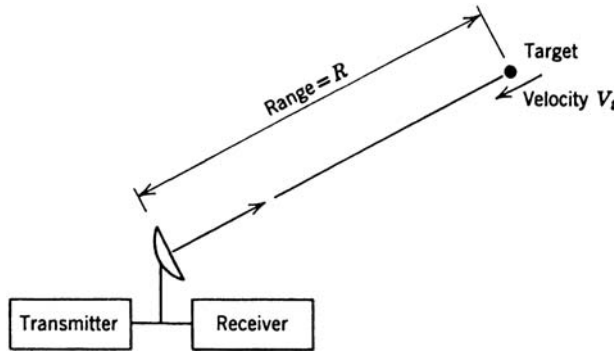


Figure 7.8: Radar system diagram.

The returned signal is delayed by the round-trip time to the target. If the target is moving, there is Doppler shift. Finally there is a random amplitude and phase due to the target fluctuation. The received signal in the absence of noise is

$$s_r(t) = \begin{cases} v\sqrt{2E_t} \sin[(\omega_c + \omega_D)(t - \tau) + \phi], & \tau \leq t \leq \tau + T, \\ 0, & \text{Elsewhere.} \end{cases} \quad (7.4)$$

Here, we estimate τ and ω_D (or, equivalently, target range and velocity). Once again, there are obvious similarities between the communication and radar/sonar problem. The basic differences are the following:

1. In the communications context A_i is a random variable with a probability density that is usually known. In radar, the range or velocity limits of interest are known. The parameters, however, are best treated as nonrandom variables.
2. In the radar case, the difficulty may be compounded by a lack of knowledge regarding the target's presence. Thus, the detection and estimation problem may have to be combined.
3. In almost all radar problems a phase reference is not available.

Other models of interest will appear naturally in the course of our discussion.

7.1.2 Format

Because this chapter is long, it is important to understand the overall structure. The basic approach has three steps:

1. The observation consists of a waveform $r(t)$. Thus, the observation space may be infinite dimensional. Our first step is to map the received signal into some convenient decision or estimation space. This will reduce the problem to ones studied in Chapters 2–5.
2. In the detection problem, we then select decision regions and compute the ROC or $Pr(\epsilon)$. In the estimation problem, we evaluate the variance or mean-square error.
3. We examine the results to see what they imply about system design and performance.

Channel	Signal Detection	Signal Parameter Estimation
Additive white noise	Simple binary	Single parameter, linear
Additive colored noise	General binary	Single parameter, nonlinear
Simple random	M -ary	Multiple parameter
Multiple channels		

Figure 7.9: Sequence of models.

We carry out these steps for a sequence of models of increasing complexity (Figure 7.9) and develop the detection and estimation problem in parallel. By emphasizing their parallel nature for the simple cases, we can save appreciable effort in the more complex cases by considering only one problem in the text and leaving the other as an exercise. We start with the simple models and then proceed to the more involved.

In Section 7.2, we develop the optimum detectors and estimators for the case of known signals in additive white Gaussian noise (AWGN). In Section 7.3, we extend these results to the case of nonwhite (colored) noise or interference. In Section 7.4, we study the case of signals with unknown parameters in additive Gaussian noise. We consider both random and nonrandom parameters. In Section 7.5, we extend these results to multiple received waveforms that we encounter both in multiple channel systems and in arrays. In Section 7.6, we study the multiple parameter estimation. In Section 7.7, we summarize our results.

In the text, we focus on real random processes. The extension to circular complex Gaussian random processes is straightforward and is developed primarily in the problems. We consider the complex model in several examples because it is more realistic.

A logical question is If the problem is so simple, why is the chapter so long? This is a result of our efforts to determine how the model and its parameters affect the design and performance of the system. We feel that only by examining some representative problems in detail we can acquire an appreciation for the implications of the theory.

Before proceeding to the solution, a brief historical comment is in order. The mathematical groundwork for our approach to this problem was developed by Grenander [Gre50]. The detection problem relating to optimum radar systems was developed at the MIT Radiation Laboratory, (e.g. [LU50]) in the early 1940s. Somewhat later Woodward and Davies [WD52, Woo55] approached the radar problem in a different way. The detection problem was formulated at about the same time in a manner similar to ours by both Peterson et al. [PBF54] and Middleton and Van Meter [MM55], whereas the estimation problem was first done by Slepian [Sle54]. Parallel results with a communications emphasis were developed by Kotelnikov [Kot47, Kot59] in Russia. Books that deal almost exclusively with radar include Helstrom [Hel60] and Wainstein and Zubakov [WZ62]. Books that deal almost exclusively with communication include Kotelnikov [Kot59], Harman [Har63], Baghdady (ed.) [Bag61], Wozencraft and Jacobs [WJ65], and Golomb et al. [GBE⁺64]. The last two parts of Middleton [Mid60a] cover a number of topics in both areas. By presenting the problems side by side, we hope to emphasize their inherent similarities and contrast their differences.

7.2 DETECTION AND ESTIMATION IN WHITE GAUSSIAN NOISE

In this section, we formulate and solve the detection and estimation problems for the case in which the interference is additive white Gaussian noise.

We consider the detection problem first: the simple binary case, the general binary case, and the M -ary case are discussed in that order. By using the concept of a sufficient statistic, the optimum receiver structures are simply derived and the performances for a number of important cases are evaluated. Finally, we study the sensitivity of the optimum receiver to the detailed assumptions of our model.

As we have seen in the classical context, the decision and estimation problems are closely related; linear estimation will turn out to be essentially the same as simple binary detection. When we proceed to the nonlinear estimation problem, new issues will develop, both in specifying the estimator structure and in evaluating its performance.

7.2.1 Detection of Signals in Additive White Gaussian Noise

7.2.1.1 Simple Binary Detection

In the simplest binary decision problem the received signal under one hypothesis consists of a completely known signal, $\sqrt{E}s(t)$, corrupted by an additive zero-mean white Gaussian noise $w(t)$ with spectral height $N_0/2$; the received signal under the other hypothesis consists of the noise $w(t)$ alone. Thus,

$$r(t) = \begin{cases} H_1 : \sqrt{E}s(t) + w(t), & 0 \leq t \leq T, \\ H_0 : w(t), & 0 \leq t \leq T. \end{cases} \quad (7.5)$$

For convenience we assume that

$$\int_0^T s^2(t) dt = 1, \quad (7.6)$$

so that E represents the received signal energy. The problem is to observe $r(t)$ over the interval $[0, T]$ and decide whether H_0 or H_1 is true. The criterion may be either Bayes or Neyman–Pearson.

The following ideas will enable us to solve this problem easily:

1. Our observation is a time-continuous random waveform. The first step is to reduce it to a set of random variables (possibly a countably infinite set).
2. One method is the series expansion of Chapter 6:

$$r(t) = \text{l. i. m.}_{K \rightarrow \infty} \sum_{i=1}^K r_i \phi_i(t), \quad 0 \leq t \leq T. \quad (7.7)$$

When $K = K'$, there are K' coefficients in the series, $r_1, \dots, r_{K'}$ that we could denote by the vector $\mathbf{r}_{K'}$. In our subsequent discussion we suppress the K' subscript and denote the coefficients by \mathbf{r} .

3. In Chapter 2, we saw that if we transformed \mathbf{r} into two independent vectors, \mathbf{l} (the sufficient statistic) and \mathbf{y} , as shown in Figure 7.10, our decision could be based only

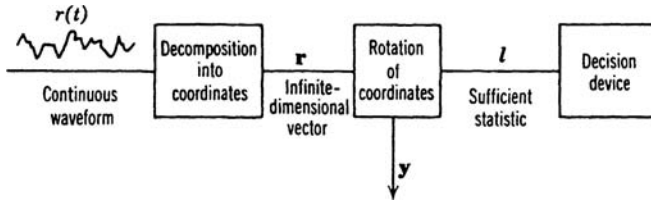


Figure 7.10: Generation of sufficient statistics.

on \mathbf{l} , because the values of \mathbf{y} did not depend on the hypothesis. The advantage of this technique was that it reduced the dimension of the decision space to that of \mathbf{l} . Because this is a binary problem we know that \mathbf{l} will be one dimensional.

Here, the method is straightforward. If we choose the first orthonormal function to be $s(t)$, the first coefficient in the decomposition is the Gaussian random variable,

$$r_1 = \begin{cases} H_0 : \int_0^T s(t)w(t) dt \triangleq w_1 \\ H_1 : \int_0^T s(t) [\sqrt{E}s(t) + w(t)] dt = \sqrt{E} + w_1. \end{cases} \quad (7.8)$$

The remaining $r_i (i > 1)$ are Gaussian random variables that can be generated by using some arbitrary orthonormal set whose members are orthogonal to $s(t)$.

$$r_i = \begin{cases} H_0 : \int_0^T \phi_i(t) w(t) dt \triangleq w_i, & i \neq 1, \\ H_1 : \int_0^T \phi_i(t) [\sqrt{E}s(t) + w(t)] dt = w_i, & i \neq 1. \end{cases} \quad (7.9)$$

From Chapter 6 (6.47), we know that

$$E(w_i w_j) = 0, \quad i \neq j.$$

Because w_i and w_j are jointly Gaussian, they are statistically independent.

We see that *only* r_1 depends on which hypothesis is true. Further, all $r_i (i > 1)$ are statistically independent of r_1 . Thus, r_1 is a sufficient statistic ($r_1 = \mathbf{l}$). The other r_i correspond to \mathbf{y} . Because they will not affect the decision, there is no need to compute them.

Several equivalent receiver structures follow immediately. The structure in Figure 7.11 is called a *correlation receiver*. It correlates the input $r(t)$ with a stored replica of the signal $s(t)$. The output is r_1 , which is a sufficient statistic ($r_1 = \mathbf{l}$) and is a Gaussian random variable. Once we have obtained r_1 , the decision problem will be identical to the classical problem in Chapter 2 (specifically, Example 2.1). We compare \mathbf{l} to a threshold in order to make a decision.

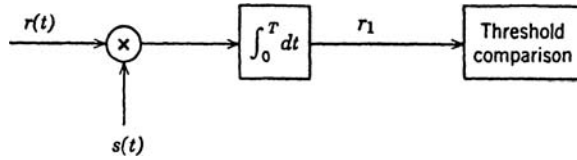


Figure 7.11: Correlation receiver.

An equivalent realization is shown in Figure 7.12. The impulse response of the linear system is simply the signal reversed in time and shifted,

$$h(\tau) = s(T - \tau). \quad (7.10)$$

The output at time T is the desired statistic l . This receiver is called a *matched filter receiver*. (It was first derived by North [Nor43, Nor63].) The two structures are mathematically identical; the choice of which structure to use depends solely on ease of realization.

Just as in Example 2.1 of Chapter 2, the sufficient statistic l is Gaussian under either hypothesis. Its mean and variance follow easily:

$$\begin{aligned} E(l|H_1) &= E(r_1|H_1) = \sqrt{E}, \\ E(l|H_0) &= E(r_1|H_0) = 0, \end{aligned} \quad (7.11)$$

$$\text{Var}(l|H_0) = \text{Var}(l|H_1) = \frac{N_0}{2}. \quad (7.12)$$

Thus, we can use the results of Chapter 2, (2.82)–(2.87), with

$$d = \left(\frac{2E}{N_0} \right)^{1/2}. \quad (7.13)$$

The curves in Figure 2.12a and b of Chapter 2 are directly applicable and are reproduced as Figures 7.13 and 7.14. We see that the performance depends only on the received signal energy E and the noise spectral height N_0 —the signal shape is not important. This is intuitively logical because the noise is the same along any coordinate.

The key to the simplicity in the solution was our ability to reduce an infinite-dimensional observation space to a one-dimensional decision space by exploiting the idea of a sufficient statistic. Clearly, we should end up with the same receiver even if we do not recognize that a sufficient statistic is available. To demonstrate this we construct the likelihood ratio directly. Three observations lead us easily to the solution.

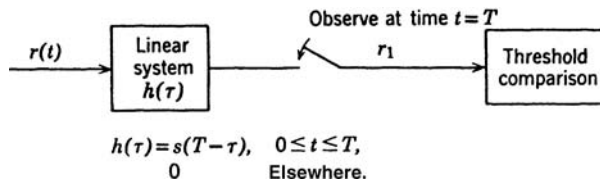


Figure 7.12: Matched filter receiver.

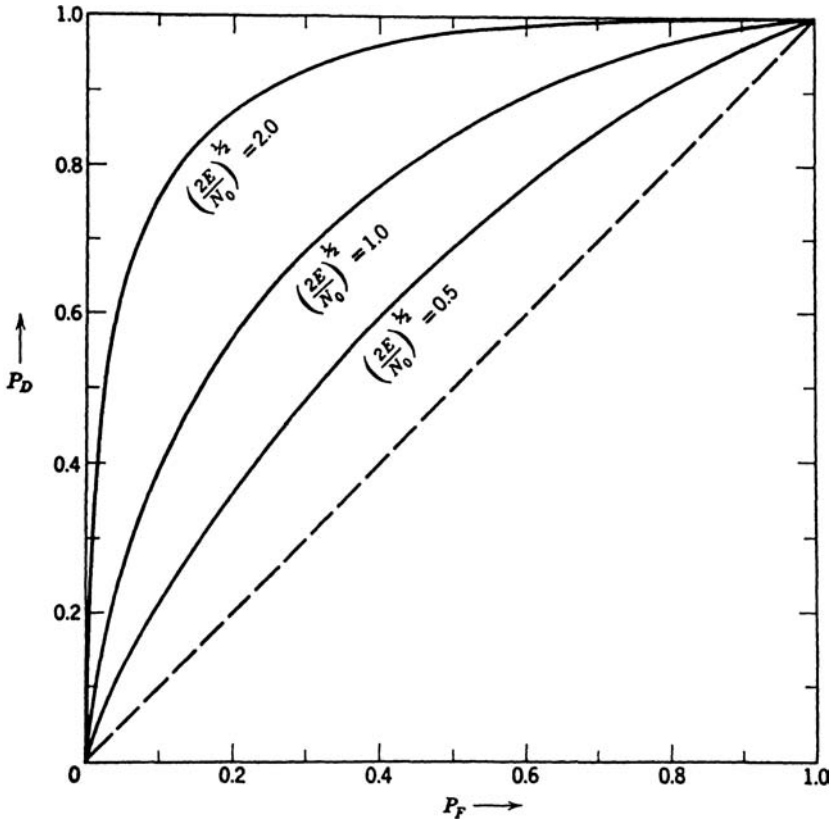


Figure 7.13: Receiver operating characteristic: known signal in additive white Gaussian noise.

1. If we approximate $r(t)$ in terms of some finite set of numbers, r_1, \dots, r_K , (\mathbf{r}), we have a problem in classical detection theory that we can solve.
2. If we choose the set r_1, r_2, \dots, r_K so that

$$p_{r_1, r_2, \dots, r_K | H_i}(R_1, R_2, \dots, R_K | H_i) = \prod_{j=1}^K p_{r_j | H_i}(R_j | H_i), \quad i = 0, 1, \quad (7.14)$$

that is, the observations are conditionally independent, we have an *easy* problem to solve.

3. Because we know that it requires an infinite set of numbers to represent $r(t)$ completely, we want to get the solution in a convenient form so that we can let $K \rightarrow \infty$.

We denote the approximation that uses K coefficients as $r_K(t)$. Thus,

$$r_K(t) = \sum_{i=1}^K r_i \phi_i(t), \quad 0 \leq t \leq T, \quad (7.15)$$

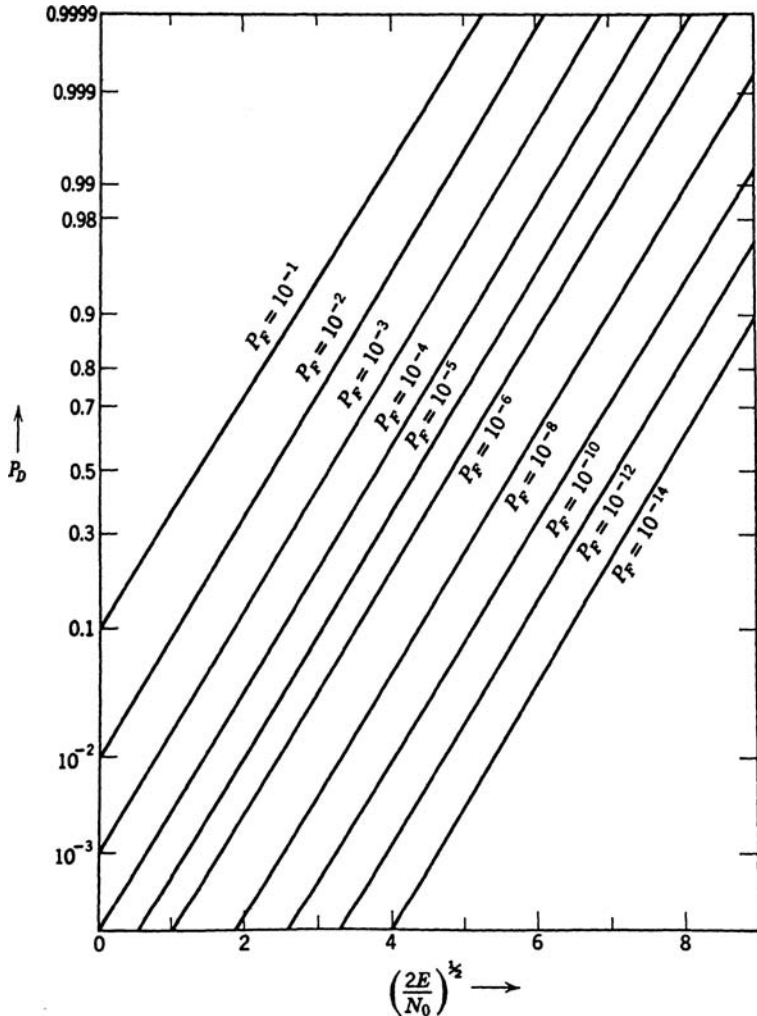


Figure 7.14: Probability of detection versus $\left(\frac{2E}{N_0}\right)^{1/2}$.

where

$$r_i = \int_0^T r(t) \phi_i(t) dt, \quad i = 1, 2, \dots, K, \quad (7.16)$$

and the $\phi_i(t)$ belong to an *arbitrary* complete orthonormal set of functions. Using (7.16), we see that under H_0

$$r_i = \int_0^T w(t) \phi_i(t) dt = w_i, \quad (7.17)$$

and under H_1

$$r_i = \int_0^T \sqrt{E}s(t) \phi_i(t) dt + \int_0^T w(t) \phi_i(t) dt = s_i + w_i. \quad (7.18)$$

The coefficients s_i correspond to an expansion of the signal

$$s_K(t) \triangleq \sum_{i=1}^K s_i \phi_i(t), \quad 0 \leq t \leq T \quad (7.19)$$

and

$$\sqrt{E}s(t) = \lim_{K \rightarrow \infty} s_K(t). \quad (7.20)$$

The r_i s are Gaussian with known statistics:

$$\begin{aligned} E(r_i | H_0) &= 0, \\ E(r_i | H_1) &= s_i, \\ \text{Var}(r_i | H_0) &= \text{Var}(r_i | H_1) = \frac{N_0}{2}. \end{aligned} \quad (7.21)$$

Because the noise is “white,” these coefficients are independent along any set of coordinates. The likelihood ratio is

$$\Lambda [r_K(t)] = \frac{p_{\mathbf{r}|H_1}(\mathbf{R}|H_1)}{p_{\mathbf{r}|H_0}(\mathbf{R}|H_0)} = \frac{\prod_{i=1}^K \frac{1}{\sqrt{\pi N_0}} \exp\left(-\frac{1}{2} \frac{(R_i - s_i)^2}{N_0/2}\right)}{\prod_{i=1}^K \frac{1}{\sqrt{\pi N_0}} \exp\left(-\frac{1}{2} \frac{R_i^2}{N_0/2}\right)}. \quad (7.22)$$

Taking the logarithm and canceling common terms, we have

$$\ln \Lambda [r_K(t)] = \frac{2}{N_0} \sum_{i=1}^K R_i s_i - \frac{1}{N_0} \sum_{i=1}^K s_i^2. \quad (7.23)$$

The two sums are easily expressed as integrals. From Parseval’s theorem,

$$\sum_{i=1}^K R_i s_i = \int_0^T r_K(t) s_K(t) dt, \quad (7.24a)$$

and

$$\sum_{i=1}^K s_i^2 = \int_0^T s_K^2(t) dt. \quad (7.24b)$$

We now have the log-likelihood ratio in a form in which it is convenient to pass to the limit:

$$\text{l. i. m. } \ln \Lambda [r_K(t)] \stackrel{K \rightarrow \infty}{\triangleq} \ln \Lambda [r(t)] = \frac{2\sqrt{E}}{N_0} \int_0^T r(t) s(t) dt - \frac{E}{N_0}. \quad (7.25)$$

The first term is just the sufficient statistic we obtained before. The second term is a bias. The resulting likelihood ratio test is

$$\frac{2\sqrt{E}}{N_0} \int_0^T r(t) s(t) dt \stackrel{H_1}{\underset{H_0}{\gtrless}} \ln \eta + \frac{E}{N_0}. \quad (7.26)$$

(Recall from Chapter 2 that η is a constant that depends on the costs and *a priori* probabilities in a Bayes test and the desired P_F in a Neyman–Pearson test.) It is important to observe that even though the probability density $p_{r(t)|H_i}(r(t)|H_i)$ is not well defined for either hypothesis, the likelihood ratio is.

Before going on to more general problems it is important to emphasize the two separate features of the signal detection problem:

1. First we reduce the received waveform to a single number that is a point in a decision space. This operation is performed physically by a correlation operation and is invariant to the decision criterion that we plan to use. This invariance is important because it enables us to construct the waveform processor without committing ourselves to a particular criterion.
2. Once we have transformed the received waveform into the decision space we have only the essential features of the problem left to consider. Once we get to the decision space the problem is the same as that studied in Chapter 2. The actual received waveform is no longer important and all physical situations that lead to the same picture in a decision space are identical for our purposes. In our simple example we saw that all signals of equal energy map into the same point in the decision space. It is therefore obvious that the signal shape is unimportant.

The separation of these two parts of the problem leads to a clearer understanding of the fundamental issues.

7.2.1.2 General Binary Detection in White Gaussian Noise

The results for the simple binary problem extend easily to the general binary problem. Let

$$r(t) = \begin{cases} H_1 : \sqrt{E_1} s_1(t) + w(t), & 0 \leq t \leq T, \\ H_0 : \sqrt{E_0} s_0(t) + w(t), & 0 \leq t \leq T, \end{cases} \quad (7.27)$$

where $s_0(t)$ and $s_1(t)$ are normalized but are *not* necessarily orthogonal. We denote the correlation between the two signals as

$$\rho \triangleq \int_0^T s_0(t) s_1(t) dt.$$

(Note that $|\rho| \leq 1$ because the signals are normalized.)

We choose our first two orthogonal functions as follows:

$$\phi_1(t) = s_1(t), \quad 0 \leq t \leq T, \quad (7.28)$$

$$\phi_2(t) = \frac{1}{\sqrt{1 - \rho^2}} [s_0(t) - \rho s_1(t)], \quad 0 \leq t \leq T. \quad (7.29)$$

We see that $\phi_2(t)$ is obtained by subtracting out the component of $s_0(t)$ that is correlated with $\phi_1(t)$ and normalizing the result. The remaining $\phi_i(t)$ consist of an arbitrary orthonormal set whose members are orthogonal to $\phi_1(t)$ and $\phi_2(t)$ and are chosen so that the entire set is complete. The coefficients are

$$r_i = \int_0^T r(t) \phi_i(t) dt, \quad i = 1, 2, \dots \quad (7.30)$$

All of the r_i except r_1 and r_2 do not depend on which hypothesis is true and are statistically independent of r_1 and r_2 . Thus, a two-dimensional decision region, shown in Figure 7.15a, is adequate. The mean value of r_i along each coordinate is

$$H_0 : E[r_i|H_0] = \sqrt{E_0} \int_0^T s_0(t) \phi_i(t) dt \triangleq s_{0i}, \quad i = 1, 2 \quad (7.31)$$

and

$$H_1 : E[r_i|H_1] = \sqrt{E_1} \int_0^T s_1(t) \phi_i(t) dt \triangleq s_{1i}, \quad i = 1, 2, \quad (7.32)$$

directly from Section 3.2

$$\ln \Lambda = -\frac{1}{N_0} \sum_{i=1}^2 (R_i - s_{1i})^2 + \frac{1}{N_0} \sum_{i=1}^2 (R_i - s_{0i})^2 \stackrel{H_1}{\gtrless} \stackrel{H_0}{\ln \eta} \quad (7.33)$$

$$= -\frac{1}{N_0} |\mathbf{R} - \mathbf{s}_1|^2 + \frac{1}{N_0} |\mathbf{R} - \mathbf{s}_0|^2 \stackrel{H_1}{\gtrless} \stackrel{H_0}{\ln \eta}, \quad (7.34)$$

or, canceling common terms and rearranging the result,

$$\mathbf{R}^T (\mathbf{s}_1 - \mathbf{s}_0) \stackrel{H_1}{\gtrless} \stackrel{H_0}{\frac{N_0}{2} \ln \eta + \frac{1}{2} (|\mathbf{s}_1|^2 - |\mathbf{s}_0|^2)}. \quad (7.35)$$

Thus, only the product of \mathbf{R}^T with the difference vector $\mathbf{s}_1 - \mathbf{s}_0$ is used to make a decision. Therefore, the decision space is divided into two parts by a line perpendicular to $\mathbf{s}_1 - \mathbf{s}_0$ as shown in Figure 7.15b. The noise components along the r_1 and r_2 axes are independent and identically distributed.

Now observe that we can transform the coordinates as shown in Figure 7.15b. The noises along the new coordinates are still independent, but only the coefficient along the l coordinate depends on the hypothesis and the y coefficient may be disregarded. Therefore, we can simplify our receiver by generating l instead of r_1 and r_2 . The function needed

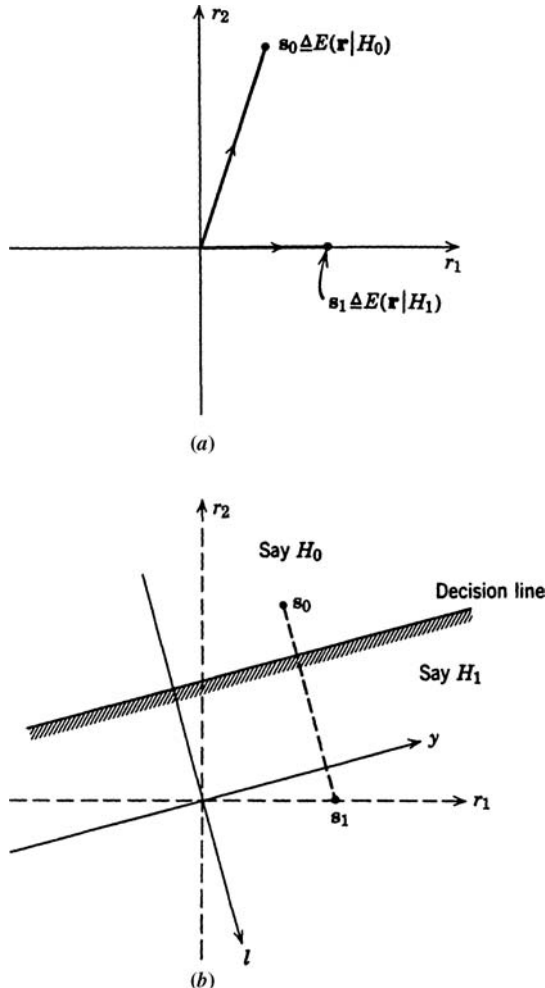


Figure 7.15: Decision spaces.

to generate the statistic is just the normalized version of the difference signal. Denote the difference signal by $s_\Delta(t)$:

$$s_\Delta(t) \triangleq \sqrt{E_1}s_1(t) - \sqrt{E_0}s_0(t). \quad (7.36)$$

The normalized function is

$$f_\Delta(t) = \frac{\sqrt{E_1}s_1(t) - \sqrt{E_0}s_0(t)}{(E_1 - 2\rho\sqrt{E_0E_1} + E_0)^{1/2}}. \quad (7.37)$$

The receiver is shown in Figure 7.16. (Note that this result could have been obtained directly by choosing $f_\Delta(t)$ as the first orthonormal function.)

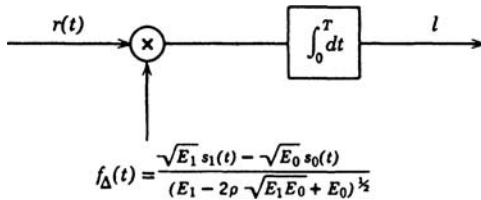


Figure 7.16: Optimum correlation receiver, general binary problem.

Thus, once again the binary problem reduces to a one-dimensional decision space. The statistic l is Gaussian:

$$E(l|H_1) = \frac{E_1 - \sqrt{E_0 E_1} \rho}{(E_1 - 2\rho\sqrt{E_0 E_1} + E_0)^{1/2}}, \quad (7.38)$$

$$E(l|H_0) = \frac{\sqrt{E_0 E_1} \rho - E_0}{(E_1 - 2\rho\sqrt{E_0 E_1} + E_0)^{1/2}}. \quad (7.39)$$

The variance is $N_0/2$ as before. Thus,

$$d^2 = \frac{2}{N_0} (E_1 + E_0 - 2\rho\sqrt{E_0 E_1}). \quad (7.40)$$

Observe that if we normalized our coordinate system so that noise variance was unity then d would be the distance between the two signals. The resulting probabilities are

$$P_F = \text{erfc}_* \left(\frac{\ln \eta}{d} + \frac{d}{2} \right), \quad (7.41)$$

$$P_D = \text{erfc}_* \left(\frac{\ln \eta}{d} - \frac{d}{2} \right). \quad (7.42)$$

[These equations are just (2.84) and (2.85).]

The best choice of signals follows easily. The performance index d is monotonically related to the distance between the two signals in the decision space. For fixed energies the best performance is obtained by making $\rho = -1$. In other words,

$$s_0(t) = -s_1(t). \quad (7.43)$$

Once again the signal shape is not important.

When the criterion is minimum probability of error (as would be the logical choice in a binary communication system) *and* the *a priori* probabilities of the two hypotheses are equal, the decision region boundary has a simple interpretation. It is the perpendicular bisector of the line connecting the signal points (Figure 7.17). Thus, the receiver under these circumstances can be interpreted as a *minimum-distance* receiver and the error probability is

$$\Pr(\epsilon) = \int_{d/2}^{\infty} \frac{1}{\sqrt{2\pi}} \exp\left(-\frac{x^2}{2}\right) dx = \text{erfc}_* \left(\frac{d}{2} \right). \quad (7.44)$$

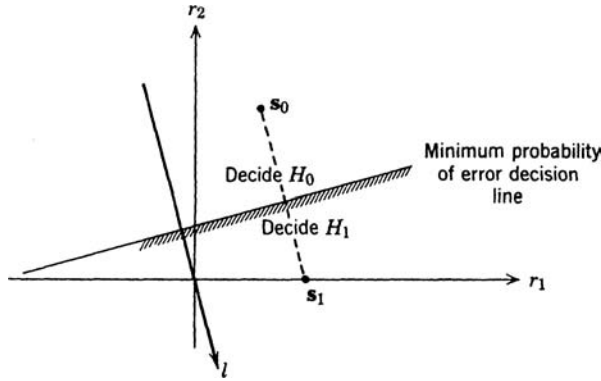


Figure 7.17: Decision space.

If, in addition, the signals have *equal energy*, the bisector goes through the origin and we are simply choosing the signal that is most correlated with $r(t)$. This can be referred to as a “largest of” receiver (Figure 7.18).

The discussion can be extended to the M -ary problem in a straightforward manner.

7.2.1.3 M -ary Detection in White Gaussian Noise

Assume that there are M hypotheses:

$$H_i : r(t) = \sqrt{E_i} s_i(t) + w(t), \quad 0 \leq t \leq T. \quad (7.45)$$

The $s_i(t)$ all have unit energy but may be correlated:

$$\int_0^T s_i(t) s_j(t) dt = \rho_{ij}, \quad i, j = 1, 2, \dots, M. \quad (7.46)$$

This problem is analogous to the M hypothesis problem in Chapter 2. We saw that the main difficulty for a likelihood ratio test with arbitrary costs was the specification of the boundaries of the decision regions. We shall devote our efforts to finding a suitable set of sufficient statistics and evaluating the minimum probability of error for some interesting cases.

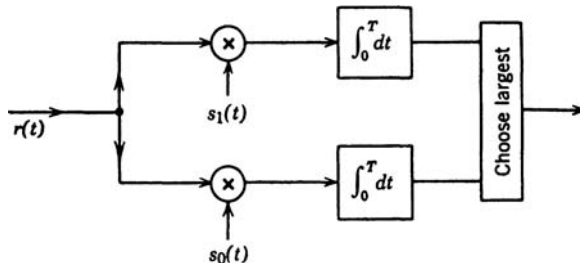


Figure 7.18: “Largest of” receiver.

First we construct a suitable coordinate system to find a decision space with the minimum possible dimensionality. The procedure is a simple extension of the method used for two dimensions. The first coordinate function is just the first signal. The second coordinate function is that component of the second signal that is linearly independent of the first and so on. We let

$$\phi_1(t) = s_1(t), \quad (7.47)$$

$$\phi_2(t) = (1 - \rho_{12}^2)^{-\frac{1}{2}} [s_2(t) - \rho_{12} s_1(t)]. \quad (7.48)$$

To construct the third coordinate function, we write

$$\phi_3(t) = c_3 [s_3(t) - c_1 \phi_1(t) - c_2 \phi_2(t)], \quad (7.49)$$

and find c_1 and c_2 by requiring orthogonality and c_3 by requiring $\phi_3(t)$ to be normalized. (This is called the Gram–Schmidt procedure and is developed in detail in Problem 7.2.7.) We proceed until one of two things happens:

1. M orthonormal functions are obtained.
2. $N < M$ orthonormal functions are obtained and the remaining signals can be represented by linear combinations of these orthonormal functions. Thus, the decision space will consist of *at most* M dimensions and fewer if the signals are linearly dependent.¹

We then use this set of orthonormal functions to generate N coefficients ($N \leq M$)

$$r_i \triangleq \int_0^T r(t) \phi_i(t) dt, \quad i = 1, 2, \dots, N. \quad (7.50)$$

These are statistically independent Gaussian random variables with variance $N_0/2$ whose means depend on which hypothesis is true.

$$E[r_i | H_j] \triangleq m_{ij}, \quad \begin{matrix} i = 1, 2, \dots, N, \\ j = 1, 2, \dots, M. \end{matrix} \quad (7.51)$$

The likelihood ratio test follows directly from our results in Chapter 2. When the criterion is minimum $\Pr(\epsilon)$, we compute

$$l_j = \ln P_j - \frac{1}{N_0} \sum_{i=1}^N (R_i - m_{ij})^2, \quad j = 1, 2, \dots, M, \quad (7.52)$$

and choose the largest. The modification for other cost assignments is also given in Chapter 2 (2.156).

¹Observe that we are talking about algebraic dependence.

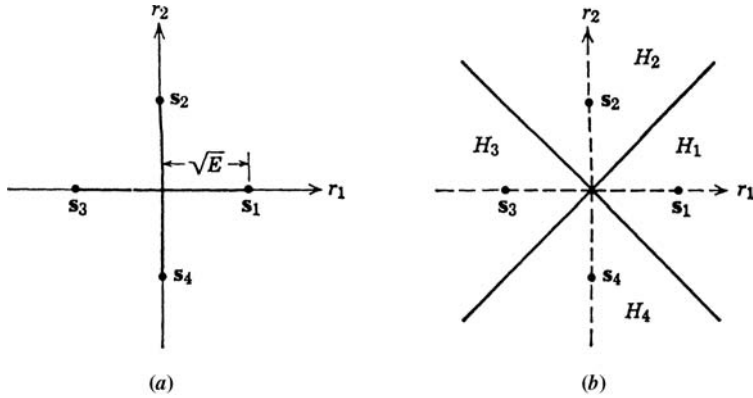


Figure 7.19: Decision space.

Two examples illustrate these ideas.

Example 7.1. Let

$$\begin{aligned}s_i(t) &= \left(\frac{2}{T}\right)^{\frac{1}{2}} \sin\left[\omega_c t + (i-1)\frac{\pi}{2}\right], & i = 1, 2, 3, 4, & 0 \leq t \leq T, \\ E_i &= E, & i = 1, 2, 3, 4,\end{aligned}\tag{7.53}$$

and

$$\omega_c = \frac{2\pi n}{T}$$

(n is an arbitrary integer). We see that

$$\phi_1(t) = \left(\frac{2}{T}\right)^{\frac{1}{2}} \sin \omega_c t, \quad 0 \leq t \leq T, \tag{7.54}$$

$$\phi_2(t) = \left(\frac{2}{T}\right)^{\frac{1}{2}} \cos \omega_c t, \quad 0 \leq t \leq T. \tag{7.55}$$

We see $s_3(t)$ and $s_4(t)$ are $-\phi_1(t)$ and $-\phi_2(t)$, respectively. Thus, in this case, $M = 4$ and $N = 2$. The decision space is shown in Figure 7.19a. The decision regions follow easily when the criterion is minimum probability of error and the *a priori* probabilities are equal. Using the result in (7.52), we obtain the decision regions in Figure 7.19b. ■

Example 7.2. Let

$$\begin{aligned}s_1(t) &= \left(\frac{2}{T}\right)^{\frac{1}{2}} \sin \frac{2\pi n}{T} t, & 0 \leq t \leq T, \\ s_2(t) &= \left(\frac{2}{T}\right)^{\frac{1}{2}} \sin \frac{4\pi n}{T} t, & 0 \leq t \leq T, \\ s_3(t) &= \left(\frac{2}{T}\right)^{\frac{1}{2}} \sin \frac{6\pi n}{T} t & 0 \leq t \leq T\end{aligned}\tag{7.56}$$

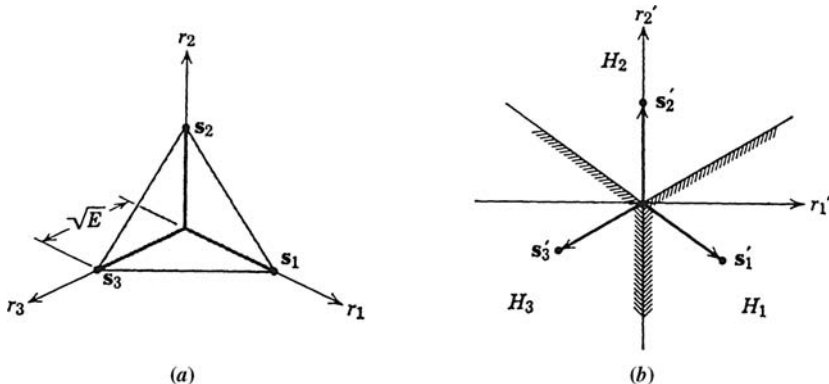


Figure 7.20: Decision space: orthogonal signals.

(n is an arbitrary integer) and

$$E_i = E, \quad i = 1, 2, 3.$$

Now

$$\phi_i(t) = s_i(t). \quad (7.57)$$

In this case, $M = N = 3$ and the decision space is three dimensional, as shown in Figure 7.20a. For $\min \Pr(\epsilon)$ and equal *a priori* probabilities the decision regions follow easily from (7.52). The boundaries are planes perpendicular to the plane through s_1, s_2 , and s_3 . Thus, it is only the projection of \mathbf{R} on this plane that is used to make a decision, and we can reduce the decision space to two dimensions as shown in Figure 7.20b. (The coefficients r'_1 and r'_2 are along the two orthonormal coordinate functions used to define the plane.) ■

Note that in Examples 7.1 and 7.2 the signal sets were so simple that the Gram–Schmidt procedure was not needed.

It is clear that these results are directly analogous to the M hypothesis case in Chapter 2. As we have already seen, the calculation of the errors is conceptually simple but usually tedious for $M > 2$. To illustrate the procedure, we compute the $\Pr(\epsilon)$ for Example 7.1.

Example 7.3 (Continuation of Example 7.1). We assume that the hypotheses are equally likely. Now the problem is symmetric. Thus, it is sufficient to assume that $s_1(t)$ was transmitted and compute the resulting $\Pr(\epsilon)$. (Clearly, $\Pr(\epsilon) = \Pr(\epsilon|H_i)$, $i = 1, 2, \dots, 4$.) We also observe that the answer would be invariant to a 45° rotation of the signal set because the noise is circularly symmetric.

Thus, the problem of interest reduces to the simple diagram shown in Figure 7.21.

The $\Pr(\epsilon)$ is simply the probability that \mathbf{r} lies outside the first quadrant when H_1 is true.

Now r_1 and r_2 are independent Gaussian variables with identical means and variances:

$$E(r_1|H_1) = E(r_2|H_1) = \left(\frac{E}{2}\right)^{1/2} \quad (7.58)$$

and

$$\text{Var}(r_1|H_1) = \text{Var}(r_2|H_1) = \frac{N_0}{2}. \quad (7.59)$$

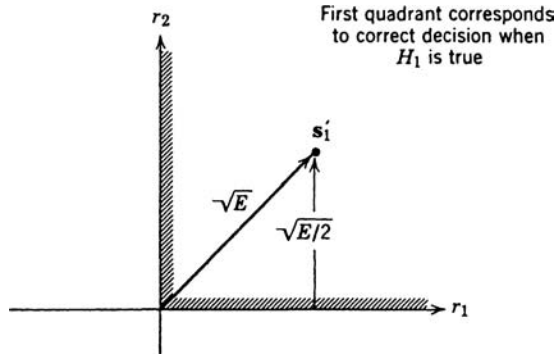


Figure 7.21: Rotation of signal.

The $\text{Pr}(\epsilon)$ can be obtained by integrating $p_{r_1, r_2 | H_1}(R_1, R_2 | H_1)$ over the area outside the first quadrant. Equivalently, $\text{Pr}(\epsilon)$ is the integral over the first quadrant subtracted from unity.

$$\text{Pr}(\epsilon) = 1 - \left[\int_0^\infty \left(2\pi \frac{N_0}{2} \right)^{-\frac{1}{2}} \exp\left(-\frac{(R_1 - \sqrt{E/2})^2}{N_0}\right) dR_1 \right]^2. \quad (7.60)$$

Changing variables, we have

$$\text{Pr}(\epsilon) = 1 - \left(\int_{-\sqrt{E/N_0}}^\infty \frac{1}{\sqrt{2\pi}} \exp\left(-\frac{x^2}{2}\right) dx \right)^2 = 1 - \left(\text{erfc}_* \left[-\left(\frac{E}{N_0}\right)^{\frac{1}{2}} \right] \right)^2, \quad (7.61)$$

which is the desired result. ■

Another example of interest is a generalization of Example 7.2.

Example 7.4. Let us assume that

$$H_i : r(t) = \sqrt{E}s_i(t) + w(t), \quad 0 \leq t \leq T, \quad i = 1, 2, \dots, M \quad (7.62)$$

and

$$\rho_{ij} = \delta_{ij}, \quad (7.63)$$

and the hypotheses are equally likely. Because the energies are equal, it is convenient to implement the LRT as a “greatest of” receiver as shown in Figure 7.22. Once again the problem is symmetric, so we may assume H_1 is true. Then an error occurs if any $l_j > l_1 : j \neq 1$, where

$$l_j \triangleq \int_0^T r(t)s_j(t) dt, \quad j = 1, 2, \dots, M.$$

Thus,

$$\text{Pr}(\epsilon) = \text{Pr}(\epsilon | H_1) = 1 - \text{Pr}(\text{all } l_j < l_1 : j \neq 1 | H_1) \quad (7.64)$$

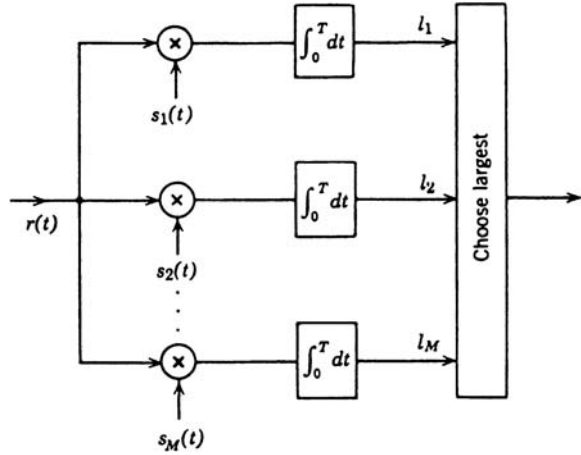


Figure 7.22: “Largest of” receiver.

or, noting that the $l_j (j \neq 1)$ have the same density on H_1 ,

$$\Pr(\epsilon) = 1 - \int_{-\infty}^{\infty} p_{l_1|H_1}(L_1|H_1) \left[\int_{-\infty}^{L_1} p_{l_2|H_1}(L_2|H_1) dL_2 \right]^{M-1} dL_1. \quad (7.65)$$

In this particular case, the densities are

$$p_{l_1|H_1}(L_1|H_1) = \frac{1}{\sqrt{\pi N_0}} \exp \left\{ -\frac{1}{2} \frac{(L_1 - \sqrt{E})^2}{N_0/2} \right\} \quad (7.66)$$

and

$$p_{l_j|H_1}(L_j|H_1) = \frac{1}{\sqrt{\pi N_0}} \exp \left\{ -\frac{1}{2} \frac{L_j^2}{N_0/2} \right\}, \quad j \neq 1. \quad (7.67)$$

Substituting these densities into (7.65) and normalizing the variables, we obtain

$$\Pr(\epsilon) = 1 - \int_{-\infty}^{\infty} dx \frac{1}{\sqrt{2\pi}} \exp \left\{ -\frac{[x - (2E/N_0)^{1/2}]^2}{2} \right\} \left(\int_{-\infty}^x \frac{1}{\sqrt{2\pi}} \exp \left[-\frac{y^2}{2} \right] dy \right)^{M-1}. \quad (7.68)$$

Unfortunately, we cannot integrate this analytically. Numerical results for certain values of M and E/N_0 are tabulated in [Urb55] and shown in Figure 7.23. For some of our purposes an *approximate* analytical expression is more interesting. We derive a very simple bound. Some other useful bounds are derived in the problems. Looking at (7.64), we see that we could rewrite the $\Pr(\epsilon)$ as

$$\Pr(\epsilon) = \Pr(\text{any } l_j > l_1 : j \neq 1 | H_1), \quad (7.69)$$

$$\Pr(\epsilon) = \Pr(l_2 > l_1 \text{ or } l_3 > l_1 \text{ or } \dots \text{ or } l_M > l_1 | H_1). \quad (7.70)$$

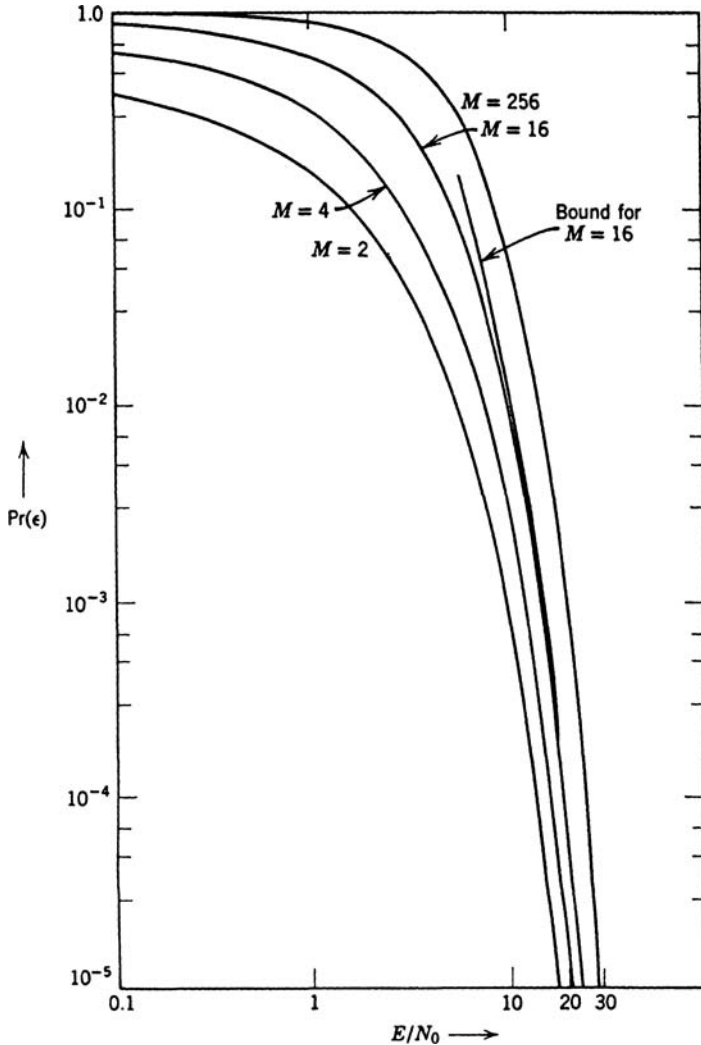


Figure 7.23: Error probability: M orthogonal signals.

Now, several l_j can be greater than l_1 . (The events are not mutually exclusive.) Thus,

$$\Pr(\epsilon) \leq \Pr(l_2 > l_1) + \Pr(l_3 > l_1) + \dots + \Pr(l_M > l_1), \quad (7.71a)$$

$$\Pr(\epsilon) \leq (M-1) \left\{ \int_{-\infty}^{\infty} \frac{1}{\sqrt{2\pi}} \exp \left[-\frac{(x - \sqrt{2E/N_0})^2}{2} \right] \left(\int_x^{\infty} \frac{1}{\sqrt{2\pi}} \exp \left(-\frac{y^2}{2} \right) dy \right) dx \right\}, \quad (7.71b)$$

but the term in the bracket is just the expression of the probability of error for two orthogonal signals. Using (7.40) with $\rho = 0$ and $E_1 = E_0 = E$ in (7.44), we have

$$\Pr(\epsilon) \leq (M-1) \int_{\sqrt{E/N_0}}^{\infty} \frac{1}{\sqrt{2\pi}} \exp\left(-\frac{y^2}{2}\right) dy. \quad (7.72a)$$

[Equation (7.72a) also follows directly from (7.71b) by a change of variables.] We can further simplify this equation by using (2.89):

$$\Pr(\epsilon) \leq \frac{(M-1)}{\sqrt{2\pi}\sqrt{E/N_0}} \exp\left(-\frac{E}{2N_0}\right). \quad (7.72b)$$

We observe that the upper bound increases linearly with M . The bound on the $\Pr(\epsilon)$ given by this expression is plotted in Figure 7.23 for $M = 16$. ■

A related problem in which M orthogonal signals arise is that of transmitting a sequence of binary digits.

Example 7.5. Sequence of digits. Consider the simple digital system shown in Figure 7.24, in which the source puts out a binary digit every T seconds. The outputs 0 and 1 are equally likely. The available transmitter power is P . For simplicity we assume that we are using orthogonal signals. The following choices are available:

1. Transmit one of two orthogonal signals every T seconds. The energy per signal is PT .
2. Transmit one of four orthogonal signals every $2T$ seconds. The energy per signal is $2PT$. For example, the encoder could use the mapping,

$$\begin{aligned} 00 &\rightarrow s_0(t), \\ 01 &\rightarrow s_1(t), \\ 10 &\rightarrow s_2(t), \\ 11 &\rightarrow s_3(t). \end{aligned}$$

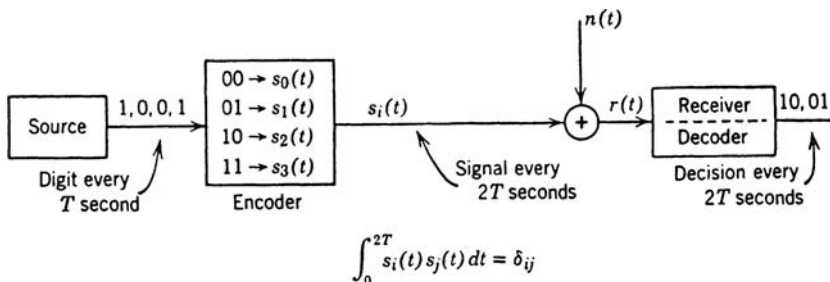


Figure 7.24: Digital communication system.

3. In general, we could transmit one of M orthogonal signals every $T \log_2 M$ seconds. The energy per signal is $TP \log_2 M$. To compute the probability of error, we use (7.68):

$$\begin{aligned} \Pr(\epsilon) &= 1 - \int_{-\infty}^{\infty} dx \frac{1}{\sqrt{2\pi}} \exp \left\{ -\frac{1}{2} \left[x - \left(\frac{2PT \log_2 M}{N_0} \right)^{\frac{1}{2}} \right]^2 \right\} \\ &\times \left[\int_{-\infty}^x \frac{1}{\sqrt{2\pi}} \exp \left(-\frac{y^2}{2} \right) dy \right]^{M-1}. \end{aligned} \quad (7.73)$$

The results have been calculated numerically [GBE⁺64] and are plotted in Figure 7.25. The behavior is quite interesting. Above a certain value of PT/N_0 the error probability decreases with increased M . Below this value the converse is true. It is instructive to investigate the behavior as $M \rightarrow \infty$. We obtain from (7.73), by a simple change of variables,

$$\lim_{M \rightarrow \infty} (1 - \Pr(\epsilon)) = \int_{-\infty}^{\infty} dy \frac{e^{-y^2/2}}{\sqrt{2\pi}} \lim_{M \rightarrow \infty} \left\{ \operatorname{erf}_*^{M-1} \left[y + \left(\frac{2PT \log_2 M}{N_0} \right)^{\frac{1}{2}} \right] \right\}. \quad (7.74)$$

Now consider the limit of the logarithm of the expression in the brace:

$$\lim_{M \rightarrow \infty} \frac{\ln \operatorname{erf}_* \left[y + \left(\frac{2PT \log_2 M}{N_0} \right)^{\frac{1}{2}} \right]}{(M-1)^{-1}}. \quad (7.75)$$

Evaluating the limit by treating M as a continuous variable and using L'Hospital's rule, we find that (see Problem 7.2.15)

$$\lim_{M \rightarrow \infty} \ln \approx \begin{cases} -\infty & \frac{PT}{N_0} < \ln 2, \\ 0 & \frac{PT}{N_0} > \ln 2. \end{cases} \quad (7.76)$$

Thus, from the continuity of logarithm,

$$\lim_{M \rightarrow \infty} \Pr(\epsilon) = \begin{cases} 0 & \frac{PT}{N_0} > \ln 2, \\ 1 & \frac{PT}{N_0} < \ln 2. \end{cases} \quad (7.77)$$

Thus, we see that there is a definite threshold effect. The value of T is determined by how fast the source produces digits. Specifically, the rate in binary digits per second is

$$R \triangleq \frac{1}{T} \text{ binary digits/s.} \quad (7.78)$$

Using orthogonal signals, we see that if

$$R < \frac{1}{\ln 2} \frac{P}{N_0}, \quad (7.79)$$

the probability of error will go to zero. The obvious disadvantage is the bandwidth requirement. As $M \rightarrow \infty$, the transmitted bandwidth goes to ∞ . ■

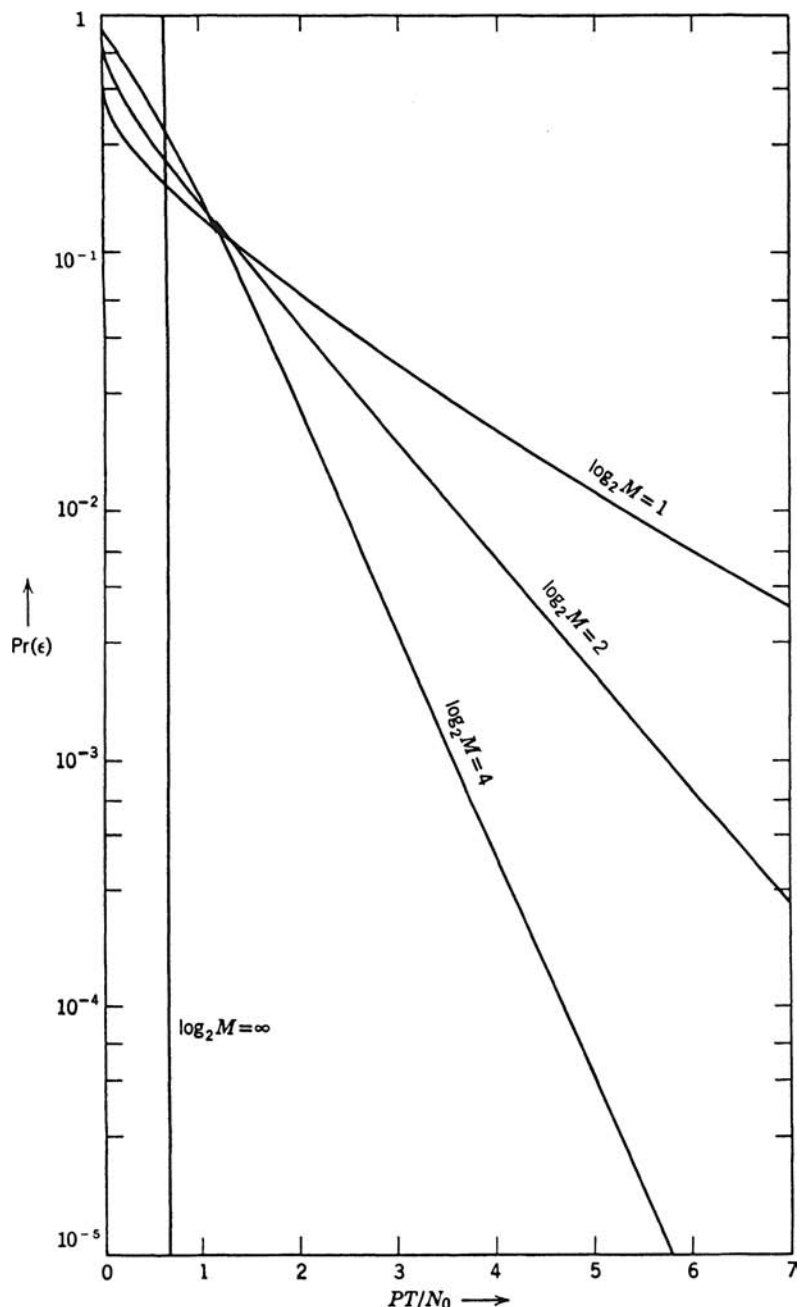


Figure 7.25: Probability of decision error: M orthogonal signals, power constraint.

The result in (7.79) was derived for a particular set of signals. Shannon has shown (e.g., [SW49] or [Sha49]) that the right-hand side is the bound on the rate for error-free transmission for any communication scheme. This rate is referred to as the capacity of an infinite bandwidth, additive white Gaussian noise channel,

$$C_{\infty} = \frac{1}{\ln 2} \frac{P}{N_0} \text{ bits/s.} \quad (7.80)$$

Shannon has also derived an expression for a bandlimited channel (W_{ch} : single sided):

$$C = W_{\text{ch}} \log_2 \left(1 + \frac{P}{W_{\text{ch}} N_0} \right). \quad (7.81)$$

These capacity expressions are fundamental to the problem of sending sequences of digits. We shall not consider this problem, for an adequate discussion would take us too far afield.

In this section, we have derived the canonic receiver structures for the M -ary hypothesis problem in which the received signal under each hypothesis is a known signal plus additive white Gaussian noise. The simplicity resulted because we were always able to reduce an infinite-dimensional observation space to a finite ($\leq M$) dimensional decision space.

In the problems we consider some of the implications of these results. Specific results derived in the problems include the following:

1. The probability of error for any set of M equally correlated signals can be expressed in terms of an equivalent set of M orthogonal signals (Problem 7.2.9).
2. The lowest value of uniform correlation is $-(M - 1)^{-1}$. Signals with this property are optimum when there is no bandwidth restriction (Problems 7.2.9–7.2.12). They are referred to as Simplex signals.
3. For large M , orthogonal signals are essentially optimum.

7.2.1.4 Sensitivity

Before leaving the problem of detection in the presence of white noise, we shall discuss an important issue that is frequently overlooked. We have been studying the mathematical model of a physical system and have assumed that we know the quantities of interest such as $s(t)$, E , and N_0 exactly. In an actual system these quantities will vary from their nominal values. It is important to determine how the performance of the optimum receiver will vary when the nominal values are perturbed. If the performance is highly sensitive to small perturbations, the validity of the nominal performance calculation is questionable. We shall discuss sensitivity in the context of the simple binary detection problem.

The model for this problem is

$$\begin{aligned} H_1 : r(t) &= \sqrt{E} s(t) + w(t), & 0 \leq t \leq T, \\ H_0 : r(t) &= w(t), & 0 \leq t \leq T. \end{aligned} \quad (7.82)$$

The receiver consists of a matched filter followed by a decision device. The impulse response of the matched filter depends on the shape of $s(t)$. The energy and noise levels affect the decision level in the general Bayes case. (In the Neyman–Pearson case only the noise level

affects the threshold setting.) There are several possible sensitivity analyses. Two of these are the following:

1. Assume that the actual signal energy and signal shape are identical to those in the model. Calculate the change in P_D and P_F due to a change in the white noise level.
2. Assume that the signal energy and the noise level are identical to those in the model. Calculate the change in P_D and P_F due to a change in the signal.

In both cases, we can approach the problem by first finding the change in d due to the changes in the model and then seeing how P_D and P_F are affected by a change in d . In this section, we shall investigate the effect of an inaccurate knowledge of signal shape on the value of d . The other questions mentioned above are left as an exercise. We assume that we have designed a filter that is matched to the assumed signal $s(t)$,

$$h(T-t) = s(t), \quad 0 \leq t \leq T, \quad (7.83)$$

and that the received waveform on H_1 is

$$r(t) = s_a(t) + w(t), \quad 0 \leq t \leq T, \quad (7.84)$$

where $s_a(t)$ is the actual signal received. There are two general methods of relating $s_a(t)$ to $s(t)$. We call the first the function-variation method.

Function-Variation Method. Let

$$s_a(t) = \sqrt{E} s(t) + \sqrt{E_\epsilon} s_\epsilon(t), \quad 0 \leq t \leq T, \quad (7.85)$$

where $s_\epsilon(t)$ is a normalized waveform representing the inaccuracy. The energy in the error signal is constrained to equal E_ϵ .

The effect can be most easily studied by examining the decision space (more precisely an augmented decision space). To include all of $s_\epsilon(t)$ in the decision space we *think* of adding another matched filter,

$$h_2(T-t) = \phi_2(t) = \frac{s_\epsilon(t) - \rho_\epsilon s(t)}{\sqrt{1 - \rho_\epsilon^2}}, \quad 0 \leq t \leq T, \quad (7.86)$$

where ρ_ϵ is the correlation between $s_\epsilon(t)$ and $s(t)$. (Observe that we do not do this physically.) We now have a two-dimensional space. The effect of the constraint is clear. Any $s_a(t)$ will lead to a point on the circle surrounding s , as shown in Figure 7.26. Observe that the decision still uses only the coordinate along $s(t)$. The effect is obvious. The error signal that causes the largest performance degradation is

$$s_\epsilon(t) = -s(t). \quad (7.87)$$

Then

$$d_a^2 = \frac{2}{N_0} \left(\sqrt{E} - \sqrt{E_\epsilon} \right)^2. \quad (7.88)$$

To state the result another way,

$$\frac{\Delta d}{d} = -\frac{\sqrt{2E_\epsilon/N_0}}{\sqrt{2E/N_0}} = -\left(\frac{E_\epsilon}{E}\right)^{1/2}, \quad (7.89)$$

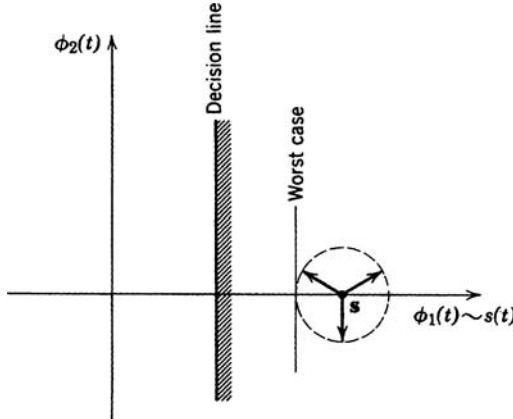


Figure 7.26: Signal locus: fixed energy in error signal.

where

$$\Delta d \triangleq d_a - d. \quad (7.90)$$

We see that small energy in the error signal implies a small change in performance. Thus, the test is insensitive to small perturbations. The second method is called the parameter-variation method.

Parameter-Variation Method. This method can best be explained by an example. Let

$$s(t) = \left(\frac{2}{T}\right)^{\frac{1}{2}} \sin \omega_c t, \quad 0 \leq t \leq T \quad (7.91)$$

be the nominal signal. The actual signal is

$$s_a(t) = \left(\frac{2}{T}\right)^{\frac{1}{2}} \sin(\omega_c t + \theta), \quad 0 \leq t \leq T, \quad (7.92)$$

which, for $\theta = 0$, corresponds to the nominal signal. The augmented decision space is shown in Figure 7.27. The vector corresponding to the actual signal moves on a circle around the origin.

$$d_a = \left(\frac{2E}{N_0}\right)^{\frac{1}{2}} \cos \theta, \quad (7.93)$$

and

$$\frac{\Delta d}{d} = -(1 - \cos \theta). \quad (7.94)$$

Once again we see that the test is insensitive to small perturbations.

The general conclusion that we can infer from these two methods is that the results of detection in the presence of white noise are insensitive to the detailed assumptions. In other words, small perturbations from the design assumptions lead to small perturbations in

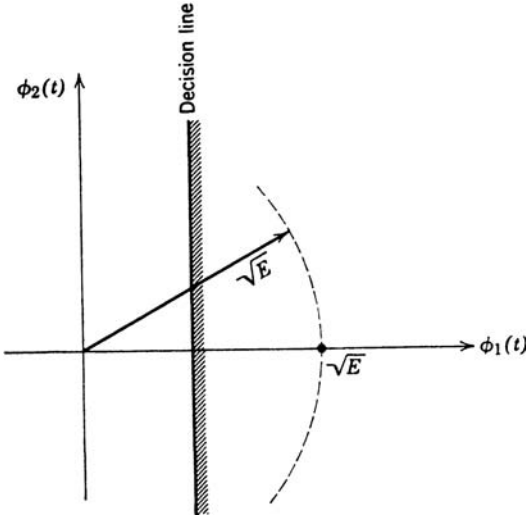


Figure 7.27: Signal locus: fixed energy in total signal.

performance. In almost all cases this type of insensitivity is necessary if the mathematical model is going to predict the actual system performance accurately.

Many statistical analyses tend to ignore this issue. The underlying reason is probably psychological. After we have gone through an involved mathematical optimization, it would be pleasant to demonstrate an order-of-magnitude improvement over the system designed by using an intuitive approach. Unfortunately, this does not always happen. When it does, we must determine whether the mathematical result is sensitive to some detailed assumption. In the sequel we shall encounter several examples of this sensitivity.

We now turn to the problem of linear estimation.

7.2.2 Linear Estimation

In Section 7.1.1, we formulated the problem of estimating signal parameters in the presence of additive noise. For the case of additive white noise the received waveform is

$$r(t) = s(t, A) + w(t), \quad 0 \leq t \leq T, \quad (7.95)$$

where $w(t)$ is a sample function from a white Gaussian noise process with spectral height $N_0/2$. The parameter A is the quantity we wish to estimate. If it is a random parameter we will assume that the *a priori* density is known and use a Bayes estimation procedure. If it is a nonrandom variable we will use ML estimates. The function $s(t, A)$ is a deterministic mapping of A into a time function. If $s(t, A)$ is a linear mapping (in other words, superposition holds), we refer to the system using the signal as a *linear signaling* (or *linear modulation*) system. Furthermore, for the criterion of interest the estimator will turn out to be linear so we refer to the problem as a *linear estimation* problem. In this section, we

study linear estimation and in Section 7.2.3, nonlinear estimation. A representative linear estimation problem is

$$r(t) = \sum_{j=1}^D A_j s_j(t) + w(t), \quad 0 \leq t \leq T, \quad (7.96)$$

where the $s_j(t)$ are linearly independent and have unit energy.

We can solve the linear estimation problem easily by exploiting its similarity to the detection problem that we just solved. We know that the likelihood function is needed. We recall, however, that the problem is greatly simplified if we can find a sufficient statistic and work with it instead of the received waveform. If we compare (7.96) and (7.8), it is clear that a sufficient statistic is

$$\begin{aligned} r_i &= \int_0^T r(t)s_i(t) dt \\ &= \int_0^T \sum_{j=1}^D A_j s_j(t)s_i(t) dt + w_i, \quad i = 1, 2, \dots, D, \end{aligned} \quad (7.97)$$

where the w_i are IID $N(0, N_0/2)$.

We define a $D \times D$ matrix \mathbf{V} ,

$$[\mathbf{V}]_{ij} \triangleq \int_0^T s_i(t)s_j(t) dt, \quad (7.98)$$

and a $D \times 1$ parameter vector \mathbf{A} ,

$$\mathbf{A} = [A_1 \ A_2 \ \cdots \ A_D]^T. \quad (7.99)$$

Then

$$\mathbf{r} = \mathbf{VA} + \mathbf{w}. \quad (7.100)$$

If \mathbf{A} is nonrandom, (7.100) is identical to (5.85) with $\mathbf{K} = \frac{N_0}{2}\mathbf{I}$. If \mathbf{A} is a random Gaussian vector then (7.100) is identical to (5.628) with $\mathbf{K} = \frac{N_0}{2}\mathbf{I}$. Therefore,

$$\hat{\mathbf{a}}_{\text{ml}} = [\mathbf{V}^T \ \mathbf{V}]^{-1} \mathbf{V}^T \mathbf{R}, \quad (7.101)$$

which is an unbiased efficient estimate, where the error covariance matrix is

$$\Lambda_\epsilon = \frac{N_0}{2} [\mathbf{V}^T \ \mathbf{V}]^{-1}.$$

Similarly,

$$\hat{\mathbf{a}}_{\text{map}} = \hat{\mathbf{a}}_{\text{ms}} = \mathbf{K}_a \mathbf{V}^T \left[\mathbf{V} \mathbf{K}_a \mathbf{V}^T + \frac{N_0}{2} \mathbf{I} \right]^{-1} \mathbf{R} \quad (7.102)$$

is a Bayesian efficient estimate whose MSE matrix is

$$\Sigma_\epsilon = \left[\mathbf{K}_a^{-1} + \frac{2}{N_0} \mathbf{V}^T \mathbf{V} \right]^{-1} \quad (7.103)$$

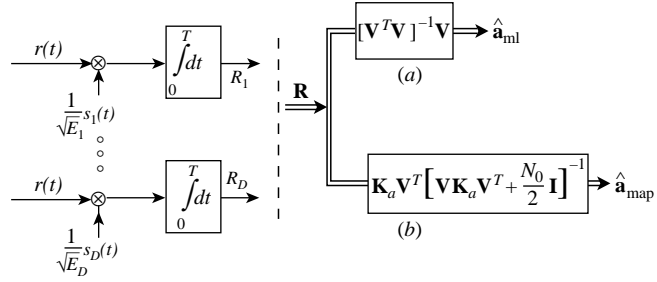


Figure 7.28: Optimum estimator: D signals in white Gaussian noise.

The receiver is shown in Figure 7.28. The only difference between the two receivers is the matrix gain.

For the case when the $s_i(t)$ are orthogonal with equal energy, $\mathbf{V} = \sqrt{E}\mathbf{I}$ and \mathbf{K}_a is $N(0, \sigma_a^2\mathbf{I})$

$$\hat{\mathbf{a}}_{ml} = \frac{1}{\sqrt{E}} \mathbf{R}, \quad (7.104)$$

$$\Lambda_\epsilon = \frac{N_0}{2E} \mathbf{I}, \quad (7.105)$$

$$\hat{\mathbf{a}}_{map} = \hat{\mathbf{a}}_{ms} = \frac{\sigma_a^2}{\sigma_a^2 + \frac{N_0}{2E}} \left(\frac{1}{\sqrt{E}} \mathbf{R} \right), \quad (7.106)$$

and

$$\Sigma_\epsilon = \left(\frac{1}{\sigma_a^2} + \frac{2E}{N_0} \right)^{-1} \mathbf{I}. \quad (7.107)$$

In both cases, we see that the only way to decrease the mean-square error is to increase the energy-to-noise ratio. In many situations the available energy-to-noise ratio is not adequate to provide the desired accuracy. In these situations we try a nonlinear signaling scheme in an effort to achieve the desired accuracy. In the next section, we discuss the nonlinear estimation.

Before leaving linear estimation, we should point out that the MAP estimate is also the Bayes estimate for a large class of criteria. Whenever \mathbf{a} is Gaussian, the *a posteriori* density is Gaussian. This invariance to criterion depends directly on the linear signaling model.

7.2.3 Nonlinear Estimation

The system in Figure 7.7 illustrates a typical nonlinear estimation problem. The received signal is

$$r(t) = s(t, A) + w(t), \quad 0 \leq t \leq T. \quad (7.108)$$

From our results in the classical case we know that a sufficient statistic does not exist in general. As before, we can construct the likelihood function. We approach the problem by making a K -coefficient approximation to $r(t)$. By proceeding as in Section 7.2.1 with

obvious notation, we have

$$\Lambda [r_K(t), A] = p_{\mathbf{r}|a}(\mathbf{R}|A) = \prod_{i=1}^K \frac{1}{\sqrt{\pi N_0}} \exp \left(-\frac{1}{2} \frac{[R_i - s_i(A)]^2}{N_0/2} \right), \quad (7.109)$$

where

$$s_i(A) \triangleq \int_0^T s(t, A) \phi_i(t) dt.$$

Now, if we let $K \rightarrow \infty$, $\Lambda [r_K(t), A]$ is not well defined. We recall from Chapter 2 that we can divide a likelihood function by anything that does not depend on A and still have a likelihood function. In Section 7.2.1, we avoided the convergence problem by dividing by

$$p_{r_K(t)|H_0}(r_K(t)|H_0) = \prod_{i=1}^K \frac{1}{\sqrt{\pi N_0}} \exp \left(-\frac{1}{2} \frac{R_i^2}{N_0/2} \right),$$

before letting $K \rightarrow \infty$. Because this function does not depend on A , it is legitimate to divide by it here. Define

$$\Lambda_1 [r_K(t), A] = \frac{\Lambda [r_K(t), A]}{p_{r_K(t)|H_0}(r_K(t)|H_0)}. \quad (7.110)$$

Substituting into this expression, canceling common terms, letting $K \rightarrow \infty$, and taking the logarithm we obtain

$$\ln \Lambda_1[r(t), A] = \frac{2}{N_0} \int_0^T r(t) s(t, A) dt - \frac{1}{N_0} \int_0^T s^2(t, A) dt. \quad (7.111)$$

To find \hat{a}_{ml} we must find the absolute maximum of this function. To find \hat{a}_{map} , we add $\ln p_a(A)$ to (7.111) and find the absolute maximum. The basic operation on the received data consists of generating the first term in (7.111) as a function of A . The physical device that we actually use to accomplish it will depend on the functional form of $s(t, A)$. We shall consider some specific cases and find the actual structure.

Before doing so we shall derive a result for the general case that will be useful in the sequel. Observe that if the maximum is interior and $\ln \Lambda_1(A)$ is differentiable at the maximum, then a necessary, but not sufficient, condition is obtained by first differentiating (7.111):

$$\frac{\partial \ln \Lambda_1(A)}{\partial A} = \frac{2}{N_0} \int_0^T [r(t) - s(t, A)] \frac{\partial s(t, A)}{\partial A} dt \quad (7.112)$$

(assuming that $s(t, A)$ is differentiable with respect to A). For \hat{a}_{ml} , a necessary condition is obtained by setting the right-hand side of (7.112) equal to zero. For \hat{a}_{map} , we add $d \ln p_a(A)/dA$ to the right-hand side of (7.112) and set the sum equal to zero. In the special

case in which $p_a(A)$ is Gaussian, $N(0, \sigma_a)$, we obtain

$$\hat{a}_{\text{map}} = \frac{2\sigma_a^2}{N_0} \int_0^T [r(t) - s(t, A)] \frac{\partial s(t, A)}{\partial A} dt \Big|_{A=\hat{a}_{\text{map}}}. \quad (7.113)$$

In the linear case (7.113) gives a unique solution. A number of solutions may exist in the nonlinear case and we must examine the sum of (7.111) and $\ln p_a(A)$ to guarantee an absolute maximum.

However, just as in Chapter 4, (7.112) enables us to find a bound on the variance of any unbiased estimate of a nonrandom variable and the addition of $d^2 \ln p_a(A)/dA^2$ leads to a bound on the mean-square error in estimating a random variable. For nonrandom variables we differentiate (7.112) and take the expectation

$$E \left[\frac{\partial^2 \ln \Lambda_1(A)}{\partial A^2} \right] = \frac{2}{N_0} \left\{ E \int_0^T [r(t) - s(t, A)] \frac{\partial^2 s(t, A)}{\partial A^2} dt - E \int_0^T \left[\frac{\partial s(t, A)}{\partial A} \right]^2 dt \right\}, \quad (7.114)$$

where we assume the derivatives exist. In the first term, we observe that

$$E[r(t) - s(t, A)] = E[w(t)] = 0. \quad (7.115)$$

In the second term, there are no random quantities; therefore, the expectation operation gives the integral itself.

Substituting into (4.96), we have

$$\text{Var}(\hat{a} - A) \geq \frac{N_0}{2 \int_0^T \left[\frac{\partial s(t, A)}{\partial A} \right]^2 dt} \quad (7.116)$$

for any unbiased estimate \hat{a} . Equality holds in (7.116) if and only if

$$\frac{\partial \ln \Lambda_1(A)}{\partial A} = k(A) \{\hat{a}[r(t)] - A\} \quad (7.117)$$

for all A and $r(t)$. Comparing (7.112) and (7.117), we see that this will hold only for linear modulation. Then \hat{a}_{ml} is the minimum variance estimate.

Similarly, for random variables

$$E[\hat{a} - a]^2 \geq \left(E_a \left\{ \frac{2}{N_0} \int_0^T \left[\frac{\partial s(t, A)}{\partial A} \right]^2 dt - \frac{d^2 \ln p_a(A)}{dA^2} \right\} \right)^{-1}, \quad (7.118)$$

where E_a denotes an expectation over the random variable a . Defining

$$\gamma_a^2 \triangleq E_a \int_0^T \left[\frac{\partial s(t, A)}{\partial A} \right]^2 dt, \quad (7.119)$$

we have

$$E(\hat{a} - a)^2 \geq \left(\frac{2}{N_0} \gamma_a^2 - E_a \left[\frac{d^2 \ln p_a(A)}{dA^2} \right] \right)^{-1}. \quad (7.120)$$

Equality will hold if and only if (see 4.185)

$$\frac{\partial^2 \ln \Lambda_1(A)}{\partial A^2} + \frac{d^2 \ln p_a(A)}{dA^2} = \text{constant}. \quad (7.121)$$

Just as in Chapter 4, in order for (7.121) to hold it is necessary and sufficient that $p_{a|r(t)}(A|r(t)), 0 \leq t \leq T$ be a Gaussian probability density. This requires a linear signaling scheme and a Gaussian *a priori* density.

What is the value of the bound if it is satisfied only for linear signaling schemes?

As in the classical case, it has two principal uses:

1. It always provides a lower bound.
2. In many cases, the actual variance (or mean-square error) in a nonlinear signaling scheme will approach this bound under certain conditions. These cases are the analogs to the *asymptotically efficient* estimates in the classical problem. We shall see that they correspond to large E/N_0 values.

To illustrate some of the concepts in the nonlinear case, we consider two simple examples.

Example 7.6. Let $s(t)$ be the pulse shown in Figure 7.29a. The parameter a is the arrival time of the pulse. We want to find a MAP estimate of a . We know a range of values χ_a that a may assume (Figure 7.29b). Inside this range the probability density is uniform. For simplicity we let the observation interval $[-T, T]$ be long enough to completely contain the pulse.

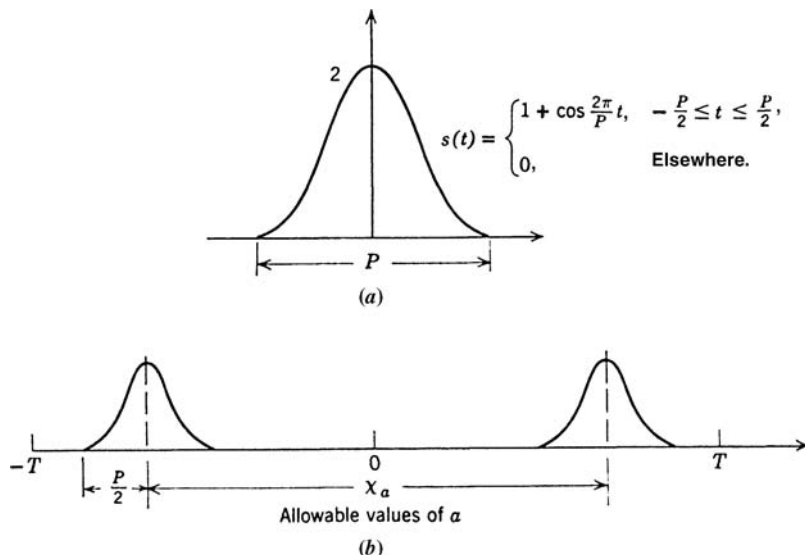


Figure 7.29: (a) Pulse shape; (b) allowable parameter range.

From (7.111) we know that the operation on the received waveform consists of finding $\ln \Lambda_1[r(t), A]$. Here

$$\ln \Lambda_1[r(t), A] = \frac{2}{N_0} \int_{-T}^T r(u)s(u - A) du - \frac{1}{N_0} \int_{-T}^T s^2(u - A) du. \quad (7.122)$$

For this particular case the second term does not depend on A , for the entire pulse is always in the interval. The first term is a convolution operation. The output of a linear filter with impulse response $h(\tau)$ and input $r(u)$ over the interval $[-T, T]$ is

$$y(t) = \int_{-T}^T r(u)h(t-u) du, \quad -T \leq t \leq T. \quad (7.123)$$

Clearly, if we let

$$h(\tau) = s(-\tau), \quad (7.124)$$

the output as a function of time over the range x_a will be identical to the likelihood function as a function of A . We simply pick the peak of the filter output as a function of time. The time at which the peak occurs is \hat{a}_{map} . The filter is the matched filter that we have already encountered in the detection problem.

In Figure 7.30, we indicate the receiver structure. The output due to the signal component is shown in line (a). Typical total outputs for three noise levels are shown in lines (b), (c), and (d). In line (b) we see that the peak of $\ln \Lambda(A)$ is large compared to the noise background. The actual peak is near the correct peak, and we can expect that the error will be accurately predicted by using the expression in (7.120). In line (c), the noise has increased and large subsidiary peaks that have no relation to the correct value of A are starting to appear. Finally, in line (d) the noise has reached the point at which the maximum bears no relation to the correct value. Thus two questions are posed:

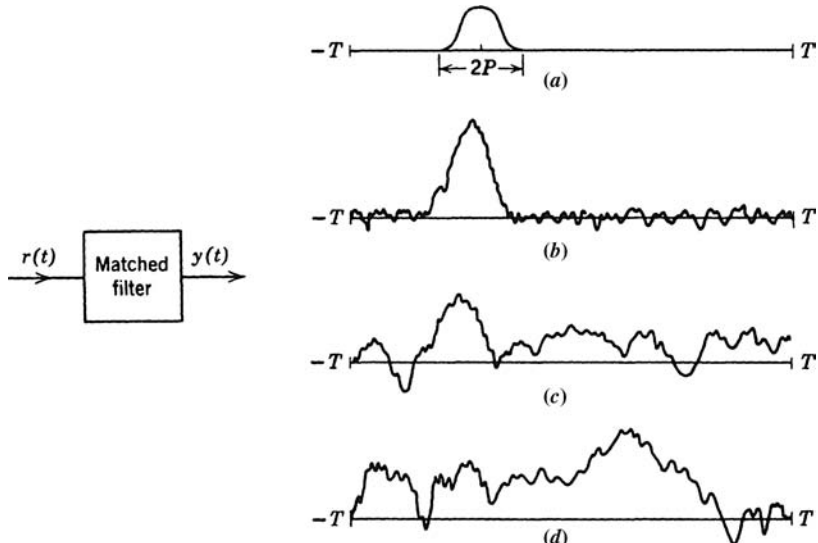


Figure 7.30: Receiver outputs [arrival time estimation]: (a) signal component; (b) low-noise level; (c) moderate-noise level; (d) high-noise level.

1. Under what conditions does the lower bound given by (7.120) accurately predict the error?
2. How can one predict performance when (7.120) is not useful? ■

Before answering these questions, we consider a second example to see if similar questions arise.

Example 7.7. Another common example of a nonlinear signaling technique is discrete frequency modulation (also referred to as pulse frequency modulation, PFM). Every T seconds the source generates a new value of the parameter a . The transmitted signal is $s(t, A)$, where

$$s(t, A) = \left(\frac{2E}{T} \right)^{\frac{1}{2}} \sin(\omega_c + \beta A)t, \quad -\frac{T}{2} \leq t \leq \frac{T}{2}. \quad (7.125)$$

Here ω_c is a known carrier frequency, β is a known constant, and E is the transmitted energy (also the received signal energy). We assume that $p_a(A)$ is a uniform variable over the interval $(-\sqrt{3}\sigma_a, \sqrt{3}\sigma_a)$.

To find \hat{a}_{map} , we construct the function indicated by the first term in (7.111) (The second term in (7.111) and the *a priori* density are constant and may be discarded.)

$$l_1(A) = \begin{cases} \int_{-T/2}^{T/2} r(t) \sin(\omega_c t + \beta At) dt, & -\sqrt{3}\sigma_a \leq A \leq \sqrt{3}\sigma_a, \\ 0, & \text{Elsewhere.} \end{cases} \quad (7.126)$$

One way to construct $l_1(A)$ would be to record $r(t)$ and perform the multiplication and integration indicated by (7.126) for successive values of A over the range. This is obviously a time-consuming process. An alternate approach² is to divide the range into increments of length Δ and perform the parallel processing operation shown in Figure 7.31 for discrete values of A :

$$\begin{aligned} A_1 &= -\sqrt{3}\sigma_a + \frac{\Delta}{2}, \\ A_2 &= -\sqrt{3}\sigma_a + \frac{3\Delta}{2}, \\ &\vdots \\ A_M &= -\sqrt{3}\sigma_a + \left(m - \frac{1}{2} \right) \Delta, \end{aligned} \quad (7.127a)$$

where

$$M = \left\lfloor \frac{2\sqrt{3}\sigma_a}{\Delta} + \frac{1}{2} \right\rfloor, \quad (7.127b)$$

and

$\lfloor \cdot \rfloor$ denotes the largest integer smaller than or equal to the argument. The output of this preliminary processing is M numbers. We choose the largest and assume that the correct value of A is in that region.

²This particular type of approach and the resulting analysis were first done by Woodward (radar range measurement [Woo55]) and Kotelnikov (PPM and PFM [Kot59]). Subsequently, they have been used with various modifications by a number of authors (e.g., Darlington [Dar64], Akima [Aki63], Wozencraft and Jacobs [WJ65], Wainstein and Zubakov [WZ62]). Our approach is similar to [WJ65]. A third way to estimate A is discussed in [Dar64].

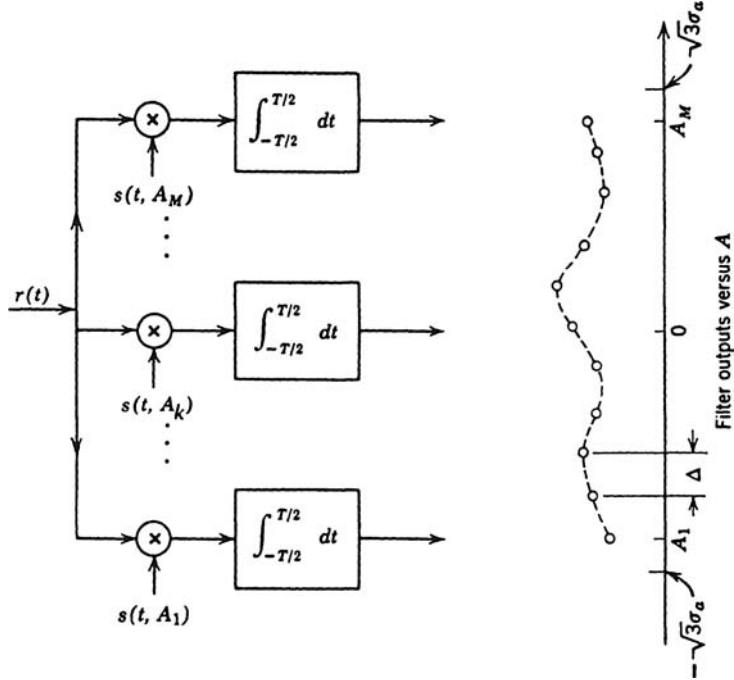


Figure 7.31: Receiver structure (frequency estimation).

To get the final estimate we conduct a local maximization by using the condition

$$\int_{-T/2}^{T/2} [r(t) - s(t, A)] \frac{\partial s(t, A)}{\partial A} dt \Big|_{A=\hat{a}_{\text{map}}} = 0. \quad (7.127c)$$

(This assumes the maximum is interior.)

A possible way to accomplish this maximization is given in the block diagram in Figure 7.32. We expect that if we chose the correct interval in our preliminary processing the final accuracy would be closely approximated by the bound in (7.116). This bound can be evaluated easily. The partial derivative of the signal is

$$\frac{\partial s(t, A)}{\partial A} = \left(\frac{2E}{T} \right)^{1/2} \beta t \cos(\omega_c t + \beta A t), \quad -T/2 \leq t \leq T/2 \quad (7.128)$$

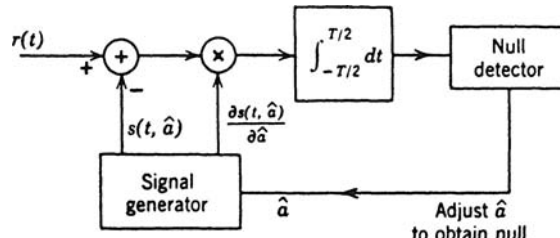


Figure 7.32: Local estimator.

and

$$\gamma_a^2 = \frac{2E}{T} \beta^2 \int_{-T/2}^{T/2} \overline{t^2 \cos^2(\omega_c t + \beta A t)} dt \simeq \frac{ET^2}{12} \beta^2, \quad (7.129)$$

when

$$T \gg \frac{1}{\omega_c}.$$

Then the normalized mean-square error of any estimate is bounded by

$$\sigma_{a,n}^2 \triangleq \frac{\sigma_\epsilon^2}{\sigma_d^2} \geq \frac{N_0}{2\gamma_a^2 \sigma_d^2} = \frac{12}{T^2} \frac{N_0}{2E} \frac{1}{\beta^2} \frac{1}{\sigma_d^2}, \quad (7.130)$$

which seems to indicate that, regardless of how small E/N_0 is, we can make the mean-square error arbitrarily small by increasing β . Unfortunately, this method neglects an important part of the problem. How is the probability of an initial interval error affected by the value of β ?

With a few simplifying assumptions we can obtain an approximate expression for this probability. We denote the actual value of A as A_a . (This subscript is necessary because A is the argument in our likelihood function.) A plot of

$$\frac{1}{E} \int_{-T/2}^{T/2} s(t, A_a) s(t, A) dt$$

for the signal in (7.125) as a function of $A_x \triangleq A - A_a$ is given in Figure 7.33. (The double frequency term is neglected.) We see that the signal component of $l_1(A)$ passes through zero every $2\pi/\beta T$ units. This suggests that a logical value of Δ is $2\pi/\beta T$.

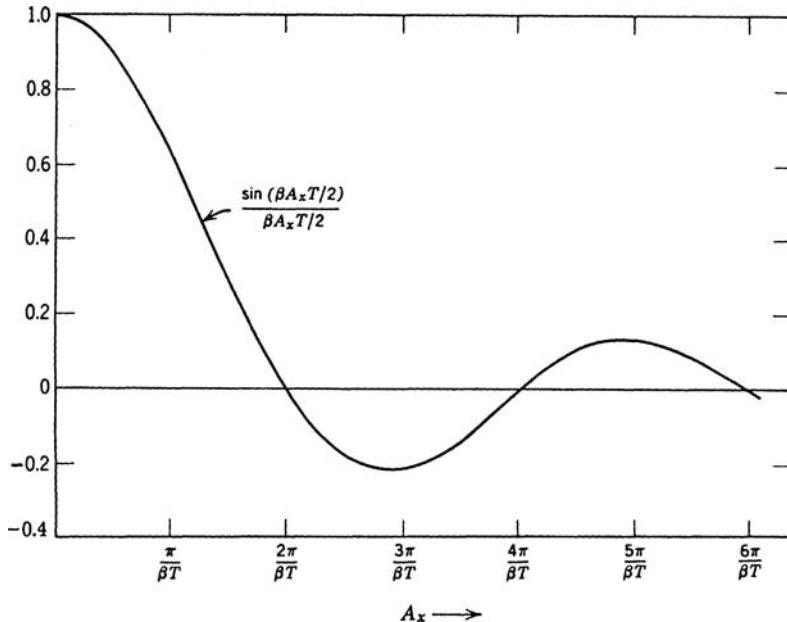


Figure 7.33: Signal component versus A_x .

To calculate the probability of choosing the wrong interval we use the approximation that we can replace all A in the first interval by A_1 and so forth. We denote the probability of choosing the wrong interval as $\Pr(\epsilon_I)$. With this approximation the problem is reduced to detect which of M orthogonal, equal energy signals is present. For large M , we neglect the residual at the end of the interval and let

$$M \cong \sqrt{3}\sigma_a\beta \frac{T}{\pi}, \quad (7.131)$$

but this is a problem we have already solved (7.72a). Because large βT is the case of interest, we may use the approximate expression in (7.72b):

$$\Pr(\epsilon_I) \leq \frac{(\sqrt{3}\sigma_a\beta T/\pi - 1)}{\sqrt{2\pi E/N_0}} \exp\left(-\frac{E}{2N_0}\right). \quad (7.132a)$$

We see that as $\sigma_a\beta T$ increases the probability that we will choose the wrong interval also increases³. The conclusion that can be inferred from this result is of fundamental importance in the nonlinear estimation problem.

For a fixed E/N_0 and T we can increase β so that the local error will be arbitrarily small if the receiver has chosen the correct interval. As β increases, however, the probability that we will be in the correct interval goes to zero. Thus, for a particular β , we must have some minimum E/N_0 to ensure that the probability of being in the wrong interval is adequately small.

The expression in (7.132a) suggests the following design procedure. We decide that a certain $\Pr(\epsilon_I)$ (say p_0) is acceptable. In order to minimize the mean-square error subject to this constraint we choose β such that (7.132a) is satisfied with equality. Substituting p_0 into the left-hand side of (7.132a), solving for $\sigma_a\beta T$, and substituting the result in (121), we obtain⁴

$$\frac{E[a_\epsilon^2]}{\sigma_a^2} = \sigma_{a_\epsilon n}^2 \simeq \frac{1}{p_0^2} \frac{9}{\pi^3} \left(\frac{N_0}{E}\right)^2 e^{-E/N_0}. \quad (7.132b)$$

The reciprocal of the normalized mean-square error as a function of E/N_0 for typical values of p_0 is shown in Figure 7.34. For reasons that will become obvious shortly, we refer to the constraint imposed by (7.132a) as a threshold constraint.

The result in (7.132a) indicates one effect of increasing β . A second effect can be seen directly from (7.125). Each value of A shifts the frequency of the transmitted signal from ω_c to $\omega_c + \beta A$. Therefore, we must have enough bandwidth available in the channel to accommodate the maximum possible frequency excursion. The pulse bandwidth is approximately $2\pi/T$ rad/s. The maximum frequency shift is $\pm\sqrt{3}\beta\sigma_a$. Therefore, the required channel bandwidth centered at ω_c is approximately

$$2\pi W_{ch} \cong 2\sqrt{3}\beta\sigma_a + \frac{2\pi}{T} = \frac{1}{T}(2\sqrt{3}\beta\sigma_a T + 2\pi) \quad (7.133)$$

When $\sigma_a\beta T$ is large we can neglect the 2π and use the approximation

$$2\pi W_{ch} \simeq 2\sqrt{3}\beta\sigma_a. \quad (7.134)$$

In many systems of interest we have only a certain bandwidth available. (This bandwidth limitation may be a legal restriction or may be caused by the physical nature of the channel.) If we assume that E/N_0 is large enough to guarantee an acceptable $\Pr(\epsilon_I)$, then (7.134) provides the constraint of the system design. We simply increase β until the available bandwidth is occupied. To find the mean-square error using this design procedure we substitute the expression for $\beta\sigma_a$ in (7.134) into

³This probability is sometimes referred to as the probability of anomaly or ambiguity.

⁴Equation (7.132b) is an approximation, for (7.132a) is a bound and we neglected the 1 in the parentheses because large βT is the case of interest.

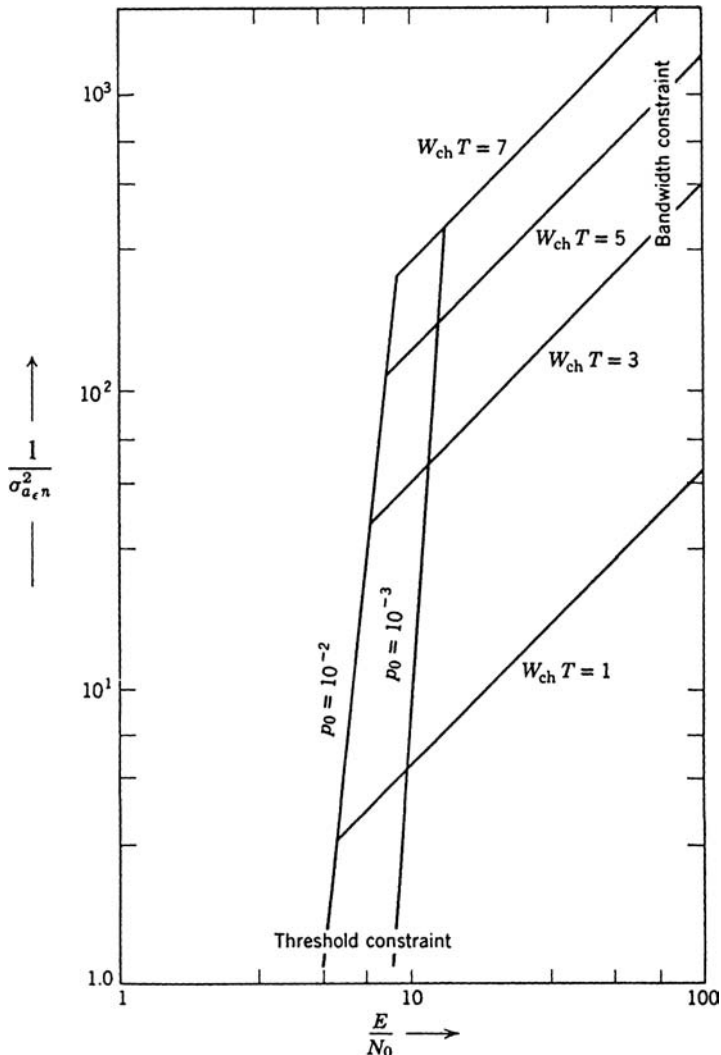


Figure 7.34: Reciprocal of the mean-square error under threshold and bandwidth constraints.

(7.130) and obtain

$$\frac{E[a_\epsilon^2]}{\sigma_a^2} = \sigma_{a_{\epsilon n}}^2 = \frac{18 N_0}{\pi^2} \frac{1}{E} \frac{1}{(W_{ch}T)^2} \quad (\text{bandwidth constraint}). \quad (7.135)$$

We see that the two quantities that determine the mean-square error are E/N_0 , the energy-to-noise ratio, and $W_{ch}T$, which is proportional to the time-bandwidth product of the transmitted pulse. The reciprocal of the normalized mean-square error is plotted in Figure 7.34 for typical values of $W_{ch}T$.

The two families of constraint lines provide us with a complete design procedure for a PFM system. For low values of E/N_0 the threshold constraint dominates. As E/N_0 increases, the MMSE moves along a fixed p_0 line until it reaches a point where the available bandwidth is a constraint. Any further increase in E/N_0 moves the MMSE along a fixed β line.

The approach in which we consider two types of error separately is useful and contributes to our understanding of the problem. To compare the results with other systems it is frequently convenient to express them as a single number, the overall mean-square error.

We can write the mean-square error as

$$\begin{aligned} E(a_\epsilon^2) = \sigma_{\epsilon_T}^2 &= E[a_\epsilon^2|\text{interval error}] \Pr(\text{interval error}) \\ &\quad + E[a_\epsilon^2|\text{no interval error}] \Pr(\text{no interval error}). \end{aligned} \quad (7.136)$$

We obtained an approximation to $\Pr(\epsilon_I)$ by collecting each incremental range of A at a single value A_I . With this approximation there is no signal component at the other correlator outputs in Figure 7.31. Thus, if an interval error is made, it is equally likely to occur in any one of the wrong intervals. Therefore, the resulting estimate \hat{a} will be uncorrelated with a .

$$\begin{aligned} E[a_\epsilon^2|\text{interval error}] &= E[(\hat{a} - a)^2|\text{interval error}] \\ &= E[\hat{a}^2|\text{interval error}] + E[a^2|\text{interval error}] - 2E[\hat{a}a|\text{interval error}]. \end{aligned} \quad (7.137)$$

Our approximation makes the last term zero. The first two terms both equal σ_a^2 . Therefore,

$$E[a_\epsilon^2|\text{interval error}] = 2\sigma_a^2. \quad (7.138)$$

If we assume that p_0 is fixed, we then obtain by using (7.132b) and (7.138) in (7.137)

$$\sigma_{\epsilon_Tn}^2 = \frac{E(a_\epsilon^2)}{\sigma_a^2} = 2p_0 + (1 - p_0) \frac{9}{\pi^3 p_0^2} \left(\frac{N_0}{E} \right)^2 e^{-E/N_0}. \quad (7.139)$$

In this case, the modulation index β must be changed as E/N_0 is changed. For a fixed β , we use (7.130) and (7.132a) to obtain

$$\sigma_{\epsilon_Tn}^2 = \frac{12}{(\sigma_a \beta t)^2} \frac{N_0}{2E} \left[1 - \frac{\sqrt{3}\sigma_a \beta T / \pi}{\sqrt{2\pi E / N_0}} e^{-E/2N_0} \right] + 2 \frac{\sqrt{3}\sigma_a \beta T / \pi}{\sqrt{2\pi E / N_0}} e^{-E/2N_0}. \quad (7.140)$$

The result in (7.140) is plotted in Figure 7.35, and we see that the mean-square error exhibits a definite threshold. The reciprocal of the normalized mean-square error for a PAM system is also shown in Figure 7.35 (from (7.107)). The magnitude of this improvement can be obtained by dividing (7.130) by (7.107).

$$\frac{\sigma_{a_{en}|\text{PFM}}^2}{\sigma_{a_{en}|\text{PAM}}^2} \cong \frac{12}{\beta^2 T^2}, \quad \frac{2\sigma_a^2 E}{N_0} \gg 1. \quad (7.141)$$

Thus, the improvement obtained from PFM is proportional to the square of βT . It is important to re-emphasize that this result assumes E/N_0 is such that the system is above threshold. If the noise level should increase, the performance of the PFM system can decrease drastically. ■

Our approach in this particular example is certainly plausible. We see, however, that it relies on a two-step estimation procedure. In discrete frequency modulation this procedure was a natural choice because it was also a logical practical implementation. In the Example 7.6, there was no need for the two-step procedure. However, in order to obtain a parallel set of results for Example 7.6 we can carry out an analogous two-step analysis and similar results. Experimental studies of both types of systems indicate that the analytical results correctly describe system performance. It would still be desirable to have a more rigorous analysis.

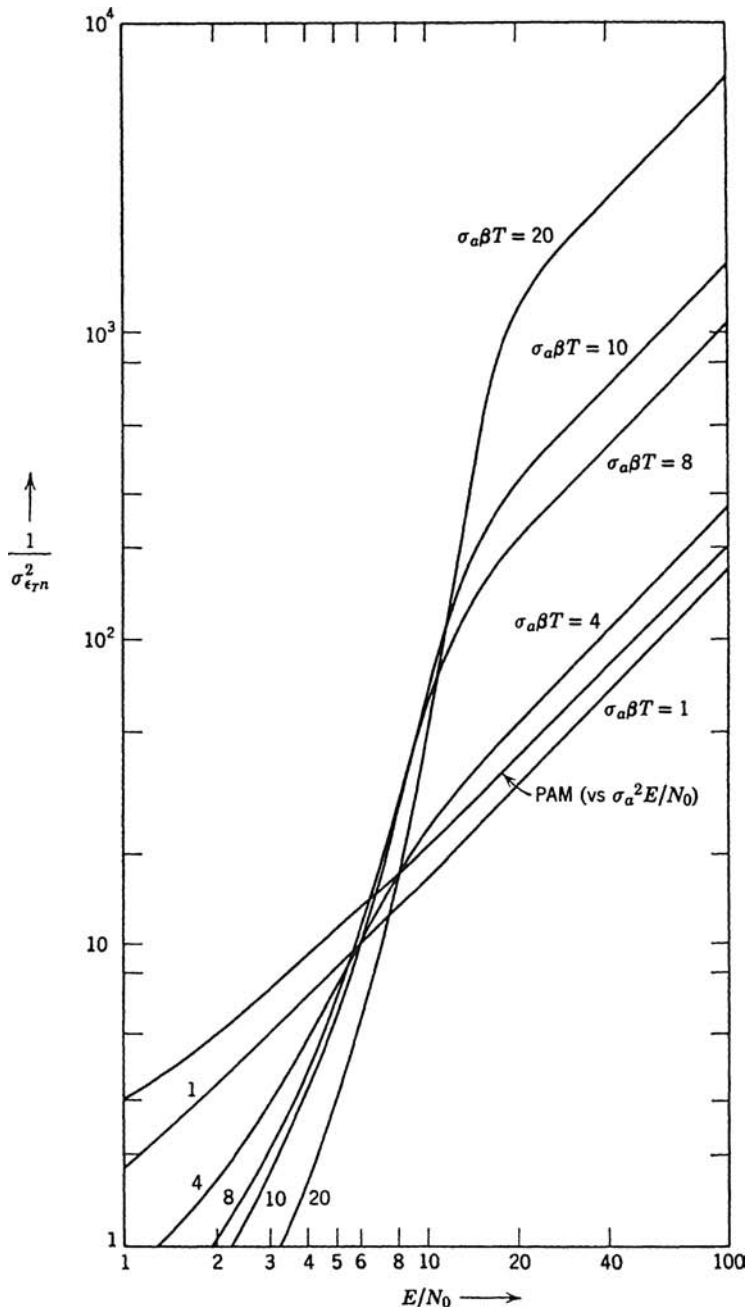


Figure 7.35: Reciprocal of the total mean-square error.

One final comment is necessary. There are some cases of interest in which the signal is not differentiable with respect to the parameter. A simple example of this type of signal arises when we approximate the transmitted signal in a radar system by an ideal rectangular pulse and want to estimate the time of arrival of the returning pulse. When the noise is weak,

formulas for these cases can be developed easily (e.g., [MS54, Kot59, Man55, Sko62]). For arbitrary noise levels we can use the global Bayesian bounds developed in Chapter 4.

7.2.4 Summary of Known Signals in White Gaussian Noise

It is appropriate to summarize some of the important results that have been derived for the problem of detection and estimation in the presence of additive white Gaussian noise.

7.2.4.1 Detection

1. For the simple binary case, the optimum receiver can be realized as a matched filter or a correlation receiver, as shown in Figures 7.11 and 7.12, respectively.
2. For the general binary case, the optimum receiver can be realized by using a single matched filter or a pair of filters.
3. In both cases, the performance is determined completely by the normalized distance d between the signal points in the decision space,

$$d^2 = \frac{2}{N_0} (E_1 + E_0 - 2\rho\sqrt{E_1 E_0}). \quad (7.142)$$

The resulting errors are

$$P_F = \operatorname{erfc}_* \left(\frac{\ln \eta}{d} + \frac{d}{2} \right), \quad (7.143)$$

$$P_M = \operatorname{erfc}_* \left(\frac{\ln \eta}{d} - \frac{d}{2} \right). \quad (7.144)$$

For equally likely hypotheses and a minimum $\Pr(\epsilon)$ criterion, the total error probability is

$$\Pr(\epsilon) = \operatorname{erfc}_* \left(\frac{d}{2} \right) \leq \left(\frac{2}{\pi d^2} \right)^{\frac{1}{2}} e^{-d^2/8}. \quad (7.145)$$

4. The performance of the optimum receiver is insensitive to small-signal variations.
5. For the M -ary case, the optimum receiver requires at most $M - 1$ matched filters, although frequently M matched filters give a simpler implementation. For M orthogonal signals a simple bound on the error probability is

$$\Pr(\epsilon) \leq \frac{M-1}{\sqrt{2\pi(E/N_0)}} \exp \left(-\frac{E}{2N_0} \right). \quad (7.146)$$

6. A simple example of transmitting a sequence of digits illustrated the idea of a channel capacity. At transmission rates below this capacity the $\Pr(\epsilon)$ approaches zero as the length of encoded sequence approaches infinity. Because of the bandwidth requirement, the orthogonal signal technique is not efficient.

7.2.4.2 Estimation

1. Linear estimation is a trivial modification of the detection problem. The optimum estimator is a set of correlators or matched filters followed by a matrix multiplication.

2. The nonlinear estimation problem introduced several new ideas. The optimum receiver is sometimes difficult to realize exactly and an approximation is necessary. Above a certain energy-to-noise level we found that we could make the estimation error appreciably smaller than in the linear estimation case that used the same amount of energy. Specifically,

$$\text{Var}[\hat{a} - A] \approx \frac{N_0/2}{\int_0^T \left[\frac{\partial s(t, A)}{\partial A} \right]^2 dt}. \quad (7.147)$$

As the noise level increased however, the receiver exhibited a *threshold* phenomenon and the error variance increased rapidly. Above the threshold we found that we had to consider the problem of a bandwidth constraint when we designed the system.

We now want to extend our model to a more general case. The next step in the direction of generality is to consider known signals in the presence of nonwhite additive Gaussian noise.

7.3 DETECTION AND ESTIMATION IN NONWHITE GAUSSIAN NOISE

Several situations in which nonwhite Gaussian interference can occur are of interest:

1. Between the actual noise source and the data-processing part of the receiver are elements (such as an antenna and RF filters) that shape the noise spectrum.
2. In addition to the desired signal at the receiver, there may be an interfering signal that can be characterized as a Gaussian process. In radar/sonar it is frequently an interfering target.

With this motivation we now formulate and solve the detection and estimation problem. As we have seen in the preceding section, a close coupling exists between detection and estimation. In fact, the development through construction of the likelihood ratio (or function) is identical. We derive the simple binary case in detail and then indicate how the results extend to other cases of interest. The first step is to specify the model.

When colored noise is present, we have to be more careful about our model. We assume that the transmitted signal on hypothesis 1 is

$$\sqrt{E}s(t) \triangleq \begin{cases} \sqrt{E}s_T(t), & 0 \leq t \leq T, \\ 0, & \text{Elsewhere.} \end{cases} \quad (7.148)$$

Observe that $s(t)$ is defined for all time. Before reception the signal is corrupted by additive Gaussian noise $n(t)$. The received waveform $r(t)$ is observed over the interval $T_i \leq t \leq T_f$. Thus,

$$\begin{aligned} H_1 : r(t) &= \sqrt{E}s(t) + n(t), & T_i \leq t \leq T_f, \\ H_0 : r(t) &= n(t), & T_i \leq t \leq T_f. \end{aligned} \quad (7.149)$$

Sometimes T_i will equal zero and T_f will equal T . In general, however, we shall let $T_i (\leq 0)$ and $T_f (\geq T)$ remain arbitrary. Specifically, we shall frequently examine the problem in

which $T_i = -\infty$ and $T_f = +\infty$. A logical question is Why should we observe the received waveform when the signal component is zero? The reason is that the noise outside the interval is correlated with the noise inside the interval, and presumably the more knowledge available about the noise inside the interval the better we can combat it and improve our system performance. A trivial case can be used to illustrate this point. Let

$$\sqrt{E}s(t) = \begin{cases} 1, & 0 \leq t \leq 1, \\ 0, & \text{Elsewhere.} \end{cases} \quad (7.150)$$

Let

$$n(t) = n, \quad 0 \leq t \leq 2, \quad (7.151)$$

where n is a Gaussian random variable. We can decide which hypothesis is true in the following way:

$$l = \int_0^1 r(t) dt - \int_1^2 r(t) dt. \quad (7.152)$$

If

$$\begin{aligned} l &= 0, && \text{say } H_0, \\ l &\neq 0, && \text{say } H_1. \end{aligned}$$

Clearly, we can make error-free decisions. Here, we used the extended interval to estimate the noise inside the interval where the signal was nonzero. Unfortunately, the actual situation is not so simple, but the idea of using an extended observation interval carries over to more realistic problems.

Initially, we shall find it useful to assume that the noise always contains an *independent* white component. Thus,

$$n(t) = w(t) + n_c(t) \quad (7.153)$$

where $n_c(t)$ is the *colored* noise component. Then,

$$K_n(t, u) = \frac{N_0}{2} \delta(t - u) + K_c(t, u) \quad (7.154)$$

We assume the $n_c(t)$ has a finite mean-square value $[E(n_c^2(t))] < \infty$ for all $T_i \leq t \leq T_f$ so $K_c(t, u)$ is a square-integrable function over $[T_i, T_f]$.

The white noise assumption is included for two reasons:

1. The physical reason is that regardless of the region of the spectrum used there will be a nonzero noise level. Extension of this level to infinity is just a convenience.
2. The mathematical reason will appear logically in our development. The white noise component enables us to guarantee that our operations will be meaningful. There are other ways to accomplish this objective but the white noise approach is the simplest.

Three logical approaches to the solution of the nonwhite noise problem are the following:

1. We choose the coordinates for the orthonormal expansion of $r(t)$ so that the coefficients are statistically independent. This will make the construction of the likelihood ratio straightforward. From our discussion in Chapter 6, we know how to carry out this procedure.
2. We operate on $r(t)$ to obtain a sufficient statistic and then use it to perform the detection.
3. We perform preliminary processing on $r(t)$ to transform the problem into a white Gaussian noise problem and then use the white Gaussian noise solution obtained in the preceding section. It is intuitively clear that if the preliminary processing is reversible it can have no effect on the performance of the system. Because we use the idea of reversibility repeatedly, however, it is worthwhile to provide a simple proof.

Reversibility. It is easy to demonstrate the desired result in a general setting. In Figure 7.36a, we show a system that operates on $r(u)$ to give an output that is optimum according to some desired criterion. The problem of interest may be detection or estimation. In system 2, shown in Figure 7.36b, we first operate on $r(u)$ with a reversible operation $k[t, r(u)]$ to obtain $z(t)$. We then design a system that will perform an operation on $z(t)$ to obtain an output that is optimum according to the same criterion as in system 1. We now claim that the performances of the two systems are identical. Clearly, system 2 cannot perform better than system 1 or this would contradict our statement that system 1 is the optimum operation on $r(u)$. We now show that system 2 cannot be worse than system 1. Suppose that system 2 were worse than system 1. If this were true, we could design the

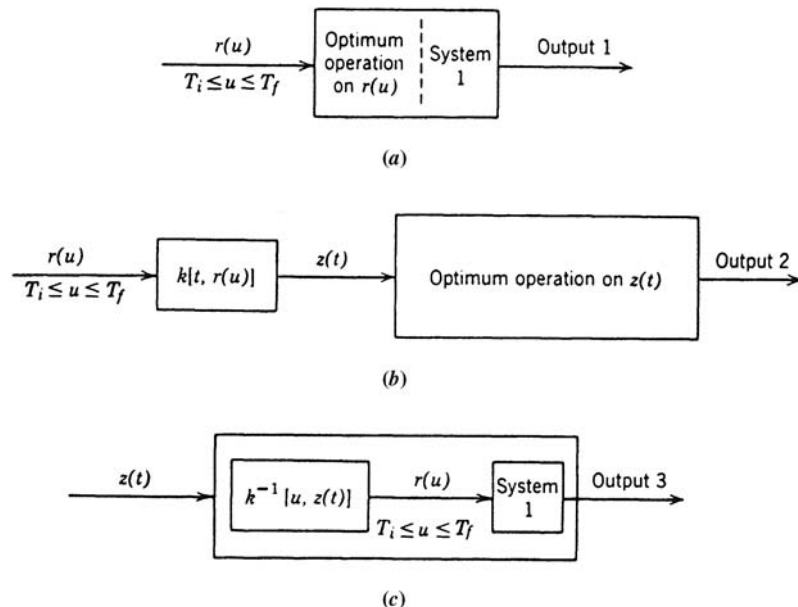


Figure 7.36: Reversibility proof: (a) system 1; (b) system 2; (c) system 3.

system shown in Figure 7.36c, which operates on $z(t)$ with the inverse of $k[t, r(u)]$ to give $r(u)$ and then passes it through system 1. This overall system will work as well as system 1 (they are identical from the input–output standpoint). Because the result in Figure 7.36c is obtained by operating on $z(t)$, it cannot be better than system 2 or it will contradict the statement that the second operation in system 2 is optimum. Thus, system 2 cannot be worse than system 1.

Therefore, *any* reversible operation can be included to facilitate the solution. We observe that linearity is not an issue, only the existence of an inverse. Reversibility is only *sufficient*, not *necessary*. (This is obvious from our discussion of sufficient statistics in Chapter 2.)

We now return to the problem of interest. The first two of these approaches involve much less work and also extend in an easy fashion to more general cases. The third approach however, using reversibility, seems to have more intuitive appeal, so we shall do it first.

7.3.1 “Whitening” Approach

First we shall derive the structures of the optimum detector and estimator. In this section, we require a nonzero white noise level.

7.3.1.1 Structures

As a preliminary operation, we shall pass $r(t)$ through a linear time-varying filter whose impulse response is $h_w(t, u)$ (Figure 7.37). The impulse response is assumed to be zero for either t or u outside the interval $[T_i, T_f]$. For the moment, we shall not worry about realizability and shall allow $h_w(t, u)$ to be nonzero for $u > t$. Later, in specific examples, we also look for realizable whitening filters. The output is

$$\begin{aligned} r_*(t) &\triangleq \int_{T_i}^{T_f} h_w(t, u) r(u) du \\ &= \int_{T_i}^{T_f} h_w(t, u) \sqrt{E}s(u) du + \int_{T_i}^{T_f} h_w(t, u) n(u) du \\ &\triangleq s_*(t) + n_*(t), \quad T_i \leq t \leq T_f, \end{aligned} \tag{7.155}$$

when H_1 is true and

$$r_*(t) = n_*(t), \quad T_i \leq t \leq T_f, \tag{7.156}$$

when H_0 is true. We want to choose $h_w(t, u)$ so that

$$K_{n\bullet}(t, u) = E[n_*(t)n_*(u)] = \delta(t - u), \quad T_i \leq t, u \leq T_f. \tag{7.157}$$

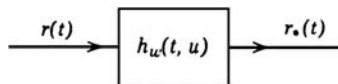


Figure 7.37: “Whitening” filter.

Observe that we have arbitrarily specified a unity spectral height for the noise level at the output of the whitening filter. This is merely a convenient normalization.

The following logical question arises:

What conditions on $K_n(t, u)$ will guarantee that a reversible whitening filter exists? Because the whitening filter is linear, we can show reversibility by finding a filter $h_w^{-1}(t, u)$ such that

$$\int_{T_i}^{T_f} h_w^{-1}(t, z) h_w(z, u) dz = \delta(t - u), \quad T_i \leq t, u \leq T_f. \quad (7.158)$$

For the moment we shall assume that we can find a suitable set of conditions and proceed with the development.

Because $n_*(t)$ is “white,” we may use (7.24a) and (7.24b) directly ($N_0 = 2$):

$$\ln \Lambda[r_*(t)] = \int_{T_i}^{T_f} r_*(u) s_*(u) du - \frac{1}{2} \int_{T_i}^{T_f} s_*^2(u) du. \quad (7.159)$$

We can also write this directly in terms of the original waveforms and $h_w(t, u)$:

$$\begin{aligned} \ln \Lambda[r(t)] &= \int_{T_i}^{T_f} du \int_{T_i}^{T_f} h_w(u, z) r(z) dz \int_{T_i}^{T_f} h_w(u, v) \sqrt{E} s(v) dv \\ &\quad - \frac{1}{2} \int_{T_i}^{T_f} du \int_{T_i}^{T_f} h_w(u, z) \sqrt{E} s(z) dz \int_{T_i}^{T_f} h_w(u, v) \sqrt{E} s(v) dv. \end{aligned} \quad (7.160a)$$

This expression can be formally simplified by defining a new function:

$$Q_n(z, v) = \int_{T_i}^{T_f} h_w(u, z) h_w(u, v) du, \quad T_i < z, v < T_f. \quad (7.160b)$$

For the moment we can regard it as a function that we accidentally stumbled on in an effort to simplify an equation.⁵ Later we shall see that it plays a fundamental role in many of our

⁵Throughout this section we must be careful about the end points of the interval. The difficulty is with factors of 2 that arise because of the delta function in the noise covariance. We avoid this by using an open interval and then show that end points are not important in this problem. We suggest that the reader ignore the comments regarding end points until he has read through Section 7.3.3. This strategy will make these sections more readable.

discussions. Rewriting (7.160a), we have

$$\begin{aligned} \ln \Lambda[r(t)] &= \int_{T_i}^{T_f} r(z) dz \int_{T_i}^{T_f} Q_n(z, v) \sqrt{E} s(v) dv \\ &\quad - \frac{E}{2} \int_{T_i}^{T_f} s(z) dz \int_{T_i}^{T_f} Q_n(z, v) s(v) dv. \end{aligned} \quad (7.161)$$

We can simplify (7.161) by writing

$$g(z) = \int_{T_i}^{T_f} Q_n(z, v) \sqrt{E} s(v) dv, \quad T_i < z < T_f. \quad (7.162)$$

We have used a strict inequality in (7.162). Looking at (7.161), we see that $g(z)$ only appears inside an integral. Therefore, if $g(z)$ does not contain singularities at the end points, we can assign $g(z)$ any finite value at the end point and $\ln \Lambda[r(t)]$ will be unchanged. Whenever there is a white noise component, we can show that $g(z)$ is square-integrable (and therefore contains no singularities). For convenience we make $g(z)$ continuous at the end points.

$$\begin{aligned} g(t_f) &= \lim_{z \rightarrow T_f^-} g(z), \\ g(t_i) &= \lim_{z \rightarrow T_i^+} g(z). \end{aligned}$$

We see that the construction of the likelihood function involves a correlation operation between the actual received waveform and a function $g(z)$. Thus, from the standpoint of constructing the receiver, the function $g(z)$ is the only one needed. Observe that the correlation of $r(t)$ with $g(t)$ is simply the reduction of the observation space to a single sufficient statistic.

Three canonical receiver structures for simple binary detection are shown in Figure 7.38. We shall see that the first two are practical implementations, whereas the third affords an interesting interpretation. The modification of Figure 7.38b to obtain a matched filter realization is obvious. To implement the receivers we must solve (7.158), (7.160b), or (7.162). Rather than finding closed-form solutions to these equations, we shall content ourselves in this section with series solutions in terms of the eigenfunctions and eigenvalues of $K_c(t, u)$. These series solutions have two purposes:

1. They demonstrate that solutions exist.
2. They are useful in certain optimization problems.

After deriving these solutions, we shall look at the receiver performance and extensions to general binary detection, M -ary detection, and estimation problems. We shall then return to the issue of closed-form solutions. The advantage of this approach is that it enables us to obtain an integrated picture of the colored noise problem and many of its important features without getting lost in the details of solving integral equations.

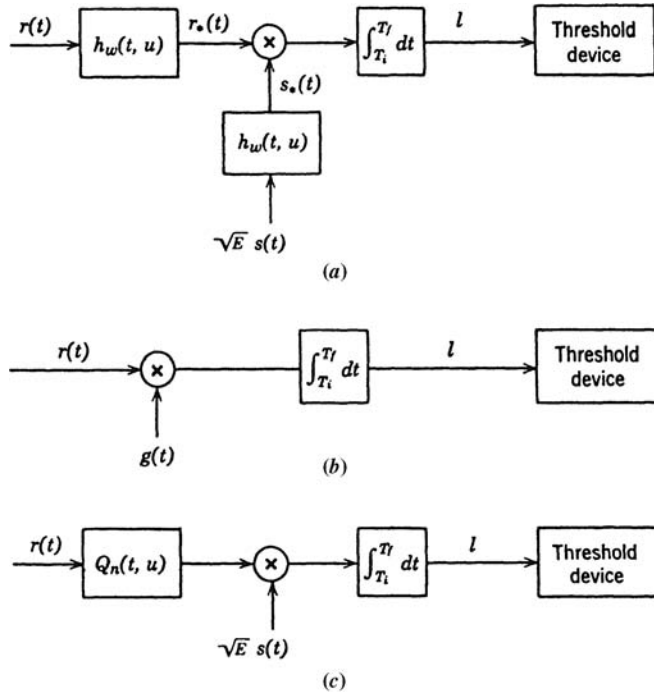


Figure 7.38: Alternate structures for colored noise problem.

7.3.1.2 Construction of $Q_n(t, u)$ and $g(t)$

The first step is to express $Q_n(t, u)$ directly in terms of $K_n(t, u)$. We recall our definition of $h_w(t, u)$. It is a time-varying linear filter chosen so that when the input is $n(t)$ the output will be $n_*(t)$, a sample function from a white Gaussian process. Thus,

$$n_*(t) = \int_{T_i}^{T_f} h_w(t, x) n(x) dx, \quad T_i \leq t \leq T_f \quad (7.163)$$

and

$$E [n_*(t)n_*(u)] = K_{n*}(t, u) = \delta(t - u), \quad T_i \leq t \leq T_f. \quad (7.164)$$

Substituting (7.163) into (7.164), we have

$$\delta(t - u) = E \int_{T_i}^{T_f} \int h_w(t, x) h_w(u, z) n(x) n(z) dx dz. \quad (7.165)$$

By bringing the expectation inside the integrals, we have

$$\delta(t - u) = \int_{T_i}^{T_f} \int h_w(t, x) h_w(u, z) K_n(x, z) dx dz, \quad T_i < t, u < T_f. \quad (7.166)$$

In order to get (7.166) into a form such that we can introduce $Q_n(t, u)$, we multiply both sides by $h_w(t, v)$ and integrate with respect to t . This gives

$$h_w(u, v) = \int_{T_i}^{T_f} dz h_w(u, z) \int_{T_i}^{T_f} K_n(x, z) dx \int_{T_i}^{T_f} h_w(t, v) h_w(t, x) dt. \quad (7.167)$$

Looking at (7.160b), we see that the last integral is just $Q_n(v, x)$. Therefore,

$$h_w(u, v) = \int_{T_i}^{T_f} dz h_w(u, z) \int_{T_i}^{T_f} K_n(x, z) Q_n(v, x) dx. \quad (7.168)$$

This implies that the inner integral must be an impulse over the open interval,

$$\delta(z - v) = \int_{T_i}^{T_f} K_n(x, z) Q_n(v, x) dx, \quad T_i < z, v < T_f. \quad (7.169)$$

This is the desired result that relates $Q_n(v, x)$ directly to the original covariance function. Because $K_n(x, z)$ is the kernel of many of the integral equations of interest to us, $Q_n(v, x)$ is frequently called the *inverse kernel*. We observe that (7.169) is analogous to the definition of an inverse matrix [e.g. (3.52)]. This parallelism will continue.

From (7.154) we know that $K_n(x, z)$ consists of an impulse and a well-behaved term. A logical approach is to try and express $Q_n(v, x)$ in a similar manner. We try a solution to (7.161) of the form

$$Q_n(v, x) = \frac{2}{N_0} [\delta(v - x) - h_o(v, x)], \quad T_i < v, x < T_f. \quad (7.170)$$

Substituting (7.152) and (7.170) into (7.169) and rearranging terms, we obtain an equation that $h_o(v, x)$ must satisfy:

$$\frac{N_0}{2} h_o(v, z) + \int_{T_i}^{T_f} h_o(v, x) K_c(x, z) dx = K_c(v, z), \quad T_i < z, v < T_f. \quad (7.171)$$

This equation is familiar to us from the section on optimum linear filters in Section 6.4.6. The significance of this similarity is seen by redrawing the system in Figure 7.38c as shown in Figure 7.39. The function $Q_n(t, u)$ is divided into two parts. We see that the output of the filter in the bottom path is precisely the minimum mean-square error estimate of the colored noise component, assuming that H_0 is true. If we knew $n_c(t)$, it is clear that the optimum processing would consist of subtracting it from $r(t)$ and passing the result into a matched filter or correlation receiver. The optimum receiver does exactly that, except that it does not

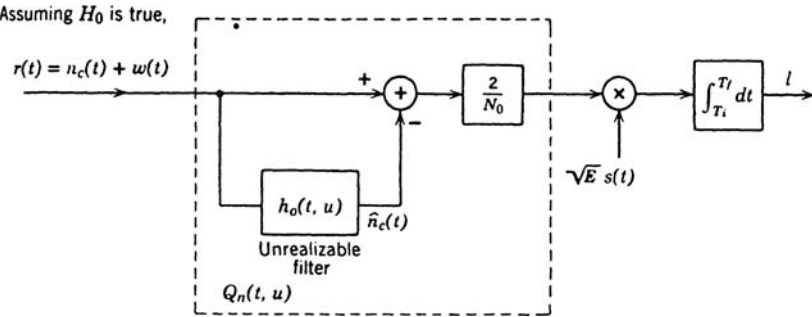


Figure 7.39: Realization of detector using an optimum linear filter.

know $n_c(t)$; therefore, it makes a MMSE estimate $\hat{n}_c(t)$ and uses it. This is an intuitively pleasing result of a type that we shall encounter frequently.⁶

From our results in Chapter 6, we can write a formal solution for $h_o(t, u)$ in terms of the eigenvalues of $K_c(t, u)$. Using (6.166),

$$h_o(t, u) = \sum_{i=1}^{\infty} \frac{\lambda_i^c}{\lambda_i^c + N_0/2} \phi_i(t) \phi_i(u), \quad T_i < t, u < T_f, \quad (7.172)$$

where λ_i^c and $\phi_i(t)$ are the eigenvalues and eigenfunctions, respectively, of $K_c(t, u)$. We can write the entire inverse kernel as

$$Q_n(t, u) = \frac{2}{N_0} \left[\delta(t - u) - \sum_{i=1}^{\infty} \frac{\lambda_i^c}{\lambda_i^c + N_0/2} \phi_i(t) \phi_i(u) \right]. \quad (7.173)$$

It is important to re-emphasize that our ability to write $Q_n(t, u)$ as an impulse function and a well-behaved function rests heavily on our assumption that there is a nonzero white noise level. This is the mathematical reason for the assumption.

We can also write $Q_n(t, u)$ as a single series. We express the impulse in terms of a series by using (6.130) and then combine the series to obtain

$$Q_n(t, u) = \sum_{i=1}^{\infty} \left(\frac{N_0}{2} + \lambda_i^c \right)^{-1} \phi_i(t) \phi_i(u) = \sum_{i=1}^{\infty} \frac{1}{\lambda_i^T} \phi_i(t) \phi_i(u), \quad (7.174)$$

where

$$\lambda_i^T \triangleq \frac{N_0}{2} + \lambda_i^c. \quad (7.175)$$

⁶The reader may wonder why we care whether a result is intuitively pleasing, if we know it is optimum. There are two reasons for this interest: (a) It is a crude error-checking device. For the type of problems of interest to us, when we obtain a mathematical result that is unintuitive it is usually necessary to go back over the model formulation and the subsequent derivation and satisfy ourselves that either the model omits some necessary feature of the problem or that our intuition is wrong. (b) In many cases the solution for the optimum receiver may be mathematically intractable. Having an intuitive interpretation for the solutions to the various Gaussian problems equips us to obtain a good receiver by using intuitive reasoning when we cannot get a mathematical solution.

(T denotes total). The series in (7.174) does not converge. However, in most cases $Q_n(t, u)$ is inside an integral and the overall expression will converge.

As a final result, we want to find an equation that will specify $g(t)$ directly in terms of $K_n(t, z)$. We start with (7.162):

$$g(z) = \int_{T_i}^{T_f} Q_n(z, v) \sqrt{E}s(v) dv, \quad T_i < z < T_f. \quad (7.176)$$

The technique that we use is based on the inverse relation between $K_n(t, z)$ and $Q_n(t, z)$, expressed by (7.169). To get rid of $Q_n(z, v)$, we simply multiply (7.176) by $K_n(t, z)$, integrate with respect to z , and use (7.169). The result is

$$\int_{T_i}^{T_f} K_n(t, z) g(z) dz = \sqrt{E}s(t), \quad T_i < t < T_f. \quad (7.177)$$

Substituting (7.154) into (7.177), we obtain an equation for the open interval (t_i, T_f) . Our continuity assumption after (7.169) extends the range to the closed interval $[T_i, T_f]$. The result is

$$\frac{N_0}{2} g(t) + \int_{T_i}^{T_f} K_c(t, z) g(z) dz = \sqrt{E}s(t), \quad T_i \leq t \leq T_f. \quad (7.178)$$

To implement the receiver, as shown in Figure 7.38b, we would solve (7.178) directly. We shall develop techniques for obtaining closed-form solutions in Section 7.3.6. A series solution can be written easily by using (7.176) and (7.173):

$$g(z) = \frac{2}{N_0} \sqrt{E}s(z) - \frac{2}{N_0} \sum_{i=1}^{\infty} \frac{\lambda_i^c s_i}{\lambda_i^c + N_0/2} \phi_i(z), \quad (7.179)$$

where

$$s_i = \int_{T_i}^{T_f} \sqrt{E}s(t) \phi_i(t) dt. \quad (7.180)$$

The first term is familiar from the white noise case. The second term indicates the effect of nonwhite noise. Observe that $g(t)$ is *always* a square-integrable function over (t_i, T_f) when a white noise component is present. We defer checking the end point behavior until Section 7.3.3.

7.3.1.3 Summary

In this section, we have derived the solution for the optimum receiver for the simple binary detection problem of a known signal in nonwhite Gaussian noise. Three realizations were the following:

1. Whitening realization (Figure 7.38a).
2. Correlator realization (Figure 7.38b).
3. Estimator–subtractor realization (Figure 7.39).

Coupled with each of these realizations was an integral equation that must be solved to build the receiver: (1) (7.158). (2) (7.169). (3) (7.171).

We demonstrated that series solutions could be obtained in terms of eigenvalues and eigenfunctions, but we postponed the problem of actually finding a closed-form solution. The concept of an “inverse kernel” was introduced and a simple application shown. The following questions remain:

1. How well does the system perform?
2. How do we find closed-form solutions to the integral equations of interest?
3. What are the analogous results for the estimation problem?

Before answering these questions, we digress briefly and rederive the results without using the idea of whitening. In view of these alternate derivations, we leave the proof that $h_w(t, u)$ is a reversible operator as an exercise for the reader (Problem 7.3.1).

7.3.2 A Direct Derivation Using the Karhunen-Loève Expansion⁷

In this section, we consider a more fundamental approach. It is not only more direct for this particular problem but also extends easily to the general case.

The reason that the solution to the white noise detection problem in Section 7.2 was so straightforward was that regardless of the orthonormal set we chose, the resulting observables r_1, r_2, \dots, r_k were conditionally independent.

From our work in Chapter 6, we know that we can achieve the same simplicity if we choose an orthogonal set in a particular manner. Specifically, we want the orthogonal functions to be the eigenfunctions of the integral equation (6.49)

$$\lambda_i^c \phi_i(t) = \int_{T_i}^{T_f} K_c(t, u) \phi_i(u) du, \quad T_i \leq t \leq T_f. \quad (7.181)$$

Observe that the λ_i^c are the eigenvalues of the colored noise process only. (If $K_c(t, u)$ is not positive definite, we augment the set to make it complete.) Then we expand $r(t)$ in this coordinate system:

$$r(t) = \lim_{K \rightarrow \infty} \sum_{i=1}^K r_i \phi_i(t) = \lim_{K \rightarrow \infty} \sum_{i=1}^K s_i \phi_i(t) + \lim_{K \rightarrow \infty} \sum_{i=1}^K n_i \phi_i(t), \quad T_i \leq t \leq T_f, \quad (7.182)$$

⁷This approach to the problem is due to Grenander [Gre50] (see also [KRR60]).

where

$$r_i = \int_{T_i}^{T_f} r(t) \phi_i(t) dt, \quad (7.183)$$

$$s_i = \int_{T_i}^{T_f} \sqrt{E} s(t) \phi_i(t) dt, \quad (7.184)$$

and

$$n_i = \int_{T_i}^{T_f} n(t) \phi_i(t) dt. \quad (7.185)$$

From (6.72), we know

$$E(n_i) = 0, \quad E(n_i n_j) = \lambda_i^T \delta_{ij}, \quad (7.186)$$

where

$$\lambda_i^T \triangleq \frac{N_0}{2} + \lambda_i^c. \quad (7.187)$$

We consider the first K coordinates. The likelihood ratio is

$$\Lambda [r_K(t)] = \frac{\prod_{i=1}^K \frac{1}{\sqrt{2\pi\lambda_i^T}} \exp\left[-\frac{1}{2} \frac{(R_i - s_i)^2}{\lambda_i^T}\right]}{\prod_{i=1}^K \frac{1}{\sqrt{2\pi\lambda_i^T}} \exp\left[-\frac{1}{2} \frac{R_i^2}{\lambda_i^T}\right]}. \quad (7.188)$$

Canceling common terms, letting $K \rightarrow \infty$, and taking the logarithm, we obtain

$$\ln \Lambda[r(t)] = \sum_{i=1}^{\infty} \frac{R_i s_i}{\lambda_i^T} - \frac{1}{2} \sum_{i=1}^{\infty} \frac{s_i^2}{\lambda_i^T}. \quad (7.189)$$

Using (7.183) and (7.184), we have

$$\begin{aligned} \ln \Lambda[r(t)] &= \int_{T_i}^{T_f} dt \int_{T_i}^{T_f} du r(t) \sum_{i=1}^{\infty} \frac{\phi_i(t) \phi_i(u)}{\lambda_i^T} \sqrt{E} s(u) \\ &\quad - \frac{E}{2} \int_{T_i}^{T_f} dt \int_{T_i}^{T_f} du s(t) \sum_{i=1}^{\infty} \frac{\phi_i(t) \phi_i(u)}{\lambda_i^T} s(u). \end{aligned} \quad (7.190)$$

From (7.174), we recognize the sum as $Q_n(t, u)$. Thus,

$$\begin{aligned}\ln \Lambda[r(t)] &= \int_{T_i}^{T_f} dt \int_{T_i}^{T_f} du r(t) Q_n(t, u) \sqrt{E}s(u) \\ &\quad - \frac{E}{2} \int_{T_i}^{T_f} dt \int_{T_i}^{T_f} du s(t) Q_n(t, u) s(u).\end{aligned}$$

This expression is identical to (7.161).⁸

Observe that if we had not gone through the whitening approach we would have simply defined $Q_n(t, u)$ to fit our needs when we arrived at this point in the derivation. When we consider more general detection problems, the direct derivation can easily be extended.

7.3.3 A Direct Derivation with a Sufficient Statistic⁹

For convenience we rewrite the detection problem of interest (7.149):

$$\begin{aligned}H_1 : r(t) &= \sqrt{E}s(t) + n(t), & T_i \leq t \leq T_f, \\ H_0 : r(t) &= n(t), & T_i \leq t \leq T_f.\end{aligned}\tag{7.191}$$

In this section, we will not require that the noise contain a white component.

From our work in Chapter 2 and Section 4.2, we know that if we can write

$$r(t) = r_1 s(t) + y(t), \quad T_i \leq t \leq T_f,\tag{7.192}$$

where r_1 is a random variable obtained by operating on $r(t)$ and demonstrate that

- (a) r_1 and $y(t)$ are statistically independent on both hypotheses,
- (b) the statistics of $y(t)$ do not depend on which hypothesis is true,

then r_1 is a sufficient statistic. We can then base our decision solely on r_1 and disregard $y(t)$. [Note that conditions (a) and (b) are sufficient, but not necessary, for r_1 to be a sufficient statistic.]

To do this we hypothesize that r_1 can be obtained by the operation

$$r_1 = \int_{T_i}^{T_f} r(u) g(u) du,\tag{7.193}$$

⁸To proceed rigorously from (7.189) to (7.190), we require $\sum_{i=1}^{\infty} (s_i^2 / \lambda_i^{T_f}) < \infty$ [Gre50, KRR60]. This is always true when white noise is present. Later, when we look at the effect of removing the white noise assumption, we shall see that the divergence of this series leads to an unstable test.

⁹This particular approach to the colored noise problem seems to have been developed independently by several people [Kai65, Yud66]. Although the two derivations are essentially the same, we follow the second.

and try to find a $g(u)$ that will lead to the desired properties. Using (7.192), we can rewrite (7.191) as

$$\begin{aligned} H_1 : r(t) &= (s_1 + n_1)s(t) + y(t), \\ H_0 : r(t) &= n_1 s(t) + y(t), \end{aligned} \quad (7.194)$$

where

$$s_1 \triangleq \int_{T_i}^{T_f} \sqrt{E} s(u) g(u) du \quad (7.195)$$

and

$$n_1 \triangleq \int_{T_i}^{T_f} n(u) g(u) du. \quad (7.196)$$

Because a sufficient statistic can be multiplied by any nonzero constant and remain a sufficient statistic we can introduce a constraint,

$$\int_{T_i}^{T_f} s(u) g(u) du = 1. \quad (7.197)$$

Using (7.197) in (7.195), we have

$$s_1 = \sqrt{E}. \quad (7.198)$$

Clearly, n_1 is a zero-mean random variable and

$$n(t) = n_1 s(t) + y(t), \quad T_i \leq t \leq T_f. \quad (7.199)$$

This puts the problem in a convenient form and it remains only to find a condition on $g(u)$ such that

$$E[n_1 y(t)] = 0, \quad T_i \leq t \leq T_f, \quad (7.200)$$

or, equivalently,

$$E\{n_1 [n(t) - n_1 s(t)]\} = 0, \quad T_i \leq t \leq T_f, \quad (7.201)$$

or

$$E[n_1 \cdot n(t)] = E[n_1^2]s(t), \quad T_i \leq t \leq T_f. \quad (7.202)$$

Using (7.196)

$$\int_{T_i}^{T_f} K_n(t, u) g(u) du = s(t) \int_{T_i}^{T_f} \int g(\sigma) K_n(\sigma, \beta) g(\beta) d\sigma d\beta, \quad T_i \leq t \leq T_f. \quad (7.203)$$

Equations (7.197) and (7.203) will both be satisfied if

$$\int_{T_i}^{T_f} K_n(t, u) g(u) du = \sqrt{E} s(t), \quad T_i \leq t \leq T_f. \quad (7.204)$$

[Substitute (7.204) into the right-hand side of (7.203) and use (7.197).] Our sufficient statistic r_1 is obtained by correlating $r(u)$ with $g(u)$. After obtaining r_1 we use it to construct a likelihood ratio test in order to decide which hypothesis is true.

We observe that (7.204) is over the closed interval $[T_i, T_f]$, whereas (7.177) was over the open interval (T_i, T_f) . The reason for this difference is that in the absence of white noise $g(u)$ may contain singularities at the end points. These singularities change the likelihood ratio so we can no longer arbitrarily choose the end point values. An advantage of our last derivation is that the correct end point conditions are included. We should also observe that if there is a white noise component (7.204) and (7.177) will give different values for $g(t_i)$ and $g(t_f)$. However, because both sets of values are finite they lead to the same likelihood ratio.

In the last two sections we have developed two alternate derivations of the optimum receiver. Other derivations are available (a mathematically inclined reader might read [Par61, Haj60, Gal63], or [Kad65]). We now return to the questions posed in the summary of Section 7.3.1.

7.3.4 Detection Performance

The next question is “How does the presence of colored noise affect performance?” In the course of answering it a number of interesting issues appear. We consider the simple binary detection case first.

7.3.4.1 Performance: Simple Binary Detection Problem

Looking at the receiver structure in Figure 7.38a, we see that the performance is identical to that of a receiver in which the input signal is $s_*(t)$ and the noise is white with a spectral height of 2. Using (7.13), we have

$$d^2 = \int_{T_i}^{T_f} [s_*(t)]^2 dt. \quad (7.205)$$

Thus, the performance index d^2 is simply equal to the energy in the whitened signal. We can also express d^2 in terms of the original signal.

$$d^2 = \int_{T_i}^{T_f} dt \left[\int_{T_i}^{T_f} h_w(t, u) \sqrt{E} s(u) du \right] \left[\int_{T_i}^{T_f} h_w(t, z) \sqrt{E} s(z) dz \right]. \quad (7.206)$$

We use the definition of $Q_n(u, z)$ to perform the integration with respect to t . This gives

$$\begin{aligned} d^2 &= E \int_{T_i}^{T_f} \int du dz s(u) Q_n(u, z) s(z), \\ d^2 &= \sqrt{E} \int_{T_i}^{T_f} du s(u) g(u). \end{aligned} \quad (7.207)$$

It is clear that the performance is no longer independent of the signal shape. The next logical step is to find the best possible signal shape. There are three cases of interest:

1. $T_i = 0, T_f = T$: the signal interval and observation interval coincide.
2. $T_i < 0, T_f > T$: the observation interval extends beyond the signal interval in one or both directions but is still finite.
3. $T_i = -\infty, T_f = \infty$: the observation interval is doubly infinite.

We consider only the first case.

7.3.4.2 Optimum Signal Design: Coincident Intervals

The problem is to constrain the signal energy E and determine how the detailed shape of $s(t)$ affects performance. The answer follows directly. Write

$$Q_n(t, u) = \sum_{i=1}^{\infty} \left(\frac{N_0}{2} + \lambda_i^c \right)^{-1} \phi_i(t) \phi_i(u). \quad (7.208)$$

Then

$$d^2 = \sum_{i=1}^{\infty} \frac{s_i^2}{N_0/2 + \lambda_i^c}, \quad (7.209)$$

where

$$s_i = \int_0^T \sqrt{E} s(t) \phi_i(t) dt. \quad (7.210)$$

Observe that

$$\sum_{i=1}^{\infty} s_i^2 = E, \quad (7.211)$$

because the functions are normalized.

Looking at (7.209), we see that d^2 is just a weighted sum of the s_i^2 . Because (7.211) constrains the sum of the s_i^2 , we want to distribute the energy so that those s_i with large weighting are large. If there exists a smallest eigenvalue, say $\lambda_j^c = \lambda_{\min}^c$, then d^2 will be maximized by letting $s_j = \sqrt{E}$ and all other $s_i = 0$. There are two cases of interest:

1. If $K_c(t, u)$ is positive definite, the number of eigenvalues is infinite. There is no smallest eigenvalue. We let $s_j = \sqrt{E}$ and all other $s_i = 0$. Then, assuming the eigenvalues

are ordered according to decreasing size,

$$d^2 \rightarrow \frac{2E}{N_0}$$

as we increase j . For many of the colored noises that we encounter in practice (e.g., the spectrum shown in Figure 6.18), the frequency of the eigenfunction increases as the eigenvalues decrease. In other words, we increase the frequency of the signal until the colored noise becomes negligible. In these cases, we obtain a more realistic signal design problem by including a bandwidth constraint.

2. If $K_c(t, u)$ is only nonnegative definite, there will be zero eigenvalues. If $s(t)$ is the eigenfunction corresponding to any one of these eigenvalues, then

$$d^2 = \frac{2E}{N_0}.$$

We see that the performance of the best signal is limited by the white noise.

7.3.4.3 Singularity

It is easy to see the effect of removing the white noise by setting N_0 equal to zero in (7.209). When the colored noise is positive definite (case 1), all eigenvalues are nonzero. We can achieve *perfect detection* ($d^2 = \infty$) if and only if the sum

$$d^2 = \sum_{i=1}^{\infty} \frac{s_i^2}{\lambda_i^c} \quad (7.212)$$

diverges.

It can be accomplished by choosing $s(t)$ so that s_i^2 is proportional to λ_i^c . We recall that

$$\sum_{i=1}^{\infty} \lambda_i^c = \int_{T_l}^{T_f} K_c(t, t) dt < M.$$

The right-hand side is finite by our assumption below (7.154). Thus, the energy in the signal ($E = \sum_{i=1}^{\infty} s_i^2$) will be finite. If there were a white noise component, we could not achieve this proportionality for all i with a finite energy signal. In (case 2) there are zero eigenvalues. Thus, we achieve $d^2 = \infty$ by choosing $s(t) = \phi_i(t)$ for any i that has a zero eigenvalue.

These two cases are referred to as *singular* detection. For arbitrarily small time intervals and arbitrarily small energy levels we achieve perfect detection. We know that this kind of performance cannot be obtained in an actual physical situation. Because the purpose of our mathematical model is to predict performance of an actual system, it is important that we make it realistic enough to eliminate singular detection. We have eliminated the possibility of singular detection by insisting on a nonzero white noise component. This accounts for the thermal noise in the receiver. Often it will appear to be insignificant. If, however, we design the signal to eliminate the effect of all other noises, it becomes the quantity that limits the performance and keeps our mathematical model from predicting results that would not occur in practice.

From (7.205) we know that d^2 is the energy in the whitened signal. Therefore, if the whitened signal has finite energy, the test is not singular. When the observation interval is

infinite and the noise process is stationary with a rational spectrum, it is easy to check the finiteness of the energy of $s_*(t)$. We first find the transfer function of the whitening filter. Recall that

$$n_*(t) = \int_{-\infty}^{\infty} h_w(u) n(t-u) du. \quad (7.213)$$

We require that $n_*(t)$ be white with unity spectral height. This implies that

$$\int_{-\infty}^{\infty} \int du dz h_w(u) h_w(z) K_n(t-u+z-v) = \delta(t-v), \quad -\infty < t, v < \infty. \quad (7.214)$$

Transforming, we obtain

$$|H_w(j\omega)|^2 S_n(\omega) = 1 \quad (7.215)$$

or

$$|H_w(j\omega)|^2 = \frac{1}{S_n(\omega)}. \quad (7.216)$$

Now assume that $S_n(\omega)$ has a rational spectrum

$$S_n(\omega) = \frac{c_q \omega^{2q} + c_{q-1} \omega^{2q-2} + \cdots + c_0}{d_p \omega^{2p} + d_{p-1} \omega^{2p-2} + \cdots + d_0}. \quad (7.217)$$

We define the difference between the order of denominator and numerator (as a function of ω^2) as r .

$$r \triangleq p - q. \quad (7.218)$$

If $n(t)$ has finite power then $r \geq 1$. However, if the noise consists of white noise plus colored noise with finite power, then $r = 0$. Using (7.217) in (7.216), we see that we can write $H_w(j\omega)$ as a ratio of two polynomials in $j\omega$.

$$H_w(j\omega) = \frac{a_p(j\omega)^p + a_{p-1}(j\omega)^{p-1} + \cdots + a_0}{b_q(j\omega)^q + b_{q-1}(j\omega)^{q-1} + \cdots + b_0}. \quad (7.219)$$

In Chapter 8, we develop an algorithm for finding the coefficients. For the moment their actual values are unimportant. Dividing the numerator by the denominator, we obtain

$$H_w(j\omega) = f_r(j\omega)^r + f_{r-1}(j\omega)^{r-1} + \cdots + f_0 + \frac{R(j\omega)}{b_q(j\omega)^q + \cdots + b_0}, \quad (7.220)$$

where f_r, \dots, f_0 are constants and $R(j\omega)$ is the remainder polynomial of order less than q . Recall that $(j\omega)^r$ in the frequency domain corresponds to taking the r th derivative in the time domain. Therefore, in order for the test to be nonsingular, the r th derivative must have finite energy. In other words, if

$$\int_{-\infty}^{\infty} \left(\frac{d^r s(t)}{dt^r} \right)^2 dt < M, \quad (7.221)$$

the test is nonsingular; for example, if

$$S_n(\omega) = \frac{2\alpha\sigma_n^2}{\omega^2 + \alpha^2}, \quad (7.222)$$

then

$$p - q = r = 1, \quad (7.223)$$

and $s'(t)$ must have finite energy. If we had modeled the signal as an ideal rectangular pulse, then our model would indicate perfect detectability. We know that this perfect detectability will not occur in practice, so we must modify our model to accurately predict system performance. In this case we can eliminate the singular result by giving the pulse a finite rise time or by adding a white component to the noise. Clearly, whenever there is finite-power colored noise plus an independent white noise component, the integral in (7.221) is just the energy in the signal and singularity is never an issue.

Our discussion has assumed an infinite observation interval. Clearly, if the test is nonsingular on the infinite interval, it is nonsingular on the finite interval because the performance is related monotonically to the length of the observation interval. The converse is not true. Singularity on the infinite interval does not imply singularity on the finite interval. In this case, we must check (7.212) or look at the finite-time whitening operation.

Throughout most of our work we retain the white noise assumption so singular tests never arise. Whenever the assumption is removed, it is necessary to check the model to ensure that it does not correspond to a singular test.

7.3.4.4 General Binary Receivers

Our discussion up to this point has considered only the simple binary detection problem. The extension to general binary receivers is straightforward. Let

$$\begin{aligned} H_1 : r(t) &= \sqrt{E_1} s_1(t) + n(t), & T_i \leq t \leq T_f, \\ H_0 : r(t) &= \sqrt{E_0} s_0(t) + n(t), & T_i \leq t \leq T_f, \end{aligned} \quad (7.224)$$

where $s_0(t)$ and $s_1(t)$ are normalized over the interval $(0, T)$ and are zero elsewhere. Proceeding in exactly the same manner as in the simple binary case, we obtain the following results. One receiver configuration is shown in Figure 7.40a. The function $g_\Delta(t)$ satisfies

$$\begin{aligned} s_\Delta(t) &\triangleq \sqrt{E_1} s_1(t) - \sqrt{E_0} s_0(t) \\ &= \int_{T_i}^{T_f} g_\Delta(u) K_n(t, u) du, \quad T_i \leq t \leq T_f. \end{aligned} \quad (7.225)$$

The performance is characterized by d^2 :

$$d^2 = \int_{T_i}^{T_f} \int s_\Delta(t) Q_n(t, u) s_\Delta(u) dt du. \quad (7.226)$$

The functions $K_n(t, u)$ and $Q_n(t, u)$ were defined in (7.154) and (7.160b), respectively. As an alternative, we can use the whitening realization shown in Figure 7.40b. Here, $h_w(t, u)$

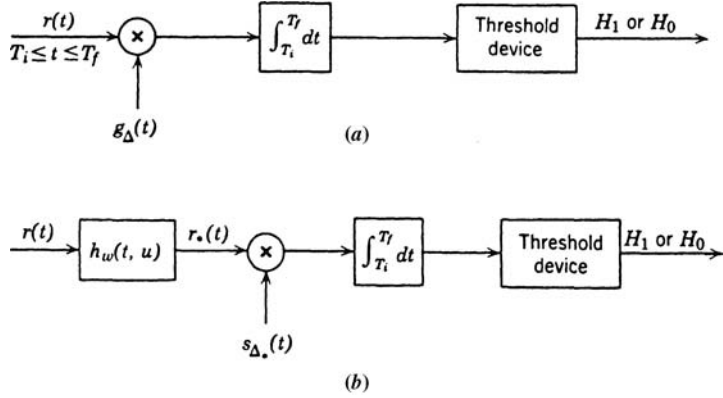


Figure 7.40: (a) Receiver configurations: general binary problem, colored noise; (b) alternate receiver realization.

satisfies (7.166) and

$$s_{\Delta*}(t) \triangleq \int_{T_i}^{T_f} h_w(t, u) s_\Delta(u) du, \quad T_i \leq i \leq T_f. \quad (7.227)$$

The performance is characterized by the energy in the whitened difference signal:

$$d^2 = \int_{T_i}^{T_f} s_{\Delta*}^2(t) dt. \quad (7.228)$$

The M -ary detection case is also a straightforward extension (see Problem 7.3.5). From our discussion of white noise, we would expect that the estimation case would also follow easily. We discuss it briefly in the next section.

7.3.5 Estimation

The model for the received waveform in the parameter estimation problem is

$$r(t) = s(t, A) + n(t), \quad T_i \leq t \leq T_f. \quad (7.229)$$

The simplest approach is to pass $r(t)$ through a whitening filter that is shown in Figure 7.3.7 and specified by (7.158). The output is

$$r_*(t) = s_*(t, A) + n_*(t), \quad (7.230)$$

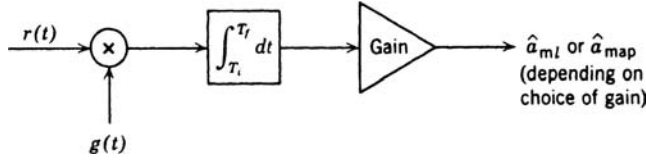


Figure 7.41: Linear estimation, colored noise.

where

$$s_*(t, A) \triangleq \int_{T_i}^{T_f} h_w(t, u)s(u, A)du, \quad (7.231)$$

$$n_*(t) = \int_{T_i}^{T_f} h_w(t, u)n(u)du, \quad (7.232)$$

and

$$E\{n_*(t)n_*(u)\} = \delta(t - u). \quad (7.233)$$

Then, all of the estimation results in Sections 7.2.2 and 7.2.3 apply. For linear estimation of a scalar parameter, the estimator is shown in Figure 7.41.

The variance and mean-square error bounds can be expressed in terms of the whitened signals or in terms of the original signals as summarized below:

1. A lower bound on the variance of any *unbiased* estimate of the nonrandom variable A :

$$\text{Var}(\hat{a} - A) \geq \left[\int_{T_i}^{T_f} \int \frac{\partial s(t, A)}{\partial A} Q_n(t, u) \frac{\partial s(u, A)}{\partial A} dt du \right]^{-1}, \quad (7.234)$$

or, equivalently,

$$\text{Var}(\hat{a} - A) \geq \left[\int_{T_i}^{T_f} \frac{\partial s(t, A)}{\partial A} \frac{\partial g(t, A)}{\partial A} dt \right]^{-1}. \quad (7.235)$$

2. A lower bound on the mean-square error in the estimate of a zero-mean Gaussian random variable a :

$$E[(\hat{a} - a)^2] \geq \left[\frac{1}{\sigma_a^2} + E_a \left(\int_{T_i}^{T_f} dt \int_{T_i}^{T_f} du \frac{\partial s(t, A)}{\partial A} Q_n(t, u) \frac{\partial s(u, A)}{\partial A} \right) \right]^{-1}. \quad (7.236)$$

3. A lower bound on the variance of any *unbiased* estimate of a nonrandom variable for the special case of an infinite observation interval and a stationary noise process:

$$\text{Var}(\hat{a} - A) \geq \left[\int_{-\infty}^{\infty} \frac{\partial S^*(j\omega, A)}{\partial A} S_n^{-1}(\omega) \frac{\partial S(j\omega, A)}{\partial A} \frac{d\omega}{2\pi} \right]^{-1}, \quad (7.237a)$$

where

$$S(j\omega, A) \triangleq \int_{-\infty}^{\infty} s(t, A) e^{-j\omega t} dt. \quad (7.237b)$$

For linear estimation, an implementation using $g(t)$ from (7.162) is shown in Figure 7.41.

The only remaining issue in the matter of colored noise is a closed-form solution for the various functions such as $Q_n(t, u)$. We consider this problem in the next section.

7.3.6 Solution Techniques for Integral Equations

As we have seen above, to specify the receiver structure completely we must solve the integral equation for $g(t)$ or $Q_n(t, u)$. In addition, if we want to use a whitening approach, we must do the factorization in (7.158) to find $h_w(t, u)$. In this section, we consider three cases of interest:

1. Infinite observation interval; stationary noise process.
2. Finite observation interval, separable kernel.
3. Finite observation interval; stationary noise process.

In Chapter 8, we will revisit the whitening filter and show that it is related to the optimum realizable filter $h_{or}(t, u)$ and develop solution techniques for processes that have a state-variable representation.

7.3.6.1 Infinite Observation Interval: Stationary Noise

In this particular case $T_i = -\infty$, $T_f = \infty$, and the covariance function of the noise is a function only of the difference in the arguments. Then (7.169) becomes

$$\delta(z - v) = \int_{-\infty}^{\infty} Q_n(x - z) K_n(v - x) dx, \quad -\infty < v, z < \infty, \quad (7.238)$$

where we assume that we can find a $Q_n(x, z)$ of this form. By denoting the Fourier transform of $K_n(\tau)$ by $S_n(\omega)$ and the Fourier transform of $Q_n(\tau)$ by $S_Q(\omega)$ and transforming both sides of (7.238) with respect to $\tau = z - v$, we obtain

$$S_Q(\omega) = \frac{1}{S_n(\omega)}. \quad (7.239)$$

We see that $S_Q(\omega)$ is just the inverse of the noise spectrum. Further, in the stationary case (7.160b) can be written as

$$Q_n(z - v) = \int_{-\infty}^{\infty} h_w(u - z) h_w(u - v) du. \quad (7.240)$$

By denoting the Fourier transform of $h_w(\tau)$ by $H_w(j\omega)$, we find that (7.240) implies

$$\frac{1}{S_n(\omega)} = S_Q(\omega) = |H_w(j\omega)|^2. \quad (7.241)$$

Finally, for the detection and linear estimation cases, (7.162) is useful. Transforming, we have

$$G_\infty(j\omega) = \sqrt{E} S_Q(\omega) S(j\omega) = \frac{S(j\omega)\sqrt{E}}{S_n(\omega)},$$

(7.242)

where the subscript ∞ indicates that we are dealing with an infinite interval.

To illustrate the various results, we consider some particular examples.

Example 7.8. We assume that the colored noise component has a rational spectrum. A typical case is

$$S_c(\omega) = \frac{2k\sigma_n^2}{\omega^2 + k^2} \quad (7.243)$$

and

$$S_n(\omega) = \frac{N_0}{2} + \frac{2k\sigma_n^2}{\omega^2 + k^2}. \quad (7.244)$$

Then

$$S_Q(\omega) = \frac{\omega^2 + k^2}{\frac{N_0}{2} [\omega^2 + k^2(1 + \Lambda)]}, \quad (7.245)$$

where $\Lambda = 4\sigma_n^2/kN_0$. Writing

$$S_Q(\omega) = \frac{(j\omega + k)(-j\omega + k)}{(N_0/2)(j\omega + k\sqrt{1 + \Lambda})(-j\omega + k\sqrt{1 + \Lambda})}, \quad (7.246)$$

we want to choose an $H_w(j\omega)$ so that (7.233) will be satisfied. To obtain a realizable whitening filter we assign the term $(j\omega + k(1 + \Lambda)^{1/2})$ to $H_w(j\omega)$ and its conjugate to $H_w^*(j\omega)$. The term $(j\omega + k)$ in the numerator can be assigned to $H_w(j\omega)$ or $H_w^*(j\omega)$.

However, we argued that the whitening filter should be reversible in order to guarantee overall optimality. To reverse $H_w(j\omega)$, we would use $H_w^{-1}(j\omega)$. If we require $H_w^{-1}(j\omega)$ to be reversible, then we also assign the zero in the left-half plane to $H_w(j\omega)$. Thus,

$$H_w(j\omega) = \left(\frac{2}{N_0} \right)^{1/2} \frac{j\omega + k}{j\omega + k(1 + \Lambda)^{1/2}}, \quad (7.247)$$

which can also be written as

$$H_w(j\omega) = \left(\frac{2}{N_0} \right)^{1/2} \left[1 - \frac{k(\sqrt{1 + \Lambda} - 1)}{j\omega + k\sqrt{1 + \Lambda}} \right]. \quad (7.248)$$

Thus, the optimum receiver (detector) can be realized in the whitening forms shown in Figures 7.42 and 7.43. The second form has an estimator-subtractor interpretation. A sketch of the waveforms for the case in which $s(t)$ is a rectangular pulse is also shown. Three observations follow:

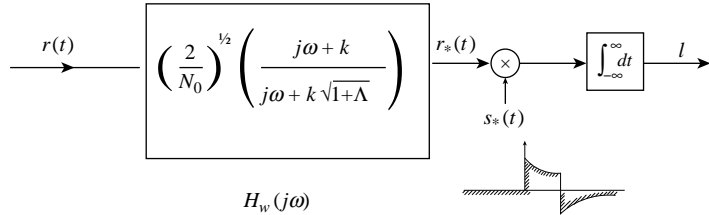


Figure 7.42: Optimum receiver: whitening implementation.

1. The whitening filter has an infinite memory. Thus, it uses the entire past of $r(t)$ to generate the input to the correlator.
2. The signal input to the multiplier will start at $t = 0$, but even after time $t = T$ the input will continue.
3. The actual integration limits are $(0, \infty)$, because one multiplier input is zero before $t = 0$. ■

In Chapter 8, we will show that these observations are true whenever the noise consists of white noise plus an independent colored noise with a rational spectrum. It is also true, but less easy to verify directly, when the colored noise has a nonrational spectrum. Thus, we conclude that under the above conditions an increase in observation interval will always improve the performance. It is also true, but less easy to verify directly, when the colored noise has a nonrational spectrum. Thus, we conclude that under the above conditions an increase in observation interval will always improve the performance. It is worthwhile to observe that if we use $H_w(j\omega)$ as the whitening filter the output of the filter in the bottom path will be $\hat{n}_{cr}(t)$, the minimum mean-square error *realizable* point estimate of $n_c(t)$. We shall verify that this result is always true when we study realizable estimators in Chapter 8.

As a second example we investigate what happens when we *remove* the white noise component.

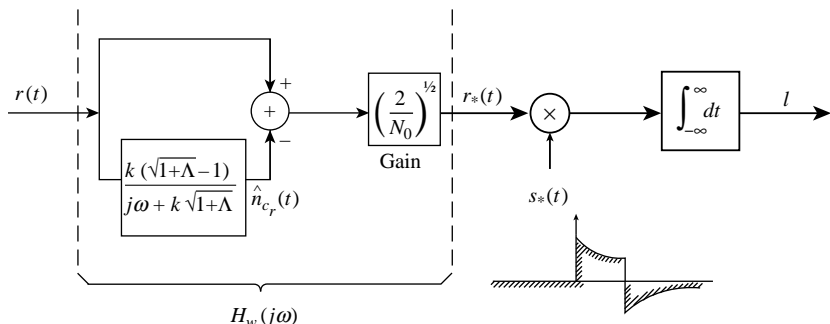


Figure 7.43: Optimum receiver: whitening implementation (estimator-subtractor).

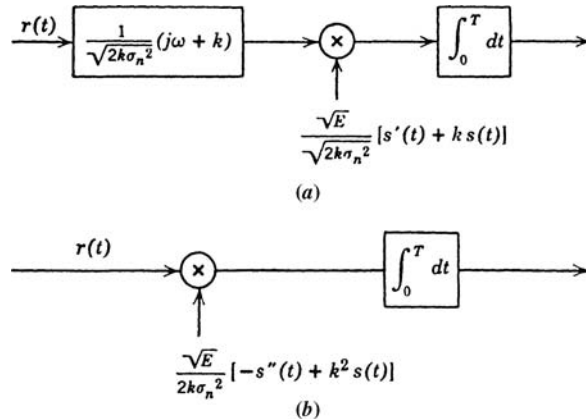


Figure 7.44: Optimum receiver: no white noise component.

Example 7.9.

$$S_n(\omega) = \frac{2k\sigma_n^2}{\omega^2 + k^2}. \quad (7.249)$$

Then

$$S_Q(\omega) = \frac{\omega^2 + k^2}{2k\sigma_n^2}. \quad (7.250)$$

The whitening filter is

$$H_w(j\omega) = \frac{1}{\sqrt{2k\sigma_n^2}}(j\omega + k). \quad (7.251)$$

Thus, the whitening filter is a differentiator and gain in parallel as shown in Figure 7.44. Observe that $s(t)$ must be differentiable everywhere in the interval $-\infty < t < \infty$; but we assume that $s(t) = 0$, $t < 0$, and $t > T$. Therefore, $s(0)$ and $s(T)$ must also be zero. This restriction is intuitively logical. Recall the loose argument we made previously: if there were a step in the signal and it was differentiated formally, the result would be an impulse plus a white noise and lead to perfect detection. This is obviously not the actual physical case. By giving the pulse a finite rise time or including some white noise we avoid this condition.

We see that the receiver does not use any of the received waveform outside the interval $0 \leq t \leq T$, even though it is available. Thus, we should expect the solution for $T_i = 0$ and $T_f = T$ to be identical. We shall see shortly that it is.

Clearly, this result will hold whenever the noise spectrum has *only poles*, because the whitening filter is a weighted sum of derivative operators. When the total noise spectrum has zeros, a longer observation time will help the detectability. Observe that when independent white noise is present, the total noise spectrum will always have zeros. ■

Before leaving the section, it is worthwhile to summarize some of the important results.

1. For rational colored noise spectra and nonzero independent white noise, the infinite-interval performance is better than any finite observation interval. Thus, the infinite-interval performance that is characterized by d_∞^2 provides a simple bound on the finite-interval performance. For the particular one-pole spectrum in Example 7.8,

a realizable, stable whitening filter can be found. This filter is *not* unique. In Chapter 8, we shall again encounter whitening filters for rational spectra. At that time we demonstrate how to find whitening filters for arbitrary rational spectra.

2. For rational colored noise spectra with no zeros and no white noise the interval in which the signal is nonzero is the only region of importance. In this case, the whitening filter is realizable but not stable (it contains differentiators).

We now consider stationary noise processes and a finite observation interval.

7.3.6.2 Finite Observation Interval: Rational Spectra¹⁰

In this section, we consider some of the properties of integral equations over a finite interval. Most of the properties have been proved in standard texts on integral equations (e.g. [CH53]). They have also been discussed in a clear manner in the detection theory context by Helstrom [Hel60]. We now state some simple properties that are useful and work some typical examples.

The first equation of interest is (7.204),

$$\sqrt{E} s(t) = \int_{T_i}^{T_f} g(u) K_n(t, u) du, \quad T_i \leq t \leq T_f, \quad (7.252)$$

where $s(t)$ and $K_n(t, u)$ are known. We want to solve for $g(t)$. Two special cases should be considered separately.

Case 1. The kernel $K_n(t, u)$ does not contain singularities. Physically, this means that there is *no white noise* present. Here, (7.252) is a *Fredholm* equation of the *first kind*, and we can show (see [CH53]) that if the range (T_i, T_f) is finite a continuous square-integrable solution will *not* exist in general. We shall find that we can always obtain a solution if we allow singularity functions (impulses and their derivatives) in $g(u)$ at the end points of the observation interval.

In Section 7.3.7, we show that whenever $g(t)$ is *not* square-integrable the test is unstable with respect to small perturbations in the model assumptions.

We have purposely excluded Case No. 1 from most of our discussion on physical grounds. In this section, we shall do a simple exercise to show the result of letting the white noise level go to zero. We shall find that in the absence of white noise we must put additional restrictions on $s(t)$ to get physically meaningful results.

Case 2. The noise contains a *nonzero* white noise term. We may then write

$$K_n(t, u) = \frac{N_0}{2} \delta(t - u) + K_c(t, u), \quad (7.253)$$

¹⁰The integral equations in Section 6.4 are special cases of the equations studied in this section. Conversely, if the equation specifying the eigenfunctions and eigenvalues has already been solved, then the solutions to the equations in the section follow easily.

where $K_c(t, u)$ is a continuous square-integrable function. Then (7.178) is the equation of interest,

$$\sqrt{E} s(t) = \frac{N_0}{2} g(t) + \int_{T_i}^{T_f} K_c(t, u) g(u) du, \quad T_i \leq t \leq T_f. \quad (7.254)$$

This equation is called a *Fredholm* equation of the *second kind*. A continuous, square-integrable solution for $g(t)$ will always exist when $K_c(t, u)$ is a continuous square-integrable function.

We now discuss two types of kernels in which straightforward procedures for solving (7.252) and (7.254) are available.

Type A (Rational Kernels). The noise $n_c(t)$ is the steady-state response of a lumped, linear passive network excited with white Gaussian noise. Here, the covariance function depends only on $(t - u)$ and we may write

$$K_c(t, u) = K_c(t - u) = K_c(\tau). \quad (7.255)$$

The transform is

$$S_c(\omega) = \int_{-\infty}^{\infty} K_c(\tau) e^{-j\omega\tau} d\tau \triangleq \frac{N(\omega^2)}{D(\omega^2)}, \quad (7.256)$$

and is a ratio of two polynomials in ω^2 . The numerator is of order q in ω^2 and the denominator is of order p in ω^2 . We assume that $n_c(t)$ has finite power so $p - q \geq 1$. Kernels whose transforms satisfy (7.256) are called *rational kernels*.

Integral equations with this type of kernel have been studied in detail in [ZR52, MZ56, You57], ([Mid60a], pp. 1082–1102; [LB56], pp. 309–329), and [Dar58]. We shall discuss a simple example that illustrates the techniques and problems involved.

Type B (separable Kernels). The covariance function of the noise can be written as

$$K_c(t, u) = \sum_{i=1}^K \lambda_i \phi_i(t) \phi_i(u), \quad T_i \leq t, u \leq T_f, \quad (7.257)$$

where K is *finite*. This type of kernel is frequently present in radar problems when there are multiple targets. As we shall see in a later section, the solution to (7.252) is straightforward. We refer to this type of kernel as *separable*. Observe that if we had allowed $K = \infty$ all kernels would be considered separable, for we can always write

$$K_c(t, u) = \sum_{i=1}^{\infty} \lambda_i \phi_i(t) \phi_i(u), \quad T_i \leq t, u \leq T_f, \quad (7.258)$$

where the λ_i and $\phi_i(t)$ are the eigenvalues and eigenfunctions. Clearly, this is *not* a practical solution technique because we have to solve another integral equation to find the $\phi_i(t)$.

We consider rational kernels in this section and separable kernels in the next.

Fredholm Equations of the First Kind: Rational Kernels. The basic technique is to find a differential equation corresponding to the integral equation. Because of the form of the kernel, this will be a differential equation with constant coefficients whose solution can be readily obtained. In fact, the particular solution of the differential equation is precisely the $g_\infty(t)$ that we derived in the last section (7.242). An integral equation with a rational kernel corresponds to a differential equation *plus* a set of boundary conditions. To incorporate the boundary conditions, we substitute the particular solution plus a weighted sum of the homogeneous solutions back into the integral equation and try to adjust the weightings so that the equation will be satisfied. It is at this point that we may have difficulty. To illustrate the technique and the possible difficulties we may meet, we consider a simple example. The first step is to show how $g_\infty(t)$ enters the picture. Assume that

$$S_n(\omega) = \frac{N(\omega^2)}{D(\omega^2)}, \quad (7.259)$$

and recall that

$$\delta(t - u) = \int_{-\infty}^{\infty} e^{j\omega(t-u)} \frac{d\omega}{2\pi}. \quad (7.260)$$

Differentiation with respect to t gives

$$p\delta(t - u) = \int_{-\infty}^{\infty} j\omega e^{j\omega(t-u)} \frac{d\omega}{2\pi}, \quad (7.261)$$

where $p \triangleq d/dt$. More generally,

$$N(-p^2)\delta(t - u) = \int_{-\infty}^{\infty} N(\omega^2) e^{j\omega(t-u)} \frac{d\omega}{2\pi}. \quad (7.262)$$

In an analogous fashion

$$D(-p^2)K_n(t - u) = \int_{-\infty}^{\infty} D(\omega^2) S_n(\omega) e^{j\omega(t-u)} \frac{d\omega}{2\pi}. \quad (7.263)$$

From (7.259), we see that the right-hand sides of (7.262) and (7.263) are identical. Therefore, the kernel satisfies the differential equation obtained by equating the left-hand sides of (7.262) and (7.263):

$$N(-p^2)\delta(t - u) = D(-p^2)K_n(t - u). \quad (7.264)$$

Now the integral equation of interest is

$$\sqrt{E}s(t) = \int_{T_i}^{T_f} K_n(t - u) g(u) du, \quad T_i \leq t \leq T_f. \quad (7.265)$$

Operating on both sides of this equation with $D(-p^2)$, we obtain

$$D(-p^2) \sqrt{E} s(t) = \int_{T_i}^{T_f} D(-p^2) K_n(t-u) g(u) du, \quad T_i \leq t \leq T_f. \quad (7.266)$$

Using (7.266) on the right-hand side, we have

$$D(-p^2) \sqrt{E} s(t) = N(-p^2) g(t), \quad T_i \leq t \leq T_f, \quad (7.267)$$

but from our previous results (7.242) we know that if the observation interval were infinite,

$$D(\omega^2) \sqrt{E} S(j\omega) = N(\omega^2) G_\infty(j\omega) \quad (7.268)$$

or

$$D(-p^2) \sqrt{E} s(t) = N(-p^2) g_\infty(t), \quad -\infty < t < \infty. \quad (7.269)$$

Thus, $g_\infty(t)$ corresponds to the *particular* solution of (7.267). There are also *homogeneous* solutions to (7.267):

$$0 = N(-p^2) g_{h_i}(t), \quad i = 1, 2, \dots, 2q. \quad (7.270)$$

We now add the particular solution $g_\infty(t)$ to a weighted sum of the $2q$ homogeneous solutions $g_{h_i}(t)$, substitute the result back into the integral equation, and adjust the weightings to satisfy the equation. At this point the discussion will be clearer if we consider a specific example.

Example 7.10. We consider the spectrum in (7.249) and use limits $[0, T]$ for algebraic simplicity.

$$K_n(t-u) = K_n(\tau) = \sigma_n^2 e^{-k|\tau|}, \quad -\infty < \tau < \infty \quad (7.271)$$

or

$$S_n(\omega) = \frac{2k\sigma_n^2}{\omega^2 + k^2}. \quad (7.272)$$

Thus,

$$N(\omega^2) = 2k\sigma_n^2 \quad (7.273)$$

and

$$D(\omega^2) = \omega^2 + k^2. \quad (7.274)$$

The differential equation (7.266) is

$$\sqrt{E} (-s''(t) + k^2 s(t)) = 2k\sigma_n^2 g(t). \quad (7.275)$$

The particular solution is

$$g_\infty(t) = \frac{\sqrt{E}}{2k\sigma_n^2} [-s''(t) + k^2 s(t)] \quad (7.276)$$

and there is no homogeneous solution as

$$q = 0. \quad (7.277)$$

Substituting back into the integral equation, we obtain

$$\sqrt{E} s(t) = \sigma_n^2 \int_0^T \exp(-k|t-u|) g(u) du, \quad 0 \leq t \leq T. \quad (7.278)$$

For $g(t)$ to be a solution, we require,

$$s(t) = \sigma_n^2 \left\{ e^{-kt} \int_0^t e^{+ku} \left[\frac{-s''(u) + k^2 s(u)}{2k\sigma_n^2} \right] du + e^{+kt} \int_t^T e^{-ku} \left[\frac{-s''(u) + k^2 s(u)}{2k\sigma_n^2} \right] du \right\}, \quad 0 \leq t \leq T. \quad (7.279)$$

Because there are no homogeneous solutions, there are no weightings to adjust. Integrating by parts we obtain the equivalent requirement,

$$0 = e^{-kt} \left\{ \frac{1}{2k} [s'(0) - ks(0)] \right\} - e^{+kt-T} \left\{ \frac{1}{2k} [s'(T) + ks(T)] \right\}, \quad 0 \leq t \leq T. \quad (7.280)$$

Clearly, the two terms in brackets must vanish independently in order for $g_\infty(t)$ to satisfy the integral equation. If they do, then our solution is complete. Unfortunately, the signal behavior at the end points often will cause the terms in the brackets to be nonzero. We must add something to $g_\infty(t)$ to cancel the e^{-kt} and e^{kt-T} terms. We denote this additional term by $g_\delta(t)$ and choose it so that

$$\sigma_n^2 \int_0^T \exp(-k|t-u|) g_\delta(u) du = -\frac{1}{2k} [s'(0) - ks(0)] e^{-kt} + \frac{1}{2k} [s'(T) + ks(T)] e^{+kt-T}, \quad 0 \leq t \leq T. \quad (7.281)$$

To generate an e^{-kt} term $g_\delta(u)$ must contain an impulse $c_1\delta(u)$. To generate an e^{+kt-T} term $g_\delta(u)$ must contain an impulse $c_2\delta(u-T)$. Thus,

$$g_\delta(u) = c_1\delta(u) + c_2\delta(u-T), \quad (7.282)$$

where

$$c_1 = \frac{ks(0) - s'(0)}{k\sigma_n^2},$$

$$c_2 = \frac{ks(T) - s'(T)}{k\sigma_n^2}, \quad (7.283)$$

to satisfy (7.280).¹¹ Thus, the complete solution to the integral equation is

$$g(t) = g_\infty(t) + g_\delta(t), \quad 0 \leq t \leq T. \quad (7.284)$$

¹¹We assume that the impulse is symmetric. Thus, only one half its area is in the interval.

From (7.161) and (7.162), we see that the output of the processor is

$$\begin{aligned} l &= \int_0^T r(t)g(t) dt \\ &= \frac{c_1}{2}r(0) + \frac{c_2}{2}r(T) + \int_0^T r(t) \left\{ \sqrt{E} \left[\frac{k^2 s(t) - s''(t)}{2k\sigma_n^2} \right] \right\} dt. \end{aligned} \quad (7.285)$$

Thus, the optimum processor consists of a *filter* and a *sampler*.

Observe that $g(t)$ will be square-integrable only when c_1 and c_2 are zero. We discuss the significance of this point in Section 7.3.7. ■

When the spectrum has more poles, higher order singularities must be added at the end points. When the spectrum has zeros, there will be homogeneous solutions, which we denote as $g_{h_i}(t)$. Then we can show that the general solution is of the form

$$g(t) = g_\infty(t) + \sum_{i=1}^{2q} a_i g_{h_i}(t) + \sum_{k=0}^{p-q-1} [b_k \delta^{(k)}(t) + c_k \delta^{(k)}(t-T)], \quad (7.286)$$

where $2p$ is the order of $D(\omega^2)$ as a function of ω and $2q$ is the order of $N(\omega^2)$ as a function of ω (e.g. [ZR52]). The function $\delta^{(k)}(t)$ is the k th derivative of $\delta(t)$. A great deal of effort has been devoted to finding efficient methods of evaluating the coefficients in (7.286) (e.g. [Wol59, Hel65]).

As we have pointed out, whenever we assume that white noise is present, the resulting integral equation will be a Fredholm equation of the second kind. For rational spectra the solution techniques are similar but the character of the solution is appreciably different.

Fredholm Equations of the Second Kind: Rational Kernels. The equation of interest is (7.254)

$$\sqrt{E} s(t) = \frac{N_0}{2} g(t) + \int_{T_i}^{T_f} K_c(t, u) g(u) du, \quad T_i \leq t \leq T_f. \quad (7.287)$$

We assume that the noise is stationary with spectrum $S_n(\omega)$,

$$S_n(\omega) = \frac{N_0}{2} + S_c(\omega) \triangleq \frac{N(\omega^2)}{D(\omega^2)}. \quad (7.288)$$

[Observe that $N(\omega^2)$ and $D(\omega^2)$ are of the same order (this is because $S_c(\omega)$ has finite power).] Proceeding in a manner identical to the preceding section, we obtain a differential equation that has a particular solution, $g_\infty(t)$, and homogeneous solutions, $g_{h_i}(t)$. Substituting

$$g(t) = g_\infty(t) + \sum_{i=1}^{2q} a_i g_{h_i}(t) \quad (7.289)$$

into the integral equation, we find that by suitably choosing the a_i we can always obtain a solution to the integral equation. [No $g_\delta(t)$ is necessary because we have enough weightings

(or degrees of freedom) to satisfy the boundary conditions.] A simple example illustrates the technique.

Example 7.11. Let

$$K_c(t, u) = \sigma_c^2 \exp(-k|t - u|), \quad (7.290)$$

the corresponding spectrum is

$$S_c(\omega) = \frac{\sigma_c^2 2k}{\omega^2 + k^2}. \quad (7.291)$$

Then

$$\begin{aligned} S_n(\omega) &= \frac{N_0}{2} + \frac{\sigma_c^2 2k}{\omega^2 + k^2} = \frac{(N_0/2)[\omega^2 + k^2(1 + 4\sigma_c^2/kN_0)]}{\omega^2 + k^2} \\ &\triangleq \frac{N(\omega^2)}{D(\omega^2)}. \end{aligned} \quad (7.292)$$

The integral equation is [using the interval $(0, T)$ for simplicity]

$$\sqrt{E}s(t) = \frac{N_0}{2}g(t) + \sigma_c^2 \int_0^T e^{-k|t-u|}g(u)du, \quad 0 \leq t \leq T. \quad (7.293)$$

The corresponding differential equation follows easily from (7.292),

$$\sqrt{E}(-s''(t) + k^2 s(t)) = \frac{N_0}{2}[-g''(t) + \gamma^2 g(t)], \quad (7.294)$$

where $\gamma^2 \triangleq k^2(1 + 4\sigma_c^2/kN_0)$. The particular solution is just $g_\infty(t)$. This can be obtained by solving the differential equation directly or by transform methods.

$$g_\infty(t) = \int_{-\infty}^{\infty} e^{+j\omega t} G_\infty(j\omega) \frac{d\omega}{2\pi}, \quad 0 \leq t \leq T, \quad (7.295)$$

$$g_\infty(t) = \frac{2\sqrt{E}}{N_0} \int_{-\infty}^{\infty} e^{+j\omega t} \left(\frac{\omega^2 + k^2}{\omega^2 + \gamma^2} \right) S(j\omega) \frac{d\omega}{2\pi}, \quad 0 \leq t \leq T. \quad (7.296)$$

The homogeneous solutions are

$$\begin{aligned} g_{h_1}(t) &= e^{\gamma t}, \\ g_{h_2}(t) &= e^{-\gamma t}. \end{aligned} \quad (7.297)$$

Then

$$g(t) = g_\infty(t) + a_1 e^{+\gamma t} + a_2 e^{-\gamma t}, \quad 0 \leq t \leq T. \quad (7.298)$$

Substitution of (7.298) into (7.293) will lead to two simultaneous equations that a_1 and a_2 must satisfy. Solving for a_1 and a_2 explicitly gives the complete solution. Several typical cases are contained in the problems.

The particular property of interest is that a solution can always be found without having to add singularity functions. Thus, the white noise assumption guarantees a square-integrable solution. (the convergence of the series in (7.172) and (7.179) implies that the solution is square-integrable.) ■

The final integral equation of interest is the one that specifies $h_o(t, u)$, (7.171). Rewriting it for the interval $[0, T]$, we have

$$h_o(t, z) + \frac{2}{N_0} \int_0^T K_c(t, u) h_o(u, z) du = \frac{2}{N_0} K_c(t, z), \quad 0 \leq t, z \leq T. \quad (7.299)$$

We observe that this is identical to (7.287) in the preceding problem, except that there is an extra variable in each expression. Thus, we can think of t as a fixed parameter and z as a variable or vice versa. In either case, we have a Fredholm equation of the second kind.

For rational kernels the procedure is identical. We illustrate this with a simple example.

Example 7.12.

$$K_c(u, z) = \sigma_s^2 \exp(-k|u - z|) h_o(t, z) + \frac{2}{N_0} \int_0^T h_o(t, u) \sigma_s^2 \exp(-k|u - z|) du \quad (7.300)$$

$$= \frac{2}{N_0} \sigma_s^2 \exp(-k|t - z|), \quad 0 \leq t, z \leq T. \quad (7.301)$$

Using the operator $k^2 - p^2$ and the results of (7.264) and (7.292), we have

$$\begin{aligned} & \left(p \triangleq \frac{d}{dz} \right), \\ & (k^2 - p^2) h_o(t, z) + \frac{2\sigma_s^2}{N_0} \cdot 2kh_o(t, z) = \frac{2\sigma_s^2}{N_0} 2k\delta(t - z), \end{aligned} \quad (7.302)$$

or

$$(1 + \Lambda) h_o(t, z) - \frac{p^2}{k^2} h_o(t, z) = \Lambda \delta(t - z), \quad (7.303)$$

where

$$\Lambda = \frac{4\sigma_s^2}{kN_0}. \quad (7.304)$$

Let $\beta^2 = k^2(1 + \Lambda)$. The particular solution is

$$h_{op}(t, z) = \frac{2\sigma_s^2}{N_0 \sqrt{1 + \Lambda}} \exp\left(-k\sqrt{1 + \Lambda}|t - z|\right), \quad 0 \leq t, z \leq T. \quad (7.305)$$

Now add homogeneous solutions $a_1(t)e^{+\beta z}$ and $a_2(t)e^{-\beta z}$ to the particular solution in (7.305) and substitute the result into (7.300). We find that we require

$$a_1(t) = \frac{2k\sigma_s^2(\beta - k)[(\beta + k)e^{+\beta t} + (\beta - k)e^{-\beta t}]e^{-\beta T}}{N_0\beta[(\beta + k)^2 e^{\beta T} - (\beta - k)^2 e^{-\beta T}]} \quad (7.306)$$

and

$$a_2(t) = \frac{2k\sigma_s^2(\beta - k)[(\beta + k)e^{+\beta(T-t)} + (\beta - k)e^{-\beta(T-t)}]}{N_0\beta[(\beta + k)^2 e^{\beta T} - (\beta - k)^2 e^{-\beta T}].} \quad (7.307)$$

The entire solution is

$$h_o(z, t) = \frac{2k\sigma_s^2 [(\beta + k)e^{+\beta z} + (\beta - k)e^{-\beta z}] [(\beta + k)e^{+\beta(T-t)} + (\beta - k)e^{-\beta(T-t)}]}{N_0\beta [(\beta + k)^2 e^{+\beta T} - (\beta - k)^2 e^{-\beta T}]}, \quad 0 \leq z \leq t \leq T. \quad (7.308)$$

The solution is symmetric in z and t . This is clearly not a very appealing function to mechanize. An important special case that we will encounter later is the one in which the colored noise component is small. Then $\beta \simeq k$ and

$$h_o(z, t) \simeq \frac{2\sigma_s^2}{N_0} \exp -\beta|t - z|, \quad 0 \leq z, t \leq T. \quad (7.309)$$

■

The important property to observe about (7.299) is that the extra variable complicates the algebra but the basic technique is still applicable.

This completes our discussion of integral equations with rational kernels and finite-time intervals.

Several observations may be made:

1. The procedure is straightforward but tedious.
2. When there is no white noise, certain restrictions must be placed on $s(t)$ to guarantee that $g(t)$ will be square-integrable.
3. When white noise is present, increasing the observation interval always improves the performance.
4. The solution for $h_o(t, u)$ for arbitrary colored noise levels appears to be too complex to implement. We can use the d^2 derived from it (7.207) as a basis of comparison for simpler mechanizations. [In Chapter 8, we discuss an easier implementation of $h_o(t, u)$.]

7.3.6.3 Finite Observation Time: Separable Kernels

As a final category, we consider integral equations with separable kernels. By contrast with the tedium of the preceding section, the solution for separable kernels follows almost by inspection. In this case

$$K_c(t, u) = \sum_{i=1}^K \lambda_i \phi_i(t) \phi_i(u), \quad T_i \leq t, u \leq T_f, \quad (7.310)$$

where λ_i and $\phi_i(t)$ are the eigenvalues and eigenfunctions of $K_c(t, u)$. Observe that (7.310) says that the noise has only K nonzero eigenvalues. Thus, unless we include a white noise component, we may have a singular problem. We include the white noise component and then observe that the solution for $h_o(t, u)$ is just a truncated version of the infinite series in (7.172). Thus,

$$h_o(t, u) = \sum_{i=1}^K \frac{\lambda_i}{N_0/2 + \lambda_i} \phi_i(t) \phi_i(u), \quad T_i \leq t, u \leq T_f, \quad (7.311)$$

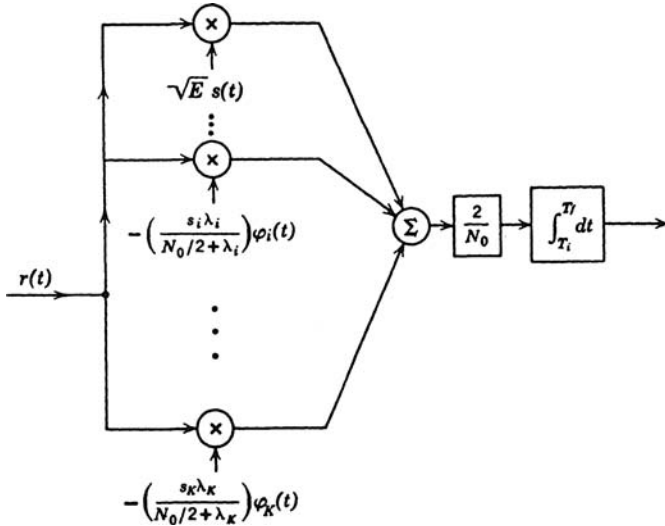


Figure 7.45: Optimum receiver: separable noise process.

The solution to (7.162) follows easily. Using (7.311) in (7.170) and the result in (7.162), we obtain

$$g(t) = \int_{T_i}^{T_f} du \sqrt{E}s(u) \frac{2}{N_0} \left[\delta(t-u) - \sum_{i=1}^K \frac{\lambda_i}{N_0/2 + \lambda_i} \phi_i(t)\phi_i(u) \right] T_i < t < T_f. \quad (7.312)$$

Recalling the definition of s_i in (7.210) and recalling that $g(t)$ is continuous at the end points, we have

$$g(t) = \begin{cases} \frac{2}{N_0} \left[\sqrt{E}s(t) - \sum_{i=1}^K \frac{s_i \lambda_i}{N_0/2 + \lambda_i} \phi_i(t) \right], & T_i \leq t \leq T_f, \\ 0, & \text{Elsewhere.} \end{cases} \quad (7.313)$$

This receiver structure is shown in Figure 7.45. Fortunately, in addition to having a simple solution, the separable kernel problem occurs frequently in practice.

A typical case is shown in Figure 7.46. Here, we are trying to detect a target in the presence of an interfering target and white noise.

Let

$$\begin{aligned} H_1 : r(t) &= \sqrt{E}s(t) + a_I s_I(t) + w(t), & T_i \leq t \leq T_f, \\ H_0 : r(t) &= a_I s_I(t) + w(t), & T_i \leq t \leq T_f. \end{aligned} \quad (7.314)$$

If we assume that a_I and $s_I(t)$ are known, the problem is trivial. The simplest nontrivial model is to assume that $s_I(t)$ is a known normalized waveform but a_I is a zero-mean Gaussian random variable, $N(0, \sigma_I^2)$.

Then

$$K_n(t, u) = \sigma_I^2 s_I(t)s_I(u) + \frac{N_0}{2} \delta(t-u), \quad T_i \leq t, u \leq T_f. \quad (7.315)$$

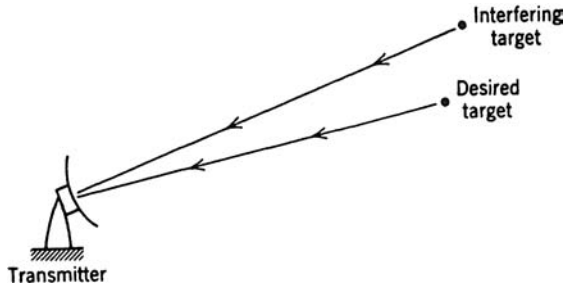


Figure 7.46: Detection in presence of interfering target.

This is a special case of the problem we have just solved. The receiver is shown in Figure 7.47a. The function $g(t)$ is obtained from (7.313). It can be redrawn, as shown in Figure 7.47b, to illustrate the estimator-subtractor interpretation (this is obviously not an efficient realization). The performance index is obtained from (7.209),

$$d^2 = \frac{2E}{N_0} \left(1 - \frac{2\sigma_I^2/N_0}{1 + 2\sigma_I^2/N_0} \rho_I^2 \right), \quad (7.316)$$

where

$$\rho_I \triangleq \int_{T_i}^{T_f} s(t) s_I(t) dt. \quad (7.317)$$

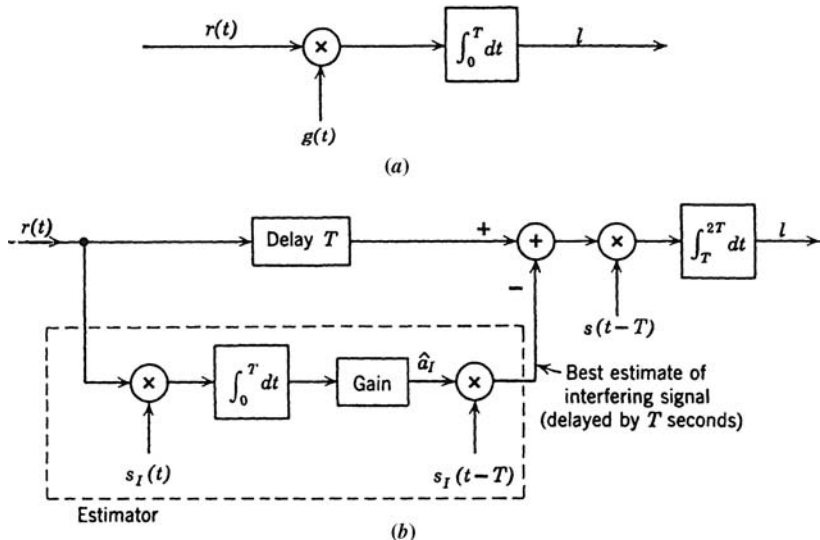


Figure 7.47: Optimum receiver: interfering targets.

Rewriting (7.316), we have

$$d^2 = \frac{2E}{N_0} \left[\frac{1 + 2\sigma_I^2/N_0(1 - \rho_I^2)}{1 + 2\sigma_I^2/N_0} \right] \quad (7.318)$$

as $\rho_I \rightarrow 0$, $d^2 \rightarrow 2E/N_0$. This result is intuitively logical. If the interfering signal is orthogonal to $s(t)$, then, regardless of its strength, it should not degrade the performance. On the other hand, as $\rho_I \rightarrow 1$,

$$d^2 \rightarrow \frac{2E/N_0}{1 + 2\sigma_I^2/N_0}. \quad (7.319)$$

Now the signals on the two hypotheses are equal and the difference in their amplitudes is the only basis for making a decision.

It is useful to discuss this model from a different viewpoint. We generalize the model. The received signal is

$$H_1 : r(t) = s(t) + \sum_{i=1}^K a_i s_i(t) + w(t), \quad T_i \leq t \leq T_f, \quad (7.320)$$

$$H_0 : r(t) = \sum_{i=1}^K a_i s_i(t) + w(t), \quad T_i \leq t \leq T_f. \quad (7.321)$$

where the $s_i(t)$ are known normalized linearly independent signals and the a_i are Gaussian random variables.

We define

$$\mathbf{s}_c(t) = [s_1 \quad s_2 \quad \cdots \quad s_K(t)]^T \quad (7.322)$$

and

$$\mathbf{a} = [a_1 \quad a_2 \quad \cdots \quad a_k]^T. \quad (7.323)$$

Now $\mathbf{s}_c(t)$ defines a K -dimensional interference subspace. Thus, we can reduce this to vector model by correlating $r(t)$ with $\mathbf{s}_c(t)$. On H_0 ,

$$r_i = \mathbf{a}^T \int_{T_i}^{T_f} r(t) s_i(t) dt \triangleq \mathbf{a}^T \rho_i + w_i. \quad (7.324)$$

We define an $N \times 1$ matrix,

$$\boldsymbol{\rho}_i \triangleq \int_{T_i}^{T_f} \mathbf{s}_c(t) s_i(t) dt, \quad (7.325)$$

$$\mathbf{r} = \begin{bmatrix} \boldsymbol{\rho}_1^T \mathbf{a} \\ \boldsymbol{\rho}_2^T \mathbf{a} \\ \vdots \\ \boldsymbol{\rho}_K^T \mathbf{a} \end{bmatrix} \triangleq \boldsymbol{\rho}_c \mathbf{a} + \mathbf{w}_c, \quad (7.326)$$

where ρ_c is $N \times N$. Therefore,

$$\mathbf{K}_{\mathbf{s}_c} = E\{\mathbf{s}_c \mathbf{s}_c^T\} = E\{\rho_c \mathbf{a} \mathbf{a}^T \rho_c^T\} = \rho_c \mathbf{K}_a \rho_c \quad (7.327)$$

since ρ_c is symmetric, and

$$\mathbf{K}_{\mathbf{w}_c} = \frac{N_0}{2} \rho_c \quad (7.328)$$

so

$$\mathbf{K}_{\mathbf{n}} = \rho_c \mathbf{K}_a \rho_c + \frac{N_0}{2} \rho_c. \quad (7.329)$$

Defining

$$\mathbf{s} = \int_{T_i}^{T_f} s(t) \mathbf{s}_c(t) dt \quad (7.330)$$

gives

$$H_1 : \mathbf{r} = \mathbf{s} + \mathbf{s}_c + \mathbf{w}_c, \quad (7.331)$$

$$H_0 : \mathbf{r} = \mathbf{s}_c + \mathbf{w}_c. \quad (7.332)$$

We have reduced the problem to the model in Section 3.2 and the optimum detector in Figure 3.4 is applicable. It is shown in Figure 7.48.

In many cases, this approach is more attractive because the mapping into the vector space only depends on $\mathbf{s}_c(t)$.

Summary of Integral Equations. In this section, we have developed techniques for solving the types of integral equation encountered in the detection and estimation problems in the presence of nonwhite noise. The character of the solution was determined by the presence or absence of a white noise component. The simplicity of the solution in the infinite-interval, stationary process case should be emphasized. Because the performance in this case always bounds the finite-interval, stationary process case, it is a useful preliminary calculation.

The extension of all three of these cases to the circular complex Gaussian model as straightforward. Fortunately, these three cases with their complex extensions cover the majority of the Gaussian problems that we encounter in practice.

As a final topic for the colored noise problem, we consider the sensitivity of the result to perturbations in the initial assumptions.

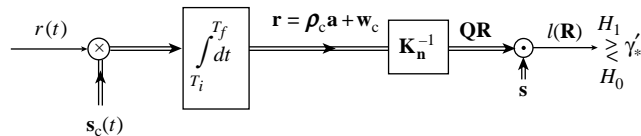


Figure 7.48: Optimum detector: separable kernel.

7.3.7 Sensitivity, Mismatch, and Diagonal Loading

In Section 7.3.7.1, we revisit the sensitivity problem that we discussed in Section 7.2.1.4. We focus our attention on worst-case analysis. In Section 7.3.7.2, we consider the case of mismatched models. The uniform linear array in Examples 5.17 and 5.18 provides a typical example.

7.3.7.1 Sensitivity

Up to this point in our discussion we have assumed that all the quantities needed to design the optimum receiver were known exactly. We want to investigate the effects of imperfect knowledge of these quantities. In order to obtain some explicit results we shall discuss the sensitivity issue in the context of the simple binary decision problem developed in Section 7.3.1. Specifically, the model assumed is

$$\begin{aligned} H_1 : r(t) &= \sqrt{E}s(t) + n(t), & T_i \leq t \leq T_f, \\ H_0 : r(t) &= n(t), & T_i \leq t \leq T_f, \end{aligned} \quad (7.333)$$

where $s(t)$, the signal, and $K_n(t, u)$, the noise covariance function, are assumed known. Just as in the white noise case, there are two methods of sensitivity analysis: the parameter variation approach and the functional variation approach. In the white noise case we varied the signal. Now the variations can include both the signal and the noise.

Typical parameter variation examples are formulated below:

1. Let the assumed signal be

$$s(t) = \begin{cases} \left(\frac{2}{T}\right)^{\frac{1}{2}} \sin \omega_c t, & 0 \leq t \leq T, \\ 0, & \text{Elsewhere,} \end{cases} \quad (7.334)$$

and the actual signal be

$$s_a(t) = \begin{cases} \left(\frac{2}{T}\right)^{\frac{1}{2}} \sin(\omega_c + \Delta\omega)t, & 0 \leq t \leq T, \\ 0, & \text{Elsewhere.} \end{cases} \quad (7.335)$$

Find $\Delta d/d$ as a function of $\Delta\omega$.

2. Let the assumed noise covariance be

$$K_n(t, u) = \frac{N_0}{2} \delta(t - u) + K_c(t, u) \quad (7.336)$$

and the actual covariance be

$$K_{na}(t, u) = \left(\frac{N_0 + \Delta N_0}{2} \right) \delta(t - u) + K_c(t, u). \quad (7.337)$$

Find $\Delta d/d$ as a function of ΔN_0 .

3. In the interfering target example of the last section (7.314) let the assumed interference signal be

$$s_I(t) = s(t - \tau). \quad (7.338)$$

In other words, it is a delayed version of the desired signal. Let the actual interference signal be

$$s_{Ia}(t) = s(t - \tau - \Delta\tau). \quad (7.339)$$

Find $\Delta d/d$ as a function of $\Delta\tau$.

These examples illustrate typical parameter variation problems. Clearly, the appropriate variations depend on the physical problem of interest. In almost all of them the succeeding calculations are straightforward. Some typical cases are included in the problems.

The functional variation approach is more interesting. As before, we do a “worst-case” analysis. Two examples are the following:

1. Let the actual signal be

$$s_a(t) = \sqrt{E}s(t) + \sqrt{E_\epsilon}s_\epsilon(t), \quad T_i \leq t \leq T_f, \quad (7.340)$$

where

$$\int_{T_i}^{T_f} s_\epsilon^2(t) dt = 1. \quad (7.341)$$

To find the worst case we choose $s_\epsilon(t)$ to make Δd as negative as possible.

2. Let the actual noise be

$$n_a(t) = n(t) + n_\epsilon(t) \quad (7.342)$$

whose covariance function is

$$K_{na}(t, u) = K_n(t, u) + K_{n\epsilon}(t, u). \quad (7.343)$$

We assume that $n_\epsilon(t)$ has finite energy in the interval

$$E \int_{T_i}^{T_f} n_\epsilon^2(t) dt \leq \Delta_n. \quad (7.344)$$

This implies that

$$\int_{T_i}^{T_f} \int_{T_i}^{T_f} K_{n\epsilon}^2(t, u) dt du \leq \Delta_n. \quad (7.345)$$

To find the worst case we choose $K_{n\epsilon}(t, u)$ to make Δd as negative as possible.

Various other perturbations and constraints are also possible. We now consider a simple version of the first problem. The second problem is developed in detail in [Roo64].

We assume that the noise process is stationary with a spectrum $S_n(\omega)$ and that the observation interval is infinite. The optimum receiver, using a whitening realization (see Figure 7.38a), is shown in Figure 7.49a. The corresponding decision space is shown in Figure 7.49b. The nominal performance is

$$d = \frac{E(l|H_1) - E(l|H_0)}{[\text{Var}(l|H_0)]^{\frac{1}{2}}} = \frac{\int_{-\infty}^{\infty} s_*^2(t) dt}{\left[\int_{-\infty}^{\infty} s_*^2(t) dt \right]^{\frac{1}{2}}} \quad (7.346)$$

or

$$d = \left[\int_{-\infty}^{\infty} s_*^2(t) dt \right]^{\frac{1}{2}}. \quad (7.347)$$

We let the actual signal be

$$s_a(t) = \sqrt{E}s(t) + \sqrt{E_\epsilon}s_\epsilon(t), \quad -\infty < t < \infty, \quad (7.348)$$

where $s(t)$ and $s_\epsilon(t)$ have unit energy. The output of the whitening filter will be

$$r_{*a}(t) \triangleq s_*(t) + s_{*\epsilon}(t) + n_*(t), \quad -\infty < t < \infty, \quad (7.349)$$

and the decision space will be as shown in Figure 7.49c. The only quantity that changes is $E(l_a|H_1)$. The variance is still the same because the noise covariance is unchanged. Thus,

$$\Delta d = \frac{1}{d} \int_{-\infty}^{\infty} s_{*\epsilon}(t)s_*(t) dt. \quad (7.350)$$

To examine the sensitivity we want to make Δd as negative as possible. If we can make $\Delta d = -d$, then the actual operating characteristic will be the $P_D = P_F$ line that is equivalent to a random test. If $\Delta d < -d$, the actual test will be worse than a random test. It is important to note that the constraint is on the energy in $s_\epsilon(t)$, not $s_{*\epsilon}(t)$. Using Parseval's theorem, we can write (7.350) as

$$\Delta d = \frac{1}{d} \int_{-\infty}^{\infty} S_{*\epsilon}(j\omega)S_*(j\omega) \frac{d\omega}{2\pi}. \quad (7.351)$$

This equation can be written in terms of the original quantities by observing that

$$S_{*\epsilon}(j\omega) = \sqrt{E_\epsilon} H_w(j\omega) S_\epsilon(j\omega) \quad (7.352)$$

and

$$S_*(j\omega) = \sqrt{E} H_w(j\omega) S(j\omega). \quad (7.353)$$

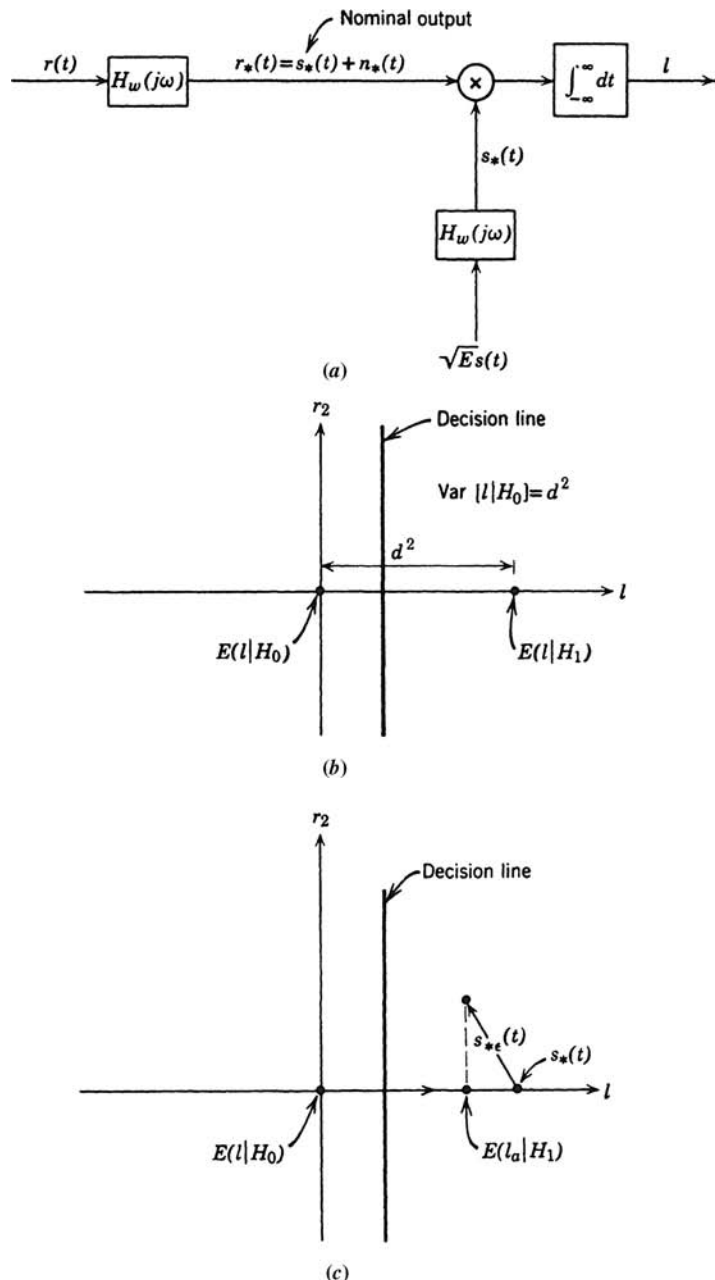


Figure 7.49: Sensitivity analysis: (a) Filter with nominal input; (b) nominal decision space; (c) actual design space.

Thus,

$$\begin{aligned}\Delta d &= \frac{\sqrt{EE_\epsilon}}{d} \int_{-\infty}^{\infty} \frac{d\omega}{2\pi} S_\epsilon(j\omega) |H_w(j\omega)|^2 S^*(j\omega) \\ &= \frac{\sqrt{EE_\epsilon}}{d} \int_{-\infty}^{\infty} S_\epsilon(j\omega) \frac{S^*(j\omega)}{S_n(\omega)} \frac{d\omega}{2\pi}.\end{aligned}\quad (7.354)$$

The constraint in (7.341) can be written as

$$\int_{-\infty}^{\infty} |S_\epsilon(j\omega)|^2 \frac{d\omega}{2\pi} = 1. \quad (7.355)$$

To perform a worst-case analysis we minimize Δd subject to the constraint in (7.355) by using Lagrange multipliers. Let

$$F = \Delta d + \lambda \left[\int_{-\infty}^{\infty} |S_\epsilon(j\omega)|^2 \frac{d\omega}{2\pi} - 1 \right]. \quad (7.356)$$

Minimizing with respect to $S_\epsilon(j\omega)$, we obtain

$$S_{\epsilon_o}(j\omega) = -\frac{\sqrt{EE_\epsilon}}{2\lambda d} \frac{S(j\omega)}{S_n(\omega)}, \quad (7.357)$$

(the subscript o denotes optimum). To evaluate λ we substitute into the constraint equation (7.355) and obtain

$$\frac{EE_\epsilon}{4\lambda^2 d^2} \int_{-\infty}^{\infty} \frac{|S(j\omega)|^2}{S_n^2(\omega)} \frac{d\omega}{2\pi} = 1. \quad (7.358)$$

If the integral exists, then

$$2\lambda = \frac{\sqrt{EE_\epsilon}}{d} \left[\int_{-\infty}^{\infty} \frac{|S(j\omega)|^2}{S_n^2(\omega)} \frac{d\omega}{2\pi} \right]^{1/2}. \quad (7.359)$$

Substituting into (7.357) and then (7.354), we have

$$\Delta d = -\left(\frac{EE_\epsilon}{d^2} \right)^{1/2} \left[\int_{-\infty}^{\infty} \frac{|S(j\omega)|^2}{S_n^2(\omega)} \frac{d\omega}{2\pi} \right]^{12}. \quad (7.360)$$

(Observe that we could also obtain (7.360) by using the Schwarz inequality in (7.354).) Using the frequency domain equivalent of (7.347), we have

$$\frac{\Delta d}{d} = -\left(\frac{E_\epsilon}{E}\right)^{\frac{1}{2}} \left\{ \frac{\left[\int_{-\infty}^{\infty} \frac{|S(j\omega)|^2}{S_n^2(\omega)} \frac{d\omega}{2\pi} \right]^{1/2}}{\left[\int_{-\infty}^{\infty} \frac{|S(j\omega)|^2}{S_n(\omega)} \frac{d\omega}{2\pi} \right]} \right\}. \quad (7.361)$$

In the white noise only case the term in the brace reduces to one and we obtain the same result as in (7.89). When the noise is not white, several observations are important:

1. If there is a white noise component, both integrals exist and the term in the braces is greater than or equal to one. (Use the Schwarz inequality on the denominator.) Thus, in the colored noise case a small-signal perturbation may cause a large change in performance.
2. If there is *no* white noise component *and* the nominal test is *not singular*, the integral in the denominator exists. Without further restrictions on $S(j\omega)$ and $S_n(\omega)$ the integral in the numerator may not exist. If it does not exist, the above derivation is not valid. In this case we can find an $S_\epsilon(j\omega)$ so that Δd will be less than any desired Δd_x . Choose

$$S_\epsilon(j\omega) = \begin{cases} k \frac{S(j\omega)}{S_n(\omega)}, & \omega \text{ in } \Omega, \\ 0, & \omega \text{ not in } \Omega, \end{cases} \quad (7.362)$$

where Ω is a region such that

$$k \frac{\sqrt{EE_\epsilon}}{d} \left(\int_{\Omega} \frac{|S(j\omega)|^2}{S_n(\omega)} \frac{d\omega}{2\pi} \right)^{1/2} = \Delta d_x \quad (7.363)$$

and k is chosen to satisfy the energy constraint on $s_\epsilon(t)$. We see that in the absence of white noise a signal perturbation exists that will make the test performance arbitrarily bad. Such tests are referred to as *unstable* (or infinitely sensitive) tests. We see that stability is a stronger requirement than nonsingularity and that the white noise assumption guarantees a nonsingular, stable test. Clearly, even though a test is stable, it may be extremely sensitive.

3. Similar results can be obtained for a finite-interval and nonstationary processes in terms of the eigenvalues. Specifically, we can show (e.g. [Roo64]) that the condition

$$\sum_{i=1}^{\infty} \frac{s_i^2}{\lambda_i^2} < \infty$$

is necessary and sufficient for stability. This is identical to the condition for $g(t)$ to be square-integrable.

In this section, we have illustrated some of the ideas involved in a sensitivity analysis of an optimum detection procedure. Although we have eliminated unstable tests by the white

noise assumption, it is still possible to encounter sensitive tests. In any practical problem it is essential to check the test sensitivity against possible parameter and function variations. We can find cases in which the test is too sensitive to be of any practical value. In these cases we try to design a test that is nominally suboptimum but less sensitive. Techniques for finding this test depend on the problem of interest. In the next section, we revisit the diagonal loading technique that is widely used in practice.

7.3.7.2 Mismatch and Diagonal Loading

In the previous section, we observed that a receiver designed assuming white noise is less sensitive than a receiver designed for a colored noise environment. The structure of the receiver is determined by (7.154)

$$K_n(t, u) = \frac{N_o}{2} \delta(t - u) + K_c(t, u) \quad (7.364)$$

or, in the stationary case,

$$S_n(\omega) = \frac{N_o}{2} + S_c(\omega). \quad (7.365)$$

We discussed this problem in the context of array processing in Part IV of DEMT, “Optimum Array Processing” [Van02] and in Chapter 5. In this case, the noise input is a vector with spectral matrix

$$\mathbf{S}_n(\omega) = \frac{N_o}{2} \mathbf{I} + \mathbf{S}_c(\omega). \quad (7.366)$$

The result is that we can design a robust receiver by assuming that

$$\mathbf{S}_n(\omega) = \frac{N_o}{2} \mathbf{I} + \sigma_L^2 \mathbf{I} + \mathbf{S}_c(\omega), \quad (7.367)$$

where $\sigma_L^2 \mathbf{I}$ is a *diagonal loading* term. By varying σ_L^2 we can trade-off robustness versus performance. The same approach applies in the scalar observation case,

$$S_n(\omega) = \left(\frac{N_o}{2} + \sigma_L^2 \right) + S_c(\omega). \quad (7.368)$$

We investigate several examples in the problems.

Before leaving the colored noise problem we consider briefly a closely related problem.

7.3.8 Known Linear Channels

There is an almost complete duality between the colored additive noise problem and the problem of transmitting through a known linear channel with memory. The latter is shown in Figure 7.50a.

The received waveform on H_1 in the simple binary problem is

$$r(t) = \int_{T_i}^{T_f} h_{ch}(t, u) \sqrt{E} s(u) du + w(t), \quad T_i \leq t \leq T_f. \quad (7.369)$$

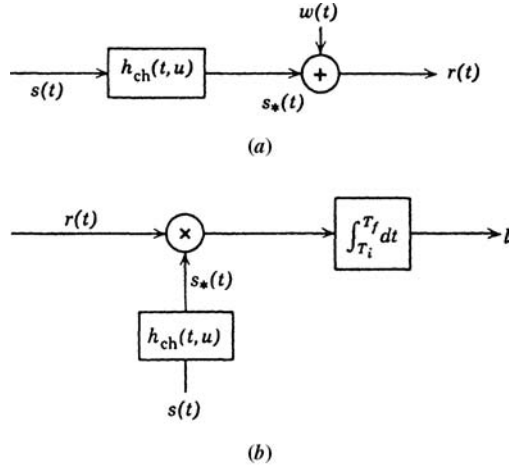


Figure 7.50: Known dispersive channel.

This is identical in form to (7.155). Thus, $h_{\text{ch}}(t, u)$ plays an analogous role to the whitening filter. The optimum receiver is shown in Figure 7.50b. The performance index is

$$\begin{aligned} d^2 &= \frac{2}{N_o} \int_{T_i}^{T_f} s_*^2(t) dt \\ &= \frac{2E}{N_o} \int_{T_i}^{T_f} dt \left[\int_a^b h_{\text{ch}}(t, u) s(u) du \int_a^b h_{\text{ch}}(t, v) s(v) dv \right], \end{aligned} \quad (7.370)$$

where the limits (a, b) depend on the channel's impulse response and the input signal duration. We assume that $T_i \leq a \leq b \leq T_f$. We can write this in a familiar quadratic form:

$$d^2 = \frac{2E}{N_0} \iint_a^b du dv s(u) Q_{\text{ch}}(u, v) s(v) \quad (7.371)$$

by defining

$$Q_{\text{ch}}(u, v) = \int_{T_i}^{T_f} h_{\text{ch}}(t, u) h_{\text{ch}}(t, v) dt, \quad a \leq u, v \leq b. \quad (7.372)$$

The only difference is that now $Q_{\text{ch}}(u, v)$ has the properties of a covariance function rather than an inverse kernel. A problem of interest is to choose $s(t)$ to maximize d^2 . The solution follows directly from our earlier signal design results. We can express d^2 in terms of the channel eigenvalues and eigenfunctions

$$d^2 = \frac{2}{N_0} \sum_{i=1}^{\infty} \lambda_i^{\text{ch}} s_i^2, \quad (7.373)$$

where

$$s_i \triangleq \int_a^b \sqrt{E} s(u) \phi_i(u) du, \quad (7.374)$$

and λ_i^{ch} and $\phi_i(u)$ correspond to the kernel $Q_{\text{ch}}(u, v)$. To maximize d^2 we choose

$$s_1 = \sqrt{E}, \quad (7.375)$$

$$s_i = 0, \quad i \neq 1, \quad (7.376)$$

because λ_1^{ch} is defined as the largest eigenvalue of the channel kernel $Q_{\text{ch}}(u, v)$. Some typical channels and their optimum signals are developed in the problems.

When we try to communicate sequences of signals over channels with memory, another problem arises. Looking at the basic communications system in Figure 7.1, we see that inside the basic interval $0 \leq t \leq T$ there is interference due to noise and there may be interference due to the sequence of signals corresponding to previous data. This second interference is referred to as the intersymbol interference and it turns out to be the major disturbance in many systems of interest. It is discussed in a number of communications books.

7.3.8.1 Summary

In this section, we have developed the optimum detectors and estimators for known signals in nonwhite Gaussian noise or interference. It is the waveform analog to the vector Gaussian model in Section 3.3 and the Gaussian estimation model in Chapter 5.

We discussed several approaches to the solution. When the nonwhite interference is full rank (infinite number of eigenvalues), the approach used most often in applications is the whitening approach. The key is finding an expression for the whitening filter, $h_w(t, u)$. For stationary processes we developed analytical techniques for both the finite and infinite observation interval. For the finite interval, we can always replace the integral equation by a matrix equation by densely sampling. We can then solve the matrix equation using Matlab to find \mathbf{Q}_n and use a Cholesky decomposition to obtain \mathbf{h}_w . In Chapter 8, we will introduce the state-variable representation of random process and derive an explicit solution for the whitening filter. For separable kernels, we can implement $Q_n(t, u)$ using a finite eigenexpansion.

In the next section, we discuss applications in which the signal contains unknown parameters.

7.4 SIGNALS WITH UNWANTED PARAMETERS: THE COMPOSITE HYPOTHESIS PROBLEM

Up to this point in Chapter 7, we have assumed that the signals of concern were completely known. The only uncertainty was caused by the additive noise. As we pointed out at the beginning of this chapter, in many physical problems of interest this assumption is not realistic. One example occurs in the radar problem. The transmitted signal is a high frequency pulse that acquires a random phase angle (and perhaps a random amplitude) when it is reflected from the target. Another example arises in the communications problem in which

there is an uncertainty in the oscillator phase. Both problems are characterized by the presence of an unwanted parameter.

Unwanted parameters appear in both detection and estimation problems. Because of the inherent similarities, it is adequate to confine our present discussion to the detection problem. In particular, we shall discuss general binary detection. In this case the received signals under the two hypotheses are

$$\begin{aligned} H_1 : r(t) &= s_1(t, \boldsymbol{\theta}) + n(t), & T_i \leq t \leq T_f, \\ H_0 : r(t) &= s_0(t, \boldsymbol{\theta}) + n(t), & T_i \leq t \leq T_f. \end{aligned} \quad (7.377)$$

The vector $\boldsymbol{\theta}$ denotes an unwanted vector parameter. The functions $s_0(t, \boldsymbol{\theta})$ and $s_1(t, \boldsymbol{\theta})$ are conditionally deterministic (i.e., if the value of $\boldsymbol{\theta}$ were known, the values of $s_0(t, \boldsymbol{\theta})$ and $s_1(t, \boldsymbol{\theta})$ would be known for all t in the observation interval). We see that this problem is just the waveform counterpart to the classical composite hypothesis testing problem discussed in Section 4.5. As we pointed out in that section, three types of situations can develop:

1. $\boldsymbol{\theta}$ is a random variable with a known *a priori* density;
2. $\boldsymbol{\theta}$ is a random variable with an unknown *a priori* density;
3. $\boldsymbol{\theta}$ is a nonrandom variable.

We focus most of our discussion here to the first situation. At the end of the section we comment briefly on the other two. The reason for this choice is that the two physical problems encountered most frequently in practice can be modeled by the first case. We discuss them in detail in Sections 7.4.1 and 7.4.2, respectively. We discuss the nonrandom case briefly in Section 7.4.3 and summarize our results in Section 7.4.4.

The technique for solving problems in the first category is straightforward. We choose a finite set of observables and denote them by the K -dimensional vector \mathbf{r} . We construct the likelihood ratio and then let $K \rightarrow \infty$.

$$\Lambda[r(t)] \triangleq \lim_{K \rightarrow \infty} \frac{p_{\mathbf{r}|H_1}(\mathbf{R}|H_1)}{p_{\mathbf{r}|H_0}(\mathbf{R}|H_0)}. \quad (7.378)$$

The only new feature is finding $p_{\mathbf{r}|H_1}(\mathbf{R}|H_1)$ and $p_{\mathbf{r}|H_0}(\mathbf{R}|H_0)$ in the presence of $\boldsymbol{\theta}$. If $\boldsymbol{\theta}$ were known, we should then have a familiar problem. Thus, an obvious approach is to write

$$p_{\mathbf{r}|H_1}(\mathbf{R}|H_1) = \int_{\chi_\theta} p_{\mathbf{r}|\boldsymbol{\theta}, H_1}(\mathbf{R}|\boldsymbol{\theta}, H_1) p_{\boldsymbol{\theta}|H_1}(\boldsymbol{\theta}|H_1) d\boldsymbol{\theta}, \quad (7.379)$$

and

$$p_{\mathbf{r}|H_0}(\mathbf{R}|H_0) = \int_{\chi_\theta} p_{\mathbf{r}|\boldsymbol{\theta}, H_0}(\mathbf{R}|\boldsymbol{\theta}, H_0) p_{\boldsymbol{\theta}|H_0}(\boldsymbol{\theta}|H_0) d\boldsymbol{\theta}. \quad (7.380)$$

Substituting (7.379) and (7.380) into (7.378) gives the likelihood ratio. The tractability of the procedure depends on the form of the functions to be integrated. In the next two sections, we consider two physical problems in which the procedure leads to easily interpretable results.

7.4.1 Random Phase Angles

In this section, we look at several physical problems in which the uncertainty in the received signal is due to a random phase angle. The first problem of interest is a radar problem. The transmitted signal is a bandpass waveform that may be both amplitude and phase modulated. We can write the transmitted waveform as

$$s_t(t) = \begin{cases} \sqrt{2E_t} f(t) \cos[\omega_c t + \phi(t)], & 0 \leq t \leq T, \\ 0, & \text{Elsewhere.} \end{cases} \quad (7.381)$$

Two typical waveforms are shown in Figure 7.51. The function $f(t)$ corresponds to the envelope and is normalized so that the transmitted energy is E_t . The function $\phi(t)$ corresponds to a phase modulation. Both functions are low frequency in comparison to ω_c .

For the present we assume that we simply want to decide whether a target is present at a particular range. If a target is present, the signal will be reflected. In the simplest case of a fixed-point target, the received waveform will be an attenuated version of the transmitted waveform with a random phase angle added to the carrier. In addition, there is an additive white noise component $w(t)$ at the receiver whether the target is present or not. If we define H_1 as the hypothesis that the target is present and H_0 as the hypothesis that the target is

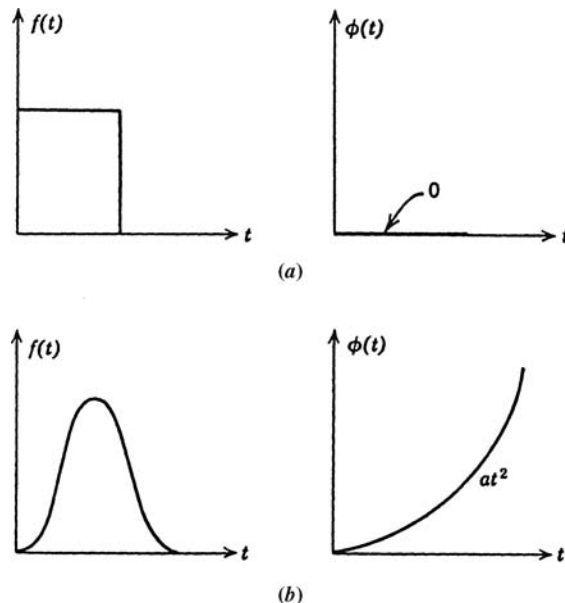


Figure 7.51: Typical envelope and phase functions.

absent, the following detection problem results:

$$\begin{aligned} H_1 : r(t) &= \sqrt{2E} f(t - \tau) \cos(\omega_c(t - \tau) \\ &\quad + \phi(t - \tau) + \theta) + w(t), & \tau \leq t \leq \tau + T \\ &= w(t), & T_i \leq t < \tau, \tau + T < t \leq T_f \\ &\triangleq s_r(t - \tau, \theta) + w(t), & T_i \leq t \leq T_f, \\ H_0 : r(t) &= w(t), & T_i \leq t \leq T_f. \end{aligned} \quad (7.382)$$

$$H_0 : r(t) = w(t), \quad T_i \leq t \leq T_f. \quad (7.383)$$

Because the noise is white, we need only observe over the interval $\tau \leq t \leq \tau + T$. Under the assumption that we are interested only in a particular τ , the model is the same if we let $\tau = 0$. Thus, we need only consider the problem

$$H_1 : r(t) = s_r(t, \theta) + w(t), \quad 0 \leq t \leq T, \quad (7.384)$$

$$H_0 : r(t) = w(t), \quad 0 \leq t \leq T. \quad (7.385)$$

Here, we have a simple binary detection problem in which the unknown parameter occurs only on one hypothesis. Before solving it we indicate how a similar problem can arise in the communications context.

In a simple on-off communication system we send a signal when the source output is “one” and nothing when the source output is “zero.” The transmitted signals on the two hypotheses are

$$\begin{aligned} H_1 : s_t(t) &= \sqrt{2E} f(t) \cos(\omega_c t + \phi(t) + \theta_a), & 0 \leq t \leq T, \\ H_0 : s_t(t) &= 0, & 0 \leq t \leq T. \end{aligned} \quad (7.386)$$

Frequently, we try to indicate to the receiver what θ_a is. One method of doing this is to send an auxiliary signal that contains information about θ_a . If this signal were transmitted through a noise-free channel, the receiver would know θ_a exactly and the problem would reduce to the known signal problem. More frequently the auxiliary signal is corrupted by noise and the receiver operates on the noise-corrupted auxiliary signal and tries to estimate θ_a . We denote this estimate by $\hat{\theta}_a$. A block diagram is shown in Figure 7.52. Now, if the estimate $\hat{\theta}_a$ equals θ_a , the problem is familiar. If they are unequal, the uncertainty is contained in the difference $\theta = \theta_a - \hat{\theta}_a$, which is a random variable. Therefore, we may consider the problem:

$$H_1 : r(t) = \sqrt{2E} f(t) \cos(\omega_c t + \phi(t) + \theta) + w(t), \quad 0 \leq t \leq T, \quad (7.387)$$

$$H_0 : r(t) = w(t), \quad 0 \leq t \leq T, \quad (7.388)$$

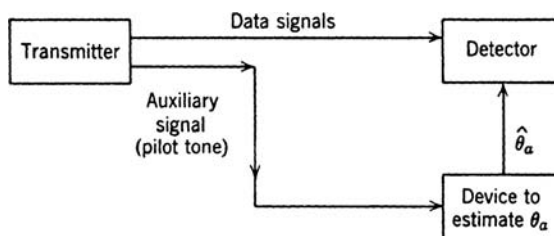


Figure 7.52: A phase estimation system.

where E_r is the actual received signal energy and θ is the phase measurement error. We see that the radar and communication problems lead to the same mathematical model.

The procedure for finding the likelihood ratio was indicated at the beginning of Section 4.4. In this particular case the model is so familiar [see (7.25)] that we can write down the form for $K \rightarrow \infty$ immediately. The resulting likelihood ratio is

$$\Lambda[r(t)] = \int_{-\pi}^{\pi} p_\theta(\theta) d\theta \exp \left[+\frac{2}{N_0} \int_0^T r(t) s_r(t, \theta) dt - \frac{1}{N_0} \int_0^T s_r^2(t, \theta) dt \right], \quad (7.389)$$

where we assume the range of θ is $[-\pi, \pi]$. The last integral corresponds to the received energy. In most cases of interest it will not be a function of the phase so we incorporate it in the threshold. To evaluate the other integral, we expand the cosine term in (7.387),

$$\cos[\omega_c t + \phi(t) + \theta] = \cos[\omega_c t + \phi(t)] \cos \theta - \sin[\omega_c t + \phi(t)] \sin \theta, \quad (7.390)$$

and define

$$L_c \triangleq \int_0^T \sqrt{2} r(t) f(t) \cos[\omega_c t + \phi(t)] dt, \quad (7.391)$$

and

$$L_s \triangleq \int_0^T \sqrt{2} r(t) f(t) \sin[\omega_c t + \phi(t)] dt. \quad (7.392)$$

Thus, the integral of interest is

$$\Lambda'[r(t)] = \int_{-\pi}^{\pi} p_\theta(\theta) d\theta \exp \left[\frac{2\sqrt{E_r}}{N_0} (L_c \cos \theta - L_s \sin \theta) \right]. \quad (7.393)$$

To proceed we must specify $p_\theta(\theta)$. Instead of choosing a particular density, we specify a family of densities indexed by a single parameter. We want to choose a family that will enable us to model as many cases of interest as possible. A family that will turn out to be useful is given in (7.394) and shown in Figure 7.53¹²:

$$p_\theta(\theta : \Lambda_m) = \frac{\exp[\Lambda_m \cos \theta]}{2\pi I_0(\Lambda_m)}, \quad -\pi \leq \theta \leq \pi. \quad (7.394)$$

The function $I_0(\Lambda_m)$ is a modified Bessel function of the first kind that is included so that the density will integrate to unity. For the present Λ_m can be regarded simply as a parameter that controls the spread of the density. When we studied phase estimators in DEMT-II [Van71a, Van03], we showed that it has an important physical significance.

Looking at Figure 7.53, we see that for $\Lambda_m = 0$

$$p_\theta(\theta) = \frac{1}{2\pi}, \quad -\pi \leq \theta \leq \pi. \quad (7.395)$$

¹²This density was first used for this application by Viterbi [Vit65].

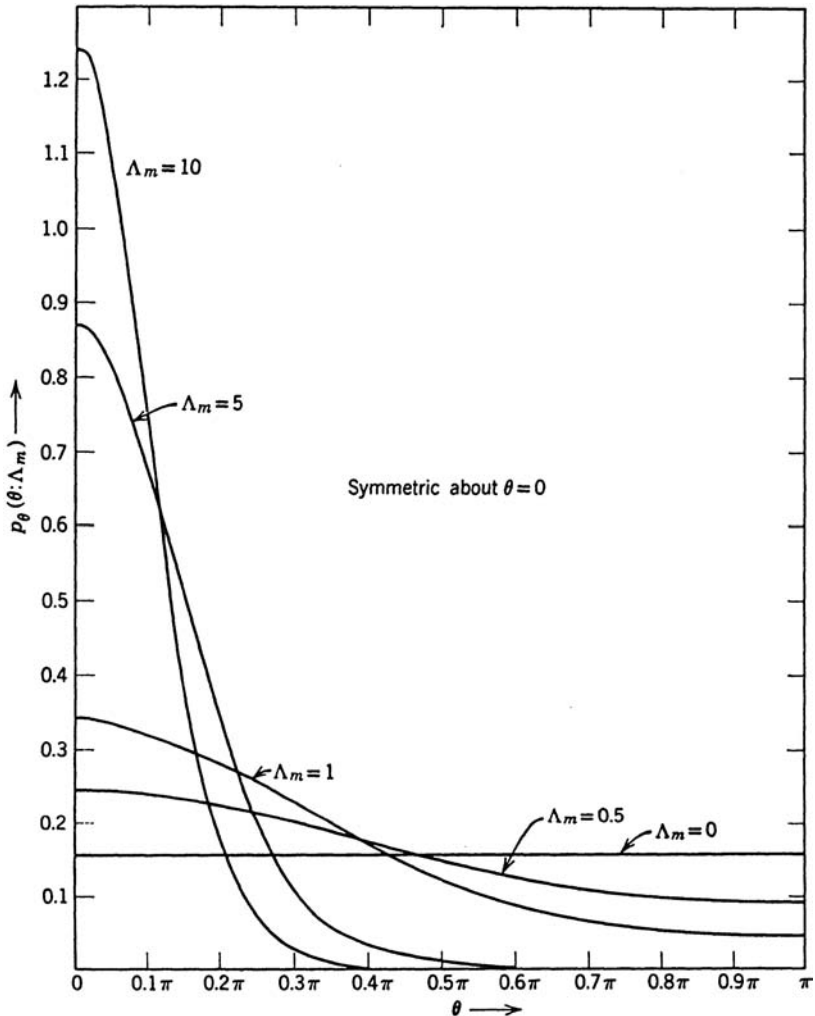


Figure 7.53: Family of probability densities for the phase angle.

This is the logical density for the radar problem. As Λ_m increases, the density becomes more peaked. Finally, as $\Lambda_m \rightarrow \infty$, we approach the known signal case. Thus, by varying Λ_m we can move continuously from the known signal problem through the intermediate case, in which there is some information about the phase, to the other extreme, the uniform phase problem.

Substituting (7.394) into (7.393), we have

$$\Lambda'[r(t)] = \int_{-\pi}^{\pi} \frac{1}{2\pi I_0(\Lambda_m)} \exp \left[\left(\Lambda_m + \frac{2\sqrt{E_r}}{N_0} L_c \right) \cos \theta - \frac{2\sqrt{E_r}}{N_0} L_s \sin \theta \right] d\theta. \quad (7.396)$$

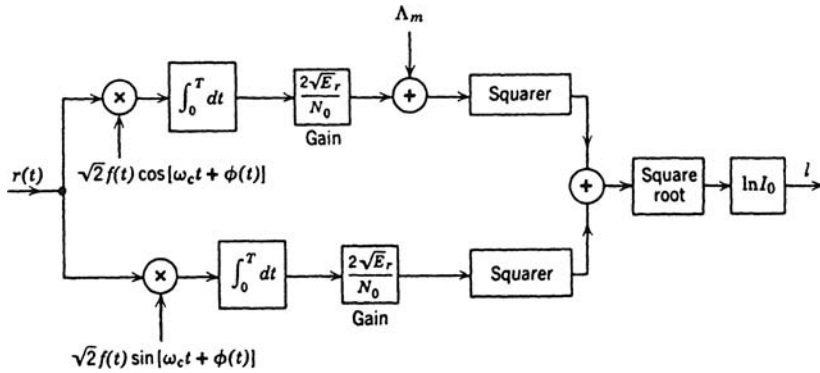


Figure 7.54: Optimum receiver: random phase angle.

This is a standard integral (e.g. [Kad65]). Thus,

$$\Lambda'[r(t)] = \frac{1}{I_0(\Lambda_m)} I_0 \left\{ \left[\left(\Lambda_m + \frac{2\sqrt{E_r}}{N_0} L_c \right)^2 + \left(\frac{2\sqrt{E_r}}{N_0} L_s \right)^2 \right]^{1/2} \right\}. \quad (7.397)$$

Substituting (7.397) into (7.389), incorporating the threshold, and taking the logarithm, we obtain

$$\ln I_0 \left\{ \left[\left(\Lambda_m + \frac{2\sqrt{E_r} L_c}{N_0} \right)^2 + \left(\frac{2\sqrt{E_r} L_s}{N_0} \right)^2 \right]^{1/2} \right\} \stackrel{H_1}{\underset{H_0}{\gtrless}} \ln \eta + \frac{E_r}{N_0} + \ln I_0(\Lambda_m). \quad (7.398)$$

The formation of the test statistic is straightforward (Figure 7.54). The function $I_0(\cdot)$ is shown in Figure 7.55. For large x

$$I_0(x) \simeq \frac{e^x}{\sqrt{2\pi x}}, \quad x \gg 1, \quad (7.399)$$

whereas for small x

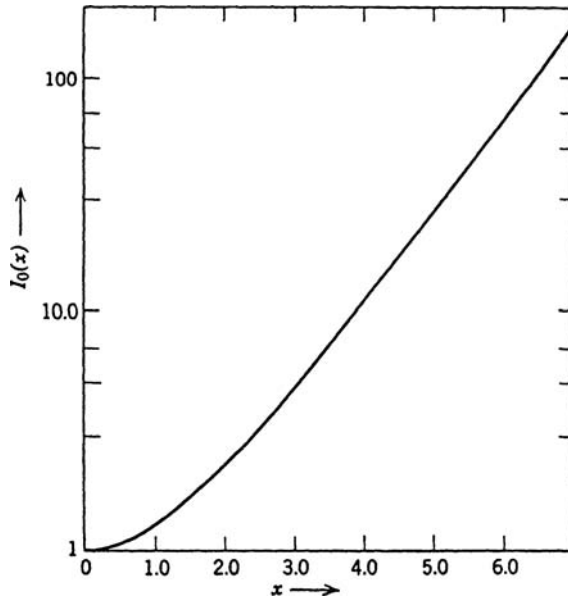
$$I_0(x) \simeq 1 + \frac{x^2}{4}, \quad x \ll 1, \quad (7.400)$$

and

$$\ln I_0(x) \simeq \frac{x^2}{4}, \quad x \ll 1. \quad (7.401)$$

Observe that because $\ln I_0(x)$ is monotone we can remove it by modifying the threshold. Thus, two tests equivalent to (7.398) are

$$\left(L_c + \frac{N_0 \Lambda_m}{2\sqrt{E_r}} \right)^2 + L_s^2 \stackrel{H_1}{\underset{H_0}{\gtrless}} \gamma \quad (7.402)$$

Figure 7.55: Plot of $I_0(x)$.

and

$$\left(\frac{2\sqrt{E_r}}{N_0}\right)^2 (L_c^2 + L_s^2) + 2\Lambda_m \frac{2\sqrt{E_r}}{N_0} L_c \stackrel{H_1}{\gtrless} \gamma'. \quad (7.403)$$

Redrawing the receiver structure as shown in Figure 7.56, we see that the optimum receiver consists of a linear component and a square-law component.

Looking at (7.402), we see that the region in the L_c, L_s plane corresponding to the decision H_0 is the interior of a circle centered at $(-N_0\Lambda_m/2\sqrt{E_r}, 0)$ with radius $\gamma^{1/2}$.

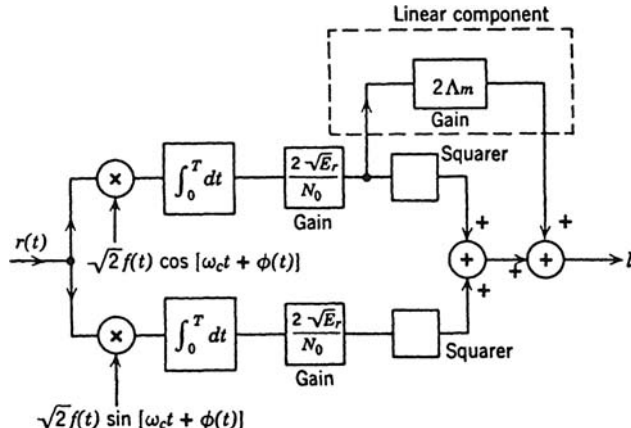


Figure 7.56: Alternate realization of optimum receiver.

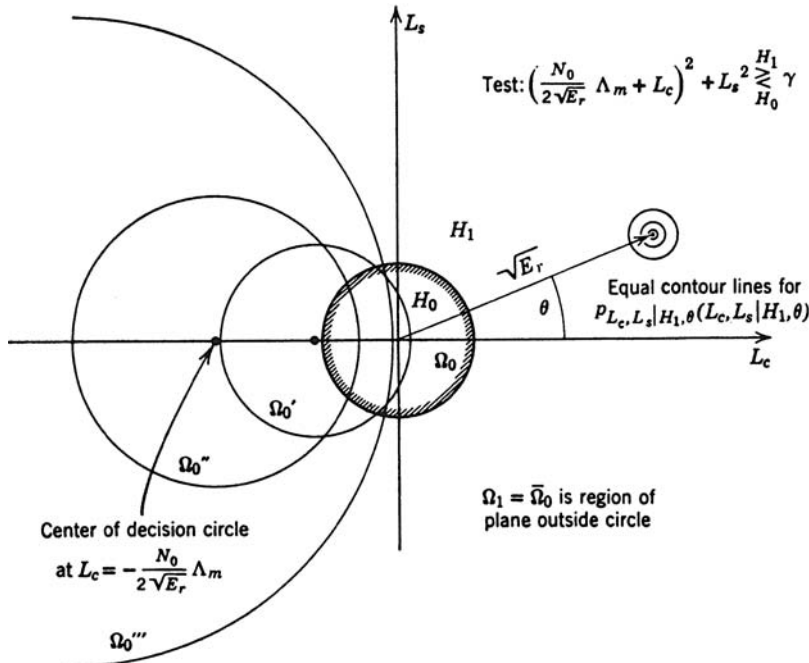


Figure 7.57: Decision regions, partially coherent case.

We denote this region as Ω_0 . The probability density of L_c and L_s under H_0 is a circularly symmetric Gaussian density centered at the origin. Therefore, if γ is fixed and Λ_m is allowed to increase, Ω_0 will move to the left and the probability of being in it on H_0 will decrease. Thus, to maintain a constant P_F we increase γ as Λ_m is increased. Several decision regions are shown in Figure 7.57. In the limit, as $\Lambda_m \rightarrow \infty$, the decision boundary approaches a straight line and we have the familiar known signal problem of Section 7.2. The probability density on H_1 depends on θ . A typical case is shown in the figure. We evaluate P_F and P_D for some interesting special cases in Examples 7.13 and 7.14 and in the problems. Before doing this it will be worthwhile to develop an alternate receiver realization for the case in which $\Lambda_m = 0$. In many cases this alternate realization will be more convenient to implement.

Matched Filter-Envelope Detector Realization. When $\Lambda_m = 0$, we must find $\sqrt{L_c^2 + L_s^2}$. We can do so by using a bandpass filter followed by an envelope detector, as shown in Figure 7.58. Because $h(t)$ is the impulse response of a bandpass filter, it is

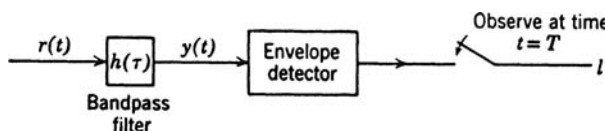


Figure 7.58: Matched filter-envelope detector for uniform phase case.

convenient to write it as

$$h(t) = h_L(t) \cos[\omega_c t + \psi_L(t)], \quad (7.404)$$

where $h_L(t)$ and $\psi_L(t)$ are low-pass functions. The output at time T is

$$y(T) = \int_0^T h(T - \tau) r(\tau) d\tau. \quad (7.405)$$

Using (7.404), we can write this equation as

$$\begin{aligned} y(T) &= \int_0^T r(\tau) h_L(T - \tau) \cos[\omega_c(T - \tau) + \psi_L(T - \tau)] d\tau \\ &= \cos \omega_c T \int_0^T r(\tau) h_L(T - \tau) \cos[\omega_c \tau - \psi_L(T - \tau)] d\tau \\ &\quad + \sin \omega_c T \int_0^T r(\tau) h_L(T - \tau) \sin[\omega_c \tau - \psi_L(T - \tau)] d\tau. \end{aligned} \quad (7.406)$$

This can be written as

$$\begin{aligned} y(T) &\triangleq y_c(T) \cos \omega_c T + y_s(T) \sin \omega_c T \\ &= \sqrt{y_c^2(T) + y_s^2(T)} \cos \left[\omega_c T - \tan^{-1} \frac{y_s(T)}{y_c(T)} \right]. \end{aligned} \quad (7.407)$$

Observing that

$$y_c(T) = \Re \int_0^T r(\tau) h_L(T - \tau) \exp[j\omega_c \tau - j\psi_L(T - \tau)] d\tau \quad (7.408)$$

and

$$y_s(T) = \Im \int_0^T r(\tau) h_L(T - \tau) \exp[j\omega_c \tau - j\psi_L(T - \tau)] d\tau, \quad (7.409)$$

we see that the output of the envelope detector is

$$\sqrt{y_c^2(T) + y_s^2(T)} = \left| \int_0^T r(\tau) h_L(T - \tau) \exp[-j\psi_L(T - \tau) + j\omega_c \tau] d\tau \right|. \quad (7.410)$$

From (7.391) and (7.392), we see that the desired test statistic is

$$\sqrt{L_c^2 + L_s^2} = \left| \int_0^T r(\tau) \sqrt{2} f(\tau) e^{+j\phi(\tau)} e^{+j\omega_c \tau} d\tau \right|. \quad (7.411)$$

We see the two expressions will be identical if

$$h_L(T - \tau) = \sqrt{2}f(\tau) \quad (7.412)$$

and

$$\psi_L(T - \tau) = -\phi(\tau). \quad (7.413)$$

This bandpass matched filter provides a simpler realization for the *uniform* phase case.

The receiver in the uniform phase case is frequently called an incoherent receiver, but the terminology tends to be misleading. We see that the matched filter utilizes all the *internal* phase structure of the signal. The only thing missing is an *absolute* phase reference. The receiver for the known signal case is called a coherent receiver because it requires an oscillator at the receiver that is coherent with the transmitter oscillator. The general case developed in this section may be termed the partially coherent case.

To complete our discussion we consider the performance for some simple cases. There is no conceptual difficulty in evaluating the error probabilities but the resulting integrals often cannot be evaluated analytically. Because various modifications of this particular problem are frequently encountered in both radar and communications, a great deal of effort has been expended in finding convenient closed-form expressions and in numerical evaluations. We have chosen two typical examples to illustrate the techniques employed.

First we consider the radar problem defined at the beginning of this section (7.381)–(7.385).

Example 7.13 (Uniform Phase). Because this model corresponds to a radar problem, the uniform phase assumption is most realistic. To construct the ROC we must compute P_F and P_D . (Recall that P_F and P_D are the probabilities that we will exceed the threshold γ when noise only and signal plus noise are present, respectively.)

Looking at Figure 7.56, we see that the test statistic is

$$l = L_c^2 + L_s^2, \quad (7.414)$$

where L_c and L_s are Gaussian random variables. The decision region is shown in Figure 7.57. We can easily verify that

$$\begin{aligned} H_0 : E(L_c) &= E(L_s) = 0, & \text{Var}(L_c) = \text{Var}(L_s) &= \frac{N_0}{2}, \\ H_1 : E(L_c|\theta) &= \sqrt{E_r} \cos \theta, & E(L_s|\theta) &= \sqrt{E_r} \sin \theta, & \text{Var}(L_c) = \text{Var}(L_s) &= \frac{N_0}{2}. \end{aligned} \quad (7.415)$$

Then

$$P_F \triangleq \Pr[l > \gamma | H_0] = \int_{\Omega_0} \int \left(2\pi \frac{N_0}{2}\right)^{-1} \exp\left(-\frac{L_c^2 + L_s^2}{N_0}\right) dL_c dL_s. \quad (7.416)$$

Changing to polar coordinates and evaluating, we have

$$P_F = \exp\left(-\frac{\gamma}{N_0}\right). \quad (7.417)$$

Similarly, the probability of detection for a particular θ is

$$P_D(\theta) = \int_{\Omega_0} \int \left(2\pi \frac{N_0}{2}\right)^{-1} \exp\left(-\frac{(L_c - \sqrt{E_r} \cos \theta)^2 + (L_s - \sqrt{E_r} \sin \theta)^2}{N_0}\right) dL_c dL_s. \quad (7.418)$$

Letting $L_c = R \cos \beta$, $L_s = R \sin \beta$, and performing the integration with respect to β , we obtain

$$P_D(\theta) = P_D = \int_{\sqrt{\gamma}}^{\infty} \frac{2}{N_0} R \exp\left(-\frac{R^2 + E_r}{N_0}\right) I_0\left(\frac{2R\sqrt{E_r}}{N_0}\right) dR. \quad (7.419)$$

As we expected, P_D does not depend on θ . We can normalize this expression by letting $z = \sqrt{2/N_0}R$. This gives

$$P_D = \int_{\sqrt{2\gamma/N_0}}^{\infty} z \exp\left(-\frac{z^2 + d^2}{2}\right) I_0(zd) dz, \quad (7.420)$$

where $d^2 \triangleq 2E_r/N_0$.

This integral cannot be evaluated analytically. It was first tabulated by Marcum [Mar48, Mar50] in terms of a function commonly called Marcum's Q -function:

$$Q(\alpha, \beta) \triangleq \int_{\beta}^{\infty} z \exp\left(-\frac{z^2 + \alpha^2}{2}\right) I_0(\alpha z) dz. \quad (7.421)$$

This function has been studied extensively and tabulated for various values of α, β (e.g. [Mar50, DJ62, Joh61]). It is also a Matlab function. Thus,

$$P_D = Q\left(d, \left(\frac{2\gamma}{N_0}\right)^{1/2}\right). \quad (7.422)$$

This can be written in terms of P_F . Using (7.416), we have

$$P_D = Q(d, \sqrt{-2 \ln P_F}). \quad (7.423)$$

The ROC is shown in Figure 7.59. The results can also be plotted in the form of P_D versus d with P_F as a parameter. This is done in Figure 7.60. Comparing Figures 7.14 and 7.60, we see that a negligible increase of d is required to maintain the same P_D for a fixed P_F when we go from the known signal model to the uniform phase model for the parameter ranges shown in Figure 7.60. ■

The second example of interest is a binary communication system in which some phase information is available.

Example 7.14: Partially coherent binary communication. The criterion is minimum probability of error and the hypotheses are equally likely. We assume that the signals under the two hypotheses are

$$H_1 : r(t) = \sqrt{2E_r} f_1(t) \cos(\omega_c t + \theta) + w(t), \quad 0 \leq t \leq T, \quad (7.424)$$

$$H_0 : r(t) = \sqrt{2E_r} f_0(t) \cos(\omega_c t + \theta) + w(t), \quad 0 \leq t \leq T, \quad (7.425)$$

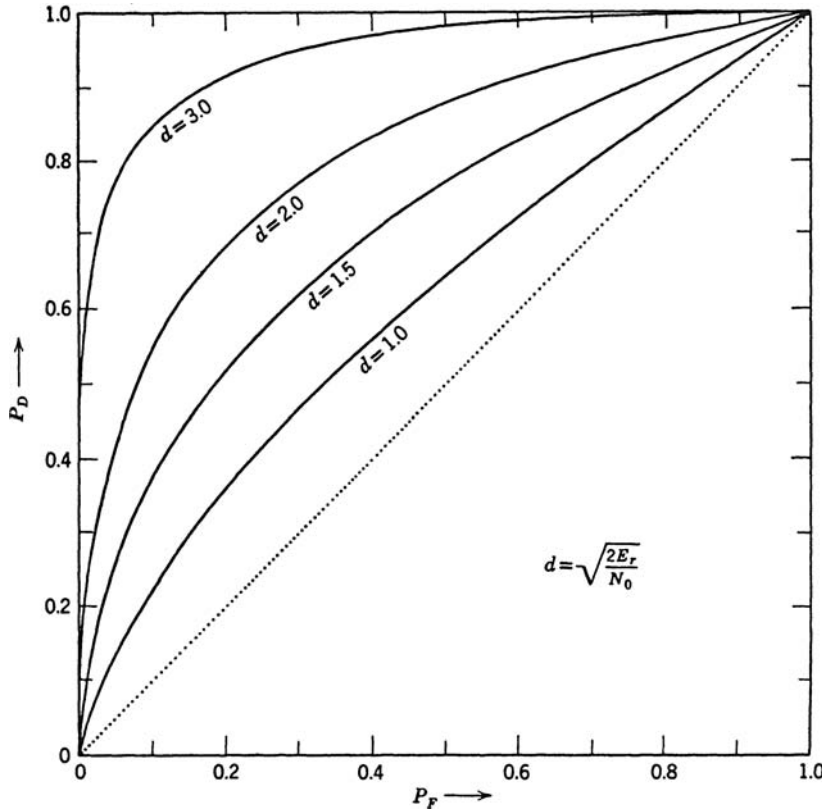


Figure 7.59: Receiver operating characteristic, random phase with uniform density.

where $f_0(t)$ and $f_1(t)$ are normalized and

$$\int_0^T f_0(t) f_1(t) dt = \rho, \quad -1 \leq \rho \leq 1. \quad (7.426)$$

The noise spectral height is $N_0/2$ and $p_\theta(\theta)$ is given by (7.394). The likelihood ratio test is obtained by an obvious modification of the simple binary problem and the receiver structure is shown in Figure 7.61.

We now look at $\Pr(\epsilon)$ as a function of ρ , d^2 , and Λ_m . Intuitively, we expect that as $\Lambda_m \rightarrow \infty$ we would approach the known signal problem, and $\rho = -1$ [the equal and opposite signals of (7.43)] would give the best result. On the other hand, as $\Lambda_m \rightarrow 0$, the phase becomes uniform. Now, any correlation (+ or -) would move the signal points closer together. Thus, we expect that $\rho = 0$ would give the best performance. As we go from the first extreme to the second, the best value of ρ should move from -1 to 0 .

We shall do only the details for the easy case in which $\rho = -1$; $\rho = 0$ is done in Problem 7.4.9. The error calculation for arbitrary ρ is done in [Vit65].

When $\rho = -1$, we observe that the output of the square-law section is identical on both hypotheses. Thus, the receiver is linear. The effect of the phase error is to rotate the signal points in the decision space as shown in Figure 7.62.

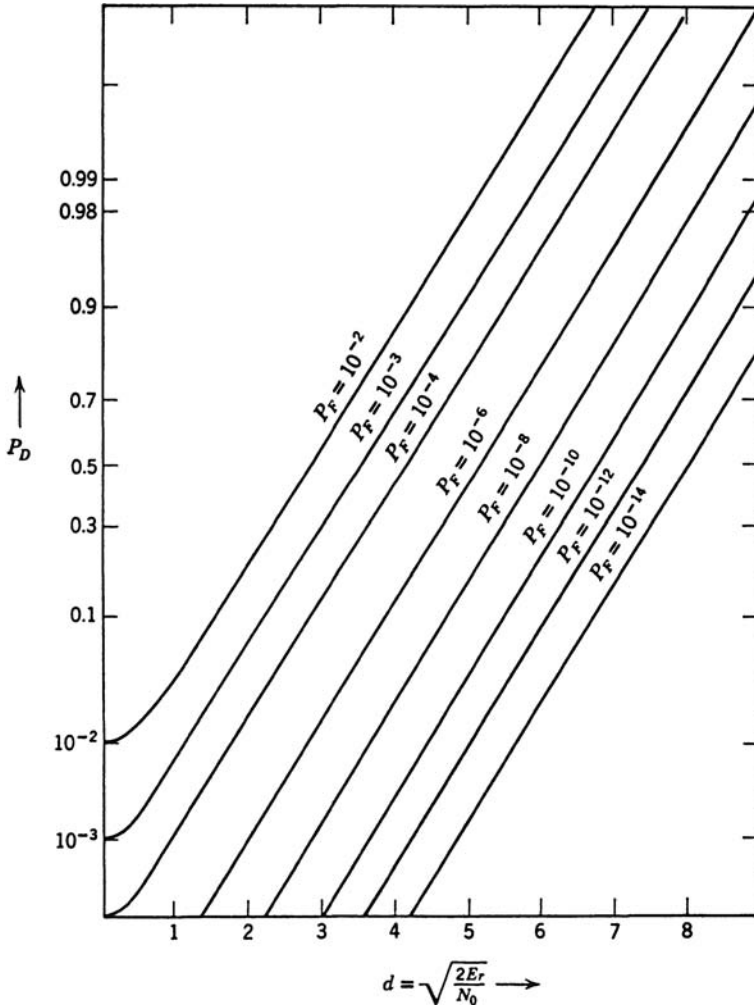


Figure 7.60: Probability of detection versus d , uniform phase.

Using the results of Section 7.2.1,

$$\Pr(\epsilon|\theta) = \int_{-\infty}^0 \left(2\pi \frac{N_0}{2}\right)^{-\frac{1}{2}} \exp\left[-\frac{(x - \sqrt{E_r} \cos \theta)^2}{N_0}\right] dx \quad (7.427)$$

or

$$\Pr(\epsilon|\theta) = \int_{-\infty}^{-\sqrt{2E_r/N_0} \cos \theta} \frac{1}{\sqrt{2\pi}} \exp\left(-\frac{z^2}{2}\right) dz. \quad (7.428)$$

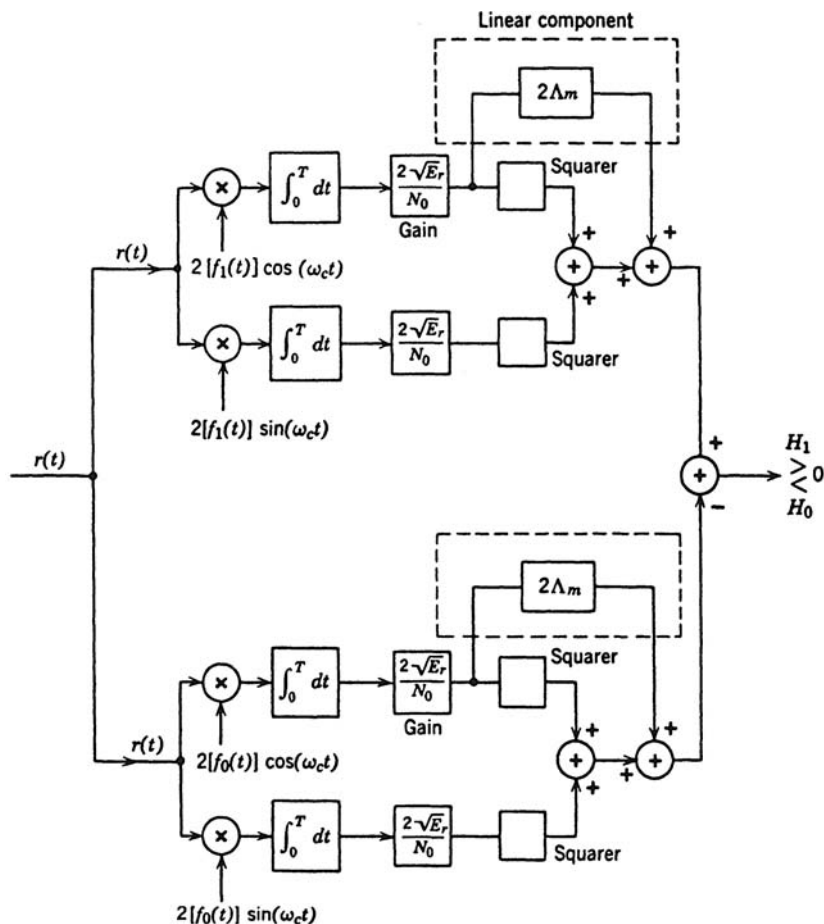


Figure 7.61: Receiver: binary communication system.

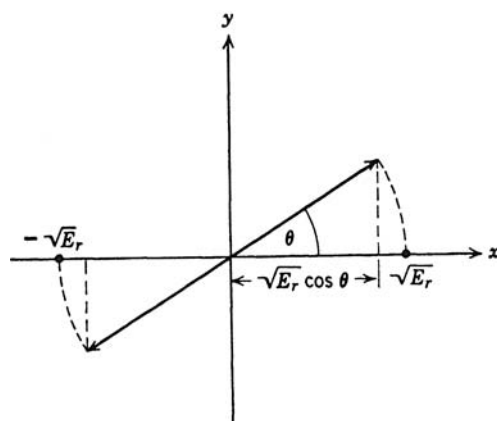


Figure 7.62: Effect of phase errors in decision space.

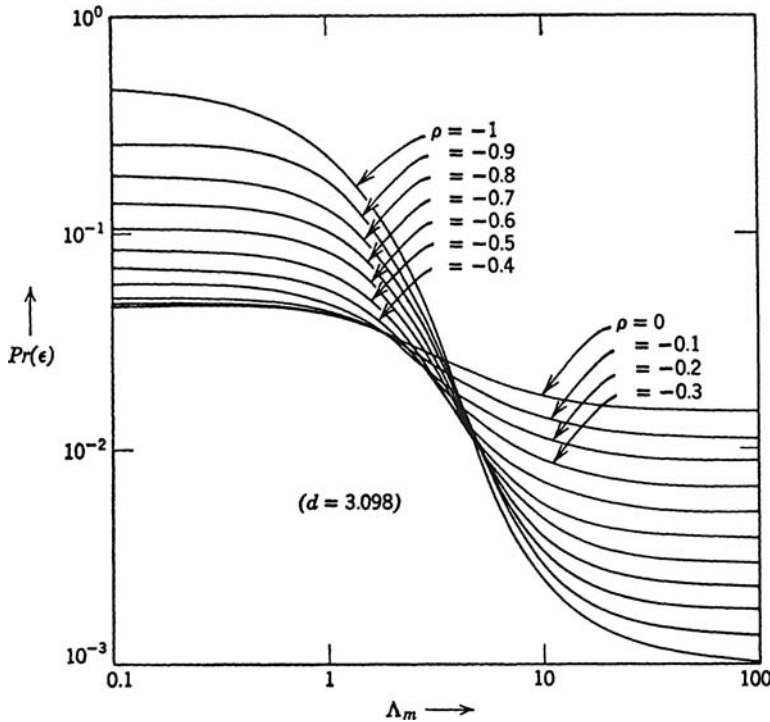


Figure 7.63: $\Pr(\epsilon)$, partially coherent binary system (10^{-3} asymptote) [Vit65].

Using (7.394),

$$\Pr(\epsilon) = \int_{-\pi}^{+\pi} \frac{\exp(\Lambda_m \cos \theta)}{2\pi I_0(\Lambda_m)} \Pr(\epsilon|\theta) d\theta. \quad (7.429)$$

This can be integrated numerically. The results for two particular values of d^2 are shown in Figures 7.63 and 7.64.¹³ The results for other ρ were also evaluated in [Vit65] and are given in these figures. We see that for Λ_m greater than about 2 the negatively correlated signals become more efficient than orthogonal signals. For $\Lambda_m \geq 10$, the difference is significant. The physical significance of Λ_m will become clearer when we study phase estimating systems in DEMT-II [Van71a, Van03]. ■

Before leaving the random phase model we revisit the radar example in Example 7.13. In many applications, we must illuminate the target with multiple pulses, a typical transmitted sequence is shown in Figure 7.65. We must now specify how the returns from successive pulses are related. There are two cases of interest.

For the case of independent phases, the optimum receiver follows easily. From (7.398), we define

$$l_i = \ln I_o \left\{ \frac{2\sqrt{E_r}}{N_o} (L_{c_i}^2 + L_{s_i}^2)^{1/2} \right\}. \quad (7.430)$$

¹³The values of d^2 were chosen to give a $\Pr(\epsilon) = 10^{-3}$ and 10^{-5} , respectively, at $\Lambda_m = \infty$.

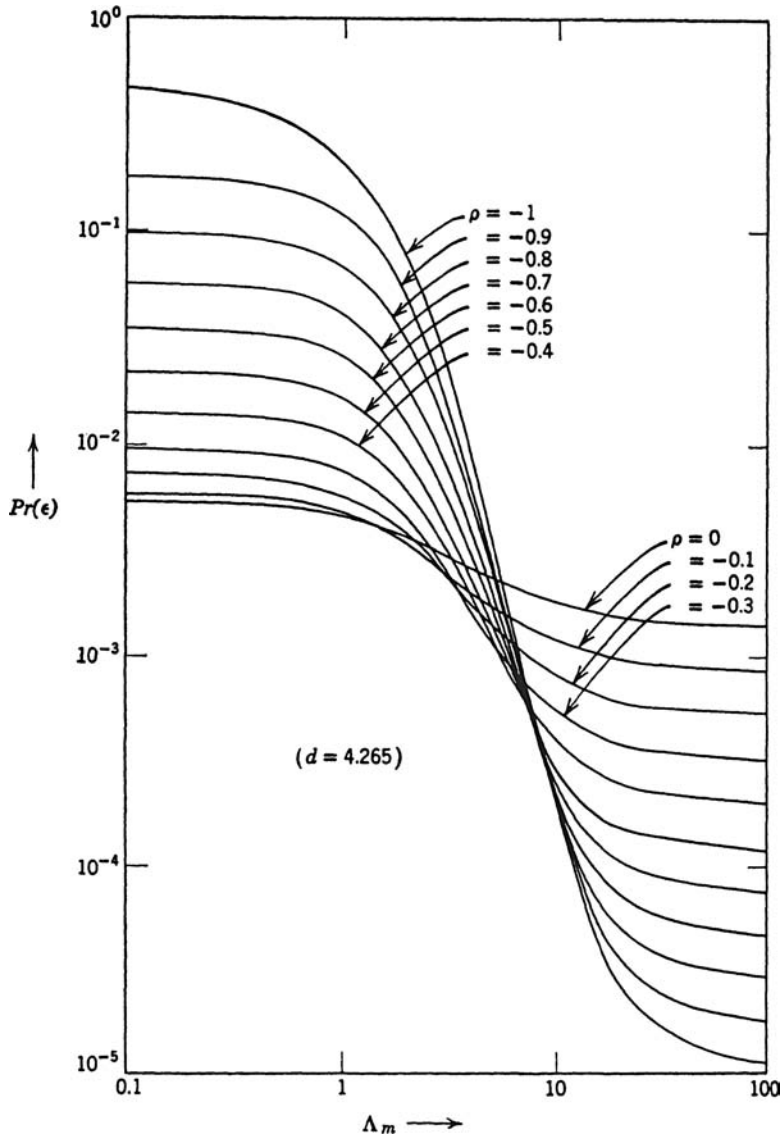


Figure 7.64: $\Pr(\epsilon)$, partially coherent binary system (10^{-5} asymptote) [Vit65].

Note that argument is just the magnitude of the output of the envelope detector in Figure 7.58 multiplied by a scalar factor. Defining

$$y_i \triangleq (L_{c_i}^2 + L_{s_i}^2)^{1/2}, \quad (7.431)$$

$$l_i = \ln I_o \left\{ \frac{2\sqrt{E_r}}{N_o} y_i \right\}, \quad (7.432)$$

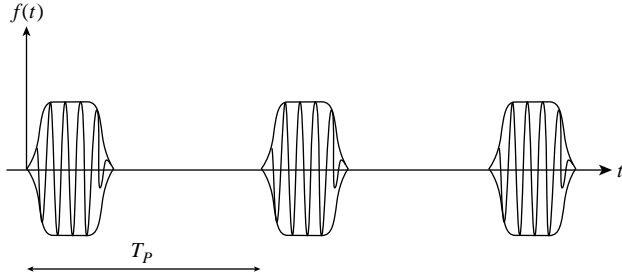


Figure 7.65: Transmitted sequence.

and the optimum receiver is

$$l = \sum_{i=1}^M l_i \stackrel{H_1}{\gtrless} \gamma. \quad (7.433)$$

The performance is difficult to analyze. The usual approach is to consider two approximations in order to assess the performance.

For large values of the argument we use the approximation in (7.399). Then

$$l = \sum_{i=1}^M \left\{ \frac{2\sqrt{E_r}}{N_o} y_i - \frac{1}{2} \ln \frac{4\pi\sqrt{E_r} y_i}{N_o} \right\} \stackrel{H_1}{\gtrless} \gamma. \quad (7.434)$$

The second term is small and can be dropped. Then (7.434) reduces to

$$\sum_{i=1}^M y_i \stackrel{H_1}{\gtrless} \gamma', \quad (7.435)$$

which corresponds to a linear envelope detector followed by a summation, which is referred to in the literature a *postdetection integration*.

For small values of the argument, we use (7.401) and the test becomes

$$\sum_{i=1}^M y_i^2 \stackrel{H_1}{\gtrless} \gamma''. \quad (7.436)$$

The performance of the quadratic detector follows easily.¹⁴ The probability density of l on H_1 is a Noncentral Chi-square density

$$p_{l|H_1}(L|H_1) = \frac{1}{2} \left(\frac{L}{\alpha^2} \right)^{(M-1)/2} \exp \left\{ -\frac{L + \alpha^2}{2} \right\} I_{M-1}(\alpha L^{1/2}) \quad (7.437)$$

where the noncentrality parameter is

$$\alpha^2 = \frac{2ME_r}{N_o}, \quad (7.438)$$

¹⁴Our discussion follows Section 8.3 of [MW95].

the M -pulse energy-to-noise density ratio.

The probability of detection is

$$P_D = \int_{\gamma''}^{\infty} p_{l|H_1}(L|H_1) dL = Q_M \left(\alpha, \sqrt{\gamma''} \right),$$

where $Q_M(\alpha, \beta)$ is Marcum's Q -function that is a Matlab function.

On H_0 , the probability density is a central Chi-square density

$$p_{l|H_0}(L|H_0) = \frac{1}{2^M \Gamma(M)} L^{M-1} \exp \left\{ -\frac{L}{2} \right\}. \quad (7.439)$$

The probability of false alarm is

$$P_F = \int_{\gamma}^{\infty} p_{l|H_0}(L|H_0) dL = 1 - \int_0^{\gamma} p_{l|H_0}(L|H_0) dL = 1 - \Gamma_M \left(\frac{\gamma''}{2} \right), \quad (7.440)$$

where $\Gamma_M(x)$ is the incomplete Gamma function that is a Matlab function. In Figure 7.66, we plot P_D versus α for various M and $P_F = 10^{-6}$.

In order to achieve a desired P_D , it requires a larger total SNR as M increases.

The performance analysis for the linear envelope detector is more difficult. Helstrom (Chapter 6 in [Hel60] and Chapter 4 in [Hel95]) provides a derivation based on Marcum's work [Mar48] and [Mar50]. He also compares the performance of linear and quadratic detectors based on his work in [Hel90].

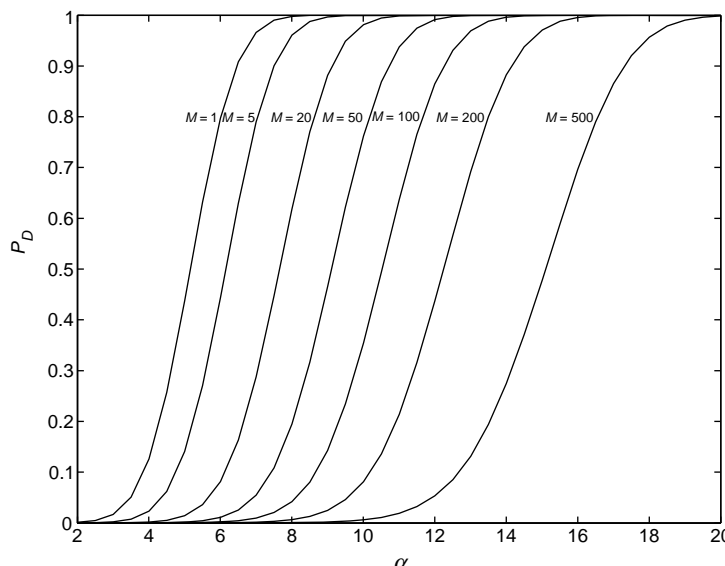


Figure 7.66: P_D versus $\alpha = \sqrt{M \left(\frac{2E_x}{N_0} \right)}$.

Another tutorial discussion is given in Sections 8.4 and 8.5 of McDonough and Whalen [MW95, MW71] and performance curves due to Robertson [Rob67] are given in the appendix to Chapter 8.

Other discussions are given in DiFrauco and Rubin [DR68] and Meyer and Mayor [MM73]. In many applications, the performance of the linear and quadratic detectors are similar but the reader should consult some of the above references if he is going to make system design decisions.

In this section, we have studied a particular case of an unwanted parameter, a random phase angle. By using a family of densities we were able to demonstrate how to progress smoothly from the known signal case to the uniform phase case. The receiver consisted of a weighted sum of a linear operation and a quadratic operation. We observe that the specific receiver structure is due to the precise form of the density chosen. In many cases the probability density for the phase angle would not correspond to any of these densities. Intuitively we expect that the receiver developed here should be “almost” optimum for *any* single-peaked density with the same variance as the member of the family for which it was designed.

We now turn to a case of equal (or perhaps greater) importance in which both the amplitude and phase of the received signal vary.

7.4.2 Random Amplitude and Phase

As we discussed in Section 7.1, there are cases in which both the amplitude and phase of the received signal vary. In the communication context this situation is encountered in ionospheric links operating above the maximum usable frequency (e.g. [SB54]) and in some tropospheric links (e.g. [BID55]). In the radar context it is encountered when the target’s aspect or effective radar cross section changes from pulse to pulse (e.g. [Swe54]).

Experimental results for a number of physical problems indicate that when the input is a sine wave, $\sqrt{2} \sin \omega_c t$, the output (in the absence of additive noise) is

$$r(t) = v_{\text{ch}}(t) \sin[\omega_c t + \theta_{\text{ch}}(t)]. \quad (7.441)$$

An exaggerated sketch is shown in Figure 7.67a. The envelope and phase vary continuously. The envelope $v_{\text{ch}}(t)$ has the Rayleigh probability density shown in Figure 7.67b and that the phase angle $\theta_{\text{ch}}(t)$ has a uniform density.

There are several ways to model this channel. The simplest technique is to replace the actual channel functions by piecewise constant functions (Figure 7.68). This would be valid when the channel does not vary significantly in a T second interval. Given this “slow-fading” model, two choices are available. We can process each signaling interval independently or exploit the channel continuity by measuring the channel and using the measurements in the receiver. We now explore the first alternative.

For the simple binary detection problem in additive white Gaussian noise we may write the received signal under the two hypotheses as¹⁵

$$\begin{aligned} H_1 : r(t) &= v\sqrt{2}f(t) \cos[\omega_c(t) + \phi(t) + \theta] + w(t), & 0 \leq t \leq T, \\ H_0 : r(t) &= w(t), & 0 \leq t \leq T. \end{aligned} \quad (7.442)$$

where v is a Rayleigh random variable and θ is a uniform random variable.

¹⁵For simplicity, we assume that the transmitted signal has unit energy and adjust the received energy by changing the characteristics of v .

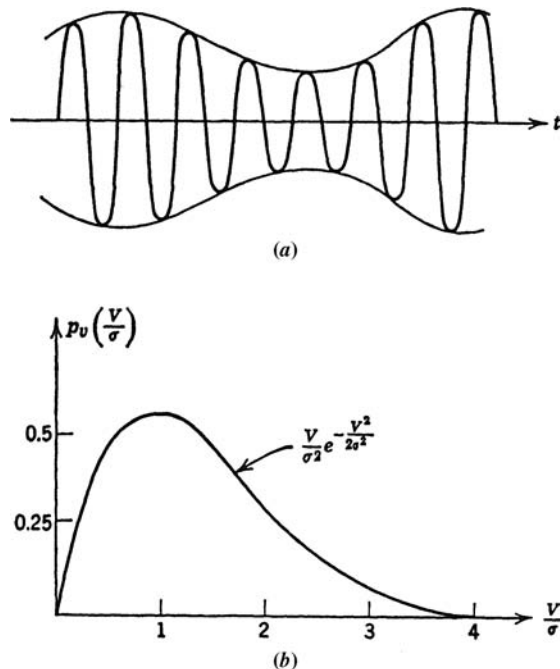


Figure 7.67: Narrow-band process at output of channel, and the probability of its envelope.

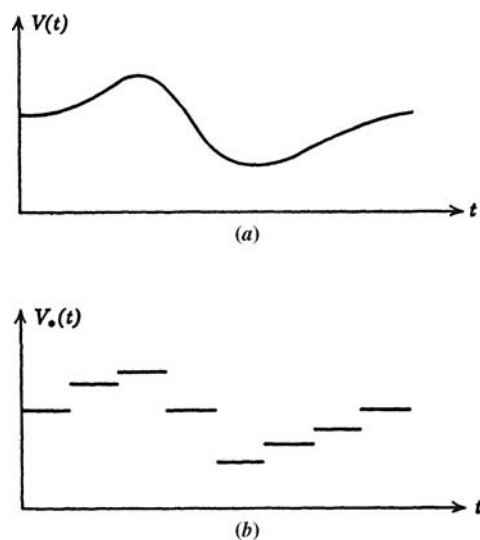


Figure 7.68: Piecewise constant approximation: (a) actual envelope; (b) piecewise constant model.

We can write the signal component equally well in terms of its quadrature components:

$$\begin{aligned} \sqrt{2} v f(t) \cos[\omega_c(t) + \phi(t) + \theta] &= a_1 \sqrt{2} f(t) \cos[\omega_c(t) + \phi(t)] \\ &+ a_2 \sqrt{2} f(t) \sin[\omega_c(t) + \phi(t)] \quad 0 \leq t \leq T, \end{aligned} \quad (7.443)$$

where a_1 and a_2 are independent zero-mean Gaussian random variables with variance σ^2 (where $E[v^2] = 2\sigma^2$; see pp. 158–161 of Davenport and Root [DR58]). We also observe that the two terms are *orthogonal*. Thus, the signal out of a Rayleigh fading channel can be viewed as the sum of two orthogonal signals, each multiplied by an independent Gaussian random variable. This seems to be an easier way to look at the problem. As a matter of fact, it is just as easy to solve the more general problem in which the received waveform on H_1 is,

$$r(t) = \sum_{i=1}^M a_i s_i(t) + w(t), \quad 0 \leq t \leq T, \quad (7.444)$$

where the a_i are independent, zero-mean Gaussian variables $N(0, \sigma_{a_i})$ and

$$\int_0^T s_i(t) s_j(t) dt = \delta_{ij}. \quad (7.445)$$

The likelihood ratio is

$$\Lambda[r(t)] = \underbrace{\int_{-\infty}^{\infty} \cdots \int_{-\infty}^{\infty}}_M p_{a_1}(A_1) p_{a_2}(A_2) \cdots p_{a_M}(A_M) \exp \left[+ \frac{2}{N_0} \int_0^T r(t) \sum_{i=1}^M A_i s_i(t) dt \right. \quad (7.446)$$

$$\left. - \frac{1}{N_0} \int_0^T \sum_{i=1}^M \sum_{j=1}^M A_i A_j s_i(t) s_j(t) dt \right] dA_1 dA_2 \cdots dA_M. \quad (7.447)$$

Defining

$$L_i = \int_0^T r(t) s_i(t) dt, \quad (7.448)$$

using the orthogonality of the $s_i(t)$, and completing the square in each of the M integrals, we find the test reduces to

$$l \triangleq \sum_{i=1}^M L_i^2 \left(\frac{\sigma_{a_i}^2}{\sigma_{a_i}^2 + N_0/2} \right) \stackrel{H_1}{\gtrless} \stackrel{H_0}{\lessgtr} \gamma. \quad (7.449)$$

Two receivers corresponding to (7.450) and shown in Figure 7.69 are commonly called a correlator-squarer receiver and a filter-squarer receiver, respectively. Equation (7.449) can

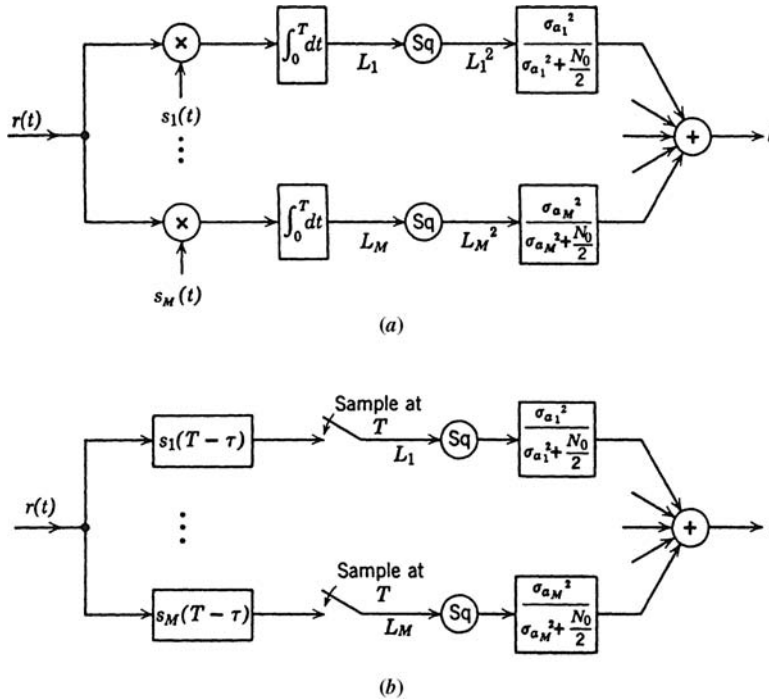


Figure 7.69: Receivers for Gaussian amplitude signals: (a) Correlation-squarer receiver; (b) filter-squarer receiver.

be rewritten as

$$l = \sum_{i=1}^M L_i \left(\frac{\sigma_{a_i}^2 L_i}{\sigma_{a_i}^2 + N_0/2} \right) \sum_{i=1}^M L_i \hat{a}_i. \quad (7.450)$$

This structure, as shown in Figure 7.70, can be interpreted as an estimator–correlator receiver (i.e., we are correlating $r(t)$ with our estimate of the received signal.) The identification of the term in braces as \hat{a}_i follows from our estimation discussion in Section 7.2. It is both a minimum mean-square error estimate and a maximum *a posteriori* probability estimate. In Figure 7.70a, we show a practical implementation. The realization in Figure 7.70b shows that we could actually obtain the estimate of the signal component as a waveform in the optimum receiver. This interpretation is quite important in later applications.¹⁶

We now apply these results to the original problem in (7.442). If we relate L_1 to L_c and L_2 to L_s , we see that the receiver is

$$L_c^2 + L_s^2 \stackrel{H_1}{\underset{H_0}{\gtrless}} \gamma, \quad (7.451)$$

¹⁶Note that we could have also obtained (7.450) by observing that the L_i are jointly Gaussian on both hypotheses and are sufficient statistics. Thus, the results of Chapter 3 are directly applicable. Whenever the L_i have nonzero means or are correlated, the use of those results is the simplest method (e.g., Problem 7.4.21). Note that we could also done the derivation using complex Gaussian variables.

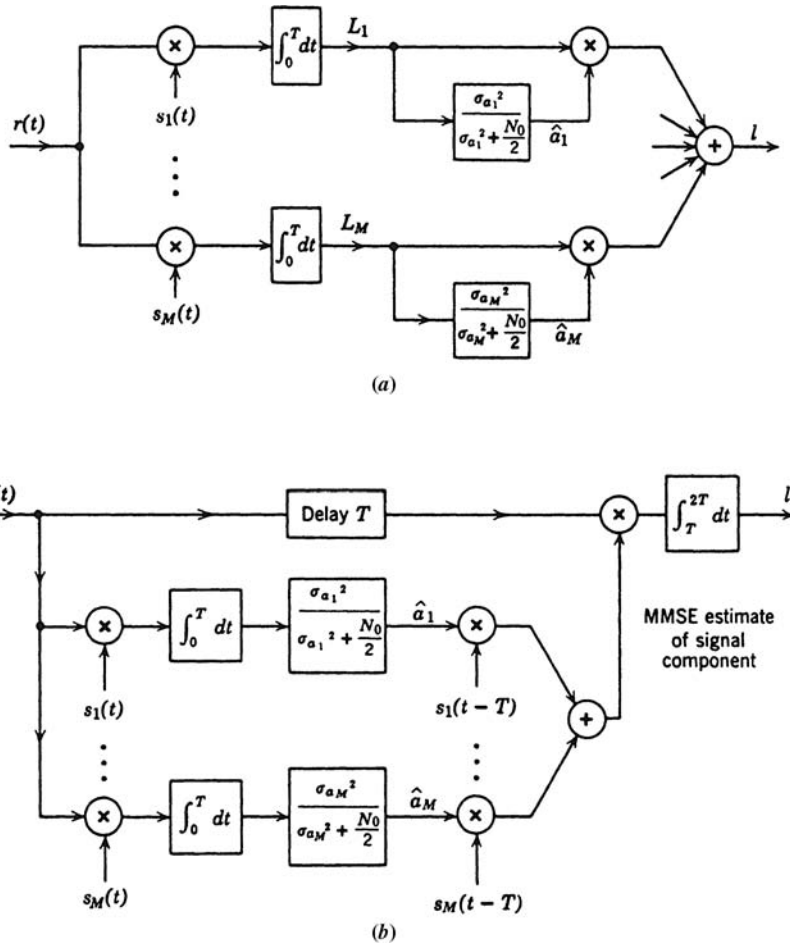


Figure 7.70: Estimator–correlator receiver.

(where L_c and L_s were defined in the random phase example). This can be realized, as shown in the preceding section, by a bandpass matched filter followed by an envelope detector. The two alternate receiver realizations are shown in Figure 7.71a and b.

The next step is to evaluate the performance. We observe that L_c and L_s are Gaussian random variables with identical distributions. Thus, the Rayleigh channel corresponds exactly to Example 2.2 of Chapter 2. In equation (2.98), we showed that

$$P_D = (P_F)^{\sigma_0^2/\sigma_1^2}, \quad (7.452)$$

where σ_0^2 is the variance of L_c on H_0 and σ_1^2 is the variance of L_c on H_1 .

$$\sigma_0^2 = \frac{N_o}{2} \quad (7.453)$$

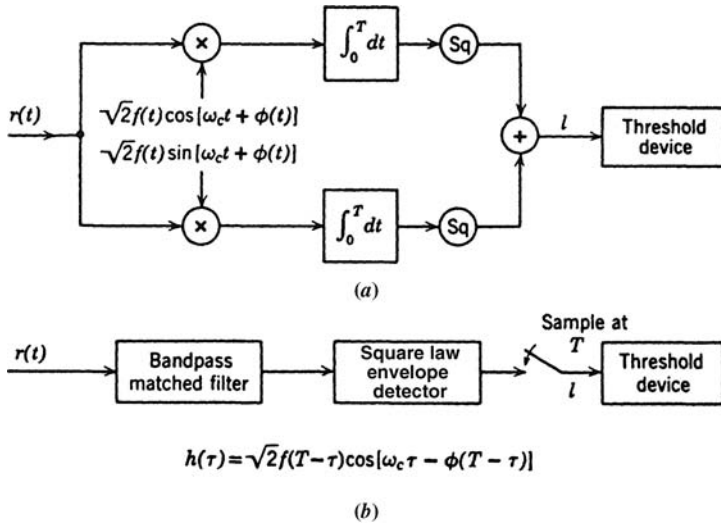


Figure 7.71: Optimum receivers, Rayleigh channel: (a) squarer realization; (b) matched filter-envelope detector realization.

and

$$\sigma_1^2 = \frac{N_o}{2} + \sigma^2 E_t \triangleq \frac{N_0}{2} + \frac{\bar{E}_r}{2}, \quad (7.454)$$

where $\bar{E}_r \triangleq 2\sigma^2 E_t$ is the average received signal energy because v^2 is the received signal energy. Substituting (7.453) and (7.454) into (2.98), we obtain

$$P_F = (P_D)^{1+\bar{E}_r/N_o}. \quad (7.455)$$

The ROC is plotted in Figure 7.72a. In Figure 7.72b, we plot P_D versus $2\bar{E}_r/N_o$ for various P_F . Comparing Figure 7.72b with the nonfading case in Figure 7.59, we see that the performance difference increases dramatically as $2\bar{E}_r/N_o$ increases. This is because, regardless of the mean of the Rayleigh density there will be a nonnegligible number of outcomes where E_r is close to zero and P_D will be very low. From our discussion of Figure 2.15, we know that the way to improve performance is to transmit multiple pulses.

We encountered the multiple pulse model in Section 7.4.1. We now assume each pulse exhibits Rayleigh fading.

For the case in which we transmit a sequence of M pulses we must specify how the fading/target reflection changes from pulse to pulse. The most common model assumes that the amplitude and phase are IID from pulse to pulse. Then, we can use (7.449) with the summation going to $2M$. Thus,

$$l = \sum_{i=1}^{2M} L_i^2 \left(\frac{\sigma^2}{\sigma^2 + \frac{N_o}{2}} \right) \stackrel{H_1}{\gtrless} \stackrel{H_0}{\gtrless} \gamma \quad (7.456)$$

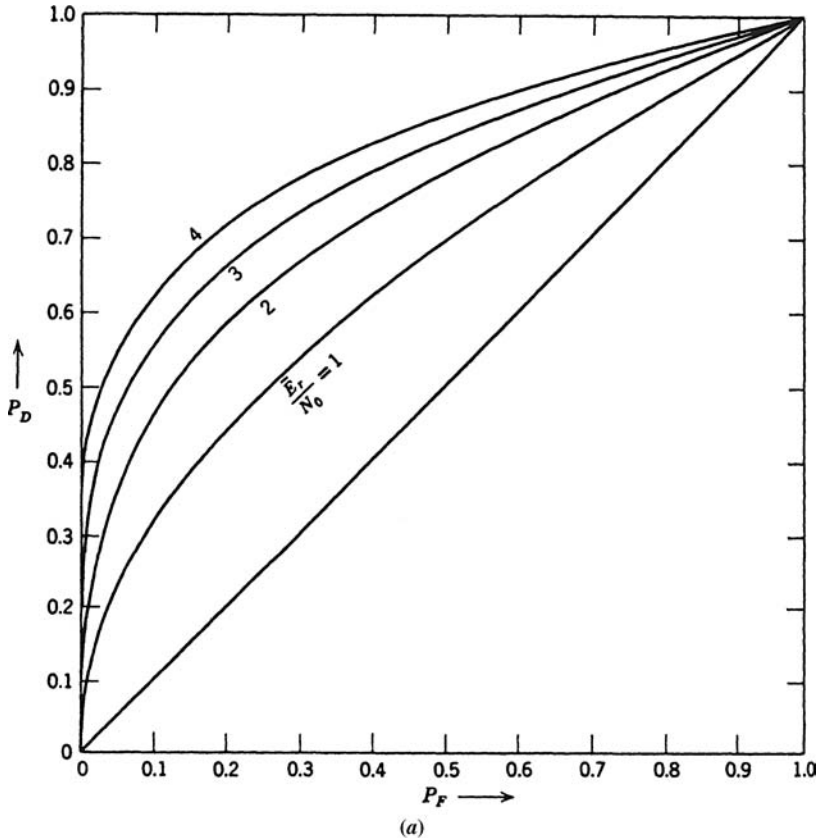


Figure 7.72: (a) Receiver operating characteristic, Rayleigh channel.

or

$$l = \sum_{i=1}^{2M} L_i^2 \frac{H_1}{H_0} \gtrless \gamma. \quad (7.457)$$

We recognize this as the model in Section 3.3.1.1 using (3.361)–(3.362). To use those results we define

$$\bar{E}_r = \sigma_s^2 \quad (7.458)$$

and

$$N_o = \sigma_n^2, \quad (7.459)$$

$$P_D = 1 - \Gamma_M \left(\frac{\gamma''}{\bar{E}_r + N_o} \right), \quad (7.460)$$

$$P_F = 1 - \Gamma_M \left(\frac{\gamma''}{N_o} \right), \quad (7.461)$$

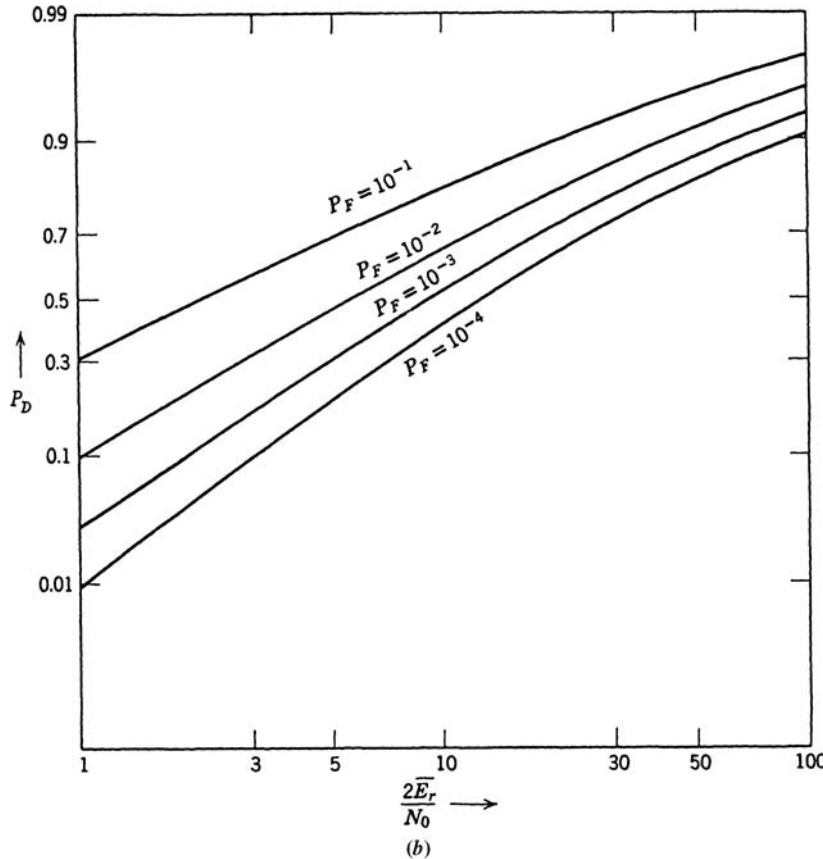


Figure 7.72: (b) Probability of detection versus $2\bar{E}_r/N_0$.

where

$$\tilde{\gamma}'' = \frac{N_o(\bar{E}_r + N_o)}{\bar{E}_r} \tilde{\gamma}' \quad (7.462)$$

and Γ_M is the incomplete Gamma function. The results can be plotted in various forms using Matlab.

The primary performance gain for the multiple pulse model with the independent fading/target reflection is due to the reduced probability that will have a deep fade on all M pulses. In addition, if the transmitted energy per pulse remains constant, the total energy/noise density increases, will improve monotonically with M .

A more interesting trade-off is to constrain the total transmitted energy in the CPI (coherent pulse interval) and look at the effect of M on the P_D for a given P_F . We have already done this trade-off in Example 2.2. Figure 2.16 is applicable if we let $N = 2M$ on the horizontal axis and replace $N\sigma_s^2/\sigma_n^2$ in the curve labels with $2M\bar{E}_r/N_o$. We see that, for each value of $2M\bar{E}_r/N_o$ there is an optimum number of pulses. This is the same as saying there is an optimum energy per pulse as M increases the \bar{E}_r/N_o per pulse decreases. We are using a quadratic detector on each pulse. When \bar{E}_r/N_o becomes too small, we encounter a *small-signal suppression effect* (e.g. [DR58]) that has been recognized since mid-1940s

[Ric45]. When the system is below the optimum energy/pulse this effect is stronger than the gain from diversity.

In some applications, the fading may be correlated from pulse to pulse. This corresponds to model in Sections 3.3.1.3 and 3.3.1.4. We will discuss this case in the problems.

The solution to the analogous binary communication problem for arbitrary signals follows in a similar fashion (e.g. [Mas56, Tur58]). We discuss a typical system briefly. Recall that the phase angle θ has a uniform density. From our results in the preceding section (Figures 7.63 and 7.64) we would expect that orthogonal signals would be optimum. We discuss briefly a simple FSK system using orthogonal signals. The received signals under the two hypotheses are

$$H_1 : r(t) = \sqrt{2} v f(t) \cos[\omega_1 t + \phi(t) + \theta] + w(t), \quad 0 \leq t \leq T, \quad (7.463)$$

$$H_0 : r(t) = \sqrt{2} v f(t) \cos[\omega_0 t + \phi(t) + \theta] + w(t), \quad 0 \leq t \leq T. \quad (7.464)$$

The frequencies are separated enough to guarantee orthogonality. Assuming equal *a priori* probabilities and a minimum probability of error criterion, $\eta = 1$. The likelihood ratio test follows directly (see Problem 7.4.24).

$$L_{c_1}^2 + L_{s_1}^2 \stackrel{H_1}{\underset{H_0}{\gtrless}} L_{c_0}^2 + L_{s_0}^2. \quad (7.465)$$

The receiver structure is shown in Figure 7.73. The probability of error can be evaluated analytically:

$$\Pr(\epsilon) = \frac{1}{2} \left[1 + \frac{1}{2} \frac{\bar{E}_r}{N_0} \right]^{-1}. \quad (7.466)$$

(See Problem 7.4.24.)

In Figure 7.74, we have plotted the $\Pr(\epsilon)$ as a function of \bar{E}_r/N_0 . For purposes of comparison we have also shown the $\Pr(\epsilon)$ for the known signal case and the uniform random phase case. We see that for both nonfading cases the probability of error decreases exponentially for large \bar{E}_r/N_0 , whereas the fading case decreases only linearly. This is intuitively logical. Regardless of how large the average received energy becomes, during a deep signal fade the probability of error is equal or nearly equal to 1/2. Even though this does not occur often,

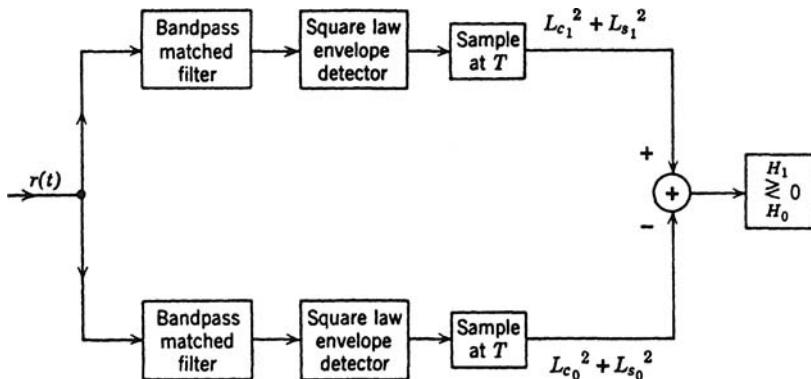


Figure 7.73: Optimum receiver: binary communication system with orthogonal signals.

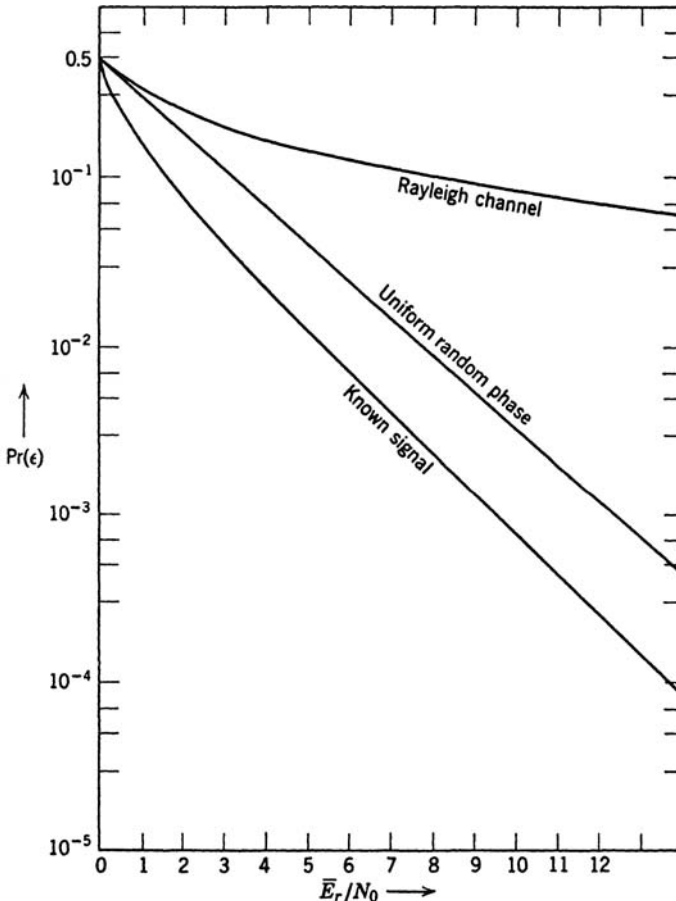


Figure 7.74: Probability of error, binary orthogonal signals, Rayleigh channel.

its occurrence keeps the probability of error from improving exponentially. One can show that by using diversity (e.g., sending the signal over several independent Rayleigh channels in parallel) we can achieve an exponential decrease (e.g., p. 381 in DEMT-III [Van71b, Van01c]). The curves have the same general behavior as Figure 2.15.

As we have already pointed out, an alternate approach is to measure the channel characteristics and use this measurement in the receiver structure. We can easily obtain an estimate of the possible improvement available by assuming that the channel measurement is *perfect*. If the measurement is perfect, we can use a coherent receiver. The resulting $Pr(\epsilon)$ is easy to evaluate. First we write the error probability conditioned on the channel variable v being equal to V . We then average over the Rayleigh density in Figure 7.67b. Using coherent or known signal reception and orthogonal signals the probability of error for a given value V is given by (7.44),

$$Pr(\epsilon|V) = \int_{V\sqrt{1/N_0}}^{\infty} \frac{1}{\sqrt{2\pi}} e^{-y^2/2} dy, \quad V \geq 0 \quad (7.467)$$

and

$$p_v(V) = \begin{cases} \frac{V}{\sigma^2} e^{-V^2/2\sigma^2}, & V \geq 0, \\ 0, & V < 0. \end{cases} \quad (7.468)$$

Thus,

$$\Pr(\epsilon) = \int_0^\infty dV \frac{V}{\sigma^2} e^{-V^2/2\sigma^2} \int_{V\sqrt{1/N_0}}^\infty \frac{1}{\sqrt{2\pi}} e^{-y^2/2} dy. \quad (7.469)$$

Changing to polar coordinates and integrating, we obtain

$$\Pr(\epsilon) = \frac{1}{2} \left[1 - \left(\frac{\bar{E}_r/N_0}{1 + \bar{E}_r/N_0} \right)^{\frac{1}{2}} \right]. \quad (7.470)$$

The result is shown in Figure 7.75.

Comparing (7.470) and (7.466) (or looking at Figure 7.75), we see that perfect measurement gives about a 3 dB improvement for high \bar{E}_r/N_0 values and orthogonal signals. In addition, if we measured the channel, we could use equal-and-opposite signals to obtain another 3 dB.

Rician Channel.¹⁷ In many physical channels there is a fixed (or “specular”) component in addition to the Rayleigh component. A typical example is an ionospheric radio link operated below the maximum usable frequency (e.g. [McN49, BP57], or [Pri57]). Such channels are called Rician channels, in honor of S.O. Rice for his pioneering work on the analysis of random processes [Ric45]. In radar systems, we encounter it where the reflection from the target consists of a strong specular component plus a number of small Rayleigh reflectors.

We now illustrate the behavior of this type of channel for a binary communication system, using orthogonal signals. The received signals on the two hypotheses are

$$\begin{aligned} H_1 : r(t) &= \sqrt{2} \alpha f_1(t) \cos[\omega_c t + \phi_1(t) + \delta] \\ &\quad + \sqrt{2} v f_1(t) \cos[\omega_c t + \phi_1(t) + \theta] + w(t), \quad 0 \leq t \leq T, \\ H_0 : r(t) &= \sqrt{2} \alpha f_0(t) \cos[\omega_c t + \phi_0(t) + \delta] \\ &\quad + \sqrt{2} v f_0(t) \cos[\omega_c t + \phi_0(t) + \theta] + w(t), \quad 0 \leq t \leq T, \end{aligned} \quad (7.471)$$

where α and δ are the amplitude and phase of the specular component. The transmitted signals are orthonormal. In the simplest case α and δ are assumed to be known (see Problem 7.5.26 for unknown δ). Under this assumption, with no loss in generality, we can let $\delta = 0$. We may now write the signal component on H_i as

$$a_1 \{ \sqrt{2} f_i(t) \cos[\omega_c t + \phi_i(t)] \} + a_2 \{ \sqrt{2} f_i(t) \sin[\omega_c t + \phi_i(t)] \}, \quad i = 0, 1. \quad (7.472)$$

¹⁷This section is the waveform analog to Section 3.4. We focus on specific examples rather than the general case.

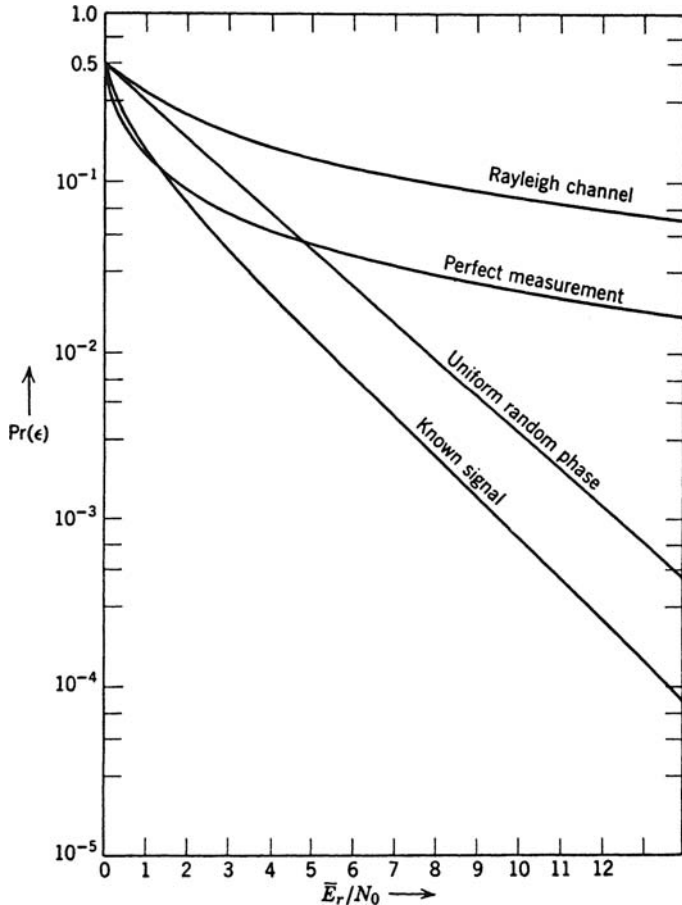


Figure 7.75: Probability of error, Rayleigh channel with perfect measurement.

Once again, a_1 and a_2 are independent Gaussian random variables:

$$\begin{aligned} E(a_1) &= \alpha, & E(a_2) &= 0, \\ \text{Var}(a_1) = \text{Var}(a_2) &= \sigma^2. \end{aligned} \quad (7.473)$$

The expected value of the received energy in the signal component on either hypothesis is

$$E(E_r) = 2\sigma^2 + \alpha^2 \triangleq \sigma^2(2 + \gamma^2), \quad (7.474)$$

where γ^2 is twice the ratio of the energy in the specular component to the average energy in the random component.

If we denote the total received amplitude and phase angle as

$$v' = \sqrt{a_1^2 + a_2^2}, \quad \theta' = \tan^{-1} \frac{a_2}{a_1}. \quad (7.475)$$

then

$$\begin{aligned} p_{v'} &= \frac{V}{\sigma^2} \exp \left\{ -\frac{1}{2\sigma^2}(V^2 + \alpha^2) \right\} I_o \left(\frac{\alpha V}{\sigma^2} \right) \\ &= \frac{V}{\sigma^2} \exp \left\{ -\frac{1}{2} \left(\frac{V^2}{\sigma^2} + \gamma^2 \right) \right\} I_o \left(\gamma \frac{V}{\sigma} \right). \end{aligned} \quad (7.476)$$

The density of the normalized envelope ($V'_n = V/\sigma$) is

$$p_{v'_n}(V_n) = V_n \exp \left\{ -\frac{1}{2}(V_n^2 + \gamma^2) \right\} I_o(\gamma V_n). \quad (7.477)$$

These densities are shown in Figure 7.76a and b ([Ric45], and [Tur58]). As we would expect, the phase angle probability density becomes quite peaked as γ increases.

The receiver structure is obtained by a straightforward modification of (7.443)–(7.451). The likelihood ratio test is

$$\left(\frac{\alpha}{2\sigma^2} + \frac{1}{N_0} L_{c_1} \right)^2 + \left(\frac{1}{N_0} L_{s_1} \right)^2 \stackrel{H_1}{\gtrless} \stackrel{H_0}{\lesssim} \left(\frac{\alpha}{2\sigma^2} + \frac{1}{N_0} L_{c_0} \right)^2 + \left(\frac{1}{N_0} L_{s_0} \right)^2. \quad (7.478)$$

The receiver structure is shown in Figure 7.77. The calculation of the error probability is tedious (e.g. [Tur58]), but the result is

$$\begin{aligned} \Pr(\epsilon) &= Q \left[\frac{\gamma}{(\beta + \frac{1}{2})^{\frac{1}{2}} \beta^{\frac{1}{2}}}, \frac{\gamma(\beta + 1)}{(\beta + 2)^{\frac{1}{2}} \beta^{\frac{1}{2}}} \right] \\ &\quad - \left(\frac{\beta + 1}{\beta + 2} \right) \exp \left[-\frac{\gamma^2}{2} \left(\frac{\beta^2 + 2\beta + 2}{\beta^2 + 2\beta} \right) \right] I_0 \left[\gamma^2 \frac{\beta + 1}{\beta(\beta + 2)} \right]. \end{aligned} \quad (7.479)$$

where $\beta \triangleq 2\sigma^2/N_0$ is the expected value of the received signal energy in the random component divided by N_0 . The probability of error is plotted for typical values of γ in Figure 7.78. Observe that $\gamma = 0$ is the Rayleigh channel and $\gamma = \infty$ is the completely known signal. We see that even when the power in the specular component is twice that of the random component the performance lies close to the Rayleigh channel performance. Once again, because the Rician channel is a channel of practical importance, considerable effort has been devoted to studying its error behavior under various conditions (e.g. [Tur58]).

7.4.3 Other Target Models

In many applications, the two fluctuation models that we have discussed are not adequate to model target fluctuation or channel fading characteristics. Much of the early radar analysis used four models originated by Swerling in Refs [Swe54, Swe60]. The Swerling I and II models are the same as the Rayleigh model. Swerling I assumes that the M signal amplitudes fade together with a Rayleigh distribution. Swerling II assumes that the M signal amplitudes fade independently with Rayleigh densities. Swerling III and IV utilize a Chi-square density of order 4 for the radar cross section of the target. It is used to model reflections from targets with a few dominant scatterers plus a number of small scatterers. Swerling III assumes that the M signal amplitudes fade together and Swerling IV assumes that they fade independently. The Swerling III and IV are similar to the Rician but the tail of the density decays more slowly. Swerling [Swe66] generalized his models in a Aerospace Corp. report that was

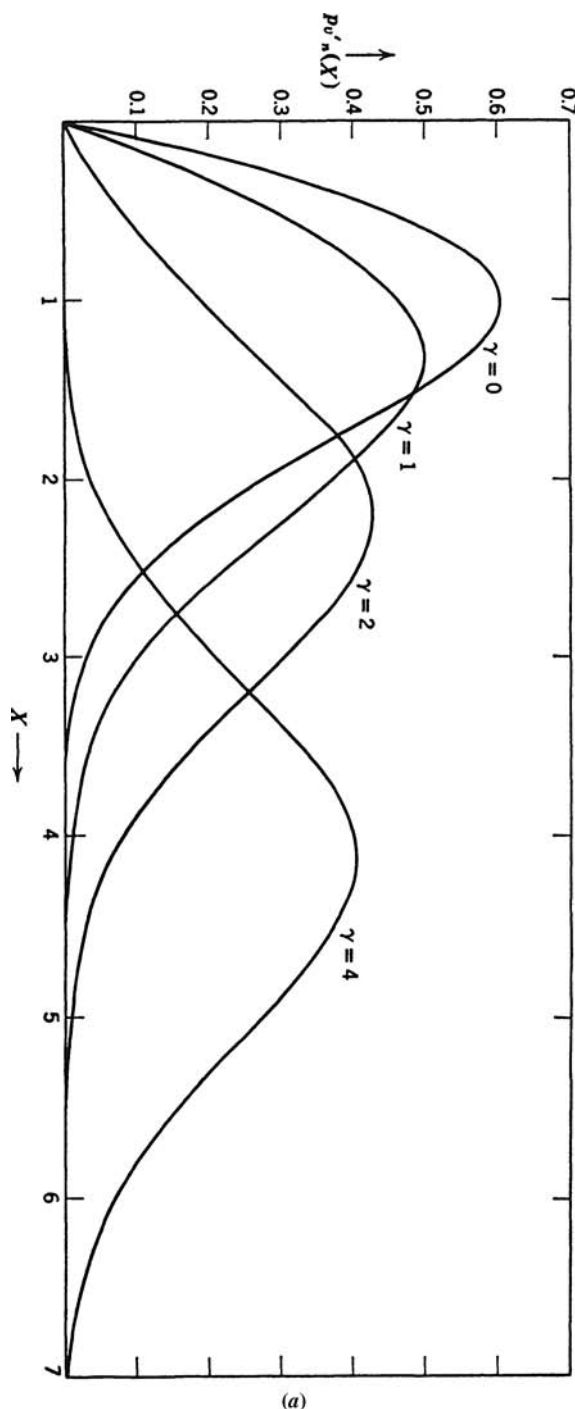


Figure 7.76: (a) Probability density for envelope, Rician channel.

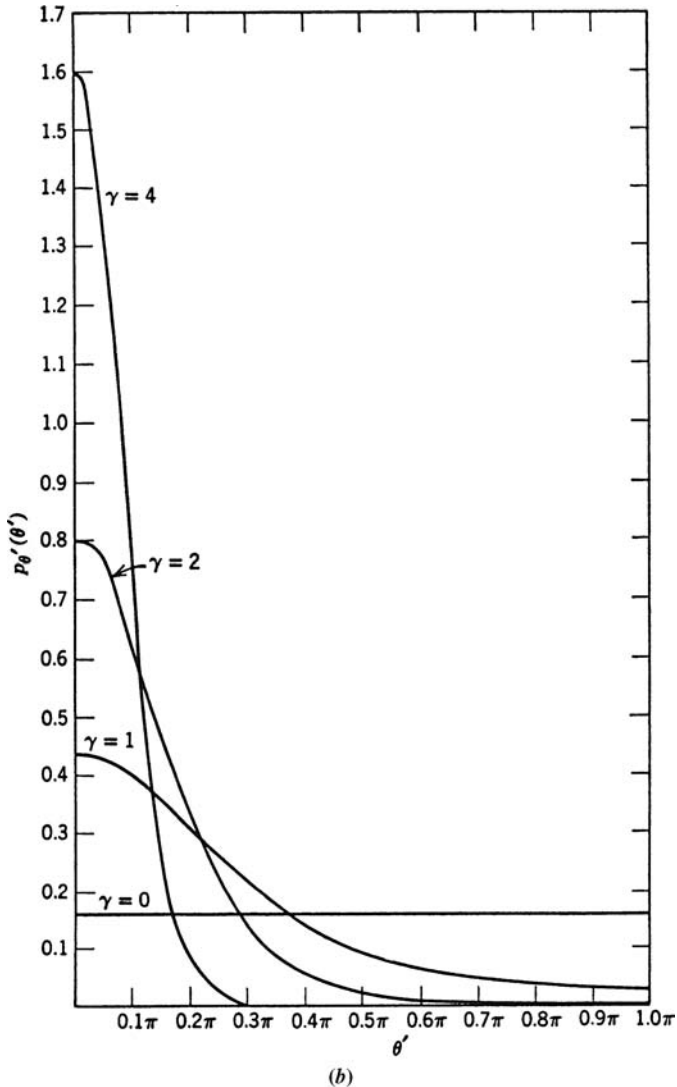


Figure 7.76: (b) Probability density for phase angle, Rician channel.

not cleared for public distribution until 1996 [Swe97]. The generalized models replaced the Chi-square densities with Gamma densities and incorporated models originated by Weinstock [Wei56]. Other target models used the log-normal density to characterize the amplitude of the envelope (e.g. [HM67, Shn91]) and the Weibull density (e.g. [Sch76]). The motivation for this collection of models is that they can produce widely varied results for the probability of detection (e.g. [Joh97]). This family of models are discussed in most radar texts (e.g. [Sko01]).

More recent work has generalized the target models by characterizing some of the parameters in the densities as random variables. Shnidman [Shn03] has good discussions of these approaches. We will develop some of those models in the problems but the reader needs to go to some of the above references for a fuller understanding.

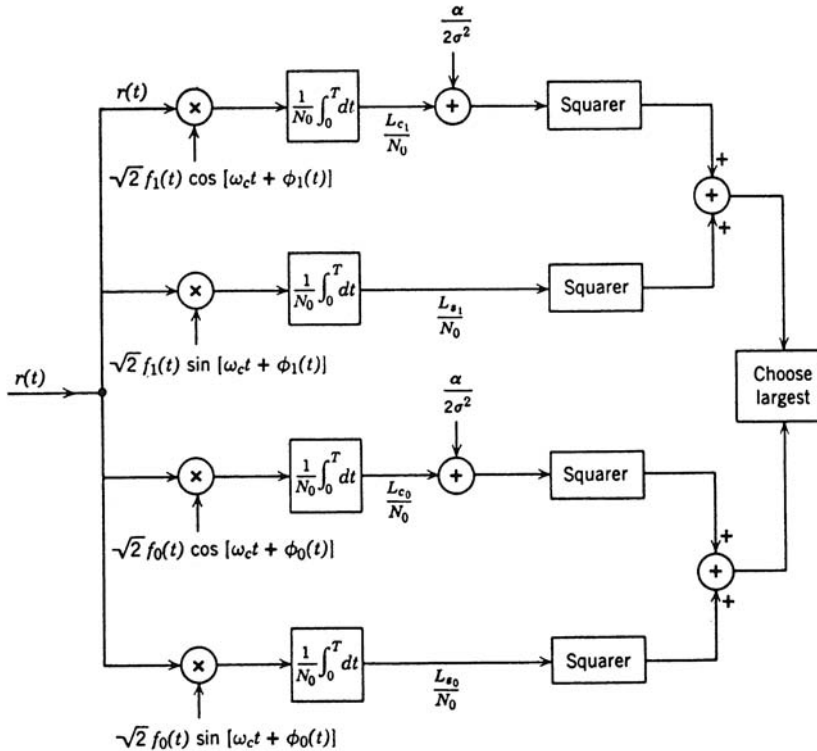


Figure 7.77: Optimum receiver for binary communication over a Rician channel.

These expanded target models get us into a non-Gaussian detection problem. However, if we assume that the reflections from successive pulses are statistically independent and we use a matched filter-envelope detector then we have reduced the model to a vector problem similar to Example 2.4 in Chapter 2.

7.4.4 Nonrandom Parameters

As discussed in the introduction, there are applications in which the parameters should be modeled as an unknown random vectors. In this case, we extend the results in Section 4.5 and Chapter 5 to the waveform model. We consider a simple example to illustrate the techniques. We use the circular complex Gaussian model to match the examples in Chapter 5.

We consider the model in which we transmit M identical pulses. We can write the received signal in complex notation as

$$\tilde{r}(t) = \sum_{i=1}^M \tilde{a}_i \tilde{s}_i(t) + \tilde{w}(t). \quad (7.480)$$

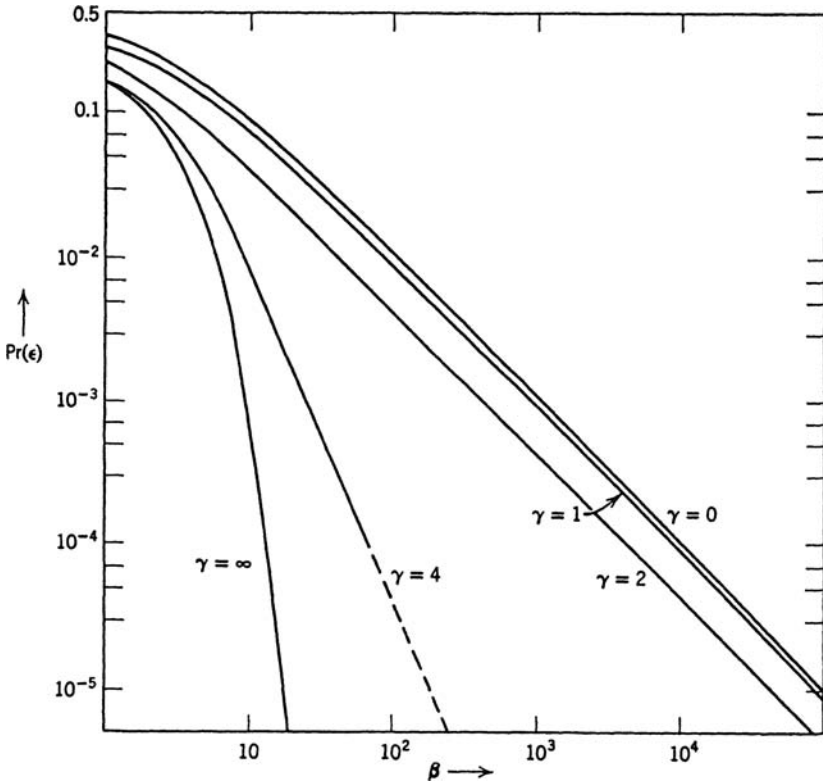


Figure 7.78: Probability of error for binary orthogonal signals, Rician channel.

The complex envelope of the output of the bandpass matched filter in Figure 7.71 can be written in complex notation¹⁸

$$\tilde{r}_i = \int_0^T \sum_{j=1}^M \tilde{a}_j \tilde{s}_j(t) \tilde{s}_i^*(t) dt + \tilde{w}_i, \quad i = 1, 2, \dots, M, \quad (7.481)$$

where the \tilde{w}_i are IID $CN(0, N_0)$. We can assume the signals are orthonormal by absorbing the transmitted energy in \tilde{a}_i .

We define

$$[\tilde{\mathbf{V}}]_{ij} \triangleq \int_0^T \tilde{s}_i^*(t) \tilde{s}_j(t) dt = \delta_{ij}, \quad (7.482)$$

because the signals are orthonormal. The \tilde{a}_i are nonrandom parameters

$$\tilde{\mathbf{a}} = [\tilde{a}_1 \ \tilde{a}_2 \ \cdots \ \tilde{a}_M]^T. \quad (7.483)$$

¹⁸This assumes we reverse the sampler and the squarer.

Then

$$\tilde{\mathbf{r}} = \tilde{\mathbf{V}}\tilde{\mathbf{a}} + \tilde{\mathbf{w}}, \quad (7.484)$$

From (5.144),

$$\hat{\mathbf{a}}_{\text{ml}} = [\tilde{\mathbf{V}}^H \tilde{\mathbf{V}}]^{-1} \tilde{\mathbf{V}}^H \tilde{\mathbf{R}} = \tilde{\mathbf{V}}^\dagger \tilde{\mathbf{R}}. \quad (7.485)$$

From Section 4.5, the generalized likelihood ratio test is

$$\Lambda_g = |\mathbf{P}_{\tilde{\mathbf{V}}} \tilde{\mathbf{R}}|^2 \begin{matrix} \stackrel{H_1}{\gtrless} \\ H_0 \end{matrix} \gamma, \quad (7.486)$$

where

$$\mathbf{P}_{\tilde{\mathbf{V}}} = \tilde{\mathbf{V}} [\tilde{\mathbf{V}}^H \tilde{\mathbf{V}}]^{-1} \tilde{\mathbf{V}}^H = \mathbf{I}. \quad (7.487)$$

Thus,

$$\Lambda_g = |\tilde{\mathbf{R}}|^2 = \sum_{i=1}^M |\tilde{R}_i|^2 \begin{matrix} \stackrel{H_1}{\gtrless} \\ H_0 \end{matrix} \gamma, \quad (7.488)$$

which corresponds to the receiver in Figure 7.71.

Most of the other ideas in Section 4.5 can be applied to the waveform problem.

7.4.4.1 Summary

As we would expect, the formulation for the M -ary signaling problem is straightforward. Probability of error calculations are once again involved (e.g. [Pro63] or [WZ62]). In this chapter, we have seen that both the Rayleigh and Rician channels are special cases of the *general Gaussian* problem.

In this section, we have studied in detail two important cases in which unwanted random parameters are contained in the signal components. Because the probability density was known, the optimum test procedure followed directly from our general likelihood ratio formulation. The particular examples of densities we considered gave integrals that could be evaluated analytically and consequently led to explicit receiver structures. Even when we could not evaluate the integrals, the method of setting up the likelihood ratio was clear.

When the probability density of θ is unknown, the best procedure is not obvious. There are two logical possibilities:

1. We can hypothesize a density and use it as if it were correct. We can investigate the dependence of the performance on the assumed density by using sensitivity analysis techniques analogous to those we have demonstrated for other problems.
2. We can use a minimax procedure. This is conceptually straightforward. For example, in a binary communication problem we find the $\Pr(\epsilon)$ as a function of $p_\theta(\theta)$ and then choose the $p_\theta(\theta)$ that maximizes $\Pr(\epsilon)$ and design for this case. The two objections to this procedure are its difficulty and the conservative result.

In Section 7.4.4, we gave a brief discussion of the nonrandom parameter case. One important parameter that we have not discussed is the $N_0/2$, the white noise level is unknown.

Most of the CFAR results in Section 4.5 map into the waveform problem in a reasonably obvious manner.

7.5 MULTIPLE CHANNELS

In Chapter 6, we introduced the idea of a vector random process. We now want to solve the detection and estimation problems for the case in which the received waveform is a sample function from a vector random process.

In the simple binary detection problem, the received waveforms are¹⁹

$$H_1 : \mathbf{r}(t) = \mathbf{s}(t) + \mathbf{n}(t), \quad T_i \leq t \leq T_f, \quad (7.489)$$

$$H_0 : \mathbf{r}(t) = \mathbf{n}(t), \quad T_i \leq t \leq T_f. \quad (7.490)$$

In the estimation case, the received waveform is

$$\mathbf{r}(t) = \mathbf{s}(t, \mathbf{A}) + \mathbf{n}(t), \quad T_i \leq t \leq T_f. \quad (7.491)$$

Two issues are involved in the vector case:

1. The first is a compact formulation of the problem. By using the vector Karhunen–Loéve expansion with scalar coefficients introduced in Chapter 6 we show that the construction of the likelihood ratio is a trivial extension of the scalar case. (This problem has been discussed in great detail by Wolf [Wol59] and Thomas and Wong [TW60].)
2. The second is to study the performance of the resulting receiver structures to see whether problems appear that did *not* occur in the scalar case. We discuss only a few simple examples in this section.

7.5.1 Vector Karhunen–Loéve

We assume that $\mathbf{s}(t)$ is a known vector signal. The additive noise $\mathbf{n}(t)$ is a sample function from an M -dimensional Gaussian random process. We assume that it contains a white noise component:

$$\mathbf{n}(t) = \mathbf{w}(t) + \mathbf{n}_c(t), \quad (7.492)$$

where

$$E [\mathbf{w}(t)\mathbf{w}^T(u)] = \frac{N_0}{2} \mathbf{I} \delta(t - u). \quad (7.493)$$

A more general case is

$$E [\mathbf{w}(t)\mathbf{w}^T(u)] = \mathbf{N} \delta(t - u). \quad (7.494)$$

The matrix \mathbf{N} contains only numbers. We assume that it is *positive definite*. Physically this means that all components of $\mathbf{r}(t)$ or any linear transformation of $\mathbf{r}(t)$ will contain a white

¹⁹In the scalar case we wrote the signal energy separately and worked with normalized waveforms. In the vector case this complicates the notation needlessly, and we use unnormalized waveforms.

noise component. The general case is done in Problem 7.5.2. We consider the case described by (7.493) in the text. The covariance function matrix of the colored noise is

$$E[\mathbf{n}_c(t)\mathbf{n}_c^T(u)] \triangleq \mathbf{K}_c(t, u). \quad (7.495)$$

We assume that each element in $\mathbf{K}_c(t, u)$ is square-integrable and that the white and colored components are independent. Using (7.492)–(7.495), we have

$$\mathbf{K}_n(t, u) = \frac{N_0}{2} \mathbf{I} \delta(t - u) + \mathbf{K}_c(t, u). \quad (7.496)$$

To construct the likelihood ratio we proceed as in the scalar case. Under hypothesis H_1

$$\begin{aligned} r_i &\triangleq \int_{T_i}^{T_f} \mathbf{r}^T(t) \boldsymbol{\phi}_i(t) dt \\ &= \int_{T_i}^{T_f} \mathbf{s}^T(t) \boldsymbol{\phi}_i(t) dt + \int_{T_i}^{T_f} \mathbf{n}^T(t) \boldsymbol{\phi}_i(t) dt \\ &= s_i + n_i. \end{aligned} \quad (7.497)$$

Notice that all of the coefficients are scalars. Thus (7.189) is directly applicable:

$$\ln \Lambda[\mathbf{r}(t)] = \sum_{i=1}^{\infty} \frac{R_i s_i}{\lambda_i} - \frac{1}{2} \sum_{i=1}^{\infty} \frac{s_i^2}{\lambda_i}. \quad (7.498)$$

Substituting (7.497) into (7.498), we have

$$\begin{aligned} \ln \Lambda[\mathbf{r}(t)] &= \iint_{T_i}^{T_f} \mathbf{r}^T(t) \sum_{i=1}^{\infty} \frac{\boldsymbol{\phi}_i(t) \boldsymbol{\phi}_i^T(u)}{\lambda_i} \mathbf{s}(u) dt du \\ &\quad - \frac{1}{2} \iint_{T_i}^{T_f} \mathbf{s}^T(t) \sum_{i=1}^{\infty} \frac{\boldsymbol{\phi}_i(t) \boldsymbol{\phi}_i^T(u)}{\lambda_i} \mathbf{s}(u) dt du. \end{aligned} \quad (7.499)$$

Defining

$$\mathbf{Q}_n(t, u) = \sum_{i=1}^{\infty} \frac{\boldsymbol{\phi}_i(t) \boldsymbol{\phi}_i^T(u)}{\lambda_i}, \quad T_i < t, u < T_f, \quad (7.500)$$

we have

$$\begin{aligned} \ln \Lambda[\mathbf{r}(t)] &= \iint_{T_i}^{T_f} \mathbf{r}^T(t) \mathbf{Q}_n(t, u) \mathbf{s}(u) dt du \\ &\quad - \frac{1}{2} \iint_{T_i}^{T_f} \mathbf{s}^T(t) \mathbf{Q}_n(t, u) \mathbf{s}(u) dt du. \end{aligned} \quad (7.501)$$

Using the vector form of Mercer's theorem, we observe that

$$\boxed{\int_{T_i}^{T_f} \mathbf{K}_n(t, u) \mathbf{Q}_n(u, z) du = \delta(t - z) \mathbf{I}, \quad T_i < t, z < T_f.} \quad (7.502)$$

By analogy with the scalar case, we write

$$\mathbf{Q}_n(t, u) = \frac{2}{N_0} \mathbf{I}[\delta(t - u) - \mathbf{h}_o(t, u)] \quad (7.503)$$

and show that $\mathbf{h}_o(t, u)$ can be represented by a convergent series. The details are in Problem 7.5.1. As in the scalar case, we simplify (7.501) by defining,

$$\mathbf{g}(t) = \int_{T_i}^{T_f} \mathbf{Q}_n(t, u) \mathbf{s}(u) du, \quad T_i < t < T_f. \quad (7.504)$$

The optimum receiver is just a vector correlator or vector matched filter, as shown in Figure 7.79. The double lines indicate vector operations and the symbol \odot denotes the dot product of the two input vectors. We can show that the performance index is

$$\begin{aligned} d^2 &= \iint_{T_i}^{T_f} \mathbf{s}^T(t) \mathbf{Q}_n(t, u) \mathbf{s}(u) dt du \\ &= \int_{T_i}^{T_f} \mathbf{s}^T(t) \mathbf{g}(t) dt. \end{aligned} \quad (7.505)$$

7.5.1.1 Application

Consider a simple example.

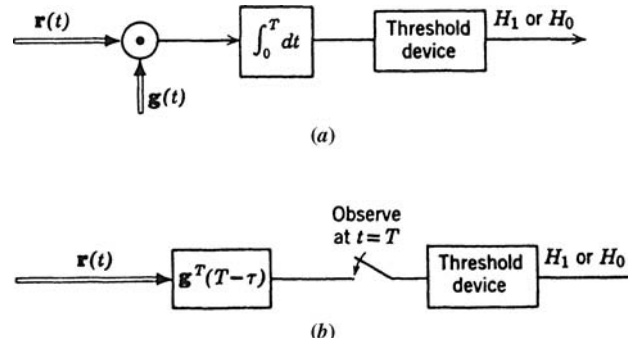


Figure 7.79: Vector receivers: (a) matrix correlator; (b) matrix matched filter.

Example 7.15.

$$\mathbf{s}(t) = \begin{bmatrix} \sqrt{E_1} s_1(t) \\ \sqrt{E_2} s_2(t) \\ \vdots \\ \sqrt{E_M} s_M(t) \end{bmatrix}, \quad 0 \leq t \leq T, \quad (7.506)$$

where the $s_i(t)$ are orthonormal.

Assume that the channel noises are independent and white:

$$E[\mathbf{w}(t)\mathbf{w}^T(u)] = \begin{bmatrix} \frac{N_0}{2} & & & & & \\ & \mathbf{0} & & & & \\ & & \frac{N_0}{2} & & & \\ & & & \ddots & & \\ & & & & \frac{N_0}{2} & \\ & \mathbf{0} & & & & \frac{N_0}{2} \end{bmatrix} \delta(t-u). \quad (7.507)$$

Then

$$\mathbf{g}(t) = \begin{bmatrix} \frac{2\sqrt{E_1}}{N_0} s_1(t) \\ \frac{2\sqrt{E_1}}{N_0} s_1(t) \\ \vdots \\ \frac{2\sqrt{E_M}}{N_0} s_M(t) \end{bmatrix}. \quad (7.508)$$

The resulting receiver is the vector correlator shown in Figure 7.80 and the performance index is

$$d^2 = \sum_{i=1}^M \frac{2E_i}{N_0}. \quad (7.509)$$

This receiver is commonly called a maximal ratio combiner [Bre55] because the inputs are weighted to maximize the output signal-to-noise ratio. The appropriate combiners for colored noise are developed in the problems. ■

Most of the techniques of the scalar case carry over directly to the vector case at the expense of algebraic complexity. For the colored noise case, the key is to find $\mathbf{h}_0(t, u)$. Just as in the scalar case, $\mathbf{h}_0(t, u)$ corresponds to the optimum unrealizable filter for estimating $\mathbf{n}_c(t)$. In Chapter 10, we will derive another form of the likelihood ratio that which contains $\mathbf{h}_{0r}(t, u)$, the optimum realizable filter and develop explicit techniques for finding $\mathbf{h}_{0r}(t, u)$. The modifications for linear and nonlinear estimation are straightforward. The modifications

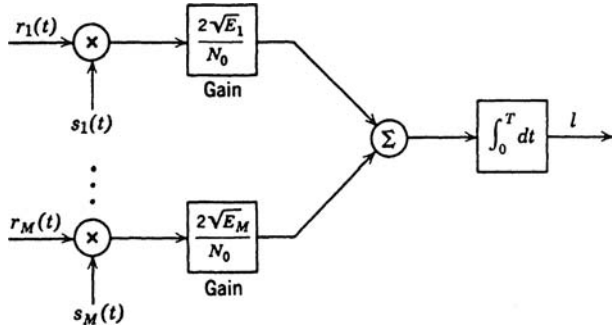


Figure 7.80: Maximal ratio combiner.

for unwanted parameters can also be extended to the vector case. The formulation for M channels of the random phase, Rayleigh, and Rician types is carried out in the problems.

7.6 MULTIPLE PARAMETER ESTIMATION

In Section 7.2.2, we considered linear estimation of multiple parameters. In this section, we revisit the general multiple parameter estimation problem.

The general model that we will start with is

$$r(t) = s(t, \theta_s) + n_c(t, \theta_c) + w(t), \quad T_i \leq t \leq T_f, \quad (7.510)$$

where $s(t, \theta_s)$ is a known signal that depends on a $D_s \times 1$ vector parameter θ_s .

The colored noise term is a zero-mean Gaussian random process whose covariance function $K_c(t, u : \theta_c)$ depends on $D_c \times 1$ vector, θ_c .

The white noise term is a zero-mean white Gaussian random process where the spectral height is a scalar parameter θ_w .

Thus, we have to estimate a $(D_s + D_c + 1) \times 1$ parameter vector, θ , where

$$\theta = \begin{bmatrix} \theta_s \\ \theta_c \\ \theta_w \end{bmatrix}.$$

If we model θ as a nonrandom vector then this model is the waveform analogy to the model in Section 5.2 and we shall exploit the parallels. If we model θ as a random vector then this is the waveform analogy to the models in Section 5.3. For hybrid models, we would use the results in Section 4.3.6. There is also a similar model for a circular complex Gaussian process. In most applications, only a subset of these parameters are unknown.

We will look at the two cases where progress can be made. Other cases are developed in the problems and in various references that we will discuss in Section 7.6.3. In Section 7.6.1, we consider the case where θ_s is the only unknown parameter. In Section 7.6.2, we develop the separable parameter model. In Section 7.6.3, we summarize our results and discuss various extensions.

7.6.1 Known Signal in Additive White Gaussian Noise

We assume that the signal depends on the parameter values $\theta_1, \theta_2, \dots, \theta_M$. Then, for the additive channel, we may write the received signal as

$$r(t) = s(t, \boldsymbol{\theta}) + w(t), \quad T_i \leq t \leq T_f, \quad (7.511)$$

where the $\boldsymbol{\theta}$ is a column matrix:

$$\boldsymbol{\theta} = \begin{bmatrix} \theta_1 \\ \vdots \\ \theta_M \end{bmatrix}. \quad (7.512)$$

We consider both random and nonrandom parameters. Proceeding as in Section 7.2.3, we find the log-likelihood function

$$\ln \Lambda_1(r(t), \boldsymbol{\theta}) = \frac{2}{N_o} \int_{T_i}^{T_f} r(t)s(t, \boldsymbol{\theta}) dt - \frac{1}{N_o} \int_{T_i}^{T_f} s^2(t, \boldsymbol{\theta}) dt. \quad (7.513)$$

To find $\hat{\boldsymbol{\theta}}_{ml}$, we must find the maximum of this M -dimensional function. The various computational algorithms in Section 5.2.8 are applicable.

The MAP estimate is found by maximizing

$$\ln p_{\boldsymbol{\theta}, r(t)}(\boldsymbol{\theta}, r(t)) = \ln \Lambda_1(r(t), \boldsymbol{\theta}) + \ln p_{\boldsymbol{\theta}}(\boldsymbol{\theta}). \quad (7.514)$$

The likelihood equation is

$$\frac{2}{N_0} \int_{T_i}^{T_f} \frac{\partial s(t, \boldsymbol{\theta})}{\partial \theta_i} [r(t) - s(t, \boldsymbol{\theta})] dt = 0. \quad (7.515)$$

The Fisher information is

$$\mathbf{J}_{F_{ij}} = -E \left(\frac{\partial^2 \ln \Lambda_1(\boldsymbol{\theta})}{\partial \theta_i \partial \theta_j} \right), \quad (7.516)$$

which reduces to

$$\mathbf{J}_{F_{ij}} = \frac{2}{N_0} \left[\int_{T_i}^{T_f} \frac{\partial s(t, \boldsymbol{\theta})}{\partial \theta_i} \frac{\partial s(t, \boldsymbol{\theta})}{\partial \theta_j} dt \right]. \quad (7.517)$$

For random variables, the Bayesian information matrix is

$$\mathbf{J}_B = \mathbf{J}_F + \mathbf{J}_P, \quad (7.518)$$

where

$$\mathbf{J}_{P_{ij}} = -E_{\boldsymbol{\theta}} \left\{ \frac{\partial^2 \ln p_{\boldsymbol{\theta}}(\boldsymbol{\theta})}{\partial \theta_i \partial \theta_j} \right\}. \quad (7.519)$$

In the next section, we consider the separable parameter model.

7.6.2 Separable Models

In this section, we consider a special case that occurs frequently in practice. It is the waveform analogy to the separable model in Section 5.2.5.

The received signal is

$$r(t) = \sum_{i=1}^M \theta_{l_i} s_i(t, \theta_{nl_i}) + w(t), \quad T_i \leq t \leq T_f. \quad (7.520)$$

We have changed the parameter notation to match Section 5.2.5. We define a $1 \times M$ vector

$$\mathbf{s}(t, \theta_{nl}) \triangleq [s_1(t, \theta_{nl_1}) \quad s_2(t, \theta_{nl_2}) \quad \cdots \quad s_M(t, \theta_{nl_M})], \quad (7.521)$$

an $M \times 1$ vector of the linear parameters

$$\boldsymbol{\theta}_l = [\theta_{l_1} \quad \theta_{l_2} \quad \cdots \quad \theta_{l_M}]^T \quad (7.522)$$

and an $M \times 1$ vector of the nonlinear parameters

$$\boldsymbol{\theta}_{nl} = [\theta_{nl_1} \quad \theta_{nl_2} \quad \cdots \quad \theta_{nl_M}]^T. \quad (7.523)$$

The $\mathbf{s}(t, \theta_{nl})$ vector is analogous to $\mathbf{V}(\theta_{nl})$ in Section 5.2.5.

The likelihood function is

$$\ln \Lambda(r(t), \boldsymbol{\theta}_l, \boldsymbol{\theta}_{nl}) = -\frac{2}{N_o} \int_{T_i}^{T_f} [r(t) - \boldsymbol{\theta}_l^T \mathbf{s}^T(t, \boldsymbol{\theta}_{nl})] [r(t) - \mathbf{s}(t, \boldsymbol{\theta}_{nl}) \boldsymbol{\theta}_l] dt. \quad (7.524)$$

Differentiating with respect to $\boldsymbol{\theta}_l^T$ and setting the result equal to zero gives

$$\hat{\boldsymbol{\theta}}_l = \left[\int_{T_i}^{T_f} \mathbf{s}^T(t, \boldsymbol{\theta}_{nl}) \mathbf{s}(t, \boldsymbol{\theta}_{nl}) dt \right]^{-1} \int_{T_i}^{T_f} \mathbf{s}^T(t, \boldsymbol{\theta}_{nl}) r(t) dt. \quad (7.525)$$

This is analogous to the $\mathbf{V}^\dagger(\boldsymbol{\theta}_{nl}) \mathbf{R}$ term in (5.229). Substituting (7.525) into (7.524) and multiplying the terms out we have

$$\hat{\boldsymbol{\theta}}_{nl} = \underset{\boldsymbol{\theta}_{nl}}{\operatorname{argmax}} \left[\int_{T_i}^{T_f} r(u) \mathbf{s}(u, \boldsymbol{\theta}_{nl}) du \right] \left[\int_{T_i}^{T_f} \mathbf{s}^T(t, \boldsymbol{\theta}_{nl}) \mathbf{s}(t, \boldsymbol{\theta}_{nl}) dt \right]^{-1} \left[\int_{T_i}^{T_f} \mathbf{s}^T(t, \boldsymbol{\theta}_{nl}) r(t) dt \right]. \quad (7.526)$$

We are projecting $r(t)$ into the signal subspace defined by $\mathbf{s}(t, \boldsymbol{\theta}_{nl})$ and choosing the value of $\boldsymbol{\theta}_{nl}$ that maximizes the resulting energy. Note that (7.526) defines an M -dimensional space and that all of the computational algorithms in Section 5.2.8 are available to do the maximization.

The information matrix follows from (7.517). We partition the total parameter vector

$$\boldsymbol{\theta} = [\boldsymbol{\theta}_l^T \quad \boldsymbol{\theta}_{nl}^T]^T. \quad (7.527)$$

Then

$$\frac{\partial s(t, \boldsymbol{\theta})}{\partial \theta_{nl_i}} = \mathbf{s}(t, \boldsymbol{\theta}_{nl}) \mathbf{e}_i = \mathbf{e}_i^T \mathbf{s}^T(t, \boldsymbol{\theta}_{nl}) \quad (7.528)$$

and

$$[\mathbf{J}(\boldsymbol{\theta}_l)]_{ij} = \frac{2}{N_o} \mathbf{e}_i^T \int_{T_i}^{T_f} \mathbf{s}^T(t, \boldsymbol{\theta}_{nl}) \mathbf{s}(t, \boldsymbol{\theta}_{nl}) dt \mathbf{e}_j, \quad (7.529)$$

$$\frac{\partial s(t, \boldsymbol{\theta})}{\partial \theta_{nl_i}} = \frac{\partial \mathbf{s}(t, \boldsymbol{\theta}_{nl})}{\partial \theta_{nl_i}} \boldsymbol{\theta}_l = \boldsymbol{\theta}_l^T \frac{\partial \mathbf{s}^T(t, \boldsymbol{\theta}_{nl})}{\partial \theta_{nl_i}}. \quad (7.530)$$

Then

$$[\mathbf{J}(\boldsymbol{\theta}_{nl})]_{ij} = \frac{2}{N_o} \boldsymbol{\theta}_l^T \left\{ \int_{T_i}^{T_f} \frac{\partial \mathbf{s}^T(t, \boldsymbol{\theta}_{nl})}{\partial \theta_{nl_i}} \frac{\partial \mathbf{s}(t, \boldsymbol{\theta}_{nl})}{\partial \theta_{nl_j}} \right\} \boldsymbol{\theta}_l \quad (7.531)$$

and the cross-term is

$$[\mathbf{J}(\boldsymbol{\theta}_l, \boldsymbol{\theta}_{nl})]_{ij} = \frac{2}{N_o} \mathbf{e}_i^T \left\{ \int_{T_i}^{T_f} \mathbf{s}^T(t, \boldsymbol{\theta}_{nl}) \frac{\partial \mathbf{s}(t, \boldsymbol{\theta}_{nl})}{\partial \theta_{nl_j}} \right\} \boldsymbol{\theta}_j. \quad (7.532)$$

We consider a simple example to illustrate the technique.

Example 7.16. We want to estimate the amplitude and frequency of a sinusoid. Thus,

$$s(t, \mathbf{A}) \triangleq s(t, A, B) = \left(\frac{2E}{T} \right)^{1/2} B \sin(\omega_c t + At), \quad -\frac{T}{2} \leq t \leq \frac{T}{2} \quad (7.533)$$

and

$$r(t) = s(t, \mathbf{A}) + w(t), \quad -\frac{T}{2} \leq t \leq \frac{T}{2}. \quad (7.534)$$

The likelihood function is

$$\begin{aligned} \ln \Lambda[r(t)|A, B] &= \frac{1}{N_0} \int_{-T/2}^{T/2} \left[2r(t) - \left(\frac{2E}{T} \right)^{1/2} B \sin(\omega_c t + At) \right] \left(\frac{2}{T} \right)^{1/2} B \sin(\omega_c t + At) dt \\ &\cong \frac{2E}{N_0} \int_{-T/2}^{T/2} r(t) \left(\frac{2E}{T} \right)^{1/2} B \sin(\omega_c t + At) dt - \frac{B^2 E}{N_0}. \end{aligned} \quad (7.535)$$

We see that this is a separable problem. Differentiating (7.535) with respect to B and setting the result to zero gives

$$\widehat{B}_{ml}(r(t)) = \left(\frac{E}{T} \right)^{1/2} \int_{-T/2}^{T/2} r(t) \sin(\omega_c t + At) dt. \quad (7.536)$$

We implement the technique in Section 7.2.3 to find $\hat{A}_{\text{ml}}(r(t))$. To find the FIM, we write

$$\frac{\partial s(t, A, B)}{\partial A} = \left(\frac{2E}{T}\right)^{1/2} Bt \cos(\omega_c t + At) \quad (7.537)$$

and

$$\frac{\partial s(t, A, B)}{\partial B} = \left(\frac{2E}{T}\right)^{1/2} \sin(\omega_c t + At). \quad (7.538)$$

The elements of \mathbf{J} are

$$\begin{aligned} J_{11} &= \frac{2}{N_0} \int_{-T/2}^{T/2} \frac{2E}{T} B^2 t^2 \cos^2(\omega_c t + At) dt \\ &\cong \sigma_b^2 \frac{T^2}{12} \frac{2E}{N_0}, \end{aligned} \quad (7.539)$$

$$J_{22} = \frac{2}{N_0} \int_{-T/2}^{T/2} \frac{2E}{T} \sin^2(\omega_c t + At) dt \cong \frac{2E}{N_0}, \quad (7.540)$$

and

$$\begin{aligned} J_{12} &= \frac{2}{N_0} \left[\int_{-T/2}^{T/2} \frac{\partial s(t, A, B)}{\partial A} \cdot \frac{\partial s(t, A, B)}{\partial B} dt \right] \\ &= \frac{2}{N_0} \left[\int_{-T/2}^{T/2} \frac{2E}{T} Bt \sin(\omega_c t + At) \cos(\omega_c t + At) dt \right] \cong 0. \end{aligned} \quad (7.541)$$

Thus, the \mathbf{J} matrix is diagonal. This means that

$$E[(\hat{a} - a)^2] \geq \left(\frac{T^2}{12} \frac{2E}{N_0}\right)^{-1} \quad (7.542)$$

and

$$E[(\hat{b} - b)^2] \geq \left(\frac{2E}{N_0}\right)^{-1}. \quad (7.543)$$

Thus, we observe that the *bounds* on the estimates of a and b are uncorrelated. We can show that for large E/N_0 the actual variances approach these bounds. ■

7.6.3 Summary

In this section, we have formulated the multiple parameter estimation problem but only developed one case in detail. When the parameter is in the covariance function the solution is more complicated. Several examples are developed in the problems.

7.7 SUMMARY

In this chapter, we have covered a wide range of problems. The central theme that related them was an additive Gaussian noise component. Using this theme as a starting point, we examined different types of problems and studied their solutions and the implications of these solutions. It turned out that the formal solution was the easiest part of the problem and that investigating the implications consumed most of our efforts. It is worth while to summarize some of the more general results.

In Section 7.2, we studied detection and estimation in white Gaussian noise. The simplest detection problem was binary detection of a known signal in the presence of white Gaussian noise. The optimum receiver could be realized as a matched filter or a correlation receiver. The performance depended only on the normalized distance between the two signal points in the decision space. This distance was characterized by the signal energies, their correlation coefficient, and the spectral height of the additive noise. For equal energy signals, a correlation coefficient of -1 was optimum. In all cases the signal shape was unimportant. The performance was insensitive to the detailed assumptions of the model.

The solution for the M signal problem followed easily. The receiver structure consisted of at most $M - 1$ matched filters or correlators. Except for a few special cases, performance calculations for arbitrary cost assignments and *a priori* probabilities were unwieldy. Therefore, we devoted our attention to minimum probability of error decisions. For arbitrary signal sets the calculation of the probability of error was still tedious. For orthogonal and nonorthogonal equally correlated signals simple expressions could be found and evaluated numerically. Simple bounds on the error probability were derived that were useful for certain ranges of parameter values. The question of the optimum signal set was discussed briefly in the text and in more detail in the problems. We found that for large M , orthogonal signals were essentially optimum.

In Section 7.3, we generalized the simple detection problem by allowing a nonwhite additive Gaussian noise component. This generalization also included known linear channels. The formal extension by means of the whitening approach or a suitable set of observable coordinates was easy. As we examined the result, some issues developed that we had not encountered before. By including a nonzero white noise component we guaranteed that the matched filter would have a square-integrable impulse response and that perfect (or singular) detection would be impossible. The resulting test was stable, but its sensitivity depended on the white noise level. In the presence of a white noise component, the performance could always be improved by extending the observation interval. In radar this was easy because of the relatively long time between successive pulses. Next we studied the effect of removing the white noise component. We saw that unless we put additional “smoothness” restrictions on the signal shape our mathematical model could lead us to singular and/or unstable tests.

In Section 7.4, we further generalized the model by allowing for uncertainties in the signal even in the absence of noise. For the case in which these uncertainties could be parameterized by random variables with known densities, the desired procedure was clear. We considered in detail the random phase case and the random amplitude and phase case. In the random phase problem, we introduced the idea of a simple estimation system that measured the phase angle and used the measurement in the detector. This gave us a method of transition from the known signal case to situations, such as the radar problem, in which the phase is uniformly distributed. For binary signals we found that the optimum signal set depended on the quality of the phase measurement. As we expected, the optimum correlation coefficient ranged from $\rho = -1$ for perfect measurement to $\rho = 0$ for the uniform density.

The random amplitude and phase case enabled us to model a number of communication links that exhibited Rayleigh and Rician fading. Here, we examined channel measurement receivers and perfect measurement receivers. We found that perfect measurement offered a 6 dB improvement. However, even with perfect measurement, the channel fading caused the error probability to decrease linearly with \bar{E}_r/N_0 instead of exponentially as in a nonfading channel.

In Section 7.5, we considered the problem of multiple channel systems. The vector Karhunen–Loève expansion enabled us to derive the likelihood ratio test easily.

We studied the estimation problem in Sections 7.2 and 7.6. The *basic* ideas in the *estimation* problem were similar, and the entire formulation up through the likelihood function was identical. For linear estimation, the resulting receiver structures were identical to those obtained in the simple binary problem. The mean-square estimation error in white noise depended only on E/N_0 .

The nonlinear estimation problem gave rise to a number of issues. The first difficulty was that a sufficient statistic did not exist, which meant that the mapping from the observation space to the estimation space depended on the parameter we were trying to estimate. In some cases this could be accommodated easily. In others, approximate techniques were necessary. The resulting function in the estimation space had a number of local maxima and we had to choose the absolute maximum. Given that we were near the correct maximum, the mean-square error could be computed easily. The error could be reduced significantly over the linear estimation error by choosing a suitable signaling scheme. If we tried to reduce the error too far, however, a new phenomenon developed, which we termed threshold. In the cascade approximation to the optimum estimator the physical mechanism for the occurrence of a threshold was clear. The first stage chose the wrong interval in which to make its local estimate. In the continuous realization (such as range estimation), the occurrence was clear but a quantitative description was more difficult. Because the actual threshold level will depend on the signal structure, the quantitative results for the particular example discussed are less important than the realization that whenever we obtain an error decrease without an increase in signal energy or a decrease in noise level a threshold effect will occur at some signal-to-noise level.

7.8 PROBLEMS

The problems are divided according to sections in the text. Unless otherwise stated, all problems use the model from the corresponding section of the text; for example, the received signals are corrupted by additive zero-mean Gaussian noise that is independent of the hypotheses.

P7.2 Additive White Gaussian Noise

BINARY DETECTION

Problem 7.2.1. Derive an expression for the probability of detection P_D , in terms of d and P_F , for the known signal in the additive white Gaussian noise detection problem (see [You57]).

Problem 7.2.2. In a binary FSK system, one of two sinusoids of different frequencies is transmitted; for example,

$$\begin{aligned}s_1(t) &= f(t) \cos 2\pi f_c t, & 0 \leq t \leq T, \\ s_2(t) &= f(t) \cos 2\pi(f_c + \Delta f)t, & 0 \leq t \leq T,\end{aligned}$$

where $f_c \gg 1/T$ and Δf . The correlation coefficient is

$$\rho = \frac{\int_0^T f^2(t) \cos(2\pi\Delta f t) dt}{\sqrt{\int_0^T f^2(t) dt}}.$$

The transmitted signal is corrupted by additive white Gaussian noise ($N_0/2$).

- (a) Evaluate ρ for a rectangular pulse; that is,

$$f(t) = \begin{cases} \left(\frac{2E}{T}\right)^{1/2}, & 0 \leq t \leq T, \\ 0, & \text{Elsewhere.} \end{cases}$$

Plot the result as a function of $\Delta f T$.

- (b) Assume that we require $\Pr(\epsilon) = 0.01$. What value of E/N_0 is necessary to achieve this if $\Delta f = \infty$? Plot the *increase* in E/N_0 over this asymptotic value that is necessary to achieve the same $\Pr(\epsilon)$ as a function of $\Delta f T$.

Problem 7.2.3. The risk involved in an experiment is

$$\mathcal{R} = C_F P_F P_0 + C_M P_M P_1.$$

The applicable ROC is Figure 2.9. You are given (a) $C_M = 2$; (b) $C_F = 1$; (c) P_1 may vary between 0 and 1. Sketch the line on the ROC that will minimize your maximum possible risk (i.e., assume P_1 is chosen to make \mathcal{R} as *large* as possible. Your line should be a locus of the thresholds that will cause the maximum to be as small as possible).

Problem 7.2.4. Consider the linear feedback system in Figure P7.1.

The function $x(t)$ is a known deterministic function that is zero for $t < 0$. Under H_1 , $A_i = A_1$. Under H_0 , $A_i = A_0$. The noise $w(t)$ is a sample function from a white Gaussian process of spectral

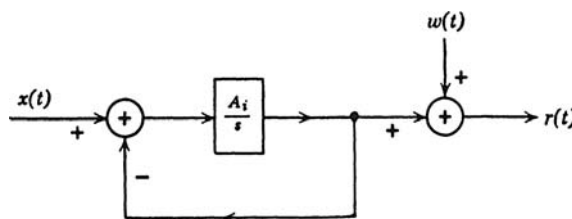


Figure P7.1

height $N_0/2$. We observe $r(t)$ over the interval $(0, T)$. All initial conditions in the feedback system are zero.

- (a) Find the likelihood ratio test.
- (b) Find an expression for P_D and P_F for the special case in which $x(t) = \delta(t)$ (an impulse) and $T = \infty$.

Problem 7.2.5. Three commonly used methods for transmitting binary signals over an additive Gaussian noise channel are on-off keying (ASK), frequency-shift keying (FSK), and phase-shift keying (PSK):

$$\begin{aligned} H_0 : r(t) &= s_0(t) + w(t), & 0 \leq t \leq T, \\ H_1 : r(t) &= s_1(t) + w(t), & 0 \leq t \leq T, \end{aligned}$$

where $w(t)$ is a sample function from a white Gaussian process of spectral height $N_0/2$. The signals for the three cases are as follows:

	ASK	FSK	PSK
$s_0(t)$	0	$\sqrt{2E/T} \sin \omega_1 t$	$\sqrt{2E/T} \sin \omega_0 t$
$s_1(t)$	$\sqrt{2E/T} \sin \omega_1 t$	$\sqrt{2E/T} \sin \omega_0 t$	$\sqrt{2E/T} \sin(\omega_0 t + \pi)$

where $\omega_0 - \omega_1 = 2\pi n/T$ for some nonzero integer n and $w_0 = 2\pi m T$ for some nonzero integer m .

- (a) Draw appropriate signal spaces for the three techniques.
- (b) Find d^2 and the resulting probability of error for the three schemes (assume that the two hypotheses are equally likely).
- (c) Comment on the relative efficiency of the three schemes (a) with regard to utilization of transmitter energy, (b) with regard to ease of implementation.
- (d) Give an example in which the model of this problem does not accurately describe the actual physical situation.

Problem 7.2.6. Suboptimum Receivers. In this problem, we investigate the degradation in performance that results from using a filter other than the optimum receiver filter. A reasonable performance comparison is the increase in transmitted energy required to overcome the decrease in d^2 that results from the mismatching. We would hope that for many practical cases the equipment simplification that results from using other than the matched filter is well worth the required increase in transmitted energy. The system of interest is shown in Figure P7.2, in which

$$\int_0^T s^2(t) dt = 1 \quad \text{and} \quad E[w(t)w(\tau)] = \frac{N_0}{2} \delta(t - \tau).$$

The received waveform is

$$\begin{aligned} H_1 : r(t) &= \sqrt{E}s(t) + w(t), & -\infty < t < \infty, \\ H_0 : r(t) &= w(t), & -\infty < t < \infty. \end{aligned}$$

We know that

$$h_o(t) = \begin{cases} s(T-t), & 0 \leq t \leq T, \\ 0, & \text{Elsewhere} \end{cases}$$

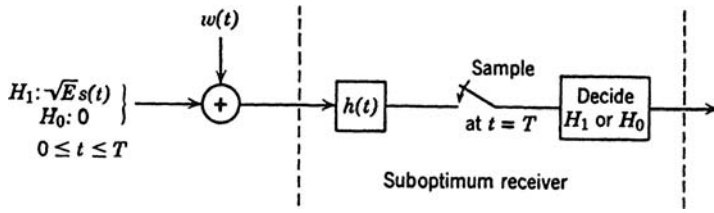


Figure P7.2

and

$$d_o^2 = \frac{2E}{N_0}.$$

Suppose that

$$h(t) = e^{-at} u_{-1}(t), \quad -\infty < t < \infty,$$

$$s(t) = \begin{cases} \left(\frac{1}{T}\right)^{1/2}, & 0 \leq t \leq T, \\ 0, & \text{Elsewhere.} \end{cases}$$

- (a) Choose the parameter a to maximize the output signal-to-noise ratio d^2 .
- (b) Compute the resulting d^2 and compare with d_o^2 . How many decibels must the transmitter energy be increased to obtain the same performance?

M-ARY SIGNALS

Problem 7.2.7. Gram–Schmidt. In this problem we go through the details of the geometric representation of a set of M waveforms in terms of N ($N \leq M$) orthogonal signals.

Consider the M signals $s_1(t), \dots, s_M(t)$ that are either linearly independent or linearly dependent. If they are linearly dependent, we can write (by definition)

$$\sum_{i=1}^M a_i s_i(t) = 0.$$

- (a) Show that if M signals are linearly dependent, then $s_M(t)$ can be expressed in terms of $s_i(t)$: $i = 1, 2, \dots, M-1$.
- (b) Continue this procedure until you obtain N linearly independent signals and $M-N$ signals expressed in terms of them. N is called the *dimension* of the signal set.
- (c) Carry out the details of the Gram–Schmidt procedure.

Problem 7.2.8. Translation/Simplex Signals [WJ65]. For maximum *a posteriori* reception, the probability of error is not affected by a linear translation of the signals in the decision space; for example, the two decision spaces in Figure P7.3a and b have the same $\Pr(\epsilon)$. Clearly, the sets do not require the same energy. Denote the average energy in a signal set as

$$\bar{E} \triangleq \sum_{i=1}^M \Pr(H_i) |s_i|^2 = \sum_{i=1}^M \Pr(H_i) E_i \int_0^T s_i^2(t) dt.$$

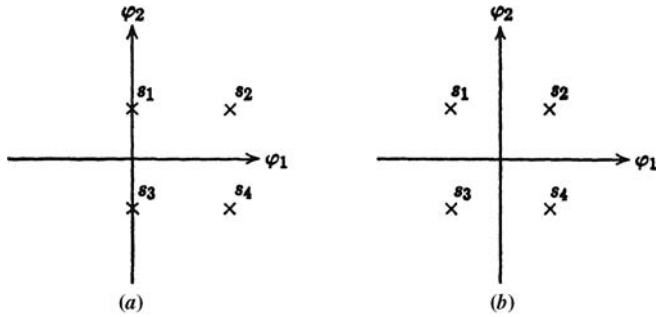


Figure P7.3

- (a) Find the linear translation that minimizes the average energy of the translated signal set; that is, minimize

$$\bar{E} \triangleq \sum_{i=1}^M \Pr(H_i) |s_i - m|^2.$$

- (b) Explain the geometric meaning of the result in part 1.
 (c) Apply the result in part 1 to the case of M orthogonal equal-energy signals representing equally likely hypotheses. The resulting signals are called *Simplex* signals. Sketch the signal vectors for $M = 2, 3, 4$.
 (d) What is the energy required to transmit each signal in the Simplex set?
 (e) Discuss the energy reduction obtained in going from the orthogonal set to the Simplex set while keeping the same $\Pr(\epsilon)$.

Problem 7.2.9. Equally Correlated Signals. Consider M equally correlated signals

$$E \int_0^T s_i(t) s_j(t) dt = \begin{cases} E, & i = j, \\ \rho E, & i \neq j. \end{cases}$$

- (a) Prove

$$-\frac{1}{M-1} \leq \rho \leq 1.$$

- (b) Verify that the left inequality is given by a Simplex set.
 (c) Prove that an equally correlated set with energy E has the same $\Pr(\epsilon)$ as an orthogonal set with energy $E_{\text{orth}} = E(1 - \rho)$.
 (d) Express the $\Pr(\epsilon)$ of the Simplex set in terms of the $\Pr(\epsilon)$ for the orthogonal set and M .

Problem 7.2.10. M Signals, Arbitrary Correlation. Consider an M -ary system used to transmit equally likely messages. The signals have equal energy and may be correlated:

$$\rho_{ij} = \int_0^T s_i(t) s_j(t) dt, \quad i, j = 1, 2, \dots, M.$$

The channel adds white Gaussian noise with spectral height $N_0/2$. Thus,

$$H_i : r(t) = \sqrt{E}s_i(t) + w(t), \quad 0 \leq t \leq T, \quad i = 1, \dots, M.$$

- (a) Draw a block diagram of an optimum receiver containing M matched filters. What is the minimum number of matched filters that can be used?
- (b) Let ρ be the signal correlation matrix. The ij element is ρ_{ij} . If ρ is nonsingular, what is the dimension of the signal space?
- (c) Find an expression for $\Pr(\epsilon|H_1)$, the probability of error, assuming H_1 is true. Assume that ρ is nonsingular.
- (d) Find an expression for $\Pr(\epsilon)$.
- (e) Is this error expression valid for Simplex signals? (Is ρ singular?)

Problem 7.2.11 (continuation). Error Probability [Vit66]. In this problem, we derive an alternate expression for the $\Pr(\epsilon)$ for the system in Problem 7.2.10. The desired expression is

$$1 - \Pr(\epsilon) = \frac{1}{M} \exp\left(-\frac{E}{N_0}\right) \int_{-\infty}^{\infty} \exp\left[\left(\frac{2E}{N_0}\right)^{\frac{1}{2}} x\right] \left[\frac{d}{dx} \int_{-\infty}^x \cdots \int_{-\infty}^x \frac{\exp\left(-\frac{1}{2}y^T \rho^{-1} y\right)}{(2\pi)^{M/2} |\rho|^{\frac{1}{2}}} dy \right] dx. \quad (\text{P.1})$$

Develop the following steps:

- (a) Rewrite the receiver in terms of M orthonormal functions $\phi_i(t)$. Define

$$\begin{aligned} s_i(t) &= \sum_{k=1}^M s_{ik} \phi_k(t), \quad i = 1, 2, \dots, M, \\ r(t) &= \sum_{k=1}^{\infty} r_k \phi_k(t). \end{aligned}$$

Verify that the optimum receiver forms the statistics

$$l_i = \int_0^T r(t) s_i(t) dt = \sum_{k=1}^M s_{ik} R_k$$

and chooses the greatest.

- (b) Assume that $s_m(t)$ is transmitted. Show

$$\begin{aligned} \Pr(\epsilon|m) &\triangleq \Pr(\mathbf{R} \text{ in } \mathbf{Z}_m) \\ &= \Pr\left(\sum_{k=1}^M s_{mk} R_k = \max_j \sum_{k=1}^M s_{jk} R_k\right). \end{aligned}$$

- (c) Verify that

$$\Pr(\epsilon) = \frac{1}{M} \exp\left(-\frac{E}{N_0}\right) \sum_{m=1}^M \int_{-\infty}^{\infty} \cdots \int_{-\infty}^{\infty} \frac{\exp\left[-(1/N_0) \sum_{k=1}^M R_k^2\right]}{(\pi N_0)^{M/2}} \exp\left(\frac{2}{N_0} \max_j \sum_{k=1}^M R_k s_{jk}\right). \quad (\text{P.2})$$

(d) Define

$$f(\mathbf{R}) = \exp \left\{ \max_j \left[\left(\frac{2}{EN_0} \right)^{\frac{1}{2}} \sum_{k=1}^M s_{jk} R_k \right] \right\}$$

and observe that (P.2) can be viewed as the expectation of $f(\mathbf{R})$ over a set of statistically independent, zero-mean Gaussian variables, R_k , with variance $N_0/2$. To evaluate this expectation, define

$$z_j \triangleq \left(\frac{2}{EN_0} \right)^{\frac{1}{2}} \sum_{k=1}^M s_{jk} R_k, \quad j = 1, 2, \dots, M,$$

and

$$\mathbf{z} = \begin{bmatrix} z_1 \\ z_2 \\ \vdots \\ z_M \end{bmatrix}.$$

Find $p_z(z)$. Define

$$x = \max z_j.$$

Find $p_x(x)$.

(e) Using the results in (d), we have

$$1 - \Pr(\epsilon) = \frac{1}{M} \exp \left(-\frac{E}{N_0} \right) \int_{-\infty}^{\infty} \exp \left[\left(\frac{2E}{N_0} \right)^{\frac{1}{2}} X \right] p_x(X) dX.$$

Use $p_x(X)$ from (d) to obtain the desired result.

Problem 7.2.12 (continuation).

- (a) Using the expression in (P.1) of Problem 7.2.11, show that $\partial \Pr(\epsilon) / \partial \rho_{12} > 0$. Does your derivation still hold if $1 \rightarrow i$ and $2 \rightarrow j$?
- (b) Use the results of part 1 and Problem 7.2.9 to develop an intuitive argument that the Simplex set is locally optimum.

Comment. The proof of local optimality is contained in [Bal61]. The proof of global optimality is contained in [LS66].

Problem 7.2.13. Consider the system in Problem 7.2.10. Define

$$\rho_{\max} = \max_{i \neq j} \rho_{ij}.$$

- (a) Prove that $\Pr(\epsilon)$ on any signal set is less than the $\Pr(\epsilon)$ for a set of equally correlated signals with correlation equal to ρ_{\max} .
- (b) Express this in terms of the error probability for a set of orthogonal signals.

- (c) Show that the $\Pr(\epsilon)$ is upper bounded by

$$\Pr(\epsilon) \leq (M-1) \left\{ \operatorname{erfc}_* \left(\left[\frac{E}{N_0} (1 - \rho_{\max}) \right]^{\frac{1}{2}} \right) \right\}.$$

Problem 7.2.14 [AD62]. Consider the system in Problem 7.2.10. Define d_i : distance between the i th message point and the nearest neighbor.

Observe

$$\begin{aligned} d_i &= \min_j 2\sqrt{(1 - \rho_{ij}) E/N_0}, \\ \bar{d} &= \frac{1}{M} \sum_{i=1}^M d_i, \\ d_{\min} &= \min_i d_i. \end{aligned}$$

Prove

$$\operatorname{erfc}_*(\bar{d}) \leq \Pr(\epsilon) \leq (M-1) \operatorname{erfc}_*(d_{\min}).$$

Note that this result extends to signals with unequal energies in an obvious manner.

Problem 7.2.15. In (7.75) of the text we used the limit

$$\lim_{M \rightarrow \infty} \frac{\ln \operatorname{erfc}_* \left[y + \left(\frac{2PT \log_2 M}{N_0} \right)^{\frac{1}{2}} \right]}{1/(M-1)}.$$

Use l'Hospital's rule to verify the limits asserted in (7.76) and (7.77).

Problem 7.2.16. The error probability in (7.73) is the probability of error in deciding which signal was sent. Each signal corresponds to a sequence of digits; for example, if $M = 8$,

$$\begin{array}{ll} 000 \rightarrow s_0(t) & 100 \rightarrow s_4(t) \\ 001 \rightarrow s_1(t) & 101 \rightarrow s_5(t) \\ 010 \rightarrow s_2(t) & 110 \rightarrow s_6(t) \\ 011 \rightarrow s_3(t) & 111 \rightarrow s_7(t) \end{array}$$

Therefore, an error in the signal decision does not necessarily mean that all digits will be in error. Frequently the digit (or bit) error probability $\Pr_B(\epsilon)$ is the error of interest.

- (a) Verify that if an error is made any of the other $M-1$ signals are equally likely to be chosen.
- (b) Verify that the expected number of bits in error, given a signal error is made, is

$$\left[\frac{\sum_{i=1}^{\log_2 M} i \binom{\log_2 M}{i}}{\sum_{i=1}^{\log_2 M} \binom{\log_2 M}{i}} \right] = \frac{(\log_2 M) M}{2(M-1)}.$$

(c) Verify that the bit error probability is

$$\Pr_B(\epsilon) = \frac{M}{2(M-1)} \Pr(\epsilon).$$

(d) Sketch the behavior of the bit error probability for $M = 2, 4$, and 8 (use Figure 7.25).

Problem 7.2.17. Biorthogonal Signals. Prove that for a set of M biorthogonal signals with energy E and equally likely hypotheses the $\Pr(\epsilon)$ is

$$\Pr(\epsilon) = 1 - \int_0^{\infty} \frac{1}{\sqrt{\pi N_0}} \exp \left[-\frac{1}{N_0} (x - \sqrt{E})^2 \right] \left[\int_{-x}^x \frac{1}{\sqrt{\pi N_0}} \exp \left(-\frac{y^2}{N_0} \right) dy \right]^{M/2-1} dx.$$

Verify that this $\Pr(\epsilon)$ approaches the error probability for orthogonal signals for large M and d^2 . What is the advantage of the biorthogonal set?

Problem 7.2.18. Consider the following digital communication system. There are four equally probable hypotheses. The signals transmitted under the hypotheses are

$$\begin{aligned} H_1 &: \left(\frac{2}{T} \right)^{\frac{1}{2}} A \sin \omega_c t, & 0 \leq t \leq T, \\ H_2 &: \frac{1}{3} \left(\frac{2}{T} \right)^{\frac{1}{2}} A \sin \omega_c t, & 0 \leq t \leq T, \\ H_3 &: -\frac{1}{3} \left(\frac{2}{T} \right)^{\frac{1}{2}} A \sin \omega_c t, & 0 \leq t \leq T, \\ H_4 &: -\left(\frac{2}{T} \right)^{\frac{1}{2}} A \sin \omega_c t, & 0 \leq t \leq T, \end{aligned}$$

where $\omega_c = 2\pi n/T$. The signal is corrupted by additive Gaussian white noise $w(t)$, $(N_0/2)$.

- (a) Draw a block diagram of the minimum probability of error receiver and the decision space and compute the resulting probability of error.
- (b) How does the probability of error behave for large A^2/N_0 ?

Problem 7.2.19. M-ary ASK [AD62]. An ASK system is used to transmit equally likely messages

$$s_i(t) = \sqrt{E_i} \phi(t), \quad i = 1, 2, \dots, M,$$

where

$$\sqrt{E_i} = (i-1)\Delta, \quad \int_0^T \phi^2(t) dt = 1.$$

The received signal under the i th hypothesis is

$$H_i : r(t) = s_i(t) + w(t), \quad 0 \leq t \leq T, \quad i = 1, 2, \dots, M,$$

where $w(t)$ is a white noise with spectral height $N_0/2$.

- (a) Draw a block diagram of the optimum receiver.
- (b) Draw the decision space and computer the $\Pr(\epsilon)$.
- (c) What is the average transmitted energy?

$$\text{Note. } \sum_{j=1}^{n-1} j^2 = \frac{(n-1)n(2n-1)}{6}.$$

- (d) What translation of the signal set in the decision space would maintain the $\Pr(\epsilon)$ while minimizing the average transmitted energy?

Problem 7.2.20 (continuation). Use the sequence transmission model in Example 7.4 with the ASK system in part (d) of Problem 7.2.19. Consider specifically the case in which $M = 4$. How should the digit sequence be mapped into signals to minimize the bit error probability? Compute the signal error probability and the bit error probability.

Problem 7.2.21. M -ary PSK [AD62]. A communication system transmitter sends one of M messages over an additive white Gaussian noise channel (spectral height $N_0/2$) using the signals

$$s_i(t) = \begin{cases} \left(\frac{2E}{T}\right)^{\frac{1}{2}} \cos\left(2\pi\frac{n}{T}t + \frac{2\pi i}{M}\right), & 0 \leq t \leq T, \quad i = 0, 1, 2, \dots, M-1 \\ 0, & \text{Elsewhere,} \end{cases}$$

where n is an integer. The messages are equally likely. This type of system is called an M -ary PSK system.

- (a) Draw a block diagram of the optimum receiver. Use the minimum number of filters.
- (b) Draw the decision-space and decision lines for various M .
- (c) Prove

$$\alpha \leq \Pr(\epsilon) \leq 2\alpha,$$

where

$$\alpha = \operatorname{erfc}_* \left[\left(\frac{2E}{N_0} \right)^{\frac{1}{2}} \sin \frac{\pi}{M} \right].$$

Problem 7.2.22 (continuation). Optimum PSK [Cah59]. The basic system is shown in Figure 7.24. The possible signaling strategies are the following:

- (a) Use a binary PSK set with the energy in each signal equal to PT .
- (b) Use an M -ary PSK set with the energy in each signal equal to $PT \log_2 M$.

Discuss how you would choose M to minimize the digit error probability. Compare biphase and four phase PSK on this basis.

Problem 7.2.23 (continuation). In the context of an M -ary PSK system discuss qualitatively the effect of an incorrect phase reference. In other words, the nominal signal set is given in

Problem 7.2.22 and the receiver is designed on that basis. The actual signal set, however, is

$$s_i(t) = \begin{cases} \left(\frac{2E}{T}\right)^{1/2} \cos\left(\frac{2\pi n}{T}t + \frac{2\pi i}{M} + \theta\right), & 0 \leq t \leq T, \\ 0, & \text{Elsewhere,} \end{cases} \quad i = 1, 2, \dots, M, \quad n \text{ is an integer}$$

where θ is a random phase angle. How does the importance of a phase error change as M increases?

ESTIMATION

Problem 7.2.24. Bhattacharyya Bound. Let

$$r(t) = s(t, A) + w(t), \quad 0 \leq t \leq T,$$

where $s(t, A)$ is differentiable k times with respect to A . The noise has spectral height $N_0/2$.

- (a) Extend the Bhattacharyya bound technique developed in Problem 4.2.24 to the waveform for the $n = 2$ case. Assume that A is nonrandom variable.
- (b) Repeat for the case in which A is a Gaussian random variable; $N(0, \sigma_a^2)$.
- (c) Extend the results in parts 1 and 2 to the case in which $n = 3$.

Problem 7.2.25. Consider the problem in Example 7.5. In addition to the unknown time of arrival, the pulse has an unknown amplitude. Thus,

$$r(t) = bs(t - a) + w(t), \quad -T \leq t \leq T,$$

where a is a uniformly distributed random variable and b is Gaussian, $N(0, \sigma_b^2)$.

Draw a block diagram of a receiver to generate the joint MAP estimates, \hat{a}_{map} and \hat{b}_{map} .

Problem 7.2.26. The known signal $s(t)$, $0 \leq t \leq T$, is transmitted over a channel with unknown *nonnegative* gain A and additive Gaussian noise $n(t)$:

$$\int_0^T s^2(t) dt = E,$$

$$K_n(t, \tau) = \frac{N_0}{2} \delta(t - \tau).$$

- (a) What is the maximum likelihood estimate of A ?
- (b) What is the bias in the estimate?
- (c) Is the estimate asymptotically unbiased?

Problem 7.2.27. Consider the stationary Poisson random process $x(t)$. A typical sample function is shown in Figure P7.4.

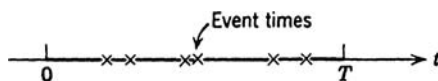


Figure P7.4

The probability of n events in any interval τ is

$$\Pr(n, \tau) = \frac{(k\tau)^n}{n!} e^{-k\tau}.$$

The parameter k of the process is an unknown nonrandom variable that we want to estimate. We observe $x(t)$ over an interval $(0, T)$.

- (a) Is it necessary to record the event times or is it adequate to count the number of events that occur in the interval? Prove that n^* , the number of events that occur in the interval $(0, T)$ is a sufficient statistic.
- (b) Find the Cramér–Rao inequality for any unbiased estimate of k .
- (c) Find the maximum-likelihood estimate of k . Call this estimate \hat{k} .
- (d) Prove that \hat{k} is unbiased.
- (e) Find $\text{Var}(\hat{k} - k)$.
- (f) Is the maximum-likelihood estimate efficient?

Problem 7.2.28. When a signal is transmitted through a particular medium, the amplitude of the output is inversely proportional to the murkiness of the medium. Before observation the output of the medium is corrupted by additive, white Gaussian noise. (Spectral height $N_0/2$, double sided.) Thus,

$$r(t) = \frac{1}{M} f(t) + w(t), \quad 0 \leq t \leq T,$$

where $f(t)$ is a known signal and

$$\int_0^T f^2(t) dt = E.$$

We want to design an optimum Murky–Meter.

- (a) Assume that M is a nonrandom variable. Derive the block diagram of a system whose output is the maximum-likelihood estimate of M (denoted by \hat{m}_{ml}).
- (b) Now assume that M is a Gaussian random variable with zero mean and variance σ_M^2 . Find the equation that specifies the maximum *a posteriori* estimate of M (denoted by \hat{m}_{map}).
- (c) Show that

$$\hat{m}_{\text{map}} \rightarrow \hat{m}_{\text{ml}}$$

as

$$\sigma_M^2 \rightarrow \infty.$$

P7.3 Nonwhite Additive Gaussian Noise

MATHEMATICAL PRELIMINARIES

Problem 7.3.1. Reversibility. Prove that $h_w(t, u)$ [defined in (7.157)] is a reversible operation by finding an $h_w^{-1}(t, u)$ such that

$$\int_{T_i}^{T_f} h_w(t, u) h_w^{-1}(u, z) du = \delta(t - z).$$

What restrictions on the noise are needed?

Problem 7.3.2. We saw in (7.171) that the integral equation

$$\frac{N_0}{2} h_o(z, v) + \int_{T_i}^{T_f} h_o(v, x) K_c(x, z) dx = K_c(z, v), \quad T_i \leq z, v \leq T_f$$

specifies the inverse kernel

$$Q_n(t, \tau) = \frac{2}{N_0} [\delta(t - \tau) - h_o(t, \tau)].$$

Show that an equivalent equation is

$$\frac{N_0}{2} h_o(z, v) + \int_{T_i}^{T_f} h_o(z, v) K_c(x, v) dx = K_c(z, v), \quad T_i \leq z, v \leq T_f.$$

Problem 7.3.3 [Col66a]. We saw in Problem 7.3.2 that the inverse kernel $Q_n(t, \tau)$ can be obtained from the solution to an integral equation:

$$\frac{N_0}{2} h_o(t, \tau) + \int_{T_i}^{T_f} h_o(t, u) K_c(u, \tau) du = K_c(t, \tau), \quad T_i \leq t, \tau \leq T_f.$$

where

$$Q_n(t, \tau) = \frac{2}{N_0} [\delta(t - \tau) - h_o(t, \tau)].$$

Suppose we let T_f , the end point of the interval, be a variable. We indicate this by writing $h_o(t, \tau : T_f)$ instead of $h_o(t, \tau)$:

$$\frac{N_0}{2} h_o(t, \tau : T_f) + \int_{T_i}^{T_f} h_o(t, u : T_f) K_c(u, \tau) du = K_c(t, \tau), \quad T_i \leq t, \tau \leq T_f.$$

Now differentiate this equation with respect to T_f and show that

$$\frac{\partial h_o(t, \tau : T_f)}{\partial T_f} = -h_o(t, T_f : T_f) h_o(T_f, \tau : T_f).$$

Hint.

$$\int_{T_i}^{T_f} f(\tau) K_c(t, \tau) d\tau = \lambda f(t), \quad T_i \leq t \leq T_f$$

has no solution for $\lambda < 0$.

Problem 7.3.4. Realizable Whitening Filters [Col66b]. In the text, two equivalent realizations of the optimum receiver for the colored noise problem were given in Figure 7.38a and b. We also saw that $Q_n(t, u)$ was an unrealizable filter specified by (7.170) and (7.171). Furthermore, we found one solution for $h_w(t, \tau)$, the whitening filter, in terms of eigenfunctions that was an unrealizable filter. We want to investigate the possibility of finding a *realizable* whitening filter.

- (a) Write down the log-likelihood ratio in terms of $h_o(t, \tau) = h_o(t, \tau : T_f)$ (see Problem 7.3.3).
- (b) Write

$$\ln \Lambda(r(t)) = \int_{T_i}^{T_f} dt \left[\int_{T_i}^{T_f} h_{wr}(t, u) \sqrt{E_s(u)} du \right] \left[\int_{T_i}^{T_f} h_{wr}(t, z) r(z) dz \right] \triangleq L(T_j) = \int_{T_i}^{T_f} \frac{\partial L(t)}{\partial t} dt.$$

The additional subscript r denotes realizable.

- (c) Use the result from Problem 7.3.3 that

$$\frac{\partial h_o(u, v : t)}{\partial t} = -h_o(t, u : t) h_o(t, v : t)$$

to show that

$$h_{wr}(t, u) = \left(\frac{2}{N_0} \right)^{\frac{1}{2}} [\delta(t - u) - h_o(t, u : t)].$$

Observe that $h_o(t, u : t)$ is a *realizable* filter.

- (d) Write down the integral equation satisfied by $h_o(t, \tau : t)$. In Chapter 8, we discuss techniques for solving this equation.

Problem 7.3.5. M -ary Signals, Colored Noise. Let the received signal on the i th hypothesis be

$$H_i : r(t) = \sqrt{E_i} s_i(t) + n_c(t) + w(t), \quad T_i \leq t \leq T_f, \quad i = 1, 2, \dots, M,$$

where $w(t)$ is zero-mean white Gaussian noise with spectral height $N_0/2$ and $n_c(t)$ is independent zero-mean colored noise with covariance function $K_c(t, u)$. The signals $s_i(t)$ are normalized over $(0, T)$ and are zero outside that interval. Assume that the hypotheses are equally likely and that the criterion is minimum $\Pr(\epsilon)$. Draw a block diagram of the optimum receiver.

ESTIMATION

Problem 7.3.6. Consider the following estimation problem:

$$r(t) = As(t) + \sum_{i=1}^3 b_i s_i(t) + w(t), \quad 0 \leq t \leq T,$$

where A is a nonrandom variable, b_i are independent, zero-mean, Gaussian random variables $E(b_i^2) = \sigma_i^2$, $w(t)$ is white noise ($N_0/2$), $s(t) = \sum_{i=1}^3 c_i s_i(t)$,

$$\int_0^T s_i(t) s_j(t) dt = \delta_{ij}, \text{ and } \int_0^T s^2(t) dt = 1.$$

- (a) Draw a block diagram of the maximum-likelihood estimator of A , \hat{a}_{ml} .
- (b) Choose c_1, c_2, c_3 to minimize the variance of the estimate.

INTEGRAL EQUATION SOLUTIONS

Problem 7.3.7. In this problem we solve a simple Fredholm equation of the second kind,

$$\sqrt{E}s(t) = \frac{N_0}{2} g(t) + \int_{T_i}^{T_f} K_c(t, u) g(u) du, \quad T_i \leq t \leq T_f,$$

where

$$\begin{aligned} K_c(t, u) &= \sigma_c^2 \exp[-k|t - u|], \\ s(t) &= \frac{1}{\sqrt{T}}, \quad 0 \leq t \leq T, \\ T_i &= 0, \\ T_f &= T. \end{aligned}$$

- (a) Find $g(t)$.
- (b) Evaluate the performance index d^2 .

Problem 7.3.8 (continuation). Solve Problem 7.3.7 for the case in which $T_i = -\infty$ and $T_f = \infty$. Compare the value of d^2 that you obtain with the value obtained in that problem.

Problem 7.3.9. Solve the Fredholm equation of the first kind,

$$\int_0^T K(t, u) g(u) = s(t), \quad 0 \leq t \leq T,$$

for the triangular kernel

$$K(t, u) = \begin{cases} 1 - |t - u|, & \text{for } |t - u| < 1, \\ 0, & \text{Elsewhere.} \end{cases}$$

Assume that $s(t)$ is twice differentiable and that $T < 1$.

Now apply this result to the problem of detecting a known signal $s(t)$, $0 \leq t \leq T$, which is observed in additive Gaussian noise with covariance

$$K_n(t, u) = \begin{cases} 1 - |t - u|, & \text{for } |t - u| \leq 1, \\ 0, & \text{Elsewhere.} \end{cases}$$

- (a) What is the optimum receiver? Note that we cannot physically generate impulses so that correlation with $g(t)$ is not a satisfactory answer.
- (b) Calculate d^2 .

What is a necessary and sufficient condition for singular detection in this problem if $s(t)$ is bounded?

Problem 7.3.10.

- (a) Evaluate d^2 for Example 7.10.
- (b) Provided that $s(t)$ is bounded and has finite energy, what is a necessary and sufficient condition on $s(t)$ for a nonsingular test?

Problem 7.3.11 (continuation). The optimum receiver for Problem 7.3.10 includes a matched filter plus a sampler. Find d^2 for the suboptimum receiver that has the matched filter but not the sampler.

Problem 7.3.12. The opposition is using a binary communication system to transmit data. The two signals used are the following:

$$\begin{aligned} s_1(t) &= \sin^2 \frac{2\pi}{T} t, & 0 \leq t \leq T, \\ s_0(t) &= -\sin^2 \frac{2\pi}{T} t, & 0 \leq t \leq T. \end{aligned}$$

The received signal is either

$$\begin{aligned} H_1 : r(t) &= s_1(t) + n(t), & 0 \leq t \leq T, \\ H_0 : r(t) &= s_0(t) + n(t), & 0 \leq t \leq T, \end{aligned}$$

where $n(t)$ is a sample function from a zero-mean Gaussian random process with covariance function

$$K_n(\tau) = e^{-\alpha|\tau|}.$$

Assume that he knows α and builds a min $\Pr(\epsilon)$ receiver. Choose α to minimize his performance.

SENSITIVITY AND SINGULARITY

Problem 7.3.13. Singularity [DR58]. Consider the simple binary detection problem shown in Figure P7.5. On H_1 the transmitted signal is a finite energy signal $x(t)$. On H_0 there is no transmitted signal. The additive noise $w(t)$ is a sample function from a white process $1v^2/cps$. The received waveform $r(t)$ is passed through a filter whose transfer function is $H(j\omega)$. The output $y(t)$, $0 \leq t \leq T$ is the signal available for processing. Let λ_k and $\phi_k(t)$ be the eigenvalues and eigenfunctions, respectively,

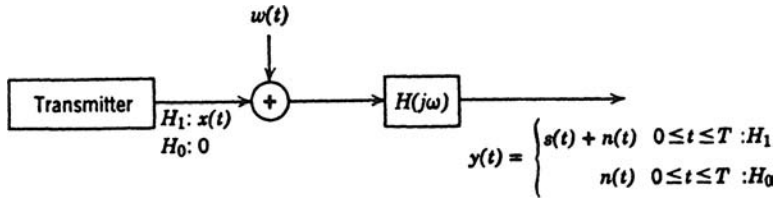


Figure P7.5

of $n(t)$, $0 \leq t \leq T$. To have singular detection, we require

$$\sum_{k=1}^{\infty} \frac{s_k^2}{\lambda_k} = \infty.$$

We want to prove that this cannot happen in this case.

(a) From

$$s_k = \int_0^T \phi_k(t) s(t) dt$$

show that

$$s_k = \int_{-\infty}^{\infty} X(f) H(j2\pi f) \Phi_k^*(f) df$$

where

$$X(f) = \int_{-\infty}^{\infty} x(t) e^{-j2\pi ft} dt$$

and

$$\Phi_k(f) = \int_{-\infty}^{\infty} \phi_k(t) e^{-j2\pi ft} dt = \int_0^T \phi_k(t) e^{-j2\pi ft} dt.$$

(b) Show that

$$\int_{-\infty}^{\infty} [H^*(j2\pi f) \Phi_m(f)] [H(j2\pi f) \Phi_k^*(f)] dt = \begin{cases} \lambda_k & \text{if } m = k \\ 0 & \text{if } m \neq k. \end{cases}$$

(c) Observe from part (b) that for some set of numbers c_k

$$X(f) = \sum_{k=1}^{\infty} \frac{c_k}{\lambda_k} H^*(j2\pi f) \Phi_k(f) + U(f),$$

where

$$\int_{-\infty}^{\infty} U(f) H(j2\pi f) \Phi_k^*(f) df = 0.$$

(d) Using (a), (b), and (c), show that

$$\sum_{k=1}^{\infty} \frac{s_k^2}{\lambda_k} \leq \int_{-\infty}^{\infty} x^2(t) dt,$$

hence that perfect detection is impossible in this situation.

Problem 7.3.14. Consider the following system:

$$\begin{aligned} H_1 : r(t) &= s_1(t) + n(t), & 0 \leq t \leq T, \\ H_0 : r(t) &= n(t), & 0 \leq t \leq T. \end{aligned}$$

It is given that

$$n(t) = \sum_{n=1}^6 a_n \cos n \frac{2\pi}{T} t,$$

where a_n are zero-mean random variables. The signal energy is

$$\int_0^T s_1^2(t) dt = E.$$

Choose $s_1(t)$ and the corresponding receiver so that perfect decisions can be made with probability 1.

Problem 7.3.15. Because white noise is a mathematical fiction (it has infinite energy, which is physically impossible), we sometimes talk about bandlimited white noise; that is,

$$S_n(\omega) = \begin{cases} \frac{N_0}{2}, & \text{If } \omega_1 \leq |\omega| \leq \omega_2, \\ 0, & \text{Otherwise.} \end{cases}$$

Now suppose that we wish to detect a strictly time-limited signal

$$s(t) = \begin{cases} \left(\frac{E}{T}\right)^{1/2}, & 0 \leq t \leq T, \\ 0, & \text{Otherwise.} \end{cases}$$

Is this a good mathematical model for a physical problem? Justify your answer.

Problem 7.3.16. Sensitivity to White Noise Level. The received waveforms under the two hypotheses are

$$\begin{aligned} H_1 : r(t) &= s(t) + n_c(t) + w(t), & -\infty < t < \infty, \\ H_0 : r(t) &= n_c(t) + w(t), & -\infty < t < \infty. \end{aligned}$$

The signal waveform $s(t)$ and the colored noise spectrum $S_n(\omega)$ are known exactly. The white noise level is

$$\frac{N_a}{2} = \frac{N_0}{2}(1+x),$$

where $N_0/2$ is the nominal value and x is a small variation. Assume that the receiver is designed on the basis of the nominal white noise level.

- (a) Find an expression for

$$\frac{\partial d/\partial x}{d} \Big|_{x=0} = \frac{\partial \ln d}{\partial x} \Big|_{x=0} \triangleq \Delta.$$

- (b) Assume that

$$s(t) = \begin{cases} \sqrt{2kP} e^{-kt}, & t \geq 0, \\ 0, & t < 0, \end{cases}$$

and

$$S_{n_c}(\omega) = \frac{2k\sigma_c^2}{\omega^2 + k^2}.$$

Evaluate Δ as a function of $\Lambda \triangleq 4\sigma_c^2/kN_0$.

Problem 7.3.17. Sensitivity to Noise Spectrum. Assume the same nominal model as in Problem 7.3.16.

- (a) Now let

$$\frac{N_a}{2} = \frac{N_0}{2}$$

and

$$S_{n_c}(\omega) = \frac{2k_a\sigma_a^2}{\omega^2 + k_a^2},$$

where

$$\begin{aligned} k_a &= k(1+y), \\ \sigma_a^2 &= \sigma_c^2(1+z). \end{aligned}$$

Find

$$\frac{\partial d/\partial y}{d} \Big|_{z=0} \stackrel{\triangle}{=} \Delta_y \quad \text{and} \quad \frac{\partial d/\partial z}{d} \Big|_{y=0} \stackrel{\triangle}{=} \Delta_z.$$

- (b) Evaluate Δ_y and Δ_z for the signal shape in Problem 7.3.16.

Problem 7.3.18. Sensitivity to Delay and Gain. The received waveforms under the two hypotheses are

$$\begin{aligned} H_1 : r(t) &= \sqrt{E} s(t) + b_I s(t - \tau) + w(t), & -\infty < t < \infty, \\ H_0 : r(t) &= b_I s(t - \tau) + w(t), & -\infty < t < \infty, \end{aligned}$$

where b_I is $N(0, \sigma_I^2)$ and $w(t)$ is white with spectral height $N_0/2$. The signal is

$$s(t) = \begin{cases} \left(\frac{1}{T}\right)^{1/2}, & 0 \leq t \leq T, \\ 0, & \text{Elsewhere.} \end{cases}$$

- (a) Design the optimum receiver, assuming that τ is known.
- (b) Evaluate d^2 as a function of τ and σ_I .
- (c) Now assume

$$\tau_a = \tau(1 + x).$$

Find an expression for d^2 of the nominal receiver as a function of x . Discuss the implications of your results.

- (d) Now we want to study the effect of changing σ_I . Let

$$\sigma_{la}^2 = \sigma_I^2(1 + y),$$

and find an expression for d^2 as a function of y .

LINEAR CHANNELS

Problem 7.3.19. Optimum Signals. Consider the system shown in Figure 7.50a. Assume that the channel is time invariant with impulse response $h(\tau)$ [or transfer function $H(f)$]. Let

$$H(f) = \begin{cases} 1, & |f| < W, \\ 0, & \text{Otherwise.} \end{cases}$$

The output observation interval is infinite. The signal input is $s(t)$, $0 \leq t \leq T$ and is normalized to have unity energy. The additive white Gaussian noise has spectral height $N_0/2$.

- (a) Find the optimum receiver.
- (b) Choose $s(t)$, $0 \leq t \leq T$, to maximize d^2 .

Problem 7.3.20. Repeat Problem 7.3.19 for the $h(t, \tau)$ given below:

$$h(t, \tau) = \begin{cases} \delta(t - \tau), & 0 \leq \tau \leq \frac{T}{4}, \frac{T}{2} \leq \tau \leq \frac{3T}{4}, -\infty < t < \infty, \\ 0, & \text{Elsewhere.} \end{cases}$$

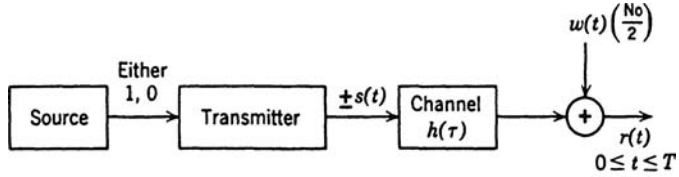


Figure P7.6

Problem 7.3.21 The system of interest is shown in Figure P7.6. Design an optimum *binary* signaling system subject to the constraints:

$$\int_0^T s^2(t) dt = E_t,$$

$$s(t) = \begin{cases} 0, & t < 0, \\ t < T, \end{cases}$$

$$h(\tau) = \begin{cases} e^{-k\tau}, & \tau \geq 0, \\ 0, & \tau < 0. \end{cases}$$

P7.4 Signals with Unwanted Parameters

MATHEMATICAL PRELIMINARIES

Formulas. Some of the problems in this section require the manipulation of Bessel functions and Q functions. A few convenient formulas are listed below. Other relations can be found in [Erd54] and the appendices of [Mid60a] and [SBS66].

I. Modified Bessel Functions.

$$I_n(z) \triangleq \frac{1}{2\pi} \int_0^{2\pi} \exp(\pm jn\theta) \exp(z \cos \theta) d\theta, \quad (\text{F.1.1})$$

$$I_n(z) = I_{-n}(z), \quad (\text{F.1.2})$$

$$I_v(z) \simeq \frac{(\frac{1}{2}z)^v}{\Gamma(v+1)}, \quad v \neq -1, -2, \dots, z \ll 1, \quad (\text{F.1.3})$$

$$I_v(z) \simeq \frac{e^z}{\sqrt{2\pi z}} \left[1 - \frac{4v^2 - 1}{8z} \right], \quad z \gg 1, \quad (\text{F.1.4})$$

$$\frac{1}{z^k} \frac{d^k}{dz^k} (z^{-v} I_v(z)) = z^{-v-k} I_{v+k}(z), \quad (\text{F.1.5})$$

$$\frac{1}{z^k} \frac{d^k}{dz^k} (z^v I_v(z)) = z^{v-k} I_{v-k}(z). \quad (\text{F.1.6})$$

II. Marcum's Q -function [SBS66].

$$Q(\sqrt{2a}, \sqrt{2b}) = \int_b^\infty \exp(-a+x) I_0(2\sqrt{ax}) dx, \quad (\text{F.2.1})$$

$$Q(a, a) = \frac{1}{2} [1 + I_0(a^2) \exp(-a^2)], \quad (\text{F.2.2})$$

$$1 + Q(a, b) - Q(b, a) = \frac{b^2 - a^2}{b^2 + a^2} \int_{a^2+b^2/2}^\infty e^{-x} I_0\left(\frac{2abx}{a^2+b^2}\right) dx, \quad 0 < a < b, \quad (\text{F.2.3})$$

$$\begin{aligned} & \int_0^\infty Q\left(\frac{\alpha_2}{\sigma_2}, \frac{R_1}{\sigma_2}\right) \frac{R_1}{\sigma_1^2} \exp\left[-\frac{\alpha_1^2 + R_1^2}{2\sigma_1^2}\right] I_0\left(\frac{\alpha_1 R_1}{\sigma_1^2}\right) dR_1 = \frac{\sigma_1^2}{\sigma_1^2 + \sigma_2^2} \\ & \times \left[1 - Q\left(\sqrt{\frac{\alpha_1^2}{\sigma_1^2 + \sigma_2^2}}, \sqrt{\frac{\alpha_2^2}{\sigma_1^2 + \sigma_2^2}}\right) \right] \\ & + \frac{\sigma_2^2}{\sigma_1^2 + \sigma_2^2} Q\left(\sqrt{\frac{\alpha_2^2}{\sigma_1^2 + \sigma_2^2}}, \sqrt{\frac{\alpha_1^2}{\sigma_1^2 + \sigma_2^2}}\right), \end{aligned} \quad (\text{F.2.4})$$

$$Q(a, b) \simeq \operatorname{erfc}_*(b-a), \quad b \gg 1, b \gg b-a. \quad (\text{F.2.5})$$

III. Rician Variables [Ste64]. Consider the two statistically independent Rician variables, x_1 and x_2 with probability densities,

$$p_{x_k}(X_k) = \frac{X_k}{\sigma_k^2} \exp\left(-\frac{a_k^2 + X_k^2}{2\sigma_k^2}\right) I_0\left(\frac{a_k X_k}{\sigma_k^2}\right), \quad 0 < a_k, X_k < \infty, \quad k = 1, 2. \quad (\text{F.3.1})$$

The probability of interest is

$$P_* = \Pr[x_2 > x_1].$$

Define the constants

$$a = \frac{a_2^2}{\sigma_1^2 + \sigma_2^2}, \quad b = \frac{a_1^2}{\sigma_1^2 + \sigma_2^2}, \quad c = \frac{\sigma_1}{\sigma_2}.$$

Then

$$P_* = Q(\sqrt{a}, \sqrt{b}) - \frac{c^2}{1+c^2} \exp\left(-\frac{a+b}{2}\right) I_0(\sqrt{ab}) \quad (\text{F.3.2})$$

or

$$P_* = \frac{c^2}{1+c^2} \left[1 - Q(\sqrt{b}, \sqrt{a}) \right] + \frac{1}{1+c^2} Q(\sqrt{a}, \sqrt{b}) \quad (\text{F.3.3})$$

or

$$P_* = \frac{1}{2} \left[1 - Q(\sqrt{b}, \sqrt{a}) + Q(\sqrt{a}, \sqrt{b}) \right] - \frac{1}{2} \frac{c^2 - 1}{c^2 + 1} \exp\left(-\frac{a+b}{2}\right) I_0(\sqrt{ab}). \quad (\text{F.3.4})$$

Problem 7.4.1. *Q*-function Properties. Marcum's *Q*-function appears frequently in the calculation of error probabilities:

$$Q(\alpha, \beta) = \int_{\beta}^{\infty} x \exp \left[-\frac{1}{2} (x^2 + \alpha^2) \right] I_0(\alpha x) dx.$$

Verify the following properties:

$$Q(\alpha, 0) = 1,$$

$$Q(0, \beta) = e^{-\beta^2/2},$$

$$Q(\alpha, \beta) = e^{-(\alpha^2 + \beta^2)/2} \sum_{n=0}^{\infty} \left(\frac{\alpha}{\beta} \right)^n I_n(\alpha\beta), \quad \alpha < \beta,$$

$$Q(\alpha, \beta) = 1 - e^{-(\alpha^2 + \beta^2)/2} \sum_{n=1}^{\infty} \left(\frac{\beta}{\alpha} \right)^n I_n(\alpha\beta), \quad \beta < \alpha,$$

$$Q(\alpha, \beta) + Q(\beta, \alpha) = 1 + e^{-(\alpha^2 + \beta^2)/2} I_0(\alpha\beta),$$

$$Q(\alpha, \beta) \simeq 1 - \frac{1}{\alpha - \beta} \left(\frac{\beta}{2\pi\alpha} \right)^{\frac{1}{2}} e^{-(\alpha-\beta)^2/2}, \quad \alpha \gg \beta \gg 1,$$

$$Q(\alpha, \beta) \simeq \frac{1}{\beta - \alpha} \left(\frac{\beta}{2\pi\alpha} \right)^{\frac{1}{2}} e^{-(\beta-\alpha)^2/2}, \quad \beta \gg \alpha \gg 1.$$

Problem 7.4.2. Let x be a Gaussian random variable $N(m_x, \sigma_x^2)$.

(a) Prove that

$$M_{x^2}(jv) \triangleq E[\exp(+jvx^2)] = \frac{\exp[jvm_x^2 / (1 - 2jv\sigma_x^2)]}{(1 - 2jv\sigma_x^2)^{1/2}}.$$

Hint.

$$M_{x^2}(jv) = [M_{x^2}(jv) M_{y^2}(jv)]^{1/2},$$

where y is an independent Gaussian random variable with identical statistics.

(b) Let z be a complex number. Modify the derivation in part (a) to show that

$$E[\exp(+zx^2)] = \frac{\exp[zm_x^2 / (1 - 2za\sigma_x^2)]}{(1 - 2za\sigma_x^2)^{\frac{1}{2}}}, \quad \Re(z) < \frac{1}{2\sigma_x^2}.$$

(c) Let

$$y^2 = \sum_{i=1}^{2M} \lambda_i x_i^2,$$

where the x_i are statistically independent Gaussian variables, $N(m_i, \sigma_i^2)$.

- Find $M_y^2(jv)$ and $E[\exp(+zy^2)]$. What condition must be imposed on $\Re(z)$ in order for the latter expectation to exist.
- (d) Consider the special case in which $\lambda_i = 1$ and $\sigma_i^2 = \sigma^2$. Verify that the probability density of y^2 is

$$p_{y^2}(Y) = \begin{cases} \frac{1}{2\sigma^2} \left(\frac{Y}{S}\sigma^2\right)^{\frac{M-1}{2}} \exp\left(-\frac{Y+S\sigma^2}{2\sigma^2}\right) I_{M-1}\left[\left(\frac{YS^2}{\sigma}\right)^{\frac{1}{2}}\right], & Y \geq 0, \\ 0, & \text{Elsewhere,} \end{cases}$$

where $S = \sum_{i=1}^{2M} m_i^2$ [see [Erd54], p. 197, equation (18)].

Problem 7.4.3. Let $Q(\mathbf{x})$ be a quadratic form of correlated Gaussian random variables,

$$Q(\mathbf{x}) \triangleq \mathbf{x}^T \mathbf{A} \mathbf{x}.$$

- (a) Show that the characteristic function of Q is

$$M_Q(jv) \triangleq E(e^{jvQ}) = \frac{\exp\left\{-\frac{1}{2}\mathbf{m}_x^T \mathbf{\Lambda}^{-1} [\mathbf{I} - (\mathbf{I} - 2jv\mathbf{\Lambda}\mathbf{A})^{-1}] \mathbf{m}_x\right\}}{|\mathbf{I} - 2jv\mathbf{\Lambda}\mathbf{A}|^{1/2}}.$$

- (b) Consider the special case in which $\mathbf{\Lambda}^{-1} = \mathbf{A}$ and $\mathbf{m}_x = \mathbf{0}$. What is the resulting density?
(c) Extend the result in part (a) to find $E(e^{zQ})$, where z is a complex number. What restrictions must be put on $\Re(z)$?

Problem 7.4.4 [Ste64]. Let x_1, x_2, x_3, x_4 be statistically independent Gaussian random variables with identical variances. Prove

$$\Pr(x_1^2 + x_2^2 \geq x_3^2 + x_4^2) = \frac{1}{2}[1 - Q(\beta, \alpha) + Q(\alpha, \beta)],$$

where

$$\alpha = \left(\frac{\bar{x}_1^2 + \bar{x}_2^2}{2\sigma^2}\right)^{1/2},$$

$$\beta = \left(\frac{\bar{x}_3^2 + \bar{x}_4^2}{2\sigma^2}\right)^{1/2}.$$

RANDOM PHASE CHANNELS

Problem 7.4.5. On-Off Signaling: Partially Coherent Channel. Consider the hypothesis testing problem stated in (7.387) and (7.388) with the probability density given by (7.394). From (7.402), we see that an equivalent test statistic is

$$(\beta + L_c)^2 + L_s^2 \stackrel{H_1}{\underset{H_0}{\gtrless}} \gamma,$$

where

$$\beta \triangleq \frac{N_0}{2} \frac{\Lambda_m}{\sqrt{E_r}}.$$

- (a) Express P_F as a Q -function.
- (b) Express P_D as an integral of a Q -function.

Problem 7.4.6. M orthogonal Signals: Partially Coherent Channel. Assume that each of the M hypotheses are equally likely. The received signals at the output of a random phase channel are

$$H_i : r(t) = \sqrt{2E_r} f_i(t) \cos[\omega_c t + \phi_i(t) + \theta] + w(t), \quad 0 \leq t \leq T, \quad i = 1, 2, \dots, M,$$

where $p_\theta(\theta)$ satisfies (7.394) and $w(t)$ is white with spectral height $N_0/2$. Find the LRT and draw a block diagram of the minimum probability of error receiver.

Problem 7.4.7 (continuation). Error Probability; Uniform Phase [WJ65]. Consider the special case of the above model in which the signals are orthogonal and θ has a uniform density.

- (a) Show that

$$\Pr(\epsilon|\theta) = 1 - E \left\{ \left[1 - \exp \left(-\frac{x^2 + y^2}{2} \right) \right]^{M-1} \right\},$$

where x and y are statistically independent Gaussian random variables with unit variance.

$$E[x|\theta] = \sqrt{2E_r/N_0} \cos \theta,$$

$$E[y|\theta] = \sqrt{2E_r/N_0} \sin \theta.$$

The expectation is over x and y , given θ .

- (b) Show that

$$\Pr(\epsilon) = \sum_{k=1}^{M-1} \binom{M-1}{k} (-1)^{k+1} \left(\frac{\exp[-(E_r/N_0)k/(k+1)]}{k+1} \right).$$

Problem 7.4.8. In the binary communication problem in Example 7.14, we assumed that the signals on the two hypotheses were *not* phase modulated. The general binary problem in white noise is

$$H_1 : r(t) = \sqrt{2E_r} f_1(t) \cos[\omega_c t + \phi_1(t) + \theta] + w(t), \quad 0 \leq t \leq T,$$

$$H_0 : r(t) = \sqrt{2E_r} f_0(t) \cos[\omega_c t + \phi_0(t) + \theta] + w(t), \quad 0 \leq t \leq T,$$

where E_r is the energy received in the signal component. The noise is white with spectral height $N_0/2$, and $p_\theta(\theta)$ satisfies (7.394). Verify that the optimum receiver structure is as shown in Figure P7.7 for $i = 0, 1$, and that the minimum probability of error test is

$$z_1^2 \stackrel{H_1}{\underset{H_0}{\gtrless}} z_0^2.$$

Problem 7.4.9 (continuation) [Vit65]. Assume that the signal components on the two hypotheses are orthogonal.

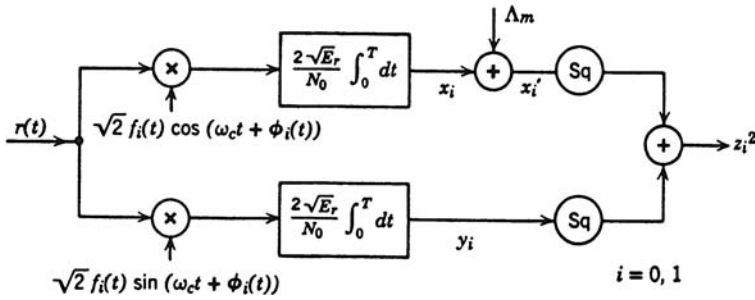


Figure P7.7

(a) Assuming that H_0 is true, verify that

$$E(x'_0) = \Lambda_m + d^2 \cos \theta,$$

$$E(y_0) = d^2 \sin \theta,$$

$$E(x'_1) = \Lambda_m,$$

$$E(y_1) = 0,$$

where $d^2 \triangleq 2E_r/N_0$ and

$$\text{Var}(x'_0) = \text{Var}(y_0) = \text{Var}(x'_1) = \text{Var}(y_1) = d^2.$$

(b) Prove that

$$p_{z_0|H_0,\theta}(Z_0|H_0, \theta) = \frac{Z_0}{d^2} \exp\left(-\frac{Z_0^2 + \Lambda_m^2 + d^4 + 2\Lambda_m d^2 \cos \theta}{2d^2}\right) \\ \times \left\{ I_0\left(\frac{\left[\left(\Lambda_m^2 + d^4 + 2\Lambda_m d^2 \cos \theta\right)^{\frac{1}{2}} Z_0\right]}{d^2}\right)\right\}$$

and

$$p_{z_1|H_0,\theta}(Z_1|H_0, \theta) = \frac{Z_1}{d^2} \exp\left(-\frac{z_1^2 + \Lambda_m^2}{2d^2}\right) I_0\left(\frac{\Lambda_m}{d^2} Z_1\right).$$

(c) Show that

$$\Pr(\epsilon) = \Pr(\epsilon|H_0) = \Pr(z_0 < z_1|H_0) \\ = \int_{-\pi}^{\pi} p_\theta(\theta) d\theta \int_0^\infty p_{z_0|H_0,\theta}(Z_0|H_0, \theta) dZ_0 \int_{z_0}^\infty p_{z_1|H_1,\theta}(Z_1|H_1, \theta) dZ_1.$$

(d) Prove that the inner two integrals can be rewritten as

$$\Pr(\epsilon|\theta) = Q(a, b) - \frac{1}{2} \exp\left(\frac{a^2 + b^2}{2}\right) I_0(ab),$$

where

$$a = \frac{\sqrt{2}\Lambda_m}{d},$$

$$b = \frac{[2(\Lambda_m^2 + d^4 + 2\Lambda_m d^2 \cos \theta)]^{1/2}}{d}.$$

- (e) Check your result for the two special cases in which $\Lambda_m \rightarrow 0$ and $\Lambda_m \rightarrow \infty$. Compare the resulting $\Pr(\epsilon)$ for these two cases in the region where d is large.

Problem 7.4.10 (continuation). Error Probability, Binary Nonorthogonal Signals [Hel55]. When bandpass signals are not orthogonal, it is conventional to define their correlation in the following manner:

$$\tilde{f}_1(t) \triangleq f_1(t)e^{j\phi_1(t)},$$

$$\tilde{f}_1(t) \triangleq f_0(t)e^{j\phi_0(t)},$$

$$\tilde{p} \triangleq \int_0^T \tilde{f}_0(t)\tilde{f}_1^*(t) dt,$$

which is a complex number.

- (a) Express the actual signals in terms of $\tilde{f}_i(t)$.
(b) Express the actual correlation coefficient of two signals in terms of \tilde{p} .
(c) Assume $\Lambda_m = 0$ (this corresponds to a uniform density) and define the quantity

$$\lambda = (1 - |\tilde{p}|^2)^{1/2}.$$

Show that

$$\Pr(\epsilon) = Q\left(\frac{d}{2}\sqrt{1-\lambda}, \frac{d}{2}\sqrt{1+\lambda}\right) - \frac{1}{2} \exp\left(-\frac{d^2}{2}\right) I_0\left(\frac{d^2}{4}|\tilde{p}|\right).$$

Problem 7.4.11 (continuation). When $p_\theta(\theta)$ is nonuniform and the signals are nonorthogonal, the calculations are much more tedious. Set up the problem and then refer to [Vit65] for the detailed manipulations.

Problem 7.4.12. M-ary PSK. Consider the M -ary PSK communication system in Problem 7.2.21. Assume that

$$p_\theta(\theta) = \frac{\exp(\Lambda_m \cos \theta)}{2\pi I_0(\Lambda_m)}, \quad -\pi \leq \theta \leq \pi.$$

- (a) Find the optimum receiver.
(b) Write an expression for the $\Pr(\epsilon)$.

Problem 7.4.13. ASK: Incoherent Channel [AD62]. An ASK system transmits equally likely messages

$$s_i(t) = \sqrt{2E_t} f(t) \cos \omega_c t, \quad i = 1, 2, \dots, M, \quad 0 \leq t \leq T,$$

where

$$\sqrt{E_i} = (i - 1)\Delta,$$

$$\int_0^T f^2(t) dt = 1,$$

and

$$(M - 1)\Delta \triangleq E.$$

The received signal under the i th hypothesis is

$$H_i : r(t) = \sqrt{2E_i} f(t) \cos(\omega_c t + \theta) + w(t), \quad 0 \leq t \leq T, \quad i = 1, 2, \dots, M,$$

where $w(t)$ is white noise ($N_0/2$). The phase θ is a random variable with a uniform density $(0, 2\pi)$.

- (a) Find the minimum $\Pr(\epsilon)$ receiver.
- (b) Draw the decision space and compute the $\Pr(\epsilon)$.

Problem 7.4.14. Asymptotic Behavior of Incoherent M -ary Systems [Tur59]. In the text we saw that the probability of error in a communication system using M orthogonal signals approached zero as $M \rightarrow \infty$ as long as the rate in digits per second was less than $P/N_0 \ln 2$ (the channel capacity). Use exactly the same model as in Example 7.4. Assume, however, that the channel adds a random phase angle. Prove that exactly the same results hold for this case.

Comment. The derivation is somewhat involved. The result is due originally to Turin [Tur59]. A detailed derivation is given in Section 8.10 of [Vit66].

Problem 7.4.15 [Col67]. Calculate the moment generating function, mean, and variance of the test statistic $G = L_c^2 + L_s^2$ for the uniform random phase problem of Section 7.4.1 under the hypothesis H_1 .

Problem 7.4.16 (continuation) [Col67]. We can show that for $d \gtrsim 3$ the equivalent test statistic

$$R = \sqrt{L_c^2 + L_s^2}$$

is approximately Gaussian. Assuming that this is true, find the mean and variance of R .

Problem 7.4.17 (continuation) [Col67]. Now use the result of Problem 7.4.16 to derive an approximate expression for the probability of detection. Express the result in terms of d and P_F and show that P_D is approximately a straight line when plotted versus d on probability paper. Compare a few points with Figure 7.60. Evaluate the increase in d over the known signal case that is necessary to achieve the same performance.

Problem 7.4.18. Amplitude Estimation. We consider a simple estimation problem in which an unwanted parameter is present. The received signal is

$$r(t) = A\sqrt{E} s(t, \theta) + w(t),$$

where A is a nonrandom parameter we want to estimate (assume that it is nonnegative):

$$s(t, \theta) = f(t) \cos[\omega_c t + \phi(t) + \theta],$$

where $f(t)$ and $\phi(t)$ are slowly varying known functions of time and θ is a random variable whose probability density is

$$p_\theta(\theta) = \begin{cases} \frac{1}{2\pi}, & -\pi < \theta < \pi, \\ 0, & \text{Otherwise.} \end{cases}$$

$w(t)$ is white Gaussian noise of spectral height $N_0/2$.

Find the transcendental equation satisfied by the maximum-likelihood estimate of A .

Problem 7.4.19. Frequency Estimation: Random Phase Channel. The received signal is

$$r(t) = \sqrt{2E} f(t) \cos(\omega_c t + \phi(t) + \omega t + \theta) + w(t), \quad 0 \leq t \leq T,$$

where $\int_0^T f^2(t)dt = 1$ and $f(t)$, $\phi(t)$, and E are known. The noise $w(t)$ is a sample function from a white Gaussian noise process ($N_0/2$). The frequency shift ω is an unknown nonrandom variable.

- (a) Find $\Lambda[r(t)|\omega]$.
- (b) Find the likelihood equation.
- (c) Draw a receiver whose output is a good approximation to $\hat{\omega}_{ml}$.

Problem 7.4.20 (continuation). Estimation Errors.

- (a) Compute a bound on the variance of any unbiased estimate of ω .
- (b) Compare the variance of $\hat{\omega}_{ml}$ under the assumption of a small error. Compare the result with the bound in part (a).
- (c) Compare the result of this problem with Example 7.6.

RANDOM AMPLITUDE AND PHASE

Problem 7.4.21. Consider the detection problem in which

$$\begin{aligned} H_1 : r(t) &= \sum_{i=1}^M a_i s_i(t) + n(t), & 0 \leq t \leq T, \\ H_0 : r(t) &= n(t), & 0 \leq t \leq T. \end{aligned}$$

The a_i are jointly Gaussian variables that we denote by the vector \mathbf{a} . The signals are denoted by the vector $s(t)$.

$$\begin{aligned} E(\mathbf{a}) &\triangleq \mathbf{m}_a, \\ E[(\mathbf{a} - \mathbf{m}_a)(\mathbf{a}^T - \mathbf{m}_a^T)] &\triangleq \Lambda_a, \end{aligned}$$

and

$$\begin{aligned} \rho &= \int_0^T \mathbf{s}(t) \mathbf{s}^T(t) dt, \\ E[n(t)n(u)] &= \frac{N_0}{2} \delta(t-u). \end{aligned}$$

- (a) Find the optimum receiver structure. Draw the various interpretations analogous to Figures 7.70 and 7.71.
- (b) Find $\mu(s)$ for this system.

Problem 7.4.22 (continuation). Extend the preceding problem to the case in which

$$E[n(t)n(u)] = \frac{N_0}{2} \delta(t - u) + K_c(t, u).$$

Problem 7.4.23. Consider the ASK system in Problem 7.4.13, operating over a Rayleigh channel. The received signal under the k th hypothesis is

$$H_k : r(t) = \sqrt{2\bar{E}_k} v f(t) \cos(\omega_c(t) + \theta) + w(t), \quad 0 \leq t \leq T, \quad k = 1, 2, \dots, M.$$

All quantities are described in Problem 7.4.13 except v :

$$p_v(V) = \begin{cases} V \exp\left(-\frac{V^2}{2}\right), & V \geq 0, \\ 0, & \text{Elsewhere} \end{cases}$$

and is independent of H_k . The hypotheses are equally likely.

- (a) Find the minimum $\Pr(\epsilon)$ receiver.
- (b) Find the $\Pr(\epsilon)$.

Problem 7.4.24. *M Orthogonal Signals: Rayleigh Channel [Pie58].* One of M orthogonal signals is used to transmit equally likely hypotheses over a Rayleigh channel. The received signal under the i th hypothesis is

$$H_i : r(t) = \sqrt{2v} f(t) \cos(\omega_i t + \theta) + w(t), \quad 0 \leq t \leq T, \quad i = 1, 2, \dots, M,$$

where v is Rayleigh with variance \bar{E}_r , θ is uniform, $w(t)$ is white ($N_0/2$), and $f(t)$ is normalized.

- (a) Draw a block diagram of the minimum probability of error receiver.
- (b) Show that

$$\Pr(\epsilon) = \sum_{n=1}^{M-1} \binom{M-1}{n} \frac{(-1)^{n+1}}{n+1+n\beta},$$

where

$$\beta \triangleq \frac{\bar{E}_r}{N_0}.$$

Problem 7.4.25 [Sus64]. In this problem, we investigate the improvement obtained by using M orthogonal signals instead of two orthogonal signals to transmit information over a Rayleigh channel.

- (a) Show that

$$\Pr(\epsilon) = 1 - \frac{\Gamma[1/(\beta+1)+1]\Gamma(M)}{\Gamma[1/(\beta+1)+M]}.$$

Hint. Use the familiar expression

$$\frac{\Gamma(z)\Gamma(a+1)}{\Gamma(z+a)} = \sum_{n=0}^{a-1} (-1)^n \frac{a(a-1)\cdots(a-n)}{n!} \frac{1}{z+n}.$$

- (b) Consider the case in which $\beta \gg 1$. Use a Taylor series expansion and the properties of $\psi(x) \triangleq \Gamma'(x)/\Gamma(x)$ to obtain the approximate expression

$$\Pr(\epsilon) \simeq \frac{1}{\beta} \left(\ln M - \frac{1}{2M} + 0.577 \right).$$

Recall that

$$\begin{aligned}\psi(1) &= 0.577 \\ \psi(z) &= \ln z - \frac{1}{2z} + o(z).\end{aligned}$$

- (c) Now assume that the M hypotheses arise from the simple coding system in Figure 7.24. Verify that the bit error probability is $\Pr_B(\epsilon) = \frac{1}{2} \frac{M}{M-1} \Pr(\epsilon)$.
- (d) Find an expression for the ratio of the $\Pr_B(\epsilon)$ in a binary system to the $\Pr_B(\epsilon)$ in an M -ary system.
- (e) Show that $M \rightarrow \infty$, the power saving resulting from using M orthogonal signals, approaches $2/\ln 2 = 4.6$ dB.

Problem 7.4.26. *M Orthogonal Signals: Rician Channel.* Consider the same system as in Problem 7.4.24, but assume that v is Rician.

- (a) Draw a block diagram of the minimum $\Pr(\epsilon)$ receiver.
 (b) Find the $\Pr(\epsilon)$.

Problem 7.4.27. *Binary Orthogonal Signals: Square-Law Receiver [WJ65].* Consider the problem of transmitting two equally likely bandpass orthogonal signals with energy E_i over the Rician channel defined in (7.477). Instead of using the optimum receiver shown in Figure 7.77, we use the receiver for the Rayleigh channel (i.e., let $\alpha = 0$ in Figure 7.77). Show that

$$\Pr(\epsilon) = \left[2 \left(1 + \frac{\bar{E}_r}{2N_0} \right) \right]^{-1} \exp \left[\frac{-\alpha^2 E_i}{2N_0(1 + \bar{E}_r/2N_0)} \right].$$

Problem 7.4.28. Repeat Problem 7.4.27 for the case of M orthogonal signals.

COMPOSITE SIGNAL HYPOTHESES

Problem 7.4.29. *Detecting One of M Orthogonal Signals.* Consider the following binary hypothesis testing problem. Under H_1 the signal is one of M orthogonal signals $\sqrt{E_1} s_1(t), \sqrt{E_2} s_2(t), \dots, \sqrt{E_M} s_M(t)$:

$$\int_0^T s_i(t) s_j(t) dt = \delta_{ij}, \quad i, j = 1, 2, \dots, M.$$

Under H_1 the i th signal occurs with probability $p_i \left(\sum_{i=1}^M p_i = 1 \right)$. Under H_0 there is no signal component. Under both hypotheses there is additive white Gaussian noise with spectral height $N_0/2$:

$$\begin{aligned} H_1 : r(t) &= \sqrt{E_i} s_i(t) + w(t), & 0 \leq t \leq T \text{ with probability } p_i, \\ H_0 : r(t) &= w(t), & 0 \leq t \leq T. \end{aligned}$$

- (a) Find the likelihood ratio test.
- (b) Draw a block diagram of the optimum receiver.

Problem 7.4.30 (continuation). Now assume that

$$\begin{aligned} p_i &= \frac{1}{M}, & i = 1, 2, \dots, M, \\ E_i &= E. \end{aligned}$$

One method of approximating the performance of the receiver was developed in Problem 2.2.14. Recall that we computed the variance of Λ (not $\ln \Lambda$) on H_0 and used the equation

$$d^2 = \ln(1 + \text{Var}[\Lambda|H_0]). \quad (\text{P.1})$$

We then used these values of d on the ROC of the known signal problem to find P_F and P_D .

- (a) Find $\text{Var}[\Lambda|H_0]$.
- (b) Using (P.1), verify that

$$\frac{2E}{N_0} = \ln \left(1 - M + Me^{d^2} \right). \quad (\text{P.2})$$

- (c) For $2E/N_0 \gtrsim 3$ verify that we may approximate (P.2) by

$$\frac{2E}{N_0} \simeq \ln M + \ln \left(e^{d^2} - 1 \right). \quad (\text{P.3})$$

The significance of (P.3) is that if we have a certain performance level (P_F, P_D) for a single known signal then to maintain the performance level when the signal is equally likely to be any one of M orthogonal signals requires an increase in the energy-to-noise ratio of $\ln M$. This can be considered as the cost of signal uncertainty.

- (d) Now remove the equal probability restriction. Show that (P.3) becomes

$$\frac{2E}{N_0} \simeq -\ln \left(\sum_{i=1}^M p_i^2 \right) + \ln \left(e^{d^2} - 1 \right).$$

What probability assignment maximizes the first term? Is this result intuitively logical?

Problem 7.4.31 (alternate continuation). Consider the special case of Problem 7.4.29 in which $M = 2$, $E_1 = E_2 = E$, and $p_1 = p_2 = \frac{1}{2}$. Define

$$l_i[r(t)] = \left[\frac{2\sqrt{E}}{N_0} \int_0^T dt r(t) s_i(t) - \frac{E}{N_0} \right], \quad i = 1, 2. \quad (\text{P.4})$$

- (a) Sketch the optimum decision boundary in l_1, l_2 -plane for various values of η .
- (b) Verify that the decision boundary approaches the asymptotes $l_1 = 2\eta$ and $l_2 = 2\eta$.
- (c) Under what conditions would the following test be close to optimum.
Test. If either $l_1 \geq 2\eta$ or $l_2 \geq 2\eta$, say H_1 is true. Otherwise say H_0 is true.
- (d) Find P_D and P_F for the suboptimum test in part (c).

Problem 7.4.32 (continuation). Consider the special case of Problem 7.4.29 in which $E_i = E$, $i = 1, 2, \dots, M$ and $p_i = 1/M$, $i = 1, 2, \dots, M$. Extending the definition of $l_i[r(t)]$ in (P.4) to $i = 1, 2, \dots, M$, we consider the suboptimum test.

Test. If one or more $l_i \geq \ln M\eta$, say H_1 . Otherwise say H_0 .

- (a) Define

$$\begin{aligned}\alpha &= \Pr[l_1 > \ln M\eta | s_1(t) \text{ is not present}], \\ \beta &= \Pr[l_1 < \ln M\eta | s_1(t) \text{ is present}].\end{aligned}$$

Show

$$\begin{aligned}P_F &= 1 - (1 - \alpha)^M, \\ P_D &= 1 - \beta(1 - \alpha)^{M-1}.\end{aligned}$$

- (b) Verify that

$$\begin{aligned}P_F &\leq M\alpha \\ P_D &\leq \beta.\end{aligned}$$

When are these bounds most accurate?

- (c) Find α and β .
- (d) Assume that $M = 1$ and E/N_0 gives a certain P_F , P_D performance. How must E/N_0 increase to maintain the same performance at M increases? (Assume that the relations in part (b) are exact.) Compare these results with those in Problem 7.4.30.

Problem 7.4.33. A similar problem is encountered when each of the M orthogonal signals has a random phase.

Under H_1 :

$$r(t) = \sqrt{2E} f_i(t) \cos[\omega_c t + \phi_i(t) + \theta_i] + w(t), \quad 0 \leq t \leq T, \quad (\text{with probability } p_i).$$

Under H_0 :

$$r(t) = w(t), \quad 0 \leq t \leq T.$$

The signal components are orthogonal. The white noise has spectral height $N_0/2$. The probabilities, $p_i = 1/M$, $i = 1, 2, \dots, M$. The phase term in each signal θ_i is an independent, uniformly distributed random variable $(0, 2\pi)$.

- (a) Find the likelihood ratio test and draw a block diagram of the optimum receiver.
- (b) Find $\text{Var}(\Lambda | H_0)$.
- (c) Using the same approximation techniques as in Problem 7.4.30, show that the correct value of d to use on the known signal ROC is

$$d \triangleq \ln[1 + \text{Var}(\Lambda | H_0)] = \ln \left[1 - \frac{1}{M} + \frac{1}{M} I_0 \left(\frac{2E}{N_0} \right) \right].$$

Problem 7.4.34 (continuation). Use the same reasoning as in Problem 7.4.31 to derive a sub-optimum test and find an expression for its performance.

Problem 7.4.35. Repeat Problems 7.4.33(a) and 7.4.34 for the case in which each of M orthogonal signals is received over a Rayleigh channel.

Problem 7.4.36. In Problem 7.4.30 we saw in the “one-of- M ” orthogonal signal problem that to maintain the same performance we had to increase $2E/N_0$ by $\ln M$. Now suppose that under H_1 one of N ($N > M$) equal-energy signals occurs with equal probability. The N signals, however, lie in an M -dimensional space. Thus, if we let $\phi_j(t)$, $j = 1, 2, \dots, M$, be a set of orthonormal functions $(0, T)$, then

$$s_i(t) = \sum_{j=1}^M a_{ij}\phi_j(t), \quad i = 1, 2, \dots, N,$$

where

$$\sum_{j=1}^M a_{ij}^2 = 1, \quad i = 1, 2, \dots, N.$$

The other assumptions in Problem 7.4.29 remain the same.

- (a) Find the likelihood ratio test.
- (b) Discuss qualitatively (or quantitatively, if you wish) the cost of uncertainty in this problem.

CHANNEL MEASUREMENT RECEIVERS

Problem 7.4.37. Channel Measurement [WJ65]. Consider the following approach to exploiting the phase stability in the channel. Use the first half of the signaling interval to transmit a channel measuring signal $\sqrt{2}s_m(t)\cos\omega_c t$ with energy E_m . Use the other half to send one of two equally likely signals $\pm\sqrt{2}s_d(t)\cos\omega_c t$ with energy E_d . Thus,

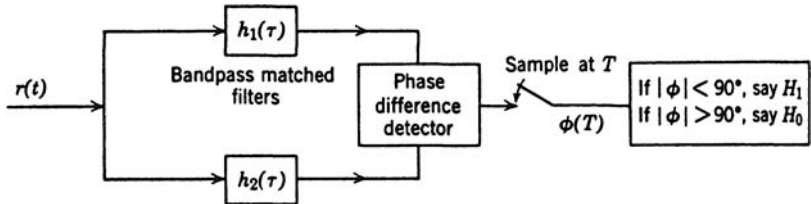
$$\begin{aligned} H_1 : r(t) &= [s_m(t) + s_d(t)]\sqrt{2}\cos(\omega_c t + \theta) + w(t), & 0 \leq t \leq T, \\ H_0 : r(t) &= [s_m(t) - s_d(t)]\sqrt{2}\cos(\omega_c t + \theta) + w(t), & 0 \leq t \leq T, \end{aligned}$$

and

$$p_\theta(\theta) = \frac{1}{2\pi}, \quad 0 \leq \theta \leq 2\pi.$$

- (a) Draw the optimum receiver and decision rule for the case in which $E_m = E_d$.
- (b) Find the optimum receiver and decision rule for the case in part (a).
- (c) Prove that the optimum receiver can also be implemented as shown in Figure P7.8.
- (d) What is the $\Pr(\epsilon)$ of the optimum system?

Problem 7.4.38 (continuation) Kineplex [DHM57]. A clever way to take advantage of the result in Problem 7.4.37 is employed in the Kineplex system. The information is transmitted by the phase relationship between successive bauds. If $s_d(t)$ is transmitted in one interval, then to send H_1 in the next interval we transmit $+s_d(t)$; and to send H_0 , we transmit $-s_d(t)$. A typical sequence is shown in Figure P7.9.



$$h_1(\tau) = \sqrt{2} s_m(T - \tau) \cos \omega_c \tau$$

$$h_2(\tau) = \sqrt{2} s_d(T - \tau) \cos \omega_c \tau$$

Figure P7.8

Source		1	1	0	0	0	1	1
Trans. sequence	$+s_m(t)$	$+s_m(t)$	+	-	+	-	-	-
(Initial reference)								

Figure P7.9

- (a) Assuming that there is no phase change from baud to baud, adapt the receiver in Figure P7.8 to this problem. Show that the resulting $\Pr(\epsilon)$ is

$$\Pr(\epsilon) = \frac{1}{2} \exp\left(-\frac{E}{N_0}\right),$$

(where E is the energy per baud, $E = E_d = E_m$).

- (b) Compare the performance of this system with the optimum coherent system in the text for large E/N_0 . Are decision errors in the Kineplex system independent from baud to baud?
(c) Compare the performance of Kineplex to the partially coherent system performance shown in Figures 7.63 and 7.64.

Problem 7.4.39 (continuation). Consider the signal system in Problem 7.4.37 and assume that $E_m \neq E_d$.

- (a) Is the phase-comparison receiver of Figure P7.8 optimum?
(b) Compute the $\Pr(\epsilon)$ of the optimum receiver.

Comment. It is clear that the ideas of phase comparison can be extended to M -ary systems. [AD62, BL64], and [LP64] discuss systems of this type.

MISCELLANEOUS

Problem 7.4.40. Consider the communication system described below. A known signal $s(t)$ is transmitted. It arrives at the receiver through *one* of two possible channels. The output is corrupted by additive white Gaussian noise $w(t)$. If the signal passes through channel 1, the input to the receiver is

$$r(t) = a s(t) + w(t), \quad 0 \leq t \leq T,$$

where a is constant over the interval. It is the value of a Gaussian random variable $N(0, \sigma_a^2)$. If the signal passes through channel 2, the input to the receiver is

$$r(t) = s(t) + w(t), \quad 0 \leq t \leq T.$$

It is given that

$$\int_0^T s^2(t) dt = E.$$

The probability of passing through channel 1 is equal to the probability of passing through channel 2 (i.e., $P_1 = P_2 = \frac{1}{2}$).

- (a) Find a receiver that decides which channel the signal passed through with minimum probability of error.
- (b) Compute the $\Pr(\epsilon)$.

Problem 7.4.41. A new engineering graduate is told to design an optimum detection system for the following problem:

$$\begin{aligned} H_1 : r(t) &= s(t) + w(t), & T_i \leq t \leq T_f, \\ H_0 : r(t) &= n(t), & T_i \leq t \leq T_f. \end{aligned}$$

The signal $s(t)$ is known. To find a suitable covariance function $K_n(t, u)$ for the noise, he asks several engineers for an opinion.

Engineer A says

$$K_n(t, u) = \frac{N_0}{2} \delta(t - u).$$

Engineer B says

$$K_n(t, u) = \frac{N_0}{2} \delta(t - u) + K_c(t, u),$$

where $K_c(t, u)$ is a known, square-integrable, positive definite function.

He must now reconcile these different opinions in order to design a signal detection system. He decides to combine their opinions probabilistically. Specifically,

$$\begin{aligned} \Pr(\text{Engineer A is correct}) &= P_A, \\ \Pr(\text{Engineer B is correct}) &= P_B, \end{aligned}$$

where $P_A + P_B = 1$.

- (a) Construct an optimum Bayes test (threshold η) to decide whether H_1 or H_0 is true.
- (b) Draw a block diagram of the receiver.
- (c) Check your answer for $P_A = 0$ and $P_B = 0$.
- (d) Discuss some other possible ways you might reconcile these different opinions.

Problem 7.4.42. Resolution. The following detection problem is a crude model of a simple radar resolution problem:

$$\begin{aligned} H_1 : r(t) &= b_d s_d(t) + b_I s_I(t) + w(t), & T_i \leq t \leq T_f, \\ H_0 : r(t) &= b_I s_I(t) + w(t), & T_i \leq t \leq T_f. \end{aligned}$$

1. $\int_{T_i}^{T_f} s_d(t) s_I(t) dt = \rho$.
2. $s_d(t)$ and $s_I(t)$ are normalized to unit energy.
3. The multipliers b_d and b_I are *independent* zero-mean Gaussian variables with variances σ_d^2 and σ_I^2 , respectively.
4. The noise $w(t)$ is white Gaussian with spectral height $N_0/2$ and is independent of the multipliers.

Find an explicit solution for the optimum likelihood ratio receiver. You do *not* need to specify the threshold.

P7.5. Multiple Channels

MATHEMATICAL DERIVATIONS

Problem 7.5.1. The definition of a matrix inverse kernel given in (7.502) is

$$\int_{T_i}^{T_f} \mathbf{K}_n(t, u) \mathbf{Q}_n(u, z) du = \mathbf{I} \delta(t - z).$$

- (a) Assume that

$$\mathbf{K}_n(t, u) = \frac{N_0}{2} \mathbf{I} \delta(t - u) + \mathbf{K}_c(t, u).$$

Show that we can write

$$\mathbf{Q}_n(t, u) = \frac{2}{N_0} [\mathbf{I} \delta(t - u) - \mathbf{h}_o(t, u)],$$

where $\mathbf{h}_o(t, u)$ is a square-integrable function. Find the matrix integral equation that $\mathbf{h}_o(t, u)$ must satisfy.

- (b) Consider the problem of a matrix linear filter operating on $\mathbf{n}(t)$.

$$\mathbf{d}(t) = \int_{T_i}^{T_f} \mathbf{h}(t, u) \mathbf{n}(u) du,$$

where

$$\mathbf{n}(t) = \mathbf{n}_c(t) + \mathbf{w}(t)$$

has the covariance function given in part 1. We want to choose $\mathbf{h}(t, u)$ so that

$$\xi_I \triangleq E \int_{T_i}^{T_f} [\mathbf{n}_c(t) - \mathbf{d}(t)]^T [\mathbf{n}_c(t) - \mathbf{d}(t)] dt$$

is minimized. Show that the linear matrix filter that does this is the $\mathbf{h}_o(t, u)$ found in part (a).

Problem 7.5.2 (continuation). In this problem we extend the derivation in Section 7.5 to include the case in which

$$\mathbf{K}_n(t, u) = \mathbf{N} \delta(t - u) + \mathbf{K}_c(t, u), \quad T_i \leq t, u \leq T_f,$$

where \mathbf{N} is a positive definite matrix of numbers. We denote the eigenvalues of \mathbf{N} as $\lambda_1, \lambda_2, \dots, \lambda_M$ and define a diagonal matrix,

$$\mathbf{I}_\lambda^k = \begin{bmatrix} \lambda_1^k & & & & \\ & \lambda_2^k & & & \\ & & \mathbf{0} & & \\ & & & \ddots & \\ & & & & \lambda_{M-1}^k \\ & & & & & \lambda_M^k \end{bmatrix}.$$

To find the LRT we first perform two preliminary transformations on \mathbf{r} as shown in Figure P7.10.

The matrix \mathbf{W} is an orthogonal matrix defined in (3.187) and has the properties

$$\begin{aligned} \mathbf{W}^T &= \mathbf{W}^{-1}, \\ \mathbf{N} &= \mathbf{W}^{-1} \mathbf{I}_\lambda \mathbf{W}. \end{aligned}$$

- (a) Verify that $\mathbf{r}''(t)$ has a covariance function matrix that satisfies (7.496).
- (b) Express l in terms of $\mathbf{r}''(t)$, $\mathbf{Q}_n''(t, u)$, and $\mathbf{s}''(t)$.
- (c) Prove that

$$l = \int_{T_i}^{T_f} \int \mathbf{r}^T(t) \mathbf{Q}_n(t, u) \mathbf{s}(u) dt du,$$

where

$$\mathbf{Q}_n(t, u) \triangleq \mathbf{N}^{-1} [\delta(t - u) - \mathbf{h}_o(t, u)],$$

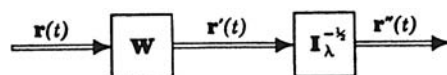


Figure P7.10

and $\mathbf{h}_o(t, u)$ satisfies the equation

$$\mathbf{K}_c(t, u) = \mathbf{h}_o(t, u)\mathbf{N} + \int_{T_i}^{T_f} \mathbf{h}_o(t, z)\mathbf{K}_c(z, u)dz, \quad T_i \leq t, u \leq T_f.$$

(d) Repeat part (b) of Problem 7.5.1.

Problem 7.5.3. Consider the vector detection problem defined in (7.489) and (7.490). Assume that $\mathbf{K}_c(t, u) = 0$ and that \mathbf{N} is not positive-definite. Find a signal vector $\mathbf{s}(t)$ with total energy E and a receiver that leads to perfect detectability.

Problem 7.5.4. Let

$$\begin{aligned} H_1 : r_i(t) &= \sum_{j=1}^k a_{ij} s_{ij}(t) + w_i(t), & i &= 1, 2, \dots, M, \\ H_0 : r_i(t) &= w_i(t), & i &= 1, 2, \dots, M. \end{aligned}$$

The noise in each channel is a sample function from a zero-mean white Gaussian random process

$$E[\mathbf{w}(t)\mathbf{w}^T(u)] = \frac{N_0}{2}\mathbf{I}\delta(t-u).$$

The a_{ij} are jointly Gaussian and zero-mean. The $s_{ij}(t)$ are orthogonal. Find an expression for the optimum Bayes receiver.

Problem 7.5.5. Consider the binary detection problem in which the received signal is an M -dimensional vector:

$$\begin{aligned} H_1 : \mathbf{r}(t) &= \mathbf{s}(t) + \mathbf{n}_c(t) + \mathbf{w}(t), & -\infty < t < \infty \\ H_0 : \mathbf{r}(t) &= \mathbf{n}_c(t) + \mathbf{w}(t), & -\infty < t < \infty. \end{aligned}$$

The total signal energy is ME :

$$\int_0^T \mathbf{s}^T(t)\mathbf{s}(t)dt = ME.$$

The signals are zero outside the interval $(0, T)$.

- (a) Draw a block diagram of the optimum receiver.
- (b) Verify that

$$d^2 = \int_{-\infty}^{\infty} \mathbf{S}^T(j\omega)\mathbf{S}_n^{-1}(\omega)\mathbf{S}(j\omega)\frac{d\omega}{2\pi}.$$

Problem 7.5.6. Maximal-Ratio Combiners. Let

$$\mathbf{r}(t) = \mathbf{s}(t) + \mathbf{w}(t), \quad 0 \leq t \leq T.$$

The received signal $\mathbf{r}(t)$ is passed into a time-invariant matrix filter with M inputs and one output $y(t)$:

$$y(t) = \int_0^T \mathbf{h}(t - \tau) \mathbf{r}(\tau) d\tau.$$

The subscript s denotes the output due to the signal. The subscript n denotes the output due to the noise. Define

$$\left(\frac{S}{N} \right)_{\text{out}} \triangleq \frac{y_s^2(T)}{E[y_n^2(T)]}.$$

- (a) Assume that the covariance matrix of $\mathbf{w}(t)$ satisfies (7.493). Find the matrix filter $\mathbf{h}(\tau)$ that maximizes $(S/N)_{\text{out}}$. Compare your answer with (7.508).
- (b) Repeat part (a) for a noise vector with an arbitrary covariance matrix $\mathbf{K}_c(t, u)$.

Problem 7.5.7. Consider the vector version of the simple binary detection problem. The received waveforms on the two hypotheses are

$$\begin{aligned} H_1 : \mathbf{r}(t) &= \mathbf{s}(t) + \mathbf{w}(t), & T_i \leq t \leq T_f, \\ H_0 : \mathbf{r}(t) &= \mathbf{w}(t), & T_i \leq t \leq T_f. \end{aligned} \quad (\text{P.1})$$

where $\mathbf{s}(t)$ and $\mathbf{w}(t)$ are sample functions of zero-mean, statistically independent, N -dimensional, vector Gaussian processes with covariance matrices

$$\mathbf{K}_s(t, u) \triangleq E[\mathbf{s}(t)\mathbf{s}^T(u)] \quad (\text{P.2})$$

and

$$\mathbf{K}_w(t, u) \triangleq E[\mathbf{w}(t)\mathbf{w}^T(u)] = \frac{N_0}{2} \delta(t - u) \mathbf{I}. \quad (\text{P.3})$$

- (a) Derive the optimum receiver for this problem.
- (b) Derive the equations specifying the three canonical realizations. Draw a block diagram of the three realizations.
- (c) Consider the special case in which

$$\mathbf{K}_s(t, u) = K_s(t, u) \mathbf{I}. \quad (\text{P.4})$$

Explain what the condition in (P.4) means. Give a physical situation that would lead to this condition. Simplify the optimum receiver in part (a).

- (d) Consider the special case in which

$$\mathbf{K}_s(t, u) = K_s(t, u) \begin{bmatrix} 1 & 1 & \cdots & 1 \\ 1 & 1 & & 1 \\ \vdots & & \ddots & \cdots \\ 1 & 1 & & 1 \\ 1 & 1 & & 1 \end{bmatrix}. \quad (\text{P.5})$$

Repeat part (c).

Problem 7.5.8. Consider the model in Problem 7.5.7. The covariance of $\mathbf{w}(t)$ is

$$\mathbf{K}_w(t, u) = N \delta(t - u),$$

where \mathbf{N} is a nonsingular matrix.

- (a) Repeat parts (a) and (b) of Problem 7.5.7.
- (b) Why do we assume that \mathbf{N} is nonsingular?
- (c) Consider the special case in which

$$\mathbf{K}_s(t, u) = K_s(t, u)\mathbf{I}$$

and \mathbf{N} is diagonal. Simplify the results in part (a).

Problem 7.5.9. Consider the model in Problem 7.5.7. Assume

$$E[\mathbf{s}(t)] = \mathbf{m}(t).$$

All of the other assumptions in Problem 7.5.7 are still valid. Repeat Problem 7.5.7.

MULTIPLE INDEPENDENT CHANNELS

In this set of problems, the statistics in the i th channel are statistically independent of the statistics in the j th channel for $j \neq i$. For the radar model, the statistics of different pulses are statistically independent.

RANDOM PHASE CHANNELS

Problem 7.5.10 [Hel60]. Let

$$x = \sum_{i=1}^M a_i^2,$$

where each a_i is an independent random variable with the probability density

$$p_{a_i}(A) = \begin{cases} \frac{A}{\sigma^2} \exp\left(-\frac{A^2 + \alpha_i^2}{2\sigma^2}\right) I_0\left(\frac{\alpha_i A}{\sigma^2}\right), & 0 \leq A < \infty, \\ 0, & \text{Elsewhere.} \end{cases}$$

Show that

$$p_x(X) = \begin{cases} \frac{1}{2\sigma^2} \left(\frac{X}{P}\right)^{\frac{M-1}{2}} \exp\left(-\frac{X+P}{2\sigma^2}\right) I_{M-1}\left(\frac{\sqrt{PX}}{\sigma^2}\right), & 0 \leq X < \infty, \\ 0, & \text{Elsewhere,} \end{cases}$$

where

$$P = \sigma^2 \sum_{i=1}^M \alpha_i^2.$$

Problem 7.5.11. Generalized Q-Function. The generalization of the Q -function to M channels is

$$Q_M(\alpha, \beta) = \int_{\beta}^{\infty} x \left(\frac{x}{\alpha}\right)^{M-1} \exp\left(-\frac{x^2 + \alpha^2}{2}\right) I_{M-1}(\alpha x) dx.$$

- (a) Verify the relation

$$Q_M(\alpha, \beta) = Q(\alpha, \beta) + \exp\left(-\frac{\alpha^2 + \beta^2}{2}\right) \sum_{k=1}^{M-1} \left(\frac{\beta}{\alpha}\right)^k I_k(\alpha\beta).$$

- (b) Find $Q_M(\alpha, 0)$.

- (c) Find $Q_M(0, \beta)$.

Problem 7.5.12. On-Off Signaling: N Incoherent Channels. Consider an on-off communication system that transmits over N fixed-amplitude random phase channels. When H_1 is true, a bandpass signal is transmitted over each channel. When H_0 is true, no signal is transmitted. The received waveforms under the two hypotheses are

$$\begin{aligned} H_1 : r_i(t) &= \sqrt{2E_i} f_i(t) \cos(\omega_i t + \phi_i(t) + \theta_i) + w(t), & 0 \leq t \leq T, & i = 1, 2, \dots, N, \\ H_0 : r_i(t) &= w(t), & 0 \leq t \leq T, & i = 1, 2, \dots, N. \end{aligned}$$

The carrier frequencies are separated enough so that the signals are in disjoint frequency bands. The $f_i(t)$ and $\phi_i(t)$ are known low-frequency functions. The amplitudes $\sqrt{E_i}$ are known. The θ_i are statistically independent phase angles with a uniform distribution. The additive noise $w(t)$ is a sample function from a white Gaussian random process ($N_0/2$) that is independent of the θ_i .

- (a) Show that the likelihood ratio test is

$$\Lambda = \prod_{i=1}^N \exp\left(-\frac{E_i}{N_0}\right) I_0\left[\frac{2E_i^{\frac{1}{2}}}{N_0} (L_{c_i}^2 + L_{s_i}^2)^{\frac{1}{2}}\right] \stackrel{H_1}{\gtrless} \eta, \stackrel{H_0}{\lessgtr} \eta,$$

where L_{c_i} and L_{s_i} are defined as in (7.391) and (7.392).

- (b) Draw a block diagram of the optimum receiver based on $\ln \Lambda$.
(c) Using (7.401), find a good approximation to the optimum receiver for the case in which the argument of $I_0(\cdot)$ is small.
(d) Repeat for the case in which the argument is large.
(e) If the E_i are unknown nonrandom variables, does a UMP test exist?

Problem 7.5.13 (continuation). In this problem we analyze the performance of the suboptimum receiver developed in part (c) of the preceding problem. The test statistic is

$$l = \sum_{i=1}^N (L_{c_i}^2 + L_{s_i}^2) \stackrel{H_1}{\gtrless} \gamma, \stackrel{H_0}{\lessgtr} \gamma.$$

- (a) Find $E[L_{c_i}|H_0]$, $E[L_{s_i}|H_0]$, $\text{Var}[L_{c_i}|H_0]$, $\text{Var}[L_{s_i}|H_0]$, $E[L_{c_i}|H_1, \theta]$, $E[L_{s_i}|H_1, \theta]$, $\text{Var}[L_{c_i}|H_1, \theta]$, $\text{Var}[L_{s_i}|H_1, \theta]$.
(b) Show that

$$\begin{aligned} M_{l|H_1}(jv) &= (1 - jvN_0)^{-N} \exp\left(\frac{jv \sum_{i=1}^N E_i}{1 - jvN_0}\right), \\ M_{l|H_0}(jv) &= (1 - jvN_0)^{-N}. \end{aligned}$$

- (c) What is $p_{i|H_0}(X|H_0)$? Write an expression for P_F . The probability density of H_1 can be obtained from Fourier transform tables (e.g. [Erd54], p. 197). It is

$$p_{i|H_1}(X|H_1) = \begin{cases} \frac{1}{N_0} \left(\frac{X}{E_T} \right)^{\frac{N-1}{2}} \exp\left(-\frac{X+E_T}{N_0}\right) I_{N-1}\left(\frac{2\sqrt{XE_T}}{N_0}\right), & X \geq 0, \\ 0, & \text{Elsewhere,} \end{cases}$$

where

$$E_T \triangleq \sum_{i=1}^N E_i.$$

- (d) Express P_D in terms of the generalized Q -function.

Comment. This problem was first studied by Marcum [Mar60].

Problem 7.5.14 (continuation). Use the bounding and approximation techniques of Section 2.4 to evaluate the performance of the square-law receiver in Problem 7.5.12. Observe that the test statistic l is *not* equal to $\ln \Lambda$, so that the results in Section 2.4 must be modified.

Problem 7.5.15. N Pulse Radar: Nonfluctuating Target. In a conventional pulse radar the target is illuminated by a sequence of pulses, as shown in Figure 7.5. If the target strength is constant during the period of illumination, the return signal will be

$$H_1 : r(t) = \sqrt{2E} \sum_{k=1}^M f(t - \tau - kT_p) \cos(\omega_c t + \theta_i) + w(t), \quad -\infty < t < \infty,$$

where τ is the round-trip time to the target, which is assumed known; and T_p is the interpulse time, which is much larger than the pulse length $T[f(t) = 0 : t < 0, t > T]$. The phase angles of the received pulses are statistically independent random variables with uniform densities. The noise $w(t)$ is a sample function of a zero-mean white Gaussian process ($N_0/2$). Under H_0 no target is present and

$$H_0 : r(t) = w(t), \quad -\infty < t < \infty.$$

- (a) Show that the LRT for this problem is identical to that in Problem 7.5.12 (except for notation). This implies that the results of Problems 7.5.12 and 7.5.13 apply to this model also.
(b) Draw a block diagram of the optimum receiver. Do not use more than one bandpass filter.

Problem 7.5.16. Orthogonal Signals: N Incoherent Channels. An alternate communication system to the one described in Problem 7.5.12 would transmit a signal on both hypotheses. Thus,

$$\begin{aligned} H_1 : r_i(t) &= \sqrt{2E_{1i}} f_{1i}(t) \cos[\omega_i t + \phi_{1i}(t) + \theta_i] + w(t), & 0 \leq t \leq T, \\ &i = 1, 2, \dots, N, \\ H_0 : r_i(t) &= \sqrt{2E_{0i}} f_{0i}(t) \cos[\omega_i t + \phi_{0i}(t) + \theta_i] + w(t), & 0 \leq t \leq T, \\ &i = 1, 2, \dots, N. \end{aligned}$$

All of the assumptions in 7.5.12 are valid. In addition, the signals on the two hypotheses are orthogonal.

- (a) Find the likelihood ratio test under the assumption of equally likely hypotheses and minimum $\text{Pr}(\epsilon)$ criterion.
- (b) Draw a block diagram of the suboptimum square-law receiver.
- (c) Assume that $E_i = E$. Find an expression for the probability of error in the square-law receiver.
- (d) Use the techniques of Section 2.4 to find a bound on the probability of error and an approximate expression for $\text{Pr}(\epsilon)$.

Problem 7.5.17 (continuation). N Partially Coherent Channels.

- (a) Consider the model in Problem 7.5.12. Now assume that the phase angles are independent random variables with probability density

$$p_{\theta_i}(\theta) = \frac{\exp(\Lambda_m \cos \theta)}{2\pi I_0(\Lambda_m)}, \quad -\pi < \theta < \pi, \quad i = 1, 2, \dots, N.$$

Do parts (a), (b), and (c) of Problem 7.5.12, using this assumption.

- (b) Repeat part (a) for the model in Problem 7.5.16.

RANDOM AMPLITUDE AND PHASE CHANNELS

Problem 7.5.18. Density of Rician Envelope and Phase. If a narrow-band signal is transmitted over a Rician channel, the output contains a specular component and a random component. Frequently it is convenient to use complex notation. Let

$$s_t(t) \triangleq \sqrt{2} \Re [f(t)e^{j\phi(t)}e^{j\omega_c t}]$$

denote the transmitted signal. Then, using (7.471), the received signal (without the additive noise) is

$$s_r(t) \triangleq \sqrt{2} \Re \{v' f(t) \exp[j\phi(t) + j\theta' + j\omega_c t]\},$$

where

$$v' e^{j\theta'} \triangleq \alpha e^{j\delta} + v e^{j\theta}$$

in order to agree with (7.471).

- (a) Show that

$$p_{v',\theta'}(V', \theta') = \begin{cases} \frac{V'}{2\pi\sigma^2} \exp\left(-\frac{V'^2 + \alpha^2 - 2V'\alpha \cos(\theta' - \delta)}{2\sigma^2}\right), & 0 \leq V' < \infty, \quad 0 \leq \theta' - \delta \leq 2\pi, \\ 0, & \text{Elsewhere.} \end{cases}$$

- (b) Show that

$$p_{v'}(V') = \begin{cases} \frac{V'}{\sigma^2} \exp\left(-\frac{V'^2 + \alpha^2}{2\sigma^2}\right) I_0\left(\frac{\alpha V'}{\sigma^2}\right), & 0 \leq V' < \infty, \\ 0 & \text{Elsewhere.} \end{cases}$$

- (c) Find $E(v')$ and $E(v'^2)$.

- (d) Find $p_{\theta'}(\theta')$, the probability density of θ' .

The probability densities in parts (b) and (d) are plotted in Figure 7.76.

Problem 7.5.19. On-Off Signaling: N Rayleigh Channels. In an on-off communication system a signal is transmitted over each of N Rayleigh channels when H_1 is true. The received signals are

$$\begin{aligned} H_1 : r_i(t) &= v_i \sqrt{2} f_i(t) \cos[\omega_i t + \phi_i(t) + \theta_i] + w_i(t), & 0 \leq t \leq T, \quad i = 1, 2, \dots, N, \\ H_0 : r_i(t) &= w_i(t), & 0 \leq t \leq T, \quad i = 1, 2, \dots, N, \end{aligned}$$

where $f_i(t)$ and $\phi_i(t)$ are known waveforms, the v_i are statistically independent Rayleigh random variables with variance E_i , the θ_i are statistically independent random variables uniformly distributed $0 \leq \theta \leq 2\pi$, and $w_i(t)$ are independent white Gaussian noises ($N_0/2$).

- (a) Find the LRT.
- (b) Draw a block diagram of the optimum receiver. Indicate both a bandpass filter realization and a filter-squarer realization.

Problem 7.5.20. N Pulse Radar: Fluctuating Target. Consider the pulsed model developed in Problem 7.5.15. If the target fluctuates, the amplitude of the reflected signal will change from pulse to pulse. A good model for this fluctuation is the Rayleigh model. Under H_1 the received signal is

$$r(t) = \sqrt{2} \sum_{i=1}^N v_i f(t - \tau - kT_p) \cos(\omega_c t + \theta_i) + w(t), \quad -\infty < t < \infty,$$

where v_i , θ_i , and $w(t)$ are specified in Problem 7.5.19.

- (a) Verify that this problem is mathematically identical to Problem 7.5.19.
- (b) Draw a block diagram of the optimum receiver.
- (c) If the required $P_F = 10^{-4}$ and the total average received energy is constrained $E[Nv_i^2] = 64$, what is the optimum number of pulses to transmit in order to maximize P_D ?

Problem 7.5.21. Binary Orthogonal Signals: N Rayleigh Channels. Consider a binary communication system using orthogonal signals and operating over N Rayleigh channels. The hypotheses are equally likely and the criterion is minimum $\Pr(\epsilon)$. The received waveforms are

$$\begin{aligned} H_1 : r_i(t) &= \sqrt{2} v_i f_1(t) \cos[\omega_{1i} t + \phi_1(t) + \theta_i] + w_i(t), & 0 \leq t \leq T, \quad i = 1, 2, \dots, N, \\ H_0 : r_i(t) &= \sqrt{2} v_i f_0(t) \cos[\omega_{0i} t + \phi_0(t) + \theta_i] + w_i(t), & 0 \leq t \leq T, \quad i = 1, 2, \dots, N. \end{aligned}$$

The signals are orthogonal. The quantities v_i , θ_i , and $w_i(t)$ are described in Problem 7.5.18. The system is an FSK system with diversity.

- (a) Draw a block diagram of the optimum receiver.
- (b) Assume $E_i = E$, $i = 1, 2, \dots, N$. Verify that this model is mathematically identical to the model in Section 3.3.1.5. The resulting $\Pr(\epsilon)$ is given in (3.444). Express this result in terms of E and N_0 .

Problem 7.5.22 (continuation). Error Bounds: Optimal Diversity. Now assume the E_i may be different.

- (a) Compute $\mu(s)$.
- (b) Find the value of s that corresponds to the threshold $\gamma = \mu(s)$ and evaluate $\mu(s)$ for this value.
- (c) Evaluate the upper bound on the $\Pr(\epsilon)$ that is given by the Chernoff bound.

- (d) Express the result in terms of the probability of error in the individual channels:

$$P_i \triangleq \Pr(\epsilon \text{ on the } i\text{th diversity channel})$$

$$P_i = \frac{1}{2} \left[\left(1 + \frac{E_i}{2N_0} \right)^{-1} \right].$$

- (e) Find an approximate expression for $\Pr(\epsilon)$ using a central limit theorem argument.

Problem 7.5.23. *M*-ary Orthogonal Signals: *N* Rayleigh Channels. A generalization of the binary diversity system is an M -ary diversity system. The M hypotheses are equally likely. The received waveforms are

$$H_k : r_i(t) = \sqrt{2} v_i f k(t) \cos[\omega_{ki} t + \phi_k(t) + \theta_i] + w_i(t), \quad 0 \leq t \leq T, \quad i = 1, 2, \dots, N, \\ k = 1, 2, \dots, M.$$

The signals are orthogonal. The quantities v_i , θ_i , and $w_i(t)$ are described in Problem 7.5.19. This type of system is usually referred to as multiple FSK (MFSK) with diversity.

- (a) Draw a block diagram of the optimum receiver.
(b) Find an expression for the probability of error in deciding which hypothesis is true.

Comment. This problem is discussed in detail in Hahn [Hah62] and results for various M and N are plotted.

Problem 7.5.24 (continuation). Bounds.

- (a) Combine the bounding techniques of Section 2.4 with the simple bounds in (7.71b) through (7.72b) to obtain a bound on the probability of error in the preceding problem.
(b) Use a central limit theorem argument to obtain an approximate expression.

Problem 7.5.25. *M* Orthogonal Signals: *N* Rician Channels. Consider the M -ary system in Problem 7.5.23. All the assumptions remain the same except now we assume that the channels are independent Rician instead of Rayleigh (see Problem 7.5.18). The amplitude and phase of the specular component are known.

- (a) Find the LRT and draw a block diagram of the optimum receiver.
(b) What are some of the difficulties involved in implementing the optimum receiver?

Problem 7.5.26 (continuation). Frequently the phase of specular component is not accurately known. Consider the model in Problem 7.5.25 and assume that

$$p_{\delta_i}(X) = \frac{\exp(\Lambda_m \cos X)}{2\pi I_0(\Lambda_m)}, \quad \pi \leq X \leq \pi,$$

and that the δ_i are independent of each other and all the other random quantities in the model.

- (a) Find the LRT and draw a block diagram of the optimum receiver.
(b) Consider the special case where $\Lambda_m = 0$. Draw a block diagram of the optimum receiver.

Commentary. The preceding problems show the computational difficulties that are encountered in evaluating error probabilities for multiple channel systems. There are two general approaches to the

problem. The direct procedure is to set up the necessary integrals and attempt to express them in terms of Q -functions, confluent hypergeometric functions, Bessel functions, or some other tabulated function. Over the years a large number of results have been obtained. A summary of solved problems and an extensive list of references are given in [Vit66]. A second approach is to try to find analytically tractable bounds to the error probability. The bounding technique derived in Section 2.4 is usually the most fruitful. The next two problems consider some useful examples.

Problem 7.5.27. Rician Channels: Optimum Diversity [Jac66].

- (a) Using the approximation techniques of Section 2.4, find $\Pr(\epsilon)$ expressions for binary orthogonal signals in N Rician channels.
- (b) Conduct the same type of analysis for a suboptimum receiver using square-law combining.
- (c) The question of optimum diversity is also appropriate in this case. Check your expressions in parts (a) and (b) with [Jac66] and verify the optimum diversity results.

Problem 7.5.28. In part (c) of Problem 7.5.27, it was shown that if the ratio of the energy in the specular component to the energy in the random component exceeded a certain value, then infinite diversity was optimum. This result is not practical because it assumes perfect knowledge of the phase of the specular component. As N increases, the effect of small phase errors will become more important and should always lead to a finite optimum number of channels. Use the phase probability density in Problem 7.5.27 and investigate the effects of imperfect phase knowledge.

P7.6 Multiple Parameter Estimation

Problem 7.6.1. The received signal is

$$r(t) = s(t, \mathbf{A}) + w(t), \quad 0 \leq t \leq T.$$

The parameter \mathbf{a} is a Gaussian random vector with probability density

$$p_{\mathbf{a}}(\mathbf{A}) = \left[(2\pi)^{M/2} |\Lambda_{\mathbf{a}}|^{\frac{1}{2}} \right]^{-1} \exp\left(-\frac{1}{2} \mathbf{A}^T \Lambda_{\mathbf{a}}^{-1} \mathbf{A}\right).$$

Using the derivative matrix notation of Chapter 4, derive an integral equation for the MAP estimate of \mathbf{a} .

Problem 7.6.2. Modify the result in Problem 7.6.1 to include the case in which $\Lambda_{\mathbf{a}}$ is singular.

Problem 7.6.3. Modify the result in part 1 of Problem 7.6.1 to include the case in which $E(\mathbf{a}) = \mathbf{m}_{\mathbf{a}}$.

Problem 7.6.4. Consider Example 7.16. Show that the actual mean-square errors approach the bound as E/N_0 increases.

Problem 7.6.5. Let

$$r(t) = s(t, a(t)) + n(t), \quad 0 \leq t \leq T.$$

Assume that $a(t)$ is a zero-mean Gaussian random process with covariance function $K_a(t, u)$. Consider the function $a^*(t)$ obtained by sampling $a(t)$ every T/M seconds and reconstructing a waveform from

the samples.

$$a^*(t) = \sum_{t=1}^M a(t_i) \frac{\sin[(\pi M/T)(t - t_i)]}{(\pi M/T)(t - t_i)}, \quad t_i = 0, \frac{T}{M}, \frac{2T}{M}, \dots$$

(a) Define

$$\hat{a}^*(t) = \sum_{i=1}^M \hat{a}(t_i) \frac{\sin[(\pi M/T)(t - t_i)]}{(\pi M/T)(t - t_i)}.$$

Find an equation for $\hat{a}^*(t)$.

(b) Proceeding formally, show that as $M \rightarrow \infty$ the equation for the MAP estimate of $a(t)$ is

$$\hat{a}(t) = \frac{2}{N_0} \int_0^T [r(u) - s(u, \hat{a}(u))] \frac{\partial s(u, \hat{a}(u))}{\partial \hat{a}(u)} K_a(t, u) du, \quad 0 \leq t \leq T.$$

Problem 7.6.6. Let

$$r(t) = s(t, \mathbf{A}) + n(t), \quad 0 \leq t \leq T,$$

where \mathbf{a} is a zero-mean Gaussian vector with a diagonal covariance matrix and $n(t)$ is a sample function from a zero-mean Gaussian random process with covariance function $K_n(t, u)$. Find the equation that specifies the MAP estimate of \mathbf{a} .

Problem 7.6.7. The multiple channel estimation problem is

$$\mathbf{r}(t) = \mathbf{s}(t, \mathbf{A}) + \mathbf{n}(t), \quad 0 \leq t \leq T,$$

where $\mathbf{r}(t)$ is an N -dimensional vector and \mathbf{a} is an M -dimensional parameter. Assume that \mathbf{a} is a zero-mean Gaussian vector with a diagonal covariance matrix. Let

$$E [\mathbf{n}(t)\mathbf{n}^T(u)] = \mathbf{K}_n(t, u).$$

Find an equation that specifies the MAP estimate of \mathbf{a} .

Problem 7.6.8. Let

$$r(t) = \sqrt{2} v f(t, \mathbf{A}) \cos[\omega_c t + \phi(t, \mathbf{A}) + \theta] + w(t), \quad 0 \leq t \leq T,$$

where v is a Rayleigh variable and θ is a uniform variable. The additive noise $w(t)$ is a sample function from a white Gaussian process with spectral height $N_0/2$. The parameter \mathbf{a} is a zero-mean Gaussian vector with a diagonal covariance matrix; \mathbf{a} , v , θ , and $w(t)$ are statistically independent. Find the likelihood function as a function of \mathbf{a} .

Problem 7.6.9. Let

$$r(t) = \sqrt{2} v f(t - \tau) \cos[\omega_c t + \phi(t - \tau) + \omega t + \theta] + w(t), \quad -\infty < t < \infty,$$

where $w(t)$ is a sample function from a zero-mean white Gaussian noise process with spectral height $N_0/2$. The functions $f(t)$ and $\phi(t)$ are deterministic functions that are low-pass compared with ω_c . The random variable v is Rayleigh and the random variable θ is uniform. The parameters τ and ω are nonrandom.

- (a) Find the likelihood function as a function of τ and ω .
- (b) Draw the block diagram of a receiver that provides an approximate implementation of the maximum likelihood estimator.

Problem 7.6.10. A sequence of amplitude modulated signals is transmitted. The signal transmitted in the k th interval is

$$s_k(t, A) = A_k s(t), \quad (k-1)T \leq t \leq kT, \quad k = 1, 2, \dots$$

The sequence of random variables is zero-mean Gaussian; the variables are related in the following manner:

$$\begin{aligned} a_1 &\text{ is } N(0, \sigma_a^2), \\ a_2 &= \Phi a_1 + u_1, \\ &\vdots \\ a_k &= \Phi a_{k-1} + u_{k-1}. \end{aligned}$$

The multiplier Φ is fixed. The u_i are independent, zero-mean Gaussian random variables, $N(0, \sigma_u^2)$. The received signal in the k th interval is

$$r(t) = s_k(t, A) + w(t), \quad (k-1)T \leq t \leq kT, \quad k = 1, 2, \dots$$

Find the MAP estimate of a_k , $k = 1, 2, \dots$

8

Estimation of Continuous-Time Random Processes

In this chapter, we shall study the linear estimation problem in detail. We first consider a simple example and then formulate the general problem of interest. In Section 8.4, we give a brief introduction to Bayesian estimation of non-Gaussian models.

8.1 OPTIMUM LINEAR PROCESSORS

The message process of interest is $a(t)$. It is transmitted over a channel embedded in a modulation function $s(t, a(t))$ and is observed in the presence of additive white noise $n(t)$. Thus,

$$r(t) = s(t, a(t)) + n(t), \quad T_i \leq t \leq T_f \quad (8.1)$$

If the mapping $s(t, a(t))$ is a linear mapping (in other words, superposition holds), we refer to the system as a *linear signaling (or linear modulation)* system.

We would like to find the minimum mean-square error estimate of $a(t)$ where t is a specific time of interest that is not necessarily in $[T_i, T_f]$. Thus, we want to minimize

$$\xi_P(t) \triangleq E \{ [\hat{a}(t) - a(t)]^2 \} .$$

There are two approaches to this minimization problem. The first is the nonstructured approach in which we assume that $a(t)$ and $n(t)$ are jointly Gaussian processes. We then find the *a posteriori* probability density of $a(t)$ given $r(u)$, $T_i \leq u \leq T_f$ and set $\hat{a}(t)$ equal to the conditional mean. From our results in Chapters 5 and 7, we would anticipate that the resulting estimate would be a linear function of $r(u)$, $T_i \leq u \leq T_f$.

The second approach is a structured approach that we discussed briefly in Chapter 1. We assume that we only know the second moments of $a(t)$ and $n(t)$. Assuming zero means, this would correspond to $K_a(t, u)$, $K_n(t, u) = \frac{N_0}{2} \delta(t - u)$, and $K_{an}(t, u)$. We restrict our processor to be a time-varying linear filter $h(t, u)$ and find the $h(t, u)$ that minimizes $\xi_P(t)$. In this chapter, we develop both approaches and show that they lead to the same linear processor.

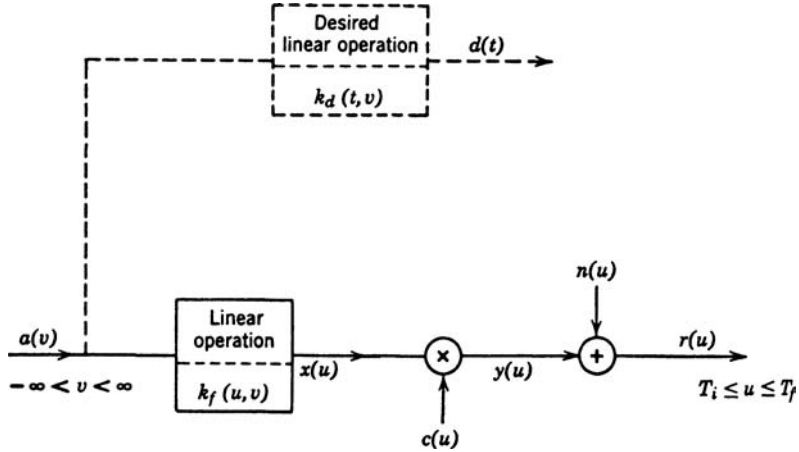


Figure 8.1: Typical estimation problem.

The point estimation problem of interest is shown in Figure 8.1. The signal available at the receiver for processing is $r(u)$. It is obtained by performing a linear operation on $a(v)$ to obtain $x(u)$, which is then multiplied by a *known* modulation function. A noise $n(u)$ is added to the output $y(u)$ before it is observed. The dotted lines represent some linear operation (not necessarily time-invariant nor realizable) that we should like to perform on $a(v)$ if it were available (possibly for all time). The output is the desired signal $d(t)$ at some *particular* time t . The time t *may or may not* be included in the observation interval.

Common examples of desired signals are

$$(i) \quad d(t) = a(t).$$

Here, the output is simply the message. Clearly, if t were included in the observation interval, $x(u) = a(u)$, $n(u)$ were zero, and $c(u)$ were a constant, we could obtain the signal exactly. In general, this will not be the case.

$$(ii) \quad d(t) = a(t + \alpha).$$

Here, if α is a positive quantity, we wish to predict the value of $a(t)$ at some time in the future. Now, even in the absence of noise the estimation problem is nontrivial if $t + \alpha > T_f$. If α is a negative quantity, we shall want the value at some previous time.

$$(iii) \quad d(t) = \frac{d}{dt} a(t).$$

Here, the desired signal is the derivative of the message. Other types of operations follow easily.

We shall assume that the linear operation is such that $d(t)$ is defined in the mean-square sense [i.e., if $d(t) = \dot{a}(t)$, as in (iii), we assume that $a(t)$ is a mean-square differentiable process]. Our discussion has been in the context of the linear modulation system in Figure 8.1. We have not yet specified the statistics of the random processes.

We consider two process models:

1. Second-Moment Model

The $a(t)$ and $n(t)$ processes are zero mean and their covariance functions, $K_a(t, u)$, $K_n(t, u)$, and $K_{an}(t, u)$ are known. We require the estimator to be linear.

2. Gaussian Assumption

The message $a(t)$, the desired signal $d(t)$, and the received signal $r(t)$ are jointly Gaussian processes. The structure of the processor is not specified.

We now return to the optimum processing problem and discuss the structured approach first. We want to operate on $r(u)$, $T_i \leq u \leq T_f$ to obtain an estimate of $d(t)$. We denote this estimate as $\hat{d}(t)$ and choose our processor so that the quantity

$$\xi_P(t) \triangleq E \{ [d(t) - \hat{d}(t)]^2 \} = E [e^2(t)] \quad (8.2)$$

is minimized. First, observe that this is a *point* estimate (therefore the subscript P). Second, we observe that we are minimizing the mean-square error between the desired signal $d(t)$ and the estimate $\hat{d}(t)$.

We shall now find the optimum processor. The approach is as follows:

1. First, we shall find the optimum *linear* processor. Properties 1, 2, 3 and 4 deal with this problem. We shall see that the Gaussian assumption is not used in the derivation of the optimum linear processor.
2. Next, by including the Gaussian assumption, Properties 5 and 6 show that a linear processor is the best of *all possible* processors for the mean-square error criterion.
3. Property 7 demonstrates that under the Gaussian assumption the linear processor is optimum for a large class of error criteria.
4. Finally, Properties 8 and 9 show the relation between point estimators and interval estimators.

Property 1. The minimum mean-square *linear* estimate is the output of a linear processor whose impulse response is a solution to the integral equation

$$K_{dr}(t, u) = \int_{T_i}^{T_f} h_o(t, \tau) K_r(\tau, u) d\tau, \quad T_i < u < T_f. \quad (8.3)$$

Proof. The output of a linear processor can be written as

$$\hat{d}(t) = \int_{T_i}^{T_f} h(t, \tau) r(\tau) d\tau, \quad (8.4)$$

where $h(t, \tau)$ is the impulse response, the value of the output at time t when the input is an impulse at time τ . If the system is physically realizable, then

$$h(t, \tau) = 0, \quad t < \tau \quad (8.5)$$

for the output cannot precede the input. If the system is time-invariant, then $h(t, \tau)$ depends only on the difference $(t - \tau)$.

We assume that $h(t, \tau) = 0$, $\tau < T_i$, $\tau > T_f$. In our basic derivation we do not require that $h(t, \tau)$ be realizable. The mean-square error at time t is

$$\begin{aligned}\xi_P(t) &= E \left\{ [d(t) - \hat{d}(t)]^2 \right\} \\ &= E \left\{ \left[d(t) - \int_{T_i}^{T_f} h(t, \tau) r(\tau) d\tau \right]^2 \right\}. \end{aligned}\quad (8.6)$$

We want to choose $h(t, \tau)$ to minimize $\xi_P(t)$. One way to solve this minimization problem is to use standard variational techniques (e.g. [Hil52], Chapter 2). Our approach is less formal and leads directly to a necessary and sufficient condition. We require the filter $h(t, \tau)$ to be a continuous function in both variables over the area $T_i \leq t, \tau \leq T_f$ and denote the $h(t, \tau)$ that minimizes $\xi_P(t)$ as $h_o(t, \tau)$. Any other filter function $h(t, \tau)$ in the allowed class can be written as

$$h(t, \tau) = h_o(t, \tau) + \epsilon h_\epsilon(t, \tau), \quad T_i \leq t, \tau \leq T_f, \quad (8.7)$$

where ϵ is a real parameter and $h_\epsilon(t, \tau)$ is in the allowable class of filters. Taking the expectation of (8.6), substituting (8.7) into the result, and grouping terms according to the power of ϵ , we obtain

$$\xi_P(t : \epsilon) = K_d(t, t) - 2 \int_{T_i}^{T_f} h(t, \tau) K_{dr}(t, \tau) d\tau + \int_{T_i}^{T_f} dv \int_{T_i}^{T_f} d\tau h(t, v) h(t, \tau) K_r(\tau, v) \quad (8.8)$$

or

$$\begin{aligned}\xi_P(t : \epsilon) &= K_d(t, t) - 2 \int_{T_i}^{T_f} h_o(t, \tau) K_{dr}(t, \tau) d\tau \\ &\quad + \int_{T_i}^{T_f} dv \int_{T_i}^{T_f} d\tau h_o(t, \tau) h_o(t, v) K_r(\tau, v) \\ &\quad - 2\epsilon \int_{T_i}^{T_f} d\tau h_\epsilon(t, \tau) \left[K_{dr}(t, \tau) - \int_{T_i}^{T_f} h_o(t, v) K_r(\tau, v) dv \right] \\ &\quad + \epsilon^2 \int_{T_i}^{T_f} \int_{T_i}^{T_f} h_\epsilon(t, v) h_\epsilon(t, \tau) K_r(\tau, v) d\tau dv. \end{aligned}\quad (8.9)$$

If we denote the first three terms as $\xi_{P_o}(t)$ and the last two terms as $\Delta\xi(t : \epsilon)$, then (8.9) becomes

$$\xi_P(t : \epsilon) = \xi_{P_o}(t) + \Delta\xi(t : \epsilon). \quad (8.10)$$

Now, if $h_o(t, \tau)$ is the optimum filter, then $\Delta\xi(t : \epsilon)$ must be greater than or equal to zero for all allowable $h_\epsilon(t, \tau)$ and all $\epsilon \neq 0$. We show that a necessary and sufficient condition for this to be true is that

$$\boxed{K_{dr}(t, \tau) - \int_{T_i}^{T_f} h_o(t, v) K_r(\tau, v) dv = 0, \quad T_i \leq t \leq T_f, \\ T_i < \tau < T_f.} \quad (8.11)$$

The equation for $\Delta\xi(t : \epsilon)$ is

$$\begin{aligned} \Delta\xi(t : \epsilon) = & -2\epsilon \int_{T_i}^{T_f} d\tau h_\epsilon(t, \tau) \left[K_{dr}(t, \tau) - \int_{T_i}^{T_f} h_o(t, v) K_r(\tau, v) dv \right] \\ & + \epsilon^2 \int_{T_i}^{T_f} \int_{T_i}^{T_f} h_\epsilon(t, v) h_\epsilon(t, \tau) K_r(\tau, v) d\tau dv. \end{aligned} \quad (8.12)$$

Three observations are needed:

1. The second term is nonnegative for any choice of $h_\epsilon(t, v)$ and ϵ because $K_r(t, \tau)$ is nonnegative definite.
2. Unless

$$\int_{T_i}^{T_f} h_\epsilon(t, \tau) \left[K_{dr}(t, \tau) - \int_{T_i}^{T_f} h_o(t, v) K_r(\tau, v) dv \right] d\tau = 0, \quad (8.13)$$

there exists for every continuous $h_\epsilon(t, \tau)$ a range of values of ϵ that will cause $\Delta\xi(t : \epsilon)$ to be negative. Specifically, $\Delta\xi(t : \epsilon) < 0$ for all

$$0 < \epsilon < \frac{2 \int_{T_i}^{T_f} h_\epsilon(t, \tau) \left[K_{dr}(t, \tau) - \int_{T_i}^{T_f} h_o(t, v) K_r(\tau, v) dv \right] d\tau}{\int_{T_i}^{T_f} \int_{T_i}^{T_f} h_\epsilon(t, v) h_\epsilon(t, \tau) K_r(\tau, v) d\tau dv} \quad (8.14)$$

if the numerator on the right-hand side of (8.14) is positive. $\Delta\xi(t : \epsilon)$ is negative for all negative ϵ greater than the right-hand side of (8.14) if the numerator is negative.

3. In order that (8.13) may hold, it is necessary and sufficient that the term in the bracket be identically zero for all $T_i < \tau < T_f$. Thus,

$$K_{dr}(t, \tau) - \int_{T_i}^{T_f} h_o(t, v) K_r(\tau, v) dv = 0, \quad \begin{aligned} T_i &\leq t \leq T_f, \\ T_i &< \tau < T_f. \end{aligned} \quad (8.15)$$

The inequality on τ is strict if there is a white noise component in $r(t)$ because the second term is discontinuous at $\tau = T_i$ and $\tau = T_f$. If (8.15) is not true, we can make the left-hand side of (8.13) positive by choosing $h_\epsilon(t, \tau) > 0$ for those values of τ

in which the left-hand side of (8.15) is greater than zero and $h_\epsilon(t, \tau) < 0$ elsewhere. These three observations complete the proof of (8.11).

Observe that $h_o(t, T_i)$ and $h_o(t, T_f)$ are uniquely specified by the continuity requirement

$$h_o(t, T_i) = \lim_{\tau \rightarrow T_i^+} h_o(t, \tau), \quad (8.16)$$

$$h_o(t, T_f) = \lim_{\tau \rightarrow T_f^-} h_o(t, \tau). \quad (8.17)$$

In Property 1A we shall show that the solution to (8.11) is unique iff $K_r(t, \tau)$ is positive definite.

We observe that the only quantities needed to design the optimum linear processor for minimizing the mean-square error are the covariance function of the received signal $K_r(t, \tau)$ and the cross-covariance between the desired signal and the received signal, $K_{dr}(t, \tau)$. We emphasize that we have *not* used the Gaussian assumption.

Several special cases are important enough to be mentioned explicitly.

Property 1A. When $d(t) = a(t)$ and $T_f = t$, we have a realizable filtering problem, and (8.11) becomes

$$K_{ar}(t, u) = \int_{T_i}^t h_o(t, \tau) K_r(\tau, u) d\tau, \quad T_i < u < t. \quad (8.18)$$

We use the term realizable because the filter indicated by (8.18) operates only on the past [i.e., $h_o(t, \tau) = 0$ for $\tau > t$].

Property 1B. Let $r(t) = c(t)x(t) + n(t) \triangleq y(t) + n(t)$. If the noise is white with spectral height $N_0/2$ and uncorrelated with $a(t)$, (8.11) becomes

$$K_{dy}(t, u) = \frac{N_0}{2} h_o(t, u) + \int_{T_i}^{T_f} h_o(t, \tau) K_y(\tau, u) d\tau, \quad T_i \leq u \leq T_f. \quad (8.19)$$

Property 1C. When the assumptions of both 1A and 1B hold, and $x(t) = a(t)$, (8.11) becomes

$$K_a(t, u) = \frac{N_0}{2} h_o(t, u) + \int_{T_i}^t h_o(t, \tau) c(\tau) K_a(\tau, u) c(u) d\tau, \quad T_i \leq u \leq t. \quad (8.20)$$

[The end point equalities were discussed in (8.16) and (8.17).]

Returning to the general case, we want to find an expression for the minimum mean-square error.

Property 2. The minimum mean-square error with the optimum linear processor is

$$\xi_{P_o}(t) \triangleq E[e_o^2(t)] = K_d(t, t) - \int_{T_i}^{T_f} h_o(t, \tau) K_{dr}(t, \tau) d\tau. \quad (8.21)$$

This follows by using (8.11) in (8.6). Hereafter we suppress the subscript o in the optimum error.

The error expressions for several special cases are also of interest. They all follow by straightforward substitution.

Property 2A. When $d(t) = a(t)$ and $T_f = t$, the minimum mean-square error is

$$\xi_P(t) = K_a(t, t) - \int_{T_i}^t h_o(t, \tau) K_{ar}(t, \tau) d\tau. \quad (8.22)$$

Property 2B. If the noise is white and uncorrelated with $a(t)$, the error is

$$\xi_P(t) = K_d(t, t) - \int_{T_i}^{T_f} h_o(t, \tau) K_{dy}(t, \tau) d\tau. \quad (8.23)$$

Property 2C. If the conditions of 2A and 2B hold and $x(t) = a(t)$, then

$$h_o(t, t) = \frac{2}{N_0} c(t) \xi_P(t). \quad (8.24)$$

If $c^{-1}(t)$ exists, (8.24) can be rewritten as

$$\xi_P(t) = \frac{N_0}{2} c^{-1}(t) h_o(t, t). \quad (8.25)$$

We may summarize the knowledge necessary to find the optimum linear processor in the following property:

Property 3. $K_r(t, u)$ and $K_{dr}(t, u)$ are the only quantities needed to find the MMSE point estimate when the processing is restricted to being linear. Any further statistical information about the processes cannot be used. All processes, Gaussian or non-Gaussian, with the same $K_r(t, u)$ and $K_{dr}(t, u)$ lead to the same processor and the same mean-square error if the processing is *required* to be linear.

Property 4. The error at time t using the optimum linear processor is uncorrelated with the input $r(u)$ at every point in the observation interval. This property follows directly from (8.15). Thus

$$E[e_o(t)r(u)] = 0, \quad T_i < u < T_f. \quad (8.26)$$

We should observe that (8.26) can also be obtained by a simple heuristic geometric argument. In Figure 8.2, we plot the desired signal $d(t)$ as a point in a vector space. The shaded plane area χ represents those points that can be achieved by a linear operation on the given input

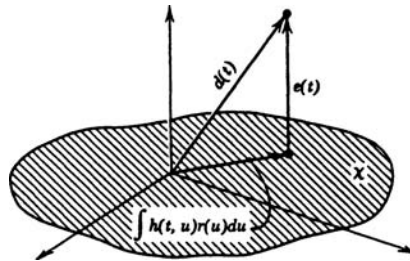


Figure 8.2: Geometric interpretation of the optimum linear filter.

$r(u)$. We want to choose $\hat{d}(t)$ as the point in χ closest to $d(t)$. Intuitively, it is clear that we must choose the point directly under $d(t)$. Therefore, the error vector is perpendicular to χ (or, equivalently, every vector in χ); that is, $e_o(t) \perp \int h(t, u)r(u) du$ for every $h(t, u)$.

The only difficulty is that the various functions are random. A suitable measure of the squared-magnitude of a vector is its mean-square value. The squared magnitude of the vector representing the error is $E[e^2(t)]$. Thus, the condition of perpendicularity is expressed as an expectation:

$$E \left[e_o(t) \int_{T_i}^{T_f} h(t, u)r(u) du \right] = 0 \quad (8.27)$$

for every continuous $h(t, u)$; this implies

$$E[e_o(t)r(u)] = 0, \quad T_i < u < T_f, \quad (8.28)$$

which is (8.26).¹

Property 4A. If the processes of concern $d(t)$, $r(t)$, and $a(t)$ are jointly Gaussian, the error using the optimum linear processor is *statistically independent* of the input $r(u)$ at every point in the observation interval.

This property follows directly from the fact that uncorrelated Gaussian variables are statistically independent.

Property 5. When the Gaussian assumption holds, the minimum mean-square error estimate is the conditional mean of the *a posteriori* probability density $p_{d(t)|r(u), T_i \leq u \leq T_f}(d(t)|r(u))$. The output $\hat{d}_o(t)$ of the optimum linear filter $h_o(t, u)$ is the required conditional mean.

We consider the case where $n(t)$ is white Gaussian noise with spectral height $N_0/2$ and is statistically independent of $a(t)$. This is not a restriction because we can always find a linear whitening filter.²

¹Our discussion is obviously heuristic. It is easy to make it rigorous by introducing a few properties of linear vector spaces, but this is not necessary for our purposes.

²We derive explicit formulas in Sections 8.2 and 8.3

We first rewrite the equation for the optimum linear filter (8.11)

$$K_{dr}(t, u) = \int_{T_i}^{T_f} h_o(t, \tau) K_r(\tau, u) d\tau, \quad T_i \leq u \leq T_f. \quad (8.29)$$

We define an inverse kernel $Q_r(z, u)$

$$\int_{T_i}^{T_f} Q_r(z, u) K_r(\tau, u) du = \delta(z - \tau). \quad (8.30)$$

This is just the functional equivalent of an inverse matrix.

Multiplying both sides of (8.29) by $Q_r(z, u)$ and integrating with respect to u gives

$$\int_{T_i}^{T_f} K_{dr}(t, u) Q_r(z, u) du = \int_{T_i}^{T_f} h_o(t, \tau) d\tau \int_{T_i}^{T_f} Q_r(z, u) K_r(\tau, u) du. \quad (8.31)$$

Using (8.30) in (8.31) gives

$$h_o(t, z) = \int_{T_i}^{T_f} K_{dr}(t, u) Q_r(z, u) du. \quad (8.32)$$

This appears to be an explicit solution, however we have to solve the integral equation in (8.30) to implement it.

From Figure 8.1

$$K_r(t, u) = K_y(t, u) + \frac{N_0}{2} \delta(t - u). \quad (8.33)$$

We expand $r(t)$ in a Karhunen–Loève expansion using the eigenfunctions of $y(t)$. The N -term approximation to $r(t)$ is

$$r_N(t) = \sum_{i=1}^N r_i \phi_i(t), \quad (8.34)$$

where the $\phi_i(t)$ satisfy

$$\lambda_i^y \phi_i(t) = \int_{T_i}^{T_f} K_y(t, u) \phi_i(u) du, \quad T_i \leq t \leq T_f, \quad (8.35)$$

$$r_i = \int_{T_i}^{T_f} r(t) \phi_i(t) dt, \quad (8.36)$$

and

$$\mathbf{r}_N \triangleq [r_1 \quad r_2 \quad \cdots \quad r_N]^T. \quad (8.37)$$

We want to find the conditional mean of $p_{d(t)|\mathbf{R}_N}(d(t)|\mathbf{R}_N)$ and then study the behavior as $N \rightarrow \infty$. However, this is just the vector problem we solved in Section 5.3. From (5.659)

$$\hat{\theta}_{\text{ms}} = \mathbf{K}_{\theta\mathbf{r}} \mathbf{K}_{\mathbf{r}}^{-1} \mathbf{R}. \quad (8.38)$$

Letting

$$\hat{d}(t) = \hat{\theta}_{\text{ms}} \quad (8.39)$$

in (8.38), we have

$$\hat{d}_N^g(t) = \mathbf{K}_{d\mathbf{r}_N}(t) \mathbf{K}_{\mathbf{r}_N}^{-1} \mathbf{R}_N. \quad (8.40)$$

The superscript “g” denotes this is a Gaussian model estimate. The first term in (8.40) is a $1 \times N$ matrix

$$\mathbf{K}_{d\mathbf{r}_N}(t) = [K_{dr_1}(t) \ K_{dr_2}(t) \ \cdots \ K_{dr_N}(t)], \quad (8.41)$$

where

$$\begin{aligned} K_{dr_i}(t) &= E \left\{ d(t) \int_{T_i}^{T_f} r(u) \phi_i(u) du \right\} \\ &= \int_{T_i}^{T_f} K_{dr}(t, u) \phi_i(u) du. \end{aligned} \quad (8.42)$$

The second term is an $N \times N$ matrix that is the inverse of $\mathbf{K}_{\mathbf{r}_N}$. The ij component of $\mathbf{K}_{\mathbf{r}_N}$ is

$$[\mathbf{K}_{\mathbf{r}_N}]_{ij} = E \left\{ \int_{T_i}^{T_f} r(\alpha) \phi_i(\alpha) d\alpha \int_{T_i}^{T_f} r(\beta) \phi_j(\beta) d\beta \right\}. \quad (8.43)$$

Using (6.48)

$$[\mathbf{K}_{\mathbf{r}_N}]_{ij} = \left(\lambda_i^y + \frac{N_0}{2} \right) \delta_{ij} \quad (8.44)$$

and

$$[\mathbf{K}_{\mathbf{r}_N}^{-1}]_{ij} = \left(\frac{1}{\lambda_i^y + \frac{N_0}{2}} \right) \delta_{ij}. \quad (8.45)$$

The product of first two terms in (8.40) is a $1 \times N$ matrix,

$$[\mathbf{K}_{d\mathbf{r}_N}(t) \mathbf{K}_{\mathbf{r}_N}^{-1}]_i = \int_{T_i}^{T_f} \left(\frac{K_{dr}(t, u)}{\lambda_i^y + \frac{N_0}{2}} \right) \phi_i(u) du. \quad (8.46)$$

The last term is a $N \times 1$ vector whose i th component is

$$[\mathbf{r}_N]_i = \int_{T_i}^{T_f} r(v) \phi_i(v) dv. \quad (8.47)$$

Therefore,

$$\hat{d}_N^g(t) = \int_{T_i}^{T_f} \sum_{i=1}^N \frac{K_{dr}(t, u)}{\lambda_i^y + \frac{N_0}{2}} \phi_i(u) du \int_{T_i}^{T_f} r(v) \phi_i(v) dv. \quad (8.48)$$

Rearranging gives

$$\hat{d}_N^g(t) = \int_{T_i}^{T_f} \int_{T_i}^{T_f} K_{dr}(t, u) r(v) \sum_{i=1}^N \frac{\phi_i(u) \phi_i(v)}{\lambda_i^y + \frac{N_0}{2}} du dv. \quad (8.49)$$

As $N \rightarrow \infty$, the summation approaches $Q_r(u, v)$,

$$Q_r(u, v) = \sum_{i=1}^{\infty} \frac{\phi_i(u) \phi_i(v)}{\lambda_i^y + \frac{N_0}{2}}. \quad (8.50)$$

Thus,

$$\hat{d}^g(t) = \int_{T_i}^{T_f} dv r(v) \int_{T_i}^{T_f} K_{dr}(t, u) Q_r(u, v) du. \quad (8.51)$$

From (8.32), the inner integral is $h_o(t, v)$, so

$$\hat{d}^g(t) = \int_{T_i}^{T_f} h_o(t, v) r(v) dv = \hat{d}_o(t), \quad (8.52)$$

which is the desired result.

The next property exploits Property 4A to show that a nonlinear processor cannot provide a smaller mean-square error.

Property 6. When the Gaussian assumption holds, the optimum *linear* processor for minimizing the mean-square error is the best of *any* type. In other words, a nonlinear processor cannot give an estimate with a smaller mean-square error.

Proof. Let $d_*(t)$ be an estimate generated by an arbitrary continuous processor operating on $r(u)$, $T_i \leq u \leq T_f$. We can denote it by

$$d_*(t) = f(t : r(u), T_i \leq u \leq T_f). \quad (8.53)$$

Denote the mean-square error using this estimate as $\xi_*(t)$. We want to show that

$$\xi_*(t) \geq \xi_P(t), \quad (8.54)$$

with equality holding when the arbitrary processor is the optimum linear filter:

$$\begin{aligned} \xi_*(t) &= E \{ [d_*(t) - d(t)]^2 \} \\ &= E \{ [d_*(t) - \hat{d}(t) + \hat{d}(t) - d(t)]^2 \} \\ &= E \{ [d_*(t) - \hat{d}(t)]^2 \} + 2E \{ [d_*(t) - \hat{d}(t)] e_o(t) \} + \xi_P(t). \end{aligned} \quad (8.55)$$

The first term is nonnegative. It remains to show that the second term is zero. We can write the second term as

$$E \left\{ \left[f(t : r(u), T_i \leq u \leq T_f) - \int_{T_i}^{T_f} h_o(t, u) r(u) du \right] e_o(t) \right\}. \quad (8.56)$$

This term is zero because $r(u)$ is *statistically independent* of $e_o(t)$ over the appropriate range, except for $u = T_f$ and $u = T_i$. (Because both processors are continuous, the expectation is also zero at the end point.) Therefore, the optimum linear processor is as good as any other processor. The final question of interest is the uniqueness. To prove uniqueness, we must show that the first term is strictly positive unless the two processors are equal. We discuss this issue in two parts.

Property 6A. First assume that $f(t : r(u), T_i \leq u \leq T_f)$ corresponds to a *linear* processor that is *not* equal to $h_o(t, u)$. Thus,

$$f(t : r(u), T_i \leq u \leq T_f) = \int_{T_i}^{T_f} (h_o(t, u) + h_*(t, u)) r(u) du, \quad (8.57)$$

where $h_*(t, u)$ represents the difference in the impulse responses.

Using (8.50)–(8.57) to evaluate the first term in (8.55), we have

$$E \{ [d_*(t) - \hat{d}(t)]^2 \} = \iint_{T_i}^{T_f} du dz h_*(t, u) K_r(u, z) h_*(t, z). \quad (8.58)$$

From (6.37) we know that if $K_r(u, z)$ is positive definite, the right-hand side will be positive for every $h_*(t, u)$ that is not identically zero. On the other hand, if $K_r(t, u)$ is only nonnegative definite, then from our discussion in Chapter 6 we know there exists an $h_*(t, u)$ such that

$$\int_{T_i}^{T_f} h_*(t, u) K_r(u, z) du = 0, \quad T_i \leq z \leq T_f. \quad (8.59)$$

Because the eigenfunctions of $K_r(u, z)$ do not form a complete orthonormal set we can construct $h_*(t, u)$ out of functions that are orthogonal to $K_r(u, z)$.

Note that our discussion in 6A has not used the Gaussian assumption and that we have derived a necessary and sufficient condition for the uniqueness of the solution of (8.11). If $K_r(u, z)$ is not positive definite, we can add an $h_*(t, u)$ satisfying (8.59) to any solution of (8.11) and still have a solution. Observe that the estimate $\hat{d}(t)$ is unique even if $K_r(u, z)$ is not positive definite. This is because any $h_*(t, u)$ that we add to $h_o(t, u)$ must satisfy (8.59) and therefore cannot cause an output when the input is $r(t)$.

Property 6B. Now assume that $f(t : r(u), T_i \leq u \leq T_f)$ is a continuous nonlinear functional unequal to $\int h_o(t, u)r(u)du$. Thus,

$$f(t : r(u), T_i \leq u \leq T_f) = \int_{T_i}^{T_f} h_o(t, u)r(u)du + f_*(t : r(u), T_i \leq u \leq T_f). \quad (8.60)$$

Then

$$E\left\{\left[d_*(t) - \hat{d}(t)\right]^2\right\} = E\left[f_*(t : r(u), T_i \leq u \leq T_f)f_*(t : r(z), T_i \leq z \leq T_f)\right]. \quad (8.61)$$

Because $r(u)$ is Gaussian and the higher moments factor, we can express the expectation on the right in terms of combinations of $K_r(u, z)$. Carrying out the tedious details gives the result that if $K_r(u, z)$ is positive definite the expectation will be positive unless $f_*(t : r(z), T_i \leq z \leq T_f)$ is identically zero.

Property 6 is obviously quite important. It enables us to achieve two sets of results simultaneously by studying the linear processing problem.

1. If the Gaussian assumption holds, we are studying the best possible processor.
2. Even if the Gaussian assumption does not hold (or we cannot justify it), we shall have found the best possible linear processor.

In our discussion of waveform estimation we have considered only minimum mean-square error and MAP estimates. The next property generalizes the criterion.

Property 7A. Let $e(t)$ denote the error in estimating $d(t)$, using some estimate $\hat{d}(t)$.

$$e(t) = d(t) - \hat{d}(t). \quad (8.62)$$

The error is weighted with some cost function $C(e(t))$. The risk is the expected value of $C(e(t))$,

$$\mathcal{R}(\hat{d}(t), t) = E[C(e(t))] = E[C(d(t) - \hat{d}(t))]. \quad (8.63)$$

The Bayes point estimator is the estimate $\hat{d}_B(t)$ that minimizes the risk. If we assume that $C(e(t))$ is a symmetric convex upward function and the Gaussian assumption holds, the Bayes estimator is equal to the MMSE estimator.

$$\hat{d}_B(t) = \hat{d}_o(t). \quad (8.64)$$

Proof. The proof consists of three observations.

1. Under the Gaussian assumption the MMSE point estimator at any time (say t_1) is the conditional mean of the *a posteriori* density $p_{d_{t_1}|r(u)}[D_{t_1} | R(u) : T_i \leq u \leq T_f]$. Observe that we are talking about a single random variable d_{t_1} so that this is a legitimate density (see Problem 8.1.1).
2. The *a posteriori* density is unimodal and symmetric about its conditional mean.
3. Property 1 on page 239 in Chapter 4 is therefore applicable and gives the above conclusion.

Property 7B. If, in addition to the assumptions in Property 7A, we require the cost function to be *strictly convex*, then

$$\hat{d}_B(t) = \hat{d}_o(t) \quad (8.65)$$

is the unique Bayes point estimator.

This result follows from (4.47) in the derivation in Chapter 4.

Property 7C. If we replace the convexity requirement on the cost function with a requirement that it be a symmetric nondecreasing function such that

$$\lim_{x \rightarrow \infty} C(X)p_{d_{t_1}|r(u)}[X|R(u) : T_i \leq u \leq T_f] = 0 \quad (8.66)$$

for all t_1 and $r(t)$ of interest, then (8.65) is still valid.

These properties are important because they guarantee that the processors we are studying in this chapter are optimum for a large class of criteria when the Gaussian assumption holds.

Finally, we can relate our results with respect to point estimators and MMSE and MAP interval estimators.

Property 8. A minimum mean-square error interval estimator is just a collection of point estimators. Specifically, suppose we observe a waveform $r(u)$ over the interval $T_i \leq u \leq T_f$ and want a signal $d(t)$ over the interval $T_\alpha \leq t \leq T_\beta$ such that the mean-square error averaged over the interval is minimized.

$$\xi_I \triangleq E \left\{ \int_{T_\alpha}^{T_\beta} [d(t) - \hat{d}(t)]^2 dt \right\}. \quad (8.67)$$

Clearly, if we can minimize the expectation of the bracket for each t then ξ_I will be minimized. This is precisely what a MMSE point estimator does. Observe that the point estimator uses $r(u)$ over the entire observation interval to generate $\hat{d}(t)$.

Property 9. Under the Gaussian assumption the minimum mean-square error point estimate and MAP point estimate are identical. This is just a special case of Property 7C. Because the MAP interval estimate is a collection of MAP point estimates, the interval estimates also coincide.

These 9 properties serve as background for our study of the linear estimation case. Properties 5 and 6 enable us to concentrate our efforts in this chapter on the *optimum linear processing* problem. When the Gaussian assumption holds, our results will correspond to the

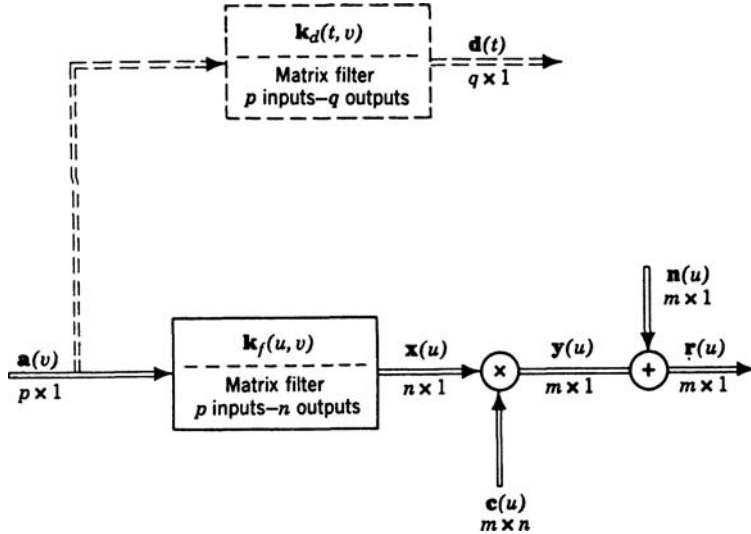


Figure 8.3: Vector estimation problem.

best possible processor (for the class of criterion described above). For arbitrary processes the results will correspond to the best linear processor.

We observe that all results carry over to the vector case with obvious modifications. Some properties, however, are used in the sequel and therefore we state them explicitly. A typical vector problem is shown in Figure 8.3.

The message $\mathbf{a}(v)$ is a p -dimensional vector. We operate on it with a matrix linear filter that has p inputs and n outputs.

$$\mathbf{x}(u) = \int_{-\infty}^{\infty} \mathbf{k}_f(u, v) \mathbf{a}(v) dv, \quad T_i \leq u \leq T_f. \quad (8.68)$$

The vector $\mathbf{x}(u)$ is multiplied by an $m \times n$ modulation matrix to give the m -dimensional vector $\mathbf{y}(t)$ that is transmitted over the channel. Observe that we have generated $\mathbf{y}(t)$ by a cascade of a linear operation with a memory and no-memory operation. The reason for this two-step procedure will become obvious later. The desired signal $\mathbf{d}(t)$ is a $q \times 1$ -dimensional vector that is related to $\mathbf{a}(v)$ by a matrix filter with p inputs and q outputs. Thus,

$$\mathbf{d}(t) = \int_{-\infty}^{\infty} \mathbf{k}_d(t, v) \mathbf{a}(v) dv. \quad (8.69)$$

We shall encounter some typical vector problems later. Observe that p, q, m , and n , the dimensions of the various vectors, may all be different.

The desired signal $\mathbf{d}(t)$ has q components. Denote the estimate of the i th component as $\hat{d}_i(t)$. We want to minimize simultaneously

$$\xi_{P_i}(t) \triangleq E \left\{ [d_i(t) - \hat{d}_i(t)]^2 \right\}, \quad i = 1, 2, \dots, q. \quad (8.70)$$

The message $\mathbf{a}(v)$ is a zero-mean vector Gaussian process and the noise is an m -dimensional Gaussian random process. In general, we assume that it contains a white component $\mathbf{w}(t)$:

$$E [\mathbf{w}(t)\mathbf{w}^T(u)] \triangleq \mathbf{R}(t)\delta(t-u), \quad (8.71)$$

where $\mathbf{R}(t)$ is positive definite. We assume also that the necessary covariance functions are known. We shall use the same property numbers as in the scalar case and add a V . We shall not restate the assumptions.

Property 1V.

$$\mathbf{K}_{\text{dr}}(t, u) = \int_{T_i}^{T_f} \mathbf{h}_o(t, \tau) \mathbf{K}_r(\tau, u) d\tau, \quad T_i < u < T_f. \quad (8.72)$$

Proof. See Problem 8.1.2.

Property 1A–V.

$$\mathbf{K}_{\text{ar}}(t, u) = \int_{T_i}^t \mathbf{h}_o(t, \tau) \mathbf{K}_r(\tau, u) d\tau, \quad T_i < u < t. \quad (8.73)$$

Property 2C–V.

$$\mathbf{h}_o(t, t) = \xi_P(t) \mathbf{C}^T(t) \mathbf{R}^{-1}(t), \quad (8.74)$$

where $\xi_P(t)$ is the error covariance matrix whose elements are

$$\xi_{P_{ij}}(t) \triangleq E \{ [a_i(t) - \hat{a}_i(t)] [a_j(t) - \hat{a}_j(t)] \}. \quad (8.75)$$

(Because the errors are zero mean, the correlation and covariance are identical.)

Proof. See Problem 8.1.3.

Other properties of the vector case follow by direct modification.

Summary. In this section, we have introduced the linear estimation problem and derived the optimum linear processor.

Up to this point we have restricted neither the processes nor the observation interval. In other words, the processes were stationary or nonstationary, the initial observation time T_i was arbitrary, and $T_f (\geq T_i)$ was arbitrary. Now we shall consider specific solution techniques. The easiest approach is by means of various special cases.

Throughout the rest of the chapter we shall be dealing with linear processors. In general, we do not specify explicitly that the Gaussian assumption holds. It is important to re-emphasize that in the absence of this assumption we are finding only the best *linear* processor (a nonlinear processor might be better). Corresponding to each problem we discuss there is another problem in which the processes are Gaussian, and for which the processor is the optimum of all processors for the given criterion.

It is also worthwhile to observe that the remainder of the chapter could have been studied directly after Chapter 1 if we had approached it as a “structured” problem and not used the Gaussian assumption. We feel that this places the emphasis incorrectly and that the linear processor should be viewed as a device that is generating the conditional mean. This viewpoint puts it into its proper place in the overall statistical problem.

8.2 REALIZABLE LINEAR FILTERS: STATIONARY PROCESSES, INFINITE PAST: WIENER FILTERS

In this section, we discuss an important case relating to (8.11). First, we assume that the final observation time corresponds to the time at which the estimate is desired. Thus $t = T_f$ and the upper limit on (8.11) becomes t . Second, we assume that $T_i = -\infty$. This assumption means that we have the infinite past available to operate on to make our estimate. From a practical standpoint it simply means that the past is available beyond the significant memory time of our filter. In a later section, when we discuss finite T_i , we shall make some quantitative statements about how large $t - T_i$ must be in order to be considered infinite.

Third, we assume that the received signal is a sample function from a stationary process and that the desired signal and the received signal are jointly stationary. Then, we may write

$$K_{dr}(t - \sigma) = \int_{-\infty}^t h_o(t, u) K_r(u - \sigma) du, \quad -\infty < \sigma < t. \quad (8.76)$$

Because the processes are stationary and the interval is infinite, let us try to find a solution to (8.76) that is time invariant.

$$K_{dr}(t - \sigma) = \int_{-\infty}^t h_o(t - u) K_r(u - \sigma) du, \quad -\infty < \sigma < t. \quad (8.77)$$

If we can find a solution to (8.77), it will also be a solution to (8.76). If $K_r(u - \sigma)$ is positive definite, (8.76) has a unique solution. Thus, if (8.77) has a solution, it will be unique and will also be the only solution to (8.76). Letting $\tau = t - \sigma$ and $v = t - u$, we have

$$K_{dr}(\tau) = \int_0^\infty h_o(v) K_r(\tau - v) dv, \quad 0 < \tau < \infty, \quad (8.78)$$

which is commonly referred to as the Wiener–Hopf equation. It was derived and solved by Wiener [Wie49]. (The linear processing problem was studied independently by Kolmogoroff [Kol41].)

Professor Wiener’s book was sometimes referred to as “The Yellow Peril” because of its yellow cover and difficult mathematics. One of his students, Professor Y. W. Lee introduced a graduate course at MIT in 1947 that evolved into his course, “Statistical Theory of Communication.” His course and later his book [Lee60] introduced Wiener filtering to several generations of students in a clear manner.

8.2.1 Solution of Wiener–Hopf Equation

Our solution to the Wiener–Hopf equation is analogous to the approach by Bode and Shannon [BS50]. Although the amount of manipulation required is identical to that in Wiener’s solution, the present procedure is more intuitive. We restrict our attention to the case in which the Fourier transform of $K_r(\tau)$, the input correlation function, is a rational function. This is not really a practical restriction because most spectra of interest can be approximated by a rational function. The general case is discussed by Wiener [Wie49] but does not lead to a practical solution technique.

The first step in our solution is to observe that $r(t)$ were white the solution to (8.78) would be trivial. If

$$K_r(\tau) = \delta(\tau), \quad (8.79)$$

then (8.78) becomes

$$K_{dr}(\tau) = \int_0^\infty h_o(v)\delta(\tau - v)dv, \quad 0 < \tau < \infty, \quad (8.80)$$

and

$$h_o(\tau) = \begin{cases} K_{dr}(\tau), & \tau \geq 0, \\ 0, & \tau < 0, \end{cases} \quad (8.81)$$

where the value at $\tau = 0$ comes from our continuity restriction.

It is unlikely that (8.79) will be satisfied in many problems of interest. If, however, we could perform some preliminary operation on $r(t)$ to transform it into a white process, as shown in Figure 8.4, the subsequent filtering problem in terms of the whitened process would be trivial. We show the following property:

Whitening Property. For all rational spectra there exists a realizable, time-invariant linear filter whose output $z(t)$ is a white process when the input is $r(t)$ and whose inverse is a realizable linear filter.

If we denote the impulse response of the whitening filter as $w(\tau)$ and the transfer function as $W(j\omega)$, then the property says:

$$(i) \quad \iint_{-\infty}^{\infty} w(u)w(v)K_r(\tau - u - v)dudv = \delta(\tau), \quad -\infty < \tau < \infty.$$

or

$$(ii) \quad |W(j\omega)|^2 S_r(\omega) = 1.$$

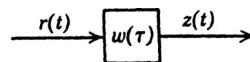


Figure 8.4: Whitening filter.

If we denote the impulse response of the inverse filter as $w^{-1}(\tau)$, then

$$(iii) \quad \int_{-\infty}^{\infty} w^{-1}(u-v)w(v) dv = \delta(u)$$

or

$$(iv) \quad \mathcal{F}[w^{-1}(\tau)] = \frac{1}{W(j\omega)} = W^{-1}(j\omega)$$

and $w^{-1}(\tau)$ must be the impulse response of a realizable filter.

We derive this property by demonstrating a constructive technique for a simple example and then extending it to arbitrary rational spectra.

Example 8.1. Let

$$S_r(\omega) = \frac{2k}{\omega^2 + k^2}. \quad (8.82)$$

We want to choose the transfer function of the whitening filter so that it is realizable and the spectrum of its output $z(t)$ satisfies the equation

$$S_z(\omega) = S_r(\omega) |W(j\omega)|^2 = 1. \quad (8.83)$$

To accomplish this we divide $S_r(\omega)$ into two parts,

$$S_r(\omega) = \left(\frac{\sqrt{2k}}{j\omega + k} \right) \left(\frac{\sqrt{2k}}{-j\omega + k} \right) \triangleq [G^+(j\omega)][G^+(j\omega)]^*. \quad (8.84)$$

We denote the first term by $G^+(j\omega)$ because it is zero for negative time. The second term is its complex conjugate. Clearly, if we let

$$W(j\omega) = \frac{1}{G^+(j\omega)} = \frac{j\omega + k}{\sqrt{2k}}, \quad (8.85)$$

then (8.83) will be satisfied.

We observe that the whitening filter consists of a differentiator and a gain term in parallel. Because

$$W^{-1}(j\omega) = G^+(j\omega) = \frac{\sqrt{2k}}{j\omega + k}, \quad (8.86)$$

it is clear that the inverse is a realizable linear filter and therefore $W(j\omega)$ is a legitimate reversible operation. Thus, we could operate on $z(t)$ in either of the two ways shown in Figure 8.5 and if we choose $h_o'(\tau)$ in an optimum manner the output of both systems will be $\hat{d}(t)$. ■

In this particular example, the selection of $W(j\omega)$ was obvious. We now consider a more complicated example.

Example 8.2. Let

$$S_r(\omega) = \frac{c^2(j\omega + \alpha_1)(-j\omega + \alpha_1)}{(j\omega + \beta_1)(-j\omega + \beta_1)}. \quad (8.87)$$

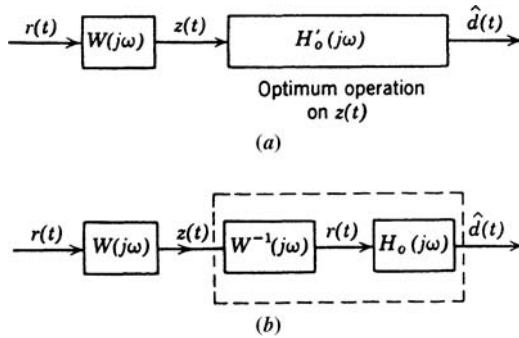


Figure 8.5: Optimum filter: (a) approach no. 1; (b) approach no. 2.

We must choose $W(j\omega)$ so that

$$S_r(\omega) = |W^{-1}(j\omega)|^2 = |G^+(j\omega)|^2 \quad (8.88)$$

and both $W(j\omega)$ and $W^{-1}(j\omega)$ [or equivalently $G^+(j\omega)$ and $W(j\omega)$] are realizable. When discussing realizability, it is convenient to use the complex s -plane. We extend our functions to the entire complex plane by replacing $j\omega$ by s , where $s = \sigma + j\omega$. In order for $W(s)$ to be realizable, it cannot have any poles in the right half of the s -plane. Therefore, we must assign the $(j\omega + \alpha_1)$ term to it. Similarly, for $W^{-1}(s)$ [or $G^+(s)$] to be realizable we assign to it the $(j\omega + \beta_1)$ term. The assignment of the constant is arbitrary because it adjusts only the white noise level. For simplicity, we assume a unity level spectrum for $z(t)$ and divide the constant evenly. Therefore,

$$G^+(j\omega) = c \frac{(j\omega + \alpha_1)}{(j\omega + \beta_1)}. \quad (8.89)$$

■

To study the general case we consider the pole-zero plot of the typical spectrum shown in Figure 8.6. Assuming that this spectrum is typical, we then find that the procedure is clear. We factor $S_r(\omega)$ and assign all poles and zeros in the left-half plane (and half of each pair of zeros on the axis) to $G^+(j\omega)$. The remaining poles and zeros will correspond exactly to the conjugate $[G^+(j\omega)]^*$. The fact that every rational spectrum can be divided in this manner follows directly from the fact that $S_r(\omega)$ is a real, even, nonnegative function of ω whose inverse transform is a correlation function. This implies the modes of behavior for the pole-zero plot shown in Figure 8.7a-c:

1. Symmetry about the σ -axis. Otherwise $S_r(\omega)$ would not be real.
2. Symmetry about the $j\omega$ -axis. Otherwise $S_r(\omega)$ would not also be even.
3. Any zeros on the $j\omega$ -axis occur in pairs. Otherwise $S_r(\omega)$ would be negative for some value of ω .
4. No poles on the $j\omega$ -axis. This would correspond to a $1/\omega^2$ term whose inverse is not the correlation function of a stationary process.

The verification of these properties is a straightforward exercise (see Problem 8.2.1).

We have now proved that we can always find a realizable, reversible whitening filter. The processing problem is now reduced to that shown in Figure 8.8. We must design $H'_o(j\omega)$

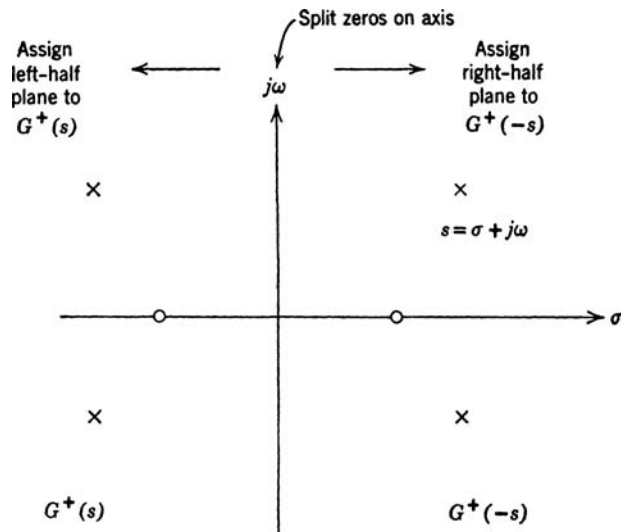
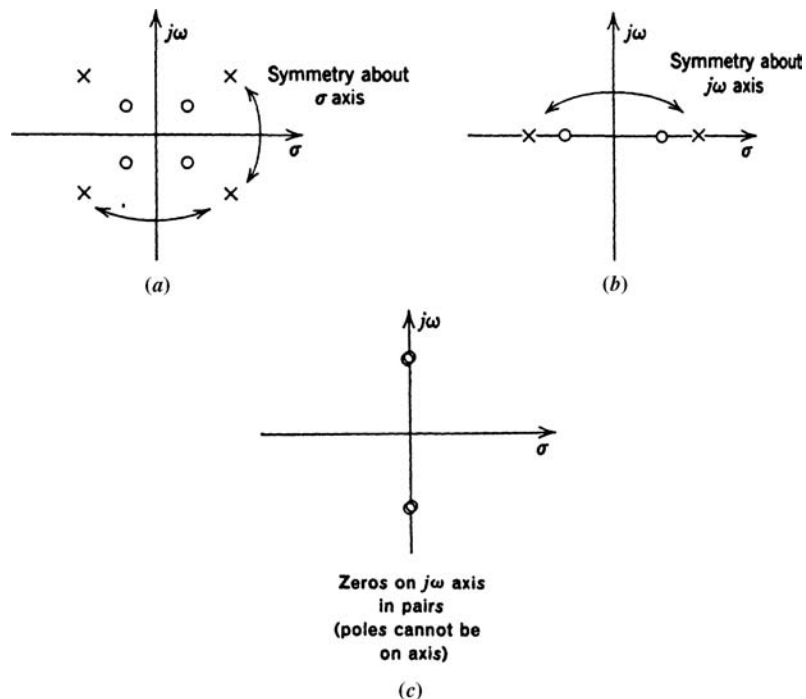


Figure 8.6: A typical pole-zero plot.

Figure 8.7: Possible pole-zero plots in the s -plane.

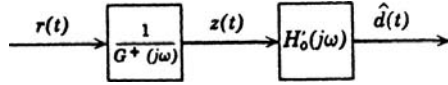


Figure 8.8: Optimum filter.

so that it operates on $z(t)$ in such a way that it produces the minimum mean-square error estimate of $d(t)$. Clearly, then, $h'_o(\tau)$ must satisfy (8.78) with r replaced by z ,

$$K_{dz}(\tau) = \int_0^\infty h'_o(v) K_z(\tau - v) dv, \quad 0 < \tau < \infty. \quad (8.90)$$

However, we have forced $z(t)$ to be white with unity spectral height. Therefore,

$$h'_o(\tau) = K_{dz}(\tau), \quad \tau \geq 0. \quad (8.91)$$

Thus, if we knew $K_{dz}(\tau)$, our solution would be complete. Because $z(t)$ is obtained from $r(t)$ by a linear operation, $K_{dz}(\tau)$ is easy to find,

$$\begin{aligned} K_{dz}(\tau) &\triangleq E \left[d(t) \int_{-\infty}^{\infty} w(v) r(t - \tau - v) dv \right] \\ &= \int_{-\infty}^{\infty} w(v) K_{dr}(\tau + v) dv = \int_{-\infty}^{\infty} w(-\beta) K_{dr}(\tau - \beta) d\beta. \end{aligned} \quad (8.92)$$

Transforming,

$$S_{dz}(j\omega) = W^*(j\omega) S_{dr}(j\omega) = \frac{S_{dr}(j\omega)}{[G^+(j\omega)]^*}. \quad (8.93)$$

We simply find the inverse transform of $S_{dz}(j\omega)$, $K_{dz}(\tau)$, and retain the part corresponding to $\tau \geq 0$. A typical $K_{dz}(\tau)$ is shown in Figure 8.9a. The associated $h'_o(\tau)$ is shown in Figure 8.9b.

We can denote the transform of $K_{dz}(\tau)$ for $\tau \geq 0$ by the symbol³

$$[S_{dz}(j\omega)]_+ \triangleq \int_0^\infty K_{dz}(\tau) e^{-j\omega\tau} d\tau = \int_0^\infty h'_o(\tau) e^{-j\omega\tau} d\tau. \quad (8.94)$$

Similarly,

$$[S_{dz}(j\omega)]_- \triangleq \int_{-\infty}^{0-} K_{dz}(\tau) e^{-j\omega\tau} d\tau. \quad (8.95)$$

Clearly,

$$S_{dz}(j\omega) = [S_{dz}(j\omega)]_+ + [S_{dz}(j\omega)]_-, \quad (8.96)$$

³In general, the symbol $[\sim]_+$ denotes the transform of the realizable part of the inverse transform of the expression inside the bracket.

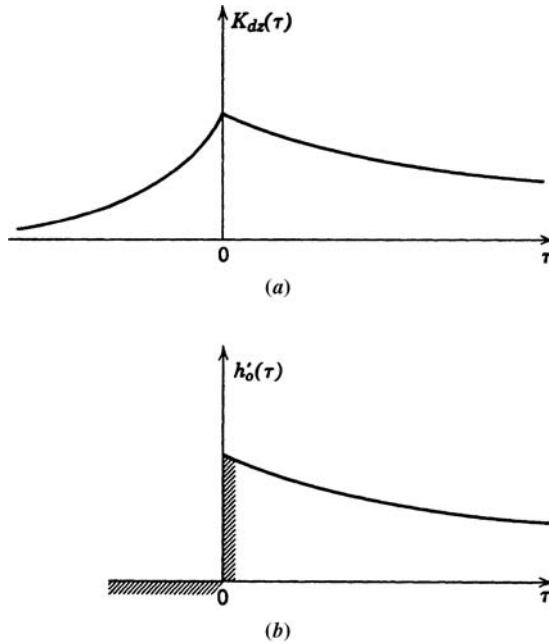


Figure 8.9: Typical functions: (a) a typical covariance function; (b) corresponding $h'_o(\tau)$.

and we may write

$$H'_o(j\omega) = [S_{dz}(j\omega)]_+ = [W^*(j\omega) S_{dr}(j\omega)]_+ = \left[\frac{S_{dr}(j\omega)}{[G^+(j\omega)]^*} \right]_+. \quad (8.97)$$

Then the entire optimum filter is just a cascade of the whitening filter and $H'_o(j\omega)$,

$$H_o(j\omega) = \left[\frac{1}{G^+(j\omega)} \right] \left[\frac{S_{dr}(j\omega)}{[G^+(j\omega)]^*} \right]_+. \quad (8.98)$$

We see that by a series of routine, conceptually simple operations we have derived the desired filter. We summarize the steps briefly.

1. We factor the *input* spectrum into two parts. One term, $G^+(s)$, contains all the poles and zeros in the left half of the *s*-plane. The other factor is its mirror image about the $j\omega$ -axis.
2. The cross-spectrum between $d(t)$ and $z(t)$ can be expressed in terms of the original cross-spectrum divided by $[G^+(j\omega)]^*$. This corresponds to a function that is nonzero for both positive and negative time. The realizable part of this function ($\tau \geq 0$) is $h'_o(\tau)$ and its transform is $H'_o(j\omega)$.
3. The transfer function of the optimum filter is a simple product of these two transfer functions. We shall see that the composite transfer function corresponds to a realizable system. Observe that we actually build the optimum linear filter as single system. The division into two parts is for conceptual purposes only.

Before we discuss the properties and implications of the solution, it will be worthwhile to consider a simple example to guarantee that we all agree on what (8.98) means.

Example 8.3. Assume that

$$r(t) = \sqrt{P} a(t) + n(t), \quad (8.99)$$

where $a(t)$ and $n(t)$ are uncorrelated zero-mean stationary processes and

$$S_a(\omega) = \frac{2k}{\omega^2 + k^2}. \quad (8.100)$$

[We see that $a(t)$ has unity power so that P is the transmitted power.]

$$S_n(\omega) = \frac{N_0}{2}. \quad (8.101)$$

The desired signal is

$$d(t) = a(t + \alpha), \quad (8.102)$$

where α is a constant.

By choosing α to be positive we have the prediction problem, choosing α to be zero gives the conventional filtering problem, and choosing α to be negative gives the filtering-with-delay problem.

The solution is a simple application of the procedure outlined in the preceding section:

$$S_r(\omega) = \frac{2kP}{\omega^2 + k^2} + \frac{N_0}{2} = \frac{N_0}{2} \frac{\omega^2 + k^2(1 + 4P/kN_0)}{\omega^2 + k^2}. \quad (8.103)$$

It is convenient to define

$$\Lambda = \frac{4P}{kN_0}. \quad (8.104)$$

(This quantity has a physical significance we shall discuss later. For the moment, it can be regarded as a useful parameter.) First we factor the spectrum

$$S_r(\omega) = \frac{N_0}{2} \frac{\omega^2 + k^2(1 + \Lambda)}{\omega^2 + k^2} = G^+(j\omega)[G^+(j\omega)]^*. \quad (8.105)$$

So

$$G^+(j\omega) = \left(\frac{N_0}{2} \right)^{1/2} \left(\frac{j\omega + k\sqrt{1 + \Lambda}}{j\omega + k} \right). \quad (8.106)$$

Now

$$\begin{aligned} K_{dr}(\tau) &= E[d(t)r(t - \tau)] = E \left\{ a(t + \alpha) \left[\sqrt{P} a(t - \tau) + n(t - \tau) \right] \right\} \\ &= \sqrt{P} E[a(t + \alpha)a(t - \tau)] = \sqrt{P} K_a(\tau + \alpha). \end{aligned} \quad (8.107)$$

Transforming,

$$S_{dr}(j\omega) = \sqrt{P} S_a(\omega) e^{+j\omega\alpha} = \frac{2k\sqrt{P} e^{+j\omega\alpha}}{\omega^2 + k^2} \quad (8.108)$$

and

$$S_{dz}(j\omega) = \frac{S_{dr}(j\omega)}{[G^+(j\omega)]^*} = \frac{2k\sqrt{P} e^{+j\omega\alpha}}{\omega^2 + k^2} \cdot \frac{-j\omega + k}{\sqrt{N_0/2} (-j\omega + k\sqrt{1 + \Lambda})}. \quad (8.109)$$

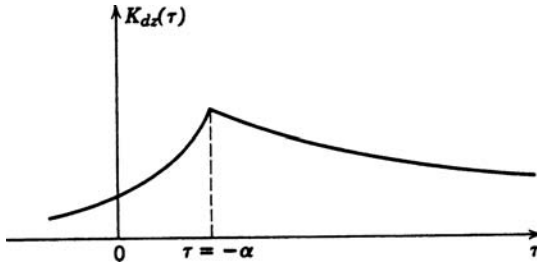


Figure 8.10: Cross-covariance function.

To find the realizable part, we take the inverse transform:

$$K_{dz}(\tau) = \mathcal{F}^{-1} \left\{ \frac{S_{dr}(j\omega)}{[G^+(j\omega)]^*} \right\} = \mathcal{F}^{-1} \left[\frac{2k\sqrt{P} e^{+j\omega\alpha}}{(j\omega + k)\sqrt{N_0/2}(-j\omega + k\sqrt{1+\Lambda})} \right]. \quad (8.110)$$

The inverse transform can be evaluated easily (either by residues or a partial fraction expansion and the shifting theorem). The result is

$$K_{dz}(\tau) = \begin{cases} \frac{2\sqrt{P}}{\sqrt{N_0/2}} \frac{1}{1 + \sqrt{1 + \Lambda}} e^{-k(\tau + \alpha)}, & \tau + \alpha \geq 0, \\ \frac{2\sqrt{P}}{\sqrt{N_0/2}} \frac{1}{1 + \sqrt{1 + \Lambda}} e^{+k\sqrt{1 + \Lambda}(\tau + \alpha)}, & \tau + \alpha < 0. \end{cases} \quad (8.111)$$

The function is shown in Figure 8.10.

Now $h'_o(\tau)$ depends on the value α . In other words, the amount of $K_{dz}(\tau)$ in the range $\tau \geq 0$ is a function of α . We consider three types of operations:

Case 1. $\alpha = 0$: Filtering with zero delay. Letting $\alpha = 0$ in (8.111), we have

$$h'_o(\tau) = \frac{2\sqrt{P}}{\sqrt{N_0/2}} \frac{1}{1 + \sqrt{1 + \Lambda}} e^{-k\tau} u_{-1}(\tau) \quad (8.112)$$

or

$$H'_o(j\omega) = \frac{1}{1 + \sqrt{1 + \Lambda}} \frac{2\sqrt{P}}{\sqrt{N_0/2}} \frac{1}{j\omega + k}. \quad (8.113)$$

Then

$$H_o(j\omega) = \frac{H'_o(j\omega)}{G^+(j\omega)} = \frac{2\sqrt{P}}{(N_0/2)(1 + \sqrt{1 + \Lambda})} \frac{1}{j\omega + k\sqrt{1 + \Lambda}}. \quad (8.114)$$

We see that our result is intuitively logical. The amplitude of the filter response is shown in Figure 8.11. The filter is a simple low-pass filter whose bandwidth varies as a function of k and Λ .

We now want to attach some physical significance to the parameter Λ . The bandwidth of the message process is directly proportional to k , as shown in Figure 8.12a. The 3 dB bandwidth is k/π cps. Another common bandwidth measure is the equivalent rectangular bandwidth (ERB), which is the bandwidth of a rectangular spectrum with height $S_a(0)$ and the same total power of the actual message as shown in Figure 8.12b. Physically, Λ is the signal-to-noise ratio in the message ERB. This ratio is most natural for most of our work. The relationship between Λ and the signal-to-noise ratio in the 3 dB bandwidth depends on the particular spectrum. For *this particular case* $\Lambda_{3dB} = (\pi/2)\Lambda$.

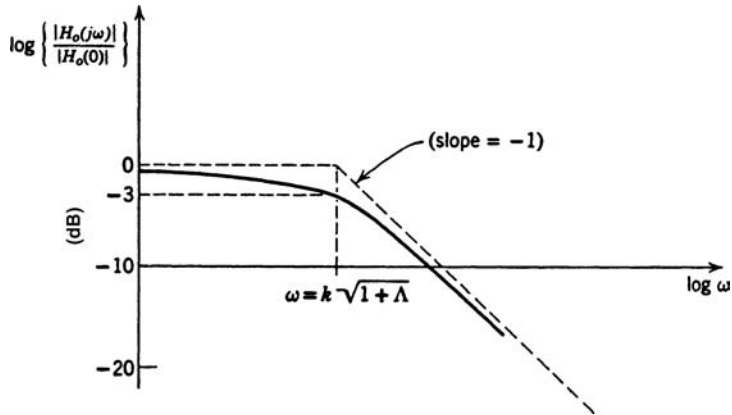


Figure 8.11: Magnitude plot for optimum filter.

We see that for a fixed k the optimum filter bandwidth increases as Λ , the signal-to-noise ratio, increases. Thus, as $\Lambda \rightarrow \infty$, the filter magnitude approaches unity for all frequencies and it passes the message component without distortion. Because the noise is unimportant in this case, this is intuitively logical. On the other hand, as $\Lambda \rightarrow 0$, the filter 3 dB point approaches k . The gain, however, approaches zero. Once again, this is intuitively logical. There is so much noise that, based on the mean-square error criterion, the best filter output is zero (the mean value of the message).

Case 2. α is negative: Filtering with delay. Here $h'_o(\tau)$ has the impulse response shown in Figure 8.13. Transforming, we have

$$H'_o(j\omega) = \frac{2k\sqrt{P}}{\sqrt{N_0/2}} \left[\frac{e^{\alpha j\omega}}{(j\omega + k)(-j\omega + k\sqrt{1+\Lambda})} - \frac{-e^{\alpha k\sqrt{1+\Lambda}}}{k(1+\sqrt{1+\Lambda})(-j\omega + k\sqrt{1+\Lambda})} \right] \quad (8.115)$$

and

$$H_o(j\omega) = \frac{H'_o(j\omega)}{G^+(j\omega)} = \frac{2k\sqrt{P}}{N_0/2} \left\{ \frac{e^{\alpha j\omega}}{[\omega^2 + k^2(1+\Lambda)]} - \frac{e^{\alpha k\sqrt{1+\Lambda}}(j\omega + k)}{k(1+\sqrt{1+\Lambda})[\omega^2 + k^2(1+\Lambda)]} \right\}. \quad (8.116)$$

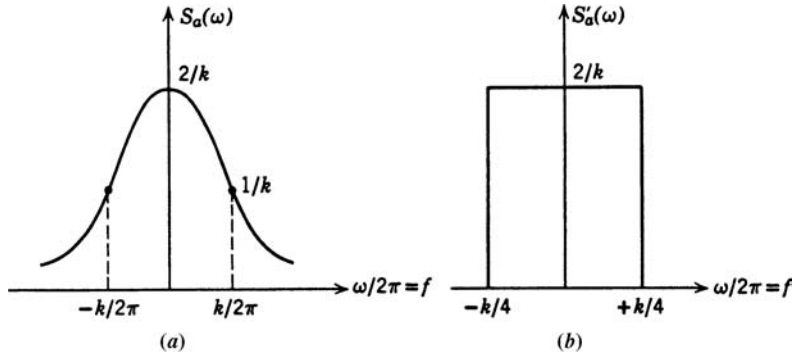


Figure 8.12: Equivalent rectangular spectrum.

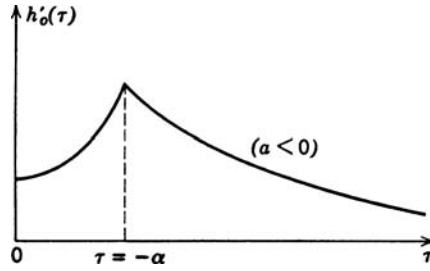


Figure 8.13: Filtering with delay.

This can be rewritten as

$$H_o(j\omega) = \frac{2k\sqrt{P} e^{\alpha j\omega}}{(N_0/2)[\omega^2 + k^2(1 + \Lambda)]} \left[1 - \frac{(j\omega + k) e^{\alpha(k\sqrt{1+\Lambda}-j\omega)}}{k(1 + \sqrt{1 + \Lambda})} \right]. \quad (8.117)$$

We observe that the expression outside the bracket is just

$$\frac{S_{dr}(j\omega)}{S_r(\omega)} e^{\alpha j\omega}. \quad (8.118)$$

We see that when α is a large negative number the second term in the bracket is approximately zero. Thus, $H_o(j\omega)$ approaches the expression in (8.118). This is just the ratio of the cross-spectrum to the total input spectrum, with a delay to make the filter realizable.

We also observe that the impulse response in Figure 8.13 is difficult to realize with conventional network synthesis techniques.

Case 3. α is positive: Filtering with prediction. Here,

$$h'_o(\tau) = \left(\frac{2\sqrt{P}}{\sqrt{N_0/2}} \frac{1}{1 + \sqrt{1 + \Lambda}} e^{-k\tau} \right) e^{-k\alpha}. \quad (8.119)$$

Comparing (8.119) with (8.112), we see that the optimum filter for prediction is just the optimum filter for estimating $a(t)$ multiplied by a gain $e^{-k\alpha}$, as shown in Figure 8.14. The reason for this is that $a(t)$ is a first-order wide-sense Markov process and the noise is white. We obtain a similar result for more general processes in Section 8.3. ■

Before concluding our discussion we amplify a point that was encountered in Case 1 of Example 8.3. One step of the solution is to find the realizable part of a function. Frequently it is unnecessary to find the time function and then retransform. Specifically, whenever $S_{dr}(j\omega)$ is a ratio of two polynomials in $j\omega$, we may write

$$\frac{S_{dr}(j\omega)}{[G^+(j\omega)]^*} = F(j\omega) + \sum_{i=1}^N \frac{c_i}{j\omega + p_i} + \sum_{j=1}^N \frac{d_j}{-j\omega + q_j}, \quad (8.120)$$

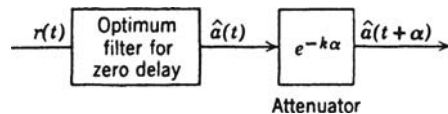


Figure 8.14: Filtering with prediction.

where $F(j\omega)$ is a polynomial, the first sum contains all terms corresponding to poles in the left half of the s -plane (including the $j\omega$ -axis), and the second sum contains all terms corresponding to poles in the right half of the s -plane. In this expanded form the realizable part consists of the first two terms. Thus,

$$\left[\frac{S_{dr}(j\omega)}{[G^+(j\omega)]^*} \right]_+ = F(j\omega) + \sum_{i=1}^N \frac{c_i}{j\omega + p_i}. \quad (8.121)$$

The use of (8.121) reduces the required manipulation.

In this section, we have developed an algorithm for solving the Wiener–Hopf equation and presented a simple example to demonstrate the technique. Next we investigate the resulting mean-square error.

8.2.2 Errors in Optimum Systems

In order to evaluate the performance of the optimum linear filter, we calculate the minimum mean-square error. The minimum mean-square error for the general case was given in (8.21) of Property 2. Because the processes are stationary and the filter is time-invariant, the mean-square error will not be a function of time. Thus, (8.21) reduces to

$$\xi_P = K_d(0) - \int_0^\infty h_o(\tau) K_{dr}(\tau) d\tau. \quad (8.122)$$

Because $h_o(\tau) = 0$ for $\tau < 0$, we can equally well write (8.122) as

$$\xi_P = K_d(0) - \int_{-\infty}^\infty h_o(\tau) K_{dr}(\tau) d\tau. \quad (8.123)$$

Now

$$H_o(j\omega) = \frac{1}{G^+(j\omega)} \int_0^\infty K_{dz}(t) e^{-j\omega t} dt, \quad (8.124)$$

where

$$K_{dz}(t) = \mathcal{F}^{-1} \left\{ \frac{S_{dr}(j\omega)}{[G^+(j\omega)]^*} \right\} = \frac{1}{2\pi} \int_{-\infty}^\infty \frac{S_{dr}(j\omega)}{[G^+(j\omega)]^*} e^{j\omega t} d\omega. \quad (8.125)$$

Substituting the inverse transform of (8.124) into (8.123), we obtain,

$$\xi_P = K_d(0) - \int_{-\infty}^\infty K_{dr}(\tau) d\tau \left[\frac{1}{2\pi} \int_{-\infty}^\infty e^{j\omega\tau} d\omega \cdot \frac{1}{G^+(j\omega)} \int_0^\infty K_{dz}(t) e^{-j\omega t} dt \right]. \quad (8.126)$$

Changing orders of integration, we have

$$\xi_P = K_d(0) - \int_0^\infty K_{dz}(t) dt \left[\frac{1}{2\pi} \int_{-\infty}^\infty e^{-j\omega t} d\omega \cdot \frac{1}{G^+(j\omega)} \int_{-\infty}^\infty K_{dr}(\tau) e^{j\omega\tau} d\tau \right]. \quad (8.127)$$

The part of the integral inside the brackets is just $K_{dz}^*(t)$. Thus, since $K_{dz}(t)$ is real,

$$\xi_P = K_d(0) - \int_0^\infty K_{dz}^2(t) dt. \quad (8.128)$$

The result in (8.128) is a convenient expression for the mean-square error. Observe that we must factor the input spectrum and perform an inverse transform in order to evaluate it. (The same shortcuts discussed above are applicable.)

We can use (8.128) to study the effect of α on the mean-square error. Denote the desired signal when $\alpha = 0$ as $d_0(t)$ and the desired signal for arbitrary α as $d_\alpha(t) \triangleq d_0(t + \alpha)$. Then

$$E[d_0(t)z(t - \tau)] = K_{d_0 z}(\tau) \triangleq \phi(\tau) \quad (8.129)$$

and

$$E[d_\alpha(t)z(t - \tau)] = E[d_0(t + \alpha)z(t - \tau)] = \phi(\tau + \alpha). \quad (8.130)$$

We can now rewrite (8.128) in terms of $\phi(\tau)$. Letting

$$K_{dz}(t) = \phi(t + \alpha) \quad (8.131)$$

in (8.128), we have

$$\xi_P^\alpha = K_d(0) - \int_0^\infty \phi^2(t + \alpha) dt = K_d(0) - \int_\alpha^\infty \phi^2(u) du. \quad (8.132)$$

Note that $\phi(u)$ is not a function of α . We observe that because the integrand is a positive quantity the error is monotone increasing with increasing α . Thus, the smallest error is achieved when $\alpha = -\infty$ (infinite delay) and increases monotonely to unity as $\alpha \rightarrow +\infty$. This result says that for *any* desired signal the minimum mean-square error will decrease if we allow delay in the processing. The mean-square error for infinite delay provides a lower bound on the mean-square error for any finite delay and is frequently called the *irreducible error*. A more interesting quantity in some cases is the normalized error. We define the normalized error as

$$\xi_{Pn}^\alpha \triangleq \frac{\xi_P^\alpha}{K_d(0)} \quad (8.133)$$

or

$$\xi_{Pn}^\alpha = 1 - \frac{1}{K_d(0)} \int_\alpha^\infty \phi^2(u) du. \quad (8.134)$$

We may now apply our results to Example 8.3.

Example 8.4 (continuation of Example 8.3). For our example

$$\xi_{Pn}^{\alpha} = \begin{cases} 1 - \frac{8P}{N_0} \frac{1}{(1 + \sqrt{1 + \Lambda})^2} \left(\int_{\alpha}^0 dt e^{+2k\sqrt{1+\Lambda}t} + \int_0^{\infty} e^{-2kt} dt \right), & \alpha \leq 0, \\ 1 - \frac{8P}{N_0} \frac{1}{(1 + \sqrt{1 + \Lambda})^2} \int_{-\alpha}^{\infty} e^{-2kt} dt, & \alpha \geq 0. \end{cases} \quad (8.135)$$

Evaluating the integrals, we have

$$\xi_{Pn}^{\alpha} = \frac{1}{\sqrt{1 + \Lambda}} + \frac{\Lambda e^{+2k\sqrt{1+\Lambda}\alpha}}{(1 + \sqrt{1 + \Lambda})^2 \sqrt{1 + \Lambda}}, \quad \alpha \leq 0 \quad (8.136)$$

$$\xi_{Pn}^0 = \frac{2}{1 + \sqrt{1 + \Lambda}}, \quad (8.137)$$

and

$$\xi_{Pn}^{\alpha} = \frac{2}{(1 + \sqrt{1 + \Lambda})} + \frac{\Lambda [1 - e^{-2k\alpha}]}{(1 + \sqrt{1 + \Lambda})^2}, \quad \alpha \geq 0. \quad (8.138)$$

The two limiting cases for (8.136) and (8.138) are $\alpha = -\infty$ and $\alpha = \infty$, respectively.

$$\xi_{Pn}^{-\infty} = \frac{1}{\sqrt{1 + \Lambda}}, \quad (8.139)$$

$$\xi_{Pn}^{\infty} = 1. \quad (8.140)$$

A plot of ξ_{Pn}^{α} versus $(k\alpha)$ is shown in Figure 8.15. Physically, the quantity $k\alpha$ is related to the reciprocal of the message bandwidth. If we define

$$\tau_c = \frac{1}{k}, \quad (8.141)$$

the units on the horizontal axis are α/τ_c , which corresponds to the delay measured in correlation times. We see that the error for a delay of one time constant is approximately the infinite delay error. Note that the error is not a symmetric function of α . ■

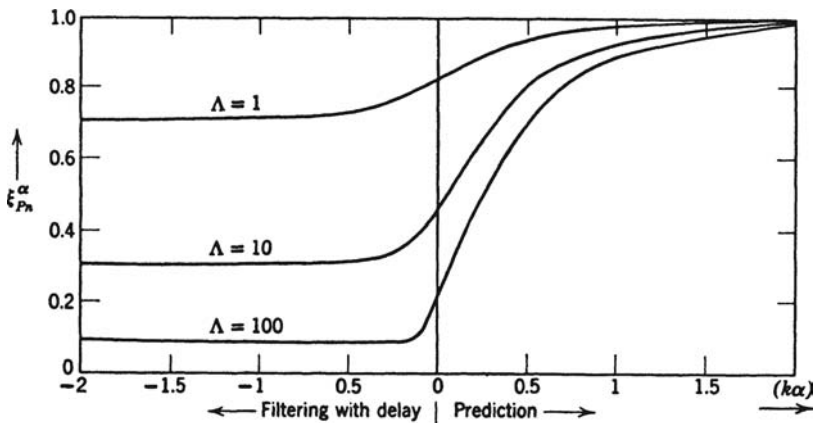


Figure 8.15: Effect of time-shift on filtering error.

Before summarizing our discussion of realizable filters, we discuss the related problem of unrealizable filters.

8.2.3 Unrealizable Filters

Instead of requiring the processor to be realizable, let us consider an optimum *unrealizable* system. This corresponds to letting $T_f > t$. In other words, we use the input $r(u)$ at times *later* than t to determine the estimate at t .

For the case in which $T_f > t$, we can modify (8.76) to obtain

$$K_{dr}(\tau) = \int_{t-T_f}^{\infty} h_o(t, t-v) K_r(\tau-v) dv, \quad t - T_f < \tau < \infty. \quad (8.142)$$

In this case $h_o(t, t-v)$ is nonzero for all $v \geq t - T_f$. Because this includes values of v less than zero, the filter will be unrealizable. The case of most interest to us is the one in which $T_f = \infty$. Then (8.142) becomes

$$K_{dr}(\tau) = \int_{-\infty}^{\infty} h_{ou}(v) K_r(\tau-v) dv, \quad -\infty < \tau < \infty. \quad (8.143)$$

We add the subscript u to emphasize that the filter is unrealizable. Because the equation is valid for all τ , we may solve by transforming

$$H_{ou}(j\omega) = \frac{S_{dr}(j\omega)}{S_r(\omega)}. \quad (8.144)$$

The mean-square error is

$$\xi_u = K_d(0) - \int_{-\infty}^{\infty} h_{ou}(\tau) K_{dr}(\tau) d\tau. \quad (8.145)$$

Note that ξ_u is a mean-square *point* estimation error. By Parseval's Theorem,

$$\xi_u = \frac{1}{2\pi} \int_{-\infty}^{\infty} [S_d(\omega) - H_{ou}(j\omega) S_{dr}^*(j\omega)] d\omega. \quad (8.146)$$

Substituting (8.144) into (8.146), we obtain

$$\xi_u = \int_{-\infty}^{\infty} \frac{S_d(\omega) S_r(\omega) - |S_{dr}(j\omega)|^2}{S_r(\omega)} \frac{d\omega}{2\pi}. \quad (8.147)$$

For the special case in which

$$\begin{aligned} d(t) &= s(t), \\ r(t) &= s(t) + n(t), \end{aligned} \quad (8.148)$$

and the message and noise are uncorrelated, (8.147) reduces to

$$\boxed{\xi_u = \int_{-\infty}^{\infty} \frac{S_n(\omega)S_s(\omega)}{S_s(\omega) + S_n(\omega)} \frac{d\omega}{2\pi}} \quad (8.149)$$

In Example 8.3, the noise is white. Therefore,

$$H_{ou}(j\omega) = \frac{\sqrt{P}S_s(\omega)}{S_r(\omega)} \quad (8.150)$$

and

$$\xi_u = \frac{N_0}{2} \int_{-\infty}^{\infty} H_{ou}(j\omega) \frac{d\omega}{2\pi} = \frac{N_0}{2} \int_{-\infty}^{\infty} \frac{\sqrt{P}S_s(\omega)}{S_r(\omega)} \frac{d\omega}{2\pi}. \quad (8.151)$$

We now return to the general case. It is easy to demonstrate that the expression in (8.146) is also equal to

$$\xi_u = K_d(0) - \int_{-\infty}^{\infty} \phi^2(t) dt. \quad (8.152)$$

Comparing (8.152) with (8.132), we see that the effect of using an unrealizable filter is the same as allowing an infinite delay in the desired signal. This result is intuitively logical. In an unrealizable filter we allow ourselves (fictitiously, of course) to use the entire past and future of the input and produce the desired signal at the present time. A practical way to approximate this processing is to wait until more of the future input comes in and produce the desired output at a later time. In many, if not most, communications problems it is the unrealizable error that is a fundamental system limitation.

The essential points to remember when discussing unrealizable filters are the following:

1. The mean-square error using an unrealizable linear filter ($T_f = \infty$) provides a lower bound on the mean-square error for any realizable linear filter. It corresponds to the *irreducible* (or infinite delay) error. The computation of ξ_u (8.149) is usually easier than the computation of ξ_P (8.122) or (8.128). Therefore, it is a logical preliminary calculation even if we are interested only in the realizable filtering problem.
2. We can build a realizable filter whose performance approaches the performance of the unrealizable filter by allowing delay in the output. We can obtain a mean-square error that is arbitrarily close to the irreducible error by increasing this delay. From the practical standpoint a delay of several times the reciprocal of the effective bandwidth of $[S_s(\omega) + S_n(\omega)]$ will usually result in a mean-square error close to the irreducible error.

We now return to the realizable filtering problem. In Sections 8.2.1 and 8.2.2, we devised an algorithm that gave us a constructive method for finding the optimum realizable filter and the resulting mean-square error. In other words, given the necessary information, we can always (conceptually, at least) proceed through a specified procedure and obtain the optimum filter and resulting performance. In practice, however, the algebraic complexity

has caused most engineers studying optimum filters to use the one-pole spectrum as the canonic message spectrum. The lack of a closed-form mean-square error expression that did not require a spectrum factorization made it essentially impossible to study the effects of different message spectra.

In the next section, we discuss a special class of linear estimation problems and develop a *closed-form* expression for the minimum mean-square error.

8.2.4 Closed-Form Error Expressions

In this section, we shall derive some useful closed-form results for a special class of optimum linear filtering problems. The case of interest is when

$$r(u) = s(u) + n(u), \quad -\infty < u \leq t. \quad (8.153)$$

In other words, the received signal consists of the message plus additive noise. The desired signal $d(t)$ is the message $s(t)$. We assume that the noise and message are uncorrelated. The message spectrum is rational with a finite variance. Our goal is to find an expression for the error that does not require spectrum factorization. The major results in this section were obtained originally by Yovits and Jackson [YJ55]. It is convenient to consider white and nonwhite noise separately.

Errors in the Presence of White Noise. We assume that $n(t)$ is white with spectral height $N_0/2$. Although the result was first obtained by Yovits and Jackson, appreciably simpler proofs have been given by Viterbi and Cahn [VC64] and Snyder [Sny65]. We follow a combination of these proofs. From (8.153)⁴

$$S_r(\omega) = S_s(\omega) + \frac{N_0}{2}, \quad (8.154)$$

and

$$G^+(j\omega) = \left[S_s(j\omega) + \frac{N_0}{2} \right]^+. \quad (8.155)$$

From (8.98)

$$H_o(j\omega) = \frac{1}{[S_s(\omega) + N_0/2]^+} \left\{ \frac{S_s(\omega)}{[S_s(\omega) + N_0/2]^-} \right\}_+ \quad (8.156)$$

or

$$H_o(j\omega) = \frac{1}{[S_s(\omega) + N_0/2]^+} \left\{ \frac{S_s(\omega) + N_0/2}{[S_s(\omega) + N_0/2]^-} - \frac{N_0/2}{[S_s(\omega) + N_0/2]^-} \right\}_+. \quad (8.157)$$

⁴To avoid a double superscript we introduce the notation

$$G^-(j\omega) = [G^+(j\omega)]^*.$$

Recall that conjugation in the frequency domain corresponds to reversal in the time domain. The time function corresponding to $G^+(j\omega)$ is zero for negative time. Therefore, the time function corresponding to $G^-(j\omega)$ is zero for positive time.

Now, the first term in the bracket is just $[S_s(\omega) + N_0/2]^+$, which is realizable. Because the realizable part operator is linear, the first term comes out of the bracket without modification. Therefore

$$H_o(j\omega) = 1 - \frac{1}{[S_s(\omega) + N_0/2]^+} \left\{ \frac{N_0/2}{[S_s(\omega) + N_0/2]^-} \right\}_+. \quad (8.158)$$

We take $\sqrt{N_0/2}$ out of the brace and put the remaining $\sqrt{N_0/2}$ inside the $[\cdot]^-$. The operation $[\cdot]^-$ is a factoring operation so we obtain $N_0/2$ inside.

$$H_o(j\omega) = 1 - \frac{\sqrt{N_0/2}}{[S_s(\omega) + N_0/2]^+} \left\{ \frac{1}{\left[\frac{S_s(\omega) + N_0/2}{N_0/2} \right]^-} \right\}_+. \quad (8.159)$$

The next step is to prove that the realizable part of the term in the brace equals one.

Proof. Let $S_s(\omega)$ be a rational spectrum. Thus,

$$S_s(\omega) = \frac{N(\omega^2)}{D(\omega^2)}, \quad (8.160)$$

where the denominator is a polynomial in ω^2 whose order is at least one higher than the numerator polynomial. Then

$$\frac{S_s(\omega) + N_0/2}{N_0/2} = \frac{N(\omega^2) + (N_0/2)D(\omega^2)}{(N_0/2)D(\omega^2)} \quad (8.161)$$

$$= \frac{D(\omega^2) + (2/N_0)N(\omega^2)}{D(\omega^2)} \quad (8.162)$$

$$= \prod_{i=1}^n \frac{\omega^2 + \alpha_i^2}{\omega^2 + \beta_i^2}. \quad (8.163)$$

Observe that there is no additional multiplier because the highest order term in the numerator and denominator are identical.

The α_i and β_i may always be chosen so that their real parts are positive. If any of the α_i or β_i are complex, the conjugate is also present. Inverting both sides of (8.163) and factoring the result, we have

$$\left\{ \left[\frac{S_s(\omega) + N_0/2}{N_0/2} \right]^- \right\}^{-1} = \prod_{i=1}^n \frac{(-j\omega + \beta_i)}{(-j\omega + \alpha_i)} \quad (8.164)$$

$$= \prod_{i=1}^n \left[1 + \frac{\beta_i - \alpha_i}{(-j\omega + \alpha_i)} \right]. \quad (8.165)$$

The transform of all terms in the product except the unity term will be zero for positive time (their poles are in the right-half s -plane). Multiplying the terms together corresponds to convolving their transforms. Convolving functions that are zero for positive time always

gives functions that are zero for positive time. Therefore, only the unity term remains when we take the realizable part of (8.165). This is the desired result. Therefore,

$$\boxed{H_o(j\omega) = 1 - \frac{\sqrt{N_0/2}}{[S_s(j\omega) + N_0/2]^+}.} \quad (8.166)$$

The next step is to derive an expression for the error. From Section 8.2.1 we know that

$$\xi_P = \frac{N_0}{2} \lim_{\tau \rightarrow t^-} h_o(t, \tau) = \frac{N_0}{2} \lim_{\epsilon \rightarrow 0^+} h_o(\epsilon) \triangleq \frac{N_0}{2} h_o(0^+) \quad (8.167)$$

for the time-invariant case. We also know that

$$\int_{-\infty}^{\infty} H_o(j\omega) \frac{d\omega}{2\pi} = \frac{h_o(0^+) + h_o(0^-)}{2} = \frac{h_o(0^+)}{2}, \quad (8.168)$$

because $h_o(\tau)$ is realizable. Combining (8.167) and (8.168), we obtain

$$\xi_P = N_0 \int_{-\infty}^{\infty} H_o(j\omega) \frac{d\omega}{2\pi}. \quad (8.169)$$

Using (8.166) in (8.159), we have

$$\xi_P = N_0 \int_{-\infty}^{\infty} \left(1 - \left\{ \left[\frac{S_s(\omega) + N_0/2}{N_0/2} \right]^+ \right\}^{-1} \right) \frac{d\omega}{2\pi}. \quad (8.170)$$

Using the conjugate of (8.164) in (8.170), we obtain

$$\xi_P = N_0 \int_{-\infty}^{\infty} \left[1 - \prod_{i=1}^n \frac{(j\omega + \beta_i)}{(j\omega + \alpha_i)} \right] \frac{d\omega}{2\pi} \quad (8.171)$$

$$= N_0 \int_{-\infty}^{\infty} \left[1 - \prod_{i=1}^n \left(1 + \frac{\beta_i - \alpha_i}{j\omega + \alpha_i} \right) \right] \frac{d\omega}{2\pi}. \quad (8.172)$$

Expanding the product, we have

$$\begin{aligned} \xi_P &= N_0 \int_{-\infty}^{\infty} \left\{ 1 - \left[1 + \sum_{i=1}^n \frac{\beta_i - \alpha_i}{j\omega + \alpha_i} + \sum_{i=1}^n \sum_{j=1}^n \frac{\gamma_{ij}}{(j\omega + \alpha_i)(j\omega + \alpha_j)} + \sum_{i=1}^n \sum_{j=1}^n \sum_{k=1}^n \dots \right] \right\} \frac{d\omega}{2\pi} \end{aligned} \quad (8.173)$$

$$\begin{aligned} &= N_0 \int_{-\infty}^{\infty} \sum_{i=1}^n \frac{(\alpha_i - \beta_i)}{(j\omega + \alpha_i)} \frac{d\omega}{2\pi} - N_0 \int_{-\infty}^{\infty} \left[\sum_{i=1}^n \sum_{j=1}^n \frac{\gamma_{ij}}{(j\omega + \alpha_i)(j\omega + \alpha_j)} + \sum_{i=1}^n \sum_{j=1}^n \sum_{k=1}^n \dots \right] \frac{d\omega}{2\pi}. \end{aligned} \quad (8.174)$$

The integral in the first term is just one half the sum of the residues (this result can be verified easily). We now show that the second term is zero. Because the integrand in the second term is analytical in the right half of the s -plane, the integral $[-\infty, \infty]$ equals

the integral around a semicircle with infinite radius. All terms in the brackets, however, are at least of order $|s|^{-2}$ for large $|s|$. Therefore, the integral on the semicircle is zero, which implies that the second term is zero. Therefore,

$$\xi_P = \frac{N_0}{2} \sum_{i=1}^n (\alpha_i - \beta_i). \quad (8.175)$$

The last step is to find a closed-form expression for the sum of the residues. This follows by observing that

$$\int_{-\infty}^{\infty} \ln \left(\frac{\omega^2 + \alpha_i^2}{\omega^2 + \beta_i^2} \right) \frac{d\omega}{2\pi} = (\alpha_i - \beta_i). \quad (8.176)$$

(To verify this equation integrate the left-hand side by parts with $u = \ln[(\omega^2 + \alpha_i^2)/(\omega^2 + \beta_i^2)]$ and $dv = d\omega/2\pi$.)

Comparing (8.175), (8.176), and (8.163), we have

$$\xi_P = \frac{N_0}{2} \int_{-\infty}^{\infty} \ln \left[1 + \frac{S_s(\omega)}{N_0/2} \right] \frac{d\omega}{2\pi}, \quad (8.177)$$

which is the desired result. Both forms of the error expressions (8.175) and (8.177) are useful. The first form is often the most convenient way to actually evaluate the error. The second form is useful when we want to find the $S_s(\omega)$ that minimizes ξ_P subject to certain constraints. In the problems, we will evaluate the mean-square error for various signals.

The result in (8.166) has another important interpretation (e.g. [Sny65]). Writing (8.166) as

$$1 - H_o(jw) = \frac{\sqrt{N_0/2}}{[S_s(w) + N_0/2]^+} \quad (8.178)$$

shows that, if we pass $r(t)$ into a filter whose transfer function is $1 - H_o(jw)$, then the output is a white noise process with unity spectrum height. This is shown in Figure 8.16. We added an r to the subscript to emphasize that the filter is realizable. This is an important concept that we will revisit later.

In the next section, we study state-variable models and the Kalman filter. We should note that any rational spectrum process model that we can solve by the Wiener filter can also be solved by the Kalman filter.

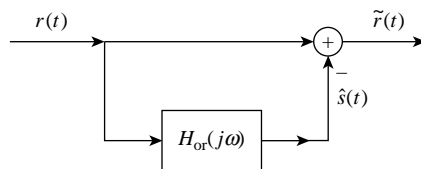


Figure 8.16: Realizable whitening filter.

8.3 GAUSSIAN-MARKOV PROCESSES: KALMAN FILTER

Once again the basic problem of interest is to operate on a received waveform $r(u)$, $T_i \leq u \leq t$, to obtain a minimum mean-square error *point* estimate of some desired waveform $d(t)$. In a simple scalar case the received waveform is

$$r(u) = c(u)a(u) + n(u), \quad T_i \leq u \leq t, \quad (8.179)$$

where $a(t)$ and $n(t)$ are zero-mean random processes with covariance functions $K_a(t, u)$ and $(N_0/2)\delta(t - u)$, respectively, and $d(t) = a(t)$. The problem is much more general than this example, but the above case is adequate for motivation purposes.

The optimum processor consists of a linear filter that satisfies the equation

$$K_{ar}(t, \sigma) = \int_{T_i}^t h_o(t, \tau) K_r(\tau, \sigma) d\tau, \quad T_i < \sigma < t. \quad (8.180)$$

In Section 8.2, we discussed a special case in which $T_i = -\infty$ and the processes were stationary. As part of the solution procedure we found a function $G^+(j\omega)$. We observed that if we passed white noise through a linear system whose transfer function was $G^+(j\omega)$ the output process had a spectrum $S_r(\omega)$.

For the finite interval it is necessary to solve (8.180). In Chapter 6, we dealt with similar equations and observed that the conversion of the integral equation to a differential equation with a set of boundary conditions is a useful procedure.

We also observed in several examples that when the message is a scalar Markov process [recall that for a stationary Gaussian process this implies that the covariance had the form $A \exp(-B|t - u|)$] the results were simpler. These observations (plus a great deal of hindsight) lead us to make the following conjectures about an alternate approach to the problem that might be fruitful:

1. Instead of describing the processes of interest in terms of their covariance functions, characterize them in terms of the linear (possibly time-varying) systems that would generate them when driven with white noise.⁵
2. Instead of describing the linear system that generates the message in terms of a time-varying impulse response, describe it in terms of a differential equation whose solution is the signal. The most convenient description will turn out to be a first-order vector differential equation.
3. Instead of specifying the optimum estimate as the output of a linear system that is specified by an integral equation, specify the optimum estimate as the solution to a differential equation whose coefficients are determined by the statistics of the processes. An obvious advantage of this method of specification is that even if we cannot solve the differential equation analytically, we can always solve it easily with an analog or digital computer.

⁵The advantages to be accrued by this characterization were first recognized and exploited by Dolph and Woodbury in 1948 [DW48].

In this section, we make these observations more precise and investigate the results. First, we discuss briefly the state-variable representation of linear, time-varying systems and the generation of random processes. Second, we derive a differential equation that is satisfied by the optimum estimate. Finally, we discuss some applications of the technique.

The discrete-time Kalman filter is due to Kalman [Kal60] and we will discuss it in Section 9.3. The continuous-time Kalman and Bucy filter is derived in [KB61, Kal63]. A recursive estimation algorithm was published earlier by Swerling [Swe59]. Another early paper by Ho and Lee [HL64] approaches the problem from a Bayesian viewpoint. Early books and papers that discuss the Kalman filter include Van Trees [Van68, Van01a], Jazwinski [Jaz70], Gelb [Gel74], Anderson and Moore [AM79], Aoki [Aok67], Bryson and Ho [BH69], Kailath [Kai80], Meditch [Med69], Sage and Melsa [SM71], Lawson and Hanson [LH74], Lee [Lee64], and Maybeck [May79]. More recent books include Grewal and Andrews [GA93], Kay [Kay93], Kailath et al. [KSH00], Hays [Hay96], Moon and Stirling [MS00], and Manolakis et al. [MIK00].

The bibliography by Mendel and Gretesbing [MG71] and the survey paper by Kailath [Kai74] provide other references to early work. Sorensen provides a comprehensive discussion of the history of recursive algorithms from Gauss [Gau63] to Kalman in his paper [Sor70] and his reprint book [Sor85]. The second section of [Sor85] reproduces the March 1983 issue of the *IEEE Transactions on Automatic Control* that was a special issue on applications. Recent books that discuss Kalman filters include Mendel [Men95], Grewal and Andrews [GA93], Bar-Shalom et al. [BSLK01], Levy [Lev08], and Kailath et al. [KSH00].

8.3.1 Differential Equation Representation of Linear Systems and Random Process Generation⁶

In our previous discussions, we have characterized linear systems by an impulse response $h(t, u)$ [or simply $h(\tau)$ in the time-invariant case]. Implicit in this description was the assumption that the input was known over the interval $-\infty < t < \infty$. Frequently this method of description is the most convenient. Alternately, we can represent many systems in terms of a differential equation relating its input and output. Indeed, this is the method by which one is usually introduced to linear system theory. The impulse response $h(t, u)$ is just the solution to the differential equation when the input is an impulse at time u .

Three ideas of importance in the differential equation representation are presented in the context of a simple example.

The first idea of importance to us is the idea of initial conditions and state variables in dynamic systems. If we want to find the output over some interval $t_0 \leq t < t_1$, we must know not only the input over this interval but also a certain number of initial conditions that must be adequate to describe how any past inputs ($t < t_0$) affect the output of the system in the interval $t \geq t_0$.

We define the *state* of the system as the minimal amount of information about the effects of past inputs necessary to describe completely the output for $t \geq t_0$. The variables that

⁶In this section, we develop the background needed to solve the problems of immediate interest. A number of books cover the subject in detail (e.g. [ZD63, Gup66, AF66, DRC65, SF65]). Our discussion is self-contained, but some results are stated without proof.

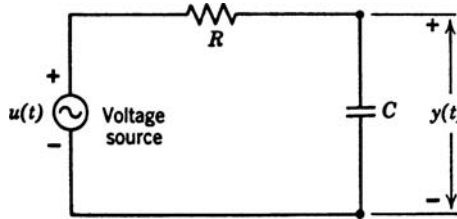


Figure 8.17: An RC circuit.

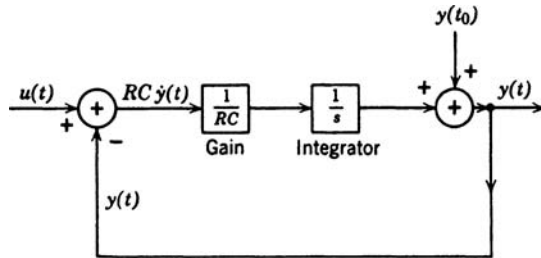


Figure 8.18: An analog computer realization.

contain this information are the *state variables*⁷ There must be enough states that every input–output pair can be accounted for. When stated with more mathematical precision, these assumptions imply that, given the state of the system at t_0 and the input from t_0 to t_1 , we can find both the *output* and the *state* at t_1 . Note that our definition implies that the dynamic systems of interest are deterministic and realizable (future inputs cannot affect the output). If the state can be described by a finite-dimensional vector, we refer to the system as a finite-dimensional dynamic system. In this section, we restrict our attention to finite-dimensional systems.

We can illustrate this with a simple example:

Example 8.5. Consider the RC circuit shown in Figure 8.17. The output voltage $y(t)$ is related to the input voltage $u(t)$ by the differential equation

$$(RC)\dot{y}(t) + y(t) = u(t). \quad (8.181)$$

To find the output $y(t)$ in the interval $t \geq t_0$ we need to know $u(t)$, $t \geq t_0$, and the voltage across the capacitor at t_0 . Thus, a suitable state variable is $y(t)$. ■

The second idea is realizing (or simulating) a differential equation by using an analog computer. For our purposes we can visualize an analog computer as a system consisting of integrators, time-varying gains, adders, and nonlinear no-memory devices joined together to produce the desired input–output relation.

For the simple RC circuit example an analog computer realization is shown in Figure 8.18. The initial condition $y(t_0)$ appears as a bias at the output of the integrator. This biased integrator output is the state variable of the system.

⁷Zadeh and DeSoer [ZD63].

The third idea is that of random process generation. If $u(t)$ is a random process or $y(t_0)$ is a random variable (or both), then $y(t)$ is a random process. Using the system described by (8.181), we can generate both nonstationary and stationary processes. As an example of a nonstationary process, let $y(t_0)$ be $N(0, \sigma_0)$, $u(t)$ be zero, and $k = 1/RC$. Then $y(t)$ is a zero-mean Gaussian random process with covariance function

$$K_y(t, u) = \sigma_0^2 e^{-k(t+u-2t_0)}, \quad t, u \geq t_0. \quad (8.182)$$

As an example of a stationary process, consider the case in which $u(t)$ is a sample function from a white noise process of spectral height q . If the input starts at $-\infty$ (i.e., $t_0 = -\infty$) and $y(t_0) = 0$, the output is a stationary process with a spectrum

$$S_y(\omega) = \frac{2k\sigma_y^2}{\omega^2 + k^2}, \quad (8.183)$$

where

$$q = 2\sigma_y^2/k. \quad (8.184)$$

We now explore these ideas in a more general context. Consider the system described by a differential equation of the form

$$y^{(n)}(t) + p_{n-1}y^{(n-1)}(t) + \cdots + p_0y(t) = b_0u(t), \quad (8.185)$$

where $y^{(n)}(t)$ denotes the n th derivative of $y(t)$. Recall that to specify the solution to an n th-order equation we need the values of $y(t), \dots, y^{(n-1)}(t)$ at t_0 . This observation will be the key to finding the state representation for this system. The first step in finding an analog computer realization is to generate the terms on the left-hand side of the equation. This is shown in Figure 8.19a. The next step is to interconnect these various quantities so that the differential equation is satisfied. The differential equation specifies the inputs to the summing point and gives the block diagram shown in Figure 8.19b. Finally, we include the initial conditions by allowing for a bias on the integrator outputs and obtain the realization shown in Figure 8.19c. The state variables are the biased integrator outputs.

It is frequently easier to work with a first-order vector differential equation than an n th-order scalar equation. For (8.185), the transformation is straightforward. Let

$$\begin{aligned} x_1(t) &= y(t) \\ x_2(t) &= \dot{y}(t) = \dot{x}_1(t) \\ &\vdots \\ x_n(t) &= y^{(n-1)}(t) = \dot{x}_{n-1}(t). \\ \dot{x}_n(t) &= y^{(n)}(t) = -\sum_{k=1}^n p_{k-1}y^{(k-1)}(t) + b_0u(t) = -\sum_{k=1}^n p_{k-1}x_k(t) + b_0u(t). \end{aligned} \quad (8.186)$$

Denoting the set of $x_i(t)$ by a column matrix, we see that the following first-order n -dimensional vector equation is equivalent to the n th-order scalar equation.

$$\frac{d\mathbf{x}(t)}{dt} \triangleq \dot{\mathbf{x}}(t) = \mathbf{F}\mathbf{x}(t) + \mathbf{G}u(t), \quad (8.187)$$

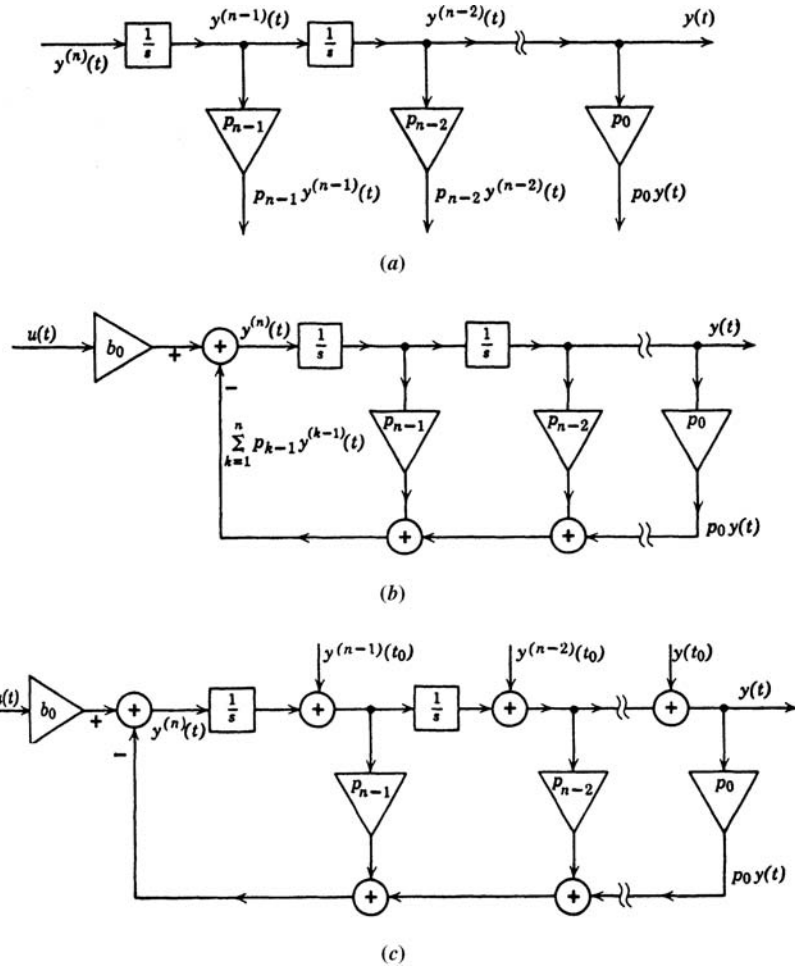


Figure 8.19: Analog computer realization.

where

$$\mathbf{F} = \begin{bmatrix} 0 & 1 & & & & \\ 0 & & 1 & 0 & & \\ 0 & & & 1 & & \\ \vdots & & 0 & & \ddots & \\ 0 & & & & & 1 \\ -p_0 & -p_1 & -p_2 & -p_3 & \cdots & -p_{n-1} \end{bmatrix} \quad (8.188)$$

and

$$\mathbf{G} = \begin{bmatrix} 0 \\ 0 \\ \vdots \\ 0 \\ b_0 \end{bmatrix}. \quad (8.189)$$

The vector $\mathbf{x}(t)$ is called the *state vector* for this linear system and (8.187) is called the *state equation* of the system. Note that the state vector $\mathbf{x}(t)$ we selected is not the only choice. Any nonsingular linear transformation of $\mathbf{x}(t)$ gives another state vector. The output $y(t)$ is related to the state vector by the equation

$$y(t) = \mathbf{C}\mathbf{x}(t), \quad (8.190)$$

where \mathbf{C} is a $1 \times n$ matrix

$$\mathbf{C} = [1 \ 0 \ 0 \ 0 \ \cdots \ 0]. \quad (8.191)$$

Equation (8.190) is called the *output equation* of the system. The two equations (8.187) and (8.190) completely characterize the system.

Just as in the first example we can generate both nonstationary and stationary random processes using the system described by (8.187) and (8.190). For stationary processes it is clear (8.185) that we can generate any process with a rational spectrum in the form of

$$S_y(\omega) = \frac{k}{d_{2n}\omega^{2n} + d_{2n-2}\omega^{2n-2} + \cdots + d_0} \quad (8.192)$$

by letting $u(t)$ be a white noise process and $t_0 = -\infty$. In this case the state vector $\mathbf{x}(t)$ is a sample function from a vector random process and $y(t)$ is one component of this process.

The next more general differential equation is

$$y^{(n)}(t) + p_{n-1}y^{(n-1)}(t) + \cdots + p_0y(t) = b_{n-1}u^{(n-1)}(t) + \cdots + b_0u(t). \quad (8.193)$$

The first step is to find an analog computer-type realization that corresponds to this differential equation. We illustrate one possible technique by looking at a simple example.

Example 8.6. Consider the case in which $n = 2$ and the initial conditions are zero. Then (8.193) is

$$\ddot{y}(t) + p_1\dot{y}(t) + p_0y(t) = b_1\dot{u}(t) + b_0u(t). \quad (8.194)$$

Our first observation is that we want to avoid actually differentiating $u(t)$ because in many cases of interest it is a white noise process. Comparing the order of the highest derivatives on the two sides of (8.194), we see that this is possible. An easy approach is to assume that $\dot{u}(t)$ exists as part of the input to the first integrator in Figure 8.20 and examine the consequences. To do this we rearrange terms as shown in (8.195):

$$[\ddot{y}(t) - b_1\dot{u}(t)] + p_1\dot{y}(t) + p_0y(t) = b_0u(t). \quad (8.195)$$

The result is shown in Figure 8.20. Defining the state variables as the integrator outputs, we obtain

$$x_1(t) = y(t) \quad (8.196)$$

and

$$x_2(t) = \dot{y}(t) - b_1u(t). \quad (8.197)$$

Using (8.195) and (8.196), we have

$$\begin{aligned} \dot{x}_1(t) &= x_2(t) + b_1u(t), \\ \dot{x}_2(t) &= -p_0x_1(t) - p_1(x_2(t) + b_1u(t)) + b_0u(t) \\ &= -p_0x_1(t) - p_1x_2(t) + (b_0 - b_1p_1)u(t). \end{aligned} \quad (8.198)$$

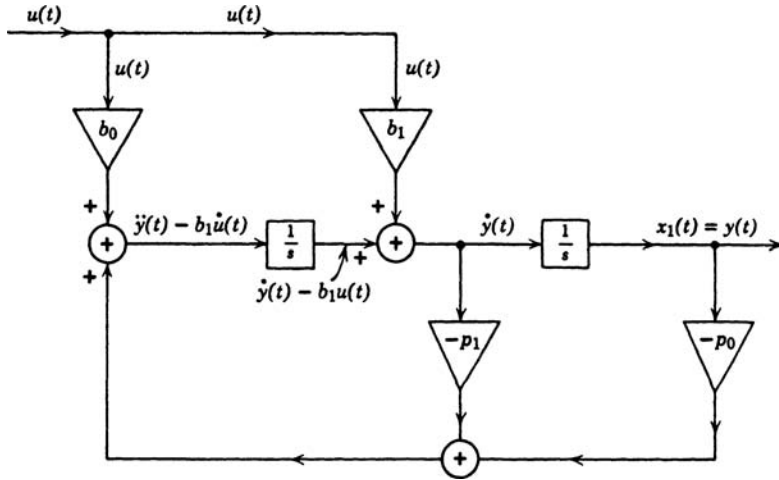


Figure 8.20: Analog realization.

We can write (8.198) as a vector-state equation by defining

$$\mathbf{F} = \begin{bmatrix} 0 & 1 \\ -p_0 & -p_1 \end{bmatrix} \quad (8.199)$$

and

$$\mathbf{G} = \begin{bmatrix} b_1 \\ b_0 - p_1 b_1 \end{bmatrix}. \quad (8.200)$$

Then

$$\mathbf{x}(t) = \mathbf{F}\mathbf{x}(t) + \mathbf{G}u(t). \quad (8.201)$$

The output equation is

$$y(t) = [1 \ 0]\mathbf{x}(t) \triangleq \mathbf{C}\mathbf{x}(t). \quad (8.202)$$

Equations (8.201) and (8.202) plus the initial condition $\mathbf{x}(t_0) = \mathbf{0}$ characterize the system. ■

It is straightforward to extend this particular technique to the n th order (see Problem 8.3.1). We refer to it as canonical realization No. 1. Our choice of state variables was somewhat arbitrary. To demonstrate this, we reconsider Example 8.6 and develop a different state representation.

Example 8.7. Once again

$$\ddot{y}(t) + p_1\dot{y}(t) + p_0y(t) = b_1\dot{u}(t) + b_0u(t). \quad (8.203)$$

As a first step we draw the two integrators and the two paths caused by b_1 and b_0 . This partial system is shown in Figure 8.21a. We now want to introduce feedback paths and identify state variables in such a way that the elements in \mathbf{F} and \mathbf{G} will be one of the coefficients in the original differential equation, unity, or zero. Looking at Figure 8.21a, we see that an easy way to do this is to feed back a

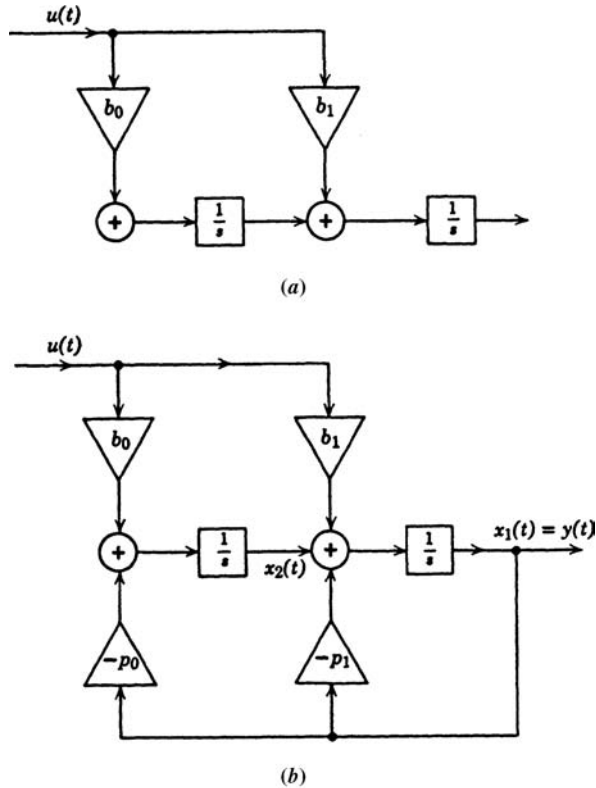


Figure 8.21: Analog realization of (8.204)–(8.206).

weighted version of $x_1(t)(= y(t))$ into each summing point as shown in Figure 8.21b. The equations for the state variables are

$$x_1(t) = y(t), \quad (8.204)$$

$$\dot{x}_1(t) = x_2(t) - p_1 y(t) + b_1 u(t), \quad (8.205)$$

$$\dot{x}_2(t) = -p_0 y(t) + b_0 u(t). \quad (8.206)$$

The **F** matrix is

$$\mathbf{F} = \begin{bmatrix} -p_1 & +1 \\ -p_0 & 0 \end{bmatrix} \quad (8.207)$$

and the **G** matrix is

$$\mathbf{G} = \begin{bmatrix} b_1 \\ b_0 \end{bmatrix}. \quad (8.208)$$

We see that the system has the desired property. ■

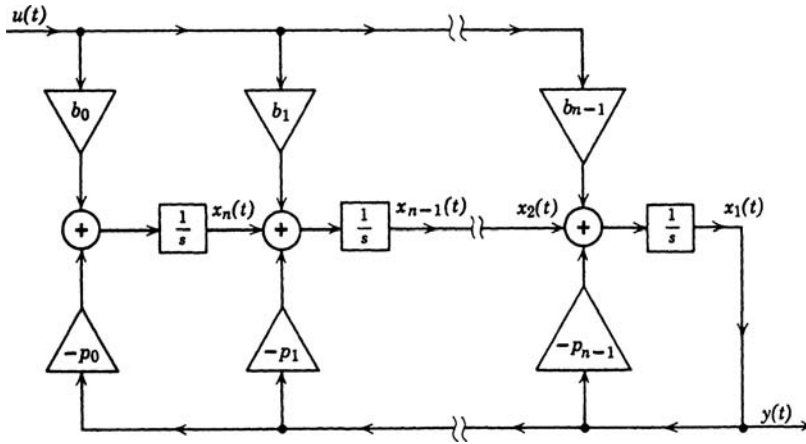


Figure 8.22: Canonic realization No. 2: state variables.

The extension to the original n th-order differential equation is straightforward. The resulting realization is shown in Figure 8.22. The equations for the state variables are

$$\begin{aligned} x_1(t) &= y(t) \\ x_2(t) &= \dot{x}_1(t) + p_{n-1}y(t) - b_{n-1}u(t) \\ &\vdots \\ x_n(t) &= \dot{x}_{n-1}(t) + p_1y(t) - b_1u(t) \\ \dot{x}_n(t) &= -p_0y(t) + b_0u(t). \end{aligned} \tag{8.209}$$

The matrix for the vector differential equation is

$$\mathbf{F} = \begin{bmatrix} -p_{n-1} & 1 & 0 & & & \\ -p_{n-2} & 0 & 1 & & & 0 \\ & & & 1 & & \\ \vdots & & & & \ddots & \\ & & & 0 & & \\ -p_1 & 0 & \cdots & & & 1 \\ -p_0 & 0 & & & & 0 \end{bmatrix} \tag{8.210}$$

and

$$\mathbf{G} = [b_{n-1} \quad b_{n-2} \quad \cdots \quad b_0]^T. \tag{8.211}$$

We refer to this realization as canonical realization No. 2.

There is still a third useful realization to consider. The transfer function corresponding to (8.193) is

$$\frac{Y(s)}{X(s)} = \frac{b_{n-1}s^{n-1} + \cdots + b_0}{s^n + p_{n-1}s^{n-1} + \cdots + p_0} \triangleq H(s). \tag{8.212}$$

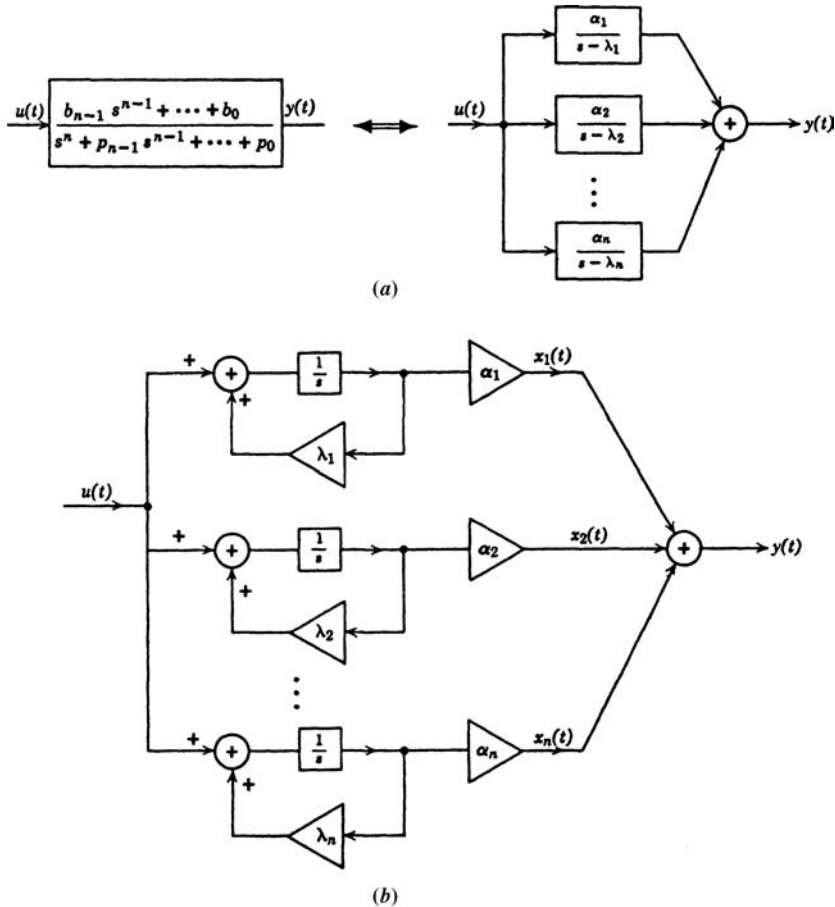


Figure 8.23: Canonic realization No. 3: (a) transfer function; (b) analog computer realization.

We can expand this equation in a partial fraction expansion

$$H(s) = \sum_{i=1}^n \frac{\alpha_i}{s - \lambda_i}, \quad (8.213)$$

where the λ_i are the roots of the denominator that are assumed to be distinct and the α_i are the corresponding residues. The system is shown in transform notation in Figure 8.23a. Clearly, we can identify each subsystem output as a state variable and realize the overall system as shown in Figure 8.23b. The \mathbf{F} matrix is diagonal.

$$\mathbf{F} = \begin{bmatrix} \lambda_1 & & & \\ & \lambda_2 & & 0 \\ & & \lambda_3 & \\ 0 & & & \ddots \\ & & & \lambda_n \end{bmatrix} \quad (8.214)$$

and the elements in the \mathbf{G} matrix are the residues

$$\mathbf{G} = \begin{bmatrix} \alpha_1 \\ \alpha_2 \\ \vdots \\ \alpha_n \end{bmatrix}. \quad (8.215)$$

Now the original output $y(t)$ is the sum of the state variables

$$y(t) = \sum_{i=1}^n x_i(t) = \mathbf{1}^T \mathbf{x}(t), \quad (8.216)$$

where

$$\mathbf{1}^T \triangleq [1 \ 1 \cdots 1]. \quad (8.217)$$

We refer to this realization as canonical realization No. 3. (The realization for repeated roots is derived in Problem 8.3.2.)

Canonical realization No. 3 requires a partial fraction expansion to find \mathbf{F} and \mathbf{G} . Observe that the state equation consists of n uncoupled first-order scalar equations

$$\dot{x}_i = \lambda_i x_i(t) + \alpha_i u(t), \quad i = 1, 2, \dots, n. \quad (8.218)$$

The solution of this set is appreciably simpler than the solution of the vector equation. On the other hand, finding the partial fraction expansion may require some calculation whereas canonical realizations No. 1 and No. 2 can be obtained by inspection.

We have now developed three different methods for realizing a system described by an n th-order constant coefficient differential equation. In each case the state vector was different. The \mathbf{F} matrices were different, but it is easy to verify that they all have the same eigenvalues. It is worthwhile to emphasize that even though we have labeled these realizations as canonical some other realization may be more desirable in a particular problem. Any nonsingular linear transformation of a state vector leads to a new state representation.

We now have the capability of generating *any* stationary random process with a rational spectrum and finite variance by exciting any of the three realizations with white noise. In addition, we can generate a wide class of nonstationary processes.

Up to this point we have seen how to represent linear time-invariant systems in terms of a state-variable representation and the associated vector-differential equation. We saw that this could correspond to a physical realization in the form of an analog computer, and we learned how we could generate a large class of random processes.

The next step is to extend our discussion to include time-varying systems and multiple input–multiple output systems.

For time-varying systems we, consider the vector equations

$$\begin{aligned} \frac{d\mathbf{x}(t)}{dt} &= \mathbf{F}(t)\mathbf{x}(t) + \mathbf{G}(t)\mathbf{u}(t) \\ y(t) &= \mathbf{C}(t)\mathbf{x}(t), \end{aligned} \quad (8.219)$$

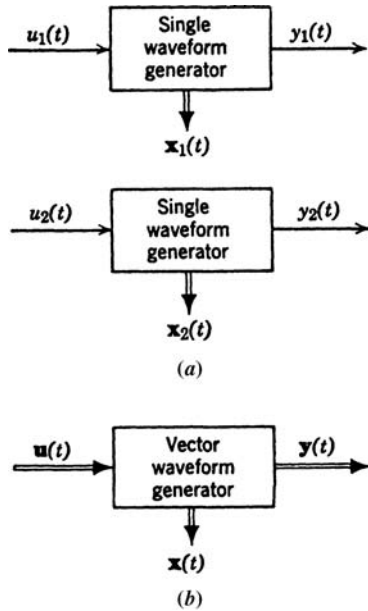


Figure 8.24: Generation of two messages.

as the basic representation.⁸ The matrices $\mathbf{F}(t)$, $\mathbf{G}(t)$, and $\mathbf{C}(t)$ may be functions of time. We can also use a white noise input

$$E [\mathbf{u}(t)\mathbf{u}^T(\tau)] = \mathbf{Q}(t)\delta(t - \tau), \quad (8.220)$$

we have the ability to generate nonstationary random processes. It is worthwhile to observe that a nonstationary process can result even when \mathbf{F} and \mathbf{G} are constant and $\mathbf{x}(t_0)$ is deterministic. The Wiener process, defined in Chapter 6, is a good example.

Example 8.8. Here, $\mathbf{F}(t) = 0$, $\mathbf{G}(t) = \sigma$, $\mathbf{C}(t) = 1$, and (8.220) becomes

$$\frac{dx(t)}{dt} = \sigma u(t). \quad (8.221)$$

Assuming that $x(0) = 0$, this gives the Wiener process. ■

Other specific examples of time-varying systems are discussed in later sections and in the problems.

The motivation for studying multiple input–multiple output systems follows directly from our discussions in earlier chapters. Consider the simple system in Figure 8.24a in

⁸The canonic realizations in Figures 8.20 and 8.22 may still be used. It is important to observe that they do not correspond to the same n th-order differential equation as in the time-invariant case. See Problem 8.3.13.

which we generate two outputs $y_1(t)$ and $y_2(t)$. We assume that the state representation of system 1 is

$$\begin{aligned}\dot{\mathbf{x}}_1(t) &= \mathbf{F}_1(t)\mathbf{x}_1(t) + \mathbf{G}_1(t)u_1(t), \\ y_1(t) &= \mathbf{C}_1(t)\mathbf{x}_1(t),\end{aligned}\quad (8.222)$$

where $\mathbf{x}_1(t)$ is an n -dimensional state vector. Similarly, the state representation of system 2 is

$$\begin{aligned}\dot{\mathbf{x}}_2(t) &= \mathbf{F}_2(t)\mathbf{x}_2(t) + \mathbf{G}_2(t)u_2(t), \\ y_2(t) &= \mathbf{C}_2(t)\mathbf{x}_2(t),\end{aligned}\quad (8.223)$$

where $\mathbf{x}_2(t)$ is an m -dimensional state vector. A more convenient way to describe these two systems is as a single vector system with an $(n+m)$ -dimensional state vector (Figure 8.24b).

$$\mathbf{x}(t) = \begin{bmatrix} \mathbf{x}_1(t) \\ \mathbf{x}_2(t) \end{bmatrix}, \quad (8.224)$$

$$\mathbf{F}(t) = \begin{bmatrix} \mathbf{F}_1(t) & \mathbf{0} \\ \mathbf{0} & \mathbf{F}_2(t) \end{bmatrix}, \quad (8.225)$$

$$\mathbf{G}(t) = \begin{bmatrix} \mathbf{G}_1(t) & \mathbf{0} \\ \mathbf{0} & \mathbf{G}_2(t) \end{bmatrix}, \quad (8.226)$$

$$\mathbf{u}(t) = \begin{bmatrix} u_1(t) \\ u_2(t) \end{bmatrix}, \quad (8.227)$$

$$\mathbf{C}(t) = \begin{bmatrix} \mathbf{C}_1(t) & \mathbf{0} \\ \mathbf{0} & \mathbf{C}_2(t) \end{bmatrix}, \quad (8.228)$$

and

$$\mathbf{y}(t) = \begin{bmatrix} y_1(t) \\ y_2(t) \end{bmatrix}. \quad (8.229)$$

We have considered several examples of different equation models to generate random processes. The general process generator model is shown in Figure 8.25. The driving function is a vector. We assume that the driving function is a white process with a matrix covariance function

$$E[\mathbf{u}(t)\mathbf{u}^T(\tau)] \triangleq \mathbf{Q}(t)\delta(t-\tau), \quad (8.230)$$

where $\mathbf{Q}(t)$ is a nonnegative definite matrix.

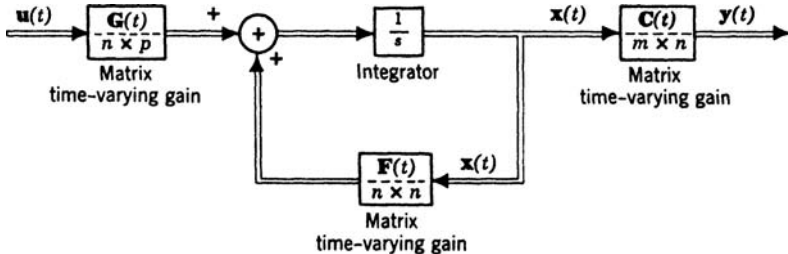


Figure 8.25: Message generation process.

It is passed through an $n \times p$ matrix. The output goes into the feedback system shown in Figure 8.25. The state vector of the system is $\mathbf{x}(t)$ and it can be described by the differential equation

$$\dot{\mathbf{x}}(t) = \mathbf{F}(t)\mathbf{x}(t) + \mathbf{G}(t)\mathbf{u}(t). \quad (8.231a)$$

The transmitted signal $\mathbf{y}(t)$ is an $m \times 1$ vector obtained by an $m \times n$ matrix operation on the state vector $\mathbf{x}(t)$

$$\mathbf{y}(t) = \mathbf{C}(t)\mathbf{x}(t). \quad (8.231b)$$

Observe that in general the initial conditions may be random variables. Then, to specify the second-moment characteristics we must know the covariance at the initial time

$$\mathbf{K}_{\mathbf{x}}(t_0, t_0) \triangleq E[\mathbf{x}(t_0)\mathbf{x}^T(t_0)] \quad (8.232a)$$

and the mean value $E[\mathbf{x}(t_0)]$.

The next step in our discussion is to consider the solution to (8.231a). We begin our discussion with the *homogeneous time-invariant* case. Then (8.231a) reduces to

$$\dot{\mathbf{x}}(t) = \mathbf{F}\mathbf{x}(t), \quad (8.232b)$$

with initial condition $\mathbf{x}(t_0)$. If $\mathbf{x}(t)$ and \mathbf{F} are scalars, the solution is familiar,

$$x(t) = e^{F(t-t_0)}x(t_0). \quad (8.233a)$$

For the vector case we can show that (e.g. [DRC65, SF65, CL55], or [Bel53])

$$\mathbf{x}(t) = e^{\mathbf{F}(t-t_0)}\mathbf{x}(t_0), \quad (8.233b)$$

where $e^{\mathbf{F}t}$ is defined by the infinite series

$$e^{\mathbf{F}t} \triangleq \mathbf{I} + \mathbf{F}t + \frac{\mathbf{F}^2 t^2}{2!} + \dots. \quad (8.233c)$$

The function $e^{\mathbf{F}(t-t_0)}$ is denoted by $\phi(t - t_0) \triangleq \phi(\tau)$. The function $\phi(t - t_0)$ is called the *state transition matrix* of the system. Two properties can easily be verified for the time-invariant case.

Property 10. The state transition matrix satisfies the equation

$$\frac{d\phi(t - t_0)}{dt} = \mathbf{F}\phi(t - t_0) \quad (8.234)$$

or

$$\frac{d\phi(\tau)}{d\tau} = \mathbf{F}\phi(\tau). \quad (8.235)$$

[Use (8.233c) and its derivative on both sides of (8.233b).]

Property 11. The initial condition

$$\phi(t_0 - t_0) = \phi(0) = \mathbf{I} \quad (8.236)$$

follows directly from (8.233b). The homogeneous solution can be rewritten in terms of $\phi(t - t_0)$:

$$\mathbf{x}(t) = \phi(t - t_0)\mathbf{x}(t_0). \quad (8.237)$$

The solution to (8.235) is easily obtained by using conventional Laplace transform techniques. Transforming (8.235), we have

$$s\Phi(s) - \mathbf{I} = \mathbf{F}\Phi(s), \quad (8.238)$$

where the identity matrix arises from the initial condition in (8.236). Rearranging terms, we have

$$[s\mathbf{I} - \mathbf{F}]\Phi(s) = \mathbf{I} \quad (8.239)$$

or

$$\Phi(s) = (s\mathbf{I} - \mathbf{F})^{-1}. \quad (8.240)$$

The state transition matrix is

$$\phi(\tau) = \mathcal{L}^{-1}[\Phi(s)] = \mathcal{L}^{-1}[(s\mathbf{I} - \mathbf{F})^{-1}]. \quad (8.241)$$

A simple example illustrates the technique.

Example 8.9. Consider the system in which the transform of the transition matrix is,

$$\Phi(s) = \left[s \begin{bmatrix} 1 & 0 \\ 0 & 1 \end{bmatrix} - \begin{bmatrix} -p_1 & 1 \\ -p_0 & 0 \end{bmatrix} \right]^{-1} \quad (8.242)$$

$$= \begin{bmatrix} s + p_1 & -1 \\ p_0 & s \end{bmatrix}^{-1} \quad (8.243)$$

$$= \frac{1}{s^2 + p_1 s + p_0} \begin{bmatrix} s & 1 \\ -p_0 & s + p_1 \end{bmatrix}. \quad (8.244)$$

To find $\phi(\tau)$ we take the inverse transform. For simplicity we let $p_1 = 3$ and $p_0 = 2$. Then

$$\phi(\tau) = \begin{bmatrix} 2e^{-2\tau} - e^{-\tau} & e^{-\tau} - e^{-2\tau} \\ 2[e^{-2\tau} - e^{-\tau}] & 2e^{-\tau} - e^{-2\tau} \end{bmatrix}. \quad (8.245)$$

■

It is important to observe that the complex natural frequencies involved in the solution are determined by the denominator of $\Phi(s)$. This is just the determinant of the matrix $s\mathbf{I} - \mathbf{F}$. Therefore these frequencies are just the roots of the equation

$$\det[s\mathbf{I} - \mathbf{F}] = 0. \quad (8.246)$$

For the time-varying case the basic concept of a state-transition matrix is still valid, but some of the above properties no longer hold. From the scalar case we know that $\phi(t, t_0)$ will be a function of two variables instead of just the difference between t and t_0 .

Definition. The state transition matrix is defined to be a function of two variables $\phi(t, t_0)$ that satisfies the differential equation

$$\dot{\phi}(t, t_0) = \mathbf{F}(t)\phi(t, t_0) \quad (8.247)$$

with initial condition $\phi(t_0, t_0) = \mathbf{I}$. The solution at any time is

$$\mathbf{x}(t) = \phi(t, t_0)\mathbf{x}(t_0). \quad (8.248)$$

An analytical solution is normally difficult to obtain. Fortunately, in most of the cases in which we use the transition matrix an analytical solution is not necessary. Usually, we need only to know that it exists and that it has certain properties. In the cases in which it actually needs evaluation, we shall do it numerically.

Two properties follow easily:

$$\phi(t_2, t_0) = \phi(t_2, t_1)\phi(t_1, t_0), \quad \text{for all } t_0, t_1, t_2 \quad (8.249)$$

and

$$\phi^{-1}(t_1, t_0) = \phi(t_0, t_1). \quad (8.250)$$

For the nonhomogeneous case the equation is

$$\dot{\mathbf{x}}(t) = \mathbf{F}(t)\mathbf{x}(t) + \mathbf{G}(t)\mathbf{u}(t). \quad (8.251)$$

The solution contains a homogeneous part and a particular part:

$$\mathbf{x}(t) = \phi(t, t_0)\mathbf{x}(t_0) + \int_{t_0}^t \phi(t, \tau)\mathbf{G}(\tau)\mathbf{u}(\tau) d\tau. \quad (8.252)$$

[Substitute (8.252) into (8.251) to verify that it is the solution.] The output $\mathbf{y}(t)$ is

$$\mathbf{y}(t) = \mathbf{C}(t)\mathbf{x}(t). \quad (8.253)$$

In our earlier work, we characterized time-varying linear systems by their impulse response $\mathbf{h}(t, \tau)$. This characterization assumes that the input is known from $-\infty$ to t . Thus,

$$\mathbf{y}(t) = \int_{-\infty}^t \mathbf{h}(t, \tau)\mathbf{u}(\tau) d\tau. \quad (8.254)$$

For most cases of interest the effect of the initial condition $\mathbf{x}(-\infty)$ will disappear in (8.252). Therefore, we may set them equal to zero and obtain,

$$\mathbf{y}(t) = \mathbf{C}(t) \int_{-\infty}^t \phi(t, \tau)\mathbf{G}(\tau)\mathbf{u}(\tau) d\tau. \quad (8.255)$$

Comparing (8.254) and (8.255), we have

$$\mathbf{h}(t, \tau) = \begin{cases} \mathbf{C}(t)\phi(t, \tau)\mathbf{G}(\tau), & t \geq \tau, \\ \mathbf{0}, & \text{Elsewhere.} \end{cases} \quad (8.256)$$

It is worthwhile to observe that the three matrices on the right will depend on the state representation that we choose for the system, but the matrix impulse response is unique. As pointed out earlier, the system is realizable. This is reflected by the $\mathbf{0}$ in (8.256).

For the time-invariant case

$$\mathbf{Y}(s) = \mathbf{H}(s)\mathbf{U}(s), \quad (8.257)$$

and

$$\mathbf{H}(s) = \mathbf{C}\Phi(s)\mathbf{G}. \quad (8.258)$$

Equation (8.257) assumes that the input has a Laplace transform.

Most of our discussion up to this point has been valid for an arbitrary driving function $\mathbf{u}(t)$. We now derive some statistical properties of vector processes $\mathbf{x}(t)$ and $\mathbf{y}(t)$ for the specific case in which $\mathbf{u}(t)$ is a sample function of a vector white noise process.

$$E[\mathbf{u}(t)\mathbf{u}^T(\tau)] = \mathbf{Q}\delta(t - \tau). \quad (8.259)$$

Property 12. The cross-correlation between the state vector $\mathbf{x}(t)$ of a system driven by a zero-mean white noise $\mathbf{u}(t)$ and the input $\mathbf{u}(\tau)$ is

$$\mathbf{K}_{\mathbf{xu}}(t, \tau) \triangleq E[\mathbf{x}(t)\mathbf{u}^T(\tau)]. \quad (8.260)$$

It is a discontinuous function that equals

$$\mathbf{K}_{\mathbf{xu}}(t, \tau) = \begin{cases} \mathbf{0}, & \tau \geq t, \\ \frac{1}{2}\mathbf{G}(t)\mathbf{Q}, & \tau = t, \\ \boldsymbol{\phi}(t, \tau)\mathbf{G}(\tau)\mathbf{Q}, & t_0 < \tau < t. \end{cases} \quad (8.261)$$

Proof. Substituting (8.252) into the definition in (8.260), we have

$$\mathbf{K}_{\mathbf{xu}}(t, \tau) = E\left\{\left[\boldsymbol{\phi}(t, t_0)\mathbf{x}(t_0) + \int_{t_0}^t \boldsymbol{\phi}(t, \alpha)\mathbf{G}(\alpha)\mathbf{u}(\alpha)d\alpha\right]\mathbf{u}^T(\tau)\right\}. \quad (8.262)$$

Bringing the expectation inside the integral and assuming that the initial state $\mathbf{x}(t_0)$ is independent of $\mathbf{u}(\tau)$ for $\tau > t_0$, we have

$$\begin{aligned} \mathbf{K}_{\mathbf{xu}}(t, \tau) &= \int_{t_0}^t \boldsymbol{\phi}(t, \alpha)\mathbf{G}(\alpha)E[\mathbf{u}(\alpha)\mathbf{u}^T(\tau)]d\alpha \\ &= \int_{t_0}^t \boldsymbol{\phi}(t, \alpha)\mathbf{G}(\alpha)\mathbf{Q}\delta(\alpha - \tau)d\alpha. \end{aligned} \quad (8.263)$$

If $\tau > t$, this expression is zero. If $\tau = t$ and we assume that the delta function is symmetric because it is the limit of a covariance function, we pick up only one half the area at the right end point. Thus,

$$\mathbf{K}_{\mathbf{xu}}(t, t) = \frac{1}{2}\boldsymbol{\phi}(t, t)\mathbf{G}(t)\mathbf{Q}. \quad (8.264)$$

Using the result following (8.247), we obtain the second line in (8.261)

If $\tau < t$, we have

$$\mathbf{K}_{\mathbf{xu}}(t, \tau) = \phi(t, \tau)\mathbf{G}(\tau)\mathbf{Q}, \quad \tau < t \quad (8.265)$$

which is the third line in (8.261). A special case of (8.265) that we shall use later is obtained by letting τ approach t from below.

$$\lim_{\tau \rightarrow t^-} \mathbf{K}_{\mathbf{xu}}(t, \tau) = \mathbf{G}(t)\mathbf{Q}. \quad (8.266)$$

The cross-correlation between the output vector $\mathbf{y}(t)$ and $\mathbf{u}(\tau)$ follows easily.

$$\mathbf{K}_{\mathbf{yu}}(t, \tau) = \mathbf{C}(t)\mathbf{K}_{\mathbf{xu}}(t, \tau). \quad (8.267)$$

Property 13. The variance matrix of the state vector $\mathbf{x}(t)$ of a system

$$\dot{\mathbf{x}}(t) = \mathbf{F}(t)\mathbf{x}(t) + \mathbf{G}(t)\mathbf{u}(t) \quad (8.268)$$

satisfies the differential equation

$$\dot{\Lambda}_{\mathbf{x}}(t) = \mathbf{F}(t)\Lambda_{\mathbf{x}}(t) + \Lambda_{\mathbf{x}}(t)\mathbf{F}^T(t) + \mathbf{G}(t)\mathbf{Q}\mathbf{G}^T(t), \quad (8.269)$$

with the initial condition

$$\Lambda_{\mathbf{x}}(t_0) = E[\mathbf{x}(t_0)\mathbf{x}^T(t_0)]. \quad (8.270)$$

[Observe that $\Lambda_{\mathbf{x}}(t) = \mathbf{K}_{\mathbf{x}}(t, t)$.]

Proof.

$$\Lambda_{\mathbf{x}}(t) \triangleq E[\mathbf{x}(t)\mathbf{x}^T(t)]. \quad (8.271)$$

Differentiating, we have

$$\frac{d\Lambda_{\mathbf{x}}(t)}{dt} = E\left[\frac{d\mathbf{x}(t)}{dt}\mathbf{x}^T(t)\right] + E\left[\mathbf{x}(t)\frac{d\mathbf{x}^T(t)}{dt}\right]. \quad (8.272)$$

The second term is just the transpose of the first. [Observe that $\mathbf{x}(t)$ is not mean-square differentiable: Therefore, we will have to be careful when dealing with (8.272).]

Substituting (8.268) into the first term in (8.272) gives

$$E\left[\frac{d\mathbf{x}(t)}{dt}\mathbf{x}^T(t)\right] = E\{[\mathbf{F}(t)\mathbf{x}(t) + \mathbf{G}(t)\mathbf{u}(t)]\mathbf{x}^T(t)\}. \quad (8.273)$$

Using Property 12 on the second term in (8.273), we have

$$E\left[\frac{d\mathbf{x}(t)}{dt}\mathbf{x}^T(t)\right] = \mathbf{F}(t)\Lambda_{\mathbf{x}}(t) + \frac{1}{2}\mathbf{G}(t)\mathbf{Q}\mathbf{G}^T(t). \quad (8.274)$$

Using (8.274) and its transpose in (8.272) gives

$$\dot{\Lambda}_{\mathbf{x}}(t) = \mathbf{F}(t)\Lambda_{\mathbf{x}}(t) + \Lambda_{\mathbf{x}}(t)\mathbf{F}^T(t) + \mathbf{G}(t)\mathbf{Q}\mathbf{G}^T(t), \quad (8.275)$$

which is the desired result.

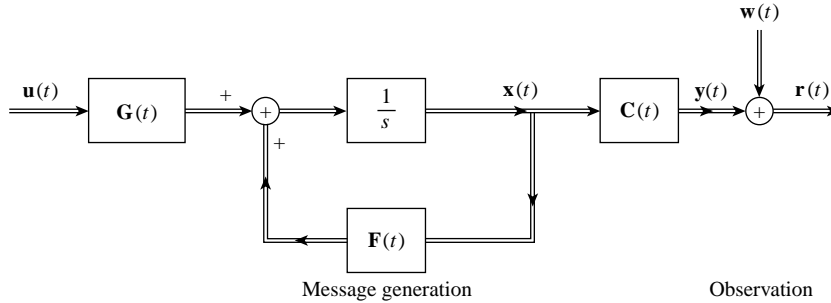


Figure 8.26: Message generation and observation processes.

We now have developed the following ideas:

1. State variables of a linear dynamic system.
2. Analog computer realizations.
3. First-order vector differential equations and state-transition matrices.
4. Random process generation.

The final step is to define the observation model.

The vector $\mathbf{y}(t)$ is transmitted over a channel where it is corrupted by additive white Gaussian noise $\mathbf{w}(t)$, where

$$E [\mathbf{w}(t)\mathbf{w}^T(t)] = \mathbf{R}(t) \delta(t - u). \quad (8.276)$$

The observation noise $\mathbf{w}(t)$ is statistically independent of $\mathbf{y}(t)$. The second vector is

$$\mathbf{r}(t) = \mathbf{C}(t) \mathbf{x}(t) + \mathbf{w}(t). \quad (8.277)$$

The signal generation and observation processes are shown in Figure 8.26. The complete model is summarized in (8.231a), (8.231b), (8.230), (8.276) and (8.277).

The next step is to show how we can modify the optimum linear filtering results we previously obtained to take advantage of this method of representation.

8.3.2 Kalman Filter

In this section, we derive a differential equation whose solution is the minimum mean-square estimate of the message (or messages). We recall that the MMSE estimate of a vector $\mathbf{x}(t)$ is a vector $\hat{\mathbf{x}}(t)$ whose components $\hat{x}_i(t)$ are chosen so that the mean-square error in estimating each component is minimized. In other words, $E [(\hat{x}_i(t) - x_i(t))^2]$, $i = 1, 2, \dots, n$ is minimized. This implies that the sum of the mean-square errors, $E \{[\hat{\mathbf{x}}^T(t) - \mathbf{x}^T(t)][\hat{\mathbf{x}}(t) - \mathbf{x}(t)]\}$ is also minimized. The derivation is straightforward but somewhat lengthy. It consists of four parts.

1. Starting with the vector Wiener–Hopf equation for realizable estimation, we derive a differential equation in t , with τ as a parameter, that the optimum filter $\mathbf{h}_o(t, \tau)$ must satisfy. This is (8.288).

2. Because the optimum estimate $\hat{\mathbf{x}}(t)$ is obtained by passing the received signal into the optimum filter, (8.288) leads to a differential equation that the optimum estimate must satisfy. This is (8.294). It turns out that all the coefficients in this equation are known except $\mathbf{h}_o(t, t)$.
3. The next step is to find an expression for $\mathbf{h}_o(t, t)$. Property 2C–V expresses $\mathbf{h}_o(t, t)$ in terms of the error matrix $\xi_P(t)$. Thus, we can equally well find an expression for $\xi_P(t)$. To do this we first find a differential equation for the error $\mathbf{x}_e(t)$. This is (8.298).
4. Finally, because

$$\xi_P(t) \triangleq E [\mathbf{x}_e(t) \mathbf{x}_e^T(t)], \quad (8.278)$$

we can use (8.299) to find a matrix differential equation that $\xi_P(t)$ must satisfy. This is (8.304). We now carry out these four steps in detail.

Step 1. We start with the integral equation obtained for the optimum finite time point estimator. We are estimating the entire vector $\mathbf{x}(t)$

$$\mathbf{K}_x(t, \sigma) \mathbf{C}^T(\sigma) = \int_{T_i}^t \mathbf{h}_o(t, \tau) \mathbf{K}_r(\tau, \sigma) d\tau, \quad T_i < \sigma < t, \quad (8.279)$$

where

$$\mathbf{K}_r(\tau, \sigma) = \mathbf{C}(\tau) \mathbf{K}_x(\tau, \sigma) \mathbf{C}^T(\sigma) + \mathbf{R}(\tau) \delta(\tau - \sigma). \quad (8.280)$$

Differentiating both sides with respect to t , we have

$$\frac{\partial \mathbf{K}_x(t, \sigma)}{\partial t} \mathbf{C}^T(\sigma) = \mathbf{h}_o(t, t) \mathbf{K}_r(t, \sigma) + \int_{T_i}^t \frac{\partial \mathbf{h}_o(t, \tau)}{\partial t} \mathbf{K}_r(\tau, \sigma) d\tau, \quad T_i < \sigma < t. \quad (8.281)$$

First we consider the first term on the right-hand side of (8.281). For $\sigma < t$, we see from (8.280) that

$$\mathbf{K}_r(t, \sigma) = \mathbf{C}(t) [\mathbf{K}_x(t, \sigma) \mathbf{C}^T(\sigma)], \quad \sigma < t. \quad (8.282)$$

The term inside the bracket is just the left-hand side of (8.279). Therefore,

$$\mathbf{h}_o(t, t) \mathbf{K}_r(t, \sigma) = \int_{T_i}^t \mathbf{h}_o(t, \tau) \mathbf{C}(t) \mathbf{h}_o(t, \tau) \mathbf{K}_r(\tau, \sigma) d\tau, \quad \sigma < t. \quad (8.283)$$

Now consider the first term on the left-hand side of (8.281),

$$\frac{\partial \mathbf{K}_x(t, \sigma)}{\partial t} = E \left[\frac{d\mathbf{x}(t)}{dt} \mathbf{x}^T(\sigma) \right]. \quad (8.284)$$

Using (8.219), we have

$$\frac{\partial \mathbf{K}_x(t, \sigma)}{\partial t} = \mathbf{F}(t) \mathbf{K}_x(t, \sigma) + \mathbf{G}(t) \mathbf{K}_{ux}(t, \sigma), \quad (8.285)$$

but the second term is zero for $\sigma < t$ [see (8.261)]. Using (8.279), we see that

$$\mathbf{F}(t)\mathbf{K}_x(t, \sigma)\mathbf{C}^T(\sigma) = \int_{T_i}^t \mathbf{F}(t)\mathbf{h}_o(t, \tau)\mathbf{K}_r(\tau, \sigma)d\tau. \quad (8.286)$$

Substituting (8.286) and (8.283) into (8.281), we have

$$\begin{aligned} \mathbf{0} = \int_{T_i}^t & \left[-\mathbf{F}(t)\mathbf{h}_o(t, \tau) + \mathbf{h}_o(t, t)\mathbf{C}(t)\mathbf{h}_o(t, \tau) + \frac{\partial \mathbf{h}_o(t, \tau)}{\partial t} \right] \mathbf{K}_r(\tau, \sigma)d\tau \\ T_i < \sigma < t. \end{aligned} \quad (8.287)$$

Clearly, if the term in the bracket is zero for all $\tau, T_i \leq \tau \leq t$, (8.287) will be satisfied. Because $\mathbf{R}(t)$ is positive definite the condition is also necessary. Thus, the differential equation satisfied by the optimum impulse response is

$$\frac{\partial \mathbf{h}_o(t, \tau)}{\partial t} = \mathbf{F}(t)\mathbf{h}_o(t, \tau) - \mathbf{h}_o(t, t)\mathbf{C}(t)\mathbf{h}_o(t, \tau). \quad (8.288)$$

Step 2. The optimum estimate is obtained by passing the input through the optimum filter. Thus

$$\hat{\mathbf{x}}(t) = \int_{T_i}^t \mathbf{h}_o(t, \tau)\mathbf{r}(\tau)d\tau. \quad (8.289)$$

We assumed in (8.289) that the MMSE realizable estimate of $\mathbf{x}(T_i) = \mathbf{0}$. Because there is no received data, our estimate at T_i is based on our *a priori* knowledge. If $\mathbf{x}(T_i)$ is a random variable with a mean-value vector $E[\mathbf{x}(T_i)]$ and a covariance matrix $\mathbf{K}_x(T_i, T_i)$, then the MMSE estimate is

$$\hat{\mathbf{x}}(T_i) = E[\mathbf{x}(T_i)]. \quad (8.290)$$

If $\mathbf{x}(T_i)$ is a deterministic quantity, say $\mathbf{x}_D(T_i)$, then we may treat it as a random variable whose mean equals $\mathbf{x}_D(t)$

$$E[\mathbf{x}(T_i)] \triangleq \mathbf{x}_D(t) \quad (8.291)$$

and whose covariance matrix $\mathbf{K}_x(T_i, T_i)$ is identically zero.

$$\mathbf{K}_x(T_i, T_i) \triangleq \mathbf{0}. \quad (8.292)$$

In both cases (8.289) assumes $E[\mathbf{x}(T_i)] = \mathbf{0}$. The modification for other initial conditions is straightforward. Differentiating (8.289), we have

$$\frac{d\hat{\mathbf{x}}(t)}{dt} = \mathbf{h}_o(t, t)\mathbf{r}(t) + \int_{T_i}^t \frac{\partial \mathbf{h}_o(t, \tau)}{\partial t} \mathbf{r}(\tau)d\tau. \quad (8.293)$$

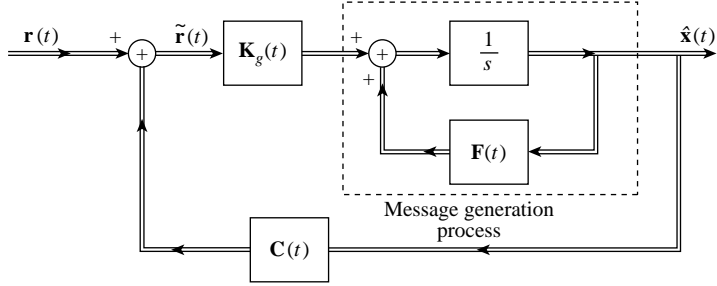


Figure 8.27: Kalman filter structure.

Substituting (8.288) into the second term on the right-hand side of (8.293) and using (8.289), we obtain

$$\frac{d\hat{\mathbf{x}}(t)}{dt} = \mathbf{F}(t)\hat{\mathbf{x}}(t) + \mathbf{h}_o(t, t)[\mathbf{r}(t) - \mathbf{C}(t)\hat{\mathbf{x}}(t)]. \quad (8.294)$$

It is convenient to introduce a new symbol for $\mathbf{h}_o(t, t)$ to indicate that it is only a function of one variable

$$\mathbf{K}_g(t) \triangleq \mathbf{h}_o(t, t). \quad (8.295)$$

which is referred to as the Kalman gain in the literature. The input to the Kalman gain is denoted by $\tilde{\mathbf{r}}(t)$ and we will discuss its significance later.

The operations in (8.294) can be represented by the matrix block diagram of Figure 8.27. We see that all the coefficients are known except $\mathbf{K}_g(t)$, but (8.74) expresses $\mathbf{h}_o(t, t)$ in terms of the error matrix,

$$\mathbf{K}_g(t) = \mathbf{h}_o(t, t) = \xi_P(t)\mathbf{C}^T(t)\mathbf{R}^{-1}(t). \quad (8.296)$$

Thus, (8.294) will be completely determined if we can find an expression for $\xi_P(t)$, the error covariance matrix for the optimum realizable point estimator.

Step 3. We first find a differential equation for the error $\mathbf{x}_\epsilon(t)$, where

$$\mathbf{x}_\epsilon(t) \triangleq \mathbf{x}(t) - \hat{\mathbf{x}}(t). \quad (8.297)$$

Differentiating, we have

$$\frac{d\mathbf{x}_\epsilon(t)}{dt} = \frac{d\mathbf{x}(t)}{dt} - \frac{d\hat{\mathbf{x}}(t)}{dt}. \quad (8.298)$$

Substituting (8.231a) for the first term on the right-hand side of (8.298), substituting (8.294) for the second term, and using (8.277), we obtain the desired equation

$$\frac{d\mathbf{x}_\epsilon(t)}{dt} = [\mathbf{F}(t) - \mathbf{K}_g(t)\mathbf{C}(t)]\mathbf{x}_\epsilon(t) - \mathbf{K}_g(t)\mathbf{w}(t) + \mathbf{G}(t)\mathbf{u}(t). \quad (8.299)$$

The last step is to derive a differential equation for $\xi_P(t)$.

Step 4. Differentiating

$$\xi_P(t) \triangleq E[\mathbf{x}_\epsilon(t)\mathbf{x}_\epsilon^T(t)], \quad (8.300)$$

we have

$$\frac{d\xi_P(t)}{dt} = E\left[\frac{d\mathbf{x}_\epsilon(t)}{dt}\mathbf{x}_\epsilon^T(t)\right] + E\left[\mathbf{x}_\epsilon(t)\frac{d\mathbf{x}_\epsilon^T(t)}{dt}\right]. \quad (8.301)$$

Substituting (8.299) into the first term of (8.301), we have

$$E\left[\frac{d\mathbf{x}_\epsilon(t)}{dt}\mathbf{x}_\epsilon^T(t)\right] = E\{[\mathbf{F}(t) - \mathbf{K}_g(t)\mathbf{C}(t)]\mathbf{x}_\epsilon(t)\mathbf{x}_\epsilon^T(t) - \mathbf{K}_g(t)\mathbf{w}(t)\mathbf{x}_\epsilon^T(t) + \mathbf{G}(t)\mathbf{u}(t)\mathbf{x}_\epsilon^T(t)\}. \quad (8.302)$$

Looking at (8.299), we see $\mathbf{x}_\epsilon(t)$ is the state vector for a system driven by the weighted sum of two independent white noises $\mathbf{w}(t)$ and $\mathbf{u}(t)$. Therefore, the expectations in the second and third terms are precisely the same type as we evaluated in Property 12 [second line of (8.261)].

$$E\left[\frac{d\mathbf{x}_\epsilon(t)}{dt}\mathbf{x}_\epsilon^T(t)\right] = \mathbf{F}(t)\xi_P(t) - \mathbf{K}_g(t)\mathbf{C}(t)\xi_P(t) + \frac{1}{2}\mathbf{K}_g(t)\mathbf{R}(t)\mathbf{K}_g^T(t) + \frac{1}{2}\mathbf{G}(t)\mathbf{Q}\mathbf{G}^T(t). \quad (8.303)$$

Adding the transpose and replacing $\mathbf{K}_g(t)$ with the right-hand side of (8.296), we have

$$\frac{d\xi_P(t)}{dt} = \mathbf{F}(t)\xi_P(t) + \xi_P(t)\mathbf{F}^T(t) - \xi_P(t)\mathbf{C}^T(t)\mathbf{R}^{-1}(t)\mathbf{C}(t)\xi_P(t) + \mathbf{G}(t)\mathbf{Q}\mathbf{G}^T(t), \quad (8.304)$$

which is called the *variance equation*. This equation and the initial condition

$$\xi_P(T_i) = E[\mathbf{x}_\epsilon(T_i)\mathbf{x}_\epsilon^T(T_i)] \quad (8.305)$$

determine $\xi_P(t)$ uniquely. Using (8.296) we obtain $\mathbf{K}_g(t)$, the gain in the optimal filter.

Observe that the variance equation does not contain the received signal. Therefore, it may be solved before any data is received and used to determine the gains in the optimum filter. The variance equation is a matrix equation equivalent to n^2 scalar differential equations. However, because $\xi_P(t)$ is a symmetric matrix, we have $\frac{1}{2}n(n+1)$ scalar nonlinear coupled differential equations to solve. In the general case it is impossible to obtain an explicit analytical solution, but this is unimportant because the equation is in a form that may be integrated using either an analog or digital computer. The optimal estimation for the linear Gaussian model is a Bayesian efficient estimation so the variance equations is also a differential equation for the Bayesian Cramér–Rao bound. We will revisit this relationship later.

The variance equation is a matrix Riccati equation whose properties have been studied extensively in other contexts (e.g. [McL50, Lev59, Rei59, Rei46], or [Col65]). To study its behavior adequately requires more background than we have developed. A property that deals with the infinite memory, stationary process case (the Wiener problem) is of interest.

Property 14. Assume that T_i is fixed and that the matrices \mathbf{F} , \mathbf{G} , \mathbf{C} , \mathbf{R} , and \mathbf{Q} are constant. Under certain conditions, as t increases there will be an initial transient period after which the filter gains will approach constant values. Looking at (8.296) and (8.304), we see that as $\dot{\xi}_P(t)$ approaches zero the error covariance matrix and gain matrix will approach constants. We refer to the problem when the condition $\dot{\xi}_P(t) = \mathbf{0}$ is true as the *steady-state estimation problem*.

The left-hand side of (8.304) is then zero and the variance equation becomes a set of $\frac{1}{2}n(n + 1)$ quadratic algebraic equations. The nonnegative definite solution is ξ_P .

Some comments regarding this statement are necessary.

1. How do we tell if the steady-state problem is meaningful? To give the *best* general answer requires notions that we have not developed [KB61] or [KS72]. A *sufficient* condition is that the message correspond to a stationary random process.
2. For small n it is feasible to calculate the various solutions and select the correct one. For even moderate n (e.g., $n = 2$), it is more practical to solve (8.304) numerically. We may start with some arbitrary nonnegative definite $\xi_P(T_i)$ and let the solution converge to the steady-state result (once again see [KB61], Theorem 4, p. 8, for a precise statement).
3. Once again we observe that we can generate $\xi_P(t)$ before the data is received or in real time. We must specify $\xi_P(T_i)$. If we assume that the message process has reached steady state, then $\dot{\Lambda}_x = \mathbf{0}$ and

$$\dot{\xi}_P(T_i) = \Lambda_x(T_i), \quad (8.306)$$

which is given by the steady-state solution to (8.275)

$$\mathbf{F}\Lambda_x + \Lambda_x\mathbf{F}^T + \mathbf{G}\mathbf{Q}\mathbf{G}^T = \mathbf{0}. \quad (8.307)$$

4. Once the filter reaches a statistical steady state, (8.304) reduces to

$$\mathbf{F}\xi_P + \xi_P\mathbf{F}^T - \xi_P\mathbf{C}^T\mathbf{R}^{-1}\mathbf{C}\xi_P^T + \mathbf{G}\mathbf{Q}\mathbf{G}^T = \mathbf{0}. \quad (8.308)$$

This is an algebraic equation whose solution is ξ_P .

A great amount of effort has been devoted to solving the algebraic Riccati equation (8.308). Laub in [Lau79] develops a technique called the Schur method that has better numerical properties than earlier eigenvector methods. He also suggests other references for a broader discussion of the problem (e.g. [Won68, Rei72, Wil71, Lai76, Pot66]). We will discuss the problem in a little more detail in Chapter 9, but we recommend [Lau79].

Property 15. This property relates to $\tilde{\mathbf{r}}(t)$, the output of the summing node in Figure 8.27. Consider a specific time t_1 . The input to the bottom of the summer represents our MMSE

of $\mathbf{y}(t)$ before we have observed $\mathbf{r}(t)$ that we denote as $\hat{\mathbf{y}}(t^-)$. The output of the summer is

$$\tilde{\mathbf{r}}(t) = \mathbf{r}(t) - \hat{\mathbf{y}}(t^-) \quad (8.309)$$

and represents the new information provided by the input and is referred as the *innovations* process. We can show that it is a white noise processes

$$E \{ \tilde{\mathbf{r}}(t) \tilde{\mathbf{r}}^T(u) \} = \tilde{\mathbf{P}}(t) \delta(t - u), \quad (8.310)$$

where

$$\tilde{\mathbf{P}}(t) = \mathbf{R}(t). \quad (8.311)$$

We carry out the proof in Section 8.3.3.

In this section, we have transformed the optimum linear filtering problem into a state-variable formulation. All the quantities of interest are expressed as outputs of dynamic systems. The three equations that describe these dynamic systems are our principal results.

Estimator equation

$$\boxed{\frac{d\hat{\mathbf{x}}(t)}{dt} = \mathbf{F}(t)\hat{\mathbf{x}}(t) + \mathbf{K}_g(t)[\mathbf{r}(t) - \mathbf{C}(t)\hat{\mathbf{x}}(t)]}. \quad (8.312)$$

Gain equation

$$\boxed{\mathbf{K}_g(t) = \xi_P(t)\mathbf{C}^T(t)\mathbf{R}^{-1}(t)}. \quad (8.313)$$

Variance equation

$$\boxed{\frac{d\xi_P(t)}{dt} = \mathbf{F}(t)\xi_P(t) + \xi_P(t)\mathbf{F}^T(t) - \xi_P(t)\mathbf{C}^T(t)\mathbf{R}^{-1}(t)\mathbf{C}(t)\xi_P(t) + \mathbf{G}(t)\mathbf{Q}\mathbf{G}^T(t)}. \quad (8.314)$$

The complete model is shown in Figure 8.28. We consider an example to illustrate the application of these results.

Example 8.10. Consider the first-order message spectrum

$$S_s(\omega) = \frac{2kP}{\omega^2 + k^2}. \quad (8.315)$$

In this case $\mathbf{x}(t)$ is a scalar; $x(t) = s(t)$.

$$r(t) = x(t) + w(t). \quad (8.316)$$

The necessary quantities follow by inspection:

$$\begin{aligned} \mathbf{F}(t) &= -k, \\ \mathbf{G}(t) &= \mathbf{1}, \\ \mathbf{C}(t) &= \mathbf{1}, \\ \mathbf{Q} &= 2kP, \\ \mathbf{R}(t) &= \frac{N_0}{2}. \end{aligned} \quad (8.317)$$

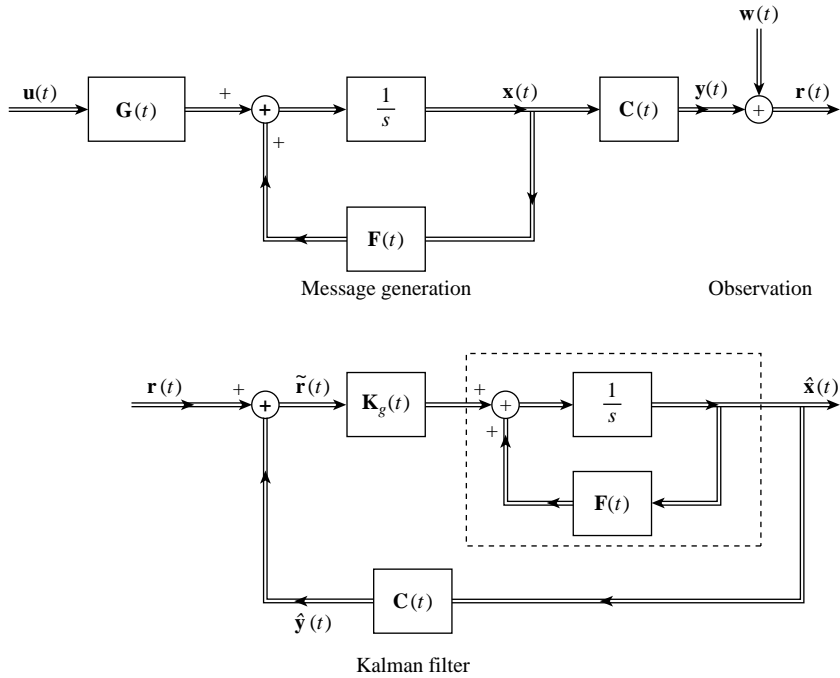


Figure 8.28: System model: message generation, observation, Kalman filter.

Substituting these quantities into (8.312), we obtain the differential equation for the optimum estimate:

$$\frac{d\hat{x}(t)}{dt} = -k\hat{x}(t) + K_g(t)[r(t) - \hat{x}(t)]. \quad (8.318)$$

The resulting filter is shown in Figure 8.29. The value of the gain $K_g(t)$ is determined by solving the variance equation.

First, we assume that the estimator has reached steady state. Then the steady-state solution to the variance equation can be obtained easily. Setting the left-hand side of (8.314) equal to zero, we obtain

$$0 = -2k\xi_{P_\infty} - \xi_{P_\infty}^2 \frac{2}{N_0} + 2kP. \quad (8.319)$$

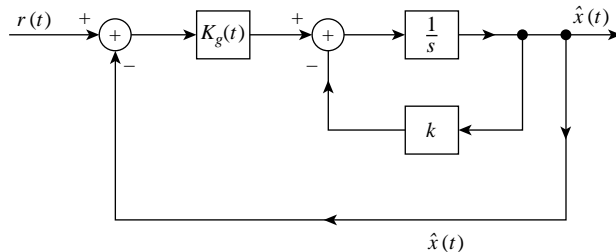


Figure 8.29: Optimum filter: Example 8.10.

where $\xi_{P\infty}$ denotes the steady-state variance.

$$\xi_{P\infty} \triangleq \lim_{t \rightarrow \infty} \xi_P(t). \quad (8.320)$$

There are two solutions to (8.319); one is positive and one is negative. Because $\xi_{P\infty}$ is a mean-square error it must be positive. Therefore,

$$\xi_{P\infty} = k \frac{N_0}{2} (-1 + \sqrt{1 + \Lambda}) \quad (8.321)$$

(recall that $\Lambda = 4P/kN_0$). From (8.313)

$$K_g(\infty) = \xi_{P\infty} R^{-1} = k(-1 + \sqrt{1 + \Lambda}). \quad (8.322)$$

Clearly, the filter must be equivalent to the one obtained in Example 8.3. The closed loop transfer function is

$$H_o(j\omega) = \frac{K_g(\infty)}{j\omega + k + K_g(\infty)}. \quad (8.323)$$

Substituting (8.322) in (8.323), we have

$$H_o(j\omega) = \frac{k(\sqrt{1 + \Lambda} - 1)}{j\omega + k\sqrt{1 + \Lambda}}, \quad (8.324)$$

which is the same as (8.114) with $P = 1$.

In Figure 8.30, we show the transient behavior of $\xi_P(t)$

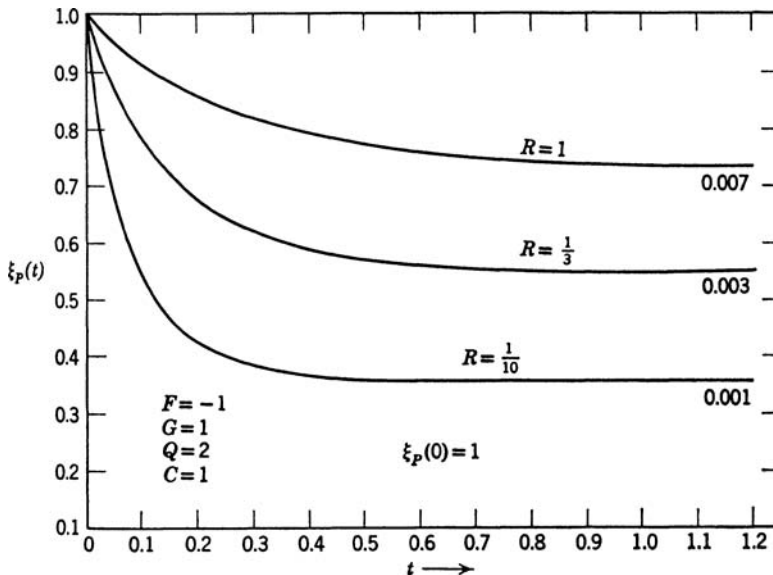


Figure 8.30: $\xi_P(t)$ versus t ; $R = 1, 0.33, 0.1$.

Example 8.11. A logical generalization of the one-pole case is the Butterworth family defined in (8.325):

$$S_a(\omega : n) = \frac{2n P}{k} \frac{\sin(\pi/2n)}{(1 + (\omega/k)^{2n})}. \quad (8.325)$$

To formulate this equation in state-variable terms we need the differential equation of the message generation process.

$$a^{(n)}(t) + p_{n-1}a^{(n-1)}(t) + \cdots + p_0a(t) = u(t). \quad (8.326)$$

The coefficients are tabulated for various n in circuit theory texts (e.g. [Gui57]). The values for $n = 1, \dots, 7$ are shown in Figure 8.31. If we are interested only in the message process, we can choose any convenient state representation. We use the (8.186),

$$\begin{aligned} x_1(t) &= a(t) \\ x_2(t) &= \dot{a}(t) = \dot{x}_1(t) \\ x_3(t) &= \ddot{a}(t) = \dot{x}_2(t) \\ &\vdots \\ x_n(t) &= a^{(n-1)}(t) = \dot{x}_{n-1}(t) \\ \dot{x}_n(t) &= -\sum_{k=1}^n p_{k-1}a^{(k-1)}(t) + u(t) \\ &= -\sum_{k=1}^n p_{k-1}x_k(t) + u(t). \end{aligned} \quad (8.327)$$

n	p_{n-1}	p_{n-2}	p_{n-3}	p_{n-4}	p_{n-5}	p_{n-6}	p_{n-7}
2	1.414	1.000					
3	2.000	2.000	1.000				
4	2.613	3.414	2.613	1.000			
5	3.236	5.236	5.236	3.236	1.000		
6	3.864	7.464	9.141	7.464	3.864	1.000	
7	4.494	10.103	14.606	14.606	10.103	4.494	1.000

$$a^{(n)}(t) + p_{n-1}a^{(n-1)}(t) + \cdots + p_0a(t) = u(t)$$

Figure 8.31: Coefficients in the differential equation describing the Butterworth spectra [Wei75].

The resulting \mathbf{F} matrix for any n is given by using (8.326) and (8.188). The other quantities needed are

$$\mathbf{G}(t) = \begin{bmatrix} 0 \\ 0 \\ \vdots \\ 1 \end{bmatrix}, \quad (8.328)$$

$$\mathbf{C}(t) = [1|0|\cdots|0], \quad (8.329)$$

$$\mathbf{Q} = 2n P k^{2n-1} \sin\left(\frac{\pi}{2n}\right), \quad (8.330)$$

$$\mathbf{R}(t) = \frac{N_0}{2}. \quad (8.331)$$

We observe that $\mathbf{K}_g(t)$ is an $n \times 1$ matrix,

$$\mathbf{K}_g(t) = \frac{2}{N_0} \begin{bmatrix} \xi_{11}(t) \\ \xi_{12}(t) \\ \vdots \\ \xi_{1n}(t) \end{bmatrix}, \quad (8.332)$$

$$\dot{\hat{x}}_1(t) = \hat{x}_2(t) + \frac{2}{N_0} \xi_{11}(t)[r(t) - \hat{x}_1(t)],$$

$$\dot{\hat{x}}_2(t) = \hat{x}_3(t) + \frac{2}{N_0} \xi_{12}(t)[r(t) - \hat{x}_1(t)]$$

•
•
•

$$\dot{\hat{x}}_n(t) = -p_0\hat{x}_1(t) - p_1\hat{x}_2(t) - \cdots - p_{n-1}\hat{x}_n(t) + \frac{2}{N_0}\xi_{ln}(t)[r(t) - \hat{x}_1(t)].$$

The block diagram is shown in Figure 8.32.

To find the values of $\xi_{11}(t), \dots, \xi_{ln}(t)$, we solve the variance equation. This could be done analytically but a numerical solution is much more practical. We assume that $T_i = 0$ and that the unobserved process is in a statistical steady state. In Figure 8.33a, we show the error as a function of time for the

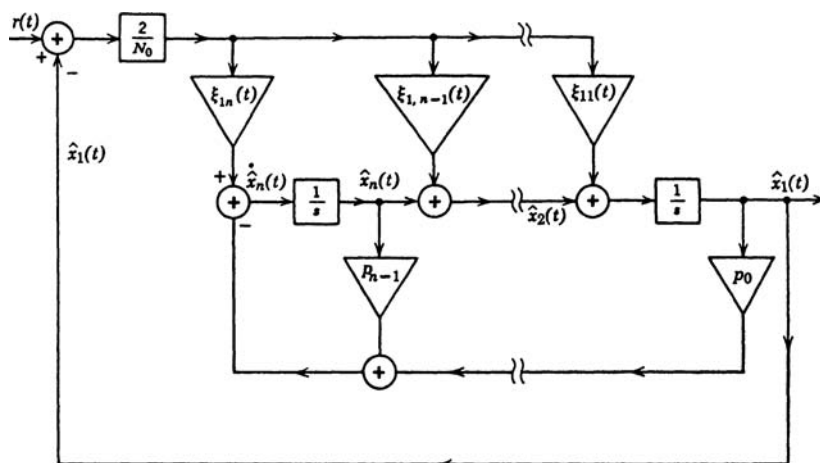


Figure 8.32: Optimum filter: n th-order Butterworth message.

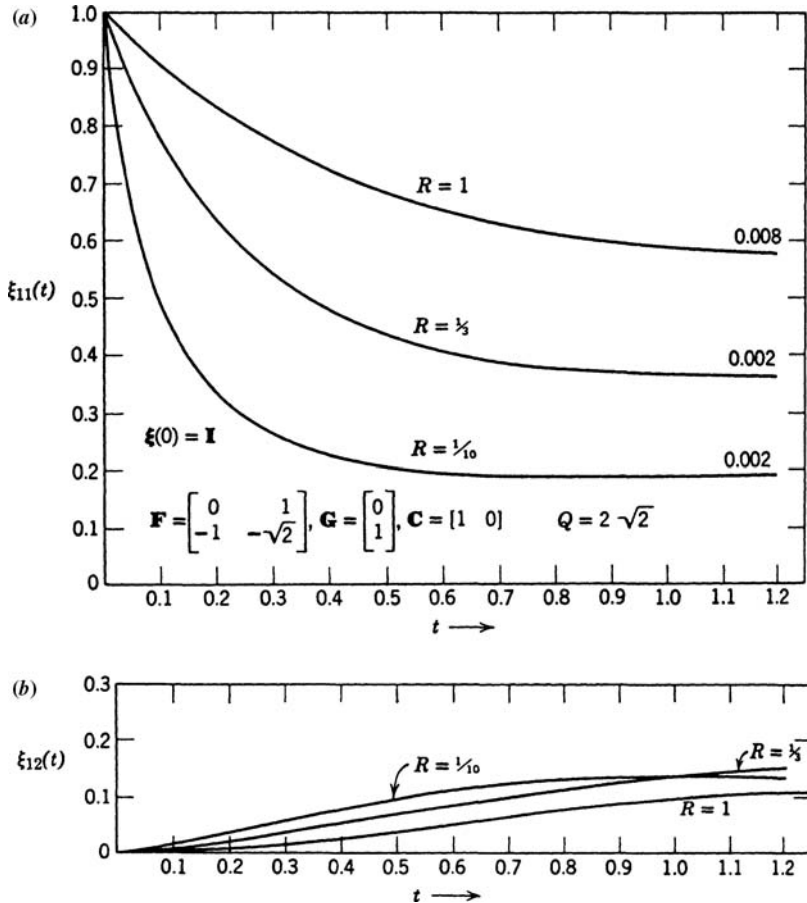


Figure 8.33: (a) Mean-square error, second-order Butterworth; (b) filter gains, second-order Butterworth.

two-pole case. The number on the right end of each curve is $\xi_P(1.2) - \xi_{P\infty}$. We see that for $t = 1$ the error has essentially reached its steady-state value. In Figure 8.33b, we show the term $\xi_{12}(t)$ ⁹. In all cases steady state is essentially reached by $t = 1$. ■

Example 8.12. The two preceding examples dealt with stationary processes. A simple nonstationary process is the Wiener process. It can be represented in differential equation form as

$$\dot{x}(t) = Gu(t), \quad (8.333)$$

$$x(0) = 0. \quad (8.334)$$

Observe that even though the coefficients in the differential equation are constant the process is nonstationary. If we assume that

$$r(t) = x(t) + w(t), \quad (8.335)$$

⁹The numerical results in Figure 8.30 are due to Baggeroer [Bag66].

the estimator follows easily

$$\dot{\hat{x}}(t) = K_g(t)[r(t) - \hat{x}(t)], \quad (8.336)$$

where

$$K_g(t) = \frac{2}{N_0} \xi_P(t) \quad (8.337)$$

and

$$\xi_P(t) = -\frac{2}{N_0} \xi_P^2(t) + G^2 Q. \quad (8.338)$$

The transient problem can be solved easily. The result is

$$\xi_P(t) = \left(\frac{N_0}{2} G^2 Q \right)^{1/2} \left(\frac{e^{\gamma t} - e^{-\gamma t}}{e^{\gamma t} + e^{-\gamma t}} \right) = \left(\frac{N_0 G^2 Q}{2} \right)^{1/2} \left(\frac{1 - e^{-2\gamma t}}{1 + e^{-2\gamma t}} \right), \quad (8.339)$$

where $\gamma = [2G^2 Q / N_0]^{1/2}$. As $t \rightarrow \infty$, the error approaches steady state.

$$\xi_{P\infty} = \left(\frac{N_0}{2} G^2 Q \right)^{1/2} \quad (8.340)$$

[(8.340) can also be obtained directly from (8.338) by letting $\xi_P(t) = 0$.]

The steady-state filter is shown in Figure 8.34. It is interesting to observe that this problem is not included in the Wiener–Hopf model in Section 8.2. A heuristic way to include it is to write

$$S_x(\omega) = \frac{G^2 Q}{\omega^2 + \epsilon^2}, \quad (8.341)$$

solve the problem by using spectral factorization techniques, and then let $\epsilon \rightarrow 0$. It is easy to verify that this approach gives the system shown in Figure 8.34. ■

Example 8.13. In this example we derive a canonic receiver model for the following problem:

1. The message has a rational spectrum in which the order of the numerator as a function of ω^2 is at least one smaller than the order of the denominator. We use the state-variable model described in Figure 8.22. The \mathbf{F} and \mathbf{G} matrices are given by (8.210) and (8.211), respectively (Canonic Realization No. 2).
2. The received signal is scalar function.

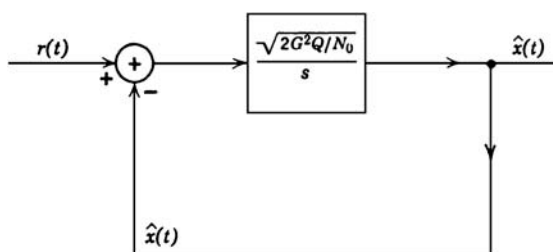


Figure 8.34: Steady-state filter: Example 8.12.

3. The observation matrix has unity in its first column and zero elsewhere. In other words, only the signal would be observed in the absence of measurement noise,

$$\mathbf{C}(t) = [1|0 \cdots 0]. \quad (8.342)$$

The equation describing the estimator is obtained from (8.312),

$$\dot{\hat{\mathbf{x}}}(t) = \mathbf{F}\hat{\mathbf{x}}(t) + \mathbf{K}_g(t)[r(t) - \hat{x}_1(t)] \quad (8.343)$$

and

$$\mathbf{K}_g(t) = \frac{2}{N_0} \xi_P(t) \mathbf{C}^T(t). \quad (8.344)$$

As in Example 8.11, the gains are simply $2/N_0$ times the first row of the error matrix. The resulting filter structure is shown in Figure 8.35. As $t \rightarrow \infty$, the gains become constant.

For the constant-gain case, by comparing the system inside the block to the two diagrams in Figures 8.22 and 8.23a, we obtain the equivalent filter structure shown in Figure 8.36.

Writing the loop filter in terms of its transfer function, we have

$$G_{lo}(s) = \frac{2}{N_0} \frac{\xi_{11}s^{n-1} + \cdots + \xi_{1n}}{s^n + p_{n-1}s^{n-1} + \cdots + p_0}. \quad (8.345)$$

Thus, the coefficients of the numerator of the loop-filter transfer function correspond to the first column in the error matrix. The poles (as we have seen before) are identical to those of the message spectrum. Observe that we still have to solve the variance equation to obtain the numerator coefficients. ■

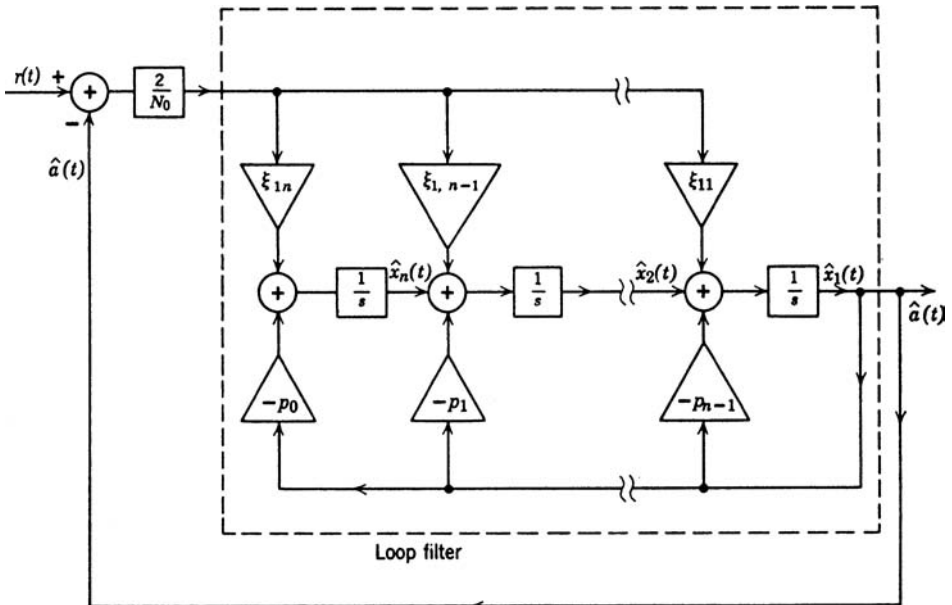


Figure 8.35: Canonic estimator: stationary messages, statistical steady state.

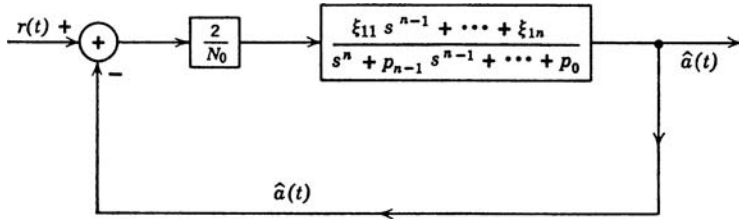


Figure 8.36: Canonic estimator: stationary messages, statistical steady state.

8.3.3 Realizable Whitening Filter

In Section 8.2, we developed a realizable whitening filter for the case of stationary processes and $T_i = -\infty$. In this section we show that¹⁰

$$h_w(t, \tau) = \delta(t - \tau) - h_{or}(t, \tau) \quad (8.346)$$

is a realizable whitening filter for the case of finite observation intervals and possibly nonstationary processes, where $h_{or}(t, \tau)$ denotes the optimum realizable time-varying linear filter for estimating $n_c(t)$ over the observation interval, $T_i \leq \tau \leq t$, assuming $r(\tau) = n_c(\tau) + w(\tau)$. In the case of stationary processes with rational spectra and a residual white noise component where the observation interval is infinite, this is readily verified by taking Fourier transforms and substituting the expression for $H_o(j\omega)$.

We assume that the colored component of the noise may be obtained as the output of a linear (possibly time-varying) dynamic system that is driven with white Gaussian noise. Moreover, we assume that this system has a state-variable representation.

$$\dot{\mathbf{x}}(t) = \mathbf{F}(t)\mathbf{x}(t) + \mathbf{G}(t)\mathbf{u}(t), \quad (8.347)$$

$$n_c(t) = \mathbf{C}_n(t)\mathbf{x}(t), \quad (8.348)$$

$$\begin{aligned} r(t) &= n_c(t) + w(t), \\ &= \mathbf{C}_n(t)\mathbf{x}(t) + w(t). \end{aligned} \quad (8.349)$$

These assumptions are not very restrictive for they enable us to discuss a wide class of problems of real interest. Moreover, they enable us to implicitly describe $h_{or}(t, \tau)$ in terms of a second dynamic system that has a state-variable representation (the Kalman-Bucy filter).

$$\dot{\hat{\mathbf{x}}}(t) = [\mathbf{F}(t) - \xi_p(t)\mathbf{C}_n^T(t)R^{-1}(t)\mathbf{C}_n(t)]\hat{\mathbf{x}}(t) + \xi_p(t)\mathbf{C}_n^T(t)R^{-1}(t)r(t), \quad (8.350)$$

$$\hat{\mathbf{x}}(T_i) = \mathbf{0}, \quad (8.351)$$

$$\hat{n}_c(t) = \mathbf{C}_n(t)\hat{\mathbf{x}}(t), \quad (8.352)$$

$$\dot{\xi}_p(t) = \mathbf{F}(t)\xi_p(t) + \xi_p(t)\mathbf{F}^T(t) - \xi_p(t)\mathbf{C}_n^T(t)R^{-1}(t)\mathbf{C}_n(t)\xi_p(t) + \mathbf{G}(t)\mathbf{Q}(t)\mathbf{G}^T(t), \quad (8.353)$$

$$\xi_p(T_i) = \mathbf{K}_x(T_i, T_i). \quad (8.354)$$

¹⁰This section is taken from Collins [Col68c]

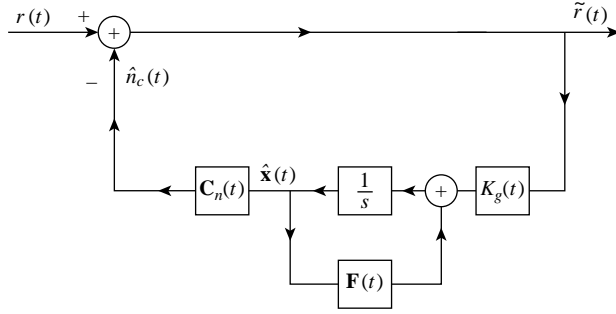


Figure 8.37: Realizable whitening filter

After a little block-diagram manipulation, the alleged whitening filter is as shown in Figure 8.37. We now calculate the covariance function at its output.

$$K_{\tilde{r}}(t, \tau) = E[\tilde{r}(t)\tilde{r}(\tau)] = K_w(t, \tau) + \mathbf{C}_n(t)\mathbf{K}_{x_\epsilon w}(t, \tau) + \mathbf{K}_{w x_\epsilon}(t, \tau)\mathbf{C}_n^T(\tau) + \mathbf{C}_n(t)\mathbf{K}_{x_\epsilon}(t, \tau)\mathbf{C}_n^T(\tau), \quad (8.355)$$

where $\mathbf{x}_\epsilon = \mathbf{x}(t) - \hat{\mathbf{x}}(t)$.

We compute each term separately.

$$K_w(t, \tau) = R(t)\delta(t - \tau)$$

$$\mathbf{C}_n(t)\mathbf{K}_{x_\epsilon w}(t, \tau) = \begin{cases} -\mathbf{C}_n(t)\Psi(t, \tau)\xi_p(\tau)\mathbf{C}_n^T(\tau), & T_i < \tau < t, \\ -\frac{1}{2}\mathbf{C}_n(t)\xi_p(t)\mathbf{C}_n^T(t), & t = \tau, \\ 0, & t < \tau, \end{cases} \quad (8.356)$$

where $\Psi(t, \tau)$ is the fundamental transition matrix for the Kalman filter; that is,

$$\dot{\Psi}(t, T_i) = [\mathbf{F}(t) - \xi_p(t)\mathbf{C}_n^T(t)\mathbf{R}^{-1}(t)\mathbf{C}_n(t)]\Psi(t, T_i), \quad (8.357)$$

$$\Psi(T_i, T_i) = \mathbf{I}. \quad (8.358)$$

Similarly,

$$\mathbf{K}_{w x_\epsilon}(t, \tau)\mathbf{C}_n^T(\tau) = \begin{cases} -\mathbf{C}_n(t)\xi_p(t)\Psi^T(\tau, t)\mathbf{C}_n^T(\tau), & T_i < t < \tau, \\ -\frac{1}{2}\mathbf{C}_n(t)\xi_p(t)\mathbf{C}_n^T(t), & t = \tau, \\ 0, & \tau < t. \end{cases} \quad (8.359)$$

Finally,

$$\mathbf{K}_{x_\epsilon}(t, \tau) = \begin{cases} \xi_p(t)\Psi^T(\tau, t), & T_i < t < \tau, \\ \xi_p(t), & t = \tau, \\ \Psi(t, \tau)\xi_p(\tau), & T_i < \tau < t. \end{cases} \quad (8.360)$$

These results are immediate consequences of the transition properties of state-variable dynamic systems and can be readily verified. Substituting, we find that

$$K_{\tilde{r}}(t, \tau) = R(t)\delta(t - \tau), \quad (8.361)$$

so that we indeed have found a realizable whitening filter.

We can normalize the white noise process by multiplying by $R^{-\frac{1}{2}}(t)$,

$$\tilde{r}_*(t) = R^{-\frac{1}{2}}(t)\tilde{r}(t). \quad (8.362)$$

The generalization of the above results to include vector received signals $\mathbf{r}(t)$ having a vector white noise component $\mathbf{w}(t)$, where

$$\mathbf{K}_w(t, \tau) = \mathbf{R}(t)\delta(t - \tau) \quad (8.363)$$

and $\mathbf{R}(t)$ is positive definite is straightforward [Col66c, Col66b]. Having thus whitened the received signal, a linear transformation on its components yields a diagonal white noise covariance.

Second, the requirement that the colored noise component have a state-variable representation is a sufficient, but not a necessary, condition for (8.346) to hold. An alternative derivation based on the impulse response characterization requires that the integral equation

$$K_{nc}(t, \tau) = \frac{N_0}{2}h_o(t, \tau) + \int_{T_i}^t h_o(t, z)K_{nc}(z, \tau)dz \quad (8.364)$$

have a solution [Col66c].

8.3.4 Generalizations

Several generalizations are necessary in order to include other problems of interest. We discuss them briefly in this section.

Prediction. In this case $\mathbf{d}(t) = \mathbf{x}(t + \alpha)$, where α is positive. We can show easily that

$$\hat{\mathbf{d}}(t) = \phi(t + \alpha, t)\hat{\mathbf{x}}(t), \quad \alpha > 0, \quad (8.365)$$

where $\phi(t, \tau)$ is the transition matrix of the system,

$$\dot{\mathbf{x}}(t) = \mathbf{F}(t)\mathbf{x}(t) + \mathbf{G}(t)\mathbf{u}(t) \quad (8.366)$$

(see Problem 8.3.29).

When we deal with a constant parameter system,

$$\phi(t + \alpha, t) = e^{\mathbf{F}\alpha}, \quad (8.367)$$

and (8.365) becomes

$$\hat{\mathbf{d}}(t) = e^{\mathbf{F}\alpha}\hat{\mathbf{x}}(t). \quad (8.368)$$

Filtering with Delay. In this case $\mathbf{d}(t) = \mathbf{x}(t + \alpha)$, but α is negative. From our discussions we know that considerable improvement is available and we would like to include it. The modification is not so straightforward as the prediction case. It turns out that the canonic receiver first finds the realizable estimate and then uses it to obtain the desired estimate. A good reference for this type of problem is Baggeroer [Bag66].

The problem of estimating $\mathbf{x}(t_1)$, where t_1 is a point interior to a fixed observation interval, is also discussed in this reference. These problems are the state-variable counterparts to the unrealizable filters discussed in Section 8.2.3. The solution is referred to as the Kalman smoother in the literature. There is good discussion in Chapter 5 of Gelb [Gel74].

Linear Transformations on the State Vector. If $\mathbf{d}(t)$ is a linear transformation of the state variables $\mathbf{x}(t)$, that is,

$$\mathbf{d}(t) = \mathbf{k}_d(t)\mathbf{x}(t), \quad (8.369)$$

then

$$\hat{\mathbf{d}}(t) = \mathbf{k}_d(t)\hat{\mathbf{x}}(t). \quad (8.370)$$

Observe that $\mathbf{k}_d(t)$ is *not* a linear filter. It is a linear transformation of the state variables. This is simply a statement of the fact that minimum mean-square estimation and linear transformation commute. The error matrix follows easily,

$$\xi_{\mathbf{d}}(t) \triangleq E[(\mathbf{d}(t) - \hat{\mathbf{d}}(t))(\mathbf{d}^T(t) - \hat{\mathbf{d}}^T(t))] = \mathbf{k}_d(t)\xi_P(t)\mathbf{k}_d^T(t). \quad (8.371)$$

A number of examples are given in the problems to illustrate these generalizations. We will revisit the Kalman filter when we discuss discrete-time processes in Chapter 9.

8.3.5 Implementation Issues

In the examples that we used in the text and in the problems the state vector $\mathbf{x}(t)$ and observation vector $\mathbf{r}(t)$ were low dimension. In practice, one may be dealing with filters with state vectors in the 100 s. We have to be aware of a number of issues that include the following:

- (a) Computational complexity due to matrix inversions.
- (b) The $\xi_P(t)$ matrix losing its positive definiteness due to round-off errors.
- (c) Sensitivity to model mismatch.

Since our filters will be implemented digitally, it is more logical to discuss these issues in the context of discrete-time systems. We do that in Section 9.3.2.

8.4 BAYESIAN ESTIMATION OF NON-GAUSSIAN MODELS

Up to this part in Chapter 8, we have considered the linear estimation problem. If the process model and observation model were Gaussian, then the optimum MSE estimation was a linear

processor, either a Wiener or Kalman filter. If only a second-moment characterization was available, we found the linear filter that minimized the MSE.

In this section, we consider the problem in which both the process model and the observation model may be non-Gaussian.

Our objective is to provide an introduction to the nonlinear filter/tracking problem. We will provide just enough background to motivate the development of *extended Kalman filter* (EKF). The EKF is an extension of the Kalman filter that works well in a number of applications, but has no claim to optimality. There are a number of algorithms that work better than the EKF in some applications.

A detailed discussion of a particular nonlinear estimation algorithm is beyond the scope of our book. We have tried to give adequate references so that the reader can obtain more detailed explanations.

The nonlinear filtering/tracking problem has a long history and there have been a number of books that include discussions of the topic. A representative list includes Jazwinski [Jaz70], Sage and Melsa [SM71], Gelb [Gel74], Anderson and Moore [AM79], Maybeck [May82], Spall [Spa88], Tanizaki [Tan96], Stone et al. [SBC99], Bar-Shalom et al. [BSLK01], and Ristic et al. [RAG04]. There have also been a large number of papers that we will cite at various points.

In this section, we consider continuous-time processes and continuous-time observations. In Section 9.3.5, we consider two other cases: continuous-time processes and discrete-time observations and discrete-time processes and discrete-time observations.

In Section 8.4.1, we develop a hierarchy of models and the corresponding extended Kalman filters. In Section 8.4.2, we discuss a Bayesian Cramér–Rao bound that bounds the MSE of any estimator. In Section 8.4.3, we summarize our results.

8.4.1 The Extended Kalman Filter

We consider models with a nonlinear process equation

$$\dot{\mathbf{x}}(t) = \mathbf{f}(\mathbf{x}(t), \mathbf{u}(t), t) \quad (8.372)$$

and a nonlinear observation equation,

$$\mathbf{r}(t) = \mathbf{c}(\mathbf{x}(t), \mathbf{w}(t), t). \quad (8.373)$$

The functions $\mathbf{u}(t)$ and $\mathbf{w}(t)$ are white, but not necessarily Gaussian, and may not appear as additive terms.

We derive a hierarchy of models that will enable us to model a large number of applications. The hierarchy is shown in Table 8.1. We start with the simplest model (linear Gaussian process and linear observations) and work our way upward in difficulty. Our models will emphasize the state-variable approach but we will include the correlation function approach where appropriate.¹¹

¹¹The Appendix in Part II of *Detection, Estimation, and Modulation Theory* [Van71a, Van03], which was written by Arthur Baggeroer, has a detailed discussion of how one maps one representation into the other.

Table 8.1: Hierarchy of models

Level	Process model	Observation model
1	$\dot{\mathbf{x}}(t) = \mathbf{F}(t)\mathbf{x}(t) + \mathbf{G}(t)\mathbf{u}(t)$ $\mathbf{u}(t) \sim N(\mathbf{0}, \mathbf{Q}(t))$	$\mathbf{r}(t) = \mathbf{C}(t)\mathbf{x}(t) + \mathbf{w}(t)$ $\mathbf{w}(t) \sim N(\mathbf{0}, \mathbf{R}(t))$
2	$\dot{\mathbf{x}}(t) = \mathbf{F}(t)\mathbf{x}(t) + \mathbf{G}(t)\mathbf{u}(t)$ $\mathbf{u}(t) \sim N(\mathbf{0}, \mathbf{Q}(t))$	$\mathbf{r}(t) = \mathbf{c}(\mathbf{x}(t), t) + \mathbf{w}(t)$ $\mathbf{w}(t) \sim N(\mathbf{0}, \mathbf{R}(t))$
3	$\dot{\mathbf{x}}(t) = \mathbf{f}(\mathbf{x}(t), t) + \mathbf{G}(t)\mathbf{u}(t)$ $\mathbf{u}(t) \sim N(\mathbf{0}, \mathbf{Q}(t))$	$\mathbf{r}(t) = \mathbf{c}(\mathbf{x}(t), t) + \mathbf{w}(t)$ $\mathbf{w}(t) \sim N(\mathbf{0}, \mathbf{R}(t))$
4	$\dot{\mathbf{x}}(t) = \mathbf{f}(\mathbf{x}(t), \mathbf{u}(t), t)$ $\mathbf{u}(t)$ is white (not necessarily Gaussian)	$\mathbf{r}(t) = \mathbf{c}(\mathbf{x}(t), \mathbf{w}(t), t)$ $\mathbf{w}(t)$ is white (not necessarily Gaussian)

8.4.1.1 Linear AWGN Process and Observations

The first-level model assumes a linear AWGN process model and a linear AWGN observation model.

This is the model that we have developed in Section 8.3. We repeat the equations for convenience.

The process model equation is

$$\dot{\mathbf{x}}(t) = \mathbf{F}(t)\mathbf{x}(t) + \mathbf{G}(t)\mathbf{u}(t), \quad T_i \leq t, \quad (8.374)$$

where $\mathbf{x}(t)$ is $n \times 1$, $\mathbf{F}(t)$ is $n \times n$, $\mathbf{G}(t)$ is $n \times p$, and $\mathbf{u}(t)$ is an $p \times 1$ zero-mean WGN process with covariance matrix $\mathbf{Q}(t)$. The observation process is an m -dimensional vector process,

$$\mathbf{r}(t) = \mathbf{C}(t)\mathbf{x}(t) + \mathbf{w}(t), \quad T_i \leq t, \quad (8.375)$$

where $\mathbf{C}(t)$ is an $m \times n$ matrix and $\mathbf{w}(t)$ is an $m \times 1$ zero-mean WGN process with covariance matrix $\mathbf{R}(t)$. The $\mathbf{u}(t)$ and $\mathbf{w}(t)$ processes are statistically independent.

The MMSE and MAP estimators are the same and are obtained using a Kalman filter, and the resulting MSE matrix can be calculated before any data is received. The Kalman filter equations are

Estimator equation

$$\dot{\hat{\mathbf{x}}}(t) = \mathbf{F}(t)\hat{\mathbf{x}}(t) + \mathbf{K}_g(t)[\mathbf{r}(t) - \mathbf{C}(t)\hat{\mathbf{x}}(t)]. \quad (8.376)$$

Gain equation

$$\mathbf{K}_g(t) = \xi_P(t)\mathbf{C}^T(t)\mathbf{R}^{-1}(t). \quad (8.377)$$

The MSE equation

$$\dot{\xi}_P(t) = \mathbf{F}(t)\xi_P(t) + \xi_P(t)\mathbf{F}^T(t) - \xi_P(t)\mathbf{C}^T(t)\mathbf{R}^{-1}(t)\mathbf{C}(t)\xi_P(t) + \mathbf{G}(t)\mathbf{Q}\mathbf{G}^T(t). \quad (8.378)$$

These results are due to Kalman [Kal60] and Kalman and Bucy [KB61], and are discussed in a large number of references.

Since the output of the Kalman filter is the conditional mean of the *a posteriori* probability density of the state vector, the estimate is efficient and the Bayesian Cramér–Rao bound equals $\xi_P(t)$. To emphasize this equality, we can rewrite (8.378) as a BCRB equation,

$$\dot{\mathbf{B}}_l(t) = \mathbf{F}(t)\mathbf{B}_l(t) + \mathbf{B}_l(t)\mathbf{F}^T(t) - \mathbf{B}_l(t)\mathbf{C}^T(t)\mathbf{R}^{-1}(t)\mathbf{C}(t)\mathbf{B}_l(t) + \mathbf{G}(t)\mathbf{Q}(t)\mathbf{G}^T(t), \quad (8.379)$$

where the subscript “*l*” denotes a linear model.

We will also find that many of the Bayesian bound equations have a similar structure to (8.379).

Later in our discussion of bounds, it will be useful to have a differential equation for the Bayesian information matrix. From the definition of the BIM,

$$\mathbf{J}_{Bl}(t)\mathbf{B}_l(t) = \mathbf{I}. \quad (8.380)$$

Differentiating gives

$$\dot{\mathbf{J}}_{Bl}(t)\mathbf{B}_l(t) + \mathbf{J}_{Bl}(t)\dot{\mathbf{B}}_l(t) = \mathbf{0}, \quad (8.381)$$

or

$$\dot{\mathbf{J}}_{Bl}(t) = -\mathbf{J}_{Bl}(t)\dot{\mathbf{B}}_l(t)\mathbf{B}_l^{-1}(t) = -\mathbf{J}_{Bl}(t)\dot{\mathbf{B}}_l(t)\mathbf{J}_{Bl}(t). \quad (8.382)$$

Substituting (8.379) into (8.382) and using (8.380) gives

$$\dot{\mathbf{J}}_{Bl}(t) = -\mathbf{J}_{Bl}(t)\mathbf{F}(t) - \mathbf{F}^T(t)\mathbf{J}_{Bl}(t) + \mathbf{C}^T(t)\mathbf{R}^{-1}\mathbf{C}(t) - \mathbf{J}_{Bl}(t)\mathbf{G}(t)\mathbf{Q}(t)\mathbf{G}^T(t)\mathbf{J}_{Bl}(t). \quad (8.383)$$

The result in (8.383) is the \mathbf{J}_{Bl} recursion for the *information version* of the Kalman filter. We discuss the information version in Chapter 9.

8.4.1.2 Linear AWGN Process, Nonlinear AWGN Observations

The second-level model assumes the linear AWGN process model in (8.374) but assumes a nonlinear AWGN observation model,

$$\mathbf{r}(t) = \mathbf{c}(\mathbf{x}(t), t) + \mathbf{w}(t), \quad T_i \leq t, \quad (8.384)$$

where $\mathbf{c}(\mathbf{x}(t), t)$ is an m -dimensional nonlinear function of $\mathbf{x}(t)$ and $\mathbf{w}(t)$ is an $m \times 1$ zero-mean WGN process with covariance matrix $\mathbf{R}(t)$. The noise processes $\mathbf{u}(t)$ and $\mathbf{w}(t)$ are statistically independent.

Two application areas in which this model is appropriate are communications systems and tracking in radar/sonar systems. In a frequency-modulation system, the transmitted signal is

$$s(y(t), t) = \sqrt{2P} \sin [\omega_c t + \beta y(t)], \quad (8.385)$$

where ω_c is the carrier frequency, β is the modulation index, and

$$y(t) = \mathbf{C}\mathbf{x}(t), \quad (8.386)$$

where $\mathbf{x}(t)$ is modeled as a Gaussian random process. Thus,

$$c(\mathbf{x}(t), t) = \sqrt{2P} \sin [\omega_c t + \beta \mathbf{C}\mathbf{x}(t)]. \quad (8.387)$$

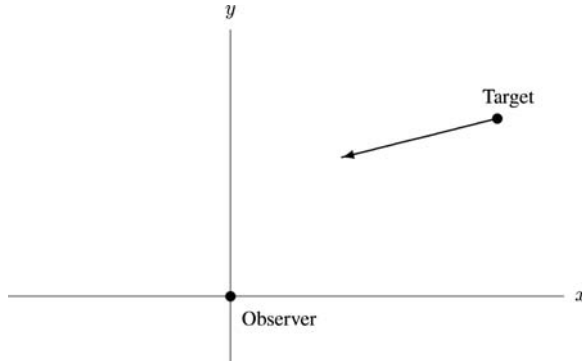


Figure 8.38: Two-dimensional tracking scenario.

To illustrate the nonlinear tracking problem, consider a two-dimensional model in which the target has nominal constant-velocity path as shown in Figure 8.38. Then

$$\mathbf{x}(t) = \begin{bmatrix} x(t) \\ \dot{x}(t) \\ y(t) \\ \dot{y}(t) \end{bmatrix}, \quad (8.388)$$

where the scalar terms denote the position and velocity of the target in the $x - y$ plane as a function of time, and

$$\dot{\mathbf{x}}(t) = \mathbf{F}\mathbf{x}(t) + \mathbf{G}\mathbf{u}(t), \quad (8.389)$$

where

$$\mathbf{F} = \left[\begin{array}{cc|cc} 0 & 1 & 0 & 0 \\ 0 & 0 & 0 & 0 \\ \hline 0 & 0 & 0 & 1 \\ 0 & 0 & 0 & 0 \end{array} \right] \quad (8.390)$$

$$\mathbf{G} = \left[\begin{array}{cc|cc} 0 & 1 & 0 & 1 \end{array} \right]^T \quad (8.391)$$

and

$$E[\mathbf{w}(t)\mathbf{w}(u)] = \mathbf{Q}(t)\delta(t-u). \quad (8.392)$$

The $\mathbf{u}(t)$ corresponds to white acceleration noise. The term introduces uncertainty into the normal constant-velocity model ($\ddot{x}(t) = u_x(t)$; $\ddot{y}(t) = u_y(t)$). This model, as well as other models, are discussed in Chapter 6 of Bar-Shalom et al. [BSLK01].

The observer is located at the origin and can estimate the range and bearing to the target. Thus,

$$\mathbf{c}(\mathbf{x}(t), t) = \begin{bmatrix} \sqrt{x^2(t) + y^2(t)} \\ \tan^{-1}\left(\frac{y(t)}{x(t)}\right) \end{bmatrix} \quad (8.393)$$

is a 2×1 vector. The received waveform is the output of a radar and $\mathbf{w}(t)$ is modeling the range and bearing errors

$$\mathbf{r}(t) = \mathbf{c}(\mathbf{x}(t), t) + \mathbf{w}(t) \quad (8.394)$$

and

$$E[\mathbf{w}(t)\mathbf{w}(u)^T] = \begin{bmatrix} \sigma_r^2 & 0 \\ 0 & \sigma_b^2 \end{bmatrix} \delta(t, u). \quad (8.395)$$

In order to find the MAP or MMSE estimate, we must first find a differential equation for the conditional probability density function of the state vector given the observations, and then find the conditional mean or the conditional mode. Kushner [Kus64b] was the first to derive the equation for the conditional probability density function (e.g. [Kus64a, Kus67a]).¹² This nonlinear equation can be mapped into a linear stochastic partial differential equation (SPDE) known as the Zakai equation, derived by Zakai [Zak69]. Kunita [Kun82] showed that there is a one-to-one correspondence between the equations. The Zakai equation is discussed in detail in Haykin et al. [HYD97]. Daum [Dau87] develops solutions for a class of nonlinear models. The reader is referred to these references for discussion of this model.

Kushner [Kus67b] also derived the exact equations for the conditional mode that is the MAP estimate. As Kushner points out, the difficulty is that a system corresponding to the exact equation cannot be built with a finite number of components.

One approach to obtaining an approximate MMSE or MAP estimate is to linearize around the current estimate.

This approach leads to the *extended Kalman filter* that is due to Swerling [Swe59] (e.g. [Sor85]).

We define

$$\left[\tilde{\mathbf{C}}(\hat{\mathbf{x}}(t), t) \right]_{ij} = \left[\frac{\partial c_i(\mathbf{x}(t), t)}{\partial x_j} \right]_{\mathbf{x}(t)=\hat{\mathbf{x}}(t)}. \quad (8.396)$$

The recursive equations for the EKF are

State estimation equation

$$\dot{\hat{\mathbf{x}}}(t) = \mathbf{F}(t)\hat{\mathbf{x}}(t) + \mathbf{K}_g(t)[\mathbf{r}(t) - \mathbf{c}(\hat{\mathbf{x}}(t), t)]. \quad (8.397)$$

¹²There was parallel work by Stratonovich, which is described in [Str59b, Str59a, Str60b, Str60a, Str66].

MSE equation

$$\dot{\xi}_P(t) = \mathbf{F}(t)\xi_P(t) + \xi_P(t)\mathbf{F}(t)^T + \mathbf{G}(t)\mathbf{Q}(t)\mathbf{G}^T(t) - \xi_P(t)\tilde{\mathbf{C}}^T(\hat{\mathbf{x}}(t), t)\mathbf{R}^{-1}(t)\tilde{\mathbf{C}}(\hat{\mathbf{x}}(t), t)\xi_P(t). \quad (8.398)$$

Gain equation

$$\mathbf{K}_g(t) = \xi_P(t)\tilde{\mathbf{C}}^T(\hat{\mathbf{x}}(t), t)\mathbf{R}^{-1}(t). \quad (8.399)$$

Initial condition

$$\hat{\mathbf{x}}(0) \sim N(\hat{\mathbf{x}}_0, \xi_0). \quad (8.400)$$

For the model in (8.388)–(8.393)

$$\tilde{\mathbf{C}}(\hat{\mathbf{x}}(t), t) = \begin{bmatrix} \frac{\hat{x}(t)}{\hat{R}(t)} & 0 & \frac{\hat{y}(t)}{\hat{R}(t)} & 0 \\ \frac{-\hat{y}(t)}{\hat{R}^2(t)} & 0 & \frac{\hat{x}(t)}{\hat{R}^2(t)} & 0 \end{bmatrix}, \quad (8.401)$$

where

$$\hat{R}(t) \triangleq \sqrt{\hat{x}^2(t) + \hat{y}^2(t)}. \quad (8.402)$$

We consider several examples in the problems. Note that the EKF has no claim to optimality.

8.4.1.3 Nonlinear AWGN Process and Observations

The third-level process model assumes that $\mathbf{x}(t)$ is a nonlinear Markov process of the form

$$\dot{\mathbf{x}}(t) = \mathbf{f}(\mathbf{x}(t), t) + \mathbf{G}(t)\mathbf{u}(t), \quad (8.403)$$

where $\mathbf{f}(\mathbf{x}(t), t)$ is an n -dimensional nonlinear function and $\mathbf{u}(t)$ is a zero-mean WGN process with covariance matrix $\mathbf{Q}(t)$. The nonlinear observation model is given by (8.384).

We expand $\mathbf{f}(\mathbf{x}(t), t)$ and $\mathbf{c}(\mathbf{x}(t), t)$ in a Taylor series around the current estimate $\hat{\mathbf{x}}(t)$ and retain the first-order terms. Then we have

$$[\tilde{\mathbf{F}}(\hat{\mathbf{x}}(t), t)]_{ij} = \left. \frac{\partial f_i(\mathbf{x}(t), t)}{\partial x_j} \right|_{\mathbf{x}(t)=\hat{\mathbf{x}}(t)}, \quad (8.404)$$

and $\tilde{\mathbf{C}}(\hat{\mathbf{x}}(t), t)$ was defined in (8.396). The continuous-time EKF equations are

Estimator equation

$$\dot{\hat{\mathbf{x}}}(t) = \mathbf{f}(\hat{\mathbf{x}}(t), t) + \mathbf{K}_g(t)[\mathbf{r}(t) - \mathbf{c}(\hat{\mathbf{x}}(t), t)] \quad (8.405)$$

with $\hat{\mathbf{x}}(0) \sim N(\hat{\mathbf{x}}_0, \xi_0)$.

Gain equation

$$\mathbf{K}_g(t) = \xi_P(t)\tilde{\mathbf{C}}^T(\hat{\mathbf{x}}(t), t)\mathbf{R}^{-1}(t). \quad (8.406)$$

MSE equation

$$\begin{aligned}\dot{\xi}_P(t) &= \tilde{\mathbf{F}}(\hat{\mathbf{x}}(t), t)\xi_P(t) + \xi_P(t)\tilde{\mathbf{F}}^T(\hat{\mathbf{x}}(t), t) + \mathbf{G}(t)\mathbf{Q}(t)\mathbf{G}^T(t) \\ &\quad - \xi_P(t)\tilde{\mathbf{C}}^T(\hat{\mathbf{x}}(t), t)\mathbf{R}^{-1}(t)\tilde{\mathbf{C}}(\hat{\mathbf{x}}(t), t)\xi_P(t).\end{aligned}\quad (8.407)$$

Note that the MSE equation is coupled with the estimator equation and cannot be precomputed.

An example of this model occurs in [AH83] (by Aidala and Hammel), where the process is modeled using modified polar coordinates,¹³

$$\mathbf{x}(t) = \begin{bmatrix} \dot{\theta}(t) \\ \dot{R}(t)/R(t) \\ \theta(t) \\ 1/R(t) \end{bmatrix}. \quad (8.408)$$

For the case in which we observe the bearing angle in the presence of noise, the observation equation is linear,

$$\mathbf{r}(t) = \mathbf{Cx}(t) + \mathbf{w}(t), \quad (8.409)$$

where

$$\mathbf{C} = \begin{bmatrix} 0 & 0 & 1 & 0 \end{bmatrix}. \quad (8.410)$$

This coordinate system is useful in the bearings-only tracking problem. The process equation is nonlinear and the observation equation is linear. Chapter 6 of [RAG04] contains a discussion of an EKF implementation in this coordinate system for the discrete-time process model.

8.4.1.4 General Nonlinear Process and Observations

The fourth-level model is the general nonlinear model that has a nonlinear process equation,

$$\dot{\mathbf{x}}(t) = \mathbf{f}(\mathbf{x}(t), \mathbf{u}(t), t) \quad (8.411)$$

and a nonlinear observation equation,

$$\dot{\mathbf{r}}(t) = \mathbf{c}(\mathbf{x}(t), \mathbf{w}(t), t). \quad (8.412)$$

The functions $\mathbf{u}(t)$ and $\mathbf{w}(t)$ are white and independent, but not necessarily Gaussian and may not appear as additive terms. This is the most general model but most applications do not require this level of generality.

Just as in the parameter estimation case, it is important to establish bounds of the performance of the estimator. We derive Bayesian Cramér–Rao bounds in Section 8.4.2.

8.4.2 Bayesian Cramér–Rao Bounds: Continuous-Time

The first application of Bayesian Cramér–Rao bounds to random processes is due to Van Trees [Van66b]. The problem of interest is

$$r(t) = c(y(t), t) + n(t), \quad T_i \leq t \leq T_f, \quad (8.413)$$

¹³A complete discussion of this model is given on pp. 114–118 in Chapter 6 of Ristic et al. [RAG04].

where $y(t)$ is a zero-mean Gaussian random process with covariance function $K_y(t, u)$ and $n(t)$ is a statistically independent zero-mean Gaussian random process with covariance function $K_n(t, u)$.

Previous work by Lehan and Parks [LP53] and Youla [You54] had derived the equations specifying the MAP estimate of $y(t)$, $T_i \leq t \leq T_f$ (an interval estimate). The mean-square interval error is defined as

$$\xi_I = \frac{1}{T_f - T_i} E \left\{ \int_{T_i}^{T_f} [y(t) - \hat{y}(t)]^2 dt \right\}. \quad (8.414)$$

The Bayesian CRB derived in [Van66a, VB07] is

$$\xi_I \geq \int_{T_i}^{T_f} \gamma(t, t) dt, \quad (8.415)$$

where $\gamma(t, x)$ is the solution to an integral equation.

For the white noise case, the noise covariance function is

$$K_n(t, u) = \frac{N_0}{2} \delta(t - u), \quad (8.416)$$

and the integral equation is

$$\gamma(t, x) + \int_{T_i}^{T_f} \frac{2}{N_0} \gamma(t, u) R_{d_s}(u, u) K_y(u, x) du = K_y(t, x), \quad T_i \leq t, x \leq T_f, \quad (8.417)$$

where

$$R_{d_s}(t, u) \triangleq E \{ d_s(y(t), t) d_s(y(u), u) \} \quad (8.418)$$

and

$$d_s(y(t), t) = \frac{\partial c(y(t), t)}{\partial y(t)}. \quad (8.419)$$

For a bandpass signal such as

$$c(y(t), t) = \sqrt{2P} \sin(\omega_c t + \beta y(t)), \quad (8.420)$$

$R_{d_s}(u, u)$ can be approximated by a constant $R_{d_s}(0) = \beta^2 P$. Then, (8.417) reduces to

$$\gamma(t, x) + \frac{2R_{d_s}(0)}{N_0} \int_{T_i}^{T_f} \gamma(t, u) K_y(u, x) du = K_y(t, x), \quad T_i \leq t, x \leq T_f, \quad (8.421)$$

which is familiar as the equation specifying the optimum linear filter. Thus, the Bayesian CRB corresponds to the MSE in an optimum linear filter with the white noise level reduced by $R_{d_s}(0)$. Van Trees also indicated, but did not prove, the same result for a realizable estimator.

Snyder ([SR72] and [VB07]) derived the Bayesian Cramér–Rao bound for the causal (realizable) estimate for the Level 2 model in (8.374) and (8.384). Snyder shows that

$$\xi_P(t) \geq \mathbf{B}_g(t), \quad (8.422)$$

where the subscript “ g ” denotes that the process model is a linear Gaussian model. The matrix $\mathbf{B}_g(t)$ satisfies the matrix differential equation

$$\dot{\mathbf{B}}_g(t) = \mathbf{F}(t)\mathbf{B}_g(t) + \mathbf{B}_g(t)\mathbf{F}^T(t) + \mathbf{G}(t)\mathbf{Q}\mathbf{G}^T(t) - \mathbf{B}_g(t)\mathbf{P}(t)\mathbf{B}_g(t), \quad (8.423)$$

where

$$\mathbf{P}(t) \triangleq E_{\mathbf{x}} \left\{ \tilde{\mathbf{C}}^T(\mathbf{x}(t), t)\mathbf{R}^{-1}(t)\tilde{\mathbf{C}}(\mathbf{x}(t), t) \right\}. \quad (8.424)$$

Note that the expectation in (8.424) is with respect to the state vector $\mathbf{x}(t)$ and will usually have to be evaluated by a Monte Carlo simulation.

The first three terms indicate how the bound matrix is propagated due to the process dynamics and the last term incorporates the reduction in the bound due to the observation. Comparing (8.423) with the linear Bayesian CRB equation (8.379), we see that they have the same structure with the $\mathbf{C}^T(t)\mathbf{R}^{-1}(t)\mathbf{C}(t)$ term replaced by $\mathbf{P}(t)$. Thus, the effect is to create a new additive noise covariance matrix. This is just the matrix analog to the scalar result in (8.421).

Note that in the linear observation case,

$$\mathbf{c}(\mathbf{x}(t), t) = \mathbf{C}(t)\mathbf{x}(t) \quad (8.425)$$

and

$$\tilde{\mathbf{C}}(\mathbf{x}(t), t) = \mathbf{C}(t). \quad (8.426)$$

Then, (8.423) reduces to (8.379) and no expectation is required because the term in the braces does not depend on $\mathbf{x}(t)$.

The Bayesian information matrix equation is obtained by substituting (8.423) into (8.382),

$$\mathbf{J}_{Bg}(t) = -\mathbf{J}_{Bg}(t)\mathbf{F}(t) - \mathbf{F}^T(t)\mathbf{J}_{Bg}(t) - \mathbf{J}_{Bg}(t)\mathbf{G}(t)\mathbf{Q}(t)\mathbf{G}^T(t)\mathbf{J}_{Bg}(t) + \mathbf{P}(t). \quad (8.427)$$

In nonlinear tracking problems, we are often interested in how well we can estimate a specific track. In this case, we set $\mathbf{Q}(t) = 0$. The resulting equations are identical to the EKF equations in (8.396)–(8.400) except that the terms are evaluated at the true value of $\mathbf{x}(t)$ instead of the estimated value.

The results in (8.427) have been applied to various analog communication problems in [Sny69] and optimum demodulators have been compared to the BCRBs.

The Bayesian CRB for the third-level process model for the one-dimensional case was derived by Bobrovsky and Zakai in [BZ75] and [BZ76] (the formulation is for the vector case but the detailed results are for the scalar case). [BZ75] considers both the discrete-time case and continuous-time case. They derive the bound by defining an equivalent linear system whose error correlation matrix provides a lower bound on the actual correlation matrix. In [BZ76], they use the Bayesian version of the Barankin bound in the derivation but only consider the case when $h \rightarrow 0$, which gives the BCRB in most of their work. For the linear Gaussian process model, their result reduces to those of Snyder and Rhodes [SR72].

The Bayesian CRB is most useful when the SNR is high. Bobrovsky et al. [BZZ88] derive upper and lower bounds for the small measurement noise case.

8.4.3 Summary

In this section, we have given a brief introduction to the estimation of nonlinear processes and nonlinear observations. We derived the extended Kalman filter and a Bayesian CRB on the performance of any estimator.

In almost all tracking applications the observations will be discrete time. We will discuss that case in Section 9.3.5. The continuous-time observation model provide a bound on the discrete-time model.

8.5 SUMMARY

In this chapter, we have studied the linear estimation of continuous-time random processes. If the random processes are Gaussian, then the optimum MMSE linear estimator is also the optimum Bayes estimator for either a MMSE or MAP criterion.

Section 8.1 developed the equations specifying the optimum linear filter for processes described by a second-moment characterization. The key result was the integral equation (8.3) whose solution was the impulse response of the optimum filter

$$K_{dr}(t, u) = \int_{T_i}^{T_f} h_o(t, \tau) K_r(\tau, u) d\tau, \quad T_i < u < T_f, \quad (8.428)$$

where $K_{dr}(t, u)$ is the cross-covariance function between the desired signal $d(t)$ and the observed input $r(u)$.

The mean-square error of the optimum was given by (8.21)

$$\xi_{P_o}(t) \triangleq E[e_o^2(t)] = K_d(t, t) - \int_{T_i}^{T_f} h_o(t, \tau) K_{dr}(t, \tau) d\tau. \quad (8.429)$$

An important result was that the error at time t using the optimum linear processor is uncorrelated with the input $r(u)$ at every point in the observation interval.

$$E[e_o(t)r(u)] = 0, \quad T_i < u < T_f. \quad (8.430)$$

If the Gaussian assumption was satisfied, then $e_o(t)$ and $r(u)$ were statistically independent.

Section 8.2 developed the Wiener filter for the case in which $T_i = -\infty$ and the random processes were stationary. In this case (8.428) reduces to (8.78)

$$K_{dr}(\tau) = \int_0^\infty h_o(v) K_r(\tau - v) dv, \quad 0 < \tau < \infty, \quad (8.431)$$

which is the Wiener–Hopf equation. We solved (8.431) using spectrum factorization. The optimum realizable filter was given by (8.98)

$$\boxed{H_o(j\omega) = \left[\frac{1}{G^+(j\omega)} \right] \left[\frac{S_{dr}(j\omega)}{[G^+(j\omega)]^*} \right]_+} \quad (8.432)$$

and the minimum mean-square error was given by (8.128)

$$\xi_P = K_d(0) - \int_0^\infty K_{dz}^2(t) dt. \quad (8.433)$$

In the special case where the desired signal is $s(t)$ and the noise is white noise, a closed form expression for ξ_P was given by (8.177)

$$\boxed{\xi_P = \frac{N_0}{2} \int_{-\infty}^\infty \ln \left[1 + \frac{S_s(\omega)}{N_0/2} \right] \frac{d\omega}{2\pi},} \quad (8.434)$$

which is twice the mutual information (as defined by Shannon) between $r(t)$ and $s(t)$.

We also considered optimum unrealizable filters which are given by (8.144)

$$\boxed{H_{ou}(j\omega) = \frac{S_{dr}(j\omega)}{S_r(\omega)}} \quad (8.435)$$

and the mean-square error is given by (8.147)

$$\boxed{\xi_u = \int_{-\infty}^\infty \frac{S_d(\omega)S_r(\omega) - |S_{dr}(j\omega)|^2}{S_r(\omega)} \frac{d\omega}{2\pi}.} \quad (8.436)$$

The essential points to remember when discussing unrealizable filters are the following:

1. The mean-square error using an unrealizable linear filter ($T_f = \infty$) provides a lower bound on the mean-square error for any realizable linear filter. It corresponds to the *irreducible* (or infinite delay) error. The computation of ξ_u (8.436) is usually easier than the computation of ξ_P (8.433) or (8.434). Therefore, it is a logical preliminary calculation even if we are interested only in the realizable filtering problem.
2. We can build a realizable filter whose performance approaches the performance of the unrealizable filter by allowing delay in the output. We can obtain a mean-square error that is arbitrarily close to the irreducible error by increasing this delay. From the practical standpoint a delay of several times the reciprocal of the effective bandwidth of $[S_d(\omega) + S_n(\omega)]$ will usually result in a mean-square error close to the irreducible error.

The second part of the chapter studied the continuous-time Kalman filter. The processes were characterized by a linear differential equations (8.231a) and (8.231b)

$$\dot{\mathbf{x}}(t) = \mathbf{F}(t)\mathbf{x}(t) + \mathbf{G}(t)\mathbf{u}(t), \quad (8.437)$$

$$\mathbf{y}(t) = \mathbf{C}(t)\mathbf{x}(t). \quad (8.438)$$

The resulting Kalman filter was specified by three equations:

Estimator equation

$$\boxed{\frac{d\hat{\mathbf{x}}(t)}{dt} = \mathbf{F}(t)\hat{\mathbf{x}}(t) + \mathbf{K}_g(t)[\mathbf{r}(t) - \mathbf{C}(t)\hat{\mathbf{x}}(t)].} \quad (8.439)$$

Gain equation

$$\boxed{\mathbf{K}_g(t) = \xi_P(t)\mathbf{C}^T(t)\mathbf{R}^{-1}(t).} \quad (8.440)$$

Variance equation

$$\boxed{\frac{d\xi_P(t)}{dt} = \mathbf{F}(t)\xi_P(t) + \xi_P(t)\mathbf{F}^T(t) - \xi_P(t)\mathbf{C}^T(t)\mathbf{R}^{-1}(t)\mathbf{C}(t)\xi_P(t) + \mathbf{G}(t)\mathbf{Q}\mathbf{G}^T(t)} \quad (8.441)$$

with initial conditions $\hat{\mathbf{x}}(0)$ and $\xi_P(0)$.

If \mathbf{F} , \mathbf{G} , \mathbf{C} , and \mathbf{R} were constants and the system generation model were stable, the Kalman filter approached a steady-state filter that was identical to the Wiener filter.

We also derived a state-variable implementation of a realizable whitening filter that could be used in the colored noise detector of Chapter 7.

We described several generalizations; the Kalman predictor and the Kalman filter with lag, but did not develop them in detail. We will give a complete discussion in Chapter 9.

Section 8.4 introduced Bayesian estimation of non-Gaussian models. Our objective was to provide just enough background to motivate the development of the intended Kalman filter and the Bayesian Cramér–Rao bound.

The Bayesian information matrix was given by (8.427) and (8.424)

$$\dot{\mathbf{J}}_{Bg}(t) = -\mathbf{J}_{Bg}(t)\mathbf{F}(t) - \mathbf{F}^T(t)\mathbf{J}_{Bg}(t) - \mathbf{J}_{Bg}(t)\mathbf{G}(t)\mathbf{Q}(t)\mathbf{G}^T(t)\mathbf{J}_{Bg}(t) + \mathbf{P}(t), \quad (8.442)$$

where

$$\mathbf{P}(t) \triangleq E_{\mathbf{x}} \left\{ \tilde{\mathbf{C}}^T(\mathbf{x}(t), t)\mathbf{R}^{-1}(t)\tilde{\mathbf{C}}(\mathbf{x}(t), t) \right\}. \quad (8.443)$$

The expectation in (8.443) is with respect to the state vector $\mathbf{x}(t)$ and will usually have to be evaluated by a Monte Carlo simulation.

There are implementation issues for both the Kalman filter and the extended Kalman filter. These issues include the following:

- (a) Computational complexity due to matrix inversions.
- (b) The $\xi_p(t)$ matrix losing its positive definiteness due to round-off errors.
- (c) Sensitivity to model mismatch.

Optimum linear filters, particularly Kalman filters, are used in a diverse variety of applications. An Internet search will reveal a surprising number of disciplines in which the linear filter plays a key role.

8.6 PROBLEMS

P8.1 Optimum Linear Processors

Problem 8.1.1. Let

$$r(t) = a(t) + n(t), \quad T_i \leq t \leq T_f,$$

where $a(t)$ and $n(t)$ are uncorrelated Gaussian zero-mean processes with covariance functions $K_a(t, u)$ and $K_n(t, u)$, respectively. Find $p_{a(t_1)|r(t):T_i \leq t \leq T_f}(A|R(t) : T_i \leq t \leq T_f)$.

Problem 8.1.2. Consider the model in Figure 8.3. Prove

$$\mathbf{K}_{\text{dr}}(t, u) = \int_{T_i}^{T_f} \mathbf{h}_o(t, \tau) \mathbf{K}_r(\tau, u) d\tau, \quad T_i < u < T_f.$$

Problem 8.1.3. Consider the vector model in Figure 8.3. Prove that

$$\mathbf{h}_o(t, t) \mathbf{R}(t) = \xi_P(t) \mathbf{C}^T(t).$$

Comment. Problems 8.1.4–8.1.9 illustrate cases in which the observation is a finite set of random variables. In addition, the observation noise is zero.

Problem 8.1.4. Consider a simple prediction problem. We observe $a(t)$ at a *single time*. The desired signal is

$$d(t) = a(t + \alpha),$$

where α is a positive constant. Assume that

$$\begin{aligned} E[a(t)] &= 0, \\ E[a(t)a(u)] &= K_a(t - u) \triangleq K_a(\tau). \end{aligned}$$

- (a) Find the best linear MMSE estimate of $d(t)$.
- (b) What is the mean-square error?
- (c) Specialize to the case $K_a(\tau) = e^{-k|\tau|}$.
- (d) Show that, for the correlation function in part (c), the MMSE estimate would not change if the entire past were available.
- (e) Is this true for any other correlation function? Justify your answer.

Problem 8.1.5. Consider the following interpolation problem. You are given the values $a(0)$ and $a(t)$:

$$\begin{aligned} E[a(t)] &= 0, & -\infty < t < \infty, \\ E[a(t)a(u)] &= K_a(t - u), & -\infty < t, u < \infty. \end{aligned}$$

- (a) Find the MMSE estimate of $a(t)$.
- (b) What is the resulting mean-square error?
- (c) Evaluate for $t = T/2$.
- (d) Consider the special case, $K_a(\tau) = e^{-k|\tau|}$, and evaluate the processor constants

Problem 8.1.6. [Pap65]. We observe $a(t)$ and $\dot{a}(t)$. Let $d(t) = a(t + \alpha)$, where α is a positive constant.

- (a) Find the MMSE linear estimate of $d(t)$.
- (b) State the conditions on $K_a(\tau)$ for your answer to be meaningful.
- (c) Check for small α .

Problem 8.1.7. [Pap65]. We observe $a(0)$ and $a(t)$. Let

$$d(t) = \int_0^t a(u) du.$$

- (a) Find the MMSE linear estimate of $d(t)$.
- (b) Check your result for $t \ll 1$.

Problem 8.1.8. Generalize the preceding model to $n + 1$ observations; $a(0), a(t), a(2t), \dots, a(nt)$.

$$d(t) = \int_0^{nt} a(u) du.$$

- (a) Find the equations that specify the optimum linear processor.
- (b) Find an explicit solution for $nt \ll 1$.

Problem 8.1.9. [Pap65]. We want to reconstruct $a(t)$ from an infinite number of samples; $a(nT)$, $n = \dots, -1, 0, +1, \dots$, using a MMSE linear estimate:

$$\hat{a}(t) = \sum_{n=-\infty}^{\infty} c_n(t) a(nT).$$

- (a) Find an expression that the coefficients $c_n(t)$ must satisfy.
- (b) Consider the special case in which

$$S_a(\omega) = 0 \quad |\omega| > \frac{\pi}{T}.$$

Evaluate the coefficients.

- (c) Prove that the resulting mean-square error is zero. (Observe that this proves the sampling theorem for random processes.)

Problem 8.1.10. In (8.26) we saw that

$$E[e_o(t)r(u)] = 0, \quad T_i < u < T_f.$$

- (a) In our derivation we assumed $h_o(t, u)$ was continuous and defined $h_o(t, T_i)$ and $h_o(t, T_f)$ by the continuity requirement. Assume $r(u)$ contains a white noise component. Prove

$$\begin{aligned} E[e_o(t)r(T_i)] &\neq 0, \\ E[e_o(t)r(T_f)] &\neq 0. \end{aligned}$$

- (b) Now remove the continuity assumption on $h_o(t, u)$ and assume $r(u)$ contains a white noise component. Find an equation specifying an $h_o(t, u)$, such that

$$E[e_o(t)r(u)] = 0, \quad T_i \leq u \leq T_f.$$

Are the mean-square errors for the filters in parts (a) and (b) the same? Why?

- (c) Discuss the implications of removing the white noise component from $r(u)$. Will $h_o(t, u)$ be continuous? Do we use strict or nonstrict inequalities in the integral equation?

P8.2 Stationary Processes, Infinite Past (Wiener Filters)

REALIZABLE AND UNREALIZABLE FILTERING

Problem 8.2.1. We have restricted our attention to rational spectra. We write the spectrum as

$$S_r(\omega) = c \frac{(\omega - n_1)(\omega - n_2) \cdots (\omega - n_N)}{(\omega - d_1)(\omega - d_2) \cdots (\omega - d_M)}, \quad n_i \neq d_j,$$

where N and M are even. We assume that $S_r(\omega)$ is integrable on the real line. Prove the following statements:

- (a) $S_r(\omega) = S_r^*(\omega)$.
- (b) c is real.
- (c) All n_i 's and d_i 's with nonzero imaginary parts occur in conjugate pairs.
- (d) $S_r(\omega) \geq 0$.
- (e) Any real roots of numerator occur with even multiplicity.
- (f) No root of the denominator can be real.
- (g) $N < M$.

Verify that these results imply all the properties indicated in Figure 8.7.

Problem 8.2.2. Let

$$r(u) = a(u) + n(u), \quad -\infty < u \leq t.$$

The waveforms $a(u)$ and $n(u)$ are sample functions from uncorrelated zero-mean processes with spectra

$$S_a(\omega) = \frac{2k\sigma_a^2}{\omega^2 + k^2}$$

and

$$S_n(\omega) = N_2\omega^2,$$

respectively.

- (a) The desired signal is $a(t)$. Find the realizable linear filter that minimizes the mean-square error.
- (b) What is the resulting mean-square error?
- (c) Repeat parts (a) and (b) for the case in which the filter may be unrealizable and compare the resulting mean-square errors.

Problem 8.2.3. Consider the model in Problem 8.2.2. Assume that

$$S_n(\omega) = N_0 + N_2\omega^2.$$

- (a) Repeat Problem 8.2.2.
- (b) Verify that your answers reduce to those in Problem 8.2.2 when $N_0 = 0$ and to those in the text when $N_2 = 0$.

Problem 8.2.4. Let

$$r(u) = a(u) + n(u), \quad -\infty < u \leq t.$$

The functions $a(u)$ and $n(u)$ are sample functions from independent zero-mean Gaussian random processes.

$$\begin{aligned} S_a(\omega) &= \frac{2k\sigma_a^2}{\omega^2 + k^2}, \\ S_n(\omega) &= \frac{2c\sigma_n^2}{\omega^2 + c^2}. \end{aligned}$$

We want to find the MMSE point estimate of $a(t)$.

- (a) Set up an expression for the optimum processor.
- (b) Find an explicit expression for the special case

$$\begin{aligned} \sigma_n^2 &= \sigma_a^2, \\ c &= 2k. \end{aligned}$$

- (c) Look at your answer in (b) and check to see if it is intuitively correct.

Problem 8.2.5. Consider the model in Problem 8.2.4. Now let

$$S_n(\omega) = \frac{N_0}{2} + \frac{2c\sigma_n^2}{\omega^2 + c^2}.$$

- (a) Find the optimum realizable linear filter (MMSE).
- (b) Find an expression for ξ_{Ph} .
- (c) Verify that the result in (a) reduces to the result in Problem 8.2.4 when $N_0 = 0$ and to the result in the text when $\sigma_n^2 = 0$.

Problem 8.2.6. Let

$$r(u) = a(u) + w(u), \quad -\infty < u \leq t.$$

The processes are uncorrelated with spectra

$$S_a(\omega) = \frac{2\sqrt{2}P/k}{1 + (\omega^2/k^2)^2}$$

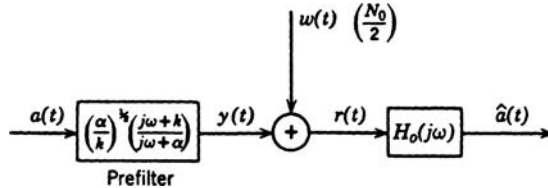


Figure P8.1

and

$$s_w(\omega) = \frac{N_0}{2}.$$

The desired signal is $a(t)$. Find the optimum realizable linear filter (MMSE).

Problem 8.2.7. The message $a(t)$ is passed through a linear network before transmission as shown in Figure P8.1. The output $y(t)$ is corrupted by uncorrelated white noise ($N_0/2$). The message spectrum is $S_a(\omega)$.

$$S_a(\omega) = \frac{2k\sigma_a^2}{\omega^2 + k^2}.$$

- (a) A minimum mean-square error realizable estimate of $a(t)$ is desired. Find the optimum linear filter.
- (b) Find ξ_{p_n} as a function of α and $\Lambda \triangleq 4\sigma_a^2/kN_0$.
- (c) Find the value of α that minimizes ξ_{p_n} .
- (d) How do the results change if the zero in the prefilter is at $+k$ instead of $-k$.

Pure Prediction. The next four problems deal with pure prediction. The model is

$$r(u) = a(u), \quad -\infty < u \leq t,$$

and

$$d(t) = a(t + \alpha),$$

where $\alpha \geq 0$. We see that there is no noise in the received waveform. The object is to *predict* $a(t)$.

Problem 8.2.8. Let

$$S_a(\omega) = \frac{2k}{\omega^2 + k^2}.$$

- (a) Find the optimum (MMSE) realizable filter.
- (b) Find the normalized prediction error $\xi_{p_n}^\alpha$.

Problem 8.2.9. Let

$$S_a(\omega) = \frac{1}{(1 + \omega^2)^2}.$$

Repeat Problem 8.2.8.

Problem 8.2.10. Let

$$S_a(\omega) = \frac{1 + \omega^2}{1 + \omega^4}.$$

Repeat Problem 8.2.8.

Problem 8.2.11.

- (a) The received signal is $a(u)$, $-\infty < u \leq t$. The desired signal is

$$d(t) = a(t + \alpha), \quad \alpha > 0.$$

Find $H_o(j\omega)$ to minimize the mean-square error

$$E \{ [\hat{d}(t) - d(t)]^2 \},$$

where

$$d(t) = \int_{-\infty}^t h_o(t-u)a(u) du.$$

The spectrum of $a(t)$ is

$$S_a(\omega) = \prod_{i=1}^n \frac{A^2}{\omega^2 + k_i^2},$$

where $k_i \neq k_j; i \neq j$ for $i = 1, 2, \dots, n; j = 1, 2, \dots, n$.

- (b) Now assume that the received signal is $a(u)$, $T_i \leq u \leq t$, where T_i is a *finite* number. Find $h_o(t, \tau)$ to minimize the mean-square error.

$$\hat{d}(t) = \int_{T_i}^t h_o(t, u)a(u) du.$$

- (c) Do the answers to parts (a) and (b) enable you to make any general statements about pure prediction problems in which the message spectrum has no zeros?

Problem 8.2.12. The message is generated as shown in Figure P8.2, where $u(t)$ is a white noise process (unity spectral height) and $\alpha_i, i = 1, 2$, and $\lambda_i, i = 1, 2$, are known positive constants. The additive white noise $w(t)(N_0/2)$ is uncorrelated with $u(t)$.

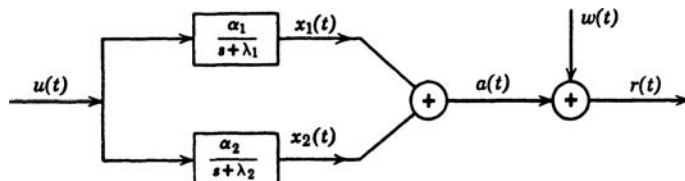


Figure P8.2

- (a) Find an expression for the linear filters whose outputs are the MMSE realizable estimates of $x_i(t)$, $i = 1, 2$.
 (b) Prove that

$$\hat{a}(t) = \sum_{i=1}^2 \hat{x}_i(t).$$

- (c) Assume that

$$d(t) = \sum_{i=1}^2 d_i x_i(t).$$

Prove that

$$\hat{d}(t) = \sum_{i=1}^2 d_i \hat{x}_i(t).$$

Problem 8.2.13. Let

$$r(u) = a(u) + n(u), \quad -\infty < u \leq t,$$

where $a(u)$ and $n(u)$ are uncorrelated random processes with spectra

$$S_a(\omega) = \frac{\omega^2}{\omega^4 + 1},$$

$$S_n(\omega) = \frac{1}{\omega^2 + \epsilon^2}.$$

The desired signal is $a(t)$. Find the optimum (MMSE) linear filter and the resulting error for the limiting case in which $\epsilon \rightarrow 0$. Sketch the magnitude and phase of $H_o(j\omega)$.

Problem 8.2.14. The received waveform $r(u)$ is

$$r(u) = a(u) + w(u), \quad -\infty < u \leq t,$$

where $a(u)$ and $w(u)$ are uncorrelated random processes with spectra

$$S_a(\omega) = \frac{2k\sigma_a^2}{\omega^2 + k^2},$$

$$S_w(\omega) = \frac{N_0}{2}.$$

Let

$$d(t) \triangleq \int_t^{t+\alpha} a(u) du, \quad \alpha > 0.$$

- (a) Find the optimum (MMSE) linear filter for estimating $d(t)$.
 (b) Find ξ_p^α .

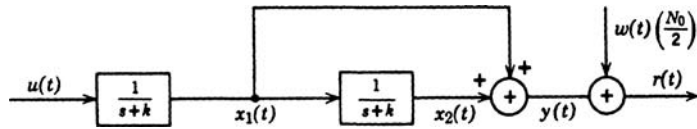


Figure P8.3

Problem 8.2.15 (continuation). Consider the same model as Problem 8.2.14. Repeat that problem for the following desired signals:

$$(a) \quad d(t) = \frac{1}{\alpha} \int_{t-\alpha}^t a(u) du, \quad \alpha > 0.$$

$$(b) \quad d(t) = \frac{1}{\beta - \alpha} \int_{t+\alpha}^{t+\beta} a(u) du, \quad \alpha > 0, \beta > 0, \beta \geq \alpha.$$

What happens as $(\beta - \alpha) \rightarrow 0$?

$$(c) \quad d(t) = \sum_{n=-1}^{+1} k_n a(t - n\alpha), \quad \alpha > 0.$$

Problem 8.2.16. Consider the model in Figure P8.3. The function $u(t)$ is a sample function from a white process (unity spectral height). Find the MMSE realizable linear estimates, $\hat{x}_1(t)$ and $\hat{x}_2(t)$. Compute the mean-square errors and the cross-correlation between the errors ($T_i = -\infty$).

Problem 8.2.17. Consider the communication problem in Figure P8.4. The message $a(t)$ is a sample function from a stationary, zero-mean Gaussian process with unity variance. The channel $k_f(\tau)$ is a linear, time-invariant, not necessarily realizable system. The additive noise $n(t)$ is a sample function from a zero-mean white Gaussian process ($N_0/2$).

- (a) We process $r(t)$ with the optimum unrealizable linear filter to find $\hat{a}(t)$. Assuming

$$\int_{-\infty}^{\infty} |K_f(j\omega)|^2 (d\omega / 2\pi) = 1.$$

Find the $k_f(\tau)$ that minimizes the minimum mean-square error.

- (b) Sketch $|H_{ou}(j\omega)|$ for

$$S_a(\omega) = \frac{2k}{\omega^2 + k^2}.$$

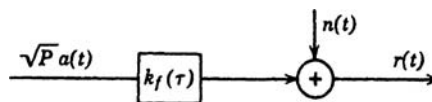


Figure P8.4

CLOSED FORM ERROR EXPRESSIONS

Problem 8.2.18. We want to integrate

$$\xi_P = \frac{N_0}{2} \int_{-\infty}^{\infty} \frac{d\omega}{2\pi} \ln \left[1 + \frac{2c_n/N_0}{1 + (\omega/k)^{2n}} \right].$$

- (a) Do this by letting $y = 2c_n/N_0$. Differentiate with respect to y and then integrate with respect to ω . Integrate the result from 0 to y .
- (b) Discuss the conditions under which this technique is valid.

Problem 8.2.19. Evaluate

$$\xi_u = \int_{-\infty}^{\infty} \frac{d\omega}{2\pi} \frac{c_n}{1 + (\omega/k)^{2n} + (2/N_0)c_n}.$$

Comment. In the next seven problems we develop closed-form error expressions for some interesting cases. In most of these problems the solutions are difficult. In all problems

$$r(u) = a(u) + n(u), \quad -\infty < u \leq t,$$

where $a(u)$ and $n(u)$ are uncorrelated. The desired signal is $a(t)$ and optimum (MMSE) linear filtering is used. The optimum realizable linear filter is $H_o(j\omega)$ and

$$G_o(j\omega) \triangleq 1 - H_o(j\omega).$$

Most of the results were obtained in Yovits and Jackson [YJ55].

Problem 8.2.20. Let

$$S_n(\omega) = \frac{N_0 a^2}{\omega^2 + a^2}.$$

Show that

$$H_o(j\omega) = 1 - k \frac{[S_n(\omega)]^+}{[S_a(\omega) + S_n(\omega)]^+},$$

where

$$k = \exp \left[\frac{2}{N_0 a} \int_0^{\infty} S_n(\omega) \ln \frac{S_n(\omega)}{S_a(\omega) + S_n(\omega)} \frac{d\omega}{2\pi} \right].$$

Problem 8.2.21. Show that if $\lim_{\omega \rightarrow \infty} S_n(\omega) \rightarrow 0$. Then

$$\xi_P = 2 \int_0^{\infty} \left\{ S_n(\omega) - |G_o(j\omega)|^2 [S_a(\omega) + S_n(\omega)] \right\} \frac{d\omega}{2\pi}.$$

Use this result and that of the preceding problem to show that for one-pole noise

$$\xi_P = \frac{N_0 a}{2} (1 - k^2).$$

Problem 8.2.22. Consider the case

$$S_n(\omega) = N_0 + N_2\omega^2 + N_4\omega^4.$$

Show that

$$|G_o(j\omega)|^2 = \frac{S_n(\omega) + K}{S_n(\omega) + S_a(\omega)},$$

where

$$\int_0^\infty \ln \left[\frac{S_n(\omega) + K}{S_n(\omega) + S_a(\omega)} \right] d\omega = 0$$

determines K .

Problem 8.2.23. Show that when $S_n(\omega)$ is a polynomial

$$\xi_P = -\frac{1}{\pi} \int_0^\infty d\omega \left\{ S_n(\omega) - |G_o(j\omega)|^2 [S_a(\omega) + S_n(\omega)] + S_n(\omega) \ln |G_o(j\omega)|^2 \right\}.$$

Problem 8.2.24. As pointed out in the text, we can double the size of the class of problems for which these results apply by a simple observation. Figure P8.5a represents a typical system in which the message is filtered before transmission.

Clearly the mean-square error in this system is identical to the error in the system in Figure P8.5b. Using Problem 8.2.23, verify that

$$\begin{aligned} \xi_P &= -\frac{1}{\pi} \int_0^\infty \left[\frac{N_0}{2\beta^2} \omega^2 - \left[\frac{N_0}{2\beta^2} \omega^2 + K \right] + \frac{N_0 \omega^2}{2\beta^2} \ln |G_o(j\omega)|^2 \right] d\omega \\ &= \frac{1}{\pi} \int_0^\infty \left[K - \frac{N_0 \omega^2}{2\beta^2} \ln \left(\frac{S_n(\omega) + K}{S_a(\omega) + S_n(\omega)} \right) \right] d\omega. \end{aligned}$$

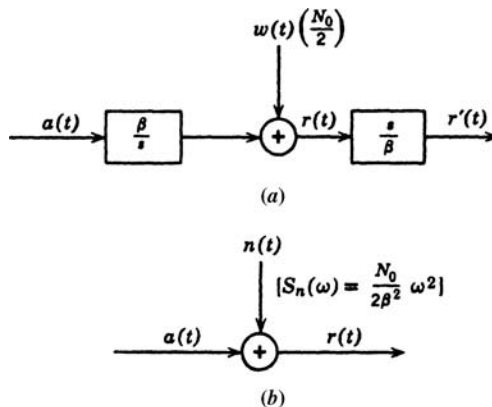


Figure P8.5

Problem 8.2.25 (continuation). [Sny66]. Using the model of Problem 8.2.24, show that

$$\xi_P = \frac{N_0}{6} [f(0)]^3 + F(0),$$

where

$$f(0) = \int_{-\infty}^{\infty} \ln \left[1 + \frac{2\beta^2 S_a(\omega)}{\omega^2 N_0} \right] \frac{d\omega}{2\pi}$$

and

$$F(0) = \int_{-\infty}^{\infty} \omega^2 \frac{N_0}{2\beta^2} \ln \left[1 + \frac{2\beta^2 S_a(\omega)}{\omega^2 N_0} \right] \frac{d\omega}{2\pi}.$$

Problem 8.2.26. [Moh68]. Extend the results in Problem 8.2.20 to the case

$$S_n(\omega) = \frac{N_0}{2} + \frac{N_1 a^2}{\omega^2 + a^2}$$

to find $|G_o(j\omega)|^2$ and ξ_P .

GENERALIZATIONS

Problem 8.2.27. Consider the simple unrealizable filter problem in which

$$r(u) = a(u) + n(u), \quad -\infty < u < \infty$$

and

$$d(t) = a(t).$$

Assume that we design the optimum unrealizable filter $H_{ou}(j\omega)$ using the spectrum $S_a(\omega)$ and $S_n(\omega)$. In practice, the noise spectrum is

$$S_{np}(\omega) = S_{nd}(\omega) + S_{ne}(\omega).$$

(a) Show that the mean-square error using $H_{ou}(j\omega)$ is

$$\xi_{up} = \xi_{uo} + \int_{-\infty}^{\infty} |H_{ou}(j\omega)|^2 S_{ne}(\omega) \frac{d\omega}{2\pi},$$

where up denotes unrealizable mean-square error in practice and uo denotes unrealizable mean-square error in the optimum filter when the design assumptions are exact.

(b) Show that the change in error is

$$\Delta \xi_u = \int_{-\infty}^{\infty} \left[\frac{S_a(\omega)}{S_a(\omega) + S_{nd}(\omega)} \right]^2 S_{ne}(\omega) \frac{d\omega}{2\pi}.$$

(c) Consider the case

$$S_{nd}(\omega) = \frac{N_0}{2},$$

$$S_{ne}(\omega) = \epsilon \frac{N_0}{2}.$$

The message spectrum is flat and bandlimited. Show that

$$\Delta\xi_u = \frac{\epsilon\Lambda}{(1+\Lambda)^2},$$

where Λ is the signal-to-noise ratio in the message bandwidth.

Problem 8.2.28. Derive an expression for the change in the mean-square error in an optimum unrealizable filter when the actual message spectrum is different from the design message spectrum.

Problem 8.2.29. Repeat Problem 8.2.28 for an optimum realizable filter and white noise.

Problem 8.2.30. Let

$$r(u) = a(u) + n(u), \quad -\infty < u \leq t,$$

where $a(u)$ and $n(u)$ are uncorrelated. Let

$$S_a(\omega) = \frac{1}{1+\omega^2}, \quad S_n(\omega) = \epsilon^2.$$

The desired signal is $d(t) = (d/dt)a(t)$.

(a) Find $H_o(j\omega)$.

(b) Discuss the behavior of $H_o(j\omega)$ and ξ_p as $\epsilon \rightarrow 0$. Why is the answer misleading?

Problem 8.2.31. Repeat Problem 8.2.30 for the case

$$S_a(\omega) = \frac{1}{1+\omega^4} \quad S_n(\omega) = \epsilon^4.$$

What is the important difference between the message random processes in the two problems? Verify that differentiation and optimum realizable filtering do not commute.

Problem 8.2.32. Let

$$g^+(\tau) = \mathcal{F}^{-1}[G^+(j\omega)].$$

Prove that the MMSE error for *pure* prediction is

$$\xi_p^\alpha = \int_0^\alpha [g^+(\tau)]^2 d\tau.$$

Problem 8.2.33. [Wie49]. Consider the message spectrum

$$S_a(\omega) = \left[\left(1 + \frac{\omega^2}{n} \right)^n \right]^{-1}.$$

(a) Show that

$$g^+(\tau) = \frac{\tau^{n-1} \exp(-\tau\sqrt{n})}{n^{-n/2}(n-1)!}.$$

(b) Show that (for large n)

$$\xi_P^\alpha \simeq \int_0^\alpha \frac{1}{2\pi} \exp \left[-2 \left(t - \frac{n-1}{\sqrt{n}} \right)^2 \right] dt.$$

(c) Use part (b) to show that for any ϵ^2 and α we can make

$$\xi_P^\alpha < \epsilon^2$$

by increasing n sufficiently. Explain why this result is true.

Problem 8.2.34. The message $a(t)$ is a zero-mean process observed in the absence of noise. The desired signal $d(t) = a(t + \alpha)$, $\alpha > 0$.

(a) Assume

$$K_a(\tau) = \frac{1}{\tau^2 + k^2}.$$

Find $\hat{d}(t)$ by using $a(t)$ and its derivatives. What is the mean-square error for $\alpha < k$?

(b) Assume

$$K_a(\tau) = e^{-k\tau^2}.$$

Show that

$$\hat{a}(t + \alpha) = \sum_{n=0}^{\infty} \left[\frac{d^n}{dt^n} a(t) \right] \frac{\alpha^n}{n!},$$

and that the mean-square error is zero for all α .

Problem 8.2.35. Consider a simple diversity system,

$$r_1(t) = a(t) + n_1(t),$$

$$r_2(t) = a(t) + n_2(t),$$

where $a(t)$, $n_1(t)$, and $n_2(t)$ are independent zero-mean, stationary Gaussian processes with finite variances. We wish to process $r_1(t)$ and $r_2(t)$, as shown in Figure P8.6. The spectra $S_{n_1}(\omega)$ and $S_{n_2}(\omega)$ are known; $S_a(\omega)$, however, is *unknown*. We require that the message $a(t)$ be undistorted. In other words, if $n_1(t)$ and $n_2(t)$ are zero, the output will be exactly $a(t)$.

- (a) What condition does this impose on $H_1(j\omega)$ and $H_2(j\omega)$?
- (b) We want to choose $H_1(j\omega)$ to minimize $E[n_c^2(t)]$, subject to the constraint that $a(t)$ be reproduced exactly in the absence of input noise. The filters must be realizable and may operate on the infinite past. Find an expression for $H_{1o}(j\omega)$ and $H_{2o}(j\omega)$ in terms of the given quantities.
- (c) Prove that the $\hat{a}(t)$ obtained in part (b) is an unbiased, efficient estimate of the sample function $a(t)$. [Therefore, $\hat{a}(t) = \hat{a}_{ml}(t)$.]

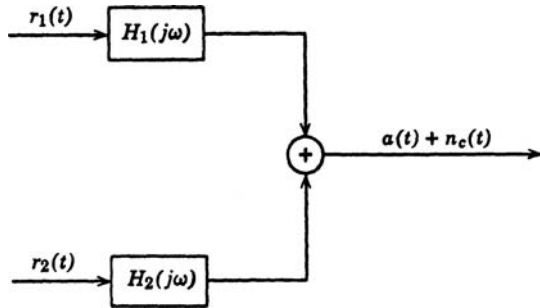


Figure P8.6

This is an example of what is referred to in the literature as a *minimum variance distortionless response* filter that we encountered previously in Section 5.2.9.

Problem 8.2.36. Generalize the result in Problem 8.2.35 to the n -input problem. Prove that any n -dimensional distortionless filter problem may be recast as an $(n - 1)$ -dimensional Wiener filter problem.

P8.3 Gaussian-Markov Processes: Kalman Filter

STATE-VARIABLE REPRESENTATIONS

Problem 8.3.1. Consider the differential equation

$$y^{(n)}(t) + p_{n-1}y^{(n-1)}(t) + \cdots + p_0y(t) = b_{n-1}u^{(n-1)}(t) + \cdots + b_0u(t).$$

Extend Canonical Realization 1 to include this case. The desired \mathbf{F} is

$$\mathbf{F} = \begin{bmatrix} 0 & 1 & & 0 \\ \vdots & & \ddots & \\ 0 & 0 & & 1 \\ -p_0 & -p_1 & \cdots & -p_{n-1} \end{bmatrix}.$$

Draw an analog computer realization and find the \mathbf{G} matrix.

Problem 8.3.2. Consider the differential equation in Problem 8.3.1. Derive Canonical Realization 3 for the case of repeated roots.

Problem 8.3.3. [DRC65]. Consider the differential equation

$$y^{(n)}(t) + p_{n-1}y^{(n-1)}(t) + \cdots + p_0y(t) = b_{n-1}u^{(n-1)}(t) + \cdots + b_0u(t).$$

- (a) Show that the system in Figure P8.7 is a correct analog computer realization.
- (b) Write the vector differential equation that describes the system.

Problem 8.3.4. Draw an analog computer realization for the following systems:

- (a) $\ddot{y}(t) + 3\dot{y}(t) + 4y(t) = \dot{u}(t) + u(t),$

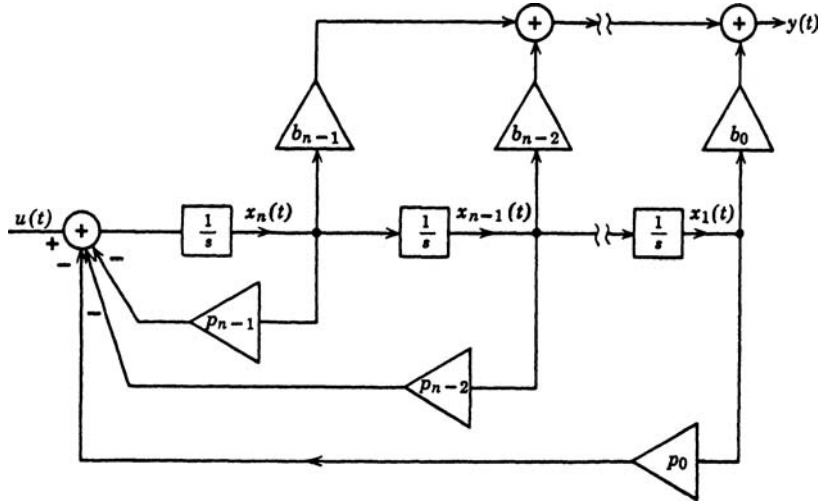


Figure P8.7

(b)

$$\begin{aligned}\ddot{y}_1(t) + 3\dot{y}_1(t) + 2y_1(t) &= u_1(t) + 2\dot{u}_2(t) + 2u_2(t), \\ \ddot{y}_2(t) + 4\dot{y}_1(t) + 3y_2(t) &= 3u_2(t) + u_1(t).\end{aligned}$$

Write the associated vector differential equation.

Problem 8.3.5. [DRC65]. Find the transfer function matrix and draw the transfer function diagram for the systems described below. Comment on the number of integrators required.

- (a) $\ddot{y}_1(t) + 3\dot{y}_1(t) + 2y_1(t) = \dot{u}_1(t) + 2u_1(t) + \dot{u}_2(t) + u_2(t)$
 $\dot{y}_2(t) + 2y_2(t) = -\dot{u}_1(t) - 2u_1(t) + u_2(t).$
- (b) $\dot{y}_1(t) + y_1(t) = u_1(t) + 2u_2(t)$
 $\dot{y}_2(t) + 3\dot{y}_2(t) + 2y_2(t) = \dot{u}_2(t) + u_2(t) - u_1(t).$
- (c) $\ddot{y}_1(t) + 2\dot{y}_2(t) + y_1(t) = \dot{u}_1(t) + u_1(t) + u_2(t)$
 $\dot{y}_2(t) + \dot{y}_1(t) + y_2(t) = u_2(t) + u_1(t).$
- (d) $\ddot{y}_1(t) + 3\dot{y}_1(t) + 2y_1(t) = 3\dot{u}_1(t) + 4\dot{u}_2(t) + 8u_2(t)$
 $\dot{y}_2(t) + 3y_2(t) - 4y_1(t) - \dot{y}_1(t) = \dot{u}_1(t) + 2\dot{u}_2(t) + 2u_2(t).$

Problem 8.3.6. [DRC65]. Find the vector differential equations for the following systems, using the partial fraction technique.

- (a) $\ddot{y}(t) + 3\dot{y}(t) + 2y(t) = u(t).$
- (b) $\ddot{y}(t) + 4\dot{y}(t) + 5\dot{y}(t) + 2y(t) = u(t).$
- (c) $\ddot{y}(t) + 4\dot{y}(t) + 6\dot{y}(t) + 4y(t) = u(t).$
- (d) $\ddot{y}_1(t) - 10\dot{y}_2(t) + y_1(t) = u_1(t).$
 $\dot{y}_2(t) + 6y_2(t) = u_2(t).$

Problem 8.3.7. Compute $e^{\mathbf{F}t}$ for the following matrices:

$$(a) \mathbf{F} = \begin{bmatrix} 1 & 1 \\ 1 & 1 \end{bmatrix}.$$

$$(b) \mathbf{F} = \begin{bmatrix} 3 & 2 \\ -1 & 6 \end{bmatrix}.$$

$$(c) \mathbf{F} = \begin{bmatrix} -2 & 5 \\ -4 & -3 \end{bmatrix}.$$

Problem 8.3.8. Compute $e^{\mathbf{F}t}$ for the following matrices:

$$(a) \mathbf{F} = \begin{bmatrix} 0 & 1 & 0 \\ 0 & 0 & 1 \\ 0 & 0 & 0 \end{bmatrix}.$$

$$(b) \mathbf{F} = \begin{bmatrix} 0 & 1 & 0 \\ 0 & 0 & 1 \\ 0 & 0 & -1 \end{bmatrix}.$$

$$(c) \mathbf{F} = \begin{bmatrix} 0 & 1 & 0 \\ 0 & 0 & 1 \\ -6 & -11 & -6 \end{bmatrix}.$$

Problem 8.3.9. Given the system with state representation as follows,

$$\dot{\mathbf{x}}(t) = \mathbf{F}\mathbf{x}(t) + \mathbf{G}u(t),$$

$$y(t) = \mathbf{C}\mathbf{x}(t),$$

$$\mathbf{x}(0) = \mathbf{0}.$$

Let $U(s)$ and $Y(s)$ denote the Laplace transform of $u(t)$ and $y(t)$, respectively. We found that the transfer function was

$$\begin{aligned} H(s) &= \frac{Y(s)}{U(s)} = \mathbf{C}\Phi(s)\mathbf{G} \\ &= \mathbf{C}(s\mathbf{I} - \mathbf{F})^{-1}\mathbf{G}. \end{aligned}$$

Show that the poles of $H(s)$ are the eigenvalues of the matrix \mathbf{F} .

Problem 8.3.10. Consider the control system shown in Figure P8.8. The output of the system is $a(t)$. The two inputs, $b(t)$ and $n(t)$, are sample functions from zero-mean, uncorrelated, stationary random processes. Their spectra are

$$S_b(\omega) = \frac{2\sigma_b^2 k}{\omega^2 + k^2}$$

and

$$S_n(\omega) = \frac{N_0}{2}.$$

Write the vector differential equation that describes a mathematically equivalent system whose input is a vector white noise $\mathbf{u}(t)$ and whose output is $a(t)$.

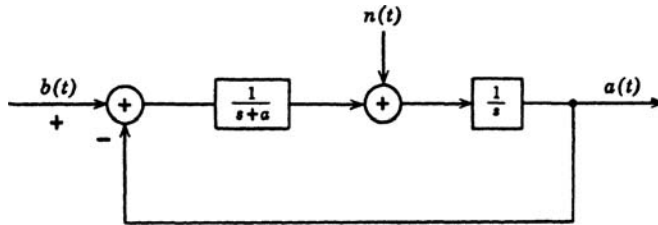


Figure P8.8

Problem 8.3.11. Consider the discrete multipath model shown in Figure P8.9. The time delays are assumed known. The channel multipliers are independent, zero-mean processes with spectra

$$S_{b_j}(\omega) = \frac{2k_j\sigma_j^2}{\omega^2 + k_j^2}, \quad \text{for } j = 1, 2, 3.$$

The additive white noise is uncorrelated and has spectral height $N_0/2$. The input signal $s(t)$ is a known waveform.

- (a) Write the state and observation equations for the process.
- (b) Indicate how this would be modified if the channel gains were correlated.

Problem 8.3.12. In the text we considered in detail state representations for time invariant systems.

Consider the time varying system

$$\ddot{y}(t) + p_1(t)\dot{y}(t) + p_0(t)y(t) = b_1(t)\dot{u}(t) + b_0(t)u(t).$$

Show that this system has the following state representation

$$\begin{aligned} \frac{d}{dt}\mathbf{x}(t) &= \begin{bmatrix} 0 & 1 \\ -p_0(t) & -p_1(t) \end{bmatrix} \mathbf{x}(t) + \begin{bmatrix} h_1(t) \\ h_2(t) \end{bmatrix} u(t), \\ y(t) &= \begin{bmatrix} 1 & 0 \end{bmatrix} \mathbf{x}(t) = x_1(t), \end{aligned}$$

where $h_1(t)$ and $h_2(t)$ are functions that you must find.

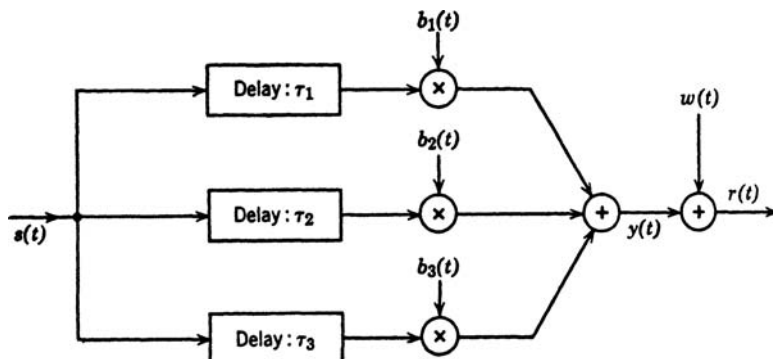


Figure P8.9

Problem 8.3.13. [DRC65]. Given the system defined by the time-varying differential equation

$$y^{(n)}(t) + \sum_{k=0}^{n-1} p_{n-k}(t)y^{(k)}(t) = \sum_{k=0}^n b_{n-k}(t)u^{(k)}(t).$$

Show that this system has the state equations

$$\begin{bmatrix} \dot{x}_1(t) \\ \dot{x}_2(t) \\ \vdots \\ \vdots \\ \dot{x}_n(t) \end{bmatrix} = \begin{bmatrix} 0 & 1 & 0 & \cdots & 0 \\ 0 & 0 & 1 & \cdots & 0 \\ \cdot & \cdot & \cdot & \cdots & \cdot \\ \cdot & \cdot & \cdot & \cdots & \cdot \\ -p_n(t) & -p_{n-1}(t) & \cdot & \cdots & -p_1(t) \end{bmatrix} \begin{bmatrix} x_1(t) \\ x_2(t) \\ \vdots \\ \vdots \\ x_n(t) \end{bmatrix} + \begin{bmatrix} g_1(t) \\ g_2(t) \\ \vdots \\ \vdots \\ g_n(t) \end{bmatrix} u(t),$$

$$y(t) = x_1(t) + g_0(t)u(t),$$

where

$$g_0(t) = b_0(t),$$

$$g_i(t) = b_i(t) - \sum_{r=0}^{i-1} \sum_{m=0}^{i-r} \binom{n+m-i}{n-i} p_{i-r-m}(t) g_r^{(m)}(t).$$

Problem 8.3.14. Demonstrate that the following is a solution to (8.275).

$$\Lambda_x(t) = \Phi(t, t_0) \left[\Lambda_x(t_0) + \int_{t_0}^t \Phi(t_0, \tau) \mathbf{G}(\tau) \mathbf{Q}(\tau) \mathbf{G}^T(\tau) \Phi^T(t_0, \tau) d\tau \right] \Phi^T(t, t_0),$$

where $\Phi(t, t_0)$ is the fundamental transition matrix; that is,

$$\begin{aligned} \frac{d}{dt} \Phi(t, t_0) &= \mathbf{F}(t) \Phi(t, t_0), \\ \Phi(t_0, t_0) &= \mathbf{I}. \end{aligned}$$

Demonstrate that this solution is unique.

Problem 8.3.15. Evaluate $\mathbf{K}_y(t, \tau)$ in terms of $\mathbf{K}_x(t, t)$ and $\Phi(t, \tau)$, where

$$\begin{aligned} \dot{\mathbf{x}}(t) &= \mathbf{F}(t)\mathbf{x}(t) + \mathbf{G}(t)\mathbf{u}(t), \\ \mathbf{y}(t) &= \mathbf{C}(t)\mathbf{x}(t), \\ E[\mathbf{u}(t)\mathbf{u}^T(\tau)] &= \mathbf{Q}\delta(t-\tau). \end{aligned}$$

Problem 8.3.16. Consider the first-order system defined by

$$\begin{aligned} \frac{dx(t)}{dt} &= -k(t)x(t) + g(t)u(t), \\ y(t) &= x(t). \end{aligned}$$

- (a) Determine a general expression for the transition matrix for this system.
- (b) What is $h(t, \tau)$ for this system?
- (c) Evaluate $h(t, \tau)$ for

$$\begin{aligned} k(t) &= k(1 + m \sin(\omega_0 t)), \\ g(t) &= 1. \end{aligned}$$

- (d) Does this technique generalize to vector equations?

Problem 8.3.17. Show that for constant parameter systems the steady-state variance of the unobserved process is given by

$$\lim_{t \rightarrow \infty} \mathbf{K}_x(t, t) = \int_0^{\infty} e^{+\mathbf{F}\tau} \mathbf{G} \mathbf{Q} \mathbf{G}^T e^{\mathbf{F}^T \tau} d\tau,$$

where

$$\begin{aligned} \dot{\mathbf{x}}(t) &= \mathbf{F}\mathbf{x}(t) + \mathbf{G}\mathbf{u}(t), \\ E[\mathbf{u}(t)\mathbf{u}^T(\tau)] &= \mathbf{Q}\delta(t - \tau), \end{aligned}$$

or, equivalently,

$$\lim_{t \rightarrow \infty} \mathbf{K}_x(t, t) = \frac{1}{2\pi j} \int_{-j\infty}^{j\infty} [s\mathbf{I} - \mathbf{F}]^{-1} \mathbf{G} \mathbf{Q} \mathbf{G}^T [-s\mathbf{I} - \mathbf{F}^T]^{-1} ds.$$

Problem 8.3.18. Consider the second-order system illustrated in Figure P8.10, where

$$\begin{aligned} E[u(t)u(\tau)] &= 2Pab(a + b)\delta(t - \tau), \\ E[w(t)w(\tau)] &= \frac{N_0}{2}\delta(t - \tau). \end{aligned}$$

(a, b are possibly complex conjugates.) The state variables are

$$\begin{aligned} x_1(t) &= y(t), \\ x_2(t) &= \dot{y}(t). \end{aligned}$$

- (a) Write the state equation and the output equation for the system.
- (b) For this state representation determine the steady-state variance matrix Λ_x of the unobserved process. In other words, find

$$\Lambda_x = \lim_{t \rightarrow \infty} E[\mathbf{x}(t)\mathbf{x}^T(t)],$$

where $\mathbf{x}(t)$ is the state vector of the system.

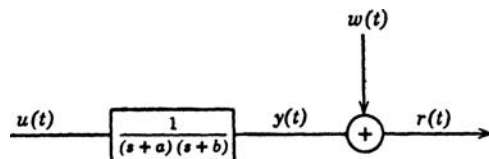


Figure P8.10

- (c) Find the transition matrix $\mathbf{T}(t, T_i)$ for the equation,

$$\frac{d\mathbf{T}(t, T_i)}{dt} = \begin{bmatrix} \mathbf{F} & \mathbf{GQG}^T \\ \mathbf{C}^T \mathbf{R}^{-1} \mathbf{C} & -\mathbf{F}^T \end{bmatrix} \mathbf{T}(t, T_i),$$

by using Laplace transform techniques. (Depending on the values of a , b , q , and $N_0/2$, the exponentials involved will be real, complex, or both.)

- (d) Find $\xi_P(t)$ when the initial condition is

$$\xi_P(T_i) = \Lambda_x.$$

Comment. Although we have an analytical means of determining $\xi_P(t)$ for a system of any order, this problem illustrates that numerical means are more appropriate.

Problem 8.3.19. Because of its time-invariant nature, the optimal linear filter, as determined by Wiener spectral factorization techniques, will lead to a nonoptimal estimate when a finite observation interval is involved. The purpose of this problem is to determine how much we degrade our estimate by using a Wiener filter when the observation interval is finite. Consider the first order system.

$$\dot{x}(t) = -kx(t) + u(t),$$

where

$$\begin{aligned} r(t) &= x(t) + w(t), \\ E[u(t)u(\tau)] &= 2kP\delta(t - \tau), \\ E[w(t)w(\tau)] &= \frac{N_0}{2}\delta(t - \tau), \\ E[x(0)] &= 0, \\ E[x^2(0)] &= P_0, \\ T_i &= 0. \end{aligned}$$

- (a) What is the variance of error obtained by using Kalman–Bucy filtering?
 (b) Show that the steady-state filter (i.e., the Wiener filter) is given by

$$H_o(j\omega) = \frac{4kP/N_0}{(k + \gamma)(j\omega + \gamma)},$$

where $\gamma = k(1 + 4P/kN_0)^{1/2}$. Denote the output of the Wiener filter as $\hat{x}_{w_o}(t)$.

- (c) Show that a state representation for the Wiener filter is

$$\dot{\hat{x}}_{w_o}(t) = -\gamma\hat{x}_{w_o}(t) + \frac{4Pk}{N_0(k + \gamma)}r(t),$$

where

$$\hat{x}_{w_o}(0) = 0.$$

- (d) Show that the error for this system is

$$\begin{aligned} \dot{\epsilon}_{w_o}(t) &= -\gamma\epsilon_{w_o}(t) - u(t) + \frac{4Pk}{N_0(k + \gamma)}w(t), \\ \epsilon_{w_o}(0) &= -x(0). \end{aligned}$$

(e) Define

$$\xi_{w_o}(t) = E[\epsilon_{w_o}^2(t)].$$

Show that

$$\begin{aligned}\dot{\xi}_{w_o}(t) &= -2\gamma\xi_{w_o}(t) + \frac{4kP\gamma}{\gamma+k}, \\ \xi_{w_o}(0) &= P_o\end{aligned}$$

and verify that

$$\xi_{w_o}(t) = \xi_{P\infty}(1 - e^{-2\gamma t}) + P_o e^{-2\gamma t}.$$

(f) Plot the ratio of the mean-square error using the Kalman–Bucy filter to the mean-square error using the Wiener filter. (Note that both errors are a function of time.)

$$\begin{aligned}\beta(t) &= \frac{\xi_P(t)}{\xi_{w_0}(t)}, \quad \text{for } \gamma = 1.5k, 2k, \text{ and } 3k. \\ P_0 &= 0, 0.5P, \text{ and } P.\end{aligned}$$

Problem 8.3.20. Consider the following system:

$$\begin{aligned}\dot{\mathbf{x}}(t) &= \mathbf{F}\mathbf{x}(t) + \mathbf{G}u(t), \\ y(t) &= \mathbf{C}\mathbf{x}(t),\end{aligned}$$

where

$$\mathbf{F} = \begin{bmatrix} 0 & 1 & 0 & 0 \\ 0 & 0 & 1 & 0 \\ 0 & 0 & 0 & 1 \\ -p_0 & -p_1 & -p_2 & -p_3 \end{bmatrix}, \quad \mathbf{G} = \begin{bmatrix} 0 \\ 0 \\ 0 \\ 1 \end{bmatrix}, \quad \mathbf{C} = \begin{bmatrix} 1 & 0 & 0 & 0 \end{bmatrix}$$

and

$$E[u(t)u(\tau)] = Q\delta(t - \tau).$$

Find the steady-state covariance matrix, that is,

$$\lim_{t \rightarrow \infty} \mathbf{K}_x(t, t),$$

for a fourth-order Butterworth process using the above representation.

$$S_a(\omega) = \frac{8 \sin(\pi/16)}{1 + \omega^8}.$$

Problem 8.3.21. Consider the system shown in Figure P8.11a, where

$$\begin{aligned}E[u(t)u(\tau)] &= \sigma^2 \delta(t - \tau), \\ E[w(t)w(\tau)] &= \frac{N_0}{2} \delta(t - \tau), \\ a(T_i) &= \dot{a}(T_i) = 0.\end{aligned}$$

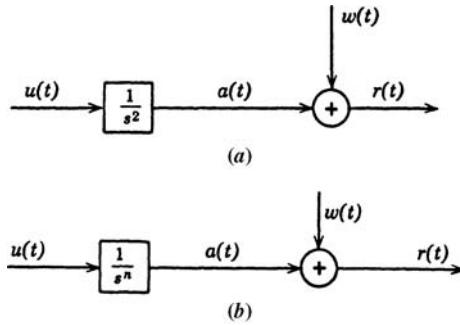


Figure P8.11

- (a) Find the optimum linear filter.
- (b) Solve the steady-state variance equation.
- (c) Verify that the “pole-splitting” technique of conventional Wiener theory gives the correct answer.

Problem 8.3.22 (continuation). A generalization of Problem 8.3.21 is shown in Figure, P8.11b. Repeat Problem 8.3.21.

Problem 8.3.23. Consider the model in Problem 8.3.21. Define the state vector as

$$\mathbf{x}(t) = \begin{bmatrix} x_1(t) \\ x_2(t) \end{bmatrix} \triangleq \begin{bmatrix} a(t) \\ \dot{a}(t) \end{bmatrix}, \quad \mathbf{x}(T_i) = \mathbf{0}.$$

- (a) Determine $\mathbf{K}_x(t, u) = E[\mathbf{x}(t)\mathbf{x}^T(u)]$.
- (b) Determine the optimum realizable filter for estimating $\mathbf{x}(t)$ (calculate the gains analytically).
- (c) Verify that your answer reduces to the answer in Problem 8.3.21 as $t \rightarrow \infty$.

Problem 8.3.24. Assume that a particle leaves the origin at $t = 0$ and travels at a constant but unknown velocity. The observation is corrupted by additive white Gaussian noise of spectral height $N_0/2$. Thus,

$$r(t) = vt + w(t), \quad t \geq 0.$$

Assume that

$$\begin{aligned} E(v) &= 0, \\ E(v^2) &= \sigma^2 \end{aligned}$$

and that v is a Gaussian random variable.

- (a) Find the equation specifying the MAP estimate of vt .
- (b) Find the equation specifying the MMSE estimate of vt .

Use the techniques of Chapter 7 to solve this problem.

Problem 8.3.25. Consider the model in Problem 8.3.24. Use a Kalman filter to solve this problem.

- (a) Find the minimum mean-square error linear estimate of the message

$$a(t) \triangleq vt.$$

- (b) Find the resulting mean-square error.
(c) Show that for large t

$$\xi_P(t) \simeq \left(\frac{3N_0}{2t} \right)^{1/2}.$$

Problem 8.3.26 (continuation).

- (a) Verify that the answers to Problems 8.3.24 and 8.3.25 are the same.
(b) Modify your estimation procedure in Problem 8.3.24 to obtain a maximum likelihood estimate (assume that v is an unknown nonrandom variable).
(c) Discuss qualitatively when the *a priori* knowledge is useful.

Problem 8.3.27 (continuation).

- (a) Generalize the model of Problem 8.3.24 to include an arbitrary polynomial message:

$$a(t) = \sum_{i=1}^K v_i t^i,$$

where

$$E(v_i) = 0,$$

$$E(v_i v_j) = \sigma_i^2 \delta_{ij}.$$

- (b) Solve for $k = 0, 1$, and 2 .

Problem 8.3.28. Consider the second-order system shown in Figure P8.10.

$$\begin{aligned} E[u(t)u(\tau)] &= Q\delta(t - \tau), \\ E[w(t)w(\tau)] &= \frac{N_0}{2}\delta(t - \tau), \\ x_1(t) &= y(t), \\ x_2(t) &= \dot{y}(t). \end{aligned}$$

- (a) Write the state equation and determine the steady-state solution to the covariance equation by setting $\dot{\xi}_P(t) = \mathbf{0}$.
(b) Do the values of a, b, Q, N_0 influence the roots we select in order that the covariance matrix will be positive definite?
(c) In general there are eight possible roots. In the a, b -plane, determine which root is selected for any particular point for fixed Q and N_0 .

Problem 8.3.29. Consider the prediction problem discussed in Section 8.3.4.

- (a) Derive the result stated in (8.365). Recall $\mathbf{d}(t) = \mathbf{x}(t + \alpha); \alpha > 0$.
- (b) Define the prediction covariance matrix as

$$\xi_P^\alpha \triangleq E \left\{ \left[\hat{\mathbf{d}}(t) - \mathbf{d}(t) \right] \left[\hat{\mathbf{d}}^T(t) - \mathbf{d}^T(t) \right] \right\}.$$

Find an expression for ξ_P^α . Verify that your answer has the correct behavior for $\alpha \rightarrow \infty$.

Problem 8.3.30 (continuation). Let

$$r(u) = a(u) + w(u), \quad -\infty < u \leq t$$

and

$$d(t) = a(t + \alpha).$$

The processes $a(u)$ and $w(u)$ are uncorrelated with spectra

$$\begin{aligned} S_a(\omega) &= \frac{2\sqrt{2}P/k}{1 + (\omega^2/k^2)^2}, \\ S_w(\omega) &= \frac{N_0}{2}. \end{aligned}$$

Use the result of Problem 8.3.29 to find $E[(\hat{d}(t) - d(t))^2]$ as a function of α .

Problem 8.3.31. Consider the following optimum realizable filtering problem:

$$\begin{aligned} r(u) &= a(u) + w(u), \quad 0 \leq u \leq t \\ S_a(\omega) &= \frac{1}{(\omega^2 + k^2)^2}, \\ S_w(\omega) &= \frac{N_0}{2}, \\ S_{aw}(\omega) &= 0. \end{aligned}$$

The desired signal $d(t)$ is

$$d(t) = \frac{da(t)}{dt}.$$

We want to find the optimum linear filter by using state-variable techniques.

- (a) Set the problem up. Define explicitly the state variables you are using and *all* matrices.
- (b) Draw an explicit block diagram of the optimum receiver. (Do not use matrix notation here.)
- (c) Write the variance equation as a set of scalar equations.
- (d) Find the steady-state solution by letting $\dot{\xi}_P(t) = \mathbf{0}$.

Problem 8.3.32. Let

$$r(u) = a(u) + w(u), \quad 0 \leq u \leq t,$$

where $a(u)$ and $n(u)$ are uncorrelated processes with spectra

$$S_a(\omega) = \frac{2k\sigma_a^2}{\omega^2 + k^2}$$

and

$$S_n(\omega) = \frac{N_0}{2}.$$

The desired signal is obtained by passing $a(t)$ through a linear system whose transfer function is

$$K_d(j\omega) = \frac{-j\omega + k}{j\omega + \beta}.$$

- (a) Find the optimum linear filter to estimate $d(t)$ and the variance equation.
- (b) Solve the variance equation for the steady-state case.

9

*Estimation of Discrete-Time Random Processes**

9.1 INTRODUCTION

In this chapter, we study the problem of linear estimation of discrete-time random processes. Our development is parallel to the development for continuous-time processes in Chapter 8. However, the chapter is self-contained and can be read independently of Chapter 8. In Section 9.2, we develop discrete-time Wiener filters and in Section 9.3, we develop discrete-time Kalman filters. In Section 9.3.5, we provide a brief introduction to Bayesian estimation for nonlinear models.

In Section 9.2, we restrict our attention to scalar stationary random processes. In Section 9.3, we consider vector random processes that may be time-varying.

For scalar random processes, the observed sequence is

$$r(k) = s(k) + n(k), \quad K_i \leq k \leq K_f. \quad (9.1)$$

There is a desired signal that is linearly related to $s(k)$,

$$d(k) = \sum_{m=K_i}^{K_f} k_d(k-m)s(m), \quad K_{di} \leq k \leq K_{df}. \quad (9.2)$$

We consider two process models for $s(k)$ and $n(k)$.

1. Second moment models The $s(k)$ and $n(k)$ processes are zero-mean and their covariance functions $k_s(k, m)$, $k_n(k, m)$, and $k_{sn}(k, m)$ are known. We minimize the mean-square error

$$\xi_n = E \left\{ |\hat{d}(k) - d(k)|^2 \right\}, \quad K_{di} \leq k \leq K_{df}, \quad (9.3)$$

and require the estimator to be linear.

2. Gaussian assumption The signal $s(k)$, the desired signal $d(k)$, and the received sequence $r(k)$ are jointly Gaussian. We minimize the mean-square error and the structure of the processor is not specified.

*Dr. Zhi Tian is the co-author for this chapter.

As expected, the two models will lead to the same processor.

In Section 9.2, we use the first model to develop discrete-time Wiener filters. We consider three cases.

1. Finite impulse response (FIR) filters

In the first case,

$$r(k) = s(k) + n(k), \quad k = 1, \dots, K, \quad (9.4)$$

and we specify a desired signal $d(k)$ where $d(k)$ is a linear function of $s(k)$. We find a finite impulse response (FIR) filter $h(m)$, $m = 0, \dots, K - 1$, which minimizes the mean-square error (MSE)

$$\xi(k) = E \left\{ |\hat{d}(k) - d(k)|^2 \right\}, \quad (9.5)$$

where

$$\hat{d}(k) = \sum_{m=0}^{K-1} h(m)r(k-m) = \sum_{m=1}^K h(k-m)r(m). \quad (9.6)$$

2. Noncausal infinite impulse response (IIR) filters

In the second case,

$$r(k) = s(k) + n(k), \quad -\infty < k < \infty, \quad (9.7)$$

and we specify a nonrealizable (noncausal) IIR filter $h(m)$, $m = -\infty, \dots, \infty$, which minimizes the MSE.

3. Causal IIR filters

In the third case,

$$r(k) = s(k) + n(k), \quad -\infty < k \leq K_f, \quad (9.8)$$

and we specify a realizable (causal) infinite impulse response (IIR) filter $h(m)$, $m = 0, 1, \dots, \infty$, which minimizes the MSE.

In all three cases, $r(k)$ and $d(k)$ are real, zero-mean, stationary random processes and their correlation functions $k_r(k)$, $k_d(k)$ and cross-correlation $k_{dr}(k)$ are known.

In Section 9.3, we develop the discrete-time Kalman filter. In this case, we assume that we have a state equation for the random process. The state equation is

$$\mathbf{x}(k) = \mathbf{F}(k-1)\mathbf{x}(k-1) + \mathbf{G}(k-1)\mathbf{u}(k-1), \quad k = 1, 2, \dots, \quad (9.9)$$

where $\mathbf{x}(k)$ is the $p \times 1$ state vector, $\mathbf{F}(k)$ is a $p \times p$ matrix whose eigenvalues all have magnitude less than one, $\mathbf{G}(k)$ is a $p \times p$ matrix, $\mathbf{u}(k)$ is a $p \times 1$ zero-mean Gaussian random vector $N(\mathbf{0}, \mathbf{Q}(k))$ and $\mathbf{u}(k)$ is statistically independent of $\mathbf{u}(m)$ for $m \neq k$. The initial state $\mathbf{x}(0)$ is modeled as a Gaussian random vector, $N(\mathbf{m}_0, \mathbf{P}_0)$. The matrices $\mathbf{F}(k)$, $\mathbf{G}(k)$, $\mathbf{Q}(k)$ are known and may be a function of k .

The observation process is

$$\begin{aligned} \mathbf{r}(k) &= \mathbf{C}(k)\mathbf{x}(k) + \mathbf{w}(k) \quad k = 1, 2, \dots, \\ &= \mathbf{s}(k) + \mathbf{w}(k) \end{aligned} \quad (9.10)$$

where $\mathbf{C}(k)$ is an $N \times p$ matrix and $\mathbf{w}(k)$ is a zero-mean Gaussian vector,

$$E[\mathbf{w}(k)\mathbf{w}^T(m)] = \mathbf{R}(k)\delta_{km}. \quad (9.11)$$

The $\mathbf{w}(k)$ and $\mathbf{u}(k)$ are statistically independent. The matrices $\mathbf{C}(k)$ and $\mathbf{R}(k)$ are known.

We find the optimum processor to minimize the MSE. One of the advantages of the Kalman filter is that it allows us to model nonstationary processes. This ability is particularly important in radar and sonar applications. When dealing with stationary processes, it allows us to model the transient behavior when we turn on the processor.

In Section 9.3, we summarize our results and discuss various extensions of the results.

9.2 DISCRETE-TIME WIENER FILTERING

The Wiener filter was developed in the early 1940s by Norbert Wiener [Wei42] and published in the literature in 1949 [Wie49]. It was developed independently in Russia by A. N. Kolmogorov [Kol41]. Professor Yuk Wing Lee at M.I.T. played a major role in making Wiener's work more understandable through his class notes and book [Lee64]. Bode and Shannon [BS50] provided a more intuitive solution to the Wiener–Hopf equation that specified the optimum realizable filter. All of their work considered stationary continuous-time processes and assumed that the infinite past was available. In addition, they assumed a linear filter and only required a second-moment characterization. Using the Bayesian linear Gaussian model and finding the conditional mean leads to the same linear processor. In Chapter 8, we developed the continuous-time model in detail. In this section, we develop the discrete-time processor.

In Section 9.2.1, we develop the model of the problem. In Section 9.2.2, we solve the equation for the FIR case and the three most common desired signals:

- (i) $d(k) = s(k)$, filtering
- (ii) $d(k) = s(k + L)$, $L \leq -1$, filter with delay
- (iii) $d(k) = s(k + L)$, $L \geq 1$, prediction

and examine the behavior as a function of K , the number of samples, the correlation between samples, and the SNR. In Section 9.2.3, we solve the equation for the IIR unrealizable (noncausal) filter. In Section 9.2.4, we solve the equation for the IIR realizable (causal) filter. In Section 9.2.5, we summarize our results.

9.2.1 Model

The received data is

$$r(k) = s(k) + n(k), \quad k = 1, \dots, K, \quad (9.12)$$

where $s(k)$ and $n(k)$ are zero-mean wide-sense stationary processes and are uncorrelated with each other. Their covariance functions are $k_s(k)$ and $k_n(k)$, respectively.

We want to design a discrete-time linear filter whose output is the minimum mean-square estimate of a desired signal $d(k)$, where $d(k)$ is a linear function of $s(k)$, $k = 1, \dots, K$.

Typical desired functions are

- (i) $d(K) = s(K)$

We have observed K samples and want to estimate the value of the signal at the current sample time. This is called “filtering.”

$$(ii) \quad d(K) = s(K + L), \quad L \geq 1,$$

We have observed K samples and want to estimate the value of the signal at some later sampling time. This is called “prediction” and is widely used in a number of applications.

$$(iii) \quad d(K) = s(K + L), \quad L \leq -1,$$

We have observed K samples and want to estimate the value of the signal at some earlier sampling time. This is called “filtering with delay.” Note that $|L|$ does not have to be less than K .

$$(iv) \quad d(K) = (s(K) - s(K - 1)) / T,$$

where T is the sampling interval. If the $s(K)$ corresponds to the range to a target, $d(K)$ would correspond to the velocity.

We consider the three cases described in Section 9.1. If K is finite, then

$$\hat{d}(k) = \sum_{m=0}^{K-1} h(m)r(k-m) = \sum_{m=1}^K h(k-m)r(m), \quad (9.13)$$

where $h(m)$ is an FIR filter.

If we assume that we have the infinite past available, then

$$\hat{d}(k) = \sum_{m=0}^{\infty} h(m)r(k-m) \quad (9.14)$$

and the filter is a realizable (causal) IIR filter.

If we assume that we have the infinite past and future available, then

$$\hat{d}(k) = \sum_{m=-\infty}^{\infty} h(m)r(k-m) \quad (9.15)$$

and the filter is a nonrealizable IIR filter.

9.2.2 Random Process Models

In order to design Wiener filters, we will find that we need to know $k_{dr}(k)$ and $k_r(k)$. If we consider the model in (9.12) and assume that $d(k)$ is a linear function of $s(k)$, then, if we know $k_s(k)$ and $k_n(k)$, we can find the necessary functions.

In many applications, we will have to measure (estimate) these functions. However, in a large number of applications, we can model the signal as an ARMA (*auto regressive moving average*) process. The system to generate an ARMA process is shown in Figure 1.¹

The input and output are related by a linear difference equation

$$x(k) = - \sum_{m=1}^p a(m)x(k-m) + \sum_{m=0}^q b(m)u(k-m), \quad 1 \leq k \leq K. \quad (9.16)$$

¹There are a number of good discussions of parametric models (for example, [Kay88, Mar87, PRLN92]). Our discussion is similar to Chapter 5 of [Kay88] and Chapter 6 of [Mar87].

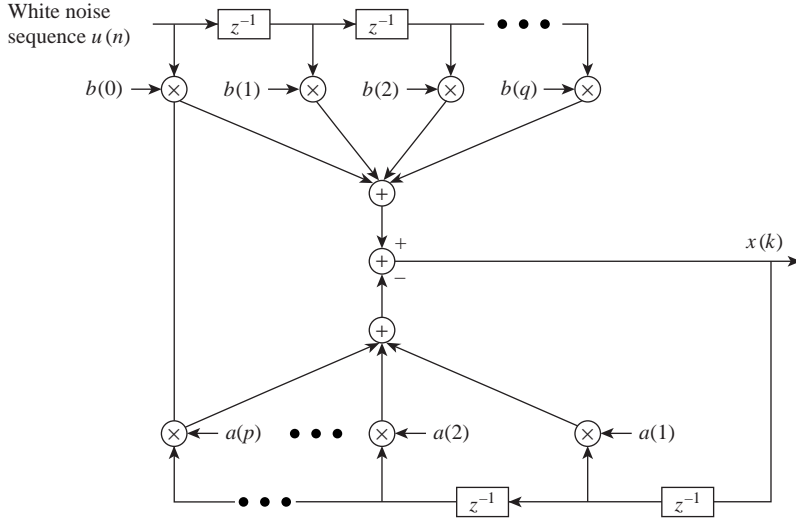


Figure 9.1: Autoregressive moving average model of random process.

The z -transform of the system is

$$H(z) = \frac{B(z)}{A(z)}, \quad (9.17)$$

where

$$A(z) = \sum_{m=0}^p a(m)z^{-m} \quad (9.18)$$

and

$$B(z) = \sum_{m=0}^q b(m)z^{-m} \quad (9.19)$$

with $a(0) = 1$ and $b(0) = 1$. We require that all the zeros of $A(z)$ be inside the unit circle. This guarantees that $H(z)$ is a stable, realizable system (e.g., [OS89]).

The output spectrum in the z -domain is

$$P_{xx}(z) = H(z)H^*\left(\frac{1}{z^*}\right) P_{uu}(z) \quad (9.20)$$

$$= \frac{B(z)B^*(\frac{1}{z^*})}{A(z)A^*(\frac{1}{z^*})} P_{uu}(z). \quad (9.21)$$

Evaluating at $z = e^{j\omega}$ gives the frequency spectrum of $x(k)$ in ω -space. Thus,

$$P_{xx}(z)|_{z=e^{j\omega}} \triangleq \tilde{P}_{xx}(e^{j\omega}) = \sigma_u^2 \left| \frac{B(e^{j\omega})}{A(e^{j\omega})} \right|^2, \quad (9.22)$$

where σ_u^2 is the variance of the input process. This model is referred to as an ARMA(p, q) process.

The corresponding covariance values are obtained by taking the inverse transform of (9.21). We write

$$P_{xx}(z)A(z) = C^* \left(\frac{1}{z^*} \right) B(z)\sigma_u^2 \quad (9.23)$$

where

$$C^* \left(\frac{1}{z^*} \right) = \frac{B^* \left(\frac{1}{z^*} \right)}{A^* \left(\frac{1}{z^*} \right)}. \quad (9.24)$$

The inverse z -transform of (9.23) is

$$\sum_{l=0}^p a(l)k_{xx}(m-l) = \sigma_u^2 \sum_{l=0}^q b(l)c^*(l-m). \quad (9.25)$$

Since $c(m) = 0$ for $m < 0$, (9.25) reduces to

$$k_{xx}(m) = \begin{cases} -\sum_{l=1}^p a(l)k_{xx}(m-l) + \sigma_u^2 \sum_{l=0}^{q-m} c^*(l)b(l+m), & 0 \leq m \leq q, \\ \sum_{l=1}^p a(l)k_{xx}(m-l), & m \geq q+1. \end{cases} \quad (9.26)$$

We focus most of our attention on processes where all of the $b(m)$ except $b(0)$ are equal to zero. In this case,

$$x(k) = -\sum_{m=1}^p a(m)x(k-m) + u(k). \quad (9.27)$$

This model is referred to as an auto-regressive (AR) process of order- p , AR(p). It is autoregressive because it is a linear regression model acting on itself. If we define

$$\bar{x}(k) = -\sum_{m=1}^p a(m)x(k-m), \quad (9.28)$$

then

$$x(k) = \bar{x}(k) + u(k) \quad (9.29)$$

so that $u(k)$ corresponds to the error between weighted sum of past values and the value $x(k)$.

The power spectral density is

$$S_x(e^{j\omega}) = \frac{\sigma_u^2}{|A(e^{j\omega})|^2}. \quad (9.30)$$

The AR process model is shown in Figure 9.2.

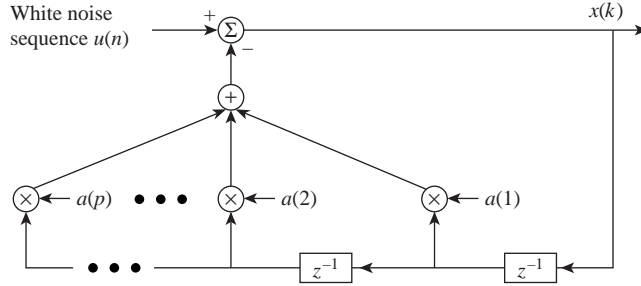


Figure 9.2: Autoregressive model of random process.

The covariance values follow directly from the process generation model. From (9.30), we have

$$\tilde{P}_{xx}(e^{j\omega})A(e^{j\omega}) = \frac{\sigma_u^2}{A^*(e^{j\omega})}. \quad (9.31)$$

Taking the inverse transform of (9.31) gives

$$k_{xx}(m) = \begin{cases} -\sum_{l=1}^p a(l)k_{xx}(m-l), & m \geq 1, \\ -\sum_{l=1}^p a(l)k_{xx}(-l) + \sigma_u^2, & m = 0, \end{cases} \quad (9.32)$$

which can be written in matrix form as

$$\begin{bmatrix} k_{xx}(0) & k_{xx}(1) & \cdots & k_{xx}(p-1) \\ k_{xx}(1) & k_{xx}(0) & \cdots & k_{xx}(p-2) \\ \vdots & \vdots & \ddots & \vdots \\ k_{xx}(p-1) & k_{xx}(p-2) & \cdots & k_{xx}(0) \end{bmatrix} \begin{bmatrix} a(1) \\ a(2) \\ \vdots \\ a(p) \end{bmatrix} = - \begin{bmatrix} k_{xx}(1) \\ k_{xx}(2) \\ \vdots \\ k_{xx}(p) \end{bmatrix}. \quad (9.33)$$

These equations are known as Yule–Walker equations (e.g. [Yul27, Wal31]). They can be efficiently solved in $O(p^2)$ operations using the Levinson algorithm [Lev47] that is a function in MATLAB. They can be augmented to include σ_u^2 ,

$$\begin{bmatrix} k_{xx}(0) & k_{xx}(1) & \cdots & k_{xx}(p) \\ k_{xx}(1) & k_{xx}(0) & \cdots & k_{xx}(p-1) \\ \vdots & \vdots & \ddots & \vdots \\ k_{xx}(p) & k_{xx}(p-1) & \cdots & k_{xx}(0) \end{bmatrix} \begin{bmatrix} 1 \\ a(1) \\ \vdots \\ a(p) \end{bmatrix} = - \begin{bmatrix} \sigma_u^2 \\ 0 \\ \vdots \\ 0 \end{bmatrix}. \quad (9.34)$$

We consider several examples to illustrate the type of frequency spectra and covariance functions that can be generated using the AR process model.

Example 9.1. Consider an AR(1) process model. We assume

$$b(0) = 1, \quad (9.35)$$

$$a(1) = -\alpha. \quad (9.36)$$

Then, from (9.27)

$$k_{xx}(k) = \alpha k_{xx}(k-1), \quad k \geq 1. \quad (9.37)$$

Solving (9.34) gives

$$k_{xx}(k) = k_{xx}(0)\alpha^{|k|} \quad (9.38)$$

and

$$k_{xx}(0) = \frac{\sigma_u^2}{1 - \alpha^2}. \quad (9.39)$$

Note that $k_{xx}(0)$ is the signal power σ_s^2 . Then

$$k_s(k) = \frac{\sigma_u^2}{1 - \alpha^2} \alpha^{|k|} = k_s(0) \alpha^{|k|} \quad (9.40)$$

and the power spectrum is

$$\begin{aligned} P_s(e^{j\omega}) &= \sum_{k=-\infty}^{\infty} k_s(k) e^{-jk\omega} \\ &= k_s(0) \sum_{k=-\infty}^{\infty} \alpha^{|k|} e^{-jk\omega} \\ &= k_s(0) \left\{ \sum_{k=-\infty}^{-1} \alpha^{-k} e^{-jk\omega} + 1 + \sum_{k=1}^{\infty} \alpha^k e^{-jk\omega} \right\} \\ &= k_s(0) \left(\frac{1 - \alpha^2}{(1 + \alpha^2) - 2\alpha \cos \omega} \right). \end{aligned} \quad (9.41)$$

The correlation $k_s(k)$ is plotted versus k in Figure 9.3 for $\alpha = 0.3, 0.5, 0.7$, and 0.9 . The power spectrum is shown in Figure 9.4. The total power, $\sigma_p^2 = k_{xx}(0)$, equals one. ■

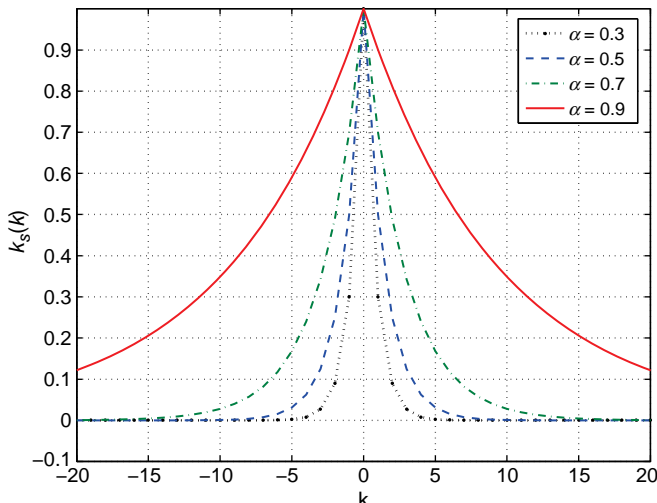


Figure 9.3: Correlation function of AR(1) process.

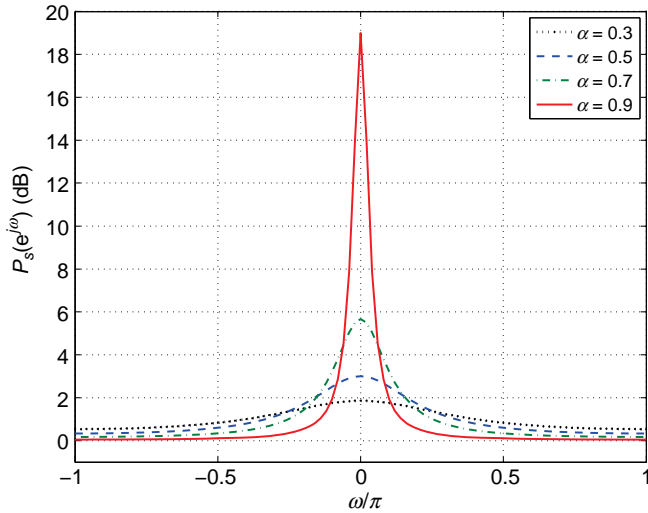


Figure 9.4: Power spectrum of AR(1) process; $\sigma_p^2 = 1$.

The next AR model of interest is the AR(2) model. We must develop some general properties of AR(2) models before we can consider examples. Our development follows Section 4.2 of Monolakis et al. [MIK00].²

If we let $b(0) = 1$, then the system function of an AR(2) model is

$$H(z) = \frac{1}{1 + a_1 z^{-1} + a_2 z^{-2}} = \frac{1}{(1 - p_1 z^{-1})(1 - p_2 z^{-1})}. \quad (9.42)$$

Multiplying the terms in the denominator of the last term and matching coefficients gives

$$a_1 = -(p_1 + p_2), \quad (9.43)$$

$$a_2 = p_1 p_2. \quad (9.44)$$

In order for $H(z)$ to be a realizable minimum phase system, p_1 and p_2 must both be inside the unit circle. This implies that a_1 and a_2 satisfy³

$$\begin{aligned} -1 &< a_2 < 1 \\ a_2 - a_1 &> -1 \\ a_2 + a_1 &> -1 \end{aligned} \quad (9.45)$$

which requires that a_1 and a_2 lie inside the triangular regions shown in Figure 9.5.

Complex roots occur when

$$\frac{a_1^2}{4} < a_2 \leq 1. \quad (9.46)$$

When $a_2 = 1$, both poles are on the unit circle.

²All of these results appeared earlier in the literature, but [MIK00] provides a concise development.

³See Problem 9.2.1.

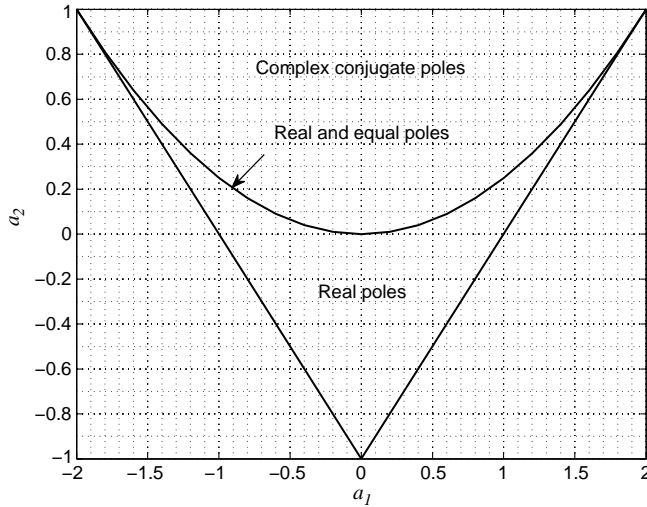


Figure 9.5: Minimum-phase region (triangle) for the AR(2) model in the (a_1, a_2) parameter space.

The complex poles can be written in polar form

$$p_i = r e^{\pm j\theta}, \quad 0 \leq r \leq 1. \quad (9.47)$$

Then,

$$a_1 = -2r \cos \theta \quad (9.48)$$

and

$$a_2 = r^2. \quad (9.49)$$

For a real process,

$$p_2 = p_1^*. \quad (9.50)$$

The system function is

$$H(z) = \frac{1}{(1 - p_1 z^{-1})(1 - p_1^* z^{-1})} = \frac{1}{1 - (2r \cos \theta)z^{-1} + r^2 z^{-2}}, \quad (9.51)$$

which r is magnitude of the pole and $\theta = \omega_p$ is the normalized frequency.

The impulse response of the AR(2) model is found by taking the inverse transform of (9.51). For $p_1 \neq p_2$,

$$h(k) = \frac{1}{p_1 - p_2} (p_1^{k+1} - p_2^{k+1}) u(k). \quad (9.52)$$

For $p_1 = p_2 = p$,

$$h(k) = (k + 1)p^k u(k). \quad (9.53)$$

For complex conjugate poles,

$$h(k) = r^k \frac{\sin[(k+1)\omega_p]}{\sin \omega_p} u(k), \quad (9.54)$$

which is a damped sinusoid of frequency ω_p .

The autocorrelation can be written as

$$k_{xx}(m) = \frac{\sigma_u^2}{(p_1 - p_2)(1 - p_1 p_2)} \left(\frac{p_1^{m+1}}{1 - p_1^2} - \frac{p_2^{m+1}}{1 - p_2^2} \right), \quad m \geq 0. \quad (9.55)$$

Therefore,

$$\sigma_p^2 = k_{xx}(0) = \frac{\sigma_u^2(1 + p_1 p_2)}{(1 - p_1 p_2)(1 - p_1^2)(1 - p_2^2)}. \quad (9.56)$$

For complex conjugate poles,

$$k_{xx}(m) = \frac{\sigma_u^2 r^m \{ \sin[(m+1)\omega_p] - r^2 \sin[(m-1)\omega_p] \}}{[(1-r^2) \sin \omega_p] (1 - 2r^2 \cos 2\omega_p + r^4)}, \quad m \geq 0, \quad (9.57)$$

and

$$\sigma_p^2 = k_{xx}(0) = \frac{\sigma_u^2(1 + r^2)}{(1 - r^2)(1 - 2r^2 \cos 2\omega_p + r^4)}. \quad (9.58)$$

The normalized autocorrelation is

$$k_{xn}(m) = \frac{k_{xx}(m)}{k_{xx}(0)} = \frac{r^m \{ \sin[(m+1)\omega_p] - r^2 \sin[(m-1)\omega_p] \}}{(1 + r^2) \sin \omega_p}, \quad m \geq 0, \quad (9.59)$$

which reduces to

$$k_{xn}(m) = \frac{1}{\cos \beta} r^m \cos(m\omega_p - \beta), \quad m \geq 0, \quad (9.60)$$

where

$$\beta = \tan^{-1} \left(\frac{(1 - r^2) \cos \omega_p}{(1 + r^2) \sin \omega_p} \right), \quad (9.61)$$

which is a damped cosine wave.

For complex conjugate poles, the spectrum can be written as

$$S_x(e^{j\omega}) = \frac{\sigma_u^2}{[1 - 2r \cos(\omega - \theta) + r^2][1 - 2r \cos(\omega + \theta) + r^2]}. \quad (9.62)$$

The peak is located at

$$\cos \omega_c = \left(\frac{1 + r^2}{2r} \right) \cos \theta. \quad (9.63)$$

Now $1 + r^2 > 2r$ for $r < 1$, so

$$\cos \omega_c > \cos \theta. \quad (9.64)$$

Therefore, $\omega_c > \omega_p$ for $0 < \omega_p < \pi/2$ and $\omega_c < \omega_p$ for $\pi/2 < \omega_p < \pi$.

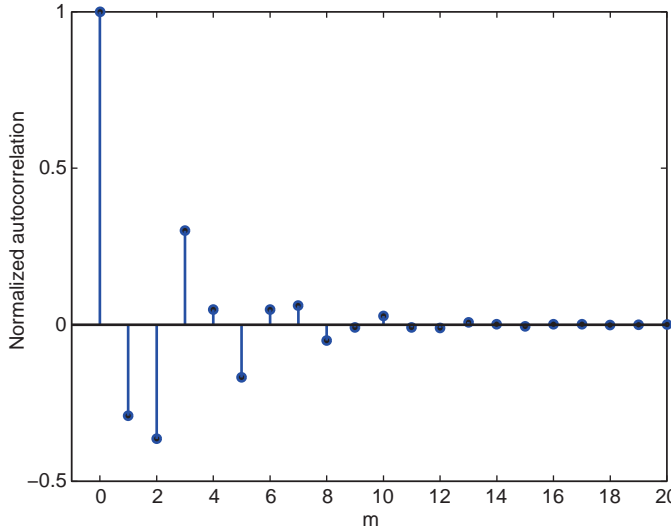


Figure 9.6: Normalized autocorrelation; AR(2), Complex conjugate poles: $0.7e^{\pm j0.6\pi}$.

Example 9.2. Consider an AR(2) process with complex conjugate poles

$$p_{1(2)} = 0.7e^{\pm j0.6\pi}. \quad (9.65)$$

From (9.44), $a_1 = -1.4 \cos(0.6\pi)$ and $a_2 = 0.49$. From (9.42),

$$\sigma_p^2 = k_{xx}(0) = \frac{\sigma_u^2(1.49)}{.51(1 - .98 \cos(1.2\pi)) + (.49)^2}. \quad (9.66)$$

The normalized autocorrelation function is given by (9.59) and is plotted in Figure 9.6. The power spectrum is given by (9.62) and is plotted in Figure 9.7. The peak of the spectrum is given by (9.63),

$$\omega_c = \cos^{-1} \left(\frac{1.49}{1.40} \cos(.6\pi) \right) = 0.6067\pi. \quad (9.67)$$

The process has a passband characteristic centered around ω_c . ■

For the general AR(p) case, we follow a similar procedure but normally rely on numerical solutions rather than analytic expressions. There are several cases that depend on the starting point.

Case 1: Poles are specified

- Find $\mathbf{a} \triangleq [a(1) \cdots a(p)]^T$ using the generalization of (9.44)

$$a(i) = (-1)^i \sum_{\{k_1 \leq k_2 \cdots \leq k_i\}} p_{k_1} p_{k_2} \cdots p_{k_i}, \quad (9.68)$$

This is implemented using .poly in MATLAB.

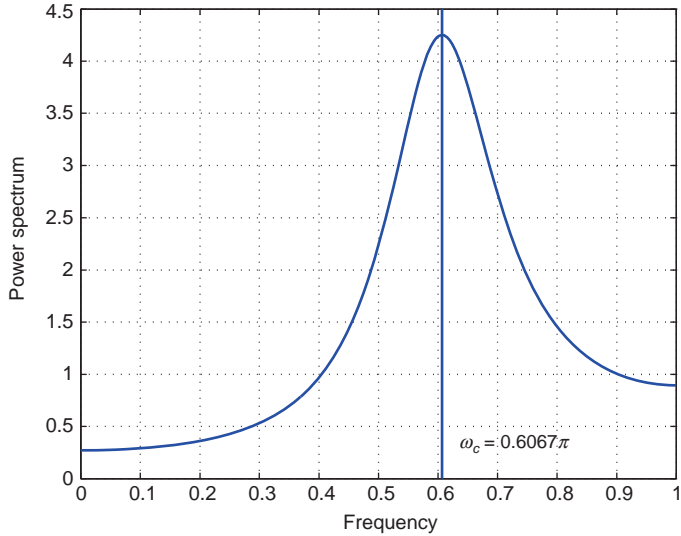


Figure 9.7: Normalized power spectrum; AR(2), Complex conjugate poles: $0.7e^{\pm j0.6\pi}$.

2. Find the spectrum using (9.22) with

$$A(z) = \prod_{i=1}^p (1 - z_i z^{-1}). \quad (9.69)$$

3. Find the autocorrelation by taking the inverse DFT of the spectrum.
4. Compute $\sigma_p^2 = k_{xx}(0)$.

Case 2: Autocorrelation function is specified

1. Find \mathbf{a} from the Yule–Walker equations (9.34).
2. Find the spectrum by taking the DFT.
3. Find the poles of $A(z)$ by using a root finding algorithm; `.roots` in MATLAB. Retain roots inside the unit circle.

Case 3: Spectrum is specified

1. Find the poles of $A(z)$.
2. Find \mathbf{a} using (9.68); `.poly` in MATLAB.
3. Find the autocorrelation function by taking the inverse transform.

Several examples are given in the problems.

The third process of interest corresponds to the case where all of the $a(k)$ coefficients are zero except for $a[0] = 1$. Then,

$$x(k) = \sum_{m=0}^q b(m)u(k-m), \quad (9.70)$$

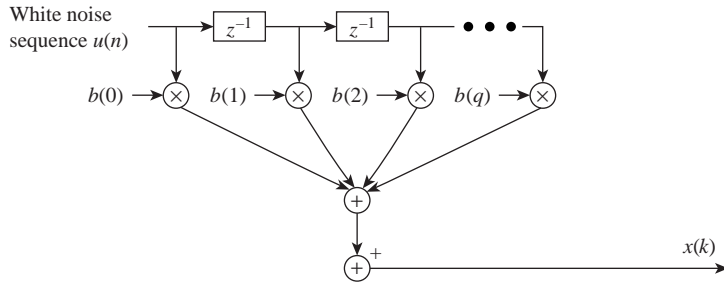


Figure 9.8: Moving average model of random process.

and the process is referred to as a moving average (MA) process.

$$S_x(e^{j\omega}) = \sigma_u^2 |B(e^{j\omega})|^2. \quad (9.71)$$

The model is shown in Figure 9.8. The corresponding covariance values can be obtained by letting $a(l) = \delta(l)$ and $c(l) = b(l)$ in (9.25). Then

$$k_x(m) = \begin{cases} \sigma_u^2 \sum_{l=0}^{q-m} b(l)b(m+l), & m = 0, 1, \dots, q, \\ 0, & m \geq q+1. \end{cases} \quad (9.72)$$

For an MA(1) process,

$$k_x(m) = \begin{cases} \sigma_u^2 [1 + |b(1)|^2], & m = 0, \\ \sigma_u^2 [|b(1)|], & m = 1, \\ 0, & m \geq 2. \end{cases} \quad (9.73)$$

For an MA(2) process,

$$k_x(m) = \begin{cases} \sigma_u^2 [1 + |b(1)|^2 + |b(2)|^2], & m = 0, \\ \sigma_u^2 [b(1) + b(1)b(2)], & m = 1, \\ \sigma_u^2 [b(2)], & m = 2, \\ 0, & m \geq 3. \end{cases} \quad (9.74)$$

Thus, the covariance matrix for an MA(2) process is a banded Toeplitz matrix,

$$\mathbf{K}_x = \begin{bmatrix} k_x(0) & k_x(1) & k_x(2) & 0 & \cdots & 0 \\ k_x(1) & k_x(0) & k_x(1) & k_x(2) & \cdots & \cdots \\ k_x(2) & k_x(1) & k_x(0) & k_x(1) & \cdots & \cdots \\ \vdots & \vdots & \vdots & \vdots & \ddots & \vdots \\ 0 & \cdots & \cdots & \cdots & k_x(1) & k_x(0) \end{bmatrix}, \quad (9.75)$$

where only the main diagonal and $2q$ adjacent diagonals are nonzero. This banded property is useful in many applications.

9.2.3 Optimum FIR Filters

We first find the optimum linear FIR filter whose output is the minimum mean-square estimate of $d(k)$. The mean-square error is

$$\xi = E \{ |e(k)|^2 \} = E \left\{ |d(k) - \hat{d}(k)|^2 \right\}. \quad (9.76)$$

Taking the derivative with respect to $h(m)$ gives

$$\frac{\partial \xi}{\partial h(m)} = E \left\{ 2e(k) \frac{\partial e(k)}{\partial h(m)} \right\} = 0. \quad (9.77)$$

Using (9.13) and (9.76) gives

$$E \{ e(k)r(k-m) \} = 0 \quad (9.78)$$

and using the definition of $e(k)$ gives

$$E \{ d(k)r(k-m) \} - \sum_{l=0}^{K-1} h(l) E \{ r(k-l)r(k-m) \} = 0, \quad m = 0, \dots, K-1. \quad (9.79)$$

The processes are wide-sense stationary, so

$$E \{ r(k-l)r(k-m) \} = k_r(l-m) \quad (9.80)$$

and

$$E \{ d(k)r(k-m) \} = k_{dr}(m). \quad (9.81)$$

Using (9.80) and (9.81) in (9.79) gives

$$k_{dr}(m) - \sum_{l=0}^{K-1} h_o(l) k_r(l-m) = 0, \quad m = 0, \dots, K-1, \quad (9.82)$$

which is a set of K equations with K unknowns, as follows:

$$\begin{bmatrix} k_r(0) & k_r(1) & \cdots & k_r(K-1) \\ k_r(1) & k_r(0) & \cdots & k_r(N-2) \\ \vdots & \ddots & \vdots & \vdots \\ k_r(K-1) & k_r(K-2) & \cdots & k_r(0) \end{bmatrix} \begin{bmatrix} h_o(0) \\ h_o(1) \\ \vdots \\ h_o(K-1) \end{bmatrix} = \begin{bmatrix} k_{dr}(0) \\ k_{dr}(1) \\ \vdots \\ k_{dr}(K-1) \end{bmatrix}. \quad (9.83)$$

The result in (9.82) and (9.83) is the *finite sample Wiener equation*. We have used the subscript “o” to denote that this is the optimum FIR filter. It can be written in matrix form as

$$\mathbf{K}_r \mathbf{h}_o = \mathbf{k}_{d(k)r}, \quad (9.84)$$

where

$$[\mathbf{h}_o]_l = h_o(l-1), \quad l = 1, \dots, K \quad (9.85)$$

and

$$[\mathbf{k}_{d(k)r}]_l = k_{dr}(l-1), \quad l = 1, \dots, K \quad (9.86)$$

are $K \times 1$ vectors and \mathbf{K}_r is the $K \times K$ matrix in (9.83).

The resulting minimum mean-square error is obtained by using (9.82) in (9.76)

$$\xi_o = E \left\{ \left(d(k) - \sum_{m=0}^{K-1} h_o(m)r(k-m) \right)^2 \right\}. \quad (9.87)$$

The cross-term is zero from (9.78), so

$$\begin{aligned} \xi_o &= k_d(0) - E \left\{ \sum_{n=0}^{K-1} h_o(n)r(k-n) \sum_{m=0}^{K-1} h_o(m)r(k-m) \right\} \\ &= k_d(0) - \sum_{n=0}^{K-1} h_o(n) \left(\sum_{m=0}^{K-1} h_o(m)k_r(m-n) \right). \end{aligned} \quad (9.88)$$

Using (9.82) gives

$$\boxed{\xi_o = k_d(0) - \sum_{n=0}^{K-1} h_o(n)k_{dr}(n).} \quad (9.89)$$

We observe that the desired signal only appears in the Wiener equation in $k_{dr}(k)$. Therefore, the filtering, filtering with delay, and prediction problems for the case where $d(k) = s(k+L)$ can be written as

$$k_{dr}(m) = E \{s(k+L)r(k-m)\}, \quad m = 0, \dots, K-1. \quad (9.90)$$

If the signal and noise are uncorrelated, then

$$\begin{aligned} k_{dr}(m) &= E \{s(k+L)s(k-m)\} \\ &= k_s(m+L), \quad m = 0, \dots, K-1. \end{aligned} \quad (9.91)$$

The Wiener filter equation in (9.83) can be written as

$$\begin{bmatrix} k_r(0) & k_r(1) & \cdots & k_r(K-1) \\ k_r(1) & k_r(0) & \cdots & k_r(K-2) \\ \vdots & & & \vdots \\ \vdots & & \ddots & \vdots \\ \vdots & & & \vdots \\ k_r(K-1) & k_r(K-2) & \cdots & k_r(0) \end{bmatrix} \begin{bmatrix} h_o(0) \\ h_o(1) \\ \vdots \\ \vdots \\ h_o(K-1) \end{bmatrix} = \begin{bmatrix} k_s(L) \\ k_s(L+1) \\ \vdots \\ k_s(0) \\ \vdots \\ k_s(L+K-1) \end{bmatrix} \quad (9.92)$$

and

$$k_s(-k) = k_s(k). \quad (9.93)$$

There is an efficient technique for solving (9.92), which is known as the Levinson–Durbin algorithm. It was invented by Levinson in a 1947 paper on Wiener filter design [Lev47] and improved by Durbin in 1960 [Dur60]. It is available as a function in the MATLAB signal processing toolbox.

The mean-square error is given by (9.89)

$$\xi_o = k_s(0) - \sum_{m=0}^{K-1} h_o(m)k_s(m+L). \quad (9.94)$$

We consider several examples to illustrate the performance of optimum filter as a function of various parameters. If we assume that the signal and noise are uncorrelated, then we must specify $k_s(k)$ and $k_n(k)$.

We use the following notation to delineate three types of Wiener FIR filters. The desired signal is $d(k) = s(K+L)$. If $L = 0$, we refer to it as an FIR Wiener filter. If $L < 0$, we refer to it as an FIR Wiener filter with lag. If $L > 0$, we refer to it as an FIR Wiener predictor.

Example 9.3: FIR Wiener filter. Consider an AR(1) process model for the signal and a white noise model for the noise. We assume

$$b(0) = 1, \quad (9.95)$$

$$a(1) = -\alpha, \quad (9.96)$$

$$k_n(k) = \sigma_w^2 \delta(0). \quad (9.97)$$

Then

$$k_s(0) = \frac{\sigma_u^2}{1 - \alpha^2} = \sigma_s^2. \quad (9.98)$$

The SNR is

$$\text{SNR} = \frac{\sigma_s^2}{\sigma_w^2}. \quad (9.99)$$

We let $\sigma_w^2 = 1$ and vary σ_u^2 to vary the SNR

$$\sigma_u^2 = \text{SNR}(1 - \alpha^2). \quad (9.100)$$

The normalized variance function was shown in Figure 9.3 and the power spectrum was shown in Figure 9.4.

The Wiener filter equation for $K = 4$ is

$$\begin{bmatrix} 1 + \sigma_\omega^2/\sigma_s^2 & \alpha & \alpha^2 & \alpha^3 \\ \alpha & 1 + \sigma_\omega^2/\sigma_s^2 & \alpha & \alpha^2 \\ \alpha^2 & \alpha & 1 + \sigma_\omega^2/\sigma_s^2 & \alpha \\ \alpha^3 & \alpha^2 & \alpha & 1 + \sigma_\omega^2/\sigma_s^2 \end{bmatrix} \begin{bmatrix} h(0) \\ h(1) \\ h(2) \\ h(3) \end{bmatrix} = \begin{bmatrix} 1 \\ \alpha \\ \alpha^2 \\ \alpha^3 \end{bmatrix}. \quad (9.101)$$

We consider the following parameter values:

- (i) $\alpha = 0.3, 0.5, 0.8, 0.95$.
- (ii) $K = 10$ and K varying.
- (iii) SNR = 0 dB, 3 dB, and 10 dB.

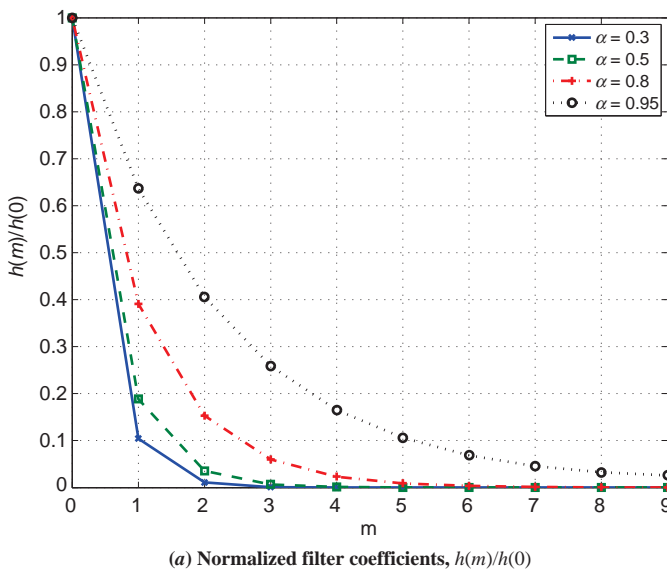
We plot three quantities in Figure 9.9 for SNR = 3 dB.

- (a) The filter coefficients $h(m)$ normalized by $h(0)$ for $K = 10$.
- (b) The frequency response of the filter for $K = 10$.
- (c) The normalized mean-square error,

$$\frac{\text{MSE}}{k_s(0)} = \frac{\text{MSE}}{\sigma_s^2}$$

as a function of K , the length of the FIR filter.

The plots for SNRs of 0 dB and 10 dB are similar except for scaling, so we do not show them.



(a) Normalized filter coefficients, $h(m)/h(0)$

Figure 9.9: AR(1) signals, SNR = 3 dB, $\alpha = 0.3, 0.5, 0.8, 0.95$.

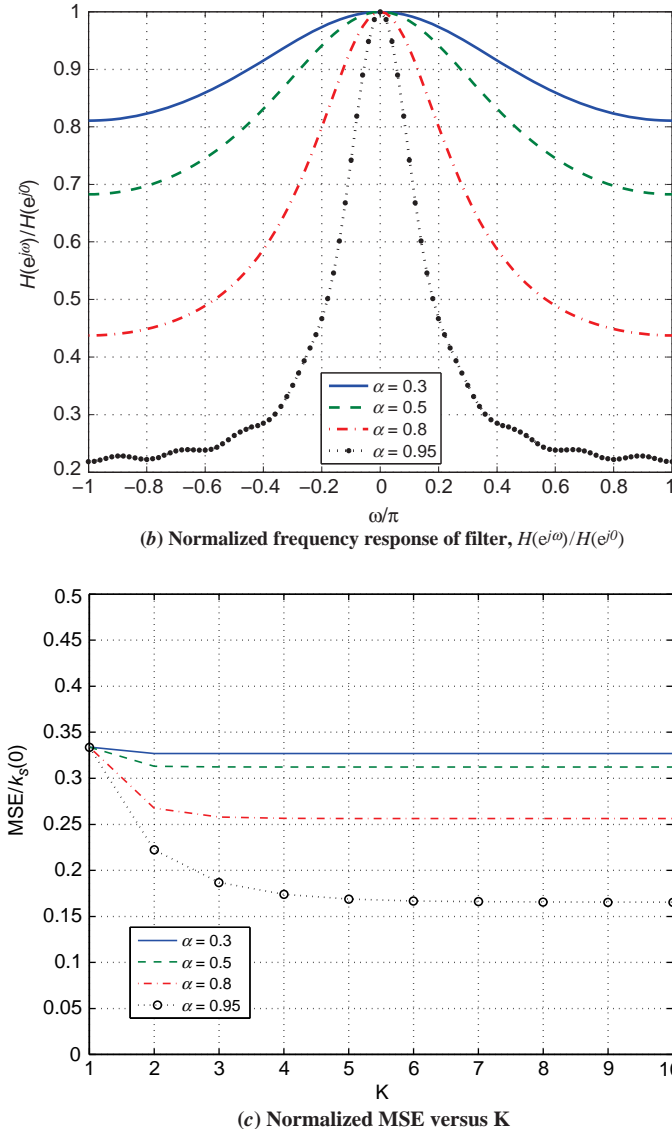


Figure 9.9: (Continued) AR(1) signals, SNR = 3 dB, $\alpha = 0.3, 0.5, 0.8, 0.95$.

We see that the filter coefficients decrease as a function of α . For $\alpha = 0.3$, $h(2) \simeq 0$. For $\alpha = 0.5$, $h(3) \simeq 0$. For $\alpha = 0.8$, $h(5) \simeq 0$. For $\alpha = 0.95$, $h(9) \simeq 0$. There is no value in including samples that are uncorrelated with the desired signal.

The frequency response becomes narrower as α increases. The MSE approaches a constant value as K increases and can be used to determine the useful length of the FIR filter. ■

We next consider the filtering with delay or smoothing problem.

Example 9.4: FIR Wiener filter with lag. We consider the same process model as in Example 9.1 and assume that L is negative. From (9.38),

$$k_s(k) = k_s(0)\alpha^{|k|}. \quad (9.102)$$

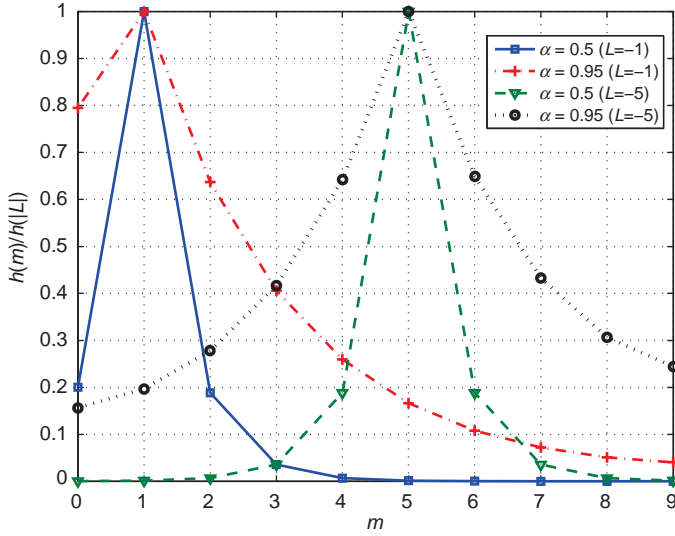


Figure 9.10: Normalized $h(m)$: AR(1), SNR = 3 dB, $N = 10$, $L = -1$ and -5 , $\alpha = 0.5$ and 0.95 .

Then (9.92) becomes

$$\begin{bmatrix} 1 + \sigma_\omega^2/\sigma_s^2 & \alpha & \alpha^2 & \alpha^3 \\ \alpha & 1 + \sigma_\omega^2/\sigma_s^2 & \alpha & \alpha^2 \\ \alpha^2 & \alpha & 1 + \sigma_\omega^2/\sigma_s^2 & \alpha \\ \alpha^3 & \alpha^2 & \alpha & 1 + \sigma_\omega^2/\sigma_s^2 \end{bmatrix} \begin{bmatrix} h(0) \\ h(1) \\ h(2) \\ h(3) \end{bmatrix} = \begin{bmatrix} \alpha^2 \\ \alpha^1 \\ 1 \\ \alpha \end{bmatrix} \quad (9.103)$$

for $K = 4$ and $L = -2$.

To illustrate the effect of the delay L , we consider the SNR = 3 dB case and $K = 10$. In Figure 9.10, we show the normalized $h(m)$ for $L = -1$ and -5 and $\alpha = 0.5$ and 0.95 . We see that, for $L = -5$, the weights are symmetric. For $L = -1$, the weights are asymmetric. The weights are proportional to the covariance so the $L = -5$ case has the benefit of more observations with higher correlation.

In Figure 9.11, we plot $\xi_0(10 : L)$ versus $|L|$ for $L \leq 0$. We see that $\xi_0(10 : L)$ decreases until it reaches a minimum at $L = -5$. The curves between 0 and 9 are symmetric about 5. As $|L|$ exceeds K , we are estimating signal values who observations did not affect the filter output. In essence, we are predicting backwards. ■

We discuss FIR Wiener predictors in the problem section. For the AR(1) case, one can show that $\hat{s}(k+L) = \alpha^L \hat{s}(k)$.

These examples illustrate the type of results that will carry over to more general process models when the noise is white, the signal is from an autoregressive process and $d(k) = d(k+L)$.

For FIR filters ($L = 0$), the decay of the filter coefficients will depend on $k_s(k)$. As $k_s(k)$ approaches zero, the filter coefficients approach zero. We can determine the length of the FIR filter that provides an MSE within a desired percentage of MSE as $N \rightarrow \infty$.

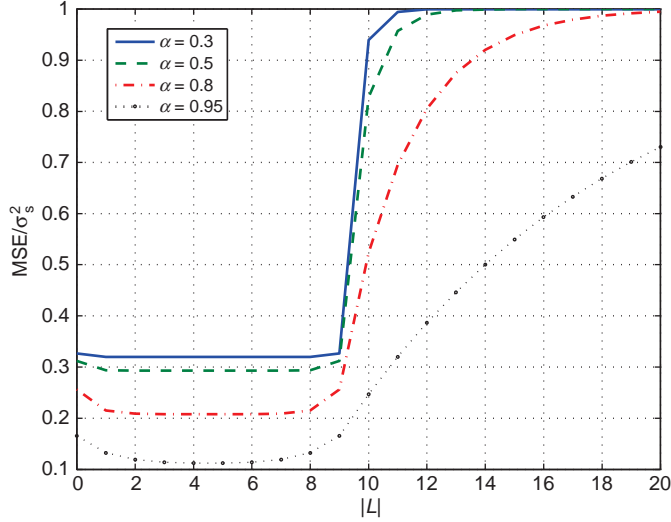


Figure 9.11: Normalized MSE versus $|L|$, $L \leq 0$, SNR = 3 dB, $\alpha = 0.3, 0.5, 0.8$, and 0.95 .

9.2.4 Unrealizable IIR Wiener Filters

In this section we derive the optimum Wiener filter assuming that we have observations from $-\infty < n < \infty$. We refer to this filter as an unrealizable or noncausal filter. The motivation for studying this filter is twofold:

- (i) It will provide a bound on the MSE of any realizable filter.
- (ii) We can approximate its performance by using filtering with delay with a suitable value of L .

The desired estimate $\hat{d}(k)$ is given

$$\hat{d}(k) = \sum_{m=-\infty}^{\infty} h_{ou}(m)r(k-m), \quad (9.104)$$

where $h_{ou}(m)$ satisfies

$$\sum_{m=-\infty}^{\infty} h_{ou}(m)k_r(k-m) = k_{dr}(k), \quad -\infty < k < \infty. \quad (9.105)$$

We have used the subscript “ou” to denote that this is the optimum unrealizable filter. We can solve (9.105) using the convolution property of Fourier transforms or z -transforms

$$H_{ou}(e^{j\omega}) = \frac{P_{dr}(e^{j\omega})}{P_r(e^{j\omega})} \quad (9.106)$$

or

$$H_{ou}(z) = \frac{S_{dr}(z)}{S_r(z)} \quad (9.107)$$

where $z = e^{j\omega}$.

The mean-square error is given by (9.89)

$$\xi_{ou} = k_d(0) - \sum_{m=-\infty}^{\infty} h_{ou}(m)k_{dr}(m), \quad (9.108)$$

which can be written in the frequency domain as

$$\xi_{ou} = \frac{1}{2\pi} \int_{-\pi}^{\pi} \left(P_d(e^{j\omega}) - H_{ou}(e^{j\omega})P_{dr}(e^{j\omega}) \right) d\omega \quad (9.109)$$

$$= \frac{1}{2\pi} \int_{-\pi}^{\pi} \left(P_d(e^{j\omega}) - \frac{P_{dr}^2(e^{j\omega})}{P_r(e^{j\omega})} \right) d\omega. \quad (9.110)$$

For the model in Section 9.1.1, with $d(k) = s(k)$,

$$r(k) = s(k) + n(k), \quad -\infty < k < \infty, \quad (9.111)$$

where $s(k)$ and $n(k)$ are uncorrelated. Then

$$P_r(e^{j\omega}) = P_s(e^{j\omega}) + P_n(e^{j\omega}) \quad (9.112)$$

and

$$P_{dr}(e^{j\omega}) = P_s(e^{j\omega}). \quad (9.113)$$

Then, (9.106) becomes

$$H_{ou}(e^{j\omega}) = \frac{P_s(e^{j\omega})}{P_s(e^{j\omega}) + P_n(e^{j\omega})}. \quad (9.114)$$

The MSE becomes

$$\xi_{ou} = \frac{1}{2\pi} \int_{-\pi}^{\pi} P_s(e^{j\omega}) \left[1 - H_{ou}(e^{j\omega}) \right] d\omega. \quad (9.115)$$

Using (9.114),

$$\xi_{ou} = \frac{1}{2\pi} \int_{-\pi}^{\pi} P_n(e^{j\omega}) H_{ou}(e^{j\omega}) d\omega. \quad (9.116)$$

The error ξ_{ou} is referred to as the *irreducible mean-square error* because it represents the MSE when an infinite amount of data is available.

An important special case occurs when the noise is white. Then

$$P_n(e^{j\omega}) = \sigma_w^2 \quad (9.117)$$

and

$$\xi_{ou} = \frac{\sigma_w^2}{2\pi} \int_{-\pi}^{\pi} H_{ou}(e^{j\omega}) d\omega = \sigma_w^2 h_{ou}(0). \quad (9.118)$$

We revisit the AR(1) model introduced in Example 9.1.

Example 9.5. We assume $\sigma_w^2 = 1$ and adjust the SNR by varying σ_u^2 . Then

$$S_{dr}(z) = S_s(z) = \frac{\sigma_u^2}{(1 - \alpha z^{-1})(1 - \alpha z)}, \quad (9.119)$$

$$S_n(z) = 1, \quad (9.120)$$

and

$$S_r(z) = 1 + \frac{\sigma_u^2}{(1 - \alpha z^{-1})(1 - \alpha z)}. \quad (9.121)$$

Then,

$$\begin{aligned} H_{ou}(z) &= \frac{\frac{\sigma_u^2}{(1 - \alpha z^{-1})(1 - \alpha z)}}{1 + \frac{\sigma_u^2}{(1 - \alpha z^{-1})(1 - \alpha z)}} \\ &= \frac{\sigma_u^2}{\sigma_u^2 + (1 - \alpha z^{-1})(1 - \alpha z)}. \end{aligned} \quad (9.122)$$

We need to put the denominator in the form

$$\text{Den}(z) = c^2(1 - \beta z^{-1})(1 - \beta z). \quad (9.123)$$

Matching the two expressions and performing some algebra, we obtain

$$\beta = \frac{1}{2\alpha} \left\{ (1 + \alpha^2 + \sigma_u^2) - ((1 + \alpha + \sigma_u^2)^2 - 4\alpha^2)^{\frac{1}{2}} \right\}, \quad (9.124)$$

and

$$c^2 = \frac{\alpha}{\beta}. \quad (9.125)$$

Then,

$$H_{ou}(z) = \frac{\sigma_u^2/c^2}{(1 - \beta z^{-1})(1 - \beta z)}. \quad (9.126)$$

Using the z -transform pair ([OS 89, p.180])

$$\beta^{|n|} \longleftrightarrow \frac{1 - \beta^2}{(1 - \beta z^{-1})(1 - \beta z)} \quad (9.127)$$

gives

$$h_{ou}(k) = \frac{\sigma_u^2 \beta}{\alpha(1 - \beta^2)} \beta^{|n|}, \quad -\infty < k < \infty. \quad (9.128)$$

Using (9.118), the MSE is

$$\xi_{ou} = h_{ou}(0) = \frac{\sigma_u^2 \beta}{\alpha(1 - \beta^2)}. \quad (9.129)$$

In Figure 9.12, we plot the normalized filter coefficients for SNR = 3 dB and $\alpha = 0.3, 0.5, 0.8$, and 0.95.

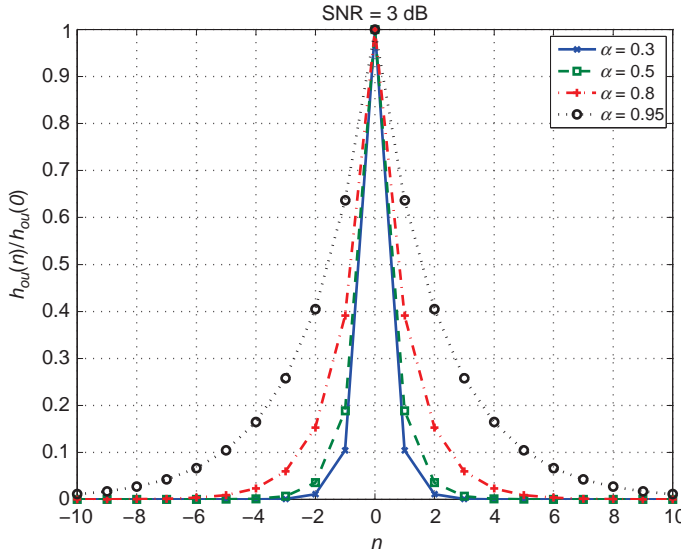


Figure 9.12: Filter coefficients for unrealizable IIR Weiner filter; SNR = 3dB, $\alpha = 0.3, 0.5, 0.8$, and 0.95 .

As expected the filter coefficients approach zero as n increases (the rate is a function of σ_u^2 and α). We would expect that we could achieve the same performance as an FIR Wiener filter with lag using $L = -K$ and choosing K to be the value where $h_{ou}(m) \approx 0$. We can quantify that by plotting the $\xi_o(K)$.

In Figure 9.13, we plot the normalized MSE for $\alpha = 0.3, 0.5, 0.7$, and 0.95 . (Recall that $\sigma_s^2 = \sigma_u^2/(1 - \alpha^2)$). ■

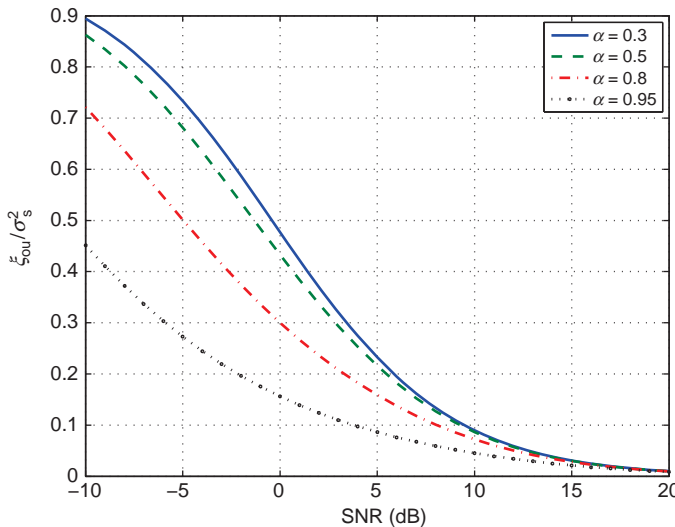


Figure 9.13: Normalized MSE versus SNR; $\alpha = 0.3, 0.5, 0.8, 0.95$.

9.2.5 Realizable IIR Wiener Filters

In this section, we derive the optimum Wiener filter assuming that we have observations from $-\infty$ up to k . Then,

$$\hat{d}(k) = \sum_{m=0}^{\infty} h_o(m)r(k-m). \quad (9.130)$$

Proceeding as in the FIR deviation, we have

$$\sum_{m=0}^{\infty} h_o(m)k_r(k-m) = k_{dr}(k), \quad 0 \leq k < \infty. \quad (9.131)$$

We cannot solve the problem by taking Fourier transforms because the restriction of $k \geq 0$. However, if the input $r(m)$ was a “white” sequence, then we could solve the problem. The first step is pass $r(m)$ through a realizable minimum phase whitening filter $W(z)$.

From our discussion in earlier chapters we know that we can whiten the input without loss of optimality as long as the whitening operation is reversible.

In this case, we must guarantee that $W^{-1}(z)$ is a realizable stable filter. The logic is illustrated in Figure 9.14. Optimizing $H'_o(z)$ in (a) will always lead to the same $\hat{d}_o(k)$. If not, then it cannot be optimum because the system in (b) would have given $\hat{d}_o(k)$.

In order to use this approach, we demonstrate that we can find a realizable whitening filter $W(z)$ whose inverse $W^{-1}(z)$ is also realizable. We assume that $r(m)$ is a real-valued random process with a rational spectrum,

$$S_r(z) = \frac{N(z)}{D(z)} \quad (9.132)$$

with no poles on the unit circle. Then, we can do a spectral factorization

$$S_r(z) = G(z)G^*(1/z^*) = c^2 \left[\frac{B(z)}{A(z)} \right] \left[\frac{B^*(1/z^*)}{A^*(1/z^*)} \right], \quad (9.133)$$

where $A(z)$ and $B(z)$ are polynomials with all of the roots inside the unit circle:

$$A(z) = 1 + a(1)z^{-1} + \cdots + a(p)z^{-p}, \quad (9.134)$$

$$B(z) = 1 + b(1)z^{-1} + \cdots + b(q)z^{-q}. \quad (9.135)$$

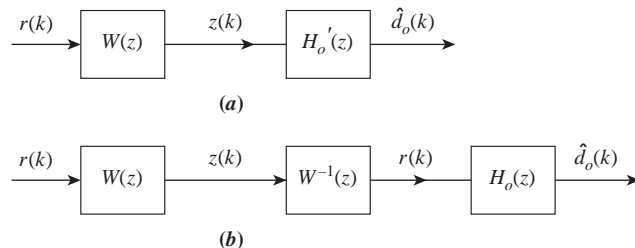


Figure 9.14: Whitening filter.

For a real-valued process, (9.133) reduces to

$$S_r(z) = G(z)G(z^{-1}) = c^2 \left[\frac{B(z)}{A(z)} \right] \left[\frac{B(z^{-1})}{A(z^{-1})} \right]. \quad (9.136)$$

We consider two simple examples.

Example 9.6. Consider the AR(1) signal model in Example 9.1 and assume $\sigma_w^2 = 0$ and $\sigma_u^2 = 1$. Then,

$$S_r(z) = S_s(z) = \frac{1 - \alpha^2}{(1 - \alpha z^{-1})(1 - \alpha z)} \quad (9.137)$$

with $\alpha < 1$. We factor this using

$$c^2 = 1 - \alpha^2, \quad (9.138)$$

$$G(z) = \frac{c}{1 - \alpha z^{-1}}, \quad (9.139)$$

and

$$G(z^{-1}) = \frac{c}{1 - \alpha z}, \quad (9.140)$$

whose poles are shown in Figure 9.15.

Thus, the z -transform of the whitening filter is

$$W(z) = \frac{1}{\sqrt{1 - \alpha^2}} (1 - \alpha z^{-1}), \quad (9.141)$$

and the filter is

$$w(k) = \frac{1}{\sqrt{1 - \alpha^2}} (\delta(k) - \alpha \delta(n - 1)). \quad (9.142)$$

■

A more realistic model is given in Example 9.7.

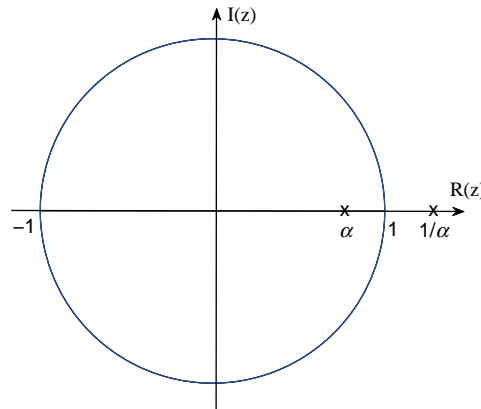


Figure 9.15: Pole-zero plot for AR(1) model.

Example 9.7. From Example 9.4,

$$S_r(z) = c^2 \frac{(1 - \beta z^{-1})(1 - \beta z)}{(1 - \alpha z^{-1})(1 - \alpha z)}, \quad (9.143)$$

where $\alpha < 1$ and $\beta < 1$.

We must choose $G^+(z)$ so that both $W(z)$ and $W^{-1}(z)$ are realizable. This means that both the poles and zeros of $G(z)$ must be inside the unit circle. Thus,

$$G(z) = c \frac{(1 - \beta z^{-1})}{(1 - \alpha z^{-1})}, \quad (9.144)$$

and

$$W(z) = \frac{1}{c} \frac{(1 - \alpha z^{-1})}{(1 - \beta z^{-1})}. \quad (9.145)$$

■

The general case is illustrated in Figure 9.16. For a real process, the power spectrum is a real-valued even function

$$P_r(e^{j\omega}) = P_r^*(e^{j\omega}) \quad (9.146)$$

and

$$S_r(z) = S_r^*(1/z^*) = S(1/z), \quad (9.147)$$

$$P_r(e^{j\omega}) = P_r(e^{-j\omega}). \quad (9.148)$$

This implies the following properties:

1. Symmetry about the real axis for poles and zero;

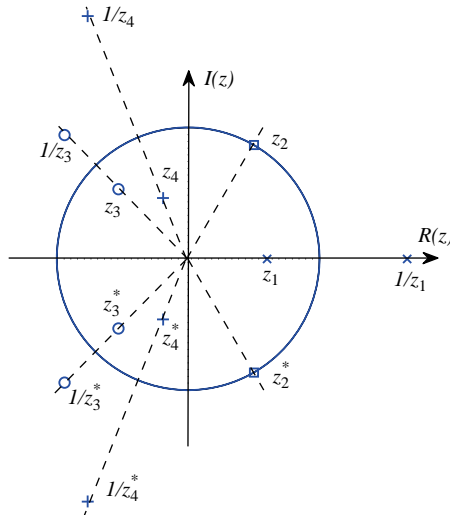
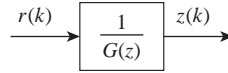


Figure 9.16: General pole-zero plot for a real process.

**Figure 9.17:** Whitening filter.

2. Symmetry about the unit circle. A pole at z_1 requires a pole at $1/z_1$. A zero at z_1 requires a zero at $1/z_1$;
3. Zeros on the unit circle must be double;
4. No poles on unit circle.

Thus, we assign all of the poles and zeros inside the unit circle and one-half of the zeros on the unit circle to $G(z)$.

Therefore, we can pass $r(m)$ through a whitening filter, $1/G(z)$ as shown in Figure 9.17.

The whitening filter is reversible, so we could process its output $z(m)$ optimally to obtain $\hat{d}(k)$.

From (9.131) and Figure 9.14(a),

$$\sum_{m=0}^{\infty} h'_o(m)k_z(k-m) = k_{dz}(k), \quad 0 \leq k < \infty. \quad (9.149)$$

Now

$$k_z(k-m) = \delta_{km}, \quad (9.150)$$

so (9.149) becomes

$$h'_o(k) = \begin{cases} k_{dz}(k) & k \geq 0, \\ 0 & k < 0. \end{cases} \quad (9.151)$$

The cross-covariance is

$$\begin{aligned} k_{dz}(l) &= E \{ d(k)z(k-l) \} \\ &= E \left\{ d(k) \sum_{m=-\infty}^{\infty} w(m)r(k-l-m) \right\} \\ &= \sum_{m=-\infty}^{\infty} w(m)k_{dr}(l+m) = \sum_{k=-\infty}^{\infty} w(-k)k_{dr}(l-k). \end{aligned} \quad (9.152)$$

The cross-spectrum is

$$S_{dz}(z) = \frac{S_{dr}(z)}{G(z^{-1})}. \quad (9.153)$$

We take the inverse z -transform of (9.153) to obtain $k_{dz}(k)$. The $k_{dz}(k)$ for the AR(1) model in Example 9.4, with SNR = 3 dB and $\alpha = 0.9$ is shown in Figure 9.18(a). We retain

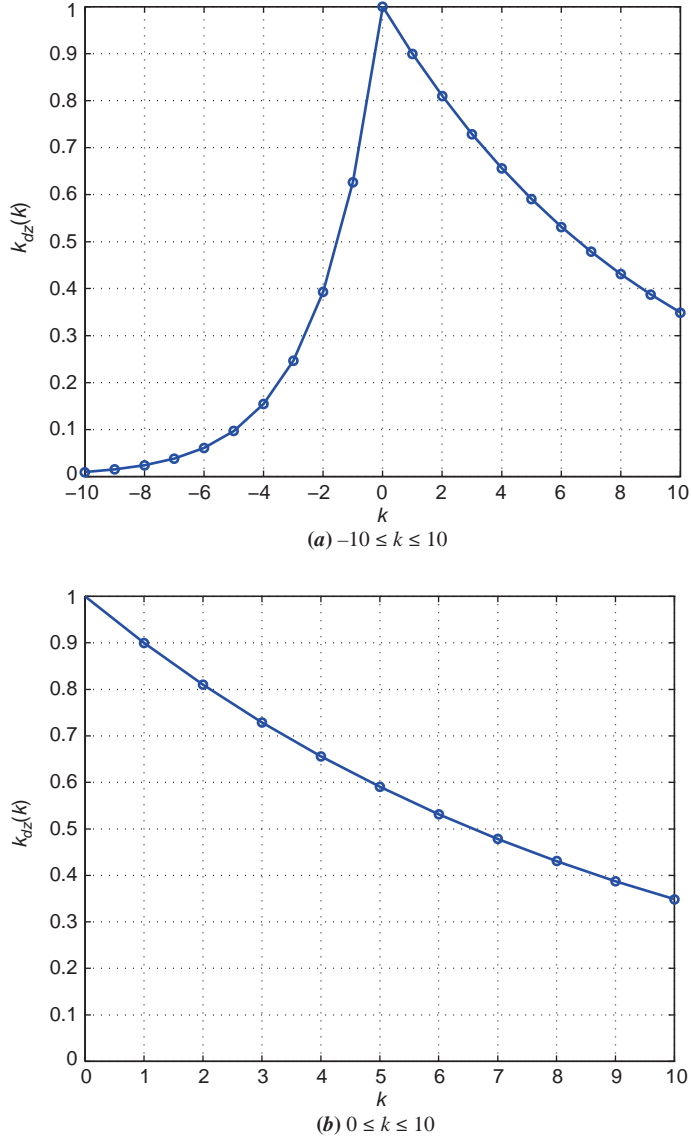


Figure 9.18: Plot of $k_{dz}(k)$; AR(1) model; SNR = 3 dB, $\alpha = 0.9$.

the coefficients corresponding to $k \geq 0$ as shown in Figure 9.18(b) and take the transform that we denote by

$$H'_o(z) \triangleq \left[\frac{S_{dr}(z)}{G(z^{-1})} \right]_+ . \quad (9.154)$$

Then, the complete optimum realizable filter is

$$H_o(z) = \frac{1}{G(z)} \left[\frac{S_{dr}(z)}{G(z^{-1})} \right]_+ . \quad (9.155)$$

We see that by a series of routine, conceptually simple operations, we have derived the optimum filter. We summaries the steps briefly.

1. We factor the input spectrum into two parts. One term $G(z)$ contains all of the poles and zeros inside the unit circle and one-half of the zeros on the unit circle. The other term $G(z^{-1})$ is its mirror image about the unit circle.
2. The cross-spectrum between $d(k)$ and $z(k)$ can be expressed in terms of the original cross-spectrum divided by $G(z^{-1})$. This corresponds to a function that is nonzero for both positive and negative k . The realizable part ($k \geq 0$) of this function is $h'_o(k)$ and its transform is $H'_o(z)$.
3. The system function of the optimum filter is the product of these two realizable system functions. Therefore, the composite system function is also realizable. Observe that we actually implement the optimum linear filter as a single system. The division into two parts is for conceptual purposes only.

We should observe that the process in Step 2 of taking the inverse z -transform, discarding the negative k terms, and taking the z -transform is unnecessary in most applications. Specifically, whenever $S_{dr}(z)/G(z^{-1})$ is a ratio of two polynomials in z , we may write

$$\frac{S_{dr}(z)}{G(z^{-1})} = F(z) + \sum_{i=1}^K \frac{c_i}{1 - p_i z^{-1}} + \sum_{j=1}^K \frac{d_j}{1 - q_j z^{-1}}, \quad (9.156)$$

where $F(z)$ is a polynomial, the first sum contains all of the poles inside or on the unit circle, and the second sum contains all of the poles outside the unit circle. In this expanded form, the realizable part consists of the first two terms. Thus,

$$\left[\frac{S_{dr}(z)}{G(z^{-1})} \right]_+ = F(z) + \sum_{i=1}^K \frac{c_i}{1 - p_i z^{-1}}. \quad (9.157)$$

The mean-square error using the optimum realizable linear filter is given by (9.89) with the summation going from 0 to ∞ ,

$$\xi_o = k_d(0) - \sum_{m=0}^{\infty} h_o(m) k_{dr}(m). \quad (9.158)$$

Because $h_o(m) = 0$ for $m < 0$, we can equally write

$$\xi_o = k_d(0) - \sum_{m=-\infty}^{\infty} h_o(m) k_{dr}(m). \quad (9.159)$$

Now, from (9.155)

$$H_o(e^{j\omega}) = \frac{1}{G(e^{j\omega})} \sum_{l=0}^{\infty} k_{dz}(l) e^{-j\omega l}, \quad (9.160)$$

where

$$k_{dz}(l) = \mathcal{F}^{-1} \left\{ \frac{P_{dr}(e^{j\omega})}{G(e^{-j\omega})} \right\} = \frac{1}{2\pi} \int_{-\pi}^{\pi} \frac{P_{dr}(e^{j\omega})}{G(e^{-j\omega})} e^{j\omega l} d\omega, \quad (9.161)$$

$$\xi_o = k_d(0) - \sum_{m=-\infty}^{\infty} k_{dr}(m) \left[\frac{1}{2\pi} \int_{-\pi}^{\pi} \frac{1}{G(e^{j\omega})} \sum_{l=0}^{\infty} k_{dz}(l) e^{-j\omega l} \cdot e^{j\omega m} d\omega \right]. \quad (9.162)$$

Changing orders of summation leads to

$$\xi_o = k_d(0) - \sum_{l=0}^{\infty} k_{dz}(l) \left[\frac{1}{2\pi} \int_{-\infty}^{\infty} \frac{1}{G(e^{j\omega})} \sum_{m=-\infty}^{\infty} k_{dr}(m) e^{j\omega m} \cdot e^{-j\omega l} d\omega \right]. \quad (9.163)$$

The term inside the bracket is $k_{dz}^*(l)$. Thus, since $k_{dz}(l)$ is real,

$$\xi_o = k_d(0) - \sum_{l=0}^{\infty} k_{dz}^2(l). \quad (9.164)$$

To illustrate these results, we consider a simple example that incorporates filtering, smoothing, and prediction.

Example 9.8. We use the same model as in Example 9.4. The signal is generated by an AR(1) process,

$$S_s(z) = \frac{\sigma_u^2}{(1 - \alpha z^{-1})(1 - \alpha z)}. \quad (9.165)$$

The noise is white with unit power,

$$S_n(z) = 1. \quad (9.166)$$

Then,

$$\begin{aligned} S_r(z) &= 1 + \frac{\sigma_u^2}{(1 - \alpha z^{-1})(1 - \alpha z)} \\ &= c^2 \frac{(1 - \beta z^{-1})(1 - \beta z)}{(1 - \alpha z^{-1})(1 - \alpha z)}, \end{aligned} \quad (9.167)$$

where β and c are given by (9.124) and (9.125).

The desired signal is

$$d(k) = s(k + L), \quad (9.168)$$

where we will consider $L = 0$, $L < 0$, and $L \geq 1$.

Then,

$$S_{dr}(z) = z^L S_s(z). \quad (9.169)$$

From (9.144),

$$G(z) = c \frac{(1 - \beta z^{-1})}{(1 - \alpha z^{-1})}, \quad (9.170)$$

$$S_{dr}(z) = z^L \frac{\sigma_u^2}{(1 - \alpha z^{-1})(1 - \alpha z)}. \quad (9.171)$$

From (9.153) and including L in the notation,

$$\begin{aligned} S_{dz}(z; L) &= \frac{1}{c} \frac{(1 - \alpha z)}{(1 - \beta z)} \cdot z^L \frac{\sigma_u^2}{(1 - \alpha z^{-1})(1 - \alpha z)} \\ &= \frac{z^L}{c} \frac{\sigma_u^2}{(1 - \beta z)(1 - \alpha z^{-1})}. \end{aligned} \quad (9.172)$$

In order to expand $S_{dz}(z; L)$ in a partial fraction expansion with recognizable terms, we rewrite (9.172) as

$$S_{dz}(z; L) = \frac{z^L}{c} \left\{ \frac{-(\sigma_u^2/\beta)z^{-1}}{(1 - \alpha z^{-1})(1 - \frac{1}{\beta}z^{-1})} \right\}. \quad (9.173)$$

We write the term in brackets as

$$\left\{ \frac{-(\sigma_u^2/\beta)z^{-1}}{(1 - \alpha z^{-1})(1 - \frac{1}{\beta}z^{-1})} \right\} = \frac{c_1}{(1 - \alpha z^{-1})} - \frac{c_2}{\left(1 - \frac{1}{\beta}z^{-1}\right)}. \quad (9.174)$$

Solving for c_1 and c_2 gives

$$c_1 = c_2 \quad (9.175)$$

and

$$c_1 = \frac{\sigma_u^2}{1 - \alpha\beta}. \quad (9.176)$$

Then,

$$S_{dz}(z; L) = \frac{z^L \sigma_u^2}{c(1 - \alpha\beta)} \left\{ \frac{1}{1 - \alpha z^{-1}} - \frac{1}{1 - \frac{1}{\beta}z^{-1}} \right\}, \quad (9.177)$$

where, from (9.125)

$$c^2 = \alpha/\beta. \quad (9.178)$$

Filtering. We first consider the case when $L = 0$.

The inverse transform for $L = 0$ is

$$K_{dz}(k; 0) = \frac{\sigma_u^2}{c(1 - \alpha\beta)} \begin{cases} \alpha^k & k \geq 0 \\ \left(\frac{1}{\beta}\right)^k = \beta^{|k|} & k < 0. \end{cases} \quad (9.179)$$

A normalized plot is shown in Figure 9.19.

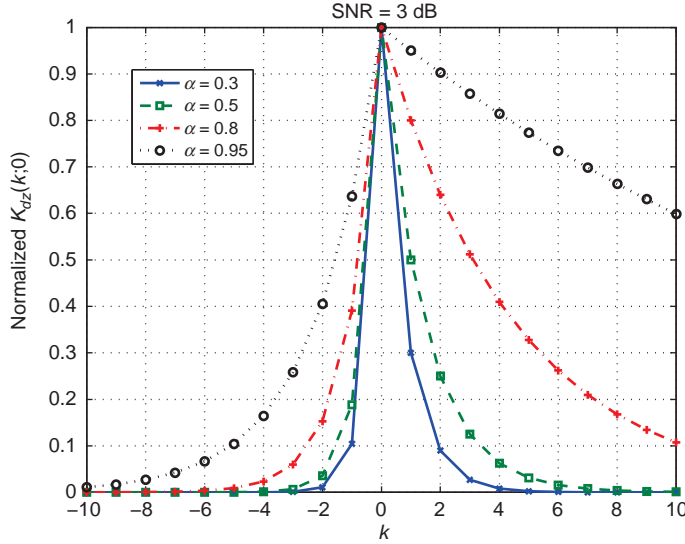


Figure 9.19: Normalized plot of $K_{dz}(k; 0)$.

Thus,

$$\left[\frac{S_{dr}(z; 0)}{G(z)} \right]_+ = \frac{\sigma_u^2}{c(1 - \alpha\beta)} \frac{1}{1 - \alpha z^{-1}}. \quad (9.180)$$

Using (9.180) and (9.170) in (9.155) gives

$$\begin{aligned} H_o(z; 0) &= \left(\frac{1}{c} \frac{(1 - \alpha z^{-1})}{(1 - \beta z^{-1})} \right) \frac{\sigma_u^2}{c(1 - \alpha\beta)} \frac{1}{(1 - \alpha z^{-1})} \\ &= \frac{1}{c^2} \frac{\sigma_u^2}{(1 - \alpha\beta)} \cdot \frac{1}{(1 - \beta z^{-1})} \end{aligned} \quad (9.181)$$

and

$$h_o(k; 0) = \left(\frac{1}{c^2} \frac{\sigma_u^2}{(1 - \alpha\beta)} \right) \beta^k, \quad k = 0, \dots, \infty, \quad (9.182)$$

$$= \left(\frac{\beta}{\alpha} \frac{\sigma_u^2}{1 - \alpha\beta} \right) \beta^k, \quad k = 0, \dots, \infty, \quad (9.183)$$

where from (9.124)

$$\beta = \frac{1}{2\alpha} \left\{ (1 + \alpha^2 + \sigma_u^2) - ((1 + \alpha + \sigma_u^2)^2 - 4\alpha^2)^{\frac{1}{2}} \right\}. \quad (9.184)$$

Thus, $H_o(z; 0)$ is a one-pole filter whose pole location β depends on α and σ_u^2 .

In Figure 9.20, we show the amplitude of the filter response. In Figure 9.21, we show how β/α behaves as a function of SNR. We see that for a fixed α , the optimum filter bandwidth which is

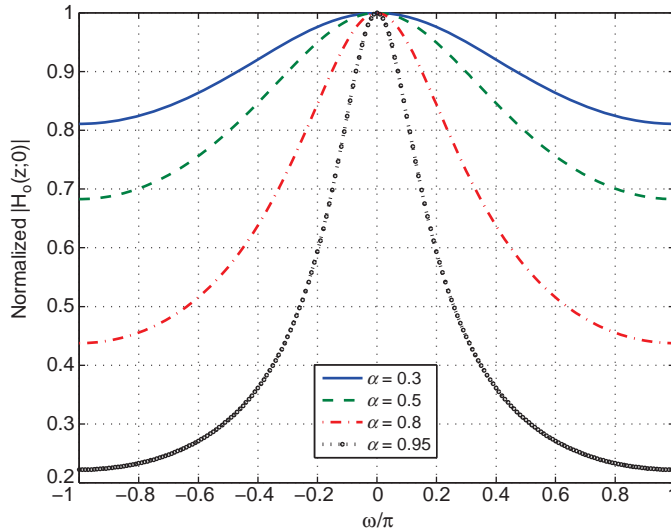


Figure 9.20: Amplitude plot of normalized $H_o(z;0)$; SNR = 3 dB.

proportional to $1/\beta$ increases as the SNR increases. Thus, as $\text{SNR} \rightarrow \infty$, the filter magnitude approaches unity for all frequencies and it passes the message component without distortion. Because the noise is unimportant in this case, this is intuitively logical. On the other hand, as the $\text{SNR} \rightarrow 0$, the finite bandwidth approaches the message bandwidth. The gain, however, approaches zero. Once again, this is intuitively logical. There is so much noise that, based on the mean-square error criterion, the best filter output is zero (the mean value of the message).

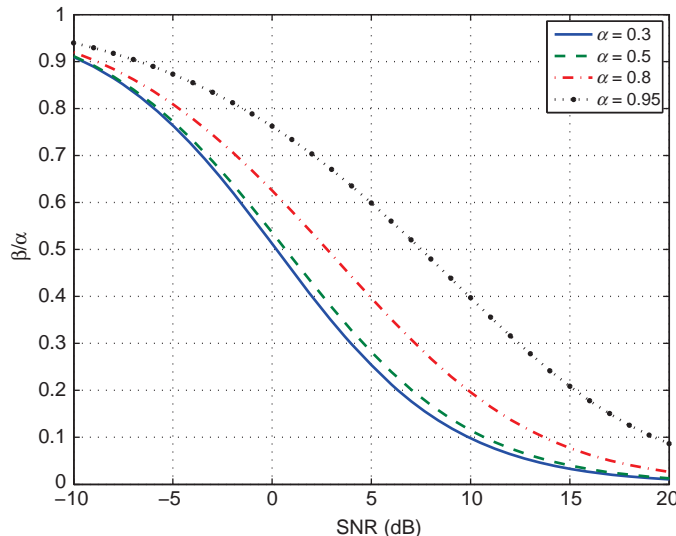


Figure 9.21: Plot of β/α versus SNR for various α .

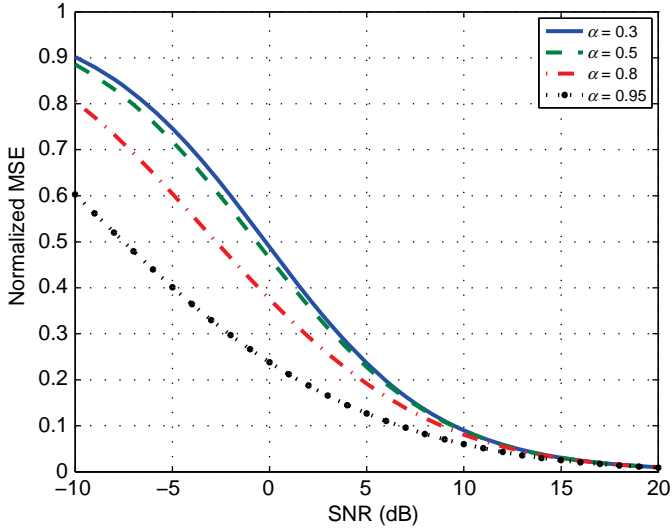


Figure 9.22: Normalized MSE for IIR realizable filter versus SNR; AR(1) model.

The MSE is given by (9.164),

$$\begin{aligned}
 \xi_o &= \frac{\sigma_u^2}{1-\alpha^2} - \sum_{n=0}^{\infty} k_{dz}^2(n) \\
 &= \frac{\sigma_u^2}{1-\alpha^2} - \left(\frac{\sigma_u^4}{\beta(1-\alpha\beta)^2} \right) \sum_{n=0}^{\infty} (\alpha^2)^n \\
 &= \frac{\sigma_u^2}{1-\alpha^2} \left\{ 1 - \frac{\beta}{\alpha} \frac{\sigma_u^2}{(1-\alpha\beta)^2} \right\}. \tag{9.185}
 \end{aligned}$$

The signal power is $\sigma_s^2 = \sigma_u^2/(1-\alpha^2)$ and since $\sigma_w^2 = 1$, the SNR $\triangleq \sigma_s^2/\sigma_w^2 = \sigma_s^2$. Then, we can rewrite (9.185) as

$$\xi_o = \text{SNR} \left\{ 1 - \frac{\beta}{\alpha} \frac{\text{SNR}(1-\alpha^2)}{(1-\alpha\beta)^2} \right\}. \tag{9.186}$$

In Figure 9.22, we plot the normalized mean-square error versus SNR for various values of α .

Prediction. We next consider the case in which L is positive.

For $L > 0$, it holds that

$$S_{dz}(z; L) = z^L S_{dz}(z; 0). \tag{9.187}$$

This corresponds to

$$k_{dz}(n; L) = k_{dz}(n + L; 0), \tag{9.188}$$

which shifts the function in Figure 9.19 to the left by L units. We show this in Figure 9.23 for $L = 3$.

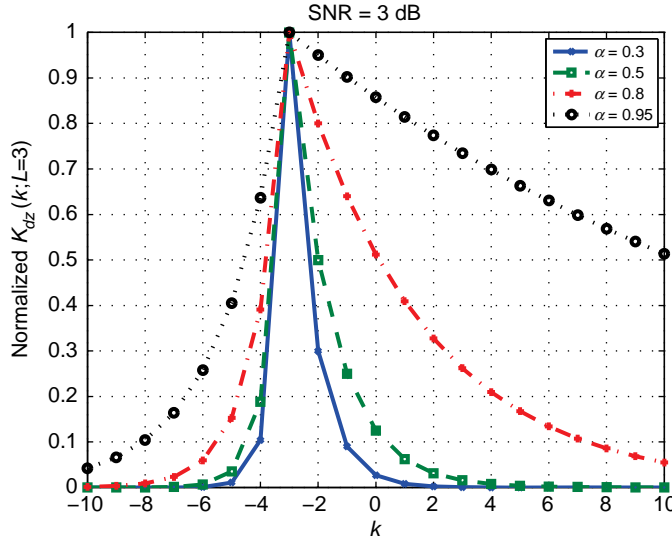


Figure 9.23: Normalized $k_{dz}(k; L)$ for $L = 3$; AR(1) model; $\alpha = 0.8$, SNR = 3 dB, $\alpha = 0.3$, 0.5, 0.8, 0.95.

The realizable part is

$$[S_{dz}(z; L)]_+ = \alpha^L [S_{dz}(z; 0)]_+. \quad (9.189)$$

The optimum predictor simply takes the output of the optimum filter $H_o(z; 0)$ and multiplies it by α^L . The mean-square error is

$$\begin{aligned} \xi_o(L) &= \frac{\sigma_u^2}{1 - \alpha^2} - \sum_{n=0}^{\infty} k_{dz}^2(n; L) \\ &= \frac{\sigma_u^2}{1 - \alpha^2} - \alpha^{2L} \sum_{n=0}^{\infty} k_{dz}^2(n; 0), \quad L \geq 0, \end{aligned} \quad (9.190)$$

which is always larger than $\xi_o(0)$.

For our example,

$$\begin{aligned} \xi_o(L) &= \frac{\sigma_u^2}{1 - \alpha^2} - \alpha^{2L} \left(\frac{\sigma_u^2}{c(1 - \alpha\beta)} \right)^2 \sum_{n=0}^{\infty} (\alpha^2)^n \\ &= \frac{\sigma_u^2}{1 - \alpha^2} - \alpha^{2L} \left(\frac{\sigma_u^4}{c^2(1 - \alpha\beta)^2} \right) \left(\frac{1}{1 - \alpha^2} \right) \\ &= \frac{\sigma_u^2}{1 - \alpha^2} \left\{ 1 - \alpha^{2L} \left(\frac{\beta}{\alpha} \right) \frac{\sigma_u^2}{(1 - \alpha\beta)^2} \right\}, \quad L \geq 0. \end{aligned} \quad (9.191)$$

In Figure 9.24, we plot the normalized MSE versus L for several values of α and SNR = 3 dB. We see that the MSE increases rapidly as a function of α^{2L} . The plots for other SNR behave in a similar manner as a function of L .

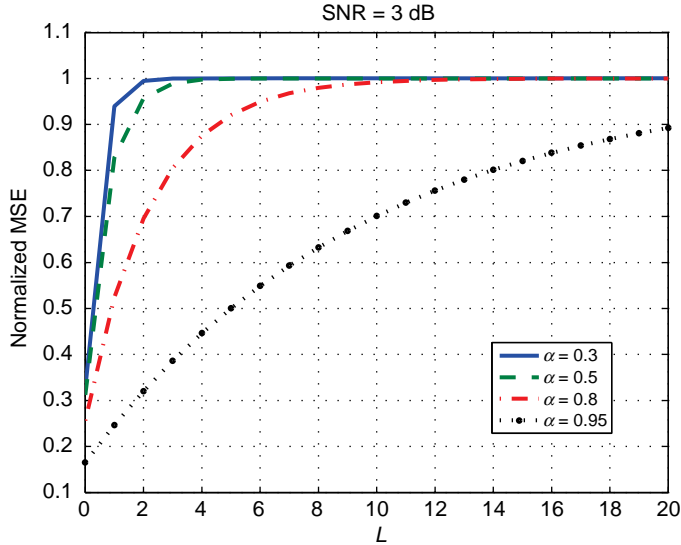


Figure 9.24: Normalized MSE versus L ; SNR = 3 dB, $\alpha = 0.3, 0.5, 0.8, 0.95$.

Filtering with Lag. We next consider the case when L is negative.

When $L < 0$, $k_{dz}(k; L)$ is shifted to right as shown in Figure 9.25 for $L = -4$.

$$k_{dz}(k; L) = \frac{\sigma_u^2}{c(1 - \alpha\beta)} \begin{cases} \beta^{|k+L|}, & k = -\infty, \dots, 0, \dots, |L|-1 \\ \alpha^{|k+L|}, & k = |L|, \dots, \infty. \end{cases} \quad (9.192)$$

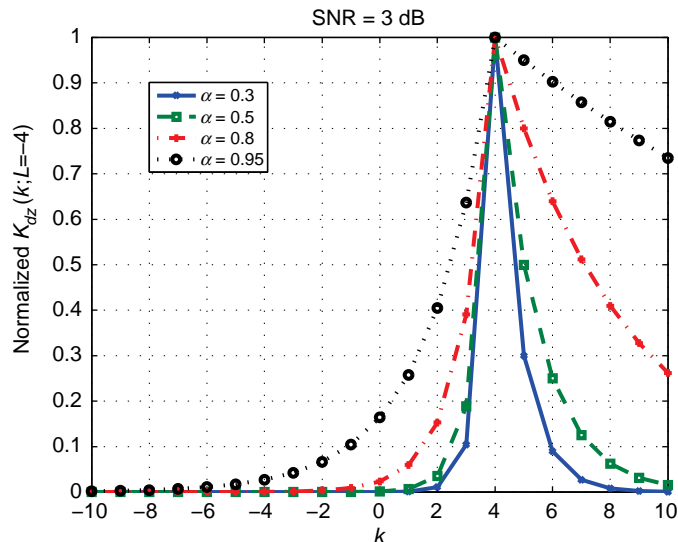


Figure 9.25: Normalized plot of $k_{dz}(k; L)$ for $L = -4$, SNR = 3 dB.

The cross-spectrum is

$$[S_{dz}(z; L)]_+ = \left(\sum_{k=0}^{|L|-1} \beta^{|k+L|} z^{-k} + \sum_{k=|L|}^{\infty} \alpha^{k+L} z^{-k} \right) \frac{\sigma_u^2}{c(1-\alpha\beta)} \quad (9.193)$$

$$= \left(\sum_{k=0}^{-L-1} \beta^{-L-k} z^{-k} + z^L \sum_{k=0}^{\infty} \alpha^k z^{-k} \right) \frac{\sigma_u^2}{c(1-\alpha\beta)}, \quad (9.194)$$

which reduces to

$$[S_{dz}(z; L)]_+ = \frac{\sigma_u^2}{c(1-\alpha\beta)} \left(\beta^{-L} \left(\frac{1 - \beta^L z^L}{1 - \beta^{-1} z^{-1}} \right) + z^L \frac{1}{(1 - \alpha z^{-1})} \right). \quad (9.195)$$

Then,

$$H_o(z; L) = \frac{1}{c} \left(\frac{1 - \alpha z^{-1}}{1 - \beta z^{-1}} \right) \frac{\sigma_u^2}{c(1-\alpha\beta)} \left(\beta^{-L} \left(\frac{1 - \beta^L z^L}{1 - \beta^{-1} z^{-1}} \right) + z^L \frac{1}{(1 - \alpha z^{-1})} \right), \quad L \leq 0, \quad (9.196)$$

which reduces to

$$H_o(z; L) = \frac{1}{c^2} \frac{\sigma_u^2}{(1-\alpha\beta)} \left\{ \frac{(\beta^{-L} - z^L)(1 - \alpha z^{-1})}{(1 - \beta^{-1} z^{-1})(1 - \beta z^{-1})} + z^L \frac{1}{(1 - \beta z^{-1})} \right\}, \quad L \leq 0. \quad (9.197)$$

The inverse transform is

$$h_0(k) = \frac{1}{c} \frac{\sigma_u^2}{(1-\alpha\beta)} \left[\left(\frac{\alpha + \beta^{-1}}{\beta + \beta^{-1}} \beta^{-(k+L)} + \frac{\alpha - \beta}{\beta + \beta^{-1}} \beta^{k-L} \right) u(k) + \frac{\alpha + \beta^{-1}}{\beta + \beta^{-1}} (\beta^{k+L} - \beta^{-(k+L)}) u(k+L) \right], \quad (9.198)$$

where $u(k)$ is a discrete unit-step function. The mean-square error is

$$\begin{aligned} \xi_o(L) &= \frac{\sigma_u^2}{1 - \alpha^2} - \sum_{k=0}^{\infty} k^2 dz(k; L) \\ &= \frac{\sigma_u^2}{1 - \alpha^2} - \left(\frac{\sigma_u^2}{c(1 - \alpha\beta)} \right)^2 \left\{ \sum_{k=0}^{|L|-1} \beta^{2(|k+L|)} + \sum_{k=|L|}^{\infty} \alpha^{2(k+L)} \right\} \end{aligned} \quad (9.199)$$

$$= \frac{\sigma_u^2}{1 - \alpha^2} - \left(\frac{\sigma_u^2}{c(1 - \alpha\beta)} \right)^2 \left\{ \sum_{k=1}^{|L|} \beta^{2k} + \sum_{k=0}^{\infty} \alpha^{2k} \right\}, \quad (9.200)$$

which reduces to

$$\xi_o(L) = \frac{\sigma_u^2}{1 - \alpha^2} - \left(\frac{\beta}{\alpha} \right) \frac{\sigma_u^4}{(1 - \alpha\beta)^2} \left\{ \frac{\beta^{-2L} - 1}{1 - \beta^{-2}} + \frac{1}{1 - \alpha^2} \right\}, \quad L < 0, \quad (9.201)$$

or

$$\xi_o(L) = \xi_o(0) - \left(\frac{\beta}{\alpha} \right) \frac{\sigma_u^2}{(1 - \alpha\beta)^2} \left(\frac{\beta^{-2L} - 1}{1 - \beta^{-2}} \right), \quad L < 0, \quad (9.202)$$

which is always less than $\xi_o(0)$. In Figure 9.26, we plot the normalized mean-square error as a function of L , $-10 \leq L \leq 10$. The MSE for $L \geq 0$ is given by (9.191). The curve is not symmetrical. This is because β is always less than or equal to α . As $L \rightarrow -\infty$, the mean-square error approaches the irreducible error given by (9.129). ■

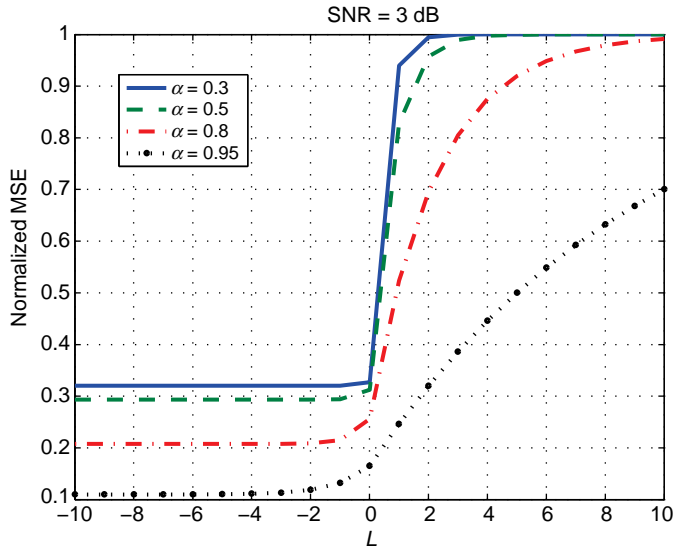


Figure 9.26: Normalized MSE versus L ; SNR = 3 dB, $\alpha = 0.3, 0.5, 0.8, 0.95$.

9.2.6 Summary: Discrete-Time Wiener Filter

In this section, we have developed several versions of the discrete-time Wiener filter. In Section 9.2.3, we developed optimum FIR filters. The key result was the optimum linear filter \mathbf{h}_o in (9.92),

$$\begin{bmatrix} k_r(0) & k_r(1) & \cdots & k_r(K-1) \\ k_r(1) & k_r(0) & \cdots & k_r(N-2) \\ \vdots & & \ddots & \vdots \\ \vdots & & & \vdots \\ k_r(K-1) & k_r(N-2) & \cdots & k_r(0) \end{bmatrix} \begin{bmatrix} h_o(0) \\ h_o(1) \\ \vdots \\ \vdots \\ h_o(K-1) \end{bmatrix} = \begin{bmatrix} k_s(L) \\ k_s(L+1) \\ \vdots \\ k_s(0) \\ \vdots \\ k_s(L+K-1) \end{bmatrix}, \quad (9.203)$$

and the resulting optimum MSE, ξ_o , given by (9.89)

$$\xi_o = k_d(0) - \sum_{n=0}^{K-1} h_o(n)k_{dr}(n). \quad (9.204)$$

We used an AR(1) process as an example and considered filtering and filtering with lag. The effective filter length depends on the correlation time of the process and the performance depends on both the correlation time and the SNR. Other examples in the problems show similar behavior.

In Section 9.2.4, we developed unrealizable IIR Wiener filters. The principal advantage is that the solution in (9.105) is simple,

$$H_{ou}(z) = \frac{S_{dr}(z)}{S_r(z)}, \quad (9.205)$$

and the irreducible mean-square error given by (9.116),

$$\xi_{ou} = \frac{1}{2\pi} \int_{-\pi}^{\pi} P_n(e^{j\omega}) H_{ou}(e^{j\omega}) d\omega \quad (9.206)$$

provides a lower bound on the MSE of any processor. Later, in Section 9.2.5, we showed that the MSE of an IIR realizable filter with lag approaches the irreducible MSE as the lag $\rightarrow \infty$.

In Section 9.2.5, we developed the optimum IIR realizable Wiener filter. By whitening the input, we were able to develop a formula (9.155) for the optimum Wiener filter,

$$H_o(z) = \frac{1}{G(z)} \left[\frac{S_{dr}(z)}{G(z^{-1})} \right]_+ \quad (9.207)$$

and the error is given by (9.164)

$$\xi_o = k_d(0) - \sum_{l=0}^{\infty} k_{dz}^2(l). \quad (9.208)$$

The AR(1) process provided examples of filtering, filtering with lag, and prediction. Other processes are studied in the problems.

In the next section, we develop the Kalman filter.

9.3 DISCRETE-TIME KALMAN FILTER

In this section, we develop discrete-time Kalman filter and study its performance in various applications. The section is organized as follows. In Section 9.3.1, we develop state-variable representations of signal random process and the observation model. In Section 9.3.2, we consider the case in which the desired signal $\mathbf{d}(k)$ is a linear transformation of the state vector $\mathbf{x}(k)$ where k denotes the latest sample time

$$\mathbf{d}(k) = \mathbf{D}\mathbf{x}(k). \quad (9.209)$$

The case is also commonly referred to as a Kalman filter.

In Section 9.3.3, we consider the case in which we want to predict a future value

$$\mathbf{d}(k) = \mathbf{D}\mathbf{x}(k + L), \quad L \geq 1. \quad (9.210)$$

This case is referred to as a Kalman predictor.

In Section 9.3.4, we consider the case in which we want the estimate of the value at a previous time

$$\mathbf{d}(k) = \mathbf{D}\mathbf{x}(k - L), \quad L \leq 0. \quad (9.211)$$

This is referred to as filtering with lag or smoothing.

In Section 9.3.5, we consider a system in which either the process model or the observation model, or both, are nonlinear and develop the extended Kalman filter (EKF).

In Section 9.3.6, we summarize our results.

The Kalman filter is a logical extension of the Bayes sequential estimator that we developed in Chapter 5. In Section 5.4.1, we derived the sequential version of the Bayes estimator of a constant parameter embedded in Bayes linear Gaussian model. The result was a linear recursive algorithm. The next step is to consider the sequential estimation of a parameter that changes with time according to a known random process model. In the Kalman model, the vector θ is modeled as the state vector of a discrete-time Gaussian–Markov process.

The Kalman filter is due to Kalman and Bucy ([Kal60, KB61, Kal63]). A recursive estimation algorithm was published earlier by Swerling [Swe59]. Sorenson provides a comprehensive discussion of the history of recursive algorithms from Gauss [Gau63] in 1793 to Kalman in his paper [Sor70] and his reprint book [Sor85]. Early books on Kalman filtering include Meditch [Med69], Jazwinski [Jaz70], Sage and Melsa [SM71], Gelb [Gel74], and Anderson and Moore [AM79].

More recent books that discuss Kalman filtering include Mendel [Men95], Manolakis et al. [MIK00], Grewal and Andrews [GA08], Kay [Kay93], Kailath et al. [KSH00], Hayes [Hay96], Levy [Lev08], Moon and Sterling [MS00], Bar-Shalom et al. [BSLK01], Helstrom [Hel95], and Scharf [Sch91].

Books that include comprehensive discussions include Mendel [Men95] and Grewal and Andrews [GA08].

Kalman filters are one of the most important discoveries of the past 50 years. They moved quickly into a number of important applications in which they play an essential role in the system. We will discuss various applications later in the section.

Our first objective is to develop the theory. In retrospect, it is a reasonably straightforward derivation. However, in applying the theory to realistic applications, various problems may arise. We will spend a fair amount of time looking at applications and possible modifications to the original filter. Thus, our second objective is to make the readers aware of the issues that are involved and discuss potential solutions.

9.3.1 Random Process Models

In order to be consistent with the literature, we denote the state vector at time k as $\mathbf{x}(k)$. Thus, $\mathbf{x}(k)$ replaces $\theta(k)$ as the vector parameter to be estimated. The state equation is

$$\mathbf{x}(k) = \mathbf{F}(k-1)\mathbf{x}(k-1) + \mathbf{G}(k-1)\mathbf{u}(k-1), \quad k = 1, \dots, \quad (9.212)$$

where $\mathbf{x}(k)$ is the $p \times 1$ state vector, $\mathbf{F}(k)$ is a $p \times p$ matrix whose eigenvalues all have magnitude less than one, $\mathbf{G}(k)$ is a $p \times q$ matrix, $\mathbf{u}(k)$ is a $q \times 1$ zero-mean Gaussian random vector $N(\mathbf{0}, \mathbf{Q}(k))$, and $\mathbf{u}(n)$ is statistically independent of $\mathbf{u}(k)$ for $n \neq k$. The initial state $\mathbf{x}(0)$ is modeled as a Gaussian random vector $N(\mathbf{m}_0, \mathbf{\Pi}_0)$. The matrices $\mathbf{F}(k)$, $\mathbf{G}(k)$, $\mathbf{Q}(k)$, \mathbf{m}_0 , and $\mathbf{\Pi}_0$ are known and the first three may be a function of k .

The observation process is

$$\begin{aligned} \mathbf{r}(k) &= \mathbf{C}(k)\mathbf{x}(k) + \mathbf{w}(k) \quad k = 1, 2, \dots, \\ &= \mathbf{s}(k) + \mathbf{w}(k), \end{aligned} \quad (9.213)$$

where $\mathbf{C}(k)$ is an $N \times p$ matrix and $\mathbf{w}(k)$ is a zero-mean Gaussian vector,

$$E[\mathbf{w}(k)\mathbf{w}^T(l)] = \mathbf{R}(k)\delta_{kl}. \quad (9.214)$$

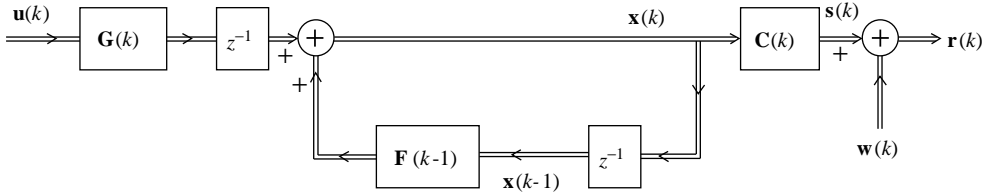


Figure 9.27: State generation and observation model.

The $\mathbf{w}(k)$ and $\mathbf{u}(k)$ are statistically independent. The matrices $\mathbf{C}(k)$ and $\mathbf{R}(k)$ are known. The state generation and observation process are shown in Figure 9.27.

The vector $\mathbf{x}(k)$ is the state vector of a Gaussian–Markov process, so $\mathbf{x}(k - 1)$ is all that is required to determine $\mathbf{x}(k)$.

The first random process model of interest is the ARMA model introduced in Figure 9.2. In Section 9.2, we used the model to obtain the covariance matrix of the process. In this section, we use it to obtain a state-variable representation of the process.

The input and output are related by a linear difference equation

$$x(k) = - \sum_{m=1}^p a(m)x(k-m) + \sum_{m=0}^q b(m)u(k-1-m), \quad 1 \leq k \leq K, \quad (9.215)$$

and $q \leq p - 1$.

We identify the components of $\mathbf{x}(k)$ as shown in Figure 9.28. The first component $x_1(k)$ is the output and the remaining components are the outputs of the delays in the lower path. Thus,

$$\mathbf{x}(k) = \begin{bmatrix} x_1(k) \\ x_1(k-1) \\ x_1(k-2) \\ \vdots \\ x_1(k-p) \end{bmatrix} \triangleq \begin{bmatrix} x_1(k) \\ x_2(k) \\ x_3(k) \\ \vdots \\ x_p(k) \end{bmatrix}. \quad (9.216)$$

Then, the output of the lower summer (including the minus sign) is a scalar

$$x_l(k) = [-a(1) \quad -a(2) \quad \cdots \quad -a(p)] \mathbf{x}(k-1) \triangleq -\mathbf{a}^T \mathbf{x}(k-1). \quad (9.217)$$

The components of the $\mathbf{u}(k)$ vector are the input $u(k)$ and the outputs of the delays in the upper path. Thus,

$$\mathbf{u}(k) = \begin{bmatrix} u(k) \\ u(k-1) \\ u(k-2) \\ \vdots \\ u(k-q) \end{bmatrix} \triangleq \begin{bmatrix} u_1(k) \\ u_2(k) \\ u_3(k) \\ \vdots \\ u_q(k) \end{bmatrix}. \quad (9.218)$$

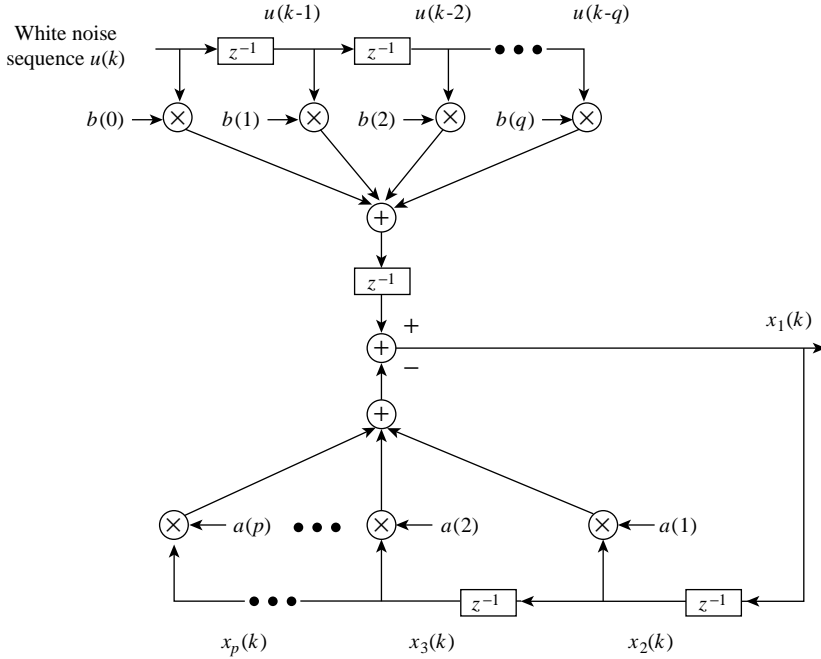


Figure 9.28: Autoregressive moving average model of a scalar random process.

Then, the output of the upper summer is a scalar

$$x_u(k) = [b(0) \ b(1) \ \dots \ b(q)] \mathbf{u}(k-1) \triangleq \mathbf{b}^T \mathbf{u}(k-1). \quad (9.219)$$

The $\mathbf{F}(k)$ and $\mathbf{G}(k)$ matrices are $p \times p$ constant matrices \mathbf{F} and \mathbf{G} . From (9.217),

$$\mathbf{F} = \begin{bmatrix} -a(1) & -a(2) & -a(3) & \cdots & -a(p) \\ 1 & 0 & 0 & \cdots & 0 \\ 0 & 1 & 0 & \cdots & 0 \\ \vdots & & \ddots & & \vdots \\ 0 & & 0 & 1 & 0 \end{bmatrix}, \quad (9.220)$$

and from (9.219)

$$\mathbf{G} = \begin{bmatrix} b(0) & b(1) & b(2) & \cdots & b(q) \\ & & & & \mathbf{0} \\ & & & & \end{bmatrix}. \quad (9.221)$$

The covariance matrix of $\mathbf{u}(k)$ is a q -dimensional identity matrix

$$E\{\mathbf{u}(k)\mathbf{u}^T(k)\} \triangleq \mathbf{Q} = \sigma_u^2 \mathbf{I}_q. \quad (9.222)$$

The signal $s(k)$ is related to $\mathbf{x}(k)$ with the observation equation (9.213), where the $1 \times p$ observation matrix is

$$\mathbf{C} = [1 \ 0 \ \cdots \ 0]. \quad (9.223)$$

We refer to the state vector model in (9.215)–(9.223) as Canonical Model 1.

A second model is also of interest.

In Example 9.2, we specified the model in terms of the zeros of $A(z)$ in (9.69). In the general case, we can write

$$H(z) = \frac{B(z)}{\prod_{i=1}^p (1 - z_i z^{-1})}. \quad (9.224)$$

We expand this using a partial fraction expansion

$$H(z) = \sum_{i=1}^p \frac{A_i}{(1 - z_i z^{-1})}, \quad (9.225)$$

where

$$A_i = [(1 - z_i z^{-1})H(z)]_{z=z_i}. \quad (9.226)$$

We can then use the state-variable model in Figure 9.29. The state vector is

$$\mathbf{x}(k) = [x_1(k) \ \cdots \ x_p(k)]^T \quad (9.227)$$

and the input $u(k)$ is a scalar. The $\mathbf{x}(k)$ differs from that in (9.216) by construction. Correspondingly,

$$\mathbf{F}(k) = \text{diag}(z_1, z_2, \dots, z_p), \quad (9.228a)$$

$$\mathbf{G}(k) = [A_1, A_2, \dots, A_p]^T, \quad (9.228b)$$

and

$$s(k) = \mathbf{C}\mathbf{x}(k) = \mathbf{1}^T \mathbf{x}(k). \quad (9.228c)$$

We refer to this as Canonical Model 2.

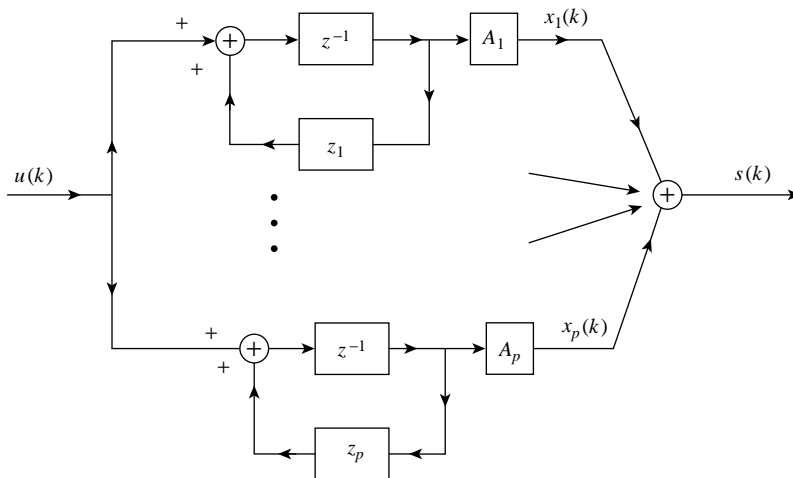


Figure 9.29: State-variable model using poles of $H(z)$.

The ARMA model is appropriate for many communication applications and we will use it in a number of examples.

The second random process models of interest are a family of kinematic models. For tracking algorithms in radar and sonar systems and for navigation applications, these kinematic models are more appropriate. We consider a one-dimensional kinematic model.

One class of kinematic models assumes that nominal trajectory can be modeled as a polynomial in $x(k)$, the position, and its derivatives. If the nominal trajectory is constant velocity, then the state vector is a 2×1 vector whose components are the position and velocity,

$$\mathbf{x}(k) = \begin{bmatrix} x(k) \\ \dot{x}(k) \end{bmatrix} = \begin{bmatrix} x(k) \\ v(k) \end{bmatrix}, \quad (9.229)$$

and \mathbf{F} is a 2×2 matrix

$$\mathbf{F} = \begin{bmatrix} 1 & T \\ 0 & 1 \end{bmatrix}, \quad (9.230)$$

where T is the sampling interval. To introduce randomness into the model, we assume that the acceleration is a zero-mean discrete-time white random process. Then,

$$\mathbf{G}(k) = \begin{bmatrix} T^2/2 \\ T \end{bmatrix}, \quad (9.231)$$

and

$$\mathbf{u}(k) = a_c(k), \quad (9.232)$$

where $a_c(k) \sim N(0, \sigma_a^2)$.

Alternatively, we can define $\mathbf{G} = \mathbf{I}$ and let

$$\mathbf{u}(k) \triangleq \begin{bmatrix} T^2/2 \\ T \end{bmatrix} a_c(k). \quad (9.233)$$

Then, the covariance matrix of $\mathbf{u}(k)$ is \mathbf{Q} ,

$$\mathbf{Q} = \sigma_a^2 \begin{bmatrix} \frac{1}{4}T^4 & \frac{1}{2}T^3 \\ \frac{1}{2}T^3 & T^2 \end{bmatrix}. \quad (9.234)$$

If the sensor only observes range, then

$$\mathbf{C} = [1 \ 0] \quad (9.235)$$

and $w(k)$ is a scalar zero-mean discrete-time white process with variance σ_w^2 .

If the sensor observes both range and velocity (e.g., a range-Doppler radar), then

$$\mathbf{C} = \mathbf{I} \quad (9.236)$$

and $\mathbf{w}(k)$ is a 2×1 vector white process with covariance matrix $\mathbf{R}(k)$.

If the nominal trajectory is constant acceleration, then the state vector is a 3×1 vector whose components are position, velocity, and acceleration

$$\mathbf{x}(k) = \begin{bmatrix} x(k) \\ \dot{x}(k) \\ \ddot{x}(k) \end{bmatrix} \triangleq \begin{bmatrix} x(k) \\ v(k) \\ a(k) \end{bmatrix}, \quad (9.237)$$

and \mathbf{F} is a 3×3 matrix

$$\mathbf{F} = \begin{bmatrix} 1 & T & \frac{1}{2}T^2 \\ 0 & 1 & T \\ 0 & 0 & 1 \end{bmatrix}. \quad (9.238)$$

To introduce randomness, we assume that $\dot{a}_c(k)$ is a white process. Then the random component of $\mathbf{x}(k)$ is

$$\mathbf{x}_r(k) = \begin{bmatrix} \frac{1}{2}T^2 \\ T \\ 1 \end{bmatrix} \dot{a}(k-1) \triangleq \mathbf{G}u(k-1), \quad (9.239)$$

where $u(k) \sim N(0, \sigma_{\dot{a}_c}^2)$ and

$$\mathbf{G} = \begin{bmatrix} \frac{1}{2}T^2 \\ T \\ 1 \end{bmatrix}. \quad (9.240)$$

The observation matrix is either

$$\mathbf{C} = [1 \ 0 \ 0] \quad (9.241)$$

for position observation, or

$$\mathbf{C} = [1 \ 1 \ 0] \quad (9.242)$$

for position and velocity observations.

As in Section 9.2, we must specify a desired signal that we want to estimate. In the Wiener filtering problem, we focused on three choices of the desired signal

$$d(k) = s(k+L), \quad (9.243)$$

where $L = 0$ was filtering, $L < 0$ was filtering with lag or smoothing, and $L \geq 1$ was prediction. Those same desired signals are still of interest in the Kalman model. In (9.223), $s(k)$ corresponds to $x_1(k)$.

We can generalize it to the case where $\mathbf{d}(k)$ is a $D \times 1$ vector,

$$\mathbf{d}(k) = \mathbf{D}\mathbf{x}(k+L), \quad (9.244)$$

where \mathbf{D} is a $D \times p$ matrix. For example, if we want to predict the position and velocity in the kinematic model in (9.237), then

$$\mathbf{D} = \begin{bmatrix} 1 & 0 & 0 \\ 0 & 1 & 0 \end{bmatrix}. \quad (9.245)$$

Because it is a linear transformation, it holds that

$$\hat{\mathbf{d}}(k) = \mathbf{D}\hat{\mathbf{x}}(k + L). \quad (9.246)$$

As expected, the algorithm will require us to estimate the entire state vector $\mathbf{x}(k + L)$. In Section 9.3.2, we focus on the case where $L = 0$ and solve the Kalman filtering problem. In Section 9.3.3, we discuss Kalman prediction. In Section 9.3.4, we discuss Kalman smoothing. We will spend a lot of time on the Kalman filtering problem because the predictors and smoothers utilize the filter.

9.3.2 Kalman Filter

In this section, we study the Kalman filter and its applications. In Section 9.3.2.1, we derive the standard Kalman filter. This version of the Kalman filter is referred to as the *covariance implementation* because it recursively computes the covariance matrix of the estimation error. This requires recursive inversion of an $N \times N$ matrix, where N is the dimension of the observation vector $\mathbf{r}(k)$.

In Section 9.3.2.2, we develop two alternative implementations that have computational advantages when $N > p$, where p is the dimension of the state vector. The derivations use the matrix inversion lemma to obtain implementations in which the recursive inversions are $p \times p$ when $\mathbf{R}(k)$ is a constant \mathbf{R} . The first implementation recursively computes the covariance matrix using a $p \times p$ inversion and we refer to it as the *reduced-dimension covariance implementation*.⁴ The second implementation recursively computes the Bayesian information matrix $\mathbf{J}_B(k)$ which is the inverse of the covariance matrix using a $p \times p$ inversion and is referred to as the *information filter*.

The three implementations are algebraically identical, but they have different computational complexity, different sensitivity to numerical errors such as round-off, and different sensitivity to model mismatch.

In Section 9.3.2.3, we study a sequence of applications in the signal processing and tracking area. These examples are consistent with the main application areas in the book but do not really illustrate the widespread usage of the Kalman filter in diverse areas.

The Kalman filters in Sections 9.3.2.1 and 9.3.2.2 assume that the observation is white Gaussian process. In Section 9.3.2.4, we show how to treat the case of colored plus white observation noise.

There is a measurement update step in the Kalman algorithm that requires processing an $N \times 1$ vector, where N is the dimension of the observation. In Section 9.3.2.5, we develop an algorithm to process the components of the vector sequentially.

In early applications, it was found that numerical round-off errors caused the covariance matrix or the Bayesian information matrix to lose its nonnegative definite property. In Section 9.3.2.6, we develop a square-root implementation of the Kalman filter that factors

⁴This implementation does not appear in most Kalman filter discussions.

the covariance matrix (or the Bayesian information matrix) into triangular matrices and updates them. This implementation guarantees a nonnegative definite matrix and improves the numerical precision.

In some applications, if there is mismatch between the mathematical model and the actual model, the Kalman filter will track the wrong model and predict a decreasing covariance matrix. However, the actual MSE is diverging. In Section 9.3.2.7, we analyze this behavior and discuss remedies.

The mismatch in Section 9.3.2.7 consists of a small bias term that is neglected in the mathematical model. In Section 9.3.2.8, we consider a more general mismatch model in which all of the matrices in the model, \mathbf{F} , \mathbf{G} , \mathbf{C} , \mathbf{Q} , \mathbf{R} , and $\mathbf{\Pi}$, may be mismatched to the actual model.

In Section 9.3.2.9, we summarize our results.

9.3.2.1 Derivation

In this section, we derive the discrete-time Kalman filter. There are two approaches to finding the Kalman filter. The first is to assume that we are dealing with the Bayesian linear Gaussian model described in Section 5.3.2. We then find $\hat{d}(k)$ as the conditional mean of the *a posteriori* density. The second is to assume that we have a process model that has the same second moments as Bayesian linear Gaussian model and find the linear filter that minimizes the mean-square error. We use the first approach in the text because it is consistent with our nonstructured approach. In addition, it shows how easy it is to extend the sequential Bayes estimation of a constant parameter to the estimation of the values of a random process.

We repeat the model in (9.212)–(9.214) for convenience

$$\mathbf{x}(k) = \mathbf{F}(k-1)\mathbf{x}(k-1) + \mathbf{G}(k-1)\mathbf{u}(k-1), \quad k = 1, \dots, \quad (9.247)$$

$$\mathbf{r}(k) = \mathbf{C}(k)\mathbf{x}(k) + \mathbf{w}(k), \quad k = 1, 2, \dots, \quad (9.248)$$

$$E \{ \mathbf{u}(k)\mathbf{u}^T(l) \} = \mathbf{Q}(k)\delta_{kl}, \quad (9.249)$$

$$E \{ \mathbf{w}(k)\mathbf{w}^T(l) \} = \mathbf{R}(k)\delta_{kl}, \quad (9.250)$$

and $\mathbf{u}(k)$ and $\mathbf{w}(k)$ are statistically independent. We assume that

$$\mathbf{x}(0) \sim N(\mathbf{m}_0, \mathbf{\Pi}_0). \quad (9.251)$$

Note that the process starts at $k = 0$ but our first observation is at $k = 1$.

The algorithm has two steps:

1. A prediction step in which we estimate the state vector $\mathbf{x}(k)$ and the received vector $\mathbf{r}(k)$ based on the state vector estimate $\hat{\mathbf{x}}(k-1)$.
2. A time-update step in which we observe $\mathbf{r}(k)$ and update our previous estimate.

We now develop these steps. We use the following notation:

- $\hat{\mathbf{x}}(k|k-1)$: the MSE estimate of $\hat{\mathbf{x}}(k)$ based on $\hat{\mathbf{x}}(k-1)$.
- $\hat{\mathbf{x}}(k) \triangleq \hat{\mathbf{x}}(k|k)$: the MSE estimate of $\hat{\mathbf{x}}(k)$ based on $\hat{\mathbf{x}}(k|k-1)$ and $\mathbf{r}(k)$.
- $\mathbf{P}(k|k-1)$: the covariance matrix of $\hat{\mathbf{x}}(k|k-1)$.
- $\mathbf{P}(k) \triangleq \mathbf{P}(k|k)$: the covariance matrix of $\hat{\mathbf{x}}(k)$.

In some sections, we will use an alternative notation to simplify the equations:

$$\begin{aligned}\hat{\mathbf{x}}_{k|k-1} &\triangleq \hat{\mathbf{x}}(k|k-1), \\ \hat{\mathbf{x}}_k &\triangleq \hat{\mathbf{x}}(k), \\ \mathbf{P}_{k|k-1} &\triangleq \mathbf{P}(k|k-1), \\ \mathbf{P}_k &\triangleq \mathbf{P}(k).\end{aligned}$$

We exploit the Gaussian assumption to update the various terms.

We initialize the algorithm with

$$\hat{\mathbf{x}}(0) = \mathbf{m}_0 \quad (9.252)$$

and

$$\mathbf{P}(0) = \mathbf{P}_0 = \mathbf{\Pi}_0. \quad (9.253)$$

Then,

$$\begin{aligned}\hat{\mathbf{x}}(k|k-1) &\triangleq E\{\mathbf{x}(k)|\hat{\mathbf{x}}(k-1)\} \\ &= E\{\mathbf{x}(k) = \mathbf{F}(k-1)\mathbf{x}(k-1) + \mathbf{G}(k-1)\mathbf{u}(k-1)|\hat{\mathbf{x}}(k-1)\}.\end{aligned} \quad (9.254)$$

Thus,

$$\boxed{\hat{\mathbf{x}}(k|k-1) = \mathbf{F}(k-1)\hat{\mathbf{x}}(k-1)}, \quad k = 1, \dots \quad (9.255)$$

The error covariance matrix is

$$\mathbf{P}(k|k-1) = E\left\{ [\hat{\mathbf{x}}(k|k-1) - \mathbf{x}(k)] [\hat{\mathbf{x}}(k|k-1) - \mathbf{x}(k)]^T \right\}, \quad (9.256)$$

which reduces to

$$\boxed{\mathbf{P}(k|k-1) = \mathbf{F}(k-1)\mathbf{P}(k-1)\mathbf{F}^T(k-1) + \mathbf{G}(k-1)\mathbf{Q}(k-1)\mathbf{G}^T(k-1)}, \quad k = 1, \dots \quad (9.257)$$

Note that

$$\hat{\mathbf{r}}(k) = \mathbf{C}(k)\hat{\mathbf{x}}(k) \quad (9.258)$$

and

$$\hat{\mathbf{r}}(k|k-1) = \mathbf{C}(k)\hat{\mathbf{x}}(k|k-1) \quad (9.259)$$

provides a prediction of the data sample at $\mathbf{r}(k)$. We define

$$\tilde{\mathbf{r}}(k) = \mathbf{r}(k) - \hat{\mathbf{r}}(k|k-1), \quad (9.260)$$

which is denoted as the innovation. This completes the prediction step.

There are several ways to develop the time-update step. The first is write the *a posteriori* density of $\mathbf{x}(k)$, given $\mathbf{r}(k)$. This follows easily because of the Gaussian assumption:

$$p_{\mathbf{x}(k)}(\mathbf{x}) = p_{(\mathbf{x}(k)|\hat{\mathbf{x}}(k|k-1))}(\mathbf{x}) \sim N(\hat{\mathbf{x}}(k|k-1), \mathbf{P}(k|k-1)), \quad (9.261)$$

$$p_{\mathbf{r}(k)|\mathbf{x}(k)}(\mathbf{x}) \sim N\left(\mathbf{C}(k)\mathbf{x}(k), \mathbf{R}(k)\right). \quad (9.262)$$

We want to find $\hat{\mathbf{x}}(k|k) \triangleq \hat{\mathbf{x}}(k)$. However, we have already solved that problem in Section 5.4.

The result is

$$\boxed{\hat{\mathbf{x}}(k) = \hat{\mathbf{x}}(k|k-1) + \mathbf{P}(k)\mathbf{C}^T(k)\mathbf{R}^{-1}(k)\tilde{\mathbf{r}}(k)} \quad (9.263)$$

and

$$\boxed{\mathbf{P}^{-1}(k) = \mathbf{P}^{-1}(k|k-1) + \mathbf{C}^T(k)\mathbf{R}^{-1}(k)\mathbf{C}(k)}. \quad (9.264)$$

We define the Kalman gain as

$$\boxed{\mathbf{K}(k) \triangleq \mathbf{P}(k)\mathbf{C}^T(k)\mathbf{R}^{-1}(k)}. \quad (9.265)$$

The covariance matrix of the innovation process, $\tilde{\mathbf{r}}(k)$, is

$$\tilde{\mathbf{P}}(k) = \mathbf{C}(k)\mathbf{P}(k|k-1)\mathbf{C}^T(k) + \mathbf{R}(k). \quad (9.266)$$

It remains to put $\mathbf{P}(k)$ in a more compact form. We first show that

$$\mathbf{P}(k) = \mathbf{P}(k|k-1) [\mathbf{I} - \mathbf{C}^T(k)\tilde{\mathbf{P}}^{-1}(k)\mathbf{C}(k)\mathbf{P}(k|k-1)]. \quad (9.267)$$

To verify this, we take the inverse of (9.264) using the matrix inversion lemma. Then,

$$\mathbf{P}(k) = \mathbf{P}(k|k-1) \left[\mathbf{I} - \mathbf{C}^T(k) (\mathbf{C}(k)\mathbf{P}(k|k-1)\mathbf{C}^T(k) + \mathbf{R}(k))^{-1} \mathbf{C}(k)\mathbf{P}(k|k-1) \right], \quad (9.268)$$

using (9.266)

$$\mathbf{P}(k) = \mathbf{P}(k|k-1) [\mathbf{I} - \mathbf{C}^T(k)\tilde{\mathbf{P}}^{-1}(k)\mathbf{C}(k)\mathbf{P}(k|k-1)]. \quad (9.269)$$

Substituting (9.269) into (9.265) gives

$$\mathbf{K}(k) = \mathbf{P}(k|k-1) [\mathbf{I} - \mathbf{C}^T(k)\tilde{\mathbf{P}}^{-1}(k)\mathbf{C}(k)\mathbf{P}(k|k-1)] \mathbf{C}^T(k)\mathbf{R}^{-1}(k) \quad (9.270)$$

$$= \mathbf{P}(k|k-1)\mathbf{C}^T(k) [\mathbf{I} - \tilde{\mathbf{P}}^{-1}(k)\mathbf{C}(k)\mathbf{P}(k|k-1)\mathbf{C}^T(k)] \mathbf{R}^{-1}(k). \quad (9.271)$$

We write the identity matrix as $\tilde{\mathbf{P}}^{-1}(k)\tilde{\mathbf{P}}(k)$ and use (9.266) again. Then,

$$\begin{aligned} \mathbf{K}(k) &= \mathbf{P}(k|k-1)\mathbf{C}^T(k)\tilde{\mathbf{P}}^{-1}(k) [\mathbf{C}(k)\mathbf{P}(k|k-1)\mathbf{C}^T(k) + \mathbf{R}(k)] \\ &\quad - \mathbf{C}(k)\mathbf{P}(k|k-1)\mathbf{C}^T(k) \mathbf{R}^{-1}(k), \end{aligned} \quad (9.272)$$

which reduces to

$$\mathbf{K}(k) = \mathbf{P}(k|k-1)\mathbf{C}^T(k)\tilde{\mathbf{P}}^{-1}(k). \quad (9.273)$$

Substituting (9.273) into (9.269) and manipulating, we have

$$\mathbf{P}(k) = [\mathbf{I} - \mathbf{K}(k)\mathbf{C}(k)] \mathbf{P}(k|k-1). \quad (9.274)$$

The steps in the Kalman filter algorithm can be summarized.

1. Initialize the algorithm with

$$\hat{\mathbf{x}}(0) = \mathbf{m}_0 \quad (9.275)$$

and

$$\mathbf{P}(0) = \mathbf{P}_0. \quad (9.276)$$

2. Calculate the prediction step

$$\hat{\mathbf{x}}(k|k-1) = \mathbf{F}(k-1)\hat{\mathbf{x}}(k-1), \quad k = 1, \dots, \quad (9.277)$$

whose covariance matrix is

$$\mathbf{P}(k|k-1) = \mathbf{F}(k-1)\mathbf{P}(k-1)\mathbf{F}^T(k-1) + \mathbf{G}(k-1)\mathbf{Q}(k-1)\mathbf{G}^T(k-1), \quad (9.278)$$

and

$$\hat{\mathbf{r}}(k|k-1) = \mathbf{C}(k)\hat{\mathbf{x}}(k|k-1), \quad (9.279)$$

and the innovation

$$\tilde{\mathbf{r}}(k) = \mathbf{r}(k) - \hat{\mathbf{r}}(k|k-1), \quad (9.280)$$

whose covariance matrix is

$$\tilde{\mathbf{P}}(k) = \mathbf{C}(k)\mathbf{P}(k|k-1)\mathbf{C}^T(k) + \mathbf{R}(k). \quad (9.281)$$

3. Compute the Kalman gain matrix

$$\mathbf{K}(k) = \mathbf{P}(k|k-1)\mathbf{C}^T(k)\tilde{\mathbf{P}}^{-1}(k). \quad (9.282)$$

4. Compute $\hat{\mathbf{x}}(k)$

$$\hat{\mathbf{x}}(k) = \hat{\mathbf{x}}(k|k-1) + \mathbf{K}(k)\tilde{\mathbf{r}}(k) \quad (9.283)$$

$$= \hat{\mathbf{x}}(k|k-1) + \mathbf{K}(k)[\mathbf{r}(k) - \mathbf{C}(k)\hat{\mathbf{x}}(k|k-1)], \quad (9.284)$$

whose error covariance matrix is

$$\mathbf{P}(k) = [\mathbf{I} - \mathbf{K}(k)\mathbf{C}(k)]\mathbf{P}(k|k-1). \quad (9.285)$$

Note that the $\mathbf{P}(k)$ and $\mathbf{K}(k)$ computation are independent of the data, so they can be calculated before the data is received.

The covariance update formula in (9.285) is sometimes referred to in the literature as the standard form. An alternative form is given in (9.286).⁵ See Problem 9.3.1.

$$\mathbf{P}(k) = [\mathbf{I} - \mathbf{K}(k)\mathbf{C}(k)]\mathbf{P}(k|k-1)[\mathbf{I} - \mathbf{K}(k)\mathbf{C}(k)]^T + \mathbf{K}(k)\mathbf{R}(k)\mathbf{K}^T(k). \quad (9.286)$$

The covariance update formula in (9.286) is referred to as the stabilized form. It requires more calculation than (9.285), but it is less sensitive to numerical errors in the calculation of the gain matrix $\mathbf{K}(k)$ in (9.282). The above references show that first-order errors in $\mathbf{K}(k)$ propagate as first-order errors in (9.285) but as second-order errors in (9.286). It will not lead to negative eigenvalues because the only subtraction is in a quadratic term.

A block diagram of Kalman Filter is shown in Figure 9.30.

⁵See discussions in Aoki [Aok67], Jazwinski [Jaz70], or Mendel [Men73, Men95].

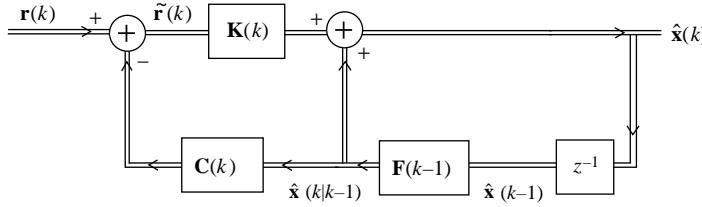


Figure 9.30: Block Diagram of Kalman Filter.

In order to relate the Kalman Filter to the fixed parameter sequential Bayes estimator in Section 5.4, we let

$$\mathbf{x}(k) = \boldsymbol{\theta}(k), \quad (9.287)$$

$$\mathbf{F}(k) = \mathbf{I}, \quad (9.288)$$

$$\mathbf{Q}(k) = \mathbf{0}, \quad (9.289)$$

$$\mathbf{C}(k) = \mathbf{V}. \quad (9.290)$$

Then, (9.277), (9.278), (9.282), (9.284), and (9.285) become

$$\hat{\boldsymbol{\theta}}(k|k-1) = \hat{\boldsymbol{\theta}}(k-1), \quad (9.291)$$

$$\mathbf{P}(k|k-1) = \mathbf{P}(k-1), \quad (9.292)$$

$$\mathbf{K}(k) = \mathbf{P}(k-1)\mathbf{V}^T [\mathbf{R} + \mathbf{V}\mathbf{P}(k-1)\mathbf{V}^T]^{-1}, \quad (9.293)$$

$$\hat{\boldsymbol{\theta}}(k) = \hat{\boldsymbol{\theta}}(k-1) + \mathbf{K}(k) [\mathbf{r}(k) - \mathbf{V}\hat{\boldsymbol{\theta}}(k-1)], \quad (9.294)$$

and

$$\mathbf{P}(k) = [\mathbf{I} - \mathbf{K}(k)\mathbf{V}] \mathbf{P}(k-1). \quad (9.295)$$

The last three equations are identical to (5.729)–(5.731).

Time-invariant Model In many applications, the various matrices $\mathbf{F}(k)$, $\mathbf{G}(k)$, $\mathbf{C}(k)$, $\mathbf{Q}(k)$, and $\mathbf{R}(k)$ are not functions of time. In this case, the Kalman filter algorithm becomes the following.

1. Initialize with

$$\hat{\mathbf{x}}(0) = \mathbf{m}_0, \quad (9.296)$$

$$\mathbf{P}(0) = \mathbf{P}_0. \quad (9.297)$$

2. Predict

$$\hat{\mathbf{x}}(k|k-1) = \mathbf{F}\hat{\mathbf{x}}(k-1), \quad (9.298)$$

$$\mathbf{P}(k|k-1) = \mathbf{F}\mathbf{P}(k-1)\mathbf{F}^T + \mathbf{G}\mathbf{Q}\mathbf{G}^T, \quad (9.299)$$

$$\tilde{\mathbf{r}}(k|k-1) = \mathbf{C}\hat{\mathbf{x}}(k|k-1), \quad (9.300)$$

$$\tilde{\mathbf{P}}(k) = \mathbf{C}\mathbf{P}(k|k-1)\mathbf{C}^T + \mathbf{R}. \quad (9.301)$$

3. Kalman gain

$$\mathbf{K}(k) = \mathbf{P}(k|k-1)\mathbf{C}^T\tilde{\mathbf{P}}^{-1}(k). \quad (9.302)$$

4. Compute $\hat{\mathbf{x}}(k)$

$$\hat{\mathbf{x}}(k) = \mathbf{F}\hat{\mathbf{x}}(k-1) + \mathbf{K}(k)[\mathbf{r}(k) - \mathbf{C}\mathbf{F}\hat{\mathbf{x}}(k-1)] \quad (9.303)$$

and

$$\mathbf{P}(k) = [\mathbf{I} - \mathbf{K}(k)\mathbf{C}]\mathbf{P}(k|k-1). \quad (9.304)$$

If the dynamic model in (9.247) has all of the eigenvalues of \mathbf{F} inside the unit circle, then we obtain the steady-state version of the update equations. We define

$$\mathbf{P}_\infty = \lim_{k \rightarrow \infty} \mathbf{P}(k), \quad (9.305)$$

$$\mathbf{P}'_\infty = \lim_{k \rightarrow \infty} \mathbf{P}(k|k-1). \quad (9.306)$$

From (9.299) and (9.304),

$$\mathbf{P}(k|k-1) = \mathbf{F}[\mathbf{I} - \mathbf{K}(k-1)\mathbf{C}]\mathbf{P}(k-1|k-2)\mathbf{F}^T + \mathbf{G}\mathbf{Q}\mathbf{G}^T. \quad (9.307)$$

Using (9.301) and (9.302),

$$\begin{aligned} \mathbf{P}(k|k-1) &= \mathbf{F} \left[\mathbf{I} - \mathbf{P}(k-1|k-2)\mathbf{C}^T \left[\mathbf{C}\mathbf{P}(k-1|k-2)\mathbf{C}^T + \mathbf{R} \right]^{-1} \mathbf{C} \right] \\ &\quad \times \mathbf{P}(k-1|k-2)\mathbf{F}^T + \mathbf{G}\mathbf{Q}\mathbf{G}^T. \end{aligned} \quad (9.308)$$

Letting $k \rightarrow \infty$ gives

$$\mathbf{P}'_\infty = \mathbf{F} \left[\mathbf{I} - \mathbf{P}'_\infty \mathbf{C}^T \left[\mathbf{C}\mathbf{P}'_\infty \mathbf{C}^T + \mathbf{R} \right]^{-1} \mathbf{C} \right] \mathbf{P}'_\infty \mathbf{F}^T + \mathbf{G}\mathbf{Q}\mathbf{G}^T, \quad (9.309)$$

which is the desired result.

From (9.299), letting $k \rightarrow \infty$ and solving for P_∞ gives

$$\mathbf{P}_\infty = \mathbf{F}^{-1} \left[\mathbf{P}'_\infty - \mathbf{G}\mathbf{Q}\mathbf{G}^T \right] \mathbf{F}^{-T}. \quad (9.310)$$

Using (9.309) in (9.310) gives

$$\mathbf{P}_\infty = \left[\mathbf{I} - \mathbf{P}'_\infty \mathbf{C}^T \left[\mathbf{C}\mathbf{P}'_\infty \mathbf{C}^T + \mathbf{R} \right]^{-1} \mathbf{C} \right] \mathbf{P}'_\infty. \quad (9.311)$$

From (9.301),

$$\tilde{\mathbf{P}}_\infty = \mathbf{C}\mathbf{P}'_\infty \mathbf{C}^T + \mathbf{R} \quad (9.312)$$

and, from (9.302),

$$\mathbf{K}_\infty = \mathbf{P}'_\infty \mathbf{C}^T \left[\mathbf{C}\mathbf{P}'_\infty \mathbf{C}^T + \mathbf{R} \right]^{-1} \quad (9.313)$$

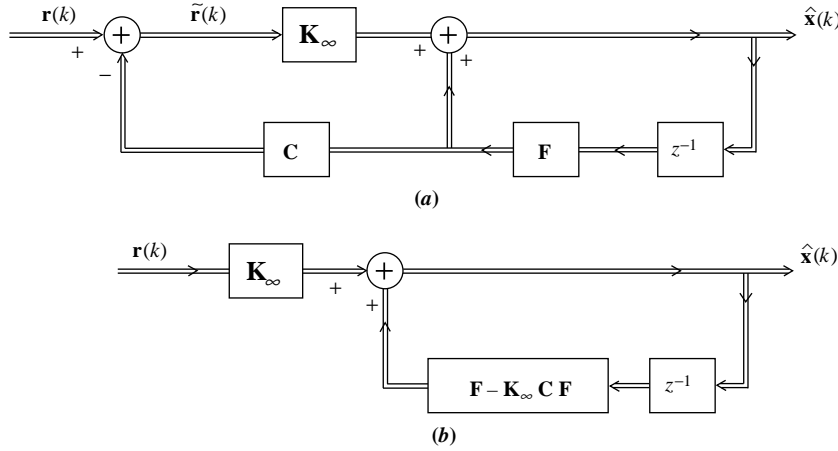


Figure 9.31: Steady-state Kalman filter.

and

$$\begin{aligned}
 \hat{x}(k) &= \mathbf{F}\hat{x}(k-1) + \mathbf{K}_\infty[\mathbf{r}(k) - \mathbf{C}\mathbf{F}\hat{x}(k-1)] \\
 &= [\mathbf{F} - \mathbf{K}_\infty \mathbf{C}\mathbf{F}]\hat{x}(k-1) + \mathbf{K}_\infty \mathbf{r}(k) \\
 &= [\mathbf{I} - \mathbf{K}_\infty \mathbf{C}]\mathbf{F}\hat{x}(k-1) + \mathbf{K}_\infty \mathbf{r}(k).
 \end{aligned} \tag{9.314}$$

The steady-state filter is shown in Figure 9.31.

Several observations about these results are useful:

- (1) The recursive equation in (9.308) is a discrete-time Riccati equations for $\mathbf{P}(k|k-1)$. The equation is nonlinear.
- (2) The equation in (9.309) is an algebraic Riccati equation for \mathbf{P}'_∞ . There has been a great deal devoted to efficient solutions to this equation. Laub [Lau79] suggests an efficient technique for solving this equation. We can always find the result by solving (9.308) recursively.
- (3) The relation between \mathbf{P}'_∞ and \mathbf{P}_∞ can be seen by considering the scalar case in Figure 9.32. We assume that the system has reached steady state at $k = k_{ss}$.

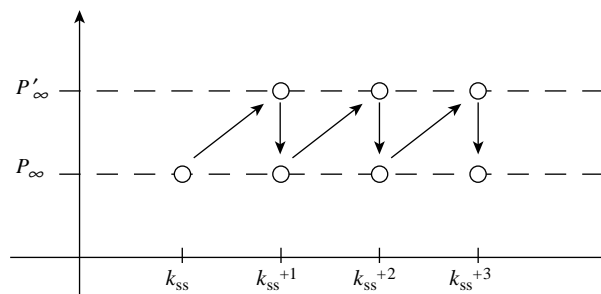


Figure 9.32: Steady-state variance behavior.

After $\mathbf{r}(k_{ss})$ is observed, the variance is given by \mathbf{P}_∞ . The system then predicts the variance at $k_{ss} + 1$, which is given by \mathbf{P}'_∞ . We then observe $\mathbf{r}(k_{ss} + 1)$ and the variance goes to \mathbf{P}_∞ . The process continues in this manner.

(4) If we define

$$\tilde{\mathbf{F}} = [\mathbf{I} - \mathbf{K}_\infty \mathbf{C}] \mathbf{F}, \quad (9.315)$$

then the eigenvalues of $\tilde{\mathbf{F}}$, particularly the dominant eigenvalues, will determine the dynamic behavior of the steady-state filter.

Note that the steady-state Kalman filter is identical to the realizable Wiener filter in Section 9.2.2.5. However, we only developed the realizable Wiener filter for scalar $r(k)$ and the Kalman filter applies to vector $\mathbf{r}(k)$.

In the standard covariance implementation of the Kalman filter we have recursively invert an $N \times N$ matrix. When $N > p$, we can obtain an alternative implementation that requires recursive inversion of a $p \times p$ matrix by applying the matrix inversion lemma to the recursion in (9.264). We carry out that development in the next section.

9.3.2.2 Reduced Dimension Implementations

In this section, we derive two alternative implementations of Kalman covariance filter that are computationally more efficient when $N > p$. The first implementation uses a $p \times p$ dimensional recursion on $\mathbf{P}(k)$. The second implementation uses a $p \times p$ dimensional recursion on the Bayesian information matrix, $\mathbf{J}_B(k) \triangleq \mathbf{P}^{-1}(k)$.

Reduced Dimension Kalman Covariance Filter. We start from the covariance matrix inverse expression in (9.264):

$$\mathbf{P}^{-1}(k) = \mathbf{P}^{-1}(k|k-1) + \mathbf{C}^T(k)\mathbf{R}^{-1}(k)\mathbf{C}(k). \quad (9.316)$$

Taking the inverse, the covariance matrix may be written as

$$\begin{aligned} \mathbf{P}(k) &= [\mathbf{P}^{-1}(k|k-1) + \mathbf{C}^T(k)\mathbf{R}^{-1}(k)\mathbf{C}(k)]^{-1} \\ &= [\mathbf{I} + \mathbf{P}(k|k-1)\mathbf{C}^T(k)\mathbf{R}^{-1}(k)\mathbf{C}(k)]^{-1}\mathbf{P}(k|k-1). \end{aligned} \quad (9.317)$$

Now define the $p \times N$ matrix

$$\mathbf{T}_p(k) \triangleq \mathbf{C}^T(k)\mathbf{R}^{-1}(k) \quad (9.318)$$

and the $p \times p$ matrix

$$\mathbf{D}(k) \triangleq \mathbf{C}^T(k)\mathbf{R}^{-1}(k)\mathbf{C}(k). \quad (9.319)$$

Then,

$$\mathbf{P}(k) = [\mathbf{I} + \mathbf{P}(k|k-1)\mathbf{D}(k)]^{-1}\mathbf{P}(k|k-1). \quad (9.320)$$

Using the Kalman gain expression in (9.265), we have

$$\mathbf{K}(k) = \mathbf{P}(k)\mathbf{T}_p(k) \quad (9.321)$$

and

$$\mathbf{K}(k)\mathbf{C}(k) = \mathbf{P}(k)\mathbf{D}(k). \quad (9.322)$$

Substituting (9.321) and (9.322) into (9.284), the state estimate becomes

$$\hat{\mathbf{x}}(k) = \hat{\mathbf{x}}(k|k-1) + \mathbf{P}(k) [\mathbf{T}_p(k)\mathbf{r}(k) - \mathbf{D}(k)\hat{\mathbf{x}}(k|k-1)]. \quad (9.323)$$

In this expression, we see that $\mathbf{r}(k)$ is transformed into a $p \times 1$ vector:

$$\mathbf{r}_p(k) \triangleq \mathbf{T}_p(k)\mathbf{r}(k) \quad (9.324)$$

and the remaining processing is p -dimensional. However, unless $\mathbf{R}(k) = \mathbf{R}$, the calculation of $\mathbf{D}(k)$ contains an $N \times N$ inverse that must be calculated for each step in the recursion. Fortunately, in most applications $\mathbf{R}(k)$ is constant. In many applications, both $\mathbf{C}(k)$ and $\mathbf{R}(k)$ are constant so that \mathbf{T}_p and \mathbf{D} are constant matrices.

We can summarize the algorithm as follows:

1. Calculate

$$\mathbf{T}_p(k) = \mathbf{C}^T(k)\mathbf{R}^{-1}(k), \quad (9.325)$$

$$\mathbf{D}(k) = \mathbf{C}^T(k)\mathbf{R}^{-1}(k)\mathbf{C}(k). \quad (9.326)$$

2. Preprocess $\mathbf{r}(k)$ to obtain

$$\mathbf{r}_p(k) = \mathbf{T}_p(k)\mathbf{r}(k). \quad (9.327)$$

3. Initialize the algorithm with $\hat{\mathbf{x}}(0)$ and $\mathbf{P}(0)$.

4. For $k = 1, \dots$, predict

$$\hat{\mathbf{x}}(k|k-1) = \mathbf{F}(k-1)\hat{\mathbf{x}}(k-1), \quad (9.328)$$

$$\mathbf{P}(k|k-1) = \mathbf{F}(k-1)\mathbf{P}(k-1)\mathbf{F}^T(k-1) + \mathbf{G}(k-1)\mathbf{Q}(k-1)\mathbf{G}^T(k-1). \quad (9.329)$$

5. Update state vector estimate and covariance matrix:

$$\mathbf{P}(k) = [\mathbf{I} + \mathbf{P}(k|k-1)\mathbf{D}(k)]^{-1}\mathbf{P}(k|k-1), \quad (9.330)$$

$$\hat{\mathbf{x}}(k) = \hat{\mathbf{x}}(k|k-1) + \mathbf{P}(k) [\mathbf{r}_p(k) - \mathbf{D}(k)\hat{\mathbf{x}}(k|k-1)]. \quad (9.331)$$

A block diagram of the reduced-dimension covariance implementation is shown in Figure 9.33.

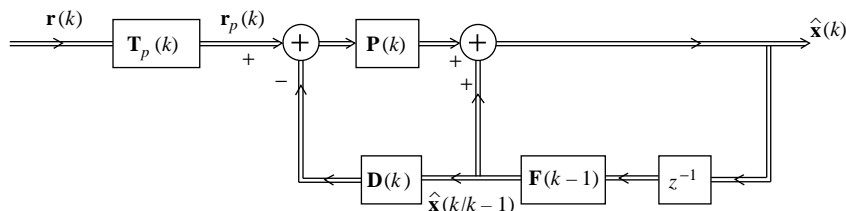


Figure 9.33: Reduced-dimension Kalman covariance filter.

Kalman Information Filter. The Kalman filter uses recursions on $\mathbf{P}(k)$ and $\mathbf{P}(k|k-1)$. There is an alternative version that uses recursions on $\mathbf{P}^{-1}(k)$ and $\mathbf{P}^{-1}(k|k-1)$. This version is called the information filter or the *Kalman information filter*. An early reference is [Fra67]. We define the information matrices:

$$\mathbf{J}(k|k-1) \triangleq \mathbf{P}^{-1}(k|k-1), \quad (9.332)$$

$$\mathbf{J}(k) \triangleq \mathbf{P}^{-1}(k). \quad (9.333)$$

Under the Bayesian linear Gaussian model, $\mathbf{J}(k)$ is the Bayesian information matrix $\mathbf{J}_B(k)$ since the Kalman filter leads to an efficient estimate that satisfies the Bayesian CRB.

We need to develop recursions for $\mathbf{J}(k|k-1)$ and $\mathbf{J}(k)$, and expressions for the Kalman gain $\mathbf{K}(k)$ and the state vector $\hat{\mathbf{x}}(k)$ that use $\mathbf{J}(k)$ and $\mathbf{J}(k|k-1)$.⁶ To find $\mathbf{J}(k|k-1)$, we define the $p \times p$ matrix

$$\begin{aligned} \mathbf{A}(k-1) &\triangleq [\mathbf{F}(k-1)\mathbf{P}(k-1)\mathbf{F}^T(k-1)]^{-1} \\ &= \mathbf{F}^{-T}(k-1)\mathbf{J}(k-1)\mathbf{F}^{-1}(k-1), \end{aligned} \quad (9.334)$$

and write (9.257) as

$$\mathbf{J}^{-1}(k|k-1) = \mathbf{A}^{-1}(k-1) + \mathbf{G}(k-1)\mathbf{Q}(k-1)\mathbf{G}^T(k-1). \quad (9.335)$$

Applying the matrix inversion lemma, we have

$$\begin{aligned} \mathbf{J}(k|k-1) &= \mathbf{A}(k-1) - \mathbf{A}(k-1)\mathbf{G}(k-1)[\mathbf{G}^T(k-1)\mathbf{A}(k-1)\mathbf{G}(k-1) \\ &\quad + \mathbf{Q}^{-1}(k-1)]^{-1}\mathbf{G}^T(k-1)\mathbf{A}(k-1) \end{aligned} \quad (9.336)$$

Now define a $p \times q$ matrix, where q is the dimension of $\mathbf{Q}(k-1)$:

$$\mathbf{B}(k-1) \triangleq \mathbf{A}(k-1)\mathbf{G}(k-1)[\mathbf{G}^T(k-1)\mathbf{A}(k-1)\mathbf{G}(k-1) + \mathbf{Q}^{-1}(k-1)]^{-1}. \quad (9.337)$$

Then, (9.336) can be simplified to

$$\begin{aligned} \mathbf{J}(k|k-1) &= \mathbf{A}(k-1) - \mathbf{B}(k-1)\mathbf{G}^T(k-1)\mathbf{A}(k-1) \\ &= [\mathbf{I} - \mathbf{B}(k-1)\mathbf{G}^T(k-1)]\mathbf{A}(k-1). \end{aligned} \quad (9.338)$$

To find expressions for $\mathbf{J}(k)$ and $\mathbf{K}(k)$, we simply use (9.264) and (9.265):

$$\mathbf{J}(k) = \mathbf{J}(k|k-1) + \mathbf{D}(k), \quad (9.339)$$

$$\mathbf{K}(k) = \mathbf{J}^{-1}(k)\mathbf{T}_p(k). \quad (9.340)$$

We can then do the state vector recursion using (9.328) and (9.331). The block diagram is the same as Figure 9.33 with $\mathbf{P}(k)$ replaced by $\mathbf{J}^{-1}(k)$. The disadvantage is that we have to take the inverse of $\mathbf{J}(k)$ at each step. Anderson and Moore [AM79] (e.g. [BSLK01]) argue that a more efficient technique is to define two new quantities:

$$\hat{\mathbf{y}}(k|k-1) = \mathbf{J}(k|k-1)\hat{\mathbf{x}}(k|k-1) \quad (9.341)$$

⁶Our development follows the derivations in [BSLK01] and [AM79].

and

$$\hat{\mathbf{y}}(k) = \mathbf{J}(k)\hat{\mathbf{x}}(k) \quad (9.342)$$

and do the recursion on them. Substituting (9.338), (9.334), and (9.328) into (9.341) gives

$$\begin{aligned} \hat{\mathbf{y}}(k|k-1) &= [\mathbf{I} - \mathbf{B}(k-1)\mathbf{G}^T(k-1)]\mathbf{F}^{-T}(k-1)\mathbf{J}(k-1)\mathbf{F}^{-1}(k-1)\mathbf{F}(k-1)\hat{\mathbf{x}}(k-1) \\ &= [\mathbf{I} - \mathbf{B}(k-1)\mathbf{G}^T(k-1)]\mathbf{F}^{-T}(k-1)\mathbf{J}(k-1)\hat{\mathbf{x}}(k-1). \end{aligned} \quad (9.343)$$

Recognizing that $\hat{\mathbf{y}}(k-1) = \mathbf{J}(k-1)\hat{\mathbf{x}}(k-1)$, we have the recursion for $\hat{\mathbf{y}}(k|k-1)$:

$$\hat{\mathbf{y}}(k|k-1) = [\mathbf{I} - \mathbf{B}(k-1)\mathbf{G}^T(k-1)]\mathbf{F}^{-T}(k-1)\hat{\mathbf{y}}(k-1). \quad (9.344)$$

To find the recursion for $\hat{\mathbf{x}}(k)$, we substitute (9.331) into (9.342) to obtain

$$\begin{aligned} \hat{\mathbf{y}}(k) &= \mathbf{J}(k)\hat{\mathbf{x}}(k|k-1) + \mathbf{J}(k)\mathbf{P}(k)[\mathbf{r}_p(k) - \mathbf{D}(k)\hat{\mathbf{x}}(k|k-1)] \\ &= \mathbf{J}(k)\hat{\mathbf{x}}(k|k-1) + \mathbf{r}_p(k) - \mathbf{D}(k)\hat{\mathbf{x}}(k|k-1). \end{aligned} \quad (9.345)$$

Substituting (9.339) into (9.345) yields

$$\begin{aligned} \hat{\mathbf{y}}(k) &= [\mathbf{J}(k|k-1) + \mathbf{D}(k)]\hat{\mathbf{x}}(k|k-1) + \mathbf{r}_p(k) - \mathbf{D}(k)\hat{\mathbf{x}}(k|k-1) \\ &= \mathbf{J}(k|k-1)\hat{\mathbf{x}}(k|k-1) + \mathbf{r}_p(k). \end{aligned} \quad (9.346)$$

Finally, using the relationship

$$\hat{\mathbf{x}}(k|k-1) = \mathbf{J}^{-1}(k|k-1)\hat{\mathbf{y}}(k|k-1), \quad (9.347)$$

this becomes

$$\hat{\mathbf{y}}(k) = \hat{\mathbf{y}}(k|k-1) + \mathbf{r}_p(k), \quad (9.348)$$

which is the desired result. A block diagram of the information filter is shown in Figure 9.34.

The Kalman information filter algorithm can be summarized as follows.

1. Calculate

$$\mathbf{T}_p(k) = \mathbf{C}^T(k)\mathbf{R}^{-1}(k) \quad (9.349)$$

$$\mathbf{D}(k) = \mathbf{C}^T(k)\mathbf{R}^{-1}(k)\mathbf{C}(k). \quad (9.350)$$

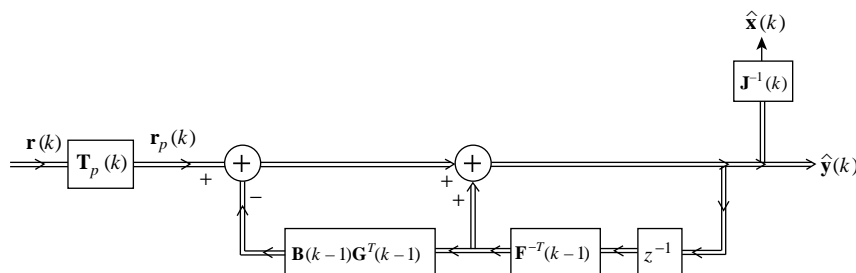


Figure 9.34: Information Filter.

2. Preprocess $\mathbf{r}(k)$ to obtain

$$\mathbf{r}_p(k) = \mathbf{T}_p(k)\mathbf{r}(k). \quad (9.351)$$

3. Initialize the algorithm with $\mathbf{J}(0)$ and

$$\hat{\mathbf{y}}(0) = \mathbf{J}(0)\hat{\mathbf{x}}(0). \quad (9.352)$$

Note that, if we have no *a priori* information, we can set $\mathbf{J}(0) = \mathbf{0}$ and then $\hat{\mathbf{y}}(0) = \mathbf{0}$.

4. For $k = 1, \dots$, calculate

$$\mathbf{A}(k-1) = \mathbf{F}^{-T}(k-1)\mathbf{J}(k-1)\mathbf{F}^{-1}(k-1), \quad (9.353)$$

$$\mathbf{B}(k-1) = \mathbf{A}(k-1)\mathbf{G}(k-1) [\mathbf{G}^T(k-1)\mathbf{A}(k-1)\mathbf{G}(k-1) + \mathbf{Q}^{-1}(k-1)]^{-1}. \quad (9.354)$$

5. Predict

$$\hat{\mathbf{y}}(k|k-1) = [\mathbf{I} - \mathbf{B}(k-1)\mathbf{G}^T(k-1)]\mathbf{F}^{-T}(k-1)\hat{\mathbf{y}}(k-1), \quad (9.355)$$

$$\mathbf{J}(k|k-1) = [\mathbf{I} - \mathbf{B}(k-1)\mathbf{G}^T(k-1)]\mathbf{A}(k-1). \quad (9.356)$$

6. Information matrix and state update:

$$\hat{\mathbf{y}}(k) = \hat{\mathbf{y}}(k|k-1) + \mathbf{r}_p(k), \quad (9.357)$$

$$\mathbf{J}(k) = \mathbf{J}(k|k-1) + \mathbf{D}(k). \quad (9.358)$$

7. To obtain the state vector estimate at each time k , we would need to calculate

$$\hat{\mathbf{x}}(k) = \mathbf{J}^{-1}(k)\hat{\mathbf{y}}(k). \quad (9.359)$$

The three forms of the Kalman filter are mathematically equivalent. However, depending on the dimension of the state vector (p), the measurement vector (N), and the process noise vector (q), one form may have computational advantages over another. In addition, when we study model mismatch in Section 9.3.2.7, we will find that the three forms have different sensitivities.

If the measurement vector is much larger than the state vector, then the alternative covariance filter and the information filter are computationally more efficient. In the standard covariance implementation, we recursively invert $\tilde{\mathbf{P}}(k)$, which is $N \times N$. In the alternative covariance implementation, we invert a $p \times p$ matrix, while in the information filter, we invert a $q \times q$ ($q \leq p$) matrix at each iteration. The alternative covariance and information filters also require inverting $\mathbf{R}(k)$, which is $N \times N$. However in many cases, $\mathbf{R}(k)$ is diagonal, so the inversion is easier, and in many cases $\mathbf{R}(k) = \mathbf{R}$, so the inversion only needs to be done once. In addition, the information filter requires inverting $\mathbf{F}(k)$ and $\mathbf{Q}(k)$, which are $p \times p$ and $q \times q$, respectively. If these are constant and/or diagonal, the computations are again simplified. In addition, as noted above, if no prior information is available, then we can initialize the information algorithm with $\mathbf{J}(0) = \mathbf{0}$.

The alternative covariance filter does not appear in most of the Kalman filter literature.⁷ However, it appears that there are applications (e.g., $q = p < N$ and constant matrices) where it is computationally more efficient.

9.3.2.3 Applications

The Kalman filter theory was published in 1961. Engineers recognized its importance and it moved quickly into many practical applications. Sorenson [Sor85] gives a summary of applications prior to 1983. Google provides an extensive list of applications. In this section, we consider four examples that illustrate the implementation of the filter.

1. An AR(1) process observed in the presence of white noise. This is the same AR(1) model we have used in previous sections.
2. The tracking problem, which we have encountered in previous chapters.
3. An AR(2) process observed in the presence of white noise. The dimension is small enough to get analytic results but new issues are introduced.
4. An array processing model to illustrate a case where the observation dimension is much larger than the state dimension. It illustrates the value of Kalman implementations in Section 9.3.2.2.

Example 9.9. We assume that the signal is an AR(1) process, so the state vector is a scalar $x(k)$. Then,

$$\mathbf{F} = -a(1) \triangleq \alpha, \quad (9.360)$$

$$\mathbf{G} = \sigma_u, \quad (9.361)$$

$$\mathbf{Q} = 1, \quad (9.362)$$

$$\mathbf{C} = 1, \quad (9.363)$$

$$\mathbf{R} = \sigma_w^2. \quad (9.364)$$

We assume $m_o = 0$ and that the *a priori* variance is

$$P(0) = \frac{\sigma_u^2}{1 - \alpha^2} = \sigma_s^2. \quad (9.365)$$

The Kalman equations are as follows:

(i) The prediction step is

$$\hat{x}(k|k-1) = \alpha\hat{x}(k-1), \quad k = 1, \dots, \quad (9.366)$$

with

$$\hat{x}(0) = 0. \quad (9.367)$$

The covariance is

$$P(k|k-1) = \alpha^2 P(k-1) + \sigma_u^2, \quad k = 1, \dots, \quad (9.368)$$

with $P(0)$ given by (9.365).

⁷In fact, we could not find it, but we suspect it is published somewhere given the extensive research on Kalman filters.

(ii) The gain equation is

$$K(k) = P(k|k-1) \left(\sigma_w^2 + P(k|k-1) \right)^{-1}. \quad (9.369)$$

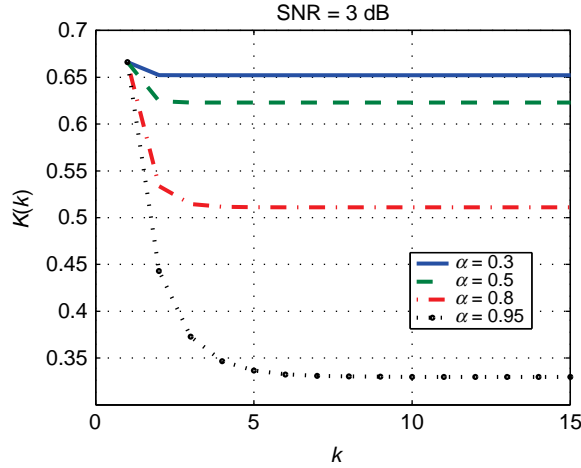
(iii) The current estimate is

$$\hat{x}(k) = \alpha \hat{x}(k-1) + K(k) [r(k) - \alpha \hat{x}(k-1)], \quad (9.370)$$

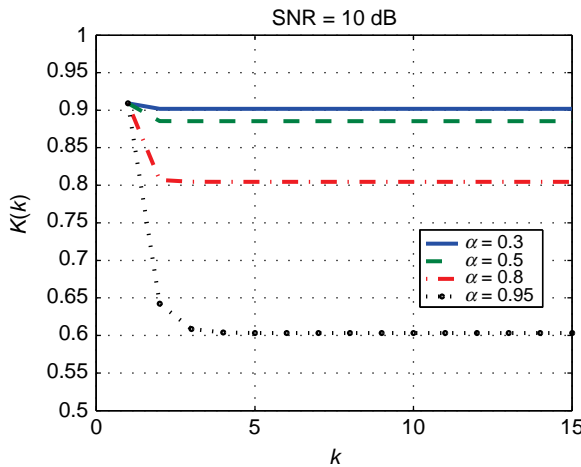
whose covariance is

$$P(k) = [1 - K(k)] P(k|k-1). \quad (9.371)$$

In Figure 9.35, we plot the Kalman gain as a function of k for $\sigma_s^2/\sigma_w^2 = 3$ dB and 10 dB for various value of α . As expected, the gain approaches a constant as k increases. The rate of approach is a



(a) Kalman gain versus k ; SNR = 3 dB, $\alpha = 0.3, 0.5, 0.8, 0.95$.



(b) Kalman gain versus k ; SNR = 10 dB, $\alpha = 0.3, 0.5, 0.8, 0.95$.

Figure 9.35: Kalman gain as a function of k .

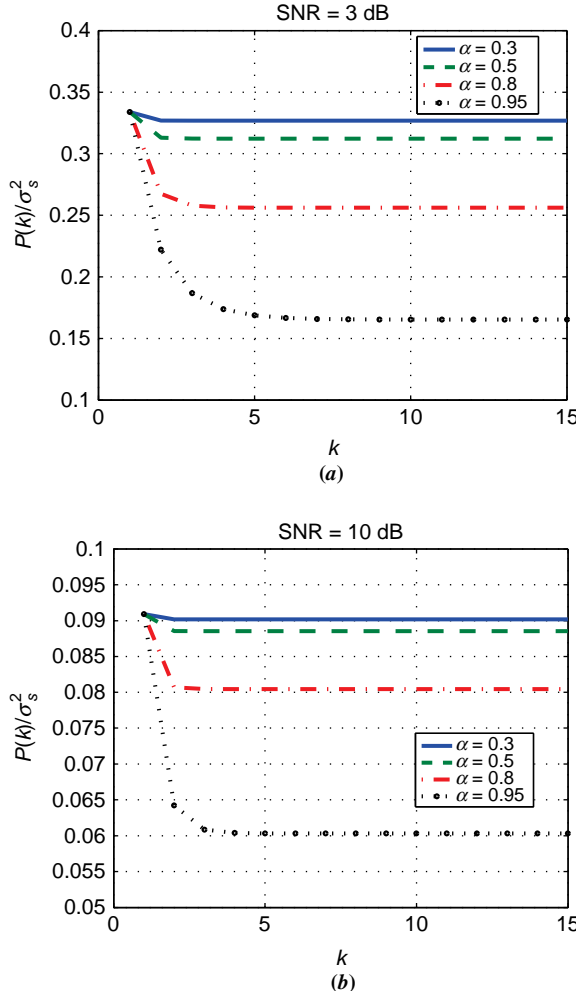


Figure 9.36: Normalized variance, $P(k)/\sigma_s^2$ versus k ; SNR = 3 dB, $\alpha = 0.3, 0.5, 0.8, 0.95$.

function of α . Meanwhile, the gain increases as the SNR increases, because we want to weight the new information, the innovation, more heavily. The increased gain increases the filter bandwidth.

One can show that for an AR(1) model with $\sigma_w^2 = 1$, that $P(k) = K(k)$. In Figure 9.36, we plot the normalized variance $P(k)/\sigma_s^2$ as a function of k . For positive values of α and $|\alpha| < 1$, the state vector process becomes stationary as $k \rightarrow \infty$. Then, as $k \rightarrow \infty$, the Kalman filter approaches steady state and the gains become constant. From (9.368),

$$P'_\infty = \alpha^2 P_\infty + \sigma_u^2, \quad (9.372)$$

and from (9.369), (9.371), and (9.372),

$$P_\infty = \left(1 - \frac{P'_\infty}{\sigma_w^2 + P'_\infty} \right) P'_\infty. \quad (9.373)$$

Using (9.372) in (9.373) gives

$$P_\infty = \frac{\sigma_w^2(\alpha^2 P_\infty + \sigma_u^2)}{\sigma_w^2 + (\alpha^2 P_\infty + \sigma_u^2)}. \quad (9.374)$$

Using (9.374), we obtain the quadratic equation,

$$\alpha^2 P_\infty^2 + P_\infty ((\sigma_s^2 + \sigma_w^2)(1 - \alpha^2)) - \sigma_w^2 \sigma_s^2 (1 - \alpha^2) = 0. \quad (9.375)$$

Solving (9.375) yields

$$P_\infty = \frac{1}{2} \sigma_w^2 \left\{ \left[\left(1 + \frac{\sigma_s^2}{\sigma_w^2} \right)^2 \left(\frac{1}{\alpha^2} - 1 \right)^2 + 4 \frac{\sigma_s^2}{\sigma_w^2} \left(\frac{1}{\alpha^2} - 1 \right) \right]^{\frac{1}{2}} - \left(1 + \frac{\sigma_s^2}{\sigma_w^2} \right) \left(\frac{1}{\alpha^2} - 1 \right) \right\}. \quad (9.376)$$

Denote the normalized mean-square error as

$$\bar{P}_\infty \triangleq \frac{P_\infty}{\sigma_s^2} \quad (9.377)$$

and the SNR as

$$\text{SNR} = \frac{\sigma_s^2}{\sigma_w^2}. \quad (9.378)$$

Then, (9.376) can be written as

$$\bar{P}_\infty = \frac{1}{2} \left\{ \left[\left(1 + \frac{1}{\text{SNR}} \right)^2 \left(\frac{1}{\alpha^2} - 1 \right)^2 + 4 \left(\frac{1}{\text{SNR}} \right) \left(\frac{1}{\alpha^2} - 1 \right) \right]^{\frac{1}{2}} - \left(1 + \frac{1}{\text{SNR}} \right) \left(\frac{1}{\alpha^2} - 1 \right) \right\}. \quad (9.379)$$

In Figure 9.37, we plot the normalized MSE versus SNR for various values of α .

The gain of the steady-state Kalman filter is

$$K_\infty = \frac{\alpha^2 P_\infty + \sigma_u^2}{\alpha^2 P_\infty + \sigma_w^2 + \sigma_u^2} \quad (9.380)$$

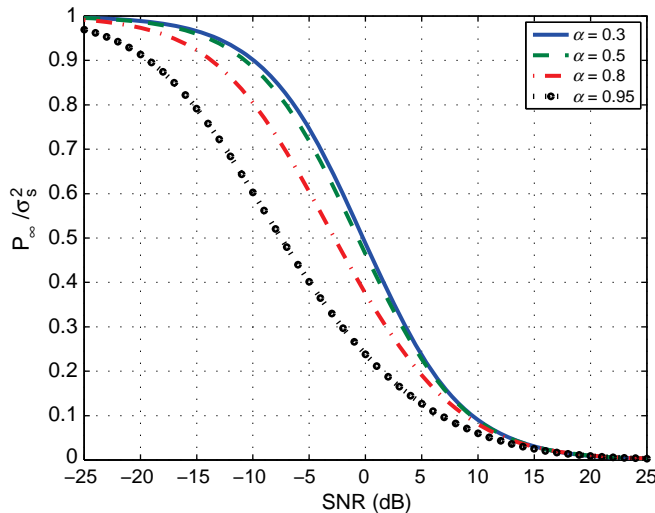


Figure 9.37: Normalized steady-state MSE versus SNR for $\alpha = 0.3, 0.5, 0.8, 0.95$.

and, from (9.370)

$$\begin{aligned}\hat{x}(k) &= \alpha\hat{x}(k-1) + K_\infty[r(k) - \alpha\hat{x}(k-1)] \\ &= \alpha[1 - K_\infty]\hat{x}(k-1) + K_\infty r(k).\end{aligned}\quad (9.381)$$

It corresponds to a system function

$$H_\infty = \frac{K_\infty}{1 - \alpha(1 - K_\infty)z^{-1}}, \quad (9.382)$$

which corresponds to the Wiener Filter in (9.181) with⁸

$$K_\infty = \frac{\beta}{\alpha} \frac{\sigma_u^2}{1 - \alpha\beta} \quad (9.383)$$

and

$$\beta = \alpha(1 - K_\infty). \quad (9.384)$$

■

The behavior in this example is representative of the behavior for any ARMA model with constant coefficients. As the observation starts, the output of the Kalman filter is identical to the output of an FIR Wiener filter. As the filter reaches steady state, it is identical to the IIR realizable Wiener filter.

Example 9.10. In this example, we consider a simple tracking problem. We use the dynamic model in (9.229)–(9.236) that we repeat for convenience. The nominal trajectory is constant velocity, so the state vector is a 2×1 vector whose components are the position and velocity:

$$\mathbf{x}(k) = \begin{bmatrix} x(k) \\ \dot{x}(k) \end{bmatrix} = \begin{bmatrix} x(k) \\ v(k) \end{bmatrix}, \quad (9.385)$$

and \mathbf{F} is a 2×2 matrix

$$\mathbf{F} = \begin{bmatrix} 1 & T \\ 0 & 1 \end{bmatrix}, \quad (9.386)$$

where T is the sampling interval. To introduce randomness into the model, we assume that the acceleration is a zero-mean discrete-time white random process. Then,

$$\mathbf{G}(k) = \begin{bmatrix} T^2/2 \\ T \end{bmatrix}, \quad (9.387)$$

and $u(k)$ is a scalar,

$$u(k) = a(k) \quad (9.388)$$

where $a(k) \sim N(0, \sigma_a^2)$. Therefore, \mathbf{Q} is a scalar

$$Q = \sigma_a^2. \quad (9.389)$$

If the sensor only observes range, then

$$\mathbf{C} = [1 \ 0] \quad (9.390)$$

⁸We leave the matching as an exercise.

and $w(k)$ is a scalar zero-mean discrete-time white process with variance σ_r^2 . Note that, the variance corresponds to the variance of the range estimate provided by the radar.

If the sensor observes both range and velocity (e.g., a range-Doppler radar)

$$\mathbf{C} = \mathbf{I}. \quad (9.391)$$

In this case

$$\mathbf{R} \triangleq \begin{bmatrix} \sigma_r^2 & 0 \\ 0 & \sigma_v^2 \end{bmatrix} \quad (9.392)$$

where σ_v^2 is the variance of the velocity estimate.

We consider the range-only case first. We assume that $x(0)$ and $v(0)$ are statistically independent Gaussian random variables $N(m_{p0}, \sigma_{p0}^2)$ and $N(m_{v0}, \sigma_{v0}^2)$, respectively.

In a typical tracking problem, we first detect a target in a range-Doppler cell. We would normally initialize the tracking filter with the center coordinates of that cell and variance proportional to the size of the cell. In this example, we assume

$$x(0) = 1,000 \text{ m}, \quad (9.393)$$

$$v(0) = -50 \text{ m/s}, \quad (9.394)$$

$$\sigma_a^2 = 40, \quad (9.395)$$

$$T = 0.1, \quad (9.396)$$

and

$$\sigma_r^2 = 100. \quad (9.397)$$

We use an initial state

$$[\hat{x}(0) \quad \hat{v}(0)]^T = [1100 \quad -100]^T \quad (9.398)$$

and

$$\mathbf{P}(0) = \text{diag}[1000, 1000]. \quad (9.399)$$

For range-only observation, we use (9.390). We show a typical realization for the range-only observation in Figure 9.38. In Figure 9.39, we show the Kalman gain. We see that the tracker has reached steady state in about 4 s. In Figure 9.40, we show the MSE for the range-only observation model. ■

We discuss the case with both range and velocity estimates in the problems.

The steady-state versions of the Kalman filter for random acceleration model in (9.385)–(9.390) are referred to as alpha-beta (α - β) trackers in the literature. Closed-form expressions for the Kalman gain \mathbf{K}_∞ and the steady-state variance \mathbf{P}_∞ are available (e.g. [BSLK01] or Problem 9.3.2.2.15).

We reparameterize the Kalman gain as

$$\mathbf{K}_\infty = [K_p \quad K_v] \triangleq \begin{bmatrix} \alpha & \frac{\beta}{T} \end{bmatrix}^T \quad (9.400)$$

and define a target maneuvering index

$$\lambda \triangleq \frac{T^2 \sigma_a}{\sigma_w}. \quad (9.401)$$

It is proportional to the ratio of the RMS value of process noise effect on the position over one sampling period ($\sigma_a T^2 / 2$) to the RMS value of the observation noise.

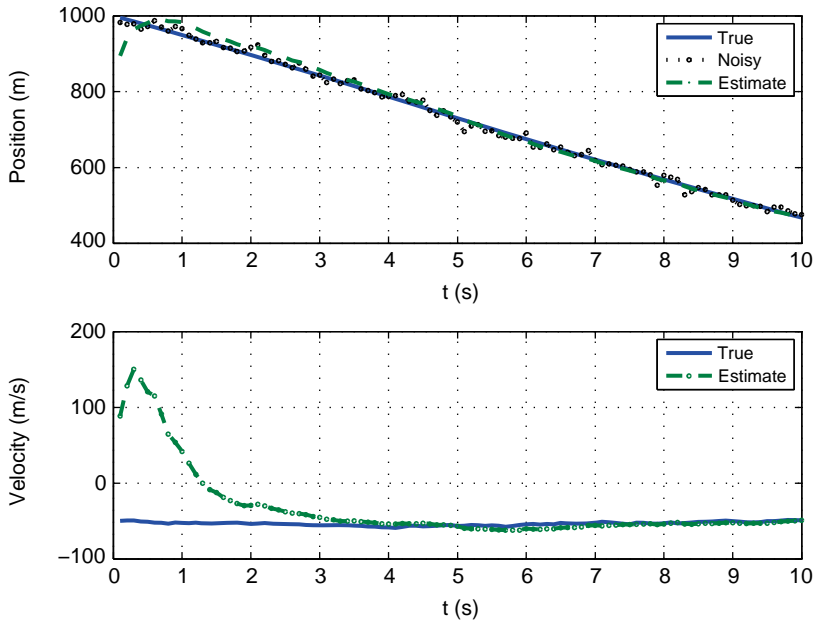


Figure 9.38: A realization of Kalman tracker with range-only observation.

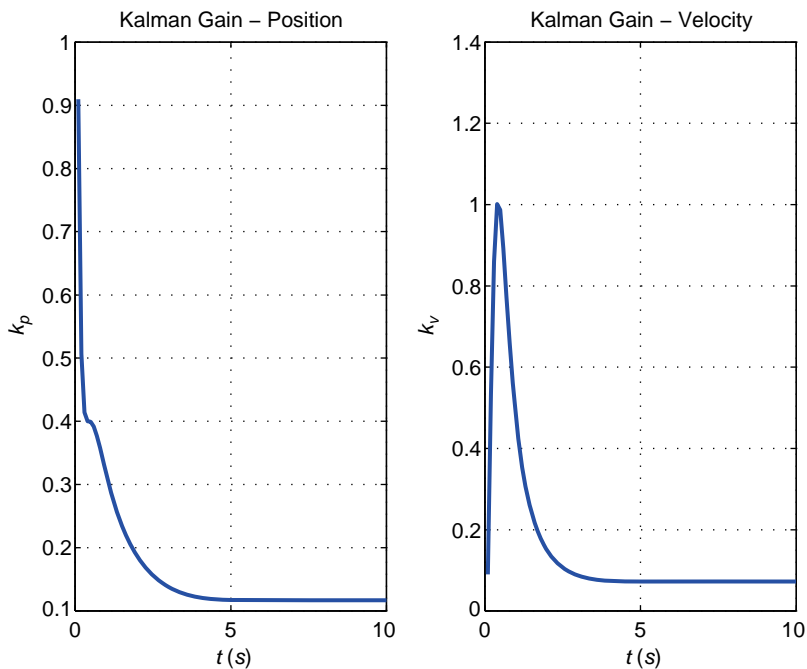


Figure 9.39: Kalman gain versus time.

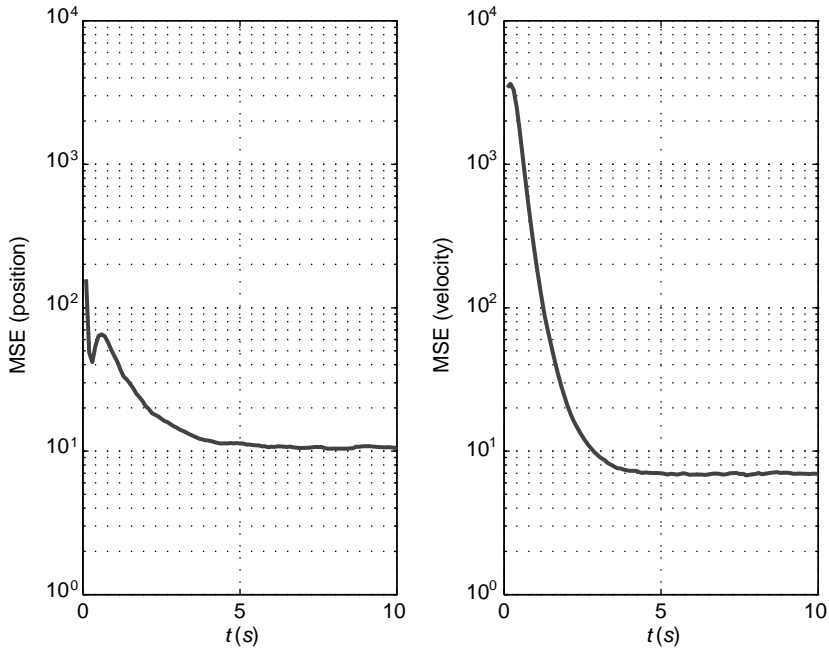


Figure 9.40: Mean-square error versus time.

Then, one can show

$$\alpha = -\frac{1}{8} \left(\lambda^2 + 8\lambda - (\lambda + 4)\sqrt{\lambda^2 + 8\lambda} \right) = K_p, \quad (9.402)$$

$$\beta = -\frac{1}{4} \left(\lambda^2 + 4\lambda - \lambda\sqrt{\lambda^2 + 8\lambda} \right) = K_v T, \quad (9.403)$$

$$\mathbf{P}_\infty = \sigma_w^2 \begin{bmatrix} \alpha & \frac{\beta}{T} \\ \frac{\beta}{T} & \frac{\beta}{T^2} \frac{\alpha - \beta/2}{1 - \alpha} \end{bmatrix}. \quad (9.404)$$

For the model in Example 9.10,

$$\alpha = 0.1064, \quad (9.405)$$

$$\beta = 0.0060, \quad (9.406)$$

$$\lambda = 0.0063, \quad (9.407)$$

$$\mathbf{P}_\infty = \begin{bmatrix} 10.6369 & 5.9790 \\ 5.9790 & 6.9168 \end{bmatrix}. \quad (9.408)$$

Example 9.11: Butterworth signals, ARMA(N, N). We introduced the continuous-time Butterworth family of signals in Chapter 8. If we sample a continuous-time Butterworth signal, we obtain a discrete-time Butterworth signal. Oppenheim and Schaefer [OS89] discuss how one

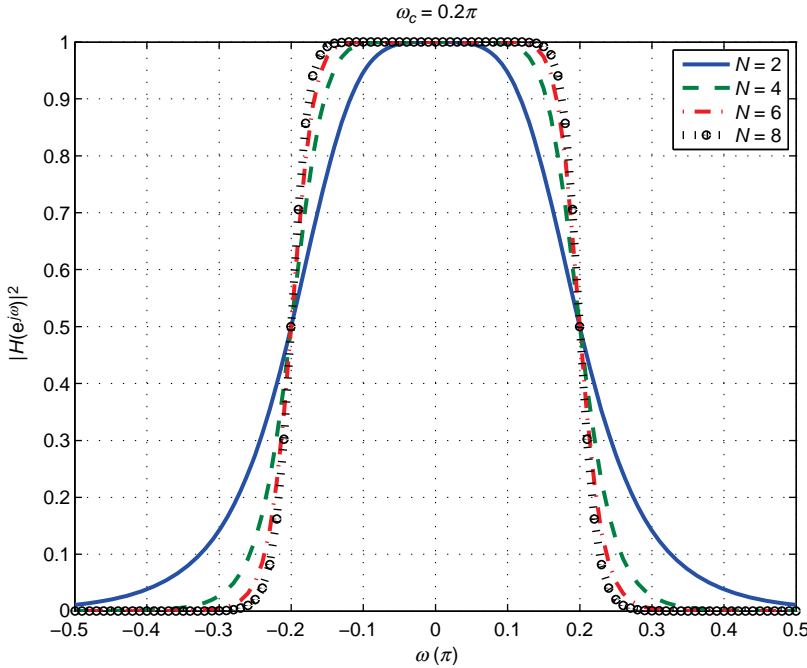


Figure 9.41: $|H(e^{j\omega})|^2$ versus ω/π ; $N = 2, 4, 6$, and 8 .

maps the continuous-time system function $H_c(s)$ into the discrete-time system function $H(z)$ using a bilinear transformation. The CT system function is

$$|H_c(s)|^2 = \frac{1}{1 + \left(\frac{s}{j\Omega_c}\right)^{2N}}, \quad (9.409)$$

where Ω_c is frequency at which $|H_c(j\omega)|^2$ is 3 dB down. Then, [OS89] shows that

$$H(z) = H_c\left(\frac{2}{T} \frac{1-z^{-1}}{1+z^{-1}}\right), \quad (9.410)$$

where T is the sampling interval. The 3 dB point of $|H(j\omega)|^2$ is given by

$$\Omega_c = \frac{2}{T} \tan\left(\frac{\omega_c}{2}\right) \quad (9.411)$$

and

$$|H(e^{j\omega})|^2 = \frac{1}{1 + \left(\frac{\tan \frac{\omega}{2}}{\tan \frac{\omega_c}{2}}\right)}. \quad (9.412)$$

In Figure 9.41, we plot $|H(e^{j\omega})|^2$ for $N = 2, 4, 6$, and 8 . As N increases, the spectrum approaches a bandlimited spectrum.⁹

⁹The theory demonstrating the use of the bilinear transform is developed in [OS89]. Kwon [Kwo98] uses their theory to develop the explicit formulas for $H(z)$. We derive some of the equations in the problems.

We consider two cases in this example. In the first case, we consider the $N = 2$ case and study the behavior as a function of ω_c , SNR, and k . In the second case, we consider the $\omega_c = 2$ case and study the behavior as a function of N , SNR, and k .

Case 1: BW(2, 2) Now define

$$\Omega'_c = \tan\left(\frac{\omega_c}{2}\right). \quad (9.413)$$

Then, for $N = 2$, one can show that the Butterworth signal is an ARMA(2, 2) process,

$$H(z) = \frac{b_0 + b_1 z^{-1} + b_2 z^{-2}}{a_0 + a_1 z^{-1} + a_2 z^{-2}} \quad (9.414)$$

with

$$b_0 = b_2 = (\Omega'_c)^2, \quad (9.415)$$

$$b_1 = 2(\Omega'_c)^2, \quad (9.416)$$

$$a_0 = 1 + 2 \cos\left(\frac{\pi}{4}\right) \Omega'_c + (\Omega'_c)^2, \quad (9.417)$$

$$a_1 = 2((\Omega'_c)^2 - 1), \quad (9.418)$$

$$a_2 = 1 - 2 \cos\left(\frac{\pi}{4}\right) \Omega'_c + (\Omega'_c)^2. \quad (9.419)$$

$H(z)$ can also be written as

$$H(z) = \frac{b_0(1 + z^{-1})^2}{a_0 + a_1 z^{-1} + a_2 z^{-2}} \quad (9.420)$$

to emphasize that there are 2 zeros at -1 . We choose ω_c , $-0.5\pi < \omega_c < 0.5\pi$, and then the state-variable model follows directly. Note that $H(e^{j\omega}) = 1$ when $\omega_c = 0$, so

$$\sum_{i=1}^2 a_i = \sum_{i=1}^2 b_i. \quad (9.421)$$

We consider $\omega_c = 0.2, 0.3, 0.4$. In Figure 9.42a, we plot the normalized variance k for SNR = 3 dB. The variance converges quickly to a steady-state value. In Figure 9.42b, we plot the normalized steady-state variance versus SNR. As we would expect, the steady-state variance decreases as ω_c decreases.

Case 2: BW(N, N) In this case, we consider Butterworth signals with $\omega_c = 0.2$ and $N = 2, 4, 6$, and 8.

For an even-order Butterworth signal, one can show that

$$H(z) = \prod_{k=0}^{N/2-1} \frac{b_0(1 + z^{-1})^2}{a_{0k} + a_{1k} z^{-1} + a_{2k} z^{-2}}, \quad (9.422)$$

where

$$a_{0k} = 1 + 2 \cos\left(\frac{\pi(2k+1)}{2N}\right) \Omega'_c + (\Omega'_c)^2, \quad (9.423)$$

$$a_{1k} = 2((\Omega'_c)^2 - 1), \quad (9.424)$$

$$a_{2k} = 1 - 2 \cos\left(\frac{\pi(2k+1)}{2N}\right) \Omega'_c + (\Omega'_c)^2. \quad (9.425)$$

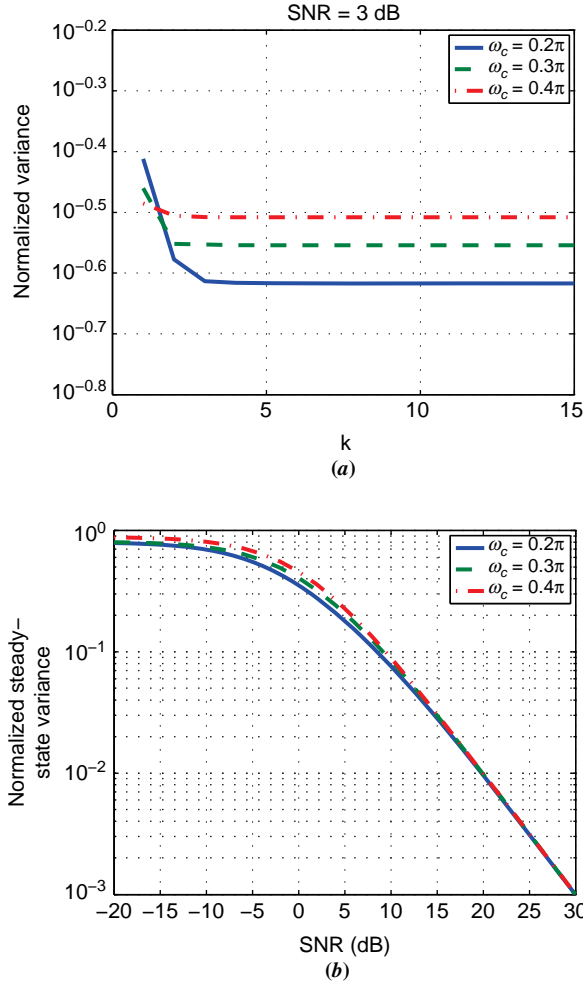


Figure 9.42: (a) Normal variance versus k ; SNR = 3 dB. (b) Normalized steady-state variance versus SNR.

In Figure 9.43a, we plot the normalized variance versus k for SNR = 3 dB, $\omega_c = 0.2\pi$, and $N = 2, 4, 6$, and 8. In Figure 9.43b, we plot the normalized steady-state variance versus SNR for the same values. As we would expect, the steady-state variance decreases as N increases. ■

Example 9.12. We consider the uniform linear array model that we encountered previously in Example 3.2. This model is repeated in Figure 9.44.

We consider a simple case where the signal arrives from broadside ($\psi = 0$) and we sample the complex envelope at the output of each sensor,

$$\tilde{r}_i(k) = \tilde{s}(k) + \tilde{w}_i(k) \quad i = 0, \dots, N-1. \quad (9.426)$$

$$k = 1, 2, \dots$$

Note that the signal samples are the same at each sensor.

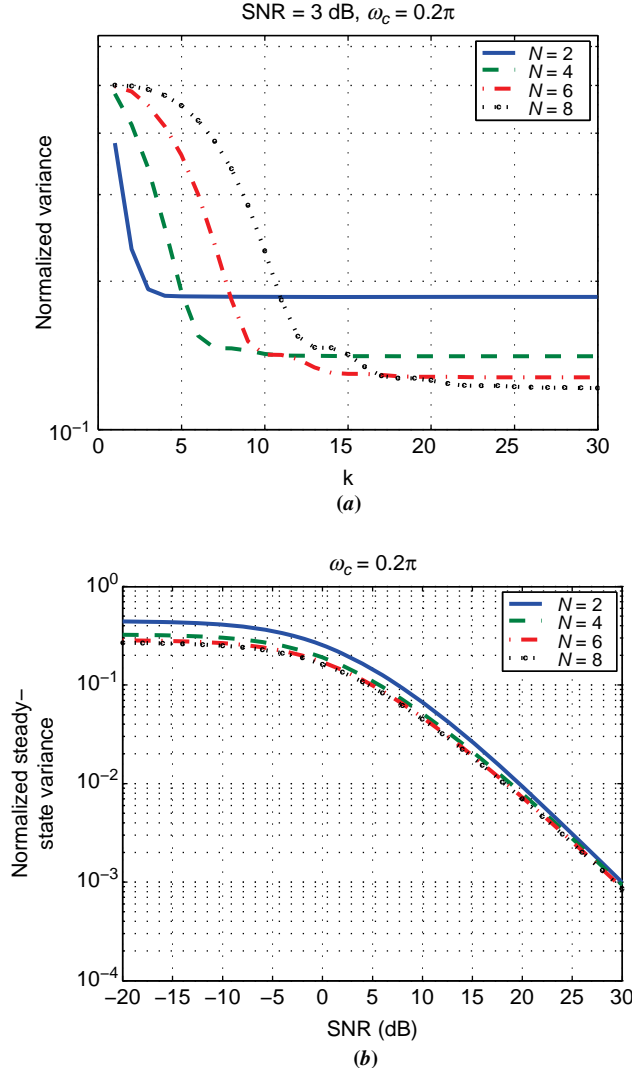


Figure 9.43: (a) Normal variance versus k ; $\text{SNR} = 3 \text{ dB}$, $\omega_c = 0.2\pi$, $N = 2, 4, 6$, and 8 .
(b) Normalized steady-state variance versus SNR; $\omega_c = 0.2\pi$, $N = 2, 4, 6$, and 8 .

We rewrite this in terms of its quadrature components¹⁰

$$\mathbf{r}_i(k) \triangleq \begin{bmatrix} r_{c_i}(k) \\ r_{s_i}(k) \end{bmatrix} = \begin{bmatrix} s_c(k) \\ s_s(k) \end{bmatrix} + \begin{bmatrix} w_{c_i}(k) \\ w_{s_i}(k) \end{bmatrix} \quad (9.427)$$

$$\triangleq \mathbf{s}(k) + \mathbf{w}_i(k). \quad (9.428)$$

The two quadrature components are modeled as statistically independent Gaussian processes with p -dimensional time-invariant state models, $p < N$.

¹⁰We could also solve the problem by introducing the complex Kalman filter.

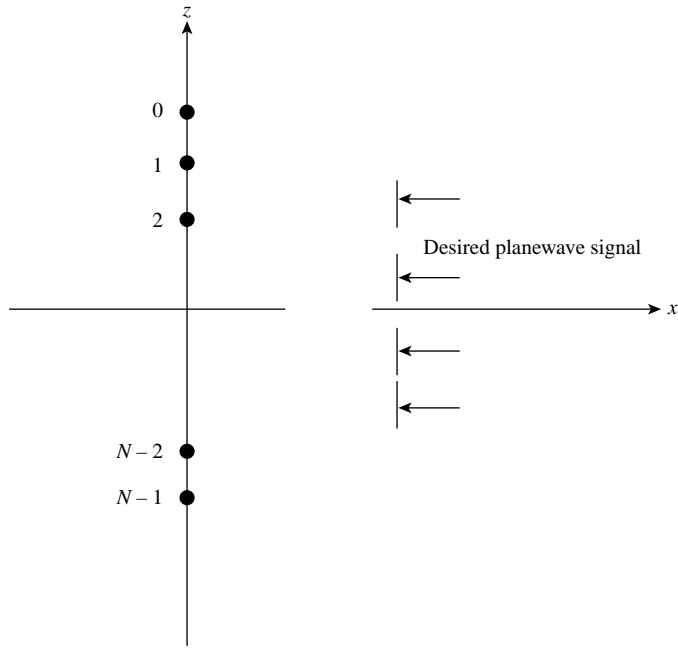


Figure 9.44: Uniform linear array with planewave input.

We define the composite state vector as

$$\mathbf{x}(k) = \begin{bmatrix} \mathbf{x}_c(k) \\ \mathbf{x}_s(k) \end{bmatrix}, \quad (9.429)$$

where \$\mathbf{x}_c(k)\$ and \$\mathbf{x}_s(k)\$ have identical state representations and

$$s_c(k) = \mathbf{C}_1 \mathbf{x}_c(k), \quad (9.430)$$

$$s_s(k) = \mathbf{C}_1 \mathbf{x}_s(k), \quad (9.431)$$

where

$$\mathbf{C}_1 = [1 \ 0 \ \cdots \ 0]. \quad (9.432)$$

Writing the model in vector notation,

$$\mathbf{r}(k) = \begin{bmatrix} \mathbf{r}_c(k) \\ \mathbf{r}_s(k) \end{bmatrix} = \begin{bmatrix} \mathbf{C} & \mathbf{0} \\ \mathbf{0} & \mathbf{C} \end{bmatrix} \begin{bmatrix} \mathbf{x}_c(k) \\ \mathbf{x}_s(k) \end{bmatrix} + \begin{bmatrix} \mathbf{w}_c \\ \mathbf{w}_s \end{bmatrix}, \quad (9.433)$$

where

$$\mathbf{C} = [\mathbf{1} \ \mathbf{0} \ \cdots \ \mathbf{0}] \triangleq [\mathbf{1}_N \ \mathbf{0}_{N,p-1}] \quad (9.434)$$

and

$$E \{ \tilde{\mathbf{w}}(k) \tilde{\mathbf{w}}^H(l) \} = \tilde{\mathbf{R}} \delta_{kl} \quad (9.435)$$

or

$$E \{ \mathbf{w}(k) \mathbf{w}^H(l) \} = \begin{bmatrix} \mathbf{R} & \mathbf{0} \\ \mathbf{0} & \mathbf{R} \end{bmatrix}. \quad (9.436)$$

We see that the estimator and variance equations are block diagonal, so we will consider only one quadrature component. Suppressing the subscript “c” we have

$$\mathbf{r}(k) = \mathbf{C}\mathbf{x}(k) + \mathbf{w}(k), \quad (9.437)$$

where

$$\mathbf{C} = \begin{bmatrix} \mathbf{1}_N & \mathbf{0}_{N,p-1} \end{bmatrix} \quad (9.438)$$

and

$$\mathbf{R} = \sigma_w^2 \mathbf{I}_N. \quad (9.439)$$

We consider the two reduced-rank models. For the reduced-dimension Kalman covariance filter from (9.318), T_p is a $p \times N$ matrix

$$\mathbf{T}_p(k) = \frac{1}{\sigma_w^2} \begin{bmatrix} \mathbf{1}_N^T \\ \mathbf{0}_{N,p-1}^T \end{bmatrix}, \quad (9.440)$$

and from (9.319), $\mathbf{D}(k)$ is a $p \times p$ matrix

$$\mathbf{D}(k) = \frac{1}{\sigma_w^2} \begin{bmatrix} \mathbf{1}_N^T \\ \mathbf{0}_{N,p-1}^T \end{bmatrix} \begin{bmatrix} \mathbf{1}_N & \mathbf{0}_{N,p-1} \end{bmatrix} = \frac{N}{\sigma_w^2} \mathbf{e}_1^T \mathbf{e}_1. \quad (9.441)$$

We preprocess $\mathbf{r}(k)$ to obtain

$$\mathbf{r}_p(k) = \frac{1}{\sigma_w^2} \begin{bmatrix} \mathbf{1}_N^T \\ \mathbf{0}_{N,p-1}^T \end{bmatrix} \mathbf{r}(k) = \frac{1}{\sigma_w^2} \begin{bmatrix} \sum_{i=1}^N r_i(k) \\ \mathbf{0}_{p-1} \end{bmatrix}. \quad (9.442)$$

For $k = 1, \dots$, we predict $\hat{\mathbf{x}}(k|k-1)$ and $\mathbf{P}(k|k-1)$ using (9.328) and (9.329). The covariance matrix updating is

$$\mathbf{P}(k) = \left[\mathbf{I}_p + \mathbf{P}(k|k-1) \frac{N}{\sigma_w^2} \mathbf{e}_1^T \mathbf{e}_1 \right]^{-1} \mathbf{P}(k|k-1), \quad (9.443)$$

and the estimate updating is

$$\begin{aligned}\hat{\mathbf{x}}(k) &= \hat{\mathbf{x}}(k|k-1) + \mathbf{P}(k) \left\{ \begin{bmatrix} \frac{1}{\sigma_w^2} \sum_{i=1}^N r_i(k) \\ \mathbf{0}_{p-1} \end{bmatrix} - \frac{N}{\sigma_w^2} \mathbf{e}_1^T \mathbf{e}_1 \hat{\mathbf{x}}(k|k-1) \right\} \\ &= \hat{\mathbf{x}}(k|k-1) + \mathbf{P}(k) \left\{ \frac{N}{\sigma_w^2} \begin{bmatrix} \frac{1}{N} \sum_{i=1}^N r_i(k) - \hat{x}_1(k|k-1) \\ \mathbf{0}_{p-1} \end{bmatrix} \right\}. \quad (9.444)\end{aligned}$$

For AR(1) model in Example 9.9,

$$T_p(k) = \frac{1}{\sigma_w^2}, \quad (9.445)$$

$$D(k) = \frac{N}{\sigma_w^2}, \quad (9.446)$$

$$r_p(k) = \frac{1}{\sigma_w^2} \sum_{i=1}^N r_i(k), \quad (9.447)$$

$$\hat{x}(k|k-1) = \alpha \hat{x}(k-1), \quad (9.448)$$

$$P(k|k-1) = \alpha^2 P(k-1) + \sigma_u^2, \quad (9.449)$$

$$P(k) = \left[1 + P(k|k-1) \frac{N}{\sigma_w^2} \right]^{-1} P(k|k-1), \quad (9.450)$$

and

$$\hat{x}(k) = \alpha \hat{x}(k-1) + P(k) \left[\frac{1}{\sigma_w^2} \sum_{i=1}^N r_i(k) - \frac{N}{\sigma_w^2} \alpha \hat{x}(k-1) \right] \quad (9.451)$$

or

$$\hat{x}(k) = \alpha \hat{x}(k-1) + P(k) \frac{N}{\sigma_w^2} \left[\frac{1}{N} \sum_{i=1}^N r_i(k) - \alpha \hat{x}(k-1) \right]. \quad (9.452)$$

We see that (9.452) is identical to (9.370), if we define the preprocessed signal

$$r_c(k) = \frac{1}{N} \sum_{i=1}^N r_i(k). \quad (9.453)$$

Thus, the effect of the array is to reduce the effective white noise level from σ_w^2 to σ_w^2/N . Similar results follow for the nondiagonal \mathbf{R} .

We next consider the information filter. The quantities $\mathbf{T}_p(k)$, $\mathbf{D}(k)$, and $\mathbf{r}_p(k)$ are given in (9.440), (9.441), and (9.442), respectively.

From (9.334),

$$\mathbf{A}(k-1) = \mathbf{F}^{-T} \mathbf{J}_B(k-1) \mathbf{F}^{-1}. \quad (9.454)$$

From (9.337),

$$\mathbf{B}(k-1) = \mathbf{A}(k-1) \left[\mathbf{A}(k-1) + \frac{1}{\sigma_u^2} \mathbf{I} \right]^{-1}. \quad (9.455)$$

From (9.338),

$$\mathbf{J}_B(k|k-1) = [\mathbf{I} - \mathbf{B}(k-1)] \mathbf{A}(k-1). \quad (9.456)$$

From (9.340), the Kalman gain is

$$\mathbf{K}(k) = \mathbf{J}_B^{-1}(k) \begin{bmatrix} \mathbf{1}_N^T \\ \mathbf{0}_{N,p-1}^T \end{bmatrix} \begin{bmatrix} \frac{1}{\sigma_w^2} \mathbf{I} \end{bmatrix} \quad (9.457)$$

$$= \frac{1}{\sigma_w^2} \mathbf{J}_B^{-1}(k) \begin{bmatrix} \mathbf{1}_N^T \\ \mathbf{0}_{N,p-1}^T \end{bmatrix}. \quad (9.458)$$

The results in (9.454)–(9.458) are valid for an arbitrary p -dimensional process with constant parameters.

For an AR(1) process in Example 9.9, they reduce to

$$J_B(k) = J_B(k|k-1) + \frac{N}{\sigma_w^2}, \quad (9.459)$$

$$A(k-1) = \frac{1}{\alpha^2} J_B(k-1), \quad (9.460)$$

$$B(k-1) = \frac{1}{\alpha^2} J_B(k-1) \left[\frac{1}{\alpha^2} J_B(k-1) + \frac{1}{\sigma_u^2} \right]^{-1}, \quad (9.461)$$

$$J_B(k|k-1) = [1 - B(k-1)] A(k-1) \quad (9.462)$$

$$= \frac{1}{\alpha^2 \sigma_u^2} J_B(k-1) \left[\frac{1}{\alpha^2} J_B(k-1) + \frac{1}{\sigma_u^2} \right]^{-1}, \quad (9.463)$$

$$\mathbf{K}(k) = \frac{1}{\sigma_w^2} J_B^{-1}(k) \mathbf{1}^T. \quad (9.464)$$

From (9.331),

$$\hat{x}(k) = \alpha \hat{x}(k-1) + J_B^{-1}(k) \frac{N}{\sigma_w^2} \left[\frac{1}{N} \sum_{i=1}^N r_i(k) - \alpha \hat{x}(k-1) \right], \quad (9.465)$$

which is the same as (9.452). ■

In many array applications, there is an interfering signal arriving from a different angle than the desired signal. If that interferer is a white process, we can include it in the \mathbf{R} matrix and the previous results can be used. However, in many cases, it is a narrowband process and we must find a state-variable model for it and treat as colored noise.

We consider the general case of estimation in the presence of colored and white noise in the next section.

9.3.2.4 Estimation in Nonwhite Noise

In this section, we consider the model in which the interference consists of a nonwhite noise component plus white noise.

$$\mathbf{r}(k) = \mathbf{s}(k) + \mathbf{n}_c(k) + \mathbf{w}(k), \quad k = 1, \dots, \quad (9.466)$$

where

$$\mathbf{s}(k) = \mathbf{C}_s(k) \mathbf{x}_s(k) \quad (9.467)$$

and

$$\mathbf{n}_c(k) = \mathbf{C}_n(k) \mathbf{x}_c(k). \quad (9.468)$$

The desired signal is $\hat{s}(k)$. We create a composite state vector, $\mathbf{x}(k)$,

$$\mathbf{x}(k) \triangleq \begin{bmatrix} \mathbf{x}_s(k) \\ \mathbf{x}_n(k) \end{bmatrix}, \quad (9.469)$$

whose state equation is

$$\mathbf{x}(k) = \begin{bmatrix} \mathbf{F}_s(k-1) & \mathbf{0} \\ \mathbf{0} & \mathbf{F}_n(k-1) \end{bmatrix} \mathbf{x}(k-1) + \begin{bmatrix} \mathbf{G}_s(k-1) & \mathbf{0} \\ \mathbf{0} & \mathbf{G}_n(k-1) \end{bmatrix} \begin{bmatrix} \mathbf{u}_s(k-1) \\ \mathbf{u}_n(k-1) \end{bmatrix}, \quad k = 1, \dots, \quad (9.470)$$

where

$$E \left\{ \begin{bmatrix} \mathbf{u}_s(k) \\ \mathbf{u}_n(k) \end{bmatrix} \begin{bmatrix} \mathbf{u}_s(l)^T & \mathbf{u}_n(l)^T \end{bmatrix} \right\} = \begin{bmatrix} \sigma_{us}^2 \delta_{kl} \mathbf{I} & \mathbf{0} \\ \mathbf{0} & \sigma_{un}^2 \delta_{kl} \mathbf{I} \end{bmatrix}. \quad (9.471)$$

We implement the Kalman filter and

$$\hat{\mathbf{s}}(k) = [\mathbf{C}_s(k) \quad \mathbf{0}] \hat{\mathbf{x}}(k). \quad (9.472)$$

We illustrate this with a simple example.

Example 9.13. The signal is the AR(1) process in Example 9.9 with parameters α_s and σ_s^2 . The nonwhite noise is an AR(1) process in Example 9.9 with parameters $\alpha_n = c\alpha_s$, $c \leq 1$, and σ_w^2 . The “ c ” parameter is ratio of the 3 dB bandwidth of the signal to the 3 dB bandwidth of the colored noise. As c decreases, the interference power is spread over a wider bandwidth and is easier to filter out. The white noise variance is $\sigma_w^2 = 1$.

We can compare the spectra of the signal and colored noise processes in Figure 9.4. We assume the system has reached steady state and define

$$\text{SNR} = \sigma_s^2 / \sigma_w^2, \quad (9.473)$$

$$\text{CWR} = \sigma_n^2 / \sigma_w^2. \quad (9.474)$$

Further, \mathbf{P}_∞ is covariance matrix of the composite state vector and that of the signal component is

$$\mathbf{P}_{\infty s} = [1 \quad 0] \mathbf{P}_\infty \begin{bmatrix} 1 \\ 0 \end{bmatrix}. \quad (9.475)$$

In Figure 9.45, we plot $\mathbf{P}_{\infty s}$ versus SNR for various c , with CWR = 10 and $\alpha_s = 0.95$.

In Figure 9.46, we plot $\mathbf{P}_{\infty s}$ versus SNR for various CWR, with $c = 0.5$ and $\alpha_s = 0.95$. ■

9.3.2.5 Sequential Processing of Estimators

In many applications, the measurement covariance matrix $\mathbf{R}(k)$ is diagonal,

$$\mathbf{R}(k) = \text{diag} [R_1(k) \quad R_2(k) \quad \dots \quad R_N(k)]. \quad (9.476)$$

If not, we can preprocess the input using a Cholesky decomposition to diagonalize it.

From (9.248), the measurement equation is

$$\mathbf{r}(k) = \mathbf{C}(k)\mathbf{x}(k) + \mathbf{w}(k). \quad (9.477)$$

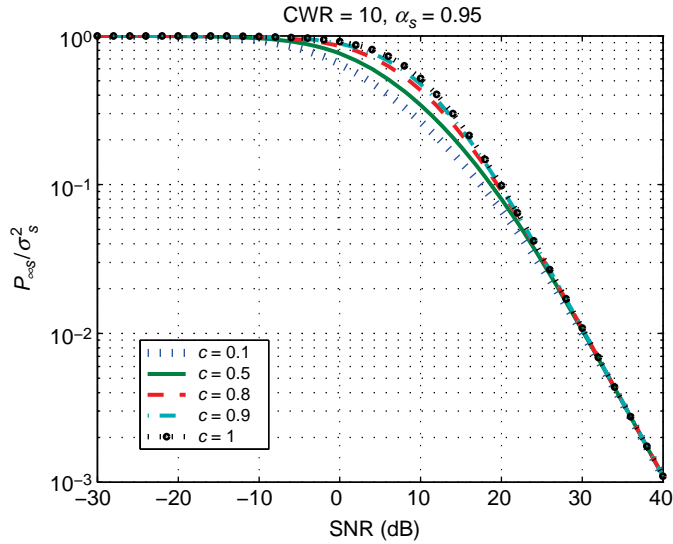


Figure 9.45: Normalized $P_{\infty s}$ versus SNR; $c = 0.1, 0.5, 0.8, 0.9, 1.0, \alpha_s = 0.95$, CWR = 10 dB.

If we identify the rows of $\mathbf{C}(k)$ as $\mathbf{C}_i(k)$, then

$$\mathbf{C}(k) = \begin{bmatrix} \mathbf{C}_1(k) \\ \mathbf{C}_2(k) \\ \vdots \\ \mathbf{C}_N(k) \end{bmatrix}. \quad (9.478)$$

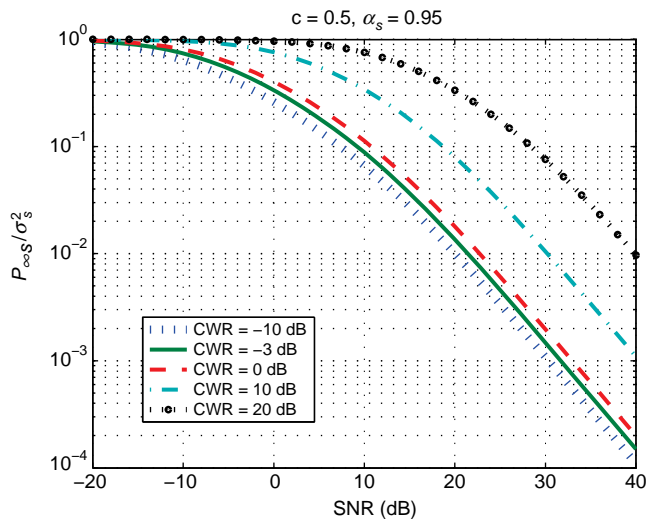


Figure 9.46: Normalized $P_{\infty s}$ versus SNR; $c = 0.5, \alpha_s = 0.95$, CWR = -10 dB, -3 dB, 0 dB, 10 dB, 20 dB.

We can write (9.477) as

$$\mathbf{r}(k) = \begin{bmatrix} r_1(k) \\ r_2(k) \\ \vdots \\ r_N(k) \end{bmatrix} = \begin{bmatrix} \mathbf{C}_1(k)\mathbf{x}(k) + w_1(k) \\ \mathbf{C}_2(k)\mathbf{x}(k) + w_2(k) \\ \vdots \\ \mathbf{C}_N(k)\mathbf{x}(k) + w_N(k) \end{bmatrix}, \quad (9.479)$$

and treat the vector measurement update at time k as a sequence of scalar updates.

We start the iteration with the predicted state $\hat{\mathbf{x}}(k|k-1)$ and the predicted covariance $\mathbf{P}(k|k-1)$. To initialize the sequential updating, we write

$$\hat{\mathbf{x}}(k|k, 0) \triangleq \hat{\mathbf{x}}(k|k-1) \quad (9.480)$$

and

$$\mathbf{P}(k|k, 0) \triangleq \mathbf{P}(k|k-1). \quad (9.481)$$

We index the updates by $i = 1, 2, \dots, N$. The innovation for the i th step is

$$\tilde{r}(k, i) = r_i(k) - \hat{r}(k|k, i), \quad (9.482)$$

where

$$\hat{r}(k|k, i) \triangleq \mathbf{C}_i(k)\hat{\mathbf{x}}(k|k, i). \quad (9.483)$$

The covariance is a scalar

$$\tilde{P}(k, i) = \mathbf{C}_i(k)\mathbf{P}(k|k, i-1)\mathbf{C}_i^T(k) + R_i(k) \quad (9.484)$$

and the gain is a $p \times 1$ vector

$$\mathbf{K}(k, i) = \frac{\mathbf{P}(k|k, i-1)\mathbf{C}_i^T(k)}{\tilde{P}(k, i)}. \quad (9.485)$$

The updated state estimate is

$$\hat{\mathbf{x}}(k|k, i) = \hat{\mathbf{x}}(k|k, i-1) + \mathbf{K}(k, i)[r_i(k) - \mathbf{C}_i(k)\hat{\mathbf{x}}(k|k, i-1)] \quad (9.486)$$

with covariance

$$\mathbf{P}(k|k, i) = \mathbf{P}(k|k, i-1) - \mathbf{K}(k, i)\mathbf{C}_i(k)\mathbf{P}(k|k, i-1), \quad (9.487)$$

whose stable form is

$$\mathbf{P}(k|k, i) = \mathbf{P}(k|k, i-1) - \frac{\mathbf{P}(k|k, i-1)\mathbf{C}_i^T(k)\mathbf{C}_i(k)\mathbf{P}(k|k, i-1)}{\mathbf{C}_i(k)\mathbf{P}(k|k, i-1)\mathbf{C}_i^T(k) + R_i(k)}. \quad (9.488)$$

After the N th iteration, we reach

$$\hat{\mathbf{x}}(k) \triangleq \hat{\mathbf{x}}(k|k, N) \quad (9.489)$$

and

$$\mathbf{P}(k) \triangleq \mathbf{P}(k|k, N). \quad (9.490)$$

Several examples of scalar updates are given in the problems.

9.3.2.6 Square-Root Filters

In many applications of Kalman filters, the propagation of the error covariance matrix using (9.278) or (9.285) results in a matrix, which is not positive definite. The source of problem is the numerical computation of ill-conditioned quantities with finite word lengths.

The Apollo project was one of the first important real-world applications of the Kalman filter and there were problems with the implementation. James Potter, a graduate student in Mathematics at M.I.T. and part-time employee of M.I.T.'s Draper Labs, invented an algorithm that factored the predicted covariance matrix $\mathbf{P}_{k+1|k}$ into

$$\mathbf{P}_{k+1|k} = \mathbf{S}_{k+1|k} \mathbf{S}_{k+1|k}^T, \quad (9.491)$$

and derived a stable algorithm to update $\mathbf{S}_{k+1|k}$. It was used on all of the Apollo missions to the moon and gave birth to a family of *square-root algorithms* that are the most reliable and numerically stable implementation of the Kalman filter (e.g. [Pot65, Bat64], or [BL70]).

The paper by Kaminski et al. [KBS71] has a survey of the early techniques and the evolution of the various algorithms due to Potter [Pot65, Bat64], Schmidt [Sch70], Bellantoni and Dodge [BD67], Dyer and McReynolds [DM69], and Andrews [And68]. In Sections 6.4 and 6.5 of their book [GA08], Grewal and Andrews give a detailed discussion of factorization methods and discuss two forms of square-root filtering: Carlson–Schmidt square-root filter [Car73] and Bierman–Thornton filter [Bie77, Tho76]. In Section 6.6, they discuss other implementations including a square-root information filter. MATLAB files are provided.

To introduce the square-root filter, we develop three algorithms. The first algorithm is the original Potter algorithm, which is easy to explain and illustrates the basic idea. The second algorithm is due to Bierman and provides a useful algorithm for the general case.¹¹ Both of these algorithms consider the covariance version of the Kalman filter. The third algorithm is a square-root version for the information filter.

The Potter algorithm is due to Potter and is given in [Bat64]. It assumes a scalar observation model and no process noise.

We define

$$\mathbf{P}_{k|k-1} = \mathbf{S}_{k|k-1} \mathbf{S}_{k|k-1}^T \quad (9.492)$$

and

$$\mathbf{P}_k = \mathbf{S}_k \mathbf{S}_k^T. \quad (9.493)$$

In the Potter algorithm, $\mathbf{S}_{k|k-1}$ and \mathbf{S}_k are not triangular. Most subsequent square-root algorithms impose that restriction.

The covariance update equation

$$\mathbf{P}_k = \mathbf{P}_{k|k-1} - \mathbf{P}_{k|k-1} \mathbf{C}_k^T \left[\mathbf{C}_k \mathbf{P}_{k|k-1} \mathbf{C}_k^T + \mathbf{R} \right]^{-1} \mathbf{C}_k \mathbf{P}_{k|k-1} \quad (9.494)$$

can be written in a partially factored form as

$$\mathbf{S}_k \mathbf{S}_k^T = \mathbf{S}_{k|k-1} \underbrace{\left\{ \mathbf{I}_p - \mathbf{V} \left[\mathbf{V}^T \mathbf{V} + \mathbf{R} \right]^{-1} \mathbf{V}^T \right\}}_{\triangleq \mathbf{W}_f \mathbf{W}_f^T} \mathbf{S}_{k|k-1}^T, \quad (9.495)$$

¹¹We use subscript notation in both examples to simply the equations.

where

$$\mathbf{V} \triangleq \mathbf{S}_{k|k-1}^T \mathbf{C}_k^T \quad (9.496)$$

is a $p \times N$ matrix.

Then,

$$\mathbf{S}_k \mathbf{S}_k^T \triangleq \mathbf{S}_{k|k-1} \mathbf{W}_f \mathbf{W}_f^T \mathbf{S}_{k|k-1}^T, \quad (9.497)$$

so

$$\mathbf{S}_k = \mathbf{S}_{k|k-1} \mathbf{W}_f. \quad (9.498)$$

Now assume \mathbf{R} is a scalar (or that we use sequential scalar updates). Then the matrix to be factored is

$$\mathbf{I}_p - \frac{\mathbf{v}\mathbf{v}^T}{R + |\mathbf{v}|^2}, \quad (9.499)$$

where \mathbf{v} is $p \times 1$.

If we define

$$s = \frac{1}{R + |\mathbf{v}|^2}, \quad (9.500)$$

then we can show that

$$\mathbf{I}_p - s\mathbf{v}\mathbf{v}^T = (\mathbf{I}_p - \gamma\mathbf{v}\mathbf{v}^T)(\mathbf{I}_p - \gamma\mathbf{v}\mathbf{v}^T), \quad (9.501)$$

where

$$\gamma = \frac{1 + \sqrt{1 - s|\mathbf{v}|^2}}{|\mathbf{v}|^2} = \frac{1 + \sqrt{R/(R + |\mathbf{v}|^2)}}{|\mathbf{v}|^2}. \quad (9.502)$$

Thus,

$$\mathbf{S}_k = \mathbf{S}_{k|k-1} [\mathbf{I}_p - \gamma\mathbf{v}\mathbf{v}^T]. \quad (9.503)$$

Although we can initialize \mathbf{S}_k with \mathbf{S}_0 as a lower triangular Cholesky factor, the triangularity is not maintained in the Potter algorithm. The triangularity is maintained in most other square-root algorithms.

Kaminski et al. [KBS71] discuss various extensions of Potter's algorithm to include matrix observations and process noise.

We provide one version of these square-root algorithms. Our derivation is taken from Moon and Sterling [MS00]. Earlier references include [Bie77], [AM79], and [VD86].

We define the Cholesky factorization of $\mathbf{P}_{k+1|k}$ as

$$\mathbf{P}_{k+1|k} = \mathbf{S}_{k+1|k} \mathbf{S}_{k+1|k}^T, \quad (9.504)$$

where $\mathbf{S}_{k+1|k}$ is the “square root” of $\mathbf{P}_{k+1|k}$. The factorization is done so that $\mathbf{S}_{k+1|k}$ is a lower triangular matrix.

We summarize the Kalman equations that we use as a starting point:

$$\tilde{\mathbf{P}}_k = \mathbf{C}_k \mathbf{P}_{k|k-1} \mathbf{C}_k^T + \mathbf{R}_k \triangleq \mathbf{W}_k, \quad (9.505)$$

$$\hat{\mathbf{x}}_{k+1|k} = \mathbf{F}_k \hat{\mathbf{x}}_k. \quad (9.506)$$

Using (9.284), we can write as

$$\hat{\mathbf{x}}_{k+1|k} = \mathbf{F}_k \left\{ \hat{\mathbf{x}}_{k|k-1} + \mathbf{K}_k [\mathbf{r}_k - \mathbf{C}_k \hat{\mathbf{x}}_{k|k-1}] \right\} \quad (9.507)$$

$$= \mathbf{F}_k \hat{\mathbf{x}}_{k|k-1} + \mathbf{F}_k \mathbf{P}_{k|k-1} \mathbf{C}_k^T \tilde{\mathbf{P}}_k^{-1} [\mathbf{r}_k - \mathbf{C}_k \hat{\mathbf{x}}_{k|k-1}] \quad (9.508)$$

and

$$\mathbf{P}_{k+1|k} = \mathbf{F}_k [\mathbf{I} - \mathbf{P}_{k|k-1} \mathbf{C}_k^T \tilde{\mathbf{P}}_k^{-1} \mathbf{C}_k] \mathbf{P}_{k|k-1} \mathbf{F}_k^T + \tilde{\mathbf{Q}}_k, \quad (9.509)$$

where $\tilde{\mathbf{Q}}_k \triangleq \mathbf{G}_k \mathbf{Q}_k \mathbf{G}_k^T$ is assumed to be positive semidefinite.

The steps in square-root Kalman filter are

1. Form the matrix

$$\mathbf{X}_k = \begin{bmatrix} \mathbf{R}_k^{1/2} & \mathbf{C}_k \mathbf{S}_{k|k-1} & \mathbf{0} \\ \mathbf{0} & \mathbf{F}_k \mathbf{S}_{k|k-1} & \tilde{\mathbf{Q}}_k^{1/2} \end{bmatrix}, \quad (9.510)$$

where the square roots are Cholesky factors. In many cases, \mathbf{R}_k is diagonal, or we can use sequential scalar updating.

2. Triangularize \mathbf{X}_k using an orthogonal matrix \mathbf{U}_k , that is, find an orthogonal matrix \mathbf{U}_k such that $\mathbf{Y}_k = \mathbf{X}_k \mathbf{U}_k$ is lower triangular. Then, identify the following components \mathbf{W}_k , \mathbf{B}_k , and $\mathbf{S}_{k+1|k}$:

$$\mathbf{X}_k \mathbf{U}_k = \begin{bmatrix} \mathbf{R}_k^{1/2} & \mathbf{C}_k \mathbf{S}_{k|k-1} & \mathbf{0} \\ \mathbf{0} & \mathbf{F}_k \mathbf{S}_{k|k-1} & \tilde{\mathbf{Q}}_k^{1/2} \end{bmatrix} \mathbf{U}_k = \begin{bmatrix} \mathbf{W}_k^{1/2} & \mathbf{0} & \mathbf{0} \\ \mathbf{B}_k & \mathbf{S}_{k+1|k} & \mathbf{0} \end{bmatrix}. \quad (9.511)$$

We use a Householder transformation to find \mathbf{U}_k . The Householder transformation is discussed in a number of references (e.g. [Van02]).

3. Update the estimate

$$\hat{\mathbf{x}}_{k+1|k} = \mathbf{F}_k \hat{\mathbf{x}}_{k|k-1} + \mathbf{B}_k \mathbf{W}_k^{-1/2} (\mathbf{r}_k - \mathbf{C}_k \hat{\mathbf{x}}_{k|k-1}). \quad (9.512)$$

To verify (9.512), we

$$\mathbf{X}_k \mathbf{X}_k^T = [\mathbf{X}_k \mathbf{U}_k] [\mathbf{X}_k \mathbf{U}_k]^T = \begin{bmatrix} \mathbf{R}_k + \mathbf{C}_k \mathbf{S}_{k|k-1} \mathbf{S}_{k|k-1}^T \mathbf{C}_k^T & \mathbf{C}_k \mathbf{S}_{k|k-1} \mathbf{S}_{k|k-1}^T \mathbf{F}_k^T \\ \mathbf{F}_k \mathbf{S}_{k|k-1} \mathbf{S}_{k|k-1}^T \mathbf{C}_k^T & \mathbf{F}_k \mathbf{S}_{k|k-1} \mathbf{S}_{k|k-1}^T \mathbf{F}_k^T + \tilde{\mathbf{Q}}_k \end{bmatrix} \quad (9.513)$$

$$= \begin{bmatrix} \mathbf{R}_k + \mathbf{C}_k \mathbf{P}_{k|k-1} \mathbf{C}_k^T & \mathbf{C}_k \mathbf{P}_{k|k-1} \mathbf{F}_k^T \\ \mathbf{F}_k \mathbf{P}_{k|k-1} \mathbf{C}_k^T & \mathbf{F}_k \mathbf{P}_{k|k-1} \mathbf{F}_k^T + \tilde{\mathbf{Q}}_k \end{bmatrix}. \quad (9.514)$$

We can also write (9.514) using the right-hand side of (9.511)

$$\mathbf{X}_k \mathbf{X}_k^T = \begin{bmatrix} \mathbf{W}_k & \mathbf{W}_k^{1/2} \mathbf{B}_k^T \\ \mathbf{B}_k \mathbf{W}_k^{1/2} & \mathbf{B}_k \mathbf{B}_k^T + \mathbf{S}_{k+1|k} \mathbf{S}_{k+1|k}^T \end{bmatrix}. \quad (9.515)$$

Evaluating the matrices in the lower left corner of (9.514) and (9.515) gives

$$\mathbf{B}_k \mathbf{W}_k^{1/2} = \mathbf{F}_k \mathbf{P}_{k|k-1} \mathbf{C}_k^T. \quad (9.516)$$

Therefore,

$$\mathbf{B}_k \mathbf{W}_k^{-1/2} = \mathbf{F}_k \mathbf{P}_{k|k-1} \mathbf{C}_k^T \mathbf{W}_k^{-1} \quad (9.517)$$

so that (9.512) and (9.508) are identical.

From the lower right corner of (9.514) and (9.515)

$$\mathbf{B}_k \mathbf{B}_k^T + \mathbf{S}_{k+1|k} \mathbf{S}_{k+1|k}^T = \mathbf{F}_k \mathbf{P}_{k|k-1} \mathbf{F}_k^T + \tilde{\mathbf{Q}}_k \quad (9.518)$$

or

$$\mathbf{S}_{k+1|k} \mathbf{S}_{k+1|k}^T = \mathbf{F}_k \mathbf{P}_{k|k-1} \mathbf{F}_k^T + \tilde{\mathbf{Q}}_k - \mathbf{B}_k \mathbf{B}_k^T. \quad (9.519)$$

Using (9.516), (9.519) can be written as

$$\mathbf{S}_{k+1|k} \mathbf{S}_{k+1|k}^T = \mathbf{F}_k \mathbf{P}_{k|k-1} \mathbf{F}_k^T + \tilde{\mathbf{Q}}_k - \mathbf{F}_k \mathbf{P}_{k|k-1} \mathbf{C}_k^T \mathbf{W}_k^{-1} \mathbf{C}_k \mathbf{P}_{k|k-1} \mathbf{F}_k^T \quad (9.520)$$

$$= \mathbf{F}_k [\mathbf{I} - \mathbf{P}_{k|k-1} \mathbf{C}_k^T \mathbf{W}_k^{-1} \mathbf{C}_k] \mathbf{P}_{k|k-1} \mathbf{F}_k^T + \tilde{\mathbf{Q}}_k. \quad (9.521)$$

which shows the $\mathbf{S}_{k+1|k}$ is the factor of $\mathbf{P}_{k+1|k}$ in (9.509).

This completes the derivation.

The square-root information filter (SRIF) was developed in 1969 for use in JPL's Mariner 10 missions to Venus (e.g., [Bie77]).

We describe a SRIF contained in [AM79]. Recall that $\mathbf{P}_k = \mathbf{S}_k \mathbf{S}_k^T$. The measurement update for the information equation is

$$\begin{bmatrix} \mathbf{S}_k^{-1} \\ \mathbf{0} \end{bmatrix} = \mathbf{T} \begin{bmatrix} \mathbf{S}_{k|k-1}^{-1} \\ \mathbf{R}_k^{-1/2} \mathbf{C}_k^T \end{bmatrix}, \quad (9.522)$$

where \mathbf{T} is an orthogonal transformation such that the right-hand side of (9.522) is upper triangular.

The update for the estimate is

$$\begin{bmatrix} \hat{\mathbf{b}}_{k|k}^{-1} \\ * \end{bmatrix} = \mathbf{T} \begin{bmatrix} \hat{\mathbf{b}}_{k|k-1}^{-1} \\ \mathbf{R}_k^{-1/2} \mathbf{r}_k \end{bmatrix}, \quad (9.523)$$

where

$$\hat{\mathbf{b}}_{k|k} = \mathbf{S}_k^{-1} \hat{\mathbf{x}}_{k|k} \quad (9.524)$$

and

$$\hat{\mathbf{b}}_{k|k-1} = \mathbf{S}_{k|k-1}^{-1} \hat{\mathbf{x}}_{k|k-1}. \quad (9.525)$$

The time-update equation is

$$\begin{bmatrix} \left[[\mathbf{Q}_k^{-1} + \mathbf{G}_k^T \mathbf{A}_k \mathbf{G}_k]^{1/2} \right]^T & \mathbf{B}_k^T \\ \mathbf{0} & \mathbf{S}_{k+1|k}^{-1} \end{bmatrix} = \bar{\mathbf{T}} \begin{bmatrix} \left[\mathbf{Q}_k^{1/2} \right]^{-1} & \mathbf{0} \\ \mathbf{S}_k^{-1} \mathbf{F}_k^{-1} \mathbf{G}_k & \mathbf{S}_k^{-1} \mathbf{F}_k^{-1} \end{bmatrix}, \quad (9.526)$$

where $\bar{\mathbf{T}}$ is orthogonal and produces the upper triangular form in (9.526). The estimate update is

$$\begin{bmatrix} * \\ \hat{\mathbf{b}}_{k+1|k} \end{bmatrix} = \bar{\mathbf{T}} \begin{bmatrix} \mathbf{0} \\ \hat{\mathbf{b}}_{k|k} \end{bmatrix}. \quad (9.527)$$

These equations can also be written in combined form as

$$\hat{\mathbf{T}} \begin{bmatrix} \left[\mathbf{Q}_k^{1/2} \right]^{-1} & \mathbf{0} & \mathbf{0} \\ \mathbf{S}_k^{-1} \mathbf{F}_k^{-1} \mathbf{G}_k & \mathbf{S}_k^{-1} \mathbf{F}_k^{-1} & \hat{\mathbf{b}}_{k|k} \\ 0 & \mathbf{R}_{k+1}^{-1/2} \mathbf{C}_{k+1}^T & \mathbf{R}_{k+1}^{-1/2} \mathbf{r}_{k+1}^T \end{bmatrix} = \begin{bmatrix} \left[\mathbf{Q}_k^{-1} + \mathbf{G}_k^T \mathbf{A}_k \mathbf{G}_k \right]^{T/2} & \mathbf{B}_k^T & * \\ \mathbf{0} & \mathbf{S}_{k+1}^{-1} & \hat{\mathbf{b}}_{k+1|k+1} \\ \mathbf{0} & \mathbf{0} & * \end{bmatrix}. \quad (9.528)$$

Several examples are given in the problems.

There have been a number of articles comparing the various forms of the Kalman in terms of computational complexity and sensitivity to numerical errors (e.g. [KBS71, Men71, BT77, Bie77], and [VD86]).

9.3.2.7 Divergence

In many applications the Kalman filters may have to operate for an extended period of time. In some of these cases, in particular, orbital navigation systems, a phenomenon called divergence occurs. The errors in the estimates are much larger than predicted by model's covariance equations [Gun63, SST67]. These errors may be caused by inaccuracies in density and gravity models, nonlinearities, biases, and round-off and truncation errors in the calculations. Jazwinski [Jaz70] and Fitzgerald [Fit71] provide excellent discussions of the problem and discuss several solutions to the problem. Jazwinski's discussion includes references to some of the earlier research on the problem. We will introduce the problem and consider a simple example, but the interested reader should consult the above references.

The two techniques to solve the problem most commonly used in applications are

1. Enhance the process noise covariance \mathbf{Q} by adding a diagonal component to the \mathbf{Q} matrix. We refer to this as remedy *I* or *diagonal loading* \mathbf{Q} (\mathbf{Q}_{DL}).
2. Because divergence is a large sample problem, another approach is to insert some type of memory limitation technique. Jazwinski [Jaz70] discusses finite memories and Sorenson and Sacks [SS71] discuss exponential fading memories.

In this case,

$$\mathbf{P}(k|k-1) = \{ \mathbf{F}(k-1) \mathbf{P}(k-1) \mathbf{F}(k-1)^T \} \exp(c_f) + \mathbf{G}(k-1) \mathbf{Q}(k-1) \mathbf{G}(k-1)^T, \quad (9.529)$$

where $c_f \geq 0$ is a constant fading coefficient. It has the effect of increasing $\mathbf{P}(k-1)$,

$$\mathbf{P}_f(k-1) = \exp(c_f) \mathbf{P}(k-1) \quad (9.530)$$

before updating.

We refer to this as remedy *II* or *exponential fading memory*.

We consider a simple example due to Jazwinski [Jaz70] (e.g. [Fit71, Men95]).

Example 9.14. The actual state equations are

$$x(k) = x(k - 1) + b, \quad (9.531)$$

$$r(k) = x(k) + w(k), \quad (9.532)$$

where b is a small bias that we neglect in the model.

The model equations are

$$x_m(k) = x_m(k - 1), \quad (9.533)$$

$$r(k) = x_m(k) + w(k), \quad (9.534)$$

where $w(k) \sim N(0, \sigma_w^2)$. Note that there is no $u(k - 1)$ term in (9.533) ($\mathbf{Q} = \sigma_u^2 = 0$), so this is really a parameter estimation problem. Then,¹²

$$\hat{x}_m(k) = \hat{x}_m(k - 1) + K(k)[r(k) - \hat{x}_m(k - 1)], \quad (9.535)$$

where

$$K(k) = \frac{P(0)}{kP(0) + \sigma_w^2}, \quad (9.536)$$

which goes to zero as $k \rightarrow \infty$ so that $\hat{x}_m(k) \rightarrow \hat{x}_m(k - 1)$ and $P_m(k) \rightarrow P_m(k - 1)$.

The actual error is

$$\tilde{x}(k) = x(k) - \hat{x}_m(k). \quad (9.537)$$

One can show that

$$\tilde{x}(k) = \frac{\sigma_w^2}{kP(0) + \sigma_w^2} \tilde{x}(0) - \frac{P(0)}{kP(0) + \sigma_w^2} \sum_{i=1}^k w(i) + \frac{[k(k-1)/2]P(0) + k\sigma_w^2}{kP(0) + \sigma_w^2} b. \quad (9.538)$$

As $k \rightarrow \infty$, $\tilde{x}(k) \rightarrow \infty$ because of the last term in (9.538).

We consider two alternative remedies.

1. We diagonally load the \mathbf{Q} matrix. In this case, we replace (9.533) by

$$x_m(k) = x_m(k - 1) + u(k - 1), \quad (9.539)$$

where $u(k) \sim N(0, \sigma_u^2)$.

We now have a familiar AR(1) problem (Example 9.9).

For the model in (9.539), the Kalman model equations are

$$\hat{x}(k|k - 1) = \hat{x}(k - 1), \quad (9.540)$$

$$P(k|k - 1) = P(k - 1) + \sigma_u^2, \quad (9.541)$$

$$\hat{r}(k|k - 1) = \hat{x}(k|k - 1), \quad (9.542)$$

$$\tilde{P}(k) = P(k|k - 1) + \sigma_w^2, \quad (9.543)$$

$$K(k) = P(k|k - 1)\tilde{P}^{-1}(k), \quad (9.544)$$

$$\hat{x}(k) = \hat{x}(k - 1) + K(k)[r(k) - \hat{x}(k - 1)], \quad (9.545)$$

$$P(k) = [1 - K(k)]P(k|k - 1). \quad (9.546)$$

We must choose a value for σ_u^2 . We would like to chose it so that the actual MSE is minimized. If we assume that the system has reached steady state, then we can find an analytic expression for the optimum σ_u^2 to minimize the actual variance; as we would expect, it depends on “ b ” and σ_w^2 and these values shall be used to optimize σ_u^2 .

¹²We leave the derivation as a problem.

2. For the exponential fading memory algorithm, we use

$$P(k|k-1) = \exp(c_f)P(k-1). \quad (9.547)$$

Once again, we choose “ b ” and σ_w^2 and find the optimum value of c_f . The use of exponential fading memory is analogous to the weighted least squares algorithm in Section 5.2.9.1.

In Figure 9.47a, we show typical realizations of the true track, the estimate using the nominal model (9.540) (no correction), and the estimate using diagonal loading Q_{DL} with $\sigma_u^2 = 0.25$ and $b = 0.2$. The initial conditions are $\hat{x}_m(0) = 0$, $x(0) = 0$, and $P(0) = 0$. The noise variance $\sigma_w^2 = 1$.

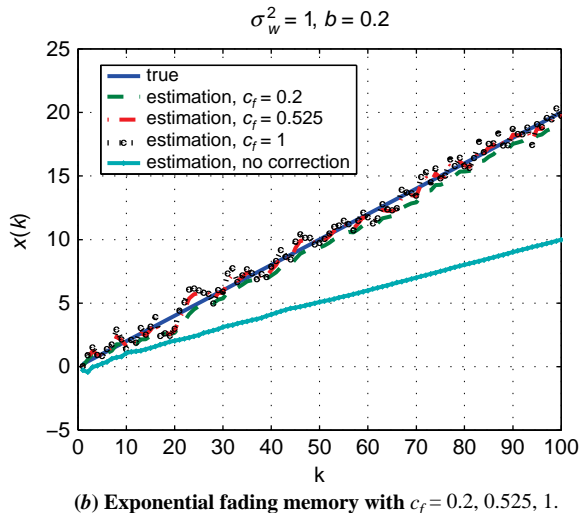
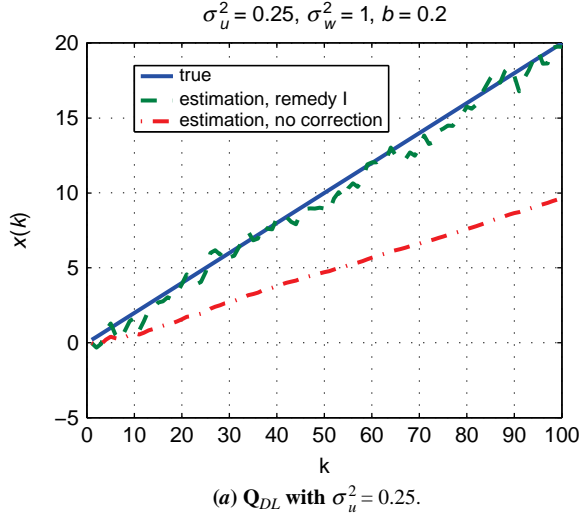


Figure 9.47: Typical realizations for bias $b = 0.2$. True values of $x(k)$, and estimated values $\hat{x}(k)$ with and without correction.

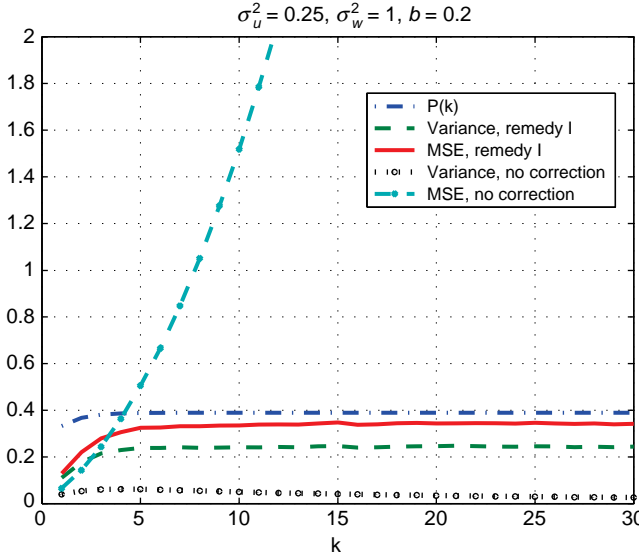


Figure 9.48: $P(k)$, MSE, and variance using model with no correction, and MSE and variance for diagonal loading Q_{DL} with $\sigma_u^2 = 0.25$.

In Figure 9.47b, we show the same quantities using exponential fading with $c_f = 0.2, 0.525, 1.0$. We see that the uncorrected estimate is diverging.

In Figure 9.48, we plot $P(k)$ from (9.546) and the actual variance and MSE with no correction. As expected from (9.538), the MSE becomes unbounded. We also show the MSE and variance using Q_{DL} with $\sigma_u^2 = 0.25$. We see that the estimator approaches steady state at $k = 7$ with an MSE of 0.3372.

In Figure 9.49, we plot the MSE, bias, and variance for the no correction case and the exponential fading model with $c_f = 0.2, 0.525$, and 1. The steady-state results are an MSE of 0.3361.

By using either of these two remedies, we have gained protection against an unknown bias that is not included in the model. To judge the cost of this protection, we compute the variance and MSE when $b = 0$. The resulting estimator is unbiased and the variance is plotted in Figure 9.50. We see that both remedies approach a steady-state variance of about 0.25, while the uncorrected model variance goes to zero.

One can show that, as b increases, the optimum values of σ_u^2 and c_f increase and the resulting MSEs increase. For example, for $b = 0.5$,

$$\text{opt } \sigma_u^2 = 1.1 \quad \text{MSE} = 0.5335 \quad (9.548)$$

$$\text{opt } c_f = 0.875 \quad \text{MSE} = 0.5312 \quad (9.549)$$

and for $b = 1.0$,

$$\text{opt } \sigma_u^2 = 2.07 \quad \text{MSE} = 0.6983 \quad (9.550)$$

$$\text{opt } c_f = 1.35 \quad \text{MSE} = 0.7019. \quad (9.551)$$

These results are specific to this example and cannot be used to compare diagonal loading and exponential fading memory algorithms for the more general case.

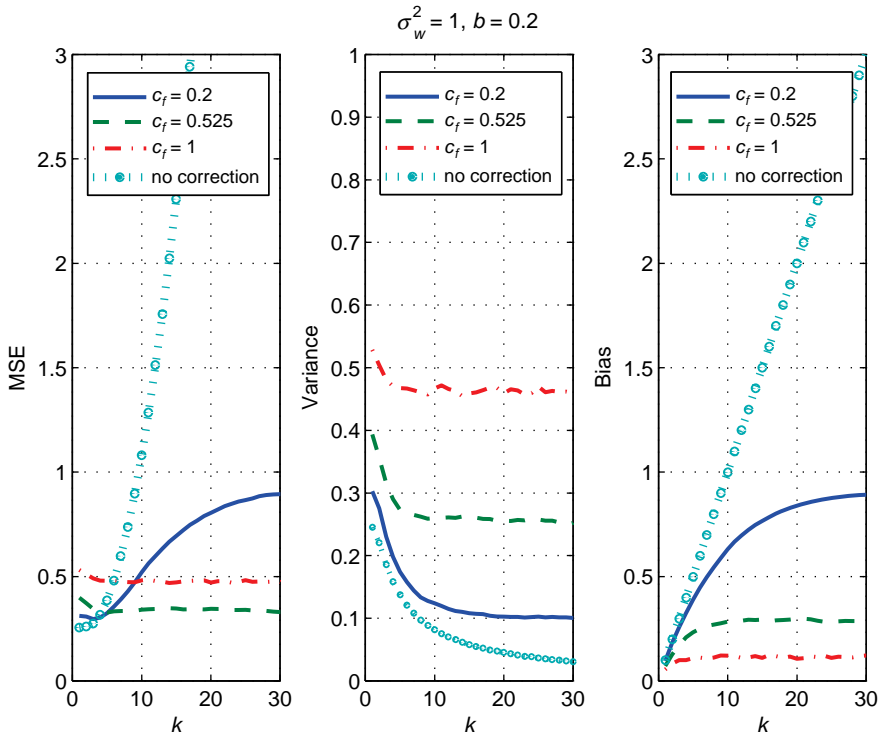


Figure 9.49: MSE, bias, and variance for model with no correction and for exponential memory with $c_f = 0.2, 0.525$, and 1.0 .

The reason that divergence occurred was that σ_u^2 was zero in our model. Whenever we have an ARMA signal model, we will not encounter the divergence phenomenon. Both Jazwinski [Jaz70] and Fitzgerald [Fit71] discuss the general case. ■

In the next section, we discuss the more general problem of model mismatch and sensitivity.

9.3.2.8 Sensitivity and Model Mismatch

As we emphasized in earlier discussions, it is important to investigate the sensitivity of the Kalman filter to model mismatch. In Section “Model Mismatch,” we develop a general approach for the case in which the actual state model and observation model are different from the one assumed to design the filter. In Section “Sensitivity,” we briefly discuss an approach that measures sensitivity by differentiating with respect to the parameters in the variance matrices. In Section “Summary,” we summarize our results.

Model Mismatch.¹³ We assume that the covariance version of Kalman filter has been designed based on the model matrices, \mathbf{F}_k , \mathbf{G}_k , \mathbf{C}_k , \mathbf{Q}_k , \mathbf{R}_k , and Π_0 . The actual system can

¹³Our equations are taken from p. 357 of [KSH00]. Similar results appeared earlier in various references (e.g., Sage and Melsa [SM71]).

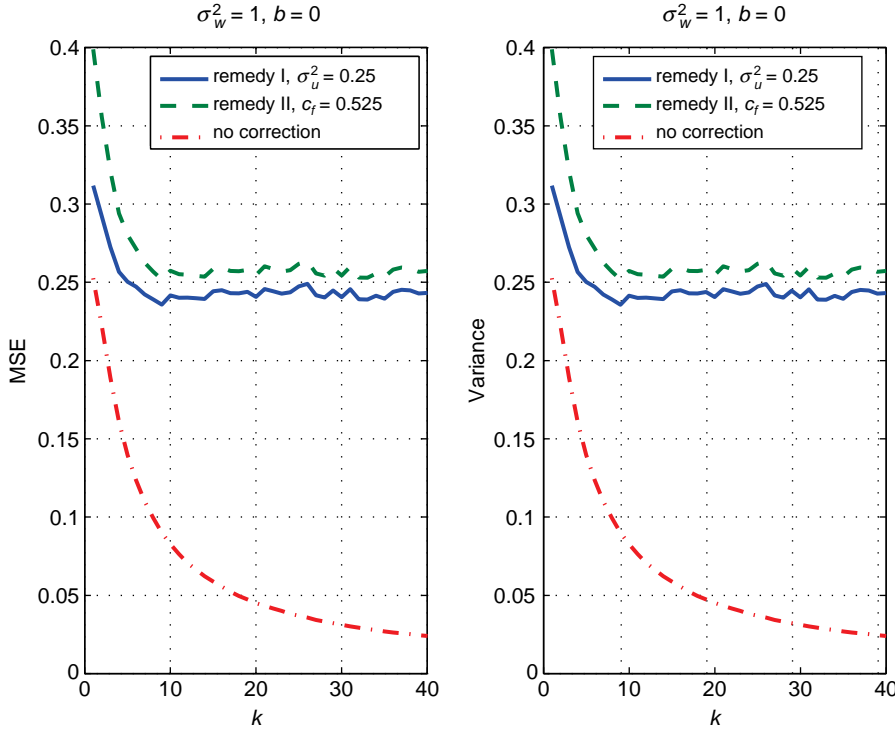


Figure 9.50: MSE and variance of estimators for $b = 0$; no correction, Q_{DL} with $\sigma_u^2 = 0.25$, exponential weighting with $c_f = 0.525$.

be described by the state and measurement vectors \mathbf{x}_k^{ac} and \mathbf{r}_k^{ac} and the noise vectors \mathbf{u}_k^{ac} and \mathbf{w}_k^{ac} , which are associated with the matrices, $\bar{\mathbf{F}}_k$, $\bar{\mathbf{G}}_k$, $\bar{\mathbf{C}}_k$, $\bar{\mathbf{Q}}_k$, $\bar{\mathbf{R}}_k$, and $\bar{\Pi}_0$. Thus,

$$\mathbf{x}_k^{ac} = \bar{\mathbf{F}}_{k-1}\mathbf{x}_{k-1}^{ac} + \bar{\mathbf{G}}_{k-1}\mathbf{u}_{k-1}^{ac}, \quad k = 1, 2, \dots, \quad (9.552)$$

$$\mathbf{r}_k^{ac} = \bar{\mathbf{C}}_k\mathbf{x}_k^{ac} + \mathbf{w}_k^{ac}, \quad k = 1, 2, \dots. \quad (9.553)$$

We assume that \mathbf{u}_k^{ac} , \mathbf{w}_k^{ac} , and \mathbf{x}_0^{ac} are zero-mean uncorrelated random variables with

$$\mathbf{u}_k^{ac}\mathbf{u}_j^{acT} = \bar{\mathbf{Q}}_k\delta_{kj}, \quad (9.554)$$

$$\mathbf{w}_k^{ac}\mathbf{w}_j^{acT} = \bar{\mathbf{R}}_k\delta_{kj}, \quad (9.555)$$

and

$$\mathbf{x}_0^{ac}\mathbf{x}_0^{acT} = \bar{\Pi}_0. \quad (9.556)$$

We also write

$$\bar{\mathbf{F}}_k = \mathbf{F}_k + \Delta\mathbf{F}_k, \quad (9.557)$$

$$\bar{\mathbf{G}}_k = \mathbf{G}_k + \Delta\mathbf{G}_k, \quad (9.558)$$

$$\bar{\mathbf{C}}_k = \mathbf{C}_k + \Delta\mathbf{C}_k. \quad (9.559)$$

The Kalman filter that is implemented is

$$\hat{\mathbf{x}}_k = \mathbf{F}_{k-1} \hat{\mathbf{x}}_{k-1} + \mathbf{K}_k \tilde{\mathbf{r}}_k^{\text{ac}}, \quad (9.560)$$

where

$$\tilde{\mathbf{r}}_k^{\text{ac}} = \mathbf{r}_k^{\text{ac}} - \mathbf{C}_k \hat{\mathbf{x}}_{k|k-1} \quad (9.561)$$

and \mathbf{K}_k , \mathbf{R}_k , and \mathbf{P}_k are computed using the assumed original model.

We now define

$$\tilde{\mathbf{x}}_k^{\text{ac}} = \mathbf{x}_k^{\text{ac}} - \hat{\mathbf{x}}_k, \quad (9.562)$$

$$\mathbf{P}_k^{\text{ac}} = E \left\{ \tilde{\mathbf{x}}_k^{\text{ac}} \tilde{\mathbf{x}}_k^{\text{ac}T} \right\}, \quad (9.563)$$

$$\boldsymbol{\Pi}_k^{\text{ac}} = E \left\{ \mathbf{x}_k^{\text{ac}} \mathbf{x}_k^{\text{ac}T} \right\}, \quad (9.564)$$

$$\mathbf{P}_k^c = E \left\{ \tilde{\mathbf{x}}_k^{\text{ac}} \mathbf{x}_k^{\text{ac}T} \right\}. \quad (9.565)$$

Using (9.557) in (9.552) gives

$$\mathbf{x}_k^{\text{ac}} = (\mathbf{F}_{k-1} + \Delta \mathbf{F}_{k-1}) \mathbf{x}_{k-1}^{\text{ac}} + \bar{\mathbf{G}}_{k-1} \mathbf{u}_{k-1}^{\text{ac}}. \quad (9.566)$$

Using (9.552) and (9.553) in (9.560) gives

$$\hat{\mathbf{x}}_k = \mathbf{F}_{k-1} \hat{\mathbf{x}}_{k-1} + \mathbf{K}_k (\mathbf{r}_k^{\text{ac}} - \mathbf{C}_k \mathbf{F}_{k-1} \hat{\mathbf{x}}_{k-1}) \quad (9.567)$$

$$= \mathbf{F}_{k-1} \hat{\mathbf{x}}_{k-1} + \mathbf{K}_k \bar{\mathbf{C}}_k \bar{\mathbf{F}}_{k-1} \mathbf{x}_{k-1}^{\text{ac}} + \mathbf{K}_k \bar{\mathbf{C}}_k \bar{\mathbf{G}}_{k-1} \mathbf{u}_{k-1}^{\text{ac}} + \mathbf{K}_k \mathbf{w}_k^{\text{ac}} - \mathbf{K}_k \mathbf{C}_k \mathbf{F}_{k-1} \hat{\mathbf{x}}_{k-1}. \quad (9.568)$$

We define

$$\mathbf{F}_{p,k-1} \triangleq \mathbf{F}_{k-1} - \mathbf{K}_k \mathbf{C}_k \mathbf{F}_{k-1}. \quad (9.569)$$

Then, (9.568) can be written as

$$\begin{aligned} \hat{\mathbf{x}}_k &= \mathbf{F}_{p,k-1} \hat{\mathbf{x}}_{k-1} + (\mathbf{K}_k \mathbf{C}_k \mathbf{F}_{k-1} + \mathbf{K}_k \Delta \mathbf{C}_k \mathbf{F}_{k-1} + \mathbf{K}_k \mathbf{C}_k \Delta \mathbf{F}_{k-1} + \mathbf{K}_k \Delta \mathbf{C}_k \Delta \mathbf{F}_{k-1}) \mathbf{x}_{k-1}^{\text{ac}} \\ &\quad + \mathbf{K}_k \bar{\mathbf{C}}_k \bar{\mathbf{G}}_{k-1} \mathbf{u}_{k-1}^{\text{ac}} + \mathbf{K}_k \mathbf{w}_k^{\text{ac}}. \end{aligned} \quad (9.570)$$

Using (9.566) and (9.570), the error $\tilde{\mathbf{x}}_k^{\text{ac}} \triangleq \mathbf{x}_k^{\text{ac}} - \hat{\mathbf{x}}_k$ can be written as

$$\begin{aligned} \tilde{\mathbf{x}}_k^{\text{ac}} &= (\mathbf{F}_{k-1} - \mathbf{K}_k \mathbf{C}_k \mathbf{F}_{k-1}) \mathbf{x}_{k-1}^{\text{ac}} - \mathbf{F}_{p,k-1} \hat{\mathbf{x}}_{k-1} + (\Delta \mathbf{F}_{k-1} - \mathbf{K}_k \Delta \mathbf{C}_k \mathbf{F}_{k-1} - \mathbf{K}_k \mathbf{C}_k \Delta \mathbf{F}_{k-1} \\ &\quad - \mathbf{K}_k \Delta \mathbf{C}_k \Delta \mathbf{F}_{k-1}) \mathbf{x}_{k-1}^{\text{ac}} + (\bar{\mathbf{G}}_{k-1} - \mathbf{K}_k \bar{\mathbf{C}}_k \bar{\mathbf{G}}_{k-1}) \mathbf{u}_{k-1}^{\text{ac}} - \mathbf{K}_k \mathbf{w}_k^{\text{ac}}. \end{aligned} \quad (9.571)$$

Now define

$$\Delta \mathbf{F}_{p,k-1} = \Delta \mathbf{F}_{k-1} - \mathbf{K}_k \Delta \mathbf{C}_k \mathbf{F}_{k-1} - \mathbf{K}_k \mathbf{C}_k \Delta \mathbf{F}_{k-1} - \mathbf{K}_k \Delta \mathbf{C}_k \Delta \mathbf{F}_{k-1}. \quad (9.572)$$

Then, (9.571) can be written as

$$\tilde{\mathbf{x}}_k^{\text{ac}} = \mathbf{F}_{p,k-1} \tilde{\mathbf{x}}_{k-1}^{\text{ac}} + \Delta \mathbf{F}_{p,k-1} \mathbf{x}_{k-1}^{\text{ac}} + (\mathbf{I} - \mathbf{K}_k \bar{\mathbf{C}}_k) \bar{\mathbf{G}}_{k-1} \mathbf{u}_{k-1}^{\text{ac}} - \mathbf{K}_k \mathbf{w}_k^{\text{ac}} \quad (9.573)$$

and

$$\mathbf{P}_k^{\text{ac}} \triangleq E \left\{ \tilde{\mathbf{x}}_k^{\text{ac}} \tilde{\mathbf{x}}_k^{\text{ac}T} \right\}. \quad (9.574)$$

Substituting (9.573) into (9.574) and evaluating the expectation, we find that there are four terms corresponding to the i th term $\tilde{\mathbf{x}}_k^{\text{ac}}$ multiplied by the i th term in $\tilde{\mathbf{x}}_k^{\text{ac}T}$. There is one nonzero cross-term and its transpose. This term is

$$\mathbf{F}_{p,k-1} E \left\{ \tilde{\mathbf{x}}_{k-1}^{\text{ac}} \mathbf{x}_{k-1}^{\text{ac}T} \right\} \Delta \mathbf{F}_{p,k-1} \triangleq \mathbf{F}_{p,k-1} \mathbf{P}_{k-1}^c \Delta \mathbf{F}_{p,k-1}^T. \quad (9.575)$$

From (9.566) and (9.573), one can show that the recursion for \mathbf{P}_k^c is

$$\mathbf{P}_k^c = \mathbf{F}_{p,k-1} \mathbf{P}_{k-1}^c \bar{\mathbf{F}}_{k-1} + \Delta \mathbf{F}_{p,k-1} \Pi_{k-1}^{\text{ac}} \bar{\mathbf{F}}_{k-1}^T + (\mathbf{I} - \mathbf{K}_k \bar{\mathbf{C}}_k) \bar{\mathbf{G}}_{k-1} \bar{\mathbf{Q}}_{k-1} \bar{\mathbf{G}}_{k-1}^T, \quad (9.576)$$

$$\mathbf{P}_0^c = \bar{\Pi}_0, \quad (9.577)$$

where Π_k^{ac} is given by the recursion

$$\begin{aligned} \Pi_k^{\text{ac}} &= \bar{\mathbf{F}}_{k-1} \Pi_{k-1}^{\text{ac}} \bar{\mathbf{F}}_{k-1}^T + \bar{\mathbf{G}}_{k-1} \bar{\mathbf{Q}}_{k-1} \bar{\mathbf{G}}_{k-1}^T, \\ \Pi_0^{\text{ac}} &= \Pi_0. \end{aligned} \quad (9.578)$$

Then, (9.574) can be written as

$$\begin{aligned} \mathbf{P}_k^{\text{ac}} &= \mathbf{F}_{p,k-1} \mathbf{P}_{k-1}^{\text{ac}} \mathbf{F}_{p,k-1}^T + \Delta \mathbf{F}_{p,k-1} \Pi_{k-1}^{\text{ac}} \Delta \mathbf{F}_{p,k-1}^T + \mathbf{F}_{p,k-1} \mathbf{P}_{k-1}^c \Delta \mathbf{F}_{p,k-1}^T \\ &\quad + \Delta \mathbf{F}_{p,k-1} (\mathbf{P}_{k-1}^c)^T \mathbf{F}_{p,k-1}^T + (\mathbf{I} - \mathbf{K}_k \bar{\mathbf{C}}_k) \bar{\mathbf{G}}_{k-1} \bar{\mathbf{Q}}_{k-1} \bar{\mathbf{G}}_{k-1}^T (\mathbf{I} - \mathbf{K}_k \bar{\mathbf{C}}_k)^T + \mathbf{K}_k \bar{\mathbf{R}}_k \mathbf{K}_k^T. \end{aligned} \quad (9.579)$$

We consider several examples to illustrate the behavior. We are interested in three quantities:

- (i) The nominal error covariance matrix \mathbf{P}_k .
- (ii) The actual error covariance matrix \mathbf{P}_k^{ac} .
- (iii) The perfect error covariance matrix, \mathbf{P}_k^{pm} . This matrix assumes that we can measure or estimate the actual matrices perfectly and we redesign (or adapt) the Kalman filter to these values.

In Section 9.3.5, after we have developed the extended Kalman filter, we will discuss joint state and parameter estimation. The result in (iii) will bound the potential performance.

Example 9.15. Consider the AR (1) model in Example 9.9. We want to look at effects of a mismatched value of α .

$$\bar{F} = \alpha + \Delta\alpha. \quad (9.580)$$

We consider the specific case where $0.11 < \alpha \leq 0.89$ and $\Delta\alpha = -0.1$ and 0.1 . We recall from (9.365) that

$$\sigma_s^2 = \frac{\sigma_u^2}{1 - \alpha^2}, \quad (9.581)$$

so that if α is changed, the SNR will change. It is more realistic to hold the SNR constant. Therefore,

$$\bar{Q} = \bar{\sigma}_u^2 = \sigma_u^2 (1 - (\alpha + \Delta\alpha)^2). \quad (9.582)$$

We assume the system has reached steady state.

In Figure 9.51a, we assume the SNR = 3 dB. We plot the nominal normalized variance $P_\infty^{\text{nom}}/\sigma_s^2$ versus α . For $\Delta\alpha = 0.1$, we plot the normalized mismatched variance $P_\infty^{\text{ac}}/\sigma_s^2$ and the normalized perfect measurement variance $P_\infty^{\text{pm}}/\sigma_s^2$. For $\Delta\alpha = -0.1$, we repeat the two preceding curves. In

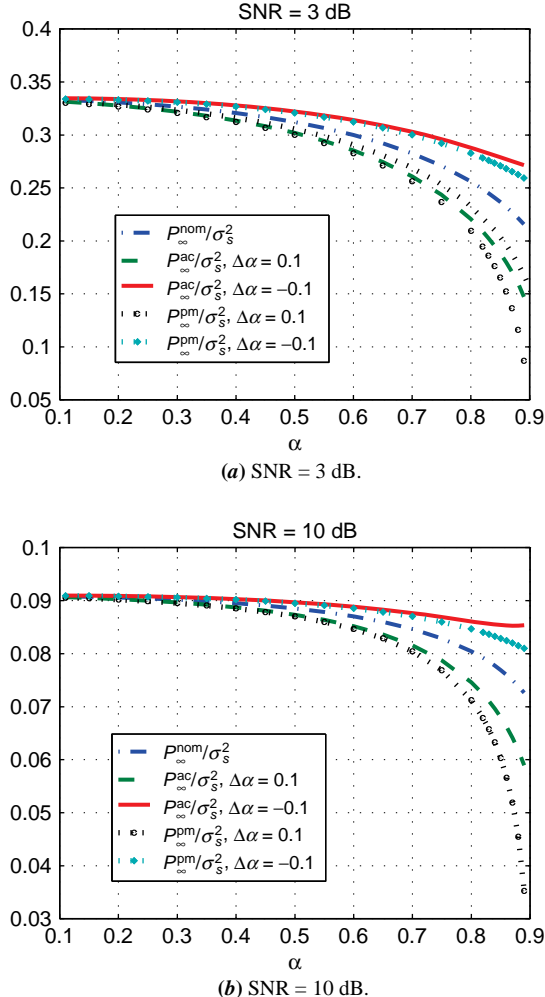


Figure 9.51: Normalized P_{∞}^{nom} , P_{∞}^{ac} , P_{∞}^{pm} versus α ; $\Delta\alpha = -0.1, 0.1$.

Figure 9.51b, we plot the same curves for SNR = 10 dB. From Example 9.9, we know that increasing α decreases the normalized variance. The $P_{\infty}^{\text{pm}}/\sigma_s^2$ curves illustrate this behavior (it corresponds to a result in Example 9.9). The $P_{\infty}^{\text{ac}}/\sigma_s^2$ curve illustrates the actual normalized variance. Similarly, decreasing α increases the normalized variance.

In Figure 9.52, we plot the same five curves versus SNR for $\alpha = 0.8$. In Figure 9.53, we plot $(\Delta P_{\infty}/P_{\infty}^{\text{nom}})/(\Delta\alpha/\alpha)$ for $\alpha = 0.8$ and SNR = 3 dB, 10 dB, where $\Delta P_{\infty} \triangleq P_{\infty}^{\text{ac}} - P_{\infty}^{\text{nom}}$. ■

When the only model mismatch is in \mathbf{Q}_k , we can find an expression for the difference between \mathbf{P}_k and \mathbf{P}_k^{ac} as a function of $\mathbf{Q}_k - \bar{\mathbf{Q}}_k$.

$$\mathbf{P}_k = (\mathbf{I} - \mathbf{K}_k \mathbf{C}_k) \mathbf{P}_{k|k-1} \quad (9.583)$$

$$= (\mathbf{I} - \mathbf{K}_k \mathbf{C}_k) \mathbf{P}_{k|k-1} (\mathbf{I} - \mathbf{K}_k \mathbf{C}_k)^T + \mathbf{P}_k (\mathbf{K}_k \mathbf{C}_k)^T \quad (9.584)$$

$$= (\mathbf{I} - \mathbf{K}_k \mathbf{C}_k) (\mathbf{F}_{k-1} \mathbf{P}_{k-1} \mathbf{F}_{k-1}^T + \mathbf{G}_k \mathbf{Q}_k \mathbf{G}_k^T) (\mathbf{I} - \mathbf{K}_k \mathbf{C}_k)^T + \mathbf{P}_k (\mathbf{K}_k \mathbf{C}_k)^T. \quad (9.585)$$

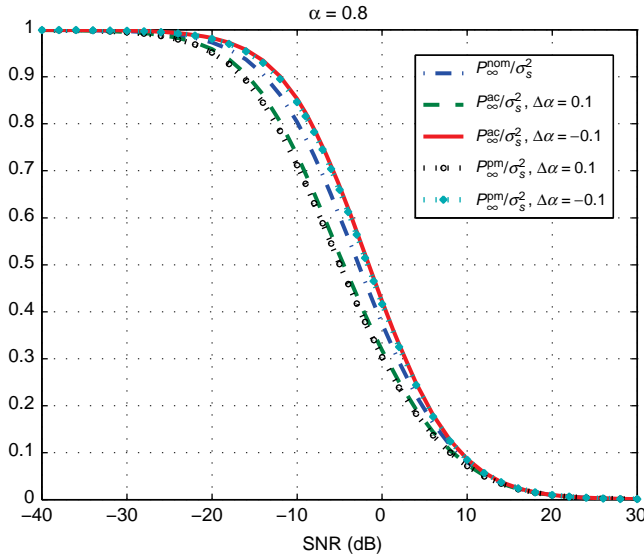


Figure 9.52: Normalized P_{∞}^{nom} , P_{∞}^{ac} , P_{∞}^{pm} versus SNR; $\alpha = 0.8$, $\Delta\alpha = -0.1, 0.1$.

When $\Delta\mathbf{F} = \mathbf{0}$, $\Delta\mathbf{C} = \mathbf{0}$, $\Delta\mathbf{G} = \mathbf{0}$, we have $\Delta\mathbf{F}_{p,k-1} = \mathbf{0}$, which simplifies (9.579) to

$$\mathbf{P}_k^{\text{ac}} = (\mathbf{I} - \mathbf{K}_k \mathbf{C}_k) (\mathbf{F}_{k-1} \mathbf{P}_{k-1}^{\text{ac}} \mathbf{F}_{k-1}^T + \mathbf{G}_{k-1} \bar{\mathbf{Q}}_{k-1} \mathbf{G}_{k-1}^T) (\mathbf{I} - \mathbf{K}_k \mathbf{C}_k)^T + \mathbf{K}_k \bar{\mathbf{R}}_k \mathbf{K}_k^T, \quad (9.586)$$

$$\begin{aligned} \mathbf{P}_k - \mathbf{P}_k^{\text{ac}} &= \mathbf{F}_{p,k-1} (\mathbf{P}_{k-1} - \mathbf{P}_{k-1}^{\text{ac}}) \mathbf{F}_{p,k-1}^T + \mathbf{G}_{p,k-1} (\mathbf{Q}_{k-1} - \bar{\mathbf{Q}}_{k-1}) \mathbf{G}_{p,k-1}^T \\ &\quad + \mathbf{P}_k (\mathbf{K}_k \mathbf{C}_k)^T - \mathbf{K}_k \bar{\mathbf{R}}_k \mathbf{K}_k^T, \end{aligned} \quad (9.587)$$

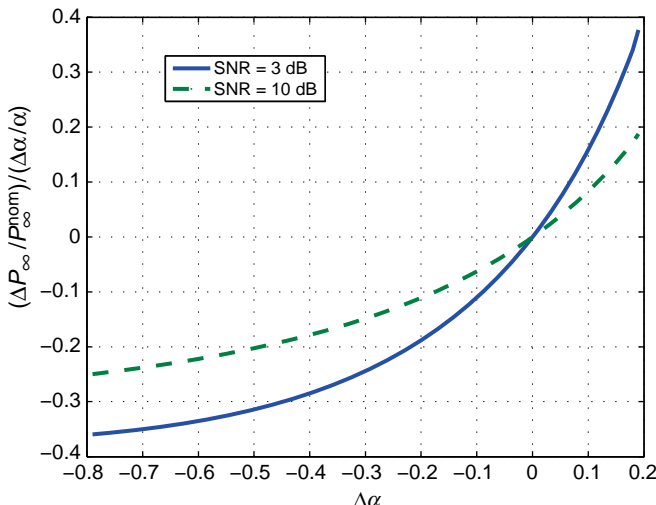


Figure 9.53: Sensitivity: $(\Delta P_{\infty} / P_{\infty}^{\text{nom}}) / (\Delta\alpha / \alpha)$ versus $\Delta\alpha$; $\alpha = 0.8$, SNR = 3 dB, 10 dB.

where

$$\mathbf{G}_{p,k-1} \triangleq (\mathbf{I} - \mathbf{K}_k \mathbf{C}_k) \mathbf{G}_{k-1}. \quad (9.588)$$

One can show that $\mathbf{P}_k (\mathbf{K}_k \mathbf{C}_k)^T - \mathbf{K}_k \bar{\mathbf{R}}_k \mathbf{K}_k^T = \mathbf{0}$, which results in the following recursion:

$$\mathbf{P}_k - \mathbf{P}_k^{\text{ac}} = \mathbf{F}_{p,k-1} (\mathbf{P}_{k-1} - \mathbf{P}_{k-1}^{\text{ac}}) \mathbf{F}_{p,k-1}^T + \mathbf{G}_{p,k-1} (\mathbf{Q}_{k-1} - \bar{\mathbf{Q}}_{p,k-1}) \mathbf{G}_{p,k-1}^T, \quad (9.589)$$

$$\mathbf{P}_0 - \mathbf{P}_0^{\text{ac}} = \mathbf{0}. \quad (9.590)$$

In addition, one can show that if $\mathbf{Q}_{k-1} \geq \bar{\mathbf{Q}}_{k-1}$, then $\mathbf{P}_k^{\text{ac}} \leq \mathbf{P}_k$.

Note that our discussion has only considered the covariance implementation of the Kalman filter. If we are using either the reduced-dimension covariance implementation or the information filter, we must repeat the analysis.

Sensitivity. In this section, we consider the approach in which we let θ denote a scalar parameter in one of the above matrices. Then for small variations, we can compute $\partial \mathbf{P}(k) / \partial \theta$ to determine the effect of small changes on the variance of the estimate.

For larger changes in θ , we would compute $\Delta \mathbf{P}(k) / \Delta \theta$ that depends on $\Delta \mathbf{K}(k) / \Delta \theta$, which depends $\Delta \mathbf{P}(k|k-1) / \Delta \theta$ that depends on $\Delta \mathbf{P}(k-1) / \Delta \theta$. Thus, we have a set of Kalman sensitivity equations to solve. Mendel [Men95] (pp. 260–265) gives a complete discussion of this approach and the interested reader should read this reference.

Summary. We consider a number of examples in the problems. The key point of the section is to emphasize that any reader who is implementing a Kalman filter in an actual application needs to investigate the sensitivity to model mismatch.

9.3.2.9 Summary: Kalman Filters

In this section, we have studied the discrete-time Kalman filter. The first four sections were devoted to developing the theory and studying some typical applications. The last four sections were devoted to introducing some of the problems that may occur when we implement the filter.

In Section 9.3.2.1, we derived the standard Kalman filter. This version of the Kalman filter is referred to as the *covariance implementation* because it recursively inverts the covariance matrix of the estimation error. The key equations are (9.275)–(9.286). The standard algorithm requires recursive inversion of an $N \times N$ matrix, where N is the dimension of the observation vector $\mathbf{r}(k)$.

In Section 9.3.2.2, we developed two alternative implementations that have computational advantage when $N \geq p$, where p is the dimension of the state vector. The derivations used the matrix inversion lemma to obtain implementations in which the recursive inversions are $p \times p$ when $\mathbf{R}(k)$ is a constant \mathbf{R} . The first implementation recursively computes the covariance matrix using a $p \times p$ inversion and we refer to it as the *reduced-dimension covariance implementation*. The key equations are (9.325)–(9.331). The second implementation recursively computes the Bayesian information matrix $\mathbf{J}_B(k)$ that is the inverse of the covariance matrix using a $p \times p$ inversion and is referred to as the *information filter*. The key equations are (9.349)–(9.359). The three implementations are algebraically identical, but they have different computational complexity, different sensitivity to numerical errors such as round-off, and different sensitivity to model mismatch.

In Section 9.3.2.3, we studied a sequence of applications in the signal processing and tracking areas. Examples 9.9 and 9.11 considered ARMA signal models of increasing

dimension of the state vector. All of them had scalar observations, so the standard covariance implementation was appropriate. Example 9.12 considered an array processing application where $N \gg p$. Both reduced-dimension algorithms used a recursive $p \times p$ inversion. Example 9.10 considered a simple one-dimensional tracking problem. The more realistic 2 or 3 dimensional tracking problem has a nonlinear observation model, so we deferred discussion until Section 9.3.5.

These examples are consistent with the main application areas in the book but did not really illustrate the widespread usage of the Kalman filter in diverse areas. An Internet search on “Kalman Filter Applications” will provide a much broader view.

The Kalman filter in Sections 9.3.2.1–9.3.2.3 assumes white Gaussian noise in the observation model. In Section 9.3.2.4, we showed how to treat the case of colored plus white observation noise. Our approach consists of augmenting the signal state vector with a colored noise state vector. This reduces the problem to a standard Kalman filtering problem with an increased dimension of the state vector.

There is a measurement update step in the Kalman filter algorithm that requires processing an $N \times 1$ vector, where N is the dimension of the observation. In Section 9.3.2.5, we developed an algorithm to process the components of the vector sequentially.

In early applications, it was found that numerical round-off errors caused the covariance matrix or the Bayesian information matrix to lose its nonnegative definite property. In Section 9.3.2.6, we developed a square-root implementation of the Kalman filter which factors the covariance matrix (or the Bayesian information matrix) into triangular matrices and updates them. This implementation guarantees a nonnegative definite matrix and improves the numerical precision. This section provided a brief introduction to square-root filtering. There are a number of different square-root algorithms and the literature should be consulted for a particular application.

In some applications, if there is mismatch between the mathematical model and the actual model, the Kalman filter will track the wrong model and predict a decreasing covariance matrix. However, the actual MSE is diverging. In Section 9.3.2.7, we analyzed this behavior and discussed remedies.

The mismatch in Section 9.3.2.7 consists of a small bias term that is neglected in the mathematical model. In Section 9.3.2.8, we considered a more general mismatch model in which all of the matrices in the model, \mathbf{F} , \mathbf{G} , \mathbf{C} , \mathbf{Q} , \mathbf{R} , and $\boldsymbol{\Pi}$ may be mismatched to the actual model. The key equations are (9.567) and (9.573)–(9.579).

It is an essential part of the design of an algorithm for a practical application to investigate its sensitivity to possible model mismatches.

We have spent a considerable amount of time studying Kalman filters. In addition to their widespread usage, they are the key building block in Kalman prediction and smoothers. We study Kalman prediction in the next section.

9.3.3 Kalman Predictors

In this section, we give a brief introduction to prediction using a Kalman filter. There are three types of prediction problems.

- (a) Fixed-lead prediction: In this case,

$$d(k) = s(k + L), \quad (9.591)$$

where L is a positive number.

(b) Fixed-point prediction: In this case,

$$d(k) = s(L_p), \quad (9.592)$$

where L_p is a fixed point, $L_p > k$.

(c) Fixed-interval prediction: In this case, the interval is fixed, $k = 1, 2, \dots, K$, and we want to predict

$$d(m) = s(m), \quad m = K + 1, K + 2, \dots \quad (9.593)$$

This is the model that we encountered in Section 9.2 using covariance functions.

In all of these cases, we assume that a Kalman filter is implemented and that we have $\hat{\mathbf{x}}(k)$ and $\mathbf{P}(k)$ available. Because we are dealing with a Markov process, these are the only quantities needed to find $\hat{d}(k)$ and its variance.

9.3.3.1 Fixed-Lead Prediction

This is simply the Kalman filtering problem where the prediction step in (9.277) is valid and there is no measurement update step. The predicted value of state variable $\mathbf{x}(k+L)$ is

$$\hat{\mathbf{x}}(k+L|k) = \prod_{j=0}^{L-1} \mathbf{F}(k+L-1-j) \hat{\mathbf{x}}(k) \quad (9.594)$$

If $\mathbf{F}(k)$ is constant, this reduces to

$$\hat{\mathbf{x}}(k+L|k) = \mathbf{F}^L \hat{\mathbf{x}}(k). \quad (9.595)$$

To find the covariance matrix, we use (9.278) recursively,

$$\mathbf{P}_p(k+1) \triangleq \mathbf{P}(k+1|k) = \mathbf{F}\mathbf{P}(k)\mathbf{F}^T + \mathbf{G}(k)\mathbf{Q}(k)\mathbf{G}^T(k) \quad (9.596)$$

until we find $\mathbf{P}_p(k+L) \triangleq \mathbf{P}(k+L|k)$.

This can be written as

$$\mathbf{P}(k+L|k) = \mathbf{F}^L \mathbf{P}(k) (\mathbf{F}^L)^T + \sum_{j=0}^{L-1} \sigma_u^2 \mathbf{F}^j (\mathbf{F}^j)^T \quad (9.597)$$

for $\mathbf{G}(k)\mathbf{Q}(k)\mathbf{G}^T(k) = \sigma_u^2 \mathbf{I}$, and

$$\mathbf{P}(k+L|k) = \mathbf{F}^L \mathbf{P}(k) (\mathbf{F}^L)^T + \sum_{j=0}^{L-1} \mathbf{F}^j \mathbf{G}(k) \mathbf{Q}(k) \mathbf{G}^T(k) (\mathbf{F}^j)^T \quad (9.598)$$

for arbitrary $\mathbf{Q}(k)$ and $\mathbf{G}(k)$.

We consider a simple example using the AR (1) model in Example 9.9.

Example 9.16 (Continuation of Example 9.9). For the AR(1) model in Example 9.9, this reduces to

$$\hat{x}(k+L) = \alpha^L \hat{x}(k). \quad (9.599)$$

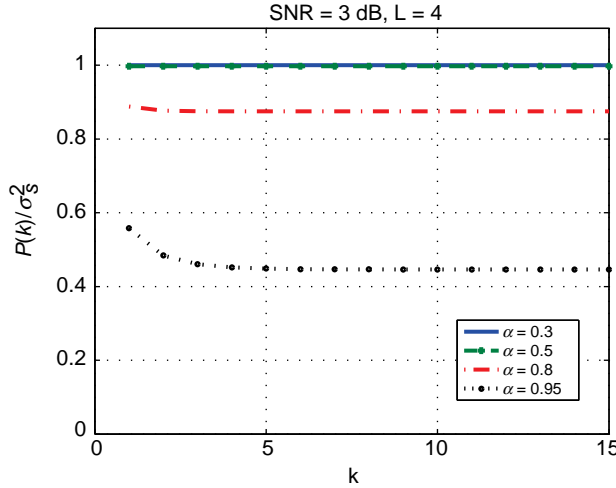


Figure 9.54: Normalized variance versus k ; SNR = 3 dB $L = 4$, $\alpha = 0.3, 0.5, 0.8$, and 0.95 .

Using (9.597), we can write the covariance matrix as

$$P(k + L|k) = \alpha^{2L} P(k) + \sum_{j=0}^{L-1} \alpha^{2j} \sigma_u^2 \quad (9.600)$$

$$= \alpha^{2L} P(k) + \left(\frac{1 - \alpha^{2L}}{1 - \alpha^2} \right) \sigma_u^2 \quad (9.601)$$

$$= \alpha^{2L} P(k) + (1 - \alpha^{2L}) \sigma_s^2. \quad (9.602)$$

In Figure 9.54, we plot the normalized covariance versus k for SNR = 3 dB for $L = 4$ and various α . When $\alpha \leq 0.8$, we have very little ability to predict for $L = 4$. We see that the error reaches steady state at $k = 5$ for $\alpha = 0.95$ and much sooner for smaller α .

In Figure 9.55, we plot the normalized steady-state variance versus L for SNR = 3 dB and various α . As expected, the figure is identical to Figure 9.24. ■

9.3.3.2 Fixed-Point Prediction

In this case,

$$d(k) = s(L_p) \quad (9.603)$$

where L_p is a fixed point, $L_p > k$. We need to estimate the state vector $\hat{\mathbf{x}}(L_p|k)$. We initialize the algorithm with $\hat{\mathbf{x}}(L_p|0)$ and $\mathbf{P}(L_p : 0)$, which are given by the fixed-lead algorithm with $L_p = L$.

First, consider the case when $L_p = 4$ and $k = 0, 1, 2, 3$.

$$\hat{\mathbf{x}}(L_p|k) = \mathbf{F}(L_p - 1)\hat{\mathbf{x}}(L_p - 1|k = L_p - 1) \quad (9.604)$$

$$= \mathbf{F}(L_p - 1) \left\{ \mathbf{F}(L_p - 2)\hat{\mathbf{x}}(L_p - 2|k = L_p - 2) \right\} \quad (9.605)$$

$$= \mathbf{F}(L_p - 1)\mathbf{F}(L_p - 2) \left\{ \mathbf{F}(L_p - 3)\hat{\mathbf{x}}(L_p - 3|k = L_p - 3) \right\} \quad (9.606)$$

$$= \mathbf{F}(L_p - 1)\mathbf{F}(L_p - 2)\mathbf{F}(L_p - 3)\mathbf{F}(L_p - 4)\hat{\mathbf{x}}(0). \quad (9.607)$$

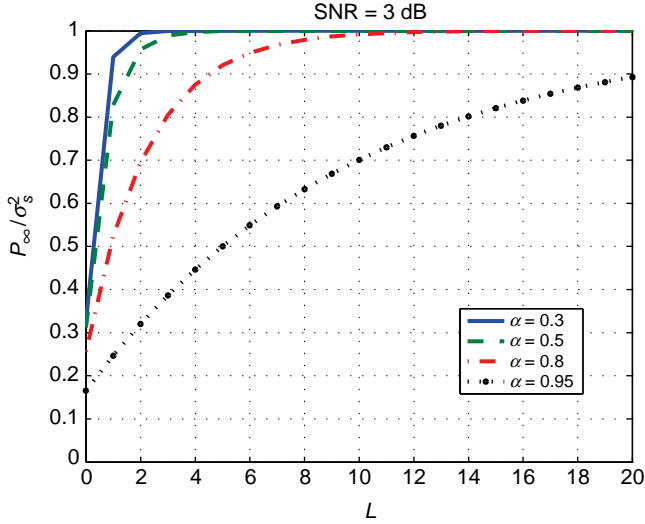


Figure 9.55: Normalized steady-state variance versus L ; $\text{SNR} = 3 \text{ dB}$, $\alpha = 0.3, 0.5, 0.8$, and 0.95 .

For the general case,

$$\hat{\mathbf{x}}(L_p|k) = \left[\prod_{j=0}^{L_p-k-1} \mathbf{F}(L_p - 1 - j) \right] \hat{\mathbf{x}}(k), \quad (9.608)$$

and for constant \mathbf{F} ,

$$\hat{\mathbf{x}}(L_p|k) = \mathbf{F}^{L_p-k} \hat{\mathbf{x}}(k). \quad (9.609)$$

Substituting (9.283) into (9.608) gives

$$\hat{\mathbf{x}}(L_p|k) = \left[\prod_{j=0}^{L_p-k-1} \mathbf{F}(L_p - 1 - j) \right] \left[\mathbf{F}(k-1) \hat{\mathbf{x}}(k-1) + \mathbf{K}(k) \tilde{\mathbf{r}}(k) \right] \quad (9.610)$$

$$= \hat{\mathbf{x}}(L_p|k-1) + \left[\prod_{j=0}^{L_p-k-1} \mathbf{F}(L_p - 1 - j) \right] \mathbf{K}(k) \tilde{\mathbf{r}}(k). \quad (9.611)$$

The covariance update equation is

$$\begin{aligned} \mathbf{P}(L_p : k | k-1) &= \mathbf{F}(L_p - (k-1)) \mathbf{P}(L_p : k-1) \mathbf{F}^T(L_p - (k-1)) \\ &\quad + \mathbf{G}(L_p - (k-1)) \mathbf{Q}(L_p - (k-1)) \mathbf{G}^T(L_p - (k-1)). \end{aligned} \quad (9.612)$$

Example 9.17 (Continuation of Example 9.9). We consider the AR(1) model in Example 9.9. The estimate is

$$\hat{x}(L_p|k) = \alpha^{L_p-k} \hat{x}(k). \quad (9.613)$$

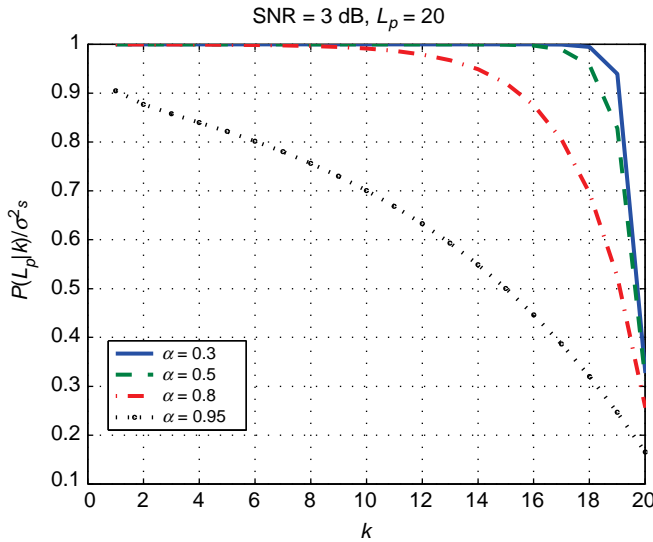


Figure 9.56: Normalized fixed-point prediction covariance, $P(L_p|k)/\sigma_s^2$, SNR = 3 dB, $\alpha = 0.3, 0.5, 0.8$, and 0.95 .

Letting $L = L_p - k$ in (9.601) yields

$$P(L_p|k) = \alpha^{2(L_p-k)} P(k) + \left(\frac{1 - \alpha^{2(L_p-k)}}{1 - \alpha^2} \right) \sigma_u^2. \quad (9.614)$$

In Figure 9.56, we plot $P(L_p|k)/\sigma_s^2$ versus k , for $L_p = 20$, SNR = 3 dB and $\alpha = 0.3, 0.5, 0.8, 0.95$. As we would expect, the curves do not start to move away from a normalized variance of 1 until $(L_p - k)\alpha < 1$.

As we would expect, the curves are the reverse of Figure 9.55. ■

9.3.3.3 Fixed-Interval Prediction

In this case,

$$\hat{\mathbf{x}}(m|K) = \mathbf{F}(m-1)\hat{\mathbf{x}}(m-1|K), \quad m = K+1, K+2, \dots, \quad (9.615)$$

which reduces to

$$\hat{\mathbf{x}}(m|K) = \prod_{j=0}^{m-K-1} \mathbf{F}(m-1-j)\hat{\mathbf{x}}(K|K). \quad (9.616)$$

These are just a set of fixed-point prediction with $L_p = m$, $m = K+1, K+2, \dots$

9.3.3.4 Summary: Kalman Predictors

In this section, we have discussed three types of Kalman predictors. All of them contain the Kalman filter as the key component. The resulting performance will depend on the correlation time of the signal process.

9.3.4 Kalman Smoothing

The smoothing problem is more complicated. There are three types of smoothing that are encountered in applications:

1. *Fixed-interval smoothing.* We have K samples, $k = 1, \dots, K$, and we want to find $\hat{\mathbf{x}}(k|K) \triangleq \hat{\mathbf{x}}(k|\mathbf{r}_K)$, where
$$\mathbf{r}_K = [\mathbf{r}(1) \quad \cdots \quad \mathbf{r}(K)].$$
2. *Fixed-lag smoothing.* We observed $\mathbf{r}(k)$, $k = 1, 2, \dots$, and we want to find $\hat{\mathbf{x}}(k+L)$, where L is negative. This case is the filtering with delay problem that we considered in the Wiener filter context.
3. *Fixed-point smoothing.* We want to find $\hat{\mathbf{x}}(k_s)$, where k_s is fixed and we observe $\mathbf{r}(k)$, $k = k_s, k_s + 1, \dots, k_s + K$, and K increases.

As we observed in our discussion of Wiener filters, smoothing has the potential to provide significant reduction in the mean-square error. Smoothing for state-space models appeared shortly after the introduction of the Kalman filter. A survey of the early work is given in Meditch [Med73]. Early textbooks include Lee [Lee64], Bryson and Ho [BH69], Meditch [Med69], and Sage and Melsa [SM71]. Two books that provide excellent presentations are Anderson and Moore [AM79] and Gelb [Gel74], and our discussion relies heavily on their work.

Early references include Rauch [Rau63], Rauch, Tung, and Streibel [RTS65], Weaver [Wea63]. Mayne [May66] and Fraser and Potter [FP69] developed the concept of implementing the smoother as a combination of forward and backward Kalman filters. We discuss this approach in Section 9.3.4.1.

References on fixed-lag filtering include Anderson and Chirattananon [AC71], Moore [Moo73], and Anderson [And69]. We discuss their models in Section 9.3.4.2.

Fixed-point smoothing is discussed in several of the above references and is developed in detail in Section 7.2 of Anderson and Moore [AM79] and in Mendel [Men95]. The reader is referred to their reference for the development.

9.3.4.1 Fixed-Interval Smoothing

The fixed-interval smoothing problem is to find $\hat{\mathbf{x}}(k|K)$ given the observation $\mathbf{r}(1), \mathbf{r}(2), \dots, \mathbf{r}(K)$. Our approach is to first solve the Kalman filtering problem and store $\hat{\mathbf{x}}(k|k)$, $\hat{\mathbf{x}}(k|k-1)$, $\mathbf{P}(k|k)$, and $\mathbf{P}(k|k-1)$, for $k = 1, \dots, K$. All these quantities have been determined in the Kalman filtering process. We refer to this filter as the *forward* Kalman filter.

We then use $\hat{\mathbf{x}}(K|K)$ and $\mathbf{P}(K)$ as initial conditions and derive a *backward* Kalman filter. The derivation is similar to the derivation of the standard Kalman filter. The steps are

1. Compute the backward gain \mathbf{K}_b ,

$$\mathbf{K}_b(k) = \mathbf{P}(k)\mathbf{F}^T(k)\mathbf{P}(k+1|k), \quad k = 0, \dots, K-1. \quad (9.617)$$

Note that all of the covariance matrices on the right-hand side of (9.617) were available from the forward Kalman filter.

2. Compute the state estimate by iterating backwards,

$$\hat{\mathbf{x}}(k|K) = \hat{\mathbf{x}}(k) + \mathbf{K}_b(k) [\hat{\mathbf{x}}(k+1|K) - \hat{\mathbf{x}}(k+1|k)], \quad k = K-1, K-2, \dots, 0, \quad (9.618)$$

with initial condition $\hat{\mathbf{x}}(K)$.

3. Compute the error covariance matrix

$$\mathbf{P}(k|K) = \mathbf{P}(k) + \mathbf{K}_b(k) [\mathbf{P}(k+1|K) - \mathbf{P}(k+1|k)] \mathbf{K}_b^T(k), \quad k = K-1, K-2, \dots, 0. \quad (9.619)$$

We illustrate this approach with the same model as Example 9.9.

Example 9.18 (Continuation of Example 9.9). The model is given in (9.360)–(9.364) and the forward Kalman filter terms are in (9.366)–(9.371). We assume that the forward Kalman filter has been implemented and quantities $\hat{\mathbf{x}}(k)$, $\hat{\mathbf{x}}(k|k-1)$, $\mathbf{P}(k)$, and $\mathbf{P}(k|k-1)$, $k = 1, \dots, K$, have been stored. We implement the backward Kalman filter for $K = 10$ so that we can compare our results to Figure 9.11 from Example 9.4. In Figure 9.57, we consider the case of SNR = 3 dB. We show the forward covariance denoted by $\xi_{of}(k)$ and the backward (smoothed) covariance denoted by $\xi_{os}(k)$.

The results are what we would expect from our FIR estimation results in Figure 9.11. The center point of the interval has the lowest variance because of the symmetry of the covariance function. ■

9.3.4.2 Fixed-Lag Smoothing

In this section, we study the fixed-lag smoothing problem in which we want to find

$$\hat{\mathbf{x}}(k-L|k) = E \{ \hat{\mathbf{x}}(k-L) | \mathbf{r}(0), \dots, \mathbf{r}(k) \} \quad (9.620)$$

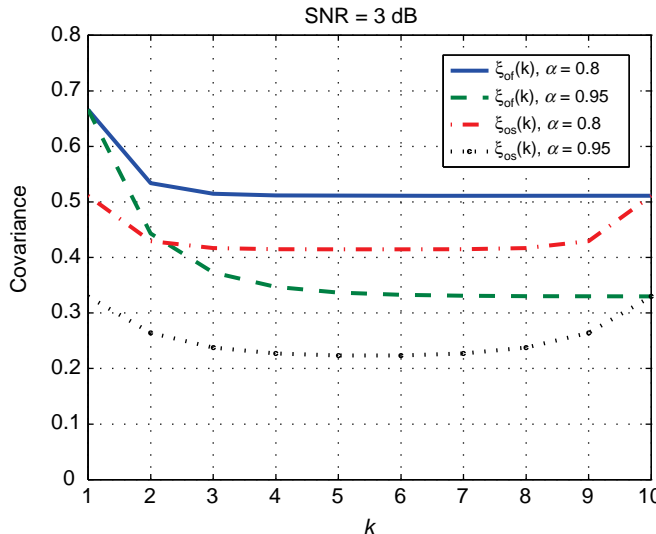


Figure 9.57: Smoothed covariance: AR (1) process; SNR = 3 dB, $K = 10$, $\alpha = 0.8$, and 0.95 .

and the covariance matrix,

$$\mathbf{P}(k-L|k) = E \left\{ [\mathbf{x}(k-L) - \hat{\mathbf{x}}(k-L|k)] [\mathbf{x}(k-L) - \hat{\mathbf{x}}(k-L|k)]^T \mid \mathbf{r}(0), \dots, \mathbf{r}(k) \right\}. \quad (9.621)$$

The earliest fixed-lag smoothing algorithm was developed by Rauch [Rau63]. Another smoothing algorithm was published by Meditch [Med69]. Kelly and Anderson [KA71] showed that these algorithms were not asymptotically stable. Biswas and Mahalanabis [BM72] formulated the smoothing problem as a standard Kalman filtering problem by augmenting the state vector with a set of delayed state vectors, $\mathbf{x}(k-1), \dots, \mathbf{x}(k-L)$. They proved the stability of their algorithm in [BM73b] and [BM73a] and showed the computational requirements. Moore [Moo73] also developed a smoother as an augmented state filter.

We derive their algorithm and our discussion follows Anderson and Moore [AM79] and Mendel [Men95]. We introduce $L+1$ state vectors

$$\mathbf{x}_1(k+1) = \mathbf{x}(k), \quad (9.622)$$

$$\mathbf{x}_2(k+1) = \mathbf{x}(k-1), \quad (9.623)$$

$$\mathbf{x}_3(k+1) = \mathbf{x}(k-2), \quad (9.624)$$

$$\vdots \quad (9.625)$$

$$\mathbf{x}_{L+1}(k+1) = \mathbf{x}(k-L). \quad (9.626)$$

The state equations are

$$\begin{bmatrix} \mathbf{x}(k+1) \\ \mathbf{x}_1(k+1) \\ \mathbf{x}_2(k+1) \\ \vdots \\ \mathbf{x}_{L+1}(k+1) \end{bmatrix} = \begin{bmatrix} \mathbf{F}(k) & 0 & \cdots & \cdots & 0 \\ \mathbf{I} & 0 & \cdots & \cdots & \vdots \\ 0 & \mathbf{I} & 0 & \cdots & \vdots \\ \vdots & 0 & \ddots & \ddots & \vdots \\ 0 & \cdots & 0 & \mathbf{I} & 0 \end{bmatrix} \begin{bmatrix} \mathbf{x}(k) \\ \mathbf{x}_1(k) \\ \mathbf{x}_2(k) \\ \vdots \\ \mathbf{x}_{L+1}(k) \end{bmatrix} + \begin{bmatrix} \mathbf{G}(k) \\ \mathbf{0} \end{bmatrix} \mathbf{u}(k), \quad (9.627)$$

$$\mathbf{r}(k) = [\mathbf{C}(k) \quad \mathbf{0} \quad \mathbf{0}] \begin{bmatrix} \mathbf{x}(k) \\ \mathbf{x}_1(k) \\ \vdots \\ \mathbf{x}_{L+1}(k) \end{bmatrix} + \mathbf{w}(k). \quad (9.628)$$

The resulting Kalman filter is

$$\begin{bmatrix} \hat{\mathbf{x}}(k+1|k+1) \\ \hat{\mathbf{x}}_1(k+1|k+1) \\ \hat{\mathbf{x}}_2(k+1|k+1) \\ \vdots \\ \hat{\mathbf{x}}_{L+1}(k+1|k+1) \end{bmatrix} = \begin{bmatrix} \mathbf{F}(k) & 0 & \cdots & \cdots & 0 \\ \mathbf{I} & 0 & \cdots & \cdots & \vdots \\ 0 & \mathbf{I} & 0 & \cdots & \vdots \\ \vdots & 0 & \ddots & \ddots & \vdots \\ 0 & \cdots & 0 & \mathbf{I} & 0 \end{bmatrix} \begin{bmatrix} \hat{\mathbf{x}}(k|k) \\ \hat{\mathbf{x}}_1(k|k) \\ \hat{\mathbf{x}}_2(k|k) \\ \vdots \\ \hat{\mathbf{x}}_{L+1}(k|k) \end{bmatrix} + \begin{bmatrix} \mathbf{K}_0(k+1) \\ \mathbf{K}_1(k+1) \\ \mathbf{K}_2(k+1) \\ \vdots \\ \mathbf{K}_{L+1}(k+1) \end{bmatrix} \cdot \tilde{\mathbf{r}}(k+1|k) \quad (9.629)$$

Using (9.622)–(9.626), we have

$$\hat{\mathbf{x}}_1(k+1|k+1) = \hat{\mathbf{x}}(k|k+1), \quad (9.630)$$

$$\hat{\mathbf{x}}_2(k+1|k+1) = \hat{\mathbf{x}}(k-1|k+1), \quad (9.631)$$

$$\hat{\mathbf{x}}_3(k+1|k+1) = \hat{\mathbf{x}}(k-2|k+1), \quad (9.632)$$

$$\vdots \quad (9.633)$$

$$\hat{\mathbf{x}}_{L+1}(k+1|k+1) = \hat{\mathbf{x}}(k-L|k+1). \quad (9.634)$$

Then, (9.629) can be written as

$$\hat{\mathbf{x}}(k+1|k+1) = \mathbf{F}(k)\hat{\mathbf{x}}(k|k) + \mathbf{K}_0(k+1)\tilde{\mathbf{r}}(k+1|k), \quad (9.635)$$

$$\hat{\mathbf{x}}(k|k+1) = \hat{\mathbf{x}}(k|k) + \mathbf{K}_1(k+1)\tilde{\mathbf{r}}(k+1|k), \quad (9.636)$$

$$\hat{\mathbf{x}}(k-1|k+1) = \hat{\mathbf{x}}(k-1|k) + \mathbf{K}_2(k+1)\tilde{\mathbf{r}}(k+1|k), \quad (9.637)$$

$$\vdots \quad (9.638)$$

$$\hat{\mathbf{x}}(k-L|k+1) = \hat{\mathbf{x}}(k-L+1|k) + \mathbf{K}_{L+1}(k+1)\tilde{\mathbf{r}}(k+1|k). \quad (9.639)$$

where the gain matrices $\mathbf{K}_0, \mathbf{K}_1, \dots, \mathbf{K}_{L+1}$ are partitions of the overall gain matrix.

The augmented Kalman filter is shown in Figure 9.58. We observe that the only feedback path is in the original Kalman filter so that, if it is stable, the augmented filter is stable.

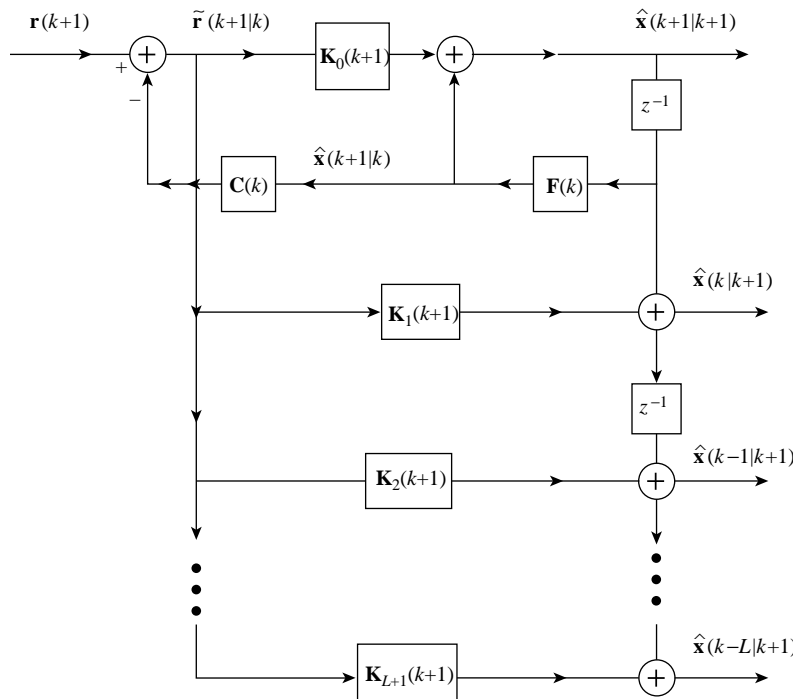


Figure 9.58: Fixed-lag smoother.

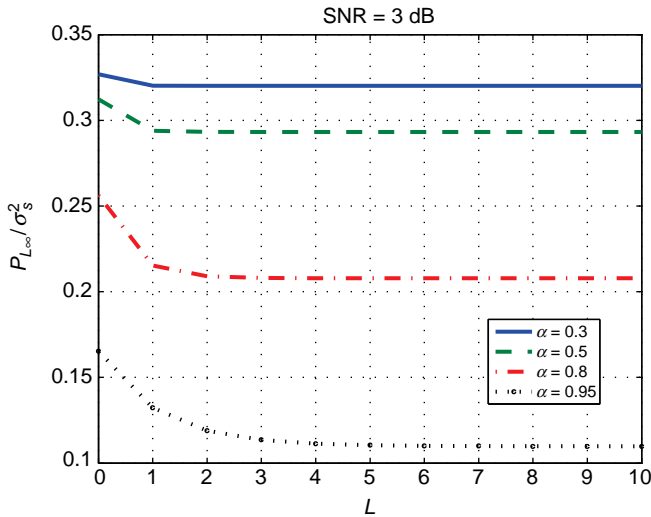


Figure 9.59: $P_{L\infty}/\sigma_s^2$ versus L for SNR = 3 dB; $\alpha = 0.3, 0.5, 0.8$, and 0.95 .

Some additional aspects of this fixed-lag smoother are

1. To compute $\hat{x}(k-L|k)$, we must also compute the $L-1$ fixed-lag estimates, $\hat{x}(k-1), \hat{x}(k-2), \dots, \hat{x}(k-L+1|k)$; this may be costly to do from a computational point of view.
2. Computation can be reduced by careful coding of the partitioned recursive predictor equations.

Example 9.19 (Continuation of Example 9.9). We use the parameter values in Example 9.9 and assume the system has reached steady state. In Figure 9.59, we plot the normalized $P_{L\infty}$ versus L for SNR = 3 dB and $\alpha = 0.3, 0.5, 0.8$, and 0.95 . As expected, the plot matches the Wiener filter result in Figure 9.26. ■

9.3.4.3 Summary: Kalman Smoothing

In this section we have discussed fixed-interval and fixed-lag smoothing. The fixed-point smoothing results follow from the fixed-lag smoothing results. For fixed-interval smoothing, we implement the smoother using a forward Kalman filter followed by a backward Kalman filter. For fixed-lag smoothing, we implement a Kalman filter for an augmented state model. Both smoothers require more computation than the corresponding filter.

9.3.5 Bayesian Estimation of Nonlinear Models

In this section, we consider the problem of Bayesian estimation of nonlinear models. We encountered this problem for continuous-time processes in Chapter 8, but this section can be read independently.¹⁴

¹⁴This section is based on our book on Bayesian Bounds [VB07].

In Section 9.3.5.1, we introduce the general nonlinear model and study MMSE and MAP estimation. In Section 9.3.5.2, we derive the extended Kalman filter. In Section 9.3.5.3, we derive a recursive Bayesian Cramér–Rao bound. In Section 9.3.5.4, we consider various applications.

This chapter has focused on discrete-time processes and discrete-time observations. In almost all tracking and navigation applications, we have continuous-time processes and discrete-time observations. Section 9.3.5.5 discusses this problem and derives the EKF and BCRB. Techniques for discretizing the continuous-time state equations are developed. In Section 9.3.5.6, we provide a brief summary.

9.3.5.1 General Nonlinear Model: MMSE and MAP Estimation

The general nonlinear filtering/tracking problem is modeled with a nonlinear process model,

$$\mathbf{x}_k = \mathbf{f}_{k-1}(\mathbf{x}_{k-1}, \mathbf{v}_{k-1}); \quad k = 1, \dots, n, \quad (9.640)$$

where $\mathbf{v}_k, k = 0, \dots, n - 1$, are statistically independent random vectors that are not necessarily Gaussian. The vector \mathbf{x}_k is the state vector of a p -dimensional Markov process, which is not necessarily a Gaussian–Markov process.

The observation equation is

$$\mathbf{r}_k = \mathbf{h}_k(\mathbf{x}_k, \mathbf{w}_k), \quad (9.641)$$

where the $\mathbf{w}_k, k = 1, \dots, n$, are statistically independent random vectors that are not necessarily Gaussian. The \mathbf{v}_k and \mathbf{w}_k are statistically independent. The observation vector \mathbf{r}_k is N -dimensional.

The discrete-time filtering problem is to find $\hat{\mathbf{x}}_n$ given $\mathbf{r}_k, k = 1, \dots, n$, where $\hat{\mathbf{x}}_n$ is the MMSE or MAP estimate of \mathbf{x}_n . In order to find the MMSE or MAP estimate of \mathbf{x}_n , we need to find the *a posteriori* probability density of \mathbf{x}_n given $\mathbf{r}_1, \mathbf{r}_2, \dots, \mathbf{r}_n$. We can formulate the problem as follows.

At the n th observation, define the $np \times 1$ vector

$$\mathbf{X}_n = \text{vec} [\mathbf{x}_1 \quad \mathbf{x}_2 \quad \cdots \quad \mathbf{x}_n] \quad (9.642)$$

and the $nN \times 1$ vector

$$\mathbf{R}_n = \text{vec} [\mathbf{r}_1 \quad \mathbf{r}_2 \quad \cdots \quad \mathbf{r}_n]. \quad (9.643)$$

Then,

$$p(\mathbf{R}_n | \mathbf{X}_n) = \prod_{k=1}^n p(\mathbf{r}_k | \mathbf{x}_k) = p(\mathbf{r}_n | \mathbf{x}_n) \prod_{k=1}^{n-1} p(\mathbf{r}_k | \mathbf{x}_k) \quad (9.644)$$

and

$$p(\mathbf{X}_n) = p(\mathbf{x}_n | \mathbf{x}_{n-1}) \int \left\{ \prod_{k=1}^{n-1} p(\mathbf{x}_k | \mathbf{x}_{k-1}) p(\mathbf{x}_0) \right\} d\mathbf{x}_0. \quad (9.645)$$

We can write the *a posteriori* density of \mathbf{X}_n as

$$p(\mathbf{X}_n | \mathbf{R}_n) = \frac{p(\mathbf{X}_n, \mathbf{R}_n)}{p(\mathbf{R}_n)} = c p(\mathbf{R}_n | \mathbf{X}_n) p(\mathbf{X}_n), \quad (9.646)$$

where c is a normalization constant such that the function is a probability density, and the posterior density of \mathbf{x}_n as

$$p(\mathbf{x}_n | \mathbf{R}_n) = \int p(\mathbf{X}_n | \mathbf{R}_n) d\mathbf{x}_1 d\mathbf{x}_2 \cdots d\mathbf{x}_{n-1} = c \int p(\mathbf{R}_n | \mathbf{X}_n) p(\mathbf{X}_n) d\mathbf{x}_1 \cdots d\mathbf{x}_{n-1}. \quad (9.647)$$

Using (9.644) and (9.645) in (9.647) gives

$$p(\mathbf{x}_n | \mathbf{R}_n) = \int \left\{ p(\mathbf{r}_n | \mathbf{x}_n) \left(\prod_{k=1}^{n-1} p(\mathbf{r}_k | \mathbf{x}_k) \right) p(\mathbf{x}_n | \mathbf{x}_{n-1}) \left(\prod_{k=1}^{n-1} p(\mathbf{x}_k | \mathbf{x}_{k-1}) \right) p(\mathbf{x}_0) \right\} d\mathbf{x}_0 \cdots d\mathbf{x}_{n-1}, \quad (9.648)$$

which can be written as

$$p(\mathbf{x}_n | \mathbf{R}_n) = p(\mathbf{r}_n | \mathbf{x}_n) \int p(\mathbf{x}_n | \mathbf{x}_{n-1}) \left\{ \int \left(\prod_{k=1}^{n-1} p(\mathbf{r}_k | \mathbf{x}_k) p(\mathbf{x}_k | \mathbf{x}_{k-1}) \right) p(\mathbf{x}_0) d\mathbf{x}_0 \cdots d\mathbf{x}_{n-2} \right\} d\mathbf{x}_{n-1}. \quad (9.649)$$

The term in the braces is $p(\mathbf{x}_{n-1} | \mathbf{R}_{n-1})$.

The recursion can be divided into two steps:

Dynamic model update:

$$p(\mathbf{x}_n | \mathbf{R}_n^-) \triangleq \int p(\mathbf{x}_n | \mathbf{x}_{n-1}) p(\mathbf{x}_{n-1} | \mathbf{R}_{n-1}) d\mathbf{x}_{n-1}. \quad (9.650)$$

The “ $-$ ” superscript denotes the probability density before the n th observation.

Observation update:

$$p(\mathbf{x}_n | \mathbf{R}_n) = c p(\mathbf{r}_n | \mathbf{x}_n) p(\mathbf{x}_n | \mathbf{R}_n^-). \quad (9.651)$$

Given the posterior density $p(\mathbf{x}_n | \mathbf{R}_n)$, the MMSE estimate is

$$\hat{\mathbf{x}}_{n,\text{MSE}} \triangleq E \{ \mathbf{x}_n | \mathbf{R}_n \} = \int \mathbf{x}_n p(\mathbf{x}_n | \mathbf{R}_n) d\mathbf{x}_n \quad (9.652)$$

and the MAP estimate is

$$\hat{\mathbf{x}}_{n,\text{MAP}} = \arg \max_{\mathbf{x}_n} \{ \ln p(\mathbf{r}_n | \mathbf{x}_n) + \ln p(\mathbf{x}_n | \mathbf{R}_n^-) \}. \quad (9.653)$$

For an estimate $\hat{\mathbf{x}}_n$, the conditional MSE matrix is

$$\mathbf{P}_n \triangleq E_{\mathbf{x}_n | \mathbf{R}_n} \{ [\mathbf{x}_n - \hat{\mathbf{x}}_n] [\mathbf{x}_n - \hat{\mathbf{x}}_n]^T \} = \int [\mathbf{x}_n - \hat{\mathbf{x}}_n] [\mathbf{x}_n - \hat{\mathbf{x}}_n]^T p(\mathbf{x}_n | \mathbf{R}_n) d\mathbf{x}_n. \quad (9.654)$$

The results in (9.650)–(9.654) are exact and have been known for a number of years. Unfortunately, an exact solution is not feasible in the general case.

There is a long history of attempts to find computationally feasible solutions to this problem; for example, Ho and Lee [HL64], Bryson and Frazier [BF63], Cox [Cox64], Jazwinski [Jaz70], Gelb [Gel74], Zadeh [Zad53], Sorenson [Sor88], and Anderson and Moore [AM79]. More recent book references include Stone et al. [SBC99], Bar-Shalom et al. [BSLK01], and Ristic et al. [RAG04].

Ristic et al. [RAG04] divides nonlinear filtering implementations into five categories:¹⁵

1. Finite-dimensional filters
2. Analytical approximations
3. Grid-based methods
4. Gaussian sum filters
5. Particle filters.

The first category contains a class of models where exact solutions are available. The next four categories describe approximate nonlinear systems.

For a certain class of nonlinear models, a finite-dimensional sufficient statistic exists and an exact finite-dimensional filter can be found. Two of these exact filters are known as Benes and Daum filters after their inventors. They are described in Benes [Ben81] and Daum [Dau86], [Dau88], [Dau95]. Brigo, Hanzon, and LeGland [BHL98] develop a projection filter approximation that results in a finite-dimensional filter.

Analytic approximations linearize the nonlinear functions in the process model and observation model. They include the extended Kalman filter (EKF), the higher-order EKF, and the iterated EKF. Derivations of the various versions of the EKF are contained in [Jaz70], [Gel74], [AM79], [Sor85], [BSLK01], and [RAG04].

We include a summary of the EKF equations because of their relationship to the recursive Bayesian CRB. The second-order EKF was derived by Athans, Wishner, and Bertolini [AWB68] for the continuous-time dynamic system and discrete-time observations. They gave examples in which the second-order EKF gives significant improvement over the first-order EKF (e.g. [BSLK01]). The second-order EKF is related to the recursive Bayesian Bhattacharyya bound.

Grid-based methods discretize the integration variable in (9.650) and replace the integral with a summation. They are discussed in [Sor74], [KS88], [Kas00], and [Sto01], and summarized in Section 2.2 of [RAG04]. The practical difficulty is that the dimension grows quickly.

Gaussian sum filters approximate $p(\mathbf{x}_k | \mathbf{R}_k)$ by a weighted sum of Gaussian probability densities. They are due to Sorenson and Alspach (e.g., [SA71, AS72], and [BSLK01]) and summarized in Section 2.3 of [RAG04].

Particle filters implement the recursive Bayesian filter using sequential Monte Carlo simulations that utilize importance sampling. Arulampalan, Maskell, Gordon, and Clapp in [AMGC02], and Doucet et al. [DGA00], [DG02] provide broad discussions of particle filters. Other references include Gordon et al. [GSS93], Doucet et al. [DdG01], and Carpenter et al. [CCF99].

In the next section, we introduce the extended Kalman filter.

9.3.5.2 Extended Kalman Filter

For the special case of nonlinear models with additive noise, we have

$$\mathbf{x}_k = \mathbf{f}_{k-1}(\mathbf{x}_{k-1}) + \mathbf{u}_{k-1}, \quad (9.655)$$

$$\mathbf{r}_k = \mathbf{c}_k(\mathbf{x}_k) + \mathbf{w}_k, \quad (9.656)$$

¹⁵Our discussion follows Chapters 2 and 3 of [RAG04]. Our goal is to introduce the ideas and direct the reader to appropriate references. One technique, the extended Kalman filter, is discussed in more detail because of its relationship to the Bayesian Cramér–Rao bound.

where the \mathbf{u}_k and \mathbf{w}_k are statistically Gaussian random vectors $N(\mathbf{0}, \mathbf{Q}_k)$ and $N(\mathbf{0}, \mathbf{R}_k)$. The nonlinearity of $\mathbf{f}_{k-1}(\cdot)$ causes the signal process to be non-Gaussian. The nonlinearity of observation causes the received process to be non-Gaussian.

The extended Kalman filter is derived by approximating the nonlinear functions by the first term in their Taylor series expansion evaluated at the estimated state vector.¹⁶

They are the Jacobians

$$\tilde{\mathbf{F}}_{k-1} = [\nabla_{\mathbf{x}_{k-1}} [\mathbf{f}_{k-1}^T(\mathbf{x}_{k-1})]]^T \Big|_{\mathbf{x}_{k-1} = \hat{\mathbf{x}}_{k-1}} \quad (9.657)$$

or

$$[\tilde{\mathbf{F}}_{k-1}]_{ij} = \frac{\partial f_{k-1,i}}{\partial x_{k-1,j}} \Big|_{\mathbf{x}_{k-1} = \hat{\mathbf{x}}_{k-1}}, \quad (9.658)$$

and

$$\tilde{\mathbf{C}}_k = [\nabla_{\mathbf{x}_k} [\mathbf{c}_k^T(\mathbf{x}_k)]]^T \Big|_{\mathbf{x}_k = \hat{\mathbf{x}}_{k|k-1}} \quad (9.659)$$

or

$$[\tilde{\mathbf{C}}_k]_{ij} = \frac{\partial c_{k,i}}{\partial x_{k,j}} \Big|_{\mathbf{x}_k = \hat{\mathbf{x}}_{k|k-1}}. \quad (9.660)$$

We can then use a standard Kalman filter on the linearized equations. The equations are referred to as the *extended Kalman filter* (EKF). A good history of the extended Kalman filter is given in Sorenson [Sor85]. He attributed the first version to Swerling [Swe59]. Gelb [Gel74] has derivations for continuous, discrete, and mixed cases. Other references include Anderson and Moore [AM79] and Athans et al. [AWB68]. A recent reference with the derivation is Bar-Shalom et al. [BSLK01] and the equations are given in Ristic et al. [RAG04].

The EKF for the covariance version follows from (9.275)–(9.286):

1. Initialize the algorithm with

$$\hat{\mathbf{x}}_0 = \mathbf{m}_0 \quad (9.661)$$

and

$$\mathbf{P}_0 = \mathbf{P}_0. \quad (9.662)$$

2. Calculate the prediction step

$$\hat{\mathbf{x}}_{k|k-1} = \mathbf{f}_{k-1}(\hat{\mathbf{x}}_{k-1}) \quad (9.663)$$

and the MSE is

$$\mathbf{P}_{k|k-1} = \tilde{\mathbf{F}}_{k-1} \mathbf{P}_{k-1} \tilde{\mathbf{F}}_{k-1}^T + \mathbf{G}_{k-1} \mathbf{Q}_{k-1} \mathbf{G}_{k-1}^T. \quad (9.664)$$

Note that the estimate may be biased.

¹⁶We have used $\mathbf{x}_{k|k-1} \triangleq \mathbf{x}(k|k-1)$ and $\hat{\mathbf{x}}_{k-1} \triangleq \hat{\mathbf{x}}(k-1)$ to make the derivative expressions more readable.

3. Calculate the EKF gain matrix

$$\mathbf{K}_k = \mathbf{P}_{k|k-1} \tilde{\mathbf{C}}_k^T [\tilde{\mathbf{C}}_k \mathbf{P}_{k|k-1} \tilde{\mathbf{C}}_k^T + \mathbf{R}_k]^{-1}. \quad (9.665)$$

4. Compute $\hat{\mathbf{x}}_k$

$$\hat{\mathbf{x}}_k = \hat{\mathbf{x}}_{k|k-1} + \mathbf{K}_k [\mathbf{r}_k - \mathbf{c}_k(\hat{\mathbf{x}}_{k|k-1})]. \quad (9.666)$$

whose MSE equation is

$$\mathbf{P}_k = [\mathbf{I} - \mathbf{K}_k \tilde{\mathbf{C}}_k] \mathbf{P}_{k|k-1} [\mathbf{I} - \mathbf{K}_k \tilde{\mathbf{C}}_k]^T + \mathbf{K}_k \mathbf{R}_k \mathbf{K}_k^T, \quad (9.667)$$

where $\tilde{\mathbf{F}}_{k-1}$ and $\tilde{\mathbf{C}}_k$ are linearizations of \mathbf{f}_{k-1} and \mathbf{c}_k in (9.657) and (9.659), respectively, about the estimated state vector. Note that \mathbf{P}_k and \mathbf{K}_k are functions of the data, so they cannot be precomputed.

The information version of the EKF follows from (9.332) to (9.340).

1. Initialize with \mathbf{J}_0 and $\hat{\mathbf{x}}_0$.
2. Predict

$$\mathbf{J}_{k|k-1} = [\mathbf{G}_{k-1} \mathbf{Q}_{k-1} \mathbf{G}_{k-1}^T + \tilde{\mathbf{F}}_{k-1} \mathbf{J}_{k-1}^{-1} \tilde{\mathbf{F}}_{k-1}^T]^{-1} \quad (9.668)$$

and

$$\hat{\mathbf{x}}_{k|k-1} = \mathbf{f}_{k-1}(\hat{\mathbf{x}}_{k-1}). \quad (9.669)$$

3. Calculate

$$\tilde{\mathbf{T}}_{p,k} = \tilde{\mathbf{C}}_k^T \mathbf{R}_k^{-1}, \quad (9.670)$$

$$\tilde{\mathbf{D}}_k = \tilde{\mathbf{C}}_k^T \mathbf{R}_k^{-1} \tilde{\mathbf{C}}_k. \quad (9.671)$$

4. Update

$$\mathbf{J}_k = \mathbf{J}_{k|k-1} + \tilde{\mathbf{D}}_k, \quad (9.672)$$

$$\mathbf{K}_k = \mathbf{J}_k^{-1} \tilde{\mathbf{T}}_{p,k}, \quad (9.673)$$

$$\hat{\mathbf{x}}_k = \hat{\mathbf{x}}_{k|k-1} + \mathbf{K}_k [\mathbf{r}_k - \mathbf{c}_k(\hat{\mathbf{x}}_{k|k-1})]. \quad (9.674)$$

It is important to note that EKF has no claim to optimality. For some applications it works well and in other cases, it is of marginal or zero value. We discuss some general guidelines after we examine some applications in Section 9.3.5.4.

With a few exceptions, all of the nonlinear filters of interest have to be evaluated by simulation. Thus, it is important to be able to find computationally feasible recursive Bayesian bounds on the MSE matrix of any nonlinear estimator. We develop one of these bounds, the recursive Bayesian CRB, in the next section.

9.3.5.3 Recursive Bayesian Cramér–Rao Bounds

In our book on Bayesian Bounds [VB07], we developed a sequence of recursive versions of the various static parameter bounds based on the covariance inequality that were derived in Chapter 5. The other two techniques (the Ziv–Zakai family and the MIE) do not appear

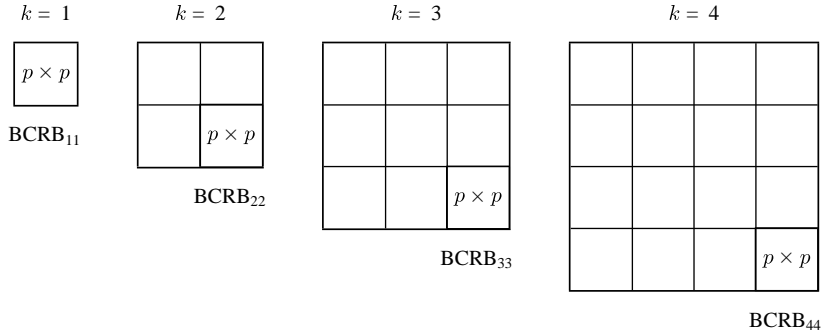


Figure 9.60: Dimensionality growth of BCRB.

to have recursive implementations. In this section, we restrict our attention to the Bayesian Cramér–Rao bound.

A sequence of papers have derived various versions of a Bayesian Cramér–Rao bound for this model. [BZ75] was the first to derive the BCRB for a scalar discrete-time system. Later papers include [Gal79] and [Doe95]. All of these papers related the nonlinear problem to an “equivalent” linear system. Finally, in 1998, [TMN98] derived an efficient recursive Bayesian Cramér–Rao bound on the MSE matrix of the state vector estimator $\hat{\mathbf{x}}_n$. This paper has become the primary reference for subsequent analyses. A subsequent paper [ŠKT01] extended the results to the smoothing and prediction problems.

Recall that \mathbf{x}_n is a $p \times 1$ vector and there are n observations. Thus, $\mathbf{J}(\mathbf{X}_n)$ is $np \times np$. We can write the Bayesian CRB using (4.513). The result will be an $np \times np$ matrix with an expectation over the entire sequence of state vectors $\mathbf{x}_1, \dots, \mathbf{x}_n$. This dimensionality growth is illustrated in Figure 9.60. If we decompose

$$\mathbf{X}_n = \begin{bmatrix} \mathbf{x}_{n-1} \\ \mathbf{x}_n \end{bmatrix}, \quad (9.675)$$

where

$$\mathbf{X}_{n-1} = \text{vec} [\mathbf{x}_1 \ \mathbf{x}_2 \ \cdots \ \mathbf{x}_{n-1}], \quad (9.676)$$

then we are only interested in the $p \times p$ matrix in the lower-right corner, BCRB_{nn} . We define

$$\mathbf{J}_n \triangleq \text{BCRB}_{nn}^{-1}. \quad (9.677)$$

The key is to find a recursion on the $p \times p$ matrix \mathbf{J}_n .

In [TMN98], Tichavský, Muravchik, and Nehorai show that

$$\mathbf{J}_{n+1} = \mathbf{D}_n^{22} - \mathbf{D}_n^{21} (\mathbf{J}_n + \mathbf{D}_n^{11})^{-1} \mathbf{D}_n^{12}, \quad (9.678)$$

where

$$\mathbf{D}_n^{11} = E_{\mathbf{x}_n, \mathbf{x}_{n+1}} [-\Delta_{\mathbf{x}_n}^{\mathbf{x}_n} \ln p(\mathbf{x}_{n+1} | \mathbf{x}_n)], \quad (9.679)$$

$$\mathbf{D}_n^{12} = E_{\mathbf{x}_n, \mathbf{x}_{n+1}} [-\Delta_{\mathbf{x}_n}^{\mathbf{x}_{n+1}} \ln p(\mathbf{x}_{n+1} | \mathbf{x}_n)], \quad (9.680)$$

$$\mathbf{D}_n^{22} = E_{\mathbf{x}_n, \mathbf{x}_{n+1}} [-\Delta_{\mathbf{x}_{n+1}}^{\mathbf{x}_n} \ln p(\mathbf{x}_{n+1} | \mathbf{x}_n)] + E_{\mathbf{x}_{n+1}, \mathbf{r}_{n+1}} [-\Delta_{\mathbf{x}_{n+1}}^{\mathbf{x}_{n+1}} \ln p(\mathbf{r}_{n+1} | \mathbf{x}_{n+1})]. \quad (9.681)$$

The gradient operators are

$$\nabla_{\alpha} = \begin{bmatrix} \frac{\partial}{\partial \alpha_1} & \frac{\partial}{\partial \alpha_2} & \cdots & \frac{\partial}{\partial \alpha_p} \end{bmatrix}^T \quad (9.682)$$

and

$$\Delta_{\beta}^{\alpha} = \nabla_{\beta} [\nabla_{\alpha}^T]. \quad (9.683)$$

The structure of recursion is

$$\mathbf{J}_{n+1} = [\mathbf{D}_n^{22}(1) - \mathbf{D}_n^{21}(\mathbf{J}_n + \mathbf{D}_n^{11})^{-1}\mathbf{D}_n^{12}] + \mathbf{D}_n^{22}(2), \quad (9.684)$$

where $\mathbf{D}_n^{22}(1)$ and $\mathbf{D}_n^{22}(2)$ are the two terms in \mathbf{D}_n^{22} in (9.681). The first term in (9.684) is the prediction of the Bayesian information matrix (BIM) using the process model and the second term incorporates the updated measurement.

It is generally useful to write the expectation in $\mathbf{D}_n^{22}(2)$ as

$$E_{\mathbf{x}_{n+1}} \left\{ E_{\mathbf{r}_{n+1}|\mathbf{x}_{n+1}} \left[-\Delta_{\mathbf{x}_{n+1}}^{\mathbf{x}_{n+1}} \ln p(\mathbf{r}_{n+1}|\mathbf{x}_{n+1}) \right] \right\}, \quad (9.685)$$

because the term inside the braces is the classic Fisher information matrix (FIM) that has been evaluated for a large number of applications. Note that this is a “static parameter” FIM so that many of the results from Chapters 4 and 5 can be used. This observation is important because the two-term structure of (9.684) allows us to turn any static parameter estimation problem into a dynamic estimation problem by defining the process model for the parameter vector and computing the first term in (9.684). The term inside the braces in (9.685) has already been computed for the static estimation problem.

We consider three special cases:

1. AWGN: $\mathbf{f}_n(\mathbf{x}_n)$ and $\mathbf{c}_n(\mathbf{x}_n)$ are both linear.
2. AWGN: $\mathbf{f}_n(\mathbf{x}_n)$ and $\mathbf{c}_n(\mathbf{x}_n)$ are nonlinear.
3. AWGN: $\mathbf{f}_n(\mathbf{x}_n)$ is linear and $\mathbf{c}_n(\mathbf{x}_n)$ is nonlinear.

In Case 1, the process and observation equations satisfy the linear Gaussian model

$$\mathbf{x}_{n+1} = \mathbf{F}_n \mathbf{x}_n + \mathbf{v}_n, \quad (9.686)$$

$$\mathbf{r}_n = \mathbf{C}_n \mathbf{x}_n + \mathbf{w}_n, \quad (9.687)$$

where \mathbf{v}_n is Gaussian $\mathbf{N}(\mathbf{0}, \mathbf{Q}_n)$ and \mathbf{w}_n is Gaussian $N(\mathbf{0}, \mathbf{R}_n)$. Writing the log of the various Gaussian densities and substituting into (9.679)–(9.681) gives

$$\mathbf{J}_{n+1} = \mathbf{Q}_n^{-1} - \mathbf{Q}_n^{-1} \mathbf{F}_n [\mathbf{J}_n + \mathbf{F}_n^T \mathbf{Q}_n^{-1} \mathbf{F}_n]^{-1} \mathbf{F}_n^T \mathbf{Q}_n^{-1} + \mathbf{C}_{n+1}^T \mathbf{R}_{n+1}^{-1} \mathbf{C}_{n+1}. \quad (9.688)$$

Using the matrix inversion lemma gives

$$\mathbf{J}_{n+1} = [\mathbf{Q}_n + \mathbf{F}_n \mathbf{J}_n^{-1} \mathbf{F}_n^T]^{-1} + \mathbf{C}_{n+1}^T \mathbf{R}_{n+1}^{-1} \mathbf{C}_{n+1}, \quad (9.689)$$

where the first term is the process prediction and the second term is the measurement update. The recursion in (9.689) is familiar from the information matrix version of the Kalman filter in (9.339).

In Case 2, $\mathbf{f}_n(\mathbf{x}_n)$ and $\mathbf{c}_n(\mathbf{x}_n)$ are nonlinear and \mathbf{v}_n and \mathbf{w}_n are AWGN. The process and observation equations are

$$\mathbf{x}_{n+1} = \mathbf{f}_n(\mathbf{x}_n) + \mathbf{v}_n, \quad (9.690)$$

$$\mathbf{z}_n = \mathbf{c}_n(\mathbf{x}_n) + \mathbf{w}_n, \quad (9.691)$$

where \mathbf{v}_n is Gaussian $N(\mathbf{0}, \mathbf{Q}_n)$ and \mathbf{w}_n is Gaussian $N(\mathbf{0}, \mathbf{R}_n)$. The \mathbf{v}_n and \mathbf{w}_n are statistically independent of each other and successive \mathbf{v}_n and \mathbf{w}_n are statistically independent. The logs of the two probability densities are

$$-\ln p(\mathbf{x}_{n+1}|\mathbf{x}_n) = c_1 + \frac{1}{2} [\mathbf{x}_{n+1} - \mathbf{f}_n(\mathbf{x}_n)]^T \mathbf{Q}_n^{-1} [\mathbf{x}_{n+1} - \mathbf{f}(\mathbf{x}_n)], \quad (9.692)$$

$$-\ln p(\mathbf{r}_{n+1}|\mathbf{x}_{n+1}) = c_2 + \frac{1}{2} [\mathbf{r}_{n+1} - \mathbf{c}_{n+1}(\mathbf{x}_{n+1})]^T \mathbf{R}_n^{-1} [\mathbf{r}_{n+1} - \mathbf{c}_{n+1}(\mathbf{x}_{n+1})]. \quad (9.693)$$

Therefore,

$$\mathbf{D}_n^{11} = E_{\mathbf{x}_n} \left\{ [\nabla_{\mathbf{x}_n} \mathbf{f}_n^T(\mathbf{x}_n)] \mathbf{Q}_n^{-1} [\nabla_{\mathbf{x}_n} \mathbf{f}^T(\mathbf{x}_n)]^T \right\}, \quad (9.694)$$

$$\mathbf{D}_n^{12} = -E_{\mathbf{x}_n} \left\{ \nabla_{\mathbf{x}_n} \mathbf{f}_n^T(\mathbf{x}_n) \right\} \mathbf{Q}_n^{-1}, \quad (9.695)$$

$$\mathbf{D}_n^{22} = \mathbf{Q}_n^{-1} + E_{\mathbf{x}_{n+1}} \left\{ [\nabla_{\mathbf{x}_{n+1}} \mathbf{c}_{n+1}^T(\mathbf{x}_{n+1})] \mathbf{R}_{n+1}^{-1} [\nabla_{\mathbf{x}_{n+1}} \mathbf{c}_{n+1}^T(\mathbf{x}_{n+1})]^T \right\}. \quad (9.696)$$

Define

$$\tilde{\mathbf{F}}_n(\mathbf{x}_n) = [\nabla_{\mathbf{x}_n} \mathbf{f}_n^T(\mathbf{x}_n)]^T, \quad (9.697)$$

$$\tilde{\mathbf{C}}_{n+1}(\mathbf{x}_{n+1}) = [\nabla_{\mathbf{x}_{n+1}} \mathbf{c}_{n+1}^T(\mathbf{x}_{n+1})]^T. \quad (9.698)$$

Note that $\tilde{\mathbf{F}}_n(\mathbf{x}_n)$ and $\tilde{\mathbf{C}}_{n+1}(\mathbf{x}_{n+1})$ are the Jacobians of $\mathbf{f}_n(\mathbf{x}_n)$ and $\mathbf{c}_{n+1}(\mathbf{x}_{n+1})$, respectively, evaluated at their true values,

$$[\tilde{\mathbf{F}}_n(\mathbf{x}_n)]_{ij} = \frac{\partial f_{ni}}{\partial x_j}, \quad (9.699)$$

$$[\tilde{\mathbf{C}}_{n+1}(\mathbf{x}_{n+1})]_{ij} = \frac{\partial c_{n+1,i}}{\partial x_j}. \quad (9.700)$$

Suppressing the arguments, we can write

$$\mathbf{D}_n^{11} = E_{\mathbf{x}_n} \left\{ \tilde{\mathbf{F}}_n^T \mathbf{Q}_n^{-1} \tilde{\mathbf{F}}_n \right\}, \quad (9.701)$$

$$\mathbf{D}_n^{12} = -E_{\mathbf{x}_n} \left\{ \tilde{\mathbf{F}}_n^T \right\} \mathbf{Q}_n^{-1}, \quad (9.702)$$

$$\mathbf{D}_n^{22} = \mathbf{Q}_n^{-1} + E_{\mathbf{x}_{n+1}} \left\{ \tilde{\mathbf{C}}_{n+1}^T \mathbf{R}_{n+1}^{-1} \tilde{\mathbf{C}}_{n+1} \right\}, \quad (9.703)$$

and

$$\begin{aligned} \mathbf{J}_{n+1} &= \mathbf{Q}_n^{-1} - \mathbf{Q}_n^{-1} E_{\mathbf{x}_n} \left\{ \tilde{\mathbf{F}}_n \right\} [\mathbf{J}_n + E_{\mathbf{x}_n} \left\{ \tilde{\mathbf{F}}_n^T \mathbf{Q}_n^{-1} \tilde{\mathbf{F}}_n \right\}]^{-1} E_{\mathbf{x}_n} \left\{ \tilde{\mathbf{F}}_n^T \right\} \mathbf{Q}_n^{-1} \\ &\quad + E_{\mathbf{x}_{n+1}} \left\{ \tilde{\mathbf{C}}_{n+1}^T \mathbf{R}_{n+1}^{-1} \tilde{\mathbf{C}}_{n+1} \right\}. \end{aligned} \quad (9.704)$$

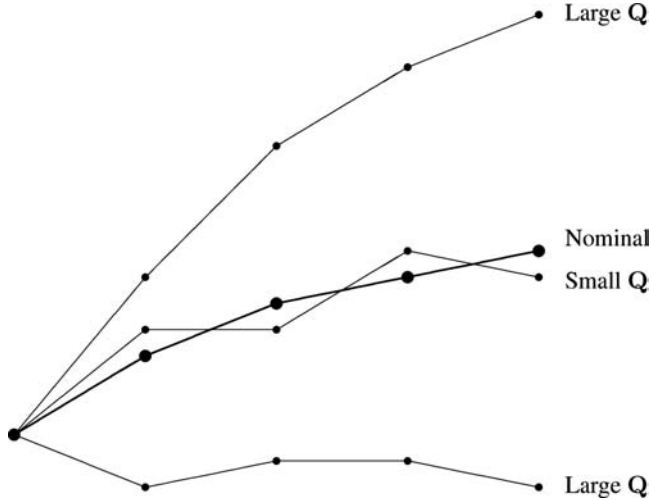


Figure 9.61: Nominal track and typical realizations.

The difficulty in evaluating (9.701)–(9.703) is performing the expectation over the state vector \mathbf{x}_n or \mathbf{x}_{n+1} . We can approximate the expectations using a Monte Carlo simulation. A number of state vector realizations are generated:

$$\mathbf{x}_0^{(i)}, \mathbf{x}_1^{(i)}, \dots, \mathbf{x}_{n+1}^{(i)}; \quad i = 1, \dots, M. \quad (9.705)$$

We then average over the \mathbf{x}_0 realizations to get \mathbf{J}_0 . We then average \mathbf{x}_1 to get the next terms and so forth.

In many applications, the process noise \mathbf{v}_k is small. A typical example is the radar/sonar tracking problem. The nominal track is shown as a thick line in Figure 9.61. A typical realization for small \mathbf{Q} is shown with a thin line. Two realizations for large \mathbf{Q} are also shown. In most cases, the actual squared error for a specific realization depends on the actual track. In the large \mathbf{Q} case, by averaging over very different track realizations, we may lose the relevant information. Thus, in most applications, the small \mathbf{Q} case is the one of interest.

In many applications, the process noise is small enough that we can approximate

$$\mathbf{D}_n^{11} \simeq \tilde{\mathbf{F}}_n^T \mathbf{Q}_n^{-1} \tilde{\mathbf{F}}_n \Big|_{\mathbf{x}_n = \mathbf{x}_{Q0n}}, \quad (9.706)$$

$$\mathbf{D}_n^{12} \simeq -\tilde{\mathbf{F}}_n^T \mathbf{Q}_n^{-1} \Big|_{\mathbf{x}_n = \mathbf{x}_{Q0n}}, \quad (9.707)$$

$$\mathbf{D}_n^{22} \simeq \mathbf{Q}_n^{-1} + \tilde{\mathbf{C}}_{n+1}^T \mathbf{R}_{n+1}^{-1} \tilde{\mathbf{C}}_{n+1} \Big|_{\mathbf{x}_{n+1} = \mathbf{x}_{Q0(n+1)}}, \quad (9.708)$$

where \mathbf{x}_{Q_0n} denotes the true state vector for the case when $\mathbf{Q}_n = \mathbf{0}$. Then,

$$\mathbf{J}_{n+1} = \mathbf{Q}_n^{-1} - \mathbf{Q}_n^{-1} \tilde{\mathbf{F}}_n [\mathbf{J}_n + \tilde{\mathbf{F}}_n^T \mathbf{Q}_n^{-1} \tilde{\mathbf{F}}_n]^{-1} \tilde{\mathbf{F}}_n^T \mathbf{Q}_n^{-1} + \tilde{\mathbf{C}}_{n+1}^T \mathbf{R}_{n+1}^{-1} \tilde{\mathbf{C}}_{n+1}. \quad (9.709)$$

Using the matrix inversion lemma gives

$$\mathbf{J}_{n+1} = [\mathbf{Q}_n + \tilde{\mathbf{F}}_n \mathbf{J}_n^{-1} \tilde{\mathbf{F}}_n^T]^{-1} + \tilde{\mathbf{C}}_{n+1}^T \mathbf{R}_{n+1}^{-1} \tilde{\mathbf{C}}_{n+1}. \quad (9.710)$$

The recursion in (9.710) still allows weak process noise. This recursion is the same as the first-order extended Kalman Filter in (9.672) except that $\tilde{\mathbf{F}}_n$ and $\tilde{\mathbf{C}}_{n+1}$ are evaluated at the true state, whereas in the EKF, they are evaluated at the estimated state.

For zero process noise, set $\mathbf{Q}_n = \mathbf{0}$ and obtain¹⁷

$$\mathbf{J}_{n+1} = [\tilde{\mathbf{F}}^{-1}]^T \mathbf{J}_n \tilde{\mathbf{F}}_n^{-1} + \tilde{\mathbf{C}}_{n+1}^T \mathbf{R}_{n+1}^{-1} \tilde{\mathbf{C}}_{n+1}. \quad (9.711)$$

Note that this result is a recursive version of the classic Cramér–Rao bound for \mathbf{x}_k .

Case 3 has a linear Gaussian process model and a nonlinear observation model with AWGN,

$$\mathbf{x}_{n+1} = \mathbf{F}_n \mathbf{x}_n + \mathbf{v}_n, \quad (9.712)$$

$$\mathbf{r}_n = \mathbf{c}_n(\mathbf{x}_n) + \mathbf{w}_n, \quad (9.713)$$

where \mathbf{v}_n is $N(\mathbf{0}, \mathbf{Q}_n)$ and \mathbf{w}_n is $N(\mathbf{0}, \mathbf{R}_n)$. The recursion in (9.704) reduces to

$$\mathbf{J}_{n+1} = [\mathbf{Q}_n + \mathbf{F}_n \mathbf{J}_n^{-1} \mathbf{F}_n^T]^{-1} + E_{\mathbf{x}_{n+1}} \{ \tilde{\mathbf{C}}_{n+1}^T \mathbf{R}_{n+1}^{-1} \tilde{\mathbf{C}}_{n+1} \}. \quad (9.714)$$

Note that (9.714) is exact and does not require a small process noise assumption.

9.3.5.4 Applications

We consider three examples to illustrate the extended Kalman filter and the recursive Bayesian Cramér–Rao bound. The first example analyzes dynamic frequency estimation and has linear state equations and nonlinear observations. It is an extension of Example 4.15 in Chapter 4. The second example is a 2D tracking application. The state equation is linear and the observation model is nonlinear. The third example analyzes tracking of a ballistic missile as it reenters the atmosphere. It has a nonlinear state model and a linear observation model. In addition, the state vector is augmented with β , the ballistic coefficient which must be estimated.

Example 9.20: Dynamic Frequency Estimation. Consider the problem of estimating the time-varying frequency of a complex sinusoidal signal. The observation equation is¹⁸

$$\tilde{r}(n) = m_0 e^{j\phi_n} + \tilde{w}_n; \quad n = 1, 2, \dots, \quad (9.715)$$

where the \tilde{w}_n are statistically independent circular complex Gaussian random variables with variance $\sigma_{\tilde{w}}^2$.

¹⁷This result was first obtained by Taylor [Tay79].

¹⁸The BCRB in this problem was solved by Tichavský et al. [TMN98]. By using (9.714), we obtain the same answer in a simpler manner. However, we should note that the \mathbf{Q} matrix in this model is singular and the derivation included a \mathbf{Q}^{-1} term.

We rewrite in real notation as

$$\mathbf{r}_n = m_0 \begin{bmatrix} \cos(\phi_n) \\ \sin(\phi_n) \end{bmatrix} + \mathbf{w}_n, \quad (9.716)$$

where

$$\mathbf{R}_n = \frac{\sigma_{\tilde{w}}^2}{2} \mathbf{I}. \quad (9.717)$$

Both m_0 and $\sigma_{\tilde{w}}^2$ are known.

The state vector is

$$\mathbf{x}_n = \begin{bmatrix} \omega_n \\ \phi_n \end{bmatrix} \quad (9.718)$$

and the state equations are

$$\omega_n = \omega_{n-1} + u_{n-1}, \quad (9.719)$$

$$\phi_n = \phi_{n-1} + \omega_n = \phi_{n-1} + \omega_{n-1} + u_{n-1}, \quad (9.720)$$

where the u_{n-1} are statistically independent Gaussian random variables with variance γ^2 . The state equation can be written as

$$\mathbf{x}_n = \begin{bmatrix} 1 & 0 \\ 1 & 1 \end{bmatrix} \mathbf{x}_{n-1} + \begin{bmatrix} u_{n-1} \\ u_{n-1} \end{bmatrix}. \quad (9.721)$$

Thus,

$$\mathbf{F}_n = \begin{bmatrix} 1 & 0 \\ 1 & 1 \end{bmatrix} = \mathbf{F} \quad (9.722)$$

and

$$\mathbf{Q}_n = \gamma^2 \begin{bmatrix} 1 & 1 \\ 1 & 1 \end{bmatrix} = \mathbf{Q}, \quad (9.723)$$

$$\mathbf{G}_n = [1 \ 1]^T = \mathbf{G}. \quad (9.724)$$

The observation matrix is

$$\mathbf{c}_n(\mathbf{x}_n) = m_0 \begin{bmatrix} \cos(\phi_n) \\ \sin(\phi_n) \end{bmatrix}, \quad (9.725)$$

so using (9.660) yields

$$\tilde{\mathbf{C}}_n = [\nabla_{\mathbf{x}_n} [\mathbf{c}_n^T(\mathbf{x}_n)]]_{\mathbf{x}_n=\hat{\mathbf{x}}_{n|n-1}}^T \quad (9.726)$$

$$= m_0 \begin{bmatrix} 0 & -\sin(\hat{\phi}_{n|n-1}) \\ 0 & \cos(\hat{\phi}_{n|n-1}) \end{bmatrix}. \quad (9.727)$$

The EKF equations (9.668)–(9.674) are

$$\hat{\mathbf{x}}_{n|n-1} = \mathbf{F}\hat{\mathbf{x}}_{n-1}, \quad (9.728)$$

$$\mathbf{J}_{n|n-1} = [\mathbf{GQG}^T + \mathbf{F}\mathbf{J}_{n-1}^{-1}\mathbf{F}^T]^{-1}, \quad (9.729)$$

$$\tilde{\mathbf{C}}_n = m_0 \begin{bmatrix} 0 & -\sin(\hat{\phi}_{n|n-1}) \\ 0 & \cos(\hat{\phi}_{n|n-1}) \end{bmatrix}, \quad (9.730)$$

$$\tilde{\mathbf{D}}_n = \frac{2m_0^2}{\sigma_w^2} \begin{bmatrix} 0 & 0 \\ 0 & 1 \end{bmatrix}, \quad (9.731)$$

$$\tilde{\mathbf{T}}_{p,n} = \frac{2}{\sigma_w^2} \tilde{\mathbf{C}}_n^T, \quad (9.732)$$

$$\mathbf{J}_n = \mathbf{J}_{n|n-1} + \tilde{\mathbf{D}}_n, \quad (9.733)$$

$$\mathbf{K}_n = \mathbf{J}_n^{-1} \tilde{\mathbf{T}}_{p,n}, \quad (9.734)$$

$$\hat{\mathbf{x}}_n = \hat{\mathbf{x}}_{n|n-1} + \mathbf{K}_n \left(\mathbf{r}_n - m_0 [\cos(\hat{\phi}_{n|n-1}) \quad \sin(\hat{\phi}_{n|n-1})]^T \right). \quad (9.735)$$

We initialize the EKF with

$$\mathbf{x}_0 = \bar{\mathbf{x}}_0, \quad (9.736)$$

$$\mathbf{J}_0 = \frac{1}{\sigma_0^2} \mathbf{I}. \quad (9.737)$$

We use $\bar{\mathbf{x}}_0 = \mathbf{0}$, $\sigma_0^2 = 0.01\pi^2$, and $m_0^2/\sigma_w^2 = 5$ for the simulation.

We run 100 simulations and compute the MSE and the variance of ω_n using $[\mathbf{P}_n]_{11}$ from (9.667). We then average over the simulations.

In order to compute the BCRB, we use (9.714) for the recursion. Define

$$\mathbf{J}_n = \begin{bmatrix} J_n^{\omega\omega} & J_n^{\omega\phi} \\ J_n^{\phi\omega} & J_n^{\phi\phi} \end{bmatrix}. \quad (9.738)$$

The first term in (9.714) is

$$[\mathbf{Q}_n + \mathbf{F}_n \mathbf{J}_n^{-1} \mathbf{F}_n^T]^{-1} = \left(\gamma^2 \begin{bmatrix} 1 & 1 \\ 1 & 1 \end{bmatrix} + \frac{1}{d_n} \begin{bmatrix} 1 & 0 \\ 1 & 1 \end{bmatrix} \begin{bmatrix} J_n^{\phi\phi} & -J_n^{\omega\phi} \\ -J_n^{\omega\phi} & J_n^{\omega\omega} \end{bmatrix} \begin{bmatrix} 1 & 1 \\ 0 & 1 \end{bmatrix} \right)^{-1}, \quad (9.739)$$

where

$$d_n = \det[\mathbf{J}_n] = J_n^{\phi\phi} J_n^{\omega\omega} - (J_n^{\omega\phi})^2. \quad (9.740)$$

The second term in (9.714) is

$$\begin{bmatrix} 0 \\ -jm_0 e^{-j\phi_n} \end{bmatrix} \cdot \frac{1}{\sigma_w^2} \begin{bmatrix} 0 & jm_0 e^{j\phi_n} \end{bmatrix} = \frac{1}{\sigma_w^2} \begin{bmatrix} 0 & 0 \\ 0 & m_0^2 \end{bmatrix}, \quad (9.741)$$

which does not depend on \mathbf{x}_{n+1} , so the expectation in (9.714) is not required. Adding (9.739) and (9.741) and simplifying gives the recursion for the Bayesian information matrix,

$$\mathbf{J}_{n+1} = \frac{1}{1 + \gamma^2 J_n^{\phi\phi}} \begin{bmatrix} \gamma^2 d_n + J_n^{\omega\omega} - 2J_n^{\omega\phi} + J_n^{\phi\phi} & -\gamma^2 d_n + J_n^{\omega\phi} - J_n^{\phi\phi} \\ -\gamma^2 d_n + J_n^{\omega\phi} - J_n^{\phi\phi} & \gamma^2 d_n + J_n^{\phi\phi} + \frac{2m_0^2}{\sigma_w^2} (1 + \gamma^2 J_n^{\omega\omega}) \end{bmatrix}, \quad (9.742)$$

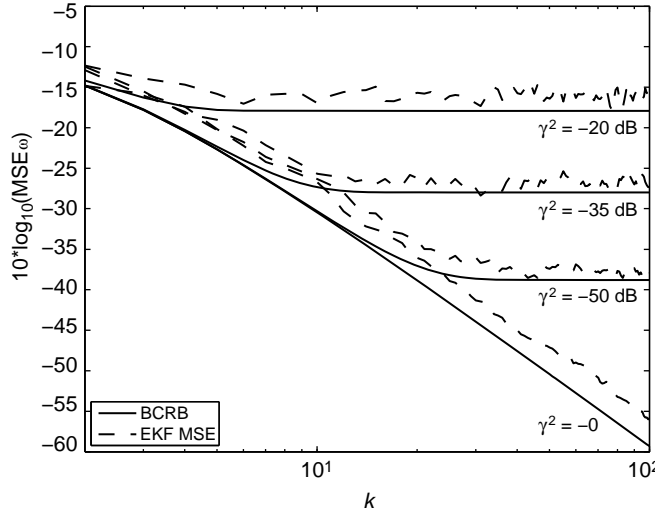


Figure 9.62: Dynamic frequency estimation versus k ; MSE and $\text{Var}(w_n)$, $m_0^2/\sigma_w^2 = 5$.

which is initialized with

$$\mathbf{J}_0 = \frac{1}{\sigma_0^2} \mathbf{I}. \quad (9.743)$$

The result in (9.742) is Equation (98) in [TMN98].

The EKF MSE and the BCRB are shown in Figure 9.62 for various values of γ^2 . The EKF is close to the BCRB but not on it. The EKF is sensitive to the variance in the initial conditions. The value $\sigma_0 = 0.1\pi$ (which is pretty large) in the simulation was the largest that we could use and have the EKF work. It was less sensitive to the value of \bar{x}_0 . We generated a starting state vector according to a uniform distortion with zero mean and variance = 0.1π and the results were similar. ■

1. For nonzero γ^2 , the BCRB approaches a steady-state value. The analytic expression for \mathbf{J}_∞ is given in [TMN98].
2. For $\gamma^2 = 0$ (constant frequency), the BCRB reduces to

$$B(\hat{\omega}_n) = \frac{6}{n(n^2 - 1)} \frac{\sigma_{\tilde{w}}^2}{m_0^2}, \quad (9.744)$$

which is the result in Example 4.29.

3. If m_0 is a zero-mean complex Gaussian random variable with unknown variance σ_m^2 and $\sigma_{\tilde{w}}^2$ is unknown, we use a 4×1 mixed parameter vector $\boldsymbol{\theta} = [\omega_n \ \phi_n \ \sigma_m^2 \ \sigma_{\tilde{w}}^2]^T$, where σ_m^2 and $\sigma_{\tilde{w}}^2$ are unknown nonrandom quantities. We use a recursive version of the hybrid CRB.
4. To study the general frequency modulation problem, we expand the state vector $\boldsymbol{\omega}_n$,

$$\boldsymbol{\omega}_n = [\omega_n \ \dot{\omega}_n \ \ddot{\omega}_n \ \dots]^T$$

to model the message process.

5. For large SNR, a phase-locked loop with the correct loop filter will approach the BCRB.

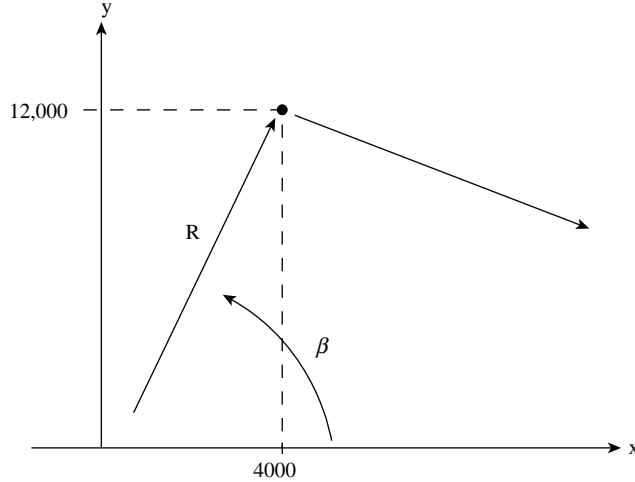


Figure 9.63: Two-dimensional tracking problem.

As in the static-parameter cases in many applications, the BCRB provides a tight bound when the SNR is high. The asymptotic case ($n \rightarrow \infty$) does not play the same role as in the static-parameter case because \mathbf{x}_n is changing. For the special case in which f_n and c_n are constant, a stationary bound is obtained as $n \rightarrow \infty$ (e.g., [TMN98]). This example is representative of many nonlinear filtering problems.

Example 9.21: Two-Dimensional Tracking. In this example, we consider the two-dimensional version of the tracking problem in Example 9.10. The nominal trajectory is a constant velocity track in the $x - y$ plane as shown in Figure 9.63.

The state vector is four-dimensional,

$$\mathbf{x}(k) = [x(k) \quad v_x(k) \quad y(k) \quad v_y(k)] \quad (9.745)$$

and

$$\mathbf{F} = \begin{bmatrix} 1 & T & 0 & 0 \\ 0 & 1 & 0 & 0 \\ 0 & 0 & 1 & T \\ 0 & 0 & 0 & 1 \end{bmatrix}, \quad (9.746)$$

where T is the sampling interval.

We assume that the acceleration in the x and y directions as statistically independent zero-mean discrete-time white processes.

We define

$$\mathbf{a}(k) \triangleq \begin{bmatrix} a_x(k) \\ a_y(k) \end{bmatrix} \quad (9.747)$$

and

$$E \{ \mathbf{a}(k) \mathbf{a}^T(k) \} = \begin{bmatrix} \sigma_x^2 & 0 \\ 0 & \sigma_y^2 \end{bmatrix}. \quad (9.748)$$

Then,

$$\mathbf{u}(k) = \begin{bmatrix} \frac{T^2}{2} & T & 0 & 0 \\ 0 & 0 & \frac{T^2}{2} & T \end{bmatrix}^T \mathbf{a}(k) \quad (9.749)$$

and

$$\mathbf{Q} = \begin{bmatrix} \sigma_x^2 \begin{bmatrix} \frac{T^4}{4} & \frac{T^3}{2} \\ \frac{T^3}{2} & T^2 \end{bmatrix} & \mathbf{0} \\ \mathbf{0} & \sigma_y^2 \begin{bmatrix} \frac{T^4}{4} & \frac{T^3}{2} \\ \frac{T^3}{2} & T^2 \end{bmatrix} \end{bmatrix}. \quad (9.750)$$

The radar observes range and bearing in the presence of white noise

$$\mathbf{C}(k) = \begin{bmatrix} (x^2(k) + y^2(k))^{\frac{1}{2}} \\ \tan^{-1} \left(\frac{y(k)}{x(k)} \right) \end{bmatrix} \quad (9.751)$$

and

$$\mathbf{R}(k) = \begin{bmatrix} \sigma_r^2 & 0 \\ 0 & \sigma_\beta^2 \end{bmatrix}. \quad (9.752)$$

Using (9.660) yields

$$\tilde{\mathbf{C}}(k) = \begin{bmatrix} \frac{x(k)}{R(k)} & 0 & \frac{y(k)}{R(k)} & 0 \\ -\frac{y(k)}{R^2(k)} & 0 & \frac{x(k)}{R^2(k)} & 0 \end{bmatrix}. \quad (9.753)$$

We use the EKF equations (9.663)–(9.667) with

$$\tilde{\mathbf{F}}(k) = \mathbf{F}, \quad (9.754)$$

$$x(0) = 4,000 \text{ m}, \quad (9.755)$$

$$y(0) = 12,000 \text{ m}, \quad (9.756)$$

$$v_x(0) = 80 \text{ m/s}, \quad (9.757)$$

$$v_y(0) = -20 \text{ m/s}, \quad (9.758)$$

$$\sigma_x^2 = \sigma_y^2 = 40 (\text{m/s}^2)^2, \quad (9.759)$$

$$\sigma_r^2 = 500 \text{ m}^2, \quad (9.760)$$

$$\sigma_\beta^2 = 0.04 \text{ rad}^2, \quad (9.761)$$

$$T = 0.1 \text{ s}. \quad (9.762)$$

We use an initial state of the estimate

$$\hat{\mathbf{x}}^T(0) = [5000 \quad 90 \quad 15,000 \quad -20], \quad (9.763)$$

with $\mathbf{P}(0) = 1000 \mathbf{I}$.

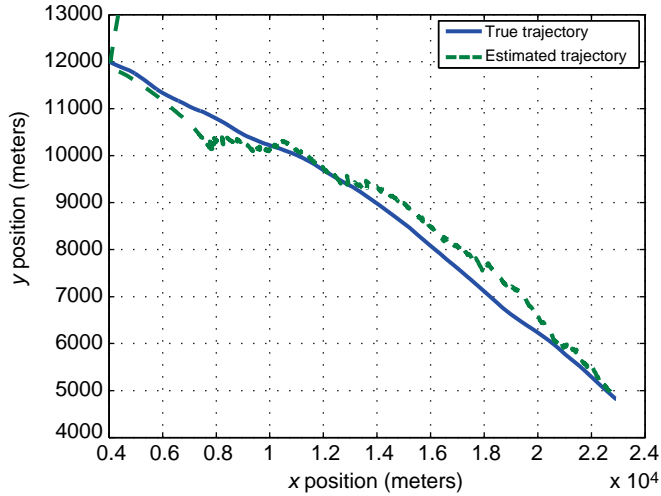


Figure 9.64: A realization of the true trajectory and the estimated trajectory.

In Figure 9.64, we show a realization of a true trajectory and an estimated trajectory. In Figure 9.65, we show realization of the true position and velocity and the estimated position and velocity. In Figure 9.66, we show the biases of the position and velocity estimates versus k . In Figure 9.67, we show the root MSE of the position and velocity estimates. To evaluate the Bayesian CRB, we observe that our model is Case 3, (9.712)–(9.714). For our model (9.714) reduces to

$$\mathbf{J}_{k+1} = (\mathbf{Q} + \mathbf{F}\mathbf{J}_k^{-1}\mathbf{F}^T) + E_{\mathbf{x}_{k+1}} \{ \tilde{\mathbf{C}}_{k+1} \mathbf{R}^{-1} \tilde{\mathbf{C}}_{k+1} \}. \quad (9.764)$$

In Figure 9.68, we plot $\sqrt{\text{MSE}}$ and $\sqrt{\text{BCRB}}$ versus k . The RMSE approaches the BCRB as k increases.

The performance is not sensitive to the initial estimates. We should note that we chose a trajectory that remained in the first quadrant. The arctangent function in (9.751) is periodic with period π . For cases where the observed values may be in a different quadrant than the true value (e.g., trajectories passing close to the origin), the algorithm must be modified. Fortunately, this is not an issue in most applications. ■

The third example considers tracking a ballistic object (e.g., missile) on reentry into the atmosphere. As we would expect, a significant amount of research has been devoted to this problem. We use a model that originally appeared in [Gel74] (Example 6.1–6.2 on page 194 and also is used in Chapter 5 of Ristic et al. [RAG04]).

In addition to being an important application, it introduces the technique of estimating a parameter in a model by augmenting the state vector.

Example 9.22: Ballistic Object Tracking. In this example,¹⁹ we consider the problem of tracking a ballistic object as it reenters the atmosphere. Its speed is high and its time to impact is

¹⁹This example is taken from Chapter 5 of Ristic, Arulampalam, and Gordon's book, "Beyond the Kalman filter", [RAG04].

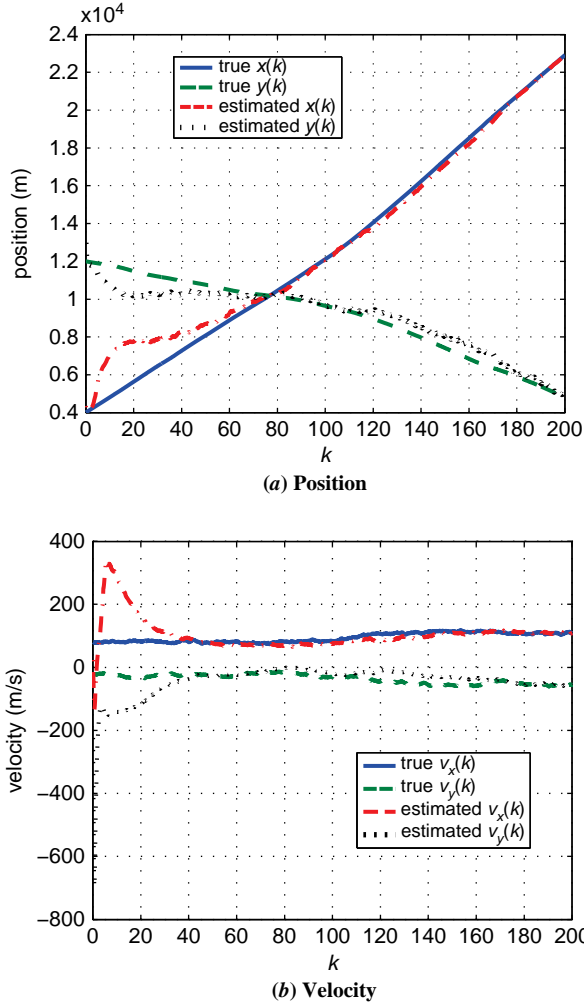


Figure 9.65: Realization of the true position and velocity and the estimated position and velocity.

short. We assume it is traveling in a vertical direction as shown in Figure 9.69 assuming that drag and gravity are the only focus acting on it, then

$$\dot{x}_1 = \dot{h} = -v, \quad (9.765)$$

$$\dot{x}_2 = \dot{v} = \frac{-\rho(h) \cdot g \cdot v^2}{2\beta} + g, \quad (9.766)$$

$$\dot{x}_3 = \dot{\beta} = 0, \quad (9.767)$$

where h is altitude, v is velocity, $\rho(h)$ is air density, $g = 9.81 \text{ m/s}^2$ is acceleration due to gravity, and β is the ballistic coefficient. Air density, measured in kg/m^3 , is modeled as an exponentially decaying function of altitude h ,

$$\rho(h) = \gamma \exp(-\eta h) \quad (9.768)$$

with $\gamma = 1.754$ and $\eta = 1.49 \times 10^{-4}$.

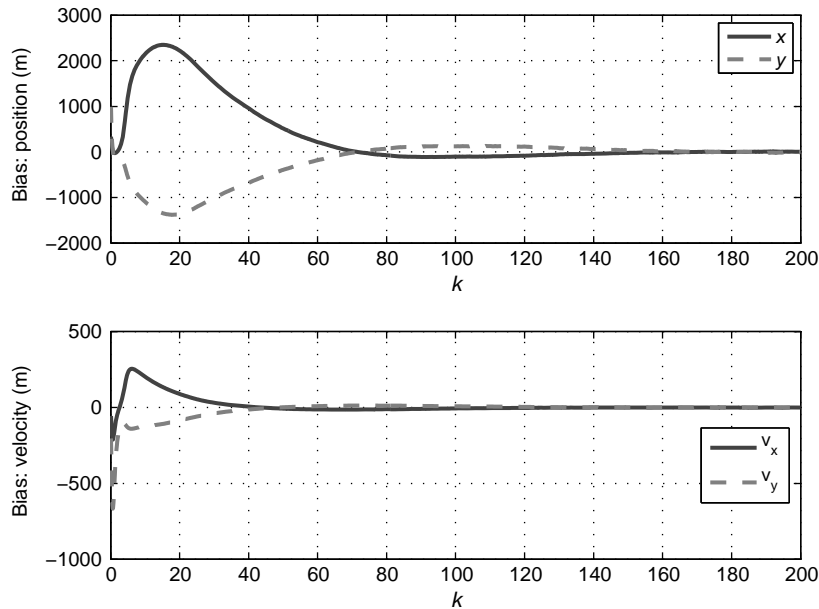


Figure 9.66: Bias of the position and velocity estimates.

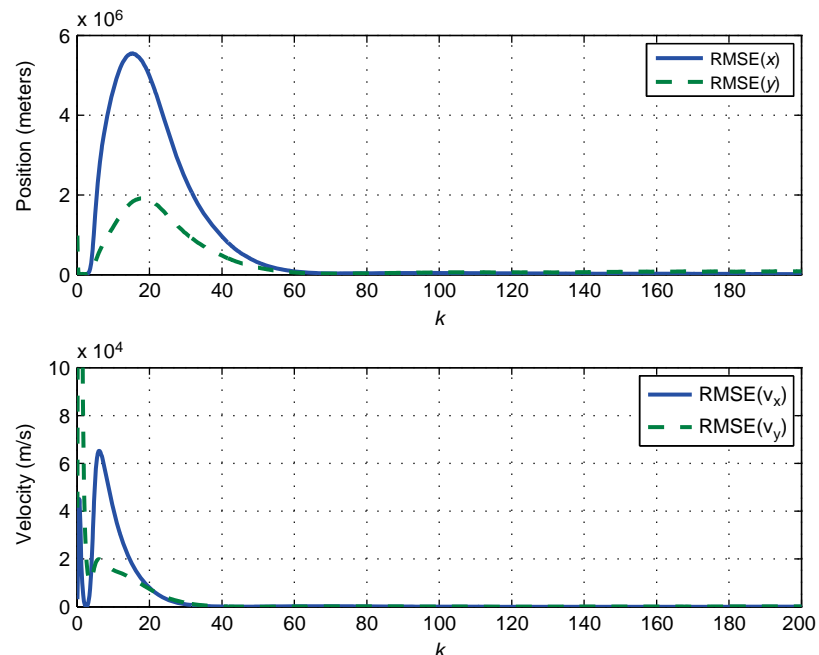


Figure 9.67: Root mean square estimates of the position and velocity.

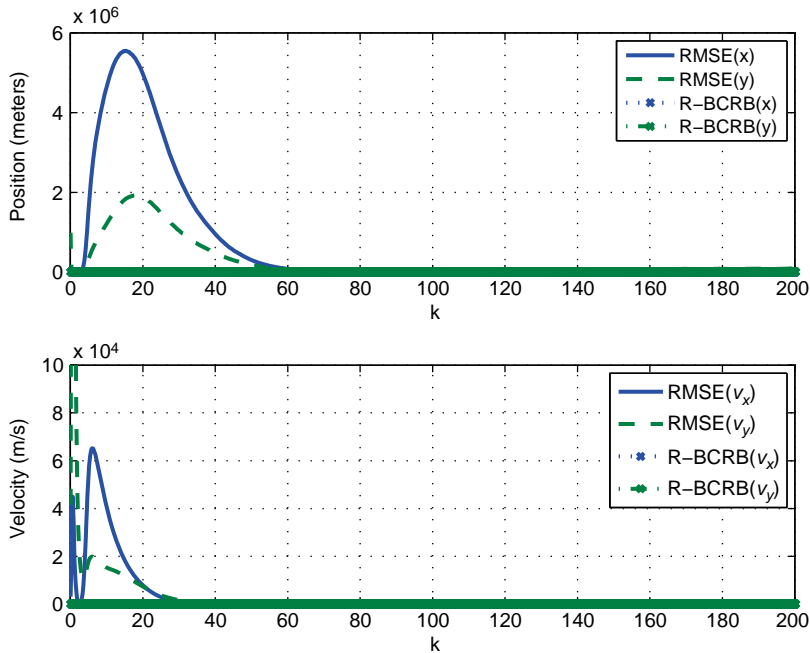


Figure 9.68: $\sqrt{\text{MSE}}$ and $\sqrt{\text{BCRB}}$ of position and velocity versus k .

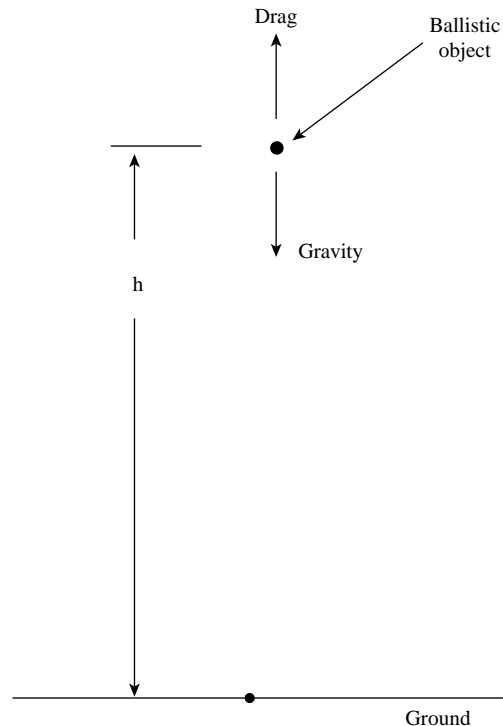


Figure 9.69: Model for ballistic target tracking.

The ballistic coefficient β depends on the object's mass, shape, and cross-section. We assume that we have *a priori* information and can model it as $N(\beta_0, \sigma_\beta^2)$ where β_0 and σ_β^2 are known. Define the state vector as

$$\mathbf{x} = [h \quad v \quad \beta]^T. \quad (9.769)$$

The state dynamics can be written as

$$\dot{\mathbf{x}}(t) = \mathbf{g}(\mathbf{x}(t)), \quad (9.770)$$

where \mathbf{g} follows from (9.765)–(9.767).

The discrete-time approximation with a small integration step is

$$\mathbf{x}(k) = [\mathbf{x}(k-1) + \tau \mathbf{g}(\mathbf{x}(k-1))] \triangleq \mathbf{f}(\mathbf{x}_{k-1}). \quad (9.771)$$

Adding process noise, we obtain the discrete-time state equation,

$$\mathbf{x}(k) = \mathbf{f}(\mathbf{x}_{k-1}) + \mathbf{u}_{k-1}, \quad (9.772)$$

where

$$\mathbf{f}(\mathbf{x}_{k-1}) = \Phi \mathbf{x}_{k-1} - \mathbf{G} [D(\mathbf{x}_{k-1}) - g] \quad (9.773)$$

and

$$\Phi = \begin{bmatrix} 1 & -\tau & 0 \\ 0 & 1 & 0 \\ 0 & 0 & 1 \end{bmatrix}, \quad (9.774)$$

$$\mathbf{G} = [0 \quad \tau \quad 0]^T, \quad (9.775)$$

and drag

$$D(\mathbf{x}_{k-1}) = \frac{g \cdot \rho(x_1(k-1)) \cdot x_2^2(k-1)}{2x_3(k-1)}. \quad (9.776)$$

Note that the drag is the only nonlinear term in the state equation. We assume the process noise is given by

$$\mathbf{Q} = \begin{bmatrix} q_1 \tau^3 / 3 & q_1 \tau^2 / 2 & 0 \\ q_1 \tau^2 / 2 & q_1 \tau & 0 \\ 0 & 0 & q_2 \tau \end{bmatrix}, \quad (9.777)$$

where q_1 and q_2 control the amount of process noise in the target dynamics and the ballistic coefficient, respectively.

A radar is positioned on the earth directly below the target and measures range (height) at intervals of T seconds,

$$r(k) = \mathbf{C} \mathbf{x}(k) + w(k), \quad (9.778)$$

where

$$\mathbf{C} = [1 \quad 0 \quad 0] \quad (9.779)$$

and $w(k) \sim N(0, \sigma_w^2)$ and is independent of the process noise.

We show a typical target trajectory in Figure 9.70 for the following parameters $h(0) = 61$ km, $v(0) = 3048$ m/s, $\beta = 19, 161$ kg/ms², $T = \tau = 0.1$, and $q_1 = q_2 = 0$. We see that the velocity is almost constant for the first 10 s and then drops quickly due to the air resistance.

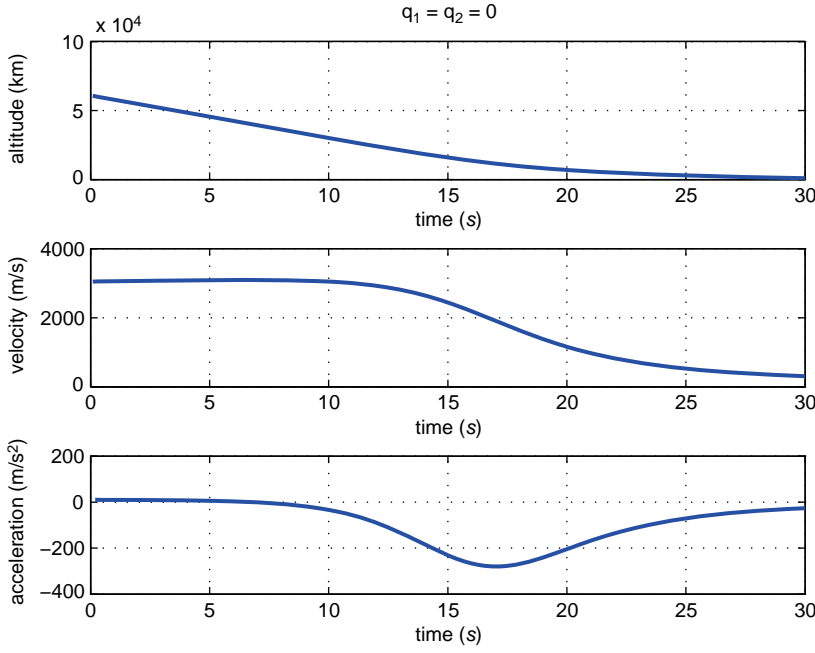


Figure 9.70: True trajectory: (a) altitude, (b) velocity, and (c) acceleration of a ballistic object versus time.

We first derive the Bayesian Cramér–Rao Bound. The measurement equation is linear, so we use (9.679), (9.680), and (9.681),

$$\mathbf{D}_k^{11} = E \{ \tilde{\mathbf{F}}_k^T \mathbf{Q}^{-1} \tilde{\mathbf{F}}_k \}, \quad (9.780)$$

$$\mathbf{D}_k^{12} = -E \{ \tilde{\mathbf{F}}_k^T \} \mathbf{Q}^{-1} = [\mathbf{D}_k^{21}]^T, \quad (9.781)$$

$$\mathbf{D}_k^{22} = \mathbf{Q}^{-1} + \mathbf{C}^T R^{-1} \mathbf{C}. \quad (9.782)$$

Substituting into (9.684) gives

$$\mathbf{J}_{k+1} = \mathbf{Q}^{-1} + \mathbf{C}^T R^{-1} \mathbf{C} - \mathbf{Q}^{-1} E \{ \tilde{\mathbf{F}}_k \} [\mathbf{J}_k + E \{ \tilde{\mathbf{F}}_k^T \mathbf{Q}^{-1} \tilde{\mathbf{F}}_k \}]^{-1} E \{ \tilde{\mathbf{F}}_k \} \mathbf{Q}^{-1}. \quad (9.783)$$

In the absence of process noise, (9.783) reduces to (9.711)

$$\mathbf{J}_{k+1} = [\tilde{\mathbf{F}}_k^{-1}]^T \mathbf{J}_k \tilde{\mathbf{F}}_k^{-1} + \mathbf{C}^T R^{-1} \mathbf{C} \quad (9.784)$$

$$= [\tilde{\mathbf{F}}_k^{-1}]^T \mathbf{J}_k \tilde{\mathbf{F}}_k^{-1} + \begin{bmatrix} \frac{1}{\sigma_w^2} & 0 & 0 \\ 0 & 0 & 0 \\ 0 & 0 & 0 \end{bmatrix}. \quad (9.785)$$

The initial information matrix \mathbf{J}_0 assumes $\mathbf{x}_0 \sim N(\hat{\mathbf{x}}_0, \mathbf{P}_0)$. We use two-point differencing of height and velocity (e.g., [BSLK01]) to obtain the upper left block in \mathbf{P}_0 . The lower right element is σ_β^2 . The

ballistic coefficient is clearly not Gaussian. We use a beta distribution whose support spans the range of β and use the resulting variance for σ_β^2 .

$$\mathbf{P}(0) = \begin{bmatrix} R & R/T & 0 \\ R/T & 2R/T^2 & 0 \\ 0 & 0 & \sigma_\beta^2 \end{bmatrix}. \quad (9.786)$$

We next find the Jacobian of $\mathbf{f}(\mathbf{x}(k))$

$$\tilde{\mathbf{F}}_k = [\nabla_{\mathbf{x}_k} \mathbf{f}^T(\mathbf{x}(k))]^T = \begin{bmatrix} 1 & -\tau & 0 \\ f_{21}\tau & 1 - f_{22}\tau & f_{23}\tau \\ 0 & 0 & 1 \end{bmatrix}, \quad (9.787)$$

where

$$f_{21} = \frac{\eta g \rho_k x_2^2(k)}{2x_3(k)}, \quad (9.788)$$

$$f_{22} = \frac{g \rho_k x_2(k)}{x_3(k)}, \quad (9.789)$$

$$f_{23} = \frac{g \rho_k x_2^2(k)}{2x_3^2(k)}, \quad (9.790)$$

where

$$\rho_k \triangleq \gamma \exp(-\eta x_1(k)). \quad (9.791)$$

We calculate the BCRB for the trajectory in Figure 9.69 with the same initial values and $R = (200\text{m})^2$, $T = \tau = 0.1$, and $\sigma_\beta = 718.4 \text{ kg/ms}^2$. In Figure 9.71, we show the BCRBs for the components of the state vector

$$\text{BCRB}(\mathbf{x}_i(k)) = \mathbf{J}_k^{-1}[i, i], \quad i = 1, 2, 3. \quad (9.792)$$

For zero process noise, we use (9.785) and the results are shown with solid lines.²⁰ For nonzero process noise, we use $q_1 = q_2 = 1$ and average over a 100 simulations. The results are shown with dotted lines.

In the first 10 s, the $\sqrt{\text{BCRB}}$ for the ballistic coefficient is almost constant because there is no drag at the higher altitude so the state equations are linear and there is no information about β . During the second 10 s, the higher air density causes the drag to increase while the velocity decreases rapidly. The bound β decreases because we have information to estimate it. The bounds of height and velocity increase. In the last 10 s all of the bounds decrease.

The EKF equations are given by (9.663)–(9.667),

$$\hat{\mathbf{x}}_{k|k-1} = \mathbf{f}(\hat{\mathbf{x}}(k-1)), \quad (9.793)$$

$$\mathbf{P}_{k|k-1} = \tilde{\mathbf{F}}_{k-1} \mathbf{P}_{k-1} \tilde{\mathbf{F}}_{k-1}^T + \mathbf{Q}. \quad (9.794)$$

Note that $\tilde{\mathbf{F}}_{k-1}$ in the EKF is evaluated at the estimated $\hat{\mathbf{x}}_{k-1}$ whereas the $\tilde{\mathbf{F}}_{k-1}$ in the BCRB is evaluated at the true \mathbf{x}_{k-1} .

²⁰We reduced σ_β significantly from the example in [RAG04] in order to improve the performance of the EKF.

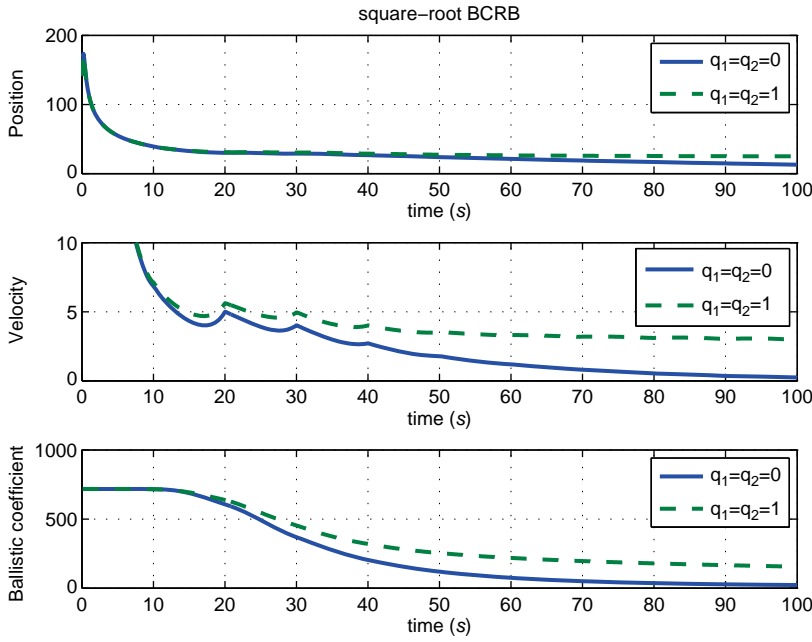


Figure 9.71: $\sqrt{\text{BCRB}}$ for (a) altitude, (b) velocity, (c) ballistic coefficient.

The measurement equations are linear, so

$$\mathbf{K}_k = \mathbf{P}_{k|k-1} \mathbf{C}^T [\mathbf{C} \mathbf{P}_{k|k-1} \mathbf{C}^T + \sigma_w^2]^{-1}, \quad (9.795)$$

$$\hat{\mathbf{x}}_k = \hat{\mathbf{x}}_{k|k-1} + \mathbf{K}_k [\mathbf{r}_k - \mathbf{C}^T \hat{\mathbf{x}}_{k|k-1}], \quad (9.796)$$

$$\mathbf{P}_k = [\mathbf{I} - \mathbf{K}_k \mathbf{C}] \mathbf{P}_{k|k-1}. \quad (9.797)$$

We implement the EKF equations (9.663)–(9.667), with the following parameters.

True Target Track: $h(0) = 61$ km, $v(0) = 3048$ m/s, $\beta = 19,161$ kg/m², $T = \tau = 0.1$, and $q_1 = q_2 = 1$.

Initialization of EKF: $\hat{x}_1(0) = \hat{h}(0) = 60.96$ km, $\hat{x}_2(0) = \hat{v}(0) = 3000$ m/s, $\hat{x}_3(0) = \hat{\beta}(0) = 18,000$ kg/ms², $\sigma_r^2 = (200m)^2$, $\sigma_\beta = 718.4$ kg/ms².

We run 100 simulations and calculate the MSE for $k = 1, \dots, 400$. We then average over the results. The bias and MSE are shown in Figures 9.72 and 9.73. ■

9.3.5.5 Joint State And Parameter Estimation

In many applications, the parameter in the state equation are not known exactly. However, we usually have *a priori* knowledge of possible values based on the physical situation. In this section, we consider the problem of jointly estimating the state and the parameter.

We modify the model in (9.655)–(9.656) to include the case where $\mathbf{f}_{k-1}(\mathbf{x}(k-1))$ depends on an unknown parameter vector that we model as random variable. We augment the

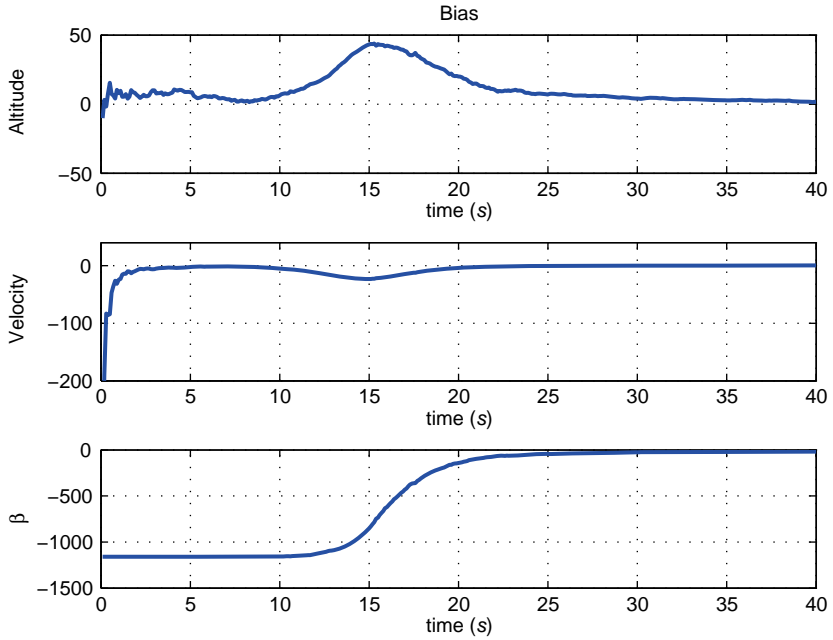


Figure 9.72: Bias of altitude, velocity, and β estimates versus time.

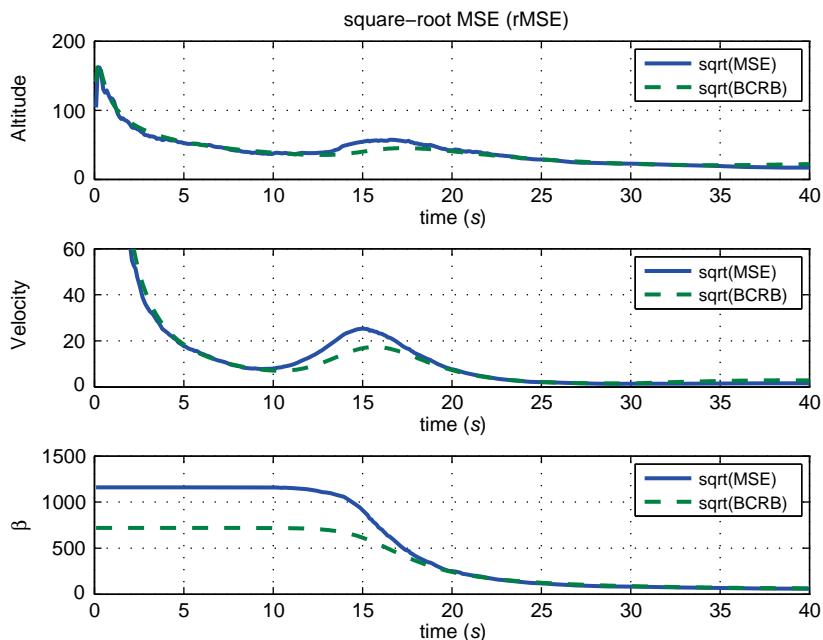


Figure 9.73: RMSE and $\sqrt{\text{BCRB}}$ of altitude, velocity and β estimates versus time.

$p \times 1$ state vector with the $m \times 1$ component vector θ . Thus,

$$\mathbf{x}_a(k) \triangleq \begin{bmatrix} \mathbf{x}(k) \\ \theta(k) \end{bmatrix}. \quad (9.798)$$

Our initial approach is to assume θ is constant, so

$$\theta(k) = \theta(k-1). \quad (9.799)$$

A problem with (9.799) is that in many cases, the Kalman gain for that component will go to zero. To counter this, we model $\theta(k)$ as

$$\theta(k) = \theta(k-1) + \mathbf{u}_\theta(k-1) \quad (9.800)$$

and choose \mathbf{Q}_θ to have a small value.

We write the state equation as

$$\mathbf{x}_a(k) = \mathbf{f}_{k-1}(\mathbf{x}_a(k-1)) + \mathbf{u}_a(k-1), \quad (9.801)$$

where

$$\mathbf{u}_a(k-1) = [\mathbf{u}^T(k-1) \quad \mathbf{u}_\theta^T(k-1)]^T. \quad (9.802)$$

We illustrate the algorithm with a simple example.

Example 9.23. Consider the AR(1) model in Example 9.9 with unknown α ,

$$x(k) = \alpha x(k-1) + u(k). \quad (9.803)$$

The augmented state vector is

$$\mathbf{x}_a(k) = \begin{bmatrix} x(k) \\ \alpha(k) \end{bmatrix} \triangleq \begin{bmatrix} x_1^a(k) \\ x_2^a(k) \end{bmatrix}. \quad (9.804)$$

The augmented state equation is

$$\mathbf{x}_a(k) = \mathbf{f}_{k-1}(\mathbf{x}_a(k-1)) + \mathbf{u}_a(k), \quad (9.805)$$

where

$$\mathbf{f}_{k-1}(\mathbf{x}_a(k-1)) = \begin{bmatrix} x_1^a(k-1)x_2^a(k-1) \\ x_2^a(k-1) \end{bmatrix} \quad (9.806)$$

and

$$\mathbf{u}_a(k) = [u(k) \quad u_\alpha(k)]^T. \quad (9.807)$$

The observation equation is linear,

$$r(k) = \mathbf{C} \mathbf{x}_a(k) + w(k) \quad (9.808)$$

where

$$\mathbf{C} = [1 \quad 0]. \quad (9.809)$$

Then,

$$\tilde{\mathbf{F}}_{k-1}^a = \nabla_{\mathbf{x}_a(k-1)} [\mathbf{f}_{k-1}^T(\mathbf{x}_a(k-1))]_{\mathbf{x}_a(k-1)=\hat{\mathbf{x}}_a(k-1)}^T \quad (9.810)$$

$$= \begin{bmatrix} \hat{x}_2^a(k-1) & \hat{x}_1^a(k-1) \\ 0 & 1 \end{bmatrix}. \quad (9.811)$$

The resulting EKF is as follows.

Initial conditions:

$$\hat{\mathbf{x}}_a(0) = \begin{bmatrix} 0 \\ \alpha_m \end{bmatrix}, \quad (9.812)$$

$$\mathbf{P}_0^a = \begin{bmatrix} P(0) & 0 \\ 0 & P_\alpha(0) \end{bmatrix}, \quad (9.813)$$

where we have modeled $\alpha_0 \sim N(\alpha_m, P_\alpha(0))$. We need to choose $P_\alpha(0)$ small enough so that the probability of $\alpha > 1$ is close to zero.

EKF update:

$$\hat{\mathbf{x}}_a(k|k-1) = \begin{bmatrix} \hat{x}_1^a(k-1) \hat{x}_2^a(k-1) \\ \hat{x}_2^a(k-1) \end{bmatrix}, \quad (9.814)$$

$$\mathbf{P}_{k|k-1}^a = \begin{bmatrix} \sigma_u^2 & 0 \\ 0 & \sigma_\alpha^2 \end{bmatrix} + \tilde{\mathbf{F}}_{k-1}^a \mathbf{P}_{k-1}^a \tilde{\mathbf{F}}_{k-1}^{aT}, \quad (9.815)$$

$$\mathbf{K}_k^a = \mathbf{P}_{k|k-1}^a \mathbf{C}^T [\mathbf{C} \mathbf{P}_{k|k-1}^a \mathbf{C}^T + \sigma_w^2]^{-1}, \quad (9.816)$$

$$\hat{\mathbf{x}}_a(k) = \hat{\mathbf{x}}_a(k|k-1) + \mathbf{K}_k^a [r(k) - \mathbf{C} \hat{\mathbf{x}}_a(k|k-1)], \quad (9.817)$$

$$\mathbf{P}_k^a = [\mathbf{I} - \mathbf{K}_k^a \mathbf{C}] \mathbf{P}_{k|k-1}^a. \quad (9.818)$$

We need to choose the initial variance of α and σ_α^2 small enough that the probability of $\hat{\alpha} \geq 1$ is negligible. We can also modify (9.817) to put a limit, say $0.05 < \hat{\alpha}_k < 0.99$, on $\hat{x}_2^a(k) = \hat{\alpha}_k$.

We consider a case with the following true values

$$x(0) = 20, \quad (9.819)$$

$$\alpha = 0.95, \quad (9.820)$$

$$\sigma_w^2 = 1.0, \quad (9.821)$$

$$\sigma_u^2 = 0.36\sigma_s^2. \quad (9.822)$$

We initialize the algorithm with

$$\mathbf{x}^a(0) = [25 \quad 0.75]^T, \quad (9.823)$$

$$P_\alpha(0) = \sigma_\alpha^2 = 0.05^2, \quad (9.824)$$

$$P(0) = 4. \quad (9.825)$$

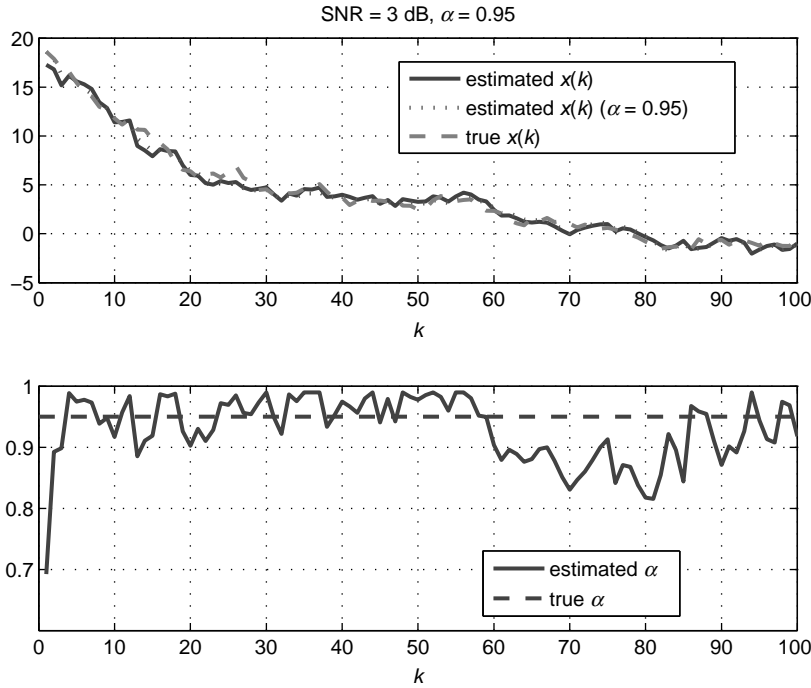


Figure 9.74: AR(1) model; $\hat{x}(k)$ and $\hat{\alpha}(k)$, SNR= 3 dB.

In Figure 9.74 we show several typical realizations for SNR = 3 dB. In Figure 9.75, we plot the $P_{11}^a(k)$, $P_{22}^a(k)$, and $P_{21}^a(k)$. ■

The technique is still valid when θ is a vector. However, implementing appropriate bounds on the parameters becomes more complicated.

9.3.5.6 Continuous-Time Processes and Discrete-Time Observations

Most tracking and navigation applications start with a continuous-time process and a discrete-time observation model. We consider the continuous-time process model in Table 8.1 in Section 8.4,

$$\dot{\mathbf{x}}(t) = \mathbf{f}(\mathbf{x}(t), t) + \mathbf{G}(t)\mathbf{u}(t), \quad (9.826)$$

where $\mathbf{u}(t)$ is a WGN process with covariance matrix $\mathbf{Q}(t)$. The observation model is discrete time,

$$\mathbf{r}_k = \mathbf{c}_k(\mathbf{x}_k) + \mathbf{w}_k, \quad (9.827)$$

where \mathbf{w}_k is $N(\mathbf{0}, \mathbf{R}_k)$. The \mathbf{w}_k , $k = 1, \dots, K$, are statistically independent of each other and $\mathbf{u}(t)$.

This model is appropriate for most radar and sonar tracking problems. One of the advantages of the mixed model is that it allows us to explore different observation time sampling strategies. Discussions of the model and applications are available in a number of references

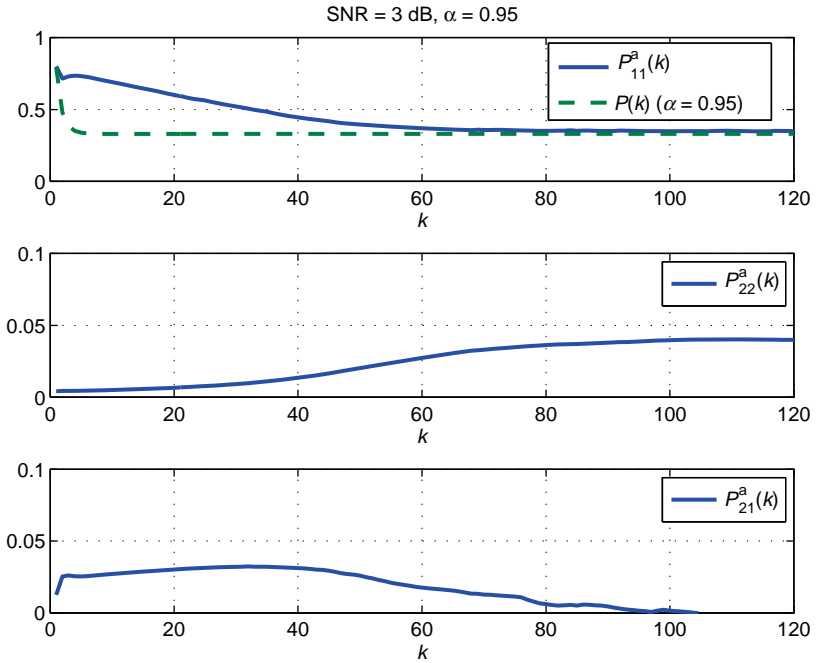


Figure 9.75: AR(1) model; $P_{11}^a(k)$, $P_{22}^a(k)$, $P_{21}^a(k)$ versus k , SNR = 3 dB.

(e.g., [Jaz70], [Gel74], or [BSLK01]). Most of the results carry over from the results in Section 8.

We discuss three topics:

1. The extended Kalman filter for the continuous-time, discrete-observation model.
2. The BCRB for the linear AWGN process model and nonlinear observation model.
3. An example of discretizing the continuous-time state equation to obtain a discrete-time state equation.

Extended Kalman Filter. We define two estimates of \mathbf{x}_k . The first is denoted by $\hat{\mathbf{x}}_k^-$ and is the estimate just prior to the observation \mathbf{r}_k . The second estimate is $\hat{\mathbf{x}}_k^+$ and is the estimate just after \mathbf{r}_k is observed. The first estimate $\hat{\mathbf{x}}_k^-$ is obtained from $\hat{\mathbf{x}}_{k-1}^+$ through the process dynamics. The second estimate, $\hat{\mathbf{x}}_k^+$ is obtained from $\hat{\mathbf{x}}_k^-$ by including the effect of \mathbf{r}_k . The resulting equations are²¹

State equation propagation:

$$\dot{\hat{\mathbf{x}}}(t) = \mathbf{f}(\hat{\mathbf{x}}(t), t). \quad (9.828)$$

This equation generates $\hat{\mathbf{x}}_k^-$ from $\hat{\mathbf{x}}_{k-1}^+$.

²¹These equations were taken from p. 188 of Gelb [Gel74].

MSE matrix propagation:

$$\dot{\mathbf{P}}(t) = \tilde{\mathbf{F}}(\hat{\mathbf{x}}(t), t)\mathbf{P}(t) + \mathbf{P}(t)\tilde{\mathbf{F}}^T(\hat{\mathbf{x}}(t), t) + \mathbf{G}(t)\mathbf{Q}(t)\mathbf{G}^T(t), \quad (9.829)$$

This equation generates \mathbf{P}_k^- from \mathbf{P}_{k-1}^+ .

Gain matrix:

$$\mathbf{K}_k = \mathbf{P}_k^- \tilde{\mathbf{C}}_k^T(\hat{\mathbf{x}}_k^-) [\tilde{\mathbf{C}}_k(\hat{\mathbf{x}}_k^-)\mathbf{P}_k^- \tilde{\mathbf{C}}_k^T(\hat{\mathbf{x}}_k^-) + \mathbf{R}_k]^{-1}, \quad (9.830)$$

State estimate update:

$$\hat{\mathbf{x}}_k^+ = \hat{\mathbf{x}}_k^- + \mathbf{K}_k [\mathbf{r}_k - \mathbf{c}_k(\hat{\mathbf{x}}_k^-)], \quad (9.831)$$

Error covariance update:

$$\mathbf{P}_k^+ = [\mathbf{I} - \mathbf{K}_k \tilde{\mathbf{C}}_k(\hat{\mathbf{x}}_k^-)] \mathbf{P}_k^-, \quad (9.832)$$

where $\tilde{\mathbf{F}}(\hat{\mathbf{x}}(t), t)$ is defined in (8.404) and

$$[\tilde{\mathbf{C}}_k(\hat{\mathbf{x}}_k^-)]_{ij} = \left. \frac{\partial c_{ij}(\mathbf{x}(t_k))}{\partial x_j(t_k)} \right|_{\mathbf{x}(t_k)=\hat{\mathbf{x}}_k^-}. \quad (9.833)$$

Bayesian Cramér–Rao Bound. We denote the Bayesian CRB and the Bayesian information matrix at time t_k^- as $\mathbf{B}_g(t_k^-)$ and $\mathbf{J}_{Bg}(t_k^-)$, respectively, for the linear AWGN process model. We denote the BCRB and BIM at t_k^+ as $\mathbf{B}_g(t_k^+)$ and $\mathbf{J}_{Bg}(t_k^+)$, respectively.

We assume that we know $\mathbf{B}_g(t_{k-1}^+)$ and $\mathbf{J}_{Bg}(t_{k-1}^+)$. Then $\mathbf{J}_{Bg}(t)$, $t_{k-1}^+ \leq t \leq t_k^-$, satisfies the differential equation (8.383) with the third term omitted because there is no observation:

$$\dot{\mathbf{J}}_{Bg}(t) = -\mathbf{J}_{Bg}(t)\mathbf{F}(t) - \mathbf{F}^T(t)\mathbf{J}_{Bg}(t) - \mathbf{J}_{Bg}(t)\mathbf{G}(t)\mathbf{Q}(t)\mathbf{G}^T(t)\mathbf{J}_{Bg}(t); \quad t_{k-1}^+ \leq t \leq t_k^-, \quad (9.834)$$

with initial conditions $\mathbf{J}_{Bg}(t_{k-1}^+)$. Integrating (9.834) gives $\mathbf{J}_{Bg}(t_k^-)$.

Incorporating the observation is a static problem, so

$$\mathbf{J}_B = \mathbf{J}_P + \mathbf{J}_D, \quad (9.835)$$

which, for our model is

$$\mathbf{J}_{Bg}(t_k^+) = \mathbf{J}_{Bg}(t_k^-) + E_{\mathbf{x}_k} \{ \tilde{\mathbf{C}}^T(t_k^-) \mathbf{R}_k^{-1} \tilde{\mathbf{C}}(t_k^-) \} \quad (9.836)$$

and

$$\mathbf{B}_g(t_k^+) = \mathbf{J}_{Bg}^{-1}(t_k^+). \quad (9.837)$$

The initial condition for the recursion is $\mathbf{J}_{Bg}(t_0)$.

Discretizing the Continuous-Time State Equation. Many of the tracking models that we used in Section 9.3.5.4 were obtained by discretizing a continuous-time state equation. We illustrate the technique with a model taken from Bar–Shalom et al. [BSLK01, pp. 268–270].

Consider a one-dimensional tracking problem where the nominal target has a constant velocity and its position at time t is denoted by $x(t)$. The state vector is

$$\mathbf{x}(t) = \begin{bmatrix} x(t) \\ v(t) \end{bmatrix} \quad (9.838)$$

and, for a nominal track,

$$\dot{v}_{nom}(t) = 0. \quad (9.839)$$

We want to model uncertainties in the track by a continuous-time, zero-mean white noise $u(t)$. We let

$$\dot{v}(t) = u(t), \quad (9.840)$$

where

$$E[u(t)] = 0 \quad (9.841)$$

and

$$E[u(t)u(\tau)] = q\delta(t - \tau). \quad (9.842)$$

Then, (9.826) can be written as

$$\dot{\mathbf{x}}(t) = \mathbf{F}_c \mathbf{x}(t) + \mathbf{G}_c \mathbf{u}(t), \quad (9.843)$$

where

$$\mathbf{F}_c = \begin{bmatrix} 0 & 1 \\ 0 & 0 \end{bmatrix}, \quad (9.844)$$

$$\mathbf{G}_c = \begin{bmatrix} 0 \\ 1 \end{bmatrix}, \quad (9.845)$$

and

$$\mathbf{u}(t) = \begin{bmatrix} 0 \\ u(t) \end{bmatrix}. \quad (9.846)$$

The subscript “*c*” denotes the continuous-time model.

The discretized state equation is

$$\mathbf{x}(k+1) = \mathbf{F}_d \mathbf{x}(k) + \mathbf{u}_d(k). \quad (9.847)$$

The solution to the continuous-time state equation is given in Sections 4.2, 4.3, and 6.2 of [BSLK01]. The result is that

$$\mathbf{F}_d = e^{\mathbf{F}_c T} \approx \mathbf{I} + \mathbf{F}_c T = \begin{bmatrix} 1 & T \\ 0 & 1 \end{bmatrix}, \quad (9.848)$$

$$\mathbf{u}_d(k) = \int_0^T e^{\mathbf{F}_c(T-\tau)} \mathbf{G}_c v(kT + \tau) d\tau. \quad (9.849)$$

The covariance matrix for $\mathbf{u}_d(k)$ is

$$\begin{aligned}
 \mathbf{Q} &= E \{ \mathbf{u}_d(k) \mathbf{u}_d^T(k) \} \\
 &= \int_0^T e^{(T-\tau)\mathbf{F}_c} \mathbf{G}_c q \mathbf{G}_c^T e^{(T-\tau)\mathbf{F}_c^T} d\tau \\
 &= q \int_0^T \begin{bmatrix} T - \tau \\ 1 \end{bmatrix} \begin{bmatrix} T - \tau & 1 \end{bmatrix} d\tau \\
 &= q \begin{bmatrix} \frac{1}{3}T^3 & \frac{1}{2}T^2 \\ \frac{1}{2}T^2 & T \end{bmatrix}
 \end{aligned} \tag{9.850}$$

and

$$E \{ \mathbf{u}_d(k) \mathbf{u}_d(j) \} = \mathbf{Q} \delta_{kj}. \tag{9.851}$$

If the continuous-time model is nonlinear, then we normally linearize it around a nominal trajectory using the techniques developed for the EKF in Section 9.3.5.2 and the proceed as in the above example. Bar-Shalom et al. [BSLK01] and Mendel [Men95] discuss these techniques.

9.3.5.7 Summary

In this section, we have introduced the problem of Bayesian estimation of nonlinear models. After discussing the general problem we restricted our discussion of actual estimation to the extended Kalman filter.

It is important to remember that the EKF has no claim to optimality and generally works well where the degree of nonlinearity is not too severe. The iterated EKF, which we did not develop, works better in some applications at the cost of additional computation. However, the most important point to remember is nonlinear filtering has progressed significantly and as discussed in Section 9.3.5.1, many better options such as particle filters are available for applications where the EKF is not useful.

The Bayesian Cramér–Rao Bound provides a useful technique to predict the potential performance of any estimator. A large number of applications of the BCRB are discussed in our book, “Bayesian Bounds” [VB07].

9.3.6 Summary: Kalman Filters

In this section, we studied the discrete-time Kalman filter in detail. In Section 9.3.1, we developed state-variable representations of signal processes and the observation model. We focused our attention to two types of processes, autoregressive moving average (ARMA) processes that are important models for communication systems and kinematic models that are important in the radar and sonar area.

In Section 9.3.2, we developed the discrete-time Kalman filter. We referred to a Kalman processor as a Kalman filter when we were estimating the state vector $\mathbf{x}(k)$ based on a sequence of received observations $\mathbf{r}(n), n = 1, \dots, k$. This section was a major part of the chapter because Kalman predictors, $\mathbf{x}(k+L)$, $L > 0$, and Kalman smoothers, $\mathbf{x}(k-L)$, $L < 0$, contained the filter.

In Section 9.3.2.1, we derived the standard Kalman filter. This version of the Kalman filter is referred to as the *covariance implementation* because it recursively inverts the covariance matrix of the estimation error. The key equations are (9.275)–(9.286). The standard algorithm requires recursive inversion of an $N \times N$ matrix, where N is the dimension of the observation vector $\mathbf{r}(k)$.

In Section 9.3.2.2, we developed two alternative implementations that have computational advantage when $N \geq p$, where p is the dimension of the state vector. The derivations used the matrix inversion lemma to obtain implementations in which the recursive inversion is $p \times p$ when $\mathbf{R}(k)$ is a constant \mathbf{R} .

The first implementation recursively computes the covariance matrix using a $p \times p$ inversion and we refer to it as the *reduced-dimension covariance implementation*. The key equations are (9.325)–(9.331). The second implementation recursively computes the Bayesian information matrix $\mathbf{J}_B(k)$, which is the inverse of the covariance matrix using a $p \times p$ inversion and is referred to as the *information filter*. The key equations are (9.349)–(9.359).

The three implementations are algebraically identical, but they have different computational complexity, different sensitivity to numerical errors such as round-off, and different sensitivity to model mismatch.

In Section 9.3.2.3, we studied a sequence of applications in the signal processing and tracking area. Examples 9.9 and 9.11 considered ARMA signal models of increasing dimension of the state vector. All of them had scalar observations, so the standard covariance implementation was appropriate. Example 9.12 considered an array processing application where $N \gg p$. Both reduced-dimension algorithms used a recursive $p \times p$ inversion.

Example 9.10 considered a simple one-dimensional tracking problem. The more realistic two- or three-dimensional tracking problem has a nonlinear observation model, so we deferred discussion until Section 9.3.5.

These examples are consistent with the main application areas in the book but did not really illustrate the widespread usage of the Kalman filter in diverse areas. An Internet search “Kalman Filter Applications” will provide a much broader view.

The Kalman filter in Sections 9.3.2.1–9.3.2.3 assumes white Gaussian noise in the observation model. In Section 9.3.2.4, we showed how to treat the case of colored plus white observation noise. Our approach consists of augmenting the signal state vector with a colored noise state vector. This reduces the problem to a standard Kalman filtering problem with increased dimension of the state vector.

There is a measurement update step in the Kalman algorithm that requires processing an $N \times 1$ vector, where N is the dimension of the observation. In Section 9.3.2.5, we developed an algorithm to process the components of the vector sequentially.

In early applications, it was found that numerical round-off errors caused the covariance matrix or the Bayesian information matrix to lose its nonnegative definite property. In Section 9.3.2.6, we developed a square-root implementation of the Kalman filter that factors the covariance matrix (or the Bayesian information matrix) into triangular matrices and updates them. This implementation guarantees a nonnegative definite matrix and improves the numerical precision. This section provided a brief introduction to square-root filtering. There are a number of different square-root algorithms and the literature should be consulted for a particular application.

In some applications, if there is mismatch between the mathematical model and the actual model, the Kalman filter will track the wrong model and predict a decreasing covariance

matrix. However, the actual MSE is diverging. In Section 9.3.2.7, we analyze this behavior and discuss remedies.

The mismatch in Section 9.3.2.7 consists of a small bias term that is neglected in the mathematical model. In Section 9.3.2.8, we considered a more general mismatch model in which all of the matrices in the model, \mathbf{F} , \mathbf{G} , \mathbf{C} , \mathbf{Q} , \mathbf{R} , and $\boldsymbol{\Pi}$ may be mismatched to the actual model. The key equations are (9.566)–(9.579).

It is an essential part of the design of an algorithm for a practical application to investigate its sensitivity to possible model mismatches.

We spent a considerable amount of time studying Kalman filters. In addition to their widespread usage, they are the key building block in Kalman prediction and smoothers.

In Section 9.3.3, we studied Kalman predictors. There are three types of prediction problems:

- (a) Fixed-lead prediction: In this case,

$$d(k) = s(k + L), \quad (9.852)$$

where L is a positive number.

- (b) Fixed-point prediction: In this case,

$$d(k) = s(L_p), \quad (9.853)$$

where L_p is a fixed point, $L_p > k$.

- (c) Fixed-interval prediction: In this case, the interval is fixed, $k = 1, 2, \dots, K$, and we want to predict

$$d(m) = s(m), \quad m = K + 1, K + 2, \dots \quad (9.854)$$

This is the model that we encountered in Section 9.2 using covariance functions.

In all of these cases, we assumed that a Kalman filter is implemented and that we have $\hat{\mathbf{x}}(k)$ and $\mathbf{P}(k)$ available. Because we are dealing with a Markov process, these are the only quantities needed to find $\hat{d}(k)$ and its variance.

The prediction part of the Kalman processor is straightforward. In all three cases, it is linear operation of $\hat{\mathbf{x}}(k)$. Thus, all of the implementation issues discussed in Section 9.3.2 must be considered. The performance of the predictors will be a function of the correlation between $\mathbf{x}(k)$ and $\mathbf{x}(k + L)$.

In Section 9.3.4, we studied the Kalman smoothing problem. There are three types of smoothing problem that are encountered in applications:

1. *Fixed-interval smoothing.* We have K samples, $k = 1, \dots, K$, and we want to find $\hat{\mathbf{x}}(k|K) \triangleq \hat{\mathbf{x}}(k|\mathbf{r}_K)$, where

$$\mathbf{r}_K = [\mathbf{r}(1) \quad \cdots \quad \mathbf{r}(K)].$$

2. *Fixed-Lag smoothing.* We observed $\mathbf{r}(k)$, $k = 1, 2, \dots$, and we want to find $\hat{\mathbf{x}}(k + L)$, where L is negative. This case is the filtering with delay problem that we considered in the Wiener filter context.

3. *Fixed-Point smoothing.* We want to find $\hat{\mathbf{x}}(k_s)$, where k_s is fixed and we observe $\mathbf{r}(k)$, $k = k_s, k_s + 1, \dots, k_s + K$, and K increases.

The Kalman smoothing processors are more complicated than the Kalman filter. Our solution for the fixed-interval smoother required a forward Kalman filter followed by a backward Kalman filter. Our solutions for fixed-lag smoothing involved augmenting the state vector such that the dimension increased from p to pL , where L was the length of the delay. However, smoothing has the potential to reduce the estimation error and is used in a number of applications.

In Section 9.3.5, we introduced the problem of Bayesian estimation of nonlinear models. Our objective was to develop a general nonlinear model and formulate the MMSE and MAP estimation problem. A detailed discussion of possible solutions was beyond the scope of the book, so we focused our attention on two topics that are useful in many applications.

In Section 9.3.5.2, we derived the extended Kalman filter that has no claim to optimality but performs adequately in many applications.

In Section 9.3.5.3, we derived the Bayesian Cramér–Rao Bound that is the dynamic version of the BCRB that we first encountered in Chapter 4. It provides a lower bound on the MSE of estimator and gives a reference that we can compare suboptimum processors to.

In Section 9.3.5.4, we studied three interesting applications. The first was dynamic frequency estimation, which was the extension of the static frequency estimation in Chapter 4 to a random process. The second was a two-dimensional tracking problem, which was a more realistic application than the one-dimensional case studied earlier. The third dealt with tracking a ballistic object upon reentry into the atmosphere. In addition to being an important application, it introduced the idea of estimating an unknown parameter in the basic dynamic model by augmenting the state vector.

In Section 9.3.5.5, we studied the problems of estimating the parameters in the model by augmenting the state vectors. Coupled with our results on model mismatch in Section 9.3.2.8, it gave us the ability to trade-off the added complexity of parameter estimation and simply using a mismatched model in terms of performance.

The collection of results should have satisfied our objective of providing a comprehensive discussion of Kalman filter at the appropriate level.

9.4 SUMMARY

In this chapter we have provided a comprehensive discussion of discrete-time Wiener and Kalman filters. The summaries in Sections 9.2.6 and 9.3.6 provide a detailed review of the results. Chapters 8 and 9 should provide adequate background to solve a large number of random process estimation problems.

9.5 PROBLEMS

In this chapter, we used the AR(1) process in a number of examples to illustrate different algorithms. In the problem section, we introduce a set of ARMA models that we use throughout the problems to illustrate the algorithms. In order to simplify cross-referencing, the problem sections are divided into smaller increments.

P9.2 Discrete-Time Wiener Filters

P9.2.2 Random Process Models

The first set of problems are ARMA processes that are specified by $H(z)$ whose input is $\mathbf{u}(k) \sim N(\mathbf{0}, \sigma_u^2 \mathbf{I})$. In each problem,

- Plot the poles and zeros.
- Plot the spectrum.
- Find the autocorrelation function and $\sigma_s^2 = K_s(0)$.

Problem 9.2.2.1. AR(2)

$$H(z) = \frac{1}{1 - 0.75z^{-1} + 0.5z^{-2}}.$$

Problem 9.2.2.2. AR(3) [Hay96]

$$H(z) = \frac{1}{(1 + 0.5z^{-1})(1 + 0.75z^{-1})(1 + 2z^{-1})}.$$

Problem 9.2.2.3. AR(4) [MIK00]

$$H(z) = \frac{1}{1 - 2.76072z^{-1} + 3.8106z^{-2} - 2.6535z^{-3} + 0.9238z^{-4}}.$$

Problem 9.2.2.4. ARMA(4, 2) [Hay96]

$$H(z) = \frac{1 - 0.9z^{-1} + 0.81z^{-2}}{1 - 1.978z^{-1} + 2.853z^{-2} - 1.877z^{-3} + 0.9036z^{-4}}.$$

Problem 9.2.2.5. ARMA(6, 6), 6th-order Butterworth [OS89]

$$H(z) = \frac{0.0007378(1 + z^{-1})^6}{(1 - 1.2686z^{-1} + 0.7051z^{-2})(1 - 1.0106z^{-1} + 0.3583z^{-2})} \times \frac{1}{(1 - 0.9044z^{-1} + 0.2155z^{-2})}.$$

Problem 9.2.2.6. ARMA(6, 6) [OS89]

$$H(z) = \frac{0.2871 - 0.4466z^{-1}}{1 - 1.2971z^{-1} + 0.6949z^{-2}} + \frac{-2.1428 + 1.1455z^{-1}}{1 - 1.0691z^{-1} + 0.3699z^{-2}} + \frac{1.8557 - 0.6303z^{-1}}{1 - 0.9972z^{-1} + 0.2570z^{-2}}.$$

In the next set of problems, the ARMA processes are specified by their poles and zeros $u(k) \sim N(0, 1)$. In each problem,

- Find $a(m)$ and $b(m)$.
- Find the autocorrelation function and $\sigma_s^2 = k_s(0)$.
- Plot the spectrum.

Problem 9.2.2.7. The signal process is the sum of 2 SI AR(2) processes. For $s_1(k)$,

$$p_{1,(2)} = 0.7 \exp(\pm 0.6\pi).$$

For $s_2(k)$,

$$p_{1,(2)} = 0.5 \exp(\pm(0.6 + \Delta)\pi).$$

Consider three cases of Δ , $\Delta = -0.3, -0.1, 0.1$.

Problem 9.2.2.8. Consider the AR(3) process with poles at

$$z_{1,(2)} = 0.9 \exp(\pm 0.8\pi), \\ z_3 = 0.9.$$

Problem 9.2.2.9. The signal process is the sum of three statistically independent AR(1) processes $s_1(k)$, $s_2(k)$, and $s_3(k)$, with following parameters:

$$\sigma_{u_1}^2 = \sigma_{u_2}^2 = \sigma_{u_3}^2 = 1, \\ \alpha_1 = 0.5, \\ \alpha_2 = 0.8, \\ \alpha_3 = 0.95.$$

Problem 9.2.2.10. ARMA (N, N), N even, Butterworth

- a. A second-order Butterworth signal is an ARMA (2, 2) process

$$H(z) = \frac{b_0 + b_1 z^{-1} + b_2 z^{-2}}{a_0 + a_1 z^{-1} + a_2 z^{-2}},$$

with

$$b_0 = b_2 = (\Omega'_c)^2, \\ b_1 = 2(\Omega'_c)^2, \\ a_0 = 1 + 2 \cos\left(\frac{\pi}{4}\right) \Omega'_c + (\Omega'_c)^2, \\ a_1 = 2((\Omega'_c)^2 - 1), \\ a_2 = 1 - 2 \cos\left(\frac{\pi}{4}\right) \Omega'_c + (\Omega'_c)^2,$$

where

$$\Omega'_c = \tan\left(\frac{\omega_c}{2}\right)$$

and ω_c is the half-power frequency of the spectrum.

- b. An even-order Butterworth signal is an ARMA(N, N) process

$$H(z) = \prod_{k=0}^{\frac{N}{2}-1} \frac{b_{0k}(1+z^{-1})^2}{a_{0k} + a_{1k}z^{-1} + a_{2k}z^{-2}},$$

where

$$a_{0k} = 1 + 2 \cos\left[\frac{\pi(2k+1)}{2N}\right] \Omega'_c + (\Omega'_c)^2, \\ a_{1k} = 2((\Omega'_c)^2 - 1), \\ a_{2k} = 1 - 2 \cos\left[\frac{\pi(2k+1)}{2N}\right] \Omega'_c + (\Omega'_c)^2.$$

Table 9.1: Table P.1

Problem	Signal Model
9.2.3.1	9.2.2.1
9.2.3.2	9.2.2.2
9.2.3.3	9.2.2.3
9.2.3.4	9.2.2.4
9.2.3.5	9.2.2.5
9.2.3.6	9.2.2.6
9.2.3.7	9.2.2.7
9.2.3.8	9.2.2.8
9.2.3.9	9.2.2.9
9.2.3.10	9.2.2.10

P9.2.3 FIR Wiener Filters

The first 10 problems in the section all have the same structure. A random process model for the signal is specified. You are asked to repeat Example 9.3.

- a. Plot the normalized filter coefficients for $K = 10$.
- b. Plot the frequency response for $K = 10$.
- c. Plot the normalized MSE as a function of K .
- d. Discuss your results.

The next 10 problems repeat Example 9.4 for the signal models in Table P.1. In each problem,

- a. Plot the normalized $h(m)$ for $K = 10$ and $L = -1$ and -5 and representative parameter values.
- b. Plot $\xi_0(10 : L)$, $L \leq 0$ versus $|L|$.
- c. Discuss your results.

Problems 9.2.3.m ($m = 11, \dots, 20$). Use the signal model in Problem 9.2.2.($m - 10$).

The next 10 problems discuss predictions for the signal models in Table P.1. In each problem,

- a. Plot the normalized $h(m)$ for $K = 10$ and $L = 1$ and 10 and representative parameter values.
- b. Plot $\xi_0(10 : L)$, $L \leq 0$ versus $|L|$.
- c. Discuss your results.

Problem 9.2.3.m ($m = 21, \dots, 30$). Use the signal model in Problem 9.2.2.($m - 20$).

P9.2.4 Unrealizable IIR Wiener Filters

In the first 10 problems, we repeat Example 9.5 for the signals in Table P.1. In each problem,

- a. Plot the normalized filter coefficients for SNR = 3 dB and representative parameter values.
- b. Plot the normalized MSE versus SNR for representative parameter values.

Problems 9.2.4.m ($m = 1, \dots, 10$). Use the signal model in Problem 9.2.2. m .

P9.2.5 Realizable IIR Wiener Filters

In the first 10 problems, we repeat Example 9.8 for the signals in Table P.1. In each problem,

- a. Plot the normalized plot of $K_{dz}(k; 0)$.
- b. Plot ξ_0 versus SNR for representative parameter values.
- c. For prediction, plot the normalized value of $K_{dz}(k; L)$, $L \geq 0$, for $L = 1$ and 10.
- d. Plot $\xi_0(L)$, $L \geq 0$ versus SNR for representative parameter values.
- e. For filtering with lag, plot the normalized value of $K_{dz}(k; L)$ and $h_0(m; L)$ for representative parameter values.
- f. Plot $\xi_0(L)$, $L \leq 0$ versus SNR for representative parameter values.
- g. Discuss your results.

Problem 9.2.5.m ($m = 1, \dots, 10$). Use the signal model in Problem 9.2.3.m.

P9.3 Discrete-Time Kalman Filters

P9.3.1 Random Process Models

ARMA models The first 10 problems consider the ARMA models in Section 9.2.2. In each problem, we want to find:

- a. The \mathbf{F} , \mathbf{G} , and \mathbf{C} matrices in Canonical Model # 1 using the $a(m)$ and $b(m)$ values in the ARMA model and the corresponding \mathbf{Q} matrices. $\mathbf{R} = \sigma_w^2 \mathbf{I}$.
- b. The state vector model in Canonical Model # 2 using the poles of the process.

Problem 9.3.1.m ($m = 1, \dots, 10$). Use the signal process model in Problem 9.2.3.m.

Kinematic models

Problem 9.3.1.11. Consider the tracking model in (9.229)–(9.236). Assume $\mathbf{x}(0)$ is a Gaussian random vector, $N(\mathbf{m}(0), \mathbf{K}(0))$.

Assume

$$\begin{aligned}\mathbf{m}(0) &= \begin{bmatrix} 0 \\ 10 \end{bmatrix}, \\ \mathbf{K}(0) &= \text{diag} [1 \quad 9],\end{aligned}$$

$$T = 1, \sigma_w^2 = 0.50, \mathbf{C} = [1 \quad 0].$$

- a. Plot a realization of the actual position and velocity and the observed position for several values of σ_a^2 , $1 \leq k \leq 30$.
- b. Repeat for $\mathbf{C} = [1 \quad 1]$ with

$$\mathbf{R}(k) = \text{diag} [\sigma_p^2 \quad \sigma_v^2]$$

where $\sigma_p^2 = 0.50$ and $\sigma_v^2 = 0.50$. Add observed velocity to the plots.

- c. Discuss your results.

Problem 9.3.1.12. Consider the constant acceleration model in (9.237)–(9.242). Assume $\mathbf{x}(0)$ is a Gaussian random vector, $N(\mathbf{m}(0), \mathbf{K}(0))$.

Assume

$$\mathbf{m}(0) = \begin{bmatrix} 0 \\ 10 \\ 0.1 \end{bmatrix},$$

$$\mathbf{K}(0) = \text{diag} [1 \ 9 \ 0.04],$$

$$T = 1, \sigma_w^2 = 0.50, \mathbf{C} = [1 \ 0].$$

- a. Plot a realization of the actual position, velocity, and acceleration and the observed position for several values of σ_a^2 .
- b. Repeat part b of Problem 9.3.1.11.
- c. Discuss your results.

P9.3.2.1 Kalman Filter Derivation

Problem 9.3.2.1.1. Consider the state variable model where

$$\mathbf{x}(k) = \mathbf{F}(k-1)\mathbf{x}(k-1) + \mathbf{G}(k-1)\mathbf{u}(k-1) + \mathbf{B}(k-1)\mathbf{v}(k-1)$$

where $\mathbf{v}(k-1)$ is a known $l \times 1$ vector input (e.g. the mean of $\mathbf{u}(k)$ process is non-zero), and $\mathbf{B}(k)$ is a known $p \times l$ matrix. The observation model remains the same.

Find the Kalman filter.

Problem 9.3.2.1.2. Specify a circular complex Gaussian state variable model and observation model and find the complex Kalman filter.

Problem 9.3.2.1.3. Consider the one-step prediction problem, where

$$\alpha(k) \triangleq \hat{\mathbf{x}}(k+1|k).$$

- a. Show that

$$\hat{\mathbf{x}}(k+1|k) = \mathbf{F}(k)\hat{\mathbf{x}}(k);$$

- b. Show that α can be written as

$$\hat{\mathbf{x}}(k+1|k) = \mathbf{F}(k)\hat{\mathbf{x}}(k|k-1) + \mathbf{F}(k)\mathbf{K}(k)\tilde{\mathbf{r}}(k).$$

- c. Draw a block diagram and identify $\hat{\mathbf{x}}(k+1|k)$ and $\hat{\mathbf{x}}(k)$ as outputs.
- d. Derive the recursion for the error covariance matrix.

P9.3.2.2 Reduced Dimension Filters

Problem 9.3.2.2.1. The one-step predictions form of the Kalman filter is given in Problem 9.3.2.1.3. Derive the one-step prediction form for the reduced-dimension covariance filter.

Problem 9.3.2.2.2. Repeat problem 9.3.2.2.1, for the information filter using the $\mathbf{y}(k)$ state estimation.

P9.3.2.3 Applications: Kalman Filter

ARMA models The first 10 problems repeat Example 9.9 for the signal models in Table P.1.

In each problem,

- Plot the Kalman gain versus k , for SNR = 3 dB and 10 dB for the various parameter values. Use the state variable model with $a(m)$ and $b(m)$.
- Plot $P_{11}(k)/\sigma_s^2$ versus k .
- Plot the normalized MSE versus SNR.

Problem 9.3.2.3.m ($m = 1, \dots, 10$). Use the signal model in Problem 9.2.2.10.

Butterworth Spectra In Example 9.11, we introduced the discrete-time Butterworth process and formed the Kalman filter for the BW(2, 2) and BW(N, N) Butterworth processes. In the next sequence of problems, we study this family of processes in more detail.

Problem 9.3.2.3.11. Consider the $N = 2$ case. Derive (9.414)–(9.419) by using (9.409)–(9.411).

Problem 9.3.2.3.12. We can normalize (9.409) by setting $\Omega_c = 1$.

- Show that the normalized $H_{cn}(s)$ can be written as

$$H_{cn}(s) = \prod_{k=1}^{\frac{N}{2}} \left[s^2 - 2s \cos \left(\frac{2k+N-1}{2N} \pi \right) + 1 \right] \quad \text{for } N \text{ even.}$$

- Show that the normalized $H_{cn}(s)$ can be written as

$$H_{cn}(s) = (s+1) \prod_{k=1}^{\frac{N-1}{2}} \left[s^2 - 2s \cos \left(\frac{2k+N-1}{2N} \pi \right) + 1 \right] \quad \text{for } N \text{ odd.}$$

- Verify the following table of factors.

N	Factors of Polynomial $H_n(s)$
1	$(s+1)$
2	$s^2 + 1.4142s + 1$
3	$(s+1)(s^2 + s + 1)$
4	$(s^2 + 0.7654s + 1)(s^2 + 1.8478s + 1)$
5	$(s+1)(s^2 + 0.6180s + 1)(s^2 + 1.6180s + 1)$
6	$(s^2 + 0.5176s + 1)(s^2 + 1.4142s + 1)(s^2 + 1.9319s + 1)$
7	$(s+1)(s^2 + 0.4450s + 1)(s^2 + 1.2470s + 1)(s^2 + 1.8019s + 1)$
8	$(s^2 + 0.3902s + 1)(s^2 + 1.1111s + 1)(s^2 + 1.6629s + 1)(s^2 + 1.9616s + 1)$

Note that $H(s)$ scales using (9.409) but that, because the bilinear transformation is nonlinear $H(z)$ does not scale linearly.

Problem 9.3.2.3.13. Consider the $N = 1$ case.

- Derive $H(z)$.
- Consider $\omega_c = 0.2\pi, 0.4\pi, 0.6\pi, 0.8\pi$. Plot the power spectra. Also, plot the power spectra of AR(1) processes with α chosen to give the same half-power point.
- Find the Kalman filter. Plot the normalized variance versus k for SNR = 3 dB.
- Plot the normalized steady state MSE versus SNR for the four values of ω_c .
- Discuss your results.

Problem 9.3.2.3.14.

- Derive the Kalman filter for the $N = 3$ case and repeat parts c of Problem 9.3.2.3.13.
- Derive the Kalman filter for the $N = 5$ case.
- Derive the Kalman filter for the $N = 7$ case.
- Derive the Kalman filter for the $N = 9$ case.
- In order to compare results across the family, consider each of the four values of ω_c separately. Plot the results from Example 9.11 and parts a–d on a separate plot for each ω_c .
- Discuss your results.

Tracking Models

Problem 9.3.2.3.15. [from [BSLK01]]

In this problem, we develop closed-form expressions for the steady-state gain \mathbf{K}_∞ and the steady-state variance \mathbf{P}_∞ for the random acceleration model in (9.229)–(9.236).

We reparameterize the steady-state Kalman gain as

$$\mathbf{K}_\infty = \begin{bmatrix} K_p & K_v \end{bmatrix}^T \triangleq \begin{bmatrix} \alpha & \frac{\beta}{T} \end{bmatrix}, \quad (\text{P.1})$$

where α and β are dimensionless.

- Using (9.312), show that the innovations covariance is

$$\tilde{\mathbf{P}}_\infty = m_{11} + \sigma_w^2, \quad (\text{P.2})$$

where

$$\mathbf{P}'_\infty \triangleq \mathbf{P}_\infty(k|k-1) \triangleq \begin{bmatrix} m_{11} & m_{12} \\ m_{21} & m_{22} \end{bmatrix}. \quad (\text{P.3})$$

- Using (9.313), (P.1), and (P.3), show that

$$K_p = \frac{m_{11}}{m_{11} + \sigma_w^2}, \quad (\text{P.4})$$

$$K_v = K_p \frac{m_{12}}{m_{11}}. \quad (\text{P.5})$$

c. Using (9.311), show that the covariance update equation is

$$\begin{aligned}\mathbf{P}_\infty &\triangleq \begin{bmatrix} P_{11} & P_{12} \\ P_{21} & P_{22} \end{bmatrix} \\ &= \begin{bmatrix} (1 - K_p)m_{11} & (1 - K_p)m_{12} \\ (1 - K_p)m_{12} & m_{22} - K_v m_{12} \end{bmatrix}. \end{aligned}\quad (\text{P.6})$$

d. Show that (9.311) can be rewritten as

$$\mathbf{P}_\infty = \mathbf{F}^{-1} [\mathbf{P}'_\infty - \mathbf{Q}] \mathbf{F}^{-T}, \quad (\text{P.7})$$

where

$$\mathbf{F}^{-1} = \begin{bmatrix} 1 & -T \\ 0 & 1 \end{bmatrix}. \quad (\text{P.8})$$

e. Using (P.7), show that

$$\mathbf{P}_\infty = \begin{bmatrix} m_{11} - 2Tm_{12} + T^2m_{22} - \frac{1}{4}T^4\sigma_a^2 & m_{12} - Tm_{22} + \frac{1}{2}T^3\sigma_a^2 \\ m_{12} - Tm_{22} + \frac{1}{2}T^3\sigma_a^2 & m_{22} - T^2\sigma_a^2 \end{bmatrix}. \quad (\text{P.9})$$

f. By equating terms in (P.6) and (P.9), show that

$$K_p m_{11} = 2Tm_{12} - T^2m_{22} + \frac{T^4}{4}\sigma_a^2, \quad (\text{P.10})$$

$$K_p m_{12} = Tm_{22} - \frac{T^3}{2}\sigma_a^2, \quad (\text{P.11})$$

$$K_v m_{11} = T^2\sigma_a^2. \quad (\text{P.12})$$

g. Using (P.4), (P.5), (P.10), (P.11), and (P.12), show that

$$m_{11} = \frac{K_p}{1 - K_p} \sigma_w^2, \quad (\text{P.13})$$

$$m_{12} = \frac{K_v}{1 - K_p} \sigma_w^2, \quad (\text{P.14})$$

$$m_{22} = \frac{K_p m_{12}}{T} + \frac{T^2}{2} \sigma_a^2 = \left(\frac{K_p}{T} + \frac{K_v}{2} \right) m_{12}. \quad (\text{P.15})$$

h. Using (P.12)–(P.15) in (P.10), show that

$$K_p^2 - 2TK_v + TK_p K_v + \frac{T^2}{4} K_v^2 = 0. \quad (\text{P.16})$$

i. Use (P.1) to rewrite this as

$$\alpha^2 - 2\beta + \alpha\beta + \frac{\beta^2}{4} = 0. \quad (\text{P.17})$$

j. Use (P.17) to show that

$$\alpha = \sqrt{2\beta} - \frac{\beta}{2}. \quad (\text{P.18})$$

k. Use (P.12) and (P.14) to show that

$$\frac{\beta^2}{1-\alpha} = \frac{T^4 \sigma_a^2}{\sigma_w^2} \triangleq \lambda^2. \quad (\text{P.19})$$

The quantity λ is called the target tracking index. It is proportional to the ratio of the RMS value of process noise effect of the position over one sampling period ($\sigma_a T^2/2$) to the RMS value of the observation noise.

l. Show that

$$\beta = \frac{1}{4} (\lambda^2 + 4\lambda - \lambda\sqrt{\lambda^2 + 8\lambda}) = K_v T \quad (\text{P.20})$$

and

$$\alpha = -\frac{1}{8} (\lambda^2 + 8\lambda - (\lambda + 4)\sqrt{\lambda^2 + 8\lambda}) = K_p. \quad (\text{P.21})$$

m. Show that

$$\mathbf{P}_\infty = \sigma_w^2 \begin{bmatrix} \alpha & \frac{\beta}{T} \\ \frac{\beta}{T} & \frac{\beta}{T^2} \frac{\alpha - \beta/2}{1-\alpha} \end{bmatrix}. \quad (\text{P.22})$$

n. Plot α and β as a function of λ .

Problem 9.3.2.3.16. Consider the tracking model in Example 9.10. Assume that the sensor measures both range and velocity. Then \mathbf{C} and \mathbf{R} are given by (9.391) and (9.392). Assume $\sigma_v^2 = 40 \text{ (m/s)}^2$. Plot Figures 9.38–9.40 for this case.

Problem 9.3.2.3.17. Consider the tracking model in which the nominal trajectory is constant acceleration. This model is described in (9.237)–(9.242). Use the same initial conditions as in Example 9.10,

$$\begin{aligned} x(0) &= 1000 \text{ m}, \\ v(0) &= -50 \text{ m/s}, \\ a(0) &= 0 \text{ m/s}^2, \\ \sigma_a &= 15 \text{ m/s}^3, \\ T &= 0.1 \text{ s}, \\ \sigma_r &= 10 \text{ m}, \\ \hat{x}(0) &= 1100, \\ \hat{v}(0) &= -100, \\ \hat{a}(0) &= 10, \\ P(0) &= \text{diag} [1000 \quad 1000 \quad 100]. \end{aligned}$$

Plot Figures 9.38–9.40 for this case.

Problem 9.3.2.3.18. Repeat Problem 9.3.2.3.17 for the case of range and velocity observation. Assume

$$\sigma_v^2 = 40 \text{ (m/s)}^2$$

Problem 9.3.2.3.19. The steady-state version of the Kalman filter in Problem 9.3.2.3.17 is referred to as an alpha-beta-gamma filter and the gains are

$$\mathbf{K}_\infty^T \triangleq \begin{bmatrix} \alpha & \frac{\beta}{T} & \frac{\gamma}{2T^2} \end{bmatrix}^T.$$

Read Section 6.5.5 (pp. 289–291) of [BSLK01] or do an Internet search to find an analysis similar to Problem 9.3.2.3.15, and then plot the steady-state gains versus the tracking index.

Reduced-Dimension Filters

The next several problems provide some familiarity with the implementation of the reduced-dimension covariance filter and the information filter.

Problem 9.3.2.3.20. Consider the model in Example 9.12. We consider only a single quadrature component. Assume $N = 20$ and $\mathbf{R} = \sigma_w^2 \mathbf{I}$. Repeat parts a–d of Problem 9.3.2.3.14 using an information filter.

Problem 9.3.2.3.21. Consider the model in Example 9.12. We consider only a single quadrature component. The input $\mathbf{r}(k)$ is given by (9.433) and \mathbf{C} is given by (9.434). The covariance matrix of $\mathbf{w}(k)$ is

$$\mathbf{R} = \sigma_w^2 \mathbf{I} + \mathbf{R}_c,$$

where

$$\mathbf{R}_c = \sigma_I^2 \begin{bmatrix} 1 & \alpha & \alpha^2 & \cdots & \alpha^N \\ \alpha & 1 & \alpha & \cdots & \alpha^{N-1} \\ \vdots & \vdots & \ddots & \cdots & \vdots \\ \alpha^N & \alpha^{N-1} & \cdots & \cdots & 1 \end{bmatrix}.$$

The $\mathbf{x}(k)$ is a 4th-order Butterworth process, BW(4,4) (See Example 9.11). The SNR = σ_s^2/σ_w^2 is 3 dB. The number of array elements is $N = 20$. Derive three implementations of the Kalman Filter:

- a. Standard covariance filter.
- b. Reduced-dimension covariance filter.
- c. Information filter, with \mathbf{y} being the state vector.
- d. Plot the same results as Figure 9.43.

Problem 9.3.2.3.22. Consider the model in Example 9.12 and review Examples 3.2 and 3.7.

- a. Find the complex Kalman information filter and plot the same results as in Example 9.12.
- b. Assume there is a single interfering signal as described in Example 3.7. Note that \tilde{a}_k is IID so that it can be included in $\tilde{\mathbf{R}}$. Repeat part a.

P9.3.2.4 Estimation in Nonwhite Noise

The next 10 problems repeat Example 9.13. The state equations are given by (9.466)–(9.471). The nonwhite noise is an AR(1) process with $\alpha_n = 0.3, 0.5, 0.8, 0.95$ and power σ_n^2 . We use the signal models in Table P.1.

In each problem,

- Find the Kalman filter.
- Plot $P_{\infty s}$ versus SNR for the 4 values of α and CWR = 10.
- Plot $P_{\infty s}$ versus SNR for various CWR and $\alpha = 0.8$.

Problem 9.3.2.4.m ($m = 1, \dots, 10$). Use signal model in Problem 9.2.2.m.

The next three problems repeat Example 9.14 for a number of Butterworth signal models. In each problem,

- Find the Kalman filter.
- Plot $P_{\infty s}$ versus SNR for various parameter combinations and CWR = 10.

We denote a Butterworth process of order N and 3 dB point of ω_c as $BW(N, \omega_c)$. We will also denote an AR(1) process with 3 dB point $\omega_c(\alpha)$ as $AR(1, \omega_c(\alpha))$.

In each problem, discuss your results.

Problem 9.3.2.4.11. Signal is $BW(2, 0.2)$. Colored noise is $AR(1, \omega_c(\alpha))$. Find behavior as a function of $\omega_c(\alpha) \geq 0.2$.

Problem 9.3.2.4.12. Repeat Problem 9.3.2.4.11 for

- $BW(4, 0.2)$.
- $BW(6, 0.2)$.
- $BW(8, 0.2)$.
- $BW(10, 0.2)$.

Problem 9.3.2.4.13. Repeat Problem 9.3.2.4.12 for colored noise of $BW(2, \omega_c(\alpha))$, where $\omega_c(\alpha) \geq 0.2$.

Problem 9.3.2.4.14.

$$r(k) = s(k) + n_c(k) + w(k).$$

The signal process $s(k)$ is an AR(2) process with poles at $0.7 \exp(\pm 0.6\pi)$. The colored noise process is an AR(2) with poles at $0.5 \exp(\pm(0.6 + \Delta_i)\pi)$, where $\Delta_i = -0.1i$, $i = 1, 2, 3$. The white noise has $\sigma_w^2 = 1.0$.

- Plot the power spectra of the two processes for the three values of i .
- Assume the process has reached steady state. Plot $P_{\infty s}$ versus SNR for CWR = 10.

Problem 9.3.2.4.15. Review Examples 9.12 and 3.7, and Problem 9.3.2.3.22. Assume that $\tilde{\mathbf{a}}_k$ in (3.318) is a complex AR(1) process with $\alpha = \alpha_I$. The signal is also a complex AR(1) process with $\alpha = \alpha_s$. Study the effect of INR, θ_I , and $(\alpha_I - \alpha_s)$. Find the optimum Kalman information filter and compare your results to Problem 9.3.2.3.22.

P9.3.2.5 Sequential Update

Problem 9.3.2.5.1. Derive the sequential update equations for the information filter.

Problem 9.3.2.5.2. Consider part d in Problem 9.3.2.3.14. Implement the Kalman information filter using sequential scalar updating and verify that your results are the same in the referenced problem.

P9.3.2.7 Divergence

Problem 9.3.2.7.1. Consider the model in Example 9.14. Assume that we know “b.” Design the optimum Kalman filter for the model (recall Problem 9.3.2.1.1). Compare the performance to the results in Example 9.14.

P9.3.2.8 Sensitivity and Model Mismatch

Problem 9.3.2.8.1. Derive the model mismatch equations (9.552)–(9.579) for the information filter version of the Kalman filter.

Problem 9.3.2.8.2. Consider the AR(1) model in Example 9.15. Assume that we increase the $Q = \sigma_u^2$ in the Kalman filter to make the model less sensitive to mismatch.

- Let

$$\sigma_{u,\text{KF}}^2 = \sigma_{u,\text{mod}}^2(1 + \beta).$$

Assume that $\alpha = 0.8$ and that the model SNR = 3 dB. Plot the normalized change in P_{ac} as a function of β

$$\frac{P_{ac} - P_{\text{nom}}}{P_{\text{nom}}}.$$

- Repeat Figure 9.51a for $\beta = 0.05, 0.10$, and 0.20 .

Problem 9.3.2.8.3. We design a Kalman filter assuming that the signal process is a second-order Butterworth BW(2, 0.4π). The actual process is BW(4, 0.5π).

- Plot $P_{11,\infty}^{\text{nom}}/\sigma_s^2$, $P_{11,\infty}^{\text{ac}}/\sigma_s^2$, $P_{11,\infty}^{\text{pm}}/\sigma_s^2$ versus SNR.
- Investigate the effects of increasing σ_u^2 as discussed in Problem 9.3.2.8.2.

P9.3.3.1 Fixed-Lead Prediction

In the next 10 problems, we repeat Example 9.16 for the signal models in Table P.1. In each problem,

- Plot the normalized variance versus k for $L = 4$ and SNR = 3 dB and 10 dB.
- Plot the normalized variance versus L for SNR = 3 dB and 10 dB.

Problem 9.3.3.1.m ($m = 1, \dots, 10$). Use the signal model in Problem 9.2.2. m . In the next set of problems, we repeat Example 9.16 for signal models we have encountered in previous problems.

Problem 9.3.3.1.11. Use the signal model in Example 9.11.

Problem 9.3.3.1.12. Use the signal model in Problem 9.3.2.3.13.

Problem 9.3.3.1.13. Use the signal models in Problem 9.3.2.3.14.

Problem 9.3.3.1.14. Use the signal model in Example 9.10.

Problem 9.3.3.1.15. Use the signal model and observation model in Problem 9.3.2.3.16.

Problem 9.3.3.1.16. Use the signal models in Problem 9.3.2.3.17.

P9.3.3.2 Fixed-Point Prediction

In the next 10 problems, we repeat Example 9.17 for the signal models in Table P.1. In each problem, plot the normalized variance $P_{11}(L_p|k)/\sigma_s^2$ versus k .

Problem 9.3.3.2.m ($m = 1, \dots, 10$). Use the signal model in Problem 9.2.2.m.

In next set of problems, we repeat Example 9.17 for the signal models we have encountered previously.

Problem 9.3.3.2.m ($m = 11, \dots, 16$). Use the signal model in Problem 9.3.2.3.m.

Problem 9.3.3.2.17. In a tracking application (e.g. Example 9.10), the fixed-point predicts the range at time $k = L_p$. In many applications, we want to predict when the target will be at a given range. Develop an algorithm to estimate the time-of-arrival at a specific point, r_p . Test it with the model in Example 9.10.

P9.3.4.1 Fixed-Interval Smoothing

In the next 10 problems, we repeat Example 9.18 for the signal models in Table P.1. In each problem, plot the forward variance $\xi_{11,f}(k)$ and the backward variance $\xi_{11,b}(k)$ for $k = 10$ and SNR = 3 dB.

Problem 9.3.4.1.m ($m = 1, \dots, 10$). Use the signal model in Problem 9.2.2.m.

In the next set of problems, repeat Example 9.18 for signal models indicated.

Problem 9.3.4.1.m ($m = 11, 12, 13$). Use the signal models in Problem 9.3.2.3.m.

P9.3.4.2 Fixed-Lag Smoothing

In the next 10 problems, we repeat Example 9.19 for the signal model in Table P.1. In each problem, assume the system has reached steady state. Plot $P_{L\infty,11}$ versus L for SNR = 3 dB and 10 dB.

Problem 9.3.4.2.m ($m = 1, \dots, 10$). Use the signal model in Problem 9.2.2.m.

In the next set of problems, we repeat Example 9.19 for signal models indicated.

Problem 9.3.4.2.m ($m = 11, 12, 13$). Use the signal models in Problem 9.3.2.3.m.

10

Detection of Gaussian Signals

10.1 INTRODUCTION

In this chapter, we consider the problem of detecting a sample function of Gaussian random process in additive Gaussian noise. We consider both continuous-time and discrete-time random processes. In both cases, we assume that the additive noise is a sample function of a white Gaussian noise process whose height is known. In Chapters 8 and 9, we developed whitening filters, so the white noise assumption does not lose any generality.

In Section 10.2, we consider continuous-time processes and develop two approaches. In the first approach, we generate a finite-dimensional vector by either temporal sampling or a Karhunen–Loëve expansion. We can choose the dimension large enough to give a vector model that is a good approximation to the original problem. We can then apply the detection theory results to solve the problem using block data processing.

In the second approach, we use the Karhunen–Loëve approach that we introduced in Chapter 6 and used for deterministic signals in Chapter 7. This leads to integral equations that we must solve to find the optimum detector. However, these equations are identical to the equations developed in Chapter 8 for the optimum smoothing filter $h_{ou}(t, u)$ or the optimum realizable filter $h_{or}(t, u)$, and we can use the solution techniques developed in Chapter 8 to specify the optimum detector. We also analyze the performance using the $\mu(s)$ function of Chapter 2 as a tool.

In Section 10.3, we consider discrete-time processes. In this case, if we use block processing, then an exact solution has already been developed in Chapter 3 if the process is modeled using a second moment characterization. In many cases, the process is described using a state variable characterization. In this case, we need an implementation using realizable estimates. We derive an implementation in which the necessary signals are generated by the discrete-time Kalman filters developed in Chapter 9.

In Section 10.4, we summarize our results and discuss related topics of interest.

A large part of this Chapter is taken from Chapters 2–4 of DEMT-III [Van71b, Van01c].

10.2 DETECTION OF CONTINUOUS-TIME GAUSSIAN PROCESSES

In this section, we consider the problem of detecting a sample function from a Gaussian random process in the presence of additive white Gaussian noise. It is characterized by

Detection, Estimation, and Modulation Theory, Second Edition. Harry L. Van Trees, Kristine L. Bell with Zhi Tian. © 2013 John Wiley & Sons, Inc. Published 2013 by John Wiley & Sons, Inc.

the property that on both hypotheses, the received waveform contains an additive noise component $w(t)$, which is a sample function from a zero-mean white Gaussian process with spectral height $N_0/2$. When H_1 is true, the received waveform also contains a signal $s(t)$, which is a sample function from a Gaussian random process whose mean and covariance function are known. Thus,

$$H_1 : r(t) = s(t) + w(t), \quad T_i \leq t \leq T_f, \quad (10.1)$$

and

$$H_0 : r(t) = w(t), \quad T_i \leq t \leq T_f. \quad (10.2)$$

The signal process has a mean value function $m(t)$,

$$E[s(t)] = m(t), \quad T_i \leq t \leq T_f, \quad (10.3)$$

and a covariance function $K_s(t, u)$,

$$E[(s(t) - m(t))(s(u) - m(u))] \triangleq K_s(t, u), \quad T_i \leq t, u \leq T_f. \quad (10.4)$$

Both $m(t)$ and $K_s(t, u)$ are known. We assume that the signal process has a finite mean-square value and is statistically independent of the additive noise. Thus, the covariance function of $r(t)$ on H_1 is

$$E[(r(t) - m(t))(r(u) - m(u))|H_1] \triangleq K_1(t, u) = K_s(t, u) + \frac{N_0}{2}\delta(t - u), \quad T_i \leq t, u \leq T_f. \quad (10.5)$$

We refer to $r(t)$ as a *conditionally Gaussian* random process. The term “conditionally Gaussian” is used because $r(t)$, given H_1 is true, and $r(t)$, given H_0 is true, are the two Gaussian processes in the model.

We observe that the mean value function can be viewed as a deterministic component in the input. When we want to emphasize this we write

$$\begin{aligned} H_1 : r(t) &= m(t) + [s(t) - m(t)] + w(t) \\ &= m(t) + s_R(t) + w(t), \quad T_i \leq t \leq T_f. \end{aligned} \quad (10.6)$$

(The subscript R denotes the random component of the signal process.) Now the waveform on H_1 consists of a known signal corrupted by two independent zero-mean Gaussian processes. If $K_s(t, u)$ is identically zero, the problem degenerates into the known signal in white noise problem of Chapter 7. As we proceed, we shall find that all of the results in Sections 7.2–7.4 except for the random phase case in Section 7.4.1 can be viewed as special cases of this detection problem.

In most of the subsequent discussion we will assume $m(t) = 0$. The restriction to white noise simplifies the discussion. As discussed in Section 7.3 and Chapter 8, we can map a colored noise problem into a white noise problem by using a whitening filter.

The continuous time model is discussed in detail in Chapters 2–5 of DEMT-III [Van71b, Van01c] and the reader is referred to that for a more complete discussion.

In this section, we will discuss two approaches to the problem. In Section 10.2.1, we map the continuous time model into a finite dimensional vector space by one of two methods. In the first, we assume the received signal is bandlimited and sample the received

process at T second intervals. This method immediately reduces the problem to the model in Chapter 3. The second method does a Karhunen–Loëve expansion of the signal process and retains the K significant eigenvalues. This method also reduces the problem to the model in Chapter 3.

In Section 10.2.2, we formulate the problem in terms of K eigenvalues and eigenvectors. We then put the likelihood ratio in a form so that we can let $K \rightarrow \infty$. This results in an integral equation that we have to solve to implement the optimum detector. We then manipulate the detector into various forms:

- a. **Estimator–correlator:** This form contains a function $h_1(t, u)$ that corresponds to the optimum linear smoothing filter.
- b. **Filter-squarer-integrator:** This form contains a functional square-root and is most practical in the SPLOT model that will discuss in Section 10.2.3.
- c. **Realizable filter detector:** This form contains the optimum realizable filter.

The motivation for developing the forms in (a) and (c) is that a large class of processes can be modeled using the state-variable techniques that were developed in Chapter 8. Then, we can implement the filter in (c) as a Kalman filter and the filter in (a) as a Kalman smoother.

In Section 10.2.3, we consider the stationary process-long observation time (SPLOT) model and analyze the resulting detectors. In Section 10.2.4, we summarize our results.

We consider real random processes in the text and develop the analogous results for circular complex Gaussian random processes in the problems.

Most of the original work on the detection of Gaussian signals is due to Price [Pri53, Pri54, Pri55, Pri56] and Middleton [Mid57, Mid60b, Mid60a], and [Mid61]. Much of the early work on state-variable realization for detection problems was done by two of my M.I.T. doctoral students: Arthur Baggeroer [Bag67a] and Lew Collins [Col66a, Col68c, Col68b, Col68a], and Fred Schweppe [Sch65] of Lincoln Labs.

10.2.1 Sampling

In this section, we reduce the problem to a K -dimensional problem that we have already solved in Chapter 3. In the first approach, we assume the signal and noise processes are bandlimited and sample every $T = 1/2W$ seconds.

Then, for zero-mean processes, the model reduces to the model in Section 3.3 and, from (3.343)

$$l(\mathbf{R}) = \frac{2}{N_0} \mathbf{R}^T \mathbf{H} \mathbf{R} \begin{matrix} H_1 \\ \geqslant \\ H_0 \end{matrix} \gamma', \quad (10.7)$$

where

$$\mathbf{H} = \frac{2}{N_0} \left[\frac{2}{N_0} \mathbf{I} + \mathbf{K}_s^{-1} \right]^{-1}. \quad (10.8)$$

We can implement the detector using (10.7) and (10.8), but in order to analyze it, we do an eigendecomposition of \mathbf{K}_s that leads to the receiver configuration in Figure 3.27, which is repeated in Figure 10.1.

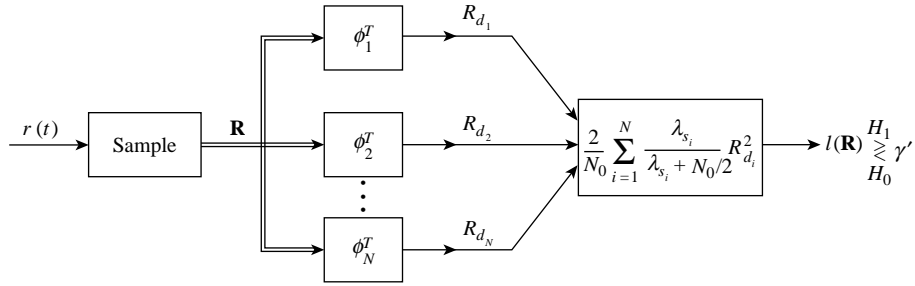


Figure 10.1: Optimum detector: sampling.

Note that the sampled model is an approximate model because the original signal is generally not completely bandlimited.

In the second approach, we do a Karhunen–Loève expansion of $K_s(t, u)$ as developed in Chapter 6. From (6.49)

$$\lambda_i \phi_i(t) = \int_0^T K_s(t, u) \phi_i(u) du, \quad (10.9)$$

we retain the K eigenvalues. We choose K so that

$$\sum_{i=1}^K \lambda_i = \alpha E_s, \quad (10.10)$$

where E_s is the signal energy and

$$\alpha \leq 1 \quad (10.11)$$

is chosen to represent the percentage of the signal energy we want to retain in our approximate model. For the low-rank model in Section 6.4.5, $\alpha = 1$.

Then, the optimum detector can be implemented as shown in Figure 10.2, which corresponds to the model in Section 3.3. In general, we will have to solve (10.9) numerically.

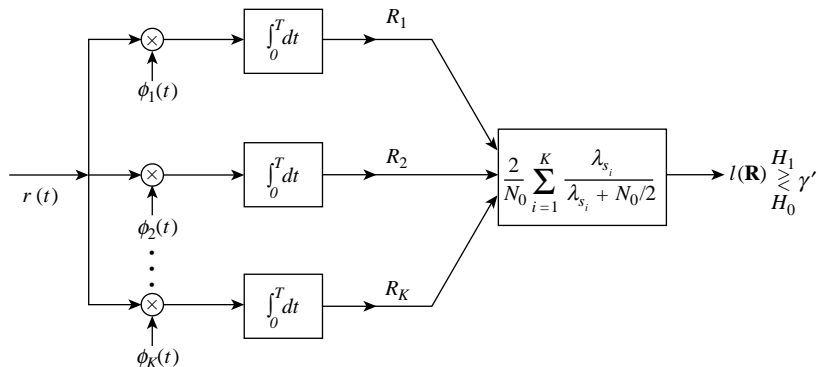


Figure 10.2: Optimum detector: Karhunen–Loève sampling.

In either approach, we have reduced the continuous-time problem to a finite-dimensional Gaussian model that we have already solved.

10.2.2 Optimum Continuous-Time Receivers

Our approach to designing the optimum receiver is analogous to the approach in the deterministic signal case. The essential steps are the following:

1. We expand $r(t)$ in a series, using the eigenfunctions of the signal process as coordinate functions. The noise term $w(t)$ is white, so the coefficients of the expansion will be conditionally uncorrelated on both hypotheses. Because the input $r(t)$ is Gaussian on both hypotheses, the coefficients are conditionally statistically independent.
2. We truncate the expansion at the K th term and denote the first K coefficients by the vector \mathbf{r} . The waveform corresponding to the sum of the first K terms in the series is $r_K(t)$.
3. We then construct the likelihood ratio,

$$\Lambda(r_K(t)) = \Lambda(\mathbf{R}) = \frac{p_{r|H_1}(\mathbf{R}|H_1)}{p_{r|H_0}(\mathbf{R}|H_0)}, \quad (10.12)$$

and manipulate it into a form so that we can let $K \rightarrow \infty$.

4. We denote the limit of $\Lambda(r_K(t))$ as $\Lambda(r(t))$. The test consists of comparing the likelihood ratio with a threshold η ,

$$\Lambda[r(t)] \stackrel{H_1}{\underset{H_0}{\gtrless}} \eta. \quad (10.13)$$

As before, the threshold η is determined by the costs and *a priori* probabilities in a Bayes test and the desired P_F in a Neyman–Pearson test.

We now carry out these steps in detail and then investigate the properties of the resulting tests.

The orthonormal functions for the series expansion are the eigenfunctions of the integral equation

$$\lambda_i^s \phi_i(t) = \int_{T_i}^{T_f} K_s(t, u) \phi_i(u) du, \quad T_i \leq t \leq T_f. \quad (10.14)$$

We shall assume that the orthonormal functions form a complete set. This will occur naturally if $K_s(t, u)$ is positive definite. If $K_s(t, u)$ is only nonnegative definite, we augment the set to make it complete.

The coefficients in the series expansion are

$$r_i \triangleq \int_{T_i}^{T_f} r(t) \phi_i(t) dt. \quad (10.15)$$

The K -term approximation is

$$r_K(t) = \sum_{i=1}^K r_i \phi_i(t), \quad T_i \leq t \leq T_f, \quad (10.16)$$

and

$$r(t) = \lim_{K \rightarrow \infty} r_K(t), \quad T_i \leq t \leq T_f. \quad (10.17)$$

The statistical properties of the coefficients on the two hypotheses follow easily.

$$E[r_i | H_0] = E \left[\int_{T_i}^{T_f} w(t) \phi_i(t) dt \right] = 0. \quad (10.18)$$

$$E[r_i r_j | H_0] = \frac{N_0}{2} \delta_{ij}. \quad (10.19)$$

$$\begin{aligned} E[r_i | H_1] &= E \left[\int_{T_i}^{T_f} s(t) \phi_i(t) dt + \int_{T_i}^{T_f} w(t) \phi_i(t) dt \right] \\ &= \int_{T_i}^{T_f} m(t) \phi_i(t) dt \triangleq m_i. \end{aligned} \quad (10.20)$$

Notice that (10.20) implies that the m_i are the coefficients of an orthogonal expansion of the mean-value function; that is,

$$m(t) = \sum_{i=1}^{\infty} m_i \phi_i(t), \quad T_i \leq t \leq T_f. \quad (10.21)$$

The covariance between coefficients is

$$E[(r_i - m_i)(r_j - m_j) | H_1] = \left(\lambda_i^s + \frac{N_0}{2} \right) \delta_{ij}, \quad (10.22)$$

where λ_i^s is the i th eigenvalue of (10.14). The superscript s emphasizes that it is an eigenvalue of the signal process $s(t)$.

Under both hypotheses, the coefficients r_i are statistically independent Gaussian random variables. The probability density of \mathbf{r} is just the product of the densities of the

coefficients. Thus,

$$\begin{aligned}\Lambda(\mathbf{R}) &\triangleq \frac{p_{r|H_1}(\mathbf{R}|H_1)}{p_{r|H_0}(\mathbf{R}|H_0)} \\ &= \frac{\left(\prod_{i=1}^K \frac{1}{[2\pi(N_0/2+\lambda_i^s)]^{\frac{1}{2}}} \right) \exp\left(-\frac{1}{2} \sum_{i=1}^K \frac{(R_i-m_i)^2}{\lambda_i^s + (N_0/2)}\right)}{\left(\prod_{i=1}^K \frac{1}{[2\pi(N_0/2)]^{\frac{1}{2}}} \right) \exp\left(-\frac{1}{2} \sum_{i=1}^K \frac{R_i^2}{N_0/2}\right)}.\end{aligned}\quad (10.23)$$

Multiplying out each term in the exponent, canceling common factors, taking the logarithm, and rearranging the results, we have

$$\begin{aligned}\ln \Lambda(\mathbf{R}) &= \frac{1}{N_0} \sum_{i=1}^K \left(\frac{\lambda_i^s}{\lambda_i^s + N_0/2} \right) R_i^2 + \sum_{i=1}^K \left(\frac{1}{\lambda_i^s + N_0/2} \right) m_i R_i \\ &\quad - \frac{1}{2} \sum_{i=1}^K \left(\frac{1}{\lambda_i^s + N_0/2} \right) m_i^2 - \frac{1}{2} \sum_{i=1}^K \ln \left(1 + \frac{2\lambda_i^s}{N_0} \right).\end{aligned}\quad (10.24)$$

The final step is to obtain closed-form expressions for the various terms when $K \rightarrow \infty$. To do this, we need the inverse kernel that was first introduced in (7.160b). The covariance function of the *entire* input $r(t)$ on H_1 is $K_1(t, u)$. The corresponding inverse kernel is defined by the relation

$$\int_{T_i}^{T_f} K_1(t, u) Q_1(u, z) du = \delta(t - z), \quad T_i < t, z < T_f. \quad (10.25)$$

In terms of eigenfunctions and eigenvalues,

$$Q_1(t, u) = \sum_{i=1}^{\infty} \frac{1}{\lambda_i^s + N_0/2} \phi_i(t) \phi_i(u), \quad T_i < t, u < T_f. \quad (10.26)$$

We also saw in (7.170) that we could write $Q_1(t, u)$ as a sum of an impulse component and a well-behaved function,

$$Q_1(t, u) = \frac{2}{N_0} (\delta(t - u) - h_1(t, u)), \quad T_i < t, u < T_f, \quad (10.27)$$

where the function $h_1(t, u)$ satisfies the integral equation

$$\frac{N_0}{2} h_1(t, u) + \int_{T_i}^{T_f} h_1(t, z) K_s(z, u) dz = K_s(t, u), \quad T_i \leq t, u \leq T_f.$$

(10.28)

Note that (10.28) is identical to (6.156b) that specified the optimum smoothing filter. The endpoint values of $h_1(t, u)$ are defined as a limit of the open-interval values because we assume that $h_1(t, u)$ is continuous. We also recall that we could write the solution to

(10.28) in terms of eigenfunctions and eigenvalues.

$$h_1(t, u) = \sum_{i=1}^{\infty} \frac{\lambda_i^s}{\lambda_i^s + N_0/2} \phi_i(t) \phi_i(u), \quad T_i \leq t, u \leq T_f. \quad (10.29)$$

We now rewrite the first three terms in (10.24) by using (10.15) and (10.20) to obtain

$$\begin{aligned} \ln \Lambda(r_K(t)) &= \frac{1}{N_0} \iint_{T_i}^{T_f} r(t) \left[\sum_{i=1}^K \left(\frac{\lambda_i^s}{\lambda_i^s + N_0/2} \right) \phi_i(t) \phi_i(u) \right] r(u) dt du \\ &\quad + \iint_{T_i}^{T_f} m(t) \left[\sum_{i=1}^K \left(\frac{1}{\lambda_i^s + N_0/2} \right) \phi_i(t) \phi_i(u) \right] r(u) dt du \\ &\quad - \frac{1}{2} \iint_{T_i}^{T_f} m(t) \left[\sum_{i=1}^K \left(\frac{1}{\lambda_i^s + N_0/2} \right) \phi_i(t) \phi_i(u) \right] m(u) dt du \\ &\quad - \frac{1}{2} \sum_{i=1}^K \ln \left(1 + \frac{2\lambda_i^s}{N_0} \right). \end{aligned} \quad (10.30)$$

We now let $K \rightarrow \infty$ in (10.30) and use (10.26) and (10.29) to evaluate the first three terms in (10.30). The result is

$$\begin{aligned} \ln \Lambda(r(t)) &= \frac{1}{N_0} \iint_{T_i}^{T_f} r(t) h_1(t, u) r(u) dt du + \iint_{T_i}^{T_f} m(t) Q_1(t, u) r(u) dt du \\ &\quad - \frac{1}{2} \iint_{T_i}^{T_f} m(t) Q_1(t, u) m(u) dt du - \frac{1}{2} \sum_{i=1}^{\infty} \ln \left(1 + \frac{2\lambda_i^s}{N_0} \right). \end{aligned} \quad (10.31)$$

We can further simplify the second and third terms on the right-hand side of (10.31) by recalling the definition of $g(u)$ in (7.162),

$$g_1(u) \triangleq \int_{T_i}^{T_f} m(t) Q_1(t, u) dt, \quad T_i < u < T_f. \quad (10.32)$$

Notice that $m(t)$ plays the role of the known signal [which was denoted by $s(t)$ in Chapter 7]. We also observe that the third and fourth term are *not* functions of $r(t)$ and may be absorbed in the threshold. Thus, the likelihood ratio test (LRT) is,

$$\boxed{\frac{1}{N_0} \iint_{T_i}^{T_f} r(t) h_1(t, u) r(u) dt du + \int_{T_i}^{T_f} g_1(u) r(u) du \stackrel{H_1}{\geq} \gamma_*}, \quad (10.33)$$

where

$$\boxed{\gamma_* \triangleq \ln \eta + \frac{1}{2} \int_{T_i}^{T_f} g_1(u)m(u) du + \frac{1}{2} \sum_{i=1}^{\infty} \ln \left(1 + \frac{2\lambda_i^s}{N_0} \right).} \quad (10.34)$$

The results in (10.33) and (10.34) are the continuous-time version of the general Gaussian problem in Section 3.4.

If we are using a Bayes test, we must evaluate the infinite sum on the right side in order to set the threshold. In (10.74), we develop a convenient closed-form expression for this sum. For the Neyman–Pearson test we adjust γ_* directly to obtain the desired P_F so that the exact value of the sum is not needed as long as we know the sum converges. The convergence follows easily.

$$\sum_{i=1}^{\infty} \ln \left(1 + \frac{2\lambda_i^s}{N_0} \right) \leq \sum_{i=1}^{\infty} \frac{2\lambda_i^s}{N_0} = \frac{2}{N_0} \int_{T_i}^{T_f} K_s(t, t) dt. \quad (10.35)$$

The integral is just the expected value of the energy in the process, which was assumed to be finite.

The first term on the left-hand side of (10.33) is a quadratic operation on $r(t)$ and arises because the signal is random. If $K_s(t, u)$ is zero (i.e., the signal is deterministic), this term disappears. We denote the first term by l_R . (The subscript R denotes random.) The second term on the left-hand side is a linear operation on $r(t)$ and arises because of the mean value $m(t)$. Whenever the signal is a zero-mean process, this term disappears. We denote the second term by l_D . (The subscript D denotes deterministic.) It is also convenient to denote the last two terms on the right-hand side of (10.34) as $(-l_B^{[2]})$ and $(-l_B^{[1]})$. Thus, we have the definitions

$$l_R \triangleq \frac{1}{N_0} \iint_{T_i}^{T_f} r(t) h_1(t, u) r(u) dt du, \quad (10.36)$$

$$l_D \triangleq \int_{T_i}^{T_f} g_1(u) r(u) du, \quad (10.37)$$

$$l_B^{[1]} \triangleq -\frac{1}{2} \sum_{i=1}^{\infty} \ln \left(1 + \frac{2\lambda_i^s}{N_0} \right), \quad (10.38)$$

$$l_B^{[2]} \triangleq -\frac{1}{2} \int_{T_i}^{T_f} g_1(u) m(u) du. \quad (10.39)$$

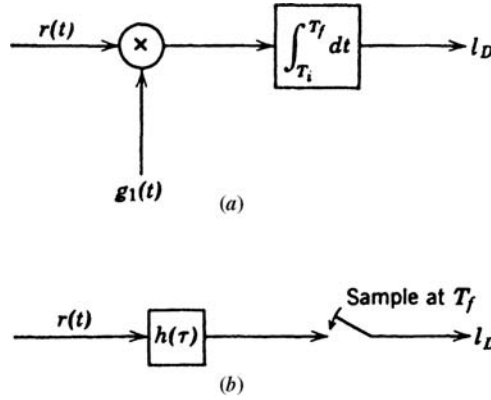


Figure 10.3: Generation of l_D .

In this notation, the LRT is

$$\boxed{l_R + l_D \stackrel{H_1}{\gtrless} \ln \eta - l_B^{[1]} - l_B^{[2]} = \gamma - l_B^{[1]} - l_B^{[2]} \triangleq \gamma_*}. \quad (10.40)$$

The second term on the left-hand side of (10.40) is generated physically by either a cross-correlation or a matched filter operation, as shown in Figure 10.3. The impulse response of the matched filter in Figure 10.3b is

$$h(\tau) = \begin{cases} g_1(T_f - \tau), & 0 \leq \tau \leq T_f - T_i, \\ 0, & \text{elsewhere.} \end{cases} \quad (10.41)$$

We previously encountered these operations in the colored noise detection problem discussed in Section 7.3. Thus, the only new component in the optimum receiver is a device to generate l_R . In the next several paragraphs we develop a number of methods of generating l_R .

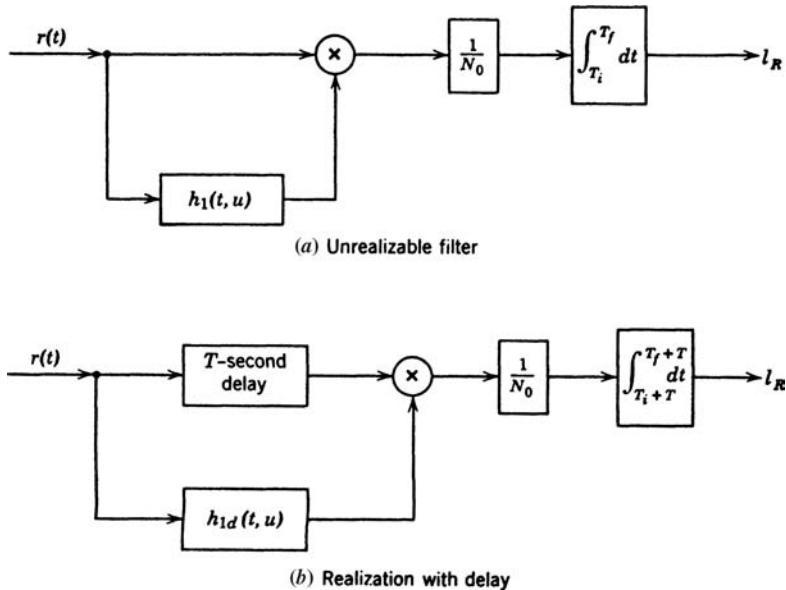
Canonical Realization No. 1: Estimator–Correlator

We want to generate l_R , where

$$l_R = \frac{1}{N_0} \int_{T_i}^{T_f} r(t) h_1(t, u) r(u) dt du, \quad (10.42)$$

and $h_1(t, u)$ satisfies (10.28). An obvious realization is shown in Figure 10.4a. Notice that $h_1(t, u)$ is an unrealizable (or noncausal) filter. Therefore, in order actually to build it, we would have to allow a delay in the filter in the system in Figure 10.4a. This is done by defining a new filter whose output is a delayed version of the output of $h_1(t, u)$,

$$h_{1d}(t, u) = \begin{cases} h_1(t - T, u), & T_i + T \leq t \leq T_f + T, T_i \leq u \leq T_f, \\ 0, & \text{elsewhere,} \end{cases} \quad (10.43)$$

Figure 10.4: Generation of l_R .

where

$$T \triangleq T_f - T_i \quad (10.44)$$

is the length of the observation interval. Adding a corresponding delay in the upper path and the integrator gives the system in Figure 10.4b.

This realization has an interesting interpretation. We first assume that $m(t)$ is zero and then recall that we have previously encountered (10.28) in the linear filter context. Specifically, if we had available a waveform

$$r(t) = s(t) + w(t), \quad T_i \leq t \leq T_f \quad (10.45)$$

and wanted to estimate $s(t)$ using a minimum mean-square error (MMSE) or maximum *a posteriori* probability (MAP) criterion, then, from (8.4), we know that the resulting estimate $\hat{s}_u(t)$ would be obtained by passing $r(t)$ through $h_1(t, u)$.

$$\hat{s}_u(t) = \int_{T_i}^{T_f} h_1(t, u) r(u) du, \quad T_i \leq t \leq T_f, \quad (10.46)$$

where $h_1(t, u)$ satisfies (10.28) and the subscript u emphasizes that the estimate is unrealizable. Looking at Figure 10.5, we see that the receiver is correlating $r(t)$ with the MMSE estimate of $s(t)$. For this reason, the realization in Figure 10.5 is frequently referred to as an estimator–correlator receiver. This is an intuitively pleasing interpretation. (This result is due to Price [Pri53, Pri54, Pri55], and [Pri56].)

Notice that the interpretation of the left-hand side of (10.46) as the MMSE estimate is only valid when $r(t)$ is zero mean. However, the output of the receiver in Figure 10.5 is l_R for either the zero-mean or the non-zero-mean case. We also obtain an estimator–correlator

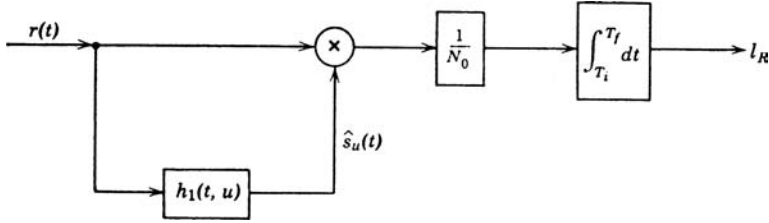


Figure 10.5: Estimator–correlator (zero-mean case).

interpretation in the nonzero-mean case by a straightforward modification of the above discussion.

It is important not to misinterpret the term “unrealizable” in our description of $h_1(t, u)$. It simply means $h_1(t, u)$ is nonzero for $t < u$. We would actually implement it using a “smoothing” filter that we will describe later.

Canonical Realization No. 2: Filter-Square-Integrator (FSI) Receiver

A second canonical form can be derived by factoring $h_1(t, u)$. We define $h_f(z, t)$ by the relation

$$h_1(t, u) = \int_{T_i}^{T_f} h_f(z, t) h_f(z, u) dz, \quad T_i \leq t, u \leq T_f. \quad (10.47)$$

If we do not require that $h_f(z, t)$ be realizable, we can find an infinite number of solutions to (10.47). From (10.29), we recall that

$$h_1(t, u) = \sum_{i=1}^{\infty} h_i \phi_i(t) \phi_i(u), \quad T_i \leq t, u \leq T_f, \quad (10.48)$$

where

$$h_i = \frac{\lambda_i^s}{\lambda_i^s + N_0/2}. \quad (10.49)$$

We see that

$$h_{fu}(z, t) = \sum_{i=1}^{\infty} \pm \sqrt{h_i} \phi_i(z) \phi_i(t), \quad T_i \leq z, t \leq T_f, \quad (10.50)$$

is a solution to (10.47) for any assignment of plus and minus signs in the series.

Using (10.47) in (10.42), l_R becomes

$$l_R = \frac{1}{N_0} \int_{T_i}^{T_f} dz \left[\int_{T_i}^{T_f} h_{fu}(z, t) r(t) dt \right]^2. \quad (10.51)$$

This can be realized by a cascade of an unrealizable filter, a square-law device, and an integrator as shown in Figure 10.6.

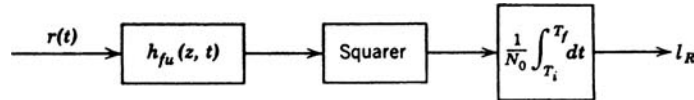


Figure 10.6: Filter-squarer receiver (unrealizable).

Alternatively, we can require that $h_1(t, u)$ be factored using realizable filters. In other words, we must find a solution $h_{fr}(z, t)$ to (10.47) that is zero for $t > z$. Then,

$$l_R = \frac{1}{N_0} \int_{T_i}^{T_f} dz \left[\int_{T_i}^z h_{fr}(z, t) r(t) dt \right]^2, \quad (10.52)$$

and the resulting receiver is shown in Figure 10.7. If the time interval is short, a realizable solution to (10.47) is difficult to find for arbitrary signal processes. Later, when we study the SPLIT problem we will be able to find a solution using spectrum factorization.

The integral equation (10.47) is a functional relationship somewhat analogous to the square-root relation. Thus, we refer to $h_f(z, t)$ as the *functional square root* of $h_1(t, u)$. We shall only define functional square roots for symmetric two-variable functions that can be expanded as in (10.48) with nonnegative coefficients. We frequently use the notation

$$h_1(t, u) = \int_{T_i}^{T_f} h_1^{[1/2]}(z, t) h_1^{[1/2]}(z, u) dz. \quad (10.53)$$

Any solution to (10.53) is called a functional square root. Notice that the solutions are not necessarily symmetric.

The difficulty with all of the configurations that we have derived up to this point is that to actually implement them we must solve (10.28).

Fortunately (6.156b) and (8.19) also specify the optimum smoothing filter for a finite observation time interval so that all of the solutions that we obtained earlier can be applied directly. However, for all of the cases we discussed, except for the low-rank model, the smoothing filter was harder to implement than the realizable filter.

This motivates finding a canonical realization that can be implemented with realizable filters.

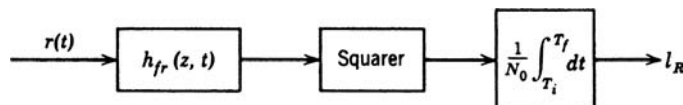


Figure 10.7: Filter-squarer receiver (realizable).

Canonical Realization No. 3: Optimum Realizable Filter Receiver

The basic concept involved in this realization is that of generating the likelihood ratio in real time as the output of a nonlinear dynamic system.¹ The derivation is of interest because the basic technique is applicable to many problems. For notational simplicity, we let $T_i = 0$ and $T_f = T$ in this section. We shall assume that $m(t) = 0$ and consider only l_R .

Clearly, l_R is a function of the length of the observation interval T . To emphasize this, we can write

$$l_R(T|r(u), 0 \leq u \leq T) \triangleq l_R(T). \quad (10.54)$$

More generally, we could define a likelihood function for any value of time t .

$$l_R(t|r(u), 0 \leq u \leq t) \triangleq l_R(t), \quad (10.55)$$

where $l_R(0) = 0$. We can write $l_R(T)$ as

$$l_R(T) = \int_0^T \frac{dl_R(t)}{dt} dt = \int_0^T \dot{l}_R(t) dt. \quad (10.56)$$

Now we want to find an easy method for generating $\dot{l}_R(t)$. Replacing T by t in (10.36), we have

$$l_R(t) = \frac{1}{N_0} \int_0^t d\tau r(\tau) \int_0^t du h_1(\tau, u : t)r(u), \quad (10.57)$$

where $h_1(\tau, u : t)$ from (10.28) satisfies the integral equation

$$\frac{N_0}{2} h_1(\tau, u : t) + \int_0^t h_1(\tau, z : t) K_s(z, u) dz = K_s(\tau, u), \quad 0 \leq \tau, u \leq t. \quad (10.58)$$

[Observe that the solution to (10.58) depends on t . We emphasize this with the notation $h_1(\cdot, \cdot : t)$.] Differentiating (10.57), we obtain

$$\begin{aligned} \dot{l}_R(t) &= \frac{1}{N_0} \left[r(t) \int_0^t du h_1(t, u : t)r(u) \right. \\ &\quad \left. + \int_0^t d\tau r(\tau) \left(h_1(\tau, t : t)r(t) + \int_0^t \frac{\partial h_1(\tau, u : t)}{\partial t} r(u) du \right) \right]. \end{aligned} \quad (10.59)$$

¹The original derivation of Canonical Realization No. 3 was done by Schweppe [Sch65]. The technique is a modification of the linear filter derivation in [KB61].

We see that the first two terms in (10.59) depend on $h_1(t, u : t)$. For this case, (10.58) reduces to²

$$\frac{N_0}{2} h_1(t, u : t) + \int_0^t h_1(t, z : t) K_s(z, u) dz = K_s(t, u), \quad 0 \leq u \leq t. \quad (10.60)$$

We know from our previous work in Section 6.4.6 that

$$\hat{s}_r(t) = \int_0^t h_1(t, u : t) r(u) du, \quad (10.61)$$

or

$$\hat{s}_r(t) = \int_0^t h_1(u, t : t) r(u) du. \quad (10.62)$$

[The subscript r means that the operation in (10.61) can be implemented with a realizable filter.] The result in (10.62) follows from the symmetry of the solution to (10.58). Using (10.61) and (10.62) in (10.59) gives

$$\hat{l}_R(t) = \frac{1}{N_0} \left[2r(t)\hat{s}_r(t) + \int_0^t d\tau \int_0^t du r(\tau) \frac{\partial h_1(\tau, u : t)}{\partial t} r(u) \right]. \quad (10.63)$$

We next show that

$$\frac{\partial h_1(\tau, u : t)}{\partial t} = -h_1(\tau, t : t) h_1(t, u : t), \quad 0 \leq \tau, u \leq t. \quad (10.64)$$

We follow Collins [Col66c].

Differentiating $h_1(\tau, u ; t)$ in (10.58) gives

$$\frac{N_0}{2} \frac{\partial h_1(\tau, u : t)}{\partial t} + \int_0^t \frac{\partial h_1(\tau, z : t)}{\partial t} K_s(z, u) dz + h_1(\tau, t : t) K_s(t, u) = 0, \quad 0 \leq \tau, u \leq t. \quad (10.65)$$

Now replace $K_s(t, u)$ with the left-hand side of (10.60) and rearrange terms. This gives

$$-\frac{N_0}{2} \left\{ \frac{\partial h_1(\tau, u : t)}{\partial t} + h_1(\tau, t : t) h_1(t, u : t) \right\} = \int_0^t \left\{ \frac{\partial h_1(\tau, z : t)}{\partial t} + h_1(\tau, t : t) h_1(t, z : t) \right\} \\ \times K_s(z, u) dz, \quad 0 \leq \tau, u \leq t. \quad (10.66)$$

We see that the terms in braces play the role of an eigenfunction with an eigenvalue of $(-N_0/2)$. However, $K_s(z, u)$ is non-negative definite, and so it cannot have a negative eigenvalue. Thus, the term in braces must be identically zero in order for (10.66) to hold. This is the desired result.

²Notice that $h_1(t, u : t) = h_{or}(t, u)$.

Substituting (10.64) into (10.63) and using (10.60), we obtain the desired result,

$$\hat{l}_R(t) = \frac{1}{N_0} [2r(t)\hat{s}_r(t) - \hat{s}_r^2(t)]. \quad (10.67)$$

Then,³

$$l_R = l_R(T) = \frac{1}{N_0} \int_0^T [2r(t)\hat{s}_r(t) - \hat{s}_r^2(t)] dt.$$

(10.68)

Before looking at the optimum receiver configuration and some examples, it is appropriate to digress briefly and demonstrate an algorithm for computing the infinite sum $\sum_{i=1}^{\infty} \ln(1 + 2\lambda_i^s/N_0)$ that is needed to evaluate the bias in the Bayes test. We do this now because the derivation is analogous to the one we just completed. Two notational comments are necessary:

- a. The eigenvalues in the sum depend on the length of the interval. We emphasize this with the notation $\lambda_i^s(T)$.
- b. The eigenfunctions also depend on the length of the interval, and so we use the notation $\phi_i(t : T)$.

This notation was used previously in Chapter 6.

We write

$$\sum_{i=1}^{\infty} \ln \left(1 + \frac{2}{N_0} \lambda_i^s(T) \right) = \int_0^T dt \left[\frac{d}{dt} \sum_{i=1}^{\infty} \ln \left(1 + \frac{2}{N_0} \lambda_i^s(t) \right) \right]. \quad (10.69)$$

Performing the indicated differentiation, we have

$$\frac{d}{dt} \sum_{i=1}^{\infty} \ln \left(1 + \frac{2}{N_0} \lambda_i^s(t) \right) = \frac{2}{N_0} \sum_{i=1}^{\infty} \frac{[d\lambda_i^s(t)]/dt}{1 + (2/N_0)\lambda_i^s(t)}. \quad (10.70)$$

In (6.175), we proved that

$$\frac{d\lambda_i^s(t)}{dt} = \lambda_i^s(t)\phi_i^2(t : t), \quad (10.71)$$

and we showed that (6.166),

$$h_1(t, t : t) = \sum_{i=1}^{\infty} \frac{\lambda_i^s(t)}{\lambda_i^s(t) + N_0/2} \phi_i^2(t : t), \quad (10.72)$$

³A result equivalent to that in (10.68) was derived independently by Stratonovich and Sosulin [SS64, SS65, SS66] and [Sos67]. The integral in (10.68) is a stochastic integral, and some care must be used when one is dealing with arbitrary (not necessarily Gaussian) random processes. For Gaussian processes it can be interpreted as a Stratonovich integral and used rigorously [Str66]. For arbitrary processes an Itô integral formulation is preferable [Doo53], [Itô61], and [Dun68]. Interested readers should consult these references or [KF69] and [Kai69]. For our purposes, it is adequate to treat (10.68) as an ordinary integral and manipulate it using the normal rules of calculus.

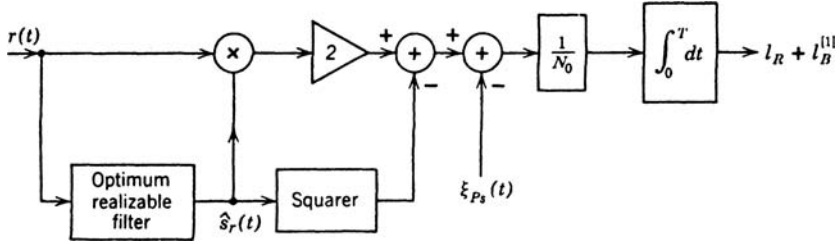


Figure 10.8: Optimum realizable filter realization (Canonical Realization No. 3).

where $h_1(t, t : t)$ is the optimum MMSE realizable linear filter specified by (10.60). From (6.161), the minimum mean-square realizable estimation error $\xi_{Ps}(t)$ is

$$\xi_{Ps}(t) = \frac{N_0}{2} h_1(t, t : t) \triangleq \frac{N_0}{2} h_{or}(t, t). \quad (10.73)$$

Thus,

$$\sum_{i=1}^{\infty} \ln \left(1 + \frac{2\lambda_i^s(T)}{N_0} \right) = \int_0^T h_{or}(t, t) dt = \frac{2}{N_0} \int_0^T \xi_{Ps}(t) dt \triangleq \ln D_{\mathcal{F}} \left(\frac{2}{N_0} \right), \quad (10.74)$$

where $D_{\mathcal{F}} \left(\frac{2}{N_0} \right)$ is the Fredholm determinant.

From (10.38),

$$l_B^{[1]} = -\frac{1}{2} \sum_{i=1}^{\infty} \ln \left(1 + \frac{2\lambda_i^s}{N_0} \right) = -\frac{1}{N_0} \int_0^T \xi_{Ps}(t) dt. \quad (10.75)$$

We see that whenever we use Canonical Realization No. 3, we obtain the first bias term needed for the Bayes test as a by-product. A block diagram of Realization No. 3 for generating l_R and $l_B^{[1]}$ is shown in Figure 10.8.

We recall from Chapter 8 that if we implement the optimum realizable filter as a Kalman filter, then $\xi_{Ps}(t)$ is part of the solution. In addition, we recall that $l_B^{[1]}$ is not needed for a Neyman–Pearson test.

10.2.3 Performance of Optimum Receivers

In this section, we study the performance of the optimum receivers.⁴ For simplicity, we assume that $m(t) = 0$. We have previously encountered this problem for finite K in Section 3.3. When the eigenvalues were equal, a closed-form expression was available. For real processes with unequal eigenvalues, we could not find an analytic expression. For complex processes, an analytic solution was available.

In this section, we focus on obtaining a closed-form expression for $\mu(s)$ and then using the results in Section 2.4 to bound the performance or obtain approximate expressions.

⁴This section is a shortened version of Section 2.2 in DEMT-III, [Van71b, Van01c].

We recall that the function $\mu_K(s)$ played the central role in our discussion. [The subscript K is added to emphasize that we are dealing with K -term approximation to $r(t)$.] From (2.199)–(2.202),

$$\mu_K(s) \triangleq \ln[\phi_{l(\mathbf{R})|H_0}(s)], \quad (10.76)$$

where $l(\mathbf{R})$ is the logarithm of the likelihood ratio

$$l(\mathbf{R}) = \ln \Lambda(\mathbf{R}) = \ln \left(\frac{p_{\text{r}|H_1}(\mathbf{R}|H_1)}{p_{\text{r}|H_0}(\mathbf{R}|H_0)} \right), \quad (10.77)$$

and $\phi_{l(\mathbf{R})|H_0}(s)$ is its moment-generating function on H_0

$$\phi_{l(\mathbf{R})|H_0}(s) = E[e^{s l(\mathbf{R})}|H_0], \quad (10.78)$$

for real s . Using the definition of $l(\mathbf{R})$ in (10.77),

$$\mu_K(s) = \ln \int_{-\infty}^{\infty} \dots \int_{-\infty}^{\infty} [p_{\text{r}|H_1}(\mathbf{R}|H_1)]^s [p_{\text{r}|H_0}(\mathbf{R}|H_0)]^{1-s} d\mathbf{R}. \quad (10.79)$$

We then developed upper bounds on P_F and P_M .

$$\begin{aligned} P_F &\leq \exp[\mu_K(s) - s\dot{\mu}_K(s)], \\ P_M &\leq \exp[\mu_K(s) + (1-s)\dot{\mu}_K(s)], \quad 0 \leq s \leq 1, \end{aligned} \quad (10.80)$$

where $\dot{\mu}_K(s) = \gamma_K$, the threshold in the LRT. By varying the parameter s , we could study threshold settings anywhere between $E[l|H_1]$ and $E[l|H_0]$. The definition of $l(\mathbf{R})$ in (10.77) guaranteed that $\mu_K(s)$ existed for $0 \leq s \leq 1$.

We now define a function $\mu(s)$,

$$\mu(s) \triangleq \lim_{K \rightarrow \infty} \mu_K(s). \quad (10.81)$$

If we can demonstrate that the limit exists, our bounds in (10.80) will still be valid. However, in order to be useful, the expression for $\mu(s)$ must be in a form that is practical to evaluate. Thus, our first goal in this section is to find a convenient closed-form expression for $\mu(s)$.

The second useful set of results in Section 2.4 was the approximate error expressions in (2.239) and (2.242),

$$P_F \simeq \frac{1}{\sqrt{2\pi s^2 \ddot{\mu}(s)}} e^{\mu(s) - s\dot{\mu}(s)}, \quad s \geq 0, \quad (10.82)$$

and

$$P_M \simeq \frac{1}{\sqrt{2\pi(1-s)^2 \ddot{\mu}(s)}} e^{\mu(s) + (1-s)\dot{\mu}(s)}, \quad s \leq 1. \quad (10.83)$$

We first evaluate $\mu_K(s)$ for finite K . Substituting (10.23) with $m_i = 0$ into (10.79) gives

$$\begin{aligned}\mu_K(s) &= \ln \int_{-\infty}^{\infty} \cdots \int_{-\infty}^{\infty} \left\{ \left[\prod_{i=1}^K \frac{1}{\sqrt{2\pi(N_0/2 + \lambda_i^s)}} \exp \left(-\frac{1}{2} \sum_{i=1}^K \frac{(R_i)^2}{(\lambda_i^s + N_0/2)} \right) \right]^s \right. \\ &\quad \times \left. \left\{ \left[\prod_{i=1}^K \frac{1}{\sqrt{2\pi(N_0/2)}} \right] \exp \left(-\frac{1}{2} \sum_{i=1}^K \frac{R_i^2}{N_0/2} \right) \right\}^{1-s} dR_1 \cdots dR_K. \quad (10.84)\right.\end{aligned}$$

Performing the integration, we have

$$\mu_K(s) = \frac{1}{2} \sum_{i=1}^K \left[(1-s) \ln \left(1 + \frac{2\lambda_i^s}{N_0} \right) - \ln \left(1 + \frac{2(1-s)\lambda_i^s}{N_0} \right) \right], \quad 0 \leq s \leq 1. \quad (10.85)$$

From our earlier discussion, we know the sum on the right-hand side of (10.85) is well behaved as $K \rightarrow \infty$.

We now take the limit of (10.85) as $K \rightarrow \infty$.

$$\boxed{\mu(s) \triangleq \frac{1}{2} \sum_{i=1}^{\infty} \left[(1-s) \ln \left(1 + \frac{2\lambda_i^s}{N_0} \right) - \ln \left(1 + \frac{2(1-s)\lambda_i^s}{N_0} \right) \right]. \quad (10.86)}$$

Using (10.75), we can write the sum of eigenvalues as an integral of the MSE

$$\sum_{i=1}^{\infty} \ln \left(1 + \frac{2\lambda_i^s}{N_0} \right) = \frac{2}{N_0} \int_{T_i}^{T_f} \xi_P \left(t | s(\cdot), \frac{N_0}{2} \right) dt. \quad (10.87)$$

Comparing (10.86) and (10.87) leads to the desired result.

$$\mu(s) = \frac{1-s}{N_0} \int_{T_i}^{T_f} dt \left[\xi_P \left(t | s(\cdot), \frac{N_0}{2} \right) - \xi_P \left(t | s(\cdot), \frac{N_0}{2(1-s)} \right) \right]. \quad (10.88)$$

Thus, to find $\mu(s)$, we must find the mean-square error for two realizable linear filtering problems. In the first, the signal is $s(\cdot)$ and the noise is white with spectral height $N_0/2$. In the second, the signal is $s(\cdot)$ and the noise is white with spectral height $N_0/2(1-s)$. An alternative expression for $\mu(s)$ also follows easily.

$$\mu(s) = \frac{1}{N_0} \int_{T_i}^{T_f} \left[(1-s) \xi_P \left(t | s(\cdot), \frac{N_0}{2} \right) - \xi_P \left(t | \sqrt{1-s} s(\cdot), \frac{N_0}{2} \right) \right] dt. \quad (10.89)$$

We can now use (10.80) with $\mu(s)$ replacing $\mu_K(s)$. We can also use (10.82) and (10.83) for approximate expressions, although we need a different argument than the one used in Section 2.4 to justify the approximation (see Section 2.2.2 of DEMT-III [Van71b, Van01c]).

Note that, in order to use (10.80), we need $\dot{\mu}(s)$ and that, in order to use (10.82) and (10.83), we need $\ddot{\mu}(s)$. In general, we cannot find an analytical expression for $\mu(s)$, so we must compute the derivatives numerically.

In the next three sections, we consider random process models where we can obtain explicit solutions for the optimum detector.

10.2.4 State-Variable Realization

In this section, we consider Gaussian-Markov processes which we introduced in Chapter 8. They can be described by a state equation

$$\dot{\mathbf{x}}(t) = \mathbf{F}(t)\mathbf{x}(t) + \mathbf{G}(t)\mathbf{u}(t), \quad (10.90)$$

where $\mathbf{F}(t)$ and $\mathbf{G}(t)$ are possibly time-varying matrices, and by an observation equation,

$$s(t) = \mathbf{C}(t)\mathbf{x}(t), \quad (10.91)$$

where $\mathbf{C}(t)$ is the observation matrix. The input $\mathbf{u}(t)$ is a sample function from a zero-mean vector white noise process,

$$E[\mathbf{u}(t)\mathbf{u}^T(\tau)] = \mathbf{Q}\delta(t - \tau), \quad (10.92)$$

and the initial conditions are

$$E[\mathbf{x}(0)] = \mathbf{0}, \quad (10.93)$$

$$E[\mathbf{x}(0)\mathbf{x}^T(0)] \triangleq \mathbf{\Pi}_0. \quad (10.94)$$

From Section 8.3, we know that the MMSE realizable estimate of $s(t)$ is given by the equations

$$\hat{s}_r(t) = \mathbf{C}(t)\hat{\mathbf{x}}(t), \quad (10.95)$$

$$\dot{\hat{\mathbf{x}}}(t) = \mathbf{F}(t)\hat{\mathbf{x}}(t) + \mathbf{K}_g(t)[r(t) - \mathbf{C}(t)\hat{\mathbf{x}}(t)]. \quad (10.96)$$

The matrix $\xi_P(t)$ is the error covariance matrix of $\mathbf{x}(t) - \hat{\mathbf{x}}(t)$.

$$\xi_P(t) \triangleq E[(\mathbf{x}(t) - \hat{\mathbf{x}}(t))(\mathbf{x}^T(t) - \hat{\mathbf{x}}^T(t))]. \quad (10.97)$$

It satisfies the nonlinear matrix differential equations,

$$\dot{\xi}_P(t) = \mathbf{F}(t)\xi_P(t) + \xi_P(t)\mathbf{F}^T(t) - \xi_P(t)\mathbf{C}^T(t)\frac{2}{N_0}\mathbf{C}(t)\xi_P(t) + \mathbf{G}(t)\mathbf{Q}\mathbf{G}^T(t). \quad (10.98)$$

The mean-square error in estimating $s(t)$ is

$$\xi_{P_s}(t) = \mathbf{C}(t)\xi_P(t)\mathbf{C}^T(t). \quad (10.99)$$

Notice that $\xi_P(t)$ is the error covariance matrix for the state vector and $\xi_{P_s}(t)$ is the scalar mean-square error in estimating $s(t)$. Both (10.98) and (10.99) can be computed either before $r(t)$ is received or simultaneously with the computation of $\hat{\mathbf{x}}(t)$.

The system needed to generate l_R follows easily and is shown in Figure 10.9. The state equation describing l_R is obtained from (10.67),

$$\dot{l}_R(t) = \frac{1}{N_0}[2r(t)\hat{s}_r(t) - \hat{s}_r^2(t)], \quad (10.100)$$

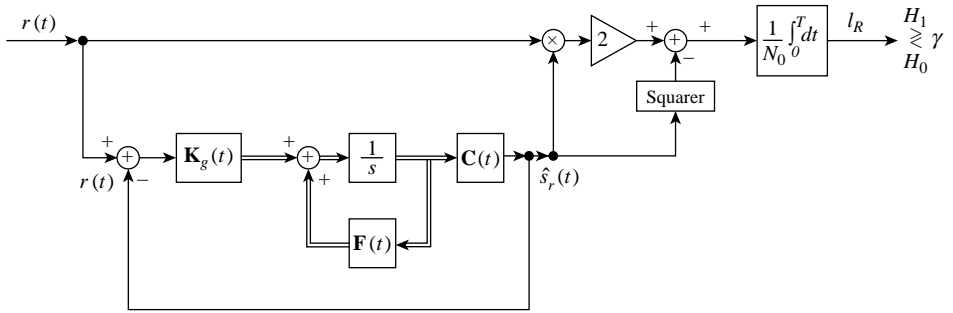


Figure 10.9: Optimum detector: State-variable processes.

where $\hat{s}_r(t)$ is the output of the Kalman filter and is defined by (10.95)–(10.96) and

$$l_R \triangleq \int_0^T \hat{l}_R(t) dt. \quad (10.101)$$

For a Neyman Pearson test, we choose γ to achieve the required P_F . For a Bayes test, we must also compute $l_B^{[1]}$ from (10.75).

The important feature of this realization is that there are *no* integral equations to solve. The likelihood ratio is generated as the output of a dynamic system. We now consider a simple example to illustrate the application of these ideas.

Example 10.1. We consider a model that corresponds to a passive sonar or passive radar system. The received waveforms on the two hypotheses are

$$\begin{aligned} H_1 : r(t) &= s(t) + w(t), & 0 \leq t \leq T, \\ H_0 : r(t) &= w(t), & 0 \leq t \leq T. \end{aligned} \quad (10.102)$$

We assume that the signal process has a state representation

$$\dot{\mathbf{x}}(t) = \mathbf{F}(t)\mathbf{x}(t) + \mathbf{G}(t)\mathbf{u}(t). \quad (10.103)$$

where $\mathbf{u}(t)$ satisfies (10.92) and

$$s(t) = \mathbf{C}(t)\mathbf{x}(t). \quad (10.104)$$

It is instructive to draw the receiver for the simple case in which $s(t)$ has a one-dimensional state equation with constant coefficients. We let

$$\mathbf{F}(t) = -k, \quad (10.105)$$

$$\mathbf{G}(t) = 1, \quad (10.106)$$

$$\mathbf{Q} = 2kP, \quad (10.107)$$

$$\mathbf{C}(t) = 1, \quad (10.108)$$

$$\mathbf{R}(t) = \frac{N_0}{2}, \quad (10.109)$$

and

$$\xi_P(0) = P. \quad (10.110)$$

Then (10.96) and (10.98) reduce to

$$\dot{\hat{x}}(t) = -k\hat{x}(t) + \frac{2}{N_0}\xi_P(t)[r(t) - \hat{x}(t)], \quad (10.111)$$

$$\dot{\xi}_P(t) = -2k\xi_P(t) - \frac{2}{N_0}\xi_P^2(t) + 2kP. \quad (10.112)$$

For this one-dimensional state model, we can get an analytic expression for $\xi_P(t)$ and its integral.⁵

$$\xi_P\left(t|s(.), \frac{N_0}{2}\right) = \frac{2\bar{E}_r}{T} \frac{1}{(1+\alpha)} \left\{ \frac{1 - [(1-\alpha)/(1+\alpha)]e^{-2k\alpha t}}{1 - [(1-\alpha)^2/(1+\alpha)^2]e^{-2k\alpha t}} \right\}, \quad 0 \leq t \leq T, \quad (10.113)$$

where

$$\bar{E}_r = PT \quad (10.114)$$

is the average received energy and

$$\alpha \triangleq \sqrt{1 + \frac{4\bar{E}_r}{kN_0}} = \sqrt{1 + \Lambda_1}. \quad (10.115)$$

Integrating, we obtain

$$\int_{T_i}^{T_f} \xi_P\left(t|s(.), \frac{N_0}{2}\right) dt = \frac{N_0}{2} \left\{ \ln \left[\frac{(1+\alpha)^2 e^{2k\alpha T} - (1-\alpha)^2}{4\alpha} \right] - (\alpha+1)kT \right\}. \quad (10.116)$$

To get the second term in (10.88), we define

$$\alpha_s \triangleq \sqrt{1 + \frac{4\bar{E}_r(1-s)}{kTN_0}} \quad (10.117)$$

and replace α by α_s in (10.116). Then

$$\mu(s) = \frac{1-s}{2} \left\{ \ln \left[\frac{[(1+\alpha)^2 e^{2k\alpha T} - (1-\alpha)^2]\alpha_s}{[(1+\alpha_s)^2 e^{2k\alpha_s T} - (1-\alpha_s)^2]\alpha} \right] - \frac{4\bar{E}_r}{N_0} \left[\frac{1}{\alpha-1} - \frac{1}{\alpha_s-1} \right] \right\}. \quad (10.118)$$

We see that $\mu(s)$ (and therefore the error expression) is a function of two quantities, \bar{E}_r/N_0 , the average energy divided by the noise spectral height and the kT product. The 3dB bandwidth of the spectrum is k radians per second so that kT is a time-bandwidth product.

We leave the simulation of the optimum receiver as an exercise (Problem 10.2.4.1). The necessary Kalman filter has been developed in Chapter 8 and the detector is shown in Figure 10.9. ■

10.2.5 Stationary Process-Long Observation Time (SPLIT) Receiver

In many physical situations of interest, the received waveforms under both hypotheses are segments of stationary processes. Thus, we can characterize the processes by their power density spectra. If the spectra are rational, they will have a finite-dimensional state representation and we can solve the problem using state-variable techniques. In our previous work with state variables, we saw that when the input was a stationary process the gains in

⁵The details are on pp. 44–46 of DEMT-III [Van71b, Van01c].

the optimum system approached constant values and the system approached a time-invariant system. In this section, we consider cases in which the observation time is *long* compared with the time necessary for the system transients to decay. By ignoring the transient, we can obtain much simpler solutions. If desired, we can always check the validity of the approximation by solving the problem with state-variable techniques. We refer to the results obtained by ignoring the transients as asymptotic results and add a subscript ∞ to the various expressions. As in the general case, we are interested in optimum receiver structures and their performance.

We discuss Canonical Realization no. 1 briefly but focus on Canonical Realization no. 2. We can also implement Canonical Realization no. 3 using a Wiener filter derived in Section 8.2 but do not discuss it in detail.

The model for the simple binary problem was given in (10.1), (10.2). For algebraic simplicity, we discuss only the zero-mean case in the text. The received waveforms are

$$\begin{aligned} H_1 : r(t) &= s(t) + w(t), & T_i \leq t \leq T_f, \\ H_0 : r(t) &= w(t), & T_i \leq t \leq T_f. \end{aligned} \quad (10.119)$$

We assume that $s(t)$ is a zero-mean Gaussian process with spectrum $S_s(\omega)$. The noise $w(t)$ is a white, zero-mean Gaussian process that is statistically independent of $s(t)$ and has a spectral height $N_0/2$. The LRT is

$$l_R + l_B \stackrel{H_1}{\gtrless} \ln \eta. \quad (10.120)$$

We first examine various receiver realizations for computing l_R . Next we derive a formula for l_B . Finally, we compute the performance.

If we use Canonical Realization No. 1,

$$l_R = \frac{1}{N_0} \iint_{T_i}^{T_f} r(t) h_1(t, u) r(u) dt du, \quad (10.121)$$

where $h_1(t, u)$ is a solution to

$$\frac{N_0}{2} h_1(t, u) + \int_{T_i}^{T_f} h_1(t, z) K_s(z - u) dz = K_s(t - u), \quad T_i \leq t, u \leq T_f. \quad (10.122)$$

From our work in Section 6.4, we know that the total solution is made up of a particular solution that does not depend on the limits and a weighted sum of bounded homogeneous solutions that give the correct endpoint conditions. These homogeneous solutions decay as we move into the interior of the interval. If the time interval is large, the particular solution will exert the most influence on l_R , so that we can obtain a good approximation to the solution by neglecting the homogeneous solutions. To accomplish this, we let $T_i = -\infty$

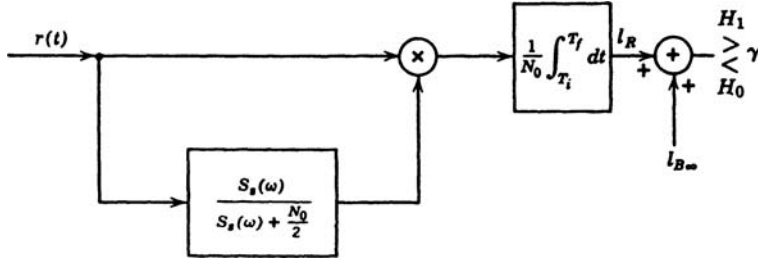


Figure 10.10: Canonical Receiver No. 1: stationary process, long observation time.

and $T_f = \infty$ in (10.122). With the infinite limits, we would assume that we could find a solution to (10.122) that corresponded to a time-invariant filter. To verify this, we let

$$h_1(t, u) = h_{1\infty}(t - u) \quad (10.123)$$

in (10.122) and try to find a solution. Rewriting (10.122), we have

$$\frac{N_0}{2} h_{1\infty}(t - u) + \int_{-\infty}^{\infty} h_{1\infty}(t - z) K_s(z - u) dz = K_s(t - u), \\ -\infty < t, u < \infty, \quad (10.124)$$

which can be solved by using Fourier transforms. Transforming, we have

$$H_{1\infty}(j\omega) = \frac{S_s(\omega)}{S_s(\omega) + (N_0/2)}, \quad (10.125)$$

which is the desired result. The resulting receiver is shown in Figure 10.10. Notice that we have used only the infinite limits to solve the integral equation. The receiver still operates on $r(t)$ over $[T_i, T_f]$. The filter in (10.125) is unrealizable, so a more attractive solution is Canonical Realization No. 2.

To implement Canonical Realization No. 2, we must solve (10.47).

$$h_1(t, u) = \int_{T_i}^{T_f} h_f(z, t) h_f(z, u) dz, \quad T_i \leq t, u \leq T_f. \quad (10.126)$$

To find the asymptotic solution, we let $T_i = -\infty$ and $T_f = \infty$. We assume that a time-invariant solution exists. The resulting equation is

$$h_{1\infty}(t - u) = \int_{-\infty}^{\infty} h_{f\infty}(z - t) h_{f\infty}(z - u) dz, \quad -\infty < t, u < \infty. \quad (10.127)$$

Transforming, we have

$$H_{1\infty}(j\omega) = |H_{f\infty}(j\omega)|^2. \quad (10.128)$$

Now $H_{1\infty}(j\omega)$ has all of the properties of a power density spectrum. Therefore, we can find a realizable $H_{f\infty}(j\omega)$ by assigning all of the poles and zeros of $H_{1\infty}(j\omega)$ that lie in the left

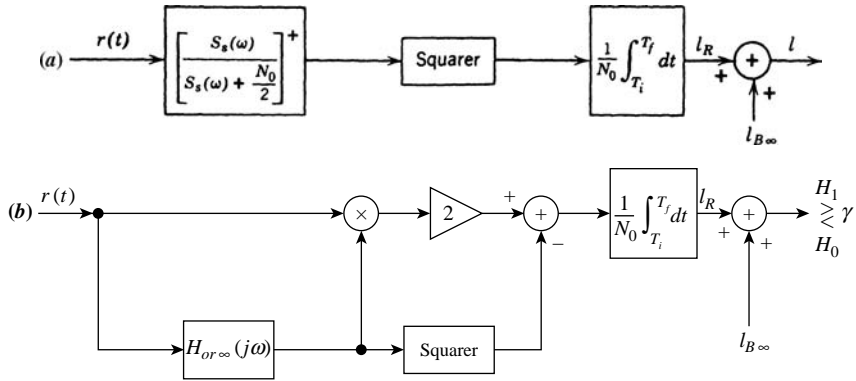


Figure 10.11: Stationary process, long-observation time (a) Canonical Realization No. 2 (b) Canonical Realization No. 3.

half of complex s -plane to $H_{fr\infty}(s)$. We denote the result as

$$H_{fr\infty}(j\omega) = [H_{1\infty}(j\omega)]^+ \quad (10.129)$$

The resulting receiver is shown in Figure 10.11a.

To implement Canonical Realization No. 3, we must solve the realizable filtering problem. By letting $T_i = -\infty$ and assuming stationarity, we obtain the Wiener filtering problem. The solution is given by

$$H_{or\infty} = \frac{1}{[S_s(\omega) + (N_0/2)]^+} \left[\frac{S_s(\omega)}{[S_s(\omega) + (N_0/2)]^-} \right]_+. \quad (10.130)$$

The receiver is shown in Figure 10.11b. Comparing Figures 10.10 and 10.11, we see that Canonical Realization No. 2 in Figure 10.11a is the simplest to implement.

Note that if we are using the state-variable model, the detector in Figure 10.9 will approach the detector in Figure 10.11b as $(T_f - T_i)$ increases.

For a Bayes detector, we need to evaluate l_B . Using (10.38) we have

$$l_{B\infty} = -\frac{1}{2} \sum_{i=1}^{\infty} \ln \left(1 + \frac{2\lambda_i^s}{N_o} \right) = -\frac{T}{2} \int_{-\infty}^{\infty} \ln \left(1 + \frac{2S_s(\omega)}{N_0} \right) \frac{d\omega}{2\pi} = -\xi_{P\infty} \frac{T}{N_0}, \quad (10.131)$$

where

$$T = T_f - T_i. \quad (10.132)$$

In order to bound or approximate the performance, we need $\mu(s)$

$$\mu_{\infty}(s) = \frac{T}{2} \left\{ (1-s) \int_{-\infty}^{\infty} \ln \left[1 + \frac{2S_s(\omega)}{N_0} \right] \frac{d\omega}{2\pi} - \int_{-\infty}^{\infty} \ln \left[1 + \frac{2(1-s)S_s(\omega)}{N_0} \right] \frac{d\omega}{2\pi} \right\}. \quad (10.133)$$

An equivalent form is

$$\mu_\infty(s) = \frac{T}{2} \int_{-\infty}^{\infty} \ln \left[\frac{[1 + (2S_s(\omega)/N_0)]^{1-s}}{[1 + (2(1-s)S_s(\omega)/N_0)]} \right] \frac{d\omega}{2\pi}. \quad (10.134)$$

To illustrate the application of these asymptotic results, we consider two simple examples.

Example 10.2: First-Order Butterworth Spectrum (continuation of Example 10.1).
The received waveforms on the two hypotheses are

$$\begin{aligned} H_1 : r(t) &= s(t) + w(t), & T_i \leq t \leq T_f, \\ H_0 : r(t) &= w(t), & T_i \leq t \leq T_f. \end{aligned} \quad (10.135)$$

The signal process $s(t)$ is a sample function from a stationary, zero-mean, Gaussian random process with spectrum $S_s(\omega)$,

$$S_s(\omega) = \frac{2kP}{\omega^2 + k^2}, \quad -\infty < \omega < \infty. \quad (10.136)$$

The noise process is a statistically independent, zero-mean white Gaussian random process with spectral height $N_0/2$.

Using (10.136) in (10.125), we obtain

$$H_{1\infty}(j\omega) = \frac{2kP/(\omega^2 + k^2)}{(2kP/(\omega^2 + k^2)) + N_0/2} = \frac{k^2 \Lambda_1}{[\omega^2 + k^2(1 + \Lambda_1)]}, \quad (10.137)$$

where

$$\Lambda_1 = \frac{4P}{kN_0} \quad (10.138)$$

is the signal-to-noise ratio in the message bandwidth. From (10.129)⁶,

$$H_{f\infty}(j\omega) = \frac{k\Lambda_1^{\frac{1}{2}}}{j\omega + k\sqrt{1 + \Lambda_1}}. \quad (10.139)$$

We obtain the bias term and $\xi_{P\infty}$ from (10.131). It was evaluated for the first-order Butterworth spectrum in Example 8.4. From (8.137),

$$\xi_{P\infty} = \frac{2P}{1 + \sqrt{1 + \Lambda_1}}. \quad (10.140)$$

Using (10.140) in (10.131), we have

$$l_{B\infty} = -\frac{2PT}{N_0[1 + \sqrt{1 + \Lambda_1}]} \quad (10.141)$$

⁶Note that $H_{f\infty}(j\omega)$ is not the same as the optimum realizable filter derived in (8.114) although it looks similar. The pole is same but the gain is smaller. For $\Lambda_1 \gg 1$ the gains converge.

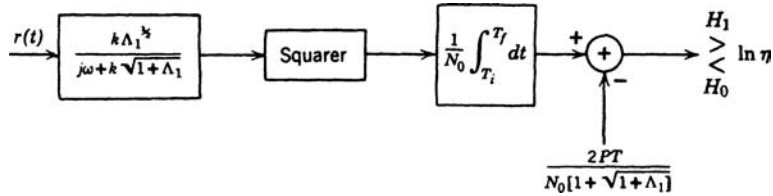


Figure 10.12: Filter-squarer receiver: First-order Butterworth spectrum, long observation time.

The resulting receiver is shown in Figure 10.12. Notice that the location of the pole of the filter depends on Λ_1 . As Λ_1 decreases, the filter pole approaches the pole of the message spectrum. As Λ_1 increases, the bandwidth of the filter increases.

To evaluate the performance, we find $\mu_\infty(s)$ by using (10.140) in (10.131) and (10.133),

$$\mu_\infty(s) = \frac{(1-s)T}{N_0} \left\{ \frac{2P}{1 + \sqrt{1 + \Lambda_1}} - \frac{2P}{1 + \sqrt{1 + (1-s)\Lambda_1}} \right\}. \quad (10.142)$$

At this point, it is useful to introduce an efficient notation to emphasize the important parameters in the performance expression.

We introduce several quantities,

$$\bar{E}_r \triangleq PT, \quad (10.143)$$

which is the average energy in the signal process, and

$$D_1 \triangleq \frac{kT}{2}, \quad (10.144)$$

which is a measure of the time-bandwidth product of the signal process. Notice that

$$\Lambda_1 = \frac{2\bar{E}_r/N_0}{D_1}. \quad (10.145)$$

Using (10.143) in (10.142), we obtain

$$\mu_\infty(s) = - \left(\frac{2\bar{E}_r}{N_0} \right) g_1(s, \Lambda_1), \quad (10.146)$$

where

$$g_1(s, \Lambda_1) \triangleq -(1-s) \left\{ \left(1 + \sqrt{1 + \Lambda_1} \right)^{-1} - \left(1 + \sqrt{1 + (1-s)\Lambda_1} \right)^{-1} \right\}. \quad (10.147)$$

The first factor in (10.146) is the average signal energy-to-noise ratio and appears in all detection problems. The second term includes the effect of the spectral shape, the signal-to-noise ratio in the message bandwidth, and the threshold. It is this term that will vary in different examples. To evaluate the approximate expressions for P_F and P_D , we need $\mu_\infty(s)$ and $\dot{\mu}_\infty(s)$. Then, from (10.82) and (10.83),

$$P_F \simeq \frac{1}{\sqrt{2\pi s^2 \ddot{\mu}_\infty(s)}} \exp [\mu_\infty(s) - s\dot{\mu}_\infty(s)] \quad (10.148)$$

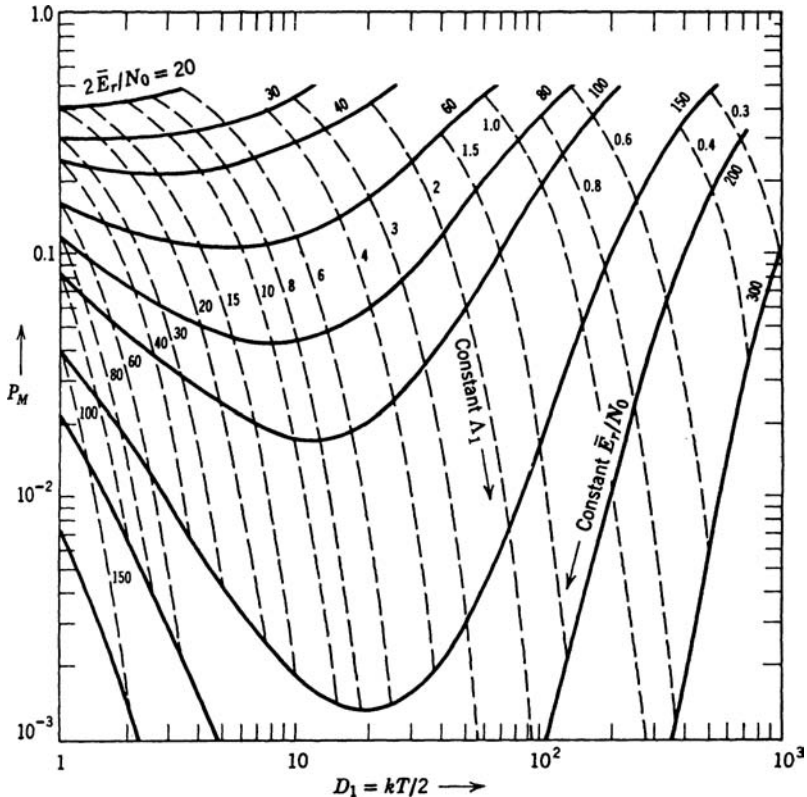


Figure 10.13: Probability of miss versus time-bandwidth product for first-order Butterworth spectrum, $P_F = 10^{-3}$.

and

$$P_M \simeq \frac{1}{\sqrt{2\pi(1-s)^2\mu_\infty(s)}} \exp [\mu_\infty(s) + (1-s)\dot{\mu}_\infty(s)]. \quad (10.149)$$

From (10.146) and (10.147), we can obtain the necessary quantities to substitute into (10.148) and (10.149). In Figures 10.13 and 10.14, we have plotted the approximate performance characteristics indicated by (10.148) and (10.149). In Figure 10.13, we have constrained P_F to equal 10^{-3} . The horizontal axis is $D_1 (= kT/2)$. The vertical axis is P_M . The solid curves correspond to constant values of $2\bar{E}_r/N_0$. We see that the performance is strongly dependent on the time-bandwidth product of the signal process. Notice that there is an optimum value of Λ_1 for each value of $2\bar{E}_r/N_0$. We recall from Chapter 6 that the kT product will determine the number of significant eigenvalues for the first-order Butterworth spectrum. On a given $2\bar{E}_r/N_0$ curve, the minimum corresponds to the optimum number of significant eigenvalues that the signal energy is divided over. This corresponds to the optimum diversity result that we encountered in Chapter 2 (Example 2.6) and Chapter 7 (Section 7.4.2, page 701). The dashed curves correspond physically to increasing the observation time. Similar results are shown for $P_F = 10^{-5}$ in Figure 10.14.

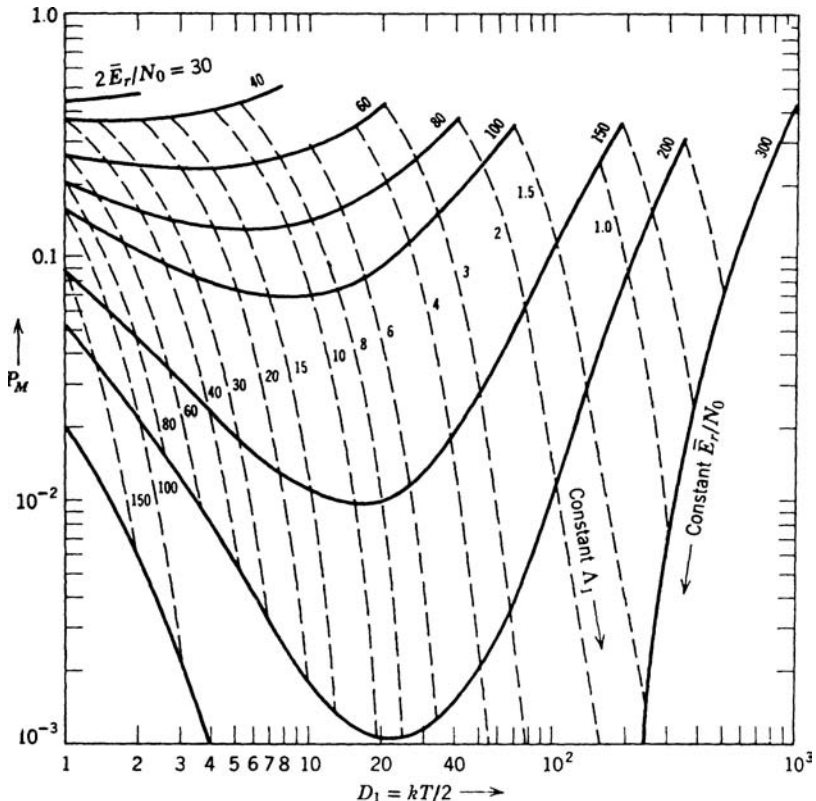


Figure 10.14: Probability of miss versus time-bandwidth product for first-order Butterworth spectrum, $P_F = 10^{-5}$.

For small values of D_1 (say, $D_1 < 2$), the curves should be checked using state-variable techniques because the SPLIT approximation may not be valid.

For larger time-bandwidth products our performance calculations give good results, for two reasons:

1. The error resulting from the large time-interval approximation decreases rapidly as kT increases.
2. The error resulting from truncating the Edgeworth series at the first term decreases as kT increases, because there are more significant eigenvalues. As the number of significant eigenvalues increases, the tilted density becomes closer to a Gaussian density.

Notice that if the system is operating close to the optimum value of Λ_1 , D_1 will be large enough to make the SPLIT approximation valid. ■

Similar results for higher-order Butterworth spectra can be obtained easily. In the next example, we consider the case in which the signal has an ideal bandlimited message spectrum.

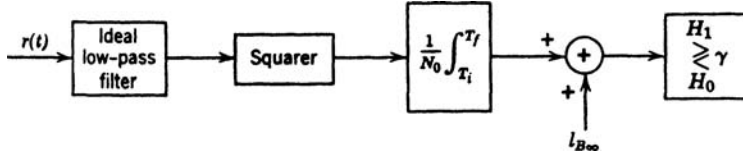


Figure 10.15: Optimum receiver: Ideal low-pass spectrum, long observation time.

Example 10.3. In this example, we assume that $S_s(\omega)$ has a bandlimited spectrum

$$S_s(\omega) = \begin{cases} \frac{P}{2W}, & -2\pi W \leq \omega \leq 2\pi W, \\ 0, & \text{elsewhere.} \end{cases} \quad (10.150)$$

From (10.150) and (10.125),

$$H_{1\infty}(j\omega) = \begin{cases} \frac{P}{P + N_0 W}, & -2\pi W \leq \omega \leq 2\pi W, \\ 0, & \text{elsewhere.} \end{cases} \quad (10.151)$$

Thus,

$$H_{f\infty}(j\omega) = \begin{cases} \frac{1}{(1 + N_0 W/P)^{\frac{1}{2}}}, & -2\pi W \leq \omega \leq 2\pi W, \\ 0, & \text{elsewhere.} \end{cases} \quad (10.152)$$

The bias term is obtained by using (10.150) in (10.131).

$$l_{B\infty} = -WT \ln \left(1 + \frac{P}{N_0 W} \right). \quad (10.153)$$

The resulting receiver is shown in Figure 10.15. Notice that we cannot realize the filter in (10.152) exactly. We can approximate it arbitrarily closely by using an n th-order Butterworth filter, where n is chosen large enough to obtain the desired approximation accuracy.

To calculate the performance, we find $\mu_\infty(s)$ from (10.133). The result is

$$\mu_\infty(s) = \frac{T(1-s)}{N_0} \left\{ N_0 W \ln \left(1 + \frac{P}{N_0 W} \right) - \frac{N_0 W}{(1-s)} \ln \left(1 + \frac{P(1-s)}{N_0 W} \right) \right\}. \quad (10.154)$$

This can be written as

$$\mu_\infty(s) = -\frac{2\bar{E}_r}{N_0} g_\infty(s, \Lambda_\infty), \quad (10.155)$$

where

$$\begin{aligned} g_\infty(s, \Lambda_\infty) &= -\frac{1}{2\Lambda_\infty} [(1-s) \ln(1 + \Lambda_\infty) - \ln(1 + (1-s)\Lambda_\infty)] \\ &= \frac{-1}{2\Lambda_\infty} \left[\ln \left[\frac{(1 + \Lambda_\infty)^{1-s}}{(1 + (1-s)\Lambda_\infty)} \right] \right] \end{aligned} \quad (10.156)$$

and

$$\Lambda_\infty = \frac{P}{N_0 W}. \quad (10.157)$$

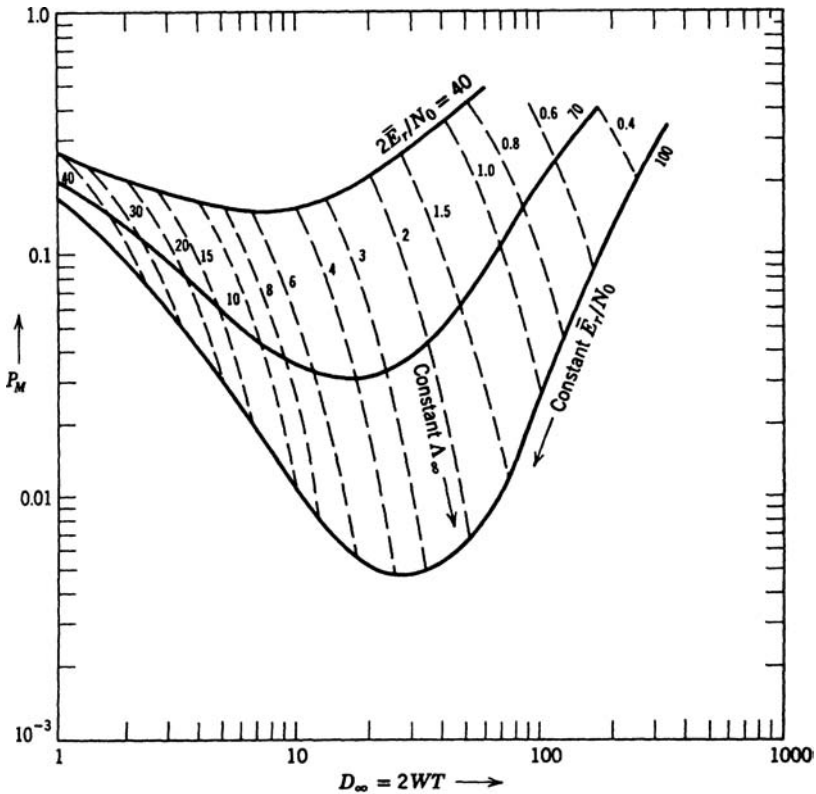


Figure 10.16: Probability of miss versus time-bandwidth product, ideal bandlimited spectrum, $P_F = 10^{-3}$.

Notice that the ∞ subscript of Λ_∞ and $g_\infty(\cdot, \cdot)$ denotes an infinite-order Butterworth spectrum. In Figure 10.16, we plot the same results as in Example 10.2 for $P_F = 10^{-3}$. We recall from Section 6.4.2 that the number of significant eigenvalues is $2WT + 1$ so that the horizontal scale in Figure 10.16 corresponds to the number of significant eigenvalues minus 1. ■

In this section, we studied the case in which the received waveform is a sample function of a stationary random process *and* the observation interval is long. By neglecting the transient effects at the ends of the observation interval, we were able to implement the receiver using time-invariant filters. The resulting receiver is suboptimum but approaches the optimum receiver rapidly as the time-bandwidth product of the signal process increases.

We have not discussed how long the observation interval must be in order for the SPLOT approximation to be valid. Whenever the processes have rational spectra, we can compute the performance of both the optimum receiver and the SPLOT receiver using state-variable techniques. Thus, in any particular situation we can check the validity of the approximation quantitatively. A conservative requirement for using the approximation is to check the time-bandwidth product at the input to the squarer in Canonical Realization No. 2. If the product is greater than 5, the approximation is almost always valid.

The performance expressions for the SPLOT case were simplified because we could use the asymptotic expressions for the Fredholm determinant.

10.2.6 Low-Rank Kernels

In this section we discuss optimum detectors for low-rank signal models. In Section 4.2.1 in DEMT-III, we referred to these models as separable kernel models. We utilize a complex Gaussian model because it is more appropriate for the applications that we are going to discuss.

The received complex envelopes on two hypothesis are

$$\begin{aligned} H_1 : \tilde{r}(t) &= \tilde{s}(t) + \tilde{w}(t), & T_i \leq t \leq T_f, \\ H_0 : \tilde{r}(t) &= \tilde{w}(t), & T_i \leq t \leq T_f. \end{aligned} \quad (10.158)$$

The noise $\tilde{w}(t)$ is a sample function from a zero-mean complex white Gaussian random process with spectral height N_0 . The signal $\tilde{s}(t)$ is a sample function from a zero-mean Gaussian random process with covariance function $\tilde{K}_{\tilde{s}}(t, u)$. The LRT is

$$l_R = \frac{1}{N_0} \iint_{T_i}^{T_f} \tilde{r}^*(t) \tilde{h}_1(t, u) \tilde{r}(u) dt du \stackrel{H_1}{\gtrless} \gamma, \quad (10.159)$$

where $\tilde{h}_1(t, u)$ is specified by the integral equation

$$N_0 \tilde{h}_1(t, u) + \int_{T_i}^{T_f} \tilde{h}_1(t, z) \tilde{K}_s(z, u) dz = \tilde{K}_{\tilde{s}}(t, u), \quad T_i \leq t, u \leq T_f. \quad (10.160)$$

A low-rank signal has a finite number of eigenvalues, so we can write

$$\tilde{K}_{\tilde{s}}(t, u) = \sum_{i=1}^K \lambda_i^s \tilde{\phi}_i(t) \tilde{\phi}_i^*(u), \quad T_i \leq t, u \leq T_f, \quad (10.161)$$

where $\tilde{\phi}_i(t)$ and λ_i^s are the eigenfunctions and eigenvalues, respectively, of the signal process. In this case the solution to (10.160) is

$$\tilde{h}_1(t, u) = \sum_{i=1}^K h_i \tilde{\phi}_i(t) \tilde{\phi}_i^*(u) = \sum_{i=1}^K \frac{\lambda_i^s}{N_0 + \lambda_i^s} \tilde{\phi}_i(t) \tilde{\phi}_i^*(u), \quad T_i \leq t, u \leq T_f. \quad (10.162)$$

For low-rank kernels, the simplest realization is Canonical Realization No. 2 (the filter-squared receiver). From (10.47),

$$\tilde{h}_1(t, u) = \int_{T_i}^{T_f} \tilde{h}_f(z, t) \tilde{h}_f^*(z, u) dz, \quad (10.163)$$

whose solution is

$$\tilde{h}_{fu}(z, t) = \sum_{i=1}^K h_i^{\frac{1}{2}} \tilde{\phi}_i(z) \tilde{\phi}_i^*(t), \quad T_i \leq t, z \leq T_f. \quad (10.164)$$

Using (10.162) in (10.159) we obtain

$$l_R = \frac{1}{N_0} \sum_{i=1}^K h_i \left| \left[\int_{T_i}^{T_f} \tilde{r}(t) \tilde{\phi}_i^*(t) dt \right] \right|^2. \quad (10.165)$$

The operation on $\tilde{r}(t)$ can be realized using either correlators or matched filters.

One of the many cases where we encounter the low-rank model is

$$\tilde{s}(t) = \sum_{i=1}^K \tilde{b}_i \tilde{s}_i(t), \quad (10.166)$$

where the $\tilde{s}_i(t)$ are normalized linearly independent signals.

Defining

$$\tilde{\mathbf{b}} = [\tilde{b}_1 \dots \tilde{b}_K]^T \quad (10.167)$$

and

$$\tilde{\mathbf{s}}(t) = [\tilde{s}_1(t) \dots \tilde{s}_K(t)]^H, \quad (10.168)$$

the signal covariance function is

$$\tilde{K}_{\tilde{s}}(t, u) = \tilde{\mathbf{s}}^H(t) \tilde{\mathbf{K}}_{\tilde{s}} \tilde{\mathbf{s}}(u) \quad (10.169)$$

and the eigenequation is

$$\lambda_i \tilde{\mathbf{c}}_i = \tilde{\mathbf{K}}_{\tilde{s}} \tilde{\rho}_{\tilde{s}} \tilde{\mathbf{c}}_i \quad (10.170)$$

and

$$\tilde{\rho}_{\tilde{s}} = \int_0^T \tilde{\mathbf{s}}(u) \tilde{\mathbf{s}}^H(u) du. \quad (10.171)$$

An important special case of this model is when the $\tilde{s}_i(t)$ are orthonormal so that

$$\tilde{\rho}_{\tilde{s}} = \mathbf{I} \quad (10.172)$$

This could occur because of time or frequency diversity. Historically, the first place that the time diversity mode arose was in pulsed radar systems. The transmitted signal is a sequence of pulsed sinusoids at a carrier frequency $\omega_c = 2n\pi/T$, where n is a large integer. The sequence shown in Figure 10.17.

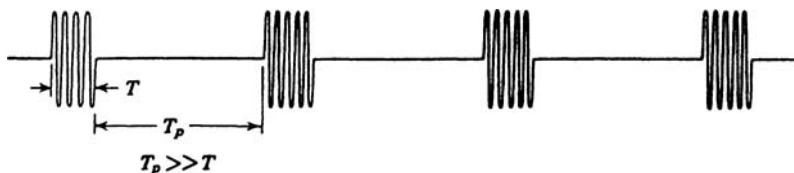


Figure 10.17: Transmitted pulse sequence.

The i th transmitted signal is

$$s_i(t) = \begin{cases} \sqrt{2}\Re(\tilde{s}_i(t)e^{j\omega t}) & (i-1)T_p \leq t \leq (i-1)T_p + T, \\ 0 & \text{elsewhere.} \end{cases} \quad (10.173)$$

where the complex transmitted envelope $\tilde{s}_i(t)$ is normalized.

If a target is present, the complex envelope of the returned signal on the pulse is

$$\tilde{s}_{ri}(t) = \begin{cases} \tilde{b}_i \tilde{s}_i(t) & (i-1)T_p \leq t \leq (i-1)T_p + T, \\ 0 & \text{elsewhere.} \end{cases} \quad (10.174)$$

where \tilde{b}_i is a zero-mean circular complex Gaussian random variable. When the signals are orthonormal and identical, the most efficient approach is to create the finite vector signal subspace first by passing the received waveform through a bandpass matched filter and sampling the output every T_p seconds to generate a complex vector $\tilde{\mathbf{r}}$ consisting of K samples. Thus,

$$\tilde{\mathbf{r}} = \begin{cases} \tilde{\mathbf{b}} + \tilde{\mathbf{w}}, & H_1 \\ \tilde{\mathbf{w}}, & H_0 \end{cases}, \quad (10.175)$$

where

$$\tilde{\mathbf{K}}_{\tilde{s}} = \tilde{\mathbf{K}}_{\tilde{b}} \quad (10.176)$$

and

$$\tilde{\mathbf{K}}_{\tilde{w}} = N_0 \mathbf{I}. \quad (10.177)$$

This is exactly the problem we solved in Section 3.3.1. From (3.350), the LRT is

$$l(\tilde{\mathbf{R}}) = \frac{1}{N_0} \tilde{\mathbf{R}}^H \tilde{\mathbf{H}} \tilde{\mathbf{R}}, \quad (10.178)$$

where

$$\tilde{\mathbf{H}} = \frac{1}{N_0} \left(\frac{1}{N_0} \mathbf{I} + \tilde{\mathbf{K}}_{\tilde{b}} \right)^{-1}. \quad (10.179)$$

The resulting receiver is shown in Figure 10.18. To evaluate the performance, we do the eigendecomposition in (3.383) and find P_F and P_D by using (3.395) and (3.397), respectively. Example 3.8 evaluates the performance for the case when

$$\tilde{\mathbf{K}}_{\tilde{b}} = \sigma_b^2 \begin{bmatrix} 1 & \tilde{\rho}^* & \dots & (\tilde{\rho}^*)^{(N-1)} \\ \tilde{\rho} & 1 & \dots & (\tilde{\rho}^*)^{(N-2)} \\ \vdots & \vdots & \ddots & \vdots \\ \tilde{\rho}^{(N-1)} & \tilde{\rho}^{(N-2)} & \dots & 1 \end{bmatrix}. \quad (10.180)$$

To use the results in Example 3.8, we set

$$\sigma_{\tilde{s}}^2 = \sigma_b^2 = \bar{E}_{r1}, \quad (10.181)$$

which is average received energy per pulse, and

$$\sigma_{\tilde{w}}^2 = N_0. \quad (10.182)$$

The results for uncorrelated signal returns is shown in Figure 10.19.

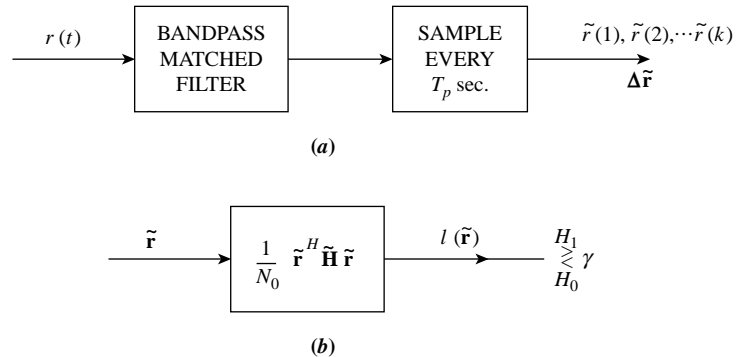


Figure 10.18: Optimum receiver for pulsed radar with correlated returns.

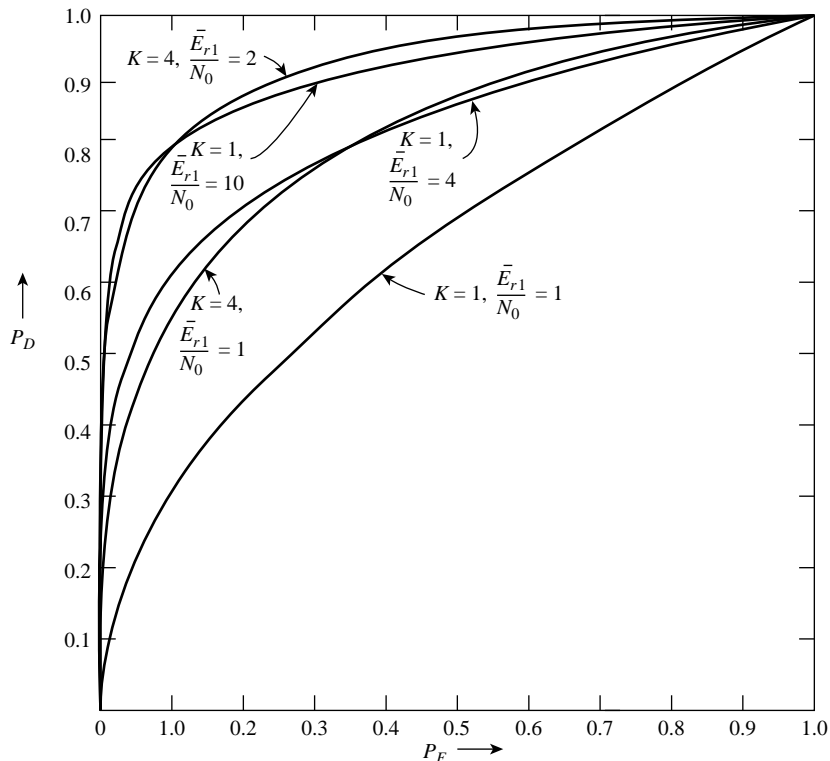


Figure 10.19: Receiver operating characteristics: pulsed radar, Rayleigh target; uncorrelated returns.

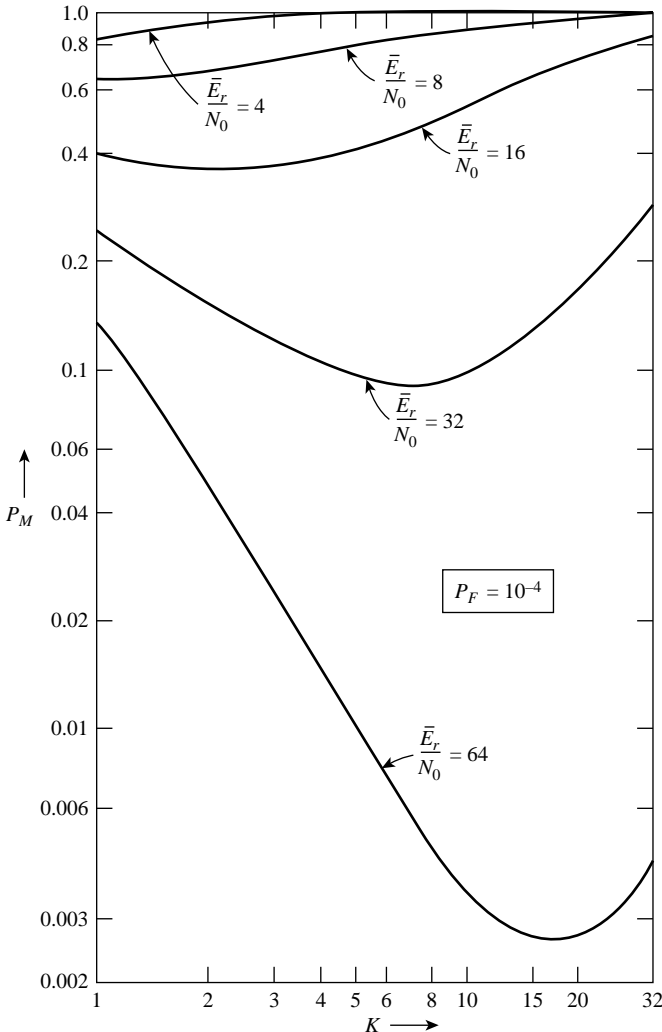


Figure 10.20: P_M as a function of the number of transmitted pulses (total energy fixed).

As we have observed previously, if the total energy is constrained then there is an optimum number of pulses to maximize P_D for a given P_F . This is shown in Figure 10.20 for $P_F = 10^{-4}$.

The results for $\tilde{\rho} \neq 0$ that correspond to correlated Rayleigh signals are shown in Figures 3.28 and 3.29.

We also encounter the low-rank model in frequency diversity communications (e.g. pp. 126–130 of DEMT-III [Van71b, Van01c])

In this section, we have studied the low-rank kernel problem. Here, the receiver output consists of a weighted sum of the squares of a finite number of statistically independent Gaussian variables. The important difference between this case and the general Gaussian problem is that we have *finite* sums rather than *infinite* sums. For the complex Gaussian model, we have an analytical expression for P_D and P_F . Note that, for the complex

Gaussian model, we can approximate analytically by using the low rank technique and increasing K by adding more eigenvalues.

10.2.7 Summary

In this section, we studied the problem of simple binary detection of a Gaussian random process in the presence of white Gaussian noise. We argued this also solved the problem of detection of Gaussian random process in the presence of colored noise because we had previously derived realizable whitening filters for three important process models: SPLOT models, state-variable models, and low-rank interference models.

In Section 10.2.1, we provided the option of reducing the problem to a finite dimensional problem by either classical sampling or a Karhunen–Loèv expansion. Then the results of Chapters 3 or 5 were directly applicable.

In Section 10.2.2, we focused our attention on the case when $K \rightarrow \infty$ and we implemented the optimum detector using continuous-time filters. We developed three canonical realizations:

- The estimator–correlator that required a smoothing filter.
- The filter-squarer that required a factorization.
- The optimum realizable filter detector that required the solution of an optimum realizable filtering problem.

In section 10.2.3, we studied the performance of the optimum detector. Except for low-rank signals, we relied on finding expressions for $\mu(s)$ and used the bounds and approximations of Section 2.4.

In the next three sections, we considered process models where we could obtain explicit solutions. In Section 10.2.4, we used the state-variable model introduced in Chapter 8. This model provided a straightforward implementation of Canonical Receiver 3 using a Kalman filter. The error expression need to find $\mu(s)$ was also generated using a Kalman filter.

In Section 10.2.5, we used the SPLOT model. We could implement Canonical Receiver 2 using spectrum factorization or Canonical Receiver 3 using a realizable Wiener filter.

In Section 10.2.6, we considered a low-rank signal model. In this case, Canonical Receives 1 and 2 reduced to a finite set of correlators or matched filters and results in Chapter 3 were directly applicable.

There are several areas that we have not discussed. The general binary detection problem in white noise is

$$\begin{aligned} H_1 : r(t) &= s_1(t) + w(t), & T_i \leq t \leq T_f, \\ H_0 : r(t) &= s_0(t) + w(t), & T_i \leq t \leq T_f, \end{aligned} \quad (10.183)$$

This is a straightforward generalization that is developed in Chapter 3 of DEMT-III [Van71b, Van01c].

The general binary detection problem in colored noise is

$$\begin{aligned} H_1 : r(t) &= s_1(t) + n_c(t) + w(t), & T_i \leq t \leq T_f, \\ H_0 : r(t) &= s_0(t) + n_c(t) + w(t), & T_i \leq t \leq T_f. \end{aligned} \quad (10.184)$$

We can solve this problem using a whitening filter. However, for the state-variable model, it may be easier to solve the problem directly by augmenting the state vector to include the colored noise.

When the noise level is unknown, we can extend the GLRT results in Section 4.5 to the waveform problem.

10.3 DETECTION OF DISCRETE-TIME GAUSSIAN PROCESSES

In this section, we discuss the binary hypothesis testing problem when the observation on the two hypotheses are discrete-time Gaussian random processes. In Section 10.3.1, we assume that we use block processing over a set of K observations and the processes are characterized by their mean value function and covariance function. In Section 10.3.2, we again use block processing but the processes are characterized by a state variable representation.

10.3.1 Second Moment Characterization

In this model, we assume that we have a set of K samples that we denote with the vector \mathbf{r} . We discuss two models. In the first model, the vectors on the two hypotheses are Gaussian random vectors with known means and covariance matrices. Thus,

$$H_0 : \mathbf{r} \sim N(\mathbf{m}_0, \mathbf{K}_0) \quad (10.185)$$

$$H_1 : \mathbf{r} \sim N(\mathbf{m}_1, \mathbf{K}_1) \quad (10.186)$$

for the real vector case and

$$H_0 : \mathbf{r} \sim CN(\tilde{\mathbf{m}}_0, \tilde{\mathbf{K}}_0) \quad (10.187)$$

$$H_1 : \mathbf{r} \sim CN(\tilde{\mathbf{m}}_1, \tilde{\mathbf{K}}_1) \quad (10.188)$$

for the complex vector case. We discuss this model in Section 10.3.1.1.

In the second model, the vectors on the two hypotheses are Gaussian random vectors whose means and/or covariance matrices contain unknown parameters. Thus,

$$H_0 : \mathbf{r} \sim N(\mathbf{m}_0(\boldsymbol{\theta}_{m_0}), \mathbf{K}_{s_0}(\boldsymbol{\theta}_{c_0})) \quad (10.189)$$

$$H_1 : \mathbf{r} \sim N(\mathbf{m}_1(\boldsymbol{\theta}_{m_1}), \mathbf{K}_{s_1}(\boldsymbol{\theta}_{c_1})) \quad (10.190)$$

for the real vector case and

$$H_0 : \tilde{\mathbf{r}} \sim CN(\tilde{\mathbf{m}}_0(\boldsymbol{\theta}_{m_0}), \tilde{\mathbf{K}}_{s_0}(\boldsymbol{\theta}_{c_0})) \quad (10.191)$$

$$H_1 : \tilde{\mathbf{r}} \sim CN(\tilde{\mathbf{m}}_1(\boldsymbol{\theta}_{m_1}), \tilde{\mathbf{K}}_{s_1}(\boldsymbol{\theta}_{c_1})) \quad (10.192)$$

for the complex vector case.

We discuss this model in Section 10.3.1.2.

In both cases, we have already solved the problems in Chapters 3–5. Therefore, our approach is to give the reader a road map to the appropriate section or example.

10.3.1.1 Known Means and Covariance Matrices

In order to minimize duplication, we use the real vector model in (10.185) and (10.186). In most of the referenced sections, we also develop the complex vector model.

Case 1A: Equal covariance matrices on both hypotheses In this case,

$$\mathbf{K}_0 = \mathbf{K}_1 \triangleq \mathbf{K} \quad (10.193)$$

and it is discussed in Section 3.2. The special cases are given in Table 10.1.

Table 10.1: Special Covariance Matrices

Section	Covariance Matrix
3.2.1	$\mathbf{K} = \sigma_w^2 \mathbf{I}$
3.2.2	$\mathbf{K} = \text{diag} [\sigma_{w_1}^2 \sigma_{w_2}^2 \cdots \sigma_{w_N}^2]$
3.2.3	\mathbf{K} is arbitrary ^a full rank
3.2.5	$\mathbf{K} = \mathbf{K}_I + \sigma_w^2 \mathbf{I}$
3.2.6	\mathbf{K}_I is low rank

^a \mathbf{K} must be a valid covariance matrix

Case 1B: Equal mean vectors on both hypotheses In this case,

$$\mathbf{m}_0 = \mathbf{m}_1 = \mathbf{0}. \quad (10.194)$$

We can set the means equal to $\mathbf{0}$ because only $\Delta\mathbf{m}$ appears in the solution. The case is discussed in Section 3.3 and the special cases are given in Table 10.2.

Case 1C: Unequal mean vectors and unequal covariance matrices This is the general Gaussian model and is discussed in Section 3.4. The structure of the detector is a combination of Case 1A and Case 1B. The performance evaluation is generally difficult.

10.3.1.2 Means and Covariance Matrices with Unknown Parameters

The model is given in (10.189)–(10.192). The previous results are contained in two places. They are discussed in the context of composite hypotheses in Section 4.5 and in the context of nonrandom parameter estimation in Section 5.2.

In Section 4.5.2, we considered the case in which θ_m is a random Gaussian vector and the covariance matrices are known. The two specific cases discussed are shown in Table 10.3. In these cases we reduce the model to a simple hypotheses problem by integrating over the probability density of the unknown parameters.

In Section 4.5.3, we considered the case in which θ_m and θ_c are unknown nonrandom vectors and focused our attention on the generalized likelihood ratio test. The specific cases are shown in Tables 10.4 and 10.5.

These various cases will solve the detection problem for large number of applications in the radar and communication area.

Table 10.2: Special Covariance Matrices

Section	Covariance Matrix
3.3.1	$\mathbf{K}_0 = \sigma_w^2 \mathbf{I}$
3.3.1.1	$\mathbf{K}_1 = \sigma_s^2 \mathbf{I} + \sigma_w^2 \mathbf{I}$
3.3.1.2	$\mathbf{K}_1 = \text{diag} [\sigma_{s_1}^2 \sigma_{s_2}^2 \cdots \sigma_{s_N}^2] + \sigma_w^2 \mathbf{I}$
3.3.1.3	\mathbf{K}_1 is arbitrary full rank + $\sigma_w^2 \mathbf{I}$
3.3.1.4	\mathbf{K}_1 is low rank + $\sigma_w^2 \mathbf{I}$
3.3.1.5	Symmetric Hypotheses
3.3.2	\mathbf{K}_0 is nondiagonal
3.3.2.1	$\mathbf{K}_0 = \mathbf{K}_n, \mathbf{K}_1 = \mathbf{K}_s + \mathbf{K}_n$
3.3.2.2	$\mathbf{K}_0 = \mathbf{K}_{s_0} + \sigma_w^2 \mathbf{I}, \mathbf{K}_1 = \mathbf{K}_{s_1} + \sigma_w^2 \mathbf{I}$

Table 10.3: Random Parameters

Example	Model
4.38	$H_0 : \mathbf{r} \sim N(\mathbf{0}, \sigma_w^2 \mathbf{I})$ $H_1 : \mathbf{r} \sim N(m\mathbf{v}, \sigma_w^2 \mathbf{I})$ $m \sim N(0, \sigma_m^2)$
4.39	$H_0 : \mathbf{r} \sim N(0, \sigma_w^2 \mathbf{I})$ $H_1 : \mathbf{r} \sim N(\mathbf{V}\boldsymbol{\theta}, \sigma_w^2 \mathbf{I})$ $\boldsymbol{\theta} \sim N(\mathbf{0}, \mathbf{K}_{\boldsymbol{\theta}})$

Table 10.4: GLRT Examples

Example	Model
4.40	$H_0 : \mathbf{r} \sim N(0, \sigma_w^2)$ $H_1 : \mathbf{r} \sim N(M, \sigma_w^2)$ $M_L \leq M \leq M_U$ σ_w^2 known
4.44	$H_0 : \mathbf{r} \sim N(\mathbf{0}, \sigma_w^2 \mathbf{I})$ $H_1 : \mathbf{r} \sim N(M\mathbf{1}, \sigma_w^2 \mathbf{I})$ $M_L \leq M \leq M_U$ σ_w^2 known
4.45	$H_0 : \mathbf{r} \sim N(\mathbf{0}, \sigma_w^2 \mathbf{I})$ $H_1 : \mathbf{r} \sim N(M\mathbf{v}, \sigma_w^2 \mathbf{I})$ $M_L \leq M \leq M_U$ σ_w^2 known
4.46	$H_0 : \mathbf{r} \sim N(\mathbf{0}, \sigma_w^2 \mathbf{I})$ $H_1 : \mathbf{r} \sim N(M\mathbf{v}, \sigma_w^2 \mathbf{I})$ $M_L \leq M \leq M_U$ $\sigma_w^2 > 0$
4.47	$H_0 : \mathbf{r} \sim N(\mathbf{0}, \sigma_w^2 \mathbf{I})$ $H_1 : \mathbf{r} \sim N(\mathbf{V}\boldsymbol{\theta}, \sigma_w^2 \mathbf{I})$ $\sigma_w^2 > 0$

Table 10.5: Fisher Linear Gaussian Model

Section	Model
5.2.4	$\mathbf{r} \sim N(\mathbf{V}\boldsymbol{\theta}_m, \mathbf{K})$
5.2.5	$\mathbf{r} \sim N(\mathbf{V}(\boldsymbol{\theta}_{m,nl})\boldsymbol{\theta}_{m,l}, \mathbf{K})$
5.2.6	$\mathbf{r} \sim N(\mathbf{0}, \mathbf{K}(\boldsymbol{\theta}_c))$
5.2.6.1	$\mathbf{K}(\boldsymbol{\theta}_c) = \sigma_w^2 \mathbf{I}$
5.2.6.2	$\mathbf{K}(\boldsymbol{\theta}_c) = \sigma_n^2 \mathbf{K}_n$
5.2.6.3	$\mathbf{K}(\boldsymbol{\theta}_c) = \sigma_s^2 \mathbf{v}_s \mathbf{v}_s^T + \sigma_w^2 \mathbf{I}$
5.2.6.4	$\mathbf{K}(\boldsymbol{\theta}_c) = \sigma_s^2 \mathbf{v}_s \mathbf{v}_s^T + \sigma_n^2 \mathbf{K}_n$
5.2.7	$\mathbf{r} \sim N(\mathbf{V}\boldsymbol{\theta}_m, \mathbf{K}(\boldsymbol{\theta}_c))$ $\boldsymbol{\theta}_m$ and $\boldsymbol{\theta}_c$ are unknown

10.3.2 State Variable Characterization

In this section, we consider the model in which the received sequences on the two hypotheses are

$$H_0 : r(k) = w(k), \quad k = 0, 1, \dots, K, \quad (10.195)$$

$$H_1 : r(k) = s(k) + w(k), \quad k = 0, 1, \dots, K. \quad (10.196)$$

The signal $s(k)$ has a state variable representation. From (9.212),

$$\mathbf{x}(k) = \mathbf{F}(k-1)\mathbf{x}(k-1) + \mathbf{G}(k-1)\mathbf{u}(k-1) \quad (10.197)$$

and, from (9.213)

$$s(k) = \mathbf{C}(k)\mathbf{x}(k). \quad (10.198)$$

The noise $w(k)$ is a white process.

We want to find the optimum detector. We can rewrite (10.195) and (10.196) as

$$H_0 : \mathbf{r} = \mathbf{w}, \quad (10.199)$$

$$H_1 : \mathbf{r} = \mathbf{s} + \mathbf{w}. \quad (10.200)$$

Thus, from Section 3.3 (3.342) and (3.343), the optimum detector is

$$l(\mathbf{R}) \triangleq \frac{1}{\sigma_w^2} \mathbf{R}^T \mathbf{H} \mathbf{R} \stackrel{H_1}{\gtrless} \stackrel{H_0}{\gtrless} \gamma_3, \quad (10.201)$$

where

$$\mathbf{H} = \frac{1}{\sigma_w^2} \left[\frac{1}{\sigma_w^2} \mathbf{I} + \mathbf{K}_s^{-1} \right]^{-1} \quad (10.202)$$

and is shown in Figure 3.25.

In the context of the current discussion, the key result is that $\hat{\mathbf{s}}$ is the noncausal estimate of \mathbf{s} . This means that we could also generate $\hat{\mathbf{s}}$ recursively using the Kalman smoother developed in Section 9.3. However, the smoothing filters are always more complex than the Kalman linear filter or linear predictor.

In Section 10.2, we derived an optimum detector structure for continuous-time processes that only required the MMSE *causal* estimate. The continuous version of this detector was derived independently by Schweppe [Sch65] and Stratonovich and Sosulin [SS65]. It was discussed in the early literature in Chapter 2 of DEMT-III [Van71b, Van01b], and Helstrom [Hel95].

We want to derive an optimum detector for discrete-time processes that uses a realizable linear filter and a realizable linear one-step prediction filter. The detector appears in Chapter 10 of Levy [Lev08] and we follow his derivation.

The input is a discrete-time scalar Gaussian random process

$$r(k) = s(k) + w(k) \quad k = 0, 1, \dots, K-1. \quad (10.203)$$

We assume that $s(k)$ has a state-variable representation so that we can use the techniques in Section 9.3 to generate the filtered estimate,

$$d(k) = s(k) \quad (10.204)$$

and the one-step prediction,

$$d(k) = s(k + 1). \quad (10.205)$$

However, all of our results are valid for the model in which we have a second-moment characterization and use an FIR Wiener processor from Section 9.2.3.

We first find the one-step prediction of $s(k)$ based on observations $r(m)$, $m = 0, 1, \dots, k - 1$. Then, $\hat{s}_p(k)$ is the conditional mean

$$\begin{aligned} \hat{s}_p(k) &= E\{s(k)|r(m), 0 \leq m \leq k - 1\} \\ &= - \sum_{m=0}^{k-1} a(k, m)r(m). \end{aligned} \quad (10.206)$$

Then, the innovations process is

$$\tilde{r}(k) \triangleq r(k) - \hat{s}_p(k) = \sum_{m=0}^k a(k, m)r(m) \quad (10.207)$$

with $a(k, k) = 1$.

Note that we are going to generate $\hat{s}_p(k)$ using a Kalman filter. We use $a(k, m)$ in our development but will not need to find it.

The predicted value of $r(k)$ is the same as $\hat{s}_p(k)$ because $w(k)$ is white Gaussian noise.

$$\hat{r}_p(k|k - 1) = E[r(k)|r(m), 0 \leq m \leq k - 1] = \hat{s}_p(k). \quad (10.208)$$

The innovation, $\tilde{r}(k)$ is a time-varying WGN process whose variance is

$$\tilde{P}(k) = E\{\tilde{r}^2(k)\} \quad (10.209)$$

and

$$E\{\tilde{r}(k)\tilde{r}(m)\} = \tilde{P}(k)\delta_{km}. \quad (10.210)$$

We can normalize the innovation, $\tilde{r}(k)$

$$\tilde{r}(k) = \tilde{P}^{-\frac{1}{2}}(k)\tilde{r}(k) = \sum_{m=0}^k f(k, m)r(m), \quad (10.211)$$

where the causal filter $f(k, m)$ is defined as

$$f(k, m) \triangleq \tilde{P}^{-\frac{1}{2}}(k)a(k, m), \quad 0 \leq m \leq k. \quad (10.212)$$

We now construct $(K + 1)$ dimensional vectors

$$\tilde{\mathbf{r}} = [\tilde{r}_0 \tilde{r}_1 \dots \tilde{r}_K]^T \quad (10.213)$$

and

$$\mathbf{r} = [r_0 \ r_1 \ \cdots \ r_K]^T \quad (10.214)$$

and the lower triangular matrix \mathbf{F} such that the entry of row $k + 1$ and column $m + 1$ is $f(k, m)$

$$\mathbf{F} = \begin{bmatrix} f(0, 0) & 0 & 0 \\ f(1, 0) & f(1, 1) & \\ f(2, 0) & & \ddots \\ \vdots & & \\ f(K, 0) & & f(K, K) \end{bmatrix} \quad (10.215)$$

Then, (10.211) can be written as

$$\tilde{\mathbf{r}} = \mathbf{Fr} \quad (10.216)$$

and since $\tilde{\mathbf{r}}$ is white Gaussian noise with unit intensity

$$\mathbf{I}_{K+1} = E \{ \tilde{\mathbf{r}} \tilde{\mathbf{r}}^T \} = \mathbf{FK}_r \mathbf{F}^T, \quad (10.217)$$

which implies that

$$\mathbf{K}_r^{-1} = \mathbf{F}^T \mathbf{F} \quad (10.218)$$

represents an upper times lower Cholesky factorization of the inverse of \mathbf{K}_r .

From (3.343), the sufficient statistic is

$$l(\mathbf{r}) = \frac{1}{2} \mathbf{r}^T \mathbf{H} \mathbf{r} \quad (10.219)$$

and using (3.342),

$$l(\mathbf{r}) = \frac{1}{2} \mathbf{r}^T \{ \mathbf{I} - \sigma_w^2 \mathbf{F}^T \mathbf{F} \} \mathbf{r} \quad (10.220)$$

$$= \frac{1}{2} \{ \mathbf{r}^T \mathbf{r} - \sigma_w^2 \mathbf{r}^T \mathbf{F}^T \mathbf{Fr} \} \quad (10.221)$$

$$= \frac{1}{2} \{ \mathbf{r}^T \mathbf{r} - \sigma_w^2 \tilde{\mathbf{r}}^T \tilde{\mathbf{r}} \}, \quad (10.222)$$

which can be written as

$$l(\mathbf{r}) = \frac{1}{2} \sum_{k=0}^K \left\{ \mathbf{r}^2(k) - \frac{\sigma_w^2}{P(k)} \tilde{r}^2(k) \right\}, \quad (10.223)$$

which depends only on the observations and the innovation process $\tilde{r}(k)$ which is generated by the Kalman filter.

We can obtain a different version of (10.223) that has a structure that allows comparison with the known signal detector.

We introduce the filtered estimate

$$\hat{s}_f(k) = E \{ s(k) | r(m) \}, \quad 0 \leq m \leq k \quad (10.224)$$

and the *a posteriori* residual,

$$\delta(k) = r(k) - \hat{s}_f(k) \quad (10.225)$$

or

$$\delta(k) = \tilde{s}_f(k) + w(k), \quad (10.226)$$

where

$$\tilde{s}_f(k) = s(k) - \hat{s}_f(k) \quad (10.227)$$

denotes the filtering error. From (10.224) and (10.225), the residual depends linearly on the observations, $r(m)$, $0 \leq m \leq k$. From (10.226), the residual is orthogonal to $r(m)$, $0 \leq m \leq k-1$. Therefore, $\delta(k)$ must be proportional to the innovations process,

$$\delta(k) = C\tilde{r}(k), \quad (10.228)$$

where

$$C = E\{\delta(k)\tilde{r}(k)\} / \tilde{P}(k), \quad (10.229)$$

From (10.207),

$$\begin{aligned} E\{\delta(k)\tilde{r}(k)\} &= E\{\delta(k)r(k)\} - E\{\delta(k)\hat{s}_p(k)\} \\ &= E\{w^2(k)\} = \sigma_w^2, \end{aligned} \quad (10.230)$$

so

$$C = \sigma_w^2 / \tilde{P}(k). \quad (10.231)$$

We make the following substitutions into (10.222)

$$\tilde{r}(k) = \frac{\tilde{P}(k)}{\sigma_w^2} \delta(k) = \frac{\tilde{P}(k)}{\sigma_w^2} (r(k) - \hat{s}_f(k)) \quad (10.232)$$

and

$$\tilde{r}(k) = r(k) - \hat{s}_p(k). \quad (10.233)$$

Then,

$$l(\mathbf{R}) = \left[\sum_{k=0}^K r(k) \left(\frac{\hat{s}_f(k) + \hat{s}_p(k)}{2} \right) - \frac{1}{2} \sum_{k=0}^K \hat{s}_f(k) \hat{s}_p(k) \right]. \quad (10.234)$$

The optimum receiver is shown in Figure 10.21. This result is analogous to the known signal result in (3.92) where

$$l(\mathbf{R}) = \sum_{k=1}^K r(k)s(k) - \frac{1}{2} \sum_{k=1}^K s(k)^2. \quad (10.235)$$

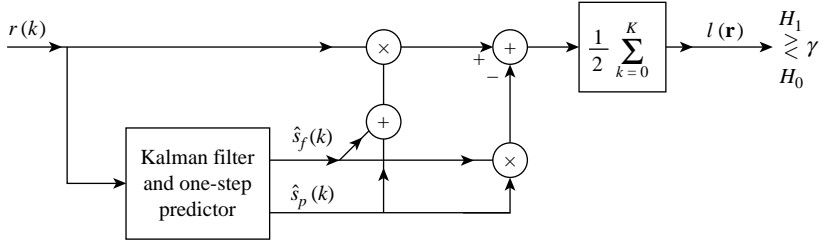


Figure 10.21: Optimum detector using causal estimators.

We see that the causal Gaussian detector replaces $s(k)$ by the arithmetic mean in the first term

$$\hat{s}_{\text{ari}}(k) \triangleq \frac{1}{2} (\hat{s}_f(k) + \hat{s}_p(k)) \quad (10.236)$$

and the geometric mean in the second term

$$\hat{s}_{\text{geo}}(k) \triangleq (\hat{s}_f(k)\hat{s}_p(k))^{\frac{1}{2}}. \quad (10.237)$$

The causal estimators can be implemented with a realizable FIR Wiener filter or a Kalman filter.

The last step in the detector is to specify the threshold. For a Neyman–Pearson test we let γ_3 control the P_F . For a Bayes test, we need to evaluate the threshold using the expression in (3.331). The last two terms on the right-hand side of (3.331) are

$$\ln |\mathbf{K}_1| - \ln |\sigma_w^2 \mathbf{I}| = \ln \left(\frac{|\mathbf{K}_r|}{\sigma_w^{2K}} \right) = \sum_{k=1}^{K+1} \ln \left(1 + \frac{\lambda_k^s}{\sigma_w^2} \right) \triangleq \ln D_F(\sigma_w^2), \quad (10.238)$$

where D_F as the same terms has the Fredholm determinant but the sum goes to $K + 1$ instead of ∞ .

$$\gamma_3 = 2 \ln \eta + \ln D_F(\sigma_w^2). \quad (10.239)$$

From (10.218),

$$|\mathbf{K}_r^{-1}| = |\mathbf{F}^T \mathbf{F}| = \prod_{k=0}^K \tilde{P}^{-1}(k) \quad (10.240)$$

because \mathbf{F} is lower triangular with diagonal terms $\tilde{P}^{-1/2}(k)$. Thus,

$$|\mathbf{K}_r| = \prod_{k=0}^K \tilde{P}(k) \quad (10.241)$$

and

$$\ln D_F(\sigma_w^2) = \sum_{k=0}^K \ln \left(\frac{\tilde{P}(k)}{\sigma_w^2} \right). \quad (10.242)$$

The $\tilde{P}(k)$ terms are computed in the Kalman filter.

We now have a complete implementation of the optimum detector including the Bayes threshold using Kalman filters. Several examples are given in the problems. Note that we have already found the necessary filters for a number of processes in Chapter 9.

We studied the performance for block processing in Section 3.3. To use these results, we must find the eigenvalues of the process over the interval $[0, K]$. Alternatively, we can use the bounds on P_D and P_F developed in Section 2.4 and that use the log of the moment-generating function.

For our model,⁷

$$\begin{aligned} \ln \int_{-\infty}^{\infty} \cdots \int_{-\infty}^{\infty} & \left\{ \left[\prod_{k=1}^{K+1} \frac{1}{(2\pi(\sigma_w^2 + \lambda_k^s))^{1/2}} \exp \left(-\frac{1}{2} \sum_{k=1}^K \frac{R_n^2}{\lambda_k^s + \sigma_w^2} \right) \right]^s \right\} \\ & \times \left\{ \prod_{k=1}^K \frac{1}{(2\pi\sigma_w^2)^{1/2}} \exp \left(-\frac{1}{2} \sum_{k=1}^K \frac{R_n^2}{\sigma_w^2} \right) \right\}^{1-s} dR_1 \cdots dR_K. \end{aligned} \quad (10.243)$$

Performing the integration, we have

$$\mu(s) = \frac{1}{2}(1-s) \sum_{k=1}^{K+1} \ln \left(1 + \frac{\lambda_k^s}{\sigma_w^2} \right) - \frac{1}{2} \sum_{k=1}^{K+1} \ln \left(1 + \frac{(1-s)\lambda_k^s}{\sigma_w^2} \right). \quad (10.244)$$

The first sum is given by (10.242). In order to evaluate the second term, we implement a Kalman filter with the white noise level set at $\sigma_w^2/(1-s)$.

We can then write

$$\mu(s) = \frac{1}{2}(1-s) \sum_{k=1}^{K+1} \ln \left(\frac{\tilde{P}(k)}{\sigma_w^2} \right) - \frac{1}{2} \sum_{k=1}^{K+1} \ln \left(\frac{\tilde{P}(k; 1-s)}{\sigma_w^2/(1-s)} \right). \quad (10.245)$$

In order to use the bound in (2.217), we need $\dot{\mu}(s)$, so we can use (2.216)

$$s_* : \dot{\mu}(s_*) = \gamma_*. \quad (10.246)$$

An analytic expression for $\dot{\mu}(s)$ is not available. One possible approach to run the error covariance of the Kalman filter for multiple values of s and find the derivative numerically. Note that this can be done in advance because it does not depend on the data. Assuming we can compute $\dot{\mu}(s)$, then we have the following bounds. From (2.217),

$$P_F \leq e^{\mu(s_*) - s_* \dot{\mu}(s_*)}, \quad (10.247)$$

and from (2.223)

$$P_M \leq e^{\mu(s_*) - (1-s_*) \dot{\mu}(s_*)}, \quad (10.248)$$

If we can compute $\dot{\mu}(s)$, then we can use the approximate formulas in (2.238) and (2.241). Note that, if K is large, we can use the steady-state value of $\tilde{P}(k) = \tilde{P}_\infty$ in (10.245).

⁷This discussion is taken from Section 2.2.1 of DEMT-III [Van71b, Van01b]

In Problem 10.3.1, we simulate the algorithm for the case when the signal is the AR(1) process in Example 9.9. We have already implemented the Kalman filter and the one-step predictor (Example 9.16).

10.3.3 Summary

In this section, we developed optimum detectors for discrete-time random processes. In Section 10.3.1, we considered Gaussian random processes that we characterized using their second moments. In this case, we can denote the K received samples by a vector \mathbf{r} and use the results from Chapters 3–5 directly. We can also use the detector in Figure 10.21 and we can use an FIR Wiener filter and one-step Wiener predictor to generate the necessary signals in the detector.

In Section 10.3.2, we considered Gaussian random processes that we characterized using a state-variable representation. We derived the discrete-time version corresponding to the Schweppe detector in continuous time. This is an important implementation in many applications.

10.4 SUMMARY

In this chapter, we considered the problem of detecting a sample function of a Gaussian random process in additive Gaussian noise. We considered both continuous-time and discrete-time random processes. In both cases, we assumed that the additive noise was a sample function of white Gaussian noise process whose height was known. In Chapters 8 and 9, we developed whitening filters so the white noise assumption does not lose any generality.

In Section 10.2, we considered continuous-time processes and developed two approaches. In the first approach, we generate a finite-dimensional vector by either temporal sampling or a Karhunen–Loëve expansion. We can choose the dimension large enough to give a vector model that is a good approximation to the original problem. We can then apply the detection theory results to solve the problem using block data processing. We revisited this approach in Section 10.3.1 and provided tables showing where to find the results in Chapters 3–5.

In the second approach in Section 10.2, we used the Karhunen–Loëve approach that we introduced in Chapter 6 and used for deterministic signals in Chapter 7. This led to integral equations that we must solve to find the optimum detector. However, these equations are identical to the equations developed in Chapter 8 for the optimum smoothing filter $h_{ou}(t, u)$ or the optimum realizable filter $h_{or}(t, u)$ and we can use the solution techniques developed in Chapter 8 to specify the optimum detector. The key result was (10.68)

$$l_R = l_R(T) = \frac{1}{N_0} \int_0^T [2r(t)\hat{s}_r(t) - \hat{s}_r^2(t)] dt \quad (10.249)$$

and the optimum detector was shown in Figure 10.8. This enabled us to find the optimum detector for any signal model where we could find the optimum linear filter. All of the models in Chapter 8 were applicable.

We also derived explicit solutions for three important classes of applications:

1. **State-variable models:** The key result was Canonical Realization 3 in Figure 10.9 where $\hat{s}_r(t)$ is generated using Kalman filters. This implementation allows us to treat nonstationary processes. We only considered the case of scalar observations, but an analogous detector can be derived for vector observations.
2. **S PLOT model:** For processes characterized by their spectrum, the key result was the filter-squarer detector in Figure 10.11a, which is obtained by spectrum factorization. For state-variable processes with constant matrices, the implementation in Figure 10.11b is the steady-state version of the detector in Figure 10.9.
3. **Low-rank kernel model:** When the signal process has a finite number of eigenvalues, the optimum detector reduces to a model in Chapter 3 and all of the results are directly applicable.

In Section 10.3, we considered discrete-time processes. In this case, if we use block processing, then an exact solution has already been developed in Chapter 3 if the process is modeled using a second moment characterization. In many cases, the process is described using a state-variable characterization. In this case, we can use an implementation using realizable estimates. The key results are the likelihood result in (10.234) and the detector in Figure 10.21.

This chapter concludes our discussion of the hierarchy of problems we set out to solve in Chapter 1. In Chapter 11, we give a brief summary of our results.

10.5 PROBLEMS

P10.2.2 Optimum Continuous-Time Receivers

Problem 10.2.2.1. Consider the model described by (10.1)–(10.6). Assume that $m(t)$ is not zero. Derive an estimator–correlator receiver analogous to that in Figure 10.5 for this case.

Problem 10.2.2.2. Consider the function $h_1(t, t|z)$, which is specified by the equation

$$zh_1(t, u|z) + \int_{T_i}^{T_f} h_1(t, y|z) K_s(y, u) dy = K_s(t, u), \quad T_i \leq t, u \leq T_f.$$

Verify that the following equation

$$\sum_{i=1}^{\infty} \ln \left(1 + \frac{2\lambda_i^s}{N_0} \right) = \int_0^{2/N_0} dz \int_{T_i}^{T_f} h_1(t, t|z) dt,$$

is true.

Problem 10.2.2.3. Consider the waveform

$$r(\tau) = n_c(\tau) + w(\tau), \quad T_i \leq \tau \leq t,$$

where $n_c(\tau)$ can be generated as the output of a dynamic system,

$$\begin{aligned}\dot{\mathbf{x}}(t) &= \mathbf{F}(t)\mathbf{x}(t) + \mathbf{G}(t)u(t), \\ n_c(t) &= \mathbf{C}(t)\mathbf{x}(t),\end{aligned}$$

driven by a statistically independent white noise $u(t)$. Denote the MMSE realizable estimate of $n_c(\tau)$ as $\hat{n}_c(\tau)$. Prove that the process

$$r_*(t) \triangleq r(t) - \hat{n}_c(t) = r(t) - \mathbf{C}(t)\hat{\mathbf{x}}(t)$$

is white.

Problem 10.2.2.4. The received waveforms on the two hypotheses are

$$\begin{aligned}H_1 : r(t) &= s(t) + w(t), \quad 0 \leq t \leq T, \\ H_0 : r(t) &= w(t), \quad 0 \leq t \leq T.\end{aligned}$$

The process $w(t)$ is a sample function of a white Gaussian random process with spectral height $N_0/2$. The process $s(t)$ is a Wiener process that is statistically independent of $w(t)$.

$$\begin{aligned}s(0) &= 0, \\ E[s^2(t)] &= \sigma^2 t.\end{aligned}$$

1. Find the likelihood ratio test.
2. Draw a realization of the optimum receiver. Specify all components completely.

Problem 10.2.2.5. The received waveforms on the two hypotheses are

$$\begin{aligned}H_1 : r(t) &= s(t) + w(t), \quad 0 \leq t \leq T, \\ H_0 : r(t) &= w(t), \quad 0 \leq t \leq T.\end{aligned}$$

The process $w(t)$ is a sample function of a white Gaussian random process with spectral height $N_0/2$. The signal $s(t)$ is a sample function of a Gaussian random process and can be written as

$$s(t) = at, \quad 0 \leq t,$$

where a is a zero-mean Gaussian random variable with variance σ_a^2 . Find the optimum receiver. Specify all components completely.

Problem 10.2.2.6. Repeat Problem 10.2.2.5 for the case in which

$$s(t) = at + b, \quad 0 \leq t,$$

where a and b are statistically independent, zero-mean Gaussian random variables with variances σ_a^2 and σ_b^2 , respectively.

Problem 10.2.2.7.

1. Repeat Problem 10.2.2.6 for the case in which a and b are statistically independent Gaussian random variables with means m_a and m_b and variances σ_a^2 and σ_b^2 , respectively.
2. Consider four special cases of part 1:
 - (i) $m_a = 0$,
 - (ii) $m_b = 0$,
 - (iii) $\sigma_a^2 = 0$,
 - (iv) $\sigma_b^2 = 0$.

Verify that the receiver for each of these special cases reduces to the correct structure.

Problem 10.2.2.8. Consider the model in Problem 10.2.2.5. Assume that $s(t)$ is a piecewise constant waveform,

$$s(t) = \begin{cases} b_1, & 0 < t \leq T_0, \\ b_2, & T_0 < t \leq 2T_0, \\ b_3, & 2T_0 < t \leq 3T_0, \\ \vdots \\ b_n, & (n-1)T_0 < t \leq nT_0, \end{cases}$$

The b_i are statistically independent, zero-mean Gaussian random variables with variances equal to σ_b^2 . Find the optimum receiver.

Problem 10.2.2.9. Consider the model in Problem 10.2.2.5. Assume

$$s(t) = \sum_{i=1}^K a_i t^i, \quad 0 \leq t,$$

where the a_i are statistically independent random variables with variances σ_i^2 . Find the optimum receiver.

Problem 10.2.2.10. Reexamine Problems 10.2.2.5–10.2.2.9. If you implemented the optimum receiver using Canonical Realization No. 3 and state variables, go back and find an easier procedure.

Problem 10.2.2.11 Consider the model in Problem 10.2.2.4. Assume that $s(t)$ is a segment of a stationary zero-mean Gaussian process with an n th-order Butterworth spectrum

$$S_s(\omega : n) = \frac{2nP}{k} \frac{\sin(\pi/2n)}{(\omega/k)^{2n} + 1}, \quad n = 1, 2, \dots$$

1. Review the state representation for these processes in Chapter 8. Make certain that you understand the choice of initial conditions.
2. Draw a block diagram of the optimum receiver.

Problem 10.2.2.12. On both hypotheses there is a sample function of a zero-mean Gaussian white noise process with spectral height $N_0/2$. On H_1 , the signal is equally likely to be a sample function from any one of M zero-mean Gaussian processes. We denote the covariance function of the i th

process as $K_{s_i}(t, u)$, $i = 1, \dots, M$. Thus,

$$\begin{aligned} H_1 : r(t) &= s_i(t) + w(t), \quad T_i \leq t \leq T_f, \quad \text{with probability } \frac{1}{M}, \quad i = 1, \dots, M. \\ H_0 : r(t) &= w(t), \quad T_i \leq t \leq T_f. \end{aligned}$$

Find the optimum Bayes receiver to decide which hypothesis is true.

Problem 10.2.2.13. Consider the vector version of the simple binary detection problem. The received waveforms on the two hypotheses are

$$\begin{aligned} H_1 : \mathbf{r}(t) &= \mathbf{s}(t) + \mathbf{w}(t), \quad T_i \leq t \leq T_f, \\ H_0 : \mathbf{r}(t) &= \mathbf{w}(t), \quad T_i \leq t \leq T_f, \end{aligned} \quad (\text{P.1})$$

where $\mathbf{s}(t)$ and $\mathbf{w}(t)$ are sample functions of zero-mean, statistically independent, N -dimensional, vector Gaussian processes with covariance matrices

$$\mathbf{K}_s(t, u) \triangleq E[\mathbf{s}(t)\mathbf{s}^T(u)] \quad (\text{P.2})$$

and

$$\mathbf{K}_w(t, u) \triangleq E[\mathbf{w}(t)\mathbf{w}^T(u)] = \frac{N_0}{2} \delta(t - u) \mathbf{I}. \quad (\text{P.3})$$

1. Derive the optimum receiver for this problem.
2. Derive the equations specifying the three canonical realizations. Draw a block diagram of the three realizations.
3. Consider the special case in which

$$\mathbf{K}_s(t, u) = K_s(t, u) \mathbf{I}. \quad (\text{P.4})$$

Explain what the condition in (P.4) means. Give a physical situation that would lead to this condition. Simplify the optimum receiver in part 1.

4. Consider the special case in which

$$\mathbf{K}_s(t, u) = K_s(t, u) \begin{bmatrix} 1 & 1 & \cdots & 1 \\ 1 & 1 & & 1 \\ \vdots & \ddots & \ddots & \vdots \\ \vdots & & \ddots & \vdots \\ 1 & & & 1 \end{bmatrix}. \quad (\text{P.5})$$

Repeat part 3.

Problem 10.2.2.14. Consider the model in Problem 10.2.2.13. The covariance of $\mathbf{w}(t)$ is

$$\mathbf{K}_w(t, u) = \mathbf{N} \delta(t - u)$$

where \mathbf{N} is a nonsingular matrix.

1. Repeat parts 1 and 2 of Problem 10.2.2.13.
2. Why do we assume that \mathbf{N} is nonsingular?
3. Consider the special case in which

$$\mathbf{K}_s(t, u) = K_s(t, u)\mathbf{I}$$

and \mathbf{N} is diagonal. Simplify the results in part 1.

Problem 10.2.2.15. Consider the model in Problem 10.2.2.13. Assume

$$E[\mathbf{s}(t)] = \mathbf{m}(t).$$

All of the other assumptions in Problem 10.2.2.13 are still valid. Repeat Problem 10.2.2.13.

Problem 10.2.2.16. Consider the Rayleigh channel model that we encountered previously in Chapter 7.

On H_1 we transmit a bandpass signal,

$$s_t(t) \triangleq \sqrt{2P}f(t)\cos\omega_c t,$$

where $f(t)$ is a slowly varying function (the envelope of the signal). The received signal is

$$H_1 : r(t) = \sqrt{2P}b_1(t)f(t)\cos\omega_c t + \sqrt{2P}b_2(t)f(t)\sin\omega_c t + w(t), \quad T_i \leq t \leq T_f.$$

The channel processes $b_1(t)$ and $b_2(t)$ are statistically independent, zero-mean Gaussian processes whose covariance functions are $K_b(t, u)$. The additive noise $w(t)$ is a sample function of a statistically independent, zero-mean Gaussian process with spectral height $N_0/2$. The channel processes vary slowly compared to ω_c . On H_0 , only white noise is present.

1. Derive the optimum receiver for this model of the Rayleigh channel.
2. Draw a filter-squared realization for the optimum receiver.
3. Draw a state-variable realization of the optimum receiver. Assume that

$$S_b(\omega) = \frac{2k\sigma_b^2}{\omega^2 + k^2}.$$

Problem 10.2.2.17. The model for a Rician channel is the same as that in Problem 10.2.2.16, except that

$$E[b_1(t)] = m$$

instead of zero. Repeat Problem 10.2.2.16 for this case.

P10.2.3. Performance of Optimum Receivers

Problem 10.2.3.1.

1. Consider the model in Problem 10.2.2.4. Evaluate $\mu(s)$ for this system.
2. Define

$$\gamma \triangleq \sqrt{\frac{2\sigma^2}{N_0}}.$$

Simplify the expression in part 1 for the case in which $\gamma T \gg 1$.

Problem 10.2.3.2.

1. Evaluate $\mu(s)$ for the system in Problem 10.2.2.5.
2. Plot the result as a function of s .
3. Find P_F and P_D .

Problem 10.2.3.3. Evaluate $\mu(s)$ for the system in Problem 10.2.2.6.

Problem 10.2.3.4. Evaluate $\mu(s)$ for the system in Problem 10.2.2.7.

Problem 10.2.3.5.

1. Evaluate $\mu(s)$ for the system in Problem 10.2.2.8.
2. Evaluate P_F and P_D .

Problem 10.2.3.6. Consider the system in Problem 10.2.2.13.

1. Assume that (P.4) in part 3 is valid. Find $\mu(s)$ for this special case.
2. Assume that (P.5) in part 4 is valid. Find $\mu(s)$ for this special case.
3. Derive an expression for $\mu(s)$ for the general case.

Problem 10.2.3.7. Find $\mu(s)$ for the Rayleigh channel model in Problem 10.2.2.16.

Problem 10.2.3.8. Find $\mu(s)$ for the Rician channel model in Problem 10.2.2.17.

P10.2.4 State Variable Realization

The first problem implements the simulation for Example 10.1. The second set of problems deals with the Butterworth family of random processes. The state-variable model is given in Example 8.11. The coefficients for the model are shown in Figure 8.31 for $n = 1-7$. The corresponding $H(s)$ function is given in Problem 9.3.2.3.12. In each problem, simulate the optimum receiver for $P_F = 10^{-5}$ and plot P_D versus \bar{E}_r/N_0 for the same values of kT as in Problem 10.2.4.1.

Problem 10.2.4.1 Simulate the optimum receiver in Figure 10.9 with the threshold set to give $P_F = 10^{-5}$. Plot P_D as \bar{E}_r/N_0 for $kT = 0.1, 1.0, 10.0$, and 100 .

Problem 10.2.4.2 $m = 2, \dots, 7$. Consider the Butterworth spectrum with order m .

P10.2.5 Stationary Process, Long Observation Time (SPLIT) Receiver

Unless otherwise indicated, you should assume that the SPLIT condition is valid in all problems in this section.

Problem 10.2.5.1. Consider the model in (10.1). Assume that $s(t)$ is a Wiener process such that

$$K_s(t, u) = \sigma^2 \min [t, u]$$

and

$$s(0) = 0.$$

1. Find the optimum receiver.
2. Evaluate $\mu_\infty(s)$.
3. Compare your result with that in Problem 10.2.2.4.

Problem 10.2.5.2. Consider the model in (10.1). Assume that

$$S_s(\omega) = \frac{2n P}{k} \frac{\sin(\pi/2n)}{1 + (\omega/k)^{2n}}.$$

Evaluate $\mu_\infty(s)$ for this case.

Problem 10.2.5.3. (continuation). In Problem 10.2.5.2, we derived an expression for $\mu_\infty(s)$. Fix s at some value s_0 , where

$$0 < s_0 < 1.$$

Study the behavior of $\mu_\infty(s_0)$ as a function of n . Consider different values of s_0 . How does

$$\Lambda_B \triangleq \frac{2\pi P}{kN_0}$$

enter into the discussion?

P10.3 Detection of Discrete-Time Gaussian Processes

Problem 10.3.1. Consider the model in (10.195)–(10.198) and (10.203)–(10.205). Assume the signal is the AR(1) process in Example 9.9. Simulate the algorithm in (10.234) and plot P_D versus $K\sigma_s^2/\sigma_w^2$ for $P_F = 10^{-5}$.

Problem 10.3.2. Consider the model in Problem 10.3.1. Assume the signal is the Butterworth process, BW(2,2), described in Case 1 of Example 9.11. Define

$$\bar{E}_r = PK$$

1. Fixed the optimum detector.
2. Simulate the detector and plot
 - (a) ROC for $2\bar{E}_r/N_0 = 0$ and 3dB.
 - (a) P_D vs P_F versus $2\bar{E}_r/N_0$ for $P_F = 10^{-5}$.

Problem 10.3.3. Repeat Problem 10.3.1 for the Butterworth process, BW(N,N), described in Case 2 of Example 9.11.

11

Epilogue

In this chapter, we provide a brief review of the key results developed in the book and reemphasize some of the fundamental themes carried throughout the book.

The book was divided into four topical areas:

- a. Chapters 2–5; Classical Detection and Estimation Theory
- b. Chapter 6; Representation of Random Processes
- c. Chapters 7 and 10; Detection of Signals and Estimation of Signal Parameters
- d. Chapters 8 and 9; Linear Estimation of Random Processes.

In the next four sections, we review the key results in each of these areas. In Section 11.5, we offer some general comments about the field.

11.1 CLASSICAL DETECTION AND ESTIMATION THEORY

11.1.1 Classical Detection Theory

In Chapter 2, we derived the essential detection theory results that provided the basis for the detection problems in the remainder of the book.

We began our discussion in Section 2.2 by considering the simple binary hypothesis testing problem. There were several key results:

- a. Using either a Bayes criterion or a Neyman–Pearson criterion, we find that the optimum test is a likelihood ratio test,

$$\Lambda(\mathbf{R}) = \frac{p_{\mathbf{r}|H_1}(\mathbf{R}|H_1)}{p_{\mathbf{r}|H_0}(\mathbf{R}|H_0)} \stackrel{H_1}{\gtrless} \eta. \quad (11.1)$$

Thus, regardless of the dimensionality of the observation space, the test consists of comparing a scalar variable $\Lambda(\mathbf{R})$ with a threshold.

- b. In many cases, construction of the LRT can be simplified if we can identify a sufficient statistic. Geometrically, this statistic is just that coordinate in a suitable coordinate

Detection, Estimation, and Modulation Theory, Second Edition. Harry L. Van Trees, Kristine L. Bell with Zhi Tian. © 2013 John Wiley & Sons, Inc. Published 2013 by John Wiley & Sons, Inc.

system that describes the observation space that contains *all* the information necessary to make a decision. (See (2.74)–(2.76)).

- c. A complete description of the LRT performance was obtained by plotting the conditional probabilities P_D and P_F as the threshold η was varied. The resulting ROC could be used to calculate the Bayes risk for any set of costs. In many cases, only one value of the threshold is of interest and a complete ROC is not necessary.

In Section 2.3, we introduced the M hypotheses problem. The key results were:

- a. The dimension of the decision space is no more than $M - 1$. The boundaries of the decision regions are hyperplanes in the $(\Lambda_1, \dots, \Lambda_{M-1})$ plane.
- b. The optimum test is straightforward to find. From (2.156), we compute

$$\beta_i(\mathbf{R}) = \sum_{j=0}^{M-1} c_{ij} \Pr(H_j | \mathbf{R}), \quad i = 0, 1, \dots, M-1, \quad (11.2)$$

and choose the smallest. The error probabilities were frequently difficult to compute.

- c. A particular test of importance is the minimum total probability of error test. Here, we compute the *a posteriori* probability of each hypothesis $\Pr(H_i | \mathbf{R})$ and choose the largest.

In Sections 2.2 and 2.3, we dealt primarily with problems in which we could derive the structure of the optimum test and obtain relatively simple analytic expressions for the receiver operating characteristic or the error probability. In Section 2.4, we developed bounds and approximate expressions for the error probabilities in the large group of problems where an exact solution is difficult. The key function in these results was the logarithm of the moment generating function of the likelihood ratio. From (2.204),

$$\mu(s) = \ln \int_{-\infty}^{\infty} [p_{\mathbf{r}|H_1}(\mathbf{R}|H_1)]^s [p_{\mathbf{r}|H_0}(\mathbf{R}|H_0)]^{1-s} d\mathbf{R}. \quad (11.3)$$

The function $\mu(s)$ plays a central role in all of the bounds and approximate expressions that are derived in Section 2.4. It is straightforward to calculate when the components of \mathbf{r} on the two hypotheses are statistically independent. Then,

$$\mu_i(s) = \ln \int_{-\infty}^{\infty} [p_{\mathbf{r}_i|H_1}(\mathbf{R}_i|H_1)]^s [p_{\mathbf{r}_i|H_0}(\mathbf{R}_i|H_0)]^{1-s} d\mathbf{R}_i, \quad i = 1, \dots, N, \quad (11.4)$$

and

$$\mu(s) = \sum_{i=1}^N \mu_i(s). \quad (11.5)$$

In many applications of interest, it is necessary to simulate the detection algorithm in order to evaluate the performance. In Section 2.5, we gave a brief introduction to Monte Carlo simulation. A key issue is the number of trials needed to have a desired level of confidence in the result. In most systems of interest, the desired P_F is very small (e.g., $P_F \leq 10^{-6}$ is frequently required). In these cases, the number of trials required to obtain a reasonable

confidence level is prohibitively large. We introduced a technique called “importance sampling” that provided a dramatic reduction in the number of trials. The key function in our approach was the $\mu(s)$ developed in Section 2.4.

11.1.2 General Gaussian Detection

In Chapter 3, we did a comprehensive study of the general Gaussian detection problem, which is an accurate model for a large number of applications. Our emphasis was on using the model to solve a wide variety of communications, radar, and sonar problems.

In Section 3.1, we derived the likelihood ratio for the real and circular complex Gaussian model. From (3.57),

$$\begin{aligned} l(\mathbf{R}) &= \frac{1}{2}(\mathbf{R} - \mathbf{m}_0)^T \mathbf{Q}_0 (\mathbf{R} - \mathbf{m}_0) - \frac{1}{2}(\mathbf{R} - \mathbf{m}_1)^T \mathbf{Q}_1 (\mathbf{R} - \mathbf{m}_1) \\ &\stackrel{H_1}{\gtrless} \ln \eta + \frac{1}{2} \ln |\mathbf{K}_1| - \frac{1}{2} \ln |\mathbf{K}_0| \triangleq \gamma_1 \end{aligned} \quad (11.6)$$

for the real case, and from (3.83)

$$l(\tilde{\mathbf{R}}) = (\tilde{\mathbf{R}} - \tilde{\mathbf{m}}_0)^H \tilde{\mathbf{Q}}_0 (\tilde{\mathbf{R}} - \tilde{\mathbf{m}}_0) - (\tilde{\mathbf{R}} - \tilde{\mathbf{m}}_1)^H \tilde{\mathbf{Q}}_1 (\tilde{\mathbf{R}} - \tilde{\mathbf{m}}_1) \stackrel{H_1}{\gtrless} \ln \eta + \ln |\tilde{\mathbf{K}}_1| - \ln |\tilde{\mathbf{K}}_0| \triangleq \gamma'_1 \quad (11.7)$$

for the circular complex case.

We derived the $\mu(s)$ function that was the key to performance bounds and simulation using importance sampling. From (3.68),

$$\mu(s) = \frac{s(s-1)}{2} \Delta \mathbf{m}^T \mathbf{K}(s)^{-1} \Delta \mathbf{m} + \frac{s}{2} \ln |\mathbf{K}_0| + \frac{1-s}{2} \ln |\mathbf{K}_1| - \frac{1}{2} \ln |\mathbf{K}(s)| \quad (11.8)$$

for the real case, and from (3.84),

$$\mu(s) = s(s-1) \Delta \tilde{\mathbf{m}}^H \tilde{\mathbf{K}}(s)^{-1} \Delta \tilde{\mathbf{m}} + s \ln |\tilde{\mathbf{K}}_0| + (1-s) \ln |\tilde{\mathbf{K}}_1| - \ln |\tilde{\mathbf{K}}(s)| \quad (11.9)$$

for the circular complex case.

These results gave us everything needed to implement the optimum test and to simulate its performance. The next three sections developed a sequence of models corresponding to important applications. By studying various models, we could find analytic performance results that enable us to understand how the components of the models affect performance.

In Section 3.2, we considered the case in which the covariance matrices on the two hypotheses are equal. We found that the likelihood ratio test was

$$l(\mathbf{R}) \triangleq \Delta \mathbf{m}^T \mathbf{Q} \mathbf{R} \stackrel{H_1}{\gtrless} \gamma_2 \quad (11.10)$$

for the real case. It is a linear multiplication of the observed Gaussian vector, so it is a scalar Gaussian variable and the performance was completely determined by using

$$d^2 = \Delta \mathbf{m}^T \mathbf{Q} \Delta \mathbf{m} \quad (11.11)$$

in (2.84) and in (2.85). Similar results were obtained for the circular complex case in (3.108), (3.118), and (3.119).

This model was encountered in Chapter 7 in communication systems in which the means represent the signal transmitted on the two hypotheses and the transmission channel attenuates the signal and adds interference and noise. We found analytic performance results and showed how to design optimum signals for a specific interference. We introduced eigendecomposition in order to better understand our analytic results.

In Section 3.3, we considered the case in which the mean vectors on the hypotheses are equal. We found that the sufficient statistic was a quadrature form. From (3.331),

$$l(\mathbf{R}) \triangleq \mathbf{R}^T \Delta \mathbf{Q} \mathbf{R} \stackrel{H_1}{\gtrless} \stackrel{H_0}{\gtrless} \gamma_3 \quad (11.12)$$

for the real case, and from (3.333)

$$l(\tilde{\mathbf{R}}) \triangleq \tilde{\mathbf{R}}^H \Delta \tilde{\mathbf{Q}} \tilde{\mathbf{R}} \stackrel{H_1}{\gtrless} \stackrel{H_0}{\gtrless} \gamma'_3 \quad (11.13)$$

for the complex case.

In order to analyze the performance, we did an eigendecomposition. We showed that by a sequence of whitening and diagonalizing transformations we could change any model to the case where $\Delta \mathbf{Q}$ was a diagonal matrix whose components were functions of the eigenvalues.

For the real Gaussian case, we found the characteristic function of $l(\mathbf{R})$ on both hypotheses but had to do a numerical integration to find the probability densities needed to calculate P_D , P_F , or $\Pr(\epsilon)$. For the complex case, we found a closed form expression for the probability densities and calculated P_D and P_F using standard mathematical functions. This model was used in Chapter 7 to study communications and radar systems where the channel (or target) introduces a complex Gaussian multiplier onto the transmitted signals (referred to as the Rayleigh model). It was used in Chapter 10 to study radar, sonar, and radio astronomy problems where we are trying to detect a sample from a Gaussian random process (either real or complex) in the presence of Gaussian interference and noise.

In Section 3.4, we returned to the general Gaussian case. We found that the sufficient statistic was the sum of a linear term and a quadratic term, which are correlated in most cases. From (3.503),

$$l(\mathbf{R}) = \frac{1}{2} \mathbf{R}^T \Delta \mathbf{Q} \mathbf{R} + \Delta \mathbf{g}^T \mathbf{R}. \quad (11.14)$$

Except for some special cases, we could not find analytic expressions for the performance. We resorted to the bounds and approximations using $\mu(s)$ and to the simulations using importance sampling developed in Section 2.5. The closed form expression for $\mu(s)$ enabled us to find the appropriate tilted density. This model was encountered in Chapter 7 in communications and radar systems where the channel (or target) introduces a complex Gaussian multiplier with a nonzero mean (the specular component) onto the transmitted signals (referred to as the Rician model).

In Section 3.5, we extended these models to the M hypotheses case. We could always find the optimum Bayes test. Except for special cases, the performance is difficult to evaluate and we resorted to bounds on the $\Pr(\epsilon)$.

In retrospect, the reader should appreciate why Chapter 3 was long and detailed. When we studied physical applications in Chapters 7 and 10, our strategy was to map the waveforms into a finite-dimensional space where we had already solved the problem in Chapter 3.

11.1.3 Classical Parameter Estimation

In Chapter 4, we discussed parameter estimation for nonrandom and random parameters. For nonrandom parameters, we emphasized maximum likelihood estimates and the Cramér–Rao bound. For random parameters, we emphasized Bayesian estimates and the Bayesian Cramér–Rao bound.

In Section 4.2, we considered scalar parameters. For nonrandom parameter estimation the key results were:

- a. The maximum likelihood estimate $\hat{a}_{\text{ml}}(\mathbf{R})$ is the value of A where the likelihood function $p_{\mathbf{r}|a}(\mathbf{R}|A)$ achieves its maximum.
- b. The variance of any unbiased estimate of A is lower bounded by the CRB.
- c. Under suitable regularity conditions, $\hat{a}_{\text{ml}}(\mathbf{R})$ is unbiased and approaches the CRB asymptotically.
- d. If the parameter is embedded in the signal in a nonlinear manner, then a threshold behavior will occur as the SNR or number of observations decreases.
- e. If the likelihood function is in the exponential family, then a number of useful properties are available.

For Bayesian estimation, the key results are:

- a. For a quadratic cost function, the MMSE estimate is the conditional mean of the *a posteriori* density.
- b. The MAP estimate is the mode of the *a posteriori* density. We often use it when $\hat{a}_{\text{ms}}(\mathbf{R})$ is difficult to find.
- c. The MSE of any Bayesian estimator is lower bounded by the Bayesian Cramér–Rao bound.
- d. The MMSE estimate, $\hat{a}_{\text{ms}}(\mathbf{R})$, and the MAP estimate, $\hat{a}_{\text{map}}(\mathbf{R})$, approach the ML estimate, $\hat{a}_{\text{ml}}(\mathbf{R})$, asymptotically and their MSE is lower bounded by the ECRB.
- e. Bayesian estimates exhibit a similar threshold behavior to ML estimates as the SNR or the number of observations decreases.
- f. The exponential family plays a key role in specifying the conjugate prior.

In Section 4.3, we developed estimators for nonrandom and random parameter vectors. The results were extensions of the results for scalar parameters in Section 4.2, and all of the comments in the preceding paragraph can be adapted to the vector case.

The difficulty arises in implementing the estimation procedures. In the case of a K -dimensional nonrandom parameter vector, we must search over a K -dimensional space to find $\hat{\mathbf{a}}_{\text{ml}}(\mathbf{R})$. For a K -dimensional random parameter, a similar search is required to find $\hat{\mathbf{a}}_{\text{map}}(\mathbf{R})$ and a K -fold integration is required to find $\hat{\mathbf{a}}_{\text{ms}}(\mathbf{R})$. In Chapter 5, we discussed several iterative techniques that can be used in certain applications.

For nonrandom parameters, the CRB provides a lower bound on the covariance matrix of any unbiased estimate. If the components of the observation \mathbf{r} are statistically independent given \mathbf{a} ,

$$p_{\mathbf{r}|\mathbf{a}}(\mathbf{R}|\mathbf{A}) = \prod_{i=1}^N p_{r_i|\mathbf{a}}(R_i|\mathbf{A}) \quad (11.15)$$

then the CRB can be evaluated by one-dimensional integrations. In the special case where $p_{\mathbf{r}|\theta}(\mathbf{R}|\mathbf{A})$ is multivariate Gaussian, we can always achieve independence by a whitening transformation.

For random parameters, the BCRB provides a lower bound of the mean-square error matrix of any estimator and the ECRB provides a lower bound on the asymptotic mean-square error. These bounds require the integration of $\mathbf{J}_F(\mathbf{A})$ or $\mathbf{J}_F^{-1}(\mathbf{A})$ over $p_{\mathbf{a}}(\mathbf{A})$.

In many applications, some of the parameters in the vector are unwanted and can be treated as nuisance parameters. We developed various techniques to solve this problem that depended on how \mathbf{a}_w and \mathbf{a}_u were modeled (random or nonrandom).

In other applications, the parameter vector contains random and nonrandom components, \mathbf{a}_r and \mathbf{a}_{nr} . We developed a hybrid estimator and a hybrid bound.

We expanded our case study of frequency estimation introduced in Section 4.2 to include joint frequency and phase estimation. As expected, we also observed the threshold behavior when we jointly estimated frequency and phase. This motivated our development of global Bayesian bounds in Section 4.4.

In Section 4.4, we developed the framework for a family of global Bayesian bounds based on the covariance inequality. We derived the Weiss–Weinstein bound and applied it to our frequency estimation case study. The WWB or a combined BCRB–WWB appear to provide the best prediction of performance for bounds in the covariance inequality family. As demonstrated by the example, choosing the test points to use in the bound requires some skill.

We also discussed the method of interval estimation, which is an approximation rather than a bound. It is motivated by an algorithm that could be used to find the maximum of the *a posteriori* density. It appears to provide good results in many applications.

We have included this discussion of global bounds in this introductory text because we feel that understanding the threshold effect and the effect of “outliers” on the system performance is an essential part of the system design problem. In addition, the issue seems to be ignored in much of the literature.

In Section 4.5, we discussed the composite hypothesis problem that we encounter frequently in practice. For random parameters with known densities, the optimum procedure is easy to formulate but may be hard to implement in practice.

For nonrandom parameters, we introduced the idea of *uniformly most powerful* (UMP) tests and the conditions for their existence. We developed the *generalized likelihood ratio test* (GLRT) and used it in many subsequent applications. We considered the case in which the white noise variance was unknown and found that the GLRT had a constant false alarm rate (CFAR) character. This result led to a brief discussion of invariant tests, but we did not pursue the topic.

11.1.4 General Gaussian Estimation

In Chapter 5, we studied the general Gaussian estimation problem in detail. The model is defined by the transition probability density in (5.1),

$$p_{\mathbf{r}|\theta}(\mathbf{R}|\theta) = \frac{1}{(2\pi)^{N/2} |\mathbf{K}(\theta)|^{1/2}} \exp \left\{ -\frac{1}{2} [\mathbf{R} - \mathbf{m}(\theta)]^T \mathbf{K}^{-1}(\theta) [\mathbf{R} - \mathbf{m}(\theta)] \right\}. \quad (11.16)$$

In Section 5.2, we considered nonrandom parameters. For the general case, this required a minimization over a D -dimensional space as shown in (5.54)

$$\hat{\theta}_{ml}(\mathbf{R}) = \operatorname{argmin}_{\theta} \left\{ \ln |\mathbf{K}(\theta)| + [\mathbf{R} - \mathbf{m}(\theta)]^T \mathbf{K}^{-1}(\theta) [\mathbf{R} - \mathbf{m}(\theta)] \right\}. \quad (11.17)$$

Before considering the solution to the minimization problem, we developed compact expressions for the Cramér–Rao bound. For real observation and real parameters, the information matrix, $\mathbf{J}_F(\boldsymbol{\theta})$ was given by (5.72)

$$\mathbf{J}_{Fij}(\boldsymbol{\theta}) = \frac{1}{2} \operatorname{tr} \left[\mathbf{K}^{-1}(\boldsymbol{\theta}) \frac{\partial \mathbf{K}(\boldsymbol{\theta})}{\partial \theta_i} \mathbf{K}^{-1}(\boldsymbol{\theta}) \frac{\partial \mathbf{K}(\boldsymbol{\theta})}{\partial \theta_j} \right] + \left[\frac{\partial \mathbf{m}^T(\boldsymbol{\theta})}{\partial \theta_i} \mathbf{K}^{-1}(\boldsymbol{\theta}) \frac{\partial \mathbf{m}(\boldsymbol{\theta})}{\partial \theta_j} \right] \quad (11.18)$$

and the CRB equaled $\mathbf{J}_F^{-1}(\boldsymbol{\theta})$.

For complex observations and real parameters, $\mathbf{J}_F(\boldsymbol{\theta})$ was given by (5.82)

$$\mathbf{J}_{Fij}(\boldsymbol{\theta}) = \operatorname{tr} \left[\tilde{\mathbf{K}}^{-1}(\boldsymbol{\theta}) \frac{\partial \tilde{\mathbf{K}}(\boldsymbol{\theta})}{\partial \theta_i} \tilde{\mathbf{K}}^{-1}(\boldsymbol{\theta}) \frac{\partial \tilde{\mathbf{K}}(\boldsymbol{\theta})}{\partial \theta_j} \right] + 2\Re \left[\frac{\partial \tilde{\mathbf{m}}^H(\boldsymbol{\theta})}{\partial \theta_i} \tilde{\mathbf{K}}^{-1}(\boldsymbol{\theta}) \frac{\partial \tilde{\mathbf{m}}(\boldsymbol{\theta})}{\partial \theta_j} \right]. \quad (11.19)$$

For complex observations and complex parameters, \mathbf{J}_F was given by (5.139)

$$\mathbf{J}_F(\boldsymbol{\theta}) = 2 \begin{bmatrix} \Re[\tilde{\mathbf{V}}^H \tilde{\mathbf{K}}^{-1} \tilde{\mathbf{V}}] & -\Im[\tilde{\mathbf{V}}^H \tilde{\mathbf{K}}^{-1} \tilde{\mathbf{V}}] \\ \Im[\tilde{\mathbf{V}}^H \tilde{\mathbf{K}}^{-1} \tilde{\mathbf{V}}] & \Re[\tilde{\mathbf{V}}^H \tilde{\mathbf{K}}^{-1} \tilde{\mathbf{V}}] \end{bmatrix}. \quad (11.20)$$

For multiple IID observations, $\mathbf{J}_F(\boldsymbol{\theta})$ was given by (5.84)

$$\mathbf{J}_F = K \mathbf{J}_F(\boldsymbol{\theta}; k). \quad (11.21)$$

It is important to remember that the CRBs are bounds on the covariance matrix and assume an unbiased estimate. For biased estimates, we added an additional term, which assumed that the bias is known.

In Section 5.2.4, we studied the Fisher linear Gaussian model which is defined by (5.85) for real parameters (or (5.86) for the complex case),

$$\mathbf{r} \sim N(\mathbf{V}\boldsymbol{\theta}_m, \mathbf{K}), \quad (11.22)$$

where the covariance matrix \mathbf{K} is known.

Then, the ML estimate is given by (5.95) for the real case

$$\hat{\boldsymbol{\theta}}_{\text{ml}}(\mathbf{R}) = [\mathbf{V}^T \mathbf{V}]^{-1} \mathbf{V}^T \mathbf{R} = \mathbf{V}^\dagger \mathbf{R} \quad (11.23)$$

and (5.130) for the complex case

$$\hat{\boldsymbol{\theta}}_{\text{ml}}(\mathbf{R}) = [\tilde{\mathbf{V}} \tilde{\mathbf{K}}^{-1} \tilde{\mathbf{V}}]^{-1} \tilde{\mathbf{V}}^H \tilde{\mathbf{K}}^{-1} \tilde{\mathbf{R}}. \quad (11.24)$$

The estimates are unbiased and efficient. Their error covariance matrix satisfies the CRB with equality.

We considered several important examples to illustrate the behavior. In Section 5.2.4.3, we considered low-rank interference and developed an eigenspace version of the ML estimator. The structure provides an efficient implementation and also allows us to implement suboptimum reduced-rank estimators.

In Section 5.2.5, we considered separable models. These models are defined by (5.223) for the real observation and the real parameter case

$$\mathbf{r} \sim N(\mathbf{V}(\boldsymbol{\theta}_{nl})\boldsymbol{\theta}_l, \mathbf{K}) \quad (11.25)$$

and (5.225) for the complex observation case.

We find an explicit expression for $\hat{\boldsymbol{\theta}}_l(\mathbf{R})$ and used it to create a compressed likelihood function. Thus, $\hat{\boldsymbol{\theta}}_{nl}(\mathbf{R})$ is given by (5.236)

$$\hat{\boldsymbol{\theta}}_{nl}(\mathbf{R}) = \underset{\boldsymbol{\theta}_{nl}}{\operatorname{argmax}} \left\{ \|\mathbf{P}_{\mathbf{V}(\boldsymbol{\theta}_{nl})}\mathbf{R}\|^2 \right\} = \underset{\boldsymbol{\theta}_{nl}}{\operatorname{argmax}} \left\{ \mathbf{R}^T \mathbf{P}_{\mathbf{V}(\boldsymbol{\theta}_{nl})} \mathbf{R} \right\}, \quad (11.26)$$

so we have reduced the problem to a maximization of a D -dimensional space instead of a $2D$ -dimensional space.

In Section 5.2.6, we considered the problem where the mean was known and the unknown parameters were in the covariance matrix. In general, $\hat{\boldsymbol{\theta}}_c$ is given by maximizing

$$\hat{\boldsymbol{\theta}}_{c,\text{ml}}(\mathbf{R}) = \underset{\boldsymbol{\theta}_c}{\operatorname{argmax}} \left\{ -\frac{1}{2} \ln |\mathbf{K}(\boldsymbol{\theta})| - \frac{1}{2} (\mathbf{R}^T \mathbf{K}^{-1}(\boldsymbol{\theta}) \mathbf{R}) \right\}. \quad (11.27)$$

We considered several cases in which the single parameter θ_c corresponded to the noise power or the 2×1 vector $\boldsymbol{\theta}_c$ corresponded to the signal and noise powers. We were able to obtain closed form expressions for the ML estimates.

In Section 5.2.7, we studied the model in which the observations satisfied the linear Gaussian model but the covariance matrix also contained unknown parameters. We found that we could project \mathbf{R} into the signal subspace to create a compressed log-likelihood function. For the white noise case with unknown variance σ_w^2 , the compressed log-likelihood function was given by (5.399)

$$l(\hat{\boldsymbol{\theta}}_{m,\text{ml}}(\mathbf{R}), \sigma_w^2; \mathbf{R}) = -\frac{N}{2} \ln \sigma_w^2 - \frac{1}{2\sigma_w^2} \{[\mathbf{P}_{\mathbf{V}}^\perp \mathbf{R}]^T [\mathbf{P}_{\mathbf{V}}^\perp \mathbf{R}]\} \quad (11.28)$$

and we could obtain an explicit answer for $\hat{\boldsymbol{\theta}}_{m,\text{ml}}(\mathbf{R})$ and $\hat{\sigma}_{w,\text{ml}}^2(\mathbf{R})$.

For the general case, we had to find the maximum of $l(\hat{\boldsymbol{\theta}}_{m,\text{ml}}(\mathbf{R}, \boldsymbol{\theta}_c), \boldsymbol{\theta}_c; \mathbf{R})$ as given by (5.413)

$$\begin{aligned} l(\hat{\boldsymbol{\theta}}_{m,\text{ml}}(\mathbf{R}, \boldsymbol{\theta}_c), \boldsymbol{\theta}_c; \mathbf{R}) &= -\frac{1}{2} \ln |\mathbf{K}(\boldsymbol{\theta}_c)| \\ &\quad - \frac{1}{2} \mathbf{R}^T \left\{ \mathbf{K}^{-1}(\boldsymbol{\theta}_c) - \mathbf{K}^{-1}(\boldsymbol{\theta}_c) \mathbf{V} [\mathbf{V}^T \mathbf{K}^{-1}(\boldsymbol{\theta}_c) \mathbf{V}]^{-1} \mathbf{V}^T \mathbf{K}^{-1}(\boldsymbol{\theta}_c) \right\} \mathbf{R}. \end{aligned} \quad (11.29)$$

In Section 5.2.8, we developed computational algorithms to solve minimization or maximization problems such as the one in (5.416). We developed three algorithms: gradient techniques, the alternating projection (AP) algorithm, and the expectation–maximization (EM) algorithm, and gave examples to illustrate their performance. The key to good performance is to start with a good set of initial conditions so that we do not converge to an incorrect local maximum or minimum.

In Section 5.2.9, we discussed equivalent algorithms and showed that the minimum variance distortionless response (MVDR) algorithm and the least squares algorithm invented by Gauss are equivalent to the ML estimator when the Fisher linear Gaussian model is applicable.

In Section 5.2.10, we provided an introduction to the important problem of the sensitivity of the optimum processor to the case where the actual model is different from the assumed model. We considered a specific example and showed that by imposing a quadratic constraint on the weight vector

$$\tilde{\mathbf{h}}^H \tilde{\mathbf{h}} \leq T_0, \quad (11.30)$$

we obtain a new estimator that introduces an artificially high noise level by loading the diagonal matrix. The resulting estimator is

$$\tilde{\mathbf{h}}^H = [\tilde{\mathbf{v}}_s^H (\tilde{\mathbf{K}} + \sigma_L^2 \mathbf{I}) \tilde{\mathbf{v}}_s]^{-1} \tilde{\mathbf{v}}_s^H [\tilde{\mathbf{K}} + \sigma_L^2 \mathbf{I}]^{-1}. \quad (11.31)$$

Diagonal loading is widely used to develop robust processors.

In Section 5.3.1, we considered random parameters and developed MAP and MMSE estimators, the Bayesian Cramér–Rao bound, and the ECRB.

The Bayesian log-likelihood function is given by (5.602)

$$l_B(\boldsymbol{\theta}; \mathbf{R}) = -\frac{1}{2} \ln |\mathbf{K}(\boldsymbol{\theta}_c)| - \frac{1}{2} \{[\mathbf{R} - \mathbf{m}(\boldsymbol{\theta}_m)]^T \mathbf{K}^{-1}(\boldsymbol{\theta}_c) [\mathbf{R} - \mathbf{m}(\boldsymbol{\theta}_m)]\} + \ln p_{\boldsymbol{\theta}}(\boldsymbol{\theta}) + \zeta, \quad (11.32)$$

which is just the nonrandom $l(\boldsymbol{\theta}; \mathbf{R})$ plus the log of the prior density.

The Bayesian information matrix is

$$\mathbf{J}_B = E_{\boldsymbol{\theta}}[\mathbf{J}_F(\boldsymbol{\theta})] + \mathbf{J}_P, \quad (11.33)$$

where \mathbf{J}_P is given by (5.605). The expected CRB is given by

$$\text{ECRB} = E_{\boldsymbol{\theta}}[\mathbf{J}_F^{-1}(\boldsymbol{\theta})] \geq \mathbf{J}_B^{-1} = \text{BCRB}. \quad (11.34)$$

The ECRB is important in the asymptotic case where

$$\lim_{K \rightarrow \infty} \hat{\boldsymbol{\theta}}_{\text{map}}(\mathbf{R}) \rightarrow \hat{\boldsymbol{\theta}}_{\text{ml}}(\mathbf{R}). \quad (11.35)$$

We considered several examples where the conjugate priors were applicable and found explicit solutions.

In Section 5.3.2, we considered the Bayesian linear Gaussian model defined by

$$\mathbf{r} = \mathbf{V}\boldsymbol{\theta} + \mathbf{n}. \quad (11.36)$$

This expression has the same form as the Fisher linear Gaussian model. However, the parameter $\boldsymbol{\theta}$ is a random $D \times 1$ vector and the *a priori* density is the conjugate prior which is $N(\mathbf{m}_{\boldsymbol{\theta}}, \mathbf{K}_{\boldsymbol{\theta}})$. For the zero-mean case, the MAP and MMSE estimates are given by

$$\hat{\boldsymbol{\theta}}_{\text{ms}}(\mathbf{R}) = \hat{\boldsymbol{\theta}}_{\text{map}}(\mathbf{R}) = \mathbf{K}_{\boldsymbol{\theta}} \mathbf{V}^T [\mathbf{V} \mathbf{K}_{\boldsymbol{\theta}} \mathbf{V}^T + \mathbf{K}_{\mathbf{n}}]^{-1} \mathbf{R}. \quad (11.37)$$

The estimates are Bayesian efficient and the MSE matrix is given by the Bayesian Cramér–Rao bound,

$$\boldsymbol{\Sigma}_{\epsilon} = \mathbf{J}_B^{-1} = [\mathbf{K}_{\boldsymbol{\theta}}^{-1} + \mathbf{V}^T \mathbf{K}_{\mathbf{n}}^{-1} \mathbf{V}]^{-1}, \quad (11.38)$$

which can also be written as

$$\boldsymbol{\Sigma}_{\epsilon} = \mathbf{K}_{\boldsymbol{\theta}} - \mathbf{K}_{\boldsymbol{\theta}} \mathbf{V}^T [\mathbf{V} \mathbf{K}_{\boldsymbol{\theta}} \mathbf{V}^T + \mathbf{K}_{\mathbf{n}}]^{-1} \mathbf{V} \mathbf{K}_{\boldsymbol{\theta}} \quad (11.39)$$

We also showed that if we defined the Bayesian linear Gaussian problem by requiring $p_{\theta|R}(\theta|R)$ to be Gaussian, then

$$\hat{\theta}_{\text{map}}(R) = \hat{\theta}_{\text{ms}}(R) = K_{\theta|R} K_{R}^{-1} R \triangleq HR. \quad (11.40)$$

In Section 5.4, we developed sequential Bayes estimation. The result was the sequential MAP/MMSE estimator shown in Figure 5.28 and specified by (5.727)–(5.731).

- (1) Initialize the algorithm with

$$\hat{\theta}(0) = m_\theta \quad (11.41)$$

and

$$\Sigma(0) = K_\theta. \quad (11.42)$$

- (2) Compute $G(1)$ using (5.729) with $k = 1$,

$$G(k) = \Sigma(k-1) V^T(k) [V(k) \Sigma(k-1) V^T(k) + K_n]^{-1}. \quad (11.43)$$

- (3) Compute $\hat{\theta}(1)$ using (5.730) with $k = 1$,

$$\hat{\theta}(k) = \hat{\theta}(k-1) + G(k) [R(k) - V(k) \hat{\theta}(k-1)]. \quad (11.44)$$

- (4) Compute $\Sigma(1)$ using (5.731) with $k = 1$,

$$\Sigma(k) = [I - G(k)V(k)]\Sigma(k-1). \quad (11.45)$$

- (5) Continue the iteration for $k = 2, 3, 4, \dots$

This sequential MAP/MMSE algorithm is important when the observations are received sequentially. In addition, it sets the stage for the discrete-time Kalman filter that we discussed in detail in Chapter 9.

We also showed that the recursive least squares algorithm had the same structure but required an initial block estimate using D samples to initialize the algorithm.

11.2 REPRESENTATION OF RANDOM PROCESSES

In the classical detection and estimation problems, the observations were modeled as finite-dimensional vectors. In the parameter estimation problem, the parameters and observations were characterized by a finite-dimensional vector.

In order to study the physical applications where the processes that we are observing are continuous functions of time (and space in some cases), we needed to find a technique to transform the problem into a model where the observations are vectors (perhaps with countably infinite dimensions) and the sufficient statistics are finite dimensional vectors.

There are several ways to characterize the random processes that facilitate the desired transformation. Chapter 6 considered real Gaussian random processes that were characterized by their mean and covariance functions. We then expanded the sample functions in a

series expansion

$$x(t) = \lim_{N \rightarrow \infty} \sum_{i=1}^N x_i \phi_i(t), \quad 0 \leq t \leq T, \quad (11.46)$$

where the $\phi_i(t)$ are a CON set and l.i.m. denotes limit in the mean. By choosing the coordinate function to satisfy

$$\lambda \phi(t) = \int_{T_i}^{T_f} K(t, u) \phi(u) du, \quad T_i \leq t \leq T_f, \quad (11.47)$$

the x_i were statistically-independent Gaussian random variables. This expansion is the Karhunen–Loëve expansion that has a number of useful properties. It is the continuous-time analog to the vector eigenequation in Chapter 3

$$\lambda \Phi = \mathbf{K} \Phi, \quad (11.48)$$

where \mathbf{K} was a symmetric nonnegative definite matrix. All of the insights that we had developed in Chapter 3 about working in an eigenspace carried over to the continuous problem. An important property was Mercer's theorem

$$K_x(t, u) = \sum_{i=1}^{\infty} \lambda_i \phi_i(t) \phi_i(u), \quad 0 \leq t, u \leq T, \quad (11.49)$$

where the convergence is uniform for $0 \leq t, u \leq T$. It allowed us to derive a number of important results.

Although we discussed analytic techniques for solving (11.49), in most cases, we would solve it numerically. In a number of important applications that we discussed in Chapters 7 and 10, the signal covariance function has a finite number of eigenvalues and the problem reduces to a classical problem in Chapters 2 or 4.

We introduced the problem of finding the MMSE estimate of the sample functions of a random process using a linear filter. The resulting integral equation is

$$K_d(t, u) - \int_0^T h_o(t, v) K_r(u, v) dv = 0, \quad \begin{aligned} 0 &\leq t \leq T \\ 0 &< u < T. \end{aligned} \quad (11.50)$$

For the case of a signal in white noise, we could write $h_o(t, u)$ and the MS error $\xi_{P_o}(t)$ using the eigenfunctions and eigenvalues,

$$h_o(t, u) = \sum_{i=1}^{\infty} \frac{\lambda_i}{\lambda_i + N_0/2} \phi_i(t) \phi_i(u) \quad (11.51)$$

and

$$\xi_{P_o}(t) = \frac{N_0}{2} \sum_{i=1}^{\infty} \frac{\lambda_i}{\lambda_i + N_0/2} \phi_i^2(t) \quad 0 \leq t \leq T, \quad (11.52)$$

The solution in (11.51) represents a practical solution only when the number of significant eigenvalues is small. In most cases, the solution in terms of eigenfunctions will be useful only for theoretical purposes. In Chapter 8, we developed more practical solutions. In addition,

we showed that, when the processes were Gaussian, the output of $h_o(t, u)$ was the optimum Bayes estimate.

We also introduced SPLOT (stationary process, long observation time) processes. In this case, the eigenvalues are approximated by

$$\lambda_n \simeq S_x(f_n) = S_x(nf_0) \quad (11.53)$$

and the eigenfunctions are approximated by

$$\phi_n(t) \simeq \frac{1}{\sqrt{T}} e^{+j2\pi f_n t} \quad -\frac{T}{2} \leq t \leq \frac{T}{2}. \quad (11.54)$$

These approximations allow us to obtain solutions in a number of whitening applications.

We used the Karhunen–Loève representation in Chapters 7 and 10 to solve a large number of communications and radar/sonar problems.

11.3 DETECTION OF SIGNALS AND ESTIMATION OF SIGNAL PARAMETERS

In Chapters 7 and 10, we applied our detection and estimation results from Chapters 2–5 to a number of important applications in the communications, radar, and sonar areas. By using the representation of continuous random processes developed in Chapter 6, we were able to go directly to a sufficient statistic and the likelihood ratio test.

In Section 7.2, we studied detection and estimation in white Gaussian noise. The simplest detection problem was binary detection of a known signal in the presence of white Gaussian noise. The optimum receiver could be realized as a matched filter or a correlation receiver. The performance depended only on the normalized distance between the two signal points in the decision space. This distance was characterized by the signal energies, their correlation coefficient, and the spectral height of the additive noise.

$$d^2 = \frac{2}{N_0} \left(E_1 + E_0 - 2\rho\sqrt{E_1 E_0} \right). \quad (11.55)$$

The resulting errors are

$$P_F = \text{erfc}_* \left(\frac{\ln \eta}{d} + \frac{d}{2} \right), \quad (11.56)$$

$$P_M = \text{erfc}_* \left(\frac{\ln \eta}{d} - \frac{d}{2} \right). \quad (11.57)$$

For equally likely hypotheses and a minimum $\Pr(\epsilon)$ criterion, the total error probability is

$$\Pr(\epsilon) = \text{erfc}_* \left(\frac{d}{2} \right) \leq \left(\frac{2}{\pi d^2} \right)^{\frac{1}{2}} e^{-d^2/8}. \quad (11.58)$$

For equal energy signals, a correlation coefficient of -1 was optimum. In all cases, the signal shape was unimportant. The performance was insensitive to the detailed assumptions of the model.

The solution for the M signal problem followed easily. The receiver structure consisted of at most $M - 1$ matched filters or correlators. Except for a few special cases, performance

calculations for arbitrary cost assignments and *a priori* probabilities were unwieldy. Therefore, we devoted our attention to minimum probability of error decisions. For arbitrary signal sets, the calculation of the probability of error was still tedious. For orthogonal and nonorthogonal equally correlated signals, simple expressions could be found and evaluated numerically. Simple bounds on the error probability were derived that were useful for certain ranges of parameter values.

$$\Pr(\epsilon) \leq \frac{M-1}{\sqrt{2\pi(E/N_0)}} \exp\left(-\frac{E}{2N_0}\right). \quad (11.59)$$

In Section 7.3, we generalized the simple detection problem by allowing a nonwhite additive Gaussian noise component. We considered two approaches to the problem. In the first approach, we found a reversible whitening filter that was the continuous-time analog to the whitening matrices in Chapter 3. We saw that it could be implemented using the optimum linear filter developed in Chapter 6. Later, in Chapter 8, we derived a realizable whitening filter. The whitening filter lead to the introduction of an inverse kernel,

$$Q_n(z, v) = \int_{T_i}^{T_f} h_w(u, z) h_w(u, v) du \quad T_i < z, v < T_f. \quad (11.60)$$

and the relationship,

$$\delta(z - v) = \int_{T_i}^{T_f} K_n(x, z) Q_n(v, x) dx \quad T_i < z, v < T_f. \quad (11.61)$$

which showed that $Q_n(v, x)$ is just the functional analog of the inverse of the covariance matrix. All of these results could also be established directly using the Karhunen–Loëve expansion. Thus, all of the applications in Sections 7.2 and 7.3 reduced to the Gaussian model in Section 3.2.

In Section 7.4, we further generalized the model by allowing for uncertainties in the signal even in the absence of noise. For the case in which these uncertainties could be parameterized by random variables with known densities, the desired procedure was clear. We considered in detail the random phase case and the random amplitude and phase case. In the random phase problem, we introduced the idea of a simple estimation system that measured the phase angle and used the measurement in the detector. This gave us a method of transition from the known signal case to situations, such as the radar problem, in which the phase is uniformly distributed. For binary signals, we found that the optimum signal set depended on the quality of the phase measurement. As we expected, the optimum correlation coefficient ranged from $\rho = -1$ for perfect measurement to $\rho = 0$ for the uniform density.

The random amplitude and phase case enabled us to model a number of communication links that exhibited Rayleigh and Rician fading. The Rayleigh channel was a special case of the circular complex Gaussian model in Section 3.3, so all of the results were directly applicable. We examined channel measurement receivers and perfect measurement receivers. We found that perfect measurement offered a 6 dB improvement. However, even with perfect measurement, the channel fading caused the error probability to decrease linearly with \bar{E}_r/N_0 instead of exponentially as in a nonfading channel. We revisited this problem in Chapter 10 and found that we could achieve exponential decrease by time diversity,

frequency diversity, or interleaving. The Rician channel was a special case of the general Gaussian problem in Section 3.4, so all of the results applied.

We studied the estimation problem in Sections 7.2 and 7.6. The *basic* ideas in the *estimation* problem were similar, and the entire formulation up through the likelihood function was identical. For linear estimation, the resulting receiver structures were identical to those obtained in the simple binary problem. The mean-square estimation error in white noise depended only on E/N_0 .

The nonlinear estimation problem gave rise to a number of issues. The first difficulty was that a sufficient statistic did not exist, which meant that the mapping from the observation space to the estimation space depended on the parameter we were trying to estimate. In some cases, this could be accommodated easily. In others, approximate techniques were necessary. The resulting function in the estimation space had a number of local maxima and we had to choose the absolute maximum. Given that we were near the correct maximum, the mean-square error could be computed easily. The error could be reduced significantly over the linear estimation error by choosing a suitable signaling scheme. If we tried to reduce the error too far, however, a new phenomenon developed, which we termed threshold. In the cascade approximation to the optimum estimator the physical mechanism for the occurrence of a threshold was clear. The first stage chose the wrong interval in which to make its local estimate. In the continuous realization (such as range estimation) the occurrence was clear but a quantitative description was more difficult. Because the actual threshold level will depend on the signal structure, the quantitative results for the particular example discussed are less important than the realization that whenever we obtain an error decrease without an increase in signal energy or a decrease in noise level a threshold effect will occur at some signal-to-noise level.

In Chapter 10, we considered the problem of detecting a sample function of Gaussian random process in additive Gaussian noise. We considered both continuous-time and discrete-time random processes. In both cases, we assumed that the additive noise was a sample function of white Gaussian noise process whose height was known. In Chapters 8 and 9, we had developed whitening filters, so the white noise assumption does not lose any generality.

In Section 10.2, we considered continuous-time processes and developed two approaches. In the first approach, we generated a finite-dimensional vector by either temporal sampling or a Karhunen–Loëve expansion. We can choose the dimension large enough to give a vector model that is a good approximation to the original problem. We can then apply the detection theory results to solve the problem using block data processing. We revisited this approach in Section 10.3.1 and provided tables showing where to find the results in Chapters 3–5.

In the second approach in Section 10.2, we used the Karhunen–Loëve approach that we introduced in Chapter 6 and used for deterministic signals in Chapter 7. This led to integral equations that we must solve to find the optimum detector. However, these equations are identical to the equations developed in Chapter 8 for the optimum smoothing filter $h_{ou}(t, u)$ or the optimum realizable filter $h_{or}(t, u)$, so we could use the solution techniques developed in Chapter 8 to specify the optimum detector. The key result was (10.68)

$$l_R = l_R(T) = \frac{1}{N_0} \int_0^T [2r(t)\hat{s}_r(t) - \hat{s}_r^2(t)] dt \quad (11.62)$$

and the optimum detector was shown in Figure 10.8. This enabled us to find the optimum detector for any signal model where we could find the optimum linear filter. All of the models in Chapter 8 were applicable.

We also derived explicit solutions for three important classes of applications:

- a. **State-variable models:** The key result was Canonical Realization 3 in Figure 10.9 where $\hat{s}_r(t)$ is generated using Kalman filters. This implementation allows us to treat nonstationary processes. We only considered the case of scalar observations, but an analogous detector can be derived for vector observations.
- b. **SPLIT model:** For processes characterized by their spectrum, the key result was the filter-squerer detector in Figure 10.11a, which is obtained by spectrum factorization. For state-variable processes with constant matrices, the implementation in Figure 10.11b is the steady-state version of the detector in Figure 10.9.
- c. **Low-rank kernel model:** When the signal process has a finite number of eigenvalues, the optimum detector reduces to a model in Chapter 3 and all of the results are directly applicable.

In Section 10.3, we considered discrete-time processes. In this case, if we use block processing, then an exact solution has already been developed in Chapter 3 if the process is modeled using a second moment characterization. In many cases, the process is described using a state-variable characterization. In this case, we can use an implementation using realizable estimates. The key results are the likelihood result in (10.234) and the detector in Figure 10.21.

11.4 LINEAR ESTIMATION OF RANDOM PROCESSES

The last topical area is the linear estimation of random processes. Linear estimation of continuous-time processes was developed in Chapter 8 and linear estimation of discrete-time processes was developed in Chapter 9. In both cases, when the processes were Gaussian, the linear estimators were the optimum Bayes estimators for a mean-square error criterion.

The chapters could have been read independently and we anticipate that most readers only read one in detail. Although the developments in the two chapters were parallel, the two chapters differed in depth. Chapter 8 developed Wiener and Kalman filter theory and worked a number of representative examples to illustrate the behavior of the filters. However, it did not discuss some of the issues that occur when the filters are implemented in actual applications. This discussion was deferred to Chapter 9 because in most cases, the filter will be implemented digitally. Chapter 9 provided a more comprehensive discussion of the implementation of the filters.

Section 8.1 developed the equations specifying the optimum linear filter for processes described by a second-moment characterization. The key result was the integral equation (8.3) whose solution was the impulse response of the optimum filter

$$K_{dr}(t, u) = \int_{T_i}^{T_f} h_o(t, \tau) K_r(\tau, u) d\tau \quad T_i < u < T_f, \quad (11.63)$$

where $K_{dr}(t, u)$ is the cross-covariance function between the desired signal $d(t)$ and the observed input $r(u)$.

The mean-square error of the optimum was given by (8.21)

$$\xi_{P_o}(t) \triangleq E[e_o^2(t)] = K_d(t, t) - \int_{T_i}^{T_f} h_o(t, \tau) K_{dr}(t, \tau) d\tau. \quad (11.64)$$

An important result was that the error at time t using the optimum linear processor is uncorrelated with the input $r(u)$ at every point in the observation interval. This property follows directly from (8.15). Thus,

$$E[e_o(t)r(u)] = 0, \quad T_i < u < T_f. \quad (11.65)$$

If the Gaussian assumption was satisfied then $e_0(t)$ and $r(u)$ were statistically independent.

Section 8.2 developed the Wiener filter for the case in which $T_i = -\infty$ and the random processes were stationary. In this case, (11.63) reduces to (8.78)

$$K_{dr}(\tau) = \int_0^\infty h_o(v) K_r(\tau - v) dv, \quad 0 < \tau < \infty, \quad (11.66)$$

which is the Wiener–Hopf equation. We solved (11.66) using spectrum factorization. The optimum realizable filter was given by (8.98)

$$H_o(j\omega) = \left[\frac{1}{G^+(j\omega)} \right] \left[\frac{S_{dr}(j\omega)}{[G^+(j\omega)]^*} \right]_+ \quad (11.67)$$

and the minimum mean-square error was given by (8.128)

$$\xi_P = K_d(0) - \int_0^\infty K_{dz}^2(t) dt. \quad (11.68)$$

For the special case where the desired signal is $s(t)$ and the noise is white noise, a closed form expression for ξ_P was given by (8.177)

$$\xi_P = \frac{N_0}{2} \int_{-\infty}^{\infty} \ln \left[1 + \frac{S_s(\omega)}{N_0/2} \right] \frac{d\omega}{2\pi}, \quad (11.69)$$

which is twice the mutual information (as defined by Shannon) between $r(t)$ and $s(t)$.

We also considered optimum unrealizable filters which are given by (8.144)

$$H_{ou}(j\omega) = \frac{S_{dr}(j\omega)}{S_r(\omega)}, \quad (11.70)$$

and the mean-square error is given by (8.147)

$$\xi_u = \int_{-\infty}^{\infty} \frac{S_d(\omega) S_r(\omega) - |S_{dr}(j\omega)|^2}{S_r(\omega)} \frac{d\omega}{2\pi}. \quad (11.71)$$

The essential points to remember when discussing unrealizable filters are the following:

1. The mean-square error using an unrealizable linear filter ($T_f = \infty$) provides a lower bound on the mean-square error for any realizable linear filter. It corresponds to the *irreducible* (or infinite delay) error. The computation of ξ_u (11.71) is usually easier than the computation of ξ_P (11.68) or (11.69). Therefore, it is a logical preliminary calculation even if we are interested only in the realizable filtering problem.
2. We can build a realizable filter whose performance approaches the performance of the unrealizable filter by allowing delay in the output. We can obtain a mean-square error that is arbitrarily close to the irreducible error by increasing this delay. From the practical standpoint a delay of several times the reciprocal of the effective bandwidth of $[S_a(\omega) + S_n(\omega)]$ will usually result in a mean-square error close to the irreducible error.

The second part of the chapter studied the continuous-time Kalman filter. The processes were characterized by linear differential equations (8.231a, b)

$$\dot{\mathbf{x}}(t) = \mathbf{F}(t)\mathbf{x}(t) + \mathbf{G}(t)\mathbf{u}(t), \quad (11.72)$$

$$\mathbf{y}(t) = \mathbf{C}(t)\mathbf{x}(t). \quad (11.73)$$

The resulting Kalman filter was specified by three equations:

Estimator Equation

$$\frac{d\hat{\mathbf{x}}(t)}{dt} = \mathbf{F}(t)\hat{\mathbf{x}}(t) + \mathbf{K}_g(t)[\mathbf{r}(t) - \mathbf{C}(t)\hat{\mathbf{x}}(t)]. \quad (11.74)$$

Gain Equation

$$\mathbf{K}_g(t) = \xi_P(t)\mathbf{C}^T(t)\mathbf{R}^{-1}(t). \quad (11.75)$$

Variance Equation

$$\frac{d\xi_P(t)}{dt} = \mathbf{F}(t)\xi_P(t) + \xi_P(t)\mathbf{F}^T(t) - \xi_P(t)\mathbf{C}^T(t)\mathbf{R}^{-1}(t)\mathbf{C}(t)\xi_P(t) + \mathbf{G}(t)\mathbf{Q}\mathbf{G}^T(t) \quad (11.76)$$

with initial conditions $\hat{\mathbf{x}}(0)$ and $\xi_P(0)$.

If \mathbf{F} , \mathbf{G} , \mathbf{C} , and \mathbf{R} were constants and the system generation model were stable, the Kalman filter approached a steady-state filter which was identical to the Wiener filter.

We also derived a state-variable implementation of a realizable whitening filter that could be used in the colored noise detector of Chapter 7.

We described several generalizations; the Kalman predictor and the Kalman filter with lag, but did not develop them in detail. We gave a complete discussion in Chapter 9.

Section 8.4 introduced Bayesian estimation of non-Gaussian models. Our objective was to provide just enough background to motivate the development the extended Kalman filter and the Bayesian Crame-Rao bound.

The extended Kalman filter was given by (8.405)–(8.407).

Estimator Equation

$$\dot{\hat{\mathbf{x}}}(t) = \mathbf{f}(\hat{\mathbf{x}}(t), t) + \mathbf{K}_g(t) [\mathbf{r}(t) - \mathbf{c}(\hat{\mathbf{x}}(t), t)] \quad (11.77)$$

with $\hat{\mathbf{x}}(0) \sim N(\hat{\mathbf{x}}_0, \xi_0)$.

Gain Equation

$$\mathbf{K}_g(t) = \xi_P(t) \tilde{\mathbf{C}}^T(\hat{\mathbf{x}}(t), t) \mathbf{R}^{-1}(t) \quad (11.78)$$

MSE Equation

$$\begin{aligned} \dot{\xi}_P(t) &= \tilde{\mathbf{F}}(\hat{\mathbf{x}}(t), t) \xi_P(t) + \xi_P(t) \tilde{\mathbf{F}}^T(\hat{\mathbf{x}}(t), t) + \mathbf{G}(t) \mathbf{Q}(t) \mathbf{G}^T(t) \\ &\quad - \xi_P(t) \tilde{\mathbf{C}}^T(\hat{\mathbf{x}}(t), t) \mathbf{R}^{-1}(t) \tilde{\mathbf{C}}(\hat{\mathbf{x}}(t), t) \xi_P(t). \end{aligned} \quad (11.79)$$

The EKF has no claim to optimality but works well in a number of applications.

The Bayesian information matrix for the linear Gaussian process model and the nonlinear observation model was given by (8.424) and (8.427)

$$\dot{\mathbf{J}}_{Bg}(t) = -\mathbf{J}_{Bg}(t) \mathbf{F}(t) - \mathbf{F}^T(t) \mathbf{J}_{Bg}(t) - \mathbf{J}_{Bg}(t) \mathbf{G}(t) \mathbf{Q}(t) \mathbf{G}^T(t) \mathbf{J}_{Bg}(t) + \mathbf{P}(t), \quad (11.80)$$

where

$$\mathbf{P}(t) \triangleq E_{\mathbf{x}} \left\{ \tilde{\mathbf{C}}^T(\mathbf{x}(t), t) \mathbf{R}^{-1}(t) \tilde{\mathbf{C}}(\mathbf{x}(t), t) \right\}. \quad (11.81)$$

The expectation in (11.81) is with respect to the state vector $\mathbf{x}(t)$ and will usually have to be evaluated by a Monte Carlo simulation.

There are implementation issues for both the Kalman filter and the extended Kalman filter. These issues include

- (a) Computational complexity due to matrix inversions.
- (b) The $\xi_P(t)$ matrix losing its positive definiteness due to round-off errors.
- (c) Sensitivity to model mismatch.

Optimum linear filters, particularly Kalman filters, are used in a diverse variety of applications. An Internet search will reveal a surprising number of disciplines in which the linear filter plays a key role.

In Chapter 9, we derived the discrete-time versions of the Wiener and Kalman filters. Except for the FIR Wiener filter, the parallelism with the continuous-time case was clear.

We first considered optimum FIR filters, the key result was the equation for the optimum linear filter \mathbf{h}_o (9.92),

$$\begin{bmatrix} k_r(0) & k_r(1) & \cdots & k_r(K-1) \\ k_r(1) & k_r(0) & \cdots & k_r(N-2) \\ \vdots & & & \vdots \\ \vdots & & \ddots & \vdots \\ \vdots & & & \vdots \\ k_r(K-1) & k_r(N-2) & \cdots & k_r(0) \end{bmatrix} \begin{bmatrix} h_o(0) \\ h_o(1) \\ \vdots \\ h_o(K-1) \end{bmatrix} = \begin{bmatrix} k_s(L) \\ k_s(L+1) \\ \vdots \\ k_s(0) \\ \vdots \\ k_s(L+K-1) \end{bmatrix} \quad (11.82)$$

and the resulting optimum MSE, ξ_o , given by (9.89)

$$\xi_o = k_d(0) - \sum_{n=0}^{K-1} h_o(n)k_{dr}(n). \quad (11.83)$$

We used an AR(1) process as an example and considered filtering and filtering with lag. The effective filter length depended on the correlation time of the process and the performance depended on both the correlation time and the SNR.

In Section 9.2.4, we developed unrealizable IIR Wiener filters. The principal advantage is that the solution to (9.105) is simple,

$$H_{ou}(z) = \frac{S_{dr}(z)}{S_r(z)} \quad (11.84)$$

and the irreducible mean-square error given by (9.116)

$$\xi_{ou} = \frac{1}{2\pi} \int_{-\pi}^{\pi} P_n(e^{j\omega}) H_{ou}(e^{j\omega}) d\omega \quad (11.85)$$

provides a lower bound on the MSE of any processor. Later, in Section 9.2.5, we showed that the MSE of an IIR realizable filter with lag approaches the irreducible MSE as the lag $\rightarrow \infty$.

In Section 9.2.5, we developed the optimum IIR realizable Wiener filter. By whitening the input, we were able to develop a formula (9.155) for the optimum Wiener filter,

$$H_o(z) = \frac{1}{G(z)} \left[\frac{S_{dr}(z)}{G(z^{-1})} \right]_+ \quad (11.86)$$

and the error is given by (9.164)

$$\xi_o = k_d(0) - \sum_{l=0}^{\infty} k_{dz}^2(l). \quad (11.87)$$

The AR(1) process provided examples of filtering, filtering with lag, and prediction.

In Section 9.3 we studied the discrete-time Kalman filter in detail. In Section 9.3.1, we developed state-variable representations of signal processes and the observation model. We focused our attention to two types of processes, autoregressive moving average (ARMA) processes that are important models for communication systems and kinematic models that are important in the radar and sonar area.

In Section 9.3.2, we developed the discrete-time Kalman filter. We referred to a Kalman processor as a Kalman filter when we were estimating the state vector $\mathbf{x}(k)$ based on a sequence of received observations $\mathbf{r}(n)$, $n = 1, \dots, k$. This section was a major part of the chapter because Kalman predictors, $\mathbf{x}(k+L)$, $L > 0$ and Kalman smoothers, $\mathbf{x}(k+L)$, $L < 0$ contained the filter.

In Section 9.3.2.1, we derived the standard Kalman filter. This version of the Kalman filter is referred to as the *covariance implementation* because it recursively inverts the covariance matrix of the estimation error. The key equations are (9.275)–(9.286). The standard algorithm requires recursive inversion of an $N \times N$ matrix, where N is the dimension of the observation vector $\mathbf{r}(k)$.

In Section 9.3.2.2, we developed two alternative implementations that have computational advantage when $N \geq p$, where p is the dimension of the state vector. The derivations used the matrix inversion lemma to obtain implementations in which the recursive inversion is $p \times p$ when $\mathbf{R}(k)$ is a constant \mathbf{R} . The first implementation recursively computes the covariance matrix using a $p \times p$ inversion and we refer to it as the *reduced dimension covariance implementation*. The key equations are (9.325)–(9.331). The second implementation recursively computes the Bayesian information matrix $\mathbf{J}_B(k)$ that is the inverse of the covariance matrix using a $p \times p$ inversion and is referred to as the *information filter*. The key equations are (9.349)–(9.359).

The three implementations are algebraically identical, but they have different computational complexity, different sensitivity to numerical errors such as round-off, and different sensitivity to model mismatch.

In Section 9.3.2.3, we studied a sequence of applications in the signal processing and tracking area.

The Kalman filter in Sections 9.3.2.1–9.3.2.3 assumed white Gaussian noise in the observation model. In Section 9.3.2.4, we showed how to treat the case of colored plus white observation noise. Our approach consisted of augmenting the signal state vector with a colored noise state vector. This reduced the problem to a standard Kalman filtering problem with increased dimension of the state vector.

In early applications, it was found that numerical round-off errors caused the covariance matrix or the Bayesian information matrix to lose its nonnegative definite property. In Section 9.3.2.6, we developed a square-root implementation of the Kalman filter that factors the covariance matrix (or the Bayesian information matrix) into triangular matrices and updates them. This implementation guarantees a nonnegative definite matrix and improves the numerical precision. This section provided a brief introduction to square-root filtering. There are a number of different square-root algorithms and the literature should be consulted for a particular application.

In Section 9.3.2.8, we considered a general mismatch model in which all of the matrices in the model, \mathbf{F} , \mathbf{G} , \mathbf{C} , \mathbf{Q} , \mathbf{R} , and $\mathbf{\Pi}$ may be mismatched to the actual model. The key equations are (9.566)–(9.579). It is an essential part of the design of an algorithm for a practical application to investigate its sensitivity to possible model mismatches.

We spent a considerable amount of time studying Kalman filters. In addition to their widespread usage, they are the key building block in Kalman prediction and smoothers.

In Section 9.3.3, we studied Kalman predictors. There are three types of prediction problems:

- (a) Fixed-lead prediction: In this case,

$$d(k) = s(k + L) \quad (11.88)$$

where L is a positive number.

- (b) Fixed-point prediction: In this case,

$$d(k) = s(L_p) \quad (11.89)$$

where L_p is a fixed-point, $L_p > k$.

- (c) Fixed-interval prediction: In this case, the interval is fixed, $k = 1, 2, \dots, K$ and we want to predict

$$d(m) = s(m), \quad m = K + 1, K + 2, \dots \quad (11.90)$$

This is the model that we encountered in Section 9.2 using covariance functions.

In all of these cases, we assume that a Kalman filter is implemented and that we have $\hat{\mathbf{x}}(k)$ and $\mathbf{P}(k)$ available. Because we are dealing with a Markov process, these are the only quantities needed to find $\hat{d}(k)$ and its variance.

The prediction part of the Kalman processor is straightforward. In all three cases, it is linear operation of $\hat{\mathbf{x}}(k)$. Thus, all of the implementations issues discussed in Section 9.3.2 must be considered. The performance of the predictors will be a functions of the correlation between $\mathbf{x}(k)$ and $\mathbf{x}(k + L)$.

In Section 9.3.4, we studied the Kalman smoothing problems. There are three types of smoothing problems that are encountered in applications:

- a. *Fixed interval smoothing*

We have K samples, $k = 1, \dots, K$ and we want to find $\hat{\mathbf{x}}(k|K) \triangleq \hat{\mathbf{x}}(k|\mathbf{r}_K)$ where

$$\mathbf{r}_K = [\mathbf{r}(1) \cdots \mathbf{r}(K)].$$

- b. *Fixed Lag smoothing*

We observed $\mathbf{r}(k)$, $k = 1, 2, \dots$ and we want to find $\hat{\mathbf{x}}(k + L)$ where L is negative.

This case is the filtering with delay problem that we considered in the Wiener filter context.

- c. *Fixed Point smoothing*

We want to find $\hat{\mathbf{x}}(k_s)$, where k_s is fixed and we observe $\mathbf{r}(k)$, $k = k_s, k_s + 1, \dots, k_s + K$, and K increases.

The Kalman smoothing processors are more complicated than the Kalman filter. Our solution for the fixed-interval smoother required a forward Kalman filter followed by a backward Kalman filter. Our solutions for fixed-lag smoothing involved augmenting the state vector such that the dimension increased from p to pL , where L was the length of the delay. However, smoothing has the potential to reduce the estimation error and is used in a number of applications.

In Section 9.3.5, we introduced the problem of Bayesian estimation of discrete-time nonlinear models. The discussion was parallel to the continuous-time process development. However, some results such as the general Bayesian Cramér–Rao bound were introduced. In addition, most of the current research in nonlinear estimation deals with discrete-time processes.

11.5 OBSERVATIONS

The previous four sections have summarized some of key results that we derived in order to solve the hierarchy of detection and estimation theory problems outlined in Chapter 1. In this section, we offer some general observations about various topics in the detection and estimation theory area.

11.5.1 Models and Mismatch

The reader should remember that the last word in the title of the book is “theory.” We have constructed mathematical models of channels or targets in the real world. However, we have not gone into detail on the physical phenomena that confirms the model or presented experimental measurements to justify the model. This is an important step in applying our theoretical results but it is so application specific that it is beyond the scope of an introductory text.

We have partially compensated for this by studying the sensitivity of the performance of the algorithm to variations in the model. This term “sensitivity” is often replaced by “environmental mismatch” in the literature. We also introduced techniques (e.g. diagonal loading) for modifying the optimum processor to make it more robust to mismatch. This type of analysis should be an essential part of the system design.

11.5.2 Bayes vis-a-vis Fisher

We have developed the Bayes approach and the Fisher approach (including Neyman–Pearson) in parallel. This is because most physical problems coupled with the system objective fit more naturally in one of the approaches. We have compared the approaches where appropriate but avoided trying to fit a Fisher model into a Bayes context.

11.5.3 Bayesian and Fisher Bounds

Most estimation texts and journal articles discuss the Cramér–Rao bound which is due to Fisher [Fis22]. We have seen that it is a tight bound for many problems when the number of independent observations approaches infinity or when the signal-to-noise ratio is high. The Bayesian CRB provides a lower bound in the random parameter case and is tight when the SNR is high and/or when the number of observation approach infinity. These bounds are useful in two ways:

- a. They are lower bounds, which serve as a check on the results of a simulation or analysis.
- b. However, they do not answer the question, “How far is infinity?” We observed that many nonlinear estimation problems exhibit a dramatic threshold when the number of observations and/or the SNR decrease. An important part of the system design is knowing where this threshold occurs and the system behavior in the transition region.

We developed a family of global Bayesian bounds to study the behavior. Similar bounds are also available for the nonrandom parameter case.

We also developed bounds for the detection theory problem. The reader should remember the central role that $\mu(s)$, the log of the moment generating function of $l(\mathbf{R})$ plays in the detection theory bound, importance sampling, and the Bayesian covariance inequality bounds.

11.5.4 Eigenspace

In various chapters, we tried to emphasize the importance of analyzing performance and designing algorithms in eigenspace. The techniques have been known for a number of years. We emphasized the application in the Gaussian model but it is also useful in second-moment analysis to generate orthogonal vectors with uncorrelated coefficients. As pointed out in [Cox99], possible disadvantages are computational complexity, $O(n^3)$, and that the vectors do not correspond to individual signals.

11.5.5 Whitening

Many of our models assumed the received signal, either a waveform or a vector, was observed the presence of white noise and, in many cases, white Gaussian noise. We were able to obtain a number of key results for these models. In many applications, the received signal also contains interfering signals and/or nonwhite noise. We demonstrated, first with vectors and then with waveforms, that we could always find a whitening transformation that mapped the original process into a signal plus white noise problem.

The reader should remember to consider this approach when dealing with more general problems.

11.5.6 The Gaussian Model

We have spent a significant portion of the book on the Gaussian model. The reasons are twofold. The first reason is that a large number of communications, radar, and sonar applications can be modeled (either exactly or approximately) by using either the real or complex Gaussian model. In the estimation problem, it serves a dual role. It provides the optimum MMSE linear estimator for any process with the same second moments as the Gaussian process. It provides the optimum Bayes estimator for the squared-error cost function. The second reason is that one can obtain solutions to almost all of the Gaussian models that are encountered in practice.

We believe that the reader should have a thorough knowledges of the Gaussian model even if he or she is primarily interested in non-Gaussian problems.

11.6 CONCLUSION

In this chapter, we summarized some of the key results in the book and offered some general observations about the field. This concludes our journey through the detection and estimation theory field. We hope the reader has enjoyed the text and will find the results useful in their career.

Appendix A

Probability Distributions and Mathematical Functions

A.1 PROBABILITY DISTRIBUTIONS

A.1.1 Continuous Univariate Distributions

For continuous univariate distributions, the probability density function (pdf), cumulative distribution function (CDF), and characteristic function (CF) are provided below, as well as the parameters that characterize the distribution, the support of the distribution, and the mean, variance, median, and mode when available.

Uniform

Parameters	pdf $p_x(X)$	Support	CDF $P_x(X)$	CF $M_x(jv)$
$a \in \mathbb{R}, b \in \mathbb{R}, b > a$	$\frac{1}{b-a}$	$a \leq X \leq b$	$\frac{x-a}{b-a}$	$\frac{e^{jbv} - e^{jav}}{jv(b-a)}$
Mean	Variance	Median	Mode	
$\frac{a+b}{2}$	$\frac{(b-a)^2}{12}$	$\frac{a+b}{2}$	—	

Gaussian (Normal)

Parameters	pdf $p_x(X)$	Support	CDF $P_x(X)$	CF $M_x(jv)$
$\mu \in \mathbb{R}, \sigma > 0$	$\frac{1}{\sqrt{2\pi}\sigma} \exp\left(-\frac{(X-\mu)^2}{2\sigma^2}\right)$	$X \in \mathbb{R}$	$1 - \text{erfc}_*(X)$	$\exp\left(j\mu v - \frac{\sigma^2 v^2}{2}\right)$
Mean	Variance	Median	Mode	
μ	σ^2	μ	μ	

Log-normal

Parameters	pdf $p_x(X)$	Support	CDF $P_x(X)$	CF $M_x(jv)$
$\mu \in \mathbb{R}, \sigma > 0$	$\frac{1}{\sqrt{2\pi}\sigma X} \exp\left(-\frac{(\ln X - \mu)^2}{2\sigma^2}\right)$	$X > 0$	$1 - \text{erfc}_*(\ln X)$	—
Mean	Variance	Median	Mode	
$e^{\mu+\sigma^2/2}$	$(e^{\sigma^2} + 2) e^{2\mu+\sigma^2}$	e^μ	$e^{\mu-\sigma^2}$	

Gamma

Parameters	pdf $p_x(X)$	Support	CDF $P_x(X)$	CF $M_x(jv)$
$a > 0, b > 0$	$\frac{X^{a-1} e^{-X/b}}{b^a \Gamma(a)}$	$X \geq 0$	$\Gamma_a(X/b)$	$(1 - jb)^{-a}$
Mean	Variance	Median	Mode	
ab	ab^2	—	$(a-1)b$ for $a \geq 1$	

Inverse Gamma

Parameters	pdf $p_x(X)$	Support	CDF $P_x(X)$	CF $M_x(jv)$
$a > 0, b > 0$	$\frac{X^{-a-1} e^{-1/Xb}}{b^a \Gamma(a)}$	$X \geq 0$	$\Gamma_a(1/Xb)$	$\frac{2\left(-\frac{jv}{b}\right)^{\frac{a}{2}}}{\Gamma(a)} K_a\left(\sqrt{-\frac{j4v}{b}}\right)$
Mean	Variance	Median	Mode	
$\frac{1}{b(a-1)}$	$\frac{1}{b^2(a-1)^2(a-2)}$	—	$\frac{1}{b(a+1)}$	

Exponential

Exponential is a special case of Gamma ($a = 1, b = 1/\lambda$) and Weibull ($\alpha = 1, b = 1/\lambda$).

Parameters	pdf $p_x(X)$	Support	CDF $P_x(X)$	CF $M_x(jv)$
$\lambda > 0$	$\lambda e^{-\lambda X}$	$X \geq 0$	$1 - e^{-\lambda X}$	$(1 - jv/\lambda)^{-1}$
Mean	Variance	Median	Mode	
$\frac{1}{\lambda}$	$\frac{1}{\lambda^2}$	$\frac{\ln 2}{\lambda}$	0	

Chi-squared

Chi-squared is a special case of Gamma ($a = n/2, b = 2$).

Parameters	pdf $p_x(X)$	Support	CDF $P_x(X)$	CF $M_x(jv)$
$n > 0$	$\frac{X^{\frac{n}{2}-1} e^{-X/2}}{2^{\frac{n}{2}} \Gamma(n/2)}$	$X \geq 0$	$\Gamma_{\frac{n}{2}}(X/2)$	$(1 - j2v)^{-\frac{n}{2}}$
Mean	Variance	Median	Mode	
n	$2n$	—	$\max(0, n - 2)$	

Noncentral Chi-squared

Parameters	pdf $p_x(X)$	Support	CDF $P_x(X)$	CF $M_x(jv)$
$n > 0, \lambda > 0$	$\frac{1}{2} \exp\left(-\frac{1}{2}(X + \lambda)\right) \cdot \left(\frac{X}{\lambda}\right)^{\frac{n-2}{2}} I_{\frac{n}{2}-1}\left(\sqrt{\lambda X}\right)$	$X \geq 0$	$1 - Q_{\frac{n}{2}}\left(\sqrt{\lambda}, \sqrt{X}\right)$	$\frac{\exp\left(\frac{j\lambda v}{1 - j2v}\right)}{(1 - j2v)^{\frac{n}{2}}}$
Mean	Variance	Median	Mode	
$n + \lambda$	$2(n + 2\lambda)$	—	—	

Central F

Parameters	pdf $p_x(X)$	Support	CDF $P_x(X)$	CF $M_x(jv)$
$n > 0, m > 0$	$\frac{X^{\frac{n}{2}-1} \left(1 + \frac{nX}{m}\right)^{-\frac{n+m}{2}}}{\left(\frac{m}{n}\right)^{\frac{n}{2}} B\left(\frac{n}{2}, \frac{m}{2}\right)}$	$X \geq 0$	$B_{\frac{n}{2}, \frac{m}{2}}\left(\frac{nX}{nX + m}\right)$	—
Mean	Variance	Median	Mode	
$\frac{m}{m-2}$	$\frac{2m^2(n+m-2)}{n(m-2)^2(m-4)}$	—	$\frac{(n-2)m}{n(m+2)}$	

Noncentral F

Parameters	pdf $p_x(X)$	CDF $P_x(X)$
$n > 0, m > 0, \lambda > 0$	$e^{-\frac{\lambda}{2}} \sum_{k=0}^{\infty} \frac{\left(\frac{\lambda}{2}\right)^k}{k!} \frac{X^{\frac{n}{2}+k-1} \left(1 + \frac{nX}{m}\right)^{-\frac{n+m}{2}-k}}{\left(\frac{m}{n}\right)^{\frac{n}{2}+k} B\left(\frac{n}{2} + k, \frac{m}{2}\right)}$	$e^{-\frac{\lambda}{2}} \sum_{k=0}^{\infty} \frac{\left(\frac{\lambda}{2}\right)^k}{k!} B_{\frac{n}{2}+k, \frac{m}{2}}\left(\frac{nX}{nX + m}\right)$
Mean	Variance	Support
$\frac{(n+\lambda)m}{n(m-2)}$	$\frac{2m^2[(n+\lambda)^2 + (n+2\lambda)(m-2)]}{n^2(m-2)^2(m-4)}$	$X \geq 0$

Generalized Gaussian

Parameters	pdf $p_x(X)$	Support	CDF $P_x(X)$	CF $M_x(jv)$
$\mu \in \mathbb{R}, \alpha > 0, b > 0$	$\frac{\alpha \exp\left(-\left \frac{X-\mu}{b}\right ^\alpha\right)}{2b\Gamma(1/\alpha)}$	$X \in \mathbb{R}$	$\frac{1}{2} + \frac{\text{sgn}(X-\mu)}{2}.$	$e^{j\mu v} \sum_{n=0}^{\infty} \frac{(jbv)^{2n}}{(2n)!} \frac{\Gamma(\frac{2n+1}{\alpha})}{\Gamma(1/\alpha)}$
Mean				$\Gamma_{\frac{1}{\alpha}}\left(\left \frac{X-\mu}{b}\right ^\alpha\right)$
Variance	$\frac{b^2\Gamma(3/\alpha)}{\Gamma(1/\alpha)}$		Median	Mode
μ			μ	μ

Laplacian

Laplacian is a special case of Generalized Gaussian ($\mu, \alpha = 1, b$).

Parameters	pdf $p_x(X)$	Support	CDF $P_x(X)$	CF $M_x(jv)$
$\mu \in \mathbb{R}, b > 0$	$\frac{1}{2b} \exp\left(-\left \frac{X-\mu}{b}\right \right)$	$X \in \mathbb{R}$	$\frac{1}{2} + \frac{\text{sgn}(X-\mu)}{2}.$	$\frac{\exp(j\mu v)}{1+b^2v^2}$
Mean				$\left[1 - \exp\left(-\left \frac{X-\mu}{b}\right \right)\right]$
Variance	$2b^2$		Median	Mode
μ			μ	μ

Weibull

Parameters	pdf $p_x(X)$	Support	CDF $P_x(X)$	CF $M_x(jv)$
$\alpha > 0, b > 0$	$\frac{\alpha}{b} \left(\frac{X}{b}\right)^{\alpha-1} e^{-(X/b)^\alpha}$	$X \geq 0$	$1 - e^{-(X/b)^\alpha}$	$\sum_{n=0}^{\infty} \frac{(jbv)^n}{n!} \Gamma\left(1 + \frac{n}{\alpha}\right)$
Mean				
$b \Gamma\left(1 + \frac{1}{\alpha}\right)$	$b^2 \left[\Gamma\left(1 + \frac{2}{\alpha}\right) - \Gamma^2\left(1 + \frac{1}{\alpha}\right) \right]$		Median	Mode
			$b (\ln 2)^{1/\alpha}$	$b \left(\frac{\alpha-1}{\alpha}\right)^{1/\alpha} \quad \alpha > 1$
			$0 \quad \alpha = 1$	

Rayleigh

Rayleigh is a special case of Weibull ($\alpha = 2, b = \sqrt{2}\sigma$) and Rician ($\sigma, \gamma = 0$).

Parameters	pdf $p_x(X)$	Support	CDF $P_x(X)$	CF $M_x(jv)$
$\sigma > 0$	$\frac{X}{\sigma^2} \exp\left(-\frac{X^2}{2\sigma^2}\right)$	$X \geq 0$	$1 - e^{-X^2/2\sigma^2}$	$\sum_{n=0}^{\infty} \frac{(j\sqrt{2}\sigma v)^n}{n!} \Gamma\left(1 + \frac{n}{2}\right)$
Mean	Variance	Median	Mode	
$\sigma\sqrt{\frac{\pi}{2}}$	$\frac{4 - \pi}{2}\sigma^2$	$\sigma\sqrt{\ln(4)}$	σ	

Rician

Parameters	pdf $p_x(X)$	Support	CDF $P_x(X)$	CF $M_x(jv)$
$\sigma > 0, \gamma > 0$	$\frac{X}{\sigma^2} \exp\left(-\frac{(X^2 + \gamma^2)}{2\sigma^2}\right) I_0\left(\frac{X\gamma}{\sigma}\right)$	$X \geq 0$	$1 - Q_1\left(\frac{\gamma}{\sigma}, \frac{X}{\sigma}\right)$	-
Mean	Variance	Median	Mode	
$\sigma\sqrt{\frac{\pi}{2}} {}_1F_1\left(-\frac{1}{2}; 1; \frac{-\gamma^2}{2\sigma^2}\right)$	$2\sigma^2 + \gamma^2$ $-\frac{\pi\sigma^2}{2} {}_1F_1^2\left(-\frac{1}{2}; 1; \frac{-\gamma^2}{2\sigma^2}\right)$	-	-	

Cauchy

Parameters	pdf $p_x(X)$	Support	CDF $P_x(X)$	CF $M_x(jv)$
$\mu \in \mathbb{R}, \gamma > 0$	$\frac{\gamma}{\pi[\gamma^2 + (X - \mu)^2]}$	$X \in \mathbb{R}$	$\frac{1}{\pi} \arctan\left(\frac{X - \mu}{\gamma}\right) + \frac{1}{2}$	$\exp(j\mu v - \gamma v)$
Mean	Variance	Median	Mode	
Does not exist	Does not exist	μ	μ	

Beta

Parameters	pdf $p_x(X)$	Support	CDF $P_x(X)$	CF $M_x(jv)$
$a > 0, b > 0$	$\frac{X^{a-1}(1-X)^{b-1}}{B(a, b)}$	$0 \leq X \leq 1$	$B_{a,b}(X)$	$\sum_{n=0}^{\infty} \frac{(jv)^n}{n!} \frac{B(a+n, b)}{B(a, b)}$
Mean	Variance	Median	Mode	
$\frac{a}{a+b}$	$\frac{ab}{(a+b)^2(a+b+1)}$	-	$\frac{a-1}{a+b-2}$ for $a, b > 1$	

Tikhonov (von Mises)

Parameters	pdf $p_x(X)$	Support	CDF $P_x(X)$	CF $M_x(jv)$
$\Lambda > 0$	$\frac{\exp(\Lambda \cos X)}{2\pi I_0(\Lambda)}$	$-\pi \leqslant X \leqslant \pi$	—	$\frac{I_{ v }(\Lambda)}{I_0(\Lambda)}$
Mean	Variance	Median	Mode	
0	$1 - \frac{I_1(\Lambda)}{I_0(\Lambda)}$	0	0 for $\Lambda > 0$	

A.1.2 Discrete Univariate Distributions

For discrete univariate distributions, the probability mass function (PMF), the parameters that characterize the distribution, the support of the distribution, and the mean and variance are provided below.

Poisson

Parameters	PMF $\Pr(x = k)$	Support	Mean	Variance
$\lambda > 0$	$\frac{\lambda^k}{k!} e^{-\lambda}$	$k = 0, 1, \dots$	λ	λ

Binomial

Parameters	PMF $\Pr(x = k)$	Support	Mean	Variance
$N \geqslant 1$ integer, $p \in [0, 1]$	$\binom{N}{k} p^k (1-p)^{N-k}$	$k = 0, 1, \dots, N$	Np	$Np(1-p)$

Bernoulli

Bernoulli is a special case of Binomial ($N = 1, p$).

Parameters	PMF $\Pr(x = k)$	Support	Mean	Variance
$p \in [0, 1]$	$p^k (1-p)^{1-k}$	$k = 0, 1$	p	$p(1-p)$

Negative Binomial

Parameters	PMF $\Pr(x = k)$	Support	Mean	Variance
$r \geqslant 1$ integer, $p \in [0, 1]$	$\binom{k-1}{r-1} p^r (1-p)^{k-r}$	$k = r, r+1, \dots$	$\frac{r}{p}$	$\frac{r(1-p)}{p^2}$

Geometric

Geometric is a special case of Negative Binomial ($r = 1, p$).

Parameters	PMF $\Pr(x = k)$	Support	Mean	Variance
$p \in [0, 1]$	$p(1-p)^{k-1}$	$k = 1, 2, \dots$	$\frac{1}{p}$	$\frac{(1-p)}{p^2}$

A.1.3 Continuous Multivariate Distributions

For continuous multivariate distributions, the pdf, the parameters that characterize the distribution, the support of the distribution, and the mean and covariance matrix are provided below.

Multivariate Gaussian (Normal)

Parameters	pdf $p_{\mathbf{x}}(\mathbf{X})$	Support	Mean	Covariance
$\mu \in \mathbb{R}^M$, $\mathbf{K}_{M \times M} > 0$	$\frac{\exp\left(-\frac{1}{2} [\mathbf{X} - \mu]^T \mathbf{K}^{-1} [\mathbf{X} - \mu]\right)}{(2\pi)^{M/2} \mathbf{K} ^{1/2}}$	$\mathbf{X} \in \mathbb{R}^M$	μ	\mathbf{K}

Multivariate Circular Complex Gaussian (Normal)

Parameters	pdf $p_{\tilde{\mathbf{x}}}(\tilde{\mathbf{X}})$	Support	Mean	Covariance
$\tilde{\mu} \in \mathbb{C}^M$, $\tilde{\mathbf{K}}_{M \times M} > 0$	$\frac{\exp\left(-[\tilde{\mathbf{X}} - \tilde{\mu}]^H \tilde{\mathbf{K}}^{-1} [\tilde{\mathbf{X}} - \tilde{\mu}]\right)}{(2\pi)^M \tilde{\mathbf{K}} }$	$\tilde{\mathbf{X}} \in \mathbb{C}^M$	$\tilde{\mu}$	$\tilde{\mathbf{K}}$

Normal-Gamma

Parameters	pdf $p_{x,y}(X, Y)$	Support	Mean	Covariance
$\mu \in \mathbb{R}$, $\sigma > 0$, $a > 0$, $b > 0$	$\frac{Y^{a-1} e^{-Y/b}}{b^a \Gamma(a)} \cdot \frac{\sqrt{Y}}{\sqrt{2\pi\sigma}} \cdot \exp\left(-\frac{Y(X-\mu)^2}{2\sigma^2}\right)$	$X \in \mathbb{R}$, $Y > 0$	$E(X) = \mu$, $E(Y) = ab$	$\text{Var}(X) = \frac{\sigma^2}{b(a-1)}$, $\text{Var}(Y) = ab^2$, $\text{Cov}(X, Y) = 0$

Normal-Inverse Gamma

Parameters	pdf $p_{x,y}(X, Y)$	Support	Mean	Covariance
$\mu \in \mathbb{R}$, $\sigma > 0$, $a > 0$, $b > 0$	$\frac{Y^{-a-1} e^{-1/bY}}{b^a \Gamma(a)} \cdot \frac{1}{\sqrt{2\pi Y \sigma}} \cdot \exp\left(-\frac{(X-\mu)^2}{2\sigma^2 Y}\right)$	$X \in \mathbb{R}$, $Y > 0$	$E(X) = \mu$, $E(Y) = \frac{1}{b(a-1)}$	$\text{Var}(X) = \frac{\sigma^2}{b(a-1)}$, $\text{Var}(Y) = \frac{1}{b^2(a-1)^2(a-2)}$, $\text{Cov}(X, Y) = 0$

Wishart

Parameters	pdf $p_{\mathbf{x}}(\mathbf{X})$	Support	Mean	Covariance
$n > M - 1$, $\mathbf{K}_{M \times M} > 0$	$\frac{ \mathbf{X} ^{\frac{n-M-1}{2}} \exp\left(-\frac{1}{2} \text{tr}(\mathbf{K}^{-1} \mathbf{X})\right)}{2^{\frac{nM}{2}} \mathbf{K} ^{\frac{n}{2}} G_M\left(\frac{n}{2}\right)}$	$\mathbf{X}_{M \times M} > 0$	$n\mathbf{K}$	$\text{Var}(X_{ij}) = n(K_{ij}^2 + K_{ii}K_{jj})$

Inverse Wishart

Parameters	pdf $p_{\mathbf{X}}(\mathbf{X})$	Support	Mean	Covariance
$n > M - 1, \quad \mathbf{Q}_{M \times M} > 0$	$\frac{ \mathbf{X} ^{-\frac{n+M+1}{2}} \exp\left(-\frac{1}{2}\text{tr}(\mathbf{Q}\mathbf{X}^{-1})\right)}{2^{\frac{nM}{2}} \mathbf{Q} ^{-\frac{n}{2}} G_M\left(\frac{n}{2}\right)}$	$\mathbf{X}_{M \times M} > 0$	$\frac{\mathbf{Q}}{n-M-1}$	$\text{Var}(X_{ij}) = \frac{(n-M+1)Q_{ij}^2 + (n-M-1)Q_{ii}Q_{jj}}{(n-M)(n-M-1)^2(n-M-3)}$

Normal-Wishart

Parameters	pdf $p_{\mathbf{x}, \mathbf{y}}(\mathbf{X}, \mathbf{Y})$	Support	Mean	Covariance
$\mu \in \mathbb{R}^m, \sigma > 0, \quad n > M - 1, \quad \mathbf{K}_{M \times M} > 0$	$\mathbf{X} \mathbf{Y} \sim N(\mu, \sigma^2 \mathbf{Y}^{-1}), \quad \mathbf{Y} \sim W(n, \mathbf{K})$	$\mathbf{X} \in \mathbb{R}^m, \quad \mathbf{Y}_{M \times M} > 0$	$E(\mathbf{X}) = \mu, \quad E(\mathbf{Y}) = n\mathbf{K}$	$\text{Cov}(\mathbf{X}) = \frac{\sigma^2 \mathbf{K}^{-1}}{(n-M-1)}, \quad \text{Var}(Y_{ij}) = n(K_{ij}^2 + K_{ii}K_{jj}), \quad \text{Cov}(X_i, Y_j) = 0$

Normal-Inverse Wishart

Parameters	pdf $p_{\mathbf{x}, \mathbf{y}}(\mathbf{X}, \mathbf{Y})$	Support	Mean	Covariance
$\mu \in \mathbb{R}^m, \sigma > 0, \quad n > M - 1, \quad \mathbf{Q}_{M \times M} > 0$	$\mathbf{X} \mathbf{Y} \sim N(\mu, \sigma^2 \mathbf{Y}), \quad \mathbf{Y} \sim W^{-1}(n, \mathbf{Q})$	$\mathbf{X} \in \mathbb{R}^m, \quad \mathbf{Y}_{M \times M} > 0$	$E(\mathbf{X}) = \mu, \quad E(\mathbf{Y}) = \frac{\mathbf{Q}}{n-M-1}$	$\text{Cov}(\mathbf{X}) = \frac{\sigma^2 \mathbf{Q}}{(n-M-1)}, \quad \text{Var}(Y_{ij}) = \frac{(n-M+1)Q_{ij}^2 + (n-M-1)Q_{ii}Q_{jj}}{(n-M)(n-M-1)^2(n-M-3)}, \quad \text{Cov}(X_i, Y_j) = 0$

A.2 CONJUGATE PRIORS

A.2.1 Parameters of Continuous Univariate Distributions

The observation consists of N IID continuous random variables: $r_i, i = 1, \dots, N$. The likelihood function is

$$p_{\mathbf{r}|\mathbf{a}}(\mathbf{R}|\mathbf{A}) = \prod_{i=1}^N p_{r|\mathbf{a}}(R_i|\mathbf{A}).$$

The sample mean and variance are

$$\begin{aligned} \bar{R} &\triangleq \frac{1}{N} \sum_{i=1}^N R_i, \\ V &\triangleq \frac{1}{N} \sum_{i=1}^N (R_i - \bar{R})^2 \end{aligned}$$

Likelihood Function	Parameter	Conjugate Prior Distribution	Prior Hyperparameters	Posterior Hyperparameters
Gaussian with known variance σ^2	Mean μ	Gaussian	μ_0, σ_0^2	$\mu_p = \sigma_p^2 \left(\frac{\mu_0}{\sigma_0^2} + \frac{N}{\sigma^2} \bar{R} \right)$, $\sigma_p^2 = \left(\frac{1}{\sigma_0^2} + \frac{N}{\sigma^2} \right)^{-1}$
Gaussian with known mean μ	Variance σ^2	Inverse Gamma	a_0, b_0	$a_p = a_0 + \frac{N}{2}$, $b_p = \left(\frac{1}{b_0} + \frac{1}{2} \sum_{i=1}^N (R_i - \mu)^2 \right)^{-1}$
Gaussian with known mean μ	Precision $\tau = \frac{1}{\sigma^2}$	Gamma	a_0, b_0	$a_p = a_0 + \frac{N}{2}$, $b_p = \left(\frac{1}{b_0} + \frac{1}{2} \sum_{i=1}^N (R_i - \mu)^2 \right)^{-1}$
Gaussian	Mean μ and variance σ^2	Normal-Inverse Gamma	$\mu_0, \sigma_0^2, a_0, b_0$	$\mu_p = \sigma_p^2 \left(\frac{\mu_0}{\sigma_0^2} + N \bar{R} \right)$, $\sigma_p^2 = \left(\frac{1}{\sigma_0^2} + N \right)^{-1}$, $a_p = a_0 + \frac{N}{2}$, $b_p = \left(\frac{1}{b_0} + \frac{N}{2} V + \frac{N \sigma_p^2}{2 \sigma_0^2} (\bar{R} - \mu_0)^2 \right)^{-1}$
Gaussian	Mean μ and precision $\tau = \frac{1}{\sigma^2}$	Normal-Gamma	$\mu_0, \sigma_0^2, a_0, b_0$	$\mu_p = \sigma_p^2 \left(\frac{\mu_0}{\sigma_0^2} + N \bar{R} \right)$, $\sigma_p^2 = \left(\frac{1}{\sigma_0^2} + N \right)^{-1}$, $a_p = a_0 + \frac{N}{2}$, $b_p = \left(\frac{1}{b_0} + \frac{N}{2} V + \frac{N \sigma_p^2}{2 \sigma_0^2} (\bar{R} - \mu_0)^2 \right)^{-1}$
Log-normal with known variance σ^2	Mean μ	Gaussian	μ_0, σ_0^2	$\mu_p = \sigma_p^2 \left(\frac{\mu_0}{\sigma_0^2} + \frac{1}{\sigma^2} \sum_{i=1}^N \ln R_i \right)$, $\sigma_p^2 = \left(\frac{1}{\sigma_0^2} + \frac{N}{\sigma^2} \right)^{-1}$
Log-normal with known mean μ	Variance σ^2	Inverse Gamma	a_0, b_0	$a_p = a_0 + \frac{N}{2}$, $b_p = \left(\frac{1}{b_0} + \frac{1}{2} \sum_{i=1}^N (\ln R_i - \mu)^2 \right)^{-1}$
Log-normal with known mean μ	Precision $\tau = \frac{1}{\sigma^2}$	Gamma	a_0, b_0	$a_p = a_0 + \frac{N}{2}$, $b_p = \left(\frac{1}{b_0} + \frac{1}{2} \sum_{i=1}^N (\ln R_i - \mu)^2 \right)^{-1}$
Exponential	Rate λ	Gamma	a_0, b_0	$a_p = a_0 + N$, $b_p = \left(\frac{1}{b_0} + N \bar{R} \right)^{-1}$
Gamma with known shape a	Scale b	Inverse Gamma	a_0, b_0	$a_p = a_0 + Na$, $b_p = \left(\frac{1}{b_0} + N \bar{R} \right)^{-1}$
Gamma with known shape a	Inverse scale $\beta = \frac{1}{b}$	Gamma	a_0, β_0	$a_p = a_0 + Na$, $\beta_p = \beta_0 + N \bar{R}$
Gamma with known scale b	Shape a		$\frac{C_0 p_0^{X-1}}{b^{X r_0} \Gamma(X)^{r_0}}$	$p_p = p_0 \prod_{i=1}^N R_i$, $r_p = r_0 + N$, $s_p = s_0 + N$

(Continued)

Likelihood Function	Parameter	Conjugate Prior Distribution	Prior Hyperparameters	Posterior Hyperparameters
Gamma	Shape a and scale b	$\frac{C_0 p_0^{X-1} e^{-q/Y}}{Y^{Xr_0} \Gamma(X)^{s_0}}$	p_0, q_0, r_0, s_0	$p_p = p_0 \prod_{i=1}^N R_i, q_p = q_0 + N\bar{R},$ $r_p = r_0 + N, s_p = s_0 + N$
Gamma	Shape a and inverse scale $\beta = \frac{1}{b}$	$\frac{C_0 p_0^{X-1} e^{-q/Y}}{Y^{-Xr_0} \Gamma(X)^{s_0}}$	p_0, q_0, r_0, s_0	$p_p = p_0 \prod_{i=1}^N R_i, q_p = q_0 + N\bar{R},$ $r_p = r_0 + N, s_p = s_0 + N$
Inverse Gamma with known shape a	Scale b	Inverse Gamma	a_0, b_0	$a_p = a_0 + Na, b_p = \left(\frac{1}{b_0} + \sum_{i=1}^N R_i^{-1}\right)^{-1}$
Inverse Gamma with known shape a	Inverse scale $\beta = \frac{1}{b}$	Gamma	a_0, β_0	$a_p = a_0 + Na, \beta_p = \beta_0 + \sum_{i=1}^N R_i^{-1}$
Inverse Gamma with known scale b	Shape a	$\frac{C_0 p_0^{X-1}}{b^{Xr_0} \Gamma(X)^{s_0}}$	p_0, r_0, s_0	$p_p = p_0 \prod_{i=1}^N R_i^{-1}, r_p = r_0 + N, s_p = s_0 + N$
Inverse Gamma	Shape a and scale $\beta = \frac{1}{b}$	$\frac{C_0 p_0^{X-1} e^{-q/Y}}{Y^{Xr_0} \Gamma(X)^{s_0}}$	p_0, q_0, r_0, s_0	$p_p = p_0 \prod_{i=1}^N R_i^{-1}, q_p = q_0 + \sum_{i=1}^N R_i^{-1},$ $r_p = r_0 + N, s_p = s_0 + N$
Inverse Gamma	Shape a and inverse scale $\beta = \frac{1}{b}$	$\frac{C_0 p_0^{X-1} e^{-q/Y}}{Y^{-Xr_0} \Gamma(X)^{s_0}}$	p_0, q_0, r_0, s_0	$p_p = p_0 \prod_{i=1}^N R_i^{-1}, q_p = q_0 + \sum_{i=1}^N R_i^{-1},$ $r_p = r_0 + N, s_p = s_0 + N$

A.2.2 Parameters of Discrete Univariate Distributions

The observation consists of M IID discrete random variables: $n_i, i = 1, \dots, M$. The likelihood function is

$$\Pr(n = \mathbf{N}|a = A) = \prod_{i=1}^M \Pr(n_i = N_i|a = A)$$

Likelihood Function	Parameter	Conjugate Prior Distribution	Prior Hyperparameters	Posterior Hyperparameters
Poisson	Rate λ	Gamma	a_0, b_0	$a_p = a_0 + \sum_{i=1}^M N_i, b_p = \frac{b_0}{Mb_0 + 1}$
Bernoulli	Probability p	Beta	a_0, b_0	$a_p = a_0 + \sum_{i=1}^M N_i, b_p = b_0 + M - \sum_{i=1}^M N_i$
Binomial with known N	Probability p	Beta	a_0, b_0	$a_p = a_0 + \sum_{i=1}^M N_i, b_p = b_0 + MN - \sum_{i=1}^M N_i$
Geometric	Probability p	Beta	a_0, b_0	$a_p = a_0 + M, b_p = b_0 - M + \sum_{i=1}^M N_i$
Negative Binomial with known r	Probability p	Beta	a_0, b_0	$a_p = a_0 + Mr, b_p = b_0 - Mr + \sum_{i=1}^M N_i$

A.2.3 Parameters of Multivariate Continuous Distributions

The observation consists of N IID continuous random vectors: $\mathbf{r}_i, i = 1, \dots, N$. The likelihood function is

$$p_{\mathbf{r}_1, \dots, \mathbf{r}_N | \mathbf{a}}(\mathbf{R}_1, \dots, \mathbf{R}_N | \mathbf{A}) = \prod_{i=1}^N p_{r_i | \mathbf{a}}(\mathbf{R}_i | \mathbf{A}).$$

The sample mean and covariance matrix are

$$\begin{aligned}\bar{\mathbf{R}} &\triangleq \frac{1}{N} \sum_{i=1}^N \mathbf{R}_i, \\ \mathbf{V} &\triangleq \frac{1}{N} \sum_{i=1}^N (\mathbf{R}_i - \bar{\mathbf{R}})(\mathbf{R}_i - \bar{\mathbf{R}})^T\end{aligned}$$

Likelihood Function	Parameters	Conjugate Prior Distribution	Prior Hyperparameters	Posterior Hyperparameters
Multivariate Gaussian with known covariance \mathbf{K}	Mean μ	Multivariate Gaussian	μ_0, \mathbf{K}_0	$\mu_p = \mathbf{K}_p (\mathbf{K}_0^{-1} \mu_0 + N \mathbf{K}^{-1} \bar{\mathbf{R}}),$ $\mathbf{K}_p = (\mathbf{K}_0^{-1} + N \mathbf{K}^{-1})^{-1}$
Multivariate Gaussian with known mean μ	Covariance \mathbf{K}	Inverse Wishart	n_0, \mathbf{Q}_0	$n_p = n_0 + N,$ $\mathbf{Q}_p = \mathbf{Q}_0 + \sum_{i=1}^N (\mathbf{R}_i - \mu)(\mathbf{R}_i - \mu)^T$
Multivariate Gaussian with known mean μ	Precision $\mathbf{Q} = \mathbf{K}^{-1}$	Wishart	n_0, \mathbf{K}_0	$n_p = n_0 + N,$ $\mathbf{K}_p = \left[\mathbf{K}_0^{-1} + \sum_{i=1}^N (\mathbf{R}_i - \mu)(\mathbf{R}_i - \mu)^T \right]^{-1}$
Multivariate Gaussian	Mean μ and covariance \mathbf{K}	Normal-Inverse Wishart	$\mu_0, \sigma_0^2, n_0, \mathbf{Q}_0$	$\mu_p = \sigma_p^2 \left(\frac{\mu_0}{\sigma_0^2} + N \bar{\mathbf{R}} \right),$ $\sigma_p^2 = \left(\frac{1}{\sigma_0^2} + N \right)^{-1}, n_p = n_0 + N,$ $\mathbf{Q}_p = \mathbf{Q}_0 + N \mathbf{V} + \frac{N \sigma_p^2}{\sigma_0^2} (\bar{\mathbf{R}} - \mu_0)(\bar{\mathbf{R}} - \mu_0)^T$
Multivariate Gaussian	Mean μ and precision \mathbf{Q}	Normal-Wishart	$\mu_0, \sigma_0^2, n_0, \mathbf{K}_0$	$\mu_p = \sigma_p^2 \left(\frac{\mu_0}{\sigma_0^2} + N \bar{\mathbf{R}} \right),$ $\sigma_p^2 = \left(\frac{1}{\sigma_0^2} + N \right)^{-1}, n_p = n_0 + N,$ $\mathbf{K}_p^{-1} = \mathbf{K}_0^{-1} + N \mathbf{V} + \frac{N \sigma_p^2}{\sigma_0^2} (\bar{\mathbf{R}} - \mu_0)(\bar{\mathbf{R}} - \mu_0)^T$

A.3 MATHEMATICAL FUNCTIONS

Function	Notation	Definition	Matlab Syntax
Error	$\text{erf}(Z)$	$\frac{2}{\sqrt{\pi}} \int_0^Z e^{-X^2} dX$	$\text{Y=erf}(Z)$ $\text{Z=erfinv}(Y)$
Complementary error	$\text{erfc}(Z)$	$\frac{2}{\sqrt{\pi}} \int_Z^\infty e^{-X^2} dX = 1 - \text{erf}(Z)$	$\text{Y=erfc}(Z)$ $\text{Z=erfcinv}(Y)$
Modified complementary error	$\text{erfc}_*(Z)$	$\int_Z^\infty \frac{1}{\sqrt{2\pi}} \exp\left(-\frac{X^2}{2}\right) dX$	$\text{P=normcdf}(-Z, 0, 1)$ $\text{Z=-norminv}(P, 0, 1)$
Gamma	$\Gamma(a)$	$\int_0^\infty X^{a-1} e^{-X} dX$	$\text{G=gamma}(a)$
Normalized incomplete Gamma	$\Gamma_a(Z)$	$\frac{1}{\Gamma(a)} \int_0^Z X^{a-1} e^{-X} dX$	$\text{P=gammainc}(Z, a)$ $\text{Z=gaminv}(P, a, 1)$
Multivariate Gamma	$G_M(a)$	$\int_{\mathbf{X}>0} \mathbf{X} ^{a-(M+1)/2} e^{-\text{tr}(\mathbf{X})} d\mathbf{X}$ $= \pi^{M(M-1)/4} \prod_{m=1}^M \Gamma(a - (M-1)/2)$	
Beta	$B(a, b)$	$\int_0^1 X^{a-1} (1-X)^{b-1} dX = \frac{\Gamma(a)\Gamma(b)}{\Gamma(a+b)}$	$\text{B=beta}(a, b)$
Normalized incomplete Beta	$B_{a,b}(Z)$	$\frac{1}{B(a, b)} \int_0^Z X^{a-1} (1-X)^{b-1} dX$	$\text{P=betainc}(Z, a, b)$ $\text{Z=betainv}(P, a, b)$
Digamma	$\psi_0(Z)$	$\frac{d}{dZ} \ln \Gamma(Z) = \frac{\Gamma'(Z)}{\Gamma(Z)}$	$\text{Y=psi}(Z)$
Polygamma	$\psi_m(Z)$	$\frac{d^m}{dZ^m} \psi_0(Z)$	$\text{Y=psi}(m, Z)$
Modified Bessel of the first kind	$I_v(Z)$	$\frac{1}{\pi} \int_0^\pi e^{Z \cos \theta} \cos(v\theta) d\theta$ $- \frac{\sin(v\pi)}{\pi} \int_0^\infty e^{-Z \cosh t - vt} dt$	$\text{Y=besseli}(nu, z)$
Modified Bessel of the second kind	$K_v(Z)$	$\int_0^\infty e^{-Z \cosh t} \cosh(vt) dt$	$\text{Y=besselk}(nu, z)$
Marcum Q	$Q_M(a, b)$	$\int_b^\infty X \left(\frac{X}{a}\right)^{M-1} \exp\left(-\frac{X^2+a^2}{2}\right) I_{M-1}(aX) dX$	$\text{P=marcumq}(a, b, M)$
Confluent hypergeometric	${}_1F_1(a; b; Z)$	$\frac{\Gamma(b)}{\Gamma(a)\Gamma(b-a)} \int_0^1 e^{ZX} X^{a-1} (1-X)^{b-a-1} dX$	
Confluent hypergeometric	${}_1F_1\left(-\frac{1}{2}; 1; Z\right)$	$e^{Z/2} \left[(1-Z) I_0\left(-\frac{Z}{2}\right) - Z I_1\left(-\frac{Z}{2}\right) \right]$	

Appendix B

Example Index

Chapter 1 Examples

No.	Section	Page	Related	Topic
1.1	1.3	11		Max SNR linear filter
1.2	1.3	12		Min MSE quadratic processor

Chapter 2 Examples

No.	Section	Page	Related	Topic
2.1	2.2.1	24		Gaussian mean binary detection
2.2	2.2.1	25		Gaussian variance binary detection
2.3	2.2.1	26		Poisson mean (rate) binary detection
2.4	2.2.1	28		Generalized Gaussian mean binary detection
2.5	2.2.2	36	2.1	ROC, Gaussian mean binary detection
2.6	2.2.2	39	2.2	ROC, Gaussian variance binary detection
2.7	2.2.2	44	2.3	ROC, Poisson mean (rate) binary detection
2.8	2.2.2	48	2.4	ROC, generalized Gaussian mean binary detection
2.9	2.3	58	2.1, 2.5	5-ary Gaussian mean, scalar observation detection
2.10	2.3	59	2.1, 2.5	4-ary Gaussian mean, vector observation detection
2.11	2.3	61	2.4	M -ary generalized Gaussian variance detection
2.12	2.4	73	2.1, 2.5	Bounds, Gaussian mean binary detection
2.13	2.4	75	2.2, 2.6	Bounds, Gaussian variance binary detection
2.14	2.4	77		Bounds, Weibull binary detection
2.15	2.5.1	84	2.1, 2.5, 2.12	Simulation, Gaussian mean binary detection
2.16	2.5.2.5	97	2.1, 2.5, 2.12, 2.15	Importance sampling, Gaussian mean binary detection
2.17	2.5.2.5	99	2.2, 2.6, 2.13	Importance sampling, Gaussian variance binary detection
2.18	2.5.2.5	102		Importance sampling, Beta binary detection
2.19	2.5.2.6	107	2.18	Iterative importance sampling, Beta binary detection

Chapter 3 Examples

No.	Section	Page	Related	Topic
3.1	3.2.1	143		Equal cov. matrix, mean = complex exponential
3.2	3.2.1	144		Equal cov. matrix, mean = planewave
3.3	3.2.3	153		Equal cov. matrix, general case, eigendecomposition
3.4	3.2.4	158		Equal cov. matrix, K Toeplitz
3.5	3.2.5	164	3.4	Equal cov. matrix, K Toeplitz + white noise
3.6	3.2.6	167	3.1	Equal cov. matrix, mean = comp. exp., cov = comp. exp., int. + white noise
3.7	3.2.6	170	3.2	Equal cov. matrix, mean = planewave, cov = planewave int. + white noise
3.8	3.3.1.3	183	3.4, 3.5	Equal mean, K0 = white noise, K1 = complex Toeplitz + white noise
3.9	3.4.2	199		General Gaussian complex
3.10	3.4.3	206		Single quadratic form

Chapter 4 Examples

No.	Section	Page	Related	Topic
4.1	4.1	230		Gaussian linear mean estimation
4.2	4.2.1	237	4.1	Gaussian linear mean Bayesian (MMSE, MAP, ABS) estimation
4.3	4.2.1	241	4.2	Gaussian nonlinear mean MAP estimation
4.4	4.2.1	241		Poisson rate Bayesian (MMSE, MAP) estimation
4.5	4.2.1	243	4.2	Gaussian linear mean conjugate prior
4.6	4.2.1	243	4.4	Poisson rate conjugate prior
4.7	4.2.2	252	4.2, 4.5	Gaussian linear mean ML estimation, estimator mean and variance, CRB
4.8	4.2.2	253	4.4, 4.6	Poisson rate ML estimation, estimator mean and variance, CRB
4.9	4.2.2	254	4.3, 4.7	Gaussian nonlinear mean ML estimation, CRB
4.10	4.2.2	255		Gamma scale (b) ML estimation, estimator mean and variance, CRB
4.11	4.2.2	256	4.10	Gamma inverse scale (beta) ML estimation, estimator mean and variance, CRB
4.12	4.2.2	258	4.10, 4.11	Gamma shape (a) ML estimation, CRB
4.13	4.2.3.1	264	4.2, 4.5, 4.7	Gaussian linear mean BCRB, MSE
4.14	4.2.3.2	266	4.4, 4.6, 4.8	Poisson rate BCRB, ECRB, MSE
4.15	4.2.4	268	3.1	Complex exponential frequency ML estimation, CRB
4.16	4.2.4	271	4.15	Complex exponential frequency, MAP estimation, BCRB, ECRB
4.17	4.2.5.1	280	4.2, 4.5, 4.7, 4.13	Gaussian linear mean, exp. family
4.18	4.2.5.1	281	4.4, 4.6, 4.8, 4.14	Poisson rate, exp. family
4.19	4.2.5.1	281	4.10, 4.11	Gamma scale (b, beta), exp. family
4.20	4.2.5.1	282		Weibull scale (b), exp. family
4.21	4.2.5.1	283	4.2, 4.5, 4.7, 4.13, 4.17	Gaussian linear mean, exp. family cumulants

(Continued)

Chapter 4 Examples (Continued)

No.	Section	Page	Related	Topic
4.22	4.2.5.1	284	4.11, 4.19	Gamma scale (beta), exp. family cumulants
4.23	4.2.5.1	285	4.2, 4.5, 4.7, 4.13, 4.17, 4.21	Gaussian linear mean, exp. family ML and CRB
4.24	4.2.5.1	286	4.10, 4.11, 4.19, 4.22	Gamma scale (b, beta), exp. family ML and CRB
4.25	4.2.5.2	288	4.10, 4.19, 4.24	Gamma scale (b), exp. family Bayesian
4.26	4.3.3.1	303	4.2, 4.5, 4.7, 4.13, 4.17, 4.21, 4.23	Gaussian mean and variance, ML, CRB, estimator mean and variance
4.27	4.3.3.1	306		Mutivariate Gaussian mean vector, ML, CRB, estimator mean and variance
4.28	4.3.3.1	307	4.10, 4.12, 4.19, 4.24, 4.25	Gamma scale (b) and shape (a), ML, CRB
4.29	4.3.3.1	310	4.15, 4.16	Complex exponential frequency and phase, ML, CRB
4.30	4.3.3.1	312	3.2, 4.29	Wavenumber, complex amplitude (mag and phase), ML, CRB
4.31	4.3.3.2	320	4.27	Multivariate Gaussian mean vector, MAP, MMSE, MSE, BCRB, conjugate prior
4.32	4.3.4.1	323	4.17, 4.21, 4.23, 4.26	Gaussian mean and variance, exp. family ML and CRB
4.33	4.3.6.1	330	4.30	Wavenumber, complex amplitude (mag and phase), array perturbations, hybrid ML/MAP
4.34	4.4.1.3	337	4.15, 4.16, 4.29	Complex exponential frequency, WWB
4.35	4.4.2	346	4.15, 4.16, 4.29, 4.34	Complex exponential frequency, MIE ML
4.36	4.4.2	347	4.15, 4.16, 4.29, 4.34, 4.35	Complex exponential frequency, MIE MAP
4.37	4.5.1	348	2.1, 2.5	Gaussian mean (unknown) binary detection
4.38	4.5.2	350	4.2, 4.37	Gaussian mean vector (unknown random magnitude) binary detection
4.39	4.5.2	351	4.37, 4.38	Gaussian mean V theta (unknown random theta) binary detection
4.40	4.5.3	352	2.1, 2.5, 4.37	Gaussian mean (unknown nonrandom) UMP test
4.41	4.5.3	357	4.40	Gaussian mean (unknown nonrandom) MLR
4.42	4.5.3	358	2.3	Poisson rate (unknown nonrandom) one-sided binary detection, MLR, UMP test
4.43	4.5.3	358	4.19	Gamma scale (b) (unknown nonrandom) binary detection, exp. fam. MLR, UMP test
4.44	4.5.3	359	4.7, 4.37, 4.40	Gaussian mean (unknown nonrandom) binary detection, GLRT
4.45	4.5.3	361	4.38, 4.44	Gaussian mean vector (unknown nonrandom magnitude) binary detection, GLRT
4.46	4.5.3	363	4.45	Gaussian mean vector (unknown nonrandom magnitude and variance) binary detection, GLRT
4.47	4.5.3	368	4.39, 4.46	Gaussian mean V theta (unknown nonrandom theta and variance) binary detection, GLRT

Chapter 5 Examples

No.	Section	Page	Related	Topic
5.1	5.2.1	402		FLG
5.1a	5.2.1	403		FLG, tracking
5.2	5.2.1	403		FLG complex
5.2a	5.2.1	404	3.1, 3.6, 4.15	FLG complex, comp. exp.
5.2b	5.2.1	404	3.2, 3.7, 4.30	FLG complex, planewave
5.3	5.2.1	405		Separable
5.4	5.2.1	405		Separable complex
5.4a	5.2.1	405	5.2a	Separable complex, $V = \text{comp. exp.}$
5.4b	5.2.1	405	5.2b	Separable complex, $V = \text{planewave}$
5.5	5.2.1	406		$K = \text{colored noise}$
5.5w	5.2.1	406	4.46	$K = \text{white noise}$
5.6	5.2.1	406		$K = \text{rank 1 interference} + \text{white noise}$
5.6a	5.2.1	406		$K = \text{rank 1 int.} + \text{white noise; comp. exp.}$
5.7	5.2.1	407	5.6a	$K = \text{rank 1 interference} + \text{white noise; comp. exp.}$
5.8	5.2.4.2	418	5.1a	FLG, tracking; ML, Cov = CRB
5.9	5.2.4.2	419	5.2	FLG complex, $D = 2$; ML, Cov = CRB
5.9a	5.2.4.2	421	5.2a, 5.9, 4.15	FLG complex, comp. exp., $D = 2$; ML, Cov = CRB
5.9b	5.2.4.2	423	5.2b, 5.9, 5.9a, 4.30	FLG complex, planewave, $D = 2$; ML, Cov = CRB
5.10	5.2.4.3	426	5.2b (3.7, 5.9b)	FLG complex, rank 1 int., planewave, $D=1$; ML, Cov=CRB
5.11	5.2.5	436	4.29, 5.4a, 5.9a	Separable, $D = 1$ comp. exp.; ML, CRB
5.12	5.2.5	437	4.29, 5.4a, 5.9a, 5.11	Separable, D comp. exp; ML, CRB
5.13	5.2.5	439	4.29, 5.4a, 5.9a, 5.11, 5.12	Separable, $D = 2$ comp. exp.; ML, CRB
5.14	5.2.6.3	449	5.6a	$K = \text{rank 1 int.} + \text{white noise, comp. exp.}$
5.15	5.2.8.3	460	5.13	Separable, $D = 2$ comp. exp.; AP Alg
5.16	5.2.8.4	467	5.13, 5.15	Separable, $D = 2$ comp. exp.; EM, SAGE Alg
5.17	5.2.10.1	474	5.10, 4.33	FLG complex, rank 1 int., planewave, $D = 1$; ML, array perturbations
5.18	5.2.10.2	480	5.10, 5.17, 4.33	FLG complex, rank 1 int., planewave, $D = 1$; array perturbations, diagonal loading
5.19	5.3.1	484	4.5	Gaussian mean MMSE, MSE
5.20	5.3.1	484	4.26	Gaussian variance MMSE, MSE
5.21	5.3.2	491	Section 3.3	BLG, MAP, MSE
5.22	5.3.2	492		BLG; MAP, MSE
5.23	5.3.2	492	5.1a, 5.8	BLG, tracking; MAP/MMSE, MSE = BCRB
5.24	5.4.1	501	5.19	Sequential Bayes, Gaussian mean; MMSE, MSE
5.25	5.4.1	502	5.1a, 5.8, 5.23	Sequential Bayes, tracking; MMSE
5.26	5.4.2	504	5.1a, 5.8, 5.23, 5.25	Sequential ML; tracking
5.27	5.4.2	505		Sequential Polynomial fitting

Chapter 6 Examples

No.	Section	Page	Related	Topic
6.1	6.3.1	529		Single-time characterization of random process
6.2	6.4.1	541		Eigendecomposition of BW1 process
6.3	6.4.3	549		Eigendecomposition of Wiener process
6.4	6.5	566		Eigendecomposition of vector process

Chapter 7 Examples

No.	Section	Page	Related	Topic
7.1	7.2.1.3	603		M -ary detection, QPSK signals in WGN
7.2	7.2.1.3	603		M -ary detection FSK signals in WGN
7.3	7.2.1.3	604	7.1	Probability of error for QPSK
7.4	7.2.1.3	605		M -ary detection, orthogonal signals
7.5	7.2.1.3	608		Sequence of digits
7.6	7.2.3	619		Arrival time estimation
7.7	7.2.3	621		Pulse frequency modulation
7.8	7.3.6.1	651		Whitening filter, SPLIT, CGN, BW1 + WGN
7.9	7.3.6.1	653		Whitening filter, SPLIT, CGN, BW1
7.10	7.3.6.2	657		Fredholm eqn., First kind
7.11	7.3.6.2	660		Fredholm eqn., Second kind
7.12	7.3.6.2	661		Optimum linear filter
7.13	7.4.1	685		BP signal w uniform phase, ROC
7.14	7.4.1	686		Partially coherent binary comm.
7.15	7.5.1.1	715		Maximal ratio combiner
7.16	7.6	719		Estimate ampl. and phase of sinusoid

Chapter 8 Examples

No.	Section	Page	Related	Topic
8.1	8.2.1	789		Realizable whitening filter, BW1
8.2	8.2.1	789		Realizable whitening filter, 1 zero, 1 pole
8.3	8.2.1	794		Wiener filter, BW 1 + WGN
8.4	8.2.2	800	8.3	Wiener filter, BW 1 + WGN, prediction/delay
8.5	8.3.1	809		Differential eqn. representation
8.6	8.3.1	812		State-variable representation
8.7	8.3.1	813		State-variable representation
8.8	8.3.1	818		State-variable representation, time varying
8.9	8.3.1	821		Solution to state eqn.
8.10	8.3.2	831		Kalman filter, BW1 + WGN
8.11	8.3.2	834		Kalman filter, BWN + WGN
8.12	8.3.2	836		Kalman filter, steady state
8.13	8.3.2	837		Kalman filter, SS, rational spectrum

Chapter 9 Examples

No.	Section	Page	Related	Topic
9.1	9.2.2	886		Autocorrelation function, AR(1)
9.2	9.2.2	891		Autocorrelation function, AR(2)
9.3	9.2.3	896	9.1	FIR Wiener filter, AR(1) + WGN
9.4	9.2.3	898	9.1	FIR Wiener filter with lag, AR(1) + WGN
9.5	9.2.4	902	9.1	Unrealizable IIR Wiener filter, AR(1) + WGN
9.6	9.2.5	905	9.1	IIR whitening filter, AR(1)
9.7	9.2.5	906	9.4	IIR whitening filter, AR(1) + WGN
9.8	9.2.5	910	9.4	IIR Wiener filter, AR(1) + WGN, $L < 0$, $L = 0$, $L > 0$
9.9	9.3.2.3	939		Kalman filter, AR(1) + WGN
9.10	9.3.2.3	943		Kalman filter, constant velocity track, WGN
9.11	9.3.2.3	946		Kalman filter, BW(N,N) + WGN
9.12	9.3.2.3	949		ULA, reduced dim. Kalman filter
9.13	9.3.2.4	955		Kalman filter, AR(1) + CGN
9.14	9.3.2.7	963		Divergence due to bias
9.15	9.3.2.8	969		Mismatched Kalman filter
9.16	9.3.3.1	974	9.9	Fixed-lead Kalman predictor, AR(1) + WGN
9.17	9.3.3.2	976	9.9	Fixed-point Kalman predictor, AR(1) + WGN
9.18	9.3.4.1	979	9.9	Fixed-interval Kalman smoother, AR(1) + WGN
9.19	9.3.4.2	982	9.9	Fixed-lag Kalman smoother, AR(1) + WGN
9.20	9.3.5.4	992		Dynamic freq. estimation, EKF + BCRB
9.21	9.3.5.4	996		2D CV tracking, EKF + BCRB
9.22	9.3.5.4	998		Ballistic missile tracking, EKF + BCRB
9.23	9.3.5.5	1007	9.9, 9.15	Joint state and parameter est., EKF, AR(1) + WGN

Chapter 10 Examples

No.	Section	Page	Related	Topic
10.1	10.2.4	1050		CT state-variable impl. of optimum detector, BW1 + WGN
10.2	10.2.5	1055	10.1	CT state-variable impl. of optimum detector, BW1 + WGN, SPLIT
10.3	10.2.5	1059		CT state-variable impl. of optimum detector, bandlimited spectrum + WGN, SPLIT

References

- Abe93. J. S. Abel. A bound on the mean-square-estimate error. *IEEE Trans. Inform. Theory*, 39(5):1675–1680, September 1993.
- AC71. B. D. O. Anderson and S. Chirarattananon. Smoothing as an improvement on filtering. *Electron. Lett.*, 7(18):524, 1971.
- AD62. E. Arthurs and H. Dym. On the optimum detection of digital signals in the presence of white Gaussian noise—a geometric interpretation and a study of three basic data transmission systems. *IRE Trans. Commun. Syst.*, 10:336–372, Dec. 1962.
- AF66. M. Athans and P. L. Falb. *Optimal Control*. McGraw-Hill, New York, 1966.
- AH83. V. Aidala and S. Hammel. Utilization of modified polar coordinates for bearings-only tracking. *IEEE Trans. Auto. Control*, AC-28(3):283–294, March 1983.
- Aki63. H. Akima. Theoretical studies on signal-to-noise characteristics of an FM system. *IEEE Trans. Space Electron. Telemetry*, SET-9:101–108, 1963.
- AM79. B. D. O. Anderson and J. B. Moore. *Optimal Filtering*. Prentice Hall, Englewood Cliffs, NJ, 1979.
- AMGC02. M. S. Arulampalam, S. Maskell, N. Gordon, and T. Clapp. A tutorial on particle filters for online nonlinear/non-Gaussian Bayesian tracking. *IEEE Trans. Sig. Process*, 50(2):174–188, 2002.
- And68. A. Andrews. A square root formulation of the Kalman covariance equation. *AIAA*, 6:1165–1166, 1968.
- And69. B. D. O. Anderson. Properties of optimal linear smoothing. *IEEE Trans. Auto. Control*, AC-14 (1):114–115, 1969.
- Aok67. M. Aoki. *Optimization of Stochastic Systems: Topics in Discrete-time Systems*. Academic Press, New York, 1967.
- AS64. M. Abramovitz and I. A. Stegun, editors. *Handbook of Mathematical Functions*. National Bureau of Standards, U.S. Government Printing Office, Washington, DC, June 1964.
- AS72. D. L. Alspach and H. W. Sorenson. Nonlinear Bayesian estimation using Gaussian sum approximations. *IEEE Trans. Auto. Control*, 17(4):439–448, 1972.
- Ath05. F. Athley. Threshold region performance of maximum likelihood direction of arrival estimators. *IEEE Trans. Sig. Process.*, 53(4):1359–1373, April 2005.
- AWB68. M. Athans, R. P. Wishner, and A. Bertolini. Suboptimal state estimation for continuous-time nonlinear systems from discrete noisy measurements. *IEEE Trans. Auto. Control*, AC-13:504–514, October 1968.
- Bag61. E. J. Baghdady. *Lectures on Communication System Theory*. McGraw-Hill, New York, 1961.

- Bag66. A. B. Baggeroer. Maximum *a posteriori* interval estimation. In *WESCON, Paper No. 7/3*, August 23–26, 1966.
- Bag67a. A. B. Baggeroer. A state-variable technique for the solution of Fredholm integral equations. In *IEEE International Conference on Communications*, Minneapolis, June 12–14, 1967.
- Bag67b. A. B. Baggeroer. A state-variable technique for the solution of Fredholm integral equations. R.L.E 459, MIT, July 15, 1967.
- Bag68. A. B. Baggeroer. *State variables, the Fredholm theory, and optimal communications*. Ph.D. thesis, Department of Electrical Engineering, Massachusetts Institute of Technology, January 1968.
- Bag69. A. B. Baggeroer. Barankin bound on the variance of estimates of Gaussian random process. Technical Report, MIT Research Laboratory of Electronics, Lexington, MA, January 1969.
- Bal61. A. V. Balakrishnan. A contribution to the sphere packing problem of communication theory. *J. Math. Anal. Appl.*, 3:485–506, December 1961.
- Ban71. W. J. Bangs. *Array processing with generalized beamformers*. Ph.D. thesis, Yale University, New Haven, CT, 1971.
- Bar49. E. W. Barankin. Locally best unbiased estimates. *Ann. Math. Stat.*, 20:477, 1949.
- Bat64. R. H. Battin. *Astronomical Guidance*. McGraw-Hill, New York, 1964.
- BD67. J. F. Bellantoni and K. W. Dodge. A square root formulation of the Kalman–Schmidt filter. *AIAA*, 5:1309–1314, 1967.
- Bel53. R. E. Bellman. *Stability Theory of Differential Equations*. McGraw-Hill, New York, 1953.
- Bel60. R. Bellman. *Introduction to Matrix Analysis*. MacGraw-Hill, New York, NY, 1960.
- Bel95. K. Bell. *Performance bounds in parameter estimation with application to bearing estimation*. Ph.D. thesis, George Mason University, Fairfax, VA, 1995.
- Ben81. V. E. Benes. Exact finite-dimensional filters with certain diffusion non linear drift. *Stochastics*, 5:65–92, 1981.
- BEV96. K. Bell, Y. Ephraim, and H. L. Van Trees. Explicit Ziv-Zakai lower bounds for bearing estimation. *IEEE Trans. Sig. Process.*, 44(11):2810–2824, November 1996.
- BF63. A. E. Bryson and M. Frazier. Smoothing for linear and nonlinear dynamic systems. Technical Report ASD-TDR-63-119, USAF, February 1963.
- BFS87. P. Bratley, B. L. Fox, and L. A. Schrage. *A Guide to Simulation*. Springer-Verlag, New York, NY, 1987.
- BH69. A. E. Bryson and Y. C. Ho. *Applied Optimal Control*. Blaisdell Publishing Company, Waltham, MA, 1969.
- Bha43. A. Bhattacharyya. On a measure of divergence between two statistical populations defined by their probability distributions. *Bull. Calcutta Math. Soc.*, 35(3):99–110, 1943.
- Bha48. A. Bhattacharyya. On some analogues of the amount of information and their use in statistical estimation. *Sankhya*, 8:1, 201, 315, 1946, 1947, 1948.
- BHL98. D. Brigo, B. Hanzon, and F. LeGland. A differential geometric approach to nonlinear filtering. *IEEE Trans. Auto. Control*, 43(2):247–252, February 1998.
- BID55. K. Bullington, W. J. Inkster, and A. L. Durkee. *Results of propagation tests at 505 Mc and 4090 Mc on beyond-horizon paths*. *Proc. IRE*, 43, 1955.
- Bie77. G. J. Bierman. *Factorization Methods for Discrete Sequential Estimation*. Academic Press, New York, 1977.
- BL64. J. J. Bussgang and M. Leiter. Error rate approximation for differential phase-shift keying. *IEEE Trans. Commun. Syst.*, 12:18–27, March 1964.
- BL70. R. H. Battin and G. M. Levine. Application of kalman filtering techniques in the Apollo program. *Theory and Applications of Kalman Filtering, NATO Advisory Group for Aerospace Research and Development, AGARDograph*, 139, February 1970.
- BM72. K. K. Biswas and A. K. Mahalanabis. Optimal fixed-lag smoothing for time-delayed systems with colored noise. *IEEE Trans. Auto. Control*, AC-17:387–388, 1972.

- BM73a. K. K. Biswas and A. K. Mahalanabis. On computational aspects of two recent smoothing algorithms. *IEEE Trans. Auto. Control*, AC-18:395–396, 1973.
- BM73b. K. K. Biswas and A. K. Mahalanabis. On the stability of a fixed-lag smoother. *IEEE Trans. Auto. Control*, AC-18:63–64, 1973.
- BMZ87. B. Z. Bobrovsky, E. Mayer-Wolf, and M. Zakai. Some classes of global Cramér–Rao bounds. *Ann. Stat.*, 15:1421–1438, 1987.
- BP57. D. G. Brennan and M. L. Philips. Phase and amplitude variability in medium-frequency ionospheric transmission. Technical Report, MIT, Lincoln Lab., September 1957.
- BR60. A. T. Bharucha-Reid. *Elements of the Theory of Markov Processes and Their Applications*. MacGraw-Hill, New York, NY, 1960.
- Bra83. D. H. Brandwood. A complex gradient operator and its application in adaptive array theory. *IEE Proc. F and H*, 130(1):11–16, 1983.
- Bre55. D. G. Brennan. On the maximum signal-to-noise ratio realizable from several noisy signals. *Proc. IRE*, 43:1530, 1955.
- BS50. H. W. Bode and C. E. Shannon. A simplified derivation of linear least-squares smoothing and prediction theory. *Proc. IRE*, 38:417–426, 1950.
- BSLK01. Y. Bar-Shalom, X. R. Li, and T. Kirubarajan. *Estimation with Applications to Tracking and Navigation*. John Wiley and Sons, New York, NY, 2001.
- BT77. G. J. Bierman and C. L. Thornton. Numerical comparison of Kalman filter algorithms: orbit determination case study. *Automatica*, 13:23–35, 1977.
- Buc90. J. A. Bucklew. *Large Detection Techniques in Decision, Simulation and Estimation*. John Wiley, New York, NY, 1990.
- BV06. K. Bell and H. L. Van Trees. Combined Cramér–Rao/Weiss–Weinstein bound for tracking target bearing. In *Fourth Annual IEEE Workshop on Sensor Array and Multi-Channel Processing (SAM 2006)*, Waltham, MA, July 2006, pp. 273–277.
- BZ75. B. Z. Bobrovsky and M. Zakai. A lower bound on the estimation error for Markov processes. *IEEE Trans. Auto. Control*, 20(6):785–788, December 1975.
- BZ76. B. Z. Bobrovsky and M. Zakai. A lower bound on the estimation error for certain diffusion processes. *IEEE Trans. Inform. Theory*, IT-22(1):45–52, January 1976.
- BZZ88. B. Bobrovsky, M. Zakai, and O. Zetouni. Error bounds for the nonlinear filtering of signals with small diffusion coefficients. *IEEE Trans. Inform. Theory*, 34(4):710–721, 1988.
- Cah59. C. R. Cahn. Performance of digital phase-modulation systems. *IRE Trans. Commun. Syst.*, 7:3–6, 1959.
- Car73. N. A. Carlson. Fast triangular formulation of the square root filter. *AIAA*, 11(9):1259–1265, 1973.
- Car88. B. D. Carlson. Covariance matrix estimation errors and diagonal loading in adaptive arrays. *IEEE Trans. Aerospace Electron. Syst.*, 24(4):397–401, July 1988.
- CCF99. J. Carpenter, P. Clifford, and P. Fearnhead. Improved particle filter for non-linear problems. *IEE Proc. Part F: Radar Sonar Navigation*, 146:2–7, February 1999.
- CFM83. M. Cottrell, J. C. Fort, and G. Malgouyres. Large deviations and rare events in the study of stochastic algorithms. *IEEE Trans. Auto. Control*, AC-28:907–920, September 1983.
- CH53. R. Courant and D. Hilbert. *Methods of Mathematical Physics*. Interscience Publishers, 1953.
- Che62. H. Chernoff. A measure of asymptotic efficiency for tests of a hypothesis based on the sum of observations. *Ann. Math. Stat.*, 23:493–507, 1962.
- CK84. T. K. Citron and T. Kailath. An improved eigenvector beamformer. In *Proceedings of the International Conference on Acoustics, Speech and Signal Processing*, 1984.
- CL55. E. A. Coddington and N. Levinson. *Theory of Ordinary Differential Equations*. McGraw-Hill, New York, 1955.
- Col65. W. J. Coles. Matrix Riccati differential equations. *J. Soc. Indust. Appl. Math.*, 13, September 1965.

- Col66a. L. Collins. An expression for $\frac{\partial h_o(s, t; t)}{\partial t}$. *Detection and Estimation Theory Group Internal Memo (April)*, IM-LDC-6, MIT, April 1966.
- Col66b. L. D. Collins. Realizable likelihood function computers for known signals in colored noise. MIT Research Lab of Electronics, Cambridge, MA, Internal Memo, IM-LDC-7, May 1966.
- Col66c. L. D. Collins. Realizable whitening filters. MIT Research Lab of Electronics, Cambridge, MA, Internal Memo, IM-LDC-5, April 1966.
- Col67. L. Collins. An asymptotic expression for the error probability for signals with random phase. Detection and Estimation Theory Group Internal Memo IM-LDC-20, MIT, February 3, 1967.
- Col68a. L. D. Collins. *Asymptotic approximation to the error probability for detecting Gaussian signals*. Sc. d., Department of Electrical Engineering, Massachusetts Institute of Technology, Cambridge, June 1968.
- Col68b. L. D. Collins. Closed-form expressions for the Fredholm determinant for state-variable covariance functions. *Proc. IEEE (Letters)*, 56:350–351, March 1968.
- Col68c. L. D. Collins. Realizable whitening filters and state-variable realizations. *Proc. IEEE (Letters)*, 56:100–101, January 1968.
- Cox73. H. Cox. Resolving power and sensitivity to mismatch of optimum array processors. *J. Acoust. Soc. Am.*, 54(3):771–785, September 1973.
- Cox99. Henry Cox. Adaptive array processing: a tour beneath the sea (Keynote Lecture). In *1999 Adaptive Sensor Array Processing (ASAP) Workshop*, M.I.T. Lincoln Laboratory, Lexington, MA, 1999.
- Cra46. H. Cramér. *Mathematical Methods of Statistics*. Princeton University Press, Princeton, NJ, 1946.
- CV07. C.-Y. Chen and P. P. Vaidyanathan. Quadratically constrained beamforming robust against direction-of-arrival mismatch. *IEEE Trans. Sig. Process.*, 55(8):4139–4150, August 2007.
- CY92. L. Chang and C. Yeh. Performance of DMI and eigenspace-based beamformers. *IEEE Trans. Ant. Prop.*, 40:1336–1347, November 1992.
- CZO87. H. Cox, R. M. Zeskind, and M. M. Owen. Robust adaptive beamforming. *IEEE Trans. Acoust., Speech, Sig. Process.*, ASSP-35(10):1365–1376, October 1987.
- Dar58. S. Darlington. Linear least-squares smoothing and prediction, with applications. *B. J. S. T.*, 37:1221–1294, September 1958.
- Dar64. S. Darlington. Demodulation of wideband, low-power FM signals. *Bell Syst. Tech. J.*, 43(1):339–374, 1964.
- Dau86. F. E. Daum. Exact finite dimensional nonlinear filters. *IEEE Trans. Auto. Control*, 31(7):616–622, 1986.
- Dau87. F. E. Daum. Solution of the Zakai equation by separation of variables. *IEEE Trans. Auto. Control*, AC-32(10):941–943, 1987.
- Dau88. F. E. Daum. *Bayesian Analysis of Time Series and Dynamic Models*, Chapter New Exact nonlinear Filters, Vol. 8. Marcel-Dekker, New York, 1988, pp. 199–226.
- Dau95. F. E. Daum. Beyond Kalman filters: practical design of nonlinear filters. *Proc. SPIE*, 31(7):252–262, 1995.
- DdG01. A. Doucet, N. de Freitas, and N. J. Gordon, editors. *Sequential Monte Carlo Methods in Practice*. Springer, New York, 2001.
- DeL93. D. F. DeLong. Use of the Weiss–Weinstein bound to compare the direction-finding performance of sparse arrays. Technical Report 982, MIT Lincoln Laboratory, Lexington, MA, 1993.
- DeV86. L. DeVroye. *Non-Uniform Random Variate Generation*. Springer-Verlag, New York, NY, 1986.
- DG02. P. M. Djuric and S. J. Godsill. Special issue on Monte Carlo methods for statistical signal processing. *IEEE Trans. Sig. Process.*, 50, February 2002.

- DGA00. A. Doucet, S. Godsill, and C. Andrieu. On Sequential Monte Carlo sampling methods for Bayesian filtering. *Stat. Comput.*, 10(3):197–208, 2000.
- DHM57. M. Doelz, E. Heald, and D. Martin. Binary data transmission techniques for linear systems. *Proc. IRE*, 45:656–661, May 1957.
- DJ62. A. R. Di Donato and M. P. Jarnagin. A method for computing the circular coverage function. *Math. Comp.*, 16:347–355, 1962.
- DLR77. A. P. Dempster, N. M. Laird, and D. B. Rubin. Maximum likelihood from incomplete data via the EM algorithm. *J. Roy. Stat. Soc.*, December 1977, pp. 1–38.
- DM69. P. Dyer and S. McReynolds. Extension of square-root filtering to include process noise. *J. Optim.: Theory Appl.*, 3:444–458, June 1969.
- Doe95. P. C. Doerschuk. Cramér–Rao bounds for discrete-time nonlinear filtering problems. *IEEE Trans. Auto. Control*, 40(8):1465–1469, 1995.
- Doo53. J. Doob. *Stochastic Processes*. John Wiley and Sons, Inc., New York, 1953.
- DR58. W. B. Davenport and W. L Root. *An Introduction to the Theory of Random Signals and Noise*. McGraw-Hill, New York, NY, 1958.
- DR68. J. V. DiFranco and W. L. Rubin. *Radar Detection*. Prentice Hall, Englewood Cliffs, NJ, 1968.
- DR87. W. B. Davenport and W. L Root. *An Introduction to the Theory of Random Signals and Noise*. IEEE Press, New York, 1987.
- DRC65. P. M. DeRusso, R. J. Roy, and C. M. Close. *State Variables for Engineers*. Wiley, New York, 1965.
- DS83. J. E. Dennis and R. B. Schnabel. *Numerical Methods for Unconstrained Optimization and Nonlinear Equations*. Prentice Hall, Englewood Cliffs, NJ, 1983.
- DS96. J. E. Dennis and R. B. Schnabel. *Numerical Methods for Unconstrained Optimization and Nonlinear Equations*. Prentice Hall, Inc., Englewood Cliffs, NJ, 1996. SIAM edition, an unabridged, corrected republication of the book in 1983.
- Dug37. D. Dugué. Applications des propriétés de la limite du sens du calcul des probabilités à l'études des diverses questions d'estimation. *Journal de l'École Polytechnique Paris*, 3(4):305–372, 1937.
- Dun68. T. Duncan. Probability densities for diffusion processes with applications to nonlinear filtering theory and detection theory. *Inform. Control*, 13:62–74, July 1968.
- Dun86. M. J. Dunn. *Sufficiency and invariance principles applied to four detection problems*. Master's thesis, University of Colorado at Boulder, 1986.
- Dur60. J. Durbin. The fitting of time series models. *Rev. Inst. Int. Stat.*, 28:233–243, 1960.
- DW48. C. L. Dolph and M. A. Woodbury. On the relation between green's functions and covariances of certain stochastic processes and its application to unbiased linear prediction. *Trans. Am. Math. Soc.*, 1948.
- Ech91. J. D. Echard. Estimation of radar detection and false alarm probabilities. *IEEE Trans. Aerospace Electron. Syst.*, 27(2):255–260, March 1991.
- Eld04. Y. C. Eldar. Minimum variance in biased estimation: Bounds and asymptotically optimal estimators. *IEEE Trans. Sig. Process.*, 52:1915–1930, July 2004.
- Erd54. A. Erdelyi et al. *Higher Transcendental Functions*. McGraw-Hill, New York, 1954.
- Ess32. F. Esscher. On the probability function in the collective theory of risk. *Scand. Actuarial J.*, 15:175–195, 1932.
- Fan61. R.M. Fano. *Transmission of Information*. MIT Press and Wiley, Cambridge, MA and New York, 1961.
- Far83. D.R. Farrier. Gain of an array of sensors subjected to processor perturbation. *Proc. Inst. Elec. Eng.*, 72(pt. H, no. 4):251–254, June 1983.
- Fel57. W. Feller. *An Introduction to Probability Theory and Its Applications*, volume I. Wiley, New York, NY, 1957.
- Fel66. W. Feller. *An Introduction to Probability Theory and Its Applications*, volume II. Wiley, New York, NY, 1966.

- Fen59. A. V. Fend. On the attainment of Cramér–Rao and Bhattacharyya bounds for the variance of an estimate. *Ann. Math. Stat.*, 30:381–388, 1959.
- Fer67. T. S. Ferguson. *Math. Stat.* Academic Press, New York, 1967.
- FH94. J. A. Fessler and A. O. Hero. A recursive algorithm for computing Cramér–Rao-type bounds on estimator covariance. *IEEE Trans. Inform. Theory*, 40(4):1205–10, July 1994.
- Fis22. R. A. Fisher. On the mathematical foundations theoretical statistics. *Phil. Trans. Royal Soc., London*, 222:309, 1922.
- Fis25. R. A. Fisher. Theory of statistical estimation. *Proc. Cambridge Phil. Soc.*, 22:700, 1925.
- Fis34. R. A. Fisher. Two new properties of mathematical likelihood. *Proc. Cambridge Phil. Soc., London*, 144:285, 1934.
- Fis35. R. A. Fisher. The logic of inductive inference. *J. Royal Stat. Soc.*, 98:39, 1935.
- Fit71. R. M. Fitzgerald. Divergence of the Kalman filter. *IEEE Trans. Auto. Control*, AC-16:736–743, 1971.
- Fla57. C. Flammer. *Spheroidal Wave Functions*. Stanford University Press, 1957.
- FP69. D. C. Fraser and J. E. Potter. The optimum linear smoother as a combination of two optimum linear filters. *IEEE Trans. Auto. Control*, AC-14 (4):387–390, 1969.
- Fra67. D. C. Fraser. A new technique for the optimal smoothing of data. Technical Report, Rep. T-474, MIT Instrumentation Lab, January 1967, p. 114.
- Fré43. M. Fréchet. Sure l’extension du certaines évaluations statistiques au cas de petits échantillons. *Rev. Int. Stat.*, 11:185–205, 1943.
- Fro72. O. L. Frost, III. An algorithm for linearly constrained adaptive array processing. *Proc. IEEE*, 60(8):926–935, August 1972.
- FW88. M. Feder and E. Weinstein. Parameter estimation of superimposed signals using the EM algorithm. *IEEE Trans. Acoust., Speech, and Sig. Proc.*, 36(4):477–489, April 1988.
- FY53. R. Fisher and F. Yates. *Statistical Tables for Biological, Agricultural, and Medical Research*. Oliver and Boyd, Edinburgh, 1953.
- GA93. M. S. Grewal and A. P. Andrews. *Kalman Filtering: Theory and Practice*. Prentice Hall, Englewood Cliffs, NJ, 1993.
- GA08. M. S. Grewal and A. P. Andrews. *Kalman Filtering: Theory and Practice using MATLAB*. Wiley, 2008.
- Gab86. W. F. Gabriel. Using spectral estimation technique in adaptive processing antenna system. *IEEE Trans. Ant. Prop.*, 1986.
- Gal63. C. A. Galtieri. *On the Characterization of Continuous Gaussian Processes*. Electronics Research Laboratory, University of California, Berkeley, Internal Tech, July 1963.
- Gal65. R.G. Gallager. Lower bounds on the tails of probability distributions. QPR 77 277-291, MIT, RLE, April 1965.
- Gal79. J. I. Galdos. A Lower bound on Filtering Error with Application to Phase Demodulation. *IEEE Trans. Inform. Theory*, 25(4):452–462, 1979.
- Gau63. K. G. Gauss. *Theory of Motion of the Heavenly Bodies*. Dover, New York, 1963.
- GBE⁺64. S. W. Golomb, L. D. Baumert, M. F. Easterling, J. J. Stiffer, and A. J. Viterbi. *Digital Communications*. Prentice Hall, Englewood Cliffs, NJ, 1964.
- GCSR04. A. Gelman, J. B. Carlin, H. S. Stern, and D. B. Rubin. *Bayesian Data Analysis*. Chapman and Hall, New York, NY, 2004.
- Gel74. A. Gelb. *Applied Optimal Estimation*. MIT Press, Cambridge, MA, 1974.
- GH62. J. A. Greenwood and H. O. Hartley. *Guides to Tables in Mathematical Statistics*. Princeton University Press, Princeton, NJ, 1962.
- GH90. J. D. Gorman and A. O. Hero. Lower bounds for parametric estimation with constraints, *IEEE. Trans. Info. Theory*, 36(6):1285–1301, 1990.
- GL95. R. D. Gill and B. Y. Levit. Applications of the Van Trees inequality: a Bayesian Cramér–Rao bound. *Bernoulli* 1, 1(2):59–79, 1995.
- GM55. E. N. Gilbert and S. P. Morgan. Optimum design of directive antenna arrays subject to random variations. *Bell Syst. Tech. J.*, 34:637–663, May 1955.

- GMW81. P. E. Gill, W. Murray, and M. H. Wright. *Practical Optimization*. Academic, London, 1981.
- God85. L.C. Godara. The effect of phase-shifter error and the performance of an antenna array beamformer. *IEEE J. Ocean. Engr.*, OE-10(3):278–284, July 1985.
- God86. L. C. Godara. Error analysis of the optimal antenna array processors. *IEEE Trans. Aerospace Electron. Syst.*, AES-22(4):395–409, July 1986.
- GP73. G. Golub and V. Pereyra. The differentiation of pseudo inverses and nonlinear least squares problems whose variables separable. *SIAM J. Numer. Anal.*, 10:413–432, 1973.
- Gre50. U. Grenander. Stochastic processes and statistical inference. *Arkiv Matematik*, 1:195–277, 1950.
- GSS93. N. J. Gordon, D. J. Salmond, and A. F. M. Smith. Novel approach to nonlinear/non-Gaussian Bayesian state estimation. *IEE Proc.-F*, 140(2):107–113, 1993.
- Gui57. E. A. Guillemin. *Synthesis of Passive Networks*. Wiley, New York, 1957.
- Gun63. T. L. Gunckel. Orbit determination using Kalman’s method. *Navigation*, 10:273–291, 1963.
- Gup66. S. C. Gupta. *Transform and State Variable Methods in Linear Systems*. Wiley, New York, 1966.
- Hah62. P. Hahn. Theoretical diversity improvement in multiple FSK. *IRE Trans. Commun. Systems.*, 10:177–184, June 1962.
- Haj60. J. Hajek. *On a Simple Linear Model in Gaussian Processes*. Transactions of the 2nd Prague Conference on Information Theory, 1960.
- Har63. W. W. Harman. *Principles of the Statistical Theory of Communication*. McGraw-Hill, New York, 1963.
- Hay96. M. H. Hayes. *Statistical Digital Signal Processing and Modeling*. Wiley, New York, 1996.
- Hel55. C. W. Helstrom. The resolution of signals in white Gaussian noise. *Proc. I.R.E*, 43:1111–1118, 1955.
- Hel60. C. W. Helstrom. *Statistical Theory of Signal detection*. Pergamon, London, 1960.
- Hel65. C. W. Helstrom. Solution of the detection integral equation for stationary filtered white noise. *IEEE Trans. Inform. Theory*, 11:335–339, July, 1965.
- Hel90. C. Helstrom. Performance of receivers with linear rectifiers. *IEEE Trans. Aerospace Electron. Syst.*, AES-26:210–217, 1990.
- Hel95. Carl W. Helstrom. *Elements of Signal Detection and Estimation*. Prentice Hall, Englewood Cliffs, NJ, 1995.
- HFU96. A. O. Hero, J. A. Fessler, and M. Usman. Exploring estimator bias-variance tradeoffs using the uniform CR bound. *IEEE Trans. Sig. Process.*, 44(8):2026–2041, August 1996.
- HH64. J. M. Hammersley and D. C. Handscomb. *Monte Carlo Methods*. Chapman and Hall, New York, NY, 1964.
- Hil52. F. B. Hildebrand. *Methods of Applied Mathematics*. Prentice-Hall, Englewood Cliffs, NJ, 1952.
- HJ63. R. Y. Huang and R. A. Johnson. Information transmission with time continuous random processes. *IEEE Trans. Inform. Theory*, 2:84–95, April 1963.
- HL64. Y. Ho and R. Lee. A Bayesian approach to problems in stochastic estimation and control. *IEEE Trans. Auto. Control*, 9(4):333–339, October 1964.
- HM67. G. R. Heidbreder and R. L. Mitchell. Detection probabilities for log-normally distributed signals. *IEEE Trans. Aerospace Electron. Syst.*, AES-3:5–13, 1967.
- HT83. E. K. L. Hung and R. M. Turner. A fast beamforming algorithm for large arrays. *IEEE Trans. Aerospace Electron. Syst.*, AES-19(4):598–607, July 1983.
- HYD97. Simon Haykin, Paul Yee, and Eric Derbez. Optimum nonlinear filtering. *IEEE Trans. Sig. Process.*, 45(11):2774–2786, 1997.
- IH81. I. A. Ibragimov and R. Z. Has’minski. *Statistical Estimation*. Springer-Verlag, New York, 1981.

- Itô61. K. Itô. *Lectures on Stochastic Processes*. Tata Institute for Fundamental Research, Bombay, 1961.
- Jac66. I. M. Jacobs. Probability-of-error bounds for binary transmission on the slow fading channel. *IEEE Trans. Inform. Theory*, IT-12(4), October 1966.
- Jaz70. A. H. Jazwinski. *Stochastic Processes and Filtering Theory*. Academic Press, New York, 1970.
- JBS92. M. C. Jeruchim, P. Balaban, and K. S. Shanmugan. *Simulation of Communication Systems*. Plenum, New York, NY, 1992.
- JKB94. N. L. Johnson, S. Kotz, and N. Balakrishnan. *Continuous Univariate Distributions*, volume 1. John Wiley and Sons, New York, NY, 1994.
- Joh61. D. E. Johansen. New techniques for machine computation of the q-functions truncated normal deviates, and matrix eigenvalues. Sylvania ARL, Waltham, MA, Sci. Rept., 2, July 1961.
- Joh97. S. L. Johnston. Target pitfalls (illness, diagnosis, and prescription). *IEEE Trans. Aerospace Electron. Syst.*, 33:715–720, 1997.
- Jos76. V. M. Joshi. On the attainment of the Cramér–Rao lower bound. *Ann. Stat.*, 4(5):998–1002, 1976.
- KA71. C. N. Kelly and B. D. O. Anderson. On the stability of fixed-lag smoothing algorithms. *J. Franklin Inst.*, 291(4):271–281, 1971.
- Kad65. T. T. Kadota. Optimum reception of M -ary Gaussian signals in Gaussian noise. *Bell Syst. Tech. J.*, 44:2187–2197, November 1965.
- Kai65. T. Kailath. The detection of known signals in colored Gaussian noise. *Proc. Natl. Electron. Conf.*, 1965.
- Kai66. T. Kailath. Some integral equations with ‘nonrational’ kernels. *IEEE Trans. Inform. Theory*, IT-12:442–447, October 1966.
- Kai69. T. Kailath. A general likelihood-ratio formula for random signals in noise. *IEEE Trans. Inform. Theory*, IT-5(3):350–361, 1969.
- Kai74. J. F. Kaiser. Nonrecursive digital filter design using the IO-Sinh window function. In *Proceedings of the IEEE International Symposium on Circuits and Systems*, San Francisco, 1974, pp. 20–23.
- Kai80. T. Kailath. *Linear Systems*. Prentice Hall, New York, NY, 1980.
- Kal60. R.E Kalman. A new approach to linear filtering and prediction problems. *J. Basic Eng., Trans. ASME, series D*, 82(1):35–45, March 1960.
- Kal63. R. E Kalman. New methods in Wiener filtering theory. In *Ist Symposium of Engineering Applications of Random function Theory and Probability*, John Wiley & Sons, Inc., New York, 1963, pp. 270–388.
- Kar47. K. Karhunen. Über linearen methoden in der wahrscheinlichkeitsrechnung. *Ann. Acad. Sci. Fennical, Ser. A, Math. Phys.*, 37:3–79, 1947.
- Kas00. K. Kastella. *Multitarget-Multisensor Tracking*, volume III, chapter Finite difference methods for nonlinear filtering and automatic target recognition. Artech House, Norwood, MA, 2000.
- Kau75. L. Kaufman. A variable projection method for solving separable nonlinear least squares problems. *BIT*, 15:49–57, 1975.
- Kay88. S. M. Kay. *Modern Spectral Estimation: Theory and Application*. Prentice Hall, Englewood Cliffs, NJ, 1988.
- Kay93. S. M. Kay. *Fundamentals of Statistical Signal Processing, Estimation Theory*. Prentice Hall, Upper Saddle River, NJ, 1993.
- Kay98. S. M. Kay. *Fundamentals of Statistical Signal Processing, Detection Theory*, volume 2. Prentice Hall, 1998.
- KB61. R. E. Kalman and R. Bucy. New results in linear filtering and prediction theory. *Trans. ASME, J. Basic Eng.*, 83:95–108, March 1961.

- KBS71. P. G. Kaminski, A. E. Bryson, and S. F. Schmidt. Discrete square root filtering: a survey of current techniques. *IEEE Trans. Auto. Control*, 6(16):727–735, December 1971.
- KF69. T. Kailath and P. A. Frost. Mathematical modeling of stochastic processes. In *JACC Control Symposium*, 1969.
- Kle80. L. I. Kleinberg. Array gain for signals and noise having amplitude and phase fluctuations. *J. Acoust. Soc. Am.*, 67(2):572–576, February 1980.
- KM53. H. Kahn and A. W. Marshall. Methods of reducing sample size in Monte Carlo computations. *J. Operations Res.*, 1(5):263–278, November 1953.
- Kol41. A. N. Kolmogorov. Interpolation and extrapolation von stationären zufälligen folgen. *Bull. Acad. Sci. USSR Ser. Math.*, 5:3–14, 1941.
- Kot47. V. A. Kotelnikov. *The Theory of Optimum Noise Immunity*. Doctoral Dissertation, Molotov Institute, Moscow, 1947.
- Kot59. V. A. Kotelnikov. *The Theory of Optimum Noise Immunity*. MacGraw-Hill, New York, NY, 1959.
- KR56. S. Karlin and H. Rubin. The theory of decision procedures for distributions with monotone likelihood ratio. *Ann. Math. Stat.*, 27:272–299, 1956.
- KR60. E. J. Kelly and W. L. Root. A representation of vector-valued random processes. Technical Report Group Rept. 55-21, Lincoln Laboratory, MIT, Lexington, MA, April 1960.
- KRR60. E. J. Kelly, I. S. Reed, and W. L. Root. The detection of radar echoes in noise, pt. i. *J. Soc. Ind. Appl. Math.*, 8(2):309–341, June 1960.
- KS61. M. G. Kendall and A. Stuart. *The Advanced Theory of Statistics, Inference and Relationship*, volume 2. Hafner, New York, NY, 1961.
- KS72. H. Kwakernaak and R. Sivan. *Linear Optimal Control Systems*. Wiley, New York, 1972.
- KS79. M. G. Kendall and A. Stuart. *The Advanced Theory of Statistics*, volume 1. Macmillan, New York, NY, 1979.
- KS88. Steven M. Kay and Arnab K. Shaw. Frequency estimation by principal component AR spectral estimation method without eigendecomposition. *IEEE Trans. Acoust., Speech, Sig. Process.*, 36(1):95–101, January 1988.
- KSH00. T. Kailath, A. H. Sayed, and B. Hassibi. *Linear Estimation*. Prentice Hall, Upper Saddle River, 2000.
- KT85. I. P. Kirsteins and D. W. Tufts. On the probability density of signal-to-noise ratio in an improved adaptive detector. In *Proceedings of International Conference on ASSP*, Tampa, FL, 1985, pp. 572–575.
- Kun82. H. Kunita. Stochastic partial differential equations connected with nonlinear filtering. In S. Mitter and A. Moro, editors, *Nonlinear Filtering Stochastic Contr*, volume 972 of *Lecture Notes Math*, Springer, Berlin 1982, pp. 163–165.
- Kus64a. H. J. Kushner. On the dynamical equations of conditional probability density functions with applications to optimal stochastic control theory. *J. Math. Anal. Appl.*, 8(2):332–344, 1964.
- Kus64b. H. J. Kushner. On the differential equations satisfied by conditional probability densities of Markov processes, with applications. *J. Siam Control*, 2(1):106–119, 1964.
- Kus67a. H. J. Kushner. Dynamical equations for optimal nonlinear filtering. *J. Differential Equations*, 3:179–190, 1967.
- Kus67b. H. J. Kushner. The exact dynamical equations satisfied by the conditional mode. *IEEE Trans. Auto. Control*, AC-12(3):262–267, 1967.
- Kwo98. <http://www.kwon3d.com/theory/filtering/sys.html>
- Lai76. D. G. Lainiotis. Partitioned Riccati solutions and integration-free doubling algorithms. *IEEE Trans. Auto. Control*, AC-21:677–689, 1976.
- Lau79. Alan J. Laub. A schur method for solving algebraic Riccati equations. *IEEE Trans. Auto. Control*, AC-24(6):913–921, 1979.

- LB56. J. H. Laning and R. H. Battin. *Random Processes in Automatic Control*. McGraw-Hill, New York, 1956.
- LB05. R. G. Lorenz and S. P. Boyd. Robust minimum variance beamforming. *IEEE Trans. Sig. Process.*, 53(5):1684–1696, May 2005.
- LC98. E. L. Lehmann and G. Castella. *Theory of Point Estimation*. Spring-Verlag, New York, 1998.
- Lee60. Y. W. Lee. *Statistical Theory of Communication*. John Wiley and Sons Inc., December 1960.
- Lee64. R. C. K. Lee. *Optimal Estimation, Identification and Control*. The MIT Press, Cambridge, MA, 1964.
- Leh50. E. L. Lehmann. Some principles of the theory of testing hypotheses. *Ann. Math. Stat.*, 20:1–26, 1950.
- Leh59. E. L. Lehmann. *Testing Statistical Hypotheses*. Wiley, New York, NY, 1959.
- Leh83. E. L. Lehmann. *Theory of Point Estimation*. John Wiley and Sons, New York, 1983.
- Lev47. N Levinson. The Wiener RMS error criterion in filter design and prediction. *J. Math Phys.*, 25:261–278, 1947.
- Lev59. J. J. Levin. On the matrix Riccati equation. *Proc. Am. Math. Soc.*, 10:519–524, 1959.
- Lev08. B. C. Levy. *Principles of Signal Detection and Parameter Estimation*. Spring-Verlag, 2008.
- LH74. C. L. Lawson and R. J. Hanson. *Solving Least Squares Problems*. Prentice Hall, Englewood Cliffs, NJ, 1974.
- Loe45. M. Loeve. Sur les fonctions aleatoires stationnaires de second ordre. In *Rev. Sci.*, volume 83, 1945, pp. 297–310.
- Loe55. M. Loeve. *Probability Theory*. Van Nostrand, Princeton, New Jersey, 1955.
- Lov24. W. V. Lovitt. *Linear Integral Equations*. McGraw-Hill, New York, 1924.
- LP53. F. W. Lehan and R. J. Parks. Optimum demodulation. *IRE Nat. Conv. Rec.*, 8:101–103, 1953.
- LP61. H. J. Landau and H. O. Pollak. Prolate spheroidal wave functions, Fourier analysis, and uncertainty: II. *Bell Syst. Tech. J.*, 40(1):65–84, January 1961.
- LP62. H. J. Landau and H. O. Pollak. Prolate spheroidal wave functions, Fourier analysis, and uncertainty: III. *Bell Syst. Tech. J.*, 41(4):1295–1336, July 1962.
- LP64. M. Leiter and J. Proakis. The equivalence of two test statistics for an optimum differential phase-shift keying receiver. *IEEE Trans. Commun. Tech.*, 4:209–210, December 1964.
- LR05. E. L. Lehmann and J. P. Romano. Generalizations of the family wise error rate. *Ann. Stat.*, 33(3):1138–1154, 2005.
- LS53. E. L. Lehmann and C. M. Stein. The admissibility of certain invariant statistical tests involving a translation parameter. *Ann. Math. Stat.*, 24:473–479, 1953.
- LS66. H. J. Landau and D. Slepian. On the optimality of the regular simplex code. *Bell System Tech. J.*, 45:1247–1272, October 1966.
- LS05. J. Li and P. Stoica. *Robust Adaptive Beamforming*. Wiley, New York, 2005.
- LSW03. J. Li, P. Stoica, and Z. Wang. On robust Capon beamforming and diagonal loading. *IEEE Trans. Sig. Process.*, 51(7):1702–1715, July 2003.
- LU50. J. L. Lawson and G. E. Uhlenbeck. *Threshold Signals*. McGraw-Hill, New York, 1950.
- Man55. R. Manasse. *Range and Velocity Accuracy from Radar Measurements*. MIT Lincoln Laboratory, February 1955.
- Mar48. J. Marcum. A statistical theory of target detection by pulsed radar. Technical Report, Math. Appendix, Report Rand Corporation, 1948. Reprinted in *IEEE Trans. Inform. Theory*, IT-6 (No. 2): 59–267, April 1960.
- Mar50. J. I. Marcum. Table of q-functions. Technical Report, Rand Corporation Rpt, January 1950.
- Mar60. M. Marcus. Basic theorems in matrix theory. Technical Report Applied Math. Ser. 57, National Bureau of Standards, January 1960.

- Mar87. S. L. Marple, Jr. *Digital Spectral Analysis*. Prentice Hall, Inc., Englewood Cliffs, NJ, 1987.
- Mar93. T. L. Marzetta. A simple derivation of the constrained multiple parameter Cramér–Rao bound, *IEEE Trans. Signal Process.*, 41(6):2247–2249, 1993.
- Mas56. M. Masonson. Binary transmission through noise and fading. *IRE Natl. Conv. Rec.*, Pt. 2:69–82, 1956.
- May66. D. Q. Mayne. A solution to the smoothing problem for linear dynamic systems. *Automatica*, 4:73–92, 1966.
- May79. J. T. Mayhan. Some techniques for evaluating the bandwidth characteristics of adaptive nulling systems. *IEEE Trans. Ant. Prop.*, AP-27:363–373, May 1979.
- May82. P. S. Maybeck. *Stochastic Models, Estimation and Control*, volume 2. Academic Press, New York, NY, 1982.
- MC78. R. Miller and C. Chang. A modified Cramér–Rao bound and its applications. *IEEE Trans. Inform. Theory*, 24(3):398–400, May 1978.
- McL50. N. W. McLachlan. *Ordinary Non-Linear Differential Equations in Engineering and Physical Sciences*. Clarendon Press, Oxford, 1950.
- McN49. R. W. E. McNicol. The fading of radio waves on medium and high frequencies. *Proc. Inst. Elec. Engrs.*, 96(Pt. 3):517–524, 1949.
- Med69. J. S. Meditch. *Stochastic Optimal Linear Estimation and Control*. McGraw-Hill, NY, 1969.
- Med73. J. S. Meditch. A survey of data smoothing for linear and nonlinear dynamic systems. *Automatica*, 9(2):151–162, March 1973.
- Men71. J. Mendel. Computational requirements for a discrete Kalman filter. *IEEE Trans. Auto. Control*, AC-16(6):748–758, 1971.
- Men73. J. M. Mendel. *Discrete Techniques of Parameter Estimation: The Equation Error Formulation*. Marcel Dekker, New York, 1973.
- Men95. J. M. Mendel. *Lessons in Estimation Theory for Signal Processing, Communications, and Control*. Prentice Hall, Englewood Cliffs, NJ, 1995.
- MF90. M. I. Miller and D. R. Fuhrmann. Maximum-likelihood narrow-band direction finding and the EM algorithm. *IEEE Trans. Acoust., Speech Sig. Process.*, 38(9), September 1990.
- MG71. J. M. Mendel and D. L. Giesecking. Bibliography on the linear-quadratic-Gaussian problem. *IEEE Trans. Auto. Control*, AC-16:847–869, 1971.
- MH71. R. J. McAulay and E. M. Hofstetter. Barankin bounds on parameter estimation. *IEEE Trans. Inform. Theory*, IT-17(6):669–676, November 1971.
- Mid57. D. Middleton. On the detection of stochastic signals in additive normal noise I. *IRE Trans. Inform. Theory*, 3:86–121, June 1957.
- Mid60a. D. Middleton. *An Introduction to Statistical Communication Theory*. McGraw-Hill Book Co., Inc, New York, 1960.
- Mid60b. D. Middleton. On the detection of stochastic signals in additive normal noise II. *IRE Trans. Inform. Theory*, 6:349–360, June 1960.
- Mid61. D. Middleton. On singular and nonsingular optimum (bayes) tests for the detection of normal stochastic signals in normal noise. *IRE Trans. Inform. Theory*, 7:105–113, April 1961.
- MIK00. D. G. Manolakis, V. K. Ingle, and S.M. Kogon. *Statistical and Adaptive Signal Processing*. McGraw-Hill, New York, 2000.
- Mit81. R. L. Mitchell. Importance sampling applied to simulation of false alarm statistics. *IEEE Trans. Aerospace Electron. Syst.*, AES-17:15–24, January 1981.
- MM55. D. Middleton and D. Van Meter. Detection and extraction of signals in noise from the point of view of statistical decision theory. *J. Soc. Ind. Appl. Math.*, (3):192, 1955. Also in 4:86, 1956.
- MM73. D. P. Meyer and H. A. Mayer. *Radar Target Detection: Handbook of Theory and Practice*. New York, Academic Press, 1973.

- Moh68. M. Mohajeri. Closed-form error expressions. Master's thesis, Department of Electrical and Computer Engineering, MIT, 1968.
- Moo73. J. B. Moore. Discrete-time fixed-lag smoothing algorithms. *Automatica*, 9(2):163–174, 1973.
- Moo96. T. K. Moon. The expectation maximization algorithm. *IEEE Sig. Process. Mag.*, 47–60, November 1996.
- MP81. R.A. Mucci and R.G. Pridham. Impact of beam steering errors on shifted sideband and phase shift beamforming techniques. *J. Acoust. Soc. Am.*, 69(5):1360–1368, May 1981.
- MS54. A. J. Mallinckrodt and T. E. Sollenberger. Optimum-pulse-time determination. *IRE Trans. Inform. Theory*, PGIT-3:151–159, March 1954.
- MS00. T. K. Moon and W. C. Stirling. *Mathematical Methods and Algorithms for Signal Processing*. Prentice Hall, 2000.
- MSK02. T. J. Moore, B. M. Sadler, and R. J. Kozick. Regularity and strict identifiability in MIMO systems. *IEEE Trans. Signal Process.*, 50(8):1831–1842, 2002.
- MW71. R. N. McDonough and A. D. Whalen. *Detection of Signals in Noise*. Academic Press, first edition, 1971.
- MW95. R. N. McDonough and A. D. Whalen. *Detection of Signals in Noise*. Academic Press, second edition, 1995.
- MZ56. K. S. Miller and L. A. Zadeh. Solution of an integral equation occurring in the expansion of second-order stationary random functions. *IRE Trans. Inform. Theory*, 3(187), June 1956; IT-2(2):72–75, June 1956.
- NALF05. L. Najjar-Atallah, P. Larzabal, and P. Forster. Threshold region determination of ML estimation in known phase data-aided frequency synchronization. *IEEE Sig. Process. Lett.*, 12(9):605–608, September 2005.
- Nit76. R. Nitzberg. Effect of errors in adaptive weights. *IEEE Trans. Aerospace Electron. Syst.*, AES-12(3):369, May 1976.
- Nor43. D. O. North. Analysis of the factors which determine signal/noise discrimination in radar. Technical Report PTR-6C, RCA Laboratories, Princeton, NJ, June 1943.
- Nor63. D. O. North. Analysis of the factors which determine signal/noise discrimination in radar. *Proc. IEEE*, 51, July 1963.
- NS96. S. G. Nash and A. Sofer. *Linear and Nonlinear Programming*. McGraw-Hill, 1996.
- NV94. H. Nguyen and H. L. Van Trees. Comparison of performance bounds for DOA estimation. *IEEE 7th SPW SSAP*, June 1994, pp. 313–316.
- Nyq24. H. Nyquist. Certain factors affecting telegraph speed. *Bell Syst. Tech. J.*, 3(2):324–346, 1924.
- OS89. A. V. Oppenheim and R. W. Schafer. *Discrete-Time Signal Processing*. Prentice-Hall, Englewood Cliffs, NJ, 1989.
- OVSN93. B. Ottersten, M. Viberg, P. Stoica, and A. Nehorai. Exact and large sample maximum likelihood techniques. *Radar Array Process.*, 99–152, January 1993.
- Ows85. N. L. Owsley. Sonar array processing. In S. Haykin, editor, *Array Signal Processing*. Prentice-Hall, Englewood Cliffs, NJ, 1985.
- Ows02. N. L. Owsley. Adventures in eigenland (Distinguished Lecture). In *2002 IEEE SAM Workshop*, Rosslyn, VA, 2002.
- Pap65. A. Papoulis. *Probability, Random Variable, and Stochastic Processes*. McGraw-Hill, 1965.
- Par61. E. Parzen. An approach to time series analysis. *Ann. Math. Stat.*, 32:951–990, December 1961.
- Par62. E. Parzen. *Stochastic Processes*. Holden-Day, San Francisco, 1962.
- PBF54. W. W. Peterson, T. G. Birdsall, and W. C. Fox. The theory of signal detectability. *IRE Trans. Inform. Theory*, 4:171, 1954.
- Pea02. K. Pearson. On the Systematic Fitting of Curves to Observations and Measurements, *Biometrika*, 1, 265 (1902).

- Pie58. J. N. Pierce. Theoretical diversity improvement in frequency-shift keying. *Proc. IRE*, 46:903–910, May 1958.
- Pot65. J. E. Potter. A matrix equation arising in statistical filter theory. Contractor Report CR-270, NASA, August 1965.
- Pot66. J. E. Potter. Matrix quadratic solutions. *SIAM J. Appl. Math.*, 14:496–501, 1966.
- Pri53. R. L. Pritchard. Optimum directivity for linear point arrays. *J. Acoust. Soc. Am.*, 25, September 1953.
- Pri54. R. Price. The detection of signals perturbed by scatter and noise. *IRE Trans.*, PGIT-4:163–170, September 1954.
- Pri55. R. Price. Notes on ideal receivers for scatter multipath. Group Report 34-39, Lincoln Laboratory, MIT, May 12, 1955.
- Pri56. R. Price. Optimum detection of random signals in noise with application to scatter-multipath communication. *IRE Trans.*, PGIT:125–135, December 1956.
- Pri57. R. Price. The autocorrelogram of a complete carrier wave received over the ionosphere at oblique incidence. *Proc. IRE*, 45, 1957.
- PRLN92. J. G. Proakis, C. M. Rader, F. Ling, and C. L. Nikias. *Advanced Digital Signal Processing*. Macmillan Publishing Company, New York, 1992.
- Pro63. J. G. Proakis. Optimum pulse transmission for multipath channels. Group Report 64-G-3, MIT Lincoln Lab, August 1963.
- PVS⁺08. A. Pezeshki, B. D. Van Veen, L. L. Scharf, H. Cox, and M. L. Nordenvaad. Eigenvalue beamforming using a multirank MVDR beamformer and subspace selection. *IEEE Trans. Sig. Process.*, 56(5):1954–1966, 2008.
- Qua82. A. H. Quazi. Array beam response in the presence of amplitude and phase fluctuations. *J. Acoust. Soc. Am.*, 72(1):171–180, July 1982.
- RAG04. B. Ristic, S. Arulampalam, and N. Gordon. *Beyond the Kalman Filter, Particle Filters for Tracking Applications*. Artech House, 2004.
- Rao45. C. R. Rao. Information and accuracy attainable in the estimation of statistical parameters. *Bull. Calcutta Math. Soc.*, 37(37):81–91, 1945.
- Rau63. H. E. Rauch. Solutions to the Linear Smoothing Problem. *IEEE Trans. Auto. Control*, AC-8 (4):371–372, 1963.
- RB74. D. Rife and R. Boorstyn. Single-tone parameter estimation from discrete-time observations. *IEEE Trans. Inform. Theory*, IT-20(5):591–598, September 1974.
- Rei46. W. T. Reid. A matrix differential equation of Riccati type. *Am. J. Math.*, 8:237–246, 1946. Addendum, *Am. J. Math.*, 70:460, 1948.
- Rei59. W. T. Reid. Solutions of a matrix Riccati differential equation as functions of initial values. *Math. Mech.*, 8, 1959.
- Rei72. W. T. Reid. *Riccati Differential Equations*. Academic Press, 1972.
- RFLR06. A. Renaux, P. Forster, P. Larzabal, and C. D. Richmond. The Bayesian Abel bound on the mean square error. In *ICASSP 2006*, volume 3, Toulouse, France, 2006, pp. III-9–III-12.
- Ric44. S. O. Rice. Mathematical analysis of random noise. *Bell Syst. Tech. J.*, 23:282–332, 1944.
- Ric45. S. O. Rice. Mathematical analysis of random noise. *Bell Syst. Tech. J.*, 24:46–156, 1945.
- Ric05. C. D. Richmond. Capon algorithm mean-squared error threshold SNR prediction and probability of resolution. *IEEE Trans. Signal Process.*, 53(8):2748–2764, August 2005.
- RM97. I. Reuven and H. Messer. A Barankin-type lower bound on the estimation error of a hybrid parameter vector. *IEEE Trans. Inform. Theory*, 43(3):1084–1093, May 1997.
- RN55. F. Riesz and B. S. Nagy. *Functional Analysis*. Ungar, New York, NY, 1955.
- RNE05. C. D. Richmond, R. R. Nadakuditi, and A. Edelman. Asymptotic mean squared error performance of diagonally loaded Capon-MVDR processor. In *Proceedings of the 39th Asilomar Conference of Signals, Systems, and Computers*, Asilomar, California, 2005, pp. 1711–1716.
- Rob67. G. H. Robertson. Operating characteristics for a linear detector of CW signals in narrow-band Gaussian noise. *Bell Syst. Tech. J.*, 46:755–774, 1967.

- Roo64. W. L Root. Stability in signal detection problems. In *Stochastic Processes in Mathematical Physics and Engineering, Proceedings of Symposia in Applied Mathematics*, 1964.
- Ros62. M. Rosenblatt. *Random Processes*. Oxford University Press, New York, 1962.
- RS87. Y. Rockah and P. M. Schultheiss. Array shape calibration using sources in unknown locations—part I: far-field sources. *IEEE Trans. Acoust., Speech Sig. Process.*, 35(3):286–299, March 1987.
- RTS65. H. E. Rauch, F. Tung, and C. T. Striebel. Maximum likelihood estimates of linear dynamical systems. *AIAA*, 3:1445–1450, 1965.
- RW80. A. Ruhe and P. A. Wedin. Algorithms for separable nonlinear least squares problems. *SIAM Rev.*, 22:318–327, July 1980.
- SA71. H. W. Sorenson and D. L. Alspach. Recursive Bayesian estimation using Gaussian sums. *Automatica*, 7:465–479, 1971.
- Sad93. J. S. Sadowsky. On the optimality and stability of exponential twisting in Monte Carlo estimation. *IEEE Trans. Inform. Theory*, 39:119–128, January 1993.
- SB54. R. A. Silverman and M. Balser. Statistics of electromagnetic radiation scattered by a turbulent medium. *Phys. Rev.*, 96:560–563, 1954.
- SB90. J. S. Sadowsky and J. A. Bucklew. On large deviations theory and asymptotically efficient Monte Carlo estimation. *IEEE Trans. Inform. Theory*, 36:579–588, March 1990.
- SBC99. L. D. Stone, C. A. Barlow, and T. L. Corwin. *Bayesian Multiple Target Tracking*. Artech House, 1999.
- SBS66. M. Schwartz, W. R. Bennett, and S. Stein. *Communication Systems and Techniques*. McGraw-Hill, New York, 1966.
- Sch65. F. Schwerpe. Evaluation of likelihood functions for Gaussian signals. *IEEE Trans.*, 11(1):61–70, January 1965.
- Sch70. S. F. Schmidt. Computational techniques in kalman filtering. *Theory and Applications of Kalman Filtering, NATO Advisory Group for Aerospace Research and Development, AGARDograph*, 139, 1970.
- Sch76. D. C. Schleher. Radar detection in Weibull clutter. *IEEE Trans. Aerospace Electron. Syst.*, 12:736–743, 1976.
- Sch87. L. L. Scharf. Signal processing in the linear statistical model. In *IEEE Workshop on Underwater Acoustic Signal Detection*, University of Rhode Island, September 1987.
- Sch91. L. L. Scharf. *Statistical Signal Processing: Detection, Estimation, and Time Series Analysis*. Addison-Wesley, Reading, MA, 1991.
- SF65. R. J. Schwartz and B. Friedland. *Linear Systems*. McGraw-Hill, New York, 1965.
- SF94. L. L. Scharf and B. Friedlander. Matched subspace detectors. *IEEE Trans. Signal Processing*, 42(8):2146–2157, August 1994.
- SGB67. C. E. Shannon, R. G. Gallager, and E. R. Berlekamp. Lower bounds to error probability for coding on discrete memoryless channels: I. *Inform. Control*, 10(1):65–103, 1967.
- Sha49. C. E. Shannon. Communication in the presence of noise. *Proc. IRE*, 37:10–21, 1949.
- Sha56. C. E. Shannon. *Seminar Notes for Seminar in Information Theory*. MIT, 1956.
- She58. S. Sherman. Non-mean-square error criteria. *IRE Trans. Inform. Theory*, IT-4(3):125–126, 1958.
- Shn91. D. A. Shnidman. Calculation of probability of detection for log-normal target fluctuations. *IEEE Trans. Aerospace Electron. Syst.*, 27:172–174, 1991.
- Shn03. D. A. Shnidman. Expanded swerling target models. *IEEE Trans. Aerospace Electron. Syst.*, 39:1059–1069, 2003.
- Shu57. M. P. Shutzenberger. A generalization of the Fréchet–Cramér inequality in the case of Bayes estimation. *Bull. Am. Math. Soc.*, 63(142), 1957.
- Sie76. D. Siegmund. Importance sampling in the Monte Carlo study of sequential tests. *Ann. Stat.*, 4(4):673–684, 1976.
- Sko62. M. I. Skolnik. *Introduction to Radar Systems*. McGraw-Hill, New York, 1962.

- Sko01. M. I. Skolnik. *Introduction to Radar Systems*. McGraw-Hill, New York, second edition, 2001.
- ŠKT01. M. Šimandl, J. Královec, and P. Tichavský. Filtering, predictive and smoothing Cramér–Rao bounds for discrete-time nonlinear dynamic systems. *Automatica*, 37:1703–1716, 2001.
- SL71. L. Scharf and D. Lytle. Signal detection in Gaussian noise of unknown level: an invariance application. *IEEE Trans. Inform. Theory*, IT-17:404–441, July 1971.
- Sle54. D. Slepian. Estimation of signal parameters in the presence of noise. *IRE Trans. Inform. Theory*, PGIT-3:68–89, 1954.
- Sle57. D. Slepian. Estimation of signal parameters in the presence of noise. *IRE Trans. Inform. Theory*, PGIT-3:68–89, 1957.
- SM71. A. P. Sage and J. L. Melsa. *Estimation Theory with Applications to Communications and Control*. McGraw-Hill, New York, NY, 1971.
- SM90. P. Stoica and R. Moses. On biased estimators and the unbiased Cramér–Rao lower bound. *Sig. Process.*, 21(4):349–350, October 1990.
- SMC⁺56. J. A. Stratton, P. M. Morse, L. J. Chu, J. D. C. Little, and F. J. Corbato. *Spheroidal Wave Functions*. MIT Press and Wiley, 1956.
- SN98. P. Stoica and B. C. Ng. On the Cramér–Rao bound under parametric constraints, *IEEE Signal Process Letters*, 5(7):177–179, 1998.
- Sny65. D. L. Snyder. Some useful expressions for optimum linear filtering in white noise. *Proc. IEEE*, 53:629–630, 1965.
- Sny66. D. L. Snyder. Optimum linear filtering of an integrated signal in white noise. *IEEE Trans. Aerospace Electron. Syst.*, AES-2, 2:231–232, 1966.
- Sny69. D. L. Snyder. *The State-Variable Approach to Continuous Estimation with Applications to Analog Communications Theory*. MIT Press, Cambridge, MA, 1969.
- Som29. A. Sommerfeld. *An Introduction to the Geometry of N Dimensions*. Dutton, New York, NY, 1929.
- Sor70. H. W. Sorenson. Least-squares estimation: from Gauss to Kalman. *IEEE Spectrum*, 7:63–68, July 1970.
- Sor74. H. W. Sorenson. On the development of practical nonlinear filters. *Inform. Sci.*, 7:253–270, 1974.
- Sor85. H. W. Sorenson. *Kalman Filtering: Theory and Application*. IEEE Press, New York, 1985.
- Sor88. H. W. Sorenson. *Bayesian Analysis of Time Series and Dynamic Models*. Marcel Dekker, New York, 1988, pp. 127–165.
- Sos67. Y. G. Sosulin. Optimum extraction of non-Gaussian signals in noise. *Radio Eng. Electron. Phys.*, 12:89–97, January 1967.
- SP61. D. Slepian and H. O. Pollak. Prolate spheroidal wave functions, Fourier analysis, and uncertainty: I. *Bell Syst. Tech. J.*, 40(1):43–64, January 1961.
- Spa88. J. C. Spall, editor. *Bayesian Analysis of Time Series and Dynamic Models*, chapter Recursive Estimation for Nonlinear Dynamic Systems. Marcel Dekker, New York, NY, 1988, pp. 127–165.
- SR72. D. L. Snyder and I. B. Rhodes. Filtering and control performance bounds with implication on asymptotic separation. *Automatica*, 8:747–753, 1972.
- Sri02. R. Srinivasan. *Importance Sampling: Applications in Communications and Detection*. Springer-Verlag, New York, NY, 2002.
- SS64. R. L. Stratonovich and Y. G. Sosulin. Optimal detection of a Markov process in Noise. *Eng. Cybernet*, 6:7–19, October 1964.
- SS65. D. Slepian and E. Sonnenblick. Eigenvalues associated with prolate spheroidal wave functions of zero order. *Bell Syst. Tech. J.*, 44(8):1745–1760, October 1965.
- SS66. R. L. Stratonovich and Y. G. Sosulin. Optimum reception of signals in non-Gaussian noise. *Rad. Eng. Electron. Phys.*, 11:497–507, April 1966.

- SS71. H. W. Sorenson and J. E. Sacks. Recursive fading memory filtering. *Inform. Sci.*, 3:101–119, 1971.
- SSG97. P. J. Smith, M. Shadi, and H. Gao. Quick simulation: a review of importance sampling techniques in communication systems. *IEEE J. Sel. Areas Commun.*, 15(4):597–613, 1997.
- SST67. F. H. Schlee, C. J. Standish, and N. F. Toda. Divergence in the Kalman filter. *AIAA*, 5:1114–1120, June 1967.
- Ste64. S. Stein. Unified analysis of certain coherent and non-coherent binary communication systems. *IEEE Trans. Inform. Theory*, 10:43–51, 1964.
- Sto01. L. D. Stone. *Handbook of Multisensor Data Fusion*, chapter A Bayesian approach to multiple-target tracking. Number 10. CRC Press, Boca Raton, FL, 2001.
- Str59a. R. L. Stratonovich. Optimum nonlinear systems which bring about a separation of a signal with constant parameters from noise. *Radiofizika*, II(6):892–901, 1959.
- Str59b. R. L. Stratonovich. On the theory of optimal nonlinear filtration of random functions. *Theory Prob. Appl.*, 4:223–225, 1959.
- Str60a. R. L. Stratonovich. Application of the theory of Markov processes to optimal signal discrimination. *Radio Eng. Electron.*, 5(11):1751–1763, 1960.
- Str60b. R. L. Stratonovich. Conditional Markov processes. *Theory Prob. Appl.*, 5(2):156–178, 1960.
- Str66. R. L. Stratonovich. A new representation for stochastic integrals and equations. *Siam J. Control*, 4(2):362–371, 1966.
- Sus64. S. M. Sussman. Simplified relations for bit and character error probabilities for M -ary transmission over Rayleigh fading channels. *IEEE Trans. Commun. Tech.*, COM-12, 4, 1964.
- SW49. C. E. Shannon and W. Weaver. *The Mathematical Theory of Communication*. University of Illinois Press, Urbana, IL, 1949.
- Swe54. P. Swerling. Probability of detection for fluctuating targets. *IRE Trans. Inform. Theory*, 2:269–308, 1954. Reprinted from Rand Corp. Report RM-1217, March 17, 1954.
- Swe59. P. Swerling. A proposed stagewise differential correction procedure for satellite tracking and prediction. *J. Astronaut. Sci.*, 6, 1959.
- Swe60. P. Swerling. Probability of detection for fluctuating targets. *IRE Trans. Inform. Theory*, 6:269–308, 1960. Reprinted from Rand Corp. Report RM-1217, March 17, 1954.
- Swe66. P. Swerling. Probability of detection for some additional fluctuating target cases. *Aerospace Corp. Report TOR-669(9990)-14*, 1966, pp. 698–709.
- Swe97. P. Swerling. Radar probability of detection for some additional fluctuating target cases. *IEEE Trans. Aerospace Electron. Syst.*, 33:698–709, 1997.
- Tal07. N. N. Taleb. *The Black Swan: The Impact of the Highly Improbable*. Random House, New York, NY, 2007.
- Tan96. H. Tanizaki. *Nonlinear Filters: Estimation and Applications*, second edition, Springer-Verlag, New York, NY, 1996.
- Tay79. J. H. Taylor. The Cramér–Rao estimation error lower bound computation for deterministic nonlinear systems. *IEEE Trans. Auto. Control*, 24:343–344, April 1979.
- The84. H. Theicher. The central limit theorem for Esscher transformed random variables. *Indian J. Stat.*, 46:35–40, 1984.
- Tho76. C. L. Thornton. *Triangular covariance factorization for Kalman filtering*. Ph.D. thesis, University of California at Los Angeles, 1976.
- TMN98. P. Tichavský, C. Muravchik, and A. Nehorai. Posterior Cramér–Rao bounds for discrete-time nonlinear filtering. *IEEE Trans. Sig. Process.*, 46(5):1386–1396, May 1998.
- Tri57. F. G. Tricomi. *Integral Equations*. Interscience Publishers, New York, 1957.
- TT10a. K. Todros and J. Tabrikian. General classes of performance lower bounds for parameter estimation—part I: Non-Bayesian bounds for unbiased estimators. *IEEE Trans. Inform. Theory*, 56(10):5045–5063, October 2010.

- TT10b. K. Todros and J. Tabrikian. General classes of performance lower bounds for parameter estimation—part II: Bayesian bounds. *IEEE Trans. Information Theory*, 56(10):5064–5082, October 2010.
- Tur58. G. L. Turin. Error probabilities for binary symmetric ideal reception through non-selective slow fading and noise. *Proc. IRE*, 46:1603–1619, 1958.
- Tur59. G. L. Turin. The asymptotic behavior of ideal M-ary systems. *Proc. IRE* (correspondence), 47, 1959.
- TW60. J. B. Thomas and E. Wong. On the statistical theory of optimum demodulation. *IRE Trans. Inform. Theory*, 6:420–425, September 1960.
- Urb55. R. H. Urbano. Analysis and tabulation of the M positions experiment integral and related error function integrals. Technical Report TR-55-100, AFCRC, Bedford, MA, April 1955.
- Van54. A. Van der Ziel. *Noise*. Prentice Hall, Englewood Cliffs, NJ, 1954.
- Van66a. H. L. Van Trees. A generalized Bhattacharyya bound. Internal memorandum, Detection and Estimation Theory Group, MIT, 1966.
- Van66b. H. L. Van Trees. A generalized Bhattacharyya bound. Internal Memo, MIT, IM-VT-6, January 1966.
- Van68. H. L. Van Trees. *Detection, Estimation, and Modulation Theory, Part I*. John Wiley and Sons, New York, NY, 1968.
- Van71a. H. L. Van Trees. *Detection, Estimation, and Modulation Theory, Part II*. John Wiley and Sons, New York, NY, 1971.
- Van71b. H. L. Van Trees. *Detection, Estimation, and Modulation Theory, Part III*. John Wiley and Sons, New York, NY, 1971.
- Van01a. H. L. Van Trees. *Detection, Estimation, and Modulation Theory, Part I*. John Wiley and Sons, New York, NY, 2001. (reprint)
- Van01b. H. L. Van Trees. *Detection, Estimation, and Modulation Theory, Part III*. Wiley Interscience, New York, NY, 2001. (reprint)
- Van02. H. L. Van Trees. *Optimum Array Processing, Part IV of Detection, Estimation, and Modulation Theory*. John Wiley and Sons, New York, NY, 2002.
- Van03. H. L. Van Trees. *Detection, Estimation, and Modulation Theory, Part II*. John Wiley and Sons, New York, NY, 2003. (reprint)
- VB07. H. L. Van Trees and K. Bell, editors. *Bayesian Bounds for Parameter Estimation and Nonlinear Filtering/Tracking*. Wiley, New York, NY, 2007.
- VC64. A. J. Viterbi and C. R. Cahn. Optimum coherent phase and frequency demodulation of a class of modulating spectra. *IEEE Trans. Space Electron. Telemetry*, SET-10, 3:95–102, September 1964.
- VD86. M. Verhaegen and P. Van Dooren. Numerical aspects of different Kalman filter implementations. *IEEE Trans. Auto. Control*, 10:907–917, October 1986.
- VGL03. S. A. Vorobyov, A. B. Gershman, and Z. Q. Luo. Robust adaptive beamforming using worst-case performance optimization: a solution to the signal mismatch problem. *IEEE Trans. Signal Process.*, 51(2):313–324, February 2003.
- Vit65. A. J. Viterbi. Optimum detection and signal selection for partially coherent binary communication. *IEEE Trans. Inform. Theory*, 11(2):239–246, April 1965.
- Vit66. A. J. Viterbi. *Principles of Coherent Communication*. McGraw-Hill, New York, NY, 1966.
- VOK91. M. Viberg, B. Ottersten, and T. Kailath. Detection and estimation in sensor arrays using weighted subspace fitting. *IEEE Trans. Sig. Proc.*, 39:2436–2449, November 1991.
- VTG68. H. L. Van Trees and H. D. Goldfein. *Solutions Manual for Selected Problems, Detection, Estimation and Modulation Theory, Part I*. John Wiley and Sons, New York, NY, 1968.
- VV88. B. D. Van Veen. Eigenstructure based partially adaptive array design. *IEEE Trans. Ant. Prop.*, 36(3):357–362, March 1988.
- VW48. G. E. Valley and H. Wallman. *Vacuum Tube Amplifiers*. McGraw-Hill, New York, 1948.

- Wal31. Gilbert Walker. On periodicity in series of related terms. *Proc. Royal Soc. London*, 131(Ser. A):518–532, 1931.
- WD52. P. M. Woodward and I. L. Davies. Information theory and inverse probability in telecommunication. *Proc. IEE - Part III: Radio Commun. Eng.*, 99:37, 1952.
- Wea63. C. S. Weaver. Estimating the output of a linear discrete system with Gaussian inputs. *IEEE Trans. Auto. Control*, AC-8:372–374, 1963.
- Wei42. N. Weiner. Extrapolation, interpolation, and smoothing of stationary time series with engineering applications. Technical Report, Nat. Defense Res., New York, February 1942. Classified.
- Wei56. W. W. Weinstock. *Target Cross Section Models for Radar Systems analysis*. Ph.D. thesis, University of Pennsylvania, Philadelphia, 1956.
- Wei75. L. Weinberg. *Network Analysis and Synthesis*. R. E. Krieger Pub. Co., 1975.
- Wei85. A. J. Weiss. *Fundamental Bounds in Parameter Estimation*. Ph.D. thesis, Tel-Aviv University, 1985.
- Wei86. A. J. Weiss. Composite bound on arrival time estimation errors. *IEEE Trans. Aero. Elec. Syst.*, AES-22:751–756, Nov. 1986.
- Wei87. Anthony J. Weiss. Bounds on time-delay estimation for monochromatic signals. *IEEE Trans. Aerospace Electron. Syst.*, AES-23(6):798–808, November 1987.
- Wie49. N. Wiener. *The Extrapolation, Interpolation and Smoothing of Stationary Time Series*. Wiley, New York, 1949.
- Wij73. R. A. Wijsman. On the attainment of the Cramér–Rao lower bound. *Ann. Stat.*, 1:538–542, 1973.
- Wil62. S. S. Wilks. *Mathematical Statistics*. John Wiley and Sons, New York, NY, 1962.
- Wil71. J. C. Willems. Least Squares Stationary Optimal Control and the Algebraic Riccati Equation. *IEEE Trans. Auto. Control*, AC-16:621–634, 1971.
- WJ65. J. M. Wozencraft and I. M. Jacobs. *Principles of Communication Engineering*. John Wiley and Sons, New York, NY, 1965.
- Wol59. J. K. Wolf. *On the detection and estimation problem for multiple non-stationary random processes*. Ph.D. thesis, Department of Electrical Engineering, Princeton University, NJ, 1959.
- Won68. W. M. Wonham. On a matrix Riccati equation of stochastic control. *SIAM J. Control*, 6:681–697, 1968.
- Woo52. P. M. Woodward. *Probability and Information Theory with Application to Radar*. McGraw-Hill, New York, NY, 1952.
- Woo55. P. M. Woodward. *Probability and Information Theory, with Application to Radar*. McGraw-Hill, New York, 1955.
- Wu83. N. L. Wu. An explicit solution and data extension in the maximum entropy method. *IEEE Trans. Acoust., Speech, Sig. Process.*, ASSP-31(2):486–491, April 1983.
- WW85. A. J. Weiss and E. Weinstein. A lower bound on the mean square error in random parameter estimation. *IEEE Trans. Inform. Theory*, 31(5):680–682, September 1985.
- WW88. E. Weinstein and A. J. Weiss. A general class of lower bounds in parameter estimation. *IEEE Trans. Inform. Theory*, IT-34:338–342, March 1988.
- WZ62. L. A. Wainstein and V. D. Zubakov. *Extraction of Signals from Noise*. Prentice-Hall, Englewood Cliffs, NJ, 1962.
- XBR04. W. Xu, A. Baggeroer, and C. Richmond. Bayesian bounds for matched-field parameter estimation. *IEEE Trans. Sig. Process.*, 52(12):3293–3305, December 2004.
- YJ55. M. C. Yovits and J. L. Jackson. Linear filter optimization with game theory considerations. *IRE Nat. Conv. Rec.*, 4:193–199, 1955.
- You54. D. C. Youla. The use of maximum likelihood in estimating continuously modulated intelligence which has been corrupted by noise. *IRE Trans. Inform. Theory*, IT-3:90–105, 1954.

- You57. D. Youla. The solution of homogeneous Wiener-Hopf integral equation occurring in the expansion of second-order stationary random functions. *IRE Trans.*, 3:187–193, 1957.
- YU94. W. S. Youn and C. K. Un. Robust adaptive beamforming based on the eigenstructure method. *IEEE Trans. Sig. Process.*, 42(6):1543–1547, June 1994.
- Yud66. H. Yudkin. A derivation of the likelihood ratio for additive colored noise, unpublished, 1966.
- Yul27. G. Udny Yule. On a method of investigating periodicities in disturbed series, with special reference to Wolfer's sunspot numbers. *Phil. Trans. Royal Soc. London*, 226(Ser. A):267–298, 1927.
- YY95. J.-L. Yu and C.-C. Yeh. Generalized eigenspace-based beamformers. *IEEE Trans. Sig. Process.*, 43(11):2453–2461, November 1995.
- Zad53. L. A. Zadeh. Optimum nonlinear filters. *J. Appl. Phys.*, 24:396–404, 1953.
- Zak69. M. Zakai. On the optimal filtering of diffusion process. *Wahrscheinlichkeits theorie verw Gebiete*, 11:230–243, 1969.
- ZD63. L. A. Zadeh and C. A. DeSoer. *Linear System Theory*. McGraw-Hill, New York, 1963.
- ZR52. L. A. Zadeh and J. R. Ragazzini. Optimum filters for the detection of signals in noise. *Proc. IRE*, 40:1223, 1952.
- ZW88. I. Ziskind and M. Wax. Maximum likelihood localization of multiple sources by alternating projection. *IEEE Trans. Acoust., Speech, Signal Process.*, 36(10):1553–1560, October 1988.

Index

Ambiguity surface

- normalized, 269
- posterior, 273

Approximate performance expressions, 63, 71, 121

Array manifold vector, 145

Array processing, 144, 170, 216

Asymptotic behavior

- MAP estimate, 265
- MMSE estimate, 265

Asymptotic behavior of ML estimate

- consistent, 260
- efficient, 260
- Gaussian, 260

Bandpass

- Gaussian random process, 128
- white noise, 131

Bayes criterion, 21, 50, 109

Bayes test, 22, 29

Bayesian Cramér-Rao bounds, discrete-time recursive, 987

Bayesian efficient estimate, 264

Bayesian estimation: continuous-time non-Gaussian processes, 842

Bayesian Cramér-Rao bound, 849

Bayesian information matrix, 845

extended Kalman filter, 843

hierarchy of models, 844

Bayesian estimation: discrete-time non-Gaussian processes, 982

applications, 992

ballistic object tracking, 998

dynamic frequency estimation, 992

tracking, 996

continuous-time processes and discrete-time observations, 1009

extended Kalman filter, 985

general nonlinear model: MMSE & MAP estimates, 983

joint state and parameter estimation, 1005

recursive Bayesian Cramér-Rao bounds, 987

Bayesian information, 263

Bayesian linear Gaussian model, 487

Bayesian log-likelihood function, 236

Beta function, 103

Bhattacharyya distance, 75

Bias

- known, 246

- unbiased, 246

- unknown, 246

Binary communication system, partially coherent, 686

Bounds

- Barankin, 261, 345, 384

- Bayesian Bhattacharyya, 345, 396

- Bayesian Cramér-Rao, 263, 345

- Bayesian lower bounds on MSE, 261

- Bhattacharyya, 261, 345, 385

- Bobrovsky-Zakai, 345, 395

- Chernoff, 68

- combined, 341, 345

- Cramér-Rao, 248, 345

- $\text{erfc}^*(X)$, 38

- expectation of CRB (ECRB), 265

- Bounds (*Continued*)
 - perfect measurement, 352
 - posterior Cramér-Rao, 263
 - Reuven-Messer, 345, 395
 - Van Trees inequality, 263
 - weighted Bayesian Cramér-Rao, 345
 - Weiss-Weinstein, 336, 340, 345
- Butterworth family, 544–545
- Central limit theorem, 70**
- Channel capacity, 611
- Channels
 - known linear, 673
 - Rayleigh, 694
 - Rician, 704
- Characteristic function, 41
 - circular complex Gaussian random vector, 130
 - real Gaussian random vector, 126
- Chernoff bound, 68, 86
- Cholesky decomposition, 176
- Classical detection theory, 17, 1084
- Classical estimation theory, 230, 1088
- Coherent pulse interval (CPI), 701
- Complementary error function, $\text{erfc}^*(X)$, 37
- Complete orthonormal set (CON), 525
- Composite hypotheses, signals with unwanted parameters, 675–706
- Composite hypothesis tests, 110, 348
 - nonrandom parameters, 352
 - generalized likelihood ratio test (GLRT), 359
 - perfect measurement bound, 352
 - uniformly most powerful (UMP) test, 353
 - random parameters, 350
- Compressed log-likelihood function, 311
- Computational algorithms, 452
 - alternating projection, 457
 - expectation-maximization, 461
 - gradient techniques, 453
- Conditional probabilities, 31, 51
- Confidence interval, 82
- Conjugate priors, 242, 379, 391, 1114
 - continuous multivariate distributions, 1117
 - continuous univariate distributions, 1114
 - discrete univariate distributions, 1116
- Constant false alarm (CFAR) test, 365
- Continuous multivariate distributions, 1113
 - Inverse Wishart, 1114
 - Multivariate circular complex Gaussian, 1113
 - Multivariate Gaussian, 1113
 - Normal Gamma, 1113
- Normal-inverse Gamma, 1113
- Normal-inverse Wishart, 1114
- Normal-Wishart, 1114
- Wishart, 1113
- Continuous univariate distributions, 1107
 - Beta, 102, 1111
 - Cauchy, 118, 1111
 - Central F, 366, 1111
 - Chi-squared, 41, 1109
 - Exponential, 41, 1108
 - Gamma, 41–42, 1108
 - Gaussian, 24, 1107
 - Generalized Gaussian, 28, 1110
 - Inverse Gamma, 289, 1108
 - Laplacian, 28, 1110
 - Log-normal, 391, 1108
 - Noncentral Chi-squared, 204, 1109
 - Noncentral F, 366, 1109
 - Rayleigh, 118, 1111
 - Rician, 1111
 - Tikhonov, 680, 1112
 - Uniform, 680, 1107
 - Weibull, 77, 1110
- Conventional beampattern, 169
- Correlation test, 60
- Cost functions
 - absolute error, 232
 - convex-upward, 239
 - definition, 232
 - squared error, 232
 - symmetric non-decreasing, 240
 - uniform error, 233
- Cramér-Rao bound, 248, 300, 345
- Decision theory problem, 17**
- Detection: continuous-time Gaussian random processes, 1030
 - estimator -correlator, 1032, 1039
 - low-rank kernels, 1061
 - optimum continuous-time receivers, 1034–1039
 - performance, 1046
 - realizable filter detector, 1032, 1043
 - sampling, 1032
 - state-variable realization, 1049
 - stationary process; long observation time (SPLIT), 1051
- Detection: discrete-time Gaussian random processes, 1067
 - Schweppé detector, 1070
 - second moment characterization, 1067
 - state variable characterization, 1070

- Detection: equal covariance circular complex Gaussian, 140
 d^2 , 142
ID, 147
IID, 143
interference matrix, 164
low-rank model, 167
- Detection: equal covariance real Gaussian, 138
 d^2 , 140
eigendecomposition, 147–156
ID, 146
IID, 142
interference matrix, 160–165
low-rank model, 165
optimum signal design, 156–160
- Detection: equal means circular complex Gaussian, 174
correlated signal components, 180
diagonal IID on H_0 , 176
low-rank signal, 185
non-diagonal matrix on H_0 , 194
signal on both hypotheses, 195
- Detection: equal means real Gaussian, 174
correlated signal components, 179
diagonal IID on H_0 , 175
IID signal, 177
ID signal, 178
low-rank signal, 184
symmetric hypotheses, 186
non-diagonal matrix on H_0 , 191
signal on H_1 only, 191
- Detection, general Gaussian, 197
circular complex Gaussian vectors, 198
 M hypotheses, 209
real Gaussian vectors, 197
- Detection of signals, 584, 1095
- Detection of signals: known signals in AWGN, 591
digital communications system, 608
general binary, 597
 M -ary, 601
ROC, 594
simple binary, 591
 correlation receiver, 593
 matched filter receiver, 593
- Detection of signals: known signals in nonwhite Gaussian noise, 629
integral equations, 650
 finite observation interval: rational spectra, 654
finite observation interval: separable kernels, 662
infinite observation interval: stationary process, 650
Karhunen-Loëve expansion, 639
known linear channels, 673
multiple channels, vector Karhunen-Loëve, 712
reversibility, 631
sensitivity and mismatch, 667, 673
simple binary detection, 643
 optimum signal design, 644
 singularity, 645
sufficient statistic derivation, 641
whitening approach, 632
- Detection of signals: signals with unknown parameters in Gaussian noise, 675–706
nonrandom parameters, GLRT, 709
random phase angles, 677
Rayleigh channel, 694
Rician channel, 704
Swerling I-IV, 706
target models, 706
- Detection theory hierarchy, 4
- Diagonal loading, 477, 673
- Digamma function, 104
- Digital communication system, 1, 4
- Discrete-time Kalman filter, 919, 926
 applications, 939
 AR models, 939
 array processing, 949
 Butterworth signals, 946
 tracking, 943
 derivation, 927
 divergence, 962
 model mismatch, 966
 nonwhite noise, 954
 random process models, 920
 canonical Model #1, 923
 canonical Model #2, 923
 kinematic models, 924
 state generation and observation model, 921
 reduced dimension implementations, 934
 covariance filter, 934
 information filter, 936
 sequential processing, 955
 square-root filters, 958
 time-invariant steady state, 931
- Discrete-time Kalman predictors, 973
 fixed-interval, 977
 fixed-lead, 974
 fixed-point, 975

- Discrete-time Kalman smoothers, 978
 fixed-interval, 978
 fixed-lag, 979
- Discrete-time Wiener filtering, 882
 model, 882
 optimum FIR filters, 894
 finite sample Wiener equation, 895
 FIR Wiener filter, 896
 FIR Wiener filter with lag, 898
 Levinson-Durbin algorithm, 896
- random process models, 883
 autoregressive model, 885
 autoregressive moving average model, 883
 moving average model, 893
 Yule-Walker equations, 886
- realizable IIR Wiener filters, 904
 filtering with lag, 916
 optimum filter, 908
 pole-zero plot, 905
 prediction, 914
 spectrum factorization, 904
 whitening filter 904
- unrealizable IIR Wiener filters, 900
- Eigenfunctions and eigenvalues, 559**
 asymptotic property, 560
 monotonic property, 559
- Eigenvalues, 149
- Eigenvectors, 149
- Estimate(s); estimation
 asymptotic behavior, 265
 Bayes, 232
 Bayesian efficient, 264
 compressed log-likelihood function, 311
 DOA, 312
 efficient, 248
 estimation rule, 231
 Fisher information, 250
 frequency and phase, 310
 frequency, 268
 hybrid parameters, 328
 MAP, 235
 maximum likelihood, 247
 minimum absolute error, 235
 minimum mean-square error, 234
 multiple nonrandom parameters, 296, 299
 concentration ellipsoid, 299
 efficiency commutation, 303
 Fisher information matrix (FIM), 300
 functions of parameters, 303
 ML, 296
 vector CRB, 300
- multiple random parameters, 293, 299, 316
 asymptotic behavior, 319
 Bayesian efficient, 319
 Bayesian Cramér-Rao bound, 317
 Bayesian information matrix (BIM), 316
 conjugate priors, 320
 cost function, 294
 functions of parameters, 319
 linear transformations, 295
 MAP, 295
 MMSE, 295
 nuisance parameters, 325
 hybrid parameters, 328
 random parameter bounds, 327
- observation space, 231
- parameter space, 230
- probabilistic mapping, 230
- scalar nonrandom parameters, 246
 Cramér-Rao bound, 248
- scalar random parameters, 232
- sufficient statistic, 238
- summary of key results, 375
- summary of scalar parameter results, 292
- Estimation: continuous-time random processes, 771
- Estimation: discrete-time random processes, 880
- Estimation of multiple signal parameters in Gaussian noise, 716
 known signal, 717
 separable models, 718
- Estimation of signal parameters in nonwhite Gaussian noise, 648
- Estimation of signal parameters in white Gaussian noise
 linear, 614
 nonlinear, 616
 nonlinear, Cramér-Rao bound, 618
 nonlinear, discrete frequency modulation, 621
 nonlinear, range estimation, 619
- Estimation of signal parameters, 1095
- Estimation theory hierarchy, 7
- Exponential family, 279, 321, 388, 393
- Exponential twisting, 108
- Filtering theory hierarchy, 10**
- Filters: continuous-time, 771
 Gaussian assumption, 778
 conditional mean, 778
 convex cost function, 783
 MAP estimator, 784

- interval estimator, 784
minimum mean-square error, 773
MMSE realizable, 776
optimum linear, 771
uncorrelated error, 777
- Filters: realizable continuous-time,
 Gaussian-Markov process, 807
Butterworth family, 834
canonical realization No. 1, 813
canonical realization No. 2, 815
canonical realization No. 3, 816
differential equation representation, 808
filtering with delay, 842
implementation issues, 842
Kalman filter, 825
linear transformation of state vector, 842
message generation process, 819
observation process, 825
prediction, 841
random process generation, 808
realizable whitening filter, 839
state transition matrix, 821
- Filters: realizable continuous-time, stationary
 process: infinite past, 787
 closed form error expressions, 803
 delay, 796
 errors in optimum systems, 798
 irreducible error, 802
 prediction, 797
 spectrum factorization, 789
 whitening filter, 788
Wiener filter, 787
Wiener-Hopf equation, 787
zero delay, 795
- Filters: unrealizable continuous-time, stationary
 process: infinite past, 801
- Fisher information, 250, 263
Fisher information matrix, 300
Fisher linear Gaussian model, 412
Fredholm equations, 654
 first kind, 654, 656
 second kind, 655, 659
Frequency estimation, 268, 310
 Bayesian, 271, 337, 346, 347
- Gamma function, 28**
- Gaussian bandpass process, 128
Gaussian circular complex random vector, 127
Gaussian estimation: nonrandom parameters,
 401
 array processing, 404, 405
 complex exponentials, 404–407
- computational algorithms, 452
alternating projection, 457
expectation-maximization, 461
gradient techniques, 453
covariance matrix parameters, 442
Cramér-Rao bound, 409
diagonal loading, 477
Fisher linear Gaussian model, 412
 array processing, 423, 426
 complex exponentials, 421
 Cramér-Rao bound, 413
 eigenspace beamformer, 429
 low-rank model, 424
 maximum likelihood estimate, 413
 tracking, 418
least squares, 470
linear Gaussian mean and covariance matrix
 parameters, 450
maximum likelihood estimation, 407
minimum variance distortionless response
 (MVDR), 470
sensitivity and mismatch, 473
separable models, 406
separable models for mean parameters, 429
tracking, 403
- Gaussian estimation: random parameters, 483
 asymptotic behavior and ECRB, 485–486
 Bayesian linear Gaussian model, 487
 Bayesian linear Gaussian model, sequential
 estimation, 495
BCRB, 484
MAP estimate, 484
- Gaussian estimation, summary of key results,
 507
- Gaussian random variable, 24, 36
Gaussian real random vector, 126
General Gaussian detection, 125, 1086
General Gaussian estimation, 400, 1089
Global Bayesian bounds, 332
 covariance inequality bounds, 333
 Bayesian CRB, 334
 combined Bayesian bounds, 341
 Weiss-Weinstein bound, 336
- Gram-Schmidt procedure, 602
- Histograms, 99**
- Homogeneous integral equations, 540
 bandlimited spectra, 545
 Gaussian white noise (GWN), 551
 low-rank kernel, 552
 optimum linear filter, 553
 rational spectra, 540–545

- Homogeneous integral equations (*Continued*)
 - white noise process, 550
 - Wiener process, 548
- Hyperparameters
 - posterior, 243
 - prior, 243
- Importance sampling, 80, 86**
- Incomplete gamma function, 42
- Independent distribution (ID) model, 27
- Inequality
 - Cramér-Rao, 248, 261
 - Jensen's, 265
 - Schwarz, 248
 - Van Trees, 263
- Innovation sequence, 498
- Invariant test, 370
- Inverse kernel, $Q_n(t, u)$, 633
- Iterative importance sampling, 106
- Karhunen-Loève expansion, 532, 535**
 - eigenfunctions, 533
 - eigenvalues, 533
- Known signal in noise, 2, 4, 6, 7
- Lagrange multiplier, 33**
- Large deviation theory, 86
- Least squares estimation, 470
- Levinson-Durbin algorithm, 896
- Likelihood equation, 247
- Likelihood ratio test (LRT), 23, 28, 34, 50, 109
 - continuous, 48
- Likelihood ratio, 23
- Linear estimation of random processes, 1098
- Log of moment generating function, $\mu(s)$, 65, 110
- Low-rank models, 165, 184, 219
- MAP equation, 236**
- MAP estimate, 235, 295
- M hypotheses, 51, 119
 - Bayes criterion, 51, 109
 - MAP test, 55, 58
 - minimum probability of error criterion, 54
- Minimax test, 33
- Marcum's Q function, 686
- Matched filter-envelope detector, 683
- Matched subspace detector, 365
- Mathematical preliminaries, 742
 - Marcum's Q function, 743
- modified Bessel functions, 742
- Rician variables, 743
- Maximum a posteriori probability (MAP) test, 31, 109
- Maximum likelihood estimate, 247, 296
- Mean-square convergence, 532
- Mercer's Theorem, 534
- Method of Interval Estimation, 345
- Minimum distance decision rule, 60
- Minimum mean-square error estimate, 234, 295
- Minimum probability of error test, 30
- Minimum variance distortionless response (MVDR) estimate, 470
- Moment generating function, 65
- Monte Carlo simulation, 80, 123
- $\mu(s)$, general Gaussian, circular complex Gaussian vectors, 137
- $\mu(s)$, general Gaussian, real Gaussian vectors, 134
- Neyman-Pearson test, 33, 50, 109**
- Non-structured approach, 13
- Nuisance parameters, 325
- Observations, 1105**
 - Bayes vis-à-vis Fisher, 1105
 - Bayesian and Fisher bounds, 1105
 - eigenspace, 1106
 - models and mismatch, 1105
 - whitening, 1106
- Optimum diversity, 44
- Orthonormal expansions: deterministic signals, 520
 - complete orthonormal set (CON), 525
 - signal as vector, 526–527
- Parseval's theorem, 525**
- Performance bounds, 63, 121
- Pole-zero plot, 791
- Polynomial fitting, 217
- Probability density. *See also* Continuous univariate distributions
 - circular complex Gaussian random vector, 130
 - conjugate prior, 242
 - non-informative priors, 253
 - nonrandom multiple parameter exponential family, 321
 - Cramér-Rao bound, 323
 - cumulants, 322
 - maximum likelihood estimate, 322
 - real Gaussian random vector, 126

- nonrandom scalar parameter exponential family, 279
 canonical form, 280
 Cramér-Rao bound, efficiency, 285
 cumulants, 282
 Gamma, 281
 Gaussian, 280
 maximum likelihood estimate, 284
 natural parameter, 279
 Poisson, 281
 Weibull, 282
 random multiple parameter exponential family, 324
 Bayesian CRB, 325
 conjugate prior, 324
 MAP estimate, 325
 random scalar parameter exponential family, 287
 Bayesian Cramér-Rao bound, 288
 conjugate prior, 287
 Gamma, 288
 MAP estimate, 288
 Probability distribution, discrete, 1112
 Binomial, 82, 1112
 Poisson, 26, 1112
 Probability of detection, P_D , 31
 Probability of false alarm, P_F , 31
 Probability of miss, P_M , 31
 Pulse frequency modulation system (PFM), 6, 7
- Quadratic forms, 134**
 Quadrature decomposition, 128
- Random process characterization, 528**
 complete, 531
 conventional, 528
 covariance stationary, 531
 Gaussian, 536–540
 Karhunen-Loëve expansion, 532, 535
 Markov, 531
 second moment, 530
 series representation, 532
 single-time, 529
 vector, 564
 Random signal in noise, 4, 6, 7, 9, 10
 Randomized decision rule, 47, 114
 Rayleigh channel, 694
 binary communication, 702
 multiple pulses, 699
 optimum diversity, 701
- perfect measurement, 703
 piecewise constant, 694
 slow-fading, 694
 Receiver operating characteristic (ROC), 35–38, 48–51
 Recursive maximum likelihood, 504
 Representation of random processes, 519, 1093
 Reversibility, 631
 Rician channels, 704
- Sampling, 5, 15, 128**
 Sequential estimation: Bayesian linear Gaussian model, 495
 innovation sequence, 498
 tracking, 502
 Signal with unknown parameters in noise, 3, 4, 6, 7, 9, 10
 Simple binary hypothesis tests, 20, 111
 Simulation of P_F , 87
 Simulation of P_M , 91
 Simulation of ROC, 94
 Spheroidal functions
 angular prolate, 546
 radial prolate, 547
 Square-root Kalman filters, 958
 Structured approach, 11
 Sufficient statistic, 25, 64, 80
- Target models**
 generalized Swerling, 706
 Rayleigh, 694, 706
 Rician, 704, 706
 Schnidman parametric, 708
- Tests
 CFAR, 367
 composite hypothesis, 348
 GLRT, 359
 UMP, 353, 396–398
 Tikhonov regularization, 480
 Tilted density, 66, 86
 Toeplitz matrix, 158
 Tracking problem, 2-dimensional, 10
 Trigamma function, 104
- Uniform linear array, 144**
- Van Trees inequality, 263**
- Wavenumber, 145**
 Weiss-Weinstein bound, 336, 340, 345
 Wiener process, 548